Multi-hazard Loss Estimation Methodology

Hurricane Model

Hazus®–MH 2.1

Technical Manual

Developed by:
Department of Homeland Security
Federal Emergency Management Agency
Mitigation Division
Washington, D.C.

This manual is available on the FEMA website at http://www.fema.gov/plan/prevent/hazus.

To order the Hazus software visit www.msc.fema.gov and go to the Product Catalog to place your order.

Hazus® is a trademark of the Federal Emergency Management Agency.

ACKNOWLEDGMENTS

Hazus-MH, Hazus-MH MR1, Hazus-MH MR2, Hazus-MH MR3, Hazus-MH MR4, Hazus-MH MR5, and Hazus-MH 2.0

Hurricane Model Methodology Development

Wind Committee

Chairman, Joseph Minor, Consultant, Rockport, Texas
Arthur Chiu, University of Hawaii, Honolulu, Hawaii
Mark Levitan, Louisiana State University, Baton Rouge, Louisiana
Richard Marshall, Consultant, Poolesville, Maryland
Robert McComb, Texas Tech University, Lubbock, Texas
Kishor Mehta, Texas Tech University, Lubbock, Texas
Dale Perry, Texas A&M University, College Station, Texas
Mark Powell, National Oceanic and Atmospheric Administration, Miami, Florida
Douglas Smits, City of Charleston, Charleston, South Carolina
Masoud Zadeh, Consultant, San Jose, California

Coastal Surge Committee

Chairman, Kishor Mehta, Texas Tech University, Lubbock, TX
Andrew Kennedy, University of Notre Dame, South Bend, IN
Mark Crowell, Department of Homeland Security, Federal Emergency Management Agency, Washington, D.C.
Jamie Rhome, National Oceanic and Atmospheric Administration, Miami, FL
Ed Laatsch, Department of Homeland Security, Federal Emergency Management Agency, Washington, D.C.
Joseph Minor, University of Missouri-Rolla, Rockport, TX
Spencer Rogers. North Carolina Sea Grant, Wilmington, NC

Applied Research Associates, Inc., Raleigh, North Carolina

Peter Vickery, Project Manager; Lawrence Twisdale, Jr., Project Manager, Francis Lavelle, Project Manager; Jason Lin, Peter Skerlj, Michael Young, Reddy Kadasani, Chris Driscoll, Kevin Huang, Peter Montpellier, Andrew Steckley, Jeffrey Sciaudone, Yingzhao Chen, Dhiraj Wadhera, Bo Yu, Sudhan Banik, Antonio Rigato

Consultants

Impact Forecasting, Chicago; Illinois, Sethu Raman, North Carolina State University, Raleigh, North Carolina; Thomas Smith, TLSmith Consulting, Rockton, Illinois; Timothy Reinhold, Clemson University, Clemson, South Carolina; Christopher P. Jones, P.E., Durham, North Carolin; Neil Blais, Blais & Associates, Rancho San Margaria, California

Hurricane Model Software Development

Software Committee

Chairman, Dick Bilden, Consultant, Reston, Virginia
Co-Chairman, Mike Haecker, Consultant, Austin, Texas
Dan Cotter, Terrapoint, The Woodlands, Texas
Gerry Key, Computer Sciences Corporation, San Diego, California
Tracy Lenocker, Lenocker and Associates, Inc., Orange, California
Ken Lewis, KVL and Associates, Inc., Scottsdale, Arizona
Frank Opporto, DHS, EP&R Directorate (FEMA), Information Services Technology Division, Washington, D.C.
Dirk Vandervoort, POWER Engineers, Inc., Boise Idaho
Leslie Weiner-Leandro, DHS, EP&R Directorate (FEMA), Information Services Technology Division, Washington, D.C.

Applied Research Associates, Inc., Raleigh, North Carolina

Francis Lavelle, Project Manager; Chris Driscoll, Peter Vickery

Beta Test Subcommittee – Hazus-MH

Darryl Davis, Corps of Engineers Hydrologic Engineering Center, Davis, California
Neil Grigg, Colorado State University, Fort Collins, Colorado
Charles Kircher, Kircher & Associates, Palo Alto, California
Tracy Lenocker, Lenocker and Associates, Inc., Orange, California
Kenneth Lewis, KVL and Associates, Inc., Scottsdale, Arizona
Masoud Zadeh, Consultant, San Jose, California

Beta Test Communities – Hazus-MH

Division of Emergency Management, Tallahassee, Florida; Washington State Emergency Management, Camp Murray, Washington; Whatcom County Public Works, Bellingham, Washington; Johnson County, Olathe, Kansas; Mecklenburg County Stormwater Services, Charolotte, North Carolina; Louisiana State University, Baton Rouge, Louisiana; Charleson County Building Services, North Charleston, South Carolina

Beta Test Subcommittee – Hazus-MH MR1

Douglas Bausch, Department of Homeland Security, Federal Emergency Management Agency, Washington, D.C.
Richard Eisner, Governor's Office of Emergency Services, Oakland, California
John Knight, South Carolina Emergency Management Division, Columbia, South Carolina
Kevin Mickey, The Polis Center, Indianapolis, Indiana
Mark Neimeister, Delaware Geological Survey, Newark, Delaware
Lynn Seirup, New York City Office of Emergency Management, New York, New York

Beta Test Subcommittee – Hazus-MH MR2

Douglas Bausch, Department of Homeland Security, Federal Emergency Management Agency, Washington, D.C.

John Knight, South Carolina Emergency Management Division, Columbia, South Carolina
Kevin Mickey, The Polis Center, Indianapolis, Indiana
Joe Rachel, Department of Homeland Security, Federal Emergency Management Agency, Washington, D.C.
Ken Wallace, Department of Homeland Security, Federal Emergency Management Agency, Washington, D.C.
Bryan Siltanen, Advanced Systems Development, Inc., Arlington, VA

Beta Test Subcommittee – Hazus-MH MR3
Douglas Bausch, Department of Homeland Security, Federal Emergency Management Agency, Washington, D.C.
John Buechler, The Polis Center, Indianapolis, IN
Susan Cutter, Hazards and Vulnerability Research Institute, University of South Carolina, Columbia, SC
Aiju Ding, CivilTech Engineering, Inc., Cypress, TXs
Craig Eissler, Geo-Tech Visual Power Tec Texas Geographic Society, Austin, TX
Melanie Gall, Hazards and Vulnerability Research Institute, University of South Carolina, Columbia, SC
Shane Hubbard, The Polis Center, Indianapolis, IN
David Maltby, Geo-Tech Visual Power Tech/First American Flood Data Services, Austin, TX
Kevin Mickey, The Polis Center, Indianapolis, IN
David Niel, APPTIS Inc., McLean, VA
Jack Schmitz, The Polis Center, Indianapolis, IN
Bryan Siltanen, APPTIS Inc., McLean, VA
Hilary Stephens, Greenhorne & O'Mara, Inc., Laurel, MD
Eric Tate, Hazards and Vulnerability Research Institute, University of South Carolina, Columbia, SC

Beta Testing – Hazus-MH MR4
Kevin Mickey, The Polis Center, Indianapolis, IN
Jack Schmitz, The Polis Center, Indianapolis, IN
Adam Campbell, The Polis Center, Indianapolis, IN
Shane Hubbard, University of Iowa, Iowa City, IA

Beta Testing – Hazus-MH MR5
Kevin Mickey, The Polis Center, Indianapolis, IN
Jack Schmitz, The Polis Center, Indianapolis, IN
Adam Campbell, Zimmerman Associates, Inc.
Shane Hubbard, University of Iowa, Iowa City, IA

Beta Testing – Hazus-MH 2.0

Adam Campbell, Zimmerman Associates Inc., Hanover, MD
Kevin Mickey, The Polis Center, Indianapolis, IN
Jack Schmitz, The Polis Center, Indianapolis, IN
Melissa Gona, The Polis Center, Indianapolis, IN
Sonia Davidson, The Polis Center, Indianapolis, IN
Shane Hubbard, University of Iowa, Iowa City, IA

IV&V Acceptance Testing – Hazus-MH 2.0

Philip Schneider, National Institute of Building Sciences, Washington, D.C.
Vanessa Glynn-Linaris, GeoRevs LLC, Grand Canyon, AZ

Hazus Shell Development

PBS&J, Atlanta, Georgia

Mourad Bouhafs,Senior Group Manager (Hazus-MH, Hazus-MH MR3), Pushpendra Johari, Program Manager (Hazus-MH MR1), Sandeep Mehndiratta

Special thanks to ESRI for its assistance in coordinating ArcGIS with Hazus-MH.

Project Sponsorhsip and Oversight

Department of Homeland Security, FEMA, Mitigation Division, Washington, D.C.

Frederick Sharrocks, Section Chief, Assessment & Plan for Risk; Cliff Oliver, Chief, Risk Assessment Branch; Edward Laatsch, Chief, Building Science and Technology; Eric Berman, Project Officer; Claire Drury, Project Officer; Paul Tertell, Michael Mahoney, Stuart Nishenko, ScottMcAfee, Paul Bryant

FEMA Technical Monitors

Douglas Bausch, FEMA Region 8; Mark Crowell, Physical Scientist; John Ingargiola, Douglas Bellemo, Allyson Lichtenfels, Divisional Coordination

Special thanks to the National Aeronautics and Space Administration for providing financial assistance for developing tree debris estimation capability in the Hurricane Model

TABLE OF CONTENTS

CHAPTER 1. INTRODUCTION 1-1

1.1 Background 1-1

1.2 Scope 1-1

1.3 Technical Approach 1-3

1.4 Technical Manual Organization 1-5

CHAPTER 2. HURRICANE RISK MODEL 2-1

2.1 Review of Hurricane Wind Models 2-1

2.2 Hurricane Wind Field Model 2-2
2.2.1 Mean Wind Field Model 2-3
2.2.2 Surface Level Winds 2-3
2.2.3 Summary 2-25

2.3 Hurricane Simulation Methodology 2-25
2.3.1 Introduction 2-25
2.3.2 Storm Track Modeling 2-26
2.3.3 Modeling of Radius to Maximum Winds 2-27
2.3.4 Pressure Profile Parameter (*B*) 2-28
2.3.5 Filling Models 2-32
2.3.6 Track and Central Pressure Model Evaluation 2-34
2.3.7 Landfalling Hurricanes 2-34
2.3.8 Predicted Wind Speeds vs. Return Period 2-43
2.3.9 Summary 2-45

2.4 Hurricane Rainfall Rate Model 2-47
2.4.1 Introduction 2-47
2.4.2 Data and Prior Studies 2-48
2.4.3 Model Development 2-49
2.4.4 Hurricane Rainfall Rate Model Implementation and Calibration 2-53
2.4.5 Summary 2-58

CHAPTER 3. SURFACE ROUGHNESS MODELING 3-1

3.1 Introduction 3-1

3.2 Land Use Databases 3-3
3.2.1 Florida Water Management District Data 3-4
3.2.2 MRLC-NLCD Database 3-7

3.3 Surface Roughness Lengths in the Southeast Florida Area 3-12

3.4 Surface Roughness Lengths in the Florida Panhandle Area 3-16

3.5 Roughness Length Database Development for All Coastal States 3-21
3.5.1 The National Land Cover Data 3-21
3.5.2 Mapping NLCD Land Cover Codes to Roughness Lengths 3-27
3.5.3 Census Tract-Averaged Roughness Length 3-34
3.5.4 Comparisons of z_o Values Computed from NLCD Data on Rectangular Grids with Empirically Assigned z_o Values 3-36

3.6 Example of Roughness Length (z_o) Calculation Using Lettau's Formula 3-40

3.7 Effect of Surface Roughness on Near Ground Gust Wind Speeds 3-49

3.8 Surface Roughness Updates for Hazus 2.0 3-55
3.8.1 LULC Codes 21 and 22 and MRLC-NLCD Data 3-56
3.8.2 Implementation in Hazus 2.0 3-59

CHAPTER 4. WIND LOADS 4-1

4.1 Introduction 4-1

4.2 Wall Pressures-Low-Rise Buildings 4-2

4.3 Roof Pressures - Low-Rise Buildings 4-4

4.4 Wind Loads on Low-Rise Buildings - Effect of Nearby Buildings 4-16

4.5 Integrated (Overall) Wind Loads on Low-Rise Buildings 4-17

4.6 Wind Loads on High-Rise Buildings 4-28

CHAPTER 5. WINDBORNE DEBRIS 5-1

5.1 Windborne Debris - Residential Missile Model 5-1

5.2 Windborne Debris - Commercial Missile Model 5-7
5.2.1 Windborne Gravel Debris Simulation and Case Studies 5-8
5.2.2 Probability of Damage to Building Envelopes by Windborne Gravel Debris 5-25

CHAPTER 6. PHYSICAL DAMAGE MODELING 6-1

6.1 General Approach 6-1

6.2 Resistance Models for Residential Buildings 6-3
6.2.1 Roof Sheathing in Wood Frame Construction 6-3
6.2.2 Air Permeable Roof Cover Systems 6-4
6.2.3 Windows and Sliding Glass Doors 6-5
6.2.4 Roof-Wall Connections 6-6
6.2.5 Masonry Walls 6-7
6.2.6 Wood Frame Walls 6-16

6.3 Damage Model Validation for Residential Buildings 6-32
6.3.1 Roof Cover and Roof Deck Damage 6-32
6.3.1.1 Hurricane Andrew (1992) 6-32
6.3.1.2 Hurricane Erin (1995) 6-42
6.3.1.3 Hurricane Fran (1996) 6-43
6.3.2 Window Damage 6-44
6.3.3 Whole Roof Failures 6-44

6.4 Damage Model Results for Residential Buildings 6-46
6.4.1 Effect of Mitigation on Residential Building Damage 6-59

6.5 Manufactured Homes 6-62
6.5.1 Resistance Models for Manufactured Homes 6-64
6.5.2 Damage Model Validation for Manufactured Homes 6-67
6.5.3 Damage Model Results for Manufactured Homes 6-72

6.6 Roof Covers on Flat Roofs 6-73
6.6.1 Resistance Model for Roof Covers on Flat Roofs 6-74
6.6.2 Damage Model Validation for Roof Covers on Flat Roofs 6-76

6.7 Open-Web Steel Joist Roof System 6-78
6.7.1 Resistance Model for Open-Web Steel Joists 6-80
6.7.2 Resistance Model for Metal Deck on Open-Web Steel Joists 6-83

6.8 Pre-Engineered Metal Buildings 6-95
6.8.1 Resistance Model for Metal Building Wall System 6-96
6.8.2 Resistance Model for Metal Building Roof System 6-101
6.9 Damage Model Results for Marginally- or Non-Engineered Hotel/Motel and Multi-Family Residential Buildings 6-102
6.10 Damage Model Results for Low-Rise Masonry Strip Mall Buildings 6-105
6.11 Damage Model Results for Pre-Engineered Metal Buildings 6-126
6.12 Damage Model Results for Engineered Residential and Commercial Buildings 6-130
6.13 Damage Model Results for Industrial Buildings 6-135
6.14 Damage Model Results for Essential Facilities 6-140
6.14.1 Damage Model Results for Fire Stations 6-143
6.14.2 Damage Model Results for Elementary Schools 6-145
6.14.3 Damage Model Results for High School 6-148
6.14.4 Damage Model Results for Hospitals 6-152

CHAPTER 7. DIRECT ECONOMIC LOSSES 7-1

7.1 Introduction 7-1
7.2 Residential Input Parameters 7-1
7.3 Residential Subassembly Costs 7-3
7.3.1 Default Residence 7-3
7.3.2 Subassembly Cost Ratios 7-4
7.4 Explicit Costing of Residental Losses 7-5
7.5 Modeling of Residential Interior and Content Losses and Loss of Use 7-7
7.5.1 Economic Damage to the Building Interior 7-7
7.5.2 Economic Damage to Contents 7-9
7.5.3 Loss of Use for Residential Buildings 7-11
7.6 Residential Loss Model Validation Examples 7-11
7.7 Loss Model Results for Residential Buildings 7-14
7.8 Manufactured Home Loss Model 7-19
7.8.1 Manufactured Home Loss Model Costing 7-19
7.8.2 Fast Running Manufactured Home Loss Functions 7-36
7.9 Economic Loss Model for Commercial Buildings 7-36
7.9.1 Subassembly Cost Ratios 7-37
7.9.2 Building Loss Model 7-39
7.9.3 Content Loss Model 7-43
7.9.4 Business Interruption Model 7-44
7.9.5 Loss of Function for Essential Facilities 7-46
7.10 Loss Model Results for Marginally-Engineered or Non-Engineered Hotel/Motel and Multi-Family Residential Buildings 7-50
7.11 Loss Model Results for Low-Rise Masonry Strip Mall Buildings 7-50
7.12 Loss Model Results for Pre-Engineered Metal Buildings 7-83
7.13 Loss Model Results for Engineered Residential and Commercial Buildings 7-83
7.14 Loss Model Results for Industrial Buildings 7-99
7.15 Loss Model Results for Essential Facilities 7-102
7.15.1 Loss Model Results for Fire Stations 7-108

7.15.2 Loss Model Results for Elemtary Schools 7-111
7.15.3 Loss Model Results for High Schools 7-114
7.15.4 Loss Model Results for Hospitals 7-119

CHAPTER 8. BUILDING STOCK CLASSIFICATION METHODS 8-1

8.1 Introduction 8-1

8.2 Aerial Photography Samples 8-1

8.3 Contractor Survey 8-4

CHAPTER 9. LOSS MODEL VALIDATION STUDIES FOR HURRICANES ANDREW, ERIN, OPAL AND HUGO 9-1

9.1 Introduction 9-1

9.2 Example Results - Hurricane Andrew 9-1

9.3 Example Results - Hurricanes Erin and Opal 9-10

9.4 Example Results - Hurricane Hugo 9-15

9.5 Summary 9-23

CHAPTER 10. DEBRIS GENERATED FROM DAMAGED BUILDINGS 10-1

10.1 Introduction 10-1

10.2 Description of Methodology 10-2

10.3 Validation Studies 10-8

10.4 Final Remarks 10-15

CHAPTER 11. SHORT TERM SHELTER REQUIREMENTS 11-1

11.1 Introduction 11-1

11.2 Description of Methodology 11-1

11.3 Simplified Methodology. 11-4

CHAPTER 12. TREE BLOWDOWN 12-1

12.1 Introduction and Background 12-1

12.2 Related Research 12-2

12.3 Wind Throw Model 12-2
12.3.1 Wind Load Response and Breakage Model 12-2
12.3.2 Wind Modeling for Simple Terrains 12-7
12.3.3 Example Tree Response - Ponderosa Pine 12-10
12.3.4 Wind Modeling in Forested Areas 12-13
12.3.4.1 Canopy Modeling 12-14
12.3.4.2 Effective Windspeeds in Forested Areas 12-16
12.3.5 Simulation Methodology 12-19

12.3 Simulation Methodology 12-20

12.4 Blowdown Results 12-20
12.4.1 Treee Blowdown Curves 12-20
12.4.2 Tree Blowdown Validation 12-20

12.5 Tree Inventory Data by County 12-24
12.5.1 Forest Inventory Analysis (FIA) Program and Database 12-24

12.5.2 Average Tree Density and Tree Height Distribution at County Level 12-25

12.6 Hazus Tree Coverage Database 12-26
12.6.1 MRLC National Land Cover Data 12-26
12.6.2 Tree Density, Tree Height, and Predominant Tree Type by Census Tract 12-26

12.7 Debris Generated from Tree Blowdown 12-28
12.7.1 Total Weight and Volume of Downed Trees 12-29
12.7.2 Tree Debris Collection Models 12-31
12.7.2.1 Tree Debris Collection Model Description 12-31
12.7.2.2 Implementing into Hazus-MH 12-35
12.7.2.3 Other Considerations for Hazus 2.0 12-37
12.7.3 Comparison of Modeled and Reported Tree Debris 12-38
12.7.3.1 Example Tree Collection Data – Hurricane Isabel, North Carolina 12-38
12.7.3.2 Example Tree Collection Data – Hurricane Isabel, Virginia 12-39
12.7.3.3 Comparison to Other Collection Data 12-43

12.8 Tree Blowdown Damage to Buildings 12-44
12.8.1 Overview 12-44
12.8.2 Tree Drop Tests 12-45
12.8.3 Relationship between Damage Severity and Impact Energy 12-45

12.9 Estimation of Direct Economic Loss from Physical Damage States 12-48

12.10 Mean Loss as a Function of Wind Speed 12-54
12.10.1 Losses Due to Tree Blow-Down 12-54
12.10.2 Loss Function for a Specific Building Type in Given Census Tract 12-55
12.10.3 Combining Tree Blowdown Normalized Loss Functions with the Basic Fast-Running Building and Contents Loss Functions 12-55

CHAPTER 13. COASTAL STORM SURGE 13-1

13.1 Introduction 13-1

13.2 Coastal Storm Surge and Wave Hazard Models 13-1
13.2.1 Wind Speed, Wind Direction, and Atmospheric Pressure Validation 13-2
13.2.2 Storm Tide Implementation and Validation 13-3
13.2.3 Wave Model Implementation and Validation 13-8
13.2.4 Coupling of SLOSH and SWAN 13-34
13.2.5 Coastal Surge Analysis for Study Regions Spanning Multiple SLOSH Basins 13-37
12.2.6 Integration with Coastal Flood Model 12-40

13.3 Combined Wind and Flood Losses for Coastal Storm Surge 12-43
13.3.1 Building Sub-Assembly Approach 13-45
13.3.2 Development of Sub-Assembly Loss Tables 13-48
13.3.3 Wave Model Implementation and Validation 13-8

13.4 Coastal Storm Surge References 13-58

CHAPTER 14. REFERENCES 14-1

APPENDIX A. Damage State Functions for Residential Buildings A-1

APPENDIX B. Damage State Functions for Manufactured Homes B-1

APPENDIX C. Damage State Functions for Marginally- or Non-Engineered Hotel/Motel and Multi-Family Residential Buildings C-1

APPENDIX D. Damage State Functions for Low Rise Masonry Strip Mall Buildings D-1

APPENDIX E. Damage State Functions for Pre-Engineered Metal Buildings E-1

APPENDIX F. Damage State Functions for Engineered Residential and Commercial Buildings F-1

APPENDIX G. Damage State Functions for Industrial Buildings G-1

APPENDIX H. Loss Functions for Residential Buildings H-1

APPENDIX I. Loss Functions for Manufactured Homes I-1

APPENDIX J. Loss Functions for Marginally- or Non-Engineered Hotel/Motel and Multi-Family Residential Buildings J-1

APPENDIX K. Loss Functions for Pre-Engineered Metal Buildings L-1

APPENDIX M. Loss Functions for Engineered Residential and Commercial Buildings M-1

APPENDIX N. Loss Functions for Industrial Buildings N-1

APPENDIX O. Comparisons of Modeled and Measured Wind Speeds, Wind Directions, and Pressures for Hurricane Isabel (2003) O-1

APPENDIX P. Comparisons of Modeled and Measured Wind Speeds, Wind Directions, and Pressures for Hurricane Ivan (2004) P-1

APPENDIX Q. Comparisons of Modeled and Measured Wind Speeds, Wind Directions, and Pressures for Hurricane Katrina (2005) Q-1

APPENDIX R. Comparisons of Modeled and Measured Wind Speeds, Wind Directions, and Pressures for Hurricane Gustav (2008) R-1

APPENDIX S. Comparisons of Modeled and Measured Wind Speeds, Wind Directions, and Pressures for Hurricane Ike (2008) S-1

APPENDIX T. Comparison of Observed and Modeled Storm Tides for Hurricane Andrew (1992) T-1

APPENDIX U. Comparison of Observed and Modeled Storm Tides for Hurricane Isabel (2003) U-1

APPENDIX V. Comparison of Observed and SLOSH Model Computed Storm Tides for Hurricane Ivan (2004) V-1

APPENDIX W. Comparison of Observed and SLOSH Model Computed Storm Tides for Hurricane Katrina (2005) W-1

APPENDIX X. Comparison of Observed and SLOSH Model Computed Storm Tides for Hurricane Gustav (2008) X-1

APPENDIX Y. Comparison of Observed and SLOSH Model Computed Storm Tides for Hurricane Ike (2008) Along the Coast of Texas Y-1

APPENDIX Z. Wind Sub-Assembly Loss Tables Z-1

APPENDIX AA. Flood Sub-Assembly Loss Tables AA-1

MESSAGE TO USERS

The Hazus Hurricane Model is designed to produce loss estimates for use by federal, state, regional and local governments in planning for hurricane risk mitigation, emergency preparedness, response and recovery. The methodology deals with important aspects of the built environment, and a wide range of different types of losses. Extensive national databases are embedded within Hazus, containing information such as demographic aspects of the population in a study region, square footage for different occupancies of buildings, and numbers and locations of bridges. Embedded parameters have been included as needed. Using this information, users can carry out general loss estimates for a region. The Hazus methodology and software are flexible enough so that locally developed inventories and other data that more accurately reflect the local environment can be substituted, resulting in increased accuracy.

Uncertainties are inherent in any loss estimation methodology. They arise in part from incomplete scientific knowledge concerning hurricanes and their effects upon buildings and facilities. They also result from the approximations and simplifications that are necessary for comprehensive analyses. Incomplete or inaccurate inventories of the built environment, demographics and economic parameters add to the uncertainty. Where inventories, demographics and economic parameters track closely those assumed and built into the basic methodology, estimates of loss should be within a factor of two. Where one or more of these parameters are incomplete or inaccurate the range of uncertainty may exceed a factor of two or more.

The hurricane loss estimation methodology is based on sound scientific and engineering principals and experimental and experience data. The methodology has been tested against the judgment of experts and, to the extent possible, against records from several past hurricanes. However, limited and incomplete data about actual hurricane damage precludes complete calibration of the methodology. Nevertheless, when used with embedded inventories and parameters, the Hazus Hurricane Model has provided a credible estimate of such aggregated losses as the total cost of damage.

Users should be aware of the following specific limitations:

- While the Hazus Hurricane Model can be used to estimate losses for an individual building, the results must be considered as average for a group of similar buildings. It is frequently noted that nominally similar buildings have experienced vastly different damage and losses during a hurricane.

- The Hurricane model contains definitions and assumptions regarding building strengths that represent a norm for construction in hurricane zones. These norms are defined in the technical manual. Where construction quality is known to be different from the defined norms, larger uncertainties in loss projections may be realized.

Hazus should still be regarded as a work in progress. Additional damage and loss data from actual hurricanes and further experience in using the software will contribute to

improvements in future releases. To assist us in further improving Hazus, users are invited to submit comments on methodological and software issues by letter, fax or e-mail to:

David Adler
Zimmerman Associates, Inc.
7390 Coca Cola Drive
Hanover, MD 21076
Tel: 410-712-7401
Fax: 800-358-9620
E-Mail: david.adler@riskmapcds.com

Eric Berman
Department of Homeland Security
Federal Emergency Management Agency
Mitigation Division
500 C Street, S.W.
Washington, DC 20472
Tel: 202-646-3427
Fax: 202-646-2787
E-Mail: Eric.Berman@dhs.gov

Chapter 1. Introduction

1.1 Background

In 1997, the National Institute of Building Sciences (NIBS), under a cooperative agreement with the Federal Emergency Management Agency (FEMA), released the first Hazus Earthquake Model, a national, standardized GIS-based tool for estimating potential losses from earthquake. Earthquake loss estimates calculated with Hazus are used by local, state, and regional officials for planning and stimulating mitigation efforts to reduce losses from earthquakes, and preparing for emergency response and recovery following earthquakes. Hazus has also been used to perform a nationwide assessment of earthquake risk (FEMA, 2001).

Hazus has now been expanded to perform similar loss evaluations for wind and flood. FEMA and NIBS initiated development of the wind and flood models in 1997 with the creation of two committees to oversee technical development of the models. The resulting Hazus software is an integrated, multi-hazard loss estimation program, packaged to run within a ArcView®, a full-featured GIS platform.

The Hazus Hurricane Model allows practitioners to estimate the economic and social losses from hurricane winds. The information provided by the model will assist state and local officials in evaluating, planning for, and mitigating the effects of hurricane winds. The Hurricane Model provides practitioners and policy makers with a tool to help reduce wind damage, reduce disaster payments, and make wise use of the nation's emergency management resources.

The Hurricane Model is the first component of a planned Hazus Wind Model. When fully implemented, the Wind Model will address the wind hazard and effects associated with hurricanes, tornadoes, thunderstorms, extratropical storms and hail. The need for Hazus to treat the different meteorological phenomena is indicated in Figure 1.1, where it is seen that different regions of the United States are affected by different types of wind storms. In many regions of the country, damaging winds are produced by more than one meteorological phenomenon.

1.2 Scope

The geographic scope of the Hazus Hurricane Model is limited to the Atlantic and Gulf coasts of the United States and Hawaii. The capabilities of the model are summarized in Table 1.1. The Hurricane Model includes a default terrain roughness based on digitized Land Use and Land Cover (LULC) data, but it does not model topographic speedups. Damage, direct economic losses, and building debris are modeled for the General Building Stock (i.e., residential, commercial, industrial, agricultural, educational, and government building occupancies). Short-term shelter requirements for displaced households and loss of function for essential facilities are also included in the model.

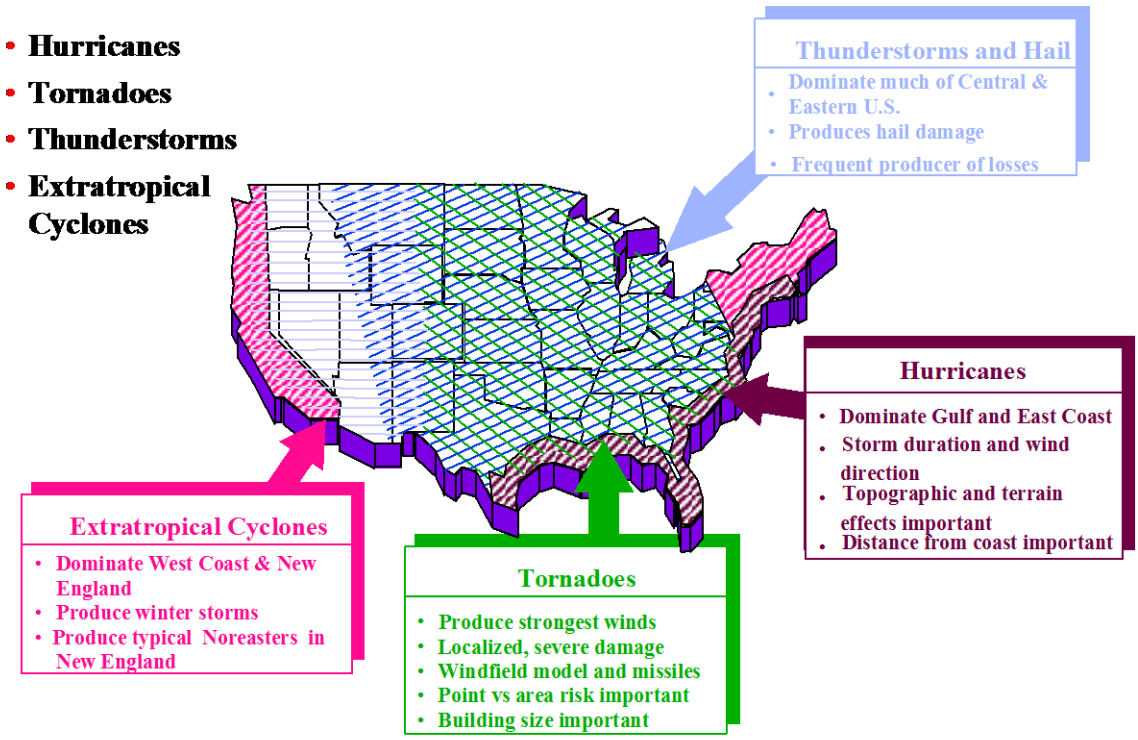

Figure 1.1. Meteorological Events Contributing to the Wind Hazard in Different Regions of the Continental United States.

Table 1.1. Summary of Hurricane Model Capabilities

Parameter/Data	Level 1 (Default Data)	Level 2 (User-Supplied Data)	Level 3 (Advanced Data)
Wind Model	Default Probabilistic	User-Defined Scenario	
Coastal Surge Model	Default Historic	User-Defined Scenario	
Building Inventory	Default	User-Supplied	
Facilities and Building Classes	Residential Commercial Industrial Essential Facilities		
Utility, Transportation, and High Potential Loss Facilities	Display/Edit Locations Only – No Damage or Loss Estimates		
Terrain	Default		Expert-Supplied
Loss Functions	Default		
Damage Functions	Default		
Shelter Requirements	Default	User-Supplied Parameters	
Debris	Default	User-Supplied Tree Coverage Parameters	

1.3 Technical Approach

The approach and framework of the Hazus Wind Model are outlined in Figure 1.2, with the elements of the present Hurricane Model indicated in bold type. The approach is based on a hazard-load-resistance-damage-loss methodology developed from an individual risk framework. The basic model components (hazard model, load model, resistance models, etc.) are developed separately. Each model component is, wherever possible, separately validated using full scale data, model scale data, or experimental data. A major factor driving the use of a first principles based hazard-load-resistance-loss model, rather than the simple wind speed dependent loss models traditionally used, is the ability for the approach to be extended to model the effects of code changes and mitigation strategies on reduction in damage and loss. Furthermore, since economic damage (loss) is modeled separately from physical damage to a building, estimates of both building damage and loss are separately modeled and predicted.

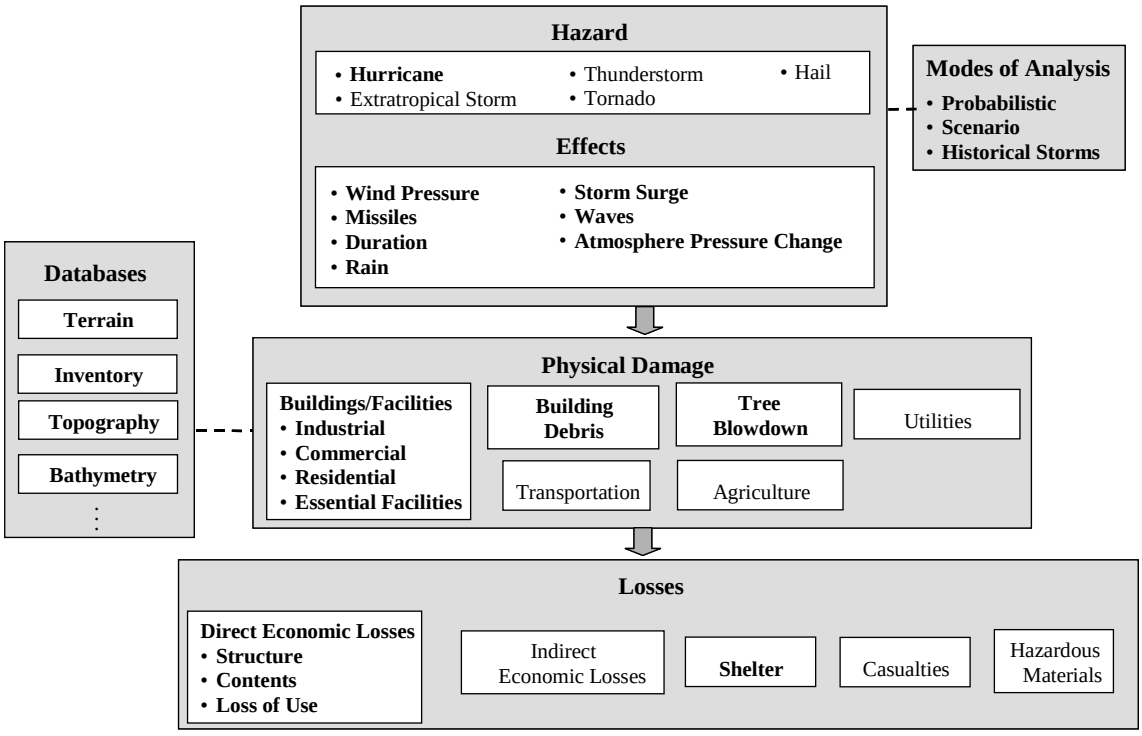

Figure 1.2. Hazus Wind Model Framework – Elements Shown in Bold are Implemented in the Current Version of the Hurricane Model.

The performance of a building class under wind loading events is formulated probabilistically using simple concepts of structural reliability. For a single failure mode,

the failure or damage probability is the probability that the wind load effect (e.g., aerodynamic pressure or impact energy) is greater than the resistance of the element. Because of uncertainties in the prediction of loads and structural response, the load effect S (e.g., the uplift pressure on a piece of roof sheathing) and structural resistance R (e.g., the pull-out resistance of the roof sheathing fasteners per unit area) are uncertain. These uncertainties are represented by probability density functions $f_S(s)$ and $f_R(r)$, respectively. The probability of damage, P_d, is simply

$$P_d = P(R - S < 0) \tag{1.1}$$

which can be expressed as

$$P_d = \int_{-\infty}^{\infty} F_R(x)\, f_S(x)\, dx \tag{1.2}$$

where $F_R(x)$ is the cumulative distribution function (e.g., the probability of sheathing failure given an uplift pressure $\geq x$). By performing simulations on representative buildings within a building class, the damage probabilities for building components are estimated and the relationships between physical damage and wind hazard are developed. Similarly, losses are estimated using repair and restoration models for physical damage states.

This approach logically leads to a simple concept of probabilistic analysis for estimating building/facility damage and loss. From Equation 1.1, the basic performance equation for reliability-based analysis is used to estimate damage probabilities for each individual building component. The probability of the building class damage states are conceptually estimated using the multivariate extension of Equation 1.1, generally expressed as a limit or damage state function, g, in terms of the basic variables, $\underline{X}$, such that

$$M = g(\underline{X}) = g(X_1, X_2, \ldots X_m). \tag{1.3}$$

Damage or failure is defined as $M < 0$; hence, $M = 0$ is the failure surface. The basic variables, $X_1, X_2, \ldots X_m$, are the load effect and resistance variables required to model all of the failure modes of interest, such as: roof sheathing uplift failures, window impact failures, wall failures, whole roof failures, etc. There are many methods to estimate P_d, including advanced first order second moment methods and Monte Carlo simulation. Simulation methods are used herein in detailed analyses to develop the damage state and loss estimation probability distributions. These results are used with simple probabilistic (numerical and analytical) methods in the Hazus software tool to compute the damage and loss estimates.

For purposes of calibration and validation of the damage and loss predictions using simplified load and resistance models, it is conceptually useful to generalize Equation 1.1 to include a factor ϕ on the nominal resistance. With this extension, damage occurs when

$$\phi R < S \ . \tag{1.4}$$

In Equation 1.4, ϕ is a factor that is developed as part of the research to calibrate predicted damage to observed damage in actual wind events. While in Load and Resistance Factor Design (LRFD) ϕ is partial safety factor on resistance (generally less than one), ϕ takes on a more general calibration interpretation for the purpose of accurate damage and loss estimation. The introduction of ϕ does not imply that all the building class damage states and loss estimates will require a calibration adjustment with non-unity ϕ. It is introduced to recognize that given the use of code-based loads and nominal resistances, along with other simplifications and approximations, a simple factored approach to calibration may be useful for certain damage or loss predictions. No factor is applied to the load side of the equation since the objective of the Hazus wind model is to predict damage and loss using standardized methods and not to attempt to develop load-factor adjustments to code-based loads.

These concepts are implemented in the model development phase to produce the fast-running damage and loss functions required in Hazus software tool. The non-technical user of Hazus is not required to understand the technical issues of the probabilistic analysis and model development. Rather, the important issues to the users center on the accuracy of the model predictions, as applied to damage and loss estimates across broad classes of buildings.

1.4 Technical Manual Organization

This manual contains 14 chapters and 27 appendices. Chapters 2-5 describe the hurricane hazard and effects models. Chapter 6 presents the methodology and results of the physical damage model for the general building stock, and Appendices A-G provide damage state functions for each of the analyzed model buildings. Chapter 7 parallels Chapter 6 by presenting the methodology and results for the direct economic loss model, and Appendices H-N provide loss functions for each of the analyzed model buildings. In Chapter 8, methods are discussed for characterizing the frequencies of various wind-resistive features in the general building stock. End-to-end validations of the Hurricane Model are presented in Chapter 9 for Hurricanes Andrew, Erin, Opal, and Hugo. Chapter 10 and 11 present the methodologies for the building debris and short-term shelter requirements models, respectively. Chapter 12 describes the tree blowdown model, which is used to estimate tree debris as well as additional building and content losses in residential areas due to tree impacts. Chapter 13 and Appendices O-AA describe the coastal storm surge methodology. The references are listed in Chapter 14.

Chapter 2. Hurricane Risk Model

2.1 Review of Hurricane Wind Models

The use of mathematical simulation methods to estimate hurricane wind speeds was first implemented by Russell (1968, 1971) for the Texas coast. Others have used this approach for portions of the United States coastline (Russell and Schueller, 1974; Tryggvason, et al., 1976; Batts, et al., 1980; Georgiou, et al., 1983; Twisdale and Dunn, 1983; Georgiou, 1985; and Vickery and Twisdale, 1995a, 1995b). The study of Batts, et al. (1980) was a milestone, being the first study to examine the entire United States Coastline, and it provided a rational means to determine design wind speeds associated with the Gulf and Atlantic coasts of the United States. At the time the Batts study was being carried out, there was relatively little good quality, full-scale data available with which to evaluate the physical models used in the simulation.

The basic approach in all these studies is the same in that site specific statistics of key hurricane parameters including central pressure difference (Δp), radius to maximum winds (R_{max}), heading (θ), translation speed (c), and the coast crossing position or distance of closest approach (d_{min}) are first obtained. Given that the statistical distributions of these key hurricane parameters are known, a Monte Carlo approach is used to sample from each distribution, and a mathematical representation of a hurricane is passed along the straight line path satisfying the sampled data, while the simulated wind speeds are recorded. The intensity of the hurricane is held constant until landfall is achieved, after which time the hurricane is decayed using filling rate models. As indicated in Vickery and Twisdale (1995b), the approaches used in the previously noted studies are similar, with the major differences being associated with the physical models used, including the filling rate models and wind field models. Other differences include the size of the region over which the hurricane climatology can be considered uniform (i.e., the extent of the area surrounding the site of interest for which the statistical distributions are derived), and the use of a coast segment crossing approach (e.g., Russell, 1971; and Batts, et al., 1980), or a circular subregion approach (e.g., Georgiou, et al., 1983; Georgiou, 1985; Neumann, 1991; Vickery and Twisdale, 1995b).

For insurance loss prediction applications, the book by Friedman (1987) discusses hurricane and loss modeling issues, and how model results can be used by the insurance industry. Other hurricane models that have been described in the literature for the purposes of loss estimation include Clarke (1986), Boissonnade and Dong (1993), and Daneshvaran and Morden (1998). The modeling approach used by Clarke considers only landfalling storms, and the wind field model is not described. In none of these papers are predictions of wind speed vs. return period given along the Gulf and Atlantic coastlines which would allow the reader to assess how the models perform against peer review and published engineering models (such as Georgiou, 1983; Batts, et al., 1980; etc.).

Under funding by the NSF, with additional support provided by the National Association of Homebuilders, as well as Applied Research Associates, Inc., an advanced hurricane

model was developed by Applied Research Associates during the period 1995-1997. This model has been reviewed by the ASCE-7 Committee in 1998 and published as two journal papers (Vickery, et al., 2000a, 2000b). Predicted hurricane wind speeds resulting from this new model are the basis of the national standard for wind load design provisions as defined in ASCE 7-98, ASCE 7-02 and ASCE 7-05.

In this model, a new simulation approach is developed where the full track of a hurricane or tropical storm is modeled, beginning with its initiation over the ocean and ending with its final dissipation. Using this approach, the central pressure is modeled as a function of sea surface temperature, and the storm heading, speed, etc., are updated at each six-hour point in the storm history. Linear interpolation is used between the six-hour points. The approach is validated by comparing the site-specific statistics of the key hurricane parameters of the simulated hurricane tracks with the statistics derived from the historical data. This model includes a numerical wind field model (Vickery, et al., 2000b) which incorporates a full nonlinear solution to the equations of motion. For use in Hazus-MH, the model described in Vickery, et al, (2000a, 2000b) has been updated to include all historical storms occurring between 1886 through 2005.The new model included improved modeling of storm weakening after landfall, an improved statistical representation of the Holland B parameter, and an updated windfield model.

2.2 Hurricane Wind Field Model

A critical component in the simulation of hurricanes is a good representation of the hurricane wind field given information regarding the storm intensity, size and translation speed. The hurricane wind field model contains two components. The first component is the overall mean flow field describing the upper level winds, and the second is the boundary layer model used to estimate wind speeds at the surface of the earth, given the upper level wind speeds.

The mean flow field model (Vickery, et al., 2000b) solves the full nonlinear equations of motion of a translating hurricane and then parameterizes these for use in fast running simulations. The use of a full numerical solution to the equations of motion for a hurricane allows the modeling of asymmetries in the storm that arise from the complex interaction of the frictional forces and the winds which vary throughout the storm. They can produce very high wind speeds wrapping around the eyewall in some small and intense storms. The use of simple empirical models to define the hurricane will not reproduce these effects.

The new hurricane boundary layer model (Vickery et al., 2008) is developed using a combination of velocity profiles computed using dropsonde data and a linear theoretical hurricane boundary layer model developed by Kepert (2001). The final hurricane boundary layer model incorporates a combined logarithmic-quadratic variation of the mean wind speed with height used to replicate the height of the low level jet observed in the hurricane boundary layer. This allows for a more realistic representation of the wind speeds near the surface, and for better estimates of the effect of the sea-land interface in reducing wind speeds near the coast.

Numerous comparisons between modeled and observed hurricane wind speed records have been performed. These include both comparisons of the mean wind speeds and the peak gust wind speeds. The resulting wind field model is the most physically based and validated model currently in use for estimating hurricane wind speed exceedance probabilities.

2.2.1 Mean Wind Field Model

The wind field model is based on a dynamic numerical model of the planetary boundary layer (PBL). The model considers the equation of horizontal motion, vertically averaged over the height of the PBL. A finite difference scheme is used to solve for the steady-state wind field over a set of nested rectangular grids. These wind fields are then fit using a Fourier fitting approach so that each wind field can be described using a relatively small number of parameters. The equations are solved for 1560 combinations of central pressure, translation speed and radius to maximum winds for hurricanes both over land and over water. Parameterizing the solved wind field models retains the more accurate modeling associated with the numerical modeling of the hurricane while still enabling rapid computational storm.

A similar approach for modeling hurricane wind fields resulting from a numerical solution to the equations of motion for a translating hurricane was first used by Georgiou (1985) and then by Vickery and Twisdale (1995a). In both of these studies the numerical model results were obtained from Shapiro's (1983) model, where the solutions to the equations of motion were themselves solved using a spectral approach employing the first two terms of the expansion. The approach used here has an advantage over the use of the Shapiro model, in that the full non-linear equations are solved, and then the results are fit to a Fourier series using more than two terms, hence maintaining a more precise solution to the equations of motion.

2.2.2 Surface Level Winds

In all hurricane simulation procedures published to date, the hurricane boundary layer has been defined using empirical relationships between the upper level winds and the surface (10 m) level winds. The ratio of the surface level winds to the upper level winds within these empirical models is very high (0.8-0.9) compared to typical values in extra-tropical storms (ratio of about 0.6 in open country terrain). The new hurricane wind field model (Vickery, et al., 2008) described here uses a more theoretically based model of the hurricane boundary layer and is developed using a combination of velocity profiles computed using dropsonde data and a linear theoretical hurricane boundary layer model developed by Kepert (2001). The final hurricane boundary layer model incorporates a combined logarithmic-quadratic variation of the mean wind speed with height used to replicate the height of the low level jet observed in the hurricane boundary layer. The empirical hurricane boundary layer model reproduced the shape of the hurricane boundary layer over the lower 1000 m. The analysis of the profiles from dropsonde data reproduce the observations noted in Powell, et al. (2003) that the sea drag coefficient reaches a maximum value. The results also suggest that the magnitude of this maximum value decreases with decreasing storm RMW.

2.2.2.1 Hurricane Boundary Layer Model

Dropsondes are dropped from reconnaissance aircraft generally from heights between 1.5-3 km. Dropsondes fall vertically downwards at a speed of about 10 m/sec measuring wind speed, temperature, humidity etc at every 0.5 sec. Dropsondes hit the sea surface after several minutes from the time of drop, drifting 10-15 km tangentially and hundreds of meters radially (Powell, et. al.. 2003). Further dropsonde details are given in Hock and Franklin (1999), and Franklin, et al. (2003). The dropsonde dataset used here was obtained from the Atlantic Oceanographic and Meteorological Laboratories -Hurricane Research Division (AOML-HRD) and consists of all profiles collected during the 1997-2003 hurricane seasons. Most of these profiles are from Atlantic and Gulf of Mexico hurricanes with a few coming from Pacific Ocean hurricanes. The dropsonde data has been previously subjected to a quality control criterion by AOML-HRD to remove any identifiable errors. All measurements have been smoothed by AOML-HRD using a 5-sec low pass filter to remove noise due to switching of the satellites.

In the analysis of the dropsonde data, the drops were separated into those associated with profiles measured at or near the radius to maximum winds (RMW) and those associated with drops away from the RMW. The assignment of a particular profile to either the RMW region or the outer vortex region was determined using comments of the flight meteorologist, an examination of concurrent flight level radial wind profiles (if available), airborne radar reflectivity imagery, and H*Wind (Powell, et al. 1996,1998) objective wind field analyses. Following the approach of Powell, et al. (2003), the wind profiles were analyzed in a composite sense, as a function of the mean boundary layer (MBL) wind speed, defined as the mean wind speed averaged over a height range of 10 m to 500 m. The six different MBL groups correspond to mean MBL wind speeds of 20 – 29 m/sec, 30 – 39 m/sec, 40 – 49 m/sec, 50 – 59 m/sec, 60 – 69 m/sec and 70-85 m/sec. Each group was divided vertically into height bins chosen to provide maximum resolution close to the sea surface. The mean wind speeds vs. height were computed by taking the average of all wind speed measurements within height bins of 10 m for heights less than 300 m, 20 m bins for heights ranging between 300 and 500 m, 50 m bins for heights between 500 m and 1000 m, and 100 m bins for heights greater than 1000 m. The single height value assigned to each bin is the mean value computed within height bin.

Figure 2.1 shows the mean velocity profiles near the RMW for each of the six MBL wind speed groups. Qualitatively, Figure 2.1 indicates that in the lower few hundred meters of the boundary layer, the mean velocity profile is approximately logarithmic, and the height at which the maximum wind speed occurs decreases with increasing wind speed, ranging from a maximum height of about 700 m for the 20 – 29 m/sec MBL case, to a minimum of about 400 m for the 60 – 69 m/sec MBL case. The lowering of the height at which the maximum wind speed occurs is consistent with the analysis described in Kepert (2001) and Kepert and Wang (2001), where the existence of a lower level “jet” is discussed. The jet strength is defined as the ratio of the maximum wind speed divided by the gradient balance wind speed. Kepert considers the jet height to be equivalent to the boundary layer height, and that concept is carried through here. Kepert (2001) demonstrates that both the magnitude and height of the jet are a function of the inertial stability, *I*, defined as:

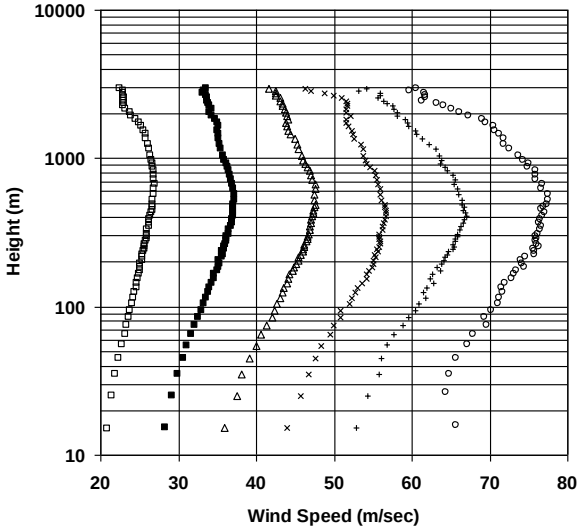

Figure 2.1. Mean Wind Profiles (20-29 m/sec, 30-39 m/sec, 40-49 m/sec, 50-59 m/sec, 60-69 m/sec, 70-85 m/sec).

$$I = \sqrt{(f + \frac{2V}{r})(f + \frac{V}{r} + \frac{\partial V}{\partial r})} \tag{2.1}$$

where, V is the azimuthally averaged tangential gradient wind speed (as computed from the surface pressure field), f is the Coriolis parameter and r is the radial distance from the center of the storm. As indicated in Equation 2.1 the inertial stability factor is a function of both wind speed and radius, and thus to take into account the effect of radius, the dropsonde data were further divided into bins having similar values of r. Two sets of radii groups were developed. The first group corresponding to drops performed at or near the radius to maximum winds, and the second group corresponding to drops performed outside of the *RMW*.

For a neutrally stable boundary layer, the increase in the mean wind speed with height near the surface is given by:

$$U(z) = \frac{u_*}{k} \ln(\frac{z}{z_o}) \tag{2.2}$$

where k is the von-Karman coefficient having a value of 0.4, u_* is the friction velocity, and, z_0 is the surface roughness.

The friction velocity is related to the surface shear stress (τ) as:

$$\tau = \rho u_*^2 \ = \rho C_d U_{10}{}^2 \tag{2.3}$$

where C_d is the surface drag coefficient and U_{10} is the mean wind speed (representative of the wind speed averaged over a period of 30 minutes to an hour) at a height of 10 m.

For each combination of *r* and MBL, an estimate of the surface roughness and sea surface drag coefficient was obtained using a least squares fit (in linear-logarithmic space) of the measured wind speeds over height ranges of 20 to 200 m, 20 to 150 m and 20 to100 m (Figure 2.2). The velocity profiles given in Figure 2.2 show a trend for the height of the mean wind speed maxima to decrease as both the *RMW* decreases and the wind speed increases, consistent with the analysis of Kepert (2001). Using the intercepts from the least squares fits, estimates of the effective surface roughness, z_0, and the associated uncertainty, were obtained for each profile. Given a value of z_0, the surface drag coefficient is computed using Equations 2.2 and 2.3.

Figure 2.3 presents the resulting C_d vs. U_{10} data for the three height ranges. Results are given for the MBL data separated by *RMW* bins, and for the case with no separation by *RMW* (as in Powell, et al., 2003). The 95% confidence bounds shown in Figure 2.3 represent a lower bound because the error in the intercept does not include any errors associated with the estimates of the dropsonde height, *z*, nor the errors in the estimates of the measured wind speed at each height. As seen in Figure 2.3, on average, the drag coefficient increases with increasing wind speed up to wind speeds of about 24-28 m/sec and then starts to level off or perhaps even decrease for higher wind speeds, consistent with the results of Powell, et al. (2003). The data suggest that the magnitude of the maximum value of C_d decreases with decreasing RMW. Also shown in Figure 2.3 is the Large and Pond (1981) drag coefficient model, modified to have a maximum value that varies with the RMW. The maximum (cap) values range from 0.0019 for the smallest storms up to 0.0024 for the largest storms.

The approach taken for examining the characteristics of the hurricane boundary layer near the *RMW* was repeated for dropsonde profiles measured outside the *RMW*. The radius groups chosen were determined based on the number of profiles associated within each MBL group. Figure 2.4 shows the resulting mean velocity profiles along with the logarithmic fits to the wind data, fit using the wind speed data for a surface layer of 20 - 200 m range. As indicated in Figure 2.4, there is a trend for the height of the wind maxima to increase as the radius increases and decrease with increase in wind speed, again, consistent with the analysis described by Kepert (2001). Figure 2.5 shows a comparison of the estimated values of C_d and the error bounds corresponding to 95% confidence interval plotted vs. U_{10}. As seen in Figure 2.5, on average, the drag coefficient increases with increasing wind speed up to about 30 m/sec and then levels off, but the apparent decrease in C_d seen in the case of the near *RMW* observations is not evident here. To incorporate the effect of radius on the limiting value of C_d, the limiting value of C_d is modeled as a function of radius, *r* in the form:

$$C_{d_{\max}} = (0.0881r + 17.66)10^{-3}; \quad 0.0019 \le C_{d_{\max}} \le 0.0025 \tag{2.4}$$

where *r* is the radial distance from the storm center (km), but is constrained to have a minimum value equal to the *RMW*.

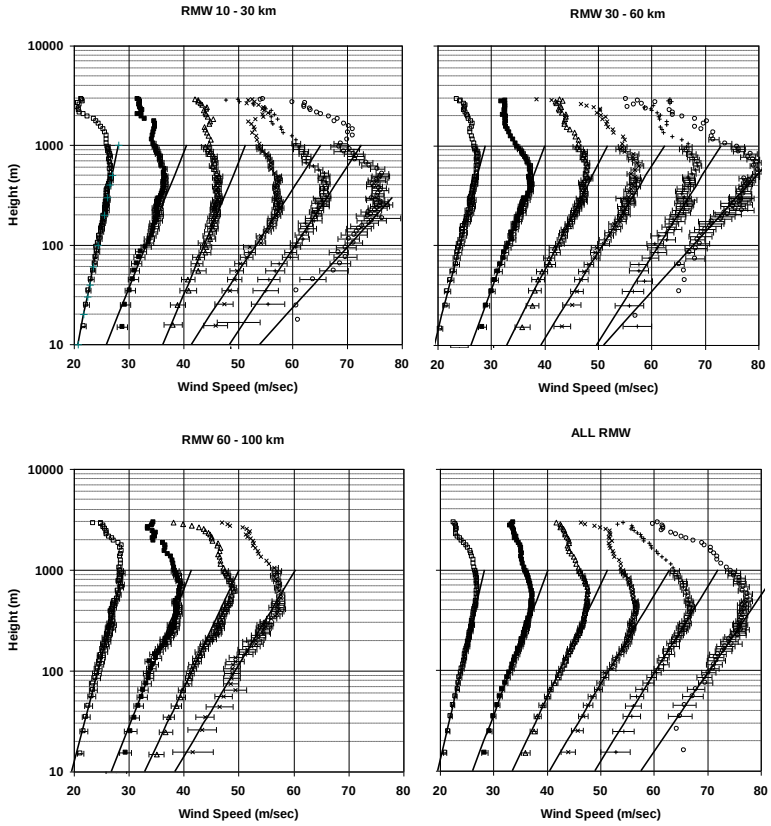

Figure 2.2. Mean and Fitted Logarithmic Profiles for Drops Near the *RMW* for all MBL Cases. Horizontal error bars represent the 95th percentile error on the estimate of the mean wind speed. LSF fits are for the 20 – 200 m case. (MBL cases correspond to 20-29 m/sec, 30-39 m/sec, 40-49 m/sec, 50-59 m/sec, 60-69 m/sec, and 70-85 m/sec).

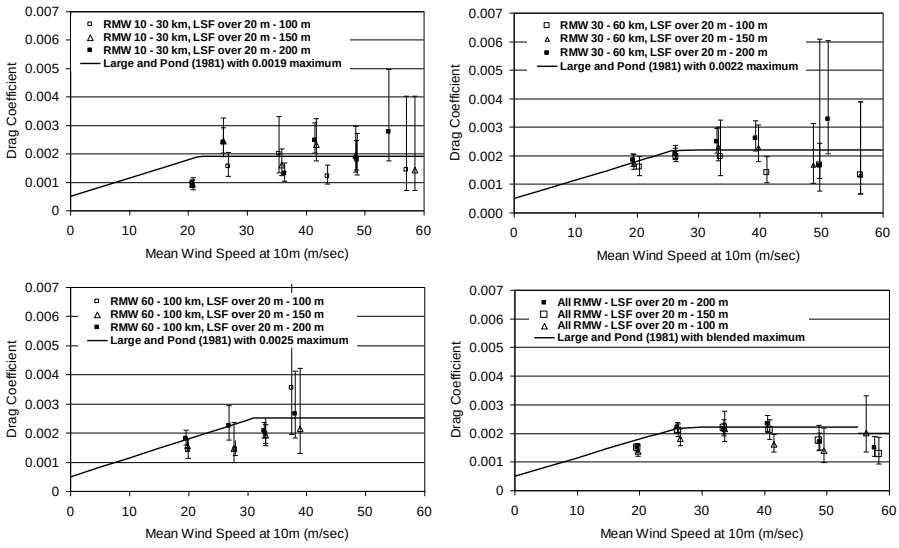

Figure 2.3. Variation of the Sea Surface Drag Coefficient with Mean Wind Speed at 10 m, Near the *RMW*.

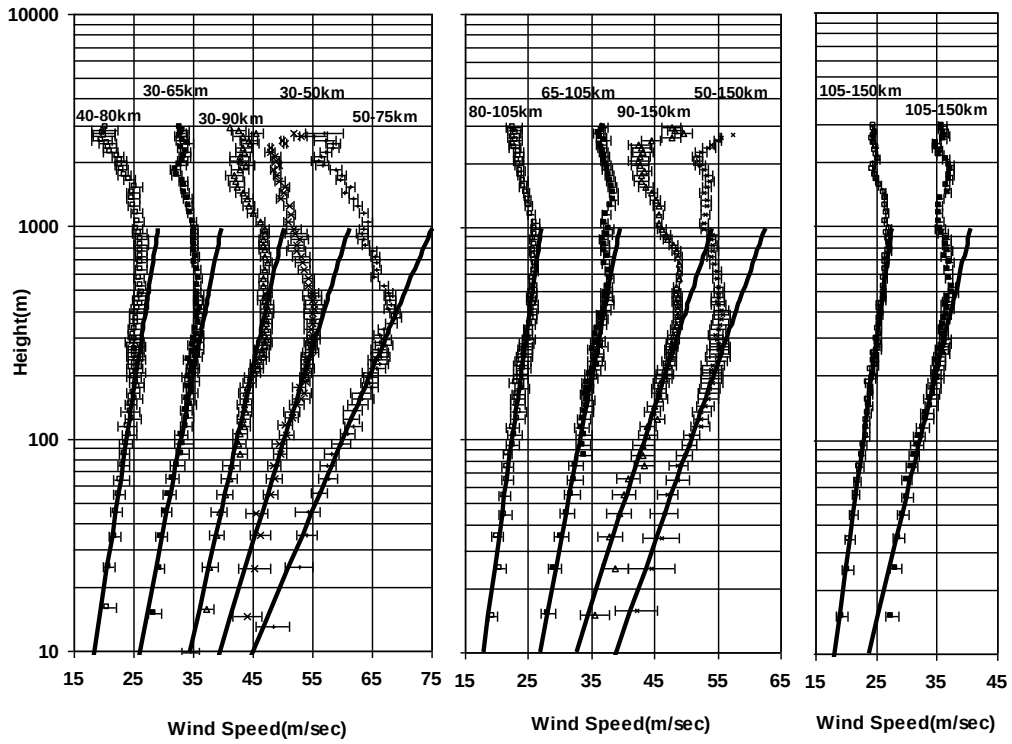

Figure 2.4. Mean Wind Profiles and Fitted Logarithmic Profiles for Outside *RMW* Case. The radius range used to compute the mean velocity profile is noted in the figure. MBL cases correspond to 20-29 m/sec, 30-39 m/sec, 40-49 m/sec, 50-59 m/sec, and 60-69 m/sec).

A possible explanation for this reduction in C_d as a function of radius is given in Makin (2005) where it is suggested that a limiting value of C_d is caused by the production of sea spray inhibiting the transfer of momentum from the wind to the sea surface. Makin suggests that most of the sea spray is produced by the mechanical tearing by the wind from steep short waves, and thus for storms with small *RMW* (and hence small wind fetches) more of the waves will be short as compared to the large RMW case.

2.2.2.1.1 Empirical Model for the Marine Hurricane Boundary Layer

In the lower few hundred meters, the atmospheric boundary layer of the hurricane is adequately modeled using the logarithmic law, however; the profiles shown in Figures 2.2 and 2.4 clearly indicate that in some cases such a model can be used well beyond heights of about 300 m, in most of the high wind speed cases, the logarithmic law breaks down, and the wind speeds begin to decrease with increasing height. The height at which the logarithmic law fails to describe the variation of the mean wind speed with height is strongly correlated with the height at which the mean wind speed reaches a maximum value (i.e., jet or boundary layer height). With this observation noted, the hurricane boundary layer was modeled in the form:

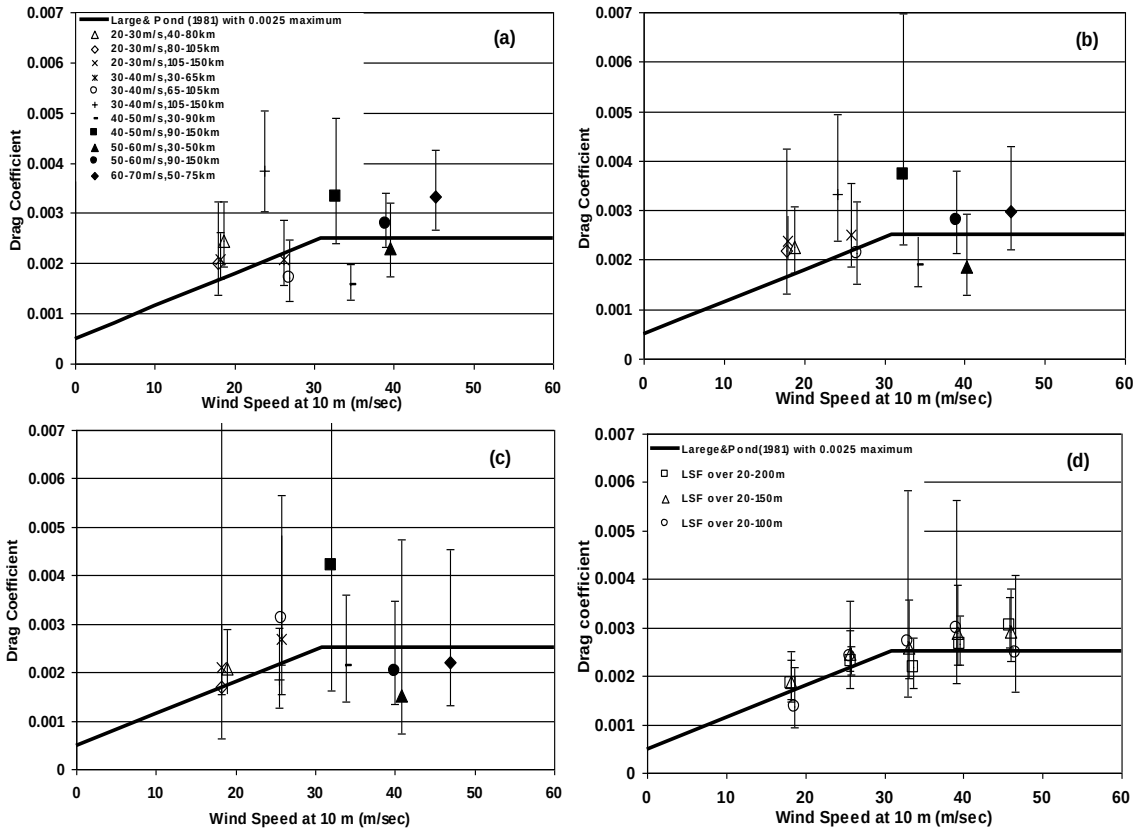

Figure 2.5. Variation of the Sea Surface Drag Coefficient with Mean Wind Speed at 10 m, Outside *RMW* case.(a) Least square fit for a height range of 20 m – 200 m (b) Least square fit for a height range of 20 m – 150 m (c) Least square fit for a height range of 20 m - 100 m (d) No separation by radius.

$$U(z) = \frac{u_*}{k}\left[\ln(\frac{z}{z_o}) - a(\frac{z}{H^*})^n\right] \tag{2.5}$$

Each of the parameters, a and n were treated as free parameters but were required to be constant for all values of r, and H^* is a boundary layer height parameter. The boundary layer or jet height was allowed to vary with each profile. To determine the appropriate parameters for use in Equation 2.5, two approaches were taken, namely:

Method 1: The values of u_* and z_0 were computed from the regression analysis and the values of u_*, a, n and H^* were selected to minimize the error over the height range of 20 m to 1000 m

Method 2: The values of z_0 were computed using the capped Large and Pond drag coefficient model and the values of u_*, a, n and H^* were selected to minimize the error over the height range of 20 m to 1000 m.

Figure 2.6 presents the observed and modeled mean velocity profiles near the *RMW* for the 10 km to 30 km and 30 to 60 km *RMW* cases. In all cases, the best values *a* and *n* were 0.4 and 2.0 respectively. By setting the derivative of Equation 2.5 with respect to *z* equal to zero it is seen that the boundary layer or jet height, *H* is equal to $1.12H^*$.

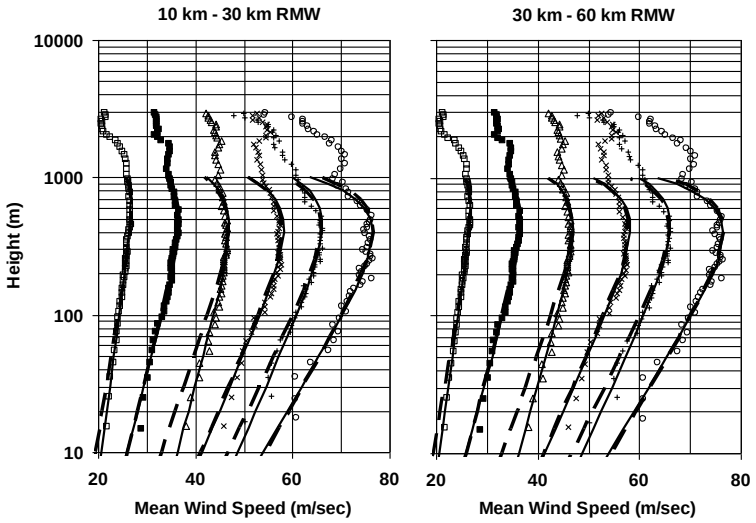

Figure 2.6. Observed and Modeled Velocity Profiles for the 10 km to 30 km and 30 km – 60 km *RMW* Cases. Solid lines represent model data derived using least squares fit values of surface roughness and friction velocity using LSF over 20 - 200 m range. Dashed lines represent model results using C_d derived from truncated Large and Pond (1981) drag coefficient model.

2.2.2.1.2 Hurricane Boundary Layer Height

According to Kepert (2001), the jet height or boundary layer height is inversely proportional to the square root of the inertial stability parameter as given by:

$$H = \sqrt{\frac{2K}{I}} \tan^{-1}\left(-1-\frac{2}{\chi}\right) \tag{2.6a}$$

$$\chi = C_d V \sqrt{\frac{2}{KI}} \tag{2.6b}$$

where *K* is the turbulent diffusivity of momentum, *I* is inertial stability, and C_d is the surface drag coefficient.

Here, the boundary layer height is also modeled as a function of *I*, where in the calculation of *I*, an average value of the radius within a radius bin is used to define *r*, and the maximum wind speed from mean velocity profile is used as a surrogate for the gradient velocity, *V*. Using the estimates of the boundary layer height, H^* for *r* both near and outside the *RMW*, a regression models for relating H^* and *I* are given by:

$$H^* = 343.7 + 0.260 / I \qquad r^2 = 0.75, \quad \sigma_e = 99m \qquad (2.7a)$$

$$H^* = 186.6 + 12.66 / \sqrt{I} \qquad r^2 = 0.70, \quad \sigma_H = 106m \qquad (2.7b)$$

The regression model for H^*, modeled as a function of $1/I$ explains 75% of the variance associated with the underlying data, whereas when H^* is modeled as a function of $1/\sqrt{I}$ the model explains 70% of the variance. The boundary layer height model is in general agreement with Kepert's (2001) analysis, where the boundary layer height scaling parameter was shown to be inversely proportional to the square root of the inertial stability. Based on the observed values of H^*, the model is capped using a lower bound of 300 m and an upper bound of 1200 m. Figure 2.7 shows a comparison of the H^* derived from the regression models, H derived using Equation 2.6 with K=75 m^2/sec (Kepert, 2001) and the observed values of H^*.

2.2.2.1.3 Marine Boundary Layer Model Verification

Using Equations 2.3 and 2.5 to define the variation of the mean wind speed with height, coupled with Equation 2.7a to define the boundary layer height, the characteristics of the boundary layer were estimated given only U_{max} and r. In the verification process, the value of U_{max} is set equal to the maximum mean wind speed obtained by the dropsondes over the range of 20 to 1000 m, and r is equal to the mean value of r used to determine the *RMW* or r bin. Figure 2.8 presents examples of the modeled and measured boundary layers for the 10 to 30 km and 30 to 60 km *RMW* cases. Figure 2.9 shows the mean error plotted vs. height (with the errors computed over ranges of heights) where it is seen that in most cases the error is less than 5%, however; there is a weak trend evident where the underestimate of wind speeds near the surface increases as *RMW* decreases. The modeled and observed wind speeds were grouped into height bins of 10 - 50 m, 50 - 100 m, 100 – 200 m, 200 - 300 m, 300 - 400 m, 400 - 500 m, 500 - 700 m and 700 - 1000 m.

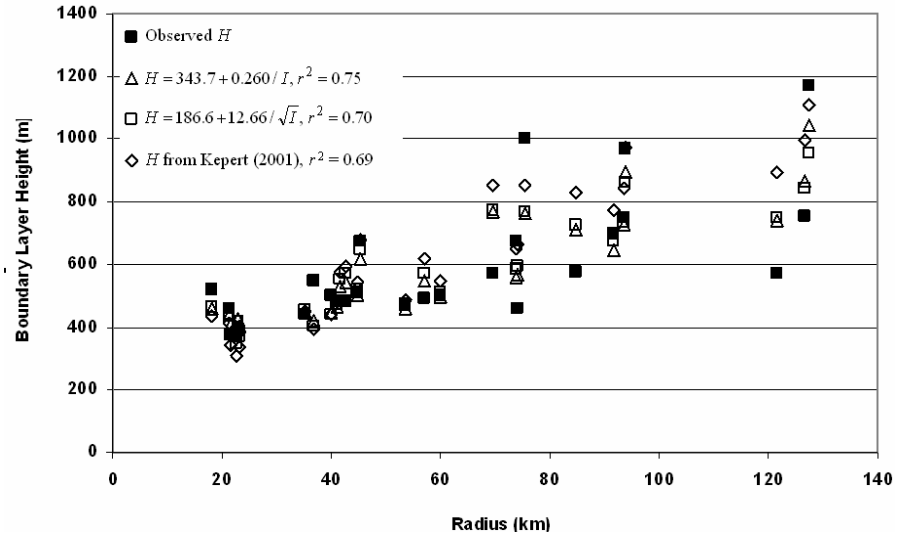

Figure 2.7. Comparison of Regression Model, Kepert (2001) Model and Observed Boundary Layer Heights.

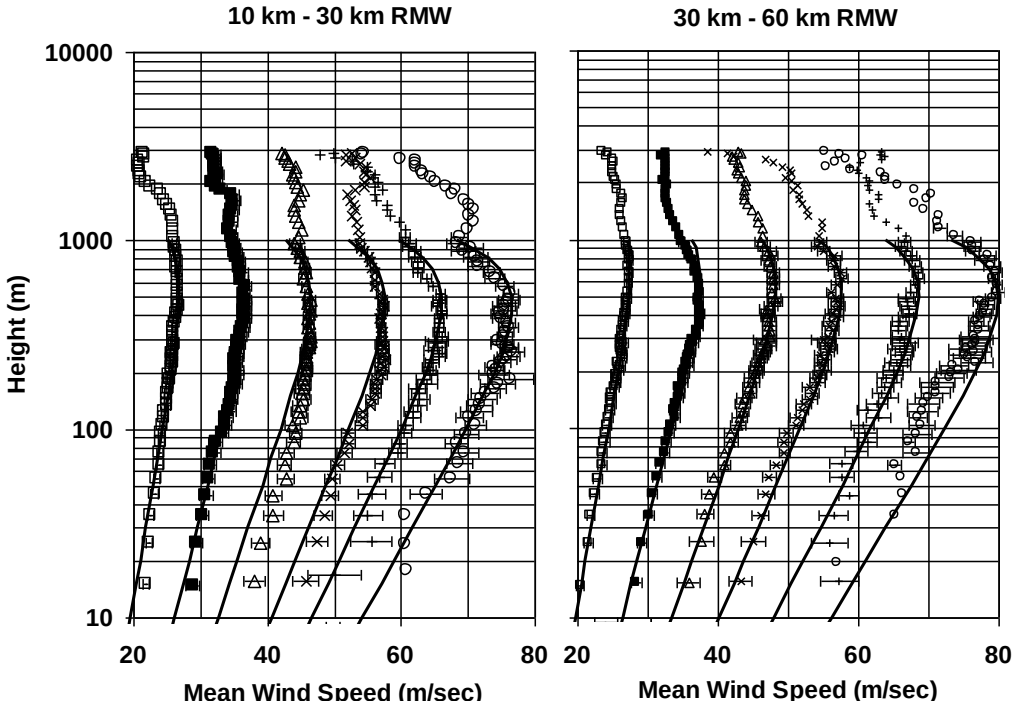

Figure 2.8 Observed and Modeled Velocity Profiles Near the *RMW* for the 10 km to 30 km and 30 km to 60 km *RMW* Cases. Solid lines represent model wind speeds computed given U_{max}, *RMW* and *f*.

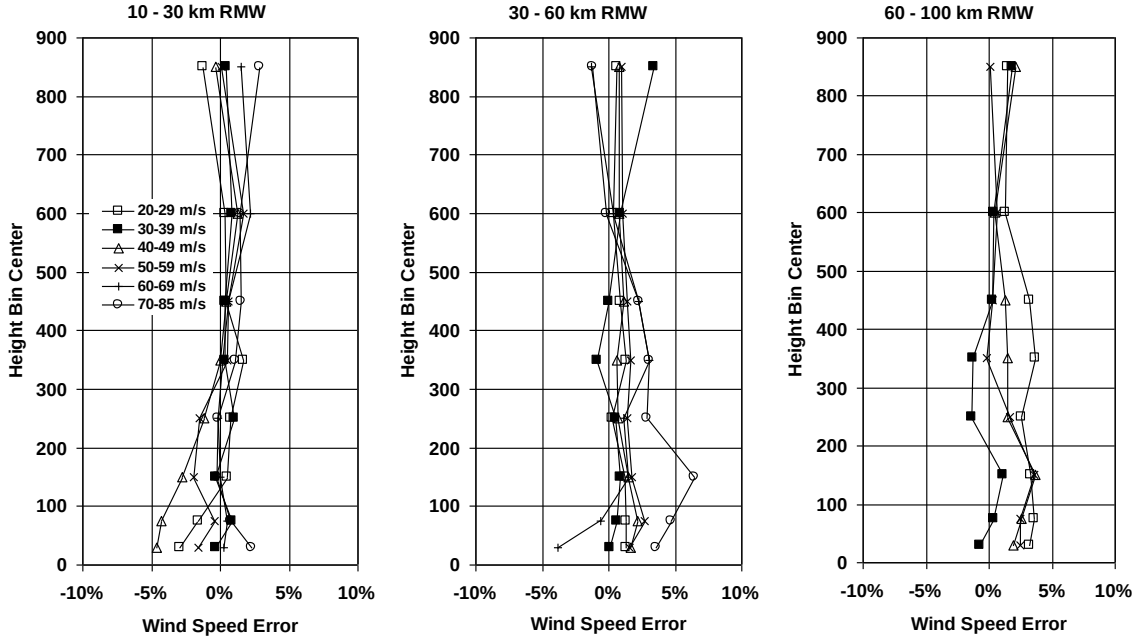

Figure 2.9. Mean Error in Modeled Wind Speeds vs. Height for Dropsonde Data Taken Near *RMW*.

Figure 2.10 presents a comparison of the modeled and observed ratios of U_{10}/U_{max} plotted vs. U_{max} for dropsonde data collected around the *RMW*. Observed values of U_{10}/U_{max} are obtained by extending the log-law velocity profiles to the 10 m level using the LSF results over the three different height ranges discussed earlier. The mean value of U_{10}/U_{max} obtained from the model is 0.716. The mean values of U_{10}/U_{max} computed from the data using a LSF over height ranges of 20-200 m, 20-150 m and 20-100 m are 0.703, 0.713 and 0.719, respectively. The corresponding r^2 values are 0.32, 0.57 and 0.65, respectively. The mean modeled value of $U_{10}/\overline{U}_{500}$, where $\overline{U}_{500}$ is the wind speed averaged over the lower 500 m of the boundary layer is 0.755, which is slightly lower than the value of 0.78 reported in Powell, et al., (2003).

Figure 2.11 presents the variation of the mean error with height for the outside *RMW* cases. It is seen that in all the cases the mean error is less than 5%. Outside of the *RMW*, the mean ratios of U_{10}/U_{max} for the observed and the modeled wind speeds are 0.698 and 0.686 respectively, implying a mean underestimate of the surface level wind speeds of about 2%. The empirical hurricane boundary layer model described here is shown to be able to reasonably well reproduce the shape of the marine hurricane boundary layer given only a wind speed at gradient or jet height, and a distance, *r*, from the center of the storm. The height of the jet is adequately described using a simple model where the jet height is inversely proportional to either, I or $\sqrt{I}$. Due to the limitation of the number of available mean velocity profiles, there was insufficient data to further separate the profiles by azimuth in addition to MBL and *r* bins, and as a result, any variation in the jet height as a function of azimuth (as is indicated by Kepert (2001) does in fact exist) is lost in the hurricane boundary layer model presented here. However, the magnitude of the jet strength and its variation with azimuth is modeled using the slab model representation of the hurricane wind field, as described later.

2.2.2.1.4 Sea Land Transition

The characteristics of the hurricane boundary layer described previously are representative of open water (marine) conditions and not for the over land case. Over land there is virtually no dropsonde data to determine the characteristics of the over land hurricane boundary layer. The approach taken here to model the sea-land transition follows the classical approach (e.g., Deaves, 1981; Kao, et al., 1974) where the wind speed at the top of the boundary layer is assumed to remain unchanged as the flow moves over a new roughness regime. The shape of the mean boundary layer over land is assumed to be adequately represented by Equation 2.5, and the methodology outlined in Kepert (2001) is used to estimate the increase in the boundary layer height associated with a change in surface roughness. The increase in the boundary layer height, H is modeled using Equation 2.6, which requires an estimate of the increase in K as a function of the increase in C_d. For estimating the increase in the value of K as the wind moves from sea to land (open terrain), K is taken as:

$$K \approx C_d U^2 / \frac{\partial U}{\partial z} = u_*^2 / \frac{\partial U}{\partial z} \approx kzu_* \qquad (2.8)$$

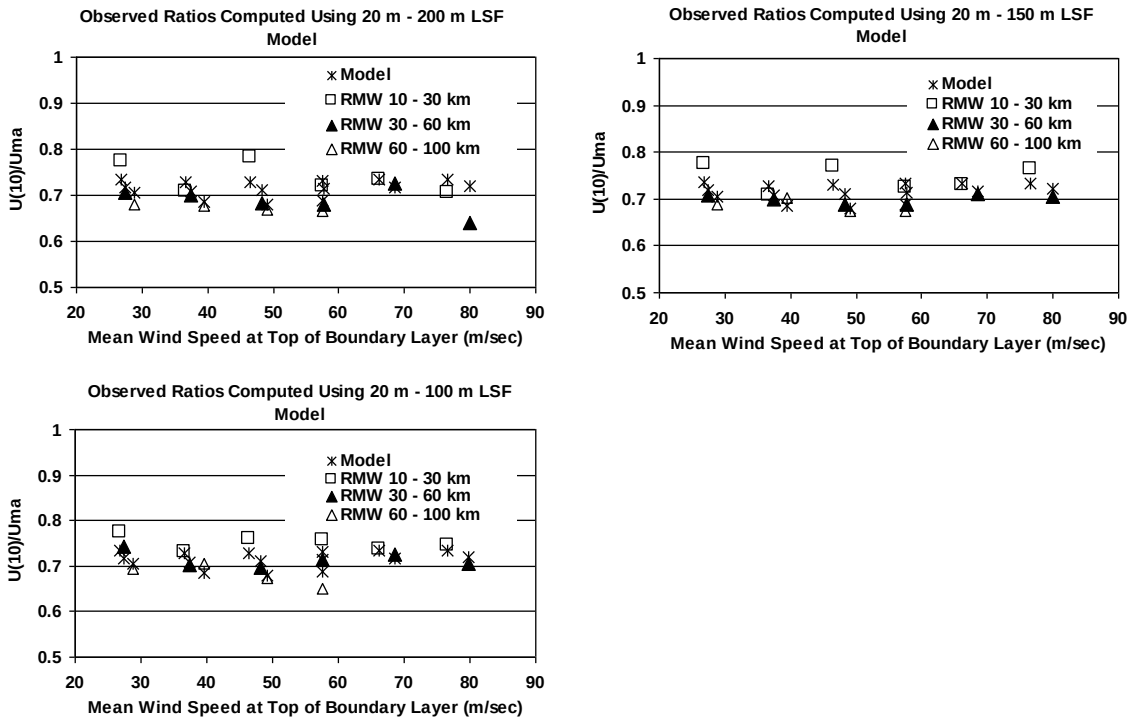

Figure 2.10. Comparison of Modeled and Observed Ratios of Mean Wind Speed at 10 m to Mean Wind Speeds at the Top of the Boundary Layer Near the *RMW*.

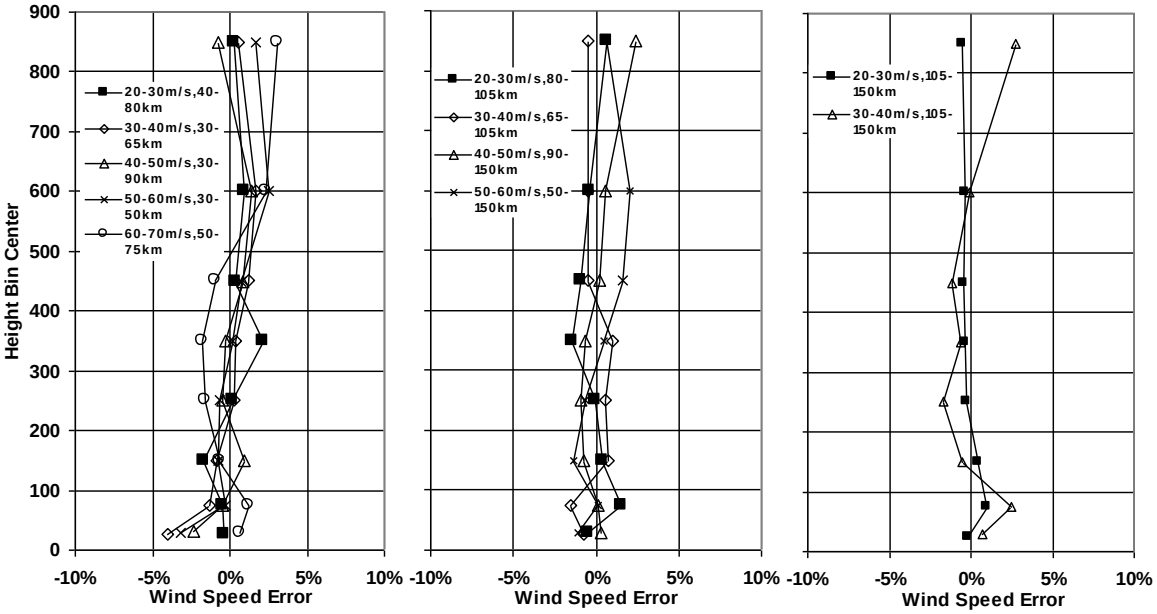

Figure 2.11. Mean Error in Modeled Wind Speeds vs. Height for Dropsonde Data Taken Outside *RMW* Region.

Equations 2.6 and 2.8 are used to estimate the increase in *H*, yielding typical estimates of the increase in *H* ranging between 20% and 30% for land defined with z_0=0.03 m, with the magnitude of the increase varying with both wind speed and radius. The value of *H* computed using Equations 2.6 and 2.8 is dependent on the value of *z* used in Equation 2.8, but the ratio of the two boundary layer heights is, for practical purposes, independent of the value of *z* used in Equation 2.8.

Figure 2.12 presents the ratio of the mean wind speed over land (z_o=0.03 m) to the mean wind speed over water (z_o=0.0013 m) as a function of the marine boundary layer height. Also shown in Figure 2.12 is the wind speed ratio computed using the ESDU (1982) transition model. Figure 2.12 shows that the reduction of the mean wind speed as the wind moves from the sea to the land associated with a hurricane is less than that estimated using the ESDU model, and that the wind speed reduction factor is dependent on *H*, and hence storm intensity and size. The wind speed reduction factors given in Figure 2.12 are larger than to those predicted by ESDU for large *H*, but match the model given in Simiu and Scanlan (1996) for large *H*. In model implementation, the increase in the boundary layer height predicted using Equations 2.6 and 2.8 is further increased so that the resulting reduction in the wind speed associated with the sea land transition matches that given in ESDU (1982) for large *H*. Using this approach, for typical values of *H* (~600 m) near the *RMW*, the predicted reduction in the mean wind speed matched that given by the model given in Simiu and Scanlan (1996). The wind speed reduction factors shown in Figure 2.12 are representative of a fully transitioned boundary layer.

As the wind moves from the sea to the land, the value of the maximum wind speed at a given height in the new rougher terrain approaches the fully transitioned value asymptotically over some fetch distance, *F*. Published estimates of the fetch length vary markedly, ranging from a few kilometers (e.g. Melbourne, 1992) to in excess of 100 km (ESDU, 1982, Deaves, 1981). Powell, et al., (1996) suggest that wind measurements at a height of 10 m taken as far as 20 km to 30 km inland are still influenced by the upstream marine roughness. For modeling the transition from sea to land, the ESDU model is used, but the limiting fetch distance is reduced to 20 km rather than the ~100 km used in ESDU (1982). The use of the smaller fetch distance is consistent with the lower boundary layer heights associated with tropical cyclones (~600 m) compared to much larger values (~3000 m) used in ESDU where *H* scales as u_*/f rather than $\sqrt{2K/I}$.

The ESDU transition model was chosen since it provides a means to transition the wind speeds associated with an arbitrary averaging time (i.e. hourly, 10 minute mean, peak gust, etc.). Figure 2.13 shows a comparison of the original and modified ESDU transition functions for the gust and hourly mean wind speeds. In either model it is evident that at a distance of about 1 km approximately 60% of the transition (or wind speed reduction) has already occurred. An exact value of *F* is considered to be difficult, if not impossible to verify, and an inspection of Figure 2.13 indicates that the error in the predicted wind speed is not particularly sensitive to the value of *F* (for *F*>10 km). For example, the difference between the model estimates of the degree to which the wind speed has reached equilibrium at 10 km, (approximately where the difference between the ESDU,

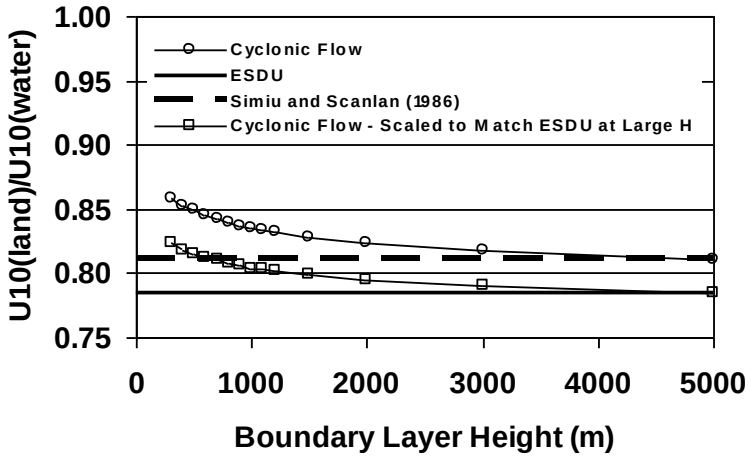

Figure 2.12. Ratio of the Fully Transitioned Mean Wind Speed Over Land (z_o=0.03m) to the Mean Wind Speed Over Water (z_o=0.0013m) as a Function of Boundary Layer Height.

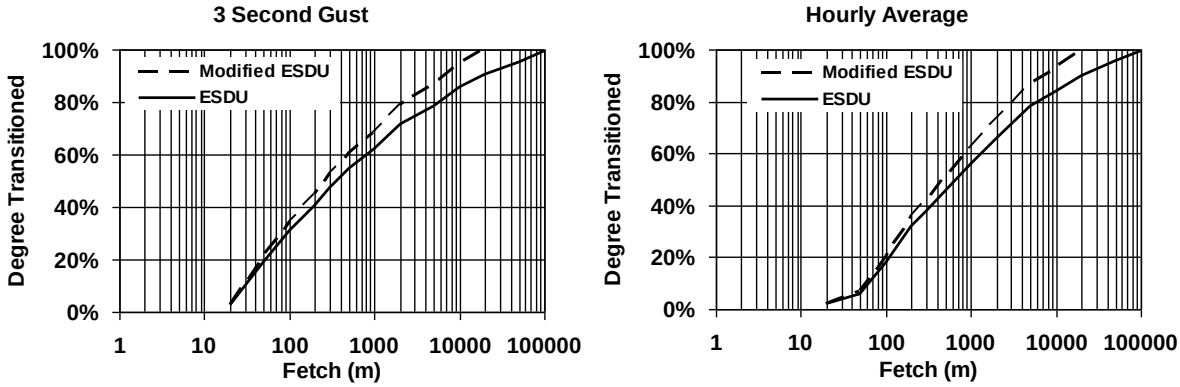

Figure 2.13. ESDU and Modified ESDU Wind Speed Transition Functions.

(*F*~100 km) and the modified ESDU, (*F*=20 km) function reaches a maximum) is about 10%. Referring to Figure 2.12 it is seen that the maximum reduction in the mean wind speed using the ESDU model is about 17% thus, the magnitude of the wind speed error associated with the assumed fetch length is about 10% of 17%, or ~1.7%. The error in the estimate of the peak gust wind speed associated with the assumed fully transitioned fetch length is even less.

2.2.2.2 Model Verification

Verification of the boundary layer model as a whole, with emphasis on the sea-land transition, is made difficult because of the paucity of measurements of both marine and near-by over land wind speeds in landfalling hurricanes. Furthermore, experimental verification of the results suggesting that the reduction in wind speed associated with the change in roughness from sea to land is less than what is expected in non-cyclonic winds,

is complicated by the fact that the reduction in wind speed as a function of distance inland includes the combined effect of the transition model and the wind speed reduction model. The approach taken here to verify the combined boundary layer-transition model uses comparisons of time series of measured mean and gust wind speeds combined with model estimates of wind speeds made using a slab representation of a hurricane coupled with the hurricane boundary layer model and terrain transition models described herein. The mean wind speeds obtained from the HBL model are converted to gust or sustained (one minute) values using the ESDU gust factor models. The ESDU models have been shown by Vickery and Skerlj (2005) to be valid for hurricanes. Details of the slab model approach are given in Thompson and Cardone (1996) and Vickery, et al. (2000). The slab model used here is a modification of the model described in Vickery, et al. (2000), where the drag coefficient used in Vickery, et al (2000) has been replaced by the truncated Large and Pond model, and the number of nested grids has been increased from 4 to 6. In the use of the slab model, the resulting integrated wind speed (mean value throughout the boundary layer) is adjusted to be representative of the maximum wind speed in the boundary layer. The difference between the maximum wind speed and the depth averaged wind speed is only a few percent, and varies dependent upon when the averaging is performed over the assumed 1000 m boundary layer height used in the slab model, or if the averaging height taken is the modeled boundary layer, or jet height. In the comparisons of modeled and observed marine and land wind speeds, an additional 2% increase in the modeled winds was required to eliminate a low overall bias in the comparisons. This small increase is consistent with the underestimate of the surface winds discussed earlier in the case of small *RMW* storms, the underestimate for winds outside the eyewall, and the difference between $U_{10}/\overline{U}_{500}$ given in Powell, et al. (2003) and that computed herein. The slab model approach to modeling the hurricane wind field brings out features of the wind field that are not reproduced in simple gradient balance vortex models or empirical models such as those described by in NWS-23 (Schwerdt, et al., 1979). For example, Figure 2.14 presents the distribution and magnitude of the jet determined (here defined as the depth average wind speed divided by the gradient balance wind speed) using the slab model. A comparison of the jet strength and its variation with azimuth resulting from the 2-D slab model with the results of a full 3-D model of a translating hurricane as presented in Kepert and Wang (2001) indicate that the 2-D numerical slab model is able to reproduce the horizontal variation and magnitude of the jet characteristics corresponding to a height of ~ 500 m produced by a full 3-D numerical model. The variation of the jet height with azimuth is not maintained using the slab model.

In the verification of the model with an emphasis on the sea-land transition, only hurricanes having continuous measurements of wind speeds both over land and over water near the land fall location are useful. The only reasonably well documented storms that meet this criterion include Hurricanes Bertha and Fran (1996), Hurricane Bonnie (1999), near the North Carolina coast, and Hurricane Ivan (2004) along the Gulf Coast. The validation approach is indirect, with the process involving a comparison of modeled and observed maximum peak gust wind speeds produced by the hurricanes over both marine and land terrains. Conclusions as to the validity of the model are inferred by

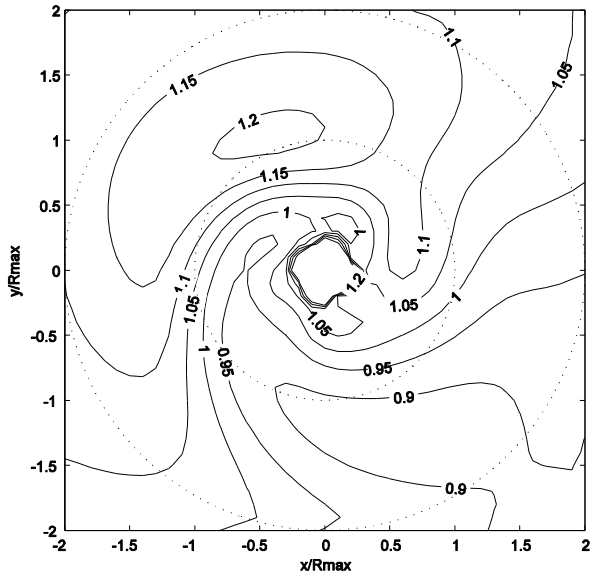

Figure 2.14. Jet Strength Computed Using the Slab Model for a Hurricane Moving Towards the Top of the Page.

determining if there is a bias in the estimates of the modeled marine winds vs. the modeled over land winds. All measured gust wind speeds have been adjusted to be representative of 3 second gust speeds at a height of 10 m, in either open terrain (z_o = 0.03 m) or marine conditions. In the case of marine wind speed measurements obtained from 3-m discus buoys, the measured wind speeds in high wind cases have been increased by 10% to account for the underestimates in the measured wind speeds as described in Gilhousen (2006). Each hurricane is modeled using information on the hurricane track (position and central pressure) obtained from the National Hurricane center, coupled with estimates of the RMW and the Holland *B* parameter. The modeled pressure field is axi-symmetric, but varies with time. The initial estimate of the RMW is usually obtained from H*Wind snapshots of the hurricane wind field at or near the time of landfall. The final estimates of *B* and the *RMW* and their variation with time after landfall are obtained through an iterative approach by reproducing the overall shapes of the wind speed and direction traces and surface pressure traces obtained from as many ground stations as possible. Figure 2.15 presents examples of comparison of wind speed and pressure data obtained from stations located near the point of land fall for different hurricanes.

An extensive set of validation studies has been performed using the hurricane windfield/boundary layer model described herein through comparisons of modeled and observed wind speed and pressure data obtained for 19 landfalling hurricanes occurring since 1985. In each validation study, estimates of RMW and *B*, and their variation in time were obtained using the iterative approach described above. The number of anemometer stations with either complete continuous records of wind speeds, or records where the maximum wind speed during the storm was measured, is given in Table 2.1. Note that in

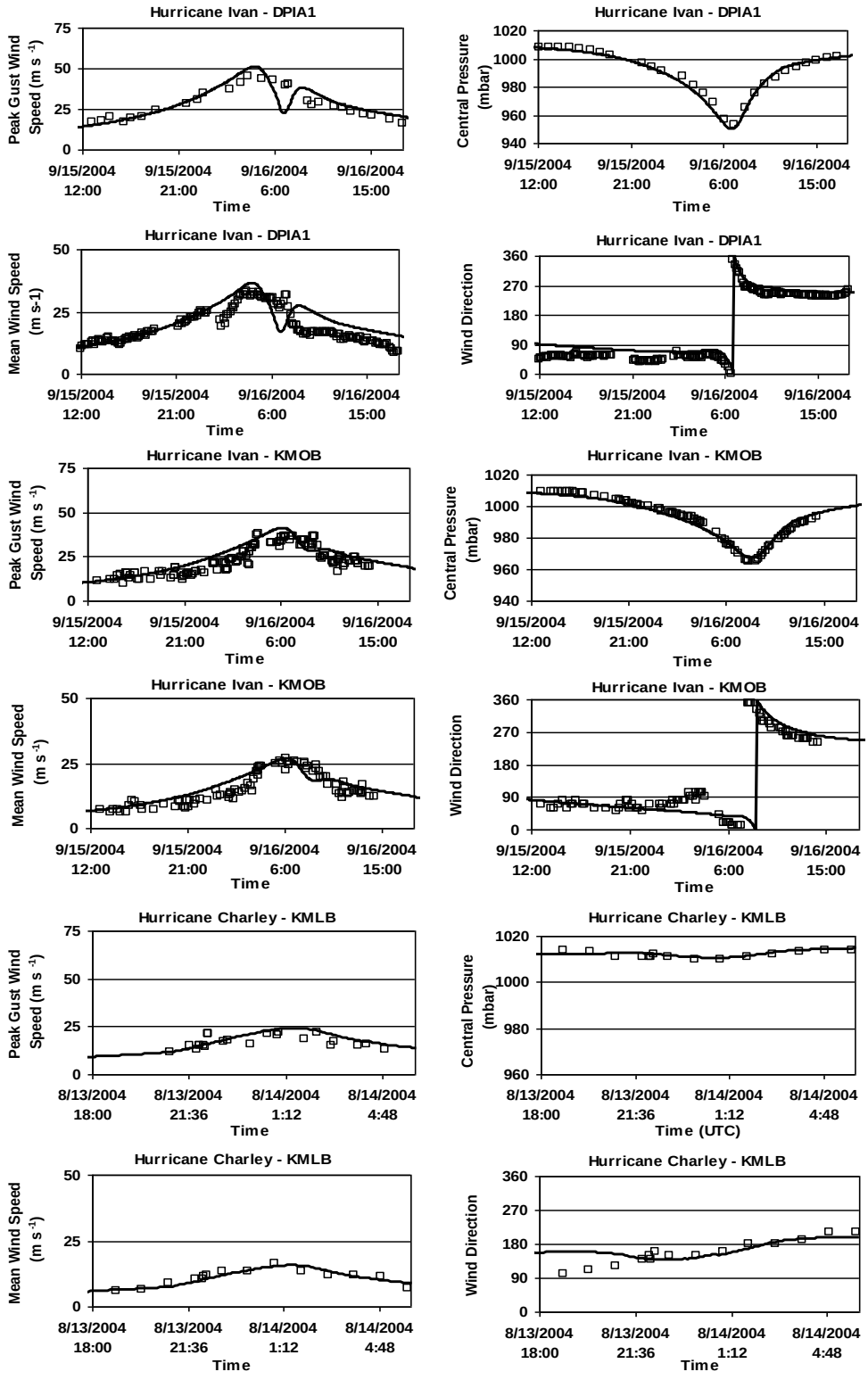

Figure 2.15. Example Plots Showing Modeled and Observed Wind Speeds, Surface Pressures and Wind Directions. Model results represented by solid line, observed values represented by the open squares.

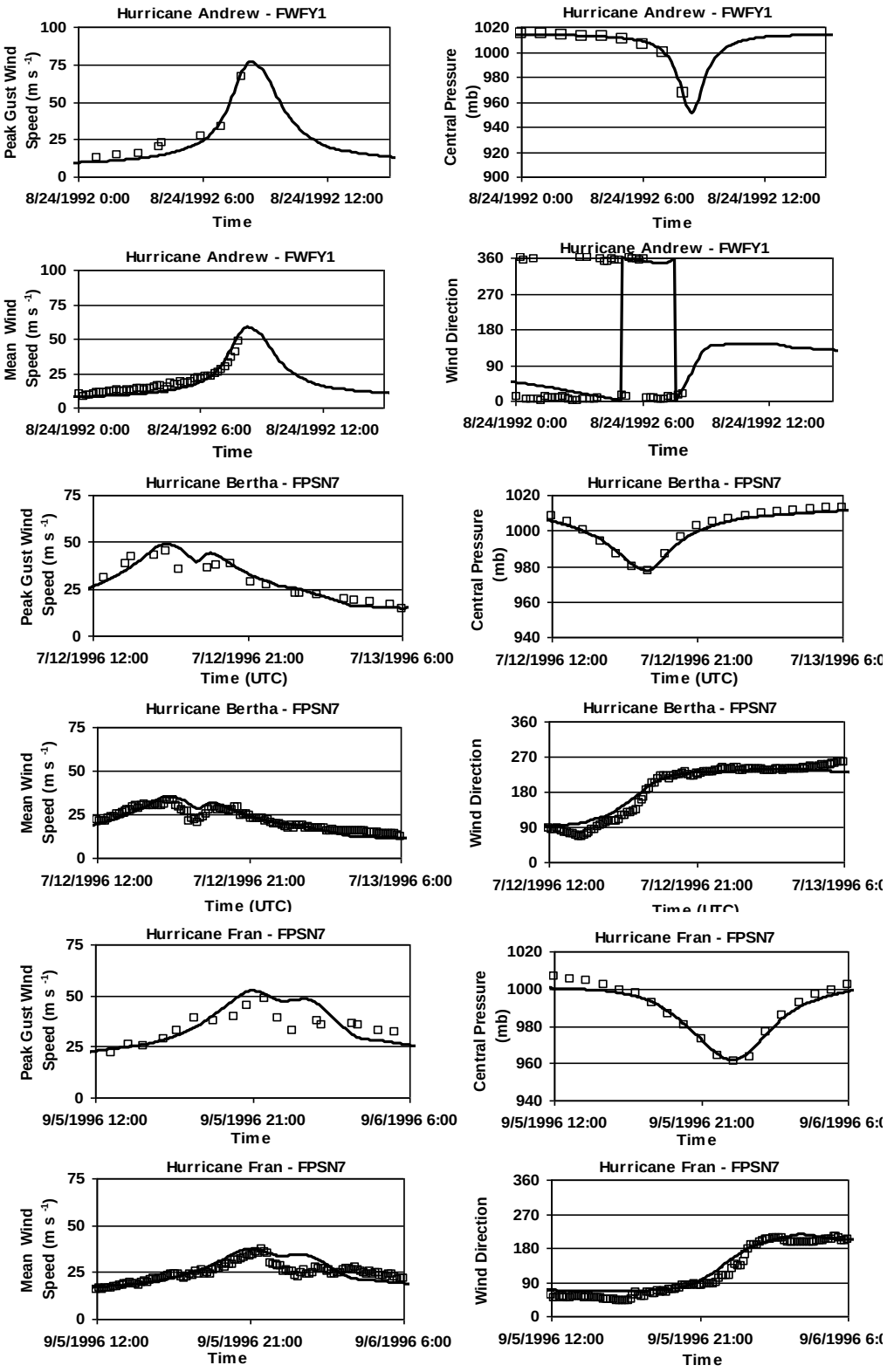

Figure 2.15. Example Plots Showing Modeled and Observed Wind Speeds, Surface Pressures and Wind Directions. Model results represented by solid line, observed values represented by the open squares. (Continued)

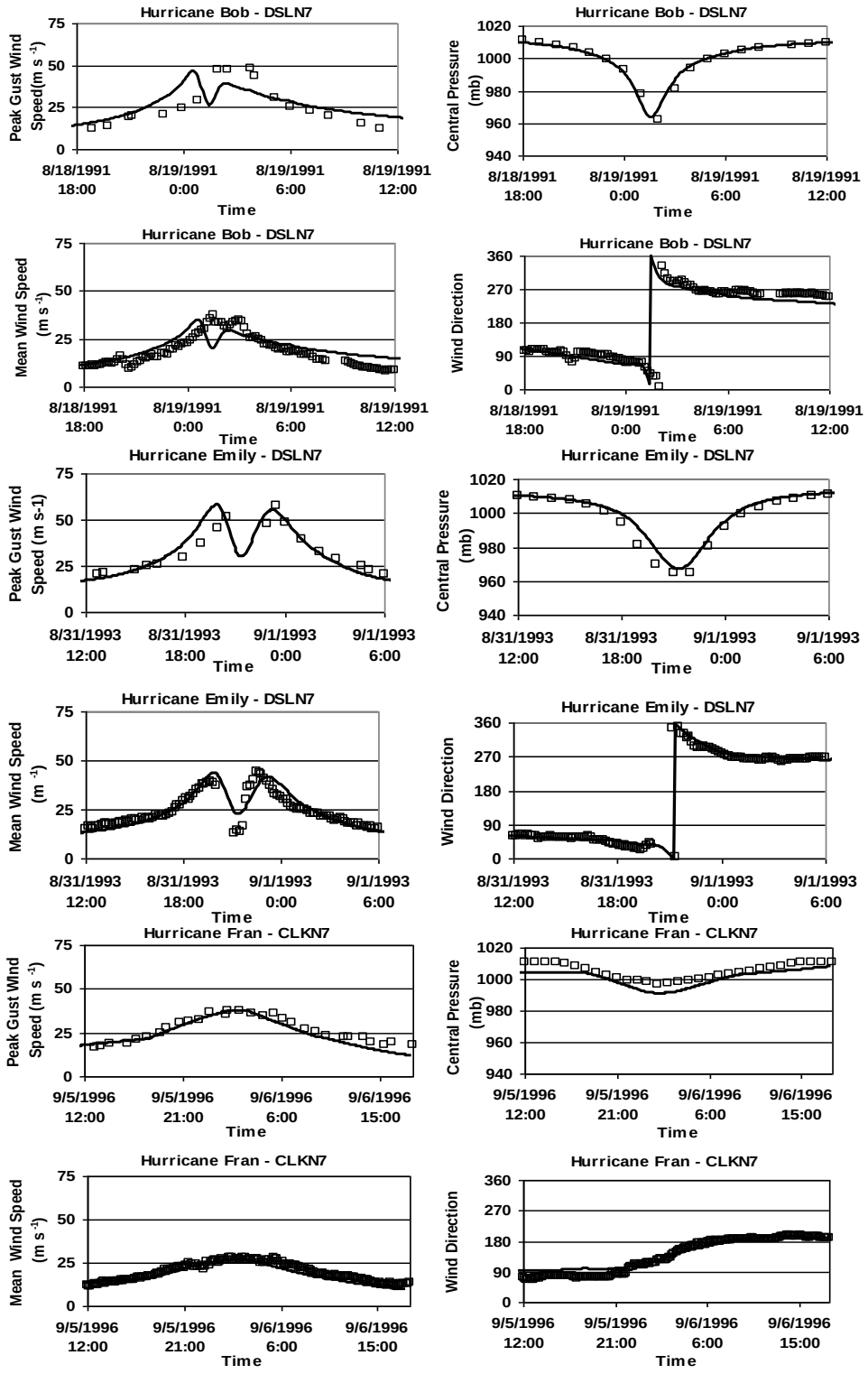

Figure 2.15. Example Plots Showing Modeled and Observed Wind Speeds, Surface Pressures and Wind Directions. Model results represented by solid line, observed values represented by the open squares. (Concluded)

Table 2.1. Number of Wind Speed Records for Each Hurricane

Year	Hurricane Name	Number of complete wind speed records		
		Land	Marine	Total
1979	Frederic	4		4
1985	Elena	3	2	5
1989	Hugo	6	1	7
1991	Bob	2	5	7
1992	Andrew	1	2	3
1993	Emily		9	9
1995	Erin	5	2	7
1996	Bertha	5	3	8
1996	Fran	9	3	12
1996	Opal	5	2	7
1998	Bonnie	2	4	6
1998	Georges	3	10	13
1999	Floyd	2	4	6
1999	Irene	4	5	9
2003	Isabel	10	7	17
2004	Charley	7		7
2004	Frances	13		13
2004	Ivan	13	6	19
2004	Jeanne	14	1	15
2005	Dennis	9	3	12
2005	Katrina	8	2	10
2005	Ophelia	5	7	12
2005	Rita	14		14
2005	Wilma	21	2	23
	Total	165	80	245

many cases, additional incomplete records of wind speeds and pressures were used to assist in estimating the variation in both RMW and *B*. Figure 2.16 presents scatter plots summarizing the comparisons of modeled and observed maximum peak gust wind speeds produced by the storms. In each plot, the slope and r^2 values are given resulting from a linear regression analysis where the regression line is forced to pass through the origin. In all cases, the regression slopes are within 3% of unity. Figure 2.17 presents a summary comparison of the maximum peak gust wind speeds computed using the wind field model described in Vickery, et al., (2008) to observations for both marine and land based anemometers. There are a total of 245 comparisons summarized in data presented in Figure 2.17 (165 land based measurements and 80 marine based measurements). The agreement between the model and observed wind speeds is good, however there are relatively few measured gust wind speeds greater than 100 mph (45 m/sec).

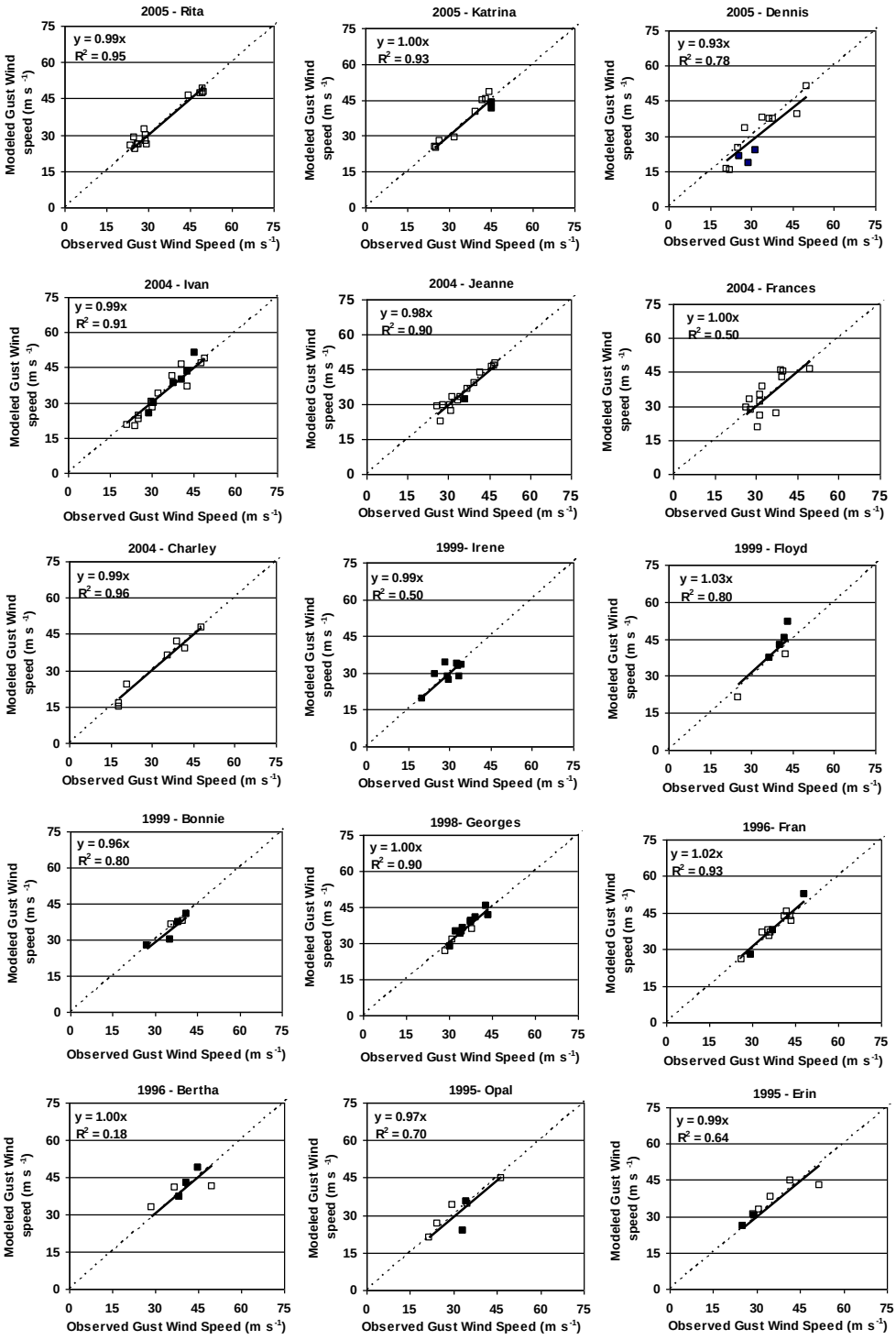

Figure 2.16. Comparison of Modeled and Observed Maximum Peak Gust Wind Speeds for 15 Land Falling Hurricanes. Open squares represent land based measurements; solid squares represent marine based measurements. All wind speeds are at a height of 10m in either open terrain or for marine conditions.

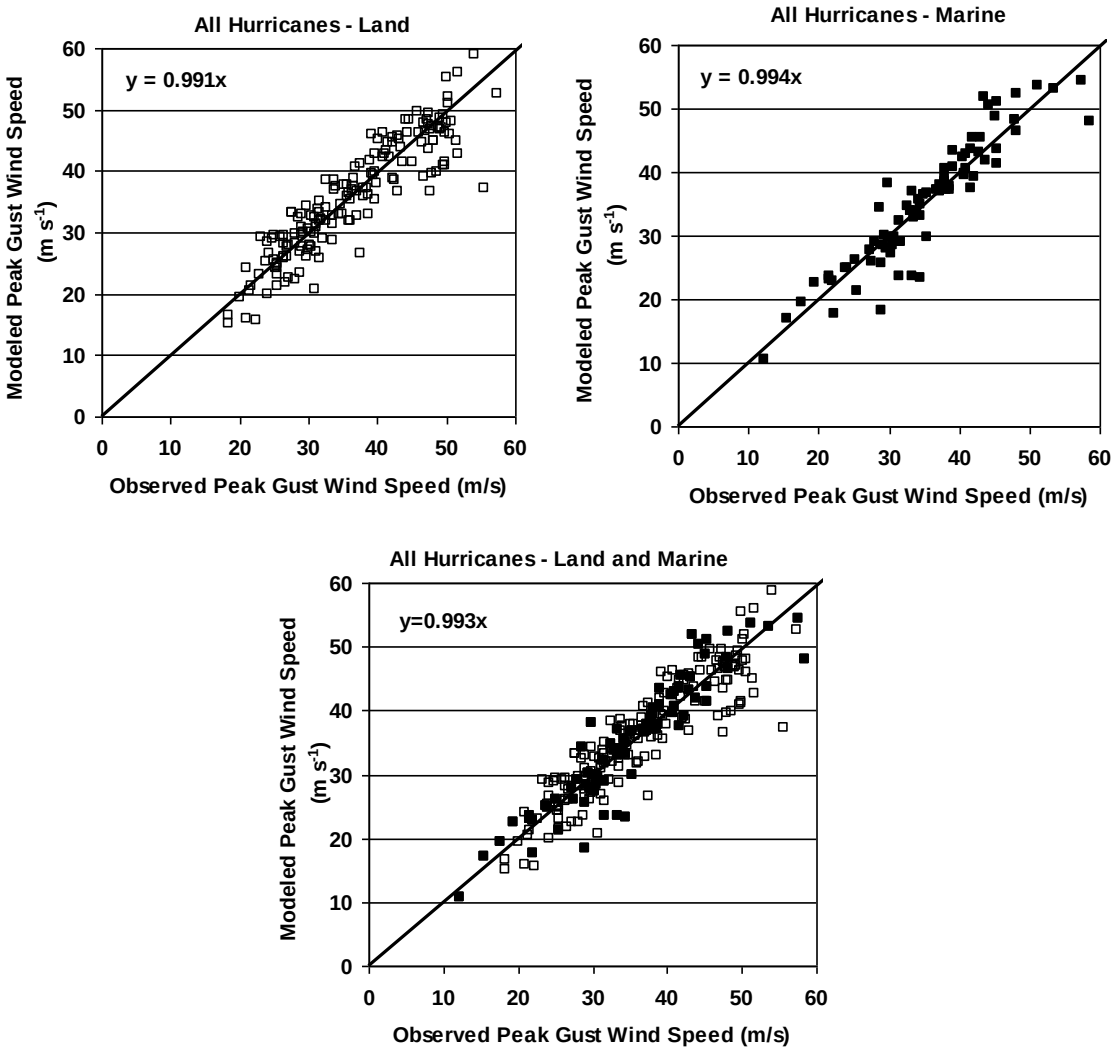

Figure 2.17. Example Comparisons of Modeled and Predicted Maximum Surface Level Peak Gust Wind Speeds in Open Terrain from US Landfalling Hurricanes. Wind speeds measured on land are given for open terrain and wind speeds measured over water are given for marine terrain.

The largest observed gust wind speed is only 128 mph (57 m/s). The differences between the modeled and observed wind speeds is caused by a combination of the inability of wind field model to be adequately described by a single value of *B* and *RMW*, errors in the modeled boundary layer, errors in height, terrain and averaging time adjustments applied to measured wind speeds (if required) as well as storm track position errors and errors in the estimated values of Δp, *RMW* and *B*.

2.2.3 Summary

The boundary layer modeling has been improved over the models used in prior hurricane risk studies, by taking into account the dropsonde data, the theoretical model of Kepert (2003), and by using a physically based gust factor model that properly models the variation in the gust factor with surface roughness.

The modeling of the hurricane wind field has also been improved in comparison to models used in previous studies. It employs the full non-linear solution to the equations of motion of a hurricane (rather than the spectral model used in Georgiou (1985) or Vickery and Twisdale (1995a), or the empirical models used in all other studies). Evaluation of the hurricane model through comparisons with real hurricane wind speed data shows that the model provides a good representation of the hurricane wind field. The hurricane wind field model relies, wherever possible, on physical models rather than empirical models to describe the wind speeds within the storm, and is the most advanced hurricane model currently in use for estimating hurricane wind speed risk.

2.3 Hurricane Simulation Methodology

2.3.1 Introduction

Mathematical simulation of hurricanes is the most accepted approach for estimating wind speeds for the design of structures and assessment of hurricane risk. The basic approach in all previously published hurricane simulation studies is the same in that site specific statistics of key hurricane parameters (including central pressure difference (Δp), Holland pressure profile parameter (B), radius to maximum winds (R_{max}), heading (θ), translation speed (c), and the coast crossing position or distance of closest approach (d_{min}) are first obtained. Given that the statistical distributions of these key hurricane parameters are known, a Monte Carlo approach is used to sample values from each of the aforementioned distributions and a mathematical representation of a hurricane is passed along the straight line path, satisfying the sampled data, while the simulated wind speeds are recorded. The intensity of the hurricane is held constant until landfall is achieved, after which time the hurricane is decayed using filling rate models.

A hurricane simulation approach has been developed where the full track of a hurricane or tropical storm is modeled, beginning with its initiation over the ocean and ending with its final dissipation (Vickery, et al., 2000a). Using this approach, the central pressure is modeled as a function of sea surface temperature and the storm heading, speed etc. are updated at each six-hour point in the storm history. Linear interpolation is used between the six-hour points. The approach is validated by comparing the site specific statistics of the key hurricane parameters of the simulated hurricane tracks with statistics derived from the historical data. When coupled with the wind field model, hurricane wind speeds can be computed at any point along or near the hurricane coastline. The model is able to reproduce the continually varying hurricane statistics along the US coastline, and can treat multiple landfalling storms, by-passing storms, storm curvature and re-intensification in cases where the storm re-enters the water before making a second or third landfall.

2.3.2 Storm Track Modeling

The storm track simulation model is initiated by randomly sampling a starting position, date, time, heading and translation speed from one of the tropical storms given in the HURDAT database. The number of storms to be simulated in any one year is obtained by sampling from a negative binomial distribution having a mean value of 8.4 storms/yr and a standard deviation of 3.56 storms/yr. Given the initial storm heading, speed, and intensity, the simulation model estimates the new position and speed of the storm based on the changes in the translation speed, *c*, and direction (or heading) of the storm, θ, over the current six-hour period. The changes in the speed and direction between times *i* and *i*+1 are obtained from:

$$\Delta \ln c = a_1 + a_2\psi + a_3\lambda + a_4 \ln c_i + a_5\theta_i + \varepsilon \tag{2.9}$$

$$\Delta\theta = b_1 + b_2\psi + b_3\lambda + b_4 c_i + b_5\theta_i + b_6\theta_{i-1} + \varepsilon \tag{2.10}$$

where a_1, a_2, etc., are constants, ψ and λ are the storm latitude and longitude, c_i is the storm translation speed at time step i, θ_i is the storm heading at time step i, θ_{i-1} is the heading of the storm at time step i-1 and ε is a random error term. The coefficients a_1, a_2 etc. have been developed using 5° by 5° grids over the entire Atlantic basin. A different set of coefficients for easterly and westerly headed storms is used. As the storm moves into a different 5° by 5° square, the coefficients used to define the changes in heading and speed change accordingly. The maximum change in the direction of a simulated storm was truncated to ensure realistic limits on the maximum change in storm direction as a function of wind speed. The bounding value of the upper limit in the change of storm direction over a six hour period is a function of storm translation speed.

The central pressure modeling method used in the approach eliminates the need to model the central pressure of the hurricane explicitly, by using a relative intensity parameter which is coupled to the sea surface temperature. This relative intensity approach is an improvement over traditional simulation techniques in that the central pressures derived are bounded by physical constraints, thus eliminating the need to artificially truncate the central pressure distribution. The method was first used in single point simulations by Darling (1991). The approach is validated by comparing the statistics of the observed and modeled hurricane central pressure statistics along the US coastline.

During the hurricane simulation process, the values of the relative intensity, *I*, at each time step are obtained from,

$$\ln(I_{i+1}) = c_0 + c_1 \ln(I_i) + c_2 \ln(I_{i-1}) + c_3 \ln(I_{i-2}) + c_4 T_s + c_5 (T_{s_{i+1}} - T_{s_i}) + \varepsilon \tag{2.11}$$

where T_s is the sea surface temperature and the coefficients c_0, c_1, etc. vary with storm latitude, basin (Gulf of Mexico or Atlantic Ocean), and heading (i.e., Easterly or Westerly direction). Near the US coastline, where more continuous pressure data are available, finer, regionally specific values of these coefficients are developed. These regionally specific coefficients take into account changes in the relationships between sea surface temperature and storm intensity that are influenced by subsurface water temperatures as

described in Cooper (1988). The maximum increase in storm intensity over a six hour period was set equal to 40 mbar, (6.7 mbar/hr) which is greater than the largest average six hour change of about 25 mbar/6hrs (4.2 mbar/hr) observed in Super Typhoon Forrest in the western Pacific in 1983, but less than the maximum rate of 7.14 mbar/hr also observed in Super Typhoon Forrest, but for a period of less than 3 hrs. Once a simulated storm makes landfall, the change in central pressure with time is modeled using the filling models described in Vickery (2005). If a storm moves back over water, Equation 2.11 is again used to model the variation in central pressure with time. Using this modeling approach, the central pressure of the storm continuously changes with time, unlike traditional hurricane simulations, where a constant value of central pressure is assumed until landfall is achieved.

2.3.3 Modeling of Radius to Maximum Winds

The statistical model describing the relationship between the radius of maximum winds and the storm central pressure and latitude is an update of the model given in Vickery, et. al (2000b). The model described in Vickery, et. al (2000b) is primarily based on information on landfalling storms provided in NWS38. The revised model has been updated to include information of the radius to maximum winds from some of the more recent storms occurring in the Atlantic Basin including hurricane Mitch (1998), Hurricane Brett (1999), Hurricane Floyd (1999), in addition to the inclusion of Hurricane Gilbert (1988).

The relationship between the radius to maximum winds, $R_{\max}$, central pressure difference, Δp, and latitude, ψ, is given as:

$$\ln R_{\max} = 2.556 - 0.000050255\Delta p^2 + 0.042243032\psi; \quad r^2=0.3249 \qquad (2.12)$$

Comparisons of the observed values of $R_{\max}$ and those predicted from the statistical model are shown in Figure 2.18. The statistical model reproduces the observations that the more intense storms have smaller values of $R_{\max}$ and that the storms located in more northern latitudes tend to have larger values of $R_{\max}$. In the simulation of hurricanes, $R_{\max}$ is constrained to have a maximum value of 150 km and a minimum value of 8 km.

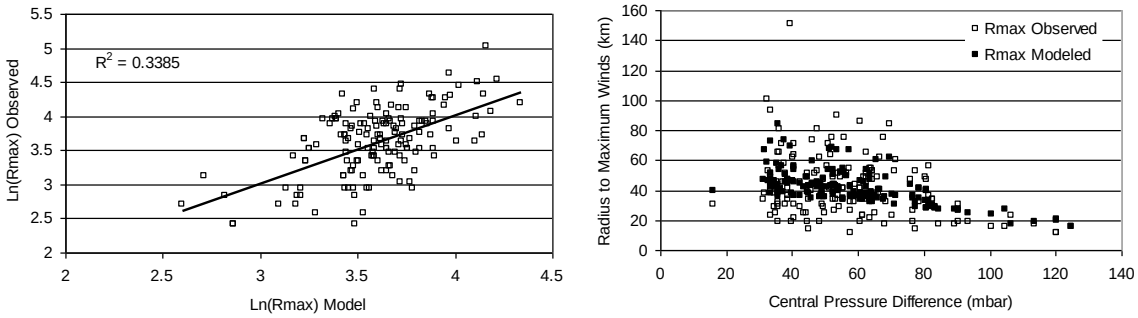

Figure 2.18. Modeled and Observed Values of Radius of Maximum Winds.

2.3.4 Pressure Profile Parameter (*B*)

Upper level aircraft data available at NOAA site were used to estimate Holland's pressure profile parameter (*B*) (Vickery and Wadhera, 2008). The upper level aircraft dataset used here contains a total of 4546 radial profiles from 62 Atlantic storms. This data is the same as that used by Willoughby, et al (2006), in their analysis of *B*, with the main difference in the analysis methodology being that pressures are used here and Willoughby, et al (2006) performed their analysis using wind speeds. For every storm, data has been organized based on the different flights that passed through the storm. For each flight, the airplane traversed through the hurricane a number of times in different directions. For every pass the data was collected from the center of the storm to a certain radius (usually 150 km). Available data is then organized according to their radial distance from the center of the storm. For each bin (based on the radius from the center of the storm) flight level pressure, flight altitude, dew point temperature, wind speed and air temperature are available. Each profile from every flight and every storm is treated as an independent observation. Holland, (1980) describes the radial distribution of surface pressure in a hurricane in the form:

$$p(r) = p_0 + \Delta p \cdot \exp - \left[\frac{RMW}{r} \right]^B \tag{2.13}$$

where $p(r)$ is the surface pressure at a distance r from the storm center, p_0 is the central pressure, Δp is the central pressure difference, A is the location parameter and B is the Holland's pressure profile parameter.

The surface pressure and radial distance are transformed to the form of Equation 2.13. The missing quantities in Equation 2.13 are *RMW* and *B*. First estimate of *RMW* is made from the recorded wind speed profile i.e. *RMW* is the radius to the measured maximum wind speed. From here on, the radius corresponding to the maximum wind speed in a profile is referred to as *RMW*. To estimate the optimum values of *B* and *RMW*, *RMW* and *B* are varied over the range [0.5*RMW*, 1.5*RMW*] and [0.5, 2.5] respectively. The algorithm calculates an optimum B value by minimizing the mean of the square differences between the measured and the modeled surface pressure in a range of 0.5*RMW* to 1.5*RMW* for different *B* and *RMW* values. Mathematically, the mean square error between the measured and the modeled surface pressure can be written as:

$$\varepsilon^2 = \frac{\sum_{i=0.5RMW}^{1.5RMW} \left(P_{obs_i} - P_{theo_i} \right)^2}{n} \tag{2.14}$$

where P_{obsi} is the measured pressure, P_{theoi} is the theoretical pressure calculated using Equation 2.13 and n is the number of data points in the range [0.5*RMW*, 1.5*RMW*]. The values of *B* and *RMW* chosen correspond to those yielding the minimum mean square error, ε^2. The corresponding r^2 value for the fit is given by:

$$r^2 = 1 - \frac{\varepsilon^2}{\sigma^2} \tag{2.15}$$

where σ is the standard deviation of the measured pressure data in the range of [0.5*RMW*, 1.5*RMW*].

A quality control criterion was used to filter out profiles. Each of the filtered profiles has at least one of the following characteristics associated with it, (a) Flight level pressure is less than 700 mbar i.e. height greater than 3000 m, (b) Central pressure difference is less than 25 mbar, (c) Radius to maximum winds is greater than two-third of the sampling domain, (d) the distance of aircrafts closest approach to the center is greater than half of the radius to maximum winds, (e) Data is available for less than one third of the sampling range i.e. less than 50 km, (f) visual inspection which involved eliminating profiles with a considerable amount of data missing in the range of interest [0.5*RMW*, 1.5*RMW*]. The rationale for using criteria (a) is that higher the measurement height, less representative measurements are of the surface observations. Criteria (b) results in the data associated with Category 1 or higher hurricanes only. The rationale for using criteria (c), (d), (e) and (f) is to ensure that there is a sufficient number of measurements on both sides of the radius to maximum winds to have a clear representation of the shape of the profile (Willoughby et al. 2006). The use of the quality control criteria eliminated a total of 2291 profiles from a set of 4556 profiles. Figure 2.19 presents a few examples of pressure profiles that were eliminated from the analysis. Both the measured pressure data and the corresponding fit to Holland's equation are shown. It is observed that each of the subplots in Figure 2.19 is compromised by at least one of the above mentioned quality control criteria.

Figure 2.20 presents examples of pressure profiles that were retained for analysis. Each row in Figure 2.20 corresponds to a complete airplane traverse in one direction. The shaded regions in Figure 2.20 represent the error minimizing range of 0.5*RMW* to 1.5*RMW*. The fit parameters i.e. the *B* value, the central pressure difference and the *RMW* are also provided in the title of every profile. For a given traverse through a hurricane, differences in the *B* values for two different profiles is due to the change in the radius to the maximum winds and the central pressure difference. The geographical distribution of the filtered profiles, based on the storm center, is shown in Figure 2.21. The filtered profiles have a wide geographical distribution and provides with a wide domain of hurricane climatic characteristics. The filtered dataset has an average *RMW* of 46 km (standard deviation of 22 km), an average central pressure difference of 51 mbar (18 mbar) and an average location of 25.84°N (5.74°N) and 74.78°W (12.82°W). 71% of the fits yield r^2 values greater than 0.95 and 80% of the fits have a mean square error less than 2.5 mbar. The maximum mean square error was 24.6 mbar which occurred for one of Hurricane Opal's profiles where Holland's equation overestimated the pressures at all points. The approach for analyzing the *B* data involved the estimation of *RMW* and *B* from each single pass of a flight through the storm.

The *B* values computed as discussed above were found to be correlated to the radius to maximum winds, central pressure difference, latitude and sea surface temperature.

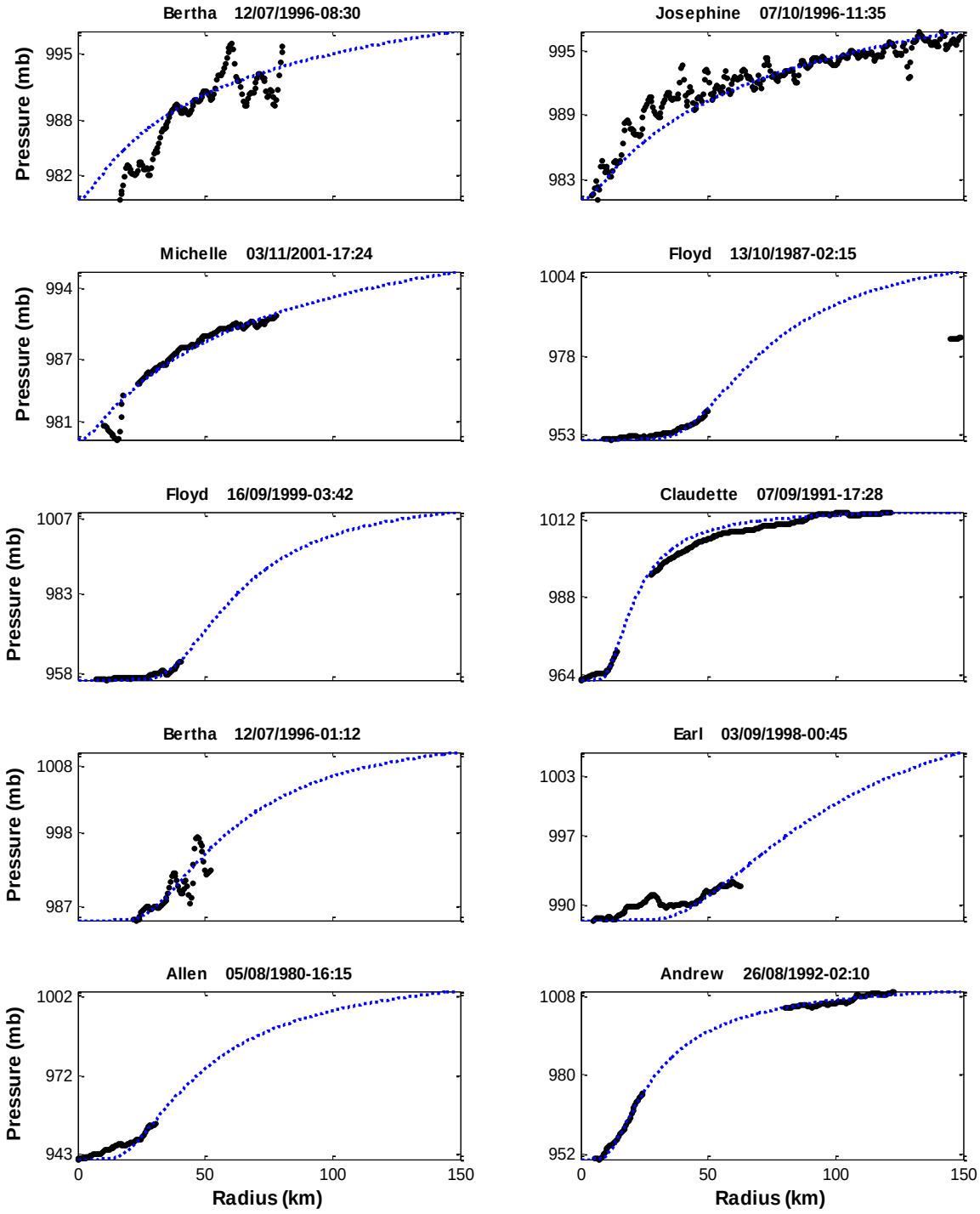

Figure 2.19. Examples of the Eliminated Profiles.

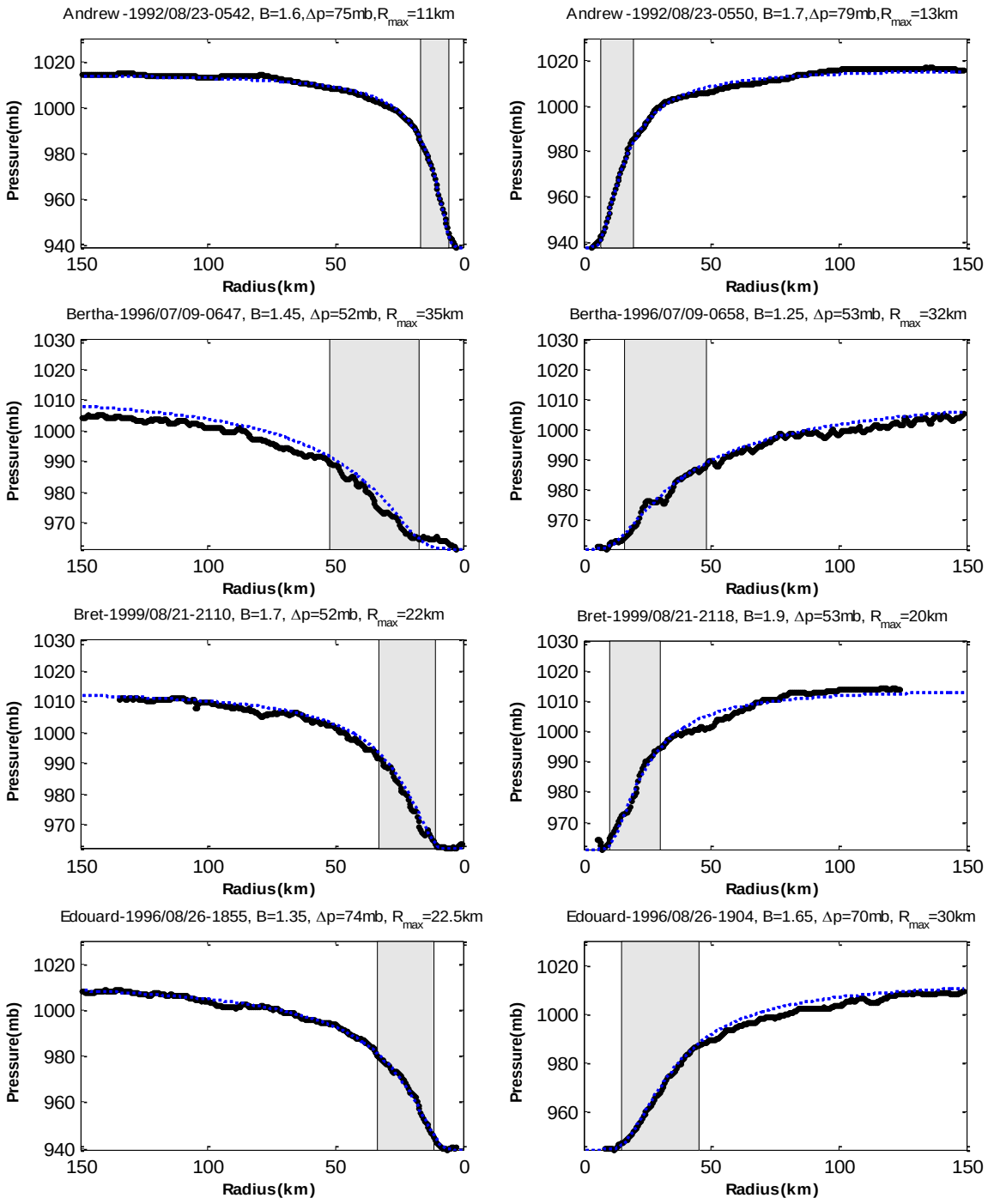

Figure 2.20. Examples of Surface Pressure Profiles for a Traverse Across a Given Hurricane.

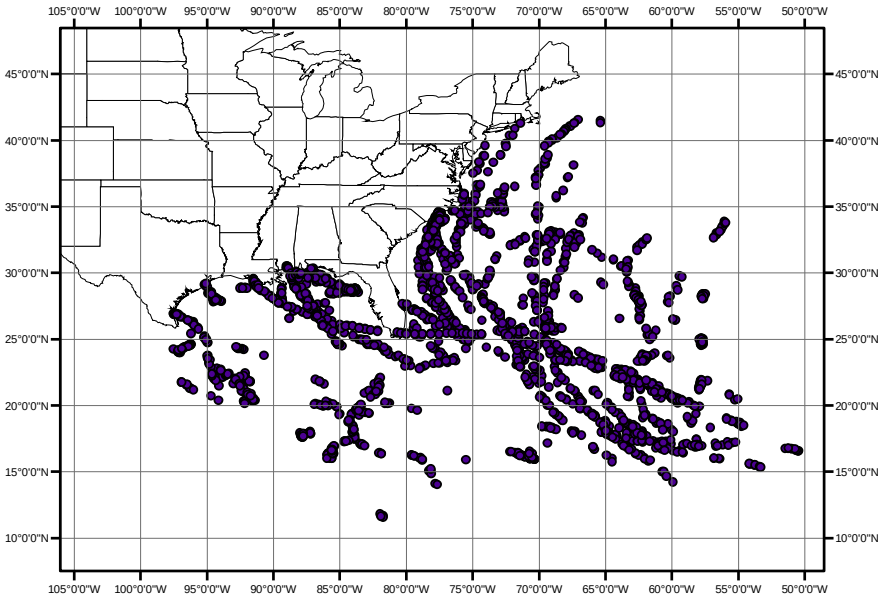

Figure 2.21. Geographical Distribution of all the Filtered Profiles.

Only points associated with central pressures less than 980 mbar are included in the analysis. The resulting model of B is

$$B = -0.36467 - 0.15182 \cdot LN(R_{\max}) + 0.081639 \cdot LN(\Delta p) - 0.11663 \cdot LN(\theta) + 0.67354 \cdot LN(T) \qquad r^2 = 0.145, \quad \sigma_e = 0.302 \tag{2.16}$$

2.3.5 Filling Models

The filling models used in Hazus-MH are described in Vickery (2005). The form of the filling models is an exponential decay function in the form

$$\Delta p(t) = \Delta p_o \exp(-at)$$

where $\Delta p(t)$, expressed in mb, is the difference between the central pressure of the storm and the far field pressure (normally taken as the as the pressure associated with the outermost closed isobar) t hours after landfall, Δp_o (mb) is the difference between the central pressure of the storm and the far field pressure at the time the storm makes landfall and a is the filling constant.

The magnitude of the filling constant used in the exponential decay function is modeled as a function of readily defined characteristics of a tropical cyclone at the time of landfall. For storms making landfall along the Gulf Coast of the United States and the Florida peninsula, the reduction in the central pressure difference following landfall is modeled as a function of $\Delta p_o c/RMW$. Along the Mid-Atlantic coast, the reduction in the central pressure difference following landfall is adequately modeled either as a function of $\Delta p_o c/RMW$ or a function of Δp_o alone. Along the New England coast, the reduction in central pressure difference following landfall is modeled with decay constant modeled as

a function of Δp_o. Figure 2.22 shows the values of decay constant versus $\Delta p_o c/RMW$ for Gulf, Florida and Mid Atlantic coast and versus Δp_o for New England coast. The models implemented in Hazus-MH are as follows:

Gulf Coast	$a = 0.0413 + 0.0018(\Delta p_0 c / RMW)$	; σ_ε=0.0169
Florida Peninsula Coast	$a = 0.0225 + 0.0017(\Delta p_0 c / RMW)$	; σ_ε=0.0158
Mid-Atlantic Coast	$a = 0.0364 + 0.0016(\Delta p_0 c / RMW)$	; σ_ε=0.0161
New England Coast	$a = 0.0034 + 0.0010\Delta p_0$	; σ_ε=0.0114

When implemented, the minimum allowable value of a sampled filling coefficient is set at 0.015, with the sampled error constrained to lie within $\pm 3\sigma_\varepsilon$.

.

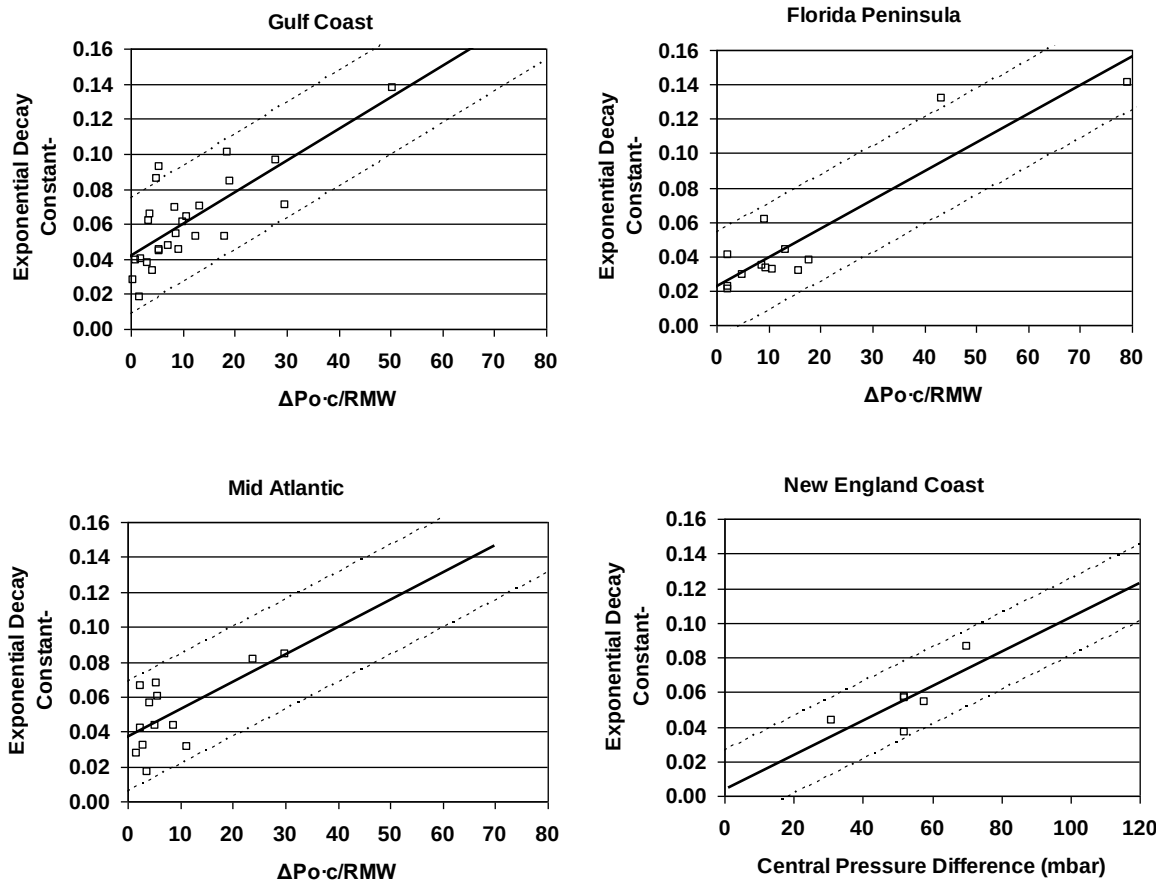

Figure 2.22. Filling Constant, *a*, vs. $\Delta p_o c/RMW$ for Gulf, Florida and Atlantic Coast and vs. Δp_o for New England Coast. Solid line represents linear regression line. Thin dashed lines represent the mean error $\pm 2\sigma_\varepsilon$

2.3.6 Track and Central Pressure Model Evaluation

The hurricane modeling methodology described above is evaluated through comparisons of observed and simulated hurricane statistics along the US coastline. The simulated statistics are derived from a 100,000 year simulation of storms occurring in the Atlantic Basin. Comparisons are given for the statistics of simulated and real storms approaching within 250 kilometers of the coastal mileposts shown in Figure 2.23. The central pressure difference statistics are computed using the minimum values observed within the 250 km radius sub-region. All other parameters are those computed or observed at the point of closest approach to the milepost.

Figure 2.24 shows comparisons of the mean and, in some cases, standard deviation of the simulated and observed values of heading, translation speed, minimum approach distance (d_{min}), occurrence rate and central pressure along the Mexican and U.S. coastlines at 50 nautical mile increments (~185 km). The HURDAT statistics given in Figure 2.24 are derived for storms occurring during the period 1886-2001. The comparison of simulated and observed hurricane statistics shown in Figure 2.24 indicates that the modeling approach provides good estimates of the five key hurricane parameters at nearly all locations along the coastline. The empirical storm track modeling approach has been shown to successfully reproduce the statistics of the key hurricane parameters along the US coastline. The approach is able to properly model the probabilities of a single storm passing near multiple sites (results not presented here). Using this simulation procedure, the storm intensities change with time, and the storms change both direction and speed as they pass by a site. The approach more realistically models storm paths when compared to traditional hurricane simulation methods.

2.3.7 Landfalling Hurricanes

The historical information on landfalling hurricanes along the coastline provides another means to evaluate the hurricane simulation model. During the simulation process when a simulated storm makes landfall, the central pressure, maximum sustained wind speed (one minute average, over water), and landfall location are retained. Using the magnitude of the central pressure and wind speed at the time of landfall, the simulated storm is assigned a category as defined by Table 2.2. Historical information on the central pressure at the time of landfall is available for all intense hurricanes, IH, as defined by Saffir-Simpson Category 3 and higher storms, and for all other landfalling hurricanes occurring since 1964. Between 1900 and 2005 there have been a total of 189 hurricane landfalls, 172 of which have central pressure data associated with the storm at the time of landfall. Note that in the counting of the 189 landfalls, each time a storm crosses land from the water, a landfall is considered to have occurred.

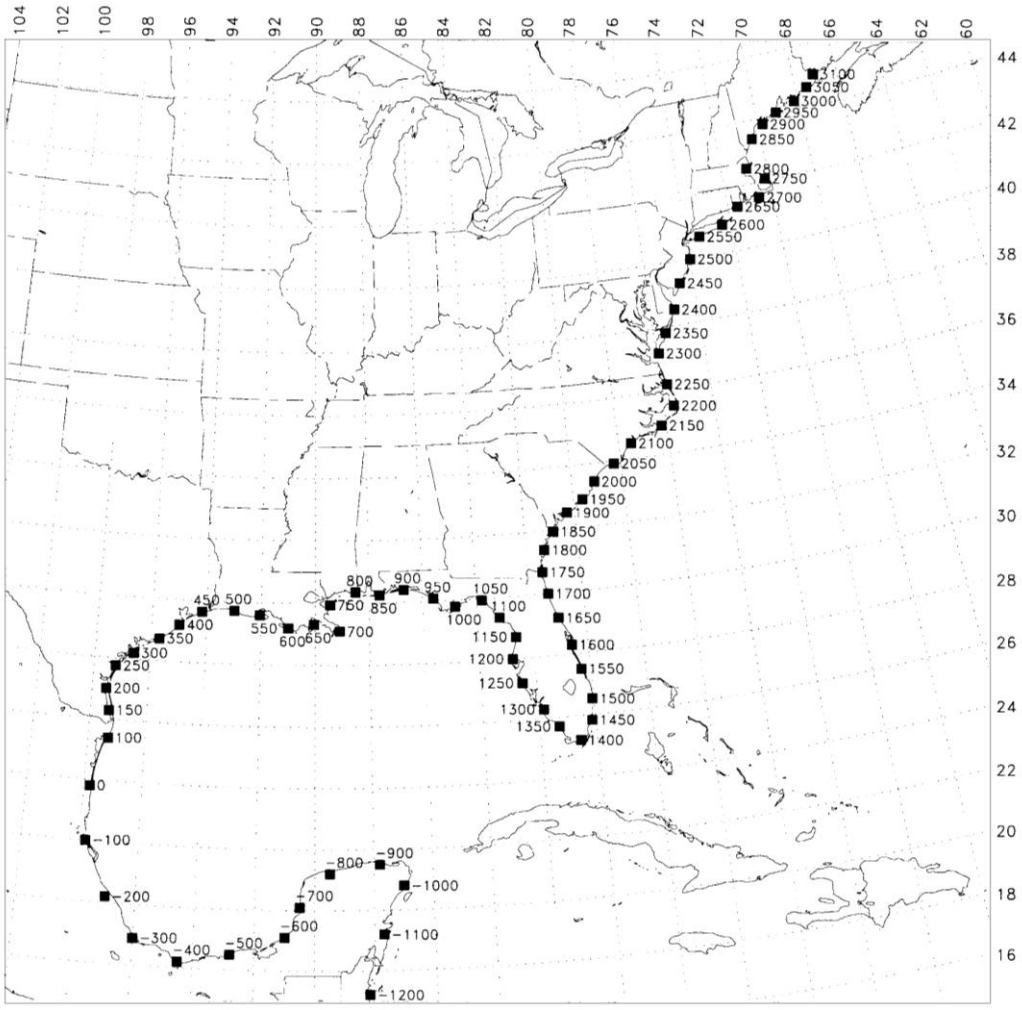

Figure 2.23. Locations of Milepost Stations Along the U.S. Coastline.

For example, Hurricane Andrew made two landfalls, once as a Category 4 storm in South Florida, and once as a Category 3 storm in Louisiana[1]. Thus, the definition of a landfalling storm used herein differs from that usually used by the NHC that scores only one landfall per storm when counting the total number of landfalls in the US. All of the 189 landfalls have a Saffir-Simpson Category, based on the *estimated* maximum sustained wind speed at the time of landfall. The comparisons of landfalling storms that follow concentrate on comparing the modeled and observed landfall intensities based on central pressure rather than wind speed. Figure 2.25 shows comparisons of the modeled and observed rates of intense hurricane landfalls, by region, for the Saffir-Simpson storm category defined by central pressure at the time of landfall. Table 2.3 presents the

1 The upgrade of Hurricane Andrew from a Category 4 to a Category 5 in South Florida occurred after the analysis presented in this section was completed.

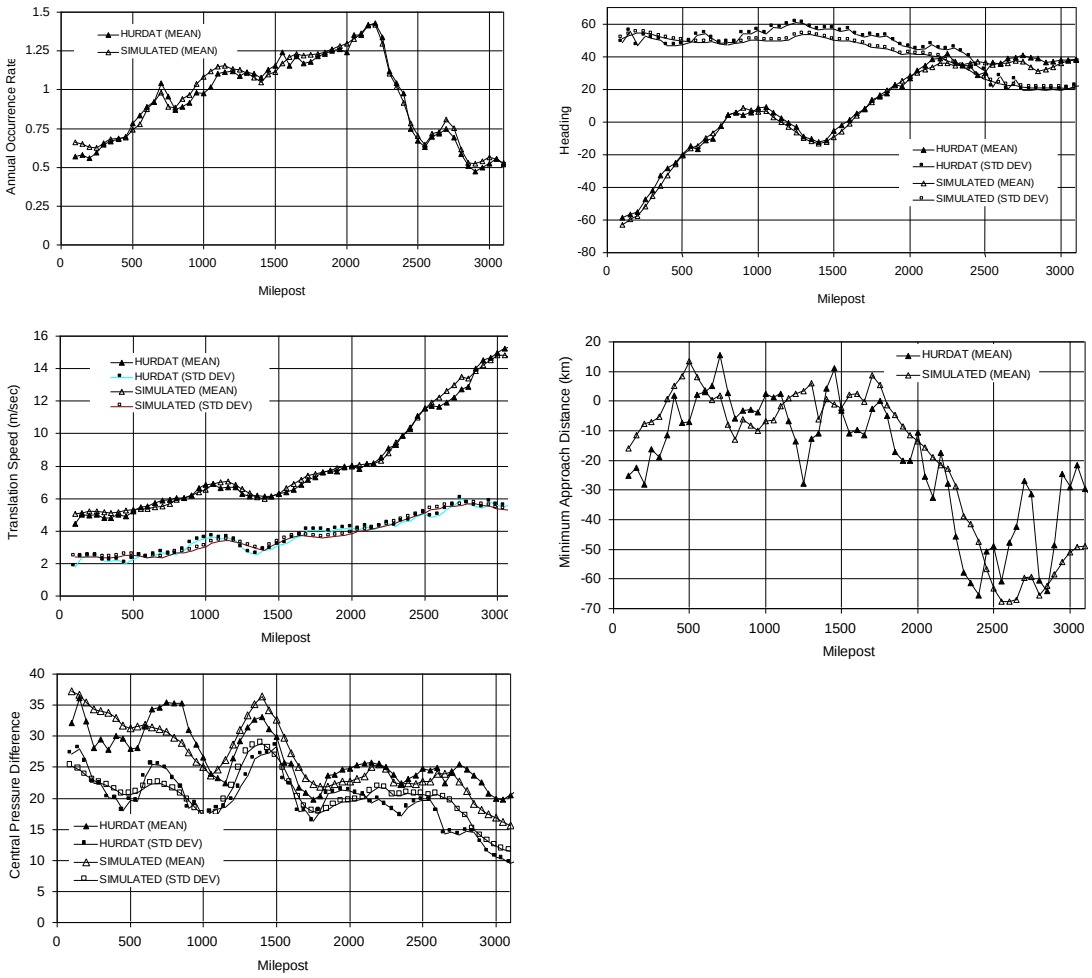

Figure 2.24. Comparison of Simulated and Observed Key Hurricane Parameters vs. Milepost.

Table 2.2. Saffir-Simpson Storm Categories

Saffir-Simpson Category	Minimum Central Pressure	Maximum Sustained Wind Speed (Over Water)		Maximum Gust Speed (Over Water)		Maximum Gust Speed (Over Land, z_0 = 0.03m)	
	(mb)	(m/s)	(mph)	(m/s)	(mph)	(m/s)	(mph)
1	≥980	33.1-42.0	74-94	40.6-51.9	91-116	36.8-48.1	82-108
2	979-965	42.0-49.6	94-110	51.9-61.7	116-140	48.1-58.1	108-130
3	964-945	49.6-58.1	110-130	61.7-72.7	140-165	58.1-69.7	130-156
4	944-920	58.1-69.3	130-155	72.7-87.3	165-195	69.7-85.5	156-191
5	<920	>69.3	>155	87.3	>195	>85.5	>191

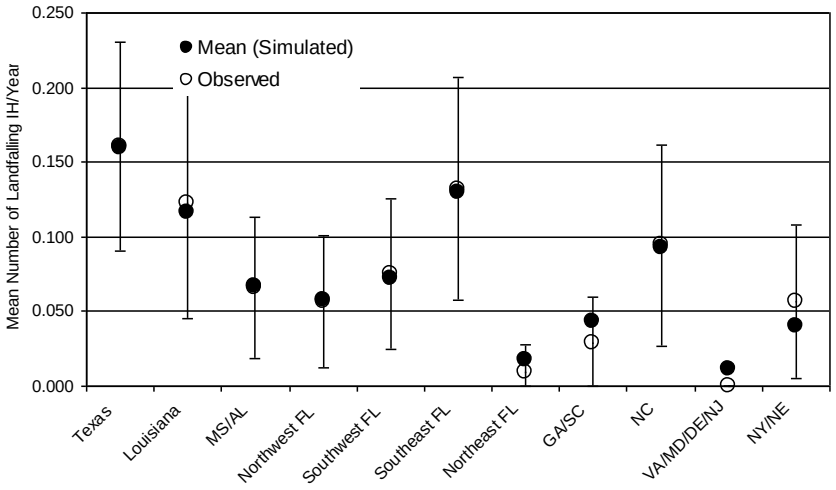

Figure 2.25. Comparison of Rate of Landfalling Intense Hurricanes by Region Along the US Coastline. (IH defined by pressure).

information used to categorize each landfalling storm, along with the category of the storm as defined by central pressure and the category of the storm as given in HURDAT. The source of the central pressure data are given for each instance where central pressure data is given, with the majority of the central pressure data obtained from the NOAA publication NWS38 (Ho, et al., 1984).

The simulated landfall rates given in Figure 2.25 have been derived from a 100,000-year simulation of storms in the Atlantic basin. The observed data are given as the mean value $\pm 1.96\sigma$ (i.e., the 95^{th} percentile confidence range) for observed IH storms categorized by central pressure. Modeled data are given as mean values only. Based on central pressure, the agreement between the observed and simulated rates of landfalling intense hurricanes is seen to be very good, with the variation of intense hurricane landfall rate with location along the coastline reproduced very well. The simulation yields a landfall rate of 0.71 intense hurricanes per year vs. and observed rate of 0.72 intense hurricanes per year.

Figure 2.26 presents similar data to that presented in Figure 2.25, except that the distribution of landfall intensity by storm category is presented without regard to the landfall region. In the case of Category 4 and higher storms, the simulation produces an average annual landfall rate, derived from central pressure, of about one Category 4 or 5 storm every 5 years. This landfall rate is slightly less than that given in Vickery, et. al (2000b), where a rate of one Category 4 or 5 storm every 4 years was simulated.

The comparison of modeled and observed intense hurricanes, where the observed hurricane intensity is based on wind speed, suggests that the model underestimates the occurrence of intense hurricanes. The apparent underestimation of the landfall rate of intense hurricanes when defined by wind speed is discussed in Vickery, et al. (2000b), where it is shown that many of the Category 3 storms (as defined in HURDAT) should have been Category 2 storms. Table 2.4 shows a comparison of the Saffir-Simpson rating

Table 2.3. Storm Category and Central Pressure at Landfall

Year	Name	Land Fall State	Category	Central Pressure	Source	HURDAT Category
1900	UN-NAMED	TX	4	936	NWS38	4
1901	UN-NAMED	LA	2			2
1901	UN-NAMED	MS	2	973	HURDAT	2
1901	UN-NAMED	NC	1	973	NWS38	1
1903	UN-NAMED	SE FL	2	977	NWS38	2
1903	UN-NAMED	NW FL	1			1
1903	UN-NAMED	NJ	1			1
1904	UN-NAMED	SC	1			1
1906	UN-NAMED	SC	3	947	NWS38	3
1906	UN-NAMED	MS	2	965	NWS38	3
1906	UN-NAMED	SW FL	2	967	NWS38	3
1906	UN-NAMED	SE FL	1	979	FCHLM	1
1908	UN-NAMED	NC	1			1
1909	UN-NAMED	LA	4	931	Hebert, et. al	4
1909	UN-NAMED	TX	3	959	NWS38	3
1910	UN-NAMED	SW FL	3	955	Hebert, et. al	3
1910	UN-NAMED	TX	2			2
1911	UN-NAMED	SC	2			2
1911	UN-NAMED	NW FL	1	990	FCHLM	1
1912	UN-NAMED	TX	1			1
1912	UN-NAMED	AL	1			1
1913	UN-NAMED	NC	2	976	NWS38	1
1913	UN-NAMED	TX	1			1
1915	UN-NAMED	LA	4	932	NWS38	4
1915	UN-NAMED	TX	3	949	NWS38	4
1915	UN-NAMED	NW FL	1			1
1916	UN-NAMED	TX	3	948	NWS38	3
1916	UN-NAMED	AL	3	950	NWS38	3
1916	UN-NAMED	NW FL	2	974	NWS38	2
1916	UN-NAMED	SE FL	1			1
1916	UN-NAMED	SC	1	982	HURDAT	1
1916	UN-NAMED	MA	1			1
1917	UN-NAMED	NW FL	3	964	NWS38	3
1918	UN-NAMED	LA	3	955	Hebert, et. al	3
1919	UN-NAMED	TX	3	948	NWS38	4
1920	UN-NAMED	LA	1	980	NWS38	2
1920	UN-NAMED	NC	1			1
1921	UN-NAMED	TX	3	954	NWS38	2
1921	UN-NAMED	SW FL	3	960	NWS38	3
1923	UN-NAMED	LA	1			1
1924	UN-NAMED	SW FL	2	978	NWS38	1
1924	UN-NAMED	NW FL	1			1
1925	UN-NAMED	SW FL	1			1
1926	UN-NAMED	SE FL	4	932	NWS38	4
1926	UN-NAMED	LA	3	955	NWS38	3
1926	UN-NAMED	MS	3			3
1926	UN-NAMED	SE FL	3	960	NWS38	2
1928	UN-NAMED	SE FL	4	935	NWS38	4
1928	UN-NAMED	SE FL	2	977	HURDAT	2
1929	UN-NAMED	SE FL	3	948	NWS38	3
1929	UN-NAMED	TX	2	970	NWS38	1
1929	UN-NAMED	NW FL	2	975	NWS38	2
1932	UN-NAMED	TX	4	942	NWS38	4
1932	UN-NAMED	AL	1			1
1933	UN-NAMED	TX	3	949	NWS38	3
1933	UN-NAMED	SE FL	3	948	NWS38	3
1933	UN-NAMED	NC	3	948	NWS38	3
1933	UN-NAMED	NC	3	957	NWS38	3

Table 2.3. Storm Category and Central Pressure at Landfall (Continued)

Year	Name	Land Fall State	Category	Central Pressure	Source	HURDAT Category
1933	UN-NAMED	SE FL	1			1
1934	UN-NAMED	TX	2			2
1934	UN-NAMED	LA	2	966	NWS38	3
1935	UN-NAMED	SW FL	5	892	NWS38	5
1935	UN-NAMED	NW FL	1	985	MWR 1935	2
1935	UN-NAMED	SE FL	2	973	NWS38	2
1936	UN-NAMED	NW FL	3	963.8	NWS38	3
1936	UN-NAMED	TX	1			1
1938	UN-NAMED	NY	3	946	NWS38	3
1938	UN-NAMED	LA	1			1
1939	UN-NAMED	NW FL	1			1
1939	UN-NAMED	SE FL	1			1
1940	UN-NAMED	LA	2	972	HURDAT	2
1940	UN-NAMED	SC	2	975	NWS38	2
1941	UN-NAMED	TX	3	959	NWS38	3
1941	UN-NAMED	SE FL	2			2
1941	UN-NAMED	NW FL	1	981	NWS38	2
1942	UN-NAMED	TX	3	951	NWS38	3
1942	UN-NAMED	TX	1			1
1943	UN-NAMED	TX	2	975	NWS38	2
1944	UN-NAMED	SW FL	3	962	NWS38	3
1944	UN-NAMED	NY	3	955	NWS38	3
1944	UN-NAMED	NC	1			1
1945	UN-NAMED	SE FL	3	951	NWS38	3
1945	UN-NAMED	TX	2	967	NWS38	2
1945	UN-NAMED	NW FL	1			1
1946	UN-NAMED	SW FL	1			1
1947	UN-NAMED	SE FL	4	940	NWS38	4
1947	UN-NAMED	LA	2	966	NWS38	2
1947	UN-NAMED	SC	2	967	NWS38	2
1947	UN-NAMED	TX	1			1
1948	UN-NAMED	SW FL	3	963	HURDAT	3
1948	UN-NAMED	SE FL	2	965	NWS38	2
1948	UN-NAMED	LA	1	989	HURDAT	1
1949	UN-NAMED	TX	3	963	NWS38	2
1949	UN-NAMED	SE FL	3	954	HURDAT	3
1950	EASY	NW FL	3	958	NWS38	3
1950	KING	SE FL	3	955	NWS38	3
1950	BAKER	AL	1	979	NWS38	1
1952	ABLE	SC	1			1
1953	FLORENCE	NW FL	1	985	HURDAT	1
1953	BARBARA	NC	1	987	HURDAT	1
1954	HAZEL	NC	4	938	NWS38	4
1954	CAROL	NY	3	962	NWS38	3
1954	EDNA	MA	3	954	Hebert, et. al	3
1954	EDNA	ME	1			1
1955	CONNIE	NC	3	963	NWS38	3
1955	IONE	NC	3	960	NWS38	3
1955	DIANE	NC	1	982	NWS38	1
1956	FLOSSY	NW FL	2	974	NWS38	2
1956	FLOSSY	LA	1	983	HURDAT	1
1957	AUDREY	LA	3	947	NWS38	4
1959	GRACIE	SC	3	951	NWS38	3
1959	DEBRA	TX	1	984	HURDAT	1
1959	CINDY	SC	1			1
1960	DONNA	SW FL	4	930	NWS38	4
1960	DONNA	NC	3	958	NWS38	3
1960	DONNA	NY	3	959	NWS38	3

Table 2.3. Storm Category and Central Pressure at Landfall (Continued)

Year	Name	Land Fall State	Category	Central Pressure	Source	HURDAT Category
1960	ETHEL	MS	1			1
1961	CARLA	TX	4	931	HURDAT	4
1963	CINDY	TX	1			1
1964	HILDA	LA	3	959	HURDAT	3
1964	DORA	NE FL	3	961	NWS38	3
1964	ISABELL	SW FL	2	969	HURDAT	2
1964	CLEO	SE FL	2	968	NWS38	2
1965	BETSY	LA	3	945	HURDAT	3
1965	BETSY	SE FL	3	952	HURDAT	3
1966	ALMA	NW FL	2	977	HURDAT	2
1966	INEZ	SW FL	1	984	HURDAT	1
1967	BEULAH	TX	3	950	Hebert, et. al	3
1968	GLADYS	NW FL	2	977	HURDAT	2
1969	CAMILLE	MS	5	909	HURDAT	5
1969	GERDA	ME	1	980	HURDAT	1
1970	CELIA	TX	3	945	HURDAT	3
1971	FERN	TX	2	978	HURDAT	2
1971	EDITH	LA	2	978	HURDAT	2
1971	GINGER	NC	1	990	HURDAT	1
1972	AGNES	NW FL	1	984	HURDAT	1
1974	CARMAN	LA	3	952	HURDAT	3
1975	ELOISE	NW FL	3	955	MWR 4/76	3
1976	BELLE	NY	1	980	MWR 4/77	1
1977	BABE	LA	1	1000	MWR 4/78	1
1979	FREDERIC	AL	3	949	HURDAT	3
1979	DAVID	SE FL	2	972	MWR 7/80	2
1979	DAVID	GA	2	970	MWR 7/80	2
1979	BOB	LA	1	986	MWR 7/80	1
1980	ALLEN	TX	3	945	MWR 7/81	3
1983	ALICIA	TX	3	962	MWR 5/84	3
1984	DIANA	NC	2	970	MWR 7/85	2
1985	ELENA	MS	3	960	HURDAT	3
1985	GLORIA	NY	3	960	HURDAT	3
1985	JUAN	LA	2	974	HURDAT	2
1985	KATE	NW FL	2	967	MWR 7/86	2
1985	DANNY	LA	1	987	MWR 7/86	1
1985	BOB	SC	1	1002	MWR 7/86	1
1986	BONNIE	TX	1	991	HURDAT	1
1986	CHARLEY	NC	1	992	HURDAT	1
1987	FLOYD	SW FL	1	993	MWR 4/88	1
1988	FLORENCE	LA	1	983	HURDAT	1
1989	HUGO	SC	4	934	MWR 5/90	4
1989	CHANTEL	TX	1	986	MWR 5/90	1
1989	JERRY	TX	1	983	MWR 5/90	1
1991	BOB	RI	2	965	MWR 11/92	2
1992	ANDREW	SE FL	4	922	MWR 3/94	4
1992	ANDREW	LA	3	956	MWR 3/94	3
1995	OPAL	NW FL	4	942	Hebert, et. al	3
1995	ERIN	NW FL	2	973	Prelim Report	2
1995	ERIN	SE FL	1	984	Prelim Report	1
1996	FRAN	NC	3	954	Prelim Report	3
1996	BERTHA	NC	2	974	Prelim Report	2
1997	DANNY	AL	1	984	Prelim Report	1
1998	GEORGES	MS	3	964	Prelim Report	2
1998	BONNIE	NC	3	964	Prelim Report	2
1998	EARL	NW FL	1	987	Prelim Report	1
1999	BRET	TX	3	951	Prelim Report	3
1999	FLOYD	NC	3	956	Prelim Report	2
1999	IRENE	SW FL	1	987	Prelim Report	1

Table 2.3. Storm Category and Central Pressure at Landfall (Concluded)

Year	Name	Land Fall State	Category	Central Pressure	Source	HURDAT Category
2003	CLAUDETTE	TX	2	979	Prelim Report	1
2003	ISABEL	NC	3	957	Prelim Report	2
2004	IVAN	MS	3	946	Prelim Report	4
2004	CHARLEY	SW FL	4	941	Prelim Report	1
2004	JEANNE	SE FL	3	950	Prelim Report	2
2004	FRANCES	SE FL	3	960	Prelim Report	1
2004	GASTON	SC	1	985	Prelim Report	3
2004	CHARLEY	SC	1	992	Prelim Report	3
2005	KATRINA	LA	4	920	Prelim Report	1
2005	RITA	LA	4	937	Prelim Report	3
2005	CINDY	LA	1	991	Prelim Report	4
2005	DENNIS	NW FL	3	946	Prelim Report	1
2005	WILMA	SW FL	3	950	Prelim Report	3
2005	KATRINA	SE FL	1	984	Prelim Report	3

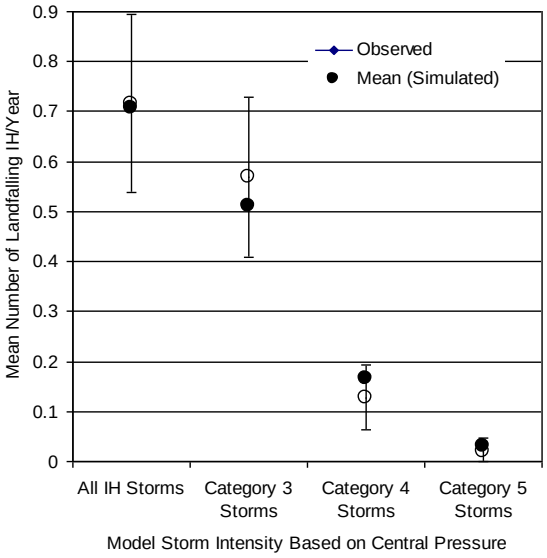

Figure 2.26. Comparison of Number of Annual Landfalling Intense Hurricanes by Storm Category (IH defined by pressure).

of recent landfalling storms that have been followed by detailed studies of the wind field at the time of landfall. All of the reconstructed wind fields were produced by NOAA/HRD. The results of these studies are given in Powell (1987), Powell, Dodge and Black (1991), Powell and Houston (1996), Powell and Houston (1998) and Houston, Powell and Dodge (1997).

As indicated in Table 2.4, the official rating (defined by wind speed) given to many of the hurricanes is high. In Table 2.4 the shaded rows indicate storms where the official landfall category is higher than that indicated by the wind speed analysis performed and published by NOAA/HRD. Most of these over-ratings occur when Category 2 storms are scored as Category 3 storms. At least 50% of the Category 3 storms given in Table 2.4

Table 2.4. Comparison of HURDAT Hurricane Classification to Classifications Resulting from Detailed Studies Performed by NOAA/HRD

Hurricane	Year	HURDAT Category at Landfall	Category by Central Pressure at Landfall	Category by Maximum Wind Speeds at Landfall (NOAA/HRD)
Frederic	1979	3	3	3
Alicia	1983	3	3	1-2
Hugo	1989	4	4	4
Andrew	1991	4	4	4
Emily	1993	3	3	3
Erin	1995	2	2	1
Opal	1995	3	4	2
Bertha	1996	2	2	2
Fran	1996	3	3	2

are over-rated by one category. In the case of the Hurricane Alicia surface wind field analysis given in Powell (1987), the averaging time is not explicitly stated, although a sustained (or one-minute average) is implied. The maximum surface level wind speed given in Powell (1987) for Alicia at landfall is 39 m/sec. If this wind speed is taken as a one-minute average then the storm would be a Category 1 hurricane. If this 39 m/s wind speed is taken to correspond to a mean hourly value, then the storm would be rated as a Category 2 storm; hence, a range of storm categories is given in Table 2.4.

If the hurricanes given in Table 2.4 had been categorized by central pressure instead of the estimated maximum wind speed at the time of landfall, there would almost be a one-to-one correspondence between the scored category and the actual category, with only Opal having a different category. Considering that the hurricane categories assigned to the storms by the National Hurricane Center (NHC) (given in Table 2.2) are based on upper level wind speeds measured by numerous aircraft, coupled with surface level wind speeds measured at data buoy and C-MAN stations, it is not unreasonable to assume that the errors in hurricane classification (as defined by the peak wind speed) in earlier years, when the quantity and quality of full scale data was not as high as today's, were even more frequent. In general, it is much simpler to determine the minimum central pressure in a hurricane than it is to reconstruct the wind field, and only over the past two decades has a significant effort gone into post-storm hurricane wind field reconstruction. Errors associated with the measurements of wind speed are much greater than those associated with the measurements of central pressure. Figure 2.27 shows comparisons of landfall rates of all hurricanes as a function of location along the coastline and storm intensity (defined by central pressures). Note that for the landfalling storms that have no value of central pressure assigned to them, it has been assumed that the landfall category of the storm as given in HURDAT (as given in Table 2.3) is consistent with the landfall category associated with the storm central pressure at the time of landfall. A simulated storm is categorized as a hurricane only if the modeled sustained wind speed at the time of landfall (one minute average over water) exceeds 74 mph, irrespective of the value of the central pressure. The model yields an average of 1.79 hurricane landfalls per year vs. a historical average of 1.72 storms per year. The histograms of landfall rates shown in

Figure 2.27 are statistically equivalent as indicated by a χ^2 test performed at a 5% significance level. Figure 2.28 shows a comparisons of the modeled and observed central pressures at landfall plotted vs. return period for storms making landfall along the Gulf coast (west of the FL-AL border), the Florida coastline, the Atlantic coastline north of Florida and for the entire Gulf and Atlantic U.S. coastline. Note that in the development of Figure 2.28, there is some uncertainty in the ranking of some of the storms having central pressures higher than Category 3 values since central pressure data is not available for all Category 1 and 2 storms. The probability distributions of the historical data used to derive the central pressure vs. return period plots given in Figure 2.28 have been developed assuming that all the storms having no central pressure data are weaker (i.e., have higher central pressures) than the strongest Category 2 storm which has central pressure data. Figure 2.28 shows excellent agreement between the modeled and observed central pressures as a function of return period for the coastal US as a whole and for the three individual regions.

The agreement is particularly good for storms having intensities of Category 3 or higher, where no assumptions have had to be made with respect to missing central pressure data. Again, the landfall statistics for the modeled data have been derived from a 100,000-year simulation of storms occurring in the Atlantic Basin. Figure 2.29 presents plots similar to those shown in Figure 2.28 except for smaller geographic areas (or coastal segments). The agreement between the modeled and observed data, while still very good, is not as good as that seen in the case of the large coastal segments primarily because the number of storms making landfall along these smaller segments is relatively small.

2.3.8 Predicted Wind Speeds vs. Return Period

Using the storm track simulation methodology combined with the wind field and gust factor models described in Vickery, et al. (2000a), 100,000 years of storms were simulated. When a simulated storm is within 250 km of a milepost, the peak gust wind speeds are recorded at 15-minute intervals, with the largest wind speed in each of 16 directions and the largest overall being retained. Upon completion of a 100,000-year simulation, the wind speed data are rank ordered and then used to define the wind speed probability distribution conditional on a storm being within 250 km of the site. The probability that the tropical cyclone wind speed (independent of direction) is exceeded during time period *t* is,

$$P_t(v > V) = 1 - \sum_{x=0}^{\infty} P(v < V \mid x)\, p_t(x) \tag{2.17}$$

where $P(v < V \mid x)$ is the probability that velocity v is less than V given that x storms occur, and $p_t(x)$ is the probability of x storms occurring during time period t. From 2. 20, with $p_t(x)$ defined as Poisson and setting t to one year, the annual probability of exceeding a given wind speed is,

$$P_a(v > V) = 1 - \exp[-\upsilon P(v > V)] \tag{2.18}$$

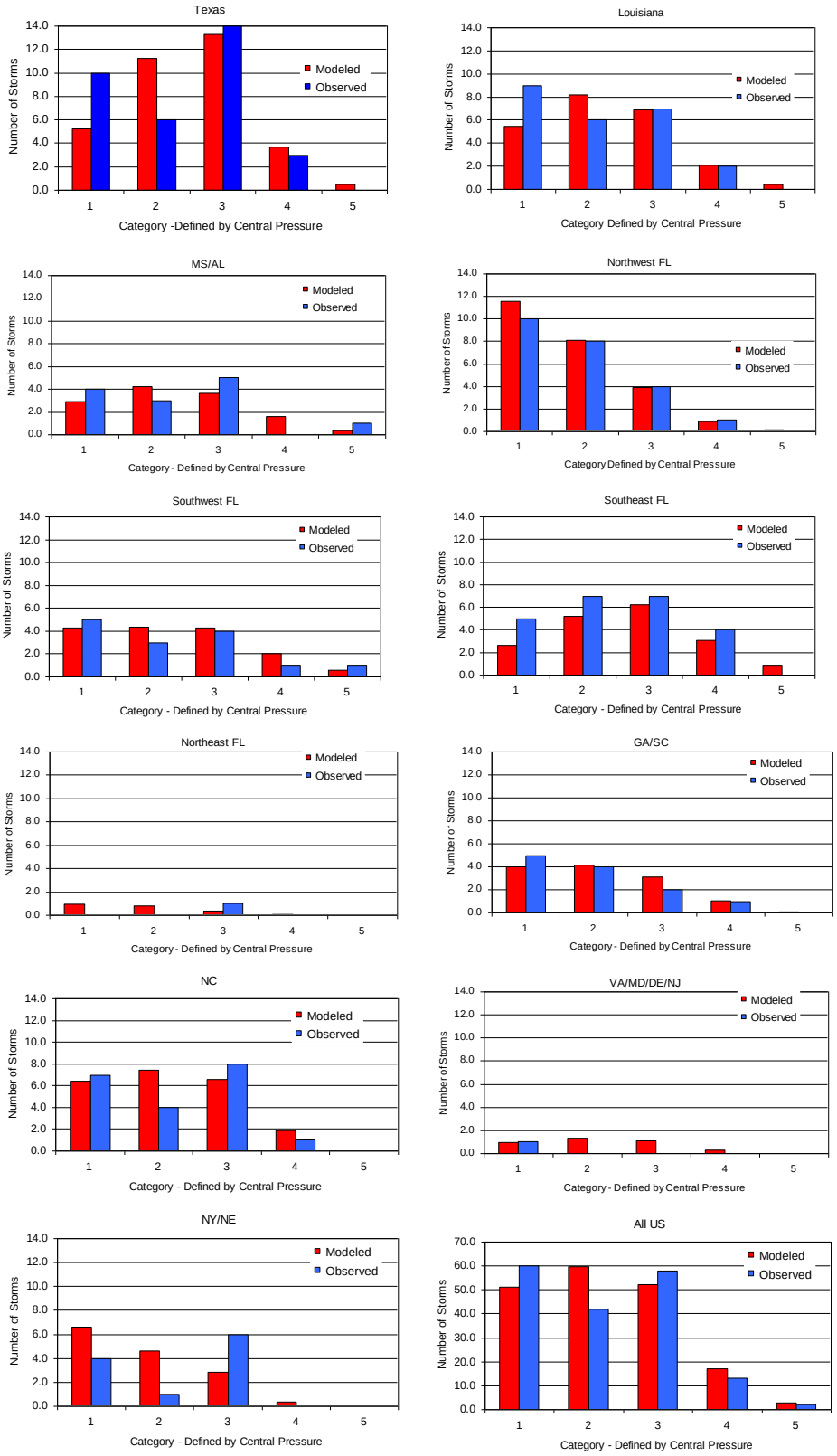

Figure 2.27. Comparisons of Modeled and Observed Hurricane Landfall Rates as a Function of Storm Category.

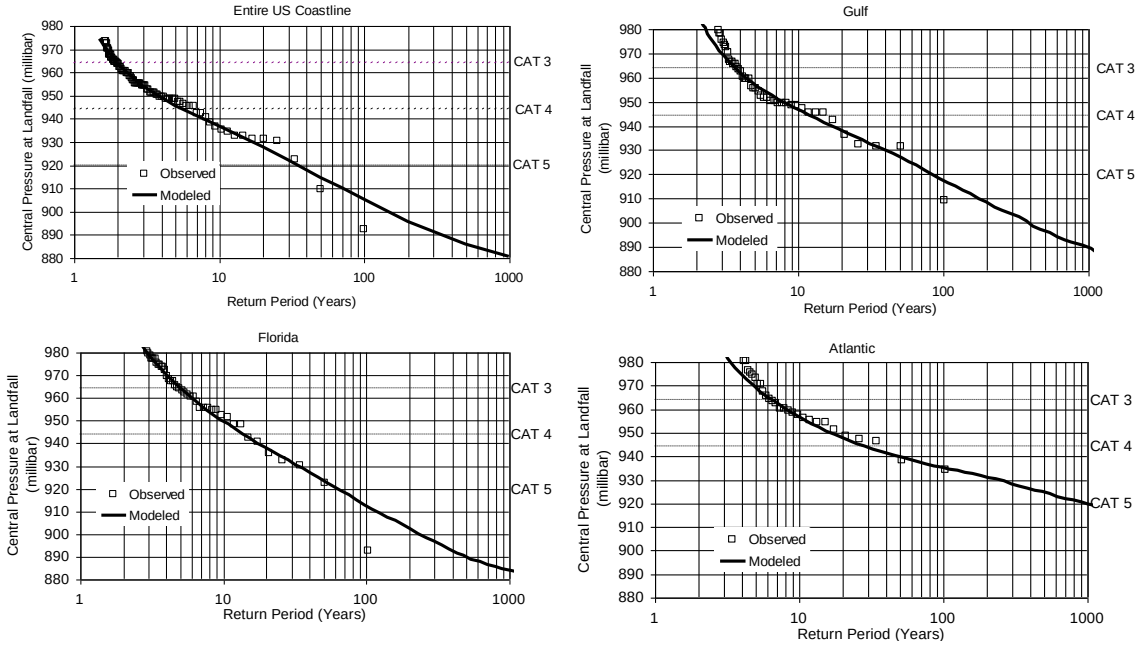

Figure 2.28. Comparison of Modeled and Observed Storm Central Pressure at Landfall vs. Return Period for Various Geographic Regions.

where υ represents the average annual number of storms approaching with 250 km of the site (i.e., the annual occurrence rate).

Figure 2.30 presents a plot of 100 year return period peak gust wind speeds along the Gulf and Atlantic coastlines derived from the updated hurricane simulation model used in Hazus. The wind speeds given in Figure 2.30 are peak gust wind speeds at a height of 10 m above ground over open terrain.

2.3.9 Summary

The hurricane simulation methodology models the entire track of a tropical storm in the Atlantic basin and has been validated through comparisons to historical data along the US coastline. The modeling approach allow the storms to curve and change speed and intensify as they move, and is able to reproduce the continually varying statistics associated with central pressure, heading, etc., along the US coastline. The model is an improvement over earlier hurricane simulation techniques since it eliminates the problems associated with the selection of a sub-region from which to derive the statistical distributions needed in traditional simulation models. In traditional models, the use of large areas to derive the hurricane statistics will smear any local climatological features that are inherently reproduced in this method. The prime advantage of this approach compared to the traditional approaches is the ability to properly model hurricane wind risk over large regions, within which the hurricane climatology can vary significantly. This improved prediction capability provides significant technical advantages for

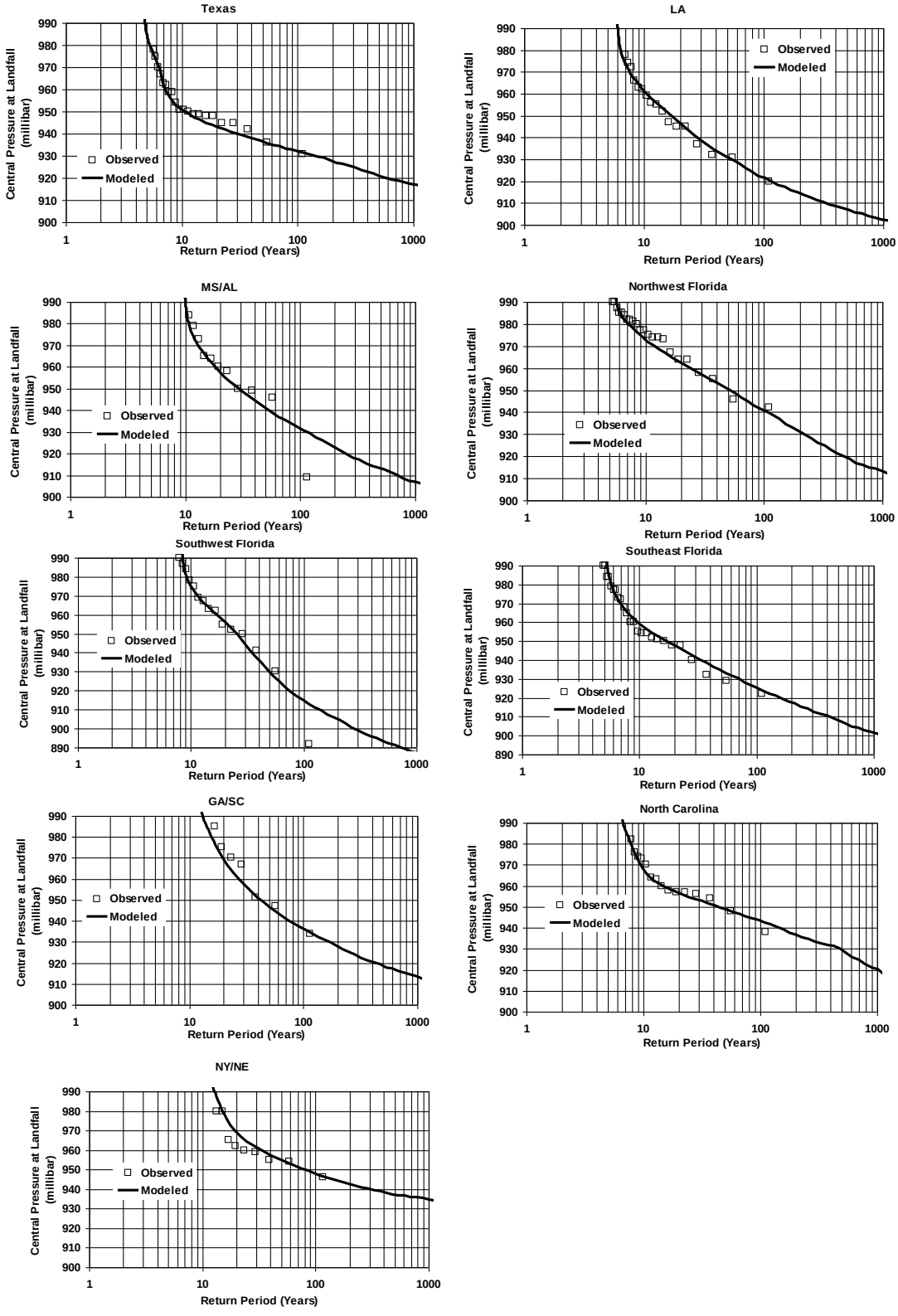

Figure 2.29. Comparison of Modeled and Observed Storm Central Pressure at Landfall vs. Return Period for Various Local Geographic Regions.

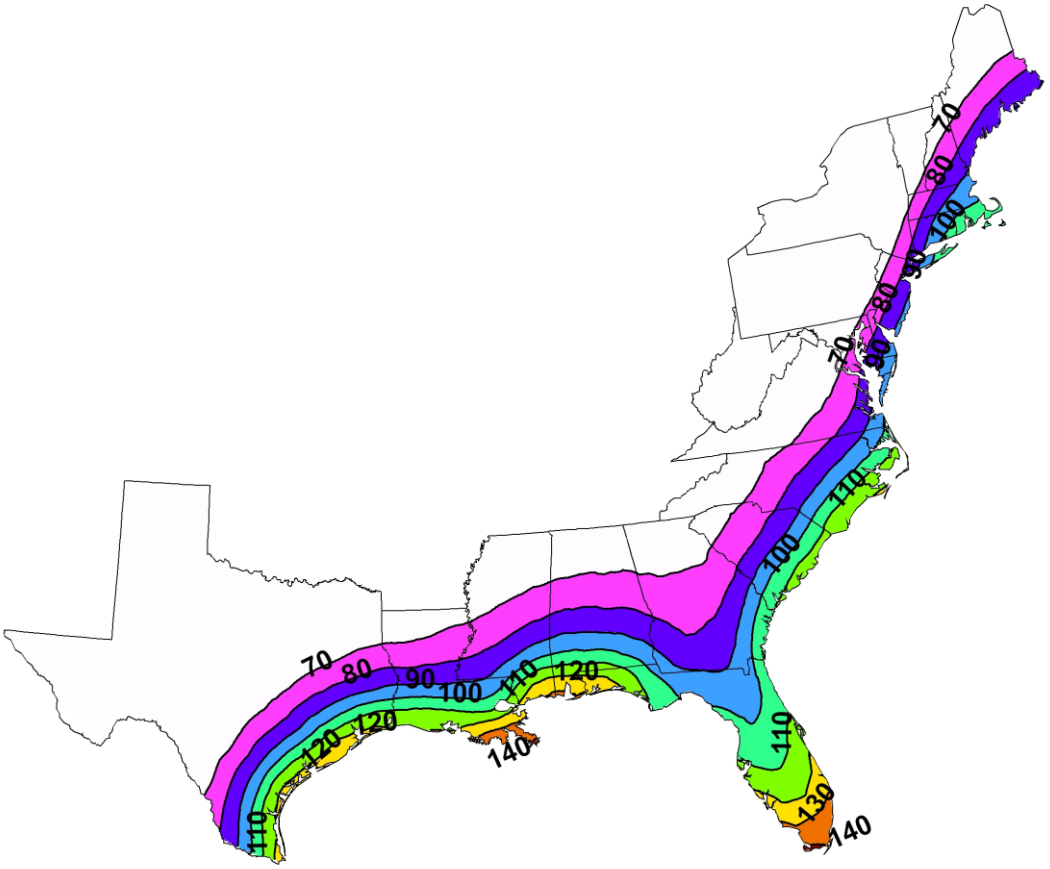

Figure 2.30. Predicted 100 Year Return Period Wind Speed for US Atlantic and Gulf Coast.

portfolio analyses which encompass large geographic areas than do the previous published and accepted models such as those described by Batts, et al. (1980), Georgiou (1985), Neumann (1991), and the NOAA publications NWS 23 and NWS 38.

2.4 Hurricane Rainfall Rate Model

2.4.1 Introduction

Hurricane flow is a complex atmospheric system comprising of multiscale systems interacting in a nonlinear and varying degree of intensity. Some of the known environmental features affecting the hurricane dynamics include: vertical wind shear, trough interactions, warm eddy core interactions, outflow patterns, eddy angular flow convergence, upper level cooling, dry air intrusions, eye wall cycles, low-level temperature advection, rain band downdrafts, and ocean currents (cf., Hong, et al., 1998). For near-land cyclonic flows, additional interactions such as fronts, coastline shape, topography and soil moisture availability play a significant role in the storm dynamics particularly during the land falling stages (Reddy and Raman, 1997a, 1997b; Schneider, 1998).

Traditionally, one of the most difficult variables to model within an atmospheric system is the rainfall. The variation of the rainfall amount within the hurricane system is a result of numerous nonlinear processes interacting simultaneously. Even the most comprehensive modeling systems, with very detailed physics, and numerical algorithms assimilating observational data, have limited success estimating the rainfall intensity and location associated with the hurricane (Elsberry, 1998).

However, rainfall rates and their locations are important variables to be considered for a risk management system. Even approximate estimates can provide vital information necessary for resource planning, flooding, erosion, as well as structural risk assessment. Hence, there is an ongoing requirement to adopt even heuristic approaches for estimating rainfall rates and distribution within the hurricane flow. To satisfy this need, an empirical approach (referred to as "HuRRDE": Hurricane Rainfall Rate and Distribution Estimator), relating the sectorial rainfall rate with annular distance from the hurricane center, has been developed and implemented in the Hazus Hurricane Model. Section 2.4.2 reviews the available data and prior studies. Section 2.4.3 discusses the model development and the corrections for intensity, translation speed, and frictional convergence during landfall. Section 2.4.4 presents the model implementation and calibration using a number of recent storms. Some comments about the rainfall model are included in Section 2.4.5.

2.4.2 Data and Prior Studies

There is a paucity of high resolution, continuous observations of rainfall rates within the hurricane flow. However, several efforts have been made to assimilate satellite information with surface and aircraft data (e.g., Shi, et al., 1997). The present model focuses on published analyses of Special Sensor Microwave/Imagery (SSM/I) (see Alliss, et al., 1992; Rodgers, et al., 1994; Ferraro, et al., 1996). The SSM/I analyses provide detailed radial rainfall rate information. Over fifty studies were evaluated for the purpose of obtaining relevant data.

The starting point for developing the model was the observational study by Rodgers, et al., in which 103 SSM/I observations for 18 western North Atlantic tropical cyclones from 1987 to 1989 were used for documenting the precipitation characteristics. The tropical cyclones used in their study were:

1987 storms: Cindy, Dennis, Emily, and Floyd;

1988 storms: Chris, Debby, Florence, Gilbert, Helene, Isacc, Joan, and Keith;

1989 storms: Dean, Felix, Gabrielle, Hugo, Iris, and Jerry.

Figure 2.31 adopted from Rogers, et al. (1994), summarizes the SSM/I derived azimuthally averaged rain rates for the eight 55 km annuli (rings) around the center. The distribution is considered robust as it is averaged over 47 depressions (P_{min} > 1000 mb), 29 tropical storms (P_{min} = 1000–977 mb), and 27 hurricanes (P_{min} < 977 mb). The radial distribution for the hurricane case is considered the first step in the model development. However, it should be noted that the Rogers, et al. (1994) data has a 55 km resolution.

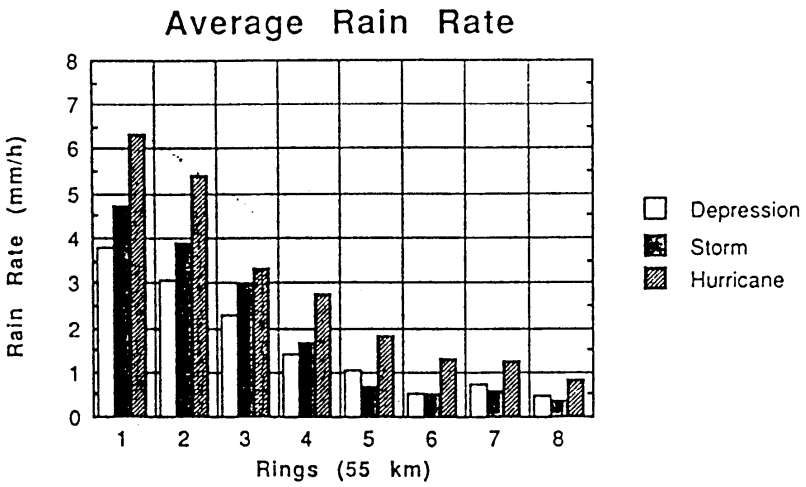

Figure 2.31. Average Rain Rate.

Evidence from both observational studies (Alliss, et al., 1994) and numerical studies (Drury and Evans, 1998) suggests there is even more intense precipitation at the inner-core than at the first 55 km annular ring. Hence, in the next step of the model development, a sharp increase from the first ring to the inner core is assumed. The inner core is assumed to be at a distance of R_{max} from the 'eye'. Though, typically R_{max} will vary for every hurricane at different stages of development, for the purpose of developing the simple rainfall rate model, R_{max} was initially assumed to be constant close to landfall. Accordingly, R_{max} was considered to be 30 km. Note that considering the overall uncertainty associated with entire system, this first-order assumption is not expected to affect the results significantly. Accordingly, Figure 2.32 shows the 'observed' or 'analyzed' radial rainfall distribution used for model development. The sharp increase in the rainfall rate from 1.83 R_{max} (55 km) to R_{max} is apparent. It should be noted that the center ('eye') generally does not experience any significant precipitation and hence the R = 0 case is assigned to be rainfall free (see also Alliss, et al., 1994, for Hurricane Florence case).

2.4.3 Model Development

For developing the relation between rainfall rate (RR) and radial distance, the first approach was to relate RR through a fifth-order polynomial to R/R_{max}. However this approach has obvious serious stability considerations. The higher order (cubic and beyond) terms are linked with increasingly larger distances (R/R_{max} increases as R increases). Thus, a small error would amplify in the system several folds making the outcome extremely sensitive and unrealistic. To overcome this, a relationship between RR and R_{max}/R was developed. Accordingly, for the data shown in Figure 2.32, the relation is of the form:

$$RR = -5.5 + 110\left(R_{\max}/R\right) - 390\left(R_{\max}/R\right)^2 + 550\left(R_{\max}/R\right)^3 - 250\left(R_{\max}/R\right)^4 \quad (2.19)$$

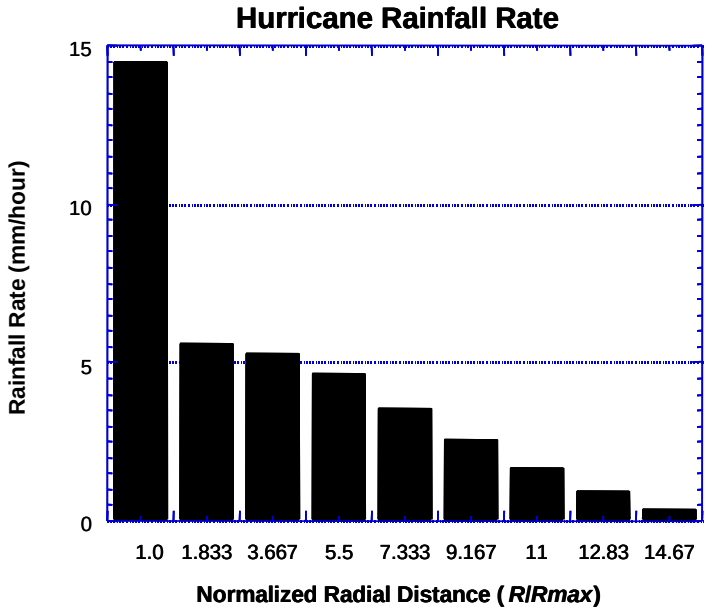

Figure 2.32. Rainfall Rate as Function of Normalized Radial Distance from the "Eye" (R_{max} is assumed to be 30 km).

Figure 2.33 shows the rainfall rates from Figure 2.32 and the rainfall rates represented by Equation 2.19. Overall there is a good agreement amongst the two (r^2 = 0.92). Some differences are also seen between the 'analyzed' data and the prediction using Equation 2.19, particularly in terms of the decreased precipitation from R_{max} to the "eye." This 'error' exists due to the approximate estimation of R_{max} in this particular case. Also, caution was exercised so as not to 'over fit' the equation to the data set, which could cause loss in predictive skills. Within these constraints, Equation 2.19 provides a reasonable means of estimating rainfall rate in the hurricane as a function of annular distance from the eye.

In order to make the empirical relation applicable to various hurricane intensities, corrections need to be made to Equation 2.19. Three corrections, as described in the following paragraphs, have been implemented.

The first correction involves the changes in the central pressure with time (dP/dt) (and, hence, the intensity of the hurricane). Note that, Equation 2.19, due to the averaging involved, may best represent Category 1-2 type-hurricanes. Typically, as the central pressure drops, a storm becomes more intense, yielding larger rainfall rates. For Equation 2.19, this correction is inherent, if R_{max} is calculated as function of ΔP.

By adopting relations between R_{max}, ΔP, and latitude, ψ, similar to Equation 2.19, changes in the rainfall rate will occur with changes in ΔP. Figure 2.34 shows a summary of a review from Rogers, et. al (1994) comparing hurricanes (P_{min} < 977 mb), storms (977 mb < P_{min} < 1000 mb), and depressions (P_{min} > 1000 mb). As seen in the figure, the hurricane rainfall rate is about 30 to 40% more than the storm rainfall rate, and about

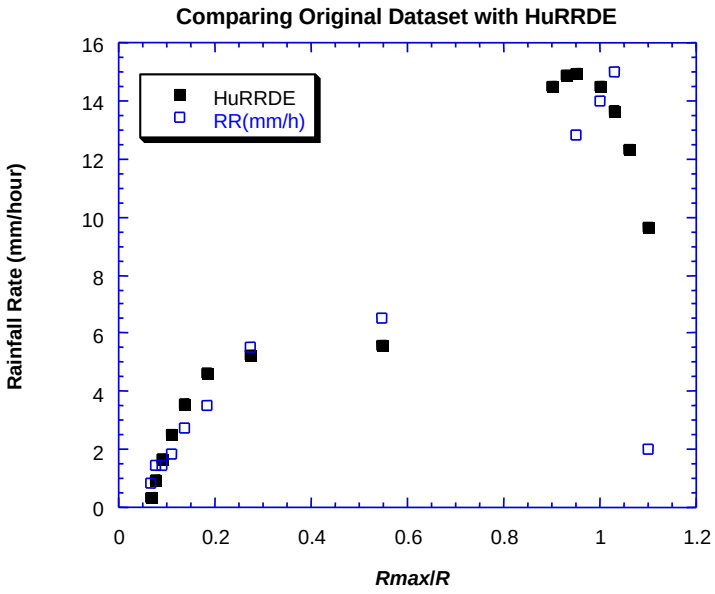

Figure 2.33. Plot Showing the Original Rainfall Rate with the Estimation from Equation 2.19.

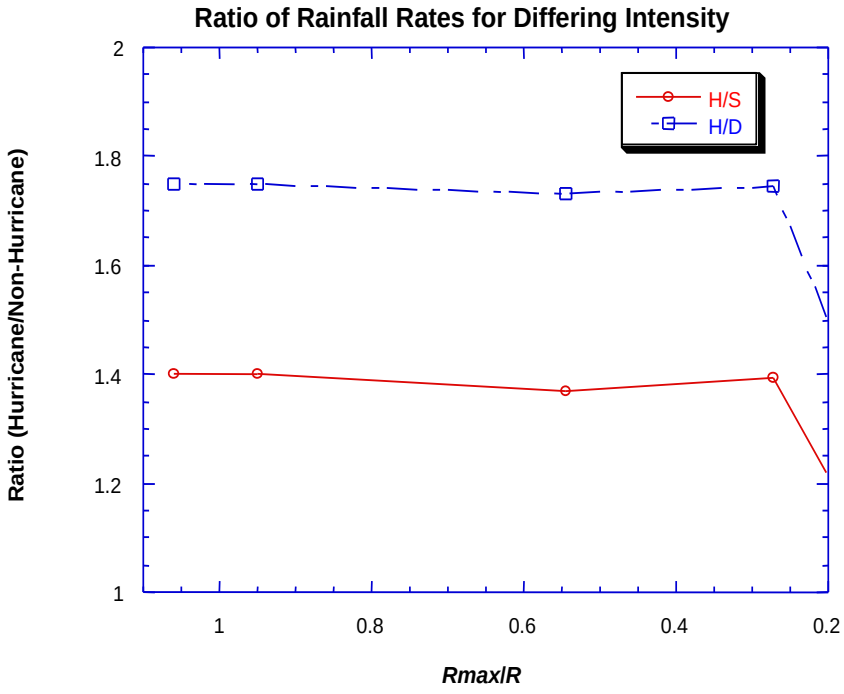

Figure 2.34. Ratio of Rainfall Rates for Hurricane Against Non-hurricane Tropical Cyclones as a Function of Normalized Radial Distance, Following Rogers, et al. (1994). (H/S refers to the ratio of hurricane (P_{min} < 977 mb) to storm (977 mb < P_{min} < 1000 mb) rainfall rates. H/D refers the ratio of hurricane to depression (P_{min} > 1000 mb) rainfall rates).

75% more than the depression rainfall rate. Extrapolating this, it is assumed that for every 20 mb drop a 35% higher effective rainfall rate for the tropical cyclone. Hence, *RR* can be corrected for the hurricane category as follows:

$$RR_e = k \cdot RR \tag{2.20}$$

The mid-values of *k* for Category 1 through 4 hurricanes are assumed to be 1, 1.35, 1.85, and 2.5. A Category 5 hurricane making landfall, will have rainfall rates that would be governed by very special forcing and cannot be estimated in any simple manner.

Additionally, for a more dynamic change in the rainfall rate, due to the rate of change of central pressure (without change in the category), it is assumed that:

$$RR_p = RR_e \left[1 - \left(dP/dt\right)/100\right] \tag{2.21}$$

Thus, for example, a 10 mb drop would lead to a change in the rainfall rate by a factor of 1.1, while a rise in the central pressure (positive dP/dt) by 5 mb would effectively decrease the rainfall rate to $0.95RR_e$. Thus, following Equations 2.19 and 2.21, an increase in the central pressure over time will lead to increased R_{max}, hence an indirect reduction in *RR*, and a direct decrease in the central pressure intensity corrected rainfall rate (RR_p).

The second correction is dependent on how fast the storm is moving. Studies suggest (see Jones, 1987; Baik, 1989, for instance) that there is an asymmetric rainfall distribution as a function of the storm motion. Once again, using the data from Rogers, et al. (1994), sectorial rainfall rate corrections can be made for slow (<8 knots) and fast (>15 knots) moving tropical systems as follows:

$$RR_{sp} = s \cdot RR_p \tag{2.22}$$

The value of the coefficient '*s*' is shown in Table 2.5.

Table 2.5. Sector Values for Rainfall Rate Parameter, *s*

Sector	*s* in slow storms	*s* in fast storms
0-45	1.45	1.15
46-90	1.05	1.15
91-135	0.55	1.35
16-180	0.65	1.15
181-225	0.85	0.85
226-270	0.95	0.65
271-335	1.15	0.8
336-359	1.35	0.95

A third potential correction is for land falling component. Studies, particularly numerical simulations, suggest that in the first sector with the onshore winds (0-45 with zero angle corresponding to the coastline) rainfall rate is increased by 25%. However, further

research is required to determine whether this correction should be included in a future update to the rainfall model.

Figure 2.35 shows an independent verification for data obtained for Hurricane Florence and Hurricane Hugo (in the developing as well as developed stage). The observations are obtained from Alliss (1992). Note that, there is lack of rainfall rate observations at higher $R_{max.}$ In this "off-line" comparison, there has been no correction for the storm speed or for the sector. Only the category change has been accounted for. Thus, for Florence, a Category 2 was assumed. For Hugo, we assumed initially a storm correction (reducing the RR_e), and for the developed hurricane, a Category 4 correction was assumed. As can be observed, there is an encouraging agreement in the 'observed' and the estimated rainfall rates.

2.4.4 Hurricane Rainfall Rate Model Implementation and Calibration

In the final hurricane simulation model, Equation 2.19 is used to determine the base rainfall rate (RR) for R/R_{max} greater than or equal to one. For values of R/R_{max} between zero and one, a linear model is used where the RR is zero at R/R_{max} equal to zero and then increases linearly up to the value of RR determined by Equation 2.19 at R/R_{max} equal to one. The base rainfall rate is adjusted for storm category. Instead of using distinct k factors for a given storm category (see Equation 2.19), k is determined using the following linear function of central pressure deficit (mb):

$$k = 0.0319\Delta p - 0.0395,\ k \geq 1k \tag{2.23}$$

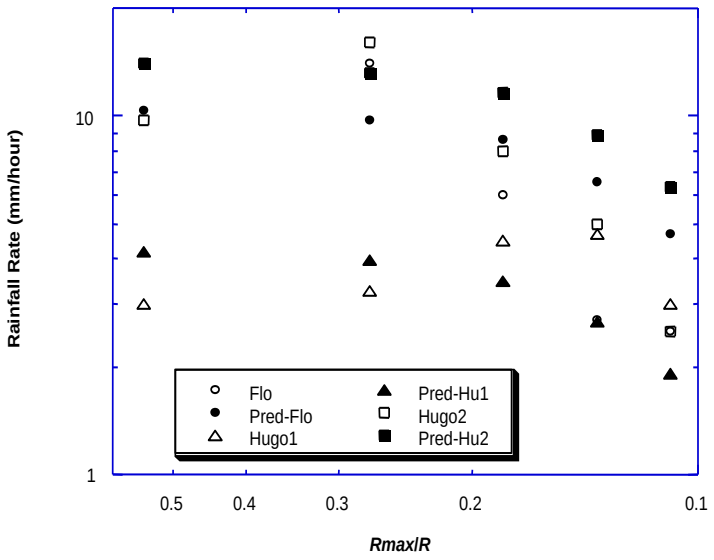

Figure 2.35. Observed and Estimated Rainfall Rates for Hurricane Florence (Flo, Pred-Flo), Hurricane Hugo in Developing Stages (Hugo1, Pred-Hu1), and in Developed Stages (Hugo2, Pred-Hu2).

This line was developed by plotting the factors given following Equation 2.19 at the middle of the range in central pressure deficit for the particular storm category and then fitting a line ($r^2 = 0.9933$).

The base rainfall rate is also adjusted for storm translation speed using the sector dependant factors given in Table 2.5. Not yet implemented into the rainfall rate model is the correction for the increase in rainfall rate within the onshore flow regime as the hurricane makes landfall. This factor, when implemented, will further increase the rainfall rate for locations on or near the coast receiving onshore winds by 25%.

Several hurricanes, including Hugo (1989), Bertha (1996), Fran (1996) and Bonnie (1998), for which relatively high quality rainfall measurements at a number of meteorological stations are available, were used to calibrate the rainfall rate model. By comparing the model predictions and the actual measurements, the rainfall rate model was found to provide reasonably accurate estimations of the peak rainfall rates for most of the stations investigated. However, the off-peak rainfall rates were significantly overestimated. A number of factors may contribute to the overestimation: (1) the drop of rainfall rate with the increase in R/R_{max} may be much faster than that predicted using Equation 2.19; (2) rain gauges located on the ground often under predict the rainfall during high winds due to the effects of the flow aerodynamics around the rain gauges; (3) other features, such as the hurricane's interaction with other weather systems, outflow patterns and sea-to-land transitions may also contribute to the inconsistency between the measured rainfall rates and the predicted ones. To overcome this problem, a modification factor (*MF*), defined as the ratio of the actual measurement to the model prediction, was developed so that the proposed model will provide the best estimation of the rainfall rate in a hurricane. Figure 2.36 shows the relationship between the modification factor and R/R_{max} for the hurricanes investigated. The modification factor is seen to decrease with the increase of R/R_{max}. To be used in the rainfall rate model, a relationship between the modification factor and R/R_{max} was determined using least square regression, which is of the form:

$$MF = -0.7 * ln\left(R / R_{max}\right) + 1.0 \ . \tag{2.24}$$

Note that when *MF* is greater than 3.0, it is taken as 3.0 and when *MF* is less than 0.2, it is taken as 0.2. Note also that when R/R_{max} is less than 1.0 (i.e., within the hurricane eye), the modification factor is greater than 1.0, which indicates the rainfall rate around the is eyewall relatively uniform (i.e., stable rainband). Accordingly, the linear model assumed previously may underestimate the rainfall rate for this region. Considering the modification factor, the final rainfall rate output from the simulation model is:

$$RR_{MFsp} = MF \cdot RR_{sp} \tag{2.25}$$

Figure 2.37 shows the comparison between the model predictions and the actual measurements for Hurricanes Hugo (1989), Bertha (1996), Fran (1996), and Bonnie (1998). Most of the sites investigated for these four storms are ordinary commercial

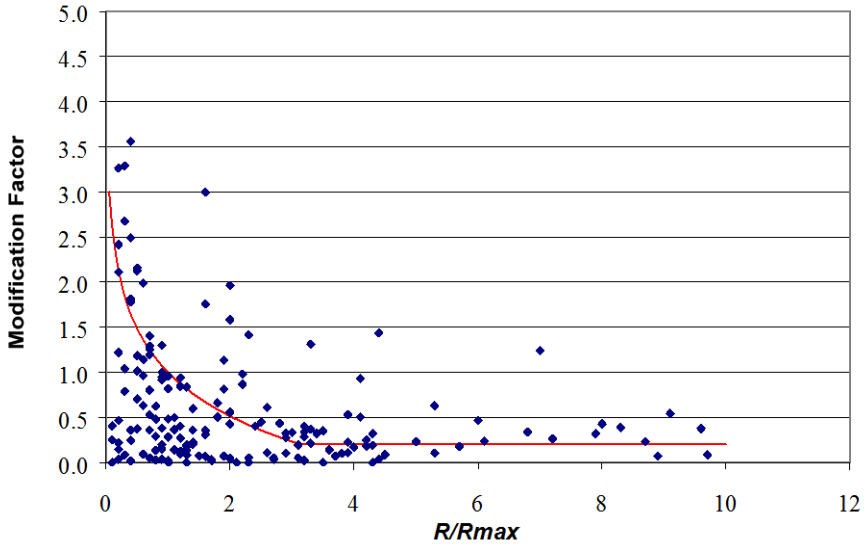

Figure 2.36. Relationship Between the Modification Factor and R/R_{max}.

airports with open terrain except Kure Beach, which is a private meteorological station located about 300 m inland. All the data collected are continuous hourly rainfall rates. The model is seen to provide reasonably accurate predictions for most of the sites investigated. However, abnormalities still exist for several sites and will be addressed individually in the following paragraphs.

The eye of Hurricane Hugo passed over the coast of South Carolina near Charleston at approximately 04:00 UTC on September 22, 1989. The model is seen to underestimate the rainfall rate when Hugo was approaching Charleston Airport. One possible explanation is that the rainfall might be intensified significantly within the onshore flow regime when Hugo made landfall and this rainfall enhancement effect was not considered in the proposed model.

Considering rainfall intensification within the onshore flow regime for a landfalling hurricane can be an area of future development. Besides the underestimation of the rainfall rate at the approaching stage of Hurricane Hugo, the peak rainfall rate at Charleston Airport was significantly overestimated by the model. The reason of the overestimation is unknown. The rainfall rate model predictions agree well with the actual measurements at Columbia Airport and Greenville/Spartanburg Airport, two inland sites located about 180 km and 330 km to the coast, respectively.

The rainfall model catches the general trend and the first peak of the rainfall rate at Wilmington Airport for Hurricane Bertha (1996). The model indicates a second peak when the backside of the storm moved across Wilmington Airport. However, this peak was not apparent on the actual records. Similar trend was also observed at Kure Beach. Moreover, at Kure beach, one extremely high peak rainfall rate (compared to the value at Wilmington Airport, which is fairly close to Kure Beach) was recorded by the rain gauge,

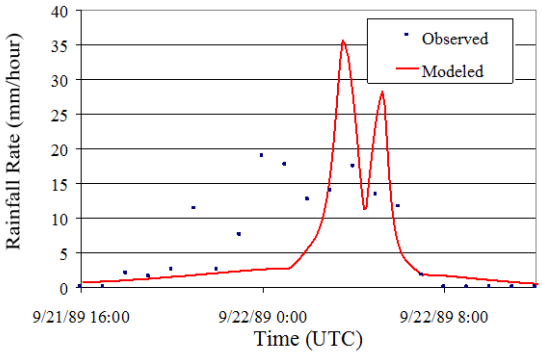

Charleston Airport, Hugo (1989)

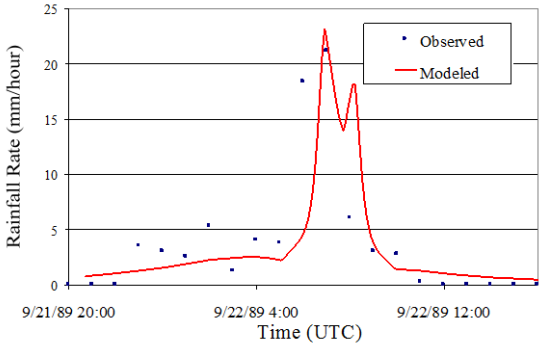

Columbia Airport, Hugo (1989)

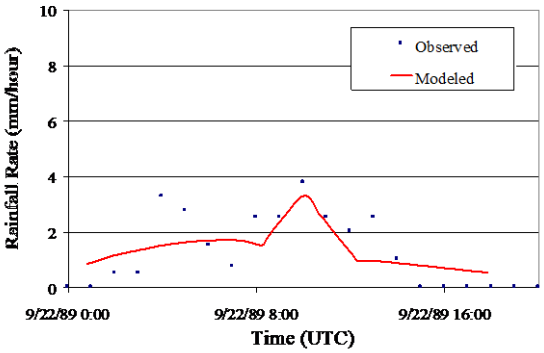

Greenville/Spartanburg Airport, Hugo (1989)

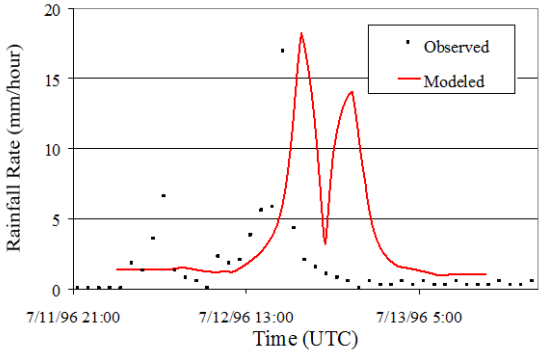

Wilmington Airport, Bertha (1996)

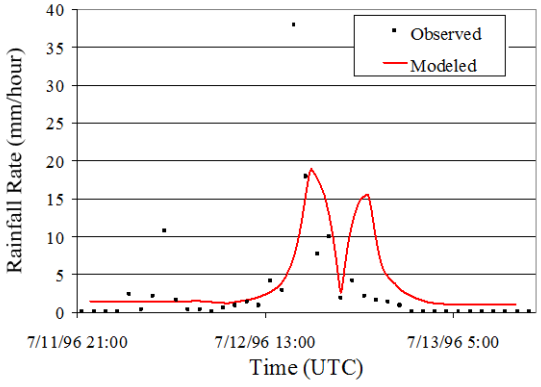

Kure Beach, Bertha (1996)

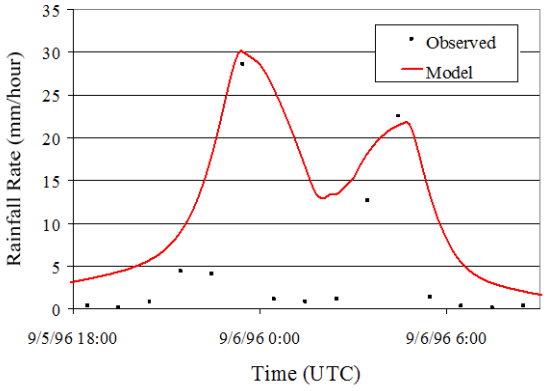

Wilmington Airport, Fran (1996)

Figure 2.37. Comparison of Observed and Modeled Hurricane Rainfall Rates.

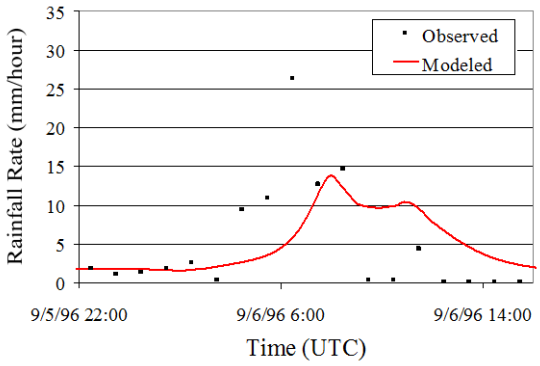

Greensboro Airport, Fran (1996)

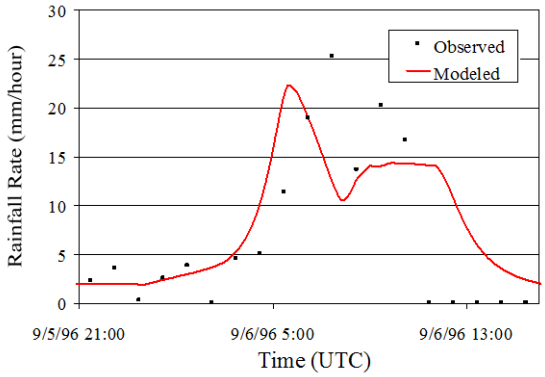

Raleigh/Durham Airport, Fran (1996)

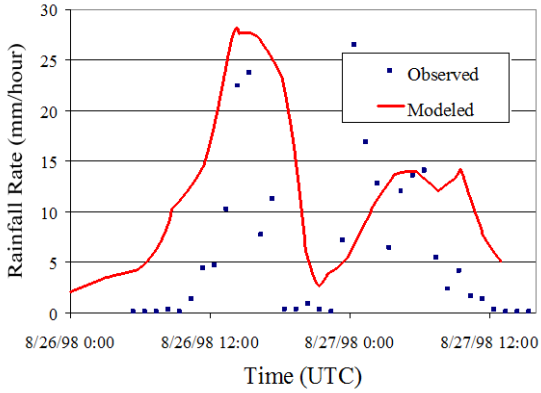

Kure Beach, Bonnie (1998)

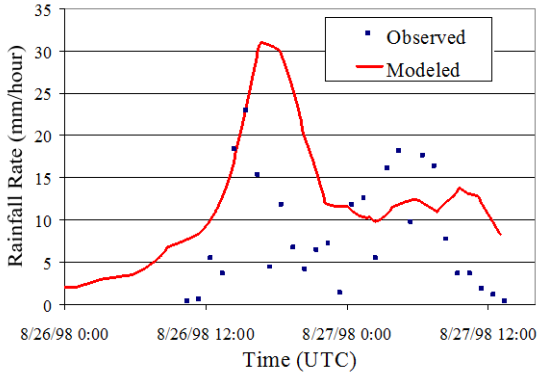

Wilmington Airport, Bonnie (1998)

Figure 2.37. Comparison of Observed and Modeled Hurricane Rainfall Rates (concluded).

which is believed to be caused by rainband downdrafts. Note that the rainfall data obtained at Kure Beach in Hurricane Bertha was not used in the calibration. Therefore, the fairly good agreement between the model predictions and the actual measurements at this site validated the rainfall rate model.

Fran was a Cape Verde hurricane that moved across the Atlantic during the peak of the hurricane season. It made landfall around 00:30 UTC on September 6, 1996, on the North Carolina coast. The model is seen to provide very good estimation of the rainfall rate during the passage of Hurricane Fran at Wilmington Airport. However, the model overestimated the rainfall rate in the eye when virtually no rain was recorded by the rain gauge. The peak rainfall rate at Greensboro Airport was underestimated by the model. The rainband shifting to the north-west quadrant may cause unusually high precipitation at Greensboro Airport. The model predictions at Raleigh/Durham Airport agree relatively well with the actual measurements.

Bonnie (1998) made landfall at almost the same location as Fran, but instead of moving straight inland, drifted along the North Carolina coast, causing difficulties in predicting

its intensity and rainfall rate. From the last two charts in Figure 2.37, the model is seen to follow the general trend of the actual measurements at Kure Beach and Wilmington Airport. However, the correlation between the model predictions and the actual measurements is poor (compared with those in Hurricanes Hugo, Bertha and Fran). When a hurricane is drifting along the coast, complex internal boundary layers and significant transverse eddies may be observed in the storm, resulting in unusually large fluctuations in the measured wind speeds and rainfall rates. Further efforts are required to model this complex situation.

Another feature to the interest of risk management is the total rainfall at a particular location during the whole event. Therefore, total rainfall data collected from eight hurricanes, i.e., Frederic (1979), Elena (1985), Hugo (1989), Erin (1995), Opal (1995), Bertha (1996), Fran (1996), and Bonnie (1998), were used to validate the rainfall model. The comparisons between the model predictions and the actual measurements are shown in Table 2.6. The total rainfalls listed in the column, Full Scale 1, were calculated from continuous hourly rainfall data shown in Figure 2.37. The values in the column, Full Scale 2, were obtained from annual Atlantic hurricane season summary for the years of 1979, 1985, 1989, and 1996 (Hebert, 1980; Case, 1986; Case and Mayfield, 1990; Pasch and Avila, 1999). Preliminary reports by the National Hurricane Center for Hurricanes Erin and Opal were used to determine the total rainfall for these two storms (Rappaport, 1995; Mayfield, 1995). Since no information about the time span for the total rainfall was given in the annual Atlantic hurricane season summaries or the preliminary reports, a period of plus and minus 12 hours from the time when peak rainfall rate occurred was assumed in the model to calculate the total rainfall, which means a 24-hour cumulative rainfall given by the model. Accordingly, the model predictions are expected to be slightly lower than the values shown in the column denoted Full Scale 2. The mean and standard deviation of the ratios of the model predictions to the full scale measurements are 0.96 and 0.50, respectively. Note that if the extremely high value (2.53) at Wilmington in Hurricane Fran is taken out from the data set, the mean and standard deviation drop to 0.91 and 0.41, respectively. Note also that when both continuous station records and total rainfall data for an event are available, the model predictions always lie in between these two values, i.e., full scale set 1 and full scale set 2.

2.4.5 Summary

The proposed rainfall rate model is capable of providing reasonable rainfall rate predictions in a hurricane. However, due to the complex nature of a hurricane, a significant degree of variability should be expected. Further development is needed to account for all possible aspects affecting rainfall rate in a hurricane. Uncertainties associated with input parameters and physical models should also be addressed to provide more reliable predictions.

Table 2.6. 24-Hour Total Rainfall Comparison

Hurricane	Location	Full Scale 1* (mm)	Full Scale 2* (mm)	Model (mm)	Model/Full Scale **
Frederic (1979)	Pensacola FSS		83	59	0.71
	Dauphin Island		215	176	0.82
	Mobile		217	167	0.77
Elena (1985)	Pensacola NAS		63	37	0.58
	Pensacola Reg. Airport		65	34	0.52
	Tallahassee		84	24	0.28
	Mobile		60	31	0.52
	Dauphin Island		76	85	1.12
Hugo (1989)	Charleston Airport	135		101	0.75
	Columbia	75		67	0.90
	GSP Airport	27		26	0.98
	Myrtle Beach		58	41	0.71
Erin (1995)	Panama City Beach		137	50	0.36
	Pensacola NAS		56	96	1.72
	Mobile		65	95	1.46
Opal (1995)	Pensacola NAS		185	93	0.50
	Pensacola NPA		176	93	0.53
	Mobile		190	48	0.25
Bertha (1996)	Wilmington	59	144	116	0.80
	Kure Beach	107		123	1.14
	Greenville		104	117	1.12
	New Bern		116	145	1.26
Fran (1996)	Wilmington	79		200	2.53
	Raleigh/Durham	128	224	161	0.72
	Greensboro	89	99	94	0.95
	Fort Bragg		119	139	1.16
	New River		179	190	1.06
	Pope AFB		171	136	0.80
	Rocky Mount		94	142	1.51
Bonnie (1998)	Kure Beach	207		351	1.70
	Wilmington	230		377	1.64

* Full scale 1 represents total rainfall calculated from continuous hourly rainfall data reported by individual stations. Full scale 2 represents total rainfall reported in annual Atlantic hurricane season summary included in Monthly Weather Review except for Hurricanes Erin and Opal, for which preliminary reports from the National Hurricane Center were used.

** In the case when both full scale data are available, the total full scale rainfall is taken as the value given in the column of full scale 2.

Chapter 3. Surface Roughness Modeling

3.1 Introduction

A critical component in the modeling of wind effects, damage, and loss to buildings and facilities is the assessment of the ground roughness. As the ground surface becomes rougher, the wind speeds near the ground decrease although the upper level wind speed remains the same. The wind loads experienced by structures located in a typical suburban, treed, or urban environment are much lower than those experienced by buildings located in relatively unobstructed regions such as waterfront and open field locations. The wind loads experienced by one- and two-story structures located in forested areas may be as low as one half of those experienced by similar structures located in an open environment.

The effect of surface roughness is treated in a simple fashion in building codes and standards using exposure categories. For example, open terrain and suburban terrain are designated as Exposures C and B, respectively, in ASCE-7. The approach taken in that standard, and most national and international standards, is to define a basic wind speed, which represents the wind speed at a height of 10 m in open terrain. The effect of the actual local terrain is then taken into account by modifying that wind speed by a factor, which is dictated by the exposure category for the local terrain.

The ground surface roughness is defined using a characteristic roughness length, denoted as z_0. This roughness length is a function of the height and spacing of the buildings, trees and other obstructions on the ground surface. Given the open terrain wind speed, the local terrain roughness length, and the fetch over which the wind has blown over the surface, it is possible to estimate the local terrain wind speeds at any height. As described in Chapter 2, the hurricane model yields estimates of wind speed at any location for open terrain conditions. Hence, given information on the upstream fetch and the associated surface roughness length, the wind speed at any location and any height can be estimated.

Numerous studies have been performed over the last several decades attempting to categorize z_0 using surface exposure description. However, up to date, no consistent agreement has been reached among researchers. Wieringa (1992,1993) summarized most of the traceable studies on roughness lengths for various terrains performed in the last thirty years (including field projects, numerical modeling studies, and wind tunnel investigations) and gave a table showing his best estimations. This table, included herein as Table 3.1, serves as a reasonable basis for determining appropriate roughness lengths for areas on the mainland. For comparison, roughness lengths given by one set of researchers, Simiu and Scanlan (1996), are shown in Table 3.2. Surface roughness lengths proposed by a number of researchers, emphasizing built-up areas, are presented in Table 3.3.

Table 3.1. Roughness Lengths of Homogeneous Surface Types (from Wieringa, 1993)

Surface Type	Roughness Length (m)
Sea, loose sand and snow	≈ 0.0002 (wind speed dependent)
Concrete, flat desert, tidal flat	0.0002 – 0.0005
Flat snow field	0.0001 – 0.0007
Rough ice field	0.001 – 0.012
Fallow ground	0.001 – 0.004
Short grass and moss	0.008 – 0.03
Long grass and heather	0.02 – 0.06
Low mature agricultural crops	0.04 – 0.09
High mature crops (“grain”)	0.12 – 0.18
Continuous bushland	0.35 – 0.45
Mature pine forest	0.8 – 1.6
Tropical forest	1.7 – 2.3
Dense low buildings (“suburb”)	0.4 – 0.7
Regularly-built large town	0.7 – 1.5

Table 3.2. Roughness Lengths For Various Surface Types (from Simiu and Scanlan, 1996)

Type of Surface	z_0 (m)
Sand	0.0001-0.001
Snow Surface	0.001-0.006
Mown Grass (~0.01m)	0.001-0.01
Low Grass, Steppe	0.01-0.04
Fallow Field	0.02-0.03
High Grass	0.04-0.10
Palmetto	0.10-0.30
Pine Forest (mean height of trees: 15 m; one tree per 10 m^2	0.90-1.00
Sparsely Built up suburbs	0.20-0.40
Densely Built up suburbs and towns	0.80-1.20
Centers of large Cities	2.00-3.00

Table 3.3. Roughness Lengths of Rather Homogeneously Built-up Areas (from Wieringa, 1993)

Surface Type	z_0 (m)	Reference
Scattered low buildings	0.5±0.2	Shiotani (1962)
Low buildings and trees	≈0.7	Duchêne-Marullaz (1979)
Regular dense low houses	0.5±0.1	Steyn (1982)
“Regular” city buildings	≈1.3	Jensen (1958)
“Regular” city buildings	1.1±0.4	Brook (1972)
“Regular” city buildings	1.0±0.6	Karlsson (1986)
“Regular” city buildings	0.9±0.3	Yersel and Goble (1986)

Note that the data in these tables are for homogeneous terrain only, which means the wind must pass several kilometers of fetch of the same terrain before it reaches the area investigated. For areas on the mainland, due to relatively homogeneous land exposure, the transition layer in the vertical wind profile can be taken as fully adapted up to the standard height of 10 m (even though local integration over an area of several square kilometers may be used to determine the effective value of heterogeneous roughness). However, this is not the case for barrier islands. Typically the overland fetch is fairly short in this case. When a hurricane moves from the open water onto the barrier island, no obvious over-land boundary layer can be developed (i.e., not enough fetch distance). Therefore, the effective roughness length will be much smaller than that for areas on the mainland for the same land use category.

As an alternative to the information given in Tables 3.1 through 3.3, the effective roughness length over a particular local area can be estimated using a simple equation proposed by Lettau (1969):

$$z_0 \approx 0.5HS / A \tag{3.1}$$

where H = average height within the area, S = total projected frontal area of the obstacles, and A = surface area.

Because the ground surface roughness has a major impact on the magnitude of the loads experienced by a structure, it is important to be able to estimate the local surface roughness. Currently, no direct databases exist describing the distribution of the surface roughness over regions within the US. Consequently, indirect methods are used to estimate the surface roughness distribution. The approach for estimating the surface roughness is to obtain information on land use and land cover (LULC), for which databases do exist, and then estimate the surface roughness for each LULC class. By assigning a value of the surface roughness associated with a given land use, a surface roughness map can be developed directly from a LULC map and the mean wind speeds and gustiness can be reasonably estimated at any surface location within a storm.

In the following sections, some of the LULC databases that are available and potentially of use in Hazus are discussed. Sections 3.1 through 3.7 provide background and details to the calculation of terrain roughness prior to Hazus 2.0. Updates developed for Hazus 2.0 are discussed in Section 3.8.

3.2 Land Use Databases

Although land cover and land use data has become increasingly available in digital format from a variety of data sources and agencies, a single source of up-to-date, nationally consistent land cover mapping at a moderate to high spatial detail had not been readily available.

The U.S. Environmental Protection Agency's Office of Water Management has researched the availability of single state and multi-state land cover data sets across the country and has compiled a summary of their findings. In all, 75 different data sets were

identified, most covering a single state or parts of a state. The national data sets that have been available to date, except for the MRLC-NLCD database discussed later, are either very coarse or are substantially out of date and thus have limited use for the purpose of Hazus.

The USGS LULC data cover most of the contiguous United States and Hawaii, and have a resolution of about 200m for most urban areas. This resolution is minimally suitable, and the data are available in both raster and vector formats; however, they are based mostly on old 1970's aerial photography. The EPA also has a vector database based on essentially the same data as the USGS LULC data.

The conterminous U.S. Land Cover Characteristics database was developed jointly by the USGS EROS Data Center and the Center for Advanced Land Management Information Technologies (CALMIT) at the University of Nebraska-Lincoln. Although it is based on more recent 1990 satellite imagery from NOAA, the resolution is rather coarse at 1 km.

The United States GAP Analysis Program of the USGS Biological Resources Division provides 30m resolution raster data based on more recent Landsat Thematic Mapper (TM) imagery augmented by several other data sources. The classification system uses the Federal Geographic Data Committee (FGDC) vegetation classification system which is very detailed for non-developed vegetated areas, but is unfortunately much less detailed for agricultural and built up areas which are of most interest for use in Hazus.

3.2.1 Florida Water Management District Data

Florida's five Water Management Districts maintain LULC databases that collectively cover the entire state. The five districts are listed below and their regions are shown in Figure 3.1:

1. Northwest Florida Water Management District
2. Suwanee River Water Management District
3. St. Johns River Water Management District
4. Southwest Water Management District
5. South Florida Water Management District.

The LULC databases from these agencies are considered a superior source for Florida terrain information because they are more recent and the classification system is more refined than, for example, the USGS LULC data.

Each water management district independently prepared their LULC databases. Although all districts worked from the same source media, and all used the same coding system, each used a different contractor to perform the work. Consequently, there are slight differences in the preparation of each database.

The source data for the versions of the databases used in Hazus was the National Aerial Photography Program's 1:40,000 scale infrared imagery of 1994/1995. The districts

intend to update their databases every five years to keep up with the changes in land use associated with urbanization.

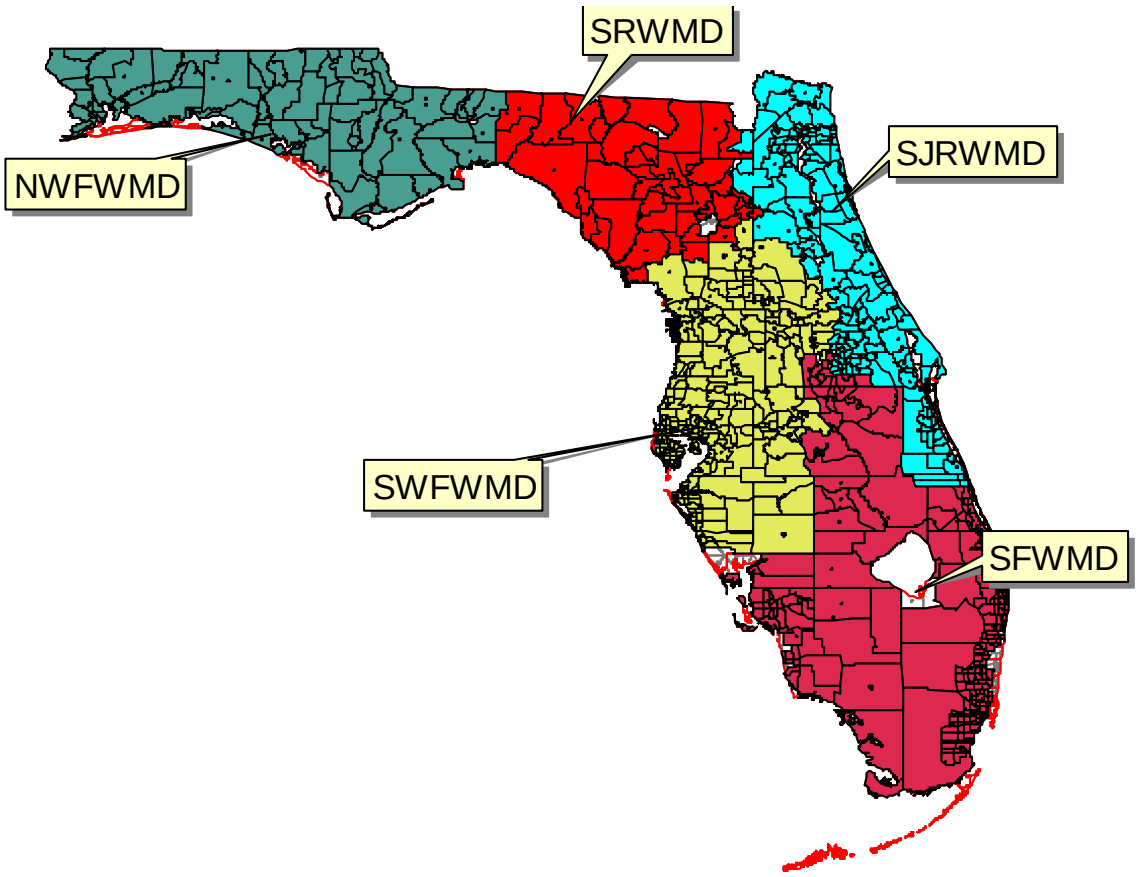

Figure 3.1. The Five Florida Water Management Districts.

All of the districts used the Florida Land Use and Land Cover Classification System (FLULCCS) developed by the Florida Department of Transportation. The system is arranged in four levels with each higher level providing more specific land information. For example, the Level I classification "Urban and Built-Up" is broken down into nine Level II classifications as shown below:

1. Residential Low Density,
2. Residential Medium Density,
3. Residential High Density,
4. Commercial and Services,
5. Industrial,
6. Extractive,
7. Institutional,
8. Recreational, and
9. Open Land.

A variable number of Level III classifications are available for each of the Level II classifications listed above, and some of these have Level IV classifications. For example, the Level II classification "Residential Low Density" is divided into the following four Level III categories:

1. Manufactured Home Units Any Density,
2. Fixed Single Family Units,
3. Mixed Units (Fixed and Manufactured Home Units), and
4. Low Density Under Construction.

There are a total of nine Level I land use classifications that can be expanded in more detailed categories, as illustrated above, through the use of the Levels II and III classification systems. The nine Level I classifications are:

1. Urban And Built-Up,
2. Agriculture,
3. Rangeland,
4. Upland Forest,
5. Water,
6. Wetlands,
7. Barren Land,
8. Transportation, Communication and Utilities, and
9. Special Classifications.

All of the districts make use of the FLULCCS to Level II, and some use it to Level III.

In general the identification of polygon regions was done manually by personnel trained to recognize and categorize the different land-use regions. This process aimed at a minimum polygon area-resolution of ½ acre to 5 acres depending on the land-use category and the particular process followed by the contractor preparing the database. Each district carried out a different degree of quality assurance and field testing on their databases. The resulting classifications have been quoted as being from 85% to 95% accurate. In general, the classification of upland areas (which are of greatest concern for the wind-hazard methodology) are considered to be of higher overall quality because they tend to be easier to identify, categorize, and delineate.

Land use databases similar to those of the Florida Water Management Districts are not available in other states along the Atlantic and Gulf Coast. There are numerous smaller databases of various qualities prepared by agencies in other states; however, these have been prepared using disparate data sources, time periods, and classification systems, and, in most cases, they are complete only for localized regions that were of concern to the agency for a particular reason. The final decision on LULC database implementation reflects the desire for a universal LULC database source for the hurricane model vs. the use of multiple databases that may have higher quality/resolution data for certain states. This decision can also be supported by an analysis of how sensitive the damage and loss predictions are to different LULC databases.

3.2.2 MRLC-NLCD Database

The most nationally consistent and up-to-date source of land-use data is the National Land Cover Data (NLCD) compiled by the Multi-Resolution Land Characteristics (MRLC) Consortium. This is a partnership of six federal environmental monitoring programs along with the EROS Data Center of the USGS. Their goal was to combine their resources in purchasing Landsat satellite imagery and to use the experience, expertise, and resources of the respective programs to generate LULC data and functional land characteristics databases for the conterminous United States.

The participating programs are:

1. Environmental Monitoring and Assessment Program (EMAP) of the US EPA
2. GAP Analysis Program of the USGS Biological Resources Division
3. National Water Quality Assessment Program (NAWQA) of the USGS
4. Coastal Change Analysis Program (C-CAP) of NOAA
5. North American Landscape Characterization (NALC) Project of the US EPA and the USGS
6. Remote Sensing Applications Center (RSAC) of the USFS

Although some of the participants have used the Landsat data for their own particular purposes, the EROS Data Center processed the data to produce a national database at 30m resolution for the entire conterminous United States and stored it in generic raster data structures. It uses a nationally consistent hierarchical land cover classification system. The sources for this system are the C-CAP Level 2 legend (Dobson, et al., 1995) reorganized to easily collapse into the level 1 classes of the Anderson System (Anderson, et al., 1976). The classification system is summarized in Table 3.4.

The primary data source is the nominally 1991 (±5 year) Landsat TM coverage purchased by the consortium members. This is augmented with ancillary data sets to help resolve uncertainties and otherwise enhance the data set. All data sets have been validated prior to release. A three-tiered validation procedure was used and includes general data integrity screening, comparisons to existing data sets, and formal accuracy assessments.

The land use categories given in the MRLC database are similar to those provided by the dated USGS database. The release notes of MRLC-NLCD data provide detailed descriptions on the land characteristics for each land category, which is helpful in defining a z_0 value for a category. However, as indicated by Table 3.4, the categorization of the developed areas is much more coarse than the categorization given in the South Florida Water District database. For example, there is a total of only 3 categories for developed areas in the MLRC whereas there are nine Level II classes in the SFWMD database with additional Level III classes for each Level II. The advantage of the MRLC database over the FWMD database is that it is a consistent data set for the entire United States.

Table 3.4. MRLC Database Classification System

Water	11	Open Water
	12	Perennial Ice/Snow
Developed	21	Low Intensity Residential
	22	High Intensity Residential
	23	Commercial/Industrial/ Transportation
Barren	31	Bare Rock/Sand
	32	Quarries/Strip Mines/Gravel Pits
	33	Transitional
Natural Forested Upland (non-wet)	41	Deciduous Forest
	42	Evergreen Forest
	43	Mixed Forest
Natural Shrubland	51	Deciduous Shrubland
Non-Natural Woody	61	Planted/Cultivated (orchards, vineyards, groves)
Herbaceous Upland Natural/ Semi-Natural Vegetation	71	Grassland/Herbaceous
Herbaceous Planted/Cultivated	81	Pasture/Hay
	82	Row Crops
	83	Small Grains
	84	Bare Soil
	85	Other Grasses (Urban/recreational; e.g. parks, lawns, golf courses)
Wetlands	91	Woody Wetlands
	92	Emergent Herbaceous Wetlands

Calibration of NLCD Land Cover Classifications against Aerial Photos. The MRLC-NLCD database is still under refinement, updating, and the resolution of confused land cover classes. There are accuracy problems recognized for the current version as of the March 2000 release. Some of these problems are acknowledged in the NLCD release notes. These include difficulties in, for example, new development since 1992 not captured in the Landsat TM images, data extraction for wetland classes, and separation of grass, shrub and woody areas, as well as location match, etc.

To ensure the overall correctness of regional roughness lengths derived from the MRLC-NLCD database, the land cover classifications have been verified and calibrated for representative roughness lengths against aerial photos. The z_0 values to be used for a land cover class have been determined by the calibration results, with adjustments based on the detailed descriptions on the land cover characteristics provided by the NLCD release notes for each land cover class. Aerial photos of twelve regions in Southeast Florida ranging from 0.2 to 0.5 square miles in area were used, with eleven of them in Dade County and one in Broward County. The photos were taken as of early 1998. Most of them are for suburban locations. The calibration process is described below. Since the land cover characteristics are expected to be different across regions, the z_0 values are valid for Southeast Florida.

Examples of the MRLC-NLCD data maps for areas corresponding to the aerial photos were displayed on a GIS system using color codes, as shown in Figures 3.2 to 3.4. Each small square block (pixel) represents a 30 m×30 m area. The data maps are overlaid with street layout data from another source to help match locations to the aerial photos. The

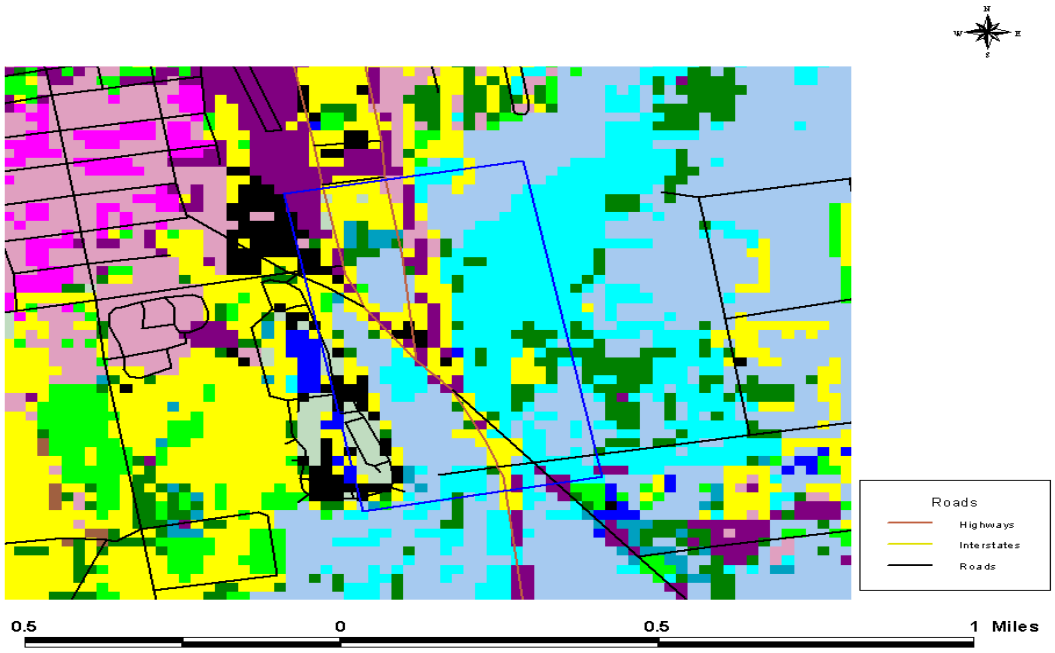

Figure 3.2. Example A of Overlaid NLCD Data Map and Street Layout (COMM 01: Dade County).

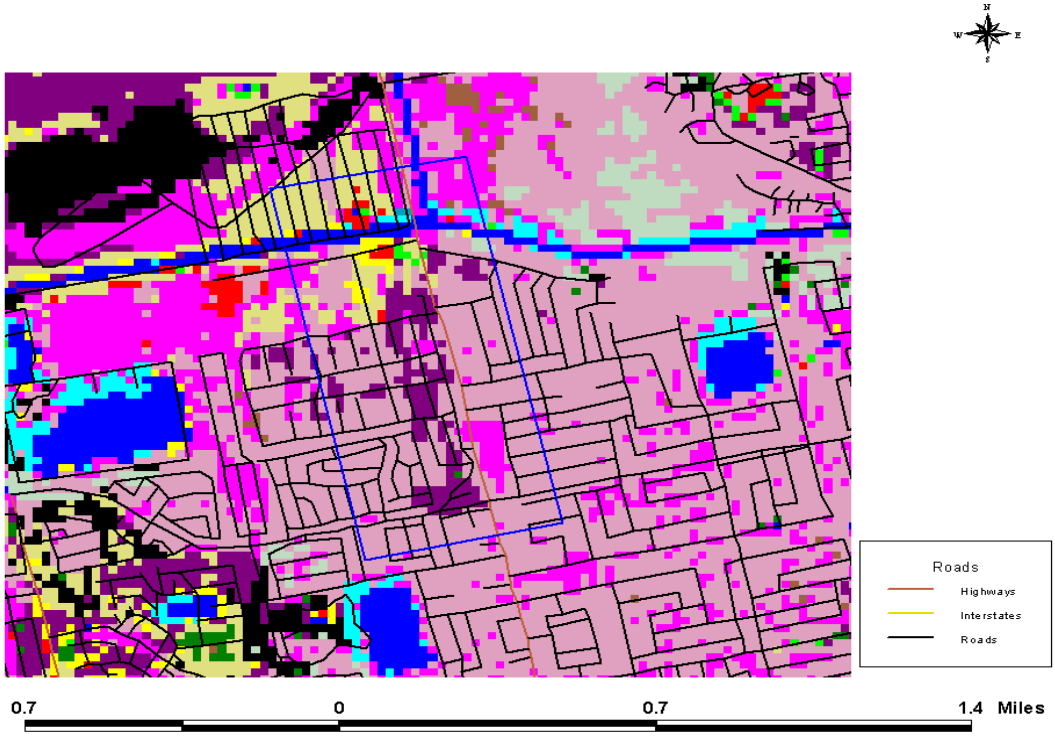

Figure 3.3. Example B of Overlaid NLCD Data Map and Street Layout (INDU01: Dade County).

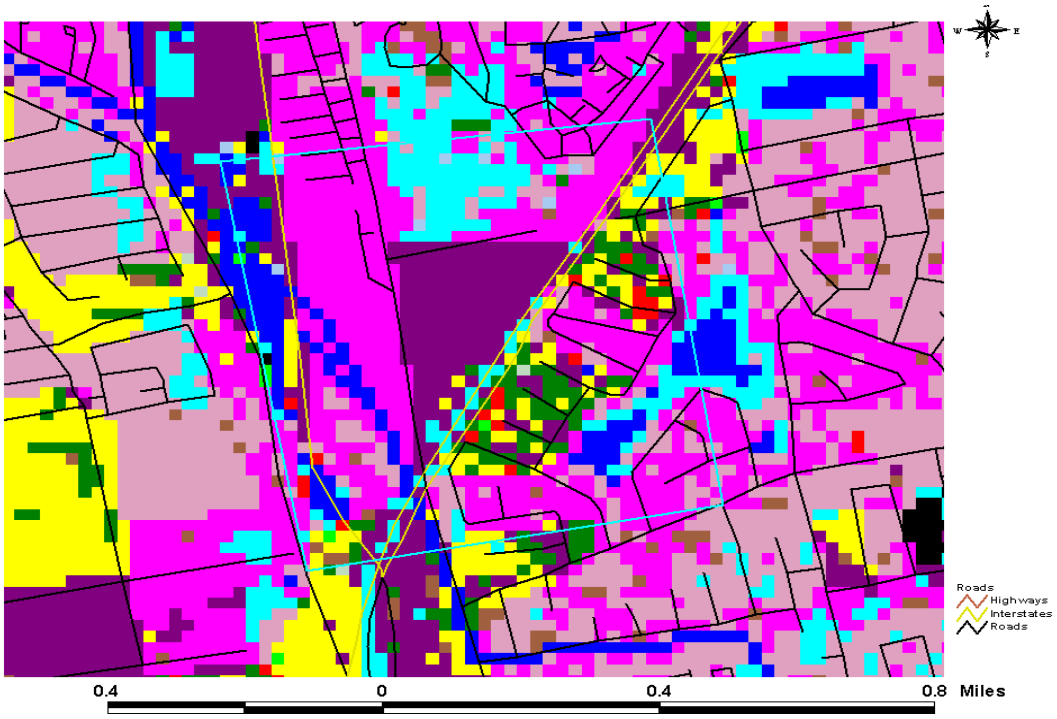

Figure 3.4. Example C of Overlaid NLCD Data Map and Street Layout (INDU06: Dade County).

boundaries of the aerial photos are identified and indicated by the polygon shown in the center of the data map. Within the polygon, each small sub-region of roughly equal area and of similar land cover characteristics as shown by the aerial photos is assigned a representative roughness length (z_0 value) empirically, consistent with the criteria for z_0 assignment used throughout this document. (Normally, the small sub-region coincides with an area represented by a cluster of 30 m×30 m NLCD pixels with the same classification code.) The statistics of the z_0 values assigned to the small sub-regions having the same NLCD classification are listed in Table 3.5, along with the number of sub-region z_0 values used for computing these statistics for each NLCD class. These statistics are derived based on all twelve aerial photos.

It was found that the general pattern of NLCD data is consistent with the land cover/land use as shown by the aerial photos. However, two types of errors were observed during the verification and calibration process, which have also been acknowledged in the NLCD release notes. The first is a location mismatch, which is estimated to be up to about 120 m from the comparison with the aerial photos and the street layout. The aerial photos and the street layout data generally correspond very well. The second type is misclassification of land cover. For example, areas shown as barren land in the NLCD map were actually residential areas in the aerial photos. This could be due to the fact that the aerial photos are more recent and showing new development not captured by NLCD data. There are also misclassifications across the three sub-classes (Low Intensity Residential, High

Table 3.5. NLCD Land Cover Classification vs Surface Roughness Length

MRLC-NLCD Land Cover Classification and Numerical Coding	Land Surface Roughness Length, z_0 (m)					Number of Sub-Regions Used
	Used	Avg.	COV	Max.	Min.	
Water						
11 Open Water	**0.010**	0.013	0.612	0.030	0.010	6
12 Perennial Ice/Snow	**0.012**					0
Developed						
21 Low Intensity Residential	**0.350**	0.307	0.496	0.600	0.010	51
22 High Intensity Residential	**0.600**	0.401	0.498	0.800	0.080	39
23 Commercial/Industrial/Transportation	**0.350**	0.265	0.605	0.600	0.030	28
Barren						
31 Bare Rock/Sand/Clay	**0.200**	0.300				1
32 Quarries/Strip Mines/Gravel Pits	**0.400**					0
33 Transitional	**0.400**	0.400	0.661	0.600	0.100	3
Forested Upland						
41 Deciduous Forest	**0.600**					0
42 Evergreen Forest	**0.600**	0.500				1
43 Mixed Forest	**0.600**					0
Shrubland						
51 Shrubland	**0.060**	0.040				1
Non-natural Woody						
61 Orchards/Vineyards/Other	**0.210**	0.213	0.777	0.400	0.050	4
Herbaceous Upland						
71 Grasslands/Herbaceous	**0.150**	0.193	0.662	0.300	0.050	4
Herbaceous Planted/Cultivated						
81 Pasture/Hay	**0.150**	0.160	1.301	0.400	0.030	3
82 Row Crops	**0.100**	0.100	0.913	0.300	0.030	8
83 Small Grains	**0.030**					0
84 Fallow	**0.030**					0
85 Urban/Recreational Grasses	**0.150**	0.155	0.514	0.250	0.030	6
Wetlands						
91 Woody Wetlands	**0.300**	0.545	0.594	1.100	0.300	10
92 Emergent Herbaceous Wetlands	**0.030**	0.188	0.959	0.600	0.050	10

Intensity Residential, and Commercial/Industrial/Transportation) under the Developed class. Less frequently, some areas that are shown to be undeveloped in the aerial photos are classified as Developed in the NLCD database. The latter two cases of errors are indications of inaccuracy in the NLCD data acquisition and processing instead of the results of new development.

Based on the calibration results, and considering other factors such as possible bias towards suburban regions with the sample aerial photos used, a set of z_0 values corresponding to specific NLCD classifications was adopted for use in estimating regional representative roughness lengths for Southeast Florida, as included in Table 3.5. In principle, the adopted z_0 values are based on the average values from the calibration with mostly minor adjustments based on the detailed descriptions on the land cover

characteristics provided by the NLCD release notes for each land cover class. However, two major adjustments from the calibrated averages, which are associated with the Developed and Wetlands classes, are worth mentioning. For the Developed class, since the aerial photos used contain only suburban developments, the z_0 values for all three sub-classes of the Developed class were adjusted upwards to accommodate those areas closer to city centers that are rougher but have the same NLCD classifications, for example, areas with many multi-story residential and commercial buildings. For the wetlands, the aerial photos do not include any everglade areas that have much lower z_0 values than those from the photos but are also classified as either Woody Wetlands or Emergent Herbaceous Wetlands. Thus, the z_0 values for Wetlands were adjusted downwards to accommodate such areas as the everglades that were not represented by the aerial photos. The adopted set of z_0 values is used for computing the zip code average z_0 values as presented in Section 3.3 for Southeast Florida. Note that zip codes are used here instead of census tracts since, as is discussed in Chapter 9 of this manual, the loss validation studies (using insurance data) were performed using zip codes.

3.3 Surface Roughness Lengths in the Southeast Florida Area

In order to estimate the surface roughness associated with a given land use category of the FWMD database, sample aerial photographs corresponding to known land use categories were obtained and calibrations similar to those for the MRLC-NLCD data were performed. Figure 3.5 shows an example of a part of one of the aerial photographs used in the roughness length determination. In the example given in Figure 3.5, most of the visible area consists of a medium density residential area. Using aerial photographs that cover the key areas of the land use database, aerodynamic roughness lengths were assigned to each of the various land use categories as given in Table 3.6. The estimates of the surface roughness were based on a combination of judgment, Equation 3.1, and the data presented later in Tables 3.7 through 3.8. The assignment of roughness lengths was performed through exact matching of the LULC database with the aerial photographs. Within each land use category a best estimate of the surface roughness has been assigned as well as a likely range. Figure 3.6 shows an example of the variation in roughness lengths for an area containing Homestead AFB in South Dade County.

Again, for many of the terrain categories, the assigned values of roughness length given in Table 3.6 for the FWMD database are applicable for the South Florida area only and cannot be used elsewhere. The major reason that the z_0 mapping developed for South Florida should not be used elsewhere is related to the height and density of trees. In the South Florida area, tree height and density was shown (from the aerial photographs) to be much less than is usually observed elsewhere (North Florida, Atlantic Coast, etc.). Trees play an important role in reducing wind speeds over the ground, and in most regions of the U.S., typical suburban areas are more heavily treed (with taller trees) and thus the wind speeds experienced by buildings (for the same hurricane) will be lower. These different terrain characteristics are discussed further in Section 3.4.

Figure 3.5. Example Aerial Photograph Used to Determine Aerodynamic Roughness Lengths in the South Florida Area. Photograph Primarily Shows a Medium Density Residential Area.

Table 3.6. Land Use Categories and Assigned Values of z_0 for Use in the Southeast Florida Region with the FWMD Data

Level II Classification Code	Description	Mid-Point Value of z_0 (m)	Range of z_0 (m)
110	Low Density Residential	0.15	0.10-0.30
120	Medium Density Residential	0.35	0.10-0.70
130	High Density Residential – Low-Rise (131)	0.30	0.10-0.50
	– High-Rise (132)	0.50	0.30-0.80
140	Commercial and Services	0.50	0.20-1.00
150	Industrial	0.50	0.20-0.70
160	Extraction	0.03	
170	Institutional	0.30	0.20-0.40
180	Recreational	0.10	0.05-0.30
190	Open Land	0.03	0.01-0.07
210	Cropland and Pasture	0.03	0.02-0.07
220	Tree Crops	0.50	0.30-0.80
230	Feeding Operations	0.03	0.02-0.07
240	Nurseries and Vineyards	0.10	0.05-0.30
250	Specialty Farms	0.05	0.03-0.08
260	Other Open Lands	0.05	0.03-0.08
310	Herbaceous Rangeland	0.10	0.05-0.20
320	Shrub and Bushland	0.10	0.05-0.20
330	Mixed Rangeland	0.10	0.05-0.20
410	Coniferous Forests	1.0	0.50-1.50
420	Hardwood Forests	1.0	0.50-1.50
430	Other Hardwood Forests	1.0	0.50-1.50
440	Tree Plantations	1.0	0.50-1.50
500	Water	Computed or 0.01	
610	Hardwood Forests – Wetlands	0.50	0.40-0.60
620	Coniferous Forests – Wetlands	0.50	0.40-0.60
630	Mixed Forests – Wetlands	0.50	0.40-0.60
640	Vegetated Non-Forest Wetlands	0.03	0.01-0.07
650	Non-Vegetated Wetlands	0.01	0.005-0.02
710	Beaches other than Swimming	0.02	0.01-0.03
720	Sand – Other than Beaches	0.02	0.01-0.03
730	Exposed Rock	0.05	0.01-0.07
740	Disturbed	0.05	0.01-0.07
810	Transportation	0.05	0.03-0.10
820	Commercial	0.05	0.03-0.10
830	Utility	0.05	0.03-0.10

Comparison Between Zip Code Average z_0 Values Derived Using FWMD and MRLC Land Cover Databases. For Southeast Florida as an example, the average z_0 values for the zip codes using the two databases are shown in Figures 3.7 and 3.8, respectively. The agreement between the two sets of results is encouraging and suggests that given the uncertainty in the estimation of z_0, either land use database can be used to define the terrain. This preliminary comparison indicates that the more refined land use categories

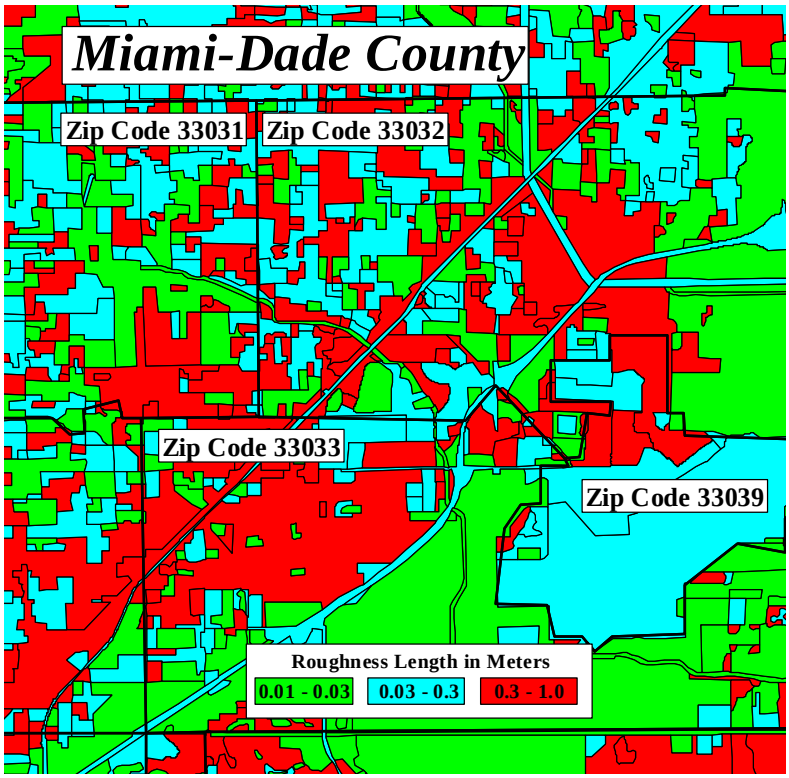

Figure 3.6. Example Roughness Length Map.

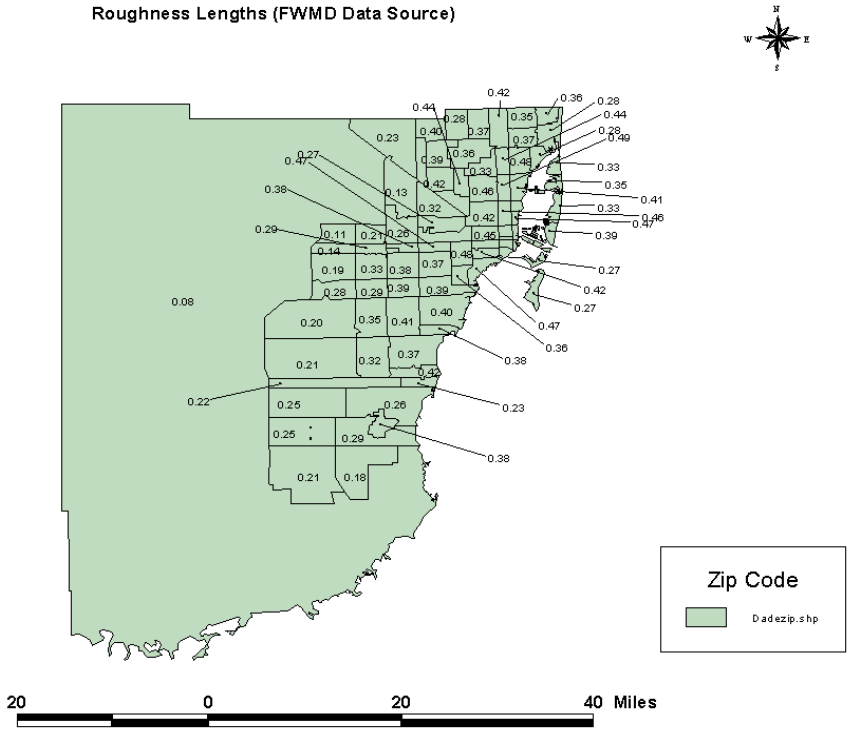

Figure 3.7. Zip Code Average Roughness Length Derived from the FWMD Database.

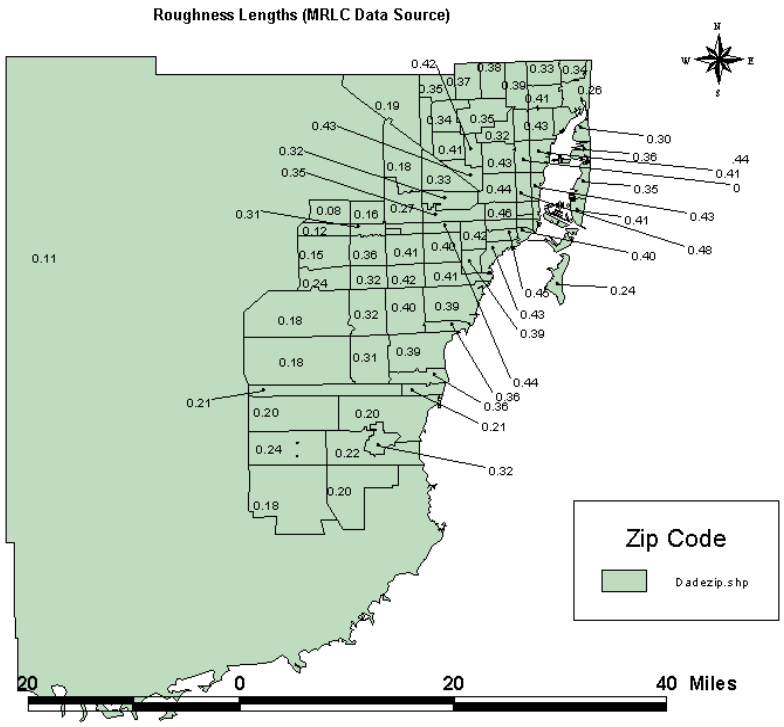

Figure 3.8. Zip Code Average Roughness Length Derived from the MRLC Database.

given in the SFWMD data may have only a moderate impact on predicted damages and losses for a regional loss study. Examples of the effect of the different LULC databases on loss estimation are provided in Chapter 9.

3.4 Surface Roughness Lengths in the Florida Panhandle Area

The aerial photography available for the Florida Panhandle area is in the format of Digital Orthophoto Quarter Quadrangles (DOQQ). The DOQQs are rectified aerial photos with 1m resolution (which is the highest resolution currently available) obtained from Florida Resources & Environmental Analysis Center at Florida State University. The mapping function for this area was developed by overlaying the DOQQs on the land use coverage obtained from the Northwest Florida Water Management District (NWFWMD). A number of aerial photo samples were then identified for each land use category, which formed the basis for the development of mapping functions (using engineering judgment and referring to the published literatures on roughness length determination, as well). The following section gives more detailed discussion about the methods and reasoning used to determine the roughness lengths. Figures 3.9 to 3.16 show some examples of the identified aerial photos for the categories of low density residential (LDR), medium density residential (MDR), high density residential (HDR), and commercial and service (C&S), for barriers islands and mainland, respectively. The land exposure differences for each land use category between the barrier island and the mainland are obvious. To reflect these differences, two distinct sets of mapping functions were developed for these two different land features.

Figure 3.9. Example DOQQ for Low Density Residential Area on Barrier Islands Located along the Florida Panhandle.

Figure 3.10. Example DOQQ for Medium Density Residential Area on Barrier Islands Located along the Florida Panhandle.

Figure 3.11. Example DOQQ for High Density Residential Area on Barrier Islands along the Florida Panhandle.

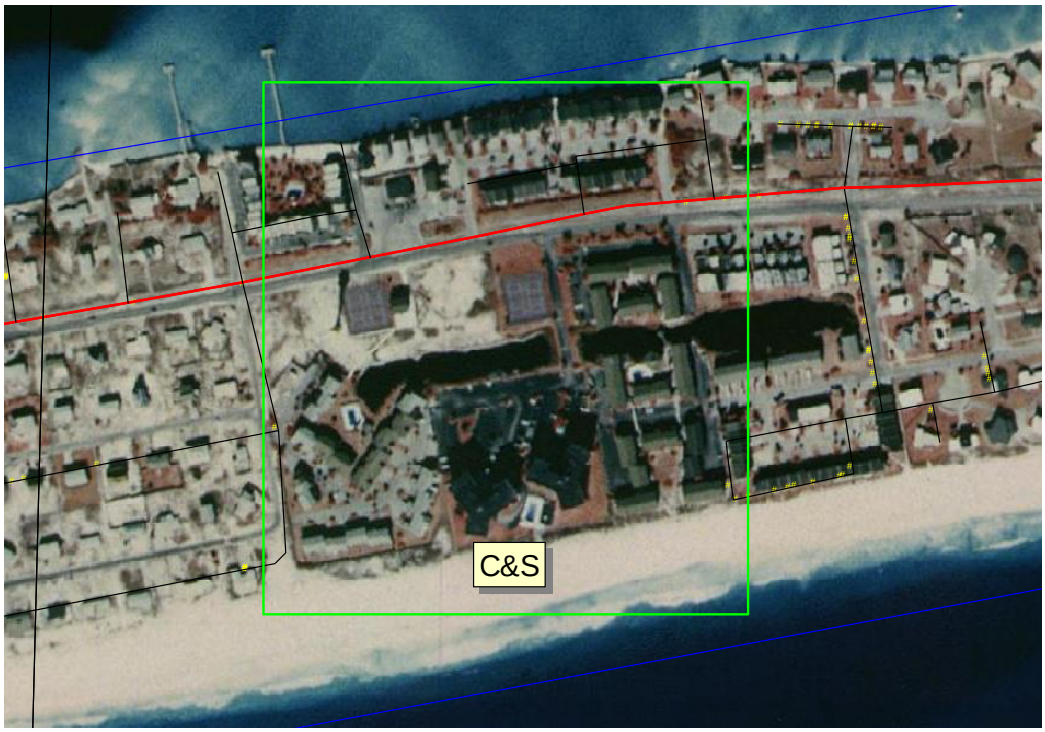

Figure 3.12. Example DOQQ for Commercial and Service Area on Barrier Islands along the Florida Panhandle.

Figure 3.13. Example DOQQ for a Low Density Residential Area on the Mainland Portion of the Florida Panhandle.

Figure 3.14. Example DOQQ for a Medium Density Residential Area on the Mainland Portion of the Florida Panhandle.

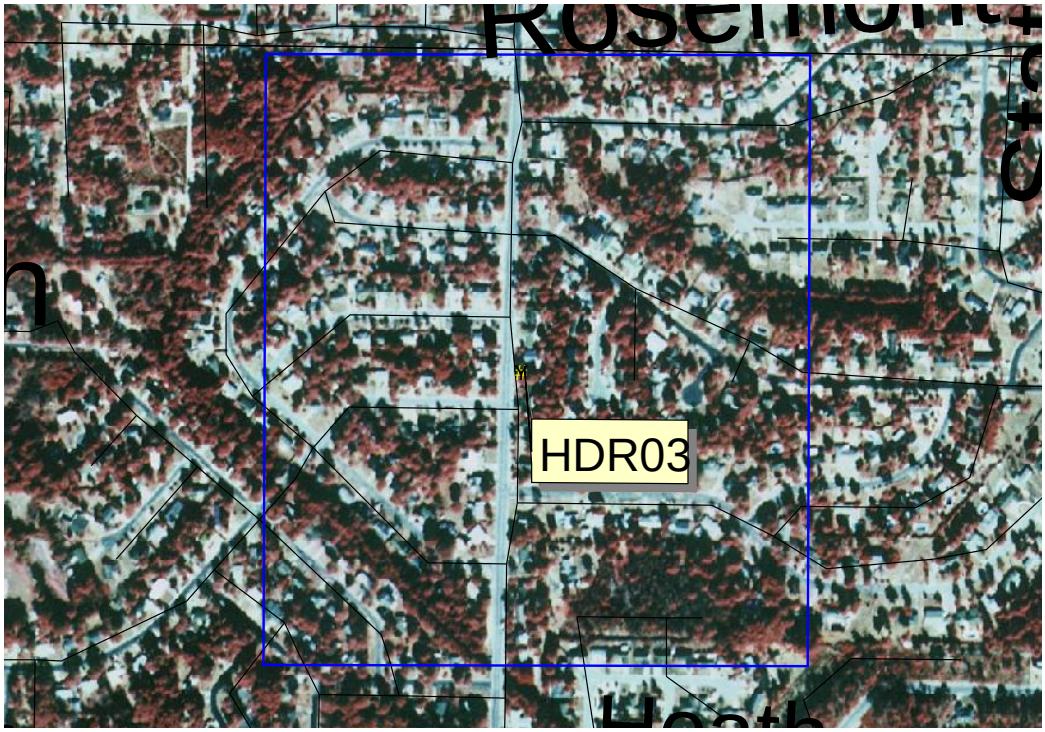

Figure 3.15. Example DOQQ for a High Density Residential Area on the Mainland Portion of the Florida Panhandle.

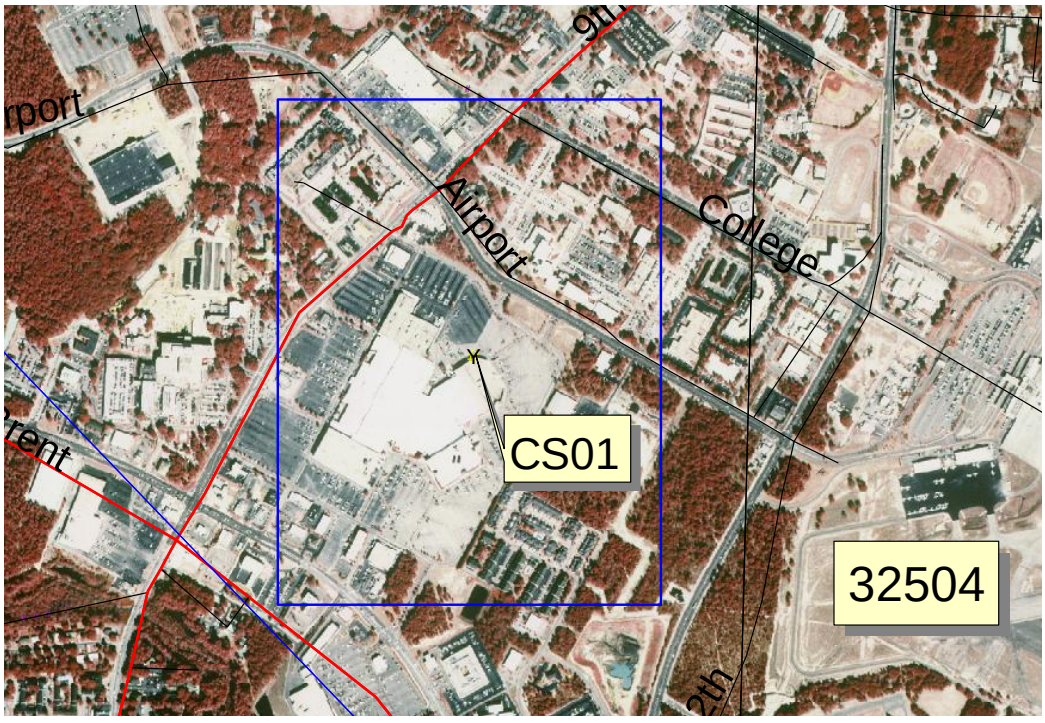

Figure 3.16. Example DOQQ for a Commercial and Services Area on the Mainland Portion of the Florida Panhandle.

Even with the help of aerial photos, it is still not trivial to define the mapping function for each land use category due to numerous factors affecting the roughness length, including primarily, the size, shape, density, and distribution of the surface obstacles and the upwind fetch distances.

Since few trees exist on the barrier islands, the total frontal area can be taken as the total area of the buildings. From the identified aerial photos, the lengths of the building can be estimated. The range and the mid-range values of z_0 were determined using engineering judgment. Other land use categories, such as cropland, forests, and wetlands, are not applicable to the areas on the barrier islands investigated. Therefore, the roughness lengths for these categories are noted as N/A. The determined roughness lengths for each land use category for barrier islands and mainland are listed in Tables 3.7 and 3.8, respectively. The mid-range values in Tables 3.7 and 3.8 serve as the mapping functions for determining appropriate roughness lengths from the land use categories for Florida Panhandle area.

Note also that for some coastal areas (such as those in Bay County), typically within one km of the coast, the land exposure is rather similar to that on a barrier island, i.e., very open and without any significant amount of trees. The roughness lengths for these areas have been assigned according to the table for barrier islands, i.e., Table 3.7.

3.5 Roughness Length Database Development for All Coastal States

3.5.1 The National Land Cover Data

Following the study to develop surface roughness length data for Southeast and Northwest Florida described in previous sections, a study for other coastal states was carried out using MRLC-NLCD land cover database, which is the most nationally consistent database available. Using the same procedure described in Section 3.2.2, a surface roughness length database has been developed for all coastal states.

To verify the accuracy of the NLCD land cover classification and map land cover codes to roughness lengths for different regions of the US, aerial photographs downloaded from Microsoft TerraServer were used to empirically determine the roughness lengths of selected areas with constant NLCD land cover codes. Some examples are presented below for North Carolina and Texas.

North Carolina. Figure 3.17 shows the land cover for the entire state of North Carolina, where the land cover codes (or pixel values) are represented with the color scheme shown in Figure 3.18, which approximately matches natural color and will be used throughout this section. It is seen that the NLCD data used reflects the characteristics of the state's general landscape. Figure 3.19 shows the aerial photograph and the NLCD land cover data for the Raleigh area of North Carolina, which demonstrates that the patterns match reasonably well. By zooming into a smaller area, Figure 3.20 shows that the accuracy of the NLCD data seems to be satisfactorily representing the true land cover types shown by the 1993 aerial photograph. (The NLCD data were derived from satellite images taken between November 1990 and June 1993). Further review was conducted in areas where

Table 3.7. Land Use Categories and Assigned Values of z_0 for Barrier Islands along the Florida Panhandle

Level II Classification Code	Description	Mid-Point Value of z_0 (m)	Range of z_0 (m)
110	Low Density Residential	0.07	0.03-0.15
120	Medium Density Residential	0.10	0.05-0.20
130	High Density Residential	0.15	0.05-0.30
140	Commercial and Services	0.15	0.05-0.35
150	Industrial	0.10	0.05-0.25
160	Extraction	0.03	
170	Institutional	0.10	0.05-0.25
180	Recreational	0.05	0.02-0.15
190	Open Land	0.03	0.01-0.07
210	Cropland and Pasture	N/A	N/A
220	Tree Crops	N/A	N/A
230	Feeding Operations	N/A	N/A
240	Nurseries and Vineyard	N/A	N/A
250	Specialty Farms	N/A	N/A
260	Other Open Lands	N/A	N/A
310	Herbaceous Rangeland	0.03	0.01-0.1
320	Shrub and Bushland	0.03	0.01-0.1
330	Mixed Rangeland	0.03	0.01-0.1
410	Coniferous Forests	N/A	N/A
420	Hardwood Forests	N/A	N/A
430	Other Hardwood Forests	N/A	N/A
440	Tree Plantations	N/A	N/A
500	Water	Computed or 0.01	
610	Hardwood Forests – Wetlands	N/A	N/A
620	Coniferous Forests – Wetlands	N/A	N/A
630	Mixed Forests – Wetland	N/A	N/A
640	Vegetated Non-Forest Wetlands	N/A	N/A
650	Non-Vegetated Wetlands	0.01	0.005-0.02
710	Beaches Other than Swimming	0.01	0.001-0.02
720	Sand – Other than Beaches	0.01	0.001-0.03
730	Exposed Rock	0.02	0.005-0.05
740	Disturbed	0.02	0.005-0.05
810	Transportation	0.05	0.03-0.10
820	Commercial	0.05	0.03-0.11
830	Utility	0.05	0.03-0.12

Table 3.8. Land Use Categories and Assigned Values of z_0 for Mainland Florida Panhandle

Level II Classification Code	Description	Mid-Point Value of z_0 (m)	Range of z_0 (m)
110	Low Density Residential	0.30	0.10-0.60
120	Medium Density Residential	0.50	0.20-1.20
130	High Density Residential	1.00	0.30-1.50
140	Commercial and Services	0.50	0.20-1.00
150	Industrial	0.30	0.10-0.60
160	Extraction	0.03	
170	Institutional	0.30	0.20-0.40
180	Recreational	0.10	0.05-0.30
190	Open Land	0.03	0.01-0.07
210	Cropland and Pasture	0.03	0.02-0.07
220	Tree Crops	0.50	0.30-0.80
230	Feeding Operations	0.03	0.02-0.07
240	Nurseries and Vineyard	0.10	0.05-0.30
250	Specialty Farms	0.05	0.03-0.08
260	Other Open Lands	0.05	0.03-0.08
310	Herbaceous Rangeland	0.10	0.05-0.20
320	Shrub and Bushland	0.10	0.05-0.21
330	Mixed Rangeland	0.10	0.05-0.22
410	Coniferous Forests	1.00	0.50-1.50
420	Hardwood Forests	1.00	0.50-1.51
430	Other Hardwood Forests	1.00	0.50-1.52
440	Tree Plantations	1.00	0.50-1.53
500	Water	Computed or 0.01	
610	Hardwood Forests – Wetlands	0.50	0.40-0.60
620	Coniferous Forests – Wetlands	0.50	0.40-0.60
630	Mixed Forests – Wetland	0.50	0.40-0.60
640	Vegetated Non-Forest Wetlands	0.03	0.01-0.07
650	Non-Vegetated Wetlands	0.01	0.005-0.02
710	Beaches Other than Swimming	0.02	0.01-0.03
720	Sand – Other than Beaches	0.02	0.01-0.04
730	Exposed Rock	0.05	0.01-0.07
740	Disturbed	0.05	0.01-0.07
810	Transportation	0.05	0.03-0.10
820	Commercial	0.05	0.03-0.11
830	Utility	0.05	0.03-0.12

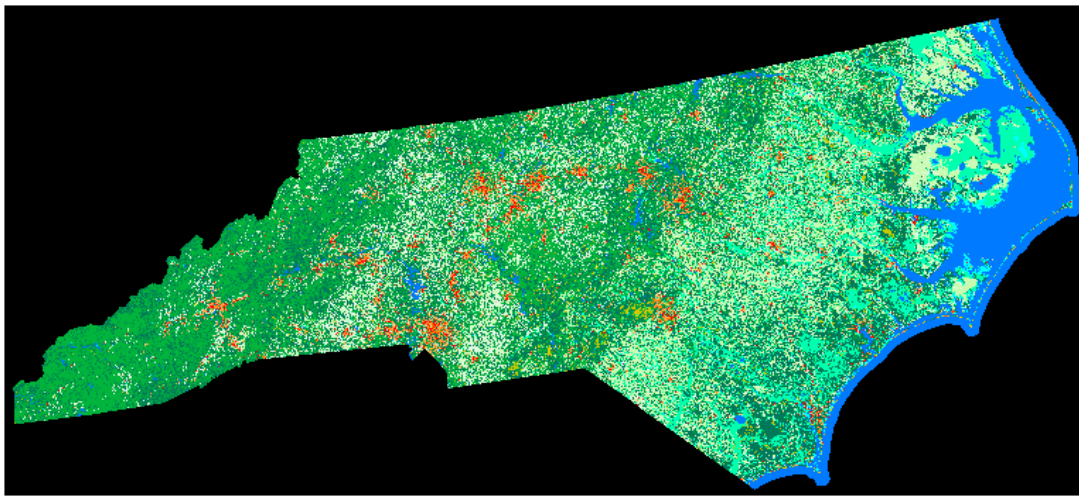

Figure 3.17. Color-Coded Land Cover Characteristics of the State of North Carolina as Derived from NLCD Database (1991).

Category Group	Class Code	Class Color	Class Name
Water	11		Water
	12		Ice / Snow
Developed	21		Low Intensity Residential
	22		High Intensity Residential
	23		Comm. / Ind. / Trans.
Barren	31		Rock / Sand / Clay
	32		Quarry / Strip Mine /Gravel Pit
	33		Transitional
Forested Upland	41		Deciduous Forest
	42		Evergreen Forest
	43		Mixed Forest
Shrubland	51		Shrubland
Non-natural Woody	61		Orchard / Vineyard / Other
Herbaceous Upland	71		Grassland / Herbaceous
Herb. Planted / Cultivated	81		Pasture / Hay
	82		Row Crop
	83		Small Grain
	84		Fallow
	85		Urban / Recreational Grass
Wetland	91		Woody Wetland
	92		Herbaceous Wetland

Figure 3.18. Color Scheme Used throughout Section 3.5.

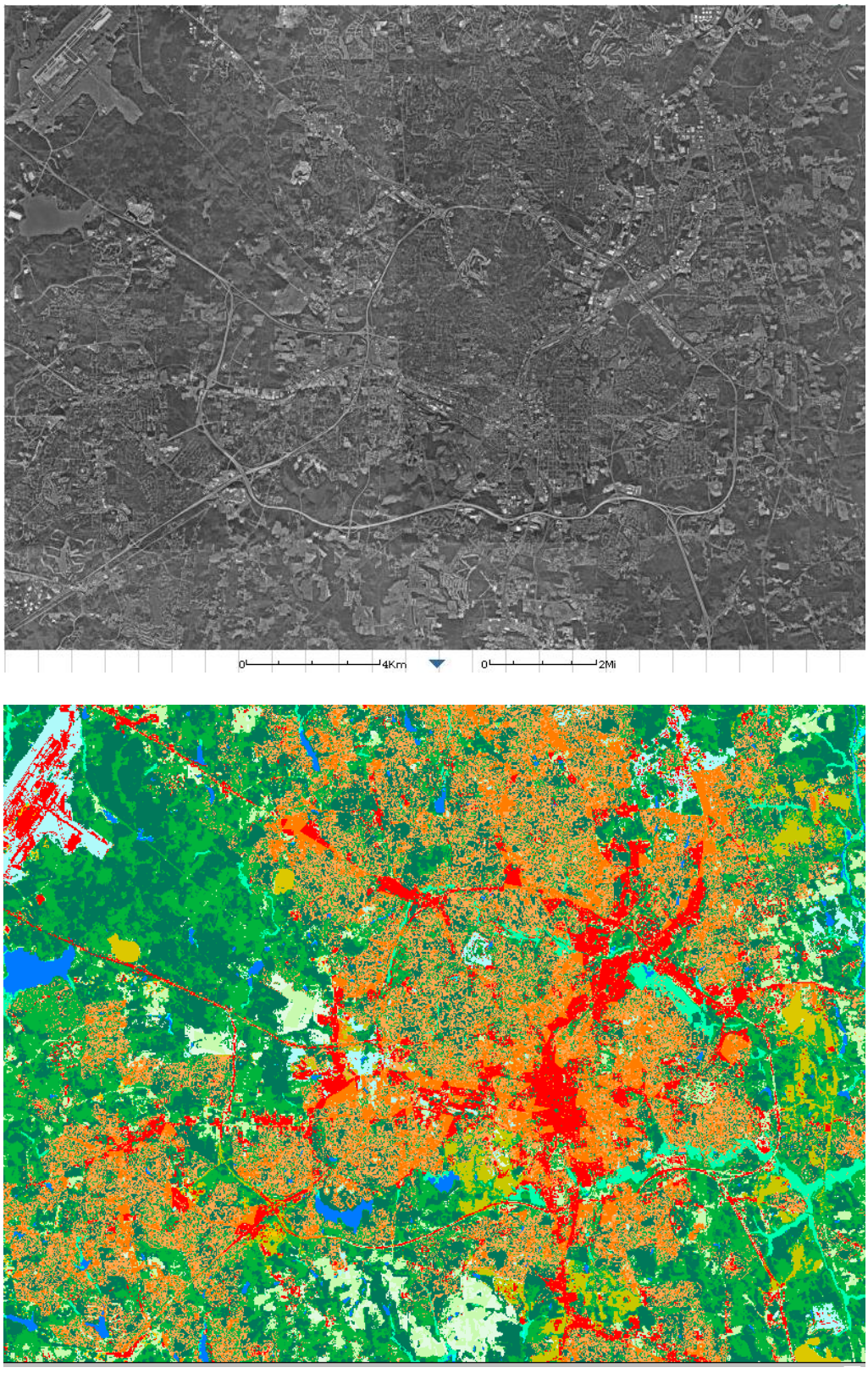

Figure 3.19. Metropolitan Raleigh, NC (upper: Aerial photograph; lower: NLCD).

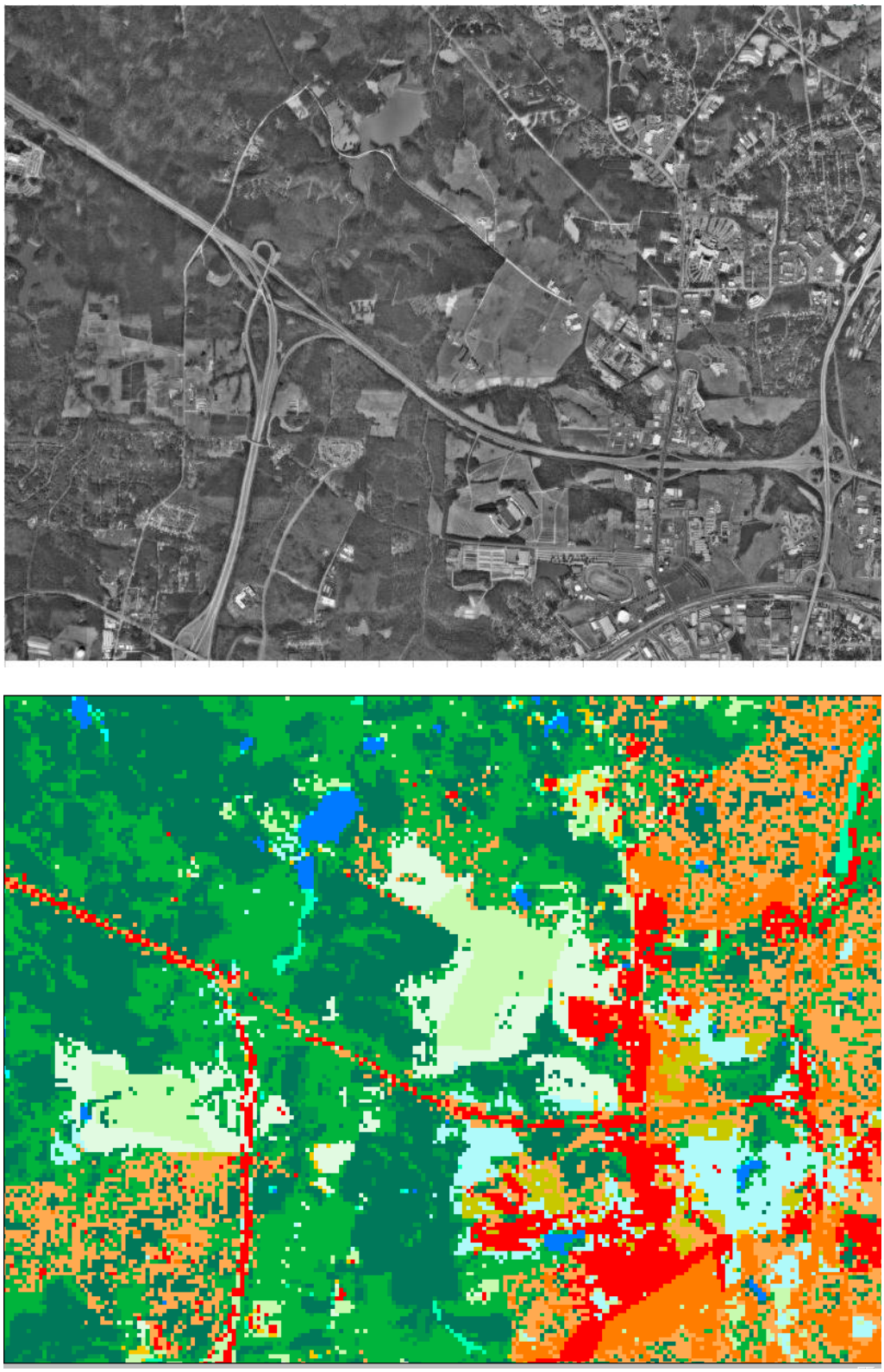

Figure 3.20. West Suburb of Raleigh, NC (upper: Aerial photograph; lower: NLCD).

doubts existed. For example, areas A and B initially appeared to be developed areas in the aerial photograph (Figure 3.5-4), but they are classified by the NLCD data as herbaceous land (Pasture/Hay and Row Crop). However, zooming in on the aerial photograph confirms that areas A and B are herbaceous land, as shown in Figure 3.21.

As examples of the empirical assignment of roughness length, a roughness length of 0.05 was assigned to these two specific areas. For the developed areas next to them, roughness lengths of 0.25 to 0.3 were assigned, while roughnesses of 0.55 to 0.7 were estimated for the surrounding forest and other woody areas.

Figure 3.22 shows downtown Wilmington, North Carolina, and the predominantly herbaceous wetland across from the river. Consistent patterns are observed between the NLCD data and the aerial photograph. Close-ups near the USS North Carolina battleship museum are presented in Figure 3.23, where a roughness length of 0.65 was assigned to the downtown portion on the right, 0.01 for the water, 0.10 for the herbaceous wetland (reed marsh) and 0.7 for the woody wetland (treed). For the highways, which are classified as comm./industrial/trans. (Coded 23), a value of 0.1 was used.

Texas. The Galveston-Texas City-Santa Fe area of Texas is presented in Figure 3.24. Again, the general patterns and detailed land cover characteristics are consistent. By zooming into sampled areas on the aerial photograph, roughness lengths were assigned. As an example, a close-up of the region corresponding to area #1 of the NLCD data map reveals that it is predominantly a cluster of residential buildings, consistent with the NLCD data, as shown in Figure 3.25. The area next to it and between the two major highways is shown as being covered by a mixture of trees, farming and other features, also consistent with the NLCD data.

Another example for Texas is shown in Figure 3.26, which is a suburban area about 40km northeast of downtown Houston. The land cover characteristics represented by NLCD data and shown by the aerial photograph are remarkably consistent for this area of complicated land covers, as interlaced with residential, commercial/industrial, highways, recreational, waters, forests, wetlands and farms. Roughness lengths were assigned to various featured areas, respectively, by zooming into corresponding regions.

3.5.2 Mapping NLCD Land Cover Codes to Roughness Lengths

With the help of aerial photographs, in addition to that of the NLCD classification descriptions, roughness lengths were empirically estimated for sampled individual areas, as illustrated in the above examples. There is variability in the assigned values for areas with the same land cover code. Area-weighted averages of the assigned values yield the representative roughness length (z_0) for a specific land cover class. The averaged value and standard deviation of z_0 are shown in Table 3.9 for all Gulf and Atlantic coastal states/regions. There are differences in the averaged value and standard deviation of z_0 among the states for a specific land cover class. For example, the values for forested upland are generally higher for North Carolina than Texas, which can be attributed to the larger tree heights commonly seen in North Carolina.

Area A

Area B

Figure 3.21. Close-Up Views of Two Areas in West Suburb of Raleigh, NC.

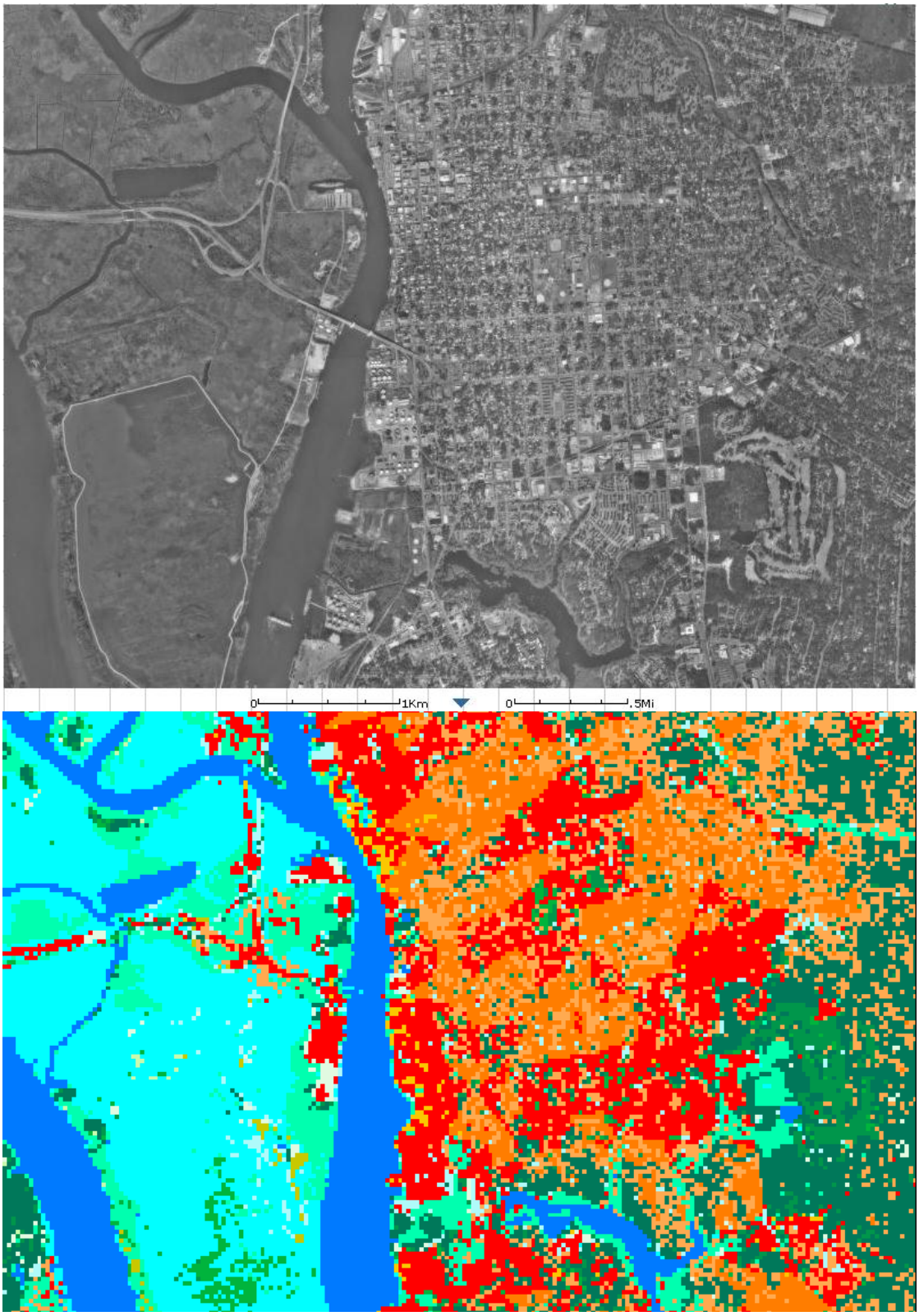

Figure 3.22. Downtown Wilmington, NC (upper: Aerial photograph; lower: NLCD).

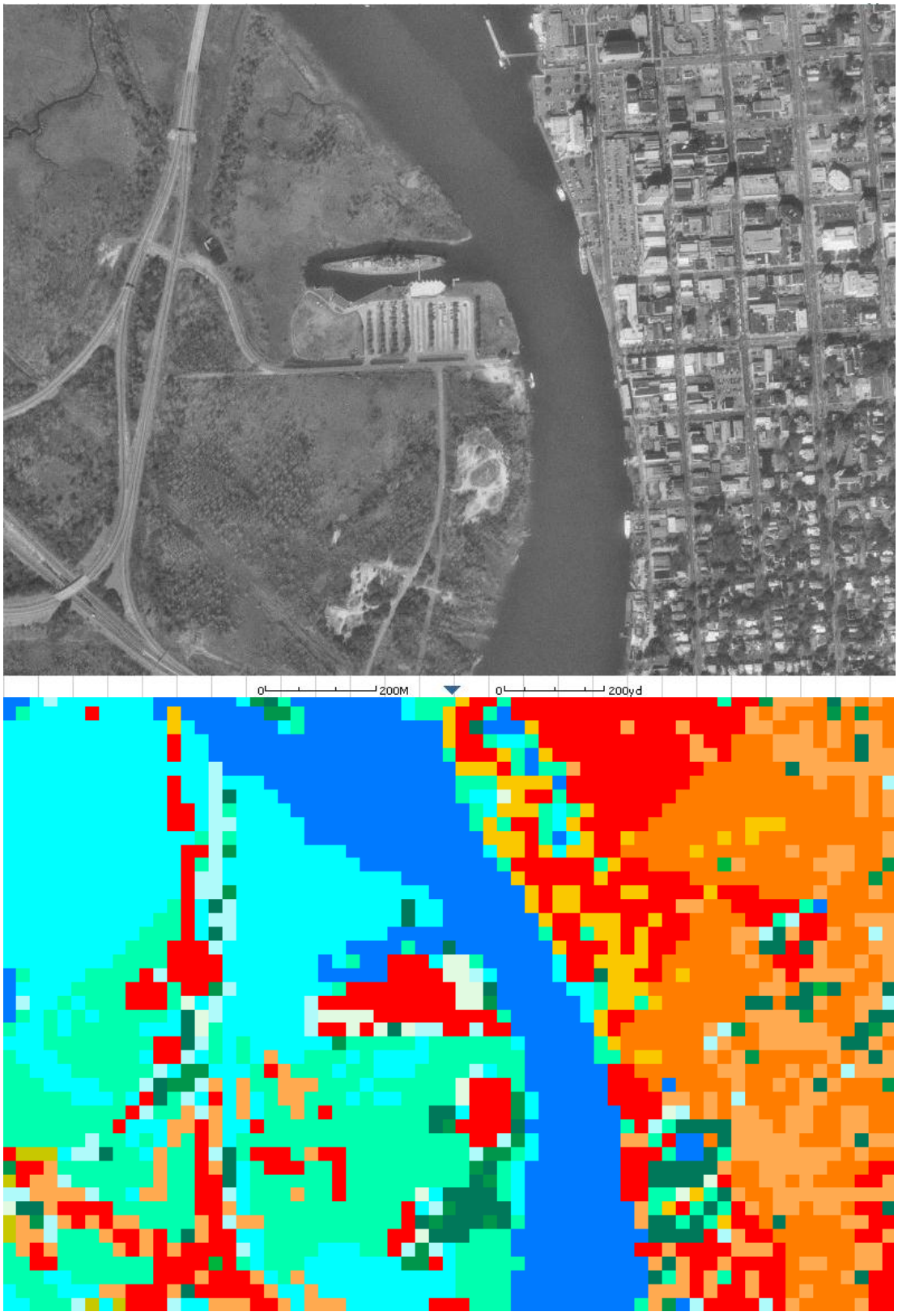

Figure 3.23. Close-Up of Downtown Wilmington, NC (upper: Aerial photograph; lower: NLCD).

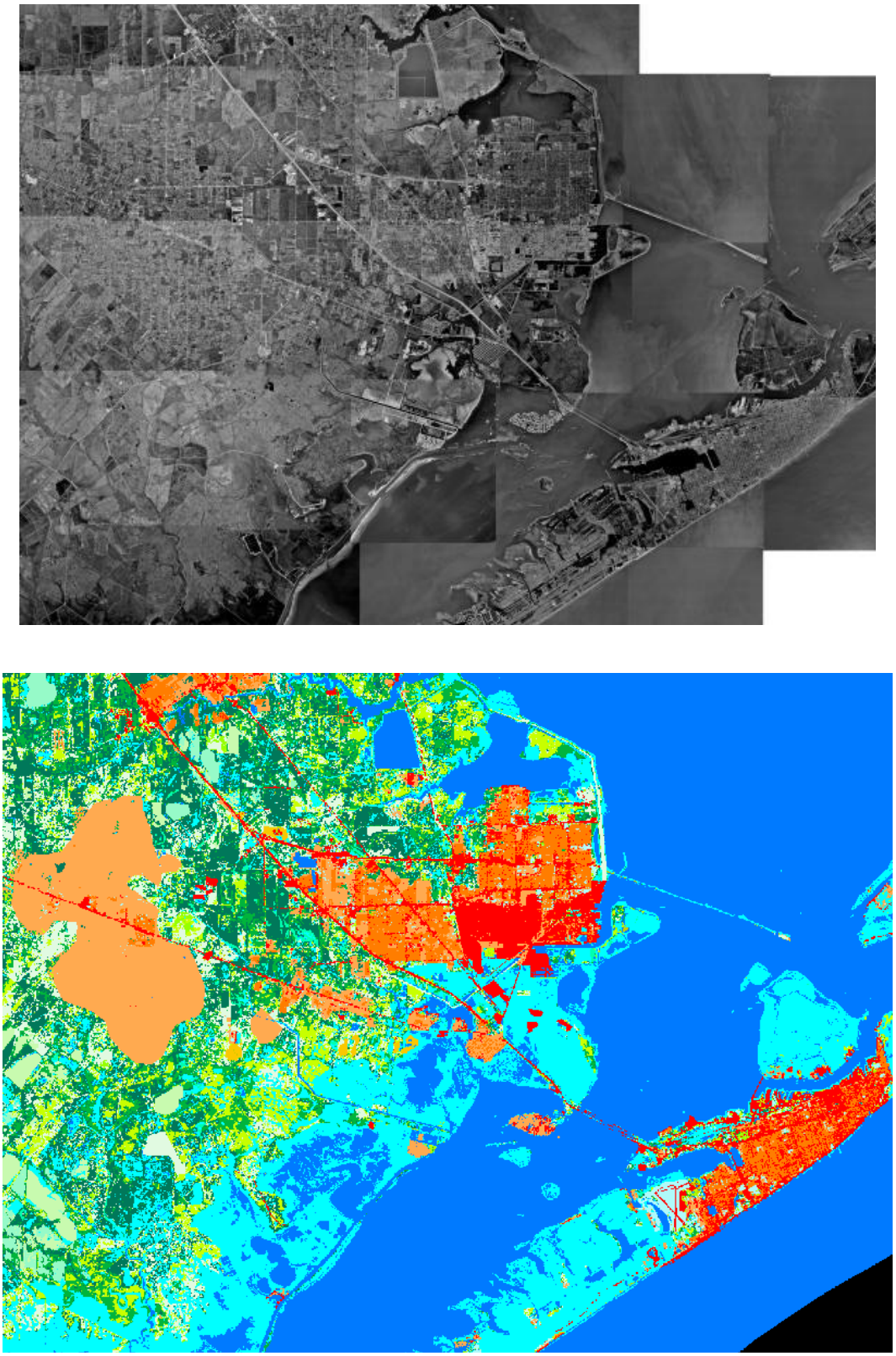

Figure 3.24. Galveston-Texas City-Santa Fe Area, TX (upper: Aerial photo; lower: NLCD).

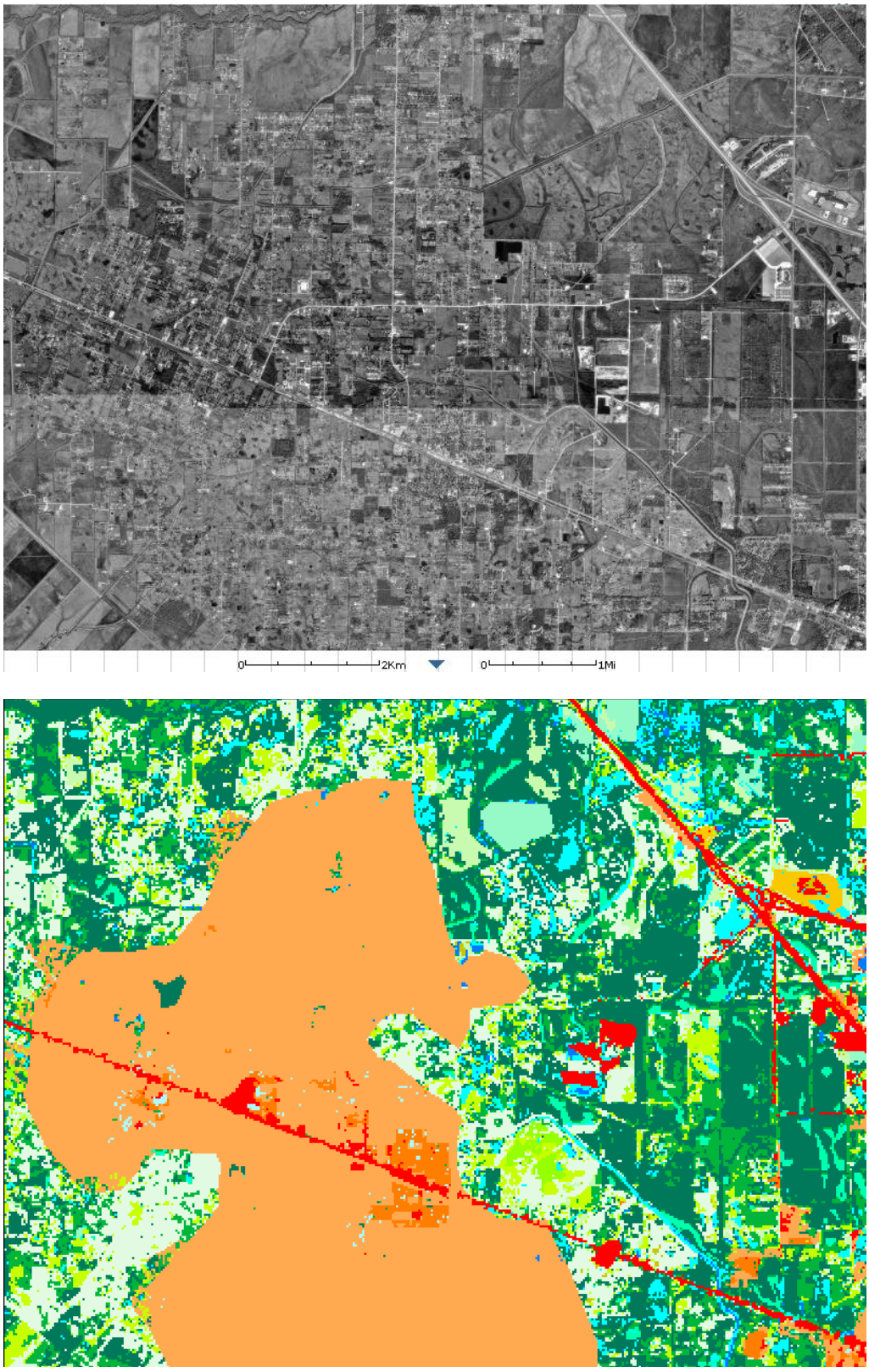

Figure 3.25. Close-up of Santa Fe Area, TX (upper: Aerial photograph; lower: NLCD).

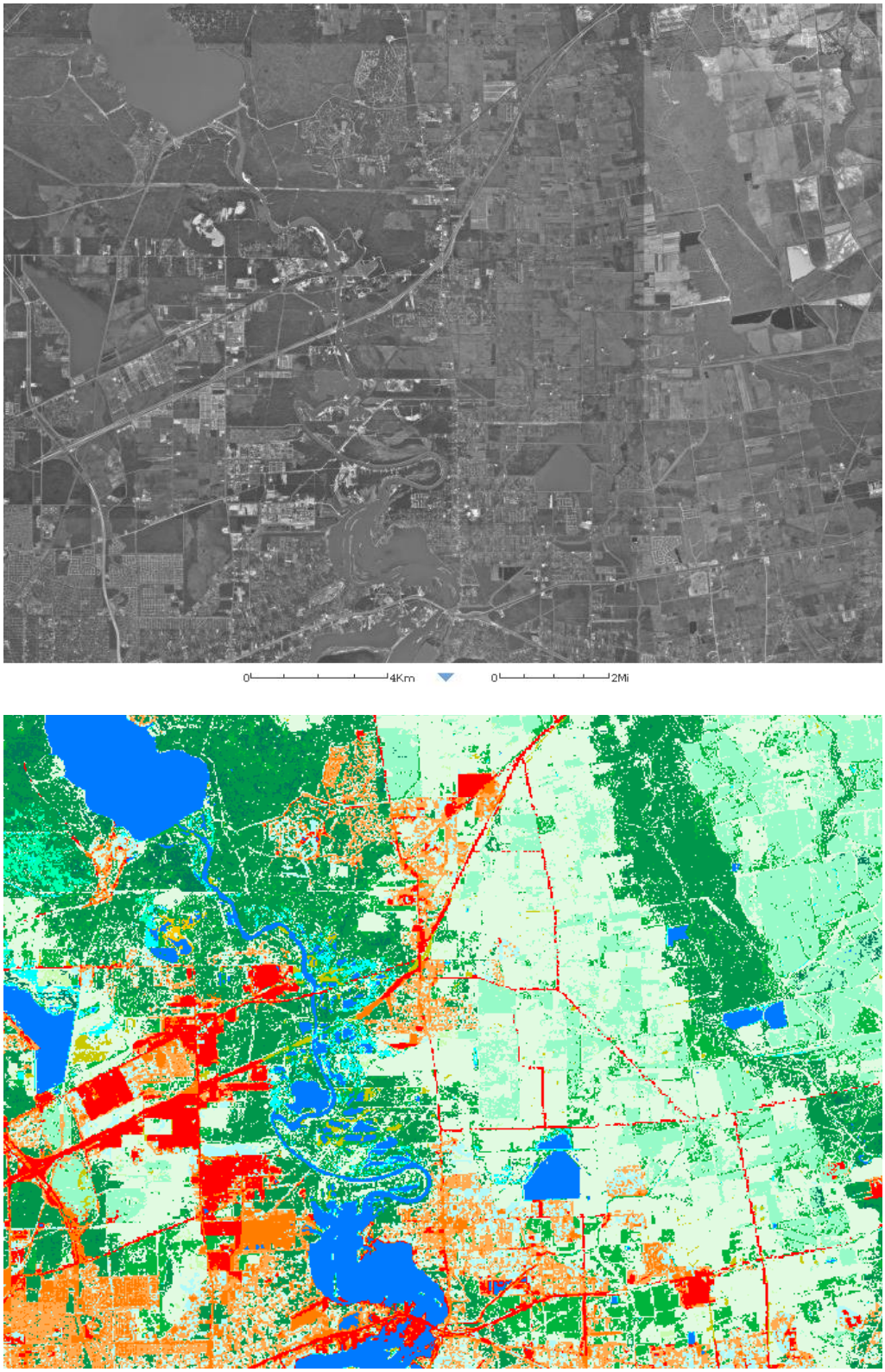

Figure 3.26. Northeast Suburb of Houston, TX (upper: Aerial photograph; lower: NLCD).

Table 3.9. Roughness Length for NLCD Land Cover Classes

State/Region	TX		LA		MS		AL		FL Pan		FL W		FL SE		FL NE		GA		SC		NC		VA	
Land Cover Class	**Ave**	Stdev	**Ave**	Stdev	**Ave**	Stdev	**Ave**	Stdev	**Ave**	Stdev	**Ave**	Stdev	**Ave**	Stdev	**Ave**	Stdev	**Ave**	Stdev	**Ave**	Stdev	**Ave**	Stdev	**Ave**	Stdev
Water																								
11 Open Water	**0.010**		**0.010**		**0.010**		**0.010**		**0.010**		**0.010**		**0.010**		**0.010**		**0.010**		**0.010**		**0.010**		**0.010**	
12 Perennial Ice/Snow	**0.012**		**0.012**		**0.012**		**0.012**		**0.012**		**0.012**		**0.012**		**0.012**		**0.012**		**0.012**		**0.012**		**0.012**	
Developed																								
21 Low Intensity Residential	**0.35**	0.10	**0.33**	0.13	**0.33**	0.11	**0.33**	0.11	**0.33**	0.11	**0.34**	0.12	**0.34**	0.11	**0.33**	0.12	**0.35**	0.11	**0.36**	0.11	**0.35**	0.10	**0.35**	0.15
22 High Intensity Residential	**0.55**	0.10	**0.50**	0.14	**0.53**	0.14	**0.53**	0.14	**0.53**	0.14	**0.54**	0.15	**0.57**	0.18	**0.54**	0.14	**0.57**	0.11	**0.57**	0.16	**0.55**	0.11	**0.53**	0.19
23 Commercial/Industrial/Transportation	**0.44**	0.38	**0.39**	0.35	**0.35**	0.21	**0.35**	0.21	**0.35**	0.21	**0.39**	0.27	**0.38**	0.26	**0.34**	0.26	**0.35**	0.20	**0.34**	0.20	**0.33**	0.21	**0.38**	0.20
Barren																								
31 Bare Rock/Sand/Clay	**0.10**	0.04	**0.09**	0.05	**0.09**	0.05	**0.09**	0.05	**0.09**	0.05	**0.10**	0.06	**0.09**	0.04	**0.09**	0.05	**0.10**	0.05	**0.10**	0.06	**0.10**	0.05	**0.10**	0.04
32 Quarries/Strip Mines/Gravel Pits	**0.14**	0.08	**0.18**	0.09	**0.18**	0.09	**0.18**	0.09	**0.18**	0.09	**0.17**	0.09	**0.20**	0.09	**0.18**	0.08	**0.17**	0.06	**0.17**	0.07	**0.17**	0.09	**0.12**	0.05
33 Transitional	**0.15**	0.09	**0.18**	0.10	**0.20**	0.07	**0.20**	0.07	**0.20**	0.07	**0.17**	0.09	**0.19**	0.08	**0.16**	0.09	**0.13**	0.06	**0.17**	0.10	**0.15**	0.09	**0.20**	0.09
Forested Upland																								
41 Deciduous Forest	**0.55**	0.16	**0.65**	0.19	**0.68**	0.17	**0.68**	0.17	**0.68**	0.17	**0.65**	0.18	**0.69**	0.13	**0.72**	0.13	**0.76**	0.15	**0.79**	0.19	**0.78**	0.15	**0.79**	0.16
42 Evergreen Forest	**0.56**	0.14	**0.72**	0.20	**0.73**	0.12	**0.73**	0.12	**0.73**	0.12	**0.76**	0.13	**0.71**	0.10	**0.74**	0.14	**0.75**	0.15	**0.82**	0.14	**0.81**	0.15	**0.82**	0.11
43 Mixed Forest	**0.55**	0.14	**0.71**	0.21	**0.71**	0.12	**0.71**	0.12	**0.71**	0.12	**0.74**	0.13	**0.71**	0.10	**0.73**	0.15	**0.76**	0.14	**0.80**	0.16	**0.80**	0.14	**0.81**	0.14
Shrubland																								
51 Shrubland	**0.10**	0.05	**0.12**	0.03	**0.12**	0.03	**0.12**	0.03	**0.12**	0.03	**0.12**	0.04	**0.12**	0.03	**0.12**	0.03	**0.11**	0.03	**0.13**	0.04	**0.10**	0.03	**0.12**	0.03
Non-Natural Woody																								
61 Orchards/Vineyards/Other	**0.25**	0.11	**0.27**	0.13	**0.25**	0.13	**0.25**	0.13	**0.25**	0.13	**0.24**	0.12	**0.27**	0.14	**0.24**	0.12	**0.26**	0.14	**0.29**	0.16	**0.25**	0.10	**0.24**	0.15
Herbaceous Upland																								
71 Grasslands/Herbaceous	**0.04**	0.02	**0.04**	0.01	**0.04**	0.01	**0.04**	0.01	**0.04**	0.01	**0.04**	0.02	**0.04**	0.02	**0.04**	0.02	**0.05**	0.02	**0.04**	0.02	**0.04**	0.02	**0.04**	0.02
Herbaceous Planted / Cultivated																								
81 Pasture/Hay	**0.04**	0.02	**0.06**	0.02	**0.05**	0.02	**0.05**	0.02	**0.05**	0.02	**0.05**	0.02	**0.05**	0.02	**0.06**	0.01	**0.05**	0.02	**0.06**	0.02	**0.06**	0.02	**0.05**	0.02
82 Row Crops	**0.06**	0.02	**0.06**	0.02	**0.05**	0.02	**0.05**	0.02	**0.05**	0.02	**0.06**	0.03	**0.06**	0.02	**0.06**	0.02	**0.06**	0.03	**0.06**	0.02	**0.06**	0.02	**0.05**	0.02
83 Small Grains	**0.04**	0.02	**0.05**	0.02	**0.06**	0.02	**0.06**	0.02	**0.06**	0.02	**0.05**	0.03	**0.06**	0.02	**0.07**	0.02	**0.06**	0.03	**0.07**	0.03	**0.06**	0.02	**0.06**	0.02
84 Fallow	**0.03**	0.02	**0.04**	0.02	**0.04**	0.02	**0.04**	0.02	**0.04**	0.02	**0.03**	0.01	**0.03**	0.02	**0.04**	0.02	**0.04**	0.02	**0.03**	0.01	**0.03**	0.02	**0.04**	0.01
85 Urban/Recreational Grasses	**0.07**	0.04	**0.05**	0.03	**0.03**	0.04	**0.03**	0.04	**0.03**	0.04	**0.04**	0.04	**0.06**	0.03	**0.06**	0.04	**0.06**	0.04	**0.06**	0.03	**0.07**	0.04	**0.05**	0.04
Wetland																								
91 Woody Wetlands	**0.50**	0.20	**0.55**	0.21	**0.58**	0.21	**0.58**	0.21	**0.58**	0.21	**0.59**	0.22	**0.54**	0.20	**0.57**	0.26	**0.60**	0.27	**0.61**	0.22	**0.60**	0.21	**0.59**	0.24
92 Emergent Herbaceous Wetlands	**0.10**	0.05	**0.11**	0.05	**0.09**	0.04	**0.09**	0.04	**0.09**	0.04	**0.08**	0.04	**0.04**	0.01	**0.09**	0.03	**0.10**	0.04	**0.10**	0.04	**0.10**	0.05	**0.10**	0.05

State/Region	MD		DE		PA		NJ		NY (Man&LI)		Manhattan		Long Is.		CT		RI		MA		NH		ME	
Land Cover Class	**Ave**	Stdev	**Ave**	Stdev	**Ave**	Stdev	**Ave**	Stdev	**Ave**	Stdev	**Ave**	Stdev	**Ave**	Stdev	**Ave**	Stdev	**Ave**	Stdev	**Ave**	Stdev	**Ave**	Stdev	**Ave**	Stdev
Water																								
11 Open Water	**0.010**		**0.010**		**0.010**		**0.010**		**0.010**		**0.010**		**0.010**		**0.010**		**0.010**		**0.010**		**0.010**		**0.010**	
12 Perennial Ice/Snow	**0.012**		**0.012**		**0.012**		**0.012**		**0.012**		**0.012**		**0.012**		**0.012**		**0.012**		**0.012**		**0.012**		**0.012**	
Developed																								
21 Low Intensity Residential	**0.35**	0.15	**0.35**	0.15	**0.36**	0.14	**0.35**	0.14	**0.43**	0.17	**0.50**	0.10	**0.42**	0.17	**0.34**	0.10	**0.34**	0.10	**0.36**	0.10	**0.29**	0.10	**0.29**	0.10
22 High Intensity Residential	**0.53**	0.19	**0.53**	0.19	**0.62**	0.17	**0.58**	0.21	**0.73**	0.34	**0.84**	0.42	**0.62**	0.18	**0.48**	0.16	**0.48**	0.16	**0.59**	0.18	**0.53**	0.08	**0.53**	0.08
23 Commercial/Industrial/Transportation	**0.38**	0.20	**0.38**	0.20	**0.44**	0.33	**0.42**	0.22	**0.92**	0.82	**1.55**	0.93	**0.44**	0.12	**0.35**	0.15	**0.35**	0.15	**0.51**	0.38	**0.31**	0.15	**0.31**	0.15
Barren																								
31 Bare Rock/Sand/Clay	**0.10**	0.04	**0.10**	0.04	**0.14**	0.04	**0.08**	0.03	**0.09**	0.04	**0.09**	0.04	**0.09**	0.04	**0.10**	0.04	**0.10**	0.04	**0.12**	0.05	**0.12**	0.05	**0.12**	0.05
32 Quarries/Strip Mines/Gravel Pits	**0.12**	0.05	**0.12**	0.05	**0.12**	0.06	**0.15**	0.08	**0.17**	0.08	**0.17**	0.08	**0.17**	0.08	**0.15**	0.08	**0.15**	0.08	**0.16**	0.10	**0.15**	0.06	**0.15**	0.06
33 Transitional	**0.20**	0.09	**0.20**	0.09	**0.14**	0.09	**0.22**	0.08	**0.21**	0.10	**0.21**	0.10	**0.21**	0.10	**0.17**	0.09	**0.17**	0.09	**0.19**	0.07	**0.13**	0.09	**0.13**	0.09
Forested Upland																								
41 Deciduous Forest	**0.79**	0.16	**0.79**	0.16	**0.77**	0.11	**0.78**	0.15	**0.78**	0.19	**0.78**	0.19	**0.78**	0.19	**0.79**	0.09	**0.79**	0.09	**0.77**	0.14	**0.78**	0.13	**0.78**	0.13
42 Evergreen Forest	**0.82**	0.11	**0.82**	0.11	**0.77**	0.16	**0.82**	0.10	**0.78**	0.12	**0.78**	0.12	**0.78**	0.12	**0.80**	0.15	**0.80**	0.15	**0.78**	0.14	**0.78**	0.13	**0.78**	0.13
43 Mixed Forest	**0.81**	0.14	**0.81**	0.14	**0.78**	0.14	**0.80**	0.12	**0.79**	0.12	**0.79**	0.12	**0.79**	0.12	**0.80**	0.16	**0.80**	0.16	**0.79**	0.12	**0.79**	0.13	**0.79**	0.13
Shrubland																								
51 Shrubland	**0.12**	0.03	**0.12**	0.03	**0.14**	0.04	**0.13**	0.04	**0.13**	0.04	**0.13**	0.04	**0.13**	0.04	**0.11**	0.02	**0.11**	0.02	**0.13**	0.03	**0.11**	0.04	**0.11**	0.04
Non-Natural Woody																								
61 Orchards/Vineyards/Other	**0.24**	0.15	**0.24**	0.15	**0.22**	0.15	**0.24**	0.16	**0.26**	0.11	**0.26**	0.11	**0.26**	0.11	**0.26**	0.12	**0.26**	0.12	**0.26**	0.14	**0.25**	0.13	**0.25**	0.13
Herbaceous Upland																								
71 Grasslands/Herbaceous	**0.04**	0.02	**0.04**	0.02	**0.04**	0.02	**0.04**	0.02	**0.05**	0.02	**0.05**	0.02	**0.05**	0.02	**0.04**	0.02	**0.04**	0.02	**0.04**	0.02	**0.04**	0.02	**0.04**	0.02
Herbaceous Planted / Cultivated																								
81 Pasture/Hay	**0.05**	0.02	**0.05**	0.02	**0.05**	0.02	**0.06**	0.02	**0.05**	0.02	**0.05**	0.02	**0.05**	0.02	**0.05**	0.02	**0.05**	0.02	**0.05**	0.02	**0.06**	0.02	**0.06**	0.02
82 Row Crops	**0.05**	0.02	**0.05**	0.02	**0.05**	0.03	**0.05**	0.01	**0.06**	0.03	**0.06**	0.03	**0.06**	0.03	**0.06**	0.03	**0.06**	0.03	**0.06**	0.03	**0.06**	0.02	**0.06**	0.02
83 Small Grains	**0.06**	0.02	**0.06**	0.02	**0.06**	0.03	**0.06**	0.02	**0.06**	0.03	**0.06**	0.03	**0.06**	0.03	**0.06**	0.02	**0.06**	0.02	**0.06**	0.02	**0.07**	0.03	**0.07**	0.03
84 Fallow	**0.04**	0.01	**0.04**	0.01	**0.04**	0.02	**0.03**	0.01	**0.04**	0.02	**0.04**	0.02	**0.04**	0.02	**0.03**	0.01	**0.03**	0.01	**0.04**	0.02	**0.04**	0.02	**0.04**	0.02
85 Urban/Recreational Grasses	**0.05**	0.04	**0.05**	0.04	**0.07**	0.05	**0.05**	0.04	**0.08**	0.03	**0.08**	0.03	**0.08**	0.03	**0.05**	0.04	**0.05**	0.04	**0.06**	0.04	**0.03**	0.04	**0.03**	0.04
Wetland																								
91 Woody Wetlands	**0.59**	0.24	**0.59**	0.24	**0.60**	0.24	**0.60**	0.24	**0.60**	0.22	**0.60**	0.22	**0.60**	0.22	**0.58**	0.22	**0.58**	0.22	**0.58**	0.21	**0.61**	0.20	**0.61**	0.20
92 Emergent Herbaceous Wetlands	**0.10**	0.05	**0.10**	0.05	**0.10**	0.04	**0.08**	0.04	**0.10**	0.04	**0.10**	0.04	**0.10**	0.04	**0.09**	0.05	**0.09**	0.05	**0.09**	0.04	**0.09**	0.04	**0.09**	0.04

3.5.3 Census Tract-Averaged Roughness Length

Using the roughness length-mapped NLCD data, census tract-averaged roughness lengths have been computed for the Year 2000 census tracts. Examples developed using the 1990 census tract shapes are presented in Figures 3.27 and 3.28 for North Carolina and Texas, respectively, where two counties are shown for each state, one coastal county and another relatively inland. For North Carolina, New Hanover County is the coastal county and Wake County is the inland county. For Texas, two adjacent counties were arbitrarily selected. The results are reasonable.

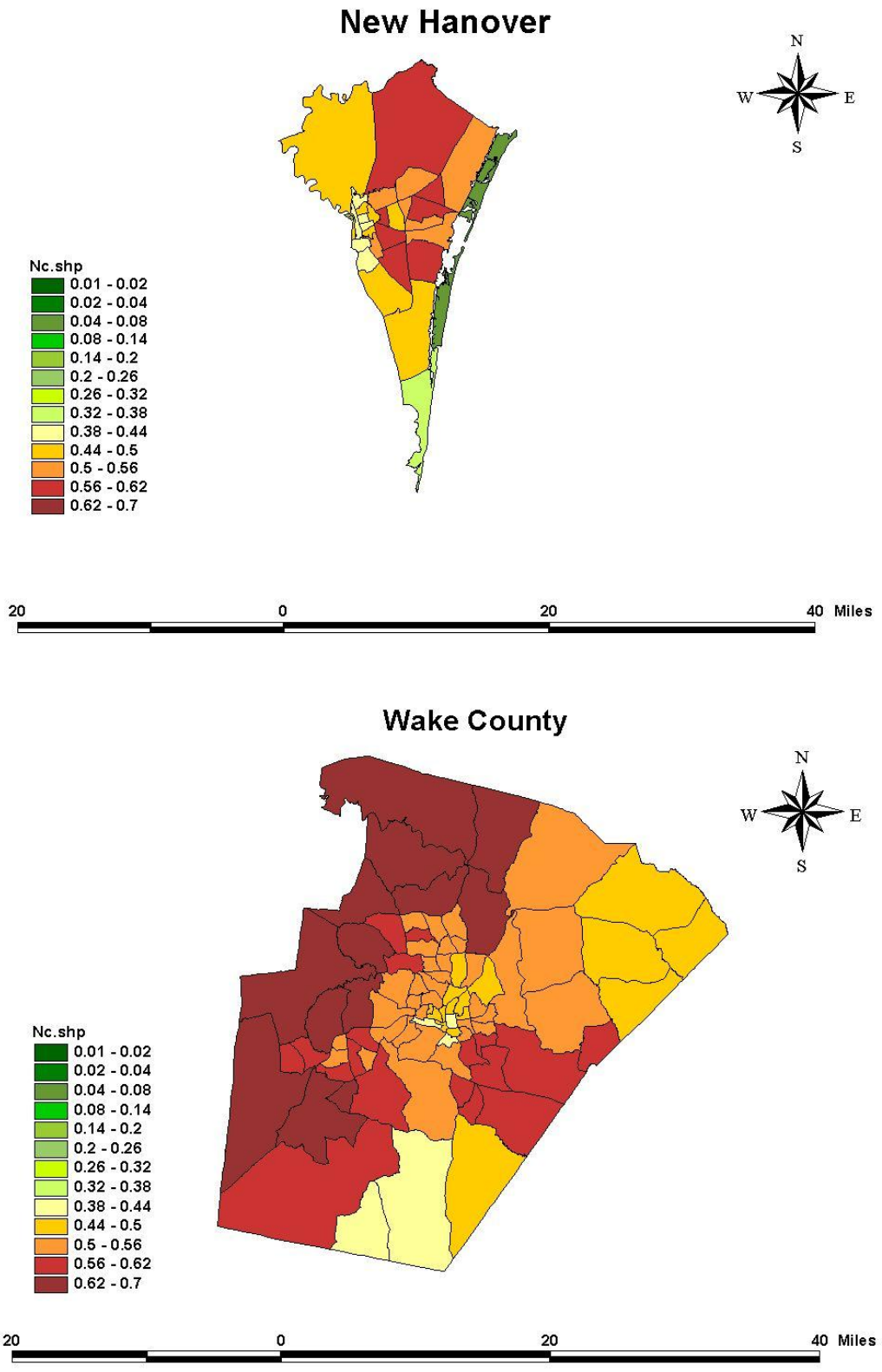

Figure 3.27. Census Tract-Averaged Roughness Length Derived from NLCD Data, NC.

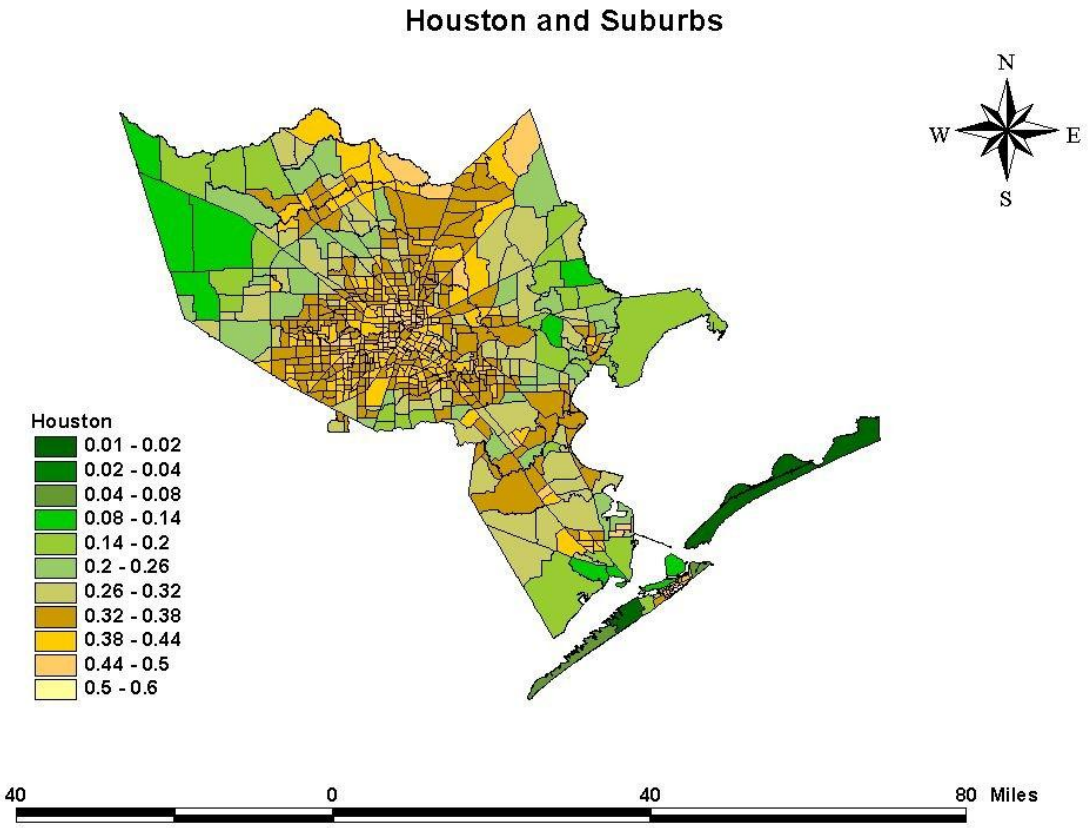

Figure 3.28. Census Tract-Averaged Roughness Length Derived from NLCD Data, Texas.

3.5.4 Comparisons of z_0 Values Computed from NLCD Data on Rectangular Grids with Empirically Assigned z_0 Values

Averaged z_0 values are also computed from NLCD data on 1.8km x 1.2km rectangular grids and compared to empirically assigned z_0 values based on observations from aerial photographs. Examples of the comparison are presented in Figures 3.29 through 3.32 for selected locations in Texas, Florida, North Carolina and Rhode Island, respectively. The correlation between the two sets of z_0 values is shown in Figures 3.33 through 3.36 for these four locations, respectively. The correlation coefficients are, respectively, 0.88, 0.93, 0.63 and 0.77 for the four locations. The results from all four locations are combined in Figure 3.37, for which the correlation coefficient is 0.926, which is higher than the average of the four individual correlation coefficients. This reflects that estimation of z_0 values using NLCD data provides better relative accuracy when involving a larger variety of land cover characteristics than for a smaller, localized land area. These comparisons serve as a check on the reasonableness of averaged z_0 values computed from NLCD data. It indicates that the degree of agreement is acceptable in general, except for a few grid cells that, in particular, involve commercial high-rise buildings in downtown areas, such as for the studied cases of Raleigh, NC, and Miami, FL.

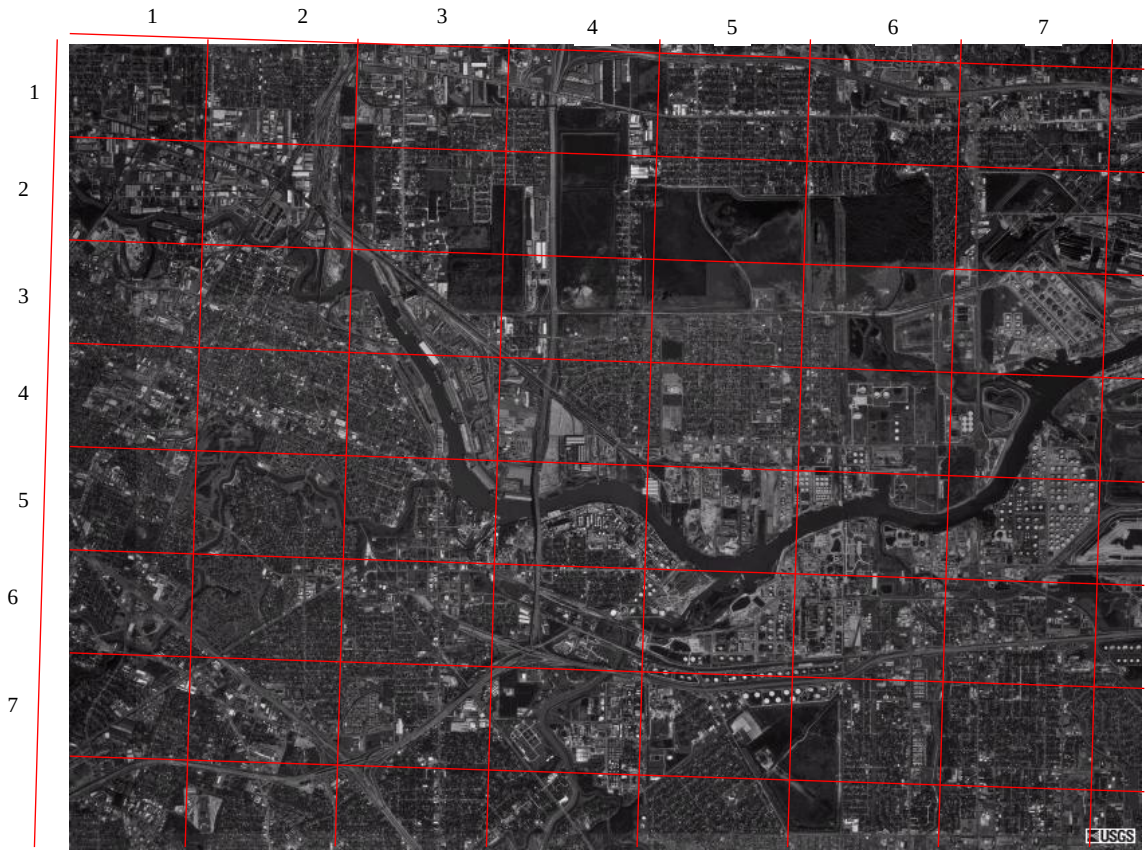

Assigned Zo	1	2	3	4	5	6	7
1	0.45	0.45	0.45	0.40	0.40	0.40	0.40
2	0.40	0.45	0.32	0.30	0.40	0.40	0.40
3	0.45	0.48	0.40	0.32	0.33	0.30	0.35
4	0.50	0.45	0.42	0.40	0.45	0.30	0.28
5	0.42	0.30	0.40	0.35	0.32	0.32	0.35
6	0.42	0.30	0.42	0.40	0.35	0.40	0.38
7	0.40	0.45	0.48	0.32	0.32	0.40	0.42

Computed Zo	1	2	3	4	5	6	7
1	0.447	0.441	0.438	0.367	0.372	0.384	0.408
2	0.418	0.428	0.372	0.320	0.414	0.341	0.414
3	0.471	0.483	0.399	0.332	0.330	0.341	0.373
4	0.491	0.468	0.429	0.403	0.421	0.339	0.305
5	0.416	0.304	0.385	0.358	0.361	0.327	0.389
6	0.448	0.319	0.409	0.410	0.397	0.429	0.418
7	0.394	0.439	0.431	0.391	0.389	0.403	0.423

Figure 3.29. z_0 Values Computed from NLCD Data and Assigned Empirically for a Location in East Suburban of Houston, TX.

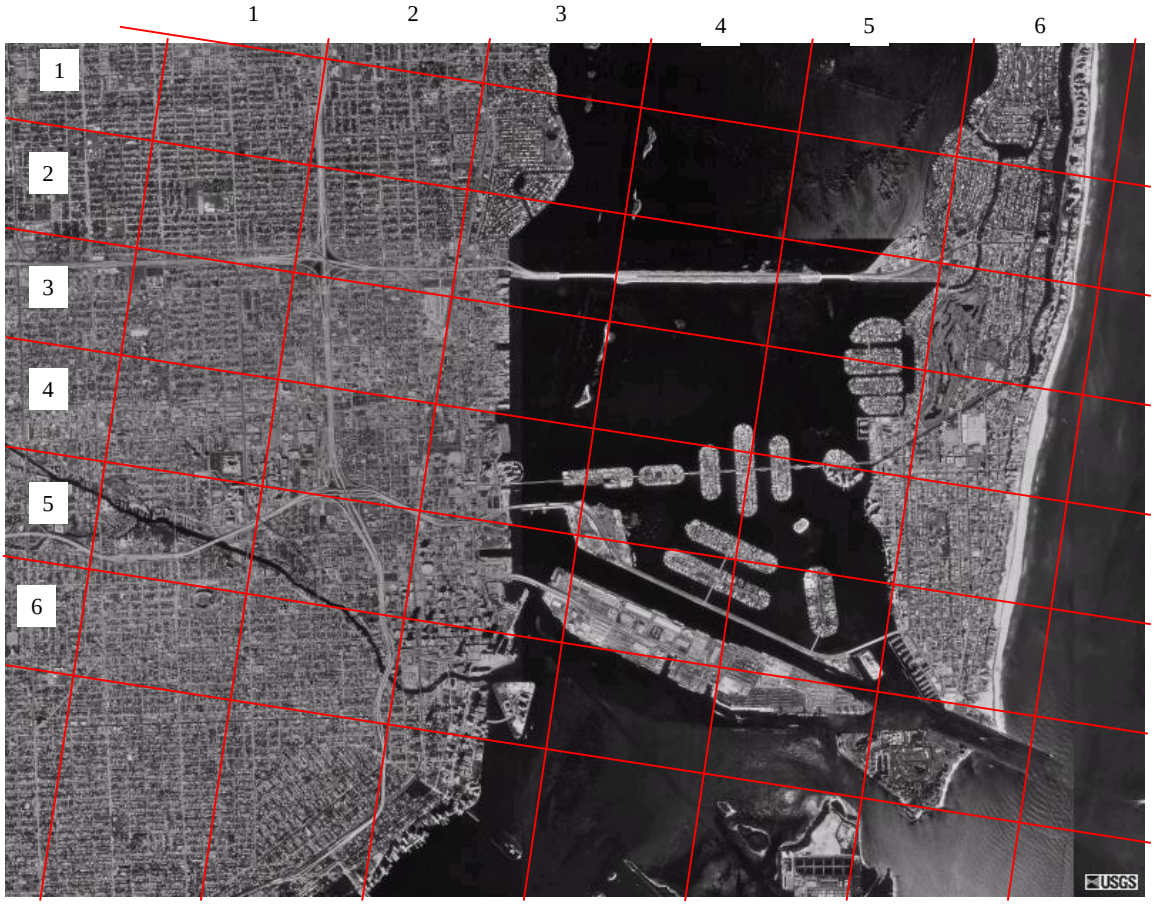

Assigned Zo	1	2	3	4	5	6
1	0.45	0.42	0.20	0.01	0.10	0.30
2	0.42	0.45	0.10	0.02	0.15	0.25
3	0.45	0.50	0.15	0.01	0.20	0.30
4	0.52	0.60	0.35	0.10	0.10	0.30
5	0.55	0.50	0.40	0.15	0.10	0.25
6	0.55	0.50	0.50	0.02	0.10	0.10

Computed Zo	1	2	3	4	5	6
1	0.472	0.470	0.192	0.014	0.113	0.300
2	0.447	0.464	0.140	0.036	0.129	0.260
3	0.494	0.463	0.178	0.017	0.160	0.290
4	0.463	0.447	0.225	0.127	0.137	0.306
5	0.423	0.426	0.255	0.196	0.093	0.266
6	0.485	0.468	0.224	0.040	0.107	0.114

Figure 3.30. z_0 Values Computed from NLCD Data and Assigned Empirically for Miami, FL, Including Downtown (Cell # 6-3).

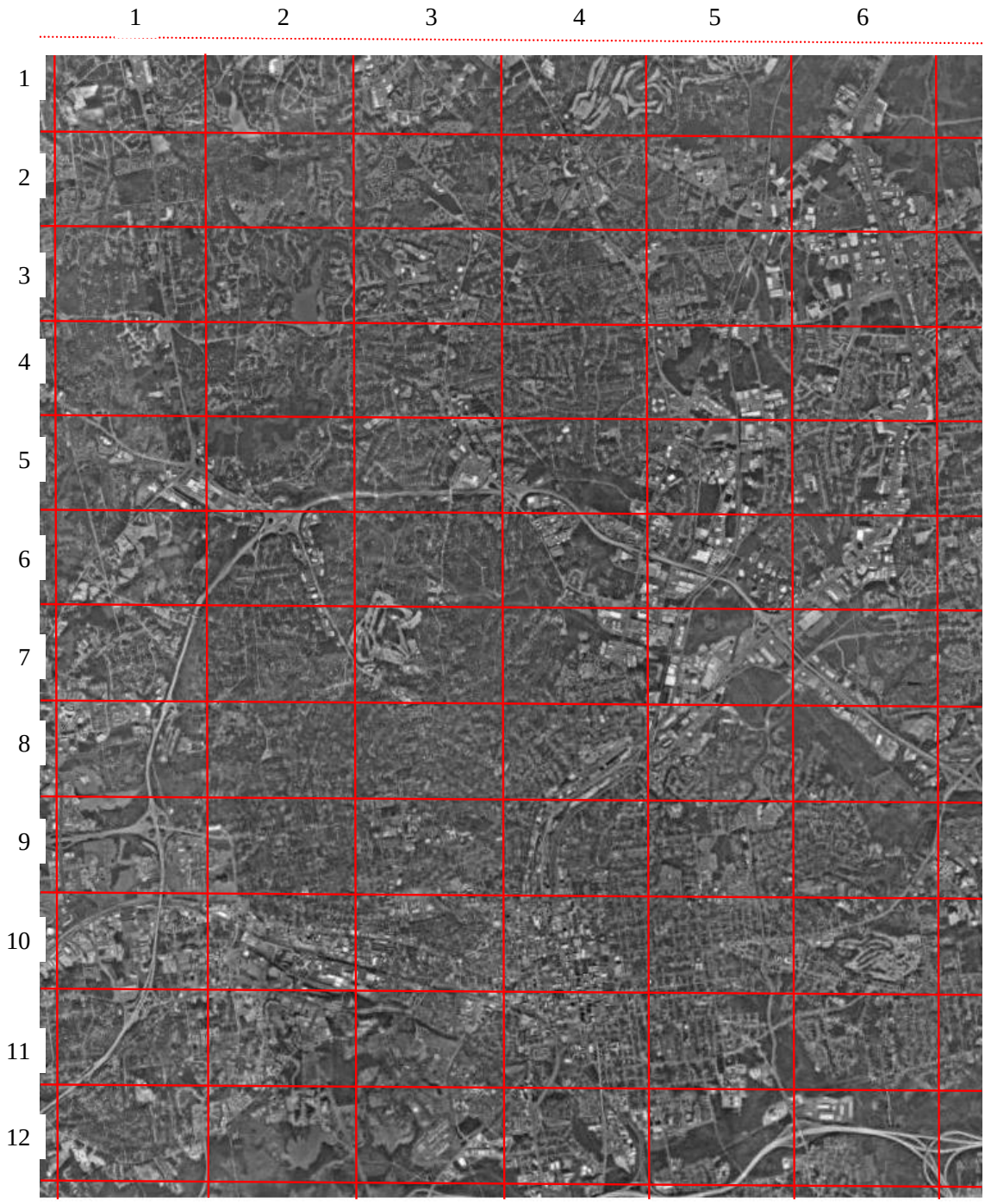

Figure 3.31. z_0 Values Computed from NLCD Data and Assigned Empirically for Raleigh, NC, Including Downtown (Cell # 10-4)

Assigned Zo	1	2	3	4	5	6
1	0.60	0.60	0.55	0.45	0.50	0.55
2	0.60	0.65	0.60	0.50	0.55	0.50
3	0.60	0.55	0.52	0.55	0.55	0.48
4	0.60	0.60	0.60	0.60	0.58	0.50
5	0.50	0.58	0.50	0.55	0.55	0.55
6	0.50	0.55	0.58	0.55	0.50	0.50
7	0.55	0.55	0.45	0.50	0.45	0.50
8	0.50	0.60	0.60	0.55	0.48	0.55
9	0.35	0.55	0.50	0.48	0.50	0.55
10	0.42	0.42	0.45	0.62	0.45	0.40
11	0.45	0.40	0.35	0.62	0.45	0.45
12	0.50	0.50	0.35	0.45	0.55	0.55

Computed Zo	1	2	3	4	5	6
1	0.557	0.546	0.518	0.482	0.619	0.666
2	0.567	0.562	0.604	0.498	0.521	0.491
3	0.622	0.580	0.514	0.535	0.534	0.479
4	0.607	0.597	0.542	0.533	0.569	0.495
5	0.519	0.587	0.524	0.522	0.525	0.520
6	0.537	0.528	0.542	0.490	0.487	0.476
7	0.573	0.572	0.499	0.529	0.448	0.500
8	0.491	0.552	0.535	0.487	0.449	0.536
9	0.365	0.521	0.489	0.465	0.513	0.524
10	0.418	0.430	0.451	0.399	0.495	0.462
11	0.527	0.466	0.428	0.411	0.508	0.539
12	0.554	0.522	0.375	0.430	0.532	0.524

Figure 3.31. z_0 Values Computed from NLCD Data and Assigned Empirically for Raleigh, NC, Including Downtown (Cell#10-4) (concluded).

3.6 Example of Roughness Length (z_0) Calculation Using Lettau's Formula

The empirical relationship between z_0 and the ground roughness physical dimensions proposed by Lettau (1969) forms the basis of the methodology given in ASCE-7-02 for the computation of the roughness length (z_0) for the purpose of determining if a building is located in Exposure B (defined as Suburban Terrain) or Exposure C (defined as Open Terrain). In ASCE-7-02, a building is considered to be located in a suburban terrain (Exposure B) if the value of z_0 computed using Lettau's method is greater than or equal to 0.15 m and less than 0.7 m. The representative value of Exposure B in ASCE-7-02 is defined with a surface roughness of 0.3 m.

Recall that Lettau's formula for estimating the surface roughness length, z_0, is:

$$z_0 \approx 0.5HS/A \tag{3.2}$$

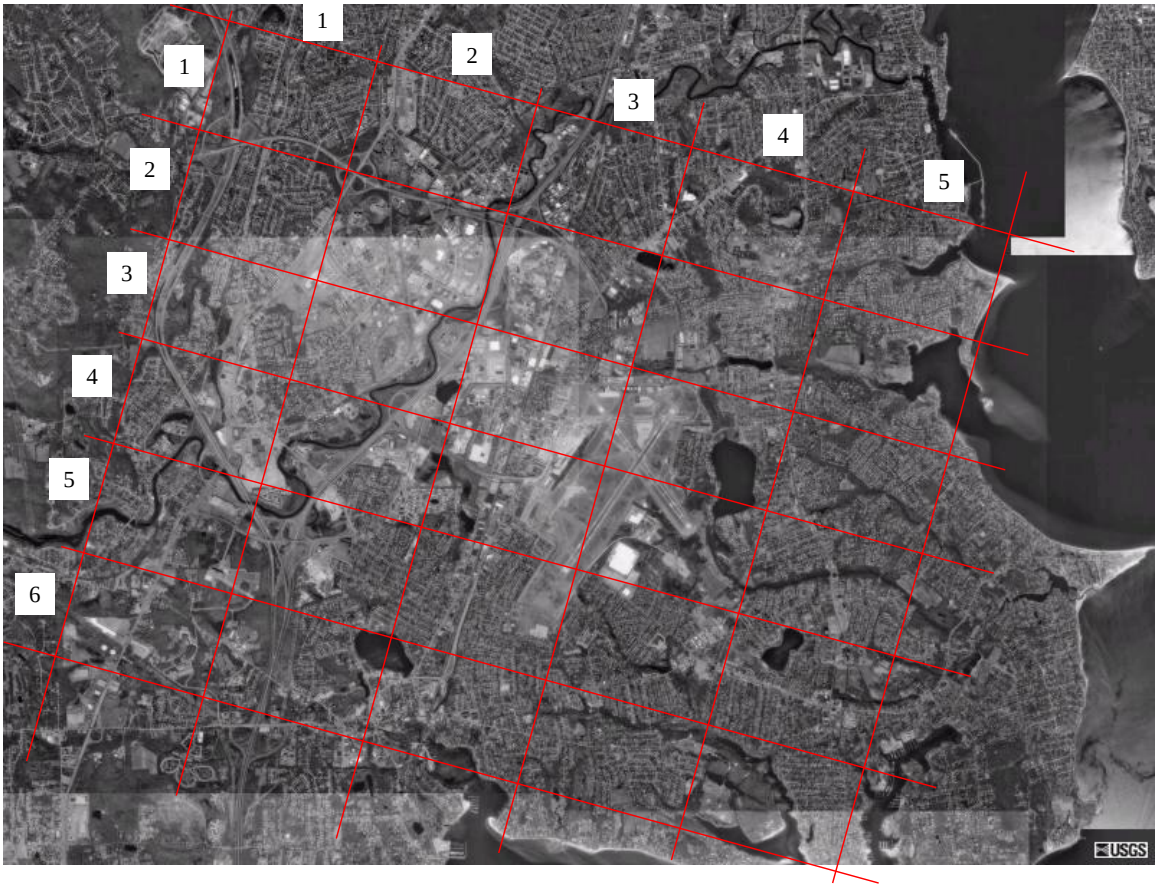

Assigned Zo	1	2	3	4	5
1	0.38	0.35	0.32	0.34	0.32
2	0.40	0.32	0.35	0.40	0.30
3	0.45	0.35	0.28	0.20	0.40
4	0.40	0.40	0.32	0.35	0.40
5	0.40	0.30	0.38	0.42	0.38
6	0.45	0.40	0.38	0.45	0.32

Computed Zo	1	2	3	4	5
1	0.409	0.368	0.367	0.397	0.318
2	0.382	0.346	0.357	0.388	0.324
3	0.406	0.354	0.312	0.250	0.419
4	0.394	0.364	0.305	0.349	0.389
5	0.427	0.381	0.330	0.380	0.367
6	0.507	0.447	0.328	0.405	0.351

Figure 3.32. z_0 Values Computed from NLCD Data and Assigned Empirically for a Location in South Suburban of Providence, RI.

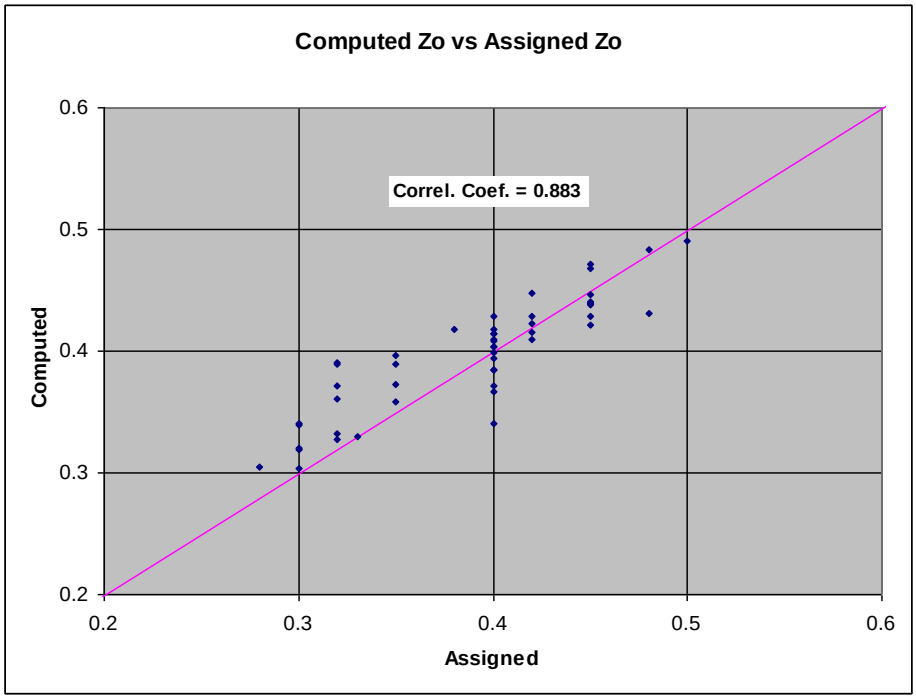

Figure 3.33. Comparison Between z_0 Values Computed from NLCD Data and Assigned Empirically for a Location in East Suburban of Houston, TX.

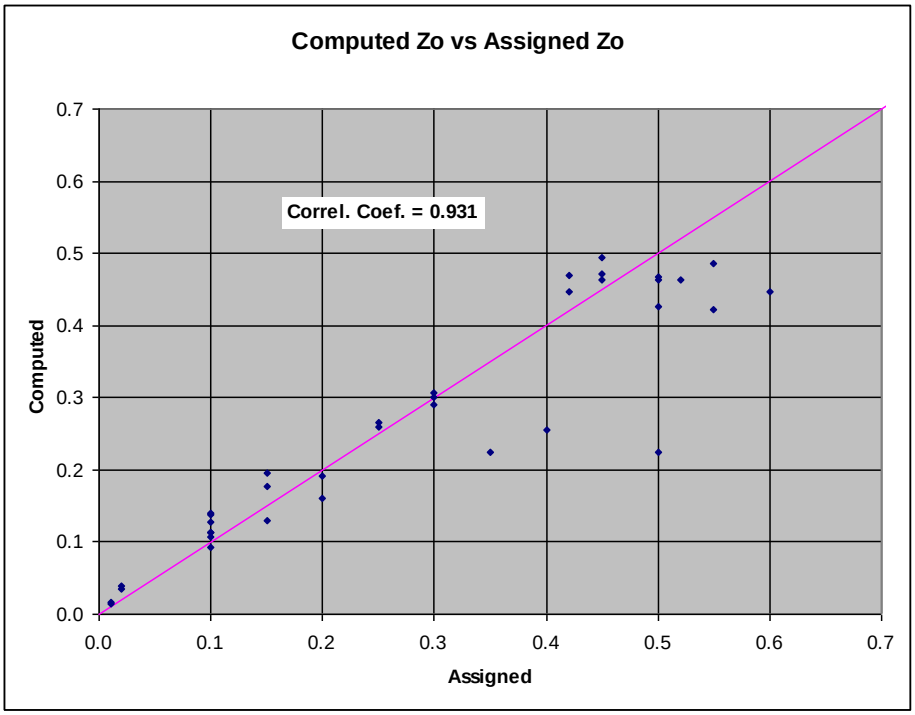

Figure 3.34. Comparison Between z_0 Values Computed from NLCD Data and Assigned Empirically for Miami, FL, Including Downtown Area.

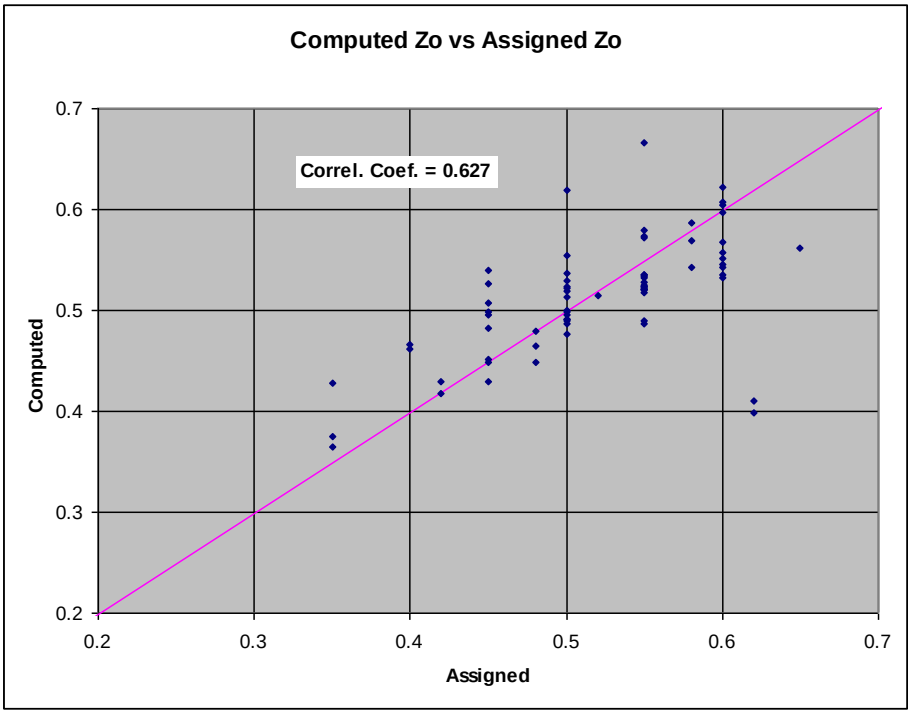

Figure 3.35. Comparison Between z_0 Values Computed from NLCD Data and Assigned Empirically for Raleigh, NC, Including Downtown Area.

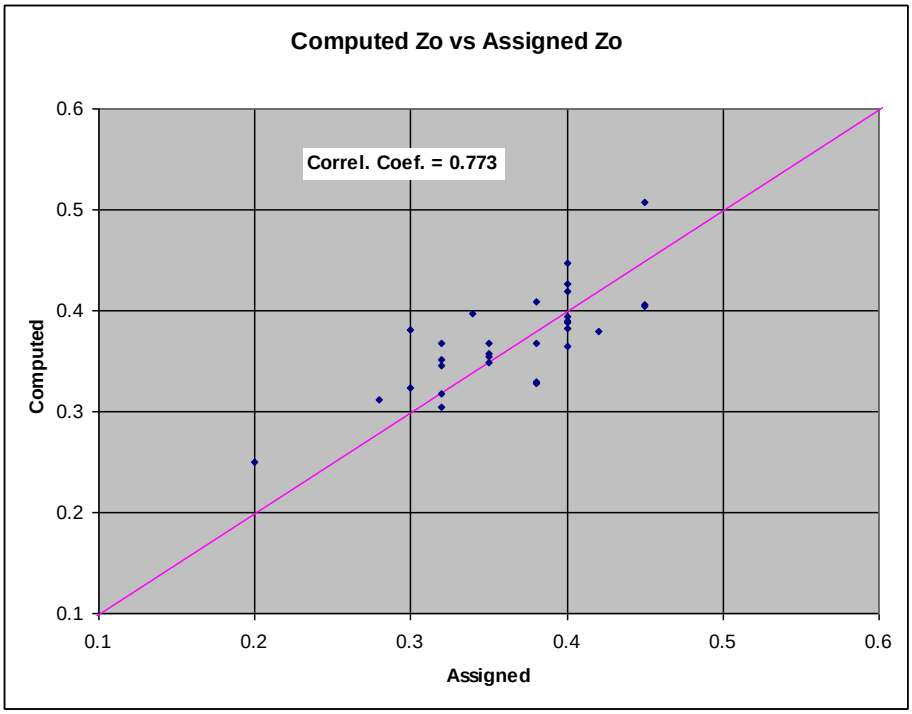

Figure 3.36. Comparison Between z_0 Values Computed from NLCD Data and Assigned Empirically for a Location in Southern Providence, RI.

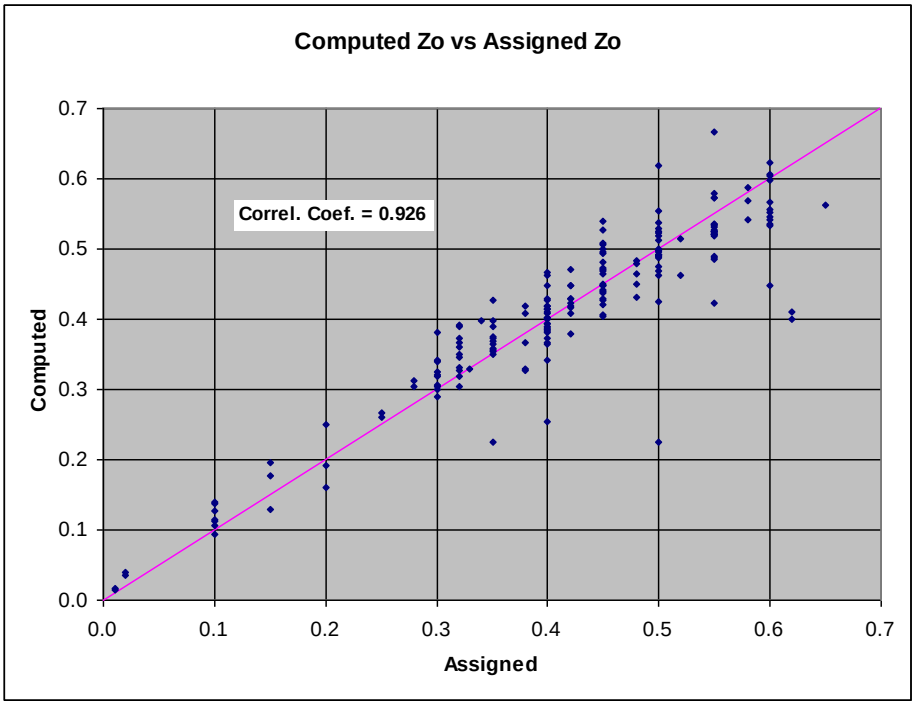

Figure 3.37. Comparison Between z_0 Values Computed from NLCD Data and Assigned Empirically for the Four Locations Studied.

where H = average height of the obstacle in the upwind terrain, S = the average projected frontal area per obstruction presented to the wind, and A = the average area of ground occupied by each obstruction (including the open area surrounding it). When calculating an average value of z_0 over a region, S and A can be substituted by the total projected frontal area of all the obstacles upwind of a site and the total ground area these obstacles collectively occupy.

When trees or bushes are present, their contribution to the frontal area must also be considered. ASCE-7-02 suggests that for conifers and other evergreens no more than 50% of their gross frontal area can be taken to be effective in obstructing the wind. For deciduous trees and bushes ASCE-7-02 states that no more than 15% of the their gross frontal area can be taken to be effective in obstructing the wind, however in hurricane prone regions, trees are generally still in full leaf during the time period hurricanes are likely to impact a region, thus an effective area of 50% is probably more appropriate. Recall, that the objective in estimating the surface roughness is to enable a realistic estimate of losses, and thus there should not be any tendency to choose a low value of frontal area in an attempt to obtain a conservative (low) value of z_0 as may be done in a building design situation.

Following is a step-by-step demonstration to show how to use the DOQQs to obtain the information required for Lettau's formula and the logic in defining the input parameters. For demonstration purpose, the DOQQs from one medium density residential area in

each of five counties in Florida (Escambia, Lee, Dade, Palm Beach, and Duval, see Figures 3.38 through 3.42) are used.

Medium density residential areas are selected because:

1. Building density is in such a range that the possibility of a building being shadowed by trees is small and ambiguity does not exist in distinguishing two separate buildings
2. Building heights for a residential area are relatively uniform and relatively easy to estimate, thus providing more reliable results.

It may be difficult to accurately determine an obstacle's height by looking at the DOQQs or aerial photography. Sometimes, the length of the sun shadow projected by an obstacle can help if any known reference object exists. Familiarity with a region will aid considerably in reducing errors associated with estimates of both building and tree heights.

Here, using Figure 3.38 as an example, the steps used to calculate the roughness length with Lettau's method are demonstrated. This is a medium density residential area in the Panhandle of Florida (Escambia County). The wind was assumed coming from the direction shown by the arrow in Figure 3.38. The study area defined by the polygon shown in Figure 3.38 has a total ground area of about 60800 m^2. By counting all the

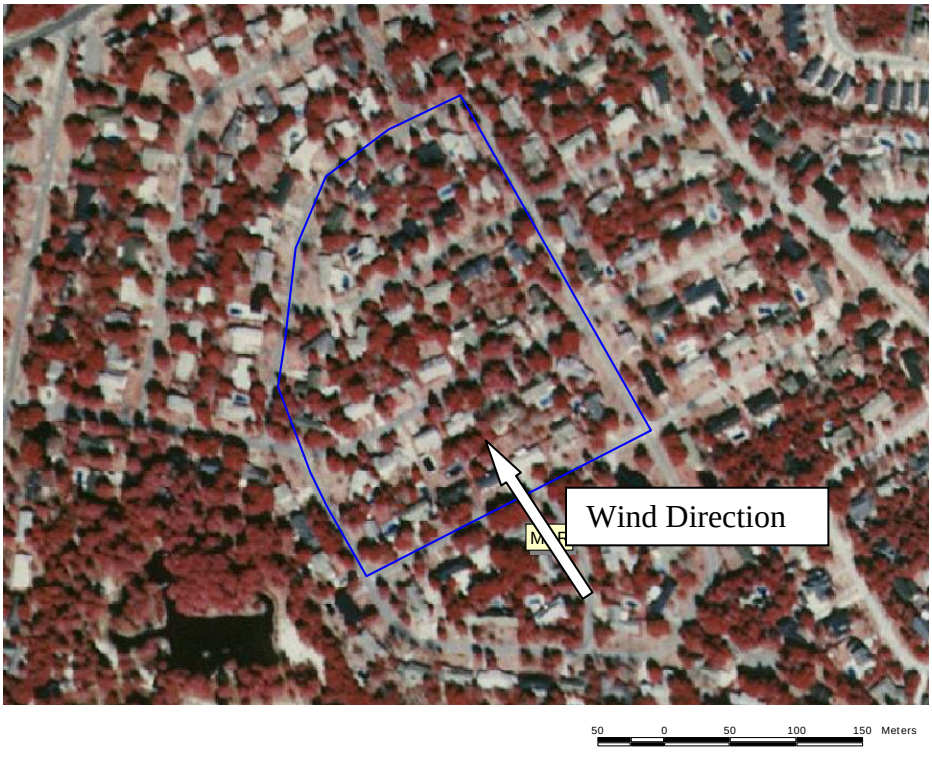

Figure 3.38. Medium Density Residential Area in Escambia County.

Figure 3.39. Medium Density Residential Area in Lee County.

Figure 3.40. Medium Density Residential Area in Dade County.

Figure 3.41. Medium Density Residential Area in Palm Beach County.

Figure 3.42. Medium Density Residential Area in Duval County.

buildings in the study area, a total frontal (perpendicular to the wind direction) length of about 630 m was estimated. In this example, the homes are assumed to exist in a subdivision having a mixture of one and two story homes, with an assumed average roof height of about 6m. Therefore, the total frontal area from all the buildings is: 6 m × 630 m = 3780 m^2.

The trees were assumed to be about 15m tall. The gross tree frontal area is estimated to be roughly 1.5 times the building frontal area by looking at Figure 3.38. Therefore, the total effective tree frontal area is about (1.5 × 3780) × 50% = 2835 m^2, given that the ratio of effective area to gross frontal area is assumed to be 50% for both deciduous and coniferous trees during hurricane seasons.

Then by using Latteus equation, the roughness length for this area is calculated from:

$$z_0 = 0.5\frac{HS}{A} = 0.5\frac{(HS)_{bldg} + (HS)_{tree}}{A} = 0.5\frac{6\times 3780 + 15\times 2835}{60800} = 0.5\frac{22680 + 42525}{60800} = 0.56m$$

Note that when the trees are the major obstacles in the areas being investigated (which is common), significant uncertainties may exist in the estimated tree heights, frontal areas, and relative densities but as seen in the example given above, trees account for about two-thirds of the surface roughness length computed using Lettau's approach.

Similar procedures have been applied to the other DOQQs included in this section. The parameter values determined at each step for the five examples are listed in Table 3.10. The assumed wind directions are shown in Figures 3.38 to 3.42, respectively. The computed roughness lengths all fall into the definition of Exposure B (as defined in ASCE 7), and all roughness lengths fall within the roughness length ranges given in Tables 3.6 and 3.8 for Medium Density Residential.

Table 3.10. Examples for Roughness Length Calculation Using Lettau's Formula

Parameter	Fig. 1(Escambia County)	Fig. 2(Lee County)	Fig. 3(Dade County)	Fig. 4(Palm Beach County)	Fig. 5(Duval County)
Ground Area (m^2)	60800	225000	77000	150000	35000
Estimated Mean Roof Height (m)	6	5	4.5	4.5	6
Building Frontal Length (m)	630	2800	1000	2900	240
Building Frontal Area (m^2)	3780	14000	4500	13050	1440
Mean Tree Height (m)	15	6	-	6	15
Tree/Building Area Ratio	1.50	0.15	0.00	0.10	3.00
Tree Frontal Area (m^2)	5670	2100	0	1305	4320
SH (building)	22680	70000	20250	58725	8640
Effective *SH* (trees)	42525	6300	0	3915	32400
Roughness Length z_0 (m)	0.56	0.17	0.13	0.21	0.59

Note that the calculated roughness length is wind-direction dependent. For uniform building orientations within a region, the difference in the computed roughness lengths for different wind directions can be significant. For instance, in the Palm Beach County

example, if the wind direction changes ±90°, the projected width of the buildings is in the range of 50% to 70% of that seen in the worked example, and thus the computed roughness length reduces to 50% to 70% of the original value. To remove the effect of directionality associated with building orientation, the frontal width of the building can be substituted with an effective width defined as the square root of the estimated plan area.

Although Lettau's method provides a convenient and quantitative means to estimate roughness length from DOQQs, aerial photography, etc., it should be used with caution. Engineering judgment needs to be applied to the results through comparisons with estimates of z_0 given in the literature. Inevitably, some variations and uncertainties are associated with the estimation of the surface roughness length in any terrain, but as will be shown later, this parameter plays a very important role in the estimation of wind induced damage and loss.

3.7 Effect of Surface Roughness on Near Ground Gust Wind Speeds

In this section, the effects of z_0 on gust wind speeds (defined as a 3 second average) near the ground surface and on the hourly mean wind speed near the ground surface are shown. It is important to note that changes in wind speeds in areas of transitioning surface roughness are not treated in the default Hazus surface roughness model. However, a discussion of transition effects is provided in this section to assist the user in understanding their possible impact on damage and loss estimates. Transition effects are illustrated using the methodology described in ESDU (1983). The ESDU methodology forms the basis of the fetch length requirements given in ASCE-7-02 to enable the user to determine what exposure category a building is in given information on the upstream fetch lengths.

Figure 3.43 shows the ratio of the wind speed, as normalized by the reference open terrain value, as a function of surface roughness and height above ground. Wind speed ratios are given for both the peak gust wind speed and the one hour mean wind speed. The data in Figure 3.43 clearly show that the effect of surface roughness is greatest near the ground (z = 3 m and z = 5 m), around the eave height of most single story buildings. Figure 3.43, also shows that the change in wind speed (with respect to the reference terrain value) is less for the peak gust wind speed than for the mean wind speed. For example, at a height of 10 m, a change in z_0 from 0.03 m (open terrain) to 0.35 m (typical suburban terrain), the peak gust wind speed reduces by about 18%, whereas the hourly average wind speed reduces by about 32%. The reduction in the wind speed associated with an averaging time of one minute is about 25%, falling almost exactly half way between the reduction in gust wind speed and the reduction in the one hour mean wind speed. In Hazus, all damage and loss functions are given as a function of peak gust wind speed, not the one minute wind speed.

The wind speed ratio data given in Figure 3.43 are for the case of a fully transitioned boundary layer (i.e., the wind has blown over a long enough fetch of new terrain that the flow characteristics are influenced only by the local terrain, and not the previous terrain). In reality, the wind at a given height does not change immediately to reflect the new

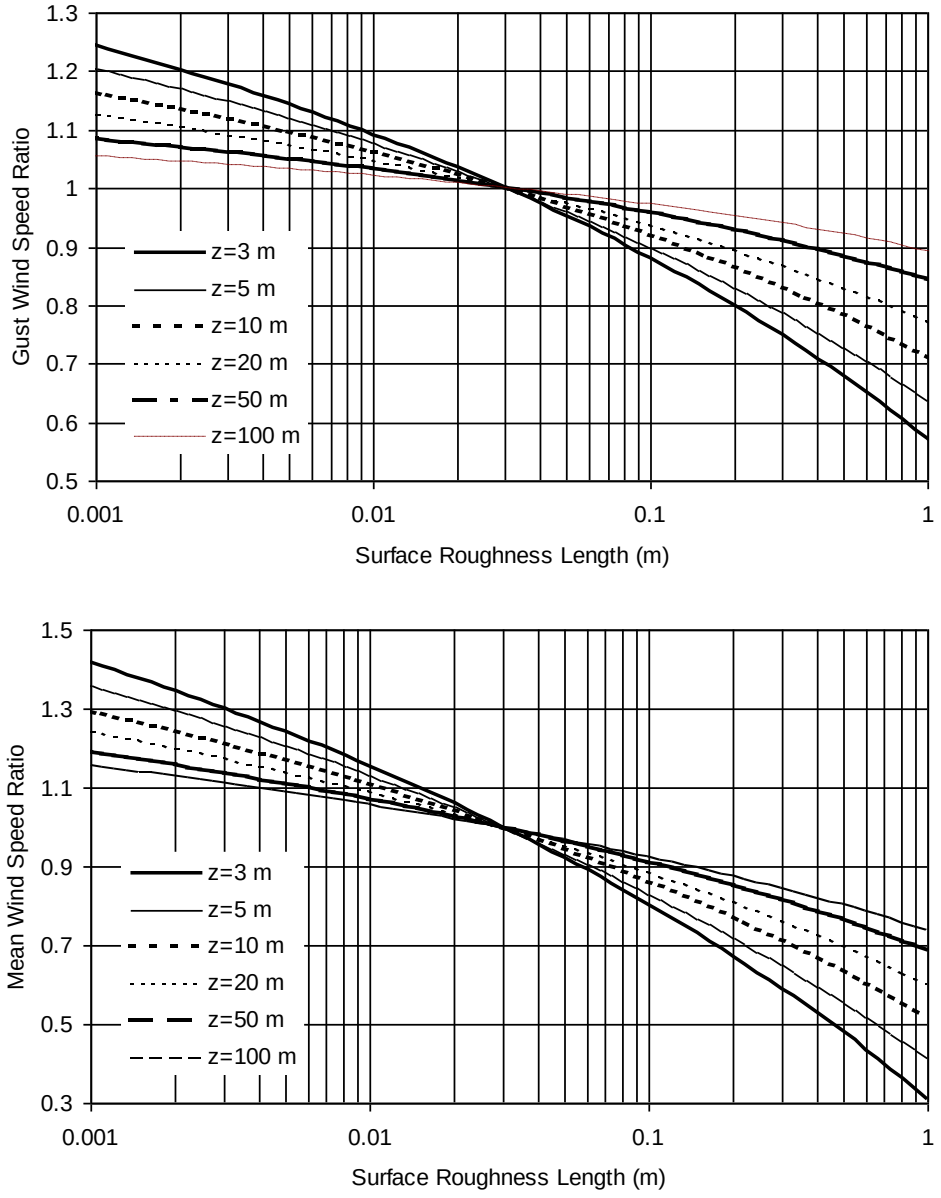

Figure 3.43. Wind Speed Ratios as a Function of Surface Roughness for Various Heights.

terrain, but rather the flow gradually makes a transition, changing to reflect the characteristics associated with the new terrain. The distance over which this transition takes place varies with height, with the wind at lower heights changing more rapidly than wind at higher levels. Figures 3.44, 3.45 and 3.46 show examples of the rates of change of the mean and gust wind speeds as the terrain changes from an open terrain (z_0 = 0.03m) to an example suburban terrain (z_0 = 0.3 m) for heights of 3 m, 10 m and 50 m, respectively. In each of Figures 3.44 through 3.46, the upper plot shows the wind speed ratio with respect to open terrain as a function of the distance into the new terrain, and the lower plot shows the percentage adjustment of the wind to the new terrain as a

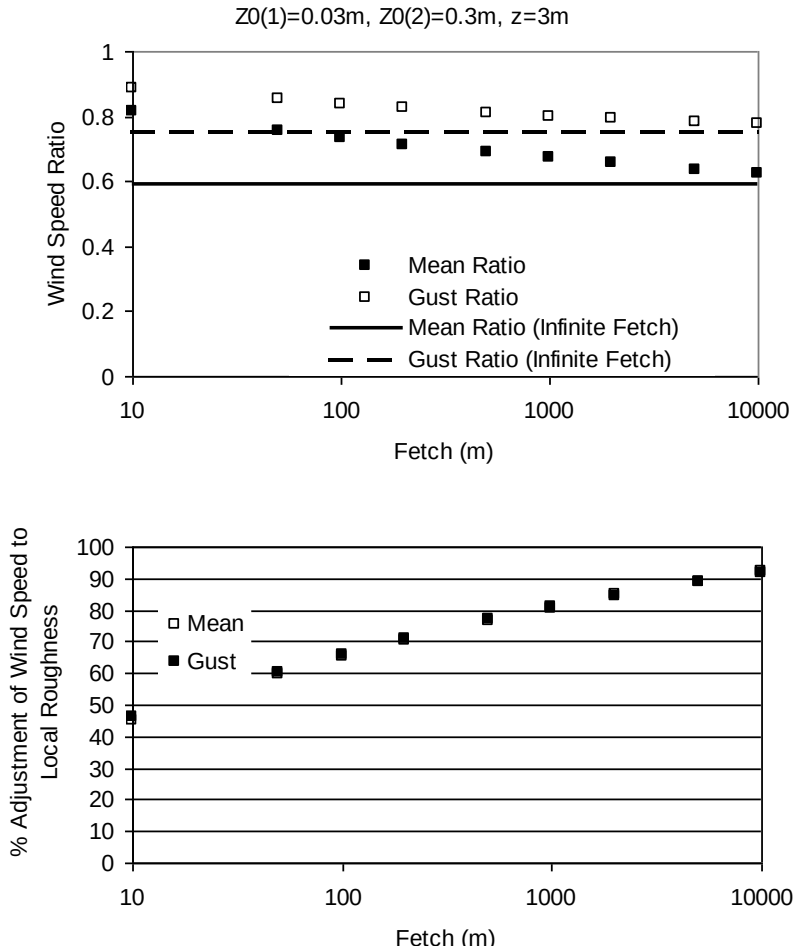

Figure 3.44. Reduction in Wind Speed at a Height of 3 m (Open Terrain to Suburban Terrain).

function of the distance. The lower plots suggest that the wind speed in the new terrain asymptotically approaches (but never reaches) the fully transitioned value. In ASCE-7-02, this problem was handled by defining the fetch required to assume a fully transitioned case as the distance over which the wind speed adjustment reaches about 80% of the fully transitioned value. Notice in the 3 m height example, about 50% of the reduction occurs within the first 10m of the terrain change. Thus, homes located on the front row of a barrier island, or the front row in a subdivision facing open farmland, are actually situated within a transition zone. The effective wind speeds that these front row structures experience will be notably higher than those experienced by homes located even as close as one row back from these front line homes.

In cases where loss studies are being performed in relatively small regions that encompass significant changes in terrain, it would be advisable to properly estimate the fraction of buildings that are likely to experience winds associated with terrains other than the default suburban values that would be appropriate for most of the building population.

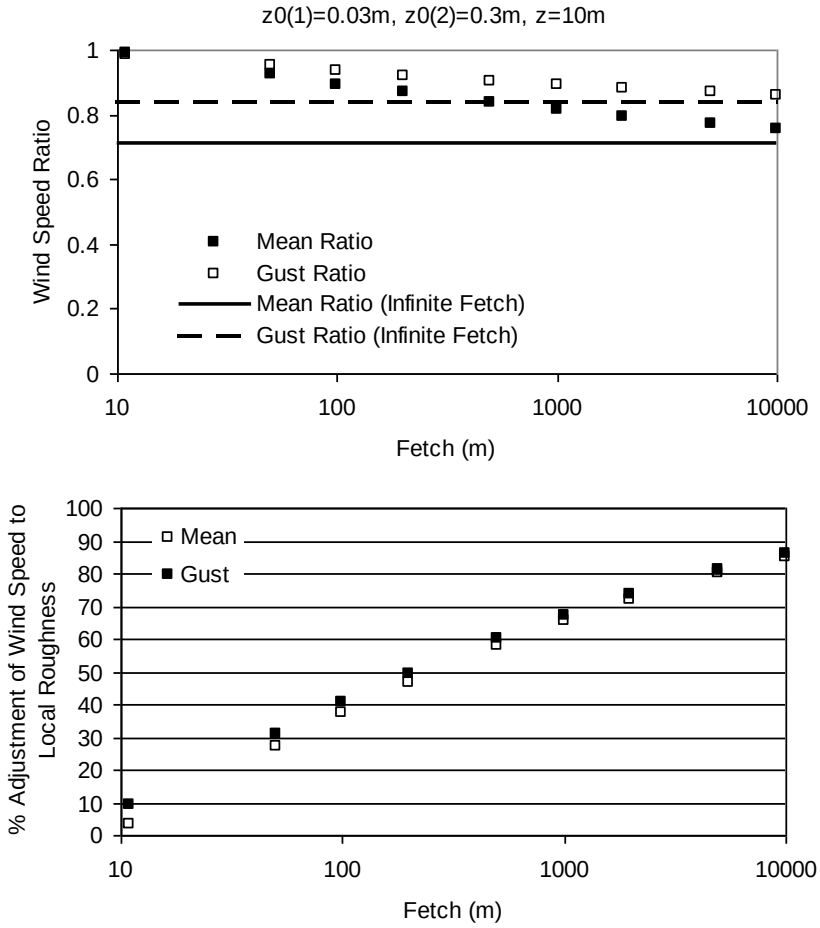

Figure 3.45. Reduction in Wind Speed at a Height of 10 m (Open Terrain to Suburban Terrain).

In the case of the 50 m height example (Figure 3.46), it is readily seen that even for a fetch distance of 1 km, the wind speed has only undergone 30% of the full adjustment. This example indicates that for taller buildings relatively isolated or in front row, the appropriate terrain selection is governed by the terrain at distances of 1km or more away from the building rather than at the location of the building itself. It should also be recognized, that the taller the building, the less the effect of terrain on the wind speeds at roof height.

Figure 3.47 shows the rapid and significant reduction in wind speed at a height of 3m associated with a change in terrain from an open terrain to a heavily treed terrain. As shown in the upper graph, a 30% reduction in the peak gust wind speed (~70% reduction in wind load) occurs within the first 100 m of the transition. This example clearly shows why significant reductions in observed damage are seen when comparing damage on barrier islands to that seen within forested regions of the mainland, even right at the coast.

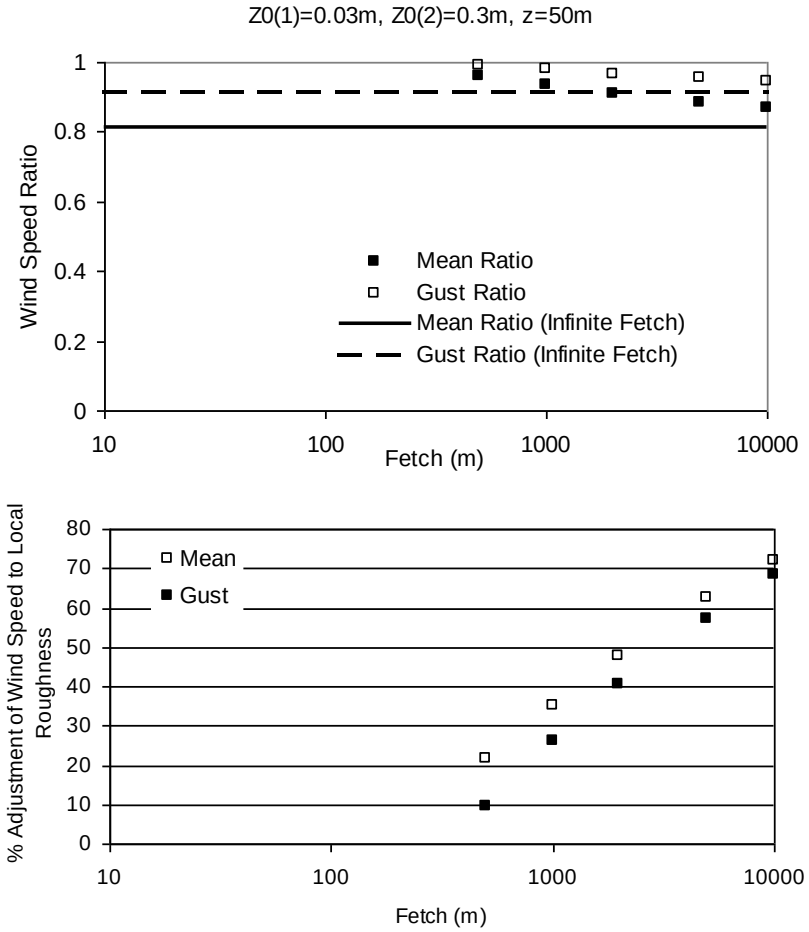

Figure 3.46. Reduction in Wind Speed at a Height of 50 m (Open Terrain to Suburban Terrain).

Large changes in roughness associated with trees located very near the intra-coastal waterways are seen in many regions along the Gulf and Atlantic coasts.

Examples of fully transitioned peak gust profiles are shown in Figure 3.48 for a range of roughness lengths. These examples are given to show the impact of z_0 on the magnitude of the peak gust wind speed as a function of height. All gust profiles given in Figure3.7-6 are referenced to the peak gust wind speed at a height of 10 m in open terrain.

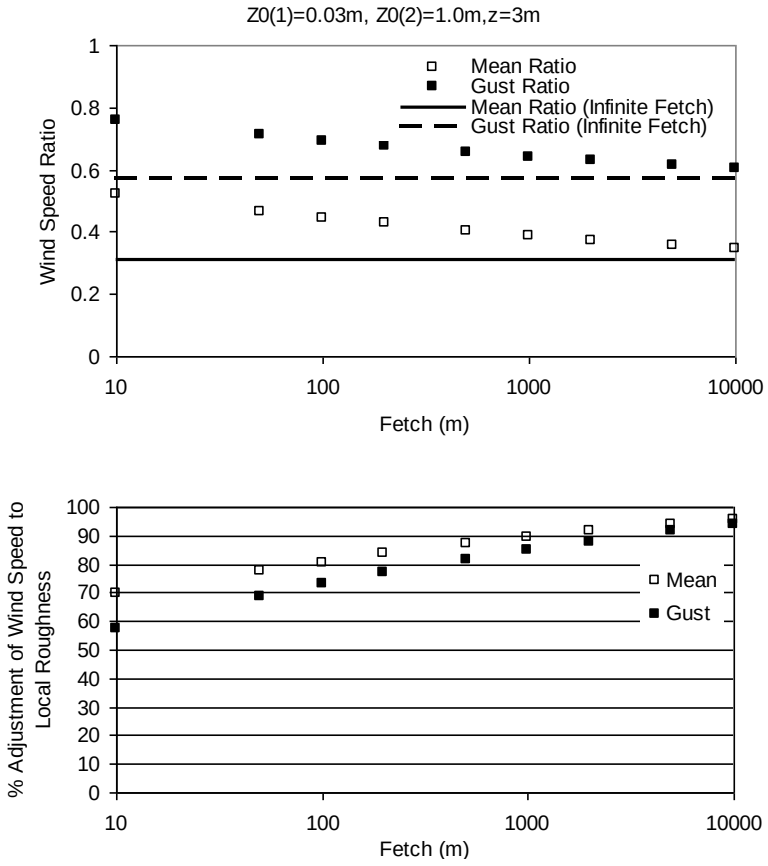

Figure 3.47. Reduction in Wind Speed at a Height of 10m (Open Terrain to Heavily Treed Terrain).

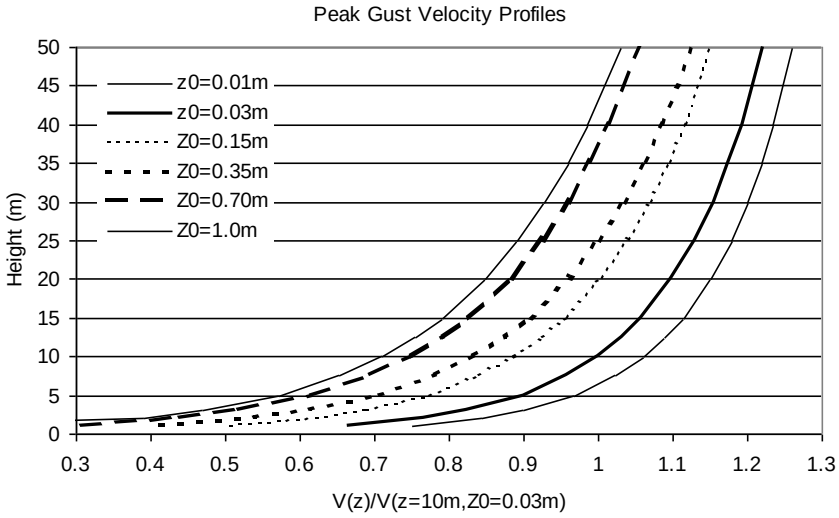

Figure 3.48. Examples of Peak Gust Velocity Profiles as a Function of z_0.

3.8 Surface Roughness Updates for Hazus 2.0

Hazus 2.0 continues to use MRLC data in determining terrain roughness for the 22 hurricane states (including Hawaii) and the District of Columbia. It employs two new data sets: (1) the NLCD 2001 Land Cover data set and (2) the NLCD 2001 Percent Tree Canopy. Both are available as digital downloads from the MRLC website. The primary components of the 2001 MRLC-NLCD data set according to the MRLC website are:

1. Normalized imagery for three time periods per path/row
2. Ancillary data including a 30 m DEM, slope, aspect and a positional index
3. Per-pixel estimates of percent imperviousness and percent tree canopy
4. 21 classes of land cover data derived from the imagery, ancillary data and derivatives using a decision tree
5. Classification rules, confidence estimates and metadata from the land cover classification.

Additional details as to how the data set was created can be found at the MRLC website. The NLCD 2001 Percent Canopy is an independent, per-pixel estimate derived from imagery and ancillary data using a regression tree used to describe tree cover. Figure 3.49 displays the percent canopy over Florida. Table 3.11 details the mapping between 2001 NLCD land use land cover (LULC) codes and 1992 NLCD LULC codes.

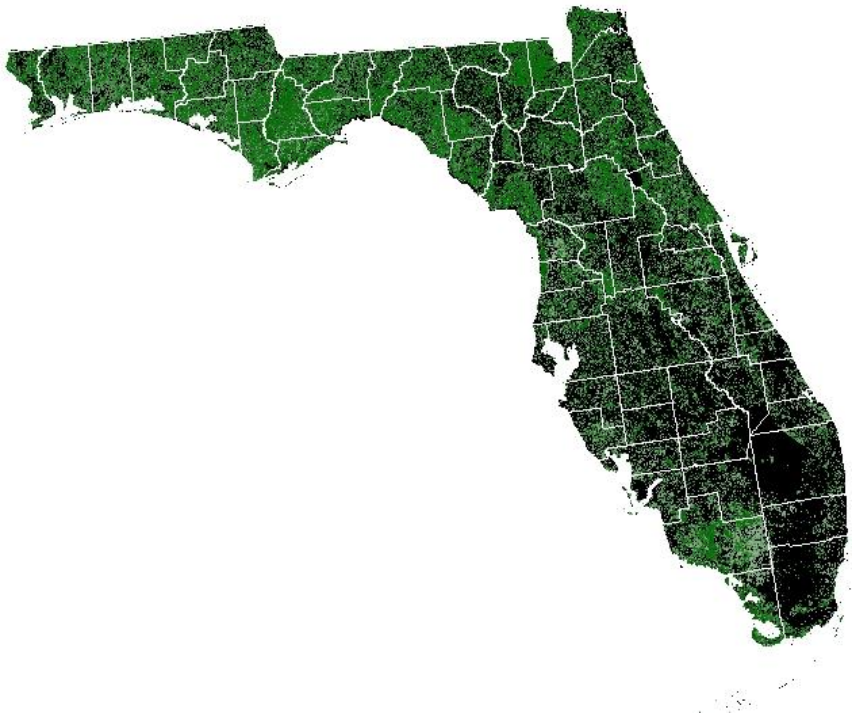

Figure 3.49. Percent (Tree) Canopy for the State of Florida

Table 3.11. 1992 to 2001 LULC Class Mapping

NLCD 2001		Mapped to NLCD 1992 Class	
Class	Description	Class	Description
11	Open Water	11	Open Water
12	Perennial Ice/Snow	12	Perennial Ice/Snow
21	Developed, Open Space**	31	Bare Rock/Sand/Clay
22	Developed, Low Intensity**	21	Low Intensity Residential
23	Developed, Medium Intensity	22	High Intensity Residential
24	Developed, High Intensity	23	Commercial/Industrial/Transportation
31	Barren Land	31	Bare Rock/Sand/Clay
32	Unconsolodated Shore*	31	Bare Rock/Sand/Clay
41	Deciduous Forest	41	Deciduous Forest
42	Evergreen Forest	42	Evergreen Forest
43	Mixed Forest	43	Mixed Forest
52	Shrub/Scrub	51	Shrubland
71	Grassland/Herbaceous	71	Grasslands/Herbaceous
81	Pasture/Hay	81	Pasture/Hay
82	Cultivated Crops	82	Row Crops
90	Woody Wetlands	91	Woody Wetlands
95	Emergent Herbaceaous Wetlan	92	Emergent Herbaceous Wetlands

* Classes not used

** This mapping used as base only for Developed, Open Space and Developed, Low Intensity

States were assigned specific terrain roughness values according to their LULC code, in tandem with aerial photography with the exception of Florida and New York. Florida was partitioned into 4 areas: panhandle, west, southeast and northeast and New York has specific values for Manhattan and Long Island. The z_0 values assigned to each LULC code are displayed in Table 3.12

3.8.1 LULC codes 21 and 22 and MRLC-NLCD Data

To account for increased terrain roughness by trees in developed open spaces and developed low intensity areas, LULC codes 21 and 22 make use of percent canopy from the MRLC according to the following equations:

For Developed, Open Space (LULC 21):

$$z_{0dos} = \sqrt{z_{0brsc}^2 + \left(z_{0ef}{}^2 - z_{0brsc}^2\right) * \left(\frac{P_{Tdos}}{P_{Tef}}\right)^2} \tag{3.3}$$

Table 3.12. Assignment of z_0 values to LULC Codes

LULC CLASS	DESCRIPTION	HI	TX	LA	MS	AL	PANHANDLE FL	WEST FL	SOUTHEAST FL	NORTHEAST FL	GA	SC	NC
11	OpenWater	0.003	0.003	0.003	0.003	0.003	0.003	0.003	0.003	0.003	0.003	0.003	0.003
12	Perennial Ice/Snow *	0.012	0.012	0.012	0.012	0.012	0.012	0.012	0.012	0.012	0.012	0.012	0.012
21	Developed, OpenSpace	0.080	0.100	0.090	0.090	0.090	0.090	0.100	0.090	0.090	0.100	0.100	0.100
22	Developed, Low Intensity	0.500	0.350	0.330	0.330	0.330	0.330	0.340	0.340	0.330	0.350	0.360	0.350
23	Developed, Medium Intensity	0.530	0.550	0.500	0.530	0.530	0.530	0.540	0.570	0.540	0.570	0.570	0.550
24	Developed, High Intensity	0.550	0.440	0.390	0.350	0.350	0.350	0.390	0.380	0.340	0.350	0.340	0.330
31	Barren Land	0.020	0.100	0.090	0.090	0.090	0.090	0.100	0.090	0.090	0.100	0.100	0.100
32	Unconsolodated Shore *	0.090	0.100	0.090	0.090	0.090	0.090	0.100	0.090	0.090	0.100	0.100	0.100
41	Deciduous Forest	0.900	0.900	0.900	0.900	0.900	0.900	0.900	0.900	0.900	0.900	0.900	0.900
42	Evergreen Forest	0.800	0.900	0.900	0.900	0.900	0.900	0.900	0.900	0.900	0.900	0.900	0.900
43	MixedForest	0.900	0.900	0.900	0.900	0.900	0.900	0.900	0.900	0.900	0.900	0.900	0.900
52	Shrubland	0.120	0.100	0.120	0.120	0.120	0.120	0.120	0.120	0.120	0.110	0.130	0.100
71	Grasslands/Herbaceous	0.085	0.040	0.040	0.040	0.040	0.040	0.040	0.040	0.040	0.050	0.040	0.040
81	Pasture/Hay	0.040	0.040	0.060	0.050	0.050	0.050	0.050	0.050	0.060	0.050	0.060	0.060
82	CultivatedCrops	0.030	0.060	0.060	0.050	0.050	0.050	0.060	0.060	0.060	0.060	0.060	0.060
90	WoodyWetlands	0.900	0.900	0.900	0.900	0.900	0.900	0.900	0.900	0.900	0.900	0.900	0.900
95	EmergentHerbaceousWetlands	0.150	0.100	0.110	0.090	0.090	0.090	0.080	0.040	0.090	0.100	0.100	0.100

* Class not used

Assignment of z_0 values to LULC Codes Continued

LULC CLASS	DESCRIPTION	VA	MD	DE	PA	NJ	NY	MAN	LONGIS	CT	RI	MA	NH	ME
11	OpenWater	0.003	0.003	0.003	0.003	0.003	0.003	0.003	0.003	0.003	0.003	0.003	0.003	0.003
12	Perennial Ice/Snow *	0.012	0.012	0.012	0.012	0.012	0.012	0.012	0.012	0.012	0.012	0.012	0.012	0.012
21	Developed, OpenSpace	0.100	0.100	0.100	0.140	0.080	0.090	0.090	0.090	0.100	0.100	0.120	0.120	0.120
22	Developed, Low Intensity	0.350	0.350	0.350	0.360	0.350	0.430	0.500	0.420	0.340	0.340	0.360	0.290	0.290
23	Developed, Medium Intensity	0.530	0.530	0.530	0.620	0.580	0.730	0.840	0.620	0.480	0.480	0.590	0.530	0.530
24	Developed, High Intensity	0.380	0.380	0.380	0.440	0.420	0.920	1.550	0.440	0.350	0.350	0.510	0.310	0.310
31	Barren Land	0.100	0.100	0.100	0.140	0.080	0.090	0.090	0.090	0.100	0.100	0.120	0.120	0.120
32	Unconsolodated Shore *	0.100	0.100	0.100	0.140	0.080	0.090	0.090	0.090	0.100	0.100	0.120	0.120	0.120
41	Deciduous Forest	0.900	0.900	0.900	0.900	0.900	0.900	0.900	0.900	0.900	0.900	0.900	0.900	0.900
42	Evergreen Forest	0.900	0.900	0.900	0.900	0.900	0.900	0.900	0.900	0.900	0.900	0.900	0.900	0.900
43	MixedForest	0.900	0.900	0.900	0.900	0.900	0.900	0.900	0.900	0.900	0.900	0.900	0.900	0.900
52	Shrubland	0.120	0.120	0.120	0.140	0.130	0.130	0.130	0.130	0.110	0.110	0.130	0.110	0.110
71	Grasslands/Herbaceous	0.040	0.040	0.040	0.040	0.040	0.050	0.050	0.050	0.040	0.040	0.040	0.040	0.040
81	Pasture/Hay	0.050	0.050	0.050	0.050	0.060	0.050	0.050	0.050	0.050	0.050	0.050	0.060	0.060
82	CultivatedCrops	0.050	0.050	0.050	0.050	0.050	0.060	0.060	0.060	0.060	0.060	0.060	0.060	0.060
90	WoodyWetlands	0.900	0.900	0.900	0.900	0.900	0.900	0.900	0.900	0.900	0.900	0.900	0.900	0.900
95	EmergentHerbaceousWetlands	0.100	0.100	0.100	0.100	0.080	0.100	0.100	0.100	0.090	0.090	0.090	0.090	0.090
	* Class not used													

where:

z_{0dos} = z_0 for Developed, Open Space

z_{0brsc} = z_0 for Bare Rock/Sand/Clay (NLCD 2001)

z_{0ef} = z_0 for Evergreen Forest

P_{Tdos} = % tree canopy in Developed, Open Space (by county)

P_{Tef} = % tree canopy in Evergreen Forest (by county)

For Developed, Low Intensity (LULC 22):

$$z_{0dli} = \sqrt{z_{0lir}^2 + \left(z_{0ef}{}^2 - z_{0lir}{}^2\right) * \left(\frac{P_{Tdli}}{P_{Tef}}\right)^2} \qquad (3.4)$$

where:

z_{0dli} = z_0 for Developed, Low Intensity

z_{0lir} = z_0 for Low Intensity Residential (NLCD 2001)

z_{0ef} = z_0 for Evergreen Forest

P_{Tdli} = % tree canopy in Developed, Low Intensity (by county)

P_{Tef} = % tree canopy in Evergreen Forest (by county)

As noted above, the variation in z_0 mapping for these two particular LULC codes is implemented at the county level.

3.8.2 Implementation in Hazus 2.0

At the census block level, terrain roughness was computed by taking the average z_0 value assigned to LULC data that overlapped the census block spatially. However, for those census blocks that had less than approximately less than one square kilometer in area, the average z_0 value computed was based on a circular area one kilometer in diameter centered at the centroid of the census block. This was done to obtain a minimum fetch of approximately 500 meters for small census blocks.

At the census tract level, z_0 values were computed by weighting census block z_0 values with building square footage as per equation 3.5.

$$Z_t = \sum_{i=1}^{n} Z_{ci} * \frac{S_{Ci}}{S_{Ti}} \tag{3.5}$$

where:

Z_t = Terrain roughness at the tract level
Z_{ci} = Terrain roughness computed for census block i
S_{Ci} = Total building square footage for census block i
S_T = Total building square footage for the census tract
n = Number of Census blocks in the tract

Weighting in this manner weights the census tract surface roughness towards those census blocks that have more buildings contained within them instead of simply taking an unweighted average of the census block surface roughnesses.

Chapter 4. Wind Loads

4.1 Introduction

Background. Wind loads on buildings are usually estimated using either boundary layer wind tunnel tests performed for a specific building or using code-specified loads that have been developed by committees from boundary layer wind tunnel test data. If wind tunnel loads are used in the design of a building or its components, the wind loading coefficients are typically measured for 36 different wind directions, with the results combined with a statistical model of the wind climate for the location where the building is to be built. Using this approach, the design loads obtained for the building take into account the effect of the variation of the wind loads with the direction of the approaching wind, and how these variations in load with direction align with the directional characteristics of the wind.

Essentially all low-rise buildings are designed using wind loads obtained from building codes. While the loading coefficients given in the codes have been developed using wind tunnel test data, the directional effects are not explicitly reproduced in North American building codes and standards. For simplicity, and ease of use, the loads given in building codes represent an estimate of the maximum load acting on a portion of the building. Different values of the loading coefficients are given in the codes for various zones on the roofs and walls. The selection of the number and size of these zones is a compromise between the true spatial variability of the maximum wind loads, and the use of as few zones as possible to simplify the design procedure. The greater the number of zones specified in a building code, the more accurate will be the final estimate of the distribution of the maximum loads acting on the building. The maximum values of the pressure coefficients given in the codes for each zone do not necessarily occur for winds approaching from the same wind direction, and therefore code-specified loads alone cannot be used to model wind loads on a building for wind approaching from a given direction.

Designers are able to take advantage of the variation of the wind loads with wind direction in both the UK and Australia, if they chose to use the detailed design procedures given in their respective building codes.

Approach. For predicting wind loads on buildings in the development of fast running damage and loss functions, it is necessary to model the variation in the wind loads acting on the building as a function of the location on the building and as a function of the direction and magnitude of the wind speed. Clearly, the best approach is to use the results from wind tunnel tests directly and combine these results with the simulated hurricane winds and directions to estimate the loads. Unfortunately, this approach is not viable since the detailed wind tunnel test data (if available) are limited by the number and locations of the pressure taps used in the models, the number of terrains in which the model buildings were tested, and the number of different geometries tested. Without the use of wind tunnel data, the next best method for developing wind loads as a function of

direction is the development of an analytic or empirical model which is able to reasonably reproduce the variation of wind loads with direction, as well as the effects of aspect ration, terrain, etc. The Australian and UK wind loading provisions represent simple examples of such an approach.

The methodology selected by the Hazus Wind Committee for developing damage and loss functions is to use code-specified loads as a the basis for the model. To treat wind directionality for roof loads, tabulated values of the pressure coefficients as a function of direction are estimated using wind tunnel data and the UK Building Code. In the case of wall loads, the pressure coefficients are modeled with cosine functions. Using this approach, the peak magnitudes of the loads correspond to the values specified in building code adopted "standards". The pressure coefficients developed using this approach are discussed in the following sections, and the results of the empirical direction model are compared to measurements of loads acting on buildings determined from wind tunnel tests. The wind loads derived using the hybrid code/directional model are applied to a number of simply shaped buildings. The shapes of the buildings considered are all either square or rectangular in plan and have either flat, hip or gable shape roofs.

4.2 Wall Pressures – Low-Rise Buildings

The magnitudes of the wall pressures used for modeling wind loads for the prediction of wind induced failures of components and cladding were derived considering the pressure coefficients given in North American wind loading standards and/or codes. The standards/codes considered in the development of the wind loads are ASCE-7-95, SBCCI (1998 Edition) and the 1995 edition of the National Building Code of Canada. In order to compare the magnitudes of the loading coefficients given in each standard/code, all coefficients were adjusted to be referenced to the mean hourly wind speed at roof height. In the case of both the NBCC and SBCCI pressure coefficients, the coefficients were divided by a value of 0.8 to remove the directionality factor that is explicitly included in the pressure coefficients given in the codes (Mehta, 1984). Additionally, in the case of the SBCCI coefficients, an internal pressure coefficient having a value of 0.2 was removed from the coefficients as given in the code before any comparisons were made. To convert the coefficients given in ASCE-7-95 from values which are normalized by the peak gust wind speed at roof height to the value which is normalized by the mean hourly wind speed, a gust factor of 1.57 was used. The gust factor (1.57) used for converting the mean hourly wind speed to a 3 second gust was derived from the ESDU (1982) gust factor models for open terrain conditions (z_0 = 0.03 m) and a mean roof height of about 4 m. In the case of the SBCCI coefficients, which are referenced to the fastest mile wind speed at roof height, a gust factor of 1.27 was used in the change of the reference dynamic pressure to a mean hourly value. The 1.27 gust factor was also computed using the ESDU (1982) gust factor model assuming open terrain conditions at a height of 4 m and an averaging time of 32 seconds (i.e., 3600/110). Tables 4.1 through 4.4 show the comparison of the peak coefficients derived from the three sources for the edge and central regions of the walls (as shown in Figure 4.1) normalized by the mean hourly wind speed at the average roof height.

Table 4.1. Comparison of Positive Wall Pressure Coefficients – Buildings with Roof Slopes Less than 10°

Pressure Zone			Pressure Coefficient		
NBCC	SBCCI	ASCE-7-95	NBCC	SBCCI	ASCE-7-95
e	e	5	2.3	2.1	2.2
w	w	4	2.3	2.1	2.2

Table 4.2. Comparison of Positive Wall Pressure Coefficients – Buildings with Roof Slopes Greater than 10°

Pressure Zone			Pressure Coefficient		
NBCC	SBCCI	ASCE-7-95	NBCC	SBCCI	ASCE-7-95
e	e	5	2.3	2.3	2.5
w	w	4	2.3	2.3	2.5

Table 4.3. Comparison of Negative Wall Pressure Coefficients – Buildings with Roof Slopes Less than 10°

Pressure Zone			Pressure Coefficient		
NBCC	SBCCI	ASCE-7-95	NBCC	SBCCI	ASCE-7-95
e	e	5	-2.6	-2.5	-3.1
w	w	4	-2.3	-2.1	-2.5

Table 4.4. Comparison of Negative Wall Pressure Coefficients – Buildings with Roof Slopes Greater than 10°

Pressure Zone			Pressure Coefficient		
NBCC	SBCCI	ASCE-7-95	NBCC	SBCCI	ASCE-7-95
e	e	5	-2.6	-2.7	-3.5
w	w	4	-2.3	-2.5	-2.7

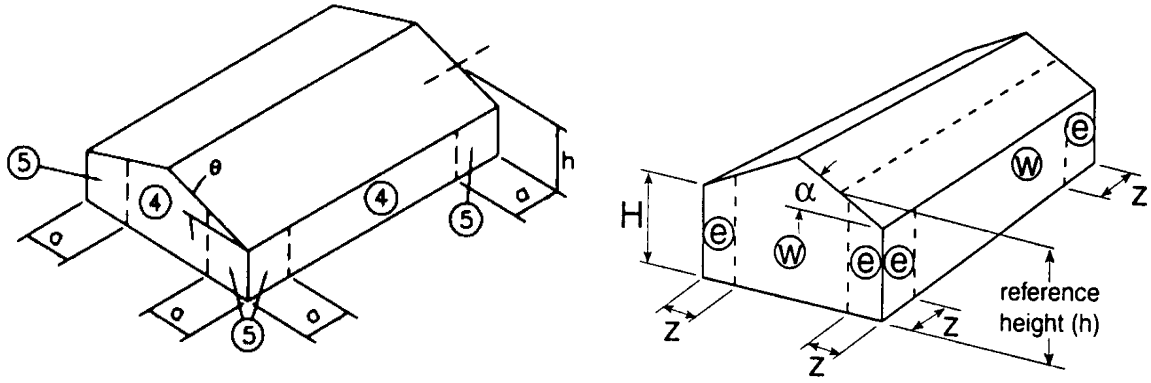

Figure 4.1. Wall Pressure Zones as Defined in ASCE-7 (Left figure) and SBCCI and NBCC (Right figure).

The coefficients given in the above tables represent the maximum (or minimum) values for design purposes and do not reflect the fact that the actual pressure coefficients vary as a function of wind direction.

Effect of Wind Direction. In order to take into account the effect of wind direction, wind tunnel data obtained from various sources including Ho (1993), Stathopoulos (1978) and Lin and Surry (1997) were used to determine the variation of the pressure coefficients with wind direction. Tables 4.5 and 4.6 shows example positive and negative pressures acting on the walls of a rectangular building for wind directions in 30° increments. The locations where the pressure coefficients are computed are given in Figure 4.2. In the example given in Tables 4.5 and 4.6 the magnitudes of the maximum (or minimum) pressures are defined using the ASCE-7-95 values for the sloped roof case.

Comparison of ASCE-7 Wall Pressures to Wind Tunnel Tests. Figures 4.3 and 4.4 show comparisons of wall pressures estimated using the ASCE-7 based model for roofs with slopes less than 10° to those obtained from boundary layer wind tunnel tests (Lin and Surry, 1997) in nominally open and suburban terrains. These plots compare pressure tap-by-pressure tap for a wind tunnel tested rectangular building, and show measured vs. ASCE-7 based-model pressure coefficients. The plot includes comparisons over the full azimuth range in 10° increments. The model building, tested at scales of 1:100 and 1:200 has an eave height of 30′ and plan dimensions of 100′×200′. The model was instrumented so that the full azimuthal range of data was available for 145 wall taps and 112 roof taps. In the comparisons given in Figures 4.3 and 4.4, the pressure coefficients are normalized by the mean hourly wind speed at roof height. Note that in the pressure modeling process, all pressure coefficients are based on the peak gust wind speed at roof height. The magnitudes of the coefficients, normalized by the mean wind speed at roof height, therefore increase with increasing surface roughness.

The banding evident in Figures 4.3 and 4.4 arises primarily from the cosine functions used in the modeling of the code based pressures and suctions that limit the value a modeled pressure can have for any given wind direction, whereas the measured peak pressure data, while following a mean trend with azimuth, are scattered about the mean azimuthal trend curve.

The agreement between the ASCE-7 based positive pressures and the measured positive pressures is reasonable. In the case of the negative pressures, there is significantly more scatter evident in the comparisons since the ASCE-7 loads for the negative pressures in Zone 4 (interior zone) have a minimum value of -2.1, whereas in reality, for long buildings, the minimum negative pressure will have a magnitude which is less than 2.1.

4.3 Roof Pressures – Low-Rise Buildings

As in the case of the wall pressures, wind loads on the roofs of low-rise buildings used for the prediction of the failure of components and cladding were derived using North American based building codes and standards. As in the case of the wall pressures, comparisons of the roof pressures specified by ASCE-7, SBCCI and NBCC were

Table 4.5. Positive Wall Pressure Coefficients Estimated for Building Shown in Figure 4.2 Given as a Function of Wind Direction

	Wind Direction (Clockwise from North)											
Location	0	30	60	90	120	150	180	210	240	270	300	330
1	0.1	0.1	0.1	0.1	1.2	2.2	2.5	2.2	1.2	0.1	0.1	0.1
2	0.1	0.1	0.1	0.1	1.2	2.2	2.5	2.2	1.2	0.1	0.1	0.1
3	0.1	0.1	0.1	0.1	1.2	2.2	2.5	2.2	1.2	0.1	0.1	0.1
4	0.1	0.1	0.1	0.1	1.2	2.2	2.5	2.2	1.2	0.1	0.1	0.1
5	0.1	0.1	0.1	0.1	1.2	2.2	2.5	2.2	1.2	0.1	0.1	0.1
6	0.1	0.1	0.1	0.1	1.2	2.2	2.5	2.2	1.2	0.1	0.1	0.1
7	0.1	0.1	0.1	0.1	1.2	2.2	2.5	2.2	1.2	0.1	0.1	0.1
8	0.1	0.1	0.1	0.1	1.2	2.2	2.5	2.2	1.2	0.1	0.1	0.1
9	0.1	0.1	0.1	0.1	1.2	2.2	2.5	2.2	1.2	0.1	0.1	0.1
10	0.1	0.1	0.1	0.1	1.2	2.2	2.5	2.2	1.2	0.1	0.1	0.1
11	0.1	0.1	0.1	0.1	1.2	2.2	2.5	2.2	1.2	0.1	0.1	0.1
12	0.1	0.1	0.1	0.1	1.2	2.2	2.5	2.2	1.2	0.1	0.1	0.1
13	0.1	0.1	0.1	0.1	1.2	2.2	2.5	2.2	1.2	0.1	0.1	0.1
14	0.1	0.1	0.1	0.1	1.2	2.2	2.5	2.2	1.2	0.1	0.1	0.1
15	0.1	0.1	0.1	0.1	1.2	2.2	2.5	2.2	1.2	0.1	0.1	0.1
16	0.1	1.2	2.2	2.5	2.2	1.2	0.1	0.1	0.1	0.1	0.1	0.1
17	0.1	1.2	2.2	2.5	2.2	1.2	0.1	0.1	0.1	0.1	0.1	0.1
18	0.1	1.2	2.2	2.5	2.2	1.2	0.1	0.1	0.1	0.1	0.1	0.1
19	0.1	1.2	2.2	2.5	2.2	1.2	0.1	0.1	0.1	0.1	0.1	0.1
20	0.1	1.2	2.2	2.5	2.2	1.2	0.1	0.1	0.1	0.1	0.1	0.1
21	0.1	1.2	2.2	2.5	2.2	1.2	0.1	0.1	0.1	0.1	0.1	0.1
22	0.1	1.2	2.2	2.5	2.2	1.2	0.1	0.1	0.1	0.1	0.1	0.1
23	0.1	1.2	2.2	2.5	2.2	1.2	0.1	0.1	0.1	0.1	0.1	0.1
24	2.5	2.2	1.2	0.1	0.1	0.1	0.1	0.1	0.1	0.1	1.2	2.2
25	2.5	2.2	1.2	0.1	0.1	0.1	0.1	0.1	0.1	0.1	1.2	2.2
26	2.5	2.2	1.2	0.1	0.1	0.1	0.1	0.1	0.1	0.1	1.2	2.2
27	2.5	2.2	1.2	0.1	0.1	0.1	0.1	0.1	0.1	0.1	1.2	2.2
28	2.5	2.2	1.2	0.1	0.1	0.1	0.1	0.1	0.1	0.1	1.2	2.2
29	2.5	2.2	1.2	0.1	0.1	0.1	0.1	0.1	0.1	0.1	1.2	2.2
30	2.5	2.2	1.2	0.1	0.1	0.1	0.1	0.1	0.1	0.1	1.2	2.2
31	2.5	2.2	1.2	0.1	0.1	0.1	0.1	0.1	0.1	0.1	1.2	2.2
32	2.5	2.2	1.2	0.1	0.1	0.1	0.1	0.1	0.1	0.1	1.2	2.2
33	2.5	2.2	1.2	0.1	0.1	0.1	0.1	0.1	0.1	0.1	1.2	2.2
34	2.5	2.2	1.2	0.1	0.1	0.1	0.1	0.1	0.1	0.1	1.2	2.2
35	2.5	2.2	1.2	0.1	0.1	0.1	0.1	0.1	0.1	0.1	1.2	2.2
36	2.5	2.2	1.2	0.1	0.1	0.1	0.1	0.1	0.1	0.1	1.2	2.2
37	2.5	2.2	1.2	0.1	0.1	0.1	0.1	0.1	0.1	0.1	1.2	2.2
38	2.5	2.2	1.2	0.1	0.1	0.1	0.1	0.1	0.1	0.1	1.2	2.2
39	0.1	0.1	0.1	0.1	0.1	0.1	0.1	1.2	2.2	2.5	2.2	1.2
40	0.1	0.1	0.1	0.1	0.1	0.1	0.1	1.2	2.2	2.5	2.2	1.2
41	0.1	0.1	0.1	0.1	0.1	0.1	0.1	1.2	2.2	2.5	2.2	1.2
42	0.1	0.1	0.1	0.1	0.1	0.1	0.1	1.2	2.2	2.5	2.2	1.2
43	0.1	0.1	0.1	0.1	0.1	0.1	0.1	1.2	2.2	2.5	2.2	1.2
44	0.1	0.1	0.1	0.1	0.1	0.1	0.1	1.2	2.2	2.5	2.2	1.2
45	0.1	0.1	0.1	0.1	0.1	0.1	0.1	1.2	2.2	2.5	2.2	1.2
46	0.1	0.1	0.1	0.1	0.1	0.1	0.1	1.2	2.2	2.5	2.2	1.2

Table 4.6. Negative Wall Pressure Coefficients Estimated for Building Shown in Figure 4.2 Given as a Function of Wind Direction

Location	Wind Direction (Clockwise from North)											
	0	30	60	90	120	150	180	210	240	270	300	330
1	-.9	-.8	-.6	-1.1	-.8	-.3	-.4	-.2	-2.0	-3.5	-2.1	-2.1
2	-.7	-.6	-.5	-.9	-.6	-.2	-.3	-.2	-1.6	-2.7	-1.6	-1.3
3	-.7	-.6	-.5	-.9	-.6	-.2	-.3	-.2	-1.6	-2.7	-1.6	-1.0
4	-.7	-.6	-.5	-.9	-.6	-.2	-.3	-.3	-1.7	-2.7	-1.7	-.8
5	-.7	-.6	-.5	-.9	-.6	-.2	-.3	-.3	-1.7	-2.7	-1.7	-.7
6	-.7	-.6	-.5	-.9	-.6	-.2	-.3	-.4	-1.8	-2.7	-1.8	-.6
7	-.7	-.6	-.5	-.9	-.6	-.2	-.3	-.4	-1.8	-2.7	-1.8	-.6
8	-.7	-.6	-.5	-.9	-.6	-.2	-.3	-.5	-1.9	-2.7	-1.9	-.6
9	-.7	-.6	-1.8	-2.7	-1.8	-.4	-.3	-.2	-.6	-.9	-.5	-.6
10	-.7	-.6	-1.8	-2.7	-1.8	-.4	-.3	-.2	-.6	-.9	-.5	-.6
11	-.7	-.7	-1.7	-2.7	-1.7	-.3	-.3	-.2	-.6	-.9	-.5	-.6
12	-.7	-.8	-1.7	-2.7	-1.7	-.3	-.3	-.2	-.6	-.9	-.5	-.6
13	-.7	-1.0	-1.6	-2.7	-1.6	-.2	-.3	-.2	-.6	-.9	-.5	-.6
14	-.7	-1.3	-1.6	-2.7	-1.6	-.2	-.3	-.2	-.6	-.9	-.5	-.6
15	-.9	-2.1	-2.1	-3.5	-2.0	-.2	-.4	-.3	-.8	-1.1	-.6	-.8
16	-3.5	-2.0	-.2	-.4	-.3	-.8	-1.1	-.5	-.7	-.7	-.7	-2.0
17	-2.7	-1.6	-.2	-.3	-.2	-.6	-.9	-.4	-.5	-.6	-.5	-1.6
18	-2.7	-1.6	-.2	-.3	-.2	-.6	-.9	-.4	-.5	-.6	-.5	-1.6
19	-2.7	-1.7	-.3	-.3	-.2	-.6	-.9	-.4	-.5	-.6	-.5	-1.7
20	-.9	-.6	-.2	-.3	-.3	-1.6	-2.7	-1.6	-.5	-.6	-.5	-.4
21	-.9	-.6	-.2	-.3	-.2	-1.6	-2.7	-1.6	-.5	-.6	-.5	-.4
22	-.9	-.6	-.2	-.3	-.2	-1.5	-2.7	-1.5	-.5	-.6	-.5	-.4
23	-1.1	-.8	-.3	-.4	-.2	-2.0	-3.5	-2.0	-.7	-.7	-.7	-.5
24	-.4	-.3	-.8	-1.1	-.6	-.8	-.9	-2.1	-2.1	-3.5	-2.0	-.2
25	-.3	-.2	-.6	-.9	-.5	-.6	-.7	-1.3	-1.6	-2.7	-1.6	-.2
26	-.3	-.2	-.6	-.9	-.5	-.6	-.7	-1.0	-1.6	-2.7	-1.6	-.2
27	-.3	-.2	-.6	-.9	-.5	-.6	-.7	-.8	-1.7	-2.7	-1.7	-.3
28	-.3	-.2	-.6	-.9	-.5	-.6	-.7	-.7	-1.7	-2.7	-1.7	-.3
29	-.3	-.2	-.6	-.9	-.5	-.6	-.7	-.6	-1.8	-2.7	-1.8	-.4
30	-.3	-.2	-.6	-.9	-.5	-.6	-.7	-.6	-1.8	-2.7	-1.8	-.4
31	-.3	-.2	-.6	-.9	-.5	-.6	-.7	-.6	-1.9	-2.7	-1.9	-.5
32	-.3	-.4	-1.8	-2.7	-1.8	-.6	-.7	-.6	-.5	-.9	-.6	-.2
33	-.3	-.4	-1.8	-2.7	-1.8	-.6	-.7	-.6	-.5	-.9	-.6	-.2
34	-.3	-.3	-1.7	-2.7	-1.7	-.7	-.7	-.6	-.5	-.9	-.6	-.2
35	-.3	-.3	-1.7	-2.7	-1.7	-.8	-.7	-.6	-.5	-.9	-.6	-.2
36	-.3	-.2	-1.6	-2.7	-1.6	-1.0	-.7	-.6	-.5	-.9	-.6	-.2
37	-.3	-.2	-1.6	-2.7	-1.6	-1.3	-.7	-.6	-.5	-.9	-.6	-.2
38	-.4	-.2	-2.0	-3.5	-2.1	-2.1	-.9	-.8	-.6	-1.1	-.8	-.3
39	-3.5	-2.0	-.7	-.7	-.7	-.5	-1.1	-.8	-.3	-.4	-.2	-2.0
40	-2.7	-1.6	-.5	-.6	-.5	-.4	-.9	-.6	-.2	-.3	-.2	-1.6
41	-2.7	-1.6	-.5	-.6	-.5	-.4	-.9	-.6	-.2	-.3	-.2	-1.6
42	-2.7	-1.7	-.5	-.6	-.5	-.4	-.9	-.6	-.2	-.3	-.3	-1.7
43	-.9	-.4	-.5	-.6	-.5	-1.6	-2.7	-1.6	-.3	-.3	-.2	-.6
44	-.9	-.4	-.5	-.6	-.5	-1.6	-2.7	-1.6	-.2	-.3	-.2	-.6
45	-.9	-.4	-.5	-.6	-.5	-1.5	-2.7	-1.5	-.2	-.3	-.2	-.6
46	-1.1	-.5	-.7	-.7	-.7	-2.0	-3.5	-2.0	-.2	-.4	-.3	-.8

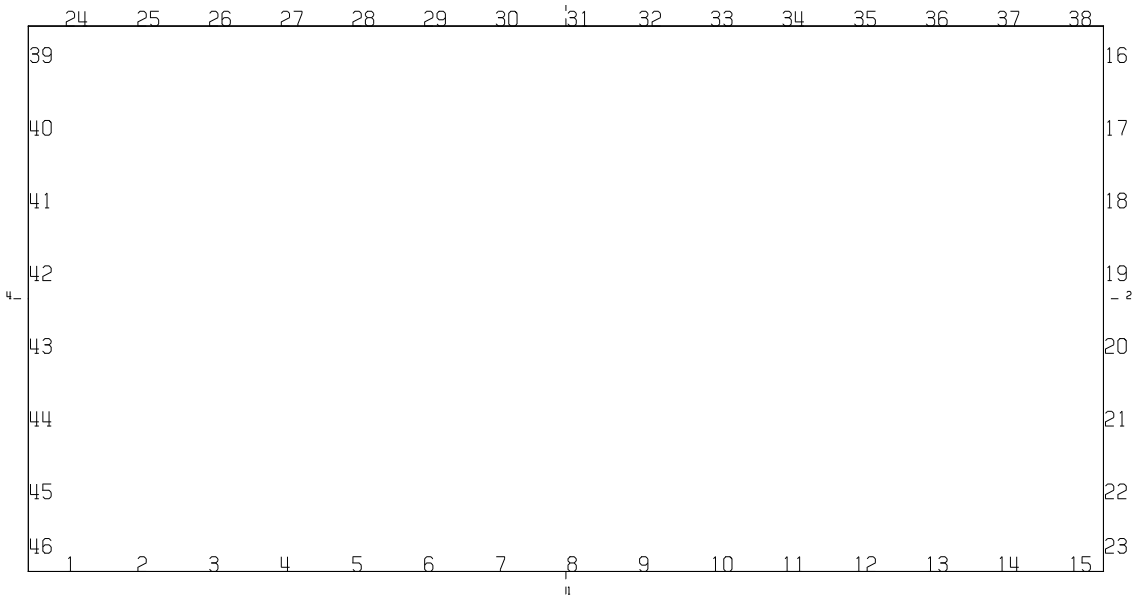

Figure 4.2. Locations of Pressure Estimates on Rectangular Building as Presented in Tables 4.5 and 4.6 (Plan View).

performed with the coefficients referenced to the mean hourly wind speed at the mean roof height. Tables 4.7 through 4.9 present comparisons of the various coefficients. Again, as in the case of wall pressures, the effect of the directionality factor has been removed from the coefficients given in the SBCCI Code and the NBCC. The pressure zones associated with each of the codes and standards are given in Figure 4.5.

Comparisons of the peak coefficients prescribed in each of the above noted standards to those produced by Meecham (1988), shown in Figure 4.3, suggest that the coefficients prescribed in ASCE-7 are generally too high along the roof ridge and eaves, whereas those prescribed by the NBCC and the SBCCI tend to be low along the roof edge and eaves. All of the above noted codes/standards appear to underestimate the wind-induced loads at the ridge/gable end corner, and this underestimation of the loads in this region is also supported in the pressure coefficient data given in Case (1996). A comparison of the SBCCI loads and the ASCE loads for hip and gable roofs suggests that the average of the two sets of pressure coefficients would yield results that most closely reproduce those obtained from the wind tunnel (except at the gable ridge). For the estimation of wind loads and resulting damage, both the SBCCI loads and the ASCE loads are investigated in the damage/loss studies.

Effect of Wind Direction. The effect of wind direction on the estimated pressure coefficients on the roofs of low-rise buildings was determined independently of the building code/standard information using the results of wind tunnel test data given in Stathopolous (1978); Meecham (1988); Ho (1993); Vickery (1984); Surry and Davenport and Mikituk (1993). This wind tunnel information was supplemented by the directional pressure coefficient data given in the United Kingdom Building Code, CP3.

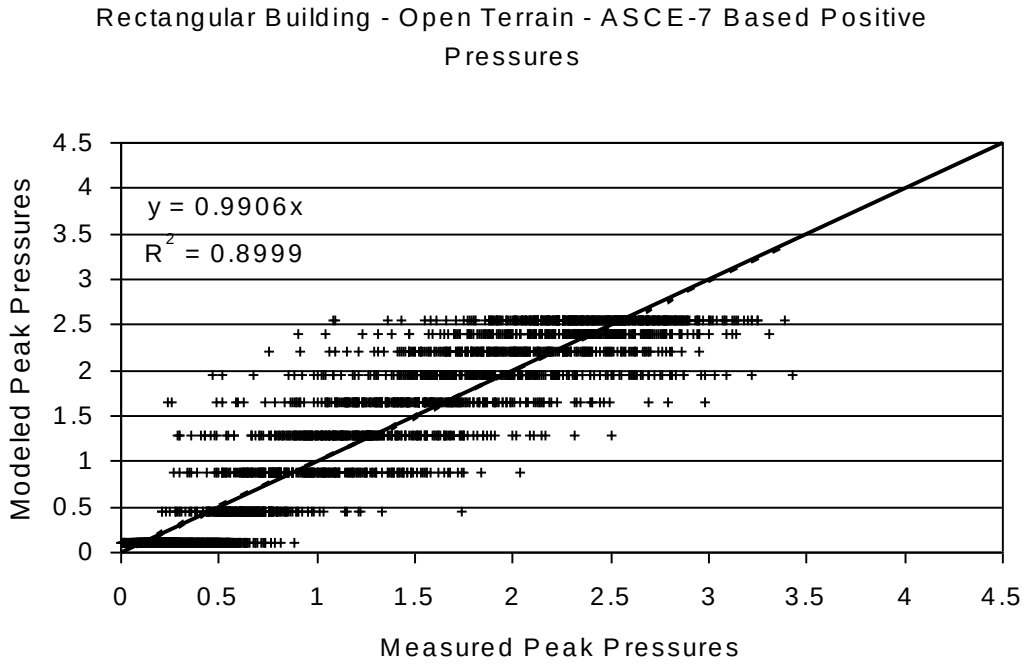

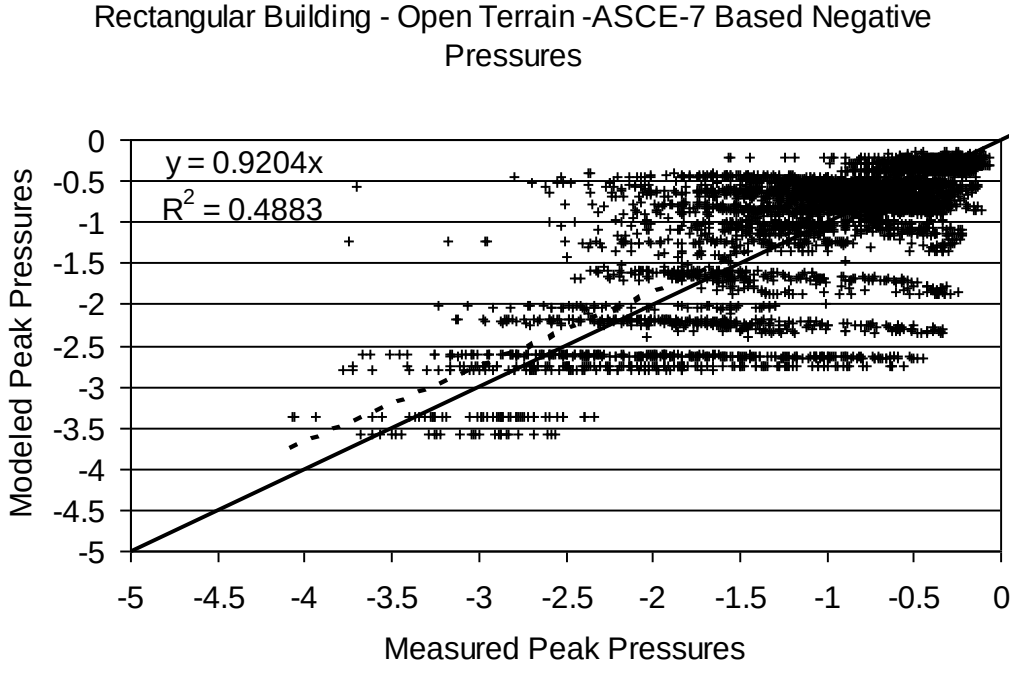

Figure 4.3. Comparison of Measured and Modeled Wall Pressure Coefficients on a Flat Roof Building in Open Terrain (z_0 = 0.1 m).

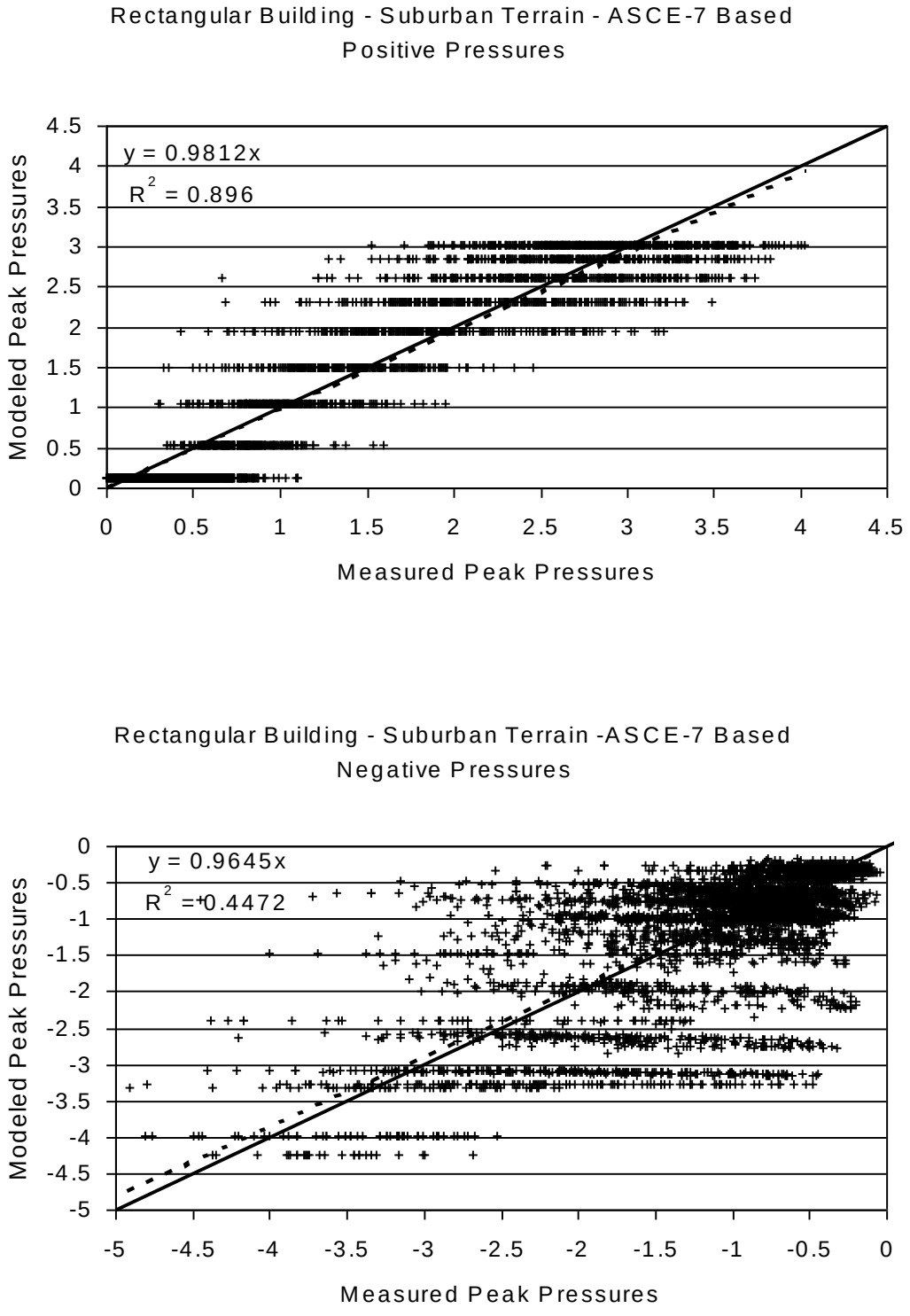

Figure 4.4. Comparison of Measured and Modeled Wall Pressure Coefficients on a Flat Roof Building in Suburban Terrain (z_0 = 0.3 m).

Table 4.7. Comparison of Negative Pressure Coefficients on Flat Roofs

Pressure Zone			Pressure Coefficient		
NBCC	SBCCI	ASCE-7-95	NBCC	SBCCI	ASCE-7-95
c	c	3	6.8	5.6	6.9
s	s_i	2	3.1	3.1	4.5
r	r_e	1	2.3	2.3	2.5

Table 4.8. Comparison of Negative Pressure Coefficients on Gable Roofs

Pressure Zone			Pressure Coefficient		
NBCC	SBCCI	ASCE-7-95	NBCC	SBCCI	ASCE-7-95
c	c	3	5.1	5.2	5.2
s	s_i	2	2.5	2.5	5.2
s’	s_e	2	3.9	4.0	5.2
r	r_e	1	2.0	2.1	2.1

Table 4.9. Comparison of Negative Pressure Coefficients on Hip Roofs

Pressure Zone			Pressure Coefficient		
NBCC	SBCCI	ASCE-7-95	NBCC	SBCCI	ASCE-7-95
c	c	3	5.1	5.2	5.2
s	s_i	2	2.5	2.5	5.2
s’	s_e	2	2.5	4.0	5.2
r	r_e	1	2.0	2.1	2.1

In the development of the wind loads as a function of direction, a zone-based approach was used for the hip and gable roofs using the data noted above. In the case of the gable roof, the zones are based on those given in the SBCCI where, because more zones exist here than in either the ASCE-7 provisions or the NBCCI provisions, the effect of wind directionality can be better modeled. For example, the largest loads on eave zone occur when the wind is blowing perpendicular to the eave or ridge), whereas the largest loads in the corner zones tend to occur when the wind is approaching from an oblique angle, and the largest loads in the center of the gable end occur when the wind is approaching in a direction which is approximately parallel to the ridge line.

In the case of the hip roof buildings, the zones (or sub-zones) used to incorporate the effect of directionality are based primarily on the UK wind loading code, CP3 as shown in Figure 4.7.

Effect of Terrain. A key assumption in the use of pressure coefficients for estimating wind loads, is that the pressure coefficients, normalized with respect to the peak gust wind speed at roof height, do not change with changes in the flow characteristics (e.g., turbulence intensity). This assumption is important because most pressure coefficient data derived from wind tunnel tests given in the literature are presented as coefficients normalized by the mean wind speed at roof height. To adjust these coefficients referenced

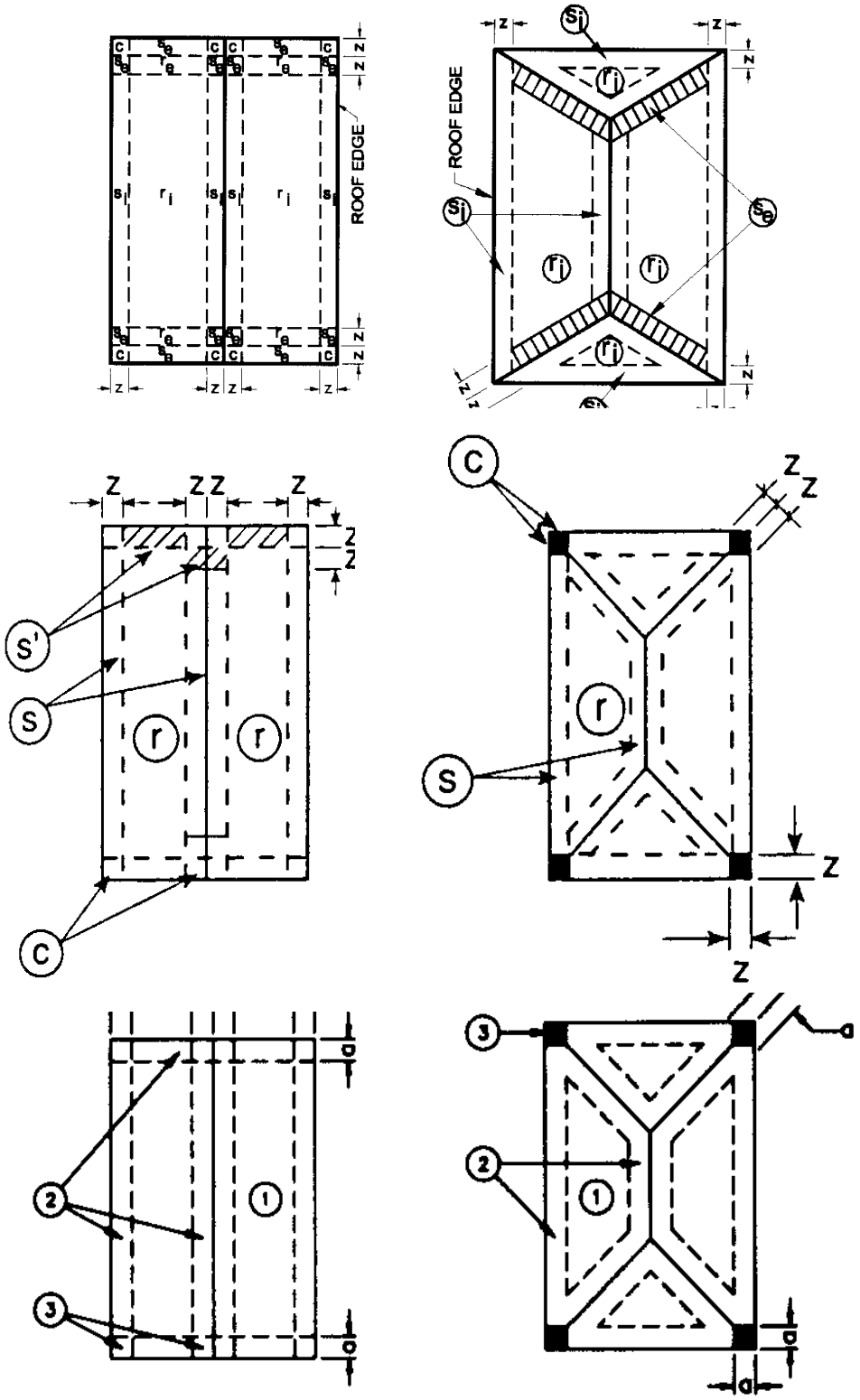

Figure 4.5. Zones used for Defining Pressure Coefficients for Gable and Hip Roofs for the SBCCI (Top Drawings), the NBCC (Middle Drawings) and ASCE-7-95 (Bottom Drawings).

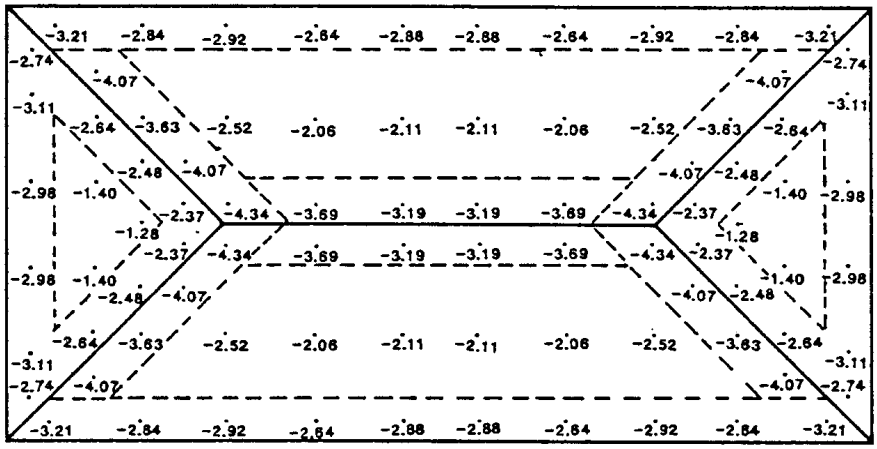

Figure 4.6. Peak Pressure Coefficients on Hip and Gable on Hip and Gable Roofs in Open Terrain (taken from Meecham, 1988).

to the mean wind speed to coefficients referenced to the peak gust speed, information on the flow characteristics used in the wind tunnel tests must be known. If the key flow parameters needed to convert the reference wind speed from mean hourly to peak gust are known (i.e., mean velocity and longitudinal turbulence intensity profiles), then the wind tunnel pressure coefficient data referenced to the mean dynamic pressure can be readily converted to a coefficient normalized to the peak gust velocity pressure. In instances when wind tunnel tests have been performed on the same building in different terrain conditions (e.g., typical open terrain and typical suburban terrain), one would expect the pressure coefficients normalized by the peak gust velocity pressure at roof height to collapse to the same value.

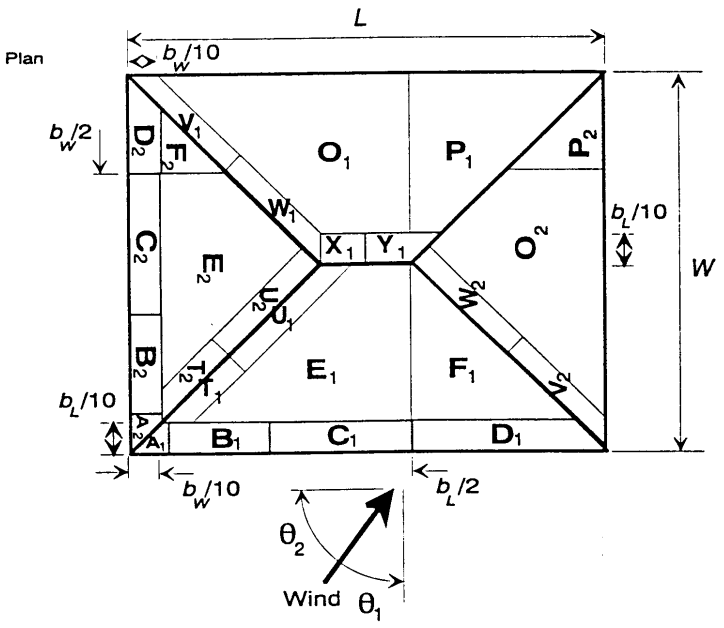

Figure 4.7. Pressure Coefficient Zones Used in the UK Wind Loading Code for Hip Roof Buildings.

Using wind tunnel data given in Monroe (1996), Ho (1992), Meecham(1988), Case (1996), Stathopolous (1978), and Lin and Surry (1997), all of which present roof pressure coefficients normalized by the mean dynamic pressure at roof height for more than one terrain condition, the coefficients were adjusted to be to be normalized with respect to the peak gust velocity pressure at roof height. The degree to which the pressure coefficients normalized by the local gust velocity pressure (at mean roof height) collapsed to yield the same negative pressure coefficient varied from study to study and building to building. In general, it was found that the peak gust pressure coefficients in the rougher terrain (normalized to the local gust velocity pressure) were higher than those at the same location in the smoother terrain.

For example, Monroe (1996) measured roof suctions on a model building with a 1:12 roof slope having an eave height of 4.9 m (full scale) in flow conditions having turbulence intensities at roof height of 12.5% and 19%. On average, the peak roof suction coefficients (normalized with respect to the mean velocity pressure at roof height) obtained in the rougher flow conditions were 75% higher than those obtained in the smoother flow conditions. By normalizing the pressures by the peak gust velocity pressure at roof height (defined as the mean wind speed plus three standard deviations of the fluctuating wind speed), the difference reduces so that the pressure coefficients in the rougher terrain are about 35% higher than those obtained in the smooth terrain. These higher coefficients suggest that using the peak gust velocity pressure to normalize the pressure coefficients is not sufficient to explain the differences in the measured pressure coefficients associated with changes in the flow characteristics.

In the case of Ho (1992), the negative pressures in the suburban terrain case do not collapse to a constant value, with the peak suction coefficients referenced to the peak gust velocity pressure being higher in suburban terrain than in open terrain. For example, converting a roof corner pressure in suburban terrain to be referenced to the peak gust velocity pressure yields a coefficient which is 15% higher than the open country value referenced to the local peak gust velocity pressure.

Similar observations were made using the Lin and Surry pressure data, the Case (1996) pressure data and a large portion of the Stathopolous (1978) data. The observation that the pressure coefficients in the rougher terrains, even when normalized with respect to the local peak gust wind, are larger (in magnitude) than those in open terrain is apparently recognized in ASCE-7-95 where the wind loads on buildings in suburban terrain (Exposure B) are limited to be no less than 85% of the value that would be computed if the building were in open terrain.

To take into account this apparent increase in the peak pressure coefficients, the basic pressure coefficient referenced to the peak gust wind speed is increased by a factor equal to the square root of the ratio of the turbulence intensity at roof height in the local terrain to the turbulence at roof height in the reference open terrain. This empirical adjustment in the pressure coefficients helps collapse the pressure coefficient data noted above, but is clearly a subject requiring more research. The use of this factor does yield estimates of pressures in low buildings in a standard suburban terrain (z_0 = 0.3 m) which are much closer to those required by ASCE-7 than if the adjustment were not made. As an illustration of the effect of the turbulence intensity, consider the following example of a building located in suburban terrain having a mean roof height of 5 m.

Using the ESDU representation of the gust velocity profile, the ratio of the 5 m gust wind speed in suburban terrain to the 5 m gust wind speed in open terrain is 0.787, implying a wind load equal to 62% of the open terrain wind load. The roof height turbulence intensities in the open and suburban terrains (from ESDU, 1992) are 18% and 29%, respectively, resulting in a 27% increase in the pressure coefficient (i.e., $100\sqrt{0.29/0.18}$). The net effect of the reduction in the peak gust velocity combined with the increase in the pressure coefficient associated with the turbulence intensity adjustment is a wind load equal to 79% of the open terrain wind load, which is comparable to the 85% factor given in ASCE-7-98.

Comparison of ASCE-7 Roof Pressure Loads to Wind Tunnel Tests. Figure 4.8 shows a comparison of the ASCE-7 based roof pressure loads to those obtained from wind tunnel tests for a relatively open terrain case and a suburban terrain case. Note that the surface roughness associated with the nominal open terrain case is described by a z_0 value of 0.1 m, which is larger than the value of about 0.03 m which is typically associated with open terrain conditions. The suburban terrain case is characterized by a roughness length of about 0.30 m. The modeled pressures (based on the ASCE-7 loads) presented in Figure 4.8 were produced using the actual values of z_0 as derived from the wind tunnel tests.

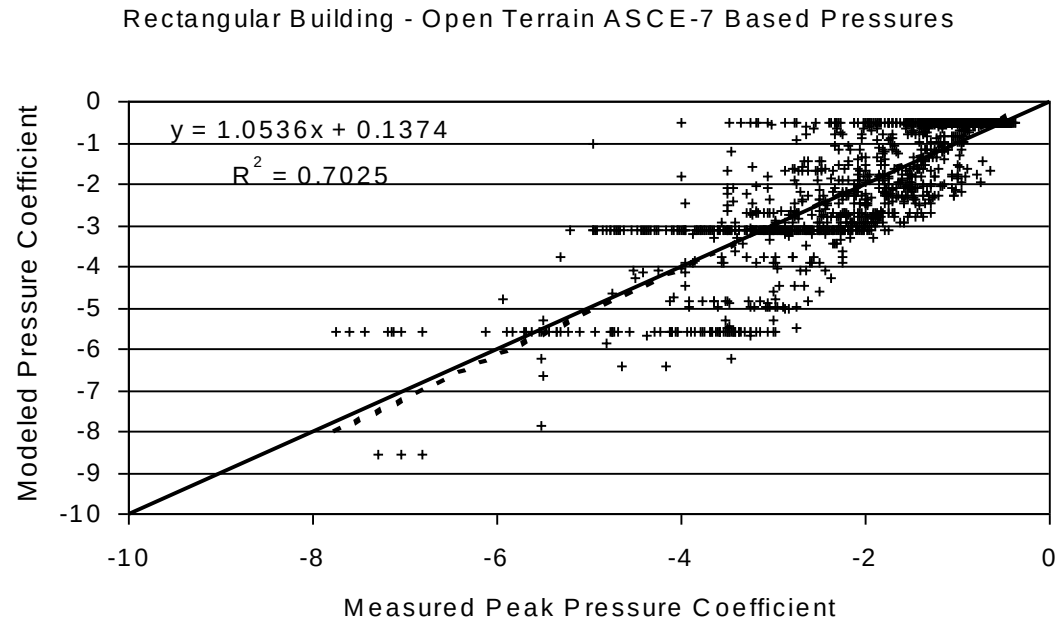

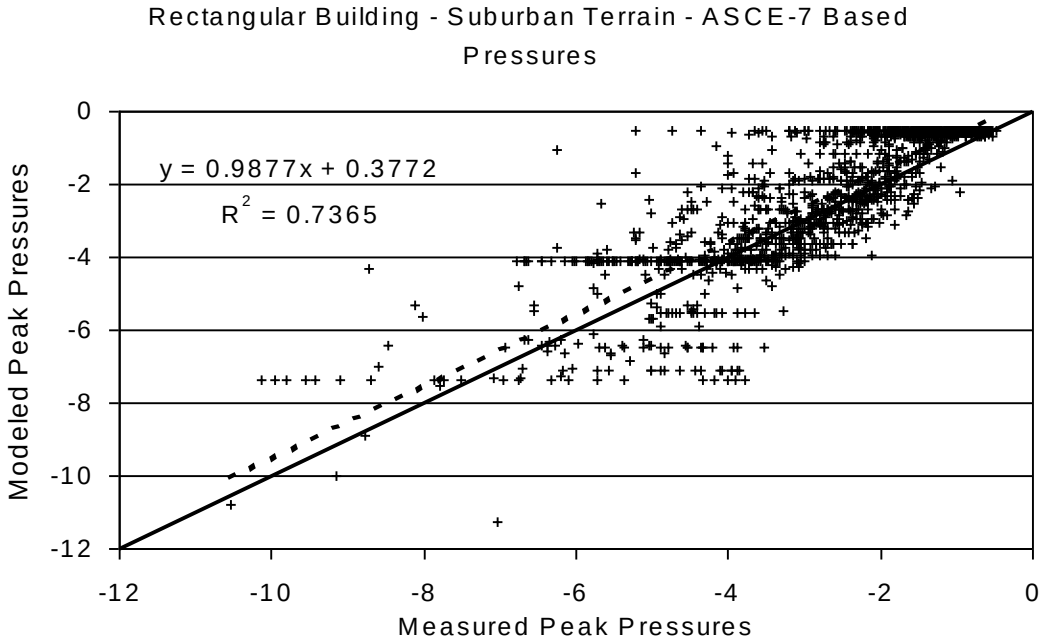

Figure 4.8. Comparison of Modeled and Measured Peak Roof Pressure Coefficients on a Flat Roof Low-Rise Building.

The comparisons of the modeled and measured wind loads suggests that the ASCE-7 based loads with the directional models and the empirical turbulence intensity adjustment factors reproduce the wind tunnel results reasonably well.

Summary. A directional pressure coefficient model has been developed using code based loads to define the maximum pressure coefficients. The roof slopes considered are in the range of 3:12 to 5:12. The effect of directionality is taken into account using available wind tunnel data, scaled (or truncated) to ensure the maximum values of the pressures are equivalent to the code specified values. The reduction in the roof loads associated with decreased wind speeds caused by increasing surface roughness is lessened through the use of a turbulence intensity adjustment factor, which yields a final reduction in wind loads comparable to that specified in ASCE-7-95.

4.4 Wind Loads on Low-Rise Buildings – Effect of Nearby Buildings

The preceding discussion of wind loads on the roofs and walls of low-rise buildings was applicable to isolated structures located within a homogeneous open or suburban terrain. In the case of real buildings situated in real environments surrounded by buildings of like size, on average there is a reduction in the loads experienced by these buildings. The reduction in load is clearly a function of both the spacing and size of the near by buildings as indicated in Holmes (1994). Comprehensive wind tunnel test data showing the effects of nearby buildings on the wind loads experienced by the test building is limited. The wind tunnel test results given in Ho (1992) are probably the most widely quoted results. In Ho (1992), low-rise, flat roofed buildings were tested in both open and suburban terrain conditions with and without the existence of nearby buildings. For the cases where nearby buildings were in place, a total of 16 different representations of surrounding buildings were modeled. The results of the Ho (1992) study indicate that the average reduction in the wind loads on the roofs is about 25% compared to the isolated building case, although the amount of the reduction varied with the location on the roof. The coefficient of variation of the reduction in wind loads was about 20%, but this value also varied with location on the roof. The reduction in the wind loads on the walls of the test building was shown to be somewhat lower, ranging between about a minimum of a 10% reduction up to a maximum of a 25% reduction in load. The coefficient of variation was about 20%. Ho made no attempt so separately examine the effects of nearby buildings on the positive and negative pressures.

In Case (1996), models of a gable roof building with a 4:12 roof slope were tested as isolated buildings and then tested for three different representations of the building surrounded by other buildings. Case found that the reduction in the negative roof and wall loads was similar to that found by Ho (1999) (i.e., a 25% reduction), but found no mean reduction in the peak positive wall pressures. Case found that the positive roof pressures actually increased in the presence of nearby buildings.

In the simulation of wind loads on low-rise buildings for the prediction of damage and loss, the effects of nearby buildings are taken into account by reducing the peak negative pressures by a mean value of 25%. No decrease in the positive wall pressures is taken.

4.5 Integrated (Overall) Wind Loads on Low-Rise Buildings

The prime thrust of this effort with respect to wind-induced damage and loss estimation is directed towards the prediction of damage to the relatively small building envelope components. Overall (large area) loads are important for the prediction of overturning and uplifting of manufactured homes, whole roof failures on residential and small commercial buildings, and failures of structural systems such as those that exist in metal buildings, roof systems, etc. The estimates of the overall loads must take into account the fact that the peak pressures which act on the exterior of buildings and other structures are not fully correlated, and as the area over which the pressures are averaged increases, the effective loading coefficient decreases. This relationship of decreasing loading coefficient with increasing area is reflected in the pressure coefficients given in wind loading codes and standards such as the SBCCI and ASCE-7, but not in the main wind force resisting calculations as defined in ASCE-7-95. The reduction in the effective pressures given in these codes/standards are based on limited wind tunnel test data. In the development of the overall loading model, a model for the prediction of the mean exterior pressures was developed using the code based wind loading model developed for components and cladding as described earlier. This mean pressure model did not exist prior to the development of the overall load model as the loading and damage models were directed towards envelope component loads and failures only.

To estimate overall loads for the prediction of overturning moments, uplift forces, etc., the modeled local pressures described earlier for the hip and gable roof buildings were integrated over the area of interest with the lack of correlation taken into account using a correlation coefficient approach similar to that originally developed by Davenport (1961). The major differences between the approach developed by Davenport and the approach used herein are: (1) Davenport properly uses the mean and standard deviations of the fluctuating pressures, whereas the present approach uses the mean and peak values (since these are estimated using the empirical pressure model) and (2) Davenport's approach was developed for line-like structures, whereas the present methodology is applied to three dimensional structures.

To estimate the peak integrated loads acting on a structure the pressures are integrated using:

$$\hat{R} = \frac{1}{2}\rho V^2 \left[\iint_A I_i \hat{C}_{p_i} I_j \hat{C}_{p_j} \, exp(-\Delta r / \lambda) dA_i dA_j \right]^{1/2} \tag{4.1}$$

where $\hat{R}$ is a peak force, moment or structural action, $\hat{C}_{p_i}$ is the peak pressure coefficient (minus the mean value) at location i, I_i is an influence coefficient converting the pressure at location i to a global force, Δr is the distance between locations i and j, and λ is a length scale which can be considered a measure of the extent over which the fluctuating pressures are correlated. In the modeling approach used for negative pressures here, the length scale decreases with increasing magnitude of the negative pressures (i.e., the very high local negative pressures are correlated over relatively small areas), and the basic value of λ is a function of the building height.

Roof Uplift Loads. Using the integration methodology described above, the code based component and cladding loads were integrated over the roof surface of a hip roof and gable roof residence. The roof slopes in both cases are 4:12, the plan dimensions of the buildings are 30′×60′ and the eave height is 9′.

As indicated in Figure 4.9, predictions of integrated loads for uplift have been compared to the results of Meecham (1988) for the uplift loads on hip and gable roofs with 4:12 roof slopes. Comparisons the uplift load estimates to those obtained from Figure 6-3 of ASCE-7-95 are also given in Figure 4.9.

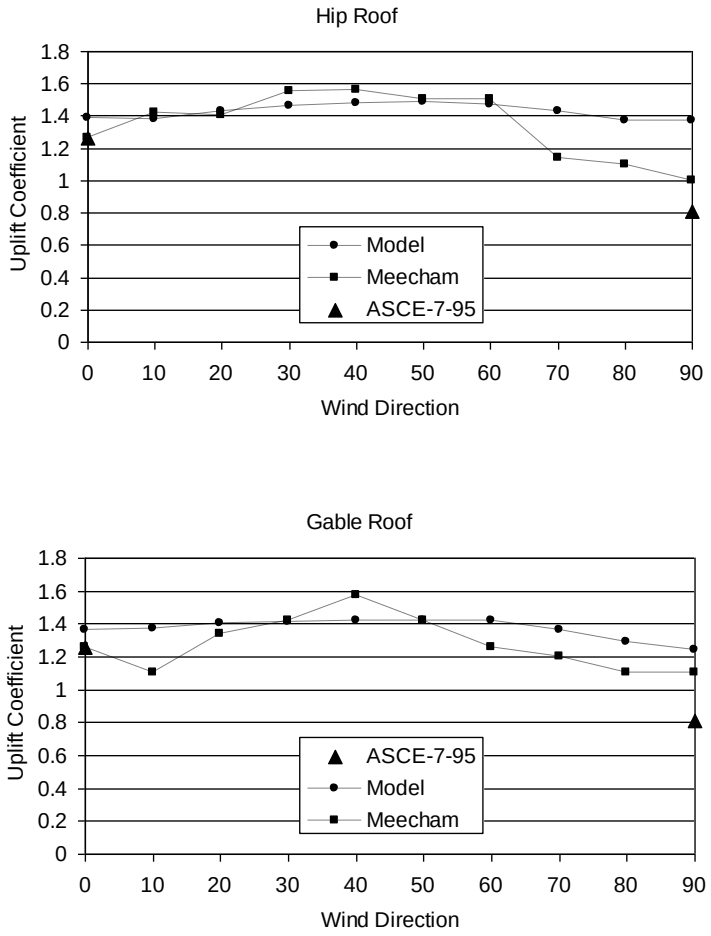

Figure 4.9. Comparisons of Modeled (Integrated) Uplift Loads on Hip and Gable Roofs to those Obtained from Wind Tunnel Experiments. Uplift Coefficients are Defined with Respect to the Mean Dynamic Pressure at Roof Height.

The comparisons of the total uplift forces given in Figure 4.9 indicate that the modeled uplift loads are in general agreement with the results given in Meecham (1988), although the variation of the uplift coefficients with wind direction is less evident in the model results.

ASCE-7 allows for the computation of overall uplift for gable and flat roofs using Figure 6-3 of the standard. The methodology allows for computation of the uplift loads for wind approaching normal to the roof ridge and parallel to the roof ridge only. The uplift loads computed for these two directions are shown in Figure 4.9, where it is seen that for winds approaching normal to the roof ridge, the ASCE-7 uplift loads obtained from Figure 6-3 of ASCE-7 agree well with the uplift loads computed by integrating the component and cladding loads discussed earlier. In the case of the hip roof, the ASCE-7 uplift loads presented in Figure 4.9 are the same as the gable values since ASCE-7 does not provide a means to compute uplift loads on roof shapes that are hip shaped. For winds approaching parallel to the roof ridge (90° as shown in Figure 4.9) the ASCE-7 uplift values are lower than either the Meecham data or the integrated uplift data.

For the prediction of roof uplift failure, the integrated loading approach is used since the methodology is based on code type loads, it produces values of uplift (for the 0° case) that are very similar to those predicted using ASCE-7. The approach allows the effect of directionality (however small in this case) to be incorporated in the damage model, consistent with the approach used throughout model development.

Integrated Roof and Wall Loads on Low-Rise Buildings with Flat Roofs. In order to further validate the pressure integration loading model, comparisons were made with integrated loads obtained directly from wind tunnel tests. The integrated wind tunnel loads were obtained by integrating the time series of wind induced pressures obtained from the wind tunnel tests of the 100′ by 200′ buildings described in Section 4.3. The individual measured pressures acting on the roof were integrated over a number of different areas as indicated in Figure 4.10. Note that in the case of the integrated wall loads, panels 1, 2 and 3 are located on the back side of the building, but are shown in Figure 4.10 as being on the front side for clarity. Comparisons of the modeled and measured force coefficients for the wall and roof sections are given in Figures 4.11 through 4.13. All force coefficients are expressed as the total wind induced force acting on the element divided by the mean dynamic pressure at roof height times the area of the element.

The model results are seen to agree reasonably well with the measured results, reproducing both the reduction in the force coefficient with increasing area, and the directional characteristics of the loads.

Overall Loads on Manufactured Homes. Using Equation 4.1, the code based roof and wall loads were integrated over the surface of a manufactured home in order to evaluate the effectiveness of the approach in estimating the lift, drag and overturning moments on manufactured homes. The results of the integration are compared to the full scale measurements described in Marshall (1977) as well as Roy (1983) and the estimates of lift, drag and overturning obtained from ASCE-7. Figure 4.14 presents the comparisons of lift, drag and overturning coefficients.

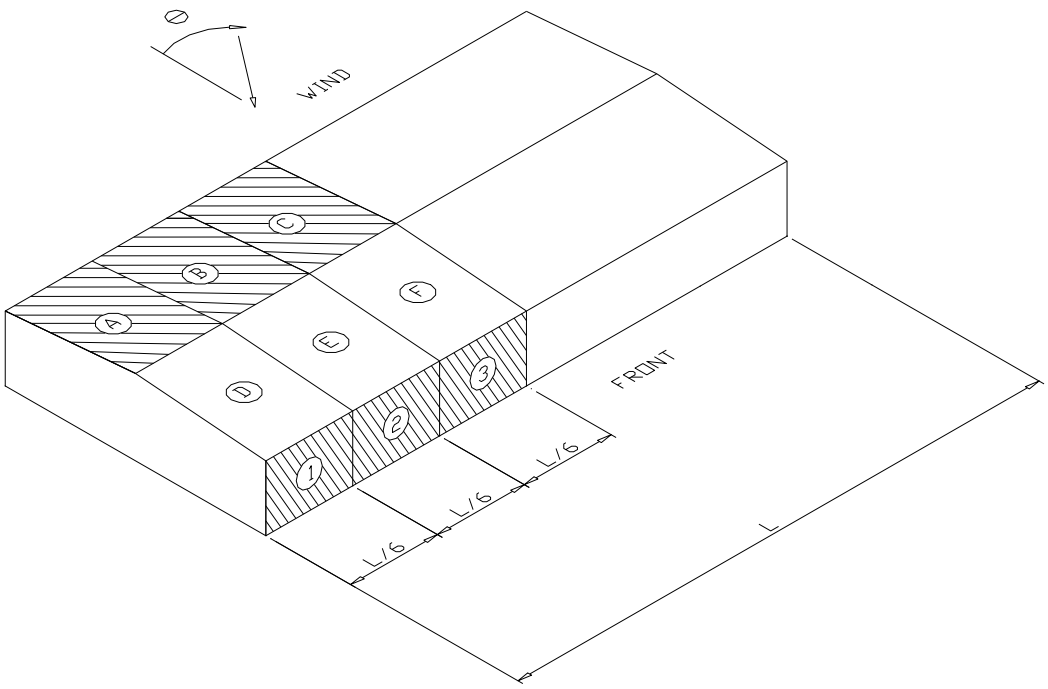

Figure 4.10. Integration Areas Used for Comparison of Overall Roof and Wall Loads.

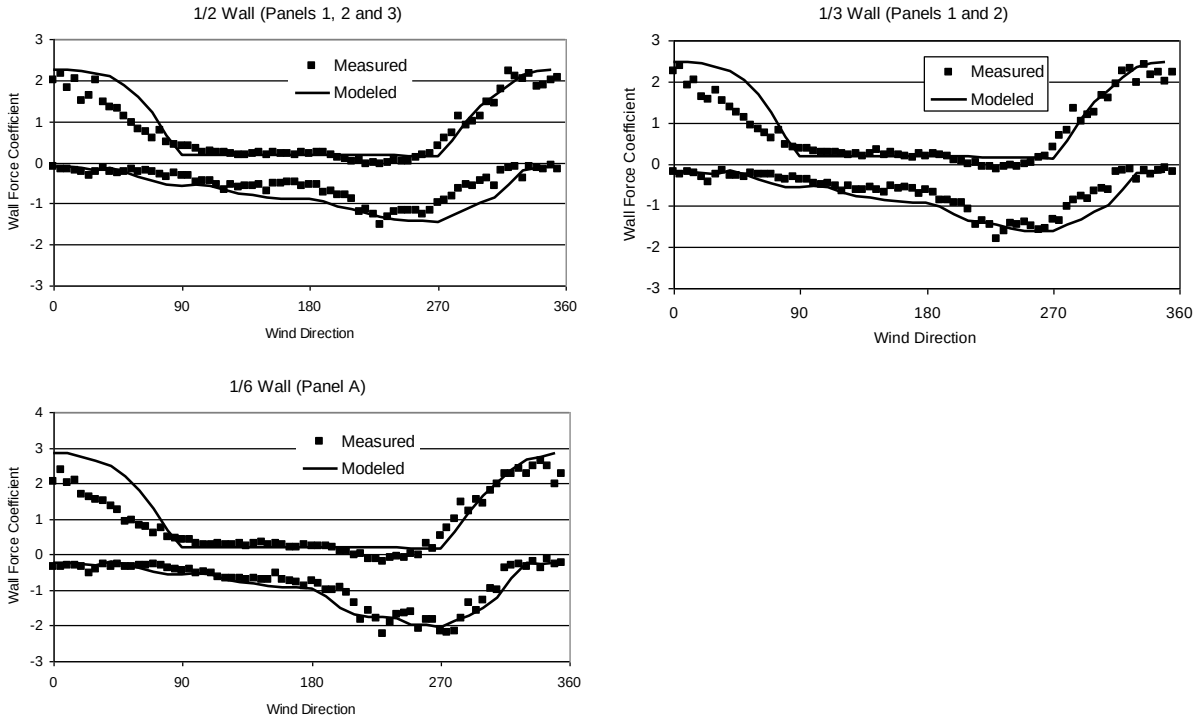

Figure 4.11. Comparison of Modeled and Measured Wall Forces on Rectangular Building in Suburban Terrain.

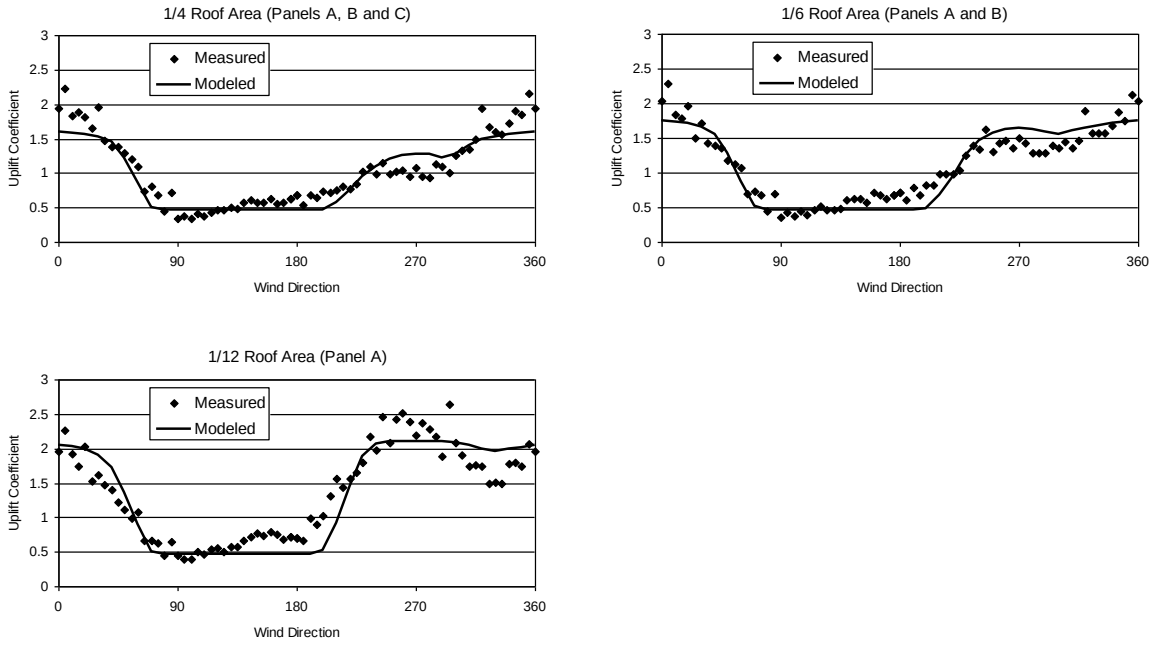

Figure 4.12. Comparison of Modeled and Observed Measured Uplift Coefficients on a Rectangular Building in Open Terrain. Roof Areas Indicated on the Graphs are Shown in Figure 4.10.

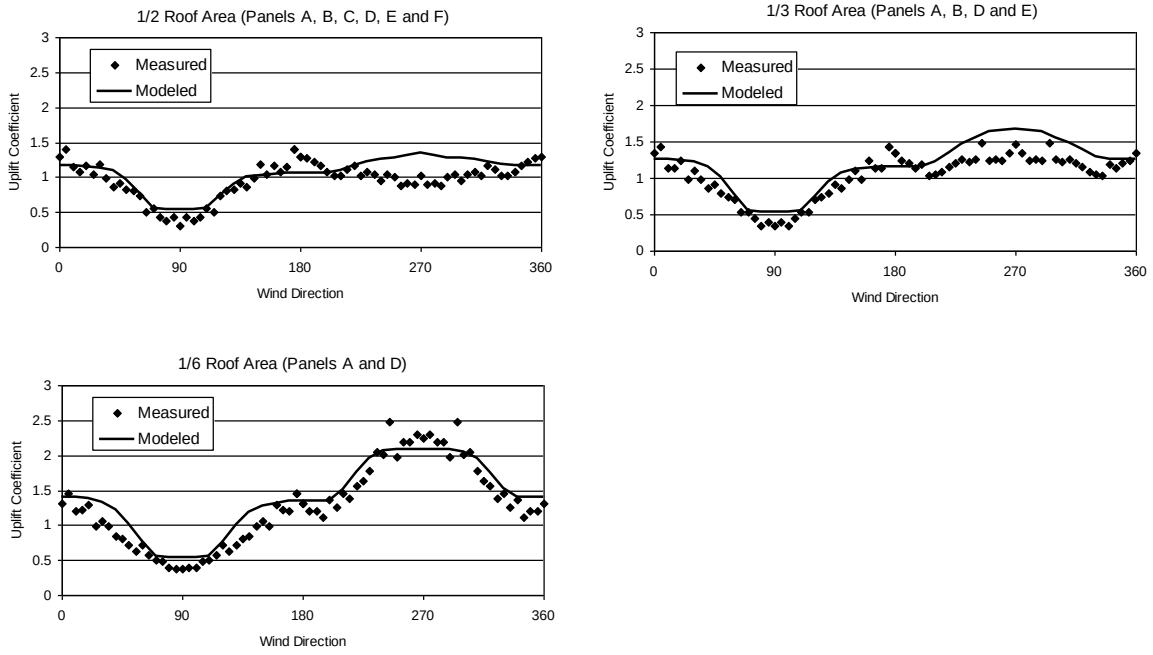

Figure 4.13. Comparison of Modeled and Observed Measured Uplift Coefficients on a Rectangular Building in Suburban Terrain. Roof Areas Indicated on the Graphs are Shown in Figure 4.11.

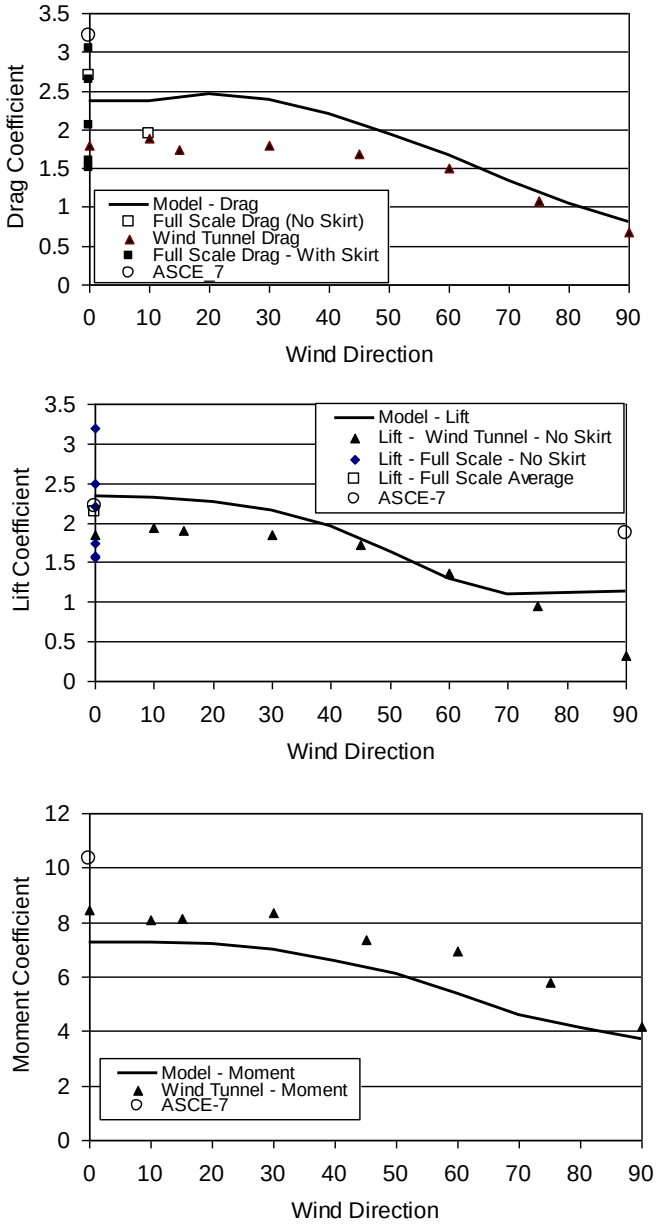

Figure 4.14. Comparison of Modeled, Wind Tunnel Measured, Full Scale Measured and ASCE-7 Estimated Drag, Lift and Moment Coefficients on a Manufactured Home.

The results given in Figure 4.14 show the modeled load estimates to be in general agreement with the limited full scale lift and drag data, as well as the wind tunnel measured lift and moment data. The drag and moment coefficients for the zero wind direction case (winds approaching the long side of a manufactured home) obtained from the model are about 20% to 30% lower than the values estimated using ASCE-7. For use in damage prediction, the modeled lift and drag forces are increased by 10% for all wind directions examined, yielding loading estimates that have maxima closer to the values

produced by ASCE-7 than indicated in Figure 4.14, but limiting the overestimate of the loads as compared to the bulk of the full scale and model scale data. This approach retains a reasonable representation of the effect of wind direction on the loads and strikes a balance between the ASCE-7-98 loads obtained using Figure 6-3 in the standard and the loads obtained from full scale and wind tunnel experiments.

Wind Loads on Long Span Roof Elements. To compute the wind induced uplift loads and bending moments acting on long span roof elements (such as trusses, open web steel joists, pre-cast concrete Tees, etc.) an influence line approach is used. Using this methodology, influence functions describing a specific structural action associated with the application of a load at a given point on the member, are used in conjunction with Equation 4.1 to produce estimates of the wind loads acting on the structural element. The influence function methodology was evaluated through comparisons of modeled and measured uplift coefficients for simply supported joists used as the primary roof system in a low-rise school building. The uplift loads at the joist supports were determined from wind tunnel tests performed at the University of Western Ontario using a 1:100 scale model of the building. Details of the wind tunnel tests and results are given in Young and Vickery (1994). Figures 4.15 and 4.16 show photographs of the model in the wind tunnel.

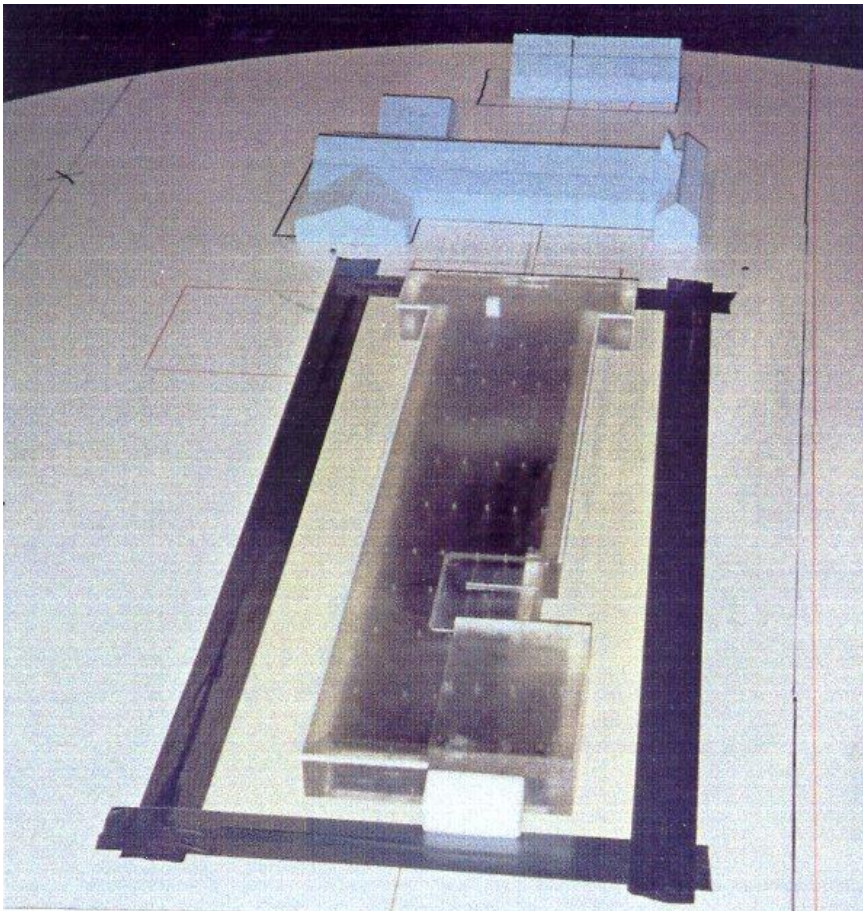

Figure 4.15. Close-up View of Model of School Building Used in Wind Tunnel Tests.

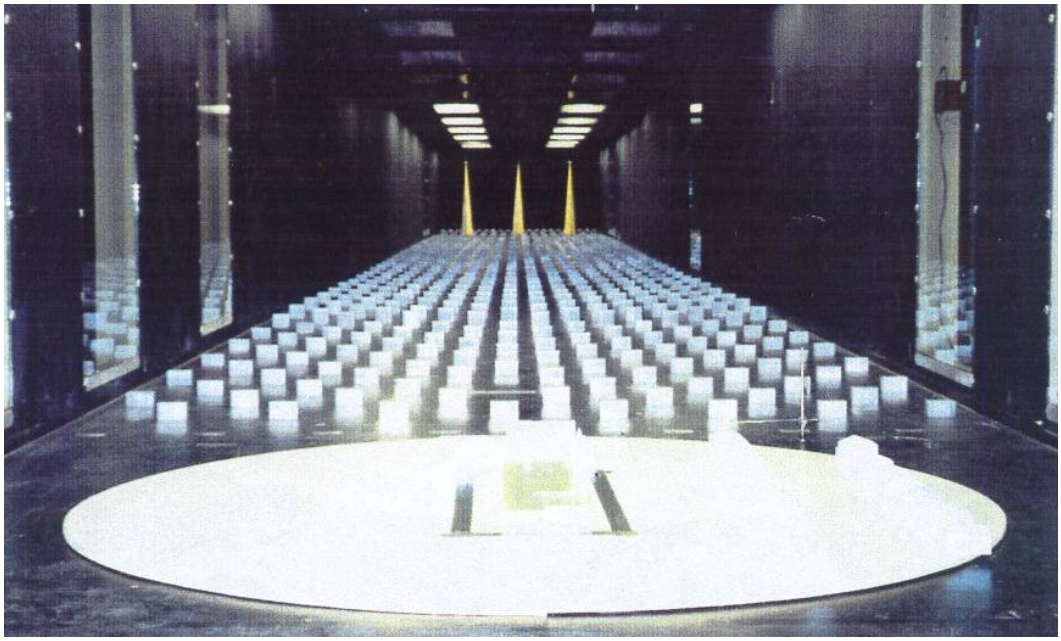

Figure 4.16. View of Model in Wind Tunnel Showing Upstream Terrain.

The roof system of the structure is comprised of open web steel joists (OWSJ) spanning the school in the North-South direction. Three trusses are used in the complete span, each supported by a masonry wall. The two longest OWSJs, spanning the classrooms (span of 25′) are supported by the outer walls and the inner hall way walls, while one shorter OWSJ truss spans the hallway. The joist layout is shown in Figure 4.17.

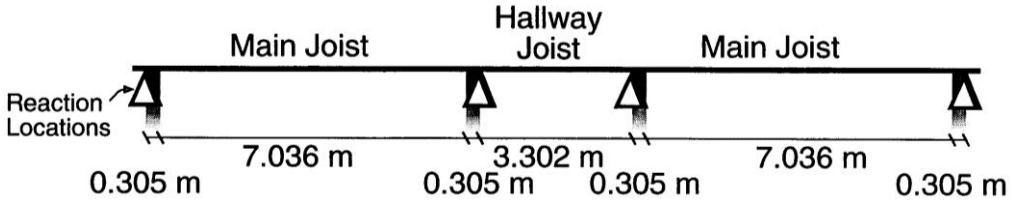

Figure 4.17. Layout of OWSJs as Modeled in Wind Tunnel Tests.

The location of the supports as modeled in the wind tunnel are shown in Figure 4.18, and Figure 4.19 shows the locations of all pressure taps used in the modeling. Comparing the layout of pressure taps to the locations of the computed up-lift points, it is evident that a total of four pressure taps are positioned along each main joist. The pressures measured at the locations of the four individual pressure taps located along the line of each main joist were combined instantaneously with pre-computed influence coefficients to obtain estimates of the uplift loads acting at the ends of each OWSJ. The uplift loads were computed for winds approaching the building for the full 360° azimuth range at intervals of 10°.

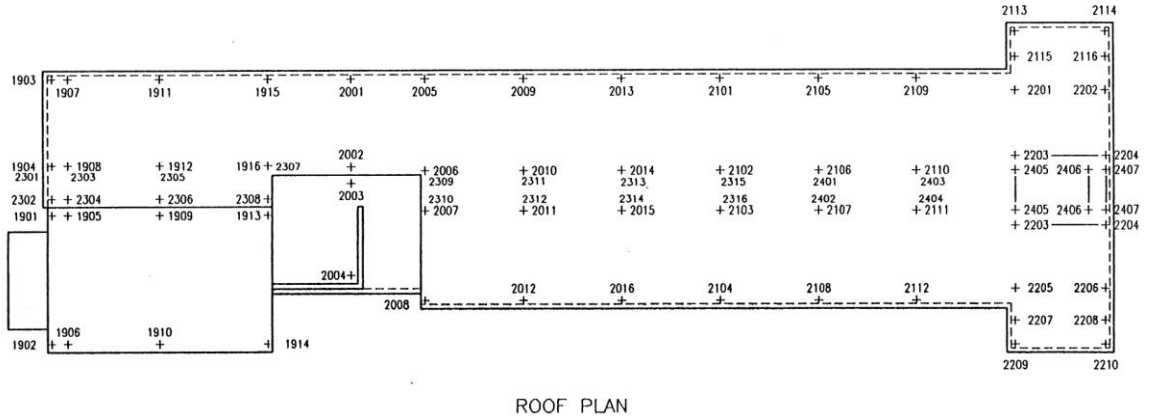

Figure 4.18. Plan View of School Showing Location of Truss Uplift Loads (North is towards top of page).

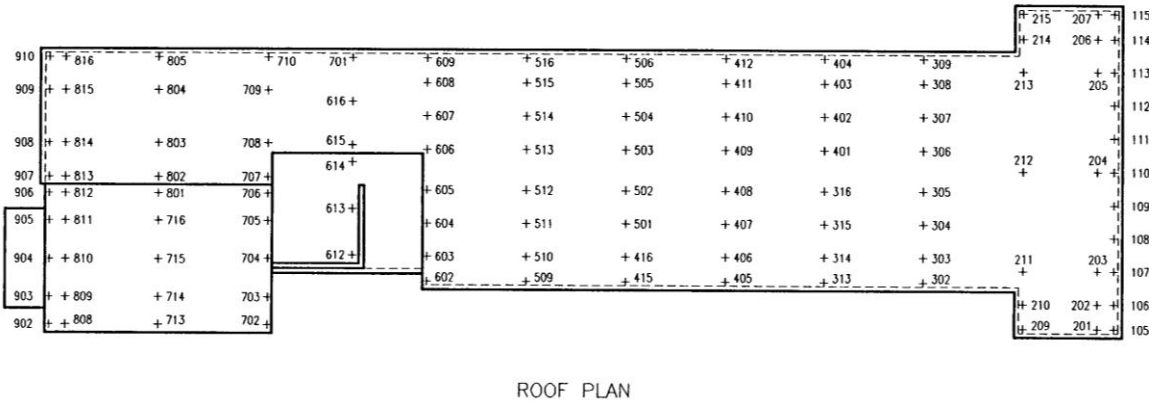

Figure 4.19. Plan View of School Showing Location of all Pressure Taps Used in the Wind Tunnel Tests (North is towards top of page).

To validate the model used to estimate OWSJ loads, comparisons of modeled and measured uplift loads were made for the uplift reactions at the points designated by the numbers 2007 through 2016, and 2101 through 2112. The measured uplift loads are compared to the modeled uplift (or reaction) loads in coefficient form, where both the wind tunnel and modeled coefficients are presented in the form:

$$C_R = \frac{R}{\frac{1}{2}\rho U_H^2 L} \tag{4.5-2}$$

where L is the length (or span) of the joist, R is the uplift load per unit width, ρ is the density of air and U_H is the mean wind speed at roof height. Figure 4.20 shows comparisons of the simulated and measured uplift coefficients as a function of wind direction for a total of 11 joists (22 reactions).

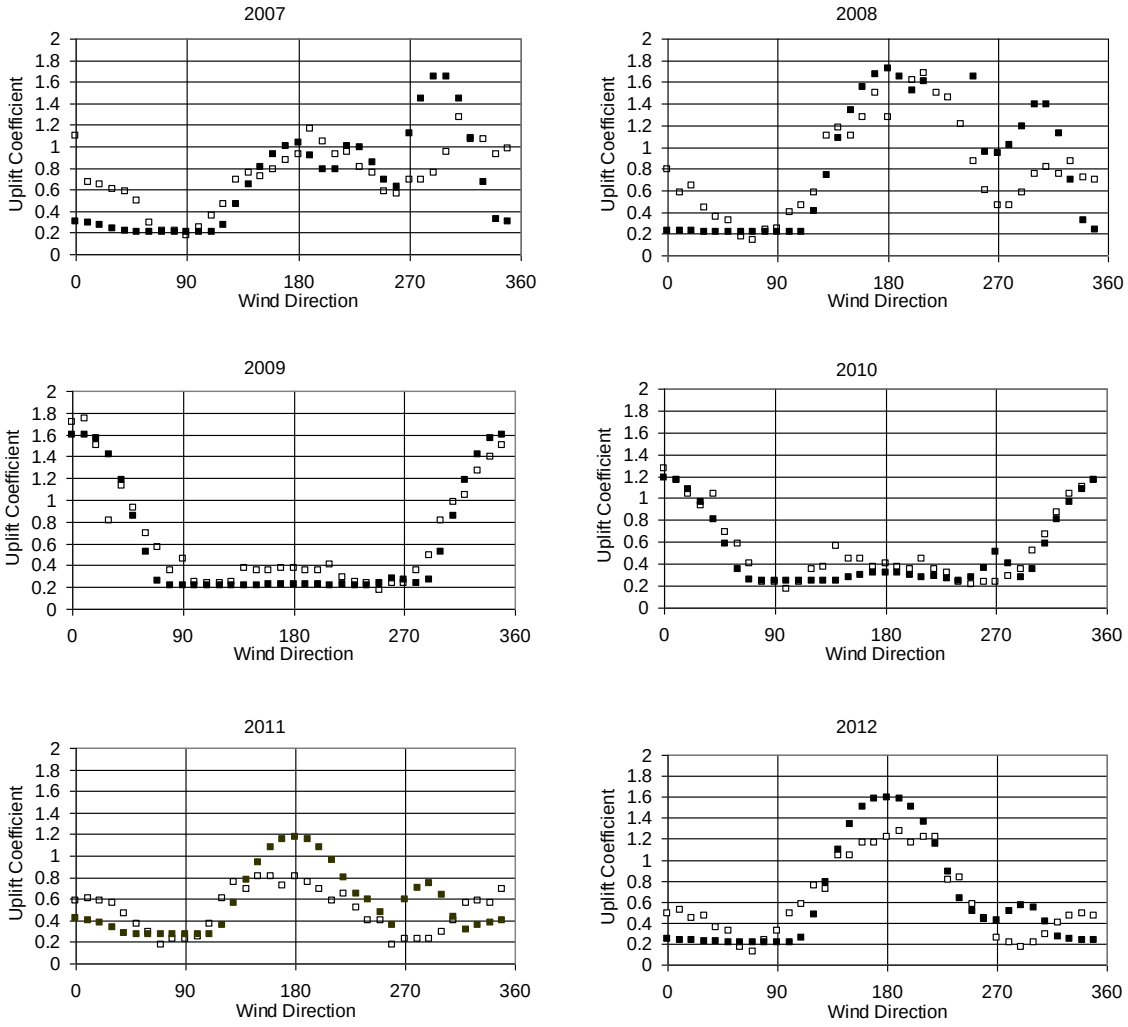

Figure 4.20. Comparison of Wind Tunnel Measured (open squares) and Simulated (solid squares) Joist Uplift Coefficients as a Function of Wind Direction.

As indicated in the comparisons between modeled and measured uplift coefficients, the agreement between the two data sets is generally quite good, particularly for OWSJs located on the north side of the building, away from the corners. The model tends to overestimate the maximum uplift loads acting on the OWSJs located on the south side of the building (denoted as 2012, 2016, 2104, 2108 and 2112) by as much as 30% (see location 2012) but this overestimate varies from joist to joist, and considering the geometry of the building, it is expected that the peak loads experienced by these joists would be nominally the same suggesting that some of the differences can be attributed to experimental variability. In the case of the OWSJs located on the north side of the building, the agreement between the measured and modeled uplift coefficients is better than for those located on the south side of the building, with the model both slightly overestimating and underestimating the magnitudes of the peak uplift coefficients at the locations of the individual joists.

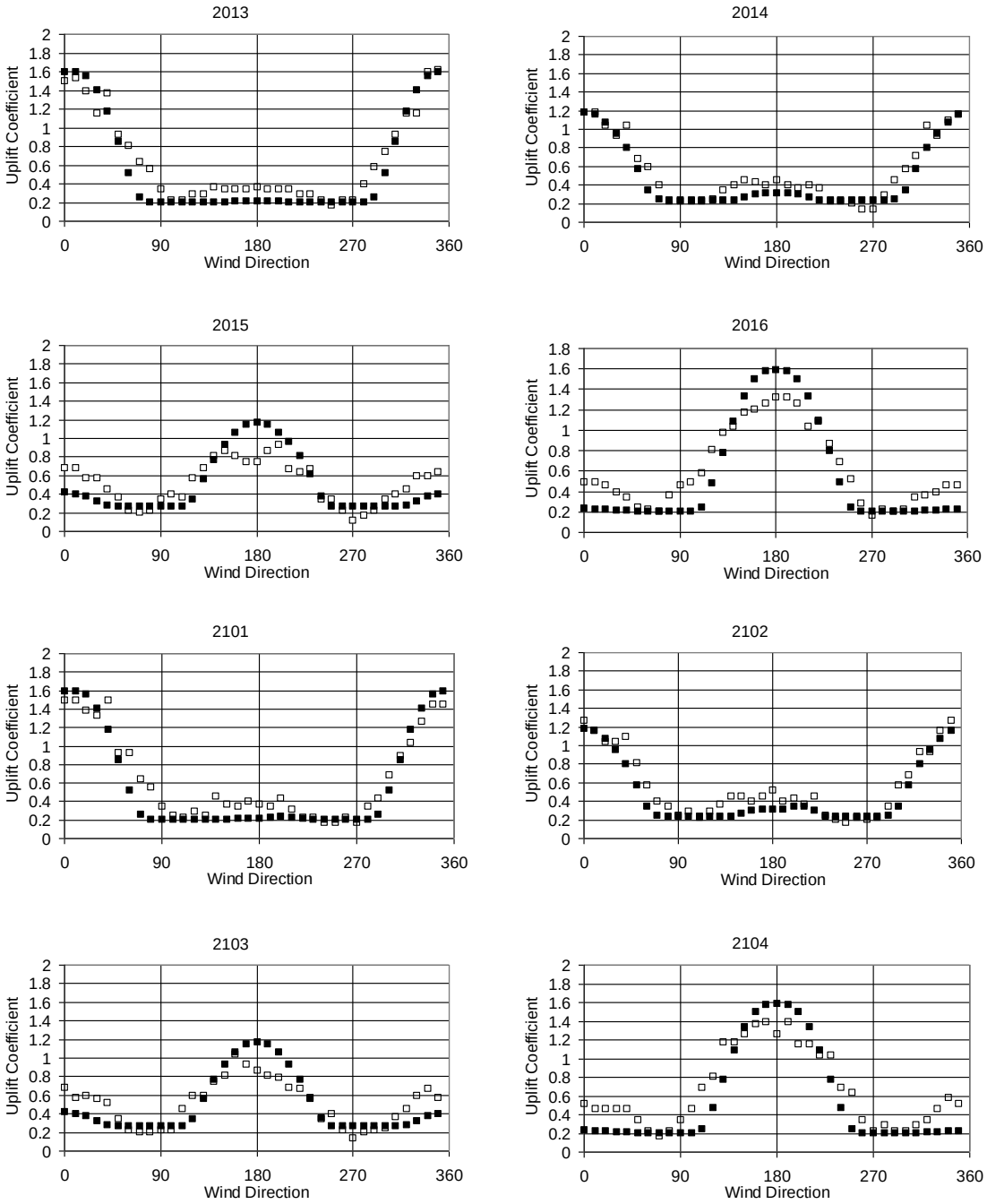

Figure 4.20. Comparison of Wind Tunnel Measured (open squares) and Simulated (solid squares) Joist Uplift Coefficients as a Function of Wind Direction (continued).

The overestimate of the wind uplift loads for joists located on the south side of the building is thought to be a result of the low buildings located to the south of the building as indicated in Figure 4.12 interfering with the flow. The net reduction in wind loads produced by these upstream buildings is consistent with the load reduction factor applied to buildings located in "real" environments as described earlier in Section 4.3.

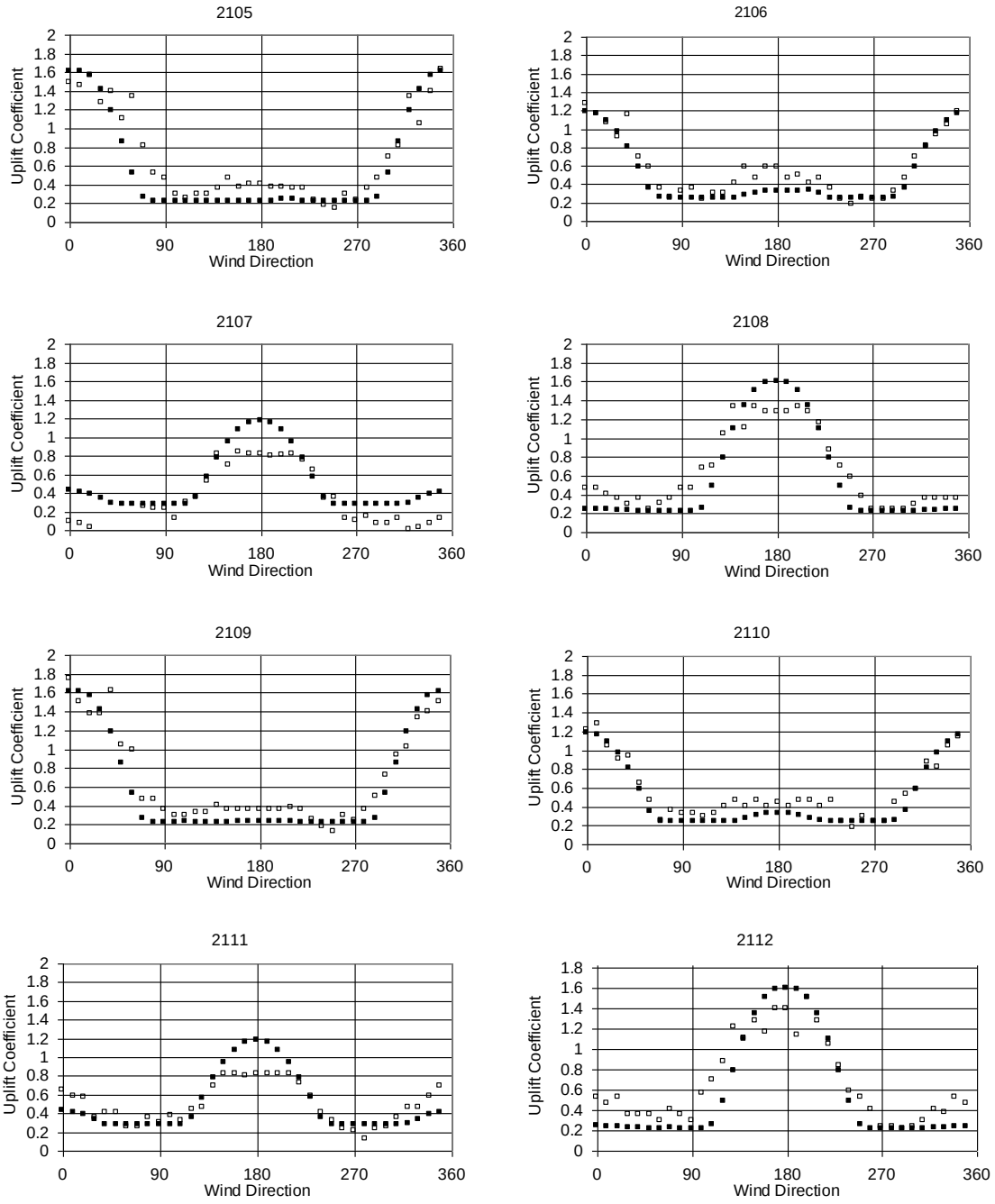

Figure 4.20. Comparison of Wind Tunnel Measured (open squares) and Simulated (solid squares) Joist Uplift Coefficients as a Function of Wind Direction (concluded).

4.6 Wind Loads on High-Rise Buildings

In the case of high-rise buildings, overall structural loads are not modeled. Wind induced damage to high-rise buildings is modeled as being associated with wind induced failure of components (i.e., windows) and damage to windows caused by windborne debris. The maximum magnitudes of the directionally dependent exterior cladding pressure load

model are set equal to the peak values given in ASCE-7-02, and information on directionality was derived using data given in Djakovich (1985) and the 1995 Version of the British Wind Loading Standard, CP3.

Example directional plots of modeled wind induced pressures and suctions have been developed for a rectangular building and a square building. The rectangular building has a length of 100′ and a width of 40′. The square building has a width of 40′. The exterior pressures are given along a ring around the building spaced a 5′ apart, with the first location positioned 2.5′ from the edge. Figures 4.21 and 4.22 indicate the locations on the model buildings for which the pressure coefficients apply.

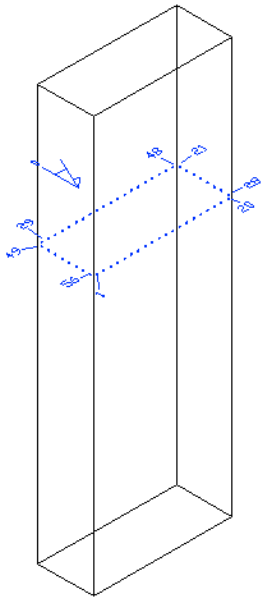

Figure 4.21. Location of Pressures Points for 2.5:1 High-Rise Building.

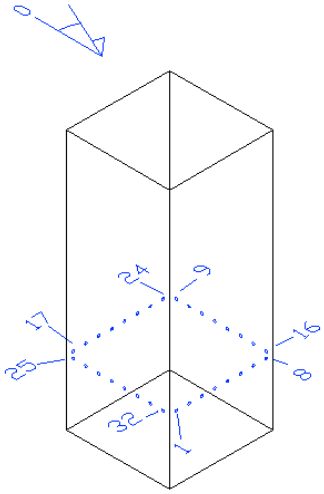

Figure 4.22. Location of Pressures Points for 1:1 High-Rise Building.

Plots of the pressure coefficients as a function of wind direction are given in Figures 4.23 and 4.24 for the buildings having length to width ratios of 2.5:1 (rectangular) and 1:1 (square), respectively. Note that in the case of the building having an aspect ratio of 2.5:1, locations on the short face experience large peak negative pressures for winds approaching from both 0° and 180°, reflecting the fact that the flow does not reattach to the short wall. In the case of winds approaching perpendicular to the short wall, the peak negative pressures on the long wall occur for one direction only, owing to the fact that the flow reattaches to the long wall.

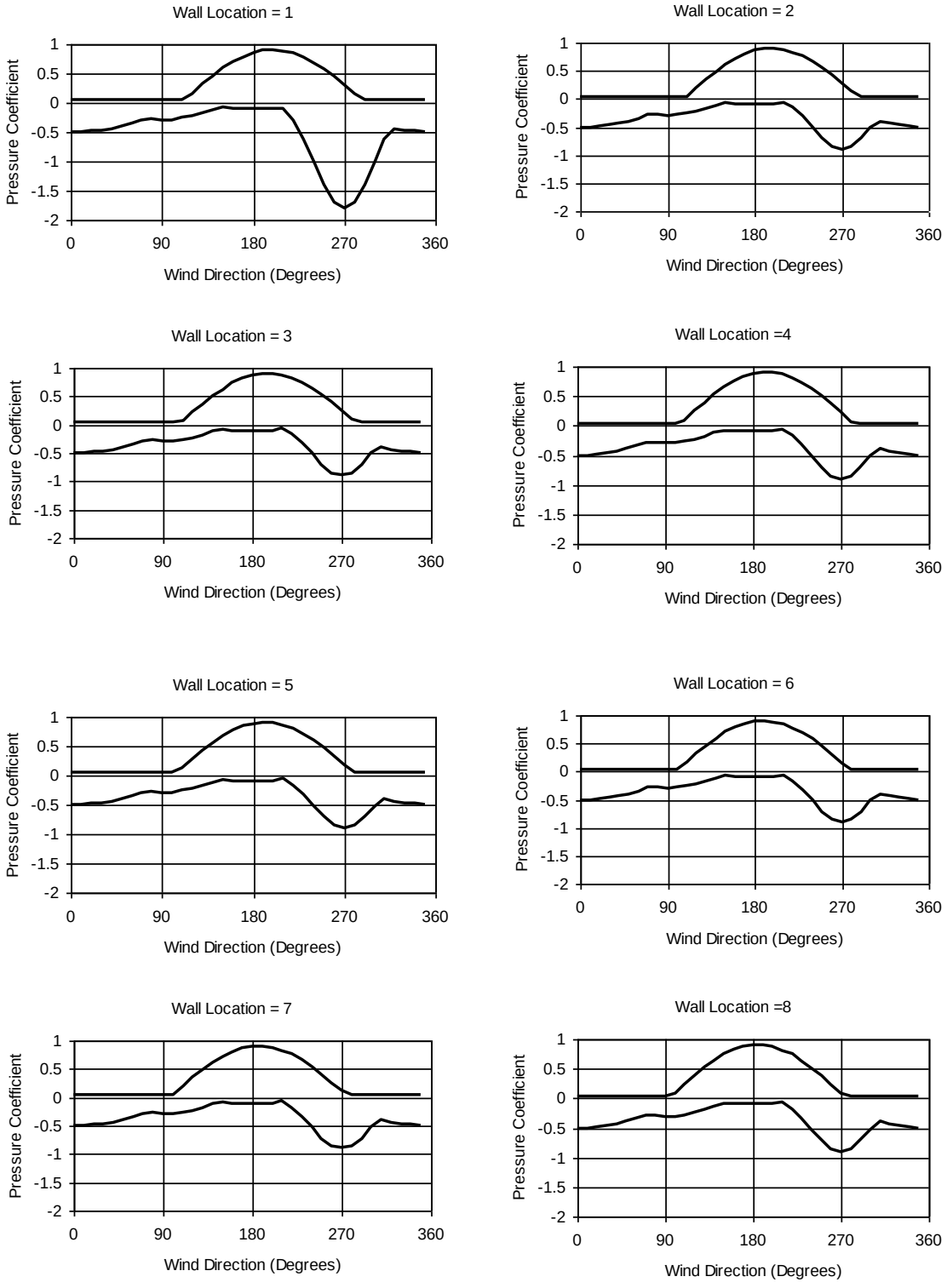

Figure 4.23. Maximum and Minimum Pressure Coefficients vs. Wind Direction Used in Modeling of a Rectangular High-Rise Building Having a Length to Width Ratio of 2.5.

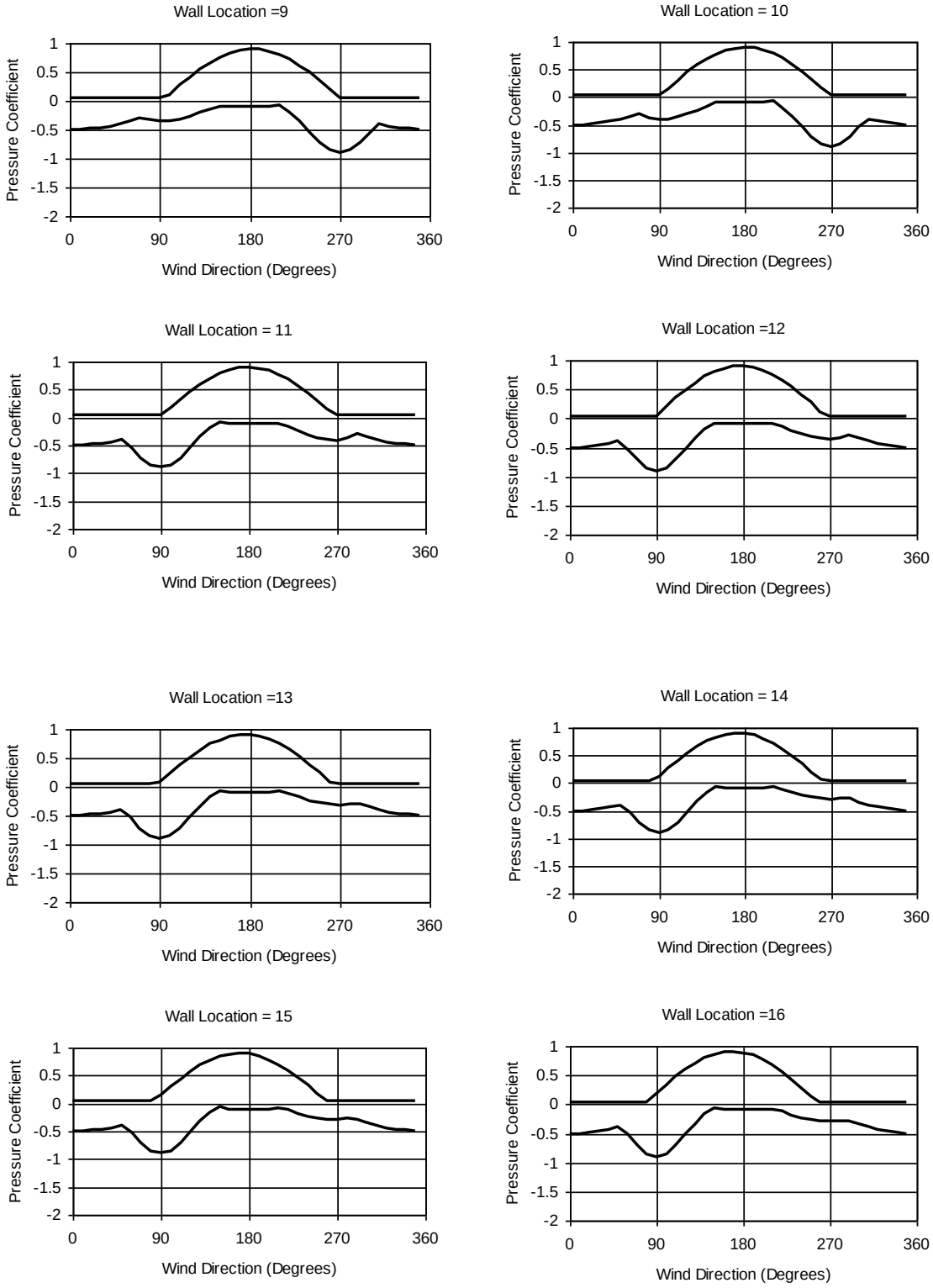

Figure 4.23. Maximum and Minimum Pressure Coefficients vs. Wind Direction Used in Modeling of a Rectangular High-Rise Building Having a Length to Width Ratio of 2.5 (continued).

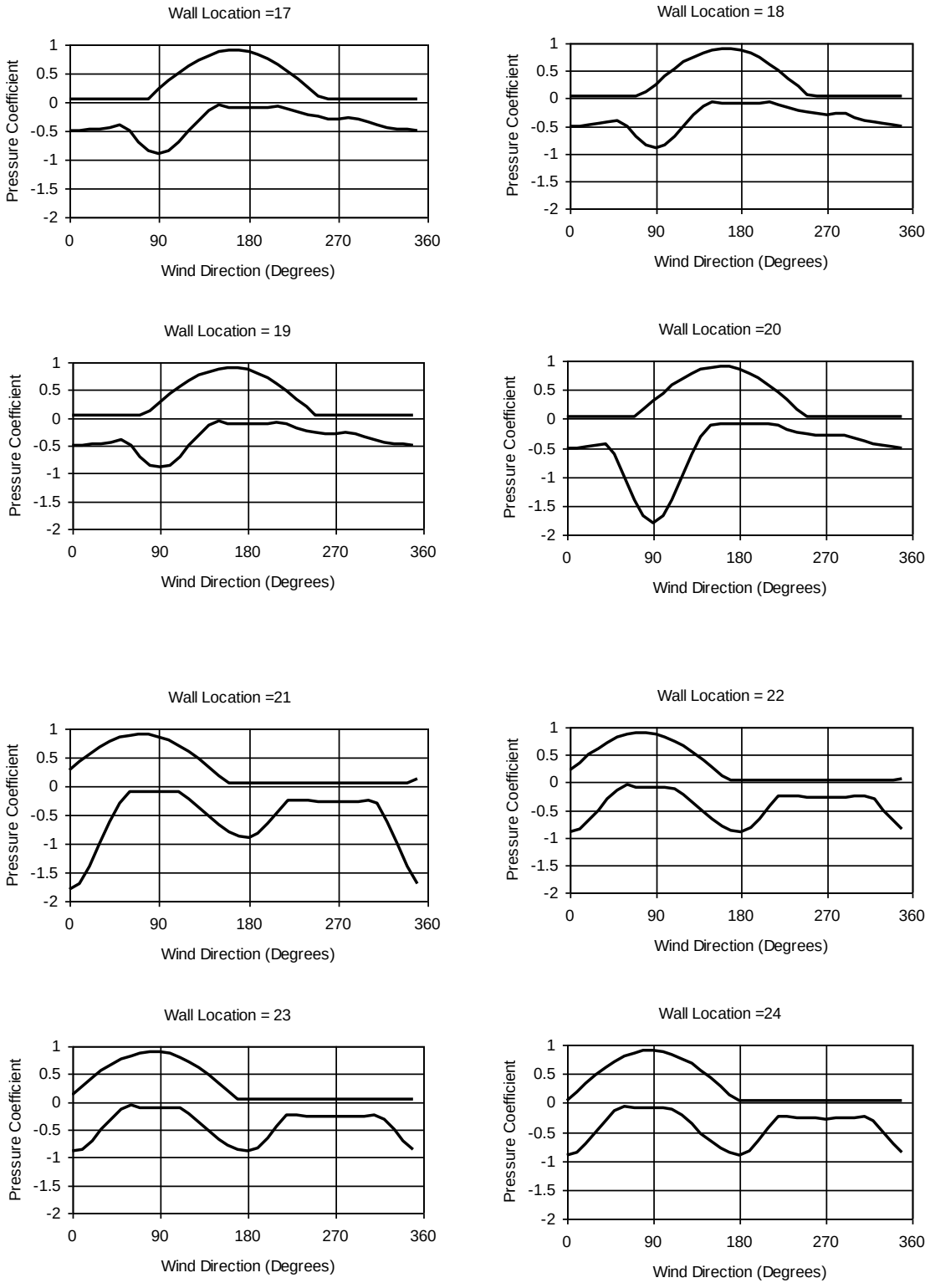

Figure 4.23. Maximum and Minimum Pressure Coefficients vs. Wind Direction Used in Modeling of a Rectangular High-Rise Building Having a Length to Width Ratio of 2.5 (continued).

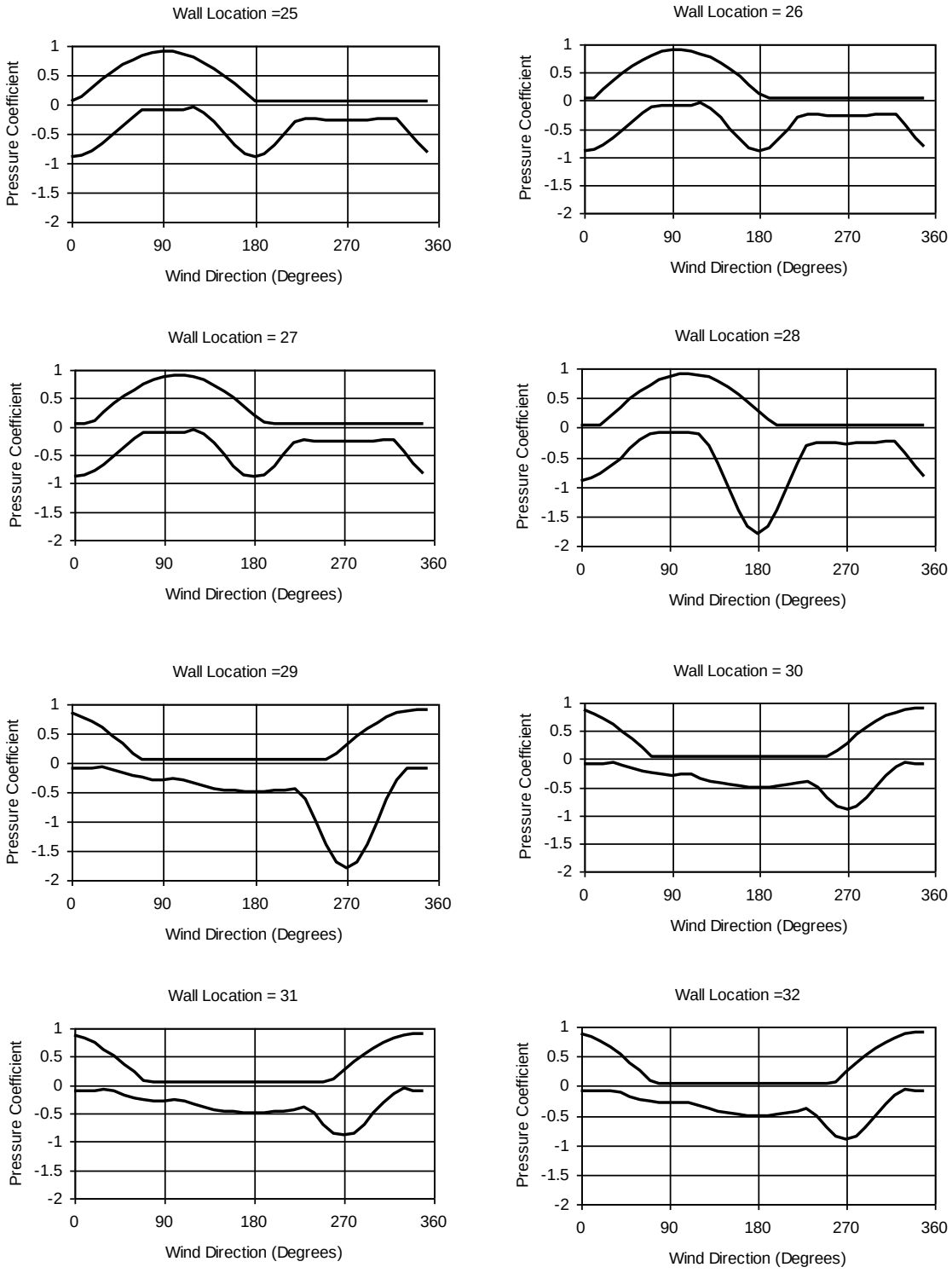

Figure 4.23. Maximum and Minimum Pressure Coefficients vs. Wind Direction Used in Modeling of a Rectangular High-Rise Building Having a Length to width Ratio of 2.5 (continued).

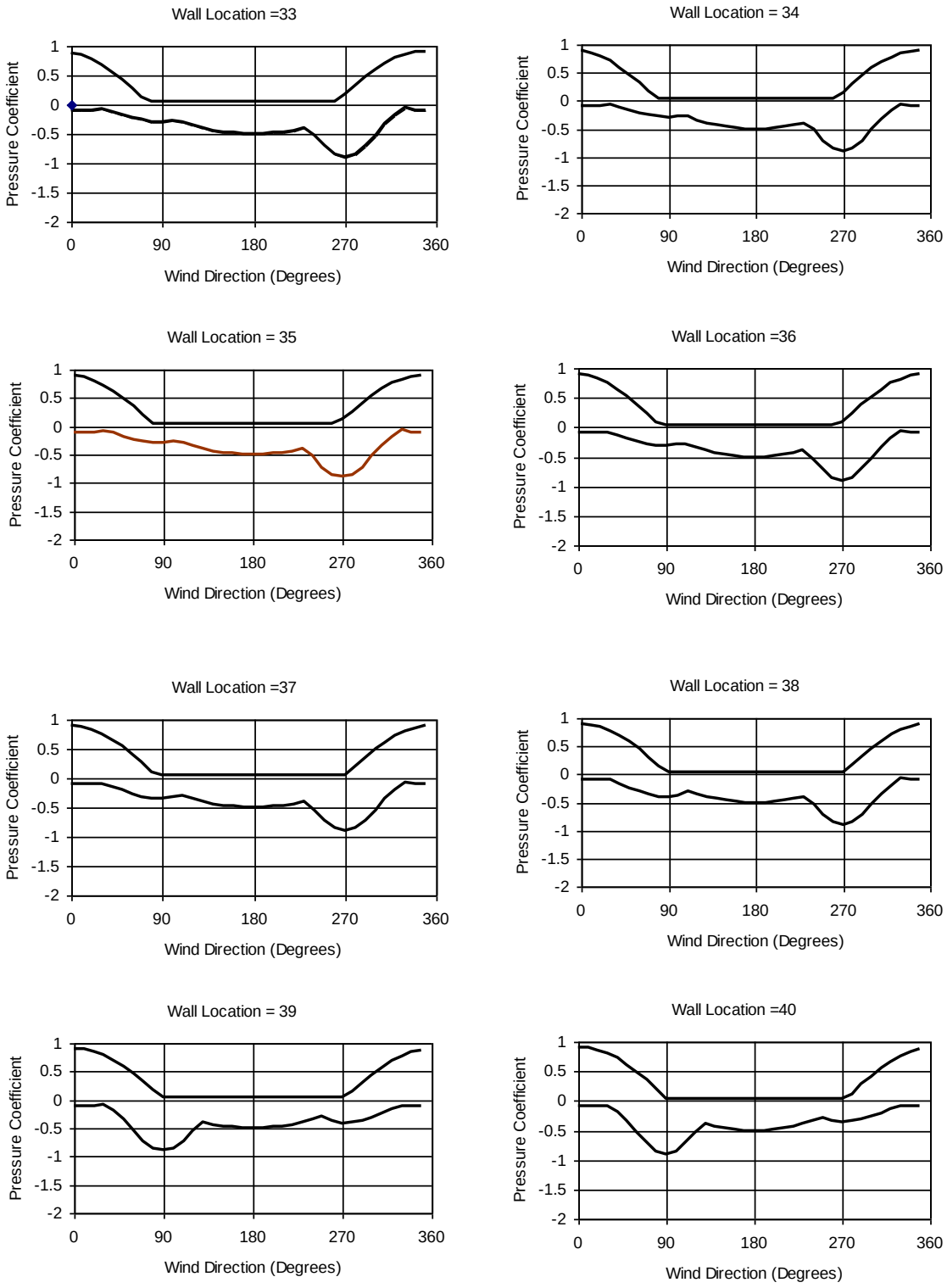

Figure 4.23. Maximum and Minimum Pressure Coefficients vs. Wind Direction Used in Modeling of a Rectangular High-Rise Building Having a Length to Width Ratio of 2.5 (continued).

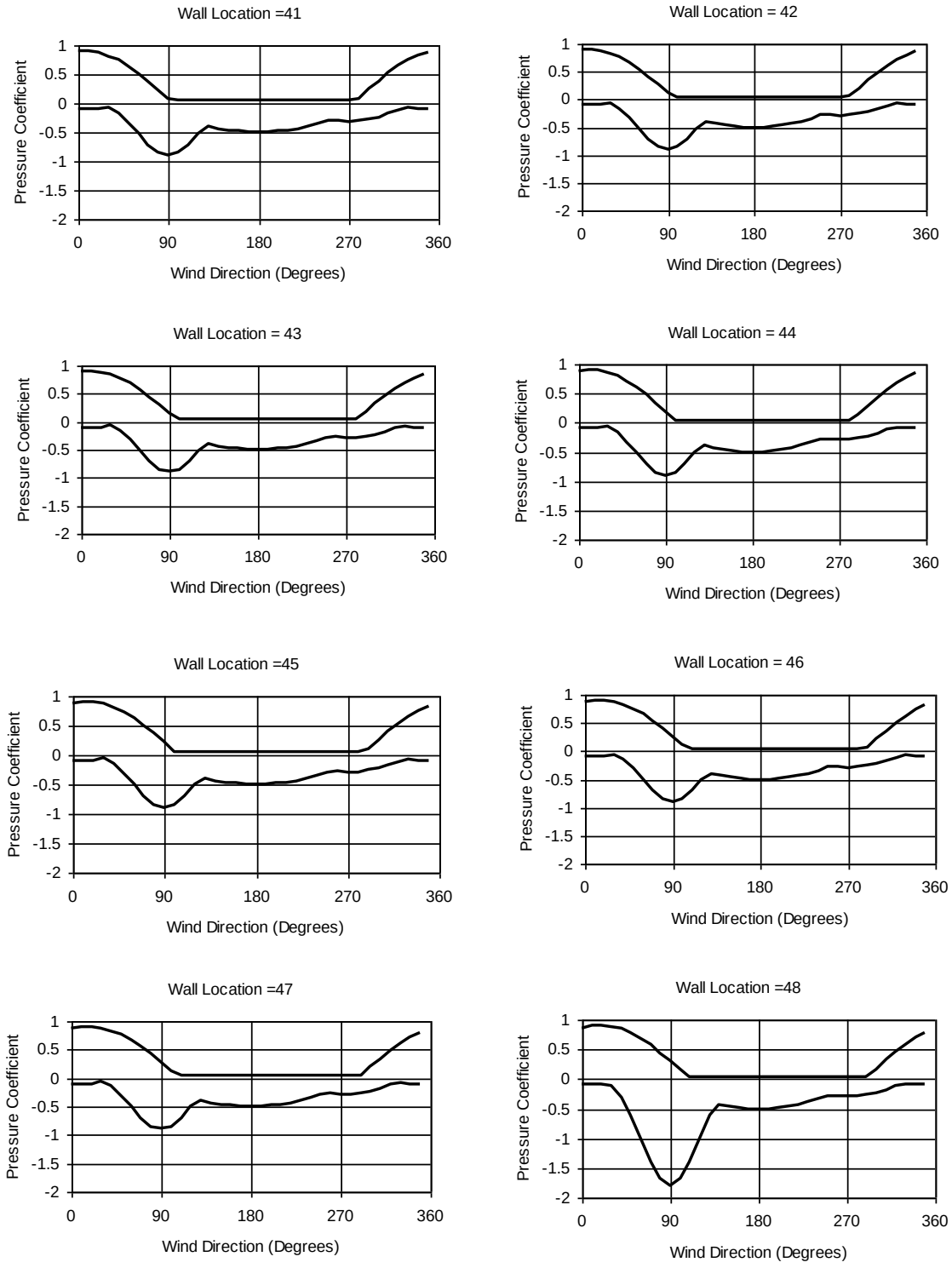

Figure 4.23. Maximum and Minimum Pressure Coefficients vs. Wind Direction Used in Modeling of a Rectangular High-Rise Building Having a Length to Width Ratio of 2.5 (continued).

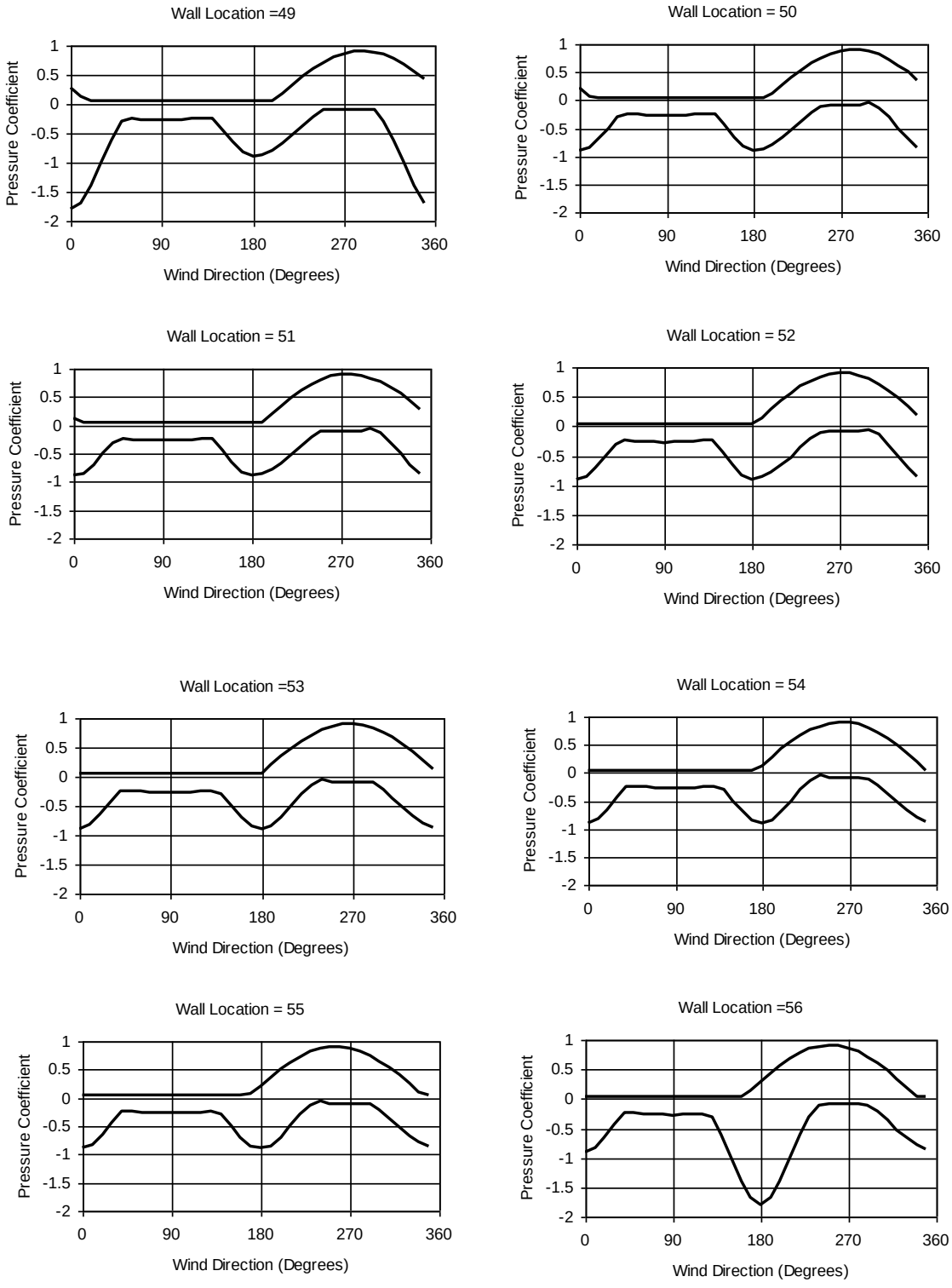

Figure 4.23. Maximum and Minimum Pressure Coefficients vs. Wind Direction Used in Modeling of a Rectangular High-Rise Building Having a Length to Width Ratio of 2.5 (concluded).

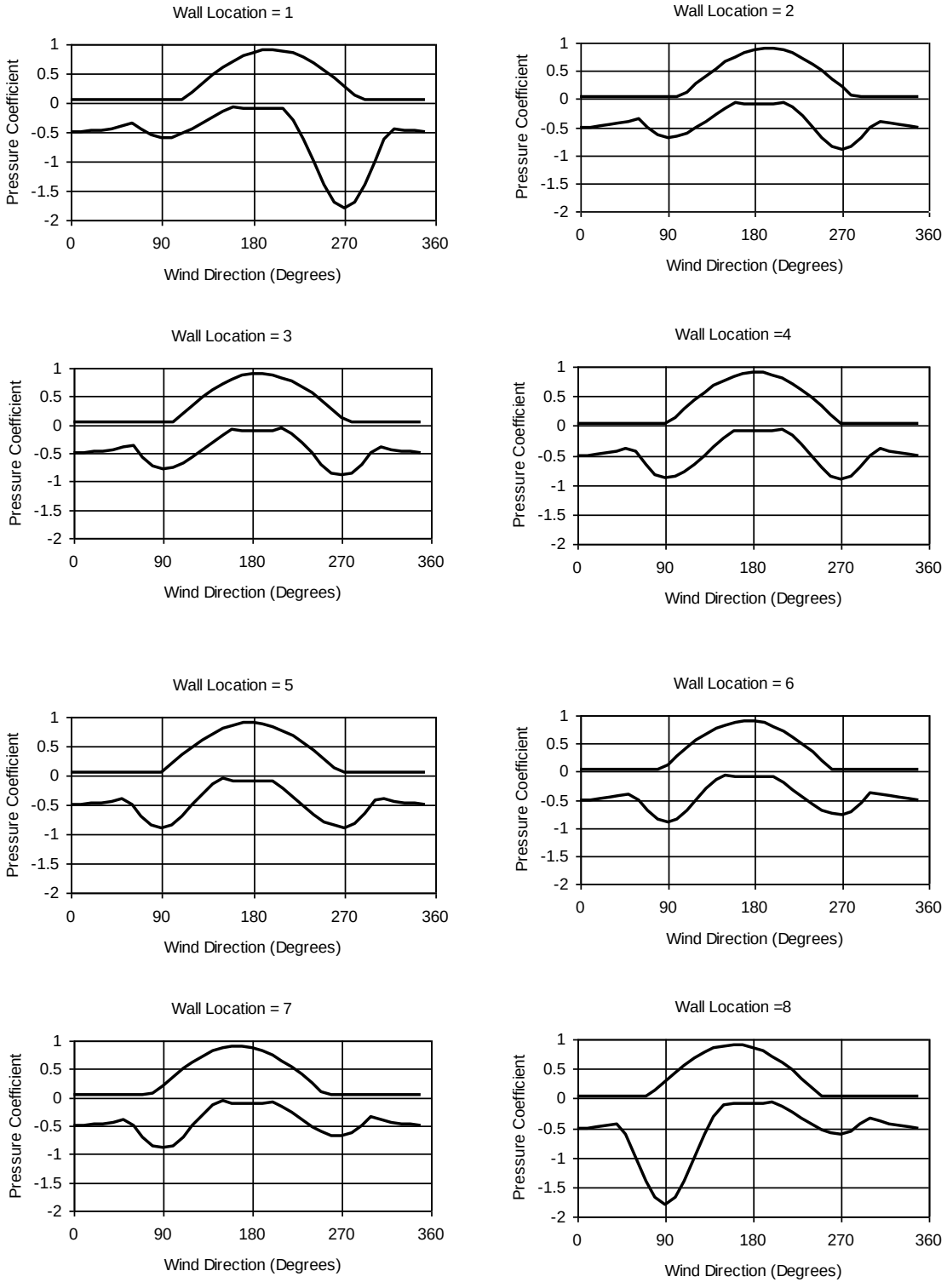

Figure 4.24. Maximum and Minimum Pressure Coefficients vs. Wind Direction Used in Modeling of a Square High-Rise Building.

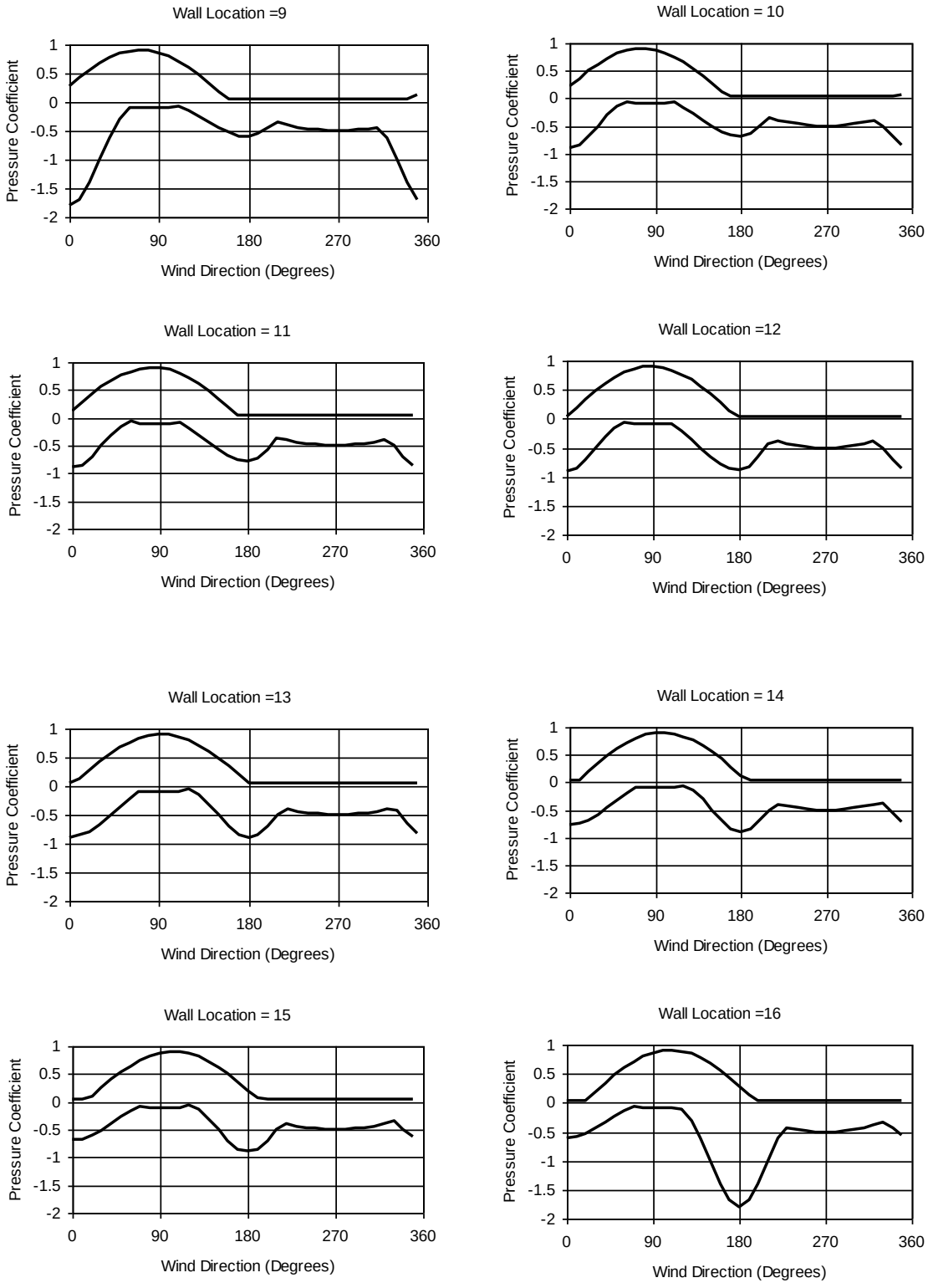

Figure 4.24. Maximum and Minimum Pressure Coefficients vs. Wind Direction Used in Modeling of a Square High-Rise Building (continued).

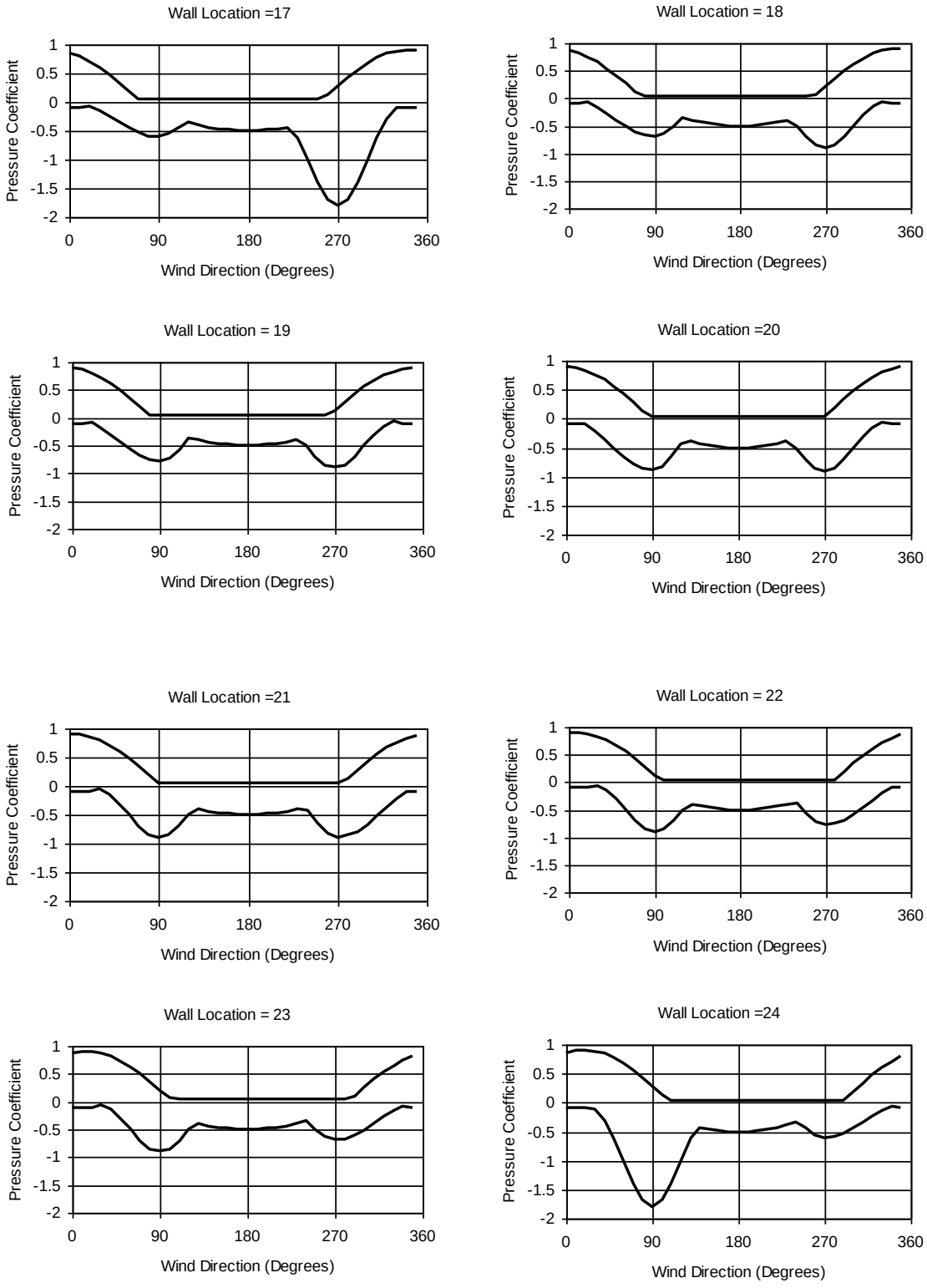

Figure 4.24. Maximum and Minimum Pressure Coefficients vs. Wind Direction Use d in Modeling of a Square High-Rise Building (continued).

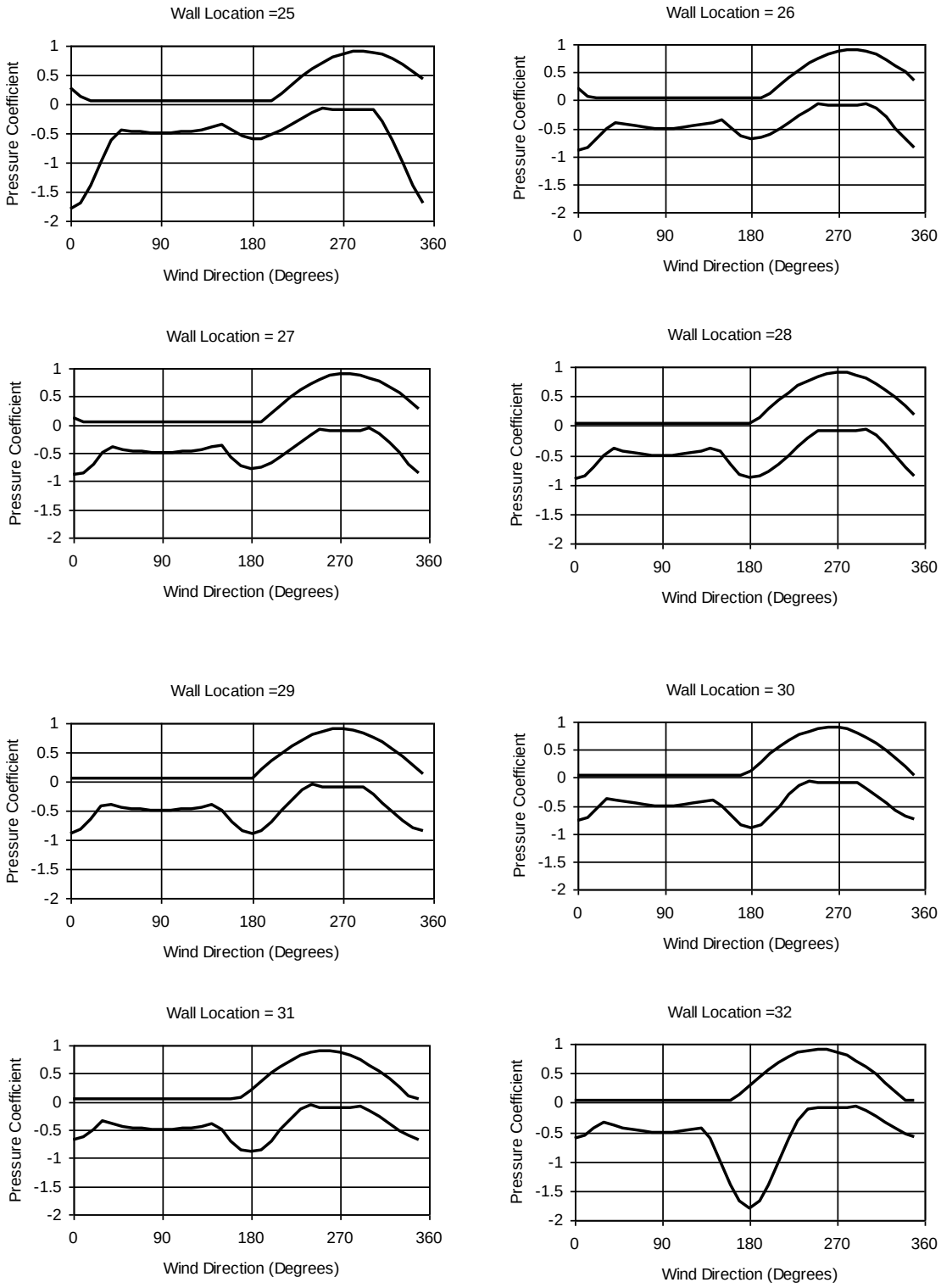

Figure 4.24. Maximum and Minimum Pressure Coefficients vs. Wind Direction Used in Modeling of a Square High-Rise Building (concluded).

Chapter 5. Windborne Debris

A significant amount of the damage to structures associated with hurricane winds is produced by windborne debris impacting the buildings and damaging the building exterior, including roof covering, windows, doors, and other openings. Two windborne debris models are used in the model. The first applies to residential environments and the second is a commercial building model for predicting the damage produced by windborne gravel. The windborne debris model used to estimate impact risk in residential environments is based on the model described in Twisdale, et al. (2000a, 2000b). The residential windborne debris model uses an explicit damage and missile transport approach. A description of the residential windborne debris model and its simplified implementation in damage simulations is provided in Section 5.1. The gravel missile model, developed to predict the damage to buildings from roof gravel missiles, is described in Section 5.2.

5.1 Windborne Debris – Residential Missile Model

Windborne Debris Simulation and Analysis. The windborne debris model developed by Twisdale, et al. (2000a, 2000b), is used to quantify the windborne debris risk in typical residential environments. The residential missile model focuses on debris produced from the roofs of residential structures since, as observed in the field after severe wind events, most of the impact damage is caused by debris that is generated from the roofs of nearby buildings. The debris types modeled include roof tiles, shingles, sheathing panels, planks (structural members) and whole roofs. The model represents the first to attempt to quantify, using physically-based models, the risk of impact damage to buildings in a residential environment.

The approach used in the residential model consists of modeling typical subdivisions, as shown for example in Figure 5.1, and impacting the buildings with debris generated from within the model subdivision. Through simulations of hurricane winds striking the subdivision, the roof components fail when the modeled wind loads exceed the component capacity. Once a component fails, it is released into the turbulent hurricane wind field, where the trajectory is computed until the component strikes either the ground or another structure. If a missile strikes the wall of another building, the impact velocity, energy and momentum are recorded. In the trajectory model, the turbulence within the hurricane wind field is modeled using an approach in which both the longitudinal and vertical components of the turbulent wind field are simulated. The missile risk simulations were performed for the subdivisions located in three different surrounding terrain environments.

For each terrain case examined, a total of 36 hurricanes were simulated for four maximum peak gust speeds of 110 mph, 130 mph, 150 mph and 170 mph, in open terrain conditions (i.e., z_0 = 0.03 m). A total of 9 different representative hurricane tracks relative to the subdivision site were simulated for each wind speed case. Typical terrain

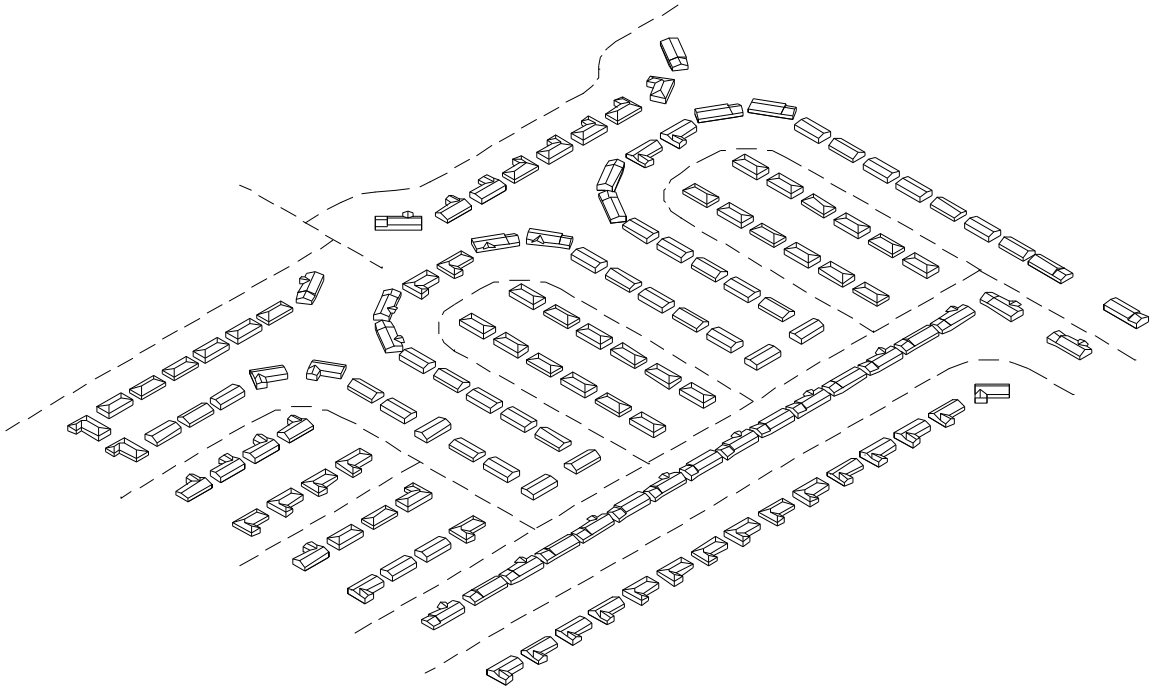

Figure 5.1. Example Model Subdivision Used in the Missile Risk Study.

conditions representative of open, suburban and treed terrain, were modeled for the wind simulation. The open terrain case was representative of the wind conditions that would be expected to be experienced on barrier islands. The suburban terrain (i.e., z_0 = 0.3 m) is representative of a residential area with relatively few tall trees to reduce the wind speeds (such as South Florida), and the treed terrain (i.e., z_0 = 1.0 m) is representative of a terrain with trees having heights greater than the heights of the buildings. This last terrain type is representative of many suburban locations along the US hurricane coastline, away from barrier islands.

Examples of the turbulent wind traces generated for open country conditions at a height of 10 m above ground are given in Figure 5.2. Also shown, in Figure 5.2, is the "gust speed envelope" represented by the solid line. This envelope is defined as the mean wind speed multiplied by the three second gust factor. A comparison of the turbulent wind trace and the theoretical envelope shows that the peak gusts produced by the turbulent model equal or slightly exceed the envelope value about three to four times per hour.

Upon completing the wind speed simulations (i.e., nine hurricanes), information on the total number of hits and associated energy and momentum levels are available. Given the information on the expected number of missile impacts on the walls of a structure, the risk of damage to an opening, $P_V(D)$ for a given wind speed, V can be obtained from:

$$P_V(D) = 1 - exp\left[-\lambda q\left(1 - P(\xi < \xi_d)\right)\right] \tag{5.1}$$

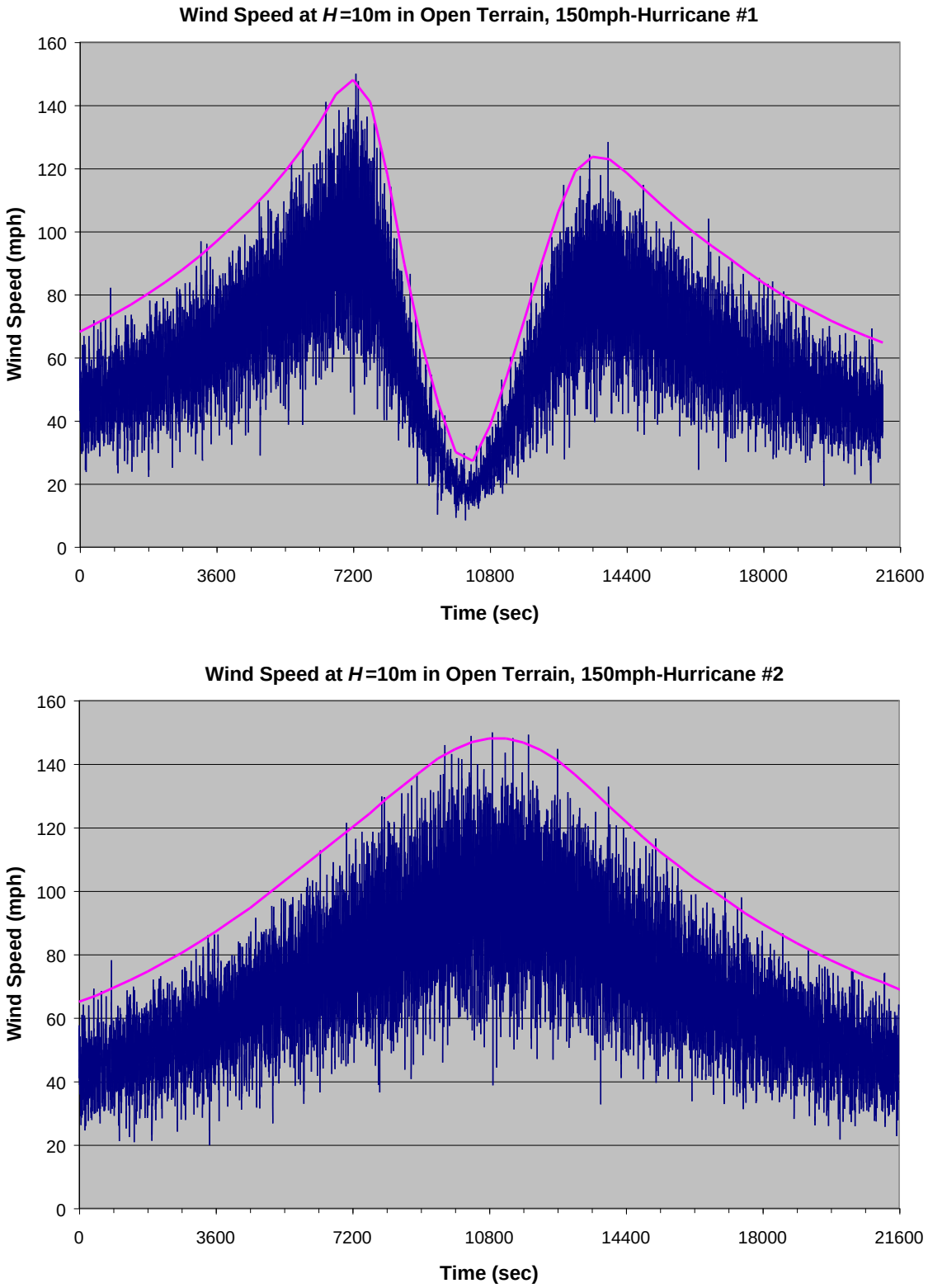

Figure 5.2. Example Hurricane Wind Speed Traces Used for the 150 mph Case.

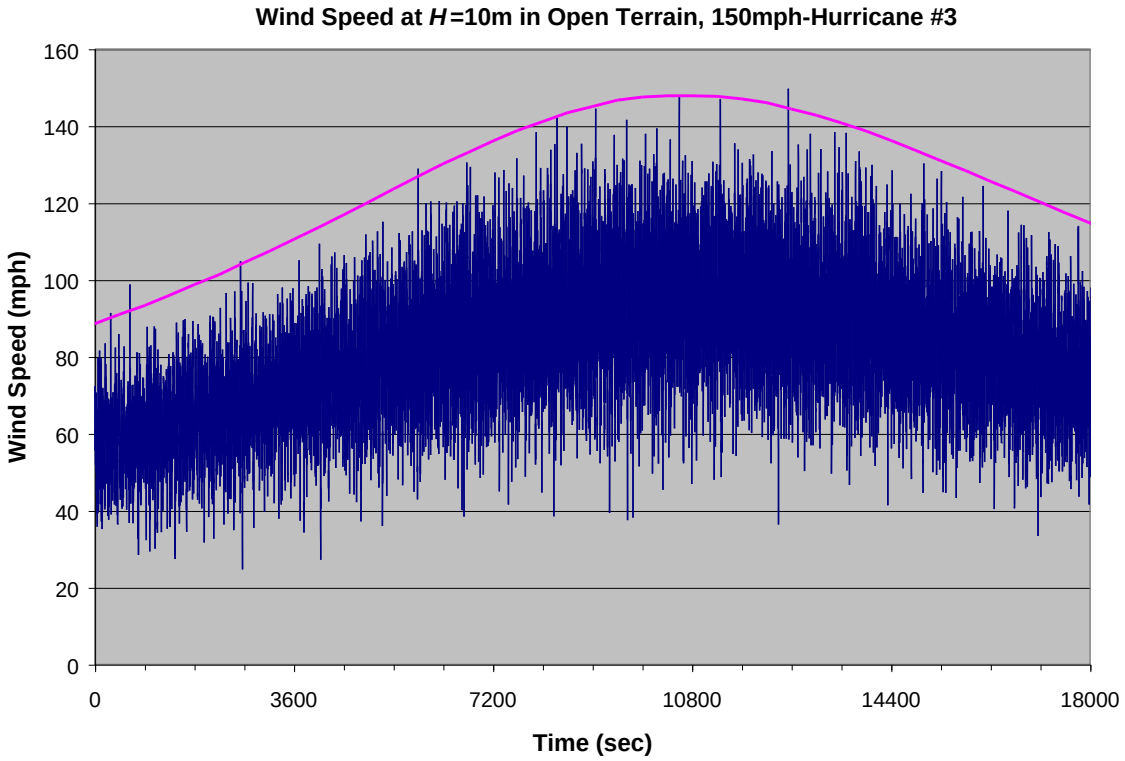

Figure 5.2 . Example Hurricane Wind Speed Traces Used for the 150 mph Case (concluded).

where ξ_d is the energy or momentum level assumed to produce damage, q is the fraction of the building surface occupied by windows and glass doors, and λ represents the mean number of missile impacts per building. $P(\xi < \xi_d)$ is the probability for the impact energy or momentum (ξ) to be less than the damage threshold value (ξ_d) given an impact. The probability of no damage, R is expressed in Equation 5.2:

$$R = 1 - P_V(D) = exp\left[-\lambda q\left(1 - P(\xi < \xi_d)\right)\right] . \quad (5.2)$$

Using Equation 5.2, probability curves for R vs. wind speed were developed, which indicate the energy or momentum level a window/door must be able to withstand in order to achieve a given probability level of no damage. Figure 5.3 shows an example of the reliability curves generated for one of the cases examined in the windborne debris risk study. The example in Figure 5.3 presents reliability curves for several impact energies and a q value of 0.2.

Implementation of the Windborne Debris Model. In the development of the damage and loss functions described herein, it is not possible to explicitly model the windborne debris on a storm-by-storm basis using the detailed first principles based trajectory and impact model described above because of computer run-time limitations. The simplified windborne debris model makes use of the results of the explicit study using an analytical model which yields results similar to those obtained from the explicit model.

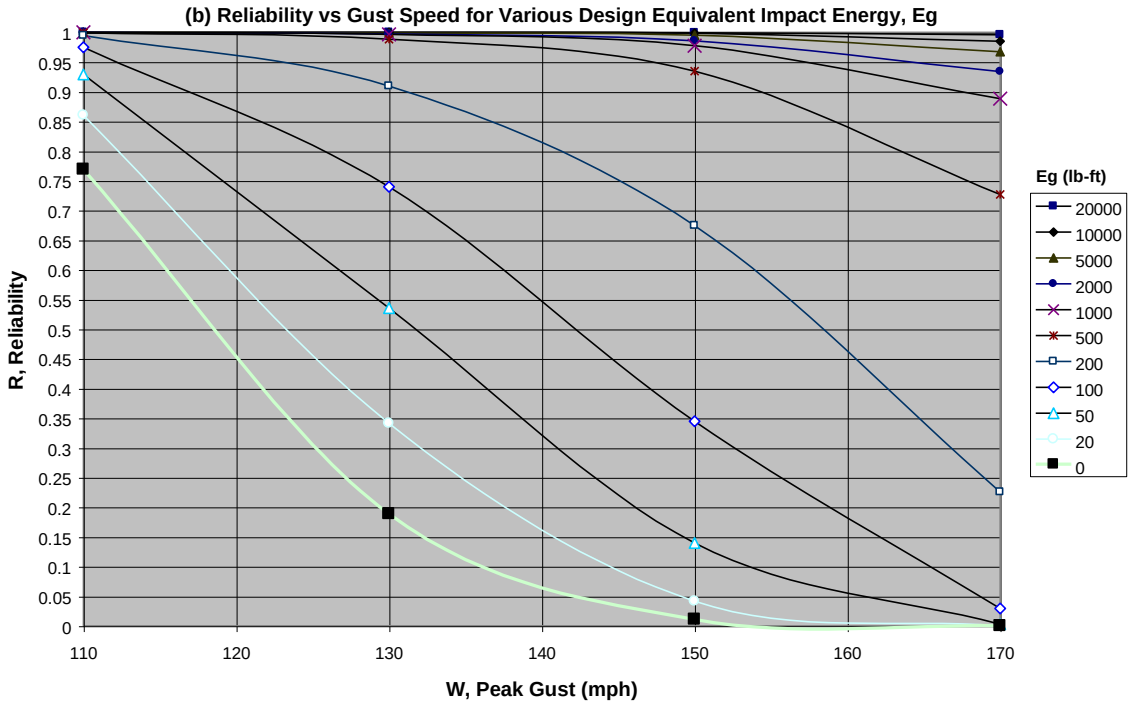

Figure 5.3. Example Energy Reliability Curves Derived for a Subdivision Comprised of Single Story Homes with Asphalt Shingle Roofs.

Using the simplified debris modeling approach, at each time step in a hurricane simulation, the number of missiles impacting the wall is given as

$$N_w = a\theta P_1(v)N_2(v) \tag{5.3}$$

where a is a constant, θ is a constant representing the number, density and size of the missile source buildings in a 45° sector, $P_1(v)$ is the fraction of missiles that hit the wall for the wind speed v, and $N_2(v)$ represents the number of missiles generated at each time step. Using a value of θ equal to unity for the eight 45° sectors represents a missile environment similar to that used in the explicit study. Increasing or decreasing θ has the effect of changing the density of the surrounding homes. The function $P_1(v)$ is obtained directly from the explicit missile simulation, whereas the function $N_2(v)$ is obtained by performing roof damage simulations using the same damage model used in the missile study, but for a larger number of wind speeds. The fraction of missiles generated that impact another building is a linear function of wind speed, whereas the number of missiles generated at each time step increases more rapidly.

Given that the building is impacted by a missile at a given time step, the impact energy is determined by sampling from Weibull distribution in the form:

$$P_e(e < E) = 1 - exp\left(-(E/C)^k\right) \tag{5.4}$$

where the Weibull parameters *C* and *k* were determined by fitting the energy exceedance data derived from the physically-based debris model. Both of the Weibull parameters are functions of the peak gust wind speed.

Note that the building can only be impacted by missiles generated from within a 90° sector, centered on a vector normal to the wall surface, and the wind must be approaching from within this sector. These criteria ensure that walls can be impacted by missiles only when the wind is blowing towards the wall, and only when there are missile sources upwind of the structure.

Figure 5.4 shows a comparison of the reliability curves generated from the physically-based model to those derived using the simplified model. In this figure, the points shown without lines connecting the data points represent those derived from the simplified model, whereas those shown with lines connecting the data points represent the original data as produced by the explicit missile simulation.

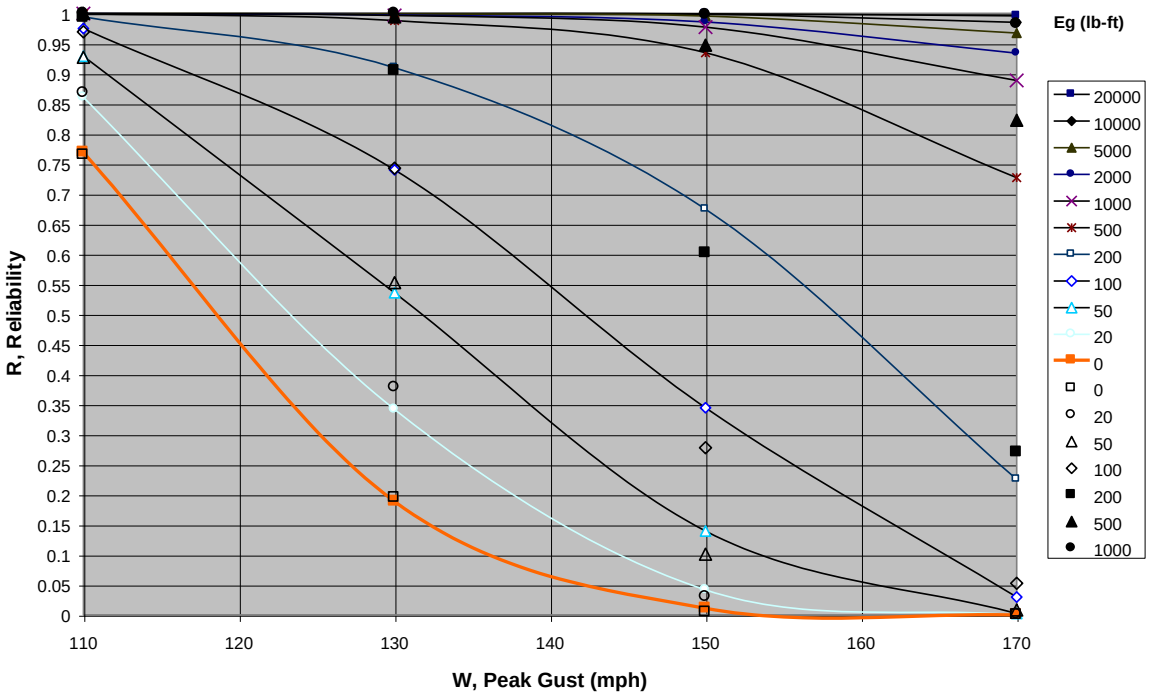

Figure 5.4. Comparison of Reliability Curves Derived from the Explicit Missile (lines) Simulation to Those Obtained from the Simplified Model (points only).

The comparisons of the two sets of reliability curves show reasonable agreement, for all impact energy levels for wind speeds less than 130 mph. In the 150 mph case, the simplified model tends to slightly underestimate the reliability (i.e., overestimate the probability of missile impact), and at a wind speed of 170 mph, the reverse is true. In general, for missile impact energies less than 500 ft-lbs, the simplified model satisfactorily reproduces the results obtained from the explicit model. For very high

impact energies (~1000 ft-lbs), the simplified model underestimates the frequency of impact, as indicated by the overestimate in the computed reliability levels. This underestimate of the frequency of very high energy impacts is not of great concern, since damage to window protection (discussed later) occurs at energies much lower than 1000 ft-lbs.

In summary, a simplified, fast running missile impact model is used which approximates the results derived with an explicit modeling approach. The simplified model, which yields reasonable estimates of the windborne debris risk, is used in the building damage model to develop the fast-running Hazus damage and loss functions.

5.2 Windborne Debris – Commercial Missile Model

The study on the risk of damage to commercial buildings by windborne gravel debris consists of two components. The first component is a mathematical simulation of the debris generation, transport and impact on building envelopes during a hurricane passage. This windborne gravel debris model simulates the characteristic layout of the gravel layers, the turbulent hurricane wind trace, local wind fields on the roof, wind action on gravel stones, gravel scour and transport, and the eventual interception of its trajectory with a building's envelope (or with the ground). Throughout a hurricane, the simulation provides detailed records of individual gravel missiles generated, their origin location, transport distance, impact location and impact momentum, as well as the characteristic layout of the gravel remaining on the roof. This model is a stand-alone program, and can be used for specific case studies or used to derive information for gravel debris risk assessment for generic settings. The development of this model, along with its validation against three field-observed cases, is described in detail in Section 5.2.1. It is demonstrated that the model agrees with field observations reasonably well.

The second component of the study aims at constructing a fast-running risk model to estimate the probability of damage to building envelope by windborne gravel debris given the impact resistance capacity of the target surfaces. The fast-running debris risk model estimates the expected number and location of fenestration elements breached by debris within each short time interval in order to interactively account for the rainwater penetration and internal pressure change in a building. The model utilizes the previous analytical formulation on debris risk (Twisdale, et. al, 2000a, 2000b) and the above physical modeling on generic configurations to provide inputs (for example, the expected number of impacts and impact momentum) required by the analytical risk formulation. From the simulation records, the number of impacts per unit area within a time interval and the impact momentum distribution for a target surface element, such as a window, with specified location and orientation relative to the source are derived. The derived number of impacts and momentum distribution are functions of the reference wind speed, wind direction, terrain, height and area of gravel source roof, depth of the gravel ballast layer and gravel size. Based on this information, a set of simplified expressions describing the relationships between the variables yields a fast-running debris module suitable for incorporation into the damage model. This second part of the model is described in Section 5.2.2.

5.2.1 Windborne Gravel Debris Simulation and Case Studies

Flat, built-up roofs and ballasted membrane roofs are commonly seen on high-rise and low-rise commercial buildings in urban and suburban areas. Gravel used on these roofs often becomes windborne missiles during high winds. This problem has been observed and reported by many field investigators (e.g., Minor, et al., 1978; Minor, 1994; Minor and Behr, 1993a, 1993b; and Behr and Minor, 1994). This section describes the computer modeling of gravel missile generation (scour and blow-off), transport trajectory and physical impact on surfaces. Three case studies are presented along with comparisons against field observations.

Scope of the Simulation. The problem of debris generation, transport and impact involves many variables. The present model includes the effects of the mean hurricane wind trace (speed and direction variation with time), correlated three-dimensional turbulence components, building geometry and street layout, roof gravel configuration (diameter distribution and thickness), as well as upstream terrain influences. Local wind velocity fields over the roof and in the wake behind the buildings are also approximated. The gravel scour pattern, trajectories and impact statistics are used to compute the information required for model calibration and for risk prediction.

Missile Generation from Roof Gravel. Within an assembly of gravel stones of nearly spherical shape and variable diameters loosely lying on a flat bed, an individual stone on the top layer will be subject to a drag, an uplift, and an overturning moment caused by the wind blowing over the surface. Gravity and the constraint of other stones balance these wind forces; however, when the wind speed increases and exceeds some threshold value, the wind forces overcome these constraints. At this point, the stone starts to intermittently rotate and shift horizontally. At another slightly higher threshold wind speed, the stone will be lifted and blown away. Both the first and second threshold wind speeds have been shown to be proportional to the square root of the stone diameter (Kind and Wardlaw, 1984). The model developed here considers the second threshold wind speed, since only at this higher wind speed is the stone released into the wind field.

In determining the local wind speeds on the roof surface, the flow separation and vortex induced velocity field is included in the model as a function of building geometry and the free stream wind speed and direction. An example of the horizontal component of the mean wind velocity on the roof surface of a cube-shaped building is shown in Figure 5.5 for an oblique on-coming wind. Figure 5.5 also shows a photograph of stream lines obtained from a flow visualization test given for comparison. The streamline patterns are in a good agreement.

The resulting scour pattern is illustrated in Figure 5.6 and compared with qualitative wind tunnel and field observations (Kind and Wardlaw, 1984). It is seen that the computer model reproduces the typical two-lobed scour pattern under oblique winds. Note that the wind tunnel model of Kind and Wardlaw has a low parapet so that the scour pattern shifts slightly downstream. Moreover, their model represents a low-rise building such that the high turbulence in the lower part of the simulated boundary layer flow reduces the sharpness of the two-lobed pattern compared to the field observation and the computer model results which are both for multi-story buildings (low turbulence intensity).

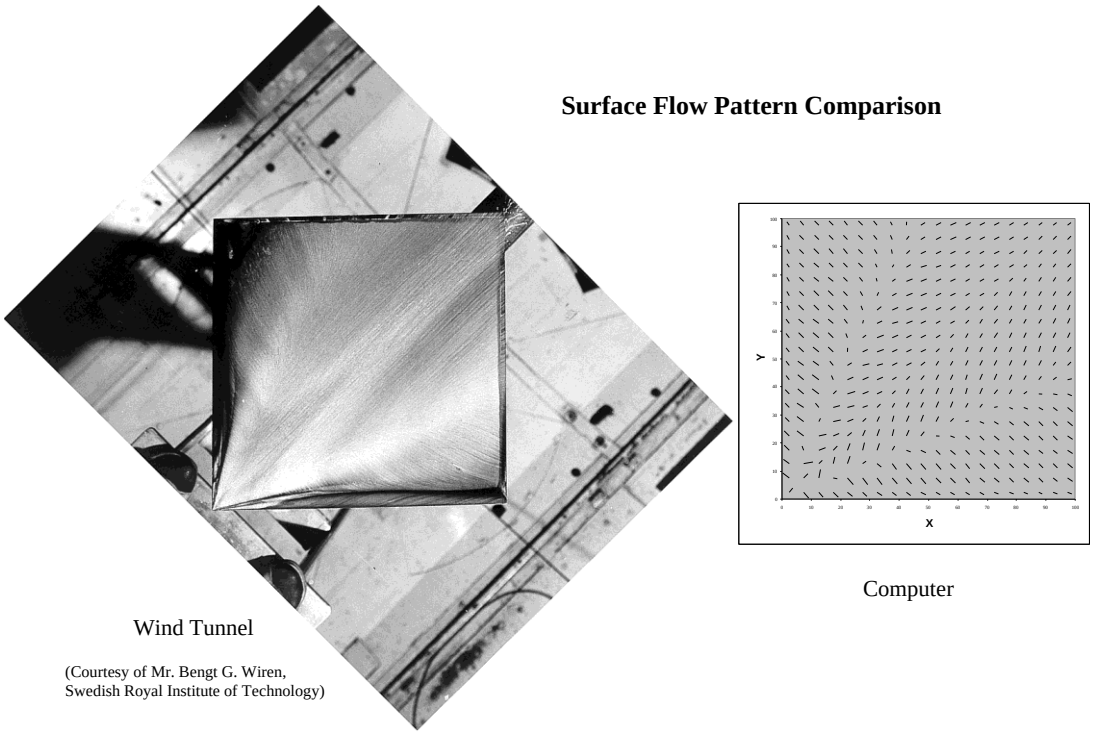

Figure 5.5. Example of Computer-Modeled Surface Flow Pattern Compared with Wind Tunnel Observation.

Missile Transport in the Wind Field. When gravel is released into the three-dimensional wind field, it is transported by the turbulent wind. This is modeled by numerically solving the equation of motion for a particle of mass, with the wind force acting on the gravel updated as a function of location and time. The influence of the vortex flow over the rooftop and the wake flow downstream of the buildings are incorporated with the on-coming turbulent wind to obtain a resultant wind field.

As an example, the computed trajectory for a sample gravel missile generated from the roof of a cube-shaped building is illustrated in Figure 5.7 for a 45° oblique wind. The gravel missile is first moved sideways toward one of the upstream roof edges by the spiral vortex flow near the roof surface. Kind and Wardlaw's (1984) wind tunnel experiments on gravel scour and blow-off also indicate that gravel missiles generated from the front portion of the roof would leave the roof over the upstream edges. After it leaves the roof, the trajectory starts to gradually bend into the on-coming wind. The gravel missiles generated from the downstream portion of the roof would have less curved trajectories since the spiral vortex flow will be weakened downstream.

Missile Impact on Building Envelopes. The trajectory of the gravel missile will eventually intersect with a surface, either the ground or a building envelope, which are geometrically defined on a global coordinate frame. The impact location and velocity are recorded. The impact momentum and energy are then calculated for each gravel missile of a given mass. This information can be used to derive statistical distributions of impact

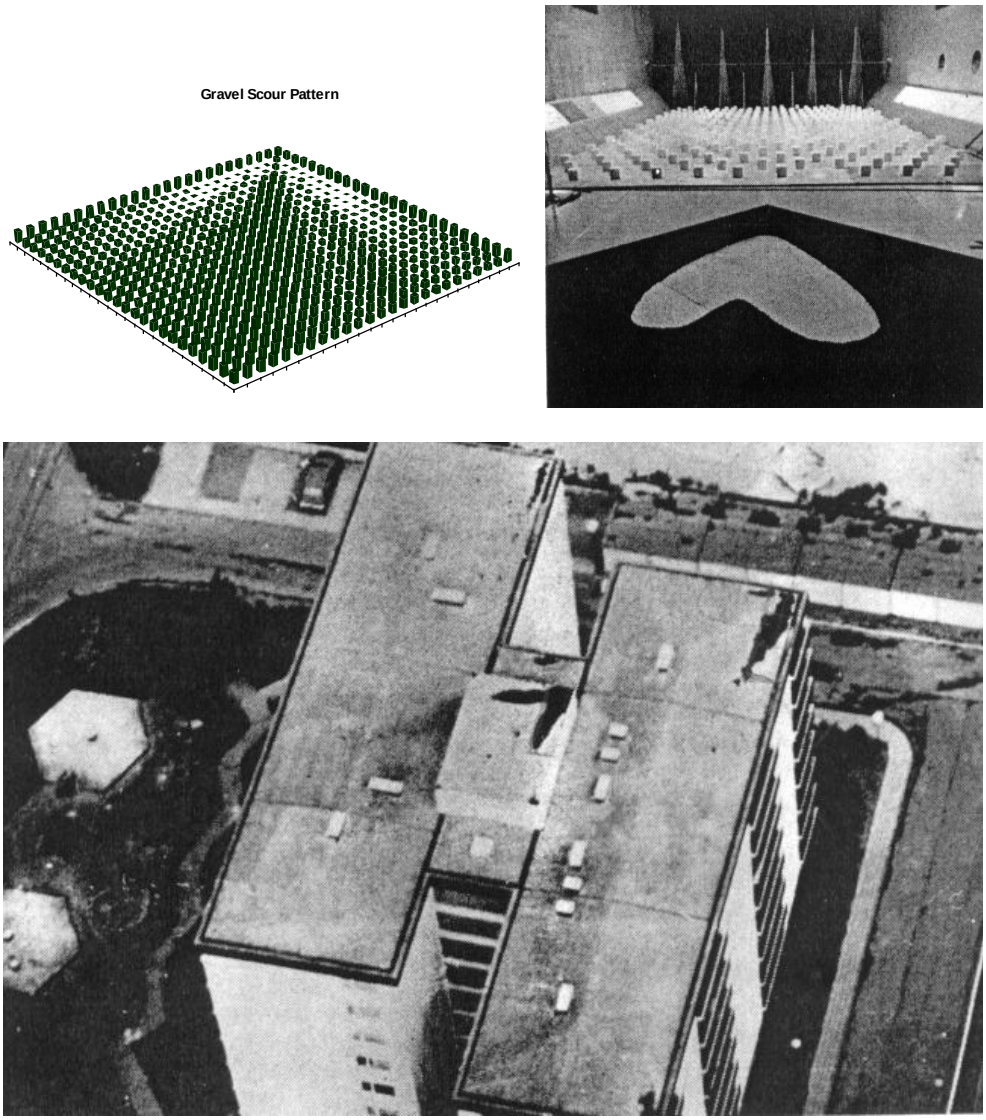

Figure 5.6. Example of Gravel Scour Pattern Compared with Field and Experimental Observations.

location, momentum or energy, and number of impacts on a specific area of the building envelope, which are subsequently used to predict the risk of building envelope breach during a storm. The recorded impact results for specific building complexes can also be used to perform model calibration and validation studies by comparing them with the field observed data for the same buildings and environments.

Case Study 1 – Kendall, Florida, Hurricane Andrew. During Hurricane Andrew, the downstream buildings in a high-rise complex in Kendall, Florida (Figure 5.8), suffered severe windborne debris impact damage to the windows, which has been investigated and documented by several researchers (e.g., Smith, 1999; Behr and Minor, 1994; and Minor, 1994). This case provides a basis for examining the results obtained with the windborne debris model.

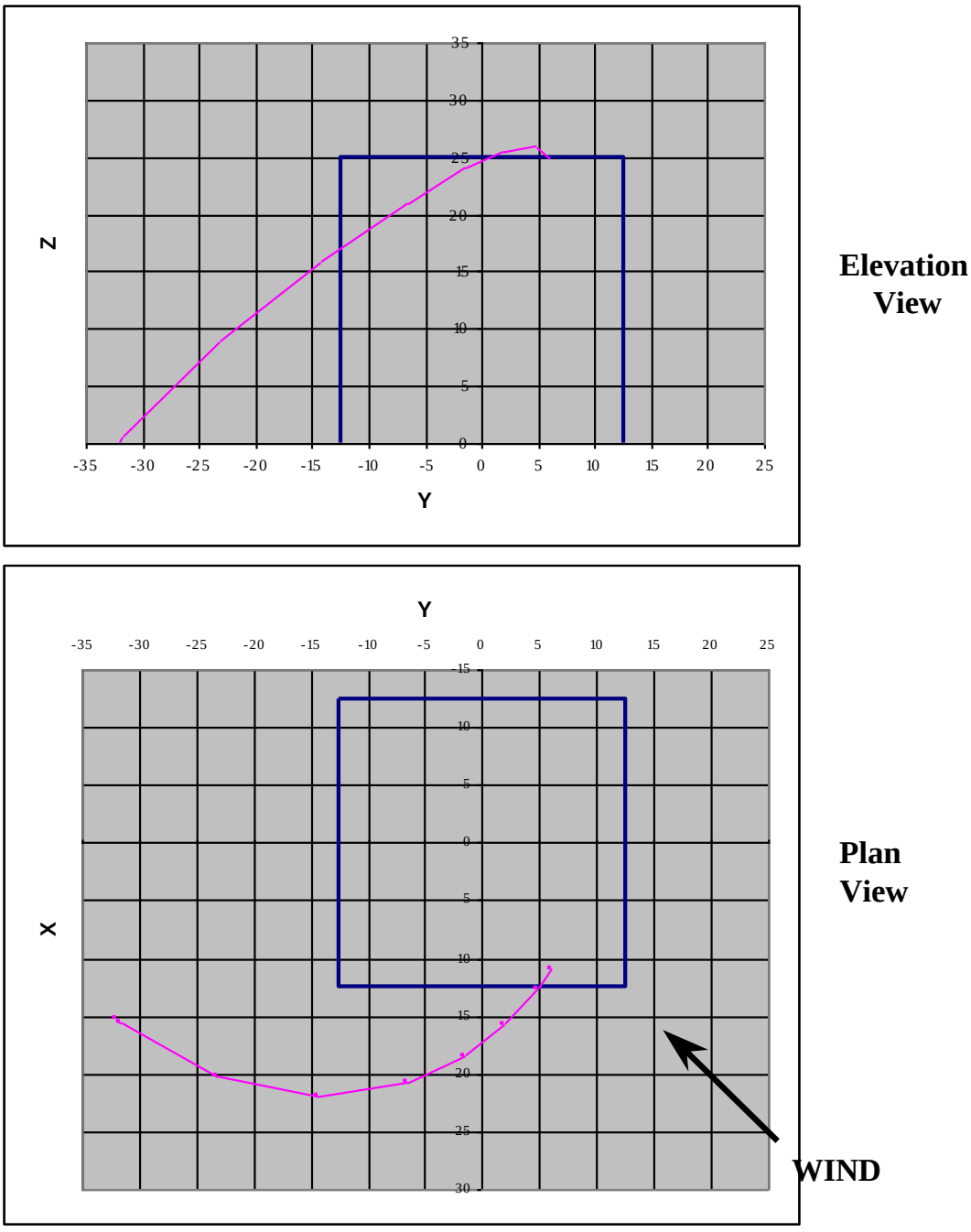

Figure 5.7. Example of Gravel Missile Trajectory.

The plan of the complex is shown in Figure 5.9. The missile source is the Marriott Hotel roof gravel ballast. The gravel missiles were generated from the two penthouse roofs only, since the other parts of the roof have tall parapets that prevented gravel from leaving the roof. For the case study, a Hurricane Andrew mean wind trace was re-created for the site using the hurricane model described in Chapter 2. The mean wind direction changed from northerly to southeasterly in a time period of about 2.5 hours during which

Figure 5.8. The Marriott-Datran Complex in Kendall, Florida.

open terrain 10 m-height peak gust winds are above 90 mph. The largest peak gusts reached 140 mph when the mean wind direction was approximately normal to the northeast walls of the buildings. Typical 3-dimensional turbulence components for a terrain roughness length of 0.5 m (slightly rougher than standard suburban) were simulated. The mean diameter of the roof gravel was determined to be 12 mm from survey records reported in Behr and Minor (1994) and Smith (1999) with a distribution given in ASTM Standards, Designation D1863-93 (Re-approved 1996) for Size # 67A. The depth of the gravel ballast layer on the roof was 76 mm (Behr and Minor, 1994). The window glass on the downstream buildings is 6 mm thick fully tempered monolithic glass (Behr and Minor, 1994) that provides an estimated threshold average breakage momentum of 0.1 kg-m/s (Minor, 1994).

The impact results obtained with the computer model are shown in Figure 5.10 for the northeast walls of the two downstream buildings, where each dot represents a damaging hit. A damaging hit is an impact by a gravel missile with its momentum's component normal to the wall being larger than the 0.1 kg-m/s threshold. The coordinate grid approximately corresponds to the window grid, one cell containing one window. One or more damaging hits within a cell yield one count of damaged window. Note that, for the case where windows occupy only a percentage of the wall area such as these buildings, only the corresponding percentage of generated gravel missiles that are randomly sampled is used for damage counts. The results shown in Figure 5.10 are these sampled hits. The photographs (Minor, 1994; Smith, 1999) documenting the window breaches are shown in Figure 5.11. For the northeast wall of Datran Tower I, the simulation yields a window failure rate of 96.7% for the upper 10 floors, in good agreement with the observed value of 97.4% as counted from Figure 5.10(a) for the same part of the wall.

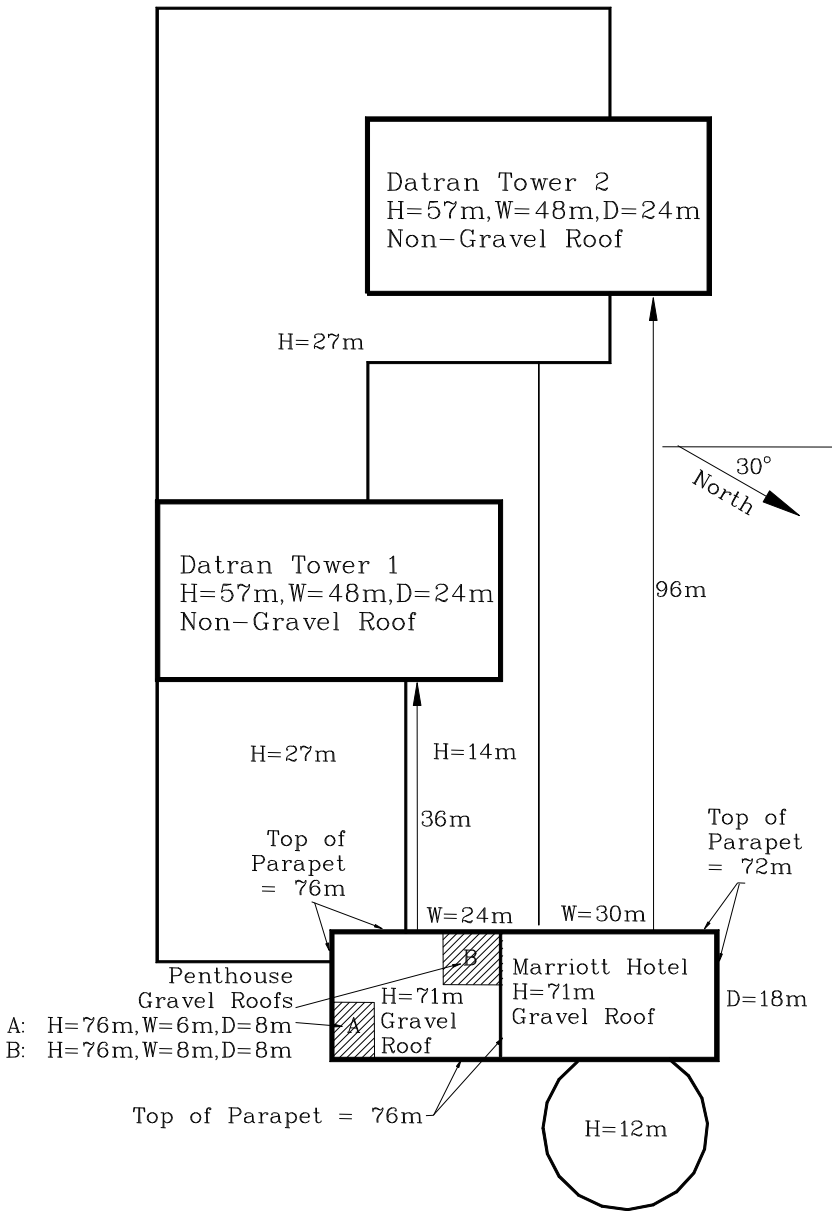

Figure 5.9. Approximate Plan of the Marriott-Datran Complex.

Other photos were used to aid the counting for the upper left corner of the wall and to confirm the counts on other parts, while the lower few floors were omitted from the counting because the damage state cannot be determined for this small area using any of the available photos or reports. For the northeast wall of Datran Tower II, the simulation shows a failure rate of 61.9% for the upper 10 stories. This is also consistent with the observed damage-state of 63.2% for the same part as determined from Figure 5.11(b). Again, window breakage on the lower right corner of Datran Tower II cannot be clearly identified from the photos presented here, nor with other available photos and reports.

It is seen that the agreement between the modeled and observed damage states are remarkably good for this case.

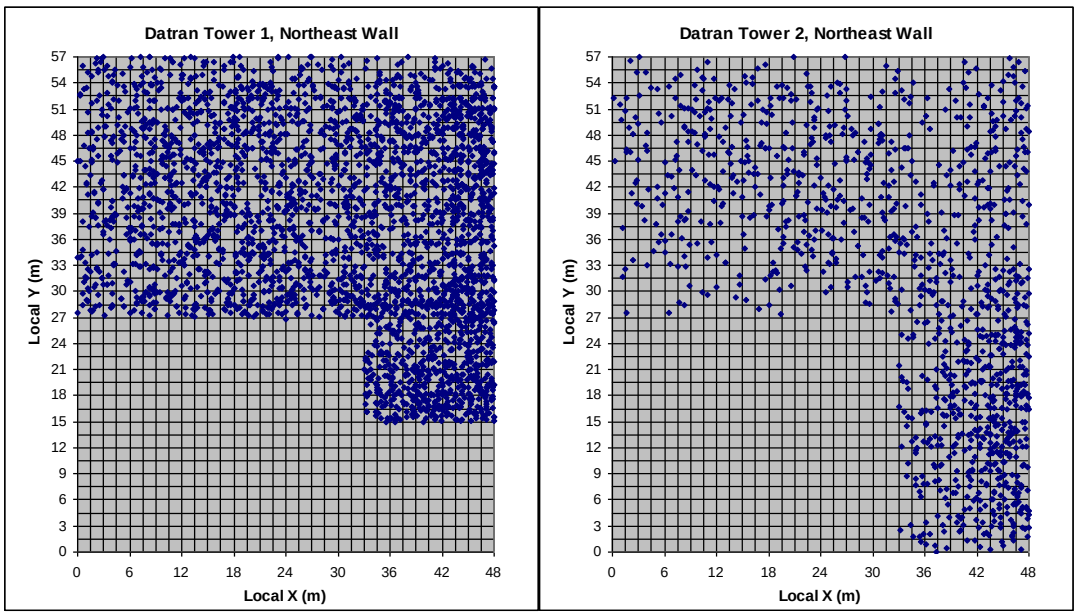

(a) (b)

Figure 5.10. Impacts on Walls with Momentum Exceeding the Threshold for Damage.

Case Study 2 – Downtown Houston, Texas, Hurricane Alicia. For this case, only partial information is available on the details of the missile sources, target glazing properties and damage states. Assumptions on some of the required information were thus made to facilitate the simulation. A qualitative comparison of simulated and observed glass damage is presented.

Figures 5.12 through 5.14 show the area in downtown Houston for which the simulations were carried out and compared with available observations. The seven buildings bounded by McKinney and Polk Streets in the NE to SW direction and by Milam and Smith Streets in the SE to NW direction were simulated for missile source and/or impact damage. The plan geometry of these buildings was modeled as shown in Figure 5.15. The available information and the assumed values of required inputs are listed in Table 5. 1.

The time-varying hurricane wind speed and direction trace at the site was re-created using the hurricane model described in Chapter 2. The site was modeled as an urban terrain with a roughness length being about 1 m for all upstream directions. The strong winds were from a quadrant centered on the east. The peak gust wind speed was estimated to be about 56 m/s (125 mph) at the roof height (110 m) of the gravel missile source buildings.

The results of the simulation are presented in Table 5.2, in comparison with the available observations. The overall agreement between the simulated results and the observations is reasonable.

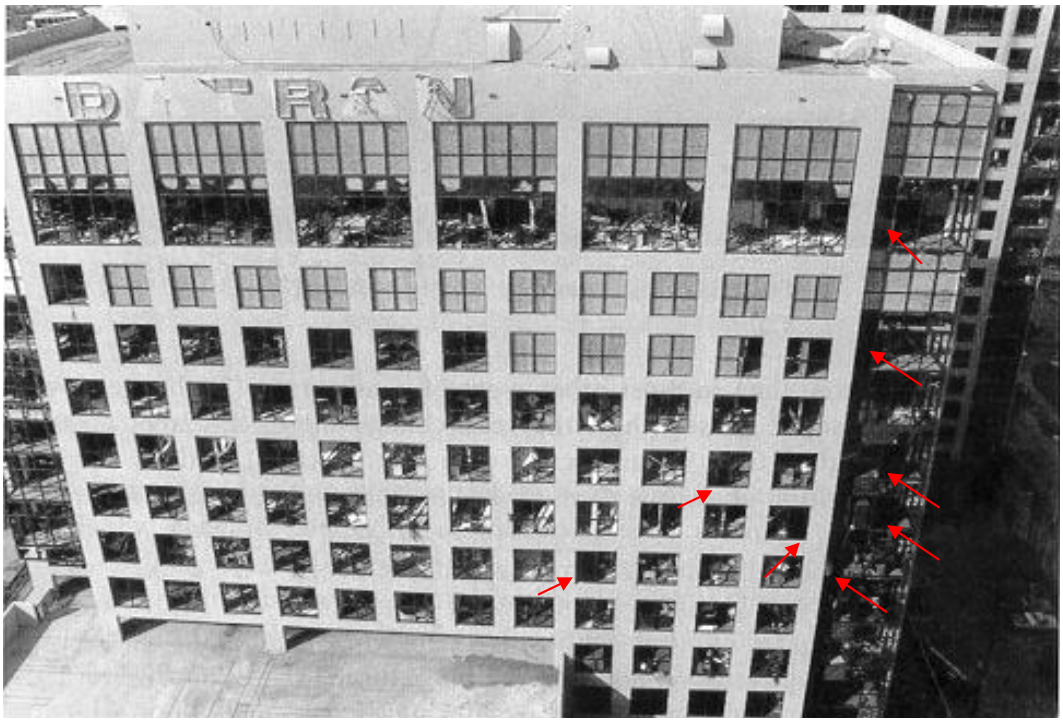

(a) Datran Tower I, Plywood Boarding of Broken Windows Underway (Picture from Minor, 1994). Arrows indicate windows that were not damaged.

(b) Datran Towers I and II, Plywood Boarding of Broken Windows Complete Except for Lower Floors (Courtesy of TLSmith Consulting).

Figure 5.11. Damage Scenarios for Datran Towers I and II Downstream of the Marriott Hotel.

Figure 5.12. General View of the Houston Central Business District (Kareem and Stevens, 1985).

Case Study 3 – Williston School, Wilmington, NC, Hurricane Bonnie. The Williston School two-building complex represents a case of low-rise buildings. Information on the details of the missile sources, target glazing properties and damage states, was collected shortly after Hurricane Bonnie's landfall at the North Carolina coast.

Figure 5.16 shows the complex (looking north). The taller portion of the building on the right (east) was the major source of gravel missiles that hit the windward face of the 2-story building on the left (west). The 3-story building located at the north end of the complex (the far end in the picture) was not a missile source, nor could it act as a shielding building, so it was not included in the simulation. Flow interference from this building was expected to be small and was neglected in the simulation. Figure 5.17 shows the windward face of the main missile source building in the complex (looking southwest), which was the upstream building during the high wind period of Hurricane Bonnie when it was hovered over the Wilmington area. Figure 5.18 indicates the sizes of the roof gravel on this building. The same type of roof gravel was also used on other buildings of the complex; however, the majority of the glass damage is believed to have been caused by gravel originating from the roof of the upstream building, as indicated by both the field observations and the simulation. Figure 19 shows the glass damage on the downstream building, in which part of the roof of the upstream building is also seen. The geometry of the modeled complex is shown in Figure 5.20. The input data for the simulation are listed in Table 5.3.

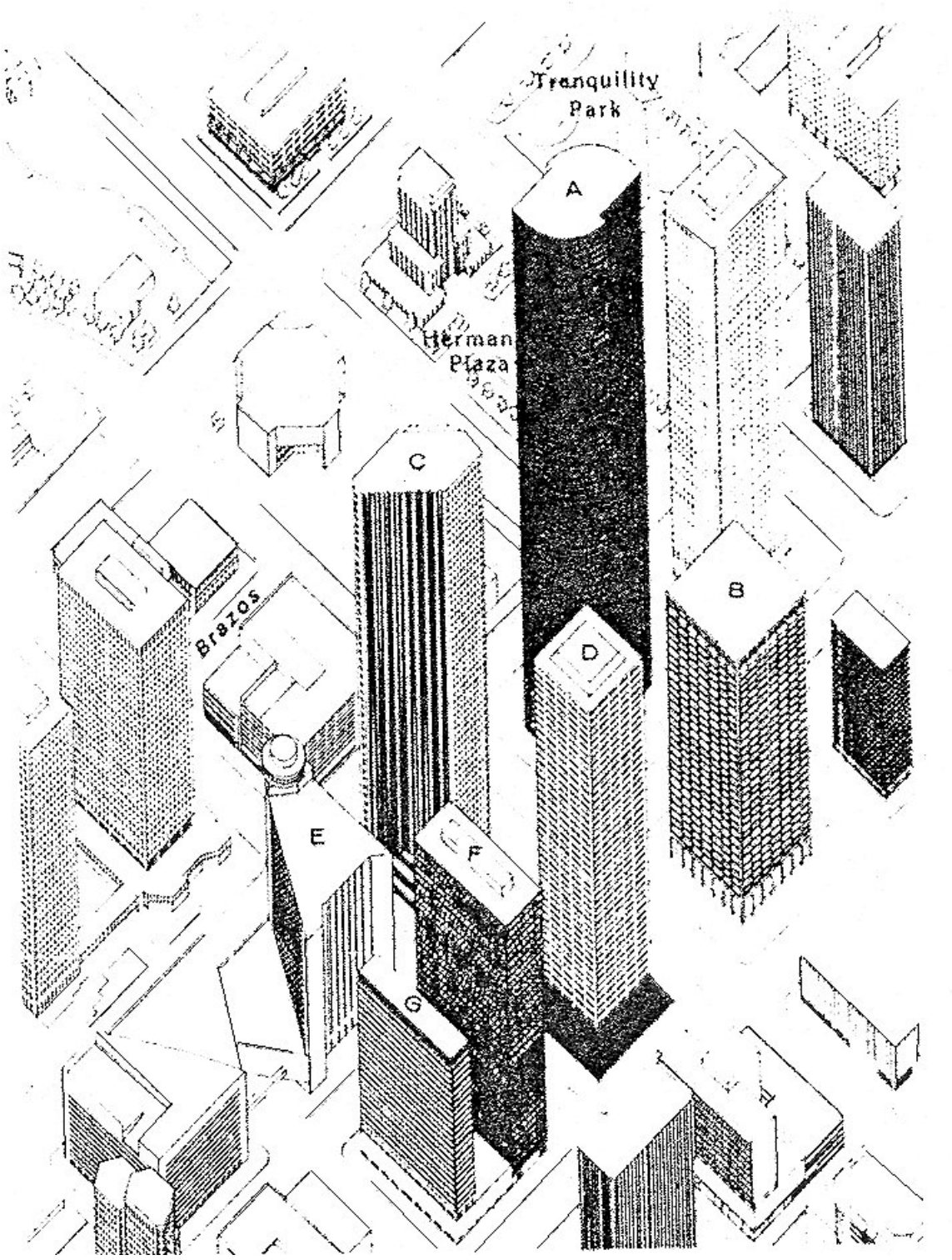

Figure 5.13. Aerial Perspective of Damaged High-Rise Buildings (Beason, et al., 1984).

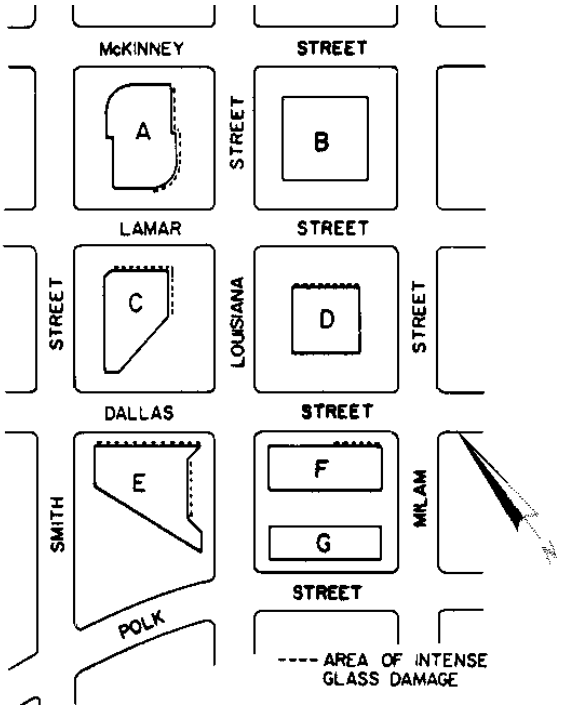

Figure 5.14. Plan View of Damaged High-Rise Building Towers (Beason, et al., 1984).

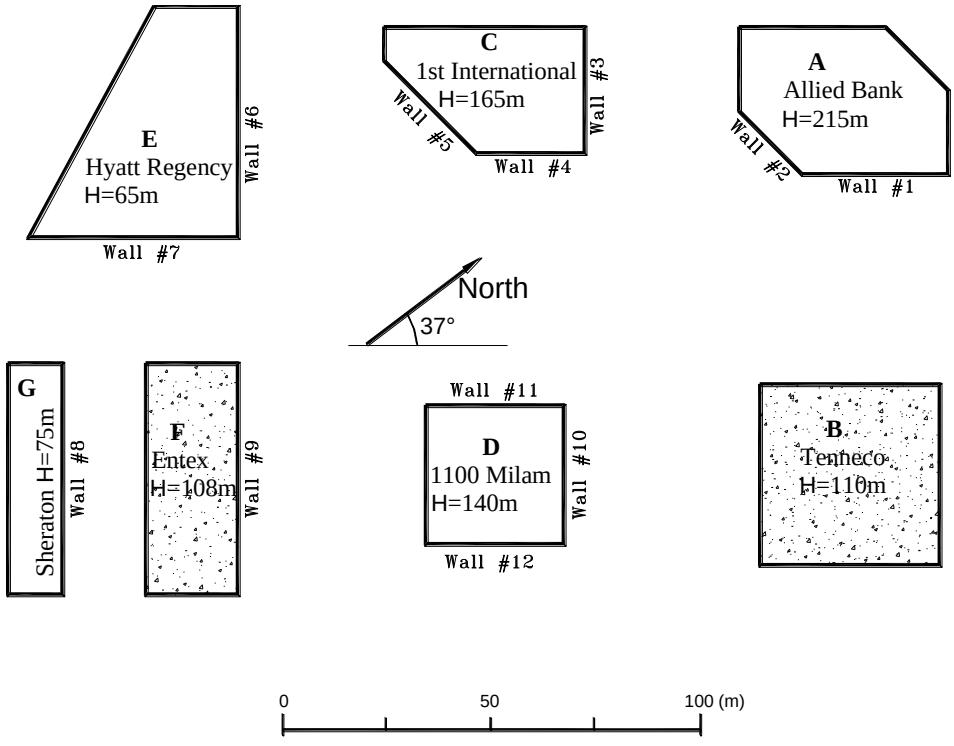

Figure 5.15. Plan Geometry of the Modeled Buildings in the Houston Downtown Central Business District.

Table 5.1. Basic Inputs of Missile Sources (Roof Gravel) and Target Glazing Properties

	Roof Gravel		Glazing					
	Mean Depth (cm)	Mean Diameter (cm)	Glaze/ Wall (%)	Ave. Size (m x m)	Thkns x Panes (cm x #)	Glass Treatment	Impact Resistance (kg-m/s)	Bldg. Height(m)
Allied Bank Plaza			100	1 x 1	0.6 x 2	T(2)	0.08	215
Tenneco Building	2(1)	1						110
First International Plaza			40	2×1.5	0.6×2	A	0.05	165
1100 Milam			60	1.8×1	0.6×2	A	0.05	140
Hyatt Regency Hotel			45	2×2	0.6×2	A	0.05	65
Entex Building	1	1	100	1.5×1	0.6×2	A	0.05	108
Sheraton Houston Hotel			40	1.2×1	0.6×2	A	0.05	75

NOTE: (1) Shaded cells indicate assumed values.
(2) T – Tempered, A – Annealed and H – Heat Strengthened.

Table 5.2. Number of Damaged Windows: Simulation vs. Available Observations

Building	Wall No.	Wall Height (m)	Wall Width (m)	Resistance (kg-m/s)	Total No. Window Panes	Simulated No. Panes Damaged	Simulated % Damaged	Total No. Simulated Damaged Panes per Building	Observed No. Panes Damaged
Allied Bank Plaza	1	215	35	0.08	7500	539	7.2		400~1000
	2	215	21	0.08	4500	258	5.7	707	(Kareem)
First International Plaza	3	165	30	0.05	1300	143	11.0		650
	4	165	25	0.05	1100	200	18.2		(Kareem)
	5	165	32	0.05	1400	0	0.0	491	
Hyatt-Regency	6	65	55	0.05	1200	36	3.0		No
	7	65	50	0.05	1100	29	2.6	65	Data
Sheraton Houston Hotel	8	75	55	0.05	1400	34	2.4	34	No Data
Entex Building	9	108	55	0.05	4000	98	2.5	98	143 (Minor)
1100 Milam Street Building	10	140	33	0.05	1550	223	14.4	247	256 (Beason, Minor, Kareem)
	11	140	33	0.05	1550	0	0.0		No Data
	12	140	33	0.05	1550	24	1.5		32 (Beason, Minor, Kareem)

Figure 5.16. A General View of the School Complex.

Figure 5.17. The Windward Face of the Main Missile Source Building (looking southwest).

Figure 5.18. Roof Gravel on the Upstream Building.

The time-varying hurricane wind trace at the site was re-created and used as the input wind speed and direction data for the missile simulation. The site was modeled as open terrain with a roughness length of 0.03 m for the strong wind directions, which was within the NE quadrant. The maximum peak gust speed was estimated to be about 40 m/s (90 mph) at roof height (11 m).

The results of the simulation are presented in Table 5.4 and compared with the observations. The overall agreement between the simulated results and the observations is reasonable. One exception is that the number of damaged window glass panes is significantly overestimated for the lower-right glazed area on the front wall of the downstream building. This may be attributed to the shielding effects provided by a row of trees in front of this glazed area, as shown in Figure 5.21, which was not modeled in the simulation.

Concluding Remarks. A first principles based model of windborne gravel debris generation and trajectory has been developed for commercial buildings in urban or suburban areas. Some qualitative comparisons with experimental and field observed data have been made for rooftop wind fields and roof gravel scour patterns. The three case studies carried out show, in general, good agreement with the field observed data for window glass breaches.

(a) Looking Southwest

(b) Looking Northwest

Figure 5.19. Glass Damage on the Windward Face of the Downstream Building.

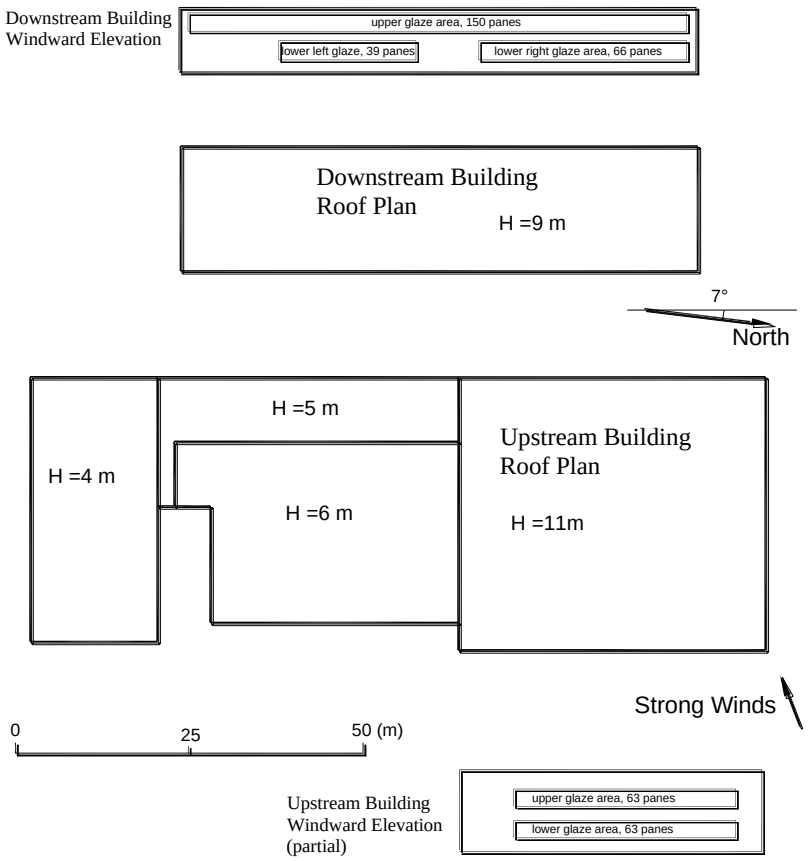

Figure 5.20. Geometry of the Modeled Complex.

Table 5.3. Basic Inputs of Missile Sources (Roof Gravel) and Target Glazing Properties

	Roof Gravel		Glazing					
	Mean Depth (cm)	Mean Diameter (cm)	Glaze/ Wall (%)	Ave. Size (m×m)	Thickness × Panes (cm×#)	Glass Treatment	Impact Resistance (kg-m/s)	Bldg. Height (m)
Upstream Bldg	3	1.2	18	1.2×0.6	0.3×2	T*	0.03	11
Downstream Bldg	3	1.2	45	1.2×0.8	0.3×2	T	0.03	9

* T – Tempered.

Table 5.4. Number of Damaged Windows: Simulation vs. Available Observations

Building	Glaze Area No. on Front Wall	Resistance (kg-m/s)	Total No. Window Panes	Modeled No. Damaged Panes	Modeled % Damaged Panes	Modeled No. Damaged Panes per Building	Observed No. Damaged Panes	Observed % Damaged Panes	Observed No. Damaged Panes per Building
Down-Stream Building	Upper	0.03	150	94	63.0		89	60.0	
	Lower left	0.03	39	8	20.5	151	13	33.3	122
	Lower right	0.03	66	49	74.2		20	30.0	
Upstream Building	Upper	0.03	63	0	0.0		0	0.0	
	Lower	0.03	63	0	0.0	0	0	0.0	0

(a) The Trees in Front of the Lower-Right Glazed Area

(b) Significantly Less Windows Damaged on the Lower-Right Glazed Area than on the Upper Glazed Area

Figure 5.21. Trees in Front of the Lower-Right Glazed Area of the Downstream Building.

5.2.2 Probability of Damage to Building Envelopes by Windborne Gravel Debris

This section describes the development of a fast-running model for estimating damage to building envelopes caused by windborne gravel debris. As a first step, the model has been developed for low-rise buildings in suburban commercial areas. The model utilizes the analytical formulation for debris impact damage risk developed previously and the physical modeling methodology described above to obtain the information required by the analytical formulation (i.e., expected number of impacts and impact momentum distribution). The general scheme and the results are presented below.

Analytical Formulation for Probability of Impact Damage. Several analytical formulations have been derived to estimate the probability of impact damage as a function of the number of impacts and the impact momentum distribution (Twisdale, et. al, 2000a and 2000b). It was found that the following simple model, which assumes mutually independent (i.e., noncontingent) impacts and uses a Poisson distribution for the number of impacts, provides a sufficiently good approximation to the results generated by the detailed model presented in Section 5.2.1. This simple model is adopted as the basic formulation for the impact damage risk and is modified to express the probability of impact damage during a hurricane for a given area of the target, *A*, and in a given time interval, *T*, as follows,

$$P_D = 1 - e^{-A \cdot T \cdot N \cdot (1 - P_m)} \tag{5.5}$$

where N is the expected number of impacts on the surface per unit area and per unit time interval and P_m is the probability of an impact having its momentum (m) less than the impact momentum resistance capacity of the surface (m_d). Many variables influence the expected number of impacts and the momentum distribution, and thus the damage probability. These variables and their effects are discussed below.

Physical Modeling to Obtain the Number of Impacts and Momentum Distribution. As mentioned above, the number of impacts and the momentum distribution are functions of many variables. The functional relationships are implicit and physical modeling is required to provide "data" for quantifying these relationships. Table 5.5 lists the set of variables that the present model considers. Also shown in the table are the values that were used as inputs for the physical modeling to develop the fast-running module for estimating the risk of windborne debris damage in suburban commercial areas.

Within the overall damage model, into which the fast-running debris model is incorporated, the values of some of the variables, such as the peak gust speeds and the location, orientation and size of the target fenestration elements, are explicitly known for each time increment. However, some variables such as the detailed configuration of the gravel sources are not specifically known and can only be accounted for generically or statistically. On the other hand, within the detailed physical modeling, millions of gravel stones are modeled and some critical records are stored for off-line analysis. Each simulation case will normally take several hours to a couple of days to complete. Hence, the number of values for each variable needs to be limited to avoid creating an unrealistically large case matrix.

Table 5.5. Variables that Influence the Number of Impacts and Momentum Distribution

	Wind Parameters				Source Parameters (Roof Gravel)				Target Parameters (Wall Fenestration)					Shielding Effects
Variable	Peak Gust	Mean Direction Relative to Source Building	Time Length for Sustained Mean Wind	Terrain	Source Roof Height	Source Roof Area	Gravel Mean Dia.	Depth of Gravel	Distance to Source	Lateral Location	Elevation above Ground	Orient-ation	Area (Size)	
Notation	V	τ	T	z_0	Hs	S	Dg	Dp	d	l	h	β	A	
Units	m/s (mph)	deg	hr	m	m (ft)	m×m (ft×ft)	cm	cm	m	m	m	deg	m×m	Accounted for with Source Reduction Factor in General Model
Values Used for Simulation	40 (90) 60 (134) 75 (168)	0 to 45 in increments of 5	0.25	0.3	6 (20) 18 (60)	15×15 (50×50) 60×60 (197×197)	1.1	4	Detailed in Figure 5.22				in Equation 5.5	

For each case, the detailed physical model was run for 15 minutes using a mean wind speed that would produce the specified open 10-meter peak gust speed when the turbulence trace is superimposed. This process was repeated for each mean wind direction relative to the upstream edge of the source building. The mean wind directions from 0 to 45° are considered the representative wind angles for a nearly square roof, due to symmetry. A roughness length for suburban terrain was modeled which is typical for areas where low-rise commercial buildings are normally located. Two source roof heights and two source roof areas were modeled, which yield four roof height-area combinations. The modeled heights and roof areas were chosen to represent lower- and upper-end values for low-rise commercial buildings. Only one value of the mean gravel diameter was used; however, the model automatically assumes a dual-linear diameter distribution bounded by zero and twice the mean diameter. The assumed depth of gravel on the roof is 4 cm. This parameter mainly affects the supply of missiles within local regions on the roof, which were modeled as 1 m by 1 m cells.

To model the targets, 12 vertical, semi-infinite planes were placed downstream of the source building as illustrated in Figure 5.22. Five of the surfaces are spaced 30 m apart to the right of the source building. The other seven surfaces are spaced 21 m apart, at 45° to the source building. The normal vectors of these planes are all within ±45° to any of the wind directions modeled. Outside this relative wind quadrant, the general model assumes no risk of debris damage. This simplification approximates the actual case since both the number of impacts and the impact momentum (the normal component of the debris' terminal momentum) decrease with increasing wind angle relative to the surface normal on both sides, forming a bell shape. The number of impacts and the impact momentum, along with the lateral impact location and its height above ground, were recorded for each modeled surface for off-line analysis.

Analysis of Modeled Results. To be suitable for use by the damage model, the modeled results have been simplified into functional relationships as described below.

Within the damage model, the values of some variables may not be specifically known. Some others may only be generically specified. For example, the exact number of buildings having gravel roofs, their detailed layout, respective heights and plan areas, will

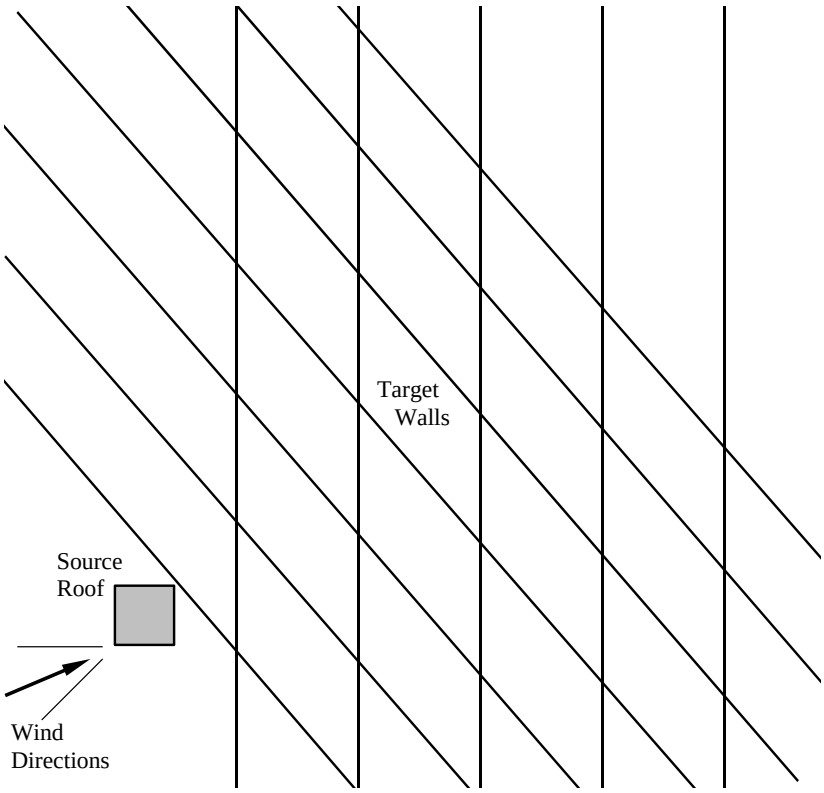

Figure 5.22. The Layout of Modeled Gravel Source Roof and Target Walls Relative to the Wind Directions Modeled.

not be specifically known, but may be reflected by reference to the geographical region, built environment or terrain type. For some of these variables, such as source building height, plan area and orientation, their effects are accounted for by averaging the results over all cases modeled. A source reduction factor is also already in place in the damage model to roughly account for the percentage of buildings having gravel roofs. Its value is empirically defined to vary between 1 and 0, where the value of 1 is typical for areas having many gravel roofs and the value of 0 is for areas having no gravel roof (e.g., open water upstream of the target building). For the areas having some gravel roofs and some non-gravel roofs, the non-gravel roofed buildings will not produce gravel missiles but are present as shielding for other buildings. In this case, the source reduction factor will be some value between 0 and 1, approximately equal to the percentage of gravel roofs in the area.

The stream-wise and lateral layout of the upstream source buildings is assumed to be homogeneous in the general model. Thus, the typical building spacing for the area becomes representative of the expected distance from the target building to the first building or the first row of buildings directly upstream, and the lateral distribution of impact locations on the target wall is treated as homogeneous. To obtain the number of impacts per unit area on the target surface as a function of wind speed, typical building spacing and the vertical location above ground, etc., the results were averaged laterally across the target wall over a defined width, which is the typical building spacing in this

case. Results for different target wall orientations relative to the wind direction were also averaged within the ±45° quadrant in consistence with the treatment by the general model as described in the previous section.

As a result of the simplifications, the expected number of impacts per unit area and the impact momentum become a function of the open-10 m peak gust speed (*V*), typical center-to-center spacing between buildings (*d*) and the vertical location above ground (*h*). The following expressions fit to the data represent the expected number of impacts on a target surface *per square meter and per hour*,

$$N = n(V,d)\cdot f(d,h)\ , \tag{5.6}$$

with $n(V, d)$ being the average over the height from ground up to 30 m, expressed by,

$$n(V,d) = 53\frac{\left(1+tanh\frac{V^{1.11}-80}{18}\right)}{\left(e^{x}+e^{-x}\right)}\ ,x=\frac{d-15}{0.33V}\ , \tag{5.7}$$

and *f(d, h)* as the height factor,

$$\begin{aligned} f(d,h) &= \frac{60}{h_o}cos^2\left(\frac{\pi}{2}\frac{h}{h_o}\right), h \le h_o\ , \\ &= 0\ , h > h_o\ ; h_o = 30-\frac{d}{10}\ . \end{aligned} \tag{5.8}$$

where *V* is the peak gust speed (m/s) in a short time interval *T*; *d* represents the estimated typical center-to-center distance (m) of buildings for the area to be modeled; and *h* the vertical location above ground (m) of the target surface element.

Equation 5.7 is illustrated in Figure 5.23 for peak gust speeds of 40, 60 and 75 m/s, where the average number of impacts per square meter per hour on the wall from 0 to 30 m is shown as the function of typical building spacing. The data derived from the physical model to which Equation 5.7 is fitted are also shown in these figures. The variation of the number of impacts with peak gust speed is illustrated in Figure 5.24, for selected center-to-center distances between buildings.

The height factors calculated from the simulated results are presented in Figure 5.25, while their empirical approximations as expressed by Equation 5.8 are shown in Figure 5.26.

The impact momentum, defined as the component of the terminal momentum perpendicular to the surface impacted, generally varies with many variables such as individual gravel diameter, terminal speed and incident angle of impact, etc. Some of these variables are in turn dependent on many other parameters, for example, wind speed,

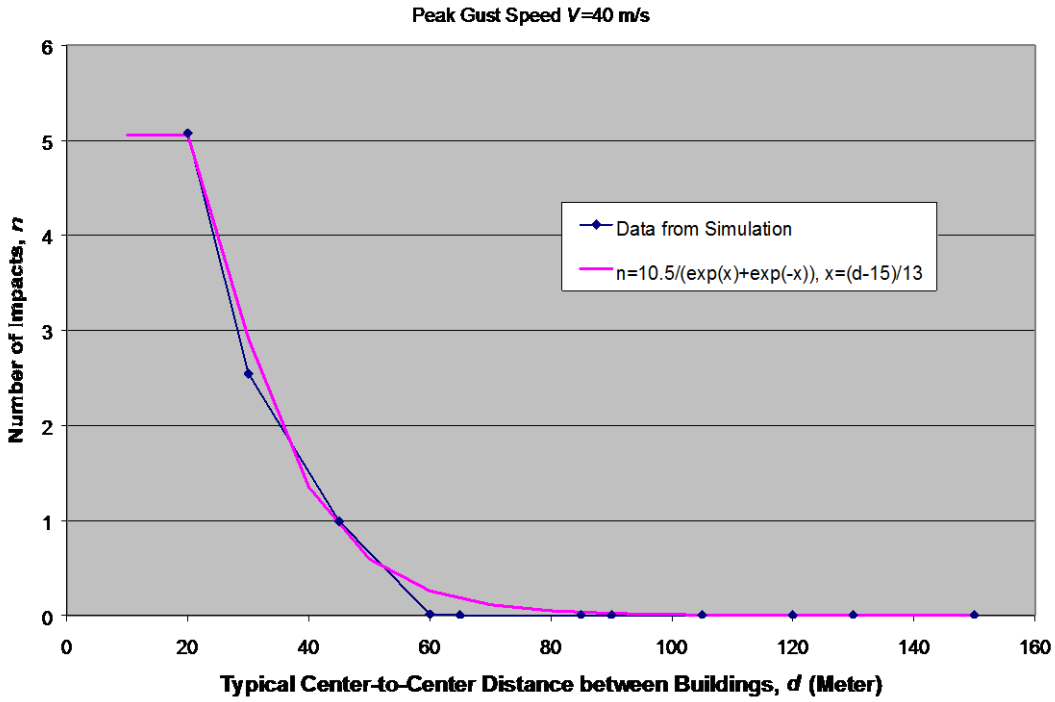

(a) For Peak Gust Speed of 40m/s (90mph)

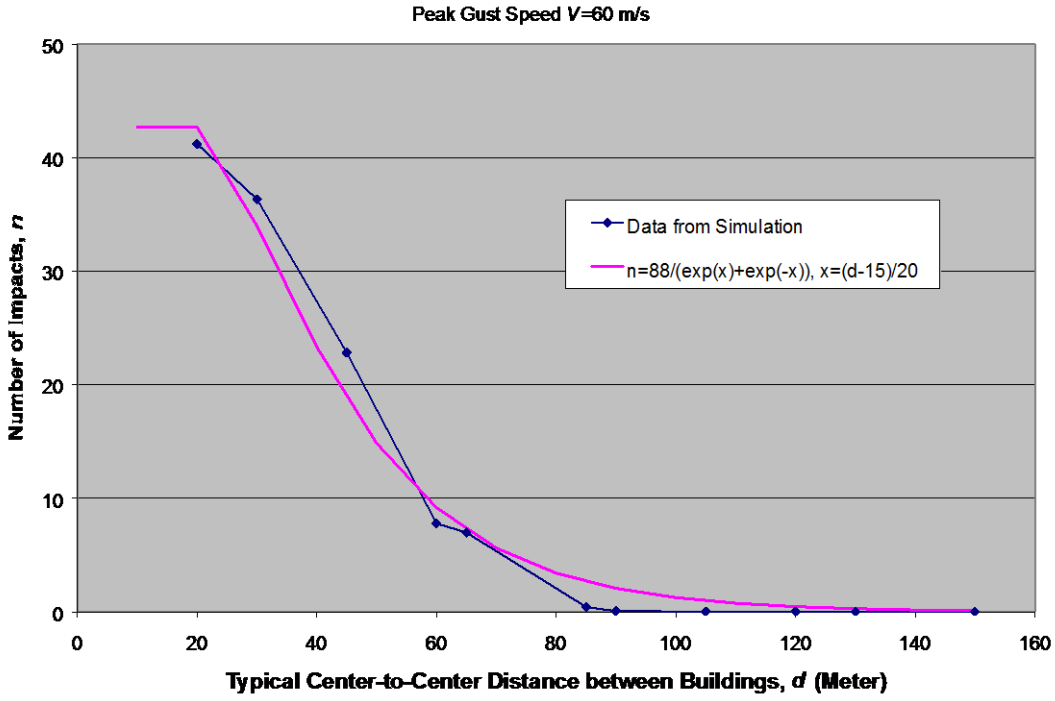

(b) For Peak Gust Speed of 60m/s (134mph)

Figure 5.23. Number of Impacts per m^2 hr on Walls Averaged Over the Lowest 30 m, as Function of Building Spacing.

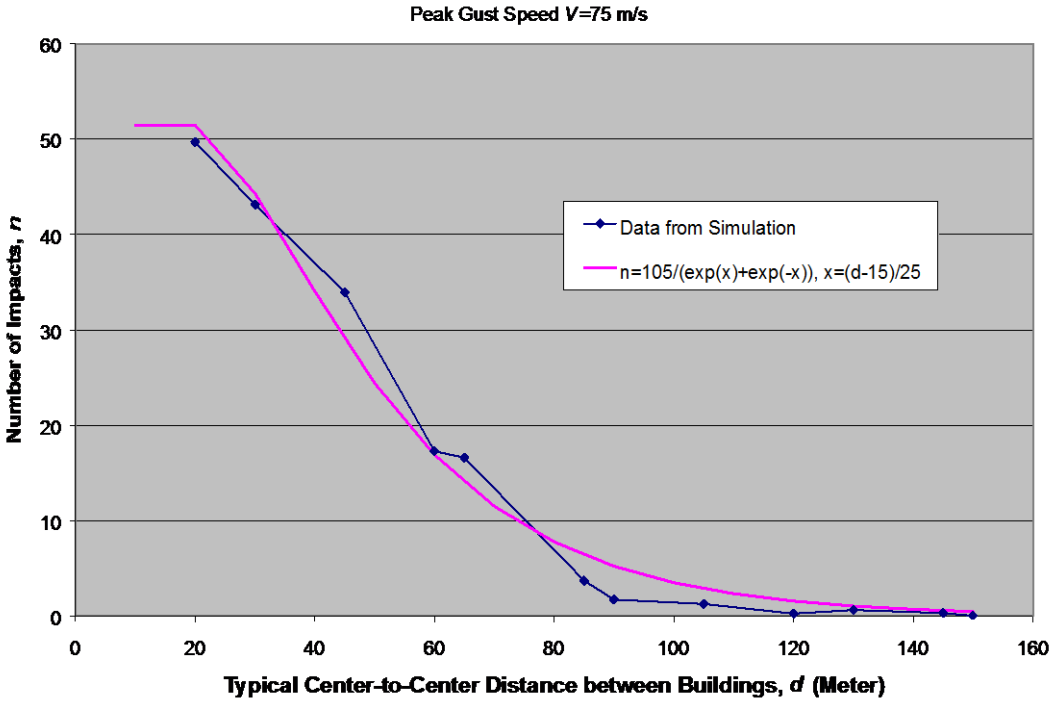

(c) For Peak Gust Speed of 75m/s (168mph).

Figure 5.23. Number of Impacts per m^2 hr on Walls Averaged Over the Lowest 30 m, as Function of Building Spacing (concluded).

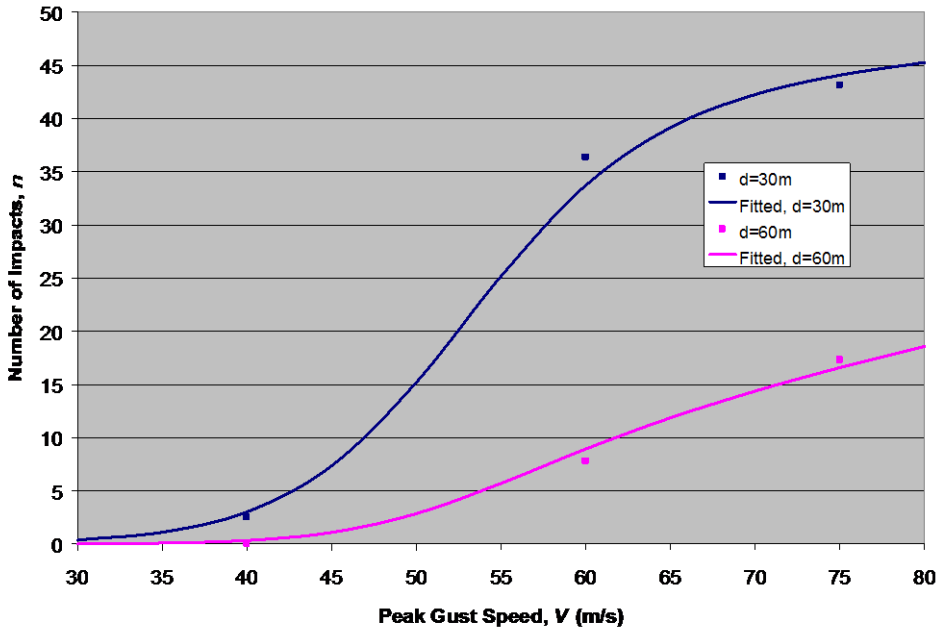

Figure 5.24. Examples of Fitted Number of Impacts Varying with Peak Gust Speed for Selected Building Spacing Cases in Comparison with Simulation Results.

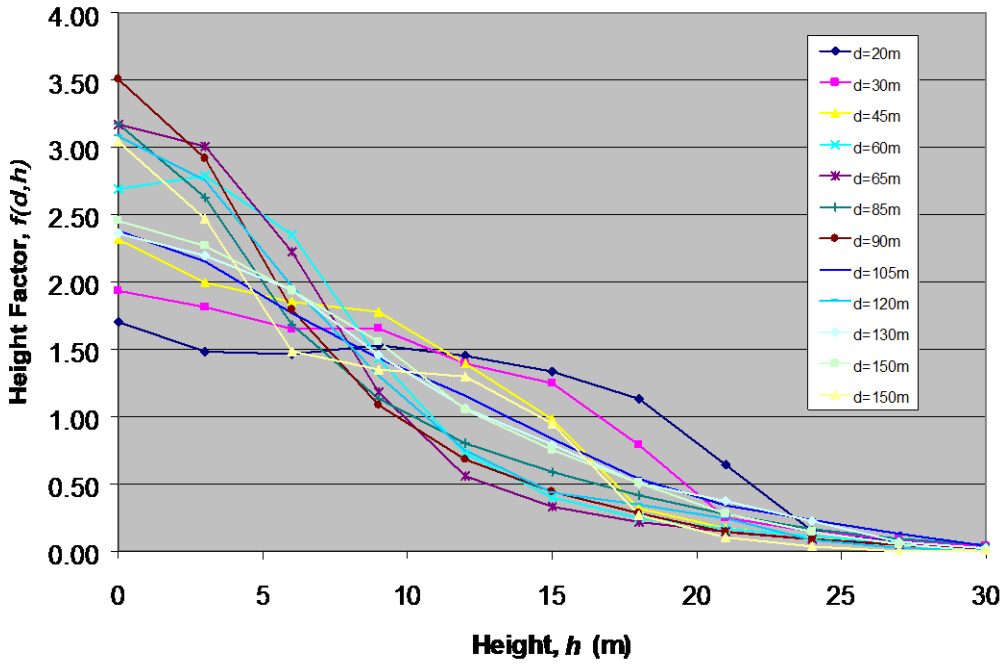

Figure 5.25. Height Factor for Number of Impacts for Various Cases with Building Spacing from 20 m to 150 m.

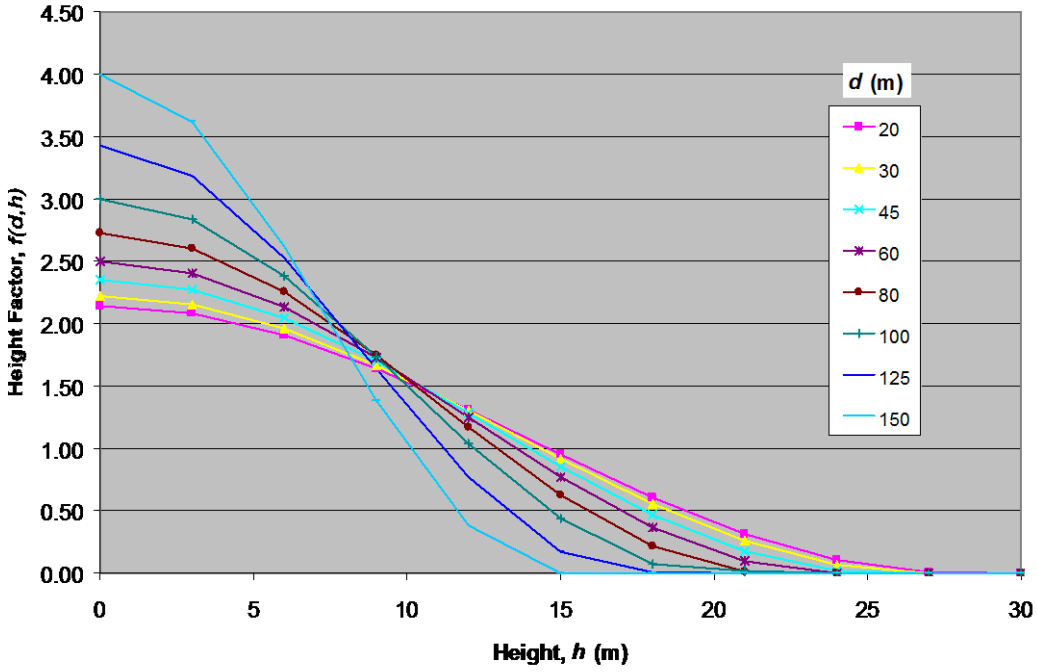

Figure 5.26. Fitted Height Factor for Number of Impacts for Building Spacing from 20 m to 150 m.

building spacing, vertical location, configuration of the source and target buildings, etc. The detailed relationships of its dependence on these parameters are rather complicated; however, as indicated by the simulation results, the statistical distributions of the impact momentum for various cases have similar shapes. When normalized by a given percentile, the distributions of the impact momentum for various cases tend to collapse. Figure 5.27 shows the averaged CDF of the impact momentum and the one standard deviation bounds over all cases, where the impact momentum is normalized by its 95th percentile.

Prior to the normalization, the distributions have been truncated at a momentum of 0.025 (kg-m/s), below which gravel missiles are considered having no damage effects on window glass products. The above results for the numbers of impacts have included only those that exceed the 0.025 kg-m/s threshold.

The 95th percentile is empirically chosen as the normalizing factor mainly because it is a convenient number and for the many cases modeled it represents a moderate value of momentum that is able to produce damage to window glass. As indicated by the results, the 95th percentile varies for different cases, dependent on various parameters mentioned above; however, there appears to be a trend of increase with wind speed, with certain variability at each wind speed. Figure 5.28 illustrates this trend and variability of the data, along with the empirical fit to their mean. Each data point plotted is derived from an individual impact momentum distribution obtained on every 25 m^2 wall area that received at least 25 hits with impact momentum larger than 0.025 kg-m/s. There are about 12,500 such data points for all cases modeled, which are all included in Figure 5.28.

Omitting the variability at each wind speed, the impact momentum distribution, simplified to be conditional on peak gust speed only, is expressed as

$$\begin{aligned} P_m = P_m(M) &= CDF\left(\frac{M - 0.025}{95th\ percentile}\right) \\ &= CDF\left(\frac{M - 0.025}{2.417\times10^{-5}V^2 - 1.379\times10^{-3}V + 6.200\times10^{-2} - 0.025}\right) \end{aligned} \tag{5.9}$$

where V (m/s) is the peak gust speed in the time interval (T), and M (kg-m/s) represents the estimated resistance capacity for impact momentum.

Equations 5.5 through 5.9, along with the mean CDF function presented in Figure 5.27, constitute the fast-running windborne gravel debris module for low-rise commercial buildings in suburban areas. It is specifically designed for the general simulation model for hurricane damages and estimates the probability of impact damage (P_D) caused by windborne gravel missiles to a vulnerable surface element of area A (m^2) during a short time interval T (hour).

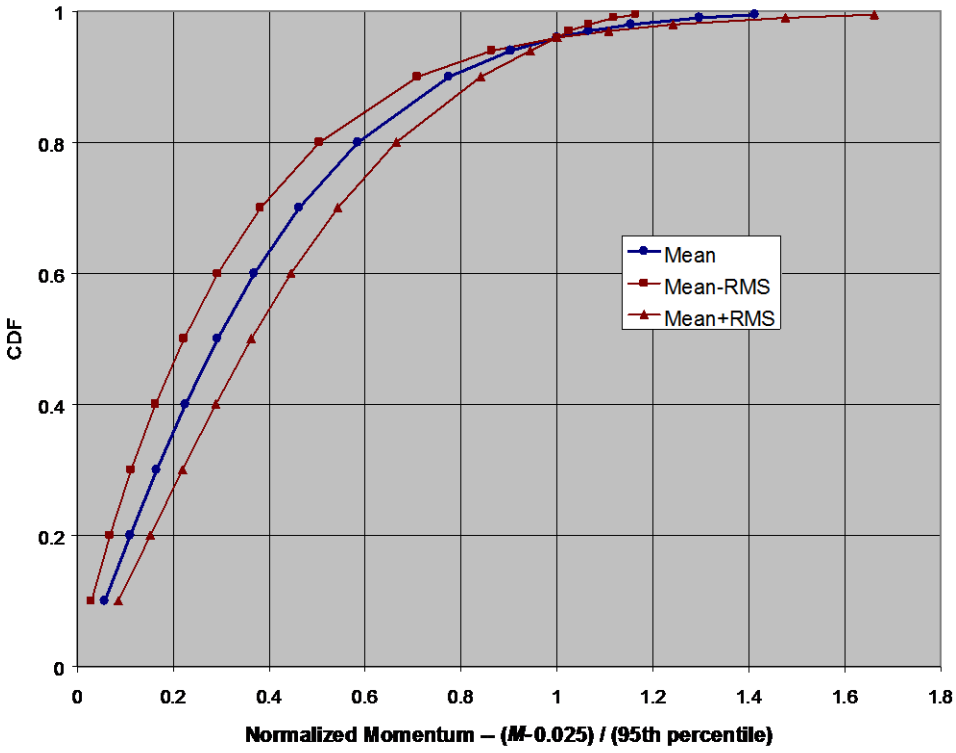

Figure 5.27. Distribution of the Normalized Impact Momentum.

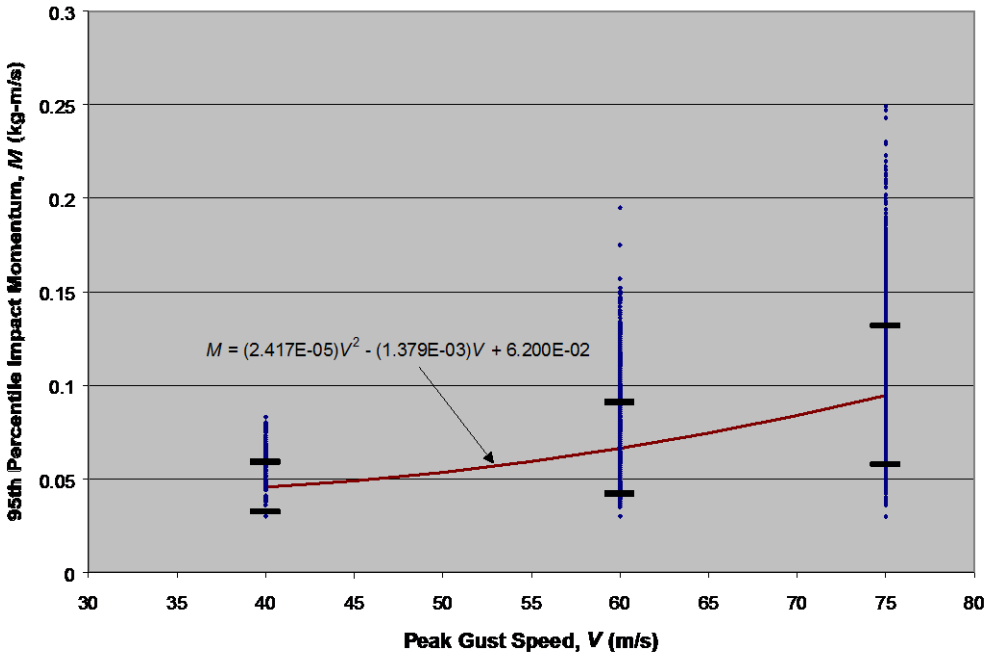

Figure 5.28. The Mean Trend of the 95th Percentile Impact Momentum with the Peak-Gust Speed, and the Variability for which the One Standard Deviation Bounds are Shown by the Short Bars.

Concluding Remark. A fast-running model has been developed to estimate the risk of damage by windborne gravel debris to low-rise buildings in suburban commercial areas. The model utilizes a previously developed analytical formulation for debris damage risk (Equation 5.5). A detailed physical modeling methodology is used to obtain the information required by the analytical formulation, including the expected number of impacts and impact momentum distribution. The detailed physical model simulates the effects of turbulent boundary layer winds, wind directionality, and the general layout of the gravel source buildings and target buildings. The output data from the detailed physical model were analyzed and simplified in accordance with the approach used in the general hurricane damage simulation model. The resulting fast-running model estimates the probability of impact damage (P_D) caused by windborne gravel missiles to a vulnerable surface element of area A during a short time interval T. Thus, it is readily integrated into the general model, which simulates the processes of a hurricane strike on a built area progressively in time and is required to estimate the number and location of fenestration elements breached by debris within each short time interval, in order to interactively account for the rainwater penetration and internal pressure change in a building.

In the development of the fast-running model, the effects of some variables, such as the detailed configurations and layout of upstream buildings, on the damage probability were averaged over an anticipated range of values since these variables are not specifically modeled in the general model. This approach provides averaged, approximate estimates of the damage probability as far as these variables are concerned. There exists propagated variability about the average resulting from such simplifications, which is undetermined at this time. The analysis of this uncertainty remains to be a future task.

Chapter 6. Physical Damage Modeling

6.1 General Approach

The physical damage model predicts wind-induced pressure damage to windows, doors, wall cladding, roof cladding and roof cover. The model also predicts glazing failure due to impacts from windborne debris. Wall failures due to inward and outward pressure loads are also modeled for masonry and wood frame walls. Failure of the connections between the roof frame and the perimeter walls are also modeled for both wood and steel roof framing systems. In addition to these failure mechanisms, the physical damage model predicts foundation failures (i.e., sliding, overturning and uplift) for manufactured homes.

The physical damage model predicts hurricane-induced building damage by comparing loads to resistances. For a given building, directionally dependent pressure coefficients are estimated (see Chapter 4) for all building components and cladding. In addition, loads acting on walls surfaces (for predicting wall failures), on roof surfaces (for predicting failure at roof/wall connections), and on the entire building (for predicting foundation failure) are computed by spatially integrating the pressure coefficients estimated at each point on a uniform grid covering the appropriate building surface. The resistance associated with each failure mechanism is defined by a probability distribution from which resistances are sampled for a given storm simulation.

Given the estimates of the loads and resistances associated with the modeled failure mechanisms, the approach used to predict building damage consists of monitoring the wind speed and direction at fifteen minute intervals over the entire duration of the storm. At each time step, wind loads are compared to resistances to predict direct wind damage. At the same time, the number of missiles impacting the building walls is computed (using the fast running missile impact model described earlier) to predict glazing damage as well as damage to the wall finish.

Internal pressurization of the building is also considered in the physical damage model. That is, the total pressure acting on a window, for example, is computed as the sum the external suction acting on the outside of the window and the internal pressure acting on the inside of the window. The internal pressure is estimated based on the number and size of wall breaches due to failed windows, doors and wall cladding. In a given time step, if additional envelope breaches occur, the internal pressure is re-computed as are the net loads associated with each of the failure mechanisms, which again are compared to the resistance in the same time step to assess additional building damage. This modeling approach is shown schematically in Figure 6.1. Note that all resistances and modeling error statistics associated with the wind loads are sampled before the storm is passed by the building and held constant for the duration of the storm. To obtain statistics on the possible damage outcomes for each storm, the component resistances and loading error statistics are re-sampled and a new damage simulation is performed using the same storm.

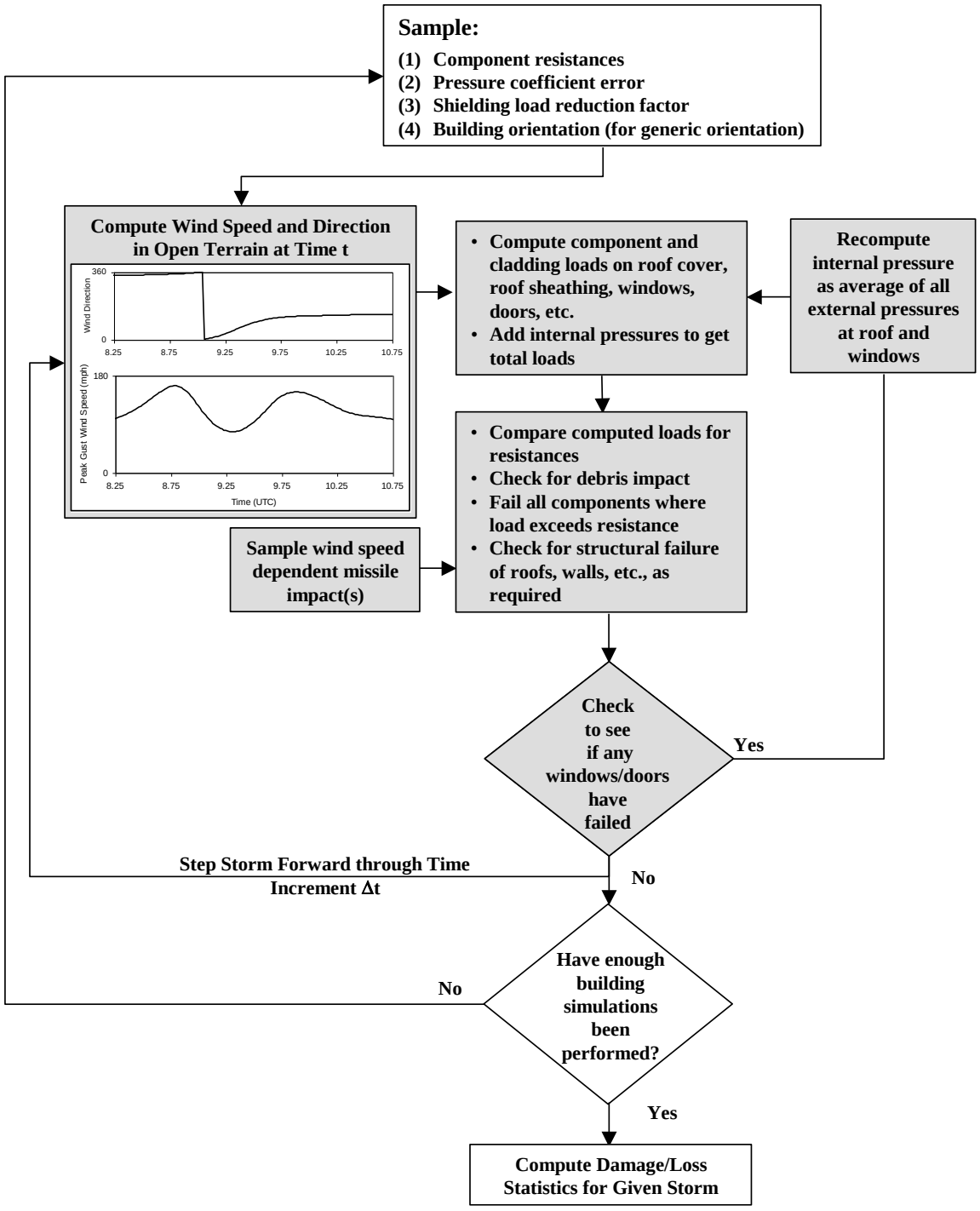

Figure 6-1. Approach Used to Simulate Damage to Buildings.

This section describes and quantifies the resistances of the various components used to model buildings and, where possible, presents examples of predicted and observed building damage states to demonstrate the suitability of the load and resistance model for estimating wind induced damage.

The following sections describe the resistances of components commonly found in residential buildings, and a validation of the load-resistance model for residential buildings. Next, the development of the manufactured home resistance and damage model is given, again followed by a validation study. Finally, descriptions of the models developed for modeling the failures of single ply membrane and built-up roofs, metal buildings, steel joists and metal roof decks are given. The suitability of this model is tested through comparisons to the limited available full scale damage data.

6.2 Resistance Models for Residential Buildings

The direct wind-induced damage (wind pressures and windborne debris) to buildings modeled herein is directed towards the performance of components and cladding, including roof covering (shingles, tiles, membrane), roof sheathing (wood frame construction only), windows and doors. Structural wall failures for masonry and wood frame walls and uplift of whole roof systems due to failure at the roof/wall connections are also modeled. Foundation failures (i.e., sliding, overturning and uplift) are considered for manufactured homes (Section 6.5).

The wind and/or missile resistance of the various components noted above have been derived from laboratory test data, engineering analyses given in the literature, and judgment based on the performance of components observed during post-hurricane damage investigations. The empirical models based on judgment and experience are required in some cases since information on the loads and failure mechanisms for some systems are simply not known. Examples of such systems are discussed later. The resistance of the cladding components used in the damage modeling are discussed in the following sections.

6.2.1 Roof Sheathing in Wood Frame Construction

The roof sheathing failure model is based primarily on the experimental uplift failure tests performed on 8′×4′ sheets of plywood and Oriented Strand Board (OSB) reported by the American Plywood Association (Cunningham, 1993), and Clemson University (Mizzel, 1994; Shane, 1996; Rosowsky, et al., 1997; Rosowsky and Schiff, 1997). Table 6.1 summarizes the relevant uplift resistance data from the various tests.

As indicated in Table 6.1, the variability of uplift capacities for a given nail size and spacing is significant. This variation is clouded by the fact that different species of wood having different specific gravities (SG) yield significantly different nail pullout resistances. The resistance of a nail to pullout varies with the specific gravity of the wood raised to the power of 2.5 (NDS-97), and the pullout capacity also varies with the moisture content of the wood.

The SG of the Douglas Fir (DF) used in the APA experiments had a reported mean value of 0.51 with a COV of 0.11. In the Clemson tests, the specific gravity of the wood is not reported, but HUD 1999 suggests a value of 0.37 would be representative of the SG for the Spruce-Pine-Fir (SPF) wood used in the Clemson tests. HUD (1999) also notes that the Southern Yellow Pine (SYP) reported in Rosowsky and Schiff (1997) was in fact

Table 6-1. Uplift Resistances of 8-by-4 Roof Sheathing Panels From Laboratory Testing

Source	Nail Size	Nail Pattern	Species[1]	Mean (psf)	COV
Cunningham	6d	6/12	DF	60	0.12
Shane	6d	6/12	Unknown	71	0.12
Mizzel	6d	6/12	SPF	25	N/S
Cunningham	8d	6/12	DF	118	0.14
Shane	8d	6/12	Unknown	90	0.20
Rosowsky, et al.. (a)	8d	6/12	SPF	72	0.19
Rosowsky, et al. (b)	8d	6/12	SPF	87	0.28
Mizzel	8d	6/12	SPF	61	N/S
Cunningham	8d	6/6	DF	218	N/A
Rosowsky and Schiff	8d	6/6	SYP	131	0.14
Mizzel (c)	8d	6/6	SPF	107	N/S
Mizzel (d)	8d	6/6	SPF	172	N/S
Mizzel (e)	8d	6/6	SPF	112	N/S

[1] DF = Douglas Fir; SPF = Spruce-Pine-Fir; SYP = Southern Yellow Pine

SPF. Thus to compare the uplift capacities of the roof sheathing panels obtained from the Clemson tests to those obtained from the APA tests, the Clemson results should be increased by a factor of about 2.2.

In the South Florida area, most homes are constructed with high density SYP lumber (HUD, 1999) (SG = 0.55) and thus the uplift resistance obtained from the APA tests are considered to be most representative of the uplift resistance of the 8′×4′ panels. Thus, for modeling the resistance of well-applied roof sheathing, a mean of 61 psf and a COV of 11% are used for the 6d nail case and a mean of 114 psf and a COV of 11% are used for the 8d case. In the implementation of the damage model, the mean uplift capacities are reduced by 10% to account for quality of installation ($\phi = 0.9$).

6.2.2 Air Permeable Roof Cover Systems

Air permeable roof cover systems include such systems as shingles (asphalt, metal, etc), tiles, wood shakes and slate. The systems are referred to as air permeable since both the upper and lower faces of the system experience wind induced pressures. The net pressure load on the system is equal to difference between the pressures acting on the top and bottom sides of the cover. The ability of the system (or components of the system) to resist wind loads is clearly a function of the hold capacity of the adhesive or mechanical attachment used to connect the roof cover to the deck. Prior to the early 1990's, no research had been performed to quantify the loads acting on an air permeable system in a wind storm or the requirements for attaching the system to the roof deck to resist these loads. The first research was performed by the Redland Roof Company in the United Kingdom (Cherry, 1991), where effective uplift and overturning coefficients on roof tiles were obtained. The effective uplift coefficients obtained in the Redland study have been incorporated in both the Standard Building Code (SBC) and the South Florida Building Code (SFBC) for use in the design of roof tile connections for both residential and commercial applications. The research program also addressed the resistance of roof tiles

against blowing off the roof by measuring the moment resistance associated with different mechanical attachment techniques. The attachment techniques examined in the Redland Study included connecting the tiles to the roof deck with one 10d nail, two 10d nails, one 8d nail, two 8d nails, one 2.5″ screw and two 2.5″ screws.

For the prediction of the performance of tile roofs, the loading and damage model incorporates the Redland roofing company results for a typical tile. The nominal resistance chosen corresponds to that of the one nail case. While it is recognized that in most of South Florida roof tiles are attached to the roof using mortar rather than mechanical connections, no data exists for a mortared connection. Thus, while the model does not properly reproduce the actual resistance of a mortared tile to be blown off in a storm, it does provide a method to enable reasonable predictions of the effective loads acting on the tiles; thus, a reasonable representation of the variation of these loads with both wind speed and location on the roof of a structure. The usefulness of the model in predicting the failure rates of tiles attached with mortar is evaluated through a calibration process.

The only available data on the effective loads acting on asphalt shingles are presented in Peterka, et al. (1998). The study by Peterka, et al., showed that, as in the case of roof tiles, the effective loads acting on shingles are reduced because negative pressures act on both the top and bottom sides of the shingle. The resistance of a shingle to the uplift pressures acting on the shingle tabs is provided by the adhesive strip on the underside of the shingle tab towards its leading edge. If the shingle tabs do lift, complete failure of the shingle occurs when the nails or staples tear from the roof or alternately, the shingle tears around the nails. To properly assess the uplift capacity of a shingle, the uplift capacity of the adhesive strip must be known, and at this point in time no public domain data are available to properly assess the uplift capacity of shingles. Thus, for the prediction of the performance of shingle roofs, the same load-resistance model are used as for the tile roof case except that the nominal resistance of the shingles have been reduced by 10% over the basic tile case. While this modeling approach is empirical, the mechanism in which either the tiles or shingle are loaded is the same; thus, as in the case of roof tiles, the approach enables a reasonable means to model the variation of the loads with both wind speed and location on the roof. Again, the usefulness of the model is evaluated through comparisons of modeled and observed roofing performance.

6.2.3 Windows and Sliding Glass Doors

The wind pressure induced failure of both windows and sliding glass doors is produced by either a failure in the glass, a failure in the frame or a failure in the frame-wall connection. The wind resistance capabilities of the above noted components can vary enormously between manufacturers and the required design pressure. For this study, the assumed failure pressure is based on the minimum loads as specified in the SBC.

Prior to 1974, the design wind pressure specified in the SBC for buildings located within 125 miles of the coast, having a mean roof height of 30′ or less, was 25 psf. The American Architectural Manufacturers Association (AAMA) requirements for windows and doors states that the product must be able to resist loads of 1.5 times the design

pressure, thus most products installed in this time period should have a minimal wind load resistance of about 38 psf. When the product is tested to meet the R25 rating, a static pressure having a magnitude of 37.5 psf is applied to the product and if it does not fail it meets the R25 specification and can be marketed as such. The ultimate capacity of the product is unknown and may be as low as 38 psf, but it could be higher.

For damage simulation purposes, it is assumed that the nominal pressure resistance of window and sliding glass door components installed in this period can be modeled using a mean resistance of 40 psf with a coefficient of variation of 0.2. The assumed distribution of the product capacity is taken as being normal. This assumption implies that about 80% of the products installed in low-rise buildings during that time period meet or exceed the minimum requirements as specified by the SBC. It is also assumed that during this time period, the same products used on low-rise buildings in Palm Beach County were installed on buildings in Dade and Broward Counties, even though the Building Code provisions were not the same.

From 1974 through to 1982, the basic design pressures in the South Florida area increased to 34 psf for buildings less than 30′ in height. For the design of windows and doors, wind loading coefficients of +1.1 and -0.55 were used to compute the design pressures, implying the products should be able to resist inward acting loads of up to 56 psf (34×1.1×1.5) and negative pressures of 28 psf.

The revision of the SBC wind load provisions in 1982 provided more realistic estimates of the pressure coefficients than the preceding versions; however, the design wind pressures for typical fenestration products on typical low-rise buildings were in the range of 30 to 40 psf depending upon the height of the building, the location of the fenestration and the size of the fenestration. The implied resistances for fenestration products meeting these load criteria range between 45 psf and 60 psf.

Although the wind load criteria for the design of windows and doors increased somewhat between the 1950's and the early 1990s, the mean resistance of 40 psf with a COV of 20% is used for all single family residential homes constructed prior to 1994.

6.2.4 Roof-Wall Connections

Since the inception of the SFBC in the late 1950's, tie down straps have been required for the roof to wall connections in both Dade and Broward Counties. In Palm Beach County, roof-wall tie downs have been required on every truss-wall connection since the late 1970's but, prior to this time, strapped connections were required only on every other truss. The uplift capacity of hurricane straps or clips varies significantly with the type of wood used to manufacture the truss, the size (thickness and width) of the strap, number of nails, etc.

Conner, et al. (1987) reported on the uplift capacity of various wood to wood connections obtained from laboratory tests using Douglas Fir wood members. For conventional toe-nail connections (three 8d nails), they reported a mean uplift capacity of 676 lbs with a COV of 8%. The strapped connection yielded a mean uplift capacity of 867 lbs with a

COV of 18%. The straps used in the experiments were 0.5″ wide (no thickness is given) with two 6d nails used for both the rafter and top plate connections. The clipped connection yielded a mean uplift capacity of 908 lbs with COV of 10%.

Reed, et al. (1997) reported test results using SPF lumber. For a toe nail connection using three 8d nails they report a mean uplift capacity of 430 lbs and for a small strap (five 8d nails in each of the rafter and top plate) they report a mean uplift capacity of 1900 lbs.

Canfield, et al. (1991) reported on the uplift capacity of a number of straps tested with SPF lumber. They reported a mean uplift capacity of 208 lbs for the three 8d toe nail case, with strapped connections yielding mean uplift capacities ranging between about 500 lbs to 1200 lbs, depending on the strap thickness and number of nails used in the connection. In the Canfield, et al. (1991) tests, the strap most closely representing that typically used in the South Florida area yielded a mean uplift resistance of 1000 lbs with a COV of 15%.

Clearly, the true uplift capacity for a field installed strap connection depends on the quality of installation, number and size of nails and the size of the strap. The South Florida Building Code requires a strap having a thickness of 0.125″ with three 8d nails be used to attach the strap to the truss or rafter. Based on the above noted experimental results, the uplift capacity of a strapped or properly clipped roof-wall connection is modeled with a mean resistance of 1200 lbs and a COV of 30%.

6.2.5 Masonry Walls

Wall failure models were developed as a step towards modeling catastrophic structural failures. The wall failure model will also be part of the casualty modeling in a future version of the hurricane model. Wall failure modeling includes failures due to both inward and outward uniform pressure loading. Two different circumstances have been considered: walls without roof support and walls with roof support. The former is for the case where the wind uplift force has already blown off the roof. The latter is for walls that are within an integrated structure. A wall within an integrated structure can become a weak link, particularly when mitigation measures have been taken to protect windows and doors, to improve roof-sheathing connections, and to strengthen roof to wall connections by using tie downs. Variability of wall resistance capacity, due to variable material and workmanship etc., is incorporated in the wall failure modeling.

For edge-supported (by roof, floor, and adjacent walls, etc.), unreinforced masonry walls under uniform lateral pressure loading, the major failure mechanism is associated with cracking due to flexural tensile stress. The cracking normally starts at, and develops along, the mortar joints (both horizontal bed joints and vertical head joints) between the concrete masonry units (CMU) owing to the failure of mortar-CMU bond as the weakest link in the wall system. Occasionally, in the vertical direction, the developing crack may proceed across a CMU from a mortar head joint to another mortar head joint. Examples of masonry wall or brick veneer damage are shown in Figure 6.2.

(a) Brick veneer (Hogan and Karwoski, 1990)

(b) Collapse of masonry walls (Zollo, 1993): A wall of 40′ span (top); Walls on a two-story building (bottom)

(c) Collapse of masonry wall and steel frame roof system (NRC, 1991)

(d) Collapse of masonry wall (HUD, 1993)

Figure 6-2. Wind-Induced Masonry Wall and Brick Veneer Damage.

Structurally, a masonry wall can be considered as an orthotropic slab with different bending moment resistance capacities in horizontal and vertical directions. Yield line theory is used to derive a wall failure model applicable for various wall spans, wall heights, cross-sectional configurations and material properties. This method has been adopted for masonry by a number of researchers (e.g., Drysdale and Essawy, 1988), as well as by the British code (BSI, 1978). While true yield-line behavior cannot be fully justified, a substantial body of data (Haseltine, 1975; Hendry and Kheir, 1976; West, et al., 1973a, 1973b) and some recent tests tend to support use of this analytical tool.

Given the edge support conditions, the accuracy of a yield-line analysis depends on the correctness of the assumed crack pattern. The resulting capacity will be the expected capacity if the assumed pattern is correct, or an upper bound value if the assumed pattern deviates from the correct one. The next section describes in detail the crack patterns observed by a number of researchers for a series of walls with varying dimensions and edge support conditions, followed by the yield-line analysis and results for the masonry wall model.

Failure Modes and Crack Patterns. Drysdale and Essawy (1988) carried out experimental investigations on the failure modes and crack patterns for a series of 9′ tall, 8″ thick, full-scale masonry walls of varying spans under uniform pressure loads. The walls were built by an experienced mason using type-S mortar and standard 8″×8″×16″ two-cell concrete blocks that are most commonly used in masonry construction. The running bond pattern, curing time and other parameters were all consistent with code requirements. The walls were investigated for different span to height ratios (i.e., aspect ratios) and various support conditions. Three repetitions for each combination of parameters were performed to provide a better statistical sample, primarily for a better measurement of the mean. The first-crack pressures and ultimate failure pressures were recorded.

The typical crack patterns observed by Drysdale and Essawy are presented in Figure 6.3 for various wall aspect ratios and support conditions. Figure 6.3(a) shows a cracking pattern for a small span wall (width W = 11.2′, aspect ratio = 1.21) simply supported along all four edges. It was observed that a vertical crack started near the middle of the wall, where maximum flexural moment is expected. The crack split diagonally and extended to the four corners of the wall under higher pressures leading to its collapse. Figure 6.3(b) shows a wider wall (W = 16.4′, aspect ratio = 1.79) where the initial crack was a horizontal one that split at its two ends under higher pressures and extended at roughly 45° to the four wall corners shortly before collapse. Wider walls supported on all four sides also generally followed the same failure pattern described in Figure 6.3(b). The wider the wall, the longer the initial horizontal crack would be. Thus, for a wall of infinitely large span, hypothetically one could only see the horizontal crack. This result agrees with Drysdale and Essawy's observations on walls with only top and bottom supports (equivalent to two-end supported beams), which resemble the middle section of a wall with an infinite span where little shear and moment load transfer would occur horizontally under uniform lateral loading. Drysdale and Essawy clearly described the horizontal crack for the top and bottom supported walls in their text although they did not reproduce the picture. Dawe and Aridru's work (1993) on prestressed masonry confirmed this cracking pattern (see Figure 6.4). It can be assumed that the side supports become no longer significant to the crack pattern and failure pressure for long span masonry walls. These observations and measured failure pressures provide an important data point for verifying the wall failure model in terms of long span masonry walls.

Figure 6.3(c) exhibits a crack pattern of a wall without top support, for a specific horizontal wall span of 16.4′ (aspect ratio = 1.79), where a vertical initial crack was joined by two diagonal cracks extending to the lower corners. It can be expected that, as

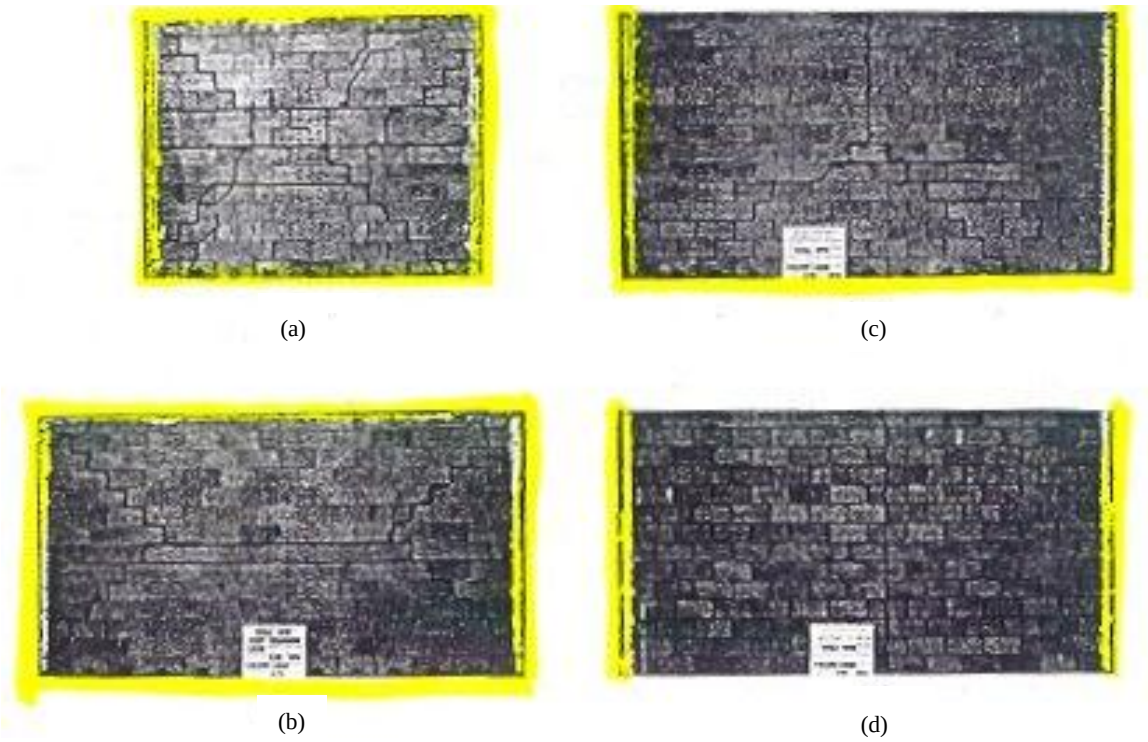

Figure 6-3. Typical Cracking Patterns for Various Wall Spans and Different Edge Support Conditions (Drysdale and Essawy, 1988).

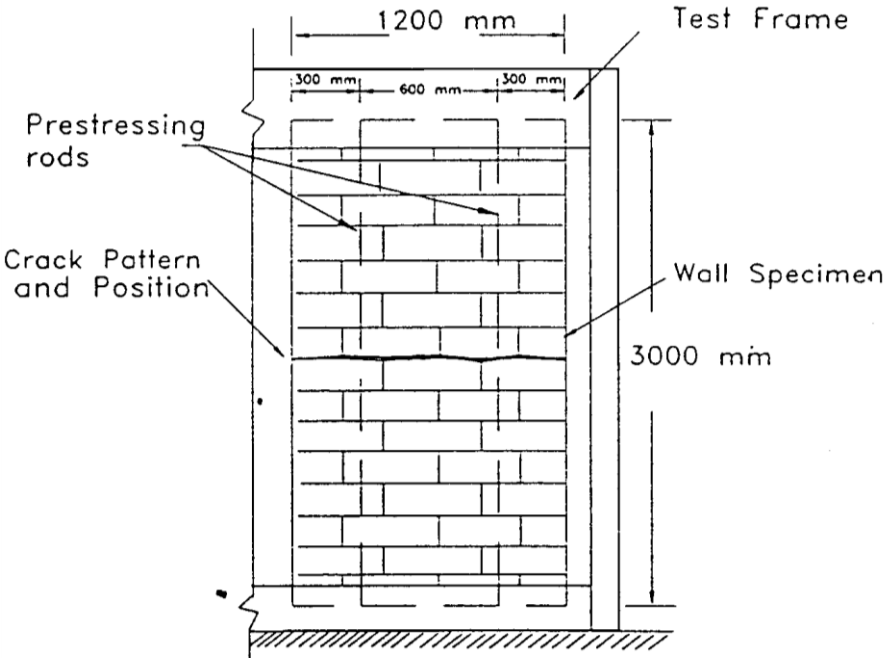

Figure 6-4. Typical Cracking Pattern for Top and Bottom Supported Prestressed Masonry Wall (Dawe and Aridru, 1993).

the aspect ratio increases, the vertical crack will shorten and the junction of the two oblique cracks will move upwards; eventually the pattern will become one with only the two oblique cracks that extend to the top edge of the wall and disjoint from each other.

The cracking pattern for walls with only two sides supported was also investigated by Drysdale and Essawy, as reproduced in Figure 6.3(d), where a vertical crack ran through the height of the wall near the mid-span, alternately passing through head joints and blocks in a nearly straight line. This would also depict the crack pattern for a wall of infinitely large height or of infinitely small aspect ratio.

The cracking patterns are summarized in Figure 6.5 for various edge support conditions and aspect ratios, based on the above observations and theoretical inferences or assumptions. The yield line analysis will either confirm or reject an assumed pattern. The correct pattern should provide the minimum capacity, while the rest will all give higher values.

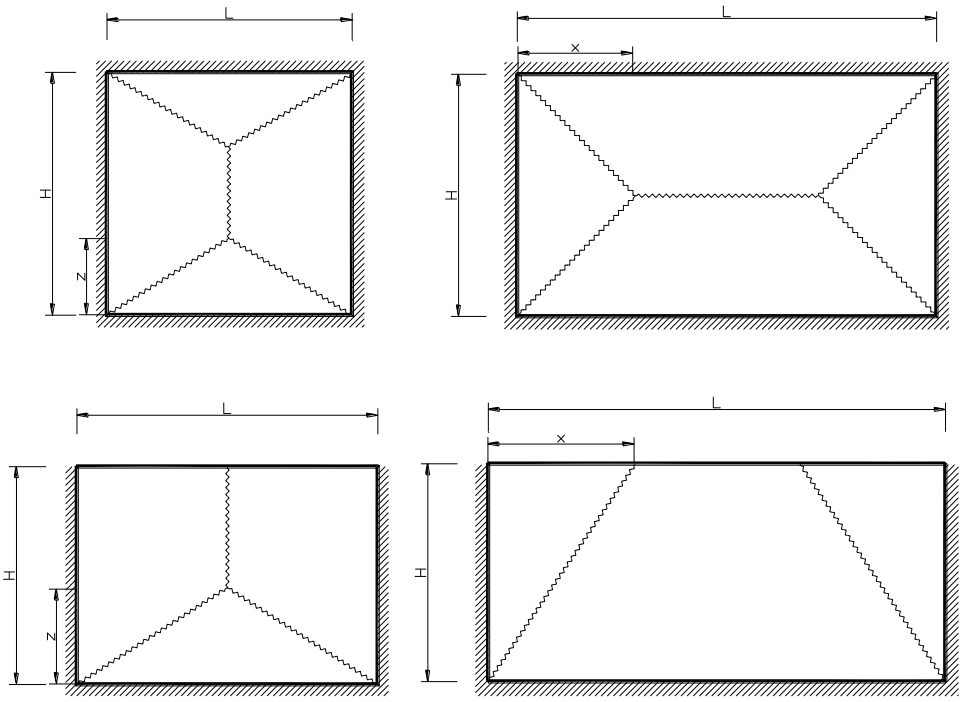

Figure 6-5. Typical Crack Patterns for Masonry Walls of Small and Large Aspect Ratios, with and without Top Supports.

Ultimate Failure Pressures. The basic fundamentals and main assumptions for yield line theory are as follows (Ghali and Neyille, 1989):

1. At fracture, the bending moment per unit length along all the fracture lines is constant and equal to the "yield" value.
2. The fractured slab parts rotate about axes along the supported edges.

3. Fractured slab parts are plane and therefore they intersect in straight lines; in other words, the "yield lines" are straight.
4. The lines of fracture on the sides of two adjacent slab parts pass through the point of intersection of their axes of rotation.

Based on these assumptions and using the energy method, the solutions for the crack pattern parameters (x or z) and corresponding ultimate pressure loads (p_r) are obtained through a series of lengthy mathematical manipulations. The results are presented in Table 6.2, in normalized form, for the walls illustrated in Figure 6.5 and with ultimate flexural moment capacities of m and ϕm for vertical and horizontal bending, respectively.

Drysdale and Essawy (1988) argued that, for walls with four simply-supported edges and moderate spans for which an initial horizontal crack occurs at mid-height and near the middle of the span at pressures significantly lower than the ultimate values, the initial horizontal crack should be treated as a free edge when estimating the ultimate failure load. This assumption results in the modified estimates of ultimate pressures shown in Table 6.3; however, the estimated failure pressures are not dramatically different than the unmodified results in Table 6.2.

For comparison, the ultimate failure pressures measured by Drysdale and Essawy are reproduced in Figure 6.6 for varying horizontal span, along with the estimated values obtained by applying the above theoretical results to their tested full-scale walls. The measured data shown are the average of three repetitions. The variation of measured failure pressures among the three repetitions is relatively small, with the coefficient of variation being in the order of 6%. The first set of data (see legend) is for walls with all four sides supported and without prestress. The three data points for spans between 11′ and 19′ are adopted directly from Drysdale and Essawy (1988). Good agreement is observed between the theoretical estimates and the measured data. The fourth point of this group, to the far end of the abscissa, is their result for walls with only top and bottom supports, hypothetically representing the case for all-side simply supported walls of infinite horizontal span. They re-tested this "extreme span"wall case using available extra specimens. The resulting average value of 47.2 psf nearly coincides with the theoretical extreme span asymptote or lower bound value. For these wall cases, the theoretical failure pressures do not significantly change for spans beyond 40′ since they are sufficiently large spans such that the side supports no longer significantly influence the expected failure pressure.

The average failure pressure measured by Drysdale and Essawy for top unsupported walls with a horizontal span of 16.4′ is also shown in Figure 6.6 in comparison with the theoretical estimate. Again, there is good agreement. This was, unfortunately, the only data they obtained for top unsupported walls.

Effects of Variable Material and Workmanship. It is recognized that relatively large variability of wall resistance capacity exists due to variable material and workmanship, versus laboratory controlled conditions (variation of laboratory measured failure pressure

Table 6-2. Failure Pressures (p_r) and Crack Pattern Parameters (x or z) Derived from Yield-Line Analysis

With Top Support	Modified Aspect Ratio $r_L = \frac{1}{r_H} = \frac{L}{\sqrt{\phi}H}$	≤1	≥1	$\rightarrow +\infty$
	Four Simple Edge Supports	$\frac{p_r HL}{m} = \frac{6\sqrt{\phi}}{r_H}\left(\frac{z}{H}\right)^{-2}$ $\frac{z}{H} = \frac{\sqrt{3r_H{}^2 + 1} - 1}{2r_H{}^2}$	$\frac{p_r HL}{m} = \frac{6\sqrt{\phi}}{r_L}\left(\frac{x}{L}\right)^{-2}$ $\frac{x}{L} = \frac{\sqrt{3r_L{}^2 + 1} - 1}{2r_L{}^2}$	$p_r \rightarrow \frac{8m}{H^2}$
	Modified Aspect Ratio $r_L = \frac{1}{r_H} = \frac{L}{\sqrt{\phi}H}$	≤1	≥1	$\rightarrow +\infty$
	Four Fixed Edge Supports	$\frac{p_r HL}{m} = \frac{12\sqrt{\phi}}{r_H}\left(\frac{z}{H}\right)^{-2}$ $\frac{z}{H} = \frac{\sqrt{3r_H{}^2 + 1} - 1}{2r_H{}^2}$	$\frac{p_r HL}{m} = \frac{12\sqrt{\phi}}{r_L}\left(\frac{x}{L}\right)^{-2}$ $\frac{x}{L} = \frac{\sqrt{3r_L{}^2 + 1} - 1}{2r_L{}^2}$	$p_r \rightarrow \frac{16m}{H^2}$
Without Top Support	Modified Aspect Ratio $r_L = \frac{1}{r_H} = \frac{L}{\sqrt{\phi}H}$	≤1.466	≥1.466	$\rightarrow +\infty$
	Three Simple Edge Supports	$\frac{p_r HL}{m} = \frac{6\sqrt{\phi}}{r_H}\left(\frac{z}{H}\right)^{-2}$ $\frac{z}{H} = \frac{\sqrt{12r_H{}^2 + 1} - 1}{4r_H{}^2}$	$\frac{p_r HL}{m} = \frac{8\sqrt{\phi}}{r_L}\left(\frac{x}{L}\right)^{-1}$ $\frac{x}{L} = \frac{\sqrt{9r_L{}^2 + 4} - 2}{3r_L{}^2}$	$(p_r \rightarrow 0)$
	Modified Aspect Ratio $r_L = \frac{1}{r_H} = \frac{L}{\sqrt{\phi}H}$	≤1.657	≥1.657	$\rightarrow +\infty$
	Three Fixed Edge Supports	$\frac{p_r HL}{m} = \frac{12\sqrt{\phi}}{r_H}\left(\frac{z}{H}\right)^{-2}$ $\frac{z}{H} = \frac{\sqrt{12r_H{}^2 + 1} - 1}{4r_H{}^2}$	$\frac{p_r HL}{m} = \frac{2\sqrt{\phi}}{r_L}\left(\frac{x}{L}\right)^{-1} \bullet \left(\frac{x}{L}r_L{}^2 + 8\right)$ $\frac{x}{L} = \frac{\sqrt{6r_L{}^2 + 4} - 2}{2r_L{}^2}$	$p_r \rightarrow \frac{2m}{H^2}$

were shown to be relatively small, as mentioned above). The effect of this variability is accounted for based on the data of Gross, et al. (1969) as quoted by Grimm (1999), which is reproduced in Figure 6.7. The data was for clay brick masonry; however, it is assumed also to be typical for the strength variability of concrete block masonry since the bond strength of the mortar, which is used for both types of masonry walls, controls in large part the ultimate resistance capacity. The data are presented as the distribution of the

Table 6-3. Failure Pressures (p_r) and Crack Pattern Parameters (x or z) Derived from Yield-Line Analysis, with the Assumption of Discontinuity at Initial Horizontal Center Crack

With Top Support	Modified Aspect Ratio $r_L = \frac{1}{r_H} = \frac{L}{\sqrt{\phi}H}$	≤0.733	≥0.733	$\rightarrow +\infty$
	FourSimple Edge Supports	$\frac{p_r HL}{m} = \frac{6\sqrt{\phi}}{r_H}\left(\frac{z}{H}\right)^{-2}$ $\frac{z}{H} = \frac{\sqrt{3r_H{}^2 + 1} - 1}{2r_H{}^2}$	$\frac{p_r HL}{m} = \frac{8\sqrt{\phi}}{r_L}\left(\frac{x}{L}\right)^{-1}$ $\frac{x}{L} = \frac{\sqrt{9r_L{}^2 + 1} - 1}{6r_L{}^2}$	Lower-Bounded by $p_r = \frac{8m}{H^2}$

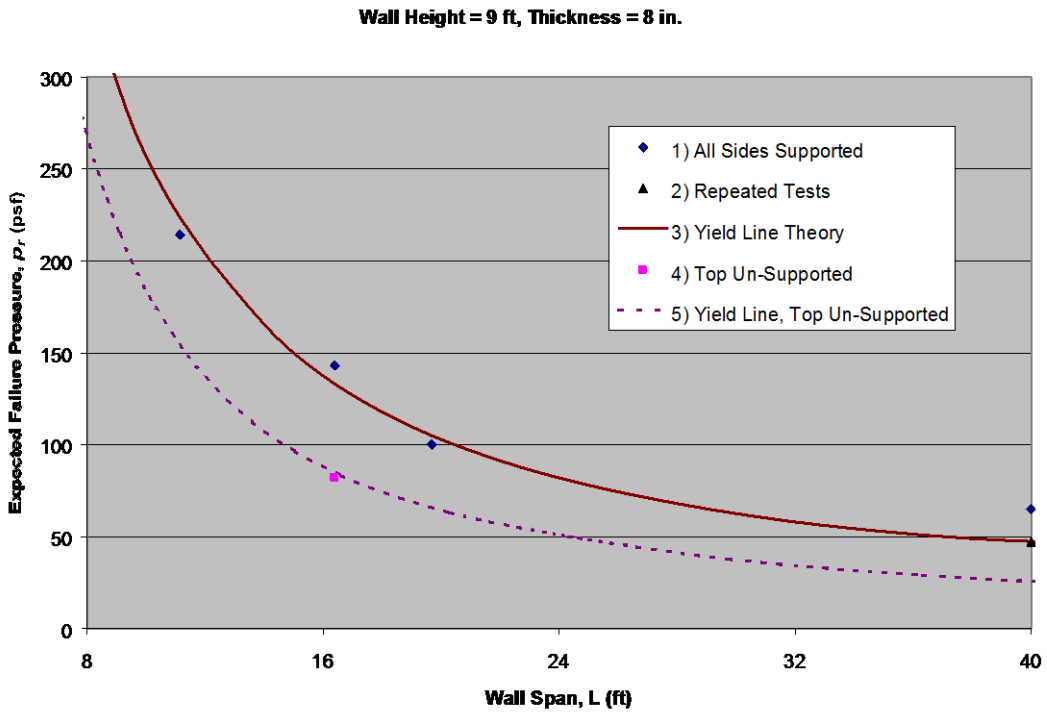

Figure 6-6. Comparison of Failure Pressure Variation with Wall Span.

flexural strength ratio between un-inspected workmanship and material and inspected or laboratory workmanship and material. Assuming a normal distribution for the resistance capacity, the mean and standard deviation of the flexural strength ratio are calculated based on the data to be about 0.8 and 0.2, respectively.

Fattal and Cattaneo (1977) discussed the effect of workmanship on masonry wall strength and recommended the use of reduction factors in estimating the strength of un-inspected masonry walls to account for variability in workmanship. They recommended a reduction factor of 0.67 to be multiplied to the mean strength obtained from laboratory or sources

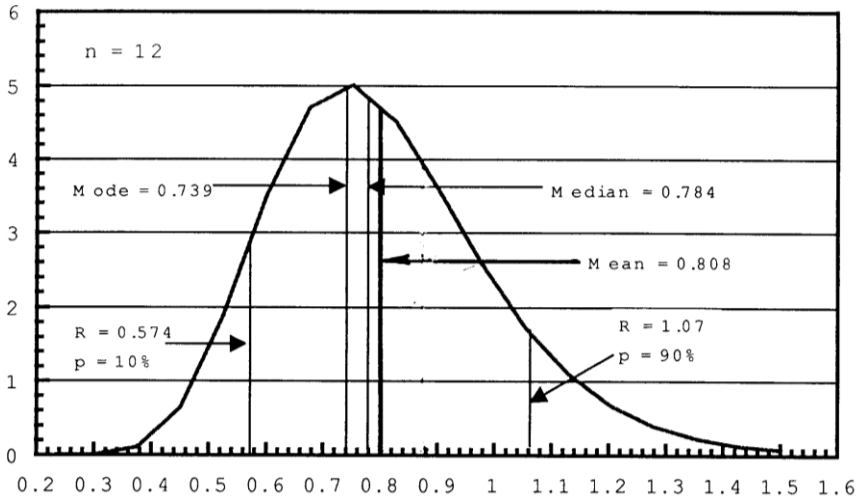

Figure 6-7. Effects of Workmanship on Actual Flexural Strength vs. Nominal Value.

other than directly measured from the wall under investigation. They also quoted code recommended workmanship reduction factors of 0.67 by BIA to 0.5 by UBC and NCMA. All these reduction factors are used as a simple method to account for the overall effect of variable workmanship on wall strength, including the effects on both the mean and the dispersion. A value of 0.67 corresponds approximately to the 25th percentile of a normal distribution of $N(0.8, 0.2)$, and 0.5 roughly to the 5th percentile. These values provide further support to the use of a mean strength ratio of 0.8 and a standard deviation of 0.2, as derived from the data reproduced in Figure 6.7.

Estimation of Wall Failure Probability. Based on the above discussions, the probability of failure, P_f, for a masonry wall of span L under uniform lateral pressure loading p is estimated as

$$P_f = \Phi\left(\frac{p - 0.8p_r(L)}{0.2p_r(L)}\right) \tag{6.1}$$

where $\Phi(*)$ denotes the standard normal cumulative distribution function. $p_r(L)$ is the laboratory measured or nominal failure pressure as a function of wall span and heights, edge supports, and ultimate flexural moments (dependent on material and concrete masonry configuration), as represented by the theoretical results in Table 6.2 for walls with and without roof support. Examples of estimated probabilities of failure are shown in Figures 6.8 and 6.9 for top supported and unsupported walls, respectively. Data are presented for simply supported, 9′ high walls of various spans.

The present model focuses on the most common failure mechanism of masonry walls that is associated with cracking of mortar joints and concrete blocks, assuming that the wall edge supports are perfect when they are present. Thus, it treats the failure probability for

walls under outward resultant pressure load the same as for walls under inward resultant pressure load, ignoring potential differences in the resistance capacities of wall anchorage along the edges between inward and outward loads. Outward loading may cause pullout of the wall anchorage while inward loading is exerted against walls presumably with edge supports closer to "perfect". It is possible that the failure probability for outward loading will be somewhat higher than for inward loading. In addition, it is assumed that there are no openings on the wall, or the openings and their perimeter framing do not decrease nor increase the wall capacity in resisting pressure loads.

Concluding Remarks. Yield-line theory is used to assess the effects of wall dimensions, support conditions and orthotropic ultimate moment capacities on the failure of masonry walls. The theoretical results agree well with experimental data. The theoretical results of expected or nominal failure pressure, along with the data on field variability of workmanship and material, provide a useful model for estimating failure probabilities of masonry walls.

6.2.6 Wood Frame Walls

For wood frame walls under lateral loads, post-storm surveys show that failures are nearly always associated with connection failures. Various examples are shown in Figures 6.10 through 6.14. This situation is similar to the observation that failures of light-frame roof systems are nearly always a result of inadequate connections rather than the capacities of the elements themselves, as shown by studies and confirmed by anecdotal evidence from post-hurricane investigation (Sparks, et al., 1994). Hence, at present, wall failure modeling for wood framed structures is focused on modeling the failure mechanism of the nail being bent and/or pulled out on wall edges that connect the wall to other parts of the structure and connect various components within the wall system.

Simplified Structural Model. The main structural components of the exterior walls include the bottom plate, studs and the double top plates, as well as bracing or sheathing. Figure 6.15 illustrates a typical wall construction. The present model deals with connections using nails only, which are typical for residential constructions. Figure 6.16 shows the most common nailing pattern as stipulated by the Wood Frame Construction Manual (1995 SBC High Wind Edition, AFPA/AWC, 1996), which is also required by many building codes. Wood frame walls are built by stories. For each story, the bottom plate of the wood frame wall is installed to the floor with two 16d face nails at each of the 16″ spaced stations. The wood studs, typically also spaced at 16″ on center, are either toe-nailed to the bottom plate with two 8d nails on each side of a stud, or end-nailed to the bottom plate using two 16d nails before it is installed onto the floor. The double top plates are end-nailed to the studs with two 16d nails on each stud. The upper and lower top plates are typically connected together with two 10d face nails at stations of 16″ spacing. Ceiling joists or roof rafters are normally toe-nailed to the double top plates of the wood frame wall, with three 8d common nails at each of the 16″ spaced stations along the top plate. At the exterior corners of the structure, and sometimes also at the intersections of exterior and interior (partition) walls, multiple studs are typically face-

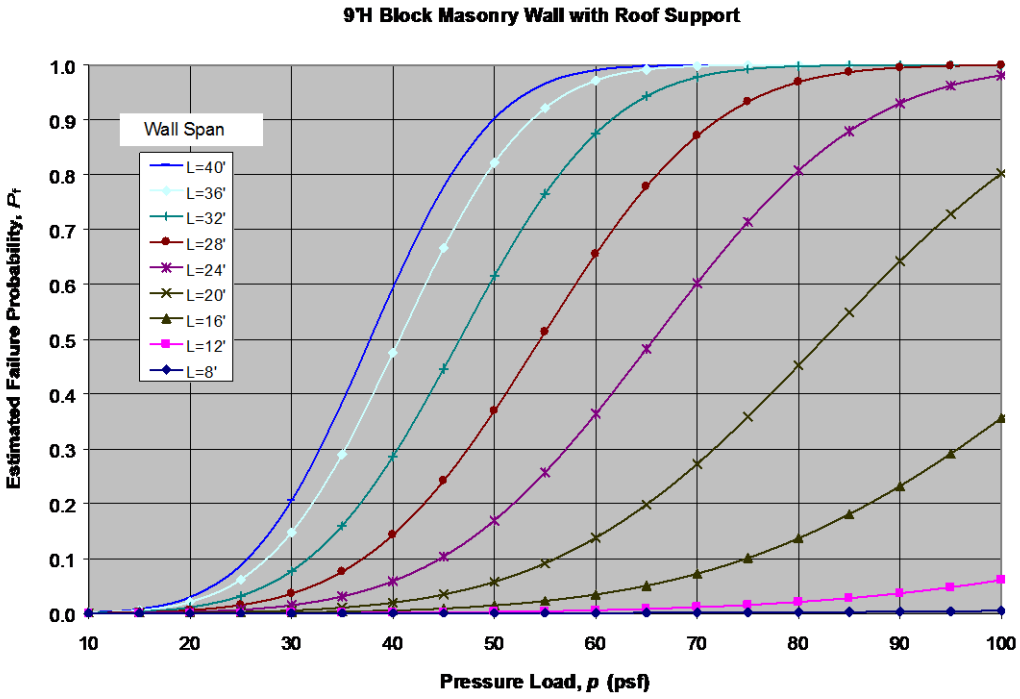

Figure 6-8. Estimated Failure Probability as a Function of Pressure Load for Various Wall Spans with Roof Support.

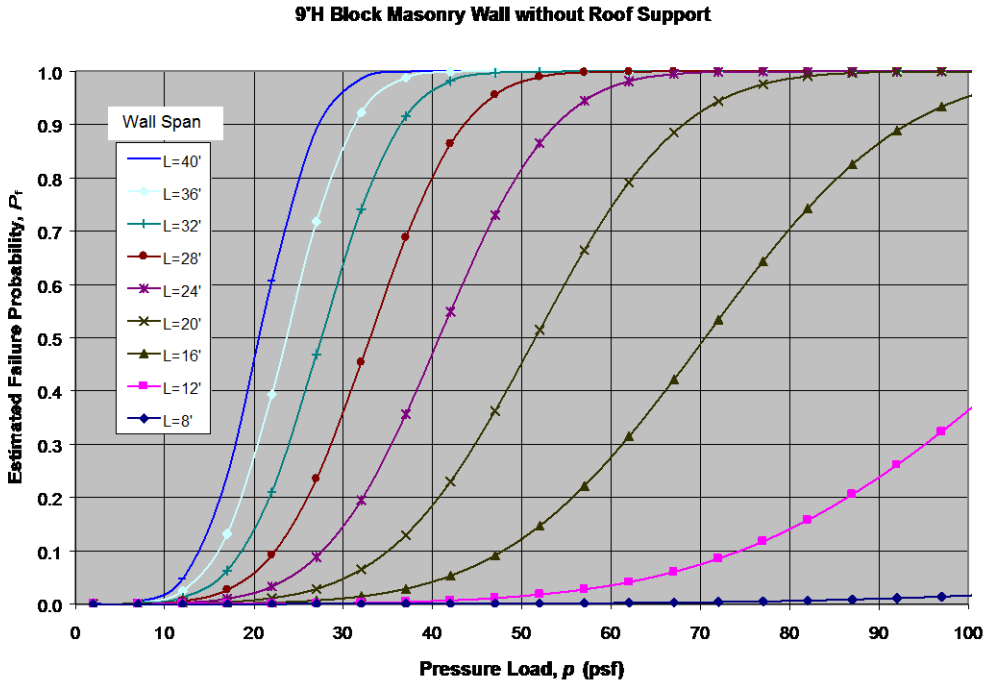

Figure 6-9. Estimated Failure Probability as a Function of Pressure Load for Various Wall Spans without Roof Support.

(a) Exterior wall fails in sections at connections to other parts of the structure

(b) Wall failure at the other side of the same building shown in (a)

Figure 6-10. Examples of Wind-Induced Damage to Residential Wood-Framed Wall System (Oklahoma Tornado Out-Break, May 1999).

(a) Wall failure while roof frame still in place

(b) This photo reveals that the wall fails at nail connections to the roof and foundation

Figure 6-11. Examples of Wind-Induced Damage to Residential Wood-Framed Wall System (Oklahoma Tornado Out-Break, May 1999).

(a) A wall section collapses

(b) Garage wall fails at the connections to the foundation

Figure 6-12. Examples of Wind-Induced Damage to Residential Wood-Framed Wall System (Oklahoma Tornado Out-Break, May 1999).

(a) A let-in braced wall section collapses, while other sections also fail at connections to gable end truss

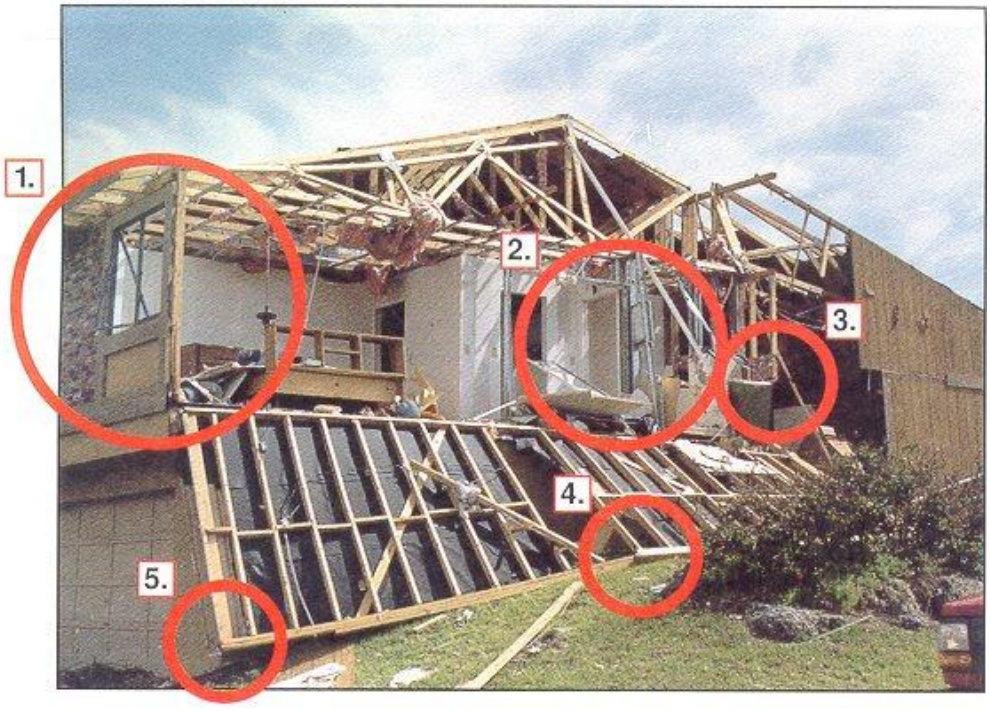

(b) Several sections of a let-in braced wall collapse, failed at connections to gable end truss

Figure 6-13. Examples of Wind-Induced Damage to Residential Wood-Framed Wall System (FEMA, 1992, Hurricane Andrew, Florida).

(c) End wall separated from end unit of a modular home

(d) Another example of gable end wall connection problem

Figure 6.13. Examples of Wind-Induced Damage to Residential Wood-Framed Wall System (FEMA, 1992, Hurricane Andrew, Florida) (concluded).

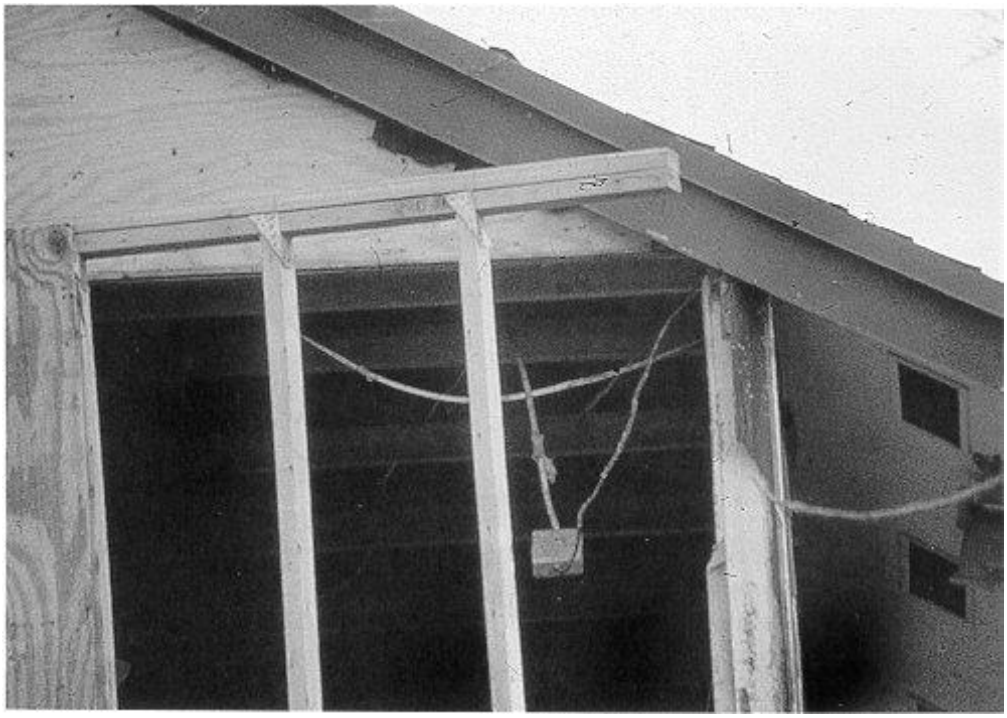

(a) Improper connection in a blown-out wall section

(b) Complete failure of a wood framing system

Figure 6-14. Examples of Wind-Induced Damage to Residential Wood-Framed Wall System (HUD, 1993, Hurricane Andrew, Florida).

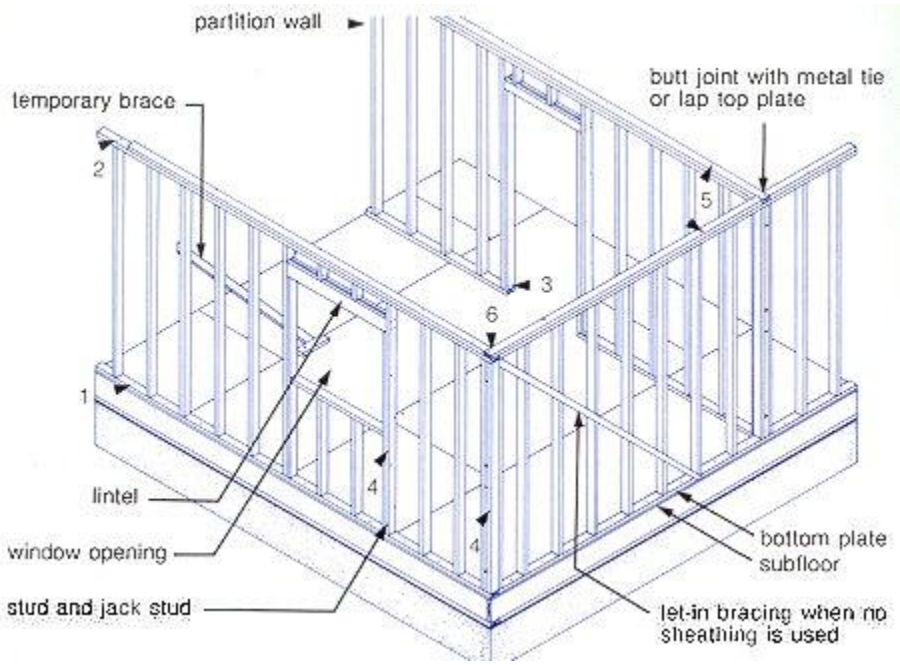

Figure 6-15. Typical Wood Frame Walls for Residential Construction (CMHC, 1989).

nailed together with 16d nails spaced at 24″. The above nailing schedule is mainly based on the Standard Building Code. There are some variations, depending on the codes/manuals used; however, the resulting variation in combined resistance capacity is expected to be relatively insignificant and can be accounted for when needed.

Wood frame walls are required to be let-in braced with 1″×4″ wood strips at about 45° to plumb or be sheathed with 4′×8′ plywood or other structural boards, at least at the corners of the structure. They are nailed to the lower top plate, studs and bottom plate of a braced wall section. Although the bracing or sheathing is intended mainly to strengthen the wall's resistance capacity for in-plane loads, it also tends to bond the wall components within its span together to react as a unit and share the lateral loads.

The present simple model treats each wall section, which is braced or sheathed together, as a structural unit, and each unit is supported only by the floor(s) and/or roof to resist uniform lateral loading, independent of other similar units. This implies that there would be perfect load sharing horizontally within the unit and no load is transferred beyond a unit. This assumption is a close approximation of the behavior of the wall sections near the mid-span of the wall under uniform pressure loading. Corner units gain additional support from the adjacent wall; however, there normally exist higher suction loads near corners that are not accounted for by the model. These effects on the corner units tend to counteract each other. Thus, corner units are treated the same as interior units in the model. Additional support by interior partition walls is ignored for walls with top support, but it is considered when dealing with walls without top support. In addition, it is assumed that wall openings and their perimeter framing do not decrease nor increase the wall capacity in resisting pressure loads.

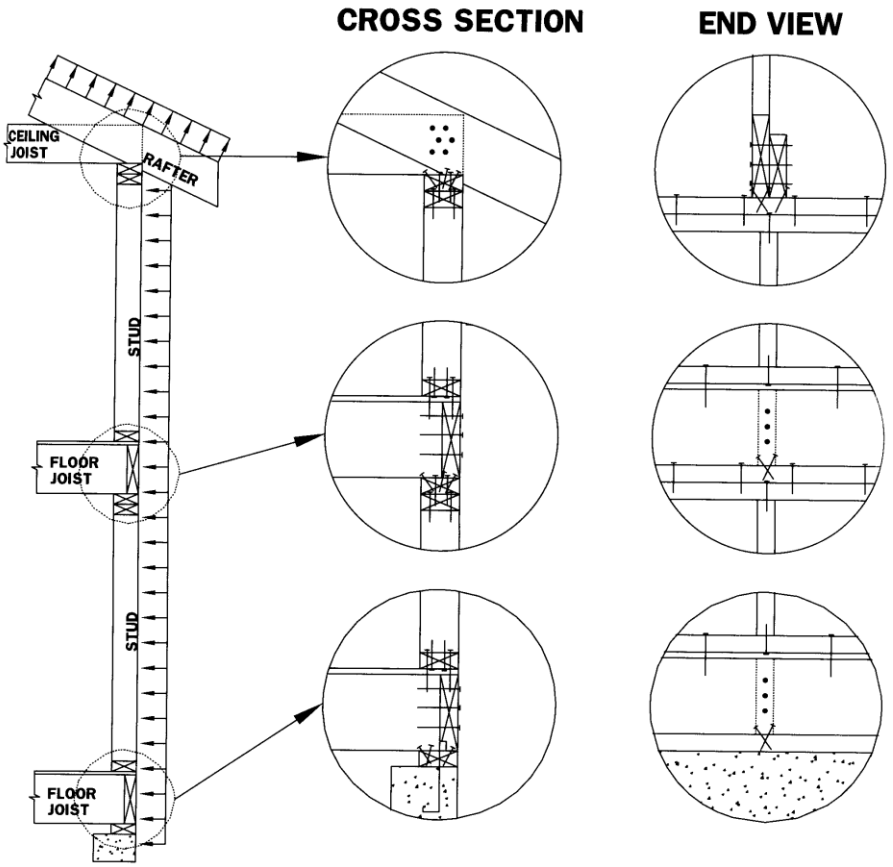

Figure 6-16. Typical Nailing Patterns for Wood Frame Wall Structure of Residential Construction (AFPA/AWC, 1996).

Such a simplified model depicts a span-wise semi-flexible wall structure, versus a completely rigid slab wall model or a completely flexible model (each individual stud reacts independently). It is deemed to be a reasonable representation of the actual system, but it could be improved by properly incorporating the effects of adjacent and partitioning wall supports. The span width of a unit somehow represents the span-wise influence width, by which a gradually varying influence function is approximated with a step function. Thus, the unit width is a critical parameter in the model and its effective value needs to be calibrated when data become available. At present, it is taken to be the bracing width for let-in braced walls, which equals the wall height (normally 8′) when 45° bracing is used. For sheathed walls, the 4′×8′ sheathing boards are used vertically and also horizontally in some occasions, which provide 4′ and 8′ bracing widths. Considering the fact that sheathing boards possess higher span-wise load transfer capability and adjacent boards are nailed to the same stud through the entire length of their edge, its effective unit width is also set to 8′ in the present model.

Post-storm surveys have indicated that wood frame walls collapse typically in sections. This observation lends some confidence in the concept for the above sectional wall model.

Lateral Failure Load for Nail Connections. A relatively simple way to estimate the resistance capacity of nail connections for various wood materials and products is to use the specified allowable design load data already compiled in the National Design Specification (AFPA/AWC, 1997) and adjust them to expected ultimate failure load with proper "safety factors." This approach is a practical alternative to collecting and analyzing a large volume of laboratory data, which would be an expensive undertaking given the large number of wood materials and products as well as their widely varying properties for different humidity, temperature and nailing application methods.

Several types of timber are more commonly used for residential constructions along the coast. These include Southern Pine (typical specific gravity, SG = 0.55), Douglas Fir-Larch (SG = 0.50), Northern Douglas Fir-Larch (SG = 0.49), Southern Douglas Fir (SG = 0.46), Spruce-Pine-Fir (SG = 0.42) and Southern Spruce-Pine-Fir (SG = 0.36). The basic lateral design loads for these timbers as compiled from NDS are listed in Table 6. 4 along with the values of the applicable adjustment factors for the nailing schedule and applications described in the last section. Since the exact proportions of these timbers' usage by the industry for residential constructions are not available, their average design value is used to estimate the anticipated ultimate load with proper safety factors. This is equivalent to assuming that the usage is equally distributed among these timbers. The associated root-mean-squared variations and the coefficients of variation due to varied timber usage are indicated in the table. The coefficients of variation range from 0.13 to 0.20.

To some extent, the design loads reflect the expected failure loads with some safety factors. The safety factors may vary from one situation to another since normally a percentile value, often the 5^{th} percentile, derived from the available distribution data of failure loads, is used as the base for determining an allowable design load. The ratio of the mean failure load to this percentile value varies with the coefficient of variation in the data. After being combined with other factors, the final basic allowable design load varies greatly relative to the actual mean failure load. For simplicity, a representative safety factor is desired in estimating the mean or expected failure load from the published allowable design load. Rosowsky and Reinhold (1999) investigated the rate-of-load effects on nail connections for wood. They presented some test results that indicate the ratio of tested lateral failure loads to the NDS allowable design value is about 4, as shown in Figure 6.17. From 16 specimens, Reed, et al. (1996) obtained an average withdrawal capacity of 350 lbs for a toe-nail connection using three 8d nails versus a NDS value of 96 lbs, indicating a factor of 3.6. Zaitz (1994) loosely suggested, by referring to the Wood Handbook ("Wood as an Engineering Material," Forest Products Laboratory, DOA, 1987), that safety factors up to a value of 6 have been used to obtain the allowable loads listed in NDS. The relatively large values of safety factors used may stem from the inherently large variability with nail connections for wood, which is a biological material having highly variable properties and strength itself.

For this present study, a basic safety factor of 4.0 is used for estimating the ultimate loads from the NDS design loads. Some other values in a range from 4.0 to 5.0 are also used depending on specific situations. For example, the safety factors used to estimate the

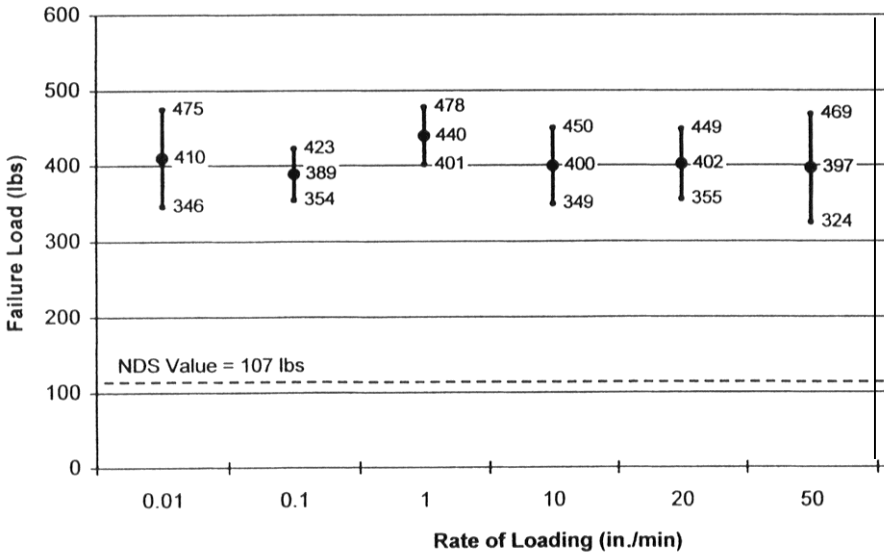

Figure 6-17. Measured Ultimate Capacity (Mean ± 1 Standard Deviation) of 8d Nail Connections for Lateral Loading in Comparison to the NDS Value, for Various Rates of Loading.

ultimate capacity of the nail connections between the studs and the top plate and those between the studs and the bottom plate are increased to 4.5 and 5.0 for let-in braced and sheathed walls, respectively. This is because the bracing and sheathing are expected to provide additional strength to the connection between these components. The resulting ultimate lateral failure loads are shown in Table 6.4 for the typical nail connections on wood frame walls.

Variability and Effects of Workmanship. There exists relatively high variability in the failure load of nail connections for wood. The overall variability in the ultimate capacity of wood structures is associated with such factors as variable properties in similar species of wood, use of different timbers, deviation of installed component's strength in a full-scale system from component test value, and variable workmanship, etc.

The variability in the strength of the same species of wood is reflected in the laboratory test result variations. For example, Rosowsky and Reinhold (1999) showed a COV of 0.13 for lateral failure load from ten 8d box nail test specimens, and 0.30 for withdrawal load from over thirty 8d common nail test specimens. Reed, et al. (1996) scored a COV of 0.23 for withdrawal load from sixteen 8d toenail specimens. The variability of strength among a number of commonly used timbers is represented by COVs ranging from 0.13 to 0.20 (with an average of 0.167) for the typical nailing applications shown in Table 6.4, assuming an equal utilization probability distribution for these timbers. Variation of the installed component's strength in a full-scale system from the component's test value will also be a significant contributing factor to the overall variability; unfortunately, it is not quantitatively known and it is difficult to estimate. Variable workmanship always plays a role in the reduction of the expected ultimate capacity and in the variability of the

Table 6-4. Estimated Resistance Capacity of Nail Connections within One Stud Spacing (Typically 16″)

Connections	Penny Weight of Nail	Thickness of Side Member (inches)	Resistance of Nail Connections (lbs)						Average (lbs)	STD (lbs)	COV
			Southern Pine (G=0.55)	Douglas Fir-Larch (G=0.50)	Northern Douglas Fir-Larch (G=0.49)	Southern Douglas Fir (G=0.46)	Spruce Pine Fir (G=0.42)	Southern Spruce Pine Fir (G=0.36)			
Joist to Top Plate	8d	0.75	104	90	87	80	70	58	81.5	16.1	0.198
Double Top Plates	10d	1.5	128	118	115	109	96	77	107.2	18.2	0.170
Top Plate to Stud	16d	1.5	154	141	138	131	120	104	131.3	17.5	0.133
Stud to Bottom Plate	8d	0.75	104	90	87	80	70	58	81.5	16.1	0.198
Bottom Plate to Floor	16d	1.5	154	141	138	131	120	104	131.3	17.5	0.133

Connections	Number of Nails per Connection	Adjustment Factors Required by NDS							Assumed Safety Factor	Reduction Factor for Workman-ship	Estimated Ultimate Failure Load (lbs)
		Duration of Load CD	Wet Service CM	Temp. Ct	Penetra-tion Depth Cd	End Grain Ceg	Diaphragm Cdi	Toe-Nail Ctn			
Joist to Top Plate	3	1	0.85	1	1	1	1	0.83	4	0.75	517
Double Top Plates	2	1	0.85	1	0.84	1	1	1	4	0.8	490
Top Plate to Stud	2	1	0.85	1	1	0.67	1	1	4.5 *	0.8	539
Stud to Bottom Plate	4	1	0.85	1	1	1	1	0.83	4.5 *	0.75	776
Bottom Plate to Floor	2	1	0.85	1	1	1	1	1	4	0.8	714

* 4.5 for Walls with Let-In Braces, and 5.0 for Walls with Sheathing Boards

ultimate capacity of a structure. For example, missing nails are frequent in residential wood construction. There are no data available for workmanship variability for wood structures, but it may be comparable to that for masonry walls, represented by a COV of 0.25.

The combined strength variability for wood structural systems is difficult to estimate. The combined COV due to the above-identified factors could approximately be a root-sum-square value of the individual COV's. This would have resulted in a combined COV somewhat larger than any individual COV, the largest of which would probably be that for variable workmanship. On the other hand, when components form a unit in resisting loads, the components of similar function share the load. For example, within a wall structural unit as described in the sectional wall model noted above, all nails connecting the bottom plate to the floor tend to share the lateral load simultaneously. Thus, their total capacity will be the sum of the individual capacities and the variability of the sum will be reduced by a factor equal to the square root of the number of nails performing the same function.

Given the above factors, a combined COV value of 0.20 is thought to be a reasonable compromise and is applied in the current version of the model.

Probability of Wall Failure. Based on the section, all wall model described above, several assumptions are made in order to derive the probability of wall failure:

1. Within a span-wise section, all nail connections for a link between any two components, such as all those between the bottom plate and the floor, simultaneously resist the load passing through this link, in such a way that the total resistance is the sum of the individual capacities;
2. All the links, such as those from studs to bottom plate, from bottom plate to floor, and from top plate to ceiling joists or roof rafters etc., form a series system of the section so that the failure of any one of these links results in failure of the section;
3. All sections are identical and form a series system of the wall so that the failure of any one of the section results in failure of the wall.

With the concept of a sectional wall and the above assumptions, the probability of wall failure, P_f, under uniform pressure load, p, can be formulated as

$$P_f = 1 - \left[\left(1 - \Phi\left(\frac{p\frac{A}{2} - R_1}{0.2R_1} \right) \right) \left(1 - \Phi\left(\frac{p\frac{A}{2} - R_2}{0.2R_2} \right) \right) \cdots\cdots \left(1 - \Phi\left(\frac{p\frac{A}{2} - R_5}{0.2R_5} \right) \right) \right]^{L/S} \quad (6.2)$$

where $\Phi(*)$ denotes the standard normal cumulative distribution function, R_1, R_2, … R_5 are the estimated total ultimate capacity of all nail connections for links 1 to 5, respectively, within a section. Estimated ultimate capacities for the individual connections are given in Table 6.4, and the number of connections equals to the effective section span (S) divided by stud spacing. $A/2$ represents half of the area of the section since the uniform pressure load is equally divided by the upper and lower supports. L is the wall span, while S represents the effective section span.

Examples of P_f versus p for various wall spans, calculated assuming an effective section span, S, of 8′, are shown in Figures 6.18 and 6.19 for let-in braced and sheathed walls, respectively.

These results are estimated ignoring the additional supports by adjacent and partition walls. This approximates the case of outward suction loads more appropriately than the case of inward pressure loads. Estimated failure probability for inward loading would be slightly lower than for outward loading of the same magnitude.

For top-unsupported walls, which models the case where the roof has been destroyed and the wall is still standing, the required supports will be transferred to the adjacent or partition walls, and the floor. Walls are normally joined through multiple studs, which are connected, typically, with 16d face nails spaced at 2′ (SBC 1977). The probability of wall failure is controlled by the failure of the upper nail connections along the joining edge of the adjacent walls. Assuming linear reaction along the height of the supporting walls, the most vulnerable top three connections (i.e., 6 nails) together will approximately share

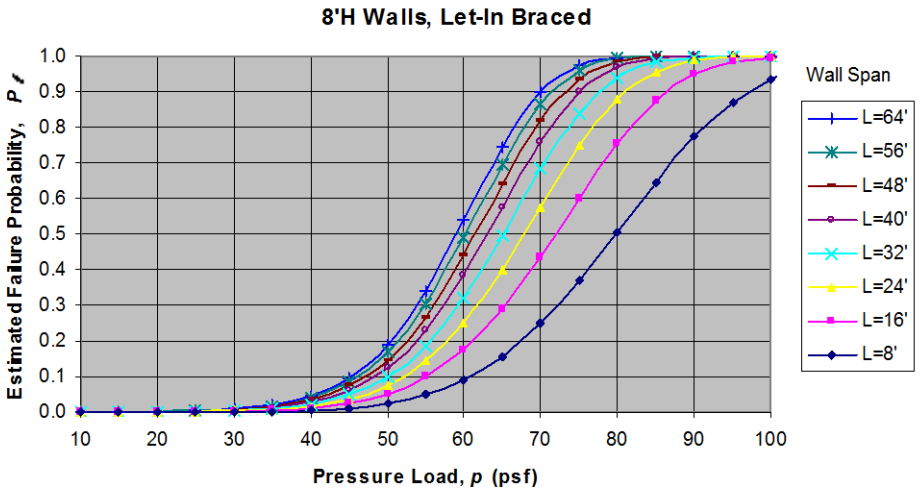

Figure 6-18. Estimated Failure Probability as a Function of Pressure Load for Various Wall Spans, Top Supported and *Let-In Braced* Wood Frame Walls.

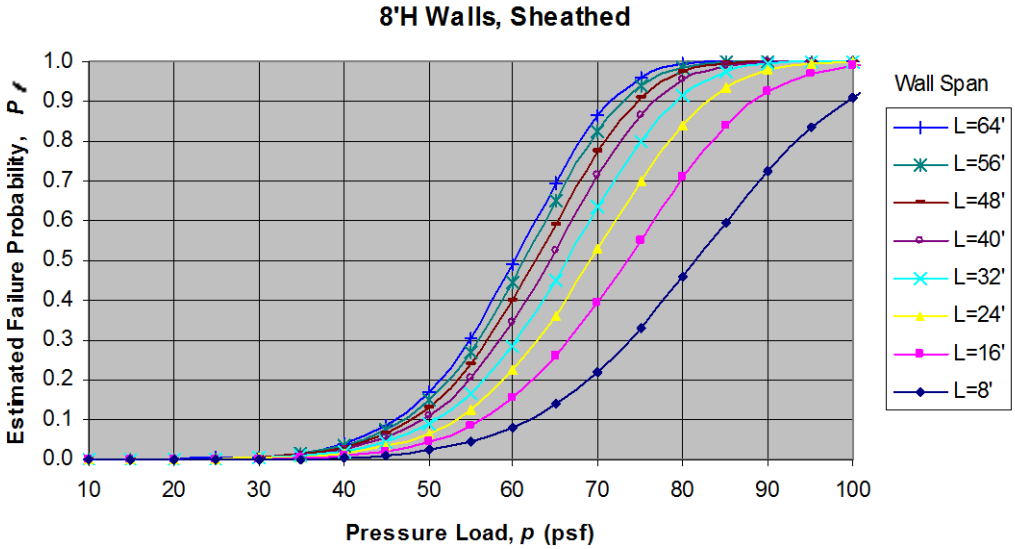

Figure 6-19. Estimated Failure Probability as a Function of Pressure Load for Various Wall Spans, Top Supported and *Sheathed* Wood Frame Walls.

9/16 of the total pressure load on the wall section spanned between the supporting walls. The failure probability is then estimated by

$$P_f = 1 - \left[1 - \Phi\left(\frac{\frac{9}{16} pHW - R}{0.25R} \right) \right]^{(L/W)+1} \tag{6.3}$$

where H is the wall height (floor to eave), W is the typical distance between supporting walls and L is the total wall span. The resistance capacity, R, is provided by six 16d face nails and is estimated to be 2142 lbs. The coefficient of variation of 0.25 used here is empirically increased from the value of 0.20 for the case of walls with a top support, due to the uncertainty anticipated with the damage states of roofs and supporting walls.

Examples of P_f versus p for various wall spans, calculated assuming a typical distance, W, of 12′, are shown in Figure 6.20.

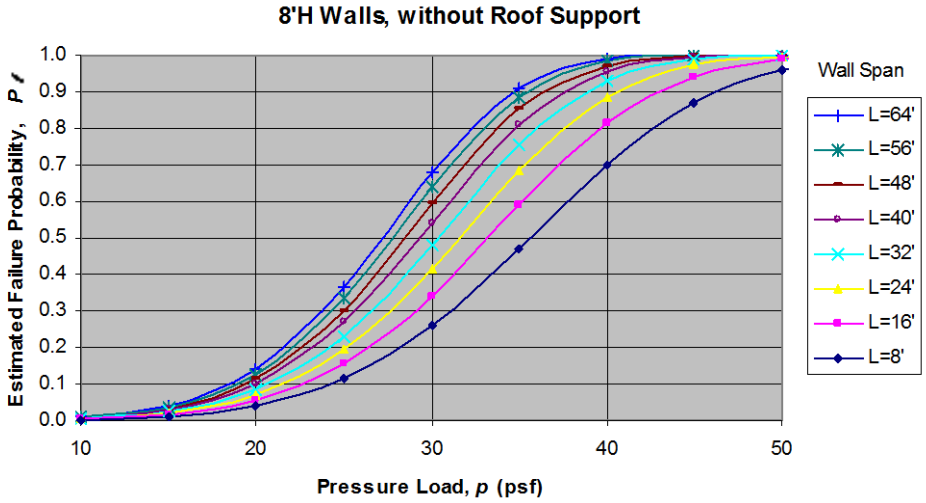

Figure 6-20. Estimated Failure Probability as a Function of Pressure Load for Various Wall Spans, Top *Unsupported* Wood Frame Walls, Let-In Braced or Sheathed.

Concluding Remarks. Based on post-storm observations and suggestions from published literature, wood frame wall failure probability is estimated based on the failure of nail connections between the wall's double top plate and ceiling joists or roof rafters, and between the bottom plate and the floor, as well as the nail connections of the wood studs to these plates. A sectional wall model, along with the concept of an effective section span, is introduced. A probabilistic failure model has been derived, relating the wall failure probability for given pressure on the wall to the mean capacity and coefficient of variation of individual connections. The mean lateral capacity and coefficient of variation of the nail connections for wood are determined from the analysis of the data available in technical papers and design manuals. For data from design manuals, conversions from the specified allowable design value to the expected ultimate capacity are made using estimated safety factors. Variability of capacity due to various effects is also modeled.

Neither roof weight nor roof uplift is included in the present wall models. It is also recognized that these models ignore some failure modes. These include, for example, the interaction of a wall-roof structural failure in which the wall and roof act as an inter-linked structural system and support each other in resisting different load effects caused by wind, such as the uplift and the lateral forces on the roof, or the lateral forces on walls.

The failure of one element may in some cases increase the likelihood of the failure of others.

6.3 Damage Model Validation for Residential Buildings

In order to validate the model's ability to predict damage to buildings, comparisons of simulated and observed damage states are performed. The damage states examined here include roof cover damage, roof sheathing damage and damage to windows. Roof cover and roof sheathing damage states are simulated and compared to roof damages experienced during Hurricanes Andrew (1992), Erin (1995) and Fran (1996). In the case of window damage to residential buildings, the information collected by HUD, as described in Crandell, et al. (1993), provides the only source of relatively unbiased statistics on window damage associated with Hurricane Andrew.

In all of the comparisons, the observed damage states are compared to those obtained by modeling the wind loads experienced by the homes using the wind loading and damage models described earlier. To obtain estimates of the wind speeds at the sites of the observed damage, a full reproduction of the wind speed and direction time history at the site are obtained using the hurricane wind field model described in Section 2.2.

6.3.1 Roof Cover and Roof Deck Damage

6.3.1.1 Hurricane Andrew (1992)

The most comprehensive existing report on the performance of roof systems for residential buildings during Hurricane Andrew is given in HUD (1993). In the HUD (1993) study, the survey team randomly selected 466 homes located in the high damage areas and then proceeded to quantify the damage states for each structure. The homes were located in nine separate clusters (A through I) as shown in Figure 6.21.

Analysis of Aerial Photographs used to Supplement the HUD Data. To expand on the HUD roof damage data, aerial photographs were obtained that correspond to four of the locations used in the HUD damage survey. The aerial photographs were produced at a scale of 1″ = 100′. This scale provides enough resolution so that the damage to the roof cover and roof sheathing can be directly estimated. The exact location of the HUD study areas is determined by geo-coding the addresses of the homes surveyed by the HUD team.

The wind speed traces at the locations of the four photographs determined from the simulation of Hurricane Andrew are given in Figure 6.22. As seen from Figure 6.22, the basic wind speeds experienced at each location are very similar. These simulated wind speeds are discussed further in Chapter 9.

The HUD building damage states were categorized into 4 distinct damage states defined as:

Damage State 0	No Damage
Damage State 1	$0 < \text{Damage} \leq 1/3$

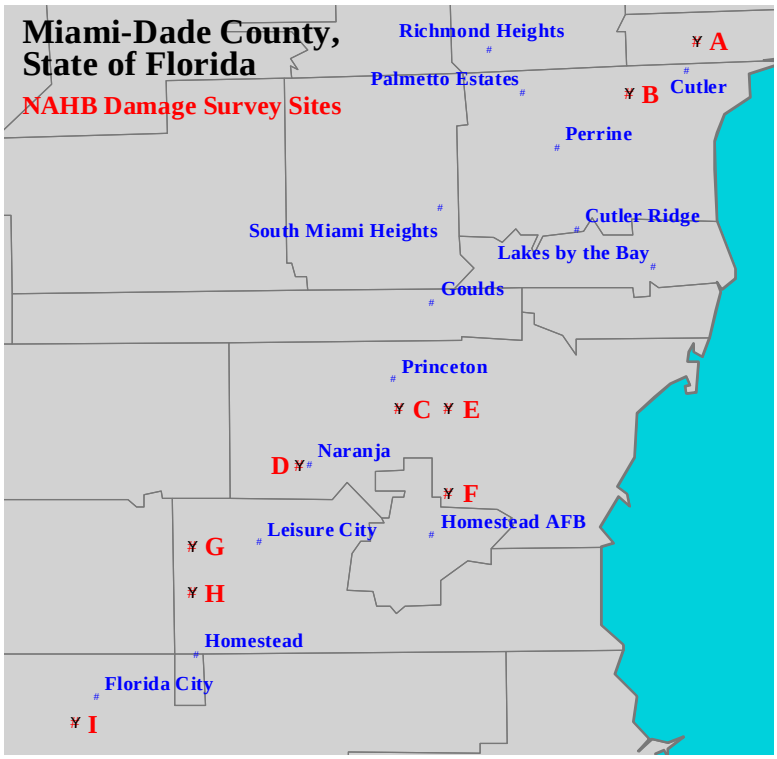

Figure 6-21. NAHB Site Locations.

Damage State 2	1/3 < Damage ≤ 2/3
Damage State 3	Damage > 2/3

The damage states recorded included roof cover damage, roof sheathing damage, roof-wall connection damage, gable end damage and window damage.

Based on conversations with members of the HUD damage team, it has been assessed that the high damage states indicated in the HUD report overstate the total damage. Thus, the roof damage states used in the analysis of the damage evident in the aerial photography are as follow:

Damage State 0:	No Damage
Damage State 1:	0.0 < Damage ≤ 0.05
Damage State 2:	0.05 < Damage ≤ 0.1
Damage State 3:	0.1 < Damage ≤0.2
Damage State 4:	0.2 < Damage ≤ 0.5
Damage State 5:	0.5 < Damage ≤ 1.0
Damage State 6:	Damage = 1.0

When examining the photographs, if uncertainty exists as to the extent of damage, because the roof was covered with a tarp or plastic, the damage state is entered as unknown. Prior to performing comparisons of simulated and observed damage states, comparisons of the damage estimates obtained from the photographs to those reported by

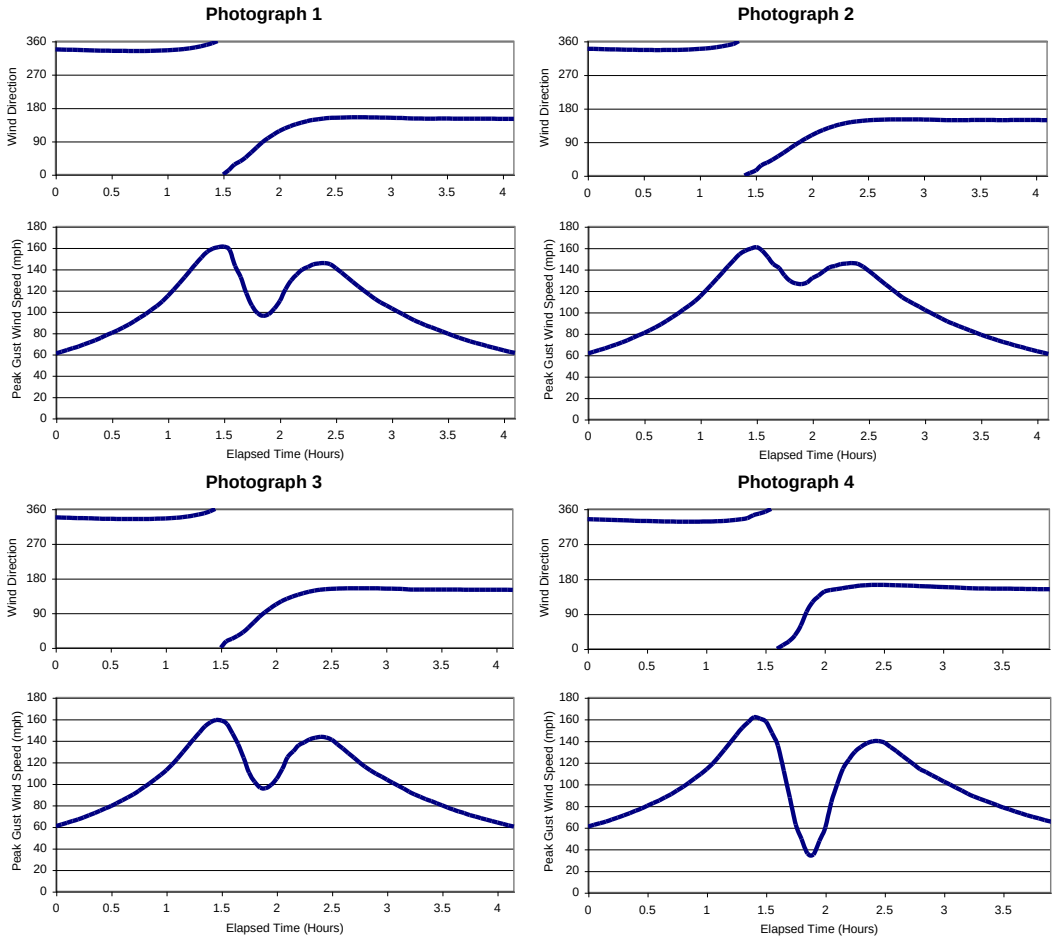

Figure 6-22. Wind Speed and Direction Traces (10m, Open Terrain) at Locations of Photographs 1, 2 3, and 4 (HUD Locations, F, E, D, and H).

HUD were made. To perform these comparisons, damage states 1, 2 and 3 observed from the aerial photographs were combined into one category, corresponding to HUD damage state 1. The four distinct damage states represent no damage, minor damage, moderate damage, and major damage, as described in Table 6.5.

Photograph 1 (HUD Location F). This subdivision was comprised of closely-spaced two story homes. The estimated value of the surface roughness within the subdivision is about 0.6 m. The surrounding terrain to the south and east of the homes is open. In the damage simulation, the subdivision was modeled with a z_0 of 0.3 m, representing a compromise between the low z_0 value around the buildings and the high z_0 value within the subdivision. Upon reviewing the aerial photography, it was obvious that the roofs of some of the homes had been repaired. All homes with repaired roofs were removed from the damage analysis. A total of 330 two-story gable homes are shown in the photograph. Of these 330 homes, 98 had obviously been repaired, leaving a total of 232 non-repaired homes. Of these 232 homes, ARA could identify the roof cover damage for 223 cases, and the roof sheathing damage in 213 cases. The HUD team surveyed 63 homes in this subdivision, and were able to identify damage for 57 of the 63 cases.

Table 6-5. Mapping Used to Match Aerial Photograph Estimated Damage States and HUD Damage States

Damage State	Aerial Photograph Estimated Damage State	HUD Damage State
0	No Damage	No Damage
1	0-20%	0-33%
2	20%-50%	33%-66%
3	>50%	>66%

The comparison of the observed damage states, shown in Figure 6.23, indicates that in the case of roof sheathing, the larger sample taken from the photograph suggests about 50% of the homes experienced the loss of a least one piece of roof sheathing whereas the HUD data suggests that about 60% of the homes experienced the loss of at least one piece of roof sheathing. The only other notable difference between the two damage state estimates is that the HUD data places a higher percentage of the homes experiencing the highest roof cover damage state than does the data obtained from the photograph, even though the highest HUD damage state begins at a higher level of damage than does the highest damage state used here.

Photograph 2 (HUD Location E). In the case of Photograph 2, 438 homes appear in the photograph. The population of these homes was made up of 308 single-story gable roof units, 97 single-story hip roof units and 30 two-story gable roof buildings. The roof shape of 3 units could not be identified. Of the 438 homes, 45 were re-roofed before the photograph was taken. Of the 393 homes that had not been re-roofed, damage states could be discerned for 239 single-story gable buildings (77% of those in the photograph), 70 single-story hip buildings (from 97 units) and 30 two-story gable buildings (from 30 units). The damage states associated with the remaining 54 homes could not be determined.

The houses within the subdivision were widely spaced. The estimated value of the surface roughness, based on the approach given by Latteu (1969), within the subdivision is about 0.15 m.

The HUD team surveyed a total of 63 homes within the area encompassed by this photograph. These 63 homes were comprised of 59 single-story gable buildings, one two-story gable, and three single-story hip roof buildings. Of the 59 single-story gable roof buildings, sheathing damage could be estimated on 42 of these (71%) and roofing damage for 45 of the homes.

Figure 6.24 compares the damage states arising from the analysis of the aerial photograph to the HUD data. A comparison of the roof sheathing damage states clearly indicate that the HUD data overestimated the true level of sheathing damage. The HUD data suggests that 89% of the single-story gable buildings experienced the loss of at least one piece of sheathing, whereas examination of the aerial photography indicates the loss of at least one piece of roof sheathing for 62% of the homes.

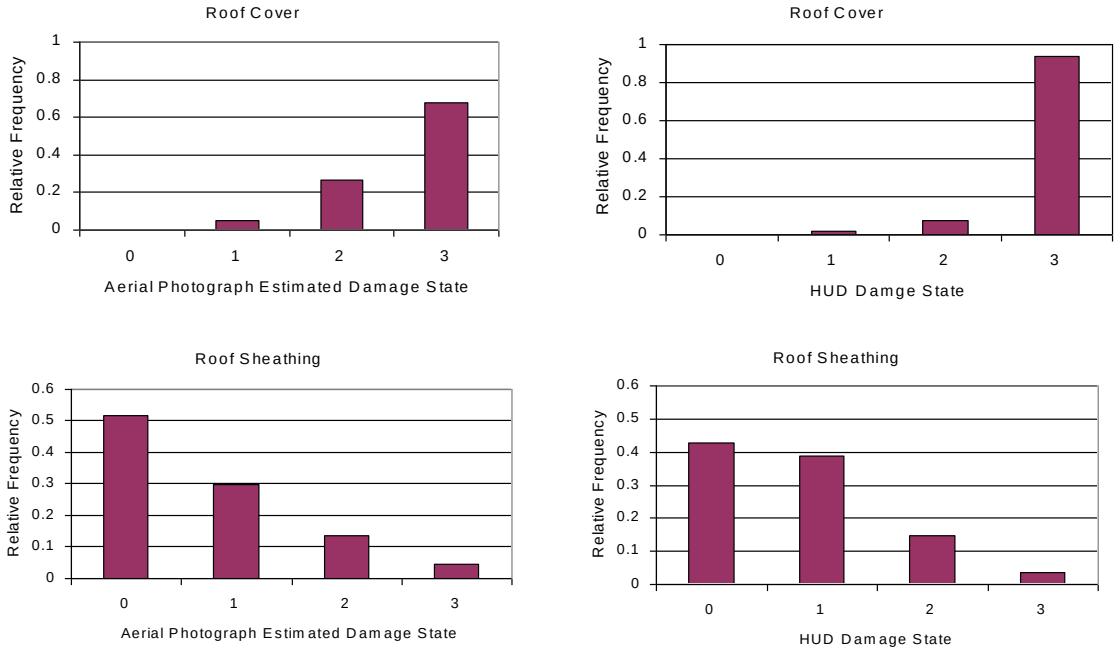

Figure 6-23. Comparison of Observed Damage States for Single Story Gable Homes Obtained from Aerial Photography and HUD Damage Survey – Location of Photograph 1 (HUD Location F).

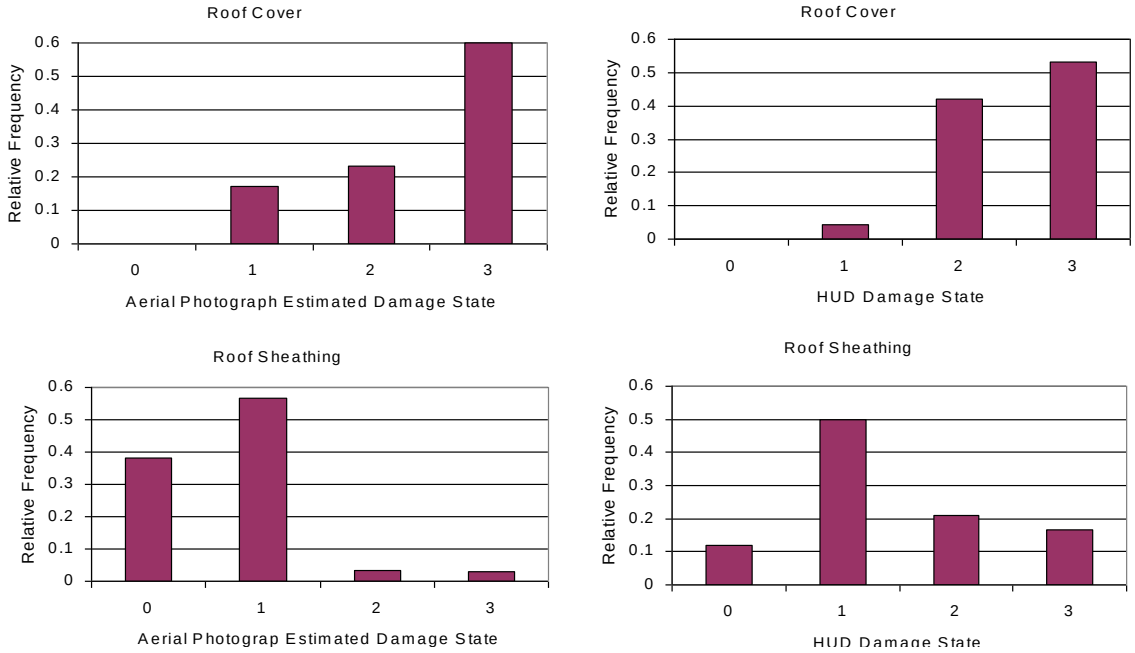

Figure 6-24. Comparison of Observed Damage States for Single Story Gable Homes Obtained from Aerial Photography and HUD Damage Survey – Location of Photograph 2 (HUD Location E).

Photograph 3 (HUD Location D). In Photograph 3, the single family home population was comprised of 193 single-story gable homes and 42 single-story hip roof homes. Of the 193 gable roof homes, 145 units (75%) had not been re-roofed and the damage could be estimated. In the case of the hip roof homes, 28 units (67%) had not been re-roofed and the damage states could be estimated.

Like the homes examined in Photograph 2, the houses within the subdivision were widely spaced. Again using the approach given in Latteu (1969), the estimated value of the surface roughness within the subdivision is 0.11 m.

Figure 6.25 presents a comparison of the HUD damage states and the damage states determined from the aerial photography. The agreement between the results obtained from the two damage surveys is reasonable. In the case of roof sheathing, both the analysis of the photography and the ground survey performed by HUD indicates that about 70% of the single-story gable homes had at least one piece of roof sheathing fail. This 70% value agrees with the results from the analysis of the homes analyzed from Photograph 2, which was subjected to nearly identical hurricane winds during the storm.

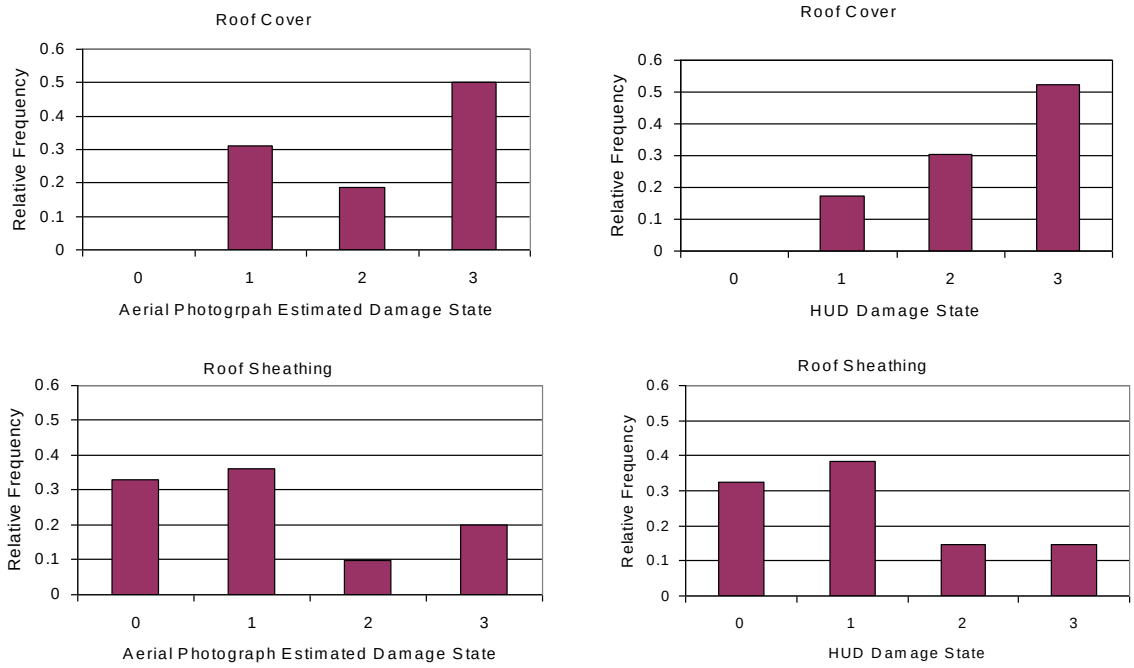

Figure 6-25. Comparison of Observed Damage States for Single Story Gable Homes Obtained from Aerial Photography and HUD Damage Survey – Location of Photograph 3 (HUD Location D).

Photograph 4 (HUD Location H). In the case of Photograph 4, too many of the homes had been repaired and thus estimates of roof damage could not be properly ascertained.

Comparison of Simulated and Observed Damage States. In the comparison of the simulated and observed roof damage states, a difficulty arises (particularly in the case of the roof sheathing) because the nail sizes used to attach the roof sheathing to the roof

trusses were not known. Prior to 1992, the South Florida Building Code required a minimum of 6d nails spaced at 6″ on center at the edges and 12″ on center in the field for sheathing less than 1/2″ thick. For a sheathing thickness greater than 1/2″, 8d nails were required using the same 6″/12″ spacing. As previously discussed, the uplift resistance of a sheathing panel attached to the rafters using 8d nails is about twice the value that is obtained using 6d nails.

In the HUD damage survey, the nail size was recorded on only two of the 466 homes examined (both had 8d nails). Data collected as part of the Residential Construction Mitigation Program under the direction of the Florida Department of Community Affairs, suggests that approximately 60% of the homes are constructed using 8d nails to attach the roof sheathing to the roof trusses, with 6d nails used in the remaining 40% of the homes. The default for characterizing the building stock is taken as 40% of the homes constructed using the code minimum requirements with a sheathing thickness of less than 1/2″ and the remaining 60% of the homes constructed using the code minimum requirements with sheathing roof panels having a thickness greater the 1/2″.

In the comparisons of simulated and observed roof damage states that follow, the comparisons are given for all buildings modeled using 6d sheathing nails, all buildings modeled using 8d sheathing nails, and the default building stock (i.e., 40% of the buildings modeled with 6d nails and 60% with 8d nails). The simulated damage are derived using the wind loads specified in ASCE-7 and assuming that the buildings are randomly oriented.

Two-Story Gable Houses. Figures 6.26 and 6.27 show comparisons of the simulated and observed damage states for the two-story gable roof homes. Figure 6.26 presents the comparisons with the data obtained from Photograph 1, whereas Figure 6.27 shows the comparisons for the damage states taken from Photograph 2. Using the default building stock (i.e., 40% of the buildings have roof decks attached with 6d nails and 60% with 8d nails) as being representative of the building stock associated with the observed damage, the comparisons given in Figures 6.26 and 6.27 suggest that modeling the loads with the ASCE-7 based pressure coefficients overestimates the damage to the roof sheathing and roof covering for two-story given in Figure 6.26 and 6.27 suggest that modeling the loads with the ASCE-7 based pressure gable houses.

Single-Story Gable Houses. Figures 6.28 and 6.29 show comparisons of the simulated and observed roof damage states for the single-story gable roof homes. For the default building stock case, the modeled roof sheathing and roof covering damage states obtained using the ASCE-7 based loads agree reasonably well with the observed damage.

Single-Story Hip Houses. Figures 6.30 and 6.31 show the roof damage state comparisons for the single-story hip roof homes. The comparison of the roof damage states derived from the observations taken from Photograph 2 (Figure 6.30) show good agreement between the observed damage states and the predicted damage states using the ASCE-7 based loads for the default building stock. On the other hand, the comparisons of predicted and observed roof damage states for Photograph 3 (Figure 6.31) show the damage model to overestimate the roof damage to the single-story hip roof homes.

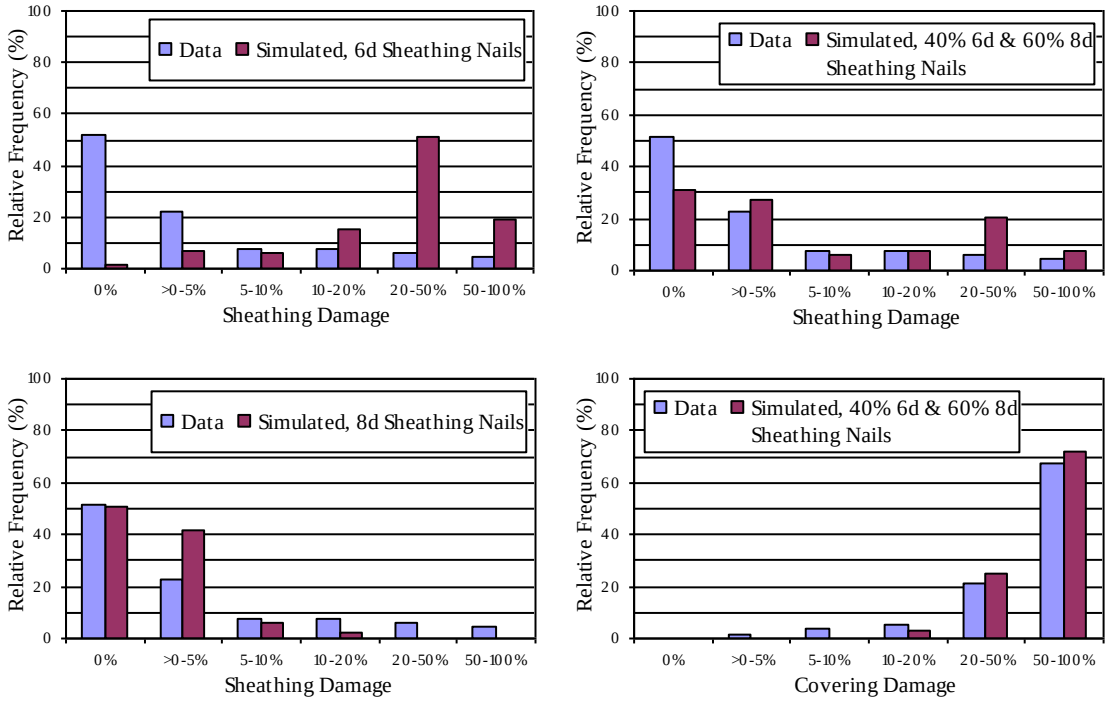

Figure 6-26. Comparison of Modeled and Observed Roof Damage States to Two-Story Gable Houses (Photograph 1).

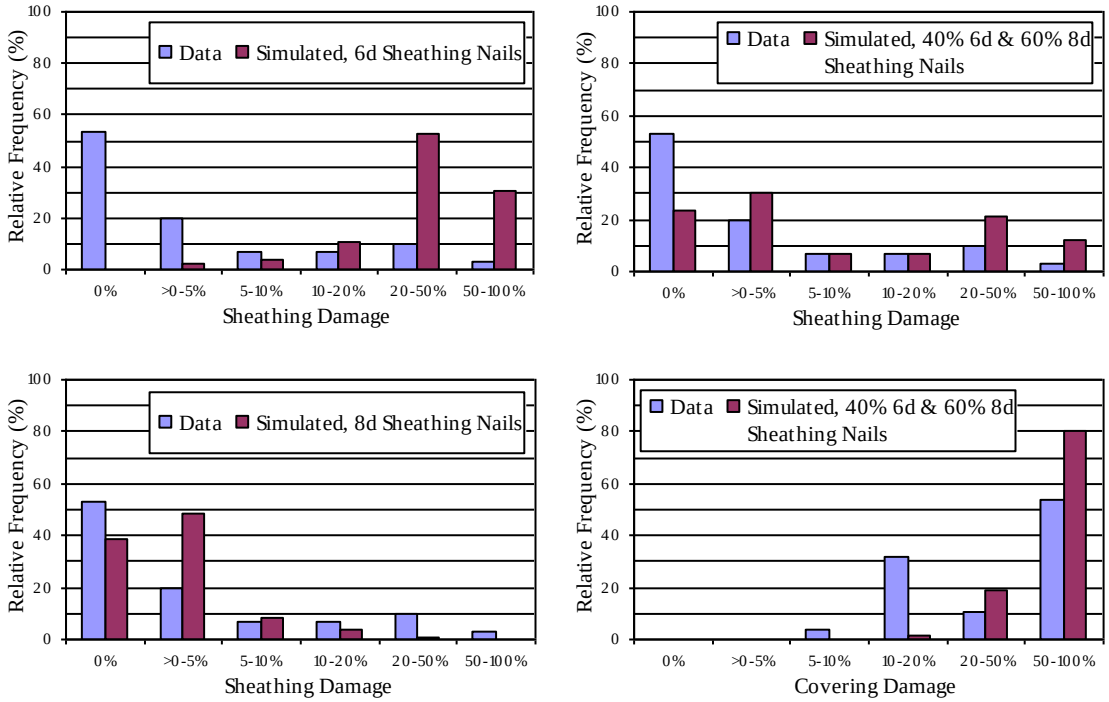

Figure 6-27. Comparison of Modeled and Observed Roof Damage States to Two-Story Gable Houses (Photograph 2).

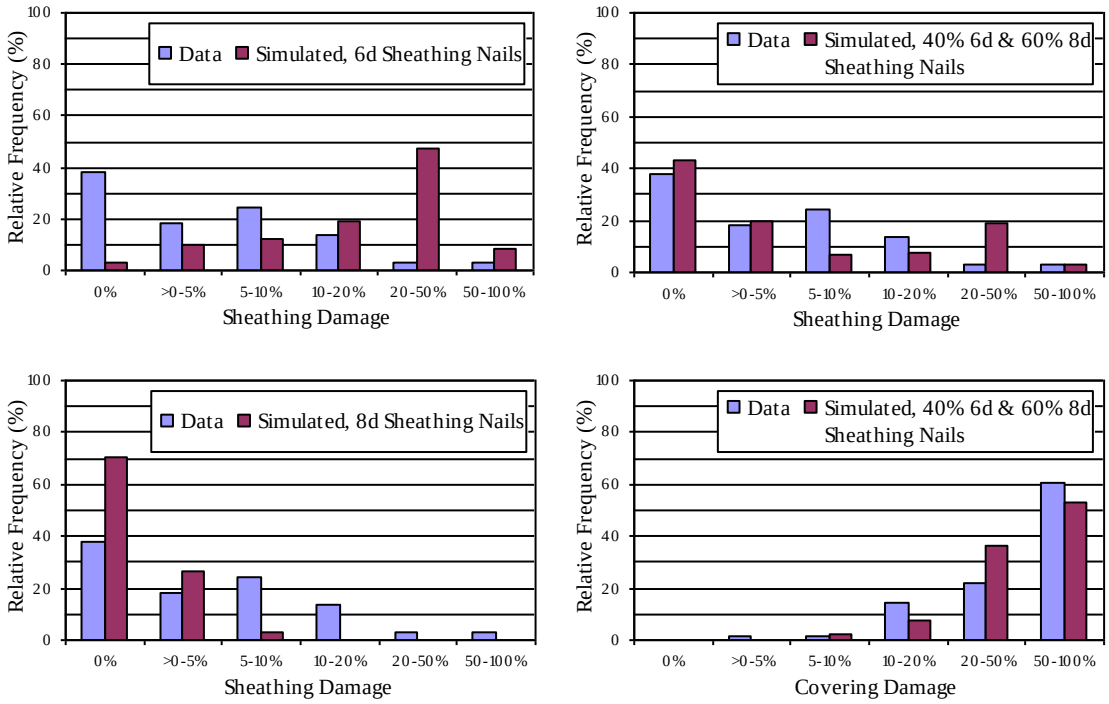

Figure 6-28. Comparison of Modeled and Observed Roof Damage States to Single-Story Gable Houses (Photograph 2).

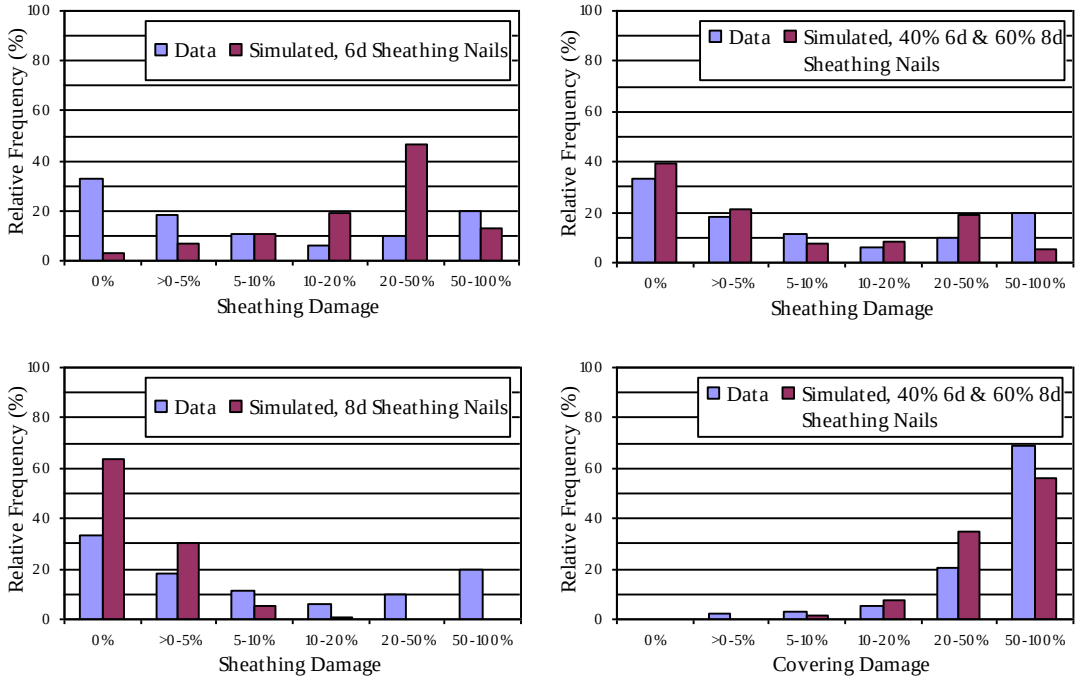

Figure 6-29. Comparison of Modeled and Observed Roof Damage States to Single-Story Gable Houses (Photograph 3).

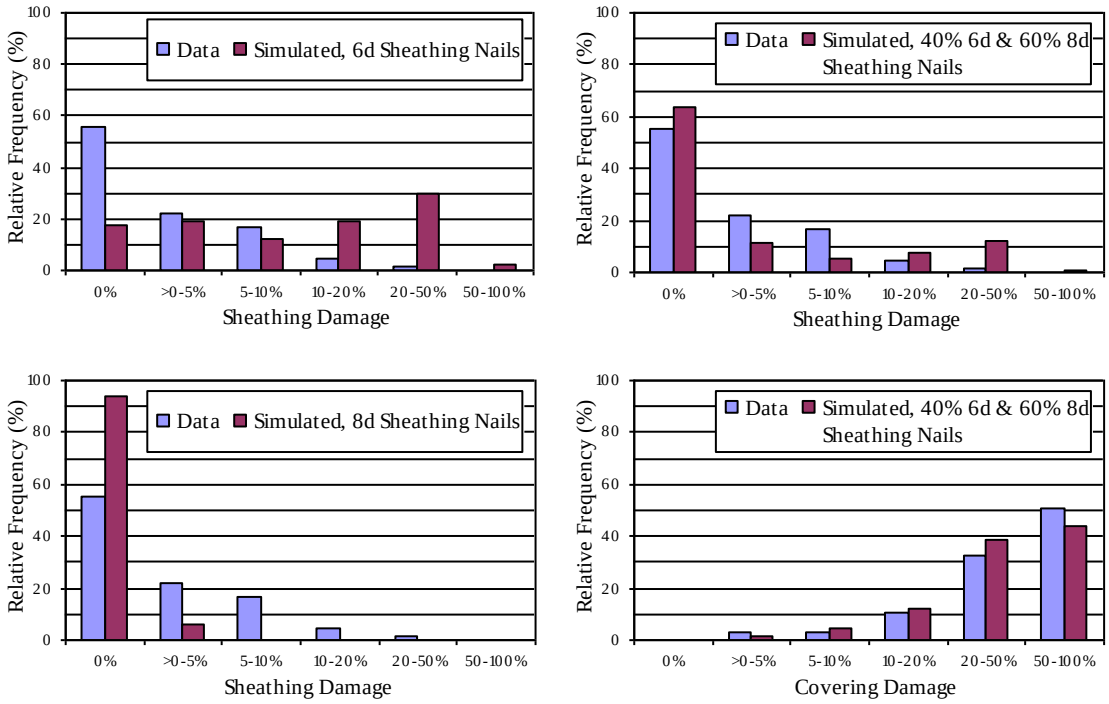

Figure 6-30. Comparison of Modeled and Observed Roof Damage States to Single-Story Hip Houses (Photograph 2).

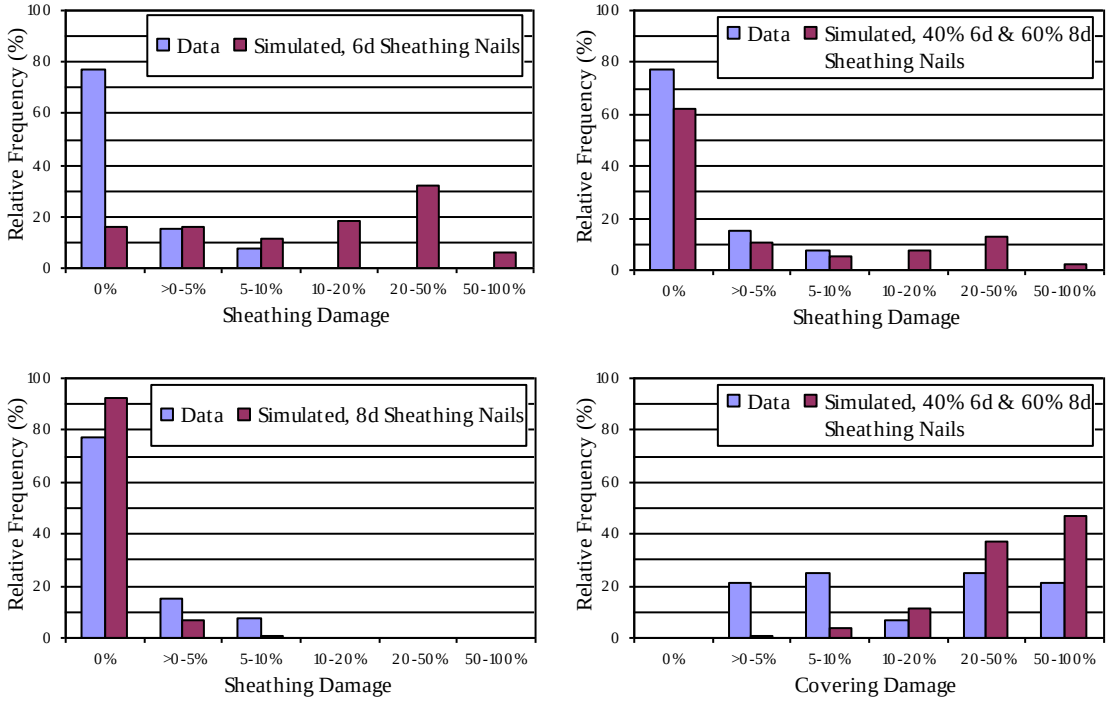

Figure 6-31. Comparison of Modeled and Observed Roof Damage States to Single-Story Hip Houses (Photograph 3).

Summary. In summary, given the assumption of the building stock with respect to the fraction of homes roofed with 6d and 8d sheathing nails, the predicted roof damage states obtained using the ASCE-7 based loads compare well with the observed roof damage states. In all cases examined, the simulated roof sheathing damage using 6d nails overestimated the observed damage and the simulated roof sheathing damage using 8d nails underestimated the observed damage – i.e., the observed data was contained within the two limiting simulations for all cases examined.

6.3.1.2 Hurricane Erin (1995)

The roof sheathing failure model is further validated through comparisons to damage sustained at Navarre Beach, Florida during Hurricane Erin. This area experienced peak gust wind speeds (open terrain at 10 m above ground) in excess of 100 mph. The damage survey includes 161 wood frame residential structures. Table 6.6 shows the surface roughness values used in the simulation. Note that the shoreline at Navarre Beach runs east-west. The roof sheathing damage simulation is performed with 30% of the homes located along the first row adjacent to the shoreline and 70% of the homes located on inside rows. The building stock with respect to sheathing attachment is also taken here as 40% of the buildings roofed with 6d sheathing nails and 60% with 8d sheathing nails.

Table 6-6. Surface Roughness Values used in Hurricane Erin Sheathing Damage Validation Study at Navarre Beach, Florida

Wind Direction	Surface Roughness (m)	
	First Row of Homes Along Shoreline	Inside Rows
Onshore	0.03	0.1
Offshore	0.2	0.2
Along Shoreline (±15°)	0.1	0.15

Of the 161 structures surveyed, 91 have gable roofs and 43 have hip roofs. The gable roof homes are further divided into categories taking into account there orientation (i.e., gable ridge parallel to the shoreline and perpendicular to the shoreline) and their height. Comparisons of the observed roof sheathing damage and the simulated roof sheathing damage are shown in Table 6.7. Note that the modeled number of homes with sheathing damage is computed as the modeled percentage multiplied by the total number of homes in the survey rounded to the nearest integer.

As seen in Table 6.7, the comparison of the observed sheathing damage and modeled sheathing damage indicates that the damage model performs reasonably well, with a bias towards overestimating the damage levels for the two-story gable roof homes oriented perpendicular to the coast and underestimating the damage levels for the two-story gable roof homes oriented parallel to the shoreline. The sheathing damage for the hip roof homes is simulated considering an equal mix of single-story and two-story homes and an equal mix of homes with roof ridges parallel and perpendicular to the shoreline.

Table 6-7. Comparison of Observed and Modeled Roof Sheathing Damage at Navarre Beach, Florida

Case	Total Number of Structures in the Survey	Observed		Modeled	
		Number of Structures with Sheathing Damage	Percentage of Structures with Sheathing Damage	Number of Structures with Sheathing Damage	Percentage of Structures with Sheathing Damage
Single Story Gable Roof Homes Oriented Parallel to Beach	10	**0**	0	**0**	0.60
Single Story Gable Roof Homes Oriented Perpendicular to Beach	5	**0**	0	**0**	0.51
Two Story Gable Roof Homes Oriented Parallel to Beach	56	**12**	21.4	**3**	4.7
Two Story Gable Roof Homes Oriented Perpendicular to Beach	20	**0**	0	**1**	4.2
Hip Roof Homes	43	**0**	0	**0**	0.07

6.3.1.3 Hurricane Fran (1996)

Using aerial photography obtained from the American Association of Wind Engineers and an aerial video obtained from the North Carolina Department of Transportation, the performance of roof covering during Hurricane Fran on hip and gable roof residential structures was reviewed. A total of 49 gable roof homes and 112 hip roof homes were identified for the study. The structures are located in North Carolina at the north end of Wrightsville Beach and at the south end of Figure Eight Island. Note that this area was chosen since it received little or no damage during Hurricane Bertha, which preceded Hurricane Fran by about two months. The study area experienced peak gust speeds (open terrain at 10 m above ground) between 105 and 110 mph during Hurricane Fran.

The shoreline at Wrightsville Beach and Figure Eight Island is oriented roughly northeast-southwest. The surface roughness values used in the simulation are the same as those used in the Hurricane Erin roof sheathing damage validation study (see Table 6.6). Consistent with that observed from the aerial photography and video, the building stock used in the roof cover damage simulation for both the hip and gable roof homes comprised an equal mix of homes with roof ridges parallel and perpendicular to the shoreline, a three to one ratio of two-story homes versus single-story homes, and a seven to three ratio of homes located immediately adjacent to the ocean versus homes located at least one row away from the ocean. Also, a 40%/60% mix of structures with 6d and 8d sheathing nails were used in the damage simulation. The results of the analysis are shown in Figure 6.32.

As seen in Figure 6.32, the agreement between the observed and modeled damage states is quite good and the small difference in the performance of hip and gable roofs is seen in both the modeled and observed data.

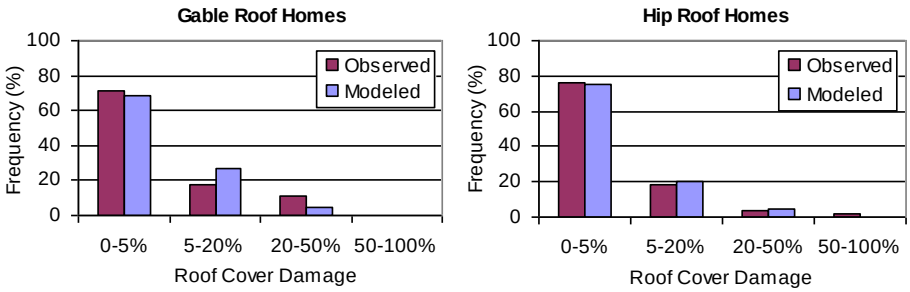

Figure 6-32. Comparison of Simulated and Observed Roof Covering Damage for Gable and Hip Roof Houses.

6.3.2 Window Damage

Figure 6.33 shows a comparison of the window damage states resulting from the HUD damage survey following Hurricane Andrew and the damage simulation using ASCE-7 loads. The data given in Figure 6.33, both observed and modeled, are for the four locations used in the roof damage validation study. The comparison of the simulated and observed damage states are reasonable, but the model tends to overestimate the number of single-story homes that experience no window damage. In the case of two-story homes, both the simulation and the observations suggest that nearly all homes experienced the loss of at least one window. The damage simulation clearly reproduces the observation that two-story homes are likely to experience more window damage than one-story homes for the same wind event.

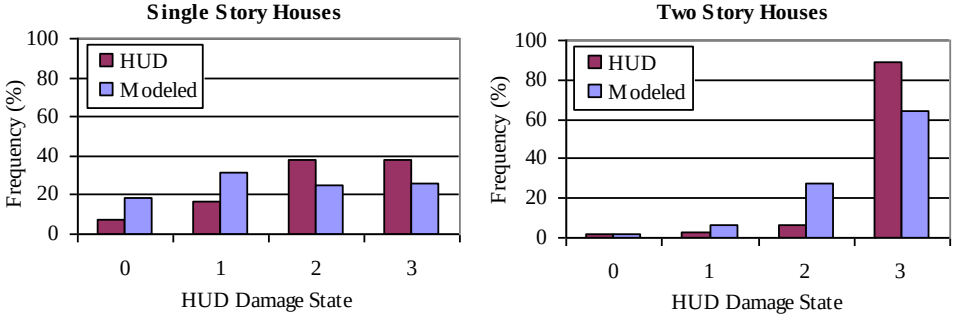

Figure 6-33. Comparison of Simulated and Observed Window Damage States for One- and Two-Story Houses, Hurricane Andrew (1992).

6.3.3 Whole Roof Failures

The whole roof failure model is a relatively simple model, where the roof is considered to fail as a complete unit if the wind induced uplift loads (computed as a combination of the internal pressure effect and the external loads) exceed the total uplift capacity of the roof provided by the roof-wall connections and the self weight. In the case of gable roofs, roof trusses (or rafters) are assumed to be spaced at 24″ on center along two walls of the building. In the case of hip roofs, a roof-wall connection is assumed to exist at 24″

intervals along the entire perimeter of the building (i.e., for a square building, the hip roof has twice as many roof-wall connections as the gable roof).

Using the data collected from the four aerial photographs of damage sustained during Hurricane Andrew discussed earlier, comparisons between the observed and modeled whole roof failure rates were performed. Observed whole roof failures from the aerial photography are assumed to be gable roofs and not hip roofs. Figure 6.34 shows a section from Photograph 3 depicting eight homes, three of which are seen to have experienced a complete (or near complete) roof failure.

Figure 6-34. Examples of Whole Roof Failures Depicted in Photograph Number 3.

All roof-wall connections were modeled as a strapped connection having a mean resistance of 1200 lbs and a coefficient of variation of 30%. Roof trusses are spaced at 24″ on center. The statistics of the modeled failure rates are computed from 1000 simulations of a randomly oriented house located at the position of the photograph. Note that these comparisons include a calibration factor of 0.8 applied to the uplift resistances. Shingle and tile roof coverings were both considered in the analysis. The self weight of the roof with shingles is estimated to be 10.4 psf and with tiles it is estimated to be 18.4 psf. The default building stock with respect to roof covers is taken as 70% with shingles and 30% with tiles after HUD (1993). Comparisons are given in Table 6.8. In the case of the observed failure rates, the fraction given in parentheses represent the number of failures over the number of buildings observed in the photograph. The comparisons given in Table 6.8 show good agreement between the modeled and observed failure rates for the default building stock for Photographs 3 and 4. The model overestimates the whole roof failure rate for Photograph 2.

Table 6-8. Comparison of Observed and Modeled Whole Roof Failures at Locations of Aerial Photographs, Hurricane Andrew (1992)

	Frequency of Whole Roof Failures – Single Story Gable Roof Homes			
		Modeled		
Photograph	Observed	Shingles	Tiles	70% Shingles/ 30% Tiles
1	-	-	-	-
2	0.65% (3/308)	8.0%	0.60%	5.8%
3	10.8% (21/193)	14.3%	1.4%	10.4%
4	0.32% (1/311)	0.50%	0.00%	0.35%
Average	3.1% (25/812)	6.6%	0.6%	4.8%

Figures 6.35 and 6.36 show modeled failure rates for strapped and toe-nailed single-story hip and gable roof homes, for three different generic terrains (open terrain, defined with z_0 = 0.03 m, standard suburban terrain, defined with z_0 = 0.35 m and treed terrain, defined with z_0 = 1.0 m) as a function of the peak gust wind speed at a height of 10 m above ground in open terrain. The mean uplift capacity and coefficient of variation of an individual toe-nailed connection are 415 lbs and 25%, respectively. Note that the experimental values of the toe-nail connections discussed in Section 6.2.4 present results with mean capacities ranging between 208 lbs up to 676 lbs, and thus the 415 lbs value used herein is simply a representative value.

The failure rates were computed using a simulation of hurricanes in the South Florida area, where for each simulation, the number of homes experiencing a whole roof failure (using 30 simulations/storm) was saved along with the peak gust wind speed (10 m in open terrain) experienced at the site. The results given in Figures 6.35 and 6.36 clearly indicate the hip roofs are less susceptible to failure than the gable roofs (as has been well documented in the literature), and that the results are very strongly dependent on the assumed terrain.

The potential for detailed validation of the non-strapped results presented in Figures 6.34 and 6.35 is limited, since there are no known systematic, statistically unbiased studies examining the performance of roofs in regions where the application of straps (or clips) at the roof-wall connections are not used. Thus the results given in Figures 6.35 and 6.36 are given primarily to assess the reasonableness of the simple uplift failure model.

6.4 Damage Model Results for Residential Buildings

Following an approach similar to that used by Vann and McDonald (1978) for defining damage states to manufactured homes, the damage state descriptions used for residential buildings are given in Table 6.9. The damage states are primarily governed by the performance of the building envelope, and are divided into five states, varying between 0 (no damage) and 4 (destruction). In Table 6.9, a building is considered to be in the higher damage state if *any* of the shaded damage indicators in the corresponding row occurs. For example, for a building to be considered to have sustained minor damage, the building must not have sustained structural failure or sheathing failure, and either one fenestration (window, door, garage door) failed or more than 2% but less than 15% of the roof cover

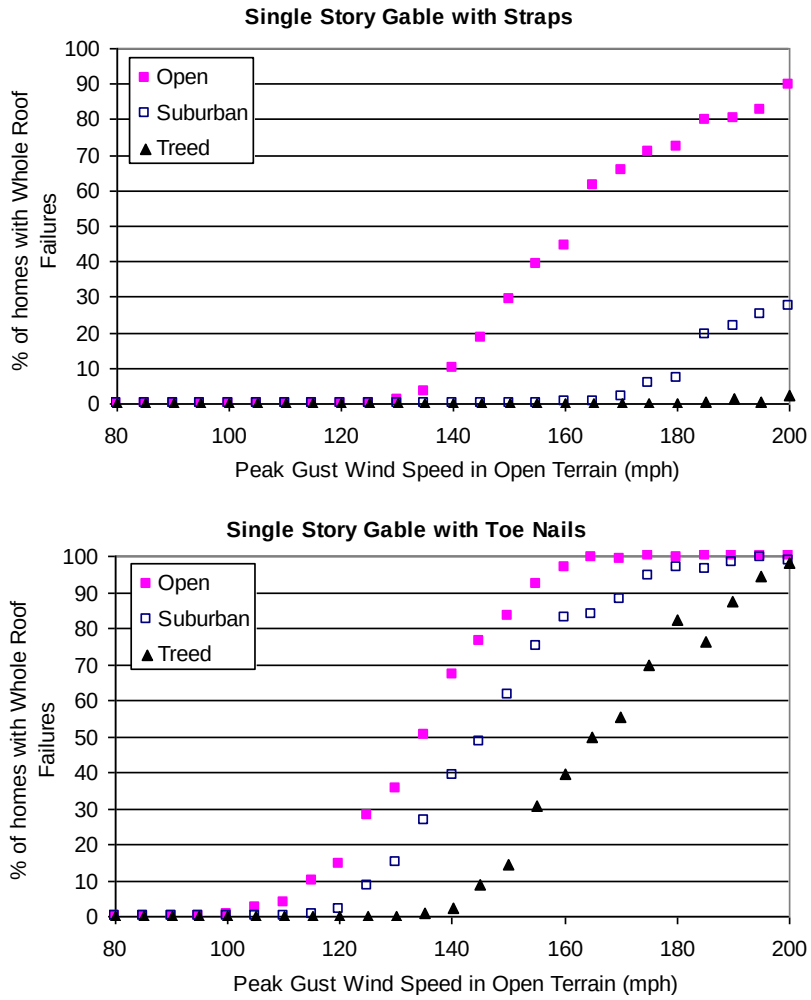

Figure 6-35. Modeled Failure Rates for Single Story Gable Roof Homes with Strapped Roof-Wall Connections and Toe Nailed Roof-Wall Connections.

failed. Photographs of buildings in each of damage states 0 through 4 are given in Figures 6.37 through 6.41.

Eight different geometric representations (4 basic shapes with both a gable roof and hip roof) of "typical" residential buildings were developed for the damage assessment. The model buildings are shown pictorially in Figure 6.42, and represent the basic building geometries used to develop the residential building classification scheme and the development of estimated damage states for each building as a function of wind speed. All buildings have been modeled as having asphalt shingle roofs. All windows are treated as being comprised of single pane annealed glass, and all sliding glass doors are considered to be comprised of tempered glass. In the case of a gable roof home, the connections between the roof and the wall are assumed to exist at the base of every truss with no connections along the gable end. In the case of the hip roof, connections between the roof and the wall are assumed to exist along the entire perimeter of the wall. During the simulation, the walls are modeled as being connected to the foundation and the roof,

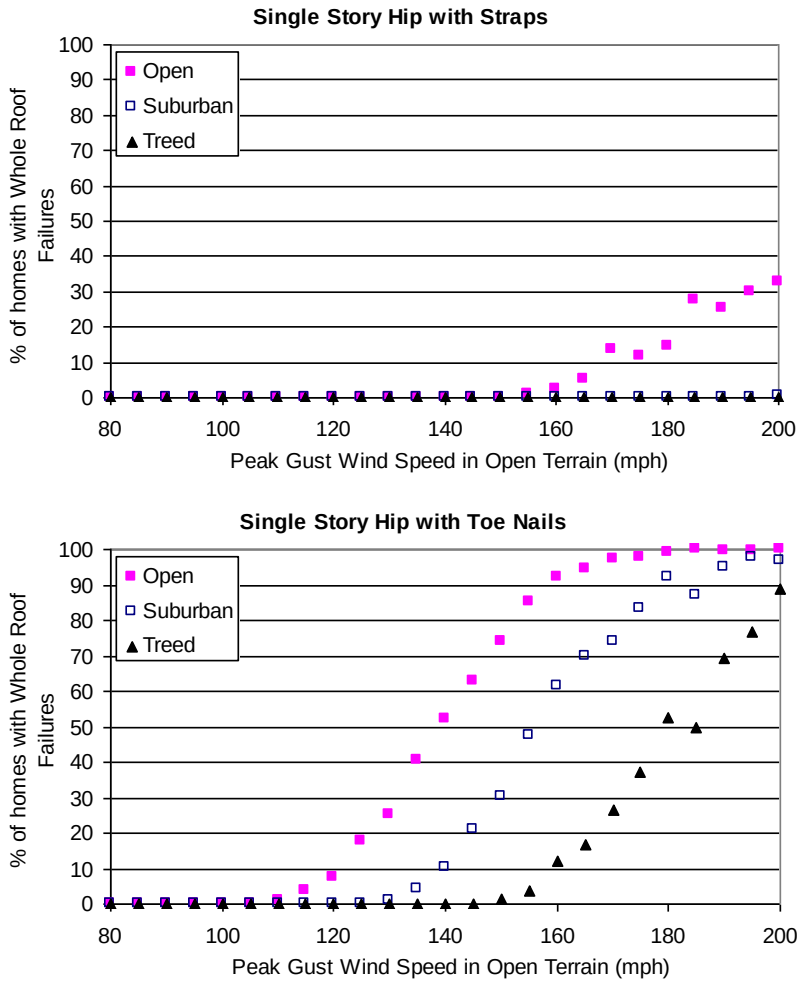

Figure 6-36. Modeled Failure Rates for Single Story Hip Roof Homes with Strapped Roof-Wall Connections and Toe Nailed Roof-Wall Connections.

until the roof fails, after which time the wall connection at the roof level is released. The model homes reflect the fact that homes with attached garages are typically bigger than those without garages. The parameters varied in the building description are as follows:

Building Size:	4 Samples as in Figure 6.42 (gable roof only shown)
Roof Shape:	Hip or Gable
Wall Construction:	Wood, Unreinforced Masonry, Reinforced Masonry
Roof Sheathing Attachment:	6d or 8d
Roof-Wall Connections:	Strapped or Toe-Nailed
Garage:	None, Strong, Weak
Number of Stories:	One or Two

Damage simulations for each of the 144 different building types have been performed for the buildings located in terrains described with z_0 = 0.03 m (open terrain), z_0 = 0.35 m (typical suburban terrain), and z_0 = 0.7 m (suburban terrain with some trees or densely spaced homes), z_0 = 1.0 m (treed suburban terrain).

Table 6-9. Damage States for Residential Construction Classes

Damage State	Qualitative Damage Description	Roof Cover Failure	Window Door Failures	Roof Deck	Missile Impacts on Walls	Roof Structure Failure	Wall Structure Failure
0	**No Damage or Very Minor Damage** Little or no visible damage from the outside. No broken windows, or failed roof deck. Minimal loss of roof over, with no or very limited water penetration.	≤2%	No	No	No	No	No
1	**Minor Damage** Maximum of one broken window, door or garage door. Moderate roof cover loss that can be covered to prevent additional water entering the building. Marks or dents on walls requiring painting or patching for repair.	>2% and ≤15%	One window, door, or garage door failure	No	<5 impacts	No	No
2	**Moderate Damage** Major roof cover damage, moderate window breakage. Minor roof sheathing failure. Some resulting damage to interior of building from water	>15% and ≤50%	> one and ≤ the larger of 20% & 3	1 to 3 panels	Typically 5 to 10 impacts	No	No
3	**Severe Damage** Major window damage or roof sheathing loss. Major roof cover loss. Extensive damage to interior from water.	>50%	> the larger of 20% & 3 and ≤50%	>3 and ≤25%	Typically 10 to 20 impacts	No	No
4	**Destruction** Complete roof failure and/or, failure of wall frame. Loss of more than 50% of roof sheathing.	Typically >50%	>50%	>25%	Typically >20 impacts	Yes	Yes

The assumed component resistances used in the simulations are given in Table 6.10. In the case of the roof-wall connections a resistance factor of 0.8 was applied. A resistance factor of 0.9 was applied to the roof sheathing uplift capacity. The resistance parameters given in Table 6.10 are the unfactored values.

Statistics on damage states have been developed through the use of a 20,000-year simulation of hurricanes (derived using the South Florida Hurricane climate) by performing 30 damage simulations for each storm. Prior to the start of each of the 30 simulations, the resistances of the individual building components are re-sampled, and the building orientation is also re-sampled. The building damage indicators including roof cover loss (as a percentage), number of failed roof sheathing panels, number of failed windows, doors, sliding glass doors, and garage doors, number of failed wall sections, and the failure of the entire roof are recorded. This individual component failure information is then used to define the final damage state of the building as defined in Table 6.9.

Appendix A shows the probabilities of achieving each building damage state and each individual component damage state as a function of wind speed. The component damage states are the thresholds that move the building damage state from one definition to another in Table 6.9. For example, in the case of roof cover, damage state 1 corresponds to roof cover loss of more than 2% but less than 15%. Only three damage states are given for roof cover, since only three roof cover damage states are used to define the total building damage state. The component damage states are presented to assist in determining which component drives the overall building damage state and to check how reasonably the damage model performs.

(a) <2% Roof Cover

(b) <2% Roof Cover

Figure 6-37. Damage State 0.

(a) 2% to 15% Roof Cover Loss, One Broken Window

(b) 2% to 15% Roof Cover Loss

Figure 6-38. Damage State 1.

(c) 2% to 15% Roof Cover Loss

(d) One Broken Window

Figure 6.38. Damage State 1 (concluded).

(a) More than One Window but less than the Greater of 3 or 20% of the Windows

(b) At least One Failed Sheathing but Less than Three Failed Pieces of Roof Sheathing

Figure 6-39. Damage State 2.

More than Three Pieces of Failed Roof Sheathing but Less than 15% of the Panels Missing

Figure 6-40. Damage State 3.

The relative performance of the different building types and the impact of terrain are shown in Table 6.11 through the use of the average per storm damage state. This average per storm damage state effectively collapses all the information obtained from the simulations into a single number, allowing a rapid evaluation of the importance of individual building parameters in assessing the damage potential of a particular building type. Note that this per storm damage state includes the effect of the hurricane climate since the modeled hurricanes are drawn directly from the 20,000-year simulation, which, of course, produces many more storms having low intensity winds than high intensity winds. In other words, the average building damage states given in Table 6.11 would be much lower if the storm simulation had been performed for a location in New England rather than South Florida.

The results shown in Table 6.11 can be used to ascertain the importance that the various building parameters and terrains have on the performance of residential buildings. The maximum and minimum changes in the per storm average damage state caused by changing a single parameter are summarized in Table 6.12. Note that the effect of any one parameter on the average damage state varies with other building parameters and with terrain.

The results clearly indicate that terrain is very important, where the average damage states are seen to increase by factors of between about 2 to 3 when moving from treed to open terrain. The impact of the number of stories on the average damage is a 35% to 75% increase in damage when the number of stories is increased from one to two.

The effect of roof shape (i.e., gable versus hip) on the damage state varies between about 11% and 33%, with the gable roof buildings experiencing more damage. The impact of changing from hip to gable is larger when the roof/wall is connected with toe-nails versus straps and is also larger when the roof sheathing is fastened with 6d nails versus 8d nails.

(a) Complete Roof Failure

(b) Complete Roof Failure, Greater than 25% Sheathing

Figure 6-41. Damage State 4.

(c) Wall Failure

(d) Whole Roof Failure, Wall Failure

Figure 6.41. Damage State 4 (concluded).

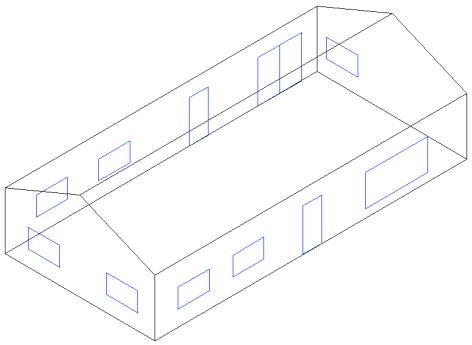

No Garage – 50′ by 24′ Plan, 9′ Eave Height

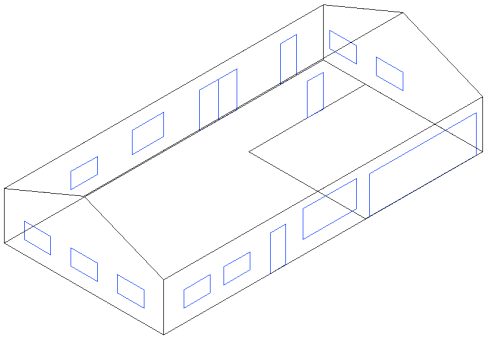

With Garage – 60′ by 30′ Plan, 9’ Eave Height

One-Story Houses

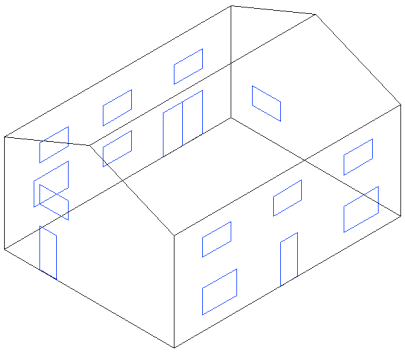

No Garage – 40′ by 30′ Plan, 17′ Eave Height

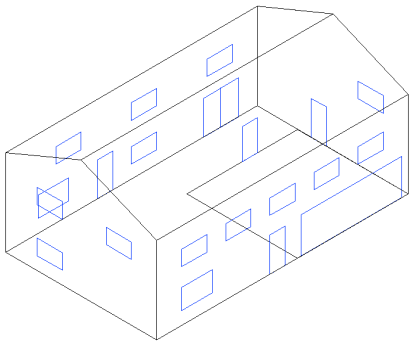

With Garage – 60′ by 30′ Plan, 17′ Eave Height

Two-Story Houses

Figure 6-42. Model House Geometries Used in Damage Simulation Study.

Table 6-10. Component Resistance Values Used to Model Residential Buildings

Component	Distribution	Distribution Parameters
Sheathing Panel (6d)	LogNormal	Mean = 54.6, COV = 0.11
Sheathing Panel (8d)	LogNormal	Mean = 103, COV = 0.11
Annealed Glass Impact	Deterministic	50 lb-ft
Tempered Glass Impact	Deterministic	100 lb-ft
Window/Sliding Glass Door Pressure	Normal	Mean = 40 psf, COV = 0.2
Window Glass (All Windows on 1 Story)	Weibull	C = 54.9 psf, k = 4.7
Window Glass (2 Large Windows on 2 Story)	Weibull	C = 38.7 psf, k = 4.8
Sliding Glass Door Glass	Weibull	C = 101.5 psf, k = 4.5
Interior Garage Door Pressure	Normal	Mean = 30 psf, COV = 0.2
Entry Door Pressure	Normal	Mean = 50 psf, COV = 0.2
Double Garage Door Pressure (weak)	Normal	Mean = 10 psf, COV = 0.2
Double Garage Door Pressure (strong)	Normal	Mean = 20 psf, COV = 0.2
Strap Up-Lift Resistance	Normal	Mean = 1200 lb, COV = 0.3
Toe-Nail Uplift Resistance	Normal	Mean = 415 lb, COV = 0.25

Table 6-11. Average Building Damage States

Building Characteristics					Hip Roof				Gable Roof			
					Terrain Surface Roughness (m)				Terrain Surface Roughness (m)			
Wall Const	No. of Stories	Roof/Wall Conn.	Sheath Nails	Garage Door	0.03	0.35	0.70	1.0	0.03	0.35	0.70	1.0
Wood Frame	One	Straps	6d	None	0.510	0.306	0.230	0.198	0.617	0.378	0.295	0.256
				Strong	0.513	0.312	0.232	0.198	0.605	0.367	0.283	0.246
				Weak	0.557	0.322	0.240	0.204	0.661	0.382	0.292	0.253
			8d	None	0.489	0.291	0.219	0.189	0.563	0.336	0.258	0.226
				Strong	0.494	0.303	0.226	0.192	0.565	0.340	0.258	0.223
				Weak	0.526	0.311	0.229	0.196	0.592	0.347	0.263	0.227
		Toe-nails	6d	None	0.536	0.331	0.246	0.210	0.646	0.422	0.318	0.275
				Strong	0.544	0.327	0.244	0.206	0.648	0.400	0.302	0.263
				Weak	0.619	0.349	0.258	0.218	0.778	0.433	0.323	0.275
			8d	None	0.531	0.327	0.243	0.206	0.619	0.403	0.304	0.262
				Strong	0.540	0.324	0.241	0.203	0.623	0.387	0.291	0.249
				Weak	0.617	0.346	0.255	0.213	0.766	0.421	0.313	0.265
	Two	Straps	6d	None	0.725	0.470	0.380	0.337	0.862	0.576	0.475	0.429
				Strong	0.717	0.465	0.374	0.332	0.837	0.554	0.455	0.408
				Weak	0.777	0.486	0.391	0.347	0.903	0.580	0.472	0.422
			8d	None	0.706	0.456	0.369	0.327	0.810	0.533	0.438	0.389
				Strong	0.693	0.449	0.361	0.319	0.793	0.522	0.425	0.381
				Weak	0.749	0.466	0.372	0.329	0.830	0.531	0.432	0.385
		Toe-nails	6d	None	0.768	0.506	0.404	0.357	0.901	0.626	0.510	0.456
				Strong	0.761	0.492	0.393	0.346	0.885	0.583	0.476	0.423
				Weak	0.848	0.519	0.413	0.364	1.058	0.651	0.524	0.459
			8d	None	0.764	0.503	0.402	0.356	0.870	0.600	0.487	0.432
				Strong	0.757	0.486	0.388	0.341	0.864	0.565	0.459	0.408
				Weak	0.841	0.514	0.408	0.360	1.035	0.633	0.507	0.448
Unreinforced Masonry	One	Straps	6d	None	0.507	0.306	0.232	0.198	0.618	0.377	0.293	0.257
				Strong	0.513	0.312	0.233	0.198	0.607	0.367	0.282	0.245
				Weak	0.561	0.324	0.239	0.204	0.659	0.384	0.292	0.254
			8d	None	0.494	0.292	0.220	0.189	0.566	0.335	0.258	0.225
				Strong	0.498	0.304	0.225	0.191	0.563	0.341	0.257	0.224
				Weak	0.528	0.309	0.230	0.196	0.592	0.347	0.263	0.225
		Toe-nails	6d	None	0.540	0.332	0.246	0.207	0.648	0.421	0.321	0.275
				Strong	0.544	0.328	0.242	0.207	0.647	0.398	0.304	0.264
				Weak	0.623	0.348	0.257	0.218	0.780	0.433	0.325	0.279
			8d	None	0.531	0.329	0.245	0.206	0.618	0.404	0.307	0.261
				Strong	0.540	0.324	0.241	0.203	0.624	0.386	0.292	0.249
				Weak	0.616	0.347	0.254	0.212	0.759	0.420	0.314	0.267
	Two	Straps	6d	None	0.724	0.470	0.378	0.337	0.861	0.577	0.476	0.429
				Strong	0.719	0.466	0.373	0.331	0.837	0.554	0.456	0.408
				Weak	0.775	0.485	0.389	0.345	0.902	0.577	0.474	0.422
			8d	None	0.708	0.459	0.370	0.329	0.812	0.531	0.439	0.391
				Strong	0.694	0.451	0.360	0.318	0.795	0.521	0.428	0.382
				Weak	0.749	0.467	0.372	0.328	0.832	0.530	0.431	0.385
		Toe-nails	6d	None	0.765	0.506	0.404	0.357	0.904	0.624	0.509	0.454
				Strong	0.761	0.491	0.391	0.346	0.885	0.584	0.477	0.427
				Weak	0.847	0.522	0.412	0.362	1.054	0.650	0.520	0.460
			8d	None	0.765	0.504	0.403	0.356	0.871	0.602	0.488	0.430
				Strong	0.759	0.487	0.386	0.340	0.862	0.567	0.458	0.409
				Weak	0.843	0.515	0.407	0.361	1.038	0.634	0.505	0.444
Reinforced Masonry	One	Straps	6d	None	0.510	0.306	0.232	0.198	0.616	0.377	0.292	0.257
				Strong	0.514	0.311	0.233	0.197	0.608	0.366	0.283	0.245
				Weak	0.560	0.323	0.239	0.204	0.662	0.382	0.293	0.253
			8d	None	0.493	0.292	0.220	0.189	0.566	0.335	0.257	0.224
				Strong	0.497	0.304	0.225	0.191	0.565	0.340	0.258	0.222
				Weak	0.527	0.309	0.231	0.195	0.592	0.346	0.264	0.225
		Toe-nails	6d	None	0.536	0.330	0.246	0.208	0.644	0.421	0.319	0.275
				Strong	0.546	0.327	0.243	0.206	0.646	0.400	0.303	0.260
				Weak	0.623	0.350	0.257	0.219	0.779	0.432	0.323	0.277
			8d	None	0.530	0.328	0.244	0.206	0.618	0.404	0.305	0.262
				Strong	0.538	0.325	0.238	0.203	0.625	0.385	0.292	0.249
				Weak	0.616	0.344	0.255	0.215	0.766	0.421	0.313	0.265
	Two	Straps	6d	None	0.724	0.470	0.378	0.336	0.860	0.575	0.476	0.429
				Strong	0.720	0.465	0.376	0.331	0.839	0.556	0.457	0.410
				Weak	0.775	0.486	0.389	0.345	0.903	0.579	0.472	0.423
			8d	None	0.710	0.459	0.369	0.327	0.811	0.538	0.438	0.392
				Strong	0.692	0.451	0.361	0.317	0.794	0.522	0.426	0.382
				Weak	0.748	0.468	0.374	0.328	0.832	0.536	0.431	0.385
		Toe-nails	6d	None	0.765	0.507	0.405	0.355	0.904	0.624	0.509	0.455
				Strong	0.757	0.488	0.393	0.345	0.885	0.583	0.478	0.423
				Weak	0.849	0.520	0.413	0.364	1.053	0.652	0.524	0.461
			8d	None	0.765	0.503	0.403	0.356	0.871	0.603	0.485	0.430
				Strong	0.756	0.485	0.387	0.341	0.861	0.567	0.460	0.409
				Weak	0.848	0.513	0.411	0.359	1.036	0.639	0.507	0.446

Table 6-12. Percent Increases in the Per Storm Average Building Damage State Due to Changes in Building Parameters (Minimum/Average/Maximum) – Residential Buildings

Parameter	Increase in Per Storm Average Damage State
Treed to Open Terrain	98% / 138% / 190%
One Story to Two Stories	35% / 55% / 75%
8d to 6d Roof Sheathing Nails	0% / 4% / 15%
Strapped to Toe-nailed Roof/Wall Connections	3% / 10% / 29%
Hip to Gable Roof	11% / 21% / 33%
No Garage to Strong Garage Door	-7% / -2% / 4%
No Garage to Weak Garage Door	-2% / 5% / 24%
Reinforced Masonry to Unreinforced Masonry Walls	-1% / 0% / 1%
Unreinforced Masonry to Wood Frame Walls	-1% / 0% / 1%

In the case of gable roof homes, the use of 6d sheathing nails versus 8d sheathing nails increases the per storm average damage state by up to 15%, with the larger increases taking place on the homes with strapped roof-wall connections. In the case of hip roof homes, the use of 6d sheathing nails increases the mean damage state by up to 6%, also with the larger increases taking place on the homes with strapped roof-wall connections.

The effect of straps on the average damage state also depends on roof shape, with the reduction in damage associated with the addition of straps being larger in the case of gable roofs. The results also indicate that the effect of roof straps in reducing damage is greater for the case where the roof sheathing is attached with 8d nails versus 6d nails. Overall, the increase in the average damage state associated with the use of toe-nail connections versus straps is in the range of 3% to 29%.

The effect of adding a garage with a strong garage door was found to be negligible in comparison to the effects of other variables. Note that the homes modeled with garages are larger than those without garages, and as a result, the average damage state values also reflect the effects of changes in building size. The effect of adding a garage with a weak garage door is seen to produce an average increase in damage ranging from 2% to 24%. The increase in damage was most pronounced for the open terrain case and for buildings with toe-nailed roof/wall connections versus strapped roof/wall connections.

The difference between wood frame walls and unreinforced masonry walls is negligible, with the differences in the average damage states being no more than 1%. The effect of reinforced masonry on resulting damage state versus unreinforced masonry is also found to be negligible. The effect of walls on the average damage state is small since other type of damage (roof sheathing, whole roof failures, etc.) are already significant by the time the walls begin to fail. Note that none of the modeled reinforced masonry walls failed in the simulations.

6.4.1 Effect of Mitigation on Residential Building Damage

Damage simulations were performed with various mitigation strategies for each of the residential buildings described in the previous section. The three mitigation strategies considered are as follows:

1. Install Dade County approved shutters
2. Upgrade roof to new Dade County (SFBC) roof sheathing nail pattern, install more wind-resistant shingles and apply secondary water resistance
3. Install Dade County approved shutters, upgrade roof to new Dade County (SFBC) roof sheathing nail pattern, install more wind-resistant shingles and apply secondary water resistance

The upgraded roof cover (shingles) are modeled as having a capacity of 120% of the base case shingles. In the case of the shutters, a shutter is considered to have failed if it is impacted by debris having an energy equal to or greater than 350 lb-ft. (i.e., a 9 lb. wood 2 by 4 impacting the shutter at a speed of 50 fps as required by the SFBC). The wind loads acting on the window behind the shutter are assumed to be reduced by 50%; however, the true amount of the reduction in the wind load is clearly dependent on the amount of leakage around the perimeter of the shutter. It is also assumed that the shutters do not fail due to pressure loading alone. In cases where shutters are added to a house and the house has a garage, the garage capacity is upgraded to meet the impact and pressure requirements of the Dade County building code. The effect of secondary water proofing is treated in the economic loss portion of the model and not in the damage portion of the model.

In the case of upgrading the roof nails, it is assumed that during re-roofing, the nail pattern on the existing roof sheathing panels is increased by nailing 8d nails in the field of the panel to achieve a 6″ on center nailing over the entire panel. In the case of a roof having 8d nails prior to re-nailing, the resulting uplift capacity is equal to that which would be provided through the use of the Dade County SFBC on a new building (i.e., 8d nails at 6″ on center in the field and along the edges).

Appendix A presents example plots showing the probabilities of achieving each building damage state and each individual component damage state as a function of wind speed for the three sets of mitigated homes. The average per storm building damage states for the three sets of buildings are given in Tables 6.13 through 6.15. Note in Tables 6.13 through 6.15, only one garage door case is given, since, when either a weak or a strong garage door is upgraded, they are upgraded to the same pressure resistance. By comparing the average damage states in Tables 6.13 through 6.15 with the average damage states given in Tables 6.11, one can see the effect of the various mitigation techniques in reducing damage. The statistics of the reductions in the average per storm damage states as a result of mitigation are summarized in Table 6.16.

The effect of adding shutters (and upgrading the garage door, if applicable) is a reduction in the average damage ranging between 6% and 23% with a mean reduction in the average damage of 15%. The effect of upgrading the roof (sheathing attachments and roof cover) yields a reduction in the average damage ranging between 18% and 44%, with an average of 27%.

Table 6-13. Average Building Damage States – Install Shutters

Building Characteristics					Hip Roof				Gable Roof			
Wall Const.	No. of Stories	Roof/Wall Conn.	Sheath Nails	Garage Door	Terrain Surface Roughness (m)				Terrain Surface Roughness (m)			
					0.03	0.35	0.70	1.0	0.03	0.35	0.70	1.0
Wood Frame	One	Straps	6d	None	0.439	0.258	0.203	0.178	0.554	0.335	0.268	0.239
				Strong	0.424	0.252	0.197	0.173	0.524	0.314	0.255	0.224
			8d	None	0.414	0.242	0.190	0.170	0.480	0.288	0.230	0.205
				Strong	0.403	0.235	0.184	0.165	0.460	0.274	0.220	0.194
		Toe-nails	6d	None	0.446	0.266	0.209	0.182	0.561	0.344	0.273	0.241
				Strong	0.436	0.259	0.202	0.179	0.533	0.327	0.262	0.231
			8d	None	0.434	0.261	0.203	0.176	0.514	0.316	0.249	0.221
				Strong	0.424	0.255	0.196	0.173	0.491	0.304	0.238	0.213
	Two	Straps	6d	None	0.605	0.410	0.343	0.310	0.747	0.518	0.437	0.398
				Strong	0.595	0.402	0.334	0.302	0.704	0.489	0.413	0.375
			8d	None	0.586	0.391	0.328	0.299	0.650	0.448	0.376	0.345
				Strong	0.567	0.378	0.316	0.286	0.629	0.430	0.361	0.328
		Toe-nails	6d	None	0.610	0.420	0.349	0.313	0.757	0.529	0.445	0.404
				Strong	0.597	0.408	0.338	0.309	0.721	0.497	0.422	0.384
			8d	None	0.603	0.414	0.344	0.307	0.695	0.483	0.404	0.369
				Strong	0.588	0.399	0.333	0.300	0.671	0.462	0.391	0.354
Unreinforced Masonry	One	Straps	6d	None	0.440	0.258	0.203	0.176	0.556	0.334	0.269	0.240
				Strong	0.424	0.250	0.198	0.173	0.522	0.318	0.253	0.226
			8d	None	0.415	0.239	0.190	0.168	0.479	0.289	0.229	0.206
				Strong	0.400	0.234	0.184	0.165	0.456	0.272	0.221	0.196
		Toe-nails	6d	None	0.444	0.267	0.208	0.181	0.561	0.345	0.271	0.241
				Strong	0.437	0.259	0.202	0.178	0.529	0.329	0.261	0.231
			8d	None	0.433	0.262	0.202	0.176	0.514	0.318	0.248	0.220
				Strong	0.422	0.251	0.198	0.173	0.490	0.302	0.240	0.213
	Two	Straps	6d	None	0.605	0.411	0.343	0.311	0.743	0.516	0.438	0.398
				Strong	0.593	0.401	0.334	0.303	0.706	0.487	0.412	0.375
			8d	None	0.583	0.389	0.328	0.296	0.646	0.448	0.376	0.342
				Strong	0.568	0.377	0.317	0.285	0.626	0.428	0.361	0.328
		Toe-nails	6d	None	0.616	0.421	0.348	0.314	0.755	0.527	0.448	0.404
				Strong	0.600	0.409	0.340	0.308	0.721	0.498	0.422	0.382
			8d	None	0.604	0.414	0.343	0.307	0.691	0.482	0.405	0.368
				Strong	0.585	0.399	0.331	0.301	0.667	0.461	0.391	0.355
Reinforced Masonry	One	Straps	6d	None	0.439	0.258	0.202	0.176	0.554	0.335	0.268	0.238
				Strong	0.426	0.251	0.197	0.173	0.523	0.316	0.253	0.227
			8d	None	0.415	0.239	0.189	0.168	0.480	0.289	0.230	0.207
				Strong	0.399	0.234	0.184	0.165	0.457	0.273	0.218	0.196
		Toe-nails	6d	None	0.444	0.266	0.207	0.182	0.560	0.344	0.273	0.241
				Strong	0.434	0.258	0.202	0.177	0.531	0.329	0.260	0.231
			8d	None	0.432	0.262	0.202	0.176	0.512	0.317	0.250	0.220
				Strong	0.421	0.252	0.195	0.171	0.491	0.304	0.240	0.212
	Two	Straps	6d	None	0.606	0.412	0.343	0.310	0.744	0.518	0.438	0.399
				Strong	0.596	0.402	0.337	0.304	0.708	0.488	0.403	0.367
			8d	None	0.582	0.390	0.327	0.298	0.649	0.450	0.378	0.343
				Strong	0.567	0.378	0.317	0.285	0.627	0.429	0.362	0.327
		Toe-nails	6d	None	0.612	0.421	0.349	0.314	0.753	0.526	0.445	0.402
				Strong	0.599	0.409	0.340	0.306	0.708	0.499	0.421	0.377
			8d	None	0.603	0.413	0.345	0.309	0.693	0.481	0.407	0.370
				Strong	0.585	0.399	0.333	0.299	0.669	0.460	0.390	0.351

The combined effect of upgrading the roof and adding window protection is a reduction in the average building damage state ranging between 45% and 59% with a mean reduction of 52%. Note that the reduction in losses associated with the application of both window protection and roof strength enhancements results in a reduction in damage (52%) which is greater than the sum of the reduction in losses of the two mitigation methods applied separately (15% + 27% = 42%). This synergistic effect is expected since the full benefits of the individual techniques cannot be realized unless other failure modes of roughly equal probability are also addressed. Simply put, the building performance is governed by the performance of the weakest link in the chain. If there are two links of roughly equal weakness, both must be strengthened.

Table 6-14. Average Building Damage States – Upgrade Roof

Building Characteristics					Hip Roof				Gable Roof			
Wall Const.	No. of Stories	Roof/Wall Conn.	Sheath Nails	Garage Door	Terrain Surface Roughness (m)				Terrain Surface Roughness (m)			
					0.03	0.35	0.70	1.0	0.03	0.35	0.70	1.0
Wood Frame	One	Straps	6d	None	0.357	0.217	0.151	0.123	0.415	0.246	0.174	0.143
				Strong	0.380	0.238	0.164	0.132	0.429	0.258	0.181	0.150
			8d	None	0.358	0.218	0.151	0.122	0.410	0.243	0.173	0.143
				Strong	0.377	0.238	0.165	0.131	0.427	0.258	0.181	0.149
		Toe-nails	6d	None	0.401	0.258	0.179	0.142	0.469	0.320	0.227	0.186
				Strong	0.425	0.263	0.182	0.146	0.495	0.310	0.220	0.178
			8d	None	0.402	0.258	0.179	0.142	0.471	0.319	0.225	0.186
				Strong	0.425	0.263	0.182	0.146	0.494	0.310	0.220	0.180
	Two	Straps	6d	None	0.550	0.338	0.256	0.219	0.648	0.405	0.316	0.275
				Strong	0.544	0.335	0.251	0.213	0.636	0.402	0.311	0.271
			8d	None	0.549	0.338	0.257	0.218	0.649	0.406	0.316	0.274
				Strong	0.546	0.337	0.252	0.213	0.638	0.401	0.311	0.269
		Toe-nails	6d	None	0.613	0.391	0.292	0.247	0.707	0.482	0.371	0.318
				Strong	0.604	0.375	0.279	0.238	0.708	0.447	0.346	0.302
			8d	None	0.613	0.391	0.292	0.248	0.708	0.479	0.373	0.318
				Strong	0.604	0.374	0.279	0.240	0.708	0.447	0.346	0.301
Unreinforced Masonry	One	Straps	6d	None	0.360	0.218	0.150	0.121	0.412	0.243	0.174	0.143
				Strong	0.379	0.238	0.165	0.132	0.429	0.258	0.181	0.148
			8d	None	0.359	0.217	0.150	0.123	0.414	0.245	0.174	0.144
				Strong	0.380	0.239	0.163	0.131	0.429	0.259	0.183	0.149
		Toe-nails	6d	None	0.401	0.258	0.178	0.141	0.470	0.320	0.227	0.186
				Strong	0.424	0.263	0.181	0.147	0.495	0.308	0.219	0.181
			8d	None	0.401	0.258	0.177	0.140	0.471	0.317	0.226	0.186
				Strong	0.424	0.263	0.183	0.147	0.495	0.309	0.217	0.180
	Two	Straps	6d	None	0.550	0.340	0.258	0.219	0.650	0.407	0.317	0.275
				Strong	0.547	0.338	0.251	0.214	0.635	0.399	0.314	0.270
			8d	None	0.549	0.337	0.256	0.219	0.646	0.408	0.317	0.275
				Strong	0.545	0.338	0.253	0.213	0.635	0.401	0.310	0.270
		Toe-nails	6d	None	0.608	0.389	0.292	0.249	0.709	0.479	0.373	0.320
				Strong	0.610	0.375	0.282	0.237	0.709	0.448	0.346	0.300
			8d	None	0.608	0.389	0.291	0.249	0.705	0.480	0.369	0.320
				Strong	0.610	0.374	0.282	0.240	0.708	0.446	0.346	0.299
Reinforced Masonry	One	Straps	6d	None	0.361	0.218	0.152	0.122	0.414	0.245	0.174	0.143
				Strong	0.380	0.236	0.165	0.134	0.430	0.258	0.181	0.149
			8d	None	0.362	0.217	0.150	0.123	0.413	0.244	0.173	0.144
				Strong	0.378	0.237	0.163	0.132	0.428	0.257	0.182	0.150
		Toe-nails	6d	None	0.402	0.258	0.178	0.141	0.471	0.317	0.226	0.185
				Strong	0.428	0.262	0.180	0.146	0.494	0.309	0.220	0.180
			8d	None	0.402	0.258	0.178	0.141	0.473	0.319	0.227	0.185
				Strong	0.427	0.263	0.181	0.145	0.496	0.309	0.220	0.180
	Two	Straps	6d	None	0.553	0.339	0.256	0.220	0.649	0.406	0.316	0.275
				Strong	0.543	0.337	0.251	0.214	0.637	0.400	0.310	0.268
			8d	None	0.548	0.338	0.257	0.218	0.646	0.407	0.317	0.274
				Strong	0.545	0.334	0.253	0.214	0.635	0.400	0.312	0.267
		Toe-nails	6d	None	0.609	0.388	0.293	0.248	0.707	0.480	0.371	0.319
				Strong	0.611	0.374	0.281	0.238	0.707	0.445	0.346	0.301
			8d	None	0.609	0.389	0.294	0.248	0.707	0.478	0.368	0.319
				Strong	0.611	0.377	0.281	0.239	0.708	0.444	0.344	0.300

Finally, it should be noted that the reduction in the average per storm building damage states presented here are valid for buildings located in the Miami area and will be different in locations having different hurricane wind climates.

6.5 Manufactured Homes

Manufactured homes are treated separately from single family homes and engineered structures. The damage model developed for manufactured homes includes a stability failure mechanism (overturning and sliding off its foundations) that is not treated for other buildings. The model also allows for frame failure, which is currently not treated in the modeling of other building types (except roof uplift failures in the case of residential buildings). This section of the report briefly reviews the history of the manufactured

Table 6-15. Average Building Damage States – Install Shutters and Upgrade Roof

Building Characteristics					Hip Roof				Gable Roof			
Wall Const.	No. of Stories	Roof/Wall Conn.	Sheath Nails	Garage Door	Terrain Surface Roughness (m)				Terrain Surface Roughness (m)			
					0.03	0.35	0.70	1.0	0.03	0.35	0.70	1.0
Wood Frame	One	Straps	6d	None	0.243	0.132	0.098	0.085	0.288	0.162	0.123	0.107
				Strong	0.237	0.133	0.096	0.083	0.275	0.156	0.119	0.102
			8d	None	0.243	0.131	0.097	0.084	0.289	0.163	0.123	0.107
				Strong	0.239	0.132	0.096	0.082	0.276	0.157	0.119	0.101
		Toe-nails	6d	None	0.266	0.158	0.114	0.095	0.333	0.200	0.148	0.125
				Strong	0.266	0.155	0.112	0.094	0.322	0.194	0.145	0.124
			8d	None	0.266	0.158	0.112	0.096	0.332	0.199	0.147	0.127
				Strong	0.265	0.156	0.111	0.094	0.321	0.193	0.144	0.125
	Two	Straps	6d	None	0.364	0.229	0.183	0.161	0.414	0.274	0.221	0.195
				Strong	0.351	0.221	0.176	0.156	0.400	0.260	0.209	0.187
			8d	None	0.363	0.228	0.184	0.164	0.412	0.272	0.218	0.196
				Strong	0.353	0.223	0.177	0.155	0.399	0.260	0.210	0.186
		Toe-nails	6d	None	0.387	0.258	0.204	0.178	0.472	0.318	0.259	0.231
				Strong	0.378	0.247	0.196	0.171	0.459	0.305	0.249	0.220
			8d	None	0.385	0.256	0.204	0.179	0.472	0.318	0.258	0.230
				Strong	0.377	0.247	0.195	0.171	0.457	0.306	0.247	0.221
Unreinforced Masonry	One	Straps	6d	None	0.241	0.133	0.097	0.085	0.288	0.163	0.123	0.107
				Strong	0.235	0.131	0.095	0.082	0.274	0.156	0.119	0.102
			8d	None	0.239	0.132	0.097	0.084	0.286	0.163	0.121	0.107
				Strong	0.235	0.132	0.096	0.082	0.273	0.156	0.118	0.102
		Toe-nails	6d	None	0.263	0.160	0.113	0.096	0.329	0.202	0.148	0.127
				Strong	0.265	0.157	0.112	0.095	0.322	0.193	0.146	0.124
			8d	None	0.263	0.159	0.113	0.095	0.330	0.197	0.147	0.126
				Strong	0.266	0.156	0.112	0.096	0.322	0.195	0.145	0.125
	Two	Straps	6d	None	0.359	0.229	0.184	0.162	0.413	0.274	0.222	0.195
				Strong	0.350	0.221	0.176	0.156	0.397	0.261	0.210	0.187
			8d	None	0.359	0.232	0.183	0.161	0.409	0.273	0.220	0.198
				Strong	0.350	0.222	0.176	0.156	0.397	0.261	0.208	0.184
		Toe-nails	6d	None	0.385	0.258	0.202	0.178	0.471	0.319	0.259	0.231
				Strong	0.377	0.248	0.194	0.173	0.454	0.303	0.247	0.223
			8d	None	0.384	0.257	0.203	0.179	0.468	0.319	0.257	0.233
				Strong	0.377	0.249	0.196	0.173	0.456	0.305	0.250	0.222
Reinforced Masonry	One	Straps	6d	None	0.241	0.133	0.098	0.085	0.288	0.163	0.123	0.107
				Strong	0.236	0.131	0.097	0.082	0.274	0.157	0.118	0.102
			8d	None	0.240	0.131	0.098	0.084	0.286	0.163	0.122	0.108
				Strong	0.236	0.131	0.096	0.082	0.275	0.156	0.119	0.101
		Toe-nails	6d	None	0.263	0.159	0.113	0.096	0.331	0.200	0.148	0.127
				Strong	0.266	0.156	0.112	0.095	0.320	0.193	0.146	0.124
			8d	None	0.263	0.157	0.113	0.096	0.328	0.198	0.148	0.126
				Strong	0.265	0.156	0.112	0.095	0.321	0.194	0.146	0.124
	Two	Straps	6d	None	0.360	0.228	0.182	0.161	0.412	0.274	0.222	0.197
				Strong	0.351	0.221	0.176	0.156	0.396	0.259	0.209	0.187
			8d	None	0.359	0.229	0.184	0.163	0.412	0.274	0.221	0.195
				Strong	0.351	0.222	0.177	0.154	0.394	0.261	0.210	0.185
		Toe-nails	6d	None	0.384	0.255	0.201	0.178	0.468	0.318	0.258	0.231
				Strong	0.376	0.247	0.198	0.172	0.454	0.304	0.246	0.221
			8d	None	0.385	0.256	0.203	0.178	0.472	0.318	0.258	0.231
				Strong	0.376	0.248	0.198	0.173	0.458	0.307	0.248	0.221

Table 6-16. Percent Decreases in the Per Storm Average Building Damage State Due to Mitigation (Minimum/Average/Maximum) – Residential Buildings

Mitigation Strategy	Decrease in Per Storm Average Damage State
Install Shutters	6% / 15% / 23%
Upgrade to Dade Roof	18% / 27% / 44%
Install Shutters and Upgrade to Dade Roof	45% / 52% / 59%

home regulatory environment, which describes how the design criteria changed with time, as well as describing the failure model and presenting examples of predicted and observed manufactured home failures.

A manufactured home is defined as: "...a structure, transportable in one or more sections, which in the traveling mode, is eight body feet or more in width and forty body feet or

more in length, or, when erected on site, is three hundred twenty or more square feet, and which is built on a permanent chassis and designed to be used as a dwelling with or without a permanent foundation when connected to the required utilities, ..." (MHCSS, 1992). A brief history of the development of manufactured housing in this country is provided in testimonies of industry leaders before congressional subcommittee hearings on raising standards (US Congress, 1981).

The design and fabrication processes are governed by U.S. Department of Housing and Urban Development regulations known as the "Manufactured Home Construction and Safety Standards (MHCSS)" 24 CFR, Part 3280. These standards went into effect in 1976. There were no national statutes covering manufactured homes. There was, however, a national standard entitled American National Standards Institute ANSI A119.1, "Standard for Manufactured Homes." Some states adopted this standard, but even in those states, enforcement was often lax. Homes built in 1976 or later are sometimes referred to as "HUD-code homes."

The original MHCSS wind load provisions were similar to those in ANSI A119.1-1973 (NFPA, 1973), defining two different wind zones (although the zone boundaries differed). Zone I was the standard zone, and Zone II was the Hurricane Zone, extending along the Gulf, Atlantic, and Alaskan coastlines. For structures located in Zone II, the wind loads given in the ANSI provisions required the unit to resist wind loads of 15 psf acting upwards on the roof surface and a wind load of 25 psf acting horizontally on one side wall. As noted above, the wind loads prescribed in the 1976 HUD code were the same as those given in ANSI A119.1-1973, the only difference between the pre- and post-1976 homes being the degree to which the provisions were enforced.

The wind loading requirements were not changed appreciably until 1994, when they were increased in response to years of excessive damage, and particularly in the wake of Hurricane Andrew (HUD, 1994). The 1994 requirements boosted wind loads to levels much closer to ASCE-7 loads, and redefined the wind zones, adding a more stringent Zone III located in southern Louisiana, southern Florida, coastal Alaska, and Hawaii.

Although home construction is regulated by HUD, installation is not. It is left to states and/or local governments. Several states have no tie-down requirements (Louisiana, for example). The manufacturer's responsibility is to provide a homeowner's manual with installation details for the specific model. The American National Standards Institute's Standard A225.1, "Manufactured Home Installations" (most recently A225.1-1994), is a consensus standard for the installation of manufactured homes and minimum construction requirements for manufactured home communities. Model building codes also address the issue of tie-down of manufactured homes (SBCCI, 1991).

6.5.1 Resistance Models for Manufactured Homes

The manufactured home damage and loss model is based primarily on the work of Vasquez (1994). The failure modes considered in the model include damage to components and cladding (roof cover, roof sheathing, windows, doors and siding), stability failures (overturning and sliding) and failure of the main wind force resisting

system (roof uplift and failure of the wall-to-floor connections). For modeling windborne debris, the same model developed for residential buildings is used.

The roof membrane systems on manufactured homes vary considerably, and may consist of metal skins attached directly to the roof trusses, or roof sheathing attached to the roof trusses where shingles provide the water proof layer. The siding of the older manufactured homes typically was comprised of either wood, vinyl, or metal panels. The model manufactured home selected for the development of a first principles based load-resistance damage model employs metal panel siding and either plywood or OSB roof sheathing.

Main Wind Force Resistance Modeling. The nominal resistance of the superstructure of the manufactured home is computed using the wind load criteria for manufactured homes located in Zone II, noted above. The factor of safety assumed in the development of the superstructure resistance functions is assigned a mean value of 1.5 and a coefficient of variation of 25%. If the load acting on the roof of the structure exceeds this nominal capacity, the roof-wall connection is considered to be damaged, but the roof does not fail. A complete roof failure is assumed to occur if the uplift forces on the roof exceed a value equal to 1.8 times the nominal resistance (i.e., 20% higher than the load used to define initial damage to the roof-wall connection). Using this approach, the mean capacity of the roof to resist uplift failure is defined as 15 psf multiplied by the safety factor.

In the estimation of the capacity of the floor-to-wall connections, a simple overturning computation was performed where the manufactured home is loaded with a vertical roof load of 15 psf and a horizontal wall load of 25 psf. The uplift forces at the floor-to-wall connections are determined using moment equilibrium. A nominal factor of safety of 1.6 (COV = 25%) is assumed to apply to the connection capacity for modeling the initial failure, and a 20% increase in this value is assumed to apply for the condition describing a complete failure of the floor-wall connection.

In cases where the roof fails, a wall is considered to fail if the load acting on the wall exceeds 12.5 psf (COV = 25%) (i.e., half the value of load used to design the manufactured home in shear). The above values all apply to post-HUD construction. In the case of pre-HUD code manufactured homes, the nominal resistances for the connections noted above are reduced by 20%.

Foundation and Tie Down Modeling. The primary method for anchoring manufactured homes against lateral and uplift loads is soil anchors. These systems have often proven to be unreliable and a major source of damage. Soil types and conditions, anchor types, installation practices, and maintenance all have a tremendous influence on the pullout capacity of the anchors. Kovacs and Yokel (1979) issued a report comparing pullout capacity of common anchors in various soil types with theoretical solutions based on the principles of soil mechanics. They concluded that the soil mechanics theories did not adequately predict pullout capacity. Given the failure of the theoretical approach, Yokel et al. (1982) performed a more systematic, empirical study. It was concluded that typical manufactured home installation practices did not yield anchor performance as required by the standards, and the capacity of the anchors varies significantly with the depth of the

anchor, and of course, the soil type. Knowledge of the anchor pullout capacity, the quality of the installation of the anchors and the capacity and corrosion states of the hardware connecting the anchor to the manufactured home unit is critical in the prediction of the performance of manufactured homes in severe wind storms.

The anchor capacity used here is derived from the Yokel, et al. (1982) data as given in Vasquez (1994), where data are given for the pullout capacity of anchors in sandy soils, silty soils and clay soils, for a range of penetration depths, and direction of applied load. The results of the Yokel, et al. (1982) study are summarized in Tables 6.17 through 6.19. As indicated in Tables 6.17 through 6.19, there is significant variability in the ultimate pullout capacity. Note that in Tables 6.17 through 6.19 the angles, β, represent the angle of the direction of the pullout force, with 90° representing a vertical load. The selection of the representative resistance characteristics of the manufactured home anchor capacity, which may be expected to realistically model the in-service characteristics of the anchor system, clearly requires significant judgment.

Table 6-17. Results of Field Pull-Out Tests on Soil Anchors Installed and Loaded at Various Angles (Yokel, et al., 1982)

Soil Type	Angles β_1/β_2 (degrees)	Load at 102 mm (4″) (lb_f)		Ultimate Load (lb_f)		Maximum Displacement (inches)	
		Mean	COV	Mean	COV	Mean	COV
Silt	60/90	2,967	0.29	7,565	0.15	10.07	0.35
Silt	45/90	1,350	0.19	7,933	0.02	13.85	0.09
Sand	40/90	2,583	0.20	6,187	0.05	9.08	0.07
Clay	40/90	767	0.15	3,267	0.21	18.60	0.20
Silt	60/135	433	0.13	3,387	0.13	25.15	0.04
Silt	45/135	413	0.08	4,243	0.03	33.80	0.04
Silt	15/135	433	0.07	4,775	0.14	54.00	0.05

Notes: Each case based on 3 tests. All tests conducted under moist soil conditions.

Table 6-18. Results of Field Pull-Out Tests on Fully Embedded Soil Anchors: $\beta_1 = 90°$, $\beta_2 = 90°$ (Yokel, et al., 1982)

Soil Type	No. of Tests	Load at 51 mm (2″) (lb_f)		Ultimate Load (lb_f)		Maximum Displacement (inches)	
		Mean	COV	Mean	COV	Mean	COV
Moist Silt	11	4,295	0.20	5,173	0.10	7.17	0.53
Wet Silt	5	2,320	0.40	3,640	0.17	11.04	0.35
Moist Sand	6	4,488	0.13	5,063	0.13	3.82	0.35
Wet Sand	3	5,100	0.17	5,953	0.18	4.35	0.25
Moist Clay	3	3,067	0.22	3,433	0.16	5.83	0.49

Table 6-19. Results of Field Pull-Out Tests on Fully Embedded Soil Anchors: $\beta_1 = 45°$, $\beta_2 = 105°$ (Pearson, et al., 1991)

Stabilizer Plates	No. of Tests	Load at 102 mm (4″) (lb_f)		Ultimate Load (lb_f)		Maximum Displacement (inches)			
						Horizontal		Vertical	
		Mean	COV	Mean	COV	Mean	COV	Mean	COV
No	5	662	0.18	2490	0.26	11.3	0.17	3.2	0.63
Yes	19	805	0.41	2578	0.22	16.1	0.26	5.1	0.57

The anchor tie down system used herein, is modeled with a mean capacity of 1500 lbs/anchor with a coefficient of variation of 35%. No reduction in the foundation capacity is used to model the foundations for pre-HUD manufactured homes. The computation of the forces required to initiate sliding or overturning are made using a static equilibrium analysis following the approach described in Vasquez (1994) and Marshall (1995). A total of five anchors are assumed to be installed for a 60′ long unit. In the stability analysis, the weight of the unit is modeled using a mean value of 25 psf (COV = 10%) and a value of 10 psf (COV = 20%) to define the weight of the contents. The combined unit weight of 35 psf is less than the 41 psf value assumed by Vasquez (1994), but higher than the 25 psf value assumed by Marshall (1995). The failure modes considered in the foundation failure analysis include sliding and overturning. Following the definition of manufactured home damage states suggested by Vann and McDonald (1978), the sliding mode of failure is broken into minor and major categories. Major sliding is considered to have occurred if the wind load required to initiate sliding exceeds 1.2 times the nominal sliding resistance.

Components and Cladding. The cladding components modeled include metal siding, windows, roof sheathing (plywood or OSB) and roof cover (shingles). The same shingle model used on single family homes is used to model the shingles on manufactured homes. The metal siding is assumed to have a mean resistance of 25 psf (COV = 15%). Failure of the cladding is considered for the case of negative loads only. The nominal resistance of the windows is taken as 32 psf (COV = 18%) for both positive and negative loads. The mean uplift capacity of the roof sheathing is taken as 45 psf.

Summary of Failure Modes Considered for Manufactured Homes. The complete list of failure modes considered for manufactured homes is as follows:

1. Roof Cover Loss
2. Roof Sheathing Loss
3. Window Breakage (Pressure and Windborne Debris)
4. Siding Failure
5. Roof-Wall Connection Failure (Minor)
6. Roof-Wall Connection Failure (Major)
7. Wall Failure Following Roof Failure
8. Floor-Wall Connection Failure (Minor)
9. Floor-Wall Connection Failure (Major)
10. Foundation Failure (Minor Sliding)
11. Foundation Failure (Major Sliding)
12. Foundation Failure (Overturning)

6.5.2 Damage Model Validation for Manufactured Homes

The manufactured home damage model has been validated through comparisons of damage states predicted from the above model to the damage states predicted from the models of Vann and McDonald (1978) and Vasquez (1994), as well as through

comparisons of observed damage from Hurricane Bertha (1996) along the North Carolina coast, Hurricane Andrew (1992) in Dade County Florida and Hurricane Elena (1986) along the Central Gulf Coast.

Comparisons of Wind Speed vs. Damage Predictions to the Vann and McDonald Model and the Vasquez Model. Table 6.20 presents a comparison of the threshold wind speeds (peak gust, 10m open terrain) associated with various damage states obtained from the load and resistance model described herein, to those given by Vann and McDonald (1978) and Vasquez (1994). The damage states given in Table 6.20 are valid for units located in open terrain. The first column in Table 6.20 presents the damage identification codes given in Vasquez (1994). The Vann and McDonald damage states are applicable to pre-HUD units only, whereas the Vasquez data likely includes a mix of pre-HUD and HUD units. Both models have been derived from wind speed versus damage data collected from post-storm damage surveys. In the case of the modeled damages, the threshold wind speeds are defined as the wind speeds where approximately 5% of the modeled units experience the indicated damage.

Table 6-20. Comparison of Threshold Velocities for Various Manufactured Home Damage States

Damage Code	Damage Description	Vann and McDonald	Vasquez	ModelPre-HUD	ModelHUD
1.1A (MI)	Minor Sliding Damage – No Anchors	60-70	<85-100	90-100	90-100
1.1A (MA)	Major Sliding Damage – No Anchors	65-90	<100-115	115-125	115-125
1.1B (MA)	Major Vaulting Damage – No Anchors				
1.1B (DE)	Total Vaulting Damage – No Anchors				
1.1C (MA)	Major Overturning Damage – No Anchors	60-70	<85-100		
1.1C (DE)	Total Overturning Damage – No Anchors	90-125	<85-100	110-120	110-120
1.2A (MA)	Total Overturning Damage – Anchor Pull Out	120-130	<120-130	130-140	130-140
1.2B (DE)	Total Overturning Damage – Tie Failure	120-130	<120-130	130-140	130-140
2A (MI)	Roof to Wall Connection Failure – Minor	60-70		100-110	100-110
2A (MA)	Roof to Wall Connection Failure – Major	90-125	110-120	100-110	110-120
2A (DE)	Roof to Wall Connection Failure – Destruction	120-130	<120-130	100-110	120-130
2B (MA)	Floor to Wall Connection Failure – Major	120-130	100-110	95-105	100-110
2B (DE)	Floor to Wall Connection Failure – Destruction		<120-130		
2C (MA)	Structural Member Failure – Major	120-130			
2C (DE)	Structural Member Failure – Total		<120-130		
2D (MA)	Tree or Large Missile Impact – Major	120-130	110-110		
2D (DE)	Tree or Large Missile Impact – Total	120-130	<120-130		
3A (MI)	Window Damage – Minor		<110-120	100-110	100-110
3B (MI)	Door Damage – Minor		<120-130		
3C (MI)	Roof Covering Damage – Minor	65-90	85-95	70-80	70-80
3C (MA)	Roof Covering Damage – Major	120-130	85-95	120-130	120-130
3C (DE)	Roof Covering Damage – Total		<120-130	120-130	120-130
3D (MI)	Wall Panel Damage – Minor		85-95	90-100	90-100
3D (MI)	Wall Panel Damage – Major		85-95	120-130	120-130
3D (DE)	Wall Panel Damage – Total	120-130	<120-130		
3E (MI)	Small Debris Damage – Minor		100-110		
3E (MA)	Small Debris Damage – Major		<85-95		

The general observation that can be made by comparing the threshold wind speeds given in Table 6.20 is that the model developed here tends to yield higher threshold wind speeds for foundation failures, but lower threshold wind speeds for the initiation of the

roof-wall connection failures. The threshold wind speeds associated with the initiation of wall-floor connection failures are comparable to those given in the Vasquez model, but lower than those suggested by the Vann and McDonald model. The wind speeds associated with the initiation of cladding failures are generally comparable between models, with the exception that the load-resistance model developed here yields higher estimates of the wind speeds required to initiate wall cladding loss.

Hurricane Bertha Validation. Following Hurricane Bertha (1996), ARA sent a team of engineers to perform a post-storm damage survey quantifying the wind induced damage to buildings along the North Carolina coast. During this damage survey, 114 manufactured home units around the Surf City area on Topsail Island were surveyed. All of the manufactured homes surveyed were tied down, and it was not determined what fraction of the homes were pre-HUD and HUD homes. The survey recorded the condition of the manufactured homes, noting damage to windows, siding and the roof system. The overall damage states of the 114 buildings are given in Table 6.21, along with the modeled damage produced by simulating the full time series of wind speed and direction produced by Hurricane Bertha at Surf City. The terrain around the manufactured home parks was typically fairly open, and thus a surface roughness of 0.1 m is used to model the basic terrain. The modeled damage states in Table 6.21 are given for both the HUD and pre-HUD model manufactured homes. The peak gust wind speed (open terrain, 10 m) resulting from the Hurricane Bertha simulation was 103 mph.

Table 6-21. Comparison of Observed and Modeled Manufactured Home Damage States on Topsail Island Produced by Hurricane Bertha (1996)

Observed Damage State	Percent Observed	HUD Home Simulation	Pre-HUD Home Simulation
No Damage	85%	85%	85%
Loss of One Metal Siding Panel	7%	10%	10%
Partial Roof Deck Failure	2.6%	0.3%	0.3%
Whole Roof Failure	1.8%	2.2%	3.7%
One Broken Window	6%	2.4%	2.4%
More than One Broken Window	0.9%	2.2%	2.2%

The comparison of the simulated and observed damage states shown in Table 6.21 indicates reasonable agreement between the modeled and observed damage states, with the model tending to slightly overestimate the number of units with minor siding damage and the number of units with whole roof damage. The overestimate of the whole roof damage is somewhat offset by the underestimate of the number of units experiencing partial roof loss. The model tends to underestimate the number of units with window damage, but the prediction of the number of units expected to sustain no damage is correct.

Hurricane Andrew Validation. Following hurricane Andrew, a report was prepared for the Manufacturing Housing Institute by Ferguson and Cardwell (1992) describing the intensity and type of damage experienced by manufactured home units located throughout the region impacted by the storm. The damage to the units in each of the surveyed parks was characterized using the damage classification system developed by Vann and McDonald (1978). To further validate the manufactured home damage model,

comparisons of simulated and observed damage states in six of the parks surveyed by Ferguson and Caldwell are performed. In order to facilitate these comparisons, the damage states predicted by the damage model had to be mapped to correspond to the damage classification scheme developed by Vann and McDonald. Table 6.22 describes the damage states associated with each of the five damage classes suggested by Vann and McDonald, along with the damage states predicted using the load and resistance based manufactured home damage model for each class. It is noteworthy that there is a fine line between the damage associated with Classes 3 and 4, and it is likely that that in both the observations and the mapping between modeled damage to Class 3 and 4 damage, there will be a number of miss-classifications.

Table 6-22. Damage Classes Described by Vann and McDonald and the Corresponding Damage States from the Damage Simulation Model

Damage Class	Description of Damage (Vann and McDonald, 1978)
0	**No Damage or Very Minor Damage** – Little or no visible damage from the outside. Slight shifting on the blocks that would suggest re-leveling, but not off the blocks. Some cracked windows, but no resulting water damage.
1	**Minor Damage** – Shifting off the blocks or so that blocks press up to the floor; re-leveling required. Walls, doors, etc., buckled slightly, but able to be corrected by re-leveling. Minor eave and upper wall damage, with slight water damage but roof not pulled all the way back. Minor pulling away of siding with slight water damage. Minor missile and/or tree damage. Slight window breakage and attendant water damage.
2	**Moderate Damage (Still Livable)** – Severe shifting off the blocks with some attendant floor and superstructure damage (punching, racking, etc). Roof removed over a portion or all of the home but the joists remain intact, walls not collapsed. Missile and/or tree damage to a section of the wall or roof, including deep dents or punctures. Serious water damage from holes in roof, walls, windows, doors or floors.
3	**Severe Damage (Not Livable, but Repairable)** – Unit rolled onto side but frame intact. Extreme shifting causing severe racking and separations in the superstructure. Roof off, joists damaged or removed, walls damaged from lack of lateral support at top. Severe tree damage, including crushing of one wall or roof section. Superstructure partially separated from under frame.
4	**Destruction (Not Livable)** – Unit rolled onto top or rolled several times. Unit tossed or vaulted through the air. Superstructure separated from the underframe or collapsed to side of the underframe. Roof off, joists removed and walls collapsed. Destruction of a major section by a falling tree.

	Modeled Damage States (If any one of the conditions in the shaded cells of a given row is true, the mobile home is placed in that damage state)					
Damage Class	Roof Cover Damage	Siding Damage	Window and Door Failures	Roof Sheathing Failures	Roof to Wall and/or Wall to Foundation Connection Failures	Foundation to Ground Anchor Failures
0	≤10%	≤1 Panel	None	None	None	None
1	>10% to ≤25%	>1 to ≤25%	1 or 2	None	None	Minor Sliding
2	>25%	>25%	>2 to ≤50%	>0% to ≤25%	Minor	Typically Minor Sliding
3	Typically >25%	Typically >25%	>50%	>25%	Typically Minor	Major Sliding
4	Typically >25%	Typically >25%	Typically >50%	Typically >25%	Major	Overturning or Uplift

The location of each manufactured home park surveyed by Ferguson and Caldwell was noted only approximately. For example, the location of the park referred to as University Lakes is given as "South side of U.S. 41, 1 mile west of the Florida Turnpike." The locations given by Ferguson and Caldwell are accurate enough to place the parks for the

purposes of performing a site specific wind speed simulation, but not accurate enough to place the parks for the purposes of estimating a surface roughness length. Damage simulations have been performed for each location using surface roughness lengths of 0.1 m and 0.3 m. All damage simulations were performed using a site specific simulation of the hurricane wind velocities, but the orientation of the units was taken as random, with a total of 1000 damage simulations performed for each park.

Table 6.23 presents the results of the damage simulations, along with a comparison of the damage descriptions for each site given by Ferguson and Caldwell. Also given in Table 6.23 are the simulated maximum peak gust wind speeds (10 m, open terrain) at each site obtained from the simulation of Hurricane Andrew.

Table 6-23. Comparison of Modeled and Observed Manufactured Home Damage States Following Hurricane Andrew in South Florida

Park Name and Number of Units	Description of Park and Damage Along with Estimated Peak Gust Wind Speed (10m, Open Terrain)	Modeled Percent of Manufactured Homes Predicted in Each Damage Class									
		Unit Class	z_0 = 0.10 m					z_0 = 0.30m				
			0	1	2	3	4	0	1	2	3	4
Courtly Manor (521 Spaces)	50% HUD-labeled; Some Class 0 and 1 damage; 1 pre-HUD Class 3 damage; Peak gust wind speed 104 mph	Pre-HUD	85	7	3	<1	5	95	3	1	<1	1
		HUD	88	7	2	<1	2	96	3	<1	<1	<1
University Lakes (1100 spaces)	40% HUD-labeled; 20 Class 3 or 4 damage, all pre-HUD; HUD Class 0 or 1 damage; Peak gust wind speed 135 mph	Pre-HUD	11	15	8	6	60	41	16	12	5	27
		HUD	13	6	10	9	52	44	18	13	6	20
Un-named Park	Old Park, no HUD units; Class 3 and 4 damage; Peak Gust Wind Speed 156 mph	Pre-HUD	4	2	1	3	94	5	11	5	6	73
		HUD										
Dadeland (Estimate 200)	50% HUD-labeled; All class 2, 3 and 4 damage; Peak gust wind speed 159 mph	Pre-HUD	0	1	<1	1	98	11	6	3	4	86
		HUD	0	1	<1	2	97	11	7	4	8	80
Redlands (Estimate 90)	Older Park, mostly pre-HUD; 1 HUD Class 1 damage, else class 3 and 4 damage; Peak gust wind speed 162 mph	Pre-HUD	0	<1	<1	1	99	1	6	2	3	88
		HUD	0	<1	<1	2	97	1	7	3	6	84
Isla Gold	50% RV, 10-20% HUD; Mostly Class 4 damage; Some HUD Class 2 and 3 damage; 1 HUD Class 1 damage; Peak gust wind speed 162 mph	Pre-HUD	<1	1	1	2	95	2	7	4	4	83
		HUD	<1	1	2	4	92	2	9	7	8	74

The overall agreement between the observed and simulated damage states is generally good, except in the case of the homes located at University Lakes, where the model overestimated the number of HUD units experiencing Class 3 and 4 level damage, and the model underestimated the number of units experiencing the lower level Class 0 and 1 damage states. In the low wind speed case (Courtly Manor), the predicted and observed percentage of units experiencing damage levels in Classes 0 and 1 is good. In the high wind speed cases (Un-named Park, Dadeland, Redlands and Isla Gold), the lack of knowledge of the true terrain at the sites, clouds the comparisons, but generally, the agreement is good.

Hurricane Elena. The damage data described in McDonald and Vann (1986) is used to validate the manufactured home damage model using the observed manufactured home damage surveyed following Hurricane Elena (1985) along the Central Gulf Coast. A total of ten parks were surveyed, but the location of only eight of the ten are given by the

authors. The description of each of the sites, in terms of the surrounding terrain, is limited with the statement made that some communities were located in heavily wooded areas while others were sited on rolling hills that were free of trees and other obstructions to the wind. The authors go on to say that the site on Dauphin Island and the one located on the west shore of Mobile Bay were the most exposed to hurricane winds. In the damage simulations, a surface roughness of 0.3 m was used for all parks, except the one located on Dauphin Island where a surface roughness of 0.1 m was used.

In McDonald and Vann (1986), the fraction of anchored homes were noted for four of the eight parks. The fraction of homes in each damage state resulting from the damage simulation was presented as a weighted average of the anchored and non-anchored cases. At the remaining four sites, no information is given as to what fraction of the units were anchored. In these latter four cases, simulated damage states are given separately for anchored and non-anchored units. The survey of the anchor systems at the first four parks suggest that, on average, 70% of the units were properly anchored. Also, no information is given in McDonald and Vann (1986) as to what fraction of the units were HUD or pre-HUD units, although the authors do note that the HUD units performed better than the pre-HUD units. In the damage simulations, only non-HUD units are modeled, and thus the model results should yield a bias towards higher than observed damage.

The comparisons of the simulated and observed damage states are given in Table 6.24. As in the case of the Hurricane Andrew data, the observed unit damage classes are defined using the Vann and McDonald damage classification system. The peak gust wind speeds given in Table 6.24 are those resulting from the simulation of Hurricane Elena, and are representative of the peak gust wind speed at a height of 10 m in open terrain.

Summary. Considering the uncertainties associated with terrain, anchor systems and age of the units, the comparison of the simulated and observed damage states given above is encouraging. Furthermore, following the discussion given in McDonald and Vann (1986), comparisons of the damage states should be made through comparisons of the total fraction of units in Classes 0, 1 and 2 combined (minor damage) and those in Classes 3 and 4 combined (major damage). With this grouping of damage states, the overall level of agreement between the simulated and observed damage states from the three validation studies is seen to be good.

6.5.3 Damage Model Results for Manufactured Homes

Using the damage model described earlier combined with the wind speed and direction traces produced for a 20,000 year simulation of hurricanes for storms in the South Florida area, estimates of manufactured home damage states as a function of peak storm wind speed are produced for manufactured homes situated in four different terrains. In the development of the damage functions, for each simulated hurricane, 90 damage simulations are performed. At the start of each of the 90 damage simulations, the manufactured home is randomly oriented, and the component resistances are sampled. Upon completion of the damage simulation, all failure modes that occurred during the passage of the storm are recorded along with the peak gust wind speed produced by the

Table 6-24. Comparison of Simulated and Observed Manufactured Home Damage States Produced by Hurricane Elena

Manufactured Home Park	Observed Percentage of Units in Each Damage Class					Modeled Percentage of Units in Each Damage Class[1]				
	0	1	2	3	4	0	1	2	3	4
Trade Winds, Dauphin Island, AL (20)Peak Gust Wind Speed 126 mph	5	35	20	0	40	16	15	7	6	55
Trav Park, West Shore of Mobile Bay, AL (12)Peak Gust Wind Speed 109 mph	75	25				89	6	1	0	4
Old Fort Village, Gautier, MS (97)Peak Gust Wind Speed 122 mph	42	39	4	3	11	54	16	7	3	13
Isle of Pines North, Gautier, MS (102)Peak Gust Wind Speed 124	48	23	6	4	19	44	17	10	4	26
Isle of Pines South, Gautier, MS (86)Peak Gust Wind Speed 124 mph	55	22	5	2	16	3847	1816	910	63	3024
Imperial Estates, North Biloxi, MS (87)Peak Gust Wind Speed 122 mph	89	3	1	3	3	6067	1513	57	40	1219
Rolling Hills, North Biloxi, MS (175)Peak Gust Wind Speed 122 mph	87	10	1	1	1	5664	1612	68	41	1916
Anchor, Gautier, MS (70)Peak Gust Wind Speed 126 mph	76	19	1	0	4	3845	1816	912	64	3024

[1] Two rows of modeled data given at sites where the fraction of anchored units is not known. The upper line represents non-anchored units and the lower line represents anchored units. When a single row of modeled data is presented, results represent a weighted average of anchored and non-anchored damage states.

storm. Following all the damage simulations for each simulated storm, the resulting damage experienced by each modeled manufactured home is categorized into one of the five damage states as defined in lower portion of Table 6.22. The fraction of manufactured homes experiencing a given damage state for a given peak gust wind speed at a height of 10 m in open terrain is then computed and tabulated. The modeled damage states are given in wind speed increments of 5 mph, such that the fraction of homes experiencing a given damage state centered on a particular wind speed are used to compute the damage statistics for that wind speed.

The resistance properties of the manufactured homes used in the development of the damage state curves are summarized in Table 6.25. The resistance values for the HUD and Pre-HUD buildings have been previously discussed. Note that the windows of the modeled manufactured homes are situated so that no windows are located in the high suction end zones along the walls and thus the siding capacity, which is at least partially located in an end zone exceeds the window capacity for the HUD Wind Zone II and Wind Zone III cases.

Appendix B shows the computed damage state curves for all terrain, HUD Code and tie-down combinations examined. Table 6.26 lists the per storm average damage states.

6.6 Roof Covers on Flat Roofs

This section describes the model used to estimate wind-induced damage to roof covers on flat roofs. The two roof cover systems modeled are built-up roof covers and single-ply membrane covers. For both roof types, the failure of roof cover system is initiated by failure of the flashing.

Table 6-25. Resistance Parameters Used to Model Manufactured Homes

Building Component	Pre-HUD	HUD	1994 HUD Wind Zone I	1994 HUD Wind Zone II	1994 HUD Wind Zone III
Roof Cover Model	Residential Shingle Model	Residential Shingle Model	Residential Shingle Model	1.2 Times Residential Shingle Model	1.2 Times Residential Shingle Model
Roof Sheathing Capacity (psf)	Mean = 45COV = 12%	Mean = 45COV = 12%	Mean = 45COV = 12%	Mean = 90COV = 12%	Mean = 90COV = 12%
Siding Resistance	Mean = 25COV = 15%	Mean = 25COV = 15%	Mean = 25COV = 15%	Mean = 72COV = 15%	Mean = 88COV = 15%
Window Resistance	Mean = 32COV = 18%	Mean = 32 COV = 18%	Mean = 32COV = 18%	Mean = 57COV = 18%	Mean = 72COV = 18%
Design Uplift Load (psf)	15	15	9	27	32
Design Drag Load (psf)	25	25	15	39	47
Roof-Wall Connection Safety Factor	Mean = 1.5COV = 25%	Mean = 1.2COV = 25%	Mean = 1.5COV = 25%	Mean = 1.5COV = 25%	Mean = 1.5COV = 25%
Floor-Wall Connection Safety Factor	Mean = 1.6COV = 24%	Mean = 1.6COV = 24%	Mean = 1.6COV = 24%	Mean = 1.6COV = 24%	Mean = 1.6COV = 24%
Anchor Pull Out Capacity (lb)	Mean = 1500COV = 35%	Mean = 1500COV = 35%	Mean = 1500COV = 35%	Mean = 1500COV = 35%	Mean = 1500COV = 35%

Table 6-26. Per Storm Average Damage States

Mobile Home Construction	Terrain Surface Roughness (m)				
	z_0 = 0.03	z_0 = 0.15	z_0 = 0.35	z_0 = 0.7	z_0 = 1.0
Pre-HUD, Not Tied Down	0.641	0.480	0.354	0.264	0.226
Pre-HUD, Tied Down	0.623	0.466	0.339	0.249	0.211
HUD, Not Tied Down	0.618	0.449	0.330	0.247	0.211
HUD, Tied Down	0.594	0.428	0.309	0.226	0.190
1994 HUD – Wind Zone I, Tied Down	0.697	0.537	0.402	0.306	0.262
1994 HUD – Wind Zone II, Tied Down	0.269	0.234	0.162	0.111	0.091
1994 HUD – Wind Zone III, Tied Down	0.249	0.214	0.151	0.106	0.087

Built-up Roof Covers. Built-up roof (BUR) covers are composed of multiple plies of roofing felts adhered to each other and to the insulation substrate with a full mop of hot asphalt, coal tar or cold adhesive. The number of plies of roofing felt ranges from three to five. Roofing felts are commonly made of polyester, organic or glass-based materials. The surfacing on BUR covers is most often gravel or slag.

Single-ply Membrane Covers. Single-ply membrane (SPM) covers are normally attached to the insulation substrate by adhesives (hot asphalt or cold applied materials) or by mechanical fasteners. Adhered SPM covers can be fully adhered or partially adhered. The adhesive in partially adhered SPM covers will typically have 50% coverage in the central portions of the roof and greater coverage at or near the edges and corners of the roof. Common membranes are thermoplastic membranes, thermoset membranes, modified bitumen membranes and liquid applied membranes.

6.6.1 Resistance Model for Roof Covers on Flat Roofs

Most wind-induced failures of BUR and SPM covers are initiated by failure of the perimeter flashing. When the flashing fails due to wind suctions, the wind can peel back the roof cover membrane at the newly exposed edge and, depending on how well the roof cover is attached to the substrate, the peeling failure can continue throughout the storm and result in large-scale damage to the roof cover system. Another failure mode is

bubbling, where the roof cover is separated from the substrate by wind-induced suctions. If the bubbled area expands to an area where the roof cover is torn or missing, the airflow may "balloon" the bubbled area and the roofing membrane may tear, provided the resultant forces exceed the tearing strength of the membrane. Subsequent damage may then occur due to peeling at the newly exposed edges of the roof membrane. A bubbled section of the roof membrane may also become breached by impact from flying debris or by tearing at the perimeter of the bubble.

The capacity of the flashing varies significantly between manufactures and mainly depends on the flashing shape and size, how the flashing is fastened to the roof (e.g., cleated versus uncleated), and the quality of installation. The flashing on a properly designed roof system complying with the minimum Factory Mutual Research Corporation roof system uplift rating (i.e., FM 1-60), should have a horizontal resistance equal to 45 psf. This equates to 22.5 plf (pounds per linear foot) for typical 6″ wide flashing. For the purposes of modeling flashing failure, the resistance of the flashing to horizontal wind suction is taken as having a mean value of 22.5 plf and a coefficient of variation of 30%.

The roof cover damage model samples resistances from normal distributions with the means and standard deviations shown in Table 6.27. These roof cover resistances are based on a combination of engineering judgment and on data obtained from a survey on roof cover types conducted in Palm-Beach, Broward and Miami-Dade counties. The survey showed that the majority of the roof covers complied only with the minimum Factory Mutual Research Corporation roof system uplift rating. The minimum uplift rating (i.e., FM 1-60) corresponds to a static test pressure of 60 psf.

Table 6-27. Roof Cover Damage Model – Normal Distribution Parameters

Roof Cover System	Roof CoverPeeling Resistance		Roof CoverBubbling Resistance		FlashingResistance	
	Mean(psf)	COV(%)	Mean(psf)	COV(%)	Mean(plf)	COV(%)
BUR Cover	50	15	150	15	22.5	30
SPM Cover (adhesive)	40	15	60	15	22.5	30
SPM Cover (mech. fasteners)	40	15	60	15	22.5	30

The flashing resistance and roof cover resistances shown in Table 6.27 are used for "average" quality construction. Another result of the roof cover survey mentioned above is that approximately 50% of the existing roof covers in Miami-Dade, Broward and Palm Beach counties are classified as being of "poor" quality. Owing to the variability in the quality of materials and installation of existing roof cover systems, an additional resistance model was added to represent "poor" quality roof covers. The resistances associated with the "poor" quality roof cover system are 30% lower than those listed in Table 6.27. Also, an additional model was added to represent "good" quality roof cover systems, which are modeled with failure capacities 50% higher than those associated with "average" quality roof covers listed in Table 6.27. Note that this 50% increase is consistent with the increase in the test pressure associated with moving the Factory Mutual Research Corporation uplift rating from the minimum rating (FM 1-60) to the next discrete level (FM 1-90).

In the roof cover damage model, the roof area is divided into square elements of equal area (e.g., 4 sq ft). The square elements are assigned directionally dependent loads according to the ASCE wind loading provisions. The loads assigned to the flashing are set according to the vertical suction loads assigned to the adjacent roof cover elements multiplied by a factor. The factor transforms the vertical suction acting upward on the roof near the edge to a horizontal suction acting outward on the wall near the same edge. A factor of one is chosen for all flashing, whether located at a corner or at edges away from the corners. The factor of unity is a simplified approximation based on full-scale measurements of flashing loads made at Texas Tech University (McDonald, et al., 1997). In the full scale flashing tests, the ratio of the horizontal force to the vertical force estimated near the roof edge varied significantly between different flashing styles.

The final estimate of both the effective loads and the resistance of the roof flashing, is subject to significant uncertainties, but the limited comparisons of simulated and modeled roof damage states performed to date, show the model yields reasonable results.

In the damage model, a failed roof cover element implies that it has been removed and the associated roof substrate area is exposed to rainwater. On the other hand, bubbled roof cover areas will not expose the underneath roof surface area to rainwater. The roof cover damage algorithm performs the following four checks at each time step within a storm simulation:

1. All non-failed flashing is checked for failure. When a piece of flashing fails, the adjacent roof cover elements also fail.
2. All non-damaged roof cover elements adjacent to failed roof cover elements are checked for peeling failure.
3. All non-damaged roof cover elements are checked for bubbling.
4. All bubbled areas that have migrated to a failed portion of the roof cover are failed.

The roof cover damage model yields failed roof cover only when the flashing fails. The only damage that results if the flashing remains intact is bubbling of the roof cover, which, as stated above, will not expose the roof substrate to rainwater. Upon further development of the roof cover damage model, bubbled roof cover areas will also be checked for tearing at the bubble perimeter and for membrane breaches caused by windborne debris impacts.

6.6.2 Damage Model Validation for Roof Covers on Flat Roofs

Two detailed validation studies have been performed for Hurricane Andrew (1992).

Hurricane Andrew (1992) – Dixie Highway. The first validation study uses an aerial photograph taken after Hurricane Andrew in a commercial area located in Miami-Dade county in the vicinity of Dixie Highway and SW 184th Street. The photograph shows an area approximately 1600′×4100′. The estimated peak gust wind speed for this area at a height of 10 m above ground is 129 mph. This translates to about 163 mph at the same

height in open country terrain. Twenty-seven buildings were identified with BUR covers and the percent roof cover damage was estimated for each of them. It is likely that the roof cover materials and installation methods vary over the buildings used in this validation study. Of the 27 buildings identified, 13 are two story commercial buildings and fourteen are one story residential structures. The majority of the two story buildings are rectangular in plan with several of them being square or comprised of two or more rectangular elements (i.e., L-shaped). The one story buildings are all rectangular in plan. The simulation is performed on a two story rectangular building (aspect ratio of 2.25) and a one story rectangular building (aspect ratio of 1.5). The aspect ratios are consistent with the those of the surveyed buildings. The building stock considered in the analysis was assumed to comprise 40% of the buildings with roof sheathing attached with 6d nails and 60% with 8d nails.

Figure 6.43 shows the histogram of observed BUR cover damage in comparison to that predicted by the model. The one-story residential buildings were modeled with "average" and "poor" quality roof cover systems while the two-story commercial building were modeled with "average" and "good" quality roof cover systems. It can be seen in Figure 6.43 that the one-story residential buildings performed consistent to that predicted using the "poor" quality BUR cover model and the two-story commercial buildings performed consistent to that predicted using the "good" quality BUR cover model.

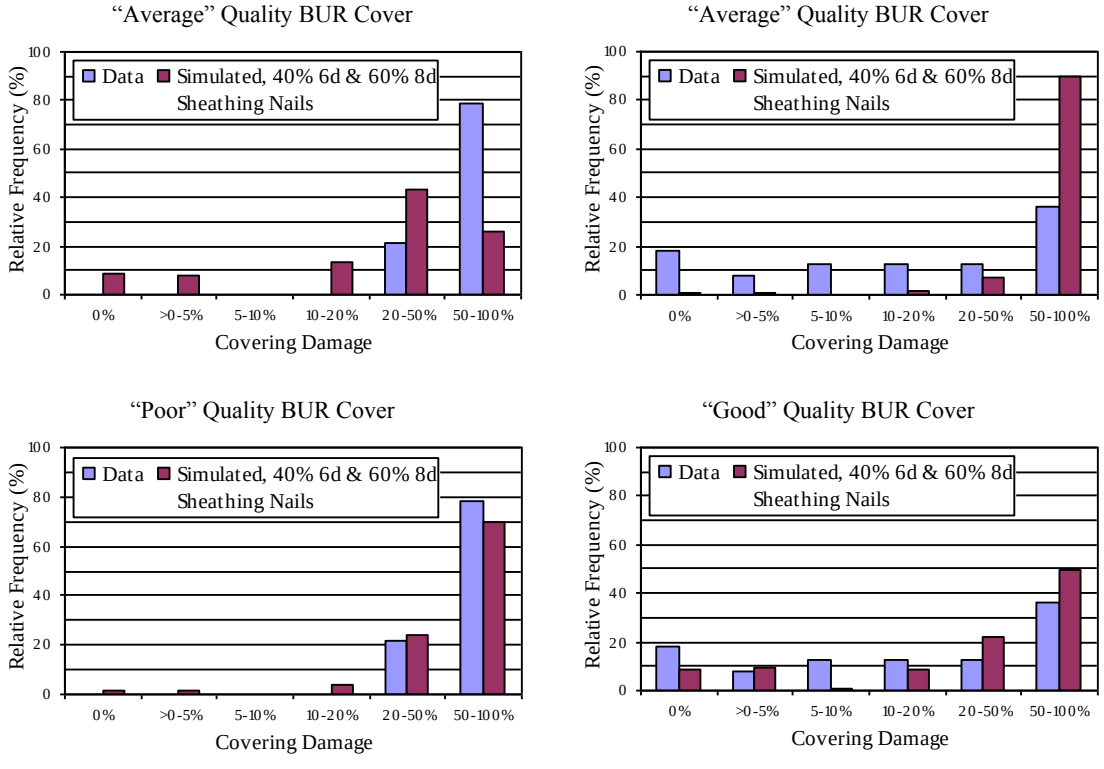

Figure 6-43. BUR Cover Damage for Hurricane Andrew – Dixie Highway.

Hurricane Andrew (1992) – Aerial Photograph 3. The second validation study for Hurricane Andrew (1992) uses damage statistics observed from Aerial Photograph 3 (see description in Section 6.3). This photograph showed 15 one-story units with square plan dimensions and 15 one-story units with rectangular plan dimensions (the aspect ratios range from approximately 3 to 5). The residential buildings were built with 4′×8′ plywood roof sheathing and BUR covers. The simulated BUR cover damage statistics are derived from 5,000 simulations using both a one-story square structure and a one-story rectangular structure (aspect ratio equal to 4). The simulations are performed considering a 40%/60% mixture of buildings with 6d and 8d sheathing nails, respectively.

The comparisons given in Figure 6.44 show that the model under-predicts the BUR cover damage observed in the aerial photograph using the "average" quality BUR cover model and performs reasonably well using the "poor" quality model.

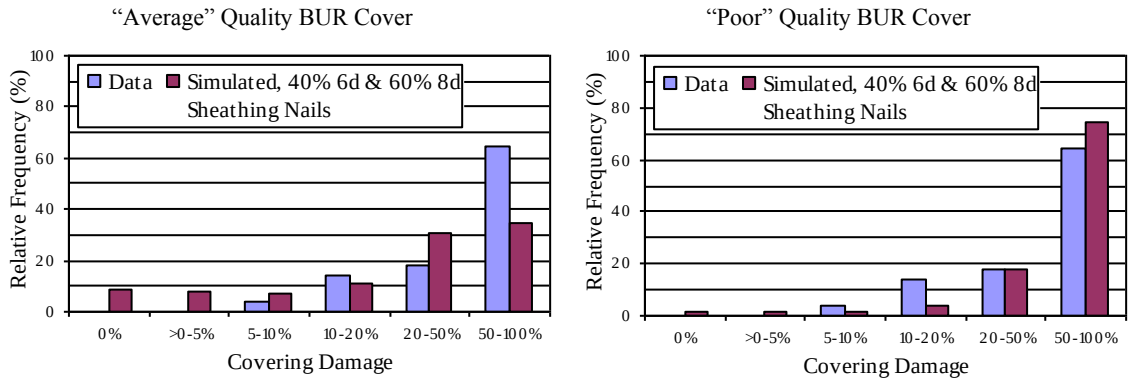

Figure 6-44. BUR Cover Damage for Hurricane Andrew – Aerial Photograph 3.

6.7 Open-Web Steel Joist Roof System

Light weight Open-Web Steel Joist (OWSJ) roof systems represent an efficient and inexpensive means to design and build a roof system to resist gravity loads. The joists consist of steel members that make up the top chord, bottom chord, and the web. The top and bottom chords are usually a set of two equal or unequal angle members. The web may either be angle or bar members depending on the span and depth of the steel joist. Under normal loading, the steel joist is designed for compression in the top chord and tension in the bottom chord (Steel Joist Institute, 1998). The top compression member is often braced by the roof deck connected to the upper chord of the joist, preventing buckling of the top chord. If the uplift pressures are greater than the dead loads of the steel joist, then the joist members undergo a stress reversal. The bottom chord members, which were designed for tension, now reverse to compression. If the bracing of the bottom chord of the joist is inadequate, this stress reversal may cause the bottom chord to buckle, failing the steel joist. The buckling of the bottom chord of an OWSJ is one of the two more commonly observed wind-induced failure modes associated with OWSJ roof systems. The other is the failure of the roof-wall connection (uplift failure), which is often associated with inadequate anchoring.

Steel joists are commonly used in light weight commercial structures, such as shopping malls, storage facilities, schools, warehouses, etc., and are usually simply supported. The OWSJ roof system can be used in combination with all steel buildings as well as buildings where the joists are supported by reinforced or unreinforced masonry walls. Different types of roof-wall connections are used to anchor steel joists, depending on the type of wall construction. The most common types of construction and anchorage are as follows:

Steel Frame Construction. For steel frame buildings, the open-web joists are usually welded to the building frame at both ends of the joist. The welded connection is designed such that the uplift capacity of the connection exceeds the design uplift load, but in no cases shall the welded connection be less than two 1″×1/8″ fillet welds. Open-web joists may also be bolted at each end using a minimum of two 1/2″ bolts on each side of the joist. Steel bearing plates are not usually used in fastening steel joist to steel frame construction.

Reinforced Masonry Construction. In buildings constructed with reinforced masonry walls, the open-web joists are anchored to a tie beam or bond beam. The anchorage consist of a minimum of 1/2″ diameter anchor bolts or 1/2″ (#4) reinforcing bars not spaced more than 6′ on center. If the beam is at least 8″ deep and has a minimum continuous reinforcement of 0.2 square inches at the top of the wall, then the anchorage is either welded to or hooked tightly around the longitudinal reinforcement in the beam. The bolts or reinforcing bars need to be extended into the wall a minimum of 6″. To complete the roof-wall connection, either the joist is bolted to the anchor bolts or the reinforcing bars are bent over each side of the joist and then welded. Steel bearing plates are not usually used when connecting steel joists to reinforced masonry walls. If the tie beam or bond beam is less than 8″ deep, then the masonry wall is considered unreinforced masonry.

Unreinforced Masonry. In buildings constructed with unreinforced masonry walls, steel bearing plates are more common due to the fact that the bearing capacity of unreinforced masonry walls is less than that of either steel frame or reinforced masonry construction. The joist is usually anchored to the wall using J-bolts with a length of 6″ or 1/2″ bolts with a length of 15″. A steel plate is attached to the head of the 15″ bolt with a minimum surface area of 6 square inches which is fully embedded into the masonry. If bearing plates are used, the plates are welded to the joist and then anchored to the masonry wall using the 6″ J-bolts or the 15″ bolts. The welding of the joist to the steel plate follows the same requirements mentioned in steel frame construction.

The uplift capacity of OWSJ anchored to unreinforced masonry walls is much less than the resistance of the joists anchored to reinforced masonry walls since the walls do not contain bond beams or tie beams with reinforcement to which the anchorage can be welded to or wrapped around (NRC, 1991).

6.7.1 Resistance Model for Open-Web Steel Joists

As discussed earlier, most steel joist failures occur due to inadequate roof-wall anchoring or from buckling of the bottom chord of the steel joist. The uplift damage model developed herein considers the failure of the roof-wall connection at the weld connecting the joist to either a steel bearing plate or a larger steel beam and the failure of unreinforced masonry walls at the mortar interface between blocks. In the case of reinforced masonry walls, the failure of the wall associated with the uplift loads acting on the joist is not considered (i.e., the welded connection will always fail before the wall fails).

Uplift Resistance. The possible failure modes modeled for the steel joist roof-wall connection are the failure of the welds between the steel joist and the steel bearing plate and the anchorage failure between the bearing plate and the unreinforced masonry wall. If a bearing plate is not present, then the failure mode is between the steel joist and the unreinforced masonry wall.

Steel Joist and Steel Bearing Plate. The steel joist is welded to the steel bearing plate using a minimum of two 1″×1/8″ fillet welds. Larger steel joists may require larger welds. The resistance of the joist/plate connection is based on the design strength of the welds using AISC Manual of Steel Construction (LRFD method) Second Edition Specifications (AISC, 1995).

The weld metal, the plate metal or the joist metal are the three possible failure modes for this type of connection. Each are calculated using the number of welds, the length of each weld and the size of the weld. The lesser of the following three resistances is used to calculate the combined resistance for this type of connection. All capacities are based on the design procedure as given in AISI 8-129.

Resistance of the Weld Metal. The nominal resistance of one weld is:

$$R_n = F_w \cdot A_w \tag{6.4}$$

where F_w is the nominal tensile strength of the weld material ($F_w = 0.60\ F_{EXX}$ in pounds per square inch), A_w is the effective area of the weld (A_w = *Length*×*Throat*) in square inches, F_{EXX} is the classification strength of the weld metal for a EXX electrode in pounds per square inch, *Throat* is the effective throat thickness (*Throat = 0.707·Size*) in inches, *Size* is the size of the fillet weld in inches.

Resistance of the Plate Base Metal. The nominal resistance of the plate metal is:

$$R_n = F_{bm} \cdot A_{bm} \tag{6.5}$$

where F_{bm} is the nominal tensile strength of the plate material in pounds per square inch, A_{bm} is the effective cross sectional area of the plate (A_{bm} = *Effective Width of Base Metal*×*Thickness*) in square inches.

Resistance of the Steel Joist Base Metal. The nominal resistance of the joist metal is:

$$R_n = F_{bm} \cdot A_{bm} \tag{6.6}$$

where F_{bm} is the nominal tensile strength of the joist material in pounds per square inch, A_{bm} is the effective cross sectional area of the joist metal (A_{bm} = *Effective Width of Base Metal*×*Thickness of Base Metal*) in square inches.

The steel bearing plate is usually A36 steel with a yield strength of 36,000 psi and the joist steel yield strength is 50,000 psi. The type of weld electrode commonly used with A36 steel is an E70 Electrode.

Example Minimum Uplift Capacity. A typical open-web steel joist with a span of 40′ normally has a chord thickness equal to 3/16″. The steel bearing plate has a thickness of 3/16″. An E70 Electrodes was used to produce 1/8″ fillet welds with a total length of 2″, 1″ on each side of the joist. The resistances of each of the three cases are as follows:

Resistance of the Weld Metal	7,424 lbs
Resistance of the Plate Base Metal	9,000 lbs
Resistance of the Steel Joist Base Metal	12,500 lbs

In this example, the limiting failure mode is the failure of the weld metal at a nominal value of 7,424 lbs.

Steel Bearing Plate/Steel Joist and the Wall Anchorage. The resistance of the wall anchorage for both the steel bearing plate and the steel joist without bearing plate are based on the same procedure. Experimental uplift failure tests have been performed at Clemson University (Leland, 1988) on anchors with embedment depths of 6″ and 15″ into walls 6′ in length. The wall length of 6′ was to simulate the Standard Building Code requirements for a maximum spacing not more than 6′ on centers. The resistances of this type of connection is highly variable because it relies on the tensile bond strength between mortar and masonry units (Leland, 1988). Table 6.28 presents a summary of the uplift test results.

Table 6-28. Uplift Resistances of an Unreinforced Roof-Wall Anchor, 6′ O.C.

Type of Roof-Wall Anchor	Mean	COV
6″ embedment J-Bolt Anchors	3312 lbs	42%
15″ embedment Anchor with 6 in^2 endplate	4868 lbs	46%

Bending Resistance. In the case of bending failures, there is not enough information on member sizes, depth of the joist, etc., to permit a detailed engineering estimate of the capacity of the joist, which would require examining the various bending failure modes (i.e., bottom flange buckling, bottom chord yielding and web members yielding or buckling). The capacity of the OWSJ to resist moments associated with the wind induced loads are based on the maximum uplift moments computed using the Standard Building

Code (UBC) wind load requirements on a simply supported steel joist. No information on the actual mode of bending failure is known, although buckling probably represents the actual limit state.

Prediction of Joist Failures. The premise behind the joist failure model is the same as the other failure models described herein, in that at each time step during a hurricane simulation the loads acting on the joists are compared to the sampled resistances, and if the load exceeds the sampled resistance, the joist is assumed to fail. In the case of moment failures, if the computed wind induced bending moment exceeds the sampled moment resistance, the joist is assumed to have buckled and can carry no more load. The portion of the wind load acting on the joist that exceeds the buckling load is then distributed to the neighboring joists. Each joist is checked to determine if failure has occurred. If failure has occurred, the excess load is redistributed. After all joists have been checked for failure, the checking process is repeated, taking into account the redistributed loads. The load redistribution process continues until all redistributed loads have been proportioned to joists that have not failed, or all joists have failed. In the case of an uplift connection failure, the joist is not able to carry any load, and thus all of the wind loads acting on the joist must be distributed to the neighboring joists.

At any time during a damage simulation, the uplift reaction loads (R_A and R_B) at either end of the joist, and the bending moment (M) at the center, are computed from the following:

$$R_A = q_H C_{F_A} lw - (L + D)lw/2 + p_i wl/2 \tag{6.7}$$

$$R_B = q_H C_{F_B} lw - (L + D)lw/2 + p_i wl/2 \tag{6.8}$$

$$M = q_H C_M l^2 w - (L + D)wl^2/8 + p_i wl^2/8 \tag{6.9}$$

where q_H is the dynamic pressure at roof height (based on the peak gust wind speed at roof height), C_{FA} and C_{FB} are the directionally dependent uplift coefficients for the reaction at each end of the joist, C_M is the directionally dependent mid-point moment coefficient, l is the span, w is the distance between joists, L and D are the live and dead loads, and p_i is the internal pressure. The uplift and moment coefficients are computed using the influence line approach described earlier.

Example OWSJ Failure Probabilities. No quantitative statistical studies examining the performance of buildings with OWSJ roofs in hurricane winds have been performed to enable the failure model to be quantitatively evaluated. Thus the modeled results presented here are not compared to any full scale performance data, and are given only to show the reasonableness of the predicted failure rates.

In the examples given, two simple rectangular buildings were modeled. Each building has a length of 180′ and a width of 40′. The 40′ width is spanned by OWSJs spaced at 6′ on center. One building has a roof height of 12′ and the other building has a roof height of 20′. On the front side of the building, there are a total of twelve windows having

dimensions of 6′ high and 12′ wide, and six glass entry doors, each of which is 6′8″ tall and 3′ wide. At the rear of the building there are six non-glazed entry doors. The roof deck is assumed to be comprised of light weight metal with a BUR cover. The roof system is designed to resist the wind loads as prescribed in the SBC Wind Load Provisions for a structure located in the 100 mph (fastest mile) wind zone. Joists designed to meet the loads applied in the more highly loaded end-zones are assumed to be used throughout the roof system. The dead and live loads used in the design of the joists are 6.25 and 25 psf, respectively. The buildings are assumed to be constructed in a terrain described by a typical suburban environment (i.e., z_0 = 0.35 m), with the windborne debris environment represented with the residential model. In the damage simulation, if a window is breached, the internal pressures are assumed to act over the entire underside of the roof. The mean value of the bending resistance of the joist is taken as 1.3 times the design value. The COV is assumed to be equal to 20%. The resistance factor associated with the welded connection for uplift is assigned a mean value of 1.5 with a COV of 20%.

The probability of joist failure as a function of wind speed is developed by passing hurricane wind speed traces past the buildings. The hurricane wind speed traces used to develop the joist failure probabilities shown in Figure 6.45 and 6.46 are the traces derived from a 20,000 year simulation of hurricanes in the South Florida area. Results are given for both the reinforced and unreinforced masonry wall case. Note that for modeling purposes, the performance of joists on steel frame buildings is the same as the performance of joists on reinforced masonry buildings. In the damage simulation model, the number of failed joists and the peak wind speed produced by the storm is retained and used to develop the damage state curves given in Figures 6.45 and 6.46. Damage states 1, 2 and 3, noted in Figures 6.45 and 6.46, represent the following:

Damage State 1	at least one failed joist, but less than 25% failed joists
Damage State 2	at least 25% failed joists but less than 50% failed joists
Damage State 3	more than 50% failed joists

Note that for a given building, the damage state curves, given in Figures 6.45 and 6.46, are very close together, indicating that once a single joist has failed, the likelihood of other joists failing immediately afterwards is high, implying a system with little redundancy.

6.7.2 Resistance Model for Metal Deck on Open-Web Steel Joists

Metal decks on steel joists are frequently used as the primary roof deck system for both steel buildings and concrete/masonry buildings. The performance of these metal decks in high wind events varies with deck size, thickness, attachment method, joist spacing, quality of installation and number of fasteners. The approach taken here to estimate the uplift capacity of a metal deck panel is to design some typical systems using the requirements given in AISI (1996) and then perform a failure analysis using a finite element model.

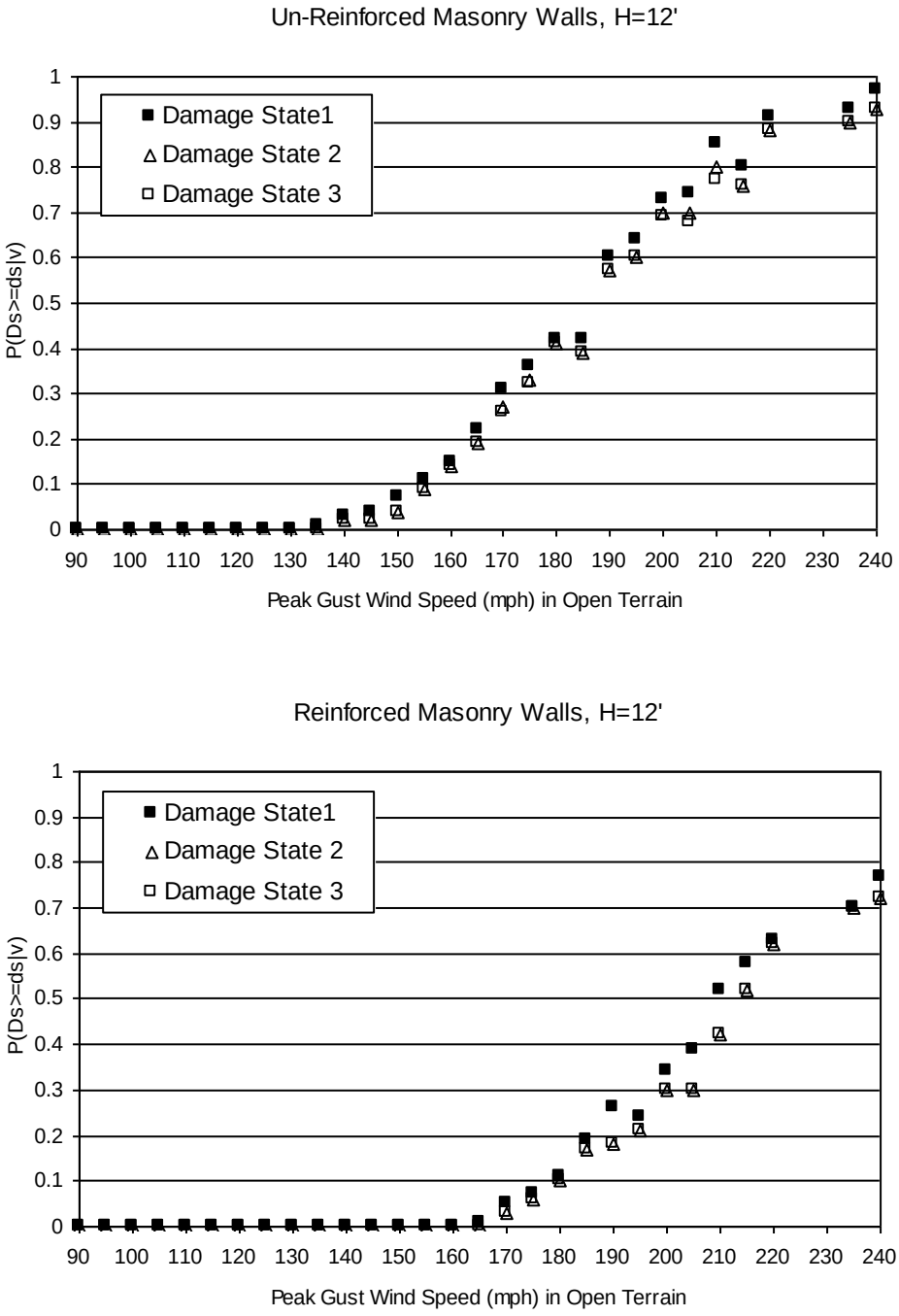

Figure 6-45. OWSJ Roof Damage States for a 12′ High Building in Suburban Terrain.

The approach involves the selection of the fastener requirements to meet the design loads, coupled with a review of recent experimental studies examining the resistance of screwed and welded connections. Given these inputs, a stochastic finite element study is used to determine the failure loads.

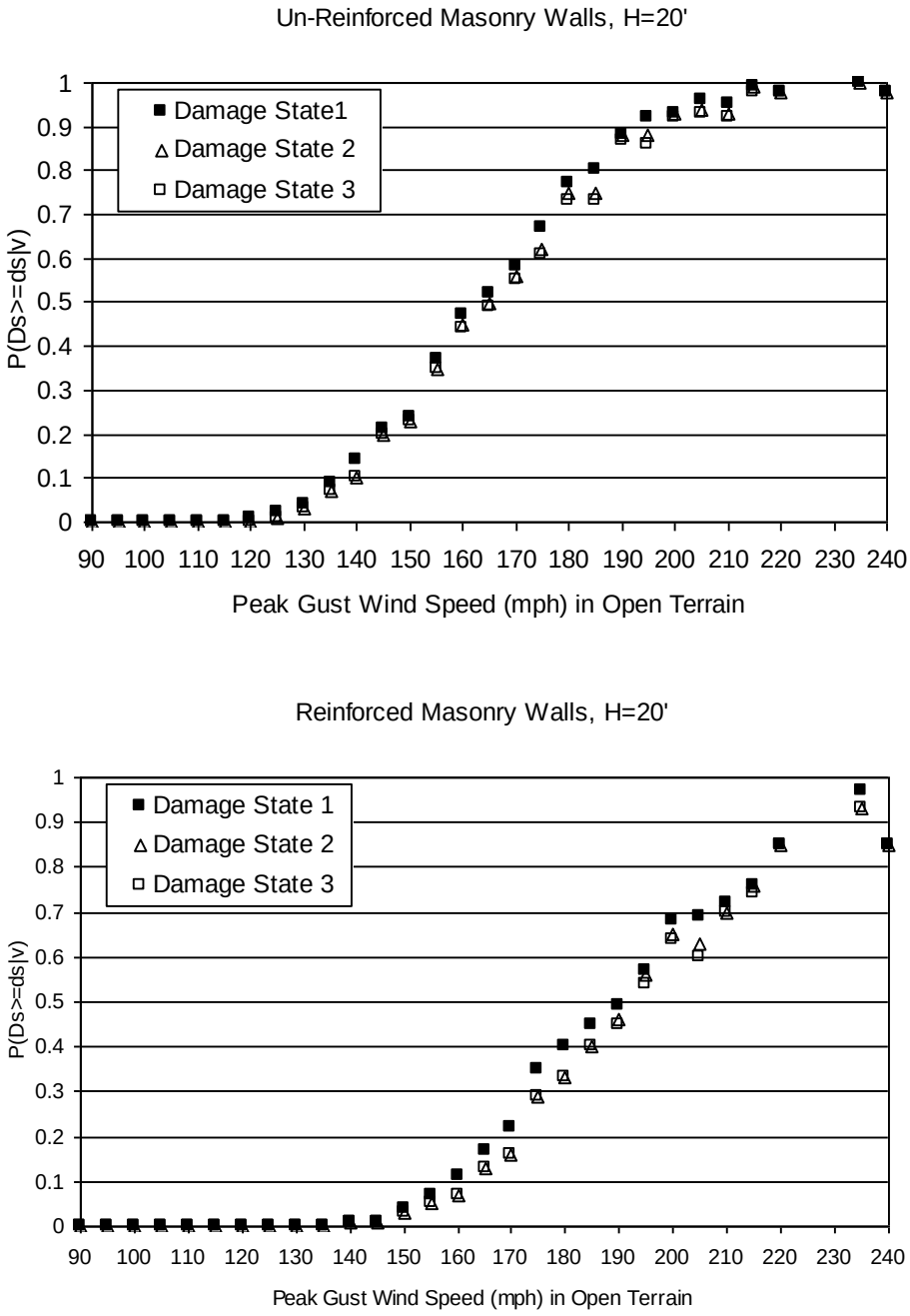

Figure 6-46. OWSJ Roof Damage States for a 20′ High Building in Suburban Terrain.

This section describes the methodology used to estimate the uplift capacity for two example cases; however, the approach is general and can be applied to any configuration of metal deck roof systems.

An Overview of Metal Decking. The metal deck is made from cold formed structural grade sheet steel that conforms to ASTM Designations A611 Grade C, D, or E (for

painted deck) or A653 Grade 33, 40, 50 or 80 (for galvanized deck) (USD, 1997). The minimum yield strength of the steel is 33 ksi. The metal deck can be categorized into 4 types (i.e., A, B, F, and N) according to different profiles of the ribs. Table 6.29 lists the profiles, nominal thickness ranges and weight ranges of these 4 deck types. Standard deck widths vary from 12″ to 36″ with an increment of 6″ (the length will vary depending on the spacing of bar joists). Typical thicknesses of the metal deck are 16, 18, 20, and 22 gage.

Table 6-29. Nominal Deck Information, from SDI (1992)

Deck Type	Name (profile)	Nominal Thickness Range	Weight Range
Type A	1-1/2″×6″ Wide Rib (WR)	0.03″ to 0.06″	2 psf to 4 psf
Type B	1-1/2″×6″ Intermediate Rib (IR)	0.03″ to 0.06″	2 psf to 4 psf
Type F	1-1/2″×6″ Narrow Rib (NR)	0.03″ to 0.06″	2 psf to 4 psf
Type N	3″×8″ Deep Rib (WR)	0.03″ to 0.06″	2 psf to 4 psf

The metal decks are attached to the building frame with arc puddle welds, self-drilling screws, or powder-actuated or pneumatically-driven pins. Sheet to sheet fastening is performed with screws, button punching (crimping) or welds. The deck is end-lapped a minimum of 2″ with the overlapping occurring at the location of the supports. The minimum end bearing is 1-1/2″. According to SDI (1992b), the common connection layout patterns are:

36″ (width) deck: 36/9, 36/7, 36/5, 36/4 for 2″or 3″ composite, and 36/3

30″ (width) deck: 30/6, 30/4 and 30/3

24″ (width) deck: 24/4

where, for example, 36/N represents the number of fasteners, N, across the 36″ width of the panel.

Screwed Decks. In determining the parameters for the case studies, two types of fasteners were considered: screws and welds. Screws are most often #12 or 1/4″ diameter when fastening the roof deck to structural members. Sheet to sheet connections (also known as stitch connections) usually use self-drilling #8 or 1/4″ diameter screws. Table 6.30 presents the properties of typical screws used to fasten the steel decks to the underlying structural roof system. Screws can be installed either at the valley or at the crest of the metal deck with or without washers (in this investigation, all the screws are assumed to be valley-fixed).

Table 6-30. Typical Screw Properties

Screw Size	d, Diameter (in)	D_w, Nominal Head Diameter (in)	Avg. Tested Tensile Strength (kips)
10	0.190	0.415 or 0.400	2.56
12	0.210	0.430 or 0.400	3.62
1/4	0.250	0.480 or 0.520	4.81

For a screw-connected roof panel, post storm damage investigations following extreme wind events have shown that the two most common steel deck failure modes are: (i) a pull over failure, where the metal deck pulls over the fastener and (ii) a pull out failure where the screw pulls out from the structural steel member. The thin steel sheathing often pulls through (pulls over) the screw heads due to either the large stress concentration around the fastener holes or fatigue under wind fluctuations. Pull through failures can occur when very thin high-strength steel battens or purlins are used and the screw fasteners can be pulled out of the steel battens or purlins. The American standard (AISI, 1996) provides two different formulas for these two failure modes:

The pull-over strength, P_{nov} (kips), is given as:

$$P_{nov} = 1.5 t_1 d_w F_{ult} \tag{6.10}$$

where t_1 = thickness of the deck (in); d_w = diameter of the washer or head of screw (in); F_{ult} = tensile strength of the deck metal (ksi).

The pull-out strength, P_{not} (kips), is given as:

$$P_{not} = 0.85 t_c d F_{ult} \tag{6.11}$$

where t_c = thickness of the support member (in); d = diameter of the screw shaft (in); F_{ult} = tensile strength of the support member (ksi).

A number of researchers have investigated pull-over and pull-out failures for a wide variety of base metal materials, deck profiles, load conditions, and test procedures (Ellifritt and Burnette, 1990; Pekoz, 1990; García, 1994; Smith, 1995; Mahendran, 1994,1997; Mahendran and Tang, 1998). In this investigation, the results summarized by Pekoz (1990) and Mahendran and Tang (1998) were used to derive the statistics of the mean to nominal ratios of the screw resistances computed using Equations 6.10 and 6.11 for the pull-over failure and pull-out failures, respectively.

Pekoz (1990) investigated more than 360 pull-over failure cases and proposed a design formula (Equation 6.10) that has been adopted by the American standard (AISI, 1996). The reported mean-to-nominal and COV are 1.027 and 0.235, respectively.

Mahendran and Tang (1998) conducted a series of pull-out tests for a range of steel battens, purlins, girts and screw fasteners commonly used in the building industry. The test results were compared with the predicted values based on current design formula (Equation 6.11) using both the measured properties and the specified properties. It was found that the current design formula used with specified properties (nominal value) provide better agreement with the test results than those predicted using the measured properties. A mean-to-nominal ratio of 1.20 and a (COV) of 0.21 were determined using all 592 test cases. The mean-to-nominal values and COVs for pull-out and pull-over failure modes form the basis for sampling screw resistances in the stochastic finite element analysis described later.

Welded Decks. In this investigation, only arc spot weld connections were considered and modeled in the finite element analysis. The supporting members were assumed to be the top chords of open-web steel joists (however, the results are applicable to hot-rolled steel beams or girders). The study by LaBoube and Yu (1993) was used to determine the resistances of the weld connections. Based on more than 260 tension tests of arc spot weld connections with variations in steel thickness, tensile strength, weld process, loading condition, and geometry, LaBoube and Yu (1993) developed equations to predict the tension capacity of an arc spot weld connection. The following equations have been adopted in the current American standard (AISI, 1996):

when $F_u/E < 0.00187$

$$P_n = \left[6.59 - 3150\left(\frac{F_u}{E}\right)\right] t d_a F_u \leq 1.46 t d_a F_u \tag{6.12}$$

when $F_u/E \geq 0.00187$

$$P_n = 0.70 t d_a F_u \tag{6.13}$$

where P_n = nominal tension capacity; F_u = tensile strength of the sheet steel; t = sheet steel thickness; d_a = average weld diameter at mid-thickness of t, where $d_a = (d–t)$ for a single sheet and $(d–2t)$ for a double sheet; E = Young's modulus of the sheet steel. Based on concentric loading cases, LaBoube and Yu (1993) found the ratio of the failure load (P_u) to the predicted load (P_n) to have a mean value of 1.18 and a COV of 0.242.

At the perimeter of a steel deck roof system where there may be strong spatial gradients in the uplift loads, the arc spot welds may experience eccentric loading conditions, and the weld capacities in these cases can be significantly lower than those under concentric loads. Based on the 34 eccentric test results reported by LaBoube and Yu (1993), a mean-to-nominal value of 0.617 and a COV of 0.242 were determined, indicating a strength reduction of about 40% compared to the behavior of a concentrically loaded connection. In the finite element analysis, for welded connections, the relative location of the metal deck panel was considered and the resistances were sampled from the eccentric load conditions for panels located at the edge of a roof system.

Case Studies. For the purpose of estimating the resistances of metal deck configurations used in engineering practice, the two most widely used building codes in southeastern United States (ASCE 7-88 and SBCCI 1988) were adopted to design the metal deck roofs of two baseline buildings (a one-story building and a two-story building). These two buildings were assumed to be located in hurricane-prone regions with design fastest mile wind speeds of 90 mph, 100 mph, and 110 mph. The mean roof heights for the flat-roof model buildings were 15′ (one-story) and 25′ (two-story). The metal roof system is comprised of 3′ by 8′ metal deck panels and supported by open-web steel joists spaced at 4′. Table 6.31 lists the calculated design wind pressures obtained from ASCE 7-88 and SBCCI 1988. An importance factor of 1.05 was used with the ASCE loads.

Table 6-31. Design Wind Pressures Calculated Using ASCE 7-88 and SBCCI 1988

Code	Number of Stories	Zone	Wind Pressure for Components & Cladding (psf)		
			90 mph	100 mph	110 mph
ASCE	1-Story	1	-28.71	-35.45	-42.89
		2	-44.26	-54.64	-66.12
		3	-59.44	-73.38	-88.79
	2-Story	1	-33.38	-41.21	-49.86
		2	-51.45	-63.52	-76.86
		3	-69.10	-85.31	-103.22
SBCCI	1-Story	r	-20.74	-25.62	-30.50
		s	-28.90	-35.70	-42.50
		z	-39.10	-48.30	-57.50
	2-Story	r	-24.40	-29.59	-35.99
		s	-34.00	-41.23	-50.15
		z	-46.00	-55.78	-67.85

The variables considered in the design were fastener size, layout, steel deck gage, steel deck strength, base metal thickness and base metal strength. The current American standard for cold-formed steel structures (AISI, 1996) was used to select appropriate designs for the calculated design loads. The deck resistances were calculated for six different layouts of fastener attachment schemes for both welded and screwed connections. Both load and resistance factor design (LRFD) and allowable stress design (ASD) were used to select the appropriate fastener layout. Tables 6.32 and 6.33 lists the six different attachment layouts for the screw connections and for the welded connections, respectively.

Table 6-32. Determined Case Studies for Screw Connections

Case	Screw Size	Layout	Installation	Steel Deck			Base Metal		
				Gage	F_y(ksi)	F_u(ksi)	Thickness (in.)	F_y(ksi)	F_u(ksi)
s1	#10	36/3	Valley-Fixed	22	40	55	0.125	33	45
s2	#10	36/4	Valley-Fixed	22	50	60	0.125	33	45
s3	#10	36/5	Valley-Fixed	22	50	60	0.125	33	45
s4	#12	36/5	Valley-Fixed	20	50	60	0.125	40	55
s5	#10	36/7	Valley-Fixed	20	50	60	0.125	40	55
s6	#12	36/7	Valley-Fixed	20	50	60	0.125	40	55

Table 6-33. Determined Case Studies for Weld Connections

Case	WeldSize	Layout	Installation	Steel Deck			Base Metal		
				Gage	F_y(ksi)	F_u(ksi)	Thickness (in.)	F_y(ksi)	F_u(ksi)
w1	0.500	36/3	Valley-Fixed	22	40	55	0.125	33	45
w2	0.500	36/3	Valley-Fixed	22	50	60	0.125	33	45
w3	0.625	36/3	Valley-Fixed	22	50	60	0.125	33	45
w4	0.625	36/3	Valley-Fixed	20	50	60	0.125	40	55
w5	0.625	36/4	Valley-Fixed	20	50	60	0.125	40	55
w6	0.850	36/4	Valley-Fixed	20	50	60	0.125	40	55

A total of 12 cases were used in the finite element analysis (6 screw connections and 6 weld connections). Recall the layout pattern of 36/*N* means *N* fasteners across the 36″ width of the metal deck panel. Since a 3′ by 8′ panel covers two spans of the bar joists, there will be a total of 3*N*+4 fasteners on the panel (4 fasteners connecting adjacent roof panels at the middle of the span). The deck profile was assumed to be an intermediate rib type B and the deck gage was selected from the manufacture's manual. Figures 6.47 through 6.50 show the metal deck profile and the different fastener patterns (layouts) used in the case studies.

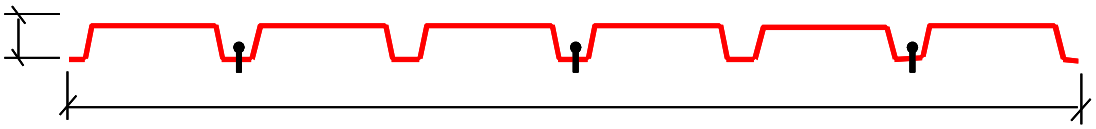

Figure 6-47. Metal Deck Profile with 3 Fasteners.

Figure 6-48. Metal Deck Profile with 4 Fasteners.

Figure 6-49. Metal Deck Profile with 5 Fasteners.

Figure 6-50. Metal Deck Profile with 7 Fasteners.

Probabilistic Finite Element Analyses. Isoparametric shell elements were used to model the metal deck. The shell element was a four-node quadrilateral element with six degrees of freedom at each node. The 3′×8′ metal deck panel was divided into 1600 (32×50) shell elements, detailed enough to give accurate fastener forces and still allowing the analysis to be run in a relatively short time period. Figure 6.51 shows the plan view of the mesh grids for the metal deck panel along with the fastener locations (denoted using stars) for a 36/4 fastener pattern. A previous study (Mahendran, 1994) suggested that despite the occasional local metal deck failure around the fasteners, the majority of the metal deck was still in elastic range when the fasteners failed, and thus the metal deck was modeled here as a linear elastic material with a Young's modulus of 29000 ksi and a Poisson's ratio of 0.29.

The fasteners used to attach the deck panel to the bar joists were modeled as a fixed support with restrictions in the *x, y* and *z* directions. No moment resistance was assumed for these fasteners. For the fasteners on the lap joints, the movements in the *x* and *y* directions were restrained, but the fasteners were allowed to move freely in the *z* direction.

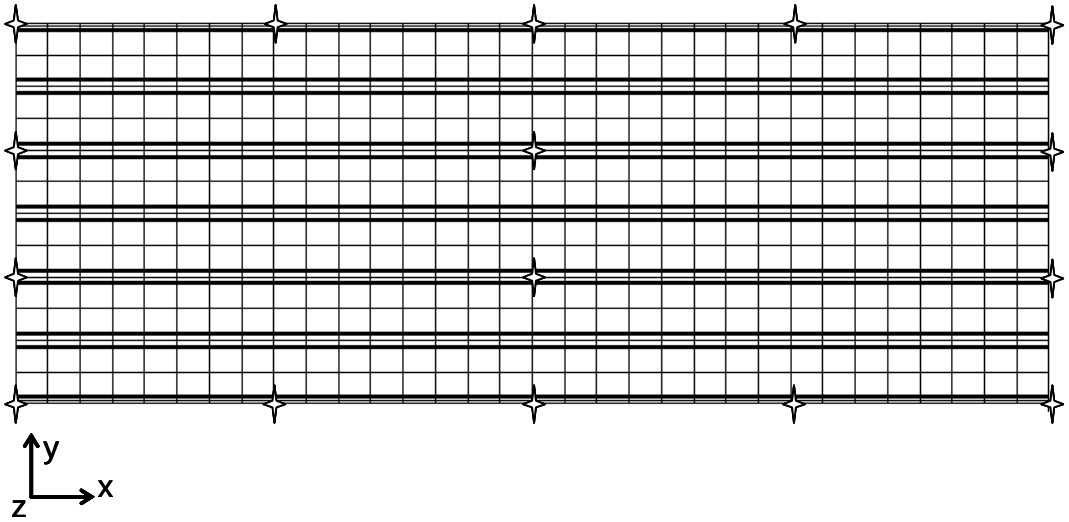

Figure 6-51. Finite Element Model of the 3′ by 8′ Panel.

The metal deck was subjected to a uniform pressure with both the ultimate tensile strength and serviceability being considered in determining the failure of a panel. Failures caused by shear and local buckling were not modeled in the finite element analysis. If screws are used, both pull-out and pull-over strengths were sampled and the resistance was taken as the smaller of the two sampled strengths. Failure of a fastener occurs when the computed fastener load exceeds the sampled fastener resistance. For the complete failure of the whole panel, the failure criteria are: (1) less than 3 fasteners remain on the panel (all the other fasteners have failed); or (2) all the remaining fasteners align in a pattern such that the panel can rotate; or (3) the maximum deflection of the panel is greater than 2′.

A Monte Carlo simulation was used to determine the statistics of the failure pressure for the metal deck (considering the randomness in the material properties and the fastener strengths). Figure 6.52 shows the flowchart of the probabilistic finite element analysis. In the simulation, for each fastener, the nominal value (i.e., design value) was calculated first using the appropriate design formula. The statistics (i.e., mean and standard deviation) of the fastener resistance were obtained by multiplying the calculated design value by the mean-to-nominal ratio statistics. The resistance of each screw was then obtained by sampling from the resulting normally distributed resistance. For screw connections, both pull-out strength and pull-over strength were sampled and the resistance was taken as the smaller of the two values. Similar procedures were also applied to the base metal properties of the metal deck (e.g., F_y and F_u). The finite element mesh, material properties, boundary conditions, fastener's strengths, and initial loads on the metal deck were generated automatically by a program written specifically for the Monte Carlo simulation. Then, a full finite element analysis was carried out to calculate the reaction in each fastener and the maximum deformation of the metal deck. Failure criteria were then checked against the calculated reactions and deformation. If the failure state was reached, the load (pressure) was then recorded as the failure load and a new simulation would start. Otherwise, failure of individual fasteners were checked and any

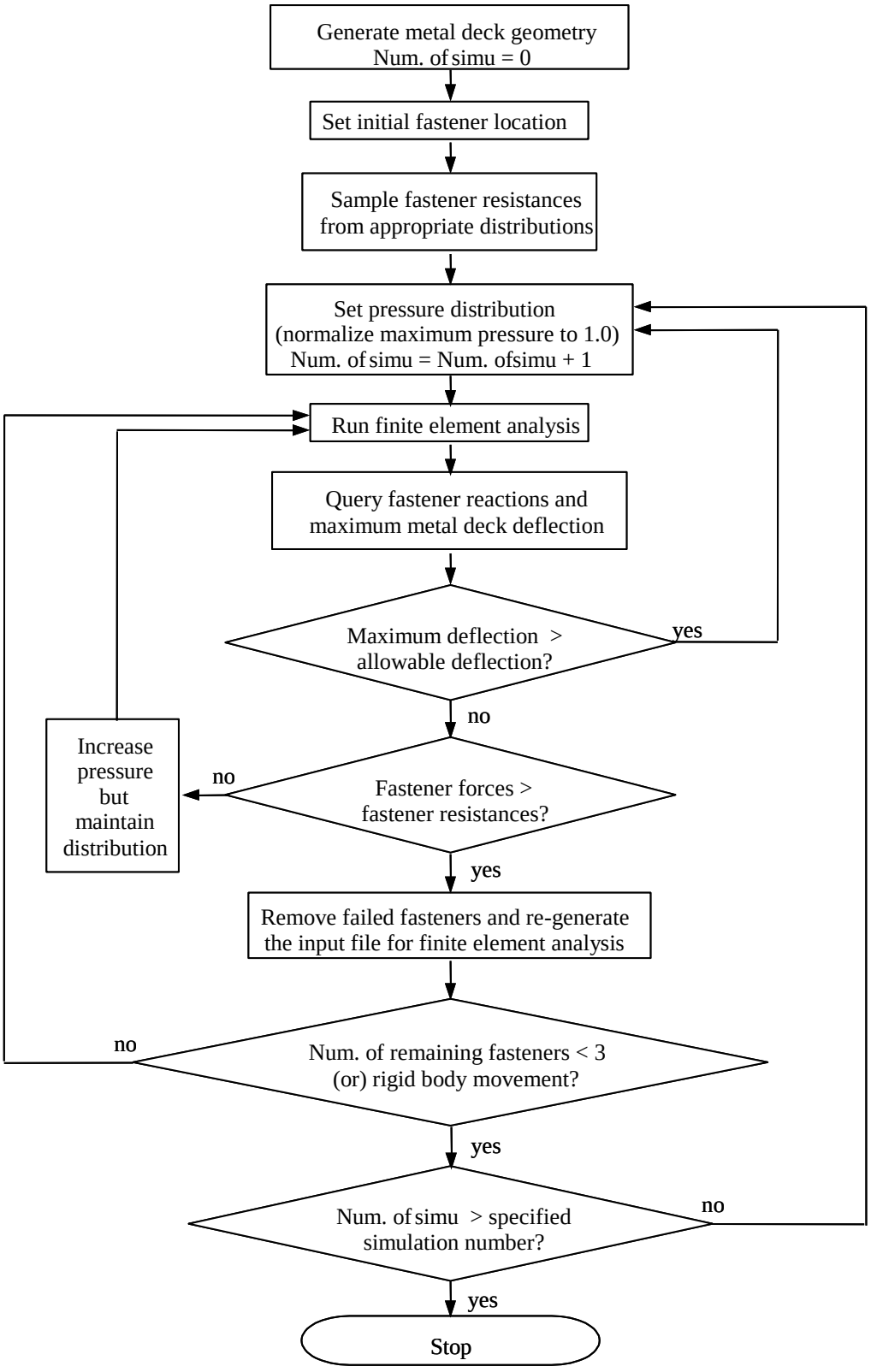

Figure 6-52. Flowchart of the Probabilistic Finite Element Analysis.

failed fasteners were removed from the analysis. The boundary conditions were then re-generated and a new finite element analysis was carried on the modified sets of the fasteners while the pressure remained the same (i.e., considering progressive failure). If no more fasteners fail, the pressure was increased and the procedure was repeated until failure of the metal deck panel was reached. The output from the finite element analysis were the initial failure pressure (i.e., the pressure at which any one of the fasteners fails) and the final failure pressure (i.e., the pressure at which the whole metal deck panel fails according to the failure criteria). After 100 simulations had been performed, the simulation results were used to characterize the statistics of the metal deck uplift capacity.

FEM Results. For each example, 100 finite element analyses were performed, from which the statistics of the failure pressure were computed. Table 6.34 lists the resulting means and standard deviations of the failure loads for selected case studies (associated with the design loads for different regions of the baseline model buildings). Note that the design pressures listed in Table 6.34 are different from the wind pressures calculated previously (see Table 6.31) because of the inclusion of dead load (for both ASD and LRFD) and the application of load factors (for LRFD only) in calculating the design pressures. In most cases, a lognormal distribution was found to provide the best fit to the failure pressures. Figures 6.53 and 6.54 show the CDFs of the failure pressures for the metal deck with screw connections and welded connections, respectively. For screw connections, the increase in resistance with higher design values and stronger designs (in a sequence of case 1 to case 6) is clear. The coefficient of variation of the failure loads is seen to be relatively constant throughout the case studies (in a range of 10-15%).

However, for welded connections, the resistances do not increase monotonically with stronger designs, and cases 3 and 6 have larger variations than the other cases. Note that for welded connections, cases 1 and 2 are assumed to be in the middle of a roof system, cases 3 and 4 are assumed to be along one edge of a roof system, and cases 5 and 6 are assumed to be at the corner of a roof system. The welds along the edge of a roof system will experience eccentric loads which have lower resistances than the welds experiencing concentric loads. Therefore, the relative location of the roof deck panel has a significant impact on the panel uplift capacity.

Note that due to the relatively small coefficient of variation (less than 20%) of the simulated failure pressures, the potential sampling error of the estimated mean failure pressure will be less than 2% of the mean value (i.e., $20\%/\sqrt{n} = 20\%/\sqrt{100} = 2\%$). Therefore, 100 simulations provide sufficient accuracy.

Summary. A damage model for metal decks on open-web steel joists has been developed by combining a finite element analysis of a deck subject to a uniform pressure load, with the results of experimental data for fastener uplift resistance. Note that a number of parameters or factors that may contribute to the failure probability, such as fatigue, local buckling, membrane strength, workmanship, and deterioration were not explicitly considered. The potential impact of the reduction in deck capacity due to fatigue, corrosion, etc. is addressed in the building damage simulation results.

Table 6-34. Simulated Failure Loads for Different Designs

Code	No. of Story	Wind Speed (mph)	Zone	Design Pressure (psf)	Screw Design			Weld Design		
					Case	Mean (psf)	Std (psf)	Case	Mean (psf)	Std (psf)
ASCE 7-88	1	90	1	-34.6	s1	187.3	24.7	w1	168.8	22.3
			2	-54.8	s1	187.3	24.7	w1	168.8	22.3
			3	-74.6	s2	212.4	23.0	w1	168.8	22.3
		100	1	-43.4	s1	187.3	24.7	w1	168.8	22.3
			2	-68.3	s2	212.4	23.0	w1	168.8	22.3
			3	-92.7	s3	233.5	30.9	w1	168.8	22.3
		110	1	-53.1	s1	187.3	24.7	w1	168.8	22.3
			2	-83.3	s3	233.5	30.9	w1	168.8	22.3
			3	-112.7	s4	299.0	37.1	w3	222.0	40.3
	2	90	1	-40.7	s1	187.3	24.7	w1	168.8	22.3
			2	-64.2	s2	212.4	23.0	w1	168.8	22.3
			3	-87.1	s3	233.5	30.9	w1	168.8	22.3
		100	1	-50.9	s1	187.3	24.7	w1	168.8	22.3
			2	-79.9	s3	233.5	30.9	w1	168.8	22.3
			3	-108.2	s4	299.0	37.1	w3	222.0	40.3
		110	1	-62.1	s2	212.4	23.0	w1	168.8	22.3
			2	-97.2	s4	299.0	37.1	w3	222.0	40.3
			3	-131.5	s5	435.8	42.0	w4	305.2	40.4
SBCCI	1	90	r	-17.7	s1	187.3	24.7	w1	168.8	22.3
			s	-25.9	s1	187.3	27.7	w1	168.8	22.3
			z	-36.1	s1	187.3	24.7	w1	168.8	22.3
		100	r	-22.6	s1	187.3	24.7	w1	168.8	22.3
			s	-32.7	s1	187.3	24.7	w1	168.8	22.3
			z	-45.3	s1	187.3	24.7	w1	168.8	22.3
		110	r	-27.5	s1	187.3	24.7	w1	168.8	22.3
			s	-39.5	s1	187.3	24.7	w1	168.8	22.3
			z	-54.5	s2	212.4	23.0	w1	168.8	22.3
	2	90	r	-21.4	s1	187.3	24.7	w1	168.8	22.3
			s	-31.0	s1	187.3	24.7	w1	168.8	22.3
			z	-43.0	s1	187.3	24.7	w1	168.8	22.3
		100	r	-26.6	s1	187.3	24.7	w1	168.8	22.3
			s	-38.2	s1	187.3	24.7	w1	168.8	22.3
			z	-52.8	s2	212.4	23.0	w1	168.8	22.3
		110	r	-33.0	s1	187.3	24.7	w1	168.8	22.3
			s	-47.2	s1	187.3	24.7	w1	168.8	22.3
			z	-64.9	s2	212.4	23.0	w1	168.8	22.3

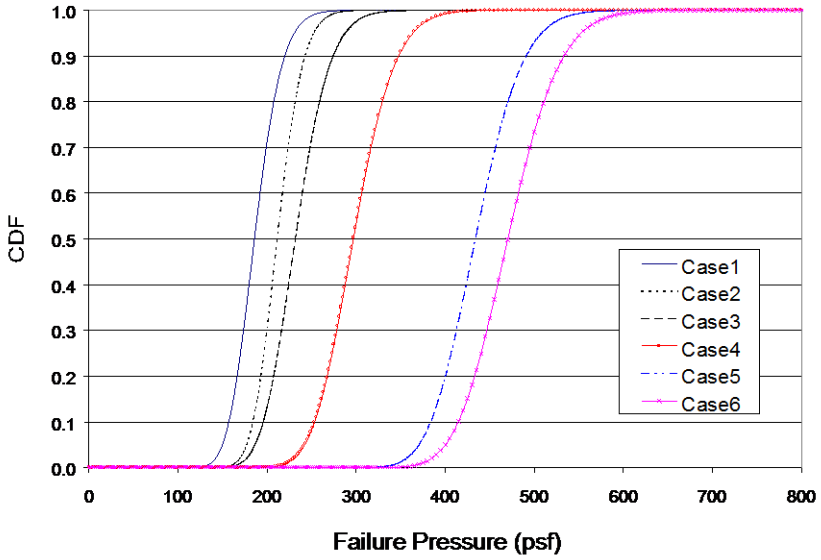

Figure 6-53. CDFs of Metal Deck Failure Pressures (Screw Connections).

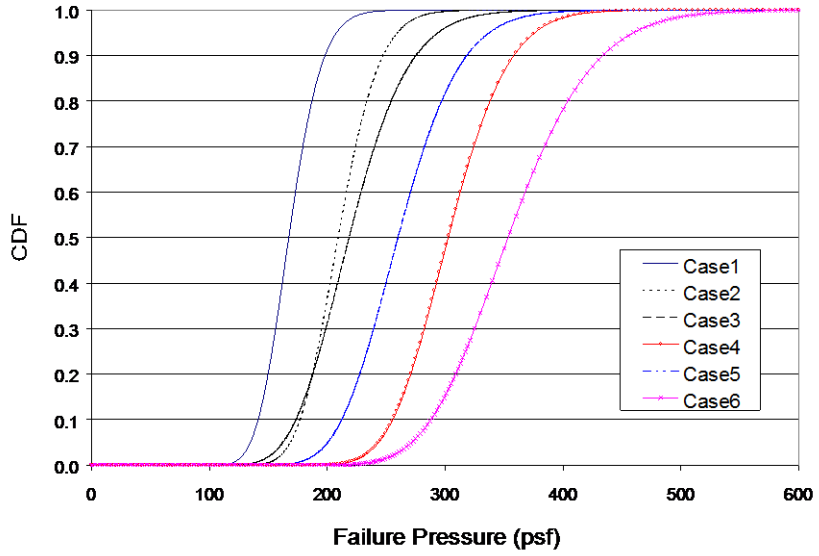

Figure 6-54. CDFs of Metal Deck Failure Pressures (Weld Connections).

6.8 Pre-Engineered Metal Buildings

Because of their fast erection, flexible expansion capability, and low maintenance, metal building systems dominate the low-rise non-residential market. For example, according to MBMA, 65% of the new one- and two-story buildings were built using metal building structures in 1995. Pre-engineered metal building systems are found in many applications, including warehouses, small office buildings, garages, supermarkets, retail stores, industrial factories, schools, town halls, and even churches (Newman, 1997). A

metal building system is typically comprised of primary frames (hot-rolled wide-flange beams and girders, hot-rolled steel rigid frame, or steel trusses), secondary frames (purlins and girts), endwall posts, roof system, wall system, foundation, and bracing.

In this analysis, as in the low-rise residential building analysis, the physical damage modeling for metal buildings is limited to modeling the damage to components and cladding, specifically the metal wall system, the metal roof system, and the entry doors and overhead doors.

6.8.1 Resistance Model for Metal Building Wall System

Wall panels on metal buildings are normally supported on cold-formed C or Z girts. The thickness of the galvanized-steel siding ranges from 18 to 29 gage, with the midrange gages being the most popular (Newman, 1997). Exposed-fastener wall panels behave similarly to through-fastened roofing and some products can be used for both wall and roof systems. Figure 6.55 shows one section of a typical exposed-fastener wall system. The wall panels are attached to the supporting members using self-drilling screws. Two adjacent panels are overlapped and joined together with side-lap fasteners, which are typically spaced at 24″ O.C.

The development of the damage model for metal wall system follows a similar procedure to that used for the metal deck systems. That is, the model development entails case study selections, probabilistic finite element analyses, and evaluation of simulation results. Two case studies (both are one-story buildings) were selected for the metal wall system: one with a design pressure of 20 psf and the other with a design pressure of 40 psf. The wall section for these two case studies is composed of two over-lapped corrugated USD C36 panels with exposed fasteners (screw connections). Note that this kind of panel can be used for both wall systems and roof systems. Figure 6.56 shows the profile of the metal panel. Each panel is 3′ wide by 10′ tall with a supporting girt at 7′ from the ground (see Figure 6.55). Each panel in case 1 has 3 size 10 screws (12″ O.C.) at both ends and 3 size 10 screws (12″ O.C.) on the girt. Each panel in case 2 has 5 size-10 screws (7.2″ O.C.) at both ends and 3 size 10 screws (12″O.C.) on the girt. The panel steel conforms to ASTM A653 Grade 33 sheet steel (F_y = 33 ksi and F_u = 50 ksi) for case 1 and Grade 37 sheet steel (F_y = 37 ksi and F_u = 58 ksi) for case 2. The girt was assumed to be a gage 16 (0.06″ thickness) cold-formed Z section with a 10″ depth. The ultimate strength of the base metal was slightly less than that of the panel. The two panels for the metal wall section are joined together using 6 lap-joint screws spaced at 24″ O.C.

Finite Element Model. A major concern regarding the finite element analysis of the wall system lies in how to model the lap joints. When subjected to a pressure load, the two panels of the wall section tend to move away from each other, resulting in significant tension forces at the lap joints. Because of the restraints provided by the lap-joint screws, the upper and bottom panels around the screw will move together until yield stress is reached. To simulate this phenomenon, a number of methods were investigated, including slave nodes, rigid beams, and rigid shell elements. The final modeling of the lap joint was accomplished by placing a small steel member with the same properties as those of

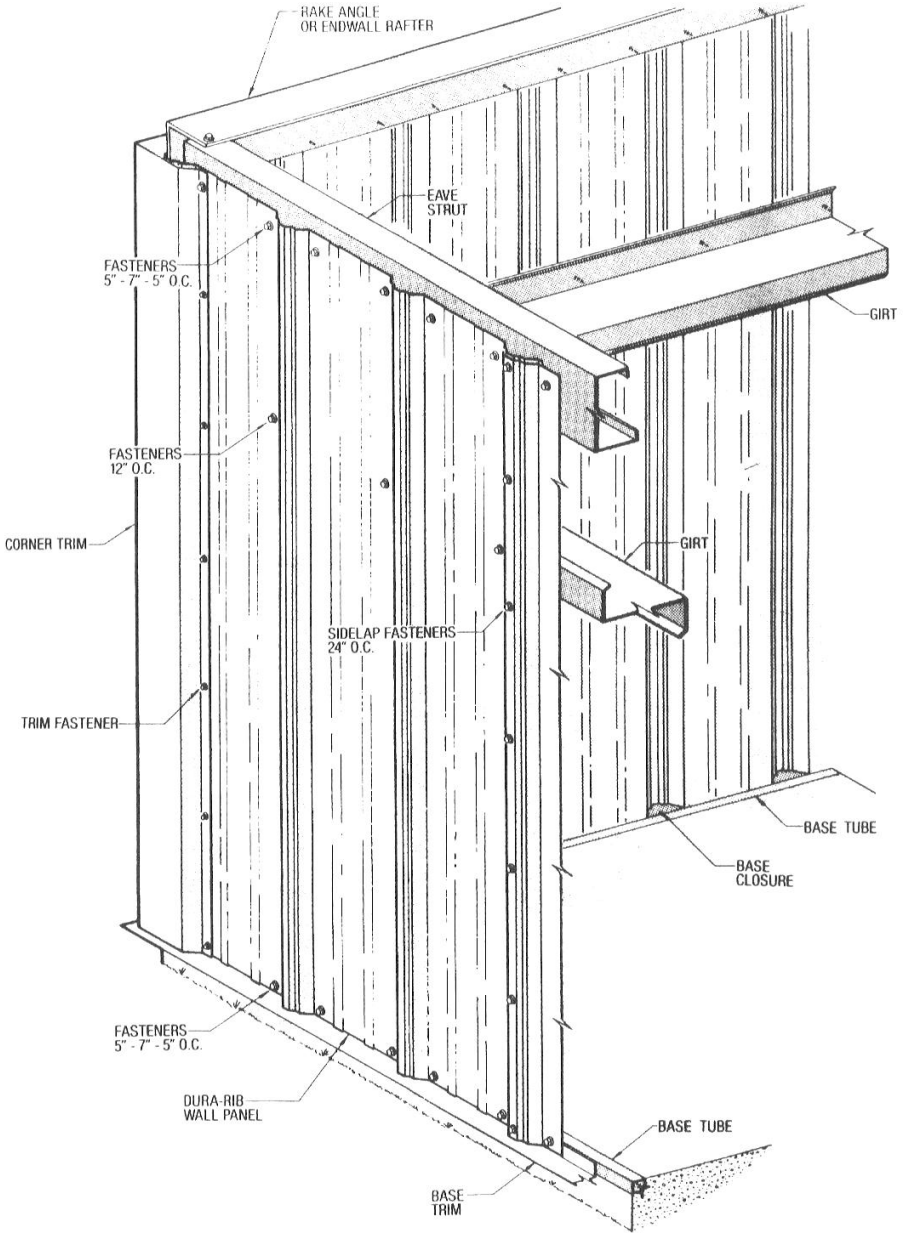

Figure 6-55. Example of a Metal Wall System with Exposed Fasteners (Newman, 1997).

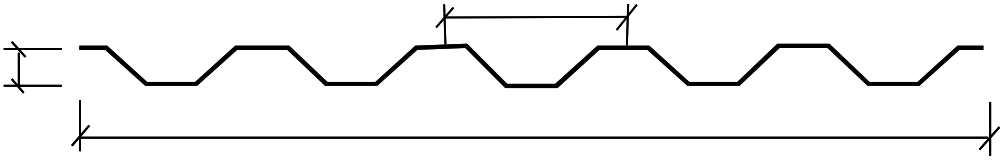

Figure 6-56. Metal Deck Profile for Wall and Roof Systems.

the panel connecting the two separate panels. Figure 6.57 shows the finite element mesh of the wall section. Note that there is a gap between the two wall panels (i.e., no connection between the wall panels except at the lap joints). Mesh grid refinement was made at each fastener and at each lap joint. Figure 6.58 shows the refined mesh around one fastener. Four nodes surrounding each fastener were fixed to model the boundary conditions (denoted as stars in Figure 6.58).

In the FEM analysis, once an element reaches yield stress, its modulus of elasticity (E) is reduced a certain percentage to simulate the plastic behavior of the element. If during the following runs that element reaches yield stress again, another percentage of reduction is applied until the whole wall section fails. However, for the lap joint elements that reach yield stress, the modulus of elasticity is dropped to near zero (to model the weak link between the two panels).

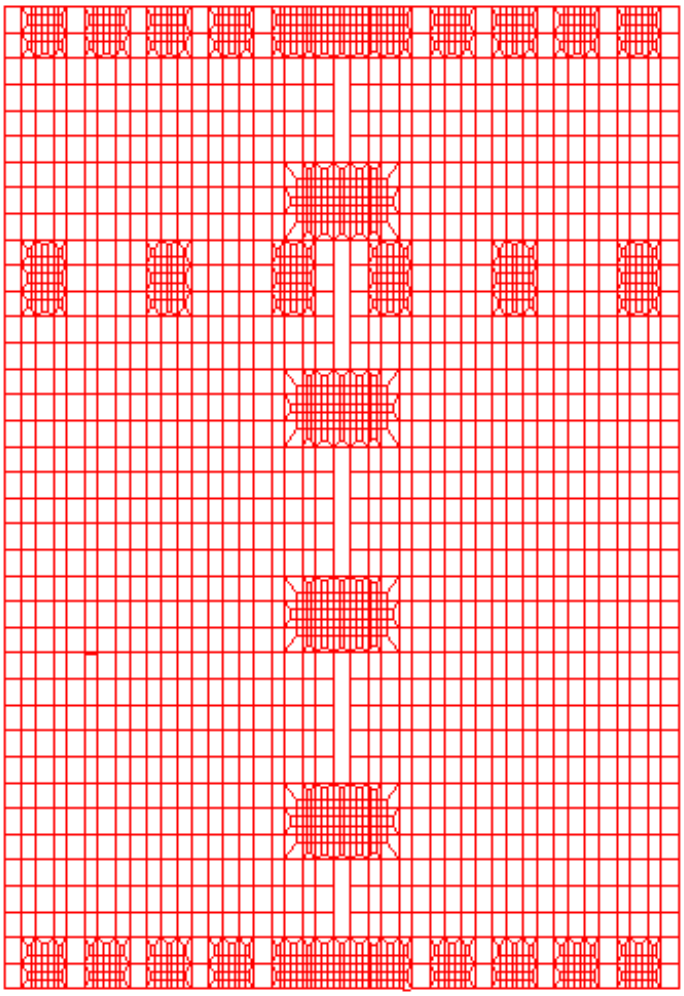

Figure 6-57. Finite Element Mesh of the Wall Panels.

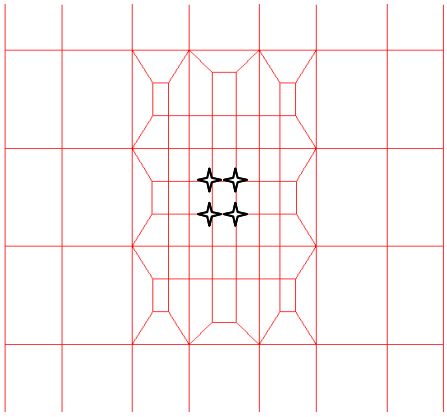

Figure 6-58. Refined Mesh around the Fastener.

As in the FEM analysis of the metal deck on steel joists, the panel-to-support connection failure was modeled as a major failure mode. Both pull-over and pull-out strengths were considered and modeled as random variables with the resistance of the fastener taken as the smaller of the two sampled values. All the other properties, such as the steel strength and panel dimensions are assumed to be deterministic (due to their relatively small variation). Once again, a number of other parameters (such as workmanship, fatigue and corrosion) that may produce significant effects on the pressure resistance of the panel, were not explicitly considered.

The wall section is considered to have failed once any of the following criteria are met:

1. less than 3 fasteners remain on the panel (all the other fasteners have failed); or
2. all the remaining fasteners align in a pattern such that the panel can rotate; or
3. the maximum vertical deflection (*z* direction) of the panel is greater than 1′; or
4. the maximum horizontal deflection (*x* direction) of the panel is greater than 0.5′.

A more stringent restriction on the vertical deflection was applied to wall systems compared to the metal deck on steel joists. Horizontal deflection was added to the failure criteria for the consideration of internal pressurization if an opening develops between the wall panels.

Simulation Results. Following the procedures described in Section 6.7.2 and shown with the flowchart in Figure 6.52, probabilistic finite element analyses were performed for the two example cases. Figure 6.59 shows one example of the stress distribution computed in the wall panels under a uniform suction of 200 psf. The stress concentrations around the fasteners are obvious. Moderate stresses are also seen around one or two lap joints. Under this high pressure, a number of elements have reached their yield stress and most of the screws have already failed.

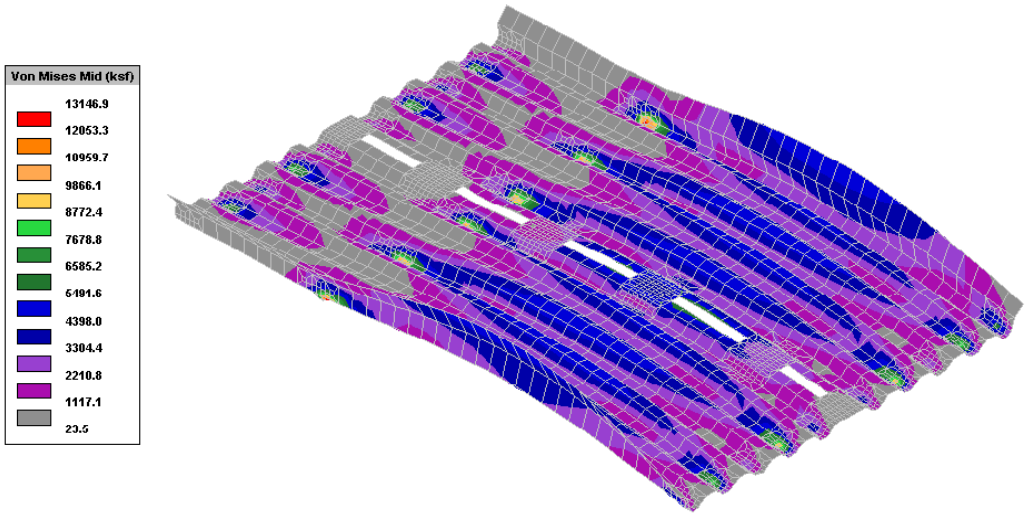

Figure 6-59. Stress Distribution of Wall Panels with Superimposed Deformation.

A total of 50 simulations were performed for each case and the statistics of the wall panel failure pressures were determined from the simulation results. As expected, the load resistance capability of case 1 is smaller than that of case 2. The mean and the standard deviation of the computed failure pressure for case 1 are 84.0 psf and 7.5 psf, respectively. The mean and the standard deviation of the computed failure pressure for case 2 are 124.2 psf and 16.5 psf, respectively. Figure 6.60 shows the CDFs of the failure pressures for these two case studies, which form the basis for the development of the damage model for metal wall systems.

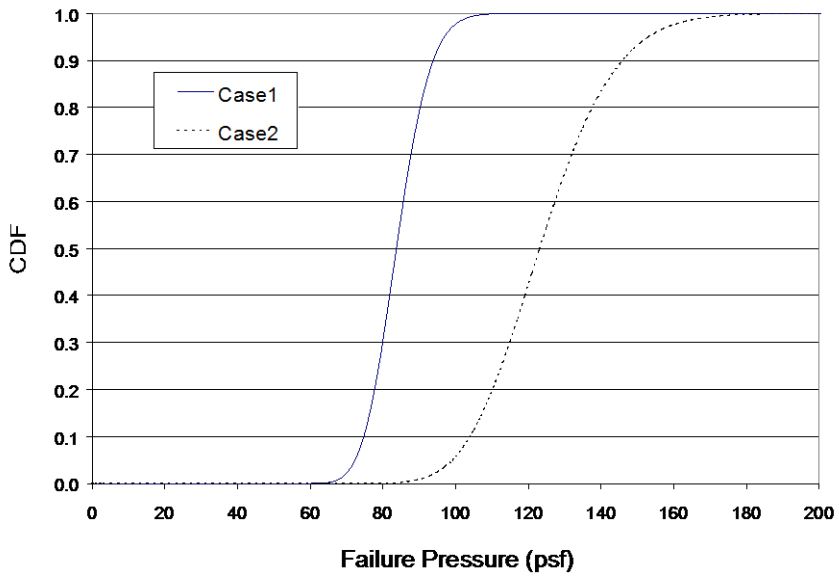

Figure 6-60. CDFs of Wall System Failure Pressures.

6.8.2 Resistance Model for Metal Building Roof System

The metal roofs investigated herein are similar to the metal decks on open-web steel joists except that the metal roof is fastened to C or Z purlins rather than steel joists. The 1996 Metal Building Manufacturers Association (MBMA) design manual was used to determine the design loads for two example buildings. The metal roof panel was assumed to be a USD C36 roof panel (USD, 1998) 3′ wide and 10′ long (covering 2 spans). Refer to Figure 6.56 for its profile. The purlin was assumed to be a cold-formed Z section with a 10″ depth, a gage of 14 (0.075″ thickness), and spaced at 5′ on the primary frame. As noted by Newman (1997), purlin spacing is controlled by the load-carrying capacity of the roof panels, with a 5′ spacing being the most common. Table 6.35 shows the calculated design pressures for the two example buildings. The metal roof failure analysis followed the same procedure used to develop the model for decks on OWSJ, with the joist properties replaced by the purlin properties. The statistics of the metal roof failure pressures from 100 probabilistic finite element runs are given in Table 6.35. The CDFs of the failure pressures for the seven screw connection design cases (Table 6.36) used in the two example buildings are shown in Figure 6.61. Note that the failure pressures for cases 4 and 5 are almost identical, since the only difference between case 4 and case 5 is the metal panel gage.

Table 6-35. Calculated Design Pressure Using MBMA and Simulated Failure Pressure Statistics from FEM Analysis

Building Code	Roof Height (ft)	Wind Speed (mph)	Zone	Design Pressure (psf)	Screw Design[1]	Failure Pressure (psf)	
						Mean	Std
MBMA	15	90	r	-21.7	s1	88.5	9.7
			s	-29.0	s1	88.5	9.7
			c	-51.0	s2	104.4	11.6
		100	r	-27.2	s1	88.5	9.7
			s	-36.1	s1	88.5	9.7
			c	-63.1	s3	119.8	14.3
		110	r	-33.3	s1	88.5	9.7
			s	-44.2	s1	88.5	9.7
			c	-76.8	s4	151.4	16.1
	30	90	r	-25.3	s1	88.5	9.7
			s	-33.7	s1	88.5	9.7
			c	-58.9	s3	119.8	14.3
		100	r	-31.0	s1	88.5	9.7
			s	-41.2	s1	88.5	9.7
			c	-71.7	s5	151.0	16.2
		110	r	-38.9	s1	88.5	9.7
			s	-51.5	s6	109.1	13.6
			c	-89.2	s7	176.9	18.6

[1] See Table 6.36

Table 6-36. Connection Layout for Example Metal Roofs

Design Case	Screw Size	Layout	Installation	Roof Panel			Girt		
				Thickness	F_y (ksi)	F_u (ksi)	Thickness (in.)	F_y (ksi)	F_u (ksi)
s1	#10	36/3	Valley-Fixed	0.024 (gage 24)	40	55	0.075	33	45
s2	#10	36/3	Valley-Fixed	0.024 (gage 24)	50	60	0.075	40	55
s3	#12	36/3	Valley-Fixed	0.030 (gage 22)	50	60	0.075	40	55
s4	#10	36/5	Valley-Fixed	0.036 (gage 20)	40	55	0.075	33	45
s5	#10	36/5	Valley-Fixed	0.030 (gage 22)	40	55	0.075	33	45
s6	#10	36/3	Valley-Fixed	0.030 (gage 22)	50	60	0.075	40	55
s7	#10	36/5	Valley-Fixed	0.036 (gage 20)	50	60	0.075	40	55

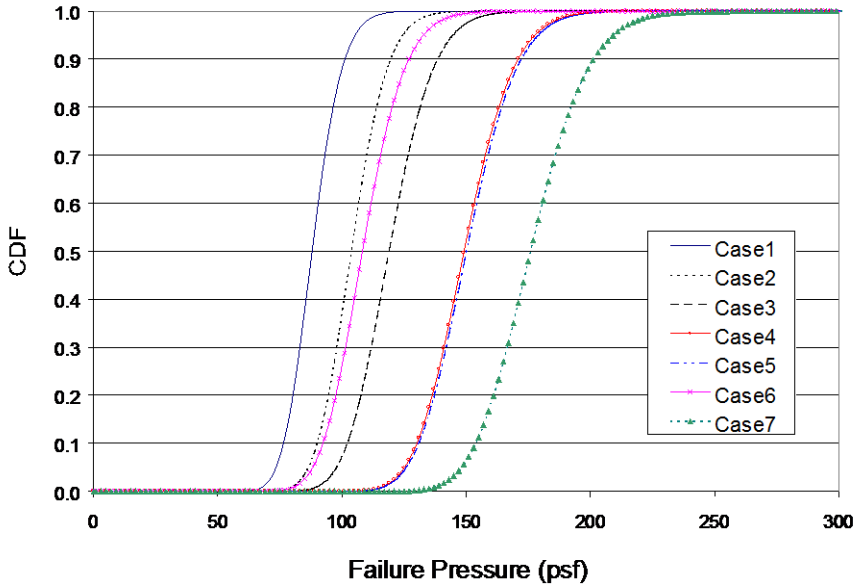

Figure 6-61. CDFs of Metal Roof Failure Pressures.

6.9 Damage Model Results for Marginally- or Non-Engineered Hotel/Motel and Multi-Family Residential Buildings

Nine different geometric representations of marginally-engineered or non-engineered hotels/motels and multi-family residential buildings were developed, as shown pictorially in Figure 6.62. Using the wind loading models and the resistance models described earlier, damage states for each building as a function of wind speed have been estimated. All buildings with sloped roofs have been modeled as having asphalt shingle roofs, and the flat roof buildings are modeled as having either a built-up roof (BUR) or a single ply EPDM roof. The BUR and EPDM roofs are each modeled as being of "poor" quality and "average" quality. All windows are treated as being comprised of single pane annealed

glass, and all sliding glass doors are modeled with tempered glass. In the case of gable

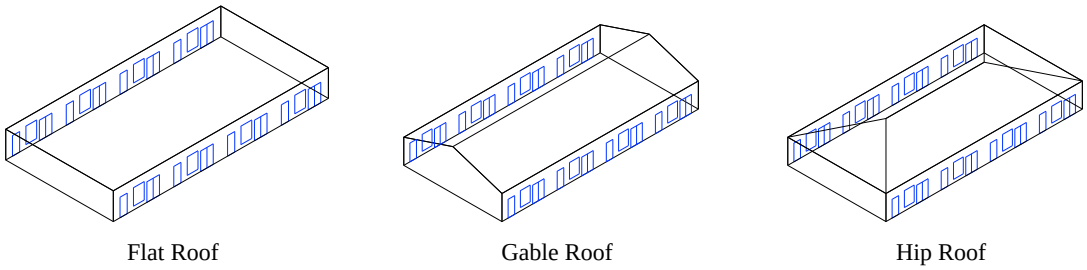

Figure 6-62. Model Building Geometries Used in Building Simulation Study.

and flat roof structures, the connections between the roof and the wall are assumed to exist at the base of every truss with no connections along the short end wall. In the case of the hip roof structures, connections between the roof and the wall are assumed to exist along the entire perimeter of the wall. Whole roof failure is modeled in such a way that it fails as an entire unit. Each building has eight independent occupancy units on each floor (four at the front and four at the back). If a window or door breach occurs in any unit, the

internal pressures are constrained to that unit. Each wall is modeled as having a horizontal span of 20′ and a vertical span of 8′, and is unsupported within the spans.

The parameters varied in the buildings are as follows:

Roof Shape:	Hip, Gable and Flat
Roof Cover:	Asphalt Shingles (Hip and Gable Roofs) and BUR/EPDM (Flat Roofs, Examined for "Average" and "Poor" Quality)
Wall Construction:	Wood Frame (All Buildings) and Unreinforced/ Reinforced Masonry (One, Two and Three Story Buildings)
Roof Deck Attach.:	6d and 8d Nails
Roof/Wall Conn.:	Strapped and Toe-Nailed
Number of Stories:	One, Two, Three and Four

The assumed component resistances used in the simulations are given in Table 6.37. Damage simulations for each basic building type were performed for terrains described with z_0 = 0.03 m (open terrain), z_0 = 0.35 m (typical suburban terrain), z_0 = 0.7 m (suburban terrain with some trees), and z_0 = 1.0 m (treed suburban terrain). All buildings are assumed to be exposed to a residential missile environment.

Table 6-37. Component Resistance Values Used to Model Marginally-Engineered or Non-Engineered Hotel/Motel and Multi-Family Residential Buildings

Component	Distribution	Distribution Parameters
Sheathing Panel (6d)	LogNormal	Mean = 54.6 psf, COV = 0.11
Sheathing Panel (8d)	LogNormal	Mean = 103 psf, COV = 0.11
Annealed Glass Impact	Deterministic	50 lb-ft
Tempered Glass Impact	Deterministic	100 lb-ft
Window/SG Door Pressure	Normal	Mean = 40 psf, COV = 0.2
Entry Door Pressure	Normal	Mean = 50 psf, COV = 0.2
Strap Up-Lift Resistance	Normal	Mean =1200 lb, COV = 0.30
Toe-Nail Uplift Resistance	Normal	Mean = 415 lb, COV = 0.25

The damage state definitions for marginally-engineered or non-engineered hotels/motels and multi-family residential buildings are the same as those for the single family residential buildings, which have been outlined in Table 6.9. Except, to make the damage state definitions with respect to roof damage (i.e., roof cover and roof deck) consistent between buildings with different numbers of stories, the threshold damage levels defining the roof damage states are modified by a factor which is a function of the number of stories. The concept is that 5% roof deck damage, for example, will have a greater effect in terms of economic losses on a one-story building compared to a two-story building. That is, in the case of the two-story building, only the top floor will experience similar damage due to the water infiltration associated with 5% roof deck loss to that experienced by the single-story building. The assumption made here for the purpose of the roof damage state definitions is that the intensity of damage on the bottom floor of the two- to the interior of the single-story building is arbitrarily set to 1, then the damage intensity to the two-story building will be (1+0.5)/2 = 0.75 (i.e., 1 represents the damage intensity story building will be half as much as that on the top floor. Thus, if the damage intensity of the top floor and 0.5 represents the damage intensity of the bottom floor). Therefore, to

achieve a similar damage intensity to that associated with 5% roof deck damage on a single-story building, an otherwise similar two-story building would require 6.7% roof deck damage (i.e., 5%/0.75). The thresholds used to define the roof damage states listed in Table 6.9 were modified in the same manner as described above for the two-, three- and four-story buildings. The multiplicative factors are 1.33, 1.71 and 2.13, respectively. It can be seen, for example, that the four-story building cannot achieve a building damage state 3 (i.e., severe damage) based on roof cover loss since the 50% threshold increases to more than 100% (i.e., 2.13*50% > 100%). Also note that the two- and three-story buildings will be placed in damage state 3 when the roof cover loss exceeds 67% and 86%, respectively.

Damage state versus wind speed plots have been developed using the same approach used for the single family residential buildings. Example building and component damage state plots are given in Appendix C. The average per storm damage states are given in Tables 6.38 through 6.40 and the impacts of the various building features on the average per storm damage are summarized in Table 6.41.

The results summarized in Table 6.41 indicate that the two parameters having the greatest impact on the average damage state for these buildings are the number of stories and, in the case of a flat roof, the change from modeling the roof cover as "average" quality versus "poor" quality. In the case of the poor quality roof, the change from a built-up roof cover to a single ply membrane has a significant impact on the building damage state. Recall, however, that both the poor quality roof cover model and the average quality roof cover model used in modeling both the BUR and the EPDM have been derived empirically using limited information obtained from post-storm damage data. The performance of either a built-up roof or a single ply roof in high wind events is subject to significant uncertainty, and is heavily influenced by the quality of installation. In the case of a poor quality flat roof cover, the results given here indicate that the performance of the single ply membrane roof cover model governs the final damage state of the building.

The change from gable to flat (flat with a built up roof) has an effect that is dependent on the number of stories and the assumed quality of the flat roof cover. A direct comparison of the performance of the flat roof building to that of the gable or hip buildings is made difficult because of the different roof covers; however, in general (for buildings other than single story) the flat roof buildings tend to perform worse than the gable or hip roof buildings.

6.10 Damage Model Results for Low-Rise Masonry Strip Mall Buildings

Small office and retail buildings are often constructed with units separated by fire walls, each having separate roof structures but a common roof cover. These low-rise buildings typically have flat roofs and are one story high. They are usually built with a masonry or concrete wall system. The roof structures are typically constructed using wood trusses and a plywood deck, open web steel joists and a metal deck, or a cast-in-place concrete deck. Because the units are separated by firewalls and have separate roof systems, window breaches in one unit do not impact either the internal pressure or the water infiltration of the adjacent unit(s). This building class is treated here as a separate

building class from those constructed as a single unit, but of comparable size and usage. The damage state definitions for low-rise masonry strip mall buildings type are described in Table 6.42.

Table 6-38. Average Building Damage States – Marginally- or Non-Engineered Hotel/Motel and Multi-Family Residential Buildings – Gable/Hip Roof with Shingles.

Building Characteristics				Strapped Roof-Wall Connections Terrain Surface Roughness (m)				Toe-Nailed Roof-Wall Connections Terrain Surface Roughness (m)			
No. of Stories	Wall Const.	Roof Shape	Roof Deck Nails	0.03	0.35	0.70	1.0	0.03	0.35	0.70	1.0
One	Wood Frame	Gable	6d	0.565	0.356	0.284	0.250	0.593	0.375	0.298	0.260
			8d	0.494	0.316	0.244	0.216	0.542	0.349	0.272	0.237
		Hip	6d	0.455	0.284	0.217	0.187	0.476	0.301	0.228	0.197
			8d	0.428	0.271	0.206	0.178	0.459	0.291	0.221	0.190
	Unreinf. Masonry	Gable	6d	0.566	0.358	0.282	0.248	0.594	0.376	0.298	0.260
			8d	0.488	0.314	0.245	0.216	0.542	0.350	0.273	0.236
		Hip	6d	0.453	0.282	0.217	0.186	0.472	0.300	0.228	0.194
			8d	0.417	0.267	0.206	0.178	0.456	0.292	0.222	0.189
	Reinf. Masonry	Gable	6d	0.563	0.357	0.282	0.248	0.592	0.376	0.297	0.260
			8d	0.488	0.314	0.245	0.216	0.541	0.348	0.270	0.235
		Hip	6d	0.453	0.282	0.218	0.186	0.473	0.298	0.229	0.196
			8d	0.416	0.267	0.206	0.178	0.456	0.291	0.219	0.189
Two	Wood Frame	Gable	6d	0.755	0.522	0.436	0.393	0.788	0.548	0.454	0.410
			8d	0.674	0.459	0.376	0.337	0.718	0.497	0.407	0.365
		Hip	6d	0.658	0.447	0.366	0.326	0.682	0.471	0.385	0.343
			8d	0.627	0.422	0.345	0.306	0.662	0.456	0.373	0.330
	Unreinf. Masonry	Gable	6d	0.743	0.515	0.431	0.389	0.780	0.545	0.453	0.409
			8d	0.656	0.450	0.371	0.331	0.711	0.498	0.408	0.366
		Hip	6d	0.641	0.441	0.362	0.323	0.677	0.468	0.381	0.342
			8d	0.606	0.414	0.336	0.300	0.658	0.458	0.373	0.328
	Reinf. Masonry	Gable	6d	0.741	0.515	0.429	0.390	0.781	0.544	0.454	0.409
			8d	0.657	0.452	0.368	0.330	0.713	0.496	0.409	0.366
		Hip	6d	0.643	0.440	0.362	0.323	0.678	0.469	0.385	0.343
			8d	0.606	0.413	0.336	0.300	0.658	0.458	0.370	0.328
Three	Wood Frame	Gable	6d	0.876	0.630	0.543	0.497	0.904	0.655	0.564	0.517
			8d	0.783	0.553	0.462	0.421	0.831	0.593	0.500	0.455
		Hip	6d	0.810	0.572	0.487	0.442	0.828	0.595	0.503	0.456
			8d	0.772	0.545	0.460	0.417	0.804	0.575	0.486	0.441
	Unreinf. Masonry	Gable	6d	0.847	0.617	0.530	0.487	0.894	0.653	0.560	0.516
			8d	0.748	0.533	0.449	0.406	0.813	0.587	0.497	0.451
		Hip	6d	0.779	0.558	0.475	0.433	0.817	0.586	0.498	0.456
			8d	0.728	0.519	0.439	0.401	0.788	0.571	0.479	0.440
	Reinf. Masonry	Gable	6d	0.848	0.616	0.531	0.488	0.895	0.651	0.558	0.515
			8d	0.749	0.533	0.447	0.406	0.814	0.587	0.497	0.450
		Hip	6d	0.778	0.558	0.473	0.433	0.819	0.589	0.501	0.456
			8d	0.729	0.517	0.439	0.398	0.789	0.568	0.481	0.436
Four	Wood Frame	Gable	6d	0.980	0.727	0.636	0.590	1.005	0.754	0.658	0.611
			8d	0.884	0.636	0.543	0.498	0.927	0.675	0.581	0.535
		Hip	6d	0.881	0.639	0.549	0.506	0.910	0.657	0.567	0.520

			8d	0.853	0.609	0.518	0.472	0.881	0.636	0.546	0.502

Table 6-39. Average Building Damage States – Marginally- or Non-Engineered Hotel/Motel and Multi-Family Residential Buildings – Flat Roofs with BUR.

Building Characteristics				Strapped Roof-Wall Connections Terrain Surface Roughness (m)				Toe-Nailed Roof-Wall Connections Terrain Surface Roughness (m)			
No. of Stories	Wall Const.	Roof Quality	Roof Deck Nails	0.03	0.35	0.70	1.0	0.03	0.35	0.70	1.0
One	Wood Frame	Average	6d	0.387	0.242	0.176	0.150	0.397	0.248	0.181	0.153
			8d	0.342	0.221	0.164	0.137	0.364	0.238	0.169	0.144
		Poor	6d	0.596	0.371	0.290	0.257	0.607	0.377	0.294	0.263
			8d	0.580	0.362	0.288	0.255	0.602	0.372	0.292	0.261
	Unreinf. Masonry	Average	6d	0.383	0.240	0.178	0.148	0.393	0.249	0.182	0.155
			8d	0.338	0.221	0.163	0.137	0.365	0.237	0.171	0.141
		Poor	6d	0.594	0.366	0.290	0.258	0.606	0.377	0.299	0.265
			8d	0.575	0.360	0.286	0.254	0.602	0.373	0.292	0.258
	Reinf. Masonry	Average	6d	0.384	0.240	0.178	0.148	0.396	0.249	0.182	0.155
			8d	0.336	0.223	0.163	0.137	0.362	0.237	0.171	0.143
		Poor	6d	0.595	0.368	0.290	0.258	0.604	0.377	0.296	0.265
			8d	0.574	0.360	0.286	0.254	0.601	0.370	0.292	0.258
Two	Wood Frame	Average	6d	0.654	0.444	0.359	0.315	0.675	0.463	0.376	0.335
			8d	0.616	0.418	0.334	0.296	0.650	0.451	0.360	0.319
		Poor	6d	0.982	0.698	0.594	0.544	1.008	0.723	0.616	0.561
			8d	0.976	0.691	0.591	0.539	1.005	0.717	0.612	0.559
	Unreinf. Masonry	Average	6d	0.642	0.435	0.353	0.312	0.670	0.464	0.373	0.334
			8d	0.601	0.409	0.330	0.292	0.640	0.446	0.360	0.320
		Poor	6d	0.972	0.691	0.589	0.539	1.004	0.718	0.613	0.560
			8d	0.962	0.684	0.584	0.535	1.001	0.716	0.612	0.558
	Reinf. Masonry	Average	6d	0.644	0.437	0.352	0.315	0.668	0.463	0.376	0.332
			8d	0.600	0.410	0.332	0.293	0.642	0.446	0.361	0.318
		Poor	6d	0.974	0.691	0.588	0.541	1.005	0.719	0.610	0.560
			8d	0.965	0.684	0.583	0.532	0.999	0.715	0.611	0.557
Three	Wood Frame	Average	6d	0.874	0.631	0.539	0.493	0.909	0.661	0.562	0.516
			8d	0.841	0.603	0.514	0.472	0.881	0.642	0.546	0.496
		Poor	6d	1.311	1.000	0.886	0.827	1.343	1.032	0.913	0.853
			8d	1.305	0.994	0.884	0.828	1.341	1.032	0.911	0.850
	Unreinf. Masonry	Average	6d	0.852	0.619	0.532	0.484	0.898	0.659	0.562	0.514
			8d	0.816	0.592	0.506	0.460	0.872	0.636	0.542	0.497
		Poor	6d	1.288	0.991	0.876	0.819	1.337	1.025	0.910	0.852
			8d	1.282	0.985	0.877	0.816	1.333	1.025	0.912	0.850
	Reinf. Masonry	Average	6d	0.851	0.620	0.530	0.478	0.898	0.656	0.563	0.513
			8d	0.814	0.593	0.502	0.461	0.871	0.637	0.540	0.496
		Poor	6d	1.289	0.988	0.883	0.819	1.333	1.025	0.911	0.850
			8d	1.282	0.983	0.876	0.822	1.333	1.029	0.911	0.852
Four	Wood Frame	Average	6d	0.955	0.706	0.609	0.563	1.001	0.745	0.654	0.602
			8d	0.897	0.650	0.561	0.513	0.968	0.719	0.625	0.579
		Poor	6d	1.291	1.003	0.900	0.847	1.334	1.048	0.939	0.884
			8d	1.255	0.974	0.864	0.809	1.326	1.038	0.933	0.874

Table 6-40. Average Building Damage States – Marginally- or Non-Engineered Hotel/Motel and Multi-Family Residential Buildings – Flat Roofs with EPDM.

Building Characteristics				Strapped Roof-Wall Connections Terrain Surface Roughness (m)				Toe-Nailed Roof-Wall Connections Terrain Surface Roughness (m)			
No. of Stories	Wall Const.	Roof Quality	Roof Deck Nails	0.03	0.35	0.70	1.0	0.03	0.35	0.70	1.0
One	Wood Frame	Average	6d	0.430	0.264	0.198	0.170	0.442	0.273	0.201	0.174
			8d	0.405	0.252	0.188	0.164	0.425	0.266	0.198	0.168
		Poor	6d	0.968	0.623	0.515	0.471	0.984	0.632	0.518	0.475
			8d	0.962	0.623	0.511	0.465	0.983	0.631	0.519	0.472
	Unreinf. Masonry	Average	6d	0.424	0.264	0.199	0.169	0.437	0.270	0.203	0.174
			8d	0.395	0.253	0.189	0.163	0.421	0.265	0.196	0.170
		Poor	6d	0.974	0.625	0.517	0.468	0.982	0.630	0.519	0.476
			8d	0.952	0.616	0.516	0.468	0.980	0.632	0.519	0.472
	Reinf. Masonry	Average	6d	0.427	0.265	0.199	0.169	0.437	0.270	0.203	0.174
			8d	0.395	0.251	0.189	0.163	0.420	0.263	0.196	0.170
		Poor	6d	0.971	0.625	0.517	0.468	0.979	0.630	0.520	0.476
			8d	0.954	0.616	0.516	0.468	0.979	0.633	0.519	0.472
Two	Wood Frame	Average	6d	0.732	0.500	0.412	0.370	0.757	0.525	0.433	0.383
			8d	0.714	0.489	0.403	0.363	0.747	0.519	0.427	0.384
		Poor	6d	1.419	1.054	0.922	0.853	1.443	1.080	0.940	0.878
			8d	1.421	1.049	0.923	0.854	1.438	1.078	0.940	0.874
	Unreinf. Masonry	Average	6d	0.722	0.498	0.408	0.366	0.752	0.526	0.433	0.387
			8d	0.703	0.482	0.402	0.359	0.745	0.515	0.426	0.380
		Poor	6d	1.419	1.049	0.922	0.853	1.444	1.080	0.942	0.873
			8d	1.409	1.049	0.919	0.851	1.440	1.078	0.941	0.871
	Reinf. Masonry	Average	6d	0.727	0.497	0.409	0.366	0.754	0.527	0.431	0.387
			8d	0.702	0.483	0.402	0.360	0.742	0.517	0.425	0.382
		Poor	6d	1.411	1.052	0.922	0.855	1.441	1.076	0.941	0.867
			8d	1.409	1.055	0.915	0.849	1.443	1.073	0.943	0.874
Three	Wood Frame	Average	6d	1.024	0.753	0.654	0.602	1.051	0.782	0.675	0.627
			8d	1.011	0.749	0.649	0.593	1.043	0.775	0.673	0.621
		Poor	6d	1.767	1.418	1.282	1.211	1.805	1.446	1.312	1.233
			8d	1.769	1.417	1.281	1.204	1.801	1.445	1.307	1.232
	Unreinf. Masonry	Average	6d	1.000	0.743	0.646	0.594	1.046	0.779	0.676	0.623
			8d	0.985	0.734	0.635	0.585	1.044	0.771	0.672	0.622
		Poor	6d	1.754	1.406	1.270	1.202	1.795	1.439	1.305	1.231
			8d	1.746	1.405	1.272	1.199	1.797	1.445	1.306	1.231
	Reinf. Masonry	Average	6d	0.997	0.741	0.647	0.592	1.045	0.780	0.665	0.613
			8d	0.989	0.730	0.638	0.584	1.035	0.776	0.672	0.624
		Poor	6d	1.748	1.405	1.272	1.200	1.795	1.446	1.309	1.233
			8d	1.745	1.408	1.269	1.196	1.798	1.444	1.309	1.235
Four	Wood Frame	Average	6d	1.046	0.782	0.685	0.638	1.089	0.824	0.727	0.675
			8d	1.005	0.747	0.650	0.603	1.076	0.814	0.716	0.664
		Poor	6d	1.591	1.294	1.181	1.119	1.631	1.335	1.216	1.154
			8d	1.543	1.260	1.149	1.088	1.620	1.328	1.213	1.148

Table 6-41. Percent Increases in the Per Storm Average Building Damage State Due to Changes in Building Parameters (Minimum/Average/Maximum) – Marginally- or Non-Engineered Hotel/Motel and Multi-Family Residential Buildings.

Gable and Hip Roofs With Singles					
	Number of Stories				
Parameter	All	One	Two	Three	Four
Unreinforced Masonry to Wood Frame Walls	-1% / 1% / 6%	-1% / 0% / 3%	0% / 1% / 3%	0% / 2% / 6%	N/A
Reinforced Masonry to Unreinforced Masonry Walls	-1% / 0% / 1%	-1% / 0% / 1%	-1% / 0% / 1%	-1% / 0% / 1%	
Hip to Gable Roof Shape	0% / 14% / 34%	16% / 24% / 34%	7% / 13% / 21%	0% / 7% / 13%	4% / 10% / 17%
8d to 6d Roof Deck Nails	2% / 9% / 20%	2% / 8% / 16%	2% / 9% / 18%	3% / 10% / 20%	3% / 9% / 19%
Strapped to Toe-Nailed Roof/Wall Connections	2% / 7% / 11%	4% / 7% / 11%	4% / 7% / 11%	2% / 7% / 11%	3% / 4% / 7%
One to Two Stories	31% / 53% / 76%	N/A			
Two to Three Stories	14% / 24% / 36%				
Three to Four Stories	9% / 14% / 19%				
Flat Roofs With BUR					
	Number of Stories				
Parameter	All	One	Two	Three	Four
Unreinforced Masonry to Wood Frame Walls	-1% / 1% / 3%	-1% / 0% / 2%	0% / 1% / 3%	0% / 1% / 3%	N/A
Reinforced Masonry to Unreinforced Masonry Walls	-1% / 0% / 1%	-1% / 0% / 1%	-1% / 0% / 1%	-1% / 0% / 1%	
Average to Poor Quality Cover	33% / 62% / 86%	51% / 66% / 86%	49% / 64% / 83%	48% / 63% / 78%	33% / 45% / 58%
8d to 6d Roof Deck Nails	0% / 3% / 14%	1% / 5% / 14%	0% / 3% / 7%	0% / 2% / 6%	1% / 4% / 10%
Strapped to Toe-Nailed Roof/Wall Connections	1% / 5% / 13%	1% / 3% / 8%	3% / 5% / 9%	2% / 5% / 8%	3% / 7% / 13%
One to Two Stories	64% / 94% / 127%	N/A			
Two to Three Stories	32% / 45% / 60%				
Three to Four Stories	-4% / 6% / 17%				
Flat Roofs With EPDM					
	Number of Stories				
Parameter	All	One	Two	Three	Four
Unreinforced Masonry to Wood Frame Walls	-1% / 0% / 3%	-1% / 0% / 3%	-1% / 0% / 2%	0% / 1% / 3%	N/A
Reinforced Masonry to Unreinforced Masonry Walls	-1% / 0% / 2%	-1% / 0% / 1%	-1% / 0% / 1%	-1% / 0% / 2%	
Average to Poor Quality Cover	50% / 114% / 188%	123% / 153% / 188%	91% / 115% / 137%	72% / 90% / 105%	50% / 66% / 80%
8d to 6d Roof Deck Nails	-2% / 1% / 8%	-1% / 2% / 8%	-1% / 1% / 4%	-2% / 0% / 2%	0% / 2% / 6%
Strapped to Toe-Nailed Roof/Wall Connections	0% / 4% / 10%	0% / 3% / 7%	1% / 4% / 7%	2% / 4% / 7%	2% / 6% / 10%
One to Two Stories	45% / 85% / 128%	N/A			
Two to Three Stories	24% / 43% / 64%				

Three to Four Stories	-13% / -2% / 8%	

Table 6-42. Damage States for Low-Rise Masonry Strip Mall Construction

Damage State	Qualitative Damage Description	Roof Cover Failure	Window and Door Failures	Roof Deck Failure	Whole Roof Failure 6 Units 1 Unit	Joist Failure 6 Units 1 Unit	Wall Failure
0	**No Damage or Very Minor Damage** Little or no visible damage from the outside. No broken windows, or failed roof deck. Minimal loss of roof cover, with no or very limited water penetration.	≤2%	No	No	No No	No No	No
1	**Minor Damage** Maximum of one broken window or door. Moderate roof cover loss that can be covered to prevent additional water entering the building. Marks or dents on walls requiring painting or patching for repair.	>2% to≤15%	1 window or door failure	No	No No	No No	No
2	**Moderate Damage** Major roof cover damage, moderate window breakage. Minor roof sheathing failure. Some resulting damage to interior of building from water.	>15%to ≤50%	2 to≤ the greater of 20% and 3	1 to 3 panels	No No	No No	No
3	**Severe Damage** Major window damage or roof sheathing loss. Major roof cover loss. Extensive damage to interior from water. Limited, local joist failures. Failure of one wall.	>50%	> the greater of 20% and 3 to ≤50%	>3 to≤25%	1 unit No	1 Unit to 1/3 of the units with joist failures >0% to ≤25% joist failures	1 wall
4	**Destruction** Complete roof failure on 1/3 or more of the units and/or failure of more than one wall. Loss of more than 25% of roof sheathing.	Typically >50%	>50%	>25%	2 or more units Yes	>1/3 of the units with joist failures >25% joist failures	2 or more walls

The representative low-rise building used for small offices and retail is modeled here with masonry walls (either reinforced or unreinforced) and with either a light weight open web steel joist (OWSJ) roof system or a wood roof system. The model buildings have a length of 184′, a width of 40′ and a roof height of either 12′ or 20′. The overall building geometry, along with the placement and relative size of the windows and doors is shown in Figure 6.63 for the building with a 12′ roof height. The building with the 20′ roof height is otherwise the same as that shown in Figure 6.63. The different building configurations (with respect to building height, number of units and roof system) modeled in this section are shown in Table 6.43.

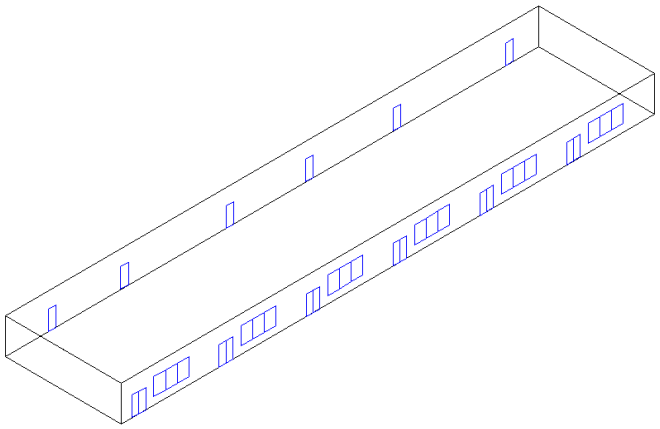

Figure 6-63. Model Building for One Story Low-Rise Masonry Strip Mall Building with Roof Height = 12′.

Table 6-43. Description of Low-Rise Masonry Strip Mall Buildings

Building Designation	Roof Height (ft)	No. of Units	Roof System(s)
A	12	6	Steel Deck on Steel Roof JoistsJoist Spacing = 4′ Joist Span = 30′ (5 Units) and 34′ (1 Unit)Joists Parallel to Long Building Edge
			Wood Deck on Wood Roof Trusses
B	20	6	Steel Deck on Steel Roof Joists Joist Spacing = 4′Joist Span = 30′ (5 Units) and 34′ (1 Unit)Joists Parallel to Long Building Edge
			Wood Deck on Wood Roof Trusses
C	20	6	Steel Deck on Steel Roof JoistsJoist Spacing = 6′Joist Span = 30′ (5 Units) and 34′ (1 Unit)Joists Parallel to Long Building Edge
D	20	1	Steel Deck on Steel Roof JoistsJoist Spacing = 6′Joist Span = 40′Joists Parallel to Short Building Edge

The multi-unit buildings have five units with a width of 30′ and one end-unit with a width of 34′. Each of these units has three 6′×4′ tempered glass windows and one tempered double glass entry door. The rear entry doors are modeled as standard residential type metal doors. The entire building has a total of 30 fenestrations, 24 of which have glazing and therefore can be broken by missile impact. The roof cover is modeled as BUR or as EPDM single ply membrane (“average” quality in both cases).

For the buildings with wood roof structures, the wood roof trusses are spaced at 2′ on center and the roof-wall connections are modeled using either toe-nailed connections or strapped connections. The plywood roof sheathing is modeled as being attached to the roof trusses using either 6d or 8d nails with a standard 6″/12″ spacing.

The OWSJs are designed to resist the uplift forces and moments computed using both ASCE-7-88 and the 1988 Version of SBC, as described in Section 6.7.2, for a design wind speed of 100 mph. In the case of the ASCE-7 loads, the building is assumed to be designed for open terrain (Exposure C) conditions. The metal deck is modeled as being connected to the joists using either screws or welds. The weld and screw designs are

assumed to meet the loading requirements as given in ASCE-7 and SBC and are designed using the methods outlined in Section 6.7.3.

The assumed component resistances are given in Table 6.44. The very high uplift capacities associated with the steel deck are brought about by the minimum requirements for connection fastening, and the short (4′) distance between joists. These uplift values are for the as-installed roof, but a sensitivity study was performed where the uplift capacities of the screwed and welded connections were reduced by 50% to allow for the effect of age and fatigue. This 50% reduction is comparable to the reduction in the pullout capacity of fasteners in metal decks as reported by Baskaran and Dutt (1995).

Four different missile environments are considered in the analysis. The missile environments include combinations of residential-type missiles (i.e., roof shingles, roof tiles and roof sheathing) and commercial-type missiles (i.e., roof gravel). Details on the windborne debris models are given in Chapter 5. In the case of the high-density commercial missile environment, the buildings from which the roof gravel originate are modeled as having a mean roof height of about 15′ and mean building spacing of about 200′. The different missile environments are examined to determine the impact of the missile modeling on the building damage states. Table 6.45 gives descriptions of the four missile environments considered in the analysis.

Example building and component damage state plots are given in Appendix D. The storm average damage states are given in Tables 6.46 and 6.47 for buildings with a wood roof system and Tables 6.48 through 6.50 for buildings with a steel roof system.

The effects of the various building parameters on the storm-average damage states for the buildings with a wood roof system are summarized in Table 6.52. It is evident that the missile environment has a large impact on the overall building damage state, increasing the mean per storm damage by 23% to 106% for the 12′ high building and by 9% to 46% for the 20′ high building when the missile environment changes from no windborne debris (Missile Environment D) to a mixed residential/commercial type environment (Missile Environment A). The effect of using toe-nails for the roof wall connections (versus straps) is a 4% to 29% increase in damage. Using 6d roof sheathing nails in place of 8d nails increases the storm average damage state by up to 15%. The relatively small effect of roof nails in these examples is associated with the fact that other severe damage states, which drive the overall building damage state, have already occurred before a significant amount of roof sheathing is lost. The effect of EPDM roof cover versus BUR roof cover is a 4% to 32% increase in the average damage state. This increase in damage is attributed to the fact that the modeling of the EPDM roof allows the entire roof membrane to fail more readily than the BUR roof, once the initial local failure has occurred.

The building parameter sensitivity results for buildings with steel roof systems are shown in Table 6.53. The results show that when the uplift capacity of the steel roof deck is reduced by 50% to account for age and fatigue, the storm average damage state increases by as much as 31% when the joist spacing is 6′ (Buildings C and D) and has a negligible

Table 6-44. Component Resistance Values Used for Strip-Mall Type Building

Fenestrations		
Component	Distribution	Distribution Parameters
Tempered Glass Small Missile Impact	Deterministic	0.01 slug-ft/sec (Momentum)
Tempered Glass Large Missile Impact	Deterministic	100 lb-ft (Energy)
Window/SG Door System Pressure	Normal	Mean = 40 psf, COV = 0.2
Entry Door System Pressure	Normal	Mean = 50 psf, COV = 0.2
Tempered Glass Pressure (Windows)	Weibull	C = 168 psf, k = 4.8
Tempered Glass Pressure (SG Doors)	Weibull	C = 175 psf, k = 6.1
Wood Deck on Wooden Roof Trusses		
Component	Distribution	Distribution Parameters
Sheathing Panel (6d)	LogNormal	Mean = 54.6 psf, COV = 0.11
Sheathing Panel (8d)	LogNormal	Mean = 103 psf, COV = 0.11
Strap Uplift Resistance	Normal	Mean = 1200 lb, COV = 0.3
Toe-Nail Uplift Resistance	Normal	Mean = 415 lb, COV = 0.25
Steel Deck on Steel Roof Joists – Building Height = 12′, Joist Spacing = 4′		
Component	Distribution	Distribution Parameters (Field, Edge, Corner)
Screwed Steel Deck – SBCCI 100mph	LogNormal	Mean = 187, 187, 187 psf, COV = 0.13, 0.13, 0.13
Screwed Steel Deck – ASCE 100mph	LogNormal	Mean = 187, 187, 212 psf, COV = 0.13, 0.13, 0.11
Welded Steel Deck – SBCCI 100mph	LogNormal	Mean = 169, 169, 169 psf, COV = 0.13, 0.13, 0.13
Welded Steel Deck – ASCE 100mph	LogNormal	Mean = 169, 169, 222 psf, COV = 0.13, 0.13, 0.18
Steel Deck on Steel Roof Joists – Building Height = 20′, Joist Spacing = 4′		
Component	Distribution	Distribution Parameters (Field, Edge, Corner)
Screwed Steel Deck – SBCCI 100mph	LogNormal	Mean = 187, 187, 187 psf, COV = 0.13, 0.13, 0.13
Screwed Steel Deck – ASCE 100mph	LogNormal	Mean = 187, 187, 212 psf, COV = 0.13, 0.13, 0.11
Welded Steel Deck – SBCCI 100mph	LogNormal	Mean = 169, 169, 169 psf, COV = 0.13, 0.13, 0.13
Welded Steel Deck – ASCE 100mph	LogNormal	Mean = 169, 169, 222 psf, COV = 0.13, 0.13, 0.18
Steel Deck on Steel Roof Joists – Building Height = 20′, Joist Spacing = 6′		
Component	Distribution	Distribution Parameters (Field, Edge, Corner)
Screwed Steel Deck – SBCCI 100mph	LogNormal	Mean = 109, 109, 109 psf, COV = 0.21, 0.21, 0.21
Screwed Steel Deck – ASCE 100mph	LogNormal	Mean = 109, 127, 165 psf, COV = 0.21, 0.21, 0.21
Welded Steel Deck – SBCCI 100mph	LogNormal	Mean = 91, 91, 97 psf, COV = 0.19, 0.19, 0.19
Welded Steel Deck – ASCE 100mph	LogNormal	Mean = 91, 123, 155 psf, COV = 0.19, 0.19, 0.19

Table 6-45. Description of Missile Environments

Missile Environment Designation	Missile Source EnvironmentC = Commercial Type Missiles, R = Residential Type Missiles,M = Equal Mix of Commercial and Residential Type Missiles, N = No Missiles							
	Center of 45° Directional Sector							
	N	NE	E	SE	S	SW	W	NW
A	M	M	M	M	M	M	M	M
B	R	C	R	R	C	R	R	R
C	R	R	R	R	R	R	R	R
D	N	N	N	N	N	N	N	N

effect when the joist spacing is 4′ (Buildings A and B). The effect of using welds versus screws to fasten the steel roof deck to the joists ranges from a 2% decrease to a 9% increase in the average damage for the buildings having a 6′ joist spacing. The effect of the roof deck fastener is negligible when the joist spacing is 4′. Similarly, the result of using the SBCCI versus the ACSE metal roof design criteria (both with a 100 mph design speed) ranges from a 1% decrease to a 23% increase in the average damage state for the buildings having a 6′ joist spacing. The effect of the metal deck design criteria is negligible when the joist spacing is 4′. The impact of metal deck quality, installation and design criteria on the storm average damage states, as discussed above, is more significant when the joist spacing is larger because the larger spacing reduces the uplift capacity of the roof panels (see Table 6.54) and therefore the metal deck damage has a larger weight in the overall damage state.

The use of EPDM roof cover versus BUR roof cover increases the overall storm average damage states by 5% to 34%. The effect of the roof cover type is similar for each of the four buildings examined. Walls constructed with unreinforced masonry versus reinforced masonry yield mean damage states which are up to 15% larger for the buildings with a roof height of 20′ (Buildings B, C and D) and has a much less significant effect (2% decrease to 4% increase) when the roof height is 12′ (Building A). Again, the different missile environments have a large impact on the storm average damage states as seen from the last three rows of Table 6.53. The largest effect is found when changing from no windborne missiles (Missile Environment D) to a mixed residential/commercial type environment (Missile Environment A) where the storm average damage states increased from between 24% and 115% for the 12′ high building cases and from between 8% and 39% for the 20′ high building cases. The elimination of glass breakage associated with windborne debris (i.e., as produced when changing the modeled Missile Environment from A to D) has a smaller impact on the overall damage state for the 20′ high building cases compared to the 12′ high building cases since the overall damage state is more influenced by roof damage compared to fenestration damage for the taller buildings.

Table 6.54 summarizes the influence of building height, joist spacing and number of units on the storm average damage state. The building height is shown to have the most significant effect, increasing the damage states from between 25% and 126% when the building height increases from 12′ to 20′. Increasing the joist spacing from 4′ to 6′

Table 6-46. Average Damage States for Building A – Twelve Foot High Strip Mall Building with Six Units and Wood Deck with Two Foot Truss Spacing

Building Characteristics				Toe-Nailed Roof-Wall Connection				Strapped Roof-Wall Connection			
				Terrain Surface Roughness (m)				Terrain Surface Roughness (m)			
Wall Type	Missile Environ.	Wood Deck Nail Size	Roof Cover	0.03	0.35	0.70	1.0	0.03	0.35	0.70	1.0
Unreinforced Masonry	A	6d	EPDM	0.694	0.459	0.340	0.285	0.571	0.425	0.314	0.267
			BUR	0.660	0.440	0.319	0.267	0.531	0.405	0.296	0.248
		8d	EPDM	0.688	0.454	0.338	0.282	0.555	0.414	0.310	0.260
			BUR	0.641	0.431	0.314	0.263	0.506	0.392	0.288	0.239
	B	6d	EPDM	0.600	0.391	0.291	0.249	0.525	0.361	0.267	0.230
			BUR	0.560	0.369	0.271	0.226	0.478	0.332	0.245	0.206
		8d	EPDM	0.594	0.386	0.291	0.246	0.508	0.353	0.264	0.222
			BUR	0.545	0.359	0.263	0.221	0.449	0.318	0.233	0.193
	C	6d	EPDM	0.518	0.331	0.249	0.214	0.475	0.288	0.221	0.190
			BUR	0.468	0.301	0.225	0.186	0.423	0.254	0.190	0.163
		8d	EPDM	0.508	0.324	0.247	0.209	0.459	0.275	0.211	0.182
			BUR	0.452	0.291	0.211	0.180	0.390	0.232	0.173	0.148
	D	6d	EPDM	0.483	0.267	0.211	0.188	0.459	0.253	0.198	0.177
			BUR	0.428	0.227	0.177	0.155	0.408	0.215	0.164	0.146
		8d	EPDM	0.478	0.261	0.206	0.180	0.450	0.246	0.190	0.167
			BUR	0.408	0.213	0.164	0.142	0.372	0.192	0.147	0.129
Reinforced Masonry	A	6d	EPDM	0.683	0.458	0.340	0.284	0.565	0.429	0.315	0.268
			BUR	0.655	0.432	0.320	0.269	0.530	0.404	0.298	0.247
		8d	EPDM	0.686	0.453	0.333	0.279	0.548	0.417	0.311	0.259
			BUR	0.644	0.429	0.316	0.261	0.499	0.391	0.287	0.239
	B	6d	EPDM	0.595	0.388	0.290	0.246	0.519	0.355	0.270	0.229
			BUR	0.553	0.363	0.266	0.226	0.474	0.330	0.244	0.205
		8d	EPDM	0.589	0.387	0.288	0.244	0.499	0.344	0.262	0.222
			BUR	0.539	0.358	0.260	0.217	0.444	0.315	0.232	0.193
	C	6d	EPDM	0.510	0.327	0.248	0.213	0.470	0.284	0.219	0.191
			BUR	0.463	0.302	0.219	0.187	0.417	0.254	0.190	0.163
		8d	EPDM	0.505	0.324	0.245	0.208	0.451	0.271	0.210	0.182
			BUR	0.442	0.288	0.214	0.179	0.381	0.230	0.171	0.147
	D	6d	EPDM	0.475	0.263	0.209	0.186	0.457	0.253	0.199	0.179
			BUR	0.419	0.223	0.176	0.153	0.402	0.213	0.164	0.145
		8d	EPDM	0.468	0.258	0.204	0.180	0.443	0.242	0.190	0.166
			BUR	0.396	0.209	0.162	0.142	0.367	0.189	0.147	0.126

Table 6-47. Average Damage States for Building B – Twenty Foot High Strip Mall Building with Six Units and Wood Deck with Two Foot Truss Spacing

Building Characteristics				Toe-Nailed Roof-Wall Connection				Strapped Roof-Wall Connection			
				Terrain Surface Roughness (m)				Terrain Surface Roughness (m)			
Wall Type	Missile Environ.	Wood Deck Nail Size	Roof Cover	0.03	0.35	0.70	1.0	0.03	0.35	0.70	1.0
Unreinforced Masonry	A	6d	EPDM	0.933	0.666	0.531	0.463	0.835	0.585	0.466	0.414
			BUR	0.863	0.620	0.485	0.422	0.757	0.533	0.419	0.365
		8d	EPDM	0.928	0.665	0.532	0.460	0.822	0.579	0.465	0.409
			BUR	0.852	0.613	0.477	0.415	0.733	0.523	0.407	0.350
	B	6d	EPDM	0.861	0.596	0.486	0.430	0.792	0.546	0.443	0.392
			BUR	0.795	0.546	0.433	0.380	0.715	0.486	0.390	0.341
		8d	EPDM	0.859	0.601	0.483	0.428	0.785	0.539	0.438	0.387
			BUR	0.775	0.537	0.421	0.373	0.692	0.468	0.372	0.326
	C	6d	EPDM	0.800	0.548	0.448	0.400	0.763	0.503	0.415	0.374
			BUR	0.719	0.484	0.393	0.346	0.673	0.435	0.355	0.316
		8d	EPDM	0.798	0.543	0.444	0.401	0.757	0.496	0.412	0.369
			BUR	0.703	0.470	0.378	0.337	0.651	0.418	0.335	0.301
	D	6d	EPDM	0.789	0.510	0.428	0.390	0.758	0.490	0.409	0.368
			BUR	0.705	0.441	0.365	0.330	0.667	0.416	0.343	0.307
		8d	EPDM	0.785	0.506	0.427	0.386	0.753	0.484	0.404	0.364
			BUR	0.681	0.425	0.353	0.316	0.649	0.396	0.326	0.290
Reinforced Masonry	A	6d	EPDM	0.903	0.659	0.524	0.460	0.789	0.567	0.458	0.401
			BUR	0.838	0.609	0.479	0.412	0.708	0.516	0.406	0.352
		8d	EPDM	0.897	0.653	0.523	0.457	0.769	0.560	0.448	0.396
			BUR	0.821	0.598	0.472	0.404	0.674	0.493	0.382	0.337
	B	6d	EPDM	0.832	0.590	0.480	0.426	0.751	0.526	0.431	0.381
			BUR	0.764	0.534	0.425	0.372	0.667	0.466	0.372	0.325
		8d	EPDM	0.829	0.585	0.475	0.424	0.735	0.514	0.418	0.374
			BUR	0.746	0.521	0.415	0.365	0.630	0.441	0.352	0.308
	C	6d	EPDM	0.761	0.533	0.440	0.397	0.719	0.484	0.403	0.361
			BUR	0.684	0.470	0.382	0.340	0.631	0.417	0.342	0.303
		8d	EPDM	0.763	0.531	0.436	0.392	0.708	0.471	0.394	0.355
			BUR	0.666	0.459	0.370	0.332	0.596	0.383	0.314	0.282
	D	6d	EPDM	0.755	0.497	0.417	0.382	0.718	0.468	0.395	0.359
			BUR	0.661	0.423	0.358	0.324	0.626	0.393	0.327	0.295
		8d	EPDM	0.745	0.492	0.413	0.378	0.706	0.458	0.383	0.349
			BUR	0.641	0.411	0.344	0.309	0.590	0.367	0.303	0.273

Table 6-48. Average Damage States for Building A – Twelve Foot High Strip Mall Building with Six Units and Metal Deck with Four Foot Joist Spacing

Building Characteristics					No Reduction in Metal Deck Capacity				50% Reduction in Metal Deck Capacity			
					Terrain Surface Roughness (m)				Terrain Surface Roughness (m)			
Wall Type	Missile Environ	Design Code	Metal Deck Attach	Roof Cover	0.03	0.35	0.70	1.0	0.03	0.35	0.70	1.0
Unreinforced Masonry	A	SBCCI	Screws	EPDM	0.540	0.421	0.312	0.259	0.537	0.418	0.310	0.261
				BUR	0.490	0.391	0.287	0.237	0.489	0.392	0.284	0.235
			Welds	EPDM	0.538	0.419	0.312	0.260	0.540	0.419	0.312	0.261
				BUR	0.487	0.393	0.286	0.240	0.487	0.392	0.286	0.237
		ASCE	Screws	EPDM	0.540	0.419	0.313	0.262	0.539	0.418	0.309	0.258
				BUR	0.490	0.394	0.287	0.236	0.487	0.394	0.288	0.236
			Welds	EPDM	0.536	0.420	0.310	0.260	0.537	0.416	0.312	0.261
				BUR	0.488	0.394	0.286	0.237	0.488	0.394	0.289	0.236
	B	SBCCI	Screws	EPDM	0.494	0.349	0.262	0.223	0.489	0.348	0.261	0.223
				BUR	0.433	0.310	0.229	0.194	0.432	0.314	0.231	0.196
			Welds	EPDM	0.489	0.346	0.261	0.222	0.491	0.346	0.262	0.222
				BUR	0.431	0.315	0.230	0.194	0.433	0.314	0.231	0.191
		ASCE	Screws	EPDM	0.489	0.350	0.260	0.221	0.489	0.346	0.260	0.220
				BUR	0.429	0.314	0.231	0.195	0.428	0.315	0.231	0.194
			Welds	EPDM	0.491	0.348	0.262	0.223	0.489	0.348	0.261	0.223
				BUR	0.431	0.315	0.231	0.194	0.431	0.313	0.230	0.195
	C	SBCCI	Screws	EPDM	0.441	0.269	0.208	0.181	0.441	0.270	0.207	0.180
				BUR	0.372	0.230	0.172	0.145	0.369	0.228	0.170	0.146
			Welds	EPDM	0.441	0.271	0.208	0.181	0.442	0.271	0.207	0.180
				BUR	0.370	0.227	0.168	0.144	0.373	0.226	0.171	0.145
		ASCE	Screws	EPDM	0.441	0.268	0.209	0.180	0.439	0.270	0.209	0.183
				BUR	0.369	0.227	0.169	0.145	0.369	0.227	0.171	0.144
			Welds	EPDM	0.439	0.269	0.209	0.179	0.439	0.270	0.207	0.180
				BUR	0.368	0.226	0.170	0.145	0.369	0.228	0.171	0.146
	D	SBCCI	Screws	EPDM	0.430	0.240	0.191	0.170	0.431	0.242	0.190	0.169
				BUR	0.359	0.188	0.145	0.128	0.359	0.188	0.147	0.129
			Welds	EPDM	0.431	0.241	0.191	0.170	0.431	0.239	0.191	0.168
				BUR	0.356	0.187	0.146	0.128	0.358	0.189	0.147	0.129
		ASCE	Screws	EPDM	0.431	0.240	0.191	0.170	0.433	0.239	0.189	0.169
				BUR	0.354	0.187	0.145	0.128	0.353	0.187	0.146	0.128
			Welds	EPDM	0.432	0.239	0.191	0.170	0.432	0.240	0.190	0.169
				BUR	0.354	0.187	0.145	0.128	0.354	0.187	0.146	0.129

Table 6.48. Average Damage States for Building A – Twelve Foot High Strip Mall Building with Six Units and Metal Deck with Four Foot Joist Spacing (concluded)

Building Characteristics					No Reduction in Metal Deck Capacity				50% Reduction in Metal Deck Capacity			
					Terrain Surface Roughness (m)				Terrain Surface Roughness (m)			
Wall Type	Missile Environ	Design Code	Metal Deck Attach.	Roof Cover	0.03	0.35	0.70	1.0	0.03	0.35	0.70	1.0
Reinforced Masonry	A	SBCCI	Screws	EPDM	0.532	0.418	0.313	0.260	0.531	0.416	0.310	0.260
				BUR	0.481	0.391	0.289	0.237	0.483	0.390	0.287	0.240
			Welds	EPDM	0.534	0.419	0.310	0.262	0.534	0.420	0.311	0.259
				BUR	0.479	0.390	0.286	0.236	0.484	0.391	0.283	0.236
		ASCE	Screws	EPDM	0.533	0.417	0.308	0.258	0.535	0.420	0.310	0.261
				BUR	0.478	0.391	0.287	0.237	0.482	0.390	0.286	0.236
			Welds	EPDM	0.533	0.418	0.313	0.258	0.533	0.418	0.311	0.258
				BUR	0.482	0.390	0.284	0.237	0.483	0.392	0.283	0.237
	B	SBCCI	Screws	EPDM	0.485	0.347	0.262	0.217	0.483	0.346	0.263	0.221
				BUR	0.423	0.312	0.230	0.191	0.424	0.314	0.231	0.193
			Welds	EPDM	0.484	0.347	0.260	0.221	0.483	0.343	0.260	0.220
				BUR	0.424	0.311	0.227	0.191	0.425	0.313	0.229	0.195
		ASCE	Screws	EPDM	0.481	0.346	0.261	0.222	0.483	0.346	0.261	0.220
				BUR	0.425	0.313	0.228	0.190	0.423	0.313	0.228	0.192
			Welds	EPDM	0.485	0.346	0.261	0.219	0.487	0.345	0.260	0.222
				BUR	0.423	0.311	0.229	0.192	0.426	0.311	0.228	0.191
	C	SBCCI	Screws	EPDM	0.433	0.266	0.207	0.179	0.432	0.268	0.207	0.180
				BUR	0.360	0.226	0.167	0.144	0.361	0.224	0.169	0.144
			Welds	EPDM	0.429	0.267	0.205	0.179	0.431	0.267	0.205	0.180
				BUR	0.360	0.226	0.169	0.144	0.363	0.226	0.168	0.145
		ASCE	Screws	EPDM	0.433	0.269	0.207	0.180	0.433	0.268	0.208	0.178
				BUR	0.360	0.226	0.169	0.144	0.361	0.226	0.168	0.144
			Welds	EPDM	0.432	0.268	0.206	0.179	0.433	0.269	0.208	0.178
				BUR	0.361	0.225	0.168	0.144	0.363	0.224	0.171	0.144
	D	SBCCI	Screws	EPDM	0.423	0.239	0.189	0.167	0.422	0.237	0.188	0.168
				BUR	0.345	0.184	0.144	0.126	0.348	0.183	0.144	0.126
			Welds	EPDM	0.425	0.239	0.189	0.167	0.427	0.236	0.188	0.167
				BUR	0.346	0.185	0.143	0.125	0.350	0.182	0.144	0.125
		ASCE	Screws	EPDM	0.425	0.237	0.189	0.167	0.424	0.237	0.187	0.167
				BUR	0.347	0.184	0.143	0.126	0.346	0.184	0.143	0.127
			Welds	EPDM	0.421	0.237	0.189	0.167	0.421	0.237	0.191	0.168
				BUR	0.344	0.183	0.143	0.126	0.349	0.184	0.143	0.127

Table 6-49. Average Damage States for Building B – Twenty Foot High Strip Mall Building with Six Units and Metal Deck with Four Foot Joist Spacing

Building Characteristics					No Reduction in Metal Deck Capacity				50% Reduction in Metal Deck Capacity			
					Terrain Surface Roughness (m)				Terrain Surface Roughness (m)			
Wall Type	Missile Environ	Design Code	Metal Deck Attach.	Roof Cover	0.03	0.35	0.70	1.0	0.03	0.35	0.70	1.0
Unreinforced Masonry	A	SBCCI	Screws	EPDM	0.813	0.574	0.463	0.406	0.813	0.575	0.464	0.406
				BUR	0.724	0.519	0.406	0.352	0.724	0.515	0.404	0.352
			Welds	EPDM	0.815	0.574	0.457	0.407	0.809	0.576	0.464	0.406
				BUR	0.726	0.517	0.402	0.350	0.725	0.519	0.404	0.350
		ASCE	Screws	EPDM	0.814	0.577	0.461	0.407	0.814	0.579	0.465	0.409
				BUR	0.725	0.517	0.405	0.351	0.726	0.517	0.404	0.348
			Welds	EPDM	0.814	0.578	0.463	0.408	0.812	0.581	0.462	0.410
				BUR	0.725	0.517	0.408	0.350	0.723	0.518	0.404	0.352
	B	SBCCI	Screws	EPDM	0.781	0.532	0.435	0.385	0.773	0.534	0.434	0.387
				BUR	0.680	0.465	0.366	0.325	0.677	0.464	0.368	0.323
			Welds	EPDM	0.776	0.534	0.433	0.387	0.772	0.537	0.431	0.384
				BUR	0.682	0.466	0.366	0.324	0.684	0.466	0.368	0.322
		ASCE	Screws	EPDM	0.775	0.535	0.433	0.383	0.775	0.534	0.434	0.386
				BUR	0.680	0.464	0.367	0.322	0.680	0.465	0.369	0.323
			Welds	EPDM	0.772	0.536	0.434	0.385	0.775	0.535	0.433	0.387
				BUR	0.681	0.467	0.367	0.321	0.683	0.461	0.369	0.322
	C	SBCCI	Screws	EPDM	0.745	0.491	0.408	0.363	0.746	0.492	0.406	0.364
				BUR	0.641	0.408	0.334	0.296	0.641	0.408	0.333	0.295
			Welds	EPDM	0.742	0.492	0.409	0.365	0.743	0.493	0.406	0.364
				BUR	0.640	0.408	0.333	0.296	0.640	0.408	0.335	0.298
		ASCE	Screws	EPDM	0.742	0.491	0.409	0.366	0.744	0.493	0.406	0.367
				BUR	0.637	0.411	0.332	0.297	0.641	0.410	0.333	0.297
			Welds	EPDM	0.744	0.489	0.407	0.364	0.742	0.491	0.403	0.365
				BUR	0.643	0.412	0.336	0.298	0.640	0.410	0.335	0.294
	D	SBCCI	Screws	EPDM	0.747	0.480	0.400	0.362	0.740	0.478	0.399	0.365
				BUR	0.633	0.392	0.323	0.289	0.636	0.391	0.323	0.290
			Welds	EPDM	0.744	0.477	0.399	0.362	0.743	0.479	0.401	0.358
				BUR	0.635	0.391	0.322	0.286	0.637	0.391	0.323	0.289
		ASCE	Screws	EPDM	0.749	0.478	0.397	0.363	0.744	0.479	0.400	0.359
				BUR	0.635	0.392	0.322	0.286	0.632	0.391	0.319	0.287
			Welds	EPDM	0.743	0.478	0.398	0.361	0.742	0.479	0.399	0.360
				BUR	0.637	0.392	0.322	0.286	0.637	0.392	0.321	0.287

Table 6.49. Average Damage States for Building B – Twenty Foot High Strip Mall Building with Six Units and Metal Deck with Four Foot Joist Spacing (concluded)

Building Characteristics					No Reduction in Metal Deck Capacity				50% Reduction in Metal Deck Capacity			
					Terrain Surface Roughness (m)				Terrain Surface Roughness (m)			
Wall Type	Missile Environ	Design Code	Metal Deck Attach.	Roof Cover	0.03	0.35	0.70	1.0	0.03	0.35	0.70	1.0
Reinforced Masonry	A	SBCCI	Screws	EPDM	0.739	0.555	0.443	0.394	0.739	0.555	0.445	0.393
				BUR	0.634	0.489	0.384	0.330	0.638	0.491	0.382	0.332
			Welds	EPDM	0.739	0.556	0.443	0.392	0.738	0.556	0.444	0.389
				BUR	0.638	0.492	0.384	0.331	0.640	0.492	0.383	0.334
		ASCE	Screws	EPDM	0.739	0.554	0.443	0.392	0.736	0.554	0.444	0.395
				BUR	0.640	0.490	0.386	0.332	0.640	0.494	0.385	0.332
			Welds	EPDM	0.735	0.554	0.445	0.392	0.740	0.555	0.443	0.393
				BUR	0.640	0.491	0.383	0.332	0.640	0.492	0.384	0.332
	B	SBCCI	Screws	EPDM	0.707	0.506	0.415	0.369	0.706	0.507	0.417	0.371
				BUR	0.601	0.438	0.344	0.301	0.599	0.438	0.345	0.304
			Welds	EPDM	0.708	0.509	0.414	0.371	0.708	0.508	0.415	0.369
				BUR	0.602	0.433	0.345	0.302	0.602	0.435	0.345	0.303
		ASCE	Screws	EPDM	0.704	0.508	0.413	0.368	0.707	0.506	0.415	0.369
				BUR	0.601	0.434	0.346	0.305	0.602	0.434	0.346	0.303
			Welds	EPDM	0.711	0.508	0.416	0.369	0.710	0.506	0.414	0.369
				BUR	0.601	0.435	0.347	0.302	0.603	0.432	0.344	0.300
	C	SBCCI	Screws	EPDM	0.677	0.457	0.384	0.345	0.677	0.460	0.384	0.345
				BUR	0.561	0.370	0.303	0.273	0.562	0.372	0.304	0.273
			Welds	EPDM	0.679	0.457	0.382	0.346	0.680	0.457	0.382	0.348
				BUR	0.562	0.374	0.306	0.274	0.565	0.375	0.305	0.273
		ASCE	Screws	EPDM	0.679	0.458	0.380	0.347	0.677	0.461	0.380	0.345
				BUR	0.562	0.371	0.304	0.273	0.562	0.373	0.306	0.274
			Welds	EPDM	0.677	0.456	0.383	0.344	0.679	0.459	0.381	0.346
				BUR	0.562	0.371	0.305	0.272	0.565	0.371	0.303	0.272
	D	SBCCI	Screws	EPDM	0.676	0.446	0.378	0.347	0.674	0.452	0.378	0.345
				BUR	0.555	0.356	0.297	0.267	0.557	0.356	0.295	0.266
			Welds	EPDM	0.679	0.448	0.378	0.345	0.676	0.447	0.376	0.344
				BUR	0.558	0.355	0.296	0.268	0.561	0.357	0.296	0.267
		ASCE	Screws	EPDM	0.677	0.446	0.379	0.346	0.677	0.447	0.375	0.344
				BUR	0.557	0.357	0.294	0.268	0.558	0.355	0.296	0.267
			Welds	EPDM	0.680	0.446	0.378	0.346	0.678	0.446	0.377	0.343
				BUR	0.559	0.355	0.295	0.268	0.559	0.355	0.296	0.267

Table 6-50. Average Damage States for Building C – Twenty Foot High Strip Mall Building with Six Units and Metal Deck with Six Foot Joist Spacing

Building Characteristics					No Reduction in Metal Deck Capacity				50% Reduction in Metal Deck Capacity			
					Terrain Surface Roughness (m)				Terrain Surface Roughness (m)			
Wall Type	Missile Environ	Design Code	Metal Deck Attach.	Roof Cover	0.03	0.35	0.70	1.0	0.03	0.35	0.70	1.0
Unreinforced Masonry	A	SBCCI	Screws	EPDM	0.816	0.577	0.462	0.408	0.852	0.602	0.487	0.430
				BUR	0.729	0.521	0.403	0.351	0.792	0.559	0.444	0.389
			Welds	EPDM	0.816	0.579	0.461	0.407	0.880	0.620	0.502	0.445
				BUR	0.729	0.523	0.402	0.349	0.827	0.587	0.468	0.412
		ASCE	Screws	EPDM	0.810	0.578	0.465	0.409	0.827	0.587	0.472	0.416
				BUR	0.725	0.520	0.402	0.351	0.747	0.529	0.415	0.364
			Welds	EPDM	0.812	0.580	0.462	0.405	0.827	0.584	0.470	0.415
				BUR	0.722	0.517	0.402	0.350	0.750	0.526	0.414	0.362
	B	SBCCI	Screws	EPDM	0.778	0.536	0.436	0.387	0.814	0.563	0.462	0.409
				BUR	0.682	0.464	0.368	0.322	0.747	0.513	0.412	0.365
			Welds	EPDM	0.775	0.535	0.436	0.387	0.836	0.574	0.476	0.424
				BUR	0.679	0.467	0.369	0.324	0.782	0.540	0.437	0.387
		ASCE	Screws	EPDM	0.772	0.535	0.431	0.388	0.790	0.544	0.442	0.395
				BUR	0.677	0.466	0.368	0.325	0.702	0.481	0.382	0.336
			Welds	EPDM	0.774	0.536	0.429	0.386	0.789	0.542	0.441	0.390
				BUR	0.679	0.462	0.368	0.321	0.696	0.475	0.377	0.330
	C	SBCCI	Screws	EPDM	0.747	0.493	0.405	0.368	0.784	0.521	0.433	0.393
				BUR	0.643	0.414	0.335	0.296	0.712	0.465	0.382	0.343
			Welds	EPDM	0.746	0.496	0.407	0.366	0.805	0.540	0.449	0.404
				BUR	0.641	0.414	0.333	0.296	0.746	0.493	0.408	0.366
		ASCE	Screws	EPDM	0.748	0.490	0.409	0.366	0.756	0.501	0.417	0.373
				BUR	0.642	0.412	0.333	0.297	0.665	0.430	0.349	0.313
			Welds	EPDM	0.747	0.490	0.408	0.364	0.753	0.498	0.414	0.371
				BUR	0.643	0.411	0.334	0.294	0.659	0.425	0.348	0.308
	D	SBCCI	Screws	EPDM	0.746	0.479	0.399	0.361	0.780	0.509	0.428	0.389
				BUR	0.635	0.391	0.322	0.288	0.709	0.447	0.371	0.335
			Welds	EPDM	0.744	0.477	0.399	0.359	0.798	0.526	0.443	0.401
				BUR	0.636	0.391	0.320	0.288	0.742	0.475	0.399	0.359
		ASCE	Screws	EPDM	0.744	0.479	0.397	0.363	0.754	0.488	0.407	0.367
				BUR	0.634	0.392	0.323	0.289	0.658	0.409	0.336	0.302
			Welds	EPDM	0.740	0.478	0.397	0.360	0.748	0.486	0.405	0.369
				BUR	0.637	0.391	0.321	0.288	0.653	0.405	0.333	0.295

Table 6.50. Average Damage States for Building C – Twenty Foot High Strip Mall Building with Six Units and Metal Deck with Six Foot Joist Spacing (concluded)

Building Characteristics					No Reduction in Metal Deck Capacity				50% Reduction in Metal Deck Capacity			
					Terrain Surface Roughness (m)				Terrain Surface Roughness (m)			
Wall Type	Missile Environ	Design Code	Metal Deck Attach.	Roof Cover	0.03	0.35	0.70	1.0	0.03	0.35	0.70	1.0
Reinforced Masonry	A	SBCCI	Screws	EPDM	0.738	0.554	0.443	0.395	0.811	0.587	0.474	0.418
				BUR	0.638	0.493	0.382	0.333	0.746	0.544	0.431	0.379
			Welds	EPDM	0.737	0.557	0.448	0.393	0.847	0.607	0.492	0.437
				BUR	0.644	0.494	0.384	0.333	0.793	0.569	0.457	0.402
		ASCE	Screws	EPDM	0.740	0.553	0.445	0.395	0.776	0.565	0.456	0.404
				BUR	0.640	0.492	0.384	0.332	0.694	0.510	0.401	0.350
			Welds	EPDM	0.738	0.554	0.445	0.392	0.786	0.566	0.455	0.402
				BUR	0.642	0.489	0.385	0.333	0.697	0.509	0.401	0.348
	B	SBCCI	Screws	EPDM	0.707	0.511	0.413	0.372	0.771	0.546	0.449	0.399
				BUR	0.603	0.434	0.347	0.305	0.702	0.495	0.401	0.353
			Welds	EPDM	0.706	0.508	0.414	0.372	0.805	0.564	0.464	0.413
				BUR	0.602	0.437	0.347	0.304	0.752	0.526	0.425	0.379
		ASCE	Screws	EPDM	0.708	0.508	0.413	0.371	0.743	0.523	0.428	0.382
				BUR	0.604	0.436	0.346	0.305	0.646	0.458	0.366	0.323
			Welds	EPDM	0.708	0.509	0.417	0.370	0.748	0.522	0.433	0.380
				BUR	0.601	0.436	0.345	0.303	0.655	0.458	0.363	0.318
	C	SBCCI	Screws	EPDM	0.679	0.461	0.382	0.347	0.741	0.504	0.419	0.380
				BUR	0.564	0.374	0.308	0.273	0.671	0.445	0.369	0.330
			Welds	EPDM	0.678	0.461	0.381	0.343	0.773	0.526	0.439	0.398
				BUR	0.560	0.375	0.307	0.275	0.712	0.484	0.398	0.358
		ASCE	Screws	EPDM	0.674	0.460	0.382	0.346	0.713	0.480	0.402	0.362
				BUR	0.564	0.375	0.307	0.274	0.611	0.406	0.330	0.294
			Welds	EPDM	0.675	0.459	0.382	0.347	0.714	0.481	0.402	0.361
				BUR	0.563	0.374	0.306	0.274	0.613	0.404	0.332	0.294
	D	SBCCI	Screws	EPDM	0.679	0.447	0.379	0.344	0.741	0.490	0.414	0.375
				BUR	0.559	0.356	0.295	0.267	0.660	0.428	0.356	0.325
			Welds	EPDM	0.676	0.448	0.379	0.345	0.768	0.510	0.432	0.390
				BUR	0.560	0.357	0.296	0.269	0.708	0.463	0.388	0.348
		ASCE	Screws	EPDM	0.676	0.446	0.376	0.343	0.709	0.464	0.390	0.356
				BUR	0.562	0.358	0.296	0.268	0.606	0.382	0.317	0.289
			Welds	EPDM	0.678	0.446	0.376	0.343	0.709	0.467	0.392	0.358
				BUR	0.556	0.357	0.296	0.267	0.607	0.380	0.318	0.285

Table 6-51. Average Damage States for Building D – Twenty Foot High Strip Mall Building with One Unit and Metal Deck with Six Foot Joist Spacing

Building Characteristics					No Reduction in Metal Deck Capacity				50% Reduction in Metal Deck Capacity			
					Terrain Surface Roughness (m)				Terrain Surface Roughness (m)			
Wall Type	Missile Environ	Design Code	Metal Deck Attach.	Roof Cover	0.03	0.35	0.70	1.0	0.03	0.35	0.70	1.0
Unreinforced Masonry	A	SBCCI	Screws	EPDM	0.829	0.583	0.468	0.410	0.876	0.612	0.495	0.435
				BUR	0.744	0.521	0.411	0.354	0.813	0.569	0.450	0.395
			Welds	EPDM	0.832	0.583	0.467	0.409	0.896	0.628	0.508	0.453
				BUR	0.746	0.522	0.408	0.353	0.851	0.594	0.473	0.417
		ASCE	Screws	EPDM	0.831	0.581	0.469	0.412	0.845	0.592	0.474	0.418
				BUR	0.746	0.524	0.408	0.355	0.771	0.540	0.421	0.368
			Welds	EPDM	0.828	0.583	0.466	0.409	0.844	0.587	0.472	0.416
				BUR	0.743	0.521	0.410	0.352	0.765	0.533	0.419	0.364
	B	SBCCI	Screws	EPDM	0.792	0.542	0.436	0.392	0.832	0.572	0.466	0.415
				BUR	0.700	0.472	0.375	0.327	0.766	0.525	0.420	0.372
			Welds	EPDM	0.791	0.542	0.437	0.391	0.856	0.588	0.482	0.428
				BUR	0.701	0.472	0.374	0.329	0.807	0.545	0.442	0.391
		ASCE	Screws	EPDM	0.796	0.538	0.436	0.388	0.806	0.548	0.447	0.398
				BUR	0.697	0.472	0.375	0.328	0.722	0.490	0.390	0.342
			Welds	EPDM	0.788	0.542	0.438	0.387	0.807	0.546	0.445	0.397
				BUR	0.704	0.470	0.375	0.329	0.718	0.486	0.383	0.338
	C	SBCCI	Screws	EPDM	0.763	0.500	0.416	0.372	0.805	0.532	0.442	0.397
				BUR	0.666	0.422	0.341	0.305	0.729	0.476	0.391	0.350
			Welds	EPDM	0.764	0.501	0.411	0.370	0.817	0.554	0.455	0.414
				BUR	0.662	0.422	0.345	0.299	0.765	0.506	0.413	0.374
		ASCE	Screws	EPDM	0.763	0.499	0.413	0.374	0.775	0.511	0.423	0.378
				BUR	0.661	0.419	0.342	0.303	0.684	0.441	0.356	0.317
			Welds	EPDM	0.762	0.498	0.415	0.370	0.771	0.507	0.422	0.379
				BUR	0.661	0.420	0.340	0.303	0.681	0.434	0.355	0.318
	D	SBCCI	Screws	EPDM	0.763	0.488	0.405	0.370	0.798	0.515	0.433	0.391
				BUR	0.656	0.403	0.330	0.298	0.722	0.458	0.377	0.342
			Welds	EPDM	0.760	0.487	0.408	0.370	0.818	0.532	0.446	0.401
				BUR	0.655	0.400	0.329	0.298	0.755	0.482	0.403	0.363
		ASCE	Screws	EPDM	0.764	0.484	0.409	0.367	0.773	0.495	0.413	0.372
				BUR	0.660	0.398	0.330	0.295	0.674	0.416	0.343	0.307
			Welds	EPDM	0.762	0.486	0.407	0.369	0.766	0.491	0.411	0.372
				BUR	0.655	0.399	0.329	0.296	0.670	0.414	0.341	0.303

Table 6.51. Average Damage States for Building D – Twenty Foot High Strip Mall Building with One Unit and Metal Deck with Six Foot Joist Spacing (concluded)

Building Characteristics					No Reduction in Metal Deck Capacity				50% Reduction in Metal Deck Capacity			
					Terrain Surface Roughness (m)				Terrain Surface Roughness (m)			
Wall Type	Missile Environ	Design Code	Metal Deck Attach.	Roof Cover	0.03	0.35	0.70	1.0	0.03	0.35	0.70	1.0
Reinforced Masonry	A	SBCCI	Screws	EPDM	0.757	0.563	0.452	0.399	0.827	0.598	0.480	0.426
				BUR	0.660	0.499	0.389	0.340	0.760	0.550	0.438	0.384
			Welds	EPDM	0.752	0.560	0.452	0.394	0.865	0.615	0.499	0.442
				BUR	0.660	0.499	0.388	0.337	0.812	0.580	0.464	0.405
		ASCE	Screws	EPDM	0.752	0.562	0.448	0.397	0.788	0.572	0.460	0.404
				BUR	0.658	0.499	0.386	0.336	0.707	0.518	0.406	0.355
			Welds	EPDM	0.752	0.560	0.448	0.395	0.798	0.571	0.456	0.405
				BUR	0.657	0.502	0.388	0.337	0.714	0.516	0.403	0.349
	B	SBCCI	Screws	EPDM	0.722	0.519	0.419	0.374	0.789	0.550	0.454	0.407
				BUR	0.622	0.443	0.354	0.310	0.720	0.503	0.406	0.361
			Welds	EPDM	0.726	0.515	0.421	0.375	0.824	0.573	0.470	0.422
				BUR	0.622	0.443	0.352	0.307	0.768	0.532	0.432	0.382
		ASCE	Screws	EPDM	0.721	0.519	0.420	0.376	0.752	0.529	0.432	0.389
				BUR	0.620	0.443	0.349	0.310	0.669	0.465	0.372	0.327
			Welds	EPDM	0.722	0.517	0.414	0.371	0.764	0.530	0.433	0.387
				BUR	0.617	0.445	0.350	0.309	0.669	0.465	0.372	0.328
	C	SBCCI	Screws	EPDM	0.694	0.468	0.392	0.350	0.758	0.512	0.428	0.384
				BUR	0.584	0.381	0.314	0.282	0.685	0.455	0.374	0.339
			Welds	EPDM	0.694	0.467	0.391	0.350	0.794	0.536	0.447	0.402
				BUR	0.583	0.386	0.314	0.280	0.729	0.488	0.406	0.364
		ASCE	Screws	EPDM	0.694	0.467	0.388	0.353	0.730	0.489	0.405	0.366
				BUR	0.585	0.383	0.312	0.279	0.631	0.414	0.339	0.302
			Welds	EPDM	0.691	0.468	0.388	0.350	0.735	0.490	0.406	0.366
				BUR	0.579	0.384	0.313	0.279	0.632	0.416	0.340	0.302
	D	SBCCI	Screws	EPDM	0.696	0.457	0.385	0.349	0.754	0.497	0.415	0.378
				BUR	0.582	0.367	0.306	0.275	0.673	0.434	0.362	0.325
			Welds	EPDM	0.698	0.456	0.385	0.348	0.779	0.517	0.436	0.391
				BUR	0.585	0.367	0.306	0.273	0.716	0.469	0.394	0.355
		ASCE	Screws	EPDM	0.691	0.458	0.384	0.348	0.722	0.474	0.399	0.360
				BUR	0.576	0.365	0.304	0.274	0.621	0.393	0.328	0.294
			Welds	EPDM	0.691	0.455	0.382	0.349	0.727	0.474	0.398	0.359
				BUR	0.574	0.365	0.305	0.274	0.621	0.390	0.324	0.290

Table 6-52. Percent Increases in the Per Storm Average Building Damage State due to Changes in Building Parameters (Minimum/Average/Maximum) – Strip Mall Building with Wood Roof System

Building Parameter	Building Designation	
	Building A	Building B
8d to 6d Roof Deck Nails	0% / 4% / 15%	-1% / 3% / 9%
Strap to Toe-Nail Roof/Wall Connections	4% / 12% / 29%	4% / 12% / 24%
Built-up to Single ply Membrane Roof Cover	4% / 13% / 32%	7% / 15% / 28%
Reinforced to Unreinforced Masonry Walls	-2% / 1% / 3%	1% / 4% / 10%
Missile Environment D to C	2% / 16% / 38%	0% / 4% / 12%
Missile Environment C to B	10% / 22% / 37%	4% / 9% / 15%
Missile Environment B to A	9% / 18% / 24%	5% / 9% / 15%

Table 6-53. Percent Increases in the Per Storm Average Building Damage State due to Changes in Building Parameters (Minimum/Average/Maximum) – Strip Mall Building with Steel Roof System

Building Parameter	Building Designation			
	Building A	Building B	Building C	Building D
0% to 50% Reduction in Metal Roof Deck Resistance	-2% / 0% / 2%	-1% / 0% / 1%	1% / 9% / 31%	1% / 9% / 30%
Screwed to Welded Metal Roof Deck	-2% / 0% / 2%	-2% / 0% / 1%	-2% / 1% / 9%	-2% / 1% / 9%
ASCE to SBCCI Metal Roof Deck Design Criteria	-2% / 0% / 2%	-2% / 0% / 2%	-1% / 5% / 22%	-1% / 5% / 23%
Built-up to Single ply Membrane Roof Cover	6% / 18% / 34%	11% / 20% / 30%	6% / 17% / 29%	5% / 16% / 27%
Reinforced to Unreinforced Masonry Walls	-2% / 1% / 4%	3% / 8% / 14%	1% / 6% / 15%	1% / 6% / 15%
Missile Environment D to C	1% / 11% / 24%	-1% / 2% / 5%	-1% / 2% / 6%	-1% / 2% / 7%
Missile Environment C to B	11% / 27% / 40%	4% / 9% / 18%	3% / 8% / 17%	3% / 7% / 16%
Missile Environment B to A	9% / 19% / 26%	3% / 8% / 14%	4% / 8% / 14%	4% / 7% / 13%

Table 6-54. Percent Increases in the Per Storm Average Building Damage State Due to Changes in Building Configuration (Minimum/Average/Maximum)

Building Configuration	Increase in Average Annual Building Loss
Building A to B – Wood Roof System (12′ to 20′ Roof Height)	26% / 67% / 125%
Building A to B – Steel Roof System (12′ to 20′ Roof Height)	25% / 69% / 126%
Building B to C – Steel Roof System (4′ to 6′ Joist Spacing)	-1% / 5% / 31%
Building C to D – Steel Roof System (6 Units to 1 Unit)	-1% / 2% / 4%

increases the mean damage state by up to 31%. It is also shown in Table 6.54 that by going from the multi-unit buildings to the single unit buildings, the mean per storm damage state increases by no more than 4%.

6.11 Damage Model Results for Pre-Engineered Metal Buildings

Three metal buildings were modeled as shown in Figure 6.64. The building damage states associated with the metal buildings are defined in Table 6.55. Note that no frame failures

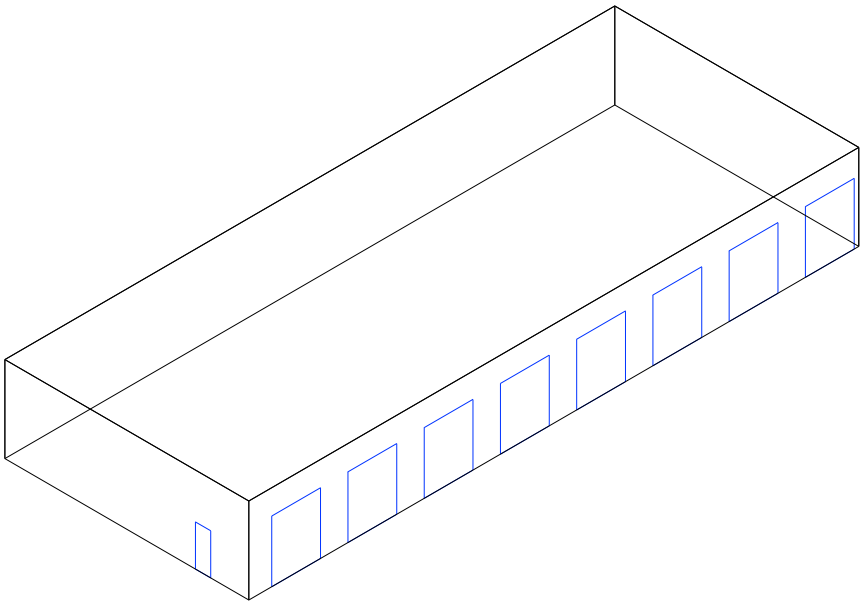

Small Metal Building, L = 100′, W = 40′, H = 14′

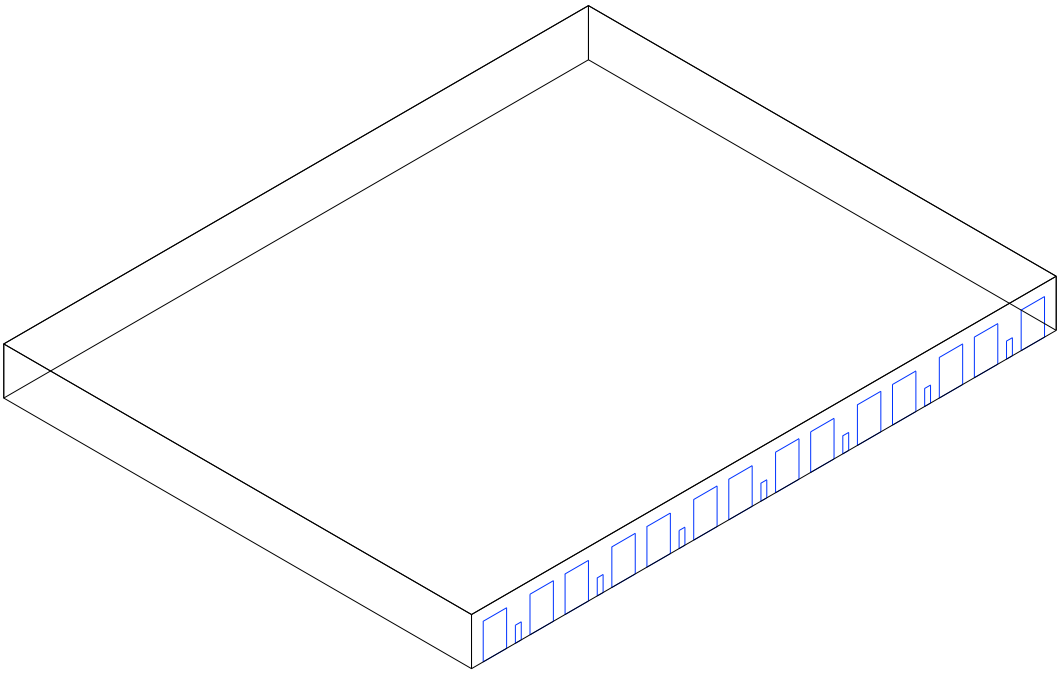

Medium Metal Building, L = 250′, W = 200′, H = 25′

Figure 6-64. Geometries of Metal Buildings Used in Study.

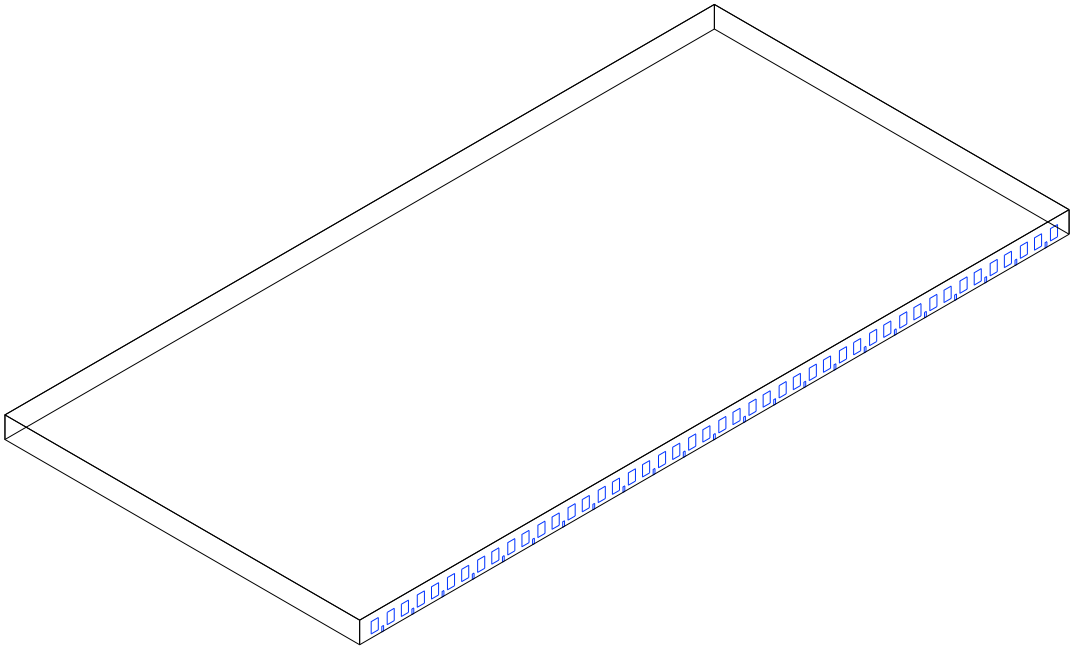

Large Metal Building, L = 1000′, W = 500′, H = 30′

Figure 6.64 . Geometries of Metal Buildings Used in Study (concluded).

Table 6-55. Damage States Metal Buildings

Damage State	Qualitative Damage Description	Entry/Over-head Door Failures	Metal Roof Deck Failures	Metal Wall Siding Failures	Missile Impacts on Walls
0	**No Damage or Very Minor Damage** Little or no visible damage from the outside. No broken windows, or failed roof deck. None or very limited water penetration.	No	No	No	No
1	**Minor Damage** Maximum of one broken window or, door or wall panel. Marks or dents on walls requiring painting or patching for repair.	One door	No	One panel	Typically<5 impacts
2	**Moderate Damage** Moderate fenestration failures. Minor roof panel failures, or wall panel failures. Some resulting damage to interior of building from water.	>One to≤33%	One totwo panels	>One to≤15%	Typically5 to 10 impacts
3	**Severe Damage** Major window damage or roof sheathing loss. Extensive damage to the interior from water. Some frame damage likely.	>33% to≤75%	>2 to≤10%	>15% to≤33%	Typically 10 to 20 impacts
4	**Destruction** Significant failures of fenestrations, significant roof and wall panel failures. Significant frame damage likely.	>75%	>10%	>33%	Typically>20 impacts

are modeled, with the entire performance of the building governed by the performance of the cladding and the fenestrations. The degrees of roof sheathing damage required to move the building from one damage state to another are similar to those used for the residential buildings. The fenestration damage requirements are less stringent than those used in the case of residential buildings, where here, 75% of the fenestrations must fail to enter damage state four, versus only 50% in the residential building case. The resistance parameters are given for all components in Table 6.56.

Table 6-56. Component Resistances for Pre-Engineered Metal Buildings

Component	Distribution	Distribution Parameters
Metal Roof Deck – 100mph Design Speed (Corner, Edge, Field)	Normal	Mean = 151,89,89 psf, COV = 0.11,0.11,0.11
Metal Roof Deck – 90 mph Design Speed (Corner, Edge, Field)	Normal	Mean = 104,89,89 psf, COV = 0.11,0.11,0.11
Metal Wall Cladding	Normal	Mean = 84 psf, COV = 0.09
Overhead Roll-Up Doors	Normal	Mean = 15 psf, COV = 0.2
Entry Door Pressure	Normal	Mean = 50 psf, COV = 0.2

Two analyses were performed for each building, one with the resistance of the metal cladding modeled as given in Table 6.56, and the second analysis with the resistance of the metal components reduced by 50%, to account for aging and fatigue.

Example building and component damage state plots are given in Appendix E. The results presented in Appendix E indicate that the performance of the model buildings is governed by the performance of the fenestrations. This is particularly evident in the case of the large metal building, which has more doors than either the small or medium-sized building. The failure sequence of the doors is such that more than one door often fails during the storm, and there is consequently little distinction between damage states 1, 2 and 3. In the examples presented herein, the weak overhead doors (modeled as having a mean failure capacity of 15 psf) represent the first mode of failure. The wall cladding failures are infrequent compared to field observations, suggesting the modeled wall capacity may be too high.

The average per storm damage states are summarized in Table 6.57. The impact of changing the various building parameters is summarized in Table 6.58. The results indicate that the size of the building has a significant impact on the average per storm damage state. On average, the per storm average damage states increased by 20% for the medium-sized building versus the small building and 57% for the large building versus the medium-sized building. Note that the size effect is coupled with the effect of the increased number of overhead doors associated with the larger buildings. Metal roof decks which have experienced age and fatigue (modeled with a 50% reduction in the uplift capacity) were found to have average per storm damage states 6% to 53% higher than new metal roof decks with all else being the same. Of the building parameters considered, the roof design code was found to have the smallest impact on building damage (see Table 6.58).

Table 6-57. Average Per Storm Damage States for Pre-Engineered Metal Buildings

Building Characteristics		No Reduction in Metal Panel Capacity				50% Reduction in Metal Panel Capacity			
		Terrain Surface Roughness (m)				Terrain Surface Roughness (m)			
Design Speed	Plan Size	0.03	0.35	0.70	1.0	0.03	0.35	0.70	1.0
90 mph	Small	0.765	0.382	0.287	0.245	0.843	0.450	0.350	0.305
	Med.	0.763	0.427	0.332	0.291	0.964	0.607	0.497	0.446
	Large	1.087	0.709	0.588	0.525	1.232	0.835	0.710	0.647
100 mph	Small	0.765	0.385	0.289	0.245	0.813	0.433	0.335	0.287
	Med.	0.761	0.424	0.332	0.289	0.890	0.534	0.433	0.386
	Large	1.086	0.704	0.588	0.526	1.225	0.827	0.698	0.638

Table 6-58. Percent Increases in the Per Storm Average Building Damage State Due to Changes in Building Parameters (Minimum/Average/Maximum) – Pre-Engineered Metal Buildings

Parameter	Change in Average Per Storm Damage
Small to Medium-sized Building	-1% / 20% / 46%
Medium-sized to Large Building	28% / 57% / 82%
100 mph to 90 mph Roof Design Code	-1% / 3% / 16%
0% to 50% Reduction in Metal Deck Capacity (i.e., Age and Fatigue)	6% / 23% / 53%

6.12 Damage Model Results for Engineered Residential and Commercial Buildings

The fully engineered buildings being considered have a structural system comprised of either concrete or steel. In the case of the concrete buildings it has been assumed that the roof slab is a poured concrete slab that can not be penetrated by water if the roof cover fails. Thus, in the case of concrete buildings, the damage state of the building is driven entirely by the performance of the windows. The damage state definitions proposed for the steel buildings are given in Table 6.59.

The steel buildings are modeled as having an open web steel joist roof system with a metal deck welded to the joists. The uplift capacities of the metal roof panels are estimated based on the ASCE design code for a 100 mph fastest mile design speed (see Section 6.7.3). The roof cover is modeled as either a good quality single ply membrane or a good quality built-up roof. The prime variables being altered for the engineered buildings are the fraction of the walls covered by glass (nominally 20%, 33% and 50%) and the number of stories (two, five and eight). The building models are shown in Figures 6.65 through 6.67. The environmental variables considered in the analysis are missile source environment and terrain exposure. The four missile environments used for the strip-mall study (see Table 6.45) are used again here for the engineered-building study. The four terrain environments considered are open (z_0 = 0.03 m), suburban (z_0 = 0.35 m), lightly treed suburban (z_0 = 0.7 m), and heavily treed suburban (z_0 = 1.0 m).

Table 6-59. Damage State Definitions for Engineered Steel Buildings

Damage State	Qualitative Damage Description	Roof Cover Failure	Window/ Door Failures	Roof Deck Failure	Missile Impacts on Walls	Joist Failures
0	**No Damage or Very Minor Damage** Little or no visible damage from the outside. No broken windows, or failed roof deck. Minimal loss of roof cover, with no or very limited water penetration.	≤2%	No	No	No	No
1	**Minor Damage** Maximum of one broken window or door. Moderate roof cover loss that can be covered to prevent additional water entering the building. Marks or dents on walls requiring painting or patching for repair.	>2% to≤15%	One window or door	No	Typically <5 impacts	No
2	**Moderate Damage** Major roof cover damage, moderate window breakage. Minor roof deck failure. Some resulting damage to interior of building from water.	>15% to≤50%	>One to ≤2%	One or two panels	Typically 5 to 10 impacts	No
3	**Severe Damage** Major window damage or roof sheathing loss. Major roof cover loss. Extensive damage to interior from water. Limited, local joist failures.	>50%	>2% to ≤25%	>Two to ≤25%	Typically 10 to 20 impacts	One Joist to ≤25%
4	**Destruction** Essentially complete roof failure and/or of more than 25% of roof sheathing. Significant amount of the wall envelope opened through windows failure. Extensive damage to interior	Typically >50%	>25%	>25%	Typically >20 impacts	>25%

The residential buildings have eight separate units per floor and the commercial buildings have a single unit per floor. The internal pressure associated with glass breakage is confined to the unit in which the window damage occurs. That is, it is assumed that no air leakage occurs between the adjacent units on the same floor and that no air leakage occurs between the adjacent units on different floors.

All glass is modeled as single pane (non-insulated) tempered glass. The window frame system is modeled with a mean failure pressure of 75 psf and a coefficient of variation of 20%. The metal deck failure pressures are modeled with normal distributions. The distribution parameters are listed in Table 6.60.

The results of the damage simulations show that the building performance is strongly driven by the performance of the roof cover. Recalling that the single ply membrane and the built-up roof cover models were developed using limited empirical data, it appears that the damage results given here overestimate the failure rates for these roof covers. To obtain a better understanding of the effect of the other parameters (window area, missile environment, number of units per floor, etc.) on the average per storm damage states, the effect of the roof cover damage was removed from the building damage state definitions and the damage analysis was re-run. Damage state results have been presented either including or excluding the roof cover effect on the overall damage state.

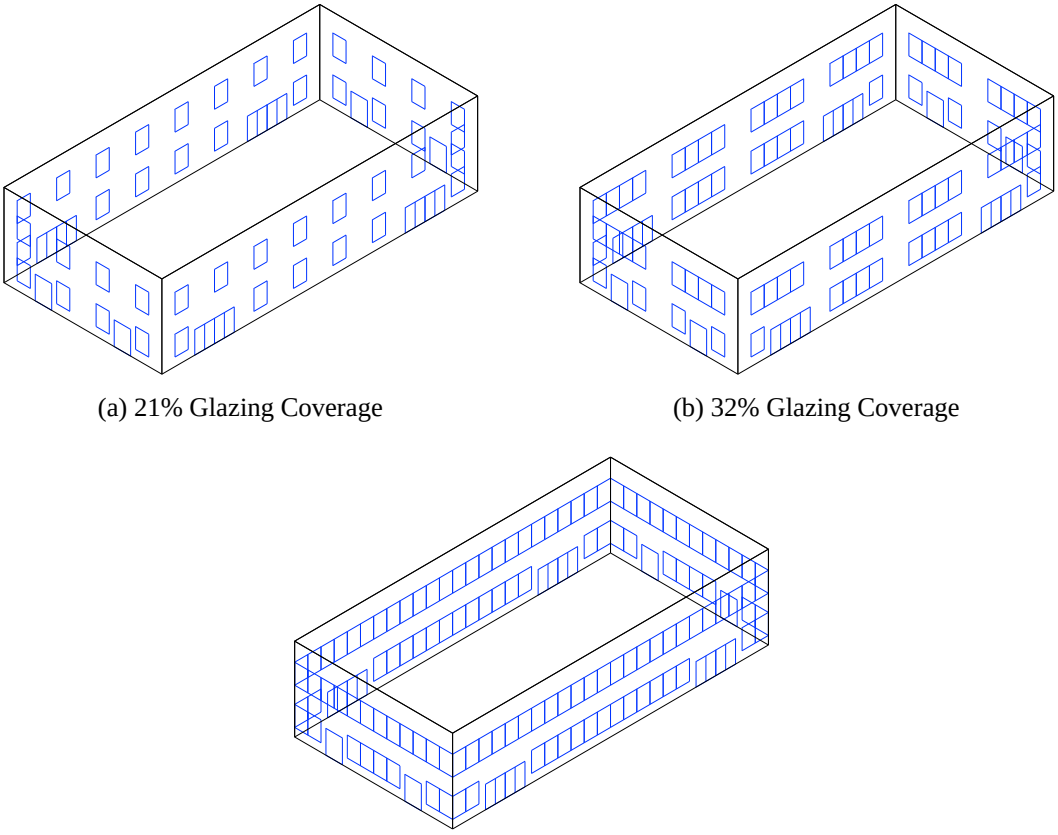

(a) 21% Glazing Coverage

(b) 32% Glazing Coverage

(c) 46% Glazing Coverage

Figure 6-65. Modeled Two-Story Fully-Engineered Buildings.

To make the damage state definitions with respect to roof damage (i.e., roof cover, roof deck and roof joists) consistent between the buildings with a different number of stories, the threshold damage levels defining the damage states are modified by a factor which is a function of the number of stories. The concept is that 5% roof deck damage, for example, will have a greater effect in terms of economic losses on a one-story building compared to a two-story building. That is, in the case of the two-story building, only the top floor will experience similar damage due to the water infiltration associated with 5% roof deck loss to that experienced by the single-story building. The assumption made here for the purpose of the roof damage state definitions is that the intensity of damage on the bottom floor of the two-story building will be half as much as that on the top floor. Thus, if the damage intensity to the interior of the single-story building is arbitrarily set to 1, then the damage intensity to the two-story building will be (1+0.5)/2 = 0.75 (i.e., 1 represents the damage intensity of the top floor and 0.5 represents the damage intensity of the bottom floor). Therefore, to achieve a similar damage intensity to that associated with 5% roof deck damage on a single-story building, an otherwise similar two-story building would require 6.7% roof deck damage (i.e., 5%/0.75). The thresholds used to define the roof damage states listed in Table 6.59 where modified in the same manner as described

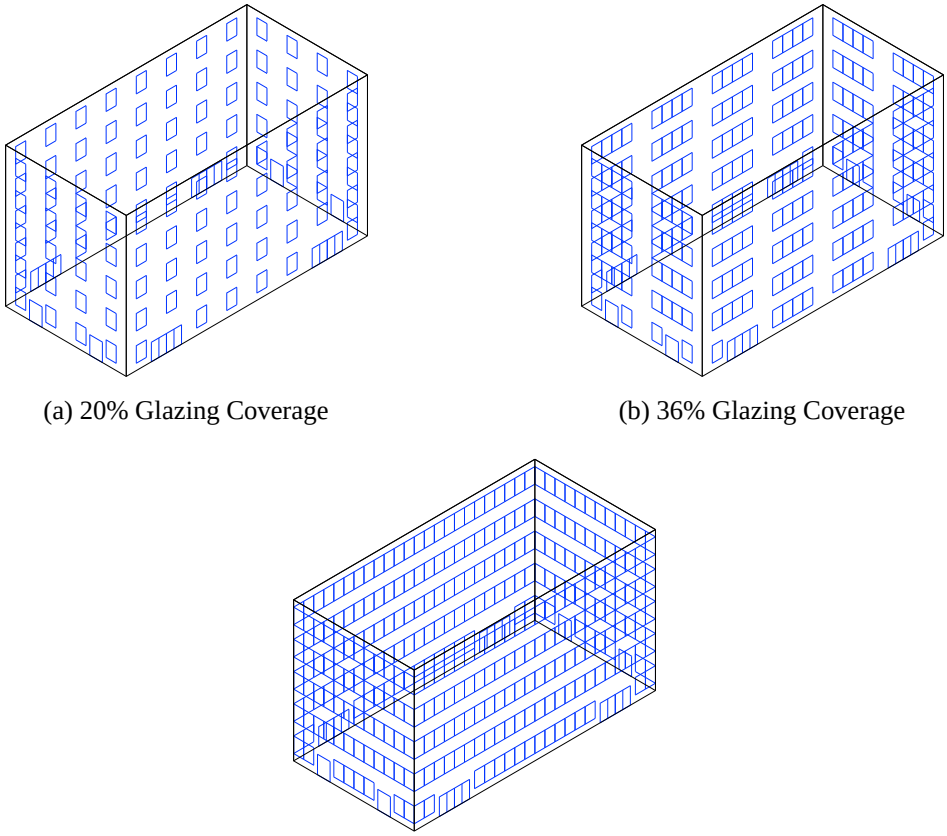

(a) 20% Glazing Coverage

(b) 36% Glazing Coverage

(c) 54% Glazing Coverage

Figure 6-66. Modeled Five-Story Fully-Engineered Buildings.

above for the two-, five- and eight-story buildings. The multiplicative factors are 1.33, 2.58 and 4.02, respectively. It can be seen, for example, that the five- and eight-story building cannot achieve a building damage state 3 (i.e., severe damage) based on roof cover loss since the 50% threshold increases to more than a 100% in both cases. Also note that the two-story building will be placed in damage state 3 when the roof cover loss exceeds 67%.

Example building and component damage state plots are given in Appendix F. Tables 6.61 through 6.63 list the average per storm damage states for the two-, five- and eight-story buildings, respectively. A summary of the effects of the various parameters on the average per storm damage states is given in Table 6.64. The average per storm damage states presented in Tables 6.61 through 6.62 were computed with the roof cover damage criteria included and excluded. As noted above, the roof cover was found to govern the overall building damage state in many of the cases and thus, to better examine the effects of the other variables, both sets of damage states have been given.

The average per storm damage states are found to increase by up to 33% when the roof cover is modeled with a EPDM single ply membrane versus a built-up roof cover. The effect of having a single unit per floor (commercial usage) compared to multi-units per floor (residential usage) is at most an 8% increase in the mean per storm damage state.

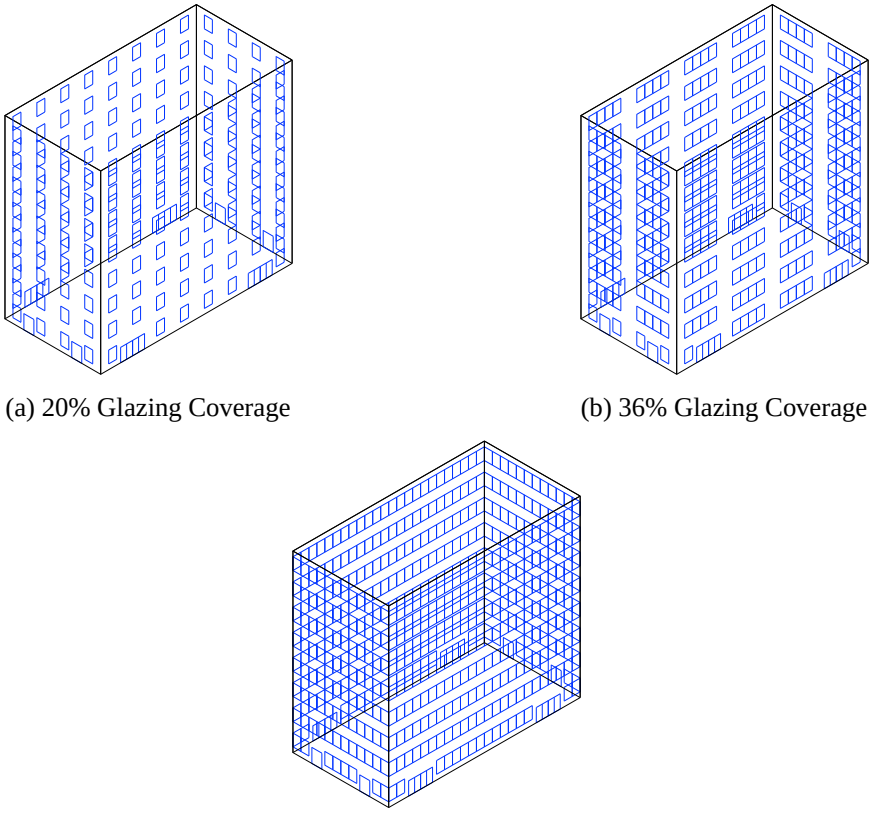

(a) 20% Glazing Coverage

(b) 36% Glazing Coverage

(c) 54% Glazing Coverage

Figure 6-67. Modeled Eight-Story Fully-Engineered Buildings.

Table 6-60. Failure Pressure Models for Metal Deck on Steel Joists

Number of Stories	Mean Failure Pressure (Standard Deviation), psf ACSE Design, 100 mph Wind Speed Zone, Welded Deck			
	Roof Zone 1	Roof Zone 2	Roof Zone 3	Roof Zone 4*
2	91 (17)	145 (27)	155 (29)	-
5	123 (23)	155 (29)	214 (41)	-
8	145 (27)	155 (29)	214 (41)	285 (45)

* Roof Zone 4 only applicable for buildings more than 60′ high

The average per storm damage states increased by as much as 13% when the glazing coverage changed from 20% to 33% and by as much as 18% when the glazing coverage changed from 33% to 50%. The impact of the missile environment on building damage states is more pronounced on the two-story buildings than it is on either the five- or eight-story buildings. This trend results from the fact that the modeled average heights of the buildings from which the commercial and residential type missiles originate are lower than the five- and eight-story engineered buildings. Thus, the glazing on the upper floors of the five- and eight-story buildings are less susceptible to missile damage than the glazing on the lower floors.

Table 6-61. Average Building Damage States – Two-Story Engineered Building

Building Characteristics				Residential Buildings (8 Units per Floor)				Commercial Buildings (1 Unit per Floor)			
Roof Cover Effect	Missile Environ.	Glazing Coverage	Roof Cover	Terrain Roughness (m)				Terrain Roughness (m)			
				0.03	0.35	0.70	1.0	0.03	0.35	0.70	1.00
Included	A	20%	BUR	0.607	0.542	0.393	0.322	0.610	0.541	0.392	0.322
			EPDM	0.629	0.548	0.403	0.335	0.629	0.547	0.401	0.334
		33%	BUR	0.684	0.593	0.433	0.356	0.684	0.593	0.434	0.356
			EPDM	0.699	0.598	0.439	0.365	0.695	0.598	0.439	0.364
		50%	BUR	0.769	0.663	0.484	0.397	0.768	0.664	0.485	0.396
			EPDM	0.776	0.667	0.488	0.403	0.774	0.669	0.489	0.405
	B	20%	BUR	0.470	0.415	0.303	0.252	0.476	0.413	0.304	0.250
			EPDM	0.512	0.433	0.322	0.272	0.516	0.435	0.325	0.272
		33%	BUR	0.525	0.458	0.333	0.277	0.529	0.455	0.333	0.275
			EPDM	0.557	0.472	0.351	0.291	0.560	0.468	0.351	0.293
		50%	BUR	0.595	0.510	0.370	0.305	0.597	0.512	0.373	0.308
			EPDM	0.620	0.520	0.387	0.323	0.624	0.521	0.387	0.323
	C	20%	BUR	0.364	0.312	0.231	0.194	0.373	0.312	0.232	0.192
			EPDM	0.422	0.339	0.260	0.223	0.430	0.339	0.260	0.222
		33%	BUR	0.400	0.346	0.254	0.213	0.409	0.349	0.255	0.211
			EPDM	0.448	0.371	0.281	0.237	0.457	0.368	0.279	0.239
		50%	BUR	0.450	0.386	0.284	0.233	0.456	0.388	0.282	0.235
			EPDM	0.487	0.403	0.304	0.256	0.492	0.405	0.303	0.258
	D	20%	BUR	0.279	0.181	0.152	0.137	0.284	0.182	0.153	0.138
			EPDM	0.356	0.238	0.202	0.182	0.360	0.238	0.201	0.184
		33%	BUR	0.279	0.182	0.153	0.138	0.286	0.185	0.153	0.139
			EPDM	0.359	0.237	0.202	0.183	0.362	0.242	0.203	0.185
		50%	BUR	0.291	0.187	0.158	0.143	0.305	0.196	0.161	0.147
			EPDM	0.363	0.243	0.204	0.184	0.376	0.249	0.208	0.189
Excluded	A	20%	N/A	0.580	0.530	0.378	0.305	0.584	0.529	0.377	0.304
		33%		0.665	0.583	0.419	0.340	0.666	0.583	0.420	0.341
		50%		0.755	0.654	0.473	0.384	0.754	0.655	0.474	0.383
	B	20%		0.409	0.390	0.272	0.217	0.419	0.387	0.275	0.217
		33%		0.479	0.437	0.308	0.248	0.484	0.434	0.307	0.247
		50%		0.562	0.493	0.350	0.282	0.565	0.495	0.352	0.285
	C	20%		0.270	0.272	0.184	0.144	0.285	0.273	0.188	0.144
		33%		0.326	0.315	0.217	0.171	0.339	0.317	0.217	0.171
		50%		0.397	0.361	0.254	0.200	0.403	0.364	0.254	0.203
	D	20%		0.092	0.041	0.030	0.025	0.098	0.042	0.031	0.025
		33%		0.096	0.041	0.030	0.025	0.104	0.043	0.032	0.026
		50%		0.145	0.075	0.060	0.050	0.160	0.085	0.067	0.059

6.13 Damage Model Results for Industrial Buildings

Large industrial buildings typically have flat roofs and are usually built with a masonry wall system. The roof structure is typically constructed using open web steel joists and a metal deck. The damage states for large industrial buildings are described in Table 6.65.

The representative industrial building is modeled here with masonry walls (either reinforced or unreinforced) and with a light weight open web steel joist (OWSJ) roof system. The model building has a length of 200′, a width of 120′ and a roof height of 20′.

Table 6-62. Average Building Damage States – Five-Story Engineered Building

Building Characteristics				Residential Buildings (8 Units per Floor)				Commercial Buildings (1 Unit per Floor)			
Roof Cover Effect	Missile Environ	Glazing Coverage	Roof Cover	Terrain Roughness (m)				Terrain Roughness (m)			
				0.03	0.35	0.70	1.0	0.03	0.35	0.70	1.00
Included	A	20%	BUR	0.628	0.562	0.428	0.367	0.643	0.566	0.433	0.372
			EPDM	0.667	0.591	0.467	0.410	0.681	0.597	0.471	0.411
		33%	BUR	0.711	0.618	0.469	0.399	0.724	0.624	0.472	0.399
			EPDM	0.741	0.644	0.501	0.437	0.754	0.645	0.506	0.442
		50%	BUR	0.795	0.677	0.512	0.436	0.805	0.681	0.518	0.440
			EPDM	0.817	0.695	0.542	0.470	0.826	0.697	0.546	0.474
	B	20%	BUR	0.542	0.477	0.372	0.324	0.557	0.482	0.376	0.331
			EPDM	0.598	0.516	0.420	0.375	0.612	0.523	0.426	0.379
		33%	BUR	0.604	0.524	0.407	0.351	0.623	0.528	0.409	0.355
			EPDM	0.649	0.560	0.448	0.400	0.668	0.565	0.453	0.403
		50%	BUR	0.682	0.576	0.446	0.384	0.700	0.580	0.452	0.392
			EPDM	0.719	0.608	0.484	0.426	0.734	0.612	0.490	0.432
	C	20%	BUR	0.481	0.416	0.334	0.297	0.502	0.425	0.341	0.302
			EPDM	0.546	0.467	0.388	0.351	0.566	0.474	0.398	0.361
		33%	BUR	0.534	0.459	0.364	0.318	0.554	0.466	0.369	0.324
			EPDM	0.594	0.505	0.415	0.370	0.610	0.509	0.417	0.376
		50%	BUR	0.599	0.506	0.399	0.349	0.616	0.508	0.404	0.355
			EPDM	0.648	0.543	0.442	0.398	0.670	0.549	0.448	0.403
	D	20%	BUR	0.400	0.302	0.268	0.250	0.417	0.304	0.273	0.254
			EPDM	0.489	0.376	0.337	0.317	0.503	0.379	0.342	0.320
		33%	BUR	0.407	0.305	0.269	0.254	0.425	0.311	0.275	0.256
			EPDM	0.496	0.378	0.338	0.318	0.511	0.384	0.345	0.321
		50%	BUR	0.447	0.342	0.303	0.285	0.479	0.368	0.324	0.303
			EPDM	0.528	0.411	0.369	0.345	0.563	0.437	0.391	0.364
Excluded	A	20%	N/A	0.572	0.522	0.373	0.301	0.589	0.527	0.378	0.307
		33%		0.669	0.586	0.423	0.343	0.682	0.591	0.425	0.345
		50%		0.763	0.650	0.475	0.388	0.774	0.654	0.480	0.393
	B	20%		0.448	0.412	0.292	0.235	0.466	0.418	0.295	0.239
		33%		0.529	0.472	0.338	0.272	0.551	0.476	0.340	0.277
		50%		0.627	0.533	0.390	0.320	0.645	0.537	0.396	0.326
	C	20%		0.355	0.332	0.234	0.185	0.378	0.339	0.239	0.192
		33%		0.433	0.392	0.280	0.223	0.456	0.398	0.283	0.230
		50%		0.523	0.450	0.330	0.272	0.543	0.454	0.335	0.278
	D	20%		0.151	0.083	0.066	0.057	0.164	0.086	0.068	0.059
		33%		0.160	0.088	0.069	0.059	0.179	0.094	0.073	0.063
		50%		0.273	0.188	0.164	0.150	0.303	0.216	0.185	0.170

The overall building geometry, along with the placement and relative size of the overhead rollup doors and entry doors is shown in Figure 6.68. The roof is divided into three sections each being 200′ long and 40′ wide. The joists span 40′ with their ends supported by a perimeter wall or a main structural beam and are spaced at 6′. Note that the entrydoors and overhead rollup doors are not glazed and thus no envelope breaches can be caused by missile impacts. The roof cover is modeled as an average quality EPDM single ply membrane.

The OWSJs are designed to resist the uplift forces and moments computed using ASCE-7-88, as described in Section 6.7.2, for a fastest-mile design wind speed of 100 mph. The building is assumed to be designed for open terrain (Exposure C) conditions. The metal

Table 6-63. Average Building Damage States – Eight-Story Engineered Building

Building Characteristics				Residential Buildings (8 Units per Floor)				Commercial Buildings (1 Unit per Floor)			
Roof Cover Effect	Missile Environ.	Glazing Coverage	Roof Cover	Terrain Roughness (m)				Terrain Roughness (m)			
				0.03	0.35	0.70	1.0	0.03	0.35	0.70	1.00
Included	A	20%	BUR	0.761	0.684	0.598	0.557	0.768	0.682	0.599	0.560
			EPDM	0.857	0.770	0.691	0.653	0.861	0.773	0.692	0.652
		33%	BUR	0.809	0.724	0.620	0.575	0.821	0.727	0.625	0.577
			EPDM	0.900	0.801	0.711	0.666	0.912	0.811	0.712	0.668
		50%	BUR	0.896	0.780	0.667	0.613	0.922	0.802	0.690	0.635
			EPDM	0.978	0.862	0.752	0.704	1.001	0.879	0.771	0.728
	B	20%	BUR	0.729	0.640	0.574	0.545	0.732	0.640	0.574	0.547
			EPDM	0.832	0.734	0.670	0.640	0.839	0.737	0.671	0.639
		33%	BUR	0.759	0.673	0.591	0.556	0.773	0.676	0.594	0.558
			EPDM	0.856	0.762	0.686	0.647	0.870	0.765	0.689	0.653
		50%	BUR	0.833	0.722	0.634	0.593	0.866	0.747	0.656	0.614
			EPDM	0.929	0.811	0.724	0.684	0.960	0.831	0.750	0.707
	C	20%	BUR	0.706	0.616	0.562	0.535	0.711	0.619	0.565	0.537
			EPDM	0.814	0.717	0.661	0.634	0.818	0.717	0.663	0.633
		33%	BUR	0.729	0.641	0.574	0.540	0.743	0.642	0.577	0.547
			EPDM	0.836	0.737	0.672	0.639	0.850	0.737	0.675	0.645
		50%	BUR	0.792	0.683	0.610	0.577	0.827	0.706	0.636	0.604
			EPDM	0.898	0.780	0.709	0.674	0.928	0.797	0.732	0.696
	D	20%	BUR	0.685	0.590	0.551	0.530	0.688	0.590	0.552	0.532
			EPDM	0.801	0.694	0.652	0.628	0.806	0.696	0.654	0.629
		33%	BUR	0.694	0.590	0.552	0.533	0.708	0.596	0.557	0.532
			EPDM	0.808	0.697	0.655	0.631	0.823	0.704	0.656	0.629
		50%	BUR	0.738	0.627	0.588	0.563	0.785	0.669	0.627	0.599
			EPDM	0.856	0.735	0.686	0.663	0.902	0.775	0.727	0.697
Excluded	A	20%	N/A	0.554	0.496	0.368	0.307	0.560	0.496	0.370	0.312
		33%		0.631	0.559	0.411	0.343	0.645	0.561	0.414	0.346
		50%		0.746	0.637	0.482	0.406	0.776	0.660	0.501	0.430
	B	20%		0.458	0.405	0.309	0.265	0.464	0.408	0.309	0.266
		33%		0.521	0.459	0.344	0.292	0.538	0.462	0.346	0.293
		50%		0.631	0.537	0.415	0.357	0.667	0.561	0.437	0.381
	C	20%		0.388	0.342	0.267	0.235	0.394	0.345	0.270	0.234
		33%		0.444	0.390	0.300	0.256	0.461	0.395	0.302	0.259
		50%		0.547	0.468	0.367	0.322	0.587	0.489	0.390	0.350
	D	20%		0.278	0.220	0.199	0.187	0.281	0.221	0.201	0.188
		33%		0.286	0.223	0.200	0.188	0.304	0.227	0.204	0.190
		50%		0.382	0.306	0.277	0.263	0.433	0.347	0.320	0.301

deck is modeled as being connected to the joists using welds. The weld design is assumed to meet the loading requirements as given in ASCE-7 and is designed using the methods outlined in Section 6.7.3.

The assumed component resistances are given in Table 6.66. The uplift values are for the as-installed roof, but a sensitivity study was performed where the uplift capacities of the welded connections were reduced by 50% to allow for the effect of age and fatigue. This 50% reduction is comparable to the reduction in the pullout capacity of fasteners in metal decks as reported by Baskaran and Dutt (1995).

Example building and component damage state plots are given in Appendix G. The average per storm damage states are given in Table 6.67. Reviewing the data in Table 6.67, it can be seen that per storm average building damage states vary by no more than 5% over the entire range of building parameters examined. As expected there are negligible differences between the per storm average building damage states due to the different missile environments since the structure does not have any glazing. The different missile environments were included, however, since they will have an impact on the losses associated with refinishing the masonry wall surfaces and replacing damaged overhead/entry doors due to damage by missile impacts. It is evident from the damage state plots shown in Appendix F that building damage state 1 is driven primarily by roof cover damage and that building damage states 3 and 4 are driven primarily by entry/overhead door damage. The entry/overhead door damage states are primarily governed by the overhead garage doors which are modeled as having a mean pressure resistance of 15 psf.

Table 6-64. Percent Increases in the Per Storm Average Building Damage State Due to Changes in Building Parameters (Minimum/Average/Maximum) – Engineered Residential and Commercial Buildings

Building Parameter	Roof Cover Effect Included	Roof Cover Effect Excluded
Two-Story Engineered Buildings		
Residential to Commercial Building Class	-1% / 1% / 5%	-1% / 2% / 16%
Built-up to Single Ply Membrane Roof Cover	1% / 12% / 33%	N/A
20% to 33% Glazing Coverage	0% / 7% / 13%	-2% / 11% / 21%
33% to 50% Glazing Coverage	0% / 9% / 13%	12% / 34% / 128%
Missile Environment D to C	19% / 49% / 107%	152% / 406% / 664%
Missile Environment C to B	20% / 28% / 33%	36% / 43% / 52%
Missile Environment B to A	22% / 27% / 31%	32% / 36% / 42%
Five-Story Engineered Buildings		
Residential to Commercial Building Class	0% / 2% / 8%	0% / 4% / 15%
Built-up to Single Ply Membrane Roof Cover	2% / 13% / 26%	N/A
20% to 33% Glazing Coverage	0% / 7% / 13%	3% / 14% / 23%
33% to 50% Glazing Coverage	6% / 10% / 18%	11% / 43% / 171%
Missile Environment D to C	11% / 25% / 51%	63% / 195% / 349%
Missile Environment C to B	5% / 10% / 15%	17% / 21% / 27%
Missile Environment B to A	9% / 14% / 18%	20% / 24% / 30%
Eight-Story Engineered Buildings		
Residential to Commercial Building Class	0% / 2% / 7%	-1% / 3% / 16%
Built-up to Single Ply Membrane Roof Cover	9% / 15% / 19%	N/A
20% to 33% Glazing Coverage	0% / 3% / 7%	0% / 10% / 17%
33% to 50% Glazing Coverage	5% / 8% / 13%	14% / 28% / 58%
Missile Environment D to C	0% / 3% / 9%	15% / 42% / 75%
Missile Environment C to B	1% / 3% / 6%	9% / 15% / 19%
Missile Environment B to A	2% / 5% / 8%	13% / 19% / 22%
All Engineered Buildings		
Two to Five Stories	2% / 36% / 105%	-2% / 41% / 198%
Five to Eight Stories	13% / 54% / 112%	-6% / 35% / 233%

Table 6-65. Damage States for Industrial Buildings

Damage State	Qualitative Damage Description	Roof Cover Failure	Door Failures	Roof Deck Failures	Missile Impacts on Walls	Joist Failures	Wall Failures
0	**No Damage or Very Minor Damage** Little or no visible damage from the outside. No failed doors or roof deck. Minimal loss of roof cover, with no or very limited water penetration.	≤2%	No	No	No	No	No
1	**Minor Damage** Maximum of one failed door. Moderate roof cover loss that can be covered to prevent additional water entering the building. Marks or dents on walls requiring painting or patching for repair.	>2% to≤15%	1 door	No	Typically <5 impacts	No	No
2	**Moderate Damage** Major roof cover damage, moderate window breakage. Minor roof sheathing failure. Some resulting damage to interior of building from water.	>15%to ≤50%	2 to ≤ the greater of 15% & 3	1 or 2 panels	Typically 5 to 10 impacts	No	No
3	**Severe Damage** Major window damage or roof sheathing loss. Major roof cover loss. Extensive damage to interior from water. Limited, local joist failures. Failure of one wall.	>50%	> the greater of 15% & 3 to ≤50%	3 to ≤25%	Typically 10 to 20 impacts	1 joistto ≤25%	1 wall
4	**Destruction** Complete roof failure on 1/3 or more of the units and/or failure of more than one wall. Loss of more than 25% of roof sheathing.	Typically >50%	>50%	>25%	Typically >20 impacts	>25%	2 or more

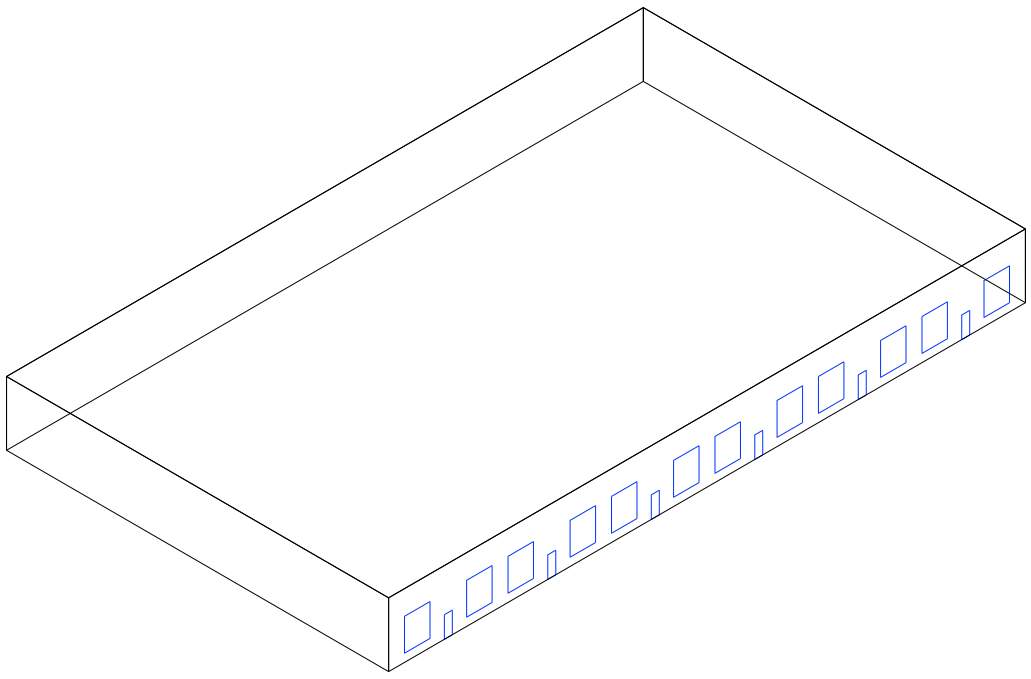

Figure 6-68. Model Building for Large Industrial Building – 200′×120′×20′ High.

Table 6-66. Component Resistance Values Used for Strip-Mall Type Building

Fenestrations		
Component	Distribution	Distribution Parameters
Entry Door Pressure	Normal	Mean = 50 psf, COV = 0.2
Overhead Rollup Garage Door Pressure	LogNormal	Mean = 15 psf, COV = 0.2
Steel Deck on Steel Roof Joists – Building Height = 20′, Joist Spacing = 6′		
Component	Distribution	Distribution Parameters (Field, Edge, Corner)
Welded Steel Deck – ASCE 100mph	Normal	Mean = 91, 123, 155 psf, COV = 0.19, 0.19, 0.19

Table 6-67. Per Storm Average Building Damage States – Industrial Building

Building Characteristics		100% Roof Deck Capacity				50% Roof Deck Capacity			
		Terrain Surface Roughness (m)				Terrain Surface Roughness (m)			
Wall Construction	Missile Environment	0.03	0.35	0.70	1.0	0.03	0.35	0.70	1.0
Unreinforced Masonry	A	1.152	0.688	0.560	0.498	1.157	0.695	0.564	0.504
	B	1.155	0.691	0.559	0.496	1.157	0.696	0.564	0.501
	C	1.149	0.689	0.558	0.499	1.159	0.694	0.566	0.506
	D	1.151	0.690	0.561	0.497	1.159	0.695	0.565	0.505
Reinforced Masonry	A	1.105	0.678	0.554	0.493	1.115	0.680	0.560	0.498
	B	1.108	0.674	0.549	0.493	1.112	0.683	0.558	0.502
	C	1.103	0.678	0.553	0.492	1.112	0.682	0.555	0.502
	D	1.107	0.674	0.553	0.492	1.113	0.684	0.561	0.499

6.14 Damage Model Results for Essential Facilities

Essential facilities consist of police stations, fire stations, schools, hospitals and emergency operation center (EOC). Of these, fire stations, schools and hospitals have been explicitly modeled. Fire stations and schools are often low-rise structures and have been modeled as such, while hospitals can be low-rise or high-rise in nature.

For the purpose of this analysis, essential facility damage is limited to entry doors and windows, overhead doors (fire station only), and metal roof systems. All essential facilities were modeled assuming that whole wall failure and roof framing member failure would not occur. Other damage characteristics specific to each model is described below.

While damage data for essential facilities is scarce, Figure 6-70 through Figure 6-73 show examples of wind-induced damage to several fire stations in the Houston area as a result of Hurricane Ike (2008).

Figure 6-69. Water Damage to Interior Ceiling of a Fire Station in the Houston Area as a Result of Roof Damage (2008, Hurricane Ike).

Figure 6-70. Water Damage to Interior Ceiling of a Fire Station in the Houston Area as a Result of Roof Damage (2008, Hurricane Ike) Continued.

Figure 6-71. Bent Bay Door Rollers for a Fire Station in the Houston Area (2008, Hurricane Ike).

Figure 6-72. Torn Awning over Rear Entry Door for a Fire Station in the Houston Area (2008, Hurricane Ike).

Figure 6-73. Panel Damage to Bay Doors for a Fire Station in the Houston Area (2008, Hurricane Ike).

6.14.1 Damage Model Results for Fire Stations

Fire stations are often one-story structures with flat roofs that house both vehicles and personnel. The portion housing vehicles tends to have a separate roof, but shares the same roof cover type as the rest of the building. Fire stations been modeled with two compartments that can communicate to each other in the event of a window breach via internal doors that allow internal pressure and water infiltration to occur between the two. Two large overhead doors that measure 12’ by 12’ have also been modeled. The damage state definitions are the same as those as strip malls as described in Table 6-42.

The modeled fire station measures 75’ wide and 85’ long, with a 14’ roof height for the portion housing vehicles and 10’ roof height for the portion over personnel as shown in Figure 6-74. The fire station was sized as a representative case from RS Means (~6,000 square feet). The windows measure 4’-6”x9’ long, and together with the entry doors and overhead doors give a total of 15 fenestrations along the building envelope. The welded metal roof deck, roof cover, terrain exposure, fenestration resistances and missile environment are as per the 12’ strip mall with joist spacing of 4’. The storm average damage states are given in Table 6-68. Average **Damage States for the Fire Station Building**

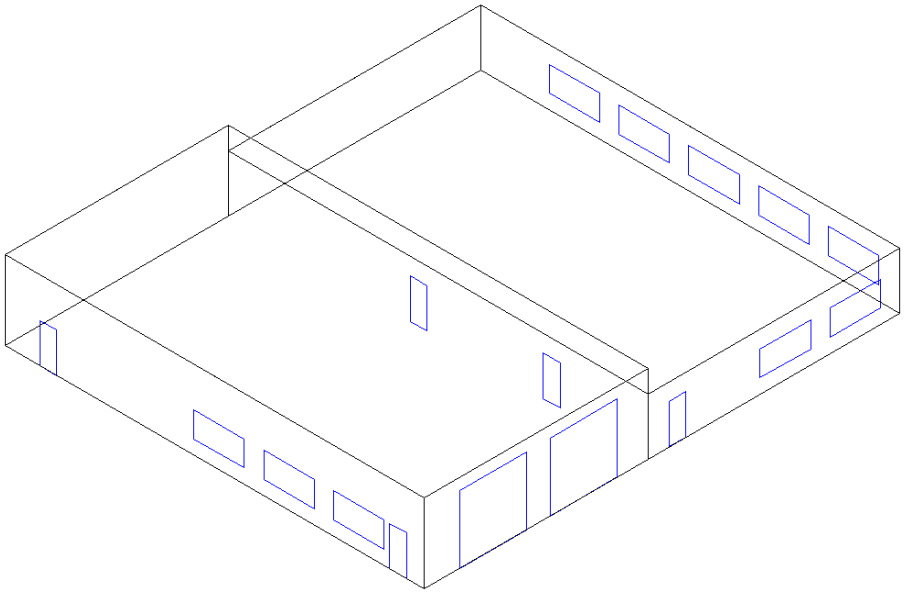

Figure 6-74. Fire Station Geometry Used in Study.

Table 6-68. Average Damage States for the Fire Station Building

Deck Mitigation	Metal Panel Capacity	Shutters	Missile Environment	Roof Cover	Terrain Surface Roughness (m)				
					0.03	0.15	0.35	0.7	1
Mitigated	100%	No	A	BUR	0.42869	0.55799	0.40415	0.28428	0.22585
				EPDM	0.43299	0.56102	0.40639	0.28565	0.22944
			B	BUR	0.38577	0.47137	0.3372	0.23635	0.18664
				EPDM	0.3925	0.47347	0.3377	0.23366	0.18814
			C	BUR	0.27711	0.28658	0.19669	0.1294	0.10087
				EPDM	0.28628	0.28824	0.20034	0.13484	0.10522
			D	BUR	0.22723	0.13327	0.08965	0.06106	0.05031
				EPDM	0.24016	0.14552	0.10052	0.07038	0.05838
		Yes	A	BUR	0.14379	0.11498	0.0798	0.05502	0.04484
				EPDM	0.16564	0.12861	0.09088	0.06533	0.05304
			B	BUR	0.1457	0.11669	0.08156	0.05679	0.04566
				EPDM	0.16653	0.13133	0.09126	0.06474	0.05451
			C	BUR	0.15244	0.13213	0.08991	0.06113	0.0499
				EPDM	0.17322	0.14456	0.10008	0.06959	0.05752
			D	BUR	0.13926	0.08964	0.06543	0.04797	0.04102
				EPDM	0.16077	0.10718	0.08055	0.05867	0.05079
Unmitigated	100%	No	A	BUR	0.49778	0.57617	0.41953	0.2992	0.24089
				EPDM	0.50138	0.57564	0.41979	0.2977	0.24367
			B	BUR	0.4616	0.4989	0.36182	0.25821	0.21245
				EPDM	0.46749	0.49933	0.36432	0.25773	0.21264
			C	BUR	0.37853	0.33419	0.24132	0.17264	0.14252
				EPDM	0.3815	0.33588	0.24385	0.17337	0.14435
			D	BUR	0.34276	0.22748	0.16667	0.12785	0.11137
				EPDM	0.3473	0.22993	0.16948	0.12938	0.11182
		Yes	A	BUR	0.32366	0.23251	0.17281	0.13011	0.11362
				EPDM	0.32842	0.23406	0.17665	0.13192	0.11323
			B	BUR	0.32558	0.23105	0.17432	0.13041	0.11194
				EPDM	0.32836	0.23746	0.1744	0.13361	0.11422
			C	BUR	0.32968	0.24238	0.18047	0.13346	0.11457
				EPDM	0.33188	0.2419	0.18178	0.13664	0.11681
			D	BUR	0.32064	0.21836	0.16256	0.12542	0.10925
				EPDM	0.32382	0.22137	0.16756	0.12711	0.10998
	50%	No	A	BUR	0.53576	0.58656	0.43066	0.30825	0.25189
				EPDM	0.53796	0.58919	0.43536	0.31094	0.25384
			B	BUR	0.50517	0.51398	0.37852	0.27338	0.22291
				EPDM	0.50772	0.51556	0.37931	0.27268	0.22361
			C	BUR	0.42656	0.3608	0.2686	0.19474	0.16423
				EPDM	0.4283	0.36454	0.26812	0.19631	0.16516
			D	BUR	0.39271	0.26599	0.20279	0.15556	0.13648
				EPDM	0.39468	0.2685	0.2042	0.1586	0.13714
		Yes	A	BUR	0.38017	0.27281	0.20794	0.15923	0.13717
				EPDM	0.38471	0.27574	0.20239	0.16015	0.13741
			B	BUR	0.38002	0.27407	0.20584	0.15926	0.13843
				EPDM	0.3842	0.27628	0.20826	0.16011	0.13925
			C	BUR	0.38212	0.28139	0.2124	0.16334	0.14068
				EPDM	0.38801	0.28486	0.21331	0.16249	0.14017
			D	BUR	0.37603	0.25864	0.19916	0.15379	0.13497
				EPDM	0.37802	0.26195	0.20061	0.15687	0.13582

The building parameter sensitivity results for fire stations are shown in Table 6-69. It is evident that the missile environment has a large impact on the overall building damage state, increasing the mean per storm damage by 89% on average when the missile environment changes from no windborne debris (Missile Environment D) to a mixed residential/commercial type environment (Missile Environment A).

The use of EPDM roof cover versus BUR roof cover increases the overall storm average damage states by 4% on average, while a resistance reduction of 50% in the metal deck increases the damage state by 15%.

Mitigation techniques such as shutters have a great effect in reducing damage in this analysis since window breakage and metal deck failure are the primary drivers of damage. Damage increases by 95% when the shutter to no shutter case is considered, and increases by 72% when the deck is no longer mitigated.

Table 6-69. Percent Increases in the Per Storm Average Building Damage State due to Changes in Building Parameters (Minimum/Average/Maximum) – Fire Station

Building Parameter	Min	Avg	Max
Built-up to Single ply Membrane Roof Cover	-3%	4%	24%
Missile Environment D to C	2%	30%	119%
Missile Environment C to B	-3%	36%	85%
Missile Environment B to A	-3%	7%	22%
Mitigated Deck to Unmitigated Deck	3%	72%	166%
0% to 50% Reduction in Metal Roof Deck Resistance	2%	15%	24%
Shutters Vs. No shutters	1%	95%	417%

6.14.2 Damage Model Results for Elementary Schools

Elementary schools are often low-rise structures with flat roofs being common. Gyms are typically taller than the rest of the building containing offices and class rooms, but shares the same roof cover. Wide hallways connect classrooms, offices, and open gathering spaces such as the gym. In this one-story building, the gym has its own compartment with no glazed openings, and can communicate with the rest of the building in the event of a window breach, allowing internal pressure and water infiltration to occur via internal doors. The damage state definitions are the same as those as strip malls as described in Table 6-42.

The elementary school measures 140’ wide by 330’ long, with a 12’ roof height for the portion over the class rooms and offices and 20’ for the portion over the gym as shown Figure 6-75. The elementary school was sized as a representative case from RS Means (~45,000 square feet). The windows measure 4’x6’ long, and together with the entry doors give a total of 148 fenestrations along the building envelope. The welded metal roof deck, roof cover, terrain exposure, and missile environment are as per the 12’ strip mall with joist spacing of 4’. The storm average damage states are given in Table 6-70.

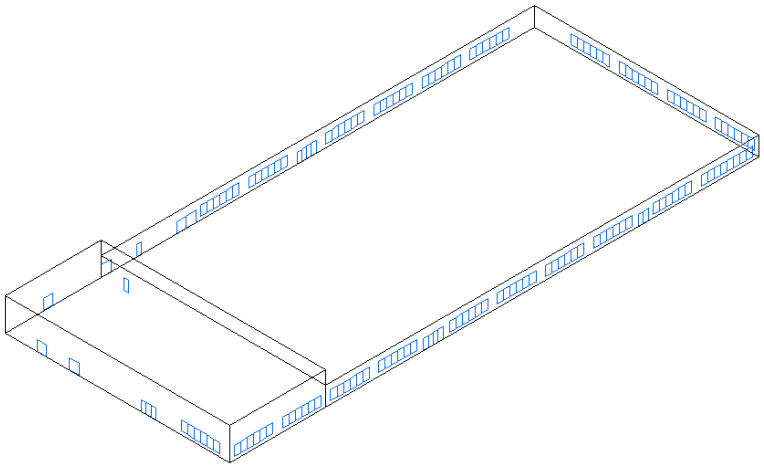

Figure 6-75. Elementary School Geometry Used in Study.

Table 6-70. Average Damage States for the Elementary School Building

Deck Mitigation	Metal Panel Capacity	Shutters	Missile Environment	Roof Cover	Terrain Surface Roughness (m)				
					0.03	0.15	0.35	0.7	1
Mitigated	100%	No	A	BUR	0.75096	0.82905	0.61976	0.44837	0.3645
				EPDM	0.74851	0.82863	0.6218	0.44924	0.36551
			B	BUR	0.61843	0.64647	0.47383	0.34033	0.27309
				EPDM	0.62214	0.64583	0.47635	0.33923	0.27363
			C	BUR	0.4865	0.47303	0.33976	0.23833	0.19146
				EPDM	0.48722	0.47378	0.34009	0.23921	0.19409
			D	BUR	0.37386	0.22972	0.16321	0.11623	0.09983
				EPDM	0.37781	0.23007	0.16365	0.11908	0.10138
		Yes	A	BUR	0.19481	0.18925	0.12737	0.08323	0.06494
				EPDM	0.20242	0.19273	0.13291	0.08817	0.0684
			B	BUR	0.20672	0.19893	0.13606	0.0897	0.06951
				EPDM	0.21397	0.20364	0.14025	0.09327	0.07296
			C	BUR	0.22599	0.21929	0.14961	0.10084	0.07694
				EPDM	0.23107	0.2243	0.15594	0.1038	0.08032
			D	BUR	0.1317	0.08157	0.05582	0.03999	0.03483
				EPDM	0.14645	0.08945	0.06417	0.04577	0.04011
Unmitigated	100%	No	A	BUR	0.78946	0.83582	0.62646	0.45707	0.37375
				EPDM	0.79177	0.839	0.62686	0.45671	0.37387
			B	BUR	0.66381	0.66583	0.493	0.35738	0.2923
				EPDM	0.66629	0.66492	0.49311	0.35844	0.29387
			C	BUR	0.54062	0.50653	0.3714	0.26799	0.21884
				EPDM	0.54301	0.50712	0.37136	0.26662	0.21769
			D	BUR	0.43734	0.28523	0.21311	0.16044	0.13837
				EPDM	0.44088	0.28455	0.2142	0.1606	0.13837
		Yes	A	BUR	0.35125	0.29503	0.22041	0.16432	0.13885
				EPDM	0.35445	0.29517	0.22256	0.16492	0.14071
			B	BUR	0.35965	0.30449	0.22641	0.16665	0.14239
				EPDM	0.36281	0.30763	0.22835	0.16952	0.14346
			C	BUR	0.3698	0.31865	0.23693	0.17395	0.14702
				EPDM	0.37486	0.32245	0.23736	0.17572	0.14813
			D	BUR	0.31751	0.22732	0.17645	0.13873	0.12255
				EPDM	0.31867	0.22686	0.17699	0.13832	0.12261
	50%	No	A	BUR	0.82432	0.84703	0.63872	0.4668	0.38213
				EPDM	0.82648	0.84803	0.6394	0.4673	0.38308
			B	BUR	0.70266	0.68438	0.51195	0.37274	0.30674
				EPDM	0.70432	0.68312	0.51411	0.37308	0.3068
			C	BUR	0.57873	0.53351	0.39392	0.28679	0.23964
				EPDM	0.58032	0.53463	0.39587	0.28637	0.23896
			D	BUR	0.48232	0.32321	0.24414	0.18851	0.1609
				EPDM	0.48417	0.32496	0.2476	0.1894	0.16307
		Yes	A	BUR	0.41067	0.33756	0.25539	0.19538	0.1676
				EPDM	0.41107	0.34166	0.26064	0.19614	0.16913
			B	BUR	0.4165	0.34846	0.26333	0.19887	0.16924
				EPDM	0.41701	0.35345	0.26374	0.19968	0.17071
			C	BUR	0.42788	0.36287	0.27179	0.20524	0.17532
				EPDM	0.42978	0.36441	0.27568	0.20754	0.17624
			D	BUR	0.37753	0.27566	0.21282	0.17335	0.15182
				EPDM	0.37573	0.27644	0.21664	0.17356	0.15182

Table 6-71. shows the building parameter sensitivity results for elementary schools. Missile environment has a large impact on the overall building damage state, in particular increasing the mean per storm damage by 103% on average when the missile environment changes from no windborne debris (Missile Environment D) to a residential type environment (Missile Environment A).

The use of EPDM roof cover versus BUR roof cover increases the overall storm average damage states by 1% on average, while a 50% reduction in metal deck resistance increases the damage state by 13%.

Mitigation techniques such as shutters have a great effect in reducing damage in this analysis since window breakage and metal deck failure are the primary drivers of damage. Damage increases by 128% on average when shutters are not part of the analysis, and increases by 57% on average when the deck is not mitigated.

Table 6-71. Percent Increases in the Per Storm Average Building Damage State due to Changes in Building Parameters (Minimum/Average/Maximum) – Elementary School

Building Parameter	Min	Avg	Max
Built-up to Single ply Membrane Roof Cover	-1%	1%	15%
Missile Environment D to C	13%	62%	169%
Missile Environment C to B	-11%	13%	43%
Missile Environment B to A	-7%	11%	34%
Mitigated Deck to Unmitigated Deck	1%	57%	252%
0% to 50% Reduction in Metal Roof Deck Resistance	1%	13%	25%
Shutters Vs. No shutters	6%	128%	461%

6.14.3 Damage Model Results for High Schools

Like elementary schools, high schools are often low-rise structures with flat roofs. Gyms can be taller than the remaining portion of the building depending on the height, and typically share the same roof cover as the remainder of the building. Wide hallways connect class rooms, offices, and open gathering spaces such as the gym, while stairs ways connect floors. For this two- or three-story building, the gym has its own compartment, and can communicate with the rest of the first floor in the event of a window breach, allowing internal pressure and water infiltration to occur via internal doors. The remaining floors have been modeled as separate compartments, and the damage state definitions are the same as those as strip malls as described in Table 6-42.

The high school measures 135’ wide and 330’ long, with 12’ stories and a gym height of 27’ feet for the two-story case as shown in Figure 6-76 and is 36’ for the three-story case as shown in Figure 6-77. The high school school was sized as a representative case from RS Means (~90,000 and ~135,000 square feet for the two- and three-story model respectively). The windows measure 4’x6’ long, and together with the entry doors give

a total of 165 fenestrations along the building envelope for the two-story case, and 243 for the three-story case. The welded metal roof deck, roof cover, fenestration resistances, terrain exposure, and missile environment are as per the two-story steel commercial building. The storm average damage states are given in Table 6-72 and Table 6-73.

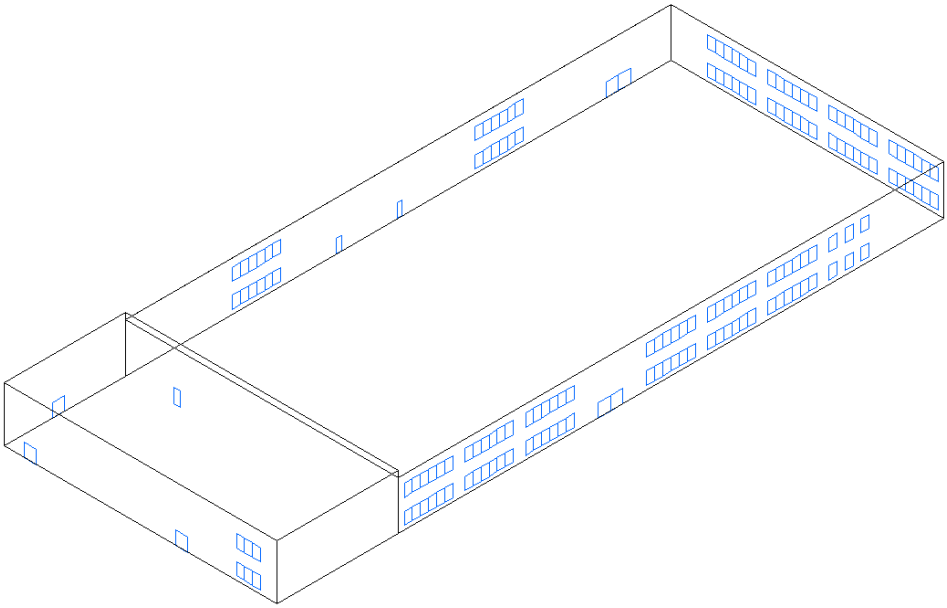

Figure 6-76. High School (Two-Story) Geometry Used in Study.

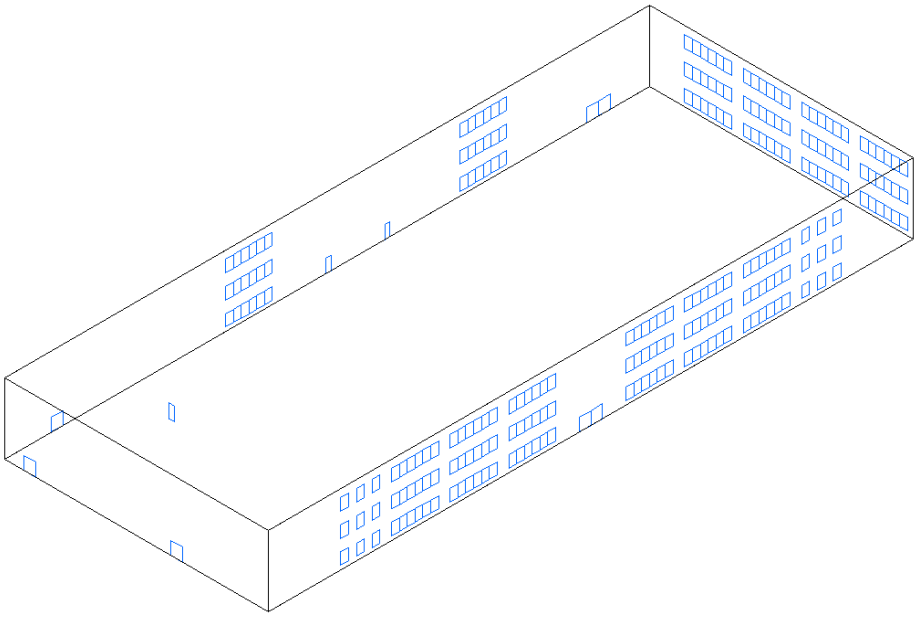

Figure 6-77. Large High School (Three-Story) Geometry Used in Study.

Table 6-72. Average Damage States – Two-Story High School

Deck Mitigation	Shutters	Missile Environment	Roof Cover	Terrain Surface Roughness (m)				
				0.03	0.15	0.35	0.7	1
Mitigated	No	A	BUR	0.67186	0.80224	0.60161	0.43648	0.35559
			EPDM	0.68212	0.80353	0.60386	0.44358	0.36508
		B	BUR	0.55919	0.64976	0.48395	0.35271	0.28849
			EPDM	0.57799	0.65923	0.49452	0.36195	0.30065
		C	BUR	0.42036	0.46728	0.34561	0.25212	0.20573
			EPDM	0.45158	0.48146	0.36107	0.26874	0.22523
		D	BUR	0.26964	0.19959	0.16215	0.13217	0.11867
			EPDM	0.33094	0.25426	0.2109	0.17403	0.15931
	Yes	A	BUR	0.26432	0.24527	0.18903	0.14773	0.12928
			EPDM	0.32436	0.28466	0.22751	0.18382	0.16305
		B	BUR	0.27116	0.24955	0.19315	0.14941	0.13141
			EPDM	0.32907	0.28774	0.23008	0.18582	0.16443
		C	BUR	0.28234	0.26885	0.2051	0.15722	0.13546
			EPDM	0.33769	0.30396	0.23983	0.19044	0.16661
		D	BUR	0.23648	0.186	0.15379	0.12719	0.11647
			EPDM	0.30407	0.24224	0.20403	0.17133	0.15653
Unmitigated	No	A	BUR	0.8967	0.90475	0.70044	0.53837	0.46166
			EPDM	0.89984	0.90634	0.70477	0.54238	0.46256
		B	BUR	0.80375	0.78192	0.6122	0.48061	0.41337
			EPDM	0.81195	0.78436	0.61694	0.48284	0.41593
		C	BUR	0.7016	0.65594	0.52102	0.41516	0.36382
			EPDM	0.7116	0.65893	0.52392	0.41966	0.36869
		D	BUR	0.61324	0.49053	0.42077	0.35565	0.32438
			EPDM	0.62073	0.49885	0.42227	0.35675	0.33087
	Yes	A	BUR	0.61114	0.51728	0.43178	0.36474	0.32645
			EPDM	0.61725	0.52611	0.43851	0.37053	0.33399
		B	BUR	0.61494	0.52514	0.43625	0.36517	0.33022
			EPDM	0.62452	0.53175	0.4431	0.3696	0.33431
		C	BUR	0.62457	0.53345	0.44441	0.36918	0.33178
			EPDM	0.63513	0.53992	0.44836	0.37363	0.33837
		D	BUR	0.58318	0.47643	0.4125	0.35126	0.32074
			EPDM	0.5923	0.48197	0.41347	0.35454	0.32747

Table 6-73. Average Damage States – Three-Story High School

Deck Mitigation	Shutters	Missile Environment	Roof Cover	Terrain Surface Roughness (m)				
				0.03	0.15	0.35	0.7	1
Mitigated	No	A	BUR	0.70836	0.79869	0.60794	0.45635	0.37703
			EPDM	0.73306	0.81141	0.62426	0.47528	0.40224
		B	BUR	0.62106	0.67441	0.51602	0.3873	0.32678
			EPDM	0.65841	0.69898	0.5408	0.41875	0.35982
		C	BUR	0.51119	0.53448	0.41079	0.31516	0.27021
			EPDM	0.56381	0.56501	0.44642	0.35446	0.31225
		D	BUR	0.3745	0.30315	0.25802	0.22173	0.20127
			EPDM	0.46151	0.38276	0.33025	0.28779	0.26391
	Yes	A	BUR	0.36412	0.33213	0.27377	0.22831	0.20746
			EPDM	0.44993	0.39624	0.33875	0.28894	0.26454
		B	BUR	0.36653	0.33341	0.27618	0.23071	0.207
			EPDM	0.45343	0.39899	0.33776	0.28801	0.26502
		C	BUR	0.37907	0.35306	0.28653	0.2352	0.21162
			EPDM	0.45766	0.4088	0.34467	0.29443	0.26849
		D	BUR	0.33937	0.28523	0.24718	0.21619	0.19818
			EPDM	0.43302	0.36683	0.32113	0.28219	0.26017
Unmitigated	No	A	BUR	1.05657	1.02453	0.83326	0.68062	0.60362
			EPDM	1.0682	1.0287	0.83976	0.68618	0.61131
		B	BUR	0.97653	0.93028	0.76959	0.63581	0.57192
			EPDM	0.98622	0.93776	0.77327	0.64251	0.57734
		C	BUR	0.90133	0.842	0.70154	0.59629	0.54307
			EPDM	0.91521	0.84686	0.71309	0.6037	0.54935
		D	BUR	0.82344	0.69825	0.62004	0.54644	0.50787
			EPDM	0.83247	0.70395	0.62653	0.5545	0.5107
	Yes	A	BUR	0.81908	0.71974	0.62872	0.5527	0.51202
			EPDM	0.82317	0.72628	0.63556	0.55644	0.51751
		B	BUR	0.81921	0.72496	0.63349	0.55183	0.51922
			EPDM	0.82813	0.7323	0.64115	0.56189	0.51791
		C	BUR	0.8234	0.73382	0.63811	0.56265	0.51065
			EPDM	0.83382	0.74615	0.64535	0.56306	0.51843
		D	BUR	0.79499	0.68135	0.60849	0.53883	0.50191
			EPDM	0.80365	0.68762	0.6154	0.54607	0.50515

The building parameter sensitivity results for high schools are shown in Table 6-74. Changing the missile environments between no windborne debris (Missile Environment D) to a mixed residential/commercial type environment (Missile Environment A) increases observed damage 56% on average for the two-story case, 30% for the three-story case, and increases the observed damage 43% overall. This trend results from the fact that the modeled average heights of the buildings from which the commercial and residential type missiles originate are lower than the three-story buildings. Thus, the

glazing on the upper floors of the three-story buildings are less susceptible to missile damage than the glazing on the lower floors.

The use of EPDM roof cover versus BUR roof cover increases the overall storm average damage states by 9%-10% on average for both the two- and three-story case.

Mitigation techniques such as shutters have a great effect in reducing damage in this analysis since window breakage and metal deck failure are the primary drivers of damage. Damage increases by 31% on average for the three-story case, 56% for the two-story case, and 44% overall when shutters are not in place.

The mitigated deck to unmitigated deck scenario increases damage by 88% and 91% for the two- and three- story case respectively and 89% overall. The three-story case is more influenced by roof damage compared to fenestration damage.

Over all, increasing story height from two to three increases average damage by 38% on average.

Table 6-74. Percent Increases in the Per Storm Average Building Damage State due to Changes in Building Parameters (Minimum/Average/Maximum) – High School

	Number of Stories								
	All			Two			Three		
Building Parameter	Min	Avg	Max	Min	Avg	Max	Min	Avg	Max
Built-up to Single ply Membrane Roof Cover	0%	9%	35%	0%	9%	35%	0%	10%	31%
Missile Environment D to C	2%	24%	134%	3%	31%	134%	2%	16%	76%
Missile Environment C to B	-7%	9%	40%	-7%	12%	40%	-6%	6%	26%
Missile Environment B to A	-3%	7%	24%	-3%	8%	24%	-1%	6%	18%
Mitigated Deck to Unmitigated Deck	13%	89%	176%	13%	88%	176%	27%	91%	153%
Shutters Vs. No shutters	1%	44%	227%	1%	56%	227%	1%	31%	140%
Two to Three Stories	0%	38%	70%	NA					

6.14.4 Damage Model Results for Hospitals

Hospitals are often designed as both low-rise and high-rise structures. Wide hallways connect open spaces such as waiting rooms and cafeterias, as well as offices and laboratories. Elevators in addition to stairwells connect floors. For the one-, four- and eight-story building, each floor has been given its own compartment. Damage state definitions are the same as those as strip malls as described in Table 6.42.

The hospital measures 180’ wide and 180’ long, with 12’ stories as shown in Figure 6-78-Figure 6-80. Based on a brief internet search, hospital dimensions were determined by the number of beds it contains. The small hospital model (~41 beds) was sized assuming that each bed corresponded to 800 square feet of facility space, while larger hospitals (~93 and ~185 beds) corresponded to 1400 square feet. The windows measure 4’x6’ long, and together with the entry doors give a total of 61, 234, and 462 fenestrations along the building envelope for the one, four and eight-story case respectively. The

welded metal roof deck, roof cover, fenestration resistances, terrain exposure, and missile environment for the one-, four-, and eight-story hospitals correspond to the two-, five- and eight-story steel commercial building respectively. Table 6-75 through Table 6-77 list the average per storm damage states for the small, medium, and large hospitals.

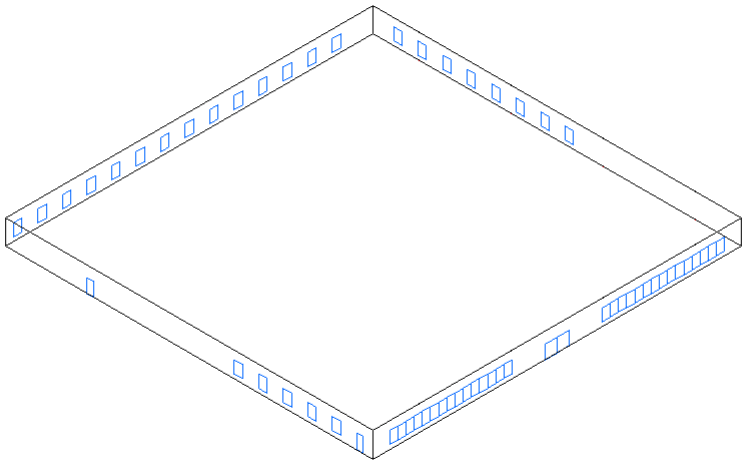

Figure 6-78. Small Hospital (<50 beds) Geometry Used in Study.

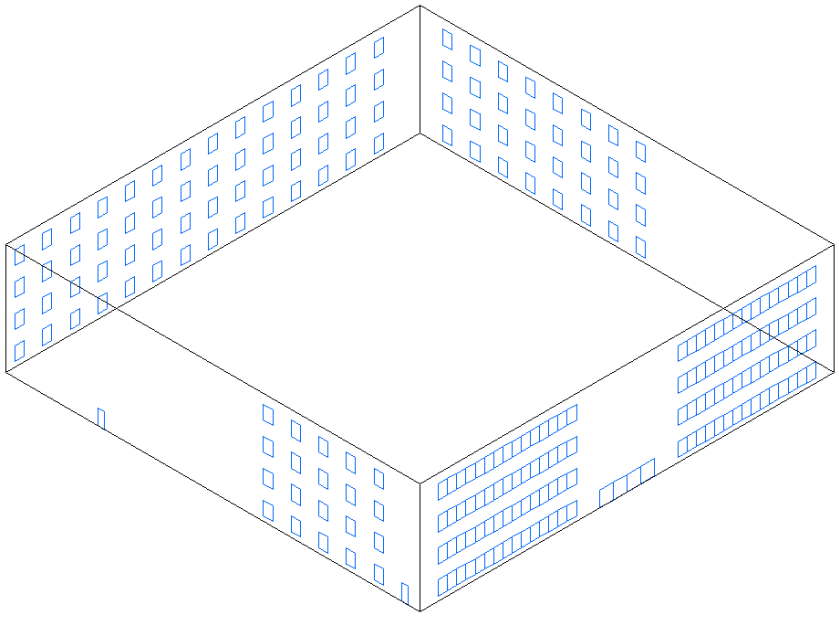

Figure 6-79. Medium Hospital (50-150 beds) Geometry Used in Study.

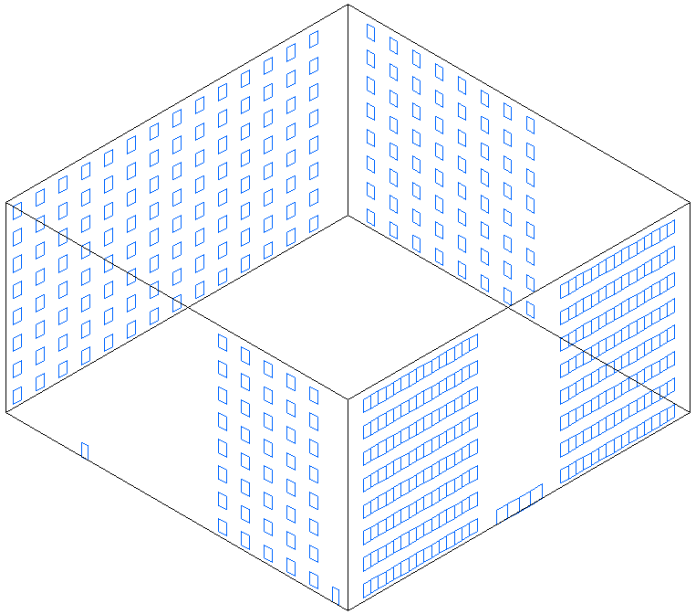

Figure 6-80. Large Hospital (>150 beds) Geometry Used in Study.

Table 6-75. Average Damage States – Small Hospital

Deck Mitigation	Shutters	Missile Environment	Roof Cover	Terrain Surface Roughness (m)				
				0.03	0.15	0.35	0.7	1
Mitigated	No	A	BUR	0.53515	0.7173	0.52765	0.37512	0.30187
			EPDM	0.54212	0.71762	0.52786	0.37617	0.30299
		B	BUR	0.39694	0.5275	0.38221	0.26931	0.21386
			EPDM	0.40924	0.53092	0.38436	0.27265	0.21717
		C	BUR	0.26149	0.35077	0.2463	0.16756	0.13243
			EPDM	0.27994	0.35647	0.25157	0.17299	0.13815
		D	BUR	0.12796	0.0801	0.05796	0.04267	0.0383
			EPDM	0.16496	0.10936	0.08147	0.0607	0.05454
	Yes	A	BUR	0.13542	0.13488	0.09276	0.0626	0.05005
			EPDM	0.16997	0.15192	0.10853	0.07741	0.06371
		B	BUR	0.14444	0.14881	0.10217	0.06884	0.05421
			EPDM	0.17827	0.16564	0.11714	0.08211	0.06712
		C	BUR	0.15327	0.16124	0.11246	0.07543	0.05882
			EPDM	0.18401	0.17673	0.1254	0.08814	0.07131
		D	BUR	0.11399	0.07705	0.05679	0.04215	0.0381
			EPDM	0.15523	0.10762	0.08008	0.06049	0.05428
Unmitigated	No	A	BUR	0.6617	0.73827	0.54451	0.39045	0.31594
			EPDM	0.66912	0.74078	0.54891	0.39224	0.3185
		B	BUR	0.54613	0.57654	0.42151	0.30029	0.24375
			EPDM	0.55203	0.58146	0.42459	0.30358	0.24859
		C	BUR	0.42903	0.42213	0.3069	0.21881	0.1785
			EPDM	0.43823	0.42913	0.31296	0.22255	0.18135
		D	BUR	0.29521	0.20264	0.15725	0.12441	0.10701
			EPDM	0.30401	0.21308	0.16447	0.12934	0.11174
	Yes	A	BUR	0.31209	0.25749	0.19054	0.14064	0.11977
			EPDM	0.31909	0.26479	0.19465	0.14558	0.12348
		B	BUR	0.32268	0.27041	0.19772	0.14422	0.12181
			EPDM	0.32886	0.27796	0.20196	0.14921	0.12678
		C	BUR	0.33025	0.27938	0.20406	0.14918	0.12429
			EPDM	0.34136	0.28715	0.20975	0.15409	0.13091
		D	BUR	0.28612	0.20046	0.15646	0.1241	0.10679
			EPDM	0.2952	0.21066	0.16366	0.12902	0.11154

Table 6-76. Average Damage States – Medium Hospital

Deck Mitigation	Shutters	Missile Environment	Roof Cover	Terrain Surface Roughness (m)				
				0.03	0.15	0.35	0.7	1
Mitigated	No	A	BUR	0.76204	0.80196	0.63255	0.49689	0.43369
			EPDM	0.82269	0.83636	0.67733	0.54761	0.48984
		B	BUR	0.69405	0.70588	0.56451	0.45126	0.40081
			EPDM	0.76361	0.75264	0.61756	0.51515	0.46124
		C	BUR	0.62957	0.62335	0.50553	0.41721	0.37374
			EPDM	0.70909	0.68067	0.56819	0.48134	0.4385
		D	BUR	0.53881	0.45676	0.40539	0.35945	0.3363
			EPDM	0.64216	0.55155	0.49286	0.44034	0.41307
	Yes	A	BUR	0.51743	0.46606	0.40879	0.36131	0.33492
			EPDM	0.6209	0.55531	0.49485	0.44177	0.4124
		B	BUR	0.52288	0.47382	0.41179	0.36212	0.33704
			EPDM	0.62812	0.55979	0.49766	0.44474	0.41197
		C	BUR	0.52683	0.48078	0.4186	0.36229	0.33756
			EPDM	0.62787	0.56821	0.50246	0.44291	0.41367
		D	BUR	0.50556	0.43454	0.39233	0.35075	0.331
			EPDM	0.61466	0.53282	0.48216	0.4318	0.40996
Unmitigated	No	A	BUR	1.09688	1.05042	0.88944	0.76403	0.70147
			EPDM	1.11041	1.06524	0.90475	0.77781	0.71733
		B	BUR	1.06321	1.0053	0.8615	0.7488	0.69249
			EPDM	1.08321	1.0222	0.87841	0.76714	0.711
		C	BUR	1.04137	0.96514	0.84232	0.73518	0.68932
			EPDM	1.06186	0.98392	0.85804	0.7544	0.70154
		D	BUR	0.97706	0.85388	0.77333	0.69744	0.65818
			EPDM	0.98787	0.86997	0.78788	0.71364	0.67317
	Yes	A	BUR	0.96006	0.86795	0.77961	0.70133	0.66277
			EPDM	0.9804	0.88002	0.79064	0.71364	0.67444
		B	BUR	0.96219	0.86946	0.78128	0.70298	0.65856
			EPDM	0.98697	0.88878	0.79792	0.71721	0.67386
		C	BUR	0.97228	0.88066	0.78467	0.70831	0.66276
			EPDM	0.98626	0.89219	0.80146	0.71922	0.67651
		D	BUR	0.95823	0.84369	0.76674	0.69339	0.65507
			EPDM	0.96787	0.85987	0.78093	0.70978	0.67004

Table 6-77. Average Damage States – Large Hospital

Deck Mitigation	Shutters	Missile Environment	Roof Cover	Terrain Surface Roughness (m)				
				0.03	0.15	0.35	0.7	1
Mitigated	No	A	BUR	1.47749	1.39787	1.31212	1.23114	1.18719
			EPDM	1.69973	1.61168	1.52916	1.45089	1.40664
		B	BUR	1.47115	1.39001	1.29864	1.23061	1.18727
			EPDM	1.69654	1.60876	1.52197	1.45175	1.40751
		C	BUR	1.46244	1.37401	1.29392	1.22661	1.18765
			EPDM	1.69195	1.60045	1.51904	1.44819	1.40749
		D	BUR	1.45898	1.36587	1.29344	1.22209	1.18682
			EPDM	1.69194	1.59499	1.51899	1.44446	1.40633
	Yes	A	BUR	1.42472	1.3405	1.27732	1.21155	1.17513
			EPDM	1.66053	1.56967	1.50355	1.43359	1.3944
		B	BUR	1.42443	1.33897	1.2733	1.21239	1.17397
			EPDM	1.65819	1.56833	1.50067	1.43241	1.39308
		C	BUR	1.42421	1.3394	1.27227	1.20951	1.17263
			EPDM	1.65701	1.56999	1.5002	1.4347	1.39144
		D	BUR	1.42303	1.33874	1.27796	1.20761	1.17443
			EPDM	1.65681	1.56787	1.5027	1.43	1.39376
Unmitigated	No	A	BUR	2.61524	2.52409	2.44647	2.36823	2.31407
			EPDM	2.62952	2.53423	2.45794	2.38246	2.32672
		B	BUR	2.61823	2.52233	2.44615	2.36741	2.32017
			EPDM	2.63052	2.53946	2.46025	2.37442	2.33058
		C	BUR	2.62113	2.52074	2.44507	2.36467	2.31584
			EPDM	2.62804	2.53359	2.45592	2.37901	2.32897
		D	BUR	2.61834	2.52722	2.44351	2.36518	2.31828
			EPDM	2.62967	2.53571	2.45723	2.37825	2.32858
	Yes	A	BUR	2.61338	2.51701	2.43979	2.36654	2.31556
			EPDM	2.62655	2.53452	2.4516	2.37543	2.32807
		B	BUR	2.61717	2.51934	2.44319	2.36414	2.31612
			EPDM	2.62176	2.53359	2.45546	2.37908	2.33063
		C	BUR	2.61185	2.51829	2.44441	2.36483	2.31765
			EPDM	2.62319	2.53414	2.45968	2.37883	2.32931
		D	BUR	2.61337	2.5252	2.44253	2.36456	2.31792
			EPDM	2.62496	2.53377	2.45605	2.37769	2.32824

Table 6-78 displays the building parameter sensitivity results for hospital buildings. Changing the missile environments between no windborne debris (Missile Environment D) to a mixed residential/commercial type environment (Missile Environment A) increases observed damage between 165%, 13%, and less than 1% on average for the

one-, four- and eight-story case respectively and 51% overall. This trend results from the fact that the modeled average heights of the buildings from which the commercial and residential type missiles originate are lower than the four- and eight-story buildings. Thus, the glazing on the upper floors of the four and Eight-story buildings are less susceptible to missile damage than the glazing on the lower floors.

The use of EPDM roof cover versus BUR roof cover increases the overall storm average damage states by 9%-10% on average for all cases.

Mitigation techniques such as shutters tend to have a large effect in reducing damage in this analysis since window breakage and metal deck failure are the primary drivers of damage. Damage increases by 1% on average for the eight-story case, 15% for the two-story case, 129% for the one-story case and 48% overall when shutters are not in place. The mitigated deck to unmitigated deck increases damage by 66% and 76% for all cases. The taller cases are more influenced by roof damage compared to fenestration damage.

Over all, damage is most sensitive to story height. Increasing story height from one to four increases average damage by 278%, and increases by 193% when increasing story height from four stories to eight stories.

Table 6-78. Percent Increases in the Per Storm Average Building Damage State due to Changes in Building Parameters (Minimum/Average/Maximum) – Hospital

	Number of Stories											
	All			One			Four			Eight		
Building Parameter	Min	Avg	Max	Min	Avg	Max	Min	Avg	Max	Min	Avg	Max
Built-up to Single ply Membrane Roof	0%	10%	44%	0%	10%	44%	1%	10%	24%	0%	9%	19%
Missile Environment D to C	0%	34%	338%	15%	94%	338%	1%	8%	36%	0%	0%	1%
Missile Environment C to B	-9%	7%	61%	-9%	20%	61%	-2%	2%	13%	0%	0%	1%
Missile Environment B to A	-9%	5%	41%	-9%	14%	41%	-2%	3%	14%	0%	0%	1%
Mitigated Deck to Unmitigated Deck	3%	73%	194%	3%	76%	194%	27%	66%	98%	55%	76%	98%
Shutters Vs. No shutters	0%	48%	503%	0%	129%	503%	0%	15%	72%	0%	1%	4%
One to Four stories	12%	278%	778%	NA								
Four to Eight stories	74%	193%	255%									

Chapter 7. Direct Economic Losses

7.1 Introduction

The loss model is a physically-based, damage-to-loss model that computes direct economic losses using a combination of explicit and implicit costing techniques. The loss model subdivides buildings into costing subassemblies. This approach provides significant costing flexibility and the capability to process a wide range of building types. The loss model is designed to process detailed building envelope damage states, and it provides the added capability of estimating building interior and content dollar losses by directly taking into account the volume of water penetrating through failed fenestrations (windows, doors, garage doors, etc.). The modeling approach is also well-suited for estimating loss of use and repair time.

The methodology, validation and results of the loss model are described in this section of the technical manual. The order of presentation parallels the discussion of the damage models in Chapter 6. Sections 7.2 through 7.7 deal with residential buildings, Section 7.8 covers manufactured homes, Sections 7.9 through 7.15 deal with commercial buildings and essential facilities

7.2 Residential Input Parameters

A schematic representation of the residential loss model is given in Figure 7.1. Cost data are obtained from RSMeans Residential Cost Data (2001). These data are based on national averages and require certain adjustments that take into account the specific geographical location of the loss, the level of work difficulty associated with repair and remodeling work, and contractor's overhead and profit. Cost adjustment indices are not applied to content or loss of use dollars. Default subassembly cost ratios are modified by the building characterization inputs and reflect actual building materials and construction types.

Loss model input parameters are grouped into two basic categories: building characterization parameters and building envelope damage parameters. Building characterization parameters include building material, building construction, fenestration, basic geometry, and building/content value information. Building envelope damage parameters include roof cover, roof deck, window damage, building missile hits, etc. Table 7.1 lists model input parameters as a function of input category.

The roof type input parameter is used to categorize the overall roof geometry and modifies the base square foot costs of installed roofing materials. The roof type parameter takes into account the decrease in labor output as the level of work difficulty increases. Roof type cost adjustment factors are listed in Table 7.2. The roof slope parameter modifies the base cost of installed roofing materials and also reflects the increase in work difficulty.

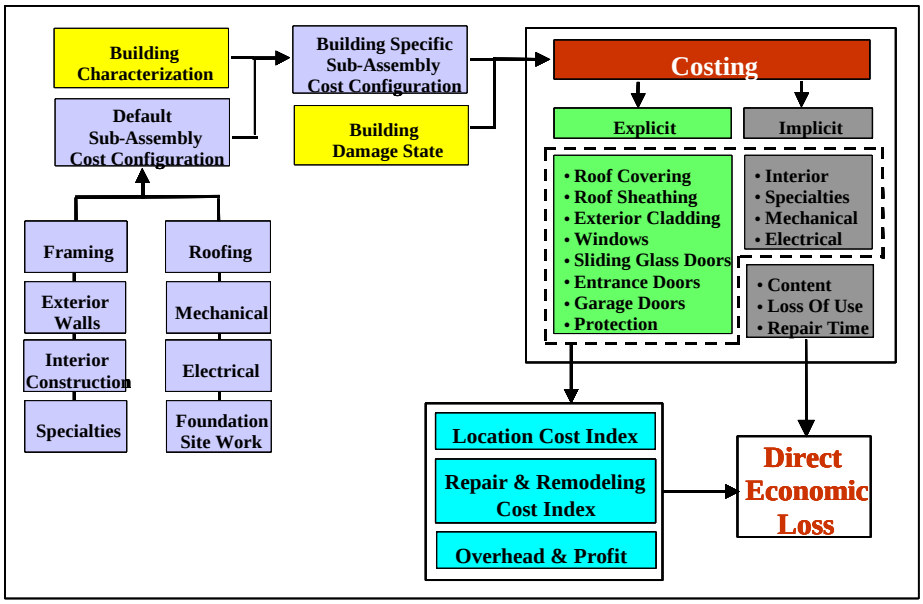

Figure 7.1. Schematic Representation of the Residential Damage-to-Loss Model.

Table 7.1. Model Parameters

Building Characterization	Damage State
ZIP Code	Percent Roof Covering Damaged
Value Group	Percent Roof Sheathing Damaged
Number of Floors	Missile Hits to Exterior Cladding
Plan Area	Volume of Water Penetrating Envelope
Wall Area	Door
Roof Type	Window
Roof Slope	Sliding Glass Door
Roof Area	Skylight
Roof Cover Material	Garage Door
Exterior Construction	Protection
Exterior Cladding	
Entrance Door	
Window	
Sliding Glass Door	
Skylight	
Garage Door	
Protection (e.g., Shutters)	

Table 7.2. Roof Installed Materials Cost Modification Factors

Roof Type	Difficulty Index
Shed	0.90
Gable	1.00
Gambrel	1.14
Hip	1.26
Mansard	1.49
Complex	1.49

7.3 Residential Subassembly Costs

Residential structures are grouped into four classes according to square foot value: economy, average, custom, and luxury. The square foot value grouping of residential structures is primarily used to reflect quality of construction, uniqueness of design, overall living area, and cost. The loss model can estimate the cost of residential structures falling into any of the above value groups. This is possible since the large majority of all residential structures, regardless of square foot value classification, consist of nine basic subassemblies: site work, foundation, framing, exterior walls, roofing, interiors, specialties, mechanical, and electrical. These nine basic subassemblies are used throughout the industry for both the costing of installed materials and the scheduling of labor and tasks.

The loss model is designed to take advantage of the construction subassembly concept by assigning a cost ratio to each of the subassemblies within the default building. The cost ratio of a subassembly is defined as the ratio of the cost to complete the subassembly to the total cost of the entire residential building.

7.3.1 Default Residence

The default economy house is a masonry single story building having a living area of approximately 1200 sq ft and an overall value of $68,940, or $57.45 per sq ft of living space. The economy residence is mass-produced from stock plans. The materials and workmanship are sufficient only to satisfy minimum building codes. Low construction cost is more important than distinctive features. The design is seldom other than square or rectangular.

Site work consists of preparation for a poured slab and excavation of a 4′ deep trench for a foundation wall. The foundation is typically a continuous concrete footing 8″ deep by 18″ wide. The foundation wall is built with 8″ thick concrete block and is 4′ deep. A 4″ trowel finished concrete slab is poured onto a 4″ crushed stone base.

Roof framing costs are based on a 4:12 pitch roof using 2×4 wood trusses spaced 24″ on center with 3/8″ plywood sheathing. Exterior walls are constructed of 8″ concrete block sealed and painted on the exterior with furring on the interior for drywall. The residence will typically have 2 flush solid core wood exterior doors and aluminum or wood awning windows.

Roof covering consists of 14 squares of asphalt shingles with 15 lb roofing paper, aluminum flashing, and attic insulation.

The interiors are constructed with ½″ drywall taped and finished and painted with primer and one finish coat. Softwood baseboard and trim are used and painted with primer and one finish coat. Floor finishes consists of rubber backed carpeting over 80% of floor area and tile over the remainder. There are typically 15 to 20 hollow core wood interior doors.

Specialties include 6 linear ft of kitchen wall and base cabinets with laminated plastic counter top.

Mechanical considerations consist of one wall hung lavatory, one water closet, one porcelain enamel steel bathtub, one stainless steel kitchen sink, a 30 gallon gas fired water heater, and gas fired forced hot air heat.

The electrical subassembly consists of a 100 ampere service with romex wiring, incandescent lighting fixtures, switches, and receptacles.

7.3.2 Subassembly Cost Ratios

Default residential subassembly cost ratios are given as a function of the number of stories in Table 7.3. For residential structures falling outside of the default building definition, cost ratios are easily modified to accommodate departures from the default material and construction configurations. A comparison between subassembly cost ratios for homes having tile versus asphalt shingle roof covering is provided in Table 7.4. For one story homes with tile roofing, the cost ratio increases significantly for the roofing subassembly and the ratios for other subassemblies decrease. The impact of this roofing material change is less for two and three story residences.

Table 7.3. Default Residential Subassembly Cost Ratios

Subassembly	1 Story	2 Story	3 Story
Site Work	1%	1%	1%
Foundation	13%	8%	5%
Framing	13%	11%	14%
Exterior Wall	22%	25%	26%
Roofing	3%	2%	1%
Interiors	32%	38%	39%
Specialties	4%	4%	4%
Mechanical	9%	8%	7%
Electrical	3%	3%	3%
Total	100%	100%	100%

Table 7.4. Subassembly Cost Ratios – Tiles versus Shingle

	1 Story		2 Story		3 Story	
Assembly	Shingle	Tile	Shingle	Tile	Shingle	Tile
Site Work	1%	1%	1%	1%	1%	1%
Foundation	13%	11%	8%	7%	5%	5%
Framing	13%	13%	11%	11%	14%	11%
Exterior Wall	22%	17%	25%	23%	26%	26%
Roofing	3%	13%	2%	7%	1%	5%
Interiors	32%	30%	38%	36%	39%	38%
Specialties	4%	4%	4%	4%	4%	4%
Mechanical	9%	8%	8%	8%	7%	7%
Electrical	3%	3%	3%	3%	3%	3%
Total	100%	100%	100%	100%	100%	100%

Table 7.5 shows a comparison between cost ratios for the default single story home and a modified single story home (brick veneer and tile roof). Using preprocessed cost data, the square foot cost of exterior wall and roofing subassemblies are adjusted to take into account the increase in cost of using brick and tile. Modified cost ratios are then easily computed as shown.

Table 7.5. Cost Ratio Comparison for Brick and Tile Modification

Subassembly	Default	Modified	Default	Modified
Site Work	$0.60	$0.60	1%	1%
Foundation	$7.19	$7.19	13%	10%
Framing	$7.83	$7.83	13%	11%
Exterior Wall	$12.10	$18.60	22%	28%
Roofing	$1.79	$7.17	3%	10%
Interiors	$18.42	$18.42	32%	27%
Specialties	$2.52	$2.52	4%	4%
Mechanical	$4.92	$4.92	9%	7%
Electrical	$1.65	$1.65	3%	2%
Sub	$57.02	$68.90	100%	100%
Profit & Overhead	$2.86	$3.46		
Total	$59.88	$72.36	100%	100%

If the modified building of Table 7.5 has a value of $65,000 and were to suffer damage to 50% of its interior subassembly, the base cost to repair the interior subassembly only (excluding city cost index, repair and remodeling adjustments, and overhead and profit) is approximately 0.5×0.27×$65,000 or $8,775.

Using the above approach, all residential structures can easily be sub-divided into their subassemblies and their respective cost ratios computed. For buildings falling outside the scope of the default building definition, modified cost ratios are easily computed as shown in Table 7.5. This approach provides the loss model with an extraordinary degree of flexibility for costing. Once the cost ratios are computed the building value is used to assign dollar values to the various subassemblies. Given a damage state to a particular subassembly, the cost to repair is easily computed as follows:

$$C = D \cdot C_R \cdot V \tag{7.1}$$

where C is the base cost to repair, D is a the fraction of the subassembly to be replaced or repaired, C_R is the cost ratio for the subassembly, and V is the building value. The base cost, C, is then adjusted to take into account city cost index, repair and remodeling adjustments, and overhead and profit.

7.4 Explicit Costing of Residential Losses

The explicit costing method directly calculates the repair and replacement costs for damaged building envelope components using a combination of RSMeans unit, linear foot, and square foot costs. Explicit costing is used within the model for several building envelope components, such as roof covering, roof sheathing, windows, entrance doors,

garage doors, fenestration protection, etc. Dollar losses associated with these components are directly calculated using actual building damage states and damage replacement thresholds. Damage replacement thresholds are the minimum damage levels at which building components are completely replaced. Replacement thresholds are an important model parameter and can significantly impact final losses, this is especially true of tile roof coverings. Replacement thresholds will typically vary between building component type and insurance companies; however, in the present loss model, damage replacement thresholds are currently set at a 0.5% damage state for both asphalt roof covering and tile roof covering. A 5% threshold for roof sheathing is used. In addition to replacement thresholds, the loss model also takes into account building component replacement based on serviceability considerations. For those building envelope components (windows, entrance doors, garage doors, and fenestration protection) that do not fail under applied load, they may still require replacement after undergoing thousands of load cycles as they become prone to permanent set. This is especially true when load cycles approach the ultimate capacity of the component. The loss model takes serviceability considerations into account by replacing those components that sustain loads exceeding 85% of their ultimate capacity.

The cost data used in the explicit costing portion of the loss model is derived from the RSMeans Residential Cost Data and is based on national averages for new construction materials and installation. Continuous deterministic functions are used to cost windows, doors, protection, garage doors, skylights, etc., as a function of type, material, and size. For example, for double hung wood windows, the following functions are used to estimate the replacement cost:

Standard glass: Replacement Cost = 10.00 · (AREA – 12.00)+225.00
Insulating glass: Replacement Cost = 14.40 · (AREA – 12.00)+270.00

where *AREA* is the overall area of the window unit. All building envelope fenestration (windows, entrance doors, garage doors, and protection) have conceptually similar functions. Roof covering costs are calculated as

$$RC = R_A \cdot (C_C + C_O) \tag{7.2}$$

where *RC* is the base roof cost, R_A is the roof area to replace, C_C is the covering cost, and C_O are other roofing costs. Roof sheathing costs are determined similarly.

The loss model cost data are obtained from new construction RSMeans Residential Cost Data. These data are based on national averages and require certain adjustments which take into account the specific geographical location of the loss, the level of work difficulty, and contractor's overhead and profit. Consequently, the model uses a city cost index to modify losses as a function of ZIP Code. A partial listing of city cost indices is provided in Table 7.6. Furthermore, loss model cost data are based on new construction costs and it is essential to adjust the computed base costs to take into account the repair and remodeling nature of the work. Costs are typically increased due to the decrease in labor output typically associated with repair and remodeling work. Additional costs also

Table 7.6. Location Index Factor – Florida

ZIP Code	City	Index
320, 322	Jacksonville	0.85
321	Daytona Beach	0.89
323	Tallahassee	0.78
324	Panama City	0.72
325	Pensacola	0.87
326	Gainesville	0.86
327, 328, 347	Orlando	0.88
329	Melbourne	0.89
330, 331, 332, 340	Miami	0.85
333	Fort Lauderdale	0.85
334, 349	West Palm Beach	0.86
335, 336, 346	Tampa	0.82
337	St. Petersburg	0.83
338	Lakeland	0.82
339	Fort Myers	0.82
342	Sarasota	0.81

arise when protecting existing work. To account for these increases in cost, base costs are adjusted using a repair and remodeling cost adjustment factor of 1.25. This factor is determined using expert judgment, field observation, and literature review (RSMeans).

7.5 Modeling of Residential Interior and Content Losses and Loss of Use

Unlike the case of the building exterior, where the cost associated with the predicted or modeled damage can be explicitly estimated, the interior damage and, hence, resulting loss, is estimated using an implicit model. In this model, the economic loss is estimated using simple functions developed primarily on the basis of experience and judgment. The economic damage to the interior of the building is a function of the damage to the roof cover, roof sheathing, roof structure and the windows and doors. The basic premise used in the development of these simple models is that once the envelope is breached, most of the damage to the interior of the building is a function of the amount of water that enters the building.

7.5.1 Economic Damage to the Building Interior

The economic damage to the interior of the building is taken as the maximum of the economic damage estimated to be a result of roof cover damage, roof sheathing damage and window damage. The interior economic damage associated with loss of roof cover, L_{RC}, is given as:

$$L_{RC} = f_1(R_{RC})(1 - f_2(A_{RC}))f_3(R_{RC})V_I \quad (7.3)$$

where, R_{RC}, is the fraction of failed roof cover, A_{RC}, is the area of failed roof cover (square feet) and V_I is the value of the interior of the building. The functions, f_1, f_2, and f_3 are described below.

The function f_1 is expressed as:

$$f_1(R_{RC}) = 1.11R_{RC}, \quad \text{for } R_R \leq 0.9$$
$$f_1(R_{RC}) = 1.0, \quad \text{for } R_R > 0.9 \tag{7.4}$$

where R_C is the fraction of failed or missing roof cover. The function f_1 represents the fractional amount of the interior area affected by the loss of a fraction of the roof cover.

The function f_2 is expressed as:

$$f_2(A_{RC}) = 1 - 0.005A_{RC}, \quad \text{for } A_{RC} \leq 200 \text{ ft}^2$$
$$f_2(A_{RC}) = 0, \quad \text{for } A_{RC} > 200 \text{ ft}^2 \tag{7.5}$$

where A_{RC} is the area of failed roof cover. The function f_2 represents a term that accounts for the fact that when the amount of roof cover damage is relatively small, in many cases water is not able to enter the building because the underlayment remains intact, or no gaps in the roof sheathing are exposed.

The third function, f_3 is expressed as:

$$f_3(R_{RC}) = 0.1, \quad \text{for } R_{RC} \leq 0.05$$
$$f_3(R_{RC}) = 2.0R_{RC}, \quad \text{for } 0.05 < R_{RC} \leq 0.5 \tag{7.6}$$
$$f_3(R_{RC}) = 1.0, \quad \text{for } R_{RC} < 0.5$$

The function f_3 represents a term that accounts for the fact that the resulting interior economic damage becomes more severe as the area of interior damage becomes larger. Examples of severe damage include ceiling sheet rock collapsing and damaging, flooring, cabinets, etc., or water migrating behind walls and damaging the electrical systems, etc. The three functions noted above are shown in graphical form in Figure 7.2.

The implicit economic damage caused by failure of the roof sheathing is modeled in the form:

$$L_S = (3.6R_S + 0.1)V_I + R_S V_{RF}, \quad \text{for } 0 < R_s < 0.25 \tag{7.7}$$

where L_S is the economic damage associated with loss of roof sheathing, R_S is the fraction of missing roof sheathing and V_{RF} is the value of the roof framing (V_{RF} typically represents only 4%-5% of the total value of a house). This equation, derived primarily from experience, in addition to the damage and loss data for individual buildings given in Bhinderwala (1995), yields an interior loss of approximately 10-15% (depending on the size of the house and the size of the sheathing) following failure of the first piece of sheathing. The interior of the house is assumed to require replacement when 25% of the roof sheathing has failed. These two points (the first sheathing failure and the 25% loss of sheathing) were used to bound the linear model for the prediction of interior loss given sheathing failure.

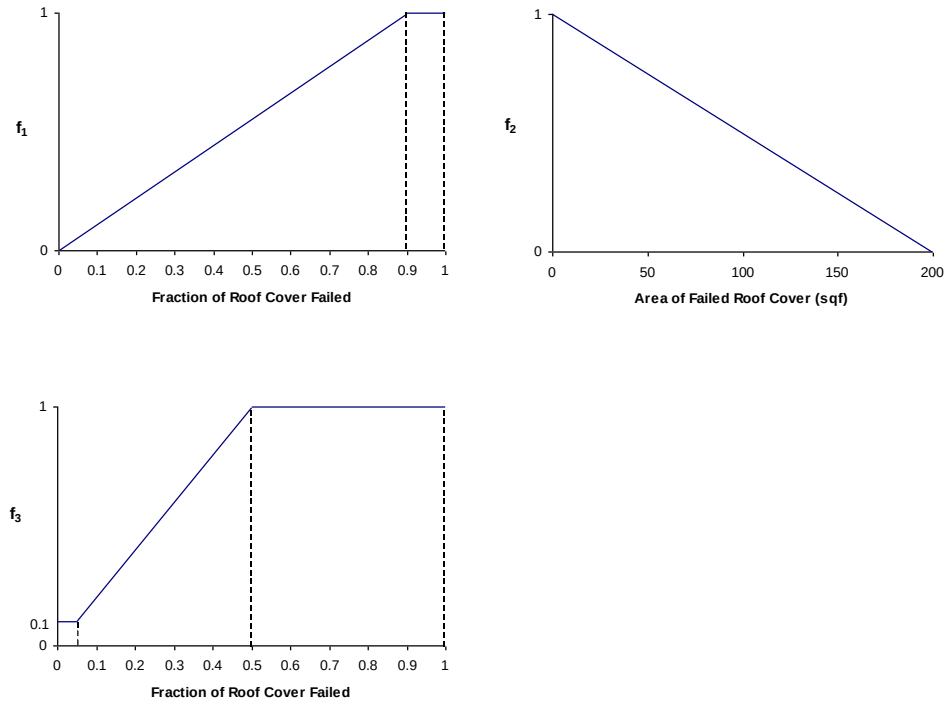

Figure 7.2. Implicit Loss Functions Associated with Damage to the Roof Cover.

The economic damage produced by the failure of windows and doors is modeled as

$$L_F = (4D_W)V_I \quad \text{, for } 0'' \leq D_W \leq 0.25'' \tag{7.8}$$

where D_W is the depth of water, in inches, averaged over the floor area of the building. The simple loss model associated with water entering through failed fenestration was developed with the assumption that the losses increase linearly with an increasing amount of water entering the building, and that 1/4″ of water (distributed uniformly over the floor area of the house) is sufficient to produce a 100% loss to the interior of the building.

The estimates of losses produced to the interior of the building are adjusted to take into account the additional costs associated with repair and replacement, and to include an allowance for overhead and profit. The total economic loss of the building, including both the exterior losses and the interior losses is constrained not to exceed the assumed value of the building.

7.5.2 Economic Damage to Contents

Content losses are modeled using the assumption that the damage to contents is highly correlated with damage to the interior of the building, but begins to occur after at least some damage has been done to the interior of the building. The model assumes that losses are associated with water entering the building. Figures 7.3 and 7.4 show examples of content damage produced by roof and window failures. Note that in the roof failure example (Figure 7.3), the damage to the contents is ultimately caused by failure of the interior (i.e., ceiling) of the building.

Figure 7.3. Content and Interior Losses Associated with Roof Sheathing Failure.

Figure 7.4. Content Losses Due to Fenestration Breach.

Content losses associated with roof cover loss are accrued at one half the rate associated with losses to the interior of the building, except that in the case of roof cover loss, no contents are damaged until a threshold of 20% roof cover loss has occurred. This jump at 20% is based on the premise that there must be water collected above the ceiling to cause the ceiling to fail, and initiate content damage. The content loss associated with fenestration failure is accrued at the same rate as the economic loss associated with the interior of the building. The content loss associated with sheathing loss is given as:

$$L_C = 4R_S, \qquad R_S<0.25$$
$$L_C = 1.0, \qquad R_S>0.25 \qquad (7.9)$$

The economic loss associated with damage to the contents of the building is taken to be the maximum among the losses produced by roof cover damage, roof sheathing damage or fenestration damage.

7.5.3 Loss of Use for Residential Buildings

Loss of use estimates for residential buildings are based on the approach used in the Hazus Earthquake Model for estimating recovery (reconstruction) time as a function of the building damage state (FEMA, 1999). Five damage states (none, slight, moderate, extensive, and complete) are employed in the earthquake model, with damage states defined as 0%, 2%, 10%, 50%, and 100%, respectively. In the hurricane model, the loss ratio is used as the indicator of reconstruction time, providing a continuous curve varying between 0% and 100%.

The recovery time for the 5 key damage states in the Earthquake Model are 0, 5, 120, 360, and 720 days, respectively, and these points define the recovery time for the Hurricane Model, with loss used instead of damage. Linear interpolation is used to obtain the actual recovery time for buildings with loss ratios other than the 5 key values.

The economic losses associated with building recovery time consider the amount of time persons in a damaged home will require temporary lodging. A loss of use multiplier is applied to the obtained recovery time to take into account the fact that homeowners can remain in their homes when buildings have slight to moderate damage. The loss of use multipliers for none, slight, moderate, extensive, and complete damage states are 0, 0, 0.5, 1, and 1, respectively (FEMA, 1999).

7.6 Residential Loss Model Validation Examples

The residential damage-to-loss model has been validated using a set of residential claim folders which document wind-induced economic losses following Hurricanes Erin, Opal, Bertha, and Fran. The houses analyzed are screened from over 140 individual claim folders. Individual claim folders were considered only if there exist a minimal degree of uncertainty with respect to the characterization of the building and the associated loss, that is, insured value, roof type, roof area, plan area, etc., building damage state, and dollar loss. Files containing information which suggests flooding may have occurred are rejected as are those files having insufficient data to explicitly rule out the possibility of flooding. The initial selection criteria were constrained to include only those claim folders having a damage state limited to roof covering and roof sheathing.

Model losses were obtained by running the model with observed damage states and building-specific information such as insured value, roof type, roof area, plan area, etc. These data are gathered by carrying out a careful study of the claim folder documentation. The documentation typically includes loss estimatics, claim folder damage pictures, a written description of the damage state, and sketches showing a plan

view of the building and the damage locations on the roof. A rigorous investigation of the claim pictures provides an estimate of the building envelop damage and characterization of the building in general. The insurance policy provides the building insured value while the estimatics are used to obtain the actual dollar loss information.

Table 7.7 summarizes the compiled data and associated losses reported as a ratio of building value. The average prediction error ratio (defined as the actual loss divided by the predicted loss) is 0.83. This suggests reasonable agreement between the predicted and actual losses. Figure 7.5 compares predicted losses and actual loss data. In some cases the actual loss dollars are adjusted to eliminate the contribution of loss dollars from components which are not explicitly modeled. For example, costs associated with outside deck repairs are omitted since the residential damage and loss models do not model these components. Hence, if the total loss for a given building was $10,000 but $3500 of the loss originated from deck and sprinkler system damage, the overall dollar loss would be adjusted by subtracting from the total loss those loss dollars associated with non-modeled components (i.e., deck and sprinkler).

Table 7.7. Predicted and Actual Losses

Case Number	Building Characteristics				Building Losses			Content Losses	
	Value ($)	Roof Area	Roof Cover*	Damage (%)	Actual	Model	Ratio	Actual	Model
1	281,000	3,125	AS	2.5	0.037	0.023	1.59	0.00	0.00
2	57,600	770	BUR	50.0	0.502	0.493	1.02	0.00	0.14
3	199,000	3,300	AS	1.0	0.017	0.029	0.60	0.00	0.00
4	230,000	3,200	AS	2.5	0.029	0.022	1.31	0.00	0.00
5	191,000	2,100	AS	2.5	0.025	0.020	1.25	0.00	0.00
6	452,200	3,500	AS	2.5	0.016	0.016	0.98	0.00	0.00
7	375,000	3,500	AS	7.5	0.041	0.027	1.53	0.00	0.00
8	226,000	2,150	AS	0.5	0.019	0.018	1.03	0.00	0.00
9	212,000	4,800	AS	4.0	0.039	0.038	1.03	0.00	0.00
10	506,000	3,100	AS	0.5	0.009	0.011	0.82	0.00	0.00
11	302,200	3,600	AS	2.0	0.012	0.019	0.61	?	0.00
12	152,000	2,750	AS	2.5	0.027	0.028	0.94	0.00	0.00
13	74,737	1,205	AS	2.5	0.013	0.025	0.52	0.00	0.00
14	245,000	2,640	TILE	2.5	0.048	0.068	0.70	0.00	0.00
15	137,000	1,650	AS	2.5	0.004	0.019	0.24	0.00	0.00
16	68,000	1,800	AS	10.0	0.066	0.057	1.14	0.00	0.00
17	153,400	1,900	AS	10.0	0.030	0.037	0.81	0.00	0.00
18	81,000	1,900	AS	5.0	0.054	0.038	1.42	?	0.00
19	253,000	4,000	AS	3.0	0.057	0.026	2.20	0.00	0.00
20	537,000	7,000	WS	3.0	0.058	0.050	1.15	0.00	0.00
21	508,000	2,000	AS	0.5	0.006	0.006	1.05	0.00	0.00
22	178,000	2,000	BUR	5.0	0.077	0.024	3.19	0.00	0.00
23	120,000	2,000	BUR	60.0	0.154	0.592	0.26	?	0.17
24	119,000	1,100	BUR	20.0	0.095	0.093	1.03	0.06	0.06
25	156,000	2,300	AS	1.0	0.059	0.023	2.59	0.00	0.00
Average					0.060	0.072	0.83	0.003	0.014

*AS = Asphalt Shingle, BUR = Built-Up Roof, Tile = Tile Roof

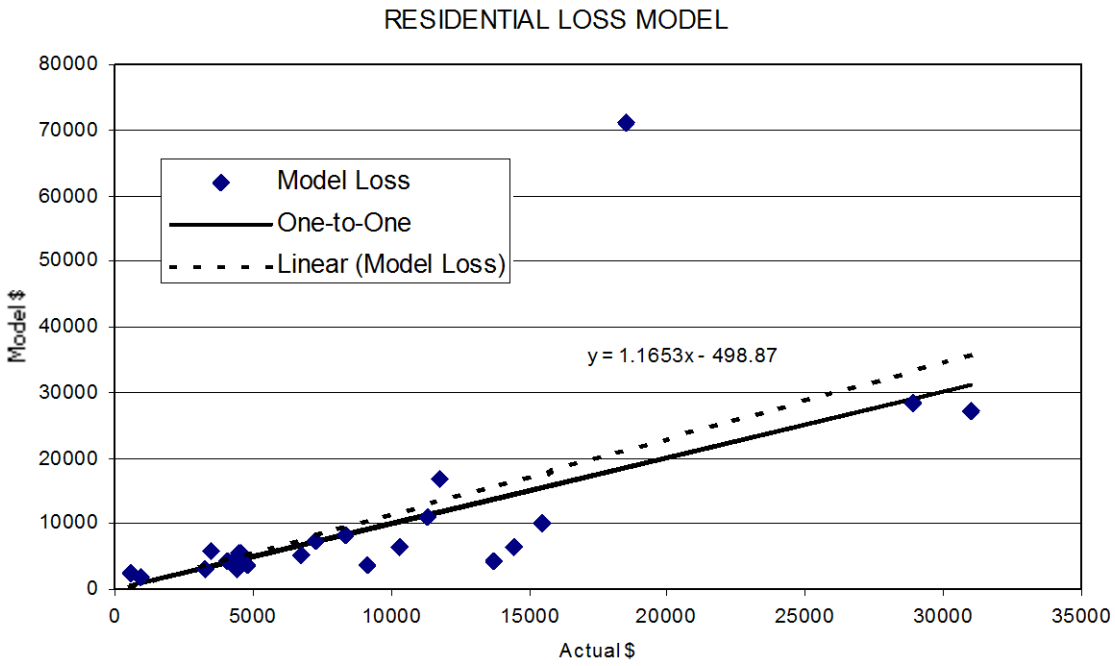

Figure 7.5. Actual and Predicted Losses.

For the 25 validation cases considered, Table 7.7 lists the actual and predicted loss ratios for both building and content losses. The case-by-case variability is not unexpected given that the majority of cases are at the low end of the loss curve. In such circumstances, the governing damage state is usually roof cover damage and is generally limited to less than10%. The variability seen in Table 7.7 is primarily linked to the total replacement threshold. If the computed cost is less than the default minimum repair cost of $250, the default minimum is registered. Roof cover damage states which do not exceed 0.5% will typically correspond to roof cover tab damage in the case of shingles, or in the case of tile roofs, scattered individual tiles, typically located at the ridges. These types of damage can usually be repaired with minimal effort. However, if the roof cover damage exceeds 0.5%, claim folder data has suggested that the repair costs are often based on a complete or partial re-roofing of the entire roof surface. For example, a gable receiving minimal damage to one side may have the entire cover replaced. The decision to replace the entire roof cover or a portion of the roof cover is at the discretion of the claim adjuster. Factors which are taken into account when making this decision are the age of the roof, color compatibility issues, discontinuation of or availability of the existing roofing materials, etc. As a result, the adjuster may or may not sanction a total or partial replacement of roofing materials depending on the overall circumstances. The loss model replaces the total roof surface given a damage state exceeding 0.5%.

Table 7.7 also list comparisons of actual and predicted content losses. The table entries denoted by the question mark symbol (?), correspond to cases where the content loss was ambiguous. The model accurately predicted zero content losses for the majority of cases. For case 23, a 17% of building value content loss was predicted. The claim folder did not report the actual content dollar loss since the content losses were below the 15%

deductible. However, it was reported that there was extensive content damage which approached the 15% deductible, suggesting the predicted 17% content loss is not unreasonable.

7.7 Loss Model Results for Residential Buildings

Using the same hurricane wind speed and direction data used in the development of the damage curves for residential buildings, per storm losses were estimated using the building and content loss models described earlier (and validated on an end-to-end basis as described in Chapter 9). Loss functions have been produced for the basic, unmitigated buildings (one story or two story, hip or gable, 6d or 8d sheathing nails, straps or toe-nails, wood frame, reinforced masonry or unreinforced masonry, no garage, 20 psf garage door or 10 psf garage door) for the four basic terrain categories.

Example plots of building loss versus wind speed are given in Appendix H where the building loss is expressed as a fraction of the total value of the building, and thus ranges between zero and one. Also included in Appendix H are loss functions associated with contents loss expressed as a fraction of the assumed content value (taken as 50% of the value of the building).

Tables 7.8, 7.9 and 7.10 present the average annual building loss, content loss and total loss, respectively, for all of the 144 residential buildings. Note that the losses are normalized by the building value in all cases and that the total loss represents the sum of building, contents and alternate living expenses. The average annual loss is simply the sum of all losses produced during the 20,000-year simulation of hurricanes divided by 20,000 years. Again, the values given in Tables 7.8 through 7.10 reflect the average annual losses for structures located in the South Florida area.

Mitigation. In order to examine the effect of mitigation on residential building losses, five different mitigation cases were examined as indicated below:

1. Install shutters.
2. Upgrade roof (roof sheathing and roof cover).
3. Upgrade roof and apply secondary water resistance.
4. Install shutters and upgrade roof.
5. Install shutters, upgrade roof and apply secondary water resistance.

The upgraded roof is modeled assuming that the existing roof (nailed with either 6d nails or 8d nails with a 6″/12″ spacing), is upgraded by adding 8d nails so the deck is connected to the roof trusses with a 6″/6″ pattern. At the same time it is assumed that a more wind resistant roof shingles are installed. These upgraded shingles are modeled by increasing the resistance of the basic shingles by 20%.

Secondary water resistance is provided by applying a waterproof seal, or cover, over the spaces between the roof sheathing panels that prevents water from entering the building through the roof if the roof cover fails in a storm. Methods for applying secondary water

Table 7.8. Average Annual Building Loss Normalized by Building Value

Building Characteristics					Hip Roof				Gable Roof			
Wall Const.	No. of Stories	Roof/Wall Conn.	Sheath Nails	Garage Door	Terrain Surface Roughness (m)				Terrain Surface Roughness (m)			
					0.03	0.35	0.70	1.0	0.03	0.35	0.70	1.0
Wood Frame	One	Straps	6d	None	0.0172	0.0092	0.0064	0.0053	0.0195	0.0107	0.0078	0.0065
				Strong	0.0167	0.0084	0.0058	0.0047	0.0185	0.0095	0.0068	0.0056
				Weak	0.0178	0.0089	0.0060	0.0049	0.0199	0.0102	0.0071	0.0059
			8d	None	0.0162	0.0083	0.0058	0.0047	0.0175	0.0089	0.0063	0.0051
				Strong	0.0158	0.0081	0.0055	0.0044	0.0171	0.0086	0.0059	0.0047
				Weak	0.0164	0.0083	0.0056	0.0045	0.0177	0.0088	0.0060	0.0049
		Toe-nails	6d	None	0.0186	0.0107	0.0074	0.0060	0.0214	0.0138	0.0097	0.0080
				Strong	0.0186	0.0095	0.0065	0.0053	0.0216	0.0119	0.0083	0.0069
				Weak	0.0217	0.0106	0.0073	0.0058	0.0281	0.0139	0.0096	0.0078
			8d	None	0.0184	0.0106	0.0073	0.0058	0.0206	0.0133	0.0093	0.0076
				Strong	0.0186	0.0094	0.0064	0.0052	0.0210	0.0117	0.0081	0.0066
				Weak	0.0217	0.0106	0.0073	0.0057	0.0280	0.0137	0.0094	0.0075
	Two	Straps	6d	None	0.0240	0.0136	0.0103	0.0087	0.0279	0.0163	0.0125	0.0108
				Strong	0.0241	0.0138	0.0103	0.0087	0.0268	0.0156	0.0119	0.0103
				Weak	0.0264	0.0146	0.0109	0.0093	0.0281	0.0163	0.0124	0.0108
			8d	None	0.0229	0.0129	0.0096	0.0082	0.0264	0.0148	0.0112	0.0094
				Strong	0.0232	0.0132	0.0098	0.0083	0.0253	0.0146	0.0110	0.0095
				Weak	0.0254	0.0140	0.0104	0.0087	0.0259	0.0150	0.0113	0.0096
		Toe-nails	6d	None	0.0268	0.0159	0.0119	0.0101	0.0307	0.0201	0.0152	0.0130
				Strong	0.0268	0.0152	0.0114	0.0096	0.0304	0.0178	0.0136	0.0116
				Weak	0.0304	0.0164	0.0124	0.0105	0.0388	0.0216	0.0163	0.0136
			8d	None	0.0265	0.0159	0.0118	0.0100	0.0300	0.0195	0.0147	0.0126
				Strong	0.0267	0.0151	0.0112	0.0094	0.0301	0.0175	0.0132	0.0114
				Weak	0.0303	0.0164	0.0122	0.0104	0.0382	0.0211	0.0159	0.0135
Unreinforced Masonry	One	Straps	6d	None	0.0172	0.0092	0.0064	0.0052	0.0196	0.0107	0.0078	0.0065
				Strong	0.0166	0.0085	0.0058	0.0047	0.0185	0.0096	0.0067	0.0056
				Weak	0.0177	0.0089	0.0060	0.0049	0.0198	0.0102	0.0071	0.0059
			8d	None	0.0163	0.0083	0.0057	0.0047	0.0176	0.0089	0.0062	0.0052
				Strong	0.0159	0.0081	0.0055	0.0044	0.0171	0.0086	0.0058	0.0047
				Weak	0.0164	0.0083	0.0056	0.0045	0.0177	0.0089	0.0060	0.0049
		Toe-nails	6d	None	0.0187	0.0106	0.0074	0.0059	0.0214	0.0137	0.0098	0.0079
				Strong	0.0187	0.0095	0.0065	0.0053	0.0215	0.0119	0.0084	0.0069
				Weak	0.0219	0.0106	0.0073	0.0058	0.0282	0.0139	0.0097	0.0079
			8d	None	0.0185	0.0106	0.0073	0.0058	0.0206	0.0133	0.0094	0.0076
				Strong	0.0186	0.0095	0.0065	0.0052	0.0210	0.0116	0.0082	0.0066
				Weak	0.0217	0.0106	0.0072	0.0057	0.0277	0.0136	0.0095	0.0076
	Two	Straps	6d	None	0.0240	0.0136	0.0103	0.0087	0.0277	0.0163	0.0125	0.0108
				Strong	0.0241	0.0138	0.0103	0.0087	0.0267	0.0155	0.0119	0.0102
				Weak	0.0263	0.0146	0.0110	0.0092	0.0280	0.0162	0.0125	0.0107
			8d	None	0.0229	0.0129	0.0096	0.0082	0.0263	0.0148	0.0112	0.0094
				Strong	0.0231	0.0132	0.0098	0.0082	0.0251	0.0145	0.0110	0.0094
				Weak	0.0254	0.0140	0.0103	0.0086	0.0259	0.0149	0.0113	0.0095
		Toe-nails	6d	None	0.0266	0.0159	0.0118	0.0101	0.0308	0.0199	0.0153	0.0129
				Strong	0.0268	0.0152	0.0113	0.0096	0.0304	0.0177	0.0135	0.0117
				Weak	0.0304	0.0166	0.0123	0.0104	0.0386	0.0215	0.0162	0.0136
			8d	None	0.0267	0.0159	0.0118	0.0100	0.0300	0.0195	0.0147	0.0124
				Strong	0.0268	0.0151	0.0111	0.0094	0.0300	0.0175	0.0132	0.0114
				Weak	0.0304	0.0164	0.0123	0.0104	0.0384	0.0212	0.0159	0.0135
Reinforced Masonry	One	Straps	6d	None	0.0173	0.0091	0.0064	0.0052	0.0195	0.0108	0.0077	0.0065
				Strong	0.0167	0.0084	0.0058	0.0047	0.0185	0.0096	0.0068	0.0056
				Weak	0.0177	0.0089	0.0060	0.0049	0.0199	0.0101	0.0072	0.0059
			8d	None	0.0162	0.0083	0.0057	0.0047	0.0175	0.0089	0.0062	0.0051
				Strong	0.0159	0.0081	0.0055	0.0044	0.0171	0.0086	0.0059	0.0047
				Weak	0.0163	0.0083	0.0056	0.0045	0.0177	0.0088	0.0061	0.0048
		Toe-nails	6d	None	0.0185	0.0106	0.0074	0.0060	0.0214	0.0138	0.0097	0.0080
				Strong	0.0187	0.0095	0.0066	0.0053	0.0215	0.0119	0.0084	0.0068
				Weak	0.0218	0.0106	0.0073	0.0059	0.0282	0.0139	0.0096	0.0078
			8d	None	0.0185	0.0105	0.0073	0.0058	0.0205	0.0133	0.0094	0.0077
				Strong	0.0185	0.0094	0.0064	0.0052	0.0211	0.0116	0.0081	0.0066
				Weak	0.0217	0.0105	0.0072	0.0058	0.0280	0.0137	0.0095	0.0076
	Two	Straps	6d	None	0.0239	0.0136	0.0102	0.0086	0.0277	0.0162	0.0125	0.0108
				Strong	0.0242	0.0137	0.0103	0.0087	0.0267	0.0156	0.0119	0.0102
				Weak	0.0263	0.0146	0.0109	0.0092	0.0281	0.0163	0.0125	0.0107
			8d	None	0.0229	0.0129	0.0096	0.0081	0.0263	0.0150	0.0112	0.0095
				Strong	0.0230	0.0131	0.0098	0.0082	0.0251	0.0146	0.0110	0.0094
				Weak	0.0253	0.0139	0.0103	0.0086	0.0258	0.0150	0.0112	0.0095
		Toe-nails	6d	None	0.0265	0.0159	0.0119	0.0099	0.0308	0.0199	0.0153	0.0131
				Strong	0.0267	0.0151	0.0114	0.0096	0.0305	0.0177	0.0137	0.0116
				Weak	0.0304	0.0165	0.0124	0.0105	0.0386	0.0217	0.0163	0.0138
			8d	None	0.0266	0.0160	0.0118	0.0100	0.0302	0.0196	0.0147	0.0124
				Strong	0.0266	0.0149	0.0112	0.0094	0.0300	0.0175	0.0133	0.0113
				Weak	0.0305	0.0164	0.0123	0.0104	0.0383	0.0215	0.0160	0.0135

Table 7.9. Average Annual Content Loss Normalized by Building Value

Building Characteristics					Hip Roof				Gable Roof			
Wall Const.	No. of Stories	Roof/Wall Conn.	Sheath Nails	Garage Door	Terrain Surface Roughness (m)				Terrain Surface Roughness (m)			
					0.03	0.35	0.70	1.0	0.03	0.35	0.70	1.0
Wood Frame	One	Straps	6d	None	0.0086	0.0041	0.0023	0.0016	0.0099	0.0049	0.0031	0.0023
				Strong	0.0087	0.0041	0.0023	0.0016	0.0100	0.0047	0.0028	0.0020
				Weak	0.0092	0.0042	0.0024	0.0017	0.0106	0.0050	0.0030	0.0022
			8d	None	0.0082	0.0038	0.0020	0.0013	0.0093	0.0043	0.0024	0.0017
				Strong	0.0083	0.0039	0.0022	0.0015	0.0095	0.0043	0.0025	0.0017
				Weak	0.0086	0.0040	0.0022	0.0015	0.0098	0.0045	0.0026	0.0018
		Toe-nails	6d	None	0.0101	0.0059	0.0037	0.0027	0.0119	0.0081	0.0053	0.0041
				Strong	0.0108	0.0053	0.0033	0.0024	0.0130	0.0072	0.0046	0.0036
				Weak	0.0132	0.0062	0.0039	0.0028	0.0180	0.0086	0.0057	0.0043
			8d	None	0.0100	0.0059	0.0036	0.0026	0.0117	0.0079	0.0052	0.0041
				Strong	0.0108	0.0053	0.0033	0.0024	0.0128	0.0071	0.0046	0.0036
				Weak	0.0132	0.0062	0.0040	0.0029	0.0180	0.0086	0.0056	0.0043
	Two	Straps	6d	None	0.0142	0.0075	0.0052	0.0041	0.0170	0.0096	0.0069	0.0057
				Strong	0.0141	0.0077	0.0053	0.0041	0.0161	0.0091	0.0066	0.0055
				Weak	0.0162	0.0084	0.0058	0.0045	0.0168	0.0094	0.0068	0.0057
			8d	None	0.0138	0.0073	0.0049	0.0039	0.0167	0.0092	0.0066	0.0053
				Strong	0.0139	0.0075	0.0050	0.0040	0.0156	0.0088	0.0063	0.0052
				Weak	0.0159	0.0081	0.0056	0.0043	0.0161	0.0090	0.0064	0.0052
		Toe-nails	6d	None	0.0162	0.0096	0.0068	0.0055	0.0191	0.0125	0.0092	0.0077
				Strong	0.0165	0.0091	0.0064	0.0051	0.0192	0.0112	0.0082	0.0068
				Weak	0.0195	0.0102	0.0073	0.0059	0.0257	0.0140	0.0103	0.0084
			8d	None	0.0161	0.0096	0.0067	0.0054	0.0190	0.0124	0.0091	0.0076
				Strong	0.0165	0.0091	0.0063	0.0050	0.0192	0.0111	0.0081	0.0068
				Weak	0.0195	0.0102	0.0073	0.0059	0.0253	0.0138	0.0101	0.0084
Unreinforced Masonry	One	Straps	6d	None	0.0085	0.0041	0.0023	0.0016	0.0100	0.0049	0.0031	0.0023
				Strong	0.0087	0.0041	0.0024	0.0016	0.0100	0.0047	0.0028	0.0021
				Weak	0.0092	0.0043	0.0024	0.0017	0.0105	0.0050	0.0030	0.0022
			8d	None	0.0082	0.0038	0.0020	0.0013	0.0094	0.0043	0.0024	0.0017
				Strong	0.0084	0.0039	0.0022	0.0015	0.0095	0.0043	0.0025	0.0017
				Weak	0.0086	0.0040	0.0022	0.0015	0.0098	0.0045	0.0026	0.0018
		Toe-nails	6d	None	0.0102	0.0059	0.0036	0.0026	0.0120	0.0081	0.0054	0.0041
				Strong	0.0109	0.0053	0.0032	0.0024	0.0129	0.0072	0.0047	0.0036
				Weak	0.0133	0.0062	0.0039	0.0029	0.0180	0.0086	0.0057	0.0044
			8d	None	0.0101	0.0059	0.0037	0.0026	0.0118	0.0079	0.0053	0.0040
				Strong	0.0109	0.0053	0.0033	0.0024	0.0127	0.0071	0.0046	0.0035
				Weak	0.0132	0.0062	0.0039	0.0028	0.0178	0.0085	0.0057	0.0044
	Two	Straps	6d	None	0.0142	0.0076	0.0052	0.0041	0.0170	0.0095	0.0069	0.0057
				Strong	0.0141	0.0077	0.0052	0.0041	0.0161	0.0091	0.0066	0.0054
				Weak	0.0161	0.0084	0.0058	0.0045	0.0167	0.0094	0.0068	0.0056
			8d	None	0.0139	0.0073	0.0049	0.0039	0.0167	0.0092	0.0067	0.0053
				Strong	0.0139	0.0075	0.0050	0.0039	0.0156	0.0088	0.0063	0.0052
				Weak	0.0159	0.0082	0.0056	0.0043	0.0161	0.0090	0.0065	0.0052
		Toe-nails	6d	None	0.0161	0.0096	0.0067	0.0055	0.0192	0.0124	0.0092	0.0076
				Strong	0.0165	0.0091	0.0063	0.0051	0.0193	0.0111	0.0082	0.0069
				Weak	0.0195	0.0103	0.0073	0.0059	0.0255	0.0140	0.0102	0.0084
			8d	None	0.0162	0.0096	0.0067	0.0055	0.0190	0.0125	0.0091	0.0075
				Strong	0.0165	0.0091	0.0063	0.0050	0.0191	0.0111	0.0081	0.0068
				Weak	0.0195	0.0103	0.0073	0.0059	0.0255	0.0139	0.0101	0.0084
Reinforced Masonry	One	Straps	6d	None	0.0086	0.0041	0.0023	0.0016	0.0099	0.0049	0.0030	0.0023
				Strong	0.0087	0.0041	0.0023	0.0016	0.0099	0.0047	0.0028	0.0021
				Weak	0.0092	0.0042	0.0024	0.0017	0.0105	0.0049	0.0030	0.0022
			8d	None	0.0082	0.0038	0.0020	0.0013	0.0093	0.0043	0.0024	0.0017
				Strong	0.0083	0.0039	0.0022	0.0015	0.0095	0.0043	0.0025	0.0017
				Weak	0.0085	0.0040	0.0022	0.0015	0.0098	0.0045	0.0026	0.0017
		Toe-nails	6d	None	0.0100	0.0059	0.0037	0.0027	0.0119	0.0081	0.0053	0.0041
				Strong	0.0109	0.0053	0.0033	0.0024	0.0129	0.0071	0.0047	0.0036
				Weak	0.0133	0.0062	0.0039	0.0029	0.0180	0.0086	0.0057	0.0044
			8d	None	0.0100	0.0058	0.0037	0.0026	0.0117	0.0079	0.0053	0.0041
				Strong	0.0108	0.0054	0.0032	0.0024	0.0128	0.0070	0.0046	0.0036
				Weak	0.0132	0.0062	0.0039	0.0029	0.0180	0.0086	0.0057	0.0043
	Two	Straps	6d	None	0.0142	0.0076	0.0052	0.0040	0.0169	0.0095	0.0069	0.0057
				Strong	0.0141	0.0076	0.0052	0.0041	0.0161	0.0092	0.0066	0.0055
				Weak	0.0161	0.0084	0.0058	0.0045	0.0168	0.0095	0.0068	0.0056
			8d	None	0.0140	0.0073	0.0049	0.0039	0.0167	0.0093	0.0066	0.0053
				Strong	0.0139	0.0074	0.0050	0.0039	0.0156	0.0088	0.0063	0.0052
				Weak	0.0159	0.0082	0.0056	0.0043	0.0161	0.0091	0.0064	0.0052
		Toe-nails	6d	None	0.0161	0.0096	0.0068	0.0054	0.0192	0.0124	0.0092	0.0077
				Strong	0.0164	0.0090	0.0064	0.0051	0.0193	0.0111	0.0083	0.0068
				Weak	0.0195	0.0102	0.0073	0.0059	0.0255	0.0141	0.0103	0.0085
			8d	None	0.0162	0.0097	0.0067	0.0055	0.0191	0.0125	0.0091	0.0075
				Strong	0.0164	0.0090	0.0063	0.0051	0.0192	0.0111	0.0081	0.0067
				Weak	0.0196	0.0102	0.0073	0.0059	0.0254	0.0140	0.0102	0.0084

Table 7.10. Average Annual Total Loss Normalized by Building Value

Building Characteristics					Hip Roof				Gable Roof			
Wall Const.	No. of Stories	Roof/Wall Conn.	Sheath Nails	Garage Door	Terrain Surface Roughness (m)				Terrain Surface Roughness (m)			
					0.03	0.35	0.70	1.0	0.03	0.35	0.70	1.0
Wood Frame	One	Straps	6d	None	0.0283	0.0145	0.0095	0.0076	0.0322	0.0172	0.0120	0.0097
				Strong	0.0278	0.0137	0.0089	0.0069	0.0311	0.0155	0.0105	0.0083
				Weak	0.0295	0.0144	0.0093	0.0073	0.0333	0.0166	0.0111	0.0089
			8d	None	0.0266	0.0132	0.0085	0.0066	0.0293	0.0144	0.0095	0.0075
				Strong	0.0264	0.0132	0.0084	0.0065	0.0291	0.0141	0.0092	0.0071
				Weak	0.0273	0.0134	0.0085	0.0066	0.0301	0.0145	0.0094	0.0073
		Toe-nails	6d	None	0.0313	0.0181	0.0121	0.0095	0.0364	0.0238	0.0164	0.0133
				Strong	0.0322	0.0161	0.0107	0.0084	0.0377	0.0208	0.0142	0.0114
				Weak	0.0381	0.0183	0.0121	0.0094	0.0503	0.0245	0.0166	0.0132
			8d	None	0.0311	0.0179	0.0118	0.0092	0.0354	0.0231	0.0158	0.0127
				Strong	0.0322	0.0161	0.0106	0.0082	0.0370	0.0205	0.0139	0.0111
				Weak	0.0381	0.0183	0.0122	0.0093	0.0503	0.0243	0.0164	0.0129
	Two	Straps	6d	None	0.0417	0.0231	0.0169	0.0140	0.0491	0.0282	0.0212	0.0181
				Strong	0.0418	0.0235	0.0171	0.0141	0.0469	0.0270	0.0203	0.0172
				Weak	0.0465	0.0251	0.0182	0.0151	0.0490	0.0281	0.0209	0.0180
			8d	None	0.0402	0.0221	0.0159	0.0132	0.0471	0.0262	0.0195	0.0161
				Strong	0.0405	0.0225	0.0162	0.0134	0.0447	0.0255	0.0188	0.0160
				Weak	0.0450	0.0241	0.0174	0.0142	0.0458	0.0262	0.0193	0.0161
		Toe-nails	6d	None	0.0470	0.0278	0.0204	0.0170	0.0545	0.0357	0.0266	0.0226
				Strong	0.0473	0.0265	0.0194	0.0161	0.0542	0.0316	0.0237	0.0201
				Weak	0.0544	0.0290	0.0215	0.0179	0.0704	0.0389	0.0290	0.0241
			8d	None	0.0466	0.0279	0.0202	0.0169	0.0535	0.0349	0.0260	0.0221
				Strong	0.0471	0.0263	0.0192	0.0158	0.0539	0.0312	0.0232	0.0198
				Weak	0.0543	0.0291	0.0213	0.0178	0.0694	0.0381	0.0284	0.0240
Unreinforced Masonry	One	Straps	6d	None	0.0281	0.0145	0.0095	0.0075	0.0325	0.0172	0.0119	0.0097
				Strong	0.0277	0.0137	0.0089	0.0068	0.0312	0.0156	0.0104	0.0084
				Weak	0.0294	0.0144	0.0093	0.0073	0.0332	0.0167	0.0111	0.0089
			8d	None	0.0268	0.0132	0.0084	0.0066	0.0294	0.0144	0.0094	0.0075
				Strong	0.0265	0.0131	0.0083	0.0064	0.0291	0.0142	0.0091	0.0071
				Weak	0.0273	0.0133	0.0086	0.0065	0.0301	0.0145	0.0094	0.0072
		Toe-nails	6d	None	0.0316	0.0179	0.0120	0.0093	0.0365	0.0238	0.0165	0.0131
				Strong	0.0323	0.0162	0.0106	0.0084	0.0375	0.0208	0.0143	0.0116
				Weak	0.0384	0.0183	0.0122	0.0095	0.0504	0.0245	0.0169	0.0134
			8d	None	0.0312	0.0180	0.0119	0.0092	0.0354	0.0231	0.0160	0.0127
				Strong	0.0322	0.0161	0.0106	0.0082	0.0369	0.0204	0.0140	0.0110
				Weak	0.0381	0.0183	0.0121	0.0093	0.0497	0.0241	0.0165	0.0131
	Two	Straps	6d	None	0.0418	0.0231	0.0169	0.0140	0.0488	0.0282	0.0212	0.0181
				Strong	0.0419	0.0234	0.0170	0.0141	0.0468	0.0270	0.0203	0.0171
				Weak	0.0463	0.0251	0.0183	0.0150	0.0489	0.0279	0.0211	0.0179
			8d	None	0.0402	0.0222	0.0159	0.0132	0.0470	0.0263	0.0195	0.0160
				Strong	0.0404	0.0226	0.0162	0.0132	0.0445	0.0254	0.0189	0.0158
				Weak	0.0449	0.0242	0.0173	0.0141	0.0458	0.0260	0.0194	0.0160
		Toe-nails	6d	None	0.0468	0.0279	0.0202	0.0170	0.0546	0.0353	0.0268	0.0224
				Strong	0.0473	0.0264	0.0193	0.0160	0.0543	0.0314	0.0237	0.0203
				Weak	0.0544	0.0293	0.0214	0.0178	0.0700	0.0387	0.0288	0.0240
			8d	None	0.0469	0.0278	0.0203	0.0169	0.0536	0.0349	0.0260	0.0218
				Strong	0.0473	0.0264	0.0189	0.0158	0.0537	0.0313	0.0233	0.0198
				Weak	0.0545	0.0291	0.0213	0.0178	0.0697	0.0382	0.0283	0.0239
Reinforced Masonry	One	Straps	6d	None	0.0283	0.0144	0.0095	0.0075	0.0322	0.0172	0.0118	0.0097
				Strong	0.0278	0.0137	0.0089	0.0068	0.0312	0.0156	0.0106	0.0084
				Weak	0.0295	0.0143	0.0093	0.0073	0.0332	0.0165	0.0112	0.0089
			8d	None	0.0267	0.0131	0.0085	0.0066	0.0293	0.0144	0.0094	0.0074
				Strong	0.0265	0.0131	0.0084	0.0064	0.0290	0.0141	0.0091	0.0070
				Weak	0.0271	0.0134	0.0086	0.0065	0.0300	0.0145	0.0094	0.0072
		Toe-nails	6d	None	0.0311	0.0180	0.0120	0.0094	0.0363	0.0239	0.0164	0.0132
				Strong	0.0323	0.0161	0.0107	0.0084	0.0375	0.0208	0.0143	0.0114
				Weak	0.0382	0.0184	0.0122	0.0096	0.0504	0.0245	0.0167	0.0133
			8d	None	0.0311	0.0178	0.0120	0.0092	0.0352	0.0231	0.0159	0.0128
				Strong	0.0320	0.0161	0.0105	0.0083	0.0371	0.0203	0.0139	0.0112
				Weak	0.0381	0.0183	0.0122	0.0095	0.0502	0.0243	0.0165	0.0131
	Two	Straps	6d	None	0.0416	0.0231	0.0168	0.0139	0.0488	0.0281	0.0213	0.0181
				Strong	0.0419	0.0234	0.0170	0.0141	0.0468	0.0271	0.0203	0.0172
				Weak	0.0463	0.0251	0.0183	0.0150	0.0491	0.0281	0.0211	0.0178
			8d	None	0.0402	0.0220	0.0158	0.0131	0.0470	0.0265	0.0193	0.0161
				Strong	0.0403	0.0224	0.0162	0.0133	0.0445	0.0255	0.0189	0.0160
				Weak	0.0448	0.0241	0.0173	0.0141	0.0457	0.0263	0.0193	0.0161
		Toe-nails	6d	None	0.0466	0.0278	0.0204	0.0167	0.0547	0.0353	0.0267	0.0227
				Strong	0.0471	0.0263	0.0195	0.0161	0.0544	0.0315	0.0240	0.0201
				Weak	0.0545	0.0291	0.0214	0.0179	0.0699	0.0390	0.0291	0.0243
			8d	None	0.0469	0.0280	0.0202	0.0169	0.0538	0.0351	0.0260	0.0218
				Strong	0.0471	0.0261	0.0191	0.0158	0.0538	0.0311	0.0233	0.0197
				Weak	0.0547	0.0290	0.0213	0.0177	0.0696	0.0387	0.0286	0.0239

resistance include hot-mopping the entire roof deck with tar prior to the application of the roof cover, or covering the spaces between sheathing panels with bitumous strips, usually manufactured for use as ice guards.

There are several products on the market now that are used in roofing of commercial and residential buildings to stop the formation of ice dams. This class of products is correctly referred to as "Self Adhering Modified Bitumen" products, but is generically referred to as Ice & Water shields. These products are an asphalt product with a polymer modifier added to give it a rubber gasket texture. The backing has an adhesive with paper covering that is removed upon application. The top of the sheet is often a sand roughened surface or plastic film that keeps the product from sticking to itself during shipping and also provides a skid resistant surface to work on after application.

This product is installed after the old roofing material is removed down to the deck and before the new roofing material is installed. It should be installed along all edges of the roof and along *all* joints between the plywood sheets. This will prevent water from penetrating through the joints after loss of the roof covering occurs. The product is manufactured in various widths. An economical use of the product for plywood joint sealing is the 6″ width rather than the 3′ width typical of many of the products. An example of the application of this type of secondary water protection is shown in Figure 7.6.

In order to model the effect of secondary water resistance, it is assumed that this mitigation approach is 95% effective, thus when the roof cover fails, the ensuing losses associated with roof cover failure (described in Section 7.6) are reduced to 5% of the baseline (no secondary water resistance) estimates.

Figure 7.6. Example of Self-Adhering Waterproof Underlayment Used to Tape Plywood Joints, Ridges and Eaves. Photo Depicts Use Around Fenestrations.

The loss analysis performed for the unmitigated buildings is repeated for the mitigated buildings to produce loss versus wind speed curves as well as average annual losses. Example loss function plots are given in Appendix H. Average annual losses (building, contents and total) are given in Tables 7.11 through 7.25 for the five mitigation strategies listed above. Table 7.26 summarizes the effect of the various building parameters on the average annual building loss and Table 7.27 gives ranges of the reductions in total loss associated with the five mitigation strategies.

7.8 Manufactured Home Loss Model

The manufactured home (MH) loss model is a physically-based damage-to-loss model that computes building economic losses using a combination of explicit and implicit costing techniques. The loss model uses the same modeling approach as the residential loss model (i.e., subdividing the structure into costing subassemblies). Eight basic subassemblies are used, they are foundation, framing, exterior walls, roofing, interiors, specialties, mechanical, and electrical. The prototypical MH is defined as having an average cost of $35 per sq ft.

7.8.1 Manufactured Home Loss Model Costing

***Losses Associated with Exterior Damage*.** Losses associated with damage to the building exterior are computed using an explicit costing technique. The explicit costing method directly calculates the repair and replacement costs for damaged MH envelope components using a combination of RSMeans unit, linear foot, and square foot costs. Explicit costing within the model is carried out for several envelope components such as roof covering, roof decking, windows, entrance doors, fenestration protection, exterior siding, etc. Dollar losses associated with these components are directly calculated using actual damage states and damage replacement thresholds. Damage replacement thresholds are the minimum damage levels at which a building component is completely replaced. Damage replacement thresholds are currently set at a 2.5% damage state for roof covering (rather than 0.5% for site built homes) and 5% for roof sheathing, which are determined from field observations and judgment. In addition to replacement thresholds, the loss model also takes into account building component replacement based on serviceability considerations. For those MH envelope components (windows, entrance doors, garage doors, and fenestration protection) that do not fail under applied load, they may still require replacement after undergoing thousands of load cycles as they become prone to permanent set. The loss model takes serviceability considerations into account by replacing those components that sustain loads exceeding 85% of their ultimate capacity.

As in the residential case, the cost data used in the explicit costing portion of the loss model are derived from the RSMeans Residential Cost Data and are based on national averages for new construction materials and installation. These data are adjusted to take into account the specific geographical location of the loss, the level of work difficulty, and contractor’s overhead and profit.

Table 7.11. Average Annual Building Loss Normalized by Building Value – Install Shutters

Building Characteristics					Hip Roof				Gable Roof			
					Terrain Surface Roughness (m)				Terrain Surface Roughness (m)			
Wall Const.	No. of Stories	Roof/ Wall Conn.	Deck Nails	Garage Door	0.03	0.35	0.70	1.0	0.03	0.35	0.70	1.0
Wood Frame	One	Straps	6d	None	0.0131	0.0072	0.0053	0.0045	0.0154	0.0086	0.0066	0.0057
				Strong	0.0122	0.0066	0.0049	0.0041	0.0137	0.0076	0.0058	0.0049
			8d	None	0.0122	0.0065	0.0049	0.0042	0.0128	0.0071	0.0053	0.0045
				Strong	0.0116	0.0061	0.0045	0.0038	0.0119	0.0065	0.0048	0.0041
		Toe-nails	6d	None	0.0135	0.0077	0.0057	0.0048	0.0159	0.0093	0.0070	0.0060
				Strong	0.0128	0.0072	0.0052	0.0044	0.0145	0.0084	0.0063	0.0054
			8d	None	0.0129	0.0074	0.0054	0.0045	0.0143	0.0084	0.0062	0.0053
				Strong	0.0125	0.0071	0.0051	0.0043	0.0137	0.0079	0.0058	0.0050
	Two	Straps	6d	None	0.0169	0.0106	0.0085	0.0074	0.0197	0.0127	0.0102	0.0091
				Strong	0.0168	0.0107	0.0085	0.0074	0.0186	0.0120	0.0096	0.0084
			8d	None	0.0163	0.0100	0.0079	0.0070	0.0169	0.0108	0.0085	0.0076
				Strong	0.0160	0.0100	0.0079	0.0069	0.0164	0.0105	0.0082	0.0072
		Toe-nails	6d	None	0.0173	0.0112	0.0088	0.0077	0.0208	0.0136	0.0110	0.0098
				Strong	0.0172	0.0110	0.0087	0.0078	0.0200	0.0129	0.0105	0.0093
			8d	None	0.0170	0.0110	0.0086	0.0075	0.0193	0.0126	0.0100	0.0089
				Strong	0.0170	0.0107	0.0086	0.0075	0.0189	0.0121	0.0097	0.0087
Unreinforced Masonry	One	Straps	6d	None	0.0131	0.0072	0.0054	0.0045	0.0154	0.0087	0.0066	0.0058
				Strong	0.0121	0.0066	0.0049	0.0041	0.0136	0.0076	0.0058	0.0049
			8d	None	0.0122	0.0065	0.0048	0.0041	0.0128	0.0070	0.0053	0.0045
				Strong	0.0114	0.0061	0.0045	0.0039	0.0117	0.0064	0.0048	0.0041
		Toe-nails	6d	None	0.0133	0.0077	0.0056	0.0048	0.0158	0.0093	0.0069	0.0060
				Strong	0.0128	0.0072	0.0052	0.0045	0.0144	0.0085	0.0064	0.0053
			8d	None	0.0129	0.0075	0.0054	0.0045	0.0144	0.0085	0.0062	0.0053
				Strong	0.0125	0.0070	0.0051	0.0043	0.0136	0.0079	0.0059	0.0051
	Two	Straps	6d	None	0.0168	0.0107	0.0085	0.0074	0.0195	0.0127	0.0103	0.0091
				Strong	0.0168	0.0107	0.0084	0.0075	0.0186	0.0119	0.0096	0.0085
			8d	None	0.0161	0.0100	0.0080	0.0070	0.0167	0.0107	0.0085	0.0074
				Strong	0.0160	0.0100	0.0079	0.0069	0.0164	0.0104	0.0082	0.0072
		Toe-nails	6d	None	0.0174	0.0112	0.0088	0.0077	0.0207	0.0136	0.0110	0.0097
				Strong	0.0173	0.0111	0.0088	0.0077	0.0200	0.0129	0.0105	0.0092
			8d	None	0.0170	0.0110	0.0086	0.0075	0.0192	0.0125	0.0100	0.0088
				Strong	0.0168	0.0108	0.0085	0.0075	0.0187	0.0121	0.0098	0.0087
Reinforced Masonry	One	Straps	6d	None	0.0131	0.0072	0.0053	0.0045	0.0153	0.0087	0.0066	0.0057
				Strong	0.0122	0.0066	0.0049	0.0041	0.0135	0.0076	0.0057	0.0049
			8d	None	0.0122	0.0065	0.0048	0.0042	0.0128	0.0070	0.0053	0.0046
				Strong	0.0114	0.0062	0.0045	0.0039	0.0119	0.0065	0.0048	0.0041
		Toe-nails	6d	None	0.0134	0.0076	0.0056	0.0048	0.0159	0.0093	0.0070	0.0059
				Strong	0.0127	0.0072	0.0052	0.0044	0.0144	0.0085	0.0063	0.0054
			8d	None	0.0129	0.0075	0.0054	0.0046	0.0143	0.0085	0.0063	0.0053
				Strong	0.0123	0.0070	0.0050	0.0043	0.0136	0.0080	0.0059	0.0050
	Two	Straps	6d	None	0.0168	0.0107	0.0084	0.0074	0.0196	0.0127	0.0103	0.0091
				Strong	0.0168	0.0107	0.0084	0.0074	0.0186	0.0119	0.0095	0.0085
			8d	None	0.0160	0.0100	0.0079	0.0070	0.0167	0.0108	0.0085	0.0075
				Strong	0.0160	0.0100	0.0080	0.0068	0.0164	0.0104	0.0082	0.0072
		Toe-nails	6d	None	0.0173	0.0112	0.0087	0.0077	0.0206	0.0136	0.0109	0.0097
				Strong	0.0173	0.0110	0.0088	0.0077	0.0198	0.0129	0.0105	0.0092
			8d	None	0.0170	0.0110	0.0086	0.0075	0.0192	0.0125	0.0101	0.0090
				Strong	0.0169	0.0108	0.0085	0.0075	0.0189	0.0120	0.0098	0.0084

Table 7.12. Average Annual Content Loss Normalized by Building Value – Install Shutters

Building Characteristics					Hip Roof				Gable Roof			
					Terrain Surface Roughness (m)				Terrain Surface Roughness (m)			
Wall Const.	No. of Stories	Roof/ Wall Conn.	Deck Nails	Garage Door	0.03	0.35	0.70	1.0	0.03	0.35	0.70	1.0
Wood Frame	One	Straps	6d	None	0.0040	0.0021	0.0013	0.0010	0.0054	0.0029	0.0020	0.0016
				Strong	0.0038	0.0019	0.0012	0.0009	0.0048	0.0025	0.0017	0.0013
			8d	None	0.0031	0.0015	0.0008	0.0007	0.0035	0.0019	0.0011	0.0008
				Strong	0.0032	0.0015	0.0009	0.0007	0.0036	0.0017	0.0010	0.0008
		Toe-nails	6d	None	0.0047	0.0029	0.0018	0.0014	0.0064	0.0039	0.0027	0.0021
				Strong	0.0050	0.0029	0.0018	0.0014	0.0063	0.0038	0.0026	0.0021
			8d	None	0.0043	0.0027	0.0017	0.0012	0.0059	0.0036	0.0024	0.0019
				Strong	0.0049	0.0029	0.0018	0.0014	0.0061	0.0036	0.0025	0.0020
	Two	Straps	6d	None	0.0061	0.0038	0.0026	0.0022	0.0080	0.0051	0.0038	0.0033
				Strong	0.0061	0.0037	0.0026	0.0021	0.0074	0.0047	0.0034	0.0029
			8d	None	0.0054	0.0032	0.0021	0.0017	0.0062	0.0039	0.0027	0.0022
				Strong	0.0054	0.0031	0.0021	0.0016	0.0060	0.0037	0.0025	0.0021
		Toe-nails	6d	None	0.0070	0.0046	0.0033	0.0027	0.0099	0.0065	0.0050	0.0044
				Strong	0.0071	0.0046	0.0033	0.0028	0.0097	0.0062	0.0049	0.0043
			8d	None	0.0068	0.0045	0.0032	0.0026	0.0095	0.0062	0.0048	0.0042
				Strong	0.0070	0.0044	0.0032	0.0026	0.0092	0.0060	0.0046	0.0040
Unreinforced Masonry	One	Straps	6d	None	0.0039	0.0021	0.0013	0.0010	0.0054	0.0029	0.0020	0.0016
				Strong	0.0037	0.0019	0.0012	0.0009	0.0047	0.0025	0.0016	0.0013
			8d	None	0.0029	0.0015	0.0008	0.0006	0.0034	0.0018	0.0011	0.0008
				Strong	0.0031	0.0016	0.0009	0.0007	0.0034	0.0017	0.0010	0.0008
		Toe-nails	6d	None	0.0045	0.0029	0.0018	0.0014	0.0064	0.0040	0.0026	0.0021
				Strong	0.0050	0.0029	0.0018	0.0014	0.0063	0.0038	0.0027	0.0021
			8d	None	0.0043	0.0028	0.0016	0.0012	0.0059	0.0037	0.0024	0.0019
				Strong	0.0048	0.0028	0.0018	0.0014	0.0060	0.0036	0.0025	0.0020
	Two	Straps	6d	None	0.0061	0.0038	0.0027	0.0021	0.0078	0.0050	0.0038	0.0033
				Strong	0.0061	0.0037	0.0026	0.0022	0.0074	0.0046	0.0034	0.0029
			8d	None	0.0052	0.0031	0.0021	0.0017	0.0061	0.0039	0.0027	0.0022
				Strong	0.0053	0.0031	0.0021	0.0016	0.0059	0.0036	0.0025	0.0020
		Toe-nails	6d	None	0.0070	0.0046	0.0033	0.0027	0.0099	0.0065	0.0051	0.0044
				Strong	0.0071	0.0046	0.0033	0.0027	0.0096	0.0062	0.0048	0.0042
			8d	None	0.0068	0.0046	0.0032	0.0027	0.0095	0.0063	0.0048	0.0042
				Strong	0.0069	0.0044	0.0031	0.0026	0.0091	0.0059	0.0047	0.0040
Reinforced Masonry	One	Straps	6d	None	0.0039	0.0021	0.0013	0.0010	0.0054	0.0029	0.0020	0.0016
				Strong	0.0037	0.0019	0.0011	0.0009	0.0047	0.0025	0.0016	0.0013
			8d	None	0.0030	0.0015	0.0008	0.0007	0.0033	0.0018	0.0011	0.0008
				Strong	0.0030	0.0016	0.0009	0.0007	0.0034	0.0017	0.0010	0.0008
		Toe-nails	6d	None	0.0046	0.0029	0.0018	0.0014	0.0064	0.0039	0.0027	0.0021
				Strong	0.0049	0.0029	0.0018	0.0014	0.0063	0.0038	0.0026	0.0021
			8d	None	0.0043	0.0028	0.0017	0.0012	0.0059	0.0037	0.0024	0.0019
				Strong	0.0046	0.0028	0.0017	0.0014	0.0060	0.0037	0.0025	0.0020
	Two	Straps	6d	None	0.0060	0.0038	0.0026	0.0021	0.0079	0.0051	0.0038	0.0033
				Strong	0.0062	0.0037	0.0026	0.0022	0.0074	0.0046	0.0034	0.0029
			8d	None	0.0052	0.0031	0.0021	0.0017	0.0061	0.0039	0.0027	0.0022
				Strong	0.0052	0.0031	0.0021	0.0016	0.0060	0.0036	0.0025	0.0020
		Toe-nails	6d	None	0.0069	0.0046	0.0033	0.0028	0.0098	0.0066	0.0050	0.0044
				Strong	0.0071	0.0045	0.0033	0.0028	0.0094	0.0063	0.0049	0.0042
			8d	None	0.0068	0.0045	0.0032	0.0026	0.0094	0.0062	0.0049	0.0043
				Strong	0.0069	0.0044	0.0032	0.0026	0.0092	0.0059	0.0046	0.0038

Table 7.13. Average Annual Total Loss Normalized by Building Value – Install Shutters

Building Characteristics					Hip Roof				Gable Roof			
					Terrain Surface Roughness (m)				Terrain Surface Roughness (m)			
Wall Const.	No. of Stories	Roof/ Wall Conn.	Deck Nails	Garage Door	0.03	0.35	0.70	1.0	0.03	0.35	0.70	1.0
Wood Frame	One	Straps	6d	None	0.0189	0.0102	0.0073	0.0061	0.0229	0.0127	0.0094	0.0080
				Strong	0.0176	0.0094	0.0067	0.0056	0.0203	0.0111	0.0082	0.0068
			8d	None	0.0169	0.0089	0.0063	0.0053	0.0181	0.0098	0.0070	0.0059
				Strong	0.0165	0.0084	0.0059	0.0050	0.0172	0.0091	0.0064	0.0054
		Toe-nails	6d	None	0.0199	0.0116	0.0082	0.0067	0.0245	0.0145	0.0107	0.0089
				Strong	0.0195	0.0110	0.0077	0.0064	0.0229	0.0134	0.0097	0.0083
			8d	None	0.0190	0.0111	0.0078	0.0063	0.0222	0.0132	0.0094	0.0079
				Strong	0.0191	0.0110	0.0076	0.0063	0.0217	0.0126	0.0091	0.0077
	Two	Straps	6d	None	0.0254	0.0159	0.0123	0.0106	0.0305	0.0197	0.0155	0.0136
				Strong	0.0254	0.0159	0.0123	0.0105	0.0287	0.0184	0.0144	0.0125
			8d	None	0.0240	0.0146	0.0111	0.0096	0.0255	0.0162	0.0124	0.0108
				Strong	0.0237	0.0146	0.0110	0.0095	0.0248	0.0157	0.0118	0.0103
		Toe-nails	6d	None	0.0267	0.0174	0.0134	0.0114	0.0338	0.0221	0.0176	0.0156
				Strong	0.0267	0.0172	0.0132	0.0117	0.0326	0.0209	0.0168	0.0149
			8d	None	0.0262	0.0171	0.0131	0.0111	0.0317	0.0206	0.0163	0.0143
				Strong	0.0264	0.0166	0.0130	0.0111	0.0309	0.0199	0.0157	0.0139
Unreinforced Masonry	One	Straps	6d	None	0.0187	0.0102	0.0073	0.0061	0.0230	0.0128	0.0095	0.0081
				Strong	0.0175	0.0094	0.0067	0.0055	0.0202	0.0112	0.0082	0.0069
			8d	None	0.0167	0.0089	0.0062	0.0053	0.0179	0.0097	0.0070	0.0059
				Strong	0.0161	0.0085	0.0059	0.0050	0.0168	0.0090	0.0065	0.0054
		Toe-nails	6d	None	0.0196	0.0116	0.0082	0.0067	0.0244	0.0146	0.0105	0.0089
				Strong	0.0196	0.0110	0.0078	0.0064	0.0227	0.0135	0.0099	0.0081
			8d	None	0.0188	0.0112	0.0077	0.0063	0.0222	0.0133	0.0094	0.0079
				Strong	0.0190	0.0108	0.0076	0.0062	0.0215	0.0126	0.0091	0.0078
	Two	Straps	6d	None	0.0253	0.0160	0.0123	0.0105	0.0302	0.0195	0.0156	0.0137
				Strong	0.0253	0.0159	0.0121	0.0106	0.0287	0.0183	0.0144	0.0126
			8d	None	0.0236	0.0145	0.0112	0.0096	0.0252	0.0161	0.0125	0.0106
				Strong	0.0235	0.0145	0.0111	0.0094	0.0247	0.0155	0.0119	0.0103
		Toe-nails	6d	None	0.0269	0.0174	0.0133	0.0114	0.0336	0.0221	0.0178	0.0155
				Strong	0.0269	0.0172	0.0133	0.0115	0.0325	0.0210	0.0168	0.0147
			8d	None	0.0262	0.0171	0.0130	0.0111	0.0315	0.0206	0.0163	0.0143
				Strong	0.0261	0.0167	0.0128	0.0111	0.0306	0.0197	0.0159	0.0140
Reinforced Masonry	One	Straps	6d	None	0.0187	0.0103	0.0072	0.0060	0.0228	0.0128	0.0095	0.0081
				Strong	0.0175	0.0094	0.0066	0.0055	0.0201	0.0112	0.0081	0.0069
			8d	None	0.0167	0.0088	0.0063	0.0053	0.0178	0.0098	0.0070	0.0060
				Strong	0.0159	0.0086	0.0059	0.0050	0.0169	0.0091	0.0064	0.0054
		Toe-nails	6d	None	0.0198	0.0115	0.0081	0.0067	0.0245	0.0145	0.0106	0.0088
				Strong	0.0194	0.0110	0.0077	0.0064	0.0228	0.0135	0.0098	0.0082
			8d	None	0.0189	0.0112	0.0078	0.0064	0.0222	0.0133	0.0095	0.0079
				Strong	0.0186	0.0107	0.0074	0.0062	0.0216	0.0127	0.0091	0.0077
	Two	Straps	6d	None	0.0252	0.0160	0.0122	0.0106	0.0303	0.0196	0.0156	0.0137
				Strong	0.0254	0.0159	0.0122	0.0106	0.0286	0.0182	0.0143	0.0126
			8d	None	0.0235	0.0145	0.0111	0.0096	0.0252	0.0163	0.0124	0.0107
				Strong	0.0235	0.0145	0.0112	0.0094	0.0247	0.0155	0.0119	0.0102
		Toe-nails	6d	None	0.0266	0.0174	0.0133	0.0115	0.0334	0.0221	0.0175	0.0154
				Strong	0.0269	0.0172	0.0132	0.0115	0.0321	0.0211	0.0168	0.0147
			8d	None	0.0262	0.0170	0.0129	0.0111	0.0314	0.0205	0.0165	0.0145
				Strong	0.0262	0.0167	0.0129	0.0112	0.0308	0.0196	0.0158	0.0135

Table 7.14. Average Annual Building Loss Normalized by Building Value – Upgrade Roof

Building Characteristics					Hip Roof				Gable Roof			
					Terrain Surface Roughness (m)				Terrain Surface Roughness (m)			
Wall Const.	No. of Stories	Roof/ Wall Conn.	Deck Nails	Garage Door	0.03	0.35	0.70	1.0	0.03	0.35	0.70	1.0
Wood Frame	One	Straps	6d	None	0.0133	0.0063	0.0038	0.0028	0.0146	0.0070	0.0042	0.0032
				Strong	0.0133	0.0063	0.0037	0.0027	0.0147	0.0068	0.0041	0.0030
			8d	None	0.0134	0.0063	0.0038	0.0028	0.0145	0.0069	0.0042	0.0032
				Strong	0.0132	0.0063	0.0037	0.0027	0.0147	0.0068	0.0041	0.0030
		Toe-nails	6d	None	0.0158	0.0090	0.0058	0.0043	0.0181	0.0120	0.0080	0.0063
				Strong	0.0167	0.0082	0.0052	0.0039	0.0194	0.0106	0.0071	0.0054
			8d	None	0.0159	0.0090	0.0058	0.0043	0.0181	0.0120	0.0079	0.0063
				Strong	0.0167	0.0082	0.0052	0.0039	0.0194	0.0107	0.0071	0.0055
	Two	Straps	6d	None	0.0204	0.0106	0.0073	0.0058	0.0242	0.0129	0.0092	0.0075
				Strong	0.0205	0.0110	0.0074	0.0059	0.0229	0.0126	0.0091	0.0074
			8d	None	0.0203	0.0106	0.0074	0.0058	0.0242	0.0129	0.0092	0.0075
				Strong	0.0205	0.0110	0.0075	0.0059	0.0229	0.0126	0.0090	0.0074
		Toe-nails	6d	None	0.0244	0.0142	0.0099	0.0080	0.0280	0.0181	0.0132	0.0109
				Strong	0.0243	0.0132	0.0093	0.0076	0.0284	0.0160	0.0117	0.0100
			8d	None	0.0244	0.0141	0.0099	0.0080	0.0281	0.0181	0.0133	0.0109
				Strong	0.0243	0.0132	0.0093	0.0076	0.0284	0.0160	0.0118	0.0099
Unreinforced Masonry	One	Straps	6d	None	0.0133	0.0063	0.0038	0.0027	0.0146	0.0069	0.0042	0.0031
				Strong	0.0132	0.0062	0.0037	0.0027	0.0147	0.0068	0.0041	0.0030
			8d	None	0.0133	0.0063	0.0038	0.0028	0.0146	0.0069	0.0042	0.0032
				Strong	0.0132	0.0063	0.0037	0.0027	0.0147	0.0068	0.0041	0.0030
		Toe-nails	6d	None	0.0158	0.0091	0.0058	0.0043	0.0182	0.0120	0.0081	0.0063
				Strong	0.0167	0.0081	0.0052	0.0040	0.0194	0.0105	0.0071	0.0056
			8d	None	0.0159	0.0091	0.0058	0.0043	0.0181	0.0119	0.0080	0.0063
				Strong	0.0166	0.0082	0.0052	0.0040	0.0194	0.0106	0.0070	0.0056
	Two	Straps	6d	None	0.0201	0.0106	0.0073	0.0057	0.0241	0.0129	0.0091	0.0074
				Strong	0.0205	0.0110	0.0074	0.0060	0.0227	0.0125	0.0091	0.0074
			8d	None	0.0201	0.0105	0.0072	0.0058	0.0240	0.0129	0.0092	0.0074
				Strong	0.0204	0.0109	0.0075	0.0059	0.0227	0.0126	0.0090	0.0074
		Toe-nails	6d	None	0.0242	0.0140	0.0099	0.0081	0.0281	0.0180	0.0133	0.0109
				Strong	0.0246	0.0132	0.0094	0.0075	0.0285	0.0161	0.0118	0.0099
			8d	None	0.0242	0.0140	0.0098	0.0081	0.0279	0.0181	0.0132	0.0109
				Strong	0.0246	0.0132	0.0094	0.0076	0.0285	0.0160	0.0118	0.0098
Reinforced Masonry	One	Straps	6d	None	0.0134	0.0063	0.0038	0.0028	0.0146	0.0069	0.0042	0.0031
				Strong	0.0132	0.0063	0.0037	0.0027	0.0146	0.0068	0.0041	0.0030
			8d	None	0.0133	0.0062	0.0038	0.0028	0.0146	0.0069	0.0042	0.0032
				Strong	0.0131	0.0063	0.0037	0.0027	0.0146	0.0068	0.0041	0.0030
		Toe-nails	6d	None	0.0159	0.0091	0.0058	0.0043	0.0181	0.0119	0.0080	0.0063
				Strong	0.0168	0.0081	0.0051	0.0039	0.0194	0.0106	0.0071	0.0055
			8d	None	0.0159	0.0091	0.0058	0.0043	0.0183	0.0119	0.0080	0.0063
				Strong	0.0168	0.0081	0.0051	0.0039	0.0195	0.0106	0.0071	0.0055
	Two	Straps	6d	None	0.0202	0.0106	0.0072	0.0057	0.0240	0.0128	0.0092	0.0074
				Strong	0.0203	0.0110	0.0075	0.0060	0.0229	0.0126	0.0089	0.0074
			8d	None	0.0200	0.0105	0.0073	0.0057	0.0240	0.0129	0.0091	0.0074
				Strong	0.0204	0.0108	0.0075	0.0060	0.0228	0.0125	0.0090	0.0073
		Toe-nails	6d	None	0.0242	0.0140	0.0099	0.0080	0.0281	0.0181	0.0132	0.0109
				Strong	0.0247	0.0132	0.0093	0.0076	0.0284	0.0160	0.0118	0.0099
			8d	None	0.0242	0.0140	0.0099	0.0080	0.0280	0.0180	0.0131	0.0109
				Strong	0.0247	0.0133	0.0093	0.0076	0.0284	0.0159	0.0117	0.0099

Table 7.15. Average Annual Content Loss Normalized by Building Value – Upgrade Roof

Building Characteristics					Hip Roof				Gable Roof			
					Terrain Surface Roughness (m)				Terrain Surface Roughness (m)			
Wall Const.	No. of Stories	Roof/ Wall Conn.	Deck Nails	Garage Door	0.03	0.35	0.70	1.0	0.03	0.35	0.70	1.0
Wood Frame	One	Straps	6d	None	0.0078	0.0036	0.0019	0.0012	0.0089	0.0041	0.0022	0.0014
				Strong	0.0081	0.0037	0.0020	0.0013	0.0092	0.0041	0.0023	0.0015
			8d	None	0.0079	0.0036	0.0019	0.0011	0.0088	0.0041	0.0021	0.0014
				Strong	0.0080	0.0037	0.0020	0.0013	0.0092	0.0041	0.0023	0.0015
		Toe-nails	6d	None	0.0096	0.0057	0.0035	0.0024	0.0113	0.0078	0.0051	0.0039
				Strong	0.0107	0.0053	0.0032	0.0022	0.0126	0.0071	0.0046	0.0034
			8d	None	0.0097	0.0057	0.0035	0.0024	0.0114	0.0078	0.0050	0.0039
				Strong	0.0106	0.0053	0.0032	0.0023	0.0126	0.0071	0.0046	0.0035
	Two	Straps	6d	None	0.0136	0.0070	0.0047	0.0035	0.0164	0.0090	0.0063	0.0050
				Strong	0.0136	0.0072	0.0047	0.0036	0.0154	0.0086	0.0061	0.0049
			8d	None	0.0136	0.0070	0.0047	0.0035	0.0164	0.0091	0.0063	0.0050
				Strong	0.0136	0.0072	0.0048	0.0036	0.0154	0.0086	0.0060	0.0049
		Toe-nails	6d	None	0.0160	0.0094	0.0064	0.0050	0.0187	0.0123	0.0089	0.0073
				Strong	0.0160	0.0088	0.0060	0.0048	0.0191	0.0110	0.0079	0.0067
			8d	None	0.0160	0.0094	0.0064	0.0051	0.0187	0.0123	0.0090	0.0073
				Strong	0.0160	0.0088	0.0061	0.0049	0.0191	0.0110	0.0080	0.0066
Unreinforced Masonry	One	Straps	6d	None	0.0078	0.0036	0.0018	0.0011	0.0089	0.0041	0.0022	0.0014
				Strong	0.0080	0.0037	0.0020	0.0013	0.0092	0.0041	0.0023	0.0015
			8d	None	0.0078	0.0036	0.0018	0.0011	0.0089	0.0041	0.0022	0.0014
				Strong	0.0080	0.0037	0.0020	0.0013	0.0092	0.0041	0.0023	0.0015
		Toe-nails	6d	None	0.0097	0.0057	0.0034	0.0024	0.0114	0.0078	0.0051	0.0039
				Strong	0.0107	0.0053	0.0032	0.0023	0.0126	0.0070	0.0046	0.0035
			8d	None	0.0097	0.0057	0.0034	0.0024	0.0114	0.0077	0.0050	0.0039
				Strong	0.0106	0.0053	0.0032	0.0023	0.0126	0.0070	0.0045	0.0035
	Two	Straps	6d	None	0.0136	0.0070	0.0047	0.0035	0.0165	0.0090	0.0063	0.0050
				Strong	0.0136	0.0073	0.0047	0.0037	0.0153	0.0085	0.0061	0.0049
			8d	None	0.0136	0.0070	0.0046	0.0035	0.0164	0.0090	0.0063	0.0050
				Strong	0.0135	0.0072	0.0048	0.0036	0.0153	0.0086	0.0061	0.0049
		Toe-nails	6d	None	0.0158	0.0093	0.0064	0.0051	0.0187	0.0122	0.0090	0.0073
				Strong	0.0162	0.0089	0.0061	0.0048	0.0191	0.0110	0.0080	0.0066
			8d	None	0.0158	0.0093	0.0064	0.0051	0.0186	0.0123	0.0089	0.0073
				Strong	0.0162	0.0089	0.0061	0.0048	0.0191	0.0109	0.0080	0.0066
Reinforced Masonry	One	Straps	6d	None	0.0079	0.0036	0.0018	0.0011	0.0089	0.0041	0.0022	0.0014
				Strong	0.0080	0.0037	0.0020	0.0013	0.0092	0.0041	0.0023	0.0015
			8d	None	0.0078	0.0035	0.0018	0.0011	0.0088	0.0041	0.0022	0.0014
				Strong	0.0079	0.0037	0.0020	0.0013	0.0091	0.0041	0.0023	0.0015
		Toe-nails	6d	None	0.0097	0.0057	0.0034	0.0024	0.0114	0.0078	0.0051	0.0039
				Strong	0.0108	0.0053	0.0031	0.0023	0.0126	0.0070	0.0046	0.0035
			8d	None	0.0097	0.0057	0.0034	0.0024	0.0115	0.0078	0.0051	0.0039
				Strong	0.0108	0.0053	0.0032	0.0022	0.0127	0.0070	0.0046	0.0035
	Two	Straps	6d	None	0.0136	0.0071	0.0046	0.0035	0.0164	0.0089	0.0063	0.0050
				Strong	0.0135	0.0073	0.0047	0.0036	0.0154	0.0086	0.0060	0.0049
			8d	None	0.0135	0.0070	0.0047	0.0035	0.0164	0.0090	0.0063	0.0050
				Strong	0.0136	0.0071	0.0048	0.0037	0.0153	0.0085	0.0061	0.0049
		Toe-nails	6d	None	0.0158	0.0093	0.0065	0.0051	0.0187	0.0123	0.0089	0.0073
				Strong	0.0163	0.0088	0.0061	0.0048	0.0190	0.0109	0.0080	0.0066
			8d	None	0.0158	0.0093	0.0065	0.0051	0.0187	0.0122	0.0088	0.0073
				Strong	0.0163	0.0089	0.0061	0.0048	0.0191	0.0109	0.0079	0.0067

Table 7.16. Average Annual Total Loss Normalized by Building Value – Upgrade Roof

Building Characteristics					Hip Roof				Gable Roof			
					Terrain Surface Roughness (m)				Terrain Surface Roughness (m)			
Wall Const.	No. of Stories	Roof/ Wall Conn.	Deck Nails	Garage Door	0.03	0.35	0.70	1.0	0.03	0.35	0.70	1.0
Wood Frame	One	Straps	6d	None	0.0229	0.0107	0.0062	0.0043	0.0257	0.0120	0.0069	0.0050
				Strong	0.0232	0.0108	0.0062	0.0043	0.0261	0.0119	0.0070	0.0049
			8d	None	0.0232	0.0107	0.0062	0.0043	0.0255	0.0119	0.0069	0.0050
				Strong	0.0232	0.0109	0.0062	0.0043	0.0261	0.0118	0.0070	0.0049
		Toe-nails	6d	None	0.0278	0.0160	0.0101	0.0074	0.0321	0.0216	0.0143	0.0111
				Strong	0.0299	0.0146	0.0091	0.0066	0.0350	0.0193	0.0128	0.0096
			8d	None	0.0278	0.0160	0.0101	0.0074	0.0322	0.0216	0.0141	0.0111
				Strong	0.0298	0.0147	0.0091	0.0067	0.0349	0.0194	0.0128	0.0098
	Two	Straps	6d	None	0.0370	0.0192	0.0130	0.0102	0.0444	0.0238	0.0169	0.0136
				Strong	0.0372	0.0198	0.0132	0.0104	0.0417	0.0231	0.0165	0.0135
			8d	None	0.0369	0.0192	0.0131	0.0102	0.0442	0.0239	0.0169	0.0136
				Strong	0.0371	0.0198	0.0134	0.0103	0.0418	0.0231	0.0164	0.0133
		Toe-nails	6d	None	0.0441	0.0257	0.0178	0.0142	0.0510	0.0332	0.0241	0.0199
				Strong	0.0441	0.0240	0.0167	0.0135	0.0518	0.0294	0.0214	0.0181
			8d	None	0.0441	0.0256	0.0178	0.0143	0.0511	0.0331	0.0243	0.0198
				Strong	0.0440	0.0240	0.0167	0.0136	0.0519	0.0294	0.0215	0.0180
Unreinforced Masonry	One	Straps	6d	None	0.0230	0.0107	0.0060	0.0042	0.0256	0.0119	0.0069	0.0049
				Strong	0.0231	0.0108	0.0062	0.0043	0.0260	0.0118	0.0070	0.0048
			8d	None	0.0230	0.0107	0.0061	0.0043	0.0257	0.0119	0.0069	0.0050
				Strong	0.0231	0.0109	0.0062	0.0043	0.0261	0.0119	0.0070	0.0049
		Toe-nails	6d	None	0.0278	0.0161	0.0100	0.0073	0.0322	0.0216	0.0144	0.0111
				Strong	0.0298	0.0146	0.0090	0.0068	0.0350	0.0191	0.0127	0.0099
			8d	None	0.0278	0.0161	0.0100	0.0073	0.0322	0.0214	0.0142	0.0111
				Strong	0.0298	0.0147	0.0092	0.0068	0.0350	0.0192	0.0125	0.0099
	Two	Straps	6d	None	0.0367	0.0191	0.0131	0.0100	0.0443	0.0238	0.0167	0.0135
				Strong	0.0372	0.0198	0.0132	0.0105	0.0415	0.0229	0.0165	0.0134
			8d	None	0.0367	0.0191	0.0128	0.0101	0.0440	0.0238	0.0169	0.0135
				Strong	0.0370	0.0197	0.0134	0.0104	0.0415	0.0231	0.0164	0.0134
		Toe-nails	6d	None	0.0437	0.0255	0.0178	0.0144	0.0511	0.0330	0.0243	0.0199
				Strong	0.0446	0.0241	0.0169	0.0134	0.0520	0.0295	0.0216	0.0180
			8d	None	0.0437	0.0255	0.0177	0.0144	0.0508	0.0332	0.0240	0.0198
				Strong	0.0445	0.0241	0.0169	0.0136	0.0519	0.0293	0.0216	0.0179
Reinforced Masonry	One	Straps	6d	None	0.0231	0.0107	0.0061	0.0042	0.0256	0.0119	0.0069	0.0049
				Strong	0.0231	0.0108	0.0062	0.0044	0.0260	0.0119	0.0069	0.0049
			8d	None	0.0230	0.0106	0.0060	0.0043	0.0255	0.0119	0.0070	0.0050
				Strong	0.0229	0.0109	0.0062	0.0043	0.0259	0.0119	0.0069	0.0049
		Toe-nails	6d	None	0.0279	0.0161	0.0100	0.0073	0.0322	0.0214	0.0142	0.0110
				Strong	0.0301	0.0146	0.0090	0.0067	0.0350	0.0192	0.0128	0.0098
			8d	None	0.0279	0.0161	0.0100	0.0073	0.0324	0.0215	0.0143	0.0110
				Strong	0.0301	0.0146	0.0090	0.0066	0.0351	0.0192	0.0127	0.0098
	Two	Straps	6d	None	0.0368	0.0192	0.0129	0.0101	0.0440	0.0237	0.0169	0.0135
				Strong	0.0368	0.0198	0.0133	0.0104	0.0418	0.0231	0.0163	0.0133
			8d	None	0.0365	0.0190	0.0130	0.0101	0.0440	0.0238	0.0168	0.0134
				Strong	0.0371	0.0195	0.0133	0.0105	0.0415	0.0229	0.0164	0.0133
		Toe-nails	6d	None	0.0437	0.0254	0.0179	0.0144	0.0511	0.0331	0.0241	0.0198
				Strong	0.0447	0.0240	0.0167	0.0135	0.0518	0.0293	0.0216	0.0180
			8d	None	0.0437	0.0254	0.0179	0.0143	0.0510	0.0330	0.0239	0.0199
				Strong	0.0447	0.0242	0.0167	0.0135	0.0519	0.0292	0.0213	0.0181

Table 7.17. Average Annual Building Loss Normalized by Building Value – Upgrade Roof and Add Secondary Water Resistance

Building Characteristics					Hip Roof				Gable Roof			
					Terrain Surface Roughness (m)				Terrain Surface Roughness (m)			
Wall Const.	No. of Stories	Roof/ Wall Conn.	Deck Nails	Garage Door	0.03	0.35	0.70	1.0	0.03	0.35	0.70	1.0
Wood Frame	One	Straps	6d	None	0.0127	0.0059	0.0034	0.0023	0.0140	0.0065	0.0037	0.0026
				Strong	0.0127	0.0059	0.0033	0.0023	0.0142	0.0064	0.0037	0.0026
			8d	None	0.0129	0.0059	0.0034	0.0023	0.0139	0.0064	0.0037	0.0026
				Strong	0.0127	0.0059	0.0033	0.0023	0.0142	0.0063	0.0037	0.0025
		Toe-nails	6d	None	0.0154	0.0089	0.0056	0.0041	0.0176	0.0118	0.0078	0.0061
				Strong	0.0165	0.0080	0.0050	0.0036	0.0191	0.0105	0.0069	0.0052
			8d	None	0.0154	0.0089	0.0056	0.0041	0.0177	0.0118	0.0077	0.0061
				Strong	0.0164	0.0080	0.0050	0.0037	0.0191	0.0105	0.0069	0.0053
	Two	Straps	6d	None	0.0199	0.0101	0.0067	0.0051	0.0238	0.0125	0.0088	0.0070
				Strong	0.0200	0.0105	0.0069	0.0054	0.0224	0.0121	0.0086	0.0069
			8d	None	0.0198	0.0101	0.0068	0.0051	0.0238	0.0126	0.0087	0.0070
				Strong	0.0200	0.0105	0.0070	0.0053	0.0224	0.0121	0.0085	0.0068
		Toe-nails	6d	None	0.0240	0.0138	0.0095	0.0075	0.0277	0.0179	0.0129	0.0106
				Strong	0.0240	0.0129	0.0089	0.0072	0.0281	0.0158	0.0115	0.0097
			8d	None	0.0240	0.0138	0.0095	0.0076	0.0277	0.0178	0.0130	0.0106
				Strong	0.0240	0.0129	0.0089	0.0072	0.0282	0.0158	0.0115	0.0096
Unreinforced Masonry	One	Straps	6d	None	0.0127	0.0059	0.0033	0.0023	0.0140	0.0064	0.0037	0.0026
				Strong	0.0126	0.0058	0.0033	0.0023	0.0141	0.0063	0.0037	0.0025
			8d	None	0.0128	0.0059	0.0033	0.0023	0.0140	0.0064	0.0037	0.0026
				Strong	0.0126	0.0059	0.0033	0.0023	0.0142	0.0063	0.0037	0.0025
		Toe-nails	6d	None	0.0154	0.0089	0.0056	0.0041	0.0177	0.0118	0.0078	0.0061
				Strong	0.0164	0.0080	0.0050	0.0037	0.0192	0.0104	0.0069	0.0054
			8d	None	0.0154	0.0089	0.0055	0.0041	0.0176	0.0117	0.0077	0.0061
				Strong	0.0164	0.0080	0.0050	0.0037	0.0191	0.0104	0.0068	0.0054
	Two	Straps	6d	None	0.0196	0.0100	0.0067	0.0051	0.0237	0.0125	0.0087	0.0069
				Strong	0.0200	0.0105	0.0069	0.0054	0.0222	0.0120	0.0086	0.0068
			8d	None	0.0196	0.0100	0.0066	0.0051	0.0236	0.0125	0.0087	0.0069
				Strong	0.0199	0.0104	0.0070	0.0053	0.0222	0.0121	0.0085	0.0068
		Toe-nails	6d	None	0.0238	0.0137	0.0095	0.0076	0.0277	0.0177	0.0130	0.0106
				Strong	0.0243	0.0129	0.0090	0.0071	0.0282	0.0158	0.0115	0.0096
			8d	None	0.0238	0.0137	0.0094	0.0076	0.0276	0.0178	0.0129	0.0106
				Strong	0.0242	0.0129	0.0090	0.0072	0.0282	0.0157	0.0115	0.0095
Reinforced Masonry	One	Straps	6d	None	0.0128	0.0059	0.0033	0.0023	0.0140	0.0064	0.0037	0.0026
				Strong	0.0126	0.0059	0.0033	0.0023	0.0141	0.0064	0.0036	0.0025
			8d	None	0.0127	0.0059	0.0033	0.0023	0.0140	0.0064	0.0037	0.0026
				Strong	0.0125	0.0059	0.0033	0.0023	0.0141	0.0063	0.0036	0.0025
		Toe-nails	6d	None	0.0155	0.0089	0.0056	0.0041	0.0177	0.0117	0.0078	0.0060
				Strong	0.0165	0.0079	0.0049	0.0037	0.0192	0.0104	0.0070	0.0053
			8d	None	0.0155	0.0089	0.0056	0.0041	0.0178	0.0117	0.0078	0.0060
				Strong	0.0165	0.0080	0.0049	0.0036	0.0192	0.0104	0.0069	0.0053
	Two	Straps	6d	None	0.0196	0.0101	0.0066	0.0051	0.0236	0.0124	0.0087	0.0069
				Strong	0.0198	0.0105	0.0069	0.0053	0.0223	0.0121	0.0084	0.0068
			8d	None	0.0195	0.0100	0.0067	0.0051	0.0235	0.0125	0.0087	0.0068
				Strong	0.0199	0.0103	0.0069	0.0054	0.0222	0.0120	0.0085	0.0068
		Toe-nails	6d	None	0.0238	0.0136	0.0096	0.0076	0.0277	0.0178	0.0129	0.0106
				Strong	0.0243	0.0129	0.0089	0.0072	0.0281	0.0157	0.0115	0.0096
			8d	None	0.0238	0.0136	0.0095	0.0076	0.0277	0.0178	0.0128	0.0106
				Strong	0.0243	0.0130	0.0089	0.0072	0.0282	0.0157	0.0114	0.0096

Table 7.18. Average Annual Content Loss Normalized by Building Value – Upgrade Roof and Add Secondary Water Resistance

Building Characteristics					Hip Roof				Gable Roof			
					Terrain Surface Roughness (m)				Terrain Surface Roughness (m)			
Wall Const.	No. of Stories	Roof/ Wall Conn.	Deck Nails	Garage Door	0.03	0.35	0.70	1.0	0.03	0.35	0.70	1.0
Wood Frame	One	Straps	6d	None	0.0077	0.0035	0.0018	0.0011	0.0088	0.0041	0.0021	0.0014
				Strong	0.0080	0.0037	0.0019	0.0012	0.0091	0.0041	0.0022	0.0014
			8d	None	0.0078	0.0035	0.0018	0.0011	0.0087	0.0040	0.0021	0.0013
				Strong	0.0079	0.0037	0.0019	0.0012	0.0091	0.0041	0.0022	0.0014
		Toe-nails	6d	None	0.0096	0.0057	0.0034	0.0024	0.0112	0.0078	0.0050	0.0039
				Strong	0.0106	0.0053	0.0032	0.0022	0.0126	0.0070	0.0046	0.0034
			8d	None	0.0096	0.0057	0.0034	0.0024	0.0113	0.0078	0.0050	0.0038
				Strong	0.0106	0.0053	0.0032	0.0022	0.0126	0.0071	0.0046	0.0034
	Two	Straps	6d	None	0.0135	0.0070	0.0046	0.0035	0.0164	0.0089	0.0063	0.0050
				Strong	0.0135	0.0071	0.0046	0.0036	0.0153	0.0085	0.0060	0.0049
			8d	None	0.0135	0.0070	0.0046	0.0034	0.0163	0.0090	0.0062	0.0050
				Strong	0.0135	0.0072	0.0047	0.0035	0.0153	0.0085	0.0060	0.0048
		Toe-nails	6d	None	0.0159	0.0094	0.0064	0.0050	0.0186	0.0123	0.0089	0.0072
				Strong	0.0160	0.0088	0.0060	0.0048	0.0190	0.0109	0.0079	0.0066
			8d	None	0.0159	0.0093	0.0064	0.0050	0.0186	0.0122	0.0089	0.0072
				Strong	0.0160	0.0088	0.0060	0.0048	0.0190	0.0109	0.0079	0.0066
Unreinforced Masonry	One	Straps	6d	None	0.0077	0.0035	0.0018	0.0011	0.0088	0.0040	0.0021	0.0013
				Strong	0.0079	0.0036	0.0019	0.0012	0.0091	0.0041	0.0022	0.0014
			8d	None	0.0078	0.0035	0.0018	0.0011	0.0088	0.0040	0.0021	0.0014
				Strong	0.0079	0.0037	0.0019	0.0012	0.0091	0.0041	0.0022	0.0014
		Toe-nails	6d	None	0.0096	0.0057	0.0034	0.0024	0.0113	0.0078	0.0051	0.0039
				Strong	0.0106	0.0053	0.0031	0.0023	0.0126	0.0070	0.0045	0.0035
			8d	None	0.0096	0.0057	0.0034	0.0024	0.0113	0.0077	0.0050	0.0039
				Strong	0.0106	0.0053	0.0032	0.0023	0.0126	0.0070	0.0045	0.0035
	Two	Straps	6d	None	0.0135	0.0069	0.0046	0.0034	0.0164	0.0089	0.0062	0.0050
				Strong	0.0135	0.0072	0.0046	0.0036	0.0152	0.0084	0.0060	0.0048
			8d	None	0.0135	0.0069	0.0045	0.0035	0.0163	0.0089	0.0063	0.0050
				Strong	0.0135	0.0071	0.0047	0.0035	0.0152	0.0085	0.0060	0.0048
		Toe-nails	6d	None	0.0157	0.0093	0.0064	0.0050	0.0187	0.0122	0.0089	0.0072
				Strong	0.0162	0.0088	0.0061	0.0047	0.0191	0.0110	0.0080	0.0066
			8d	None	0.0157	0.0093	0.0063	0.0050	0.0186	0.0123	0.0088	0.0072
				Strong	0.0161	0.0088	0.0061	0.0048	0.0191	0.0109	0.0080	0.0065
Reinforced Masonry	One	Straps	6d	None	0.0078	0.0035	0.0018	0.0011	0.0088	0.0040	0.0021	0.0013
				Strong	0.0079	0.0037	0.0019	0.0013	0.0091	0.0041	0.0022	0.0014
			8d	None	0.0077	0.0035	0.0018	0.0011	0.0087	0.0040	0.0022	0.0014
				Strong	0.0078	0.0037	0.0019	0.0012	0.0090	0.0041	0.0022	0.0014
		Toe-nails	6d	None	0.0096	0.0057	0.0034	0.0024	0.0113	0.0077	0.0050	0.0038
				Strong	0.0107	0.0052	0.0031	0.0022	0.0126	0.0070	0.0046	0.0034
			8d	None	0.0096	0.0057	0.0034	0.0024	0.0114	0.0077	0.0051	0.0038
				Strong	0.0107	0.0053	0.0031	0.0022	0.0126	0.0070	0.0045	0.0034
	Two	Straps	6d	None	0.0135	0.0070	0.0045	0.0034	0.0163	0.0089	0.0063	0.0049
				Strong	0.0134	0.0072	0.0047	0.0035	0.0153	0.0085	0.0059	0.0048
			8d	None	0.0134	0.0069	0.0046	0.0034	0.0163	0.0090	0.0062	0.0049
				Strong	0.0135	0.0071	0.0047	0.0036	0.0152	0.0085	0.0060	0.0048
		Toe-nails	6d	None	0.0158	0.0092	0.0064	0.0051	0.0187	0.0122	0.0089	0.0072
				Strong	0.0162	0.0088	0.0060	0.0047	0.0190	0.0109	0.0079	0.0066
			8d	None	0.0158	0.0092	0.0064	0.0050	0.0186	0.0122	0.0087	0.0072
				Strong	0.0162	0.0089	0.0060	0.0048	0.0190	0.0109	0.0079	0.0066

Table 7.19. Average Annual Total Loss Normalized by Building Value – Upgrade Roof and Add Secondary Water Resistance

Building Characteristics					Hip Roof				Gable Roof			
					Terrain Surface Roughness (m)				Terrain Surface Roughness (m)			
Wall Const.	No. of Stories	Roof/ Wall Conn.	Deck Nails	Garage Door	0.03	0.35	0.70	1.0	0.03	0.35	0.70	1.0
Wood Frame	One	Straps	6d	None	0.0222	0.0102	0.0056	0.0037	0.0248	0.0115	0.0063	0.0043
				Strong	0.0225	0.0103	0.0057	0.0037	0.0254	0.0113	0.0064	0.0043
			8d	None	0.0225	0.0102	0.0056	0.0036	0.0247	0.0113	0.0062	0.0042
				Strong	0.0224	0.0104	0.0057	0.0038	0.0254	0.0113	0.0064	0.0043
		Toe-nails	6d	None	0.0272	0.0158	0.0098	0.0071	0.0314	0.0213	0.0140	0.0108
				Strong	0.0296	0.0144	0.0089	0.0063	0.0346	0.0191	0.0125	0.0094
			8d	None	0.0273	0.0158	0.0098	0.0071	0.0316	0.0213	0.0138	0.0108
				Strong	0.0295	0.0144	0.0089	0.0064	0.0346	0.0191	0.0125	0.0095
	Two	Straps	6d	None	0.0364	0.0186	0.0123	0.0093	0.0438	0.0233	0.0163	0.0129
				Strong	0.0365	0.0191	0.0125	0.0097	0.0410	0.0224	0.0158	0.0127
			8d	None	0.0363	0.0186	0.0124	0.0093	0.0437	0.0235	0.0162	0.0130
				Strong	0.0365	0.0192	0.0126	0.0096	0.0411	0.0224	0.0157	0.0126
		Toe-nails	6d	None	0.0436	0.0253	0.0173	0.0136	0.0505	0.0328	0.0238	0.0195
				Strong	0.0436	0.0236	0.0162	0.0130	0.0515	0.0291	0.0211	0.0177
			8d	None	0.0436	0.0252	0.0173	0.0137	0.0506	0.0327	0.0239	0.0194
				Strong	0.0436	0.0236	0.0162	0.0131	0.0515	0.0291	0.0212	0.0177
Unreinforced Masonry	One	Straps	6d	None	0.0223	0.0102	0.0055	0.0036	0.0248	0.0114	0.0063	0.0042
				Strong	0.0223	0.0103	0.0057	0.0038	0.0253	0.0113	0.0063	0.0042
			8d	None	0.0223	0.0102	0.0055	0.0037	0.0248	0.0113	0.0063	0.0043
				Strong	0.0223	0.0103	0.0057	0.0038	0.0254	0.0113	0.0064	0.0043
		Toe-nails	6d	None	0.0272	0.0158	0.0097	0.0070	0.0316	0.0213	0.0141	0.0108
				Strong	0.0295	0.0144	0.0088	0.0065	0.0346	0.0189	0.0125	0.0096
			8d	None	0.0273	0.0158	0.0097	0.0070	0.0315	0.0211	0.0139	0.0108
				Strong	0.0294	0.0145	0.0089	0.0065	0.0346	0.0189	0.0123	0.0096
	Two	Straps	6d	None	0.0361	0.0185	0.0123	0.0092	0.0437	0.0233	0.0161	0.0129
				Strong	0.0365	0.0192	0.0125	0.0097	0.0408	0.0223	0.0159	0.0127
			8d	None	0.0360	0.0184	0.0120	0.0093	0.0435	0.0233	0.0163	0.0128
				Strong	0.0363	0.0190	0.0126	0.0096	0.0408	0.0225	0.0157	0.0127
		Toe-nails	6d	None	0.0431	0.0251	0.0173	0.0138	0.0507	0.0327	0.0239	0.0195
				Strong	0.0442	0.0237	0.0164	0.0129	0.0516	0.0292	0.0212	0.0176
			8d	None	0.0431	0.0250	0.0172	0.0138	0.0504	0.0329	0.0237	0.0194
				Strong	0.0440	0.0237	0.0165	0.0130	0.0516	0.0290	0.0212	0.0175
Reinforced Masonry	One	Straps	6d	None	0.0224	0.0102	0.0055	0.0036	0.0248	0.0113	0.0063	0.0042
				Strong	0.0223	0.0103	0.0057	0.0039	0.0252	0.0113	0.0063	0.0043
			8d	None	0.0223	0.0102	0.0055	0.0037	0.0247	0.0113	0.0064	0.0043
				Strong	0.0221	0.0103	0.0056	0.0037	0.0252	0.0113	0.0063	0.0043
		Toe-nails	6d	None	0.0274	0.0159	0.0098	0.0070	0.0316	0.0212	0.0139	0.0107
				Strong	0.0297	0.0143	0.0087	0.0064	0.0347	0.0190	0.0126	0.0095
			8d	None	0.0274	0.0159	0.0098	0.0070	0.0318	0.0212	0.0140	0.0107
				Strong	0.0297	0.0144	0.0088	0.0063	0.0347	0.0190	0.0124	0.0095
	Two	Straps	6d	None	0.0361	0.0185	0.0121	0.0093	0.0435	0.0232	0.0163	0.0128
				Strong	0.0361	0.0192	0.0126	0.0096	0.0411	0.0224	0.0156	0.0126
			8d	None	0.0359	0.0184	0.0123	0.0093	0.0434	0.0233	0.0162	0.0127
				Strong	0.0364	0.0189	0.0126	0.0097	0.0408	0.0223	0.0157	0.0126
		Toe-nails	6d	None	0.0431	0.0249	0.0174	0.0138	0.0507	0.0328	0.0238	0.0194
				Strong	0.0443	0.0236	0.0162	0.0129	0.0514	0.0290	0.0212	0.0176
			8d	None	0.0431	0.0249	0.0174	0.0137	0.0506	0.0327	0.0235	0.0195
				Strong	0.0443	0.0238	0.0162	0.0130	0.0515	0.0289	0.0210	0.0177

Table 7.20. Average Annual Building Loss Normalized by Building Value – Install Shutters and Upgrade Roof

Building Characteristics					Hip Roof				Gable Roof			
					Terrain Surface Roughness (m)				Terrain Surface Roughness (m)			
Wall Const.	No. of Stories	Roof/ Wall Conn.	Deck Nails	Garage Door	0.03	0.35	0.70	1.0	0.03	0.35	0.70	1.0
Wood Frame	One	Straps	6d	None	0.0073	0.0037	0.0024	0.0019	0.0079	0.0040	0.0027	0.0022
				Strong	0.0070	0.0036	0.0022	0.0018	0.0075	0.0038	0.0025	0.0020
			8d	None	0.0073	0.0036	0.0024	0.0019	0.0079	0.0040	0.0027	0.0022
				Strong	0.0071	0.0035	0.0022	0.0017	0.0075	0.0038	0.0025	0.0019
		Toe-nails	6d	None	0.0085	0.0050	0.0032	0.0025	0.0104	0.0060	0.0041	0.0033
				Strong	0.0087	0.0047	0.0032	0.0025	0.0102	0.0059	0.0041	0.0033
			8d	None	0.0085	0.0050	0.0032	0.0026	0.0104	0.0061	0.0041	0.0034
				Strong	0.0086	0.0048	0.0031	0.0025	0.0101	0.0059	0.0040	0.0034
	Two	Straps	6d	None	0.0105	0.0060	0.0044	0.0036	0.0113	0.0069	0.0050	0.0041
				Strong	0.0103	0.0061	0.0044	0.0036	0.0111	0.0067	0.0048	0.0040
			8d	None	0.0105	0.0061	0.0044	0.0036	0.0113	0.0069	0.0050	0.0042
				Strong	0.0104	0.0061	0.0044	0.0036	0.0110	0.0067	0.0048	0.0040
		Toe-nails	6d	None	0.0118	0.0075	0.0054	0.0045	0.0150	0.0095	0.0074	0.0064
				Strong	0.0118	0.0072	0.0054	0.0044	0.0147	0.0093	0.0071	0.0062
			8d	None	0.0116	0.0074	0.0054	0.0046	0.0150	0.0095	0.0074	0.0064
				Strong	0.0117	0.0073	0.0053	0.0044	0.0147	0.0093	0.0071	0.0062
Unreinforced Masonry	One	Straps	6d	None	0.0072	0.0036	0.0024	0.0019	0.0078	0.0041	0.0027	0.0022
				Strong	0.0069	0.0035	0.0022	0.0018	0.0073	0.0038	0.0025	0.0019
			8d	None	0.0071	0.0036	0.0023	0.0019	0.0077	0.0040	0.0026	0.0022
				Strong	0.0069	0.0035	0.0022	0.0018	0.0073	0.0038	0.0025	0.0020
		Toe-nails	6d	None	0.0084	0.0051	0.0033	0.0026	0.0102	0.0062	0.0042	0.0033
				Strong	0.0086	0.0049	0.0032	0.0025	0.0102	0.0059	0.0041	0.0033
			8d	None	0.0084	0.0050	0.0032	0.0025	0.0102	0.0060	0.0041	0.0033
				Strong	0.0086	0.0049	0.0031	0.0026	0.0101	0.0060	0.0041	0.0034
	Two	Straps	6d	None	0.0102	0.0060	0.0043	0.0036	0.0112	0.0069	0.0051	0.0042
				Strong	0.0102	0.0060	0.0043	0.0036	0.0108	0.0067	0.0048	0.0040
			8d	None	0.0102	0.0061	0.0043	0.0036	0.0111	0.0069	0.0050	0.0042
				Strong	0.0102	0.0061	0.0043	0.0036	0.0109	0.0066	0.0048	0.0040
		Toe-nails	6d	None	0.0116	0.0074	0.0054	0.0045	0.0149	0.0096	0.0074	0.0063
				Strong	0.0117	0.0073	0.0052	0.0045	0.0145	0.0092	0.0071	0.0063
			8d	None	0.0115	0.0074	0.0054	0.0045	0.0148	0.0096	0.0073	0.0064
				Strong	0.0118	0.0073	0.0053	0.0045	0.0146	0.0093	0.0071	0.0063
Reinforced Masonry	One	Straps	6d	None	0.0072	0.0036	0.0024	0.0019	0.0077	0.0040	0.0027	0.0022
				Strong	0.0069	0.0035	0.0022	0.0018	0.0073	0.0038	0.0024	0.0019
			8d	None	0.0071	0.0036	0.0024	0.0019	0.0077	0.0040	0.0027	0.0022
				Strong	0.0069	0.0035	0.0022	0.0018	0.0073	0.0038	0.0025	0.0019
		Toe-nails	6d	None	0.0084	0.0050	0.0032	0.0025	0.0103	0.0061	0.0041	0.0033
				Strong	0.0085	0.0049	0.0032	0.0025	0.0101	0.0059	0.0042	0.0033
			8d	None	0.0084	0.0049	0.0033	0.0026	0.0102	0.0060	0.0042	0.0033
				Strong	0.0086	0.0048	0.0032	0.0025	0.0101	0.0059	0.0041	0.0033
	Two	Straps	6d	None	0.0102	0.0060	0.0043	0.0035	0.0111	0.0069	0.0051	0.0042
				Strong	0.0103	0.0060	0.0043	0.0036	0.0109	0.0066	0.0048	0.0040
			8d	None	0.0102	0.0061	0.0043	0.0036	0.0112	0.0069	0.0050	0.0042
				Strong	0.0102	0.0061	0.0043	0.0035	0.0108	0.0066	0.0048	0.0040
		Toe-nails	6d	None	0.0116	0.0073	0.0054	0.0045	0.0148	0.0095	0.0074	0.0064
				Strong	0.0118	0.0073	0.0054	0.0045	0.0146	0.0093	0.0071	0.0061
			8d	None	0.0117	0.0074	0.0054	0.0045	0.0149	0.0095	0.0073	0.0064
				Strong	0.0118	0.0073	0.0054	0.0045	0.0147	0.0094	0.0071	0.0060

Table 7.21. Average Annual Content Loss Normalized by Building Value – Install Shutters and Upgrade Roof

Building Characteristics					Hip Roof				Gable Roof			
					Terrain Surface Roughness (m)				Terrain Surface Roughness (m)			
Wall Const.	No. of Stories	Roof/ Wall Conn.	Deck Nails	Garage Door	0.03	0.35	0.70	1.0	0.03	0.35	0.70	1.0
Wood Frame	One	Straps	6d	None	0.0022	0.0011	0.0005	0.0003	0.0026	0.0013	0.0007	0.0004
				Strong	0.0024	0.0011	0.0005	0.0003	0.0027	0.0013	0.0006	0.0004
			8d	None	0.0023	0.0010	0.0005	0.0003	0.0026	0.0013	0.0007	0.0004
				Strong	0.0024	0.0012	0.0005	0.0003	0.0027	0.0013	0.0006	0.0004
		Toe-nails	6d	None	0.0036	0.0024	0.0013	0.0009	0.0053	0.0032	0.0021	0.0015
				Strong	0.0042	0.0024	0.0015	0.0011	0.0055	0.0033	0.0022	0.0017
			8d	None	0.0036	0.0024	0.0013	0.0010	0.0052	0.0033	0.0020	0.0016
				Strong	0.0042	0.0025	0.0015	0.0011	0.0055	0.0033	0.0021	0.0017
	Two	Straps	6d	None	0.0043	0.0024	0.0014	0.0010	0.0050	0.0032	0.0020	0.0015
				Strong	0.0042	0.0023	0.0014	0.0010	0.0050	0.0030	0.0018	0.0014
			8d	None	0.0043	0.0025	0.0014	0.0010	0.0050	0.0032	0.0020	0.0015
				Strong	0.0042	0.0024	0.0014	0.0010	0.0049	0.0029	0.0018	0.0014
		Toe-nails	6d	None	0.0058	0.0039	0.0026	0.0021	0.0086	0.0056	0.0043	0.0037
				Strong	0.0060	0.0037	0.0026	0.0020	0.0084	0.0055	0.0041	0.0035
			8d	None	0.0057	0.0038	0.0026	0.0021	0.0086	0.0057	0.0043	0.0037
				Strong	0.0059	0.0038	0.0025	0.0020	0.0084	0.0055	0.0041	0.0036
Unreinforced Masonry	One	Straps	6d	None	0.0020	0.0010	0.0005	0.0003	0.0025	0.0013	0.0007	0.0004
				Strong	0.0023	0.0011	0.0005	0.0003	0.0025	0.0013	0.0006	0.0004
			8d	None	0.0020	0.0010	0.0005	0.0003	0.0024	0.0013	0.0006	0.0004
				Strong	0.0022	0.0011	0.0005	0.0003	0.0026	0.0013	0.0006	0.0004
		Toe-nails	6d	None	0.0035	0.0024	0.0014	0.0009	0.0051	0.0033	0.0021	0.0016
				Strong	0.0041	0.0025	0.0015	0.0011	0.0055	0.0033	0.0022	0.0017
			8d	None	0.0035	0.0024	0.0013	0.0009	0.0052	0.0032	0.0021	0.0015
				Strong	0.0041	0.0025	0.0014	0.0011	0.0055	0.0034	0.0022	0.0017
	Two	Straps	6d	None	0.0041	0.0024	0.0014	0.0010	0.0050	0.0031	0.0021	0.0015
				Strong	0.0041	0.0023	0.0014	0.0010	0.0048	0.0029	0.0018	0.0014
			8d	None	0.0040	0.0025	0.0014	0.0010	0.0049	0.0032	0.0020	0.0016
				Strong	0.0041	0.0024	0.0014	0.0010	0.0048	0.0029	0.0018	0.0014
		Toe-nails	6d	None	0.0057	0.0038	0.0025	0.0021	0.0086	0.0057	0.0043	0.0036
				Strong	0.0059	0.0038	0.0026	0.0021	0.0083	0.0054	0.0041	0.0036
			8d	None	0.0056	0.0038	0.0026	0.0020	0.0085	0.0057	0.0043	0.0038
				Strong	0.0059	0.0038	0.0026	0.0021	0.0084	0.0055	0.0041	0.0036
Reinforced Masonry	One	Straps	6d	None	0.0020	0.0010	0.0005	0.0003	0.0024	0.0013	0.0006	0.0004
				Strong	0.0023	0.0011	0.0005	0.0003	0.0026	0.0013	0.0006	0.0004
			8d	None	0.0020	0.0010	0.0005	0.0003	0.0024	0.0013	0.0007	0.0004
				Strong	0.0022	0.0011	0.0005	0.0003	0.0026	0.0013	0.0006	0.0004
		Toe-nails	6d	None	0.0034	0.0024	0.0013	0.0009	0.0052	0.0033	0.0021	0.0016
				Strong	0.0041	0.0025	0.0015	0.0011	0.0054	0.0033	0.0022	0.0017
			8d	None	0.0034	0.0024	0.0014	0.0009	0.0051	0.0032	0.0021	0.0015
				Strong	0.0041	0.0025	0.0015	0.0011	0.0055	0.0033	0.0022	0.0017
	Two	Straps	6d	None	0.0040	0.0024	0.0014	0.0010	0.0049	0.0032	0.0021	0.0016
				Strong	0.0042	0.0023	0.0014	0.0010	0.0048	0.0028	0.0018	0.0014
			8d	None	0.0041	0.0024	0.0014	0.0011	0.0050	0.0032	0.0020	0.0016
				Strong	0.0041	0.0024	0.0014	0.0010	0.0048	0.0029	0.0018	0.0014
		Toe-nails	6d	None	0.0057	0.0038	0.0026	0.0020	0.0085	0.0057	0.0043	0.0037
				Strong	0.0059	0.0037	0.0026	0.0021	0.0084	0.0055	0.0041	0.0035
			8d	None	0.0057	0.0038	0.0026	0.0020	0.0086	0.0057	0.0043	0.0037
				Strong	0.0059	0.0038	0.0026	0.0021	0.0085	0.0055	0.0041	0.0034

Table 7.22. Average Annual Total Loss Normalized by Building Value – Install Shutters and Upgrade Roof

Building Characteristics					Hip Roof				Gable Roof			
					Terrain Surface Roughness (m)				Terrain Surface Roughness (m)			
Wall Const.	No. of Stories	Roof/ Wall Conn.	Deck Nails	Garage Door	0.03	0.35	0.70	1.0	0.03	0.35	0.70	1.0
Wood Frame	One	Straps	6d	None	0.0104	0.0052	0.0031	0.0024	0.0115	0.0059	0.0037	0.0028
				Strong	0.0104	0.0051	0.0030	0.0023	0.0112	0.0056	0.0034	0.0026
			8d	None	0.0105	0.0050	0.0031	0.0024	0.0116	0.0059	0.0037	0.0029
				Strong	0.0105	0.0051	0.0030	0.0022	0.0112	0.0056	0.0034	0.0026
		Toe-nails	6d	None	0.0131	0.0080	0.0050	0.0038	0.0171	0.0101	0.0067	0.0052
				Strong	0.0141	0.0078	0.0051	0.0038	0.0171	0.0101	0.0069	0.0055
			8d	None	0.0132	0.0080	0.0049	0.0038	0.0170	0.0102	0.0067	0.0055
				Strong	0.0140	0.0080	0.0050	0.0038	0.0171	0.0101	0.0067	0.0056
	Two	Straps	6d	None	0.0162	0.0093	0.0064	0.0051	0.0180	0.0111	0.0077	0.0062
				Strong	0.0160	0.0092	0.0063	0.0051	0.0177	0.0106	0.0073	0.0060
			8d	None	0.0163	0.0094	0.0064	0.0051	0.0179	0.0110	0.0077	0.0063
				Strong	0.0160	0.0093	0.0064	0.0050	0.0175	0.0106	0.0073	0.0059
		Toe-nails	6d	None	0.0192	0.0124	0.0088	0.0072	0.0259	0.0166	0.0127	0.0110
				Strong	0.0195	0.0120	0.0087	0.0070	0.0253	0.0162	0.0122	0.0106
			8d	None	0.0190	0.0123	0.0087	0.0073	0.0258	0.0166	0.0128	0.0110
				Strong	0.0193	0.0121	0.0086	0.0070	0.0253	0.0162	0.0123	0.0107
Unreinforced Masonry	One	Straps	6d	None	0.0101	0.0051	0.0031	0.0024	0.0113	0.0059	0.0037	0.0029
				Strong	0.0101	0.0051	0.0030	0.0023	0.0108	0.0056	0.0034	0.0026
			8d	None	0.0099	0.0050	0.0031	0.0024	0.0111	0.0058	0.0036	0.0029
				Strong	0.0100	0.0051	0.0030	0.0023	0.0108	0.0055	0.0034	0.0026
		Toe-nails	6d	None	0.0130	0.0082	0.0050	0.0038	0.0168	0.0104	0.0068	0.0054
				Strong	0.0139	0.0081	0.0051	0.0039	0.0172	0.0101	0.0069	0.0054
			8d	None	0.0129	0.0081	0.0049	0.0038	0.0168	0.0101	0.0067	0.0053
				Strong	0.0140	0.0080	0.0050	0.0040	0.0170	0.0102	0.0068	0.0056
	Two	Straps	6d	None	0.0157	0.0092	0.0063	0.0051	0.0178	0.0110	0.0078	0.0063
				Strong	0.0158	0.0091	0.0063	0.0051	0.0172	0.0105	0.0072	0.0059
			8d	None	0.0156	0.0094	0.0063	0.0051	0.0177	0.0111	0.0077	0.0064
				Strong	0.0157	0.0093	0.0062	0.0050	0.0172	0.0105	0.0073	0.0059
		Toe-nails	6d	None	0.0189	0.0123	0.0087	0.0072	0.0257	0.0167	0.0127	0.0108
				Strong	0.0192	0.0122	0.0085	0.0072	0.0249	0.0160	0.0123	0.0108
			8d	None	0.0188	0.0122	0.0088	0.0072	0.0255	0.0166	0.0126	0.0111
				Strong	0.0193	0.0122	0.0086	0.0073	0.0251	0.0161	0.0123	0.0108
Reinforced Masonry	One	Straps	6d	None	0.0102	0.0051	0.0031	0.0024	0.0112	0.0058	0.0036	0.0029
				Strong	0.0101	0.0051	0.0030	0.0024	0.0108	0.0056	0.0033	0.0026
			8d	None	0.0100	0.0050	0.0031	0.0024	0.0111	0.0058	0.0037	0.0029
				Strong	0.0100	0.0051	0.0030	0.0023	0.0109	0.0055	0.0034	0.0025
		Toe-nails	6d	None	0.0129	0.0081	0.0050	0.0038	0.0169	0.0103	0.0068	0.0053
				Strong	0.0138	0.0080	0.0051	0.0039	0.0169	0.0101	0.0070	0.0055
			8d	None	0.0129	0.0080	0.0050	0.0038	0.0167	0.0101	0.0068	0.0053
				Strong	0.0138	0.0080	0.0051	0.0039	0.0171	0.0101	0.0069	0.0055
	Two	Straps	6d	None	0.0157	0.0093	0.0063	0.0050	0.0176	0.0111	0.0078	0.0063
				Strong	0.0159	0.0092	0.0063	0.0051	0.0173	0.0104	0.0073	0.0059
			8d	None	0.0157	0.0093	0.0063	0.0052	0.0177	0.0111	0.0077	0.0064
				Strong	0.0158	0.0093	0.0063	0.0050	0.0171	0.0104	0.0073	0.0059
		Toe-nails	6d	None	0.0189	0.0122	0.0087	0.0071	0.0256	0.0166	0.0128	0.0110
				Strong	0.0193	0.0120	0.0087	0.0072	0.0251	0.0161	0.0121	0.0105
			8d	None	0.0190	0.0123	0.0088	0.0071	0.0257	0.0166	0.0127	0.0110
				Strong	0.0193	0.0122	0.0088	0.0072	0.0253	0.0163	0.0122	0.0103

Table 7.23. Average Annual Building Loss Normalized by Building Value – Install Shutters, Upgrade Roof and Add Secondary Water Resistance

Building Characteristics					Hip Roof				Gable Roof			
					Terrain Surface Roughness (m)				Terrain Surface Roughness (m)			
Wall Const.	No. of Stories	Roof/ Wall Conn.	Deck Nails	Garage Door	0.03	0.35	0.70	1.0	0.03	0.35	0.70	1.0
Wood Frame	One	Straps	6d	None	0.0048	0.0025	0.0014	0.0011	0.0054	0.0028	0.0017	0.0012
				Strong	0.0048	0.0025	0.0014	0.0010	0.0053	0.0027	0.0015	0.0011
			8d	None	0.0048	0.0024	0.0014	0.0011	0.0051	0.0027	0.0016	0.0012
				Strong	0.0048	0.0025	0.0014	0.0010	0.0050	0.0027	0.0015	0.0010
		Toe-nails	6d	None	0.0068	0.0042	0.0026	0.0020	0.0090	0.0054	0.0035	0.0027
				Strong	0.0074	0.0041	0.0027	0.0020	0.0092	0.0054	0.0037	0.0029
			8d	None	0.0068	0.0042	0.0026	0.0020	0.0090	0.0054	0.0035	0.0028
				Strong	0.0074	0.0043	0.0026	0.0020	0.0091	0.0054	0.0035	0.0029
	Two	Straps	6d	None	0.0072	0.0041	0.0025	0.0018	0.0083	0.0051	0.0032	0.0025
				Strong	0.0073	0.0041	0.0025	0.0020	0.0083	0.0049	0.0031	0.0024
			8d	None	0.0072	0.0041	0.0025	0.0018	0.0081	0.0050	0.0031	0.0024
				Strong	0.0072	0.0042	0.0026	0.0019	0.0081	0.0048	0.0031	0.0023
		Toe-nails	6d	None	0.0095	0.0061	0.0042	0.0033	0.0136	0.0086	0.0065	0.0056
				Strong	0.0099	0.0060	0.0042	0.0033	0.0133	0.0085	0.0063	0.0054
			8d	None	0.0094	0.0060	0.0041	0.0033	0.0136	0.0086	0.0065	0.0056
				Strong	0.0098	0.0061	0.0042	0.0033	0.0133	0.0085	0.0063	0.0055
Unreinforced Masonry	One	Straps	6d	None	0.0045	0.0024	0.0014	0.0011	0.0051	0.0028	0.0016	0.0012
				Strong	0.0046	0.0025	0.0013	0.0010	0.0049	0.0027	0.0015	0.0011
			8d	None	0.0044	0.0024	0.0014	0.0011	0.0047	0.0027	0.0015	0.0012
				Strong	0.0045	0.0025	0.0013	0.0010	0.0048	0.0026	0.0014	0.0010
		Toe-nails	6d	None	0.0067	0.0043	0.0026	0.0020	0.0088	0.0055	0.0035	0.0028
				Strong	0.0073	0.0043	0.0027	0.0021	0.0092	0.0054	0.0036	0.0028
			8d	None	0.0066	0.0043	0.0026	0.0020	0.0089	0.0053	0.0035	0.0027
				Strong	0.0073	0.0043	0.0026	0.0021	0.0091	0.0055	0.0036	0.0029
	Two	Straps	6d	None	0.0069	0.0040	0.0024	0.0018	0.0082	0.0050	0.0033	0.0025
				Strong	0.0071	0.0041	0.0025	0.0019	0.0080	0.0049	0.0030	0.0024
			8d	None	0.0067	0.0041	0.0024	0.0018	0.0080	0.0050	0.0032	0.0024
				Strong	0.0070	0.0041	0.0025	0.0018	0.0079	0.0048	0.0030	0.0023
		Toe-nails	6d	None	0.0093	0.0061	0.0041	0.0033	0.0135	0.0086	0.0065	0.0055
				Strong	0.0097	0.0061	0.0042	0.0034	0.0131	0.0084	0.0063	0.0055
			8d	None	0.0093	0.0060	0.0041	0.0033	0.0134	0.0086	0.0064	0.0057
				Strong	0.0097	0.0061	0.0042	0.0035	0.0133	0.0084	0.0063	0.0055
Reinforced Masonry	One	Straps	6d	None	0.0046	0.0024	0.0014	0.0011	0.0051	0.0028	0.0016	0.0012
				Strong	0.0046	0.0025	0.0014	0.0010	0.0050	0.0027	0.0015	0.0011
			8d	None	0.0044	0.0024	0.0014	0.0011	0.0047	0.0027	0.0016	0.0012
				Strong	0.0045	0.0024	0.0013	0.0010	0.0048	0.0026	0.0015	0.0010
		Toe-nails	6d	None	0.0066	0.0043	0.0026	0.0020	0.0089	0.0055	0.0035	0.0027
				Strong	0.0072	0.0043	0.0027	0.0020	0.0091	0.0054	0.0037	0.0028
			8d	None	0.0066	0.0042	0.0026	0.0020	0.0088	0.0054	0.0035	0.0027
				Strong	0.0073	0.0043	0.0027	0.0020	0.0091	0.0054	0.0036	0.0029
	Two	Straps	6d	None	0.0068	0.0040	0.0024	0.0018	0.0081	0.0050	0.0033	0.0025
				Strong	0.0072	0.0041	0.0025	0.0019	0.0081	0.0047	0.0031	0.0024
			8d	None	0.0068	0.0040	0.0024	0.0018	0.0080	0.0050	0.0032	0.0024
				Strong	0.0071	0.0041	0.0025	0.0018	0.0079	0.0047	0.0030	0.0023
		Toe-nails	6d	None	0.0093	0.0060	0.0041	0.0032	0.0134	0.0086	0.0065	0.0056
				Strong	0.0098	0.0061	0.0043	0.0034	0.0133	0.0084	0.0062	0.0053
			8d	None	0.0094	0.0060	0.0041	0.0032	0.0135	0.0086	0.0064	0.0056
				Strong	0.0098	0.0061	0.0043	0.0034	0.0134	0.0085	0.0063	0.0053

Table 7.24. Average Annual Content Loss Normalized by Building Value – Install Shutters, Upgrade Roof and Add Secondary Water Resistance

Building Characteristics					Hip Roof				Gable Roof			
					Terrain Surface Roughness (m)				Terrain Surface Roughness (m)			
Wall Const.	No. of Stories	Roof/ Wall Conn.	Deck Nails	Garage Door	0.03	0.35	0.70	1.0	0.03	0.35	0.70	1.0
Wood Frame	One	Straps	6d	None	0.0017	0.0009	0.0003	0.0001	0.0021	0.0011	0.0005	0.0002
				Strong	0.0019	0.0009	0.0003	0.0002	0.0023	0.0011	0.0004	0.0002
			8d	None	0.0017	0.0008	0.0003	0.0001	0.0020	0.0010	0.0004	0.0002
				Strong	0.0020	0.0010	0.0003	0.0002	0.0022	0.0011	0.0004	0.0002
		Toe-nails	6d	None	0.0032	0.0022	0.0012	0.0008	0.0050	0.0031	0.0019	0.0014
				Strong	0.0039	0.0023	0.0014	0.0010	0.0053	0.0032	0.0021	0.0016
			8d	None	0.0032	0.0022	0.0012	0.0009	0.0049	0.0031	0.0019	0.0015
				Strong	0.0039	0.0024	0.0014	0.0010	0.0053	0.0032	0.0020	0.0017
	Two	Straps	6d	None	0.0036	0.0020	0.0011	0.0007	0.0044	0.0028	0.0016	0.0012
				Strong	0.0035	0.0019	0.0010	0.0007	0.0044	0.0026	0.0014	0.0011
			8d	None	0.0036	0.0021	0.0010	0.0007	0.0043	0.0027	0.0016	0.0012
				Strong	0.0036	0.0020	0.0010	0.0006	0.0043	0.0025	0.0014	0.0010
		Toe-nails	6d	None	0.0053	0.0036	0.0023	0.0018	0.0083	0.0055	0.0041	0.0035
				Strong	0.0055	0.0034	0.0023	0.0018	0.0082	0.0053	0.0039	0.0034
			8d	None	0.0052	0.0035	0.0023	0.0018	0.0083	0.0055	0.0041	0.0035
				Strong	0.0055	0.0035	0.0023	0.0018	0.0081	0.0054	0.0040	0.0034
Unreinforced Masonry	One	Straps	6d	None	0.0014	0.0008	0.0003	0.0001	0.0019	0.0011	0.0004	0.0002
				Strong	0.0017	0.0009	0.0003	0.0002	0.0020	0.0011	0.0004	0.0002
			8d	None	0.0014	0.0008	0.0003	0.0001	0.0017	0.0010	0.0004	0.0002
				Strong	0.0017	0.0009	0.0003	0.0002	0.0020	0.0010	0.0004	0.0002
		Toe-nails	6d	None	0.0031	0.0023	0.0012	0.0008	0.0048	0.0032	0.0019	0.0015
				Strong	0.0038	0.0024	0.0014	0.0010	0.0053	0.0032	0.0021	0.0016
			8d	None	0.0031	0.0023	0.0012	0.0008	0.0049	0.0031	0.0019	0.0014
				Strong	0.0039	0.0024	0.0013	0.0010	0.0052	0.0033	0.0021	0.0017
	Two	Straps	6d	None	0.0034	0.0019	0.0010	0.0007	0.0043	0.0027	0.0017	0.0011
				Strong	0.0034	0.0019	0.0010	0.0006	0.0042	0.0025	0.0014	0.0010
			8d	None	0.0032	0.0020	0.0010	0.0006	0.0043	0.0028	0.0016	0.0012
				Strong	0.0034	0.0020	0.0010	0.0006	0.0042	0.0025	0.0015	0.0010
		Toe-nails	6d	None	0.0052	0.0035	0.0023	0.0018	0.0083	0.0055	0.0041	0.0034
				Strong	0.0054	0.0035	0.0023	0.0018	0.0080	0.0053	0.0040	0.0034
			8d	None	0.0052	0.0035	0.0023	0.0018	0.0082	0.0055	0.0041	0.0036
				Strong	0.0054	0.0035	0.0024	0.0019	0.0081	0.0053	0.0040	0.0034
Reinforced Masonry	One	Straps	6d	None	0.0015	0.0008	0.0003	0.0001	0.0019	0.0011	0.0004	0.0002
				Strong	0.0018	0.0009	0.0003	0.0002	0.0021	0.0011	0.0004	0.0002
			8d	None	0.0014	0.0008	0.0003	0.0001	0.0018	0.0010	0.0004	0.0002
				Strong	0.0017	0.0009	0.0003	0.0002	0.0020	0.0010	0.0004	0.0002
		Toe-nails	6d	None	0.0031	0.0023	0.0012	0.0008	0.0049	0.0032	0.0019	0.0014
				Strong	0.0038	0.0024	0.0014	0.0010	0.0052	0.0032	0.0021	0.0016
			8d	None	0.0031	0.0022	0.0012	0.0008	0.0048	0.0031	0.0019	0.0014
				Strong	0.0038	0.0024	0.0014	0.0010	0.0053	0.0032	0.0021	0.0016
	Two	Straps	6d	None	0.0033	0.0020	0.0010	0.0006	0.0042	0.0027	0.0017	0.0012
				Strong	0.0035	0.0019	0.0010	0.0006	0.0042	0.0024	0.0015	0.0010
			8d	None	0.0034	0.0020	0.0010	0.0007	0.0043	0.0028	0.0016	0.0012
				Strong	0.0034	0.0020	0.0010	0.0006	0.0041	0.0025	0.0014	0.0010
		Toe-nails	6d	None	0.0052	0.0035	0.0023	0.0017	0.0083	0.0055	0.0042	0.0035
				Strong	0.0054	0.0035	0.0024	0.0018	0.0081	0.0053	0.0039	0.0033
			8d	None	0.0052	0.0035	0.0023	0.0017	0.0083	0.0055	0.0041	0.0035
				Strong	0.0055	0.0035	0.0024	0.0018	0.0082	0.0054	0.0039	0.0033

Table 7.25. Average Annual Total Loss Normalized by Building Value – Install Shutters, Upgrade Roof and Add Secondary Water Resistance

Building Characteristics					Hip Roof				Gable Roof			
					Terrain Surface Roughness (m)				Terrain Surface Roughness (m)			
Wall Const.	No. of Stories	Roof/ Wall Conn.	Deck Nails	Garage Door	0.03	0.35	0.70	1.0	0.03	0.35	0.70	1.0
Wood Frame	One	Straps	6d	None	0.0071	0.0037	0.0018	0.0013	0.0081	0.0042	0.0023	0.0015
				Strong	0.0074	0.0037	0.0018	0.0012	0.0082	0.0041	0.0021	0.0014
			8d	None	0.0071	0.0035	0.0018	0.0013	0.0077	0.0040	0.0021	0.0015
				Strong	0.0074	0.0037	0.0018	0.0012	0.0079	0.0041	0.0020	0.0014
		Toe-nails	6d	None	0.0108	0.0070	0.0041	0.0030	0.0152	0.0092	0.0059	0.0045
				Strong	0.0123	0.0070	0.0044	0.0032	0.0157	0.0094	0.0063	0.0049
			8d	None	0.0108	0.0070	0.0040	0.0031	0.0151	0.0093	0.0058	0.0047
				Strong	0.0122	0.0072	0.0043	0.0032	0.0156	0.0094	0.0061	0.0050
	Two	Straps	6d	None	0.0117	0.0066	0.0038	0.0027	0.0139	0.0086	0.0053	0.0040
				Strong	0.0117	0.0065	0.0038	0.0028	0.0139	0.0082	0.0049	0.0038
			8d	None	0.0118	0.0067	0.0038	0.0026	0.0136	0.0084	0.0051	0.0039
				Strong	0.0117	0.0067	0.0039	0.0027	0.0134	0.0080	0.0049	0.0037
		Toe-nails	6d	None	0.0161	0.0105	0.0071	0.0055	0.0239	0.0153	0.0116	0.0099
				Strong	0.0168	0.0103	0.0071	0.0056	0.0234	0.0150	0.0111	0.0095
			8d	None	0.0160	0.0104	0.0069	0.0056	0.0239	0.0154	0.0116	0.0099
				Strong	0.0166	0.0104	0.0070	0.0055	0.0234	0.0151	0.0112	0.0097
Unreinforced Masonry	One	Straps	6d	None	0.0064	0.0035	0.0018	0.0013	0.0076	0.0042	0.0022	0.0016
				Strong	0.0068	0.0037	0.0018	0.0012	0.0076	0.0040	0.0021	0.0014
			8d	None	0.0062	0.0035	0.0018	0.0013	0.0070	0.0040	0.0021	0.0014
				Strong	0.0067	0.0037	0.0018	0.0012	0.0074	0.0039	0.0020	0.0013
		Toe-nails	6d	None	0.0106	0.0072	0.0042	0.0030	0.0149	0.0095	0.0059	0.0046
				Strong	0.0121	0.0073	0.0044	0.0033	0.0157	0.0093	0.0062	0.0048
			8d	None	0.0105	0.0072	0.0040	0.0030	0.0150	0.0091	0.0059	0.0045
				Strong	0.0122	0.0073	0.0043	0.0034	0.0156	0.0095	0.0062	0.0050
	Two	Straps	6d	None	0.0111	0.0064	0.0037	0.0026	0.0137	0.0085	0.0054	0.0039
				Strong	0.0115	0.0065	0.0038	0.0027	0.0133	0.0081	0.0049	0.0037
			8d	None	0.0108	0.0066	0.0036	0.0026	0.0133	0.0084	0.0052	0.0039
				Strong	0.0113	0.0066	0.0037	0.0026	0.0132	0.0079	0.0049	0.0036
		Toe-nails	6d	None	0.0158	0.0104	0.0069	0.0055	0.0238	0.0154	0.0116	0.0097
				Strong	0.0165	0.0105	0.0071	0.0057	0.0231	0.0148	0.0112	0.0098
			8d	None	0.0158	0.0104	0.0070	0.0055	0.0236	0.0153	0.0115	0.0101
				Strong	0.0165	0.0105	0.0071	0.0058	0.0233	0.0149	0.0112	0.0097
Reinforced Masonry	One	Straps	6d	None	0.0065	0.0035	0.0018	0.0013	0.0075	0.0042	0.0022	0.0015
				Strong	0.0069	0.0037	0.0018	0.0012	0.0077	0.0041	0.0020	0.0014
			8d	None	0.0063	0.0035	0.0018	0.0013	0.0070	0.0040	0.0021	0.0015
				Strong	0.0067	0.0036	0.0018	0.0012	0.0074	0.0039	0.0021	0.0013
		Toe-nails	6d	None	0.0105	0.0071	0.0041	0.0030	0.0150	0.0094	0.0059	0.0045
				Strong	0.0120	0.0073	0.0044	0.0033	0.0155	0.0094	0.0063	0.0048
			8d	None	0.0105	0.0070	0.0042	0.0030	0.0148	0.0092	0.0059	0.0044
				Strong	0.0120	0.0072	0.0044	0.0033	0.0156	0.0094	0.0062	0.0049
	Two	Straps	6d	None	0.0110	0.0065	0.0037	0.0026	0.0135	0.0085	0.0054	0.0040
				Strong	0.0116	0.0066	0.0038	0.0027	0.0134	0.0078	0.0050	0.0037
			8d	None	0.0110	0.0064	0.0037	0.0026	0.0134	0.0084	0.0052	0.0039
				Strong	0.0114	0.0066	0.0037	0.0026	0.0131	0.0078	0.0048	0.0035
		Toe-nails	6d	None	0.0158	0.0103	0.0070	0.0054	0.0236	0.0154	0.0116	0.0099
				Strong	0.0165	0.0104	0.0072	0.0056	0.0233	0.0149	0.0110	0.0094
			8d	None	0.0159	0.0104	0.0070	0.0054	0.0237	0.0153	0.0114	0.0099
				Strong	0.0166	0.0105	0.0073	0.0057	0.0235	0.0151	0.0111	0.0094

Table 7.26. Percent Increases in the Average Annual Total Loss Due to Changes in Building Parameters (Minimum/Average/Maximum) – Residential Buildings

Parameter	Increase in Average Annual Building Loss
Treed to Open Terrain	141% / 230% / 320%
One Story to Two Story	38% / 73% / 129%
8d to 6d Roof Sheathing Nails	-1% / 5% / 31%
Strapped to Toe-Nailed Roof/Wall Connections	10% / 31% / 82%
Hip to Gable Roof	2% / 22% / 41%
No Garage to Strong Garage Door	-14% / -5% / 5%
No Garage to Weak Garage Door	-8% / 6% / 43%
Reinforced Masonry to Unreinforced Masonry Walls	-2% / 0% / 2%
Unreinforced Masonry to Wood Frame Walls	-2% / 0% / 2%

Table 7.27. Percent Decreases in the Average Annual Total Loss Due to Mitigation Parameters (Minimum/Average/Maximum) – Residential Buildings

Mitigation Strategy	Decrease in Average Annual Building Loss
Install Shutters	17% / 33% / 46%
Upgrade Roof	3% / 16% / 49%
Add Secondary Water Resistance	3% / 12% / 35%
Install Shutters and Upgrade Roof	46% / 59% / 71%
Install Shutters, Upgrade Roof, and Add Secondary Water Resistance	51% / 68% / 85%
Upgrade Roof and Add Secondary Water Resistance	4% / 19% / 57%

***Losses Associated with Frame Damage or Foundation Failure*.** Loss ratios associated with the failure of roof-wall connections, wall failure following partial or whole roof failure, floor-wall connection failure and foundation failure through sliding or overturning, are summarized in Table 7.28. The values listed in Table 7.28 are percentages of the MH replacement cash value or the content cash value. Hence, a MH sustaining minor sliding will have a building loss of 10% and a content loss of 0%. The values used in Table 7.28 are compiled from field observations and engineering judgment.

Table 7.28. Building and Content Losses Associated with Manufactured Home Frame Damage or Foundation Failure

Modeled Structure Damage State	Structure Loss (% of Building Value)	Content Loss (% of Content Value)
Minor Roof-Wall Connection Failure	20	0
Major Roof-Wall Connection Failure	100	100
Wall Failure Following roof Failure	100	100
Minor Floor-Wall Connection Failure	30	0
Major Floor-Wall Connection Failure	100	100
Minor Sliding Failure	10	0
Major Sliding Failure	100	100
Overturning	100	100

Interior and Content Losses. The implicit costing method calculates losses to the interior and framing of the building as a function of water volume penetrating the building envelope. The functions which relate the volume of water to building losses are based on engineering judgment and field observations and are identical to the residential case.

7.8.2 Fast Running Manufactured Home Loss Functions

Using the hurricane wind speed and direction data used to develop the damage function curves for manufactured homes, per storm losses were estimated through the combination of the loss model described above and the storm-by-storm damage estimates, to produce estimates of economic loss as a function of peak gust wind speed in open terrain. The resulting loss functions, computed separately for the economic losses to the building and to the contents, are given in Appendix I. Table 7.29 lists the average annual loss data for each of the manufactured homes analyzed.

Table 7.29. Annual Average Losses – Manufactured Homes

Average Annual Building Loss Normalized by Building Value					
	Terrain Surface Roughness (m)				
Mobile Home Construction	z_0 = 0.03	z_0 = 0.15	z_0 = 0.35	z_0 = 0.7	z_0 = 1.0
Pre-HUD, Not Tied Down	0.0303	0.0225	0.0167	0.0126	0.0110
Pre-HUD, Tied Down	0.0277	0.0203	0.0147	0.0106	0.0090
HUD, Not Tied Down	0.0294	0.0211	0.0157	0.0119	0.0104
HUD, Tied Down	0.0262	0.0183	0.0131	0.0094	0.0079
1994 HUD – Wind Zone I, Tied Down	0.0314	0.0240	0.0179	0.0136	0.0117
1994 HUD – Wind Zone II, Tied Down	0.0129	0.0099	0.0069	0.0048	0.0040
1994 HUD – Wind Zone III, Tied Down	0.0121	0.0091	0.0064	0.0046	0.0038
Average Annual Content Loss Normalized by Building Value					
	Terrain Surface Roughness (m)				
Mobile Home Construction	z_0 = 0.03	z_0 = 0.15	z_0 = 0.35	z_0 = 0.7	z_0 = 1.0
Pre-HUD, Not Tied Down	0.0139	0.0102	0.0075	0.0055	0.0047
Pre-HUD, Tied Down	0.0121	0.0088	0.0061	0.0041	0.0034
HUD, Not Tied Down	0.0134	0.0095	0.0070	0.0052	0.0044
HUD, Tied Down	0.0113	0.0077	0.0052	0.0034	0.0027
1994 HUD – Wind Zone I, Tied Down	0.0139	0.0107	0.0077	0.0057	0.0047
1994 HUD – Wind Zone II, Tied Down	0.0049	0.0039	0.0025	0.0016	0.0013
1994 HUD – Wind Zone III, Tied Down	0.0044	0.0034	0.0023	0.0015	0.0012

7.9 Economic Loss Model for Commercial Buildings and Essential Facilities

Similar to the residential and manufactured home (MH) loss models, the commercial and essential facilities loss model is also developed using explicit and implicit costing techniques. The commercial and essential facilities loss model differs from the residential and MH loss models in how the total cost of the building is distributed amongst the subassemblies. Due to the scope of the current commercial model, detailed unit costs are not used to derive the explicit loss for failed components. Rather, subassemblies are cost directly from their damage ratios calculated from the damage model. Changes in cost distribution among subassemblies associated with differences in exterior wall types and

common additives are ignored. It is also noted that the commercial model described herein uses different influence functions or cost functions from those used in residential loss model. Unless noted otherwise, details regarding essential facilities are similar to those used for commercial buildings.

Due to the scarcity of high quality loss data, limited calibration has been done with the commercial and essential facilities loss model, which has been developed primarily on the basis of experience and judgment.

7.9.1 Subassembly Cost Ratios

The subassembly cost ratios for the model the buildings are based on the RSMeans Square Foot Costs for new construction. Seventy commercial/industrial building types are listed in RSMeans, including apartments, bank, church, factory, hotel, motel, department store, etc. The Hazus model buildings, which are selected to represent certain building classes, are mapped to one of those 70 building types with possible adjustments to the RSMeans cost ratios according to the number of stories, percentage of exterior door area to the total exterior wall area, and percentage of windows and glazed wall area to the total exterior wall area of the model building.

Cost Ratio Adjustment – Number of Stories. As indicated in RSMeans, for similar building types, the cost ratios for foundations, substructure, exterior closure, roofing and mechanical decrease with the increase in number of stories, whereas the cost ratios for interior construction and conveying increase with the increase in number of stories. The changes in superstructure and electrical are not monotonic. Since these changes can be significant, adjustments must be made to the cost ratios if the number of stories for selected model building is different from that for the model building listed in RSMeans. Based on the data from RSMeans, the functions shown in Equations 7.10 through 7.14 are developed to adjust the cost ratio according to the story number of the selected model building.

1. Foundation, substructure, and roofing:

$$R_c' = R_c\left(1 - 2.0\left(\frac{N_m}{N} - 1\right)\right), \qquad \text{for } N_m < N$$

$$R_c' = R_c\left(1 - 0.4\left(\frac{N_m}{N} - 1\right)\right), \qquad \text{for } N_m > N \tag{7.10}$$

2. Superstructure:

$$R_c' = R_c\left(1 + 0.6\left(\frac{N_m}{N} - 1\right)\right), \qquad \text{for } N_m < N$$

$$R_c' = R_c\left(1 - 0.08\left(\frac{N_m}{N} - 1\right)\right), \qquad \text{for } N_m > N \tag{7.11}$$

3. Exterior closure and mechanical:

$$R_c' = R_c\left(1 - 0.2\left(\frac{N_m}{N} - 1\right)\right), \quad \text{for } N_m<N$$
$$R_c' = R_c, \quad \text{for } N_m>N \tag{7.12}$$

4. Interior construction:

$$R_c' = R_c\left(1 + 0.2\left(\frac{N_m}{N} - 1\right)\right), \quad \text{for } N_m<N$$
$$R_c' = R_c\left(1 + 0.133\left(\frac{N_m}{N} - 1\right)\right), \quad \text{for } N_m>N \tag{7.13}$$

5. Conveying:

$$R_c' = R_c\left(1 + 0.6\left(\frac{N_m}{N} - 1\right)\right), \quad \text{for } N_m<N$$
$$R_c' = R_c\left(1 + 0.133\left(\frac{N_m}{N} - 1\right)\right), \quad \text{for } N_m>N \tag{7.14}$$

where N_m=number of stories for selected model building, N=number of stories for the building listed in RSMeans, R_c=unadjusted cost ratio, R_c'=adjusted cost ratio. No adjustments are made for the other subassemblies.

Cost Ratio Adjustment – Door, Window, and Glazed Wall Area. Since exterior closure plays an important role in determining losses, adjustments are made to the cost distributions among all the subassemblies based on the difference in exterior closure between Hazus model building and RSMeans model building. Specifically, the costs per square foot for walls, doors, windows and glazed walls are adjusted based on the percentage of the wall area of each subassembly. For example, if the RSMeans model building has 14% of the wall area with windows and glazed walls (cost per square foot=$1.37) and a Hazus model building has 20% of the wall area with windows and glazed walls, the adjusted cost per square foot will be $1.37/0.14*0.20=$1.96. Note that since changing cost per square foot for one subassembly will affect the cost ratio for all other subassemblies (because the subtotal changes), the cost ratios for all other subassemblies must be updated accordingly.

Even though other parameters, such as square footage of floor area, perimeter length, exterior wall type, and frame type can also change the cost ratio distribution, it is assumed that their influences can be neglected. Table 7.30 lists the comparison between the cost ratios from RSMeans (motel, 2-3 stories) and adjusted cost ratios for the selected model building (a 4-story motel). For some subassemblies, the changes in cost ratio can be substantial (e.g., roofing).

7.9.2 Building Loss Model

The damage state parameters required for the commercial loss model include damage to windows, doors, roof covering, roof decking, and roof framing, damaged wall surface area, water from fenestration damage, water from roof cover damage, and water from roof sheathing damage. It is assumed that the explicit losses are caused primarily by the damage to windows, doors, roofs, and walls while water entering the building is the major cause of losses to the interior, mechanical, electrical, and conveying systems (i.e., implicit losses). To reflect the different damage-to-loss propagation mechanisms for different components, a set of costing functions are developed based on experience and judgment. Tables 7.31 and 7.32 show the influence matrixes for explicit loss and implicit loss, respectively. Each row in Tables 7.31 and 7.32 indicates a subassembly and each column indicates an input damage state. The value in each cell of Table 7.31 or 7.32 is a cost function index, which indicates the function type used to map damage to loss for a given damage parameter. For example, damage to the roof cover, roof deck, and roof frame all can result in insulation losses. However, the insulation loss ratios due to the same damage ratios from roof cover, roof deck, and roof frame are different. The cost functions for explicit insulation losses due to roof cover, roof deck, and roof frame are determined to be type 1, type 4, and type 4, respectively (see Table 7.31 – Insulation). The cost function indices as well as their associated formulae are shown in Table 7.33. Figure 7.7 shows the plots of these influence functions. In determining the loss ratios associated with roof cover damage, the influence functions for mechanical, electrical, and special construction are multiplied by 0.1, 0.2, and 0.3, respectively, to account for the reduced damage severity than the interior construction (based on limited calibration studies).

Several repair and replacement thresholds are used in the current commercial model to reflect the fact that when a certain percentage of damage to a subassembly is achieved, the entire subassembly will be replaced. These thresholds are 5%, 10%, and 30% for roof cover, roof deck, and wall cladding, respectively.

For the subassemblies with more than one damage variable involved, the possibility of overlapping is considered using their joint probability. Hence, the resulted loss ratio (R) for a subassembly with two contributing variables is approximated by $R=R_1+R_2-R_1R_2$, with R_1=loss ratio resulted from the first variable only and R_2=loss ratio resulted from the second variable only. After the loss ratio for each subassembly has been calculated, the total building loss ratio is obtained by simply adding up the loss ratios for the subassemblies. The building loss ratio is then multiplied by a repair and replacement factor of 1.25 and an overhead and profit factor of 1.20 to account for the additional costs associated with the repair and remodeling. The total economic loss of the building is also constrained not to exceed the assumed insured value.

Figure 7.8 shows a scatter plot of the calculated building loss ratio as a function of open terrain peak gust wind speed based on 20,000 year simulation for a 4-story motel in the Miami area. The contribution to the total building loss ratio from each damage state considered is also shown in this figure. Implicit losses (interior, mechanical, and

Table 7.30. Cost Ratio – RSMeans Model Building and Hazus Model Building

Damage Variables	RSMeans Model Building(3-Story Motel)		Hazus Model Building(4-Story Motel)	
Foundations				
Footings & Foundations	2.0%	2.5%	1.7%	2.2%
Piles & Caissons	0.0%		0.0%	
Excavation & Backfill	0.5%		0.5%	
Substructures				
Slab on Grade	1.7%	1.7%	1.5%	1.5%
Special Substructures	0.0%		0.0%	
Superstructure				
Columns and Beams	0.0%	13.8%	0.0%	13.6%
Structural Walls	2.6%		2.5%	
Elevated Floors/Diaphragms	6.6%		6.5%	
Roof Decking/Framing	3.2%		3.2%	
Stairs	1.4%		1.4%	
Exterior Closure				
Walls	4.7%	10.3%	4.3%	8.8%
Exterior Wall Finishes	0.0%		0.0%	
Doors	3.9%		3.9%	
Windows & Glazed Walls	1.8%		0.6%	
Roofing				
Roof Covering	1.1%	2.1%	1.0%	1.8%
Insulation	0.7%		0.6%	
Openings & Specialties	0.3%		0.2%	
Interior Construction				
Partitions	8.9%	35.6%	9.4%	37.6%
Interior Doors	7.9%		8.3%	
Wall Finishes	3.7%		3.9%	
Floor Finishes	9.3%		9.8%	
Ceiling Finishes	4.6%		4.9%	
Interior Surface of Exterior Walls	1.2%		1.3%	
Conveying				
Elevators	2.7%	2.7%	2.8%	2.8%
Special Conveyors	0.0%		0.0%	
Mechanical				
Plumbing	15.9%	22.9%	16.1%	23.2%
Fire Protection	1.8%		1.8%	
Heating	0.0%		0.0%	
Cooling	5.2%		5.3%	
Special Systems	0.0%		0.0%	
Electrical				
Service & Distribution	0.5%	8.4%	0.5%	8.5%
Lighting & Power	7.4%		7.5%	
Special Electrical	0.5%		0.5%	
Special Construction				
Specialties (& Additives)	0.0%	0.0%	0.0%	0.0%
Total	100%	100%	100%	100%

Table 7.31. Influence Matrix for Explicit Building Loss

Damage Variables	Windows	Doors	Roof Covering	Roof Decking	Roof Framing	Wall Surf. by Missile	Wall Surf. by Pressure	Wall Structure
Superstructure								
Columns and Beams	0	0	0	0	0	0	0	5
Structural Walls	0	0	0	0	0	0	0	1
Elevated Floors/Diaphragms	0	0	0	0	0	0	0	5
Roof Decking/Framing	0	0	0	2	1	0	0	0
Stairs	0	0	0	0	0	0	0	0
Exterior Closure								
Walls	0	0	0	0	0	9	1	1
Exterior Wall Finishes	0	0	0	0	0	9	1	1
Doors	0	1	0	0	0	0	0	1
Windows & Glazed Walls	1	0	0	0	0	0	0	1
Roofing								
Roof Covering	0	0	3	0	0	0	0	0
Insulation	0	0	1	4	4	0	0	0
Openings & Specialties	0	0	1	1	4	0	0	0

Table 7.32. Influence Matrix for Implicit Building Loss

Damage Variables	Water Depth by Fen	Water Depth by Cover	Water Depth by Sheath	Wet Area by Cover	Wet Area by Sheath
Interior Construction					
Partitions	6	0	0	7	8
Interior Doors	6	0	0	7	8
Wall Finishes	6	0	0	7	8
Floor Finishes	6	0	0	7	8
Ceiling Finishes	6	0	0	7	8
Interior Surface of Exterior Walls	6	0	0	7	8
Conveying					
Elevators	0	0	0	0	0
Special Conveyors	0	0	0	0	0
Mechanical					
Plumbing	6	0	0	7	8
Fire Protection	6	0	0	7	8
Heating	6	0	0	7	8
Cooling	6	0	0	7	8
Special Systems	6	0	0	7	8
Electrical					
Service & Distribution	6	0	0	7	8
Lighting & Power	6	0	0	7	8
Special Electrical	6	0	0	7	8
Special Construction					
Specialties (& Additives)	6	0	0	7	8

Table 7.33. Influence Functions

Function Index	Formula*
1	$y = x;$
2	$y = \frac{2}{\pi} tan^{-1}(e^{0.8x} - 1)$
3	$y = \frac{2}{\pi} tan^{-1}(e^{50.0x^{1.5}} - 1)$
4	$y = \frac{2}{\pi} tan^{-1}(e^{5.0x} - 1)$
5	$y = \frac{2}{\pi} tan^{-1}(e^{0.4x} - 1)$
6	$y = \frac{2}{\pi} tan^{-1}(e^{10.0x} - 1)$
7	$y = \frac{2}{\pi} tan^{-1}(e^{3.1x^{2.0}} - 1)$
8	$y = \frac{2}{\pi} tan^{-1}(e^{8.0x} - 1)$
9	$y = \frac{2}{\pi} tan^{-1}(e^{1.4x} - 1)$

* Note: x = component damage ratio (0% – 100%) and y = calculated loss ratio (0% – 100%)

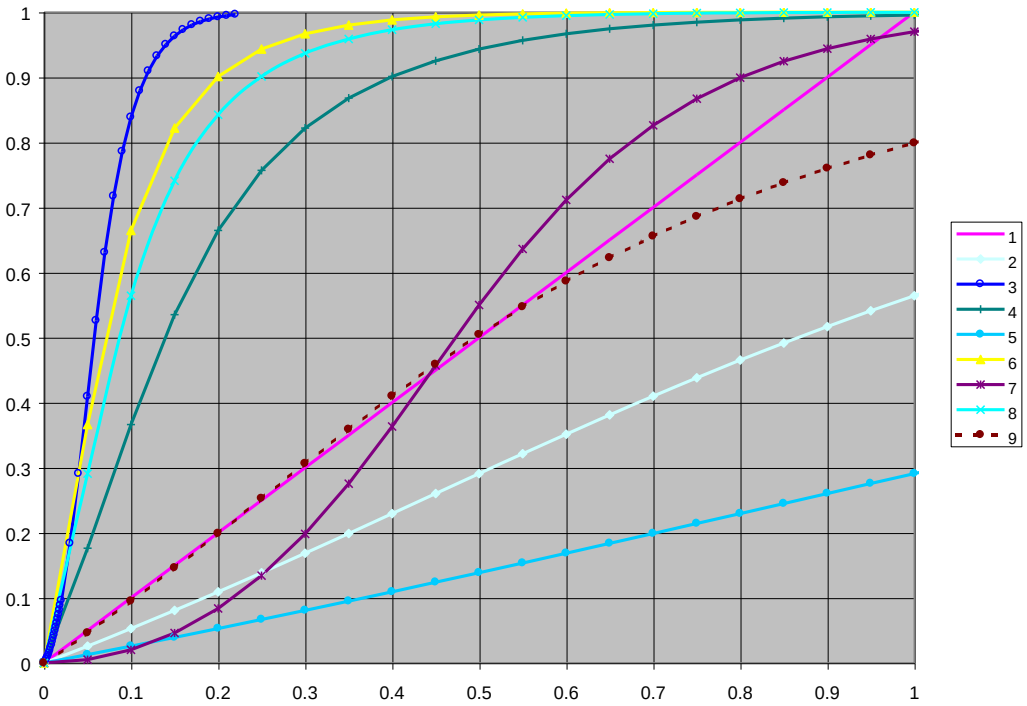

Figure 7.7. Plots of Influence Functions.

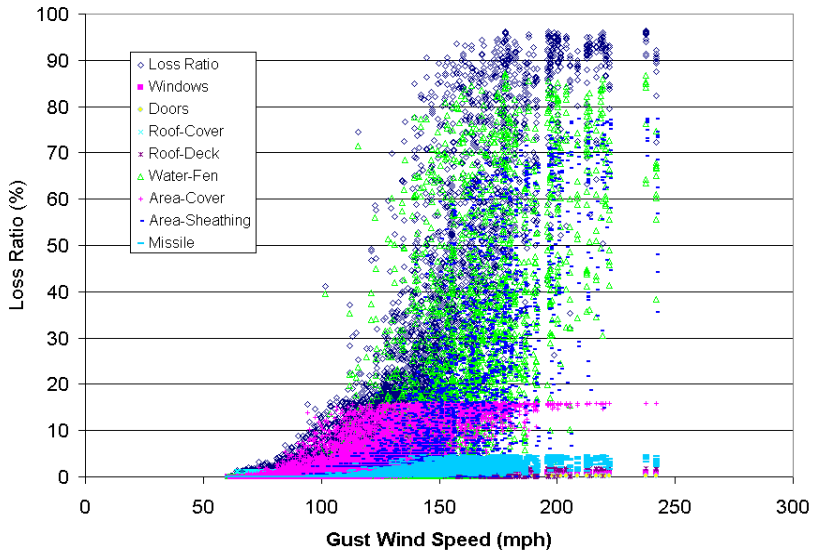

Figure 7.8. Relationship between Open Terrain Gust Wind Speed and Building Loss Ratio for a 4-Story Motel.

electrical losses due to building envelop breaches) are seen to contribute most to the total building loss. The explicit losses caused by damage to roofs, walls, and fenestration account for less than 20% of the total building loss.

7.9.3 Content Loss Model

The content loss model for commercial buildings is almost identical to the content loss model for residential buildings developed previously. Content losses are assumed to be highly correlated with the damage to the interior of the building, but begin to occur after at least some damage has been done to the interior of the building. Water entering the building is also believed to be the major cause of content loss. Three modeled damage variables (water depth due to fenestration damage, wetted interior area due to roof cover damage, and wetted interior area due to roof sheathing damage) are used to model the content loss. Note that all these three variables are related to the water entering a building after the breach of the building envelop.

Content losses due to fenestration damage are modeled as:

$$L_{c1}=4.0D_{fen}, \quad \text{for } D_{fen}<0.25'' \qquad (7.15)$$

$$L_{c1}=1.0, \quad \text{for } D_{fen}\geq 0.25''$$

where L_{c1} = content loss ratio due to fenestration damage; D_{fen} = accumulated water depth due to fenestration damage. Content losses due to roof cover damage are assumed to be accrued at one half the rate associated with losses to the interior of the building. It is also assumed that no contents are damaged until a threshold of 20% of roof cover damage has occurred. A linear approximation is made to the costing function of the interior damage due to roof cover damage to derive the costing function for content loss:

$$L_{c2}=0.0, \quad \text{for } R_{cover}<0.2$$
$$L_{c2}=1.67(R_{\text{cover}}-0.2)(0.5), \quad \text{for } R_{cover}\geq 0.2 \qquad (7.16)$$

where L_{c2} = content loss ratio due to roof over damage; R_{cover} = wetted interior ratio due to roof cover damage. The content loss associated with roof sheathing damage is modeled as:

$$L_{c3}=4.0R_{\text{sheath}}, \quad \text{for } R_{sheath}<0.25$$
$$L_{c3}=1.0, \quad \text{for } R_{sheath}\geq 0.25 \qquad (7.17)$$

where L_{c3}=content loss ratio due to roof sheathing damage; R_{sheath}=wetted interior ratio due to roof sheathing damage.

The final content loss is taken to be the maximum among the losses produced by fenestration damage, roof cover damage or roof sheathing damage, i.e., max(L_{c1}, L_{c2}, L_{c3}). Figure 7.9 shows the relationship between building loss ratio and content loss ratio for a 4-story motel located in the Miami area using 20,000 year simulation.

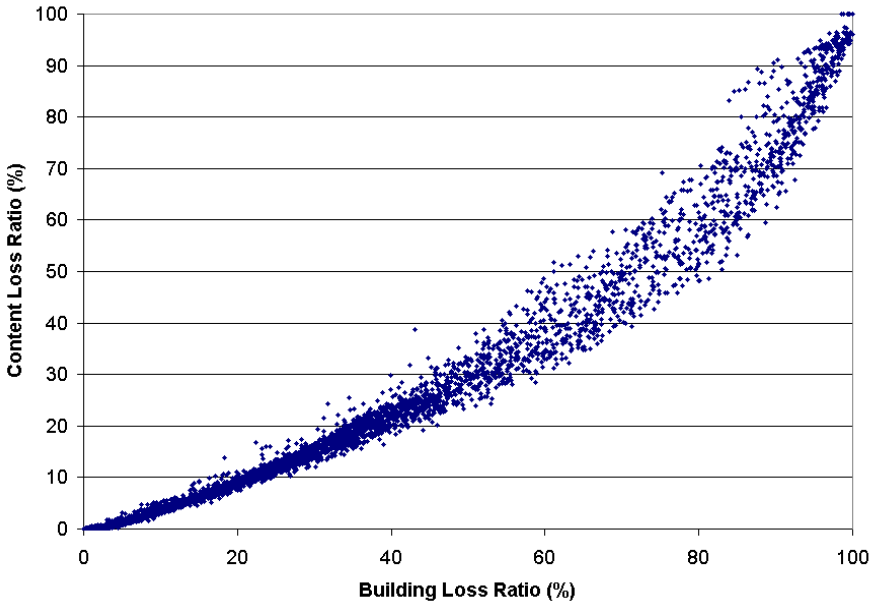

Figure 7.9. Relationship between Building Loss Ratio and Content Loss Ratio for a 4-Story Motel.

7.9.4 Business Interruption Model

The business interruption model for commercial buildings follows the business interruption model developed for earthquakes in Hazus-99 (FEMA, 1999). The model applies a multiplier to expected loss of use to estimate the duration of business interruption. The model for expected loss of use follows the approach presented in Section 7.5.3 for single-family buildings. The default multipliers for estimating business

interruption are provided in Table 7.34. As explained in Hazus-99 Technical Manual, the business interruption multiplier reflects the fact that business interruption is not directly related to loss of use for certain types of business (since they can rent alternative space or use spare industrial/commercial capacity elsewhere). The output from the business interruption model is the expected number of days for a business to be fully recovered. The relationship between the business interruption, *N* (days), and building loss ratio can be expressed as:

Table 7.34. Business Interruption Time Table

Label	Occupancy Class	Business Interruption Time Multiplier				
		Building Loss Ratio				
		0%	2%	10%	50%	100%
RES3	Multi-Family Dwelling	0	0	0.5	1	1
RES4	Temporary Lodging	0	0	0.5	1	1
RES5	Institutional Dormitory	0	0	0.5	1	1
RES6	Nursing Home	0	0	0.5	1	1
COM1	Retail Trade	0.5	0.1	0.1	0.3	0.4
COM2	Wholesale Trade	0.5	0.1	0.2	0.3	0.4
COM3	Personal and Repair Service	0.5	0.1	0.2	0.3	0.4
COM4	Professional/Technical/Business Services	0.5	0.1	0.1	0.2	0.3
COM5	Banks/Financial Institutions	0.5	0.1	0.05	0.03	0.03
COM6	Hospital	0.5	0.1	0.5	0.5	0.5
COM7	Medical Office/Clinic	0.5	0.1	0.5	0.5	0.5
COM8	Entertainment & Recreation	0.5	0.1	1	1	1
COM9	Theaters	0.5	0.1	1	1	1
COM10	Parking	0.1	0.1	1	1	1
IND1	Heavy Industrial Factory	0.5	0.5	1	1	1
IND2	Light Industrial Factory	0.5	0.1	0.2	0.3	0.4
IND3	Food/Drug/Chemicals Factory	0.5	0.2	0.2	0.3	0.4
IND4	Metals/Minerals Processing Factory	0.5	0.2	0.2	0.3	0.4
IND5	High Technology Factory	0.5	0.2	0.2	0.3	0.4
IND6	Construction	0.5	0.1	0.2	0.3	0.4
AGR	Agriculture	0	0	0.05	0.1	0.2
REL	Church/Membership Organization	1	0.2	0.05	0.03	0.03
GOV1	General Service	0.5	0.1	0.02	0.03	0.03
GOV2	Emergency Response	0.5	0.1	0.02	0.03	0.03
ED1	Schools/Libraries	0.5	0.1	0.02	0.05	0.05
ED2	College/University	0.5	0.1	0.02	0.03	0.03

$$N = N_{lou}(R_{building}) \cdot Mod(R_{building}) \tag{7.18}$$

where N_{lou}()=building loss of use (days) taking into account of delays in decision making, fiancing, inspection, etc. and *Mod*()=business interruption multiplier from Table 7.34. Both loss of use and business interruption multiplier are modeled as functions of building loss ratio ($R_{building}$). Figure 7.10 illustrates the relationship between loss of use, business interruption, and building loss for a motel (RES4).

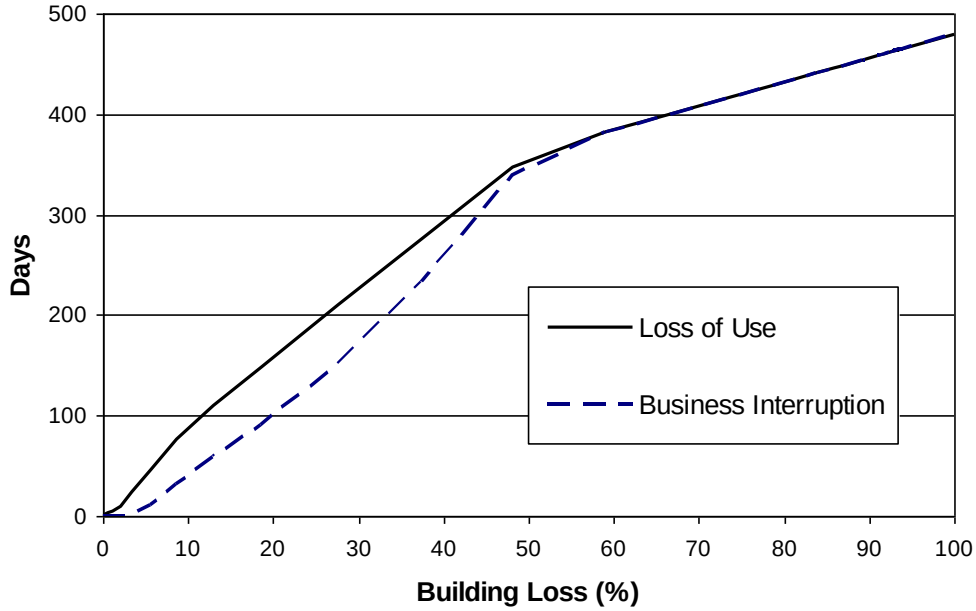

Figure 7.10. Relationship between Building Loss, Loss of Use, and Business Interruption for a Motel.

7.9.5 Loss of Function for Essential Facilities

Generally speaking, loss of function is the amount of time (days) that a facility is unable to provide the public with general services from a specific facility. This would represent the amount of time a school is closed to students, and the number of days a specific fire station cannot provide emergency fire and rescue services to its designated coverage area.

Most of the validation data obtained in developing loss of function models comes from a phone survey of individual facilities conducted in the Houston area regarding Hurricane Ike (2008) and in Escambia county in Florida after Hurricane Ivan (2004) in 2011. Data from the FEMA HMTAP 440 report was also used. Further descriptions and details are provided in the following sections. While loss of function data was obtained during the phone survey, little in the way of accompanying building loss data was obtained.

7.9.5.1 Loss of Function for Fire Stations

This represents the average amount of time (days) fire stations in a given area will not be able to provide service to the public from that facility. While an individual fire station may suffer a disruption in its ability to provide emergency services, the public as a whole may not be affected at all since equipment and resources of these disrupted facilities can be moved to other neighboring stations. Fire station loss of function is intended to alert the decision maker that facilities in a given study region may not be able to provide service after an event, and aid the decision maker in equipment and personnel re-assignment.

A phone survey of fire stations in the Houston area that were affected by Hurricane Ike (2008) showed that while fire stations can experience wind-induced damage, they typically do not close due to minor damage and power loss. For one facility, building loss was estimated to be greater than 10% when wind lifted roof panels, and allowed water to enter the facility. Despite this, the fire station did not close. Only one fire station was found to have actually suffered enough damage to close (60 days) due to wind damage among the 50+ fire stations contacted. Building loss was unknown for this case and is assumed to be an isolated case in Figure 7.10. With respect to power loss, fire stations typically have back-up generators in place or are brought to the site.

The modeled curve in Figure 7.1 represents a fire station of moderate strength in light suburban terrain, in an area that could produce a mix of residential and commercial wind-borne debris. It has been assumed that loss of function around 1 day or so starts to occur when the building experiences roughly 6% building loss (the replacement value of the roof cover).

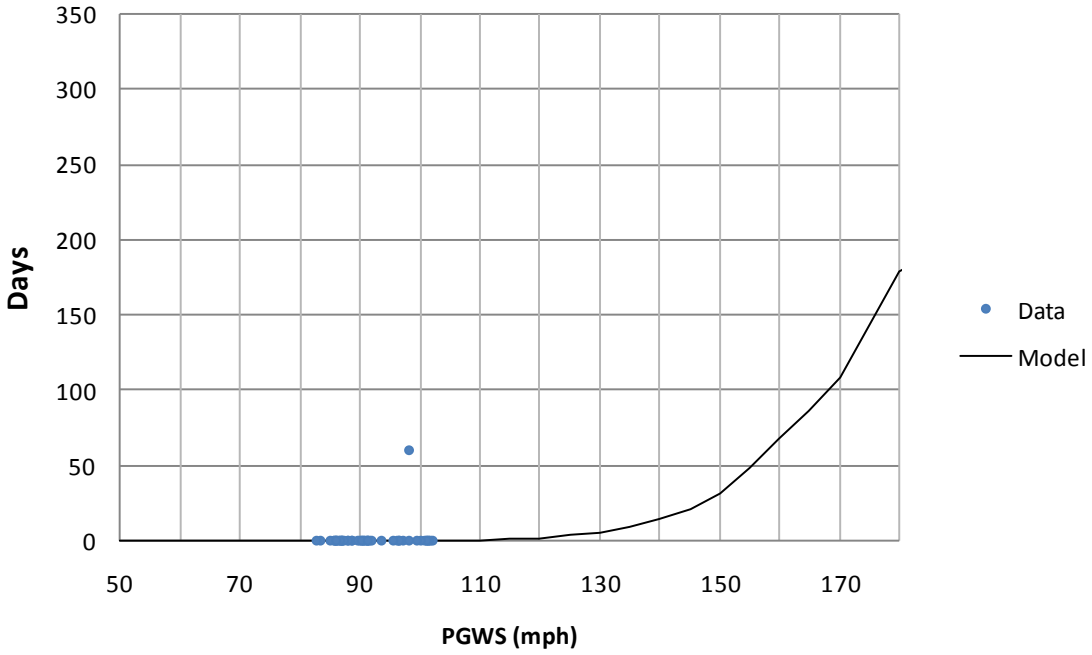

Figure 7.10. Relationship Between Modeled loss of Function and Actual loss of Function for a Given Fire Stations

7.9.5.2 Loss of Function for Schools

Loss of function for schools represents the average amount of time (days) a school will be closed to students while essential personnel may still report to the school during this period. The data displayed in Figure 7.11 are for independent school districts (ISDs) from the Houston area (Hurricane Ike, 2008) and Escambia County (Hurricane Ivan, 2004). The Loss of function model for schools was calibrated against ISD data as a whole, rather than individual schools, since decisions about school closings are typically

made at the district level, rather than at the facility level. From the phone survey conducted, ISDs typically closed due to lack of electricity.

A school in suburban terrain, susceptible to residential wind-borne debris of moderate strength was assumed when calibrating the loss of function model. Loss of function for schools is not defined by a specific building value or building feature, as is the case with fire stations, but has more to do with loss of power as a function of wind speed. At higher wind speeds it is assumed that building damage will drive the loss of function rather than power restoration. Building loss data accompanying loss of function data obtained from the phone survey for individual schools was typically less than 1% of estimated building value.

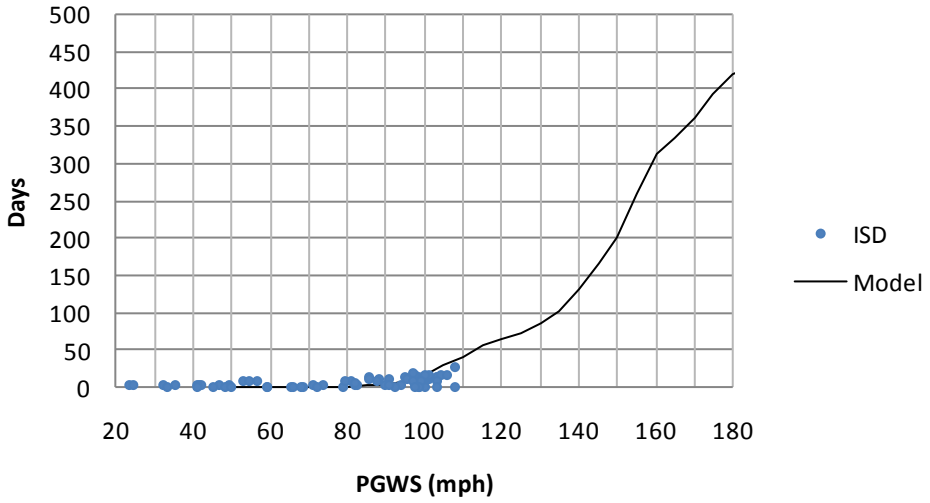

Figure 7.11. Relationship Between Modeled loss of Function and Actual loss of Function for an Elementary School of Moderate Strength located in a Residential Area

7.9.5.3 Loss of Function for Hospitals

This represents the average amount of time (days) that all beds in a hospital will be unavailable to patients. While a hospital may technically be "closed" to the general public during a hurricane, if all of its beds are still available to patients (patients were not moved from the facility), then the loss of function recorded was zero days.

Several hospitals contacted in the Houston area who were affected by Hurricane Ike (2008) were noted to have closed due to lack of power but most had emergency back-up power in place aiding in their ability to stay open. While several hospitals did experience damage, specific building loss and building value were unavailable.

Modeled loss of function of a day is assumed to occur close to 1% of the buildings value (roof cover cost). Figure 7.12 through Figure 7.14 plot modeled loss of function and phone survey data, along with FEMA HMTAP 440 data due to Hurricane Charley (2004), Ike (2008), and Ivan (2004) for small, medium, and large hospitals respectively of average strength in a suburban environment.

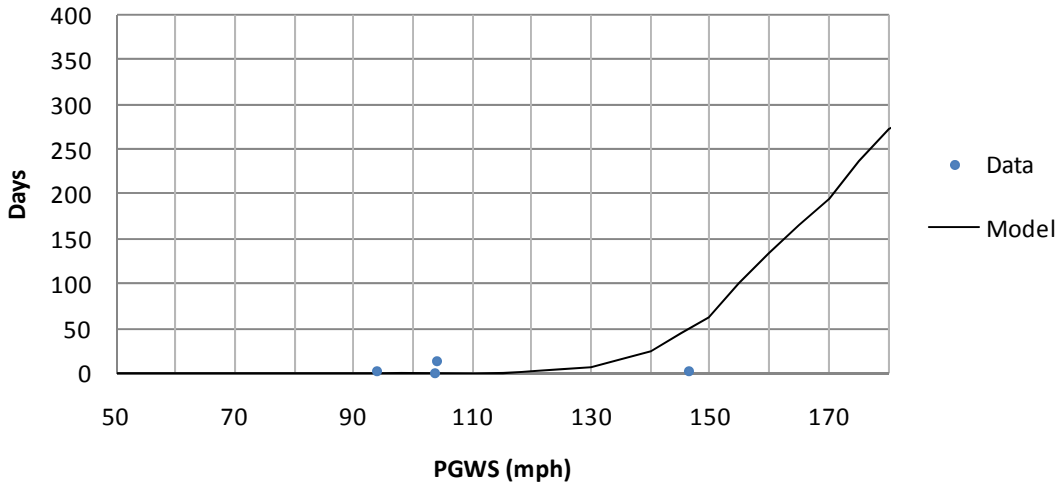

Figure 7.12. Relationship Between Modeled Loss of Function and Actual Loss of Function for a Small Hospital

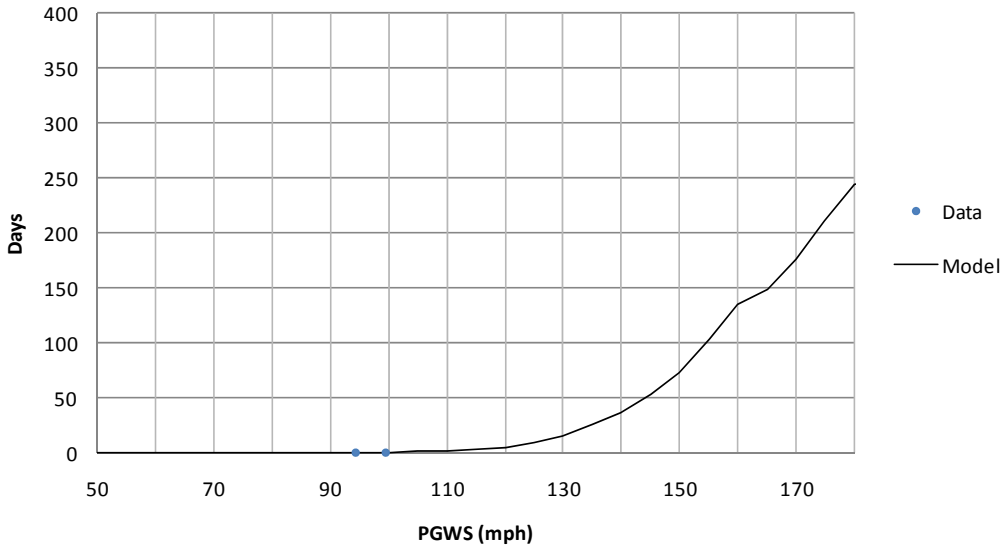

Figure 7.13. Relationship Between Modeled Loss of Function and Actual Loss of Function for a Medium Hospital

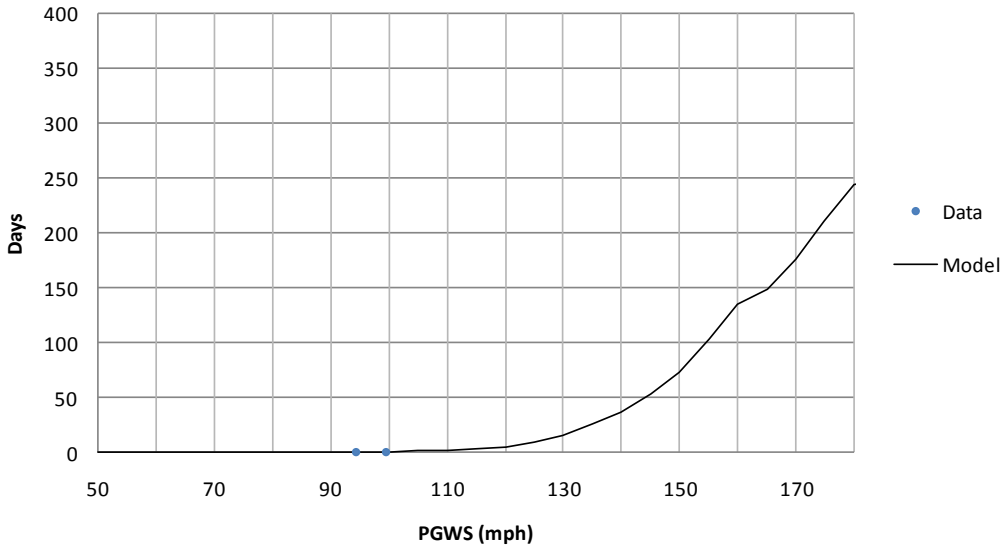

Figure 7.14. Relationship Between Modeled Loss of Function and Actual Loss of Function for a Large Hospital

7.10 Loss Model Results for Marginally-Engineered or Non-Engineered Hotel/Motel and Multi-Family Residential Buildings

The commercial loss model described in Section 7.9 has been coupled with the damage results for the multi-family residential buildings to produce estimates of losses as a function of wind speed. The same 20,000-year storm simulation used to produce the loss plots for the single family residential buildings was used for the multi-family buildings. The assumed subassembly cost distributions are listed in Tables 7.35, 7.36 and 7.37 for one-story motels, two- to three-story motels and four- to seven-story hotels, respectively.

Example building and content loss functions are given in Appendix J. Tables 7.38 through 7.40 present the average annual building loss (expressed as a fraction of the total building value) for gable/hip roofs with shingles, flat roofs with built-up roof cover and flat roofs with single ply membrane roof covers, respectively. Tables 7.41 through 7.43 present the average annual content loss (also expressed as a fraction of the building value) for the same three building classes, respectively. Table 7.44 presents a summary of the effects of various building parameters on average annual building loss.

7.11 Loss Model Results for Low-Rise Masonry Strip Mall Buildings

Loss functions have been developed for low-rise masonry strip mall buildings using the same hurricane wind speed and direction data (20,000 years of storm simulation) used in the development of the damage curves. The model buildings were assumed to be used as department stores. The assumed subassembly cost distributions are listed in Table 7.45.

Table 7.35. Subassembly Cost Distributions for One-Story Motels

Subassemblies	Cost Ratios	
Foundations		
Footings & Foundations	8.1%	9.8%
Piles & Caissons	0.0%	
Excavation & Backfill	1.6%	
Substructures		
Slab on Grade	4.7%	4.7%
Special Substructures	0.0%	
Superstructure		
Columns and Beams	0.0%	6.6%
Structural Walls	0.0%	
Elevated Floors/Diaphragms	0.0%	
Roof Decking/Framing	6.6%	
Stairs	0.0%	
Exterior Closure		
Walls	10.1%	18.4%
Exterior Wall Finishes	0.0%	
Doors	4.0%	
Windows & Glazed Walls	4.2%	
Roofing		
Roof Covering	1.6%	3.6%
Insulation	1.3%	
Openings & Specialties	0.7%	
Interior Construction		
Partitions	6.5%	25.8%
Interior Doors	1.7%	
Wall Finishes	2.7%	
Floor Finishes	8.8%	
Ceiling Finishes	4.4%	
Interior Surface of Exterior Walls	1.7%	
Conveying		
Elevators	0.0%	0.0%
Special Conveyors	0.0%	
Mechanical		
Plumbing	15.8%	23.5%
Fire Protection	3.1%	
Heating	0.0%	
Cooling	4.7%	
Special Systems	0.0%	
Electrical		
Service & Distribution	0.8%	7.6%
Lighting & Power	6.4%	
Special Electrical	0.4%	
Special Construction		
Specialties (& Additives)	0.0%	0.0%
Total	100%	100%

Table 7.36. Subassembly Cost Distributions for Two- and Three-Story Motels

Subassemblies	Cost Ratios	
Foundations		
Footings & Foundations	2.0%	2.5%
Piles & Caissons	0.0%	
Excavation & Backfill	0.5%	
Substructures		
Slab on Grade	1.7%	1.7%
Special Substructures	0.0%	
Superstructure		
Columns and Beams	0.0%	13.8%
Structural Walls	2.6%	
Elevated Floors/Diaphragms	6.6%	
Roof Decking/Framing	3.2%	
Stairs	1.4%	
Exterior Closure		
Walls	4.7%	10.3%
Exterior Wall Finishes	0.0%	
Doors	3.9%	
Windows & Glazed Walls	1.8%	
Roofing		
Roof Covering	1.1%	2.1%
Insulation	0.7%	
Openings & Specialties	0.3%	
Interior Construction		
Partitions	8.9%	35.6%
Interior Doors	7.9%	
Wall Finishes	3.7%	
Floor Finishes	9.3%	
Ceiling Finishes	4.6%	
Interior Surface of Exterior Walls	1.2%	
Conveying		
Elevators	2.7%	2.7%
Special Conveyors	0.0%	
Mechanical		
Plumbing	15.9%	22.9%
Fire Protection	1.8%	
Heating	0.0%	
Cooling	5.2%	
Special Systems	0.0%	
Electrical		
Service & Distribution	0.5%	8.4%
Lighting & Power	7.4%	
Special Electrical	0.5%	
Special Construction		
Specialties (& Additives)	0.0%	0.0%
Total	100%	100%

Table 7.37. Subassembly Cost Distributions for Four- to Seven-Story Hotels

Subassemblies	Cost Ratios	
Foundations		
Footings & Foundations	1.6%	1.8%
Piles & Caissons	0.0%	
Excavation & Backfill	0.2%	
Substructures		
Slab on Grade	0.7%	0.7%
Special Substructures	0.0%	
Superstructure		
Columns and Beams	0.0%	13.7%
Structural Walls	0.0%	
Elevated Floors/Diaphragms	12.1%	
Roof Decking/Framing	1.1%	
Stairs	0.5%	
Exterior Closure		
Walls	7.0%	10.1%
Exterior Wall Finishes	0.0%	
Doors	0.2%	
Windows & Glazed Walls	2.9%	
Roofing		
Roof Covering	0.5%	0.9%
Insulation	0.3%	
Openings & Speci alties	0.1%	
Interior Construction		
Partitions	6.0%	25.8%
Interior Doors	8.3%	
Wall Finishes	2.8%	
Floor Finishes	5.9%	
Ceiling Finishes	1.8%	
Interior Surface of Exterior Walls	1.0%	
Conveying		
Elevators	5.1%	5.1%
Special Conveyors	0.0%	
Mechanical		
Plumbing	14.5%	31.2%
Fire Protection	1.9%	
Heating	3.7%	
Cooling	10.9%	
Special Systems	0.0%	
Electrical		
Service & Distribution	1.1%	10.7%
Lighting & Power	7.2%	
Special Electrical	2.5%	
Special Construction		
Specialties (& Additives)	0.0%	0.0%
Total	100%	100%

Table 7.38. Average Annual Building Loss Normalized by Building Value – Marginally- or Non-Engineered Hotel/Motel and Multi-Family Residential Buildings – Gable/Hip Roofs with Shingles

Building Characteristics				Strapped Roof-Wall Connections				Toe-Nailed Roof-Wall Connections			
				Terrain Surface Roughness (m)				Terrain Surface Roughness (m)			
No. of Stories	Wall Constr.	Roof Shape	Roof Deck Nails	0.03	0.35	0.70	1.0	0.03	0.35	0.70	1.0
One	Wood Frame	Gable	6d	0.0120	0.0070	0.0050	0.0041	0.0151	0.0089	0.0065	0.0053
			8d	0.0093	0.0050	0.0034	0.0028	0.0141	0.0083	0.0059	0.0048
		Hip	6d	0.0090	0.0051	0.0035	0.0028	0.0119	0.0068	0.0046	0.0037
			8d	0.0077	0.0041	0.0028	0.0022	0.0117	0.0065	0.0044	0.0035
	Unreinf. Masonry	Gable	6d	0.0113	0.0069	0.0050	0.0041	0.0137	0.0085	0.0062	0.0050
			8d	0.0084	0.0048	0.0034	0.0028	0.0127	0.0079	0.0056	0.0045
		Hip	6d	0.0085	0.0050	0.0035	0.0028	0.0107	0.0065	0.0044	0.0035
			8d	0.0067	0.0040	0.0028	0.0022	0.0104	0.0063	0.0042	0.0033
	Reinf. Masonry	Gable	6d	0.0113	0.0069	0.0050	0.0041	0.0137	0.0085	0.0061	0.0050
			8d	0.0084	0.0048	0.0034	0.0028	0.0126	0.0079	0.0055	0.0044
		Hip	6d	0.0084	0.0050	0.0035	0.0028	0.0107	0.0064	0.0044	0.0035
			8d	0.0067	0.0040	0.0028	0.0022	0.0103	0.0062	0.0042	0.0033
Two	Wood Frame	Gable	6d	0.0184	0.0114	0.0089	0.0075	0.0220	0.0142	0.0110	0.0095
			8d	0.0157	0.0092	0.0068	0.0056	0.0206	0.0131	0.0101	0.0086
		Hip	6d	0.0155	0.0094	0.0072	0.0061	0.0189	0.0120	0.0092	0.0077
			8d	0.0137	0.0078	0.0057	0.0048	0.0184	0.0116	0.0088	0.0075
	Unreinf. Masonry	Gable	6d	0.0175	0.0110	0.0085	0.0074	0.0205	0.0135	0.0104	0.0090
			8d	0.0146	0.0088	0.0065	0.0054	0.0191	0.0125	0.0096	0.0083
		Hip	6d	0.0146	0.0092	0.0070	0.0059	0.0176	0.0113	0.0086	0.0074
			8d	0.0129	0.0075	0.0055	0.0046	0.0171	0.0112	0.0084	0.0070
	Reinf. Masonry	Gable	6d	0.0173	0.0111	0.0085	0.0074	0.0205	0.0134	0.0104	0.0090
			8d	0.0145	0.0088	0.0065	0.0054	0.0191	0.0124	0.0097	0.0082
		Hip	6d	0.0145	0.0092	0.0070	0.0059	0.0174	0.0114	0.0087	0.0074
			8d	0.0127	0.0075	0.0055	0.0046	0.0170	0.0111	0.0083	0.0070
Three	Wood Frame	Gable	6d	0.0217	0.0139	0.0110	0.0096	0.0261	0.0170	0.0137	0.0122
			8d	0.0186	0.0113	0.0086	0.0073	0.0248	0.0160	0.0127	0.0112
		Hip	6d	0.0195	0.0123	0.0098	0.0085	0.0235	0.0153	0.0122	0.0106
			8d	0.0171	0.0102	0.0078	0.0067	0.0229	0.0148	0.0116	0.0102
	Unreinf. Masonry	Gable	6d	0.0203	0.0132	0.0105	0.0093	0.0241	0.0161	0.0130	0.0115
			8d	0.0171	0.0105	0.0081	0.0069	0.0226	0.0149	0.0119	0.0105
		Hip	6d	0.0182	0.0118	0.0093	0.0082	0.0217	0.0142	0.0114	0.0101
			8d	0.0155	0.0095	0.0073	0.0063	0.0210	0.0138	0.0108	0.0096
	Reinf. Masonry	Gable	6d	0.0201	0.0131	0.0105	0.0092	0.0239	0.0161	0.0127	0.0115
			8d	0.0169	0.0105	0.0080	0.0068	0.0225	0.0150	0.0119	0.0104
		Hip	6d	0.0179	0.0117	0.0092	0.0082	0.0216	0.0142	0.0115	0.0100
			8d	0.0152	0.0094	0.0073	0.0062	0.0207	0.0137	0.0109	0.0094
Four	Wood Frame	Gable	6d	0.0225	0.0148	0.0120	0.0106	0.0275	0.0185	0.0151	0.0135
			8d	0.0195	0.0122	0.0094	0.0081	0.0261	0.0172	0.0140	0.0126
		Hip	6d	0.0197	0.0126	0.0100	0.0088	0.0247	0.0161	0.0130	0.0115
			8d	0.0176	0.0107	0.0083	0.0070	0.0240	0.0157	0.0126	0.0111

Table 7.39. Average Annual Building Loss Normalized by Building Value – Marginally- or Non-Engineered Hotel/Motel and Multi-Family Residential Buildings – Flat Roofs with Built-up Roof Cover

Building Characteristics				Strapped Roof-Wall Connections				Toe-Nailed Roof-Wall Connections			
				Terrain Surface Roughness (m)				Terrain Surface Roughness (m)			
No. of Stories	Wall Constr.	Roof Quality	Roof Deck Nails	0.03	0.35	0.70	1.0	0.03	0.35	0.70	1.0
One	Wood Frame	Average	6d	0.0083	0.0046	0.0031	0.0025	0.0105	0.0057	0.0037	0.0030
			8d	0.0067	0.0036	0.0024	0.0019	0.0096	0.0052	0.0033	0.0025
		Poor	6d	0.0119	0.0069	0.0050	0.0043	0.0138	0.0079	0.0056	0.0047
			8d	0.0105	0.0060	0.0044	0.0037	0.0131	0.0074	0.0052	0.0043
	Unreinf. Masonry	Average	6d	0.0078	0.0045	0.0031	0.0025	0.0095	0.0055	0.0037	0.0029
			8d	0.0059	0.0035	0.0024	0.0019	0.0087	0.0049	0.0032	0.0025
		Poor	6d	0.0114	0.0069	0.0050	0.0043	0.0129	0.0076	0.0055	0.0046
			8d	0.0098	0.0059	0.0044	0.0037	0.0123	0.0072	0.0051	0.0042
	Reinf. Masonry	Average	6d	0.0077	0.0045	0.0031	0.0025	0.0095	0.0055	0.0037	0.0029
			8d	0.0059	0.0035	0.0024	0.0019	0.0086	0.0049	0.0032	0.0025
		Poor	6d	0.0114	0.0069	0.0050	0.0043	0.0128	0.0077	0.0055	0.0046
			8d	0.0097	0.0059	0.0044	0.0037	0.0122	0.0072	0.0051	0.0042
Two	Wood Frame	Average	6d	0.0177	0.0110	0.0084	0.0070	0.0206	0.0133	0.0103	0.0089
			8d	0.0158	0.0095	0.0070	0.0059	0.0199	0.0128	0.0097	0.0083
		Poor	6d	0.0243	0.0160	0.0129	0.0115	0.0269	0.0181	0.0146	0.0129
			8d	0.0227	0.0147	0.0117	0.0104	0.0262	0.0176	0.0141	0.0125
	Unreinf. Masonry	Average	6d	0.0167	0.0104	0.0081	0.0069	0.0193	0.0127	0.0098	0.0084
			8d	0.0149	0.0091	0.0068	0.0057	0.0184	0.0122	0.0093	0.0079
		Poor	6d	0.0234	0.0157	0.0127	0.0112	0.0257	0.0174	0.0141	0.0125
			8d	0.0218	0.0143	0.0115	0.0102	0.0250	0.0170	0.0137	0.0121
	Reinf. Masonry	Average	6d	0.0167	0.0105	0.0080	0.0069	0.0192	0.0126	0.0098	0.0084
			8d	0.0149	0.0091	0.0068	0.0057	0.0183	0.0121	0.0092	0.0079
		Poor	6d	0.0234	0.0156	0.0126	0.0113	0.0256	0.0175	0.0141	0.0125
			8d	0.0218	0.0144	0.0115	0.0101	0.0248	0.0170	0.0137	0.0120
Three	Wood Frame	Average	6d	0.0245	0.0163	0.0133	0.0118	0.0285	0.0193	0.0159	0.0142
			8d	0.0220	0.0141	0.0113	0.0099	0.0276	0.0187	0.0151	0.0134
		Poor	6d	0.0327	0.0231	0.0195	0.0176	0.0364	0.0260	0.0220	0.0200
			8d	0.0301	0.0209	0.0175	0.0158	0.0355	0.0252	0.0213	0.0193
	Unreinf. Masonry	Average	6d	0.0231	0.0157	0.0129	0.0114	0.0265	0.0184	0.0151	0.0136
			8d	0.0205	0.0135	0.0108	0.0094	0.0256	0.0176	0.0144	0.0128
		Poor	6d	0.0312	0.0224	0.0190	0.0173	0.0346	0.0249	0.0212	0.0194
			8d	0.0287	0.0203	0.0171	0.0154	0.0337	0.0242	0.0206	0.0187
	Reinf. Masonry	Average	6d	0.0229	0.0157	0.0128	0.0113	0.0264	0.0183	0.0152	0.0135
			8d	0.0203	0.0135	0.0107	0.0095	0.0255	0.0176	0.0143	0.0128
		Poor	6d	0.0311	0.0223	0.0189	0.0172	0.0342	0.0248	0.0212	0.0193
			8d	0.0285	0.0203	0.0170	0.0154	0.0334	0.0243	0.0204	0.0187
Four	Wood Frame	Average	6d	0.0247	0.0168	0.0137	0.0122	0.0302	0.0212	0.0178	0.0161
			8d	0.0221	0.0144	0.0115	0.0101	0.0296	0.0204	0.0171	0.0155
		Poor	6d	0.0300	0.0212	0.0180	0.0164	0.0352	0.0256	0.0219	0.0201
			8d	0.0275	0.0192	0.0158	0.0142	0.0348	0.0249	0.0214	0.0195

Table 7.40. Average Annual Building Loss Normalized by Building Value – Marginally- or Non-Engineered Hotel/Motel and Multi-Family Residential Buildings – Flat Roofs with Single Ply Membrane Roof Cover

Building Characteristics				Strapped Roof-Wall Connections				Toe-Nailed Roof-Wall Connections			
				Terrain Surface Roughness (m)				Terrain Surface Roughness (m)			
No. of Stories	Wall Constr.	Roof Quality	Roof Deck Nails	0.03	0.35	0.70	1.0	0.03	0.35	0.70	1.0
One	Wood Frame	Average	6d	0.0095	0.0054	0.0037	0.0031	0.0115	0.0064	0.0043	0.0035
			8d	0.0081	0.0043	0.0030	0.0025	0.0109	0.0059	0.0039	0.0031
		Poor	6d	0.0206	0.0128	0.0101	0.0090	0.0223	0.0136	0.0105	0.0093
			8d	0.0193	0.0120	0.0094	0.0084	0.0216	0.0132	0.0102	0.0090
	Unreinf. Masonry	Average	6d	0.0089	0.0053	0.0037	0.0031	0.0105	0.0061	0.0041	0.0034
			8d	0.0072	0.0043	0.0030	0.0025	0.0098	0.0056	0.0038	0.0030
		Poor	6d	0.0203	0.0129	0.0101	0.0089	0.0214	0.0134	0.0104	0.0092
			8d	0.0186	0.0119	0.0095	0.0085	0.0207	0.0130	0.0101	0.0089
	Reinf. Masonry	Average	6d	0.0089	0.0053	0.0037	0.0031	0.0104	0.0061	0.0041	0.0034
			8d	0.0072	0.0043	0.0030	0.0025	0.0097	0.0056	0.0038	0.0030
		Poor	6d	0.0202	0.0129	0.0101	0.0089	0.0213	0.0134	0.0104	0.0092
			8d	0.0186	0.0119	0.0095	0.0085	0.0207	0.0130	0.0101	0.0089
Two	Wood Frame	Average	6d	0.0200	0.0126	0.0099	0.0086	0.0227	0.0149	0.0117	0.0101
			8d	0.0182	0.0113	0.0087	0.0075	0.0221	0.0145	0.0112	0.0098
		Poor	6d	0.0347	0.0244	0.0204	0.0185	0.0371	0.0263	0.0220	0.0200
			8d	0.0333	0.0230	0.0193	0.0175	0.0363	0.0258	0.0215	0.0195
	Unreinf. Masonry	Average	6d	0.0191	0.0123	0.0097	0.0085	0.0215	0.0144	0.0113	0.0098
			8d	0.0174	0.0110	0.0086	0.0073	0.0209	0.0137	0.0108	0.0093
		Poor	6d	0.0340	0.0240	0.0203	0.0184	0.0360	0.0257	0.0216	0.0196
			8d	0.0324	0.0228	0.0191	0.0173	0.0353	0.0253	0.0211	0.0191
	Reinf. Masonry	Average	6d	0.0191	0.0123	0.0097	0.0085	0.0215	0.0144	0.0113	0.0098
			8d	0.0173	0.0110	0.0085	0.0074	0.0207	0.0137	0.0107	0.0093
		Poor	6d	0.0339	0.0240	0.0203	0.0184	0.0359	0.0257	0.0216	0.0195
			8d	0.0323	0.0229	0.0190	0.0173	0.0352	0.0251	0.0211	0.0192
Three	Wood Frame	Average	6d	0.0282	0.0191	0.0159	0.0143	0.0318	0.0221	0.0184	0.0166
			8d	0.0256	0.0171	0.0140	0.0123	0.0307	0.0212	0.0177	0.0159
		Poor	6d	0.0411	0.0305	0.0265	0.0244	0.0449	0.0334	0.0290	0.0267
			8d	0.0387	0.0285	0.0245	0.0224	0.0440	0.0327	0.0283	0.0260
	Unreinf. Masonry	Average	6d	0.0266	0.0185	0.0153	0.0139	0.0300	0.0210	0.0177	0.0159
			8d	0.0240	0.0164	0.0134	0.0119	0.0291	0.0202	0.0169	0.0153
		Poor	6d	0.0398	0.0299	0.0259	0.0240	0.0430	0.0324	0.0282	0.0260
			8d	0.0372	0.0278	0.0240	0.0221	0.0422	0.0317	0.0275	0.0254
	Reinf. Masonry	Average	6d	0.0264	0.0185	0.0154	0.0138	0.0297	0.0210	0.0173	0.0156
			8d	0.0239	0.0163	0.0134	0.0119	0.0288	0.0203	0.0169	0.0153
		Poor	6d	0.0396	0.0298	0.0259	0.0239	0.0428	0.0324	0.0282	0.0261
			8d	0.0370	0.0278	0.0240	0.0220	0.0420	0.0316	0.0276	0.0254
Four	Wood Frame	Average	6d	0.0268	0.0184	0.0154	0.0139	0.0321	0.0229	0.0193	0.0176
			8d	0.0244	0.0164	0.0132	0.0118	0.0315	0.0222	0.0188	0.0170
		Poor	6d	0.0350	0.0258	0.0224	0.0205	0.0403	0.0302	0.0262	0.0243
			8d	0.0324	0.0237	0.0203	0.0185	0.0399	0.0297	0.0257	0.0237

Table 7.41. Average Annual Content Loss Normalized by Building Value – Marginally- or Non-Engineered Hotel/Motel and Multi-Family Residential Buildings – Gable/Hip Roofs with Shingles

Building Characteristics				Strapped Roof-Wall Connections				Toe-Nailed Roof-Wall Connections			
				Terrain Surface Roughness (m)				Terrain Surface Roughness (m)			
No. of Stories	Wall Constr.	Roof Shape	Roof Deck Nails	0.03	0.35	0.70	1.0	0.03	0.35	0.70	1.0
One	Wood Frame	Gable	6d	0.0047	0.0023	0.0016	0.0013	0.0065	0.0036	0.0026	0.0021
			8d	0.0030	0.0010	0.0006	0.0004	0.0059	0.0033	0.0022	0.0018
		Hip	6d	0.0031	0.0013	0.0008	0.0006	0.0049	0.0025	0.0016	0.0013
			8d	0.0022	0.0007	0.0004	0.0003	0.0047	0.0024	0.0015	0.0012
	Unreinf. Masonry	Gable	6d	0.0045	0.0023	0.0016	0.0013	0.0065	0.0036	0.0026	0.0021
			8d	0.0027	0.0009	0.0005	0.0004	0.0059	0.0032	0.0023	0.0018
		Hip	6d	0.0028	0.0013	0.0008	0.0006	0.0049	0.0025	0.0016	0.0012
			8d	0.0017	0.0006	0.0003	0.0002	0.0046	0.0024	0.0015	0.0012
	Reinf. Masonry	Gable	6d	0.0045	0.0023	0.0016	0.0013	0.0065	0.0036	0.0025	0.0021
			8d	0.0027	0.0009	0.0005	0.0004	0.0059	0.0033	0.0022	0.0017
		Hip	6d	0.0028	0.0013	0.0008	0.0006	0.0049	0.0025	0.0016	0.0012
			8d	0.0017	0.0006	0.0003	0.0002	0.0046	0.0024	0.0015	0.0012
Two	Wood Frame	Gable	6d	0.0076	0.0044	0.0033	0.0027	0.0098	0.0062	0.0047	0.0040
			8d	0.0061	0.0031	0.0021	0.0016	0.0092	0.0057	0.0043	0.0036
		Hip	6d	0.0061	0.0033	0.0024	0.0019	0.0082	0.0050	0.0037	0.0031
			8d	0.0049	0.0023	0.0014	0.0011	0.0079	0.0048	0.0036	0.0030
	Unreinf. Masonry	Gable	6d	0.0075	0.0043	0.0032	0.0027	0.0097	0.0061	0.0046	0.0040
			8d	0.0058	0.0030	0.0020	0.0016	0.0090	0.0056	0.0043	0.0036
		Hip	6d	0.0058	0.0032	0.0023	0.0019	0.0081	0.0049	0.0036	0.0031
			8d	0.0047	0.0022	0.0013	0.0010	0.0078	0.0049	0.0036	0.0029
	Reinf. Masonry	Gable	6d	0.0074	0.0044	0.0032	0.0027	0.0097	0.0061	0.0046	0.0040
			8d	0.0059	0.0030	0.0020	0.0015	0.0091	0.0056	0.0043	0.0036
		Hip	6d	0.0058	0.0032	0.0023	0.0019	0.0080	0.0050	0.0037	0.0031
			8d	0.0046	0.0021	0.0014	0.0010	0.0078	0.0049	0.0035	0.0029
Three	Wood Frame	Gable	6d	0.0092	0.0056	0.0043	0.0037	0.0119	0.0076	0.0060	0.0053
			8d	0.0077	0.0042	0.0030	0.0025	0.0113	0.0071	0.0056	0.0049
		Hip	6d	0.0079	0.0046	0.0036	0.0030	0.0104	0.0065	0.0051	0.0044
			8d	0.0065	0.0033	0.0023	0.0019	0.0101	0.0063	0.0049	0.0042
	Unreinf. Masonry	Gable	6d	0.0089	0.0054	0.0042	0.0036	0.0116	0.0074	0.0060	0.0052
			8d	0.0073	0.0040	0.0028	0.0023	0.0109	0.0069	0.0055	0.0047
		Hip	6d	0.0075	0.0044	0.0034	0.0029	0.0101	0.0063	0.0050	0.0044
			8d	0.0060	0.0031	0.0022	0.0017	0.0097	0.0061	0.0047	0.0041
	Reinf. Masonry	Gable	6d	0.0088	0.0053	0.0041	0.0036	0.0116	0.0075	0.0058	0.0052
			8d	0.0072	0.0040	0.0028	0.0023	0.0109	0.0070	0.0055	0.0047
		Hip	6d	0.0075	0.0044	0.0034	0.0029	0.0102	0.0063	0.0051	0.0043
			8d	0.0059	0.0031	0.0022	0.0017	0.0097	0.0061	0.0047	0.0040
Four	Wood Frame	Gable	6d	0.0102	0.0063	0.0050	0.0044	0.0131	0.0085	0.0069	0.0062
			8d	0.0087	0.0051	0.0038	0.0031	0.0124	0.0079	0.0064	0.0057
		Hip	6d	0.0087	0.0051	0.0040	0.0035	0.0116	0.0073	0.0058	0.0051
			8d	0.0075	0.0041	0.0030	0.0025	0.0113	0.0071	0.0056	0.0049

Table 7.42. Average Annual Content Loss Normalized by Building Value – Marginally- or Non-Engineered Hotel/Motel and Multi-Family Residential Buildings – Flat Roofs with Built-up Roof Cover

Building Characteristics				Strapped Roof-Wall Connections				Toe-Nailed Roof-Wall Connections			
				Terrain Surface Roughness (m)				Terrain Surface Roughness (m)			
No. of Stories	Wall Constr.	Roof Quality	Roof Deck Nails	0.03	0.35	0.70	1.0	0.03	0.35	0.70	1.0
One	Wood Frame	Average	6d	0.0030	0.0013	0.0008	0.0006	0.0043	0.0020	0.0012	0.0009
			8d	0.0020	0.0005	0.0003	0.0002	0.0037	0.0017	0.0009	0.0006
		Poor	6d	0.0035	0.0016	0.0010	0.0009	0.0046	0.0023	0.0014	0.0011
			8d	0.0024	0.0008	0.0005	0.0004	0.0042	0.0019	0.0012	0.0009
	Unreinf. Masonry	Average	6d	0.0028	0.0013	0.0008	0.0006	0.0042	0.0020	0.0012	0.0009
			8d	0.0016	0.0005	0.0003	0.0002	0.0037	0.0016	0.0009	0.0007
		Poor	6d	0.0032	0.0015	0.0010	0.0008	0.0046	0.0022	0.0014	0.0011
			8d	0.0021	0.0008	0.0005	0.0004	0.0041	0.0019	0.0011	0.0009
	Reinf. Masonry	Average	6d	0.0028	0.0013	0.0008	0.0006	0.0042	0.0020	0.0012	0.0009
			8d	0.0016	0.0005	0.0003	0.0002	0.0036	0.0016	0.0009	0.0007
		Poor	6d	0.0033	0.0015	0.0010	0.0008	0.0046	0.0022	0.0014	0.0011
			8d	0.0021	0.0008	0.0005	0.0004	0.0041	0.0019	0.0012	0.0009
Two	Wood Frame	Average	6d	0.0068	0.0039	0.0028	0.0022	0.0087	0.0055	0.0041	0.0035
			8d	0.0055	0.0028	0.0019	0.0014	0.0083	0.0051	0.0037	0.0031
		Poor	6d	0.0074	0.0043	0.0032	0.0027	0.0094	0.0059	0.0045	0.0038
			8d	0.0063	0.0034	0.0023	0.0019	0.0089	0.0056	0.0042	0.0036
	Unreinf. Masonry	Average	6d	0.0066	0.0037	0.0027	0.0022	0.0087	0.0054	0.0041	0.0034
			8d	0.0054	0.0028	0.0018	0.0014	0.0081	0.0051	0.0037	0.0031
		Poor	6d	0.0073	0.0043	0.0032	0.0026	0.0093	0.0059	0.0045	0.0038
			8d	0.0061	0.0033	0.0023	0.0018	0.0089	0.0056	0.0042	0.0035
	Reinf. Masonry	Average	6d	0.0066	0.0037	0.0027	0.0022	0.0086	0.0054	0.0040	0.0034
			8d	0.0054	0.0028	0.0018	0.0014	0.0080	0.0051	0.0037	0.0031
		Poor	6d	0.0073	0.0042	0.0031	0.0027	0.0093	0.0059	0.0045	0.0038
			8d	0.0061	0.0033	0.0023	0.0018	0.0088	0.0056	0.0042	0.0035
Three	Wood Frame	Average	6d	0.0092	0.0057	0.0044	0.0038	0.0120	0.0078	0.0063	0.0055
			8d	0.0077	0.0043	0.0032	0.0026	0.0115	0.0074	0.0058	0.0051
		Poor	6d	0.0101	0.0064	0.0050	0.0044	0.0128	0.0085	0.0069	0.0061
			8d	0.0085	0.0050	0.0038	0.0032	0.0123	0.0080	0.0065	0.0058
	Unreinf. Masonry	Average	6d	0.0088	0.0055	0.0043	0.0037	0.0116	0.0077	0.0062	0.0055
			8d	0.0073	0.0041	0.0030	0.0024	0.0111	0.0072	0.0058	0.0051
		Poor	6d	0.0097	0.0061	0.0049	0.0043	0.0125	0.0083	0.0068	0.0061
			8d	0.0081	0.0048	0.0037	0.0030	0.0120	0.0079	0.0064	0.0057
	Reinf. Masonry	Average	6d	0.0088	0.0055	0.0043	0.0037	0.0116	0.0077	0.0062	0.0055
			8d	0.0073	0.0041	0.0030	0.0025	0.0112	0.0073	0.0058	0.0051
		Poor	6d	0.0097	0.0062	0.0049	0.0043	0.0125	0.0083	0.0068	0.0060
			8d	0.0081	0.0048	0.0037	0.0031	0.0120	0.0080	0.0064	0.0057
Four	Wood Frame	Average	6d	0.0105	0.0066	0.0052	0.0046	0.0138	0.0093	0.0078	0.0070
			8d	0.0090	0.0053	0.0040	0.0034	0.0135	0.0090	0.0074	0.0067
		Poor	6d	0.0112	0.0072	0.0058	0.0051	0.0144	0.0099	0.0082	0.0075
			8d	0.0098	0.0060	0.0046	0.0040	0.0142	0.0095	0.0080	0.0072

Table 7.43. Average Annual Content Loss Normalized by Building Value – Marginally- or Non-Engineered Hotel/Motel and Multi-Family Residential Buildings – Flat Roofs with Single Ply Membrane Roof Cover

Building Characteristics				Strapped Roof-Wall Connections				Toe-Nailed Roof-Wall Connections			
				Terrain Surface Roughness (m)				Terrain Surface Roughness (m)			
No. of Stories	Wall Constr.	Roof Quality	Roof Deck Nails	0.03	0.35	0.70	1.0	0.03	0.35	0.70	1.0
One	Wood Frame	Average	6d	0.0032	0.0014	0.0009	0.0007	0.0044	0.0021	0.0013	0.0010
			8d	0.0022	0.0006	0.0004	0.0003	0.0039	0.0017	0.0010	0.0007
		Poor	6d	0.0047	0.0024	0.0018	0.0015	0.0059	0.0031	0.0021	0.0018
			8d	0.0038	0.0017	0.0013	0.0011	0.0054	0.0027	0.0019	0.0015
	Unreinf. Masonry	Average	6d	0.0029	0.0014	0.0009	0.0007	0.0043	0.0020	0.0013	0.0010
			8d	0.0018	0.0006	0.0004	0.0003	0.0038	0.0017	0.0010	0.0007
		Poor	6d	0.0046	0.0024	0.0018	0.0015	0.0058	0.0030	0.0021	0.0018
			8d	0.0034	0.0016	0.0013	0.0011	0.0053	0.0027	0.0019	0.0015
	Reinf. Masonry	Average	6d	0.0029	0.0014	0.0009	0.0007	0.0043	0.0020	0.0013	0.0010
			8d	0.0018	0.0006	0.0004	0.0003	0.0038	0.0017	0.0010	0.0007
		Poor	6d	0.0045	0.0024	0.0018	0.0015	0.0058	0.0031	0.0021	0.0018
			8d	0.0034	0.0016	0.0013	0.0011	0.0053	0.0027	0.0019	0.0015
Two	Wood Frame	Average	6d	0.0070	0.0040	0.0029	0.0024	0.0089	0.0056	0.0042	0.0035
			8d	0.0058	0.0031	0.0020	0.0016	0.0086	0.0054	0.0039	0.0033
		Poor	6d	0.0086	0.0053	0.0040	0.0034	0.0105	0.0069	0.0054	0.0046
			8d	0.0074	0.0043	0.0031	0.0027	0.0100	0.0065	0.0050	0.0043
	Unreinf. Masonry	Average	6d	0.0068	0.0039	0.0028	0.0024	0.0088	0.0056	0.0042	0.0035
			8d	0.0056	0.0030	0.0020	0.0016	0.0085	0.0052	0.0039	0.0033
		Poor	6d	0.0085	0.0052	0.0040	0.0034	0.0105	0.0068	0.0053	0.0046
			8d	0.0073	0.0042	0.0032	0.0026	0.0101	0.0066	0.0050	0.0043
	Reinf. Masonry	Average	6d	0.0069	0.0039	0.0028	0.0024	0.0089	0.0057	0.0042	0.0036
			8d	0.0056	0.0029	0.0020	0.0016	0.0084	0.0052	0.0039	0.0032
		Poor	6d	0.0085	0.0052	0.0040	0.0034	0.0105	0.0068	0.0053	0.0046
			8d	0.0073	0.0043	0.0031	0.0026	0.0100	0.0065	0.0049	0.0043
Three	Wood Frame	Average	6d	0.0097	0.0059	0.0047	0.0041	0.0123	0.0081	0.0066	0.0058
			8d	0.0081	0.0047	0.0035	0.0028	0.0118	0.0076	0.0062	0.0055
		Poor	6d	0.0110	0.0072	0.0058	0.0051	0.0137	0.0093	0.0076	0.0068
			8d	0.0094	0.0059	0.0045	0.0039	0.0132	0.0089	0.0072	0.0064
	Unreinf. Masonry	Average	6d	0.0092	0.0058	0.0045	0.0040	0.0121	0.0079	0.0065	0.0057
			8d	0.0076	0.0045	0.0033	0.0027	0.0115	0.0075	0.0061	0.0053
		Poor	6d	0.0106	0.0070	0.0056	0.0050	0.0134	0.0091	0.0076	0.0067
			8d	0.0090	0.0056	0.0044	0.0038	0.0129	0.0087	0.0071	0.0064
	Reinf. Masonry	Average	6d	0.0092	0.0058	0.0045	0.0039	0.0120	0.0080	0.0063	0.0056
			8d	0.0076	0.0045	0.0033	0.0027	0.0115	0.0075	0.0061	0.0054
		Poor	6d	0.0106	0.0069	0.0056	0.0049	0.0134	0.0092	0.0075	0.0068
			8d	0.0090	0.0056	0.0044	0.0038	0.0129	0.0087	0.0072	0.0064
Four	Wood Frame	Average	6d	0.0108	0.0068	0.0055	0.0048	0.0140	0.0096	0.0079	0.0072
			8d	0.0094	0.0056	0.0043	0.0037	0.0137	0.0092	0.0077	0.0069
		Poor	6d	0.0119	0.0078	0.0064	0.0057	0.0152	0.0105	0.0089	0.0080
			8d	0.0104	0.0066	0.0052	0.0046	0.0150	0.0103	0.0086	0.0078

Table 7.44. Percent Increases in the Average Annual Total Loss Due to Changes in Building Parameters (Minimum/Average/Maximum) – Marginally- or Non-Engineered Hotel/Motel and Multi-Family Residential Buildings

Parameter	Number of Stories				
	All	One	Two	Three	Four
Gable and Hip Roofs With Singles					
Unreinforced Masonry to Wood Frame Walls	0% / 5% / 18%	0% / 4% / 18%	1% / 4% / 7%	3% / 6% / 10%	N/A
Reinforced Masonry to Unreinforced Masonry Walls	-2% / 0% / 3%	-1% / 0% / 3%	-2% / 0% / 2%	-1% / 1% / 2%	
Hip to Gable Roof Shape	9% / 23% / 59%	22% / 37% / 59%	13% / 21% / 30%	9% / 13% / 17%	9% / 16% / 22%
8d to 6d Roof Deck Nails	2% / 21% / 71%	2% / 28% / 71%	2% / 19% / 46%	2% / 18% / 42%	3% / 14% / 34%
Strapped to Toe-Nailed Roof/Wall Connections	21% / 48% / 103%	27% / 61% / 103%	21% / 45% / 79%	22% / 42% / 72%	24% / 42% / 69%
One to Two Stories	48% / 91% / 135%	N/A			
Two to Three Stories	17% / 28% / 49%				
Three to Four Stories	3% / 9% / 14%				
Flat Roofs With BUR					
Unreinforced Masonry to Wood Frame Walls	0% / 4% / 15%	0% / 3% / 15%	1% / 3% / 6%	2% / 4% / 7%	N/A
Reinforced Masonry to Unreinforced Masonry Walls	-1% / 0% / 2%	-1% / 0% / 2%	-1% / 0% / 1%	-1% / 0% / 1%	
Average to Poor Quality Cover	13% / 40% / 98%	24% / 53% / 98%	24% / 40% / 69%	21% / 35% / 56%	13% / 21% / 35%
8d to 6d Roof Deck Nails	1% / 15% / 50%	6% / 24% / 50%	3% / 11% / 29%	3% / 11% / 28%	1% / 10% / 25%
Strapped to Toe-Nailed Roof/Wall Connections	12% / 31% / 68%	12% / 33% / 68%	14% / 29% / 56%	14% / 28% / 52%	21% / 37% / 65%
One to Two Stories	97% / 167% / 261%	N/A			
Two to Three Stories	31% / 49% / 70%				
Three to Four Stories	-4% / 5% / 20%				
Flat Roofs With EPDM					
Unreinforced Masonry to Wood Frame Walls	-1% / 3% / 14%	-1% / 2% / 14%	0% / 2% / 5%	2% / 3% / 7%	N/A
Reinforced Masonry to Unreinforced Masonry Walls	-1% / 0% / 2%	0% / 0% / 1%	-1% / 0% / 1%	-1% / 0% / 2%	
Average to Poor Quality Cover	20% / 87% / 246%	77% / 146% / 246%	50% / 80% / 124%	33% / 51% / 77%	20% / 32% / 48%
8d to 6d Roof Deck Nails	1% / 11% / 37%	4% / 16% / 37%	2% / 8% / 22%	2% / 9% / 23%	1% / 8% / 20%
Strapped to Toe-Nailed Roof/Wall Connections	5% / 23% / 54%	5% / 21% / 52%	9% / 21% / 44%	12% / 22% / 42%	18% / 32% / 54%
One to Two Stories	69% / 136% / 247%	N/A			
Two to Three Stories	16% / 40% / 67%				
Three to Four Stories	-12% / -1% / 12%				

Table 7.45. Subassembly Cost Distributions for Low-Rise Masonry Strip Mall

Subassemblies	Cost Ratios	
Foundations		
Footings & Foundations	2.2%	4.2%
Piles & Caissons	0.0%	
Excavation & Backfill	2.0%	
Substructures		
Slab on Grade	6.4%	6.4%
Special Substructures	0.0%	
Superstructure		
Columns and Beams	1.1%	29.2%
Structural Walls	0.0%	
Elevated Floors/Diaphragms	0.0%	
Roof Decking/Framing	28.1%	
Stairs	0.0%	
Exterior Closure		
Walls	6.2%	8.1%
Exterior Wall Finishes	0.0%	
Doors	0.5%	
Windows & Glazed Walls	1.4%	
Roofing		
Roof Covering	3.6%	6.4%
Insulation	2.6%	
Openings & Speci alties	0.2%	
Interior Construction		
Partitions	1.3%	15.7%
Interior Doors	1.8%	
Wall Finishes	0.4%	
Floor Finishes	8.6%	
Ceiling Finishes	2.6%	
Interior Surface of Exterior Walls	0.9%	
Conveying		
Elevators	0.0%	0.0%
Special Conveyors	0.0%	
Mechanical		
Plumbing	1.3%	18.2%
Fire Protection	2.8%	
Heating	0.0%	
Cooling	13.6%	
Special Systems	0.0%	
Electrical		
Service & Distribution	1.1%	12.3%
Lighting & Power	10.6%	
Special Electrical	0.6%	
Special Construction		
Specialties (& Additives)	0.0%	0.0%
Total	100%	100%

Example building and content loss functions are given in Appendix K. The average annual building and content losses (both normalized by the total building value) for all the buildings examined are presented in Tables 7.46 through 7.57. The average annual loss is obtained by summing all losses produced during the 20,000-year hurricane simulation period and then dividing by 20,000 years. The values given in the tables reflect the average annual losses for low-rise strip mall buildings located in the South Florida area. Tables 7.46 and 7.47 list building loss ratios for the buildings with a wood roof system and Tables 7.48 through 7.51 list building loss ratios for the buildings with a metal roof system. Tables 7.52 through 7.57 are the corresponding tables listing the content loss ratios.

Table 7.46. Average Annual Building Loss Normalized by Building Value for Building A – Twelve Foot High Strip Mall Building with Six Units and Wood Deck with Two Foot Truss Spacing

Building Characteristics				Toe-Nailed Roof-Wall Connection				Strapped Roof-Wall Connection			
				Terrain Surface Roughness (m)				Terrain Surface Roughness (m)			
Wall Type	Missile Environ	Wood Deck Nail Size	Roof Cover	0.03	0.35	0.70	1.0	0.03	0.35	0.70	1.0
Unreinforced Masonry	A	6d	EPDM	0.0240	0.0136	0.0094	0.0075	0.0140	0.0071	0.0049	0.0040
			BUR	0.0232	0.0131	0.0089	0.0071	0.0130	0.0064	0.0043	0.0035
		8d	EPDM	0.0237	0.0134	0.0093	0.0075	0.0125	0.0057	0.0037	0.0030
			BUR	0.0227	0.0130	0.0089	0.0071	0.0115	0.0051	0.0032	0.0024
	B	6d	EPDM	0.0197	0.0114	0.0078	0.0064	0.0131	0.0067	0.0046	0.0037
			BUR	0.0188	0.0110	0.0075	0.0059	0.0122	0.0060	0.0040	0.0032
		8d	EPDM	0.0194	0.0112	0.0078	0.0063	0.0120	0.0057	0.0036	0.0029
			BUR	0.0187	0.0109	0.0074	0.0058	0.0110	0.0049	0.0031	0.0023
	C	6d	EPDM	0.0161	0.0101	0.0071	0.0056	0.0126	0.0064	0.0044	0.0036
			BUR	0.0151	0.0096	0.0066	0.0051	0.0116	0.0057	0.0038	0.0031
		8d	EPDM	0.0157	0.0098	0.0069	0.0055	0.0118	0.0053	0.0035	0.0028
			BUR	0.0150	0.0094	0.0063	0.0051	0.0106	0.0045	0.0029	0.0022
	D	6d	EPDM	0.0138	0.0060	0.0045	0.0038	0.0120	0.0050	0.0035	0.0029
			BUR	0.0129	0.0055	0.0039	0.0032	0.0111	0.0043	0.0028	0.0024
		8d	EPDM	0.0137	0.0059	0.0043	0.0036	0.0112	0.0042	0.0027	0.0022
			BUR	0.0127	0.0053	0.0036	0.0030	0.0100	0.0034	0.0021	0.0016
Reinforced Masonry	A	6d	EPDM	0.0229	0.0135	0.0093	0.0074	0.0134	0.0070	0.0048	0.0040
			BUR	0.0224	0.0128	0.0088	0.0070	0.0123	0.0063	0.0043	0.0034
		8d	EPDM	0.0229	0.0132	0.0090	0.0072	0.0119	0.0055	0.0037	0.0029
			BUR	0.0223	0.0127	0.0089	0.0069	0.0108	0.0048	0.0031	0.0023
	B	6d	EPDM	0.0189	0.0111	0.0076	0.0062	0.0126	0.0066	0.0045	0.0037
			BUR	0.0181	0.0105	0.0072	0.0058	0.0115	0.0059	0.0040	0.0032
		8d	EPDM	0.0187	0.0110	0.0076	0.0061	0.0113	0.0053	0.0036	0.0028
			BUR	0.0178	0.0105	0.0071	0.0056	0.0104	0.0047	0.0029	0.0022
	C	6d	EPDM	0.0154	0.0099	0.0069	0.0056	0.0121	0.0062	0.0044	0.0036
			BUR	0.0145	0.0094	0.0063	0.0051	0.0110	0.0055	0.0037	0.0030
		8d	EPDM	0.0152	0.0097	0.0068	0.0054	0.0110	0.0050	0.0034	0.0027
			BUR	0.0141	0.0091	0.0063	0.0049	0.0099	0.0044	0.0027	0.0022
	D	6d	EPDM	0.0132	0.0059	0.0043	0.0037	0.0114	0.0048	0.0034	0.0029
			BUR	0.0121	0.0052	0.0037	0.0031	0.0104	0.0041	0.0028	0.0023
		8d	EPDM	0.0127	0.0056	0.0040	0.0034	0.0105	0.0040	0.0027	0.0022
			BUR	0.0118	0.0049	0.0034	0.0029	0.0094	0.0032	0.0020	0.0016

Table 7.47. Average Annual Building Loss Normalized by Building Value for Building B – Twenty Foot High Strip Mall Building with Six Units and Wood Deck with Two Foot Truss Spacing

Building Characteristics				Toe-Nailed Roof-Wall Connection Terrain Surface Roughness (m)				Strapped Roof-Wall Connection Terrain Surface Roughness (m)			
Wall Type	Missile Environ	Wood Deck Nail Size	Roof Cover	0.03	0.35	0.70	1.0	0.03	0.35	0.70	1.0
Unreinforced Masonry	A	6d	EPDM	0.0337	0.0235	0.0178	0.0151	0.0244	0.0146	0.0112	0.0098
			BUR	0.0320	0.0225	0.0169	0.0142	0.0224	0.0133	0.0100	0.0085
		8d	EPDM	0.0336	0.0234	0.0179	0.0149	0.0231	0.0132	0.0100	0.0084
			BUR	0.0319	0.0224	0.0167	0.0142	0.0212	0.0118	0.0087	0.0072
	B	6d	EPDM	0.0301	0.0200	0.0155	0.0132	0.0232	0.0138	0.0107	0.0091
			BUR	0.0288	0.0190	0.0143	0.0121	0.0212	0.0124	0.0094	0.0079
		8d	EPDM	0.0300	0.0201	0.0154	0.0132	0.0221	0.0126	0.0095	0.0080
			BUR	0.0285	0.0189	0.0141	0.0122	0.0201	0.0112	0.0081	0.0067
	C	6d	EPDM	0.0268	0.0175	0.0135	0.0117	0.0224	0.0132	0.0102	0.0088
			BUR	0.0251	0.0161	0.0124	0.0106	0.0205	0.0117	0.0089	0.0076
		8d	EPDM	0.0267	0.0173	0.0134	0.0117	0.0215	0.0121	0.0092	0.0077
			BUR	0.0250	0.0159	0.0123	0.0105	0.0196	0.0107	0.0078	0.0065
	D	6d	EPDM	0.0257	0.0147	0.0118	0.0105	0.0220	0.0120	0.0094	0.0081
			BUR	0.0238	0.0133	0.0105	0.0093	0.0199	0.0104	0.0080	0.0068
		8d	EPDM	0.0254	0.0145	0.0116	0.0103	0.0210	0.0109	0.0083	0.0070
			BUR	0.0235	0.0131	0.0104	0.0091	0.0192	0.0094	0.0069	0.0056
Reinforced Masonry	A	6d	EPDM	0.0310	0.0225	0.0170	0.0146	0.0218	0.0134	0.0105	0.0091
			BUR	0.0295	0.0213	0.0160	0.0134	0.0197	0.0119	0.0091	0.0078
		8d	EPDM	0.0306	0.0223	0.0170	0.0143	0.0200	0.0116	0.0088	0.0075
			BUR	0.0291	0.0210	0.0161	0.0133	0.0181	0.0099	0.0072	0.0062
	B	6d	EPDM	0.0275	0.0192	0.0148	0.0127	0.0207	0.0127	0.0099	0.0086
			BUR	0.0262	0.0180	0.0137	0.0116	0.0187	0.0112	0.0086	0.0073
		8d	EPDM	0.0274	0.0190	0.0147	0.0126	0.0193	0.0111	0.0084	0.0071
			BUR	0.0259	0.0177	0.0135	0.0115	0.0173	0.0096	0.0070	0.0058
	C	6d	EPDM	0.0241	0.0165	0.0129	0.0113	0.0200	0.0122	0.0096	0.0082
			BUR	0.0224	0.0152	0.0116	0.0100	0.0181	0.0107	0.0082	0.0070
		8d	EPDM	0.0240	0.0165	0.0127	0.0111	0.0189	0.0109	0.0083	0.0070
			BUR	0.0221	0.0150	0.0115	0.0100	0.0168	0.0092	0.0068	0.0057
	D	6d	EPDM	0.0228	0.0136	0.0110	0.0099	0.0195	0.0108	0.0086	0.0076
			BUR	0.0208	0.0120	0.0097	0.0087	0.0176	0.0093	0.0072	0.0063
		8d	EPDM	0.0224	0.0134	0.0108	0.0096	0.0183	0.0095	0.0072	0.0062
			BUR	0.0206	0.0119	0.0096	0.0084	0.0163	0.0079	0.0058	0.0048

Table 7.48. Average Annual Building Loss Normalized by Building Value for Building A – Twelve Foot High Strip Mall Building with Six Units and Metal Deck with Four Foot Joist Spacing

Building Characteristics					No Reduction in Metal Deck Capacity				50% Reduction in Metal Deck Capacity			
					Terrain Surface Roughness (m)				Terrain Surface Roughness (m)			
Wall Type	Missile Environ	Design Code	Metal Deck Attach.	Roof Cover	0.03	0.35	0.70	1.0	0.03	0.35	0.70	1.0
Unreinforced Masonry	A	SBCCI	Screws	EPDM	0.0100	0.0051	0.0035	0.0028	0.0100	0.0052	0.0035	0.0028
				BUR	0.0089	0.0044	0.0028	0.0022	0.0089	0.0044	0.0029	0.0022
			Welds	EPDM	0.0100	0.0051	0.0035	0.0028	0.0102	0.0053	0.0036	0.0029
				BUR	0.0088	0.0044	0.0028	0.0022	0.0092	0.0045	0.0029	0.0023
		ASCE	Screws	EPDM	0.0097	0.0050	0.0034	0.0028	0.0098	0.0051	0.0035	0.0028
				BUR	0.0086	0.0043	0.0028	0.0022	0.0087	0.0044	0.0028	0.0022
			Welds	EPDM	0.0096	0.0051	0.0034	0.0027	0.0099	0.0052	0.0035	0.0028
				BUR	0.0086	0.0043	0.0028	0.0022	0.0088	0.0045	0.0029	0.0023
	B	SBCCI	Screws	EPDM	0.0098	0.0049	0.0033	0.0026	0.0098	0.0049	0.0033	0.0027
				BUR	0.0087	0.0041	0.0027	0.0021	0.0088	0.0043	0.0027	0.0021
			Welds	EPDM	0.0097	0.0048	0.0033	0.0027	0.0100	0.0051	0.0034	0.0027
				BUR	0.0085	0.0041	0.0027	0.0021	0.0089	0.0043	0.0028	0.0022
		ASCE	Screws	EPDM	0.0094	0.0048	0.0032	0.0026	0.0095	0.0048	0.0033	0.0027
				BUR	0.0082	0.0040	0.0026	0.0021	0.0084	0.0041	0.0027	0.0021
			Welds	EPDM	0.0095	0.0048	0.0032	0.0026	0.0096	0.0049	0.0034	0.0027
				BUR	0.0083	0.0040	0.0026	0.0021	0.0085	0.0042	0.0027	0.0021
	C	SBCCI	Screws	EPDM	0.0095	0.0045	0.0031	0.0025	0.0095	0.0046	0.0031	0.0025
				BUR	0.0083	0.0038	0.0025	0.0019	0.0084	0.0038	0.0025	0.0020
			Welds	EPDM	0.0095	0.0045	0.0031	0.0025	0.0097	0.0047	0.0032	0.0026
				BUR	0.0084	0.0037	0.0024	0.0019	0.0086	0.0039	0.0026	0.0020
		ASCE	Screws	EPDM	0.0092	0.0044	0.0031	0.0025	0.0093	0.0045	0.0031	0.0025
				BUR	0.0080	0.0036	0.0024	0.0019	0.0081	0.0037	0.0024	0.0019
			Welds	EPDM	0.0092	0.0044	0.0031	0.0025	0.0094	0.0045	0.0031	0.0026
				BUR	0.0080	0.0036	0.0024	0.0019	0.0082	0.0038	0.0025	0.0020
	D	SBCCI	Screws	EPDM	0.0092	0.0037	0.0025	0.0022	0.0093	0.0038	0.0026	0.0022
				BUR	0.0081	0.0029	0.0019	0.0015	0.0082	0.0030	0.0020	0.0016
			Welds	EPDM	0.0092	0.0037	0.0026	0.0021	0.0094	0.0038	0.0027	0.0022
				BUR	0.0080	0.0029	0.0019	0.0016	0.0082	0.0030	0.0020	0.0016
		ASCE	Screws	EPDM	0.0089	0.0036	0.0025	0.0021	0.0090	0.0036	0.0026	0.0022
				BUR	0.0077	0.0028	0.0019	0.0015	0.0078	0.0029	0.0019	0.0016
			Welds	EPDM	0.0089	0.0036	0.0025	0.0021	0.0091	0.0037	0.0026	0.0022
				BUR	0.0077	0.0028	0.0019	0.0015	0.0079	0.0029	0.0019	0.0016

Table 7.48. Average Annual Building Loss Normalized by Building Value for Building A – Twelve Foot High Strip Mall Building with Six Units and Metal Deck with Four Foot Joist Spacing (concluded)

Building Characteristics					No Reduction in Metal Deck Capacity				50% Reduction in Metal Deck Capacity			
					Terrain Surface Roughness (m)				Terrain Surface Roughness (m)			
Wall Type	Missile Environ	Design Code	Metal Deck Attach.	Roof Cover	0.03	0.35	0.70	1.0	0.03	0.35	0.70	1.0
Reinforced Masonry	A	SBCCI	Screws	EPDM	0.0077	0.0046	0.0032	0.0026	0.0087	0.0048	0.0034	0.0027
				BUR	0.0066	0.0039	0.0026	0.0021	0.0076	0.0041	0.0027	0.0022
			Welds	EPDM	0.0078	0.0047	0.0032	0.0027	0.0093	0.0050	0.0034	0.0028
				BUR	0.0066	0.0039	0.0026	0.0020	0.0081	0.0043	0.0028	0.0022
		ASCE	Screws	EPDM	0.0078	0.0046	0.0032	0.0026	0.0088	0.0049	0.0034	0.0027
				BUR	0.0066	0.0039	0.0026	0.0021	0.0075	0.0041	0.0027	0.0021
			Welds	EPDM	0.0078	0.0046	0.0033	0.0026	0.0092	0.0050	0.0034	0.0028
				BUR	0.0067	0.0039	0.0026	0.0020	0.0079	0.0042	0.0028	0.0022
	B	SBCCI	Screws	EPDM	0.0075	0.0043	0.0031	0.0025	0.0086	0.0046	0.0032	0.0026
				BUR	0.0063	0.0036	0.0024	0.0019	0.0073	0.0038	0.0025	0.0020
			Welds	EPDM	0.0075	0.0044	0.0031	0.0025	0.0090	0.0047	0.0033	0.0027
				BUR	0.0063	0.0035	0.0024	0.0019	0.0078	0.0040	0.0026	0.0021
		ASCE	Screws	EPDM	0.0076	0.0043	0.0030	0.0025	0.0085	0.0046	0.0032	0.0026
				BUR	0.0065	0.0036	0.0024	0.0019	0.0073	0.0039	0.0025	0.0020
			Welds	EPDM	0.0076	0.0043	0.0031	0.0025	0.0089	0.0047	0.0032	0.0027
				BUR	0.0065	0.0036	0.0024	0.0019	0.0078	0.0040	0.0026	0.0021
	C	SBCCI	Screws	EPDM	0.0073	0.0039	0.0028	0.0024	0.0083	0.0042	0.0030	0.0025
				BUR	0.0061	0.0032	0.0021	0.0017	0.0071	0.0034	0.0023	0.0018
			Welds	EPDM	0.0072	0.0039	0.0028	0.0024	0.0087	0.0044	0.0030	0.0025
				BUR	0.0061	0.0032	0.0022	0.0018	0.0075	0.0036	0.0024	0.0019
		ASCE	Screws	EPDM	0.0073	0.0039	0.0028	0.0024	0.0082	0.0042	0.0030	0.0024
				BUR	0.0061	0.0032	0.0022	0.0018	0.0070	0.0034	0.0023	0.0019
			Welds	EPDM	0.0073	0.0040	0.0028	0.0024	0.0086	0.0043	0.0031	0.0025
				BUR	0.0062	0.0032	0.0022	0.0018	0.0075	0.0035	0.0024	0.0019
	D	SBCCI	Screws	EPDM	0.0070	0.0032	0.0024	0.0020	0.0080	0.0034	0.0025	0.0021
				BUR	0.0057	0.0024	0.0017	0.0014	0.0068	0.0026	0.0018	0.0015
			Welds	EPDM	0.0070	0.0032	0.0024	0.0020	0.0084	0.0035	0.0025	0.0021
				BUR	0.0058	0.0024	0.0017	0.0014	0.0072	0.0027	0.0019	0.0015
		ASCE	Screws	EPDM	0.0070	0.0032	0.0024	0.0020	0.0079	0.0034	0.0024	0.0021
				BUR	0.0058	0.0024	0.0017	0.0014	0.0068	0.0026	0.0018	0.0015
			Welds	EPDM	0.0071	0.0032	0.0023	0.0020	0.0082	0.0035	0.0026	0.0021
				BUR	0.0058	0.0024	0.0017	0.0014	0.0071	0.0027	0.0018	0.0015

Table 7.49. Average Annual Building Loss Normalized by Building Value for Building B – Twenty Foot High Strip Mall Building with Six Units and Metal Deck with Four Foot Joist Spacing

Building Characteristics					No Reduction in Metal Deck Capacity				50% Reduction in Metal Deck Capacity			
					Terrain Surface Roughness (m)				Terrain Surface Roughness (m)			
Wall Type	Missile Environ	Design Code	Metal Deck Attach.	Roof Cover	0.03	0.35	0.70	1.0	0.03	0.35	0.70	1.0
Unreinforced Masonry	A	SBCCI	Screws	EPDM	0.0192	0.0113	0.0087	0.0073	0.0192	0.0113	0.0087	0.0074
				BUR	0.0173	0.0099	0.0073	0.0061	0.0173	0.0099	0.0074	0.0062
			Welds	EPDM	0.0193	0.0114	0.0086	0.0074	0.0195	0.0115	0.0088	0.0075
				BUR	0.0173	0.0100	0.0073	0.0061	0.0175	0.0102	0.0076	0.0063
		ASCE	Screws	EPDM	0.0188	0.0111	0.0084	0.0072	0.0189	0.0112	0.0085	0.0073
				BUR	0.0168	0.0097	0.0071	0.0060	0.0169	0.0097	0.0072	0.0060
			Welds	EPDM	0.0188	0.0112	0.0085	0.0072	0.0190	0.0114	0.0087	0.0074
				BUR	0.0168	0.0097	0.0071	0.0060	0.0170	0.0099	0.0073	0.0062
	B	SBCCI	Screws	EPDM	0.0188	0.0108	0.0084	0.0070	0.0187	0.0110	0.0083	0.0072
				BUR	0.0166	0.0094	0.0069	0.0058	0.0166	0.0095	0.0070	0.0059
			Welds	EPDM	0.0187	0.0109	0.0082	0.0071	0.0188	0.0112	0.0084	0.0071
				BUR	0.0166	0.0095	0.0069	0.0058	0.0170	0.0096	0.0070	0.0059
		ASCE	Screws	EPDM	0.0182	0.0107	0.0081	0.0069	0.0183	0.0108	0.0082	0.0070
				BUR	0.0162	0.0092	0.0067	0.0057	0.0163	0.0093	0.0068	0.0057
			Welds	EPDM	0.0181	0.0107	0.0082	0.0069	0.0185	0.0109	0.0083	0.0071
				BUR	0.0162	0.0093	0.0067	0.0057	0.0165	0.0093	0.0069	0.0058
	C	SBCCI	Screws	EPDM	0.0182	0.0105	0.0081	0.0068	0.0183	0.0106	0.0080	0.0069
				BUR	0.0161	0.0089	0.0066	0.0055	0.0163	0.0090	0.0066	0.0056
			Welds	EPDM	0.0182	0.0105	0.0081	0.0069	0.0183	0.0107	0.0081	0.0070
				BUR	0.0162	0.0089	0.0066	0.0055	0.0164	0.0091	0.0068	0.0057
		ASCE	Screws	EPDM	0.0178	0.0103	0.0079	0.0067	0.0177	0.0104	0.0079	0.0068
				BUR	0.0157	0.0088	0.0064	0.0054	0.0159	0.0088	0.0065	0.0055
			Welds	EPDM	0.0177	0.0103	0.0079	0.0067	0.0179	0.0104	0.0079	0.0068
				BUR	0.0158	0.0087	0.0065	0.0054	0.0159	0.0088	0.0066	0.0055
	D	SBCCI	Screws	EPDM	0.0180	0.0096	0.0073	0.0063	0.0180	0.0097	0.0074	0.0064
				BUR	0.0159	0.0080	0.0060	0.0050	0.0160	0.0081	0.0060	0.0051
			Welds	EPDM	0.0179	0.0096	0.0073	0.0063	0.0181	0.0097	0.0075	0.0064
				BUR	0.0158	0.0080	0.0059	0.0050	0.0160	0.0082	0.0061	0.0052
		ASCE	Screws	EPDM	0.0175	0.0094	0.0072	0.0063	0.0175	0.0094	0.0073	0.0063
				BUR	0.0154	0.0078	0.0058	0.0049	0.0154	0.0078	0.0058	0.0049
			Welds	EPDM	0.0175	0.0094	0.0072	0.0062	0.0177	0.0095	0.0074	0.0063
				BUR	0.0155	0.0078	0.0058	0.0049	0.0156	0.0080	0.0059	0.0050

Table 7.49. Average Annual Building Loss Normalized by Building Value for Building B – Twenty Foot High Strip Mall Building with Six Units and Metal Deck with Four Foot Joist Spacing (concluded)

Building Characteristics					No Reduction in Metal Deck Capacity				50% Reduction in Metal Deck Capacity			
					Terrain Surface Roughness (m)				Terrain Surface Roughness (m)			
Wall Type	Missile Environ	Design Code	Metal Deck Attach.	Roof Cover	0.03	0.35	0.70	1.0	0.03	0.35	0.70	1.0
Reinforced Masonry	A	SBCCI	Screws	EPDM	0.0131	0.0087	0.0067	0.0059	0.0152	0.0094	0.0073	0.0063
				BUR	0.0108	0.0071	0.0053	0.0045	0.0129	0.0079	0.0058	0.0049
			Welds	EPDM	0.0132	0.0087	0.0067	0.0058	0.0158	0.0098	0.0075	0.0064
				BUR	0.0110	0.0071	0.0053	0.0045	0.0136	0.0082	0.0062	0.0052
		ASCE	Screws	EPDM	0.0132	0.0087	0.0067	0.0059	0.0150	0.0094	0.0072	0.0063
				BUR	0.0111	0.0071	0.0054	0.0045	0.0129	0.0079	0.0058	0.0049
			Welds	EPDM	0.0133	0.0087	0.0068	0.0058	0.0157	0.0097	0.0075	0.0064
				BUR	0.0111	0.0071	0.0054	0.0045	0.0135	0.0082	0.0060	0.0051
	B	SBCCI	Screws	EPDM	0.0130	0.0084	0.0066	0.0057	0.0150	0.0092	0.0071	0.0061
				BUR	0.0107	0.0068	0.0051	0.0043	0.0128	0.0076	0.0057	0.0048
			Welds	EPDM	0.0131	0.0084	0.0066	0.0058	0.0156	0.0095	0.0073	0.0063
				BUR	0.0108	0.0068	0.0051	0.0044	0.0134	0.0079	0.0059	0.0050
		ASCE	Screws	EPDM	0.0131	0.0084	0.0066	0.0057	0.0150	0.0092	0.0071	0.0061
				BUR	0.0109	0.0068	0.0052	0.0045	0.0128	0.0076	0.0057	0.0048
			Welds	EPDM	0.0132	0.0084	0.0066	0.0057	0.0156	0.0094	0.0073	0.0063
				BUR	0.0110	0.0068	0.0052	0.0044	0.0133	0.0078	0.0058	0.0049
	C	SBCCI	Screws	EPDM	0.0127	0.0081	0.0064	0.0056	0.0148	0.0089	0.0069	0.0060
				BUR	0.0105	0.0064	0.0048	0.0042	0.0126	0.0072	0.0054	0.0046
			Welds	EPDM	0.0128	0.0081	0.0064	0.0056	0.0154	0.0092	0.0071	0.0062
				BUR	0.0106	0.0065	0.0049	0.0043	0.0132	0.0076	0.0057	0.0048
		ASCE	Screws	EPDM	0.0129	0.0081	0.0063	0.0056	0.0147	0.0089	0.0068	0.0059
				BUR	0.0107	0.0064	0.0049	0.0042	0.0125	0.0072	0.0054	0.0046
			Welds	EPDM	0.0130	0.0081	0.0064	0.0056	0.0153	0.0092	0.0071	0.0061
				BUR	0.0107	0.0064	0.0049	0.0042	0.0131	0.0075	0.0056	0.0047
	D	SBCCI	Screws	EPDM	0.0125	0.0073	0.0059	0.0053	0.0145	0.0082	0.0064	0.0056
				BUR	0.0102	0.0056	0.0044	0.0039	0.0122	0.0065	0.0049	0.0042
			Welds	EPDM	0.0126	0.0074	0.0059	0.0052	0.0150	0.0084	0.0066	0.0057
				BUR	0.0103	0.0057	0.0044	0.0039	0.0130	0.0068	0.0051	0.0044
		ASCE	Screws	EPDM	0.0126	0.0074	0.0060	0.0052	0.0145	0.0081	0.0063	0.0056
				BUR	0.0104	0.0057	0.0044	0.0039	0.0122	0.0064	0.0049	0.0042
			Welds	EPDM	0.0127	0.0074	0.0060	0.0053	0.0150	0.0083	0.0065	0.0057
				BUR	0.0104	0.0057	0.0044	0.0039	0.0127	0.0066	0.0050	0.0044

Table 7.50. Average Annual Building Loss Normalized by Building Value for Building C – Twenty Foot High Strip Mall Building with Six Units and Metal Deck with Six Foot Joist Spacing

Building Characteristics					No Reduction in Metal Deck Capacity				50% Reduction in Metal Deck Capacity			
					Terrain Surface Roughness (m)				Terrain Surface Roughness (m)			
Wall Type	Missile Environ	Design Code	Metal Deck Attach.	Roof Cover	0.03	0.35	0.70	1.0	0.03	0.35	0.70	1.0
Unreinforced Masonry	A	SBCCI	Screws	EPDM	0.0199	0.0116	0.0088	0.0075	0.0242	0.0150	0.0116	0.0100
				BUR	0.0179	0.0102	0.0075	0.0063	0.0221	0.0135	0.0103	0.0088
			Welds	EPDM	0.0200	0.0118	0.0089	0.0076	0.0265	0.0169	0.0133	0.0114
				BUR	0.0181	0.0104	0.0076	0.0064	0.0245	0.0154	0.0119	0.0102
		ASCE	Screws	EPDM	0.0196	0.0116	0.0088	0.0075	0.0228	0.0139	0.0108	0.0093
				BUR	0.0176	0.0101	0.0074	0.0063	0.0209	0.0124	0.0094	0.0079
			Welds	EPDM	0.0197	0.0117	0.0088	0.0074	0.0240	0.0146	0.0114	0.0098
				BUR	0.0176	0.0101	0.0074	0.0062	0.0219	0.0132	0.0100	0.0085
	B	SBCCI	Screws	EPDM	0.0193	0.0112	0.0085	0.0072	0.0229	0.0141	0.0110	0.0094
				BUR	0.0174	0.0097	0.0071	0.0059	0.0208	0.0126	0.0096	0.0082
			Welds	EPDM	0.0193	0.0112	0.0086	0.0073	0.0249	0.0156	0.0124	0.0107
				BUR	0.0174	0.0098	0.0072	0.0060	0.0230	0.0142	0.0110	0.0094
		ASCE	Screws	EPDM	0.0190	0.0111	0.0084	0.0072	0.0219	0.0131	0.0101	0.0087
				BUR	0.0170	0.0097	0.0070	0.0059	0.0197	0.0115	0.0087	0.0074
			Welds	EPDM	0.0190	0.0111	0.0084	0.0071	0.0227	0.0138	0.0105	0.0091
				BUR	0.0170	0.0095	0.0070	0.0059	0.0205	0.0121	0.0091	0.0077
	C	SBCCI	Screws	EPDM	0.0188	0.0108	0.0082	0.0070	0.0219	0.0133	0.0103	0.0091
				BUR	0.0168	0.0093	0.0068	0.0057	0.0199	0.0118	0.0091	0.0077
			Welds	EPDM	0.0189	0.0109	0.0082	0.0071	0.0237	0.0148	0.0116	0.0101
				BUR	0.0169	0.0093	0.0069	0.0058	0.0218	0.0132	0.0103	0.0089
		ASCE	Screws	EPDM	0.0186	0.0106	0.0081	0.0069	0.0209	0.0125	0.0097	0.0083
				BUR	0.0165	0.0091	0.0067	0.0057	0.0188	0.0110	0.0083	0.0070
			Welds	EPDM	0.0186	0.0106	0.0081	0.0069	0.0215	0.0130	0.0101	0.0086
				BUR	0.0166	0.0090	0.0068	0.0056	0.0195	0.0114	0.0087	0.0073
	D	SBCCI	Screws	EPDM	0.0185	0.0098	0.0075	0.0064	0.0214	0.0120	0.0095	0.0083
				BUR	0.0165	0.0082	0.0061	0.0051	0.0196	0.0104	0.0080	0.0070
			Welds	EPDM	0.0185	0.0099	0.0075	0.0065	0.0231	0.0133	0.0106	0.0094
				BUR	0.0164	0.0083	0.0061	0.0052	0.0212	0.0118	0.0093	0.0082
		ASCE	Screws	EPDM	0.0182	0.0097	0.0074	0.0064	0.0204	0.0112	0.0086	0.0075
				BUR	0.0162	0.0081	0.0060	0.0051	0.0184	0.0095	0.0072	0.0062
			Welds	EPDM	0.0183	0.0097	0.0074	0.0063	0.0210	0.0115	0.0089	0.0078
				BUR	0.0163	0.0082	0.0060	0.0051	0.0190	0.0099	0.0075	0.0064

Table 7.50. Average Annual Building Loss Normalized by Building Value for Building C – Twenty Foot High Strip Mall Building with Six Units and Metal Deck with Six Foot Joist Spacing (concluded)

Building Characteristics					No Reduction in Metal Deck Capacity				50% Reduction in Metal Deck Capacity			
					Terrain Surface Roughness (m)				Terrain Surface Roughness (m)			
Wall Type	Missile Environ	Design Code	Metal Deck Attach.	Roof Cover	0.03	0.35	0.70	1.0	0.03	0.35	0.70	1.0
Reinforced Masonry	A	SBCCI	Screws	EPDM	0.0148	0.0092	0.0070	0.0061	0.0221	0.0141	0.0110	0.0095
				BUR	0.0125	0.0077	0.0057	0.0048	0.0200	0.0125	0.0096	0.0082
			Welds	EPDM	0.0156	0.0097	0.0074	0.0065	0.0245	0.0162	0.0126	0.0111
				BUR	0.0136	0.0081	0.0061	0.0051	0.0224	0.0145	0.0113	0.0097
		ASCE	Screws	EPDM	0.0145	0.0090	0.0070	0.0060	0.0208	0.0128	0.0100	0.0086
				BUR	0.0122	0.0075	0.0055	0.0047	0.0185	0.0112	0.0085	0.0073
			Welds	EPDM	0.0148	0.0092	0.0071	0.0060	0.0219	0.0137	0.0107	0.0092
				BUR	0.0127	0.0076	0.0057	0.0048	0.0197	0.0121	0.0093	0.0079
	B	SBCCI	Screws	EPDM	0.0146	0.0091	0.0069	0.0060	0.0209	0.0133	0.0104	0.0090
				BUR	0.0124	0.0074	0.0055	0.0047	0.0188	0.0116	0.0089	0.0076
			Welds	EPDM	0.0155	0.0095	0.0072	0.0063	0.0230	0.0149	0.0118	0.0102
				BUR	0.0133	0.0079	0.0059	0.0049	0.0212	0.0134	0.0104	0.0091
		ASCE	Screws	EPDM	0.0143	0.0088	0.0068	0.0059	0.0198	0.0122	0.0094	0.0081
				BUR	0.0121	0.0072	0.0054	0.0046	0.0174	0.0106	0.0081	0.0069
			Welds	EPDM	0.0147	0.0090	0.0070	0.0060	0.0207	0.0128	0.0100	0.0086
				BUR	0.0125	0.0074	0.0055	0.0046	0.0185	0.0112	0.0085	0.0072
	C	SBCCI	Screws	EPDM	0.0144	0.0087	0.0068	0.0058	0.0200	0.0127	0.0098	0.0086
				BUR	0.0122	0.0070	0.0053	0.0045	0.0181	0.0111	0.0084	0.0072
			Welds	EPDM	0.0152	0.0092	0.0071	0.0061	0.0219	0.0142	0.0112	0.0098
				BUR	0.0129	0.0075	0.0056	0.0048	0.0199	0.0127	0.0099	0.0084
		ASCE	Screws	EPDM	0.0139	0.0085	0.0066	0.0057	0.0190	0.0117	0.0091	0.0078
				BUR	0.0118	0.0068	0.0051	0.0044	0.0168	0.0100	0.0076	0.0065
			Welds	EPDM	0.0144	0.0087	0.0067	0.0058	0.0196	0.0122	0.0095	0.0081
				BUR	0.0123	0.0070	0.0052	0.0044	0.0175	0.0106	0.0080	0.0068
	D	SBCCI	Screws	EPDM	0.0142	0.0079	0.0063	0.0055	0.0195	0.0111	0.0089	0.0078
				BUR	0.0119	0.0062	0.0048	0.0041	0.0172	0.0095	0.0075	0.0065
			Welds	EPDM	0.0150	0.0083	0.0066	0.0057	0.0212	0.0125	0.0102	0.0089
				BUR	0.0128	0.0067	0.0050	0.0043	0.0192	0.0109	0.0087	0.0077
		ASCE	Screws	EPDM	0.0137	0.0077	0.0061	0.0054	0.0184	0.0102	0.0080	0.0070
				BUR	0.0116	0.0061	0.0046	0.0040	0.0162	0.0086	0.0066	0.0057
			Welds	EPDM	0.0143	0.0079	0.0062	0.0054	0.0190	0.0106	0.0083	0.0073
				BUR	0.0119	0.0062	0.0047	0.0041	0.0169	0.0089	0.0069	0.0059

Table 7.51. Average Annual Building Loss Normalized by Building Value for Building D – Twenty Foot High Strip Mall Building with One Unit and Metal Deck with Six Foot Joist Spacing

Building Characteristics					No Reduction in Metal Deck Capacity				50% Reduction in Metal Deck Capacity			
					Terrain Surface Roughness (m)				Terrain Surface Roughness (m)			
Wall Type	Missile Environ	Design Code	Metal Deck Attach.	Roof Cover	0.03	0.35	0.70	1.0	0.03	0.35	0.70	1.0
Unreinforced Masonry	A	SBCCI	Screws	EPDM	0.0211	0.0121	0.0092	0.0077	0.0255	0.0153	0.0118	0.0102
				BUR	0.0192	0.0106	0.0079	0.0066	0.0235	0.0136	0.0104	0.0089
			Welds	EPDM	0.0211	0.0122	0.0092	0.0078	0.0281	0.0172	0.0135	0.0118
				BUR	0.0193	0.0107	0.0079	0.0066	0.0262	0.0157	0.0121	0.0105
		ASCE	Screws	EPDM	0.0210	0.0120	0.0091	0.0078	0.0239	0.0140	0.0109	0.0093
				BUR	0.0192	0.0107	0.0078	0.0065	0.0221	0.0126	0.0095	0.0081
			Welds	EPDM	0.0209	0.0120	0.0091	0.0077	0.0252	0.0147	0.0113	0.0098
				BUR	0.0191	0.0106	0.0079	0.0065	0.0231	0.0132	0.0100	0.0086
	B	SBCCI	Screws	EPDM	0.0205	0.0118	0.0089	0.0076	0.0245	0.0148	0.0114	0.0098
				BUR	0.0187	0.0103	0.0076	0.0063	0.0226	0.0133	0.0100	0.0086
			Welds	EPDM	0.0206	0.0119	0.0090	0.0077	0.0268	0.0164	0.0129	0.0111
				BUR	0.0187	0.0104	0.0076	0.0064	0.0249	0.0148	0.0116	0.0099
		ASCE	Screws	EPDM	0.0204	0.0117	0.0089	0.0075	0.0232	0.0135	0.0105	0.0090
				BUR	0.0186	0.0103	0.0076	0.0063	0.0213	0.0121	0.0092	0.0078
			Welds	EPDM	0.0203	0.0118	0.0089	0.0075	0.0242	0.0142	0.0110	0.0094
				BUR	0.0187	0.0103	0.0076	0.0063	0.0222	0.0128	0.0095	0.0081
	C	SBCCI	Screws	EPDM	0.0201	0.0114	0.0087	0.0073	0.0239	0.0142	0.0110	0.0095
				BUR	0.0182	0.0098	0.0072	0.0061	0.0218	0.0127	0.0097	0.0083
			Welds	EPDM	0.0202	0.0115	0.0087	0.0074	0.0255	0.0159	0.0123	0.0108
				BUR	0.0182	0.0100	0.0074	0.0061	0.0238	0.0143	0.0110	0.0096
		ASCE	Screws	EPDM	0.0199	0.0113	0.0086	0.0074	0.0226	0.0132	0.0102	0.0087
				BUR	0.0182	0.0098	0.0073	0.0060	0.0206	0.0116	0.0088	0.0074
			Welds	EPDM	0.0200	0.0114	0.0086	0.0073	0.0233	0.0138	0.0106	0.0091
				BUR	0.0182	0.0098	0.0072	0.0061	0.0214	0.0122	0.0092	0.0079
	D	SBCCI	Screws	EPDM	0.0198	0.0105	0.0080	0.0070	0.0231	0.0127	0.0099	0.0086
				BUR	0.0178	0.0090	0.0067	0.0057	0.0212	0.0112	0.0085	0.0074
			Welds	EPDM	0.0198	0.0106	0.0081	0.0070	0.0248	0.0139	0.0111	0.0098
				BUR	0.0180	0.0091	0.0067	0.0057	0.0229	0.0124	0.0098	0.0086
		ASCE	Screws	EPDM	0.0197	0.0104	0.0081	0.0069	0.0221	0.0118	0.0092	0.0079
				BUR	0.0178	0.0088	0.0067	0.0056	0.0201	0.0103	0.0078	0.0067
			Welds	EPDM	0.0196	0.0105	0.0080	0.0069	0.0226	0.0121	0.0094	0.0081
				BUR	0.0178	0.0088	0.0066	0.0056	0.0207	0.0107	0.0081	0.0068

Table 7.51. Average Annual Building Loss Normalized by Building Value for Building D – Twenty Foot High Strip Mall Building with One Unit and Metal Deck with Six Foot Joist Spacing (concluded)

Building Characteristics					No Reduction in Metal Deck Capacity				50% Reduction in Metal Deck Capacity			
					Terrain Surface Roughness (m)				Terrain Surface Roughness (m)			
Wall Type	Missile Environ	Design Code	Metal Deck Attach.	Roof Cover	0.03	0.35	0.70	1.0	0.03	0.35	0.70	1.0
Reinforced Masonry	A	SBCCI	Screws	EPDM	0.0160	0.0100	0.0076	0.0065	0.0234	0.0145	0.0112	0.0098
				BUR	0.0139	0.0084	0.0061	0.0051	0.0212	0.0127	0.0099	0.0084
			Welds	EPDM	0.0165	0.0103	0.0078	0.0066	0.0264	0.0166	0.0131	0.0114
				BUR	0.0144	0.0087	0.0064	0.0053	0.0242	0.0150	0.0117	0.0100
		ASCE	Screws	EPDM	0.0152	0.0097	0.0073	0.0063	0.0216	0.0131	0.0102	0.0087
				BUR	0.0131	0.0081	0.0059	0.0049	0.0194	0.0116	0.0087	0.0075
			Welds	EPDM	0.0155	0.0098	0.0074	0.0063	0.0231	0.0139	0.0106	0.0093
				BUR	0.0134	0.0082	0.0061	0.0050	0.0208	0.0122	0.0093	0.0079
	B	SBCCI	Screws	EPDM	0.0157	0.0097	0.0074	0.0063	0.0225	0.0139	0.0108	0.0094
				BUR	0.0136	0.0081	0.0060	0.0049	0.0203	0.0123	0.0095	0.0081
			Welds	EPDM	0.0164	0.0100	0.0077	0.0065	0.0249	0.0157	0.0124	0.0109
				BUR	0.0142	0.0084	0.0062	0.0052	0.0228	0.0141	0.0110	0.0095
		ASCE	Screws	EPDM	0.0151	0.0094	0.0072	0.0062	0.0209	0.0128	0.0098	0.0085
				BUR	0.0128	0.0078	0.0057	0.0048	0.0189	0.0111	0.0084	0.0071
			Welds	EPDM	0.0153	0.0095	0.0071	0.0061	0.0220	0.0134	0.0104	0.0090
				BUR	0.0131	0.0079	0.0058	0.0049	0.0198	0.0118	0.0090	0.0076
	C	SBCCI	Screws	EPDM	0.0155	0.0092	0.0071	0.0061	0.0217	0.0135	0.0105	0.0091
				BUR	0.0133	0.0075	0.0056	0.0048	0.0195	0.0118	0.0090	0.0078
			Welds	EPDM	0.0161	0.0096	0.0074	0.0063	0.0238	0.0151	0.0120	0.0104
				BUR	0.0139	0.0080	0.0059	0.0050	0.0217	0.0135	0.0105	0.0092
		ASCE	Screws	EPDM	0.0148	0.0089	0.0068	0.0060	0.0205	0.0124	0.0095	0.0082
				BUR	0.0126	0.0072	0.0054	0.0045	0.0184	0.0108	0.0081	0.0069
			Welds	EPDM	0.0151	0.0090	0.0069	0.0060	0.0214	0.0131	0.0101	0.0086
				BUR	0.0128	0.0074	0.0054	0.0046	0.0191	0.0114	0.0086	0.0074
	D	SBCCI	Screws	EPDM	0.0152	0.0084	0.0066	0.0057	0.0210	0.0118	0.0092	0.0082
				BUR	0.0130	0.0068	0.0051	0.0044	0.0188	0.0102	0.0079	0.0068
			Welds	EPDM	0.0159	0.0088	0.0069	0.0059	0.0225	0.0132	0.0106	0.0093
				BUR	0.0137	0.0071	0.0054	0.0045	0.0206	0.0116	0.0093	0.0081
		ASCE	Screws	EPDM	0.0145	0.0081	0.0064	0.0056	0.0197	0.0108	0.0085	0.0074
				BUR	0.0123	0.0064	0.0049	0.0042	0.0177	0.0092	0.0070	0.0060
			Welds	EPDM	0.0147	0.0082	0.0064	0.0056	0.0204	0.0112	0.0088	0.0076
				BUR	0.0125	0.0066	0.0050	0.0043	0.0184	0.0095	0.0073	0.0063

Table 7.52. Average Annual Content Loss Normalized by Building Value for Building A – Twelve Foot High Strip Mall Building with Six Units and Wood Deck with Two Foot Truss Spacing

Building Characteristics				Toe-Nailed Roof-Wall Connection				Strapped Roof-Wall Connection			
				Terrain Surface Roughness (m)				Terrain Surface Roughness (m)			
Wall Type	Missile Environ.	Wood Deck Nail Size	Roof Cover	0.03	0.35	0.70	1.0	0.03	0.35	0.70	1.0
Unreinforced Masonry	A	6d	EPDM	0.0096	0.0056	0.0037	0.0029	0.0052	0.0022	0.0014	0.0011
			BUR	0.0094	0.0055	0.0036	0.0028	0.0050	0.0022	0.0014	0.0011
		8d	EPDM	0.0094	0.0055	0.0037	0.0029	0.0044	0.0016	0.0009	0.0006
			BUR	0.0092	0.0054	0.0036	0.0029	0.0043	0.0016	0.0009	0.0005
	B	6d	EPDM	0.0075	0.0043	0.0028	0.0022	0.0047	0.0021	0.0013	0.0010
			BUR	0.0074	0.0043	0.0028	0.0022	0.0046	0.0020	0.0012	0.0009
		8d	EPDM	0.0074	0.0042	0.0028	0.0022	0.0041	0.0015	0.0008	0.0006
			BUR	0.0073	0.0042	0.0027	0.0021	0.0040	0.0014	0.0008	0.0005
	C	6d	EPDM	0.0058	0.0035	0.0024	0.0018	0.0044	0.0019	0.0012	0.0009
			BUR	0.0056	0.0035	0.0023	0.0017	0.0044	0.0018	0.0011	0.0009
		8d	EPDM	0.0056	0.0034	0.0022	0.0018	0.0040	0.0013	0.0007	0.0005
			BUR	0.0055	0.0034	0.0022	0.0017	0.0038	0.0012	0.0006	0.0004
	D	6d	EPDM	0.0050	0.0019	0.0013	0.0011	0.0042	0.0014	0.0009	0.0007
			BUR	0.0049	0.0019	0.0012	0.0010	0.0042	0.0013	0.0008	0.0006
		8d	EPDM	0.0049	0.0018	0.0012	0.0010	0.0038	0.0010	0.0005	0.0004
			BUR	0.0048	0.0017	0.0011	0.0009	0.0036	0.0009	0.0004	0.0003
Reinforced Masonry	A	6d	EPDM	0.0091	0.0055	0.0036	0.0028	0.0050	0.0022	0.0014	0.0011
			BUR	0.0091	0.0053	0.0036	0.0028	0.0048	0.0021	0.0013	0.0010
		8d	EPDM	0.0091	0.0053	0.0035	0.0028	0.0041	0.0015	0.0008	0.0006
			BUR	0.0090	0.0053	0.0036	0.0027	0.0040	0.0014	0.0008	0.0005
	B	6d	EPDM	0.0072	0.0041	0.0027	0.0021	0.0046	0.0020	0.0012	0.0010
			BUR	0.0072	0.0040	0.0027	0.0021	0.0044	0.0019	0.0012	0.0009
		8d	EPDM	0.0072	0.0041	0.0027	0.0021	0.0039	0.0013	0.0007	0.0005
			BUR	0.0070	0.0040	0.0026	0.0020	0.0038	0.0013	0.0007	0.0004
	C	6d	EPDM	0.0054	0.0034	0.0022	0.0017	0.0043	0.0018	0.0012	0.0009
			BUR	0.0054	0.0034	0.0022	0.0017	0.0041	0.0017	0.0010	0.0008
		8d	EPDM	0.0054	0.0033	0.0022	0.0017	0.0037	0.0011	0.0006	0.0004
			BUR	0.0052	0.0032	0.0021	0.0016	0.0035	0.0011	0.0005	0.0004
	D	6d	EPDM	0.0047	0.0018	0.0012	0.0010	0.0040	0.0013	0.0008	0.0007
			BUR	0.0045	0.0017	0.0011	0.0009	0.0039	0.0012	0.0008	0.0006
		8d	EPDM	0.0045	0.0016	0.0010	0.0009	0.0035	0.0009	0.0005	0.0003
			BUR	0.0044	0.0015	0.0010	0.0008	0.0034	0.0008	0.0004	0.0002

Table 7.53. Average Annual Content Loss Normalized by Building Value for Building B – Twenty Foot High Strip Mall Building with Six Units and Wood Deck with Two Foot Truss Spacing

Building Characteristics				Toe-Nailed Roof-Wall Connection				Strapped Roof-Wall Connection			
				Terrain Surface Roughness (m)				Terrain Surface Roughness (m)			
Wall Type	Missile Environ.	Wood Deck Nail Size	Roof Cover	0.03	0.35	0.70	1.0	0.03	0.35	0.70	1.0
Unreinforced Masonry	A	6d	EPDM	0.0128	0.0093	0.0068	0.0057	0.0094	0.0053	0.0039	0.0033
			BUR	0.0126	0.0091	0.0068	0.0056	0.0090	0.0051	0.0037	0.0031
		8d	EPDM	0.0128	0.0093	0.0069	0.0056	0.0088	0.0047	0.0033	0.0027
			BUR	0.0125	0.0091	0.0066	0.0056	0.0084	0.0045	0.0032	0.0025
	B	6d	EPDM	0.0112	0.0075	0.0056	0.0047	0.0087	0.0047	0.0035	0.0029
			BUR	0.0111	0.0074	0.0054	0.0045	0.0084	0.0046	0.0033	0.0027
		8d	EPDM	0.0112	0.0075	0.0056	0.0047	0.0081	0.0043	0.0030	0.0024
			BUR	0.0110	0.0074	0.0054	0.0046	0.0078	0.0041	0.0027	0.0022
	C	6d	EPDM	0.0098	0.0061	0.0046	0.0039	0.0082	0.0044	0.0032	0.0027
			BUR	0.0095	0.0059	0.0044	0.0037	0.0079	0.0042	0.0031	0.0025
		8d	EPDM	0.0097	0.0060	0.0045	0.0039	0.0078	0.0039	0.0027	0.0022
			BUR	0.0094	0.0058	0.0044	0.0037	0.0075	0.0037	0.0025	0.0020
	D	6d	EPDM	0.0094	0.0050	0.0039	0.0034	0.0080	0.0039	0.0029	0.0024
			BUR	0.0091	0.0048	0.0037	0.0033	0.0076	0.0037	0.0027	0.0022
		8d	EPDM	0.0092	0.0050	0.0038	0.0034	0.0076	0.0034	0.0024	0.0019
			BUR	0.0089	0.0047	0.0036	0.0032	0.0073	0.0031	0.0021	0.0017
Reinforced Masonry	A	6d	EPDM	0.0120	0.0089	0.0066	0.0055	0.0081	0.0044	0.0033	0.0028
			BUR	0.0118	0.0087	0.0064	0.0052	0.0078	0.0042	0.0031	0.0026
		8d	EPDM	0.0118	0.0089	0.0065	0.0054	0.0070	0.0034	0.0024	0.0019
			BUR	0.0115	0.0086	0.0065	0.0052	0.0067	0.0031	0.0021	0.0017
	B	6d	EPDM	0.0103	0.0072	0.0053	0.0044	0.0074	0.0040	0.0030	0.0025
			BUR	0.0102	0.0070	0.0052	0.0043	0.0072	0.0038	0.0028	0.0023
		8d	EPDM	0.0103	0.0071	0.0053	0.0045	0.0067	0.0032	0.0022	0.0017
			BUR	0.0101	0.0069	0.0051	0.0042	0.0063	0.0029	0.0019	0.0015
	C	6d	EPDM	0.0087	0.0056	0.0042	0.0036	0.0070	0.0038	0.0028	0.0023
			BUR	0.0085	0.0054	0.0040	0.0034	0.0068	0.0035	0.0025	0.0021
		8d	EPDM	0.0086	0.0056	0.0042	0.0036	0.0064	0.0030	0.0021	0.0016
			BUR	0.0083	0.0053	0.0040	0.0034	0.0060	0.0027	0.0018	0.0014
	D	6d	EPDM	0.0082	0.0045	0.0035	0.0031	0.0069	0.0032	0.0024	0.0020
			BUR	0.0079	0.0043	0.0033	0.0029	0.0066	0.0030	0.0022	0.0018
		8d	EPDM	0.0081	0.0044	0.0035	0.0030	0.0062	0.0025	0.0017	0.0013
			BUR	0.0078	0.0042	0.0032	0.0028	0.0059	0.0023	0.0014	0.0011

Table 7.54. Average Annual Content Loss Normalized by Building Value for Building A – Twelve Foot High Strip Mall Building with Six Units and Metal Deck with Four Foot Joist Spacing

Building Characteristics					No Reduction in Metal Deck Capacity				50% Reduction in Metal Deck Capacity			
					Terrain Surface Roughness (m)				Terrain Surface Roughness (m)			
Wall Type	Missile Environ	Design Code	Metal Deck Attach.	Roof Cover	0.03	0.35	0.70	1.0	0.03	0.35	0.70	1.0
Unreinforced Masonry	A	SBCCI	Screws	EPDM	0.0035	0.0014	0.0008	0.0005	0.0035	0.0014	0.0008	0.0005
				BUR	0.0034	0.0013	0.0007	0.0005	0.0034	0.0013	0.0007	0.0005
			Welds	EPDM	0.0035	0.0013	0.0007	0.0005	0.0036	0.0014	0.0008	0.0006
				BUR	0.0033	0.0013	0.0007	0.0005	0.0035	0.0013	0.0007	0.0005
		ASCE	Screws	EPDM	0.0034	0.0013	0.0007	0.0005	0.0034	0.0013	0.0008	0.0005
				BUR	0.0033	0.0013	0.0007	0.0005	0.0033	0.0013	0.0007	0.0005
			Welds	EPDM	0.0034	0.0013	0.0007	0.0005	0.0034	0.0014	0.0008	0.0005
				BUR	0.0033	0.0013	0.0007	0.0004	0.0033	0.0013	0.0007	0.0005
	B	SBCCI	Screws	EPDM	0.0034	0.0012	0.0007	0.0004	0.0034	0.0012	0.0007	0.0005
				BUR	0.0032	0.0011	0.0006	0.0004	0.0032	0.0012	0.0006	0.0004
			Welds	EPDM	0.0033	0.0012	0.0007	0.0005	0.0034	0.0013	0.0007	0.0005
				BUR	0.0032	0.0011	0.0006	0.0004	0.0033	0.0012	0.0006	0.0004
		ASCE	Screws	EPDM	0.0032	0.0012	0.0006	0.0004	0.0032	0.0012	0.0006	0.0005
				BUR	0.0031	0.0010	0.0006	0.0004	0.0031	0.0011	0.0006	0.0004
			Welds	EPDM	0.0032	0.0012	0.0006	0.0004	0.0033	0.0012	0.0007	0.0005
				BUR	0.0031	0.0011	0.0006	0.0004	0.0032	0.0011	0.0006	0.0004
	C	SBCCI	Screws	EPDM	0.0032	0.0010	0.0005	0.0004	0.0032	0.0010	0.0006	0.0004
				BUR	0.0030	0.0009	0.0005	0.0003	0.0031	0.0009	0.0005	0.0003
			Welds	EPDM	0.0032	0.0010	0.0005	0.0004	0.0033	0.0010	0.0006	0.0004
				BUR	0.0031	0.0009	0.0004	0.0003	0.0032	0.0009	0.0005	0.0003
		ASCE	Screws	EPDM	0.0031	0.0009	0.0005	0.0004	0.0031	0.0010	0.0005	0.0004
				BUR	0.0029	0.0008	0.0004	0.0003	0.0029	0.0009	0.0004	0.0003
			Welds	EPDM	0.0031	0.0009	0.0005	0.0004	0.0032	0.0010	0.0006	0.0004
				BUR	0.0029	0.0008	0.0004	0.0003	0.0030	0.0009	0.0005	0.0003
	D	SBCCI	Screws	EPDM	0.0031	0.0008	0.0005	0.0003	0.0031	0.0009	0.0005	0.0003
				BUR	0.0030	0.0008	0.0004	0.0002	0.0030	0.0008	0.0004	0.0003
			Welds	EPDM	0.0031	0.0009	0.0005	0.0003	0.0032	0.0009	0.0005	0.0004
				BUR	0.0030	0.0007	0.0004	0.0003	0.0030	0.0008	0.0004	0.0003
		ASCE	Screws	EPDM	0.0030	0.0008	0.0004	0.0003	0.0030	0.0008	0.0005	0.0003
				BUR	0.0028	0.0007	0.0004	0.0002	0.0029	0.0007	0.0004	0.0003
			Welds	EPDM	0.0030	0.0008	0.0004	0.0003	0.0031	0.0008	0.0005	0.0004
				BUR	0.0029	0.0007	0.0004	0.0002	0.0030	0.0007	0.0004	0.0003

Table 7.54. Average Annual Content Loss Normalized by Building Value for Building A – Twelve Foot High Strip Mall Building with Six Units and Metal Deck with Four Foot Joist Spacing (concluded)

Building Characteristics					No Reduction in Metal Deck Capacity				50% Reduction in Metal Deck Capacity			
					Terrain Surface Roughness (m)				Terrain Surface Roughness (m)			
Wall Type	Missile Environ	Design Code	Metal Deck Attach.	Roof Cover	0.03	0.35	0.70	1.0	0.03	0.35	0.70	1.0
Reinforced Masonry	A	SBCCI	Screws	EPDM	0.0026	0.0011	0.0006	0.0004	0.0028	0.0011	0.0006	0.0004
				BUR	0.0025	0.0010	0.0005	0.0004	0.0027	0.0011	0.0006	0.0004
			Welds	EPDM	0.0026	0.0011	0.0006	0.0004	0.0030	0.0012	0.0007	0.0005
				BUR	0.0025	0.0010	0.0005	0.0004	0.0029	0.0011	0.0006	0.0004
		ASCE	Screws	EPDM	0.0026	0.0011	0.0006	0.0004	0.0028	0.0012	0.0006	0.0005
				BUR	0.0025	0.0010	0.0005	0.0004	0.0027	0.0011	0.0006	0.0004
			Welds	EPDM	0.0027	0.0011	0.0006	0.0004	0.0030	0.0012	0.0007	0.0005
				BUR	0.0025	0.0010	0.0005	0.0004	0.0028	0.0011	0.0006	0.0004
	B	SBCCI	Screws	EPDM	0.0025	0.0009	0.0005	0.0004	0.0027	0.0010	0.0005	0.0004
				BUR	0.0024	0.0008	0.0004	0.0003	0.0025	0.0009	0.0005	0.0003
			Welds	EPDM	0.0025	0.0009	0.0005	0.0004	0.0029	0.0010	0.0006	0.0004
				BUR	0.0024	0.0008	0.0004	0.0003	0.0027	0.0010	0.0005	0.0004
		ASCE	Screws	EPDM	0.0025	0.0009	0.0005	0.0004	0.0027	0.0010	0.0005	0.0004
				BUR	0.0024	0.0008	0.0004	0.0003	0.0026	0.0009	0.0005	0.0003
			Welds	EPDM	0.0025	0.0009	0.0005	0.0004	0.0028	0.0010	0.0006	0.0004
				BUR	0.0024	0.0008	0.0004	0.0003	0.0027	0.0010	0.0005	0.0003
	C	SBCCI	Screws	EPDM	0.0024	0.0007	0.0004	0.0003	0.0025	0.0008	0.0004	0.0003
				BUR	0.0022	0.0006	0.0003	0.0002	0.0024	0.0007	0.0004	0.0002
			Welds	EPDM	0.0023	0.0007	0.0004	0.0003	0.0027	0.0008	0.0005	0.0004
				BUR	0.0022	0.0006	0.0003	0.0002	0.0026	0.0007	0.0004	0.0003
		ASCE	Screws	EPDM	0.0024	0.0006	0.0004	0.0003	0.0025	0.0007	0.0004	0.0003
				BUR	0.0022	0.0006	0.0003	0.0002	0.0024	0.0007	0.0003	0.0002
			Welds	EPDM	0.0023	0.0007	0.0004	0.0003	0.0027	0.0008	0.0005	0.0003
				BUR	0.0022	0.0006	0.0003	0.0002	0.0026	0.0007	0.0004	0.0003
	D	SBCCI	Screws	EPDM	0.0023	0.0006	0.0003	0.0003	0.0025	0.0007	0.0004	0.0003
				BUR	0.0021	0.0005	0.0002	0.0002	0.0024	0.0005	0.0003	0.0002
			Welds	EPDM	0.0023	0.0006	0.0003	0.0003	0.0026	0.0007	0.0004	0.0003
				BUR	0.0021	0.0005	0.0002	0.0002	0.0025	0.0006	0.0003	0.0002
		ASCE	Screws	EPDM	0.0023	0.0006	0.0003	0.0003	0.0025	0.0006	0.0004	0.0003
				BUR	0.0021	0.0005	0.0002	0.0002	0.0023	0.0005	0.0003	0.0002
			Welds	EPDM	0.0023	0.0006	0.0003	0.0003	0.0026	0.0007	0.0004	0.0003
				BUR	0.0021	0.0005	0.0002	0.0002	0.0025	0.0006	0.0003	0.0002

Table 7.55. Average Annual Content Loss Normalized by Building Value for Building B – Twenty Foot High Strip Mall Building with Six Units and Metal Deck with Four Foot Joist Spacing

Building Characteristics					No Reduction in Metal Deck Capacity				50% Reduction in Metal Deck Capacity			
					Terrain Surface Roughness (m)				Terrain Surface Roughness (m)			
Wall Type	Missile Environ	Design Code	Metal Deck Attach.	Roof Cover	0.03	0.35	0.70	1.0	0.03	0.35	0.70	1.0
Unreinforced Masonry	A	SBCCI	Screws	EPDM	0.0078	0.0039	0.0028	0.0022	0.0077	0.0040	0.0028	0.0023
				BUR	0.0074	0.0038	0.0025	0.0020	0.0074	0.0038	0.0026	0.0020
			Welds	EPDM	0.0078	0.0040	0.0028	0.0023	0.0077	0.0041	0.0028	0.0022
				BUR	0.0074	0.0038	0.0026	0.0020	0.0075	0.0038	0.0026	0.0020
		ASCE	Screws	EPDM	0.0077	0.0040	0.0028	0.0022	0.0077	0.0040	0.0028	0.0022
				BUR	0.0074	0.0037	0.0025	0.0020	0.0074	0.0037	0.0025	0.0020
			Welds	EPDM	0.0077	0.0040	0.0028	0.0022	0.0078	0.0040	0.0028	0.0022
				BUR	0.0074	0.0038	0.0025	0.0020	0.0075	0.0037	0.0026	0.0020
	B	SBCCI	Screws	EPDM	0.0074	0.0036	0.0025	0.0020	0.0074	0.0036	0.0025	0.0020
				BUR	0.0070	0.0034	0.0023	0.0018	0.0070	0.0034	0.0023	0.0018
			Welds	EPDM	0.0074	0.0036	0.0025	0.0020	0.0073	0.0037	0.0025	0.0020
				BUR	0.0070	0.0034	0.0023	0.0018	0.0070	0.0034	0.0024	0.0018
		ASCE	Screws	EPDM	0.0074	0.0036	0.0025	0.0020	0.0073	0.0036	0.0026	0.0020
				BUR	0.0070	0.0034	0.0023	0.0018	0.0070	0.0034	0.0023	0.0018
			Welds	EPDM	0.0073	0.0036	0.0025	0.0020	0.0073	0.0036	0.0025	0.0020
				BUR	0.0070	0.0034	0.0023	0.0018	0.0070	0.0033	0.0023	0.0018
	C	SBCCI	Screws	EPDM	0.0072	0.0032	0.0022	0.0018	0.0072	0.0033	0.0023	0.0018
				BUR	0.0069	0.0030	0.0020	0.0016	0.0069	0.0030	0.0020	0.0016
			Welds	EPDM	0.0072	0.0032	0.0022	0.0018	0.0072	0.0033	0.0023	0.0018
				BUR	0.0069	0.0030	0.0020	0.0016	0.0069	0.0030	0.0020	0.0016
		ASCE	Screws	EPDM	0.0072	0.0032	0.0022	0.0018	0.0072	0.0032	0.0022	0.0018
				BUR	0.0068	0.0030	0.0020	0.0016	0.0068	0.0029	0.0020	0.0016
			Welds	EPDM	0.0072	0.0032	0.0022	0.0018	0.0073	0.0033	0.0023	0.0018
				BUR	0.0069	0.0029	0.0020	0.0016	0.0069	0.0030	0.0020	0.0016
	D	SBCCI	Screws	EPDM	0.0078	0.0039	0.0028	0.0022	0.0077	0.0040	0.0028	0.0023
				BUR	0.0074	0.0038	0.0025	0.0020	0.0074	0.0038	0.0026	0.0020
			Welds	EPDM	0.0078	0.0040	0.0028	0.0023	0.0077	0.0041	0.0028	0.0022
				BUR	0.0074	0.0038	0.0026	0.0020	0.0075	0.0038	0.0026	0.0020
		ASCE	Screws	EPDM	0.0077	0.0040	0.0028	0.0022	0.0077	0.0040	0.0028	0.0022
				BUR	0.0074	0.0037	0.0025	0.0020	0.0074	0.0037	0.0025	0.0020
			Welds	EPDM	0.0077	0.0040	0.0028	0.0022	0.0078	0.0040	0.0028	0.0022
				BUR	0.0074	0.0038	0.0025	0.0020	0.0075	0.0037	0.0026	0.0020

Table 7.55. Average Annual Content Loss Normalized by Building Value for Building B – Twenty Foot High Strip Mall Building with Six Units and Metal Deck with Four Foot Joist Spacing (concluded)

Building Characteristics					No Reduction in Metal Deck Capacity				50% Reduction in Metal Deck Capacity			
					Terrain Surface Roughness (m)				Terrain Surface Roughness (m)			
Wall Type	Missile Environ	Design Code	Metal Deck Attach.	Roof Cover	0.03	0.35	0.70	1.0	0.03	0.35	0.70	1.0
Reinforced Masonry	A	SBCCI	Screws	EPDM	0.0045	0.0022	0.0014	0.0011	0.0049	0.0024	0.0016	0.0013
				BUR	0.0042	0.0020	0.0012	0.0009	0.0046	0.0022	0.0014	0.0011
			Welds	EPDM	0.0045	0.0022	0.0014	0.0011	0.0051	0.0026	0.0017	0.0014
				BUR	0.0041	0.0020	0.0012	0.0009	0.0048	0.0023	0.0015	0.0012
		ASCE	Screws	EPDM	0.0045	0.0022	0.0014	0.0011	0.0049	0.0024	0.0016	0.0013
				BUR	0.0042	0.0020	0.0012	0.0009	0.0045	0.0022	0.0014	0.0011
			Welds	EPDM	0.0045	0.0022	0.0014	0.0011	0.0051	0.0025	0.0017	0.0014
				BUR	0.0042	0.0019	0.0012	0.0009	0.0048	0.0023	0.0015	0.0012
	B	SBCCI	Screws	EPDM	0.0044	0.0020	0.0013	0.0010	0.0048	0.0022	0.0015	0.0012
				BUR	0.0040	0.0018	0.0011	0.0008	0.0044	0.0020	0.0013	0.0010
			Welds	EPDM	0.0044	0.0020	0.0013	0.0011	0.0050	0.0024	0.0016	0.0013
				BUR	0.0041	0.0018	0.0011	0.0008	0.0047	0.0022	0.0014	0.0011
		ASCE	Screws	EPDM	0.0044	0.0020	0.0013	0.0010	0.0048	0.0022	0.0015	0.0012
				BUR	0.0041	0.0018	0.0011	0.0009	0.0044	0.0020	0.0013	0.0010
			Welds	EPDM	0.0044	0.0020	0.0013	0.0011	0.0050	0.0024	0.0016	0.0013
				BUR	0.0041	0.0018	0.0011	0.0008	0.0046	0.0021	0.0014	0.0011
	C	SBCCI	Screws	EPDM	0.0042	0.0018	0.0012	0.0010	0.0047	0.0020	0.0014	0.0011
				BUR	0.0039	0.0015	0.0009	0.0007	0.0043	0.0018	0.0011	0.0009
			Welds	EPDM	0.0042	0.0018	0.0012	0.0010	0.0049	0.0022	0.0015	0.0012
				BUR	0.0039	0.0015	0.0010	0.0007	0.0046	0.0019	0.0013	0.0010
		ASCE	Screws	EPDM	0.0043	0.0018	0.0012	0.0010	0.0046	0.0020	0.0014	0.0011
				BUR	0.0039	0.0015	0.0009	0.0007	0.0043	0.0018	0.0011	0.0009
			Welds	EPDM	0.0043	0.0018	0.0012	0.0010	0.0049	0.0022	0.0015	0.0012
				BUR	0.0039	0.0015	0.0009	0.0007	0.0045	0.0019	0.0013	0.0010
	D	SBCCI	Screws	EPDM	0.0042	0.0017	0.0011	0.0009	0.0046	0.0019	0.0013	0.0011
				BUR	0.0038	0.0014	0.0009	0.0007	0.0042	0.0017	0.0011	0.0008
			Welds	EPDM	0.0042	0.0017	0.0012	0.0009	0.0048	0.0021	0.0014	0.0011
				BUR	0.0039	0.0014	0.0009	0.0007	0.0045	0.0018	0.0012	0.0009
		ASCE	Screws	EPDM	0.0042	0.0017	0.0012	0.0009	0.0046	0.0019	0.0013	0.0011
				BUR	0.0039	0.0014	0.0009	0.0007	0.0042	0.0017	0.0011	0.0008
			Welds	EPDM	0.0042	0.0017	0.0012	0.0009	0.0048	0.0021	0.0014	0.0011
				BUR	0.0039	0.0014	0.0009	0.0007	0.0044	0.0018	0.0012	0.0009

Table 7.56. Average Annual Content Loss Normalized by Building Value for Building C – Twenty Foot High Strip Mall Building with Six Units and Metal Deck with Six Foot Joist Spacing

Building Characteristics					No Reduction in Metal Deck Capacity				50% Reduction in Metal Deck Capacity			
					Terrain Surface Roughness (m)				Terrain Surface Roughness (m)			
Wall Type	Missile Environ	Design Code	Metal Deck Attach.	Roof Cover	0.03	0.35	0.70	1.0	0.03	0.35	0.70	1.0
Unreinforced Masonry	A	SBCCI	Screws	EPDM	0.0083	0.0045	0.0031	0.0025	0.0096	0.0056	0.0041	0.0034
				BUR	0.0080	0.0043	0.0030	0.0023	0.0093	0.0054	0.0040	0.0033
			Welds	EPDM	0.0083	0.0045	0.0031	0.0025	0.0106	0.0064	0.0049	0.0041
				BUR	0.0080	0.0043	0.0029	0.0024	0.0103	0.0062	0.0047	0.0040
		ASCE	Screws	EPDM	0.0082	0.0044	0.0031	0.0025	0.0090	0.0051	0.0037	0.0031
				BUR	0.0080	0.0043	0.0029	0.0023	0.0088	0.0049	0.0036	0.0029
			Welds	EPDM	0.0083	0.0045	0.0031	0.0025	0.0095	0.0054	0.0041	0.0034
				BUR	0.0079	0.0042	0.0029	0.0023	0.0092	0.0052	0.0038	0.0032
	B	SBCCI	Screws	EPDM	0.0078	0.0040	0.0028	0.0022	0.0088	0.0050	0.0037	0.0031
				BUR	0.0075	0.0038	0.0026	0.0020	0.0085	0.0048	0.0035	0.0029
			Welds	EPDM	0.0078	0.0040	0.0028	0.0022	0.0096	0.0057	0.0044	0.0037
				BUR	0.0075	0.0038	0.0026	0.0020	0.0094	0.0055	0.0042	0.0035
		ASCE	Screws	EPDM	0.0078	0.0040	0.0028	0.0022	0.0085	0.0046	0.0033	0.0028
				BUR	0.0074	0.0038	0.0026	0.0020	0.0081	0.0044	0.0032	0.0026
			Welds	EPDM	0.0078	0.0040	0.0027	0.0022	0.0088	0.0049	0.0036	0.0030
				BUR	0.0074	0.0038	0.0025	0.0020	0.0084	0.0046	0.0033	0.0027
	C	SBCCI	Screws	EPDM	0.0074	0.0036	0.0025	0.0020	0.0083	0.0046	0.0033	0.0029
				BUR	0.0071	0.0034	0.0023	0.0018	0.0081	0.0044	0.0032	0.0027
			Welds	EPDM	0.0075	0.0037	0.0025	0.0021	0.0090	0.0052	0.0040	0.0034
				BUR	0.0071	0.0034	0.0024	0.0018	0.0088	0.0050	0.0038	0.0032
		ASCE	Screws	EPDM	0.0074	0.0036	0.0025	0.0020	0.0079	0.0042	0.0031	0.0025
				BUR	0.0070	0.0034	0.0022	0.0018	0.0076	0.0040	0.0029	0.0023
			Welds	EPDM	0.0074	0.0036	0.0025	0.0020	0.0081	0.0044	0.0033	0.0027
				BUR	0.0071	0.0033	0.0023	0.0018	0.0078	0.0042	0.0030	0.0025
	D	SBCCI	Screws	EPDM	0.0072	0.0032	0.0023	0.0018	0.0081	0.0040	0.0030	0.0025
				BUR	0.0069	0.0029	0.0020	0.0016	0.0079	0.0038	0.0028	0.0024
			Welds	EPDM	0.0072	0.0033	0.0023	0.0019	0.0088	0.0046	0.0035	0.0031
				BUR	0.0069	0.0030	0.0020	0.0016	0.0086	0.0044	0.0034	0.0029
		ASCE	Screws	EPDM	0.0072	0.0032	0.0022	0.0018	0.0078	0.0037	0.0027	0.0022
				BUR	0.0069	0.0030	0.0020	0.0016	0.0074	0.0034	0.0024	0.0020
			Welds	EPDM	0.0072	0.0033	0.0022	0.0018	0.0079	0.0038	0.0028	0.0023
				BUR	0.0069	0.0030	0.0020	0.0016	0.0076	0.0036	0.0026	0.0021

Table 7.56. Average Annual Content Loss Normalized by Building Value for Building C – Twenty Foot High Strip Mall Building with Six Units and Metal Deck with Six Foot Joist Spacing (concluded)

Building Characteristics					No Reduction in Metal Deck Capacity				50% Reduction in Metal Deck Capacity			
					Terrain Surface Roughness (m)				Terrain Surface Roughness (m)			
Wall Type	Missile Environ	Design Code	Metal Deck Attach.	Roof Cover	0.03	0.35	0.70	1.0	0.03	0.35	0.70	1.0
Reinforced Masonry	A	SBCCI	Screws	EPDM	0.0048	0.0023	0.0015	0.0012	0.0083	0.0048	0.0035	0.0030
				BUR	0.0044	0.0021	0.0013	0.0010	0.0080	0.0045	0.0034	0.0028
			Welds	EPDM	0.0051	0.0025	0.0017	0.0013	0.0097	0.0059	0.0045	0.0039
				BUR	0.0048	0.0023	0.0015	0.0011	0.0093	0.0056	0.0043	0.0037
		ASCE	Screws	EPDM	0.0047	0.0023	0.0015	0.0012	0.0076	0.0041	0.0031	0.0025
				BUR	0.0043	0.0021	0.0013	0.0010	0.0072	0.0039	0.0028	0.0024
			Welds	EPDM	0.0048	0.0024	0.0015	0.0012	0.0083	0.0047	0.0035	0.0030
				BUR	0.0045	0.0021	0.0013	0.0010	0.0079	0.0045	0.0033	0.0027
	B	SBCCI	Screws	EPDM	0.0047	0.0022	0.0014	0.0012	0.0077	0.0043	0.0032	0.0027
				BUR	0.0043	0.0019	0.0012	0.0009	0.0074	0.0041	0.0030	0.0025
			Welds	EPDM	0.0049	0.0024	0.0016	0.0013	0.0088	0.0052	0.0040	0.0034
				BUR	0.0046	0.0021	0.0014	0.0011	0.0086	0.0051	0.0038	0.0033
		ASCE	Screws	EPDM	0.0046	0.0021	0.0014	0.0011	0.0071	0.0038	0.0027	0.0023
				BUR	0.0043	0.0019	0.0012	0.0009	0.0067	0.0036	0.0026	0.0021
			Welds	EPDM	0.0047	0.0022	0.0015	0.0011	0.0076	0.0042	0.0031	0.0026
				BUR	0.0044	0.0019	0.0012	0.0009	0.0073	0.0040	0.0028	0.0024
	C	SBCCI	Screws	EPDM	0.0045	0.0020	0.0013	0.0011	0.0072	0.0040	0.0029	0.0025
				BUR	0.0042	0.0017	0.0011	0.0008	0.0070	0.0038	0.0027	0.0023
			Welds	EPDM	0.0048	0.0021	0.0015	0.0012	0.0082	0.0048	0.0036	0.0031
				BUR	0.0044	0.0019	0.0012	0.0010	0.0079	0.0046	0.0035	0.0030
		ASCE	Screws	EPDM	0.0044	0.0019	0.0013	0.0010	0.0067	0.0036	0.0026	0.0021
				BUR	0.0040	0.0016	0.0010	0.0008	0.0063	0.0032	0.0023	0.0019
			Welds	EPDM	0.0046	0.0020	0.0013	0.0011	0.0071	0.0039	0.0029	0.0023
				BUR	0.0042	0.0017	0.0011	0.0008	0.0067	0.0036	0.0026	0.0021
	D	SBCCI	Screws	EPDM	0.0045	0.0018	0.0013	0.0010	0.0070	0.0034	0.0026	0.0022
				BUR	0.0041	0.0016	0.0010	0.0008	0.0067	0.0032	0.0024	0.0020
			Welds	EPDM	0.0048	0.0020	0.0014	0.0011	0.0079	0.0041	0.0032	0.0028
				BUR	0.0044	0.0018	0.0011	0.0009	0.0076	0.0040	0.0030	0.0026
		ASCE	Screws	EPDM	0.0044	0.0018	0.0012	0.0010	0.0065	0.0030	0.0022	0.0018
				BUR	0.0040	0.0015	0.0010	0.0007	0.0061	0.0028	0.0019	0.0016
			Welds	EPDM	0.0046	0.0019	0.0013	0.0010	0.0068	0.0032	0.0024	0.0020
				BUR	0.0042	0.0016	0.0010	0.0008	0.0065	0.0030	0.0021	0.0018

Table 7.57. Average Annual Content Loss Normalized by Building Value for Building D – Twenty Foot High Strip Mall Building with One Unit and Metal Deck with Six Foot Joist Spacing

Building Characteristics					No Reduction in Metal Deck Capacity				50% Reduction in Metal Deck Capacity			
					Terrain Surface Roughness (m)				Terrain Surface Roughness (m)			
Wall Type	Missile Environ	Design Code	Metal Deck Attach.	Roof Cover	0.03	0.35	0.70	1.0	0.03	0.35	0.70	1.0
Unreinforced Masonry	A	SBCCI	Screws	EPDM	0.0101	0.0053	0.0036	0.0029	0.0110	0.0059	0.0043	0.0036
				BUR	0.0099	0.0050	0.0035	0.0027	0.0107	0.0057	0.0042	0.0034
			Welds	EPDM	0.0101	0.0053	0.0036	0.0029	0.0119	0.0067	0.0051	0.0043
				BUR	0.0099	0.0051	0.0035	0.0027	0.0116	0.0066	0.0049	0.0042
		ASCE	Screws	EPDM	0.0101	0.0052	0.0037	0.0029	0.0105	0.0056	0.0040	0.0033
				BUR	0.0099	0.0051	0.0035	0.0028	0.0103	0.0054	0.0038	0.0031
			Welds	EPDM	0.0101	0.0052	0.0036	0.0029	0.0109	0.0058	0.0042	0.0035
				BUR	0.0098	0.0050	0.0035	0.0027	0.0106	0.0056	0.0040	0.0033
	B	SBCCI	Screws	EPDM	0.0097	0.0049	0.0034	0.0027	0.0103	0.0056	0.0040	0.0033
				BUR	0.0094	0.0047	0.0032	0.0025	0.0101	0.0054	0.0039	0.0032
			Welds	EPDM	0.0098	0.0049	0.0034	0.0027	0.0112	0.0063	0.0047	0.0039
				BUR	0.0094	0.0048	0.0032	0.0025	0.0110	0.0061	0.0046	0.0038
		ASCE	Screws	EPDM	0.0097	0.0049	0.0034	0.0027	0.0100	0.0052	0.0037	0.0031
				BUR	0.0094	0.0047	0.0032	0.0025	0.0098	0.0050	0.0036	0.0029
			Welds	EPDM	0.0097	0.0049	0.0034	0.0027	0.0103	0.0054	0.0039	0.0032
				BUR	0.0095	0.0047	0.0032	0.0025	0.0100	0.0053	0.0037	0.0031
	C	SBCCI	Screws	EPDM	0.0094	0.0046	0.0032	0.0025	0.0099	0.0052	0.0038	0.0032
				BUR	0.0091	0.0043	0.0029	0.0023	0.0097	0.0050	0.0037	0.0030
			Welds	EPDM	0.0094	0.0046	0.0031	0.0025	0.0105	0.0060	0.0044	0.0037
				BUR	0.0091	0.0043	0.0030	0.0023	0.0104	0.0057	0.0043	0.0037
		ASCE	Screws	EPDM	0.0093	0.0045	0.0031	0.0025	0.0097	0.0049	0.0035	0.0029
				BUR	0.0091	0.0043	0.0030	0.0023	0.0094	0.0047	0.0033	0.0027
			Welds	EPDM	0.0094	0.0045	0.0031	0.0025	0.0098	0.0051	0.0037	0.0031
				BUR	0.0091	0.0043	0.0030	0.0023	0.0096	0.0049	0.0035	0.0029
	D	SBCCI	Screws	EPDM	0.0092	0.0042	0.0029	0.0023	0.0096	0.0046	0.0033	0.0028
				BUR	0.0088	0.0040	0.0027	0.0021	0.0094	0.0045	0.0032	0.0026
			Welds	EPDM	0.0092	0.0042	0.0029	0.0023	0.0102	0.0052	0.0039	0.0033
				BUR	0.0089	0.0040	0.0027	0.0021	0.0100	0.0050	0.0038	0.0032
		ASCE	Screws	EPDM	0.0092	0.0041	0.0029	0.0023	0.0094	0.0044	0.0032	0.0025
				BUR	0.0089	0.0039	0.0027	0.0021	0.0091	0.0042	0.0030	0.0024
			Welds	EPDM	0.0092	0.0042	0.0029	0.0023	0.0095	0.0045	0.0032	0.0026
				BUR	0.0089	0.0039	0.0027	0.0021	0.0092	0.0043	0.0031	0.0025

Table 7.57. Average Annual Content Loss Normalized by Building Value for Building D – Twenty Foot High Strip Mall Building with One Unit and Metal Deck with Six Foot Joist Spacing (concluded)

Building Characteristics					No Reduction in Metal Deck Capacity				50% Reduction in Metal Deck Capacity			
					Terrain Surface Roughness (m)				Terrain Surface Roughness (m)			
Wall Type	Missile Environ	Design Code	Metal Deck Attach.	Roof Cover	0.03	0.35	0.70	1.0	0.03	0.35	0.70	1.0
Reinforced Masonry	A	SBCCI	Screws	EPDM	0.0055	0.0028	0.0018	0.0014	0.0089	0.0048	0.0036	0.0030
				BUR	0.0053	0.0026	0.0016	0.0012	0.0086	0.0046	0.0035	0.0028
			Welds	EPDM	0.0056	0.0029	0.0019	0.0015	0.0107	0.0061	0.0046	0.0040
				BUR	0.0054	0.0027	0.0017	0.0013	0.0103	0.0059	0.0045	0.0038
		ASCE	Screws	EPDM	0.0053	0.0027	0.0018	0.0013	0.0080	0.0042	0.0031	0.0025
				BUR	0.0051	0.0026	0.0016	0.0011	0.0077	0.0041	0.0029	0.0024
			Welds	EPDM	0.0054	0.0028	0.0018	0.0014	0.0090	0.0048	0.0034	0.0029
				BUR	0.0051	0.0026	0.0016	0.0012	0.0086	0.0045	0.0033	0.0027
	B	SBCCI	Screws	EPDM	0.0054	0.0026	0.0017	0.0013	0.0085	0.0046	0.0034	0.0028
				BUR	0.0051	0.0024	0.0015	0.0011	0.0081	0.0044	0.0032	0.0027
			Welds	EPDM	0.0055	0.0027	0.0018	0.0014	0.0099	0.0057	0.0043	0.0037
				BUR	0.0053	0.0025	0.0016	0.0012	0.0096	0.0054	0.0041	0.0035
		ASCE	Screws	EPDM	0.0052	0.0025	0.0016	0.0012	0.0078	0.0041	0.0029	0.0024
				BUR	0.0049	0.0023	0.0014	0.0010	0.0075	0.0038	0.0027	0.0022
			Welds	EPDM	0.0053	0.0025	0.0016	0.0012	0.0085	0.0045	0.0033	0.0027
				BUR	0.0049	0.0023	0.0014	0.0011	0.0081	0.0043	0.0031	0.0025
	C	SBCCI	Screws	EPDM	0.0052	0.0022	0.0015	0.0012	0.0081	0.0043	0.0032	0.0027
				BUR	0.0049	0.0020	0.0012	0.0010	0.0078	0.0042	0.0030	0.0025
			Welds	EPDM	0.0053	0.0023	0.0016	0.0012	0.0093	0.0053	0.0041	0.0034
				BUR	0.0050	0.0021	0.0014	0.0010	0.0090	0.0051	0.0039	0.0033
		ASCE	Screws	EPDM	0.0050	0.0021	0.0014	0.0011	0.0076	0.0038	0.0028	0.0023
				BUR	0.0047	0.0019	0.0012	0.0009	0.0072	0.0036	0.0026	0.0021
			Welds	EPDM	0.0051	0.0022	0.0014	0.0011	0.0082	0.0044	0.0032	0.0026
				BUR	0.0048	0.0019	0.0012	0.0009	0.0078	0.0041	0.0029	0.0024
	D	SBCCI	Screws	EPDM	0.0051	0.0021	0.0014	0.0011	0.0079	0.0038	0.0027	0.0023
				BUR	0.0049	0.0019	0.0012	0.0009	0.0076	0.0036	0.0026	0.0021
			Welds	EPDM	0.0054	0.0023	0.0015	0.0012	0.0088	0.0045	0.0034	0.0029
				BUR	0.0051	0.0020	0.0013	0.0010	0.0086	0.0044	0.0034	0.0028
		ASCE	Screws	EPDM	0.0050	0.0020	0.0013	0.0011	0.0073	0.0033	0.0024	0.0019
				BUR	0.0047	0.0017	0.0011	0.0008	0.0070	0.0031	0.0022	0.0017
			Welds	EPDM	0.0050	0.0020	0.0014	0.0011	0.0078	0.0036	0.0026	0.0021
				BUR	0.0047	0.0018	0.0011	0.0009	0.0075	0.0034	0.0024	0.0019

Tables 7.58 through 7.60 present a summary of the effects of various building parameters on average annual total loss. The configuration of model buildings (and consequently the roof height and the joist spacing) plays a significant role in determining the average annual losses. For example, the differences in average annual total loss between Building A (Height=12′) and Building B (Height=20′), with all other parameters being equal, range from 30% to 277% for the wood roof sytem and from 65% to 266% for the steel roof system. Changing from a 4′ joist spacing to a 6′ joist spacing results in a 1% to 109% increase in average annual total loss. The effect of 6 unit versus 1 unit is a 1% decrease to an 17% increase in average annual total loss. Besides the building configuration, the missiles environment has the greatest impact on the average annual loss, increasing the average annual loss by up to 182% when the model buildings are situated in the commercial/residential missile environment (D) compared to the environment with no windborne debris (A).

Table 7.58. Percent Increases in the Average Annual Total Loss Due to Changes in Building Parameters (Minimum/Average/Maximum) – Strip Mall Building with Wood Roof System

Building Parameter	Increase in Average Annual Building Loss	
	Building A	Building B
8d to 6d Roof Deck Nails	-1% / 17% / 64%	-1% / 9% / 37%
Strap to Toe-Nail Roof/Wall Connections	15% / 92% / 239%	17% / 57% / 141%
Built-up to Single ply Membrane Roof Cover	1% / 11% / 39%	3% / 10% / 26%
Reinforced to Unreinforced Masonry Walls	-1% / 4% / 9%	3% / 12% / 27%
Missile Environment D to C	4% / 42% / 92%	2% / 13% / 26%
Missile Environment C to B	2% / 13% / 29%	2% / 11% / 21%
Missile Environment B to A	2% / 15% / 28%	4% / 12% / 21%

Table 7.59. Percent Increases in the Average Annual Total Loss Due to Changes in Building Parameters (Minimum/Average/Maximum) – Strip Mall Building with Steel Roof System

Building Parameter	Increase in Average Annual Building Loss			
	Building A	Building B	Building C	Building D
0% to 50% Reduction in Metal Roof Deck Resistance	-1% / 6% / 22%	-1% / 7% / 23%	11% / 46% / 115%	9% / 42% / 109%
Screwed to Welded Metal Roof Deck	-3% / 2% / 7%	-2% / 1% / 7%	-2% / 6% / 22%	-2% / 6% / 23%
ASCE to SBCCI Metal Roof Deck Design Criteria	-3% / 1% / 6%	-2% / 1% / 4%	0% / 9% / 34%	-2% / 9% / 33%
Built-up to Single ply Membrane Roof Cover	9% / 22% / 44%	9% / 20% / 35%	6% / 16% / 34%	5% / 14% / 31%
Reinforced to Unreinforced Masonry Walls	2% / 14% / 41%	19% / 39% / 68%	4% / 24% / 55%	3% / 27% / 60%
Missile Environment D to C	2% / 18% / 33%	1% / 8% / 13%	1% / 9% / 19%	1% / 9% / 20%
Missile Environment C to B	2% / 10% / 18%	1% / 5% / 9%	2% / 5% / 8%	2% / 5% / 11%
Missile Environment B to A	2% / 7% / 14%	1% / 5% / 10%	1% / 6% / 12%	1% / 4% / 7%

Table 7.60. Percent Increases in the Average Annual Total Loss Due to Changes in Building Configuration (Minimum/Average/Maximum)

Building Configuration	Increase in Average Annual Building Loss
Building A to B – Wood Roof System (12′ to 20′ Roof Height)	30% / 116% / 277%
Building A to B – Steel Roof System (12′ to 20′ Roof Height)	65% / 145% / 266%
Building B to C – Steel Roof System (4′ to 6′ Joist Spacing)	1% / 25% / 109%
Building C to D – Steel Roof System (6 Units to 1 Unit)	-1% / 8% / 17%

7.12 Loss Model Results for Pre-Engineered Metal Buildings

Using the same hurricane wind speed and direction data (20,000 years of storm simulation) used in the development of the damage curves for the pre-engineered metal buildings, average annual losses were estimated using the commercial loss model described in Section 7.9. The metal buildings are assumed to be used as warehouses. The assumed subassembly cost distributions are listed in Table 7.61. Even though other occupancy types are applicable and slightly different results may be obtained, a warehouse is believed to be an appropriate usage type for the model buildings used in the present simulation.

Example building and content loss functions are given in Appendix L. The avarage annual building and content losses (both normalized by the total building value) for all metal buildings examined are presented in Tables 7.62 and 7.63, respectively. The average annual loss is obtained by summing all losses produced during the 20,000-year hurricane simulation period and then dividing by 20,000 years. The values given in Tables 7.62 and 7.63 reflect the average annual losses for metal buildings located in the South Florida area.

Table 7.64 presents a summary of the effects of the various building parameters on average annual building loss. The configuration of model buildings (and consequently the size of building and the percentage of wall area covered by fenestrations) plays a significant role in determining the average annual loss. For example, the decreases in average annual total loss between small metal buildings and medium-sized metal buildings (with all other parameters being equal) range from 39% to 56%. Changing from the medium-sized metal building to the large metal buildings results in a 4% to 43% increase in average annual loss. The reduction in the metal roof panel resistance (to account for aging and fatigue) also has substantial effects on the simulated losses, where an increase of up to 55% was observed. However, the differences in total loss using different design wind speeds (90 mph vs. 100 mph) are minimal. The ±2% difference in simulated loss can be taken as randomness involved in the modeling process.

7.13 Loss Model Results for Engineered Residential and Commercial Buildings

Similar to the other model building classes, loss functions for engineered residential and commercial buildings have been developed using 20,000 years of hurricane simulations in the South Florida area. Model buildings with eight units per floor are assumed to be

Table 7.61. Subassembly Cost Distributions for Pre-Engineered Metal Buildings

Subassemblies	Cost Ratios	
Foundations		
Footings & Foundations	6.0%	8.6%
Piles & Caissons	0.0%	
Excavation & Backfill	2.6%	
Substructures		
Slab on Grade	16.6%	16.6%
Special Substructures	0.0%	
Superstructure		
Columns and Beams	0.0%	13.1%
Structural Walls	0.0%	
Elevated Floors/Diaphragms	3.0%	
Roof Decking/Framing	9.2%	
Stairs	0.9%	
Exterior Closure		
Walls	10.8%	12.4%
Exterior Wall Finishes	0.0%	
Doors	1.5%	
Windows & Glazed Walls	0.0%	
Roofing		
Roof Covering	5.1%	9.2%
Insulation	3.3%	
Openings & Specialties	0.8%	
Interior Construction		
Partitions	1.1%	8.3%
Interior Doors	0.3%	
Wall Finishes	0.4%	
Floor Finishes	2.9%	
Ceiling Finishes	0.8%	
Interior Surface of Exterior Walls	2.8%	
Conveying		
Elevators	0.0%	0.0%
Special Conveyors	0.0%	
Mechanical		
Plumbing	3.7%	18.2%
Fire Protection	4.7%	
Heating	7.9%	
Cooling	1.9%	
Special Systems	0.0%	
Electrical		
Service & Distribution	0.8%	9.4%
Lighting & Power	7.9%	
Special Electrical	0.7%	
Special Construction		
Specialties (& Additives)	4.3%	4.3%
Total	100%	100%

Table 7.62. Average Annual Building Loss Normalized by Building Value for Pre-Engineered Metal Buildings

Building Characteristics		No Reduction in Metal Panel Capacity				50% Reduction in Metal Panel Capacity			
		Terrain Surface Roughness (m)				Terrain Surface Roughness (m)			
Plan Size	Design Speed (mph)	0.03	0.35	0.70	1.0	0.03	0.35	0.70	1.0
Small	90	0.0402	0.0201	0.0147	0.0125	0.0412	0.0209	0.0155	0.0130
Med.	90	0.0187	0.0103	0.0072	0.0056	0.0222	0.0127	0.0093	0.0076
Large	90	0.0200	0.0117	0.0088	0.0071	0.0254	0.0155	0.0125	0.0109
Small	100	0.0402	0.0203	0.0149	0.0125	0.0406	0.0205	0.0155	0.0128
Med.	100	0.0187	0.0103	0.0071	0.0056	0.0220	0.0126	0.0092	0.0076
Large	100	0.0200	0.0117	0.0088	0.0072	0.0254	0.0158	0.0124	0.0108

Table 7.63. Average Annual Content Loss Normalized by Building Value for Pre-Engineered Metal Buildings

Building Characteristics		No Reduction in Metal Panel Capacity				50% Reduction in Metal Panel Capacity			
		Terrain Surface Roughness (m)				Terrain Surface Roughness (m)			
Plan Size	Design Speed (mph)	0.03	0.35	0.70	1.0	0.03	0.35	0.70	1.0
Small	90	0.0162	0.0080	0.0059	0.0050	0.0166	0.0084	0.0062	0.0052
Med.	90	0.0080	0.0041	0.0028	0.0022	0.0091	0.0050	0.0037	0.0030
Large	90	0.0080	0.0045	0.0034	0.0027	0.0102	0.0062	0.0050	0.0044
Small	100	0.0162	0.0081	0.0059	0.0050	0.0164	0.0082	0.0062	0.0051
Med.	100	0.0080	0.0041	0.0028	0.0022	0.0091	0.0050	0.0036	0.0030
Large	100	0.0080	0.0045	0.0034	0.0028	0.0103	0.0063	0.0050	0.0044

Table 7.64. Percent Increases in the Average Annual Total Loss due to Changes in Building Parameters (Minimum/Average/Maximum) – Pre-Engineered Metal Buildings

Parameter	Change in Average Building Loss Ratio
Small Building to Medium Building	-56% / -47% / -39%
Medium Building to Large Building	4% / 23% / 43%
100 mph to 90 mph Roof Design Speed	-2% / 0% / 2%
0% to 50% Reduction in Roof Deck Resistance	1% / 24% / 55%

used as apartments while model buildings with one unit per floor are assumed to be used as office buildings. Tables 7.65 through 7.70 show the assumed subassembly cost distributions for two-, five- and 8-story apartments and office buildings, respectively. The subassembly cost ratios listed in Tables 7.65 through 7.70 have already been adjusted for number of stories and glazing area according to the commercial loss model described in Section 7.9. The values included in Tables 7.65 through 7.70 correspond to the model buildings with 32% glazing coverage for two-story buildings and 36% glazing coverage for five- and eight-story buildings. Slightly different subassembly cost ratios can be expected for model buildings with higher or lower glazing coverage.

Table 7.65. Subassembly Cost Distributions for Two-Story Apartments

Subassemblies	Cost Ratios	
Foundations		
Footings & Foundations	5.1%	5.9%
Piles & Caissons	0.0%	
Excavation & Backfill	0.8%	
Substructures		
Slab on Grade	2.4%	2.4%
Special Substructures	0.0%	
Superstructure		
Columns and Beams	0.9%	11.0%
Structural Walls	0.0%	
Elevated Floors/Diaphragms	7.1%	
Roof Decking/Framing	1.7%	
Stairs	1.3%	
Exterior Closure		
Walls	8.3%	12.4%
Exterior Wall Finishes	0.0%	
Doors	0.3%	
Windows & Glazed Walls	3.9%	
Roofing		
Roof Covering	2.0%	3.0%
Insulation	1.0%	
Openings & Specialties	0.0%	
Interior Construction		
Partitions	3.7%	22.2%
Interior Doors	5.7%	
Wall Finishes	2.2%	
Floor Finishes	5.3%	
Ceiling Finishes	3.6%	
Interior Surface of Exterior Walls	1.6%	
Conveying		
Elevators	3.0%	3.0%
Special Conveyors	0.0%	
Mechanical		
Plumbing	12.9%	30.4%
Fire Protection	2.4%	
Heating	6.6%	
Cooling	8.5%	
Special Systems	0.0%	
Electrical		
Service & Distribution	1.1%	7.9%
Lighting & Power	5.9%	
Special Electrical	0.9%	
Special Construction		
Specialties (& Additives)	1.7%	1.7%
Total	100%	100%

Table 7.66. Subassembly Cost Distributions for Five-Story Apartments

Subassemblies	Cost Ratios	
Foundations		
Footings & Foundations	2.1%	2.4%
Piles & Caissons	0.0%	
Excavation & Backfill	0.3%	
Substructures		
Slab on Grade	1.0%	1.0%
Special Substructures	0.0%	
Superstructure		
Columns and Beams	1.9%	16.6%
Structural Walls	0.0%	
Elevated Floors/Diaphragms	12.1%	
Roof Decking/Framing	1.0%	
Stairs	1.4%	
Exterior Closure		
Walls	7.0%	11.8%
Exterior Wall Finishes	0.0%	
Doors	0.2%	
Windows & Glazed Walls	4.6%	
Roofing		
Roof Covering	0.8%	1.2%
Insulation	0.4%	
Openings & Specialties	0.0%	
Interior Construction		
Partitions	4.9%	25.6%
Interior Doors	7.1%	
Wall Finishes	2.8%	
Floor Finishes	5.5%	
Ceiling Finishes	3.7%	
Interior Surface of Exterior Walls	1.6%	
Conveying		
Elevators	5.2%	5.2%
Special Conveyors	0.0%	
Mechanical		
Plumbing	11.3%	26.7%
Fire Protection	2.3%	
Heating	5.6%	
Cooling	7.5%	
Special Systems	0.0%	
Electrical		
Service & Distribution	1.2%	7.6%
Lighting & Power	5.9%	
Special Electrical	0.5%	
Special Construction		
Specialties (& Additives)	2.0%	2.0%
Total	100%	100%

Table 7.67. Subassembly Cost Distributions for Eight-Story Apartments

Subassemblies	Cost Ratios	
Foundations		
Footings & Foundations	1.9%	2.1%
Piles & Caissons	0.0%	
Excavation & Backfill	0.2%	
Substructures		
Slab on Grade	0.5%	0.5%
Special Substructures	0.0%	
Superstructure		
Columns and Beams	2.5%	12.2%
Structural Walls	0.0%	
Elevated Floors/Diaphragms	8.3%	
Roof Decking/Framing	0.2%	
Stairs	1.1%	
Exterior Closure		
Walls	6.9%	12.8%
Exterior Wall Finishes	0.0%	
Doors	1.6%	
Windows & Glazed Walls	4.3%	
Roofing		
Roof Covering	0.4%	0.7%
Insulation	0.2%	
Openings & Specialties	0.0%	
Interior Construction		
Partitions	10.2%	28.6%
Interior Doors	6.4%	
Wall Finishes	2.5%	
Floor Finishes	4.9%	
Ceiling Finishes	3.3%	
Interior Surface of Exterior Walls	1.3%	
Conveying		
Elevators	5.2%	5.2%
Special Conveyors	0.0%	
Mechanical		
Plumbing	11.8%	27.8%
Fire Protection	2.8%	
Heating	5.7%	
Cooling	7.6%	
Special Systems	0.0%	
Electrical		
Service & Distribution	0.6%	8.5%
Lighting & Power	6.1%	
Special Electrical	1.8%	
Special Construction		
Specialties (& Additives)	1.8%	1.8%
Total	100%	100%

Table 7.68. Subassembly Cost Distributions for Two-Story Office Buildings

Subassemblies	Cost Ratios	
Foundations		
Footings & Foundations	3.3%	4.3%
Piles & Caissons	0.0%	
Excavation & Backfill	1.0%	
Substructures		
Slab on Grade	3.1%	3.1%
Special Substructures	0.0%	
Superstructure		
Columns and Beams	0.9%	10.7%
Structural Walls	0.0%	
Elevated Floors/Diaphragms	7.3%	
Roof Decking/Framing	1.7%	
Stairs	0.9%	
Exterior Closure		
Walls	8.8%	12.6%
Exterior Wall Finishes	0.0%	
Doors	0.4%	
Windows & Glazed Walls	3.4%	
Roofing		
Roof Covering	2.1%	3.3%
Insulation	1.3%	
Openings & Specialties	0.0%	
Interior Construction		
Partitions	2.5%	23.0%
Interior Doors	4.5%	
Wall Finishes	1.3%	
Floor Finishes	8.1%	
Ceiling Finishes	5.3%	
Interior Surface of Exterior Walls	1.4%	
Conveying		
Elevators	3.1%	3.1%
Special Conveyors	0.0%	
Mechanical		
Plumbing	2.9%	25.4%
Fire Protection	0.4%	
Heating	0.0%	
Cooling	22.1%	
Special Systems	0.0%	
Electrical		
Service & Distribution	1.6%	14.6%
Lighting & Power	12.6%	
Special Electrical	0.3%	
Special Construction		
Specialties (& Additives)	0.0%	0.0%
Total	100%	100%

Table 7.69. Subassembly Cost Distributions for Five-Story Office Buildings

Subassemblies	Cost Ratios	
Foundations		
Footings & Foundations	2.9%	3.3%
Piles & Caissons	0.0%	
Excavation & Backfill	0.4%	
Substructures		
Slab on Grade	1.1%	1.1%
Special Substructures	0.0%	
Superstructure		
Columns and Beams	2.5%	15.5%
Structural Walls	0.0%	
Elevated Floors/Diaphragms	11.2%	
Roof Decking/Framing	0.6%	
Stairs	1.1%	
Exterior Closure		
Walls	8.4%	14.8%
Exterior Wall Finishes	0.0%	
Doors	0.2%	
Windows & Glazed Walls	6.2%	
Roofing		
Roof Covering	0.8%	1.3%
Insulation	0.5%	
Openings & Specialties	0.0%	
Interior Construction		
Partitions	2.2%	19.2%
Interior Doors	2.1%	
Wall Finishes	1.0%	
Floor Finishes	7.5%	
Ceiling Finishes	4.9%	
Interior Surface of Exterior Walls	1.6%	
Conveying		
Elevators	7.6%	7.6%
Special Conveyors	0.0%	
Mechanical		
Plumbing	2.0%	23.0%
Fire Protection	0.2%	
Heating	0.0%	
Cooling	20.8%	
Special Systems	0.0%	
Electrical		
Service & Distribution	1.3%	14.2%
Lighting & Power	11.8%	
Special Electrical	1.2%	
Special Construction		
Specialties (& Additives)	0.0%	0.0%
Total	100%	100%

Table 7.70. Subassembly Cost Distributions for Eight-Story Office Buildings

Subassemblies	Cost Ratios	
Foundations		
Footings & Foundations	1.6%	1.8%
Piles & Caissons	0.0%	
Excavation & Backfill	0.2%	
Substructures		
Slab on Grade	0.6%	0.6%
Special Substructures	0.0%	
Superstructure		
Columns and Beams	3.1%	19.3%
Structural Walls	0.0%	
Elevated Floors/Diaphragms	14.0%	
Roof Decking/Framing	0.8%	
Stairs	1.4%	
Exterior Closure		
Walls	7.6%	13.5%
Exterior Wall Finishes	0.0%	
Doors	0.2%	
Windows & Glazed Walls	5.8%	
Roofing		
Roof Covering	0.5%	0.7%
Insulation	0.3%	
Openings & Specialties	0.0%	
Interior Construction		
Partitions	2.3%	20.1%
Interior Doors	2.2%	
Wall Finishes	1.1%	
Floor Finishes	7.8%	
Ceiling Finishes	5.1%	
Interior Surface of Exterior Walls	1.6%	
Conveying		
Elevators	9.4%	9.4%
Special Conveyors	0.0%	
Mechanical		
Plumbing	1.8%	20.7%
Fire Protection	0.2%	
Heating	0.0%	
Cooling	18.7%	
Special Systems	0.0%	
Electrical		
Service & Distribution	1.3%	13.8%
Lighting & Power	11.4%	
Special Electrical	1.1%	
Special Construction		
Specialties (& Additives)	0.0%	0.0%
Total	100%	100%

Example building and content loss functions are given in Appendix M. Note that the loss functions cross over between open terrain (z_0=0.03 m) and suburban terrain (z_0=0.35 m) for a number of cases. As explained in Section 6.12, wind-driven missiles are the primary cause of damage for engineered residential/commercial buildings. In an open terrain, virtually no missiles can be produced from the surrounding area of a building. On the other hand, in a suburban terrain, once the wind speed reaches a certain threshold,

significant amounts of wind-driven missiles can be produced as a result of damage sustained by surrounding buildings. Therefore, higher damages, and accordingly losses, can be expected for a building located in a suburban terrain compared to the same building situated in an open terrain (even though the local wind speed is higher in open terrain than in suburban terrain).

The average annual building losses (normalized by the total building value) for the two-, five- and eight-story engineered residential and commercial buildings are presented in Tables 7.71 through 7.73, respectively. The corresponding average annual content losses (also normalized by the total building value) are given in Tables 7.74 through 7.76. The average annual loss is obtained by summing all losses produced during the 20,000-year hurricane simulation period and then dividing the sum by 20,000 years. The average annual losses presented in Tables 7.71 through 7.72 reflect the wind climate of South Florida.

Table 7.77 presents a summary of the effects of the various building parameters on average annual total loss. Considering the buildings constructed with a metal roof deck on steel joists, the average annual losses are found to increase by up to 46% when the roof cover is modeled with a EPDM single ply membrane versus a built-up roof cover. The corresponding increase in total loss for buildings constructed with a concrete roof deck is found to be about half this value (i.e., 25%) since, in the case of the concrete deck, there is no deck failure contributing to the roof cover failure and no water can permeate the concrete deck (even when the cover has failed) to damage the interior of the building. The effect of using a metal roof deck versus a impervious concrete roof deck is an increase by up to 458% in the average annual loss.

The following discussion pertains to the engineered buildings constructed with metal roof deck on steel joists. The effect of having a single unit per floor (commercial usage) compared to multi-units per floor (residential usage) is at most a 45% increase in average annual total loss. The average annual total loss increased by as much as 28% when the glazing coverage changed from 20% to 33% and by as much as 145% when the glazing coverage changed from 33% to 50%. Also, as can be seen in Table 7.77, the surrounding missile environment has its largest impact on average annual losses for the two-story engineered buildings. This trend results from the fact that the modeled average heights of the buildings from which the commercial and residential type missiles originate are lower than the five- and eight-story engineered buildings. Thus, the glazing on the upper floors of the five- and eight-story buildings are less susceptible to missile damage than the glazing on the lower floors.

In terms of average annual loss, the effects of glazing coverage, building usage and missile environment are found to be more pronounced on the buildings constructed with concrete roof decks than they are on the buildings constructed with metal roof decks. This relates to the fact that roof deck damage is eliminated, roof cover damage is reduced (since deck failures will not contribute to roof cover failure) and interior damage is reduced (since no water infiltration through the roof system can occur) for concrete roof

Table 7.71. Average Annual Building Loss Normalized by Building Value – Two-Story Engineered Building

Building Characteristics				Residential Buildings(8 Units per Floor)				Commercial Buildings(1 Unit per Floor)			
Roof Deck	Missile Environ.	Glazing Coverage	Roof Cover	Terrain Roughness (m)				Terrain Roughness (m)			
				0.03	0.35	0.70	1.0	0.03	0.35	0.70	1.00
Metal	A	20%	BUR	0.0088	0.0084	0.0057	0.0045	0.0125	0.0114	0.0078	0.0060
			EPDM	0.0101	0.0092	0.0064	0.0051	0.0136	0.0120	0.0083	0.0066
		33%	BUR	0.0109	0.0100	0.0068	0.0054	0.0151	0.0138	0.0094	0.0074
			EPDM	0.0120	0.0107	0.0075	0.0059	0.0159	0.0142	0.0099	0.0078
		50%	BUR	0.0138	0.0124	0.0085	0.0068	0.0181	0.0159	0.0110	0.0087
			EPDM	0.0147	0.0130	0.0091	0.0073	0.0187	0.0163	0.0114	0.0091
	B	20%	BUR	0.0074	0.0071	0.0048	0.0038	0.0100	0.0086	0.0058	0.0045
			EPDM	0.0087	0.0078	0.0055	0.0044	0.0112	0.0094	0.0065	0.0051
		33%	BUR	0.0090	0.0083	0.0056	0.0044	0.0119	0.0103	0.0070	0.0054
			EPDM	0.0101	0.0090	0.0063	0.0050	0.0130	0.0109	0.0076	0.0060
		50%	BUR	0.0113	0.0099	0.0068	0.0054	0.0144	0.0121	0.0083	0.0065
			EPDM	0.0122	0.0105	0.0074	0.0060	0.0153	0.0126	0.0088	0.0070
	C	20%	BUR	0.0063	0.0055	0.0038	0.0030	0.0084	0.0069	0.0046	0.0035
			EPDM	0.0076	0.0064	0.0045	0.0037	0.0097	0.0077	0.0054	0.0043
		33%	BUR	0.0072	0.0062	0.0042	0.0033	0.0098	0.0081	0.0054	0.0042
			EPDM	0.0084	0.0071	0.0050	0.0041	0.0109	0.0088	0.0061	0.0049
		50%	BUR	0.0090	0.0076	0.0052	0.0042	0.0119	0.0095	0.0064	0.0050
			EPDM	0.0101	0.0084	0.0060	0.0049	0.0129	0.0102	0.0070	0.0057
	D	20%	BUR	0.0045	0.0025	0.0020	0.0017	0.0051	0.0026	0.0020	0.0018
			EPDM	0.0059	0.0034	0.0028	0.0025	0.0065	0.0036	0.0029	0.0026
		33%	BUR	0.0047	0.0025	0.0020	0.0018	0.0054	0.0027	0.0021	0.0018
			EPDM	0.0061	0.0035	0.0028	0.0026	0.0067	0.0037	0.0029	0.0026
		50%	BUR	0.0058	0.0033	0.0027	0.0023	0.0078	0.0044	0.0034	0.0030
			EPDM	0.0072	0.0042	0.0034	0.0030	0.0090	0.0053	0.0042	0.0037
Concrete	A	20%	BUR	0.0064	0.0074	0.0048	0.0036	0.0110	0.0108	0.0071	0.0054
			EPDM	0.0067	0.0075	0.0049	0.0036	0.0112	0.0110	0.0072	0.0055
		33%	BUR	0.0090	0.0093	0.0061	0.0046	0.0140	0.0134	0.0090	0.0070
			EPDM	0.0092	0.0094	0.0062	0.0047	0.0142	0.0135	0.0091	0.0070
		50%	BUR	0.0126	0.0119	0.0081	0.0063	0.0174	0.0157	0.0107	0.0084
			EPDM	0.0128	0.0121	0.0082	0.0064	0.0176	0.0158	0.0109	0.0085
	B	20%	BUR	0.0049	0.0058	0.0037	0.0027	0.0082	0.0077	0.0049	0.0036
			EPDM	0.0050	0.0059	0.0038	0.0028	0.0084	0.0078	0.0050	0.0037
		33%	BUR	0.0069	0.0072	0.0046	0.0035	0.0105	0.0097	0.0063	0.0047
			EPDM	0.0070	0.0073	0.0047	0.0035	0.0107	0.0098	0.0064	0.0048
		50%	BUR	0.0098	0.0092	0.0061	0.0047	0.0135	0.0117	0.0078	0.0060
			EPDM	0.0099	0.0093	0.0062	0.0049	0.0137	0.0118	0.0079	0.0061
	C	20%	BUR	0.0035	0.0040	0.0024	0.0017	0.0064	0.0058	0.0035	0.0025
			EPDM	0.0037	0.0041	0.0025	0.0018	0.0066	0.0059	0.0037	0.0026
		33%	BUR	0.0048	0.0050	0.0031	0.0022	0.0082	0.0073	0.0045	0.0033
			EPDM	0.0049	0.0051	0.0032	0.0023	0.0084	0.0074	0.0047	0.0034
		50%	BUR	0.0073	0.0068	0.0044	0.0034	0.0109	0.0089	0.0058	0.0044
			EPDM	0.0074	0.0069	0.0046	0.0035	0.0110	0.0090	0.0059	0.0045
	D	20%	BUR	0.0016	0.0006	0.0005	0.0004	0.0027	0.0008	0.0006	0.0005
			EPDM	0.0018	0.0007	0.0006	0.0005	0.0029	0.0010	0.0007	0.0006
		33%	BUR	0.0019	0.0007	0.0005	0.0004	0.0032	0.0010	0.0006	0.0005
			EPDM	0.0021	0.0008	0.0006	0.0005	0.0034	0.0011	0.0008	0.0006
		50%	BUR	0.0038	0.0018	0.0015	0.0012	0.0063	0.0033	0.0025	0.0022
			EPDM	0.0039	0.0020	0.0016	0.0013	0.0065	0.0035	0.0026	0.0022

Table 7.72. Average Annual Building Loss Normalized by Building Value – Five-Story Engineered Building

Building Characteristics				Residential Buildings(8 Units per Floor)				Commercial Buildings(1 Unit per Floor)			
Roof Deck	Missile Environ.	Glazing Coverage	Roof Cover	Terrain Roughness (m)				Terrain Roughness (m)			
				0.03	0.35	0.70	1.0	0.03	0.35	0.70	1.00
Metal	A	20%	BUR	0.0078	0.0069	0.0052	0.0044	0.0104	0.0094	0.0068	0.0056
			EPDM	0.0091	0.0080	0.0062	0.0054	0.0115	0.0103	0.0077	0.0064
		33%	BUR	0.0090	0.0080	0.0059	0.0050	0.0124	0.0109	0.0079	0.0065
			EPDM	0.0103	0.0090	0.0069	0.0059	0.0133	0.0117	0.0087	0.0073
		50%	BUR	0.0116	0.0101	0.0077	0.0067	0.0155	0.0130	0.0098	0.0083
			EPDM	0.0128	0.0111	0.0087	0.0076	0.0165	0.0138	0.0106	0.0091
	B	20%	BUR	0.0076	0.0067	0.0050	0.0043	0.0097	0.0084	0.0061	0.0050
			EPDM	0.0089	0.0077	0.0060	0.0052	0.0107	0.0093	0.0070	0.0058
		33%	BUR	0.0087	0.0076	0.0057	0.0048	0.0114	0.0096	0.0070	0.0058
			EPDM	0.0099	0.0086	0.0067	0.0057	0.0124	0.0104	0.0078	0.0065
		50%	BUR	0.0112	0.0095	0.0074	0.0064	0.0145	0.0117	0.0090	0.0077
			EPDM	0.0124	0.0105	0.0083	0.0073	0.0154	0.0125	0.0097	0.0084
	C	20%	BUR	0.0075	0.0067	0.0050	0.0043	0.0094	0.0080	0.0059	0.0048
			EPDM	0.0088	0.0078	0.0060	0.0052	0.0103	0.0089	0.0067	0.0056
		33%	BUR	0.0086	0.0076	0.0057	0.0047	0.0110	0.0092	0.0067	0.0055
			EPDM	0.0099	0.0086	0.0066	0.0057	0.0120	0.0099	0.0074	0.0063
		50%	BUR	0.0110	0.0094	0.0073	0.0063	0.0139	0.0110	0.0085	0.0073
			EPDM	0.0121	0.0104	0.0082	0.0072	0.0150	0.0118	0.0093	0.0080
	D	20%	BUR	0.0063	0.0039	0.0033	0.0030	0.0067	0.0038	0.0031	0.0027
			EPDM	0.0076	0.0050	0.0043	0.0039	0.0078	0.0047	0.0039	0.0035
		33%	BUR	0.0067	0.0041	0.0034	0.0031	0.0074	0.0041	0.0033	0.0029
			EPDM	0.0080	0.0052	0.0044	0.0040	0.0084	0.0050	0.0042	0.0037
		50%	BUR	0.0088	0.0061	0.0053	0.0049	0.0113	0.0080	0.0068	0.0063
			EPDM	0.0101	0.0071	0.0062	0.0057	0.0123	0.0088	0.0076	0.0070
Concrete	A	20%	BUR	0.0044	0.0044	0.0029	0.0022	0.0085	0.0078	0.0053	0.0041
			EPDM	0.0045	0.0045	0.0030	0.0023	0.0086	0.0079	0.0054	0.0042
		33%	BUR	0.0059	0.0058	0.0039	0.0030	0.0107	0.0096	0.0066	0.0052
			EPDM	0.0060	0.0059	0.0039	0.0031	0.0108	0.0097	0.0067	0.0053
		50%	BUR	0.0093	0.0083	0.0061	0.0051	0.0144	0.0120	0.0088	0.0073
			EPDM	0.0093	0.0085	0.0062	0.0051	0.0144	0.0121	0.0089	0.0075
	B	20%	BUR	0.0042	0.0042	0.0027	0.0021	0.0077	0.0068	0.0045	0.0035
			EPDM	0.0043	0.0043	0.0028	0.0021	0.0078	0.0069	0.0046	0.0036
		33%	BUR	0.0056	0.0054	0.0036	0.0028	0.0097	0.0083	0.0057	0.0045
			EPDM	0.0056	0.0054	0.0037	0.0028	0.0099	0.0084	0.0058	0.0045
		50%	BUR	0.0088	0.0078	0.0058	0.0048	0.0134	0.0108	0.0080	0.0067
			EPDM	0.0089	0.0079	0.0058	0.0049	0.0135	0.0109	0.0081	0.0068
	C	20%	BUR	0.0041	0.0042	0.0027	0.0021	0.0074	0.0064	0.0043	0.0033
			EPDM	0.0042	0.0043	0.0028	0.0022	0.0074	0.0065	0.0044	0.0034
		33%	BUR	0.0055	0.0054	0.0036	0.0027	0.0094	0.0079	0.0054	0.0042
			EPDM	0.0057	0.0055	0.0037	0.0028	0.0095	0.0080	0.0054	0.0043
		50%	BUR	0.0086	0.0078	0.0058	0.0047	0.0128	0.0101	0.0076	0.0064
			EPDM	0.0087	0.0079	0.0058	0.0048	0.0130	0.0102	0.0077	0.0065
	D	20%	BUR	0.0026	0.0011	0.0008	0.0007	0.0045	0.0019	0.0013	0.0011
			EPDM	0.0028	0.0012	0.0009	0.0008	0.0046	0.0020	0.0014	0.0012
		33%	BUR	0.0033	0.0014	0.0010	0.0009	0.0054	0.0024	0.0017	0.0013
			EPDM	0.0035	0.0015	0.0011	0.0009	0.0056	0.0025	0.0018	0.0014
		50%	BUR	0.0062	0.0040	0.0035	0.0031	0.0099	0.0068	0.0058	0.0053
			EPDM	0.0063	0.0041	0.0035	0.0031	0.0100	0.0069	0.0059	0.0053

Table 7.73. Average Annual Building Loss Normalized by Building Value – Eight-Story Engineered Building

Building Characteristics				Residential Buildings(8 Units per Floor)				Commercial Buildings(1 Unit per Floor)			
Roof Deck	Missile Environ.	Glazing Coverage	Roof Cover	Terrain Roughness (m)				Terrain Roughness (m)			
				0.03	0.35	0.70	1.0	0.03	0.35	0.70	1.00
Metal	A	20%	BUR	0.0106	0.0088	0.0074	0.0067	0.0113	0.0095	0.0076	0.0066
			EPDM	0.0118	0.0099	0.0085	0.0078	0.0122	0.0103	0.0084	0.0074
		33%	BUR	0.0116	0.0096	0.0079	0.0071	0.0128	0.0106	0.0084	0.0073
			EPDM	0.0128	0.0106	0.0090	0.0081	0.0138	0.0114	0.0092	0.0081
		50%	BUR	0.0148	0.0124	0.0106	0.0097	0.0170	0.0141	0.0119	0.0108
			EPDM	0.0161	0.0135	0.0117	0.0107	0.0179	0.0149	0.0127	0.0116
	B	20%	BUR	0.0103	0.0085	0.0071	0.0065	0.0108	0.0088	0.0071	0.0063
			EPDM	0.0115	0.0096	0.0082	0.0075	0.0117	0.0097	0.0079	0.0070
		33%	BUR	0.0112	0.0091	0.0076	0.0069	0.0122	0.0098	0.0078	0.0069
			EPDM	0.0124	0.0102	0.0086	0.0078	0.0130	0.0106	0.0086	0.0076
		50%	BUR	0.0143	0.0118	0.0102	0.0094	0.0163	0.0134	0.0114	0.0105
			EPDM	0.0155	0.0130	0.0112	0.0104	0.0173	0.0142	0.0122	0.0113
	C	20%	BUR	0.0102	0.0083	0.0070	0.0064	0.0105	0.0085	0.0069	0.0060
			EPDM	0.0114	0.0094	0.0081	0.0074	0.0114	0.0093	0.0077	0.0068
		33%	BUR	0.0110	0.0089	0.0074	0.0067	0.0117	0.0094	0.0075	0.0066
			EPDM	0.0123	0.0100	0.0085	0.0077	0.0126	0.0102	0.0083	0.0074
		50%	BUR	0.0140	0.0116	0.0101	0.0093	0.0161	0.0130	0.0112	0.0104
			EPDM	0.0153	0.0127	0.0111	0.0104	0.0169	0.0138	0.0120	0.0111
	D	20%	BUR	0.0096	0.0070	0.0062	0.0058	0.0094	0.0065	0.0056	0.0052
			EPDM	0.0108	0.0081	0.0073	0.0069	0.0103	0.0073	0.0064	0.0060
		33%	BUR	0.0102	0.0074	0.0065	0.0061	0.0103	0.0069	0.0060	0.0055
			EPDM	0.0115	0.0085	0.0076	0.0071	0.0112	0.0078	0.0068	0.0062
		50%	BUR	0.0134	0.0104	0.0093	0.0089	0.0150	0.0118	0.0108	0.0101
			EPDM	0.0146	0.0114	0.0104	0.0099	0.0160	0.0126	0.0115	0.0109
Concrete	A	20%	BUR	0.0051	0.0040	0.0028	0.0023	0.0080	0.0063	0.0045	0.0037
			EPDM	0.0051	0.0040	0.0029	0.0024	0.0080	0.0064	0.0046	0.0037
		33%	BUR	0.0064	0.0049	0.0036	0.0029	0.0098	0.0076	0.0056	0.0045
			EPDM	0.0065	0.0050	0.0036	0.0030	0.0098	0.0077	0.0056	0.0046
		50%	BUR	0.0105	0.0086	0.0070	0.0063	0.0146	0.0119	0.0098	0.0087
			EPDM	0.0106	0.0086	0.0071	0.0063	0.0147	0.0119	0.0098	0.0088
	B	20%	BUR	0.0048	0.0036	0.0025	0.0021	0.0075	0.0057	0.0041	0.0033
			EPDM	0.0049	0.0037	0.0026	0.0021	0.0075	0.0058	0.0041	0.0033
		33%	BUR	0.0060	0.0045	0.0032	0.0027	0.0091	0.0068	0.0050	0.0041
			EPDM	0.0060	0.0046	0.0033	0.0027	0.0091	0.0069	0.0050	0.0041
		50%	BUR	0.0100	0.0080	0.0066	0.0060	0.0139	0.0112	0.0093	0.0084
			EPDM	0.0100	0.0081	0.0067	0.0060	0.0140	0.0112	0.0094	0.0085
	C	20%	BUR	0.0047	0.0035	0.0025	0.0020	0.0072	0.0054	0.0038	0.0030
			EPDM	0.0047	0.0035	0.0025	0.0020	0.0072	0.0054	0.0039	0.0032
		33%	BUR	0.0058	0.0043	0.0031	0.0025	0.0087	0.0065	0.0046	0.0038
			EPDM	0.0059	0.0043	0.0032	0.0026	0.0087	0.0065	0.0047	0.0039
		50%	BUR	0.0096	0.0078	0.0065	0.0058	0.0136	0.0108	0.0091	0.0084
			EPDM	0.0098	0.0078	0.0065	0.0060	0.0136	0.0109	0.0092	0.0083
	D	20%	BUR	0.0040	0.0021	0.0016	0.0014	0.0060	0.0032	0.0025	0.0021
			EPDM	0.0041	0.0022	0.0017	0.0014	0.0061	0.0033	0.0025	0.0022
		33%	BUR	0.0049	0.0027	0.0021	0.0018	0.0072	0.0039	0.0031	0.0027
			EPDM	0.0052	0.0027	0.0022	0.0019	0.0072	0.0040	0.0031	0.0027
		50%	BUR	0.0090	0.0066	0.0057	0.0055	0.0126	0.0096	0.0086	0.0080
			EPDM	0.0091	0.0066	0.0059	0.0054	0.0127	0.0096	0.0086	0.0081

Table 7.74. Average Annual Content Loss Normalized by Building Value – Two-Story Engineered Building

Building Characteristics				Residential Buildings (8 Units per Floor)				Commercial Buildings(1 Unit per Floor)			
Roof Deck	Missile Environ.	Glazing Coverage	Roof Cover	Terrain Roughness (m)				Terrain Roughness (m)			
				0.03	0.35	0.70	1.0	0.03	0.35	0.70	1.00
Metal	A	20%	BUR	0.0037	0.0034	0.0022	0.0016	0.0052	0.0048	0.0030	0.0022
			EPDM	0.0039	0.0035	0.0022	0.0017	0.0053	0.0048	0.0031	0.0022
		33%	BUR	0.0049	0.0044	0.0028	0.0021	0.0068	0.0064	0.0042	0.0032
			EPDM	0.0050	0.0044	0.0029	0.0021	0.0068	0.0064	0.0042	0.0032
		50%	BUR	0.0068	0.0059	0.0039	0.0030	0.0086	0.0078	0.0052	0.0040
			EPDM	0.0069	0.0060	0.0040	0.0031	0.0086	0.0078	0.0052	0.0040
	B	20%	BUR	0.0029	0.0027	0.0017	0.0012	0.0040	0.0032	0.0019	0.0013
			EPDM	0.0031	0.0028	0.0018	0.0013	0.0041	0.0032	0.0020	0.0014
		33%	BUR	0.0039	0.0035	0.0022	0.0016	0.0051	0.0044	0.0027	0.0020
			EPDM	0.0040	0.0035	0.0023	0.0017	0.0051	0.0044	0.0028	0.0020
		50%	BUR	0.0054	0.0046	0.0030	0.0023	0.0066	0.0055	0.0036	0.0026
			EPDM	0.0055	0.0047	0.0031	0.0024	0.0066	0.0055	0.0036	0.0027
	C	20%	BUR	0.0022	0.0018	0.0011	0.0008	0.0032	0.0023	0.0013	0.0009
			EPDM	0.0024	0.0019	0.0011	0.0008	0.0033	0.0023	0.0014	0.0009
		33%	BUR	0.0028	0.0022	0.0014	0.0010	0.0040	0.0031	0.0018	0.0013
			EPDM	0.0030	0.0023	0.0014	0.0011	0.0041	0.0031	0.0019	0.0013
		50%	BUR	0.0041	0.0033	0.0021	0.0016	0.0053	0.0040	0.0025	0.0018
			EPDM	0.0042	0.0033	0.0022	0.0017	0.0053	0.0040	0.0025	0.0019
	D	20%	BUR	0.0013	0.0005	0.0003	0.0003	0.0016	0.0005	0.0003	0.0002
			EPDM	0.0015	0.0006	0.0005	0.0004	0.0018	0.0006	0.0004	0.0003
		33%	BUR	0.0014	0.0005	0.0003	0.0003	0.0018	0.0005	0.0003	0.0003
			EPDM	0.0016	0.0006	0.0005	0.0004	0.0020	0.0006	0.0004	0.0004
		50%	BUR	0.0023	0.0011	0.0008	0.0007	0.0034	0.0017	0.0013	0.0011
			EPDM	0.0025	0.0012	0.0009	0.0008	0.0036	0.0018	0.0014	0.0012
Concrete	A	20%	BUR	0.0030	0.0032	0.0020	0.0014	0.0049	0.0048	0.0030	0.0022
			EPDM	0.0030	0.0032	0.0020	0.0014	0.0049	0.0048	0.0030	0.0021
		33%	BUR	0.0044	0.0042	0.0027	0.0020	0.0066	0.0064	0.0042	0.0032
			EPDM	0.0044	0.0043	0.0027	0.0020	0.0066	0.0064	0.0042	0.0031
		50%	BUR	0.0065	0.0059	0.0039	0.0030	0.0085	0.0078	0.0052	0.0040
			EPDM	0.0065	0.0059	0.0039	0.0030	0.0085	0.0078	0.0052	0.0040
	B	20%	BUR	0.0022	0.0025	0.0015	0.0010	0.0036	0.0030	0.0018	0.0012
			EPDM	0.0021	0.0024	0.0015	0.0010	0.0036	0.0031	0.0018	0.0012
		33%	BUR	0.0033	0.0033	0.0020	0.0015	0.0048	0.0043	0.0027	0.0019
			EPDM	0.0032	0.0032	0.0020	0.0014	0.0048	0.0043	0.0027	0.0019
		50%	BUR	0.0050	0.0045	0.0029	0.0022	0.0065	0.0055	0.0036	0.0026
			EPDM	0.0050	0.0045	0.0029	0.0022	0.0065	0.0055	0.0036	0.0026
	C	20%	BUR	0.0014	0.0014	0.0008	0.0005	0.0027	0.0021	0.0011	0.0007
			EPDM	0.0014	0.0014	0.0007	0.0005	0.0027	0.0020	0.0011	0.0007
		33%	BUR	0.0021	0.0019	0.0011	0.0007	0.0037	0.0030	0.0017	0.0012
			EPDM	0.0021	0.0019	0.0011	0.0008	0.0037	0.0030	0.0017	0.0012
		50%	BUR	0.0037	0.0031	0.0019	0.0015	0.0052	0.0040	0.0025	0.0018
			EPDM	0.0036	0.0031	0.0020	0.0015	0.0051	0.0040	0.0025	0.0018
	D	20%	BUR	0.0005	0.0001	0.0000	0.0000	0.0011	0.0002	0.0001	0.0000
			EPDM	0.0005	0.0001	0.0000	0.0000	0.0011	0.0002	0.0001	0.0000
		33%	BUR	0.0007	0.0001	0.0000	0.0000	0.0014	0.0002	0.0001	0.0001
			EPDM	0.0007	0.0001	0.0000	0.0000	0.0014	0.0002	0.0001	0.0001
		50%	BUR	0.0018	0.0008	0.0006	0.0005	0.0032	0.0016	0.0012	0.0010
			EPDM	0.0018	0.0008	0.0006	0.0005	0.0032	0.0016	0.0012	0.0010

Table 7.75. Average Annual Content Loss Normalized by Building Value – Five-Story Engineered Building

Building Characteristics				Residential Buildings(8 Units per Floor)				Commercial Buildings(1 Unit per Floor)			
Roof Deck	Missile Environ.	Glazing Coverage	Roof Cover	Terrain Roughness (m)				Terrain Roughness (m)			
				0.03	0.35	0.70	1.0	0.03	0.35	0.70	1.00
Metal	A	20%	BUR	0.0031	0.0025	0.0017	0.0013	0.0050	0.0042	0.0029	0.0022
			EPDM	0.0032	0.0026	0.0018	0.0015	0.0051	0.0043	0.0030	0.0024
		33%	BUR	0.0038	0.0031	0.0022	0.0017	0.0062	0.0052	0.0036	0.0028
			EPDM	0.0040	0.0033	0.0023	0.0018	0.0063	0.0054	0.0037	0.0030
		50%	BUR	0.0055	0.0046	0.0034	0.0029	0.0083	0.0067	0.0050	0.0041
			EPDM	0.0056	0.0047	0.0035	0.0030	0.0085	0.0069	0.0051	0.0043
	B	20%	BUR	0.0029	0.0024	0.0016	0.0013	0.0045	0.0035	0.0024	0.0018
			EPDM	0.0032	0.0025	0.0018	0.0014	0.0047	0.0036	0.0025	0.0020
		33%	BUR	0.0037	0.0030	0.0020	0.0016	0.0056	0.0044	0.0030	0.0024
			EPDM	0.0038	0.0031	0.0022	0.0017	0.0058	0.0045	0.0031	0.0025
		50%	BUR	0.0053	0.0043	0.0032	0.0027	0.0078	0.0059	0.0044	0.0037
			EPDM	0.0054	0.0044	0.0034	0.0028	0.0079	0.0060	0.0045	0.0038
	C	20%	BUR	0.0029	0.0023	0.0016	0.0013	0.0044	0.0032	0.0022	0.0017
			EPDM	0.0031	0.0025	0.0017	0.0014	0.0045	0.0033	0.0023	0.0018
		33%	BUR	0.0036	0.0029	0.0021	0.0016	0.0054	0.0041	0.0028	0.0022
			EPDM	0.0038	0.0031	0.0022	0.0017	0.0056	0.0042	0.0029	0.0023
		50%	BUR	0.0052	0.0043	0.0032	0.0027	0.0074	0.0054	0.0041	0.0035
			EPDM	0.0053	0.0044	0.0033	0.0028	0.0076	0.0055	0.0042	0.0036
	D	20%	BUR	0.0023	0.0011	0.0008	0.0007	0.0031	0.0013	0.0010	0.0008
			EPDM	0.0025	0.0012	0.0010	0.0008	0.0033	0.0015	0.0011	0.0009
		33%	BUR	0.0026	0.0012	0.0009	0.0008	0.0036	0.0016	0.0012	0.0009
			EPDM	0.0028	0.0014	0.0010	0.0009	0.0038	0.0018	0.0013	0.0011
		50%	BUR	0.0040	0.0026	0.0022	0.0020	0.0061	0.0042	0.0035	0.0032
			EPDM	0.0042	0.0027	0.0023	0.0021	0.0063	0.0043	0.0036	0.0032
Concrete	A	20%	BUR	0.0021	0.0019	0.0012	0.0009	0.0045	0.0038	0.0025	0.0019
			EPDM	0.0021	0.0019	0.0012	0.0009	0.0045	0.0038	0.0025	0.0019
		33%	BUR	0.0030	0.0027	0.0017	0.0013	0.0058	0.0050	0.0033	0.0026
			EPDM	0.0030	0.0027	0.0017	0.0013	0.0058	0.0050	0.0033	0.0026
		50%	BUR	0.0050	0.0043	0.0031	0.0026	0.0081	0.0066	0.0048	0.0040
			EPDM	0.0050	0.0043	0.0031	0.0026	0.0081	0.0066	0.0048	0.0040
	B	20%	BUR	0.0020	0.0018	0.0011	0.0008	0.0040	0.0031	0.0020	0.0015
			EPDM	0.0020	0.0017	0.0011	0.0008	0.0040	0.0031	0.0020	0.0015
		33%	BUR	0.0029	0.0025	0.0016	0.0012	0.0053	0.0041	0.0028	0.0021
			EPDM	0.0028	0.0024	0.0016	0.0012	0.0053	0.0041	0.0028	0.0021
		50%	BUR	0.0048	0.0040	0.0029	0.0025	0.0076	0.0057	0.0043	0.0036
			EPDM	0.0048	0.0040	0.0029	0.0024	0.0075	0.0057	0.0043	0.0036
	C	20%	BUR	0.0019	0.0017	0.0011	0.0008	0.0038	0.0028	0.0018	0.0013
			EPDM	0.0019	0.0017	0.0011	0.0008	0.0038	0.0028	0.0018	0.0013
		33%	BUR	0.0028	0.0025	0.0016	0.0012	0.0051	0.0038	0.0025	0.0019
			EPDM	0.0028	0.0025	0.0016	0.0012	0.0051	0.0038	0.0025	0.0019
		50%	BUR	0.0047	0.0040	0.0029	0.0024	0.0072	0.0053	0.0040	0.0033
			EPDM	0.0047	0.0040	0.0029	0.0024	0.0073	0.0053	0.0040	0.0033
	D	20%	BUR	0.0013	0.0004	0.0002	0.0002	0.0026	0.0009	0.0006	0.0004
			EPDM	0.0013	0.0004	0.0003	0.0002	0.0026	0.0009	0.0006	0.0004
		33%	BUR	0.0017	0.0006	0.0004	0.0003	0.0032	0.0012	0.0008	0.0006
			EPDM	0.0017	0.0006	0.0004	0.0003	0.0032	0.0012	0.0008	0.0006
		50%	BUR	0.0034	0.0022	0.0019	0.0017	0.0058	0.0039	0.0033	0.0030
			EPDM	0.0034	0.0022	0.0018	0.0016	0.0059	0.0039	0.0033	0.0030

Table 7.76. Average Annual Content Loss Normalized by Building Value – Eight-Story Engineered Building

Building Characteristics				Residential Buildings(8 Units per Floor)				Commercial Buildings(1 Unit per Floor)			
Roof Deck	Missile Environ.	Glazing Coverage	Roof Cover	Terrain Roughness (m)				Terrain Roughness (m)			
				0.03	0.35	0.70	1.0	0.03	0.35	0.70	1.00
Metal	A	20%	BUR	0.0038	0.0028	0.0022	0.0019	0.0054	0.0041	0.0031	0.0026
			EPDM	0.0040	0.0029	0.0023	0.0021	0.0055	0.0042	0.0033	0.0027
		33%	BUR	0.0044	0.0032	0.0025	0.0022	0.0064	0.0049	0.0037	0.0031
			EPDM	0.0045	0.0033	0.0027	0.0023	0.0066	0.0051	0.0038	0.0032
		50%	BUR	0.0063	0.0050	0.0042	0.0038	0.0093	0.0074	0.0062	0.0056
			EPDM	0.0065	0.0051	0.0043	0.0039	0.0095	0.0076	0.0064	0.0057
	B	20%	BUR	0.0037	0.0026	0.0021	0.0019	0.0051	0.0037	0.0028	0.0024
			EPDM	0.0038	0.0027	0.0022	0.0019	0.0052	0.0038	0.0029	0.0025
		33%	BUR	0.0042	0.0030	0.0024	0.0021	0.0061	0.0043	0.0033	0.0028
			EPDM	0.0044	0.0031	0.0025	0.0022	0.0062	0.0045	0.0034	0.0029
		50%	BUR	0.0060	0.0047	0.0040	0.0036	0.0089	0.0070	0.0059	0.0054
			EPDM	0.0062	0.0049	0.0041	0.0037	0.0091	0.0072	0.0060	0.0055
	C	20%	BUR	0.0036	0.0025	0.0020	0.0018	0.0049	0.0034	0.0026	0.0022
			EPDM	0.0038	0.0026	0.0021	0.0019	0.0051	0.0035	0.0027	0.0023
		33%	BUR	0.0041	0.0029	0.0023	0.0020	0.0058	0.0041	0.0031	0.0026
			EPDM	0.0043	0.0030	0.0024	0.0021	0.0059	0.0042	0.0032	0.0027
		50%	BUR	0.0058	0.0046	0.0039	0.0036	0.0088	0.0067	0.0057	0.0053
			EPDM	0.0061	0.0047	0.0040	0.0037	0.0089	0.0069	0.0059	0.0054
	D	20%	BUR	0.0034	0.0021	0.0018	0.0016	0.0045	0.0026	0.0021	0.0019
			EPDM	0.0036	0.0023	0.0019	0.0018	0.0047	0.0028	0.0023	0.0020
		33%	BUR	0.0038	0.0024	0.0020	0.0018	0.0051	0.0030	0.0024	0.0022
			EPDM	0.0040	0.0025	0.0021	0.0019	0.0053	0.0032	0.0026	0.0023
		50%	BUR	0.0057	0.0042	0.0037	0.0035	0.0083	0.0063	0.0056	0.0052
			EPDM	0.0058	0.0043	0.0038	0.0036	0.0085	0.0064	0.0057	0.0054
Concrete	A	20%	BUR	0.0024	0.0016	0.0011	0.0008	0.0046	0.0033	0.0023	0.0018
			EPDM	0.0024	0.0015	0.0011	0.0009	0.0046	0.0033	0.0023	0.0018
		33%	BUR	0.0031	0.0021	0.0015	0.0012	0.0057	0.0042	0.0030	0.0024
			EPDM	0.0031	0.0021	0.0015	0.0012	0.0058	0.0042	0.0030	0.0024
		50%	BUR	0.0053	0.0042	0.0034	0.0031	0.0089	0.0070	0.0058	0.0052
			EPDM	0.0054	0.0042	0.0035	0.0031	0.0089	0.0071	0.0058	0.0052
	B	20%	BUR	0.0022	0.0014	0.0009	0.0008	0.0043	0.0029	0.0020	0.0016
			EPDM	0.0023	0.0014	0.0009	0.0007	0.0043	0.0028	0.0020	0.0016
		33%	BUR	0.0029	0.0019	0.0013	0.0011	0.0054	0.0036	0.0026	0.0021
			EPDM	0.0029	0.0019	0.0013	0.0010	0.0053	0.0036	0.0026	0.0021
		50%	BUR	0.0051	0.0039	0.0033	0.0029	0.0084	0.0066	0.0055	0.0050
			EPDM	0.0051	0.0039	0.0033	0.0029	0.0085	0.0066	0.0055	0.0050
	C	20%	BUR	0.0022	0.0013	0.0009	0.0007	0.0041	0.0026	0.0018	0.0014
			EPDM	0.0021	0.0013	0.0009	0.0007	0.0041	0.0026	0.0018	0.0014
		33%	BUR	0.0028	0.0017	0.0012	0.0010	0.0051	0.0034	0.0024	0.0019
			EPDM	0.0028	0.0017	0.0012	0.0010	0.0051	0.0034	0.0024	0.0019
		50%	BUR	0.0049	0.0038	0.0032	0.0029	0.0083	0.0063	0.0053	0.0050
			EPDM	0.0050	0.0038	0.0032	0.0029	0.0083	0.0063	0.0054	0.0049
	D	20%	BUR	0.0020	0.0009	0.0006	0.0005	0.0037	0.0018	0.0013	0.0011
			EPDM	0.0020	0.0009	0.0007	0.0005	0.0037	0.0018	0.0013	0.0011
		33%	BUR	0.0025	0.0013	0.0009	0.0008	0.0044	0.0023	0.0017	0.0015
			EPDM	0.0026	0.0012	0.0009	0.0008	0.0044	0.0023	0.0017	0.0014
		50%	BUR	0.0047	0.0034	0.0029	0.0028	0.0078	0.0058	0.0052	0.0048
			EPDM	0.0047	0.0034	0.0030	0.0027	0.0079	0.0058	0.0052	0.0048

Table 7.77. Percent Increases in the Average Annual Total Loss due to Changes in Building Parameters (Minimum/Average/Maximum) – Engineered Residential and Commercial Buildings

Two-Story Engineered Buildings		
Building Parameter	Metal Roof Deck	Concrete Roof Deck
Residential to Commercial Building Class	0% / 24% / 42%	23% / 46% / 87%
Built-up to Single Ply Membrane Roof Cover	2% / 14% / 46%	-1% / 4% / 25%
20% to 33% Glazing Coverage	0% / 16% / 28%	5% / 28% / 44%
33% to 50% Glazing Coverage	17% / 32% / 99%	18% / 90% / 435%
Missile Environment D to C	37% / 103% / 253%	66% / 368% / 808%
Missile Environment C to B	18% / 29% / 42%	25% / 44% / 72%
Missile Environment B to A	18% / 28% / 44%	28% / 37% / 58%
Concrete to Metal Roof Deck	1% / 66% / 458%	
Five-Story Engineered Buildings		
Building Parameter	Metal Roof Deck	Concrete Roof Deck
Residential to Commercial Building Class	-6% / 25% / 45%	30% / 65% / 98%
Built-up to Single Ply Membrane Roof Cover	4% / 12% / 29%	-1% / 2% / 13%
20% to 33% Glazing Coverage	3% / 14% / 21%	21% / 32% / 40%
33% to 50% Glazing Coverage	21% / 43% / 145%	28% / 92% / 321%
Missile Environment D to C	14% / 56% / 130%	18% / 142% / 294%
Missile Environment C to B	0% / 3% / 7%	-2% / 4% / 9%
Missile Environment B to A	2% / 8% / 15%	4% / 10% / 21%
Concrete to Metal Roof Deck	6% / 58% / 395%	
Eight-Story Engineered Buildings		
Building Parameter	Metal Roof Deck	Concrete Roof Deck
Residential to Commercial Building Class	-7% / 12% / 26%	47% / 61% / 76%
Built-up to Single Ply Membrane Roof Cover	4% / 9% / 16%	-3% / 1% / 6%
20% to 33% Glazing Coverage	5% / 10% / 15%	19% / 27% / 37%
33% to 50% Glazing Coverage	29% / 48% / 100%	51% / 109% / 221%
Missile Environment D to C	2% / 13% / 35%	2% / 29% / 61%
Missile Environment C to B	1% / 3% / 6%	1% / 5% / 10%
Missile Environment B to A	3% / 5% / 10%	3% / 9% / 14%
Concrete to Metal Roof Deck	12% / 82% / 334%	
All Engineered Buildings		
Building Parameter	Metal Roof Deck	Concrete Roof Deck
Two to Five Stories	-23% / 25% / 130%	-40% / 32% / 242%
Five to Eight Stories	-4% / 33% / 105%	-25% / 18% / 122%

decks, and thus losses are primarily driven by glazing damage, which is influenced by both usage, since internal pressure is confined to smaller internal areas when there are multiple units, and missile environment.

The number of stories also has a significant impact on the normalized average annual total losses (see last two rows of Table 7.77). For example, with all else being the same, the predicted average annual losses for the five-story engineered buildings are up to 242% higher than those for the two-story buildings engineered buildings.

7.14 Loss Model Results for Industrial Buildings

Loss functions for industrial buildings have been developed following the same procedure as the other model building classes (based on 20,000 years of hurricane

simulation). The model buildings are assumed to be used as factories. The assumed subassembly cost distributions are listed in Table 7.78.

Example building and content loss functions are given in Appendix N. The average annual building and content losses (both normalized by the total building value) for all industrial buildings examined are presented in Tables 7.79 and 7.80, respectively. The average annual loss is obtained by summing all losses produced during the 20,000-year hurricane simulation period and then dividing by 20,000 years. The values given in Tables 7.79 and 7.80 reflect the average annual losses for industrial buildings located in the South Florida area.

Table 7.81 presents a summary of the effects of the various building parameters on normalized average annual total loss. The wall construction has the largest impact on average annual loss with an increase of 34% on average for unreinforced masonry walls versus reinforced masonry walls. This is due to the weaker resistance of the joist/wall connections for unreinforced masonry versus reinforced masonry walls since unreinforced masonry walls do not contain bond beams or tie beams with reinforcement to which the anchorage can be welded to or wrapped around (NRC, 1991). Average annual total losses are shown to increase by 16% on average when the metal roof deck has aged and fatigued, which has been modeled with a 50% reduction in the base uplift resistance. The effect of the surrounding missile environment on building losses is small since the modeled industrial building does not comprise glazing. However, small increases were observed (up to 3%) when the missile environment changed from the no-missile environment (D) to the environment associated with a mixture of commercial and residential type missiles (A) since costs are associated with re-finishing wall surfaces and replacing entry and/or overhead doors that have been impacted by windborne debris.

Table 7.78. Subassembly Cost Distributions for Industrial Buildings

Subassemblies	Cost Ratios	
Foundations		
Footings & Foundations	4.8%	7.0%
Piles & Caissons	0.0%	
Excavation & Backfill	2.2%	
Substructures		
Slab on Grade	6.8%	6.8%
Special Substructures	0.0%	
Superstructure		
Columns and Beams	0.0%	10.5%
Structural Walls	0.0%	
Elevated Floors/Diaphragms	0.0%	
Roof Decking/Framing	10.5%	
Stairs	0.0%	
Exterior Closure		
Walls	4.7%	6.1%
Exterior Wall Finishes	0.0%	
Doors	1.4%	
Windows & Glazed Walls	0.0%	
Roofing		
Roof Covering	4.5%	7.9%
Insulation	2.7%	
Openings & Specialties	0.7%	
Interior Construction		
Partitions	4.0%	9.8%
Interior Doors	1.9%	
Wall Finishes	1.0%	
Floor Finishes	0.6%	
Ceiling Finishes	0.7%	
Interior Surface of Exterior Walls	1.6%	
Conveying		
Elevators	0.0%	0.0%
Special Conveyors	0.0%	
Mechanical		
Plumbing	6.2%	37.2%
Fire Protection	4.4%	
Heating	11.8%	
Cooling	14.8%	
Special Systems	0.0%	
Electrical		
Service & Distribution	1.7%	14.8%
Lighting & Power	12.5%	
Special Electrical	0.6%	
Special Construction		
Specialties (& Additives)	0.0%	0.0%
Total	100%	100%

Table 7.79. Average Annual Building Loss Normalized by Building Value – Industrial Building

Building Characteristics		100% Roof Deck Capacity				50% Roof Deck Capacity			
		Terrain Surface Roughness (m)				Terrain Surface Roughness (m)			
Wall Construction	Missile Environment	0.03	0.35	0.70	1.0	0.03	0.35	0.70	1.0
Unreinforced Masonry	A	0.0286	0.0147	0.0107	0.0088	0.0297	0.0155	0.0115	0.0096
	B	0.0286	0.0147	0.0107	0.0088	0.0296	0.0155	0.0116	0.0097
	C	0.0286	0.0148	0.0107	0.0089	0.0297	0.0157	0.0117	0.0098
	D	0.0285	0.0145	0.0106	0.0087	0.0295	0.0153	0.0114	0.0096
Reinforced Masonry	A	0.0200	0.0108	0.0081	0.0067	0.0231	0.0130	0.0100	0.0084
	B	0.0201	0.0109	0.0081	0.0068	0.0231	0.0131	0.0099	0.0085
	C	0.0201	0.0110	0.0081	0.0068	0.0231	0.0132	0.0100	0.0086
	D	0.0200	0.0106	0.0079	0.0066	0.0230	0.0128	0.0098	0.0084

Table 7.80. Average Annual Content Loss Normalized by Building Value – Industrial Building

Building Characteristics		100% Roof Deck Capacity				50% Roof Deck Capacity			
		Terrain Surface Roughness (m)				Terrain Surface Roughness (m)			
Wall Construction	Missile Environment	0.03	0.35	0.70	1.0	0.03	0.35	0.70	1.0
Unreinforced Masonry	A	0.0126	0.0057	0.0038	0.0029	0.0128	0.0059	0.0041	0.0032
	B	0.0126	0.0057	0.0038	0.0029	0.0128	0.0059	0.0041	0.0033
	C	0.0126	0.0057	0.0038	0.0030	0.0128	0.0060	0.0041	0.0033
	D	0.0126	0.0057	0.0038	0.0029	0.0128	0.0059	0.0041	0.0033
Reinforced Masonry	A	0.0069	0.0031	0.0021	0.0016	0.0085	0.0044	0.0032	0.0026
	B	0.0069	0.0031	0.0021	0.0016	0.0086	0.0044	0.0031	0.0026
	C	0.0069	0.0031	0.0021	0.0016	0.0086	0.0044	0.0032	0.0027
	D	0.0069	0.0031	0.0021	0.0016	0.0086	0.0044	0.0032	0.0027

Table 7.81. Percent Increase in Average Annual Total Loss Due to Changes in Building Parameters (Minimum/Average/Maximum) – Industrial Buildings

Parameter	Increase in Building Loss
Reinforced Masonry to Unreinforced Masonry Walls	16% / 34% / 53%
Missile Environment D to A	0% / 1% / 3%
0% to 50% Reduction in Roof Deck Resistance	3% / 16% / 34%

7.15 Loss Model Results for Essential Facilities

Loss functions for essential buildings have been developed following the same procedure as other model building classes (based on 20,000 years of hurricane simulation). Assumed subassembly cost distributions for fire stations, elementary schools, high schools, and hospitals are listed in Table 7.82 through Table 7.86.

Table 7.82. Subassembly Cost Distributions for Fire Stations

Subassemblies	Cost Ratios	
Foundation		
Footings & Foundations	6.4%	8.2%
Piles & Caissons	0.0%	
Excavation & Backfill	1.7%	
Substructures		
Slab on Grade	5.3%	5.3%
Special Substructures	0.0%	
Superstructure		
Columns and Beams	0.0%	3.8%
Structural Walls	0.0%	
Elevated Floors/Diaphragms	0.0%	
Roof Decking/Framing	3.8%	
Stairs	0.0%	
Exterior Closure		
Walls	15.7%	21.0%
Exterior Wall Finishes	0.0%	
Doors	3.4%	
Windows & Glazed Walls	2.0%	
Roofing		
Roof Covering	3.7%	6.6%
Insulation	1.8%	
Openings & Specialties	1.1%	
Interior Construction		
Partitions	5.1%	14.5%
Interior Doors	1.5%	
Wall Finishes	1.9%	
Floor Finishes	2.8%	
Ceiling Finishes	2.3%	
Interior Surface of Exterior Walls	0.9%	
Conveying		
Elevators	0.0%	0.0%
Special Conveyors	0.0%	
Mechanical		
Plumbing	9.4%	33.1%
Fire Protection	2.9%	
Heating	0.0%	
Cooling	20.8%	
Special Systems	0.0%	
Electrical		
Service & Distribution	1.3%	7.5%
Lighting & Power	5.8%	
Special Electrical	0.4%	
Special Construction		
Specialties (& Additives)	0.0%	0.0%
Total	100.0%	100.0%

Table 7.83. Subassembly Cost Distributions for Small Hospitals

Subassemblies	Nost Ratios	
Foundation		
Footings & Foundations	1.6%	1.9%
Piles & Caissons	0.0%	
Excavation & Backfill	0.3%	
Substructures		
Slab on Grade	1.0%	1.0%
Special Substructures	0.0%	
Superstructure		
Columns and Beams	1.3%	14.1%
Structural Walls	0.0%	
Elevated Floors/Diaphragms	8.0%	
Roof Decking/Framing	3.8%	
Stairs	0.9%	
Exterior Closure		
Walls	8.2%	9.5%
Exterior Wall Finishes	0.0%	
Doors	0.2%	
Windows & Glazed Walls	1.1%	
Roofing		
Roof Covering	0.7%	1.2%
Insulation	0.4%	
Openings & Specialties	0.1%	
Interior Construction		
Partitions	4.0%	25.1%
Interior Doors	5.9%	
Wall Finishes	5.5%	
Floor Finishes	6.2%	
Ceiling Finishes	3.1%	
Interior Surface of Exterior Walls	0.3%	
Conveying		
Elevators	2.5%	2.5%
Special Conveyors	0.0%	
Mechanical		
Plumbing	15.6%	28.1%
Fire Protection	1.4%	
Heating	2.7%	
Cooling	8.5%	
Special Systems	0.0%	
Electrical		
Service & Distribution	1.0%	10.7%
Lighting & Power	7.3%	
Special Electrical	2.4%	
Special Construction		
Specialties (& Additives)	5.9%	5.9%
Total	100.0%	100.0%

Table 7.84. Subassembly Cost Distributions for Medium and Large Hospitals

Subassemblies	Cost Ratios	
Foundation		
Footings & Foundations	6.4%	8.2%
Piles & Caissons	0.0%	
Excavation & Backfill	1.7%	
Substructures		
Slab on Grade	5.3%	5.3%
Special Substructures	0.0%	
Superstructure		
Columns and Beams	0.0%	3.8%
Structural Walls	0.0%	
Elevated Floors/Diaphragms	0.0%	
Roof Decking/Framing	3.8%	
Stairs	0.0%	
Exterior Closure		
Walls	15.7%	21.0%
Exterior Wall Finishes	0.0%	
Doors	3.4%	
Windows & Glazed Walls	2.0%	
Roofing		
Roof Covering	3.7%	6.6%
Insulation	1.8%	
Openings & Specialties	1.1%	
Interior Construction		
Partitions	5.1%	14.5%
Interior Doors	1.5%	
Wall Finishes	1.9%	
Floor Finishes	2.8%	
Ceiling Finishes	2.3%	
Interior Surface of Exterior Walls	0.9%	
Conveying		
Elevators	0.0%	0.0%
Special Conveyors	0.0%	
Mechanical		
Plumbing	9.4%	33.1%
Fire Protection	2.9%	
Heating	0.0%	
Cooling	20.8%	
Special Systems	0.0%	
Electrical		
Service & Distribution	1.3%	7.5%
Lighting & Power	5.8%	
Special Electrical	0.4%	
Special Construction		
Specialties (& Additives)	0.0%	0.0%
Total	100.0%	100.0%

Table 7.85. Subassembly Cost Distributions for Elementary Schools

Subassemblies	Cost Ratios	
Foundation		
Footings & Foundations	6.4%	8.2%
Piles & Caissons	0.0%	
Excavation & Backfill	1.7%	
Substructures		
Slab on Grade	5.3%	5.3%
Special Substructures	0.0%	
Superstructure		
Columns and Beams	0.0%	3.8%
Structural Walls	0.0%	
Elevated Floors/Diaphragms	0.0%	
Roof Decking/Framing	3.8%	
Stairs	0.0%	
Exterior Closure		
Walls	15.7%	21.0%
Exterior Wall Finishes	0.0%	
Doors	3.4%	
Windows & Glazed Walls	2.0%	
Roofing		
Roof Covering	3.7%	6.6%
Insulation	1.8%	
Openings & Specialties	1.1%	
Interior Construction		
Partitions	5.1%	14.5%
Interior Doors	1.5%	
Wall Finishes	1.9%	
Floor Finishes	2.8%	
Ceiling Finishes	2.3%	
Interior Surface of Exterior Walls	0.9%	
Conveying		
Elevators	0.0%	0.0%
Special Conveyors	0.0%	
Mechanical		
Plumbing	9.4%	33.1%
Fire Protection	2.9%	
Heating	0.0%	
Cooling	20.8%	
Special Systems	0.0%	
Electrical		
Service & Distribution	1.3%	7.5%
Lighting & Power	5.8%	
Special Electrical	0.4%	
Special Construction		
Specialties (& Additives)	0.0%	0.0%
Total	100.0%	100.0%

Table 7.86. Subassembly Cost Distributions for High Schools

Subassemblies	Cost Ratios	
Foundation		
Footings & Foundations	6.4%	8.2%
Piles & Caissons	0.0%	
Excavation & Backfill	1.7%	
Substructures		
Slab on Grade	5.3%	5.3%
Special Substructures	0.0%	
Superstructure		
Columns and Beams	0.0%	3.8%
Structural Walls	0.0%	
Elevated Floors/Diaphragms	0.0%	
Roof Decking/Framing	3.8%	
Stairs	0.0%	
Exterior Closure		
Walls	15.7%	21.0%
Exterior Wall Finishes	0.0%	
Doors	3.4%	
Windows & Glazed Walls	2.0%	
Roofing		
Roof Covering	3.7%	6.6%
Insulation	1.8%	
Openings & Specialties	1.1%	
Interior Construction		
Partitions	5.1%	14.5%
Interior Doors	1.5%	
Wall Finishes	1.9%	
Floor Finishes	2.8%	
Ceiling Finishes	2.3%	
Interior Surface of Exterior Walls	0.9%	
Conveying		
Elevators	0.0%	0.0%
Special Conveyors	0.0%	
Mechanical		
Plumbing	9.4%	33.1%
Fire Protection	2.9%	
Heating	0.0%	
Cooling	20.8%	
Special Systems	0.0%	
Electrical		
Service & Distribution	1.3%	7.5%
Lighting & Power	5.8%	
Special Electrical	0.4%	
Special Construction		
Specialties (& Additives)	0.0%	0.0%
Total	100.0%	100.0%

7.15.1 Loss Model Results for Fire Stations

The average annual building and content losses (both normalized by the total building value) for all fire stations examined are presented in Table 7.87~~Table 7.87~~ and Table 7.88~~Table 7.88~~. The average annual loss is obtained by summing all losses produced during the 20,000-year hurricane simulation period and then dividing by 20,000 years. The contents limit for fire stations has been assumed to be 20% of the building value. The values given in Table 7.87~~Table 7.87~~ and Table 7.88~~Table 7.88~~ reflect the average annual losses for fire stations located in the South Florida area.

The building parameter sensitivity results are shown in Table 7.89~~Table 7.89~~. It is evident that the missile environment has a large impact on overall loss, increasing the mean per storm loss by 121% on average when the missile environment changes from no windborne debris (Missile Environment D) to a mixed residential/commercial type environment (Missile Environment A).

The use of EPDM roof cover versus BUR roof cover increases the overall storm average loss by 6% on average, while a reduction in metal deck resistance of 50% increases losses by 46%.

Mitigation techniques such as shutters have a great effect in reducing damage in this analysis since window breakage and metal deck failure are the primary drivers of damage. Losses increases by 161% when shutters are not used, and increase by 46% when the deck is no longer mitigated.

Table 7.87. Average Annual Building Loss Normalized by Building Value – Fire Station

Deck Mitigation	Metal Panel Capacity	Shutters	Missile Environment	Roof Cover	Terrain Surface Roughness (m)				
					0.03	0.15	0.35	0.7	1
Mitigated	100%	No	A	BUR	0.0170514	0.0161	0.0109	0.0069	0.00498669
				EPDM	0.0171972	0.0162	0.011	0.0069	0.00507478
			B	BUR	0.0157124	0.013	0.0086	0.0052	0.00371321
				EPDM	0.0158897	0.0131	0.0087	0.0053	0.00382683
			C	BUR	0.0143621	0.0107	0.0068	0.004	0.00282638
				EPDM	0.0144833	0.0108	0.0069	0.0042	0.00296841
			D	BUR	0.0130329	0.0074	0.0047	0.0029	0.00220463
				EPDM	0.0132858	0.0075	0.0049	0.003	0.00231622
		Yes	A	BUR	0.0058171	0.0046	0.0026	0.0013	0.00084239
				EPDM	0.00614151	0.0048	0.0028	0.0015	0.00100789
			B	BUR	0.00618947	0.0048	0.0027	0.0014	0.000882337
				EPDM	0.00649656	0.005	0.0029	0.0016	0.0010585
			C	BUR	0.00688699	0.0053	0.0031	0.0016	0.00101328
				EPDM	0.00712358	0.0056	0.0033	0.0018	0.00118032
			D	BUR	0.00353043	0.0016	0.0009	0.0005	0.000436917
				EPDM	0.00402126	0.002	0.0012	0.0008	0.000607504
Unmitigated	100%	No	A	BUR	0.0186454	0.017	0.0117	0.0075	0.00560366
				EPDM	0.0189061	0.0173	0.0118	0.0077	0.00572873
			B	BUR	0.0175352	0.0141	0.0094	0.006	0.00440256
				EPDM	0.0177178	0.0142	0.0096	0.0061	0.00453788
			C	BUR	0.0162569	0.0117	0.0078	0.0048	0.00355456
				EPDM	0.0164464	0.0119	0.008	0.005	0.00368156
			D	BUR	0.015126	0.0088	0.0057	0.0036	0.00269041
				EPDM	0.0153974	0.0089	0.0058	0.0037	0.00282641
		Yes	A	BUR	0.0078471	0.0069	0.0044	0.0027	0.00191711
				EPDM	0.00817198	0.0071	0.0046	0.0028	0.00212245
			B	BUR	0.00829595	0.0071	0.0045	0.0027	0.00201724
				EPDM	0.00866115	0.0073	0.0047	0.0029	0.00216287
			C	BUR	0.00905946	0.0076	0.0049	0.003	0.00220119
				EPDM	0.00946218	0.008	0.0052	0.0032	0.00235777
			D	BUR	0.00520082	0.0028	0.0019	0.0013	0.0010576
				EPDM	0.00557894	0.0032	0.0021	0.0015	0.00120993
	50%	No	A	BUR	0.0196448	0.0176	0.0121	0.0079	0.00599484
				EPDM	0.0198956	0.0178	0.0123	0.0081	0.0060946
			B	BUR	0.0185656	0.0147	0.01	0.0064	0.00482461
				EPDM	0.0188125	0.0148	0.0102	0.0066	0.00493734
			C	BUR	0.0173331	0.0124	0.0083	0.0053	0.00392356
				EPDM	0.0174931	0.0126	0.0085	0.0055	0.00411666
			D	BUR	0.0161729	0.0094	0.0062	0.004	0.00298592
				EPDM	0.0163093	0.0095	0.0064	0.0041	0.0031409
		Yes	A	BUR	0.0086381	0.0079	0.0052	0.0033	0.00246454
				EPDM	0.00896467	0.0081	0.0054	0.0034	0.00262124
			B	BUR	0.00922386	0.0082	0.0054	0.0034	0.00249998
				EPDM	0.0095478	0.0085	0.0056	0.0036	0.00269934
			C	BUR	0.00998869	0.0088	0.0059	0.0037	0.00275135
				EPDM	0.0103371	0.0091	0.0062	0.0039	0.00290421
			D	BUR	0.00582516	0.0035	0.0023	0.0017	0.00133032
				EPDM	0.00624872	0.0038	0.0027	0.0019	0.00152174

Table 7.88. Average Annual Content Loss Normalized by Building Value – Fire Station

Deck Mitigation	Metal Panel Capacity	Shutters	Missile Environment	Roof Cover	Terrain Surface Roughness (m)				
					0.03	0.15	0.35	0.7	1
Mitigated	100%	No	A	BUR	0.00224182	0.002	0.0013	0.0008	0.000550166
				EPDM	0.00224161	0.002	0.0013	0.0008	0.000551257
			B	BUR	0.00208206	0.0016	0.001	0.0006	0.000385321
				EPDM	0.00208622	0.0016	0.001	0.0006	0.000387979
			C	BUR	0.00192673	0.0013	0.0008	0.0004	0.000276155
				EPDM	0.00192036	0.0013	0.0008	0.0004	0.000278679
			D	BUR	0.00183093	0.001	0.0006	0.0003	0.000241618
				EPDM	0.00184559	0.001	0.0006	0.0003	0.000242256
		Yes	A	BUR	0.000776966	0.0005	0.0002	0.0001	6.16355E-05
				EPDM	0.000783322	0.0005	0.0003	0.0001	6.43548E-05
			B	BUR	0.000810438	0.0005	0.0003	0.0001	6.07006E-05
				EPDM	0.000819764	0.0005	0.0002	0.0001	0.000065002
			C	BUR	0.00090126	0.0005	0.0003	0.0001	6.87746E-05
				EPDM	0.000896067	0.0005	0.0003	0.0001	7.01283E-05
			D	BUR	0.000473223	0.0002	9E-05	5E-05	3.47829E-05
				EPDM	0.000494645	0.0002	0.0001	6E-05	3.98822E-05
Unmitigated	100%	No	A	BUR	0.00233101	0.0021	0.0014	0.0008	0.000597136
				EPDM	0.00234296	0.0021	0.0014	0.0009	0.000605749
			B	BUR	0.00219496	0.0017	0.0011	0.0006	0.000443957
				EPDM	0.00220897	0.0017	0.0011	0.0006	0.000452487
			C	BUR	0.00206054	0.0013	0.0008	0.0005	0.000335528
				EPDM	0.00206876	0.0013	0.0009	0.0005	0.000343285
			D	BUR	0.0019977	0.0011	0.0007	0.0004	0.000282987
				EPDM	0.00202679	0.0011	0.0007	0.0004	0.000292863
		Yes	A	BUR	0.00102643	0.0008	0.0005	0.0003	0.000204343
				EPDM	0.00103759	0.0008	0.0005	0.0003	0.000220719
			B	BUR	0.00107516	0.0008	0.0005	0.0003	0.000209311
				EPDM	0.00109746	0.0008	0.0005	0.0003	0.000218945
			C	BUR	0.001167	0.0008	0.0005	0.0003	0.000222775
				EPDM	0.00119728	0.0009	0.0005	0.0003	0.000233642
			D	BUR	0.000680382	0.0003	0.0002	0.0001	0.000112458
				EPDM	0.000683975	0.0003	0.0002	0.0001	0.000112029
	50%	No	A	BUR	0.00242752	0.0021	0.0014	0.0009	0.000644602
				EPDM	0.00244479	0.0022	0.0014	0.0009	0.000649468
			B	BUR	0.00231344	0.0017	0.0011	0.0007	0.00048962
				EPDM	0.00234325	0.0017	0.0011	0.0007	0.000500986
			C	BUR	0.00219369	0.0014	0.0009	0.0005	0.00038588
				EPDM	0.00221521	0.0014	0.0009	0.0006	0.000404633
			D	BUR	0.00214237	0.0012	0.0008	0.0005	0.000324414
				EPDM	0.00215858	0.0012	0.0008	0.0005	0.000343789
		Yes	A	BUR	0.00115087	0.001	0.0006	0.0004	0.000287002
				EPDM	0.00116468	0.001	0.0006	0.0004	0.000299728
			B	BUR	0.00121833	0.001	0.0006	0.0004	0.000286715
				EPDM	0.00124155	0.001	0.0007	0.0004	0.00030336
			C	BUR	0.00131724	0.001	0.0007	0.0004	0.000311409
				EPDM	0.0013402	0.0011	0.0007	0.0004	0.000323366
			D	BUR	0.000761914	0.0004	0.0003	0.0002	0.000149517
				EPDM	0.000777079	0.0004	0.0003	0.0002	0.00015539

Table 7.89. Percent Increases in the Average Annual Total Loss due to Changes in Building Parameters (Minimum/Average/Maximum) – Fire Station

Building Parameter	Min	Avg	Max
Built-up to Single ply Membrane Roof Cover	0%	6%	42%
Missile Environment D to C	6%	79%	235%
Missile Environment C to B	-9%	13%	32%
Missile Environment B to A	-6%	9%	35%
Mitigated Deck to Unmitigated Deck	5%	46%	148%
0% to 50% Reduction in Metal Roof Deck Resistance	3%	14%	31%
Shutters Vs. No shutters	37%	161%	512%

7.15.2 Loss Model Results for Elementary Schools

The average annual building and content losses (both normalized by the total building value) for all elementary schools examined are presented in Table 7.90~~Table 7.90~~ and Table 7.91~~Table 7.91~~. The average annual loss is obtained by summing all losses produced during the 20,000-year hurricane simulation period and then dividing by 20,000 years. The contents limit for elementary schools has been assumed to be 15% of the building value. The values given in Table 7.90~~Table 7.90~~ and Table 7.91~~Table 7.91~~ reflect the average annual losses for elementary schools located in the South Florida area.

Table 7.92~~Table 7.92~~ shows the building parameter sensitivity results. Missile environment has a large impact on the overall loss, in particular increasing the mean per storm loss by 107% on average when the missile environment changes from no windborne debris (Missile Environment D) to a residential type environment (Missile Environment C).

The use of EPDM roof cover versus BUR roof cover increases the overall storm average loss by 6% on average, while a reduction in metal deck resistance of 50% increases losses by 46%.

Mitigation techniques such as shutters have a great effect in reducing damage in this analysis since window breakage and metal deck failure are the primary drivers of damage. Losses increases by 161% on average when shutters are not considered, and increase by 46% when the deck is no longer mitigated.

Table 7.90. Average Annual Building Loss Normalized by Building Value – Elementary School

Deck Mitigation	Metal Panel Capacity	Shutters	Missile Environment	Roof Cover	Terrain Surface Roughness (m)				
					0.03	0.15	0.35	0.7	1
Mitigated	100%	No	A	BUR	0.0170514	0.0161	0.0109	0.0069	0.00498669
				EPDM	0.0171972	0.0162	0.011	0.0069	0.00507478
			B	BUR	0.0157124	0.013	0.0086	0.0052	0.00371321
				EPDM	0.0158897	0.0131	0.0087	0.0053	0.00382683
			C	BUR	0.0143621	0.0107	0.0068	0.004	0.00282638
				EPDM	0.0144833	0.0108	0.0069	0.0042	0.00296841
			D	BUR	0.0130329	0.0074	0.0047	0.0029	0.00220463
				EPDM	0.0132858	0.0075	0.0049	0.003	0.00231622
		Yes	A	BUR	0.0058171	0.0046	0.0026	0.0013	0.00084239
				EPDM	0.00614151	0.0048	0.0028	0.0015	0.00100789
			B	BUR	0.00618947	0.0048	0.0027	0.0014	0.000882337
				EPDM	0.00649656	0.005	0.0029	0.0016	0.0010585
			C	BUR	0.00688699	0.0053	0.0031	0.0016	0.00101328
				EPDM	0.00712358	0.0056	0.0033	0.0018	0.00118032
			D	BUR	0.00353043	0.0016	0.0009	0.0005	0.000436917
				EPDM	0.00402126	0.002	0.0012	0.0008	0.000607504
Unmitigated	100%	No	A	BUR	0.0186454	0.017	0.0117	0.0075	0.00560366
				EPDM	0.0189061	0.0173	0.0118	0.0077	0.00572873
			B	BUR	0.0175352	0.0141	0.0094	0.006	0.00440256
				EPDM	0.0177178	0.0142	0.0096	0.0061	0.00453788
			C	BUR	0.0162569	0.0117	0.0078	0.0048	0.00355456
				EPDM	0.0164464	0.0119	0.008	0.005	0.00368156
			D	BUR	0.015126	0.0088	0.0057	0.0036	0.00269041
				EPDM	0.0153974	0.0089	0.0058	0.0037	0.00282641
		Yes	A	BUR	0.0078471	0.0069	0.0044	0.0027	0.00191711
				EPDM	0.00817198	0.0071	0.0046	0.0028	0.00212245
			B	BUR	0.00829595	0.0071	0.0045	0.0027	0.00201724
				EPDM	0.00866115	0.0073	0.0047	0.0029	0.00216287
			C	BUR	0.00905946	0.0076	0.0049	0.003	0.00220119
				EPDM	0.00946218	0.008	0.0052	0.0032	0.00235777
			D	BUR	0.00520082	0.0028	0.0019	0.0013	0.0010576
				EPDM	0.00557894	0.0032	0.0021	0.0015	0.00120993
	50%	No	A	BUR	0.0196448	0.0176	0.0121	0.0079	0.00599484
				EPDM	0.0198956	0.0178	0.0123	0.0081	0.0060946
			B	BUR	0.0185656	0.0147	0.01	0.0064	0.00482461
				EPDM	0.0188125	0.0148	0.0102	0.0066	0.00493734
			C	BUR	0.0173331	0.0124	0.0083	0.0053	0.00392356
				EPDM	0.0174931	0.0126	0.0085	0.0055	0.00411666
			D	BUR	0.0161729	0.0094	0.0062	0.004	0.00298592
				EPDM	0.0163093	0.0095	0.0064	0.0041	0.0031409
		Yes	A	BUR	0.0086381	0.0079	0.0052	0.0033	0.00246454
				EPDM	0.00896467	0.0081	0.0054	0.0034	0.00262124
			B	BUR	0.00922386	0.0082	0.0054	0.0034	0.00249998
				EPDM	0.0095478	0.0085	0.0056	0.0036	0.00269934
			C	BUR	0.00998869	0.0088	0.0059	0.0037	0.00275135
				EPDM	0.0103371	0.0091	0.0062	0.0039	0.00290421
			D	BUR	0.00582516	0.0035	0.0023	0.0017	0.00133032
				EPDM	0.00624872	0.0038	0.0027	0.0019	0.00152174

Table 7.91. Average Annual Content Loss Normalized by Building Value – Elementary School

Deck Mitigation	Metal Panel Capacity	Shutters	Missile Environment	Roof Cover	Terrain Surface Roughness (m)				
					0.03	0.15	0.35	0.7	1
Mitigated	100%	No	A	BUR	0.00224182	0.002	0.0013	0.0008	0.000550166
				EPDM	0.00224161	0.002	0.0013	0.0008	0.000551257
			B	BUR	0.00208206	0.0016	0.001	0.0006	0.000385321
				EPDM	0.00208622	0.0016	0.001	0.0006	0.000387979
			C	BUR	0.00192673	0.0013	0.0008	0.0004	0.000276155
				EPDM	0.00192036	0.0013	0.0008	0.0004	0.000278679
			D	BUR	0.00183093	0.001	0.0006	0.0003	0.000241618
				EPDM	0.00184559	0.001	0.0006	0.0003	0.000242256
		Yes	A	BUR	0.000776966	0.0005	0.0002	0.0001	6.16355E-05
				EPDM	0.000783322	0.0005	0.0003	0.0001	6.43548E-05
			B	BUR	0.000810438	0.0005	0.0003	0.0001	6.07006E-05
				EPDM	0.000819764	0.0005	0.0002	0.0001	0.000065002
			C	BUR	0.00090126	0.0005	0.0003	0.0001	6.87746E-05
				EPDM	0.000896067	0.0005	0.0003	0.0001	7.01283E-05
			D	BUR	0.000473223	0.0002	9E-05	5E-05	3.47829E-05
				EPDM	0.000494645	0.0002	0.0001	6E-05	3.98822E-05
Unmitigated	100%	No	A	BUR	0.00233101	0.0021	0.0014	0.0008	0.000597136
				EPDM	0.00234296	0.0021	0.0014	0.0009	0.000605749
			B	BUR	0.00219496	0.0017	0.0011	0.0006	0.000443957
				EPDM	0.00220897	0.0017	0.0011	0.0006	0.000452487
			C	BUR	0.00206054	0.0013	0.0008	0.0005	0.000335528
				EPDM	0.00206876	0.0013	0.0009	0.0005	0.000343285
			D	BUR	0.0019977	0.0011	0.0007	0.0004	0.000282987
				EPDM	0.00202679	0.0011	0.0007	0.0004	0.000292863
		Yes	A	BUR	0.00102643	0.0008	0.0005	0.0003	0.000204343
				EPDM	0.00103759	0.0008	0.0005	0.0003	0.000220719
			B	BUR	0.00107516	0.0008	0.0005	0.0003	0.000209311
				EPDM	0.00109746	0.0008	0.0005	0.0003	0.000218945
			C	BUR	0.001167	0.0008	0.0005	0.0003	0.000222775
				EPDM	0.00119728	0.0009	0.0005	0.0003	0.000233642
			D	BUR	0.000680382	0.0003	0.0002	0.0001	0.000112458
				EPDM	0.000683975	0.0003	0.0002	0.0001	0.000112029
	50%	No	A	BUR	0.00242752	0.0021	0.0014	0.0009	0.000644602
				EPDM	0.00244479	0.0022	0.0014	0.0009	0.000649468
			B	BUR	0.00231344	0.0017	0.0011	0.0007	0.00048962
				EPDM	0.00234325	0.0017	0.0011	0.0007	0.000500986
			C	BUR	0.00219369	0.0014	0.0009	0.0005	0.00038588
				EPDM	0.00221521	0.0014	0.0009	0.0006	0.000404633
			D	BUR	0.00214237	0.0012	0.0008	0.0005	0.000324414
				EPDM	0.00215858	0.0012	0.0008	0.0005	0.000343789
		Yes	A	BUR	0.00115087	0.001	0.0006	0.0004	0.000287002
				EPDM	0.00116468	0.001	0.0006	0.0004	0.000299728
			B	BUR	0.00121833	0.001	0.0006	0.0004	0.000286715
				EPDM	0.00124155	0.001	0.0007	0.0004	0.00030336
			C	BUR	0.00131724	0.001	0.0007	0.0004	0.000311409
				EPDM	0.0013402	0.0011	0.0007	0.0004	0.000323366
			D	BUR	0.000761914	0.0004	0.0003	0.0002	0.000149517
				EPDM	0.000777079	0.0004	0.0003	0.0002	0.00015539

Table 7.92. Percent Increases in the Average Annual Total Loss due to Changes in Building Parameters (Minimum/Average/Maximum) – Elementary School

Building Parameter	Min	Avg	Max
Built-up to Single ply Membrane Roof Cover	0%	6%	42%
Missile Environment D to C	6%	79%	235%
Missile Environment C to B	-14%	6%	32%
Missile Environment B to A	-6%	9%	35%
Mitigated Deck to Unmitigated Deck	5%	46%	148%
0% to 50% Reduction in Metal Roof Deck Resistance	3%	14%	31%
Shutters Vs. No shutters	37%	161%	512%

7.15.3 Loss Model Results for High Schools

The average annual building and content losses (both normalized by the total building value) for all high schools examined are presented in Table 7.93~~Table 7.93~~ through Table 7.96~~Table 7.96~~. The average annual loss is obtained by summing all losses produced during the 20,000-year hurricane simulation period and then dividing by 20,000 years. The contents limit for elementary schools has been assumed to be 15% of the building value.The values given in Table 7.93~~Table 7.93~~ and Table 7.96~~Table 7.96~~ reflect the average annual losses for elementary schools located in the South Florida area.

The building parameter sensitivity results for high schools are shown in

Table 7.97

~~Table 7.97~~. Changing the missile environments between no windborne debris (Missile Environment D) to a mixed residential/commercial type environment (Missile Environment A) increases losses 85% on average for the two-story case, increases losses 43% for the three-story case, and increases losses 64% overall. This trend results from the fact that the modeled average heights of the buildings from which the commercial and residential type missiles originate are lower than the three-story buildings. Thus, the glazing on the upper floors of the three-story buildings are less susceptible to missile damage than the glazing on the lower floors.

The use of EPDM roof cover versus BUR roof cover increases losses by 15%-16% on average for both the two- and three-story case.

Mitigation techniques such as shutters have a great effect in reducing damage in this analysis since window breakage and metal deck failure are the primary drivers of damage. Losses increase by 72% on average for the two-story case, 46% for the three-story case, and 59% overall when shutters are not in place. The mitigated deck to unmitigated deck increases losses by 103% and 115% for the two- and three- story case respectively and 109% overall. The three-story case is more influenced by roof damage compared to fenestration damage.

Over all, increasing story height from two to three increases average loss by 51% on average.

Table 7.93. Average Annual Building Loss Normalized by Building Value – High School

Deck Mitigation	Shutters	Missile Environment	Roof Cover	Terrain Surface Roughness (m)				
				0.03	0.15	0.35	0.7	1
Mitigated	No	A	BUR	0.007917	0.009315	0.00636	0.004164	0.00318
			EPDM	0.008661	0.009845	0.006868	0.004675	0.003627
		B	BUR	0.007164	0.007534	0.005136	0.003371	0.002543
			EPDM	0.007896	0.008181	0.005675	0.003822	0.002996
		C	BUR	0.006441	0.006212	0.004154	0.00268	0.00203
			EPDM	0.0072	0.006822	0.004729	0.003178	0.002505
		D	BUR	0.005388	0.0032	0.002207	0.001521	0.001283
			EPDM	0.006173	0.003887	0.002814	0.002058	0.001781
	Yes	A	BUR	0.003488	0.00326	0.002206	0.00149	0.001208
			EPDM	0.004355	0.003955	0.002817	0.002047	0.001704
		B	BUR	0.003586	0.003431	0.002327	0.001587	0.001293
			EPDM	0.004485	0.004136	0.002966	0.002124	0.001774
		C	BUR	0.003933	0.003816	0.002568	0.001733	0.001365
			EPDM	0.004808	0.004547	0.003193	0.002268	0.00184
		D	BUR	0.002402	0.001714	0.001337	0.001057	0.00094
			EPDM	0.00332	0.002452	0.001986	0.001606	0.001438
Unmitigat	No	A	BUR	0.013811	0.013412	0.009823	0.007055	0.005762
			EPDM	0.014469	0.013939	0.010313	0.007506	0.006132
		B	BUR	0.012246	0.011605	0.008456	0.006061	0.004951
			EPDM	0.012826	0.012117	0.008965	0.006511	0.005342
		C	BUR	0.011024	0.010358	0.007491	0.005318	0.00436
			EPDM	0.011642	0.010838	0.007962	0.005803	0.004742
		D	BUR	0.008293	0.005547	0.004208	0.003216	0.002815
			EPDM	0.008865	0.006122	0.004711	0.003646	0.003248
	Yes	A	BUR	0.007184	0.006981	0.005056	0.003722	0.003097
			EPDM	0.007868	0.007444	0.005534	0.00416	0.003495
		B	BUR	0.007475	0.007216	0.00521	0.00385	0.00321
			EPDM	0.008116	0.007742	0.005711	0.004291	0.003559
		C	BUR	0.008022	0.007862	0.005702	0.004135	0.003415
			EPDM	0.00874	0.008361	0.006195	0.004558	0.003812
		D	BUR	0.00567	0.004282	0.00352	0.002836	0.002534
			EPDM	0.006341	0.004884	0.004027	0.003349	0.002988

Table 7.94. Average Annual Content Loss Normalized by Building Value – High School

Deck Mitigation	Shutters	Missile Environment	Roof Cover	Terrain Surface Roughness (m)				
				0.03	0.15	0.35	0.7	1
Mitigated	No	A	BUR	0.000815	0.000954	0.000602	0.000356	0.000252
			EPDM	0.000822	0.000955	0.00061	0.000368	0.000262
		B	BUR	0.000727	0.000699	0.000434	0.000252	0.000173
			EPDM	0.00074	0.000712	0.000439	0.000257	0.000185
		C	BUR	0.000633	0.000514	0.0003	0.000165	0.000112
			EPDM	0.000644	0.000523	0.000314	0.000178	0.000124
		D	BUR	0.000572	0.000277	0.00016	8.9E-05	6.74E-05
			EPDM	0.000596	0.000299	0.000181	0.000109	8.5E-05
	Yes	A	BUR	0.000272	0.000206	0.00012	6.78E-05	4.85E-05
			EPDM	0.000302	0.000223	0.000137	8.68E-05	6.61E-05
		B	BUR	0.000275	0.000206	0.000122	6.97E-05	5.16E-05
			EPDM	0.000311	0.00023	0.000141	8.61E-05	6.8E-05
		C	BUR	0.000315	0.000231	0.000133	7.64E-05	5.35E-05
			EPDM	0.000344	0.000256	0.000153	9.55E-05	7.08E-05
		D	BUR	0.000133	7.52E-05	5.18E-05	3.67E-05	3.12E-05
			EPDM	0.000174	0.000105	7.88E-05	5.74E-05	4.96E-05
Unmitigat	No	A	BUR	0.001732	0.001568	0.001138	0.00081	0.000659
			EPDM	0.001784	0.001612	0.001171	0.000842	0.000679
		B	BUR	0.001542	0.001335	0.000961	0.000684	0.000557
			EPDM	0.001571	0.001363	0.000994	0.000712	0.000576
		C	BUR	0.001394	0.001177	0.000839	0.000592	0.000485
			EPDM	0.001416	0.001197	0.000865	0.000619	0.000499
		D	BUR	0.001076	0.00068	0.000495	0.000367	0.000318
			EPDM	0.001074	0.000689	0.000505	0.000374	0.000325
	Yes	A	BUR	0.000892	0.000837	0.000598	0.000433	0.000356
			EPDM	0.000911	0.000847	0.000614	0.000444	0.000364
		B	BUR	0.000929	0.000846	0.000606	0.000442	0.000364
			EPDM	0.000938	0.000865	0.000619	0.000453	0.000365
		C	BUR	0.001006	0.000919	0.00066	0.000476	0.000389
			EPDM	0.001031	0.00094	0.00068	0.000488	0.000399
		D	BUR	0.000666	0.000491	0.000397	0.000316	0.000279
			EPDM	0.000668	0.000501	0.000404	0.000332	0.000288

Table 7.95. Average Annual Building Loss Normalized by Building Value – Large High School

Deck Mitigation	Shutters	Missile Environment	Roof Cover	Terrain Surface Roughness (m)				
				0.03	0.15	0.35	0.7	1
Mitigated	No	A	BUR	0.008659	0.009232	0.006765	0.004915	0.003978
			EPDM	0.009693	0.010108	0.007565	0.005622	0.004655
		B	BUR	0.008291	0.008204	0.006057	0.004417	0.003598
			EPDM	0.009317	0.009074	0.006851	0.005141	0.004306
		C	BUR	0.007767	0.007324	0.005405	0.003899	0.003225
			EPDM	0.008795	0.008187	0.006204	0.004685	0.003941
		D	BUR	0.006799	0.004766	0.003675	0.002866	0.002484
			EPDM	0.007869	0.005735	0.004549	0.003661	0.003221
	Yes	A	BUR	0.004743	0.004557	0.003445	0.002607	0.002276
			EPDM	0.0059	0.005502	0.004314	0.003415	0.003007
		B	BUR	0.004759	0.00464	0.003557	0.002715	0.002307
			EPDM	0.00596	0.005658	0.004407	0.003471	0.003052
		C	BUR	0.005137	0.005085	0.003803	0.00286	0.002439
			EPDM	0.006251	0.006039	0.004683	0.003658	0.003192
		D	BUR	0.003899	0.003008	0.002482	0.002109	0.00189
			EPDM	0.005062	0.004017	0.003391	0.002914	0.002639
Unmitigat	No	A	BUR	0.017396	0.016201	0.012812	0.009968	0.008542
			EPDM	0.018491	0.017029	0.013614	0.010723	0.009206
		B	BUR	0.015419	0.014683	0.011586	0.008945	0.007695
			EPDM	0.016475	0.015618	0.012306	0.009684	0.008441
		C	BUR	0.014289	0.013775	0.010752	0.008349	0.007152
			EPDM	0.015338	0.014676	0.011507	0.009066	0.007916
		D	BUR	0.011387	0.008592	0.007173	0.005915	0.005288
			EPDM	0.012277	0.00948	0.007934	0.006706	0.005988
	Yes	A	BUR	0.010261	0.010008	0.007947	0.006411	0.005623
			EPDM	0.011381	0.010848	0.008724	0.0071	0.0063
		B	BUR	0.010573	0.010408	0.008198	0.006543	0.005789
			EPDM	0.011632	0.011226	0.008999	0.007317	0.006454
		C	BUR	0.01099	0.011019	0.008616	0.00689	0.005959
			EPDM	0.012065	0.011929	0.009449	0.007546	0.006614
		D	BUR	0.009048	0.007326	0.006351	0.00541	0.004905
			EPDM	0.010065	0.00826	0.00716	0.006197	0.005631

Table 7.96. Average Annual Content Loss Normalized by Building Value – Large High School

Deck Mitigation	Shutters	Missile Environment	Roof Cover	Terrain Surface Roughness (m)				
				0.03	0.15	0.35	0.7	1
Mitigated	No	A	BUR	0.000818	0.000883	0.000596	0.000389	0.000291
			EPDM	0.000835	0.000901	0.000616	0.000402	0.000301
		B	BUR	0.000766	0.000714	0.000479	0.000313	0.000232
			EPDM	0.000791	0.000731	0.000498	0.000327	0.000251
		C	BUR	0.000699	0.000582	0.000386	0.000239	0.000182
			EPDM	0.000723	0.000599	0.000402	0.000264	0.000202
		D	BUR	0.000643	0.000387	0.000266	0.00018	0.000143
			EPDM	0.000677	0.000419	0.000296	0.000207	0.000169
	Yes	A	BUR	0.000321	0.000265	0.000178	0.000122	0.000101
			EPDM	0.000363	0.000291	0.000206	0.000151	0.000128
		B	BUR	0.000315	0.00026	0.000181	0.000125	0.000101
			EPDM	0.000359	0.000292	0.000206	0.000151	0.000126
		C	BUR	0.000352	0.000293	0.000196	0.000134	0.000109
			EPDM	0.000388	0.000321	0.000225	0.000161	0.000135
		D	BUR	0.000231	0.000148	0.00011	8.77E-05	7.37E-05
			EPDM	0.000276	0.000186	0.000144	0.000118	0.000102
Unmitigat	No	A	BUR	0.002201	0.001958	0.001552	0.001209	0.001036
			EPDM	0.002302	0.00203	0.001615	0.001264	0.001077
		B	BUR	0.00193	0.001739	0.001373	0.001062	0.000912
			EPDM	0.002	0.001811	0.001418	0.001103	0.000955
		C	BUR	0.001789	0.001625	0.001267	0.000986	0.00084
			EPDM	0.001846	0.001686	0.001309	0.001015	0.000881
		D	BUR	0.00145	0.001058	0.000863	0.000697	0.000614
			EPDM	0.001451	0.001068	0.000864	0.000713	0.000625
	Yes	A	BUR	0.001241	0.001219	0.000957	0.000764	0.00066
			EPDM	0.001277	0.001245	0.000975	0.000774	0.000671
		B	BUR	0.001292	0.001264	0.000988	0.000777	0.00068
			EPDM	0.00132	0.001291	0.001012	0.000801	0.000693
		C	BUR	0.001348	0.001334	0.001034	0.000821	0.000703
			EPDM	0.001382	0.001378	0.001069	0.00083	0.000715
		D	BUR	0.001062	0.00085	0.00073	0.000615	0.000553
			EPDM	0.001069	0.000862	0.000736	0.000626	0.000567

Table 7.97. Percent Increases in the Average Annual Total Loss due to Changes in Building Parameters (Minimum/Average/Maximum) – High Schools

Building Parameter	Number of Stories								
	All			Two			Three		
	Min	Avg	Max	Min	Avg	Max	Min	Avg	Max
Built-up to Single ply Membrane Roof	0%	16%	35%	0%	16%	35%	1%	15%	24%
Missile Environment D to C	1%	50%	134%	3%	65%	134%	1%	35%	36%
Missile Environment C to B	-7%	3%	40%	-7%	5%	40%	-2%	2%	13%
Missile Environment B to A	-3%	6%	24%	-3%	7%	24%	-2%	4%	14%
Mitigated Deck to Unmitigated Deck	13%	109%	176%	13%	103%	176%	27%	115%	98%
Shutters Vs. No shutters	0%	59%	227%	1%	72%	227%	0%	46%	72%
Two to Three Stories	-2%	51%	102%	NA					

7.15.4 Loss Model Results for Hospitals

The average annual building and content losses (both normalized by the total building value) for all hospitals examined are presented in Table 7.98~~Table 7.98~~ through Table 103. The average annual loss is obtained by summing all losses produced during the 20,000-year hurricane simulation period and then dividing by 20,000 years. The contents limit for hospitals has been assumed to be 50% of the building value.The values given in Table 7.98~~Table 7.98~~ and Table 7.103 reflect the average annual losses for hospitals located in the South Florida area.

Table 7.104~~Table 7.104~~ displays the building parameter sensitivity results for hospital buildings. Changing the missile environments between no windborne debris (Missile Environment D) to a mixed residential/commercial type environment (Missile Environment A) increases losses 205%, 31%, and 3% on average for the one-, four- and eight-story case respectively and 80% overall. This trend results from the fact that the modeled average heights of the buildings from which the commercial and residential type missiles originate are lower than the four- and eight-story buildings. Thus, the glazing on the upper floors of the four- and eight-story buildings are less susceptible to missile damage than the glazing on the lower floors.

The use of EPDM roof cover versus BUR roof cover increases the overall losses between 9%, 11%, and 24% for the one-, four-, and eight-story buildings respectively and 15% on average for all cases.

Mitigation techniques such as shutters have a great effect in reducing damage in this analysis since window breakage and metal deck failure are the primary drivers of damage. Losses increase by 27% on average for the eight-story case, 45% for the two-story case, 99% for the one-story case and 57% overall when shutters are not in place. The mitigated to unmitigated deck scenario increases losses between 114% and 202%, and 149% overall. The taller cases are more influenced by roof damage compared to fenestration damage.

Over all, losses are most sensitive to story height. Increasing story height from one to four increases losses by 369% and increase by 81% when story height is changed from four to eight.

Table 7.98. Average Annual Building Loss Normalized by Building Value – Small Hospital

Deck Mitigation	Shutters	Missile Environment	Roof Cover	Terrain Surface Roughness (m)				
				0.03	0.15	0.35	0.7	1
Mitigated	No	A	BUR	0.005489	0.007745	0.004785	0.002699	0.001814
			EPDM	0.006056	0.008116	0.005071	0.002924	0.002015
		B	BUR	0.00422	0.005699	0.003376	0.001849	0.001239
			EPDM	0.004856	0.006087	0.003674	0.002103	0.001437
		C	BUR	0.00337	0.004361	0.002534	0.001339	0.000903
			EPDM	0.003968	0.004756	0.002855	0.001602	0.001128
		D	BUR	0.002155	0.000887	0.000488	0.000288	0.000238
			EPDM	0.002834	0.001409	0.000881	0.000567	0.000485
	Yes	A	BUR	0.001578	0.001739	0.001009	0.000566	0.000407
			EPDM	0.002317	0.002228	0.001386	0.000842	0.000646
		B	BUR	0.001737	0.002071	0.001212	0.000681	0.000478
			EPDM	0.002501	0.002603	0.001591	0.000966	0.00072
		C	BUR	0.001913	0.002447	0.001456	0.000817	0.000593
			EPDM	0.002652	0.00292	0.001819	0.001098	0.00083
		D	BUR	0.001085	0.000604	0.000406	0.000255	0.000226
			EPDM	0.001862	0.001149	0.000794	0.000538	0.000473
Unmitigat	No	A	BUR	0.011631	0.010652	0.006912	0.004214	0.00302
			EPDM	0.01211	0.010925	0.007209	0.004421	0.003286
		B	BUR	0.010479	0.009081	0.005808	0.003526	0.002571
			EPDM	0.010912	0.009447	0.006119	0.003774	0.00281
		C	BUR	0.009514	0.007974	0.005153	0.00307	0.00228
			EPDM	0.009799	0.00832	0.005445	0.003373	0.002476
		D	BUR	0.004439	0.002408	0.001544	0.001055	0.000833
			EPDM	0.004951	0.002849	0.001889	0.001291	0.001064
	Yes	A	BUR	0.005518	0.005635	0.003486	0.002082	0.001488
			EPDM	0.005956	0.005999	0.003796	0.002291	0.001721
		B	BUR	0.006148	0.006007	0.003754	0.002239	0.001616
			EPDM	0.006495	0.006343	0.004045	0.002448	0.001829
		C	BUR	0.006683	0.006578	0.004179	0.002474	0.001779
			EPDM	0.007175	0.006961	0.004434	0.00269	0.002011
		D	BUR	0.003603	0.002213	0.001473	0.00103	0.000816
			EPDM	0.004193	0.002672	0.001826	0.001269	0.001052

Table 7.99. Average Annual Content Loss Normalized by Building Value – Small Hospital

Deck Mitigation	Shutters	Missile Environment	Roof Cover	Terrain Surface Roughness (m)				
				0.03	0.15	0.35	0.7	1
Mitigated	No	A	BUR	0.001642	0.002273	0.00132	0.000708	0.000455
			EPDM	0.001658	0.002288	0.001337	0.000713	0.000459
		B	BUR	0.001189	0.001465	0.000803	0.000402	0.000251
			EPDM	0.001233	0.00148	0.000812	0.000411	0.00026
		C	BUR	0.000872	0.000935	0.000472	0.000209	0.000123
			EPDM	0.0009	0.000949	0.000484	0.000223	0.000138
		D	BUR	0.000633	0.000167	6.57E-05	2.89E-05	2.16E-05
			EPDM	0.000709	0.000227	0.000111	6.08E-05	4.94E-05
	Yes	A	BUR	0.000291	0.000224	0.000101	4.41E-05	2.62E-05
			EPDM	0.000376	0.000269	0.000137	7.08E-05	5.15E-05
		B	BUR	0.000328	0.000255	0.000122	4.79E-05	2.76E-05
			EPDM	0.000418	0.000308	0.000151	7.64E-05	5.31E-05
		C	BUR	0.000369	0.000307	0.000146	5.84E-05	3.63E-05
			EPDM	0.000445	0.000341	0.000174	8.57E-05	5.97E-05
		D	BUR	0.000137	6.22E-05	3.88E-05	2.12E-05	1.87E-05
			EPDM	0.000233	0.000129	8.55E-05	5.46E-05	4.72E-05
Unmitigat	No	A	BUR	0.005076	0.003844	0.002399	0.001402	0.000983
			EPDM	0.005296	0.00395	0.002504	0.001468	0.001076
		B	BUR	0.004738	0.003325	0.002038	0.001214	0.000866
			EPDM	0.004899	0.003476	0.002178	0.001292	0.000952
		C	BUR	0.004429	0.002931	0.001837	0.001057	0.000784
			EPDM	0.004501	0.00308	0.001933	0.001157	0.000838
		D	BUR	0.001989	0.000986	0.000595	0.000392	0.000304
			EPDM	0.002029	0.001027	0.000627	0.00041	0.000322
	Yes	A	BUR	0.002511	0.0024	0.001436	0.000825	0.000568
			EPDM	0.00253	0.002515	0.001526	0.000865	0.000622
		B	BUR	0.002831	0.002459	0.001477	0.000849	0.000596
			EPDM	0.002833	0.002566	0.001568	0.000886	0.000638
		C	BUR	0.003086	0.002635	0.001616	0.000928	0.00064
			EPDM	0.003191	0.002777	0.001691	0.000969	0.000692
		D	BUR	0.001459	0.000859	0.000549	0.000376	0.000293
			EPDM	0.001493	0.000897	0.000579	0.000392	0.000312

Table 7.100. Average Annual Building Loss Normalized by Building Value – Medium Hospital

Deck Mitigation	Shutters	Missile Environment	Roof Cover	Terrain Surface Roughness (m)				
				0.03	0.15	0.35	0.7	1
Mitigated	No	A	BUR	0.012282	0.012005	0.009053	0.006708	0.005592
			EPDM	0.013418	0.013003	0.010004	0.007594	0.006452
		B	BUR	0.01187	0.011078	0.008348	0.006263	0.005215
			EPDM	0.012995	0.01207	0.009308	0.007143	0.006066
		C	BUR	0.011555	0.010492	0.00797	0.005961	0.005015
			EPDM	0.012719	0.011488	0.008909	0.006856	0.005866
		D	BUR	0.010328	0.0074	0.005869	0.004591	0.004054
			EPDM	0.011479	0.008463	0.00685	0.005508	0.004929
	Yes	A	BUR	0.006497	0.006615	0.00504	0.003861	0.003283
			EPDM	0.007789	0.007718	0.00607	0.004774	0.004178
		B	BUR	0.006891	0.006929	0.005309	0.003975	0.003394
			EPDM	0.008194	0.008015	0.006289	0.004942	0.004283
		C	BUR	0.007256	0.007485	0.005606	0.004209	0.003581
			EPDM	0.00847	0.008544	0.006597	0.005134	0.004466
		D	BUR	0.005123	0.00399	0.003367	0.002899	0.002643
			EPDM	0.006397	0.005139	0.004412	0.003873	0.003542
Unmitigat	No	A	BUR	0.019701	0.019484	0.015451	0.012274	0.01075
			EPDM	0.02074	0.02043	0.016302	0.013186	0.011563
		B	BUR	0.019851	0.019279	0.015376	0.012314	0.010743
			EPDM	0.020837	0.020248	0.016238	0.013081	0.011524
		C	BUR	0.02003	0.019415	0.01553	0.012401	0.010883
			EPDM	0.021057	0.020406	0.016415	0.013227	0.011616
		D	BUR	0.016724	0.013295	0.011318	0.00962	0.008745
			EPDM	0.017687	0.014162	0.012203	0.010524	0.009516
	Yes	A	BUR	0.014395	0.013929	0.011406	0.009595	0.008601
			EPDM	0.015435	0.014915	0.012388	0.010433	0.0094
		B	BUR	0.01483	0.014451	0.011839	0.009735	0.008776
			EPDM	0.015898	0.015407	0.012729	0.010557	0.009698
		C	BUR	0.015122	0.015026	0.012235	0.01007	0.009015
			EPDM	0.016214	0.016083	0.013176	0.010911	0.009827
		D	BUR	0.013125	0.011096	0.009774	0.008582	0.007907
			EPDM	0.014214	0.011989	0.010689	0.009483	0.00868

Table 7.101. Average Annual Content Loss Normalized by Building Value – Medium Hospital

Deck Mitigation	Shutters	Missile Environment	Roof Cover	Terrain Surface Roughness (m)				
				0.03	0.15	0.35	0.7	1
Mitigated	No	A	BUR	0.003868	0.003483	0.002439	0.001663	0.001292
			EPDM	0.00396	0.00353	0.002512	0.001727	0.001361
		B	BUR	0.003727	0.003047	0.002147	0.00145	0.001142
			EPDM	0.003799	0.00312	0.0022	0.001516	0.001201
		C	BUR	0.003572	0.002775	0.001938	0.00133	0.001046
			EPDM	0.003655	0.002823	0.001999	0.00139	0.001105
		D	BUR	0.003306	0.00213	0.001506	0.001073	0.000861
			EPDM	0.003405	0.002222	0.001592	0.001152	0.000937
	Yes	A	BUR	0.001698	0.001575	0.001109	0.000772	0.000605
			EPDM	0.00181	0.001664	0.001196	0.000853	0.000683
		B	BUR	0.00182	0.001615	0.001133	0.000792	0.000645
			EPDM	0.001928	0.0017	0.001218	0.000877	0.000724
		C	BUR	0.001939	0.001741	0.001236	0.000858	0.000682
			EPDM	0.002045	0.001833	0.001319	0.000944	0.000758
		D	BUR	0.001188	0.000796	0.000621	0.000501	0.000428
			EPDM	0.001304	0.000896	0.000713	0.000585	0.000507
Unmitigat	No	A	BUR	0.007999	0.007553	0.005964	0.004711	0.004105
			EPDM	0.008124	0.007714	0.00607	0.004801	0.004169
		B	BUR	0.00815	0.007545	0.006008	0.004744	0.004158
			EPDM	0.008316	0.007782	0.006144	0.004872	0.004254
		C	BUR	0.0083	0.007669	0.00611	0.004902	0.004269
			EPDM	0.008459	0.007909	0.006284	0.004999	0.004366
		D	BUR	0.006875	0.005329	0.004453	0.003738	0.003371
			EPDM	0.006986	0.005408	0.004466	0.003787	0.003405
	Yes	A	BUR	0.005766	0.00556	0.00455	0.003761	0.003362
			EPDM	0.005819	0.005617	0.004588	0.00379	0.003395
		B	BUR	0.005969	0.005738	0.00469	0.003843	0.003426
			EPDM	0.006099	0.005836	0.004744	0.003874	0.00347
		C	BUR	0.006173	0.005957	0.004838	0.003912	0.003493
			EPDM	0.006227	0.00606	0.004924	0.003991	0.003508
		D	BUR	0.005202	0.004368	0.003832	0.003354	0.003088
			EPDM	0.00527	0.004429	0.003828	0.0034	0.003115

Table 7.102. Average Annual Building Loss Normalized by Building Value – Large Hospital

Deck Mitigation	Shutters	Missile Environment	Roof Cover	Terrain Surface Roughness (m)				
				0.03	0.15	0.35	0.7	1
Mitigated	No	A	BUR	0.022332	0.019812	0.016748	0.014241	0.012981
			EPDM	0.024169	0.0216	0.018501	0.015906	0.014657
		B	BUR	0.022205	0.019287	0.016396	0.014105	0.012889
			EPDM	0.02409	0.021089	0.018118	0.015773	0.014524
		C	BUR	0.02208	0.019057	0.016214	0.013983	0.012813
			EPDM	0.023926	0.020847	0.01795	0.015662	0.014445
		D	BUR	0.021943	0.018035	0.015622	0.013619	0.012553
			EPDM	0.023793	0.019823	0.017352	0.01529	0.014189
	Yes	A	BUR	0.014102	0.012927	0.011363	0.010113	0.009441
			EPDM	0.015998	0.014744	0.013119	0.011797	0.011086
		B	BUR	0.014334	0.013076	0.01152	0.01022	0.009649
			EPDM	0.016215	0.014887	0.013268	0.0119	0.011291
		C	BUR	0.014434	0.013341	0.011619	0.010304	0.00956
			EPDM	0.016317	0.015147	0.013362	0.012004	0.011199
		D	BUR	0.013608	0.01186	0.010714	0.009718	0.009187
			EPDM	0.015482	0.013661	0.01246	0.0114	0.010832
Unmitigat	No	A	BUR	0.038863	0.035836	0.032293	0.029269	0.027559
			EPDM	0.040418	0.037135	0.033538	0.030502	0.028763
		B	BUR	0.038794	0.035251	0.031859	0.028995	0.027453
			EPDM	0.040168	0.03673	0.03322	0.030301	0.028718
		C	BUR	0.038917	0.035115	0.031793	0.028938	0.027374
			EPDM	0.040088	0.036426	0.033157	0.030301	0.028576
		D	BUR	0.03859	0.034302	0.031282	0.028655	0.027184
			EPDM	0.039923	0.035412	0.032526	0.029885	0.028326
	Yes	A	BUR	0.033158	0.030753	0.028334	0.026257	0.025081
			EPDM	0.034505	0.032014	0.029635	0.027513	0.026304
		B	BUR	0.033307	0.031001	0.028578	0.026456	0.025254
			EPDM	0.03461	0.032277	0.029831	0.027673	0.026439
		C	BUR	0.033363	0.031077	0.028635	0.026383	0.025342
			EPDM	0.034751	0.032559	0.029937	0.027688	0.026515
		D	BUR	0.032678	0.029961	0.027886	0.026013	0.024897
			EPDM	0.033973	0.031112	0.029128	0.027225	0.026058

Table 7.103. Average Annual Content Loss Normalized by Building Value – Large Hospital

Deck Mitigation	Shutters	Missile Environment	Roof Cover	Terrain Surface Roughness (m)				
				0.03	0.15	0.35	0.7	1
Mitigated	No	A	BUR	0.005354	0.004487	0.00366	0.002988	0.002656
			EPDM	0.005473	0.004602	0.003771	0.003094	0.002779
		B	BUR	0.005303	0.004307	0.00354	0.002945	0.002626
			EPDM	0.005439	0.004424	0.003647	0.003051	0.00273
		C	BUR	0.00526	0.004206	0.003462	0.002891	0.00259
			EPDM	0.005381	0.004321	0.003573	0.002998	0.002694
		D	BUR	0.005287	0.004128	0.003428	0.002868	0.002578
			EPDM	0.005409	0.004243	0.003539	0.002974	0.002681
	Yes	A	BUR	0.003017	0.002569	0.002192	0.001899	0.001745
			EPDM	0.003139	0.002685	0.002303	0.002006	0.001849
		B	BUR	0.003069	0.002553	0.0022	0.001907	0.001792
			EPDM	0.00319	0.002669	0.002311	0.002014	0.001896
		C	BUR	0.003083	0.002585	0.002197	0.001913	0.001755
			EPDM	0.003204	0.0027	0.002308	0.002024	0.001858
		D	BUR	0.002914	0.002417	0.002099	0.001849	0.001717
			EPDM	0.003034	0.002532	0.00221	0.001956	0.00182
Unmitigat	No	A	BUR	0.010976	0.009903	0.00891	0.008066	0.007583
			EPDM	0.011088	0.009956	0.008949	0.008106	0.007628
		B	BUR	0.010955	0.009715	0.008772	0.007982	0.00755
			EPDM	0.011032	0.009819	0.008848	0.008048	0.007608
		C	BUR	0.010996	0.009649	0.00873	0.007941	0.007518
			EPDM	0.011002	0.009709	0.00881	0.00803	0.007557
		D	BUR	0.010958	0.009643	0.008739	0.007962	0.007532
			EPDM	0.011008	0.009635	0.008784	0.008009	0.007559
	Yes	A	BUR	0.009475	0.008597	0.007928	0.007354	0.007026
			EPDM	0.009521	0.008632	0.007985	0.007407	0.007075
		B	BUR	0.009495	0.008617	0.007962	0.007388	0.007062
			EPDM	0.009534	0.008651	0.008009	0.007429	0.007096
		C	BUR	0.009499	0.00859	0.007942	0.007346	0.00708
			EPDM	0.009562	0.008692	0.008007	0.007415	0.007108
		D	BUR	0.009374	0.008537	0.007913	0.007354	0.007023
			EPDM	0.009407	0.008536	0.007952	0.007394	0.007054

Table 7.104. Percent Increases in the Average Annual Total Loss due to Changes in Building Parameters (Minimum/Average/Maximum) – Hospitals

Building Parameter	Number of Stories											
	All			One			Four			Eight		
	Min	Avg	Max	Min	Avg	Max	Min	Avg	Max	Min	Avg	Max
Built-up to Single ply Membrane Roof	3%	15%	115%	3%	24%	115%	4%	11%	32%	3%	9%	18%
Missile Environment D to C	0%	71%	443%	37%	176%	443%	10%	32%	93%	0%	3%	12%
Missile Environment C to B	-20%	2%	45%	-20%	6%	45%	-7%	-1%	6%	-2%	0%	1%
Missile Environment B to A	-17%	3%	52%	-17%	10%	52%	-6%	0%	10%	-2%	0%	3%
Mitigated Deck to Unmitigated Deck	43%	149%	410%	43%	202%	410%	66%	132%	258%	67%	114%	171%
Shutters Vs. No shutters	2%	57%	458%	2%	99%	458%	10%	45%	116%	8%	27%	61%
One to Four stories	55%	369%	1794%	NA								
Four to Eight stories	28%	81%	199%									

Chapter 8. Building Stock Classification Methods

8.1 Introduction

In this section, two case studies are provided to demonstrate methods used to characterize the building stock in Southeast Florida. In Section 8.2, we show how aerial photography can be used to classify building geometries. In Section 8.3, we illustrate the use of a contractor survey to gather data on roof cover types.

8.2 Aerial Photography Samples

Commercial Building Stock. The classification of commercial buildings in Dade, Broward and Palm Beach counties is achieved by inspection of aerial photographs showing samples of the building stock within the three counties. Twenty-five aerial photographs were sampled from the three counties. The twenty-five photographs include ten random samples from areas classified as "Commercial and Services," ten random samples from areas classified as "Industrial," and five random samples from areas classified as "Institutional." The types of facilities included in these three land use categories are listed in Table 8. 1. Table 8.2 shows the photograph coverage area and the number of buildings shown within each of the randomly selected areas. Figure 8.1 shows the locations of the selected areas on a map of South Florida.

Table 8.1. Number of Aerial Photographs and Facility Type Examples by Land Use Category

Land Use Category	Number of Aerial Photographs	Facility Type Examples
Commercial and Services	10	Retail Sales and Services, Wholesale Sales and Services, Professional Services, Cultural and Entertainment, Tourist Services, and Oil and Gas Storage
Industrial	10	Food Processing, Timber Processing, Mineral Processing, and Oil and Gas Processing.
Institutional	5	Educational, Religious, Military, Medical and Health Care, Governmental, Correctional, and Commercial Child Care.

The South Florida Water Management District Land Use/Land Cover data set is used to generate the random sample. The data is in the form of a GIS polygon data layer. For example, there are 1148 polygons associated with the "Commercial and Services" category. Each of these polygons are assigned an integer number identifier from 1 to 1148. A random number generator was then used to select ten distinct integer numbers between 1 and 1148 (each number having an equal probability of being chosen) and the ten polygons associated with the randomly selected integer numbers were used.

Table 8.2. Coverage Area and Number of Buildings Within Each Photograph

Land Use Category	Photograph ID	Area(*1000 sq. ft.)	Number of Buildings
Commercialand Services	COMM01	5800	3
	COMM02	4400	18
	COMM03	9000	28
	COMM04	6600	27
	COMM05	4400	24
	COMM06	4400	15
	COMM07	4400	5
	COMM08	4600	27
	COMM09	18480	51
	COMM10	5000	14
Industrial	INDU01	9600	42
	INDU02	9800	10
	INDU03	6800	12
	INDU04	4800	33
	INDU05	22680	90
	INDU06	9900	62
	INDU07	5400	32
	INDU08	6800	25
	INDU09	8200	43
	INDU10	12600	38
Institutional	INST01	4600	53
	INST02	5000	23
	INST03	4800	14
	INST04	4600	11
	INST05	5600	23
Total		188260	723

Table 8.3 presents a breakdown of the percentage of buildings having shapes defined as L, T, C, Rectangular, Circular, Z, H, X and Triangular. Overall, the rectangular shape accounts for over three quarters of the building shapes. The rectangular shape, combined with the relatively simple L shape account for over 80% of the building shapes. The observation that the vast majority of the buildings can be described by these simple shapes indicates that modeling the overall building stock in a damage simulation can be adequately accomplished using the simple rectangular-shaped building models described in Chapters 6 and 7.

Residential Building Stock. Using the aerial photographs used to estimate roof cover damage in the Miami area, we estimated the fraction of one and two story houses, and the fraction of homes with either hip or gable roofs. We did not attempt to characterize the plan shapes of the residential buildings.

From these photographs a total of 1633 homes could be seen. Two story homes comprised 21% of the population, all of which were observed to have gable roofs. In the case of the one story homes, 23% had hip roofs, with the remainder having gable roofs. No flat-roofed homes were observed in these photographs. In cases where the homes had a roof which was a combination of a hip section and a flat section it was classified as a hip roof building. The same classification scheme was used for homes with combined flat and gable roofs. In cases where the roof was a hip/gable combination, the building was classified by the roof style that was dominant.

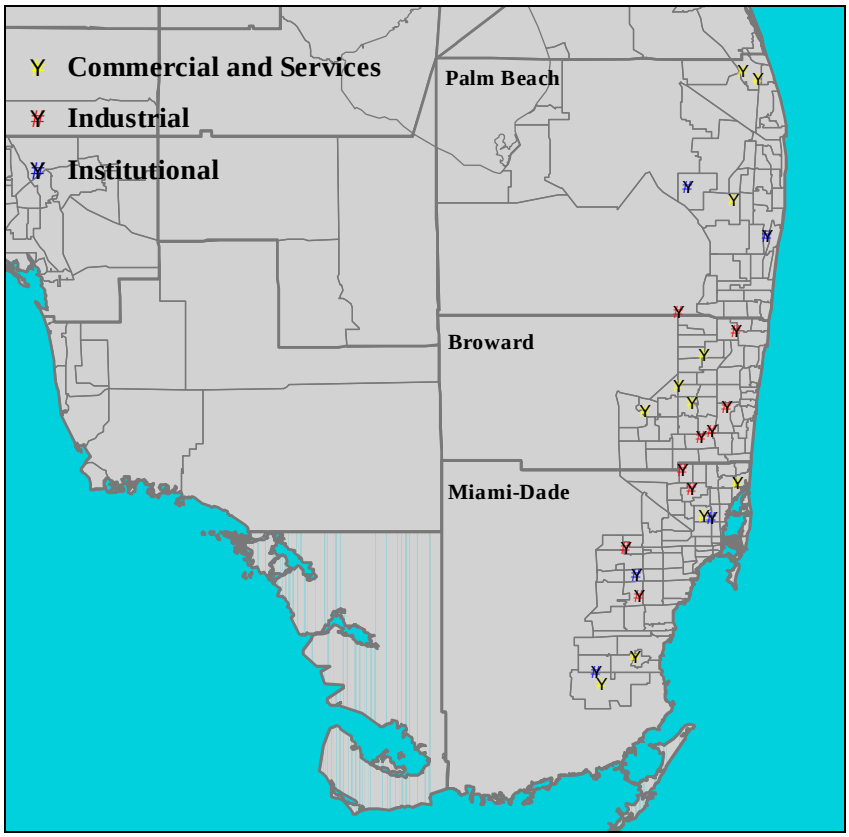

Figure 8.1. Commercial Building Stock Aerial Photograph Locations.

Table 8.3. Shapes of Institutional, Commercial and Industrial Buildings

Building Shape	% of Buildings Associated with Each Building Shape			
	Institutional	Commercial	Industrial	All
C	2.4	7.5	1.5	2.5
L	10.5	7.5	9.3	8.8
T	1.6	2.1	1.4	1.5
Complex	4.0	7.1	4.3	7.9
Rectangular	81.4	68.4	78.3	75.8
Circular	-	0.5	0.9	0.6
Z	-	-	3.5	1.8
H	-	-	0.9	0.6
X	-	0.6	-	0.1
Triangular		0.6	-	0.1

The building shape data base developed by ARA during the Florida Residential Construction Mitigation Program (RCMP) is comprised of 1103 homes. The roof shapes of these homes consists of 29% hip roof, 56% gable, 10% combination (e.g., hip/gable, hip/flat, etc.) and 5% other (e.g., flat, mansard). Single story homes comprised 85% of the total population of buildings in the RCMP building characteristics database. These proportions are comparable to the aerial photography results.

The HUD post-Andrew damage survey of 466 homes indicates that 80% are single story, and gable roofs comprise 80% of the population of one story homes. Of the two story homes, in excess of 95% had gable roofs.

The suggested simplified default building stock geometry for single family residential construction in Southeast Florida is:

Single Story Gable	60%
Single Story Hip	20%
Two Story Gable	20%

8.3 Contractor Survey

In order to estimate the distribution of roof cover types expected in the Southeast Florida area, a survey form was developed by Mr. Tom Smith, and sent to over twenty roofing contractors who do business in Palm Beach, Broward and Dade Counties. The survey form sent to the roofing contractors is shown in Figure 8.2. A total of eleven responses were received from the roofing contractors. In the brief discussion of the survey results, commercial/ industrial/institutional roof covers and residential roof cover responses are treated separately.

Commercial/Industrial/Institutional Roof Covers. The results of the survey with respect to existing roof covers and newly installed roof covers are given in Tables 8.4 and 8.5, respectively. For the existing population of buildings, the survey results clearly indicate that built-up and modified bitumen roof covers are the most commonly applied roof cover for non-residential buildings in Southeast Florida. These roof covers are expected to constitute approximately 85% of the existing population of non-residential buildings. As discussed earlier, the roof cover modeling methodology treats the failure of modified bitumen and built up roofs in the same manner.

The results of the survey with respect to new roof cover installations indicates the total combined population of built-up and modified bitumen roofs is about the same as for the existing population of roof covers, but there is a trend towards using more modified bitumen roofs than built-up with aggregate surface.

As seen in Table 8.6, the results of the survey show that existing roof covers were not typically installed such the resistance of the roofs would be higher in the more highly loaded corner regions.

The uplift capacity of the roof covers on commercial/industrial/and institutional buildings is implied by the results given in Table 8.7. Only two of the eleven respondents indicated that they felt roof covers were installed such that they met the Factory Mutual FM 1-90 standards.

Quality of installation is addressed in Table 8.8, where it is suggested that on average, prior to 1993, only 50% of the roofs were well installed. The contractors indicate that the quality of installation has improved beginning in about 1993-1994, about the time the newest edition of the South Florida Building Code was issued.

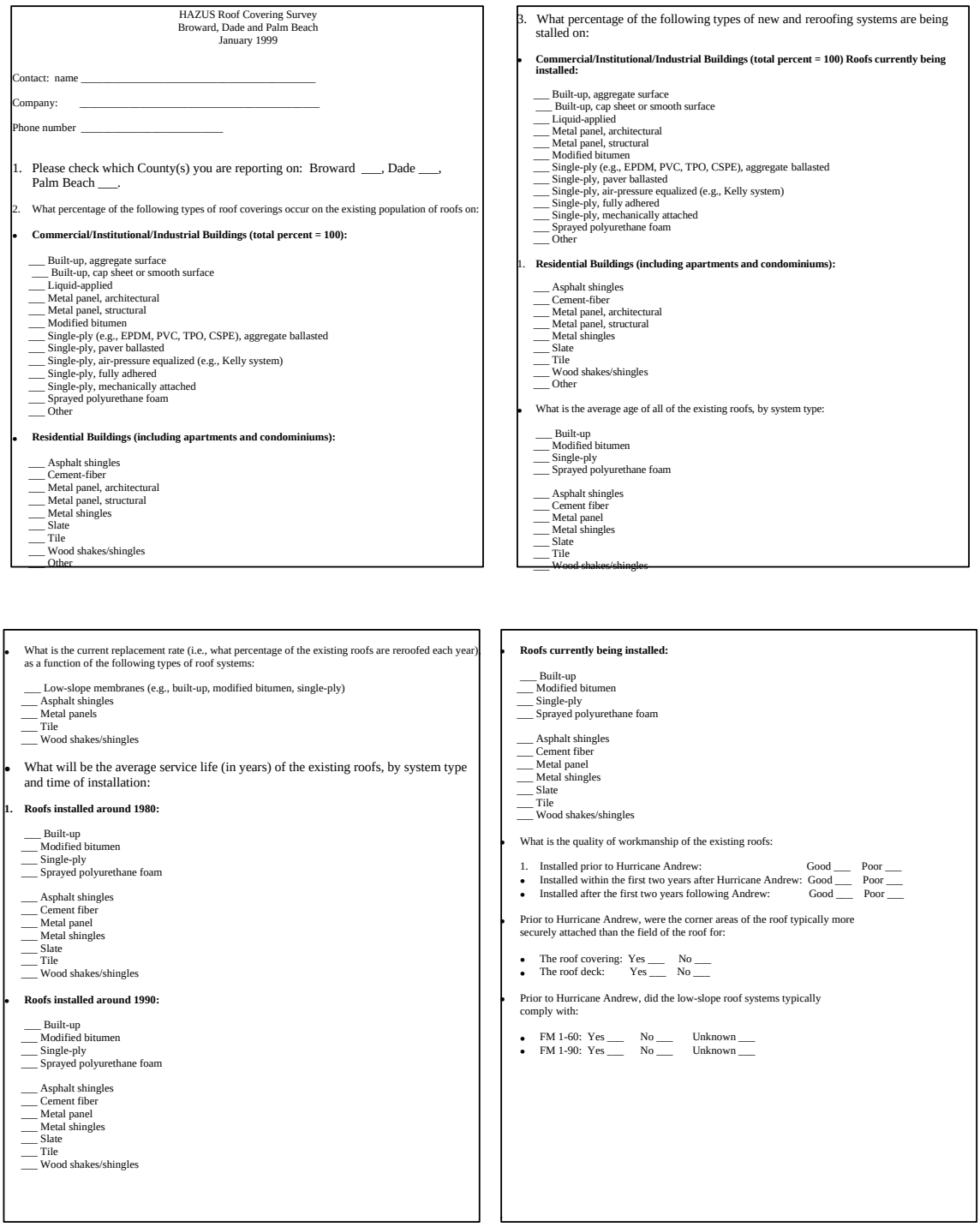

HAZUS Roof Covering Survey
Broward, Dade and Palm Beach
January 1999

Contact: name _____

Company: _____

Phone number _____

1. Please check which County(s) you are reporting on: Broward ___, Dade ___, Palm Beach ___.

2. What percentage of the following types of roof coverings occur on the existing population of roofs on:

- **Commercial/Institutional/Industrial Buildings (total percent = 100):**

___ Built-up, aggregate surface
___ Built-up, cap sheet or smooth surface
___ Liquid-applied
___ Metal panel, architectural
___ Metal panel, structural
___ Modified bitumen
___ Single-ply (e.g., EPDM, PVC, TPO, CSPE), aggregate ballasted
___ Single-ply, paver ballasted
___ Single-ply, air-pressure equalized (e.g., Kelly system)
___ Single-ply, fully adhered
___ Single-ply, mechanically attached
___ Sprayed polyurethane foam
___ Other

- **Residential Buildings (including apartments and condominiums):**

___ Asphalt shingles
___ Cement-fiber
___ Metal panel, architectural
___ Metal panel, structural
___ Metal shingles
___ Slate
___ Tile
___ Wood shakes/shingles
___ Other

3. What percentage of the following types of new and reroofing systems are being stalled on:

- **Commercial/Institutional/Industrial Buildings (total percent = 100) Roofs currently being installed:**

___ Built-up, aggregate surface
___ Built-up, cap sheet or smooth surface
___ Liquid-applied
___ Metal panel, architectural
___ Metal panel, structural
___ Modified bitumen
___ Single-ply (e.g., EPDM, PVC, TPO, CSPE), aggregate ballasted
___ Single-ply, paver ballasted
___ Single-ply, air-pressure equalized (e.g., Kelly system)
___ Single-ply, fully adhered
___ Single-ply, mechanically attached
___ Sprayed polyurethane foam
___ Other

1. **Residential Buildings (including apartments and condominiums):**

___ Asphalt shingles
___ Cement-fiber
___ Metal panel, architectural
___ Metal panel, structural
___ Metal shingles
___ Slate
___ Tile
___ Wood shakes/shingles
___ Other

- What is the average age of all of the existing roofs, by system type:

___ Built-up
___ Modified bitumen
___ Single-ply
___ Sprayed polyurethane foam

___ Asphalt shingles
___ Cement fiber
___ Metal panel
___ Metal shingles
___ Slate
___ Tile
___ Wood shakes/shingles

- What is the current replacement rate (i.e., what percentage of the existing roofs are reroofed each year) as a function of the following types of roof systems:

___ Low-slope membranes (e.g., built-up, modified bitumen, single-ply)
___ Asphalt shingles
___ Metal panels
___ Tile
___ Wood shakes/shingles

- What will be the average service life (in years) of the existing roofs, by system type and time of installation:

1. **Roofs installed around 1980:**

___ Built-up
___ Modified bitumen
___ Single-ply
___ Sprayed polyurethane foam

___ Asphalt shingles
___ Cement fiber
___ Metal panel
___ Metal shingles
___ Slate
___ Tile
___ Wood shakes/shingles

- **Roofs installed around 1990:**

___ Built-up
___ Modified bitumen
___ Single-ply
___ Sprayed polyurethane foam

___ Asphalt shingles
___ Cement fiber
___ Metal panel
___ Metal shingles
___ Slate
___ Tile
___ Wood shakes/shingles

- **Roofs currently being installed:**

___ Built-up
___ Modified bitumen
___ Single-ply
___ Sprayed polyurethane foam

___ Asphalt shingles
___ Cement fiber
___ Metal panel
___ Metal shingles
___ Slate
___ Tile
___ Wood shakes/shingles

- What is the quality of workmanship of the existing roofs:

1. Installed prior to Hurricane Andrew: Good ___ Poor ___
- Installed within the first two years after Hurricane Andrew: Good ___ Poor ___
- Installed after the first two years following Andrew: Good ___ Poor ___

- Prior to Hurricane Andrew, were the corner areas of the roof typically more securely attached than the field of the roof for:

- The roof covering: Yes ___ No ___
- The roof deck: Yes ___ No ___

- Prior to Hurricane Andrew, did the low-slope roof systems typically comply with:

- FM 1-60: Yes ___ No ___ Unknown ___
- FM 1-90: Yes ___ No ___ Unknown ___

Figure 8.2. Survey Form Sent to Roof Contractors to Ascertain Relative Frequency of Roof Cover Types.

Table 8.4. Responses to the Question: "What Percentage of the Following Types of Roof Coverings Occur on the Existing Populations of Commercial/Institutional/Industrial Buildings?"

Roof Cover Type	Response Number											
	1	2	3	4	5	6	7	8	9	10	11	AVE
Built-up, aggregate surface	20	30	50	60		60	40	30	30	55	30	41.8
Built-up, cap sheet or smooth surface	40	8	5	20		15	20	10	40	15	13	19.2
Liquid-applied	0	1	0	0		0	0	0	0	0	1	0.2
Metal panel, architectural	0	5	5	0.05		0	0	10	0	0	5	0.6
Metal panel, structural	0	3	0	0.05		0	0	0	0	0	5	0.8
Modified bitumen	40	25	30	15		25	20	18	30	25	25	26.1
Single-ply aggregate ballasted	0	10	0	0		0	5	0	0	0	2	1.8
Single-ply, paver ballasted	0	2	0	0		0	0	0	0	2	2	0.6
Single-ply, air-pressure equalized	0	1	0	0		0	0	0	0	0	1	0.2
Single-ply, fully adhered	0	5	5	0.05		0	0	10	0	0	2	2.3
Single-ply, mechanically attached	0	5	5	2		0	0	5	0	2	2	2.2
Sprayed polyurethane foam	0	5	0	0.05		0	5	2	0	1	1	1.5
Other	0	0	0	1		0	0	5	0	0	1	0.7
Total	100	100	100	98.2		100	90	90	100	100	90	100

Table 8.5. Responses to the Question: "What Percentage of the Following Types of New and Re-roofing Systems are Being Installed on Commercial/Institutional/Industrial Buildings?"

Roof Cover Type	Response Number											
	1	2	3	4	5	6	7	8	9	10	11	AVE
Built-up, aggregate surface	20	30	50	10		70	30	40	30	30	19	32.9
Built-up, cap sheet or smooth surface	40	5	0	30		4	15	20	40	10	19	18.3
Liquid-applied	0	2	0	0		0	0	0	0	0	0	0.2
Metal panel, architectural	0	7	10	5		0	0	5	0	3	1	3.1
Metal panel, structural	0	2	0	1		0	0	0	0	0	1	0.4
Modified bitumen	40	30	30	50		25	20	21	30	50	50	34.6
Single-ply aggregate ballasted	0	10	0	0		0	20	0	0	0	6	3.6
Single-ply, paver ballasted	0	3	0	0		0	0	0	0	0	1	0.4
Single-ply, air-pressure equalized	0	1	0	0		0	0	0	0	0	1	0.2
Single-ply, fully adhered	0	2	5	1		1	10	10	0	0	1	3.0
Single-ply, mechanically attached	0	3	5	2		0	0	2	0	2	1	1.5
Sprayed polyurethane foam	0	3	0	1		0	5	2	0	0	0	1.1
Other	0	2	0	0		0	0	0	0	5	0	0.7
Total	100	100	100	100		100	100	100	100	100	100	100

Table 8.6. Responses to the Question: "Prior to Hurricane Andrew, Were the Corner Areas of the Roof Typically More Securely Attached than the Field of the Roof?"

	Response Number										
	1	2	3	4	5	6	7	8	9	10	11
The roof covering	No	No	No	No	Yes	No	No	No	No	No	No
The roof deck	No	No	No	No	Yes	No	No	No	No	Yes	No

Table 8.7. Responses to the Question: "Prior to Hurricane Andrew, Did the Low Slope Roof Systems Typically Comply with FM I-60 or FM I-90?"

	Response Number										
	1	2	3	4	5	6	7	8	9	10	11
FM 1-60	Yes	Yes		No	Yes	U	No	Yes	U	U	Yes
FM 1-90	No	No	Yes	No	Yes	U	No	No	U	U	No

U = Unknown

Table 8.8. Responses to the Question: "What is the Quality of Workmanship of the Existing Roofs?"

Installation Time	Response Number											Summary
	1	2	3	4	5	6	7	8	9	10	11	
Prior to Hurricane Andrew	G	G	P	P	G	G	P	G	G	P	P	55% G, 45% P
Within first two years following Andrew	G	P	G/P	P	G	G	P	G	G	P	P	50% G, 50% P
After the first two years following Andrew	G	P	G	P	G	G	G	G	G	G	G	82% G, 18% P

Residential Roof Covers. Not surprisingly, the survey results indicate that 90% of the residential roof covers are either tile or shingle, with tile roofs being more common than shingle roofs (Table 8.9). Wood shakes and metal panels were felt to be the next most common roof cover type, representing 3.3% and 2.3% of the total roof covers in use in residential buildings.

In new construction and re-roofing (Table 8.10), shingle and tiles again are estimated to comprise about 90% of the roofs.

The RCMP data on 1100 homes in Dade, Broward, and Palm Beach counties indicates that about 47% have shingles, 45% tiles, 6% built-up, and the remaining 2% are wood shakes, slate and metal roof. These data will be used to develop the default inventory data for the South Florida regional study.

Table 8.9. Responses to the Question: "What Percentage of the Following Types of Roof Coverings Occur on the Existing Populations of Residential Buildings (Including Apartments and Condominiums)?"

Roof Cover Type	Response Number											
	1	2	3	4	5	6	7	8	9	10	11	AVE
Asphalt shingles	80	35	40	33	30	10	50		55	40	40	41.3
Cement-fiber	0	2	0	0	0	0	0		0	0	1	0.3
Metal panel, architectural	0	5	10	2	0	0	0		0	0	6	2.3
Metal panel, structural	0	1	0	1	0	0	0		0	0	1	0.3
Metal shingles	0	3	0	0	0	0	0		0	0	1	0.4
Slate	0	2	0	0	0	0	0		0	0	1	0.3
Tile	20	40	40	60	70	90	50		45	40	40	49.5
Wood shakes/shingles	0	10	10	3	0	0	0		0	0	10	3.3
Other	0	4	0	1	0	0	0		0	20	0	2.5
Total	100	102	100	100	100	100	100		100	100	100	100

Table 8.10. Responses to the Question: "What Percentage of the Following Types of New and Re-roofing Systems are Being Installed on Residential Buildings (Including Apartments and Condominiums)?"

Roof Cover Type	Response Number											
	1	2	3	4	5	6	7	8	9	10	11	AVE
Asphalt shingles	50	30	10	65	50	5	50		50	40	40	39
Cement-fiber	0	0	0	0	0	0	0		0	0	0	0
Metal panel, architectural	0	8	10	3	0	0	0		0	0	0	2.1
Metal panel, structural	0	1	0	0	0	0	0		0	0	0	0.1
Metal shingles	0	3	0	0	0	0	0		0	0	0	0.3
Slate	0	1	0	0	0	0	0		0	0	0	0.1
Tile	50	45	70	30	50	95	50		50	40	60	54
Wood shakes/shingles	0	5	10	1	0	0	0		0	0	0	1.6
Other	0	7	0	1	0	0	0		0	20	0	2.8
Total	100	100	100	100	100	100	100		100	100	100	0

Chapter 9. Loss Model Validation Studies for Hurricanes Andrew, Erin, Opal and Hugo

9.1 Introduction

The objective of the validation studies is to assess the performance of the hazard-load-resistance-damage-loss model through comparisons of simulated and observed loss statistics. The modeling approach entails selecting a population of buildings that are representative of those associated with the study regions (in these examples, South Florida, the Florida Panhandle, and South Carolina), locating these buildings within the study region, assigning the terrain values, performing the hurricane simulation, damaging the buildings during the passage of the hurricane and finally computing the losses. Each of the steps noted above requires some assumptions, particularly with respect to the building stock. The assumptions regarding the building stock are discussed on a case by case basis later in this section.

Loss model validation studies have been completed using the load, damage and loss models described in Chapters 4 through 7, coupled with the terrain modeling described in Chapter 3. The end-to-end loss validation studies are performed using ZIP Code averaged loss data for Hurricane Andrew obtained from two different sources, residential loss data provided by an insurance company for Hurricanes Erin and Opal, and residential loss data using ZIP Code averaged data for Hurricane Hugo in South Carolina.

The loss data provided for the Hurricanes Andrew and Hugo comparisons represents the total repair and replacement losses associated with the building and the contents. The ZIP Code averaged loss data are given in Bhinderwala (1995). A second set of Hurricane Andrew data is also ZIP Code averaged data for building and content losses. The loss data for Hurricanes Erin and Opal represents losses associated with damage to the building only.

Since both the actual and modeled losses are very sensitive to the wind speeds experienced at a given location, each set of loss comparisons is accompanied with a discussion of the modeled wind speeds, with comparisons of modeled and observed wind speeds presented where possible.

9.2 Example Results – Hurricane Andrew

For the Hurricane Andrew damage to loss simulation, the building stock is modeled assuming 80% of the homes were single story (25% hip, 75% gable). All two story homes are modeled as having gable roofs. 63% of the one story homes and 50% of the two story homes are assumed to have a garage. 40% of the homes use 6d roof sheathing nails spaced at 6″ on center at the edges and 12″ on center in the field, with the remaining 60% of the homes having sheathing nailed with 8d nails using the 6″/12″ spacing. All roof-wall connections are assumed to be strapped. The roof cover of the homes are modeled with 50% of the homes having a shingle roof cover and 50% of the homes

having tiles as the roof cover. All loss analyses for Hurricane Andrew are performed with the construction quality factor set equal to one. The average surface roughness at the ZIP Code level is estimated using both the FWMD data and the MRLC data. Therefore, two example sets of results are given, one using the FWMD terrain data base and the other using the MRLC terrain database. The hurricane simulation is performed with the wind speeds computed at the geographic centroid of each ZIP Code. The houses are assumed to be randomly oriented within a ZIP Code.

The loss ratios (total loss divided by the total coverage limits) are plotted vs. the maximum modeled peak gust wind speed (open terrain) computed at each ZIP Code centroid. The value of the contents in this example is taken as 70% of the value of the structure, and the losses are capped so that they cannot exceed the insured value of the structure and/or contents. It is worth noting that in many instances the cost of rebuilding a severely damaged house can exceed the replacement value of the house because it is more expensive to demolish and replace the building than it is to build a new building on a site which does not have an existing structure. Total losses exceeding the replacement value of a building occurred frequently in the heavily damaged areas associated with Hurricane Andrew.

Comparisons of the predicted and observed losses are plotted vs. the modeled peak gust wind speed at the centroid of the ZIP Code in Figure 9.1 for both terrain cases. The results indicate that using the Hazus loading, damage and loss models for residential buildings works reasonably well.

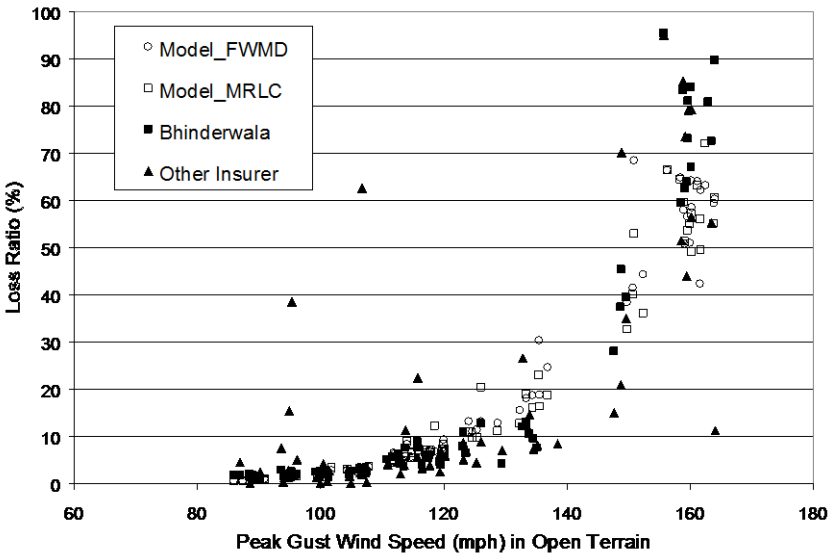

Figure 9.1. Comparison of Observed and Simulated ZIP Code Averaged Losses Produced by Hurricane Andrew in Dade County, Florida.

Figure 9.2 shows an *x-y* plot comparing modeled and observed losses for the two different terrain database cases. Results are given for losses in the range of 0 to 10%, 0 to 50% and 0 to 100%, to help visualize how the model performs for various loss ranges. To facilitate the assessment of the loss sensitivity to the assumed terrain, modeled loss ratios using the FWMD terrain data and the MRLC terrain data are compared in Figure 9.3. No significant bias is found using either of these two databases.

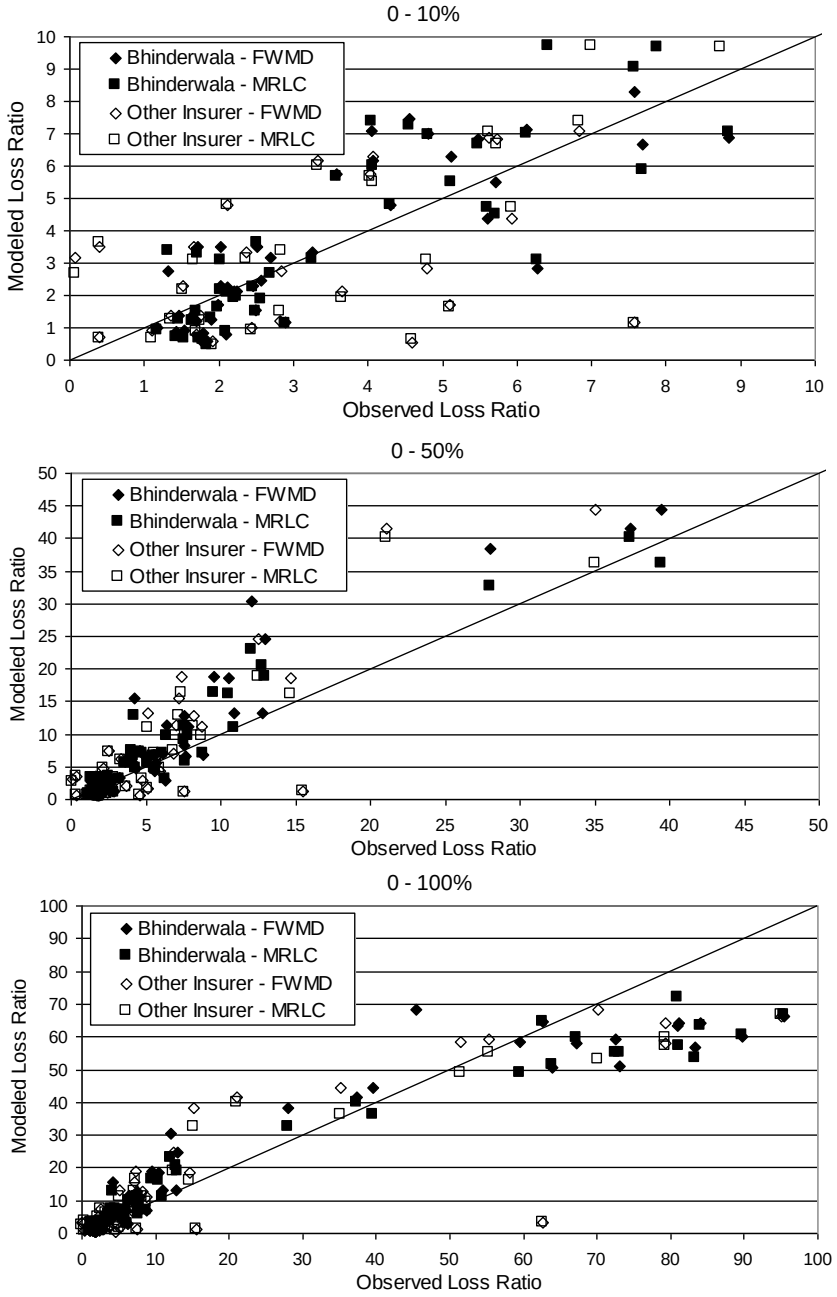

Figure 9.2. Comparison of Modeled vs. Observed Losses.

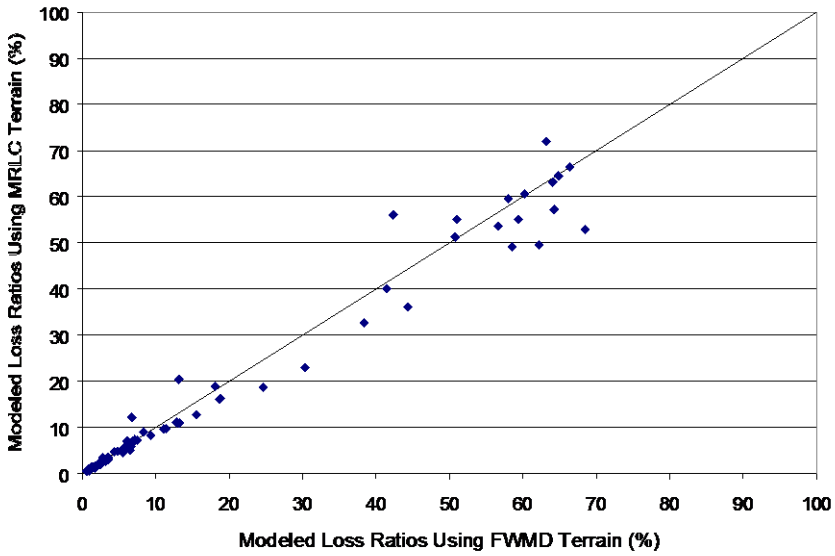

Figure 9.3. Comparison of Modeled Losses Using FWMD Terrain and MRLC Terrain.

The geographic variation of the observed and modeled losses is shown in Figures 9.4 through 9.7. Comparing the losses given in Figures 9.4 and 9.5 (both actual losses) provides an indication of the statistical variation that can be expected from the data alone, without taking into account errors introduced by wind speed modeling, terrain, etc.

Total Losses. The total loss (building plus content), summed over all of Dade County, is estimated assuming that both the number of policies and value of these policies in each ZIP Code are the same. In each case, a contribution to the estimated total loss was computed only if the insurer had policies in the given ZIP Code. This is clearly not the case in Dade County, but a comparison presented in this manner is valid, and helps mask the identity of a given insurer. The aggregate losses are given in Table 9.1. Note that the actual and modeled totals given in Table 9.1 differ between cases because the number of ZIP Codes having policies is different for the different insurers.

The results shown in Table 9.1 indicate that the modeled losses resulting from the two terrain models (FWMD and MRLC) are slightly lower than the observed losses, with the FWMD terrain model yielding the higher values of the estimated losses.

Modeled Wind Speeds in Dade County Produced by Hurricane Andrew. Figure 9.8 shows a contour representation of the maximum peak gust wind speeds produced by the hurricane model for the Hurricane Andrew simulation. The maximum wind speeds produced by the model are of the order of 165 mph, with the maximum wind speeds occurring in the same area as the maximum losses as shown in Figures 9.4 and 9.5. Figure 9.8 also shows the locations of three anemometers where wind speed and directions were recorded during the storm, as well as the location of the nine NAHB survey sites discussed in Chapter 4, for which wind speed estimates were provided by NOAA/HRD.

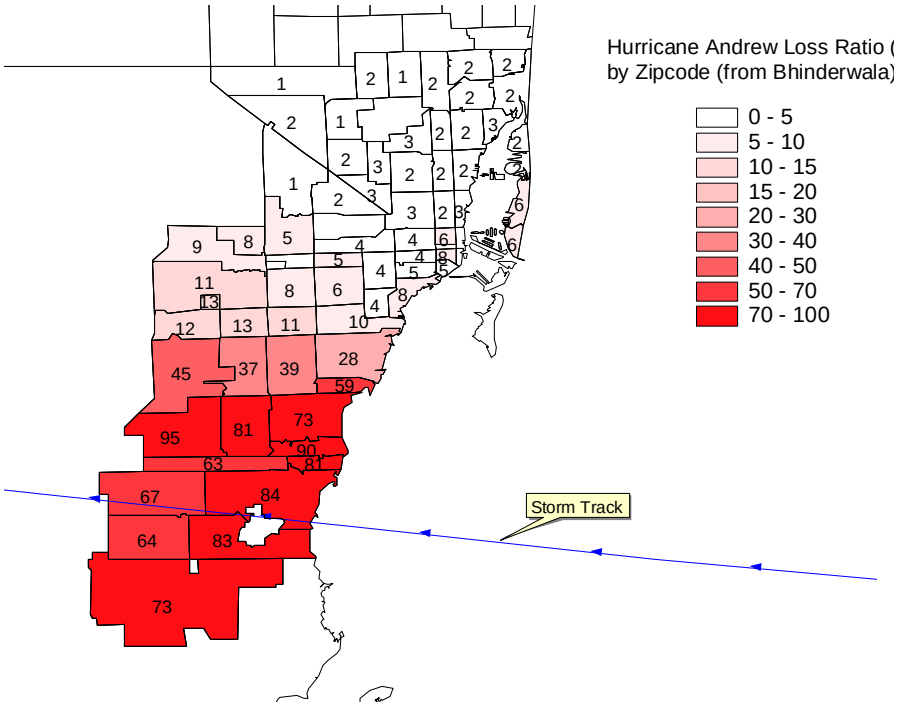

Figure 9.4. Loss Ratios by ZIP Code in Dade County (Bhinderwala Data).

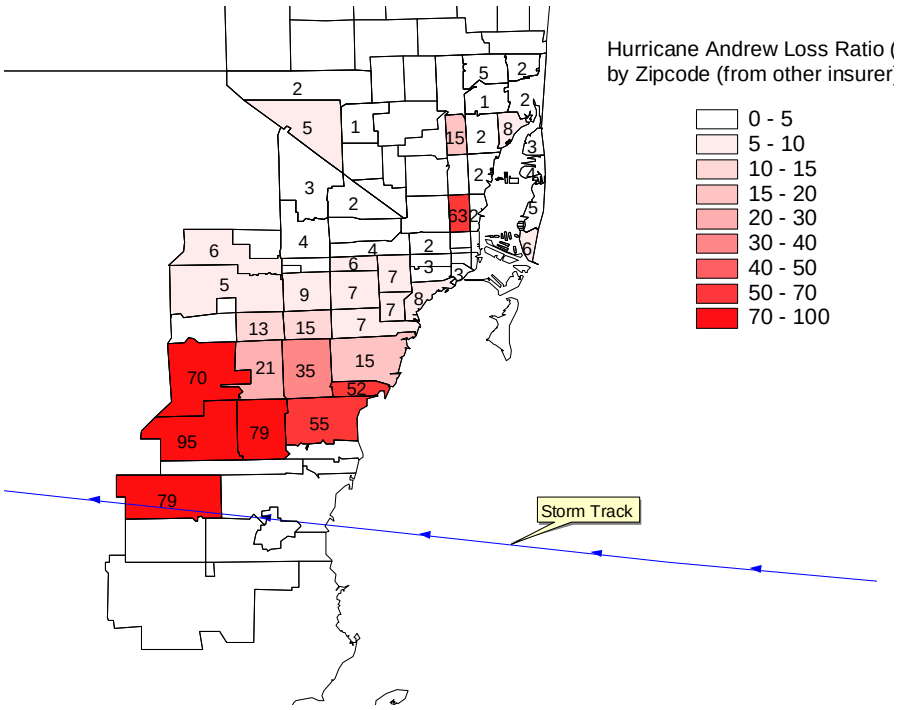

Figure 9.5. Loss Ratios by ZIP Code in Dade County (Other Insurer Data).

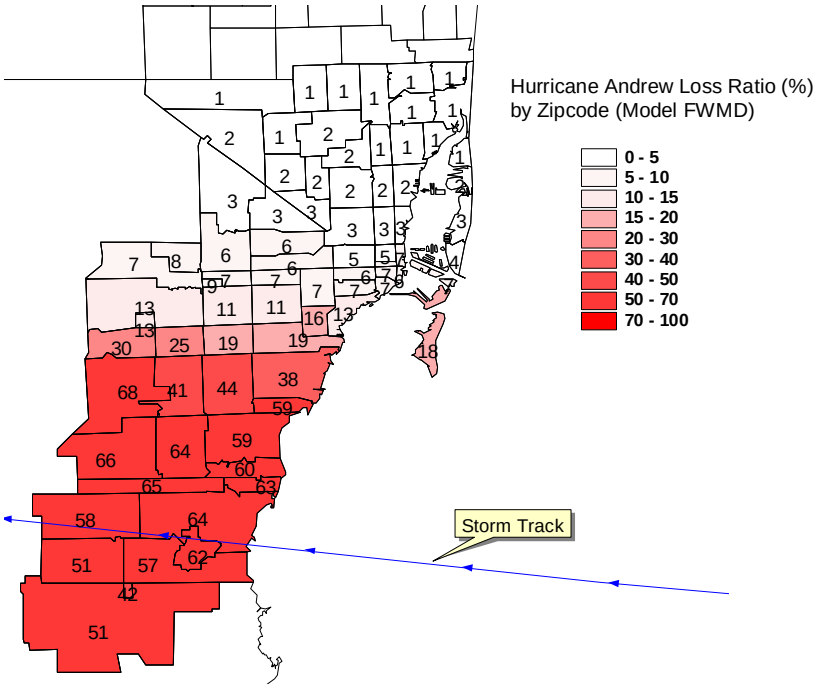

Figure 9.6. Modeled Loss Ratio (FWMD).

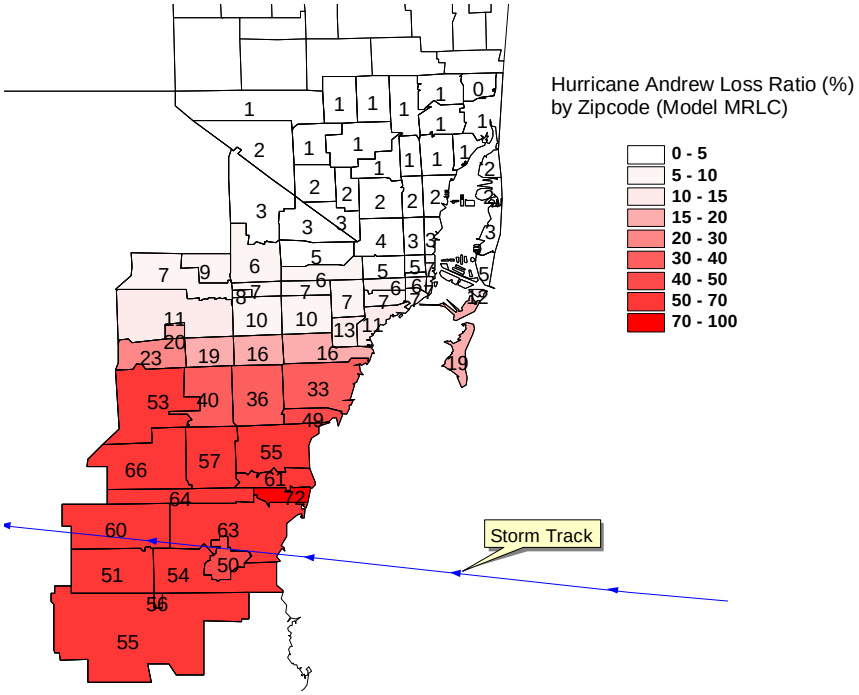

Figure 9.7. Modeled Loss Ratio (MRLC).

Table 9.1. Comparison of Modeled and Observed Losses from Hurricane Andrew

Case	Actual Loss Ratio(%)	Modeled Loss Ratio (%) (FWMD)	Modeled Loss Ratio (%) (MRLC)
Bhinderwala	19.1	18.0	17.0
Other Insurer	15.7	15.3	13.8

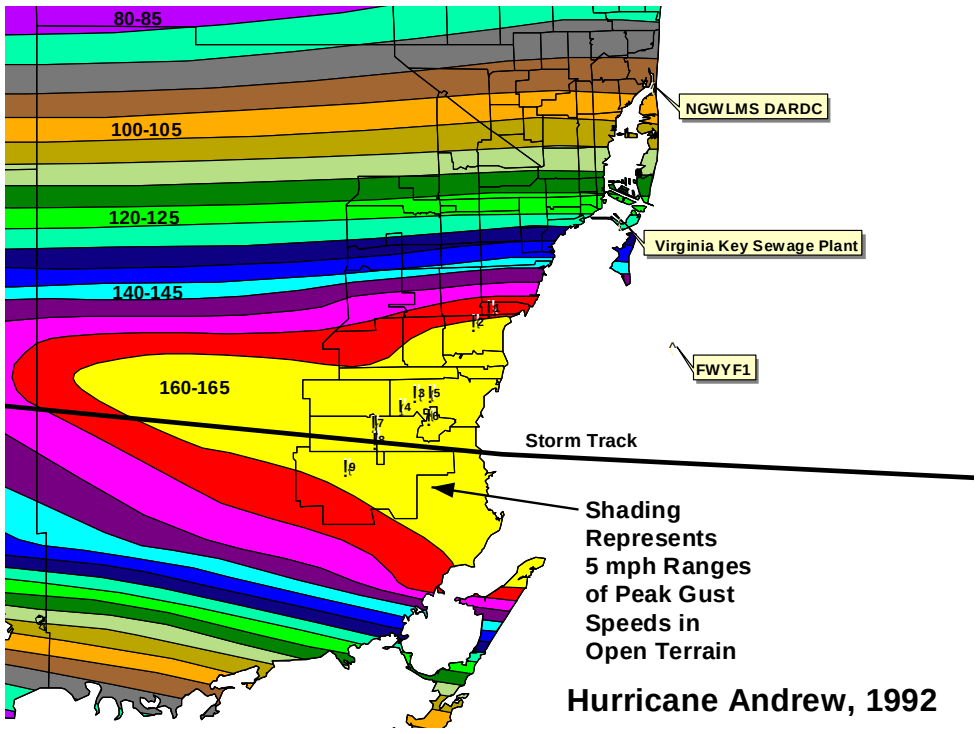

Figure 9.8. Swath of Modeled Peak Gust Wind Speeds Produced by Hurricane Andrew.

Figure 9.9 presents comparisons of the simulated and observed peak gust wind speeds and the mean wind directions at the three anemometer sites. The agreement between the observed and modeled wind speeds and directions is generally good. One major discrepancy in the comparison of the peak gust wind speed recorded at the Haulover site at 08:00 is associated with an anomalous gust. Note that the wind speeds recorded at the Virginia Key site are not from a continuous record and, thus, the peak values shown may not correspond to the maximum in the storm.

Figures 9.10 through 9.12 show comparisons of the model generated peak gust wind speeds at the locations of the nine NAHB damage surveys to the estimates of wind speeds and direction at these same sites derived by NOAA/HRD personnel. The comparisons of the wind speed traces suggest the NOAA/HRD representation of the wind field is somewhat broader than that produced by the wind field model. At the two northern locations (positions 1 and 2 as shown in Figure 9.8), the maximum values of the HRD estimated peak gust wind speeds are about 10 mph to 15 mph higher than those obtained from the wind field model.

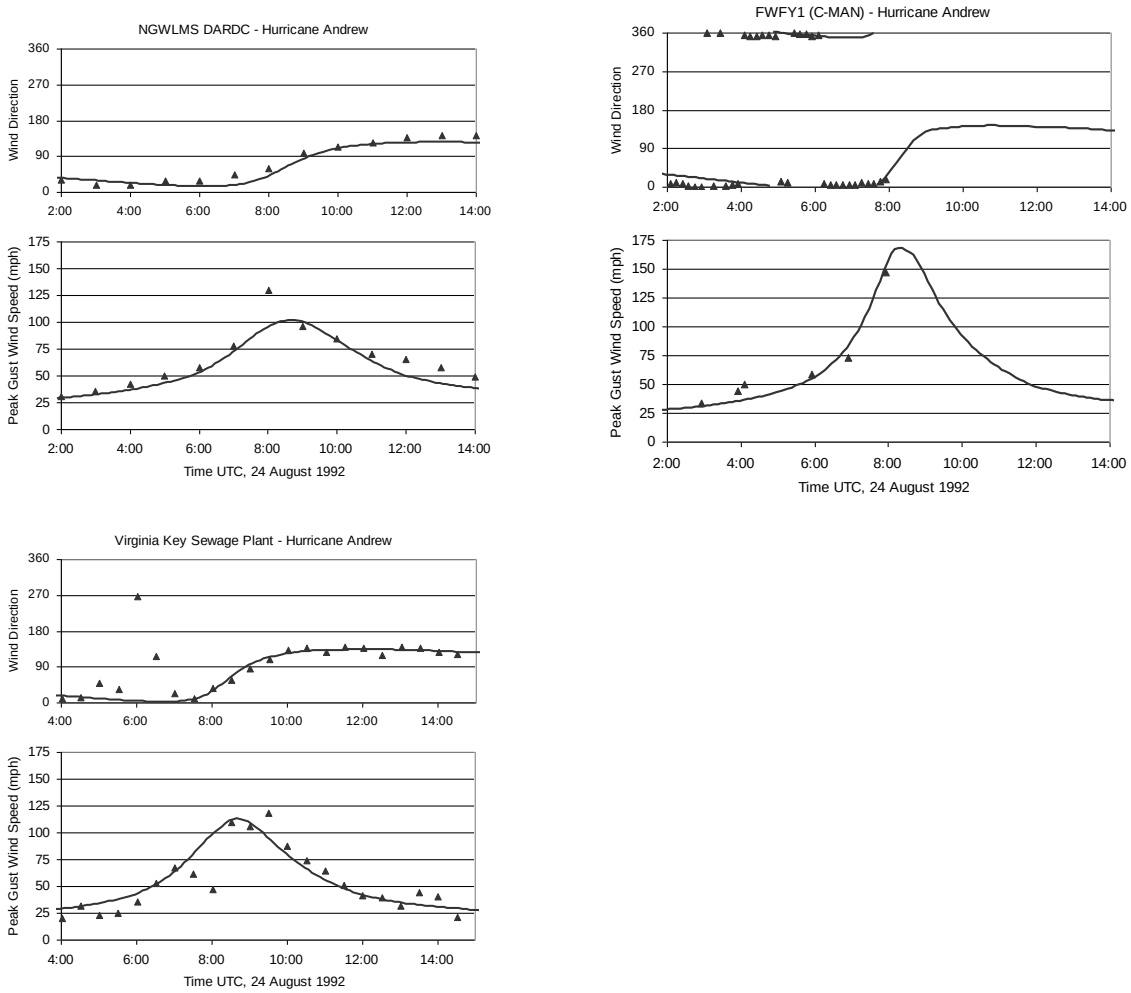

Figure 9.9. Comparison of Simulated and Observed Peak Gust Wind Speeds and Directions Produced by Hurricane Andrew. Gust Data at Virginia Key Location Derived from One Minute Mean Values. All Wind Speeds are Given for the Actual Terrain at a Height of 10 m Above Ground.

Moving towards the south, the differences in the magnitude of the HRD maximum wind speeds and the simulated wind speeds reduce, where at the southern most points, the modeled wind speeds are slightly higher (~10 mph) than the HRD values.

Overall, the differences between the modeled wind speeds and the HRD estimated wind speeds are typically less than 10%, a difference which is less than the uncertainty attributable to adjusting the aircraft measured wind speeds to surface level wind speeds as indicated in Powell and Houston (1996).

The wind speed and direction traces from the wind field model and those provided by HRD are used in the conjunction with the damage and loss models to determine the effect of these different wind speed estimates on predicted losses. The building stock used in this damage and loss analysis is the same as described earlier for the basic Hurricane

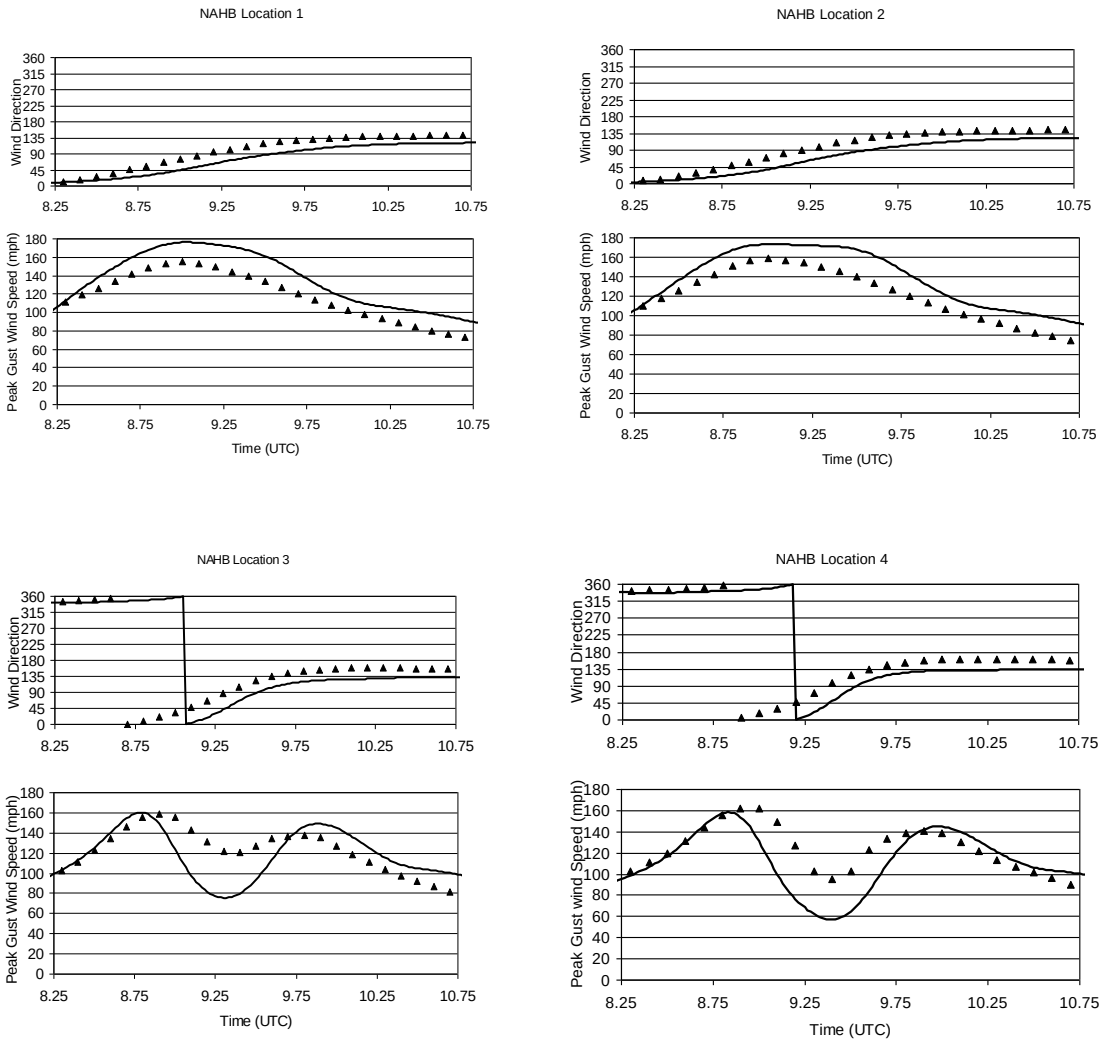

Figure 9.10. Comparison of Simulated Peak Gust Wind Speeds and Wind Direction Obtained Using the Hurricane Wind Field Model (shown as triangles) to Wind Speeds Estimated by the Hurricane Research Division (shown as continuous line) at NAHB Locations 1 through 4 as Indicated in Figure 9.8.

Andrew loss simulation example. The loss example is performed using two surface roughness (z_0 = 0.15 m and z_0 = 0.35 m). Results are given in Table 9.2, along with estimates of the observed losses near the locations of each of the nine wind speed traces (compare loss ratio data given in Figures 9.4 and 9.5 to locations 1 through 9 shown in Figure 9.8). The losses predicted using the HRD wind speeds are notably higher than those predicted using the wind speed trace produced by the wind field model at locations one and two, simply because the HRD wind speeds are consistently higher. At locations 3 through 9, the losses produced using the HRD wind speed trace are lower than those obtained using the wind field model generated wind speed trace. The high losses produced using the modeled wind speed trace are primarily a result of the high wind speeds occurring for longer periods of time and being associated with larger wind direction changes than those produced by the HRD trace.

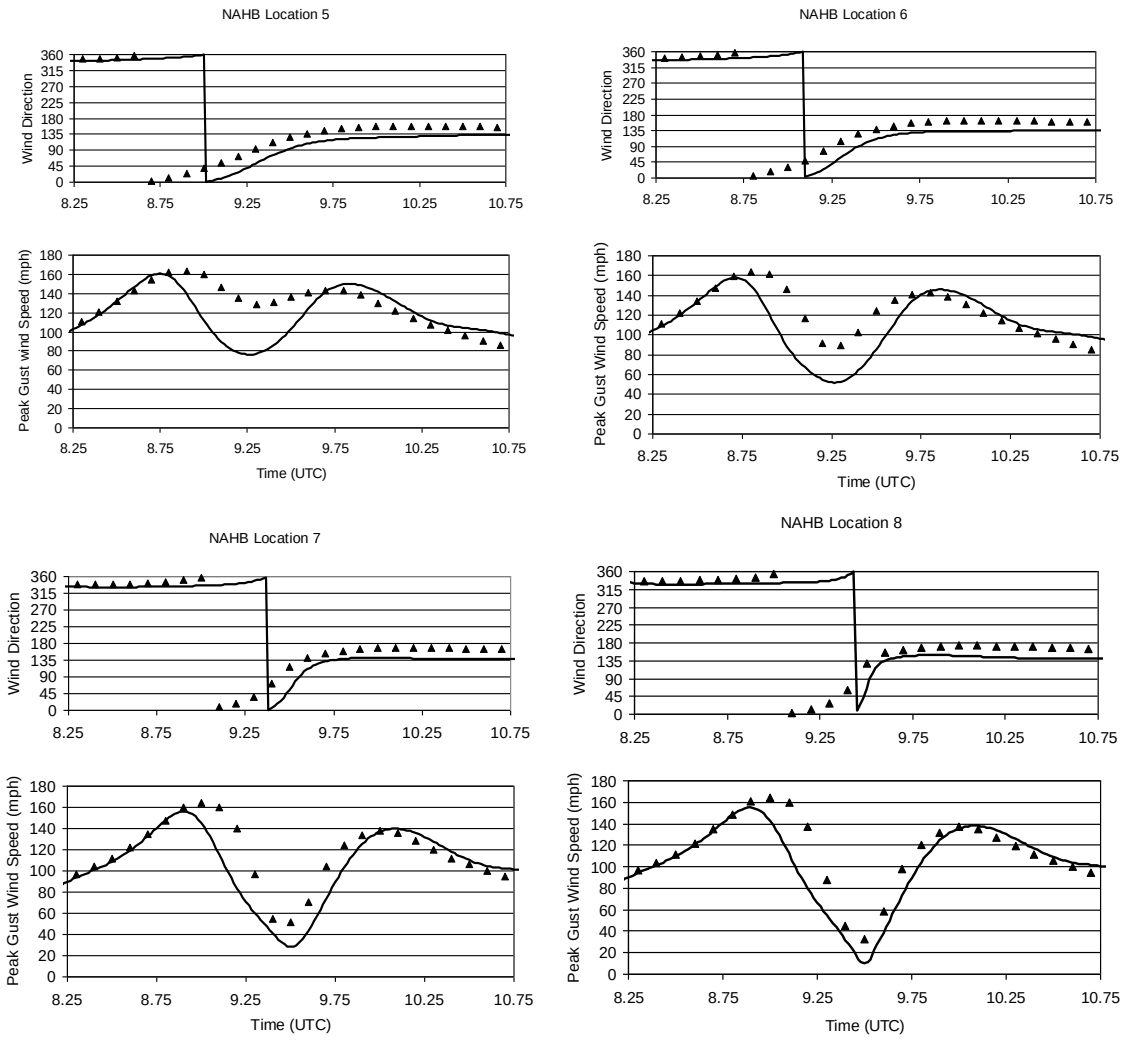

Figure 9.11. Comparison of Simulated Peak Gust Wind Speeds and Wind Direction Obtained Using the Hurricane Wind Field Model (shown as triangles) to Wind Speeds Estimated by the Hurricane Research Division (shown as continuous line) at NAHB Locations 5 through 8 as Indicated in Figure 9.8.

9.3 Example Results – Hurricanes Erin and Opal

Hurricane Erin and Opal Wind Speed Simulations. Figures 9.13 and 9.14 show contour plots of the foot print of maximum peak gust wind speeds swept out by Hurricanes Erin and Opal, as obtained from the hurricane wind field model. Figures 9.13 and 9.14 also show the locations of 4 anemometers used in the wind speed validation studies. Figures 9.15 and 9.16 show comparisons of the simulated and observed peak gust wind speeds of the four anemometer locations of both storms. In the wind speed validation examples given in Figures 9.15 and 9.16, note that the records from Eglin AFB and the Panama City Beach stations are not continuous records and, as a result, the maximum gust wind speeds produced at these sites may not have been recorded.

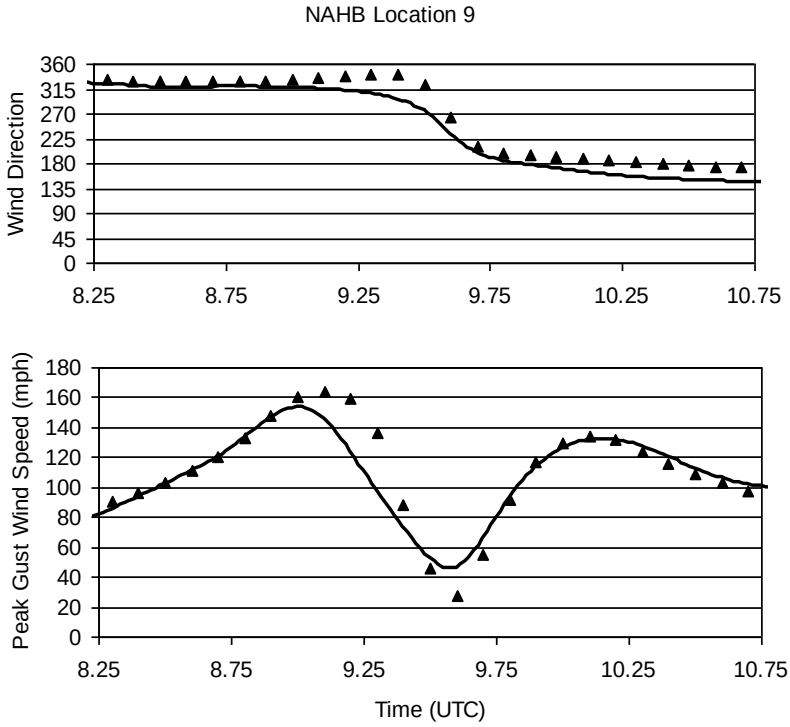

Figure 9.12. Comparison of Simulated Peak Gust Wind Speeds and Wind Direction Obtained Using the Hurricane Wind Field Model (shown as triangles) to Wind Speeds Estimated by the Hurricane Research Division (shown as continuous line) at NAHB Location 9 as Indicated in Figure 9.8.

Table 9.2. Comparisons of Loss Ratios Obtained Using the HRD Wind Speed Estimates to the Wind Field Model Wind Speed Estimates

Location	Wind Field Model Estimated Peak Gust Wind Speed (mph)	HRD Estimated Peak Gust Wind Speed (mph)	Loss Ratios Predicted Using Wind Field Model Wind Speeds (z_0=0.15 m)	Loss Ratios Predicted Using HRD Wind Speeds (z_0=0.15 m)	Actual Loss Ratios (%)	Loss Ratios Predicted Using Wind Field Model Wind Speeds (z_0=0.35 m)	Loss Ratios Predicted Using HRD Wind Speeds (z_0=0.35 m)
1	158.5	176.1	66%	85%	~50%-60%	51%	75%
2	161.4	173.2	71%	86%	~50%-60%	56%	74%
3	159.6	160.3	68%	61%	~80%	53%	44%
4	159.4	158.1	64%	55%	~80%	49%	38%
5	160.4	160.5	70%	61%	~80%	54%	44%
6	161.2	157.5	66%	54%	~80%	51%	39%
7	160	155.8	61%	49%	~60%-80%	45%	33%
8	160.6	154.9	62%	46%	~60%-80%	44%	30%
9	159.9	153.1	55%	44%	~70%	40%	30%

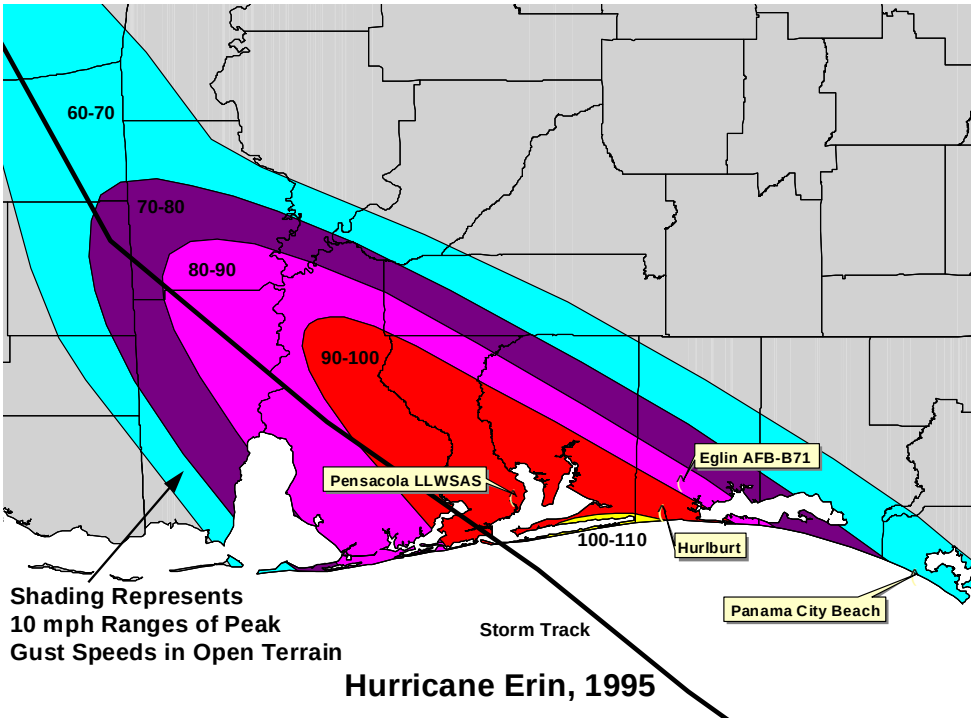

Figure 9.13. Swath of Simulated Peak Gust Wind Speeds (10 m in Open Terrain) Produced by Hurricane Erin.

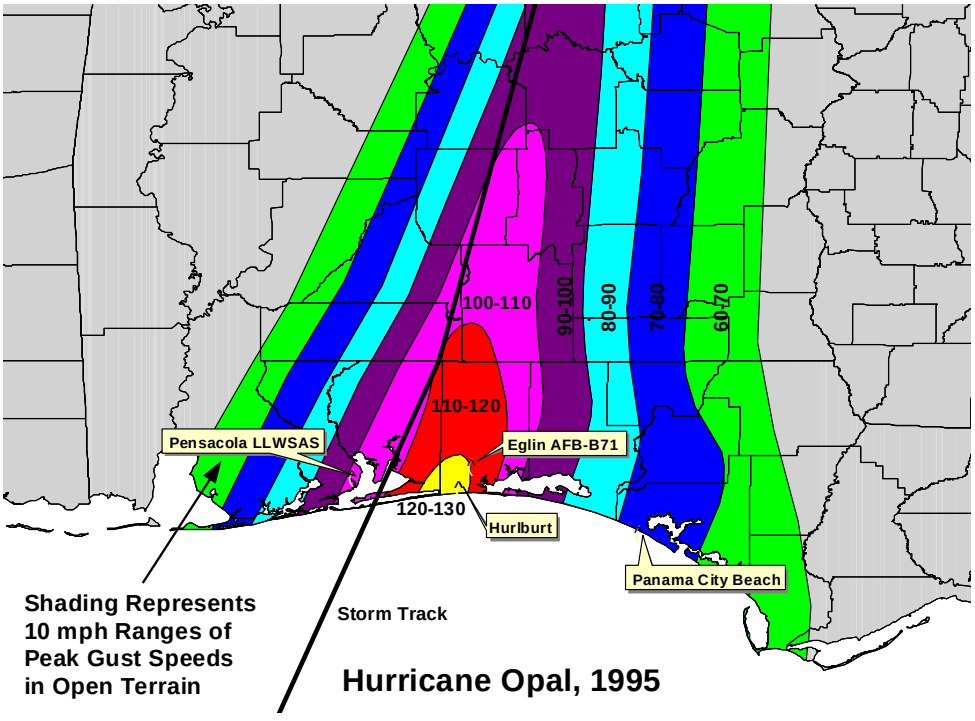

Figure 9.14. Swath of Simulated Peak Gust Wind Speeds (10 m in Open Terrain) Produced by Hurricane Opal.

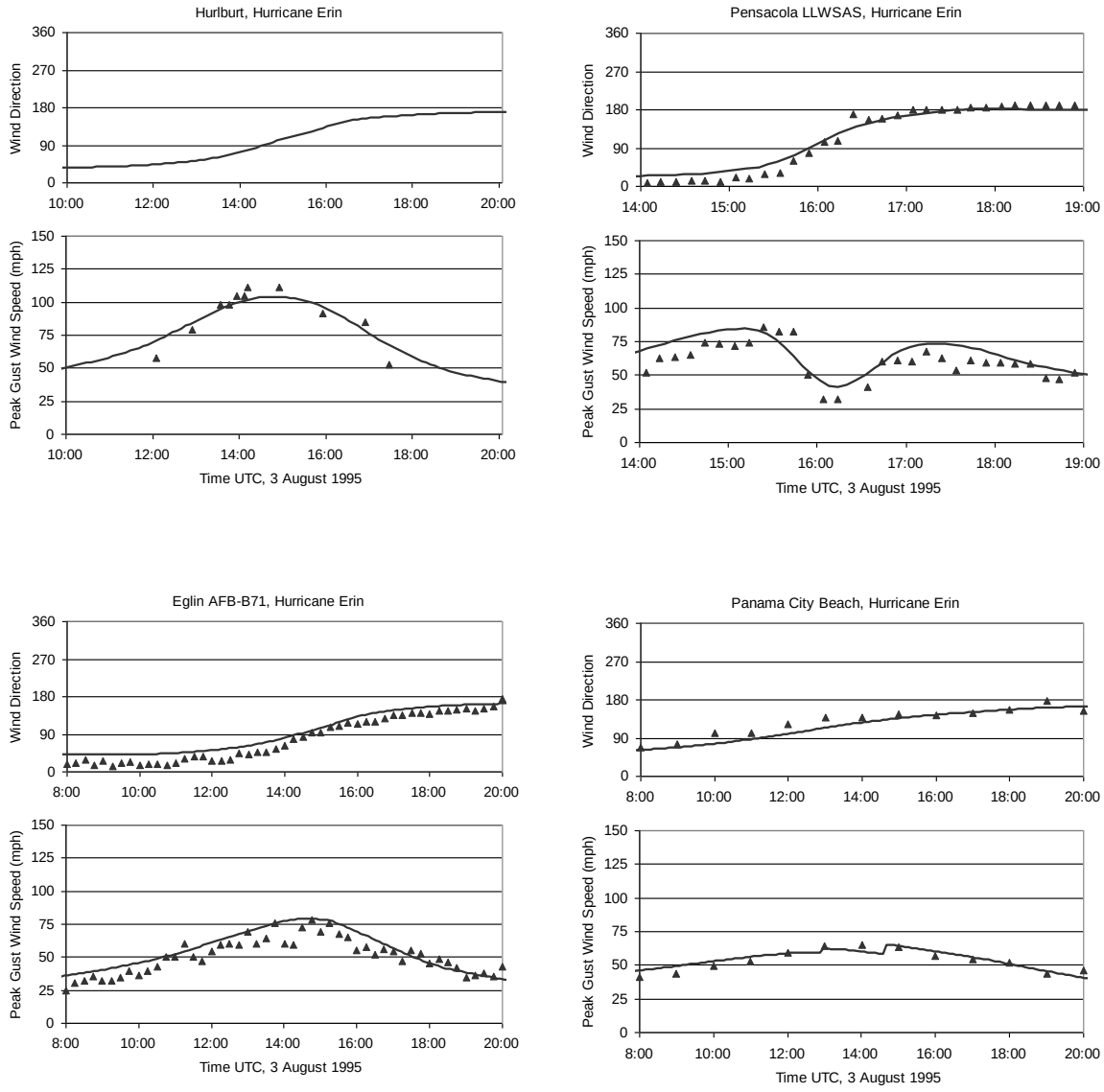

Figure 9.15. Comparison of Simulated and Observed Peak Gust Wind Speeds and Directions Produced by Hurricane Erin. Gust Data at Eglin AFB Location Derived from One Minute Mean Values. All Wind Speeds are Given for the Actual Terrain at a Height of 10 m Above Ground.

In the case of Hurricane Erin, the comparisons at the Hulburt Field station suggest that the model may be underestimating the peak gust wind speeds by about 5%, but is generally good elsewhere. In the case of Hurricane Opal, the agreement between modeled and observed wind speeds for locations on the right hand side of the storm is reasonable, but the model is overestimating the wind speeds on the left hand side of the storm as indicated by the comparison of wind speeds at the Pensacola station. The maximum simulated peak gust wind speeds are typically within about 5% to 10% of the observed values. The overall shapes of the simulated traces are similar to the observed traces indicating that the duration characteristics of the modeled and observed storms are similar.

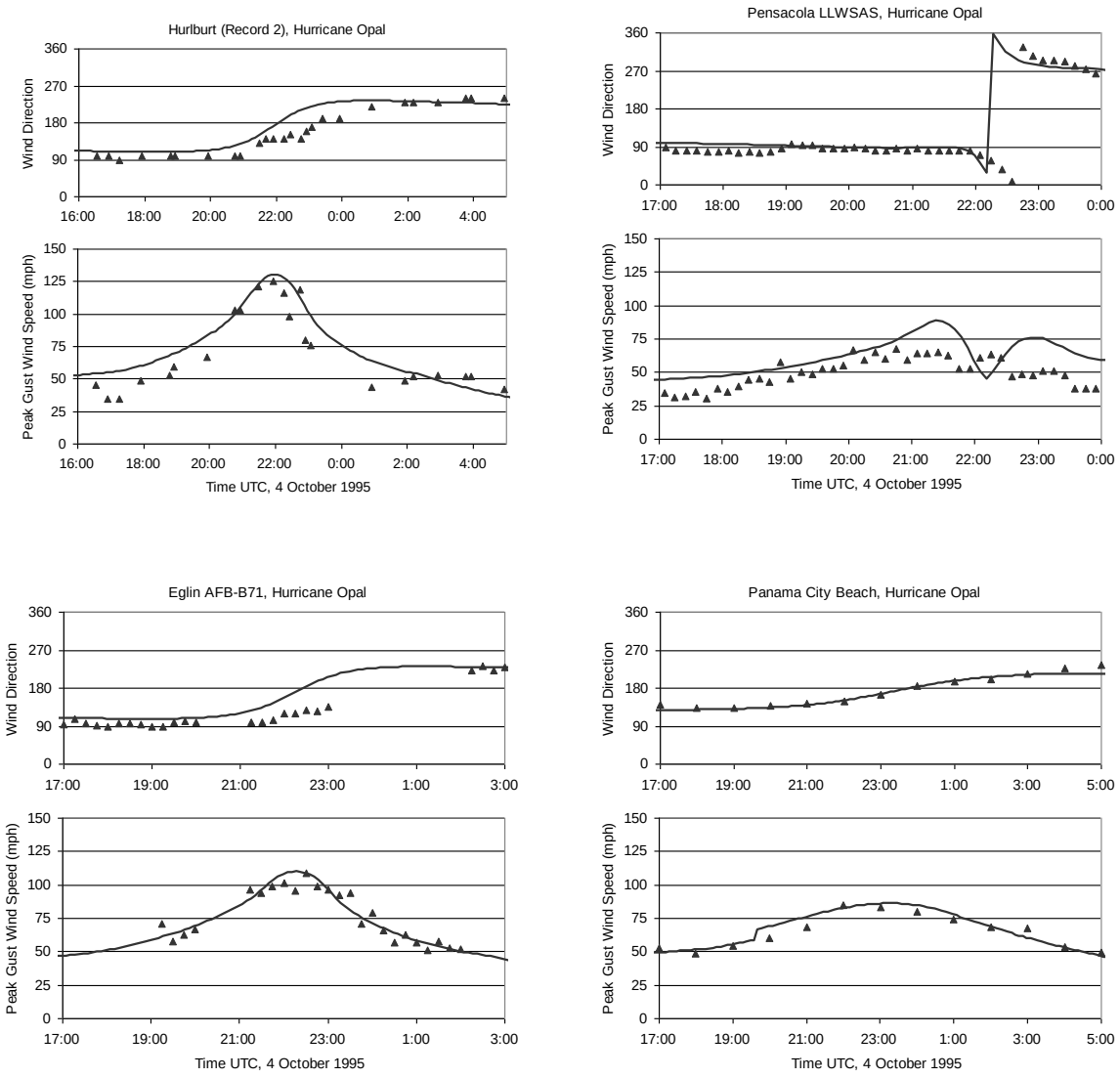

Figure 9.16. Comparison of Simulated and Observed Peak Gust Wind Speeds and Directions Produced by Hurricane Opal. All Wind Speeds are Given for the Actual Terrain at a Height of 10 m Above Ground.

Comparison of Modeled and Observed Loss Statistics. In the Erin and Opal loss validation studies, the building stock is modeled assuming 25% of the single story buildings have hip roofs and 75% have gable roofs. All two story homes are modeled as having gable roofs. 70% of the one story homes and 45% of the two story homes are assumed to have a garage. The roof deck is assumed to be attached to the roof trusses with 6d nails for 40% of the buildings and with 8d nails for 60% of the buildings. Roof-wall connections are assumed to be strapped in 80% of the cases and toe-nailed for the other 20%. The fraction of one and two story homes is estimated from statistical information provided by the insurer. All loss analyses for Hurricanes Erin and Opal are performed with the construction quality factor set equal to one. Approximately 40% of the homes were able to be geo-coded, and thus their "exact" location and hence terrain

environment could be established. Thus, for each house that could be geo-coded, the terrain is obtained by determining which land use category the house is located, and then assigning the appropriate surface roughness using the surface roughness tables given in Chapter 3. Each has been checked to determine if the unit is located on a barrier island or on the mainland. In the case of the homes that could not be geo-coded (approximately 50% of the units), the location and terrain characteristics for each house are estimated by assuming that for a given ZIP Code, the non geo-coded policies belong to the same population as the geo-coded policies.

Hurricane Erin and Opal simulations are performed with wind speed traces being recorded using grid points spaced at 0.10°. Since the wind speed grid used in the simulation of the storms does not correspond to the exact location of each home, the wind speed experienced by each house is obtained by using the wind speed and direction trace associated with the nearest grid point. Using this wind speed and direction trace, damage and ensuing losses are produced for all potential building types in the assumed building stock. The total loss ratio in each ZIP Code and county examined is estimated by summing the simulated losses weighted in proportion to the assumed number of units associated with each combination of deck thickness, roof shape, etc.

Figures 9.17 and 9.18 show the comparison of modeled and observed loss ratios at ZIP Code level for Hurricanes Erin and Opal, respectively. Only ZIP Codes with more than 10 policies are included in the comparison. The model is seen to provide reasonable agreement between modeled and actual loss ratios for Hurricane Erin. However, for Hurricane Opal, the model significantly underestimates the loss ratios of ZIP Codes with modeled peak gust wind speeds between 80 and 100 mph and overestimates the loss ratios of ZIP Codes with modeled peak gust wind speeds greater than 120 mph. In the comparison of observed and modeled losses averaged over the counties impacted by Hurricanes Erin and Opal given in Figures 9.19 through 9.22, it can be seen that near the point of landfall, the model tends to overestimate the losses in Santa Rosa County for Hurricane Opal and underestimate the losses in Santa Rosa County for Hurricane Erin, suggesting the wind field model maybe underestimating the Hurricane Erin wind speeds near the eyewall and overestimating the Hurricane Opal speeds. Besides the simulated wind speeds, a number of factors, including the assumed building stock, terrain, assumption of the non geo-coded policies belonging to the same population as geo-coded ones, can all contribute to the discrepancies between the modeled and actual loss ratios.

9.4 Example Results – Hurricane Hugo

Figure 9.23 shows the maximum peak gust wind speed contours of Hurricane Hugo produced by the hurricane model. The maximum wind speeds predicted by the model are between 130 mph and 140 mph. Figure 9.23 also shows the locations of ten anemometers and the actual and modeled maximum peak gust wind speeds at these locations where wind speeds and directions were recorded during the storm. The mean of the modeled-to-actual gust wind speed ratios is 1.02 and the COV is 0.08. Figures 9.24 through 9.26 show comparisons of the model generated peak gust wind speeds and directions to the estimates of wind speeds and directions at each of the ten locations. The overall performance of the hurricane model is, again, satisfactory.

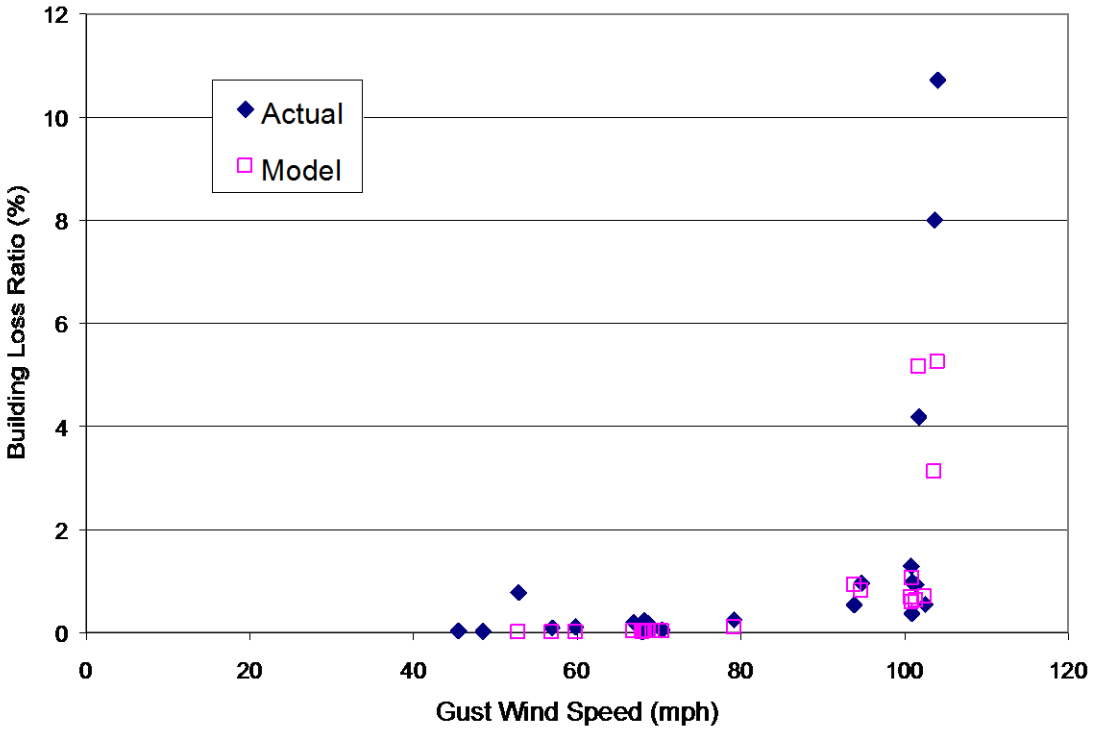

Figure 9.17. Hurricane Erin Building Loss Ratio Comparison.

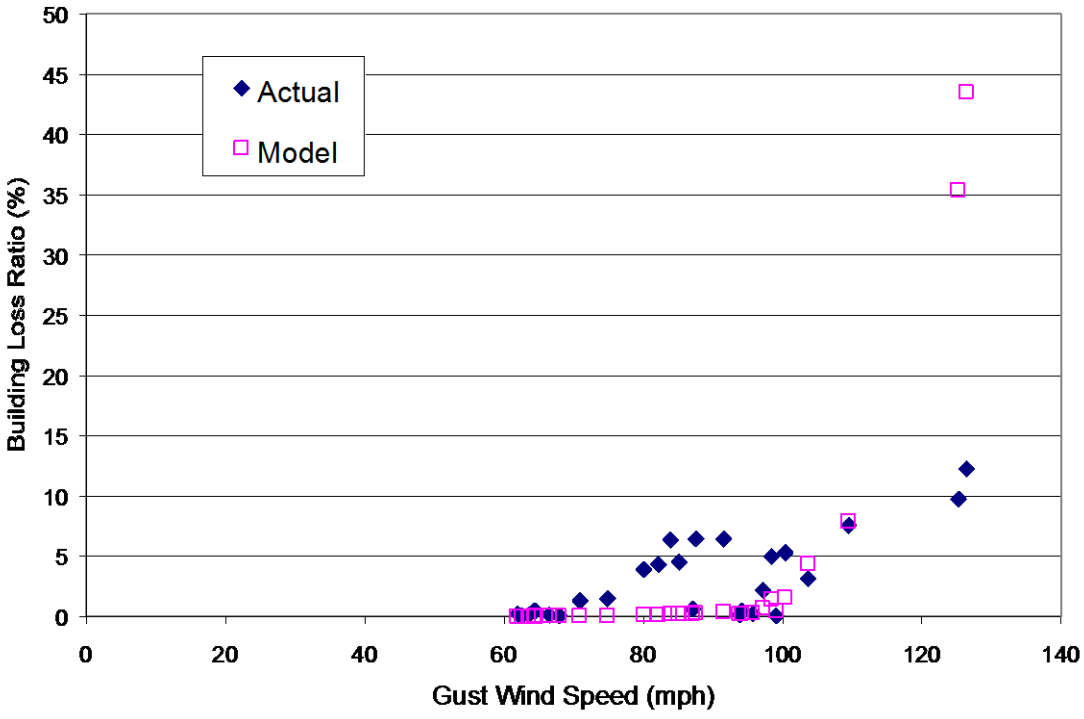

Figure 9.18. Hurricane Opal Building Loss Ratio Comparison.

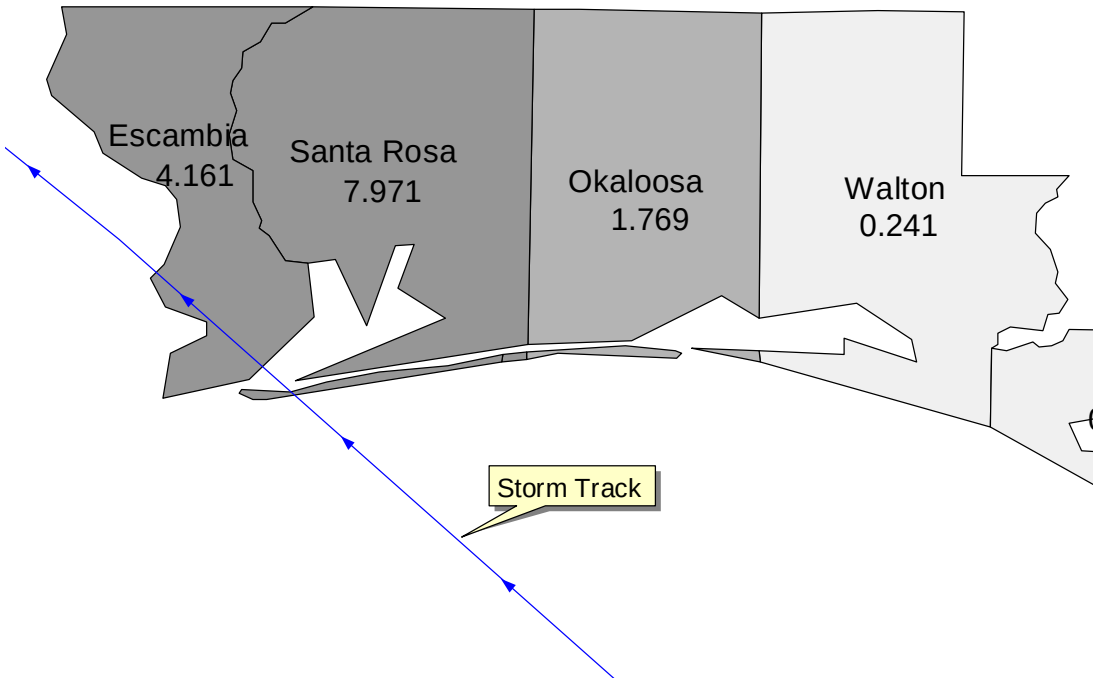

Figure 9.19. Actual Building Loss Ratios – Hurricane Erin.

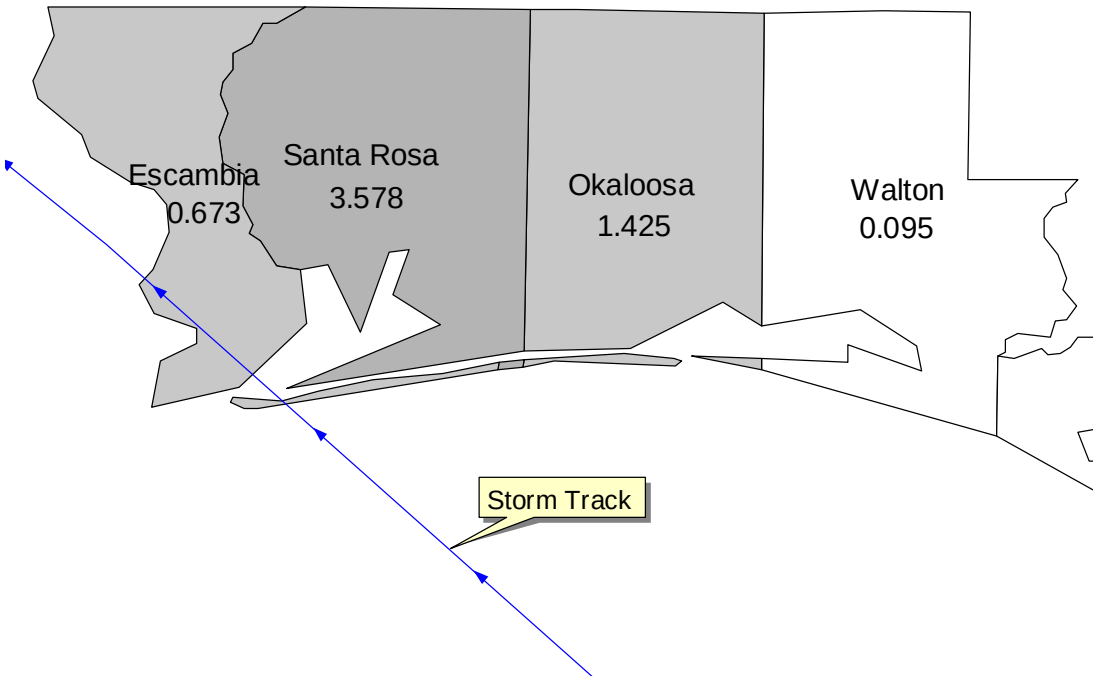

Figure 9.20. Modeled Building Loss Ratios – Hurricane Erin.

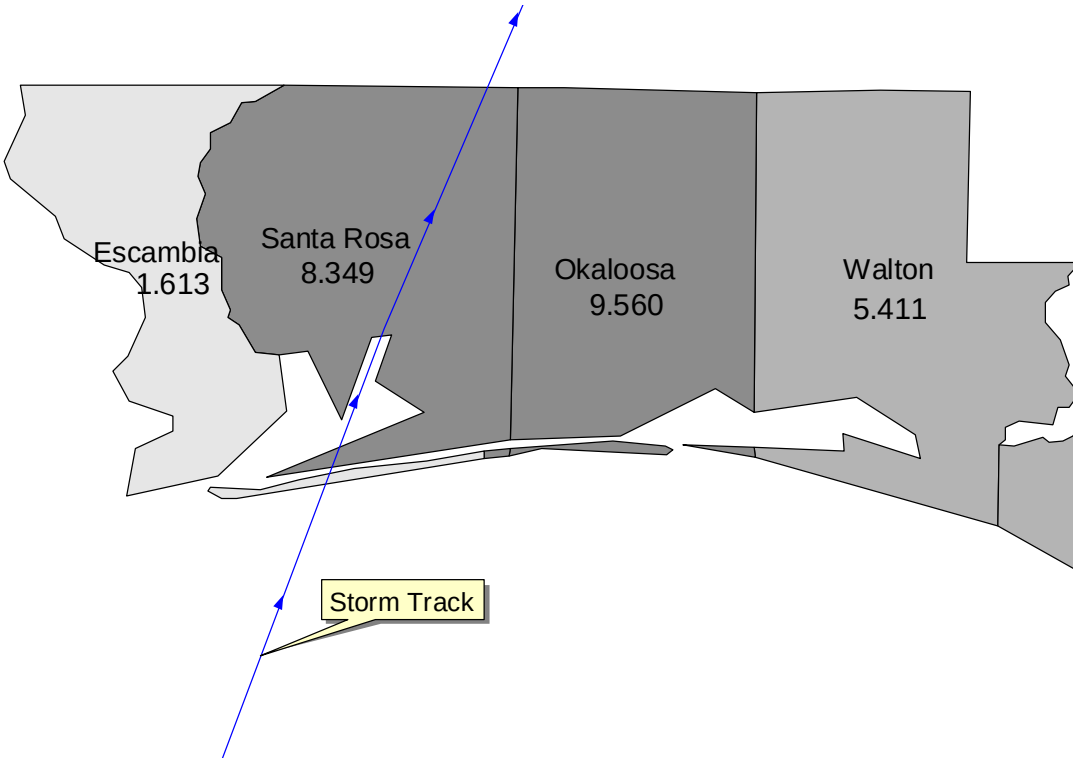

Figure 9.21. Actual Building Loss Ratios – Hurricane Opal.

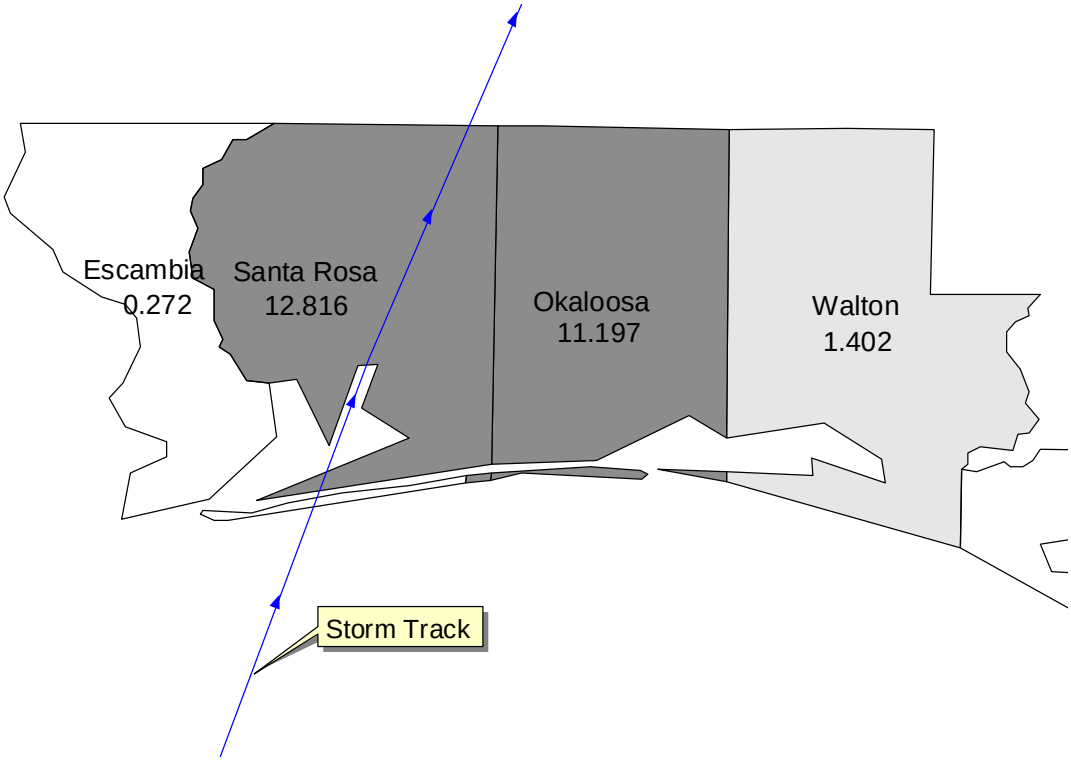

Figure 9.22. Modeled Building Loss Ratios – Hurricane Opal.

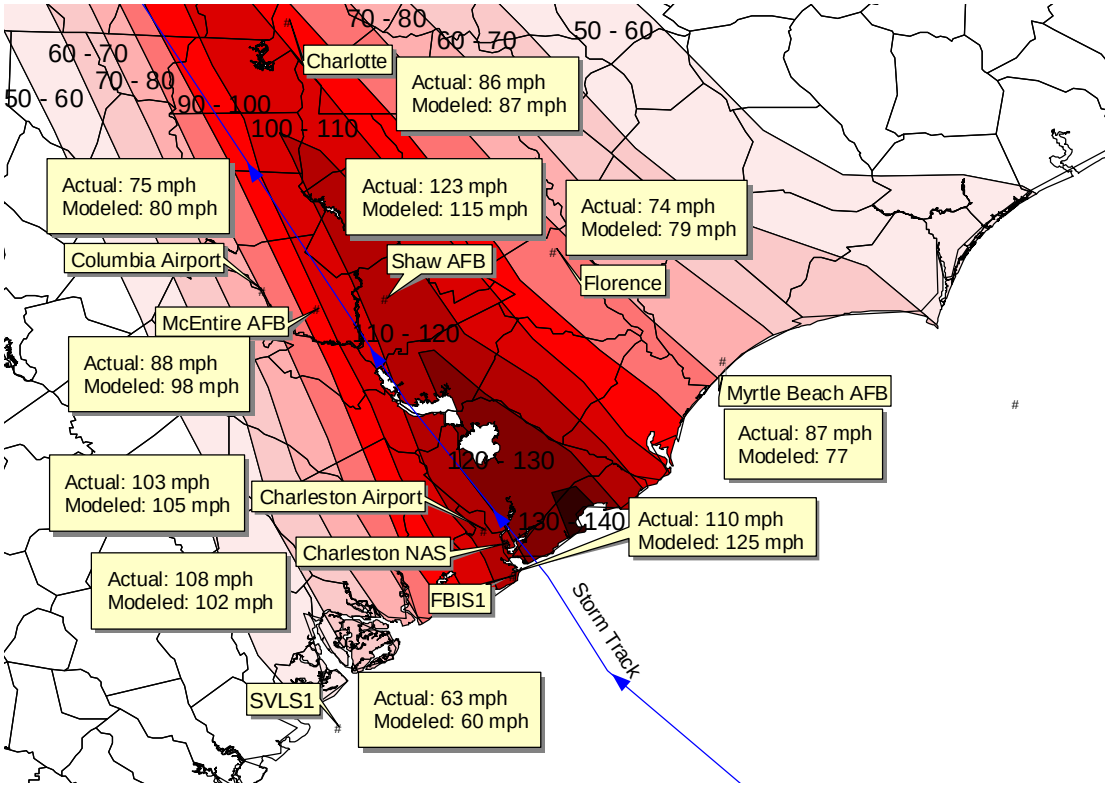

Figure 9.23. Swath of Simulated Peak Gust Wind Speeds (10 m in Open Terrain) Produced by Hurricane Hugo.

In the Hugo loss validation study, the building stock is modeled assuming 70% of the homes are single story and 30% of the homes are two stories. 71% of the one story homes and 50% of the two story homes are assumed to have a garage. 75% of the homes are assumed to have gable roofs and 25% of the homes are assumed to have hip roofs. All roof covers are assumed to be shingles. 30% of the homes are assumed to use 6d nails for roof-deck attachment, and 70% of the homes are assumed to use 8d nails. Roof-wall connections are assumed to be toe-nailed in 90% of the cases and strapped for the other 10%. The construction quality factor is set equal to one in the analysis. The average surface roughness at each ZIP Code is estimated using MRLC data. The model houses are assumed to be randomly oriented within a ZIP Codes. The insured value of the contents is taken as 70% of the insured building value.

For each ZIP Code and each building configuration, a number of simulations are performed and the average loss ratio is calculated. Then, by taking into account the assumed building stock distribution within each ZIP Code, a weighted average of the loss ratios (for all modeled building configurations) is obtained. Comparisons of the predicted and observed loss ratios are plotted vs. the modeled peak gust wind speed at the centroid of the ZIP Code in Figure 9.27, which shows reasonably good agreement between the two. The total losses (building plus contents) summed over the entire state of South Carolina was estimated assuming that both the number of policies and value of these

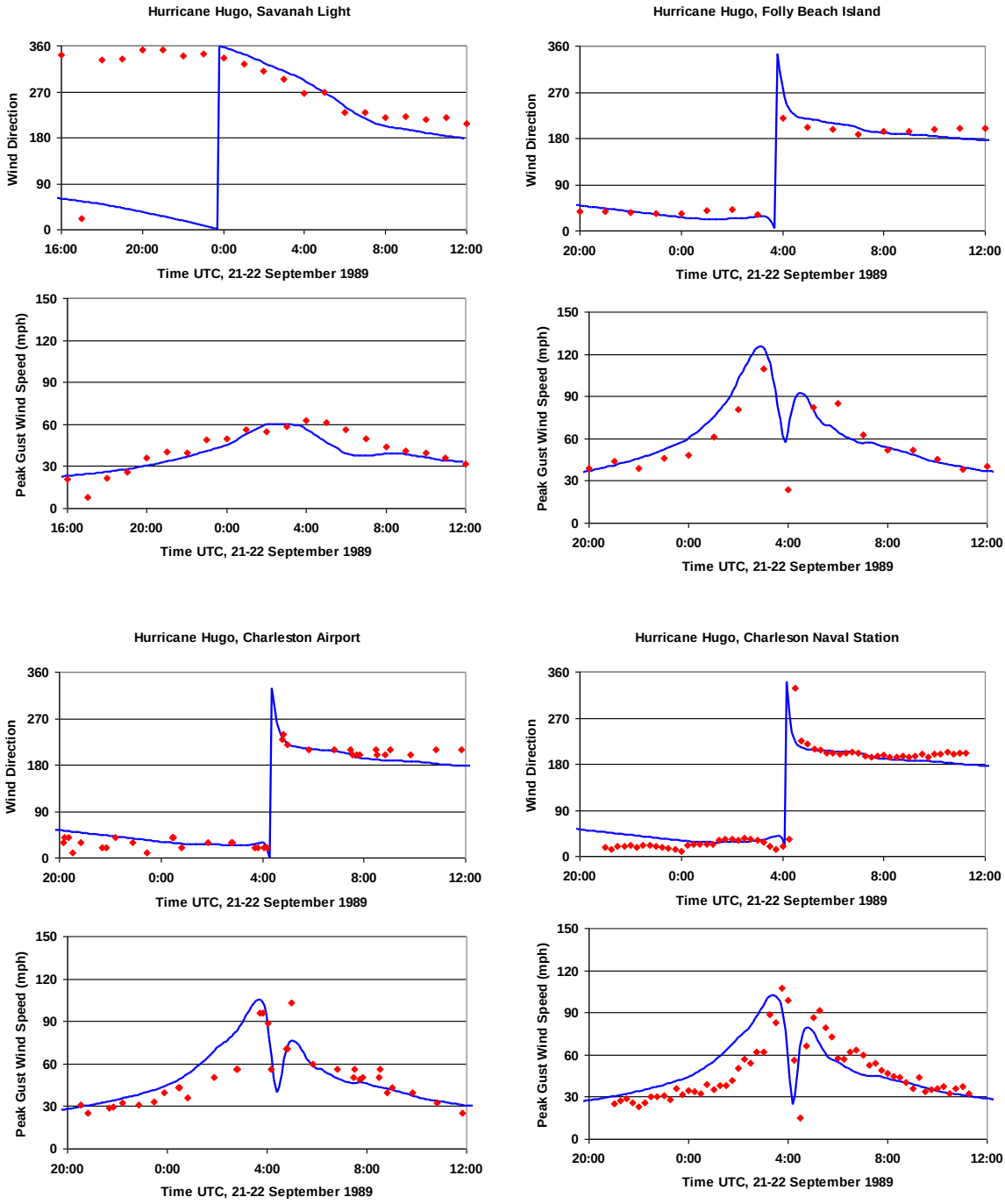

Figure 9.24. Comparison of Simulated and Observed Peak Gust Wind Speeds and Directions Produced by Hurricane Hugo. All Wind Speeds are Given for the Actual Terrain at a Height of 10 m Above Ground.

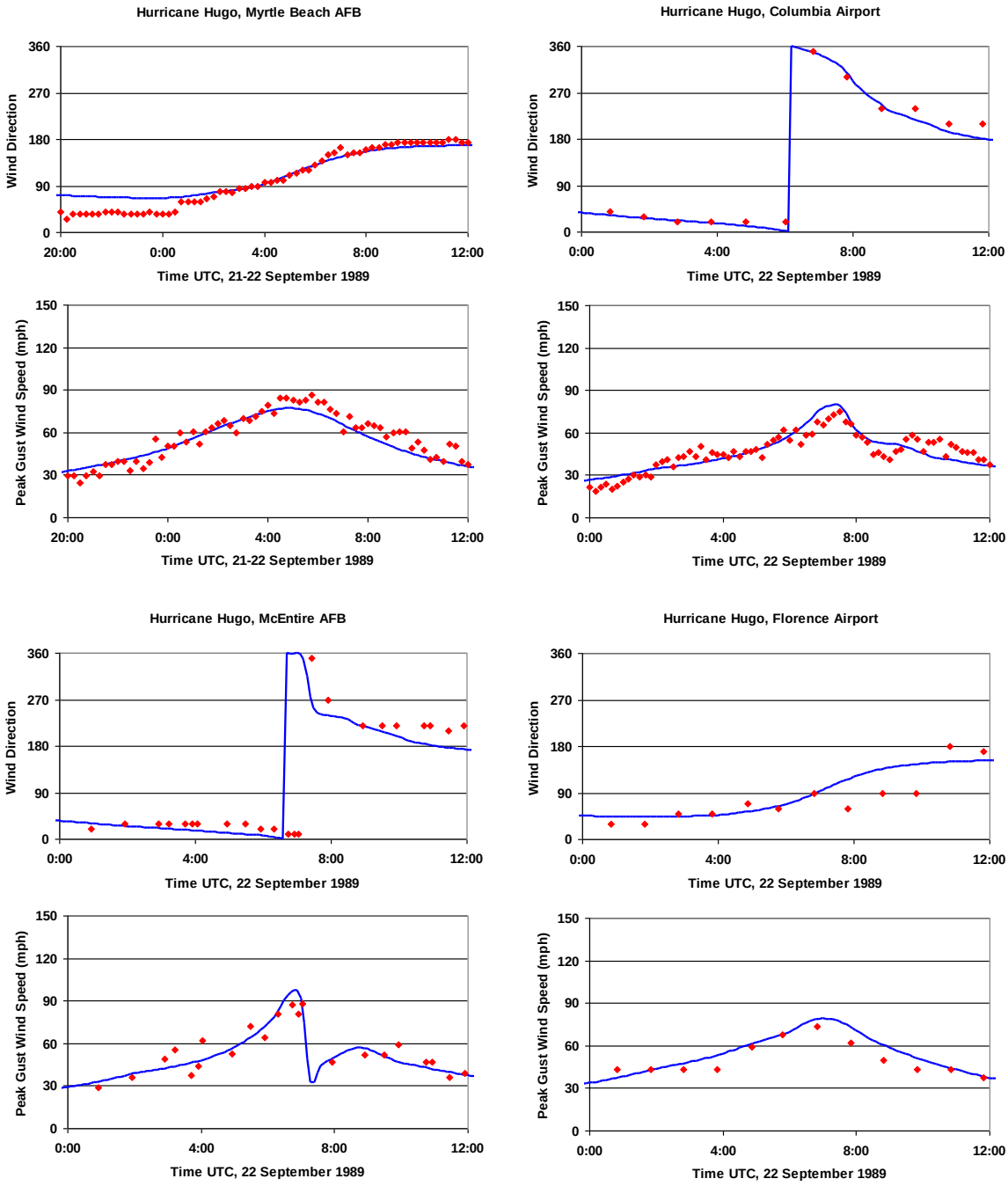

Figure 9.25. Comparison of Simulated and Observed Peak Gust Wind Speeds and Directions Produced by Hurricane Hugo. All Wind Speeds are Given for the Actual Terrain at a Height of 10 m Above Ground.

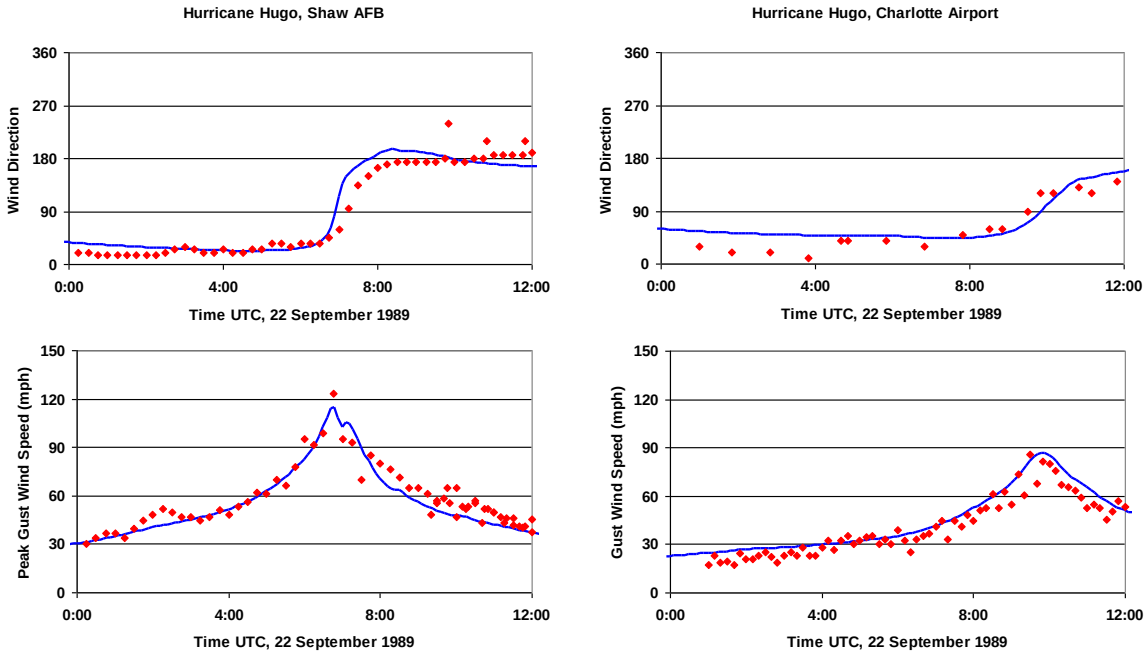

Figure 9.26. Comparison of Simulated and Observed Peak Gust Wind Speeds and Directions Produced by Hurricane Hugo. All Wind Speeds are Given for the Actual Terrain at a Height of 10 m Above Ground.

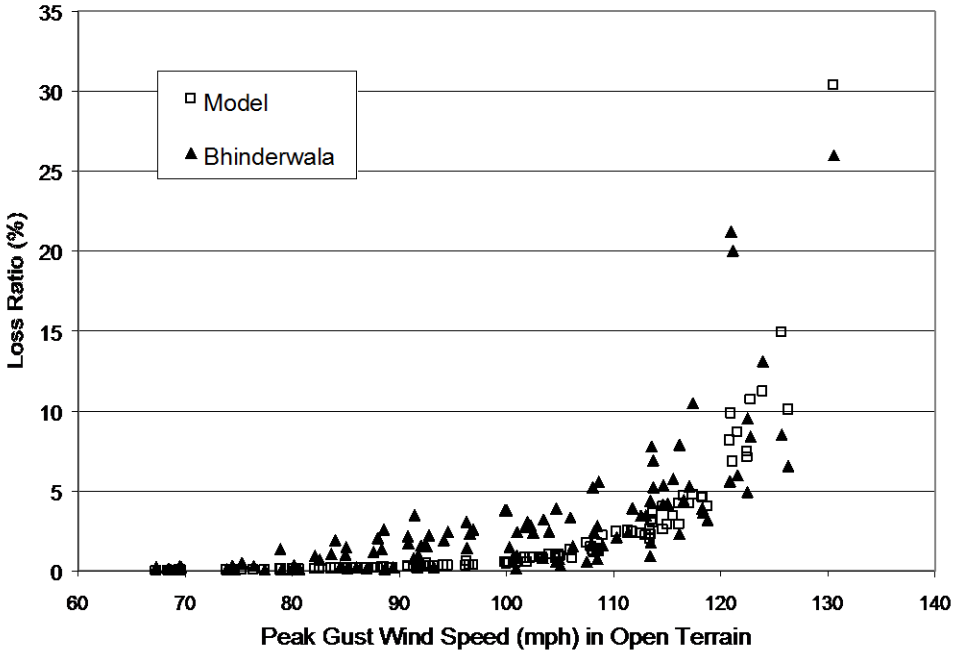

Figure 9.27. Comparison of Observed and Simulated ZIP Code Averaged Losses Produced by Hurricane Hugo in South Carolina.

policies in each ZIP Code are the same (for the same reason as in Andrew validation study). The results shown in Table 9.3 indicate that the modeled losses are slightly lower than the observed losses. The geographic variation of the observed and modeled losses are shown in Figures 9.28 and 9.29, respectively.

Table 9.3. Comparison of Modeled and Observed Aggregate Losses from Hurricane Hugo

Case	Actual Loss Ratio(%)	Modeled Loss Ratio (%)
Bhinderwala	2.96	2.32

9.5 Summary

End-to-end comparisons of modeled and observed insured losses have been presented using five different sets of insurance loss data, covering four hurricanes and three different insurers. The model validation study has been performed for residential buildings only. All modeled losses have been produced using the full load and resistance based damage and loss methodology described in Chapters 4 through 7 (as opposed to the fast-running loss curves used in the end product), and include only direct wind-induced damage to the model buildings, with no modeling of additional damage that some structures will have experienced due to falling trees, nor the inclusion of the effects of minor damage associated with wind driven rain entering a structure through non-breached windows, doors etc.

Figure 9.30 shows a comparison of the modeled and observed losses for the five data sets, plotted vs. the model estimated value of the maximum peak gust wind speed at the ZIP Code centroid. The modeled Hurricane Andrew data in Figure 9.30 are for the case with the terrain modeled using the FWMD LULC database. The losses are given as a percentage, defined as the total loss of the building and contents divided by the insured value of the building and contents. The loss ratios are plotted both on a linear scale (left plot) and on a logarithmic scale (right plot). The agreement between the modeled and the observed losses is generally good, particularly for wind speeds greater than about 100 mph. Figure 9.31 presents an *x-y* plot showing modeled losses plotted vs. the insurance loss data, where again, the agreement between the modeled and the observed losses is good. Overall, if one assumes that the value of the buildings (and contents, if applicable) in each ZIP Code plotted in Figure 9.30 is the same, the average model loss is 8.15%, compared to an observed average of 8.85%, a difference of less than 10%.

The comparisons given in Figure 9.30 and 9.31 overall show good agreement, but suggest that the damage and loss models may underestimate the small losses that occur at lower wind speeds (less than about 100 mph). This underestimate of the losses at these lower wind speeds is not unexpected since, as noted above, the damage and ensuing losses produced by tree blowdown is not modeled, nor are some other small losses associated with damage not explicitly modeled in the damage model, such as minor loss of some types of wall covering, leaking fenestrations, damage of soffits, chimneys, vents, etc.

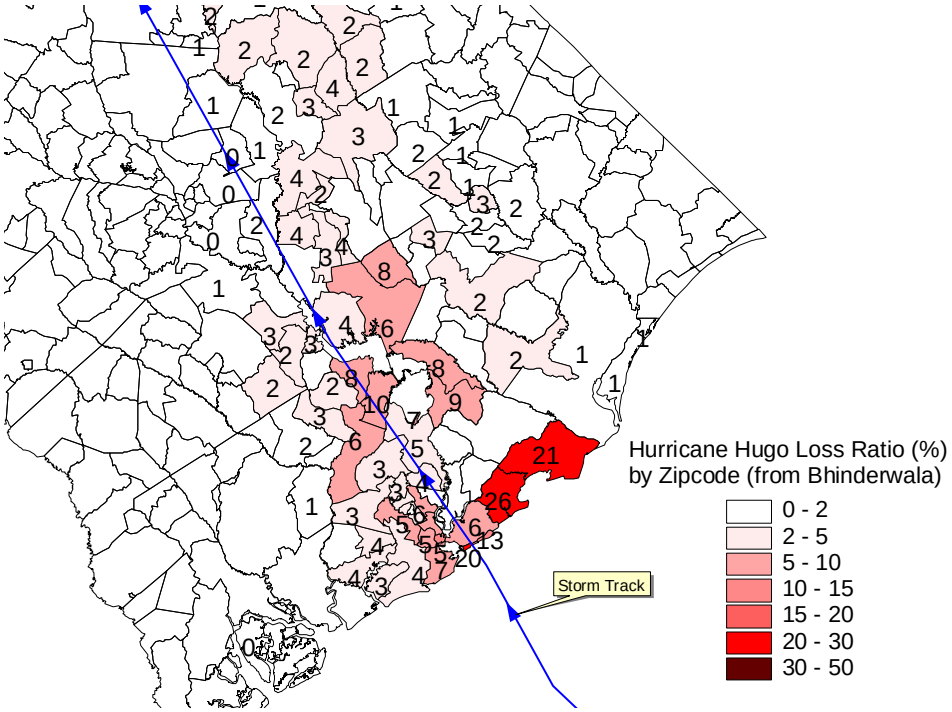

Figure 9.28. Loss Ratios by ZIP Code in South Carolina (Bhinderwala Data).

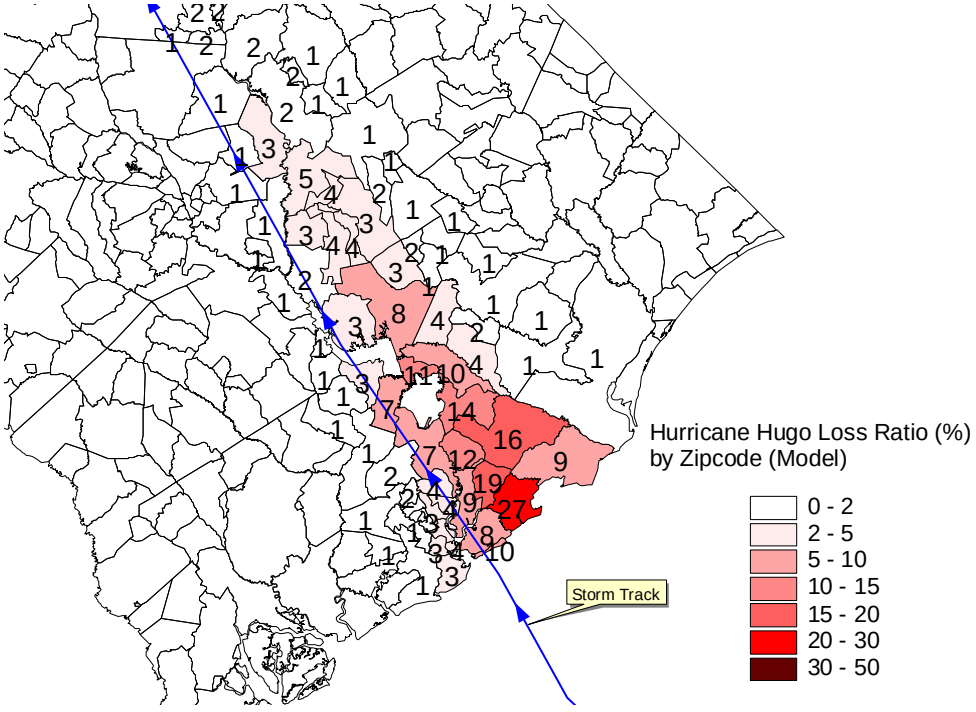

Figure 9.29. Modeled Loss Ratio (MRLC).

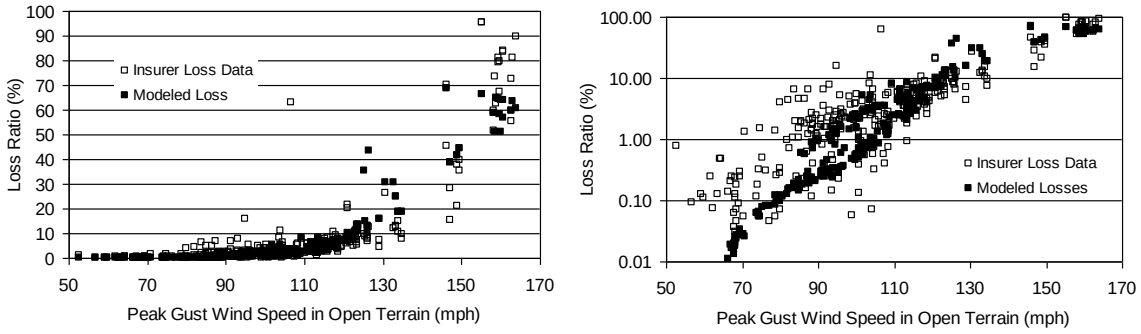

Figure 9.30. Comparison of Modeled and Observed Losses vs. Wind Speed.

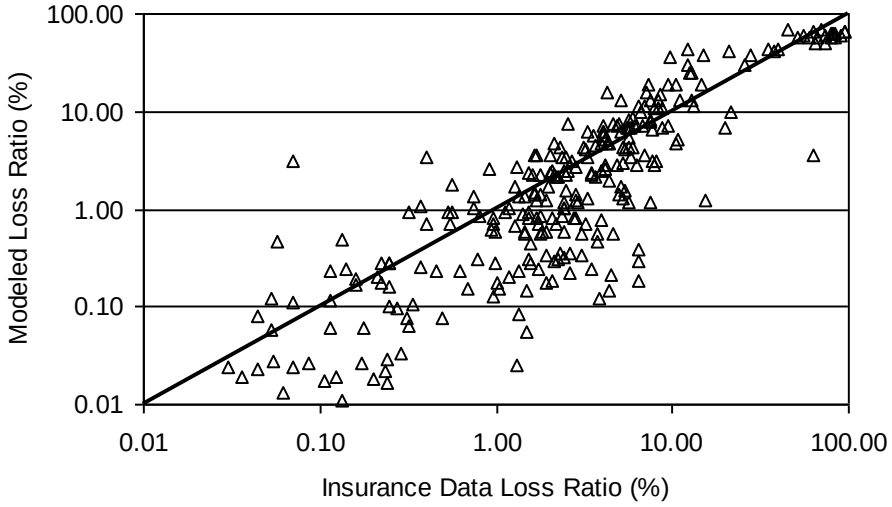

Figure 9.31. Comparison of Modeled and Observed Losses.

Furthermore, in the case of Hurricane Hugo, losses experienced by homeowners to appurtenant structures (fences, driveways, sheds, decks, etc.) were lumped into payments made for losses to the structure and cannot be separated. The loss estimation model does not account for the additional costs associated with these losses.

In summary, the loss validation studies run with the full development model have shown that the damage and loss models reproduce the observed losses reasonably well. Given the recent addition of the tree blowdown methodology (Chapter 12), an updated analysis is needed to determine whether the the losses predicted with the final version of the model are adequately estimated. The validation studies should also be re-run using the end user version of the Hazus Hurricane Model to assess whether the fast-running loss curves applied at the census tract level adequately encapsulate the details considered in the full development model (e.g., storm duration, changes in wind direction, etc.).

Chapter 10. Debris Generated from Damaged Buildings

10.1 Introduction

Debris generated by severe wind events can be categorized into five general types (Holmlin, 1993): medical (or bio-hazardous) wastes, hazardous or toxic wastes (HTW's), household garbage, burnable roadside debris, and construction and demolition debris. Burnable road side debris, which is primarily trees and other yard wastes, is often the largest among those five types of debris. Based on the scope of work specified by FEMA, only debris generated from damaged buildings (i.e., construction and demolition debris produced immediately after the event and during the rebuilding and repairing phases) and tree blow down are calculated in the current version of the model. This chapter presents the building debris model. The tree debris model is presented in Chapter 12.

Building debris consists of construction and demolition waste that is generally non-hazardous and not water soluble. Construction and demolition debris can be further categorized as wood (which is bio-degradable), masonry, metal (which is recyclable), and other (which includes gypsum board, carpet, asphalt roofing material, insulation, ceiling, pipe, etc.). Masonry and other debris are usually disposed of in authorized landfills. Debris removal is often one of the most costly and challenging operations following a natural disaster (Holmlin, 1993). Due to contamination with different types of waste materials, it is also difficult to recycle most of the structural waste (debris). Accurate and prompt estimating of the total debris generated and its distribution is vital to ensure the success of a debris removal operation after a hurricane.

A simple model for estimating the volume and type of debris has been developed by the U.S. Army Corp of Engineers (USACE) using historical data from hurricanes Frederic, Hugo, and Andrew. The USACE model was used to estimate debris produced in Escambia County for hurricanes Erin and Opal. This simple model is intended to be used for estimating debris produced by single-family residential buildings only. The model yields estimates of the expected volumes of burnable debris, landfill debris, soil debris, and metallic debris based on the category of hurricane winds occurring in a county combined with factors related to business use, number of households, vegetation density (light, medium or heavy) and a storm wet/dry multiplier. The model error is typically within ±30% (Moorse, 2001). Recent developments of this model have enabled the analysis to be done at a census track level, resulting in higher accuracy. The major limitation of this model is the inability to take into account various construction and usage classes. For example, the model significantly overestimated the building debris produced by Typhoon Paka in Guam because the model was not able to take into account the reduction in building losses associated with the large number of residential buildings having hardened concrete roofs.

To overcome the limitations of the USACE model, a new debris estimation model has been developed based on the damage states for structural and non-structural components of several model buildings. For each damaged component, the debris generated in each

category (wood, masonry, metal and other) is calculated based on the component's damage state and weight statistics. Then, by adding up the debris produced by all the damaged components, the total debris weight for that model building can be estimated. The debris volume is simply estimated by dividing the debris weight by its density. The accuracy of the new model depends heavily on the accuracy of underlying databases (which includes unit weights of the building components, debris distribution matrix, and detailed building configuration). Therefore, efforts have been devoted to the database development for the new debris model. Limited case studies have been conducted to test and calibrate the new model, and the results are summarized at the end of this section.

10.2 Description of Methodology

The form of the debris model is:

$$\mathrm{D} = \sum_{i=1}^{n} W_i \, f(d_i) \mathrm{D}_i \tag{10.1}$$

where D = debris distribution vector for the model building, which consists of debris from wood, masonry, metal and other, respectively; W_i = total weight of building component i; $f(\cdot)$ = damage intensity function, $0 \le f(\cdot) \le 1$; d_i = damage state of building component i, which is obtained from the physical damage model; D_i = debris distribution vector for building component i, which specifies the ffactions of total component weight in wood, masonry, metal and other. Since the building component weights and debris distribution vectors are available from a number of sources, the only new development needed is to define the damage intensity functions.

Similar to the economic loss model, the debris model has to produce debris estimation based on the damage states provided by the load-resistance physical damage model, which include number of damaged fenestrations, roof cover damage, roof sheathing damage, wall damage, and water damage (amount of water entering the building). The building components can be divided into two categories: those modeled explicitly by the damage model (primarily damage to the building envelope) and those modeled implicitly by the damage model (i.e., their damage states have to be estimated based on envelope damage). For components that are modeled explicitly in the damage model, it was assumed that $f(d_i) = d_i$. For components that are not modeled explicitly (e.g., building interior), the damage intensity functions were assumed to be similar in format to those used in the economic loss model, however with different parameters. For example, the interior damage due to water entering damaged fenestration was modeled as 1/4 of the rate defined by the damage intensity function in the economic loss model. Those parameters were developed using a combination of historical data and judgment. The interior damage intensity functions for roof cover, roof sheathing, and fenestration damages are defined as:

$$I_{cv} = f(d_{cv}) = \begin{cases} 0.5 d_{cv} & \text{without secondary water resistance} \\ 0.05 d_{cv} & \text{with secondary water resistance} \end{cases} \tag{10.2}$$

$$I_{sh} = f(d_{sh}) = 1.8 d_{sh} \tag{10.3}$$

$$I_{fen} = f(d_{fen}) = 1.0 d_{fen} \tag{10.4}$$

where I_{cv} = interior damage level due to roof cover damage; d_{cv} = percentage of roof cover damage; I_{sh} = interior damage level due to roof sheathing damage; d_{sh} = percentage of roof sheathing damage; I_{fen} = interior damage level due to fenestration damage; d_{fen} = the amount (in.) of wind driven rain in the interior due to fenestration damage. The final interior damage level (I) is calculated as the maximum of interior damage levels due to roof cover, roof sheathing, and fenestration damages, i.e., I = max(I_{cv}, I_{sh}, I_{fen}). The damage levels for all interior assemblies, such as partition wall, ceiling, floor finish, wall finish, content, etc., given an interior damage level, are assumed to be the same. Therefore, the total interior debris is estimated by (assuming m interior components):

$$\mathrm{D}_{int} = I \sum_{i=1}^{m} W_i \mathrm{D}_i \tag{10.5}$$

where D_{int} = interior debris distribution vector. It is further assumed that, for engineered buildings, non-modeled load-bearing structural components (such as columns and beams, concrete or metal deck floors, and load-bearing partition walls) will not be damaged and therefore no debris could be produced from those components. However, finishes on those components can be damaged by water entering the building.

For buildings that reach the destruction damage state (see definitions in Chapter 6), the entire building will be torn down and the debris produced by demolition will equal to the total building weight. In the present debris model, global damage indicators (such as total roof cover damage ratio, total roof deck damage ratio, roof frame failure, wall frame failure, etc.) are monitored and once the destruction state is reached, the total building weight will be used as the total debris weight. The total building weight is pre-calculated based on the specified construction for the model building (in the case when construction types for certain components are not given, default construction types are used in the analysis). Note that the weight of foundation is not included in the total building weight calculation. The default construction characteristics for economy, average, custom, and luxury residential buildings are defined in the residential economic loss model. The default construction characteristics for commercial buildings will be discussed later.

After total debris weight in each category (wood, masonry, metal and other) is determined, the total debris volume is estimated by dividing the total debris weight of each type by its density. However, since debris can't be fully packed, the debris density will be much less than its material's density. In the debris model, the debris density for masonry is assumed to be 2/3 of concrete masonry density (125 pcf) and the debris densities for the remaining types of debris are assumed to be 1/2 of their material densities. Due to mixture of different materials, the material density for *other* types of

debris is not readily available. It is assumed to be 70 pcf in the present debris model (between the densities of wood and masonry).

Component Unit Weight. Building component (or assembly) weights are closely related to building dead loads, while content weights are closely related to sustained live loads. Therefore, it is natural to refer to the current building code for this information. Specifically, the ASCE 7-98 Commentary (1999) is used to obtain the building component weights and live load statistics in this study. For items that are not included in the ASCE Commentary, references are made to the manufacturer's manuals. RSMeans (2001) is also used to obtain unit weights for a number of building assemblies. Table 10.1 lists the collected average building component weights. The COV for each item is assumed to be 20%. Table 10.2 lists the sustained live load statistics for residential buildings and several types of commercial buildings. For building usage types that are not listed in this table, a mean of 10 psf and standard deviation of 5 psf are assumed. Note that sustained live load statistics are based on specified areas of observation (see Table 10.2-2). The standard deviation of the average sustained load for an area greater than the observation area is:

$$\sigma_n = \sqrt{\frac{\sigma}{n}} \tag{10.6}$$

where σ_n = standard deviation of the sustained load for an area n times of the observation area and σ = observed standard deviation of the sustained load.

Debris Distribution Matrix. The debris distribution matrix defines how the debris is distributed among the four debris types (wood, masonry, metal, and other). As shown in Table 10.3, for each building component, four numbers are given, which represent the portion of debris in each debris type. For example, for combined wood and masonry exterior wall, 45% of the debris is wood, 45% of the debris is masonry, 5% of the debris is metal and the remaining 5% of the debris is other. Even though most of the time the debris distribution is intuitive and readily determined (such as metal shingle, plywood deck, and fibrous glass insulation), there are still cases that require engineering judgment. Further validation of those cases is desirable in the future.

Default Component Construction Types for Commercial Buildings. For components that are not specified in the model building, the default construction types are assumed to be the same as those specified in the RSMeans (2001). Table 10.4 lists the indices of the construction types for roof frame, insulation, partition construction, floor construction, floor finish, ceiling finish, and wall finish. The descriptions and weights for related indices are listed in Tables 10.5 through 10.11, respectively. The weights for floor finish and wall finish are calculated based on their finish composition.

Table 10.1. Component Unit Weight Used in the Debris Model

Category	Component	Unit Weight (psf)
Roof Cover	Slate, 1/4″	10
	26 gage metal shingle or metal panel	2
	Wood shingles	3
	Three-ply ready roofing	1
	Asbestos-cement shingles	4
	Slate, 3/16″	7
	Single-ply, sheet membranes	0.7
	Roman tile	12
	Ludowici tile	10
	Liquid applied membranes	1
	Five-ply felt and gravel	6
	Corrugated asbestos-cement roofing	4
	Copper or tin	1
	Cement tile	16
	Book tile, 3″	20
	Book tile, 2″	12
	Bituminous, smooth surface membranes	1.5
	Bituminous, gravel-covered membranes	5.5
	Asphalt shingles	2
	Four-ply felt and gravel	5.5
	Spanish	19
Roof Deck	Decking, 2″ wood	5
	Wood sheathing (per in. thickness)	3
	Decking, 3″ (Douglas fir)	8
	Deck, metal, 20 gage	2.5
	Deck, metal, 18 gage	3
	Plywood (per in. thickness)	3.2
Roof Frame	16″ deep @ 6' Bar Joist	17.5
	2×4 @24″ slope 4/12	2.0
	2×6 @ 48″ 2×3 batten@36″	1.2
	Metal truss	12
	Post and beam	8
Insulation	Rigid insulation, 1/2″	0.8
	Urethane foam with skin	0.5
	Polystyrene foam insulation	0.2
	Fibrous glass insulation (4″ thick)	4.4
	Fiberboard insulation	1.5
	Cellular glass insulation (4″ thick)	2.8
	Perlite insulation	0.8
Ceiling	Acoustical fiber board	1
	Gypsum Board (1/2″ thickness)	2
	Mechanical duct allowance	4
	Plaster on tile or concrete	5
	Plaster on wood lath	8
	Suspended metal lath and cement plaster	15
	Suspended metal lath and gypsum plaster	10
	Suspended steel channel system	2
	Wood furring suspension system	2.5
Coverings, Roof, and Wall	Fiberboard, 1/2″	0.8
	Gypsum sheathing, 1/2″	2
Exterior Wall	8″ medium weight hollow CMU, grout 40″ O.C.	45
	6″ normal weight solid CMU	64
	4″ normal weight solid CMU	41
	6″ light weight solid CMU	51

Table 10.1. Component Unit Weight Used in the Debris Model (continued)

Category	Component	Unit Weight (psf)
Exterior Wall	6″ medium weight hollow CMU, full grout	59
	6″ medium weight hollow CMU, grout 16″ O.C.	44
	6″ medium weight hollow CMU, grout 24″ O.C.	39
	6″ medium weight hollow CMU, grout 32″ O.C.	36
	6″ medium weight hollow CMU, grout 40″ O.C.	34
	6″. medium weight hollow CMU, grout 48″ O.C.	33
	6″. medium weight hollow CMU, no grout	28
	6″ medium weight solid CMU	60
	4″ medium weight solid CMU	38
	8″ clay brick wythes	79
	8″ light weight solid CMU	69
	8″ medium weight hollow CMU, full grout	81
	8″ medium weight hollow CMU, grout 16″ O.C.	59
	4″ medium weight hollow CMU, no grout	26
	8″ medium weight hollow CMU, grout 32″ O.C.	47
	2×6 @ 16″, 5/8″ gypsum, insulated, 3/8″ siding	12
	8″ medium weight hollow CMU, grout 48″ O.C.	44
	8″ medium weight hollow CMU, no grout	36
	8″ medium weight solid CMU	81
	8″ normal weight solid CMU	87
	Exterior stud walls with brick veneer	48
	8″ medium weight hollow CMU, grout 24″ O.C.	51
	10″ normal weight solid CMU	110
	10″ light weight solid CMU	87
	10″ medium weight hollow CMU, full grout	102
	10″ medium weight hollow CMU, grout 16″ O.C.	73
	10″ medium weight hollow CMU, grout 24″ O.C.	63
	10″ medium weight hollow CMU, grout 32″ O.C.	58
	10″ medium weight hollow CMU, grout 40″ O.C.	56
	10″ medium weight hollow CMU, grout 48″ O.C.	54
	4-″ light weight solid CMU	32
	10″ medium weight solid CMU	102
	12″ clay brick wythes	115
	12″ light weight solid CMU	105
	12″ medium weight hollow CMU, full grout	123
	2×4 @ 16″, 5/8″ gypsum, insulated, 3/8″ siding	11
	12″ medium weight hollow CMU, grout 24″ O.C.	75
	12″ medium weight hollow CMU, grout 32″ O.C.	68
	4″ clay brick wythes	39
	12″ medium weight hollow CMU, grout 40″ O.C.	65
	12″ medium weight hollow CMU, grout 48″ O.C.	62
	12″ medium weight hollow CMU, no grout	50
	12″ medium weight solid CMU	124
	12″ normal weight solid CMU	133
	16″ clay brick wythes	155
	12″ medium weight hollow CMU, grout 16″ O.C.	87
	10″ medium weight hollow CMU, no grout	44
Floors and Floor Finishes	Asphalt block (2″), 1/2″ mortar	30
	Cement finish (1″) on stone-concrete fill	32

Table 10.1. Component Unit Weight Used in the Debris Model (concluded)

Category	Component	Unit Weight (psf)
Floor and Floor Finishes	Ceramic or quarry tile (3/4″) on 1/2″ mortar bed	16
	Ceramic or quarry tile (3/4″) on 1″ mortar bed	23
	Hardwood flooring, 7/7″	4
	Linoleum or asphalt tile, 1/4″	1
	Terrazzo (1″) on stone-concrete fill	32
	Concrete floor on steel beam (Commercial)	38
	Steel deck on steel beam (Commercial)	30
	Concrete fill finish (per inch thickness)	12
	Carpet	2
	Wood block (3″) on 1/2″ mortar base	16
	Terrazzo (1″) on 2″ stone-concrete	32
	Terrazzo (1-1/2″) directly on slab	19
	Subflooring, 3/4″	3
	Solid flat tile on 1″ mortar base	23
	Slate (per mm thickness)	15
	Marble and mortar on stone-concrete file	33
	Wood block (3″ 0 on mastic, no fill	10
Floors, Wood-Joist	2×6 joists, 12″ spacing double wood floor	6
	2×8 joists, 12″ spacing double wood floor	6
	2×8 joists, 24″ spacing double wood floor	5
	2×8 joists, 16″ spacing double wood floor	8
	2×10 joists, 12″ spacing double wood floor	7
	2×10 joists, 16″ spacing double wood floor	6
	2×12 joists, 24″ spacing double wood floor	6
	2×12 joists, 16″ spacing double wood floor	7
	2×12 joists, 12″ spacing double wood floor	8
	2×10 joists, 24″ spacing double wood floor	6
	2×6 joists, 16″ spacing double wood floor	5
	2×6 joists, 24″ spacing double wood floor	5
Frame Partitions	Movable steel partitions	4
	Wood studs, 2×4, unplastered	4
	Wood studs, 2×4, plastered two sides	20
	Wood or steel studs, 1/2″ gypsum board each side	8
	Wood studs, 2×4, plastered one side	12
	Gypsum board and sound deadening board on wood or steel stud	15
Doors	Interior and Exterior	10
Garage Doors	Regular garage doors	1.6
Skylight	Skylight, metal frame, 3/8″ wire glass	8
Sliders	3/16″ tempered sliding glass door	4
Windows	Windows, glass, frame and sash	8

Table 10.2. Sustained Load Statistics

Usage Type	Occupancy	Mean (psf)	Std (psf)	Area (ft^2)
Office Building	Offices	10.9	5.9	200
Residential	Renter	6	2.6	200
Residential	Owner	6	2.6	200
Residential	Attic	2	0.87	200
Commercial	Default	10	5	200
Hotel	Guest room	4.5	1.2	200
School	Classrooms	12	2.7	1000

Table 10.3. Debris Distribution Matrix

Category	Type	Wood	Masonry	Metal	Other
Ceiling	Gypsum board (2 mm thickness)	0.00	0.00	0.00	1.00
	Gypsum board or plaster on wood furring	0.10	0.00	0.00	0.90
	Suspended metal lath and gypsum plaster	0.00	0.00	0.15	0.85
	Suspended steel channel system	0.00	0.00	1.00	0.00
Content	Commercial	0.30	0.00	0.20	0.50
	Residential	0.60	0.00	0.00	0.40
Exterior Wall	Combined wood and masonry	0.45	0.45	0.05	0.05
	Unreinforced and reinforced Masonry	0.00	0.90	0.05	0.05
	Wood	0.90	0.00	0.05	0.05
Exterior Wall Siding	Aluminum siding, metal panel	0.00	0.00	1.00	0.00
	Brick veneer, block	0.00	1.00	0.00	0.00
	NA	0.00	0.00	0.00	0.00
	Stone veneer, vinyl, stucco	0.00	0.00	0.00	1.00
	Wood	1.00	0.00	0.00	0.00
Floors	Commercial (concrete)	0.05	0.00	0.05	0.90
	Commercial (steel joist, flat form, concrete)	0.00	0.00	0.40	0.60
	Commercial (steel joist/truss)	0.00	0.00	0.80	0.20
	Residential	0.70	0.00	0.00	0.30
Garage Doors	All	0.00	0.00	1.00	0.00
Insulation	Fibrous glass, All other	0.00	0.00	0.00	1.00
Interior Partition	50% Concrete, 50% Wood Stud	0.10	0.00	0.00	0.90
	Concrete Block	0.00	0.00	0.00	1.00
	Movable Steel Partition	0.00	0.00	0.90	0.10
	Steel stud	0.00	0.00	0.20	0.80
	Wood stud	0.20	0.00	0.00	0.80
Regular Doors	All	0.90	0.00	0.00	0.10
Roof Cover	Asphalt shingle, asbestos shingle, flat tile, other tile, Slate, built-up roof, single-ply membrane, and Other	0.00	0.00	0.00	1.00
	Metal shingle, metal panel	0.00	0.00	1.00	0.00
	Wood shake	1.00	0.00	0.00	0.00
Roof Deck	Concrete	0.00	0.00	0.00	1.00
	Plywood, T&G, OSB, Dimensional lumber, Batten	1.00	0.00	0.00	0.00
Roof Frame	Metal truss	0.00	0.00	1.00	0.00
	Wood truss, wood joist, post and beam	1.00	0.00	0.00	0.00
Skylight	All	0.00	0.00	0.10	0.90
Sliders	All	0.00	0.00	0.10	0.90
Windows	All	0.20	0.00	0.10	0.70

10.3 Validation Studies

The US Army Corps of Engineers (USACE) is the principal organization responsible for debris clean-up and removal. Other local and state government agencies may also coordinate the debris clean-up efforts. USACE after action reports are the most readily available sources for model validation and testing. These reports contain information on the total amount (either by volume or by weight) of debris produced by hurricanes. However, since the after action reports don't differentiate burnable roadside debris from construction and demolition debris, assumptions have to be made to the ratio of these two types of debris (recall that only construction and demolition debris is estimated by the

Table 10.4. Default Building Component Construction Types

ID	Building Type	Roof Frame	Insul.	Partit. Const.	Floor Const.	Floor Finish	Ceiling Finish	Wall Finish
M010	Apartment, 1-3 Story	6	5	5	7	9	11	13
M020	Apartment, 4-7 Story	6	5	5	7	9	11	13
M030	Apartment, 8-24 Story	6	5	6	7	9	11	13
M040	Auditorium	9	5	4	7	23	14	14
M050	Bank	1	5	7	10	3	7	5
M060	Bowling Alley	6	5	3	10	34	14	21
M070	Bus Terminal	6	5	3	10	6	7	20
M080	Car Wash	6	5	3	10	36	17	21
M090	Church	5	7	10	10	33	17	21
M100	Club, Country	11	10	7	10	1	5	2
M110	Club, Social	6	5	3	10	10	7	10
M120	College, Classroom, 2-3 Story	6	5	3	7	22	7	19
M130	College, Dorm, 2-3 Story	2	5	6	2	24	1	19
M140	College, Dorm, 4-8 Story	3	5	3	3	24	7	19
M150	College, Laboratory	6	5	3	5	11	7	8
M160	College, Student Union	2	5	7	2	5	14	5
M170	Community Center	6	5	7	10	5	7	21
M180	Courthouse, 1 Story	1	5	10	10	12	4	12
M190	Courthouse, 2-3 Story	3	5	10	3	12	4	12
M200	Factory, 1 Story	6	5	4	10	34	2	21
M210	Factory, 3 Story	2	5	7	2	31	2	21
M220	Fire Station, 1 Story	6	5	4	10	8	2	21
M230	Fire Station, 2 Story	6	5	4	7	8	2	21
M240	Fraternity/Sorority House	10	3	7	6	16	3	21
M250	Funeral Home	11	6	5	10	18	2	7
M260	Garage, Auto Sales	6	5	7	10	8	2	21
M270	Garage, Parking	12	10	3	10	36	17	21
M280	Garage, Underground Parking	1	10	3	1	36	17	21
M290	Garage, Repair	6	5	4	10	31	3	21
M300	Garage, Service Station	11	5	4	10	34	10	21
M310	Gymnasium	5	6	4	10	30	7	4
M320	Hangar, Aircraft	6	2	4	10	36	17	21
M330	Hospital, 2-3 Story	1	5	6	1	13	15	1
M340	Hospital, 4-8 Story	6	5	5	3	13	15	1
M350	Hotel, 4-7 Story	6	5	5	3	24	7	17
M360	Hotel, 8-24 Story	6	5	5	7	24	11	17
M370	Jail	3	5	3	3	20	7	21
M380	Laundromat	6	5	7	10	34	2	21
M390	Library	4	5	7	4	4	7	21
M400	Medical Office, 1 Story	11	3	5	10	5	7	5
M410	Medical Office, 2 Story	6	5	5	7	5	7	6
M420	Motel, 1 Story	11	3	5	10	27	10	18
M430	Motel, 2-3 Story	7	5	3	28	8	18	8
M440	Movie Theatre	6	5	4	4	7	21	7
M450	Nursing Home	8	5	7	32	9	6	9
M460	Office, 2-4 Story	6	5	7	9	7	9	7
M470	Office, 5-10 Story	6	5	7	9	3	9	7
M480	Office, 11-20 Story	6	5	7	9	3	9	7
M490	Police Station	6	5	4	20	7	18	7
M500	Post Office	6	5	4	8	10	21	7
M510	Racquetball Court	6	5	6	25	7	21	7

Table 10.4. Default Building Component Construction Types (concluded)

ID	Building Type	Roof Frame	Insul.	Partit. Const.	Floor Const.	Floor Finish	Ceiling Finish	Wall Finish
M520	Religious Education	6	5	4	5	10	21	7
M530	Restaurant	11	3	7	14	10	16	7
M540	Restaurant, Fast Food	6	5	7	35	10	21	7
M550	Rink, Hockey/Indoor Soccer	6	5	3	26	10	21	7
M560	School, Elementary	6	5	4	15	10	15	7
M570	School, High, 2-3 Story	2	5	4	21	2	15	7
M580	School, Jr. High, 2-3 Story	6	5	4	7	7	3	7
M590	School, Vocational	6	5	4	21	7	3	7
M600	Store, Convenience	11	3	7	34	10	21	7
M610	Store, Department, 1 Story	7	5	7	4	10	21	7
M620	Store, Department, 3 Story	6	5	7	2	3	11	7
M630	Store, Retail	6	5	7	34	10	21	7
M640	Supermarket	6	5	2	34	10	21	7
M650	Swimming Pool, Enclosed	11	5	4	19	10	20	7
M660	Telephone Exchange	6	5	7	29	10	21	2
M670	Town hall, 1 Story	6	5	7	17	10	18	7
M680	Town Hall, 2-3 Story	6	5	7	17	7	18	7
M690	Warehouse	6	5	3	31	7	21	7
M700	Warehouse, Mini	6	5	6	36	10	21	17

Table 10.5. Roof Frame Construction Types and Unit Weights

ID	Construction Type	Weight (psf)
1	Cast-in-place concrete slab	48.0
2	Concrete flat plate (8″)	96.0
3	Concrete slab on metal deck and beam	34.0
4	Concrete waffle slab (10″)	120.0
5	Laminated wood arches	3.0
6	Open web steel joist	17.5
7	Pre-cast concrete beam and plank	80.0
8	Pre-cast double tees	42.0
9	Steel Truss	3.0
10	Wood Rafter	1.2
11	Wood Truss	2.0

Table 10.6. Insulation Types and Unit Weights

ID	Construction Type	Weight (psf)
1	Cellular glass insulation (4″ thick)	2.8
2	Fiberboard	1.5
3	Fiberglass sheets	1.5
4	Fibrous glass insulation (4″ thick)	4.4
5	Perlite/EPS composite	0.8
6	Polyisocyanurate sheets	0.4
7	Polystyrene (2″ thick)	0.4
8	Rigid insulation, 1/2″	0.8
9	Urethane foam with skin	0.5

Table 10.7. Partition Construction Types and Unit Weights

ID	Construction Type	Weight (psf)
1	2×4 unplastered wood or metal studs	4
2	50% concrete block, 505 gypsum board on metal studs	22
3	Concrete block	36
4	Concrete block and toilet partitions	26
5	Gypsum board and sound deadening board on wood or metal studs	15
6	Gypsum board on concrete block and metal studs	32
7	Gypsum board on wood or metal studs	8
8	Lightweight concrete block	24
9	Movable steel partitions	4
10	One side plaster on wood or metal studs	12
11	Two sides plaster on wood or metal studs	20

Table 10.8. Floor Finish Types and Unit Weights

ID	Finish Type	Weight (psf)
1	50% carpet, 30% hardwood, 20% ceramic tile	6.8
2	50% carpet, 40% marble tile, 10% terrazzo	17.4
3	50% carpet, 40% vinyl composition tile, 10% quarry tile	3.7
4	50% carpet, 50% ceramic tile	12.5
5	50% carpet, 50% vinyl composition tile	1.5
6	50% quarry tile, 50% vinyl composition tile	12.0
7	50% vinyl composition tile, 30% carpet, 20% terrazzo	7.5
8	50% vinyl composition tile, 50% paint	0.5
9	60% carpet, 30% vinyl composition tile, 10% ceramic tile	3.8
10	60% carpet, 35% hardwood, 5% ceramic tile	3.8
11	60% epoxy, 20% carpet, 20% vinyl composition tile	5.0
12	60% hardwood, 20% carpet, 20% terrazzo	9.2
13	60% vinyl composition tile, 20% ceramic tile, 20% terrazzo	11.6
14	65% carpet, 35% quarry tile	9.4
15	65% vinyl composition tile, 25% carpet, 10% terrazzo	4.4
16	70% carpet, 10% hardwood, 20% ceramic tile	6.4
17	70% carpet, 15% terrazzo, 15% vinyl composition tile	6.4
18	70% carpet, 30% ceramic tile	8.3
19	70% terrazzo, 30% ceramic tile	29.3
20	70% vinyl composition tile, 20% carpet, 10% ceramic tile	3.4
21	70% vinyl composition tile, 20% carpet, 10% terrazzo	4.3
22	70% vinyl composition tile, 25% carpet, 5% ceramic tile	2.4
23	70% vinyl composition tile, 30% carpet	1.3
24	80% carpet, 10% vinyl composition tile, 10% ceramic tile	4.0
25	80% carpet, 20% ceramic tile	6.2
26	80% rubber mat, 20% paint	1.6
27	85% carpet, 15% ceramic tile	5.2
28	85% carpet, 5% vinyl composition tile, 10% ceramic tile	4.1
29	90% carpet, 10% terrazzo	5.0
30	90% hardwood, 10% ceramic tile	5.9
31	90% metallic hardener, 10% vinyl composition tile	1.9
32	95% vinyl tile, 5% ceramic tile	2.1
33	Carpet	2.0
34	Vinyl composition tile	1.0
35	Quarry tile	23.0

Table 10.9. Floor Construction Types and Unit Weights

ID	Construction Type	Weight (psf)
1	Cast-in-place concrete beam and slab	120.0
2	Concrete flat plate	120.0
3	Concrete slab with metal deck and beams	38.0
4	Concrete waffle slab	120.0
5	Metal deck on open web steel joist	17.5
6	Wood joist	6.0
7	Open web steel joists, slab form, concrete	30.0
8	Pre-cast concrete beam and plank	80.0
9	Pre-cast double tees with concrete topping	58.0

Table 10.10. Wall Finish Types and Unit Weights

ID	Construction Type	Weight (psf)
1	40% vinyl wall covering, 35% ceramic tile, 25% epoxy coating	8.5
2	40% vinyl wall covering, 40% paint, 20% ceramic tile	5.0
3	50% paint, 40% glazed coating, 10% ceramic tile	2.3
4	50% paint, 50% ceramic tile	11.5
5	50% paint, 50% vinyl wall covering	0.5
6	50% vinyl wall covering, 45% paint, 5% ceramic tile	1.7
7	50% wallpaper, 25% wood paneling, 25% paint	1.1
8	60% paint, 40% epoxy coating	0.0
9	60% vinyl wall covering, 40% paint	0.6
10	65% paint, 25% vinyl wall covering, 10% ceramic tile	2.6
11	70% paint, 20% vinyl wall covering, 10% ceramic tile	2.5
12	70% paint, 20% wood paneling, 10% vinyl wall covering	0.9
13	70% paint, 25% vinyl wall covering, 5% ceramic tile	1.4
14	70% paint, 30% epoxy coating	0.0
15	75% paint, 15% glazed coating, 10% ceramic tile	2.3
16	75% paint, 25% ceramic tile	5.8
17	75% vinyl covering, 20% paint, 5% ceramic tile	1.9
18	90% paint, 10% ceramic tile	2.3
19	95% paint, 5% ceramic tile	1.2
20	Glazed coating	0.0
21	Paint	0.0

Table 10.11. Ceiling Finish Types and Unit Weights

ID	Finish Type	Weight (psf)
1	90% paint, 10% suspended fiberglass board	0.2
2	Fiberglass board on exposed grid system	3.0
3	Gypsum board on wood furring	4.5
4	Gypsum plaster on suspended metal lath	10.0
5	Gypsum plaster on wood furring	10.0
6	Mechanical duct allowance	4.0
7	Mineral fiber tile on concealed zee bars	2.0
8	Textured finish	0.2
9	Painted gypsum board	2.0
10	Painted gypsum board on furring	3.0
11	Painted gypsum board on resilient channels	2.0
12	Plaster on tile or concrete	5.0
13	Plaster on wood lath	8.0
14	Suspended fiberglass board	1.5
15	Suspended metal lath and cement plaster	15.0
16	Suspended steel channel system	2.0

present debris model), which is not ideal for a validation study. Therefore, references were made to a number of published papers on debris removal (Dowd, 1990; Tansel, 1993; Dewberry and Davis, 1993) to identify appropriate cases for model validation.

After Hurricane Andrew, Tansel (1993) carried out a detailed debris analysis for five zones with significant structural damage in Dade County. Table 10.12 lists the zone location, number of buildings, exterior wall construction distribution, average exterior damage ratio, and total structural debris for each of the five zones investigated. The amount of structural debris was estimated based on an average type of residence and structural damage states. The damage statistics in each zone were calculated using the data collected by the Metro-Dade County Building and Zoning Department. Structures with more than 50% damage were judged uninhabitable and assumed to be demolished. The debris simulation is performed using model buildings with different combinations of number of stories (1-story or 2-story), roof shape (hip or gable), wall construction (wood frame or masonry), nail size (6d or 8d), and roof cover type (shingle or tile). The total debris produced by each model building under the simulated wind speed in each zone is calculated and then aggregated within the zone to obtain the average amount of debris per building (weighted by the assumed building stock). The total amount of structural debris in each zone is calculated by multiplying the average amount of debris per building with the total number of buildings in that zone. For Dade County, the building stock is modeled assuming 80% of the homes are single story. 75% of the homes are assumed to have gable roofs and 25% of the homes are assumed to have hip roofs. The number of homes having shingle roof cover is assumed to be the same as that having tile roof cover. 40% of the homes are assumed to use 6d nails on roof deck and the remaining homes are assumed to use 8d nails. All the homes are assumed to have straps for roof-to-wall connection. The distribution of exterior wall construction types in each zone is assumed to be the same as that listed in Table 10.12. The exterior wall construction distribution for Zone 4, which is not given in the paper by Tansel (1993), is assumed to be the same as that of Zone 5 (in the same zip code). Table 10.12 also shows the simulated average debris weight per building, average debris volume per building, total structural debris weight in each zone, and the ratio between simulated and actual debris in each zone. The mean of the model-to-actual ratios is 1.05 and the standard deviation is 0.58. The result is very promising given that the debris model relies heavily on engineering judgment.

Table 10.13 shows debris comparisons for hurricanes Hugo and Andrew at a regional level. Dowd (1990) reported the debris removal and channel shoaling of USACE in hurricane Hugo. Political subdivisions made 359 requests to FEMA and an estimated 15,500,000 cubic yards of debris were removed by or for these subdivisions. USACE assisted and administrated the debris removal mission in seven counties (Berkeley, Charleston, Darlington, Dorchester, Lancaster, Orangeburg, and Sumter), with a total of 4,589,559 cubic yards of debris removed. Tansel (1993) estimated that 2.9 million tons of construction and demolition debris were generated by hurricane Andrew. The USACE after action report (USACE, 1993) gives an estimate of 40 million cubic yards of debris in Dade County. The debris simulation is performed at a zip code level. Similar to the first validation study, the average debris weight and volume per building in each zip code

Table 10.12. Structural Debris Comparison for Hurricane Andrew

Zone (zip code)	Actual Data				Simulation Results			Model / Actual
	Number of Buildings	Exterior Wall Construction Distribution	Average Exterior Damage Ratio	Structural Debris (tons)	Average Debris Weight per Building (lb)	Average Debris Volume per Building ($yard^3$)	Total Structural Debris (tons)	
Zone 1 (33186)	14,000	85% wood frame	63%	182,650	27,252	145	173,215	0.95
Zone 2 (33156)	18,000	75% concrete	24%	456,365	25,864	127	211,364	0.46
Zone 3 (33156)	604	50% wood frame; 50% concrete	53%	11,376	24,665	125	6,764	0.59
Zone 4 (33031)	2,500	-	48%	42,900	53,232	264	60,418	1.41
Zone 5 (33031)	1,100	85% wood frame	47%	14,390	53,232	264	26,584	1.85

Table 10.13. Debris Comparison for Hurricanes Hugo and Andrew

Storm	Region	Actual Weight (tons)	Actual Volume ($yard^3$)	Modeled Weight (tons)	Modeled Volume ($yard^3$)	Model/ Actual (weight)	Model/ Actual (volume)
Hugo	South Carolina	-	15,500,000	951,009	9,130,843	-	0.59
Hugo	USACE Admin. Region	-	4,589,559	782,480	7,366,394	-	1.61
Andrew	Dade County	2,900,000	40,000,000	3,396,991	35,323,080	1.17	0.88

are simulated first (using the assumed building stock). The total debris weight or volume in each zip code is then calculated by multiplying the total number of houses in each zip code with the average debris weight or volume per building. The total amount of debris in the study region is estimated by adding up the total debris in each zip code. The default building stock in Dade County is assumed to be the same as that in the first validation study and the default building stock for South Carolina is assumed to be: 70% one-story and 30% two-story; 75% gable and 25% hip; 30% using 6d nails and 70% using 8d nails; 10% using straps and 90% using toe-nails for roof-to-wall connection. The total number of houses in each zip code is estimated using 1990 census data. As shown in Table 10.13, the debris model underestimated the debris volume in South Carolina and overestimated debris volume in the regions administrated by USACE (seven counties).

For hurricane Andrew, both the modeled debris weight and debris volume are reasonably close to the actual values. It is not clear in the paper by Dowd (1990) whether all the political subdivisions that made requests to FEMA for debris removal assistance are within South Carolina. Therefore, the actual study region may cover a larger area than the state of South Carolina, which may help to explain the underestimation of debris volume by the model. The overestimation of the debris volume in the USACE administrated region may likely be to the opposite. The study region may only include portions (most likely just municipalities) of the seven counties that were mentioned in the paper.

10.4 Final Remarks

A building debris estimation model has been developed based on building component damage states and building component weight statistics. The model is capable of providing estimates of the amount (both weight and volume) of construction and demolition debris in each of the four debris types (wood, masonry, metal and other). Limited validation studies have shown that the model can produce reasonable estimates of the total building debris produced by a hurricane.

Chapter 11. Short Term Shelter Requirements

11.1 Introduction

The model for estimating the number displaced households and short term shelter needs follows that used for the Hazus Earthquake Model. The concept and formulation are described in the Hazus (Earthquake) Technical Manual (FEMA, 1999). The only modification for the Hurricane Model is that building loss ratios, instead of building damage states, are used to estimate the proportion of uninhabitable housing units.

The shelter model provides two estimates for each census tract:

1. The number of displaced households due to loss of habitability
2. The number of people requiring only short-term public shelter.

Loss of habitability is calculated from modeled damage to residential buildings, whose severity is expressed in terms of loss ratios due to physical damage, and from estimated loss of water or power supply to residential buildings or units.

11.2 Description of Methodology

The form of the displaced households model is:

$$D = \left(U_a + \beta U_b\right)\frac{H}{S+M}, \tag{11.1}$$

where

D - Number of displaced households,

U_a - Number of uninhabitable units due to damage (Equation 11.2),

U_b - Number of uninhabitable units due to loss of water or power (Equation 11.3),

H - Total number of households,

S - Total number of single-family dwelling units,

M - Total number of dwelling units in multi-family buildings,

β - Adjustment factor for household tolerance to loss of power or water (user input).

The ratio $H/(S+M)$ represents the occupancy rate averaged over the single-family and multi-family categories. U_a and U_b are estimated as follows, respectively,

$$U_a = S \cdot \int_0^1 f_s(x) \cdot w_s(x)\, dx + M \cdot \int_0^1 f_m(x) \cdot w_m(x)\, dx, \tag{11.2}$$

$$U_b = R_u[(S + M) - U_a]. \tag{11.3}$$

where,

$f_s(x)$ - Probability density function of loss ratio x for single-family buildings,

$f_m(x)$ - Probability density function of loss ratio x for multi-family buildings,

$w_s(x)$ - Un-inhabitability function in terms of loss ratio x, single-family buildings,

$w_m(x)$ - Un-inhabitability function in terms of loss ratio x, multi-family buildings,

R_u - Damage ratio to power and water facilities.

Examples of the modeled probability density function $f_s(x)$, for the case of single-family buildings for the building stock in North Florida, are shown in Figure 11.1 in the form of probability mass functions. As wind speed increases, the mass of the probability moves toward unity, indicating that all buildings experience a complete loss. Building stock data used for the loss ratio computations for Florida are presented in Figure 11.2.

Figure 11.3 shows an empirical un-inhabitability function for single-family buildings in terms of loss ratio x, where below 20% loss a building is considered still inhabitable and above 50% a building is assumed to be completely uninhabitable, while for buildings with a loss ratio between these two values a linear proportion is assumed to be uninhabitable. For multi-family buildings, as shown in Figure 11.4, the linear range is defined between 10% and 50% empirically, since some of the units in a building with relatively mild overall damage and loss may already have become uninhabitable.

Examples of computed percentage of household being displaced are shown in Figure 11.5.

Similar to the Hazus Earthquake Model, the number of people likely seeking public shelter is estimated based on the number of displaced households, D, recognizing that only a fraction of the displaced households will likely seek public shelter and this fraction is a function of several demographic variables such as income and ethnicity, as expressed below:

$$N = \frac{D \cdot P}{H} \sum_{i=1}^{5} \sum_{j=1}^{5} \sum_{k=1}^{2} \sum_{l=1}^{3} \left(\alpha_{ijkl} \cdot I_i E_j O_k A_l \right), \tag{11.4}$$

where

N - Number of people likely seeking public shelter,

D - Number of displaced households (Equation 11.1),

P - Population,

H - Total number of households,

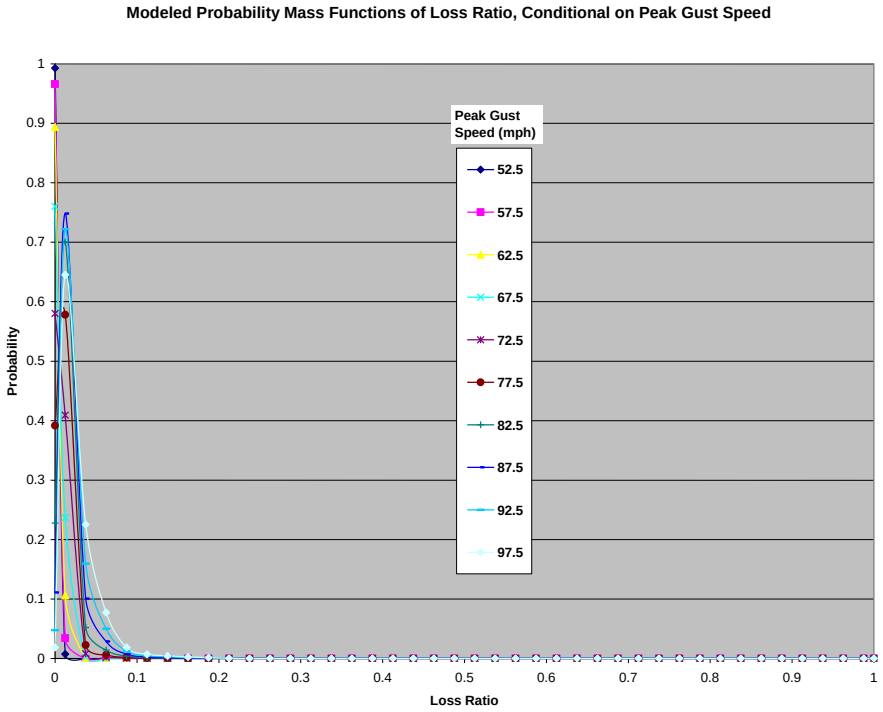

(a). Lower Peak Gust Wind Speeds (between 50 mph and 100 mph)

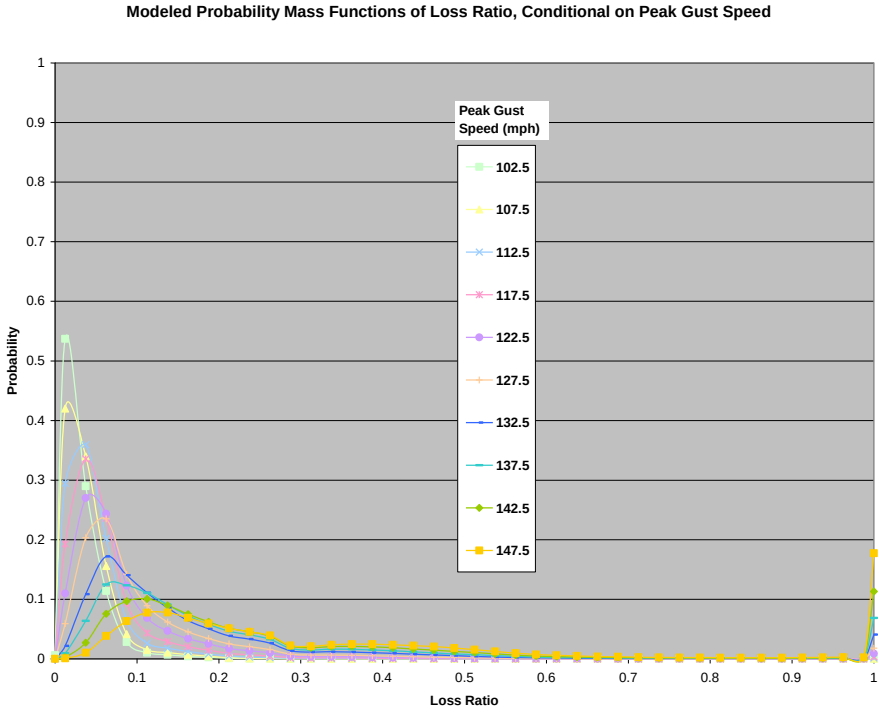

(b). Medium Peak Gust Wind Speeds (between 100 mph and 150 mph)

Figure 11.1. Modeled Probability Mass Function of Loss Ratios.

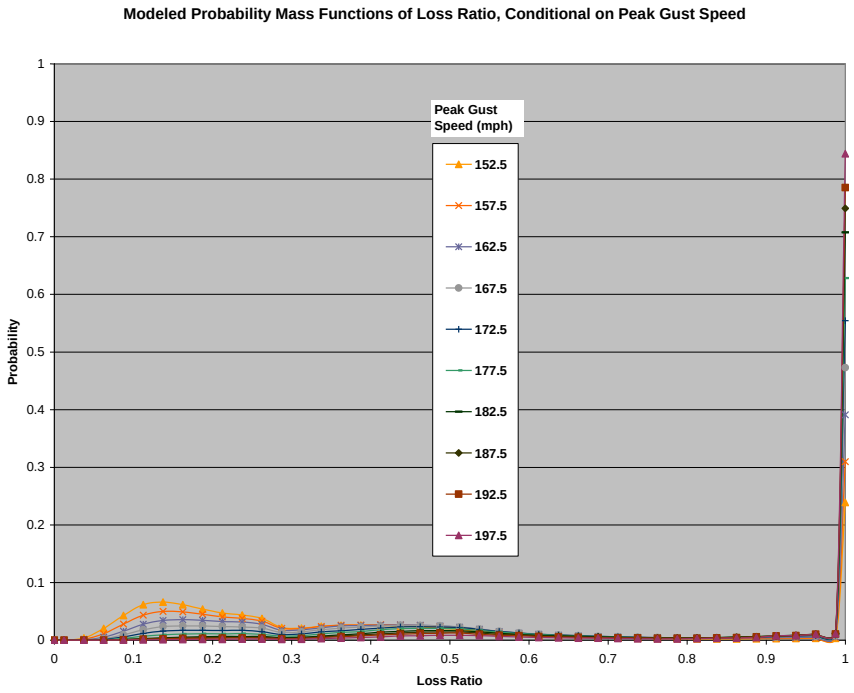

(c) High Peak Gust Wind Speeds (between 150 mph and 200 mph)

Figure 11.1. Modeled Probability Mass Function of Loss Ratios (concluded).

I_i - Percentage of population in the i^{th} income class,

E_j - Percentage of population in the j^{th} ethnic class,

O_k - Percentage of population in the k^{th} ownership class,

A_l - Percentage of population in the l^{th} age class,

α_{ijkl} - A fractional coefficient, which is a weighted average of empirical fractions of displaced households from various demographic classes who seek public shelter:

$$\alpha_{ijkl} = w_I\left(F_I\right)_i + w_E\left(F_E\right)_j + w_O\left(F_O\right)_k + w_A\left(F_A\right)_l \ , \tag{11.5}$$

where the weights and fractions are defined in Tables 11.1 and 11.2, respectively, with their default values. Note that Equations 11.4 and 11.5 are formulated assuming that the demographic variables are mutually independent and the displaced households are distributed among demographic classes in proportion to their number of households. An example of computed results is shown in Figure 11.6.

11.3 Simplified Methodology

The methodology represented by Equation 11.2 requires the full probability density function of building loss as a function of peak gust wind speed. In an effort to reduce the data storage requirements and computational requirements imposed by Equation 11.2, a

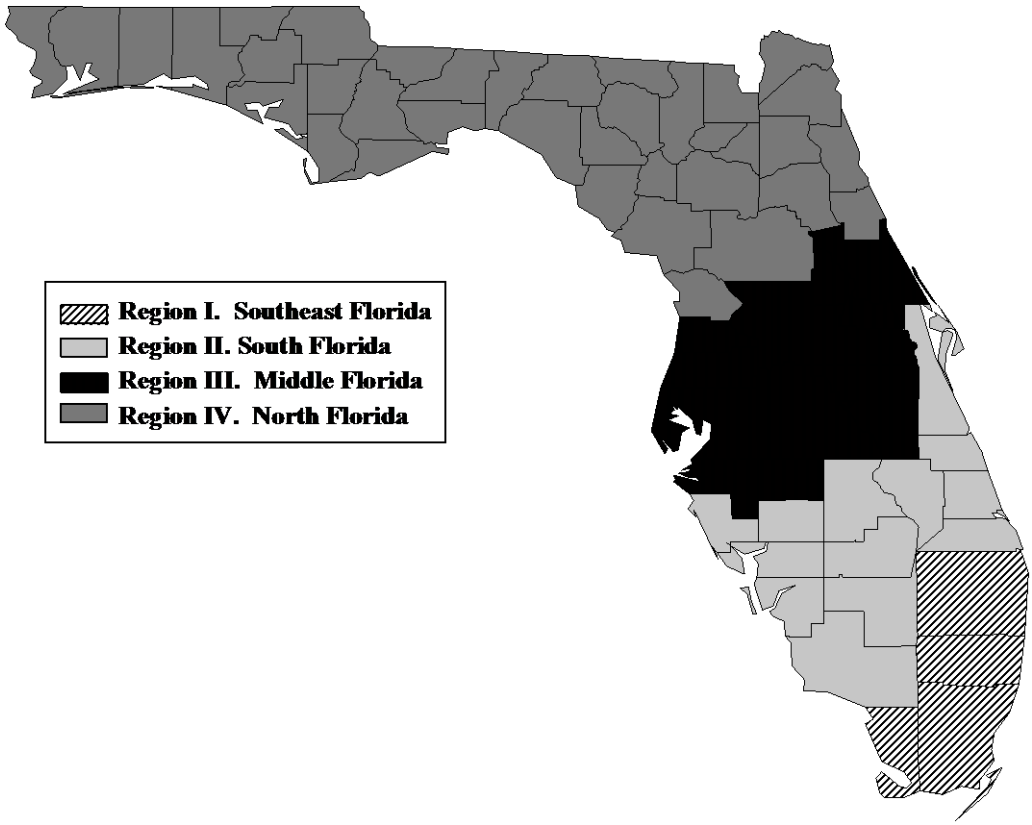

	Region I	Region II	Region III	Region IV
Roof Shape				
Gable	0.62	0.61	0.75	0.73
Hip	0.38	0.39	0.25	0.27
Roof Cover				
Regular Shingle	0.70	1.00	1.00	1.00
Hurricane Shingle	0.30	0.00	0.00	0.00
Roof-Wall Connection				
Toe Nail	0.10	0.09	0.25	0.15
Strap	0.90	0.91	0.75	0.85
Roof Deck Fastening				
6d@6/12	0.25	0.46	0.29	0.40
8d@6/12	0.32	0.32	0.29	0.35
8d@6/6	0.43	0.22	0.41	0.26
Opening Protection				
No Protection	0.70	0.85	0.95	0.92
Dade Shutter	0.30	0.15	0.05	0.08

Figure 11.2. Building Stock Data Used for the Loss Ratio Computation.

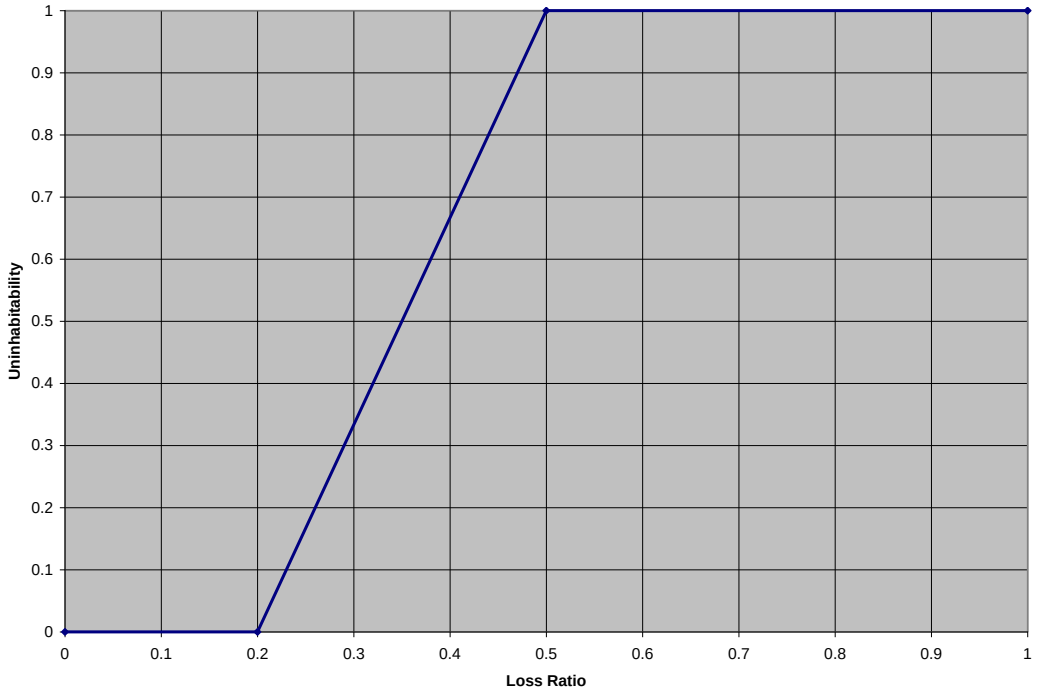

Figure 11.3. Empirical Un-Inhabitability Function for Single-Family Buildings.

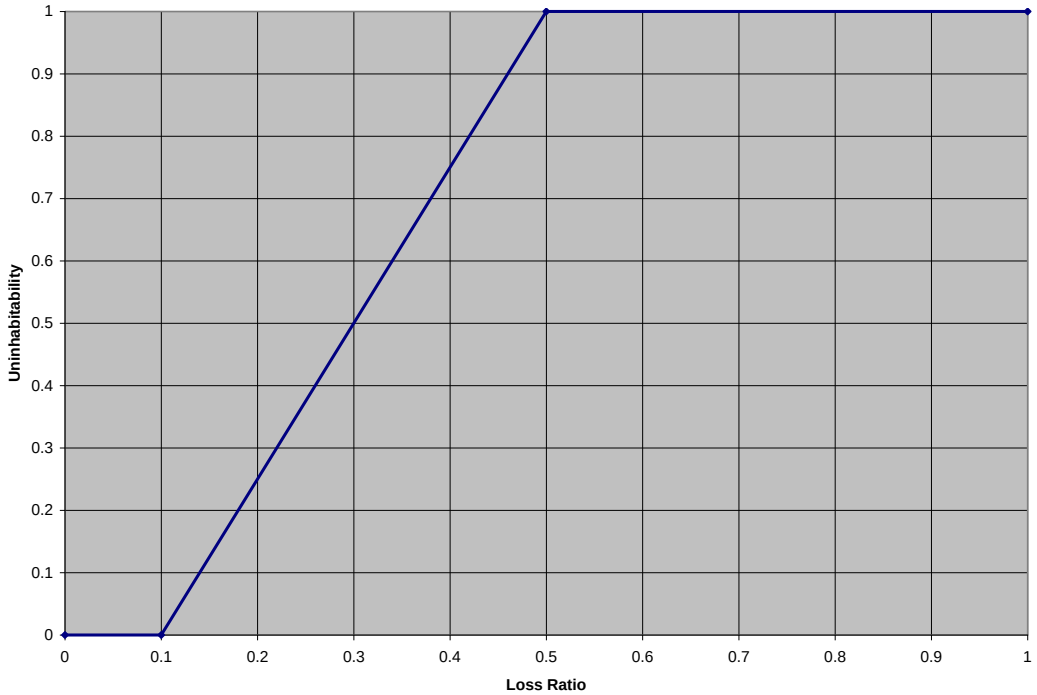

Figure 11.4. Empirical Un-Inhabitability Function for Multi-Family Buildings.

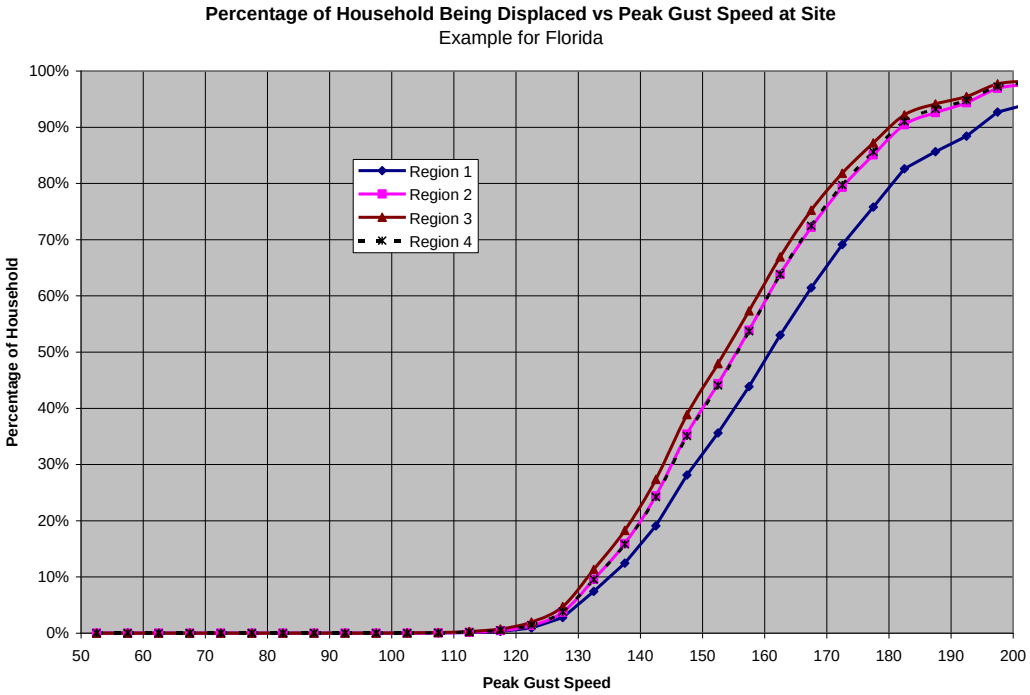

Figure 11.5. Example of Computed Percentage of Household Being Displaced as a Function of Peak Gust Wind Speed at Site.

Table 11.1. Default Weights for Demographic Variables

Symbol	Description	Default Value
w_I	Income Factor Weighting	0.73
w_E	Ethnic Factor Weighting	0.27
w_O	Ownership Factor Weighting	0.00
w_A	Age Factor Weighting	0.00
$(w_I + w_E + w_O + w_A)$	Total	1.00

implification has been developed to estimate the integrated uninhabitability ratio using mean building losses instead of the probability density functions of building loss. Mean building loss is readily available within Hazus.

A study was carried out to examine the relations between the integrated un-inhabitability ratios, which are evaluated by the integrals in Equation 11.2, and the mean building loss ratios. The results are shown in Figures 11.7 and 11.8 for single-family and multi-family buildings respectively. It is found that the scatter is very insignificant; that is, the mean building loss is a good predictor of the un-inhabitability. Fitted mean functions are also shown in Figures 11.7 and 11.8. These functions are used in Hazus in place of Equation 11.8 as follows,

$$U_a = S \cdot F_S(X_S) + M \cdot F_M(X_M), \tag{11.6}$$

where

Table 11.2. Default Fractions of Displaced Households Seeking Public Shelter

Symbol	Description	Default Value
Income		
$(F_I)_1$	Household Income < $10000	0.62
$(F_I)_2$	$10000 < Household Income < $20000	0.42
$(F_I)_3$	$20000 < Household Income < $30000	0.29
$(F_I)_4$	$30000 < Household Income < $40000	0.22
$(F_I)_5$	$40000 < Household Income	0.13
Ethnicity		
$(F_E)_1$	White	0.24
$(F_E)_2$	Black	0.48
$(F_E)_3$	Hispanic	0.47
$(F_E)_4$	Asian	0.26
$(F_E)_5$	Native American	0.26
Ownership		
$(F_O)_1$	Own Dwelling Unit	0.40
$(F_O)_2$	Rent Dwelling Unit	0.40
Age		
$(F_A)_1$	Population Under 16 Years Old	0.40
$(F_A)_2$	Population Between 16 and 65 Years	0.40
$(F_A)_3$	Population Over 65 Years Old	0.40

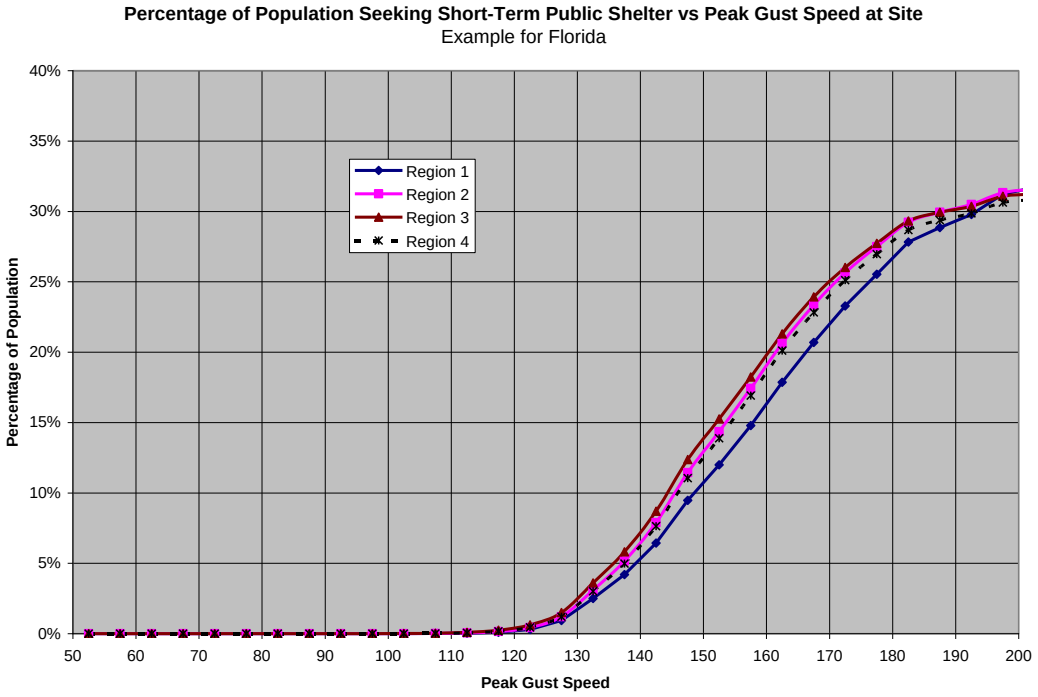

Figure 11.6. Example of Computed Percentage of Population Seeking Short-Term Public Shelter as a Function of Peak Gust Wind Speed at Site.

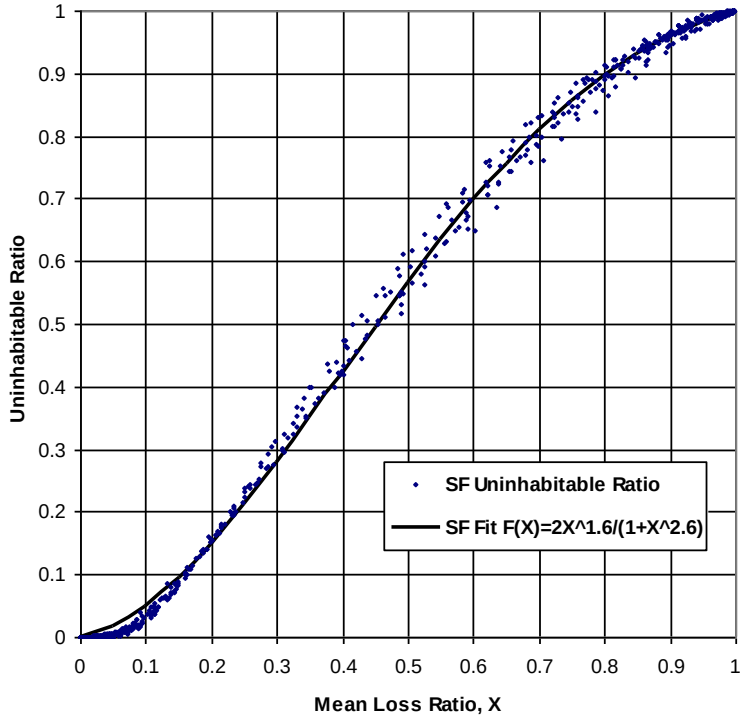

Figure 11.7. Uninhabitability as a Function of Mean Building Loss for Single-Family Buildings.

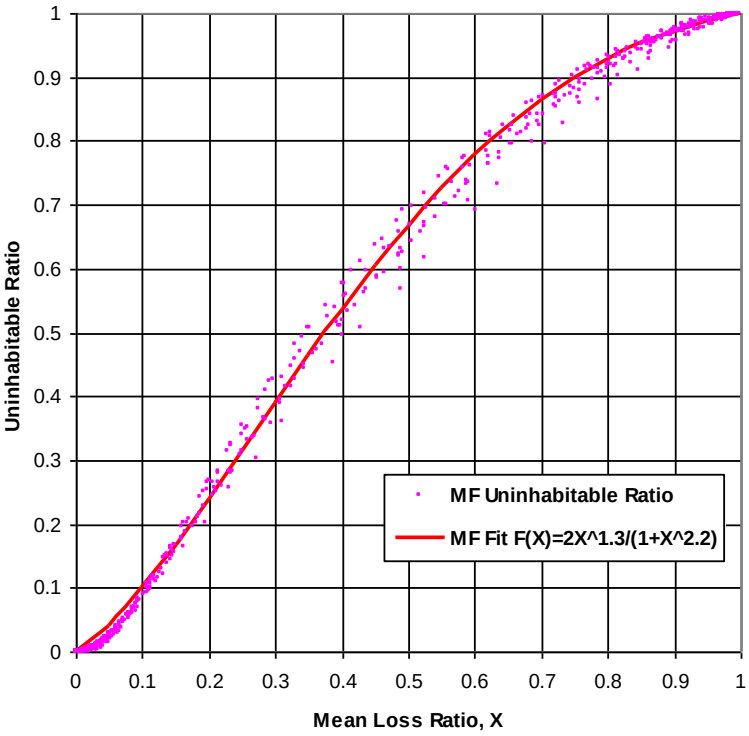

Figure 11.8. Uninhabitability as a Function of Mean Building Loss for Multi-Family Buildings.

$$F_S(X_S) = \frac{2X_S^{1.6}}{1+X_S^{2.6}} \tag{11.7}$$

$$F_M(X_M) = \frac{2X_M^{1.3}}{1+X_M^{2.2}} \tag{11.8}$$

and X_S and X_M denote the mean building loss ratios for single-family and multi-family buildings respectively. Equations 11.6 and 11.7 are plotted in Figures 11.7 and 11.8, respectively.

Because of the small amount of scatter in Figures 11.7 and 11.8, results computed using Equation 11.5 instead of Equation 11.2 are nearly identical to those shown in Figures 11.5 and 11.6. Therefore, the simplified approach is used in the fast-running implementation of the Hazus software to compute displaced households and population seeking short-term public shelters.

Chapter 12. Tree Blowdown

12.1 Introduction and Background

Damage to structures caused by windthrown trees is an ongoing problem in forested areas. In addition, during Hurricane Hugo, for example, most of the damage to the electric power distribution system was caused not by the direct action of wind but by trees falling on the distribution lines and breaking the lines (Cook, 1990). Tree debris produced by Hurricane Hugo also hampered emergency crews and delayed repairs to lifelines (Cook, 1990). At Charleston Naval Base, windthrown trees broke buried water lines, disrupting the water supply (Strehmeyer, 1990).

Extreme winds associated with thunderstorms and extratropical storms also cause extensive tree-induced damage. For example, in May 1990, there were in excess of 300 separate reports of downed trees. Of the 150 reported downed power lines, approximately 30% were caused by trees falling across the lines. Of the 100 reports of damage to structures, approximately 40% were caused by downed trees, with one case producing a fatality.

Trees have both positive and negative effects in the presence of extreme winds. On the positive side, trees provide shelter to structures, reducing the likelihood of damage produced by the direct action of wind. On the negative side, the existence of many trees surrounding a structure increases the likelihood of a tree striking and damaging the structure.

This chapter describes the tree blowdown methodology implemented in Hazus and the two damage/loss models that use the results produced by the tree blowdown methodology. The first estimates the quantity of tree debris after a hurricane. The second estimates the additional economic loss to residential buildings and contents caused by fallen trees.

Figure 12.1 shows a high-level flow chart of the data and the models. The combination of tree data by census tract and a tree blowdown probability model provide the elements needed for estimating debris quantities, while the tree data, blowdown model, hit probability and damage model, along with a cost model, yield the estimation of damage and loss to residential buildings due to tree blowdown, given a defined hurricane climate.

Section 12.2 provides a brief overview of related research. The wind throw model is described in Section 12.3, and the blowdown probability curves produced by the model are presented in Section 12.4. The development of the tree inventory database is presented in Sections 12.5 and 12.6. The tree debris model is described in Section 12.7, and the damage and loss models for residential buildings and contents are presented in Sections 12.8 through 12.10.

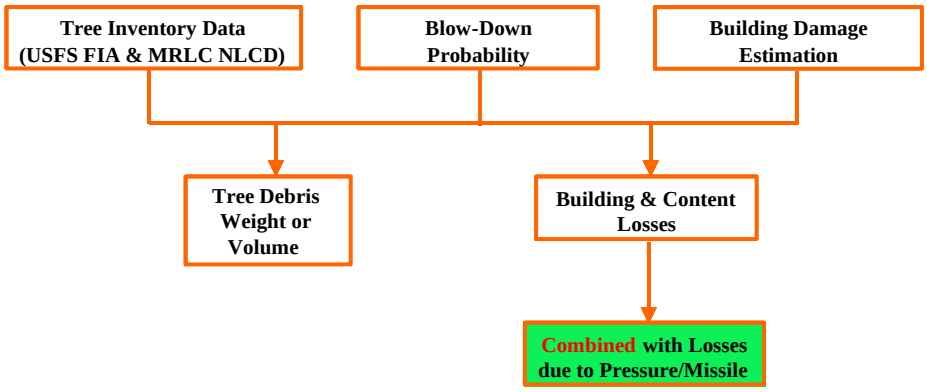

Figure 12.1. Estimation of Tree Blow-Down Debris and Damage to Buildings.

12.2 Related Research

Virtually all the research related to natural blowdown of trees has been performed by the forestry industry. This research is prompted by large annual losses of harvestable wood in many countries. In New Zealand, the average annual losses of softwood trees due to catastrophic wind events ranges between 0.02% and 3.5% (depending on the forest) of the total stock. The extent of attritional damage associated with lesser winds varies between 0% and 1% of the growing stock per annum (Somerville, 1993). Over the period 1981-1990, more than 50% of the total yield in the Czech Republic had to be cut down due to injuries produced by windthrow or snowbreak (Slodicak, 1993).

The research performed by the forestry industry (predominately in the U.K. and Europe) includes full-scale measurement of tree response due to wind action, measurements of windspeeds within canopies, static pull down tests and relatively simple mathematical models to estimate the forest blowdown potential. The model described herein draws on work done by the forestry industry in the U.K. and Europe combined with research performed in the United States. Very little research in the U. S. has been directed toward assessing the risk of forest blowdown produced by natural wind; however, the most relevant research was directed toward assessing tree blowdown probabilities associated with the effects of nuclear weapons (Twisdale, et al., 1984). The ten-year research program produced a computer simulation methodology termed BLOWTRAN (BLOWdown TRANSport) described in the section “Damage to Forests” in the EM-1 Nuclear Effects Manual. The BLOWTRAN model is adapted as described herein to obtain estimates of tree blowdown associated with natural wind.

12.3 Wind Throw Model

12.3.1 Wind Load Response and Breakage Model

The mathematical model used in BLOWTRAN to determine the drag loads acting on a tree is based on the model developed by the United States Forest Service (USFS) during the early 1950s. The drag force, F_D, acting on the tree crown is a function of the dynamic pressure acting on the tree crown combined with the effective surface area and the

effective drag coefficient. Both the drag coefficient and the effective crown area of a tree subject to strong winds decrease due to streamlining of the leaves and branches, with the end result being that the wind force acting on the tree is nearly proportional to velocity.

To determine the effect of streamlining the tree-crown system, and to develop a model to define the wind loads, the USFS conducted full-scale drag tests on 13 coniferous trees (Sauer, et al., 1951) and 18 broadleaf trees (Lai, 1955). More recent full-scale measurements on over 30 coniferous trees (Frank, et al., 1987; Frank, et al., 1989; Frank, et al., 1991) supplement the USFS data. All of the full-scale test data used herein were carried out by mounting full-size trees on the rear of a tractor trailer and driving at a constant velocity. Base overturning moments and shear forces were measured for mean velocities ranging between 6 m/s and 32 m/s in the more recent tests, and 5 m/s to 25 m/s in the USFS tests.

The drag data from these full-scale tests are correlated as functional relationships of two dimensionless parameters that describe the variation in the drag force with the bending moment at the base of the crown, as a function of the wind force, and the tree crown and stem characteristics. The drag force, F_D, in the USFS model is expressed as

$$\frac{F_D}{\frac{1}{2}\rho U^2} = \frac{d_c^3}{h}\frac{1}{W_{dbf}}\Psi_D \tag{12.1}$$

where *h is* the distance between the effective center of pressure and the base of the crown, d_c is the diameter at the base of the crown, W_{dbf} is the ratio of the weight of the dry branches to the weight of the dry foliage, and Ψ_D is a drag function. The wind velocity, U, in Equation 12.1 is the relative velocity (i.e., wind velocity minus the velocity of the tree) and, therefore, aerodynamic damping is inherently included in Equation 12.1. The drag function, Ψ_D, is given as:

$$\Psi_D = \frac{k_2 k_2 \left(\frac{R}{W_{dc}}\right)^{-1.5}}{k_1 + k_2 \left(\frac{R}{W_{dc}}\right)^{-1.5}} \tag{12.2}$$

where k_1 and k_2 are drag function parameters, W_{dc} is the dry crown weight, and R is the restoring force in the stem at the base of the crown. In the static case, the restoring force, R, is equal to the drag force, F_D. In Equation 12.2, the parameter k_1 is directly proportional to the drag coefficient for a perfectly rigid tree, and k_2 is the parameter responsible for reducing the effective drag force with increases in wind speed. Small values of k_2 describe a tree which streamlines readily; conversely, large values of k_2 describe a tree which does not readily streamline. The dry crown weight, W_{dc}, in Equation 12.2 does not need to be determined explicitly for each tree since it has been found to be strongly correlated with the height of the crown, H_c, and the stem diameter, d_c, at the base of the crown. Empirical relationships for the dry crown weight have been developed for a

number of hardwood and coniferous tree species (Storey, Fons, and Sauer, 1955; Lai, 1955; Twisdale, et al., 1989) in the form

$$ln(W_{dc}H_c) = a + b\,ln\,d_c + \varepsilon \tag{12.3}$$

where H_c is the height of the crown, a and b are regression constants, and ε is a normally distributed error term. The r^2 values for these species-dependent empirical relationships exceed 0.93 in all cases. Similar relationships for the parameter W_{dbf} have also been developed.

Because the dry crown weight, W_{dc}, and the ratio of the weight of the dry branches to the weight of the dry foliage, W_{df}. are determined through empirical relationships, the basic inputs required for the drag (or loading) side of the model are:

(i) Tree height, H_{bh};

(ii) Diameter at breast height, d_{bh} (1.3 meters above ground);

(iii) Species;

(iv) Stem form parameters, a_s and c_s, which describe the taper in the stem;

(v) Percent crown;

(vi) Drag parameters k_1 and k_2.

The species-dependent variables, a_s, c_s, k_1, and k_2, are given for a variety of conifers and broadleaf trees in Twisdale, et al. (1989) and Vickery, et al. (1993).

Statistical distributions for the drag parameter, k_1, have been developed for 12 species (three conifers and nine broadleaf trees) and a relationship between the modulus of rupture and k_1 was developed so that the value of k_1 can be estimated for species where direct measurements are not available. Figure 12.2 shows the drag parameters k_1, and k_2 plotted versus the modulus of rupture, σ_r, for broadleaf trees where it is evident that trees having higher drag coefficients (as defined using k_1) are generally stronger. In the case of conifers, no trend of increasing k_1 with increasing σ_r was observed; however a weak positive correlation between σ_r and k_2 was observed. For broadleaf trees, the drag parameter k_1 (as shown in Figure 12.3) is modeled as a lognormal distribution where

$$m_{ln\,k_1} = 7.777 + 0.04198\,\sigma_r \tag{12.4a}$$

$$\sigma_{ln\,k_2} = 0.679 \tag{12.4b}$$

are the logarithmic mean and standard deviation, respectively. The drag parameter k_2 is also lognormally distributed with the logarithmic mean and standard deviation given as

$$m_{ln\,k_1} = 12.98 + 0.0145\,\sigma_r \tag{12.5a}$$

$$\sigma_{ln\,k_2} = 0.679 \tag{12.5b}$$

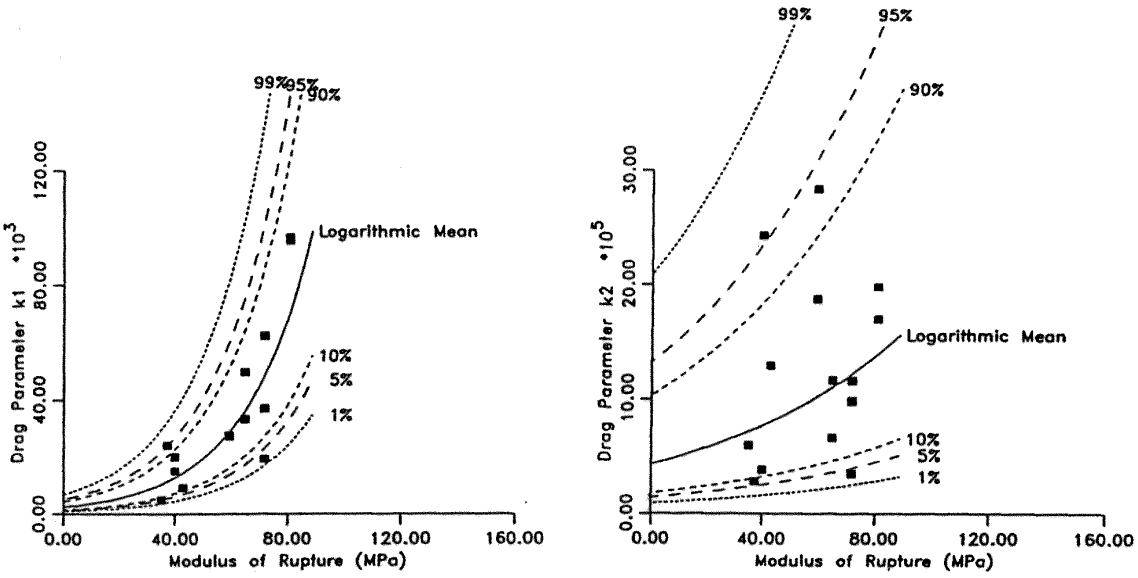

Figure 12.2. Drag Function Parameters k_1 and k_2 versus σ_r for Green Wood (Broadleaf Trees).

Tree response is modeled using a single degree of freedom model given as

$$m_e\ddot{x}+c\dot{x}+kx=F_D(t) \tag{12.6}$$

where an effective mass, m_e, located at the center of pressure, is used to predict the dynamic response of the tree subjected to either a static or dynamic wind load. The drag force is assumed to act as a point load located at the center of pressure (in the crown at a height, H_{cp} above breast height).

The linear spring stiffness for the tree is derived from small deflection theory as

$$K=\frac{3EI_{bh}}{H_{bh}^3}\overline{K}\psi\left(c_s, f_1\right) \tag{12.7}$$

where I_{bh} is the moment of inertia at breast height, H_{bh}, is the height of the tree above breast height, E is the species-dependent Young's modulus, and $\overline{K}$ is a stiffness modulus parameter which accounts for the natural variations in the stiffness from the reference (or theoretical value). Statistical distributions of $\overline{K}$ used herein have been determined from static pull-down tests on both conifers and broadleaf trees (Frank, et al., 1987, 1989; Vickery, et al., 1991). The shape function, $\psi(c_s,.f_1)$, accounts for the variable moment of inertia along the tree stem. The shape of the stem of a tree is hyperbolic in nature (Behre, 1927), such that the inside diameter, d, at any point along the stem is defined by

$$d=d_{bh}\frac{f}{a_s\left(f+c_s\right)} \tag{12.8}$$

where a_s and c_s are the species-dependent stem form parameters and f is the non-dimensional distance measured from the top of the tree. The $3EI/H^3$ term in Equation 12.7 is the stiffness of a uniform cantilever. The shape function modifies the stiffness to account for the shape of the stem.

The tree period and effective mass of the equivalent single degree of freedom system is determined using species-dependent empirical relationships for the tree period combined with the calculated spring constant, *K*. The tree period, *T*, is obtained from

$$T = a_1 + b_1 \frac{H_{bh}^2}{d_{bh}} + \varepsilon \tag{12.9}$$

where a_1 and b_1 are species-dependent regression constants, and ε is a normally distributed error term.

Bending stresses in the extreme fiber of the tree along the length of the stem prior to yielding are given by

$$\sigma = \frac{Md}{2I} \tag{12.10}$$

where $I = I_{bh}\left[\frac{1}{a_s\left(f + c_s\right)}\right]^4$, *d* is the inside diameter, and *M* is the bending moment.

The region of maximum stress, and hence the point at which the tree will likely fail, varies with the position of the applied load. In general, trees loaded near the top will tend to break in the crown, and as the effective load point moves closer to the ground, the location of maximum stress moves toward the base of the tree.

In order to determine whether or not failure occurs, a reference deflection, y_r, at the point of application of the load is determined from small deflection theory for a reference strain equal to σ_r/E, where σ_r, the modulus of rupture for green wood. The maximum linear spring resistance, R_m, is given as

$$R_m = \bar{R}_b K_r y_r \tag{12.11}$$

where $\bar{R}_b$ is a random variable representing the variability in the strength of the tree stem. Statistical distributions for $\bar{R}_b$ have been described in Frank, et al. (1987; 1989) and Vickery, et al. (1993) from the results of static pull-down tests for a number of broadleaf and coniferous trees.

In the case of conifers, $\bar{R}_b$ was found to be negatively correlated with diameter at breast height for both root and stem failures (i. e., larger diameter trees are less likely to be able to develop the theoretical maximum resistance moment). This negative correlation was less pronounced in the case of broadleaf trees.

The breakage defection, y_b, is obtained from

$$y_b = \mu y_r \tag{12.12}$$

where the ductility, μ, is a random variable whose statistical parameters have, again, been determined using the results of static tree pull-down experiments for a wide range of species. Once the breakage deflection has been reached, the tree is assumed to have failed. The height above ground at which a stem failure occurs is determined by sampling uniformly over the region where the stem bending stress exceeds 90% of the maximum calculated value.

Uprooting failures are treated similarly to stem breakage failures by replacing $\overline{R}_b$ and μ with data derived from pull-down tests, where failure occurred by uprooting. Given tree size and the modulus of rupture, σ_r, the single most important (and uncertain) parameter describing the overall resistance of the tree to blowdown is $\overline{R}_b$. Table 12.1 summarizes the basic parameters (and relationships between parameters) necessary for modeling the response of a tree to wind (or blast) loads. Information on the parameters a_s, c_s, T, μ, $\overline{K}$, $\overline{R}_b$, C_p, W_{dc}, $W_{db/f}$, and k_2 are species-dependent and are derived from experimental studies. The values of these parameters are given in Vickery, Frank, and Twisdale (1993) for a number of tree species. The information given in Vickery, Frank, and Twisdale summarizes data from a wide range of sources. In addition to species-dependent parameters, data is given for generic conifers and broadleaf trees. Information on tree height, H_{bh}, diameter, d_{bh}, and % crown, f_c, varies with species and location; however, information on typical values of H_{bh}, d_{bh}, and f_c is readily available in the forestry literature. Values of σ_r and E are given in the USDA Wood Handbook (USDA, 1974).

12.3.2 Wind Modeling for Simple Terrains

In the case of relatively open terrain, similar to open country or suburban exposures in most building codes, where the variation in windspeed with height can be adequately modeled using logarithmic or power law models, simulating the incident windfield is relatively straightforward. In these basic cases, a windspeed time history is simulated using

$$U(t) = \overline{U} + \sum_{j=1}^{N} a_j \cos\left(2\pi\Delta f_j + \phi_j\right)t \tag{12.13}$$

where $U(t)$ *is* the instantaneous windspeed at time (at the height of the center of pressure) and $\overline{U}$ is the mean windspeed at the height of the estimated center of pressure within the crown of the tree, Δf is a frequency increment, ϕ_j *is* a random phase angle sampled uniformly over the interval $0 \le \phi \le 2\pi$, and a_j *is* a frequency dependent amplitude. The amplitude term, a_j, is given as

$$a_j = \left[2S_u\left(f_j\right)\chi^2\left(f_j\right)\right]^{\frac{1}{2}}\Delta f \tag{12.14}$$

Table 12.1. Input Parameters for Modeling of Trees

Number	Variable	Description	Functional Relationship	Distribution
1	d_{bh}	Diameter at breast height	User supplied	Uniform
2	H_{bh}	Height above breast	User supplied	Truncated Normal
3	f_c	% Crown	User supplied	Truncated Normal
4	a_s	Stem form parameter	User supplied	Lognormal
5	c_s	Stem form parameter	$c_s = \frac{a}{a_s} - 1$ (1)	Normal Error Term
6	T	Fundamental period	$T = a + bH_{bh}^2 / d_{bh}$ (1)	Normal Error Term
7	μ (2)	Ductility	User supplied (1)	Lognormal
8	$\overline{K}$ (2)	Stiffness parameter	User supplied (1)	Lognormal
9	$\overline{R}_b$ (2)	Strength parameter	$ln\,\overline{R}_b = a + b\,ln\,d_{bh}$ (1)	Normal Error Term
10	C_p	Center of pressure (tree in uniform flow)	User supplied (1)	Truncated Normal
11	W_{dc}	Weight of dry crown	$ln(w_{dc}\,H_c) = a + b\,ln\,d_{bh}$ (1)	Normal Error Term
12	$W_{db/f}$	Ratio of dry branches weight to dry foliage	$ln(w_{dc/f}) = a + b\,ln\,d_{bh}$ (1)	Normal Error Term
13	K_1, k_2	Drag function parameters	User supplied (1)	Normal Error Term
14	d_c	Diameter of base of crown	$d_c = \frac{d_{bh}\,f_c}{a_s\,(f_c + c_s)}$	NA
15	σ_r	Modulus of rupture for green wood	User supplied	NA (3)
16	E	Modulus of elasticity for green wood	User supplied	NA (4)

(1) Species- (site-) dependent data derived from tests. Data available in Vickery, Frank, and Twisdale (1992).
(2) Separate distributions are given for stem failure and uprooting.
(3) Natural variation in σ_r is accounted for with $\overline{R}_b$ distribution.
(4) Natural variation in E is accounted for with K distribution.

where $S_u(f_j)$ is the value of the spectrum of longitudinal turbulence at frequency f_j and $\chi^2(f_j)$ is the magnitude of the aerodynamic admittance function at frequency f_j.

The velocity spectrum, $S_u(f)$, used in this study is based on the ESDU (1975) formulation:

$$\frac{fS_u(f)}{\sigma_u^2} = \frac{4n}{\left(1 + 70.8n^2\right)^{\frac{5}{6}}} \tag{12.15}$$

where

$$n = {}^{x}L_u\, f / \overline{U} \tag{12.16}$$

and the integral length scale ${}^{x}L_u$ is given as

$${}^{x}L_u = \frac{25z^{0.35}}{z_0{}^{0.063}} \tag{12.17}$$

where the height above ground, *z*, is equal to the height to the center of pressure of the crown, and z_0 is the aerodynamic surface roughness.

The aerodynamic admittance function, $\chi^2(f)$, is determined using the coherence function for vertical separations given in Bowen, Flay, and Panofsky (1983), where the square of the coherence function is given as

$$R_{uu}^2(z_1, z_2, f) = exp\left[-\left(12 + \frac{11\Delta z}{z}\right)\frac{f\Delta z}{z}\right] \tag{12.18}$$

and

$$\chi^2(f) = \iint_{H_c} R_{uu}(z_1, z_2, f)\, dz_1, dz_2 \tag{12.19}$$

The integral in Equation 12.19 is solved numerically for various combinations of crown height, H_c, and H_b (height to base of the crown), with the solution approximated as

$$\chi^2(f) = \frac{1.0}{1 + a_1 n + a_x n^2} \tag{12.20}$$

where

$$n = \frac{fH_c}{\overline{U}} \tag{12.21}$$

The coefficients a_1 and a_2 vary with H_c/H_b. They are evaluated for H_c/H_b ranging between 0.1 and 10 and stored for later use. Ignoring the displacement height, *d*, the mean and turbulence profiles for these "open" cases are given as (ESDU 1982)

$$\frac{\overline{U}(z)}{U_{ref}} = \frac{ln\left(\frac{z}{z_0}\right)}{ln\left(\frac{z_{ref}}{z_0}\right)} \tag{12.22}$$

and

$$\frac{\sigma_u}{\overline{U}(z)} = \frac{7.5\eta\left[0.538 + 0.09 ln\left(\frac{z}{z_0}\right)\right]^p}{1 + 0.156 ln\left(\frac{u_*}{f_c\, z_0}\right)} \tag{12.23}$$

where z_{ref} is the reference height, $\overline{U}(z)$ is the windspeed at height z, $\sigma_u(z)$ is the RMS longitudinal windspeed at height z, $\overline{U}_{ref}$ is the mean windspeed at the reference height, u_*, is the friction velocity, f_c is the coriolus parameter, and

$$\eta = 1 - \frac{6 f_c z}{u_*} \text{ and } p = \eta^{16} \tag{12.24}$$

12.3.3 Example Tree Response – Ponderosa Pine

The wind-induced response of a Ponderosa Pine tree characterized in Table 12.2 was examined in some detail, as described here. Figure 12.3 shows the input velocity spectrum at the center of pressure in conjunction with the resulting base bending moment spectrum for mean windspeeds ranging between 10 m/s and 25 m/s. The intensity of turbulence at the center of pressure is about 25%. A resonant peak is seen clearly in Figure 12.3; however, the importance of the resonant response diminishes with increasing windspeed due to increases in the aerodynamic damping. Sensitivity studies performed where the weight of the dry crown *(W_{dc})* was both increased and decreased indicate that the resonant portion of the tree response decreases with increasing crown weight. For very large values of W_{dc} the tree response is nearly quasi-static.

Table 12.2. Characteristics of Key Parameters for Example Ponderosa Pine Tree Response Estimates

Parameter	Value
Height (m)	16.4
Diameter at Breast Height (cm)	18
% Crown	56
Dry Crown Weight (N)	90
Drag Parameter k_1	8,669
Drag Parameter k_2	399,528
Period (seconds)	3.28

Figure 12.4 shows the mean, RMS, and maximum base bending moments plotted versus the mean wind speed 10 m above ground, showing the effect of dry crown weight (W_{dc}) on tree response. The windspeed is increased to the point where the tree fails. The dry crown weight has little effect on the base bending moments at low windspeeds. In this example, for a mean windspeed of 10 m/s, the peak base bending moment is proportional to W_{dc} raised to the power of 0.14, whereas for a mean windspeed of 25 m/s, the peak base bending moment is proportional to W_{dc} raised to the power 0.4. In this example, the effect of crown weight is less important than the model of Mayhead, et al. (1975), where the mass of the crown is included in the drag force model raised to the power of 0.67. It is noteworthy that the drag model proposed by Mayhead, et al. for Sitka Spruce given in the form

$$F_D = A_1 U^2 m_c^{0.67} \exp\{-0.0009779 U_2\} \tag{12.25}$$

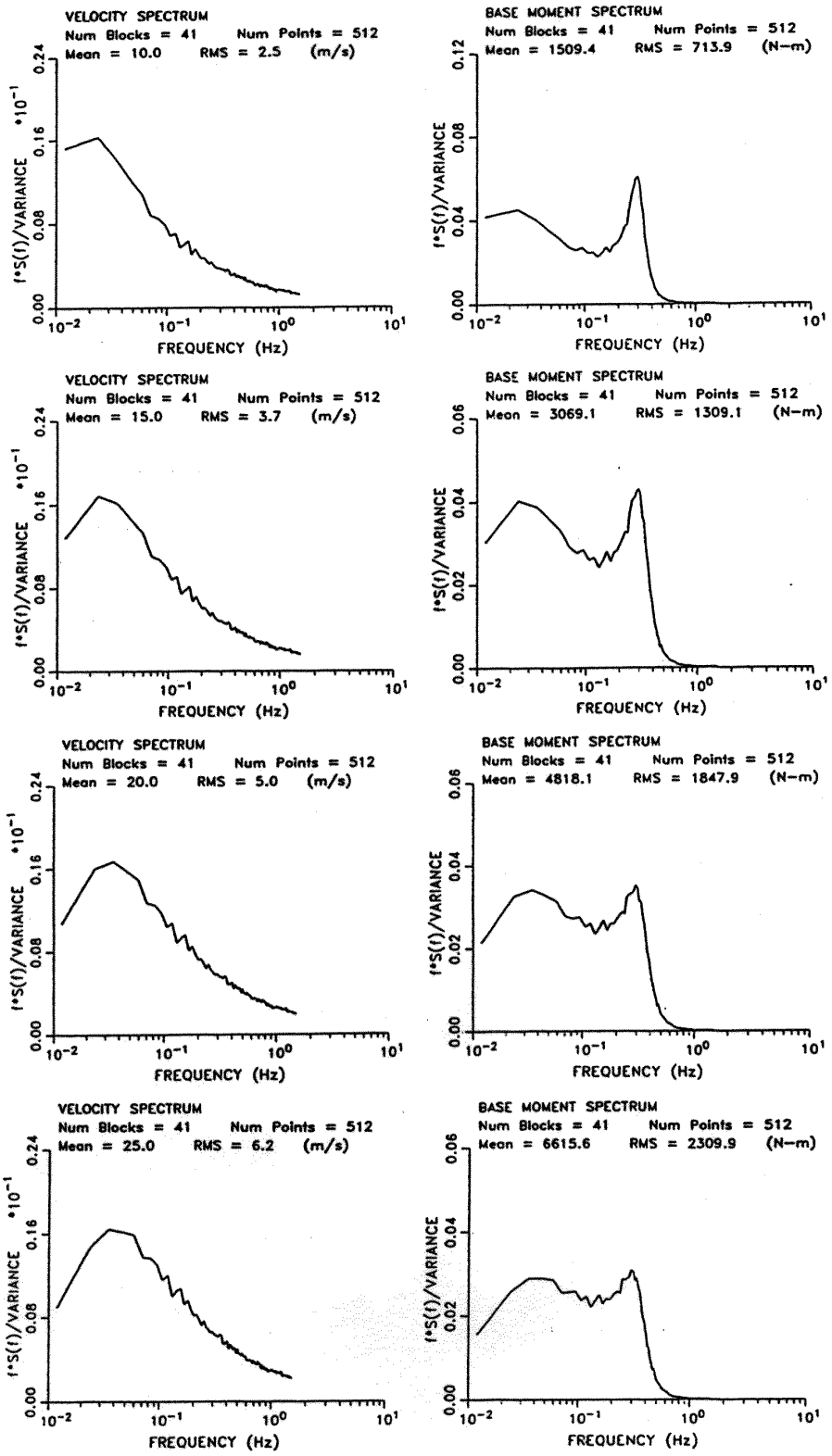

Figure 12.3. Velocity Spectra and Base Moment Spectra for Ponderosa Pine (Suburban Exposure).

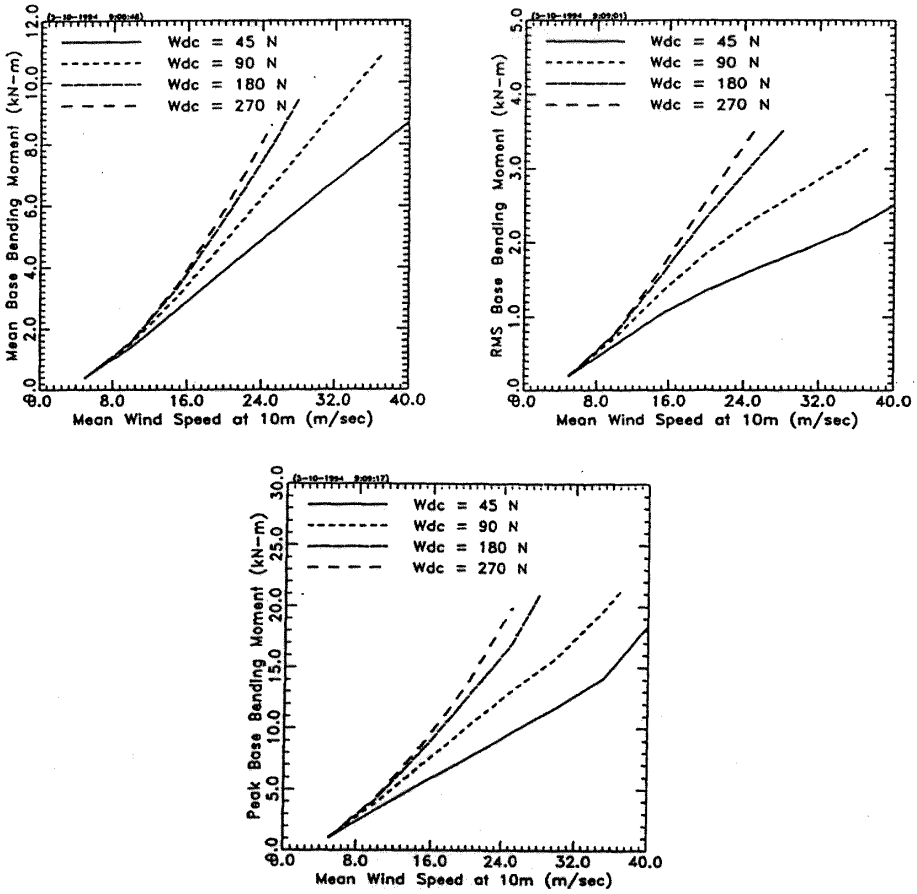

Figure 12.4. Mean, RMS, and Peak Base Bending Moment Versus Windspeed Showing Effect of Crown Weight on Tree Response.

(where m_c is the live branch weight and A_1 is a constant) yields a maximum drag force for a windspeed equal to 32 *m/s*. Higher windspeeds result in a drag force, F_D, which decreases.

Figure 12.5 shows the peak base bending moment for the Ponderosa Pine tree characterized in Table 12.2, plotted versus both the mean windspeed at 10 m and the peak windspeed at the center of the crown for typical open country (z_0 = 0.03 m) and suburban (z_0 = 0.3 m) windfields. The response of this example tree is clearly governed by the peak windspeed, and that the peak base bending moment increases approximately linearly with increases in the peak windspeed.

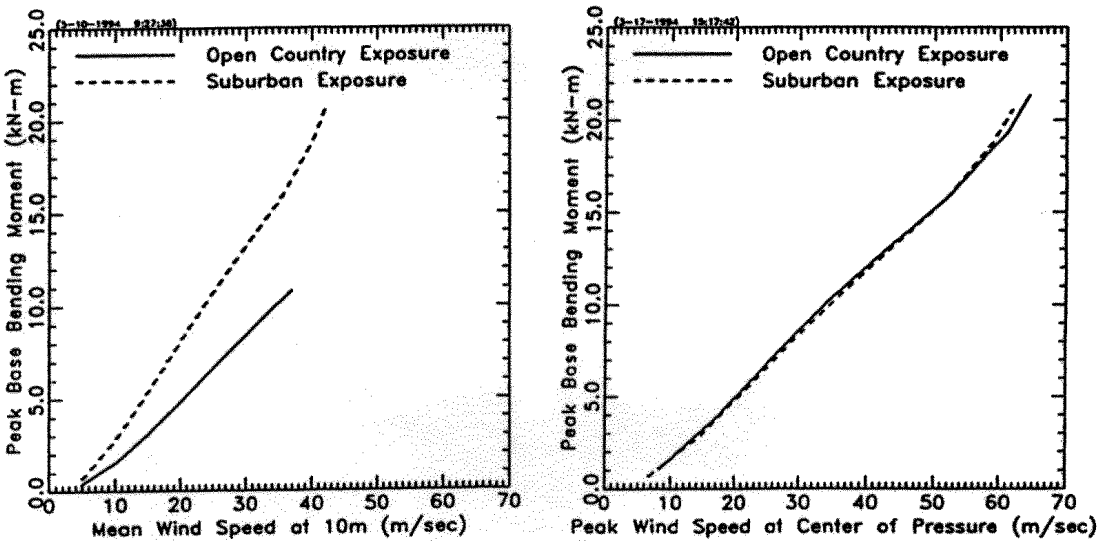

Figure 12.5. Mean and Peak Base Bending Moment Versus Peak Windspeed at Center of Pressure (Open and Suburban Terrains).

12.3.4 Wind Modeling in Forested Areas

Flow within and above plant canopies has been studied by numerous investigators over the past few decades. These studies include full-scale measurements, wind tunnel investigations, and mathematical modeling. In the case of forest flows, examples of full-scale measurements are given in Oliver and Mayhead (1974), Thompson (1979), and Bergstrom and Hogstrom (1989) for pine forests; Amiro and Davis (1988) for a Black Spruce forest; Amiro (1990a) for pine, spruce, and aspen forests; Baldocchi and Meyers (1988) for an Oak-Hickory forest; and Milne (1993) and Gardiner (1994) for a Sitka Spruce forest. Wind tunnel simulations range from very simplistic models using arrays of rigid rods to model the vegetation (Seginer, et al., 1976) to detailed aeroelastic modeling of forests (Stacey, et al., 1994). Mathematical models used to model flow within and above plant canopies include first-order closure models (e.g., Li, et al., 1985), second-order closure models (e.g., Meyers and Paw, 1986), and simplified empirical models (e.g., Cionco, 1972). A reviews of mathematical techniques used to model flow within canopies is given in Massman (1987). All of the full-scale studies noted above were carried out in relatively dense forests, so the results are not directly usable for estimating flow conditions in relatively lightly forested suburban areas, and no published measurements of wind flow conditions in lightly forested regions typical of suburban areas were found.

In the investigation described herein, the first-order closure model described in Li, et al. (1985), Li, et al. (1990), and Miller, et al. (1991) was used to describe the flow structure within and above the "forest" canopy. The computer code was provided by D. R. Miller of the University of Connecticut. The main inputs to the model include a description of the Leaf Area Index (LAI) profile of the plant canopy, defined as the leaf area per unit area of soil, an effective drag coefficient for the vegetation, and two windspeeds. Mean

windspeed and turbulence intensity profiles resulting from the model were compared to full-scale measurements in forests for cases where information on the LAI profile was also available.

Figure 12.6 shows profiles of LAI along with the measured and simulated mean, turbulence intensity, and peak windspeed profiles (peak windspeed is defined as the mean plus three standard deviations) for data given in Gardiner (1994), Stacey, et al. (1994), Baldocchi and Meyers (1988), and Amiro (1990). A drag coefficient of 0.16 (e.g., Meyers and Paw (1986) and Amiro (1990b)) was used in all cases. Figure 12.6 indicates that the first order closure model results reproduce the mean velocity profile reasonably well, through to the underside of the canopy where the secondary maxima produced by the model is greater than the maxima observed in the full-scale measurements. The RMS velocity, at height z, $\sigma_u(z)$, is estimated from

$$\sigma_u(z) = 2u_* = 2l(z)\frac{\partial u}{\partial z} \tag{12.26}$$

where $l(z)$ is the mixing length at height z above the ground surface. Details on the mixing length model are given in Miller, et al. (1991). Equation 12.26 is valid above the displacement height, d, but not beneath $z = d$. Below $z = d$ the turbulence intensity is set equal to the value computed at the lowest level in the grid. As indicated in Figure 12.6, there is no inclination for modeled local turbulence intensities to consistently overestimate or underestimate the measured intensities within the canopy; however, the modeled intensities consistently underestimate the observed intensities beneath the canopy. Within the canopy, the modeled turbulence intensities agree surprisingly well with the measured intensities. The agreement is better than the agreement between observed and modeled intensities in a Maize canopy given in Meyers and Paw (1986) using a second order closure model.

12.3.4.1 Canopy Modeling

The LAI distribution for a forested suburban region is modeled in the form

$$LAI(z) = \frac{B}{\sqrt{2\pi S}}\left[-\frac{1}{2}\left[\frac{\xi - \bar{\xi}_p}{S}\right]^2\right] \tag{12.27}$$

where S = 0.25, $\bar{\xi}_p$ is the nondimensional distance to the center of pressure measured from the base of the crown, and B is a scale factor which is a function of LAI and $\bar{\xi}_p$. A model similar to Equation 12.27 was used by Milne and Brown (1990) to describe the LAI profile in a Sitka Spruce forest. Mean and turbulence intensity profiles were developed for values of C_dLAI ranging from 0.01 and 0.3 for forests having average percentage crowns of 30%, 40%, 50%, and 60%. The mean value, $\bar{\xi}_p$, is taken as being equal to 0.5 (i.e., acting in the center of the crown).

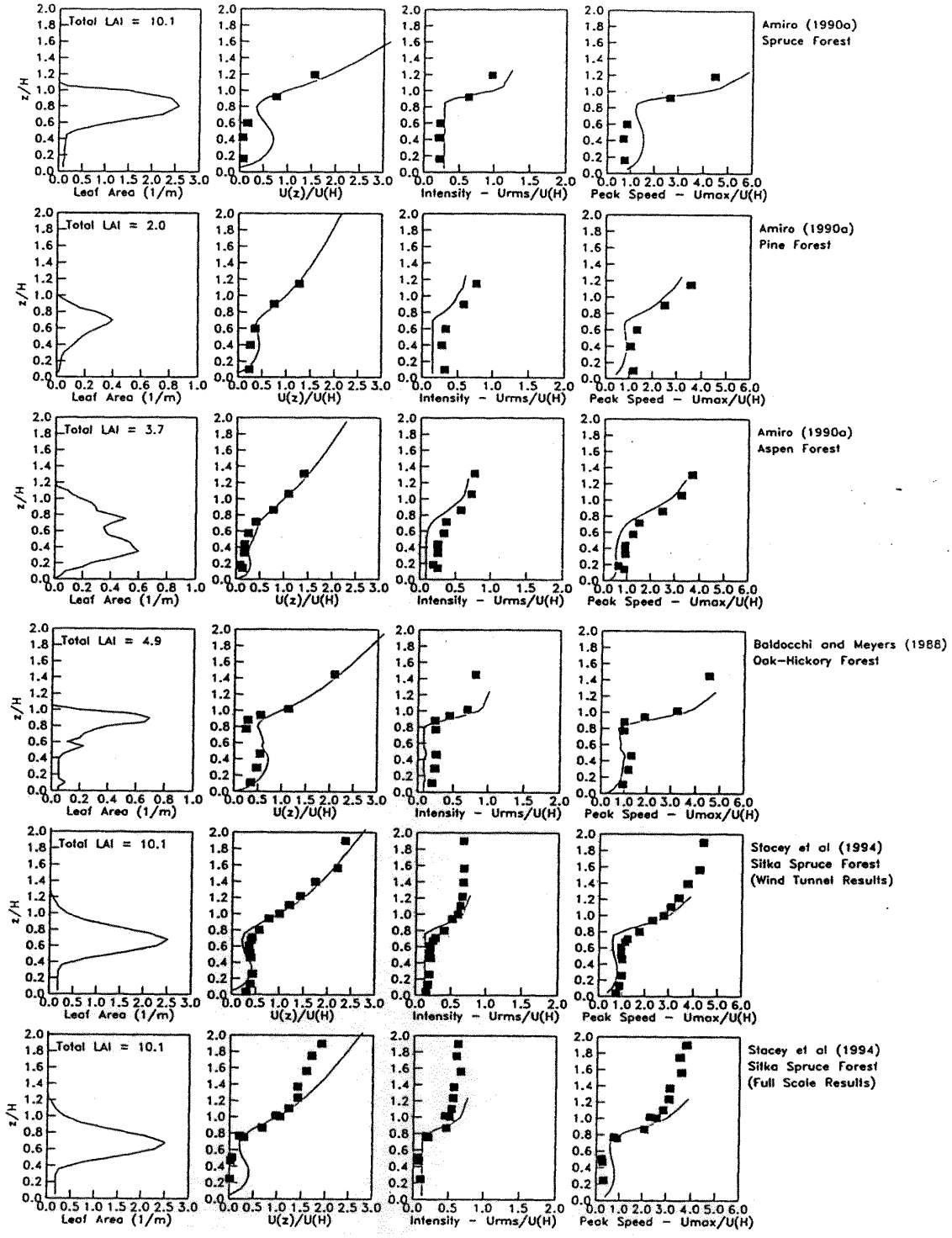

Figure 12.6. Measured Comparison of Modeled Mean and Turbulence Intensity Profiles in Forests.

Figure 12.7 shows the mean velocity and turbulence intensity profiles generated for some example C_dLAI profiles. Profiles are given for mean crown percentages within the forested area of 60%. Also shown in Figure 12.7 are the turbulence intensity and mean velocity profiles generated using the ESDU models for the atmospheric boundary layer. In developing the velocity profiles given in Figure 12.7, the displacement height, d and the surface roughness length, z_o were obtained by plotting the mean wind speed profile in semi-logarithmic space with various assumed values of d/H and selecting the combination of the two values that best fit the wind speed profile resulting from the simulation. The resulting the values of d/H and z_o/H are consistent with the information given in Shaw and Pereira (1982) and Massman (1987). The relationships between d/H and z_0/H are presented in Figure 12.8 as a function of C_dLAI. The comparison of the numerical model results with the ESDU model, show remarkable agreement above the height of the canopy for both the mean velocity and the turbulence intensity.

Given the mean velocity and turbulence intensity profiles generated for the range of C_dLAI described above, the mean wind speed at a height of (2H-d) coupled with the estimate of the local z_o is used to estimate the open terrain wind speed using the methodology given in ESDU (1982). The velocity spectrum at the center of pressure is determined using Equation 12.17, with the height replaced by $z - d$, and is combined with the admittance function defined in Equation 12.20 to develop the effective wind spectrum for use in the response estimates. In the development of the velocity profiles used herein, the influence of buildings and structures on the flow field is ignored.

12.3.4.2 Effective Windspeeds in Forested Areas

Since the tree blowdown model requires the windspeed acting at the effective center of pressure to determine the wind-induced response, effective values of $\overline{U}$ and σ_u acting at the center of pressure must be defined. These effective values are determined by integrating the product of the windspeed at height z and the frontal area at height z (assuming C_d is constant over the tree height) and equating this product with the product of an effective windspeed and the full frontal area of the tree. Effective values of the mean windspeed and turbulence intensity acting at the center of pressure were computing using two different approaches, the first of which assumes that the drag force is linearly proportional to velocity, and a second approach where the drag force is assumed to be related to the local velocity squared.

Drag Force Proportional to Velocity. Effective values of the mean velocities acting at the center of pressure of a tree in a forested area are computed as

$$\overline{U}_{eff} = U_H \frac{\int_0^H \xi(z) LAI(z) dz}{\int_0^H LAI(z) dz} \tag{12.28}$$

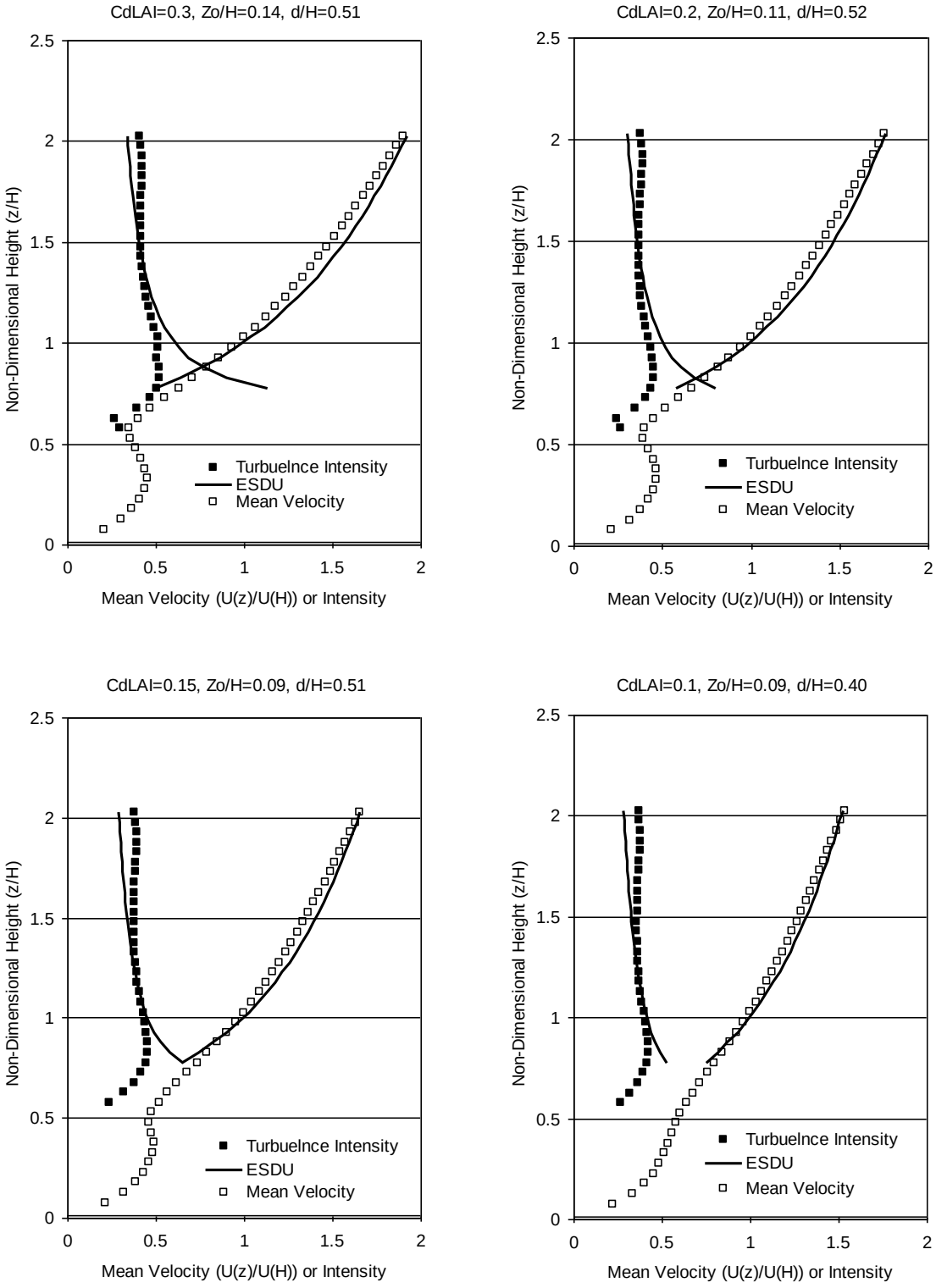

Figure 12.7. Mean and Turbulence Intensity Profiles for Various Values of C_dLAI.

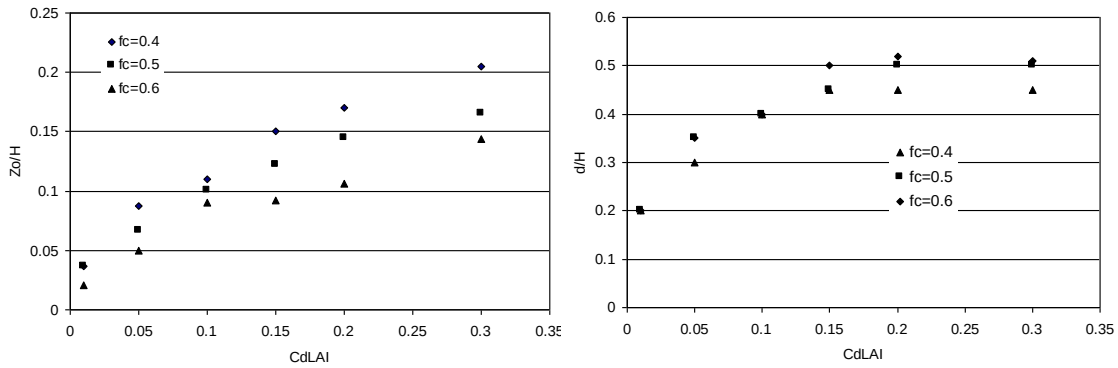

Figure 12.8. z_o/H and d/H Plotted vs. C_dLAI for Three Different Values of Crown Fraction.

where $\xi(z) = U(z)/U_H$ *is* obtained from the first order closure model and LAI(z) is the distribution of the leaf density over the height of the tree. The effective RMS velocity is computed from

$$\overline{U}_{eff}\left(1+g\frac{\sigma_{u_{eff}}}{\overline{U}_{eff}}\right)=U_H\int LAI(z)\xi(z)(1+gI_u(z))dz \tag{12.29}$$

where the peak factor, g, is taken as 3.0, and $I_u(z)$ is the turbulence intensity profile obtained from the first order closure model.

As noted earlier, the response of the tree is governed by the peak windspeed, not the mean windspeed, and as a result the effective location of the center of pressure is derived using the estimated peak wind profile.

The effective center of pressure is determined from

$$H_{cp_{eff}}=\frac{U_H\int_0^H\xi(z)(1+gI_u(z))LAI(z)z\,dz}{\hat{U}_{eff}\int_0^H LAI(z)dz} \tag{12.30}$$

where $\hat{U}_{eff}$ is the effective peak velocity given as

$$\hat{U}_{eff}=\overline{U}_{eff}\left(1+g\sigma_{u_{eff}}\right) \tag{12.31}$$

Drag Force Proportional to Velocity Squared. The effective value of the mean velocity, $\overline{U}_{eff}$, acting at the center of pressure is derived from

$$\overline{U}_{eff}^2 = U_H^2 \frac{\int_0^H \xi^2(z) LAI(z) dz}{\int_0^H LAI(z) dz} \tag{12.32}$$

The effective turbulence intensity, defined as

$$I_{u_{eff}} = \frac{\sigma_{u_{eff}}}{\overline{U}_{eff}} \tag{12.33}$$

is derived from

$$\overline{U}_{eff}^2 = \frac{U_H \int_0^H LAI(z) \xi^2(z) \left[1 + 2gI_u(z) + g^2 I_u^2(z)\right] dz}{\int_0^H LAI(z) dz} \tag{12.34}$$

the effective peak velocity $\overline{U}_{eff}^2$ is given as

$$\overline{U}_{eff}^2 = \overline{U}_{eff}^2 \left[1 + 2gI_{u_{eff}} + g^2 I_{u_{eff}}^2\right] \tag{12.35}$$

where again the peak factor, *g*, is set equal to 3. The effective height at the center of pressure is determined from

$$H_{cp_{eff}} = \frac{U_H^2 \int_0^H \xi^2(z)(1 + 2gi_u(z))^2}{\hat{U}_{eff}^2 \int_0^H LAI(z) dz} \tag{12.36}$$

The effective values, $\overline{U}_{eff}$, $\sigma_{u_{eff}}$, and $H_{cp_{eff}}$ determined using the linear and quadratic dependencies on windspeed typically vary by less than 10%, with the average of the two approaches being used to compute the tree response.

12.3.5 Simulation Methodology

In the simulation process, values of the key tree parameters given in Table 12.1 are obtained from sampling from the appropriate distributions. Using the sampled value of the center of pressure, the crown shape parameters *B* and $\overline{\xi}_p$ are determined, after which the values of U_{eff}/U_H and σ_u/U_H and effective value of center of pressure taking into account the velocity profile are calculated as described in Section 12.3.4.1. Given the new value of the center of pressure, combined with the sampled values of $\overline{R}_b$, for root and

stem failure, the failure mode (root failure or stem breakage) is determined. Given this information, time series of windspeeds (ten minutes in length) are generated, having a mean windspeed, U_H, and turbulence intensity, σ_r/U_H, and the response of the tree is calculated. Using an iterative interval halving technique, the minimum mean windspeed, U_H, required to fail the tree is determined, after which another tree is sampled and the process is repeated. The simulation process is repeated 100 times with the resulting failure windspeeds (converted to equivalent open country mean values) used to define the probability of failure distribution. Simulations for each tree examined are performed for a range of forest densities. Using the mean values of C_dA calculated for trees in a uniform wind, the average tree density, γ, *(stems/Ha)* necessary to provide the effective C_dLAI corresponding to the velocity and turbulence intensity profiles used can then be determined from

$$\gamma = \frac{10^4 C_d LAI}{C_d A} \text{ stems/}Ha \tag{12.37}$$

The information on failure windspeeds and tree density are used to determine the probabilities of trees failing and striking a typical residential structure as discussed in the following sections.

12.4 Blowdown Results

12.4.1 Tree Blowdown Curves

Simulations were performed for values of C_dLAI of 0.3, 0.2, 0.15, 0.10, 0.05 and 0.01. For each simulation, the forest canopy was approximately uniform in height (COV = 8%) and the tree diameters varied by ±1.25 cm about the mean value. Figure 12.9 shows example cumulative failure probability distribution for both homogenous deciduous and coniferous forests for three different mean values of height-diameter classes. Information on typical height and diameters and relationships between diameter and crown weight was taken from Storey and Pong (1957) for trees in a mixed hardwood forest in North Carolina. As noted in Figure 12.9, gust failure windspeed (in open country terrain) decreases with increasing forest density.

12.4.2 Tree Blowdown Validation

A validation study of the tree blowdown curves presented in Section 12.4.1 was undertaken in eight randomly selected subdivisions in eastern North Carolina immediately following Hurricane Isabel in 2003. In each of the selected residential subdivisions the survey teams counted the number of trees on each lot, counting the number of trees in each of 3 previously defined height ranges (consistent with the height ranges used in Hazus), the tree type (evergreen or deciduous) and the performance of the tree (uproot failure, stem failure or no failure). In one of the surveyed subdivisions (South Mills, NC) each tree height was estimated and the diameter at breast height was measured, and the dimensions of each lot was obtained. In all cases the address of the lot was recorded.

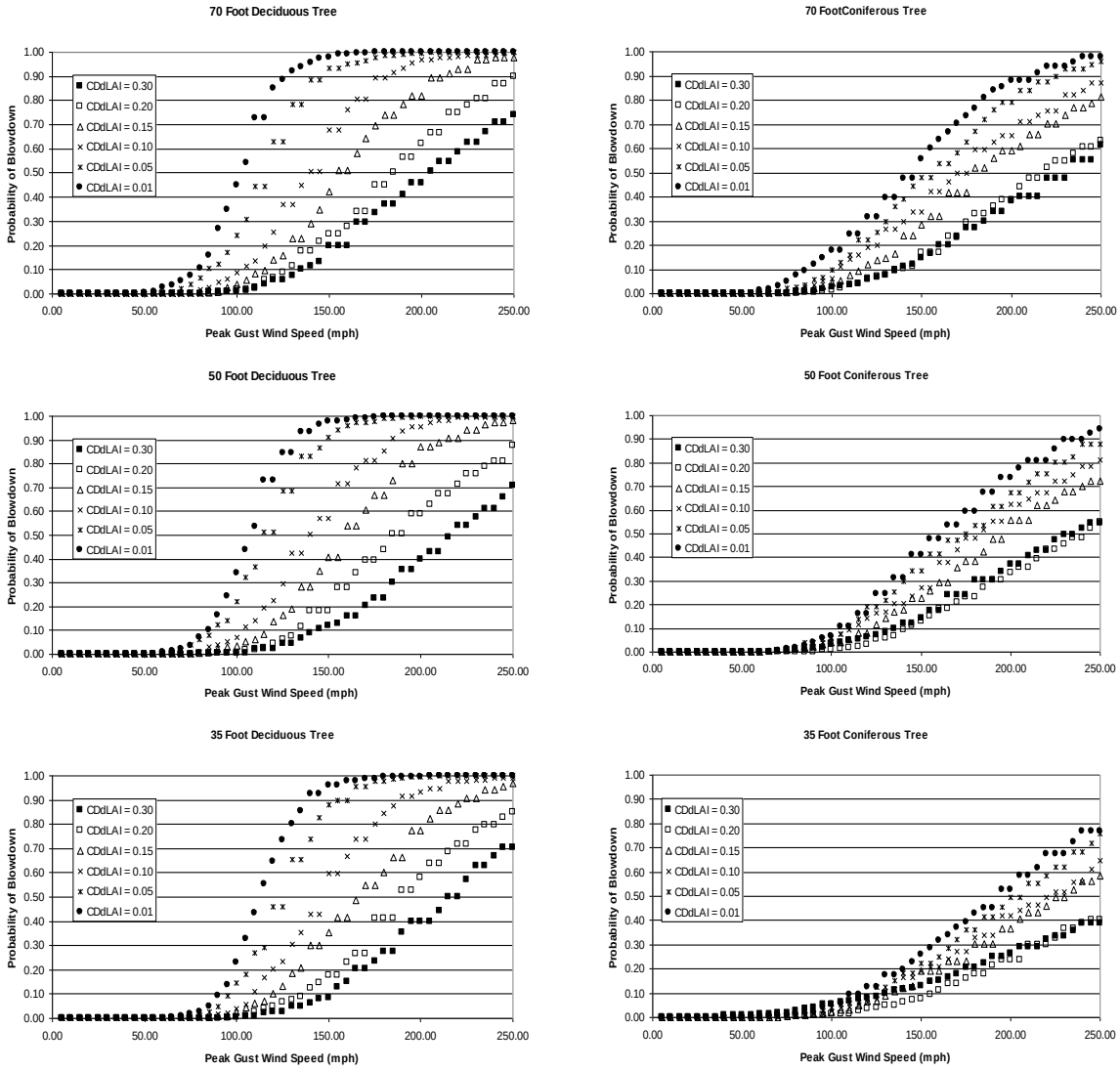

Figure 12.9. Tree Blowdown Curves.

Table 12.3 presents a summary of the data collected at the eight sites, including the estimated peak gust wind speed, the number of lots surveyed, the total number of trees surveyed, the percent of trees blown down, and the total area surveyed. A total of 1158 trees were surveyed, with the sample comprising 628 conifers and 530 deciduous trees.

Table 12.4 presents a more detailed summary presenting the number of trees in each height class as well as indicating the number of trees in each height class that fail by uprooting or through stem failure. Approximately 12% of the conifers were blown down and about 10% of the deciduous trees were blown down. The deciduous trees were more likely to fail from uprooting, whereas in the case of the conifers, stem and uprooting failures were approximately equally likely.

Table 12.3. Summary of Tree Blowdown Data

Location	Peak Gust Wind Speed (mph)	Number of Lots Surveyed	Total Number of Trees	% of Trees Blown Down
Ahoski 1	86	20	54	3.7%
Ahoski 2	86	28	113	5.3%
Elizabeth City 1	95	34	171	5.8%
Elizabeth City 2	95	45	217	8.8%
Manteo 1	92	9	178	18%
Manteo 2	92	32	150	11%
South Mills	92	27	150	19.3%
Windsor	84	28	125	8.8%
Total		223	1158	10.8%

Table 12.4. Summary of Number of Failed Trees by Height Class

		Conifers					Deciduous				
		Height Range (feet)					Height Range (feet)				
Location		<30	30-40	40-60	> 60	All	<30	30-40	40-60	> 60	All
Ahoski 1	# Trees	1	4	11	4	20	9	8	17	0	34
	# Uproot Failures	0	0	0	0	0	1	0	0	0	1
	# Stem Failures	0	1	0	0	1	0	0	0	0	0
	Total # Failures	0	1	0	0	1	1	0	0	0	1
Ahoski 2	# Trees	5	9	9	15	38	23	14	19	19	75
	# Uproot Failures	1	1	0	0	2	1	0	2	0	3
	# Stem Failures	0	0	0	1	1	0	0	0	0	0
	Total # Failures	1	1	0	1	3	1	0	2	0	3
Elizabeth City 1	# Trees	0	10	41	39	90	17	22	38	4	81
	# Uproot Failures	0	0	0	2	2	1	1	4	0	6
	# Stem Failures	0	1	0	0	1	0	0	1	0	1
	Total # Failures	0	1	0	2	3	1	1	5	0	7
Elizabeth City 2	# Trees	3	11	73	61	148	26	23	11	9	69
	# Uproot Failures	1	0	2	0	3	2	2	1	3	8
	# Stem Failures	0	0	2	3	5	2	0	1	0	3
	Total # Failures	1	0	4	3	8	4	2	2	3	11
Manteo 1	# Trees	2	4	91	0	97	26	45	10	0	81
	# Uproot Failures	0	1	6	0	7	4	3	0	0	7
	# Stem Failures	0	2	13	0	15	0	3	0	0	3
	Total # Failures	0	3	19	0	22	4	6	0	0	10
Manteo 2	# Trees	14	24	21	23	82	6	48	14	0	68
	# Uproot Failures	0	0	5	1	6	0	3	0	0	3
	# Stem Failures	0	1	3	2	6	0	1	0	0	1
	Total # Failures	0	1	8	3	12	0	4	0	0	4
Windsor	# Trees	3	6	23	23	55	25	23	12	10	70
	# Uproot Failures	0	0	1	1	2	1	1	0	0	2
	# Stem Failures	0	0	1	1	2	1	1	1	2	5
	Total # Failures	0	0	2	2	4	2	2	1	2	7
South Mills	# Trees	2	47	21	28	98	5	19	17	11	52
	# Uproot Failures	0	7	2	8	17	0	2	1	0	3
	# Stem Failures	0	1	1	1	3	0	2	2	2	6
	Total # Failures	0	8	3	9	20	0	4	3	2	9
Total	# Trees	30	115	290	193	628	137	202	138	53	530
	# Uproot Failures	2	9	16	12	39	10	12	8	3	33
	# Stem Failures	0	6	20	8	34	3	7	5	4	19
	Total # Failures	2	15	36	20	73	13	19	13	7	52

Within the Hazus tree blowdown model, each family of tree blowdown curves (probability of blowdown vs. wind speed) is stored as a function for a range of tree densities (trees/acre) for 3 pre-defined height classes for the coniferous and deciduous tree types. The original tree blowdown curves were developed by computing the probability of blowdown as a function of the effective drag per unit land are within the modeled "forest" canopy, rather than the number of trees per acre. The effective drag per unit land area is defined using a parameter referred to as C_dLAI, where C_d is a drag coefficient and *LAI* is the Leaf Area Index. The value of C_dLAI for an area is often obtained using satellite imagery to estimate the *LAI* and multiplying by a typical drag coefficient, but can also be estimated by dividing the effective total drag area in the forested region, C_dA, by the total land area covered by the trees.

The estimated values of C_dLAI at the eight sites range between 0.01 and 0.02. The lowest two values of C_dLAI used in the development of the tree blowdown curves used in Hazus are 0.01 and 0.05, and these curves are given in Figure 12.10 along with the observed blowdown data for each study region. Separate plots are given for each height class and tree type (deciduous or coniferous). The large diamond shaped point on each plot represents the weighted average probability of blowdown for all trees of the class at all sites surveyed.

From the plots, it is seen that the collected data from Hurricane Isabel agree well with the probability of blowdown curves for deciduous trees. However, less agreement is seen when coniferous trees are considered. It appears that for this case, the curves underestimate the actual probability of blowdown. In light of this comparison, the tree blowdown probabilities for coniferous trees were shifted to better agree with the available validation data.

The blowdown functions have been shifted as follows:

- All functions for short (< 40') conifers were shifted by 30 mph
- All functions for medium (40' to 60') conifers were shifted by 15 mph
- All functions for tall (> 60') conifers were shifted by 10 mph.

Figure 12.11 shows the resulting shifted functions for coniferous trees along with the validation data.

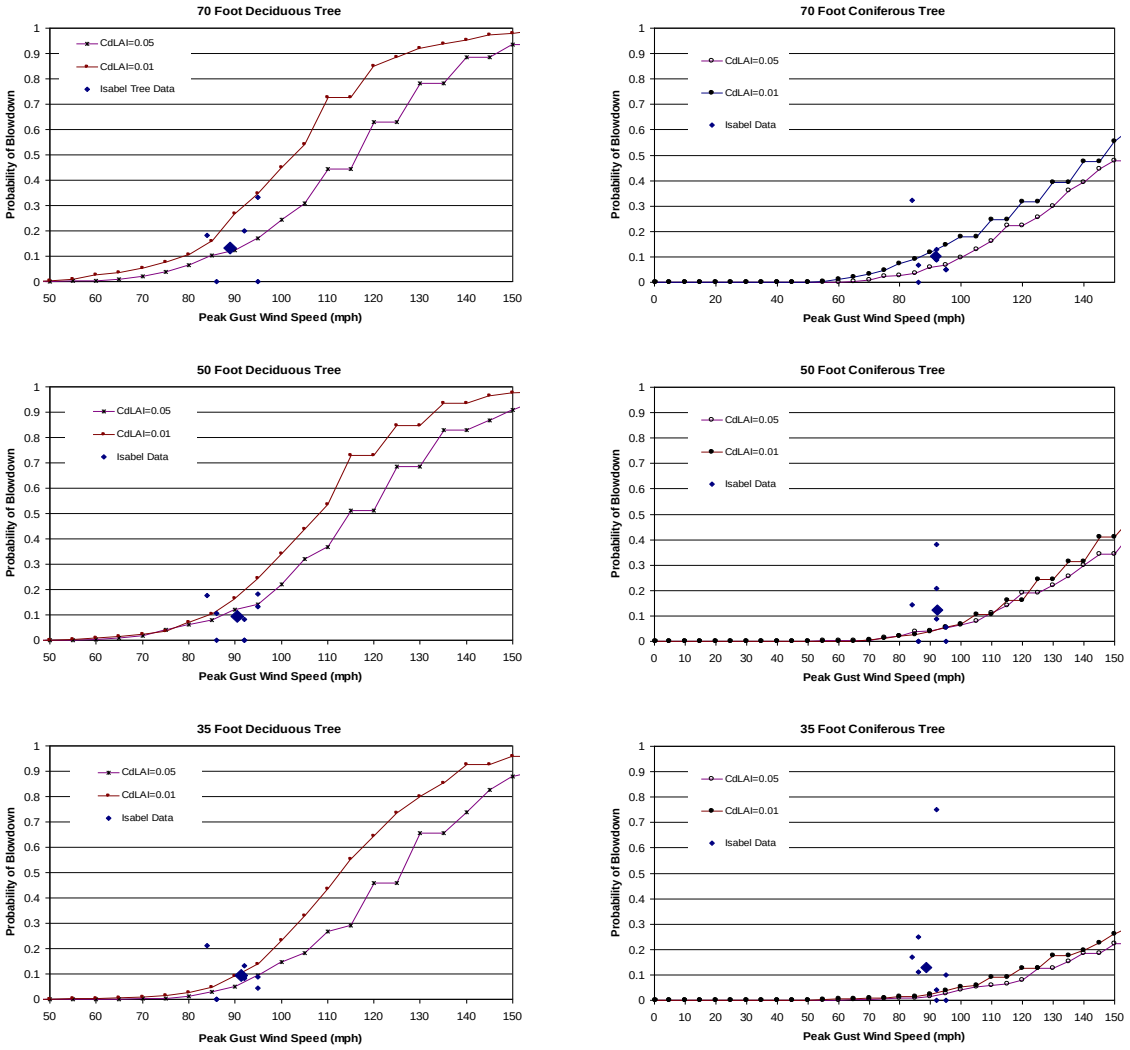

Figure 12.10. Probability of Blowdown Curves with Treefall Data Collected Following Hurricane Isabel.

12.5 Tree Inventory Data by County

12.5.1 Forest Inventory Analysis (FIA) Program and Database

The Forest Inventory Analysis (FIA) Program and Database of US Forest Service (USFS) is a nationwide tree inventory database updated on a 5-year cycle by states/regions. It is derived through a field survey and statistical analysis procedure. The database provides a spatial resolution down to the county level for the final product that is accessible in the public domain. It was initially designed for the use primarily by the lumber industry; however, it contains data such as tree count and tree diameter distribution per species in every county that are useful for the analysis described in this section. It is recognized as an authoritative source of forest/tree data on a nationwide scale. The MRLC uses FIA data to verify the accuracy of satellite imagery analysis on forest cover.

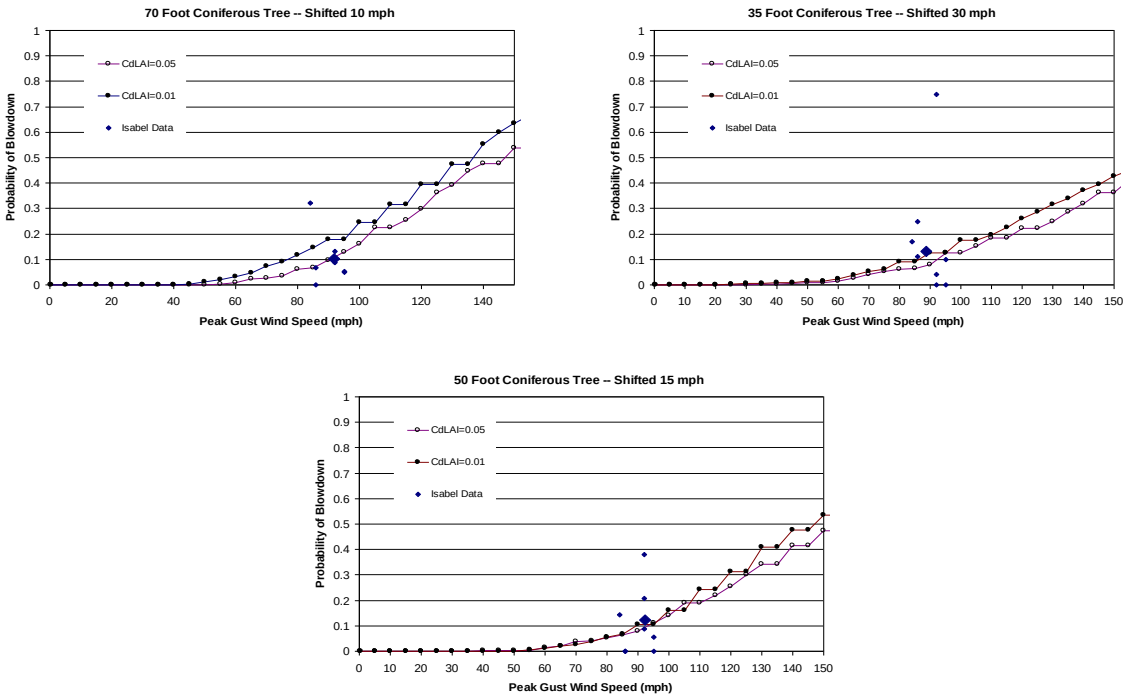

Figure 12.11. Shifted Probability of Blowdown Curves for Coniferous Trees with Treefall Data Collected Following Hurricane Isabel.

12.5.2 Average Tree Density and Tree Height Distribution at County Level

The tree blowdown methodology utilizes FIA's tree count on forest land and tree height per species per county, downloaded from the USFS website. The data incorporated into Hazus 2.0 dates between 2006 and 2010 for all states (except Hawaii which was not available at the time of this writing), with the vast majority being from 2008-2009. Prior versions of Hazus relied upon diameter distributions to determine tree height, but tree height is now readily available for most of the 1279 counties in the 22 hurricane states and the District of Columbia via download from the FIA. For those counties that did not have tree height or tree density distribution information, data from neighboring counties were used. In the case of Hawaii, data from American Samoa were used.

Using tree height information, Tree height distributions were simplified into three groups (30-40 ft, 40-60 ft, and over 60 ft tall) and summarized over all species for each county.

For each county, the average tree density is derived by dividing the tree count on forest land by the total area of forest land of the county. The forest land area used was also downloaded from the FIA database.

It should be noted that the FIA field survey and resulting database includes only contiguous tree covered areas not less than 12 acres in area. For the purpose of the Hazus model, the average tree density and tree height distribution obtained as described above are applied to all tree covered areas in a county, including smaller patches and strips of

tree covered areas embedded in residential subdivisions as identified by the MRLC land cover database.

12.6 Hazus Tree Coverage Database

The procedures carried out to derive a default tree database for Hazus from the MRLC land use database and the FIA tree database are described in this section.

12.6.1 MRLC National Land Cover Data

As described in detail in Chapter 3, the MRLC (Multi-Resolution Land Characteristics consortium) land cover database, presented in 30m resolution grids, provides relatively high spatial resolution of defined land cover types and percent tree canopy. Using the MRLC land cover database, combined with data derived from the FIA database, makes it possible to estimate the number of trees and predominant tree type at higher geographical resolutions than counties, including resolution at the census block level as required for Hazus.

12.6.2 Tree Density, Tree Height, and Predominant Tree Type by Census Tract and Census Block

For the Hazus wind risk software product, a default tree database is developed that contains variables as outlined below for each census tract.

The predominant tree type is defined in the MRLC land cover database as:

- "Coniferous" if 75% or more of the tree covered area is identified as "Evergreen" type in the MRLC land cover database;
- "Deciduous" if 75% or more of the tree covered area is identified as "Deciduous" type in the MRLC land cover database;
- "Mixed" if neither of the above two criteria holds.

Census blocks also hold to the same set of rules, however, if a census block had no forested land according the MRLC, then its predominate type defaults to the tracts predominate type.

To determine tree density at the census block level, the average tree density at the county level is first determined by dividing the tree count on forest land by the total area of forest land of the county. Second, the average canopy percentage in each county over areas determined to be evergreen forest, deciduous forest, mixed forest and woody wetlands was computed. Third, the stems per acre for 100 percent tree canopy for each county was computed assuming tree density and average canopy computed over forested areas are proportional. For example, if a county had 75 stems per acre with an average tree canopy of 50 percent, the stems per acre at 100 percent canopy was assumed to be 150 stems per acre. The maximum stems per acre was capped at 400. Finally, the average tree canopy over forested land of each census block was multiplied by its county's corresponding stems per acre for 100 percent tree canopy.

Stems per acre at the tract level is calculated by weighting the stems per acre at the census block level by area of the census block, and aggregating up to the census tract level as per Equation 12.39

$$S_t = \sum_{i=1}^{n} S_i * \frac{A_{Ci}}{A_T} \quad (12.39)$$

where:

S_t = Stems per acre at the tract level

S_i = Stems per acre at Census block *i*

A_{Ci} = Area of Census block *i*

A_T = Total area of Census tract

n = Number of Census blocks in the tract

Trees less than 30 ft tall and less than 5 inches in diameter are not included in the variable of "Forest Land Tree Density of County" or in the subsequent analysis. Trees less than 30 ft tall normally have trunk diameters less than 5 in and small crown weights. These trees are neglected in the debris volume and building damage models.

The tree height distribution represents the proportions of short (30-40 ft), medium (40-60 ft) and tall (>60 ft) trees. They sum-up to 100%. In general, tree heights rarely exceed 100 ft. which represents the 99.9th percentile height for trees over 30 ft tall in the 22 states covered by the hurricane model. On a nationwide base, the average tree heights within the three bins are 35.0, 49.7 and 74.9 ft, respectively.

The format of the Hazus tree coverage database is summarized in Table 12.5. An example of the Hazus tree data is shown in Figure 12.12 for Wake County, NC at the census tract level. A map of tree density is shown in Figure 12.13. The city of Raleigh, NC is in the lower density area in the center of the county.

Table 12.5. Hazus Tree Data Format

Census Tract	Predominant Tree Type	Stems per Acre of Land	Tree Height Distribution, %		
			30-40 ft	40-60 ft	>60 ft
xxxxxxxxxxx	Coniferous, Deciduous, or Mixed	0-400	0-100	0-100	0-100

Tree Parameters

Table:

	Census Tract	Predominate Tree Type	Stems per Acre	Tree Height Less 40 ft	Tree Height 40 ft To 60 ft	Tree Height Greater than 60 ft	Tree Collection Factor
1	37183050100	Mixed	6	11	44	45	0.80
2	37183050300	Mixed	22	11	44	45	0.92
3	37183050400	Mixed	16	11	44	45	0.75
4	37183050500	Mixed	43	11	44	45	0.75
5	37183050600	Mixed	26	11	44	45	0.75
6	37183050700	Mixed	27	11	44	45	0.80
7	37183050800	Mixed	50	11	44	45	0.44
8	37183050900	Mixed	11	11	44	45	0.77
9	37183051000	Mixed	17	11	44	45	0.90
10	37183051100	Mixed	22	11	44	45	0.22
11	37183051200	Mixed	31	11	44	45	0.85
12	37183051400	Mixed	60	11	44	45	0.99
13	37183051501	Mixed	78	11	44	45	0.87
14	37183051502	Deciduous	82	11	44	45	0.92
15	37183051600	Mixed	66	11	44	45	0.98
16	37183051700	Mixed	79	11	44	45	0.77
17	37183051800	Mixed	38	11	44	45	0.80
18	37183051900	Mixed	70	11	44	45	0.82
19	37183052001	Mixed	44	11	44	45	0.46
20	37183052002	Mixed	60	11	44	45	0.93
21	37183052101	Mixed	67	11	44	45	0.65
22	37183052102	Mixed	62	11	44	45	0.41
23	37183052201	Mixed	33	11	44	45	0.55
24	37183052202	Mixed	49	11	44	45	0.41
25	37183052301	Mixed	91	11	44	45	0.51
26	37183052302	Mixed	58	11	44	45	0.39
27	37183052401	Mixed	59	11	44	45	0.18
28	37183052402	Mixed	51	11	44	45	0.75
29	37183052404	Coniferous	72	11	44	45	0.94
30	37183052405	Coniferous	34	11	44	45	0.81
31	37183052501	Mixed	68	11	44	45	0.79
32	37183052503	Mixed	75	11	44	45	0.56
33	37183052504	Mixed	53	11	44	45	0.66
34	37183052601	Mixed	75	11	44	45	0.96
35	37183052602	Mixed	64	11	44	45	0.95
36	37183052603	Mixed	76	11	44	45	0.79
37	37183052701	Mixed	38	11	44	45	0.62

Print Map OK Cancel

Figure 12.12. Hazus Tree Coverage Data for Wake County, NC.

12.7 Debris Generated from Tree Blowdown

Hurricanes generate considerable amounts of debris from tree blowdown. In most cases, local and state governments, with federal assistance, are responsible for collecting and disposing of this debris. Tree debris disposal totals from Hurricane Isabel in North Carolina totaled over 3.2 million cubic yards and cost communities in the state over $31 million to collect and dispose of this debris. Section 12.7.1 discusses how Hazus-MH estimates the total overall tree debris generated by hurricanes. Section 12.7.2 presents the methodology for estimating the amount of tree debris to be collected as the result of hurricanes. Section 12.7.3 presents comparisons of modeled versus actual collected tree debris from several recent hurricanes including Isabel (2003), the four hurricanes that struck Florida in 2004, Wilma (2005), and Rita (2005).

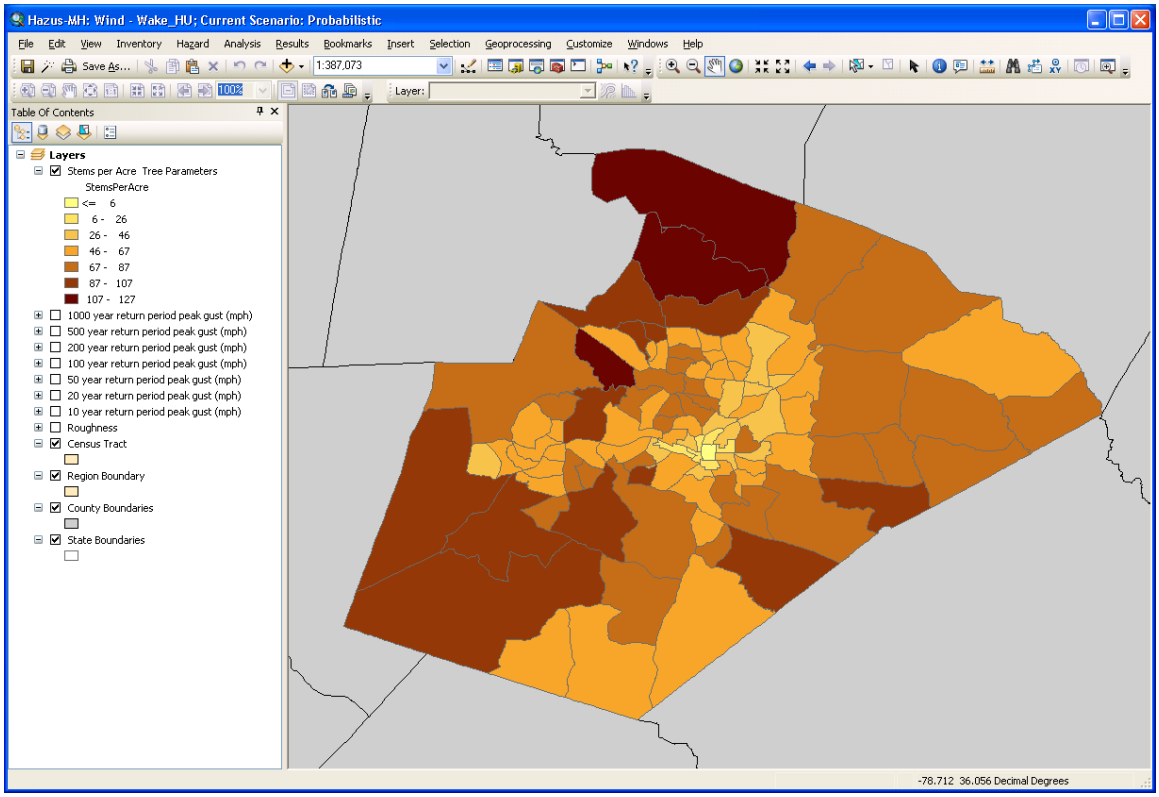

Figure 12.13. Map of Tree Density for Wake County, NC.

12.7.1 Total Weight and Volume of Downed Trees

The tree debris model combines the tree coverage database and the tree blowdown model to produce estimates of tree debris weight by census tract. The tree debris weight reported by Hazus is the expected green weight of trees greater than 30 ft tall that are expected to fail at a given windspeed for a given density of trees. The entire weight is reported as debris, even though tree debris in unpopulated areas may not be collected.

Hazus-MH computes the total weight of tree debris based on the modeled windspeed and the density of trees for the census tract (or block). The tree blowdown functions presented in Section 12.4.1 are converted to debris functions by relating the $C_D LAI$ values to number of trees per acre and multiplying the probability of blowdown values by the total expected weight of trees per acre, for the given type, height, and density of trees. Figure 12.14 shows the tree debris functions implemented in Hazus-MH.

Hazus-MH MR1 estimated the cubic yardage of tree debris using a multiplier of 3.6 cubic yards per ton based on figures reported by Escambia County, Florida after Hurricane Opal (Escambia County, 1996). Further research into appropriate bulking factors to be used to convert weight of tree debris to volume has revealed a wide range of factors used by various sources. Table 12.6 shows bulking factors developed from several different sources as a part of the development of the tree debris model for MR2.

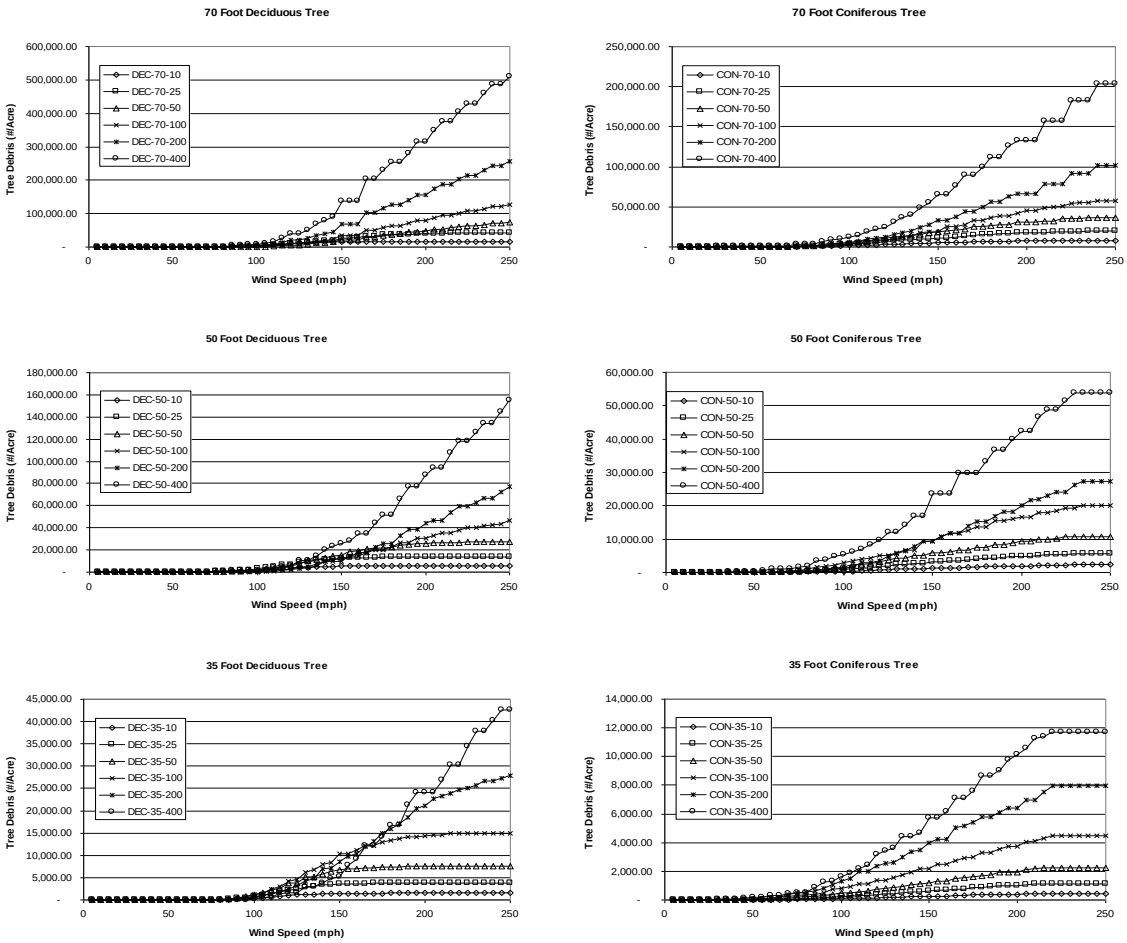

Figure 12.14. Tree Debris Functions in Pounds per Acre.

Based on the data presented in Table 12.6, it appears that the actual bulking factor should be based on a number of different types of debris – from leaves and loose brush to large limbs and stumps. It is also likely that the appropriate bulking factor will be a function of the strength of the hurricane. The majority of tree debris from weaker storms will be the result of failed limbs within the crown and will not include very many entire trees or stumps. On the other hand, stronger storms will cause more complete tree uprooting and devastating crown damage and result in denser tree debris.

A bulking factor of 4 is more appropriate for chipped or compacted tree debris, while a factor of 10 represents bulkier, uncompacted unclipped debris. For the base estimation of tree debris volume, the bulking factor in Hazus-MH is now taken as 10 CY/ton to represent uncompacted and unchipped debris. Users performing level 2 and 3 analyses are encouraged to develop their own local bulking factors based on the relationship between tree debris volume and weight from earlier or current hurricanes affecting their areas, and/or modifying the bulking factor to reflect their local debris chipping/compacting procedures.

Table 12.6. Tree Debris Related Bulking Factors from Various Sources

Source	Description	Bulking Factor (CY/ton)
FEMA 9580.1	Woody Debris	4
SC Dept of Health and Environmental Control	Wood Chips	4
MS Dept of Environmental Quality	Uncompacted Limbs and Leaves	12
CA Integrated Waste Management Board	Large Limbs and Stumps	1.85
	Mixed Yard Trimmings	18.5
	Wood Chips	4
	Prunings, Dry	54
	Prunings, Wet	43
	Prunings, Shredded	3.8
	Leaves, Dry	5.8
	Leaves	24
Solid Waste Authority of Palm Beach County, FL	Vegetative Debris	5.5
Alachua County, FL Public Works Department	Hurricane Debris from Frances and Jeanne	10.5
City of Honolulu, HI Refuse Department	Uncompacted Yard Waste	8
	Compacted Yard Waste	4.6
	Wood Chips	4
	Loose Brush	10

12.7.2 Tree Debris Collection Model

The methodology for estimating tree debris collection quantities is based on building density, length of roads, and census block shapes. This empirical method is based on the concept that trees downed in close proximity to streets, highways, or buildings make up the great majority of trees brought to the curb for collection and disposal.

12.7.2.1 Tree Debris Collection Model Description

The underlying premise of the tree debris collection model is that trees that fall in close proximity to highways, streets, and buildings are going to be collected and brought to the curb for collection. As such, an area reduction factor was developed based on a predetermined collection area around each of the streets and buildings within a study region.

The model applies a reduction factor to the overall estimate of downed trees currently produced as described in Section 12.7.1. The tree debris collection model is expressed in Equation 12.40.

$$D_c = \sum_{i=1}^{n} D_i * \frac{A_{Ci}}{A_{Ti}} \qquad (12.40)$$

where:

D_c = Tree debris collected

D_i = Total tree debris predicted by Hazus for census block i

A_{Ci} = Collection area calculated for census block i

A_{Ti} = Total area of census block *i*

n = Number of census blocks in the study region

The model was developed by running Hazus-MH at the census block level. The census block level was chosen because the boundaries of census blocks are most often represented by highways, streets, and roads with relatively few streets contained inside. A method for aggregating census block factors to the census tract level for study regions defined at the census tract level is discussed in Section 12.7.2.2.

The collection area (A_{Ci}) for each census block is first calculated based on the density of buildings within the census block (buildings per acre). As a baseline, it is assumed that downed trees will be picked up for an area of a one acre per building in the census block, with a maximum collection area set at the area of the census block. The result is that all tree debris is assumed to be collected in census blocks when the building density is equal to or greater than one building per acre.

For census blocks with building densities lower than one building per acre, the model also determines an alternative collection area along the census block perimeter and any roads within the census block. The depth of this perimeter collection area varies based on the building density of the census block because areas with little or no development will only have enough trees cleared to keep the roads safe for travel. The depth of the perimeter collection area varies from 25 to 200 feet linearly as building density varies from 0 to 1 building per acre.

25 feet was chosen as the minimum depth for the perimeter collection area to account for trees that fall into roadways and rights of way in undeveloped areas. 200 feet was chosen as the upper bound to be consistent with building-based collection area described above because a 200 foot by 200 foot square is approximately one acre in area.

The perimeter collection area is calculated in the following manner:

- The perimeter and area of each census block are calculated.
- The ratio of the square root of the area to the perimeter is then used to approximate the aspect ratio of each census block. This ratio is 0.25 for square blocks and approaches 0.0 for long slender blocks.
- From the aspect ratio and total area of each block, the width and length of an equivalent rectangle are determined.
- Perimeter collection areas are calculated for each block using the approximate length and width with the perimeter collection area depth, as shown in Figure 12.15.
- For census blocks that contain roads within their boundaries, an interior road collection area is calculated using the length of the interior roads and the depth of the perimeter collection area determined above. This area is added to the perimeter collection area.

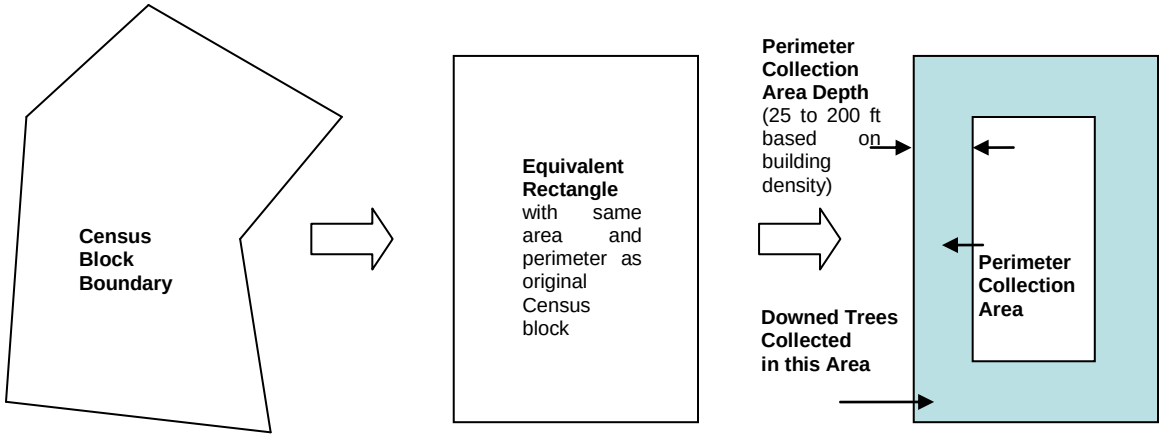

Figure 12.15. Calculation of Perimeter Collection Area for a Census Block with No Interior Roads.

- The perimeter collection area is then compared to the building based collection area (number of buildings times one acre). The larger of the two areas is retained as the total collection area (A_{Ci}), provided that the area is less than the overall census block area.

The presence and length of interior roads present inside each census block was determined by overlaying ESRI Streetmap USA data on the Hazus census blocks.

Figure 12.16 shows the relationship between equivalent census block width and building density for each census block analyzed in the Hampton Roads region of Virginia. The equivalent census block width is defined as the smaller dimension of the equivalent rectangular area calculated for each census block. The different series in the graph represent different ranges of the calculated tree debris collection factors (A_{Ci}/A_{Ti}). The collection factors are:

- Less than 0.5 for census blocks that are substantially wider than four times the perimeter collection area depth and/or that have less than 0.5 buildings per acre,
- Equal to 1.0 for census blocks with widths less than or equal to twice the perimeter collection area depth and/or with more than one building per acre, and
- Between 0.5 and 1.0 for census blocks that have widths between two and four times the perimeter collection area depth and/or building densities between 0.5 and 1.0 buildings per acre.

Thus, in Figure 12.16, we see that only wide census blocks with low building densities are assigned collection factors less than 0.5.

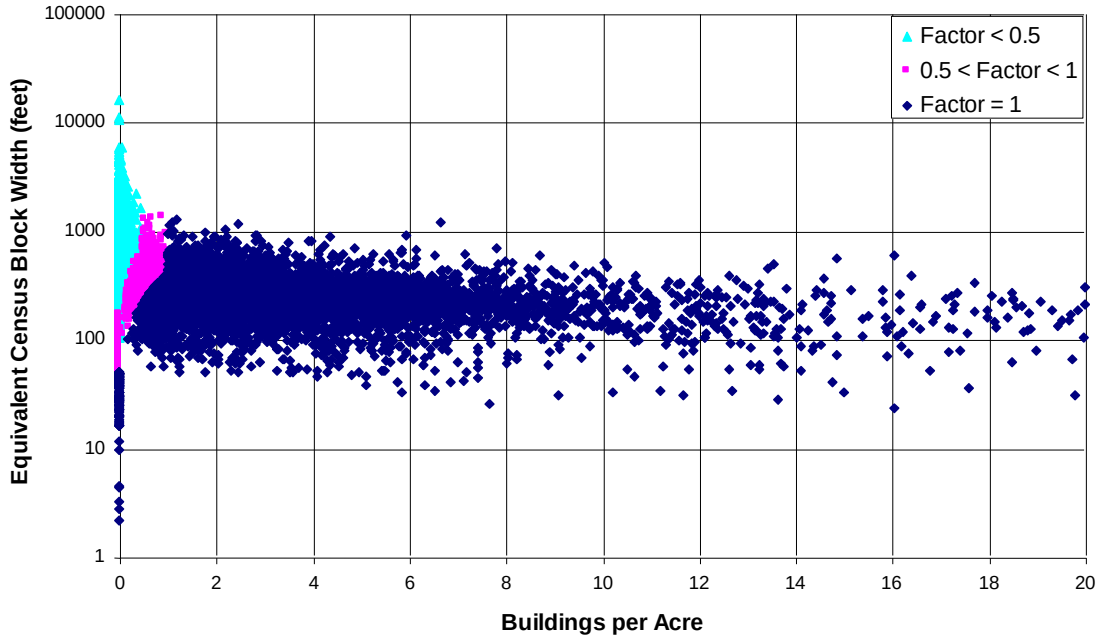

Figure 12.16. Equivalent Census Block Width versus Buildings per Acre for Hampton Roads Region of Virginia.

The resulting factors are then applied to the Hazus-MH results for tree debris quantities for each census block.

While Hazus 2.0 does not use Census 2010 blocks, collection factors were updated with 2010 Census blocks in mind. In particular, only those blocks that had less than one building per acre, did not have a collection factor of one already, or were divided into smaller portions according to the Census 2010 were updated.

Divided blocks in the 2010 Census pertain to those Census 2000 blocks that were divided into smaller portions. It was assumed that new roads were put in areas that previously did not have any. The area of these smaller portions is known, and was assumed to be square. Assuming the same building density of the Census 2000 block from which they originated, a new collection factor was determined for each of these smaller portions. These smaller portions were then area weighted and aggregating up to their original Census block to come up with a new collection factor for the original Census 2000 block (not to exceed a value of one). Figure 12.17 shows a schematic mapping of a single Census 2000 block that was divided into smaller portions and made into two Census 2010 blocks.

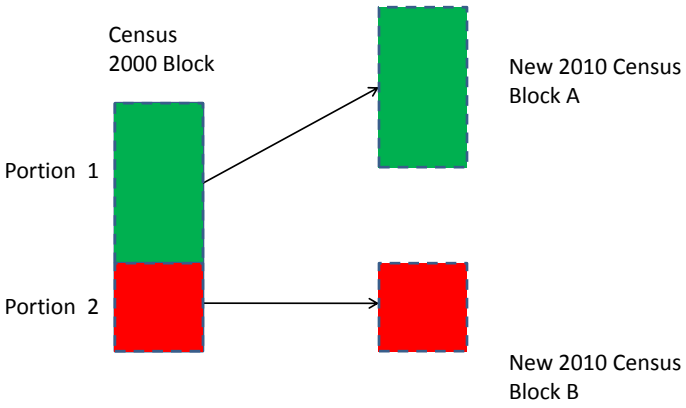

Figure 12.17. Schematic Mapping of a Census 2000 Block Partitioned into Smaller Census 2010 Blocks.

12.7.2.2 Implementing into Hazus-MH

Factors for all census blocks are pre-calculated for inclusion in Hazus-MH. These reduction values are stored in the "Tree Parameters" table in the "Tree Debris Collection Factor" column, as shown in Figure 12.18. Like the other tree parameter data, this field could also be modified by the user if more detailed information is available for individual areas at the local level.

Hazus-MH multiplies both the weight and volume of tree debris estimates in the debris analysis results table by the collection factors and presents two columns of output, as indicated in Figure 12.19.

Requiring that this analysis be completed at the census block level greatly increases the time it takes to run Hazus. In order to accommodate analyses run at the census tract level, the factors developed for individual census blocks are aggregated to the census tract level using the following equation:

$$F_{CT} = \sum_{i=1}^{n} \frac{A_{CBi} * F_{CBi}}{\sum_{i=1}^{n} A_{CBi}} \qquad (12.41)$$

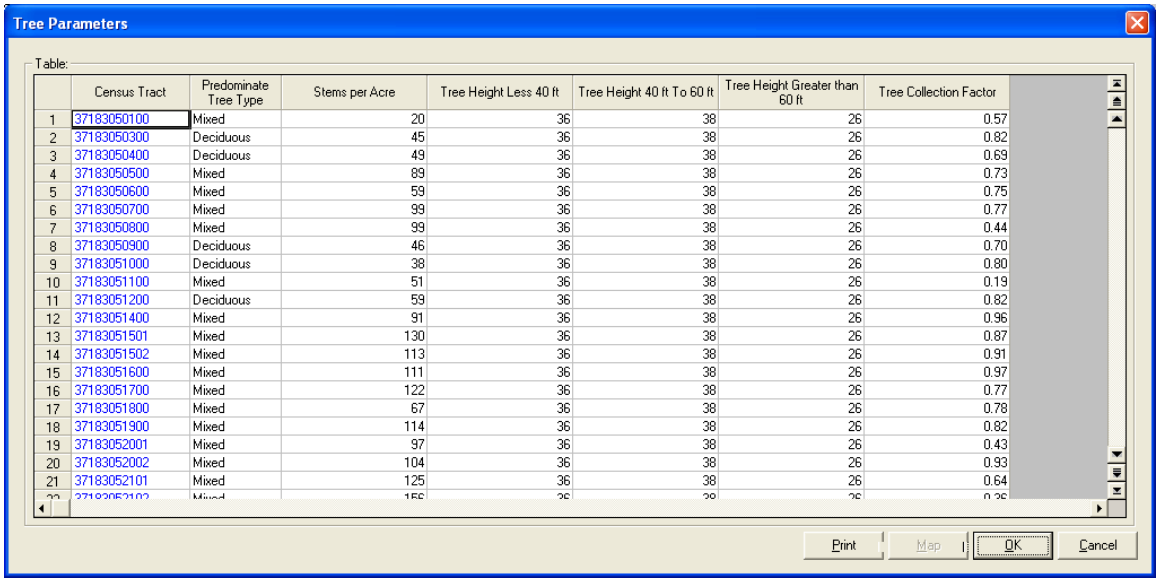

Figure 12.18. Addition of Tree Collection Factor to Tree Parameter Table in Hazus-MH

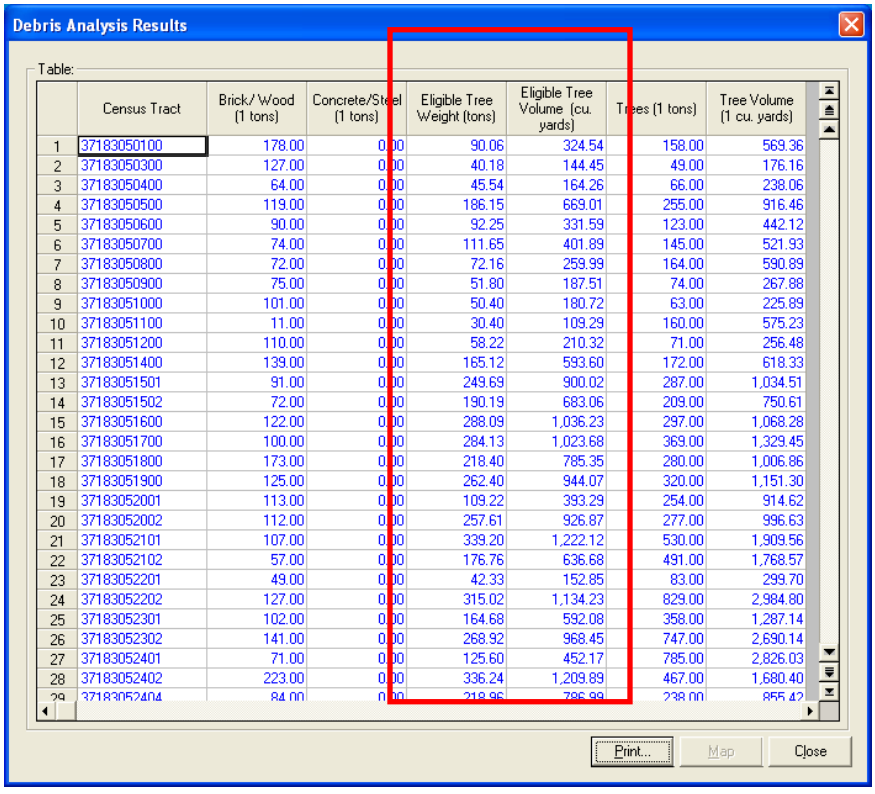

Figure 12.19. Hazus-MH Debris Results Table

where:

F_{CT} = Tree debris collection factor for a given census tract

A_{CBi} = Area of census block *i*

F_{CBi} = Tree debris collection factor for census block *i* (A_{Ci}/A_{Ti})

A_{CT} = Area of corresponding census tract

n = Number of census blocks in the current census tract

If Hazus-MH is run using uniform tree characteristics within each census tract (as is the case with the default data provided in Hazus-MH), identical estimates of tree debris generation and collection will be produced regardless of whether the analysis is run at the census tract or census block level. However, if the tree parameter data is changed such that the data vary by census block within a census tract, then results will differ and Hazus-MH must be run at the census block level for the desired results. This issue is discussed further in the next section.

12.7.2.3 Other Considerations for Hazus 2.0

While the collection factors can be aggregated to the census tract level as discussed in the previous section, the tree debris generation and collection results are sensitive to whether tree parameters are tabulated at the block or the tract level.

Prior to Hazus 2.0, the tree parameter data were assumed to be the same for every census block within a given census tract. This situation can introduce substantial biases in the tree debris generation and collection estimates for rural counties where census tracts are very large geographically and there may be only one or two census tracts for an entire county. One such area is Camden County, NC.

Tree fall frequencies surveyed in Camden County following Hurricane Isabel in 2003 demonstrated that tree coverage was scattered throughout the county with large areas of open land and smaller areas of clustered trees. Since Camden County has only one census tract, Hazus-MH considered the county to have uniform tree coverage prior to the release of Hazus 2.0.

In order to investigate further, the MRLC (Multi-Resolution Land Characteristics) land use, land cover data was revisited for a rural, four-county study region in North Carolina. Tree density statistics were re-calculated at the census block level for Camden, Chowan, Gates and Perquimans counties. The revised tree parameters were input into Hazus and the Hurricane Isabel scenario was re-run. Table 12.7 summarizes the results of this re-analysis for these four counties.

The large reductions in debris generated and collected indicate that the tree debris estimation is sensitive to the tree parameter data that is input to the tree blowdown and debris collection models. This indicates that when running level 2 or 3 analyses with refined local data, it is desirable to re-classify the land use, land cover data by census

block when using Hazus to predict tree debris generation and collection quantities. This is especially true for rural counties with large census tracts.

Table 12.7. Comparison of Modeled Tree Debris Generation and Collection Weight with Tree Parameters Compiled at the Census Tract and Census Block Levels.

	Tree Debris Generated (tons)			Tree Debris Collected (tons)		
County Name	Standard Tree Parameters	Revised Tree Parameters	Percent Reduction	Standard Tree Parameters	Revised Tree Parameters	Percent Reduction
Camden	338,711	199,911	41.0%	9,453	6,199	34.4%
Chowan	311,757	264,208	15.3%	17,539	11,276	35.7%
Gates	1,130,284	889,938	21.3%	36,609	27,493	24.9%
Perquimans	540,251	314,369	41.8%	23,386	12,631	46.0%

12.7.3 Comparison of Modeled and Reported Tree Debris

This section describes the methodology and presents a comparison of a prototype implementation of the methodology with tree debris statistics received from the North Carolina (NCDEM, 2004) and Virginia (Roarty, 2004) Departments of Emergency Management following Hurricane Isabel in 2003 (NC Department of Emergency Management, 2004; and Roarty, 2004).

12.7.3.1 Example Tree Collection Data – Hurricane Isabel, North Carolina

Tree debris collection data were obtained from the North Carolina Department of Emergency Management to assess how the methodology performs on an actual storm. Data were available for all counties in North Carolina that filed for federal assistance for debris cleanup. The data for the counties analyzed in this study are presented in Table 12.8.

These data were compiled by the North Carolina Department of Emergency Management using tree debris quantities from project worksheets completed by local governments following Hurricane Isabel. The numbers represent a combination of actual and estimated tree debris quantities by county based on their availability on the project worksheets. It is also important to note that there is a separate line noted for "State Agencies". The debris quantity reported for this entry is likely to result from additional debris collected from several of the affected counties studied. Because of this, the tree debris volumes reported by county are likely to be slightly lower than actual. However, this volume is less than 2% of the total tree debris volume reported.

Hazus-MH was run using a Hurricane Isabel scenario for the 20 North Carolina counties listed in Table 12.8. Figure 12.20 compares modeled tree debris weight (total and collected) to the actual weight of tree debris reported collected by county in North Carolina for Hurricane Isabel (reported weights calculated from reported cubic yards with an assumed bulking factor of 10 cubic yards per ton). The series labeled "All Downed Trees" represents the total tree debris estimated by Hazus before applying the collection factors.

The county names along the abscissa are ordered by increasing average census block building density. In other words, the most rural counties appear on the left and least rural

Table 12.8. North Carolina Tree Debris Collection Data for Hurricane Isabel (2003)

County	Tree Debris Volume (CY)	Collection/Disposal Cost ($)	Unit Cost ($/Cubic Yard)
Beaufort	436,323	10,781,089	24.71
Bertie	82,222	932,359	11.34
Camden	706	28,765	40.74
Carteret	135,434	802,920	5.93
Chowan	476,768	3,704,690	7.77
Craven	52,729	453,677	8.60
Currituck	60,400	402,098	6.66
Dare	220,113	1,973,850	8.97
Gates	4,094*	45,688	11.16
Hertford	58,194	400,399	6.88
Hyde	48,503	384,263	7.92
Jones	3,414	44,924	13.16
Martin	69,951	283,732	4.06
Northampton	37,747	228,001	6.04
Onslow	8,881	260,441	29.33
Pamlico	4,697	159,095	33.87
Pasquotank	773,216	3,039,044	3.93
Perquimans	33,600	239,320	7.12
Tyrrell	3,700	43,424	11.74
Washington	152,404	361,538	2.37
State Agencies	53,121	974,307	18.34
Region Total	**2,716,217**	**25,543,624**	**9.40**

* Volume estimated from cost of removal

(most urban/suburban) appear on the right. There appears to be a trend of greater over prediction of tree debris for the more rural counties. It is not possible to determine whether this trend is due to an overestimate of the number trees blown down, an overestimate of the collection factors in rural areas, an underreporting of tree debris collection in some rural counties, or some combination of the three.

The overall estimate of tree debris collected for the 20 North Carolina counties considered is about 41 percent lower than the actual totals collected by the Department of Emergency Management.

12.7.3.2 Example Tree Collection Data – Hurricane Isabel, Virginia

Data from the Virginia Department of Emergency Management were available for the 16 counties and communities that make up the Hampton Roads area. These data were compiled by the Hampton Roads Planning District for the Virginia Department of Emergency Management. The debris data for Virginia are shown in Table 12.9.

The debris data received from the Virginia Department of Emergency Management included the following caveats:

- Debris quantities from military facilities in the region are not included.

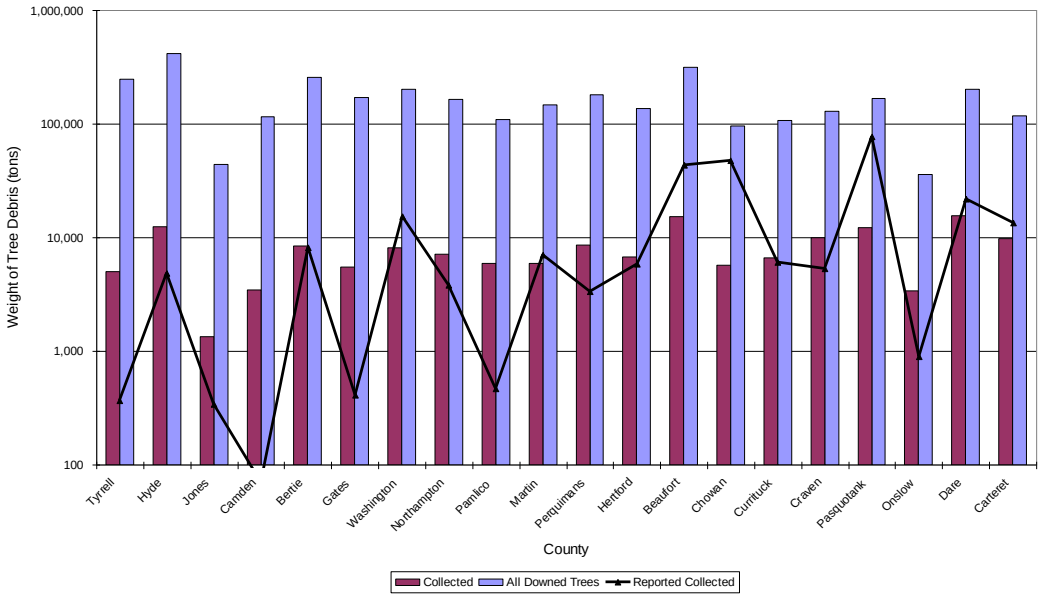

Figure 12.20. Comparison of Modeled Total and Collected Tree Debris Weight with Collection Totals Reported by NC DEM by County in North Carolina for Hurricane Isabel.

- The data shown above is for all debris, not just trees/vegetative debris. However, conversations with Virginia DEM and the Hampton Roads Planning District confirmed that over 95% of the debris reported was from vegetative sources.
- Approximately 25% of the debris was reported by the Hampton Roads District of the Virginia Department of Transportation (VDOT). This debris was collected from the study area, but the proportion belonging to each county or community is unknown and is not included in the analysis.
- VDOT is responsible for collection of vegetative debris from federal highways in the entire Hampton Roads region, as well as for the collection of debris along state roads in the counties not labeled "(city)". Debris collection from state roads in counties labeled "(city)" is the responsibility of the city government.

The modeled tree debris weight was compared directly to the data provided by the Virginia DEM without modifications for the caveats listed above, assuming a bulking factor of 10 cubic yards per ton. The counties appear in order of increasing average census block building density.

Figure 12.21 shows that for twelve of the sixteen counties, the total weight of tree debris generated by all downed trees is less than that reported by the Virginia Department of Emergency Management, indicating either that the default tree densities and/or the calculated tree blowdown rates are too low in these counties or that there are other sources of debris that are not being modeled in Hazus.

Table 12.9. Virginia Debris Collection Data for Hurricane Isabel (2003).

County	Debris Volume (CY)
Chesapeake (city)	915,101
Franklin (city)	119,000
Gloucester	190,000
Hampton (city)	749,503
Isle of Wight	152,953
James City	411,848
Newport News (city)	577,045
Norfolk (city)	1,014,000
Poquoson (city)	175,795
Portsmouth (city)	430,000
Southampton	185,200
Suffolk (city)	400,000
Surry	59,514
Virginia Beach (city)	922,000
Williamsburg (city)	79,000
York	602,830
VDOT HR District	2,365,860
Total Debris:	**9,349,649**

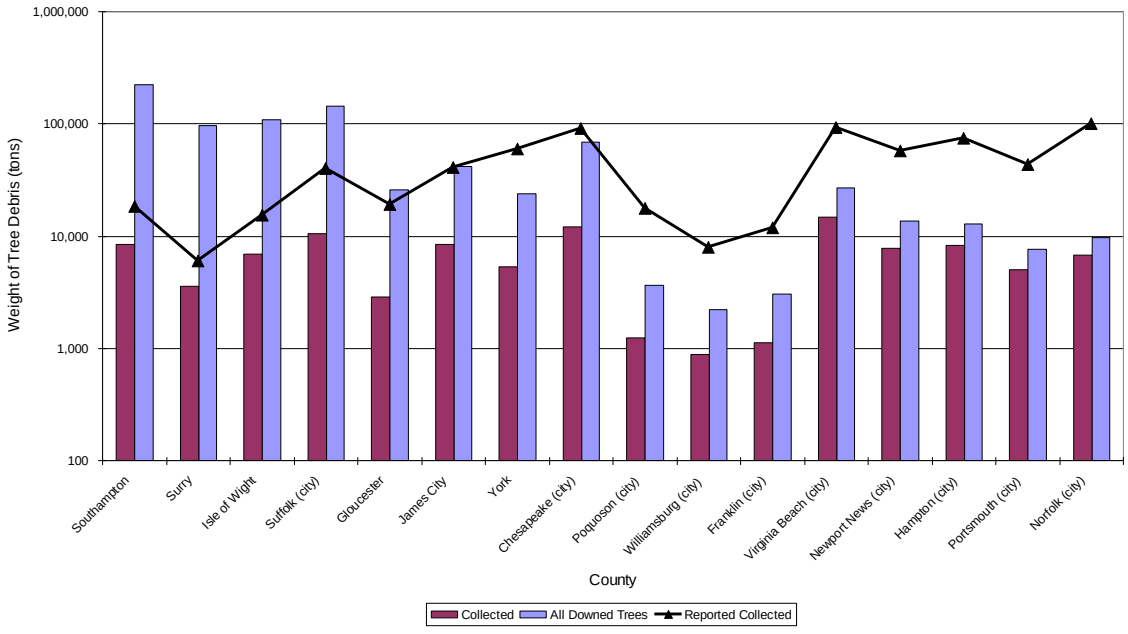

Figure 12.21. Ratio of Modeled Tree Debris to Actual Debris Collected by County in Virginia for Hurricane Isabel.

Aggregating the data over all 16 Hampton Roads communities, we find that the debris collection model underestimates the total debris collected (excluding the VDOT contribution) by about 90%. However, given that the tree blowdown model is apparently under predicting the quantity of downed trees and the various limitations of the raw data set discussed above, it is difficult to conclude that the Virginia example indicates any serious flaws in the model. The model appears to capture the proper trends and produce reasonable estimates of tree debris collection rates in rural, suburban and urban areas. Additional validation and refinement of the model is recommended as similar data sets become available for future hurricanes of varying intensities and geographic locations.

It is important to note that, in general, the Virginia Counties considered have substantially higher building densities (areas are more urban/suburban) than the counties analyzed in North Carolina. Table 12.10 lists the building densities for each of the 36 counties investigated with the average modeled tree debris collection rates. Building densities are calculated as the total number of buildings in the Hazus general building stock model divided by the land area of the county or region. Likewise, average modeled tree debris collection rates are determined by dividing the total collected tree debris volume by the total blown down tree volume modeled by Hazus for the county and region levels.

Table 12.10. Building Density and Average Tree Debris Collection Rate by County for North Carolina and Virginia.

North Carolina			Virginia		
County	Buildings per Acre	Average Tree Collection Rate (%)	County	Buildings per Acre	Average Tree Collection Rate (%)
Beaufort	0.039	4.93	Chesapeake (city)	0.308	17.88
Bertie	0.019	3.24	Franklin (city)	0.502	37.11
Camden	0.019	3.00	Gloucester	0.099	10.91
Carteret	0.113	8.33	Hampton (city)	1.325	64.92
Chowan	0.053	5.95	Isle of Wight	0.058	6.45
Craven	0.076	7.80	James City	0.220	19.99
Currituck	0.067	6.18	Newport News (city)	1.132	57.63
Dare	0.106	7.77	Norfolk (city)	1.717	69.96
Gates	0.020	3.23	Poquoson (city)	0.446	33.96
Hertford	0.039	4.92	Portsmouth (city)	1.451	66.52
Hyde	0.008	3.00	Southampton	0.017	3.79
Jones	0.015	3.00	Suffolk (city)	0.085	7.43
Martin	0.034	4.01	Surry	0.017	3.74
Northampton	0.028	4.32	Virginia Beach (city)	0.865	54.10
Onslow	0.103	9.52	Williamsburg (city)	0.496	39.54
Pamlico	0.031	5.41	York	0.306	22.12
Pasquotank	0.084	7.17			
Perquimans	0.034	4.79			
Tyrrell	0.008	2.00			
Washington	0.025	3.98			
20 NC Counties	**0.047**	**4.68**	**16 VA Counties**	**0.231**	**12.87**

For the Virginia counties considered, the tree debris collection model estimates 12.9% of the total tree debris being collected versus only about 4.7% for the much more rural counties of North Carolina. Note that although the average building density exceeds 1.0 buildings per acre for several Virginia counties, the average tress collection ratios are still

less than 100% because some of the census blocks in those counties have building densities lower than 1.0 buildings per acre.

The trend of decreased over-prediction of tree debris as building density increases may also be due in part to different disposal means used in rural versus urban areas. In rural areas, it is common to see residents and farmers burning tree debris from their property immediately following the storm, or chopping and storing the wood for use to heat their homes for the winter. This behavior reduces the amount of debris that will actually be brought to the curb for collection by local and state governments.

By contrast, residents of urban and suburban areas tend to not only bring the tree debris that falls to the curb, but actually create additional debris by removing any part of the broken trees that remained standing. These residents may also take advantage of the opportunity to dispose of other vegetative debris stored on their property. This behavior may lead to increased tree debris generated and collected in urban and suburban areas.

A potential example of this trend was discovered in the data received from the North Carolina Department of Emergency Management. One largely urban and suburban county reported over 65,000 cubic yards of vegetative debris at a removal cost of over $1.5M while Hazus-MH did not predict any downed trees for this county because the windspeeds in Hurricane Isabel did not exceed 50 mph (3 second gust).

Another observation that may lead to underestimating tree blowdown in urban/suburban areas is that the tree database and tree blowdown model only consider trees greater than 30 feet tall. The percentage of tree weight or volume coming from trees less than 30 feet tall is likely to be larger in urban/suburban areas than rural areas.

12.7.3.3 Comparison to Other Collection Data

In addition to the county data compared for Hurricane Isabel in NC and VA, tree debris estimates were also available from the following storms. Table 12.11 presents a list of areas for which estimates of tree debris collected are available for the corresponding storms.

Figure 12.22 presents a comparison of modeled tree debris collected to actual quantities reported for the hurricanes and locations mentioned above. This comparison considers the weight of tree debris in tons, however, most hurricane tree debris reports are volume (cubic yards). The vertical line for each storm-location combination represents a range of weights based on bulking factors ranging from 4 to 10 cubic yards per ton. The small horizontal line represents either the actual tonnage reported (if no vertical line is present) or tonnage estimated assuming a bulking factor of 6 cubic yards per ton.

Table 12.11. Locations of Collected Tree Debris Estimates by Hurricane Name and Year

Storm – Year	Locations with Data
Rita – 2005	State of Texas
Wilma – 2005	Palm Beach, Broward, & Miami-Dade Counties, FL
Charley + Frances + Jeanne + Ivan – 2004	State of Florida, Alachua & Orange Counties, FL
Isabel – 2003	States of North Carolina & Virginia
Erin + Opal – 1995	Escambia County, FL

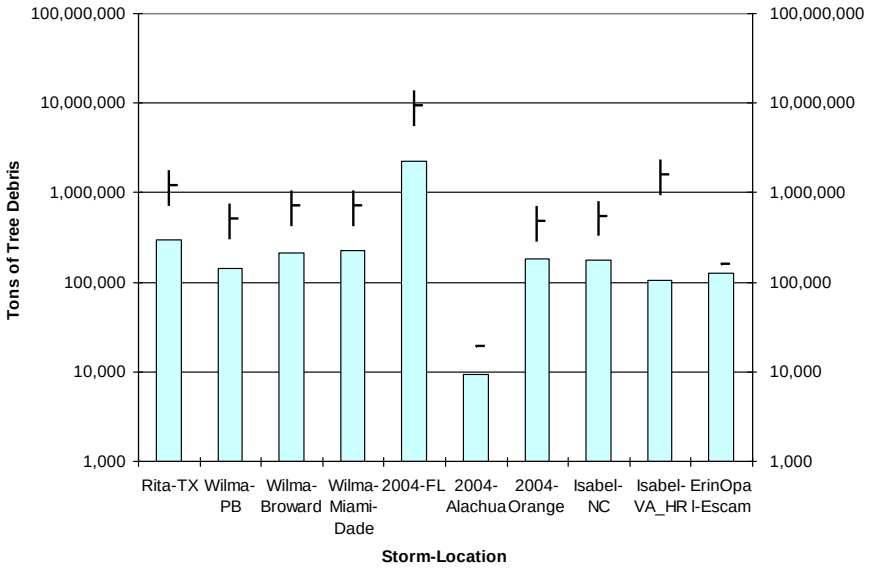

Figure 12.22. Comparison of Modeled Tree Debris Collected to Reported Amounts for Various Locations and Various Hurricanes.

12.8 Tree Blowdown Damage to Buildings

12.8.1 Overview

The building damage-to-loss model estimates expected loss as function of wind speed for 2 tree types, 3 tree height groups, 6 tree densities, 4 building geometries, and 2 wall construction types. These result in 288 normalized loss curves for tree blowdown damage to buildings, for building loss and contents loss respectively. The tree blowdown loss curves are combined with the fast-running normalized loss curves presented in Chapter 7 to form loss curves in each census tract that model wind, missile, and tree damage effects.

A Monte Carlo simulation approach is employed to derive the blowdown loss functions. A total of 10,000 simulations are performed to derive each function, which is taken to be the mean of the 10,000 simulated losses. Figure 12.23 illustrates the process for one simulation. The following sections describe the elements not presented in the previous sections.

12.8.2 Tree Drop Tests

The severity of tree damage to buildings is dependent on the tree impact energy and the structure's impact resistance. In an effort to investigate tree impact damage on residential structures, the Wind Load Test Facility at Clemson University conducted tree drop tests on modeled partial house structures. To simulate the tree trunk, the Clemson tests used two steel pipes of different weights, namely 450 lb and 950 lb, both at a length of 20 ft. The pipes were released from standing position on a rig about 18 ft from the modeled structure and free-fell to the modeled house structure. The lighter pipe hits the eave with impact energy of 3600 lb-ft, and the larger pipe hits with an impact energy of 7600 lb-ft.

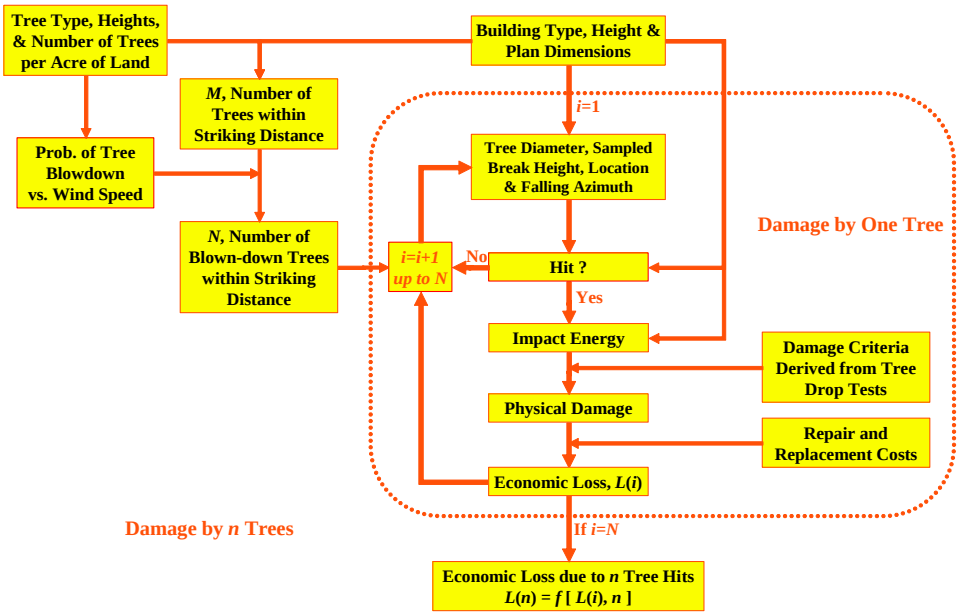

Figure 12.23. Simulation Scheme for Tree Blow-Down Damage to Building.

Video recordings were taken during the fall and impact, and still pictures were also taken of the damage after impact. Figure 12.24 to Figure 12.27 show examples of the impact damage recorded from the tests on several modeled structures with different impact resistance capacities.

12.8.3 Relationship between Damage Severity and Impact Energy

A quantitative relationship between physical damage state and the tree impact energy is essential to estimate tree blowdown damage, and ensuing economic losses, to buildings. The Clemson University tree drop test data aided in developing this relationship. The assumptions involved in establishing the damage state severity model include:

A. A tree falls solely under the action of gravity. The actions of blowing wind and the remaining resistance from root-soil interaction (for uprooting) or the

remaining resistance from wood fibers at breakpoint (for above ground breakage) are neglected.

B. A tree trunk impact is required to cause damage.

C. The tree trunk does not bounce after it hits the building.

D. If it exceeds the impact resistance of the structure, an impacting tree trunk cuts into the building until all of its kinetic energy dissipates into the structure.

E. A tree hit does not cause the complete collapse of a building.

Different building components will present different resistances to a tree trunk as it cuts through the structure. The resistance associated with a specific component of the building, such as the roof deck, top plate or bond-beam, wall sheathing, or an elevated

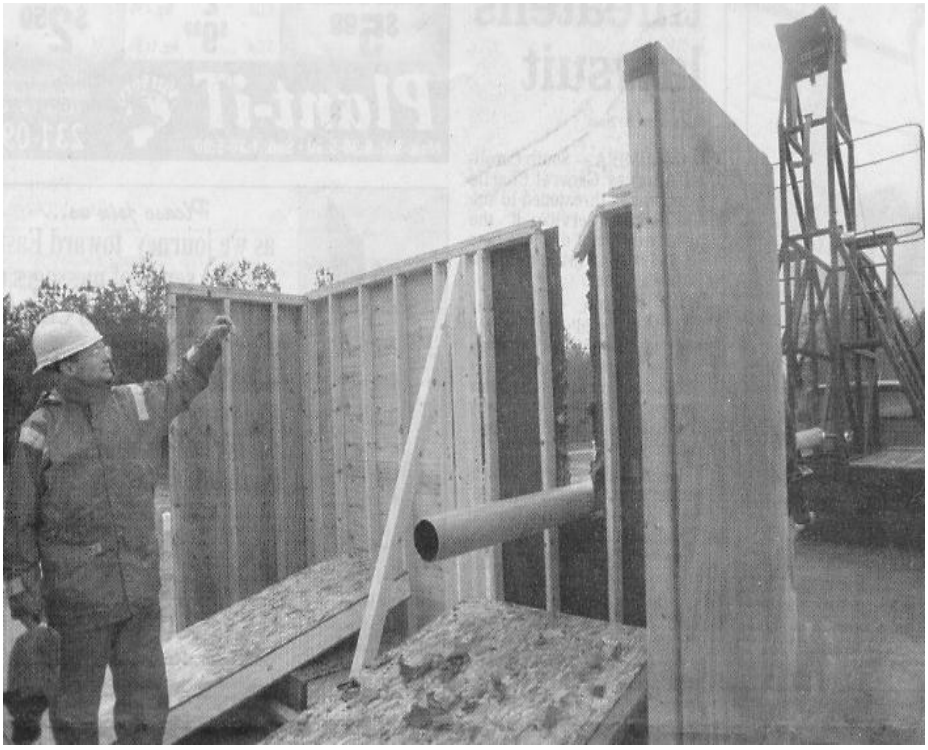

Figure 12.24. Small Pipe Impacting Wall Without Plywood Sheathing, 3600 lb-ft at Impact, Breaking Top Plates and Half-Way Cutting Into Wall.

Figure 12.25. Small Pipe Impacting Wall with Plywood Sheathing, 3600 lb-ft at Impact, Breaking Top Plates and 1/4 Cutting Into Wall.

Figure 12.26. Large Pipe Impacting Roof and Wall Without Plywood Sheathing, 7600 lb-ft at Impact, Breaking Roof, Top Plates and Entire Wall with Apparent Residual Energy Hitting Ground.

Figure 12.27. Large Pipe Impacting Roof and Wall With Plywood Sheathing, 7600 lb-ft at Impact, Breaking Roof, Top Plates and 1/8 Wall.

floor, is assumed to be constant. Based on the limited number of tree drop damage states recorded by Clemson University and additional engineering inferences, an extended number of damage states are defined for the subsequent estimation of direct economic losses, in relation to impact energy, as shown in Table 12.12. Tree heights that will potentially produce the indicated impact energy and corresponding damage states are also presented for given stand-off distance, breaking point, and fall azimuth, etc. using pine trees as an example.

12.9 Estimation of Direct Economic Loss from Physical Damage States

Cost Estimation Assumptions and Data. The cost estimates were prepared with data from RSMeans 2002 Repair and Remodeling Cost Data and the Means CostWorks 2002 software. The cost estimates have prices adjusted locally for Miami, which is consistent with the costing data of the original loss curves.

In preparing these cost estimates, the following assumptions about the construction were made:

- Roof covering is shingles
- ½" plywood roof deck
- Wood truss roof structure
- The average room size is 200 SF

Table 12.12. Damage States in Relation to Impact Energy

Damage State #		1	2	3	4	5	6	7	8
1-Story Wood	Impact Energy (lb-ft)[1]	250	2000	5600	6400	8800			
	Example Tree Height [2](ft)	30.0	46.9	57.5	59.0	62.6			
	Damage State Description	Surface damage	Roof deck crack	Top-plates rupture	¼ Cut into wall	Cut through wall			
2-Story Wood	Impact Energy (lb-ft)	250	2000	5600	6400	8800	14400	15200	17600
	Example Tree Height (ft)	32.0	50.2	61.3	62.8	66.6	72.5	73.3	75.2
	Damage State Description	Surface damage	Roof deck crack	Top-plates rupture	¼ Cut into upper wall	Cut through upper wall	Floor-plates rupture	¼ Cut into lower wall	Cut through lower wall
1-Story Masonry	Impact Energy (lb-ft)	250	2000	11000	13000	19000			
	Example Tree Height (ft)	30.0	46.9	65.2	67.2	72.0			
	Damage State	Surface damage	Roof deck crack	Bond-beam rupture	¼ Cut into wall	Cut through wall			
2-Story Masonry	Impact Energy (lb-ft)	250	2000	11000	13000	19000	30000	32000	38000
	Example Tree Height (ft)	32.0	50.2	69.3	71.4	76.2	82.1	83.0	85.3
	Damage State Description	Surface damage	Roof deck crack	Bond-beam rupture	¼ Cut into upper wall	Cut through upper wall	Floor-plates rupture	¼ Cut into lower wall	Cut through lower wall

Notes: 1. Impact Energy is defined as the energy derived from the normal component of impact velocity with respect to the eave line.
2. Assume a pine tree with stand-off distance of 30ft, breaking at ground level and hitting eave perpendicularly.

- There are 7 rooms on average in a one-story building, and 14 rooms in a two-story building
- There is 1 bathroom in a one-story building, and 2 in a two-story building
- Contents value per square foot are 50% of the building value
- Value of building is 80 dollars per SF.

The general approach consisted of estimating the size of the opening that was created for each of the damage states, then estimating the extent of damage to various components of the building such as roof covering, roof structure, walls, flooring, contents, and electrical, etc. The extent of the area damaged accounted for the replacement of "units" of a component – for example, an even number of 4x8 sheets of plywood on the roof, etc. Table 12.13 and Table 12.14 list the assumed damage areas used in the one-story and two-story cost estimates, respectively. Content damage is estimated using the areas in Table 12.13 and Table 12.14 and a simple cost per square foot valued at 50% of the assumed building value (i.e., $\$40/ft^2$).

Table 12.13. Assumed Damage Areas Used in One-Story Cost Estimates

	Damage State #			
	1	3	4	5
	Surface Damage	Roof Only	Roof and 1/4 Wall	Roof and Wall
Component				
Window (sf)	0	0	1.75 or 0	7
Roof Structure (SF)	0	200	200	200
Roof Covering(SF)	100	210	210	210
Walls(SF)	32	32	32 or 10	64
Electrical (l.f)	0	0	10	50
Flooring(SF)	0	75	200	200
Floor Structure(SF)	0	0	0	0
Contents(SF)	0	100	150	150
Partitions(SF wall)	0	200	320	400
Plumbing(each)	0	0.07	0.11	0.14
Heating(SF area)	0	100	160	200
Kitchen and Appliances(each)	0	0.07	0.12	0.14
Assumed Opening Size				
Roof (SF)	0	16	40	48
Wall (SF)	0	0	12	48

Table 12.14. Assumed Damage Areas Used in Two-Story Cost Estimates

	Damage State #			
	1	3	4	5
	Surface Damage	Roof Only	Roof and 1/4 Wall	Roof and Wall
Component				
Window (sf)	0	0	3 or 0	14
Roof Structure (SF)	0	200	200	200
Roof Covering(SF)	100	210	210	210
Walls(SF)	64	64	32 or 10	128
Electrical (l.f)	0	0	30	100
Flooring(SF)	0	300	300	400
Floor Structure(SF)	0	0	0	64
Contents(SF)	0	150	200	300
Partitions(SF wall)	0	210	420	600
Plumbing(each)	0	0.05	0.1	0.28
Heating(SF area)	0	105	210	300
Kitchen and Appliances(each)	0	0.025	0.05	0.14
Assumed Opening Size				
Roof (SF)	0	16	40	48
Wall (SF)	0	0	12	96

Additional Assumptions for One-Story. The cost estimates for Damage State 5 (roof and wall) includes 50% of a 3'x5' typical window assuming that there is a 50% chance that a window will be involved in the damaged area. The assumption is that the amount of glazing on a home is approximately 20% of the wall area, which translates to about a 50% chance that any vertical slice will involve a window. For damage state 4 (roof and 1/4 wall) the area of window was reduced further still to reflect the likelihood that the damage is only to the wall above the window, and repair to the window may be less likely. For masonry homes, it was assumed that the windows would not be affected for this damage state.

One seventh of the cost of a set of kitchen appliances and cabinets was included to reflect the fact that 1 in 7 rooms is a kitchen which is likely involved in the damaged area. Similarly for plumbing, 1/7 of a package of plumbing cost is included (which is dominated by bathroom fixtures), based on the assumption that 1 in 7 rooms is a bathroom.

The extent of required wall repair in damage state 4 for masonry walls is assumed to be less than for wood frame walls, because the CMU units are smaller, and therefore the area to be repaired can be more localized.

Additional Assumptions for Two-Story. Damage state 8 includes one full window in the cost estimate. In the same manner as the one-story building, it is assumed that there is a 50% chance that a window will be damaged on each story, or the equivalent of one full window.

For kitchens and plumbing (bathrooms) the likelihood of impacting 1 of 7 rooms on any floor was accounted for in the estimate by costing in 1/7 of the cost of a complete set of kitchen appliances/cabinets or plumbing fixtures.

The area of flooring affected in each damage state accounts for the dripping of water from one story to another.

The completed cost estimates are presented in Table 12.15. The estimates are also illustrated in Figure 12.28 to Figure 12.30 for building, contents, and combined costs as functions of impact energy. For damage states whose costs were not estimated item-by-item, overall costs were estimated based on incremental costs by comparing to the costs estimated item-by-item. Maximum potential losses resulting from *one* tree hit are also estimated to be approximately $10,000 of structure and $8,000 of contents for one-story, and $17,000 and $13,000 for two-story, all assumed to be reached at impact energy of 100,000 lb-ft.

Table 12.15. Estimated Building Repair Costs by Damage State

Damage State #		1	2	3	4	5	6	7	8
12-Story Wood	Impact Energy (lb-ft)[1]	250	2000	5600	6400	8800			
	Damage State	Surface damage	Roof deck crack	Top-plates rupture	¼ Cut into wall	Cut through wall			
	Building Cost ($)	125	800	3789	5752	6212			
	Contents Cost ($)	0	200	4000	6000	7000			
	Combined Cost ($)	125	1000	7789	11752	13212			
2-Story Wood	Impact Energy (lb-ft)	250	2000	5600	6400	8800	14400	15200	17600
	Damage State	Surface damage	Roof deck crack	Top-plates rupture	¼ Cut into upper wall	Cut through upper wall	Floor-plates rupture	¼ Cut into lower wall	Cut through lower wall
	Building Cost ($)	162	1000	3937	5923	7000	7800	9600	10283
	Contents Cost ($)	0	200	5500	8000	9000	10200	11400	12000
	Combined Cost ($)	162	1200	9437	13923	16000	18000	21000	22283
12-Story Masonry	Impact Energy (lb-ft)	250	2000	11000	13000	19000			
	Damage State	Surface damage	Roof deck crack	Bond-beam rupture	¼ Cut into wall	Cut through wall			
	Building Cost ($)	101	600	3765	5539	6692			
	Contents Cost ($)	0	200	4000	6000	7000			
	Combined Cost ($)	101	800	7765	11539	13692			
2-Story Masonry	Impact Energy (lb-ft)	250	2000	11000	13000	19000	30000	32000	38000
	Damage State	Surface damage	Roof deck crack	Bond-beam rupture	¼ Cut into upper wall	Cut through upper wall	Floor-plates rupture	¼ Cut into lower wall	Cut through lower wall
	Building Cost ($)	114	700	3888	5708	7000	7800	9600	11243
	Contents Cost ($)	0	200	5500	8000	9000	10200	11400	12000
	Combined Cost ($)	114	900	9388	13708	16000	18000	21000	23243

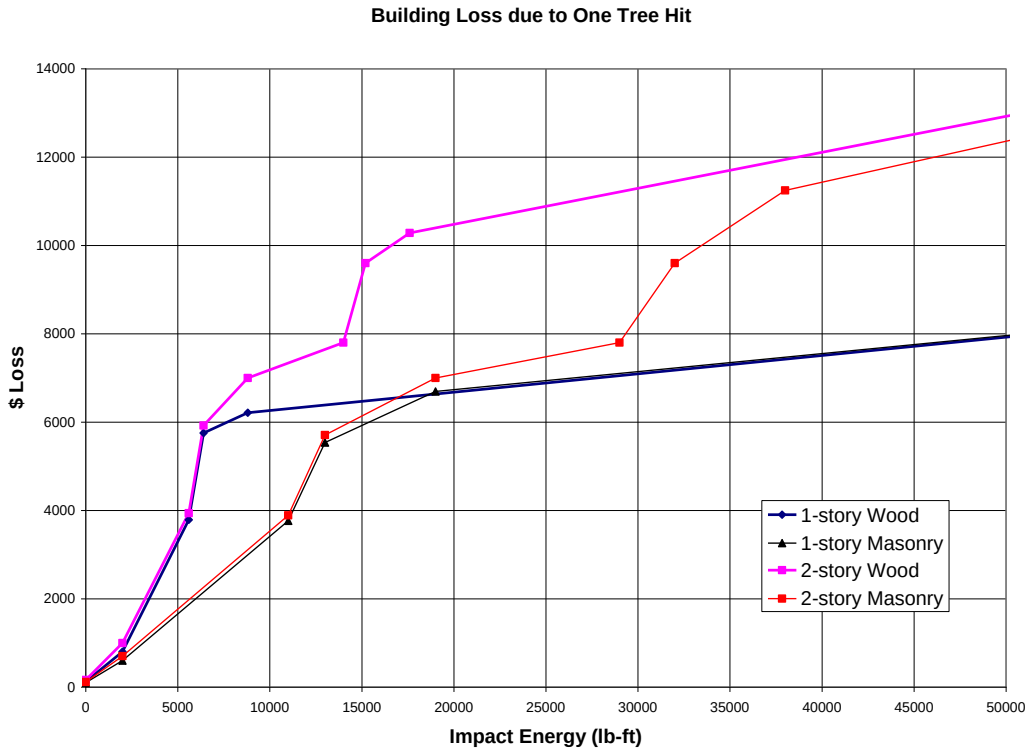

Figure 12.28. Building Repair Cost Estimates as Functions of Impact Energy.

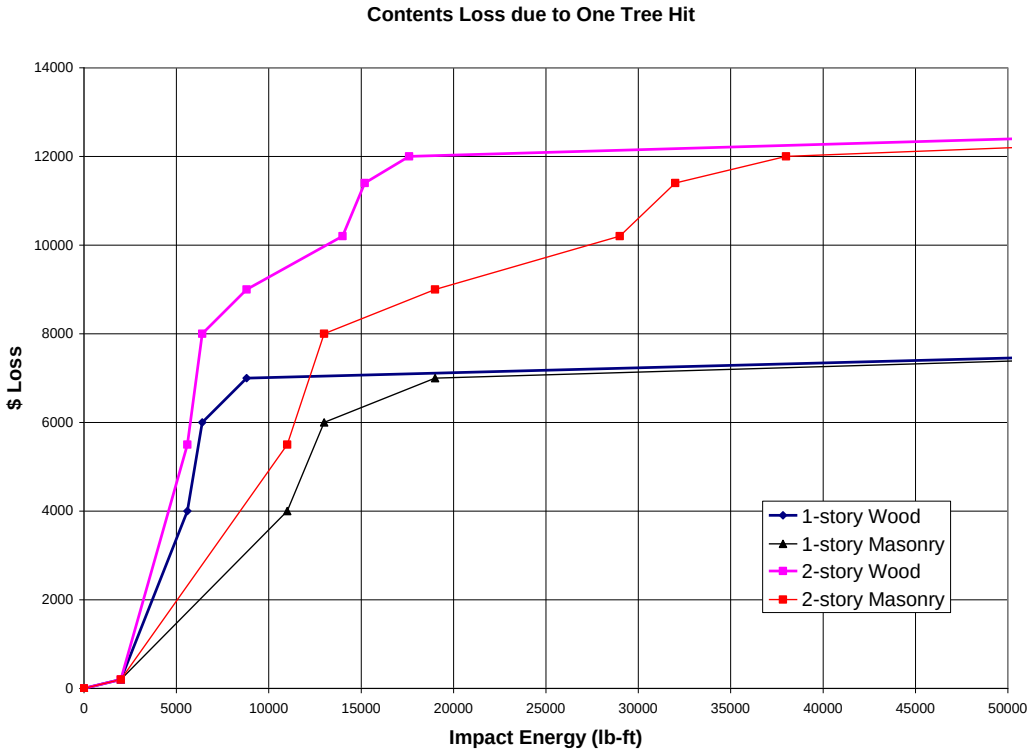

Figure 12.29. Contents Repair Cost Estimates as Functions of Impact Energy.

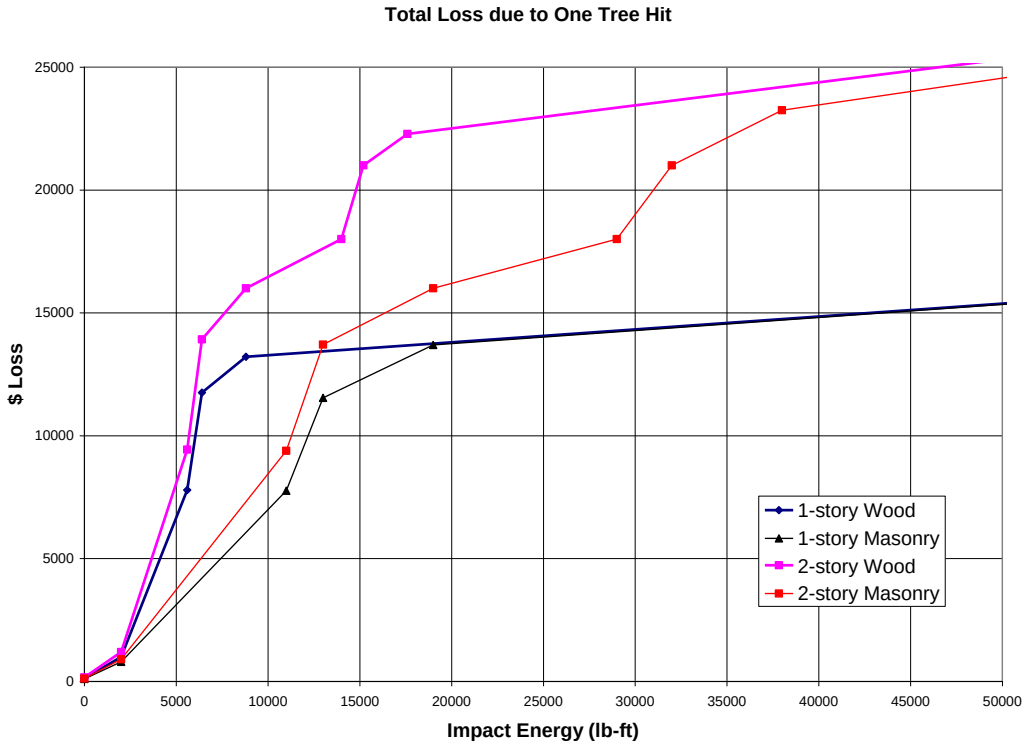

Figure 12.30. Total Repair Cost Estimates as Functions of Impact Energy.

12.10 Mean Loss as a Function of Wind Speed

12.10.1 Losses Due to Tree Blowdown

Using the methodology illustrated in Figure 12.23 and the assumptions and results discussed in the previous sections, mean building and contents losses are derived as functions of peak gust speed based on 10,000 simulations for each of the 288 cases summarized in Table 12.16. In the simulations, trees are assumed to be distributed uniformly random over areas not occupied by the building, with a 10 ft clearance from the building perimeter. The fall azimuth is also assumed to uniformly random.

Table 12.16. Parameter Matrix for the 288 Cases Studied

Parameter	Wall Type	Dimension (Value $)	Tree Type	Tree Height	Tree Density
Number of Values	2	4	2	3	6
Values	Wood	50x24x 9 (96k)	Evergreen	312-40ft	10
	Masonry	60x30x 9 (144k)	Deciduous	412-60ft	25
		40x30x17 (192k)		≥60ft	50
		50x30x17 (240k)			100
					200
		(all hip roofs)			400

For multiple impacts, each impact is assumed to damage a previously undamaged portion of the structure.

Examples of building and contents loss functions are presented in Figure 12.31 through Figure 12.35, each of which demonstrates the dependence of loss functions on one of the parameters listed in Table 12.16. Figure 12.36 compares the building and content losses for one specific combination of input parameters.

12.10.2 Loss Function for a Specific Building Type in Given Census Tract

The basic normalized loss functions and the tree inventory data are used in Hazus as follows to derive a normalized loss function for a specific building type in a specific census tract:

Input: Census tract tree inventory data: dominant tree type, tree density, and tree height distribution

For Evergreen: Census tract loss function = height group *proportion weighted average* of loss functions for the *3 height groups*, for the census tract tree type and density, and for the specific building mapped

For Deciduous: Census tract loss function = height group *proportion weighted average* of loss functions for the *3 height groups*, for the census tract tree type and density, and for the specific building mapped

For Mixed: Census tract loss function = **sum** of height group proportion weighted averages of loss functions for the 3 height groups for the *two base tree types* **divided by 2**, for the census tract tree density, and for the specific building mapped

12.10.3 Combining Tree Blowdown Normalized Loss Functions with the Basic Fast-Running Building and Contents Loss Functions

The following simplified method is used to combine the tree blowdown normalized loss with the basic fast-running loss functions described in Section 7.7 for single-family residential building and content losses:

$$\text{Total Loss} = \text{Basic Loss Ratio} + \text{Tree Damage Loss Ratio} - (\text{Basic Loss Ratio} * \text{Tree Damage Loss Ratio}) \quad (12.42)$$

The only assumption associated with deriving this equation is that the damage areas on a structure resulting from the two damage mechanisms are mutually independent.

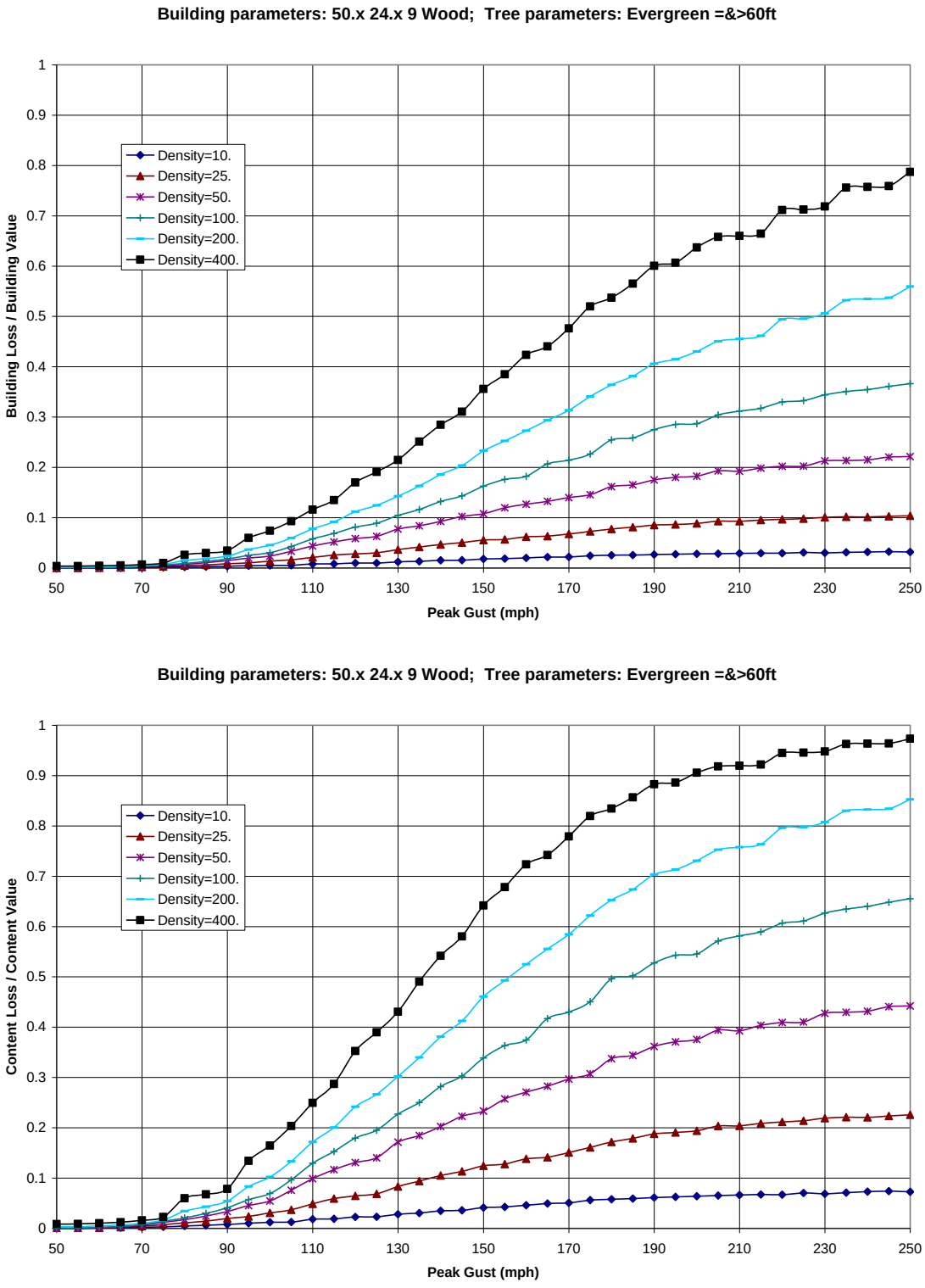

Figure 12.31. Dependence on Tree Density of Building (Upper) and Contents (Lower) Loss Functions.

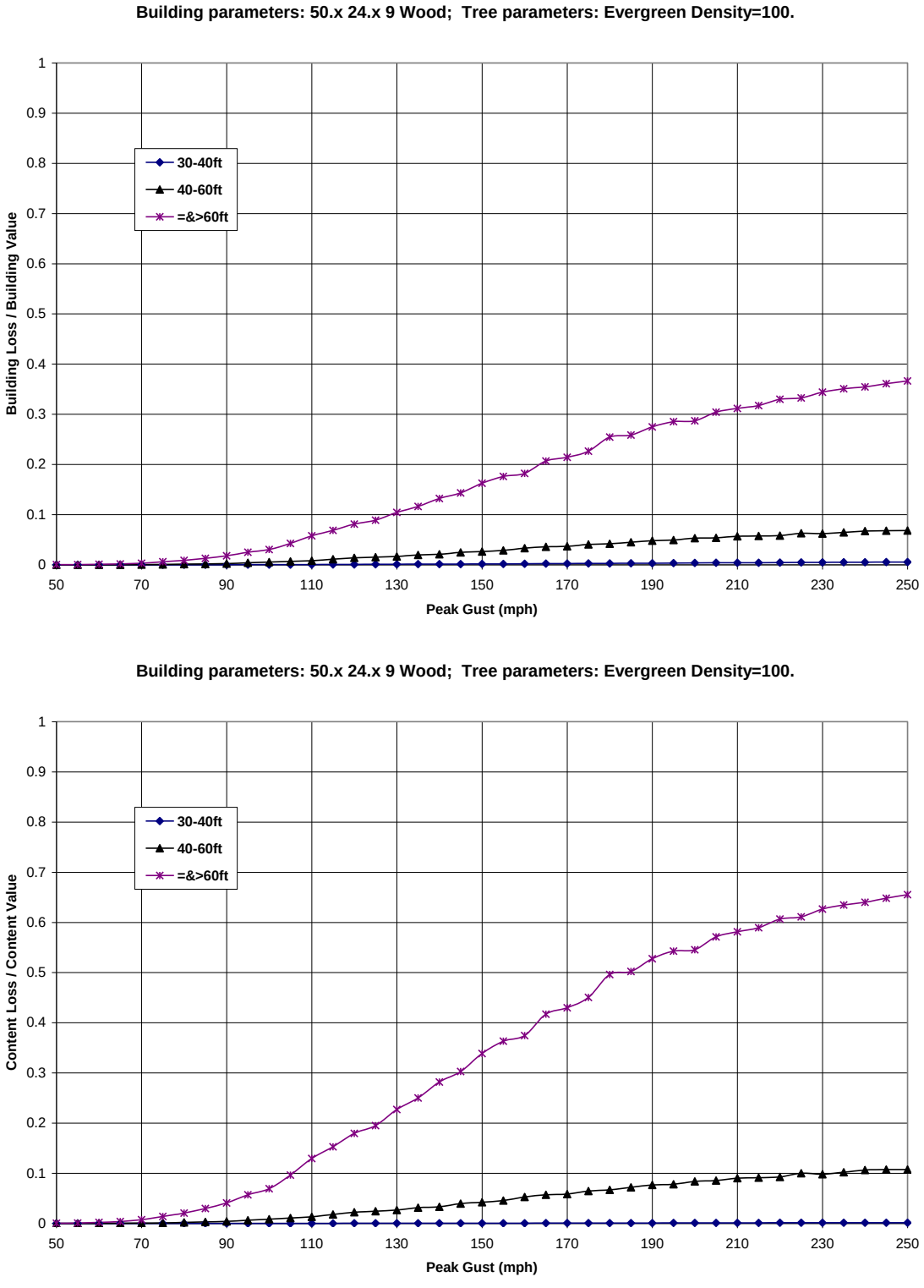

Figure 12.32. Dependence on Tree Height of Building (Upper) and Contents (Lower) Loss Functions.

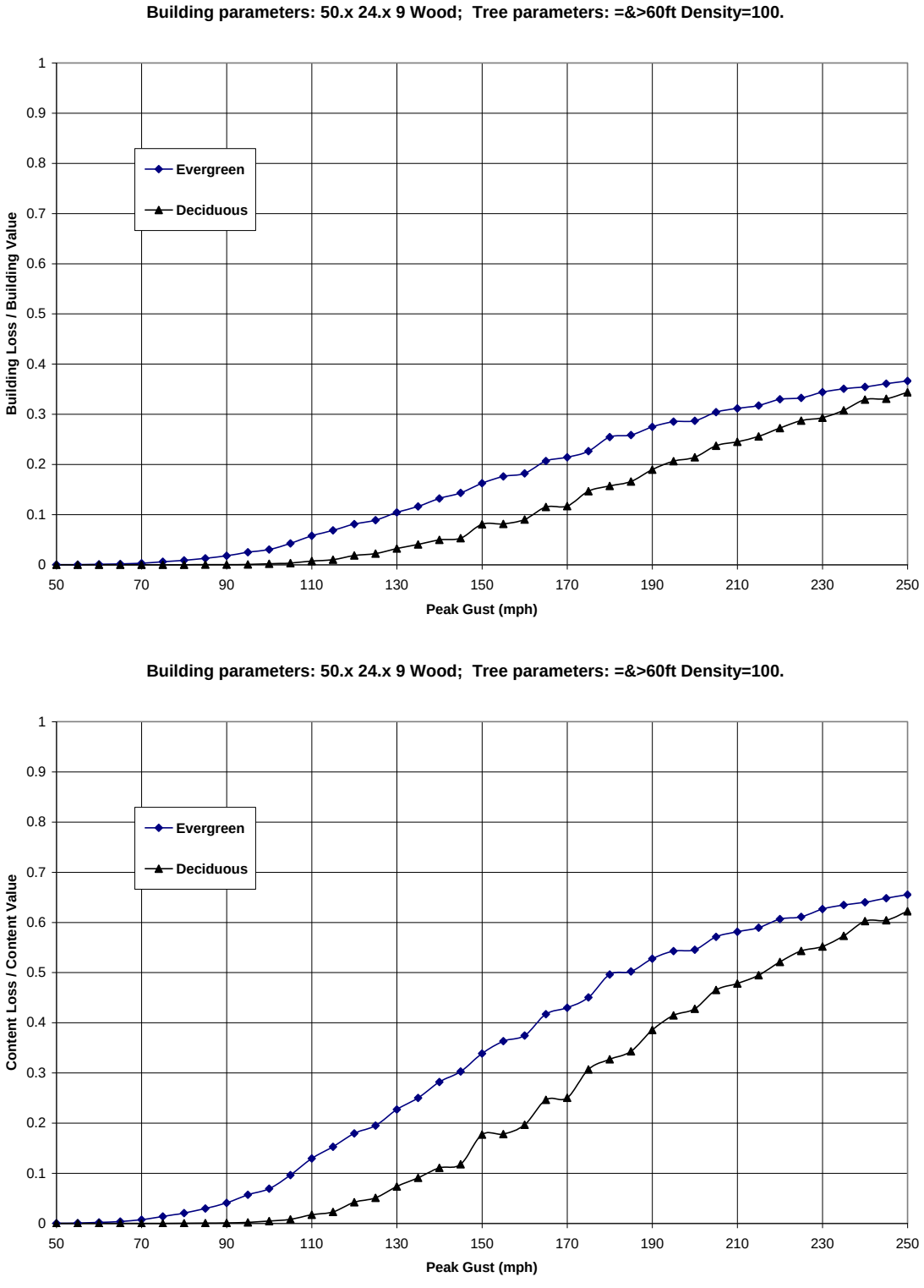

Figure 12.33. Dependence on Tree Type of Building (Upper) and Contents (Lower) Loss Functions.

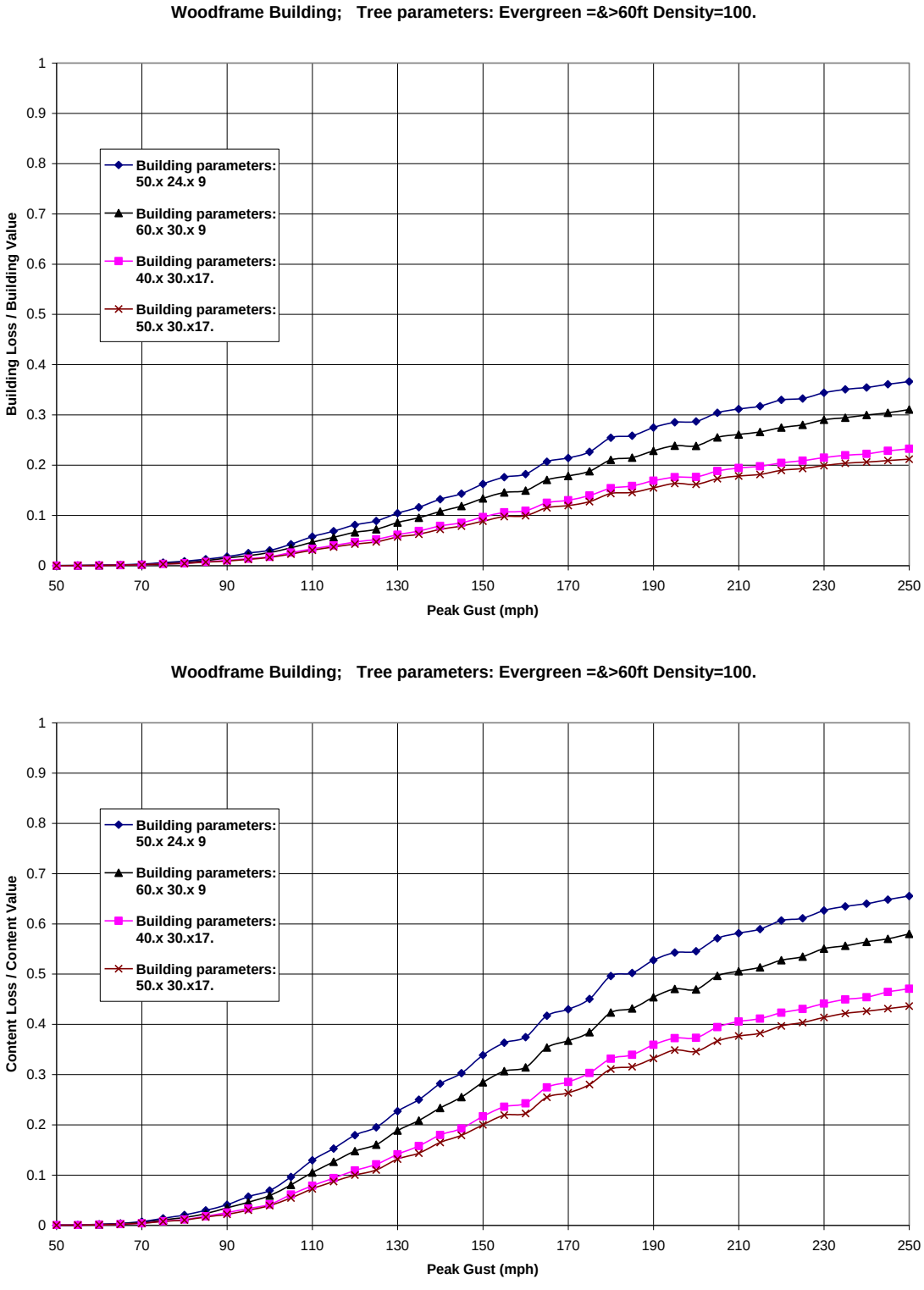

Figure 12.34. Dependence on Building Dimensions (ft) of Building (Upper) and Contents (Lower) Loss Functions.

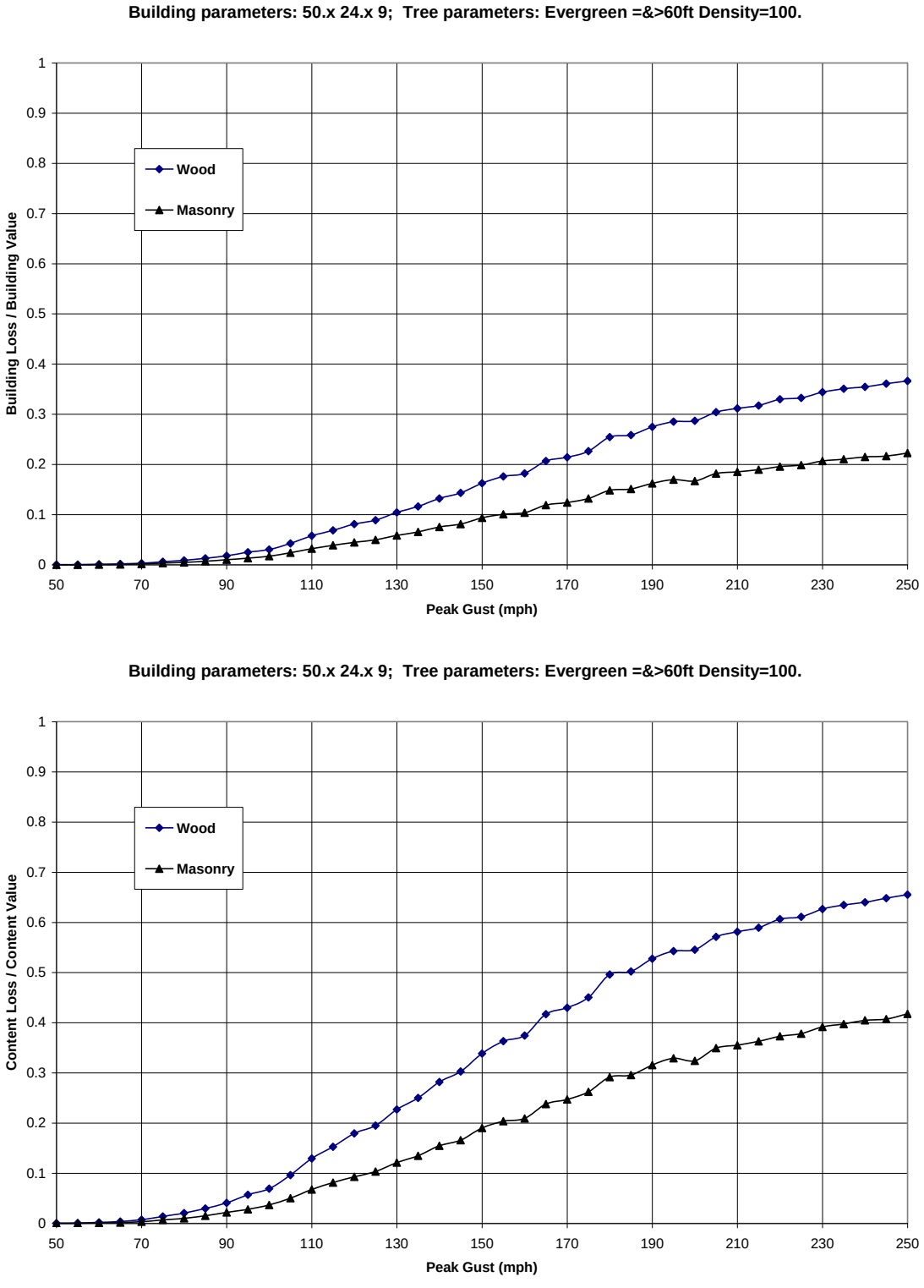

Figure 12.35. Dependence on Wall Type of Building (Upper) and Contents (Lower) Loss Functions.

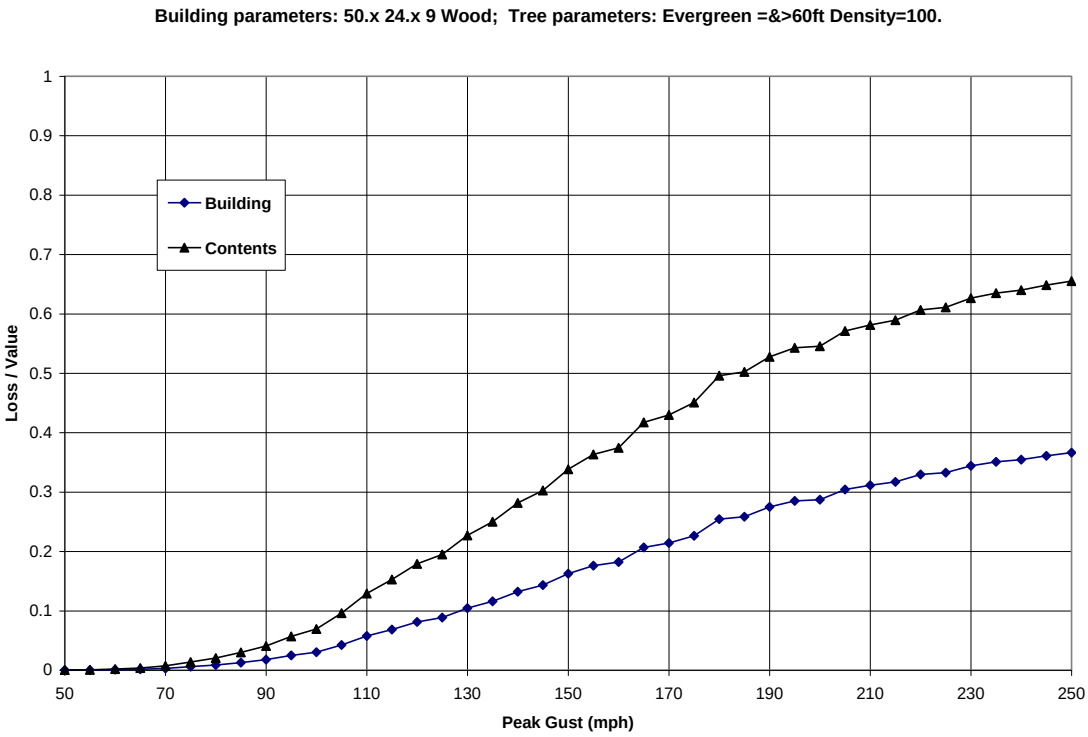

Figure 12.36. Building and Contents Loss Comparison.

Chapter 13. Coastal Storm Surge

13.1 Introduction

This chapter describes the development and validation of a hurricane storm surge and wave hazard and building loss modeling capability for Hazus-MH. The coastal surge model couples existing, publicly available hazard models estimate the storm tide and coastal wave heights produced by a single hurricane event. The storm tide model is the SLOSH (Sea, Lake, and Overland Surges from Hurricanes) methodology described in NOAA Technical Report NWS 48 (Jelesnianski et al. 1992). The wave model is the SWAN (Simulating WAves Nearshore) model developed and distributed by Delft University of Technology.

The coupled surge and wave models have been modified to use the hurricane wind field model in HAZUS-MH developed by Applied Research Associates (ARA). The primary motivation for this decision is to use the same validated and peer reviewed wind field model for predicting both direct wind damage and coastal surge damage. In addition, the storm tide estimates obtained from SLOSH using the ARA hurricane wind field model are more accurate, on average, than the storm tide estimated obtained from SLOSH using the default SLOSH wind field model.

A methodology for combining wind and flood losses to buildings at the building sub-assembly level is presented in Section 13.3. The methodology is designed to avoid "double counting" of damage to building component due to wind and flood; however, the methodology does not attempt to determine the fraction of the combined loss that is attributable to wind or flood.

Six recent hurricane events are used to throughout the report validate the wind field, storm tide, and wave models. The coastal storm surge hazard and combined wind and flood loss methodologies have been implemented in Hazus to estimate direct, building-related economic losses to the general building stock due to a user-specified hurricane scenario.

13.2 Coastal Storm Surge and Wave Hazard Models

This section describes the implementation and validation of a hurricane storm surge and wave hazard modeling capability for HAZUS-MH. The coastal surge model couples existing, publicly available hazard models to estimate the storm tide and coastal wave heights produced by a single hurricane event. The specific component models are:

1. SLOSH (Sea, Lake, and Overland Surges from Hurricanes) – FORTRAN and C source code for version 3.94 (2009) provided by National Weather Service's Meteorological Development Laboratory (NWS/MDL). The SLOSH methodology is described in NOAA Technical Report NWS 48 (Jelesnianski et al. 1992).

2. SWAN (Simulating WAves Nearshore) – Developed and distributed by Delft University of Technology. This software can be used freely under the terms of the GNU General Public License. See http://130.161.13.149/swan/support/copyright _and_ liability.htm. A listing of SWAN publications is available at http://vlm089.citg.tudelft.nl/ swan/index.htm.
3. ARA Hurricane Wind Field Model – Executable code distributed with HAZUS-MH; source code developed and owned by Applied Research Associates, Inc. The hurricane wind field model is described in Section 2 of the HAZUS-MH Hurricane Model Technical Manual (FEMA 2009a). Additional details and updates are provided in Vickery et al. (2000 and 2009).

For use in HAZUS, both SLOSH and SWAN have been modified to use the ARA hurricane wind field model. The primary motivation for this decision is to use the same validated and peer reviewed wind field model for predicting both direct wind damage and coastal surge damage.

The following recent hurricane events have been selected to validate the coastal surge models:

1. Andrew (1992) – Southeast Florida
2. Isabel (2003) – North Carolina
3. Ivan (2004) – Northwest Florida
4. Katrina (2005) – Mississippi
5. Gustav (2008) – Louisiana and Texas
6. Ike (2008) – Texas

These events are used to validate the wind field, storm tide, and wave models. The validation comparisons for Hurricane Andrew are for storm tide only.

13.2.1 Wind Speed, Wind Direction, and Atmospheric Pressure Validation

Comparisons of modeled 10-minute mean wind speeds, wind directions, and atmospheric pressures to observations from the validation events are summarized in this section. The modeled values are from the SLOSH wind field model (Jelesnianski et al. 1992) and the ARA wind field model (Vickery et al. 2000, 2009; FEMA 2009a). The modeled estimates are compared to data measured at sites located both over land and over water during the validation events.

Simulated hurricane wind speeds, wind directions, and atmospheric pressures are compared to 64 surface level records obtained from ASOS towers, C-MAN stations, buoy stations, and Florida Coastal Monitoring Program (FCMP) sites located along the hurricane tracks. Approximately 80 percent of the land based stations are located at distances of 20 km or less from the coast. Both the land based measurements of wind

speeds and the marine measurements of wind speeds have been adjusted to be representative of a height of 10 m above the local ground level or sea surface.

Summary comparisons of the observed and modeled maximum wind speeds and minimum atmospheric pressures are presented in Figure 13.1. The observed wind speeds and atmospheric pressures are compared to the simulated results obtained either from model runs using the ARA storm track and the ARA wind field model (open red circles) or from model runs using the ARA storm track and the SLOSH wind field model (filled black squares).

The comparisons indicate that the simulated wind speeds produced by the ARA wind field model are about 2% higher than the observed data, while the simulated wind speeds produced by the SLOSH wind field model are about 5% higher than the observed data. The R2 statistic for the ARA wind field model results is 73% compared to 57% for the SLOSH wind field results. The ARA and SLOSH modeled minimum atmospheric pressures are both very similar to the observed data.

Table 13.1 shows the average and root mean square (RMS) errors of the modeled wind speed, wind direction, and pressure time histories for the five hurricanes. The comparisons indicate that the ARA model provides better overall RMS estimates of wind speed and atmospheric pressure for all five hurricanes.

Appendices O through S present the modeled and observed time histories of the 10-min mean wind speeds, wind directions, and atmospheric pressures produced by Hurricane Isabel (2003), Hurricane Ivan (2004), Hurricane Katrina (2005), Hurricane Gustav (2008), and Hurricane Ike (2008), respectively. Also given in Appendices O through S are the modeled maximum 10-min mean wind speeds, as well as the landfall wind fields obtained from model runs using the ARA wind field model or the SLOSH wind field model.

In summary, the wind field validation comparisons suggest that the modeled wind speeds and atmospheric pressures produced by the ARA wind field model are generally in better agreement with the observed data than those produced by the SLOSH wind field model.

13.2.2 Storm Tide Implementation and Validation

Storm tide estimates produced by SLOSH model for the six selected validation events are compared to measurements from NOAA tide gauge stations and FEMA or USGS high water marks (HWM). Comparisons are performed for Hurricane Andrew (1992) in the Biscayne Bay area, Hurricane Isabel (2003) along the Atlantic Coast of North Carolina, Hurricane Ivan (2004) along the north central Gulf of Mexico Coast, Hurricane Katrina (2005) along the Mississippi Gulf Coast, Hurricane Gustav (2008) along the north central Gulf of Mexico Coast, and Hurricane Ike (2008) along the Texas Gulf Coast.

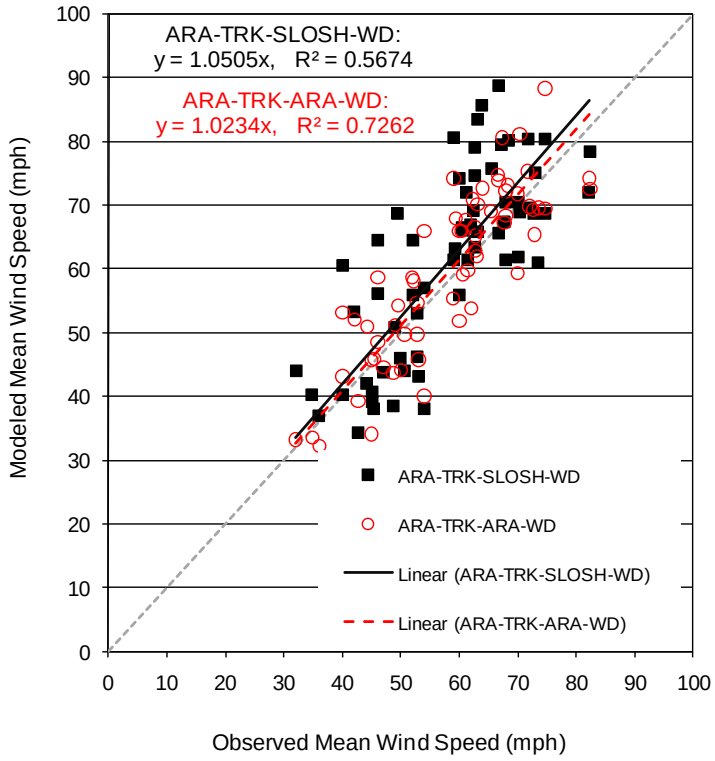

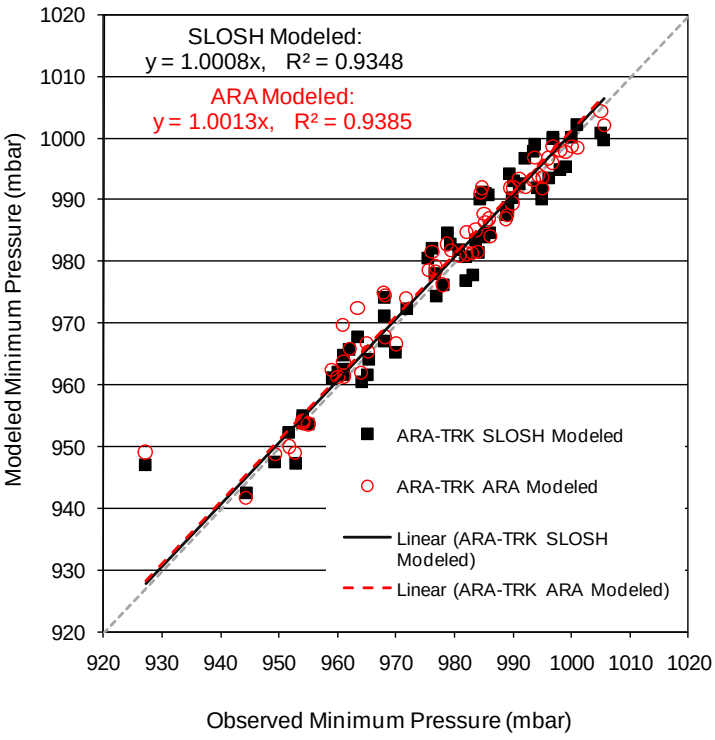

Figure 13.1. Summary Comparisons of Modeled and Observed Wind Speeds and Minimum Atmospheric Pressures.

Table 13.1. Error Analysis of Modeled Wind Speed, Wind Direction, and Atmospheric Pressure Time Histories

Hurricane	Range		Number of Data	Obs		SLOSH-Obs		ARA-Obs	
				Mean	Std	mean	RMS	mean	RMS
Isabel	Wind Speed (mph)	0-20	195	14.7	4.6	1.1	9.5	11.6	14.7
		20-40	1103	31.0	5.5	-2.6	9.8	3.5	7.5
		40-60	512	48.0	5.6	-2.3	9.0	1.3	7.6
		60-80	58	63.3	2.2	-3.3	5.5	-0.5	7.6
		all	1868	35.0	12.4	-2.2	9.4	3.6	8.6
	Wind Direction (deg)	0-45	447	27.1	12.3	16.3	19.4	41.6	43.7
		45-90	293	62.5	12.8	9.3	18.8	23.6	30.2
		90-135	214	113.3	14.1	6.9	17.6	10.8	17.7
		135-180	335	160.7	12.0	8.6	21.1	3.9	10.6
		180-225	261	198.4	12.3	-10.4	18.6	-24.9	27.7
		225-270	171	241.2	11.6	-28.4	37.2	-24.9	35.6
		270-315	65	293.2	13.3	14.5	17.6	27.0	28.6
		315-360	79	342.2	12.7	14.5	15.3	30.4	31.1
		all	1865	133.3	91.2	4.8	21.4	12.1	30.9
	Pressure (mbar)	945-965	7	963.6	0.8	0.1	1.0	5.3	5.6
		965-980	41	973.0	4.5	-2.7	3.5	3.3	4.3
		980-989	60	985.0	2.4	-5.4	6.0	0.4	2.5
		989-1030	756	1004.0	7.7	-7.4	8.2	-3.5	5.1
		all	864	1000.9	11.3	-7.0	7.8	-2.9	4.9
Ivan	Wind Speed (mph)	0-20	104	17.4	1.5	7.7	9.6	6.5	8.2
		20-40	909	32.4	5.3	1.2	9.2	2.6	7.6
		40-60	429	47.5	5.7	5.8	11.6	2.1	7.9
		60-80	88	65.8	4.1	7.2	14.8	2.0	11.8
		all	1530	37.6	12.0	3.3	10.3	2.7	8.0
	Wind Direction (deg)	0-45	228	26.0	12.7	2.8	13.7	23.5	26.9
		45-90	281	61.2	10.4	1.9	14.0	22.1	28.1
		90-135	225	109.9	12.0	9.2	21.6	21.4	29.1
		135-180	170	155.6	13.7	15.8	21.0	18.7	21.9
		180-225	109	192.2	14.1	15.1	22.1	17.7	20.5
		225-270	188	252.4	10.7	6.8	14.1	14.4	17.9
		270-315	193	285.3	12.5	2.3	13.4	11.3	26.2
		315-360	116	342.0	12.3	-6.9	15.0	11.3	17.2
		all	1510	159.9	105.5	5.6	16.8	18.3	24.8
	Pressure (mbar)	920-945	11	935.7	6.3	15.5	15.8	18.2	18.5
		945-965	21	956.3	5.0	13.2	15.3	17.5	19.5
		965-980	76	972.2	4.1	4.5	9.7	8.0	11.1
		980-989	53	984.9	2.6	-0.4	3.4	3.0	4.5
		989-1030	544	1001.6	5.6	-3.6	4.4	-0.7	2.3
		all	705	994.8	15.0	-1.7	6.1	1.3	6.0
Katrina	Wind Speed (mph)	0-20	49	15.6	3.3	13.7	13.8	10.8	11.1
		20-40	236	32.4	5.7	7.3	10.8	6.6	8.7
		40-60	402	49.2	5.9	8.5	14.7	5.4	9.1
		60-80	139	66.1	3.8	8.8	16.6	6.6	10.3
		80-100	1	81.7	0.0	6.0	6.0	12.6	12.6
		all	827	45.3	14.5	8.5	14.0	6.3	9.3
	Wind Direction (deg)	0-45	195	30.9	8.4	6.5	11.7	21.6	24.2
		45-90	222	71.3	11.2	2.0	11.5	16.7	21.5
		90-135	197	108.7	13.5	-1.5	12.5	7.6	14.1
		135-180	83	154.3	11.3	-5.9	20.2	-1.7	18.5
		180-225	60	204.8	10.8	-6.3	21.4	-6.3	18.4
		225-270	37	247.6	10.2	-8.5	21.5	5.1	27.0
		270-315	18	290.4	12.5	0.0	10.8	24.8	27.0
		315-360	14	336.7	13.6	15.0	24.5	32.9	38.4
		all	826	105.9	72.6	0.5	14.6	12.1	21.0

Table 13.1. Error Analysis of Modeled Wind Speed, Wind Direction, and Atmospheric Pressure Time Histories (Continued)

Hurricane	Range		Number of Data	Obs		SLOSH-Obs		ARA-Obs	
				Mean	Std	mean	RMS	mean	RMS
Katrina	Pressure (mbar)	920-945	4	938.1	8.0	26.0	30.7	25.5	30.6
		945-965	34	958.0	5.1	1.1	4.8	0.8	3.8
		965-980	70	974.5	4.5	0.6	3.4	0.0	2.9
		980-989	114	984.9	2.4	-0.7	2.1	-0.9	2.1
		989-1030	275	996.1	4.1	-2.1	2.6	-1.0	2.0
		all	497	987.4	12.7	-0.9	4.0	-0.5	3.6
Gustav	Wind Speed (mph)	0-20	1081	13.8	4.7	16.5	17.5	16.1	17.0
		20-40	2197	29.6	5.4	16.9	20.8	12.1	14.8
		40-60	933	47.1	4.9	11.1	16.7	5.5	12.2
		60-80	56	67.3	6.6	4.7	7.6	-1.0	7.6
		80-100	5	81.0	1.2	-2.9	3.1	-8.9	8.9
		all	4272	30.0	13.3	15.3	19.0	11.5	14.8
	Wind Direction (deg)	0-45	1811	22.8	11.9	0.3	12.9	17.4	20.7
		45-90	703	62.4	12.8	-0.7	23.3	11.4	23.0
		90-135	708	112.9	14.7	6.0	18.2	14.1	20.0
		135-180	797	158.3	14.3	-1.4	10.6	11.3	13.8
		180-225	418	195.9	15.6	-20.4	23.8	-4.3	13.6
		225-270	235	240.5	12.5	-18.1	25.2	-8.7	19.1
		270-315	67	293.1	13.4	-6.4	9.8	-9.7	17.0
		315-360	381	346.1	10.8	17.9	19.6	35.2	38.1
		all	5120	116.1	100.1	-0.5	17.4	13.4	21.5
	Pressure (mbar)	945-965	37	963.4	0.6	2.8	2.9	3.6	3.8
		965-980	523	973.2	4.1	-1.6	3.7	-0.5	3.3
		980-989	542	984.6	2.5	-1.0	3.3	-0.6	2.5
		989-1030	3725	998.6	5.4	0.1	1.8	-1.2	2.0
		all	4827	994.0	10.3	-0.2	2.3	-1.0	2.3
Ike	Wind Speed (mph)	0-20	295	12.1	4.0	13.5	16.9	5.2	7.7
		20-40	1971	32.4	5.1	18.8	21.0	15.2	17.8
		40-60	2110	48.7	5.7	8.8	13.1	7.6	12.2
		60-80	827	67.9	5.5	-4.3	8.6	-2.2	7.9
		80-100	12	81.0	0.6	-14.5	14.9	-9.6	11.6
		all	5215	43.6	15.5	10.7	16.2	8.7	13.9
	Wind Direction (deg)	0-45	1981	19.5	10.4	6.8	13.2	13.8	17.3
		45-90	524	62.8	11.3	-1.3	10.5	6.2	12.4
		90-135	338	111.3	12.5	-1.1	22.9	13.7	24.1
		135-180	454	161.1	11.6	15.5	32.8	24.1	28.9
		180-225	1005	199.7	11.8	19.3	21.9	27.8	30.0
		225-270	425	241.0	10.2	22.0	30.6	20.8	25.7
		270-315	171	292.1	13.5	21.9	27.3	30.7	33.3
		315-360	279	344.8	12.6	17.3	21.9	27.5	31.1
		all	5177	126.2	106.8	11.0	20.6	18.5	23.6
	Pressure (mbar)	945-965	982	958.1	3.3	0.2	1.4	0.4	1.6
		965-980	1346	972.1	4.5	-3.0	3.4	0.0	1.3
		980-989	1466	984.5	2.5	-4.8	5.0	-0.3	1.2
		989-1030	1474	992.5	2.9	-3.6	3.8	0.7	1.5
		all	5268	978.7	12.8	-3.1	3.8	0.2	1.4

Three sets of comparisons of the observed and modeled storm tide are performed for Hurricane Andrew and Hurricane Isabel. The first comparison uses the ARA storm track and the SLOSH wind field model (denoted as ARA-TRK-SLOSH-WD). The second comparison uses the ARA storm track and the ARA wind field model (denoted as ARA-TRK-ARA-WD). The third comparison uses the NOAA storm track and the SLOSH wind field model (denoted as NOAA-TRK-SLOSH-WD). For the remaining validation events, only the first two sets of comparisons are performed.

Detailed results for each event are provided in Appendices T through Y. The main conclusions can be summarized as follows:

- For Hurricane Andrew (Appendix T), the summary comparisons indicate that the ARA-TRK-ARA-WD model and the NOAA-TRK-SLOSH-WD model produce storm tide estimates that are 6% and 3% higher, on average, than the observations, while the values of the simulated storm tide produced by the ARA-TRK-SLOSH-WD model average about 14% higher than the observed data. In all three cases, the models tend to overestimate the smaller HWM observations (i.e., observations between 5 and 10 feet) and underestimate the larger HWM observations (i.e., observations above 12 feet).
- For Hurricane Isabel (Appendix U), the comparisons of the observed and simulated storm tide show that the ARA-TRK-ARA-WD model produces underestimates of about 11% on average, while both the ARA-TRK-SLOSH-WD model and the NOAA-TRK-SLOSH-WD model significantly underestimate the storm tide by 42% to 45%, respectively, on average. For this event, none of the three models does very well at explaining the scatter in the observed data.
- For Hurricane Ivan (Appendix V), the comparisons indicate that the values of the simulated storm tides produced by the ARA wind field model and the SLOSH wind field model both compare well to the observed data. The storm tide time series analysis for this event indicates that the ARA wind field model tends to produce lower mean and root mean square (RMS) errors than the SLOSH wind field model.
- For Hurricane Katrina (Appendix W), the comparisons indicate that the values of the simulated storm tide, for both the ARA wind field model and the SLOSH wind field model, are comparable to the observed data on average, but both models tended to over predict at the low end and under predict at the high end.
- For Hurricane Gustav (Appendix X), the SLOSH wind model and ARA wind model produce average underestimates of the observed storm tides of 24% and 20%, respectively. The underestimates are largest at the six locations with observed storm tides in excess of 10 feet. For this event, the model runs with ARA wind field model generally produce lower mean time history errors and lower RMS time history errors than the model runs using the SLOSH wind model.

- For Hurricane Ike (Appendix Y), the SLOSH wind model and ARA wind model produce average underestimates of the observed storm tides of 5% and 10%, respectively; however, the standard deviation of the errors from the ARA wind model results are smaller than the standard deviations of the errors from the SLOSH wind model results. The model runs with ARA wind field model generally produce slightly smaller mean time history errors and slightly smaller RMS time history errors than the model runs using the SLOSH wind model.

Table 13.2 summarizes the mean and RMS errors of modeled storm tide time histories for the five most recent validation events. The results show that the model run with ARA wind field model results in lower overall mean and RMS errors for four of the five hurricanes. The only exception is Hurricane Katrina, which has by a wide margin the fewest storm tide time history observation points of the five hurricanes.

In summary, comparisons suggest that the values of the model computed storm tide produced by the ARA wind field model tend to match the observed data better than those produced by the SLOSH wind field model.

13.2.3 Wave Model Implementation and Validation

For use in HAZUS, the primary purpose of the wave hazard model is to predict hurricane-induced wave heights in developed areas inundated by hurricane storm surge. A secondary purpose is to estimate wave setup stresses for coupling back into SLOSH, which will result in higher still water elevation predictions. In this section, we review the wave models considered for use in the HAZUS coastal surge methodology, discuss the computational grids used in the wave modeling methodology, show validation results for the SWAN near shore wave model, describe how the coastal surge wave model will be coupled with the storm surge model (SLOSH), and discuss how the modeled waves will ultimately be propagated into inundated areas using the transect-based approach documented in the HAZUS-MH Flood Model Technical Manual (FEMA 2009b).

13.2.3.1 Wave Models Considered

Three public-domain wave models were considered for use in the HAZUS coastal surge methodology. These models are briefly described in the following paragraphs:

13.2.3.1.1 WAVEWATCH-III

WAVEWATCH-III is a third generation deep water wave model developed by the National Centers for Environmental Predictions of the National Weather Service. This model is a product of continued development of WAVEWATCH-I developed at Delft University of Technology and WAVEWATCH-II developed at National Aeronautics and Space Administration. The model accounts for wave growth and decay due to surface wind stress, bottom friction, nonlinear wave-wave interactions and wave dissipation. Although efficient in computation in the deep water, it is not suitable for computations of wave characteristics in shallow water.

Table 13.2. Error Analysis of Modeled Storm Tides vs. Observed Time Histories

Hurricane	Unit	Surge Range	Numer Data	Obs		SLOSH-Obs		ARA-Obs	
				Mean	Std	mean	RMS	mean	RMS
Isabel 2003	(ft NAVD)	0-3	3338	1.3	0.8	0.2	0.8	0.4	1.0
		3-6	1575	4.3	0.9	-1.3	1.8	0.0	1.1
		6-9	500	6.7	0.7	-3.3	3.8	-1.0	1.8
		all	5413	2.7	2.0	-0.6	**1.6**	0.1	**1.1**
Ivan 2004	(ft NGVD)	0-3	544	2.1	0.9	-0.4	1.9	0.1	1.5
		3-6	1083	4.0	0.7	-0.9	1.2	-0.3	0.8
		6-9	52	6.5	0.2	0.8	1.1	0.2	0.6
		all	1679	3.5	1.3	-0.7	**1.4**	-0.2	**1.1**
Katrina 2005	(ft NAVD)	0-3	65	2.8	0.1	1.1	1.1	1.3	1.4
		3-6	357	4.2	0.7	0.5	1.0	0.8	1.3
		6-9	30	7.0	0.8	-0.9	1.3	0.5	0.6
		all	452	4.2	1.1	0.5	**1.0**	0.9	**1.2**
Gustav 2008	(ft NGVD)	0-3	7085	1.7	0.7	0.6	1.6	0.9	1.8
		3-6	5436	4.2	0.8	-0.7	1.8	-0.1	1.2
		6-9	2366	7.3	0.9	-2.2	3.1	-1.9	2.3
		9-12	993	10.5	0.9	-5.3	5.4	-4.0	4.0
		12-15	560	13.3	0.8	-6.4	6.5	-5.2	5.2
		all	16440	4.3	3.1	-0.8	**2.6**	-0.3	**2.1**
Ike 2008	(ft NAVD)	0-3	963	2.0	0.8	2.9	4.4	3.2	4.4
		3-6	5429	4.9	0.8	-1.5	3.1	-1.2	3.1
		6-9	11235	7.4	0.8	-1.3	3.0	-0.8	2.6
		9-12	7871	10.3	0.8	-0.2	3.3	-0.5	3.1
		12-15	3147	13.2	0.9	0.6	2.0	-0.4	1.7
		15-18	766	15.6	0.5	0.1	2.2	-1.0	2.1
		18-21	4	18.3	0.6	-6.3	6.3	-6.8	6.8
		all	29415	8.4	3.1	-0.7	**3.0**	-0.6	**2.8**

13.2.3.1.2 STWAVE

STWAVE (Steady State Spectral Wave) is a nearshore wave model developed and supported by the Coastal and Hydraulics Laboratory at the US Army Corps of Engineers Engineer Research and Development Center. The model simulates depth-induced refraction, shoaling, breaking, and diffraction. The full-plane version of STWAVE (allowing propagation and generation from all directions) is comparable to SWAN in terms of run-time and memory requirements.

13.2.3.1.3 SWAN

Simulating WAves Nearshore (SWAN) is a third-generation spectral wave model capable of generating two-dimensional wave energy spectra under specified conditions of winds, currents and bathymetry. It accounts for nearshore wave behavior such as wave breaking and wave setup and thus is suitable for shallow water computations of wave characteristics.

13.2.3.2 Computational Grids Used in the Coastal Wave Modeling Methodology

Due to time and resource limitations, it was not feasible to evaluate, implement and validate two different nearshore wave modeling options. Given the project team's previous experience with SWAN and the ability to use a SWAN to model both deep water and shallow water waves on both structured and unstructured grids, SWAN has been selected for use as the wave model in the HAZUS coastal surge methodology.

13.2.3.2.1 Implementation of SLOSH Grids and ARA Hurricane Wind Field in SWAN

For computational efficiency, SLOSH uses continuously varying grid cell sizes within each basin. It uses large grid cells near the deep water boundary and progressively smaller grid cells near the coast. In addition SLOSH uses different types of grid formats (polar, elliptical, hyperbolic, etc.) to represent a basin. To eliminate the need for duplicate and potentially conflicting bathymetry data for the storm surge and wave models, we have elected to directly use the SLOSH grids in SWAN by enabling the curvilinear grid option in the SWAN command file. The center of each SLOSH grid cell becomes a grid point in SWAN, with the average depth of the SLOSH cells used as the depth or elevation at that point. This approach is taken for two reasons: (i) to keep an identical computational grid as the input grid so that no additional interpolations are needed by SWAN, and (ii) to compute the wave parameters at the same locations in where surge is calculated in SLOSH.

The ARA hurricane wind field model is implemented in SWAN by using a nonstationary input of wind vectors at the computational grid points. These nonstationary wind vectors are computed for the duration of each SWAN run at fixed time intervals using ARA hurricane wind field model.

13.2.3.2.2 Wave Boundary Conditions for SWAN Runs on SLOSH Grids

Nonstationary wave conditions at the open ocean boundaries of a SLOSH basin are imposed in terms of wave spectra obtained through a SWAN (or WAVEWATCH III) run on a relatively large coarse grid with cells that are 20 km × 20 km in size. This grid is denoted as the Northwest Atlantic grid. The outline of this large grid is shown in red in Figure 13.2 along with the New Orleans SLOSH basin outline in blue. At first, a SWAN (or WAVEWATCH-III) run on this large grid is carried out using the nonstationary wind inputs at the coarse grid points for a given storm duration. The wave spectra obtained at the open boundary of a SLOSH basin from this run are then used as a boundary condition in the SWAN run in the SLOSH basin for the same storm duration.

13.2.3.3 Wave Model Validation Comparisons

Validation results for Hurricanes Isabel, Ivan, Katrina, Gustav and Ike are provided below. Significant wave heights, and in some cases the mean wave directions, are compared with the data obtained from the National Data Buoy Center (NDBC) and the United States Geological Survey (USGS).

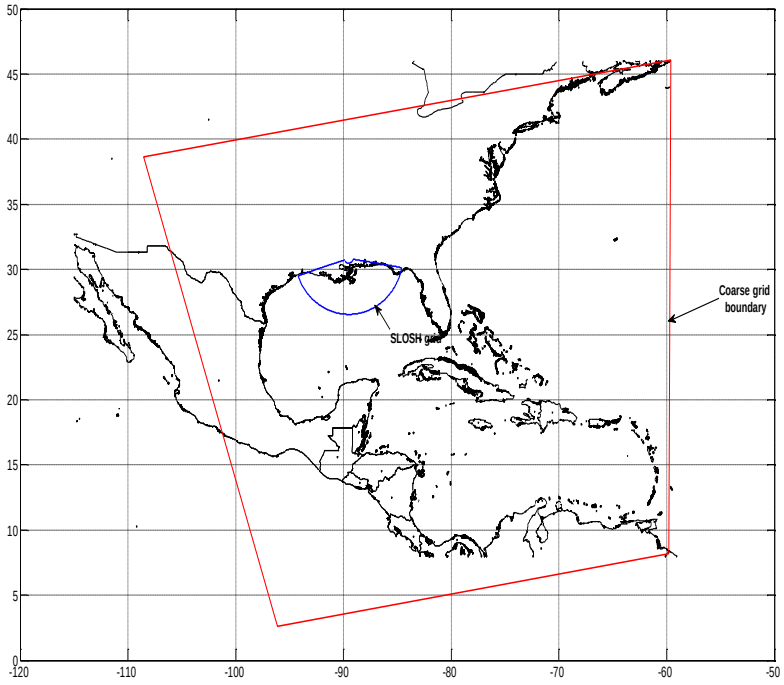

Figure 13.2. Northwest Atlantic Grid Domain.

13.2.3.3.1 Hurricane Isabel (2003)

Hurricane Isabel made landfall near Drum Inlet, North Carolina at approximately 1700 UTC on 18 September 2003 as a Category 2 hurricane.

Observed Data

One NDBC buoy (41025) is selected for validating wave heights in Hurricane Isabel, and the Pamlico Sound Hatteras basin is used in the simulation. The location of the buoy and the basin outline are shown in Figure 13.3.

Comparisons to Observed Data

Observed significant wave heights during Hurricane Isabel at buoy 42025 are compared with those obtained using SWAN. In the comparison, two cases of simulation results are shown. In the first case, the wave spectra obtained from a separate SWAN run in the Northwest Atlantic 20 km grid are used in the simulation. In the second case, the simulation is carried out without any boundary conditions.

The results are shown in Figure 13.4 where it can be seen that the boundary conditions have a substantial effect on the modeled significant wave height. Including wave boundary conditions in the simulation increases the modeled significant wave height by about 4 m. Due to the lack of a complete record at this buoy, a full comparison is not possible.

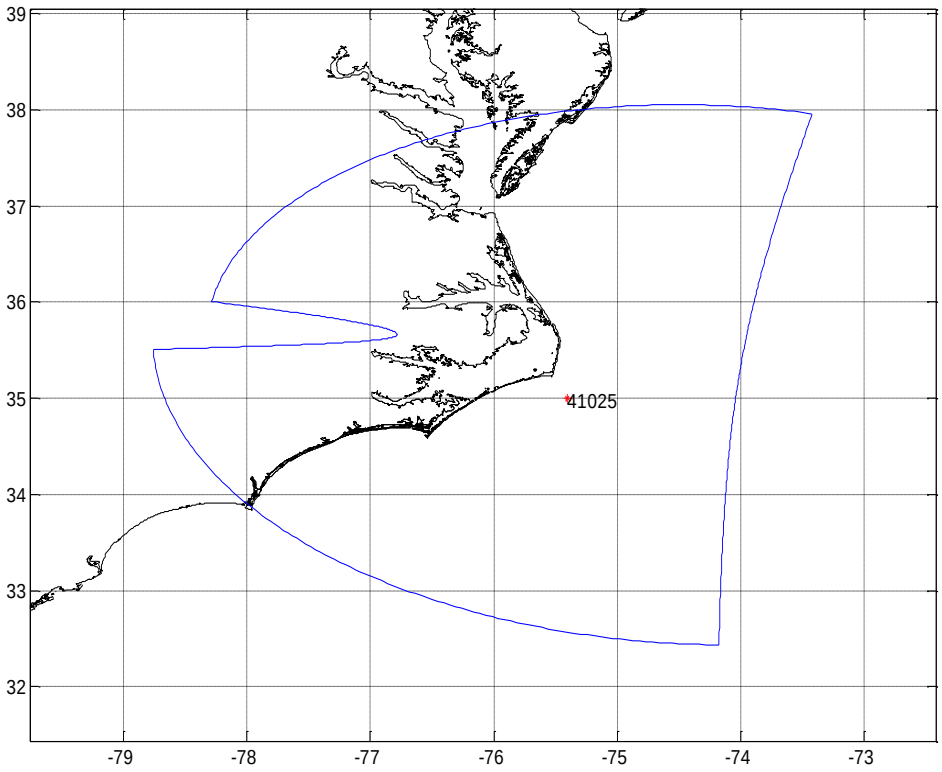

Figure 13.3. Location of NDBC Buoy in Pamlico Sound Hatteras SLOSH Basin.

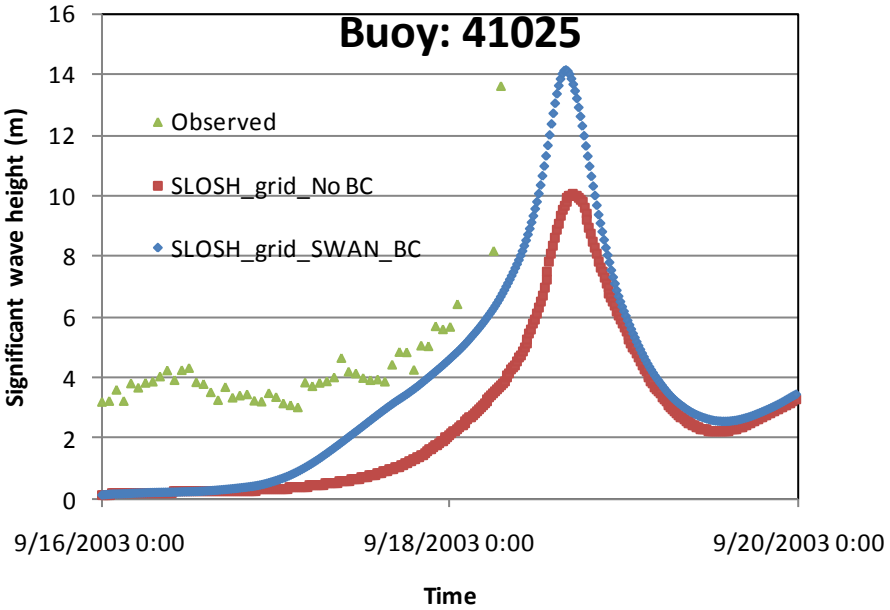

Figure 13.4. Comparison of Significant Wave Heights – Hurricane Isabel, Buoy 41025.

13.2.3.3.2 Hurricane Ivan (2004)

Hurricane Ivan made landfall as a Category 3 hurricane near Gulf Shores, Alabama at about 0650 UTC September, 2004.

Observed Data

Three NDBC buoys (42039, 42040, and 42007) are selected for validating wave heights in Hurricane Ivan, and the New Orleans SLOSH basin is used for the simulation. The location of the buoys and the basin outline are shown in Figure 13.5.

Comparisons to Observed Data

Observed significant wave heights and mean wave directions during Hurricane Ivan at NDBC buoys 42039, 42040 and 42007 are compared with those obtained from SWAN. In the comparison, two cases of simulation results are shown. In the first case, the wave spectra obtained from a separate SWAN run in the Northwest Atlantic 20 km grid are used in the simulation. In the second case, the simulation is carried out without any boundary conditions.

The comparison results are shown in Figure 13.6 and Figure 13.7. The boundary conditions have a substantial effect on the significant wave heights at the locations of the deep water buoys 42039 and 42040, whereas at the location of relatively shallow water buoy 42007, the boundary conditions do not play a significant role in the peak value of the modeled significant wave height. Including wave boundary conditions in the simulation increases the significant wave height at 42039 by about 1.5 m.

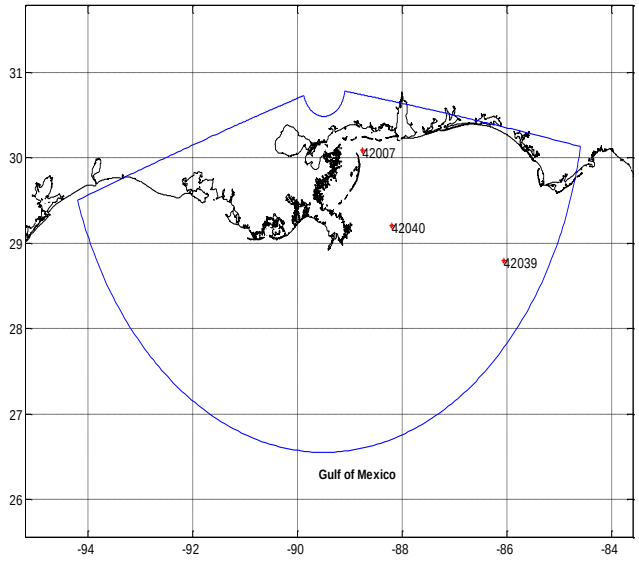

Figure 13.5. Locations of NDBC Buoys in the New Orleans SLOSH Basin.

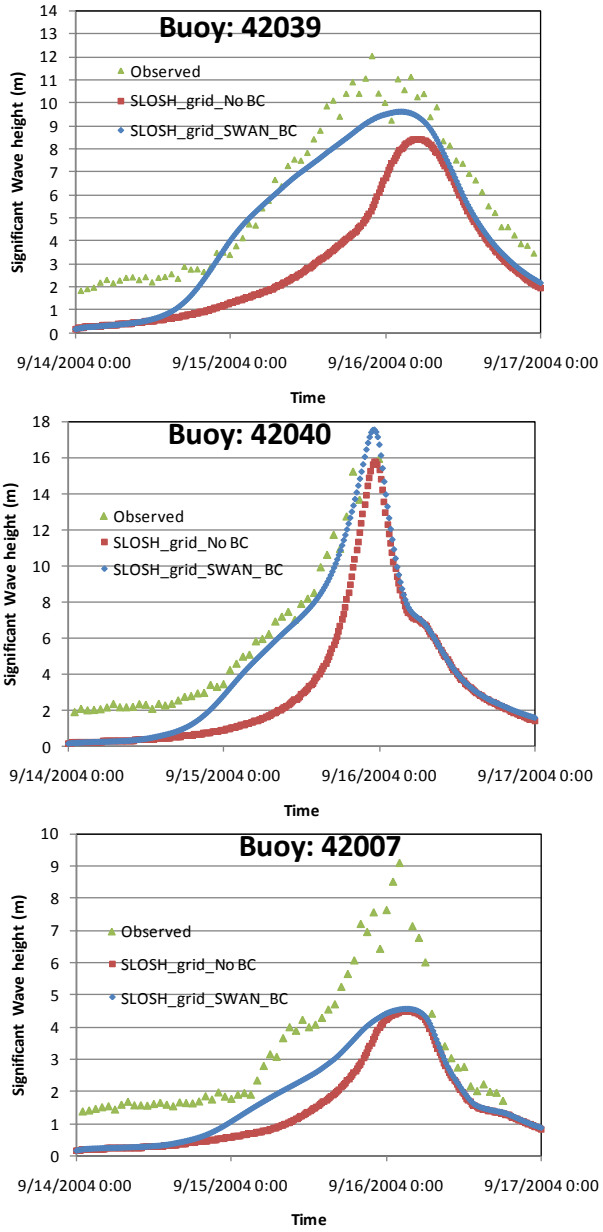

Figure 13.6. Comparison of Significant Wave Heights – Hurricane Ivan, New Orleans SLOSH Basin.

The significant wave height simulated with boundary conditions included shows reasonably good agreement with the observed data for buoys 42039 and 42040. However, there is a significant difference at buoy 42007. Possible causes include: (1) neglecting the pre-storm tide anomaly and storm surge in the simulation, (2) inaccurate bathymetry, and/or (3) insufficient grid resolution at this location.

The simulated mean wave directions at all three buoy locations shown in Figure 13.7 are in good agreement with the observations.

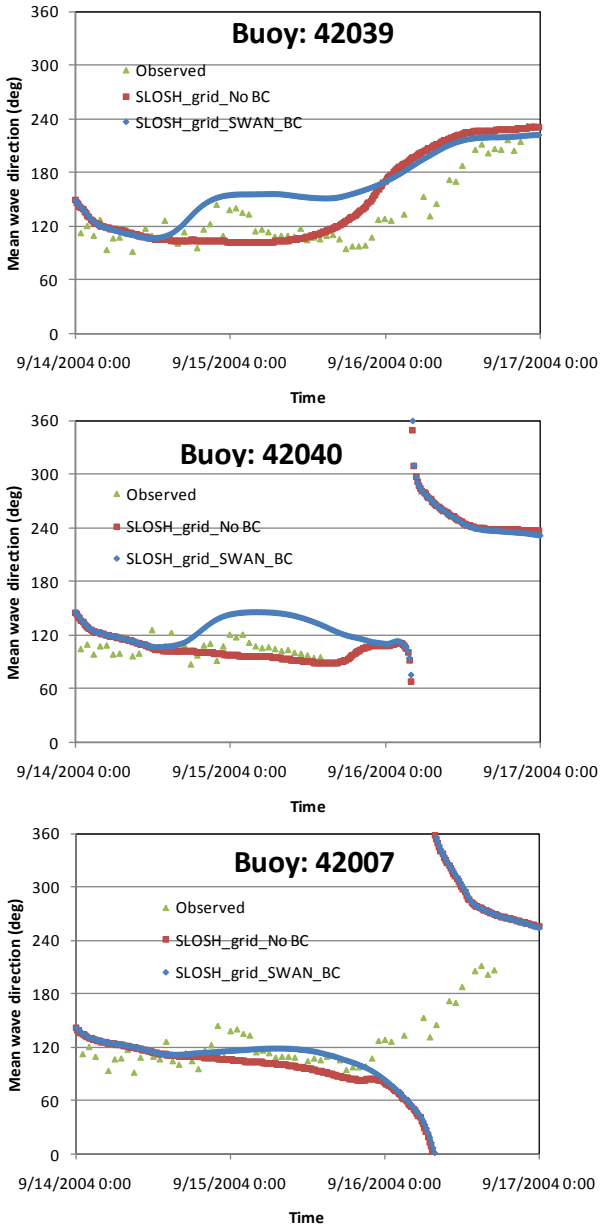

Figure 13.7. Comparison of Mean Wave Directions – Hurricane Ivan, New Orleans SLOSH Basin.

13.2.3.3.3 Hurricane Katrina (2005)

Hurricane Katrina made landfall as a Category 3 hurricane near Buras, Louisiana at 1110 UTC 29 August, 2005.

Observed Data

Three NDBC buoys (42039, 42040, and 42007) are selected for validating wave heights in Hurricane Katrina. The New Orleans, Mississippi Gulf Coast and Mobile Bay SLOSH basins are used in different SWAN runs. The locations of the three buoys relative to the three basins are shown in Figure 13.8, Figure 13.9, and Figure 13.10, respectively.

Comparisons to Observed Data

Observed significant wave heights during Hurricane Katrina at NDBC buoys 42039, 42040, and 42007 are compared with modeled results obtained from SWAN. In the comparison, two cases of simulation results are shown. In the first case, the wave spectra obtained from a separate SWAN run in the Northwest Atlantic 20 km grid are used in the simulation. In the second case, the simulation is carried out without any boundary conditions.

The comparison results are shown in Figure 13.8 through Figure 13.10. Including wave boundary conditions obtained using either SWAN or WAVEWATCH III on the Northwest Atlantic grid significantly improves the estimates at the deep water buoy locations (i.e., 42039 and 42040), with the boundary conditions obtained from the SWAN run providing better estimates than those obtained from the WAVEWATCH III run.

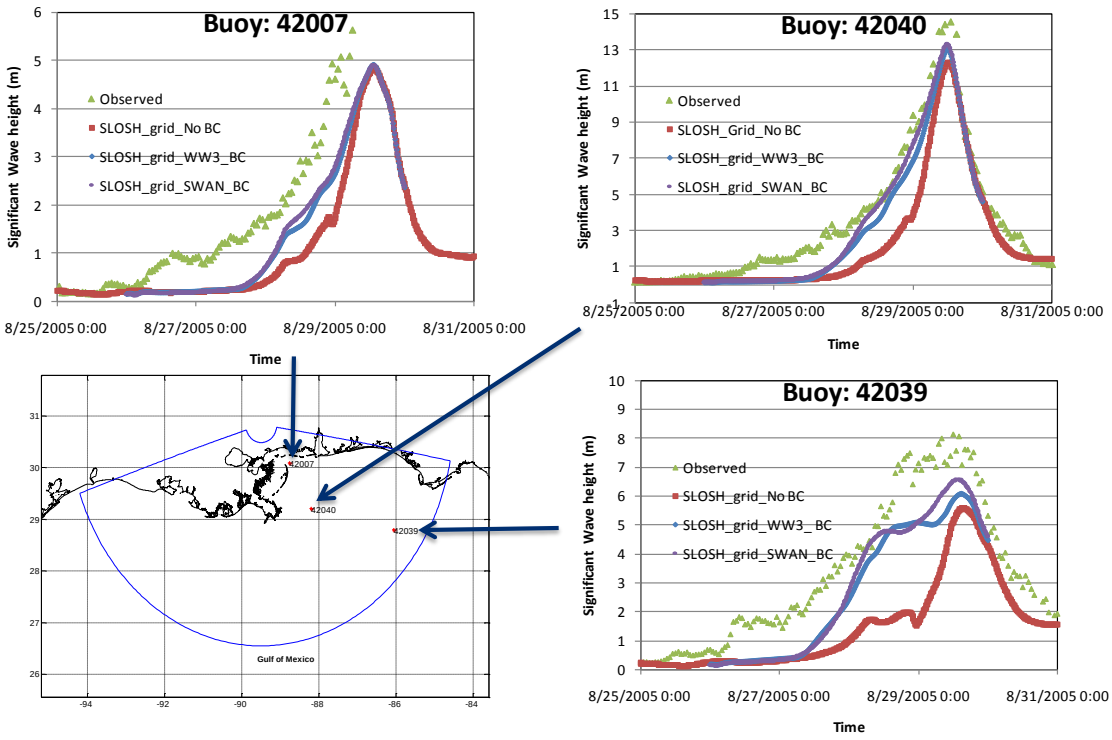

Figure 13.8. Comparison of Significant Wave Heights – Hurricane Katrina, New Orleans SLOSH Basin

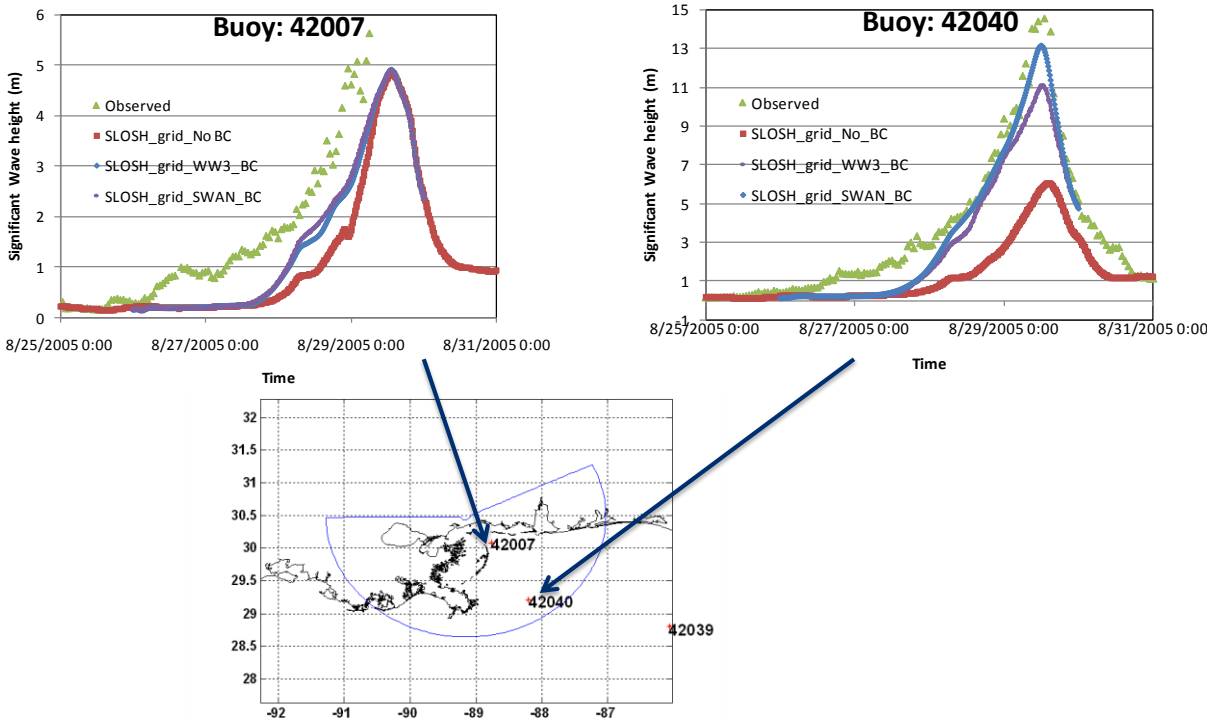

Figure 13.9. Comparison of Significant Wave Heights – Hurricane Katrina, Mississippi Gulf Coast SLOSH Basin.

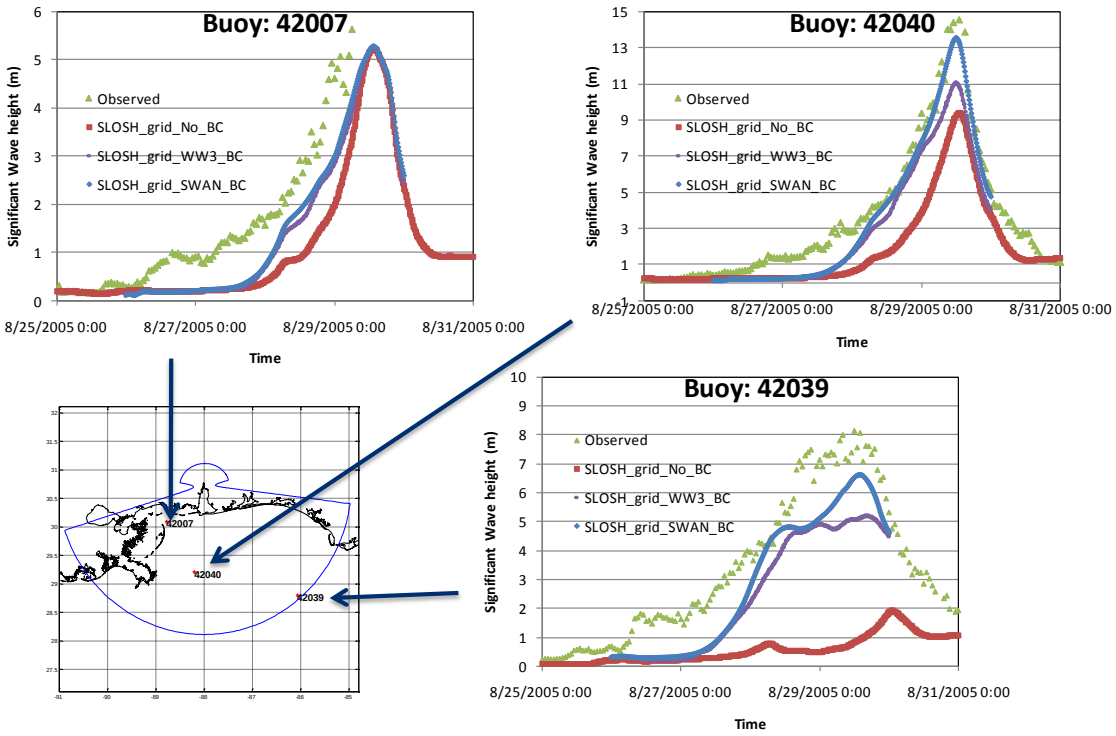

Figure 13.10. Comparison of Significant Wave Heights – Hurricane Katrina, Mobile Bay SLOSH Basin.

13.2.3.3.4 Hurricane Gustav (2008)

Hurricane Gustav made landfall as a Category 2 hurricane on the coast of Louisiana at around 1500 UTC September 1, 2008.

Observed data

Three NDBC buoys (42039, 42040, and 42007) are selected for validating wave heights in Hurricane Gustav, and the New Orleans SLOSH basin is used for the simulation. The location of the buoys and the basin outline were shown previously in Figure 13.5.

Observed nearshore wave data for 16 locations are also obtained from Dr. Andrew Kennedy of the University of Notre Dame through personal communications. These locations are plotted in Figure 13.11 along with the boundary of the New Orleans SLOSH basin.

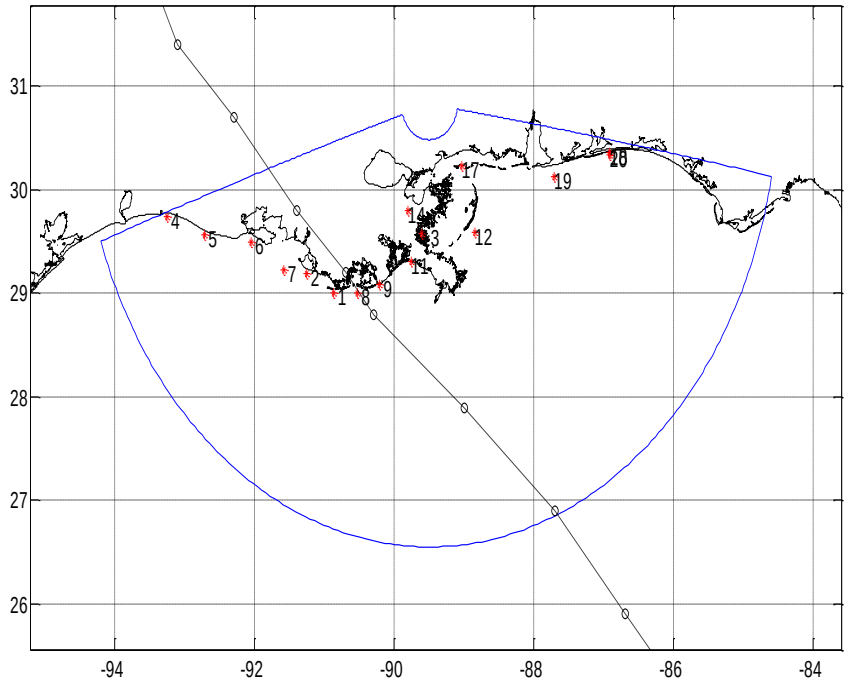

Figure 13.11. Locations of Wave Gauges inside the New Orleans SLOSH basin.

Comparisons to Observed Data

Observed significant wave heights and mean wave directions during Hurricane Gustav at NDBC buoys 42039, 42040, and 42007 are compared with modeled results obtained from SWAN. For 42039 and 42040 the observed mean wave directions are not available in the database. In the comparison, two cases of simulation results are shown. In the first case, the wave spectra obtained from a separate SWAN run in the Northwest Atlantic 20 km grid are used in the simulation. In the second case, the simulation is carried out without any boundary conditions.

The NDBC buoy comparison results are shown in Figure 13.12. Again, the boundary conditions have a substantial effect on the significant wave height at the locations of the deep water buoys (42039 and 42040), whereas at the location of relatively shallow water buoy (42007), boundary conditions do not play a significant role. For example, including wave boundary conditions in the simulation increase the peak modeled significant wave height at 42039 by about 2.5 m. The simulated mean wave directions at buoy 42007 are in reasonably good agreement with the observed mean wave directions when the wave boundary conditions are included in the simulation. The significant wave height comparisons of the observed data with those simulated including boundary conditions shows a good agreement for buoys 42039 and 42040. However, there is a significant difference in the same comparison for buoy 42007. Possible causes include: (1) neglecting the pre-storm tide anomaly and storm surge in the simulation, (2) inaccurate bathymetry, and/or (3) insufficient grid resolution at this location.

Observed significant wave heights are also compared for the locations shown in Figure 13.11. Two cases are considered. In the first case, the simulation is carried out with no surge added as an initial condition. In the second case, the maximum surge obtained from a SLOSH run for each grid cell is added as an initial condition. In both cases, the wave boundary conditions are included. The results are presented in Figure 13.13. Including surge in the simulation improves the estimates, particularly for the gauges located at the right side of the storm track. In general, the modeled results are fairly comparable with the observations. The differences in the modeled and the observed data for some gauge locations are partly due the lack of fine resolution of grid mesh at those locations. For some locations results without surge are not available since those locations are on land.

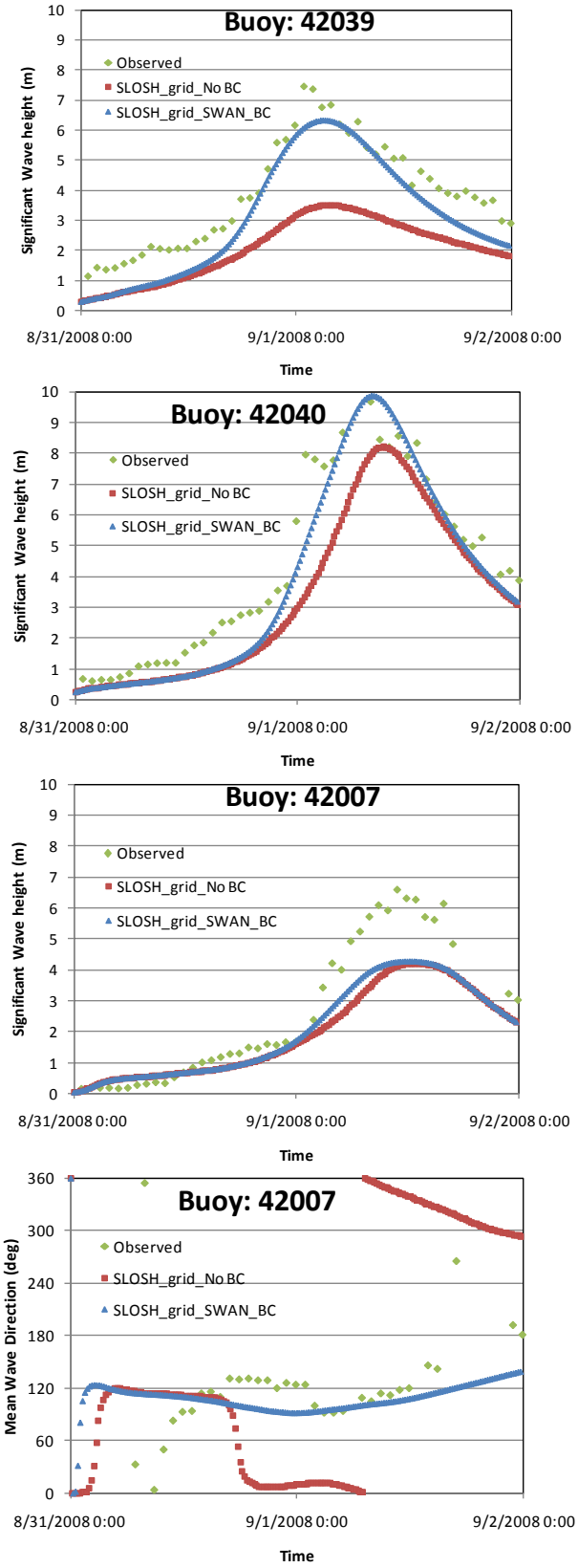

Figure 13.12. Comparison of Significant Wave Heights and Mean Wave Directions – Hurricane Gustav, NDBC Buoys

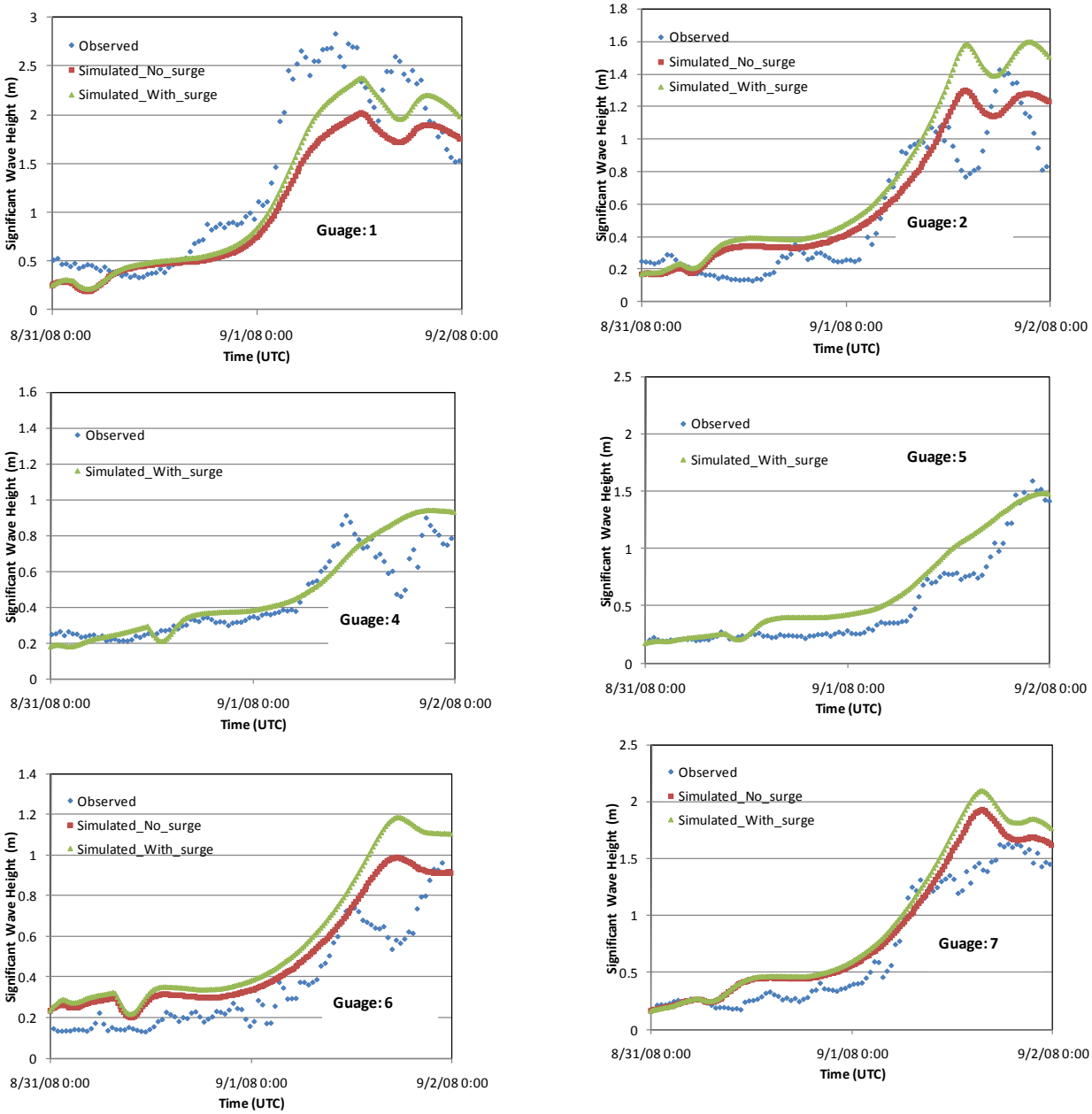

Figure 13.13. Comparison of Significant Wave Heights – Hurricane Gustav, Nearshore Wave Gauges.

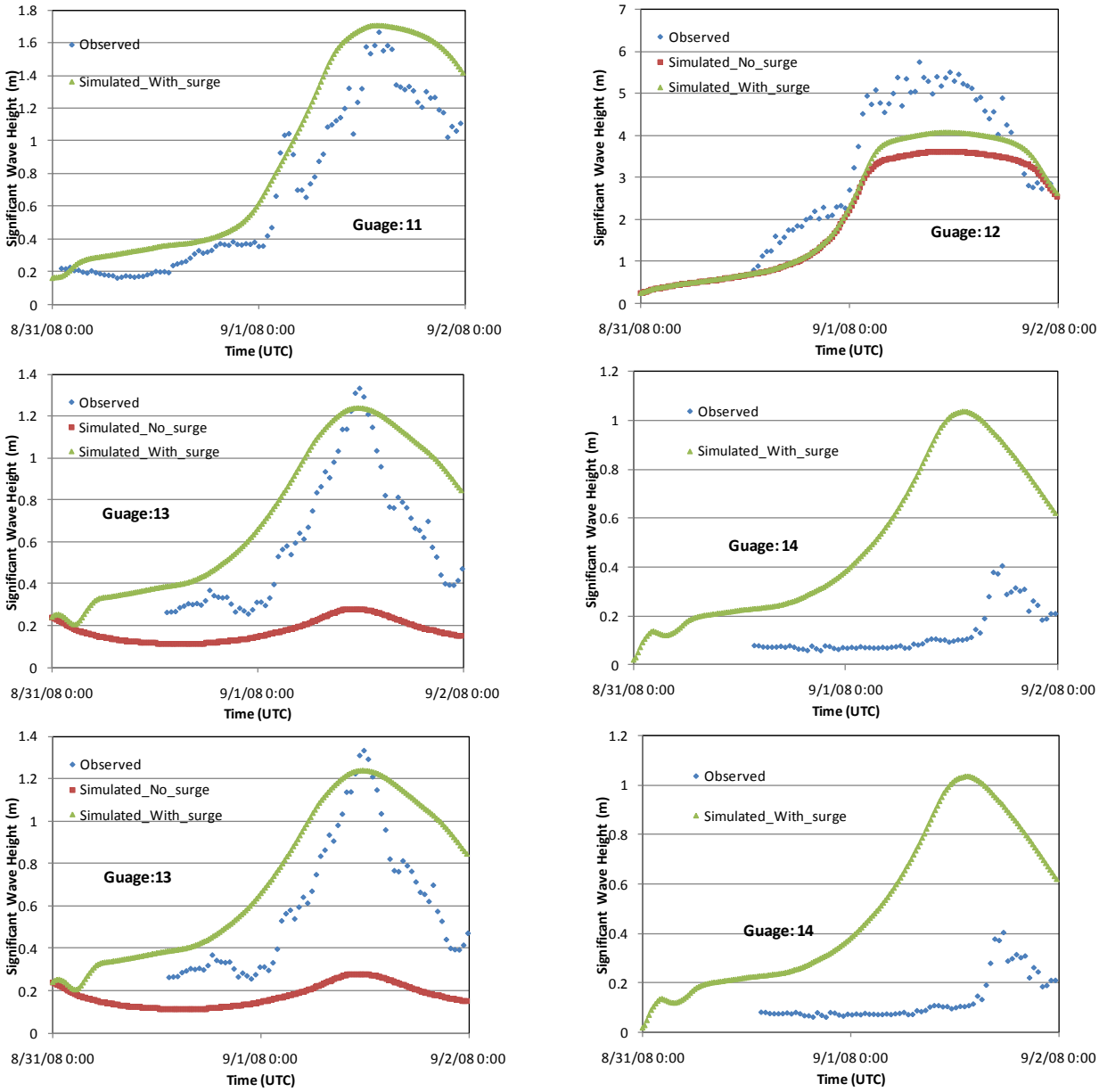

Figure 13.13. Comparison of Significant Wave Heights – Hurricane Gustav, Nearshore Wave Gauges (Continued).

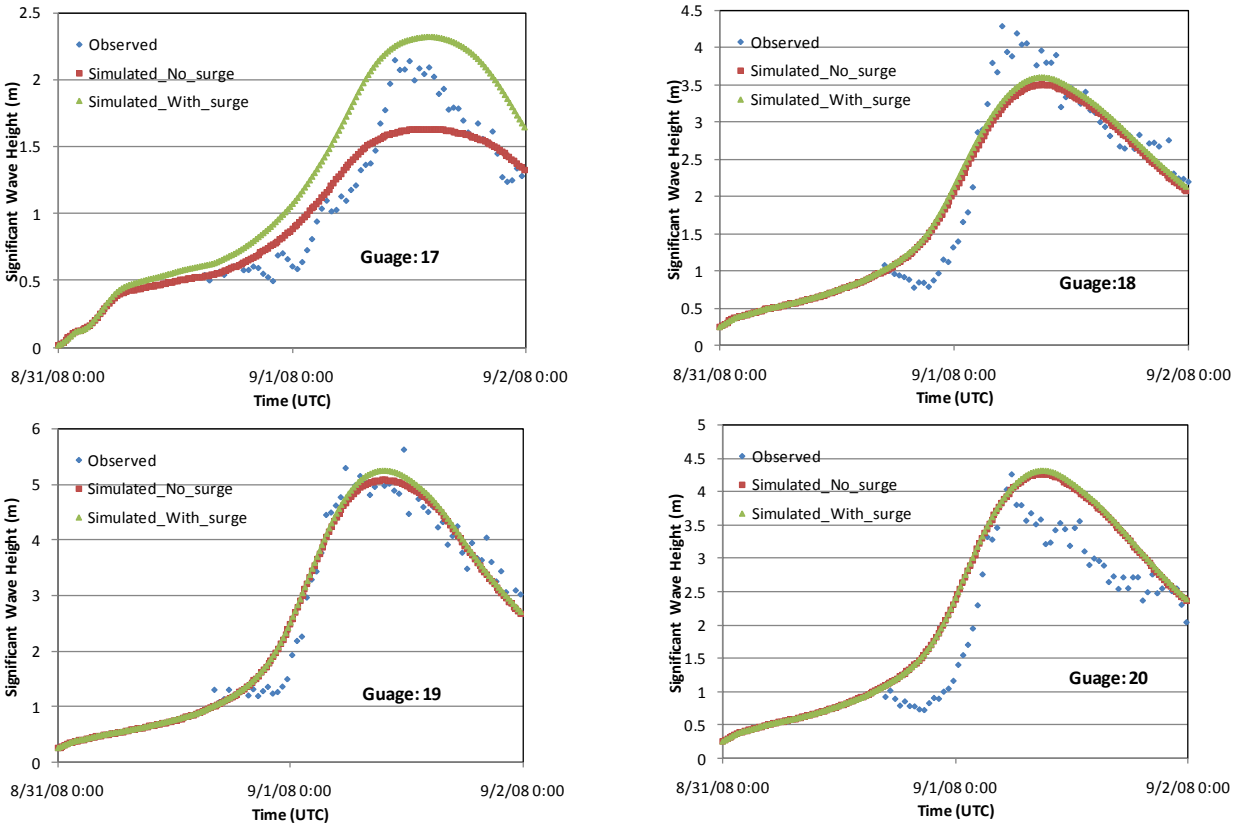

Figure 13.13. Comparison of Significant Wave Heights – Hurricane Gustav, Nearshore Wave Gauges (Continued).

13.2.3.3.5 Hurricane Ike

Hurricane Ike made landfall as a Category 2 hurricane on the coast of Texas at approximately 0700 UTC on September 13, 2008.

Observed Data

Two NDBC buoys (42019 and 42035) are selected for validating wave heights in Hurricane Ike, and the Galveston Bay SLOSH basin is used for the simulation. The location of the buoys and the basin outline are shown in Figure 13.14.

Observed nearshore wave data for eight locations along the Gulf of Mexico coast are also obtained from Dr. Andrew Kennedy of the University of Notre Dame through personal communications. These locations are plotted in Figure 13.15 along with the boundary of the Galveston Bay SLOSH basin.

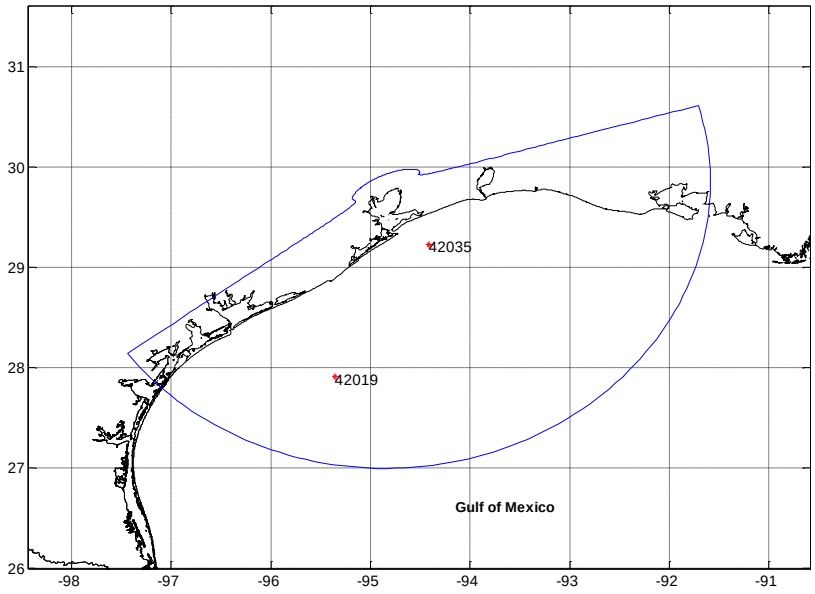

Figure 13.14. Locations of NDBC Buoys in the Galveston Bay SLOSH Basin – Hurricane Ike.

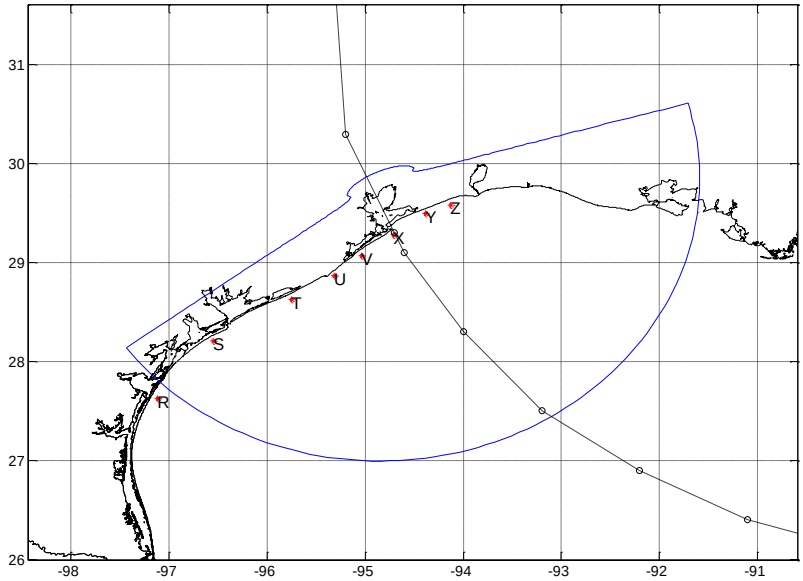

Figure 13.15. Locations of Wave Gauges in the Galveston Bay SLOSH Basin – Hurricane Ike.

Comparisons to Observed Data

Observed significant wave heights and mean wave directions during Hurricane Ike at NDBC buoys 42019 and 42035 are compared with those obtained from SWAN. In the comparisons, two cases of simulation results are used. In the first case, the wave spectra obtained from a separate SWAN run in the Northwest Atlantic 20 km grid are used in the simulation. In the second case, the simulation is carried out without any boundary conditions.

The comparison results are shown in Figure 13.16. Including boundary conditions in the simulations does not have a significant effect on the results in terms of improving the estimates of wave parameters at buoy 42035. The observed significant wave height and mean wave directions comparisons with the simulated results show better agreement for buoy 42019 than for buoy 42035. Possible causes include: (1) neglecting the pre-storm tide anomaly and storm surge in the simulation, (2) inaccurate bathymetry, and/or (3) insufficient grid resolution at this location.

Observed significant wave heights are also compared for the locations shown in Figure 13.15. Two cases are considered. In the first case, the simulation is carried out with no surge added as an initial condition. In the second case, the maximum surge obtained from a SLOSH run for each grid cell is added as an initial condition. In both cases, the wave boundary conditions are included. The results are presented in Figure 13.17. Including surge in the simulation improves the estimates significantly at the gauge locations along and to the right of the storm track. In general, the peak results are fairly comparable with observed ones, except at gauges U and V. The difference in the estimate and the observed data for some gauge locations are partly due the lack of fine resolution of grid mesh at those locations.

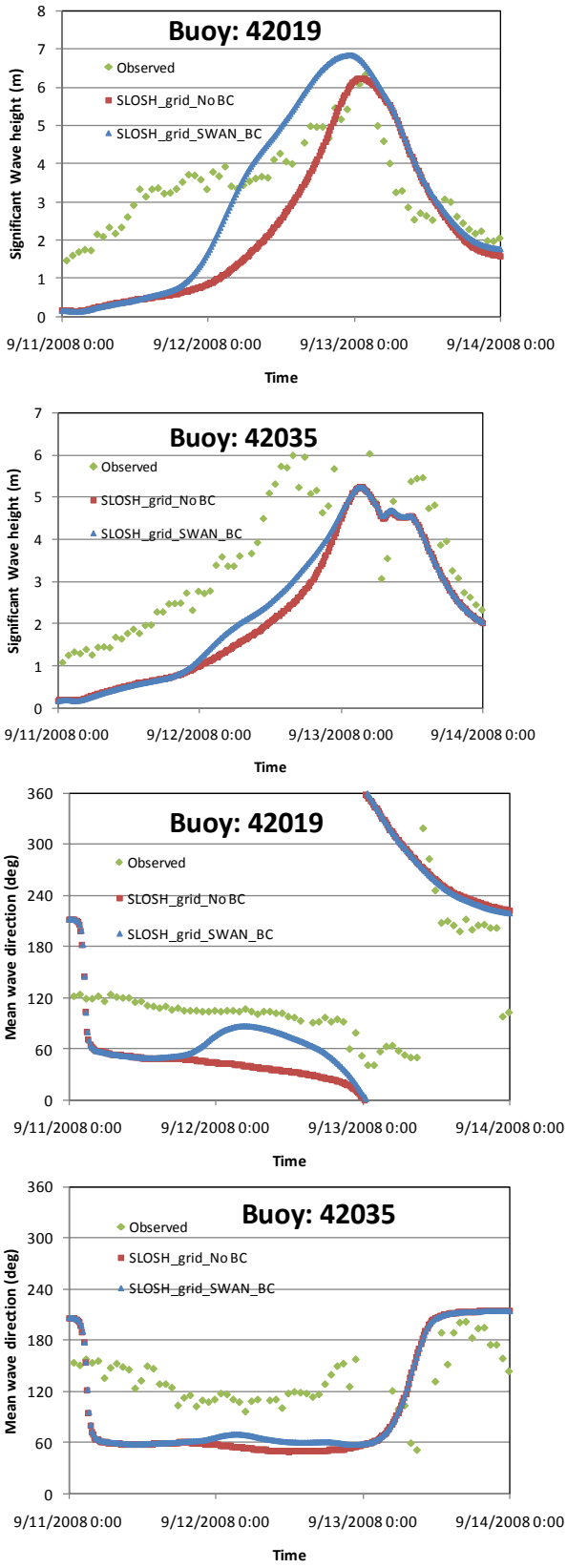

Figure 13.16. Comparison of Significant Wave Heights and Mean Wave Directions – Hurricane Ike, NDBC Buoys.

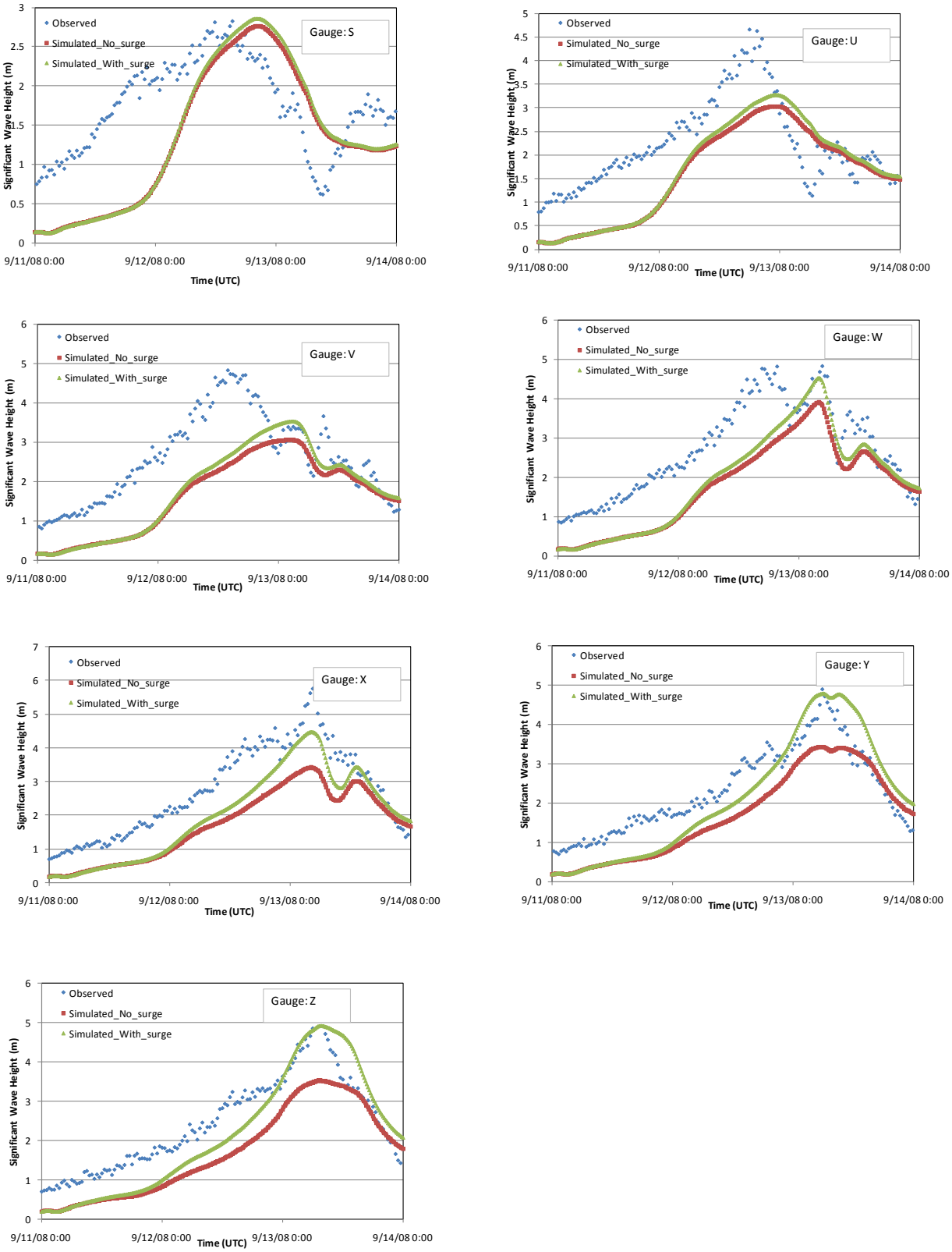

Figure 13.17. Comparison of Significant Wave Heights – Hurricane Ike, Nearshore Wave Gauges.

13.2.3.4 Run time

The SWAN run times depend on simulated storm duration, basin size, and whether wave boundary conditions are computed. A comparison of the run time of the SWAN simulations discussed in the previous sections is presented in Table 13.3. Note that the run times listed in the table is based on SWAN run on an Intel core 2 extreme 2.53 GHz processor. One can expect a significant increase in the run time for each of these runs if a single processor machine is used.

Table 13.3. Run Time Comparisons

Storm	SLOSH Basin		Simulated Hours	Boundary Condition	Run time (min)
	Name	Grid size			
Isabel	Pamlico-Sound-Hatteras	130 X 180	96	ON	75
				OFF	28
Ivan	New-Orleans	175 X 189	72	ON	59
				OFF	28
Katrina	New-Orleans	175 X 189	96	ON	68
				OFF	22
Gustav	New-Orleans	175 X 189	48	ON	56
				OFF	21
Ike	Galveston-Bay	100 X 115	72	ON	39
				OFF	8

13.2.3.5 Hurricane Ike Surge and Wave Simulations at SSS-TX-GAL-001 and -002

To further evaluate the modeling of storm tide and wave heights at the coastline, the water levels at USGS gauges SSS-TX-GAL-001 and SSS-TX-GAL-002 on the Bolivar Peninsula for Hurricane Ike are investigated (East et al. 2008).

Table 13.4 summarizes the maximum observed water levels at the two gauges and the maximum modeled storm tides using the SLOSH model and the ARA storm track for Hurricane Ike with the SLOSH wind field model (ARA-TRK, SLOSH_WD) or the ARA wind field model (ARA-TRK, ARA_WD). The default Galveston Bay SLOSH Basin model (GL2) provided by NOAA with SLOSH version 3.94 was used for the analysis.

Figure 13.18 and Figure 13.19 plot time histories of the observed water levels at the two gauges (reported as instantaneous observations at 1 minute intervals) and the modeled storm tides using the SLOSH model with the ARA storm track and the SLOSH wind field model (ARA-TRK, SLOSH_WD) or the ARA wind field model (ARA-TRK, ARA_WD). The time of landfall is shown as a dashed vertical red line in each figure.

Table 13.4. Maximum Observed Water Levels and Maximum Modeled Storm Tides at SSS-TX-GAL-001 and SSS-TX-GAL-002 for Hurricane Ike (2008)

No	ID	Lat	Lon	Obs (ft NAVD)	ARA-TRK SLOSH_WD	ARA-TRK ARA_WD
1	SSS-TX-GAL-001	29.451389	-94.634167	19.1	12.0	12.0
2	SSS-TX-GAL-002	29.465830	-94.648060	13.4	12.6	12.1

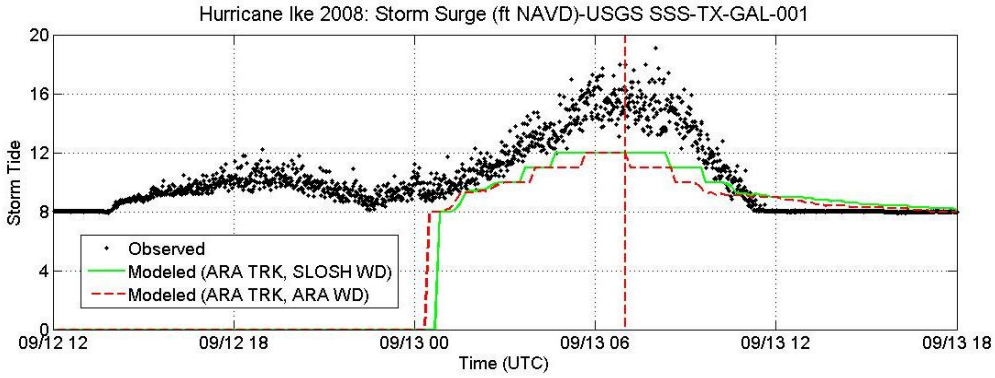

Figure 13.18. Tide Gauge Record at SSS-TX-GAL-001 Compared to the Simulated Time History of Storm Tide in the SLOSH Grid Cell Containing the Gauge Location.

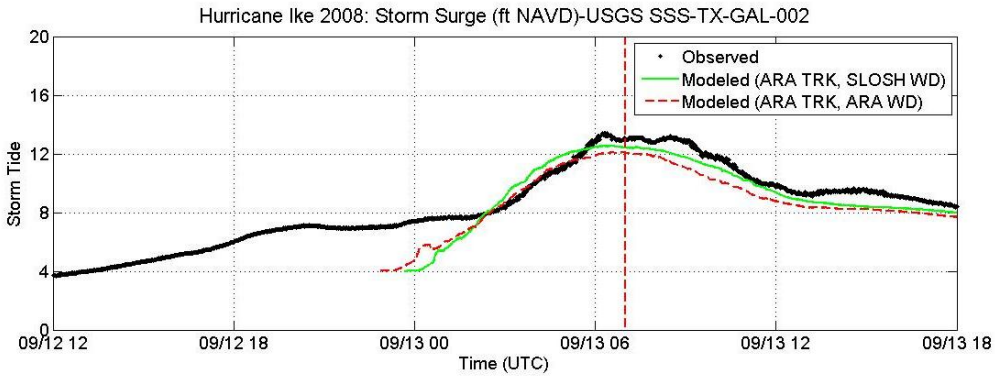

Figure 13.19. Tide Gauge Record at SSS-TX-GAL-002 Compared to the Simulated Time History of Storm Tide in the SLOSH Grid Cell Containing the Gauge Location.

SSS-TX-GAL-001 is described as a "beach/wave site" whereas SSS-TX-GAL-002 is described as a "surge site." The difference is readily apparent in the broad scatter of the SSS-TX-GAL-001 data compared to the very limited scatter of the SSS-TX-GAL-002 data.

At SSS-TX-GAL-001, the maximum storm tides from both models are both 7.1 feet below the maximum observed water level. However, the average observed water level during the 30 minutes before and 30 minutes after the peak observation is 15.1 feet. Thus, the modeled maximum storm tides are 3.1 feet below the maximum average water level. This remaining difference may be partially attributable to the lack of wave setup in the SLOSH model. At SSS-TX-GAL-002, the maximum storm tides from both models are within 10% of the maximum observed water level.

Next, the maximum SLOSH storm tide levels were used to initialize the water levels in SWAN, which was run with the ARA storm track and the ARA wind field model. The resulting time histories of significant wave height (meters) are shown in Figure 13.20 and Figure 13.21. The maximum modeled significant wave heights at SSS-TX-GAL-002 are approximately twice those at SSS-TX-GAL-001.

The maximum modeled significant wave height in each cell of the Galveston Bay SLOSH Basin is shown in Figure 13.22. Note that the modeled wave heights are generally lowest in the cells along the Gulf Coast of the peninsula where the ground elevations in the SLOSH basin model are generally highest (see Figure 13.23). The increase in modeled wave heights in the second and third rows of cells from the coast is apparently due to the decrease in ground elevation and corresponding increase in still water depth.

The modeled wave heights in Figure 13.20 and Figure 13.21 are clearly not in agreement with the rapid dissipation in wave height observed in Figure 13.18 and Figure 13.19. This disagreement is most likely due to the coarseness of the analysis grid. The relatively rapid changes in ground elevation and the significant increase in wave dissipation effects over land cannot be accurately modeled in SWAN with a coarse grid.

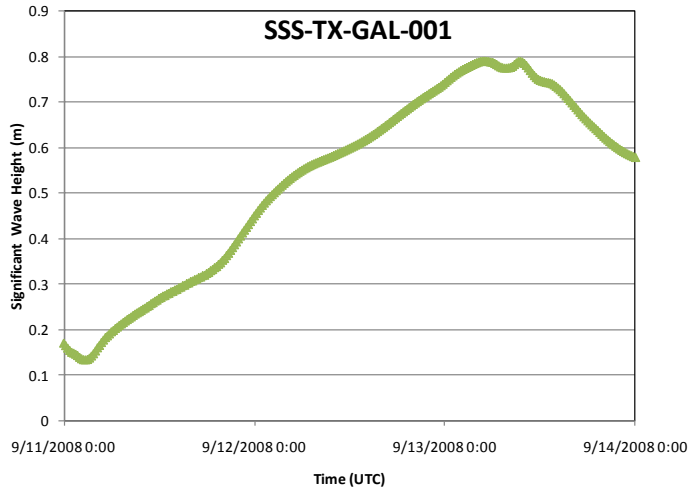

Figure 13.20. Time History of Modeled Wave Height Obtained Using SWAN at SSS-TX-GAL-001 (Note: Maximum Surge is added during the simulation).

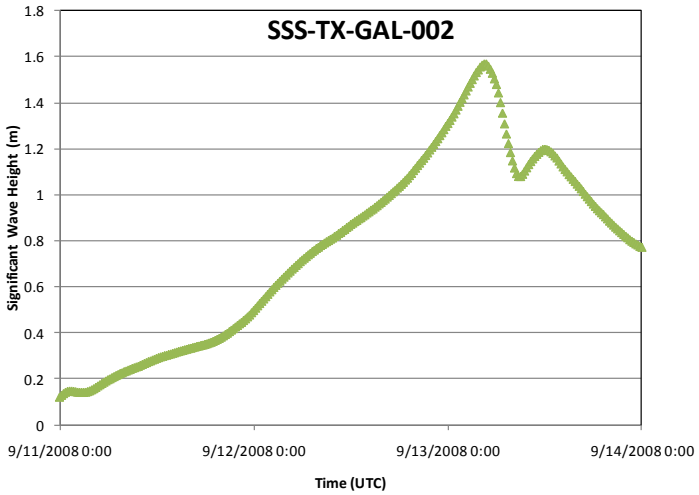

Figure 13.21. Time History of Modeled Wave Height Obtained at SSS-TX-GAL-002 Using SWAN with the Water Elevations Initialized to the Maximum Storm Tide Levels from SLOSH.

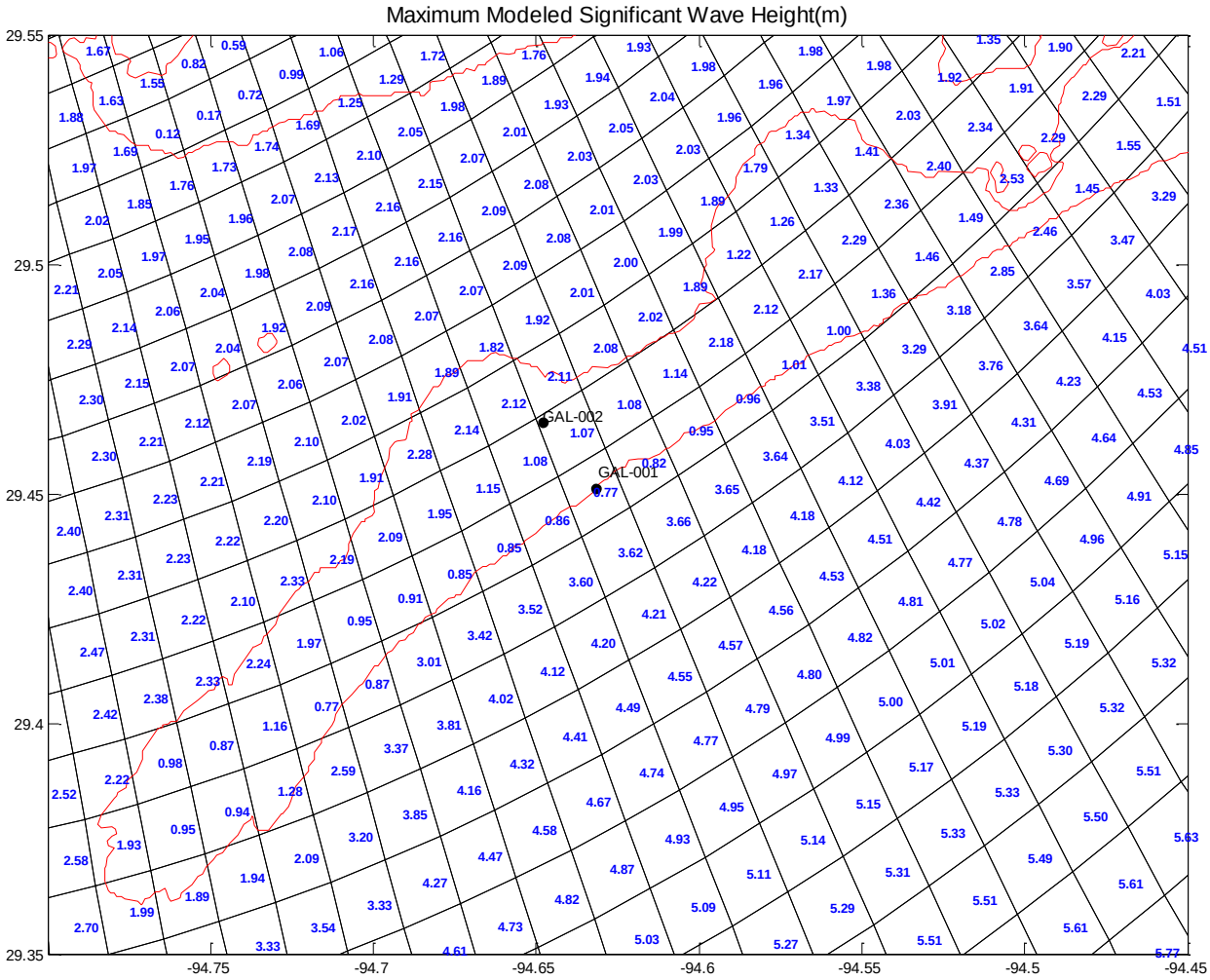

Figure 13.22. Maximum Modeled Significant Wave Heights in meters for Hurricane Ike on the Bolivar Peninsula Obtained Using SWAN with the Water Elevations Initialized to the Maximum Storm Tide Levels from SLOSH.

To deal with this limitation, the methodology implemented in HAZUS will be to model waves over land using the simplified, WHAFIS-like transect analysis methodology documented in the HAZUS-MH Flood Model Technical Manual (FEMA 2009b). The starting wave height used in the transect analysis will be the modeled significant wave height from the first completely offshore cell in the analysis grid (i.e., 3.62 m for the case shown in Figure 13.22).

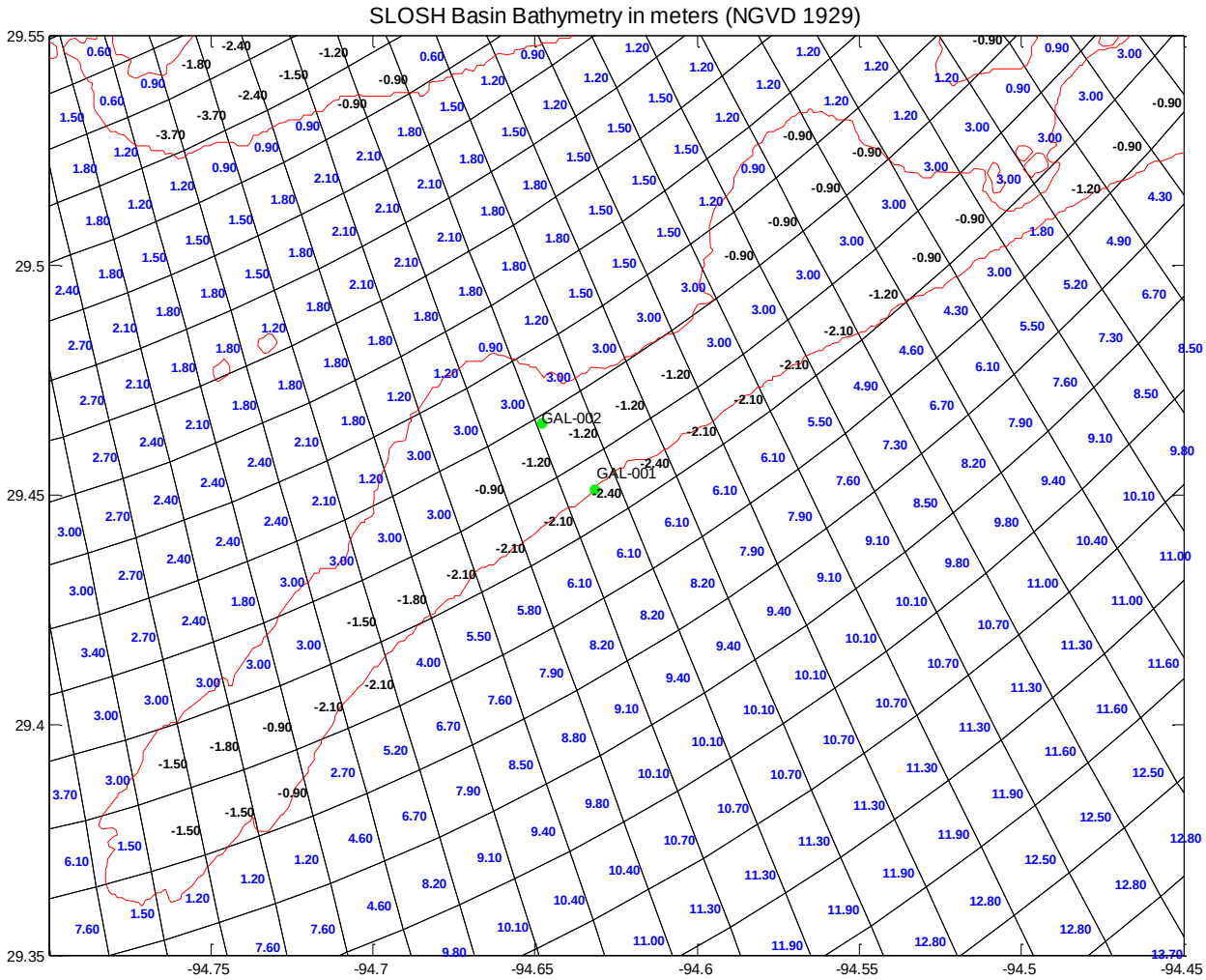

Figure 13.23. Galveston Bay SLOSH Basin Bathymetry in meters (NGVD 1929) – Positive values (blue) indicate water and negative values (black) indicate land. Positive values of 3.00 along the Bolivar Peninsula represent the Intracoastal Waterway. This figure represents an area approximately 20 statute miles in the east-west direction by approximately 13.5 statute miles in the north-south direction. In this portion of the basin, the typical cell is approximately 1 mile by 1 mile.

For the initial implementation of the overland wave model, both wave dissipation and wave regeneration effects will be neglected. No allowance is made for modeling the effects of surface roughness, vegetation, or obstructions on wave height in the current HAZUS transect analysis methodology. Developing a robust dissipation procedure would difficult given the minimal information required of Flood Model users, and given the detail that would be required to accurately capture dissipation over upland areas. Wave regeneration, on the other hand, is modeled in the current HAZUS transect analysis methodology and could be included in the coastal surge methodology. However, it is not recommended that wave regeneration be turned on in the absence of a robust wave dissipation model.

Figure 13.24 shows the modeled controlling wave heights produced by the HAZUS depth-limited wave height analysis methodology along a transect extending inland from the coastline to the location of SSS-TX-GAL-002. Results are shown with wave regeneration turn on (blue) and off (red). The results without wave regeneration are in reasonable agreement with the actual wave heights observed at SSS-TX-GAL-001 and SSS-TX-GAL-002.

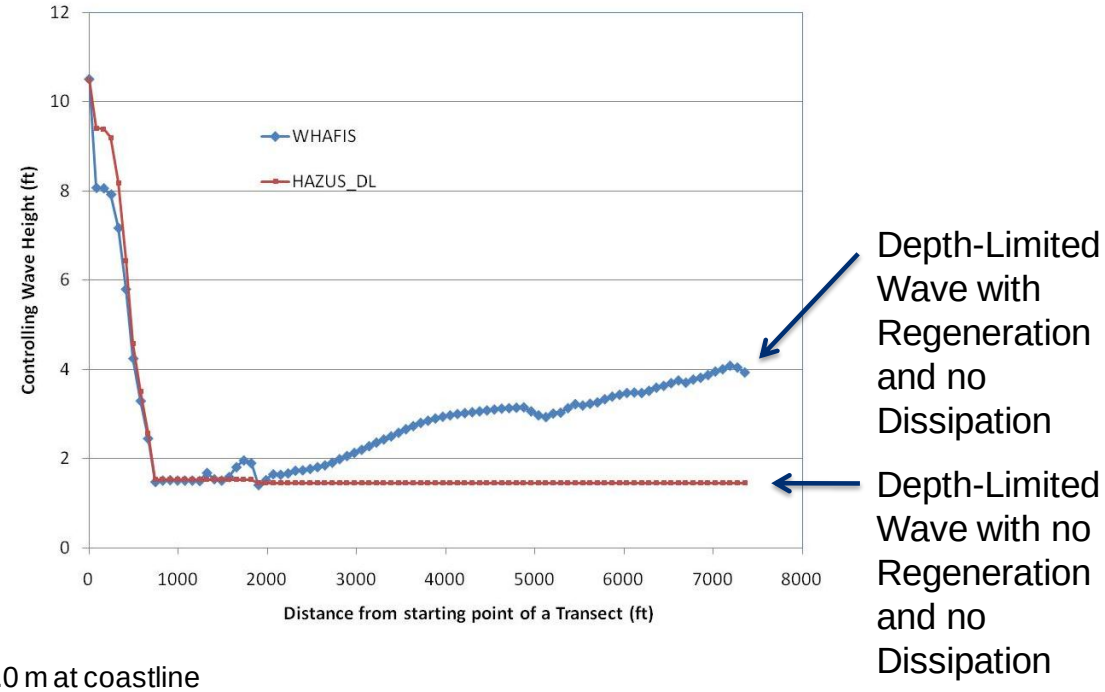

-Hsig=2.0 m at coastline
-SWEL=12.0 ft (assumed to be 100-year RP)
-All of the results from HAZUS except first point are "instantaneous" depth limited waves

Figure 13.24. Modeled Controlling Wave Heights Produced by the HAZUS Methodology for a Transect Extending Inland from the Coastline to the Location of SSS-TX-GAL-002.

13.2.4 Coupling of SLOSH and SWAN

A two-way coupling between the storm tide model and the nearshore wave model has been implemented for the HAZUS coastal surge methodology. The process is illustrated in Figure 13.25 and Figure 13.26. For a given hurricane event, the storm surge analysis is run for a fixed period of simulation time (e.g., 15 minutes) and then suspended. The new water levels from SLOSH are then passed to SWAN, and the wave model is advanced for the same fixed period of simulation time. The nearshore breaking wave stresses from SWAN are then passed back to SLOSH for the next time increment, and the simulation continues until the hurricane passes through and beyond the study region.

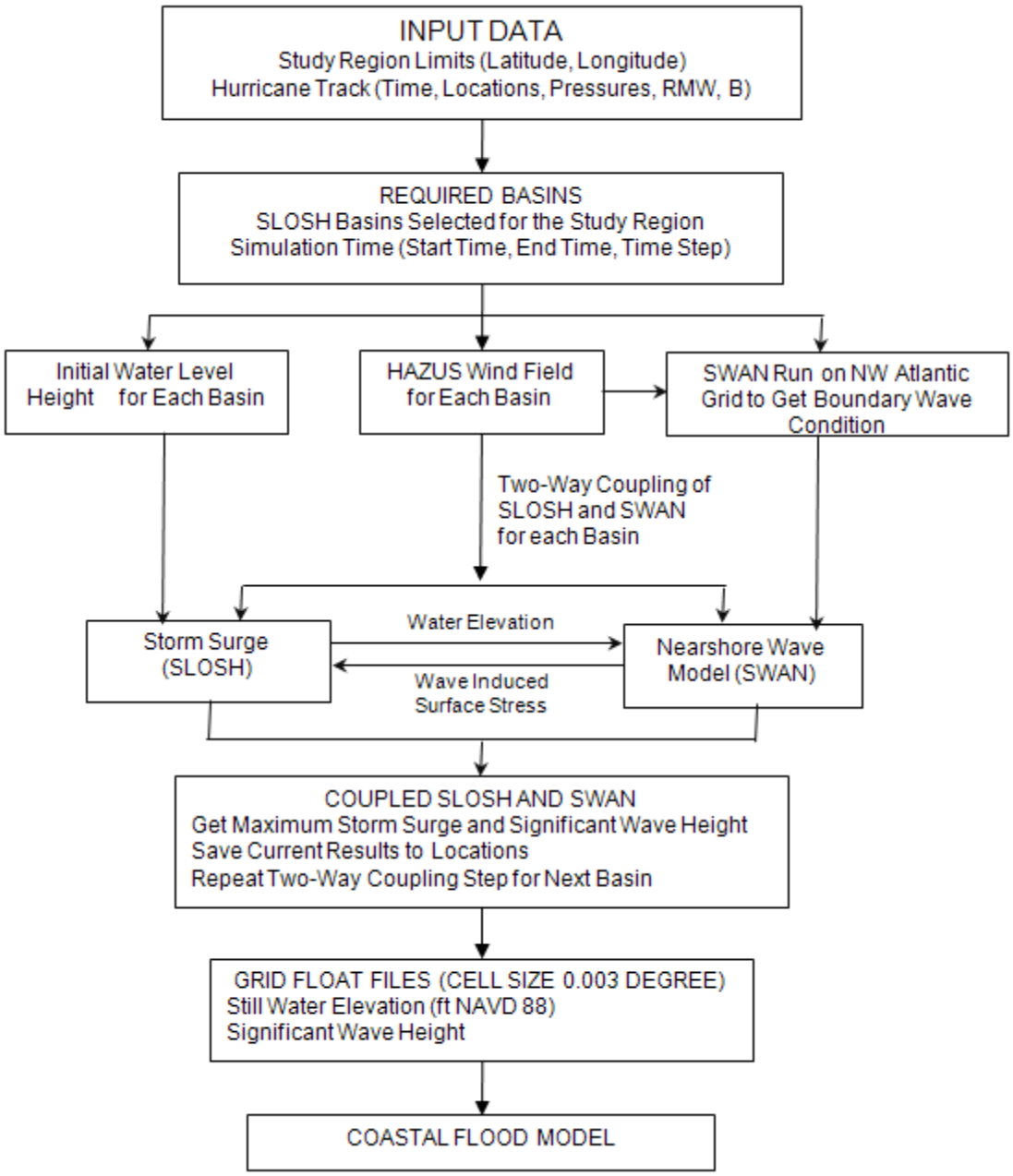

Figure 13.25. HAZUS Coast Storm Surge and Wave Model Flow Chart

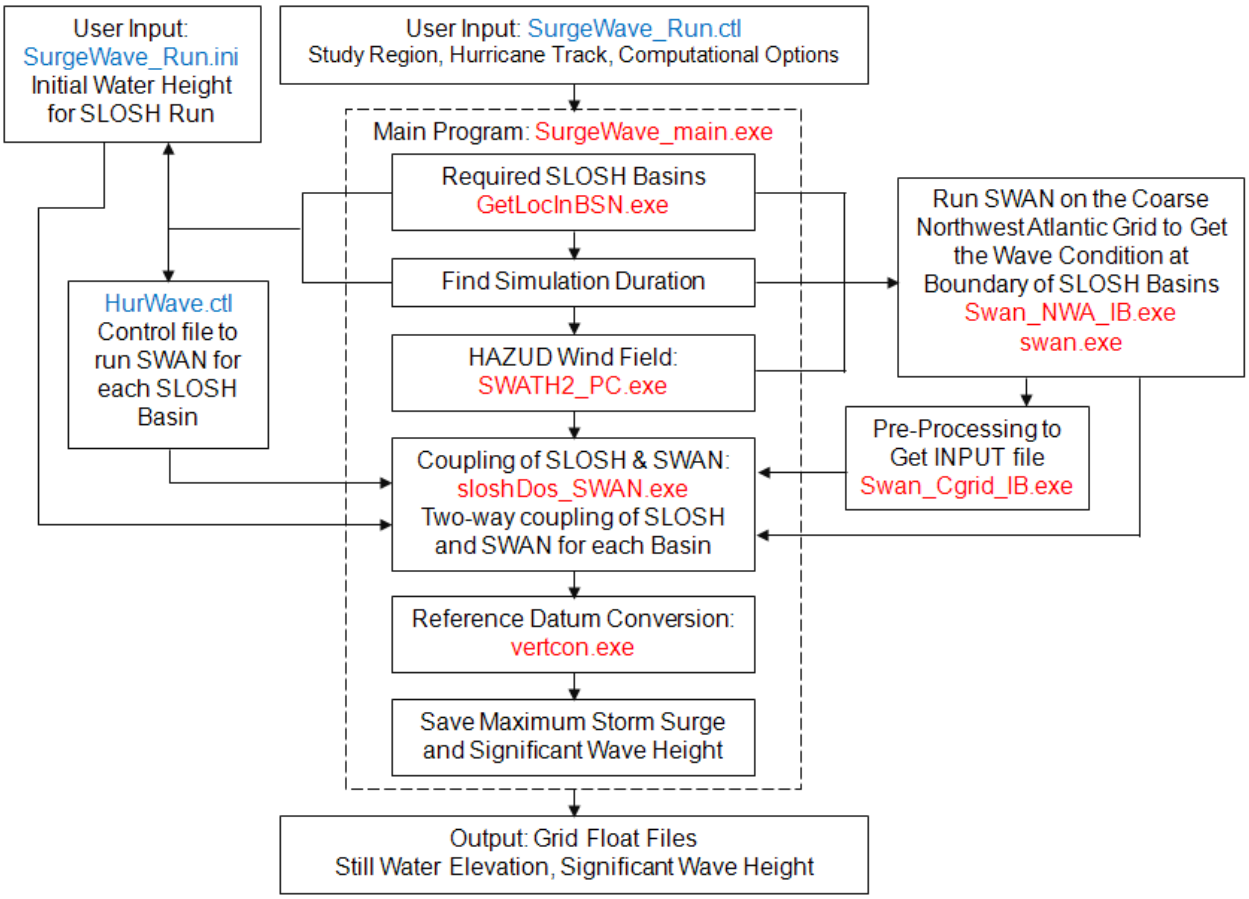

Figure 13.26. HAZUS Coast Storm Surge and Wave Model Software Components

The effect of the two-way coupling on the modeled storm surge elevation is illustrated for Hurricane Ike in Figure 13.27. In these plots, the increase in the peak modeled storm surge elevations due to the inclusion of wave stresses is shown for the Galveston Bay SLOSH Basin. For the flooded cells, the mean increase in surge elevation is 0.44 feet.

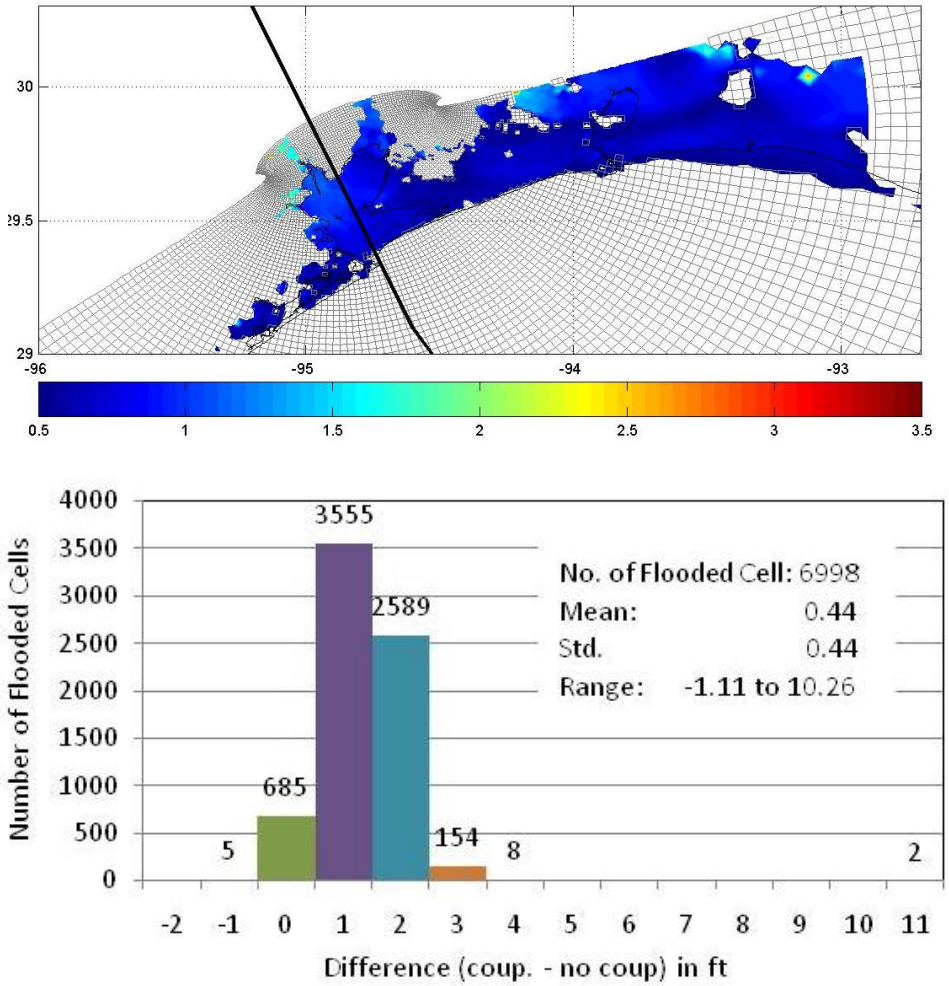

Figure 13.27. Difference (feet) in Peak Modeled Storm Tide with and without Coupling of Surge and Wave Models for Hurricane Ike.

13.2.5 Coastal Surge Analysis for Study Regions Spanning Multiple SLOSH Basins

At present, there are 32 SLOSH basins along U.S. Atlantic and Gulf of Mexico coastlines, as shown in Figure 13.28 and listed in geographical order in Table 13.5. Eleven basins were updated by NOAA in 2009 to incorporate the latest topography and bathymetric data and to provide higher grid size resolution and better representation of basin features. The updated basins also use the newer North American Vertical Datum of 1988 (NAVD 88) instead of the older National Geodetic Vertical Datum of 1929 (NGVD29) for their vertical datum. Given user-provided locations, priority for basin selection is governed by the grid resolution and the computer run time. Model run times depend on simulated storm duration, basin size, and the number of basins. For a given study region one can expect a significant increase in the run time if the number of selected basins increases.

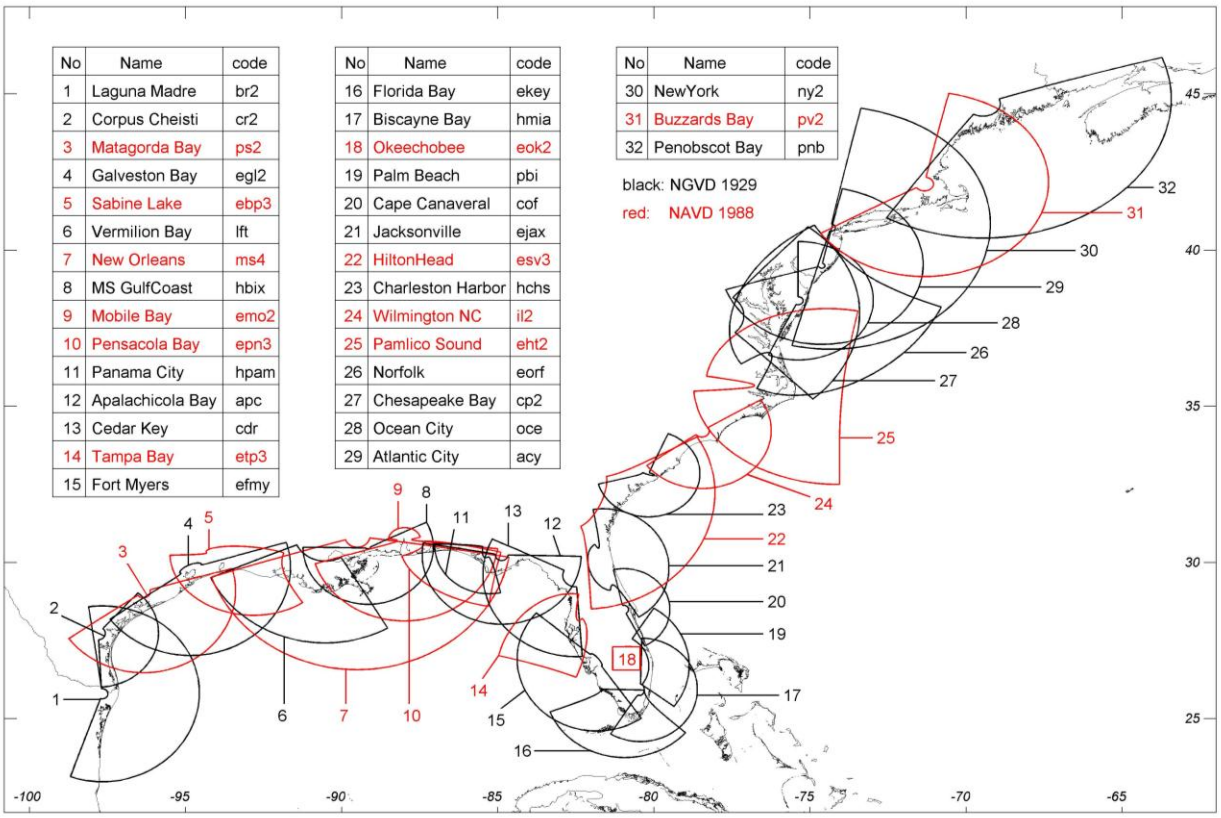

Figure 13.28. SLOSH Basins.

The following criteria are used to determine which basins will be used for a user-provided study region: (1) where multiple basins overlapped for a given location, the one with finer grid size resolution, usually the one with minimum distance from the basin origin to the location, will be used; (2) all of the 2009 updated SLOSH basins will be used to take advantage of the better representation of local features; and (3) exclude redundant basins to reduce the model run time. Following these criteria, three basins were removed: Vermilion-Bay Basin, MS-Gulf Coast Basin, and Norfolk Basin. The first two basins are overlapped by the neighboring basin of New-Orleans, and the last one is overlapped by its adjacent basins: Chesapeake Bay Basin and Pamlico Sound Basin.

The advantage of this basin selection approach is that it offers good grid resolution in areas of greatest interest while conserving computer resources by minimizing the number of basins required to simulate the storm surge and wave levels in a study region. Figure 13.29 shows an example of the polygons selected to delineate the boundaries between overlapping SLOSH basins. Each dotted polygon boundary is paired with the solid SLOSH basin of the same color. Thus, the number of basins needed to analyze a study region is simply the number of distinct polygons intersected by the study region.

Table 13.5. SLOSH Basins Used in HAZUS Coastal Surge Methodology

IDBSN	bsnname	bsncode	imxb	jmxb	Datum	Used
1	Laguna-Madre	br2	85	108	NGVD1929	✓
2	Corpus-Cheisti	cr2	67	75	NGVD1929	✓
3	Matagorda-Bay	ps2	192	211	NAVD1988	✓
4	Galveston-Bay	egl2	115	100	NGVD1929	✓
5	Sabine-Lake	ebp3	224	350	NAVD1988	✓
6	Vermilion-Bay	lft	128	156	NGVD1929	
7	New-Orleans	ms4	175	189	NAVD1988	✓
8	MS-GulfCoast	hbix	120	120	NGVD1929	
9	Mobile-Bay	emo2	229	135	NAVD1988	✓
10	Pensacola-Bay	epn3	200	330	NAVD1988	✓
11	Panama-City	hpam	105	118	NGVD1929	✓
12	Apalachicola-Bay	apc	71	93	NGVD1929	✓
13	Cedar-Key	cdr	79	85	NGVD1929	✓
14	Tampa-Bay	etp3	188	215	NAVD1988	✓
15	Fort-Myers	efmy	111	100	NGVD1929	✓
16	Florida-Bay	ekey	170	200	NGVD1929	✓
17	Biscayne-Bay	hmia	125	190	NGVD1929	✓
18	Okeechobee	eok2	129	136	NAVD1988	✓
19	Palm-Beach	pbi	71	153	NGVD1929	✓
20	Cape-Canaveral	cof	69	89	NGVD1929	✓
21	Jacksonville	ejax	84	96	NGVD1929	✓
22	HiltonHead	esv3	152	200	NAVD1988	✓
23	Charleston-Harbor	hchs	95	150	NGVD1929	✓
24	Wilmington-NC	il2	171	236	NAVD1988	✓
25	Pamlico-Sound	eht2	180	130	NAVD1988	✓
26	Norfolk	eorf	100	110	NGVD1929	
27	Chesapeake-Bay	cp2	79	84	NGVD1929	✓
28	Ocean-City	oce	75	99	NGVD1929	
29	Atlantic-City	acy	87	106	NGVD1929	✓
30	NewYork	ny2	90	83	NGVD1929	✓
31	Buzzards-Bay	pv2	183	280	NAVD1988	✓
32	Penobscot-Bay	pnb	108	115	NGVD1929	✓

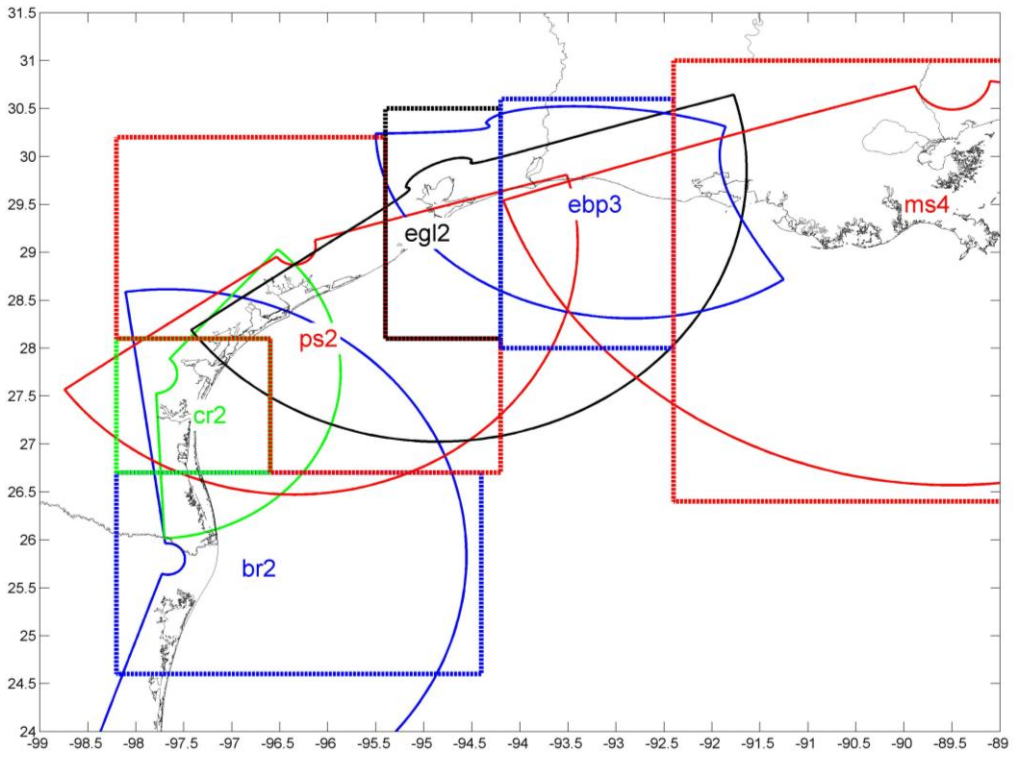

Figure 13.29. Basin Selection Regions for Texas and Louisiana.

13.2.6 Integration with Coastal Flood Model

Given a known building type (i.e., specific occupancy, foundation type, and building height grouping) at a known location, two inputs are required by the HAZUS Coastal Flood Model to estimate the extent of coastal flooding damage as a percentage of building or contents replacement value: (1) the controlling wave height at the location, and (2) the total water depth at the location (i.e., still water depth plus controlling wave height above the still water surface). The former input is used to determine the flood hazard zone (V-zone or A-zone) and, hence, the depth-damage function, while the latter input (along with the foundation type) is used to determine where to enter into the depth-damage function.

The steps for computing combined wind and flood losses are outlined below. All steps are required unless otherwise noted.

HAZUS Shell:

1. Create a coastal study region with both Hurricane and Flood hazards enabled
2. Open the study region in the Hurricane Model

HAZUS Hurricane Model:

1. Create a user-defined hurricane storm track using one of the following existing user-defined scenario options in the hurricane scenario wizard:
    a. Select a storm from the list of historic events
    b. Define storm track manually
    c. Import from exported file
    d. Import HurrEvac storm advisory
2. OPTIONAL: modify the building inventory and/or analysis parameters
    a. General Building Stock (GBS) modifications must be made at the block level to ensure compatibility between the Hurricane Model and the Flood Model.
3. Set the following analysis options
    a. Enable storm surge model
    b. OPTIONAL: Enable deep water wave model and near shore wave model with 2-way coupling
    c. OPTIONAL: Enable just the near shore wave model with 2-way coupling
4. Start the analysis
5. OPTIONAL: If deep water waves were selected in Step 3b, run SWAN on the coarse northwest Atlantic grid (~20 km cell size)
    a. Can be skipped if available time is limited
    b. Provides the wave conditions at boundary of SLOSH basin
    c. SWAN wave model is driven with HAZUS wind field model
6. Run SLOSH and SWAN codes
    a. OPTIONS:
        i. Wave model (SWAN) can be turned off if available time is limited
        ii. When the wave model is turned on, there will be two-way coupling (higher waves due to increased still water elevation from surge and higher surge due to radiation stresses from wave setup)
    b. Both models are driven with HAZUS wind field model
    c. SLOSH provides still water elevations throughout basin
        i. User can input an initial water level to approximate effect of astronomical tide at the time of hurricane landfall
        ii. Save still water elevations (feet) to a grid float file (cell size = 0.003 degrees)
    d. SWAN provides significant wave height and dominant wave periods throughout the flooded areas of the basin, but only the wave conditions near the shoreline are used in the Flood Model
        i. Save significant wave heights (feet) to a grid float file (cell size = 0.003 degrees)

7. Repeat step #6 for each required SLOSH basin
    a. The number of required basins is determined by the extent of the study region
8. Compute wind-only losses using existing methodology
9. Set flags in database to indicate:
    a. Wind results are current
    b. SLOSH results are current
    c. OPTIONAL: SWAN results are current
10. Launch the Coastal Flood Model

HAZUS Flood Model:

1. Compute the stillwater depth, d_s, in each flooded cell of the DEM:
    a. d_s = SWEL - Ground Elevation
        i. SWEL is from SLOSH (feet NAVD 88 or NGVD 29 depending on the basin)
        ii. Ground elevation is from Flood Model DEM
2. Create transects using existing methodology
3. Where each transect intersects the coastline, compute the following:
    a. Controlling wave height: $H_c = \min(0.78\ d_s, 1.6\ H_s)$ where H_s comes from the wave model
        i. NOTE: The 0.78 factor in the equation above represents the maximum depth-limited value. A more accurate wave height can be calculated if wave period is also considered – see existing WHAFIS code for wave breaking. This is where we could use the wave period information from SWAN as a future improvement.
    b. Wave crest elevation = SWEL + $0.7\ H_c$
4. Propagate the wave inland from shoreline along transects using existing methodology (simplified WHAFIS)
    a. At present, the Flood Model will ignore wave regeneration and wave dissipation.
    b. The Flood Model will not use shoreline characterization to perform wave run-up or dune erosion calculations. These will be ignored.
5. Interpolate between transects to develop the flood depth grid
6. Determine wave zone based on H_c:
    a. If $H_c \geq 1.5$ feet, then use the V-zone damage functions
    b. If $H_c < 1.5$ feet, then use the A-zone damage functions
7. For each unique combination of building type (i.e., specific occupancy, foundation type, and building height grouping) and total depth of flooding, determine the structure and contents losses by entering the appropriate depth-damage curve at the wave crest elevation minus the appropriate first floor reference elevation

8. Area weight the flood-only building and contents losses by Census block, specific occupancy, foundation type, and building height group using the existing Coastal Flood Model methodology
9. Compute the combined wind and flood losses for buildings and contents by Census block and specific building type using the combined wind and flood loss matrices.

The methodology for implementing the final step (i.e., combined wind and flood losses) is the subject of the next section.

13.3 Combined Wind and Flood Losses for Coastal Storm Surge

This section describes the methodology for combining wind and flood losses to buildings in HAZUS-MH due to hurricane storm surge and waves. The objective of the combined loss methodology is to estimate the total losses sustained by the general building stock within a region due to the winds and coastal storm surge generated by a single, user-specified hurricane scenario.

The combined wind and flood loss methodology builds upon the existing HAZUS-MH wind loss and coastal flooding loss methodologies without altering either the "wind-only" or "flood-only" loss estimates. Modifications to the existing wind-only or flood-only loss estimates are beyond to scope of this task.

The primary motivation for the combined wind and flood loss methodology is to avoid "double counting" of damage. At a minimum, the combined wind and flood loss must be at least the larger of the wind-only or the flood-only loss. At a maximum, the combined loss must be no larger than the lesser of the sum of the wind-only and flood-only losses or 100% of the building (or contents) replacement value. These constraints can be written as:

$$\max(W, F) \leq C \leq \min(W+F, 1.00) \qquad (13.1)$$

where W is the modeled wind-only building (or contents) loss ratio expressed as a fraction of the building (or contents) replacement value, F is the modeled flood-only building (or contents) loss ratio, and C is the combined wind and flood loss ratio.

As an example, consider a scenario in which the wind-only loss estimate for a single family wood frame house is 70% of the building replacement value and the flood-only loss estimate is 50%. In this situation, the lower and upper bounds on the combined wind and flood loss would be 70% and 100%, respectively, of the building replacement value.

If, as special case, we assume that the wind-induced damage and flood-induced damage are spread uniformly and randomly over a building. In this idealized case, the two damage mechanisms can be treated as independent, and the expected combined loss ratio is simply

$$C = W + F - W*F \qquad (13.2)$$

An idealized combined wind and flood loss matrix based on Equation 13.2 is shown in Figure 13.30. Note that the combined wind and flood loss estimate in each cell of the table is always less than or equal to the sum of the wind-only loss and flood-only loss shown in its column and row headings, respectively.

		Wind-Only Building Loss										
		0%	10%	20%	30%	40%	50%	60%	70%	80%	90%	100%
Flood-Only Building Loss	0%	0%	10%	20%	30%	40%	50%	60%	70%	80%	90%	100%
	10%	10%	19.0%	28.0%	37.0%	46.0%	55.0%	64.0%	73.0%	82.0%	91.0%	100%
	20%	20%	28.0%	36.0%	44.0%	52.0%	60.0%	68.0%	76.0%	84.0%	92.0%	100%
	30%	30%	37.0%	44.0%	51.0%	58.0%	65.0%	72.0%	79.0%	86.0%	93.0%	100%
	40%	40%	46.0%	52.0%	58.0%	64.0%	70.0%	76.0%	82.0%	88.0%	94.0%	100%
	50%	50%	55.0%	60.0%	65.0%	70.0%	75.0%	80.0%	85.0%	90.0%	95.0%	100%
	60%	60%	64.0%	68.0%	72.0%	76.0%	80.0%	84.0%	88.0%	92.0%	96.0%	100%
	70%	70%	73.0%	76.0%	79.0%	82.0%	85.0%	88.0%	91.0%	94.0%	97.0%	100%
	80%	80%	82.0%	84.0%	86.0%	88.0%	90.0%	92.0%	94.0%	96.0%	98.0%	100%
	90%	90%	91.0%	92.0%	93.0%	94.0%	95.0%	96.0%	97.0%	98.0%	99.0%	100%
	100%	100%	100%	100%	100%	100%	100%	100%	100%	100%	100%	100%

Figure 13.30. Combined Wind and Flood Loss Matrix for the Idealized Case of Wind and Flood Losses that are Uniformly and Randomly Distributed throughout the Building.

While the idealized combined wind and flood loss matrix shown in Figure 13.30 satisfies the constraints specified in Equation 13.1, it is nonetheless clear that neither wind nor storm surge damages are uniformly and randomly distributed throughout a structure. Wind damage is most frequently initiated at the roof and fenestrations (i.e., windows, doors, or other openings in the building envelope), whereas flood damage is most frequently initiated at the lowest elevations of the structure (e.g., basement or first finished floor) and progresses upward through the structure as the depth of flooding increases.

In the next subsection, we present an approach for incorporating the non-uniformity of wind and flood damage into the combined loss methodology. The approach is based on allocating wind and flood losses to building sub-assemblies as a function of the building type and the overall wind-only and flood-only loss estimate. The concept of building sub-assemblies is widely used in construction cost estimation and is already used in the HAZUS wind-only loss methodology. A recent U.S. Army Corps of Engineer New Orleans District study also provides guidance for allocating flood losses to building sub-assemblies.

We conclude this introduction by noting that no attempt is made in the methodology to allocate or apportion the combined loss into wind and flood loss components. While the apportioning of losses may be of great interest in situations where the financial stakeholders and/or indemnification terms for wind and flood losses differ, such situations require careful consideration of building construction details, hurricane hazard details (e.g., the magnitudes, timing, duration, and directionality of wind, surge, and

waves), and site details (e.g., aerodynamic roughness and hydrodynamic roughness) that are clearly beyond the scope of a regional loss estimation and hazard mitigation tool such as HAZUS-MH.

13.3.1 Building Sub-Assembly Approach

The existing HAZUS wind loss estimation methodology is a physically-based, damage-to-loss methodology that computes direct economic losses to buildings using a combination of explicit and implicit costing techniques. Detailed simulations of building envelope damage are used to explicitly estimate expected repair and replacement costs for the wind-damaged components of the building envelope, such as roof covering, roof sheathing, windows, doors, and wall covering. It also estimates expected losses to the building interior and contents through a combination of the roofing damage fraction and the volume of rain water penetrating through failed fenestrations (windows, doors, garage doors, etc.). The methodology is described in detail in Section 7 of the HAZUS Hurricane Technical Manual (FEMA 2009a).

A recent study for the New Orleans District of the U.S. Army Corps of Engineers (GEC 2006) provides estimates of overall building and contents losses due to flooding as a function of building type (e.g., one story house on slab foundation), type of flooding (e.g., short or long duration, freshwater or saltwater), and depth of flooding (i.e., flood level relative to first floor). The GEC study is similar to the HAZUS wind loss methodology in that it builds up the overall flood loss by summing the losses to building components, such as the structural frame, doors/trim, plumbing, cabinets, etc. For single family homes on slab foundations, the building flood loss estimates are built-up by estimating damage to a total of 20 different building components. The component loss estimates are based on interviews with homeowners and business operators and the collective judgment of nine experts in the fields of construction, repair and restoration, and insurance claims adjustment.

By grouping the wind loss components and flood loss components into a consistent set of building sub-assemblies, we can more accurately apply Equation 2 to each sub-assembly instead of applying it to the entire building. For this purpose, we define seven major building sub-assemblies:

1. Foundation: Includes site work, footings, and walls, slabs, piers or piles.
2. Below First Floor: Items other than the foundation that are located below the first floor of the structure such as mechanical equipment, stairways, parking pads, break away flood walls, etc.
3. Structure Framing: Includes all of the main load carrying structural members of the building below the roof framing and above the foundation.
4. Roof Covering: Includes the roof membrane material and flashing

5. Roof Framing: Includes trusses, rafters, and sheathing[1]
6. Exterior Walls: Includes wall covering, windows, exterior doors, and insulation
7. Interiors: Includes interior wall and floor framing, drywall, paint, interior trim, floor coverings, cabinets, counters, mechanical, and electrical

These groupings allow, for example, roof covering loss to contribute more, on average, to the overall wind-only loss than it would to same overall level of flood-only loss.

To illustrate the approach, we consider a one story, wood frame house on a slab foundation exposed to short duration coastal flooding. The default HAZUS Flood Model depth-damage curve for this specific occupancy in the Coastal A-zone is plotted in Figure 13.31. Using Table 11 from the GEC (2006) report, we can allocate the flood losses to five sub-assemblies. In this preliminary example, we choose to neglect the Below First Floor sub-assembly and merge the Structure Framing sub-assembly into the Exterior Walls sub-assembly for simplicity. The results are shown in Table 13.6.

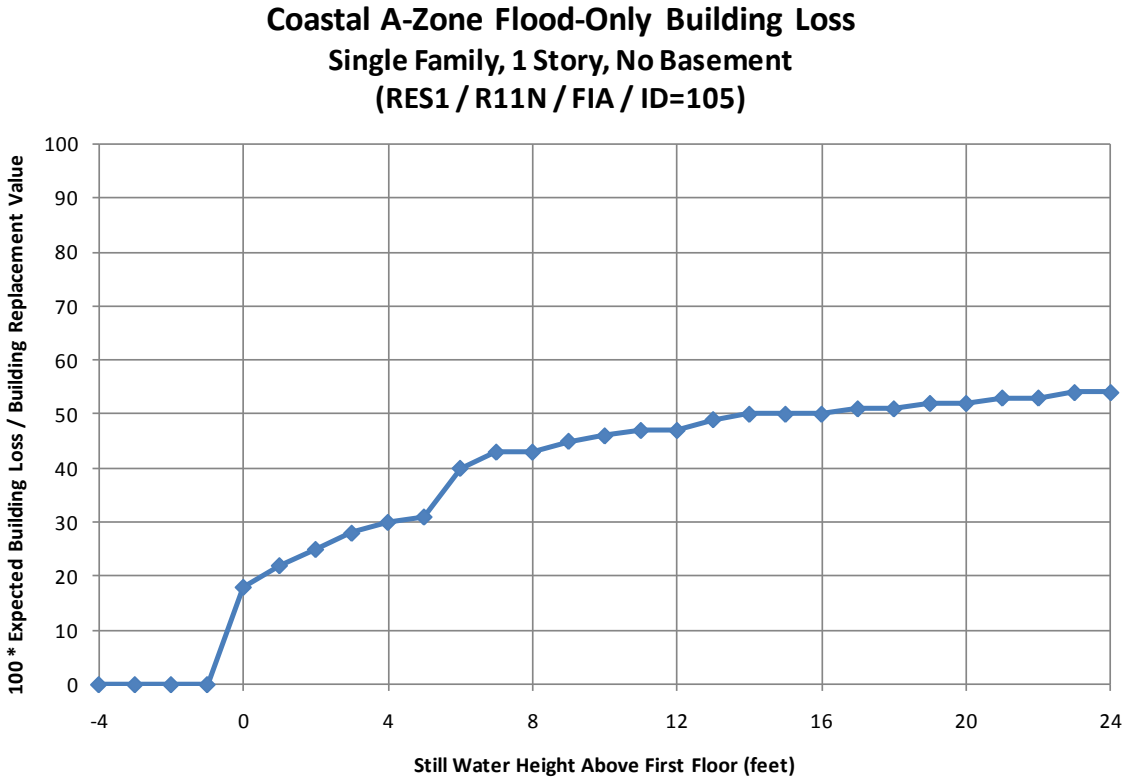

Figure 13.31. Default Depth-Damage Curve in HAZUS-MH for One Story, Single Family Houses on Slab Foundations in the Coastal A-Zone.

[1] For a one story, wood frame house on a slab foundation, the total framing cost is assumed to be distributed as 39% exterior wall framing, 26% interior wall framing, and 35% roof framing.

Using the depths associated with flood-only losses of 10%, 20%, …, 90% from Figure 13.31 and interpolating from Table 13.6, we can apportion the flood-only building loss to the five retained sub-assemblies. The results for the example house are shown in Table 13.7.

Table 13.6. Distribution of Flood Losses to Building Sub-Assemblies as a Function of Depth of Flooding for a One Story, Single Family House on Slab Foundation in a Coastal A-Zone Exposed to Short Duration Saltwater Flooding

Sub-Assembly	0.0	1.0	2.0	3.0	4.0	5.0	6.0	7.0	8.0	9.0	10.0	11.0	12.0	13.0	14.0	15.0
Foundation	0.0%	0.0%	0.0%	0.0%	0.0%	0.0%	0.0%	0.0%	0.0%	0.0%	0.0%	0.0%	0.0%	0.0%	0.0%	0.0%
Roof Covering	0.0%	0.0%	0.0%	0.0%	0.0%	0.0%	0.0%	0.0%	0.0%	0.5%	1.4%	1.6%	1.6%	2.4%	2.4%	2.4%
Roof Framing	0.0%	0.0%	0.0%	0.0%	0.0%	0.0%	0.0%	0.0%	0.0%	0.4%	0.4%	0.4%	0.4%	0.4%	0.4%	0.4%
Exterior Wall	10.0%	15.2%	18.9%	20.4%	22.5%	23.7%	24.0%	23.8%	23.6%	22.6%	22.6%	22.5%	22.5%	22.4%	22.4%	22.4%
Interiors	90.0%	84.8%	81.1%	79.6%	77.5%	76.3%	76.0%	76.2%	76.4%	76.6%	75.6%	75.5%	75.5%	74.9%	74.9%	74.9%
Total	100%	100%	100%	100%	100%	100%	100%	100%	100%	100%	100%	100%	100%	100%	100%	100%

Table 13.7. Distribution of Flood Losses to Building Sub-Assemblies as a Function of Flood-Only Building Loss for a One Story, Single Family House on Slab Foundation in a Coastal A-Zone Exposed to Short Duration Saltwater Flooding

Building Loss	Foundation	Roof Covering	Roof Framing	Exterior Walls	Interiors
10%	0.0%	0.0%	0.0%	1.0%	9.0%
20%	0.0%	0.0%	0.0%	2.5%	17.5%
30%	0.0%	0.0%	0.0%	6.7%	23.3%
40%	0.0%	0.0%	0.0%	9.6%	30.4%
50%	0.0%	1.2%	0.2%	11.2%	37.5%
60%	0.0%	1.4%	0.2%	13.4%	44.9%
70%	0.0%	1.7%	0.3%	15.7%	52.4%
80%	0.0%	1.9%	0.3%	17.9%	59.9%
90%	0.0%	2.1%	0.3%	20.1%	67.4%

The wind-only loss simulation results for the example house can likewise be distributed to the same five major sub-assemblies. The hurricane wind losses from each of 107,910 building damage simulations are grouped by overall wind-only building loss with the average contributions from each of the five major sub-assemblies. The results for the example house are shown in Table 13.8.[2]

By comparing Table 13.7 and Table 13.8, it can be seen that the roof covering and roof framing losses are bigger contributors to the wind-only losses than the flood-only losses, whereas the exterior wall and interior losses are bigger contributors the flood-only losses than the wind-only losses. This systematic difference in relative loss contributions suggests that the actual combined wind and flood losses should be higher than those shown previously in Figure 13.30.

[2] The results shown in Table 13.8 are for a one story, wood frame house located in suburban terrain with a gable roof, no garage, roof-to-wall straps, no opening protection, 8d roof deck nails at 6/12 spacing, and no secondary water resistance.

If we now apply Equation 2 to each sub-assembly with the losses expressed as a fraction of their respective sub-assembly replacement values, multiply the combined wind and flood loss for each sub-assembly by it total repair and replacement cost expressed as a fraction of the total building repair value, sum the sub-assembly losses, and apply the overall loss constraints of Equation 1, we obtain the results shown in Figure 13.32.

Table 13.8. Distribution of Wind Losses to Sub-Assemblies Relative to Building Value as a Function of Wind-Only Building Loss for a One Story, Single Family House Located in Suburban Terrain with a Gable Roof Shape and Medium Wind Resistance

Building Loss	Foundation	Roof Covering	Roof Framing	Exterior Walls	Interiors
10%	0.0%	4.3%	0.0%	0.8%	4.9%
20%	0.0%	4.7%	0.0%	1.5%	13.8%
30%	0.0%	4.7%	0.0%	2.3%	23.0%
40%	0.0%	4.8%	0.0%	2.9%	32.4%
50%	0.0%	4.8%	0.0%	3.0%	42.2%
60%	0.0%	4.9%	0.0%	3.8%	51.3%
70%	0.0%	4.9%	0.1%	4.9%	60.1%
80%	0.0%	5.2%	0.3%	14.3%	60.2%
90%	0.0%	5.2%	0.8%	23.8%	60.2%

		Wind-Only Building Loss										
		0%	10%	20%	30%	40%	50%	60%	70%	80%	90%	100%
Flood-Only Building Loss	0%	0%	10%	20%	30%	40%	50%	60%	70%	80%	90%	100%
	10%	10%	19.5%	28.7%	37.9%	47.1%	56.2%	65.3%	74.5%	84.4%	94.3%	100%
	20%	20%	29.1%	37.5%	45.9%	54.3%	62.5%	70.9%	79.4%	89.1%	98.9%	100%
	30%	30%	38.8%	46.7%	54.5%	62.3%	70.0%	77.8%	85.7%	95.0%	100.0%	100%
	40%	40%	48.4%	55.7%	62.8%	69.9%	76.9%	84.0%	91.2%	100.0%	100.0%	100%
	50%	50%	58.0%	64.6%	71.1%	77.5%	83.8%	90.3%	96.9%	100.0%	100.0%	100%
	60%	60%	67.6%	73.5%	79.3%	85.0%	90.6%	96.4%	100.0%	100.0%	100.0%	100%
	70%	70%	77.2%	82.4%	87.5%	92.5%	97.3%	100.0%	100.0%	100.0%	100.0%	100%
	80%	80%	86.8%	91.4%	95.7%	100.0%	100.0%	100.0%	100.0%	100.0%	100.0%	100%
	90%	90%	96.4%	100.0%	100.0%	100.0%	100.0%	100.0%	100.0%	100.0%	100.0%	100%
	100%	100%	100%	100%	100%	100%	100%	100%	100%	100%	100%	100%

Figure 13.32. Combined Wind and Flood Loss Matrix Assuming Wind and Flood Losses are each Uniformly Distributed within each of Five Building Sub-Assemblies

Upon reviewing the results, we see that the combined loss estimates in Figure 13.32 are indeed larger than the corresponding loss estimates in Figure 13.30, and that the 100% cap is reached in approximately 1/3 of the interior cells. We also note that the combined loss estimates in Figure 13.32 are slightly asymmetric. For example, when W=50% and F=20%, C=62.5%. On the other hand, when W=20% and F=50%, C=64.6%.

13.3.2 Development of Sub-Assembly Loss Tables

All three models in HAZUS-MH (i.e., Earthquake, Flood, and Hurricane) computes aggregate losses to the general building stock according to 33 specific occupancy (SOCC) classes and 5 general building types (GBT). The 33 SOCC classes are listed in

Table 13.9. The 5 GBT classes are Wood, Masonry, Steel, Concrete, and Manufactured Housing. To implement the combined loss methodology sub-assembly replacement values and sub-assembly loss tables are needed for each of the 33 SOCC and 5 GBT classes.

Table 13.9. HAZUS-MH Specific Occupancy Classes

Class	Description
RES1	Single Family Dwelling
RES2	Manufactured Hosuing
RES3A	Duplex
RES3B	Triplex/Quads
RES3C	Multi-dwellings (5 to 9 units)
RES3D	Multi-dwellings (10 to 19 units)
RES3E	Multi-dwellings (20 to 49 units)
RES3F	Multi-dwellings (50+ units)
RES4	Temporary Lodging
RES5	Institutional Dormitory
RES6	Nursing Home
COM1	Retail Trade
COM2	Wholesale Trade
COM3	Personal and Repair Services
COM4	Professional/ Technical Services
COM5	Banks
COM6	Hospital
COM7	Medical Office/Clinic
COM8	Entertainment & Recreation
COM9	Theaters
COM10	Parking
IND1	Heaving Industry
IND2	Light Industry
IND3	Food/Drug/Chemicals
IND4	Metals/Minerals Processing
IND5	High Technology
IND6	Construction
AGR1	Agriculture
REL1	Churches and Other non-profit Org.
GOV1	Genral Services
GOV2	Emergency Response
EDU1	Grade Schools
EDU2	Colleges Univeristies

The sub-assembly replacement values (as a percentage of total building replacement value) were developed using RS Means (2009) data for typical model buildings representing each SOCC. The GBT sub-assembly replacement values were then

estimated using a HAZUS SOCC-GBT mapping scheme for the southeastern United States. Replacement values are summarized in Table 13.10 for two cases: Pre-FIRM construction and Post-FIRM construction. As a rough rule, the foundation sub-assembly costs were typically assumed to increase by 5% when going from Pre-FIRM to Post-FIRM construction. To compensate for the increase in foundation cost, the Interiors were typically assumed to decrease by 3% and the structure frame and exterior walls sub-assemblies were each typically assumed to decrease by 1%.

Table 13.10. Sub-Assembly Replacement Values by Specific Occupancy or General Building Type as a Percentage of Total Building Replacement Value

Specific Occupancy or General Building Type		Pre-FIRM								Post-FIRM							
		Found-ation	Below First Floor	Structure Frame	Roof Covering	Roof Framing	Exterior Wall	Interiors	Total	Found-ation	Below First Floor	Structure Frame	Roof Covering	Roof Framing	Exterior Wall	Interiors	Total
RES1	Single	6%	2%	13%	5%	5%	20%	49%	100%	11%	3%	10%	5%	5%	19%	47%	100%
RES2	MH	6%	2%	10%	3%	5%	20%	54%	100%	8%	2%	10%	3%	5%	20%	52%	100%
RES3A	Duplex	6%	2%	13%	5%	5%	20%	49%	100%	11%	3%	10%	5%	5%	19%	47%	100%
RES3B	3-4 units	6%	2%	13%	5%	5%	20%	49%	100%	11%	3%	10%	5%	5%	19%	47%	100%
RES3C	5-9 units	5%	1%	10%	2%	3%	10%	69%	100%	10%	1%	9%	2%	3%	9%	66%	100%
RES3D	10-19 units	5%	1%	10%	2%	3%	10%	69%	100%	10%	1%	9%	2%	3%	9%	66%	100%
RES3E	20-49 units	5%	1%	13%	1%	3%	10%	67%	100%	10%	1%	12%	1%	3%	10%	63%	100%
RES3F	50+ units	3%	0%	13%	1%	1%	13%	69%	100%	8%	0%	12%	1%	1%	12%	66%	100%
RES4	Temp. Lodging	3%	1%	9%	1%	2%	10%	74%	100%	8%	1%	8%	1%	2%	9%	71%	100%
RES5	Instutional Dormitory	4%	0%	14%	1%	3%	14%	64%	100%	9%	0%	13%	1%	3%	13%	61%	100%
RES6	Nursing Home	5%	0%	10%	3%	2%	13%	67%	100%	10%	1%	9%	3%	2%	12%	63%	100%
COM1	Retail	6%	1%	10%	5%	5%	10%	63%	100%	11%	1%	9%	5%	5%	9%	60%	100%
COM2	Wholesale	20%	1%	7%	9%	7%	11%	45%	100%	25%	1%	6%	9%	7%	10%	42%	100%
COM3	Personal & repair services	10%	1%	8%	7%	3%	10%	61%	100%	15%	1%	7%	7%	3%	9%	58%	100%
COM4	Professional / Business	4%	1%	11%	1%	3%	17%	63%	100%	9%	1%	10%	1%	3%	16%	60%	100%
COM5	banks	6%	0%	10%	4%	9%	8%	63%	100%	11%	0%	9%	4%	9%	7%	60%	100%
COM6	Hospital	2%	0%	7%	1%	4%	7%	79%	100%	7%	0%	6%	1%	4%	6%	76%	100%
COM7	MedicalOffice	5%	1%	5%	3%	2%	12%	72%	100%	10%	1%	4%	3%	2%	11%	69%	100%
COM8	Entertainment	9%	1%	10%	4%	3%	8%	65%	100%	14%	1%	9%	4%	3%	7%	62%	100%
COM9	Theaters	6%	1%	10%	5%	6%	10%	62%	100%	11%	1%	9%	5%	6%	9%	59%	100%
COM10	Parking	12%	0%	40%	0%	10%	9%	29%	100%	17%	0%	39%	0%	10%	8%	26%	100%
IND1	Heavy	14%	1%	3%	7%	3%	10%	62%	100%	19%	1%	2%	7%	3%	9%	59%	100%
IND2	Light	15%	1%	4%	9%	7%	11%	53%	100%	20%	1%	3%	9%	7%	10%	50%	100%
IND3	Food / Chemical	11%	1%	4%	8%	6%	11%	59%	100%	16%	1%	3%	8%	6%	10%	56%	100%
IND4	Metals/Mineral Processing	7%	0%	25%	2%	6%	8%	52%	100%	12%	0%	24%	2%	6%	7%	49%	100%
IND5	High Technology	11%	0%	5%	4%	4%	4%	72%	100%	16%	0%	4%	4%	4%	3%	69%	100%
IND6	Construction	20%	1%	7%	9%	7%	11%	45%	100%	25%	1%	6%	9%	7%	10%	42%	100%
AGR1	Agriculture	26%	0%	8%	9%	9%	12%	36%	100%	31%	0%	7%	9%	9%	11%	33%	100%
REL1	Church	10%	1%	12%	4%	17%	10%	46%	100%	15%	1%	11%	4%	17%	9%	43%	100%
GOV1	General Services	10%	1%	12%	6%	4%	8%	59%	100%	15%	1%	11%	6%	4%	7%	56%	100%
GOV2	Emergency Response	6%	0%	15%	2%	2%	12%	63%	100%	11%	0%	14%	2%	2%	11%	60%	100%
EDU1	School	4%	1%	12%	3%	6%	10%	64%	100%	9%	1%	11%	3%	6%	9%	61%	100%
EDU2	College	4%	1%	10%	2%	3%	8%	72%	100%	9%	1%	9%	2%	3%	7%	69%	100%
Wood		6%	1%	13%	4%	4%	16%	56%	100%	11%	1%	12%	4%	4%	15%	53%	100%
Steel		4%	0%	12%	1%	2%	15%	66%	100%	9%	0%	11%	1%	2%	14%	63%	100%
Masonry		7%	1%	14%	3%	3%	18%	54%	100%	12%	1%	13%	3%	3%	17%	51%	100%
Concrete		4%	0%	12%	1%	2%	15%	66%	100%	11%	0%	11%	3%	2%	11%	62%	100%
MH		6%	2%	10%	3%	5%	20%	54%	100%	8%	2%	10%	3%	5%	20%	52%	100%

13.3.2.1 Development of Sub-Assembly Loss Tables for Wind Losses

To implement the combined loss methodology, wind-induced sub-assembly losses as a function of overall building loss are required at increments of 10% overall wind loss for the 5 HAZUS General Building Types (wood, concrete, masonry, steel and mobile home) and the 33 HAZUS Specific Occupancies (RES1, RES2, …). In the HAZUS Hurricane Model the 5 GBTs and 33 SOCCs are each represented by a weighted combination of the 39 Specific Building Types (SBTs) shown in Table 13.11. Although the SBT weights vary by region in HAZUS, it was found that the resulting wind sub-assembly loss tables were relatively insensitive to these regional variations. It was also found that the wind sub-assembly loss tables were relatively insensitive to variations in terrain. The primary sensitivity of the wind sub-assembly loss tables is to the wind resistive features of the SBT, such as opening protection, roof shape, roof cover strength, roof deck strength, and roof-to-wall connection strength.

Since there are typically dozens or hundreds of building variations within each HAZUS Hurricane SBT category, a limited number of specific building configurations were chosen to represent the range of building strengths present within each SBT. To select the specific configurations, each possible building configuration was first classified as being weak, medium or strong. To do this, the building configurations within a given SBT were ranked from lowest to highest in terms of expected average annual loss (AAL) at one suburban location in Florida. Within each SBT, a specific building configuration was considered to be weak if it had an AAL that was greater than the 80^{th} percentile AAL for that SBT, and it was considered to be strong if it had an AAL that was less than the 20^{th} percentile AAL for that SBT. All other buildings were considered to be medium strength. Finally, the building configuration that had an AAL closest to the 10th percentile was used to represent the strong buildings, the building configuration closest to the 90th was used to represent the weak buildings, and the one closest to the 50th percentile was used to represent a medium strength building.

Programs FEMALOSS (used for single family homes and mobile homes) and FEMACOMLOSS (for all other buildings) were used to generate sub-assembly losses for the weak, medium and strong building configurations selected for each SBT. For each simulated event in a given loss file, the overall loss relative to the building value and the sub-assembly losses were recorded. Each overall loss was binned into a 10% interval. For example, if a record in a given loss file had an overall loss of 5.9%, it would be assigned to the 10% overall loss bin. The average of all records at each 10% increment was calculated. Since sub-assembly losses do not necessarily sum up to the overall loss of their corresponding bin, sub-assembly losses were adjusted by the ratio of their loss bin and sub-assembly value sum. Loss bins that had no data were filled by interpolation. The sub-assembly wind loss table for a given SBT is then generated by weighting the full set of building configurations within the SBT using the representative weak, medium or strong sub-assembly loss distributions.

Table 13.11. HAZUS-MH Specific Building Types

SBT	Description
WSF1	Wood, Single Family, One Story
WSF2	Wood, Single Family, Two or More Stories
WMUH1	Wood, Multi-Unit Housing, One Story
WMUH2	Wood, Multi-Unit Housing, Two Stories
WMUH3	Wood, Multi-Unit Housing, Three or More Stories
MSF1	Masonry, Single Family, One Story
MSF2	Masonry, Single Family, Two or More Stories
MMUH1	Masonry, Multi-Unit Housing, One Story
MMUH2	Masonry, Multi-Unit Housing, Two Stories
MMUH3	Masonry, Multi-Unit Housing, Three or More Stories
MLRM1	Masonry, Low-Rise Strip Mall, Up to 15 Feet
MLRM2	Masonry, Low-Rise Strip Mall, More than 15 Feet
MLRI	Masonry, Low-Rise Industrial/Warehouse/Factory Buildings
MERBL	Masonry, Engineered Residential Building, Low-Rise (1-2 Stories)
MERBM	Masonry, Engineered Residential Building, Mid-Rise (3-5 Stories)
MERBH	Masonry, Engineered Residential Building, High-Rise (6+ Stories)
MECBL	Masonry, Engineered Commercial Building, Low-Rise (1-2 Stories)
MECBM	Masonry, Engineered Commercial Building, Mid-Rise (3-5 Stories)
MECBH	Masonry, Engineered Commercial Building, High-Rise (6+ Stories)
CERBL	Concrete, Engineered Residential Building, Low-Rise (1-2 Stories)
CERBM	Concrete, Engineered Residential Building, Mid-Rise (3-5 Stories)
CERBH	Concrete, Engineered Residential Building, High-Rise (6+ Stories)
CECBL	Concrete, Engineered Commercial Building, Low-Rise (1-2 Stories)
CECBM	Concrete, Engineered Commercial Building, Mid-Rise (3-5 Stories)
CECBH	Concrete, Engineered Commercial Building, High-Rise (6+ Stories)
SPMBS	Steel, Pre-Engineered Metal Building, Small
SPMBM	Steel, Pre-Engineered Metal Building, Medium
SPMBL	Steel, Pre-Engineered Metal Building, Large
SERBL	Steel, Engineered Residential Building, Low-Rise (1-2 Stories)
SERBM	Steel, Engineered Residential Building, Mid-Rise (3-5 Stories)
SERBH	Steel, Engineered Residential Building, High-Rise (6+ Stories)
SECBL	Steel, Engineered Commercial Building, Low-Rise (1-2 Stories)
SECBM	Steel, Engineered Commercial Building, Mid-Rise (3-5 Stories)
SECBH	Steel, Engineered Commercial Building, High-Rise (6+ Stories)
MHPHUD	Manufactured Home, Pre-HUD
MH76HUD	Manufactured Home, 1976 HUD
MH94HUD-I	Manufactured Home, 1994 HUD - Wind Zone I
MH94HUD-II	Manufactured Home, 1994 HUD - Wind Zone II
MH94HUD-III	Manufactured Home, 1994 HUD - Wind Zone III

Of the seven sub-assemblies, foundation and below first floor sub-assemblies are assumed to be undamaged by wind. Consistent with the original methodology used to develop the HAZUS Hurricane Model loss functions, sub-assembly losses were capped to 125% of their replacement value. The additional 25% approximates the added costs associated with repair and reconstruction compared to new construction costs.

To correct any minor reversals due to insufficient simulations at certain loss levels, the sub-assembly losses were "forced" to increase with increasing overall loss. Since the sum of the sub-assembly losses at a given loss interval may now no longer sum to the loss interval, all the sub-assemblies at this loss interval were uniformly scaled to sum the target overall loss level (e.g., 70%). Since this adjustment could again induce minor non-monotonic behaviors, the process of forcing and adjusting was repeated until the following equation was satisfied:

$$|r - \sum_{c=1}^{7} B_c(r)| \leq 0.05\% \qquad (13.3)$$

Component losses were never allowed to go beyond 125% of the component's value. Thus far, the foundation and below first floor sub-assembly losses have been null. However, it might not be possible to satisfy Equation 7 at higher levels of loss (e.g., 90% or 100%) because the remaining five components may already have of achieved maximum loss. In this case, the foundation sub-assembly loss increased from zero until Equation 13.3 was satisfied. For example, if the sum of the sub-assembly losses at the 90% loss interval comes to 88%, the foundation sub-assembly will be assumed to experience a 2% loss. This scenario did not occur at the SBT level except at 100% overall loss. Table 13.12 shows an example of the final sub-assembly loss table for a case in which the foundation sub-assembly loss had to be increased from 0% when the overall building loss reached 100%. Note that the sum of the sub-assembly caps is 125%.

Table 13.12. Sample Sub-Assembly Losses Relative to Building Value

Overall Loss	Foundation	Structure Below First Floor	Structure Frame	Roof Cover	Roof Frame	Exterior Wall	Interior
10%	0.00%	0.00%	0.00%	0.48%	0.29%	1.36%	7.87%
20%	0.00%	0.00%	0.00%	0.48%	0.29%	2.16%	17.07%
30%	0.00%	0.00%	0.00%	0.48%	0.29%	3.08%	26.16%
40%	0.00%	0.00%	0.00%	0.51%	0.29%	4.66%	34.54%
50%	0.00%	0.00%	0.00%	0.52%	0.29%	4.94%	44.26%
60%	0.00%	0.00%	0.00%	0.53%	0.29%	5.05%	54.13%
70%	0.00%	0.00%	0.00%	0.54%	0.30%	7.29%	61.87%
80%	0.00%	0.00%	0.00%	0.57%	0.34%	8.33%	70.75%
90%	0.00%	0.00%	0.00%	0.57%	0.39%	9.38%	79.66%
100%	0.13%	0.00%	1.02%	0.57%	1.26%	17.19%	79.82%
Cap	3.03%	0.00%	23.14%	0.57%	1.26%	17.19%	79.82%

Computing Sub-Assembly Wind Losses at the Specific Occupancy Level

Developing sub-assembly losses at the Specific Occupancy (SOCC) level is very similar to the SBT level, except that SBT sub-assembly loss tables are used as inputs instead of the weak, medium and strong sub-assembly loss tables.

Differences in SOCC sub-assembly values between the original wind model development effort and the values given previously in Table 13.10 for Pre-FIRM and Post-FIRM construction were addressed at this stage by multiplying the sub-assembly losses by the ratio of sub-assembly values provided in Table 13.10 to those developed through aggregation at the SOCC level from original FEMACOMLOSS and FEMALOSS values. The resulting sub-assembly losses were then forced and adjusted using Equation 3 in a similar fashion to SBT sub-assembly values.

However, unlike the SBT sub-assembly losses, it is possible to have foundation sub-assembly losses prior to 90% overall loss. This is a result of a wide variety of buildings strengths contributing to a SOC. For example, Table 13.13 shows sub-assembly losses for specific occupancy COM1 with pre-FIRM sub-assembly values. COM1 is composed of several SBTs, one of which is SPMBS (Steel, Pre-Engineer Metal Building, Small). According to Table 13.13, at an overall loss of 40%, the foundation sub-assembly starts to accumulate losses which are due to the contribution of SPMBS. Specifically, the wind speed that induces a 40% loss in COM1 is 151 mph. At this wind speed, the loss induced in SPMBS turns out to be 95%. When applying Equation 9, and examining the foundation sub-assembly losses for this SBT (Table 13.14), it is apparent that a non-zero foundation sub-assembly loss value will result when interpolating between 90% and 100%. Closer examination of Table 13.14 shows that all of the sub-assembly losses other than foundation and below first floor have reached their limits at the 90% overall wind loss level. Foundation loss is not totally unexpected given that a large portion of the building value for this SBT is in the foundation.

Computing Sub-Assembly losses at GBT Level

The development of the sub-assembly losses at the general building level is very similar to the SOCC level except that SOCC sub-assembly loss tables are used as inputs rather than SBT sub-assembly loss table, and ratios of SOCC exposure to the total exposure were used.

The resulting table is similar to Table 13.12 except that it describes sub-assembly losses at the GBT level. These values were then forced and adjusted in a similar fashion to the way SBT and SOC sub-assembly values were forced to be monotonic and adjusted to match the overall building loss.

Table 13.13. Sample Sub-Assembly Losses Relative to Building Value for COM1

Overall Loss	Foundation	Structure Below First Floor	Structure Frame	Roof Cover	Roof Frame	Exterior Wall	Interior
10%	0.0%	0.0%	0.0%	2.2%	0.2%	0.8%	6.8%
20%	0.0%	0.0%	0.0%	3.6%	0.8%	1.6%	14.0%
30%	0.0%	0.0%	0.2%	4.6%	1.3%	2.5%	21.4%
40%	0.1%	0.0%	0.4%	5.2%	1.8%	3.2%	29.3%
50%	0.2%	0.0%	0.5%	5.4%	2.0%	4.0%	38.0%
60%	0.3%	0.0%	0.7%	5.6%	2.2%	4.6%	46.6%
70%	0.3%	0.0%	0.9%	5.8%	2.5%	5.5%	55.1%
80%	0.3%	0.0%	1.1%	6.0%	2.8%	7.0%	62.8%
90%	0.3%	0.0%	3.2%	6.0%	4.2%	7.9%	68.4%
100%	0.3%	0.0%	3.6%	6.3%	4.7%	8.8%	76.4%
Cap	7.5%	1.3%	12.5%	6.3%	6.3%	12.5%	78.8%

Table 13.14. Sub-Assembly Losses Relative to Building Value for SBT SPMBS

Overall Loss	Foundation	Structure Below First Floor	Structure Frame	Roof Cover	Roof Frame	Exterior Wall	Interior
10%	0.0%	0.0%	0.0%	0.1%	0.1%	4.3%	5.5%
20%	0.0%	0.0%	0.0%	0.2%	0.1%	4.5%	15.2%
30%	0.0%	0.0%	0.0%	0.6%	0.3%	4.8%	24.3%
40%	0.0%	0.0%	0.0%	1.1%	0.4%	5.7%	32.7%
50%	0.0%	0.0%	0.0%	1.6%	2.3%	6.5%	39.6%
60%	0.0%	0.0%	0.0%	2.9%	5.7%	9.7%	41.8%
70%	0.0%	0.0%	0.5%	4.0%	8.5%	11.5%	45.4%
80%	0.0%	0.0%	1.3%	5.1%	10.8%	14.7%	48.1%
90%	0.0%	0.0%	3.3%	6.6%	14.0%	17.1%	49.0%
100%	5.9%	0.0%	4.8%	7.2%	15.3%	17.9%	49.0%
Cap	30.9%	0.0%	4.8%	7.2%	15.3%	17.9%	49.0%

Final Wind Sub-Assembly Loss Tables

The final sub-assembly loss tables for wind loss by SOCC and GBT are presented for Pre-FIRM and Post-FIRM construction in Appendix Z.

13.3.2.2 Development of Sub-Assembly Loss Tables for Flood Losses

Because flood losses by building component or building sub-assembly are only available for a handful of building types and occupancies from the GEC (2006) study, an entire set of flood sub-assembly loss tables were developed for this project based on engineering judgment. The guidelines given in Table 13.15 were used to facilitate the process and achieve consistency across Specific Occupancies and General Building Types.

Table 13.15. Guidelines for Development of Flood Sub-Assembly Loss Tables

Sub-Assembly	Pre-FIRM Foundation A Zone Conditions	Pre-FIRM Foundation CA / V Zone Conditions	Post-FIRM Foundation A Zone Conditions	Post FIRM Foundations CA / V Zone Conditions
Foundation	Start damaging foundation at 80% (first non-zero value is at 90%) damage and max damage at 50% Pre-FIRM value (e.g. 3% if foundation represents 6% of the structure value)	Start damaging foundation at 50% damage (first non-zero value is at 60%) and max at 80% Pre-FIRM value (e.g. 5% if foundation represents 6% of the structure value)	Start damaging foundation at 80% (first non-zero value is at 90%) damage and max damage at 50% Post-FIRM value (e.g. 3% if foundation represents 6% of the structure value)	Start damaging foundation at 80% (first non-zero value is at 90%) damage and max damage at 50% Post-FIRM value (e.g. 3% if foundation represents 6% of the structure value)
Below First Floor	Start damaging BFF at 0% damage (first non-zero value is 10%) and achieve 100% Pre-FIRM value by 40% building damage.	Start damaging BFF at 0% damage (first non-zero value is 10%) and achieve 100% Pre-FIRM at 20% building damage.	Start damaging BFF at 0% damage (first non-zero value is 10%) and achieve 100% Post-FIRM value by 40% building damage.	Start damaging BFF at 0% damage (first non-zero value is 10%) and achieve 100% Post-FIRM at 20% building damage.
Structure Frame	Start damaging structure frame at 70% damage (first non-zero value is 80%) and achieve 100% Pre-FIRM value at 100% building damage.	Start damaging structure frame at 10% damage (first non-zero value is 20%) and achieve 100% Pre-FIRM value at 90% building damage.	Start damaging structure frame at 70% damage (first non-zero value is 80%) and achieve 100% Post-FIRM value at 100% building damage.	Start damaging structure frame at 10% damage (first non-zero value is 20%) and achieve 100% Post-FIRM value at 90% building damage.
Roof Cover	Same as Structure	Same as Structure	Same as Structure	Same as Structure
Roof Frame	Same as Structure	Same as Structure	Same as Structure	Same as Structure
Exterior Walls	Start damaging exterior walls at 0% damage (first non-zero value at 10%) and reach maximum (100%) at 100% building damage. Ensure that exterior is always below interior.	Start damaging exterior walls at 10% damage (first non-zero value is 20%) and reach maximum (100%) Pre-FIRM value at 90% building damage.	Start damaging exterior walls at 0% damage (first non-zero value at 10%) and reach maximum (100%) at 100% building damage. Ensure that exterior is always below interior.	Start damaging exterior walls at 10% damage (first non-zero value is 20%) and reach maximum (100%) Post-FIRM value at 90% building damage.
Interiors	Start damaging interior at 0% damage (first non-zero value at 10%) and reach maximum Pre-FIRM value (100%) at 80% building damage.	Start damaging interiors at 0% (first non-zero value at 10%) and reach maximum Pre-FIRM value (100%) at 80% building damage.	Start damaging interiors at 0% damage (first non-zero value at 10%) and reach maximum Post-FIRM value (100%) at 80% building damage.	Start damaging interiors at 0% (first non-zero value at 10%) and reach maximum Post-FIRM value (100%) at 80% building damage.

As indicated in Table 13.15, separate sub-assembly loss tables were developed for Pre- and Post-FIRM construction subjected to either A Zone conditions (i.e., controlling wave heights less than 1.5 feet) or CA / V Zone conditions (i.e., controlling wave heights greater than or equal to 1.5 feet). This results in twice as many sub-assembly flood loss tables as sub-assembly wind loss tables since the wind loss tables are independent of wave conditions.

Figure 13.33 illustrates the sub-assembly losses for single-family occupancies. Separate plots are shown for each combination of construction type (Pre- or Post-FIRM) and wave conditions (A or CA / V Zone). In each plot, the horizontal axis is the overall building loss as a percentage of building replacement value and the vertical axis is the sub-assembly loss as a percentage of its own replacement value. Note that losses to the interiors sub-assembly play a relatively larger role under A Zone wave conditions, whereas losses to the below first floor and foundation sub-assemblies play larger roles under CA or V Zone wave conditions. The differences between Pre-FIRM and Post-FIRM sub-assembly loss contributions are generally less pronounced for this occupancy class than the differences between A Zone and CA / V Zone.

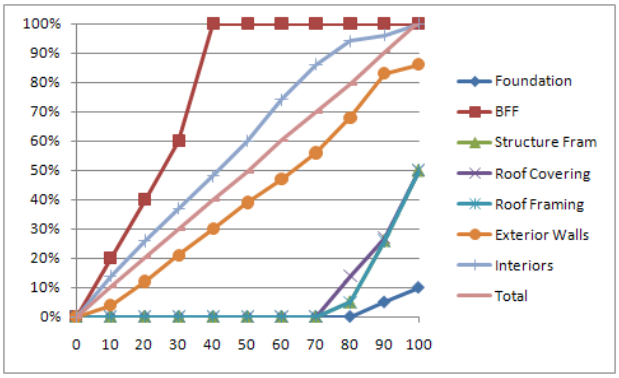

Pre-FIRM, A Zone

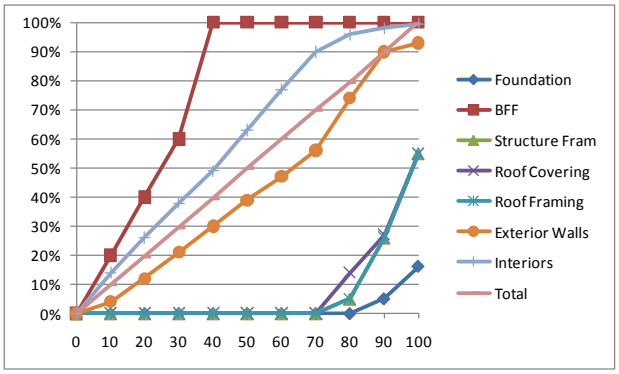

Post-FIRM, A Zone

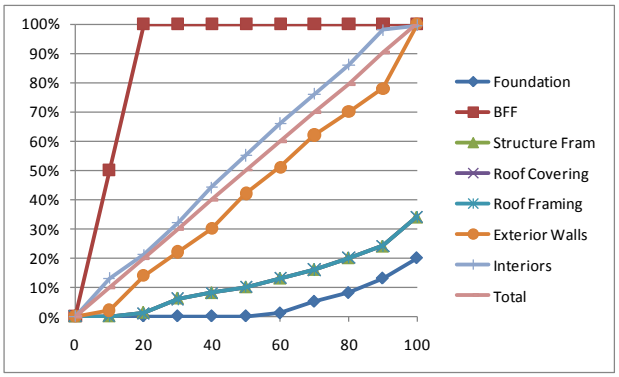

Pre-FIRM, CA or V Zone

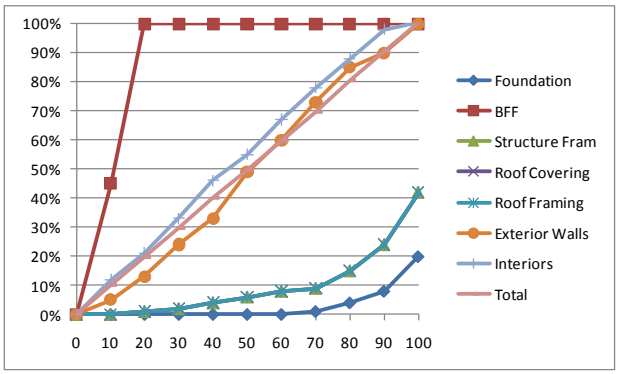

Post-FIRM, CA or Z Zone

Figure 13.33. RES1 (Single Family) Sub-Assembly Losses for Flood as a Percentage of Sub-Assembly Replacement Value.

Final Wind Sub-Assembly Loss Tables

The final sub-assembly loss tables for flood loss by SOCC and GBT are presented for Pre-FIRM and Post-FIRM construction and A Zone and CA / V Zone conditions in Appendix AA.

13.4 Coastal Storm Surge References

East, J.W., Turco, M.J., and Mason, R.R., Jr. (2008). Monitoring inland storm surge and flooding from Hurricane Ike in Texas and Louisiana, September 2008: U.S. Geological Survey Open-File Report 2008–1365 [http://pubs.usgs.gov/of/2008/1365/].

FEMA (2009a). *HAZUS-MH MR4 Hurricane Model Technical Manual*, Federal Emergency Management Agency, Mitigation Division, Washington, D.C., 2009.

FEMA (2009b). *HAZUS-MH MR4 Flood Model Technical Manual*, Federal Emergency Management Agency, Mitigation Division, Washington, D.C., 2009.

GEC (2006). *Depth-Damage Relationships for Structures, Contents, and Vehicles and Content-to-Structure Value Ratios (CSVR) in Support of the Donaldsonville to the Gulf, Louisiana, Feasibility Study*, Gulf Engineers & Consultants, Contract No. DACW29-00-D-0001, Delivery Order No. 0038, G.E.C. Project No. 22316638, prepared for U.S. Army Corps of Engineers New Orleans District, New Orleans, Louisiana, March 2006.

Jelesnianski, C.P., Chen, J., and Shaffer, W.A. (1992). *SLOSH: Sea, Lake, and Overland Surges from Hurricanes*, NOAA Technical Report NWS 48, National Weather Service, Silver Spring, MD.

RSMeans (2001). *Residential Cost Data: 20th Annual Edition*, RSMeans, Kingston, MA, 2001.

RSMeans (2009). *Square Foot Costs: 30th Annual Edition*, RSMeans, Kingston, MA, 2009.

Vickery, P.J., Wadhera, D., Powell, M.D., and Chen, Y. (2009). "A Hurricane Boundary Layer and Wind Field Model for Use in Engineering Applications," *Journal of Applied Meteorology and Climatology, 48, pp. 381-405*.

Vickery, P.J., Skerjl, P.F., Steckley, A.C., and Twisdale, L.A. (2000). "Hurricane Wind Field Model for Use in Hurricane Simulations," *Journal of Structural Engineering*, Volume 126, Number 10, pp. 1203-1221.

Chapter 14. References

AFPA/AWC (1996). "Wood Frame Construction Manual for One- and Two-Family Dwellings, 1995 SBC High Wind Edition," American Forest and Paper Association/American Wood Council, p. 71.

AFPA/AWC (1997). "National Design Specification for Wood Construction," American Forest and Paper Association/American Wood Council, August 7.

AISC (1995). *Load Resistance Factor Design*, Manual of Steel Construction 2nd Edition, American Institute of Steel Construction, Chicago, IL:, Volumes I and II, pp. 6-73 – 6-79 and pp. 8-98 – 8-130.

AISI (1996)., *Specification for the Design of Cold-Formed Steel Structural Members*, American Iron and Steel Institute Washington, DC.

Alliss, R. (1992). *The Utilization of SSM/I Data in Analysis of Tropical and Extra-Tropical Cyclones*, M.S. Thesis, Department of Marine, Earth, Atmospheric Sciences, North Carolina State University, Raleigh, NC.

Alliss, R., G.D. Sandlin, S.W. Chang, and S. Raman (1993). "Applications of SSM/I Data in the Analysis of Hurricane Florence," *Journal of Applied Meteorology*, Volume 32, pp. 1581-1591

Alliss, R.J., S. Raman, and S.W. Chang (1992). "Special Sensor Microwave/Imager (SSM/I) Observations of Hurricane Hugo (1989)," *Monthly Weather Review*, Volume 120, pp. 2723-2737.

Amiro, B.D. (1990a). "Comparison of Turbulence Statistics Within Three Boreal Forest Canopies," *Boundary-Layer Meteorology*, Volume 51, pp. 99-121.

Amiro, B.D. (1990b). "Drag Coefficients and Turbulence Spectra Within Three Boreal Forest Canopies," *Boundary-Layer Meteorology*, Volume 52, pp. 227-246.

Amiro, B.D., and P.A. Davis (1988). "Statistics of Atmospheric Turbulence Within a Natural Black Spruce Forest Canopy," *Boundary-Layer Meteorology*, Volume 44, pp. 267-283.

Arya, S.P.S. (1988). *Introduction to Micrometeorology*, Academic Press.

ASCE (1990). *Minimum Design Loads for Buildings and Other Structures ASCE 7-88*, American Society of Civil Engineers, New York, NY.

ASCE (1999). *Minimum Design Loads for Buildings and Other Structures ASCE 7-98*, American Society of Civil Engineers, New York, NY.

Baik, Jong-Jin (1989). *Tropical Cyclone Simulations with the Betts Convective Adjustment Scheme*, Ph. D. Thesis, Department of Marine, Earth, Atmospheric Sciences, North Carolina State University, Raleigh, NC, pp.159.

Baker, C.J., and H.J. Bell (1991). 'The Aerodynamics of Urban Trees," Preprints, *6th International Conference on Wind Engineering*, London, Ontario, Canada, July.

Baldocchi, D.D., and T.P. Meyers (1988). "A Spectral and Lag-Correlation Analysis of Turbulence in a Deciduous Forest Canopy," *Boundary-Layer Meteorology*, Volume 45, pp. 31-38.

Baskaran, B.A., and O. M. Dutt (1995). "Evaluation of Roof Fasteners under Dynamics Wind Loading," *Proceedings: 9th International Conference on Wind Engineering*, New Delhi, India, pp. 1207-1218.

Batts, M.E., M.R. Cordes, C.R. Russell, J.R. Shaver, and E. Simiu (1980). "Hurricane Windspeeds in The United States," National Bureau of Standards Report Number BSS-124, U.S. Dept. of Commerce, Washington, DC.

Beason, W.L., G.E. Meyers, and R.W. James (1984). "Hurricane Related Window Glass Damage in Houston," *ASCE Journal of the Structural Division*, Volume 110, Number 12, pp. 2843-2857, December.

Behr, R.A., and J.E. Minor (1994). "A Survey of Glazing System Behavior in Multi-Story Buildings During Hurricane Andrew," *The Structural Design of Tall Buildings*, Volume 3, pp.143-161.

Behr, R.A., J.E. Minor, and H.S. Norville (1993). "Structural Behavior of Architectural Laminated Glass," *Journal of Structural Engineering*, Volume 119, Number 1.

Behre, C.E. (1927). "Form-Class Taper Curves and Vol. Tables and Their Application," *Journal of Agricultural Research*, Volume 35, Number 8, Washington, DC., October.

Bergstrom, H., and U. Hogstrom, (1989). "Turbulent Exchange Above a Pine Forest, II. Organized Structures," *Boundary-Layer Meteorology*, Volume 49, pp. 231-263.

Bhinderwala, S. (1995). "Insurance Loss Analysis of Single Family Dwellings Damaged in Hurricane Andrew," M.S. Thesis, Clemson University, Clemson, SC.

Blackburn, P., and J.A. Petty (1988). "Theoretical Calculations of the Influence of Spacing on Stand Stability," *Forestry*, Volume 61, p. 3.

Boissonnade, A., and W-M. Dong (1993). "Hurricane Loss Estimation and Forecasting: Applications to Risk Management," *Proceedings 7th US National Conference on Wind Engineering*, Los Angeles, CA, pp. 115-124.

Bowen, A.J., R.G.J. Flay, and H.A. Panofsky (1983). "Vertical Coherence and Phase Delay Between Wind Components in Strong Winds Below 20 m," *Boundary Layer Meteorology*, Volume 26, pp. 313-324.

Brook, R.R. (1972). "Measurements of Turbulence in a City Environment," *Journal of Applied Meteorology*, Volume 11, pp. 443-450.

Canfield, L.R., S.H. Niu, and H. Liu (1991). "Uplift Resistance of Various Rafter-Wall Connections," *Forest Products Journal*, Volume 41, Number 7/8, July/August.

Case, P.C. (1996). "Wind Loads on Low Buildings with 4:12 Gable Roofs," M.S. Thesis, University of Western Ontario, London, Ontario, Canada, May.

Cherry, N.J. (1991). "Fixing Studies for MRTI Normal Weight Tiles" SBCCI Submission, Redland Technology Limited, New Technology & Product Development Centre, Horsham, West Sussex, England, December.

Cionco, R.M. (1965). "A Mathematical Model for Airflow in a Vegetative Canopy," *Journal of Applied Meteorology*, Volume 4, pp. 517-522.

Cionco, R.M. (1972). "A Wind-Profile Index for Canopy Flow." Boundary-Layer Meteorology, Volume 3, pp. 255-263.

Clark, K.M. (1987). "A Formal Approach to Catastrophe Risk Assessment and Management," *Proceedings November 9-11, 1986,* Volume LXXIII, Number 140, pp. 69-91.

CMHC (1989). "Canadian Wood-Frame House Construction," Canada Mortgage and Housing Corporation, p. 48.

Conner, H.W., D.S. Gromala, and D.W. Burgess (1997). "Roof Connections in Houses: Key to Wind Resistance," *Journal of Structural Engineering,* Volume 113, Number 12, pp. 2459-2474, December.

Cook, R.A. (1990). "Hurricane Hugo vs. Critical Lifelines – Lessons Learned and Implications for the Future," *Proceedings of Hurricane Hugo One Year Later*, 13-15 September.

Crandell, J.H., M. Nowak, E.M. Laatsch, A. van Overeem, C.E. Barbour, R. Dewey, H. Reigel, and H. Angleton (1993). "Assessment of Damage to Single-Family Homes Caused by Hurricanes Andrew and Iniki," Contract HC-5911, NAHB Research Center, Upper Marlboro, MD, for U.S. Department of Housing and Urban Development Office of Policy Development and Research, September.

Cunningham, T.P. (1993). "Roof Sheathing Fastening Schedules for Wind Uplift," APA Report T92-28, American Plywood Association, Tacoma, WA, March.

Daneshvaran, S., and R.E. Morden (1998). "Fast Hurricane Wind Analysis Using the Orthogonal Decomposition Method," *Journal of Wind Engineering and Industrial Aerodynamics,* Volumes 77/78 Complete, pp. 703-714.

Darling, R.W.R. (1991). "Estimating Probabilities of Hurricane Wind Speeds Using a Large-Scale Empirical Model," *Journal of Climate*, Volume 4, Number 10, pp. 1035-1046.

Davenport, A.G. (1961). "The Application of Statistical Concepts to the Wind Loading of Structures," *Proceedings Institute of Civil Engineers,* Volume 19, pp. 449-472.

Dawe, J.L., and G.G. Aridru (1993). "Prestressed Concrete Masonry Walls Subjected to Uniform Out-of-Plane Loading," *Canadian Journal of Civil Engineering,* Volume 20, pp. 969-979.

Drysdale, R.G., and A.S. Essawy (1988). "Out-of Plane Bending of Concrete Block Walls," *ASCE Journal of Structural Engineering*, Volume 114, Number 1, pp. 121-133, January.

Duchêne-Marullaz, P. (1979). "Effect of High Roughness on the Characteristics of Turbulence in Cases of Strong Winds," *Proceedings 5th International Conference on Wind Engineering*, Fort Collins, CO, p. 15.

Ellifritt, D.S., and R. Burnette (1990). "Pull-Over Strength of Screws in Simulated Building Tests," *Proceedings: 10th International Specialty Conference on Cold-Formed Steel Structures*, University of Missouri-Rolla, MO, pp. 589-603.

Elsberry, R.L, L.E Carr III, and M.A. Boothe (1998). "Progress Toward a Generalized Description of the Environment Structure Contribution to Tropical Cyclone Track Types," *Meteorological Atmospheric Physics,* Volume 67, pp. 93-115.

ESDU (1975). "Characteristics of Atmospheric Turbulence Near the Ground, Part II: Single Point Data for Strong Winds (Neutral Atmosphere)," Engineering Science Data Unit, Data Item # 86010, London, England.

ESDU (1982). "Strong Winds in the Atmospheric Boundary Layer, Part 1: Mean Hourly Wind Speed," Engineering Science Data Unit, Data Item Number 82026, London, England.

ESDU (1983). "Strong Winds in the Atmospheric Boundary Layer, Part 2: Discrete Gust Speeds," Engineering Science Data Unit, Data Item Number 83045, London, England.

Fattal, S.G., and L.E. Cattaneo (1977). "Evaluation of Structural Properties of Masonry in Extsting Buildings," U.S. Department of Commerce, National Bureau of Standards, p.13.

FEMA (1992). "Building Performance: Hurricane Andrew in Florida," Federal Emergency Management Agency, Federal Insurance Administration, FIA-22 (2/93). December 21.

FEMA (2001). "HAZUS® 99 Estimated Annualized Earthquake Losses for the United States," Federal Emergency Management Agency, Mitigation Directorate, FEMA 366, February.

Ferraro, R. (1996). "An Eight-Year (1987-1994) Time Series of Rainfall, Clouds, Water Vapor, Snow Cover, and Sea Ice Derived from SSM/I Measurements," *Bulletin of the American Meteorological Society,* Volume 77, pp. 891- 906.

Forest Products Laboratory (1987). "Wood Handbook: Wood as an Engineering Material," U.S. Department of Agriculture, Washington, DC.

Frank, R.A., C.E. Murphy, L.A. Twisdale, and T.A. Reinhold (1987). *Data Collection and Analysis for Full-Scale Drag Tests: MISTY PINE Experiment*, DAAL03-86-D-0001, Ballistic Research Laboratory, Aberdeen Proving Ground, MD, January.

Frank, R.A., M.D. Smith, L.A. Twisdale, and R.G. Pearson (1989). *Mechanical Property Tests on Selected Trees from MISTY PICTURE*, DAAA15-87-D-0008, Tasks 4 and 6, Ballistic Research Laboratory., Aberdeen Proving Ground, MD, 30 December.

Frank, R.A., M.D. Smith, P.J. Vickery, L.A. Twisdale, and M.B. Hardy (1991). *Blast Effects on Forests: MISERS GOLD Data Report (Exp. 1200)*, DAAA15-89-D-0008, Task 2, US Army Armament Research and Development Command, Ballistic Research Laboratory, Aberdeen Proving Ground, MD, 7 June.

Friedman, D.G. (1987). "US Hurricanes & Windstorms," DYP Insurance & Reinsurance Group Ltd.

Galinski, W. (1989). "A Windthrow Risk Estimation for Coniferous Trees," *Forestry*, Volume 62, Number 2.

Gardiner, B.A. (1994). "Wind and Wind Forces in a Plantation Spruce Forest," *Boundary-Layer Meteorology*, Volume 67, pp. 161-186.

García, J.M. (1994). "The Wind Loading of Fasteners, Corrugated Materials and Roofing of Low-Rise Buildings," MS Thesis, Department of Civil Engineering, The University of Western Ontario, London, Ontario, Canada.

Georgiou, P.N. (1985). "Design Windspeeds in Tropical Cyclone-Prone Regions," Ph.D. Thesis, Faculty of Engineering Science, University of Western Ontario, London, Ontario, Canada.

Georgiou, P.N., A.G. Davenport, and B.J. Vickery (1983). "Design Wind Speeds in Regions Dominated by Tropical Cyclones," *Journal of Wind Engineering and Industrial Aerodynamics*, Volume 13, Numbers 1-3, pp. 139-152.

Ghali, A., and A.M. Neville (Eds.) (1989). *Structural Analysis – A Unified Classical and Matrix Approach*, 3rd Edition, Chapman and Hall.

Grimm, C.T. (1999). "Walls May Be Half as Strong as They Say!," Southern Building, p. 19, January/February.

Gross, J.G., R.D. Dikkers, and J.C. Grogan (1969). "Recommended Practice for Engineered Brick Masonry," Brick Industry Association, Reston, VA.

Hebert, P.J., J.D. Jarrell, and B.M. Mayfield (1996). "The Deadliest, Costliest, and Most Intense United States Hurricanes of This Century (and Other Frequently Requested Hurricane Facts)," NOAA Technical Memorandum NWS-NHC-31, p. 41.

Ho, F.P., et al. (1987). "Hurricane Climatology for the Atlantic and Gulf Coasts of the United States," NOAA Technical Report NWS38, Federal Emergency Management Agency.

Ho, T.C.E. (1992). "Variability of Low Building Wind Loads," Ph.D. Thesis, Faculty of Engineering Science, University of Western Ontario, London, Ontario, Canada.

Hogan, M., and K. Karwoski (1990). "Masonry Performance in the Coastal Zone," in Proceedings "Hurricane Hugo One Year Later," B. L. Sill and P. R. Sparks (Eds.), Charleston, SC, September.

Holland, G.J. (1980). "An Analytic Model of the Wind and Pressure Profiles in Hurricanes," *Monthly Weather Review*, Volume 108, Number 8, pp. 1212-1218.

Hong, X., S.W. Chang, S. Raman, L.K. Shay, and R. Hodur (1998). "The Interaction Between Hurricane Opal (1995) and a Warm Core Eddy in the Gulf of Mexico," Submitted to *Monthly Weather Review*.

Houston, S.H., and M.D. Powell (1993). "Surface Wind Fields During Hurricane Bob's (1991) Landfall in New England," *Proceedings 20th Conference on Hurricanes and Tropical Meteorology*, American Meteorological Society, San Antonio, TX, May 10-14.

Houston, S.H., M.D. Powell, and P.P. Dodge (1997). "Surface Wind Fields in 1996 Hurricanes Bertha and Fran at Landfall," *Proceedings 22nd Conference on Hurricanes and Tropical Meteorology*, American Meteorological Society, Fort Collins, CO, May 19-23.

HUD (1980). *Economic Benefit-Cost and Risk Analysis of Mobile Home Safety Research: Wind Safety Analysis*, Office of Policy Development and Research, Department of Housing and Urban Development.

HUD (1993). "Assessment of Damage to Single-Family Homes Caused by Hurricanes Andrew and Iniki," U.S. Department of Housing and Urban Development, Office of Policy Development and Research, March.

HUD (1994). "Final Rule – Manufactured Home Construction and Safety Standards on Wind Standards," Office of the Assistant Secretary for Housing, Department of Housing and Urban Development, *Federal Register*, Volume 59, Number 10, pp. 2456-2475.

Jensen, M. (1958). "The Model-Law for Phenomena in Natural Wind," *Ingeniøren*, Volume 2, pp. 121-128.

Johnson, R.C., Jr., G.D. Ramey, and D.S. O'Hagan (1982). "Wind-Induced Forces on Trees," *Journal of Fluids Engineering*, Volume 104, March.

Jones, R. (1987). "A Simulation of Hurricane Land Fall with a Numerical Model Featuring Latent Heating by the Resolvable Scales," *Monthly Weather Review*, Volume 115, pp. 2279-2297.

Kareem, A., and J.G. Stevens (1985). "Window Glass Performance and Analysis in Hurricane Alicia," *ASCE Proceedings Specialty Conference: "Hurricane Alicia: One Year Later,"* Galveston, TX (August 1984), A. Kareem (Ed.), pp.178-186.

Karlsson, S. (1986). "The Applicability of Wind Profile Formulas to an Urban-Rural Interface Site," *Boundary Layer Meteorology*, Volume 34, pp. 333-355.

Kind, R.J., and R.L. Wardlaw (1984). "Behavior in Wind of Loose-Laid Roof Insulation Systems, Part I: Stone Scour and Blow-Off," *Proceedings 4th Canadian Workshop on Wind Engineering*, Toronto, Canada, pp. 141-149.

Kovacs, W.W., and F.Y. Yokel (1979), "Soil and Rock Anchors for Mobile Homes – A State of the Art Report", U.S. Department of Commerce, NBS Building Sciences Series 107, National Bureau of Standards, Washington, DC.

LaBoube, R.A. and W.W. Yu (1993). "Behavior of Arc Spot Weld Connections in Tension," *ASCE Journal of Structural Engineering*, Volume 119, Number 7, pp. 2187-2198.

Lai, W. (1955). *Aerodynamic Crown Drag of Several Broadleaf Tree Species*, AFSWP-863, US Forest Service, Division of Fire Research, Washington, DC.

Leland, K.B. (1988). "The Strength of Roof Anchorage in Unreinforced Concrete Masonry," Masters Thesis, Clemson University, Clemson, SC, August.

Lettau, H.H. (1969). "Note on Aerodynamic Roughness-Parameter Estimation on the Basis of Roughens-Element Description," *Journal of Applied Meteorology*, Volume 8, pp. 828-832.

Li, Z.J., D.R. Miller, and J.D. Lin (1985). "A First-Order Closure Scheme to Describe Counter-Gradient Momentum Transport in Plant Canopies," *Boundary-Layer Meteorology*, Volume 33, pp. 77-83.

Li, Z.J., J.D. Lin, and D.R. Miller (1990). "Air Flow Over and Through a Forest Edge: A Steady-State Numerical Simulation," *Boundary-Layer Meteorology*, Volume 51, pp. 179-197.

Lin, J.X., and D. Surry (1997). "Simultaneous Time Series of Pressures on the Envelope of Two Large Low-Rise Buildings," Boundary Layer Wind Tunnel Laboratory Report, BLWTL-SS7-1997, University of Western Ontario, London, Ontario, Canada, for Dr. E. Simiu, National Institute of Standards and Technology, March.

Lohmander, P., and F. Helles (1987). "Windthrow Probability as a Function of Stand Characteristics and Shelter," *Scan. Journal of Forest Research*, Volume 2, pp. 227-238.

Macha, J., J. Sevier, and J. Bertin (1983). "Comparison of Wind Pressures on a Mobile Home in Model and Full Scale," *Journal of Wind Engineering and Industrial Aerodynamics*, Volume 12, pp. 109-124.

Mahendran, M. (1994). "Behaviour and Design of Crest-Fixed Profiled Steel Roof Claddings under Wind Uplift," *Engineering Structures*, Volume 16, Number 5, pp. 368-376.

Mahendran, M. (1997). "Review of Current Test Methods for Screwed Connections," *ASCE Journal of Structural Engineering*, Volume 123, Number 3, pp. 321-325.

Mahendran, M., and R. B. Tang (1998). "Pull-Out Strength of Steel Roof and Wall Cladding Systems," *ASCE Journal of Structural Engineering*, Volume 124, Number 10, pp. 1192-1201.

Mark, F. (1985). "Evolution and Structure of Precipitation in Hurricane Allen (1980)," *Monthly Weather Review*, Volume 113, pp. 909-930.

Marshall, R. (1977). "The Measurement of Wind Loads on a Full Scale Mobile Home," NBSIR 77-1289, National Bureau of Standards, Washington, DC, p. 120.

Marshall, R.D. (1993). "Wind Load Provisions of Manufactured Home Construction and Safety Standards – A Review and Recommendation for Improvement," NISTIR 5189, Building and Fire Research Laboratory, Gaithersburg, MD, for Department of Housing and Urban Development, Washington, DC, May.

Marshall, R.D. (1994). "Manufactured Homes – Probability of Failure and the Need for Better Windstorm Protection Through Improved Anchoring Systems," NISTIR 5370, Building and Fire Research Laboratory, Gaithersburg, MD, for Department of Housing and Urban Development, Washington, DC, November.

Marshall, R.D., and F.Y. Yokel (1995). "Recommended Performance-Based Criteria for the Design of Manufactured Home Foundation Systems to Resist Wind and Seismic Loads," NISTIR 5664, Building and Fire Research Laboratory, Gaithersburg, MD, for Department of Housing and Urban Development, Washington, DC, August.

Massman, W. (1987). "A Comparative Study of Some Mathematical Models of the Mean Wind Structure and Aerodynamic Drag of Plant Canopies," *Boundary-Layer Meteorology*, Volume 40, pp. 179-197.

Mayhead, G.J., J.B.H. Gardiner, and D.W. Durant (1975). "A Report on the Physical Properties of Conifers in Relation to Plantation Stability," Forest Commission Report, Silviculture Section, Northern Research Station, Edinburgh, Scotland, June.

MBMA (1996). *Low Rise Building Systems Manual*, Metal Building Manufacturers Association, Cleveland, OH.

McDonald, J.R., and W.V. Pennington (1986). "Hurricane Damage to Manufactured Homes," *Presented at American Society of Civil Engineers Structures Congress '86*, New Orleans, LA, September.

McDonald, J.R., H. Jiang, and J. Yin (1997). "Full-Scale Measurements of Wind Loads on Metal Edge Flashings and Copings," Final Report, Institute for Disaster Research, Texas Tech University, Lubbock, TX, for Roofing Industry Consortium, February.

Meecham, D. (1988). "Wind Action on Hip and Gable Roofs," M.S. Thesis, University of Western Ontario, London, Ontario, Canada, August.

Meyers, T., and K.T. Paw (1986). "Testing of a Higher-Order Closure Model for Modeling Airflow Within and Above Plant Canopies," *Boundary-Layer Meteorology*, Volume 37, pp. 297-311.

MHCSS (1992). "Manufactured Home Construction and Safety Standards," 24 CFR Chapter XX, Part 3280.

Miller, D.R., J.D. Lin, and Z.N. Lu (1991). "Air Flow Across an Alpine Forest Clearing: A Model and Field Measurements," *Agriculture and Forest Meteorology*, Volume 56, pp. 209-225.

Milne, R., and T.A. Browne (1990). "Tree Stability and Form," Final Report CEC/NERC Contract MA-0061-UK (BA), August.

Minor, J.E. (1985). "Window Glass Performance and Hurricane Effects," *ASCE Proceedings Specialty Conference: "Hurricane Alicia: One Year Later,"* Galveston, TX (August 1984), A. Kareem (Ed.), pp.151-167

Minor, J.E. (1994). "Wind-Borne Debris and the Building Envelope," *Journal of Wind Engineering and Industrial Aerodynamics*, Volume 53, pp. 207-227.

Minor, J.E., and R.A. Behr (1993a). "Architectural Glazing Systems in Hurricanes: Performance, Design Criteria and Designs," *Proceedings 7th U.S. National Conference on Wind Engineering*, Los Angeles, CA, Volume II, pp. 453-461.

Minor, J.E., and R.A. Behr (1993b). "Improving the Performance of Architectural Glazing in Hurricanes," *Hurricanes of 1992*, R.A. Cook and M. Soltani (Eds.), ASCE, pp. 476-485.

Minor, J.E., W.L. Beason, and P.L. Harris (1978). "Designing for Wind-Borne Missiles in Urban Areas," *ASCE Journal of the Structural Division*, Volume 104, Number ST11, pp. 1749-1760.

Monroe, J.S. (1996). "Wind Tunnel Modeling of Low Rise Structures in a Validated Open Country Simulation," M.S. Thesis, Clemson University, Clemson, S, August.

National Roofing Contractors Association (1996). *NRCA Roofing and Waterproofing Manual*, Fourth Edition.

NCS BCS (1988). "Manufactured Home Installations," NCS BCS A225.1/ANSI A225.1-1987, National Conference of States on Building Codes and Standards, Inc., Herndon, VA, p. 49.

NCS BCS (1994). "Manufactured Home Installations," NCS BCS/ANSI A225.1-1994, National Conference of States on Building Codes and Standards, Inc., Herndon, VA, p. 29.

Neumann, C.J. (1991). "The National Hurricane Center Risk Analysis Program (HURISK)," NOAA Technical Memorandum NWS NHC 38, National Oceanic and Atmospheric Administration, Washington, DC.

Newman, A. (1997). *Metal Building Systems*, McGraw-Hill, New York, NY.

NFPA (1973). "Standard for Mobile Homes," NFPA Number 501B-1973/ANSI A119.1, p. 33.

NRC (1991). "Hurricane Elena, Gulf Coast August 29 – September 2, 1985, Natural Disasters Studies, Volume Two," HA 286, Committee on Natural Disasters, National Research Council, Washington, DC pp. 51-58.

Oliver, H.R., and G.J. Mayhead (1974). "Wind Measurements in a Pine Forest During a Destructive Gale," *Forestry*, Volume 47 , p. 2, 1974.

Parris, S. (1996). "Design of Wind Uplift Capacities and Retro-Fitted Adhesives," 490 and 491 Project Presentation, Clemson University, Clemson, SC, August.

Pekoz, T. (1990). "Design of Cold-Formed Steel Screw Connections," *Proceedings 10th International Specialty Conference on Cold-Formed Steel Structures*, University of Missouri-Rolla, Rolla, MO, pp. 575-587.

Powell, M.D. (1987). "Changes in the Low-Level Kinematic and Thermodynamic Structure of Hurricane Alicia (1983) of Landfall," *Monthly Weather Review*, Volume 115, pp. 75-99.

Powell, M.D., and S.H. Houston (1996). "Hurricane Andrew's Landfall in South Florida – Part II: Surface Wind Fields and Potential Real-Time Applications," *Weather and Forecasting*, Volume 11, Number 3, pp. 329-349.

Powell, M.D., and S.H. Houston (1998). "Surface Wind Fields of 1995 Hurricanes Erin, Opal, Luis, Marilyn, and Roxanne at Landfall," to appear in *Monthly Weather Review*.

Powell, M.D., P.P. Dodge, and L.B. Black (1991). "The Landfall of Hurricane Hugo in the Carolinas: Surface Wind Distribution," *Weather and Forecasting*, Volume 6, pp. 379-399.

Raman, S., and N. Reddy (1996). "Numerical Simulation of a Mesolow Over a Gulf Stream Filament," *Pure and Applied Geophysics*, Volume 147, pp. 789-819.

Reddy, N., and S. Raman (1997). "Influence of Soil Moisture Parameterization on the Simulation of a Mesoscale Coastal Front," *Pure and Applied Geophysics*, under revision.

Reed, T.D., D.V. Rosowsky, and S.D. Schiff (1996). "Roof Rafter to Top-Plate Connection in Coastal Residential Construction," *Proceedings International Wood Engineering Conference*, pp. 4-458 – 4-465.

Reed, T.D., D.V. Rosowsky, and S.D. Schiff (1997). "Uplift Capacity of Light-Frame Rafter to Top Plate Connections," *Journal of Architectural Engineering,* pp. 157-163, December.

Rodgers, E., S. Chang, and H. Pierce (1994). "A Satellite Observational and Numerical Study of Precipitation Characteristics in Western North Atlantic Cyclones," *Journal Applied Meteorology*, Volume 33, pp. 129-139.

Rosowsky, D.V., and T.A. Reinhold (1999). "Rate-of-Load and Duration-of-Load Effects for Wood Fasteners," *ASCE Journal of Structural Engineering*, Volume 125, Number 7, pp.719-724, July.

Roy, R. (1983). "Wind Tunnel Measurements of Total Loads on a Mobile Home," *Journal of Wind Engineering and Industrial Aerodynamics*, Volume 13, pp. 327-338.

Russell, L.R. (1968). "Probability Distributions for Texas Gulf Hurricane Effects of Engineering Interest," Ph.D. Thesis, Stanford University, Stanford, CA.

Russell, L.R. (1971). "Probability Distributions for Hurricane Effects," *Journal of Waterways, Harbors, and Coastal Engineering Division*, Number 1, pp. 139-154.

Russell, L.R., and G.F. Schueller (1974). "Probabilistic Models for Texas Gulf Coast Hurricane Occurrences," *Journal Petroleum Technology*, pp. 279-288.

Sauer, F.M., W.L. Fons, and K. Arnold (1951). *Experimental Investigation of Aerodynamic Drag in Tree Crowns Exposed to Steady Wind—Conifers (U),* US Department of Agriculture., Forest Service, Division of Fire Research, Washington, DC, Phase Report, 20 December 1951.

SBCCI (1988). *Standard Building Code 1988 Edition*, Southern Building Code Congress International, Birmingham, AL.

SBCCI (1991). "Standard Building Code: Appendix H, Manufactured Home Tie Down Standards," Southern Building Code Congress International, Inc., Birmingham, AL, pp. 601-606.

Schneider, D. (1998). *Structural and Intensity Changes of Hurricane Opal (1995) and Hurricane Fran (1996).* M.S. Thesis, Department of Marine, Earth, Atmospheric Sciences, North Carolina State University, pp. 80.

Seginer, I., P.J. Mulhearn, E.F. Bradley, and J.J. Finnigan (1976). "Turbulent Flow in a Model Plant Canopy," *Boundary-Layer Meteorology*, Volume 10, pp. 423-453, 1976.

Shapiro, L.J. (1983). "The Asymmetric Boundary Layer Flow Under a Translating Hurricane," *Journal of Atmospheric Science*, Volume 40, Number 8, pp. 1984-1998.

Shaw, R.H., and A.R. Pereira (1982). "Aerodynamic Roughness of a Plant Canopy: A Numerical Experiment," *Agricultural Meteorology*, Volume 26, pp. 51-65.

Shi, J., S. Chang, and S. Raman (1998). "Interaction Between Hurricane Florence (1988) and an Upper-Tropospheric Westerly Trough as Revealed by the Numerical Experiments," *Journal of Atmospheric Science*, Volume 54, pp. 1231-1240.

Shiotani, M. (1962). "The Relationship between Wind Profiles and Stabilities of the Air Layer in the Outskirts of a City," *Journal of Meteorological Society, Japan*, Volume 40, pp. 315-329.

Simiu, E., and R.H. Scanlan (1996). *Wind Effects on Structures: Fundamental and Applications to Design*, 3rd Edition, John Wiley & Sons, New York, NY.

SJI (1994). "Catalogue of Standard Specifications, Load Tables, and Weight Tables for Steel Joists and Joist Girders," Steel Joist Institute, Myrtle Beach, SC.

SJI (1998). "Structural Design of Steel Joist Roofs to Resist Uplift Loads," *Technical Digest*, Number 6, Steel Joist Institute, Myrtle Beach, SC.

Slodicak, M. (1993). "Thinning Regime in Stands of Norway Spruce Subjected to Snow and Wind Damage," *Wind-Related Damage to Trees*. IUFRO Conference, Edinburgh, Scotland, June.

Smith, T. L. (1995). "Insights on Metal Roof Performance in High-Wind Regions," Professional Roofing, pp. 12-16.

Smith, T.L. (1999). "Records of Survey on Building Damages Caused by Hurricane Andrew," Personal Communications, TLSmith Consulting.

Somerville, F. (1993). "Wind Damage to New Zealand State Plantation Forests," *Wind-Related Damage to Trees*, IUFRO Conference, Edinburgh, Scotland, June.

Sparks, P.R., S.D. Schiff and T.A. Reinhold (1994). "Wind Damage to Envelopes of Houses and Consequent Insurance Losses," *Journal of Wind Engineering and Industrial Aerodynamics*, Volume 53, pp. 145-155.

Stacey, G.R., et al. (1994) "Wind Flows and Forces in a Model Spruce Forest," *Boundary-Layer Meteorology*.

Stathopoulos, T. (1979). "Turbulent Wind Action on Low Rise Buildings," Ph.D. Thesis, University of Western Ontario, London, Ontario, Canada, February.

Steel Deck Institute (1992a). *SDI Manual of Construction with Steel Deck.*

Steel Deck Institute (1992b). *Standard Practice Details for Composite Floor Deck, Non-Composite Form Deck, and Steel Roof Deck.*

Steyn, D.G. (1982). "Turbulence in an Unstable Surface Layer over Suburban Terrain," *Boundary Layer Meteorology*, Volume 22, pp. 183-191.

Storey, T.G., and W.L. Fons (1956). *Natural Period Characteristics of Selected Tree Species*, AFSWP-864, DASIAC 06224, US Forest Service, Washington, DC, October.

Storey, T.G., and W.Y. Pong (1957). "Crown Characteristics of Several Hardwood Tree Species," AFSWP-968, US Forest Service, Division of Fire Research, Washington, DC, May.

Strehmeyer, E.H. (1990). "An Overview of Hurricane Damage to Military Facilities and the Storm Recovery Role Played by the Southern Div. Naval Facilities Engineering Command," *Proceedings of Hurricane Hugo One Year Later,* 13-15 September.

Thompson, N. (1979). "Turbulence Measurements Above a Pine Forest," *Boundary-Layer Meteorology,* Volume 16, pp. 293-310.

Tom·, A., G. Sedlacek, and K. Weynand (1993*)*. "Connections in Cold-Formed Steel," *Thin-Walled Structures,* Volume 16, pp. 219-237.

Tryggvason, B.V., D. Surry, and A.G. Davenport (1976). "Predicting Wind-Induced Response in Hurricane Zones," *Journal of Structural Division,* Volume 102, Number 12, pp. 2333-2350.

Twisdale, L.A., and W.L. Dunn (1983). "Extreme Wind Risk Analysis of the Indian Point Nuclear Generation Station," Final Rep. 44T-2491, Addendum to Rep. 44T-2171, Research Triangle Institute, Research Triangle Park, NC.

Twisdale, L.A., R.A. Frank, and C.E. Murphy (1986). *Data Collection and Analysis for Mechanical Property Tests on Selected Trees*, DAAG29-81-D-0100, Ballistic Research Laboratory, Aberdeen Proving Ground, MD, January.

Twisdale, L.A., R.A. Frank, and P.J. Vickery (1989). *Update and Application of the BLOWTRAN Methodology to Forest and Damage Prediction (Version 2.3)*, DAAA15-87-D-0008, Task 1, Ballistic Research Laboratory, Aberdeen Proving Ground, MD, December.

Twisdale, L.A., R.A. Frank, C.E. Murphy, and M.B. Hardy (1984). *Forest Blowdown and Debris Transport Methodology*, DAAK11 -84-C-0089, Ballistic Research Laboratory, Aberdeen Proving Ground, MD, May.

Twisdale, L.A., P.J. Vickery, and A.C. Steckley (1996). "Analysis of Hurricane Windborne Debris Impact Risk for Residential Structures," Applied Research Associates, Raleigh, NC, March.

Twisdale, L.A., P.J. Vickery, J.X. Lin, and A.C. Steckley (2000a). "Analysis of Hurricane Windborne Debris Impact Risk for Residential Structures: Part I," to be submitted to the *ASCE Journal of Structural Engineering*.

Twisdale, L.A., P.J. Vickery, J.X. Lin, and A.C. Steckley (2000b). "Analysis of Hurricane Windborne Debris Impact Risk for Residential Structures: Part II," to be submitted to the *ASCE Journal of Structural Engineering*.

Uematsu, Y., and N. Isyumov (1998). "Peak Gust Pressures Acting on the Roof and Wall Edges of a Low-Rise Building," *Journal of Wind Engineering and Industrial Aerodynamics*, Volumes 77 and 78, pp. 217-231.

United States Department of Agriculture, (1974). *USDA Wood Handbook: Wood as an Engineering Material*, Forest Products Laboratory, Forest Service, Agriculture Handbook No. 72, Revised August.

United Steel Deck, Inc. (1997*).* USD Catalog #303-14.

United Steel Deck, Inc. (1998*).* "Wall and Roof Systems," USD Siding Manual.

Vann, P.W., and J.R. McDonald (1978), "An Engineering Analysis: Mobile Homes in Windstorms", Report prepared for Disaster Preparedness Staff, National Weather Service, NOAA, Silver Spring, MD, Institute for Disaster Research, Lubbock, TX.

Vasquez, J.L. (1994). "Development of a Windspeed-Damage Correlation Model for Manufactured Housing Subjected to Extreme Winds," M.S. Thesis, Louisiana State University and Agricultural and Mechanical College, December.

Vickery, P.J., and L.A. Twisdale (1995a). "Wind-Field and Filling Models for Hurricane Wind-Speed Predictions," *Journal of Structural Engineering*, Volume 121, Number 11, pp. 1700-1709.

Vickery, P.J., and L.A. Twisdale (1995b). "Prediction of Hurricane Wind Speeds in The United States," *Journal of Structural Engineering*, Volume 121, Number 11, pp. 1691-1699.

Vickery, P.J., R.A. Frank, and L.A. Twisdale (1993). "Blast Effects on Forests: Forest Classification, Sensitivity Studies, and Model Evaluation," DAAA15-89-D-0008, Task Order 5, Ballistic Research Laboratory, Aberdeen Proving Ground, MD, 6 May.

Vickery, P.J., R.A. Frank, M.D. Smith, and L.A. Twisdale (1991). *Blast Effects on Forests: Hardwood Breakage Tests and Mechanical Property Tests*, DAAA15-89-D-0008, Ballistic Research Laboratory, Aberdeen Proving Ground, MD, 31 December.

Vickery, P.J., P.F. Skerjl, and L.A. Twisdale (2000a). "Simulation of Hurricane Risk in the United States Using Empirical Track Model," *Journal of Structural Engineering*, Volume 126, Number 10, pp. 1222-1237.

Vickery, P.J., P.F. Skerjl, A.C. Steckley, and L.A. Twisdale (2000b). "Hurricane Wind Field Model for Use in Hurricane Simulations," *Journal of Structural Engineering*, Volume 126, Number 10, pp. 1203-1221.

Wang, C-K, and C.G. Salmon (1997). *Reinforced Concrete Design*, Fifth Edition.

Wieringa, J. (1992). "Updating the Davenport Roughness Classification," *Journal of Wind Engineering and Industrial Aerodynamics*, Volume 41-44, pp. 357-368.

Wieringa, J. (1993). "Representative Roughness Parameters for Homogeneous Terrain," *Boundary Layer Meteorology*, Volume 63, pp. 323-363.

Yersel, M., and R. Goble (1986). "Roughness Effects on Urban Turbulence Parameters," *Boundary Layer Meteorology*, Volume 37, pp. 271-284.

Yokel, F.Y., R.M. Chung, F.A. Rankin, and C.W.C. Yancey (1982), "Load-Displacement Characteristics of Shallow Soil Anchors", U.S. Department of Commerce, NBS Building Sciences Series 142, National Bureau of Standards, Washington, DC.

Young, M.A., and B.J. Vickery (1994). "A Study of Roof Uplift Forces on Three Schools of Windsor Roman Catholic Separate School Board," Final Report BLWT-SS29-1994, The Boundary Layer Wind Tunnel Laboratory, The University of Western Ontario, Ontario, Canada.

Zaitz, M.D. (1994). "Roof Sheathing Racking Effect on Fastener Withdrawal Capacities," M.S. Thesis, Clemson University, Clemson, SC, pp.4-5, August.

Zollo, R.F. (1993). "Hurricane Andrew: August 24, 1992, Structural Performance of Buildings in Dade County, Florida," Technical Report No. CEN 93-1, University of Miami, Miami, FL, March.

Appendix A.
Damage State Functions for Residential Buildings

Appendix A.
Damage State Functions for Residential Buildings

This appendix presents damage state curves for residential buildings (see Section 6.4). The damage state curves show the probability of achieving a certain damage state versus storm-maximum peak gust speed (open terrain at 10m above ground). Plots are presented for the overall building damage states and for the individual building component damage states (refer to Table 6.4-1 for damage state definitions). Table A.1 summarizes the figures included in this appendix.

Table A.1. Sample Damage State Functions for Residential Buildings

Figure	Walls	Stories	Garage	Roof Shape	Sheathing	Roof/ Wall	Shutters	Upgraded Roof	Terrain
A.1	URM	1	No	Gable	6d	Strap	No	No	0.03
A.2	URM	1	No	Gable	6d	Strap	No	No	0.35
A.3	URM	1	No	Gable	6d	Strap	No	No	0.70
A.4	URM	1	No	Gable	6d	Strap	No	No	1.00
A.5	URM	1	No	Hip	6d	Strap	No	No	0.03
A.6	URM	1	No	Hip	6d	Strap	No	No	0.35
A.7	URM	1	No	Hip	6d	Strap	No	No	0.70
A.8	URM	1	No	Hip	6d	Strap	No	No	1.00
A.9	URM	1	No	Gable	6d	Toe-Nail	No	No	0.03
A.10	URM	1	No	Gable	6d	Toe-Nail	No	No	0.35
A.11	URM	1	No	Gable	6d	Toe-Nail	No	No	0.70
A.12	URM	1	No	Gable	6d	Toe-Nail	No	No	1.00
A.13	URM	1	No	Hip	6d	Toe-Nail	No	No	0.03
A.14	URM	1	No	Hip	6d	Toe-Nail	No	No	0.35
A.15	URM	1	No	Hip	6d	Toe-Nail	No	No	0.70
A.16	URM	1	No	Hip	6d	Toe-Nail	No	No	1.00
A.17	WFR	2	No	Gable	6d	Strap	No	No	0.03
A.18	WFR	2	No	Gable	6d	Strap	No	No	0.35
A.19	WFR	2	No	Gable	6d	Strap	No	No	0.70
A.20	WFR	2	No	Gable	6d	Strap	No	No	1.00
A.21	WFR	2	No	Hip	6d	Strap	No	No	0.03
A.22	WFR	2	No	Hip	6d	Strap	No	No	0.35
A.23	WFR	2	No	Hip	6d	Strap	No	No	0.70
A.24	WFR	2	No	Hip	6d	Strap	No	No	1.00
A.25	WFR	2	No	Gable	6d	Toe-Nail	No	No	0.03
A.26	WFR	2	No	Gable	6d	Toe-Nail	No	No	0.35
A.27	WFR	2	No	Gable	6d	Toe-Nail	No	No	0.70
A.28	WFR	2	No	Gable	6d	Toe-Nail	No	No	1.00
A.29	WFR	2	No	Hip	6d	Toe-Nail	No	No	0.03
A.30	WFR	2	No	Hip	6d	Toe-Nail	No	No	0.35
A.31	WFR	2	No	Hip	6d	Toe-Nail	No	No	0.70
A.32	WFR	2	No	Hip	6d	Toe-Nail	No	No	1.00

Table A.1. Sample Damage State Functions for Residential Buildings (continued)

Figure	Walls	Stories	Garage	Roof Shape	Sheathing	Roof/ Wall	Shutters	Upgraded Roof	Terrain
A.33	URM	2	No	Gable	6d	Strap	No	No	0.03
A.34	URM	2	No	Gable	6d	Strap	No	No	0.35
A.35	URM	2	No	Gable	6d	Strap	No	No	0.70
A.36	URM	2	No	Gable	6d	Strap	No	No	1.00
A.37	URM	2	No	Hip	6d	Strap	No	No	0.03
A.38	URM	2	No	Hip	6d	Strap	No	No	0.35
A.39	URM	2	No	Hip	6d	Strap	No	No	0.70
A.40	URM	2	No	Hip	6d	Strap	No	No	1.00
A.41	URM	2	No	Gable	6d	Toe-Nail	No	No	0.03
A.42	URM	2	No	Gable	6d	Toe-Nail	No	No	0.35
A.43	URM	2	No	Gable	6d	Toe-Nail	No	No	0.70
A.44	URM	2	No	Gable	6d	Toe-Nail	No	No	1.00
A.45	URM	2	No	Hip	6d	Toe-Nail	No	No	0.03
A.46	URM	2	No	Hip	6d	Toe-Nail	No	No	0.35
A.47	URM	2	No	Hip	6d	Toe-Nail	No	No	0.70
A.48	URM	2	No	Hip	6d	Toe-Nail	No	No	1.00
A.49	URM	1	No	Gable	8d	Strap	No	No	0.03
A.50	URM	1	No	Gable	8d	Strap	No	No	0.35
A.51	URM	1	No	Gable	8d	Strap	No	No	0.70
A.52	URM	1	No	Gable	8d	Strap	No	No	1.00
A.53	URM	1	No	Hip	8d	Strap	No	No	0.03
A.54	URM	1	No	Hip	8d	Strap	No	No	0.35
A.55	URM	1	No	Hip	8d	Strap	No	No	0.70
A.56	URM	1	No	Hip	8d	Strap	No	No	1.00
A.57	URM	1	No	Gable	8d	Toe-Nail	No	No	0.03
A.58	URM	1	No	Gable	8d	Toe-Nail	No	No	0.35
A.59	URM	1	No	Gable	8d	Toe-Nail	No	No	0.70
A.60	URM	1	No	Gable	8d	Toe-Nail	No	No	1.00
A.61	URM	1	No	Hip	8d	Toe-Nail	No	No	0.03
A.62	URM	1	No	Hip	8d	Toe-Nail	No	No	0.35
A.63	URM	1	No	Hip	8d	Toe-Nail	No	No	0.70
A.64	URM	1	No	Hip	8d	Toe-Nail	No	No	1.00
A.65	URM	1	No	Gable	8d	Strap	Yes	No	0.03
A.66	URM	1	No	Gable	8d	Strap	Yes	No	0.35
A.67	URM	1	No	Gable	8d	Strap	Yes	No	0.70
A.68	URM	1	No	Gable	8d	Strap	Yes	No	1.00
A.69	URM	1	No	Hip	8d	Strap	Yes	No	0.03
A.70	URM	1	No	Hip	8d	Strap	Yes	No	0.35
A.71	URM	1	No	Hip	8d	Strap	Yes	No	0.70
A.72	URM	1	No	Hip	8d	Strap	Yes	No	1.00
A.73	URM	1	No	Gable	8d	Toe-Nail	Yes	No	0.03
A.74	URM	1	No	Gable	8d	Toe-Nail	Yes	No	0.35
A.75	URM	1	No	Gable	8d	Toe-Nail	Yes	No	0.70
A.76	URM	1	No	Gable	8d	Toe-Nail	Yes	No	1.00

Table A.1. Sample Damage State Functions for Residential Buildings (concluded)

Figure	Walls	Stories	Garage	Roof Shape	Sheathing	Roof/ Wall	Shutters	Upgraded Roof	Terrain
A.77	URM	1	No	Hip	8d	Toe-Nail	Yes	No	0.03
A.78	URM	1	No	Hip	8d	Toe-Nail	Yes	No	0.35
A.79	URM	1	No	Hip	8d	Toe-Nail	Yes	No	0.70
A.80	URM	1	No	Hip	8d	Toe-Nail	Yes	No	1.00
A.81	URM	1	No	Gable	8d	Strap	No	Yes	0.03
A.82	URM	1	No	Gable	8d	Strap	No	Yes	0.35
A.83	URM	1	No	Gable	8d	Strap	No	Yes	0.70
A.84	URM	1	No	Gable	8d	Strap	No	Yes	1.00
A.85	URM	1	No	Hip	8d	Strap	No	Yes	0.03
A.86	URM	1	No	Hip	8d	Strap	No	Yes	0.35
A.87	URM	1	No	Hip	8d	Strap	No	Yes	0.70
A.88	URM	1	No	Hip	8d	Strap	No	Yes	1.00
A.89	URM	1	No	Gable	8d	Toe-Nail	No	Yes	0.03
A.90	URM	1	No	Gable	8d	Toe-Nail	No	Yes	0.35
A.91	URM	1	No	Gable	8d	Toe-Nail	No	Yes	0.70
A.92	URM	1	No	Gable	8d	Toe-Nail	No	Yes	1.00
A.93	URM	1	No	Hip	8d	Toe-Nail	No	Yes	0.03
A.94	URM	1	No	Hip	8d	Toe-Nail	No	Yes	0.35
A.95	URM	1	No	Hip	8d	Toe-Nail	No	Yes	0.70
A.96	URM	1	No	Hip	8d	Toe-Nail	No	Yes	1.00
A.97	URM	1	No	Gable	8d	Strap	Yes	Yes	0.03
A.98	URM	1	No	Gable	8d	Strap	Yes	Yes	0.35
A.99	URM	1	No	Gable	8d	Strap	Yes	Yes	0.70
A.100	URM	1	No	Gable	8d	Strap	Yes	Yes	1.00
A.101	URM	1	No	Hip	8d	Strap	Yes	Yes	0.03
A.102	URM	1	No	Hip	8d	Strap	Yes	Yes	0.35
A.103	URM	1	No	Hip	8d	Strap	Yes	Yes	0.70
A.104	URM	1	No	Hip	8d	Strap	Yes	Yes	1.00
A.105	URM	1	No	Gable	8d	Toe-Nail	Yes	Yes	0.03
A.106	URM	1	No	Gable	8d	Toe-Nail	Yes	Yes	0.35
A.107	URM	1	No	Gable	8d	Toe-Nail	Yes	Yes	0.70
A.108	URM	1	No	Gable	8d	Toe-Nail	Yes	Yes	1.00
A.109	URM	1	No	Hip	8d	Toe-Nail	Yes	Yes	0.03
A.110	URM	1	No	Hip	8d	Toe-Nail	Yes	Yes	0.35
A.111	URM	1	No	Hip	8d	Toe-Nail	Yes	Yes	0.70
A.112	URM	1	No	Hip	8d	Toe-Nail	Yes	Yes	1.00

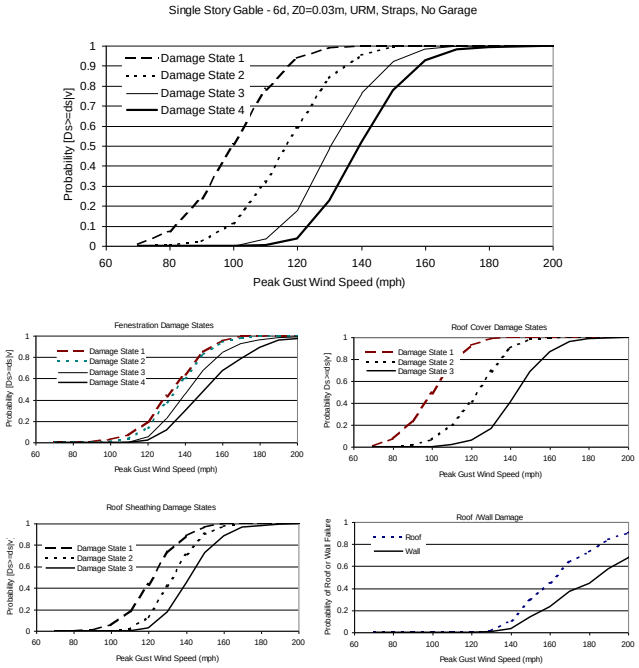

Figure A.1. Damage States versus Maximum Peak Gust Wind Speed – One Story, 6d Roof Sheathing Nails, Strapped Roof Trusses, Gable Roof, No Garage, Unreinforced Masonry Walls, z_0 = 0.03 m.

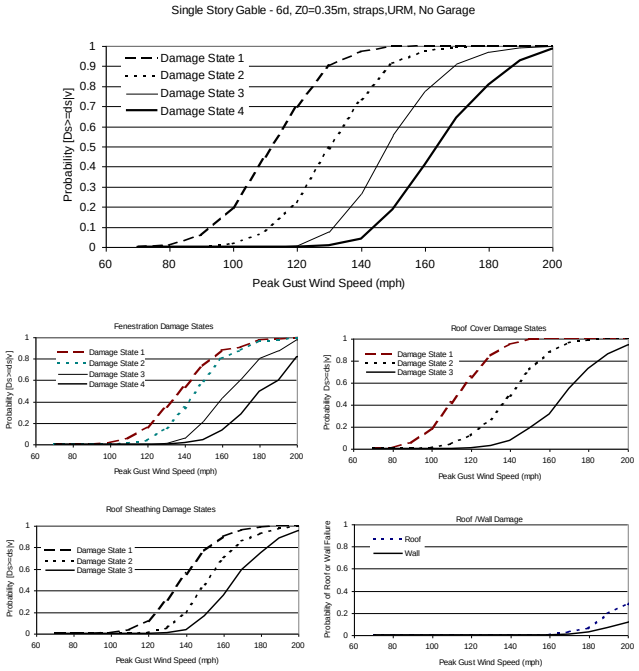

Figure A.2. Damage States versus Maximum Peak Gust Wind Speed – One Story, 6d Roof Sheathing Nails, Strapped Roof Trusses, Gable Roof, No Garage, Unreinforced Masonry Walls, z_0 = 0.35 m.

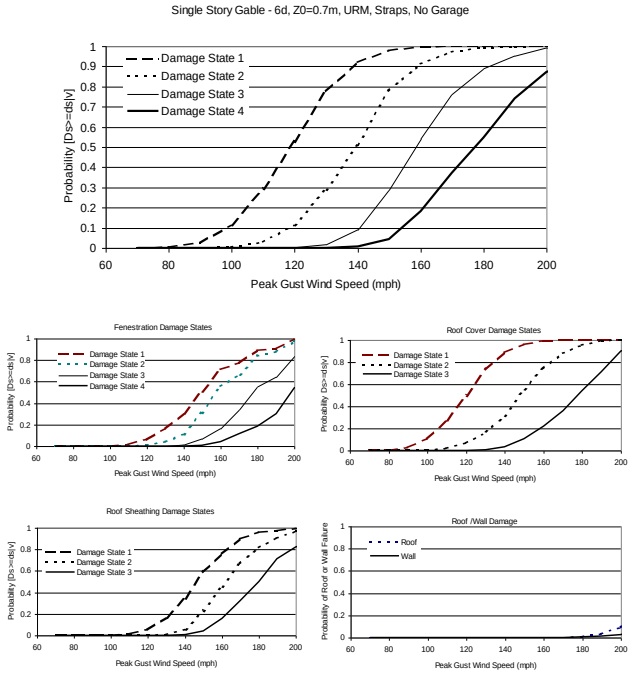

Figure A.3. Damage States versus Maximum Peak Gust Wind Speed – One Story, 6d Roof Sheathing Nails, Strapped Roof Trusses, Gable Roof, No Garage, Unreinforced Masonry Walls, z_0 = 0.70 m.

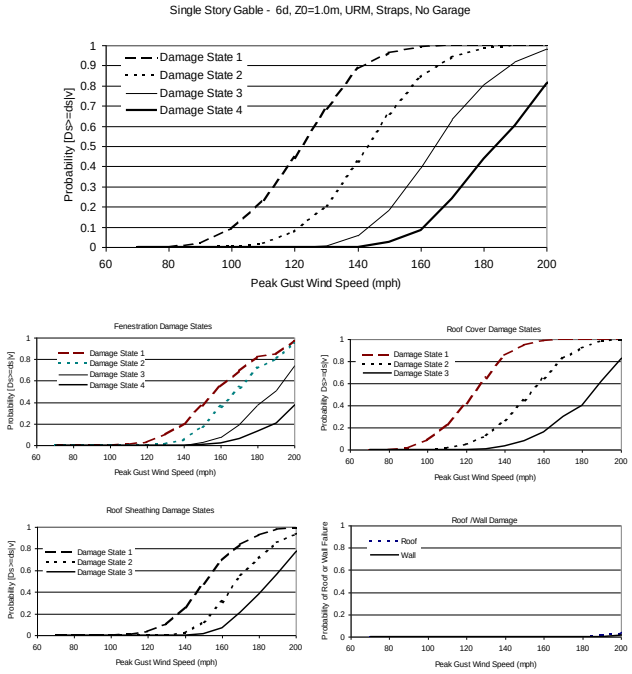

Figure A.4. Damage States versus Maximum Peak Gust Wind Speed – One Story, 6d Roof Sheathing Nails, Strapped Roof Trusses, Gable Roof, No Garage, Unreinforced Masonry Walls, z_0 = 1.0 m.

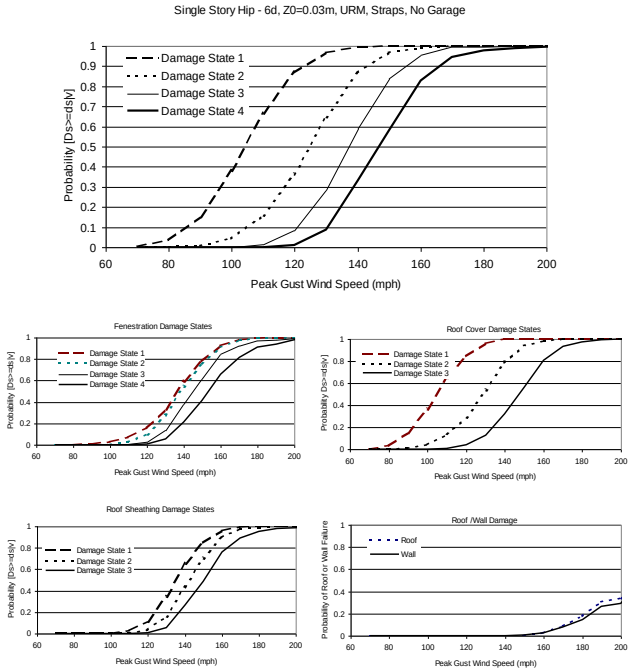

Figure A.5. Damage States versus Maximum Peak Gust Wind Speed – One Story, 6d Roof Sheathing Nails, Strapped Roof Trusses, Hip Roof, No Garage, Unreinforced Masonry Walls, z_0 = 0.03 m.

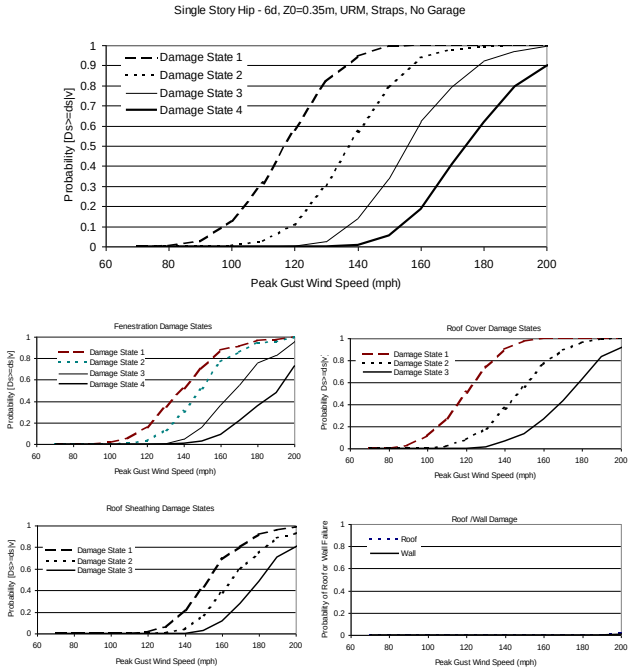

Figure A.6. Damage States versus Maximum Peak Gust Wind Speed – One Story, 6d Roof Sheathing Nails, Strapped Roof Trusses, Hip Roof, No Garage, Unreinforced Masonry Walls, z_0 = 0.35 m.

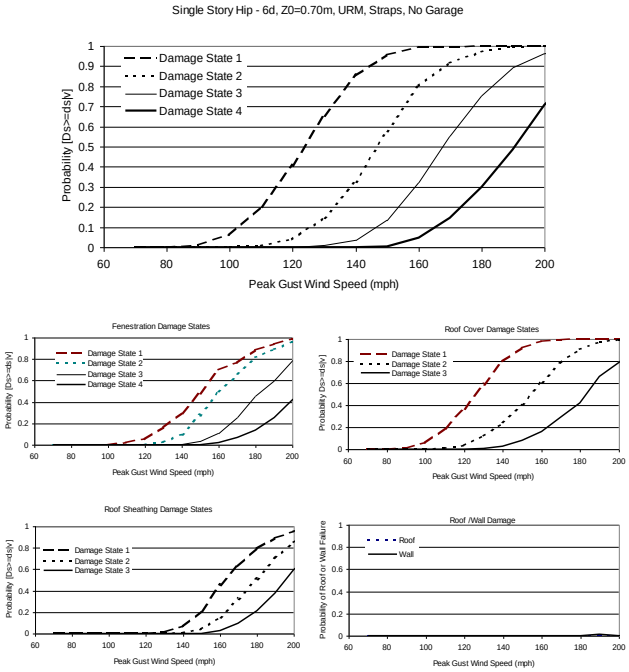

Figure A.7. Damage States versus Maximum Peak Gust Wind Speed – One Story, 6d Roof Sheathing Nails, Strapped Roof Trusses, Hip Roof, No Garage, Unreinforced Masonry Walls, z_0 = 0.70 m.

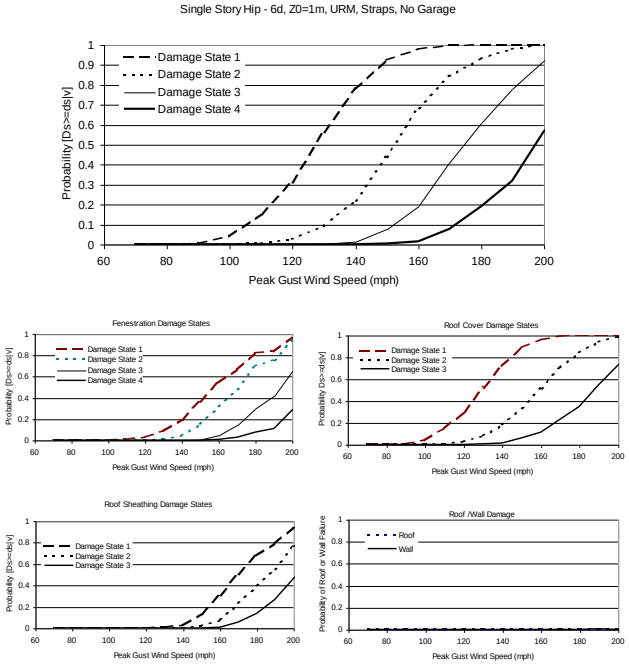

Figure A.8. Damage States versus Maximum Peak Gust Wind Speed – One Story, 6d Roof Sheathing Nails, Strapped Roof Trusses, Hip Roof, No Garage, Unreinforced Masonry Walls, z_0 = 1.0 m.

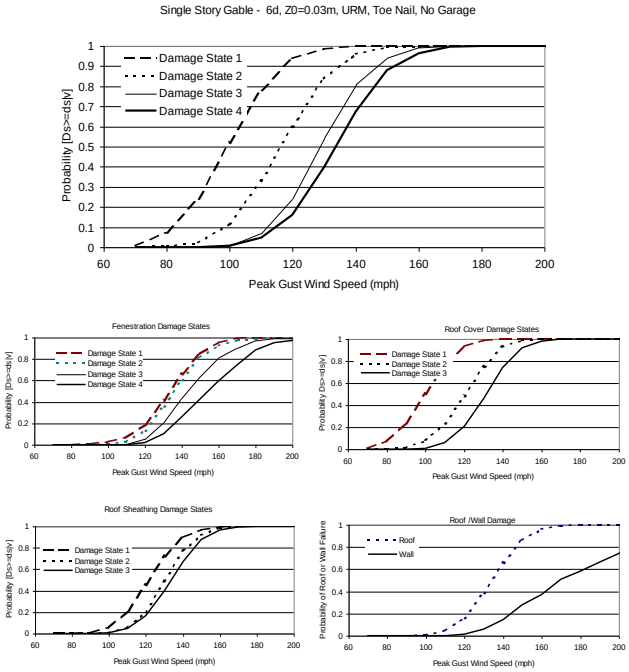

Figure A.9. Damage States versus Maximum Peak Gust Wind Speed – One Story, 6d Roof Sheathing Nails, Toe-Nailed Roof Trusses, Gable Roof, No Garage, Unreinforced Masonry Walls, z_0 = 0.03 m.

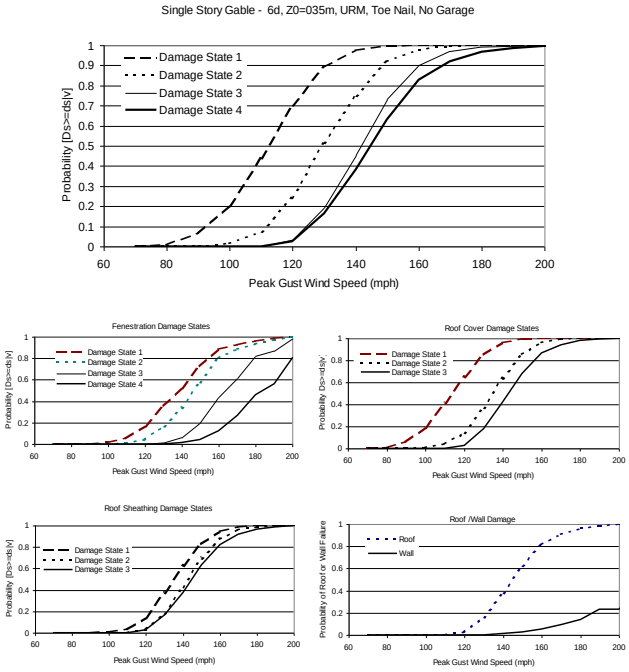

Figure A.10. Damage States versus Maximum Peak Gust Wind Speed – One Story, 6d Roof Sheathing Nails, Toe-Nailed Roof Trusses, Gable Roof, No Garage, Unreinforced Masonry Walls, z_0 = 0.35 m.

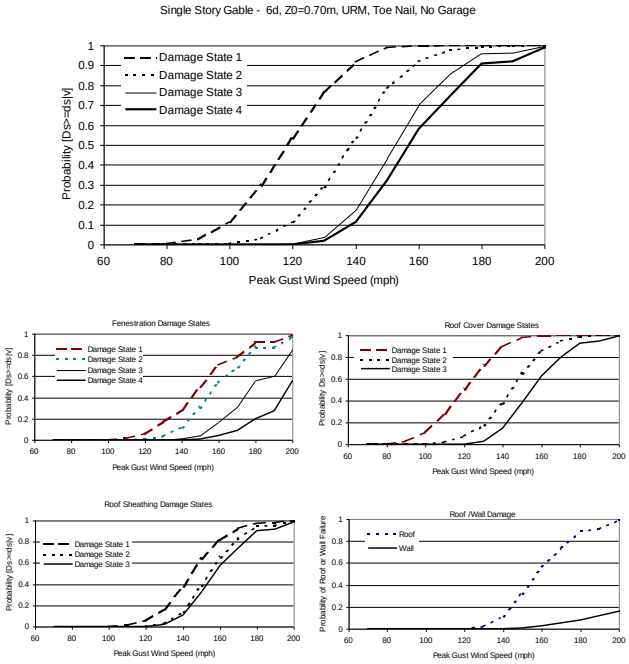

Figure A.11. Damage States versus Maximum Peak Gust Wind Speed – One Story, 6d Roof Sheathing Nails, Toe-Nailed Roof Trusses, Gable Roof, No Garage, Unreinforced Masonry Walls, z_0 = 0.70 m.

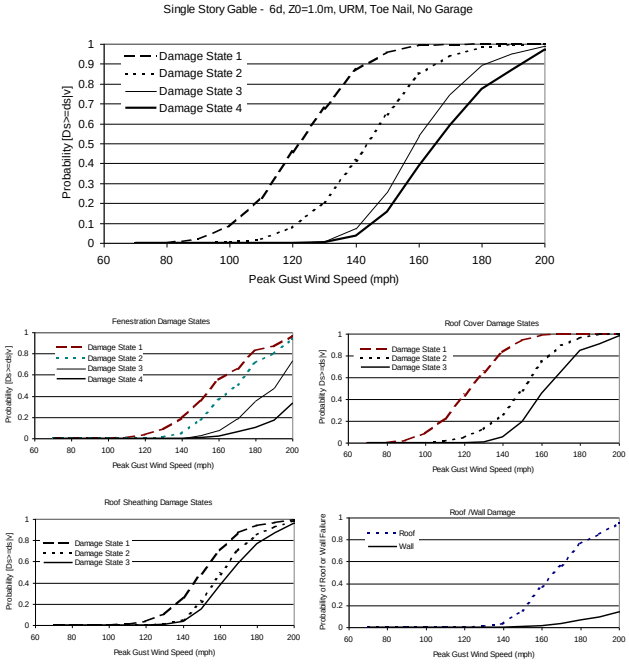

Figure A.12. Damage States versus Maximum Peak Gust Wind Speed – One Story, 6d Roof Sheathing Nails, Toe-Nailed Roof Trusses, Gable Roof, No Garage, Unreinforced Masonry Walls, z_0 = 1.0 m.

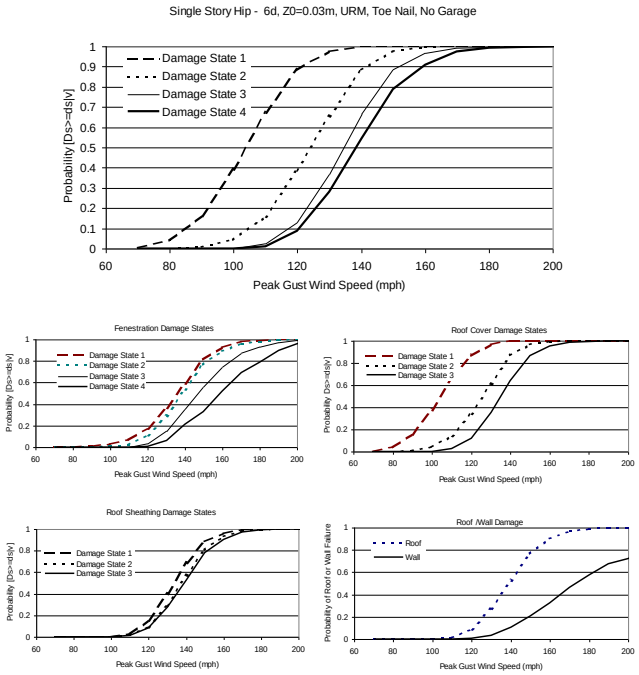

Figure A.13. Damage States versus Maximum Peak Gust Wind Speed – One Story, 6d Roof Sheathing Nails, Toe-Nailed Roof Trusses, Hip Roof, No Garage, Unreinforced Masonry Walls, z_0 = 0.03 m.

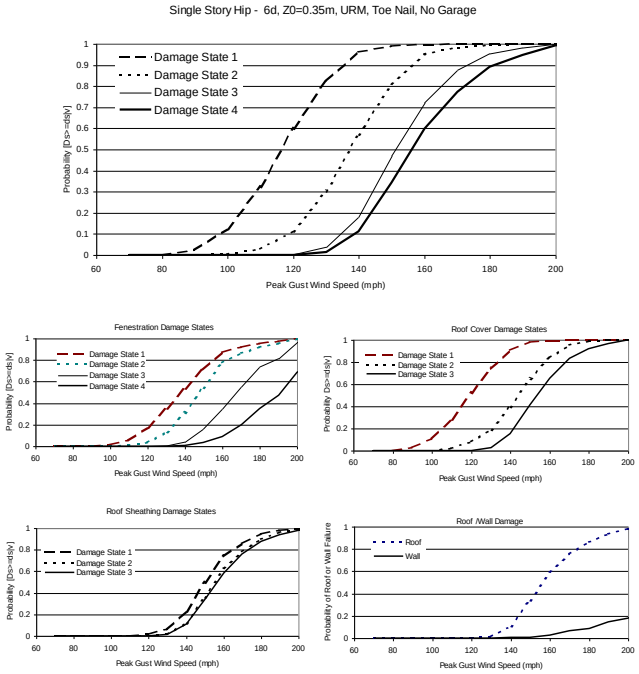

Figure A.14. Damage States versus Maximum Peak Gust Wind Speed – One Story, 6d Roof Sheathing Nails, Toe-Nailed Roof Trusses, Hip Roof, No Garage, Unreinforced Masonry Walls, z_0 = 0.35 m.

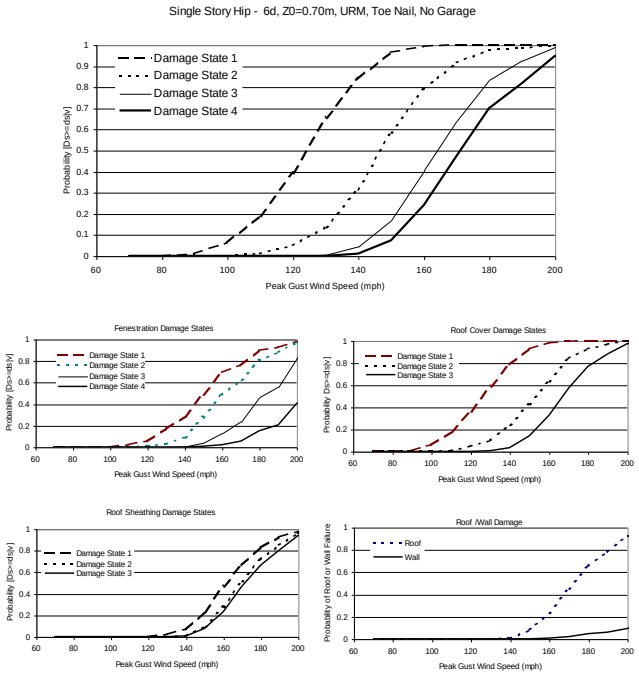

Figure A.15. Damage States versus Maximum Peak Gust Wind Speed – One Story, 6d Roof Sheathing Nails, Toe-Nailed Roof Trusses, Hip Roof, No Garage, Unreinforced Masonry Walls, z_0 = 0.70 m.

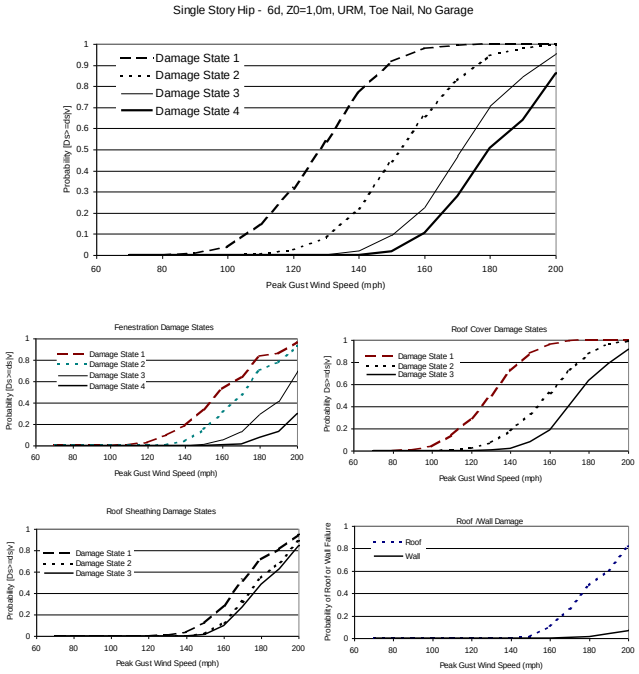

Figure A.16. Damage States versus Maximum Peak Gust Wind Speed – One Story, 6d Roof Sheathing Nails, Toe-Nailed Roof Trusses, Hip Roof, No Garage, Unreinforced Masonry Walls, z_0 = 1.0 m.

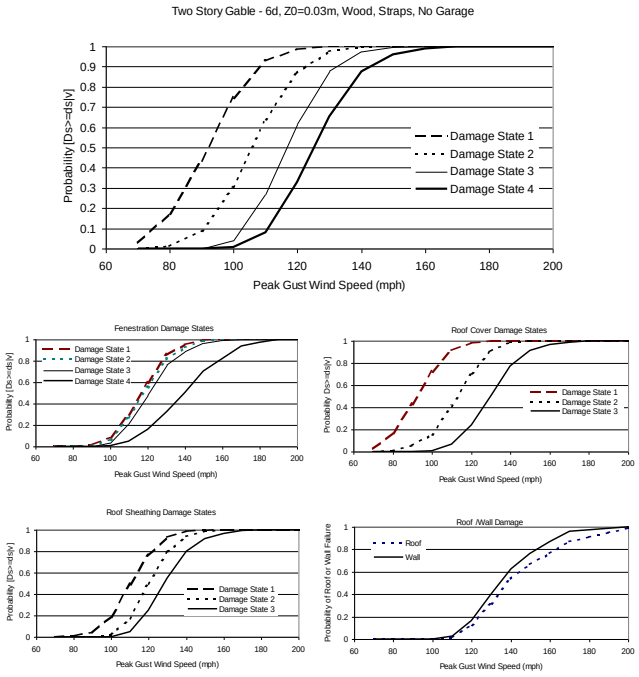

Figure A.17. Damage States versus Maximum Peak Gust Wind Speed – Two Story, 6d Roof Sheathing Nails, Strapped Roof Trusses, Gable Roof, No Garage, Wood Frame Walls, z_0 = 0.03 m.

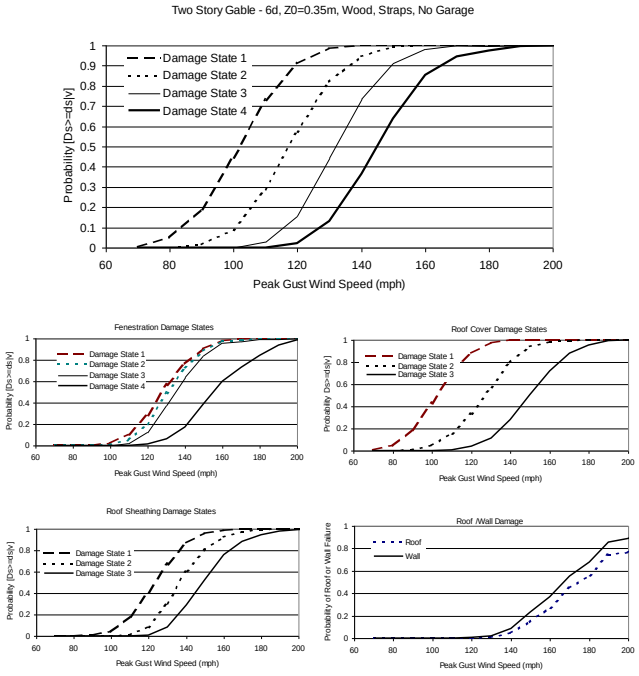

Figure A.18. Damage States versus Maximum Peak Gust Wind Speed – Two Story, 6d Roof Sheathing Nails, Strapped Roof Trusses, Gable Roof, No Garage, Wood Frame Walls, z_0 = 0.35 m.

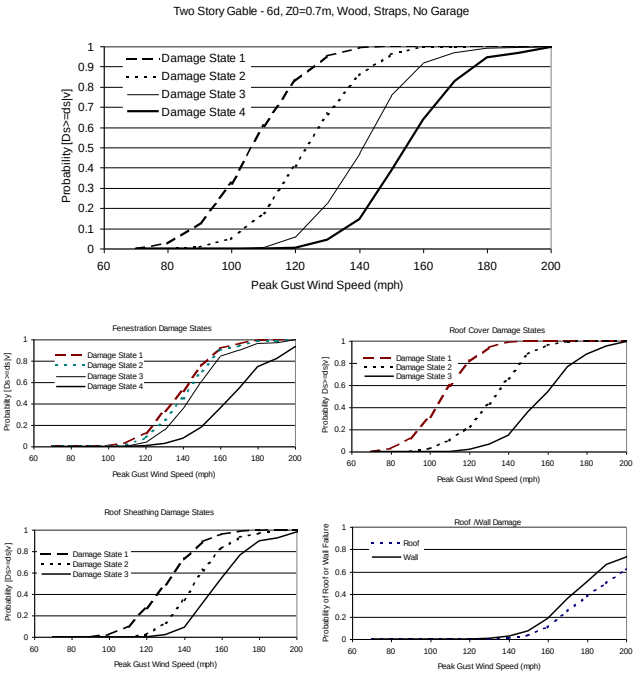

Figure A.19. Damage States versus Maximum Peak Gust Wind Speed – Two Story, 6d Roof Sheathing Nails, Strapped Roof Trusses, Gable Roof, No Garage, Wood Frame Walls, z_0 = 0.70 m.

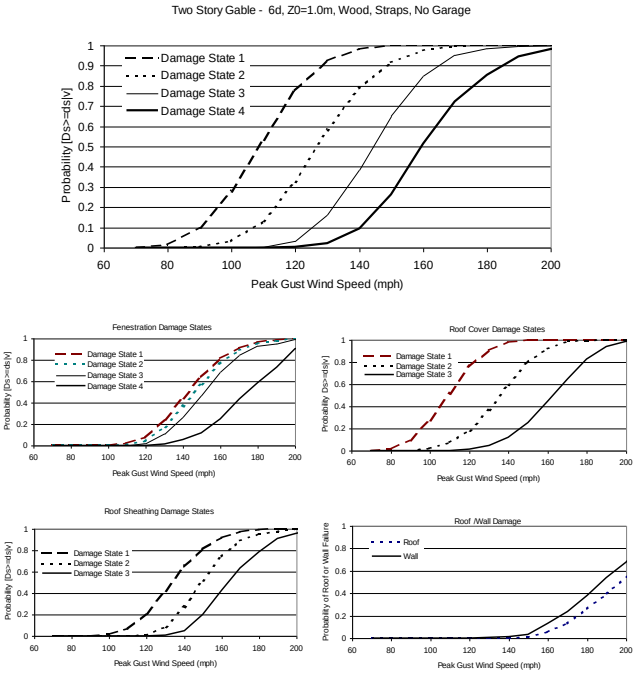

Figure A.20. Damage States versus Maximum Peak Gust Wind Speed – Two Story, 6d Roof Sheathing Nails, Strapped Roof Trusses, Hip Roof, No Garage, Wood Frame Walls, z_0 = 1.0 m.

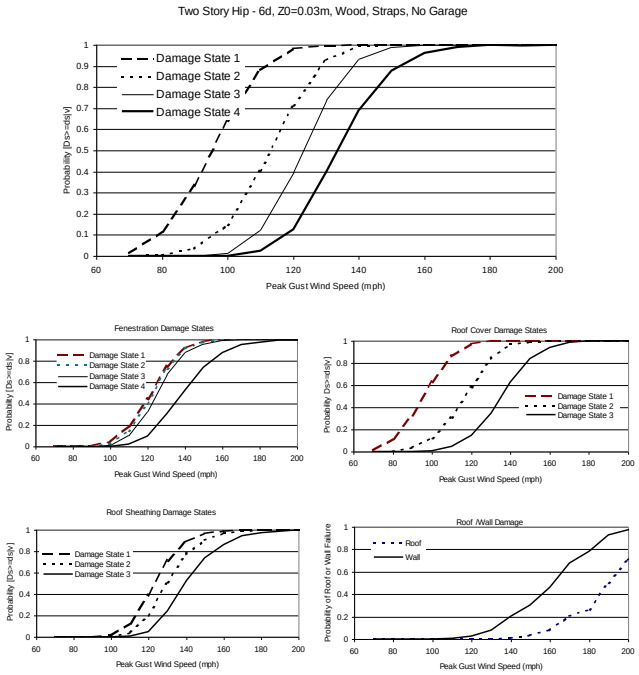

Figure A.21. Damage States versus Maximum Peak Gust Wind Speed – Two Story, 6d Roof Sheathing Nails, Strapped Roof Trusses, Hip Roof, No Garage, Wood Frame Walls, z_0 = 0.03 m.

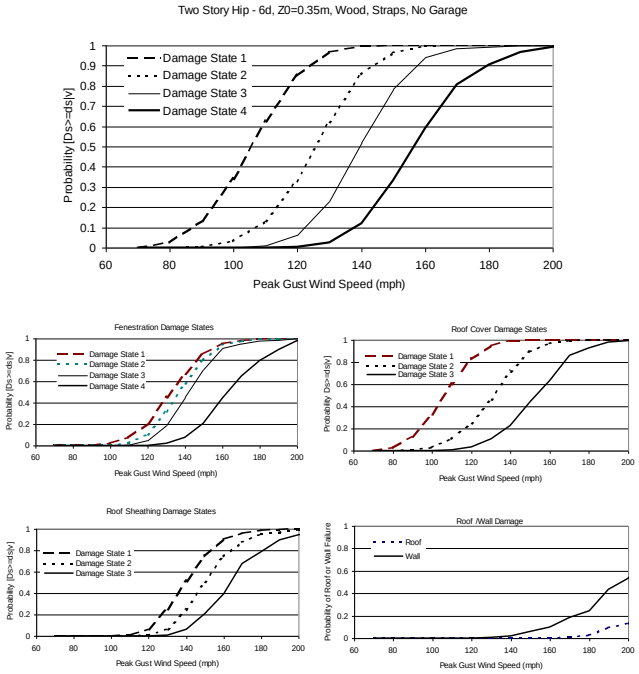

Figure A.22. Damage States versus Maximum Peak Gust Wind Speed – Two Story, 6d Roof Sheathing Nails, Strapped Roof Trusses, Hip Roof, No Garage, Wood Frame Walls, z_0 = 0.35 m.

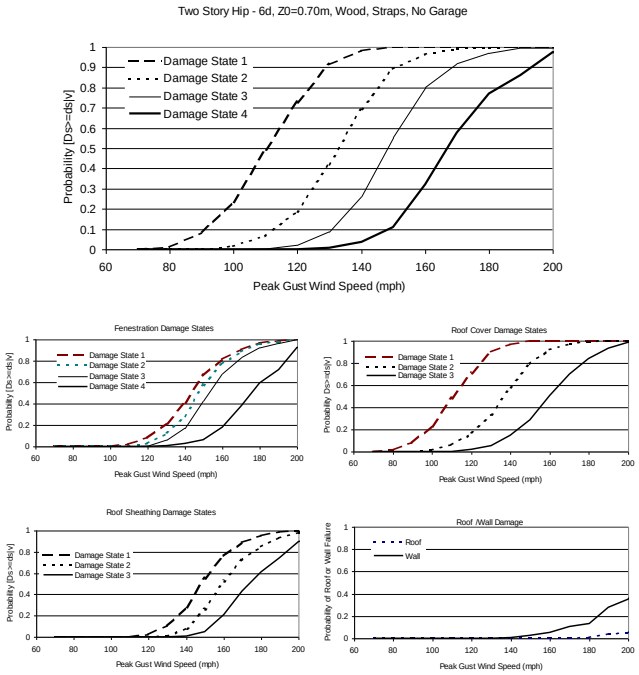

Figure A.23. Damage States versus Maximum Peak Gust Wind Speed – Two Story, 6d Roof Sheathing Nails, Strapped Roof Trusses, Hip Roof, No Garage, Wood Frame Walls, z_0 = 0.70 m.

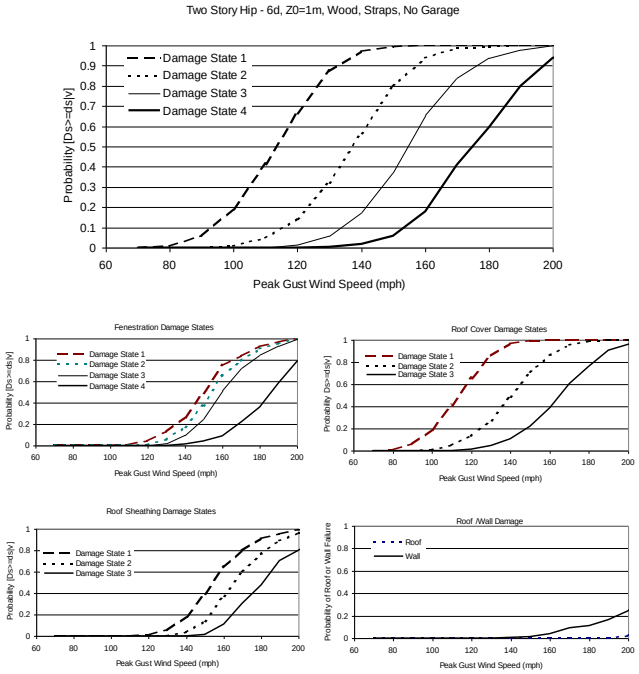

Figure A.24. Damage States versus Maximum Peak Gust Wind Speed – Two Story, 6d Roof Sheathing Nails, Strapped Roof Trusses, Hip Roof, No Garage, Wood Frame Walls, z_0 = 1.0 m.

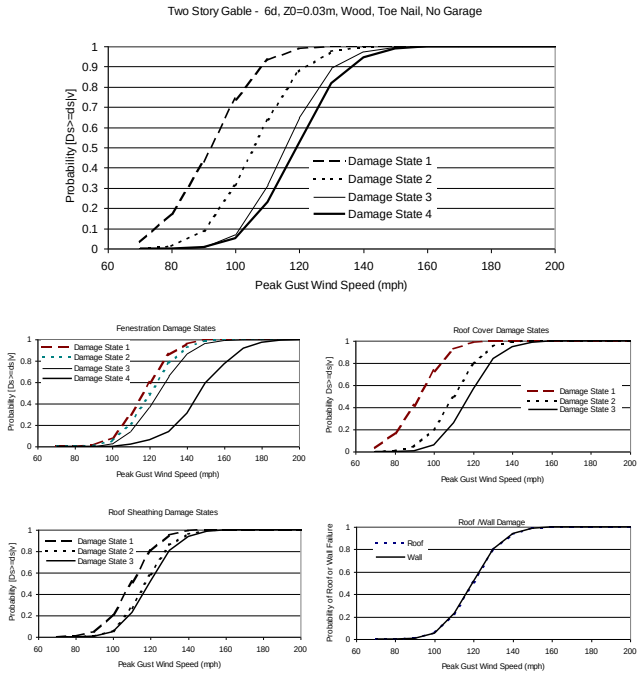

Figure A.25. Damage States versus Maximum Peak Gust Wind Speed – Two Story, 6d Roof Sheathing Nails, Toe-Nailed Roof Trusses, Gable Roof, No Garage, Wood Frame Walls, z_0 = 0.03 m.

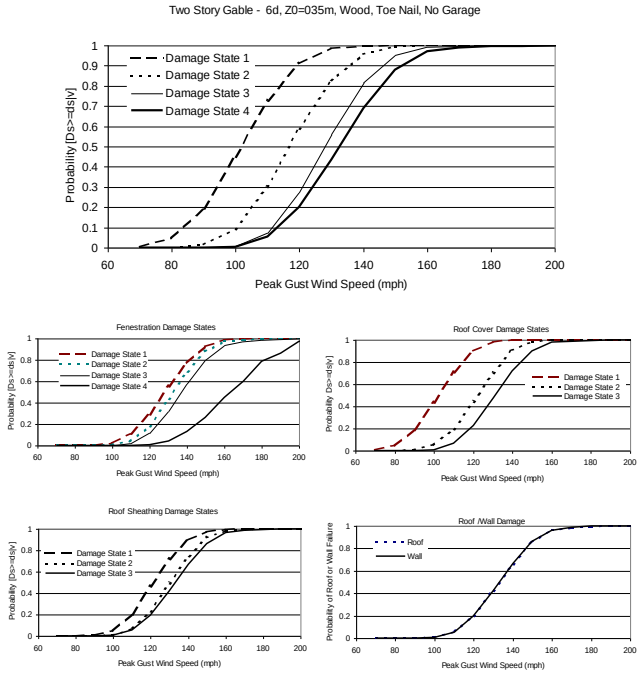

Figure A.26. Damage States versus Maximum Peak Gust Wind Speed – Two Story, 6d Roof Sheathing Nails, Toe-Nailed Roof Trusses, Gable Roof, No Garage, Wood Frame Walls, z_0 = 0.35 m.

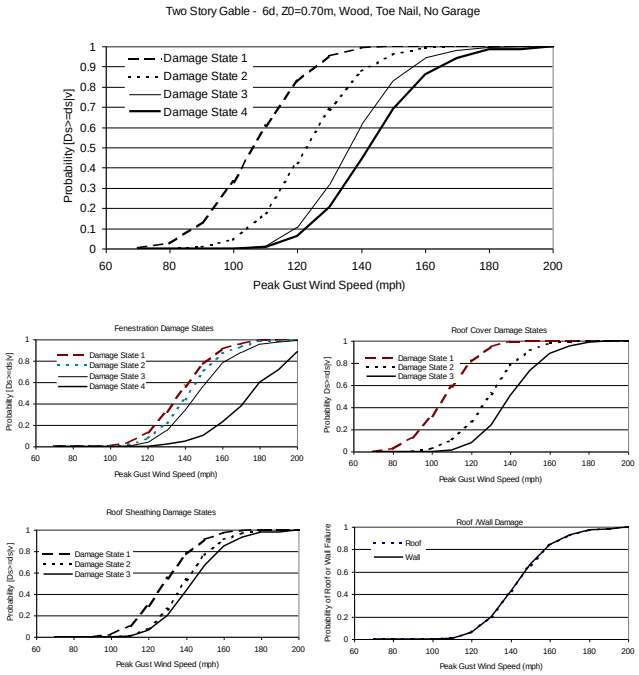

Figure A.27. Damage States versus Maximum Peak Gust Wind Speed – Two Story, 6d Roof Sheathing Nails, Toe-Nailed Roof Trusses, Gable Roof, No Garage, Wood Frame Walls, z_0 = 0.70 m.

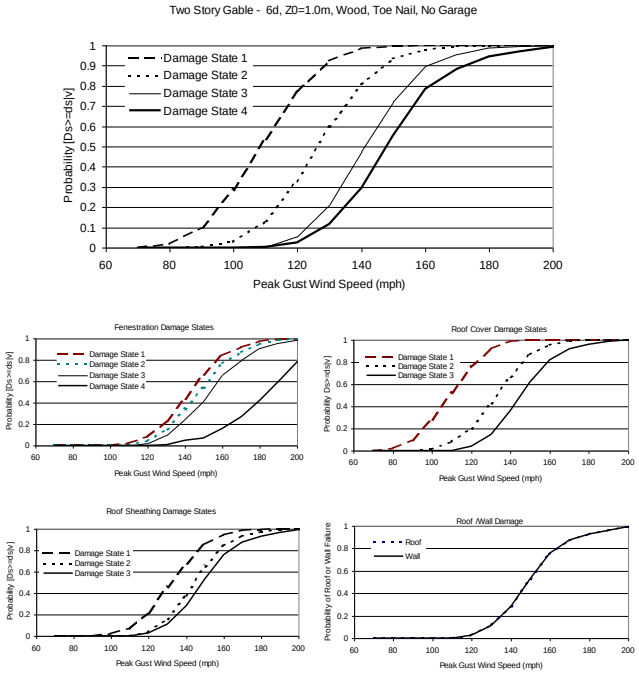

Figure A.28. Damage States versus Maximum Peak Gust Wind Speed – Two Story, 6d Roof Sheathing Nails, Toe-Nailed Roof Trusses, Gable Roof, No Garage, Wood Frame Walls, z_0 = 1.0 m.

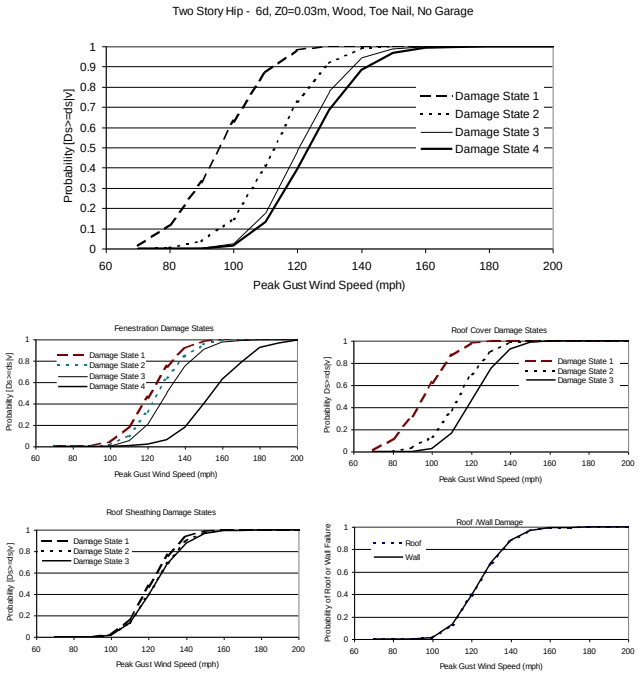

Figure A.29. Damage States versus Maximum Peak Gust Wind Speed – Two Story, 6d Roof Sheathing Nails, Toe-Nailed Roof Trusses, Hip Roof, No Garage, Wood Frame Walls, z_0 = 0.03 m.

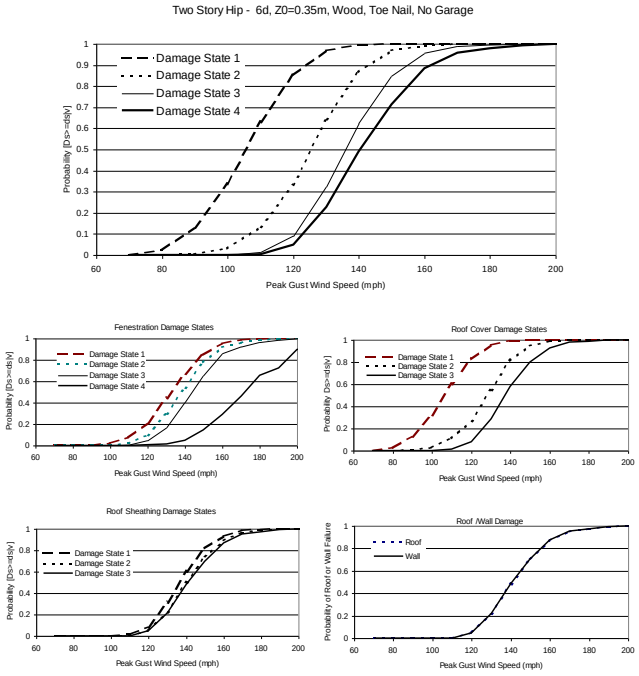

Figure A.30. Damage States versus Maximum Peak Gust Wind Speed – Two Story, 6d Roof Sheathing Nails, Toe-Nailed Roof Trusses, Hip Roof, No Garage, Wood Frame Walls, z_0 = 0.35 m.

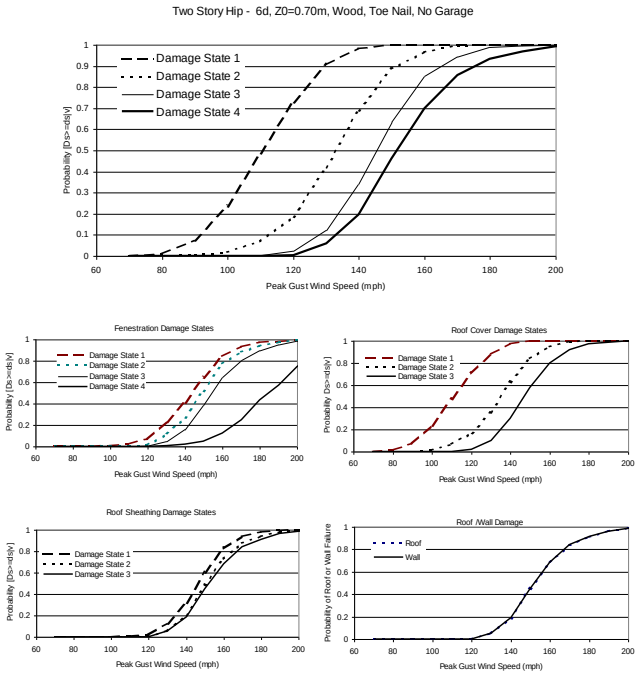

Figure A.31. Damage States versus Maximum Peak Gust Wind Speed – Two Story, 6d Roof Sheathing Nails, Toe-Nailed Roof Trusses, Hip Roof, No Garage, Wood Frame Walls, z_0 = 0.70 m.

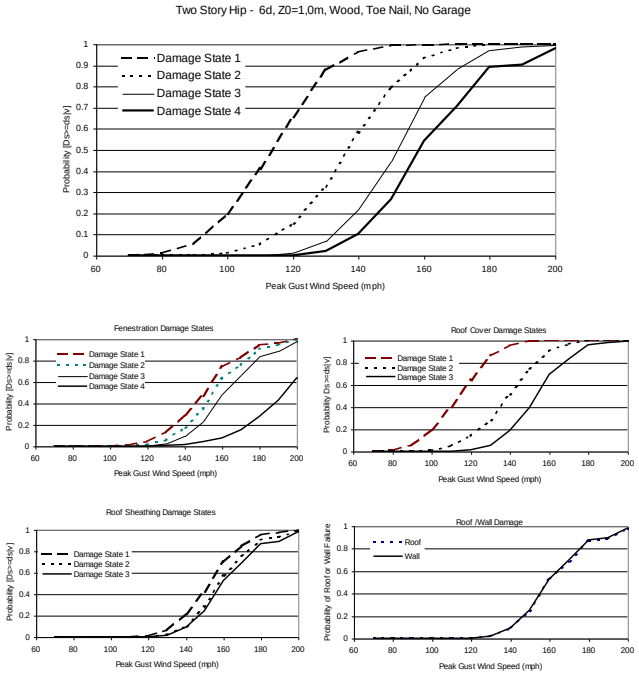

Figure A.32. Damage States versus Maximum Peak Gust Wind Speed – Two Story, 6d Roof Sheathing Nails, Toe-Nailed Roof Trusses, Hip Roof, No Garage, Wood Frame Walls, z_0 = 1.0 m.

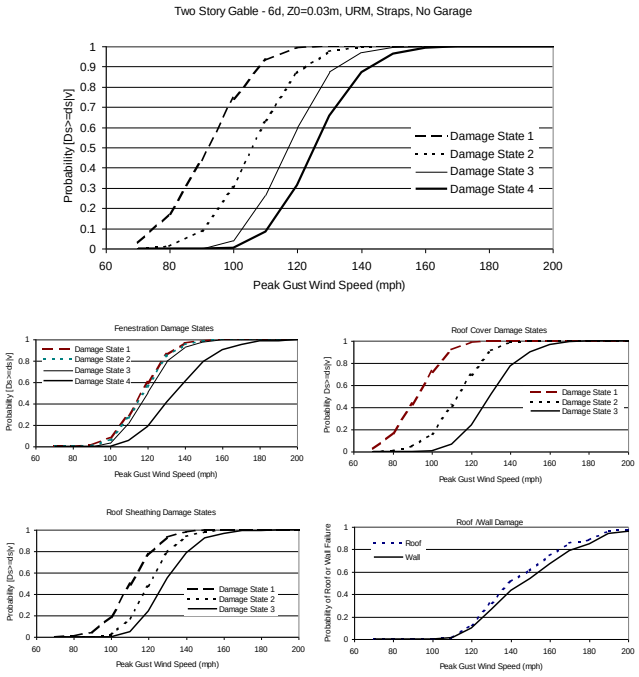

Figure A.33. Damage States versus Maximum Peak Gust Wind Speed – Two Story, 6d Roof Sheathing Nails, Strapped Roof Trusses, Gable Roof, No Garage, Unreinforced Masonry Walls, z_0 = 0.03 m.

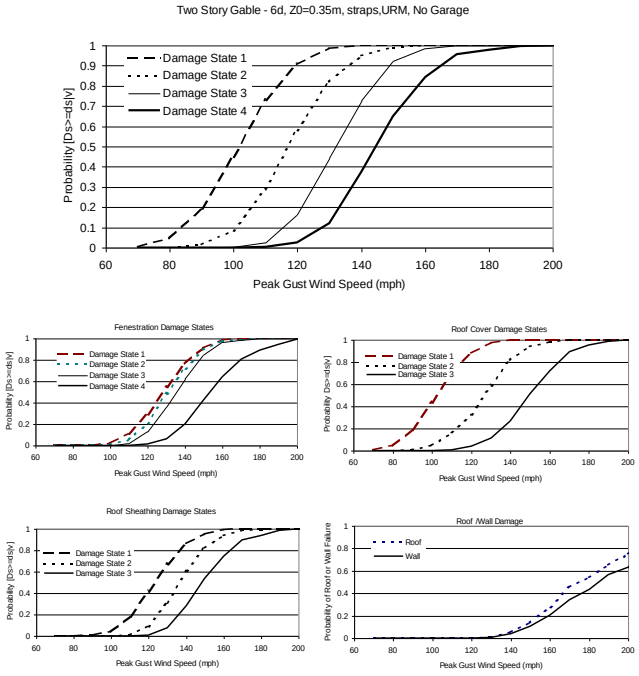

Figure A.34. Damage States versus Maximum Peak Gust Wind Speed – Two Story, 6d Roof Sheathing Nails, Strapped Roof Trusses, Gable Roof, No Garage, Unreinforced Masonry Walls, z_0 = 0.35 m.

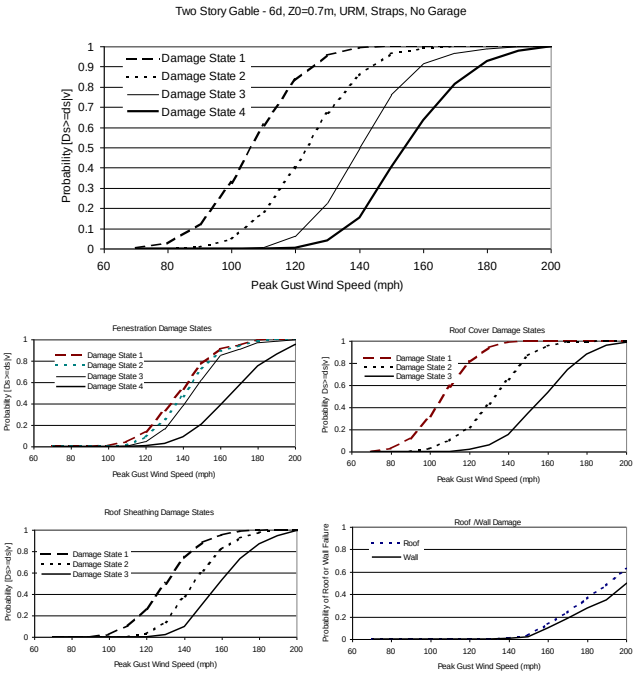

Figure A.35. Damage States versus Maximum Peak Gust Wind Speed – Two Story, 6d Roof Sheathing Nails, Strapped Roof Trusses, Gable Roof, No Garage, Unreinforced Masonry Walls, z_0 = 0.70 m.

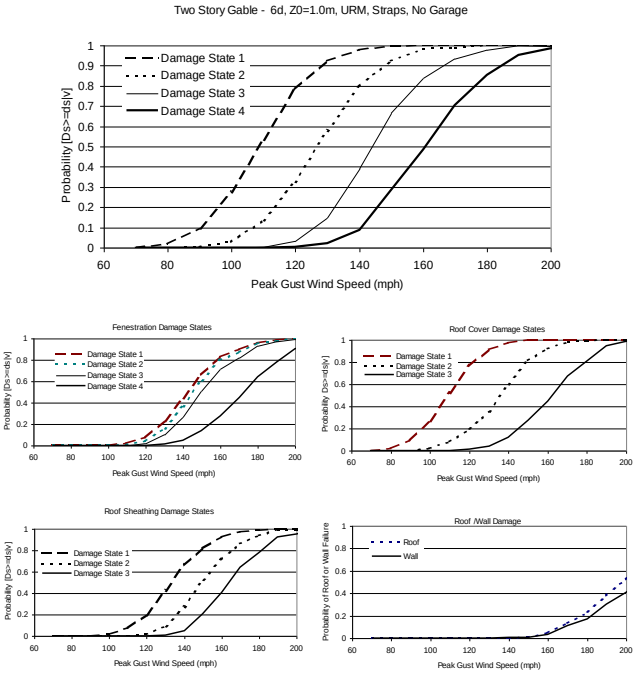

Figure A.36. Damage States versus Maximum Peak Gust Wind Speed – Two Story, 6d Roof Sheathing Nails, Strapped Roof Trusses, Gable Roof, No Garage, Unreinforced Masonry Walls, z_0 = 1.0 m.

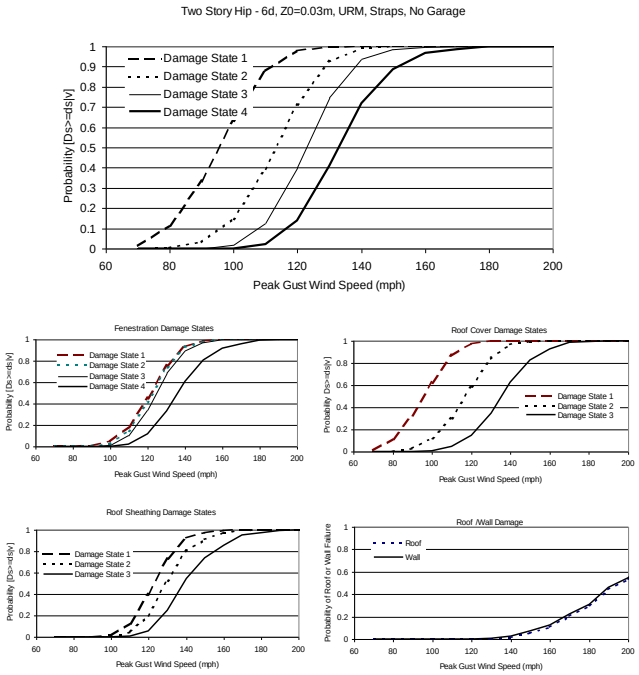

Figure A.37. Damage States versus Maximum Peak Gust Wind Speed – Two Story, 6d Roof Sheathing Nails, Strapped Roof Trusses, Hip Roof, No Garage, Unreinforced Masonry Walls, z_0 = 0.03 m.

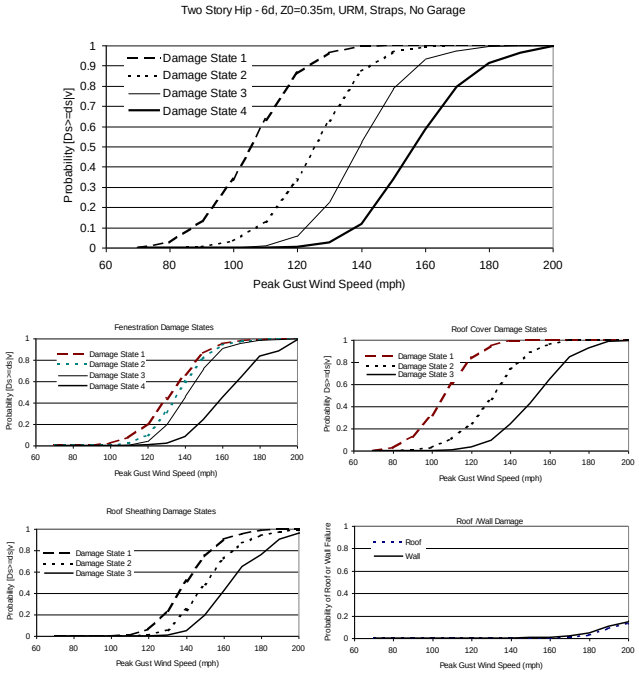

Figure A.38. Damage States versus Maximum Peak Gust Wind Speed – Two Story, 6d Roof Sheathing Nails, Strapped Roof Trusses, Hip Roof, No Garage, Unreinforced Masonry Walls, z_0 = 0.35 m.

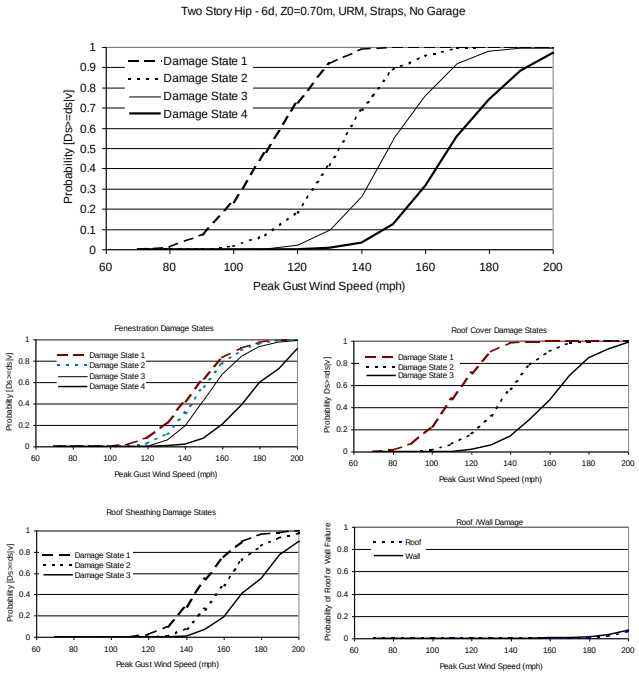

Figure A.39. Damage States versus Maximum Peak Gust Wind Speed – Two Story, 6d Roof Sheathing Nails, Strapped Roof Trusses, Hip Roof, No Garage, Unreinforced Masonry Walls, z_0 = 0.70 m.

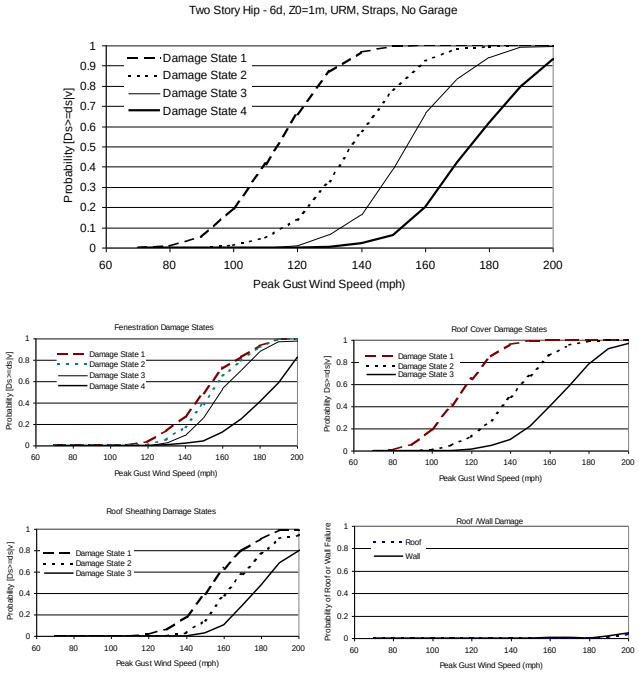

Figure A.40. Damage States versus Maximum Peak Gust Wind Speed – Two Story, 6d Roof Sheathing Nails, Strapped Roof Trusses, Hip Roof, No Garage, Unreinforced Masonry Walls, z_0 = 1.0 m.

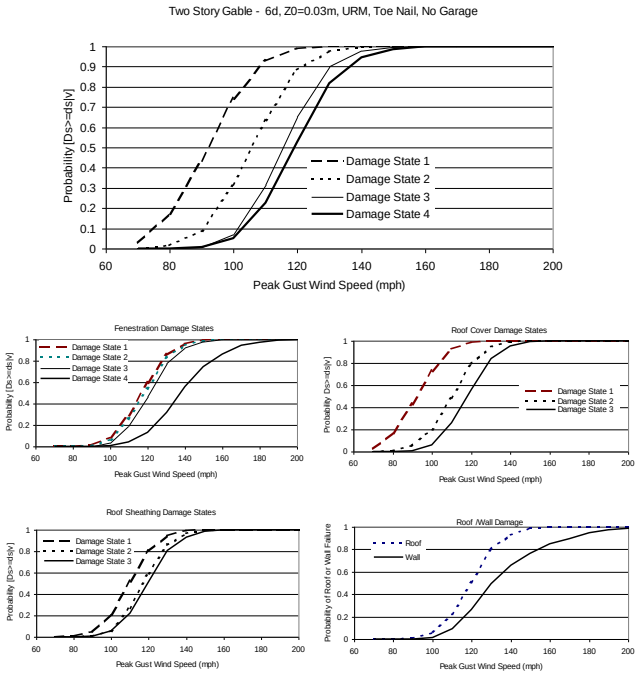

Figure A.41. Damage States versus Maximum Peak Gust Wind Speed – Two Story, 6d Roof Sheathing Nails, Toe-Nailed Roof Trusses, Gable Roof, No Garage, Unreinforced Masonry Walls, z_0 = 0.03 m.

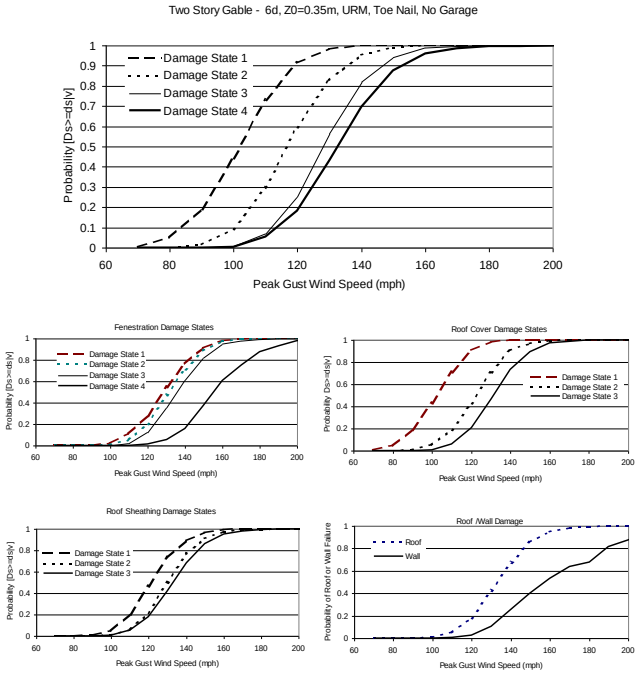

Figure A.42. Damage States versus Maximum Peak Gust Wind Speed – Two Story, 6d Roof Sheathing Nails, Toe-Nailed Roof Trusses, Gable Roof, No Garage, Unreinforced Masonry Walls, z_0 = 0.35 m.

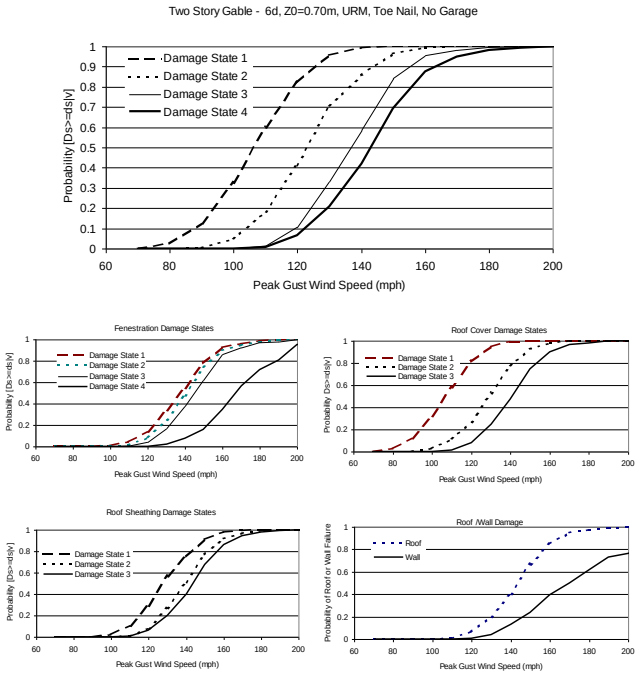

Figure A.43. Damage States versus Maximum Peak Gust Wind Speed – Two Story, 6d Roof Sheathing Nails, Toe-Nailed Roof Trusses, Gable Roof, No Garage, Unreinforced Masonry Walls, z_0 = 0.70 m.

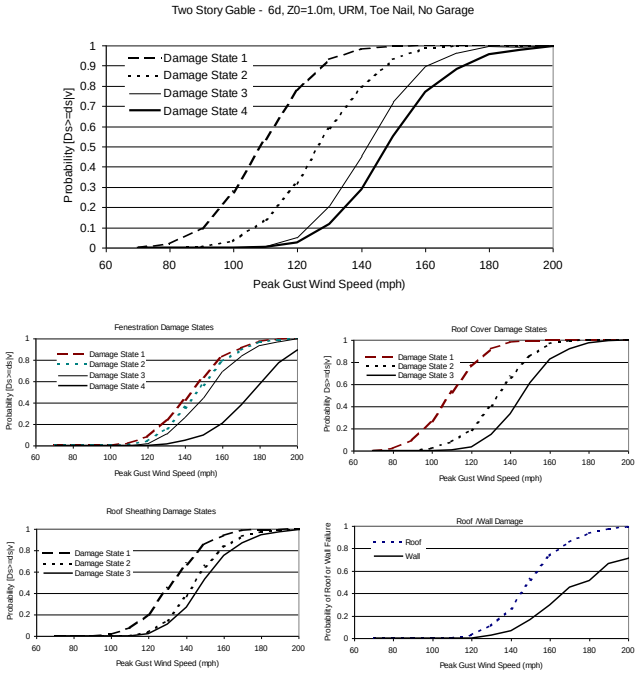

Figure A.44. Damage States versus Maximum Peak Gust Wind Speed – Two Story, 6d Roof Sheathing Nails, Toe-Nailed Roof Trusses, Gable Roof, No Garage, Unreinforced Masonry Walls, z_0 = 1.0 m.

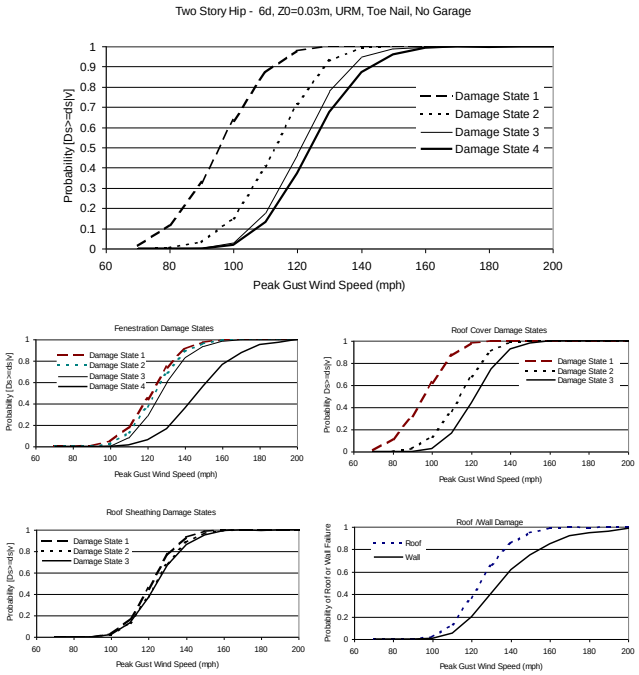

Figure A.45. Damage States versus Maximum Peak Gust Wind Speed – Two Story, 6d Roof Sheathing Nails, Toe-Nailed Roof Trusses, Hip Roof, No Garage, Unreinforced Masonry Walls, z_0 = 0.03 m.

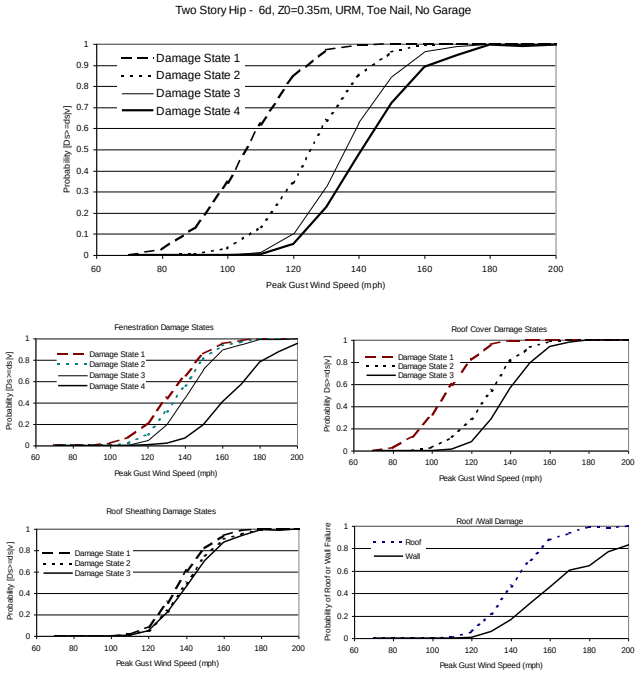

Figure A.46. Damage States versus Maximum Peak Gust Wind Speed – Two Story, 6d Roof Sheathing Nails, Toe-Nailed Roof Trusses, Hip Roof, No Garage, Unreinforced Masonry Walls, z_0 = 0.35 m.

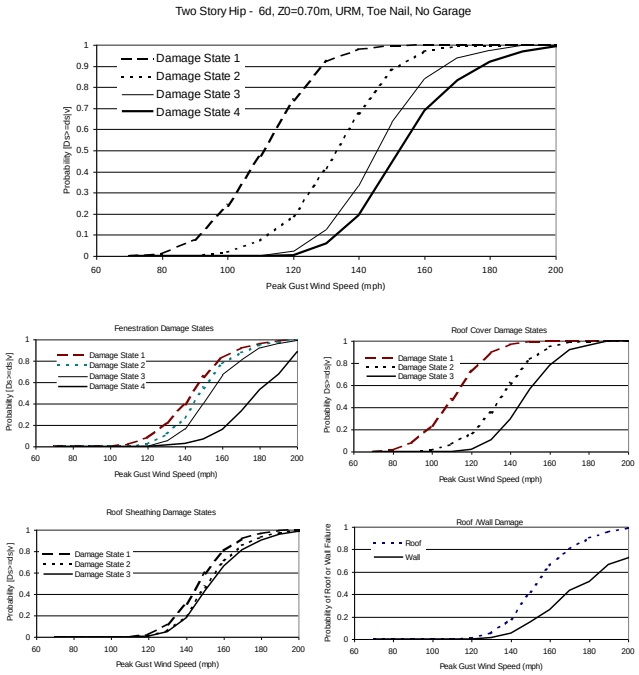

Figure A.47. Damage States versus Maximum Peak Gust Wind Speed – Two Story, 6d Roof Sheathing Nails, Toe-Nailed Roof Trusses, Hip Roof, No Garage, Unreinforced Masonry Walls, z_0 = 0.70 m.

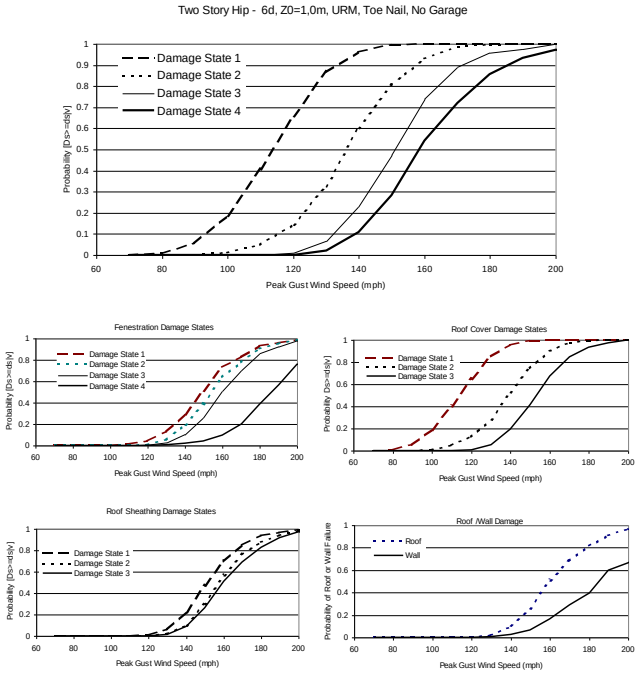

Figure A.48. Damage States versus Maximum Peak Gust Wind Speed – Two Story, 6d Roof Sheathing Nails, Toe-Nailed Roof Trusses, Hip Roof, No Garage, Unreinforced Masonry Walls, z_0 = 1.0 m.

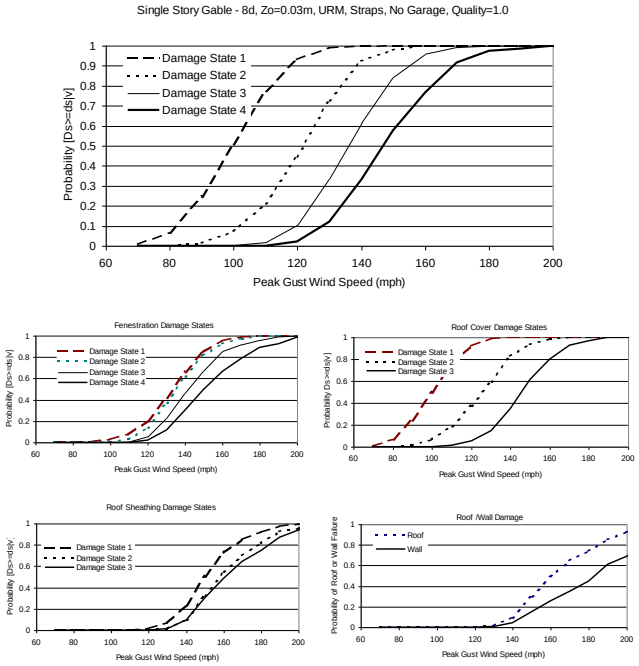

Figure A.49. Damage States versus Maximum Peak Gust Wind Speed – One Story, 8d Roof Sheathing Nails, Strapped Roof Trusses, Gable Roof, No Garage, Unreinforced Masonry Walls, z_0 = 0.03 m.

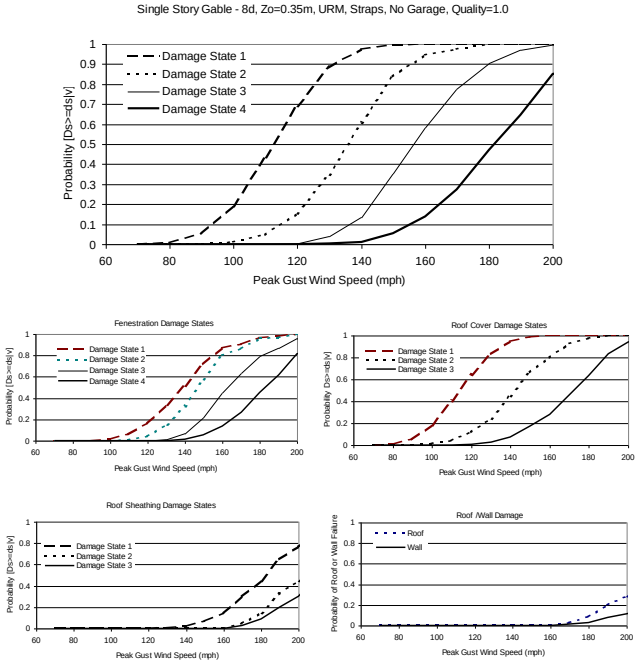

Figure A.50. Damage States versus Maximum Peak Gust Wind Speed – One Story, 8d Roof Sheathing Nails, Strapped Roof Trusses, Gable Roof, No Garage, Unreinforced Masonry Walls, z_0 = 0.35 m.

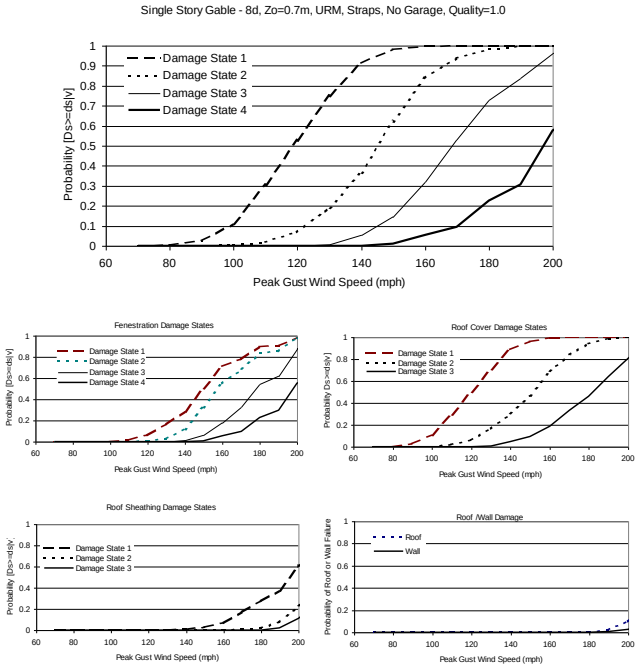

Figure A.51. Damage States versus Maximum Peak Gust Wind Speed – One Story, 8d Roof Sheathing Nails, Strapped Roof Trusses, Gable Roof, No Garage, Unreinforced Masonry Walls, z_0 = 0.70 m.

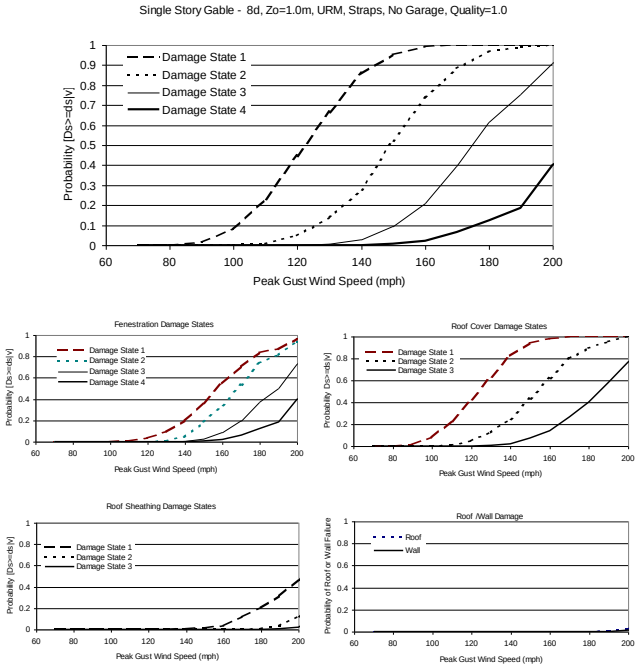

Figure A.52. Damage States versus Maximum Peak Gust Wind Speed – One Story, 8d Roof Sheathing Nails, Strapped Roof Trusses, Gable Roof, No Garage, Unreinforced Masonry Walls, z_0 = 1.0 m.

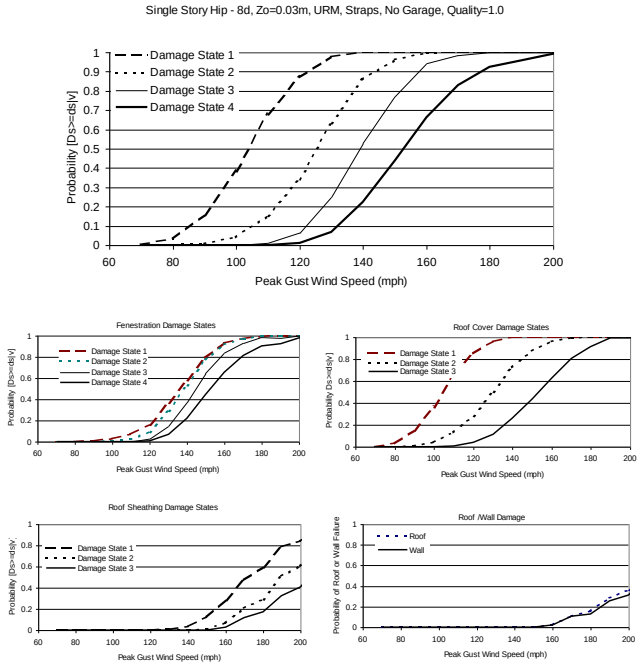

Figure A.53. Damage States versus Maximum Peak Gust Wind Speed – One Story, 8d Roof Sheathing Nails, Strapped Roof Trusses, Hip Roof, No Garage, Unreinforced Masonry Walls, z_0 = 0.03 m.

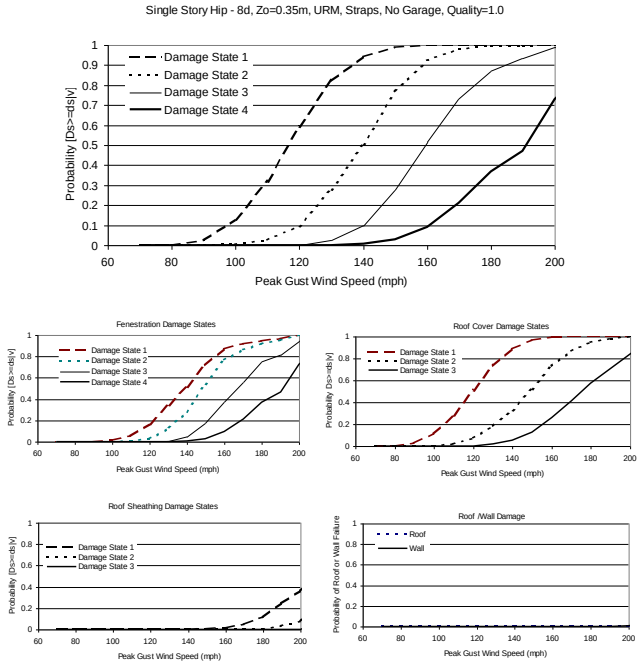

Figure A.54. Damage States versus Maximum Peak Gust Wind Speed – One Story, 8d Roof Sheathing Nails, Strapped Roof Trusses, Hip Roof, No Garage, Unreinforced Masonry Walls, z_0 = 0.35 m.

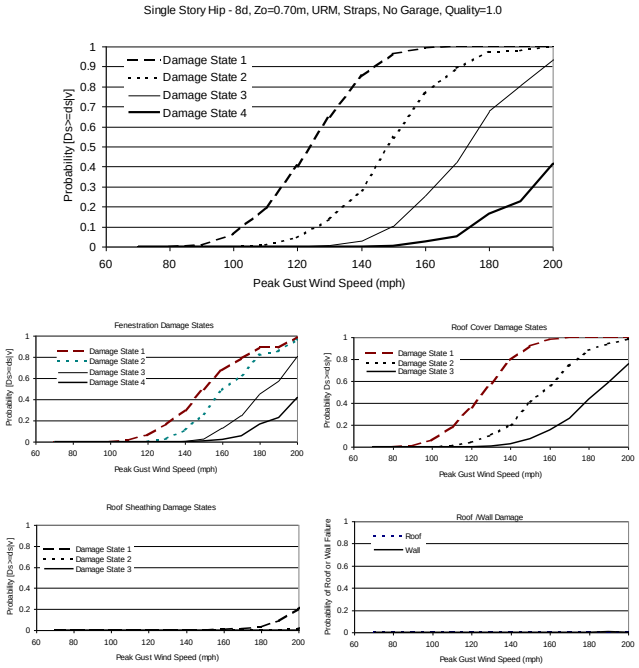

Figure A.55. Damage States versus Maximum Peak Gust Wind Speed – One Story, 8d Roof Sheathing Nails, Strapped Roof Trusses, Hip Roof, No Garage, Unreinforced Masonry Walls, z_0 = 0.70 m.

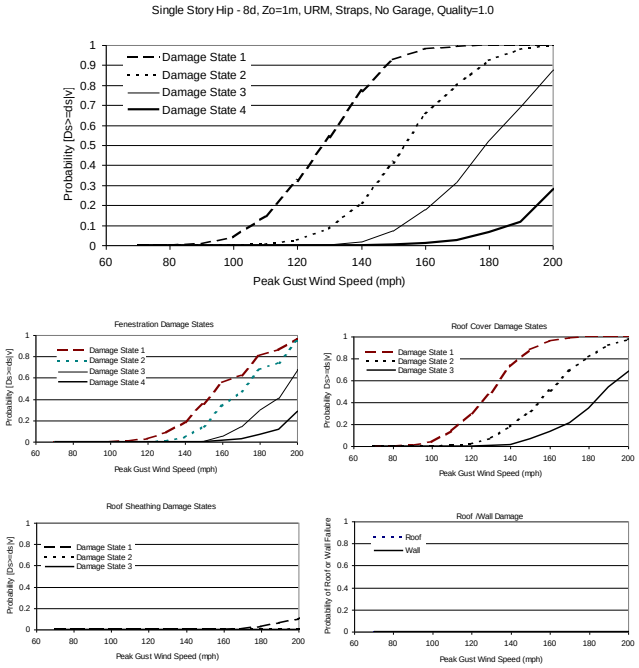

Figure A.56. Damage States versus Maximum Peak Gust Wind Speed – One Story, 8d Roof Sheathing Nails, Strapped Roof Trusses, Hip Roof, No Garage, Unreinforced Masonry Walls, z_0 = 1.0 m.

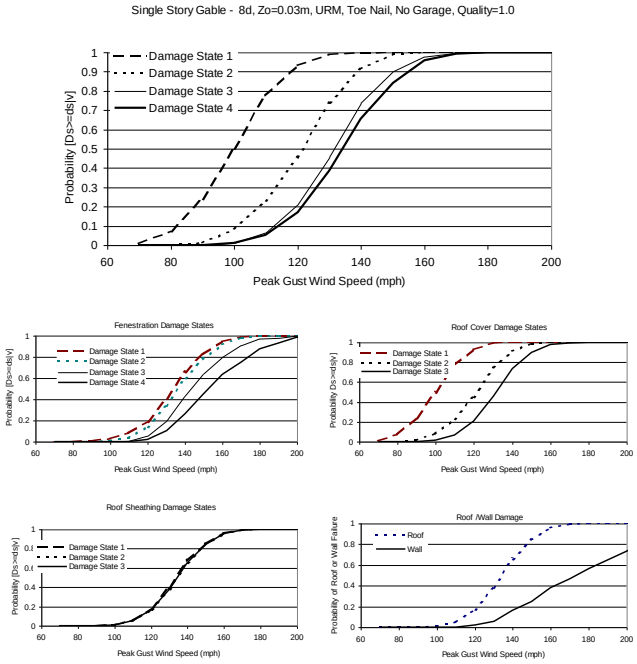

Figure A.57. Damage States versus Maximum Peak Gust Wind Speed – One Story, 8d Roof Sheathing Nails, Toe-Nailed Roof Trusses, Gable Roof, No Garage, Unreinforced Masonry Walls, z_0 = 0.03 m.

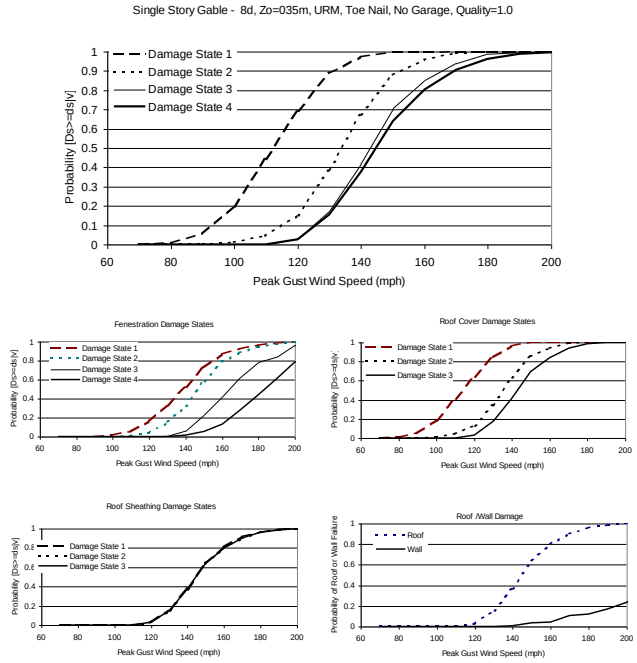

Figure A.58. Damage States versus Maximum Peak Gust Wind Speed – One Story, 8d Roof Sheathing Nails, Toe-Nailed Roof Trusses, Gable Roof, No Garage, Unreinforced Masonry Walls, z_0 = 0.35 m.

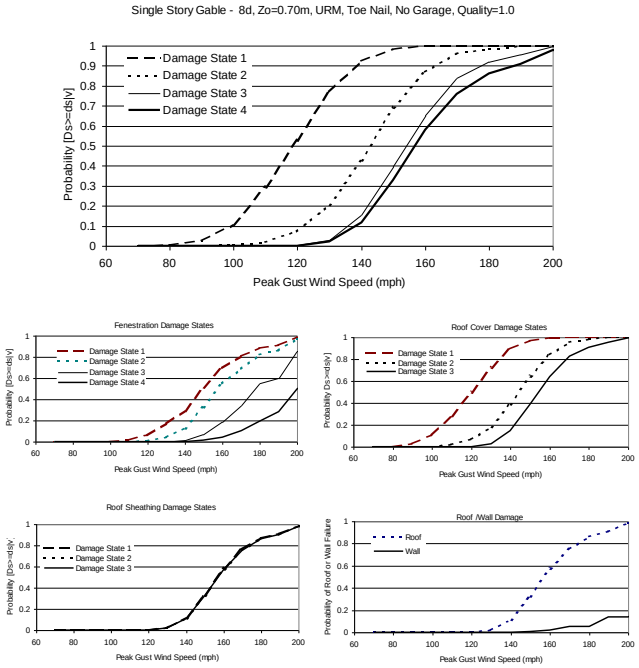

Figure A.59. Damage States versus Maximum Peak Gust Wind Speed – One Story, 8d Roof Sheathing Nails, Toe-Nailed Roof Trusses, Gable Roof, No Garage, Unreinforced Masonry Walls, z_0 = 0.70 m.

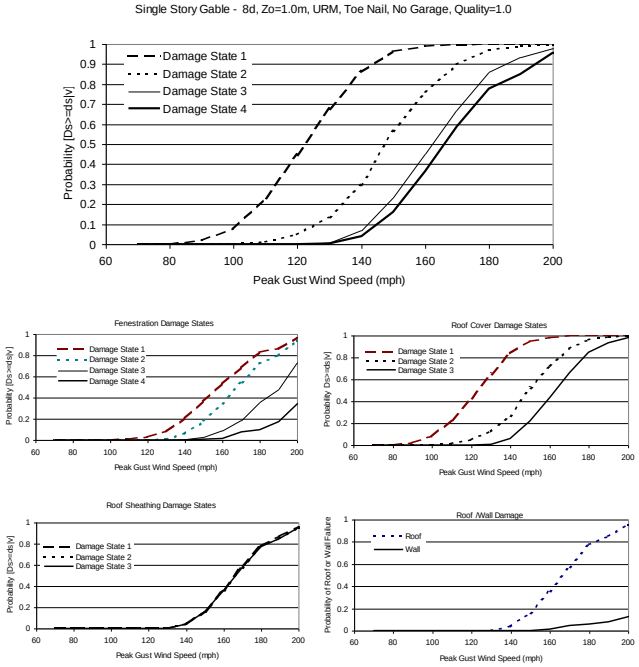

Figure A.60. Damage States versus Maximum Peak Gust Wind Speed – One Story, 8d Roof Sheathing Nails, Toe-Nailed Roof Trusses, Gable Roof, No Garage, Unreinforced Masonry Walls, z_0 = 1.0 m.

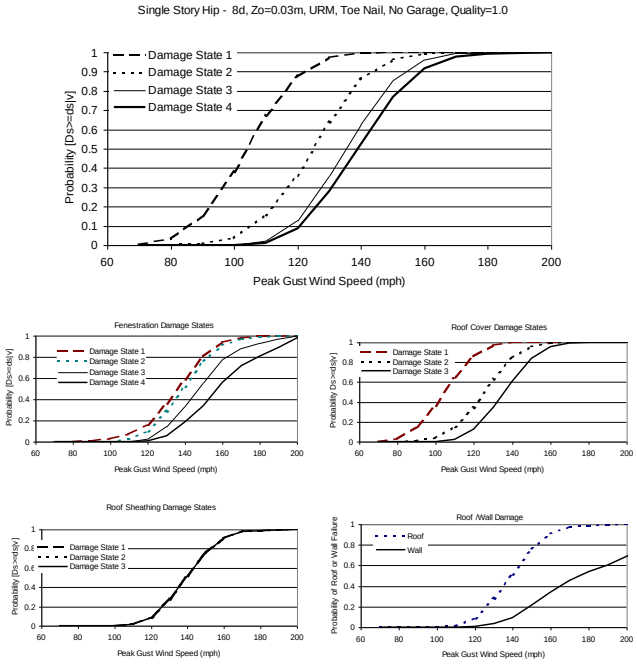

Figure A.61. Damage States versus Maximum Peak Gust Wind Speed – One Story, 8d Roof Sheathing Nails, Toe-Nailed Roof Trusses, Hip Roof, No Garage, Unreinforced Masonry Walls, z_0 = 0.03 m.

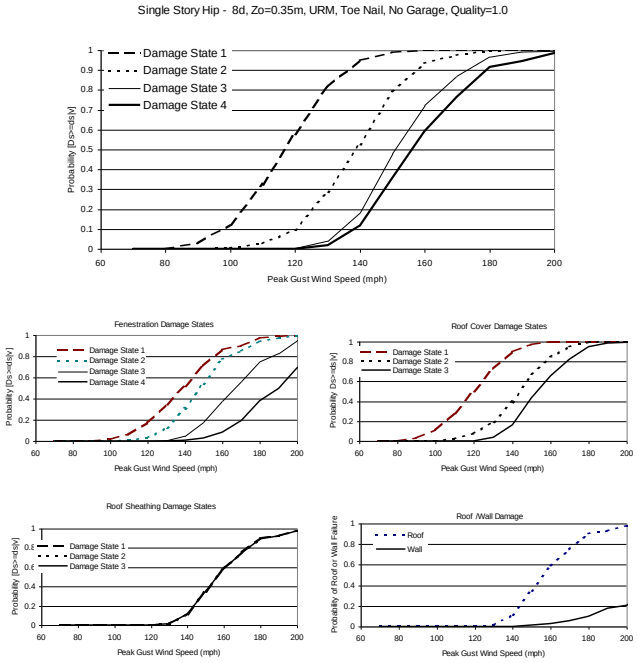

Figure A.62. Damage States versus Maximum Peak Gust Wind Speed – One Story, 8d Roof Sheathing Nails, Toe-Nailed Roof Trusses, Hip Roof, No Garage, Unreinforced Masonry Walls, z_0 = 0.35 m.

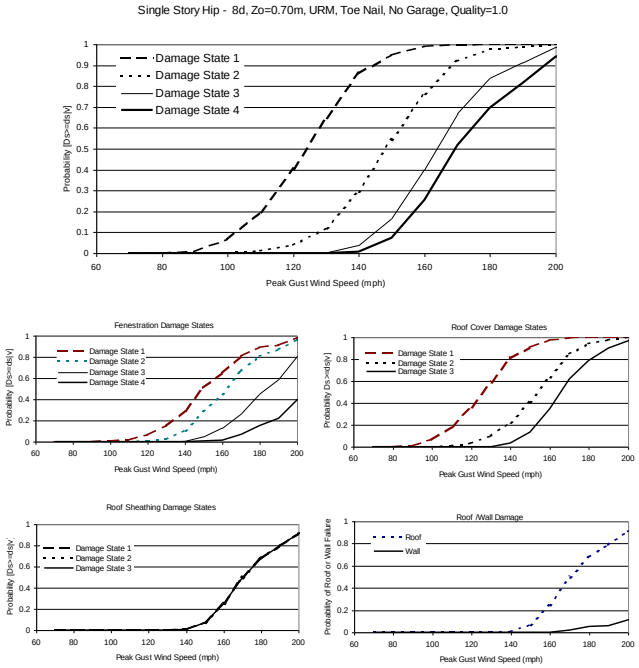

Figure A.63. Damage States versus Maximum Peak Gust Wind Speed – One Story, 8d Roof Sheathing Nails, Toe-Nailed Roof Trusses, Hip Roof, No Garage, Unreinforced Masonry Walls, z_0 = 0.70 m.

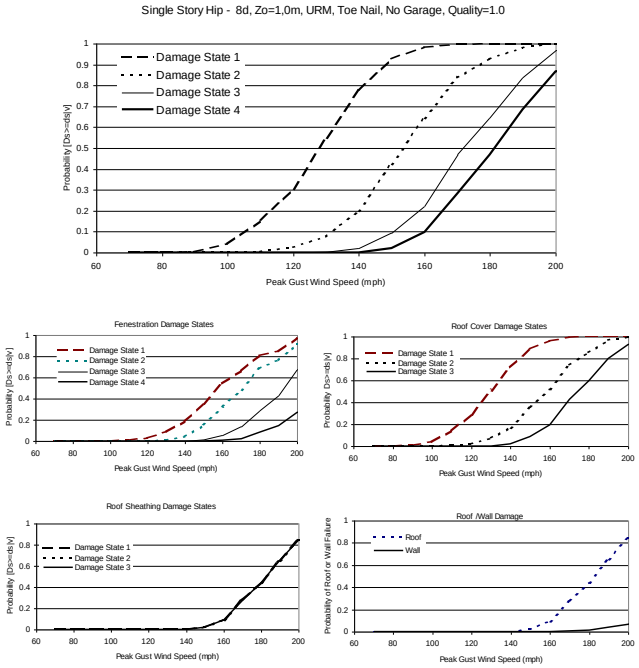

Figure A.64. Damage States versus Maximum Peak Gust Wind Speed – One Story, 8d Roof Sheathing Nails, Toe-Nailed Roof Trusses, Hip Roof, No Garage, Unreinforced Masonry Walls, z_0 = 1.0 m.

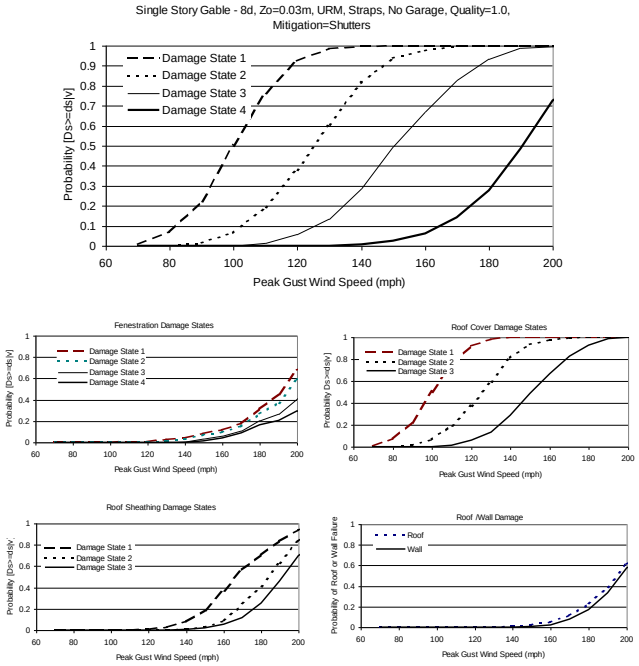

Figure A.65. Damage States versus Maximum Peak Gust Wind Speed – One Story, 8d Roof Sheathing Nails, Strapped Roof Trusses, Gable Roof, No Garage, Unreinforced Masonry Walls, z_0 = 0.03 m, Shutters

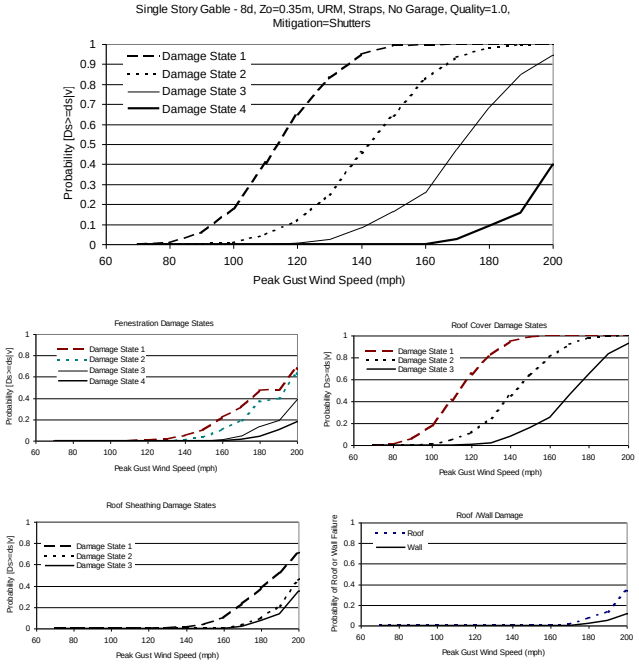

Figure A.66. Damage States versus Maximum Peak Gust Wind Speed – One Story, 8d Roof Sheathing Nails, Strapped Roof Trusses, Gable Roof, No Garage, Unreinforced Masonry Walls, z_0 = 0.35 m, Shutters

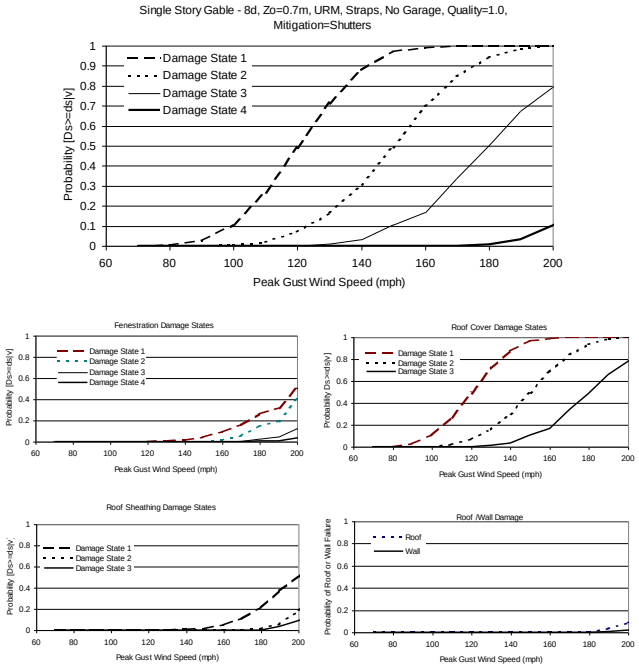

Figure A.67. Damage States versus Maximum Peak Gust Wind Speed – One Story, 8d Roof Sheathing Nails, Strapped Roof Trusses, Gable Roof, No Garage, Unreinforced Masonry Walls, z_0 = 0.70 m, Shutters

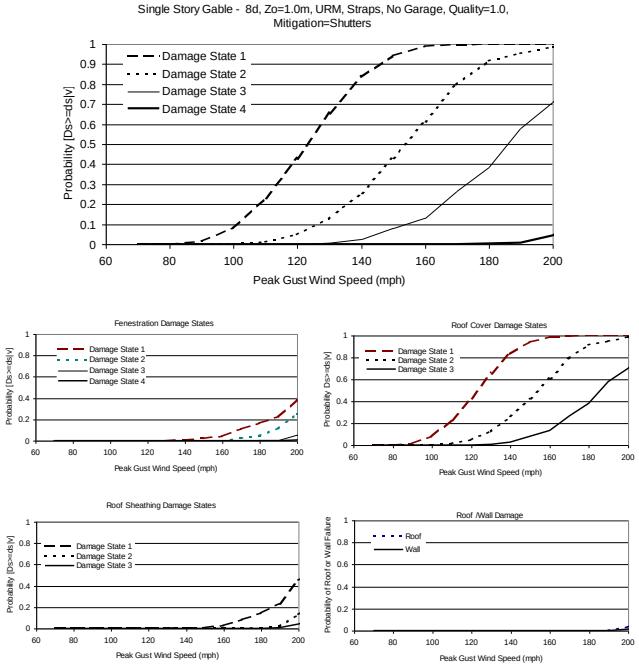

Figure A.68. Damage States versus Maximum Peak Gust Wind Speed – One Story, 8d Roof Sheathing Nails, Strapped Roof Trusses, Gable Roof, No Garage, Unreinforced Masonry Walls, z_0 = 1.0 m, Shutters

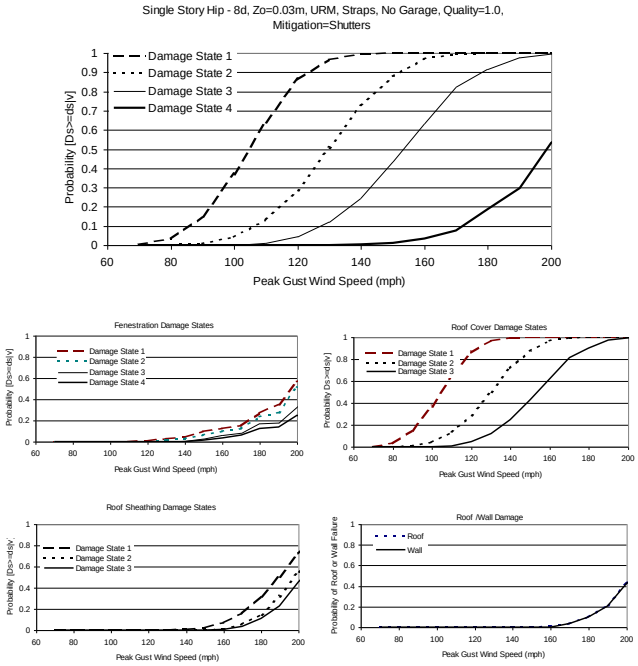

Figure A.69. Damage States versus Maximum Peak Gust Wind Speed – One Story, 8d Roof Sheathing Nails, Strapped Roof Trusses, Hip Roof, No Garage, Unreinforced Masonry Walls, z_0 = 0.03 m, Shutters

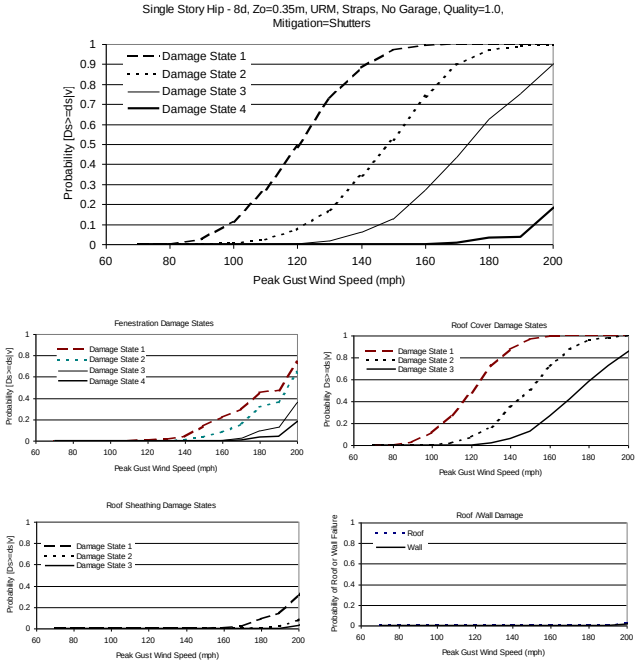

Figure A.70. Damage States versus Maximum Peak Gust Wind Speed – One Story, 8d Roof Sheathing Nails, Strapped Roof Trusses, Hip Roof, No Garage, Unreinforced Masonry Walls, z_0 = 0.35 m, Shutters

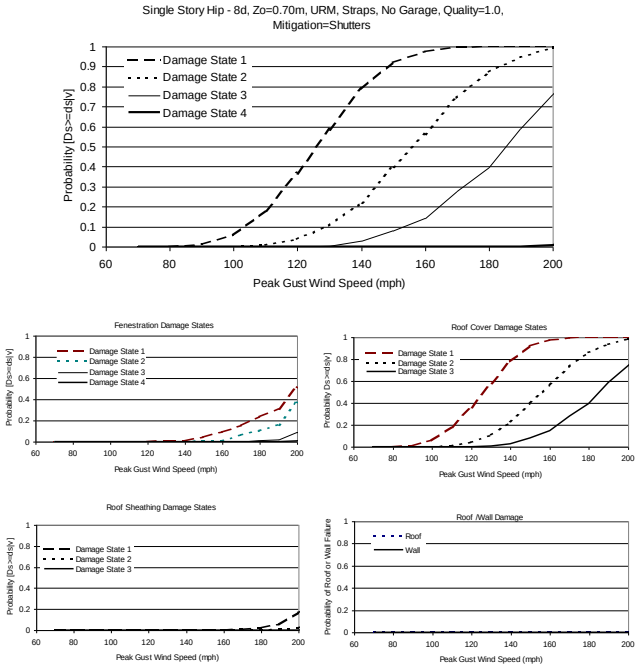

Figure A.71. Damage States versus Maximum Peak Gust Wind Speed – One Story, 8d Roof Sheathing Nails, Strapped Roof Trusses, Hip Roof, No Garage, Unreinforced Masonry Walls, z_0 = 0.70 m, Shutters

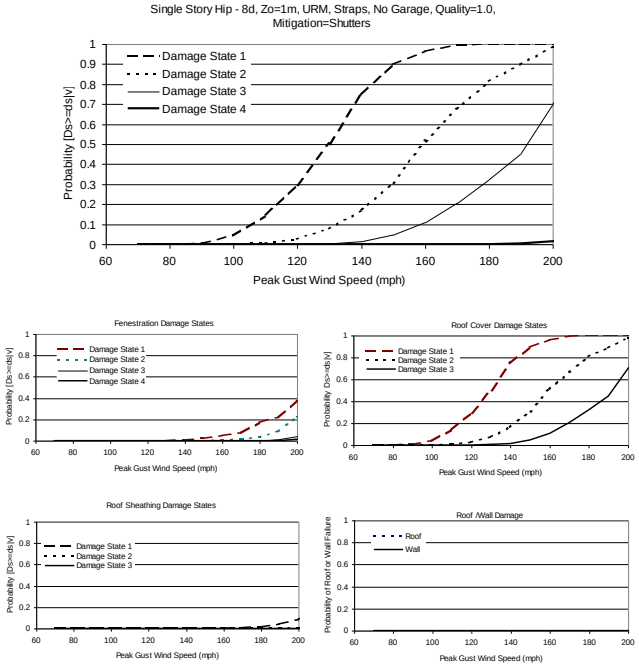

Figure A.72. Damage States versus Maximum Peak Gust Wind Speed – One Story, 8d Roof Sheathing Nails, Strapped Roof Trusses, Hip Roof, No Garage, Unreinforced Masonry Walls, z_0 = 1.0 m, Shutters

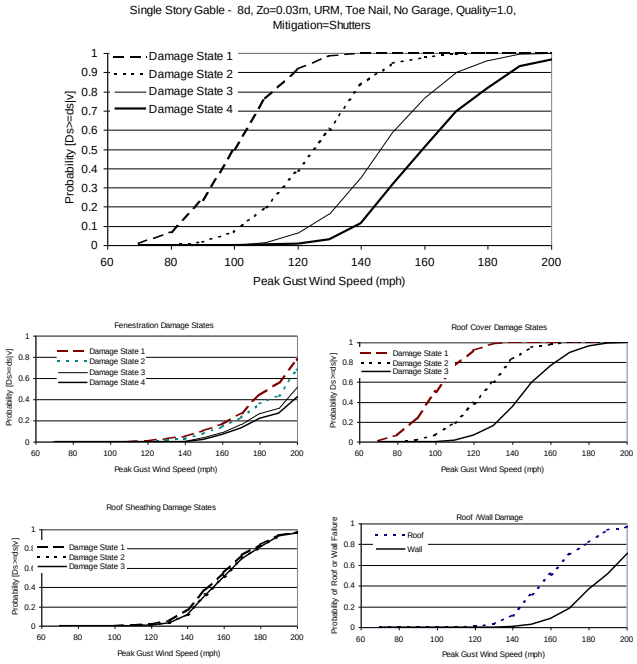

Figure A.73. Damage States versus Maximum Peak Gust Wind Speed – One Story, 8d Roof Sheathing Nails, Toe-Nailed Roof Trusses, Gable Roof, No Garage, Unreinforced Masonry Walls, z_0 = 0.03 m, Shutters

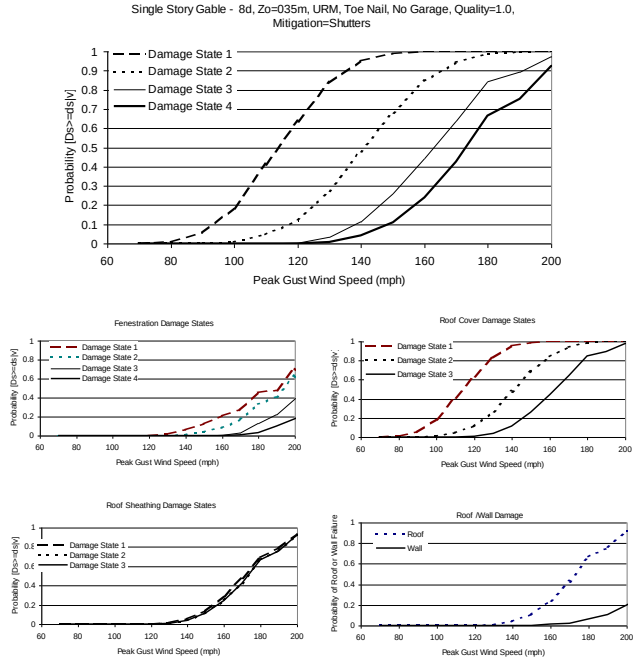

Figure A.74. Damage States versus Maximum Peak Gust Wind Speed – One Story, 8d Roof Sheathing Nails, Toe-Nailed Roof Trusses, Gable Roof, No Garage, Unreinforced Masonry Walls, z_0 = 0.35 m, Shutters

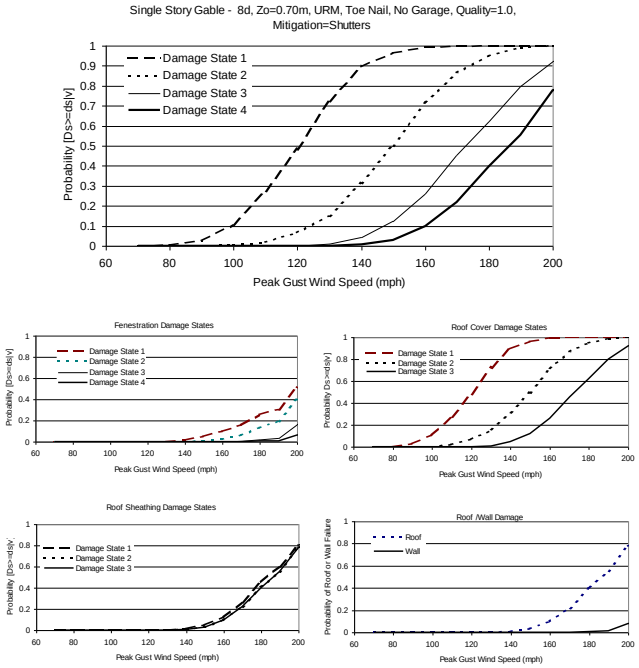

Figure A.75. Damage States versus Maximum Peak Gust Wind Speed – One Story, 8d Roof Sheathing Nails, Toe-Nailed Roof Trusses, Gable Roof, No Garage, Unreinforced Masonry Walls, z_0 = 0.70 m, Shutters

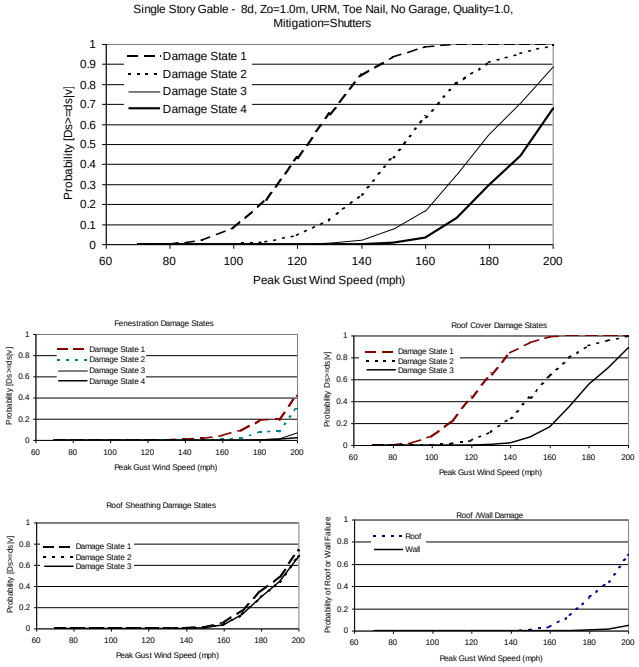

Figure A.76. Damage States versus Maximum Peak Gust Wind Speed – One Story, 8d Roof Sheathing Nails, Toe-Nailed Roof Trusses, Gable Roof, No Garage, Unreinforced Masonry Walls, z_0 = 1.0 m, Shutters

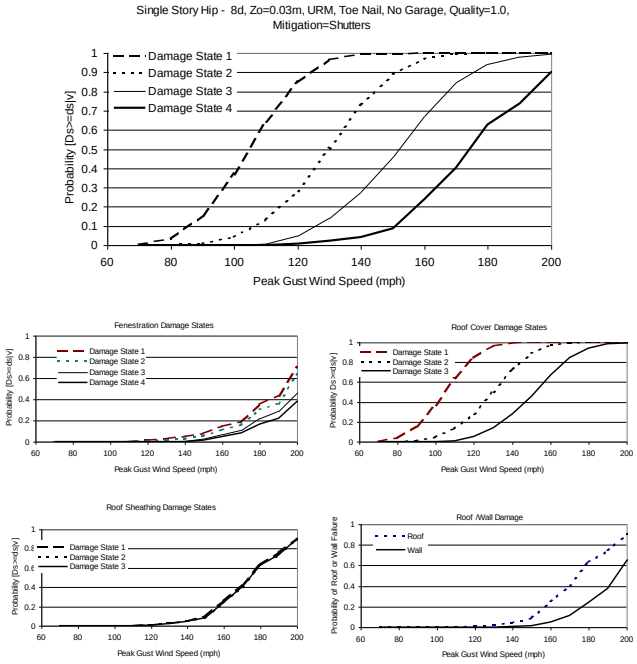

Figure A.77. Damage States versus Maximum Peak Gust Wind Speed – One Story, 8d Roof Sheathing Nails, Toe-Nailed Roof Trusses, Hip Roof, No Garage, Unreinforced Masonry Walls, z_0 = 0.03 m, Shutters

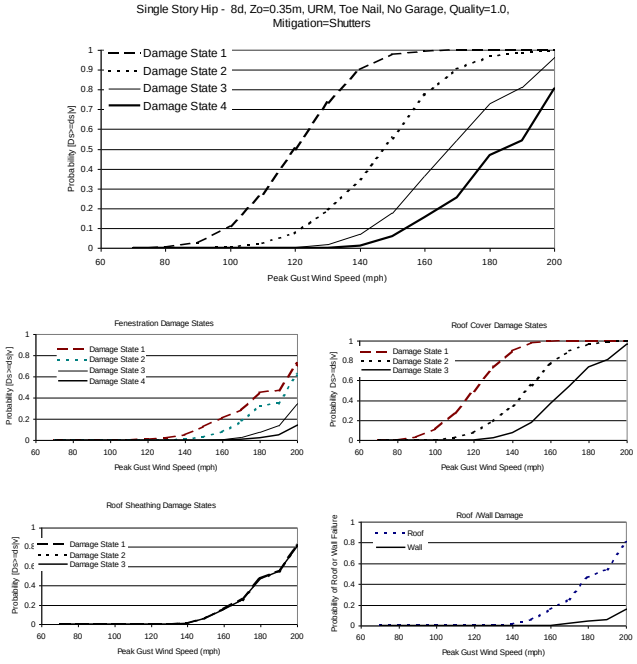

Figure A.78. Damage States versus Maximum Peak Gust Wind Speed – One Story, 8d Roof Sheathing Nails, Toe-Nailed Roof Trusses, Hip Roof, No Garage, Unreinforced Masonry Walls, z_0 = 0.35 m, Shutters

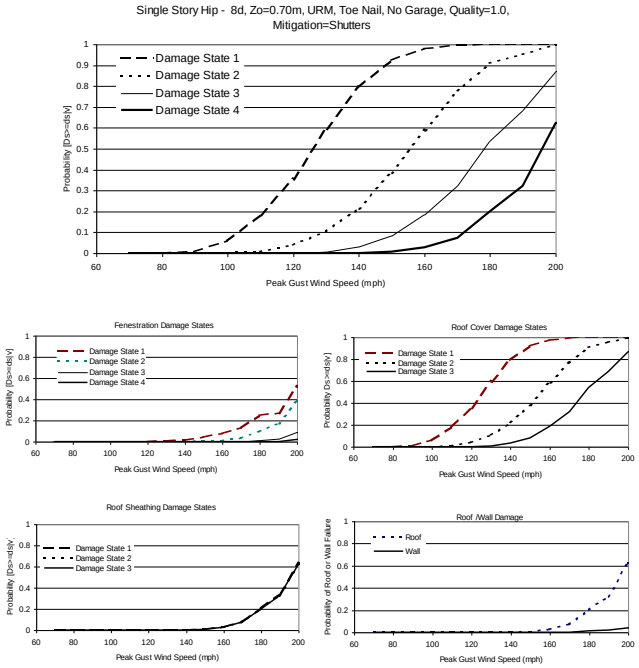

Figure A.79. Damage States versus Maximum Peak Gust Wind Speed – One Story, 8d Roof Sheathing Nails, Toe-Nailed Roof Trusses, Hip Roof, No Garage, Unreinforced Masonry Walls, z_0 = 0.70 m, Shutters

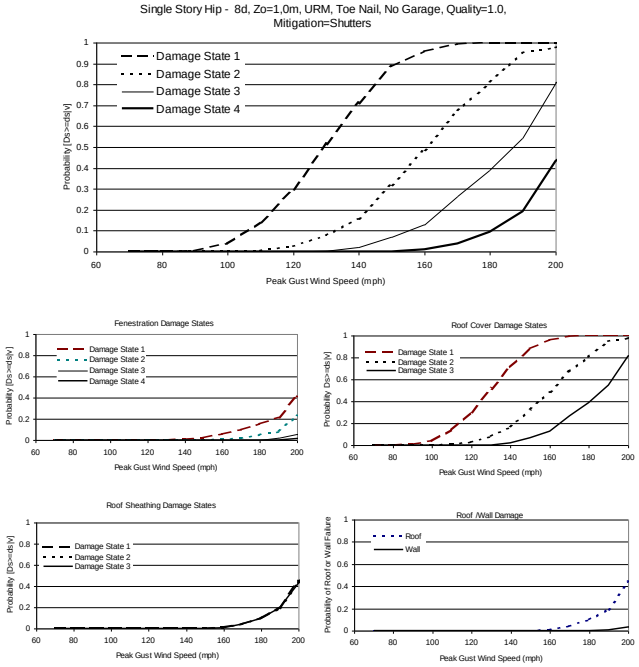

Figure A.80. Damage States versus Maximum Peak Gust Wind Speed – One Story, 8d Roof Sheathing Nails, Toe-Nailed Roof Trusses, Hip Roof, No Garage, Unreinforced Masonry Walls, z_0 = 1.0 m, Shutters

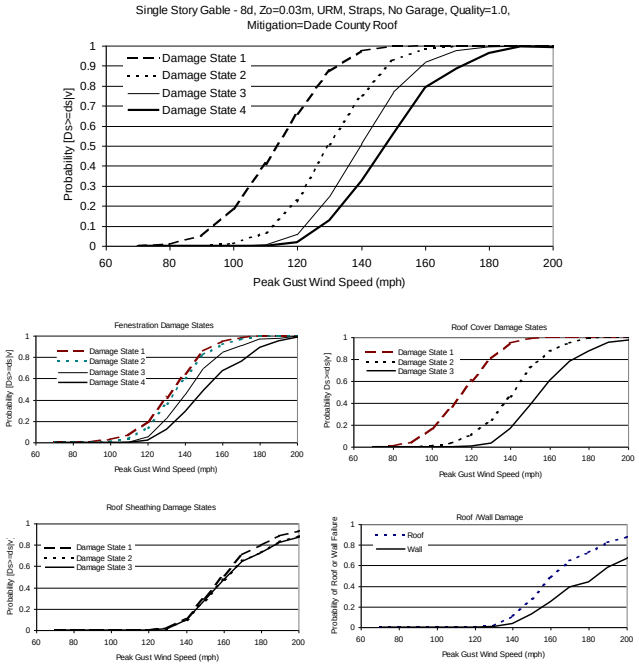

Figure A.81. Damage States versus Maximum Peak Gust Wind Speed – One Story, 8d Roof Sheathing Nails, Strapped Roof Trusses, Gable Roof, No Garage, Unreinforced Masonry Walls, z_0 = 0.03 m, Dade County Roof

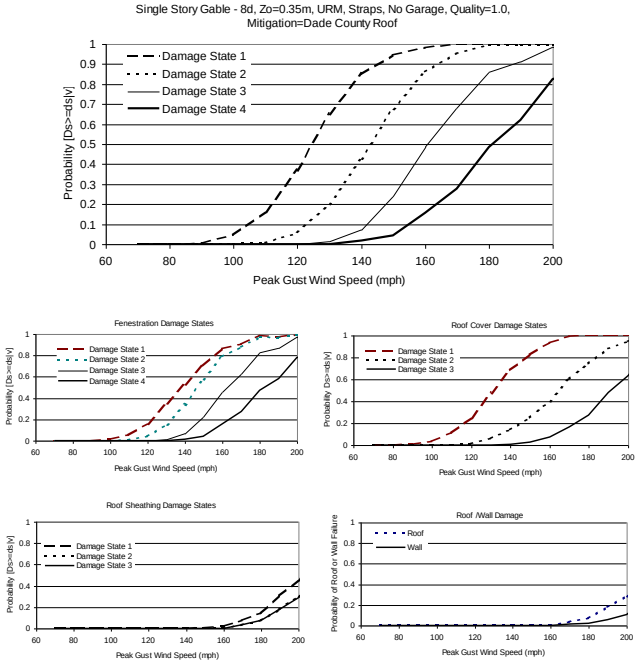

Figure A.82. Damage States versus Maximum Peak Gust Wind Speed – One Story, 8d Roof Sheathing Nails, Strapped Roof Trusses, Gable Roof, No Garage, Unreinforced Masonry Walls, z_0 = 0.35 m, Dade County Roof

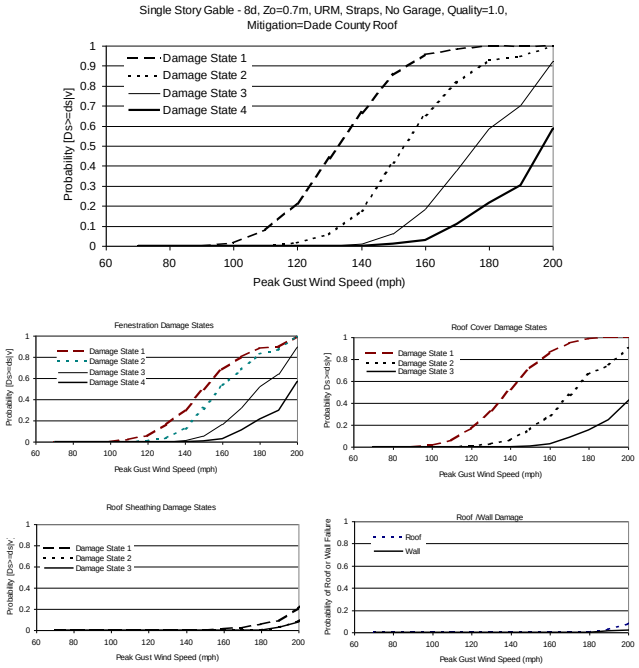

Figure A.83. Damage States versus Maximum Peak Gust Wind Speed – One Story, 8d Roof Sheathing Nails, Strapped Roof Trusses, Gable Roof, No Garage, Unreinforced Masonry Walls, z_0 = 0.70 m, Dade County Roof

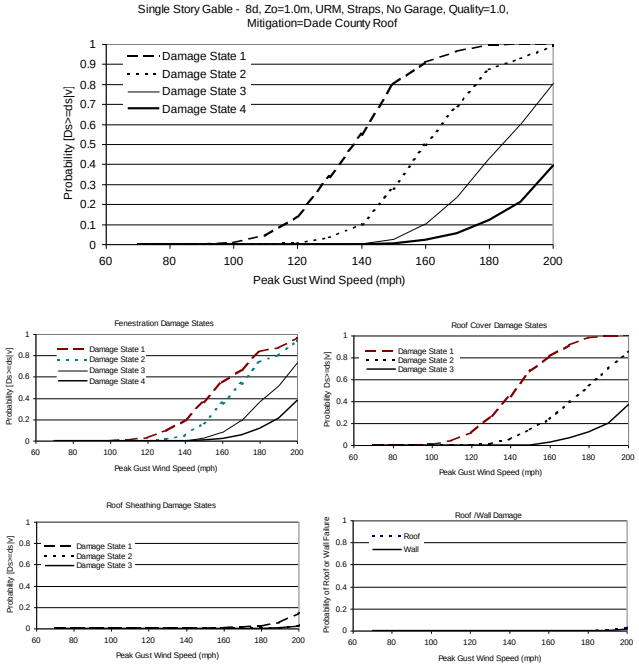

Figure A.84. Damage States versus Maximum Peak Gust Wind Speed – One Story, 8d Roof Sheathing Nails, Strapped Roof Trusses, Gable Roof, No Garage, Unreinforced Masonry Walls, z_0 = 1.0 m, Dade County Roof

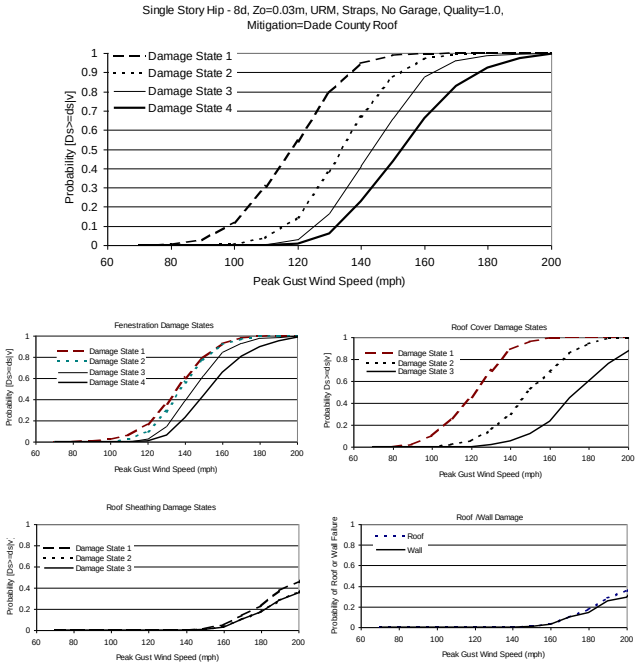

Figure A.85. Damage States versus Maximum Peak Gust Wind Speed – One Story, 8d Roof Sheathing Nails, Strapped Roof Trusses, Hip Roof, No Garage, Unreinforced Masonry Walls, z_0 = 0.03 m, Dade County Roof

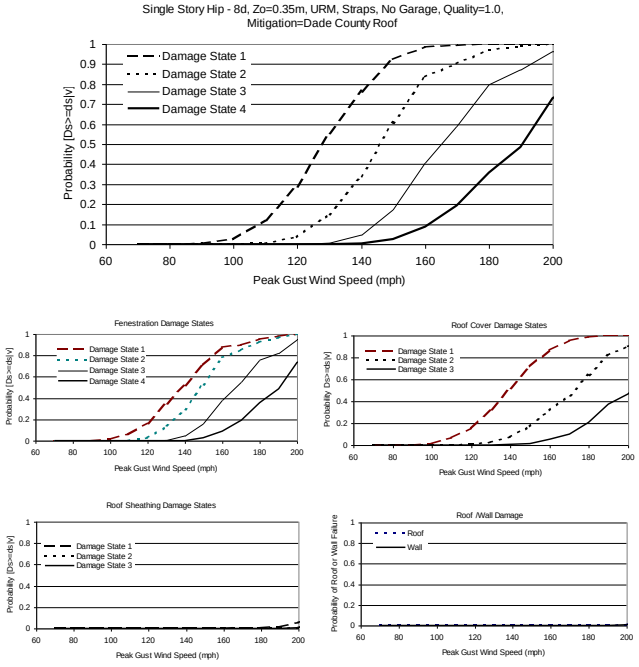

Figure A.86. Damage States versus Maximum Peak Gust Wind Speed – One Story, 8d Roof Sheathing Nails, Strapped Roof Trusses, Hip Roof, No Garage, Unreinforced Masonry Walls, z_0 = 0.35 m, Dade County Roof

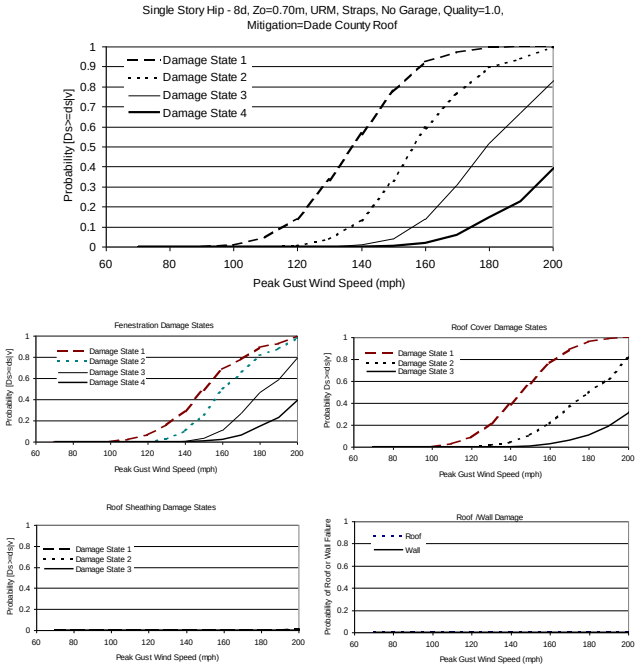

Figure A.87. Damage States versus Maximum Peak Gust Wind Speed – One Story, 8d Roof Sheathing Nails, Strapped Roof Trusses, Hip Roof, No Garage, Unreinforced Masonry Walls, z_0 = 0.70 m, Dade County Roof

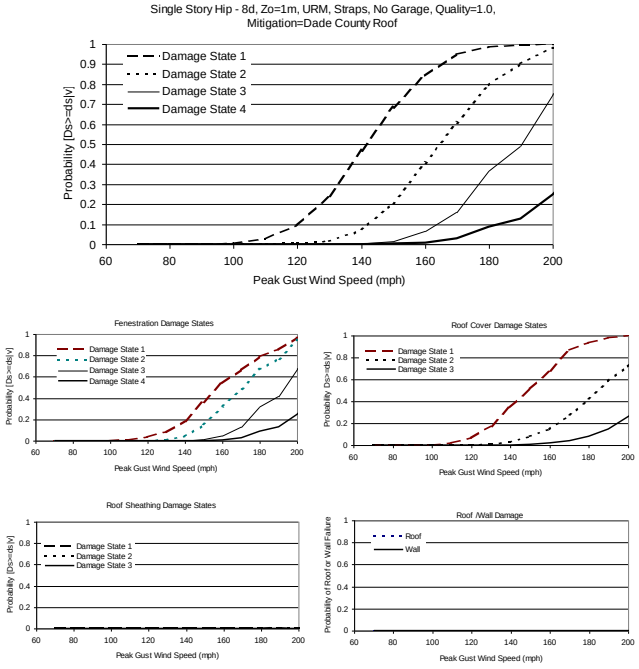

Figure A.88. Damage States versus Maximum Peak Gust Wind Speed – One Story, 8d Roof Sheathing Nails, Strapped Roof Trusses, Hip Roof, No Garage, Unreinforced Masonry Walls, z_0 = 1.0 m, Dade County Roof

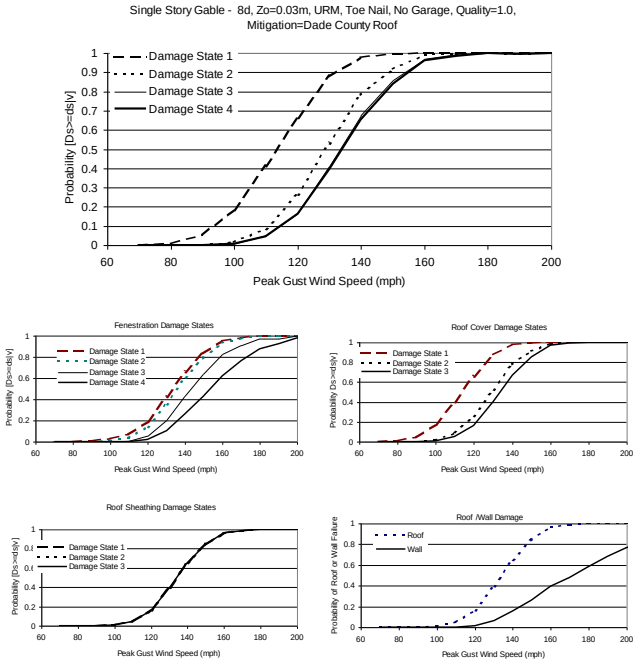

Figure A.89. Damage States versus Maximum Peak Gust Wind Speed – One Story, 8d Roof Sheathing Nails, Toe-Nailed Roof Trusses, Gable Roof, No Garage, Unreinforced Masonry Walls, z_0 = 0.03 m, Dade County Roof

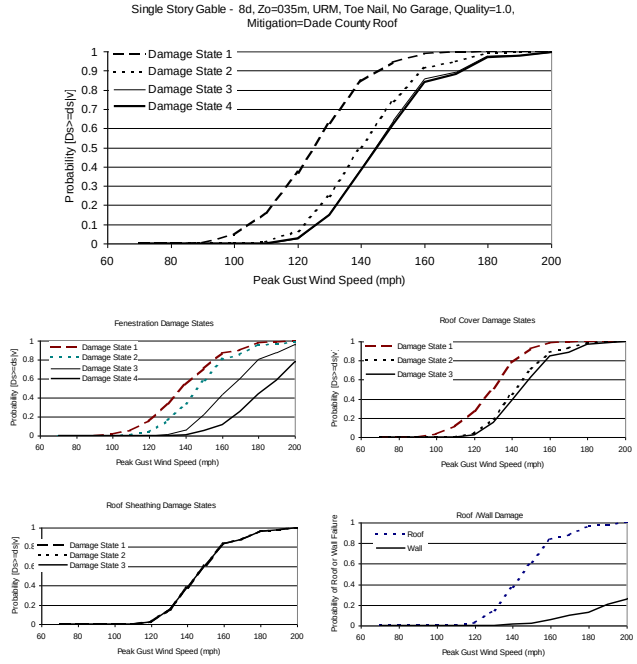

Figure A.90. Damage States versus Maximum Peak Gust Wind Speed – One Story, 8d Roof Sheathing Nails, Toe-Nailed Roof Trusses, Gable Roof, No Garage, Unreinforced Masonry Walls, z_0 = 0.35 m, Dade County Roof

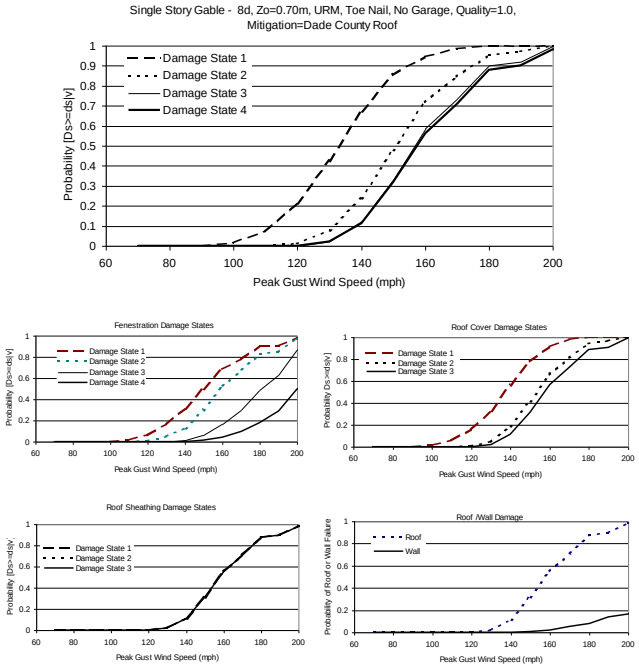

Figure A.91. Damage States versus Maximum Peak Gust Wind Speed – One Story, 8d Roof Sheathing Nails, Toe-Nailed Roof Trusses, Gable Roof, No Garage, Unreinforced Masonry Walls, z_0 = 0.70 m, Dade County Roof

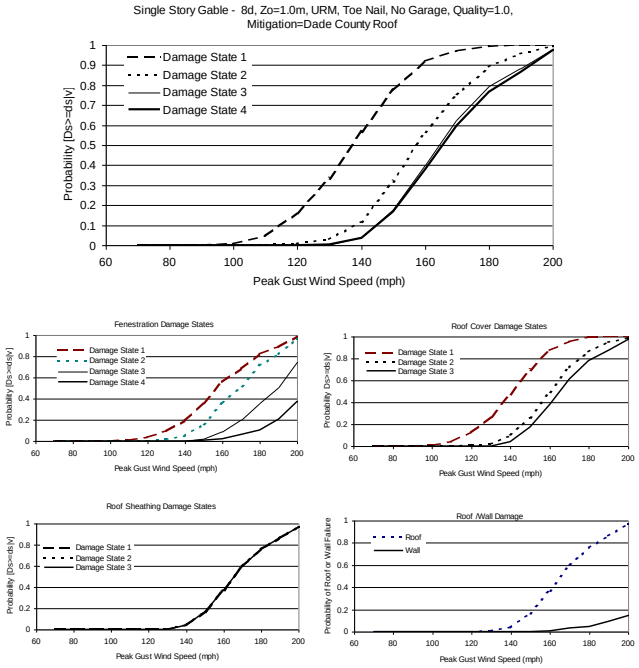

Figure A.92. Damage States versus Maximum Peak Gust Wind Speed – One Story, 8d Roof Sheathing Nails, Toe-Nailed Roof Trusses, Gable Roof, No Garage, Unreinforced Masonry Walls, z_0 = 1.0 m, Dade County Roof

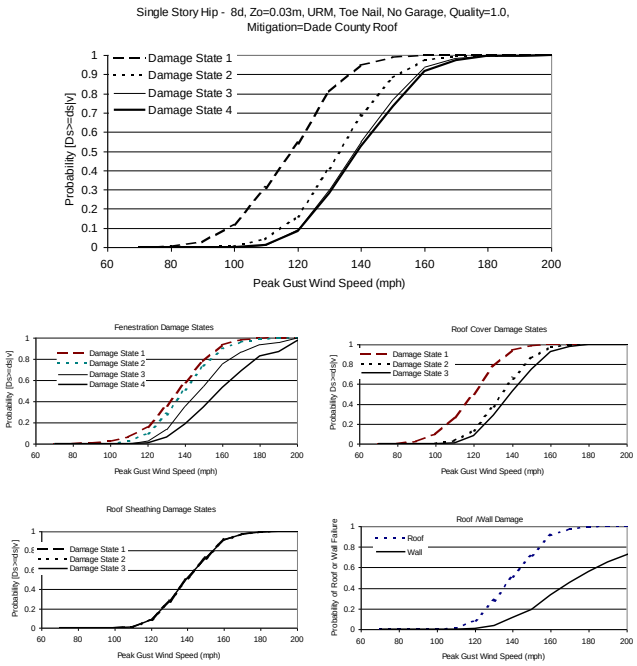

Figure A.93. Damage States versus Maximum Peak Gust Wind Speed – One Story, 8d Roof Sheathing Nails, Toe-Nailed Roof Trusses, Hip Roof, No Garage, Unreinforced Masonry Walls, z_0 = 0.03 m, Dade County Roof

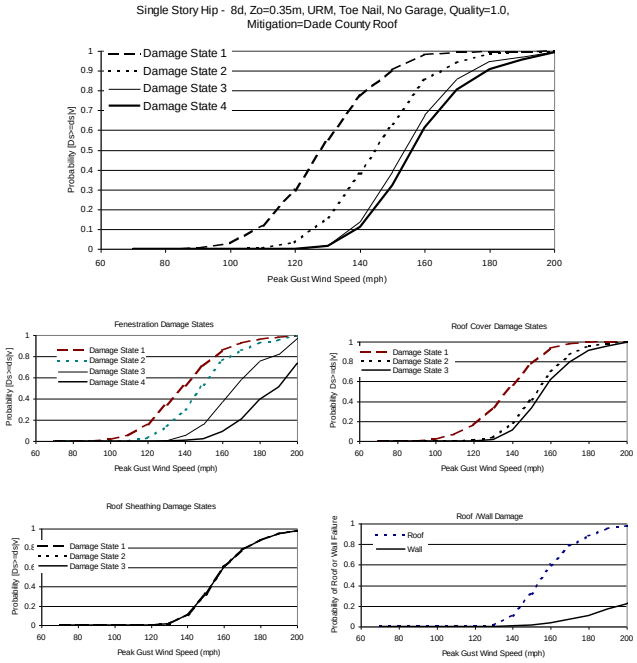

Figure A.94. Damage States versus Maximum Peak Gust Wind Speed – One Story, 8d Roof Sheathing Nails, Toe-Nailed Roof Trusses, Hip Roof, No Garage, Unreinforced Masonry Walls, z_0 = 0.35 m, Dade County Roof

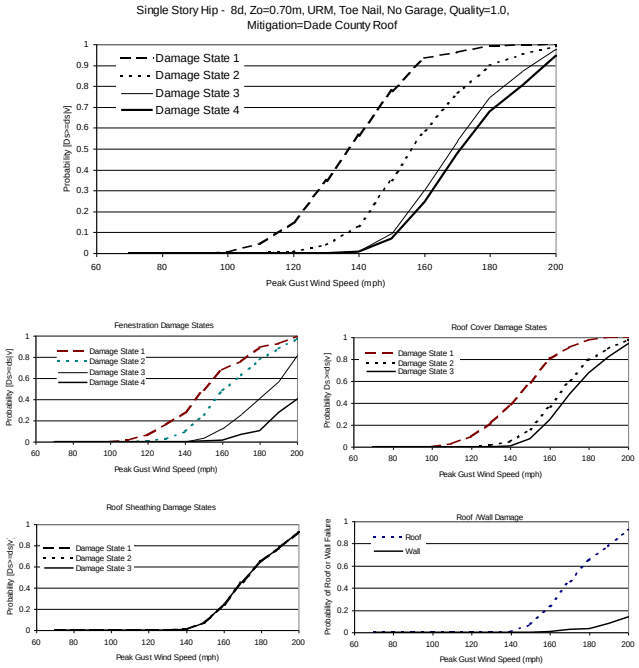

Figure A.95. Damage States versus Maximum Peak Gust Wind Speed – One Story, 8d Roof Sheathing Nails, Toe-Nailed Roof Trusses, Hip Roof, No Garage, Unreinforced Masonry Walls, z_0 = 0.70 m, Dade County Roof

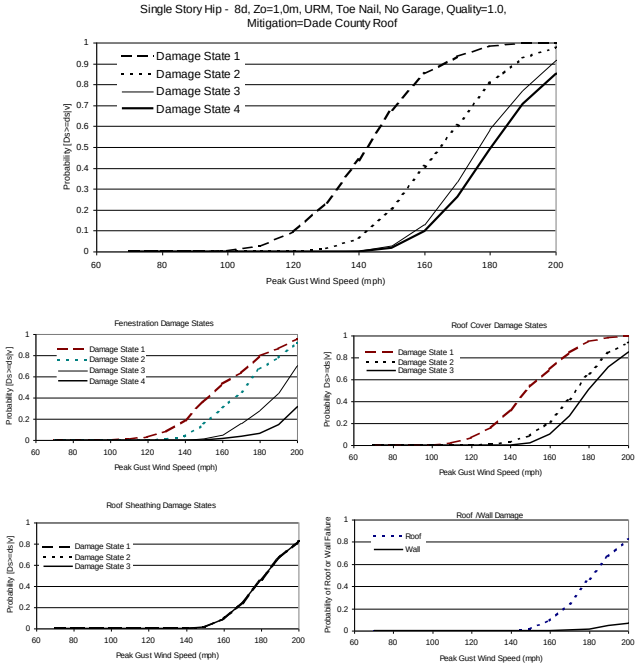

Figure A.96. Damage States versus Maximum Peak Gust Wind Speed – One Story, 8d Roof Sheathing Nails, Toe-Nailed Roof Trusses, Hip Roof, No Garage, Unreinforced Masonry Walls, z_0 = 1.0 m, Dade County Roof

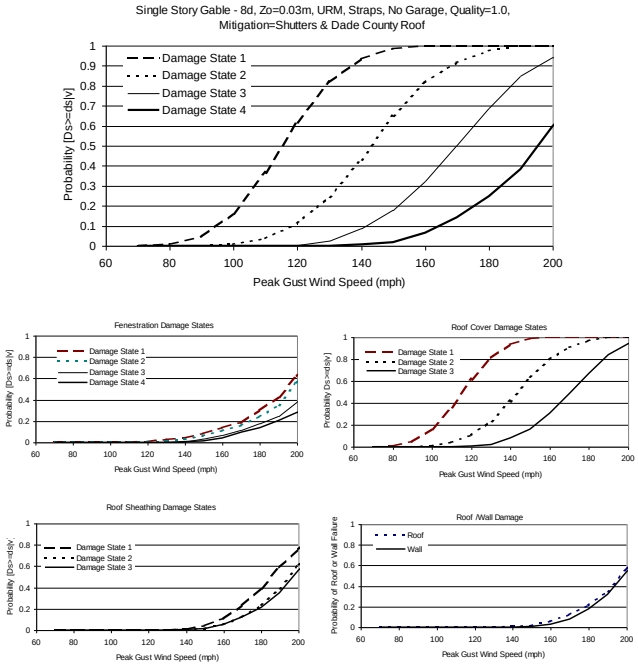

Figure A.97. Damage States versus Maximum Peak Gust Wind Speed – One Story, 8d Roof Sheathing Nails, Strapped Roof Trusses, Gable Roof, No Garage, Unreinforced Masonry Walls, z_0 = 0.03 m, Shutters and Dade County Roof

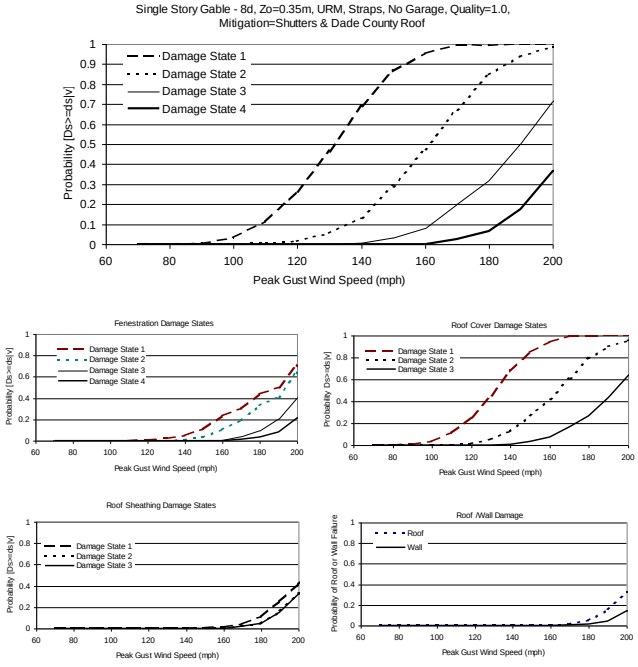

Figure A.98. Damage States versus Maximum Peak Gust Wind Speed – One Story, 8d Roof Sheathing Nails, Strapped Roof Trusses, Gable Roof, No Garage, Unreinforced Masonry Walls, z_0 = 0.35 m, Shutters and Dade County Roof

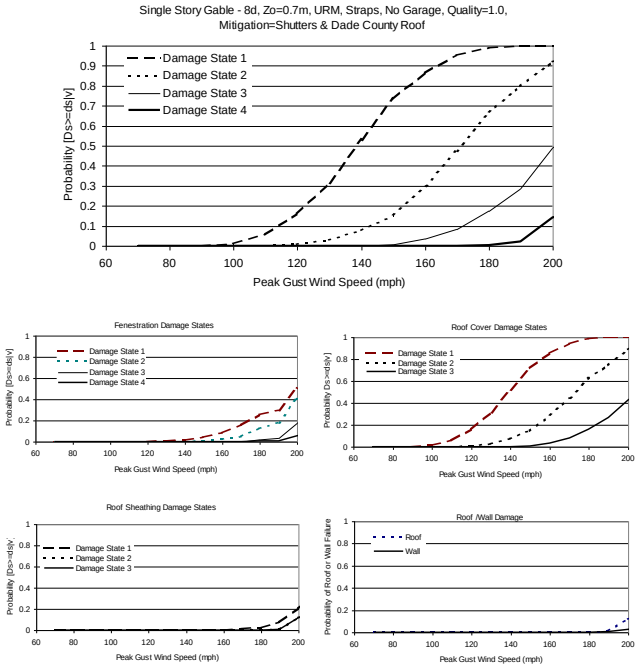

Figure A.99. Damage States versus Maximum Peak Gust Wind Speed – One Story, 8d Roof Sheathing Nails, Strapped Roof Trusses, Gable Roof, No Garage, Unreinforced Masonry Walls, z_0 = 0.70 m, Shutters and Dade County Roof

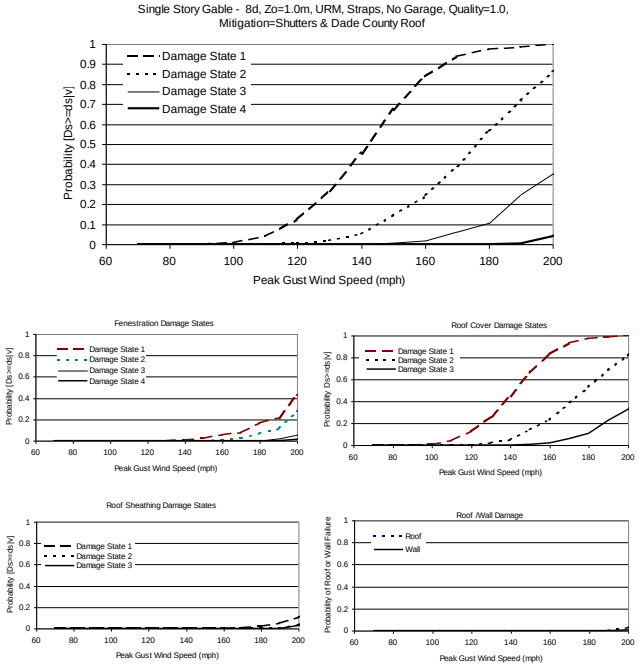

Figure A.100. Damage States versus Maximum Peak Gust Wind Speed – One Story, 8d Roof Sheathing Nails, Strapped Roof Trusses, Gable Roof, No Garage, Unreinforced Masonry Walls, z_0 = 1.0 m, Shutters and Dade County Roof

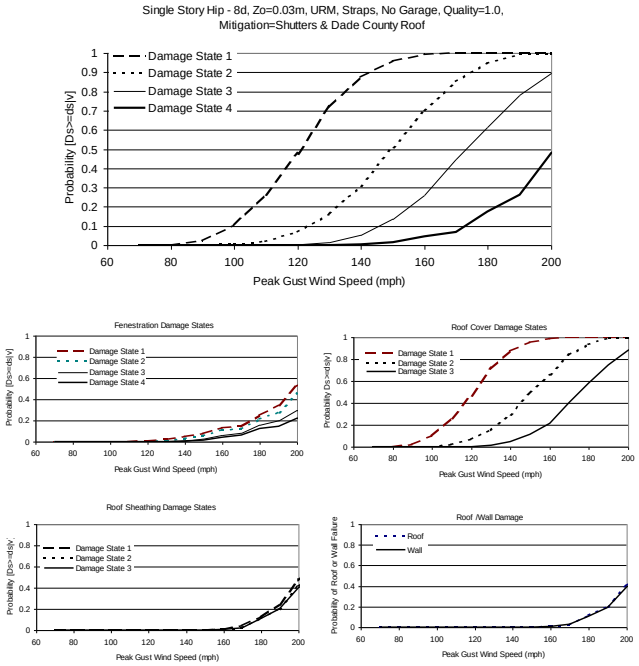

Figure A.101. Damage States versus Maximum Peak Gust Wind Speed – One Story, 8d Roof Sheathing Nails, Strapped Roof Trusses, Hip Roof, No Garage, Unreinforced Masonry Walls, z_0 = 0.03 m, Shutters and Dade County Roof

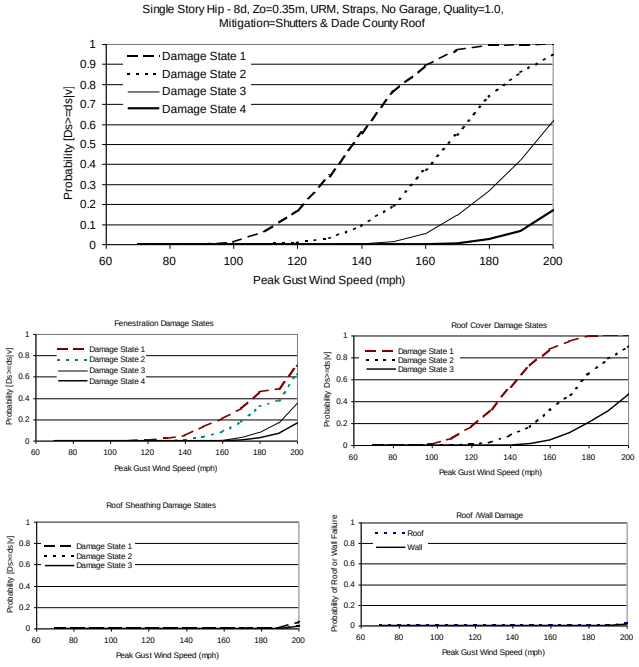

Figure A.102. Damage States versus Maximum Peak Gust Wind Speed – One Story, 8d Roof Sheathing Nails, Strapped Roof Trusses, Hip Roof, No Garage, Unreinforced Masonry Walls, z_0 = 0.35 m, Shutters and Dade County Roof

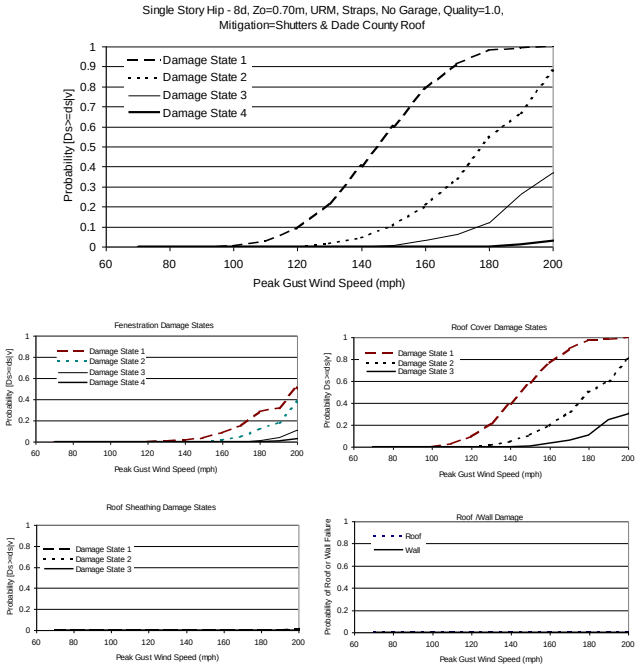

Figure A.103. Damage States versus Maximum Peak Gust Wind Speed – One Story, 8d Roof Sheathing Nails, Strapped Roof Trusses, Hip Roof, No Garage, Unreinforced Masonry Walls, z_0 = 0.70 m, Shutters and Dade County Roof

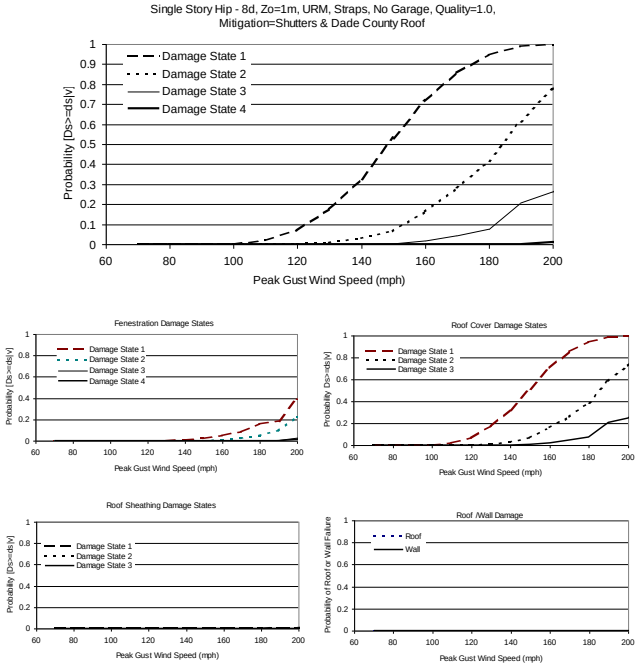

Figure A.104. Damage States versus Maximum Peak Gust Wind Speed – One Story, 8d Roof Sheathing Nails, Strapped Roof Trusses, Hip Roof, No Garage, Unreinforced Masonry Walls, z_0 = 1.0 m, Shutters and Dade County Roof

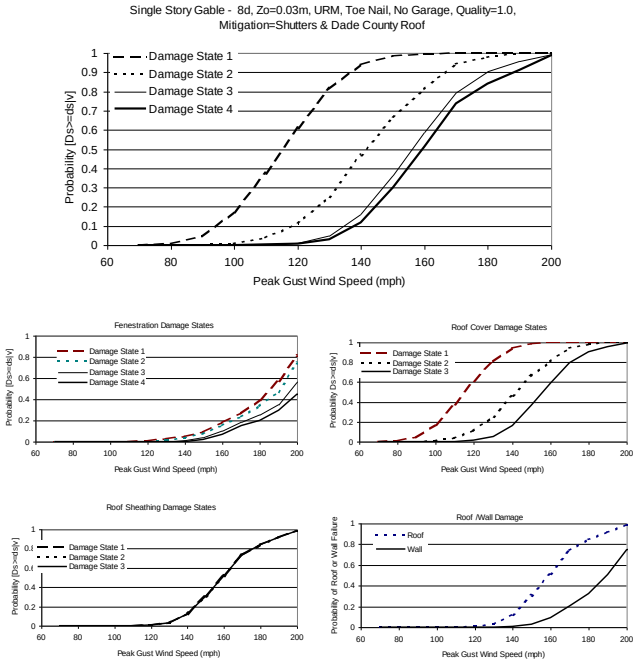

Figure A.105. Damage States versus Maximum Peak Gust Wind Speed – One Story, 8d Roof Sheathing Nails, Toe-Nailed Roof Trusses, Gable Roof, No Garage, Unreinforced Masonry Walls, z_0 = 0.03 m, Shutters and Dade County Roof

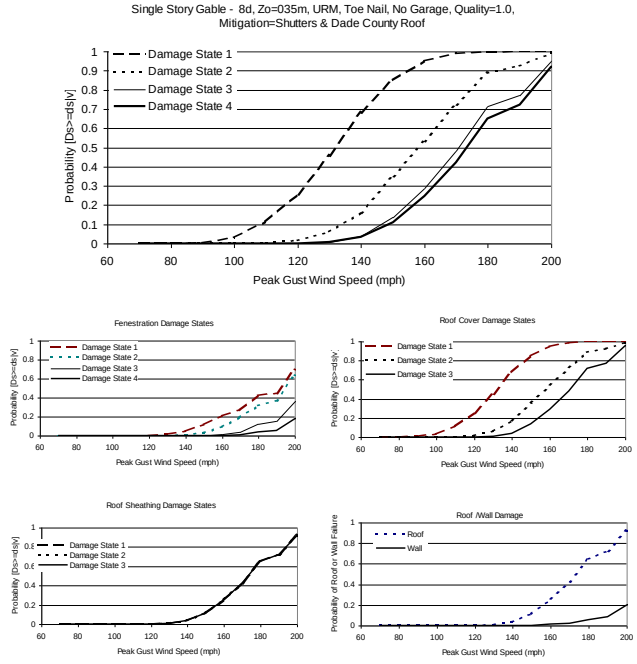

Figure A.106. Damage States versus Maximum Peak Gust Wind Speed – One Story, 8d Roof Sheathing Nails, Toe-Nailed Roof Trusses, Gable Roof, No Garage, Unreinforced Masonry Walls, z_0 = 0.35 m, Shutters and Dade County Roof

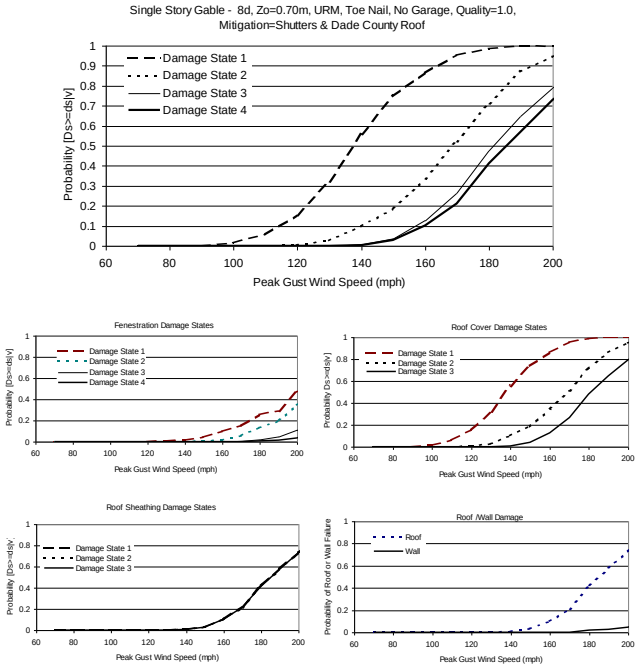

Figure A.107. Damage States versus Maximum Peak Gust Wind Speed – One Story, 8d Roof Sheathing Nails, Toe-Nailed Roof Trusses, Gable Roof, No Garage, Unreinforced Masonry Walls, z_0 = 0.70 m, Shutters and Dade County Roof

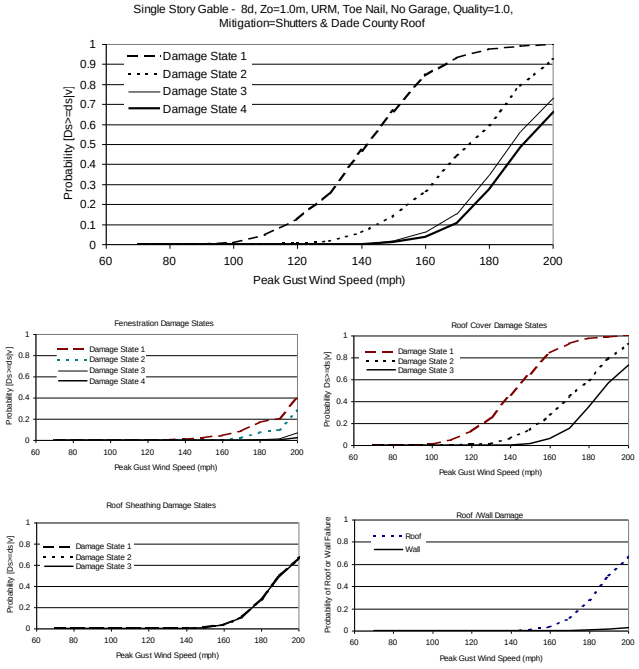

Figure A.108. Damage States versus Maximum Peak Gust Wind Speed – One Story, 8d Roof Sheathing Nails, Toe-Nailed Roof Trusses, Gable Roof, No Garage, Unreinforced Masonry Walls, z_0 = 1.0 m, Shutters and Dade County Roof

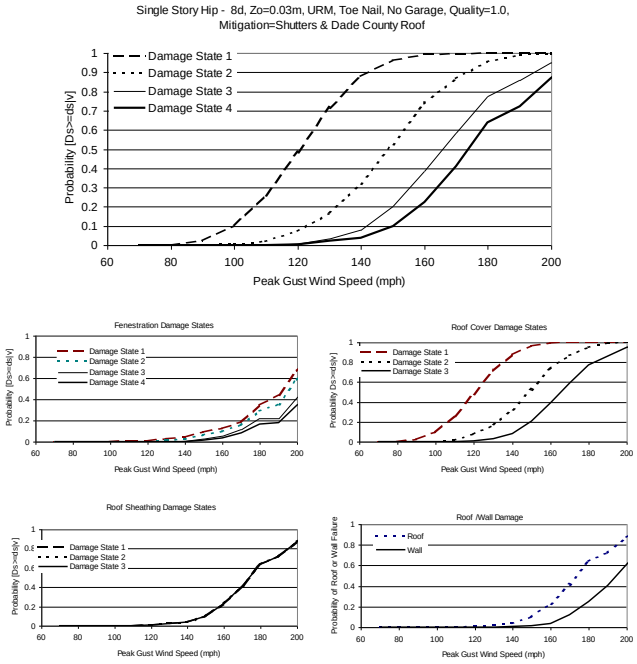

Figure A.109. Damage States versus Maximum Peak Gust Wind Speed – One Story, 8d Roof Sheathing Nails, Toe-Nailed Roof Trusses, Hip Roof, No Garage, Unreinforced Masonry Walls, z_0 = 0.03 m, Shutters and Dade County Roof

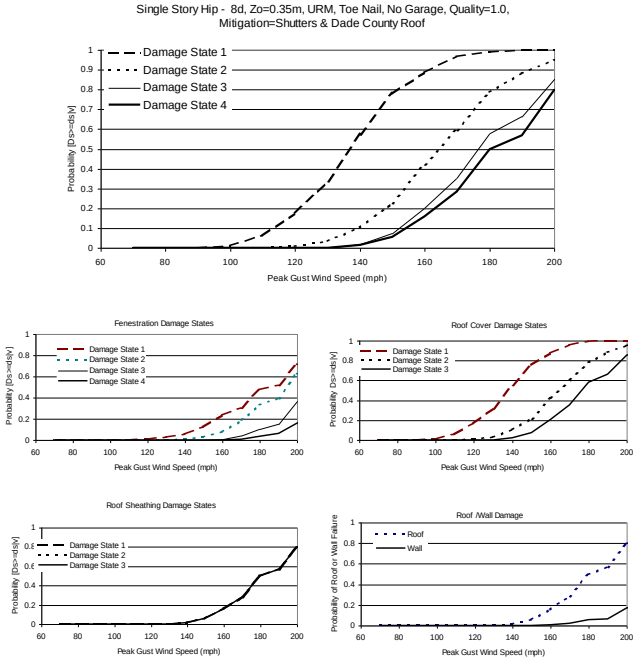

Figure A.110. Damage States versus Maximum Peak Gust Wind Speed – One Story, 8d Roof Sheathing Nails, Toe-Nailed Roof Trusses, Hip Roof, No Garage, Unreinforced Masonry Walls, z_0 = 0.35 m, Shutters and Dade County Roof

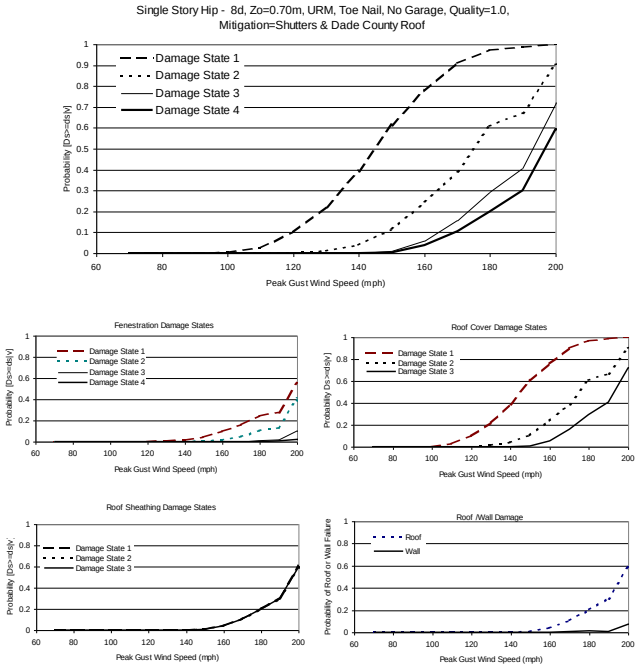

Figure A.111. Damage States versus Maximum Peak Gust Wind Speed – One Story, 8d Roof Sheathing Nails, Toe-Nailed Roof Trusses, Hip Roof, No Garage, Unreinforced Masonry Walls, z_0 = 0.70 m, Shutters and Dade County Roof

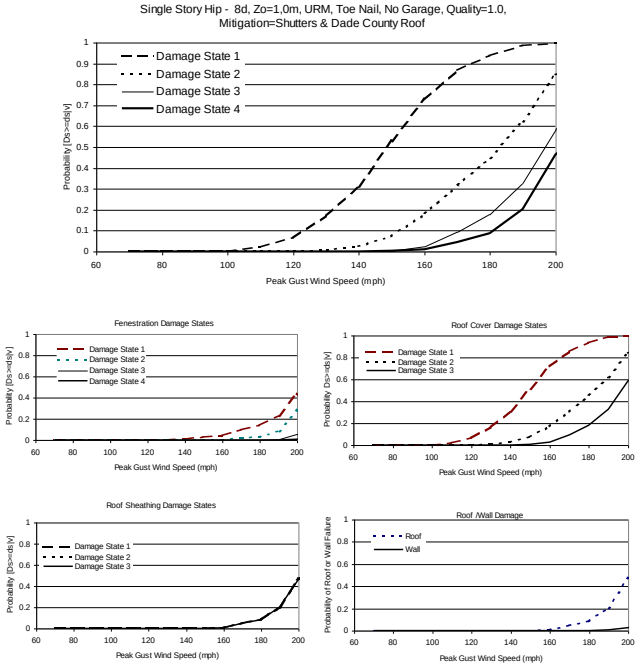

Figure A.112. Damage States versus Maximum Peak Gust Wind Speed – One Story, 8d Roof Sheathing Nails, Toe-Nailed Roof Trusses, Hip Roof, No Garage, Unreinforced Masonry Walls, z_0 = 1.0 m, Shutters and Dade County Roof

Appendix B.
Damage State Functions for Manufactured Homes

Appendix B.
Damage State Functions for Manufactured Homes

This appendix presents damage state curves for manufactured homes (see Section 6.5). The damage state curves show the probability of achieving a certain damage state versus storm-maximum peak gust speed (open terrain at 10m above ground). Plots are presented for the overall building damage states and for the individual building component damage states (refer to Table 6.5-6 for damage state definitions). As shown in Table B.1, separate figures are provided for five different terrains.

Table B.1. Damage State Functions for Manufactured Homes

Figure	Terrain
B.1	0.03
B.2	0.15
B.3	0.35
B.4	0.70
B.5	1.00

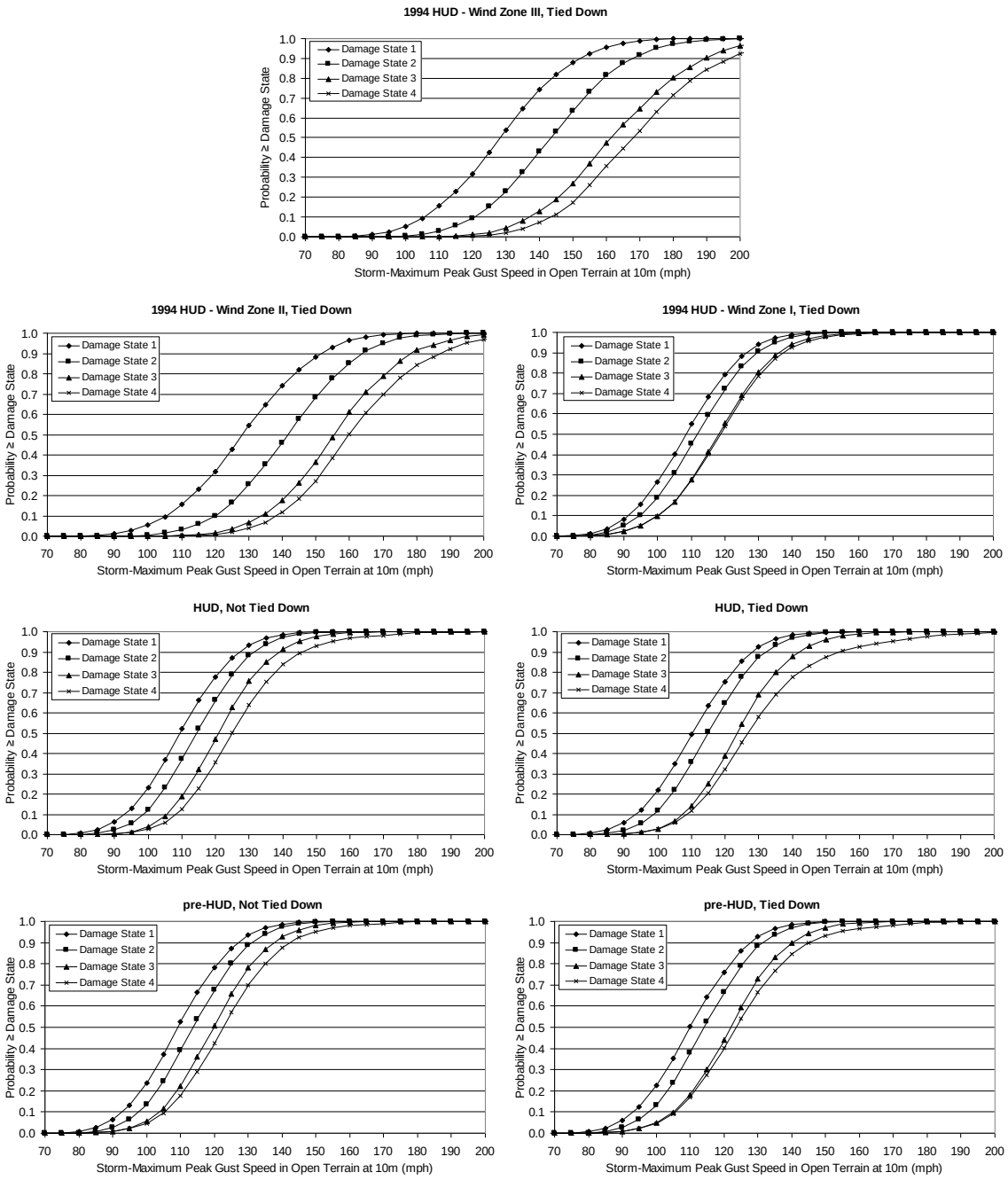

Figure B.1. Damage State Curves for Manufactured Homes Located in Typical Open Terrain described by z_0 = 0.03 m.

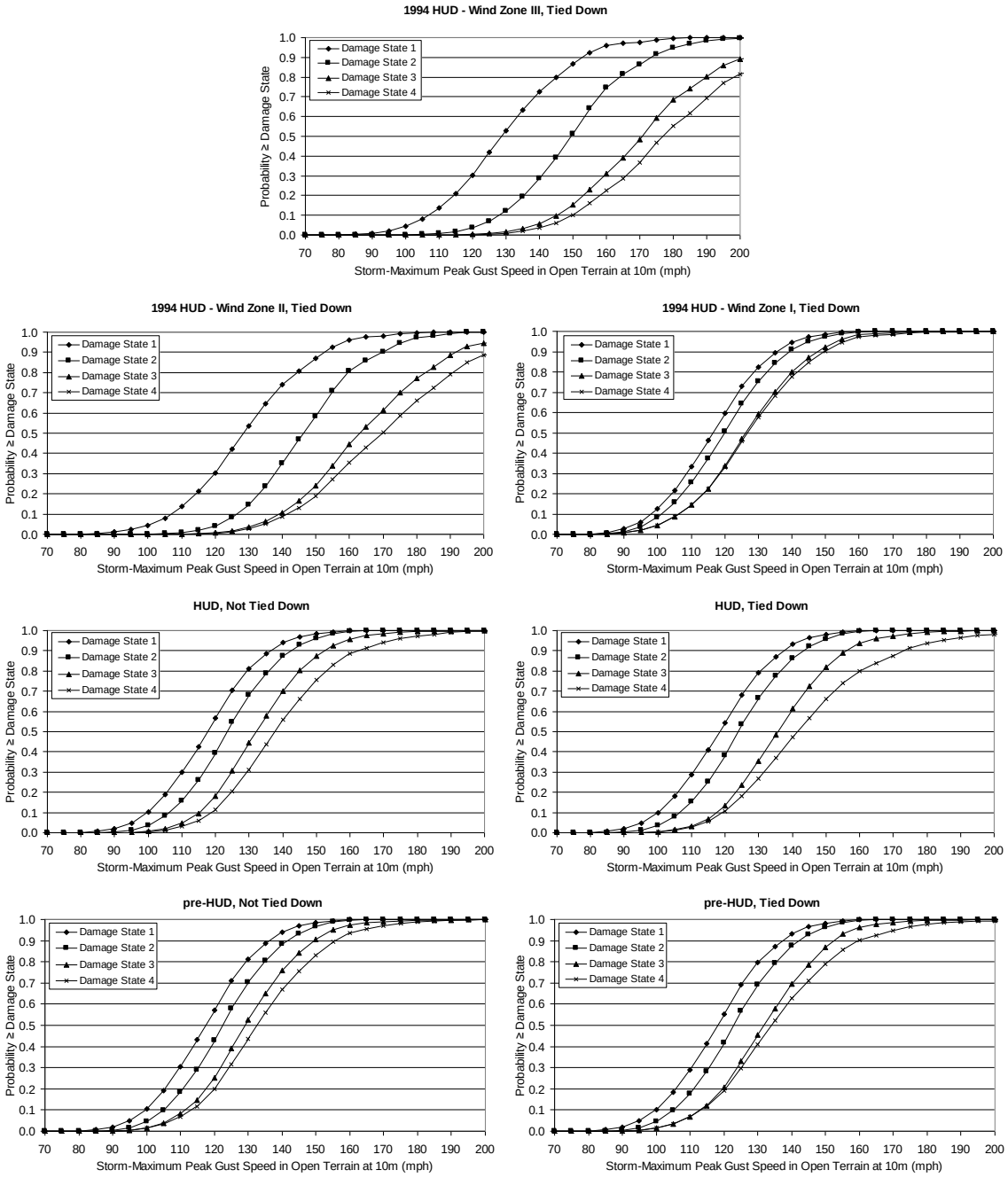

Figure B.2. Damage State Curves for Manufactured Homes Located in a Relatively Open Terrain Described by z_0 = 0.15 m.

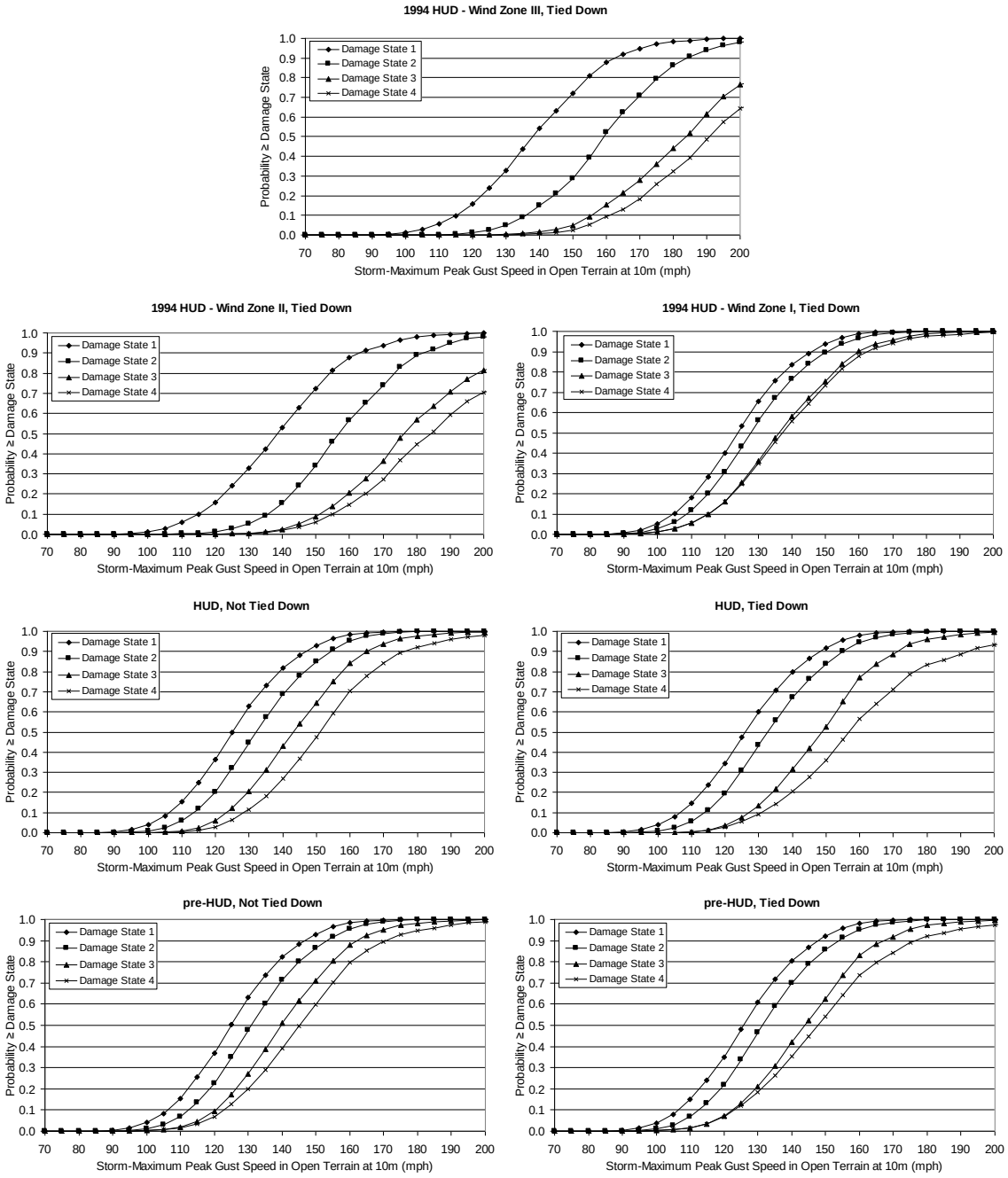

Figure B.3. Damage State Curves for Manufactured Homes Located in Typical Suburban Terrain Described by z_0 = 0.35 m.

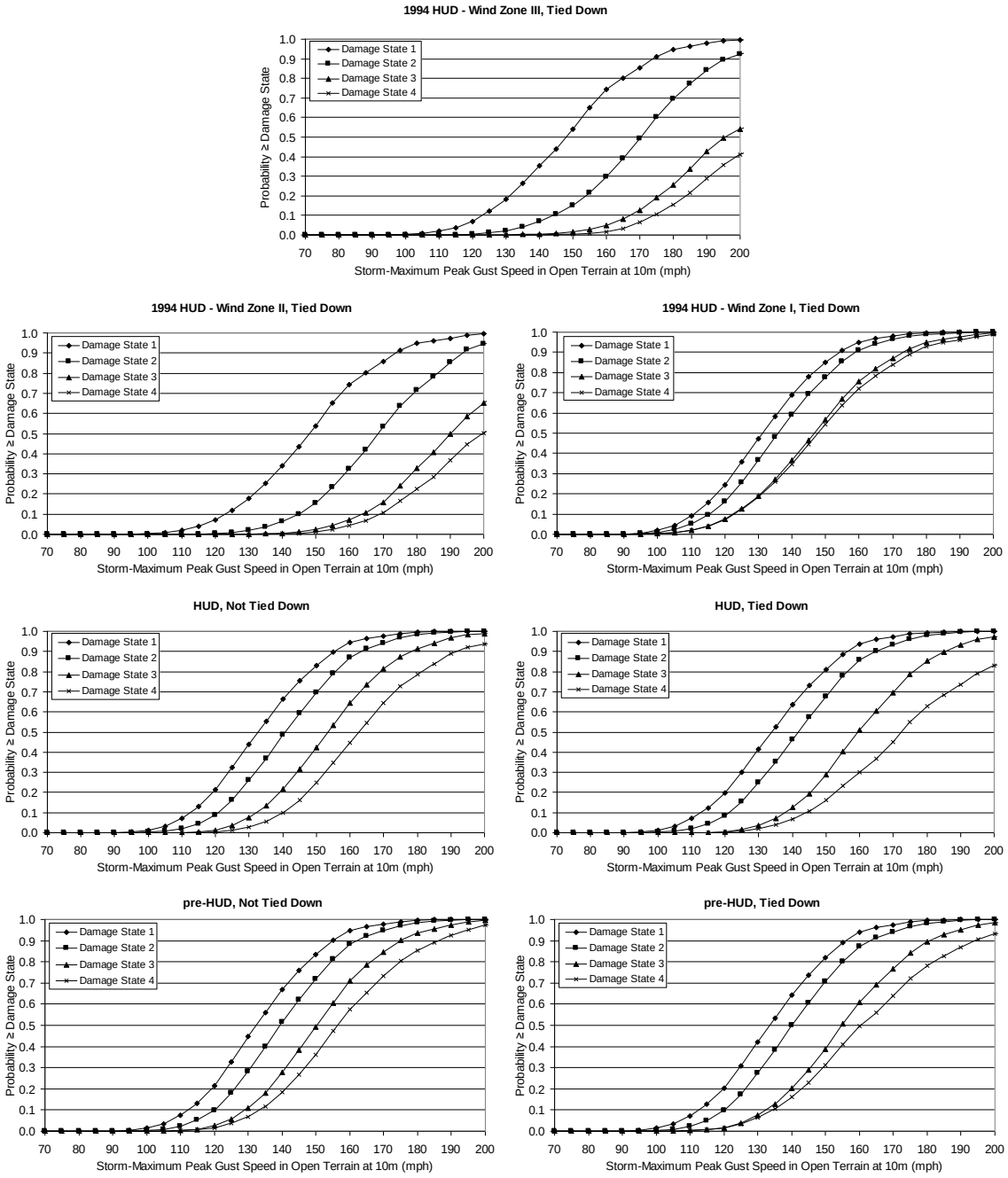

Figure B.4. Damage State Curves for Manufactured Homes Located in Lightly Treed Terrain Described with z_0 = 0.70 m.

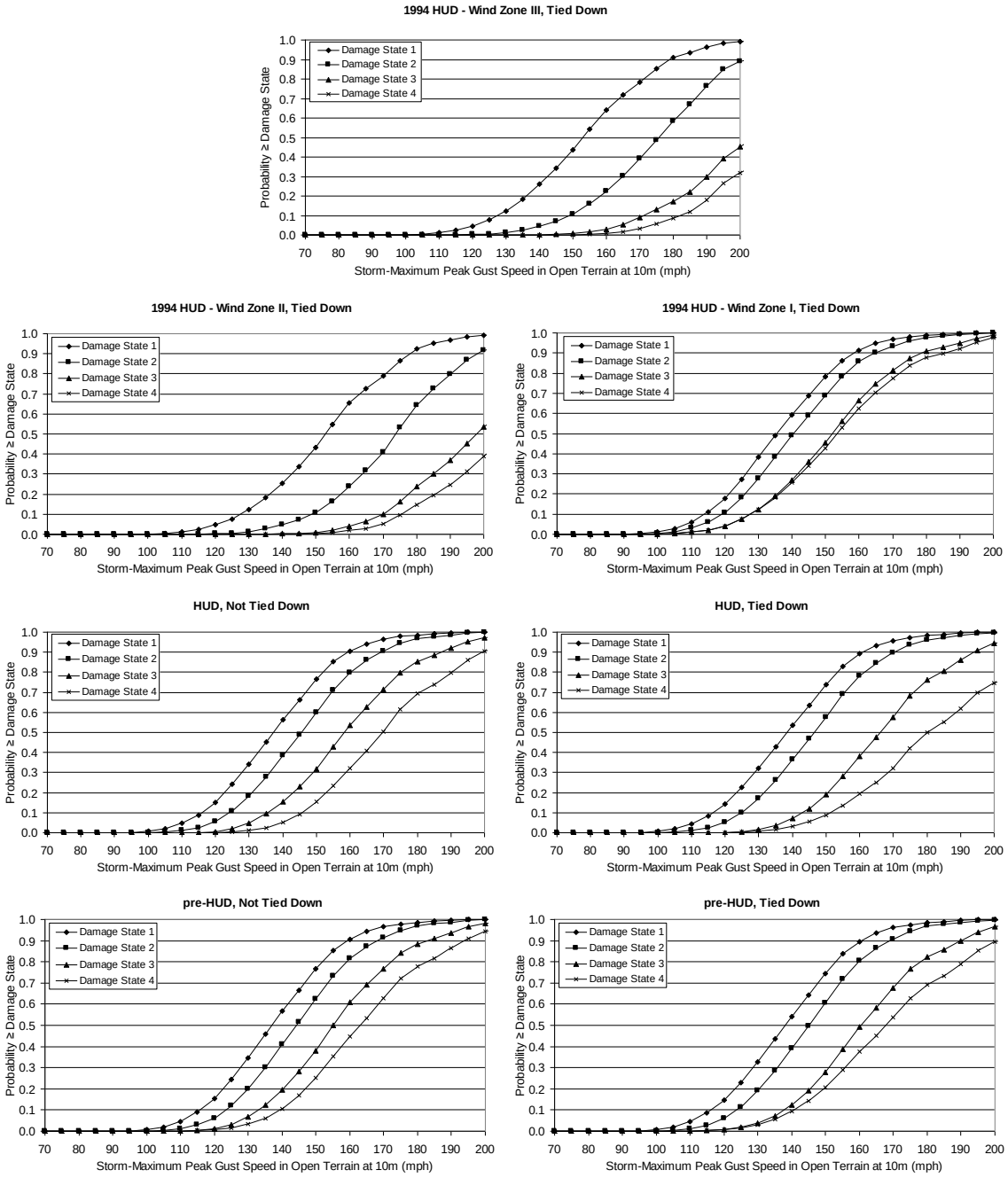

Figure B.5. Damage State Curves for Manufactured Homes Located in Typical Treed Terrain Described with z_0 = 1.0 m.

Appendix C.
Damage State Functions for Marginally- or Non-Engineered Hotel/Motel and Multi-Family Residential Buildings

Appendix C.
Damage State Functions for Marginally- or Non-Engineered Hotel/Motel and Multi-Family Residential Buildings

This appendix presents damage state curves for marginally-engineered or non-engineered hotel/motel and multi-family/residential buildings (see Section 6.9). The damage state curves show the probability of achieving a certain damage state versus storm-maximum peak gust speed (open terrain at 10m above ground). Plots are presented for the overall building damage states and for the individual building component damage states (refer to Table 6.4-1 for damage state definitions).

As shown in Table C.1, two sets of thirteen figures are given in this appendix. The first set of thirteen figures (Figures C.1 through C.13) are for buildings located in an open terrain (z =0.03 m) and the second set (Figures C.14 through C.26) are for buildings situated in a typical suburban environment (z_0=0.35 m). The first figure in each set of thirteen shows damage state results for a one-story building with 8d roof sheathing nails, strapped roof-wall connections, wood frame walls and a gable roof with shingles. The remaining twelve plots in each set show damage state results for buildings which are different by a single variable in comparison to the reference building (note that the changed variable is underlined in the figure titles). Figures C.27 and C.28 show the reference building situated in two additional terrain environments (i.e., z_0=0.7 m and 1.0 m).

Table C.1. Sample Damage State Functions for Marginally or Non-Engineered Hotel/Motel and Multi-Family Residential Buildings

Figure	Walls	Stories	Sheathing	Roof/Wall	Roof Shape	Roof Cover	Terrain
C.1	WFR	1	8d	Strap	Gable	Shingles	0.03
C.2	WFR	1	8d	Strap	**Hip**	Shingles	0.03
C.3	WFR	1	8d	Strap	**Flat**	**BUR, Average**	0.03
C.4	WFR	1	8d	Strap	**Flat**	**BUR, Poor**	0.03
C.5	WFR	1	8d	Strap	**Flat**	**EPDM, Average**	0.03
C.6	WFR	1	8d	Strap	**Flat**	**EPDM, Poor**	0.03
C.7	WFR	1	**6d**	Strap	Gable	Shingles	0.03
C.8	WFR	1	8d	**Toe-Nail**	Gable	Shingles	0.03
C.9	**URM**	1	8d	Strap	Gable	Shingles	0.03
C.10	**RM**	1	8d	Strap	Gable	Shingles	0.03
C.11	WFR	**2**	8d	Strap	Gable	Shingles	0.03
C.12	WFR	**3**	8d	Strap	Gable	Shingles	0.03
C.13	WFR	**4**	8d	Strap	Gable	Shingles	0.03

Table C.1. Sample Damage State Functions for Marginally or Non-Engineered Hotel/Motel and Multi-Family Residential Buildings (concluded)

Figure	Walls	Stories	Sheathing	Roof/Wall	Roof Shape	Roof Cover	Terrain
C.14	WFR	1	8d	Strap	Gable	Shingles	**0.35**
C.15	WFR	1	8d	Strap	**Hip**	Shingles	0.35
C.16	WFR	1	8d	Strap	**Flat**	**BUR, Average**	0.35
C.17	WFR	1	8d	Strap	**Flat**	**BUR, Poor**	0.35
C.18	WFR	1	8d	Strap	**Flat**	**EPDM, Average**	0.35
C.19	WFR	1	8d	Strap	**Flat**	**EPDM, Poor**	0.35
C.20	WFR	1	**6d**	Strap	Gable	Shingles	0.35
C.21	WFR	1	8d	**Toe-Nail**	Gable	Shingles	0.35
C.22	**URM**	1	8d	Strap	Gable	Shingles	0.35
C.23	**RM**	1	8d	Strap	Gable	Shingles	0.35
C.24	WFR	**2**	8d	Strap	Gable	Shingles	0.35
C.25	WFR	**3**	8d	Strap	Gable	Shingles	0.35
C.26	WFR	**4**	8d	Strap	Gable	Shingles	0.35
C.27	WFR	1	8d	Strap	Gable	Shingles	**0.70**
C.28	WFR	1	8d	Strap	Gable	Shingles	**1.00**

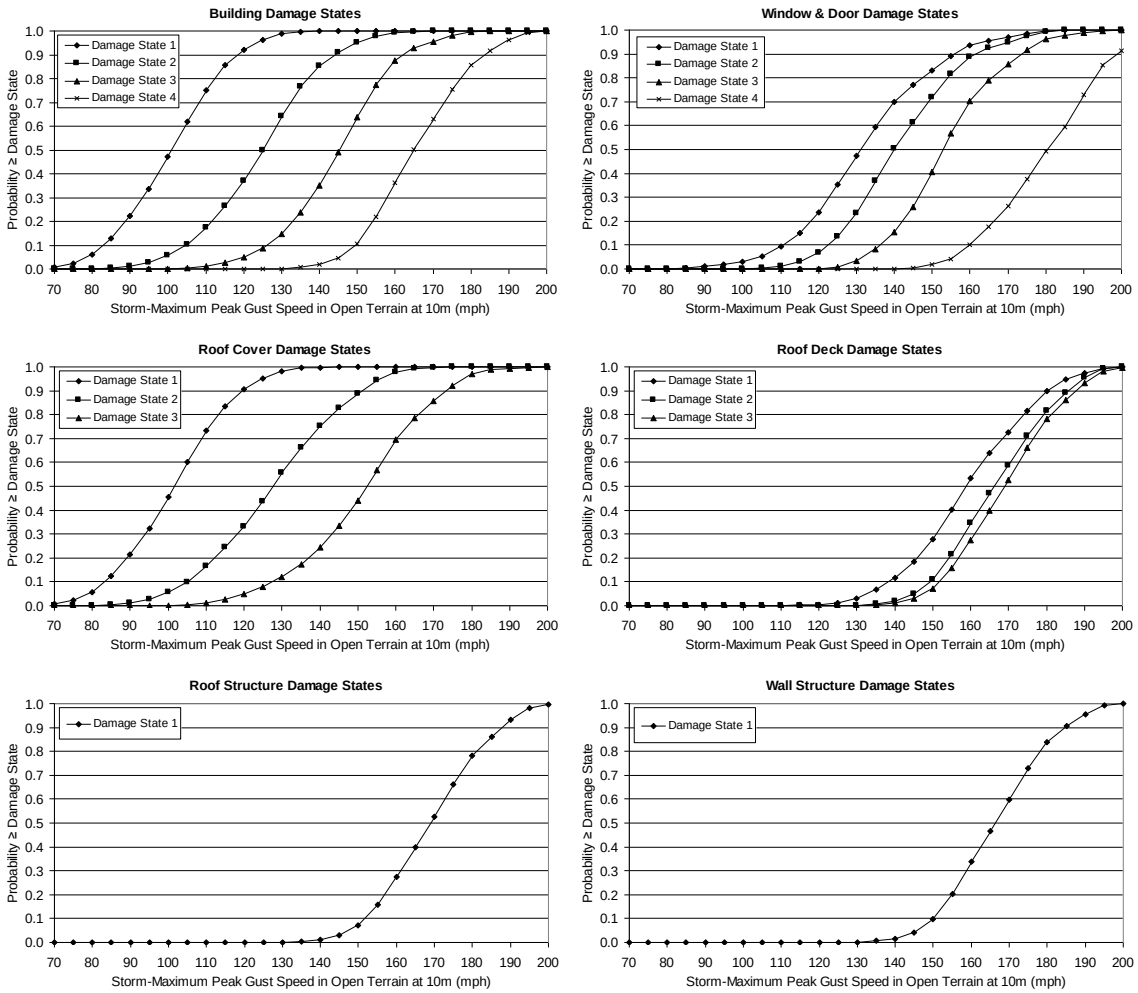

Figure C.1. Damage States vs. Maximum Peak Gust Wind Speed – One-Story, 8d Roof Deck Nails, Strapped Roof Trusses, Wood Frame Walls, Gable Roof with Shingles, z_0=0.03 m.

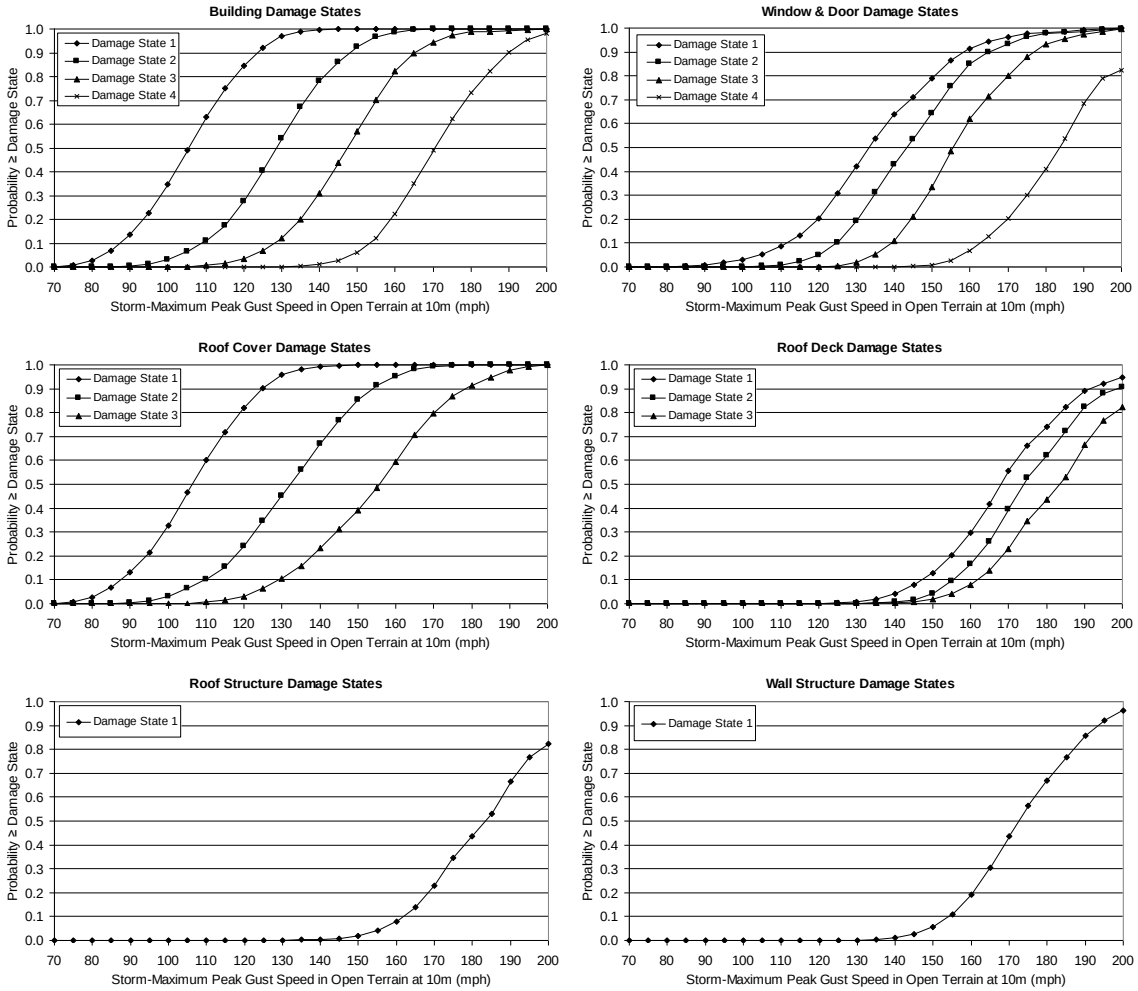

Figure C.2. Damage States vs. Maximum Peak Gust Wind Speed – One-Story, 8d Roof Deck Nails, Strapped Roof Trusses, Wood Frame Walls, Hip Roof with Shingles, z_0=0.03 m.

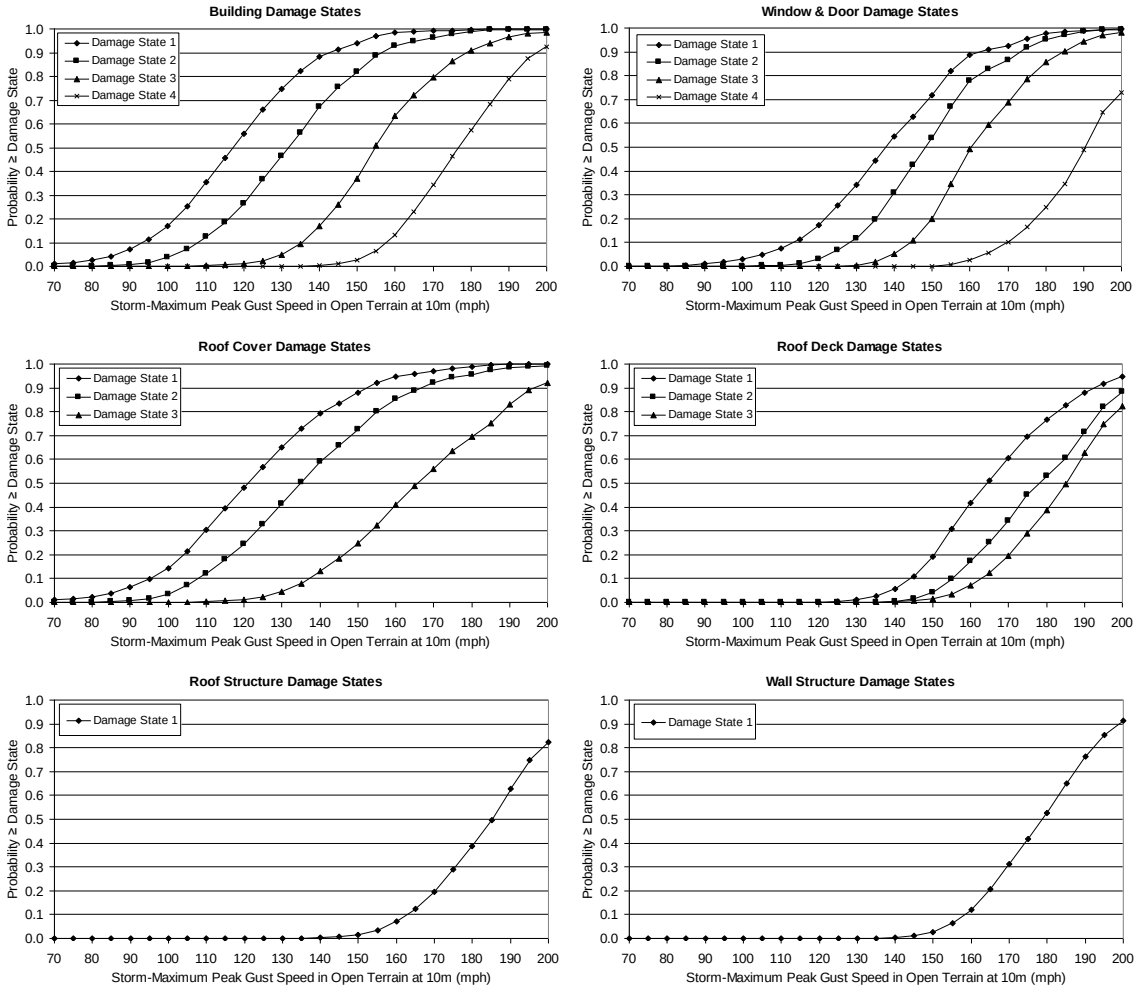

Figure C.3. Damage States vs. Maximum Peak Gust Wind Speed – One-Story, 8d Roof Deck Nails, Strapped Roof Trusses, Wood Frame Walls, <u>Flat Roof with Average Quality BUR</u>, z_0=0.03 m.

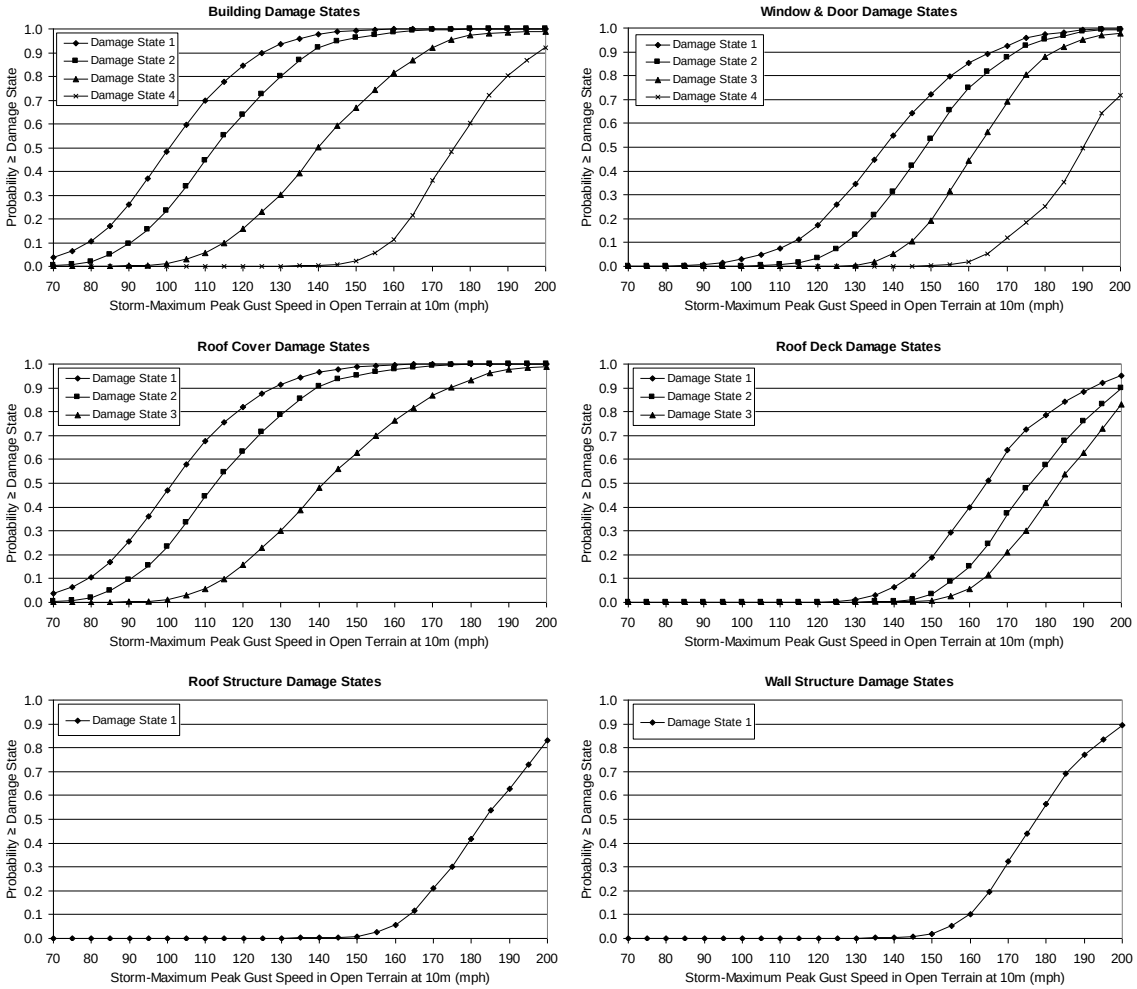

Figure C.4. Damage States vs. Maximum Peak Gust Wind Speed – One-Story, 8d Roof Deck Nails, Strapped Roof Trusses, Wood Frame Walls, <u>Flat Roof with Poor Quality BUR</u>, z_0=0.03 m.

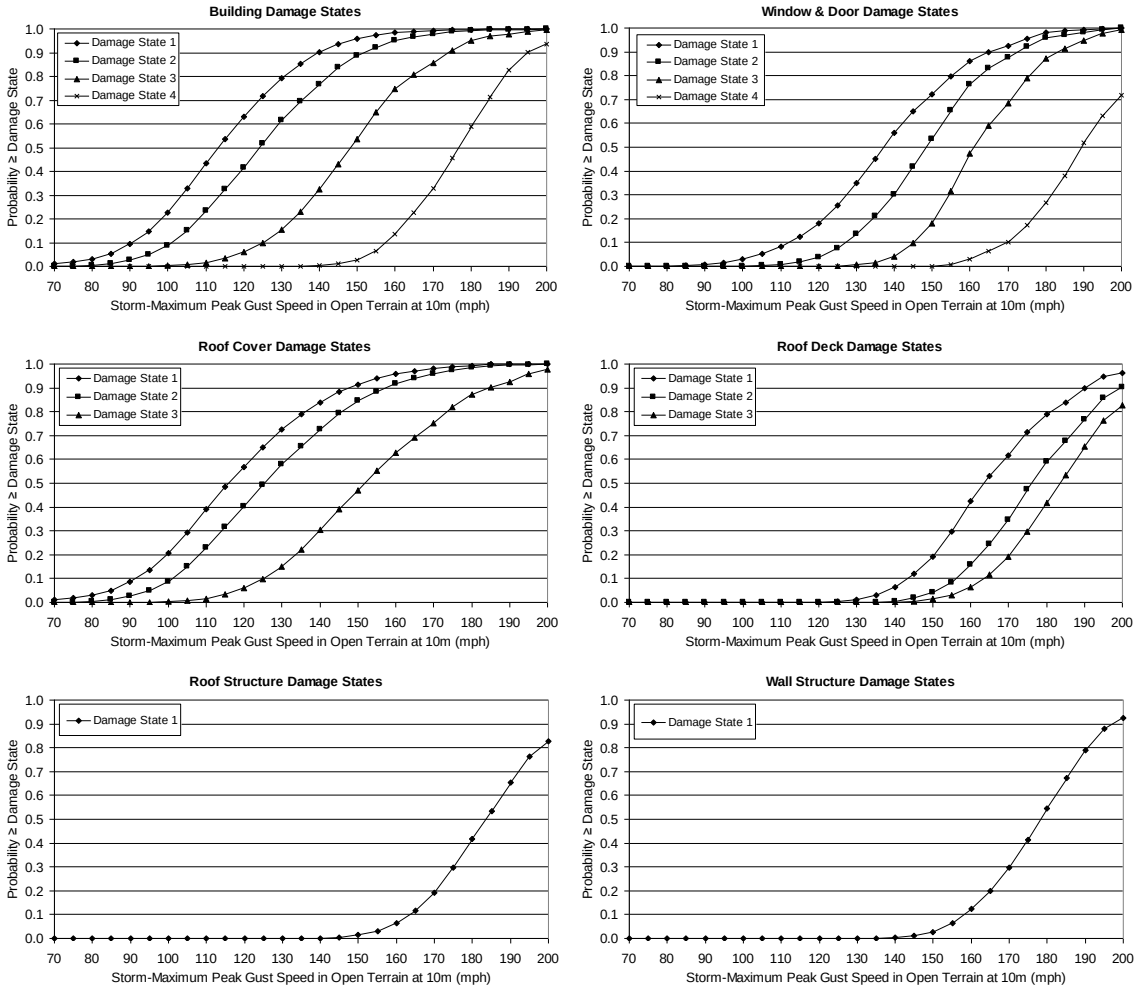

Figure C.5. Damage States vs. Maximum Peak Gust Wind Speed – One-Story, 8d Roof Deck Nails, Strapped Roof Trusses, Wood Frame Walls, <u>Flat Roof with Average Quality EPDM</u>, z_0=0.03 m.

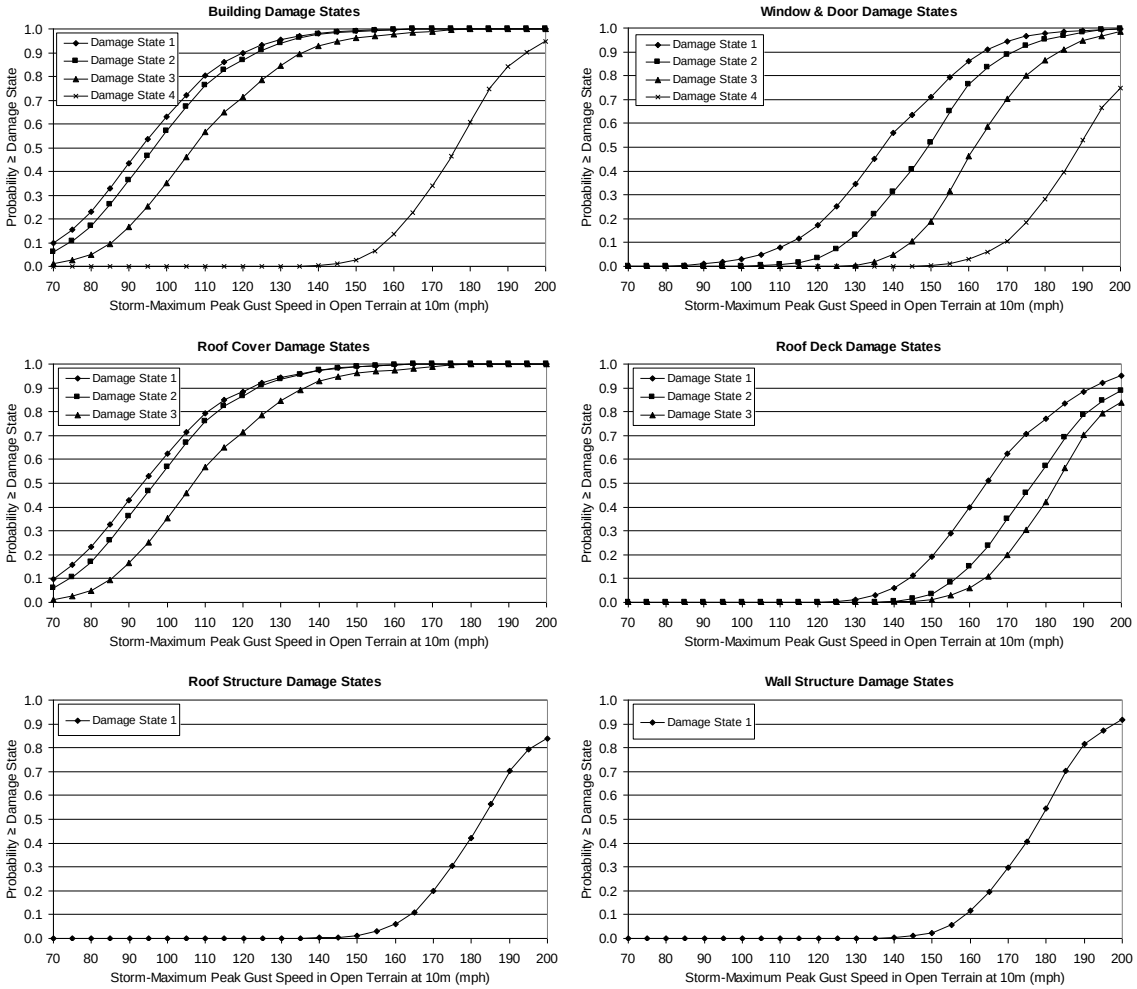

Figure C.6. Damage States vs. Maximum Peak Gust Wind Speed – One-Story, 8d Roof Deck Nails, Strapped Roof Trusses, Wood Frame Walls, Flat Roof with Poor Quality EPDM, z_0=0.03 m.

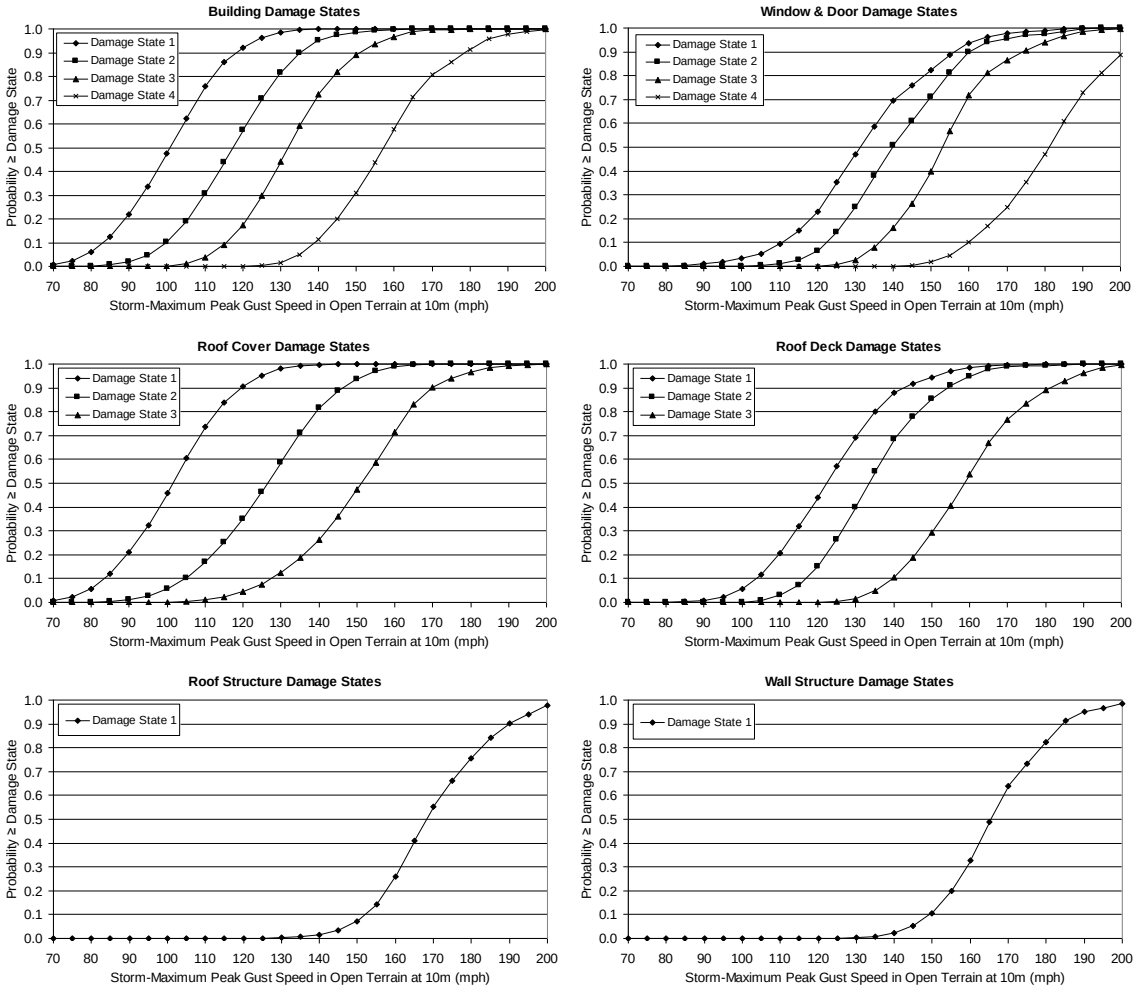

Figure C.7. Damage States vs. Maximum Peak Gust Wind Speed – One-Story, 6d Roof Deck Nails, Strapped Roof Trusses, Wood Frame Walls, Gable Roof with Shingles, z_0=0.03 m.

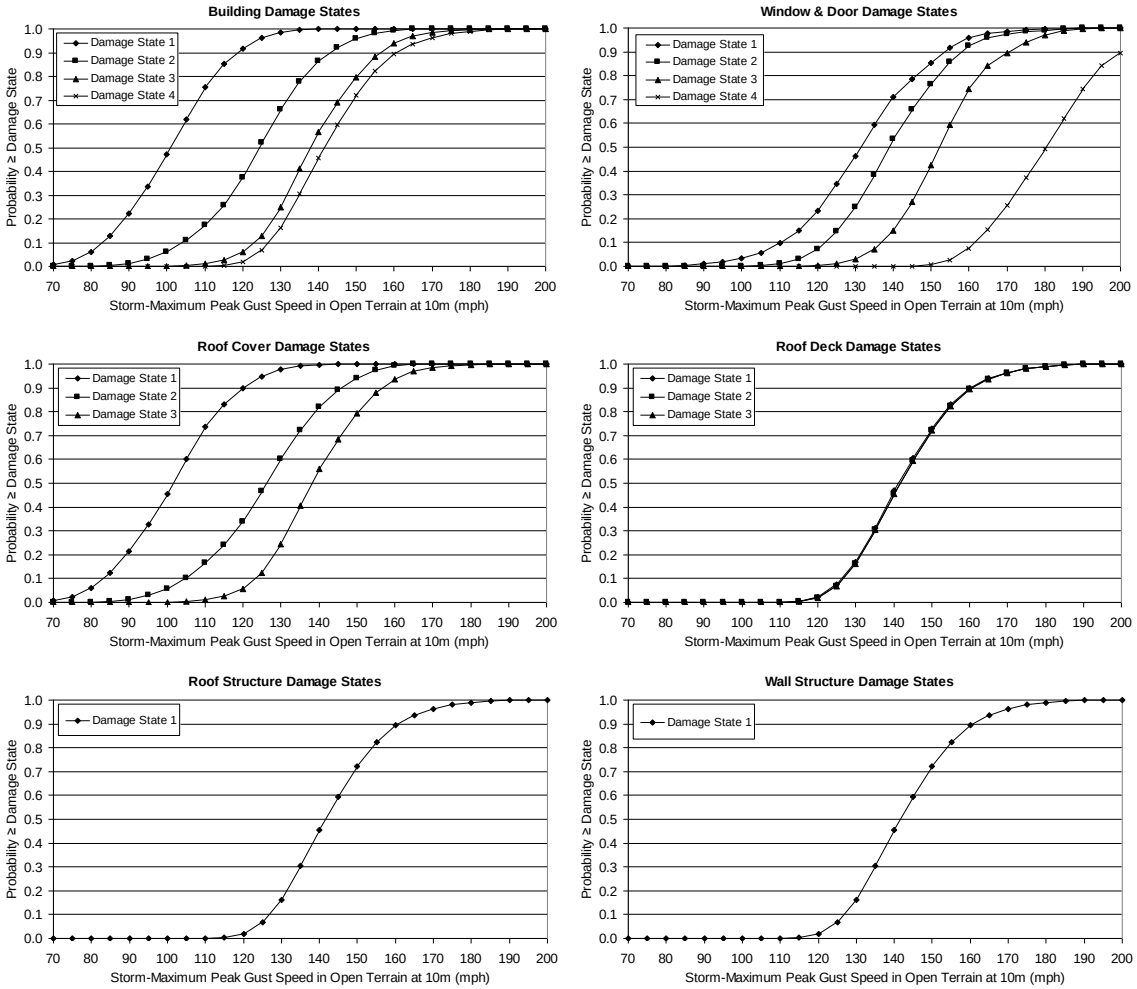

Figure C.8. Damage States vs. Maximum Peak Gust Wind Speed – One-Story, 8d Roof Deck Nails, Toe-Nnailed Roof Trusses, Wood Frame Walls, Gable Roof with Shingles, z_0=0.03 m.

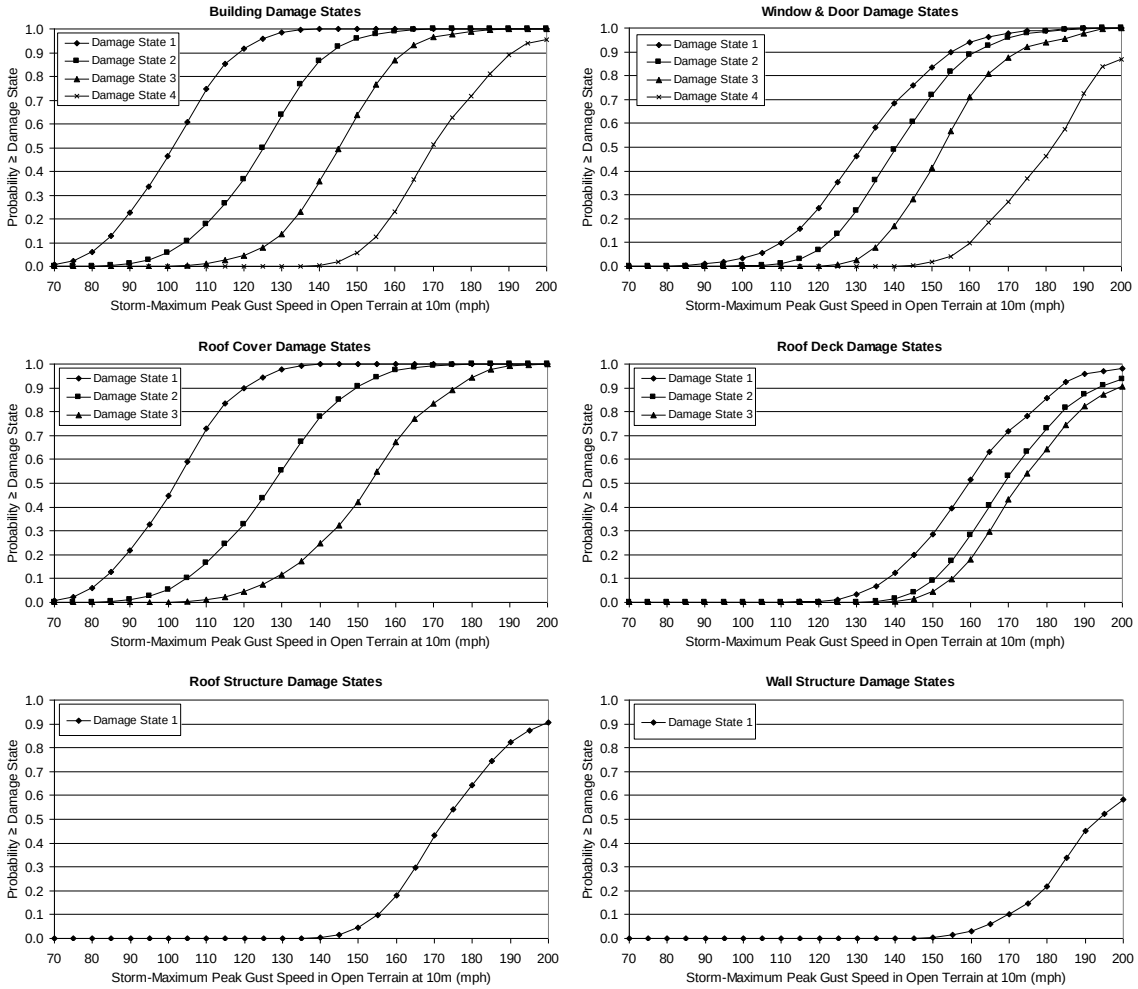

Figure C.9. Damage States vs. Maximum Peak Gust Wind Speed – One-Story, 8d Roof Deck Nails, Strapped Roof Trusses, <u>Unreinforced Masonry Walls</u>, Gable Roof with Shingles, z_0=0.03 m.

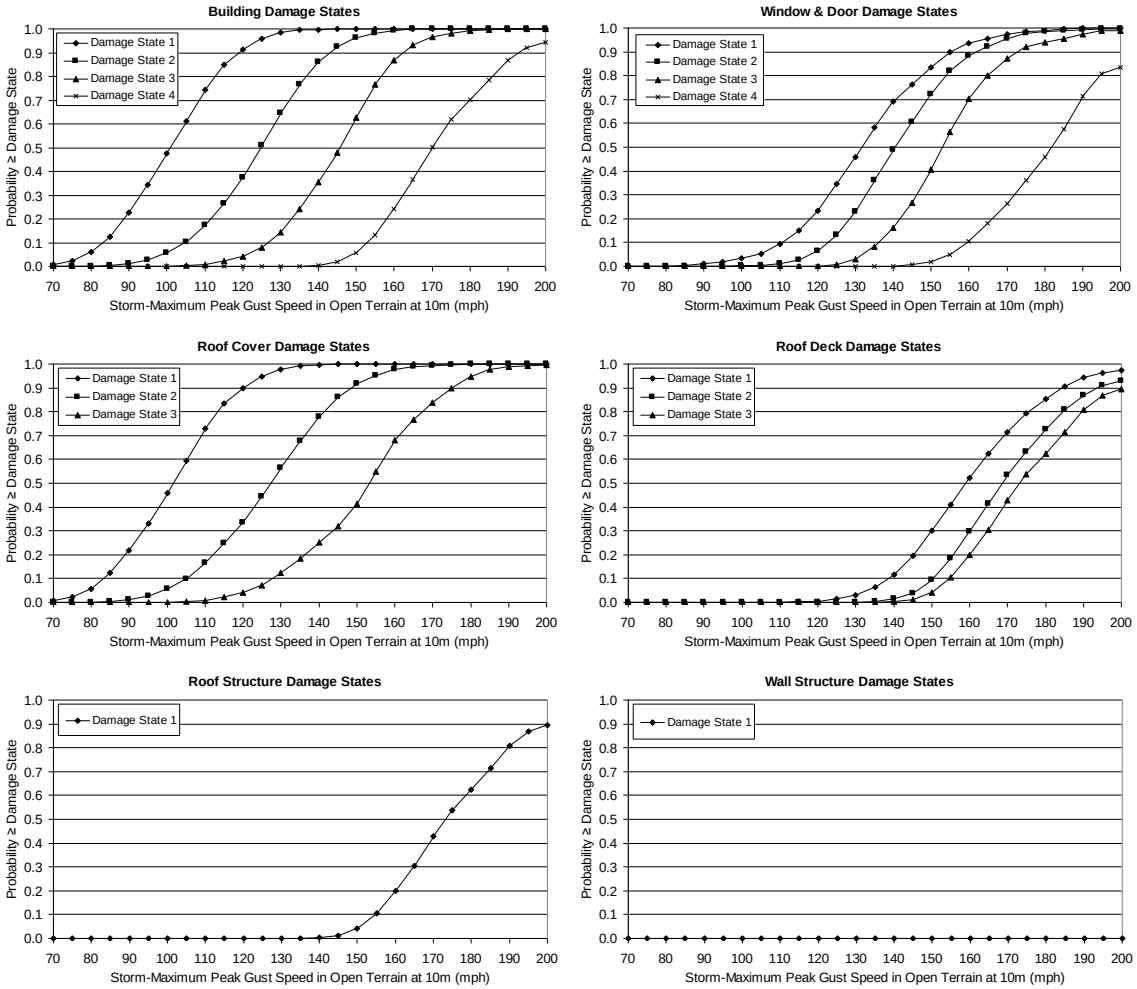

Figure C.10. Damage States vs. Maximum Peak Gust Wind Speed – One-Story, 8d Roof Deck Nails, Strapped Roof Trusses, Reinforced Masonry Walls, Gable Roof with Shingles, z_0=0.03 m.

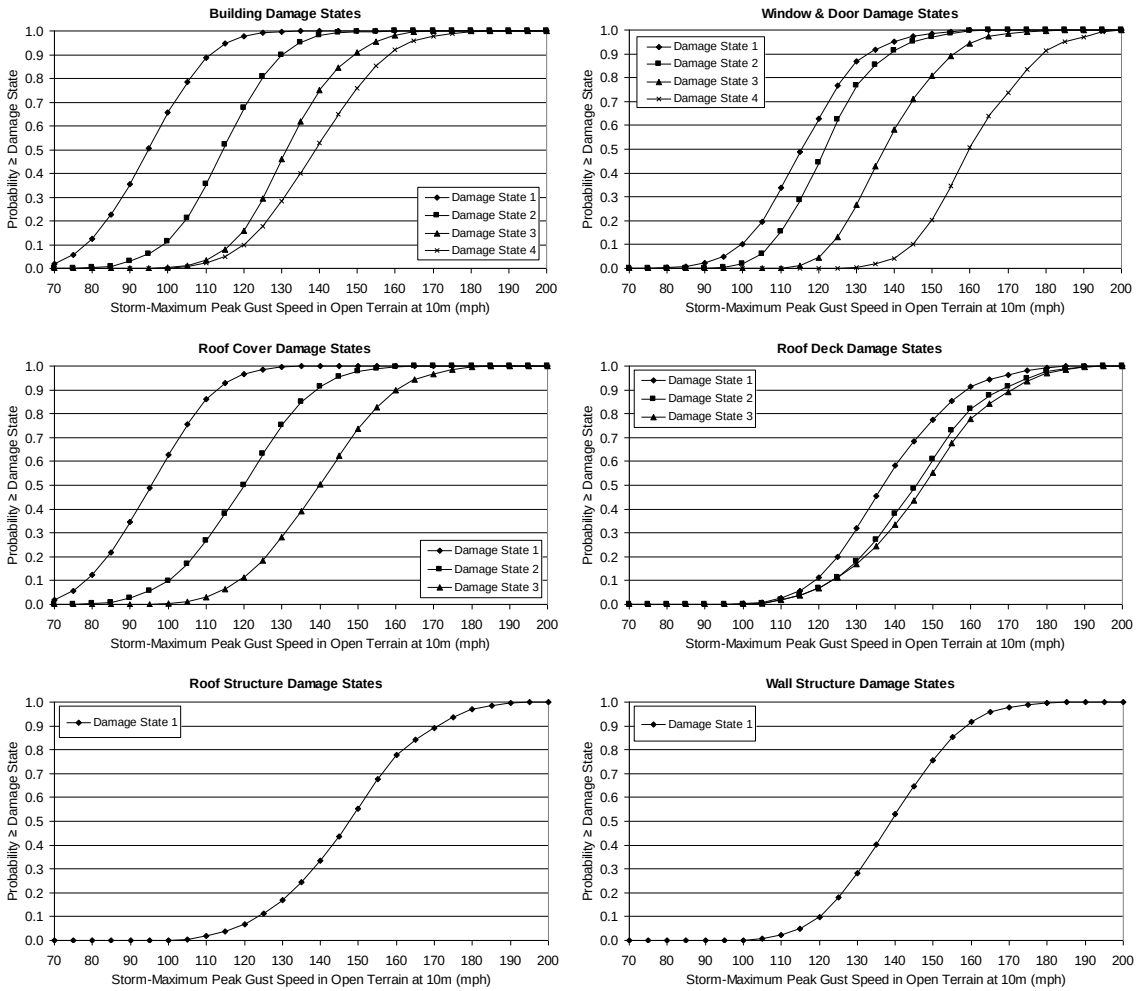

Figure C.11. Damage States vs. Maximum Peak Gust Wind Speed – <u>Two-Story</u>, 8d Roof Deck Nails, Strapped Roof Trusses, Wood Frame Walls, Gable Roof with Shingles, z_0=0.03 m.

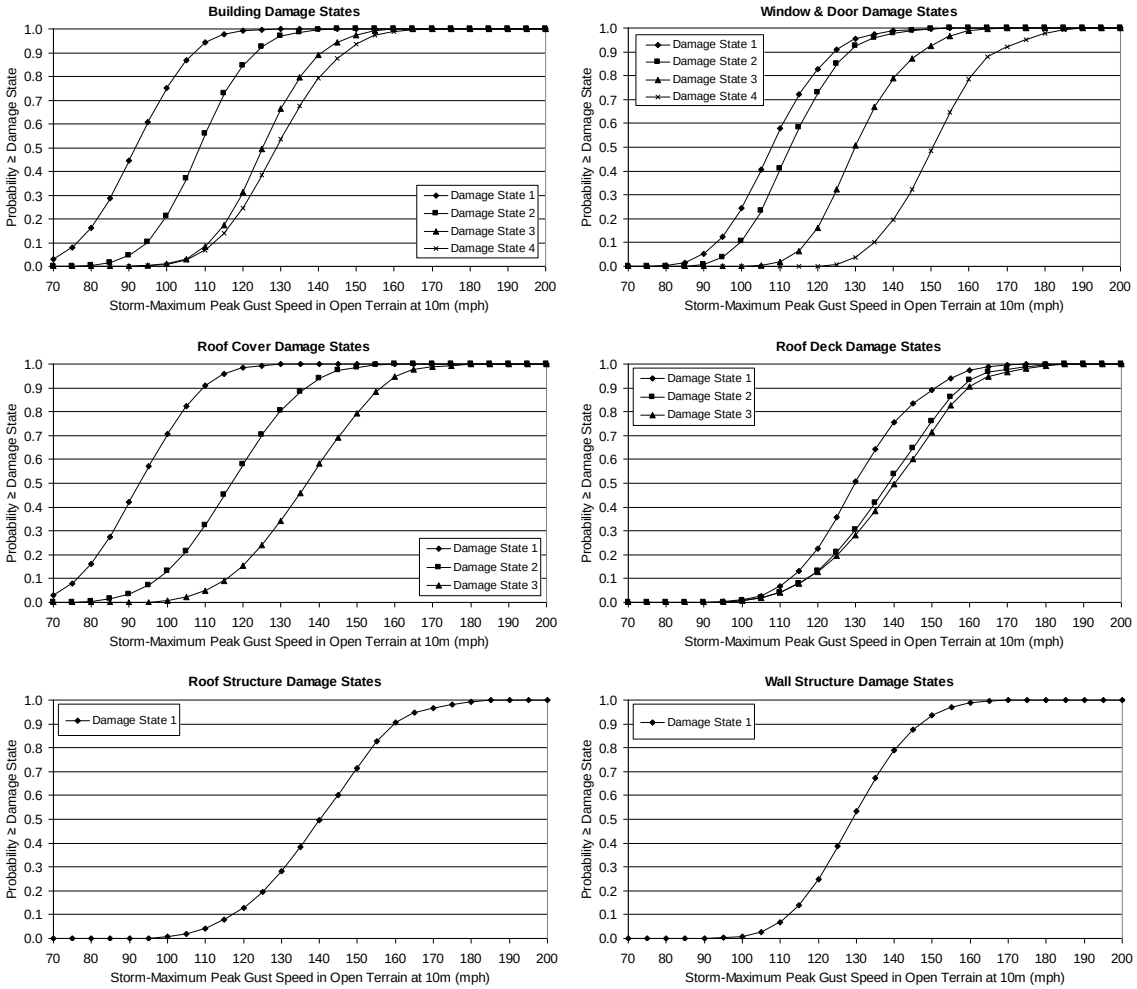

Figure C.12. Damage States vs. Maximum Peak Gust Wind Speed – <u>Three-Story</u>, 8d Roof Deck Nails, Strapped Roof Trusses, Wood Frame Walls, Gable Roof with Shingles, z_0=0.03 m.

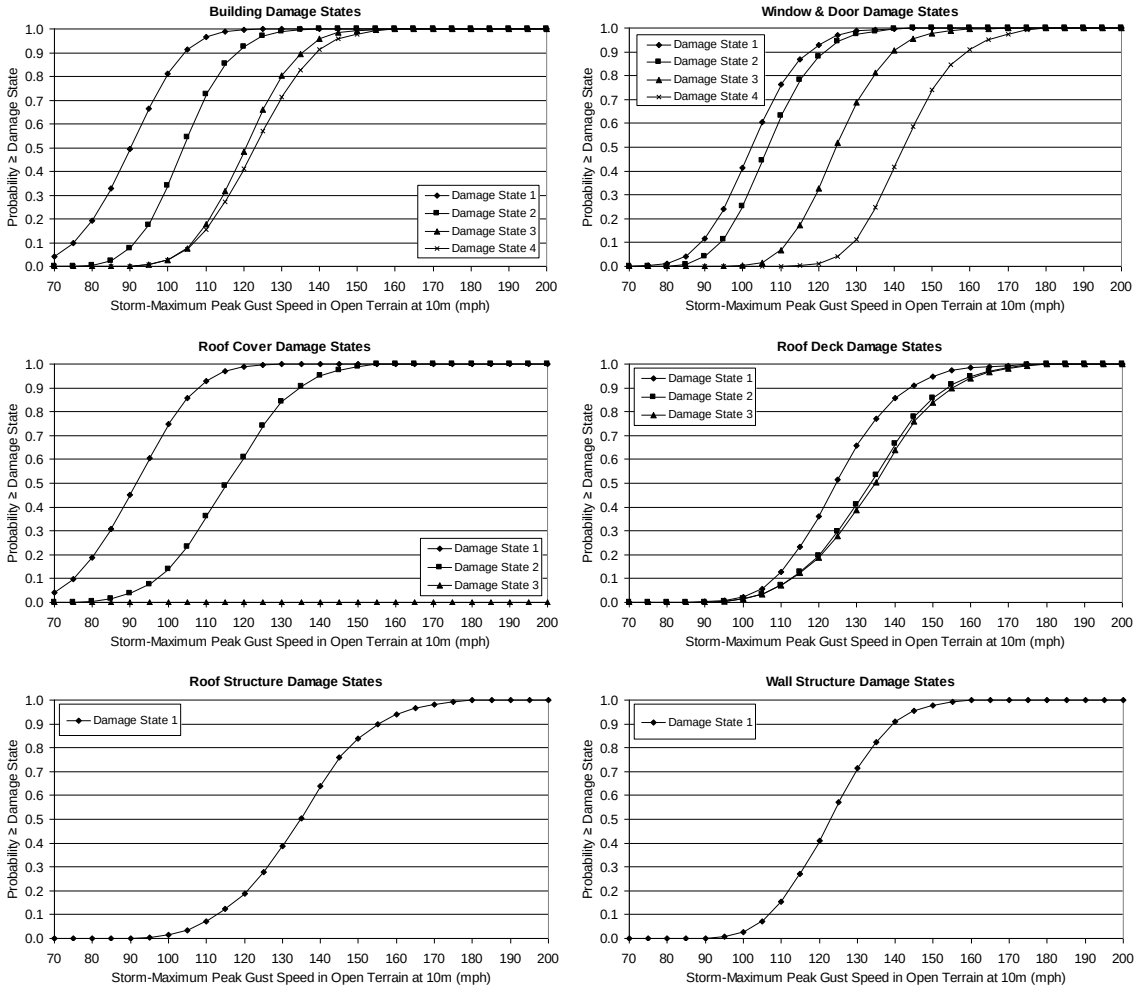

Figure C.13. Damage States vs. Maximum Peak Gust Wind Speed – <u>Four-Story</u>, 8d Roof Deck Nails, Strapped Roof Trusses, Wood Frame Walls, Gable Roof with Shingles, z_0=0.03 m.

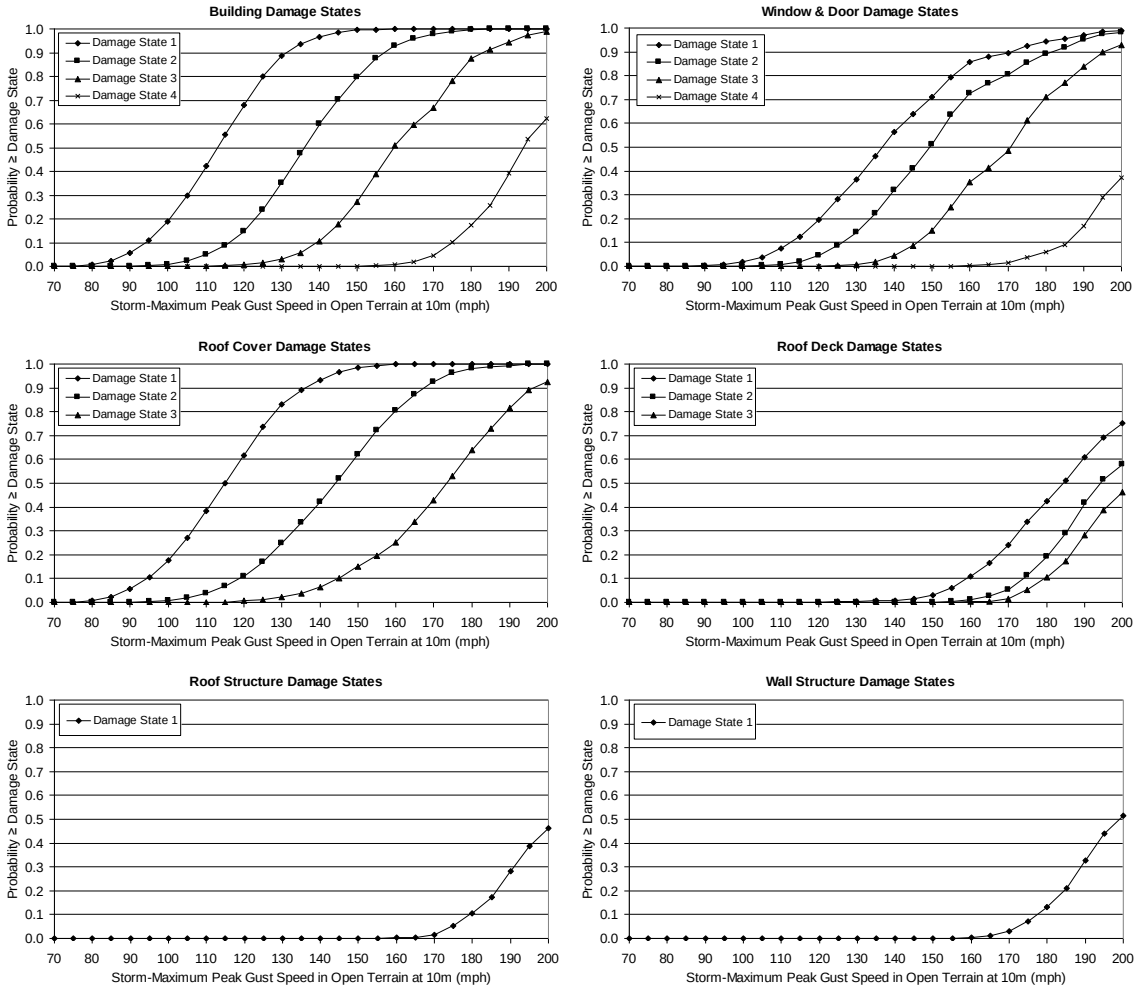

Figure C.14. Damage States vs. Maximum Peak Gust Wind Speed – One-Story, 8d Roof Deck Nails, Strapped Roof Trusses, Wood Frame Walls, Gable Roof with Shingles, z_0=0.35 m.

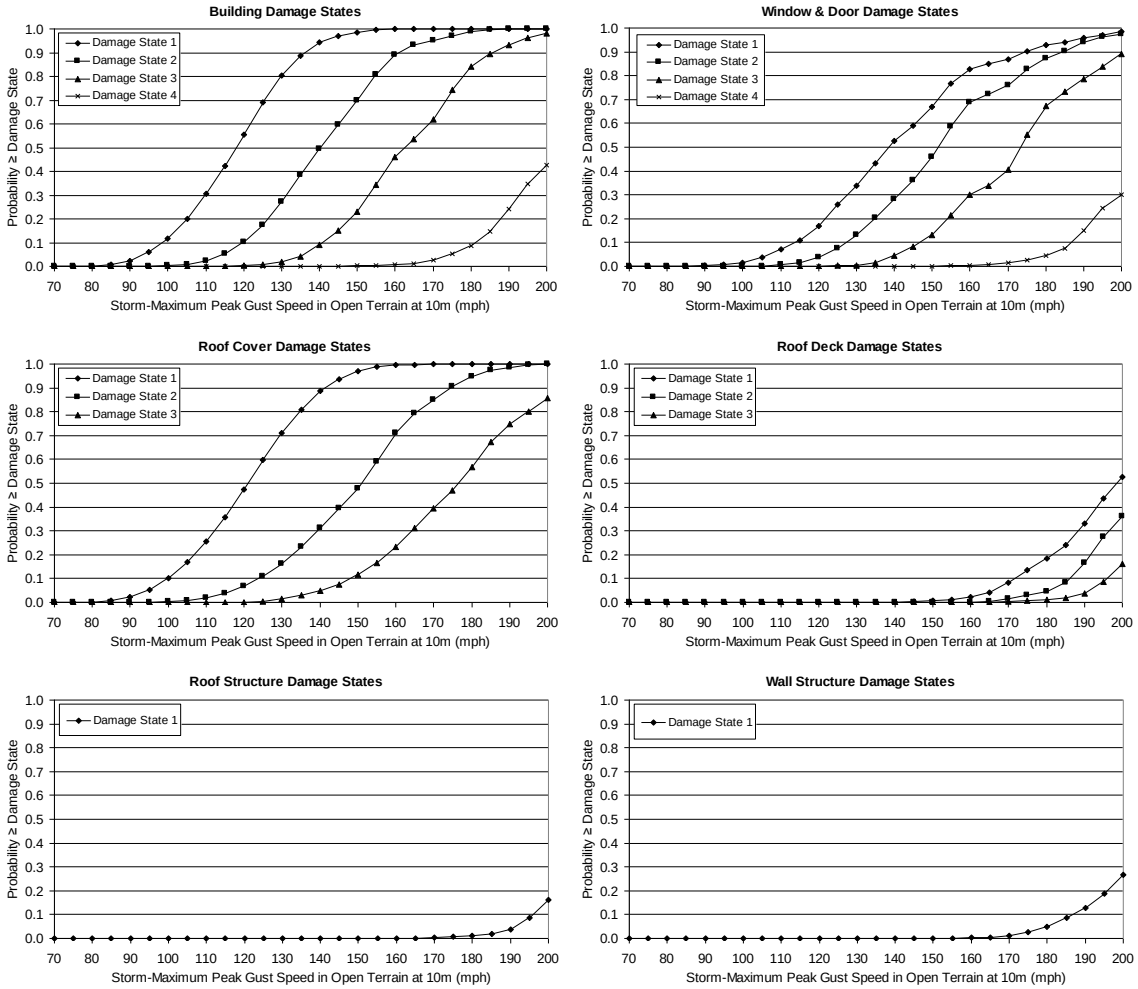

Figure C.15. Damage States vs. Maximum Peak Gust Wind Speed – One-Story, 8d Roof Deck Nails, Strapped Roof Trusses, Wood Frame Walls, <u>Hip Roof with Shingles</u>, z_0=0.35 m.

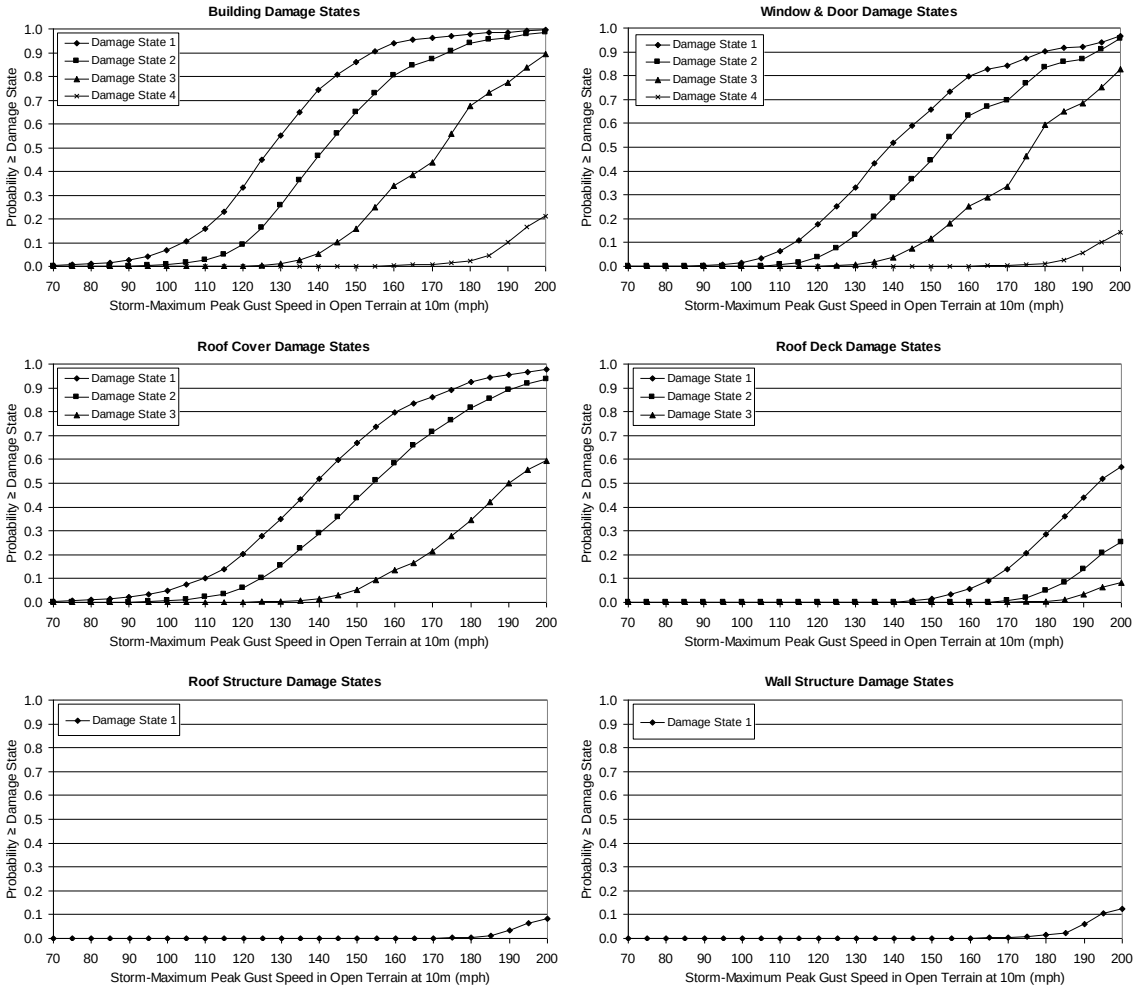

Figure C.16. Damage States vs. Maximum Peak Gust Wind Speed – One-Story, 8d Roof Deck Nails, Strapped Roof Trusses, Wood Frame Walls, <u>Flat Roof with Average Quality BUR</u>, z_0=0.35 m.

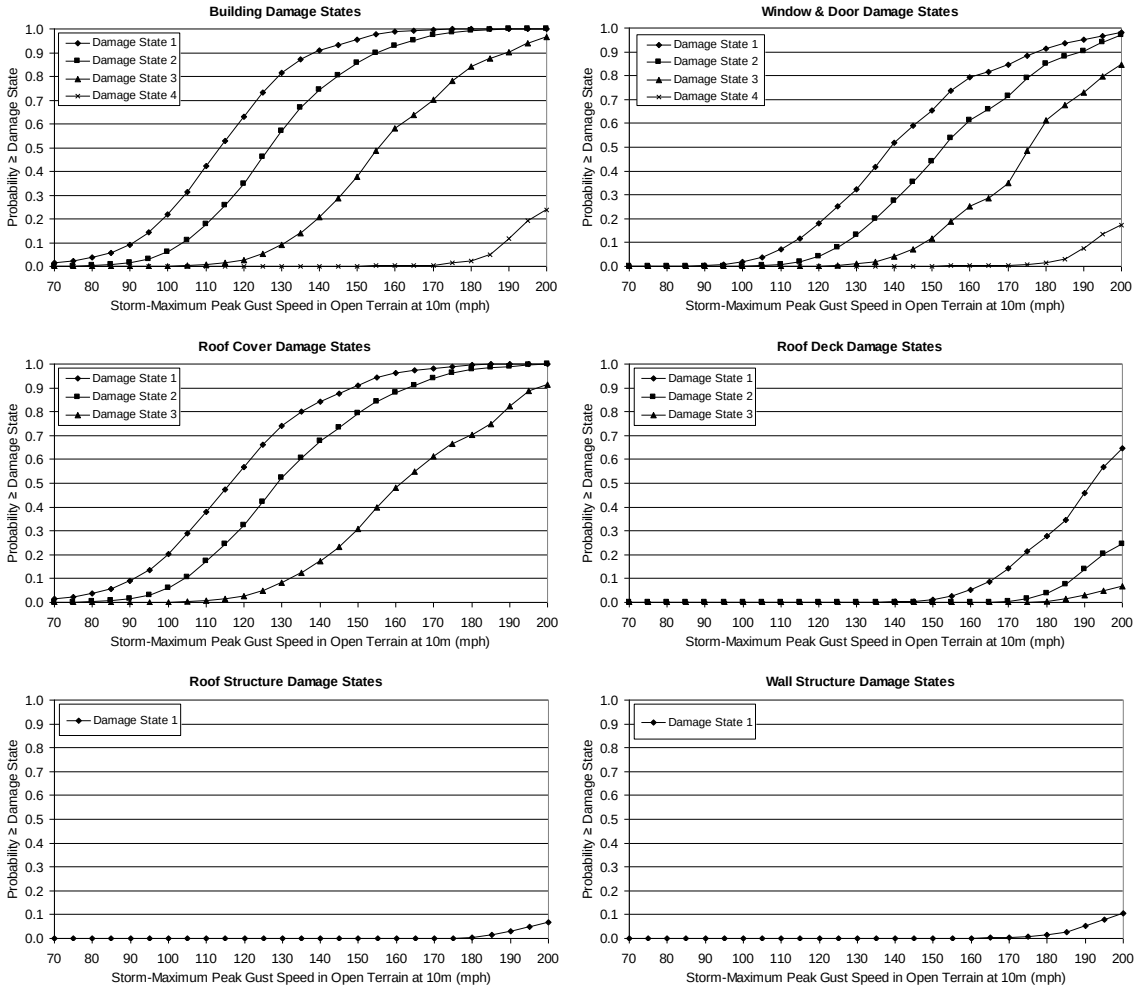

Figure C.17. Damage States vs. Maximum Peak Gust Wind Speed – One-Story, 8d Roof Deck Nails, Strapped Roof Trusses, Wood Frame Walls, Flat Roof with Poor Quality BUR, z_0=0.35 m.

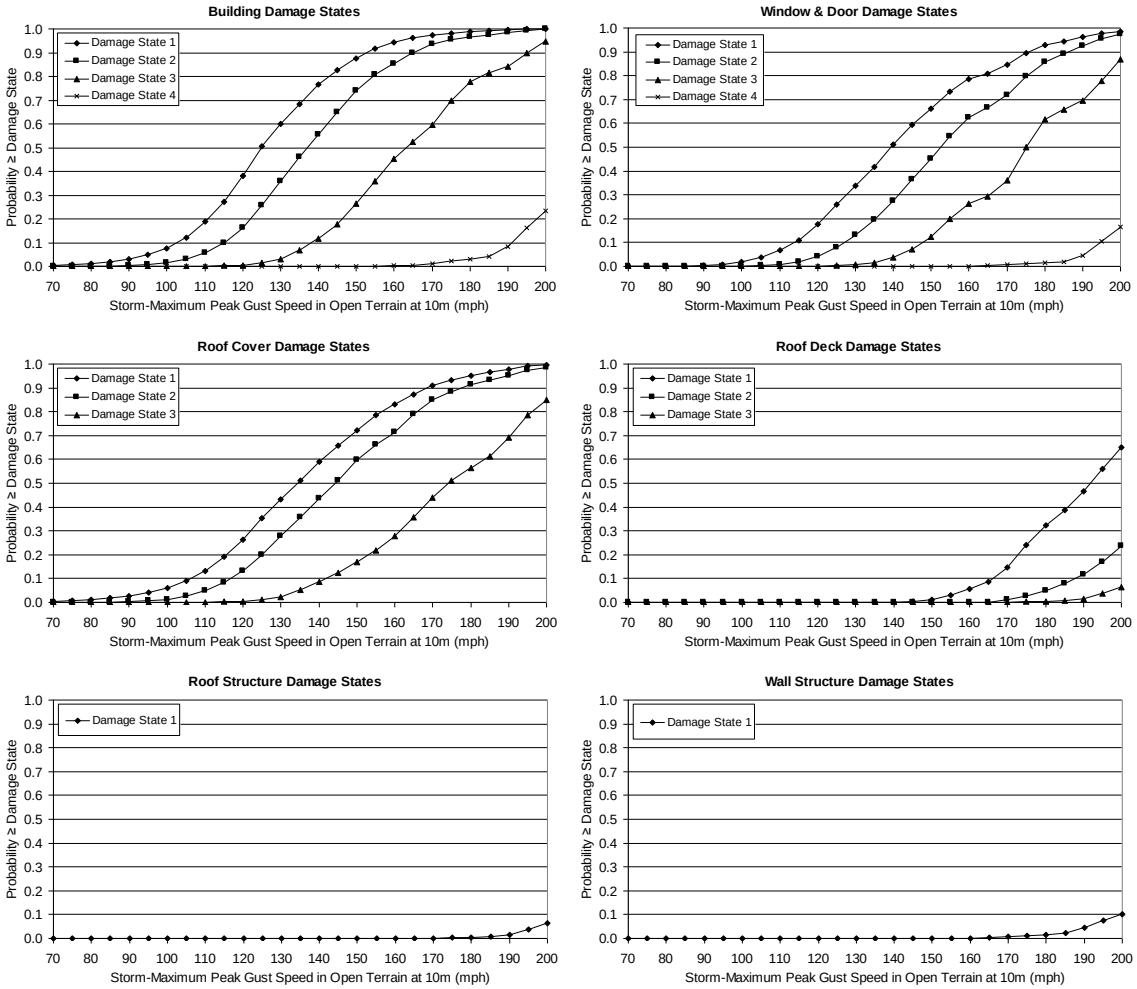

Figure C.18. Damage States vs. Maximum Peak Gust Wind Speed – One-Story, 8d Roof Deck Nails, Strapped Roof Trusses, Wood Frame Walls, Flat Roof with Average Quality EPDM, z_0=0.35 m.

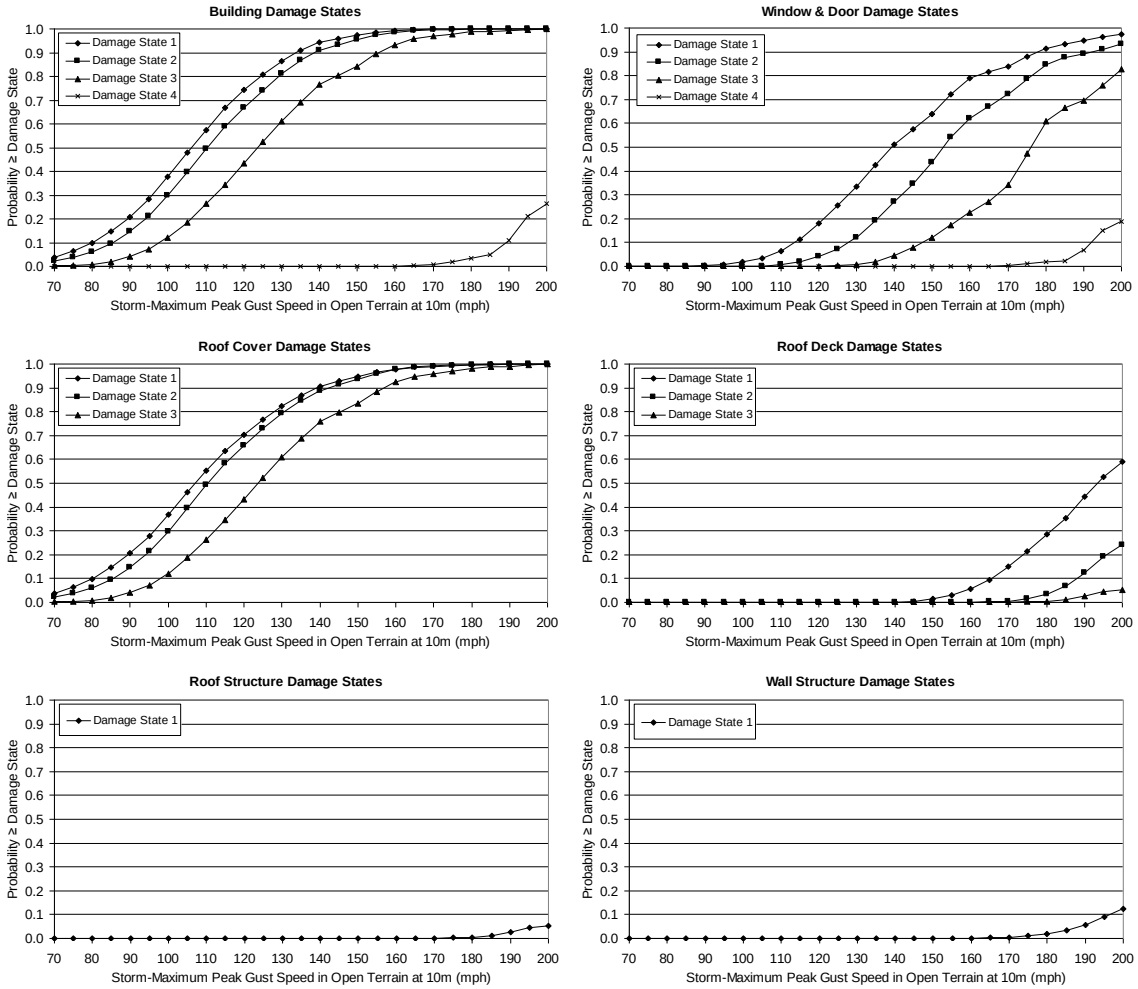

Figure C.19. Damage States vs. Maximum Peak Gust Wind Speed – One-Story, 8d Roof Deck Nails, Strapped Roof Trusses, Wood Frame Walls, <u>Flat Roof with Poor Quality EPDM</u>, z_0=0.35 m.

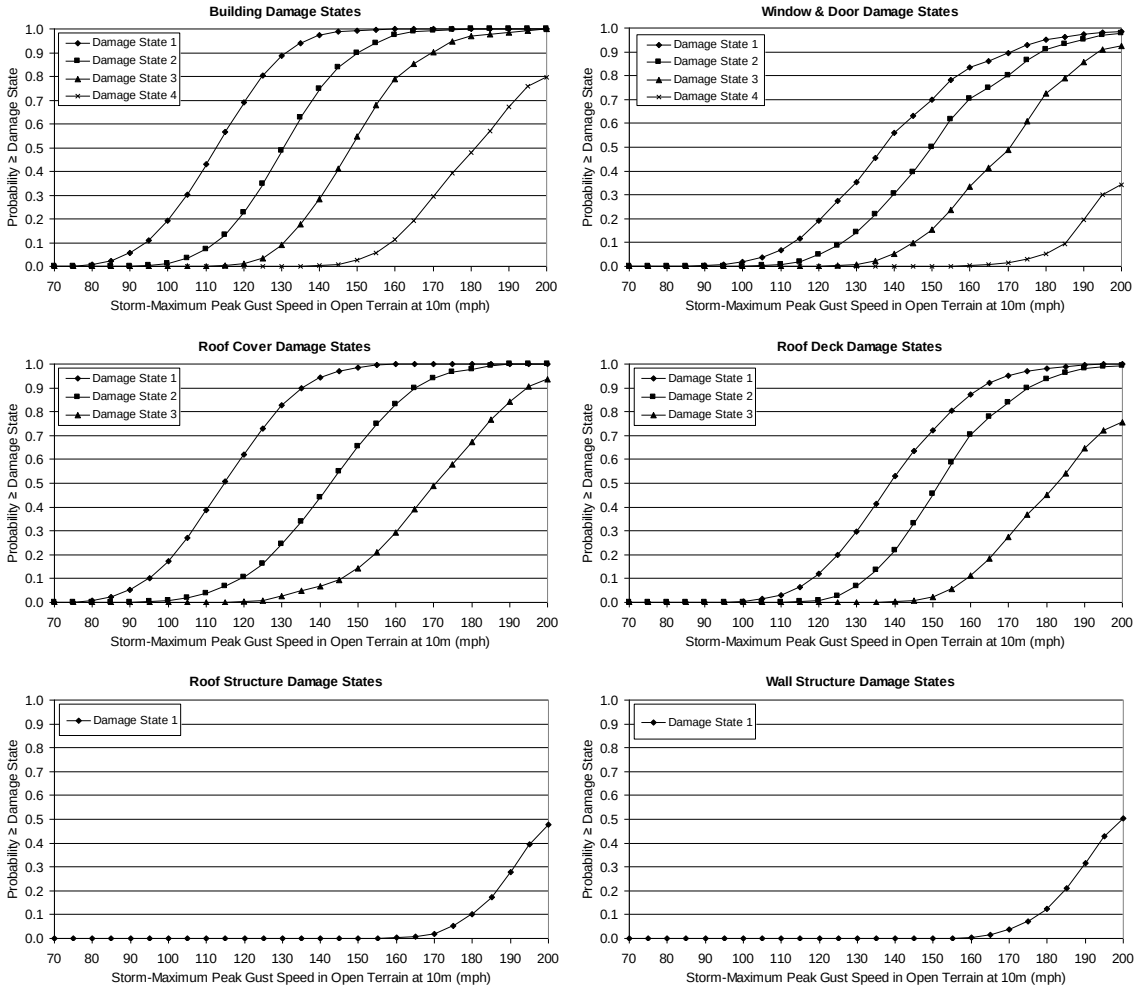

Figure C.20. Damage States vs. Maximum Peak Gust Wind Speed – One-Story, 6d Roof Deck Nails, Strapped Roof Trusses, Wood Frame Walls, Gable Roof with Shingles, z_0=0.35 m.

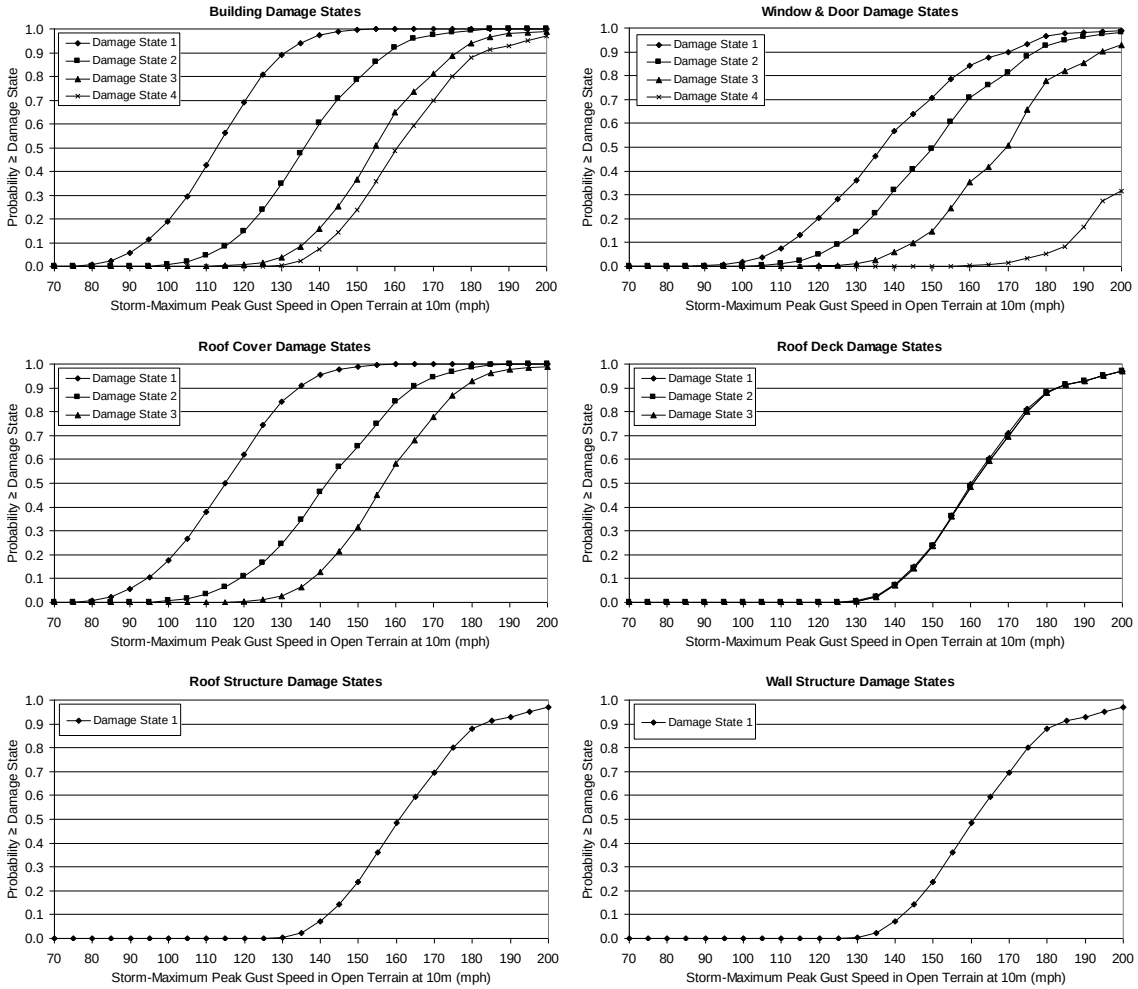

Figure C.21. Damage States vs. Maximum Peak Gust Wind Speed – One-Story, 8d Roof Deck Nails, Toe-Nailed Roof Trusses, Wood Frame Walls, Gable Roof with Shingles, z_0=0.35 m.

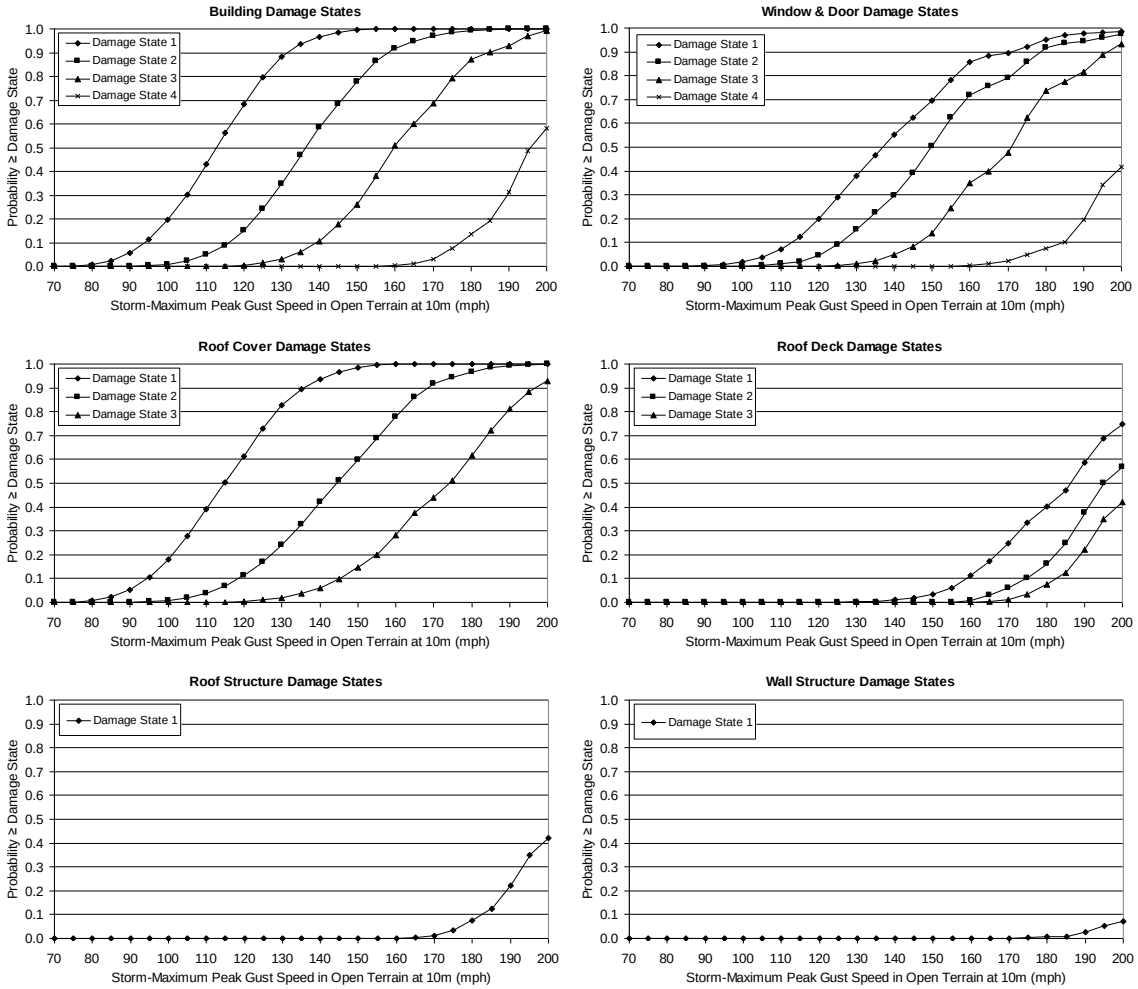

Figure C.22. Damage States vs. Maximum Peak Gust Wind Speed – One-Story, 8d Roof Deck Nails, Strapped Roof Trusses, Unreinforced Masonry Walls, Gable Roof with Shingles, z_0=0.35 m.

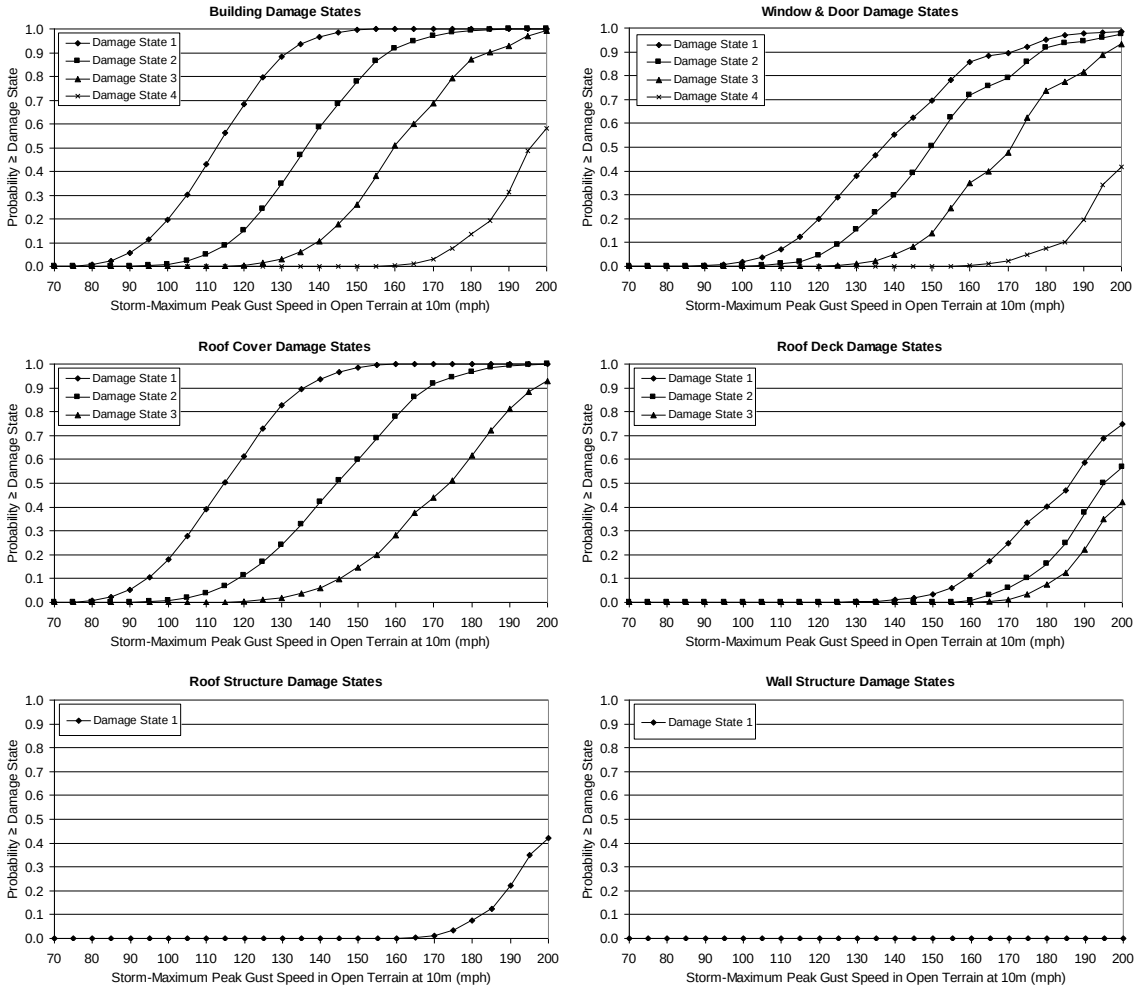

Figure C.23. Damage States vs. Maximum Peak Gust Wind Speed – One-Story, 8d Roof Deck Nails, Strapped Roof Trusses, <u>Reinforced Masonry Walls</u>, Gable Roof with Shingles, z_0=0.35 m.

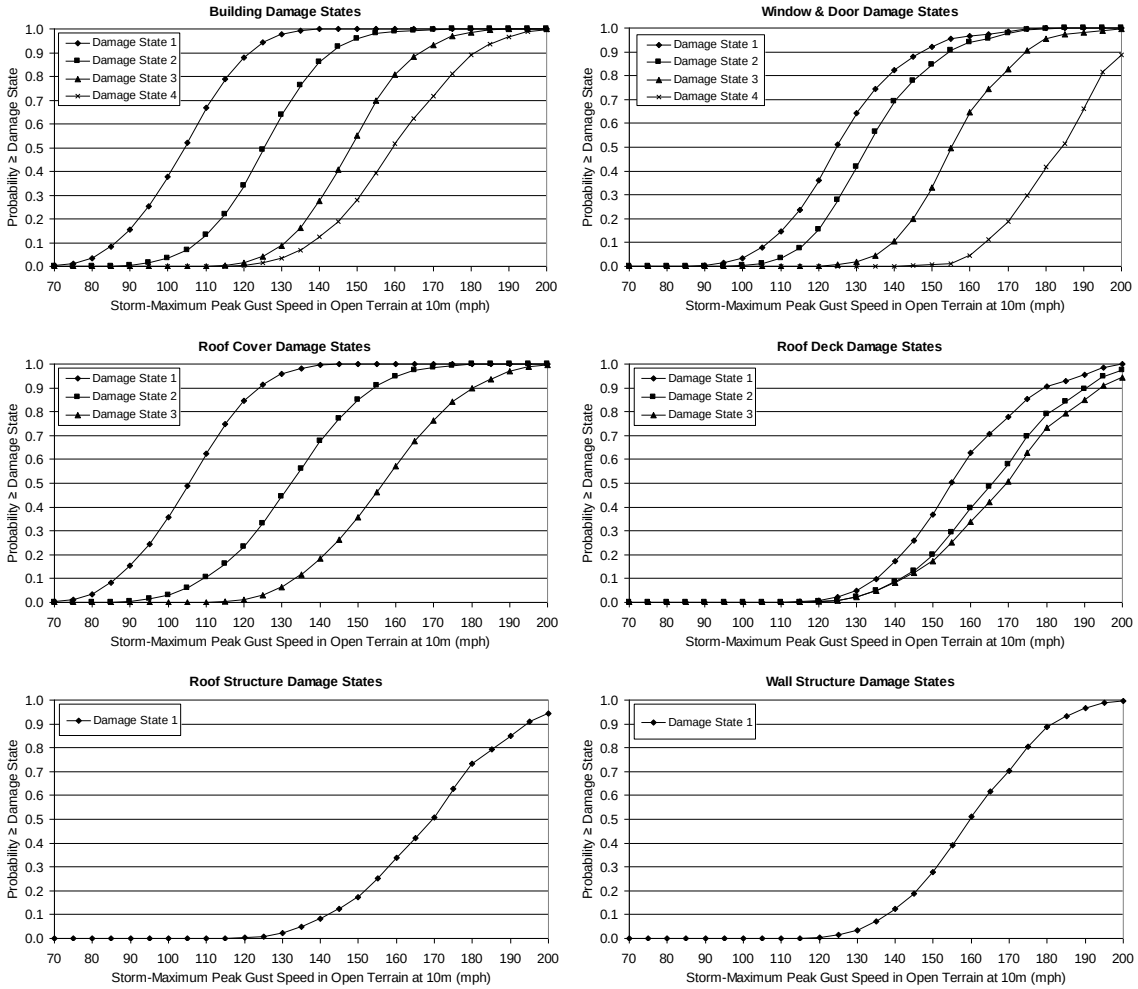

Figure C.24. Damage States vs. Maximum Peak Gust Wind Speed – <u>Two-Story</u>, 8d Roof Deck Nails, Strapped Roof Trusses, Wood Frame Walls, Gable Roof with Shingles, z_0=0.35 m.

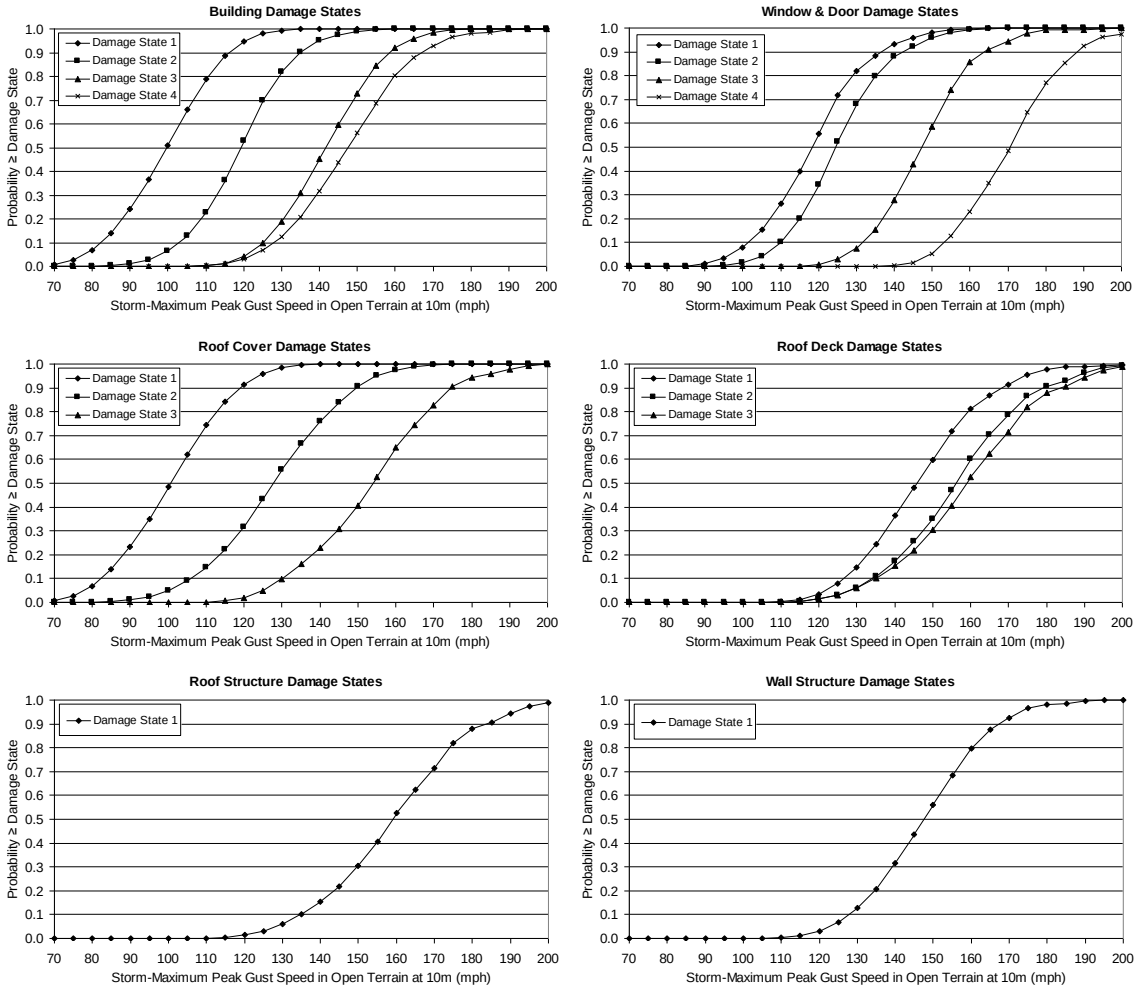

Figure C.25. Damage States vs. Maximum Peak Gust Wind Speed – <u>Three-Story</u>, 8d Roof Deck Nails, Strapped Roof Trusses, Wood Frame Walls, Gable Roof with Shingles, z_0=0.35 m.

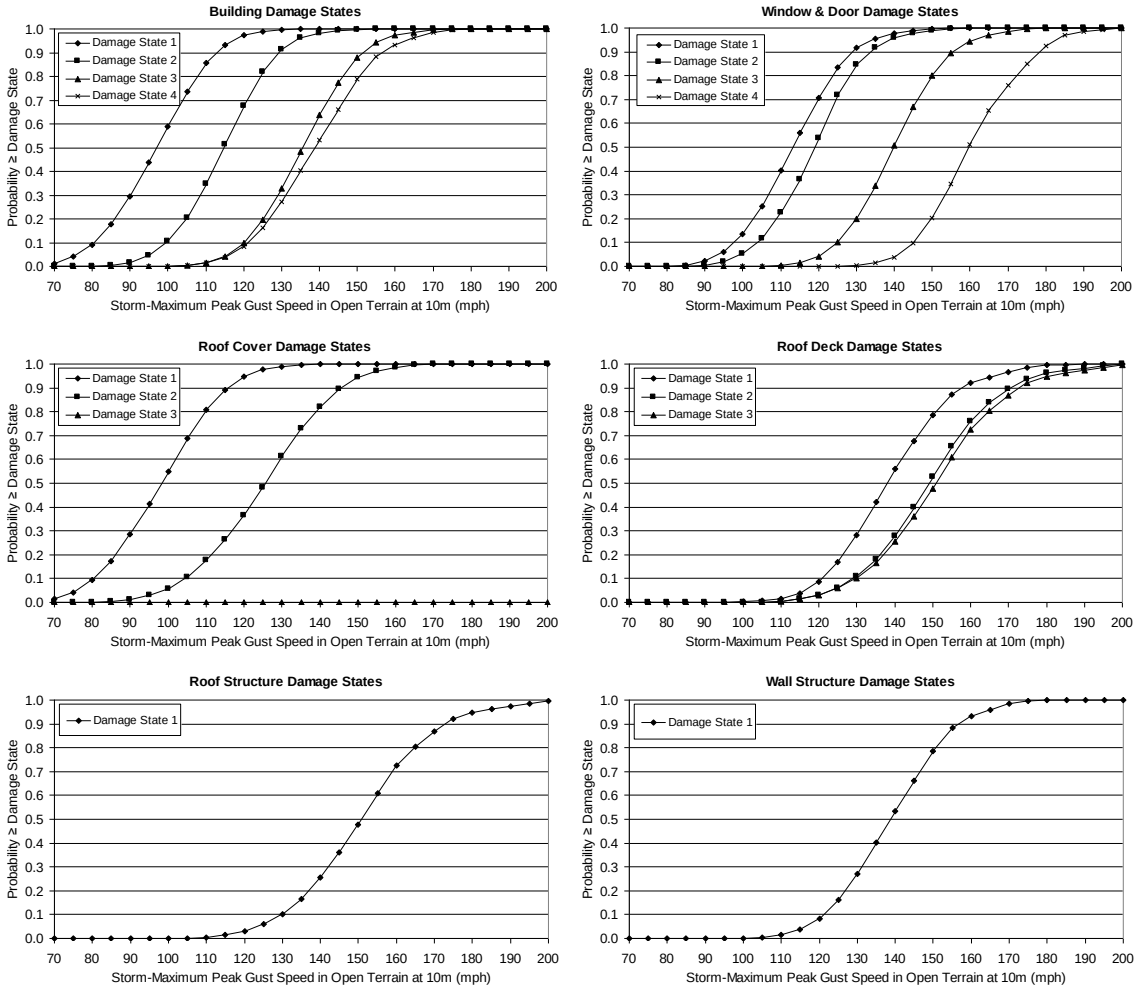

Figure C.26. Damage States vs. Maximum Peak Gust Wind Speed – <u>Four-Story</u>, 8d Roof Deck Nails, Strapped Roof Trusses, Wood Frame Walls, Gable Roof with Shingles, z_0=0.35 m.

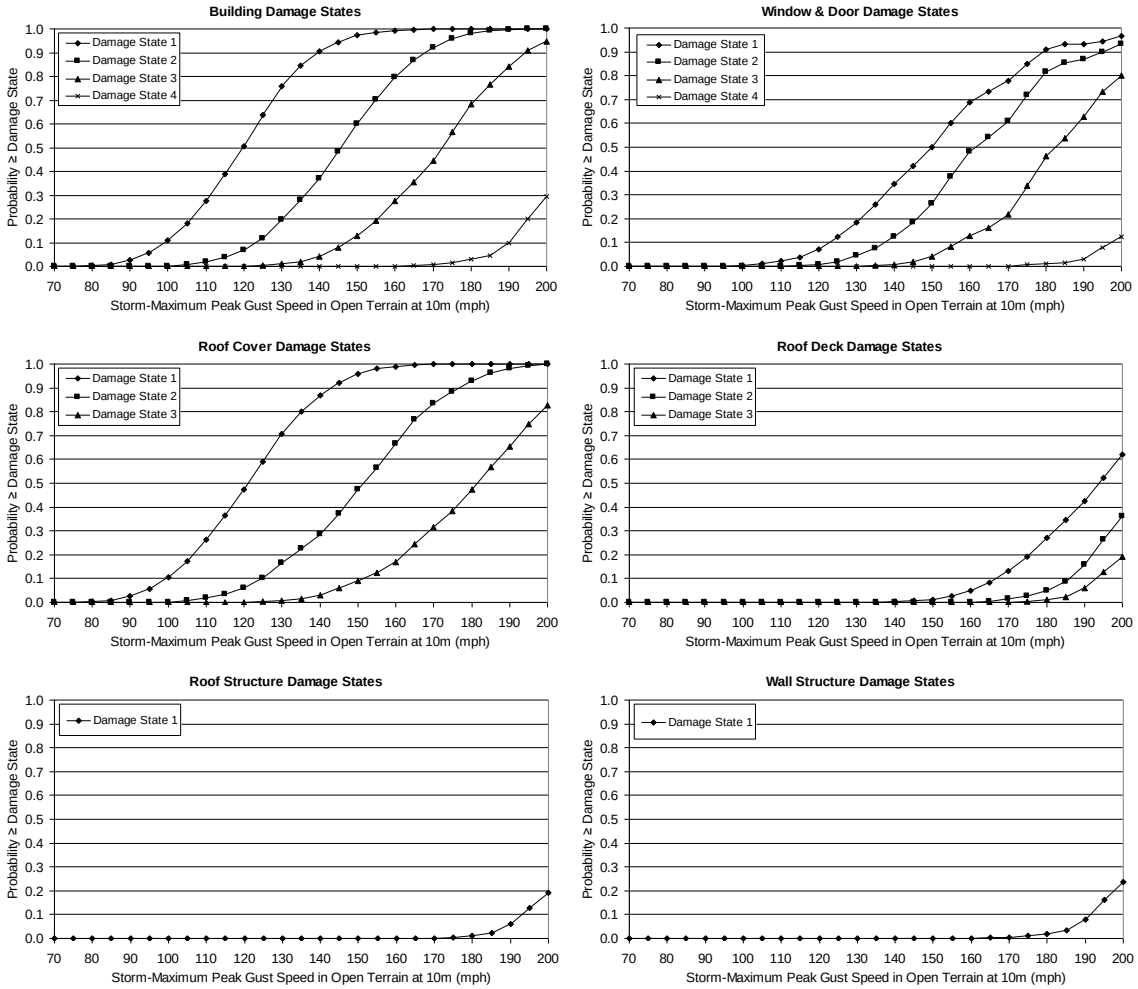

Figure C.27. Damage States vs. Maximum Peak Gust Wind Speed – One-Story, 8d Roof Deck Nails, Strapped Roof Trusses, Wood Frame Walls, Gable Roof with Shingles, z_0=0.70 m.

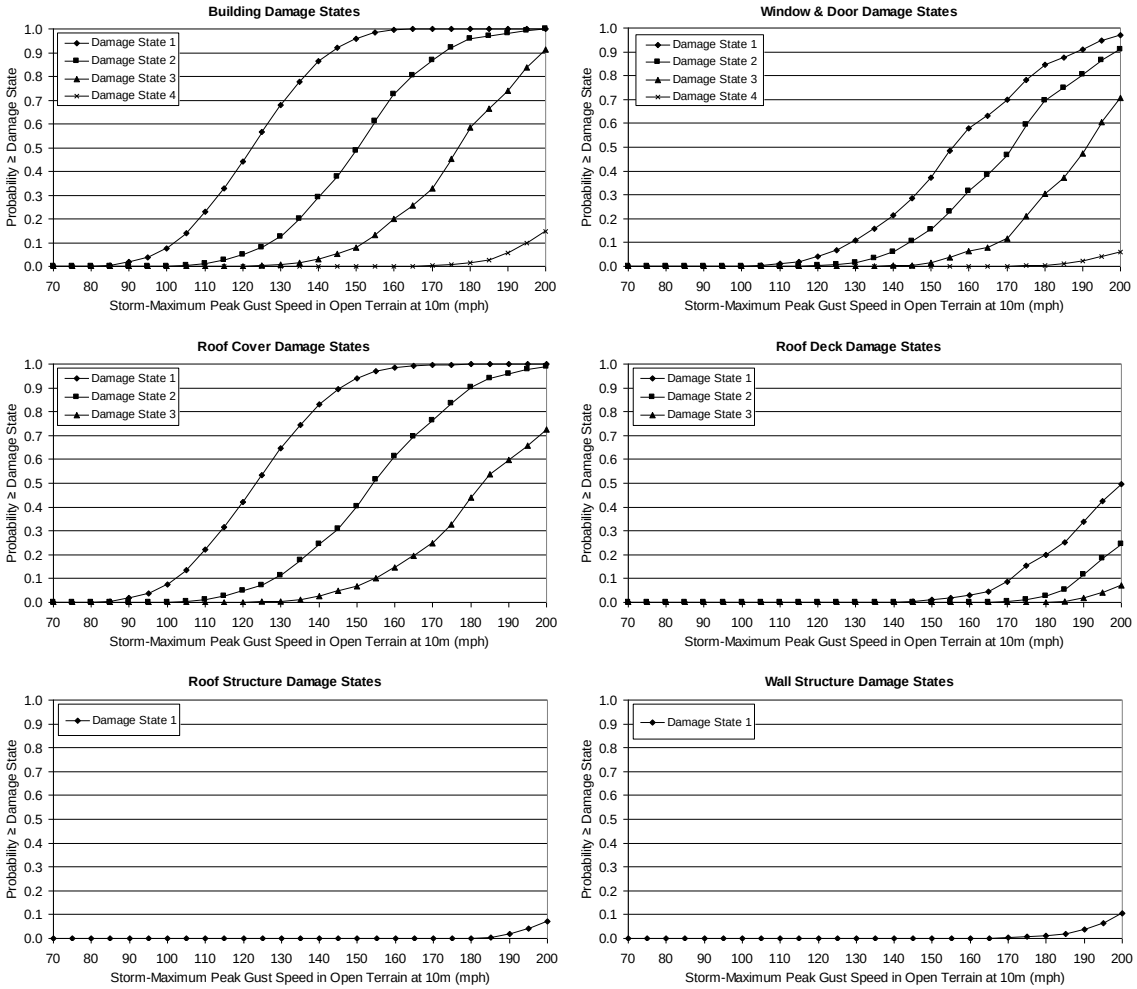

Figure C.28. Damage States vs. Maximum Peak Gust Wind Speed – One-Story, 8d Roof Deck Nails, Strapped Roof Trusses, Wood Frame Walls, Gable Roof with Shingles, z_0=1.0 m.

Appendix D.
Damage State Functions for Low Rise Masonry Strip Mall Buildings

Appendix D.
Damage State Functions for Low Rise Masonry Strip Mall Buildings

This appendix presents damage state curves for low rise masonry strip mall buildings. The damage state curves show the probability of achieving a certain damage state versus storm-maximum peak gust speed (open terrain at 10m above ground). Plots are presented for the overall building damage states and for the individual building component damage states (refer to Table 6.10-1 for damage state definitions). As shown in Table D.1, Figures D.1 through D.20 give example results for buildings modeled with a wood roof system. Figures D.21 through D.44 give example results for buildings modeled with a steel roof system.

Table D.1. Sample Damage State Functions for Low Rise Masonry Strip Mall Buildings

Figure	Walls	Height	Number of Units	Roof Frame	Frame Spacing	Roof/ Wall	Deck Mat'l.	Deck Attachment	Design Code	Roof Cover	Missile Environ.	Terrain
D.1	URM	12'	6	Wood	2'	Strap	Wood	8d	-	BUR	A	0.03
D.2	URM	12'	6	Wood	2'	Strap	Wood	8d	-	BUR	**B**	0.03
D.3	URM	12'	6	Wood	2'	Strap	Wood	8d	-	BUR	**C**	0.03
D.4	URM	12'	6	Wood	2'	Strap	Wood	8d	-	BUR	**D**	0.03
D.5	URM	12'	6	Wood	2'	Strap	Wood	8d	-	**EPDM**	A	0.03
D.6	URM	12'	6	Wood	2'	Strap	Wood	**6d**	-	BUR	A	0.03
D.7	**RM**	12'	6	Wood	2'	Strap	Wood	8d	-	BUR	A	0.03
D.8	URM	12'	6	Wood	2'	**Toe-Nail**	Wood	8d	-	BUR	A	0.03
D.9	URM	**20'**	6	Wood	2'	Strap	Wood	8d	-	BUR	A	0.03
D.10	URM	12'	6	Wood	2'	Strap	Wood	8d	-	BUR	A	**0.35**
D.11	URM	12'	6	Wood	2'	Strap	Wood	8d	-	BUR	**B**	0.35
D.12	URM	12'	6	Wood	2'	Strap	Wood	8d	-	BUR	**C**	0.35
D.13	URM	12'	6	Wood	2'	Strap	Wood	8d	-	BUR	**D**	0.35
D.14	URM	12'	6	Wood	2'	Strap	Wood	8d	-	**EPDM**	A	0.35
D.15	URM	12'	6	Wood	2'	Strap	Wood	**6d**	-	BUR	A	0.35
D.16	**RM**	12'	6	Wood	2'	Strap	Wood	8d	-	BUR	A	0.35
D.17	URM	12'	6	Wood	2'	**Toe-Nail**	Wood	8d	-	BUR	A	0.35
D.18	URM	**20'**	6	Wood	2'	Strap	Wood	8d	-	BUR	A	0.35
D.19	URM	12'	6	Wood	2'	Strap	Wood	8d	-	BUR	A	**0.70**
D.20	URM	12'	6	Wood	2'	Strap	Wood	8d	-	BUR	A	**1.00**
D.21	URM	20'	6	OWSJ	6'	-	Metal	Weld	SBCCI, 100	BUR	A	0.03
D.22	URM	20'	6	OWSJ	**4'**	-	Metal	Weld	SBCCI, 100	BUR	A	0.03
D.23	URM	20'	**1**	OWSJ	6'	-	Metal	Weld	SBCCI, 100	BUR	A	0.03
D.24	URM	**12'**	6	OWSJ	**4'**	-	Metal	Weld	SBCCI, 100	BUR	A	0.03
D.25	URM	20'	6	OWSJ	6'	-	Metal	Weld	SBCCI, 100	BUR	**B**	0.03
D.26	URM	20'	6	OWSJ	6'	-	Metal	Weld	SBCCI, 100	BUR	**C**	0.03
D.27	URM	20'	6	OWSJ	6'	-	Metal	Weld	SBCCI, 100	BUR	**D**	0.03
D.28	URM	20'	6	OWSJ	6'	-	Metal	Weld	SBCCI, 100	**EPDM**	A	0.03

Table D.1. Sample Damage State Functions for Low Rise Masonry Strip Mall Buildings (concluded)

Figure	Walls	Height	Number of Units	Roof Frame	Frame Spacing	Roof/ Wall	Deck Mat'l.	Deck Attachment	Design Code	Roof Cover	Missile Environ.	Terrain
D.29	URM	20'	6	OWSJ	6'	-	Metal	**Weld, 50%**	SBCCI, 100	BUR	A	0.03
D.30	URM	20'	6	OWSJ	6'	-	Metal	**Screw**	SBCCI, 100	BUR	A	0.03
D.31	URM	20'	6	OWSJ	6'	-	Metal	Weld	**ASCE, 100**	BUR	A	0.03
D.32	**RM**	20'	6	OWSJ	6'	-	Metal	Weld	SBCCI, 100	BUR	A	0.03
D.33	URM	20'	6	OWSJ	6'	-	Metal	Weld	SBCCI, 100	BUR	A	**0.35**
D.34	URM	20'	6	OWSJ	**4'**	-	Metal	Weld	SBCCI, 100	BUR	A	0.03
D.35	URM	20'	**1**	OWSJ	6'	-	Metal	Weld	SBCCI, 100	BUR	A	0.03
D.36	URM	**12'**	6	OWSJ	**4'**	-	Metal	Weld	SBCCI, 100	BUR	A	0.03
D.37	URM	20'	6	OWSJ	6'	-	Metal	Weld	SBCCI, 100	BUR	**B**	0.03
D.38	URM	20'	6	OWSJ	6'	-	Metal	Weld	SBCCI, 100	BUR	**C**	0.03
D.39	URM	20'	6	OWSJ	6'	-	Metal	Weld	SBCCI, 100	BUR	**D**	0.03
D.40	URM	20'	6	OWSJ	6'	-	Metal	Weld	SBCCI, 100	**EPDM**	A	0.03
D.41	URM	20'	6	OWSJ	6'	-	Metal	**Weld, 50%**	SBCCI, 100	BUR	A	0.03
D.42	URM	20'	6	OWSJ	6'	-	Metal	**Screw**	SBCCI, 100	BUR	A	0.03
D.43	URM	20'	6	OWSJ	6'	-	Metal	Weld	**ASCE, 100**	BUR	A	0.03
D.44	**RM**	20'	6	OWSJ	6'	-	Metal	Weld	SBCCI, 100	BUR	A	0.03
D.45	URM	20'	6	OWSJ	6'	-	Metal	Weld	SBCCI, 100	BUR	A	**0.70**
D.46	URM	20'	6	OWSJ	6'	-	Metal	Weld	SBCCI, 100	BUR	A	**1.00**

Two sets of nine figures are given for the buildings modeled with a wood roof system. The first set of nine figures (Figures D.1 through D.9) are for buildings located in an open terrain (z_0=0.03 m) and the second set (Figures D.10 through D.18) are for buildings situated in a typical suburban environment (z_0=0.35 m). The first figure in each set of nine shows damage state results for the 12′ high building with 6 units, 8d roof sheathing nails, strapped roof-wall connections, built-up roof cover, Unreinforced masonry walls, and situated in Missile Environment A. The remaining eight plots in each set show damage state results for buildings which are different by a single variable in comparison to the reference building (note that the changed variable is underlined in the figure titles). Figures D.19 and D.20 show results of the reference building situated in two additional terrain environments (i.e., z_0=0.70 m and 1.0 m).

Two sets of twelve figures are given for the buildings modeled with a metal roof system. The first set of twelve figures (Figures D.21 through D.32) are for buildings located in an open terrain (z_0=0.03 m) and the second set (Figures D.33 through D.44) are for buildings situated in a typical suburban environment (z_0=0.35 m). The first figure in each set of twelve shows damage state results for the 20′ high building with 6 units, a joist spacing of 6′, metal deck fastened with welds, SBCCI roof design criteria, built-up roof cover, Unreinforced masonry walls, and situated in Missile Environment A. The remaining eleven plots in each set show damage state results for buildings which are different by a single variable in comparison to the reference building (note that the changed variable is underlined in the figure titles). Figures D.45 and D.46 show results of the reference building situated in two additional terrain environments (i.e., z_0=0.70 m and 1.0 m).

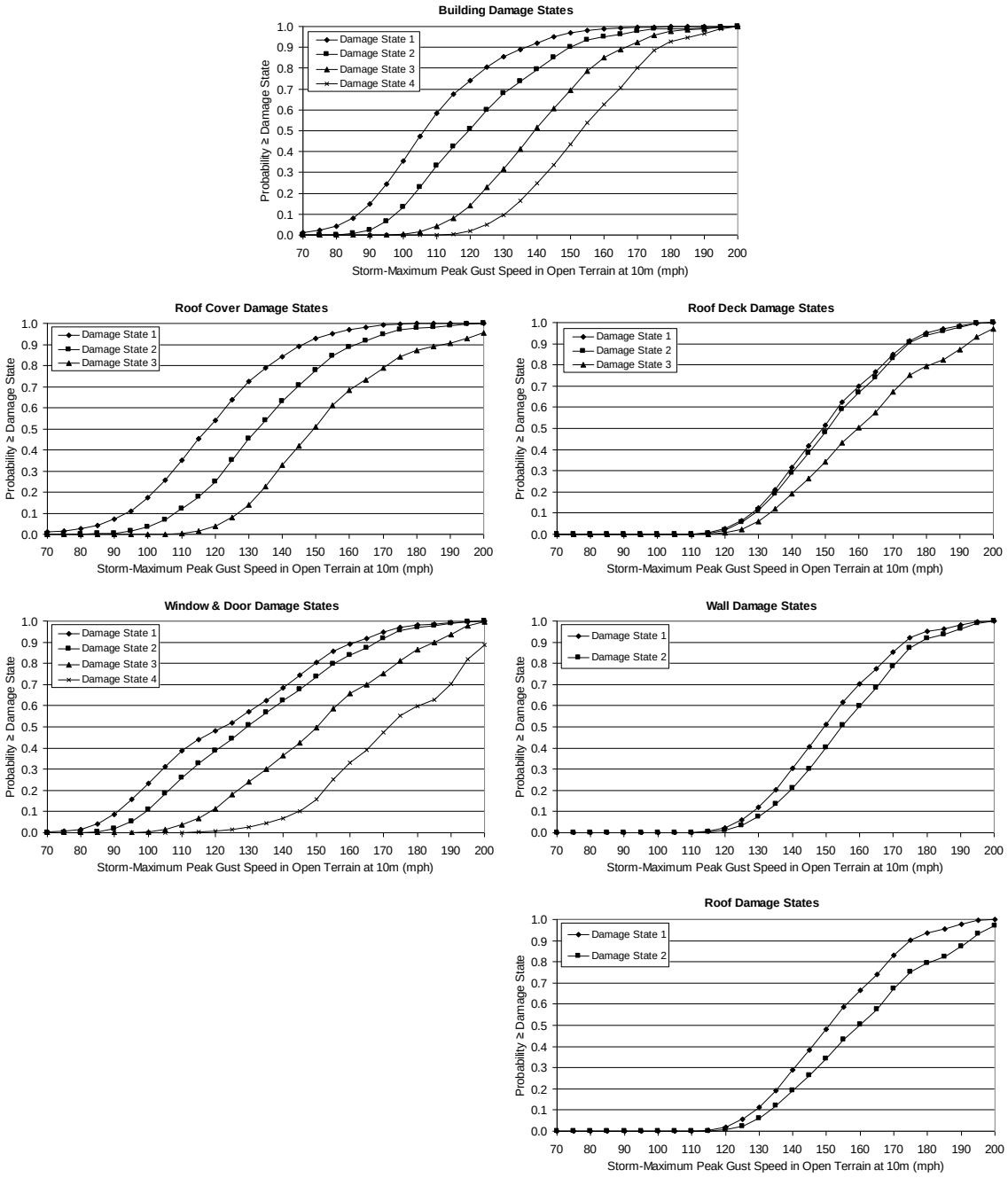

Figure D.1. Damage States vs. Peak Gust Wind Speed – Strip Mall Building A – Height=12′, No. of Units=6, Wood Deck with 8d Nails, Strapped Roof-Wall Connections, Built-up Roof Cover, Unreinforced Masonry Walls, Missile Environment A, z_0=0.03 m.

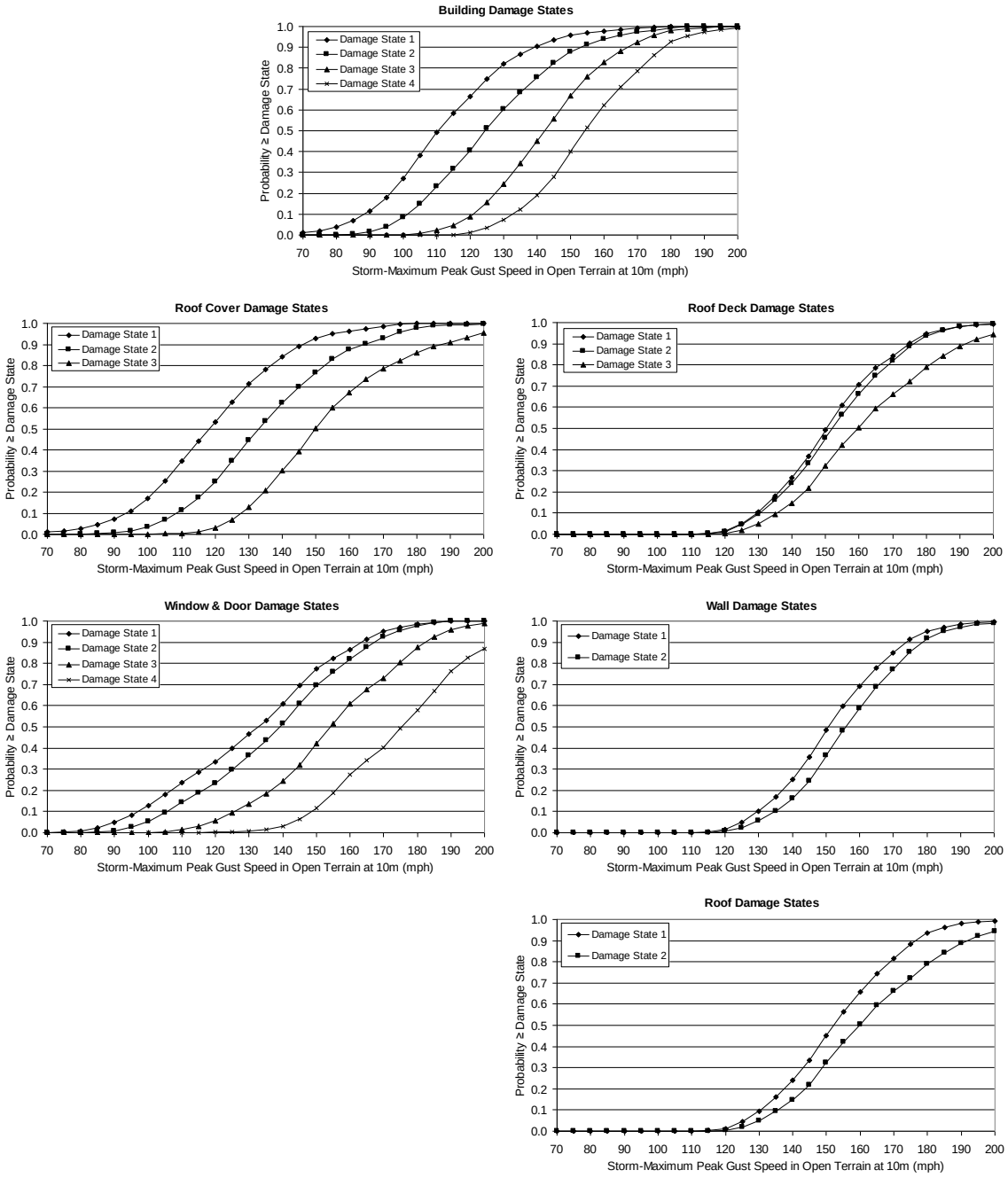

Figure D.2. Damage States vs. Peak Gust Wind Speed – Strip Mall Building A – Height=12′, No. of Units=6, Wood Deck with 8d Nails, Strapped Roof-Wall Connections, Built-up Roof Cover, Unreinforced Masonry Walls, <u>Missile Environment B</u>, z_0=0.03 m.

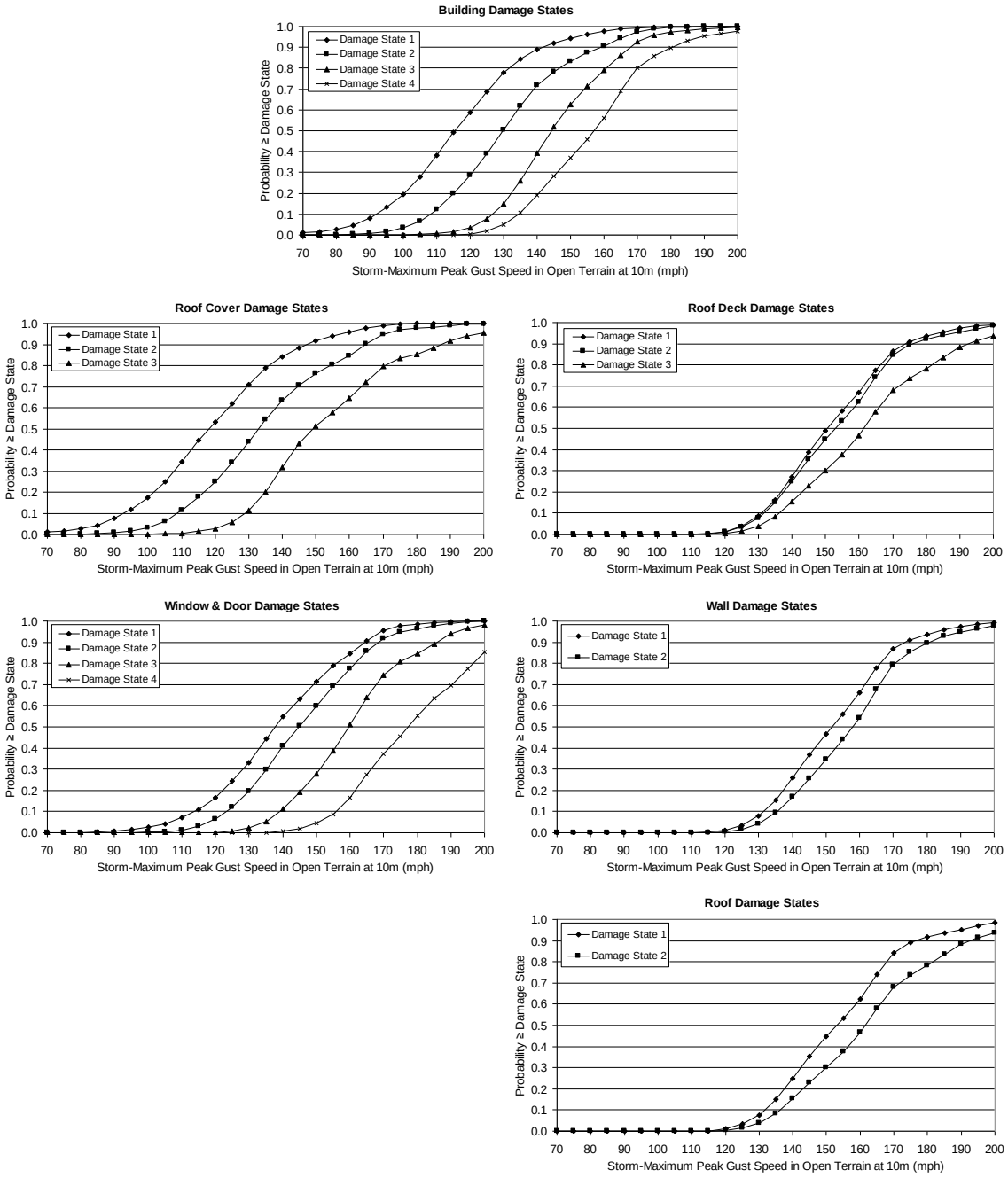

Figure D.3. Damage States vs. Peak Gust Wind Speed – Strip Mall Building A – Height=12′, No. of Units=6, Wood Deck with 8d Nails, Strapped Roof-Wall Connections, Built-up Roof Cover, Unreinforced Masonry Walls, Missile Environment C, z_0=0.03 m.

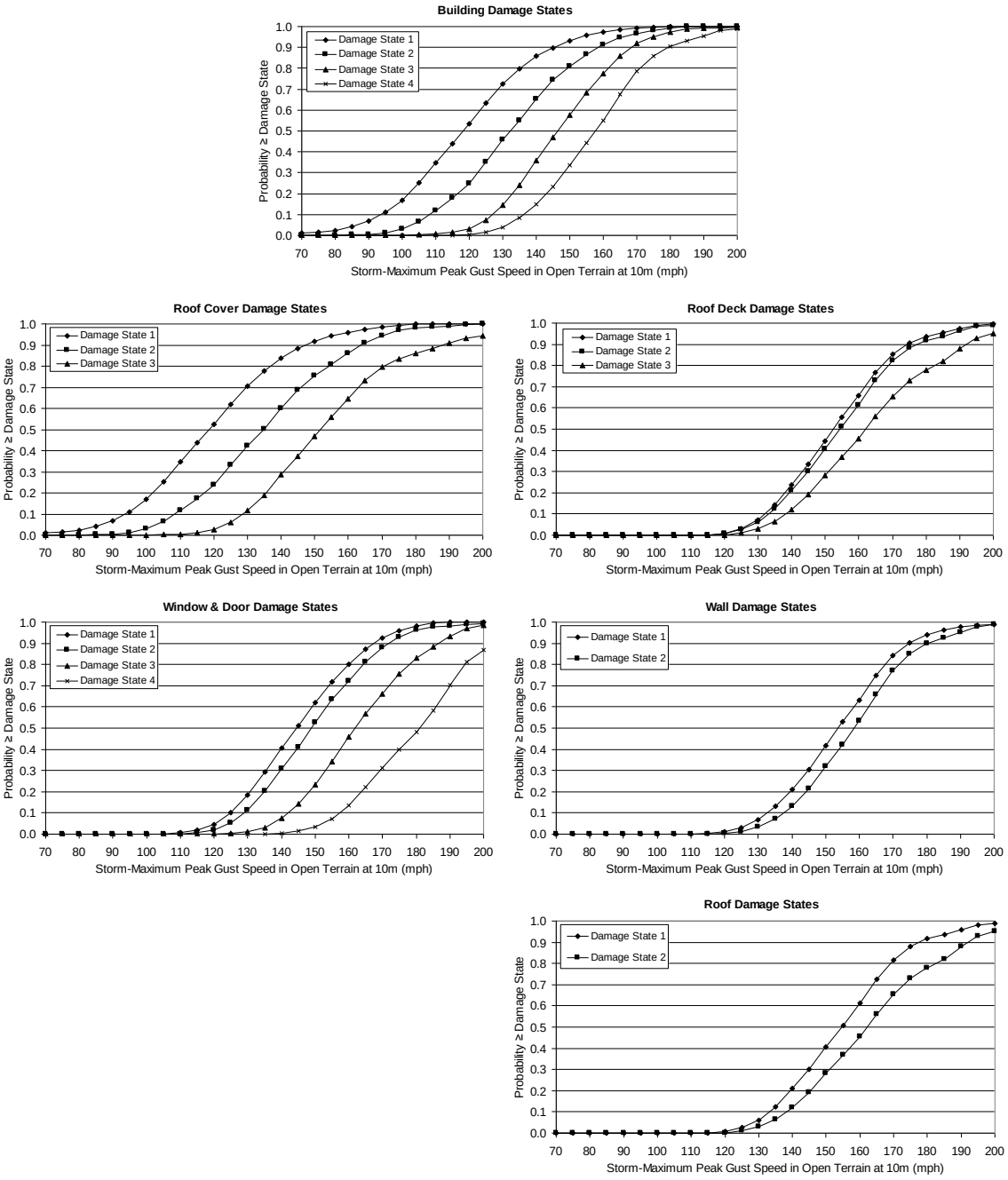

Figure D.4. Damage States vs. Peak Gust Wind Speed – Strip Mall Building A – Height=12′, No. of Units=6, Wood Deck with 8d Nails, Strapped Roof-Wall Connections, Built-up Roof Cover, Unreinforced Masonry Walls, <u>Missile Environment D</u>, z_0=0.03 m.

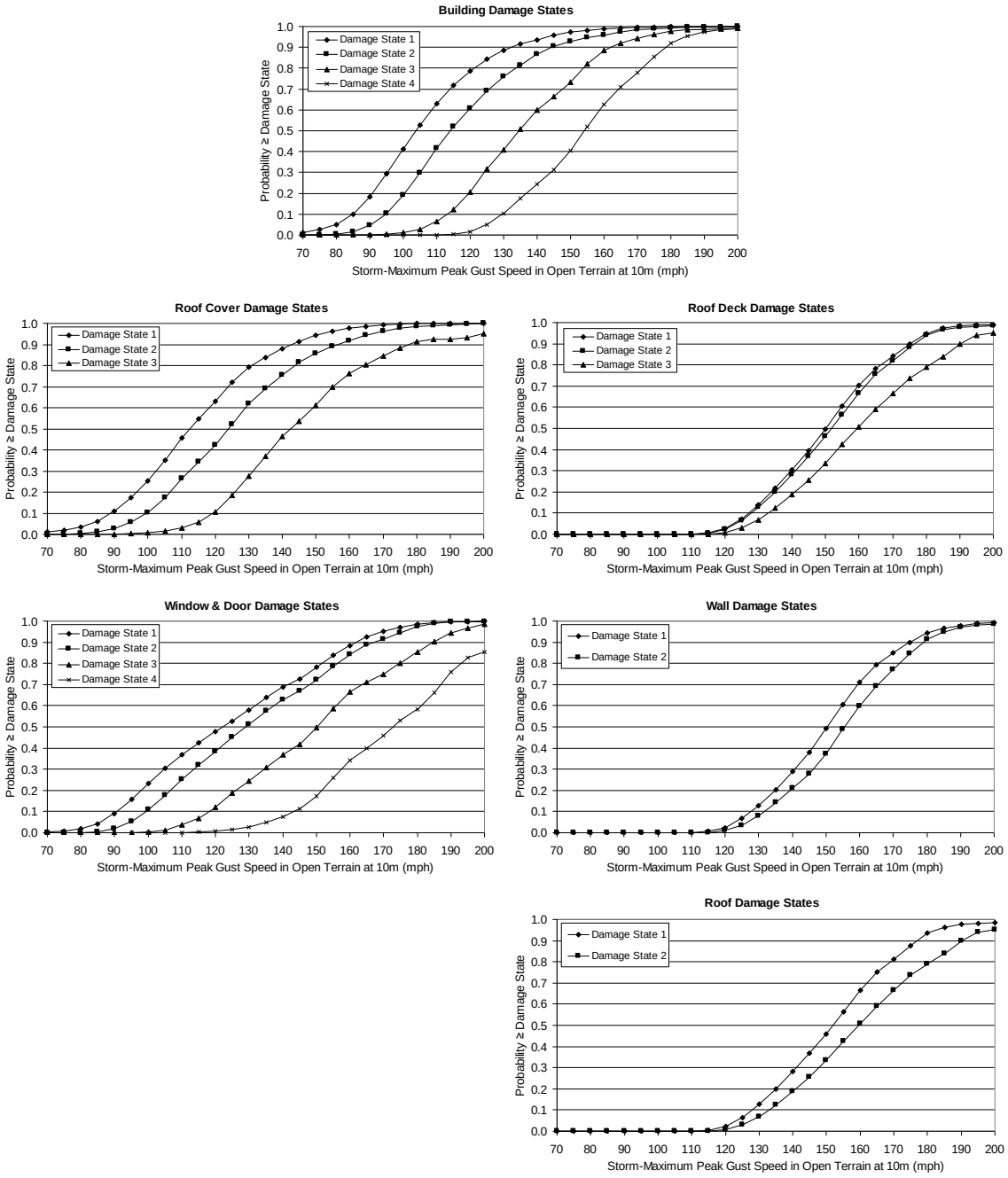

Figure D.5. Damage States vs. Peak Gust Wind Speed – Strip Mall Building A – Height=12′, No. of Units=6, Wood Deck with 8d Nails, Strapped Roof-Wall Connections, Single Ply Membrane Roof Cover, Unreinforced Masonry Walls, Missile Environment A, z_0=0.03 m.

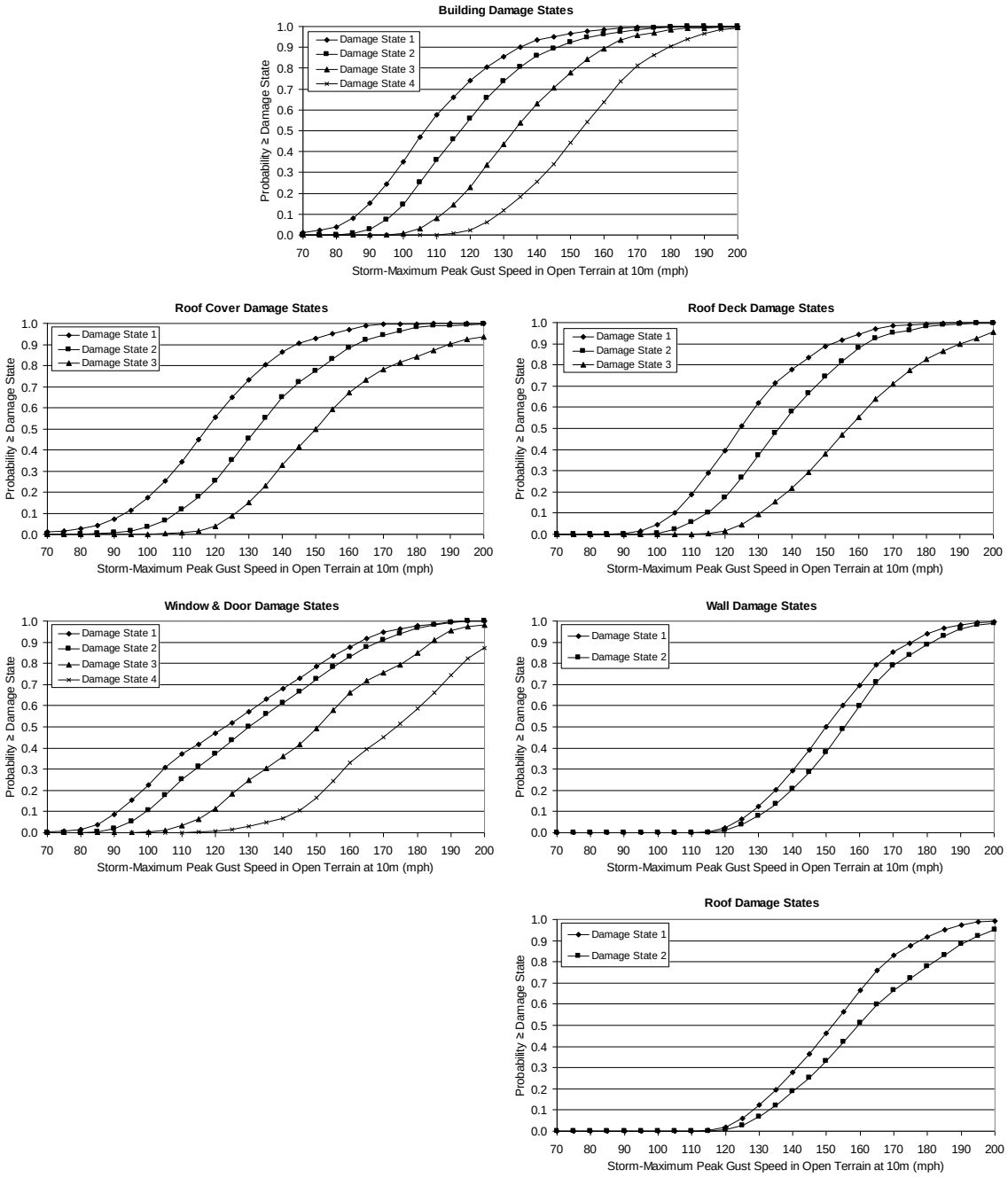

Figure D.6. Damage States vs. Peak Gust Wind Speed – Strip Mall Building A – Height=12′, No. of Units=6, Wood Deck with 6d Nails, Strapped Roof-Wall Connections, Built-up Roof Cover, Unreinforced Masonry Walls, Missile Environment A, z_0=0.03 m.

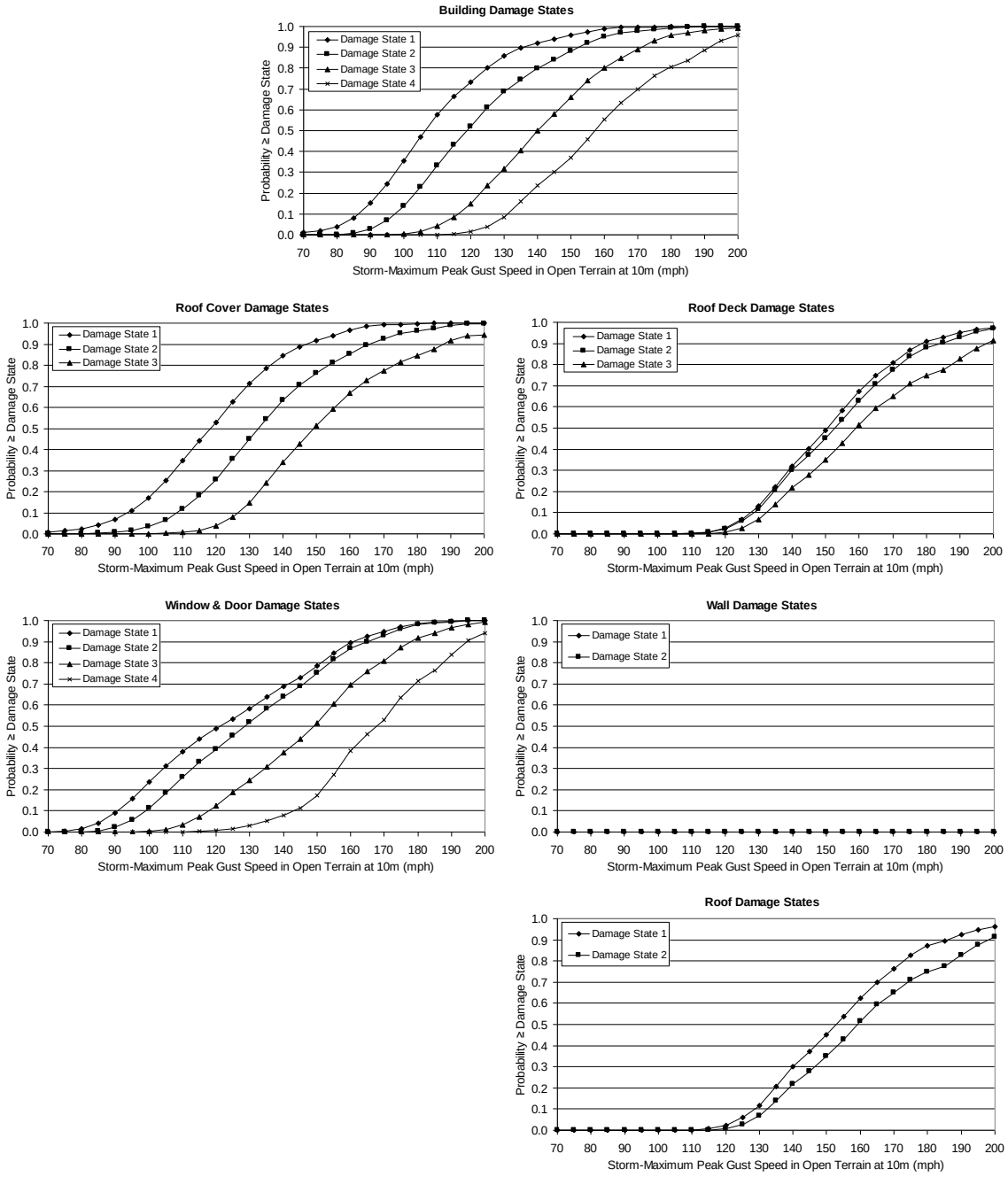

Figure D.7. Damage States vs. Peak Gust Wind Speed – Strip Mall Building A – Height=12′, No. of Units=6, Wood Deck with 8d Nails, Strapped Roof-Wall Connections, Built-up Roof Cover, Reinforced Masonry Walls, Missile Environment A, z_0=0.03 m.

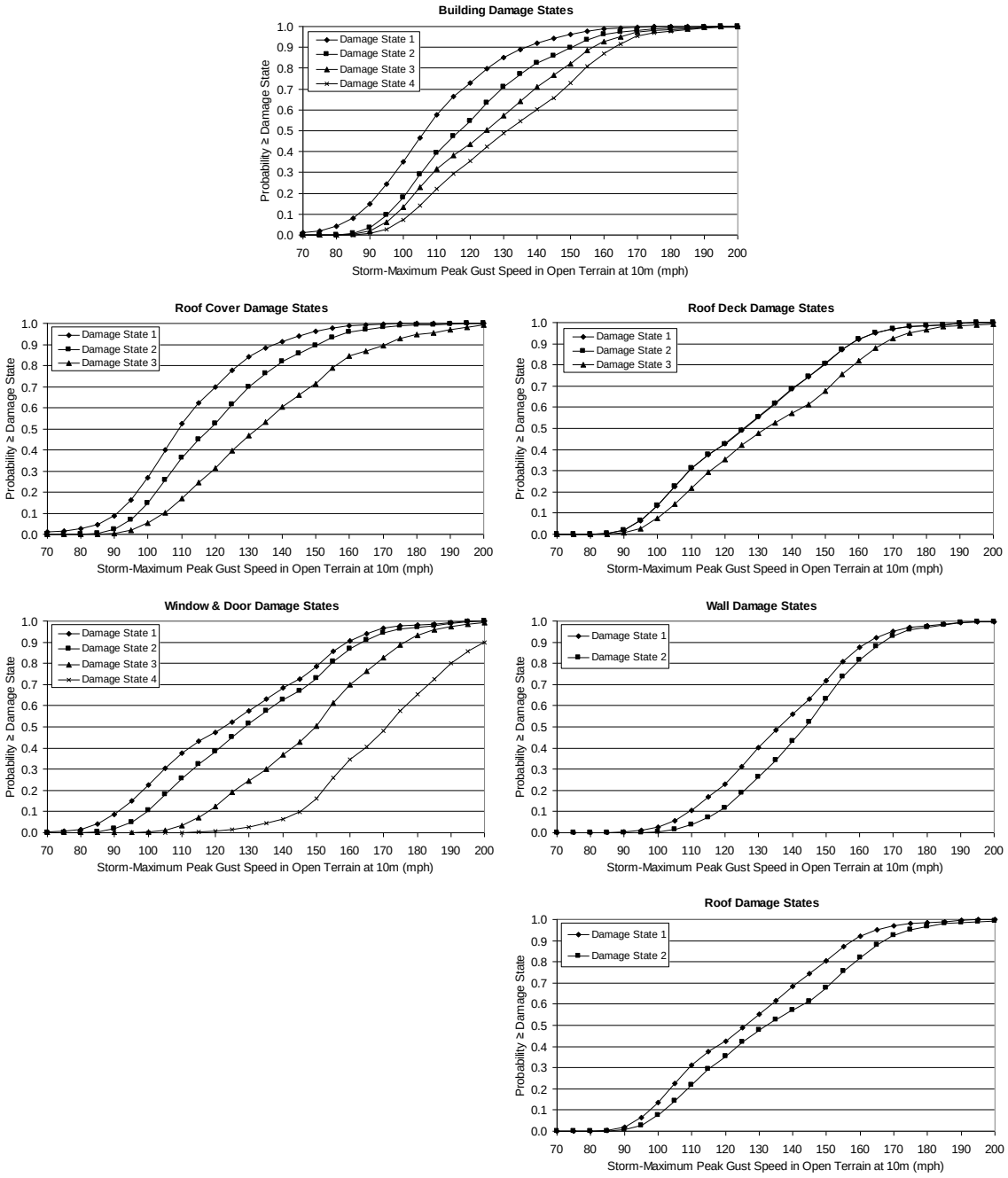

Figure D.8. Damage States vs. Peak Gust Wind Speed – Strip Mall Building A – Height=12′, No. of Units=6, Wood Deck with 8d Nails, Toe-Nailed Roof-Wall Connections, Built-up Roof Cover, Unreinforced Masonry Walls, Missile Environment A, z_0=0.03 m.

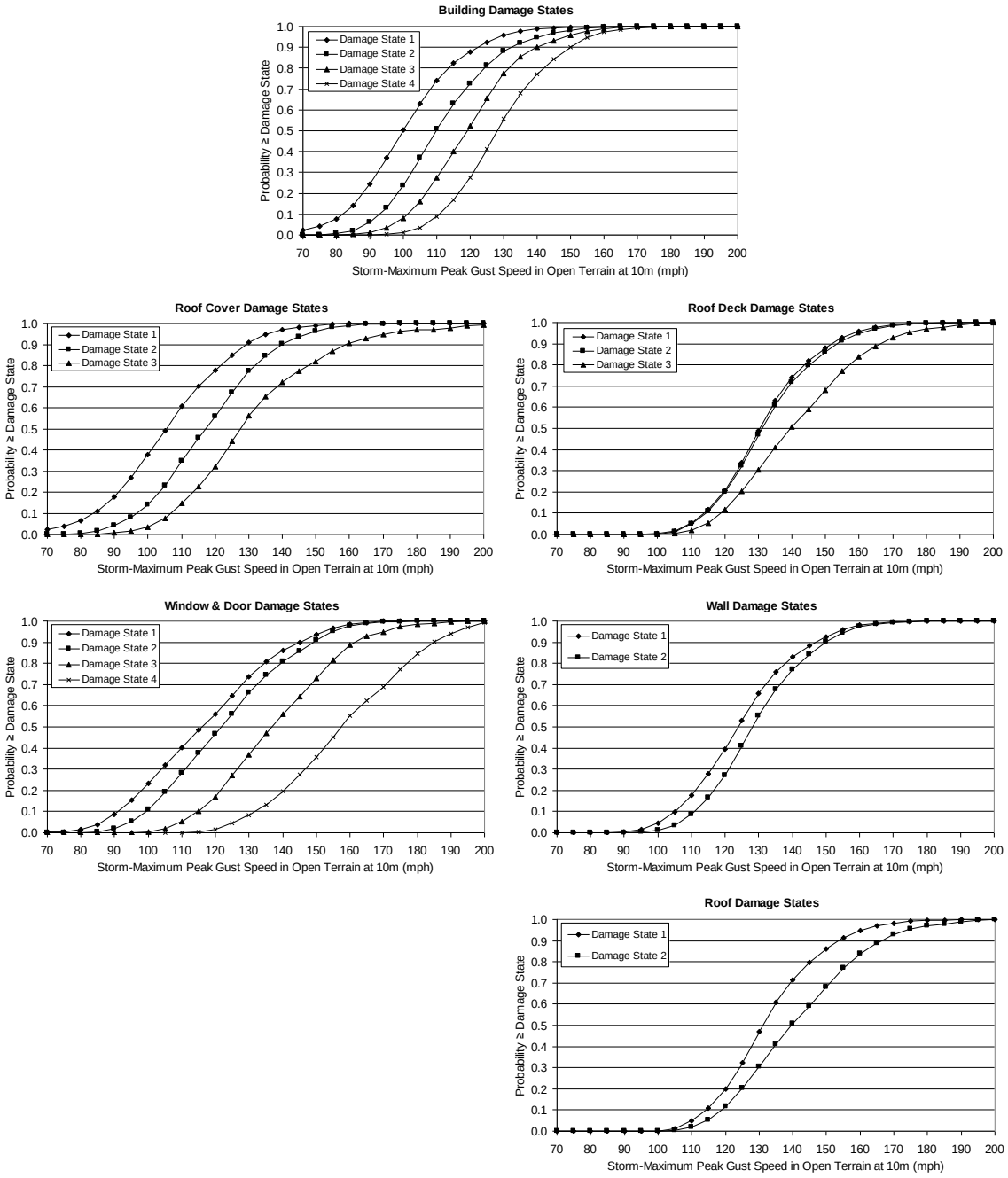

Figure D.9. Damage States vs. Peak Gust Wind Speed – Strip Mall Building B – Height=20′, No. of Units=6, Wood Deck with 8d Nails, Strapped Roof-Wall Connections, Built-up Roof Cover, Unreinforced Masonry Walls, Missile Environment A, z_0=0.03 m.

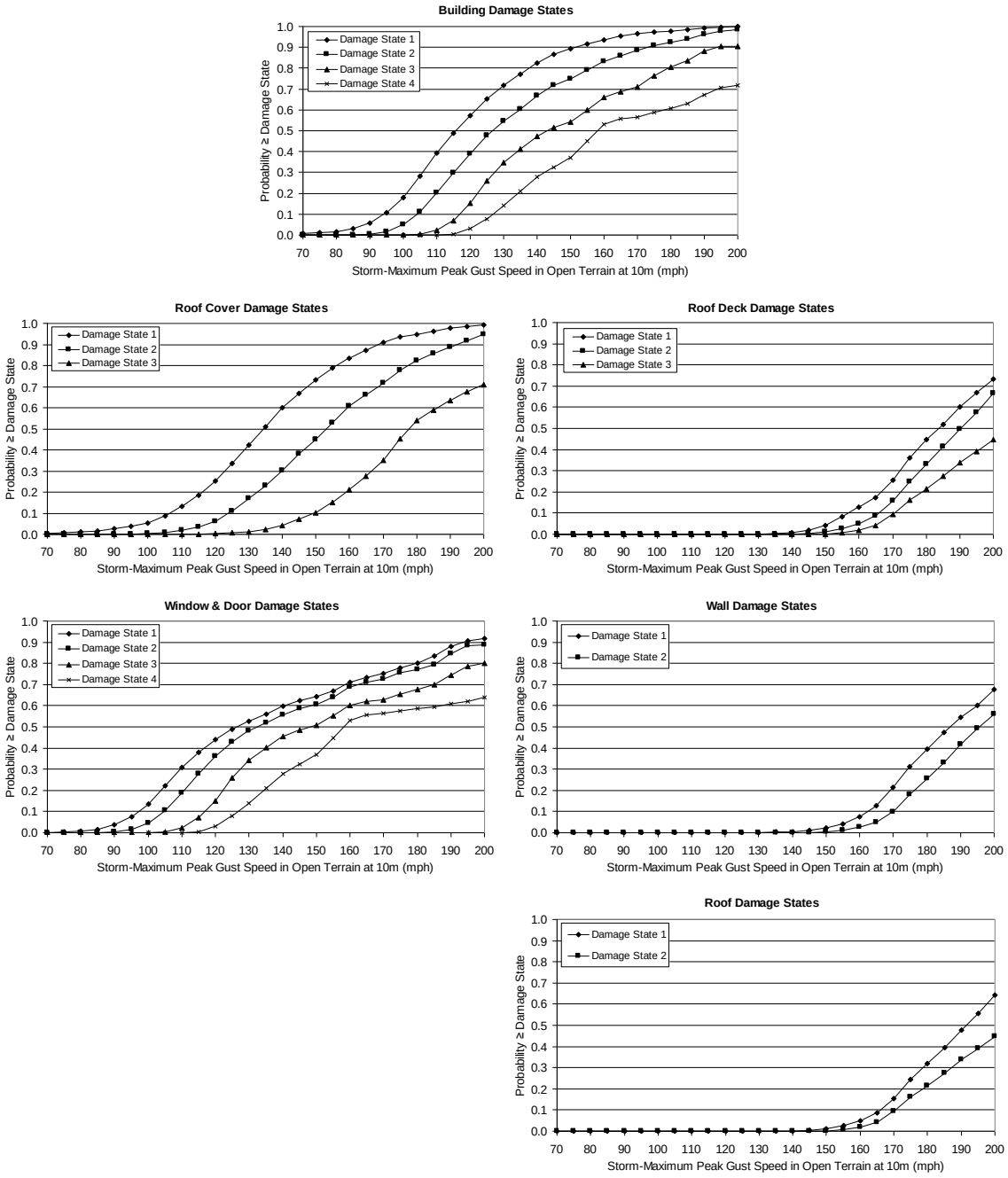

Figure D.10. Damage States vs. Peak Gust Wind Speed – Strip Mall Building A – Height=12′, No. of Units=6, Wood Deck with 8d Nails, Strapped Roof-Wall Connections, Built-up Roof Cover, Unreinforced Masonry Walls, Missile Environment A, z_0=0.35 m.

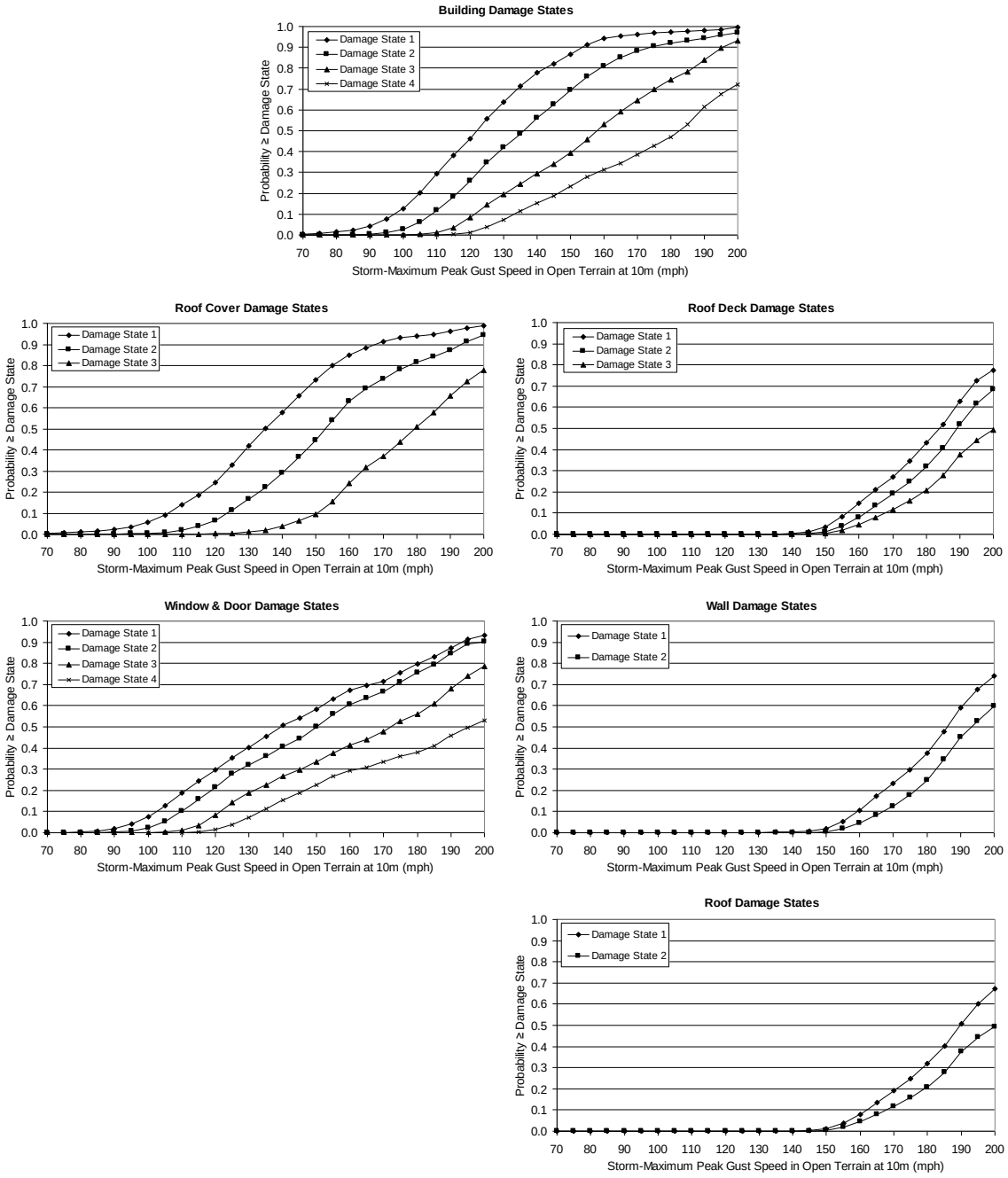

Figure D.11. Damage States vs. Peak Gust Wind Speed – Strip Mall Building A – Height=12′, No. of Units=6, Wood Deck with 8d Nails, Strapped Roof-Wall Connections, Built-up Roof Cover, Unreinforced Masonry Walls, Missile Environment B, z_0=0.35 m.

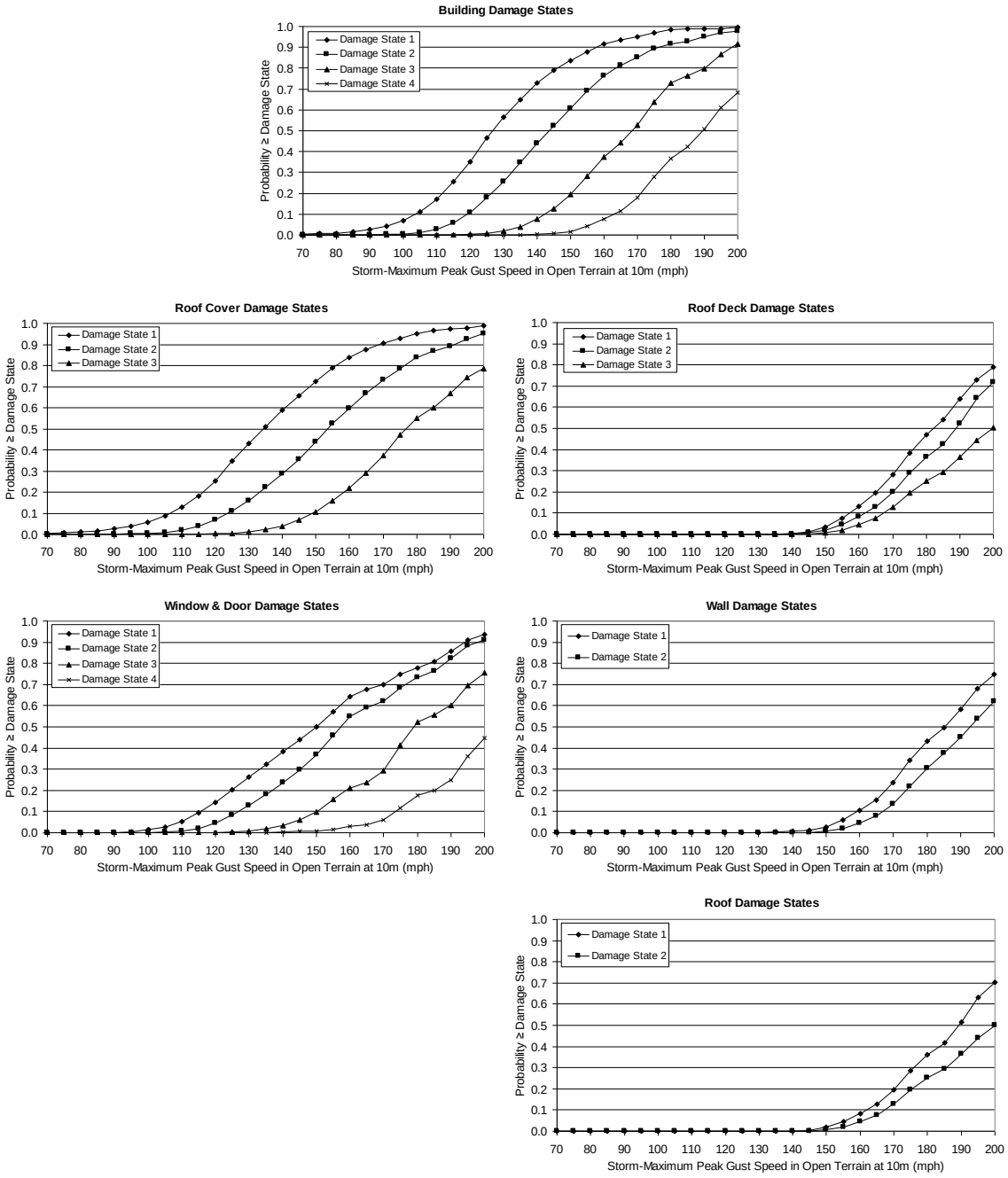

Figure D.12. Damage States vs. Peak Gust Wind Speed – Strip Mall Building A – Height=12′, No. of Units=6, Wood Deck with 8d Nails, Strapped Roof-Wall Connections, Built-up Roof Cover, Unreinforced Masonry Walls, Missile Environment C, z_0=0.35 m.

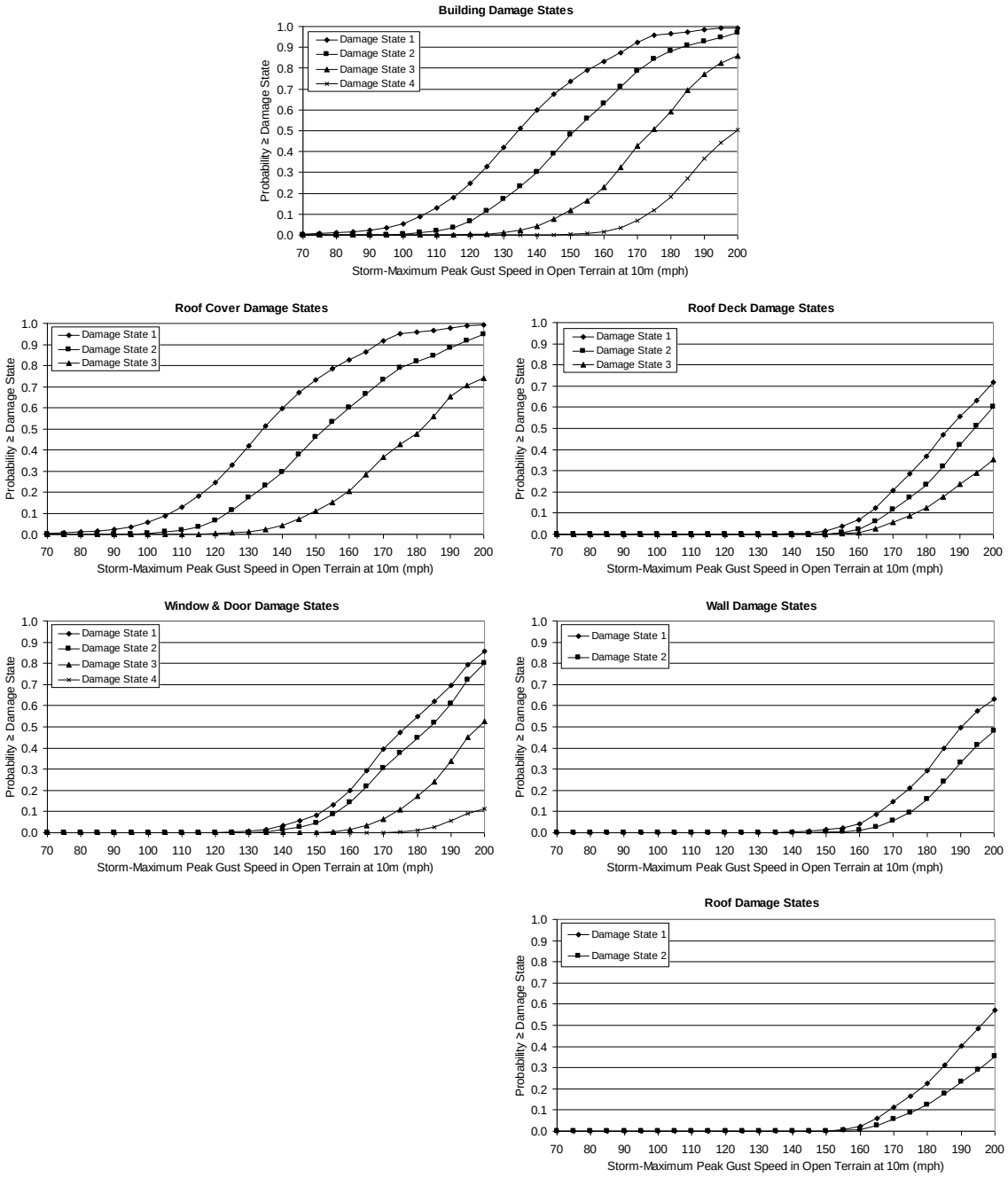

Figure D.13. Damage States vs. Peak Gust Wind Speed – Strip Mall Building A – Height=12′, No. of Units=6, Wood Deck with 8d Nails, Strapped Roof-Wall Connections, Built-up Roof Cover, Unreinforced Masonry Walls, <u>Missile Environment D</u>, z_0=0.35 m.

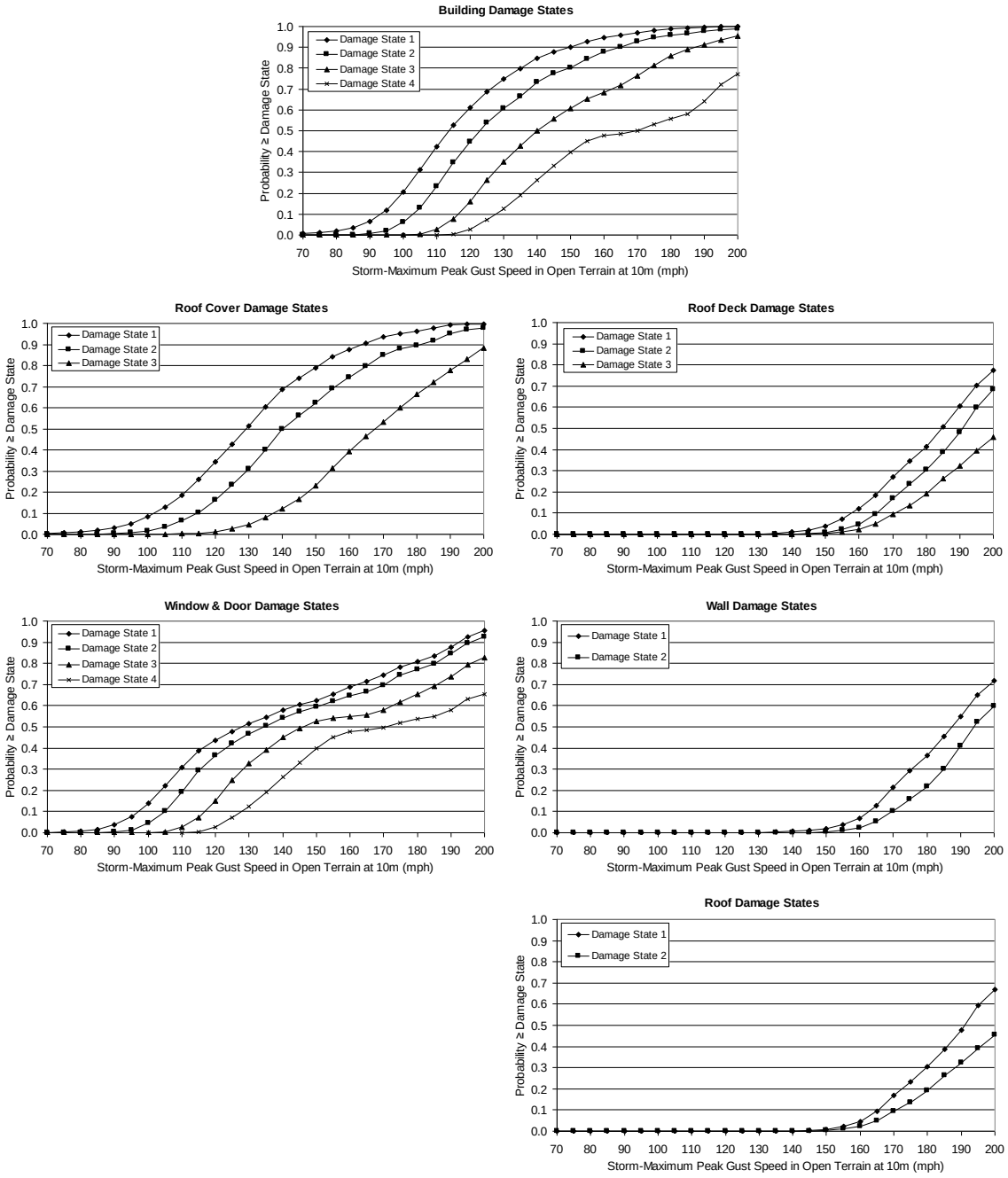

Figure D.14. Damage States vs. Peak Gust Wind Speed – Strip Mall Building A – Height=12′, No. of Units=6, Wood Deck with 8d Nails, Strapped Roof-Wall Connections, Single Ply Membrane Roof Cover, Unreinforced Masonry Walls, Missile Environment A, z_0=0.35 m.

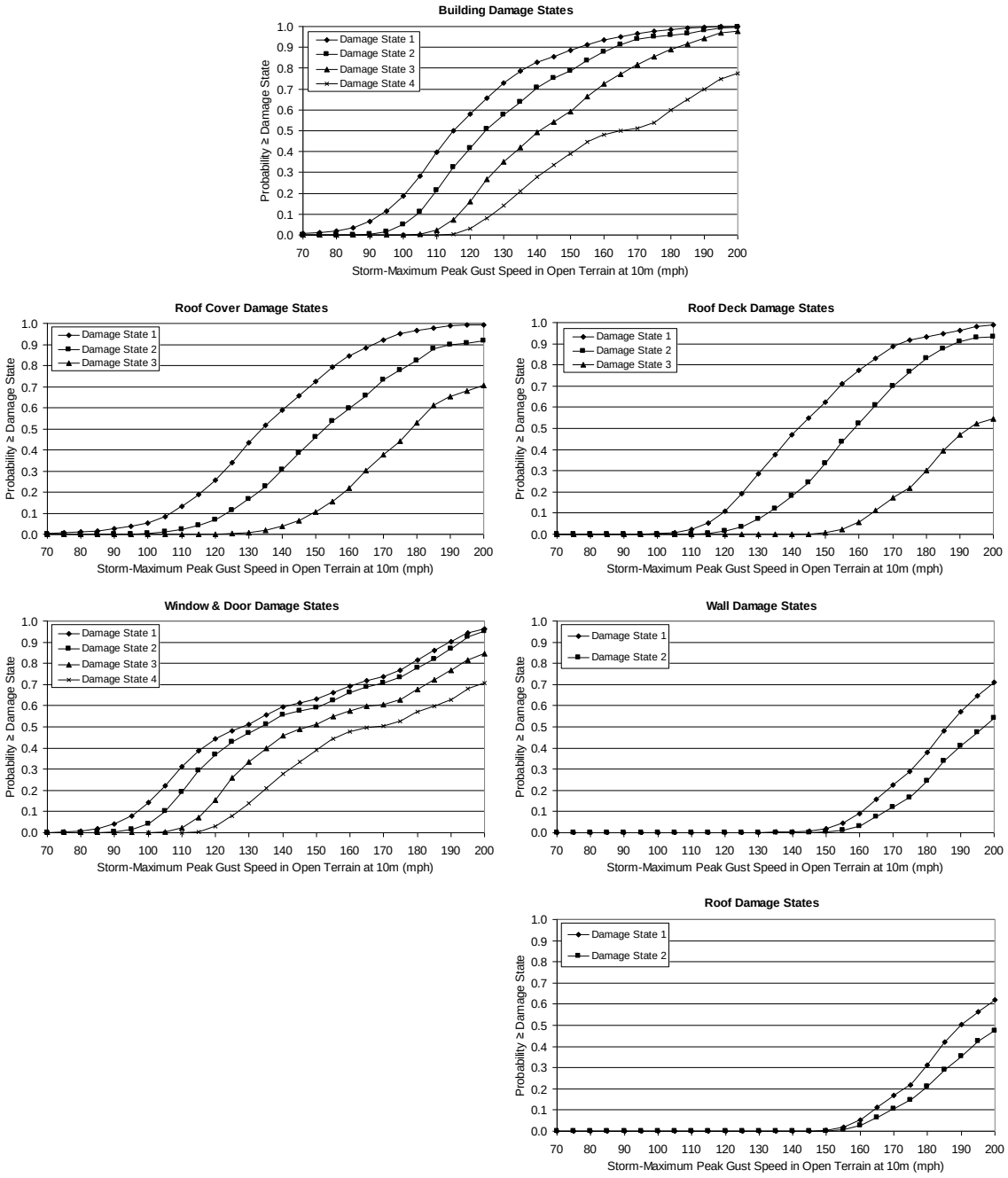

Figure D.15. Damage States vs. Peak Gust Wind Speed – Strip Mall Building A – Height=12′, No. of Units=6, Wood Deck with 6d Nails, Strapped Roof-Wall Connections, Built-up Roof Cover, Unreinforced Masonry Walls, Missile Environment A, z_0=0.35 m.

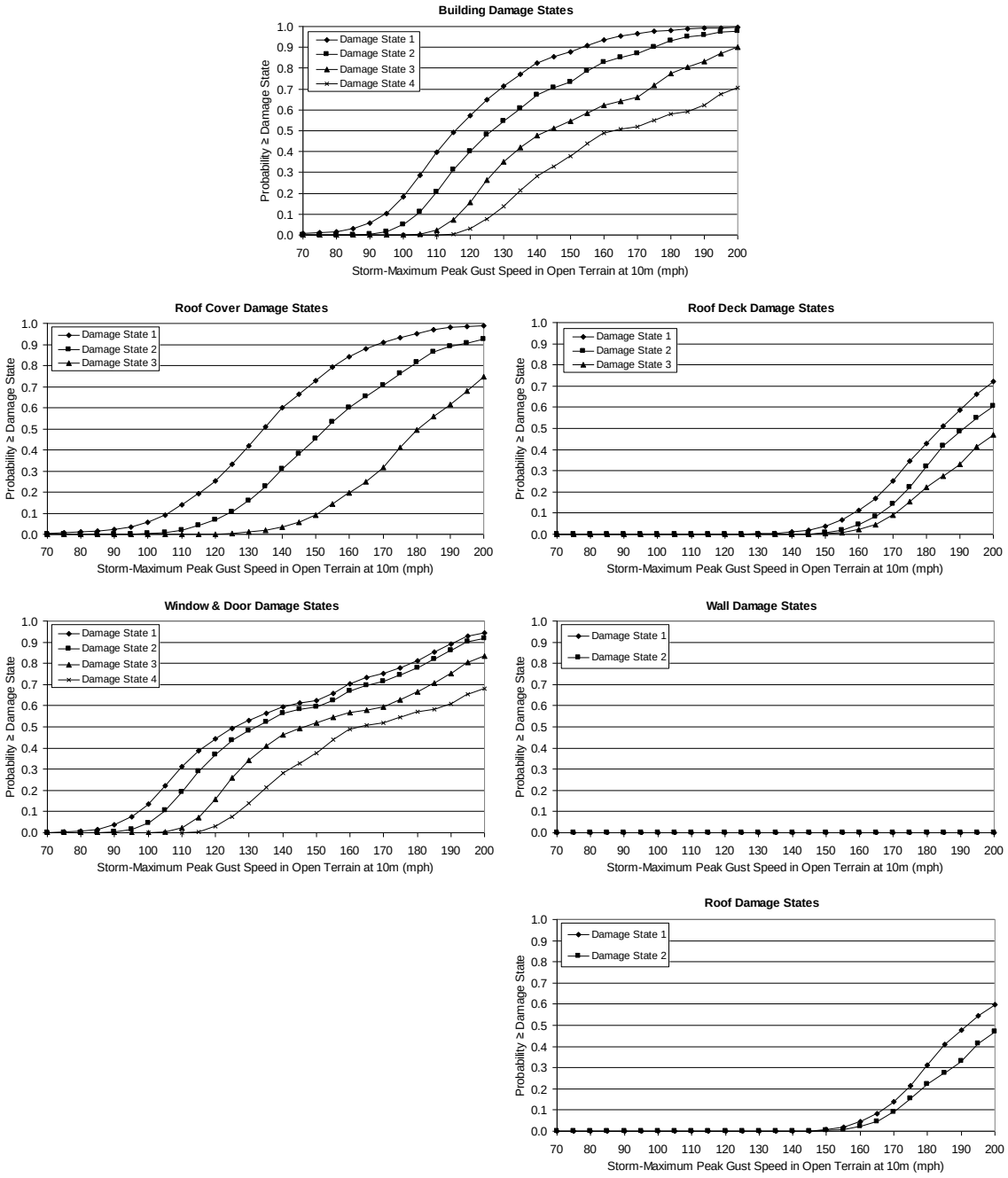

Figure D.16. Damage States vs. Peak Gust Wind Speed – Strip Mall Building A – Height=12′, No. of Units=6, Wood Deck with 8d Nails, Strapped Roof-Wall Connections, Built-up Roof Cover, Reinforced Masonry Walls, Missile Environment A, z_0=0.35 m.

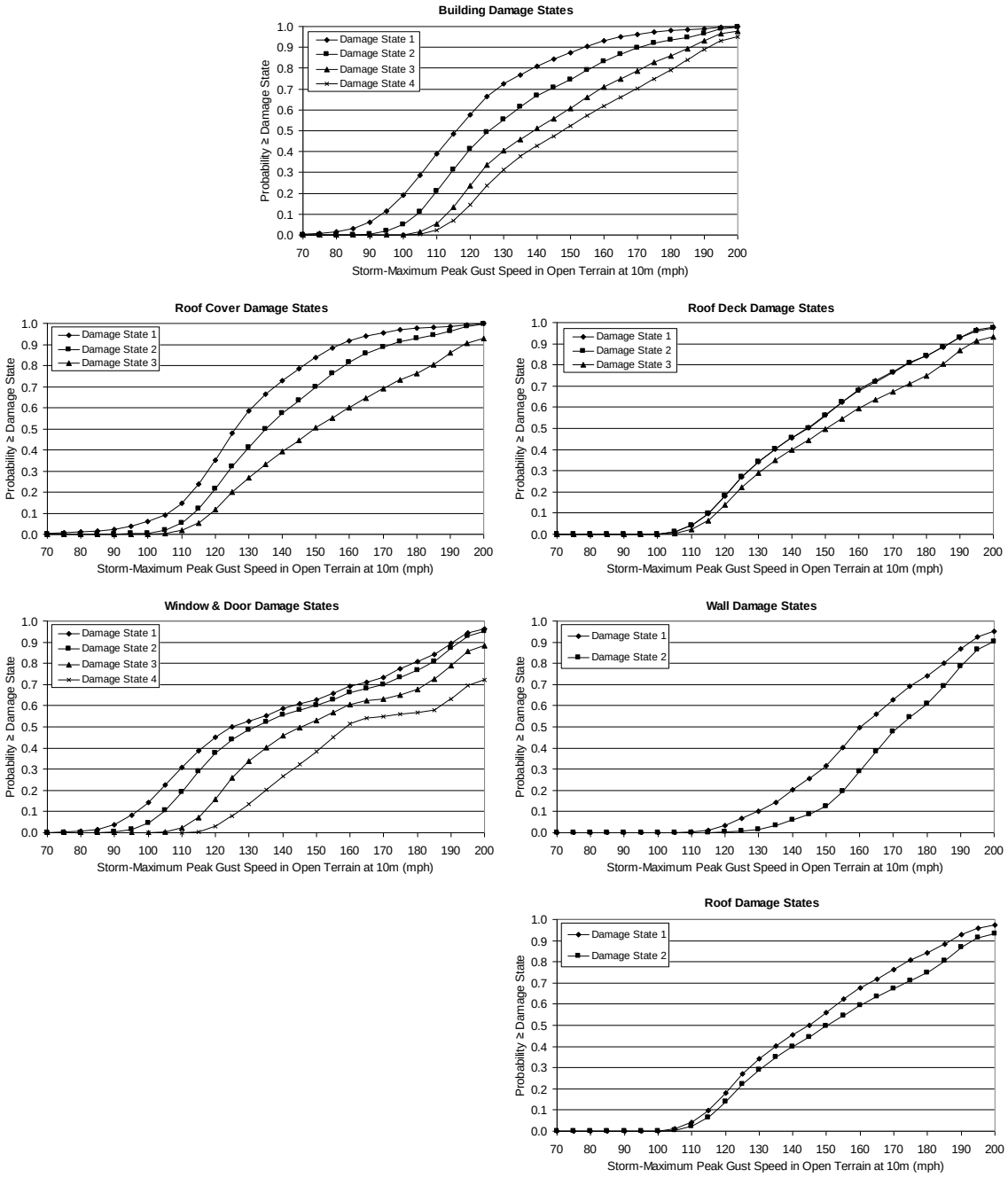

Figure D.17. Damage States vs. Peak Gust Wind Speed – Strip Mall Building A – Height=12′, No. of Units=6, Wood Deck with 8d Nails, Toe-Nailed Roof-Wall Connections, Built-up Roof Cover, Unreinforced Masonry Walls, Missile Environment A, z_0=0.35 m.

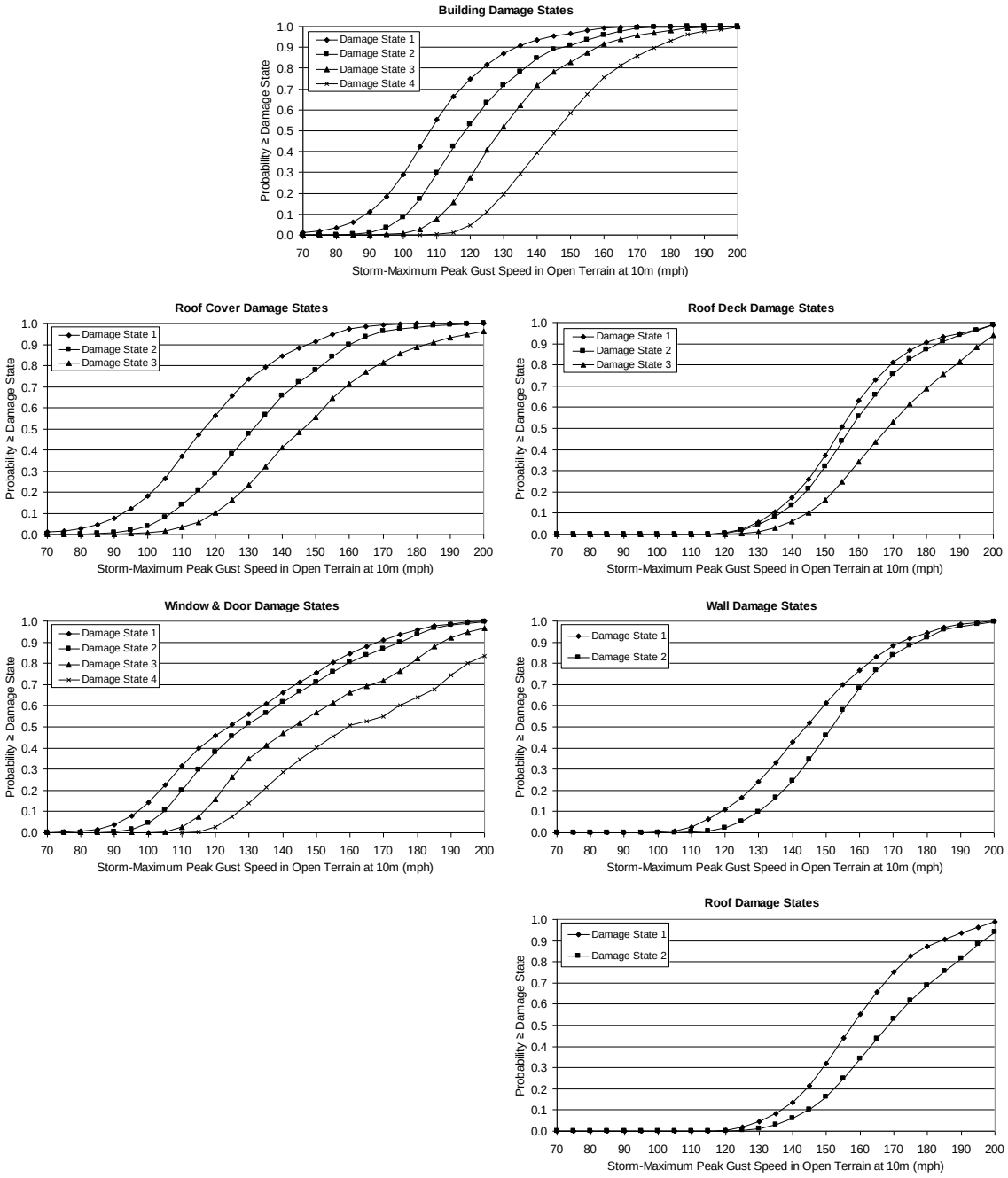

Figure D.18. Damage States vs. Peak Gust Wind Speed – Strip Mall Building B – Height=20′, No. of Units=6, Wood Deck with 8d Nails, Strapped Roof-Wall Connections, Built-up Roof Cover, Unreinforced Masonry Walls, Missile Environment A, z_0=0.35 m.

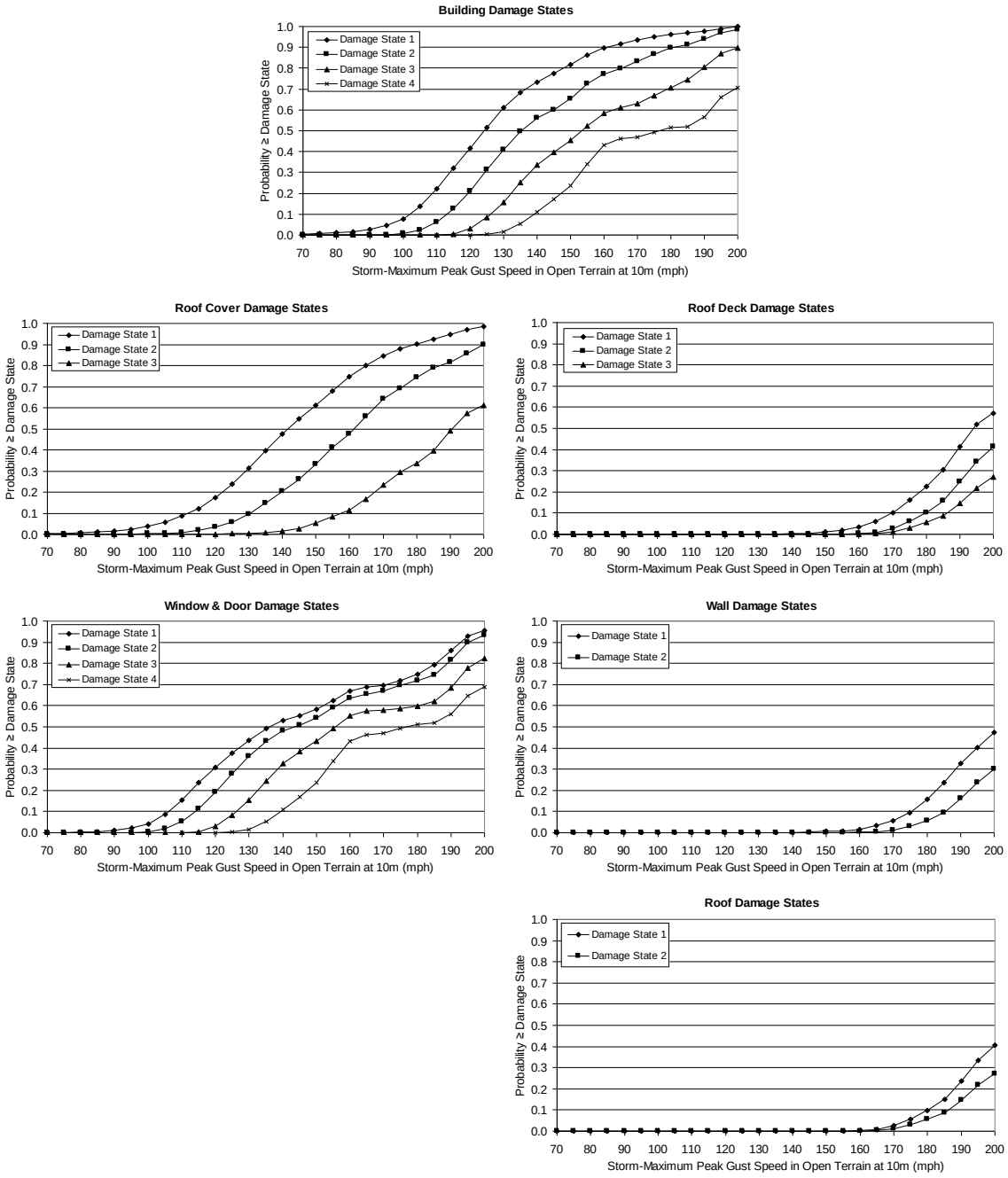

Figure D.19. Damage States vs. Peak Gust Wind Speed – Strip Mall Building A – Height=12′, No. of Units=6, Wood Deck with 8d Nails, Strapped Roof-Wall Connections, Built-up Roof Cover, Unreinforced Masonry Walls, Missile Environment A, z_0=0.70 m.

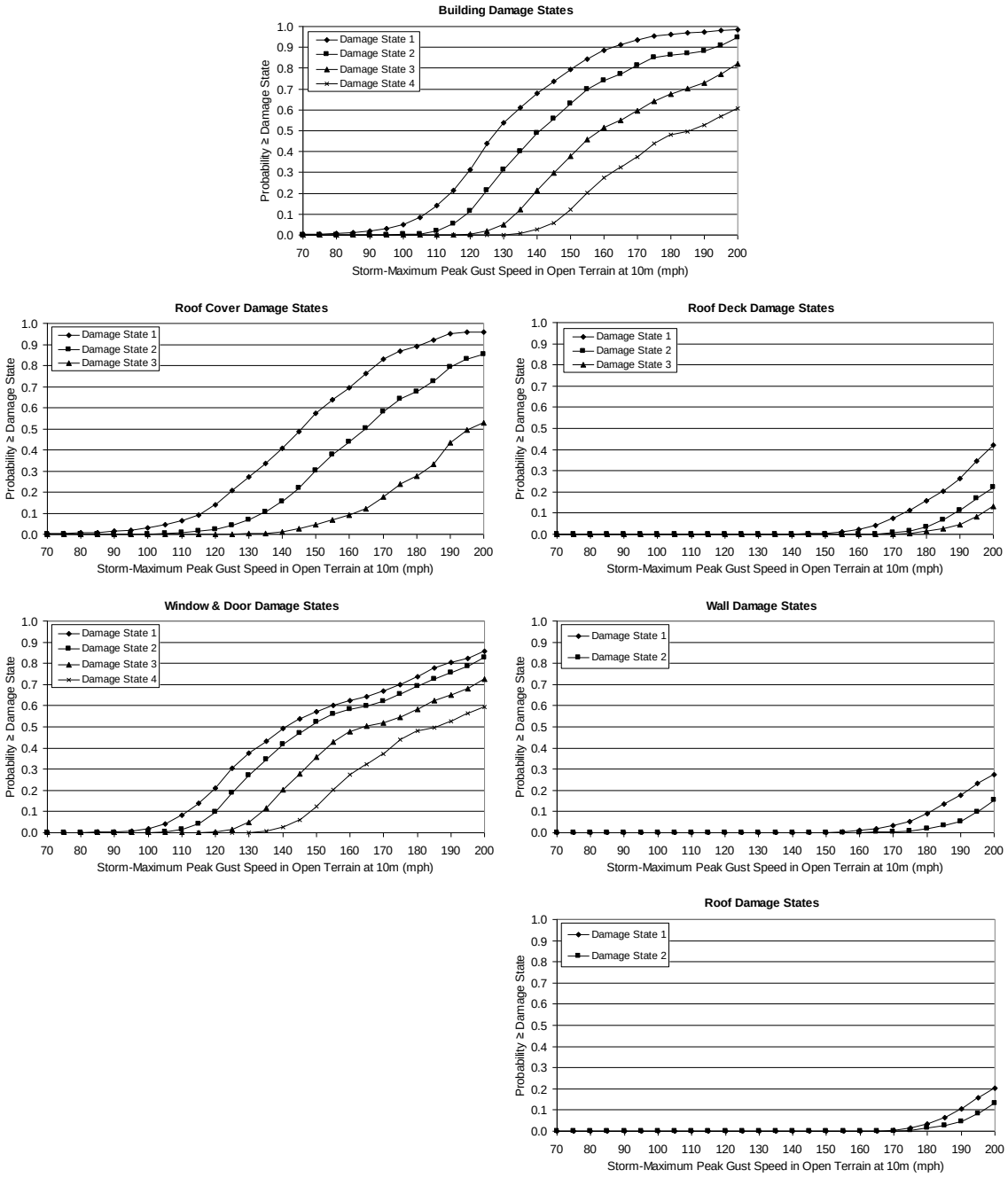

Figure D.20. Damage States vs. Peak Gust Wind Speed – Strip Mall Building A – Height=12′, No. of Units=6, Wood Deck with 8d Nails, Strapped Roof-Wall Connections, Built-up Roof Cover, Unreinforced Masonry Walls, Missile Environment A, z_0=1.0 m.

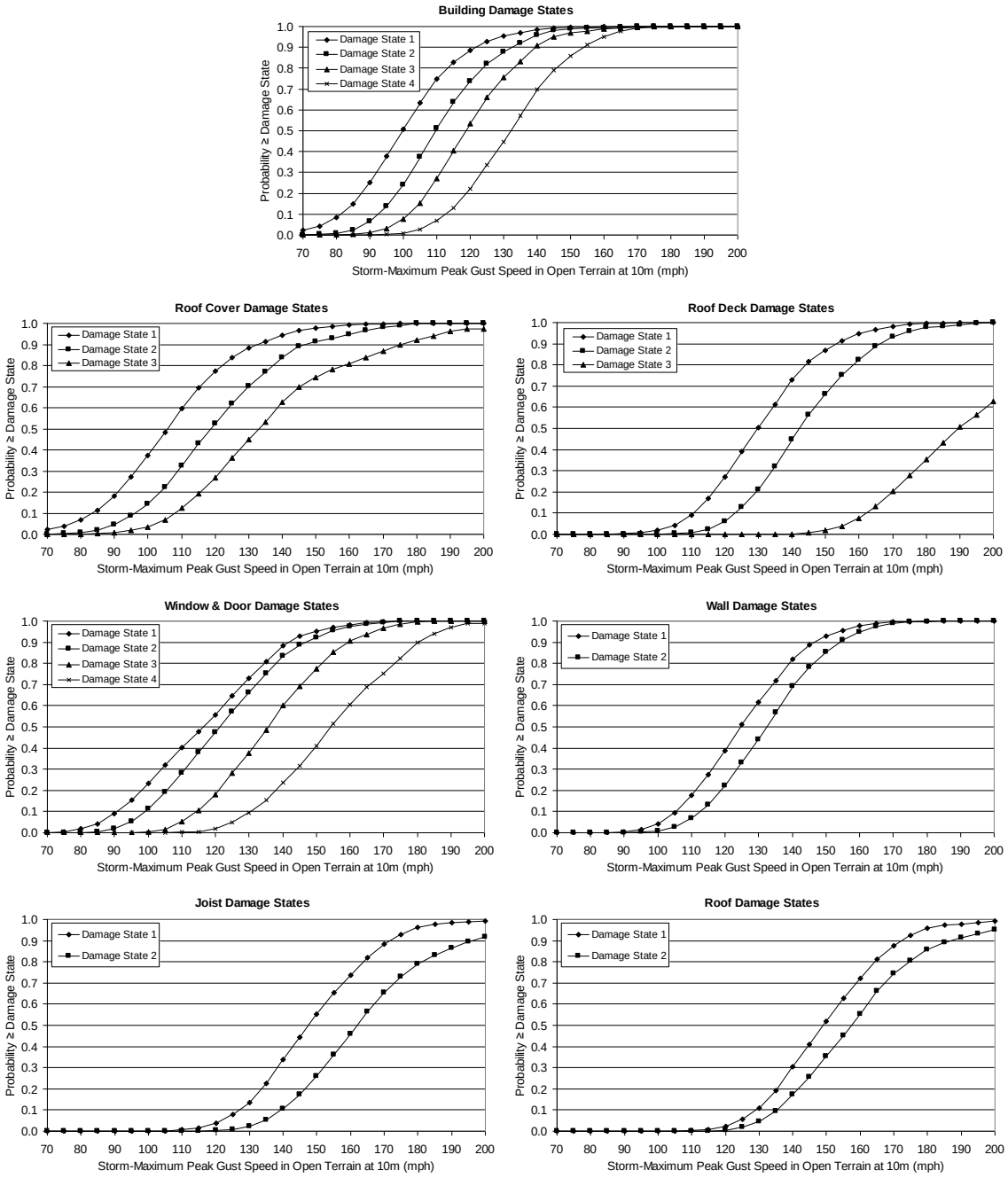

Figure D.21. Damage States vs. Peak Gust Wind Speed – Strip Mall Building C – Height=20′, No. of Units=6, Joist Spacing=6′, Metal Deck Welded to Joists, SBCCI 100 mph Design Criteria, Built-up Roof Cover, Unreinforced Masonry Walls, Missile Environment A, z_0=0.03 m.

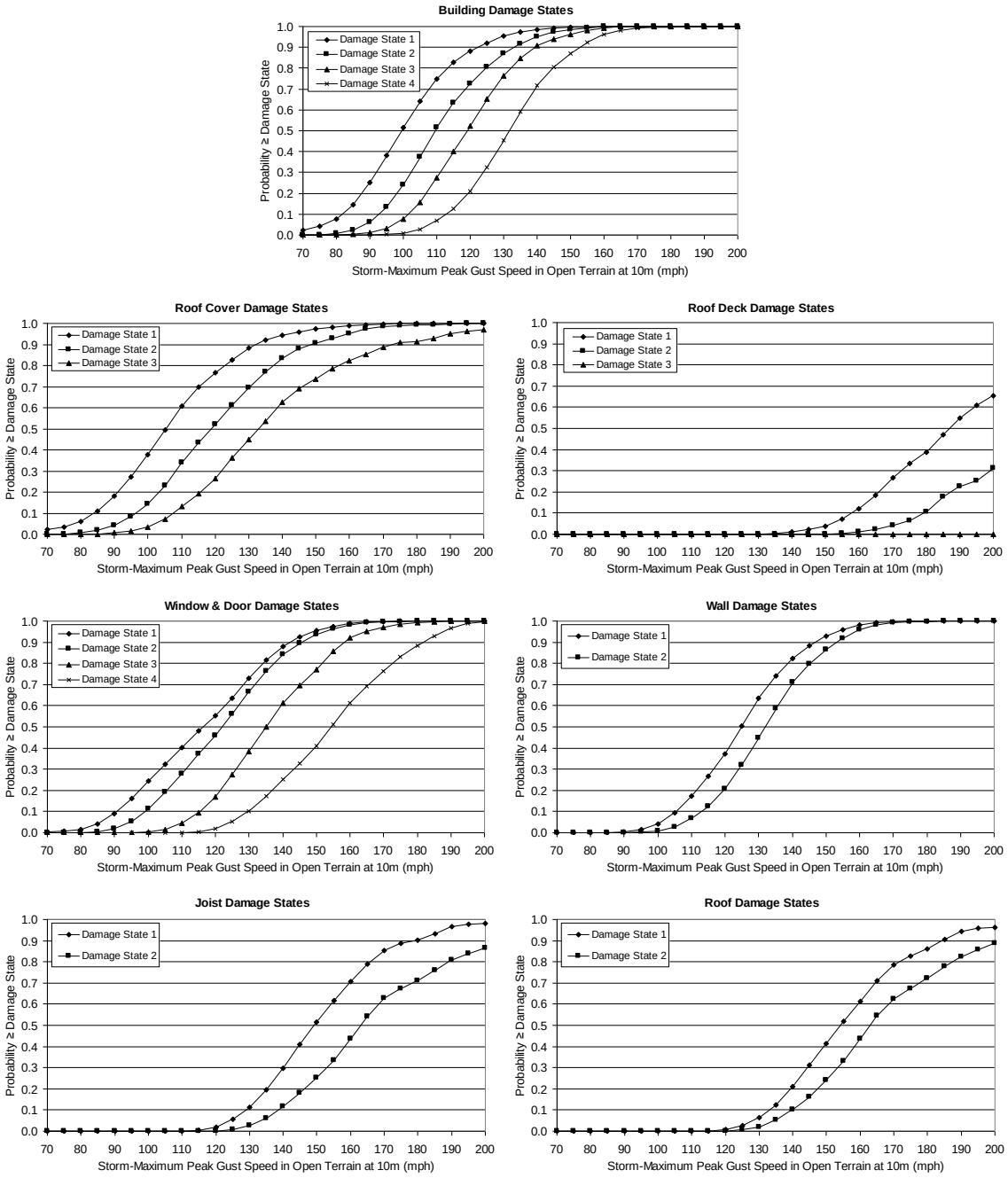

Figure D.22. Damage States vs. Peak Gust Wind Speed – Strip Mall Building B – Height=20′, No. of Units=6, Joist Spacing=4′, Metal Deck Welded to Joists, SBCCI 100 mph Design Criteria, Built-up Roof Cover, Unreinforced Masonry Walls, Missile Environment A, z_0=0.03 m.

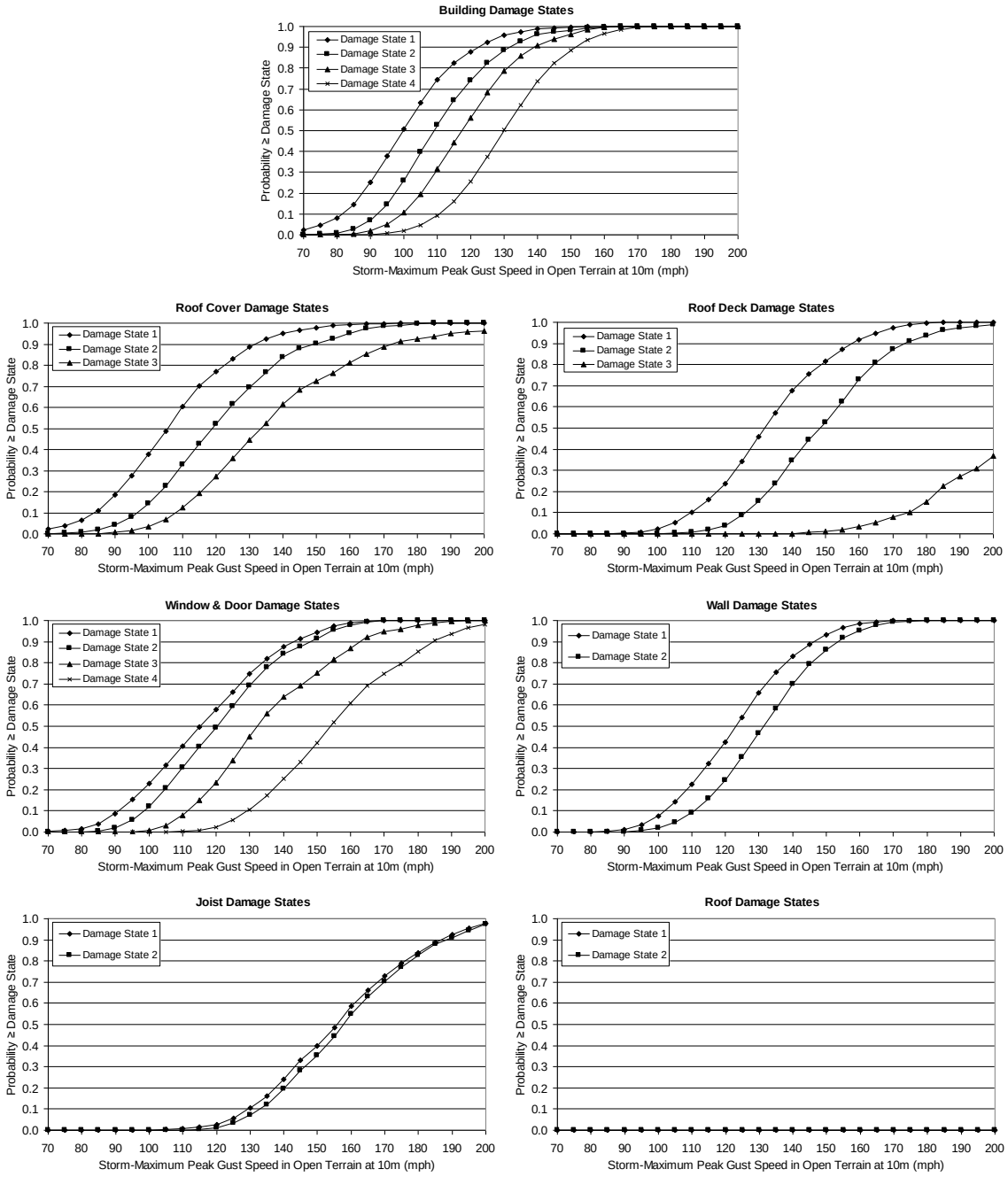

Figure D.23. Damage States vs. Peak Gust Wind Speed – Strip Mall Building D – Height=20′, No. of Units=1, Joist Spacing=6′, Metal Deck Welded to Joists, SBCCI 100 mph Design Criteria, Built-up Roof Cover, Unreinforced Masonry Walls, Missile Environment A, z_0=0.03 m.

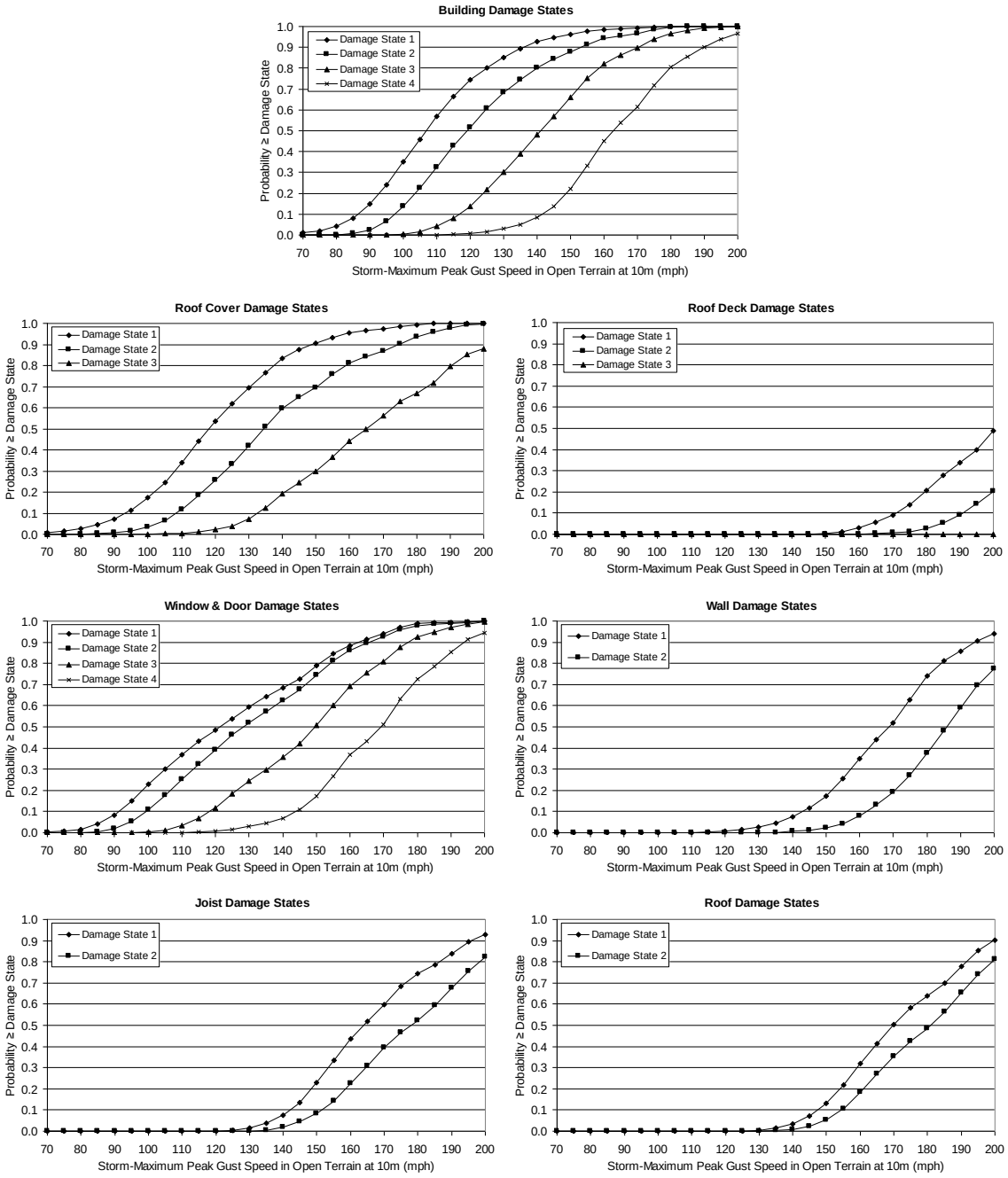

Figure D.24. Damage States vs. Peak Gust Wind Speed – Strip Mall Building A – Height=12′, No. of Units=6, Joist Spacing=4′, Metal Deck Welded to Joists, SBCCI 100 mph Design Criteria, Built-up Roof Cover, Unreinforced Masonry Walls, Missile Environment A, z_0=0.03 m.

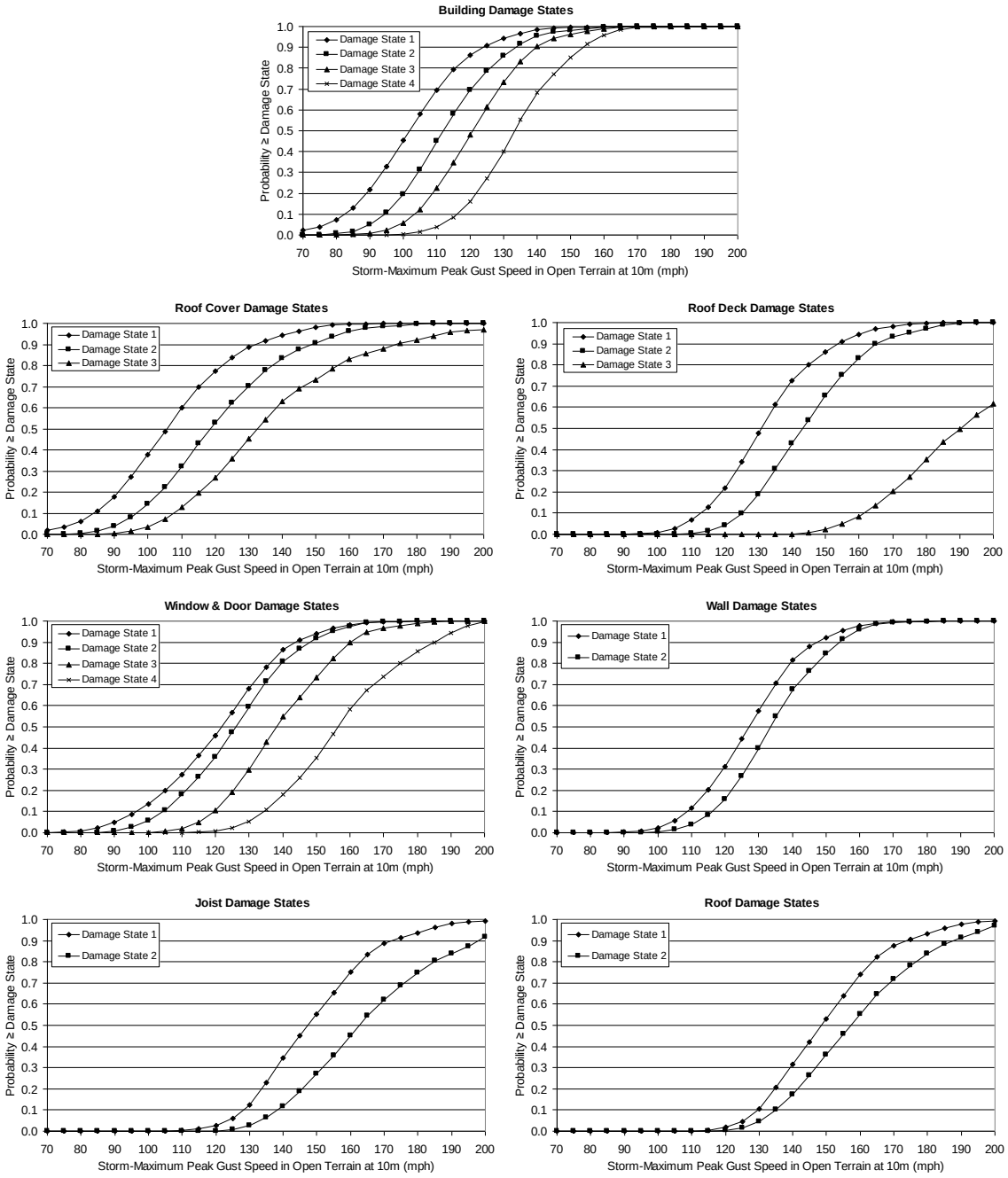

Figure D.25. Damage States vs. Peak Gust Wind Speed – Strip Mall Building C – Height=20′, No. of Units=6, Joist Spacing=6′, Metal Deck Welded to Joists, SBCCI 100 mph Design Criteria, Built-up Roof Cover, Unreinforced Masonry Walls, Missile Environment B, z_0=0.03 m.

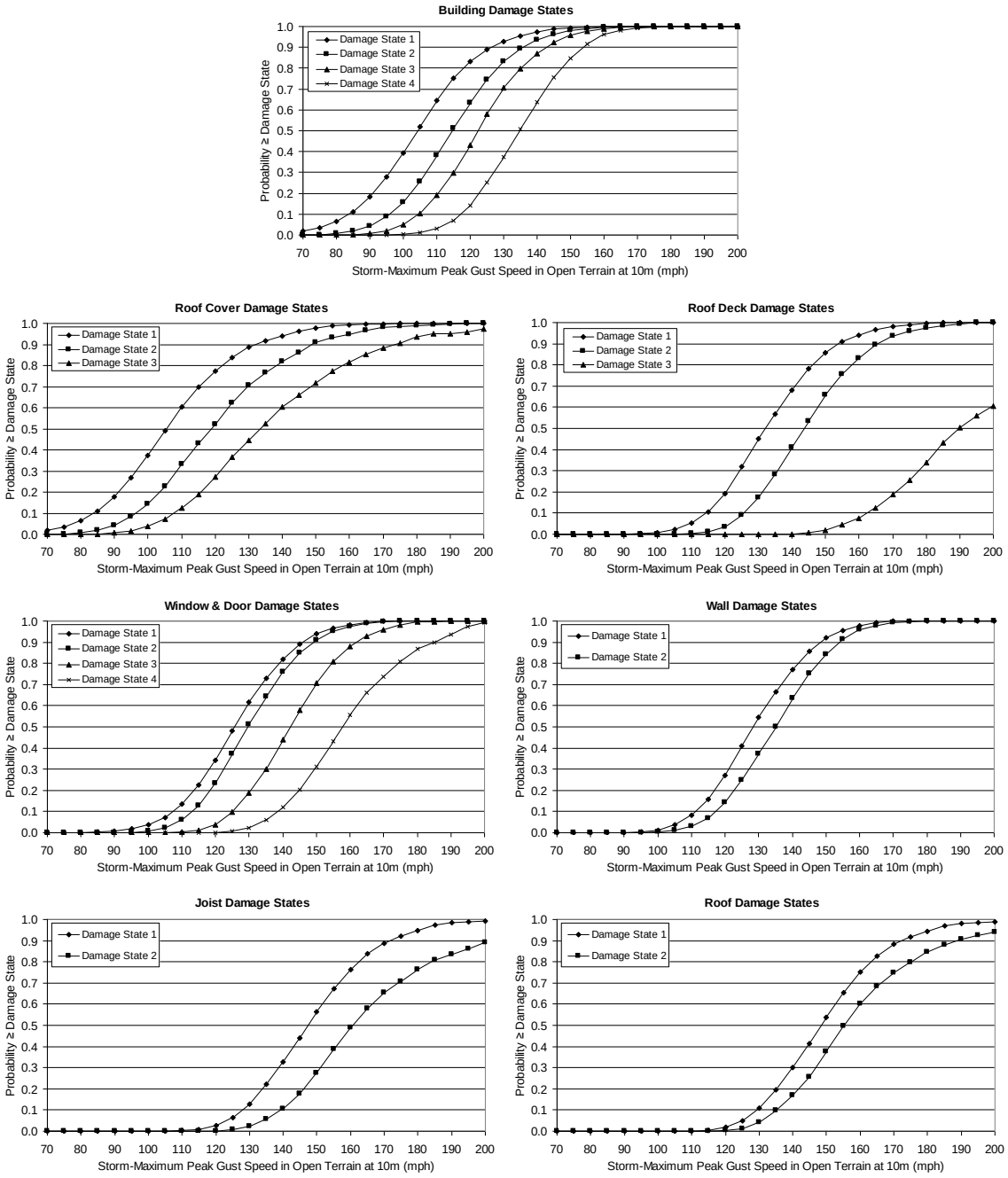

Figure D.26. Damage States vs. Peak Gust Wind Speed – Strip Mall Building C – Height=20′, No. of Units=6, Joist Spacing=6′, Metal Deck Welded to Joists, SBCCI 100 mph Design Criteria, Built-up Roof Cover, Unreinforced Masonry Walls, Missile Environment C, z_0=0.03 m.

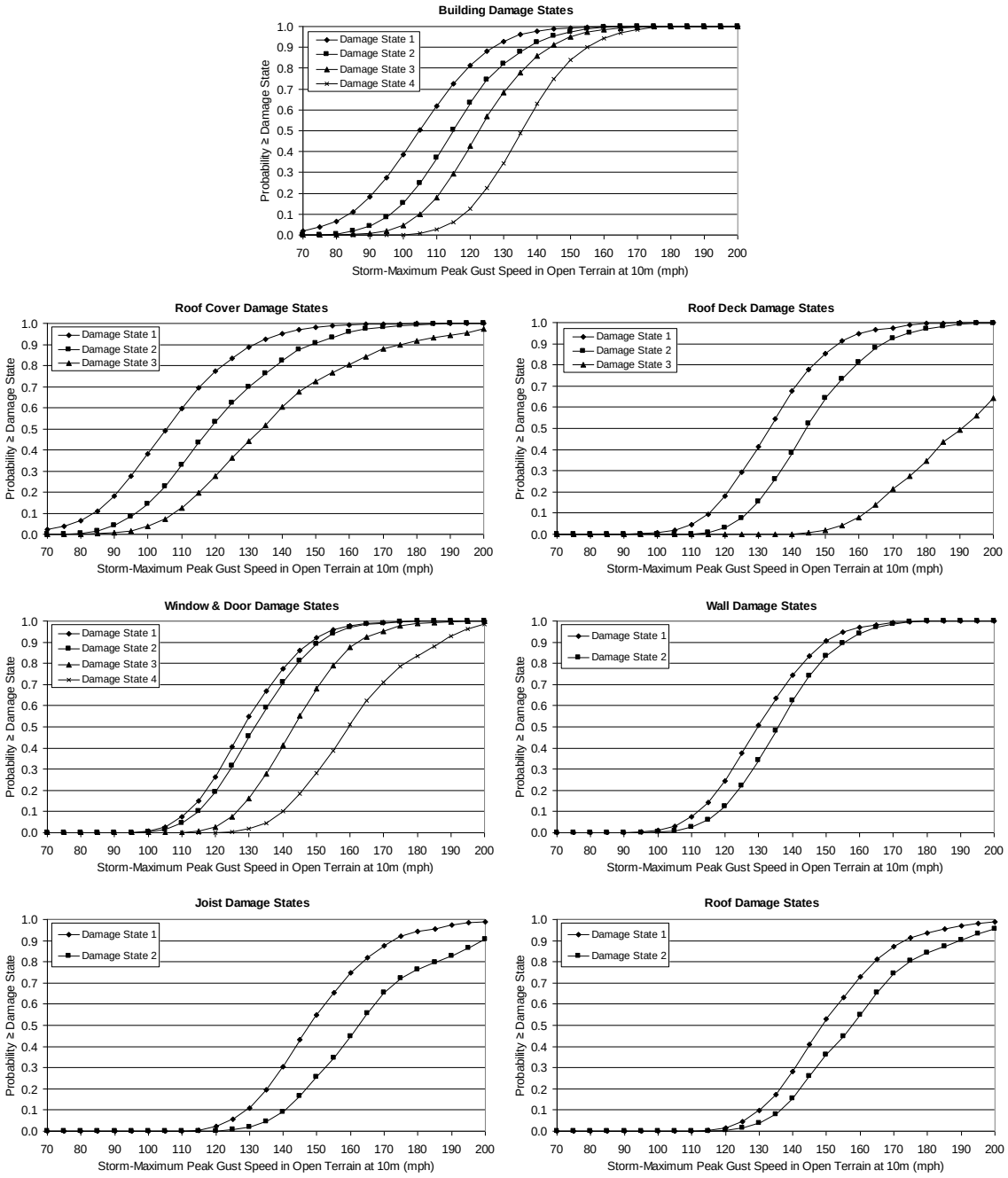

Figure D.27. Damage States vs. Peak Gust Wind Speed – Strip Mall Building C – Height=20′, No. of Units=6, Joist Spacing=6′, Metal Deck Welded to Joists, SBCCI 100 mph Design Criteria, Built-up Roof Cover, Unreinforced Masonry Walls, Missile Environment D, z_0=0.03 m.

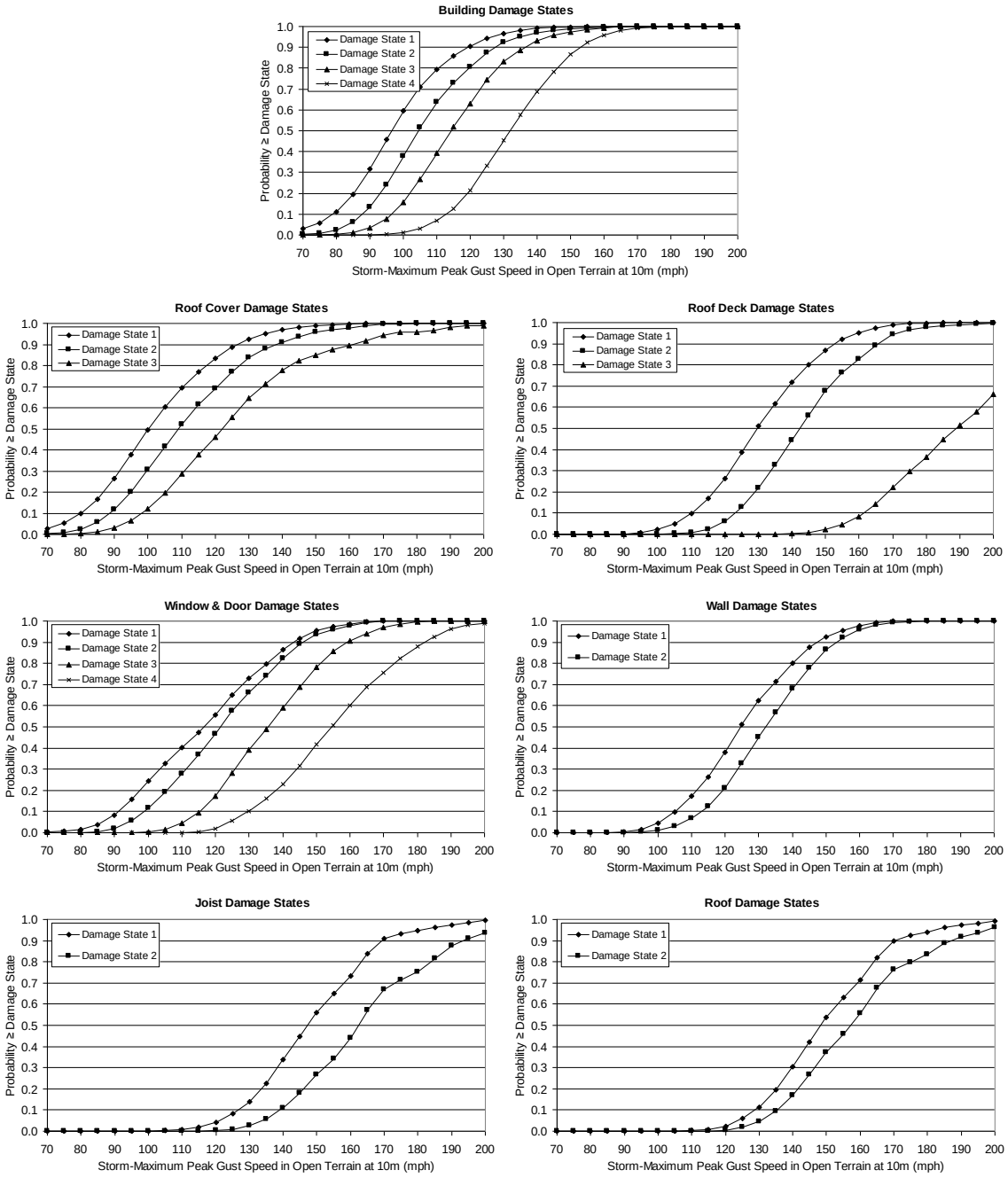

Figure D.28. Damage States vs. Peak Gust Wind Speed – Strip Mall Building C – Height=20′, No. of Units=6, Joist Spacing=6′, Metal Deck Welded to Joists, SBCCI 100 mph Design Criteria, Single Ply Membrane Roof Cover, Unreinforced Masonry Walls, Missile Environment A, z_0=0.03 m.

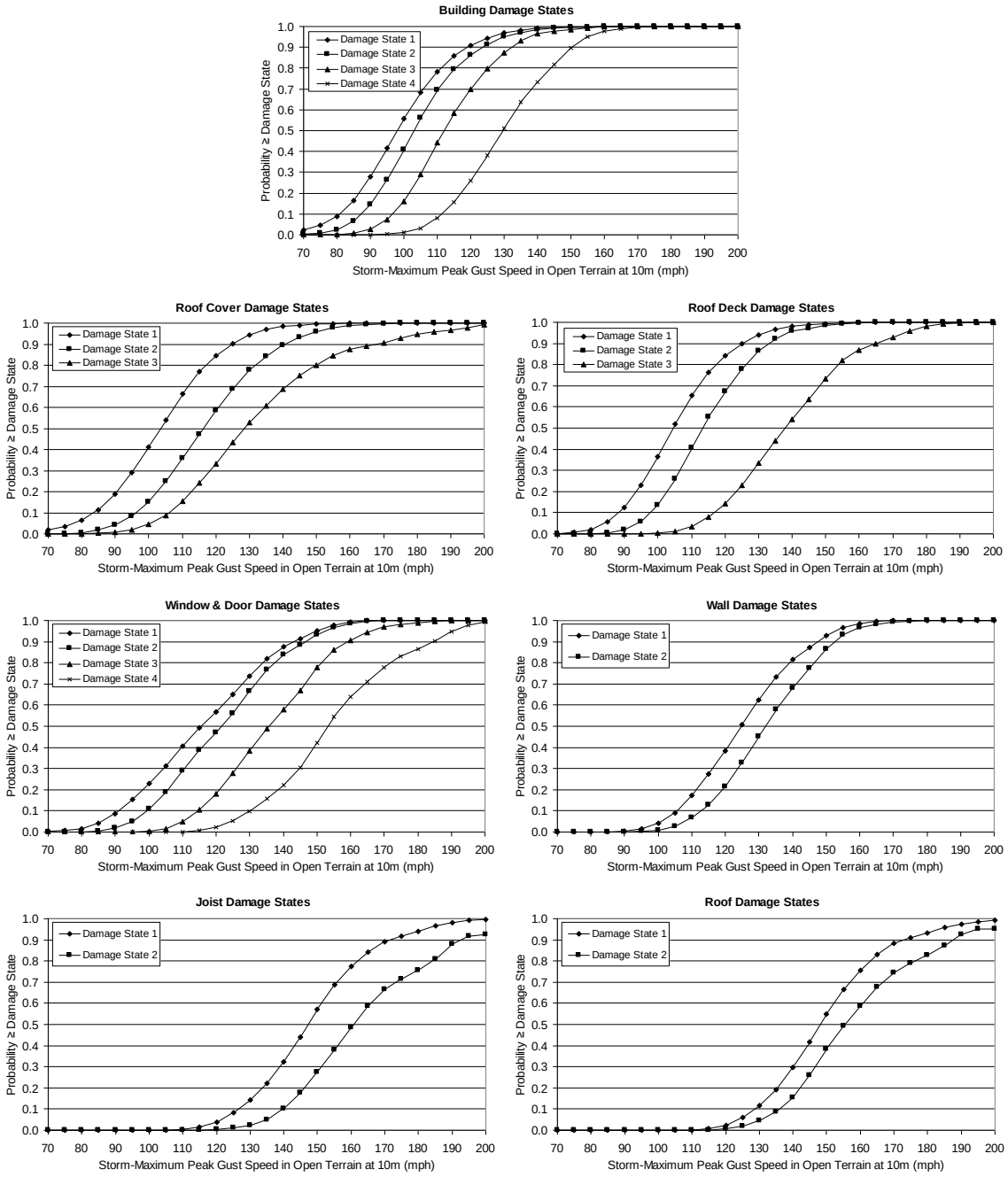

Figure D.29. Damage States vs. Peak Gust Wind Speed – Strip Mall Building C – Height=20′, No. of Units=6, Joist Spacing=6′, Metal Deck Welded to Joists with <u>50% Reduction in Resistance</u>, SBCCI 100 mph Design Criteria, Built-up Roof Cover, Unreinforced Masonry Walls, Missile Environment A, z_0=0.03 m.

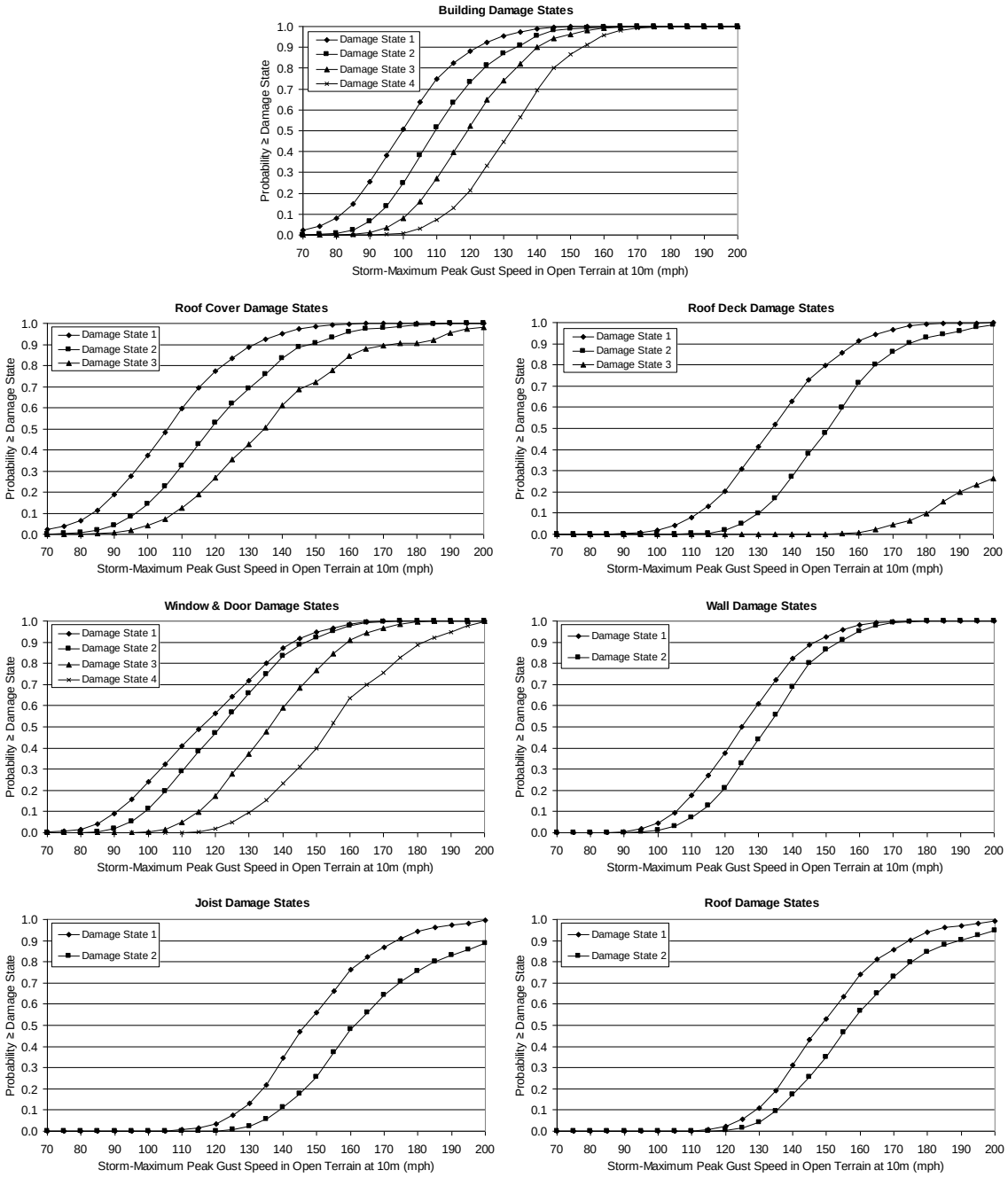

Figure D.30. Damage States vs. Peak Gust Wind Speed – Strip Mall Building C – Height=20′, No. of Units=6, Joist Spacing=6′, Metal Deck Screwed to Joists, SBCCI 100 mph Design Criteria, Built-up Roof Cover, Unreinforced Masonry Walls, Missile Environment A, z_0=0.03 m.

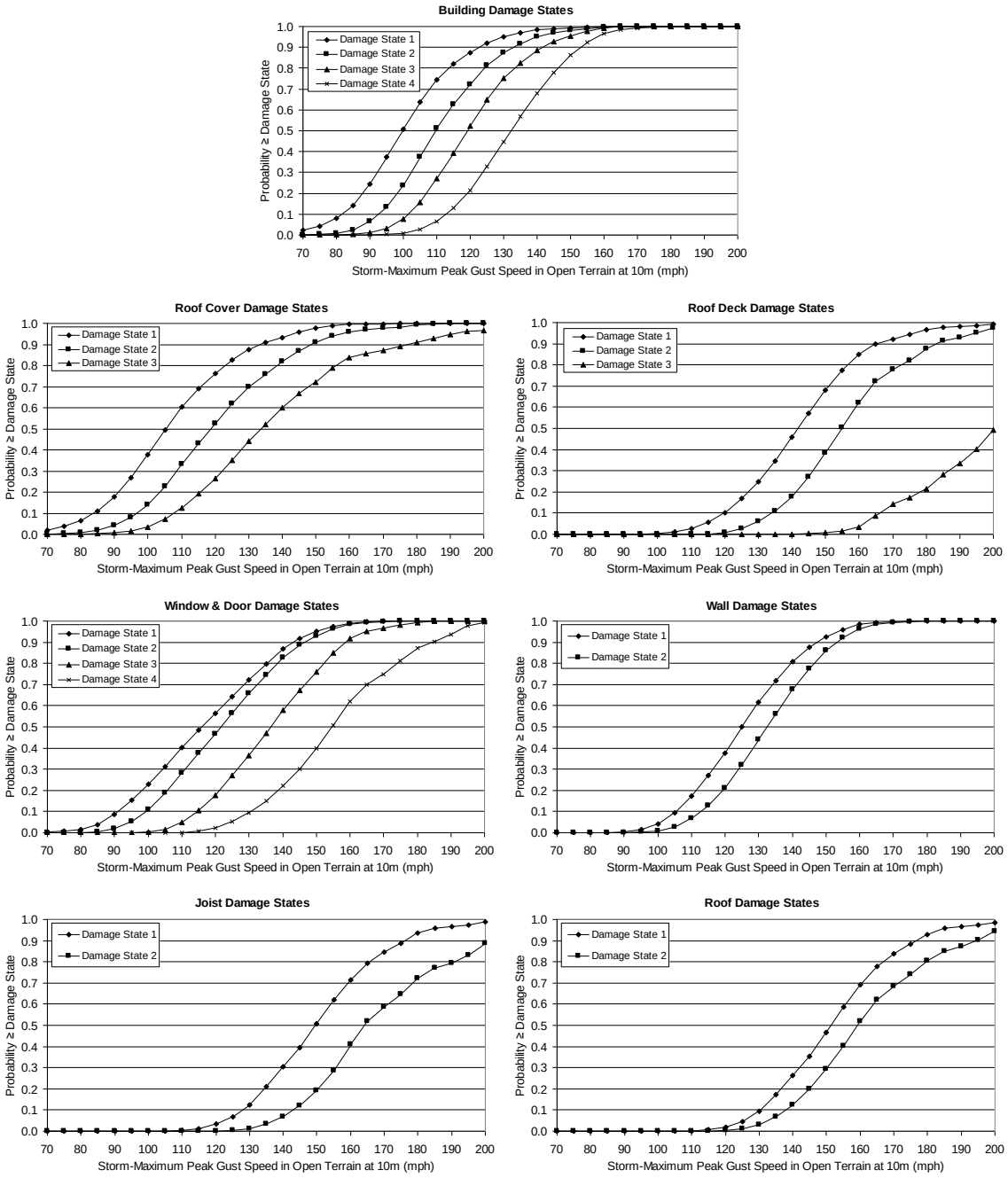

Figure D.31. Damage States vs. Peak Gust Wind Speed – Strip Mall Building C – Height=20′, No. of Units=6, Joist Spacing=6′, Metal Deck Welded to Joists, ASCE 100 mph Design Criteria, Built-up Roof Cover, Unreinforced Masonry Walls, Missile Environment A, z_0=0.03 m.

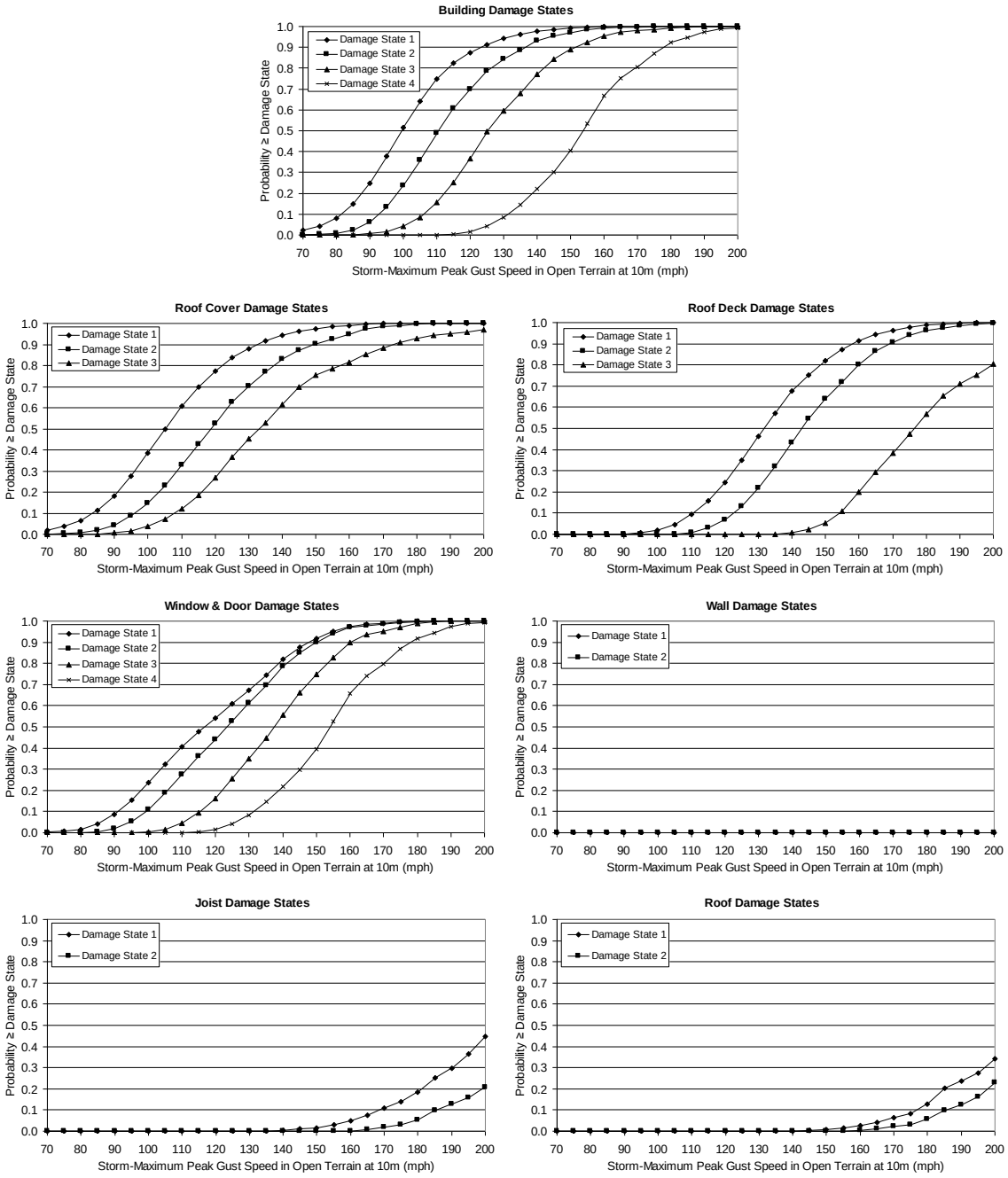

Figure D.32. Damage States vs. Peak Gust Wind Speed – Strip Mall Building C – Height=20′, No. of Units=6, Joist Spacing=6′, Metal Deck Welded to Joists, SBCCI 100 mph Design Criteria, Built-up Roof Cover, Reinforced Masonry Walls, Missile Environment A, z_0=0.03 m.

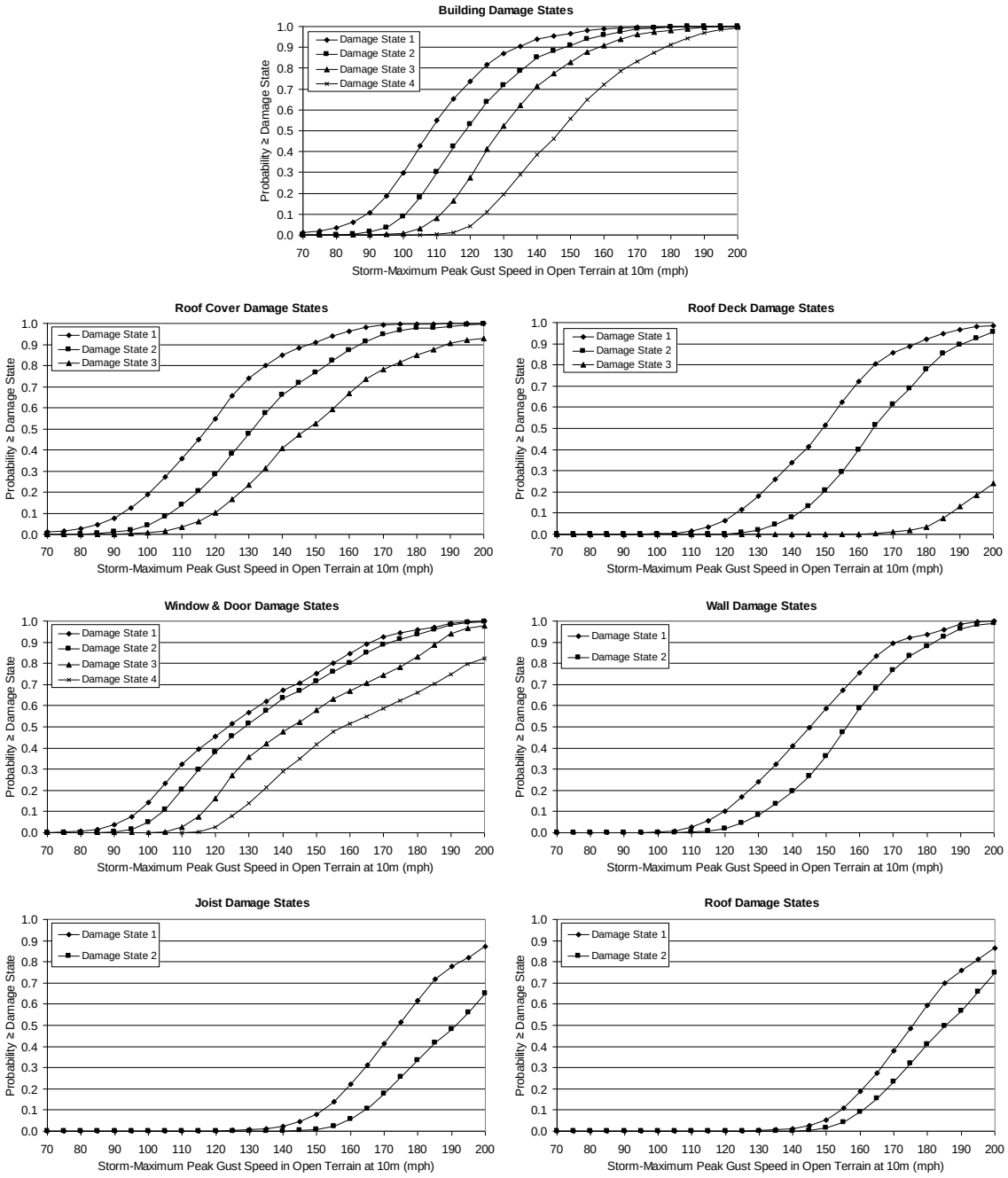

Figure D.33. Damage States vs. Peak Gust Wind Speed – Strip Mall Building C – Height=20′, No. of Units=6, Joist Spacing=6′, Metal Deck Welded to Joists, SBCCI 100 mph Design Criteria, Built-up Roof Cover, Unreinforced Masonry Walls, Missile Environment A, z_0=0.35 m.

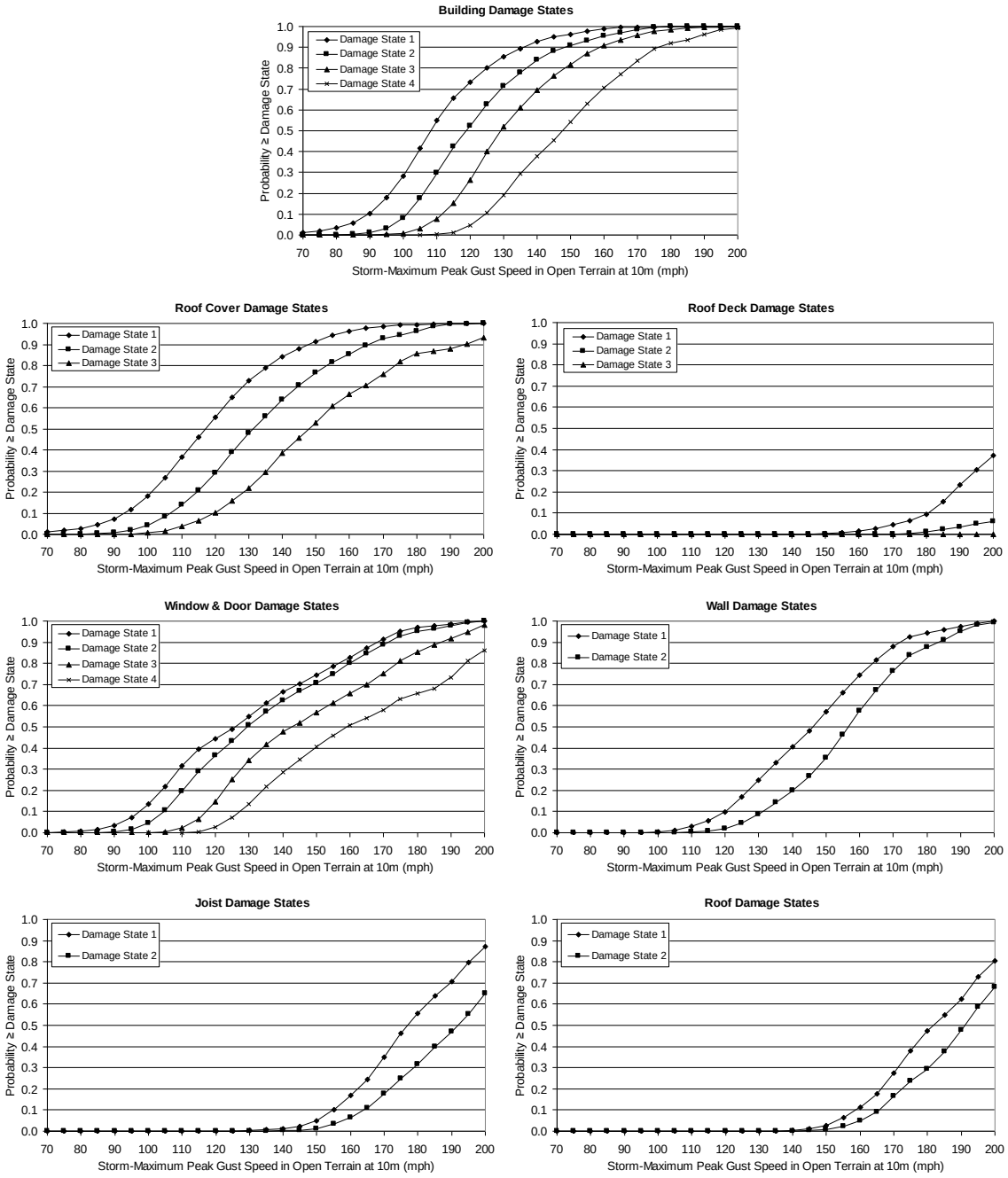

Figure D.34. Damage States vs. Peak Gust Wind Speed – Strip Mall Building B – Height=20′, No. of Units=6, Joist Spacing=4′, Metal Deck Welded to Joists, SBCCI 100 mph Design Criteria, Built-up Roof Cover, Unreinforced Masonry Walls, Missile Environment A, z_0=0.35 m.

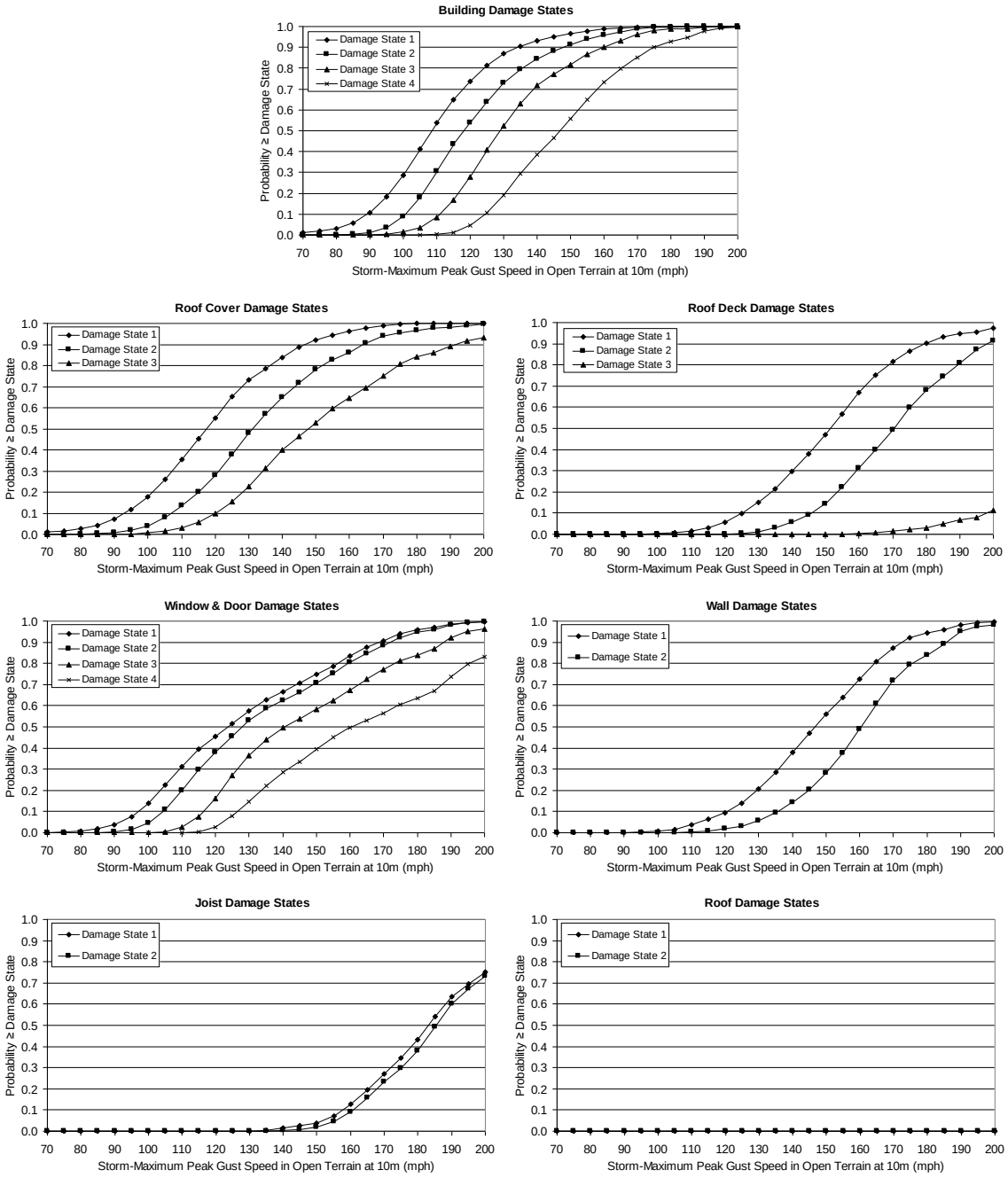

Figure D.35. Damage States vs. Peak Gust Wind Speed – Strip Mall Building D – Height=20′, No. of Units=1, Joist Spacing=6′, Metal Deck Welded to Joists, SBCCI 100 mph Design Criteria, Built-up Roof Cover, Unreinforced Masonry Walls, Missile Environment A, z_0=0.35 m.

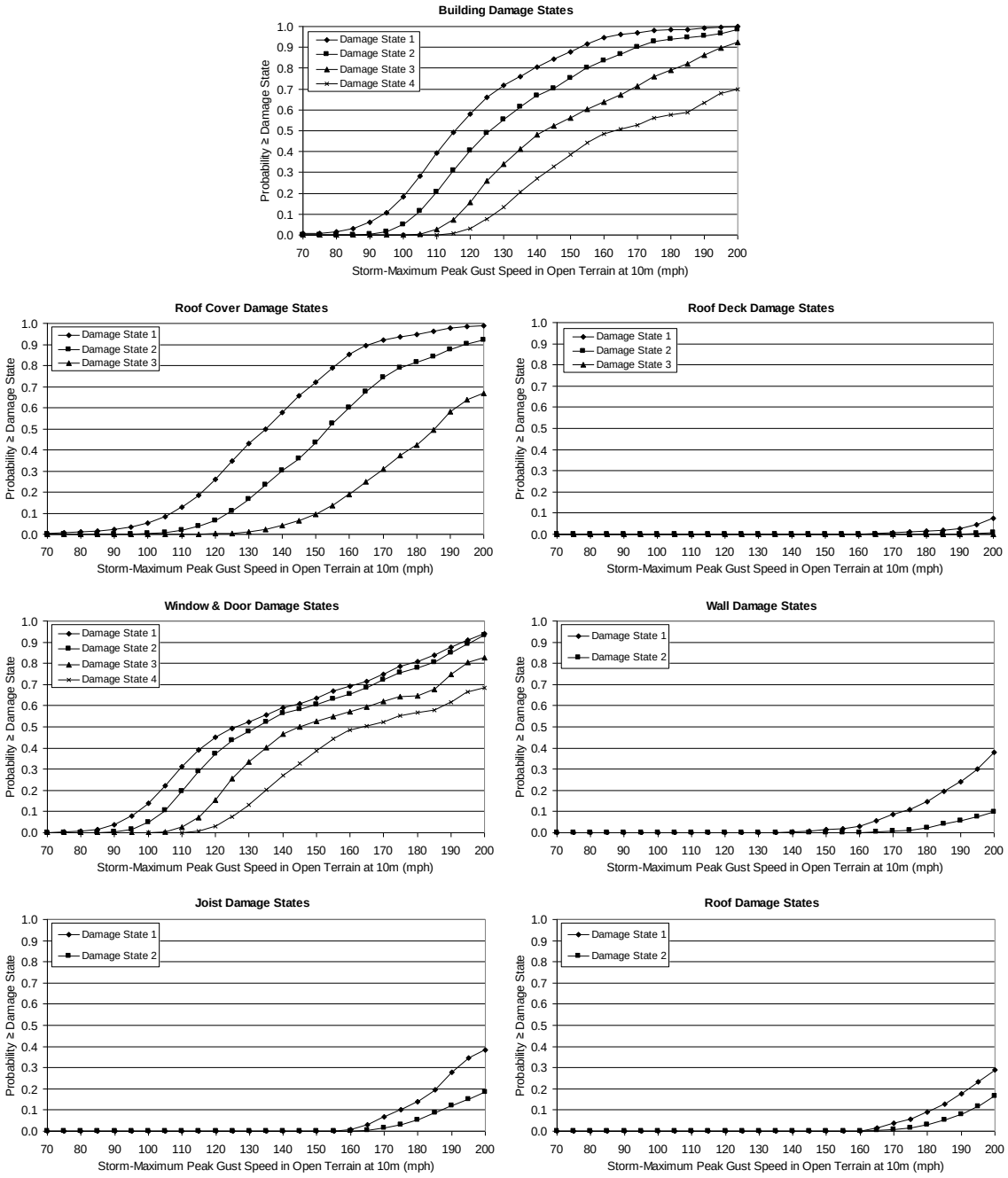

Figure D.36. Damage States vs. Peak Gust Wind Speed – Strip Mall Building A – Height=12′, No. of Units=6, Joist Spacing=4′, Metal Deck Welded to Joists, SBCCI 100 mph Design Criteria, Built-up Roof Cover, Unreinforced Masonry Walls, Missile Environment A, z_0=0.35 m.

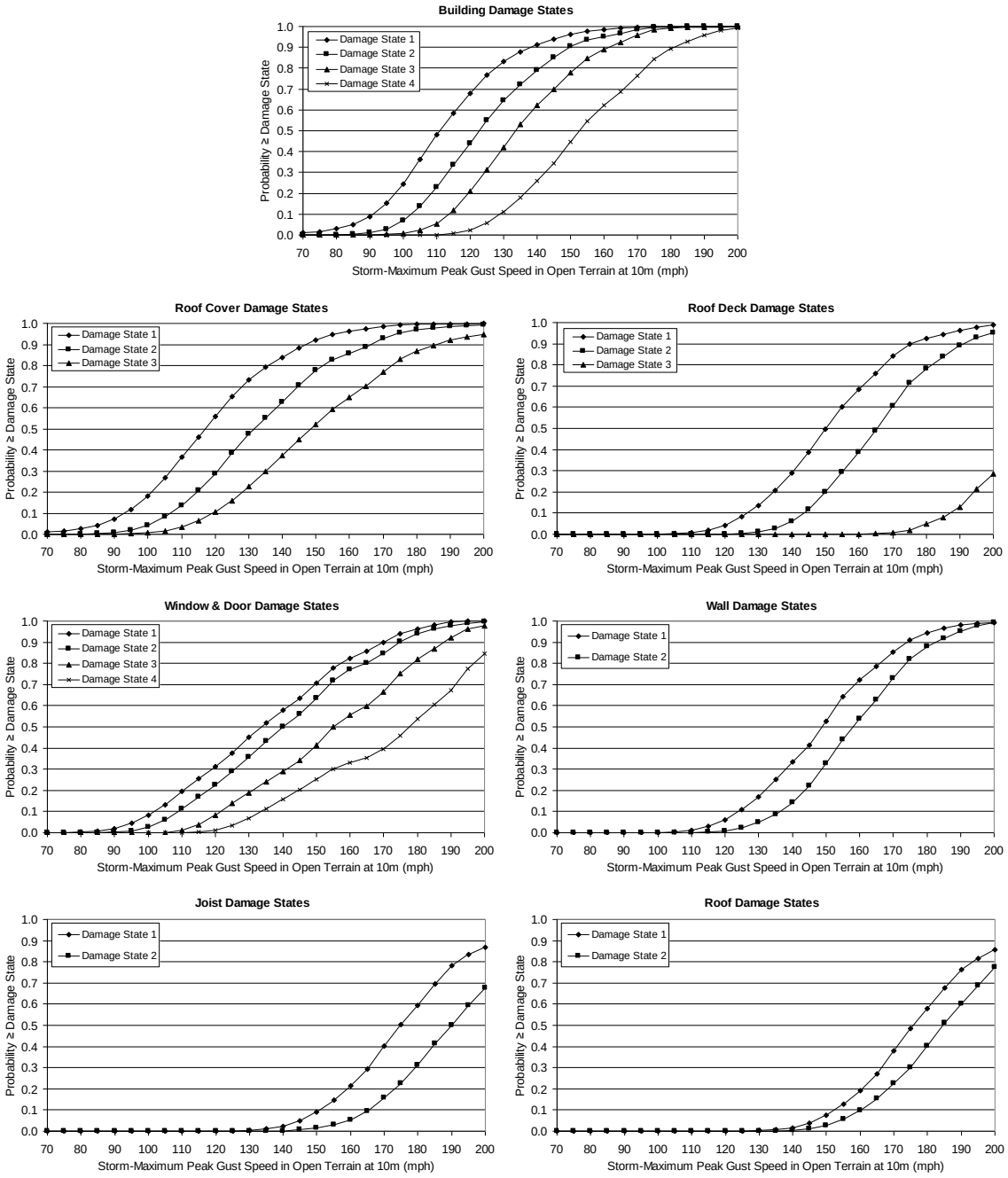

Figure D.37. Damage States vs. Peak Gust Wind Speed – Strip Mall Building C – Height=20′, No. of Units=6, Joist Spacing=6′, Metal Deck Welded to Joists, SBCCI 100 mph Design Criteria, Built-up Roof Cover, Unreinforced Masonry Walls, Missile Environment B, z_0=0.35 m.

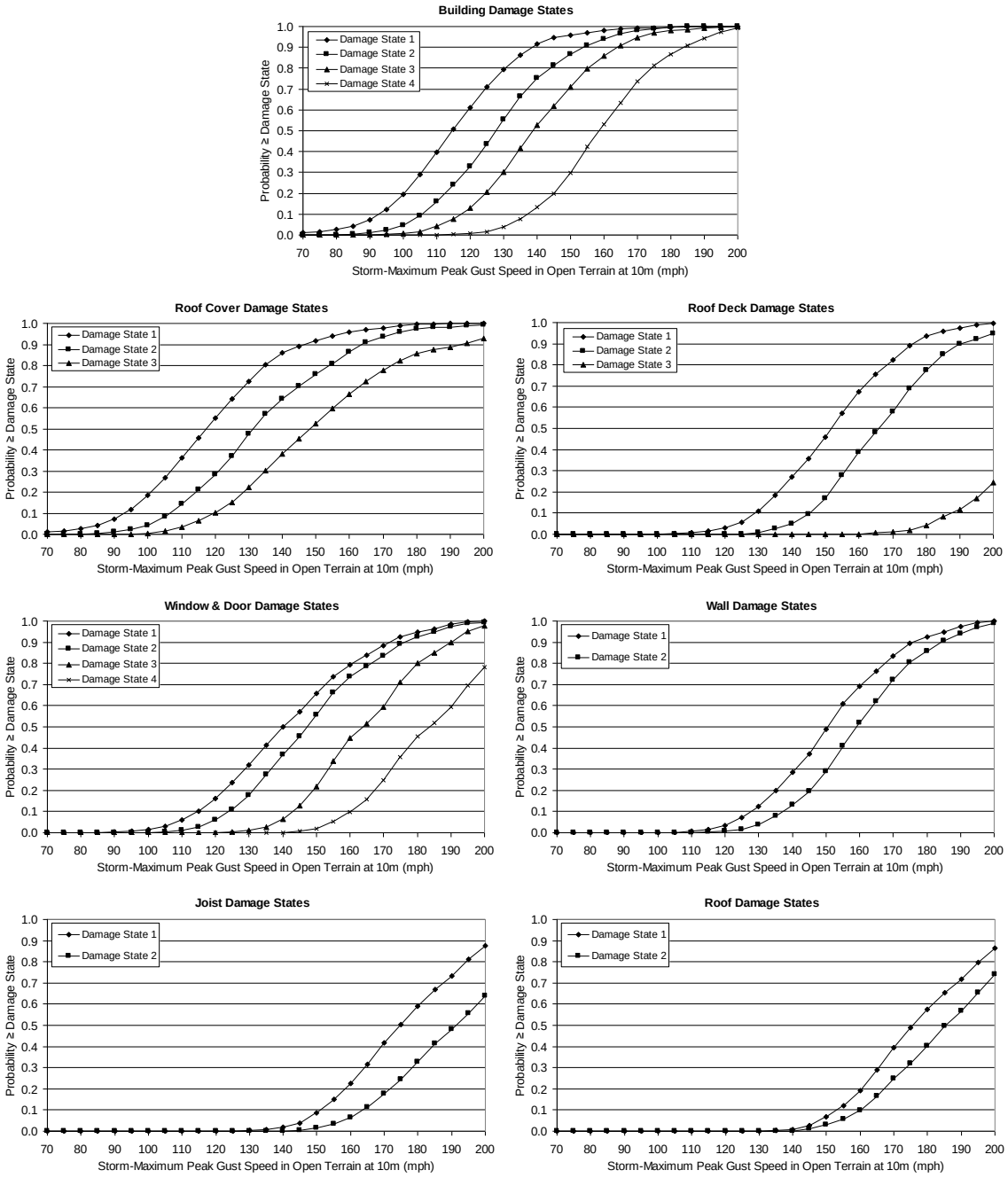

Figure D.38. Damage States vs. Peak Gust Wind Speed – Strip Mall Building C – Height=20′, No. of Units=6, Joist Spacing=6′, Metal Deck Welded to Joists, SBCCI 100 mph Design Criteria, Built-up Roof Cover, Unreinforced Masonry Walls, Missile Environment C, z_0=0.35 m.

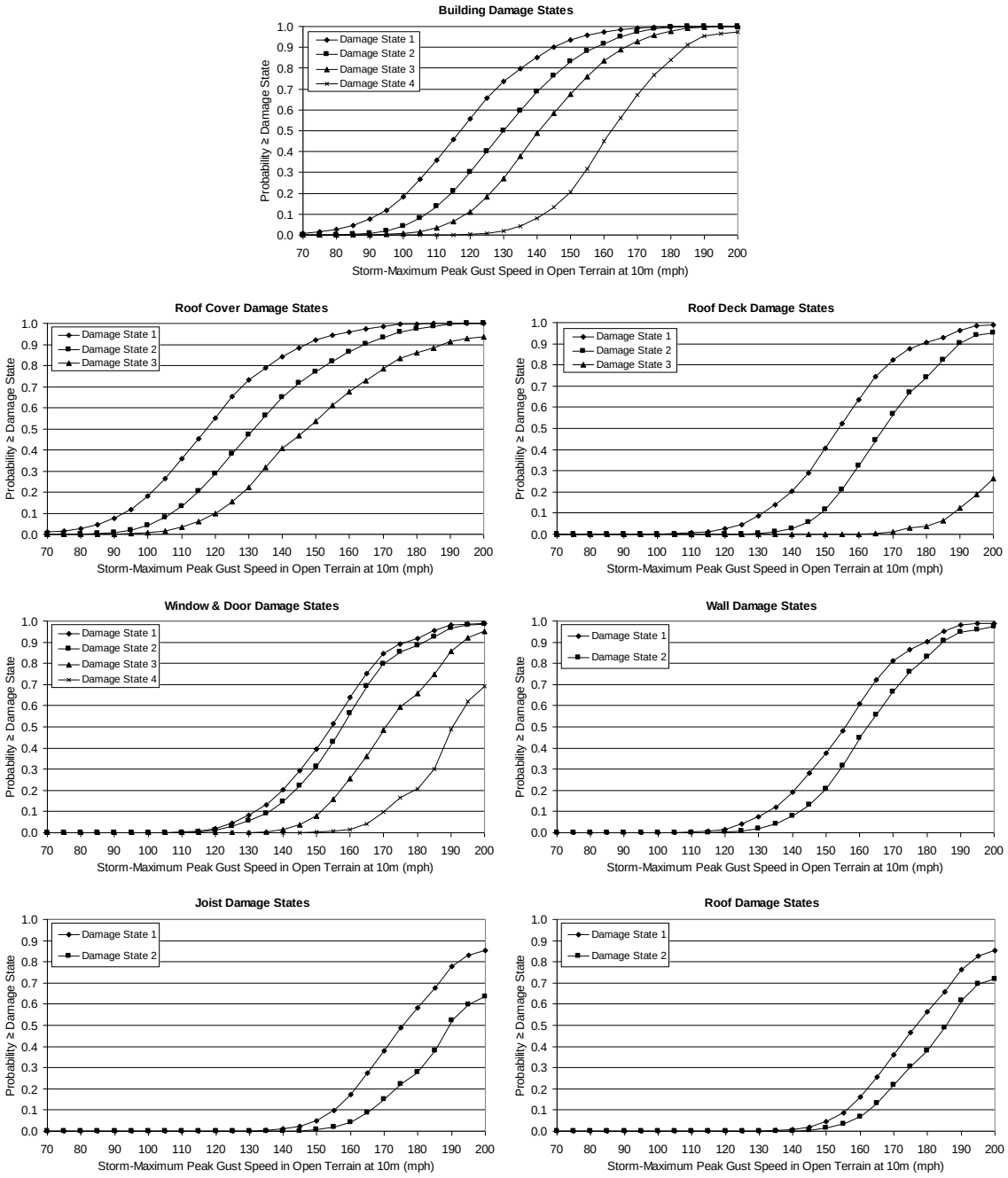

Figure D.39. Damage States vs. Peak Gust Wind Speed – Strip Mall Building C – Height=20′, No. of Units=6, Joist Spacing=6′, Metal Deck Welded to Joists, SBCCI 100 mph Design Criteria, Built-up Roof Cover, Unreinforced Masonry Walls, Missile Environment D, z_0=0.35 m.

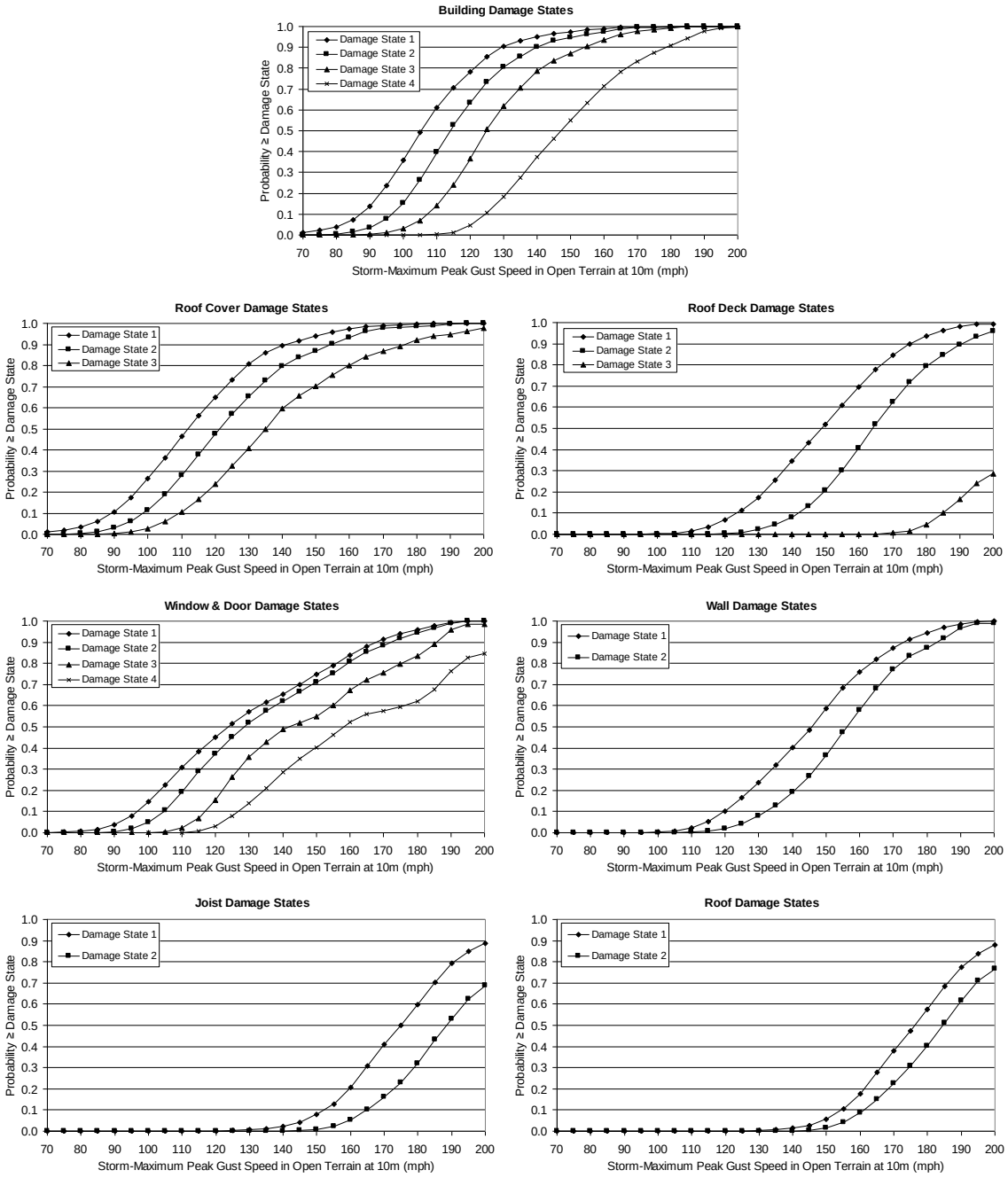

Figure D.40. Damage States vs. Peak Gust Wind Speed – Strip Mall Building C – Height=20′, No. of Units=6, Joist Spacing=6′, Metal Deck Welded to Joists, SBCCI 100 mph Design Criteria, Single Ply Membrane Roof Cover, Unreinforced Masonry Walls, Missile Environment A, z_0=0.35 m.

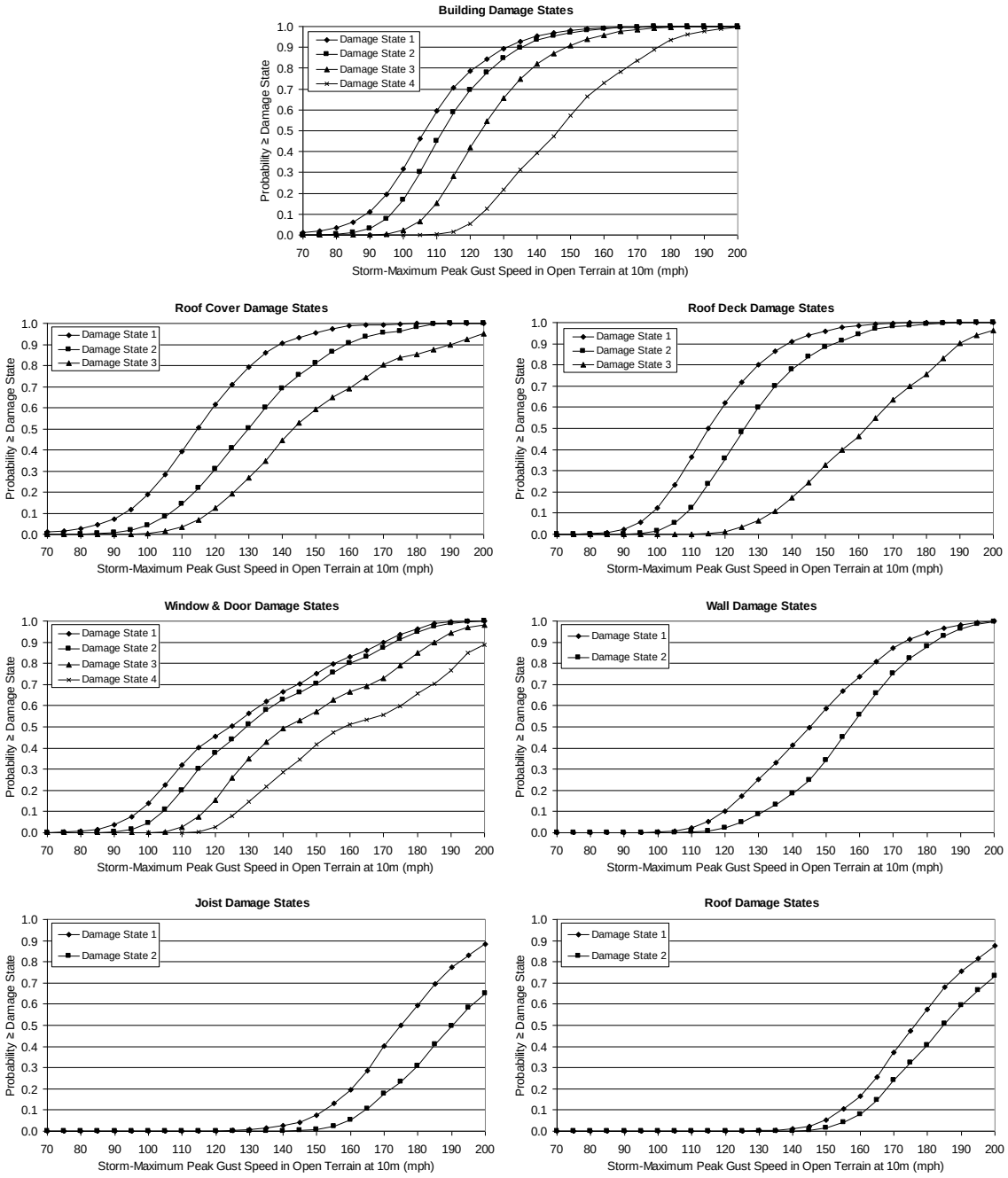

Figure D.41. Damage States vs. Peak Gust Wind Speed – Strip Mall Building C – Height=20′, No. of Units=6, Joist Spacing=6′, Metal Deck Welded to Joists with <u>50% Reduction in Resistance</u>, SBCCI 100 mph Design Criteria, Built-up Roof Cover, Unreinforced Masonry Walls, Missile Environment A, z_0=0.35 m.

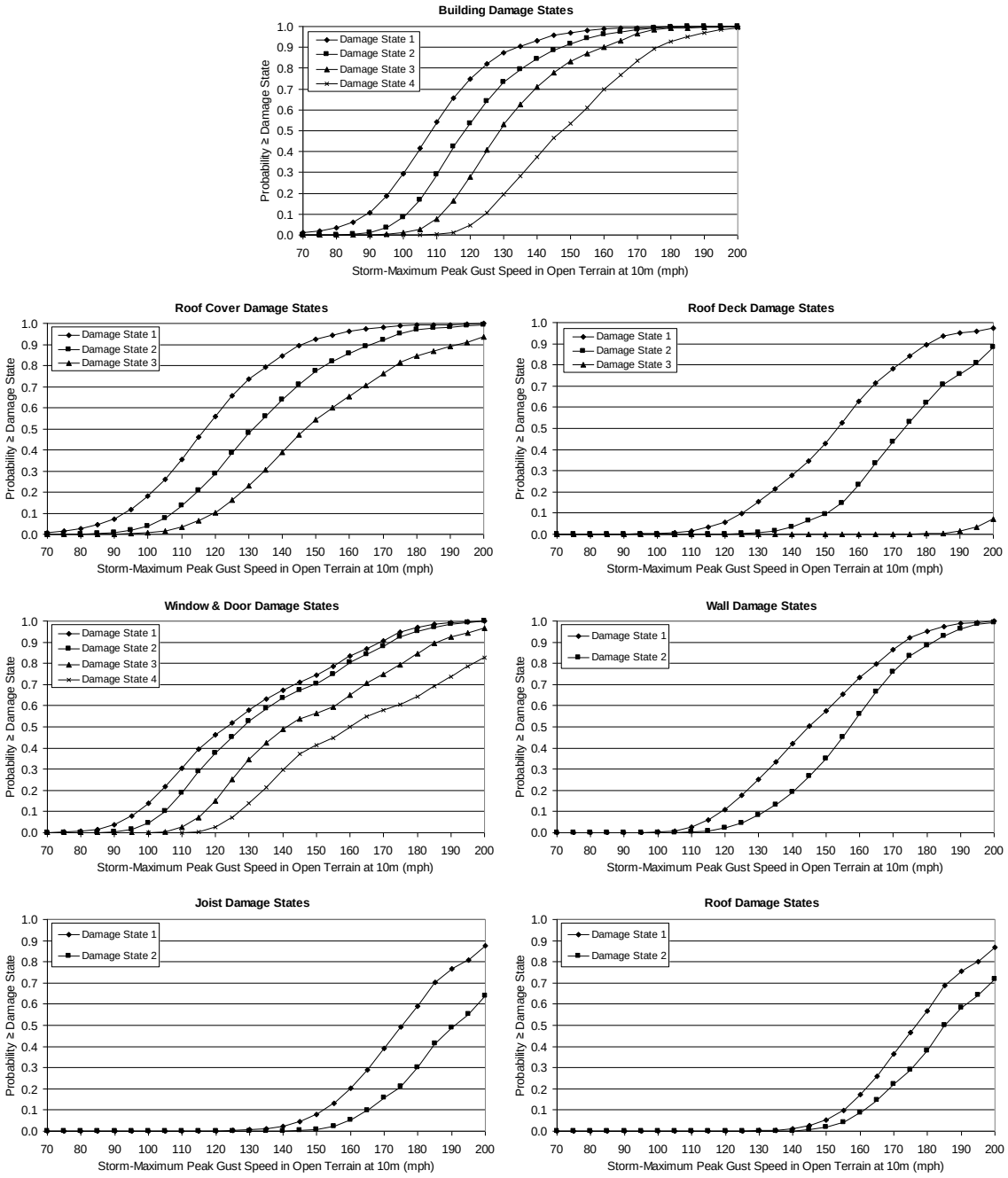

Figure D.42. Damage States vs. Peak Gust Wind Speed – Strip Mall Building C – Height=20′, No. of Units=6, Joist Spacing=6′, Metal Deck Screwed to Joists, SBCCI 100 mph Design Criteria, Built-up Roof Cover, Unreinforced Masonry Walls, Missile Environment A, z_0=0.35 m.

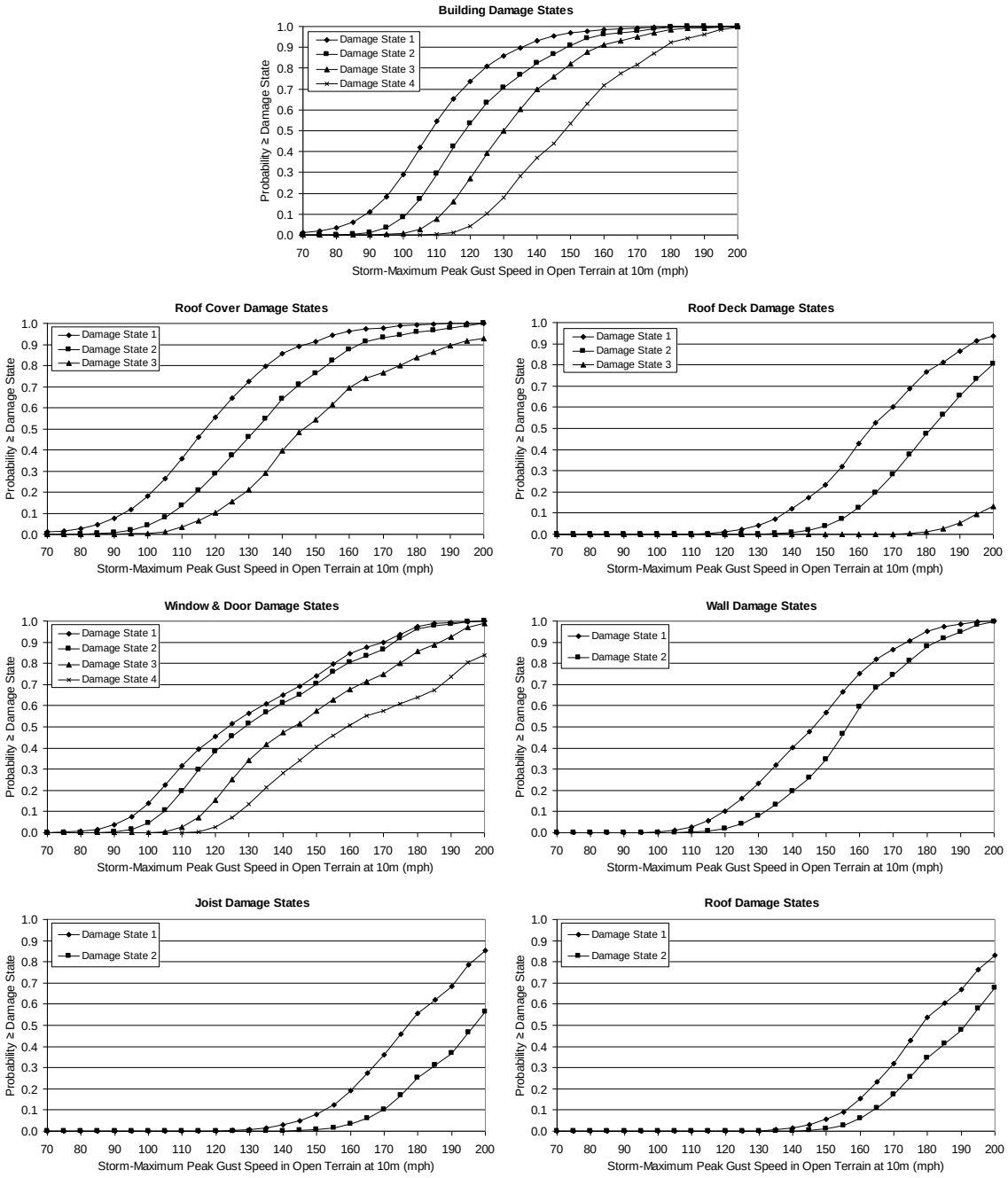

Figure D.43. Damage States vs. Peak Gust Wind Speed – Strip Mall Building C – Height=20′, No. of Units=6, Joist Spacing=6′, Metal Deck Welded to Joists, ASCE 100 mph Design Criteria, Built-up Roof Cover, Unreinforced Masonry Walls, Missile Environment A, z_0=0.35 m.

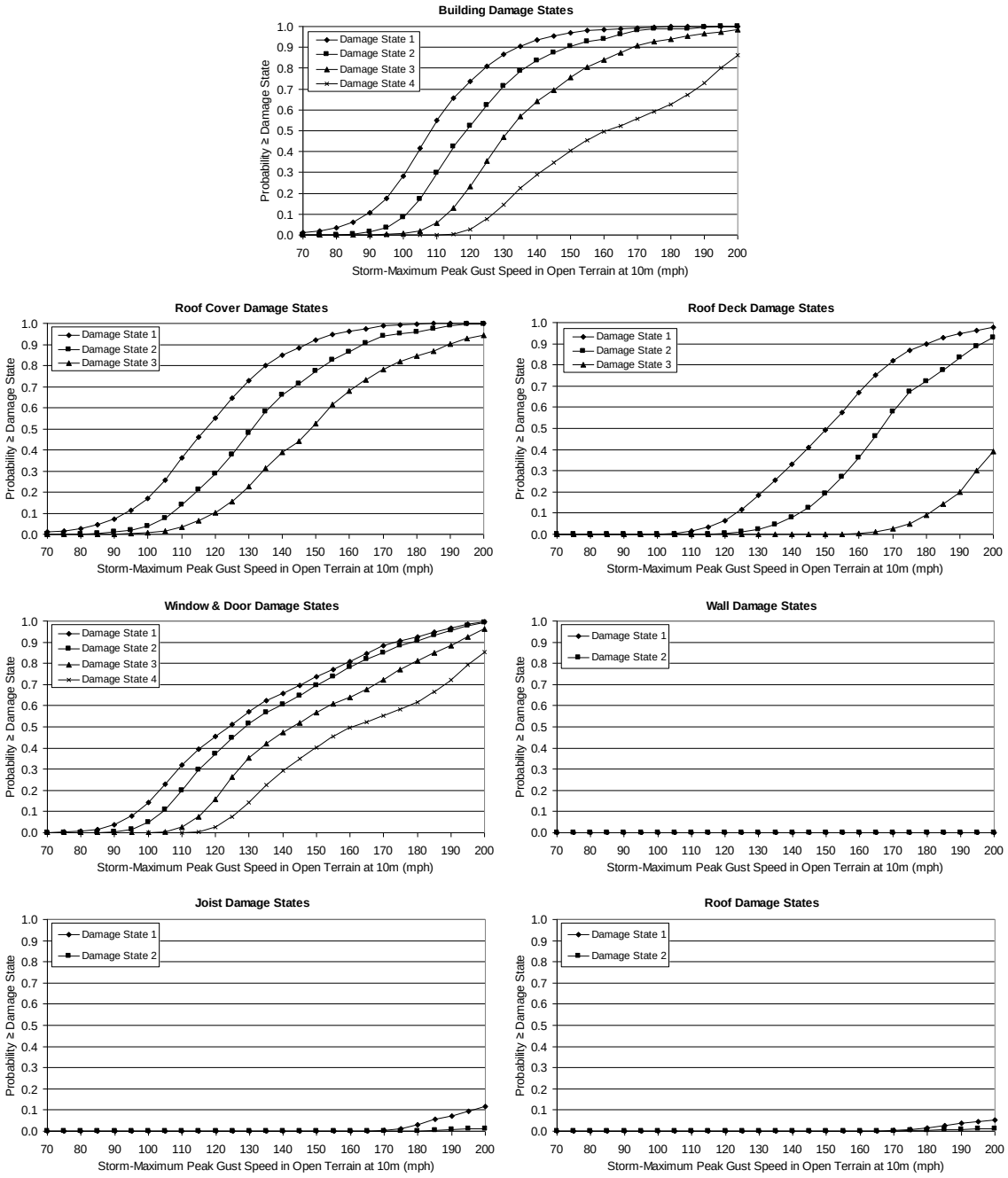

Figure D.44. Damage States vs. Peak Gust Wind Speed – Strip Mall Building C – Height=20′, No. of Units=6, Joist Spacing=6′, Metal Deck Welded to Joists, SBCCI 100 mph Design Criteria, Built-up Roof Cover, Reinforced Masonry Walls, Missile Environment A, z_0=0.35 m.

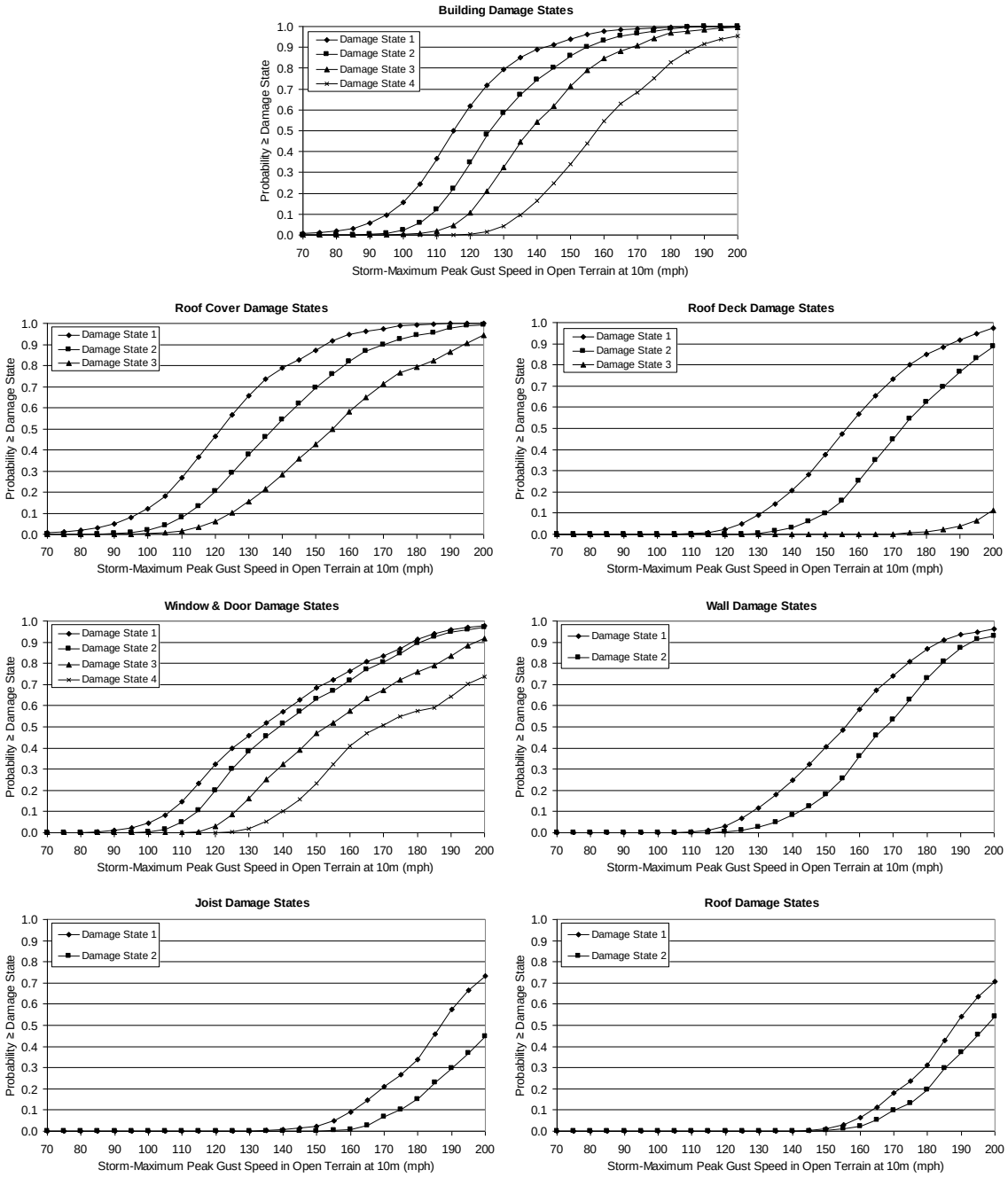

Figure D.45. Damage States vs. Peak Gust Wind Speed – Strip Mall Building C – Height=20′, No. of Units=6, Joist Spacing=6′, Metal Deck Welded to Joists, SBCCI 100 mph Design Criteria, Built-up Roof Cover, Unreinforced Masonry Walls, Missile Environment A, z_0=0.70 m.

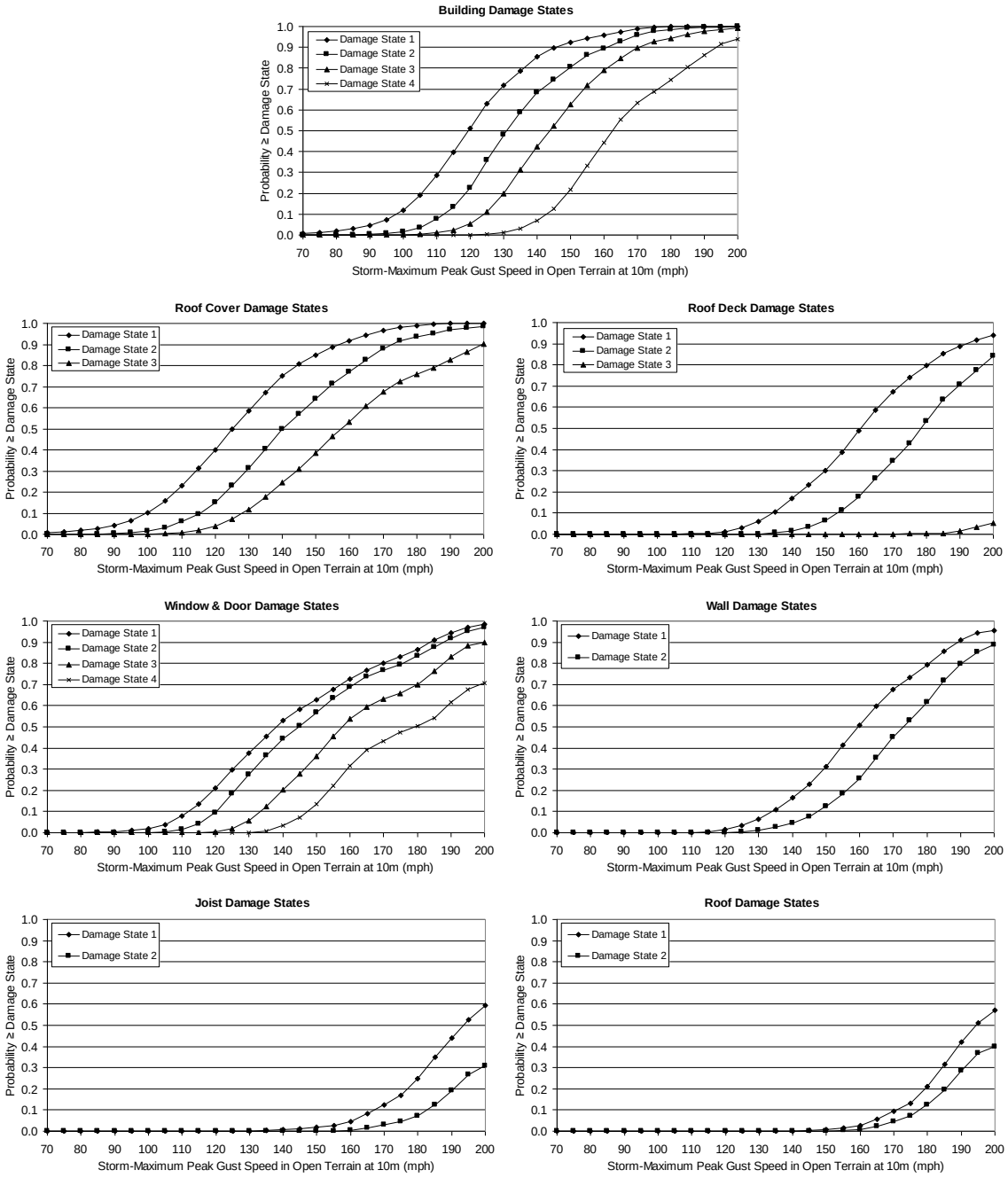

Figure D.46. Damage States vs. Peak Gust Wind Speed – Strip Mall Building C – Height=20′, No. of Units=6, Joist Spacing=6′, Metal Deck Welded to Joists, SBCCI 100 mph Design Criteria, Built-up Roof Cover, Unreinforced Masonry Walls, Missile Environment A, z_0=1.0 m.

Appendix E.
Damage State Functions for Pre-Engineered Metal Buildings

Appendix E
Damage State Functions for Pre-Engineered Metal Buildings

This appendix presents damage state curves for pre-engineered metal buildings. The damage state curves show the probability of achieving a certain damage state versus storm-maximum peak gust speed (open terrain at 10m above ground). Plots are presented for the overall building damage states and for the individual building component damage states (refer to Table 6.11-1 for damage state definitions).

As shown in Table E.1, two sets of five figures are given for the metal buildings. The first set of five figures (Figures E.1 through E.5) is for buildings located in an open terrain (z_0=0.03 m) and the second set (Figures E.6 through E.10) is for buildings situated in a typical suburban environment (z_0=0.35 m). The first figure in each set of five shows damage state results for the small metal building designed using a 100 mph design speed and with no reduction in the metal roof panel capacity. The remaining four plots in each set show damage state results for buildings which are different by a single variable in comparison to the reference building (note that the changed variable is underlined in the figure titles). Figures E.11 and E.12 show results of the reference building situated in two additional terrain environments (i.e., z_0=0.70 m and 1.0 m).

Table E.1. Damage State Functions for Pre-Engineered Metal Buildings

Figure	Model Building	Design Wind Speed	Metal Panel Capacity	Terrain
E.1	Small	100 mph	Full	0.03
E.2	**Medium**	100 mph	Full	0.03
E.3	**Large**	100 mph	Full	0.03
E.4	Small	**90 mph**	Full	0.03
E.5	Small	100 mph	**50%**	0.03
E.6	Small	100 mph	Full	**0.35**
E.7	**Medium**	100 mph	Full	0.35
E.8	**Large**	100 mph	Full	0.35
E.9	Small	**90 mph**	Full	0.35
E.10	Small	100 mph	**50%**	0.35
E.11	Small	100 mph	Full	**0.70**
E.12	Small	100 mph	Full	**1.00**

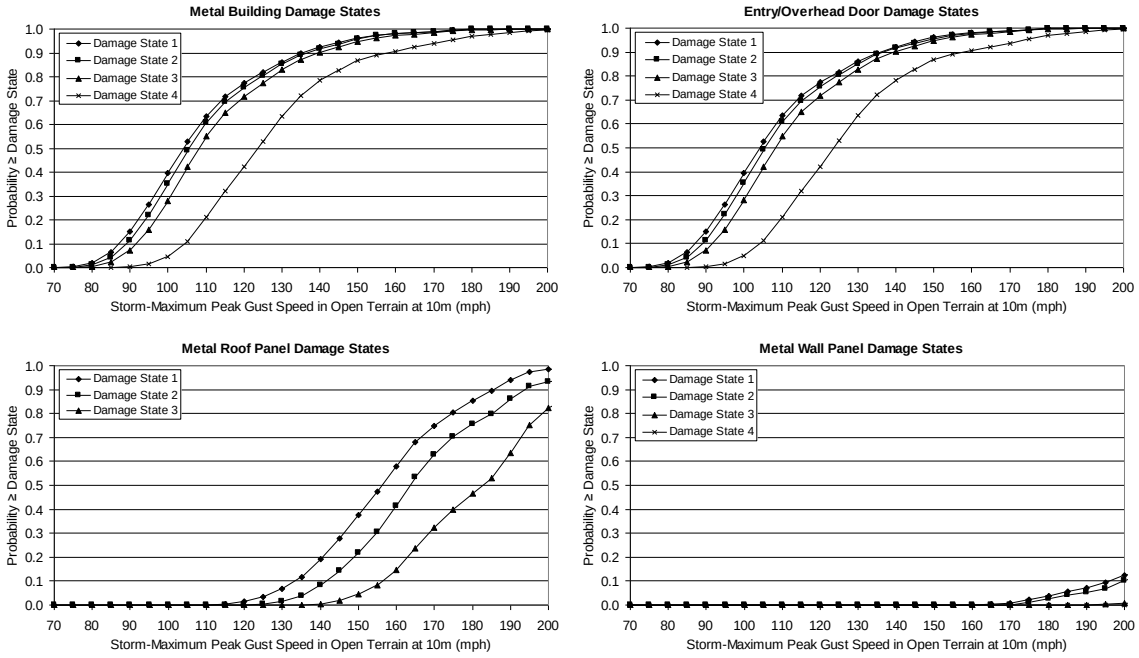

Figure E.1. Damage States vs. Peak Gust Wind Speed – Small Metal Building, 100 mph Design Speed, z_0=0.03 m, No Reduction in Metal Panel Capacity.

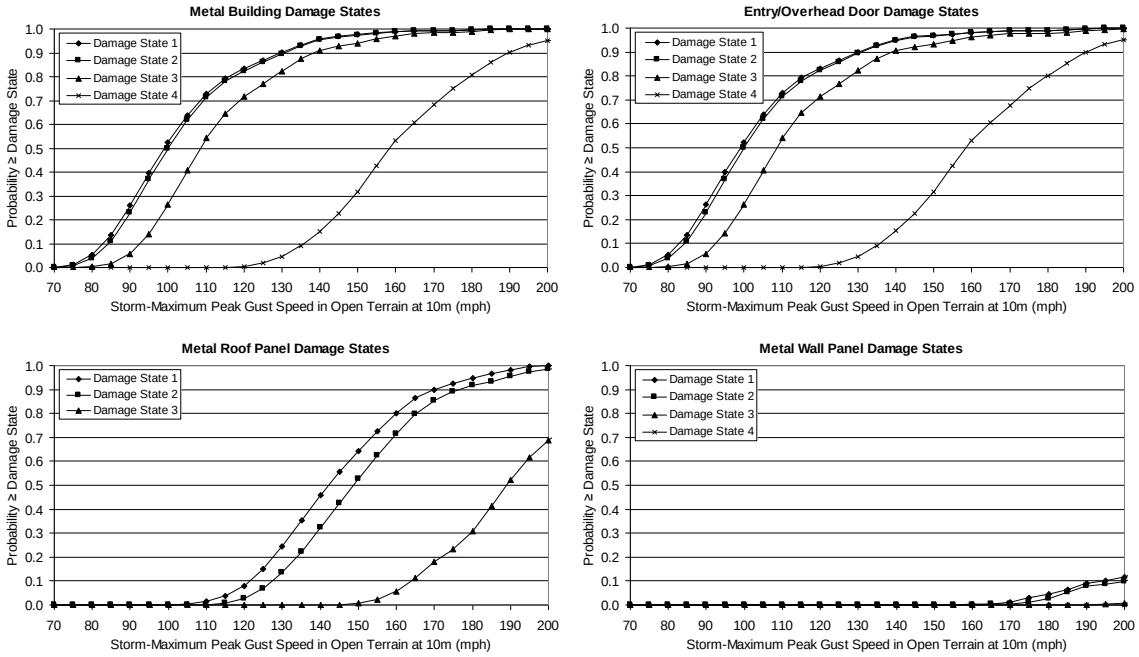

Figure E.2. Damage States vs. Peak Gust Wind Speed – <u>Medium-Sized Metal Building</u>, 100 mph Design Speed, z_0=0.03 m, No Reduction in Metal Panel Capacity..

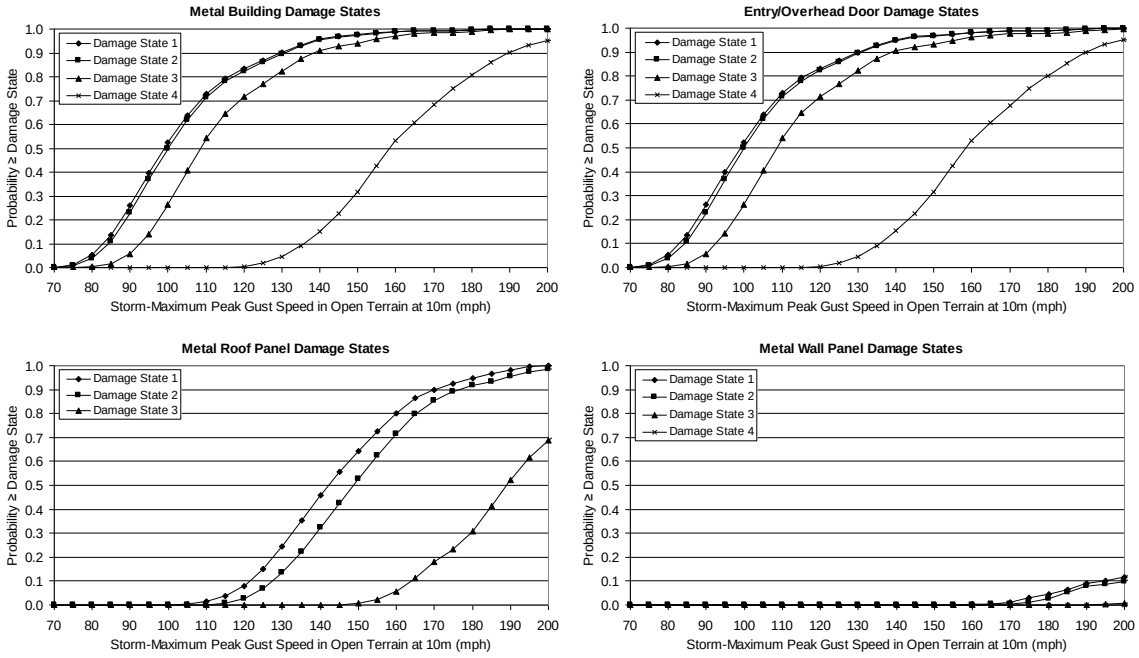

Figure E.3. Damage States vs. Peak Gust Wind Speed – <u>Large Metal Building</u>, 100 mph Design Speed, z_0=0.03 m, No Reduction in Metal Panel Capacity.

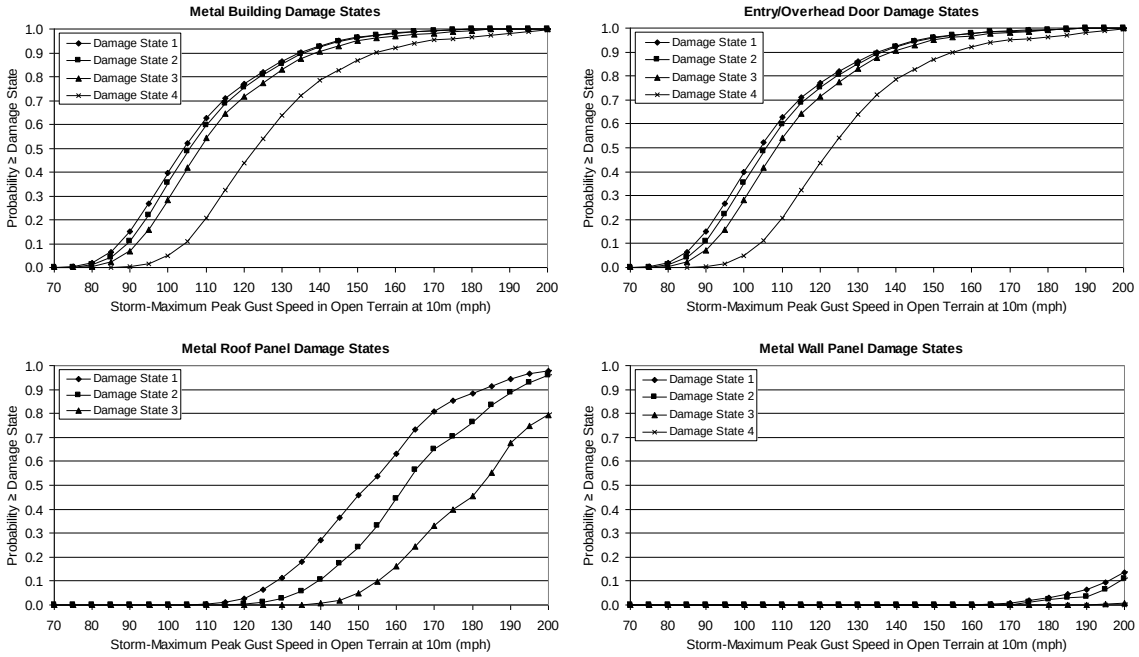

Figure E.4. Damage States vs. Peak Gust Wind Speed – Small Metal Building, <u>90 mph Design Speed</u>, z_0=0.03 m, No Reduction in Metal Panel Capacity.

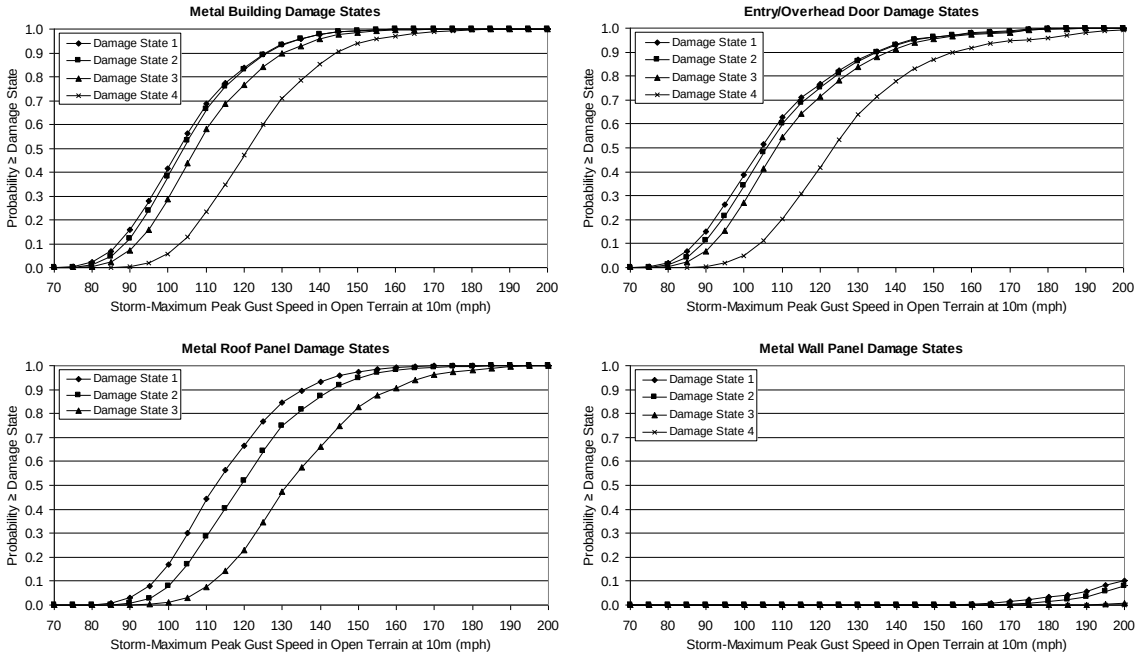

Figure E.5. Damage States vs. Peak Gust Wind Speed – Small Metal Building, 100 mph Design Speed, z_0=0.03 m, 50% Reduction in Metal Panel Capacity.

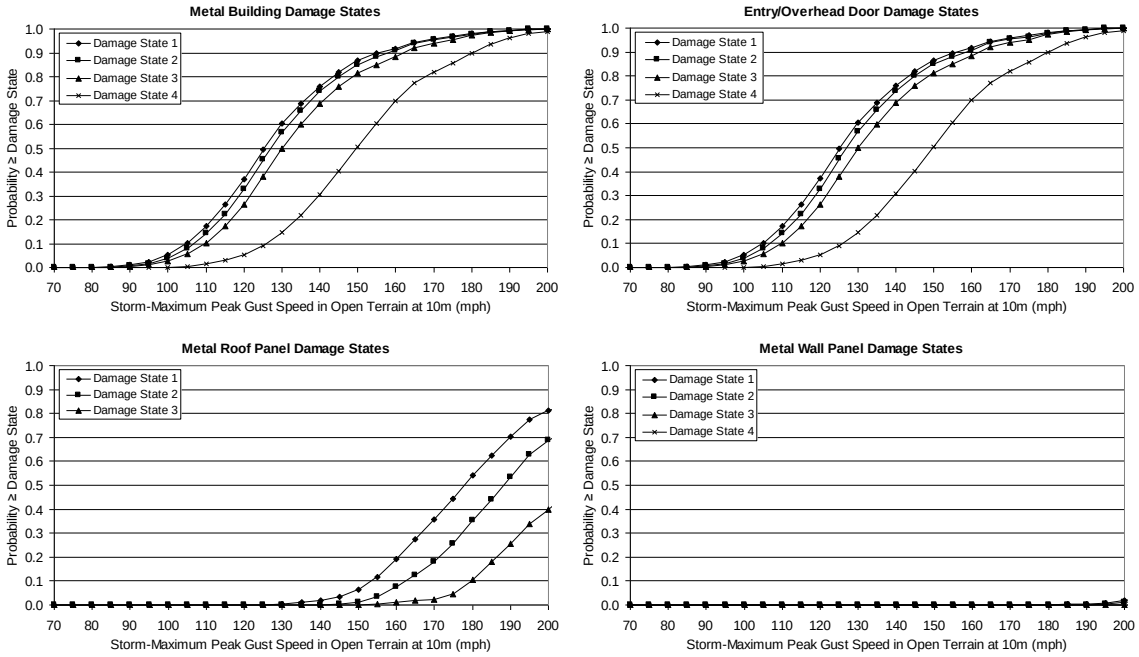

Figure E.6. Damage States vs. Peak Gust Wind Speed – Small Metal Building, 100 mph Design Speed, z_0=0.35 m, No Reduction in Metal Panel Capacity.

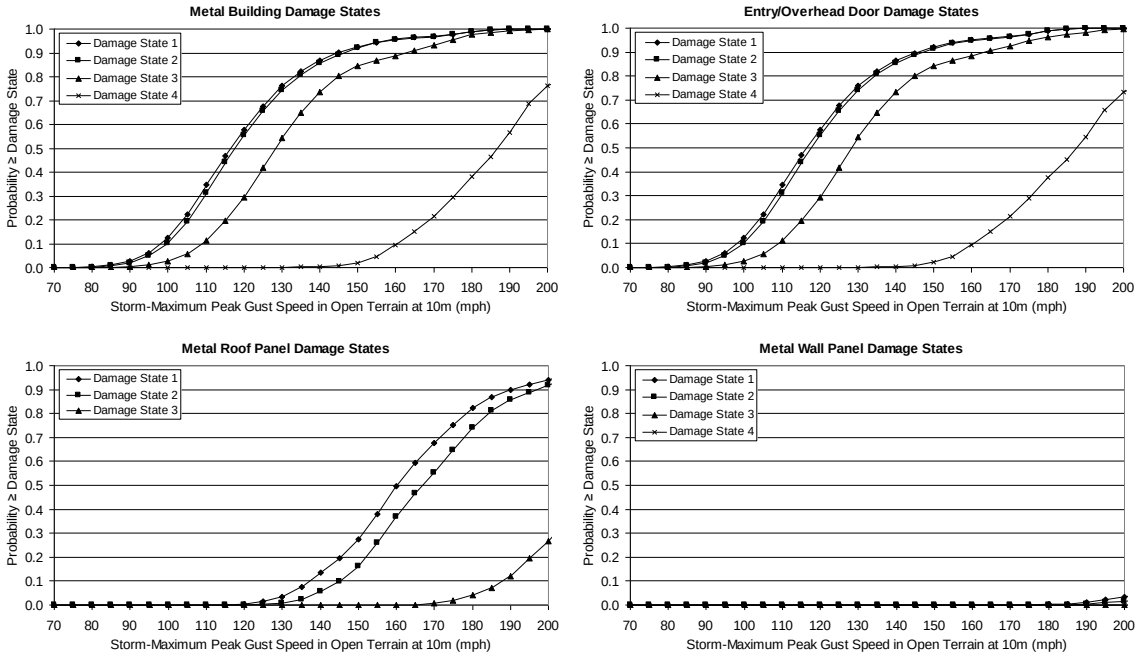

Figure E.7. Damage States vs. Peak Gust Wind Speed – Medium-Sized Metal Building, 100 mph Design Speed, z_0=0.35 m, No Reduction in Metal Panel Capacity.

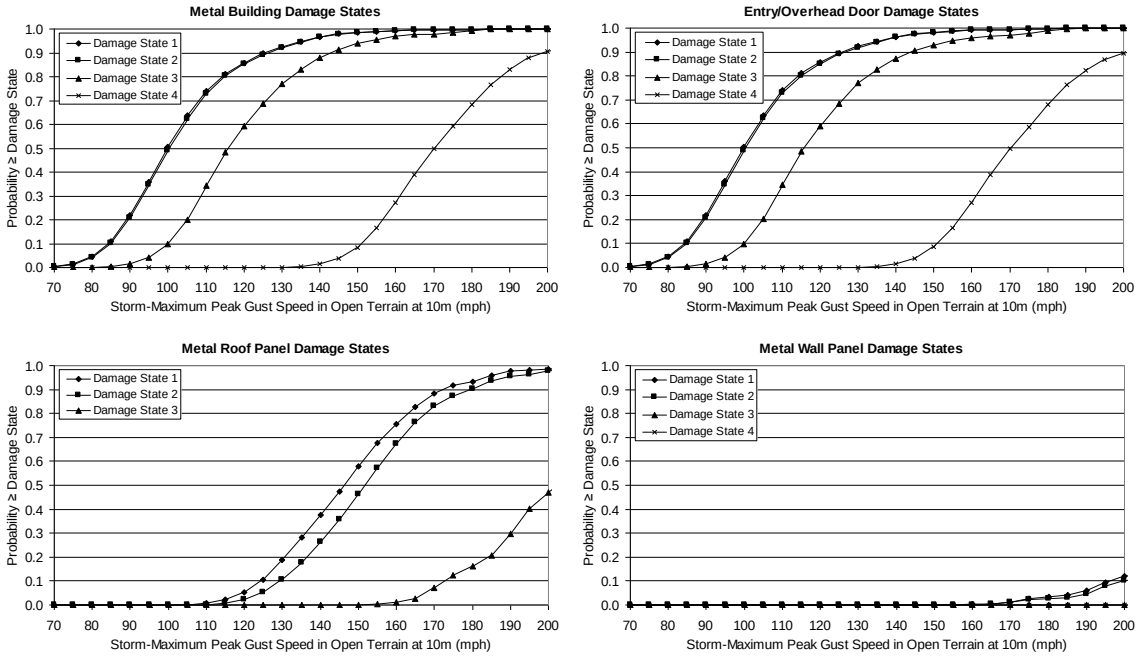

Figure E.8. Damage States vs. Peak Gust Wind Speed – Large Metal Building, 100 mph Design Speed, z_0=0.35 m, No Reduction in Metal Panel Capacity.

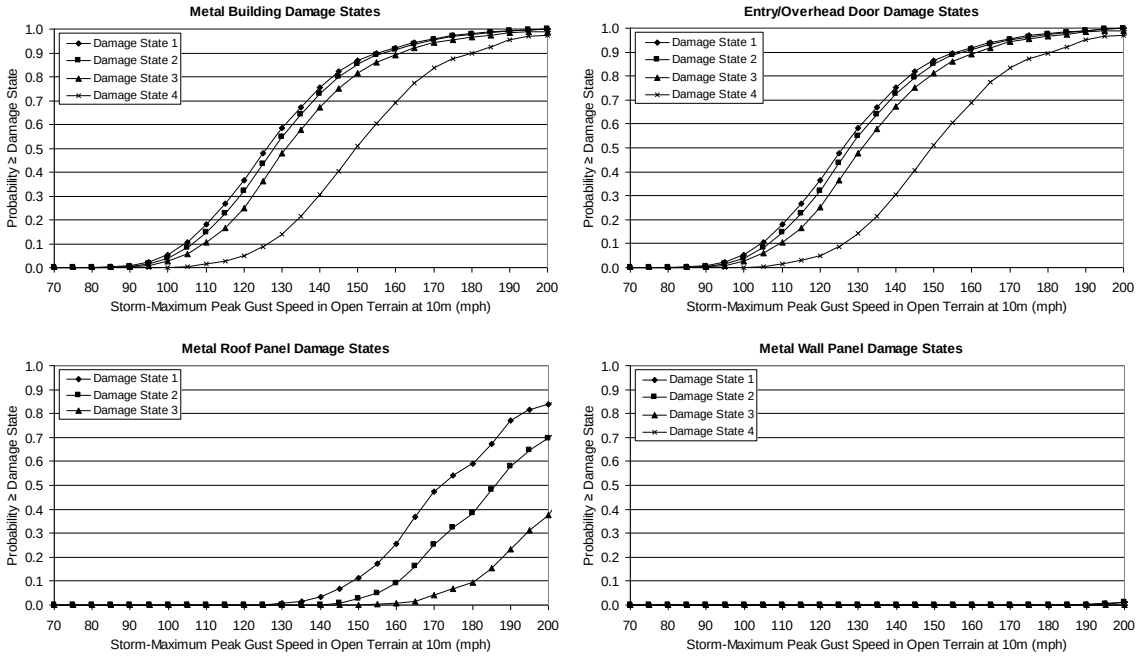

Figure E.9. Damage States vs. Peak Gust Wind Speed – Small Metal Building, 90 mph Design Speed, z_0=0.35 m, No Reduction in Metal Panel Capacity.

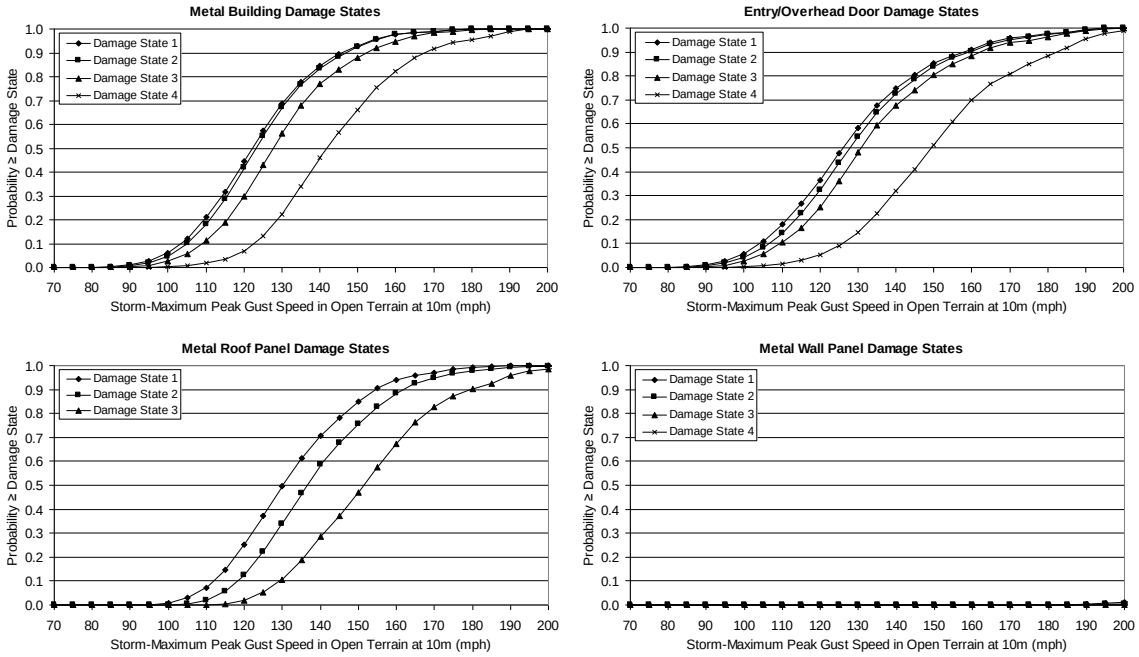

Figure E.10. Damage States vs. Peak Gust Wind Speed – Small Metal Building, 100 mph Design Speed, z_0=0.35 m, 50% Reduction in Metal Panel Capacity.

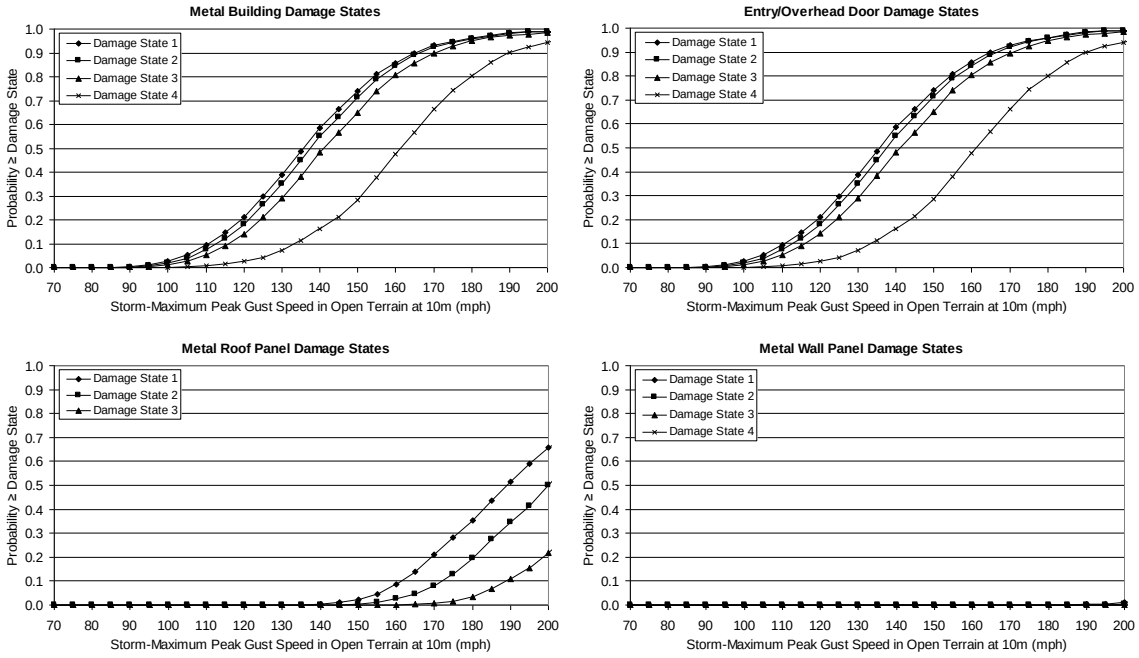

Figure E.11. Damage States vs. Peak Gust Wind Speed – Small Metal Building, 100 mph Design Speed, z_0=0.70 m, No Reduction in Metal Panel Capacity.

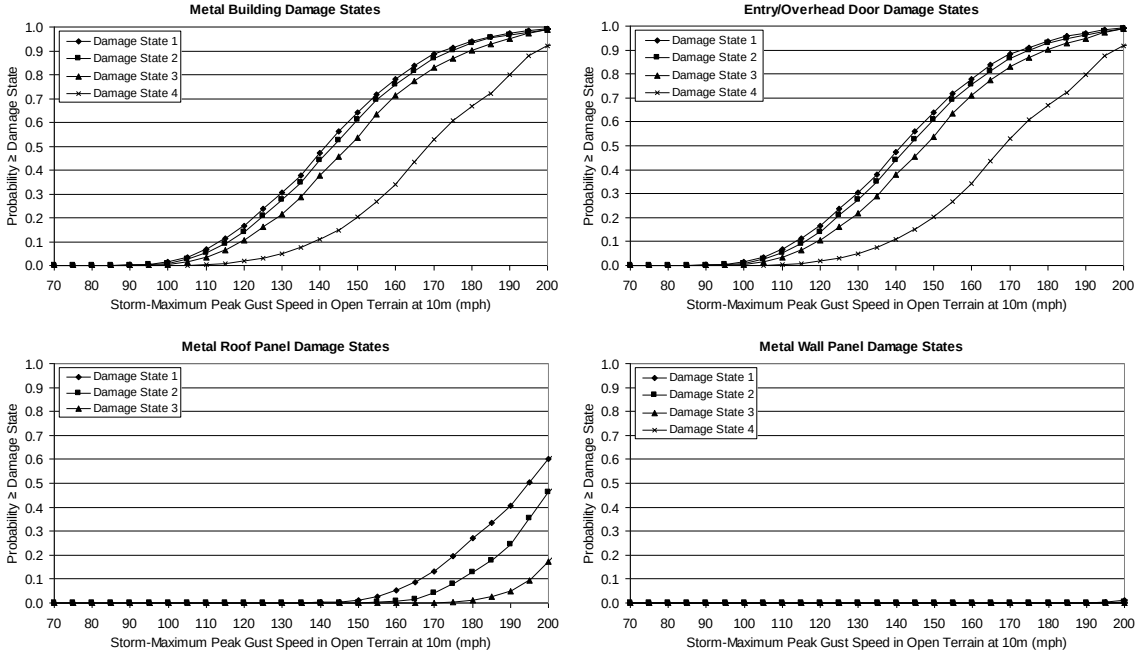

Figure E.12. Damage States vs. Peak Gust Wind Speed – Small Metal Building, 100 mph Design Speed, z_0=1.0 m, No Reduction in Metal Panel Capacity.

Appendix F.
Damage State Functions for Engineered Residential and Commercial Buildings

Appendix F.
Damage State Functions for Engineered Residential and Commercial Buildings

This appendix presents damage state curves for engineered residential and commercial buildings. The damage state curves show the probability of achieving a certain damage state versus storm-maximum peak gust speed (open terrain at 10m above ground). Plots are presented for the overall building damage states and for the individual building component damage states (refer to Table 6.12-1 for damage state definitions).

Table F.1 lists the figures provided in this appendix. Damage state plots for the two-, five- and eight-story buildings are given in Figures F.1 through F.18, F.19 through F.36 and F.37 through F.54, respectively. Two sets of eight figures are given for each of the two-, five- and eight-story engineered buildings. The first set of eight figures are for buildings located in an open terrain (z_0=0.03 m) and the second set are for buildings situated in a typical suburban environment (z_0=0.35 m). The first figure in each set of eight shows damage state results for the engineered residential building having 33% glazing coverage, a built-up roof cover and situated in Missile Environment A. The remaining seven plots in each set show damage state results for buildings which are different by a single variable in comparison to the reference building (note that the changed variable is underlined in the figure titles). The last two figures associated with the two-, five- and eight-story engineered buildings show results of the reference building situated in two additional terrain environments (i.e., z_0=0.70 m and 1.0 m).

Table F.1. Sample Damage State Functions for Engineered Residential and Commercial Buildings

Figure	Stories	Occupancy	Roof Cover	Glazing	Missile Environ.	Terrain
F.1	2	Residential	BUR	33%	A	0.03
F.2	2	Residential	BUR	**20%**	A	0.03
F.3	2	Residential	BUR	**50%**	A	0.03
F.4	2	Residential	**SPM**	33%	A	0.03
F.5	2	Residential	BUR	33%	**B**	0.03
F.6	2	Residential	BUR	33%	**C**	0.03
F.7	2	Residential	BUR	33%	**D**	0.03
F.8	2	**Commercial**	BUR	33%	A	0.03
F.9	2	Residential	BUR	33%	A	**0.35**
F.10	2	Residential	BUR	**20%**	A	0.35
F.11	2	Residential	BUR	**50%**	A	0.35
F.12	2	Residential	**SPM**	33%	A	0.35
F.13	2	Residential	BUR	33%	**B**	0.35
F.14	2	Residential	BUR	33%	**C**	0.35
F.15	2	Residential	BUR	33%	**D**	0.35
F.16	2	**Commercial**	BUR	33%	A	0.35
F.17	2	Residential	BUR	33%	A	**0.70**

Table F.1. Sample Damage State Functions for Engineered Residential and Commercial Buildings (concluded)

Figure	Stories	Occupancy	Roof Cover	Glazing	Missile Environ.	Terrain
F.18	2	Residential	BUR	33%	A	**1.00**
F.19	**5**	Residential	BUR	33%	A	0.03
F.20	5	Residential	BUR	**20%**	A	0.03
F.21	5	Residential	BUR	**50%**	A	0.03
F.22	5	Residential	**SPM**	33%	A	0.03
F.23	5	Residential	BUR	33%	**B**	0.03
F.24	5	Residential	BUR	33%	**C**	0.03
F.25	5	Residential	BUR	33%	**D**	0.03
F.26	5	**Commercial**	BUR	33%	A	0.03
F.27	5	Residential	BUR	33%	A	**0.35**
F.28	5	Residential	BUR	**20%**	A	0.35
F.29	5	Residential	BUR	**50%**	A	0.35
F.30	5	Residential	**SPM**	33%	A	0.35
F.31	5	Residential	BUR	33%	**B**	0.35
F.32	5	Residential	BUR	33%	**C**	0.35
F.33	5	Residential	BUR	33%	**D**	0.35
F.34	5	**Commercial**	BUR	33%	A	0.35
F.35	5	Residential	BUR	33%	A	**0.70**
F.36	5	Residential	BUR	33%	A	**1.00**
F.37	**8**	Residential	BUR	33%	A	0.03
F.38	8	Residential	BUR	**20%**	A	0.03
F.39	8	Residential	BUR	**50%**	A	0.03
F.40	8	Residential	**SPM**	33%	A	0.03
F.41	8	Residential	BUR	33%	**B**	0.03
F.42	8	Residential	BUR	33%	**C**	0.03
F.43	8	Residential	BUR	33%	**D**	0.03
F.44	8	**Commercial**	BUR	33%	A	0.03
F.45	8	Residential	BUR	33%	A	**0.35**
F.46	8	Residential	BUR	**20%**	A	0.35
F.47	8	Residential	BUR	**50%**	A	0.35
F.48	8	Residential	**SPM**	33%	A	0.35
F.49	8	Residential	BUR	33%	**B**	0.35
F.50	8	Residential	BUR	33%	**C**	0.35
F.51	8	Residential	BUR	33%	**D**	0.35
F.52	8	**Commercial**	BUR	33%	A	0.35
F.53	8	Residential	BUR	33%	A	**0.70**
F.54	8	Residential	BUR	33%	A	**1.00**

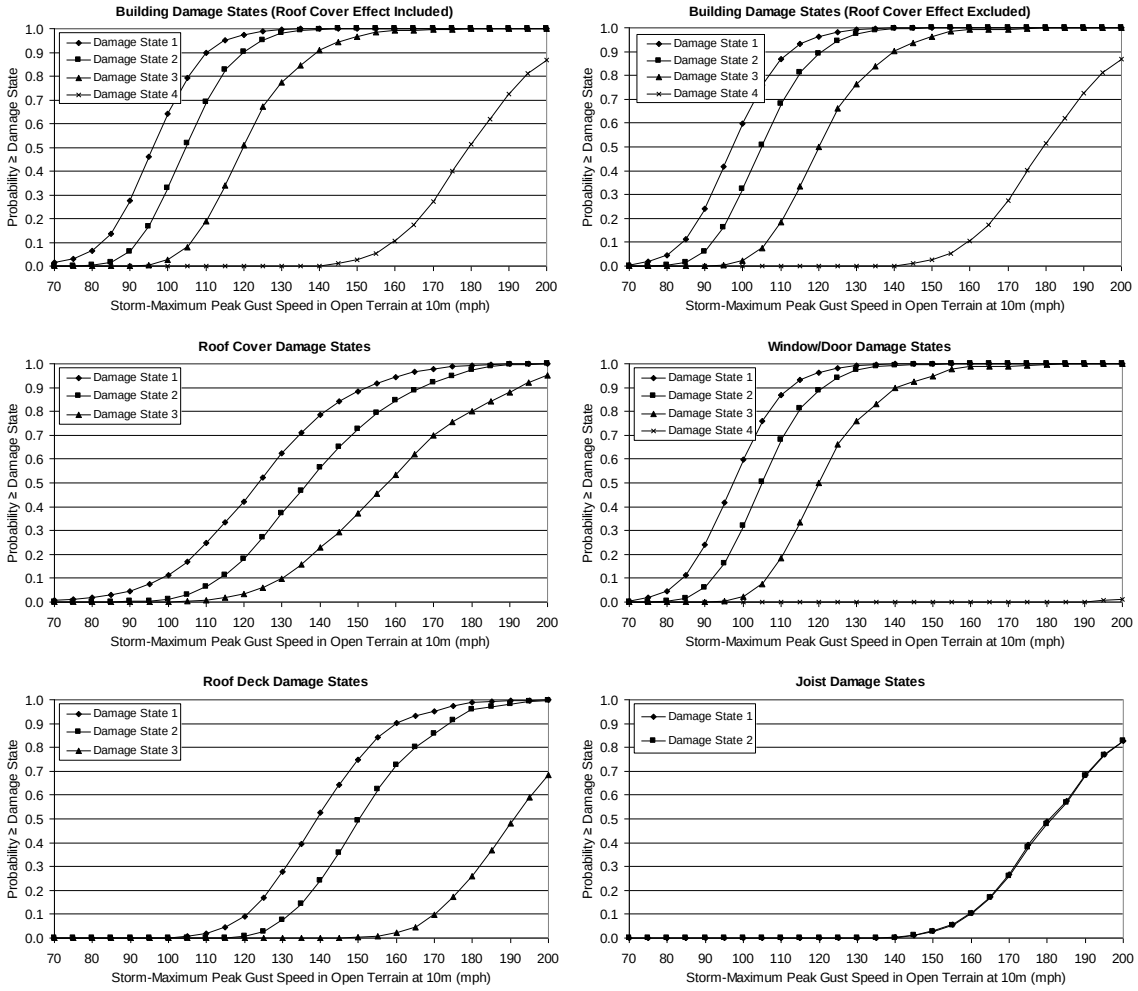

Figure F.1. Damage States vs. Peak Gust Wind Speed – Two-Story Engineered Residential Building – Built-up Roof Cover, 33% Glazing Coverage, Missile Environment A, z_0=0.03 m.

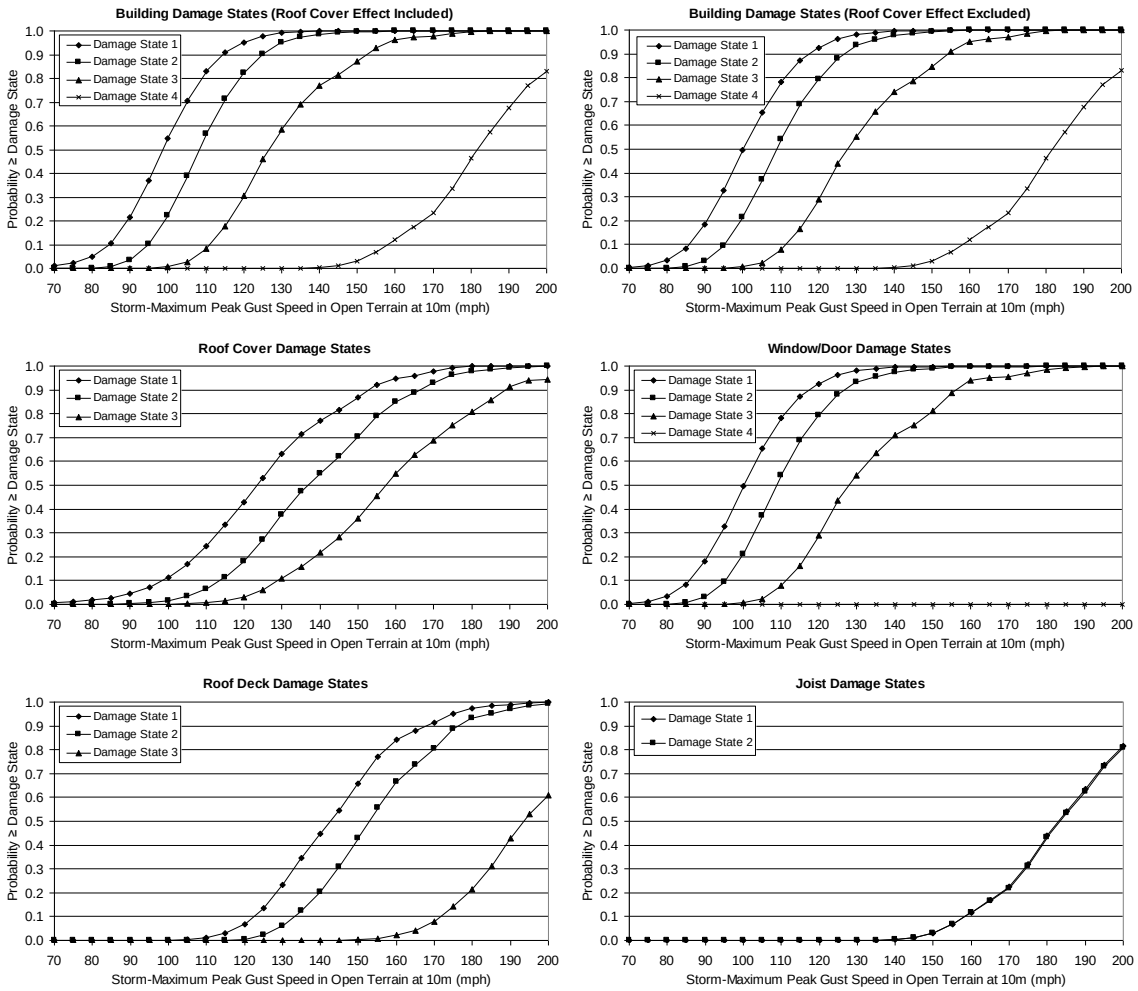

Figure F.2. Damage States vs. Peak Gust Wind Speed – Two-Story Engineered Residential Building – Built-up Roof Cover, 20% Glazing Coverage, Missile Environment A, z_0=0.03 m.

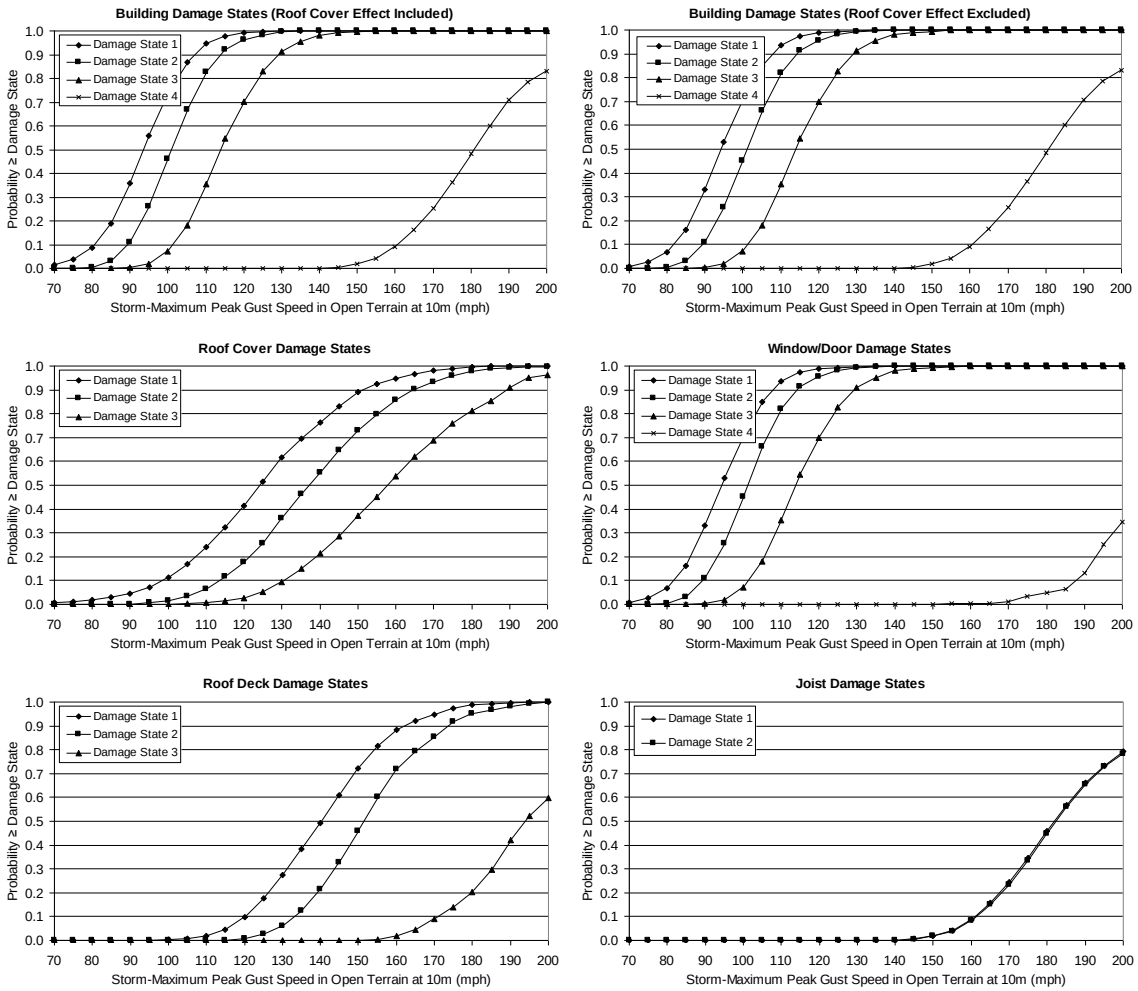

Figure F.3. Damage States vs. Peak Gust Wind Speed – Two-Story Engineered Residential Building – Built-up Roof Cover, 50% Glazing Coverage, Missile Environment A, z_0=0.03 m.

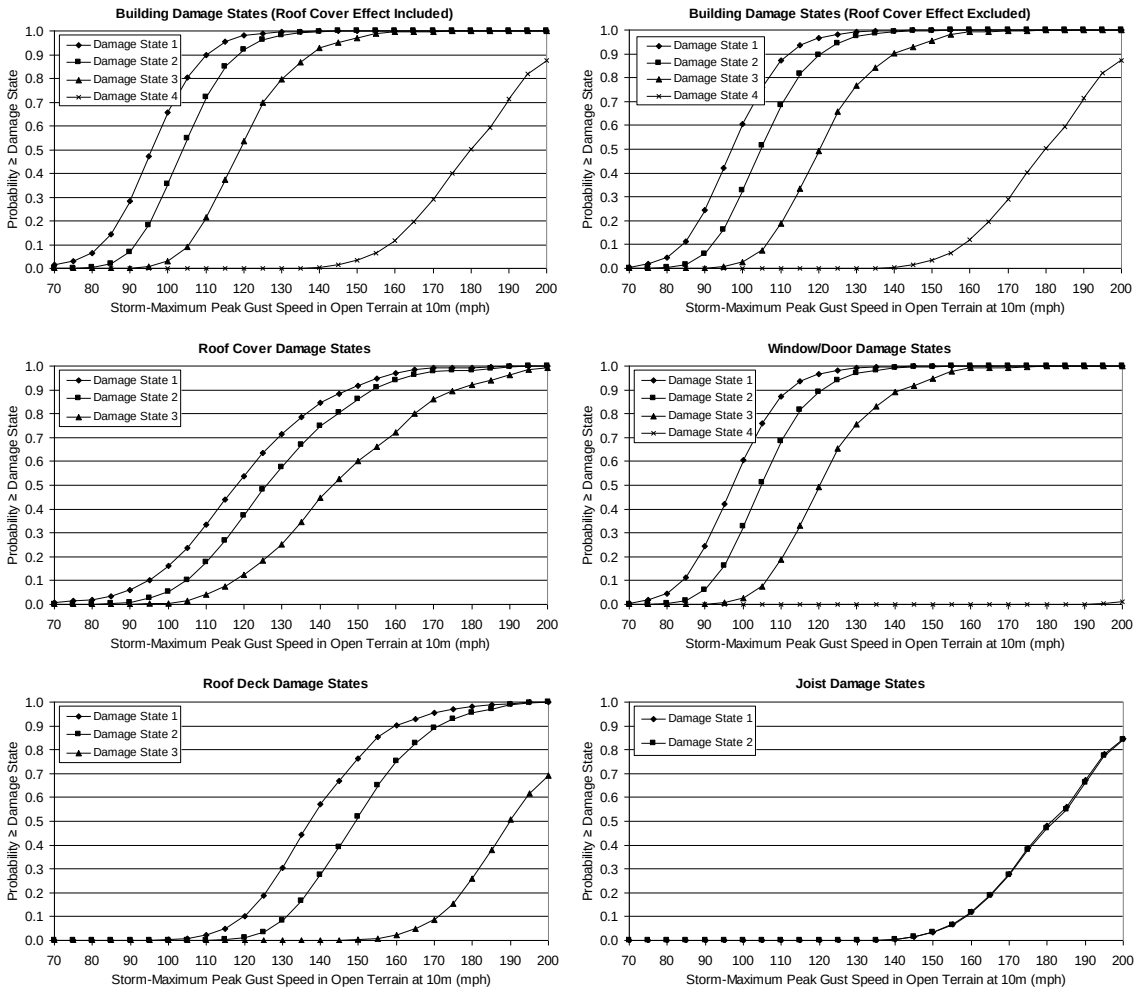

Figure F.4. Damage States vs. Peak Gust Wind Speed – Two-Story Engineered Residential Building – <u>Single Ply Membrane Roof Cover</u>, 33% Glazing Coverage, Missile Environment A, z_0=0.03 m.

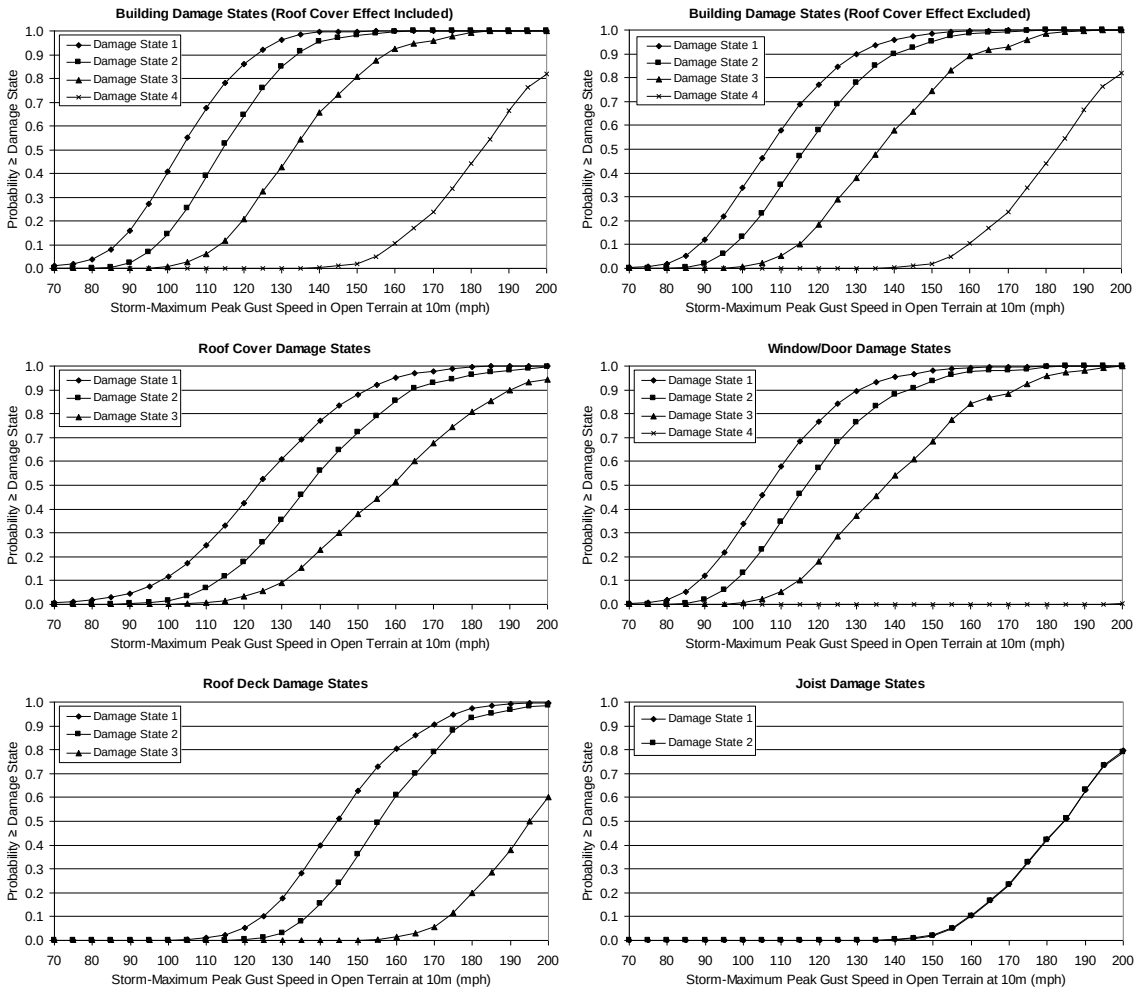

Figure F.5. Damage States vs. Peak Gust Wind Speed – Two-Story Engineered Residential Building – Built-up Roof Cover, 33% Glazing Coverage, <u>Missile Environment B</u>, z_0=0.03 m.

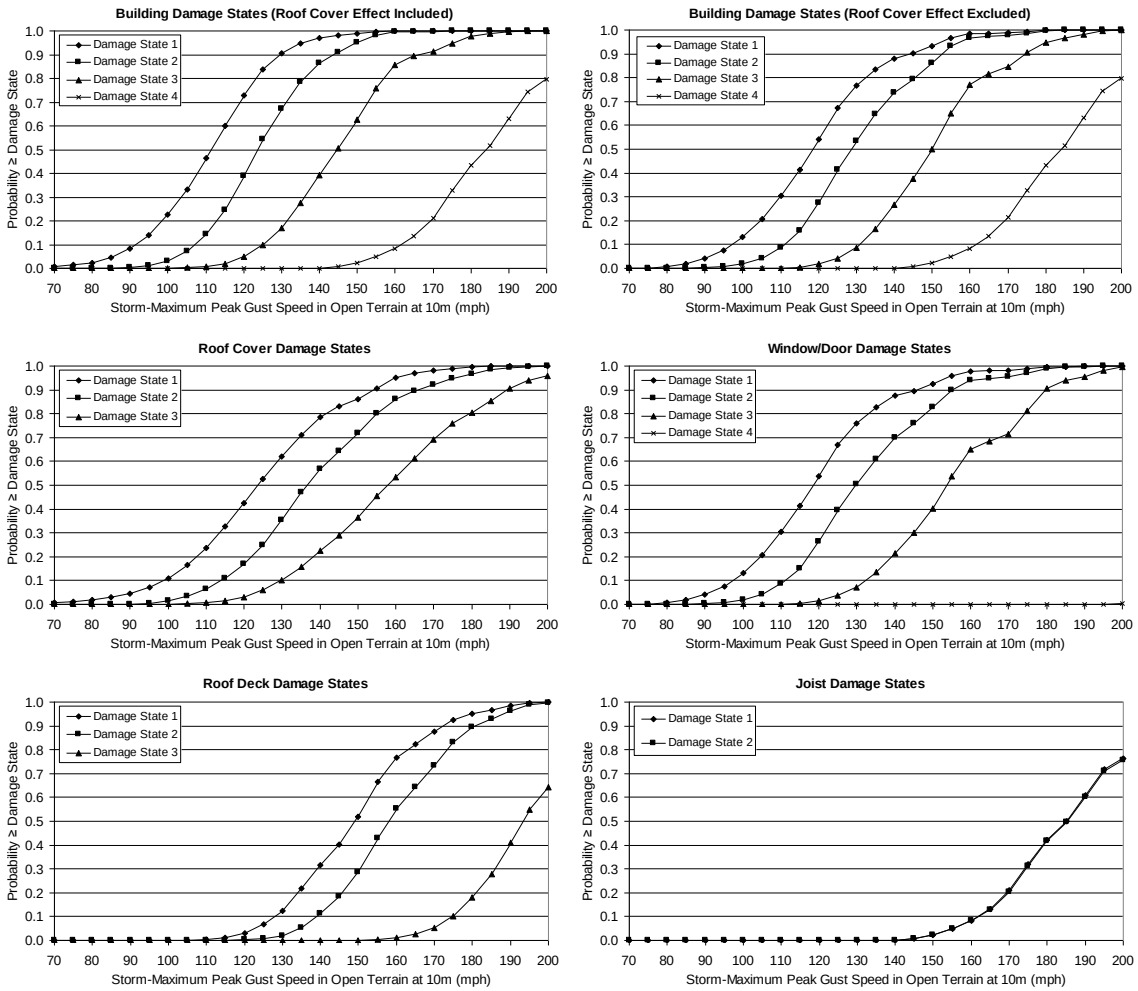

Figure F.6. Damage States vs. Peak Gust Wind Speed – Two-Story Engineered Residential Building – Built-up Roof Cover, 33% Glazing Coverage, Missile Environment C, z_0=0.03 m.

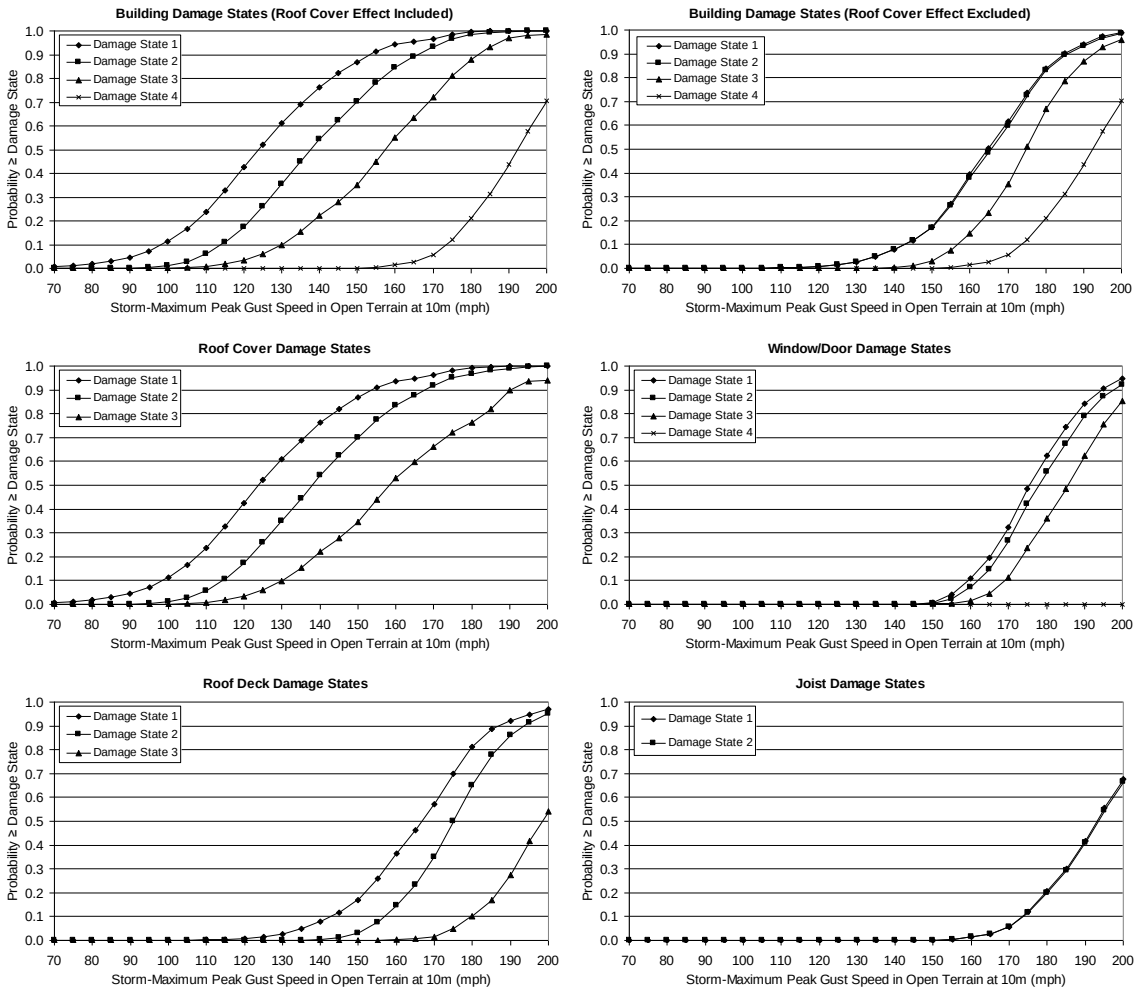

Figure F.7. Damage States vs. Peak Gust Wind Speed – Two-Story Engineered Residential Building – Built-up Roof Cover, 33% Glazing Coverage, <u>Missile Environment D</u>, z_0=0.03 m.

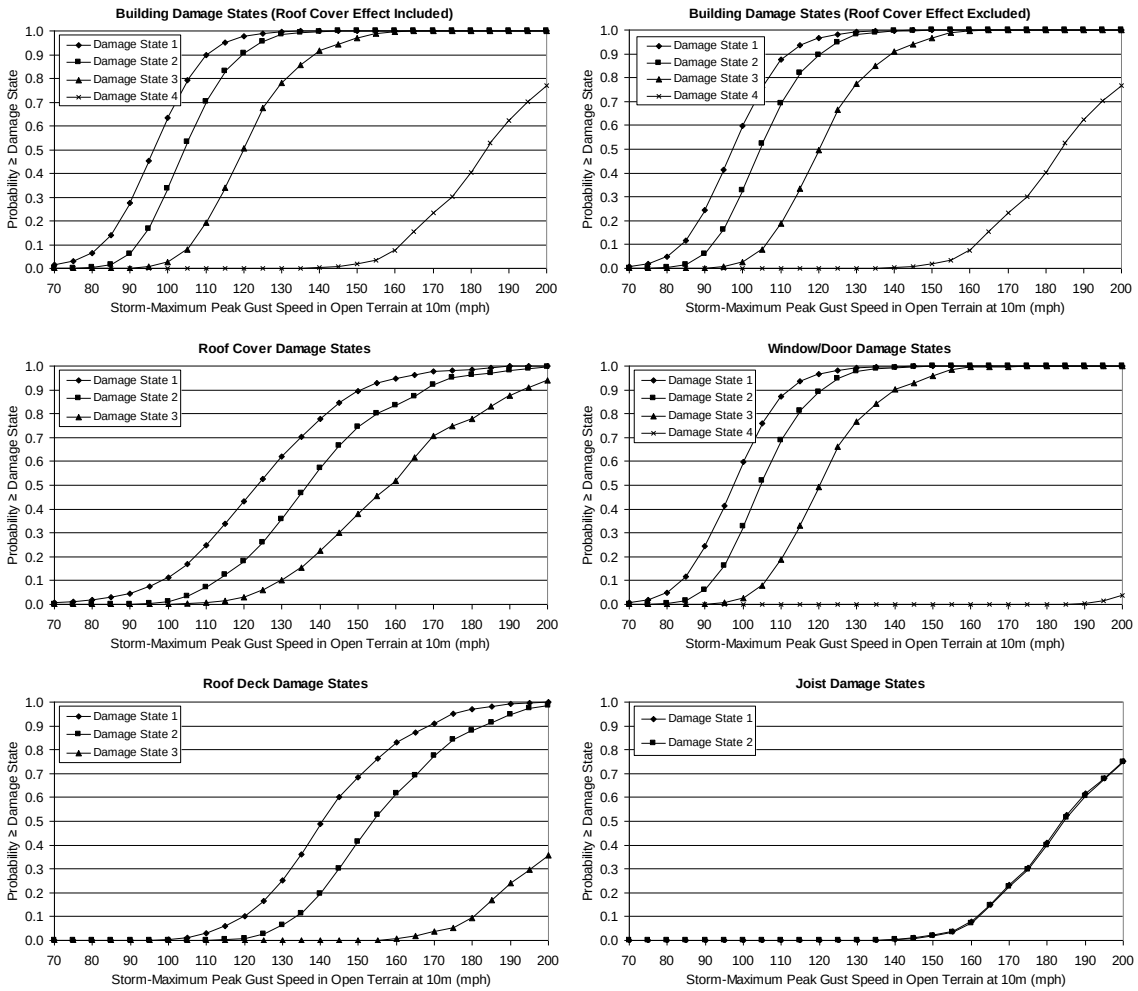

Figure F.8. Damage States vs. Peak Gust Wind Speed – Two-Story Engineered Commercial Building – Built-up Roof Cover, 33% Glazing Coverage, Missile Environment A, z_0 =0.03 m.

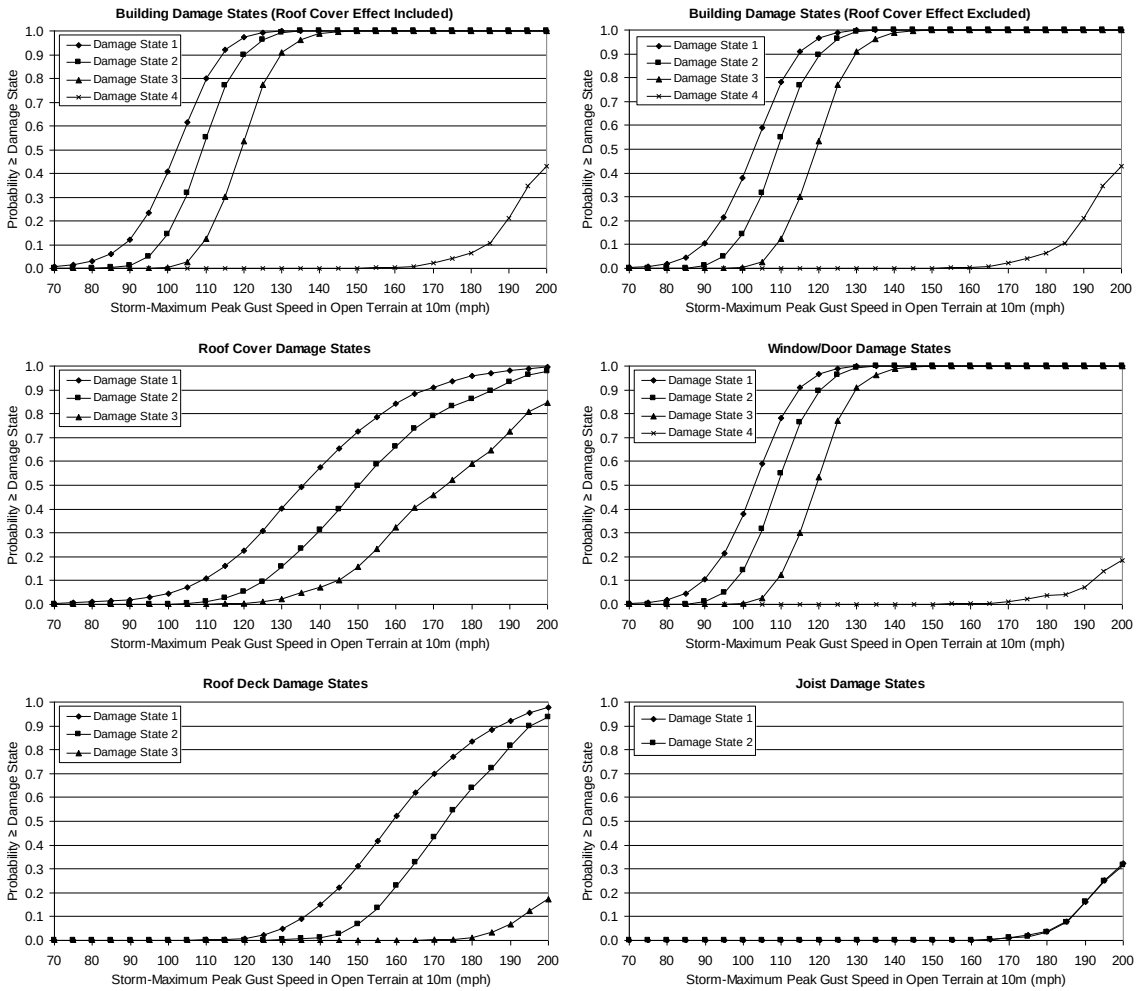

Figure F.9. Damage States vs. Peak Gust Wind Speed – Two-Story Engineered Residential Building – Built-up Roof Cover, 33% Glazing Coverage, Missile Environment A, z_0=0.35 m.

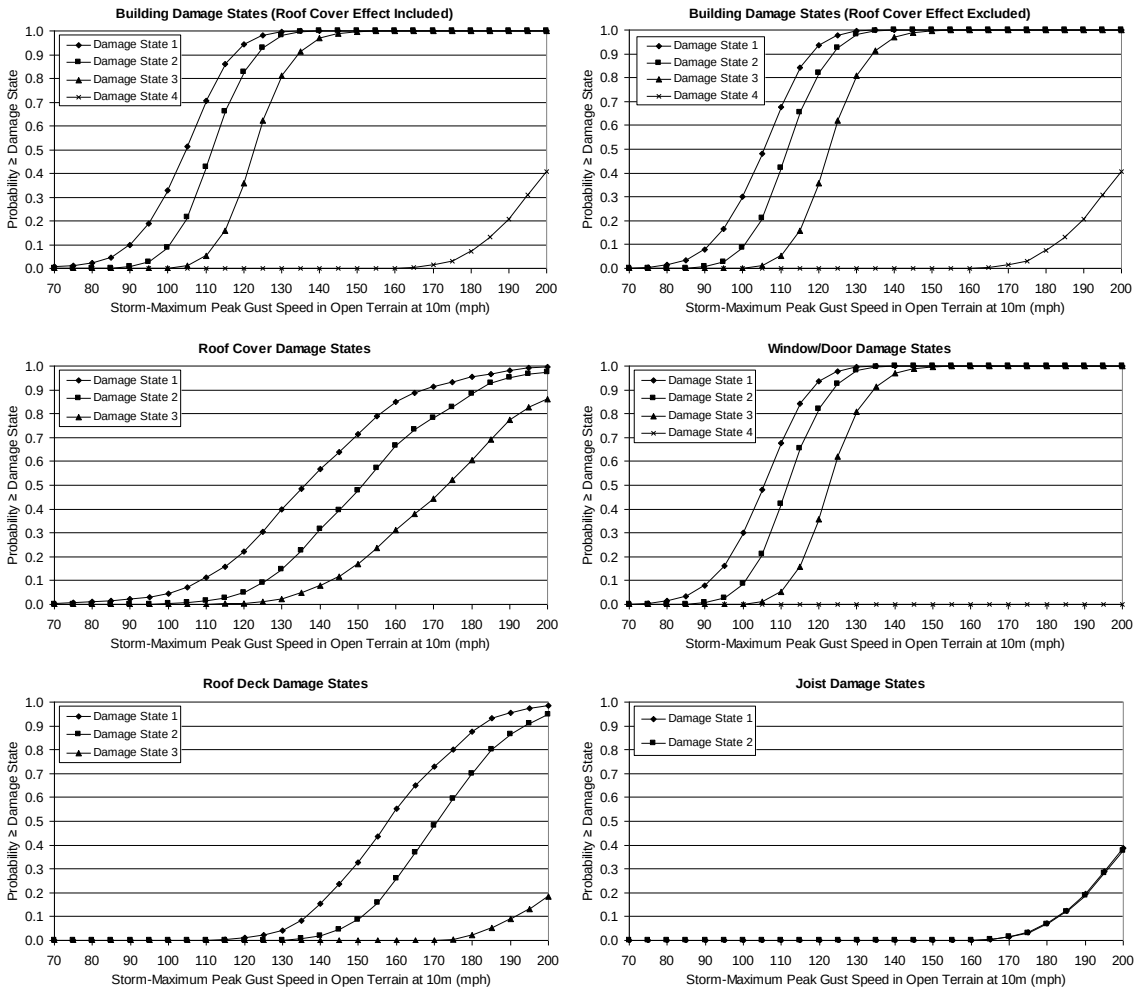

Figure F.10. Damage States vs. Peak Gust Wind Speed – Two-Story Engineered Residential Building – Built-up Roof Cover, 20% Glazing Coverage, Missile Environment A, z_0=0.35 m.

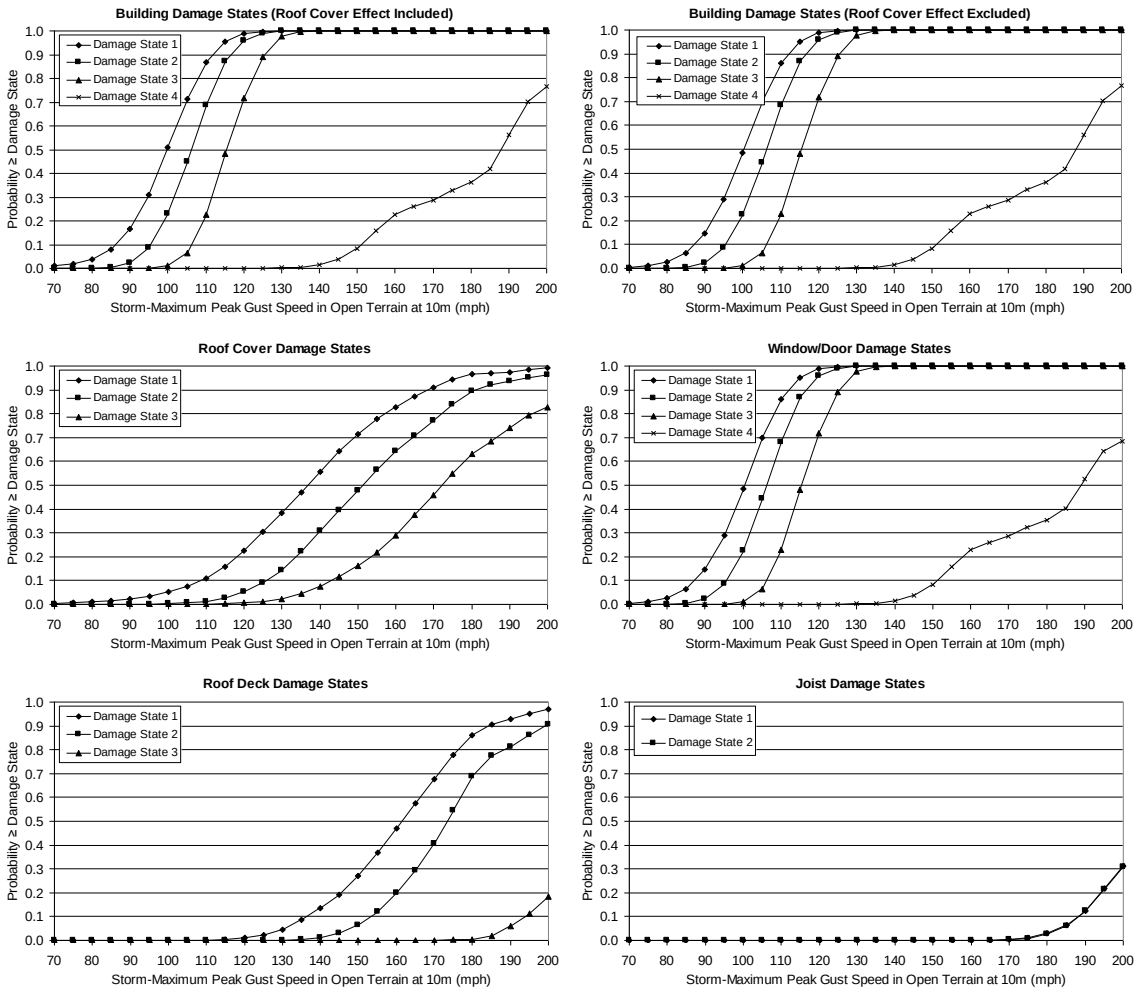

Figure F.11. Damage States vs. Peak Gust Wind Speed – Two-Story Engineered Residential Building – Built-up Roof Cover, 50% Glazing Coverage, Missile Environment A, z_0=0.35 m.

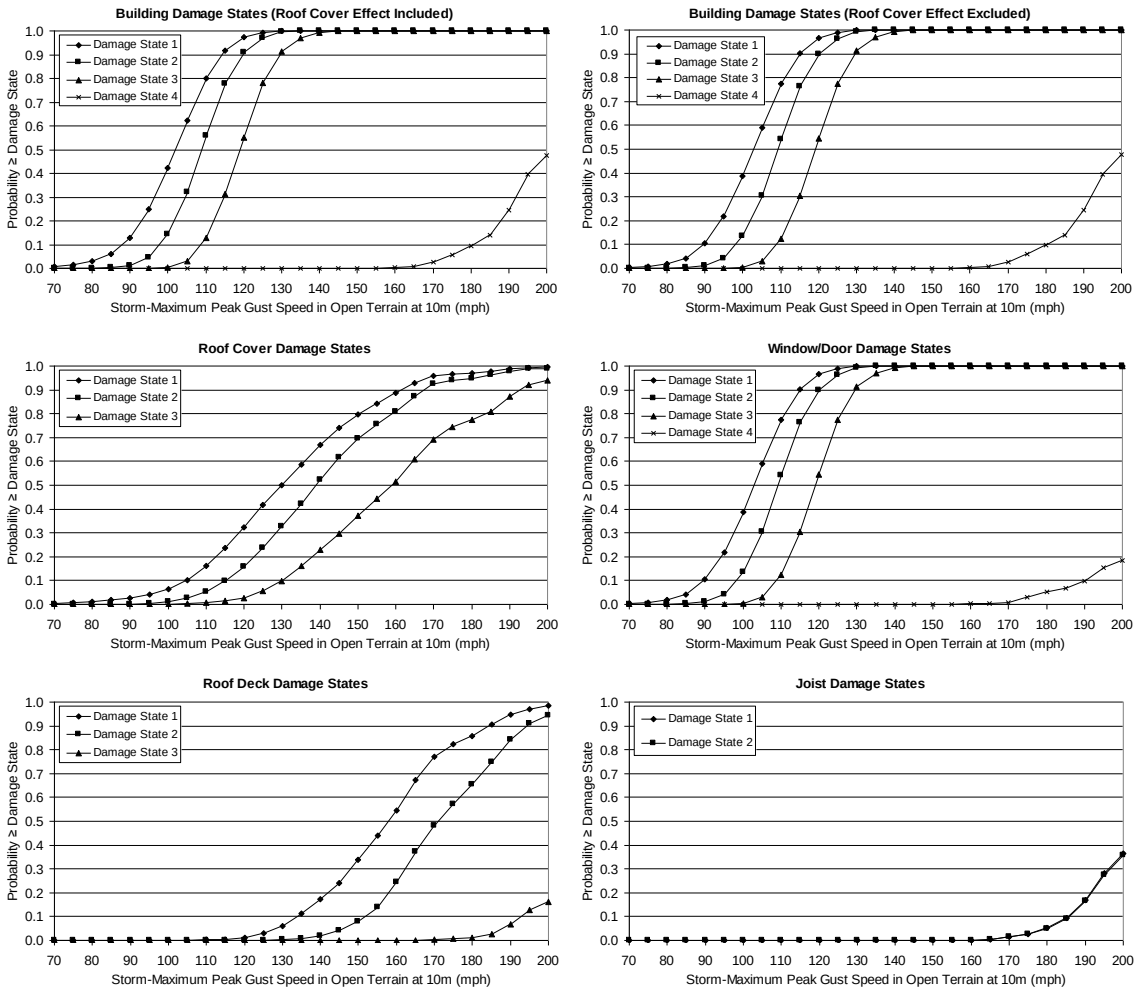

Figure F.12. Damage States vs. Peak Gust Wind Speed – Two-Story Engineered Residential Building – <u>Single Ply Membrane Roof Cover</u>, 33% Glazing Coverage, Missile Environment A, z_0=0.35 m.

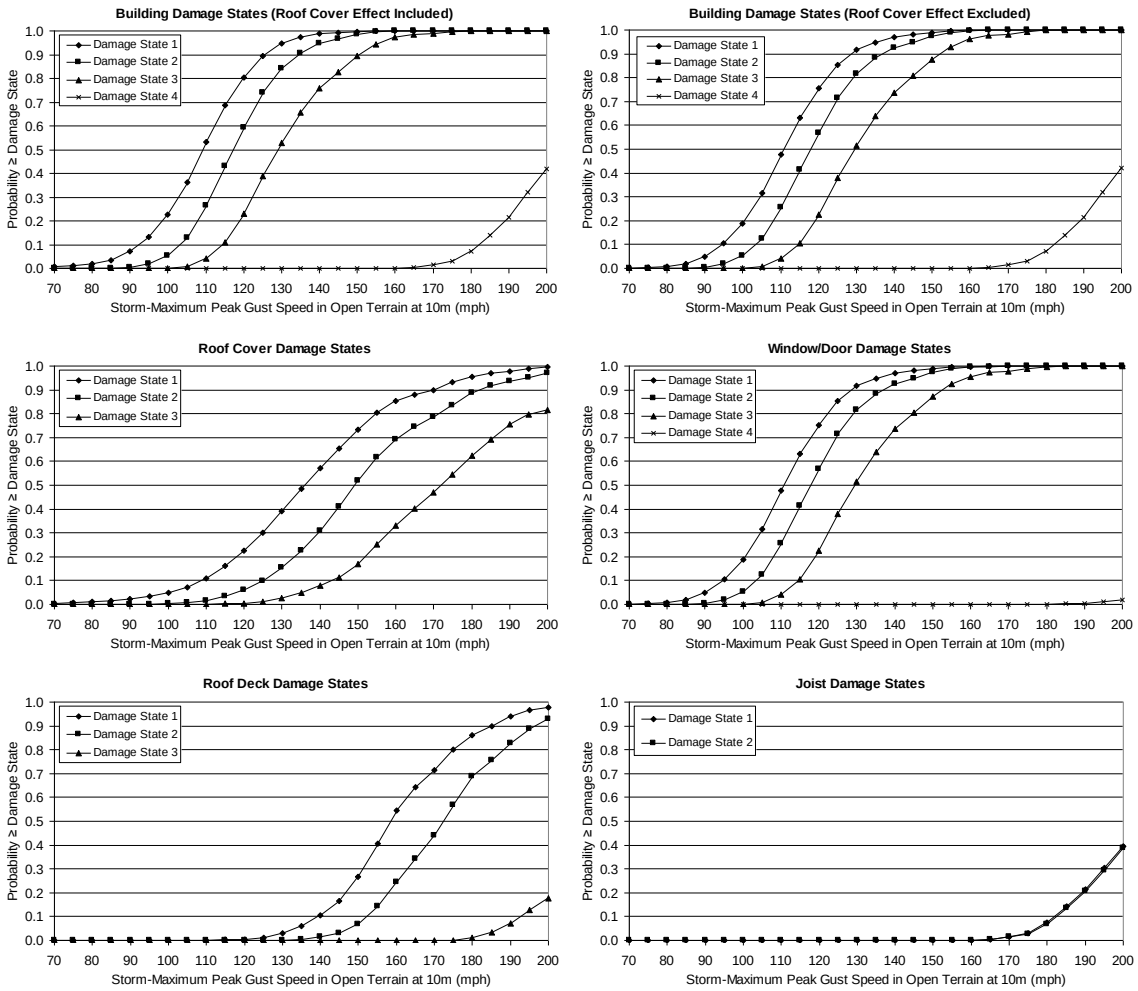

Figure F.13. Damage States vs. Peak Gust Wind Speed – Two-Story Engineered Residential Building – Built-up Roof Cover, 33% Glazing Coverage, <u>Missile Environment B</u>, z_0=0.35 m.

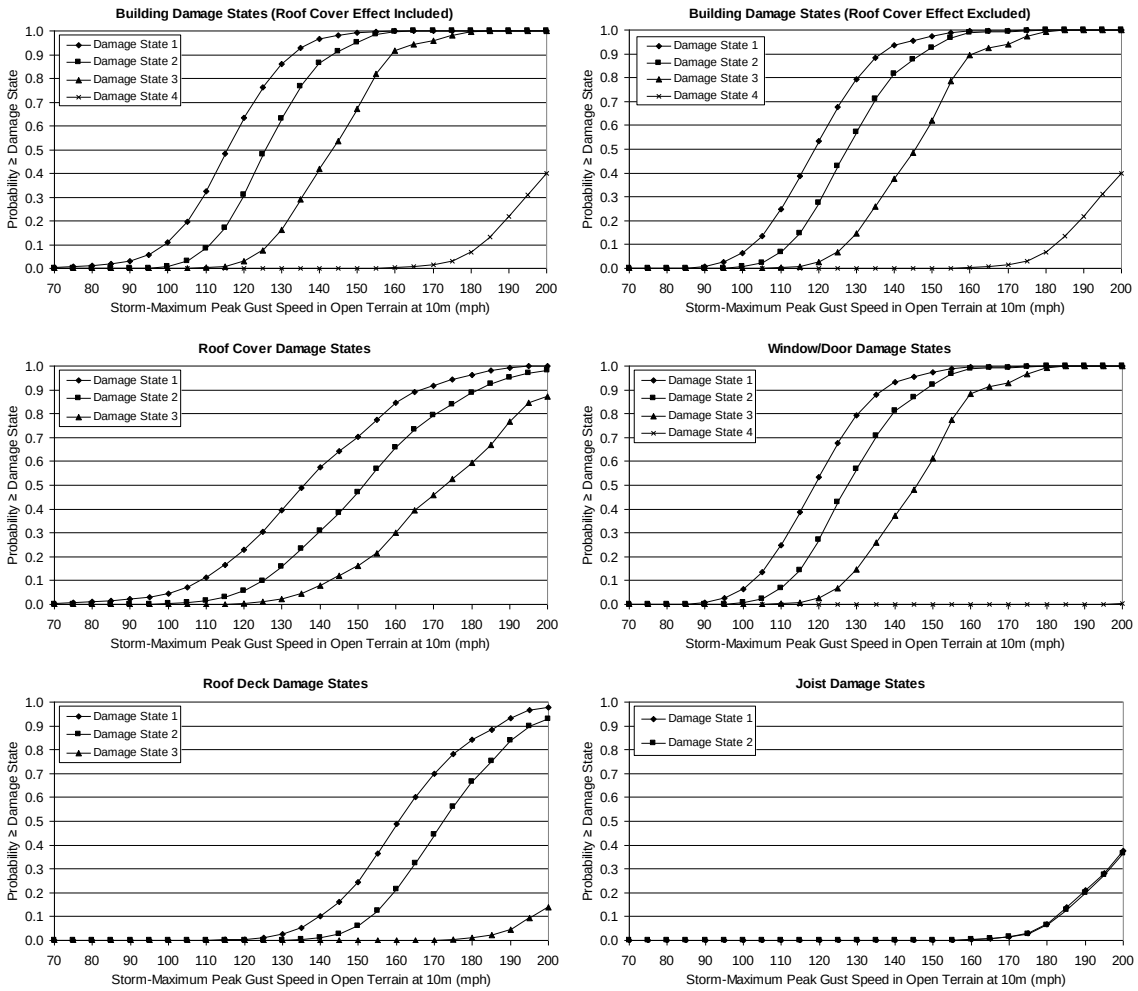

Figure F.14. Damage States vs. Peak Gust Wind Speed – Two-Story Engineered Residential Building – Built-up Roof Cover, 33% Glazing Coverage, <u>Missile Environment C</u>, z_0=0.35 m.

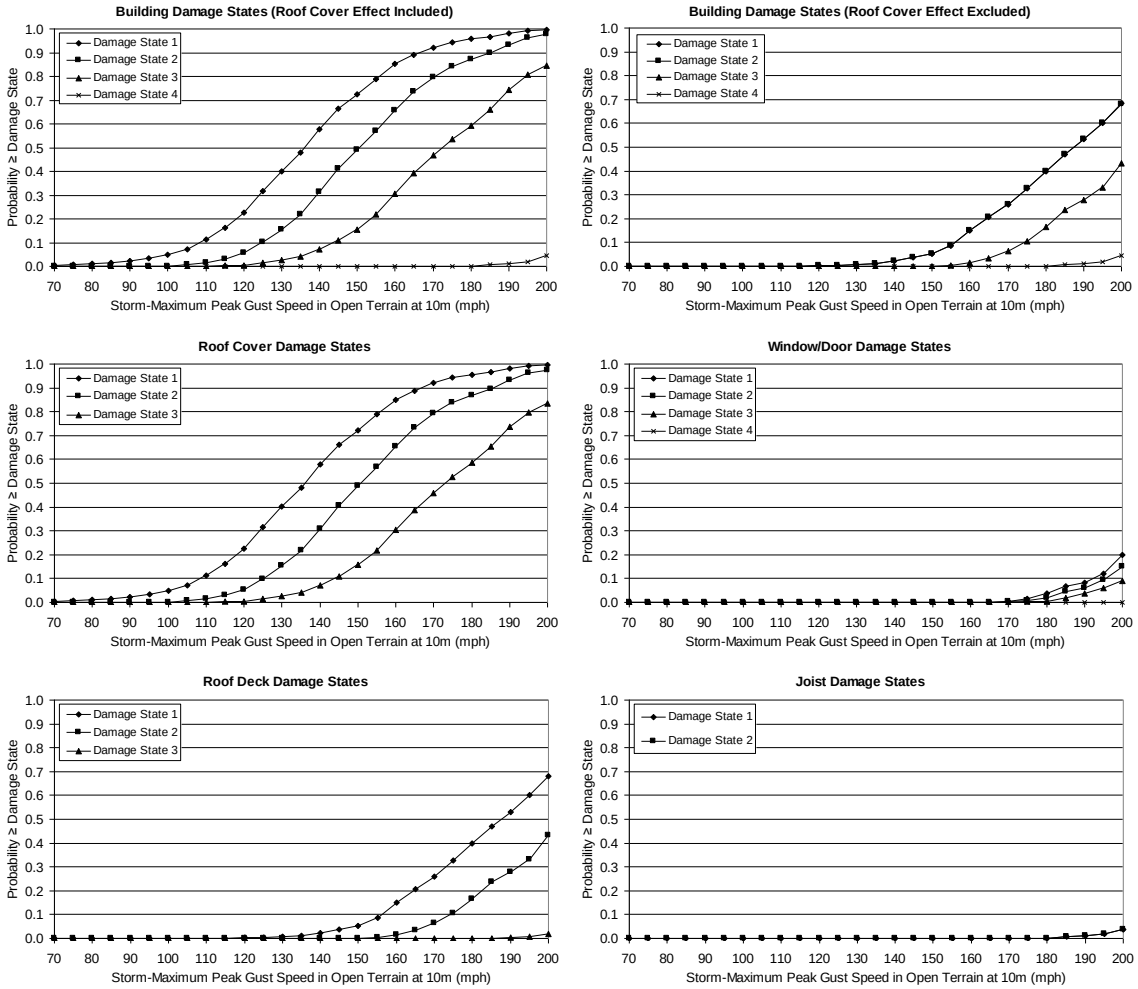

Figure F.15. Damage States vs. Peak Gust Wind Speed – Two-Story Engineered Residential Building – Built-up Roof Cover, 33% Glazing Coverage, <u>Missile Environment D</u>, z_0=0.35 m.

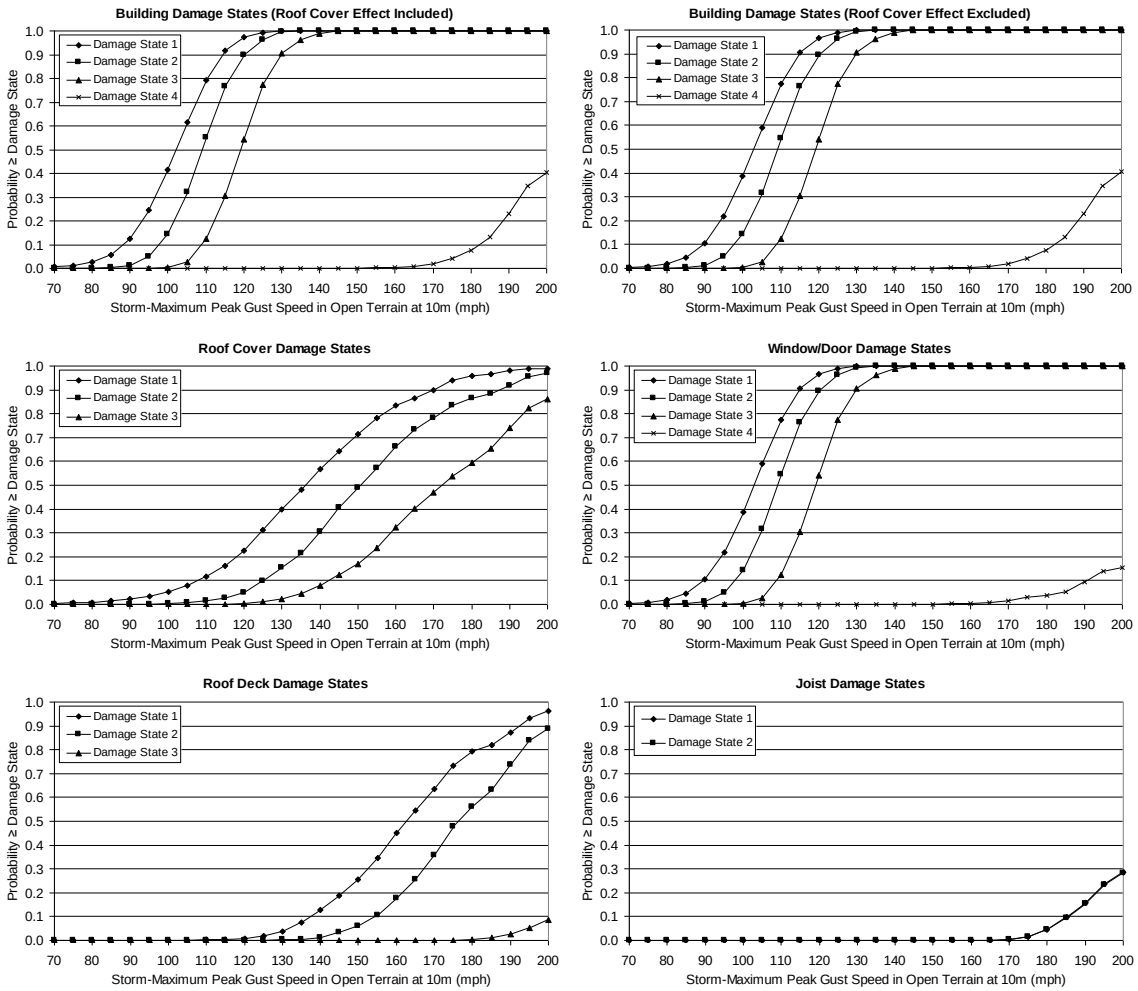

Figure F.16. Damage States vs. Peak Gust Wind Speed – Two-Story Engineered <u>Commercial Building</u> – Built-up Roof Cover, 33% Glazing Coverage, Missile Environment A, z_0=0.35 m.

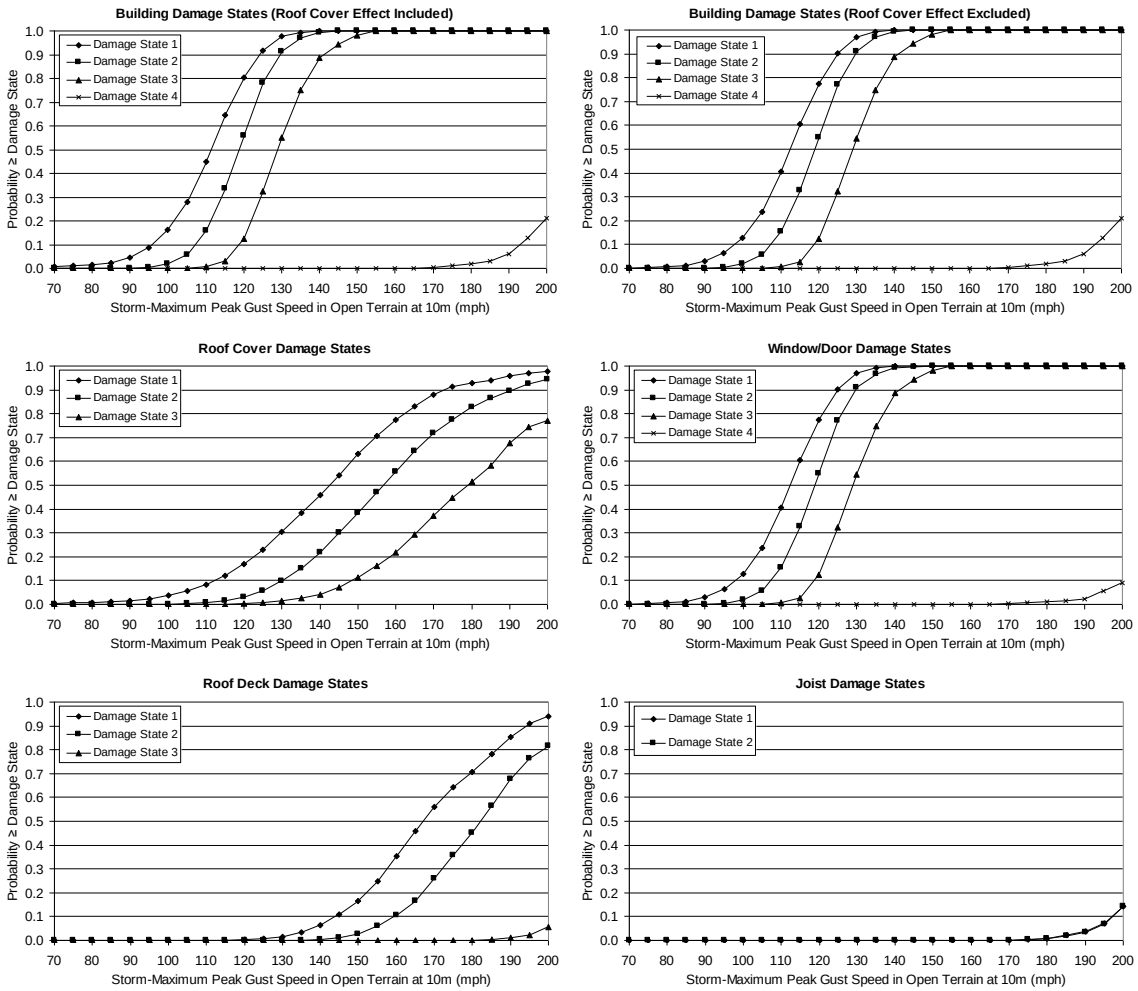

Figure F.17. Damage States vs. Peak Gust Wind Speed – Two-Story Engineered Residential Building – Built-up Roof Cover, 33% Glazing Coverage, Missile Environment A, z_0=0.70 m.

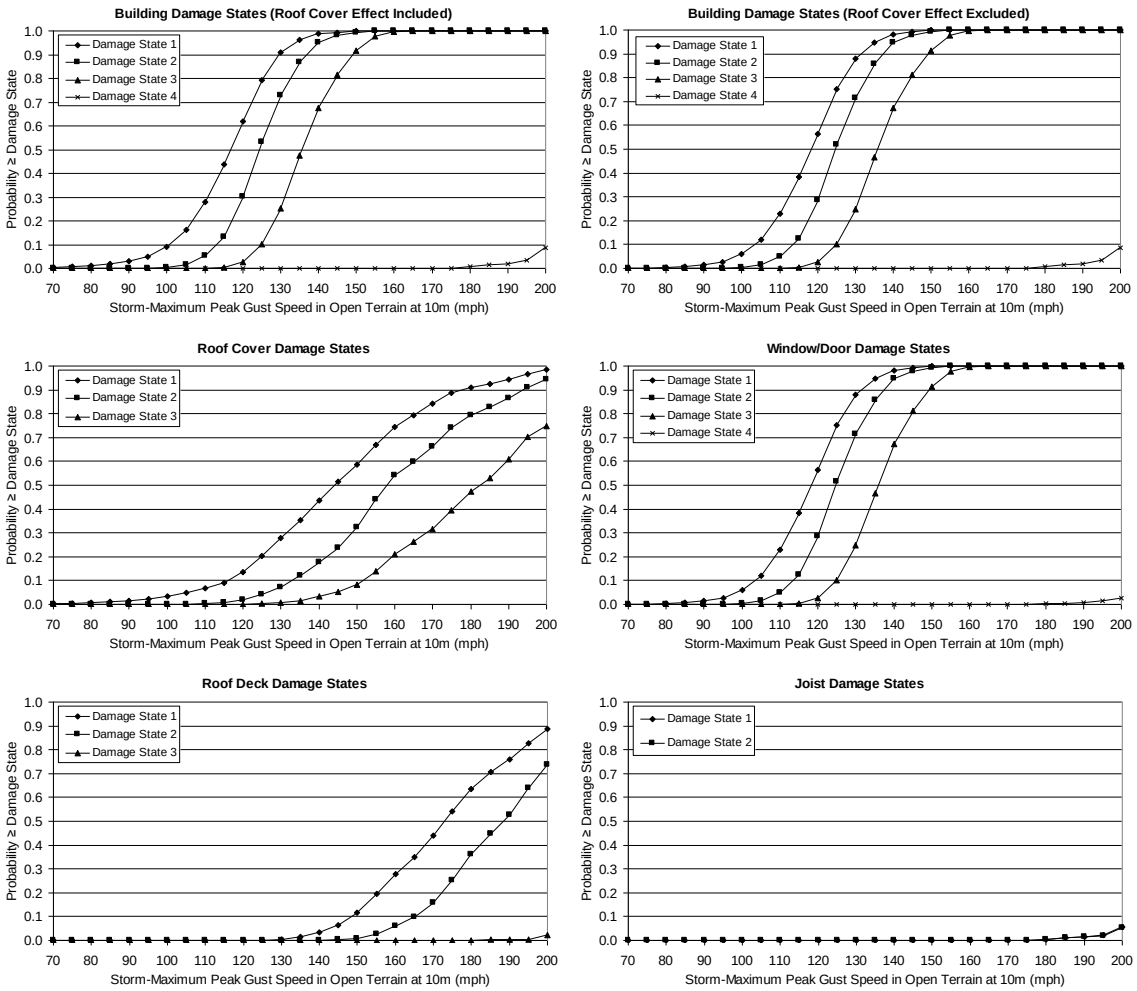

Figure F.18. Damage States vs. Peak Gust Wind Speed – Two-Story Engineered Residential Building – Built-up Roof Cover, 33% Glazing Coverage, Missile Environment A, z_0=1.0 m.

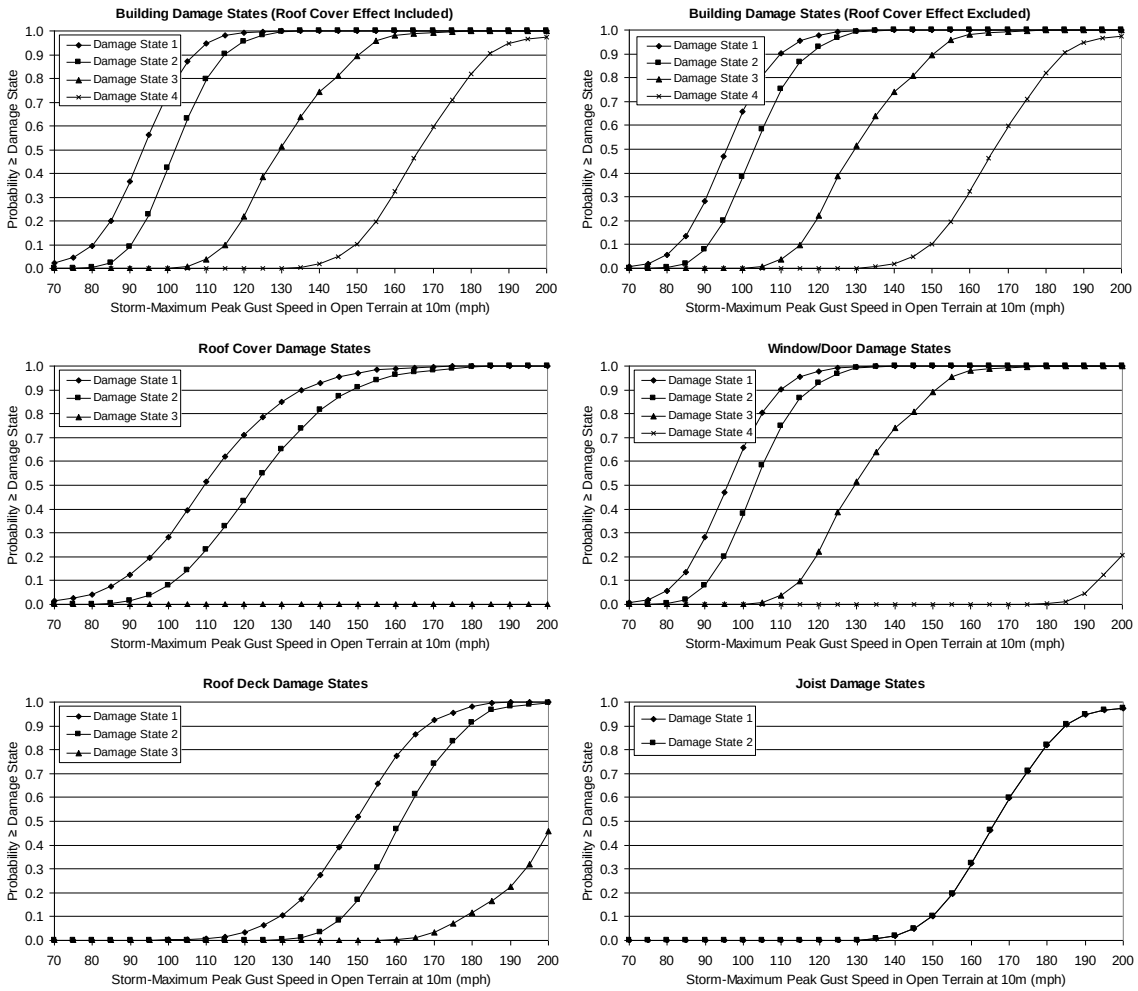

Figure F.19. Damage States vs. Peak Gust Wind Speed – Five-Story Engineered Residential Building – Built-up Roof Cover, 33% Glazing Coverage, Missile Environment A, z_0=0.03 m.

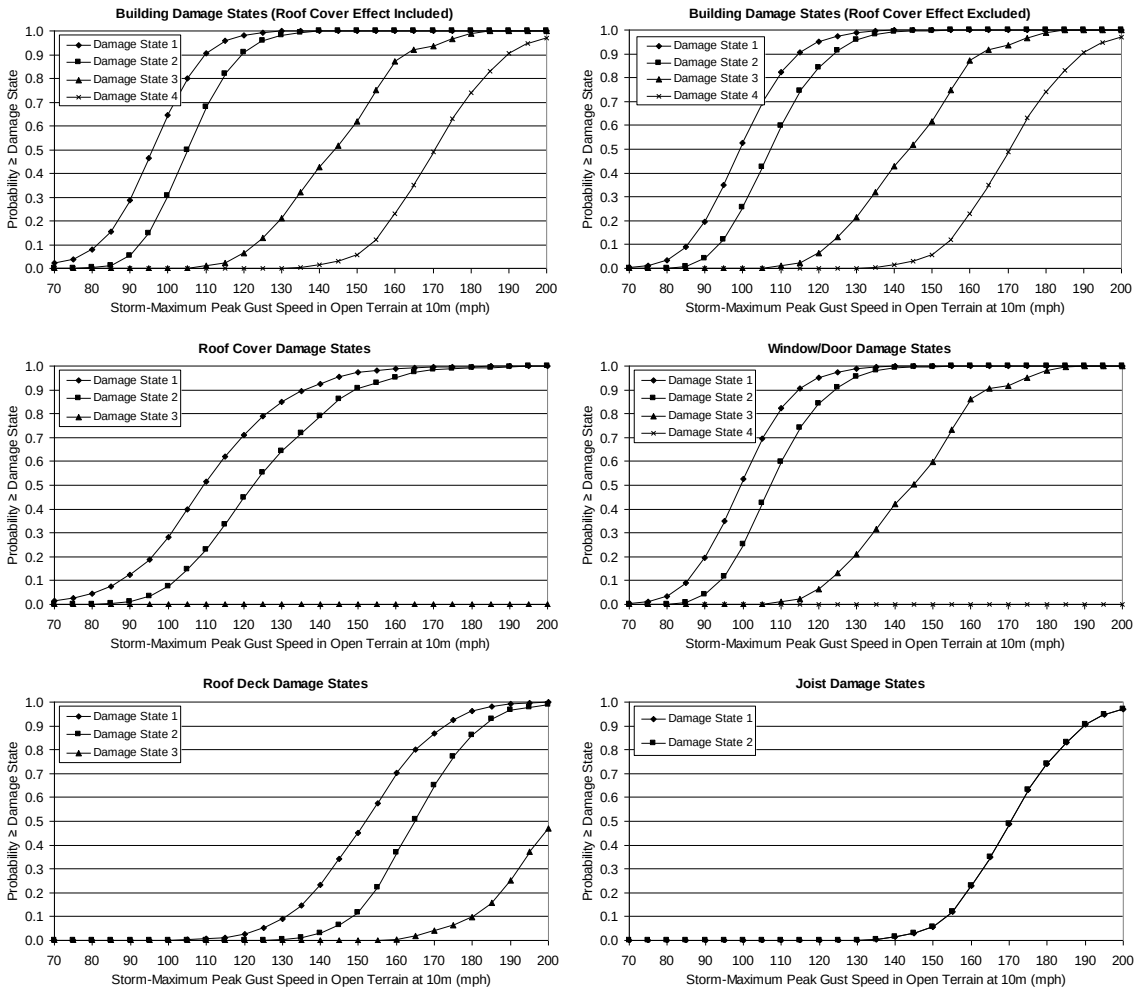

Figure F.20. Damage States vs. Peak Gust Wind Speed – Five-Story Engineered Residential Building – Built-up Roof Cover, 20% Glazing Coverage, Missile Environment A, z_0=0.03 m.

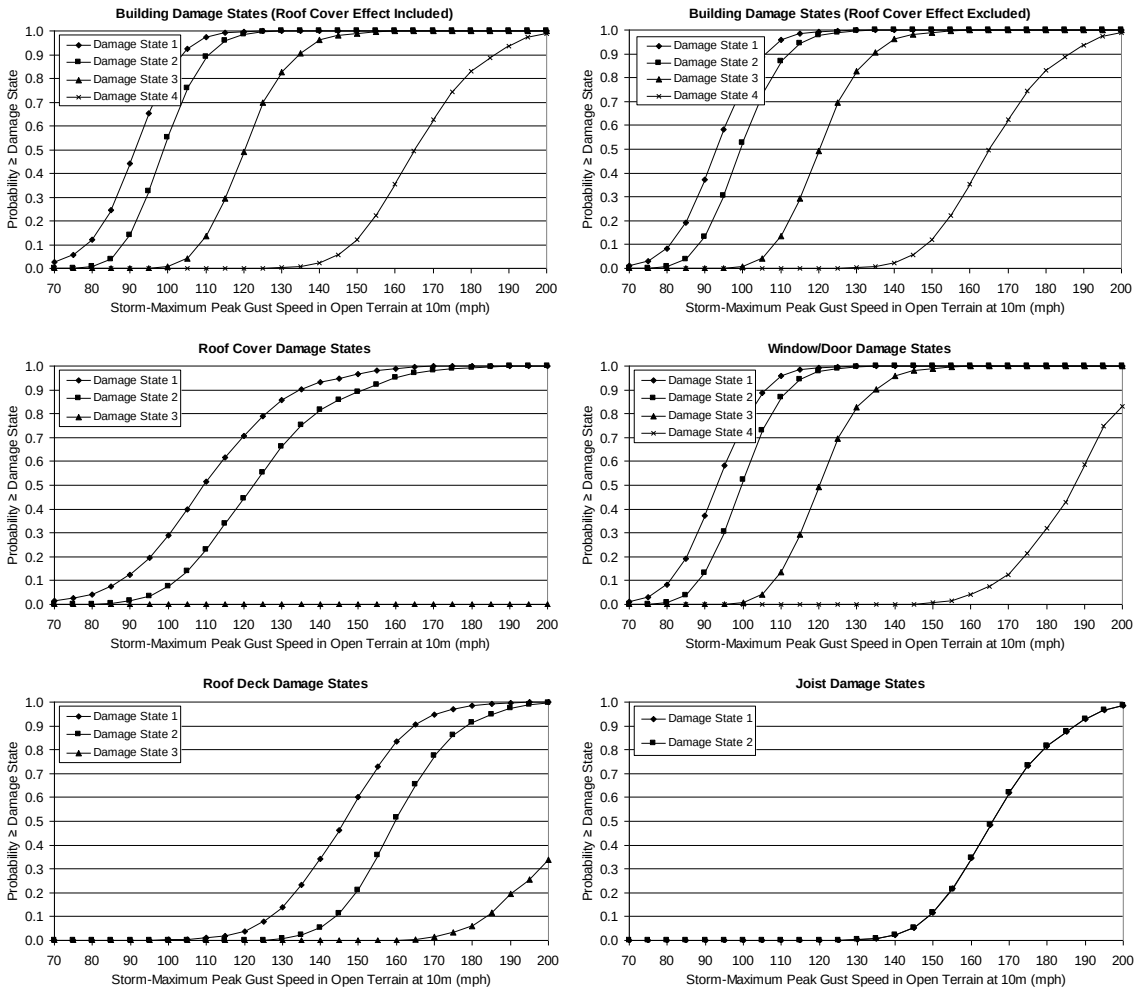

Figure F.21. Damage States vs. Peak Gust Wind Speed – Five-Story Engineered Residential Building – Built-up Roof Cover, 50% Glazing Coverage, Missile Environment A, z_0=0.03 m.

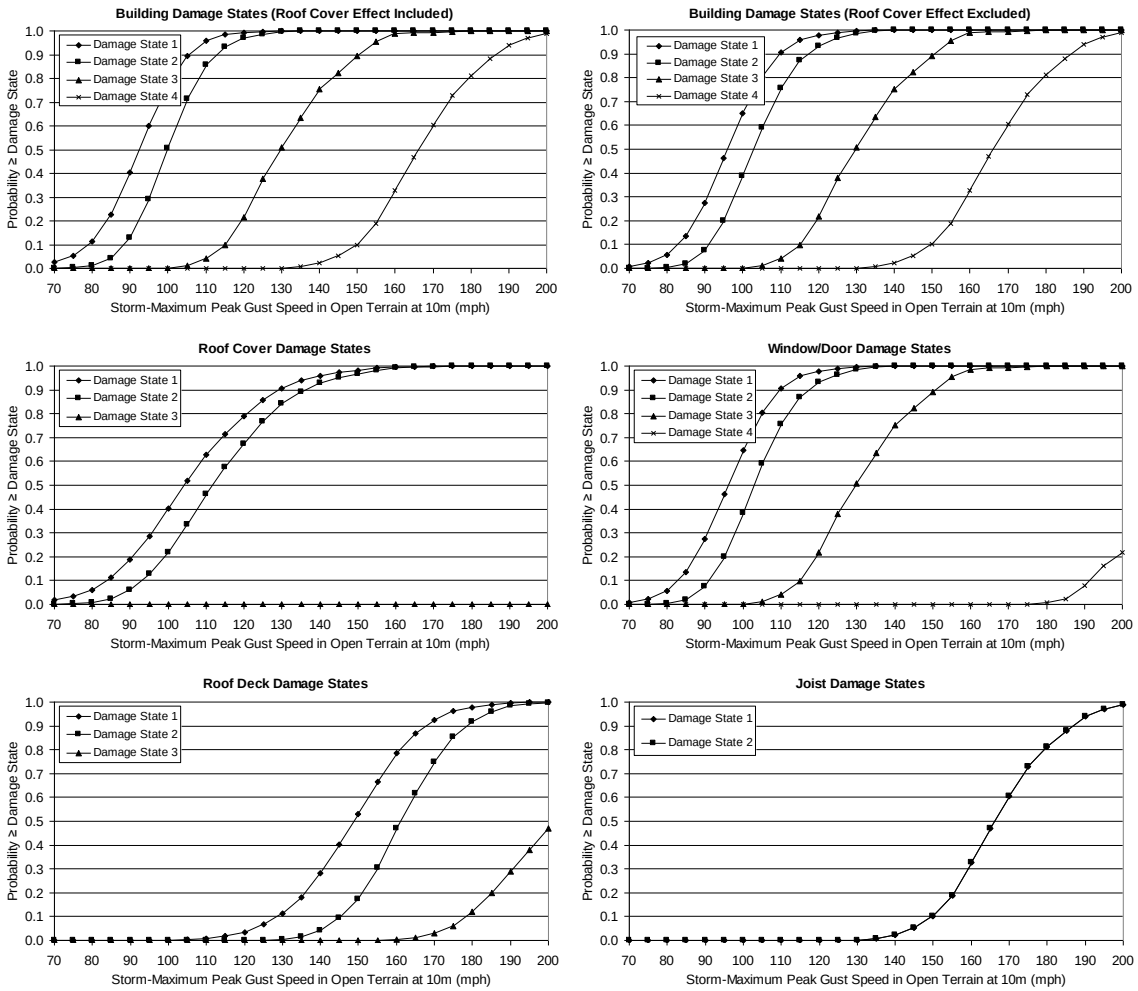

Figure F.22. Damage States vs. Peak Gust Wind Speed – Five-Story Engineered Residential Building – <u>Single Ply Membrane Roof Cover</u>, 33% Glazing Coverage, Missile Environment A, z_0=0.03 m.

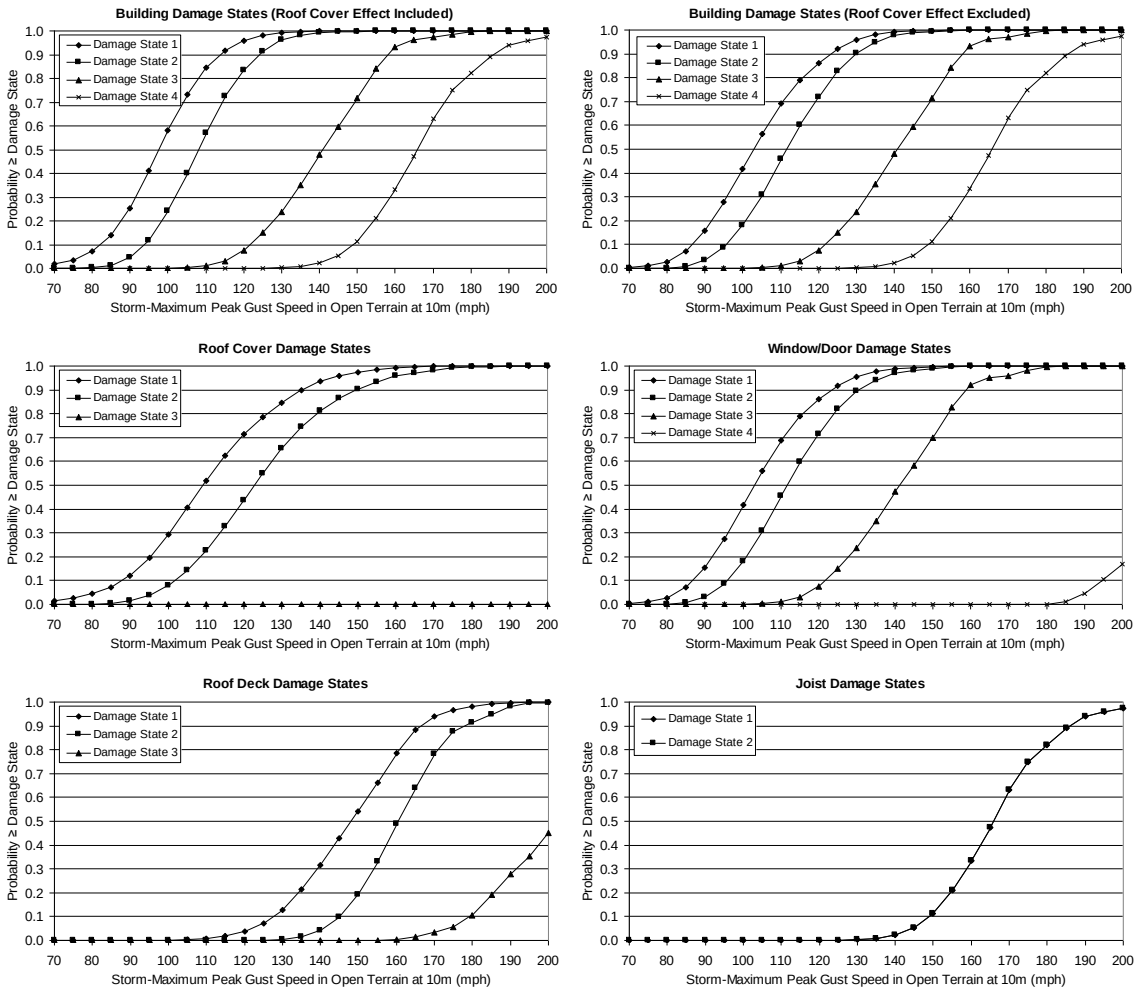

Figure F.23. Damage States vs. Peak Gust Wind Speed – Five-Story Engineered Residential Building – Built-up Roof Cover, 33% Glazing Coverage, <u>Missile Environment B</u>, z_0=0.03 m.

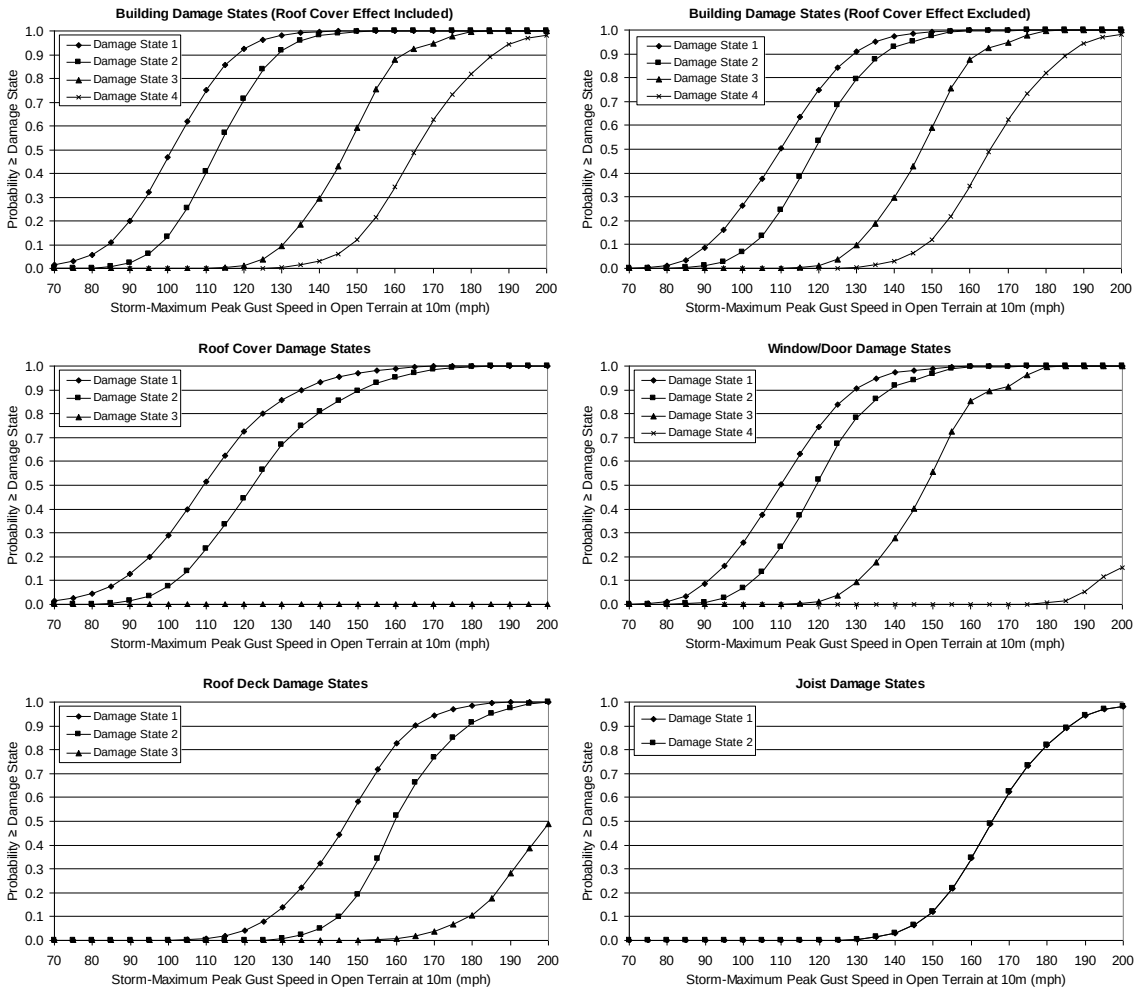

Figure F.24. Damage States vs. Peak Gust Wind Speed – Five-Story Engineered Residential Building – Built-up Roof Cover, 33% Glazing Coverage, Missile Environment C, z_0=0.03 m.

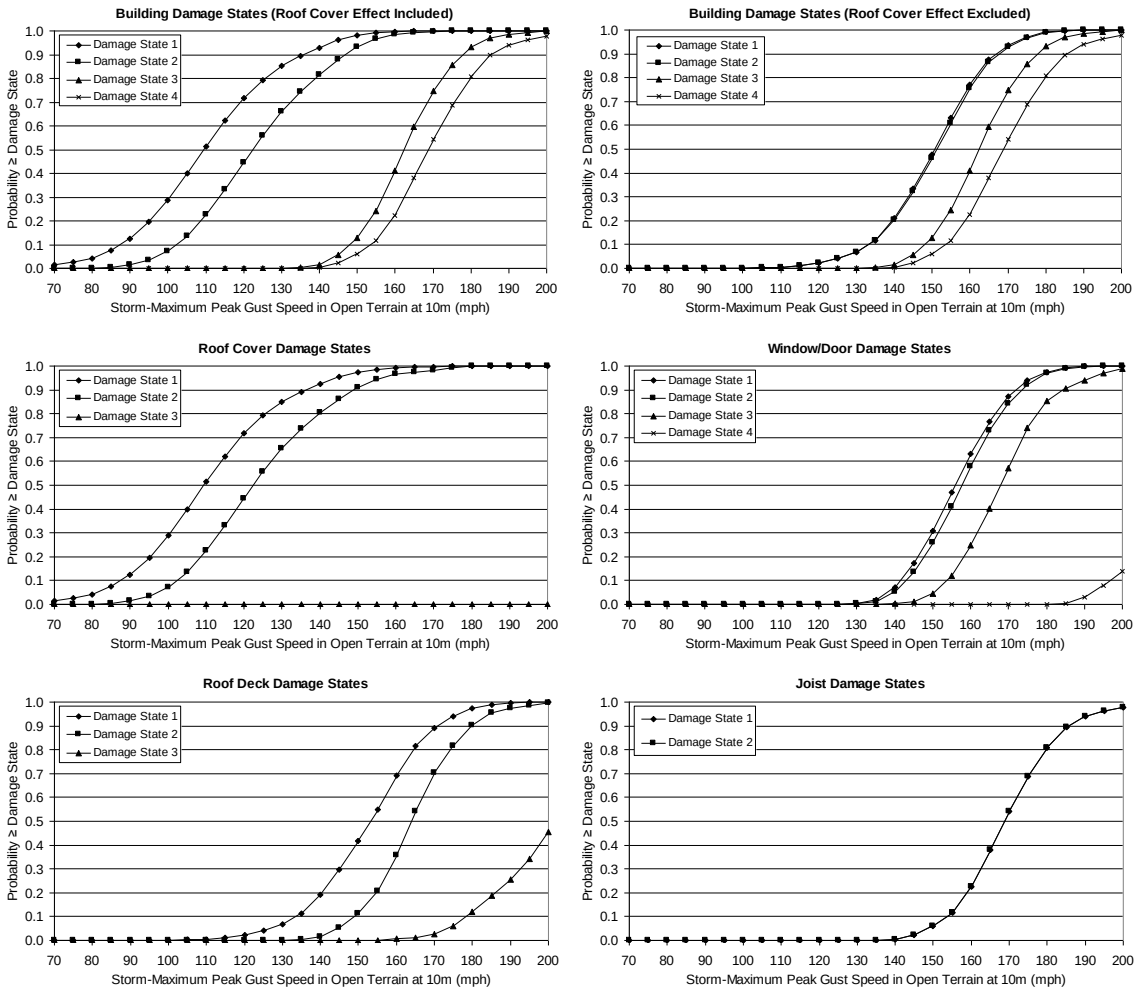

Figure F.25. Damage States vs. Peak Gust Wind Speed – Five-Story Engineered Residential Building – Built-up Roof Cover, 33% Glazing Coverage, <u>Missile Environment D</u>, z_0=0.03 m.

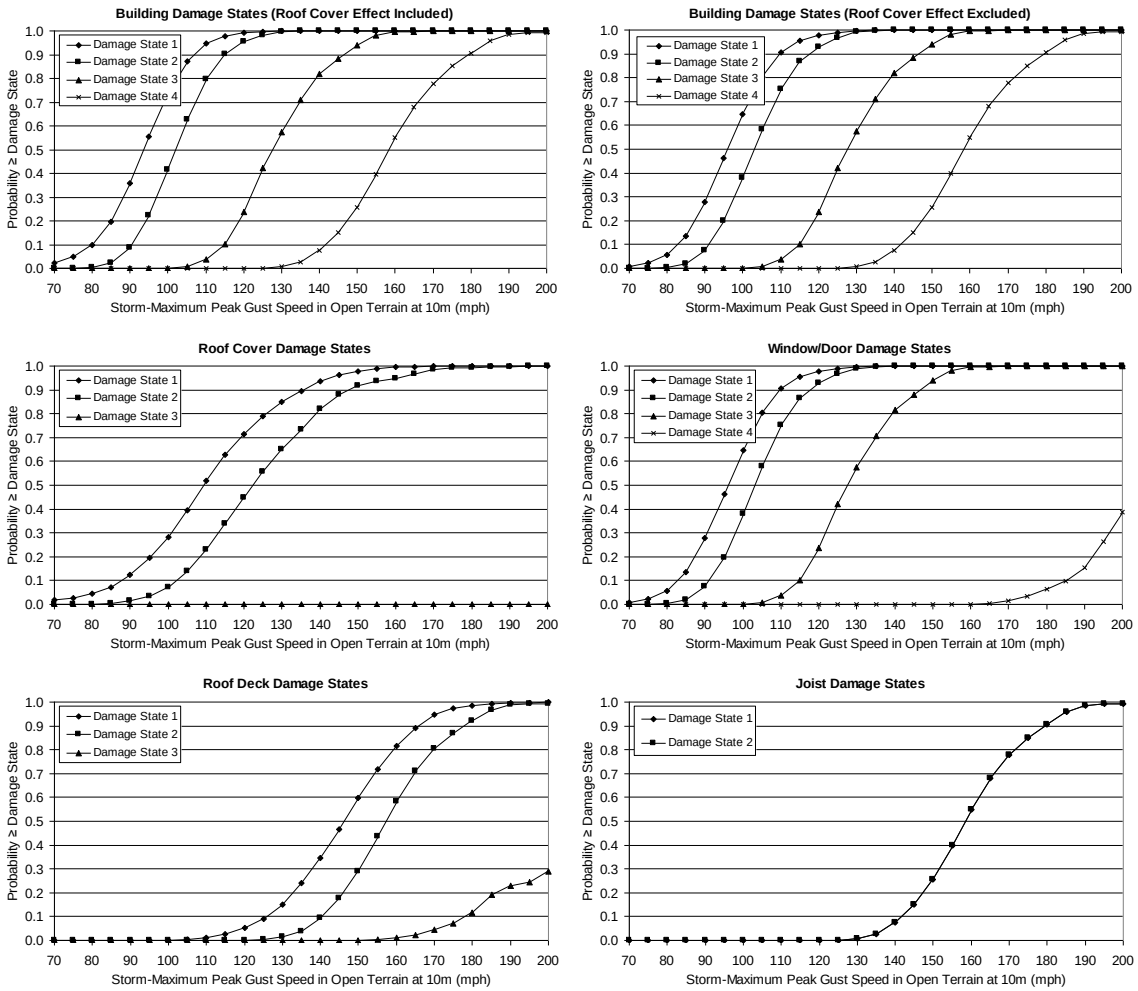

Figure F.26. Damage States vs. Peak Gust Wind Speed – Five-Story Engineered <u>Commercial Building</u> – Built-up Roof Cover, 33% Glazing Coverage, Missile Environment A, z_0=0.03 m.

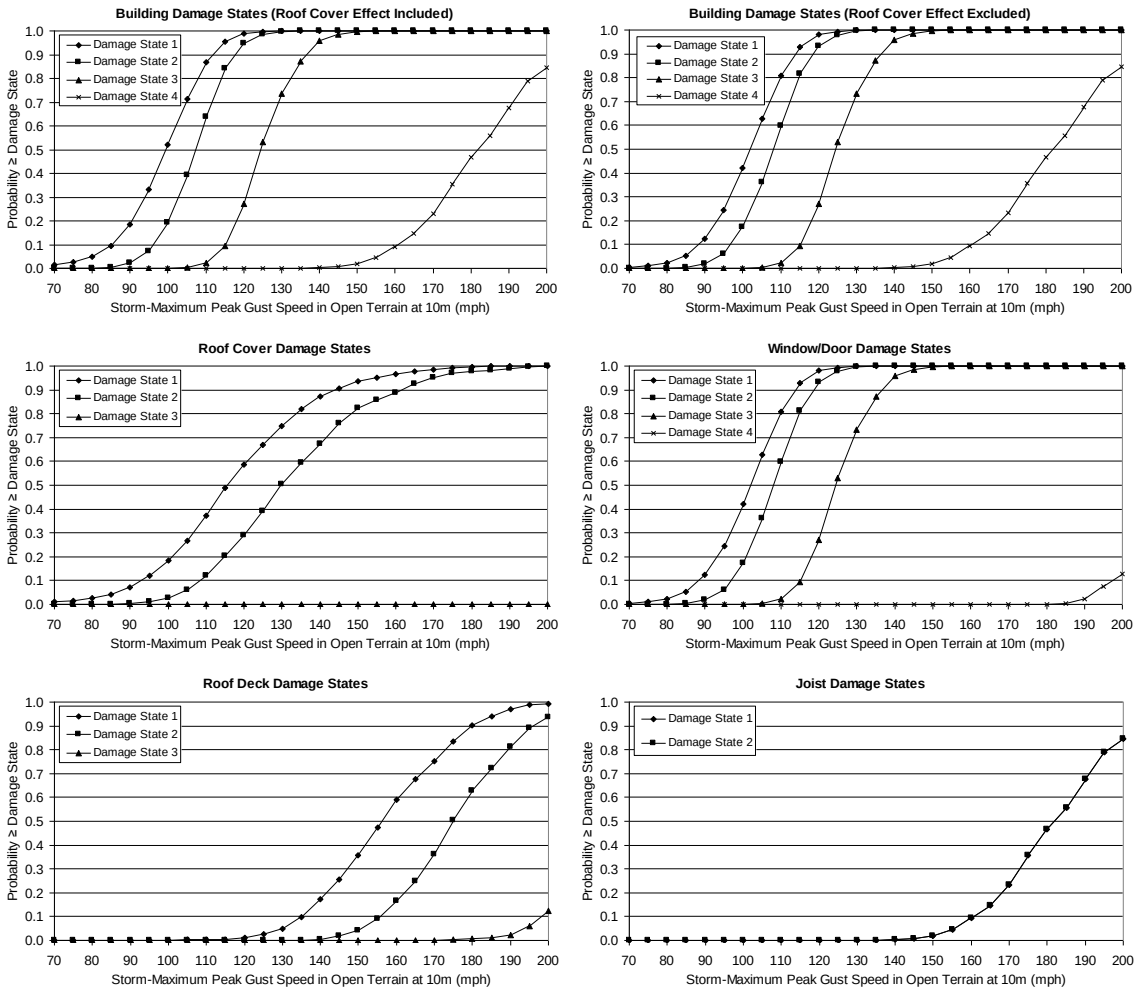

Figure F.27. Damage States vs. Peak Gust Wind Speed – Five-Story Engineered Residential Building – Built-up Roof Cover, 33% Glazing Coverage, Missile Environment A, z_0=0.35 m.

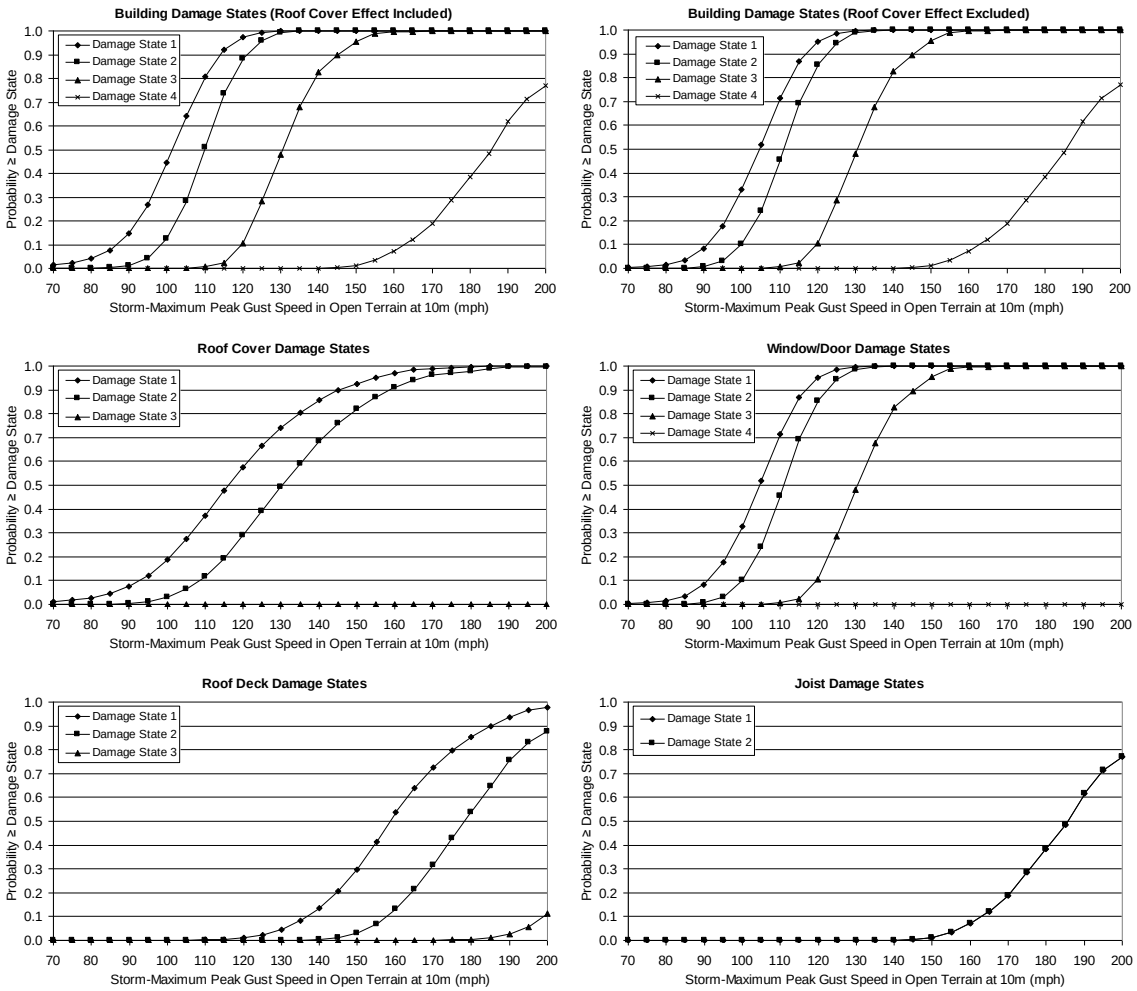

Figure F.28. Damage States vs. Peak Gust Wind Speed – Five-Story Engineered Residential Building – Built-up Roof Cover, 20% Glazing Coverage, Missile Environment A, z_0=0.35 m.

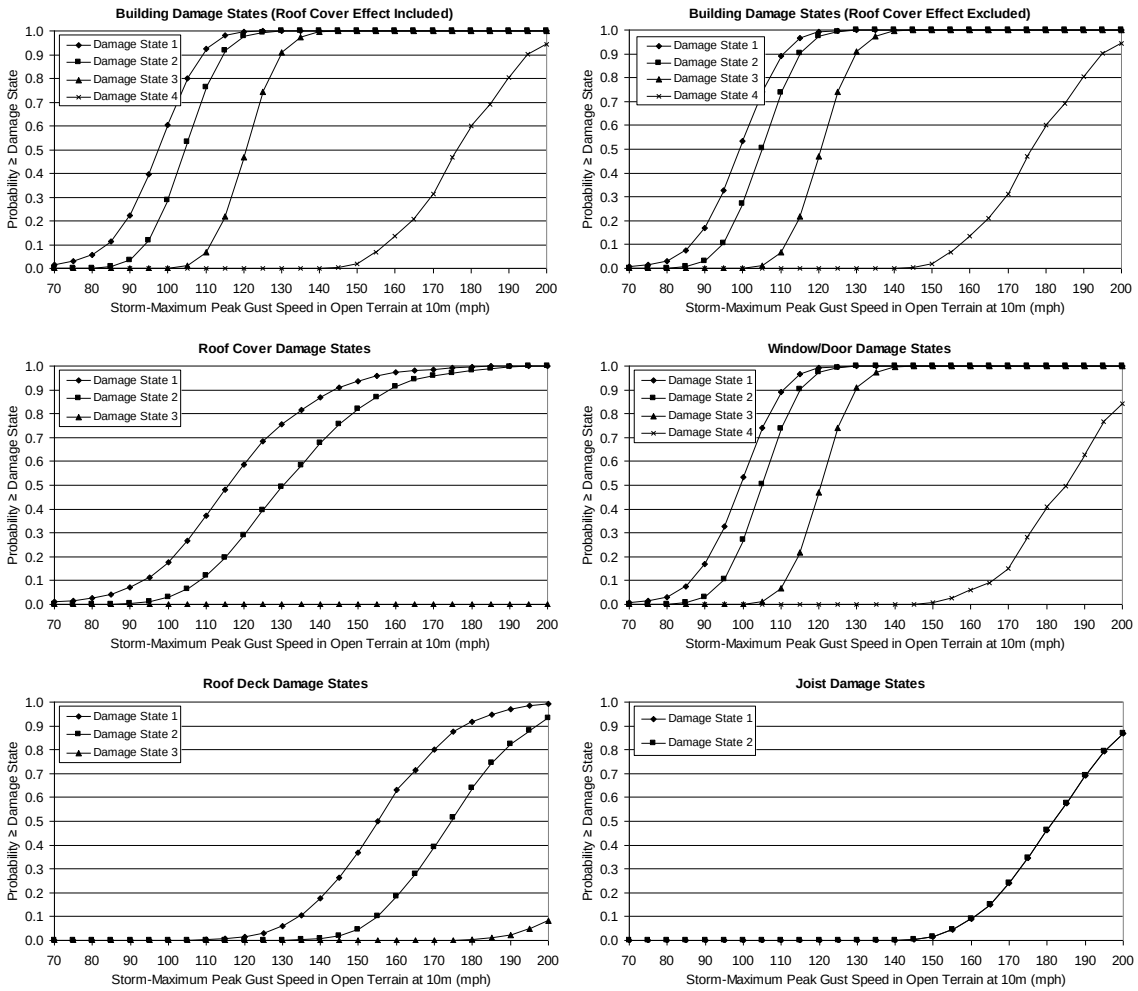

Figure F.29. Damage States vs. Peak Gust Wind Speed – Five-Story Engineered Residential Building – Built-up Roof Cover, 50% Glazing Coverage, Missile Environment A, z_0=0.35 m.

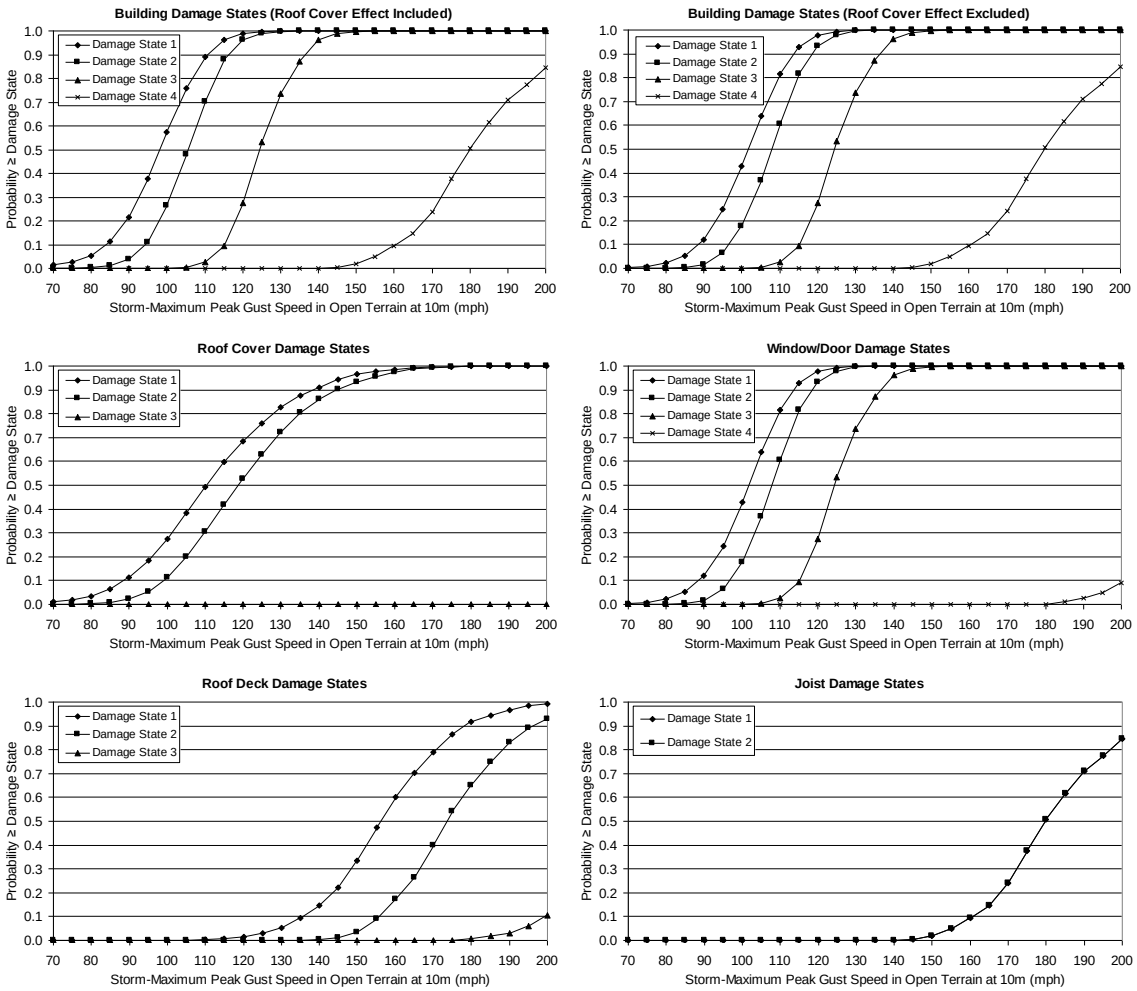

Figure F.30. Damage States vs. Peak Gust Wind Speed – Five-Story Engineered Residential Building – <u>Single Ply Membrane Roof Cover</u>, 33% Glazing Coverage, Missile Environment A, z_0=0.35 m.

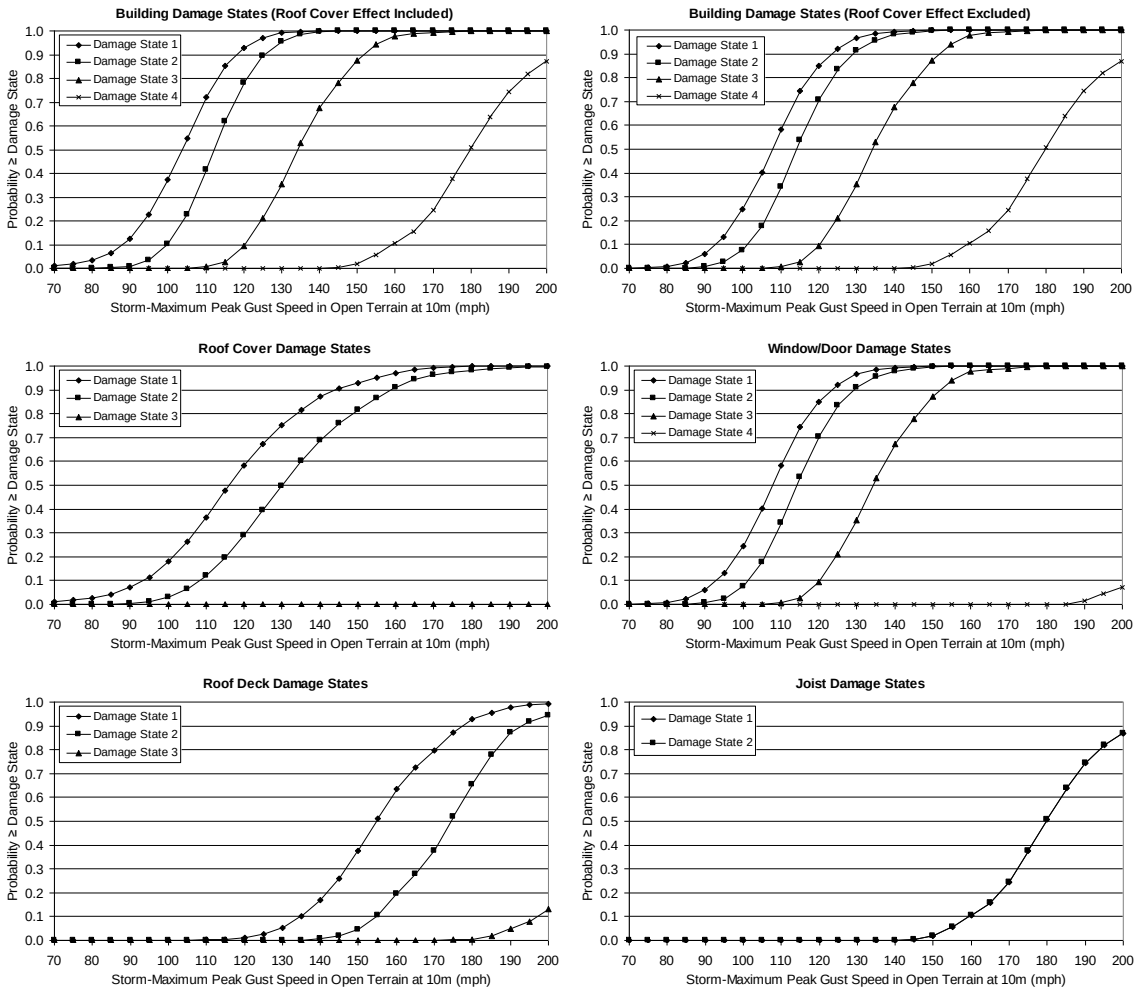

Figure F.31. Damage States vs. Peak Gust Wind Speed – Five-Story Engineered Residential Building – Built-up Roof Cover, 33% Glazing Coverage, <u>Missile Environment B</u>, z_0=0.35 m.

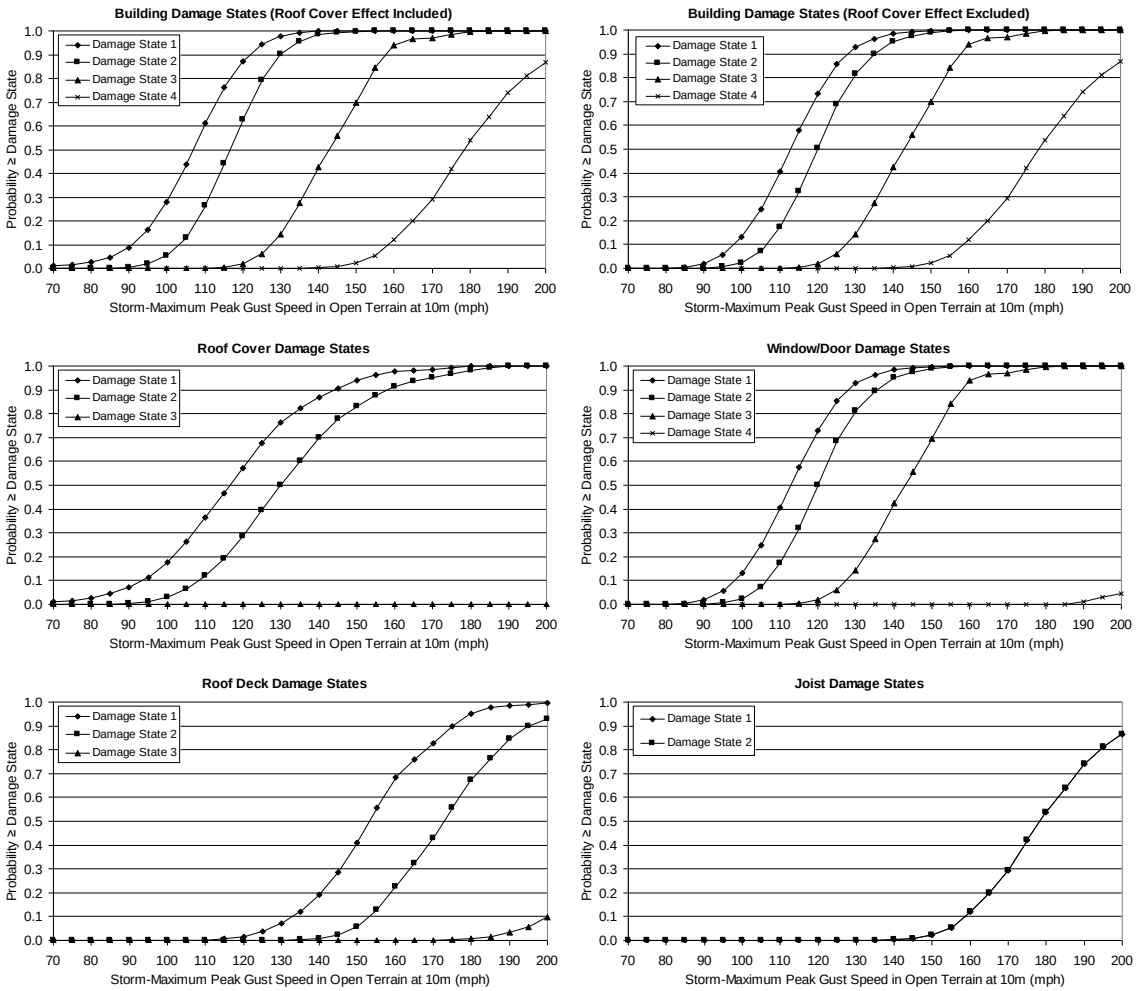

Figure F.32. Damage States vs. Peak Gust Wind Speed – Five-Story Engineered Residential Building – Built-up Roof Cover, 33% Glazing Coverage, Missile Environment C, z_0=0.35 m.

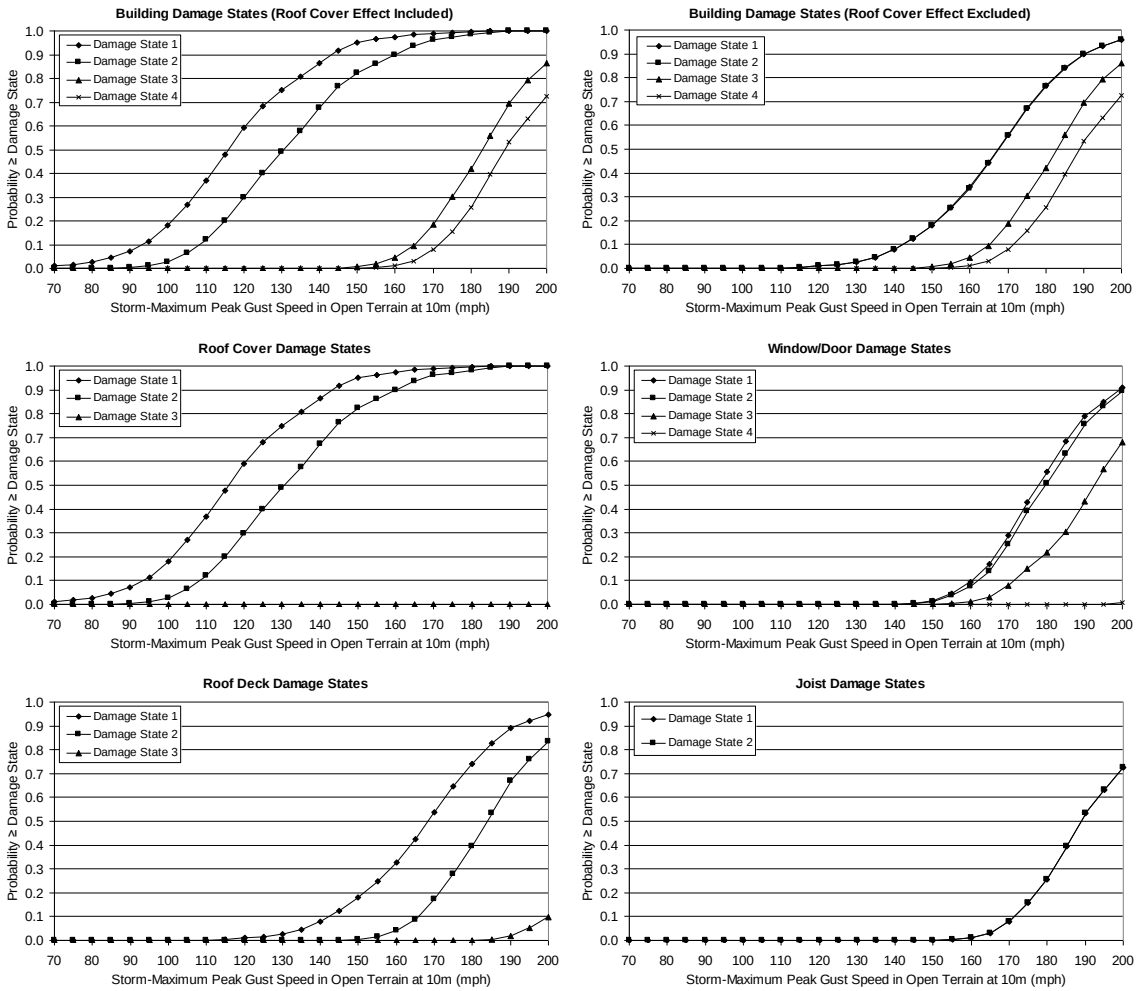

Figure F.33. Damage States vs. Peak Gust Wind Speed – Five-Story Engineered Residential Building – Built-up Roof Cover, 33% Glazing Coverage, <u>Missile Environment D</u>, z_0=0.35 m.

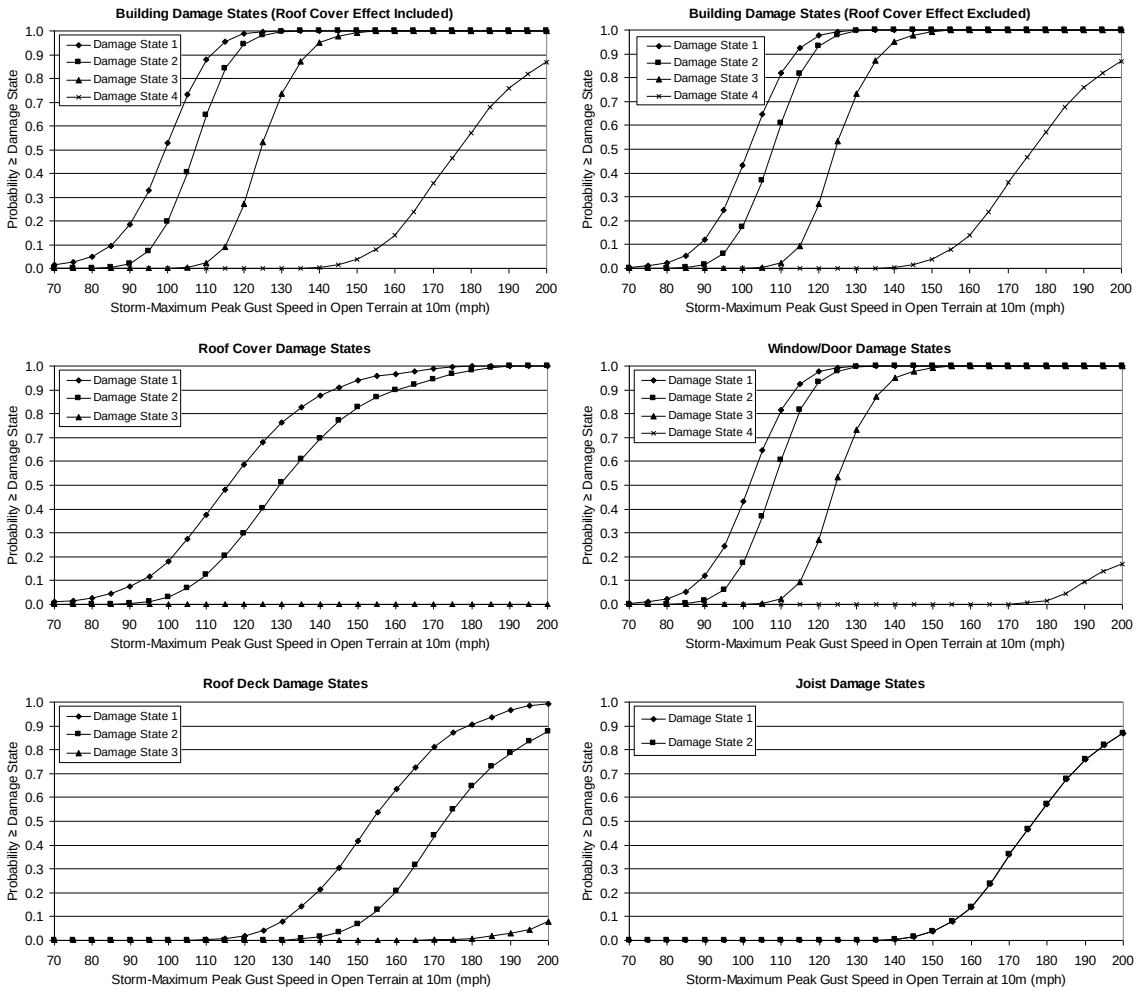

Figure F.34. Damage States vs. Peak Gust Wind Speed – Five-Story Engineered Commercial Building – Built-up Roof Cover, 33% Glazing Coverage, Missile Environment A, z_0=0.35 m.

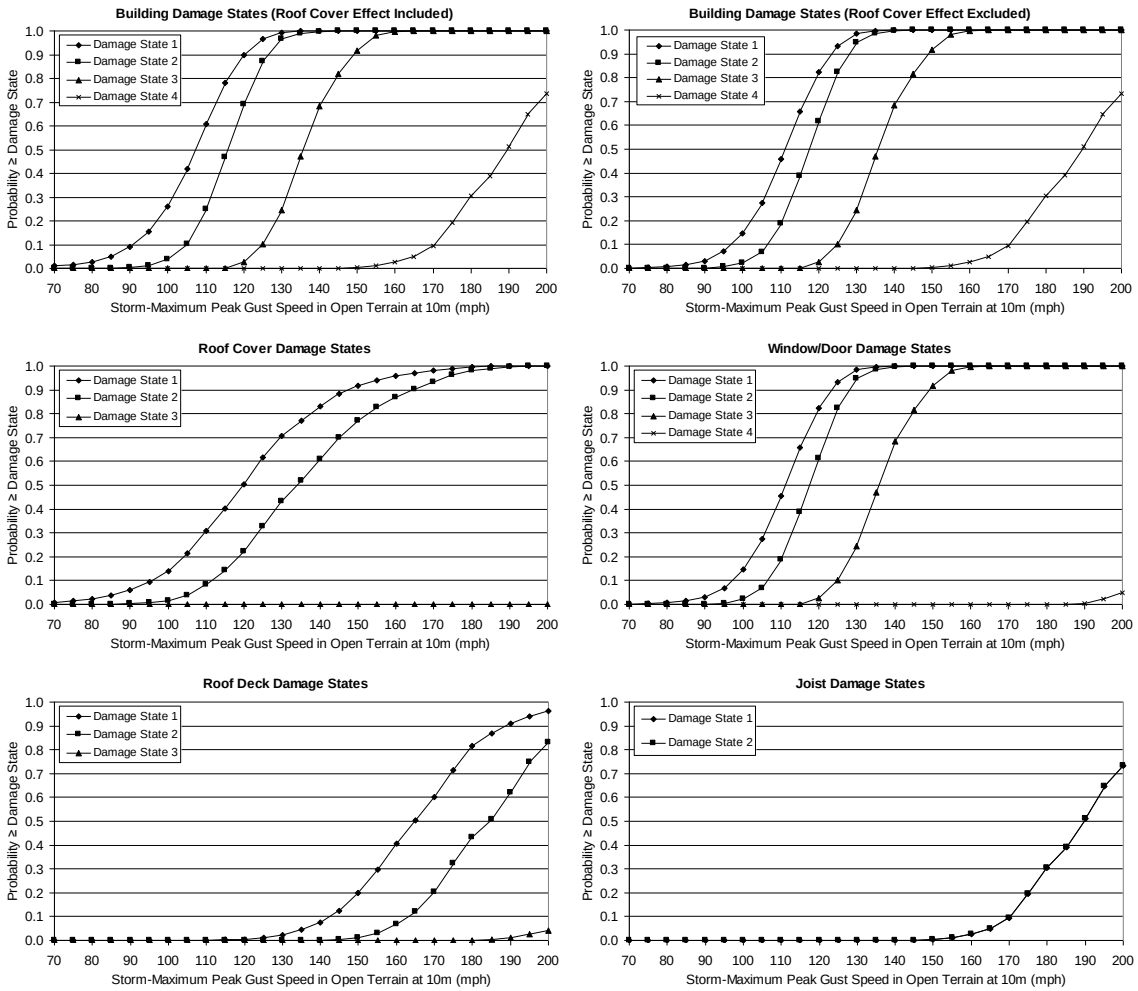

Figure F.35. Damage States vs. Peak Gust Wind Speed – Five-Story Engineered Residential Building – Built-up Roof Cover, 33% Glazing Coverage, Missile Environment A, z_0=0.70 m.

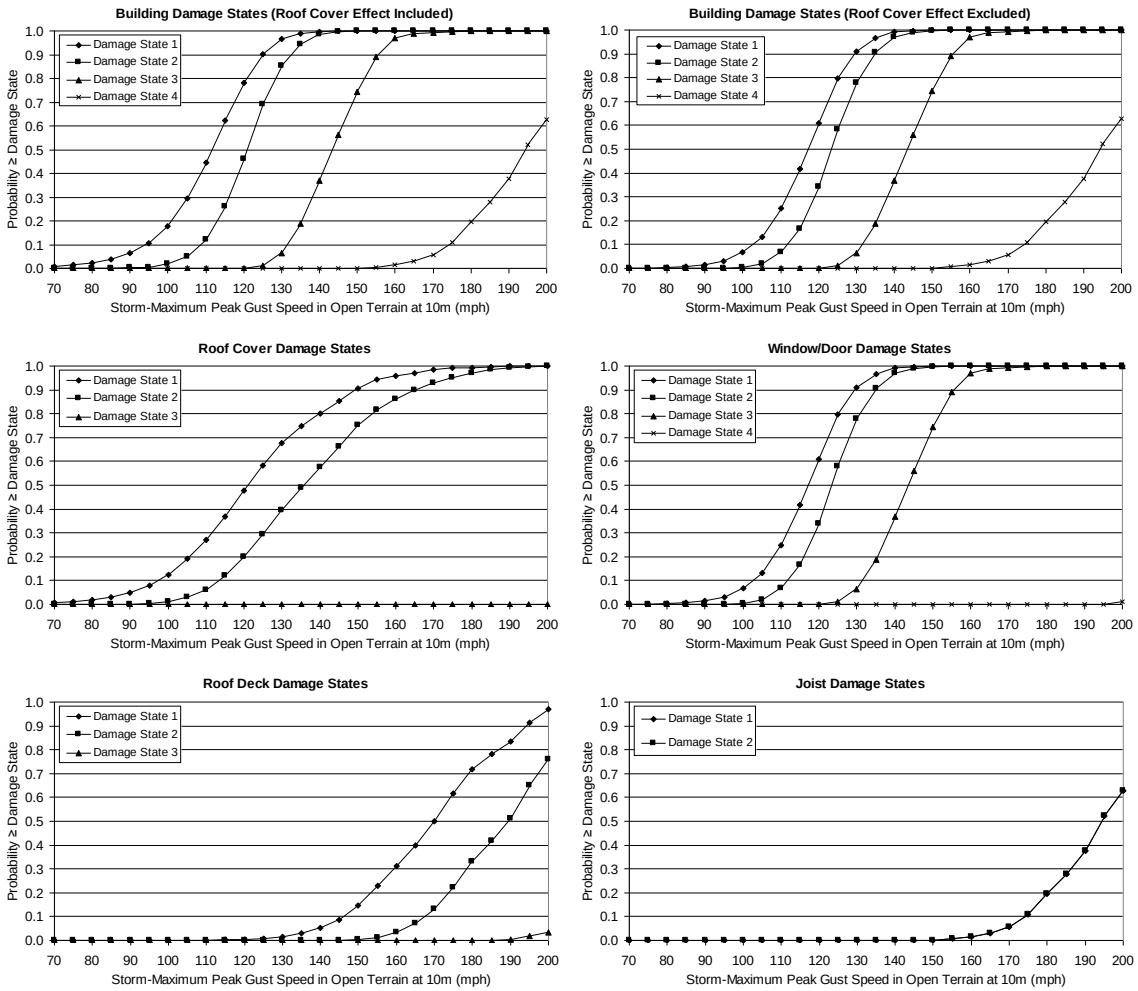

Figure F.36. Damage States vs. Peak Gust Wind Speed – Five-Story Engineered Residential Building – Built-up Roof Cover, 33% Glazing Coverage, Missile Environment A, z_0=1.0 m.

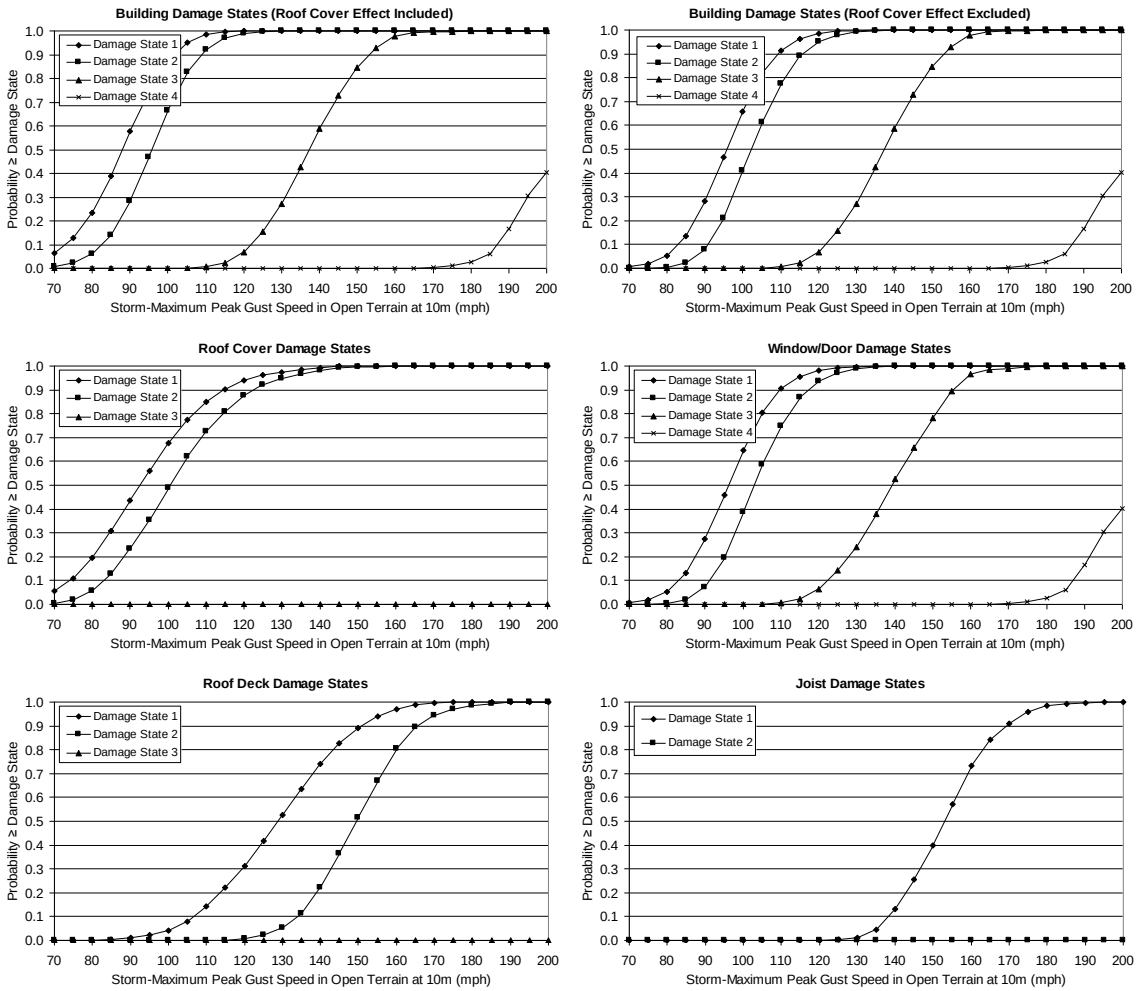

Figure F.37. Damage States vs. Peak Gust Wind Speed – Eight-Story Engineered Residential Building – Built-up Roof Cover, 33% Glazing Coverage, Missile Environment A, z_0=0.03 m.

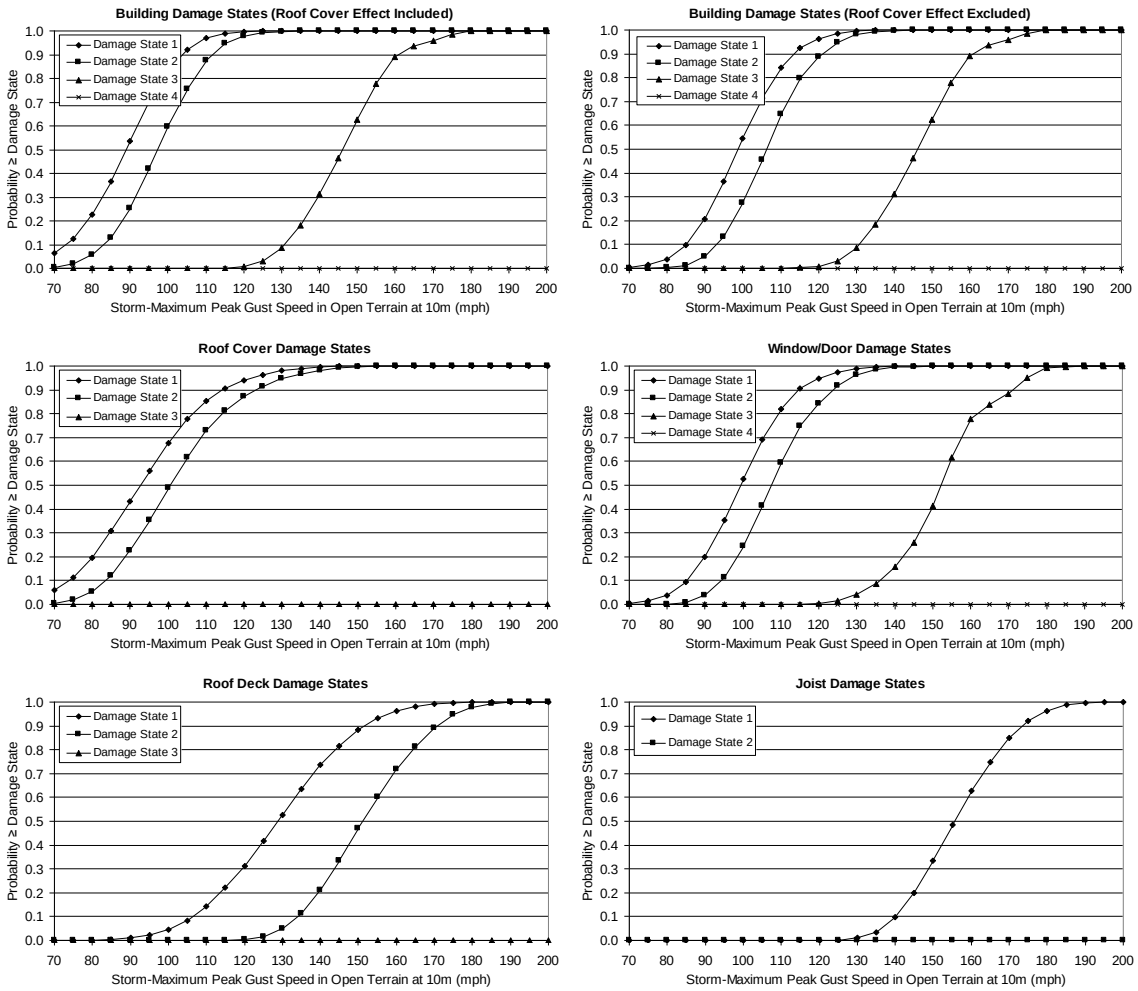

Figure F.38. Damage States vs. Peak Gust Wind Speed – Eight-Story Engineered Residential Building – Built-up Roof Cover, 20% Glazing Coverage, Missile Environment A, z_0=0.03 m.

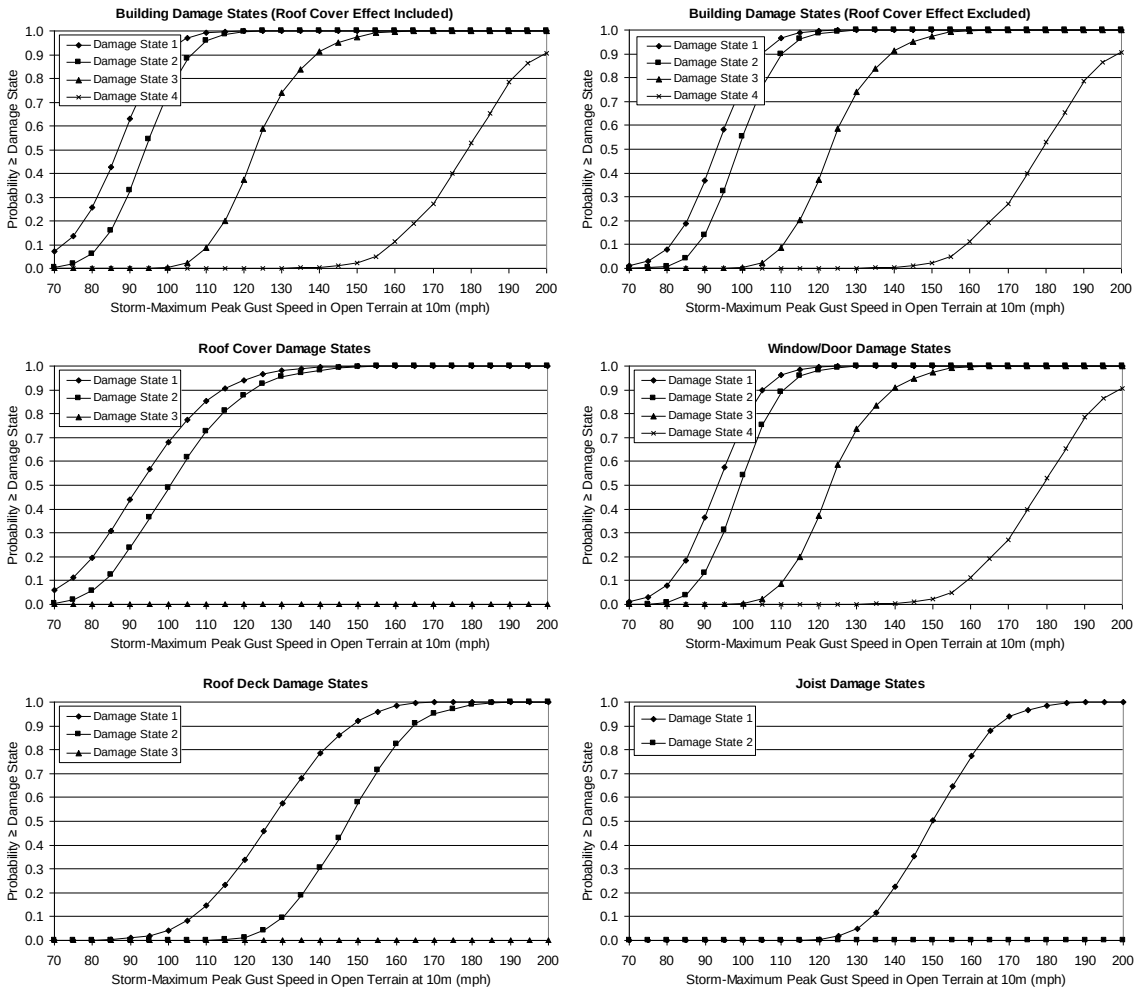

Figure F.39. Damage States vs. Peak Gust Wind Speed – Eight-Story Engineered Residential Building – Built-up Roof Cover, 50% Glazing Coverage, Missile Environment A, z_0=0.03 m.

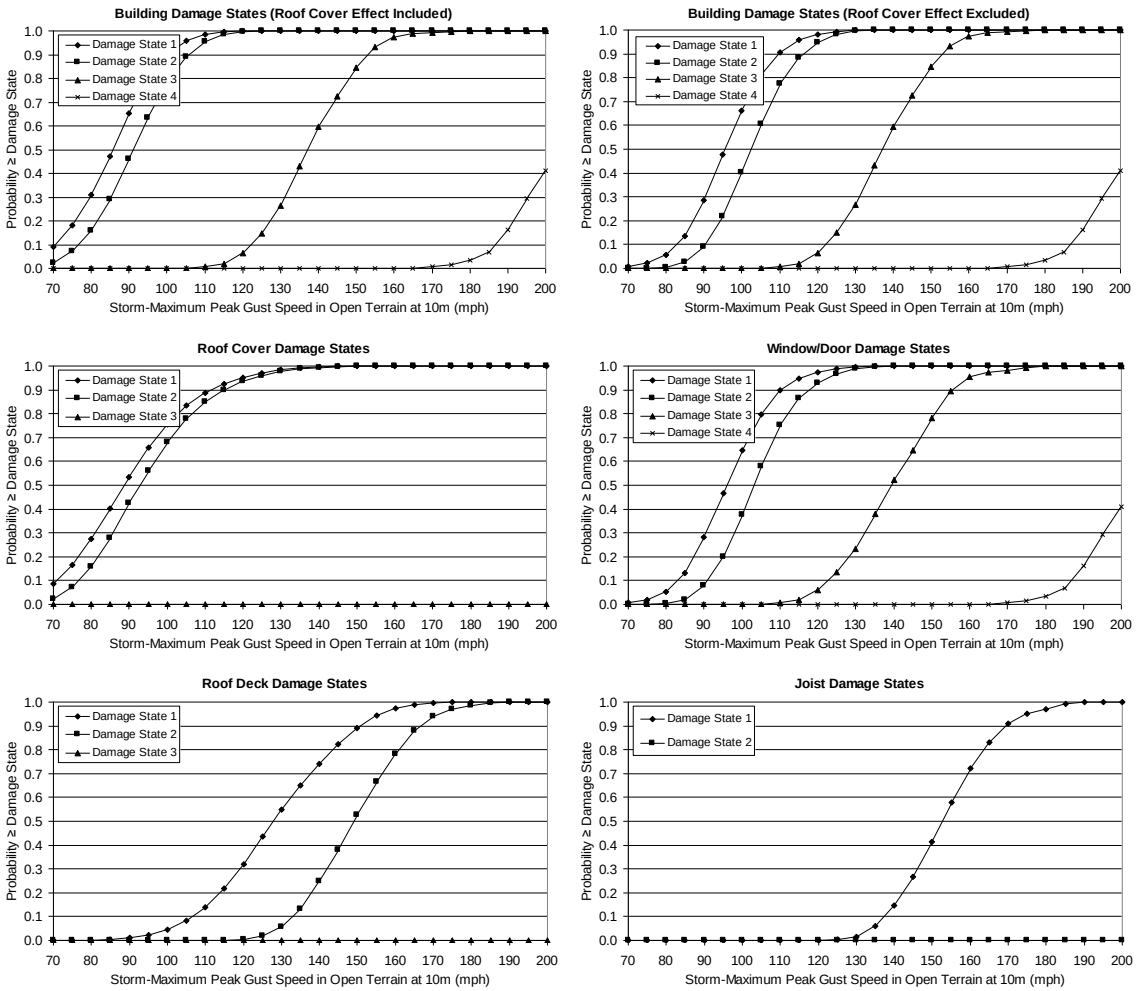

Figure F.40. Damage States vs. Peak Gust Wind Speed – Eight-Story Engineered Residential Building – <u>Single Ply Membrane Roof Cover</u>, 33% Glazing Coverage, Missile Environment A, z_0=0.03 m.

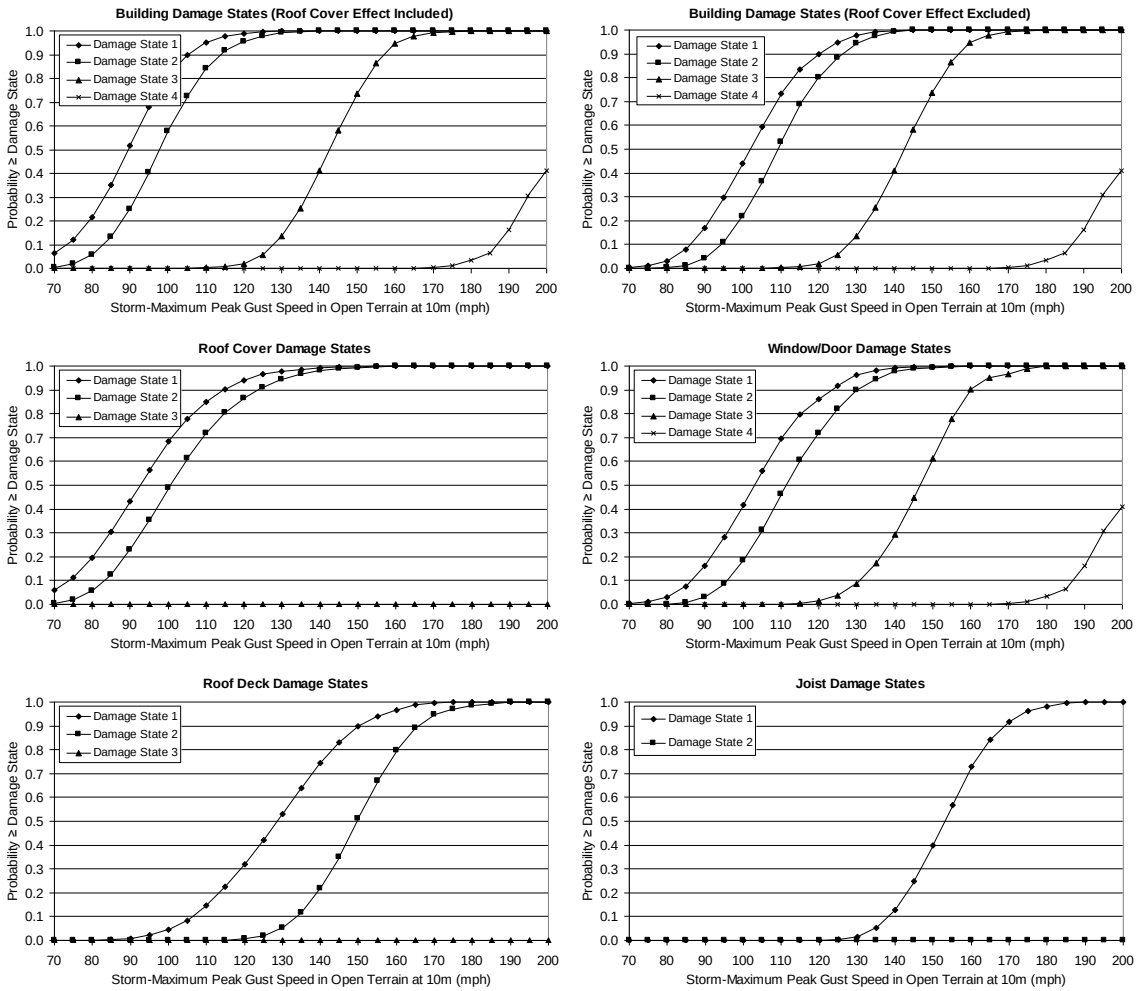

Figure F.41. Damage States vs. Peak Gust Wind Speed – Eight-Story Engineered Residential Building – Built-up Roof Cover, 33% Glazing Coverage, <u>Missile Environment B</u>, z_0=0.03 m.

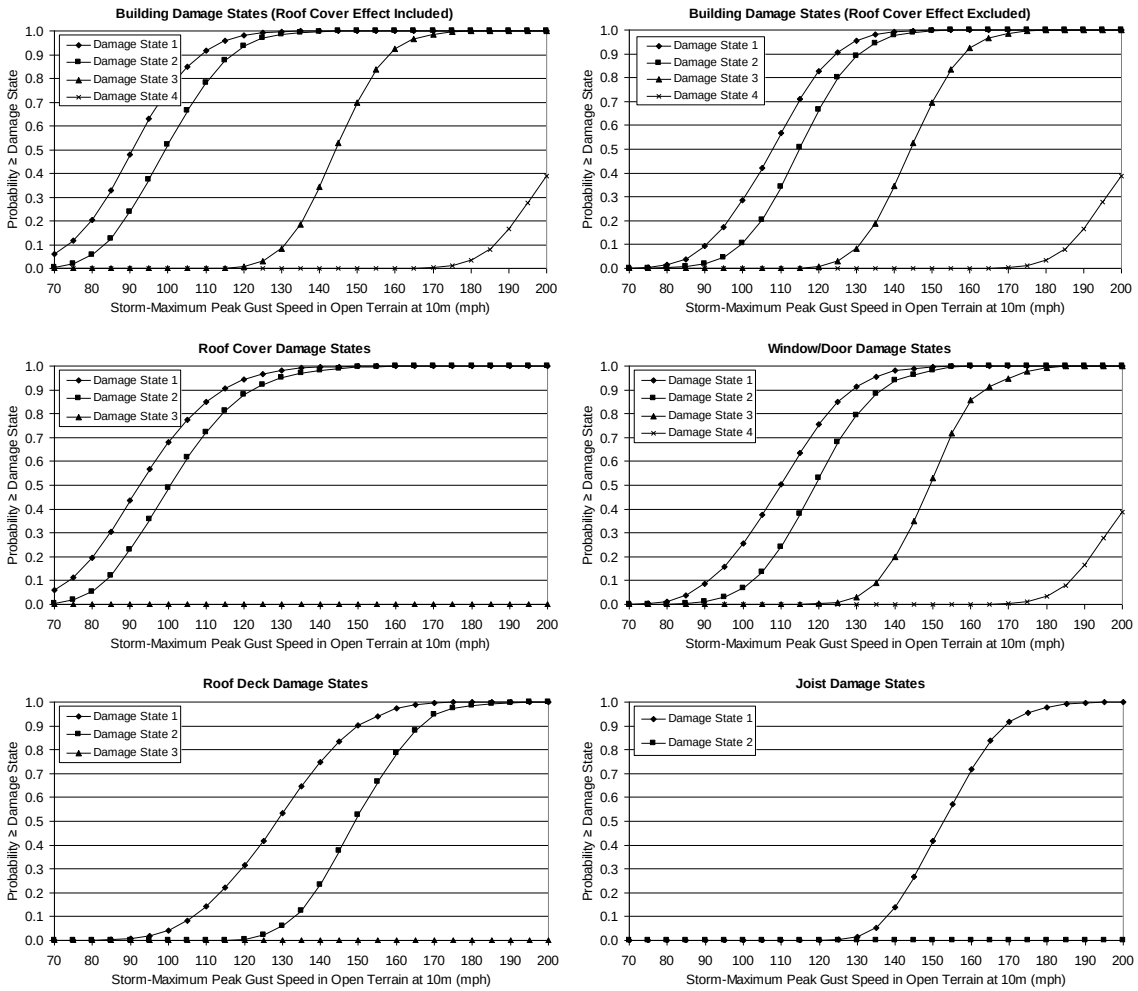

Figure F.42. Damage States vs. Peak Gust Wind Speed – Eight-Story Engineered Residential Building – Built-up Roof Cover, 33% Glazing Coverage, <u>Missile Environment C</u>, z_0=0.03 m.

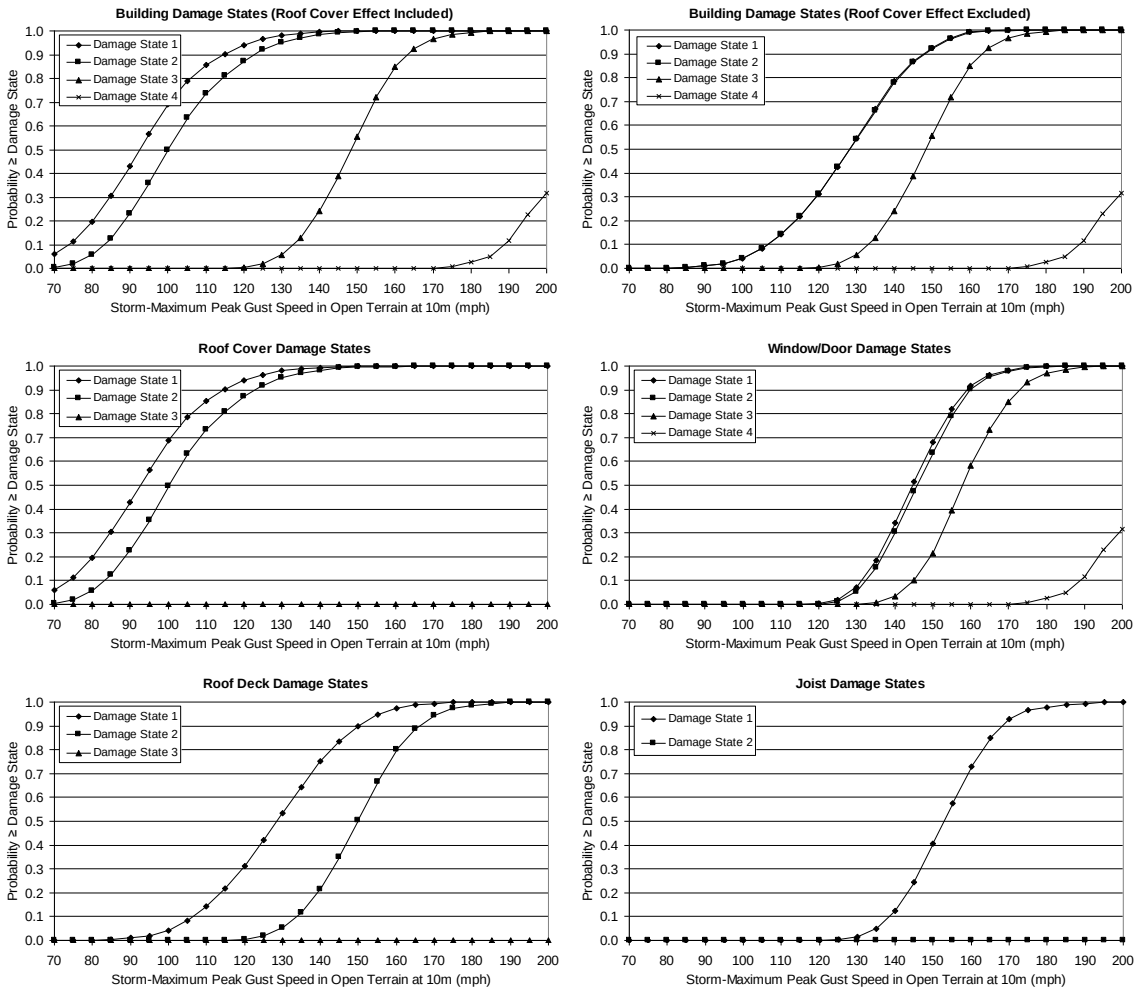

Figure F.43. Damage States vs. Peak Gust Wind Speed – Eight-Story Engineered Residential Building – Built-up Roof Cover, 33% Glazing Coverage, <u>Missile Environment D</u>, z_0=0.03 m.

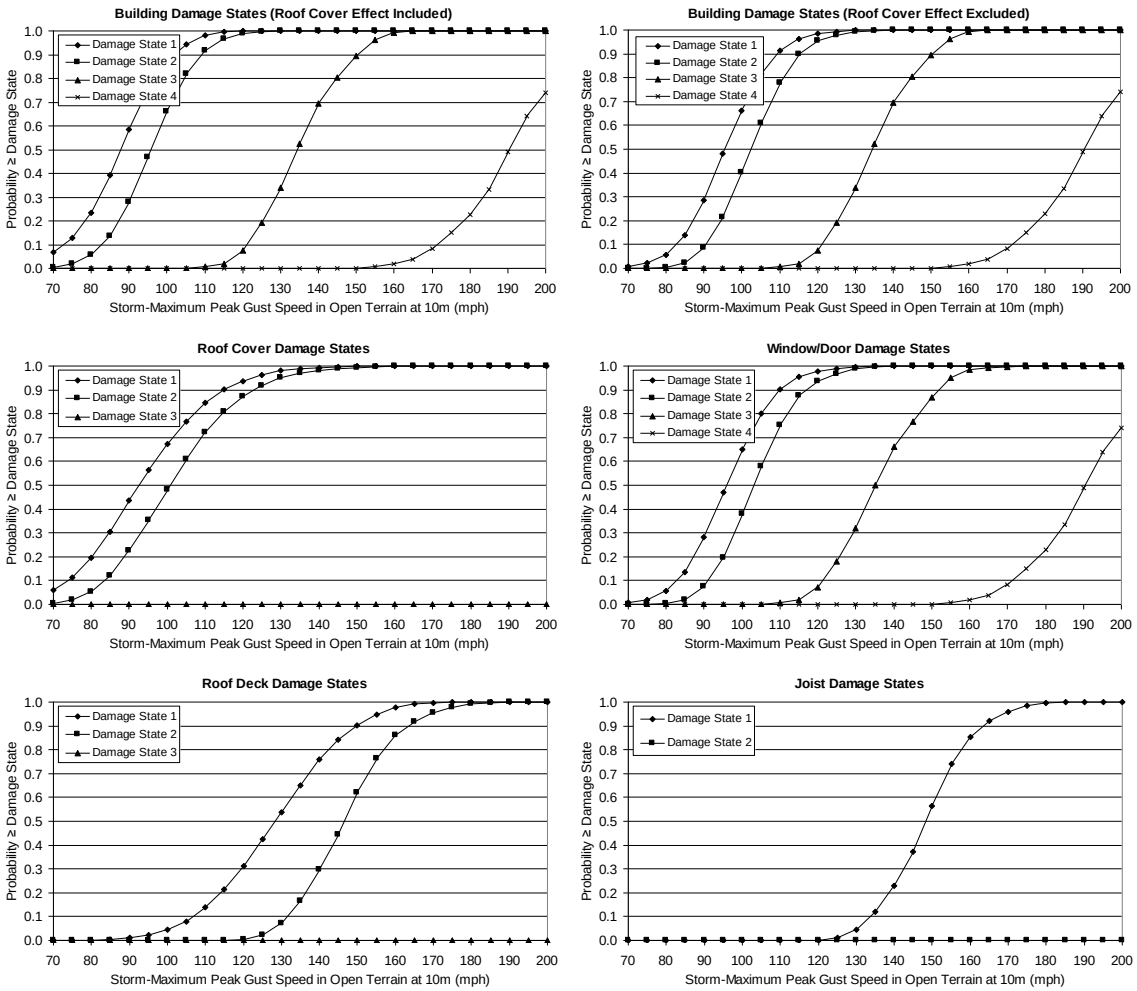

Figure F.44. Damage States vs. Peak Gust Wind Speed – Eight-Story Engineered <u>Commercial Building</u> – Built-up Roof Cover, 33% Glazing Coverage, Missile Environment A, z_0=0.03 m.

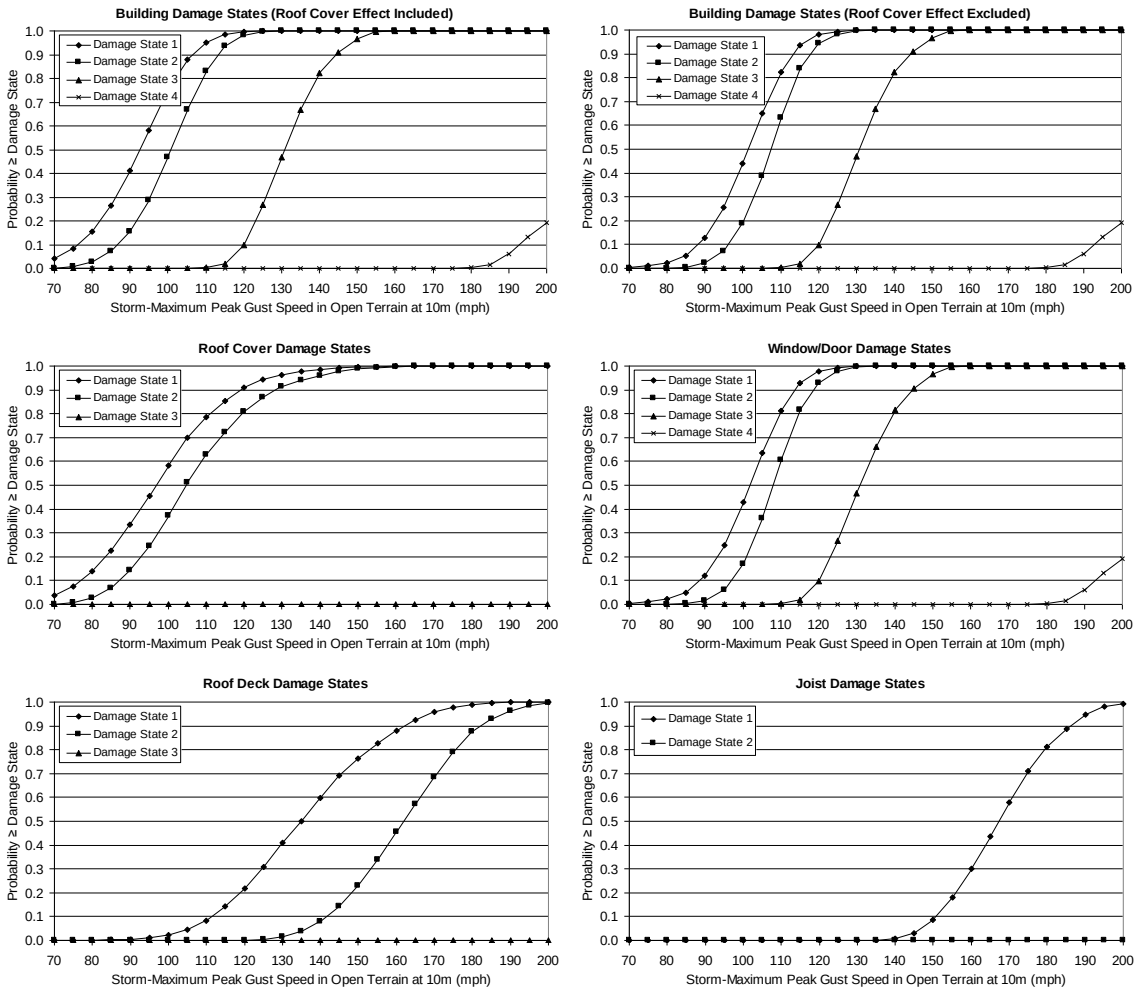

Figure F.45. Damage States vs. Peak Gust Wind Speed – Eight-Story Engineered Residential Building – Built-up Roof Cover, 33% Glazing Coverage, Missile Environment A, z_0=0.35 m.

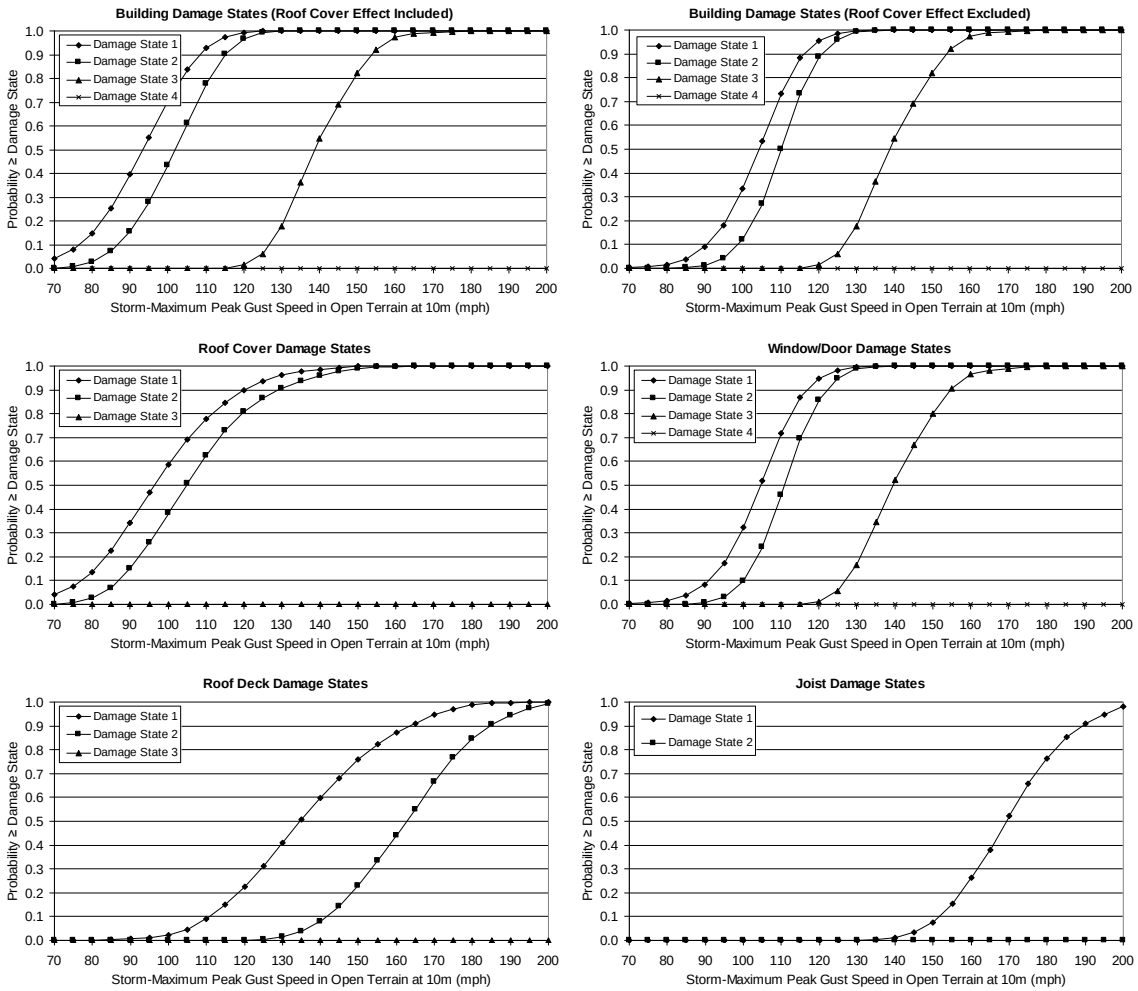

Figure F.46. Damage States vs. Peak Gust Wind Speed – Eight-Story Engineered Residential Building – Built-up Roof Cover, <u>20% Glazing Coverage</u>, Missile Environment A, z_0=0.35 m.

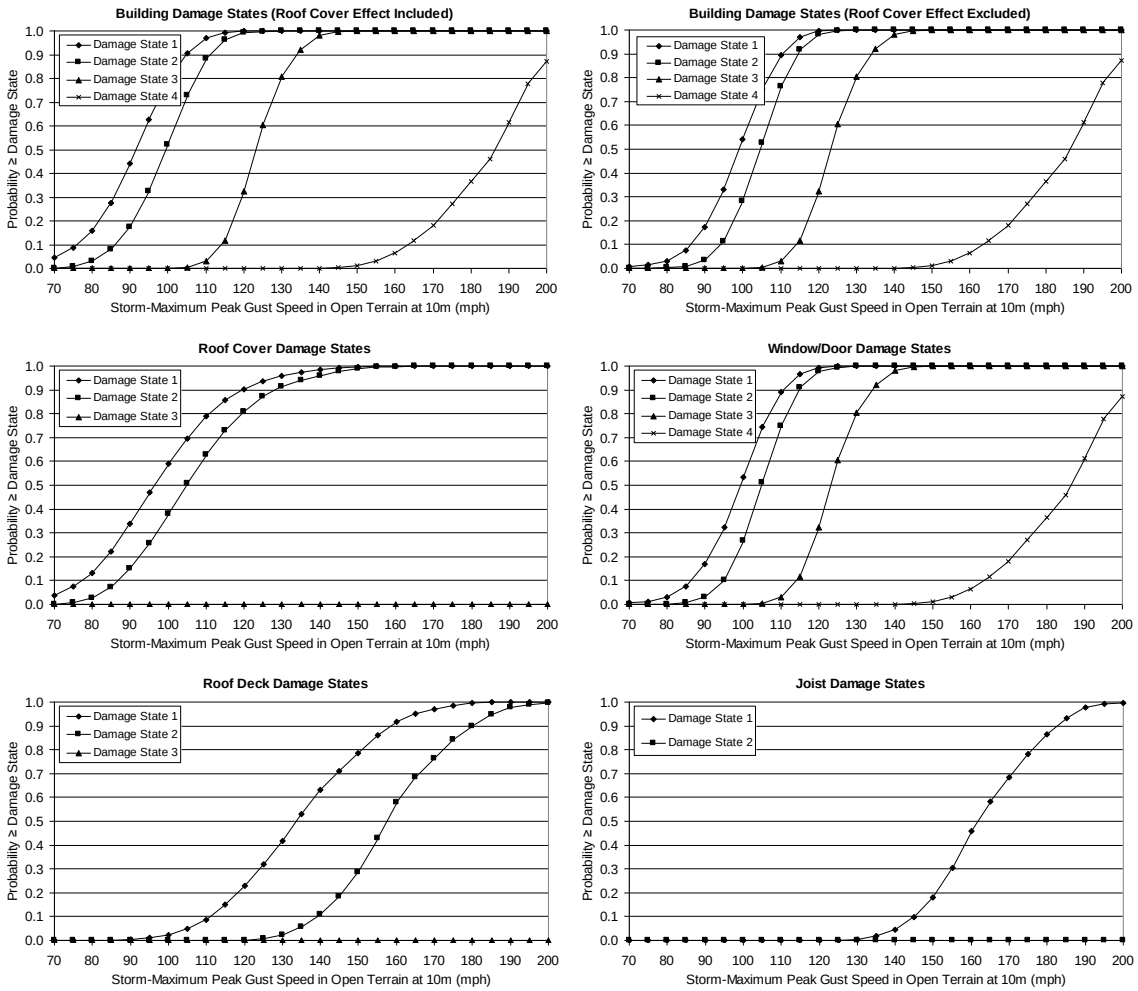

Figure F.47. Damage States vs. Peak Gust Wind Speed – Eight-Story Engineered Residential Building – Built-up Roof Cover, 50% Glazing Coverage, Missile Environment A, z_0=0.35 m.

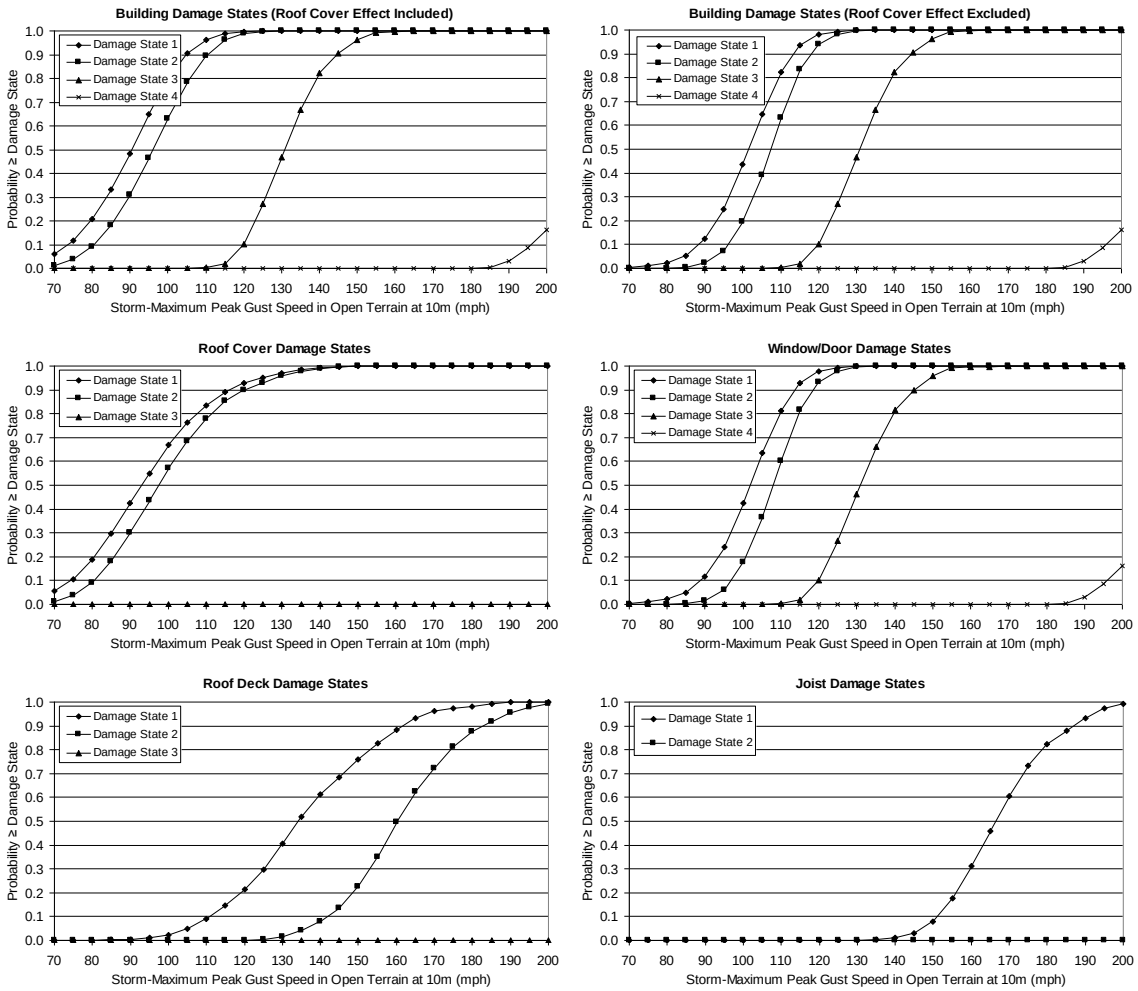

Figure F.48. Damage States vs. Peak Gust Wind Speed – Eight-Story Engineered Residential Building – <u>Single Ply Membrane Roof Cover</u>, 33% Glazing Coverage, Missile Environment A, z_0=0.35 m.

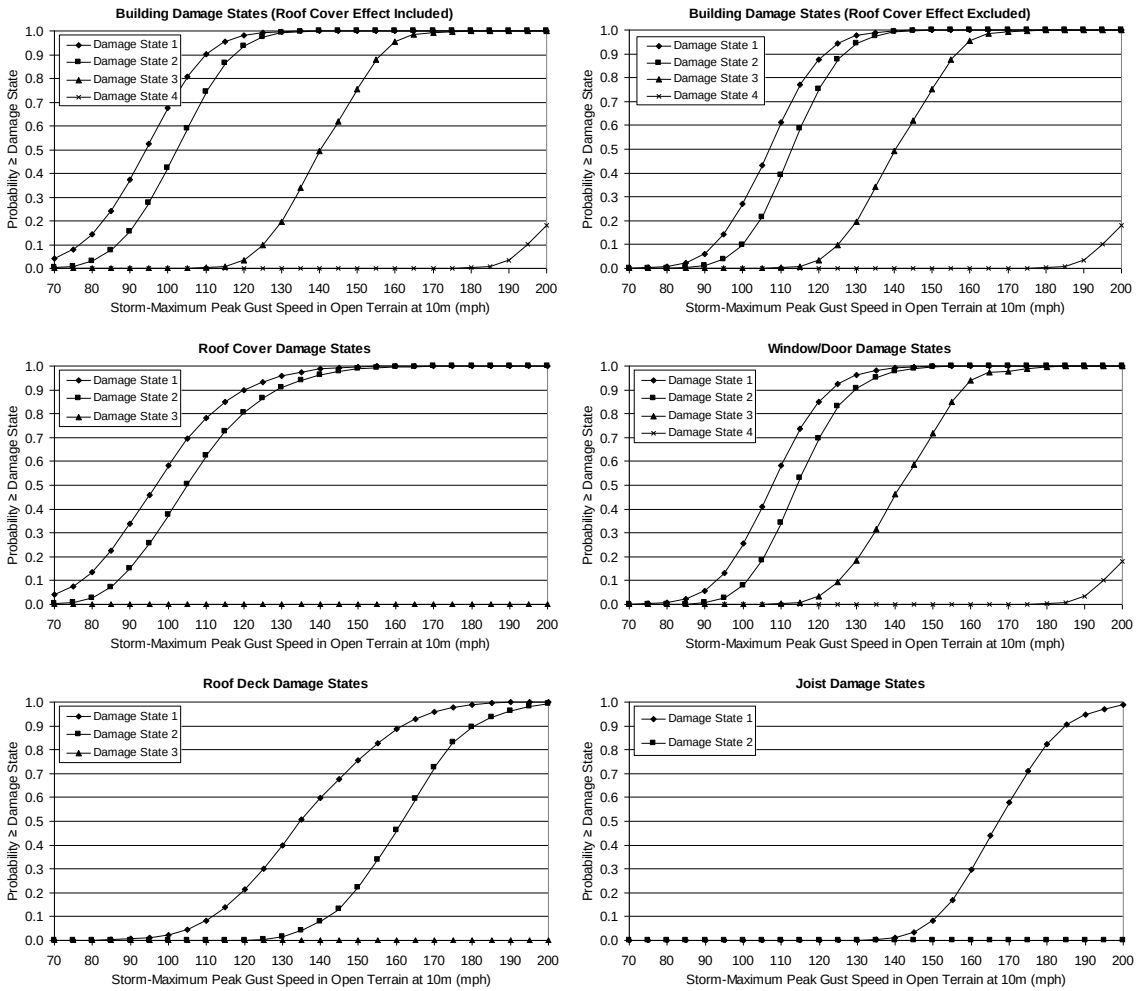

Figure F.49. Damage States vs. Peak Gust Wind Speed – Eight-Story Engineered Residential Building – Built-up Roof Cover, 33% Glazing Coverage, <u>Missile Environment B</u>, z_0=0.35 m.

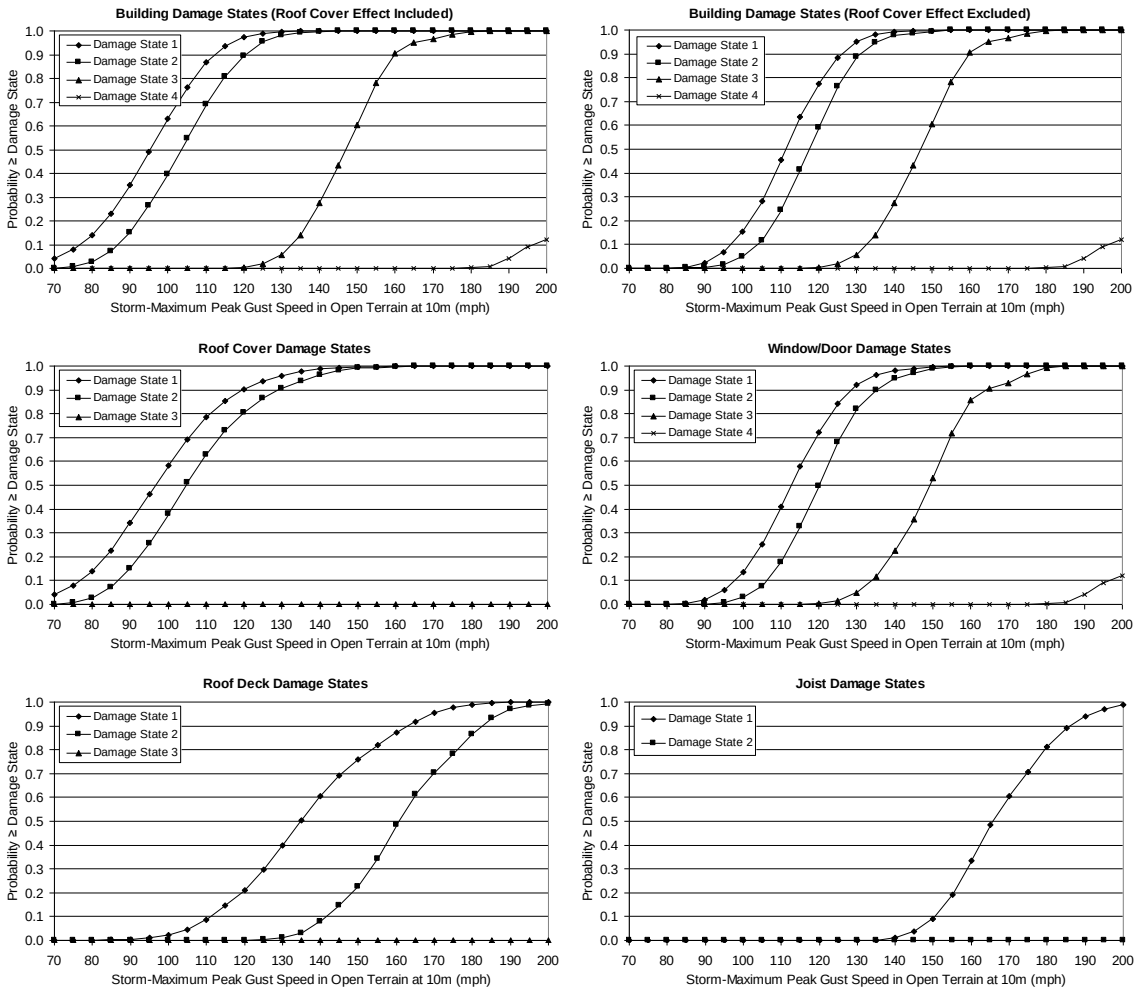

Figure F.50. Damage States vs. Peak Gust Wind Speed – Eight-Story Engineered Residential Building – Built-up Roof Cover, 33% Glazing Coverage, <u>Missile Environment C</u>, z_0=0.35 m.

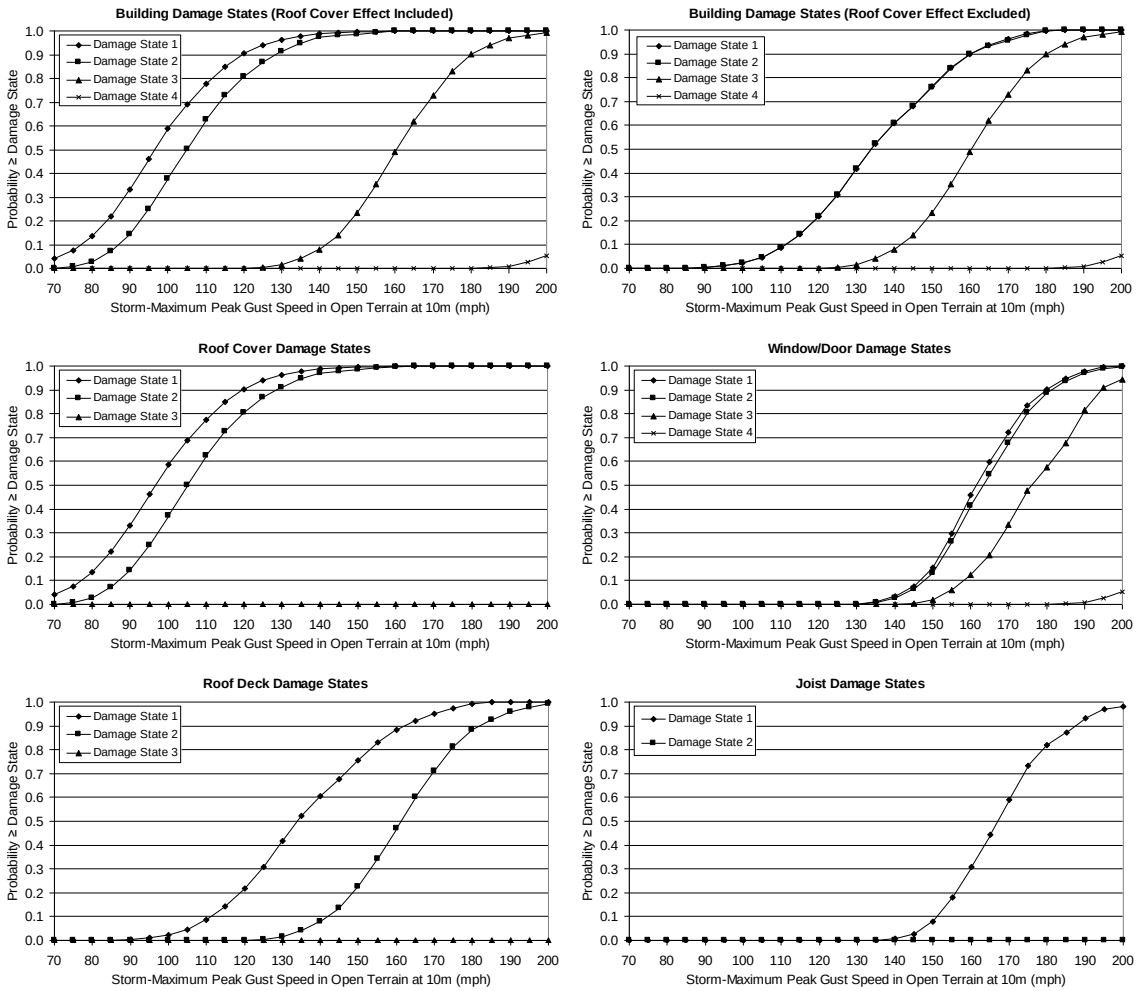

Figure F.51. Damage States vs. Peak Gust Wind Speed – Eight-Story Engineered Residential Building – Built-up Roof Cover, 33% Glazing Coverage, <u>Missile Environment D</u>, z_0=0.35 m.

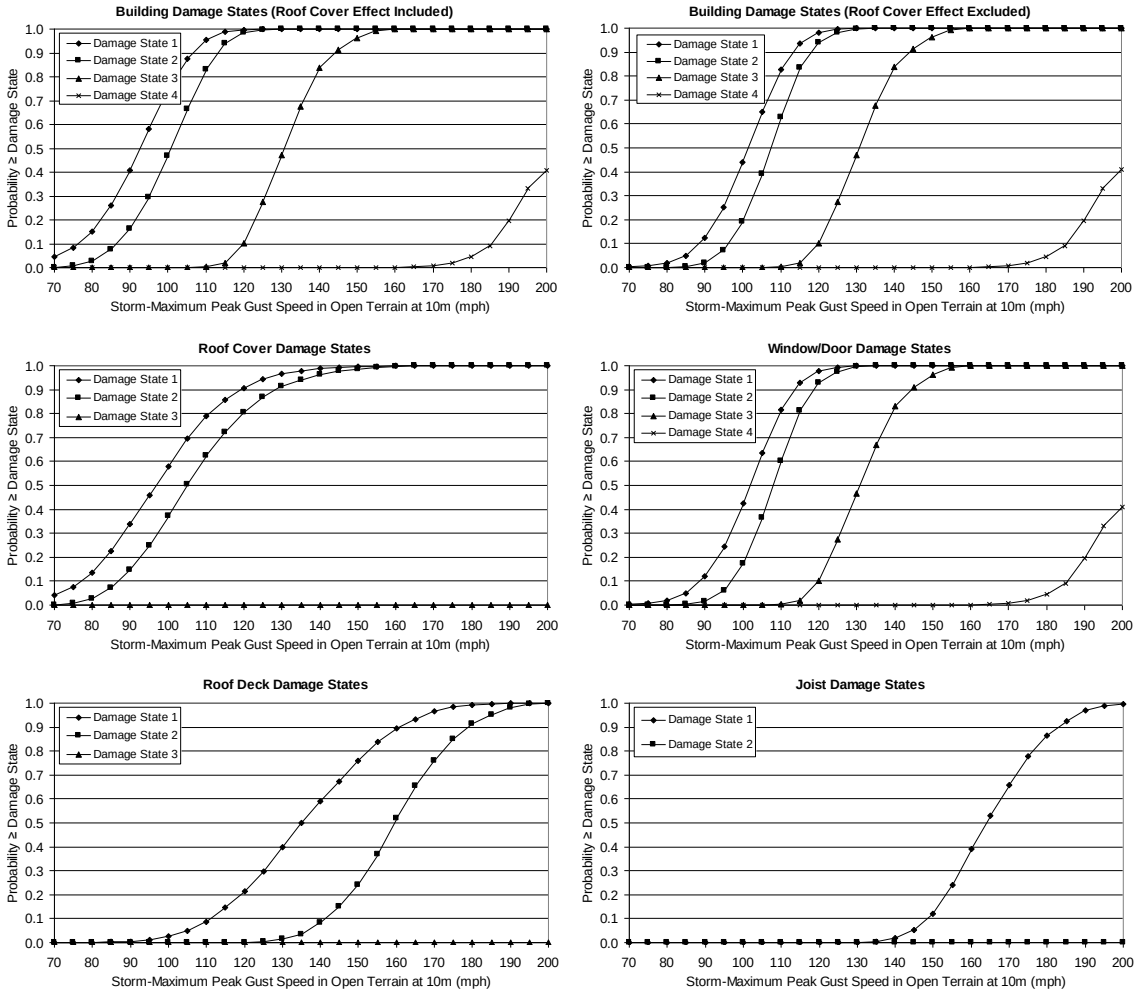

Figure F.52. Damage States vs. Peak Gust Wind Speed – Eight-Story Engineered Commercial Building – Built-up Roof Cover, 33% Glazing Coverage, Missile Environment A, z_0=0.35 m.

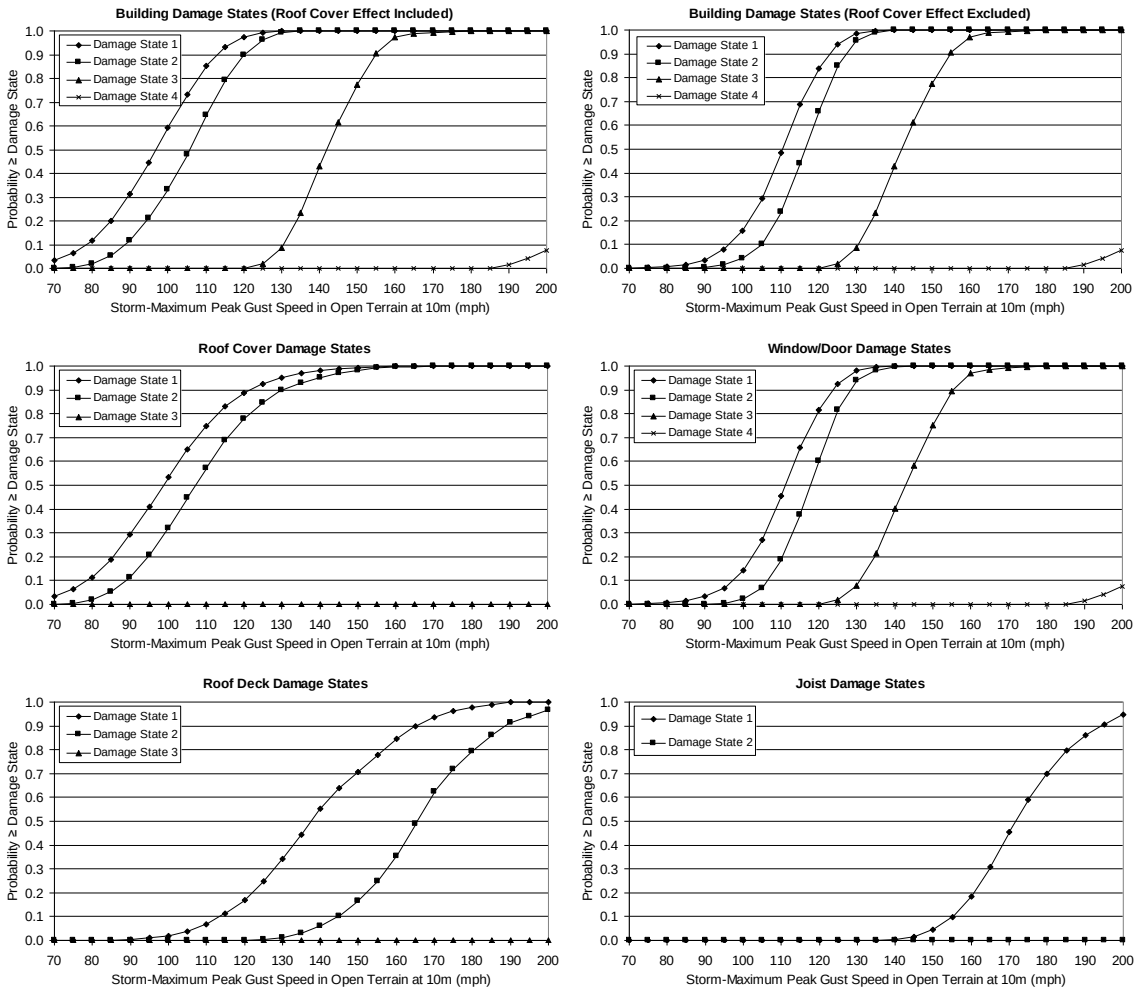

Figure F.53. Damage States vs. Peak Gust Wind Speed – Eight-Story Engineered Residential Building – Built-up Roof Cover, 33% Glazing Coverage, Missile Environment A, z_0=0.70 m.

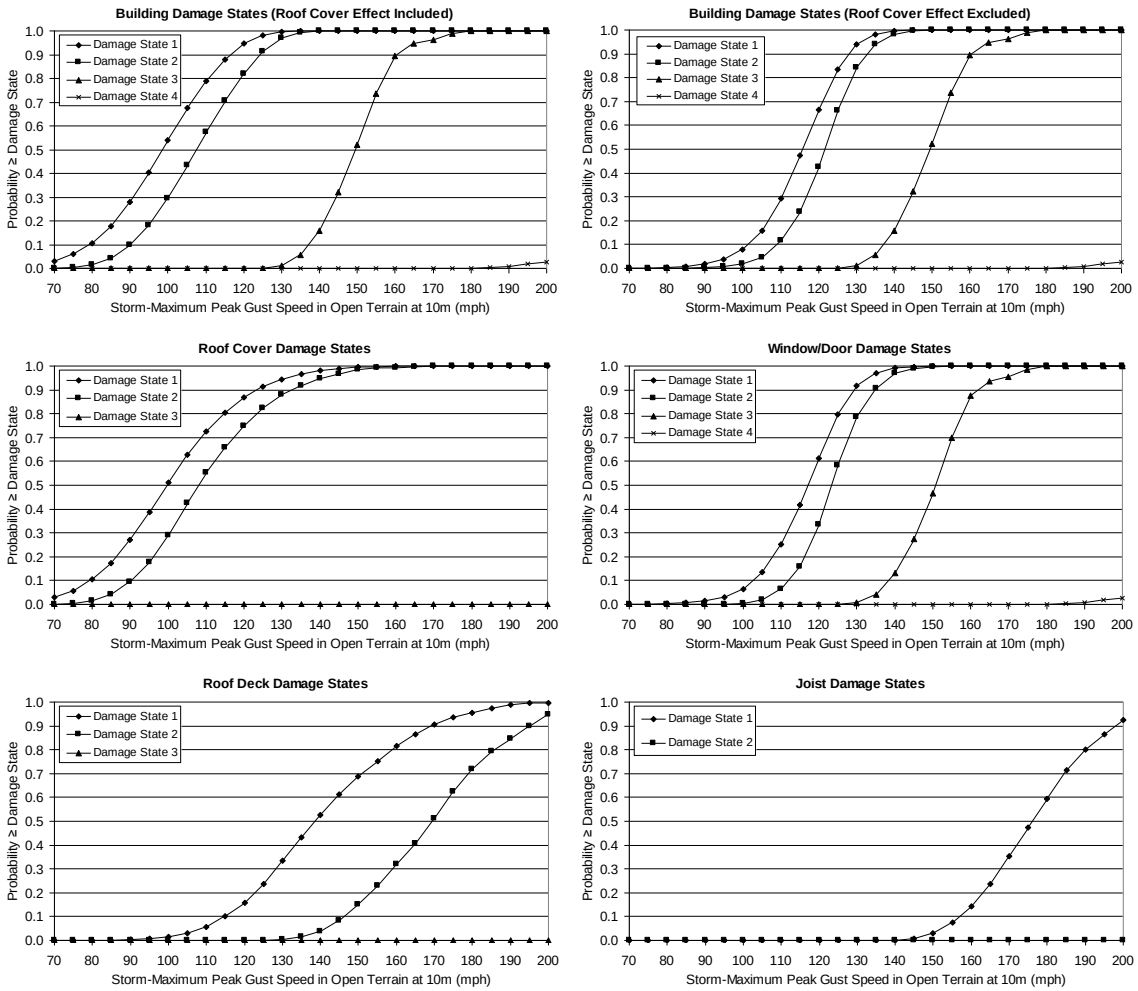

Figure F.54. Damage States vs. Peak Gust Wind Speed – Eight-Story Engineered Residential Building – Built-up Roof Cover, 33% Glazing Coverage, Missile Environment A, z_0=1.0 m.

Appendix G.
Damage State Functions for Industrial Buildings

Appendix G.
Damage State Functions for Industrial Buildings

This appendix presents damage state curves for industrial buildings. The damage state curves show the probability of achieving a certain damage state versus storm-maximum peak gust speed (open terrain at 10m above ground). Plots are presented for the overall building damage states and for the individual building component damage states (refer to Table 6.13-1 for damage state definitions).

Table G.1 lists the figures provided in this appendix. Two sets of three figures are given for the metal buildings. The first set of three figures (Figures G.1 through G.3) are for buildings located in an open terrain (z_0=0.03 m) and the second set (Figures G.4 through G.6) are for buildings situated in a typical suburban environment (z_0=0.35 m). The first figure in each set of three shows damage state results for the industrial building constructed with unreinforced masonry walls, having no reduction in the metal roof deck capacity and situated in Missile Environment A. The remaining two plots in each set show damage state results for buildings which are different by a single variable in comparison to the reference building (note that the changed variable is underlined in the figure titles). Figures G.7 and G.8 show results of the reference building situated in two additional terrain environments (i.e., z_0=0.70 m and 1.0 m).

Table G.1. Sample Damage State Functions for Industrial Buildings

Figure	Walls	Metal Deck Capacity	Missile Environ.	Terrain
G.1	URM	Full	A	0.03
G.2	**RM**	Full	A	0.03
G.3	URM	**50%**	A	0.03
G.4	URM	Full	A	**0.35**
G.5	**RM**	Full	A	0.35
G.6	URM	**50%**	A	0.35
G.7	URM	Full	A	**0.70**
G.8	URM	Full	A	**1.00**

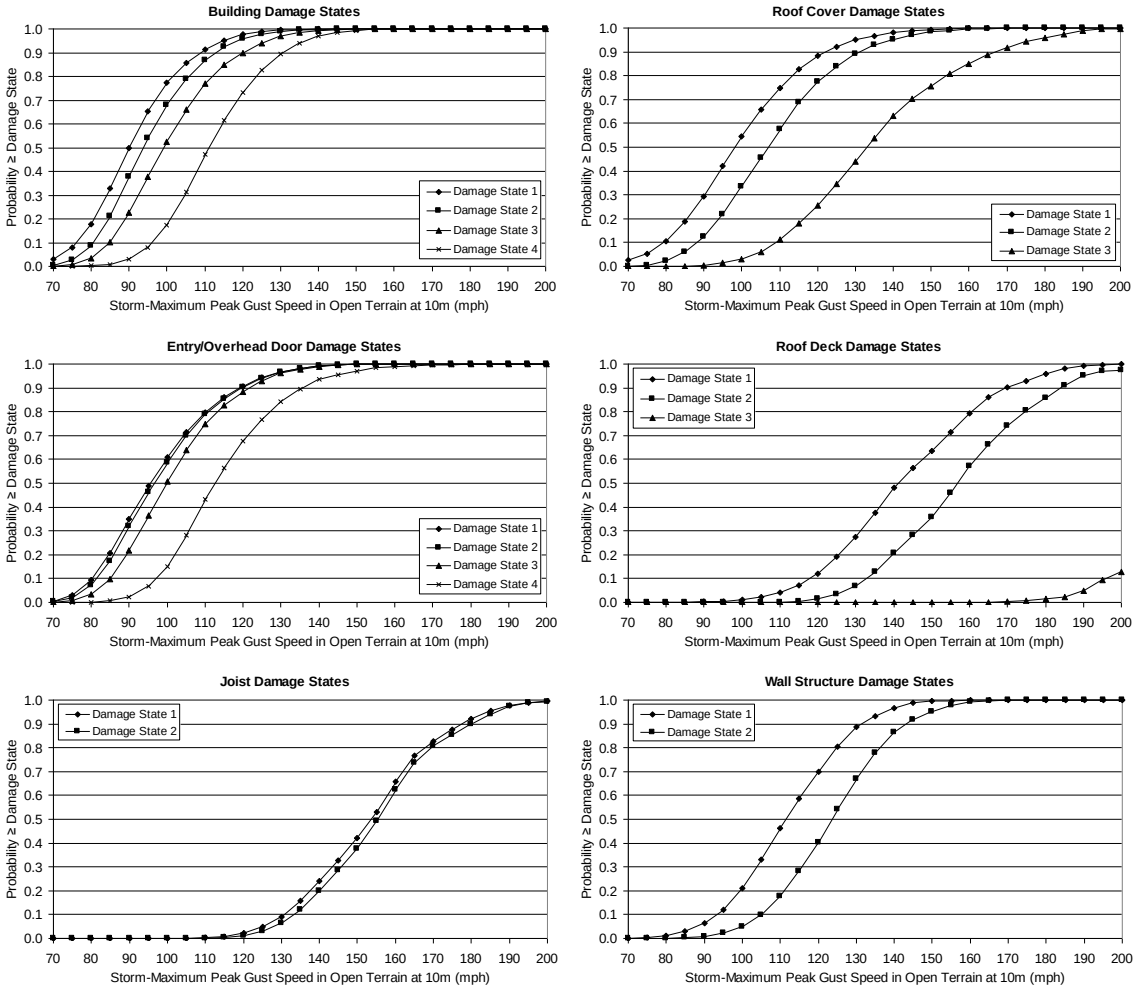

Figure G.1. Damage States vs. Maximum Peak Gust Wind Speed – Industrial Building – No Reduction in Metal Deck Capacity, Unreinforced Masonry Walls, Missile Environment A, z_0=0.03 m.

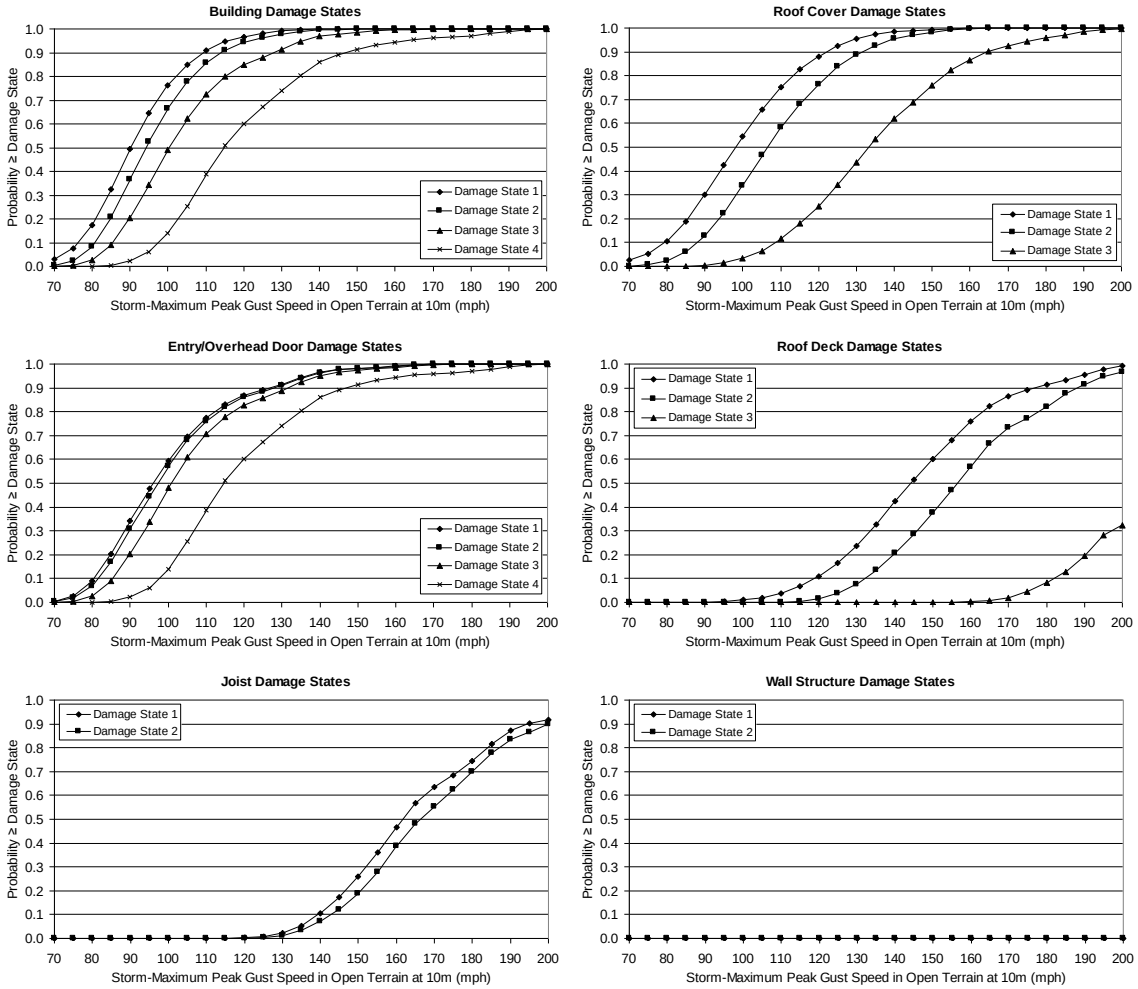

Figure G.2. Damage States vs. Maximum Peak Gust Wind Speed – Industrial Building – No Reduction in Metal Deck Capacity, <u>Reinforced Masonry Walls</u>, Missile Environment A, z_0=0.03 m.

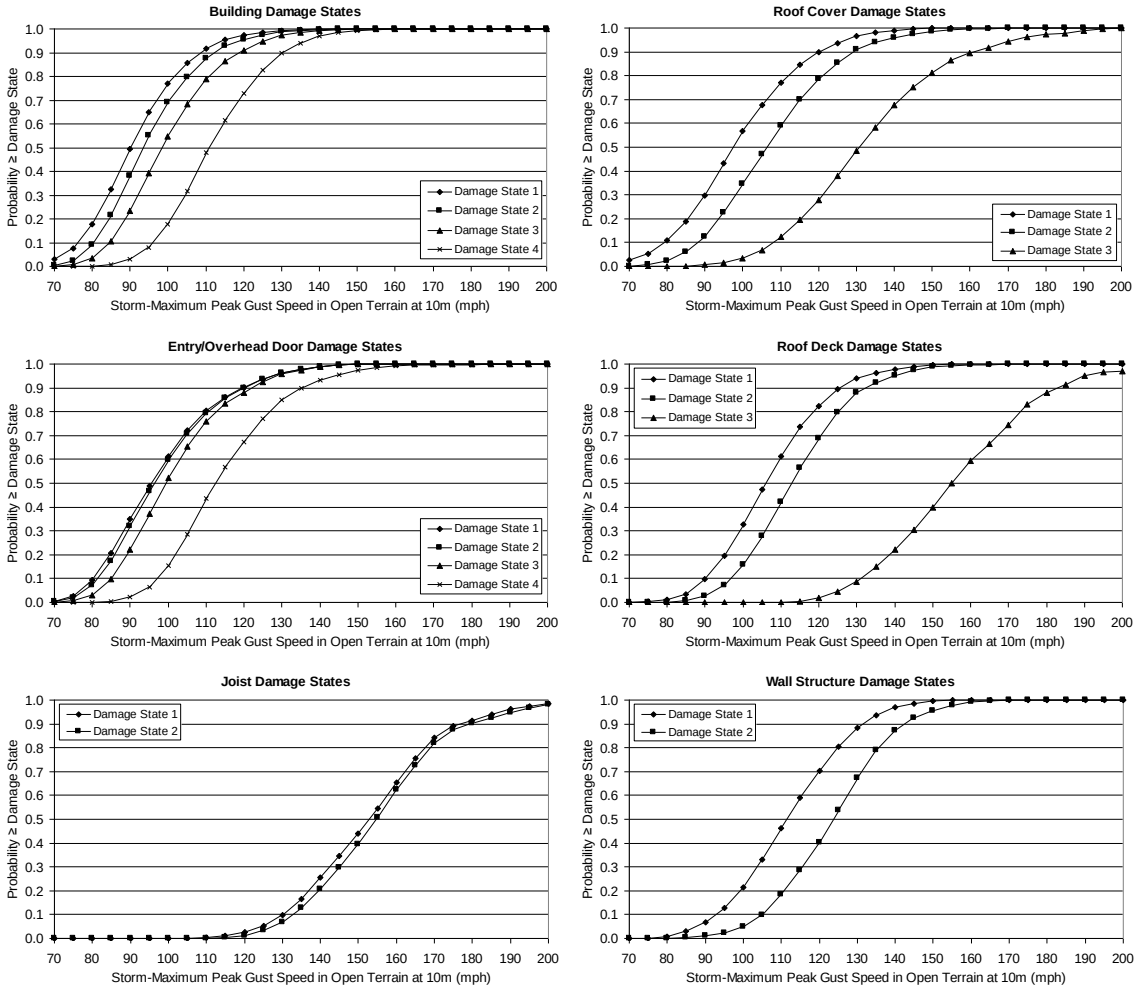

Figure G.3. Damage States vs. Maximum Peak Gust Wind Speed – Industrial Building – *50%* Reduction in Metal Deck Capacity, Unreinforced Masonry Walls, Missile Environment A, z_0=0.03 m.

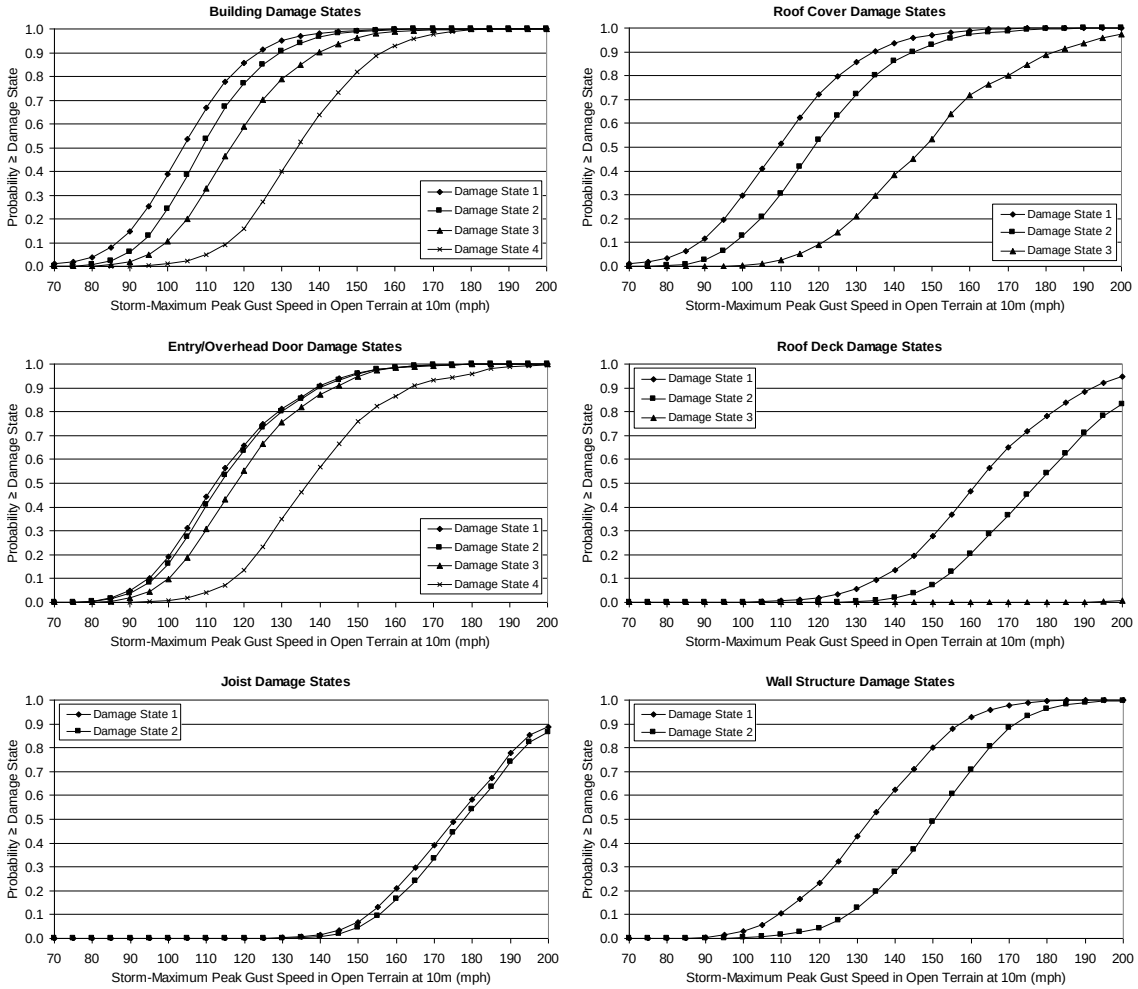

Figure G.4. Damage States vs. Maximum Peak Gust Wind Speed – Industrial Building – No Reduction in Metal Deck Capacity, Unreinforced Masonry Walls, Missile Environment A, z_0=0.35 m.

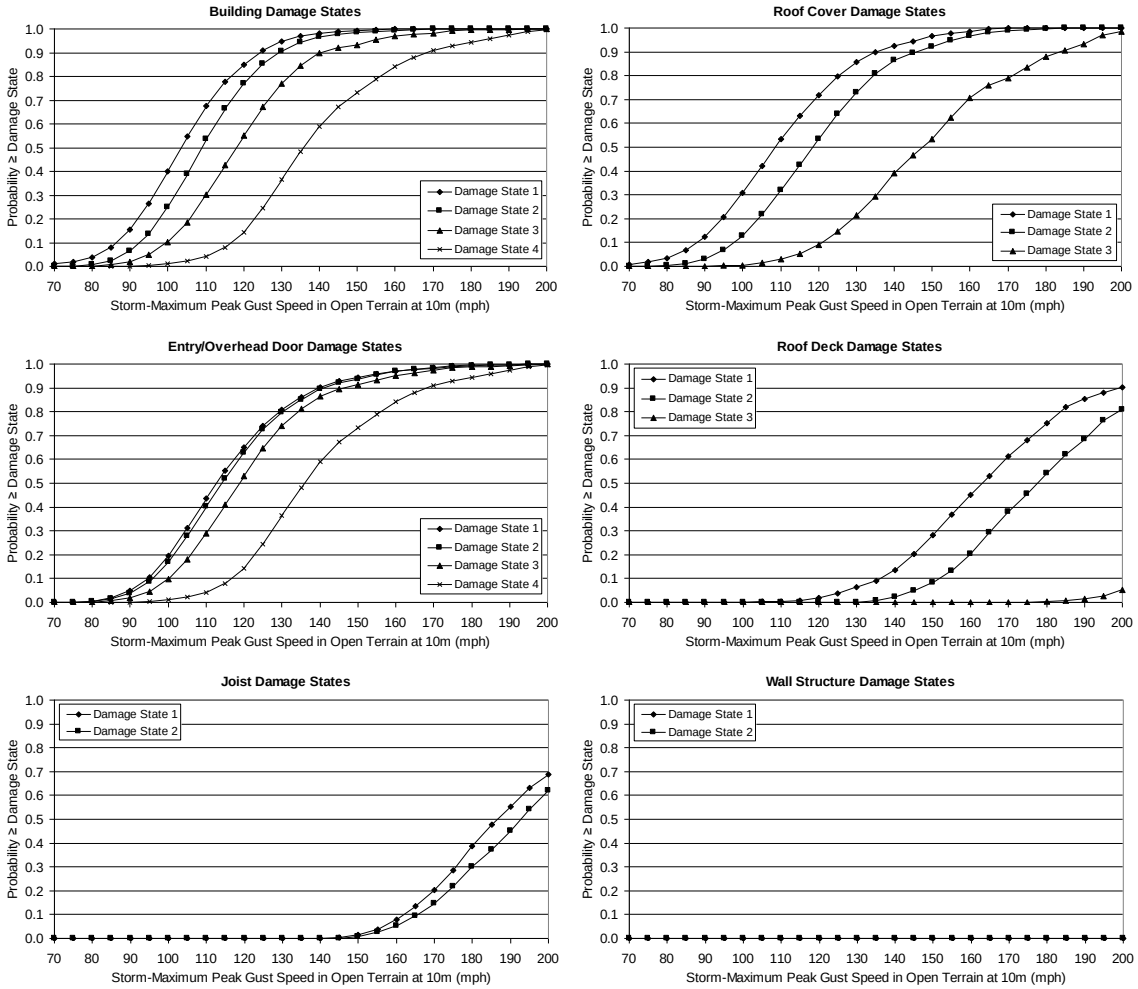

Figure G.5. Damage States vs. Maximum Peak Gust Wind Speed – Industrial Building – No Reduction in Metal Deck Capacity, Reinforced Masonry Walls, Missile Environment A, z_0=0.35 m.

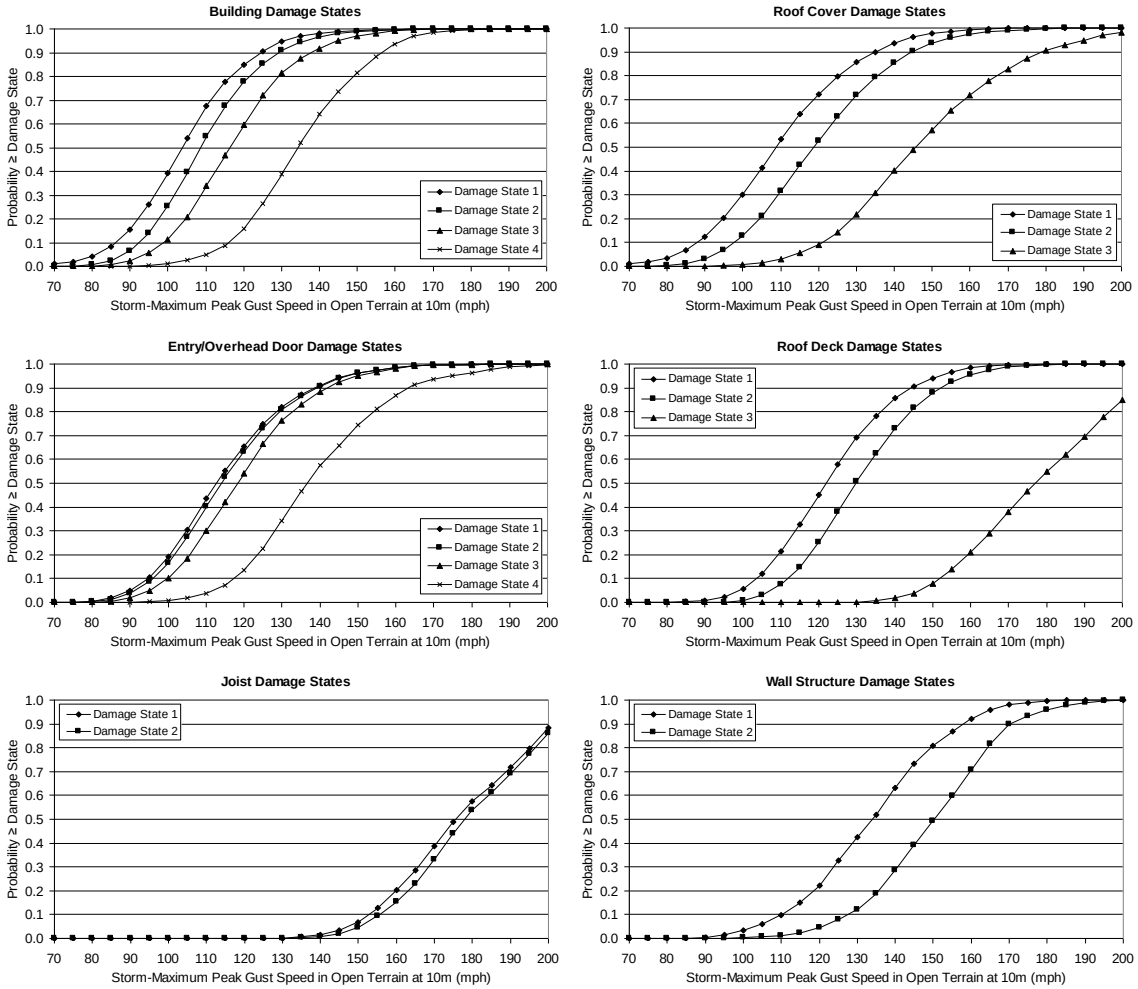

Figure G.6. Damage States vs. Maximum Peak Gust Wind Speed – Industrial Building – <u>50% Reduction in Metal Deck Capacity</u>, Unreinforced Masonry Walls, Missile Environment A, z_0=0.35 m.

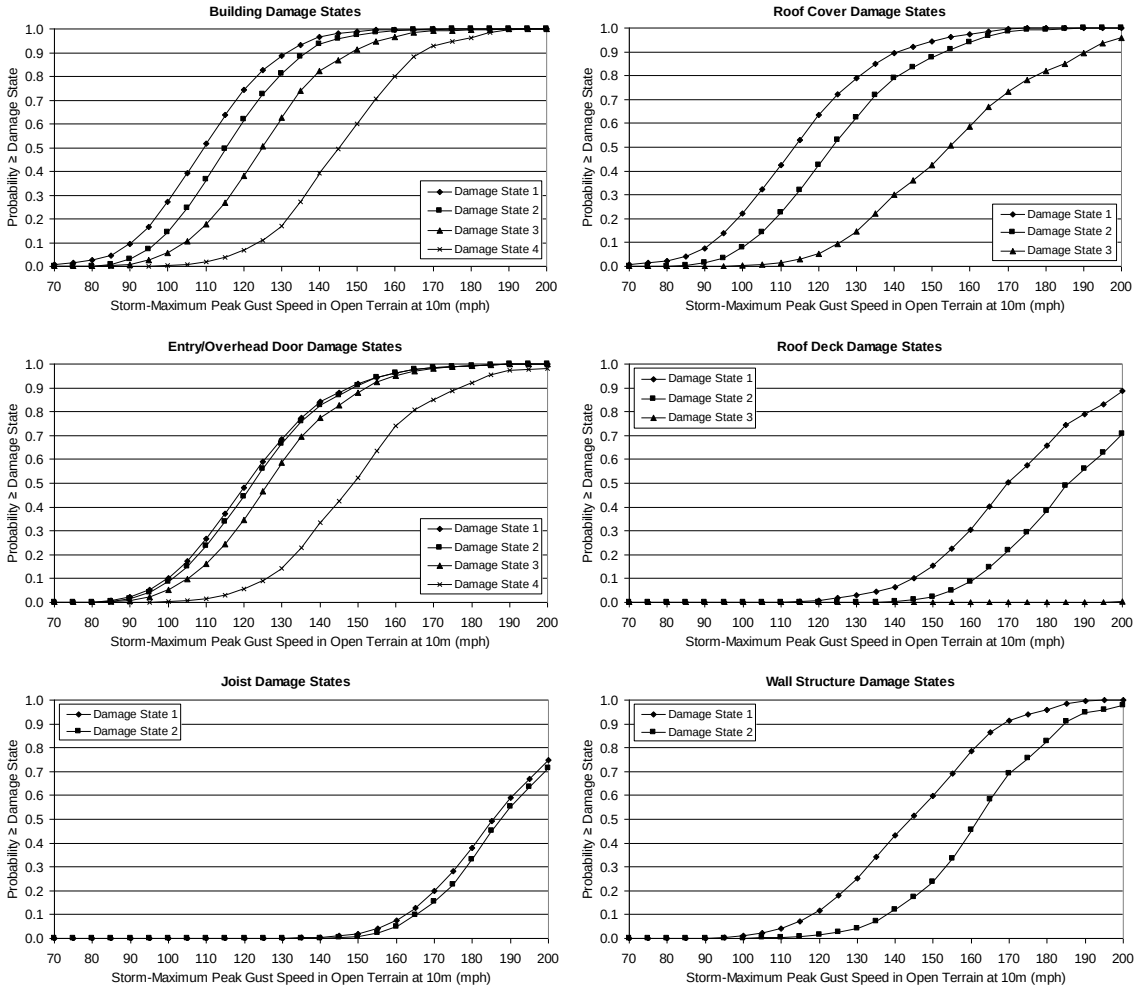

Figure G.7. Damage States vs. Maximum Peak Gust Wind Speed – Industrial Building – No Reduction in Metal Deck Capacity, Unreinforced Masonry Walls, Missile Environment A, z_0=0.7 m.

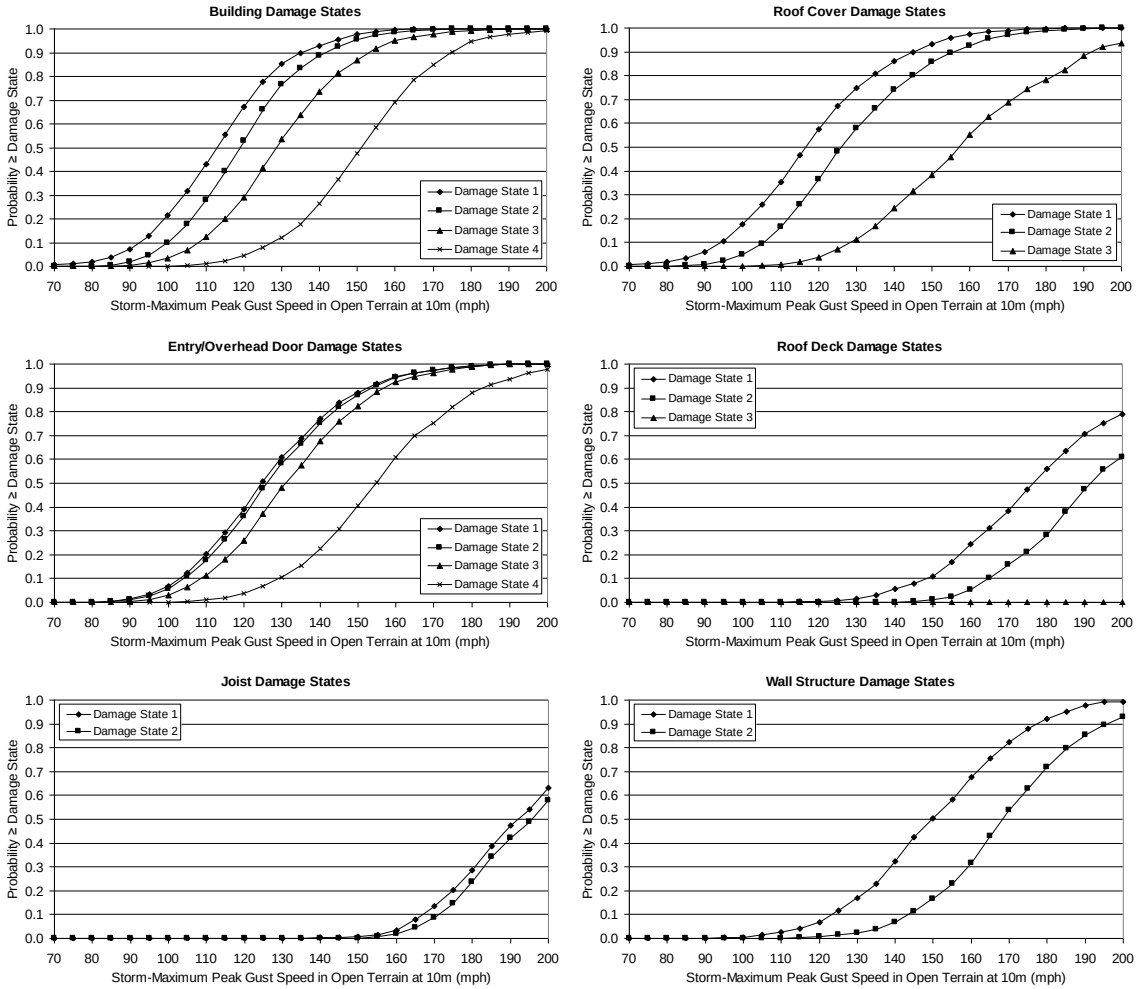

Figure G.8. Damage States vs. Maximum Peak Gust Wind Speed – Industrial Building – No Reduction in Metal Deck Capacity, Unreinforced Masonry Walls, Missile Environment A, z_0=1.0 m.

Appendix H.
Loss Functions for Residential Buildings

Appendix H.
Loss Functions for Residential Buildings

This appendix presents loss functions for residential buildings (see Section 7.7). The loss functions represent either average building loss normalized by building value or average content loss normalized by content value. Therefore, the loss ratios range between 0 and 1 in both cases. Note that the content value is set to 50% of the building value. For a given simulated storm, the building loss ratio and content loss ratio are estimated based on the modeled damage and the largest gust speed over the entire duration of the simulated storm is saved. The loss functions are then computed by averaging the loss ratios associated with the storms producing a maximum gust speed within 5 mph ranges. The average loss ratios (content or building loss) associated with each 5 mph gust speed range are then plotted at the center of that range. Note that the wind speeds are representative of open terrain at 10 m above ground.

Table H.1 lists the figures provided in this appendix. In each set of sixteen plots, the building parameters varied are: roof deck nails (6d or 8d), roof/wall connections (toE.nail or strap), number of stories (one or two), and roof shape (gable or hip). Plots are presented for the buildings constructed with wood frame walls and for the buildings having no garage.

Table H.1. Sample Loss Functions for Residential Buildings

Figure	Loss Type	Walls	Stories	Garage	Roof Shape	Sheathing	Roof/ Wall	Shutters	Upgraded Roof	Secondary Water Resistance
H.1	Building	WFR	1	No	Gable	6d	Toe-Nail	No	No	No
H.2	Building	WFR	1	No	Gable	6d	Strap	No	No	No
H.3	Building	WFR	1	No	Gable	8d	Toe-Nail	No	No	No
H.4	Building	WFR	1	No	Gable	8d	Strap	No	No	No
H.5	Building	WFR	1	No	Hip	6d	Toe-Nail	No	No	No
H.6	Building	WFR	1	No	Hip	6d	Strap	No	No	No
H.7	Building	WFR	1	No	Hip	8d	Toe-Nail	No	No	No
H.8	Building	WFR	1	No	Hip	8d	Strap	No	No	No
H.9	Building	WFR	2	No	Gable	6d	Toe-Nail	No	No	No
H.10	Building	WFR	2	No	Gable	6d	Strap	No	No	No
H.11	Building	WFR	2	No	Gable	8d	Toe-Nail	No	No	No
H.12	Building	WFR	2	No	Gable	8d	Strap	No	No	No
H.13	Building	WFR	2	No	Hip	6d	Toe-Nail	No	No	No
H.14	Building	WFR	2	No	Hip	6d	Strap	No	No	No
H.15	Building	WFR	2	No	Hip	8d	Toe-Nail	No	No	No
H.16	Building	WFR	2	No	Hip	8d	Strap	No	No	No
H.17	Content	WFR	1	No	Gable	6d	Toe-Nail	No	No	No
H.18	Content	WFR	1	No	Gable	6d	Strap	No	No	No
H.19	Content	WFR	1	No	Gable	8d	Toe-Nail	No	No	No
H.20	Content	WFR	1	No	Gable	8d	Strap	No	No	No
H.21	Content	WFR	1	No	Hip	6d	Toe-Nail	No	No	No

Table H.1. Sample Loss Functions for Residential Buildings (continued)

Figure	Loss Type	Walls	Stories	Garage	Roof Shape	Sheathing	Roof/ Wall	Shutters	Upgraded Roof	Secondary Water Resistance
H.22	Content	WFR	1	No	Hip	6d	Strap	No	No	No
H.23	Content	WFR	1	No	Hip	8d	Toe-Nail	No	No	No
H.24	Content	WFR	1	No	Hip	8d	Strap	No	No	No
H.25	Content	WFR	2	No	Gable	6d	Toe-Nail	No	No	No
H.26	Content	WFR	2	No	Gable	6d	Strap	No	No	No
H.27	Content	WFR	2	No	Gable	8d	Toe-Nail	No	No	No
H.28	Content	WFR	2	No	Gable	8d	Strap	No	No	No
H.29	Content	WFR	2	No	Hip	6d	Toe-Nail	No	No	No
H.30	Content	WFR	2	No	Hip	6d	Strap	No	No	No
H.31	Content	WFR	2	No	Hip	8d	Toe-Nail	No	No	No
H.32	Content	WFR	2	No	Hip	8d	Strap	No	No	No
H.33	Building	WFR	1	No	Gable	6d	Toe-Nail	Yes	No	No
H.34	Building	WFR	1	No	Gable	6d	Strap	Yes	No	No
H.35	Building	WFR	1	No	Gable	8d	Toe-Nail	Yes	No	No
H.36	Building	WFR	1	No	Gable	8d	Strap	Yes	No	No
H.37	Building	WFR	1	No	Hip	6d	Toe-Nail	Yes	No	No
H.38	Building	WFR	1	No	Hip	6d	Strap	Yes	No	No
H.39	Building	WFR	1	No	Hip	8d	Toe-Nail	Yes	No	No
H.40	Building	WFR	1	No	Hip	8d	Strap	Yes	No	No
H.41	Building	WFR	2	No	Gable	6d	Toe-Nail	Yes	No	No
H.42	Building	WFR	2	No	Gable	6d	Strap	Yes	No	No
H.43	Building	WFR	2	No	Gable	8d	Toe-Nail	Yes	No	No
H.44	Building	WFR	2	No	Gable	8d	Strap	Yes	No	No
H.45	Building	WFR	2	No	Hip	6d	Toe-Nail	Yes	No	No
H.46	Building	WFR	2	No	Hip	6d	Strap	Yes	No	No
H.47	Building	WFR	2	No	Hip	8d	Toe-Nail	Yes	No	No
H.48	Building	WFR	2	No	Hip	8d	Strap	Yes	No	No
H.49	Content	WFR	1	No	Gable	6d	Toe-Nail	Yes	No	No
H.50	Content	WFR	1	No	Gable	6d	Strap	Yes	No	No
H.51	Content	WFR	1	No	Gable	8d	Toe-Nail	Yes	No	No
H.52	Content	WFR	1	No	Gable	8d	Strap	Yes	No	No
H.53	Content	WFR	1	No	Hip	6d	Toe-Nail	Yes	No	No
H.54	Content	WFR	1	No	Hip	6d	Strap	Yes	No	No
H.55	Content	WFR	1	No	Hip	8d	Toe-Nail	Yes	No	No
H.56	Content	WFR	1	No	Hip	8d	Strap	Yes	No	No
H.57	Content	WFR	2	No	Gable	6d	Toe-Nail	Yes	No	No
H.58	Content	WFR	2	No	Gable	6d	Strap	Yes	No	No
H.59	Content	WFR	2	No	Gable	8d	Toe-Nail	Yes	No	No
H.60	Content	WFR	2	No	Gable	8d	Strap	Yes	No	No
H.61	Content	WFR	2	No	Hip	6d	Toe-Nail	Yes	No	No
H.62	Content	WFR	2	No	Hip	6d	Strap	Yes	No	No
H.63	Content	WFR	2	No	Hip	8d	Toe-Nail	Yes	No	No
H.64	Content	WFR	2	No	Hip	8d	Strap	Yes	No	No

Table H.1. Sample Loss Functions for Residential Buildings (continued)

Figure	Loss Type	Walls	Stories	Garage	Roof Shape	Sheathing	Roof/ Wall	Shutters	Upgraded Roof	Secondary Water Resistance
H.65	Building	WFR	1	No	Gable	6d	Toe-Nail	No	Yes	No
H.66	Building	WFR	1	No	Gable	6d	Strap	No	Yes	No
H.67	Building	WFR	1	No	Gable	8d	Toe-Nail	No	Yes	No
H.68	Building	WFR	1	No	Gable	8d	Strap	No	Yes	No
H.69	Building	WFR	1	No	Hip	6d	Toe-Nail	No	Yes	No
H.70	Building	WFR	1	No	Hip	6d	Strap	No	Yes	No
H.71	Building	WFR	1	No	Hip	8d	Toe-Nail	No	Yes	No
H.72	Building	WFR	1	No	Hip	8d	Strap	No	Yes	No
H.73	Building	WFR	2	No	Gable	6d	Toe-Nail	No	Yes	No
H.74	Building	WFR	2	No	Gable	6d	Strap	No	Yes	No
H.75	Building	WFR	2	No	Gable	8d	Toe-Nail	No	Yes	No
H.76	Building	WFR	2	No	Gable	8d	Strap	No	Yes	No
H.77	Building	WFR	2	No	Hip	6d	Toe-Nail	No	Yes	No
H.78	Building	WFR	2	No	Hip	6d	Strap	No	Yes	No
H.79	Building	WFR	2	No	Hip	8d	Toe-Nail	No	Yes	No
H.80	Building	WFR	2	No	Hip	8d	Strap	No	Yes	No
H.81	Content	WFR	1	No	Gable	6d	Toe-Nail	No	Yes	No
H.82	Content	WFR	1	No	Gable	6d	Strap	No	Yes	No
H.83	Content	WFR	1	No	Gable	8d	Toe-Nail	No	Yes	No
H.84	Content	WFR	1	No	Gable	8d	Strap	No	Yes	No
H.85	Content	WFR	1	No	Hip	6d	Toe-Nail	No	Yes	No
H.86	Content	WFR	1	No	Hip	6d	Strap	No	Yes	No
H.87	Content	WFR	1	No	Hip	8d	Toe-Nail	No	Yes	No
H.88	Content	WFR	1	No	Hip	8d	Strap	No	Yes	No
H.89	Content	WFR	2	No	Gable	6d	Toe-Nail	No	Yes	No
H.90	Content	WFR	2	No	Gable	6d	Strap	No	Yes	No
H.91	Content	WFR	2	No	Gable	8d	Toe-Nail	No	Yes	No
H.92	Content	WFR	2	No	Gable	8d	Strap	No	Yes	No
H.93	Content	WFR	2	No	Hip	6d	Toe-Nail	No	Yes	No
H.94	Content	WFR	2	No	Hip	6d	Strap	No	Yes	No
H.95	Content	WFR	2	No	Hip	8d	Toe-Nail	No	Yes	No
H.96	Content	WFR	2	No	Hip	8d	Strap	No	Yes	No
H.97	Building	WFR	1	No	Gable	6d	Toe-Nail	No	Yes	Yes
H.98	Building	WFR	1	No	Gable	6d	Strap	No	Yes	Yes
H.99	Building	WFR	1	No	Gable	8d	Toe-Nail	No	Yes	Yes
H.100	Building	WFR	1	No	Gable	8d	Strap	No	Yes	Yes
H.101	Building	WFR	1	No	Hip	6d	Toe-Nail	No	Yes	Yes
H.102	Building	WFR	1	No	Hip	6d	Strap	No	Yes	Yes
H.103	Building	WFR	1	No	Hip	8d	Toe-Nail	No	Yes	Yes
H.104	Building	WFR	1	No	Hip	8d	Strap	No	Yes	Yes
H.105	Building	WFR	2	No	Gable	6d	Toe-Nail	No	Yes	Yes
H.106	Building	WFR	2	No	Gable	6d	Strap	No	Yes	Yes
H.107	Building	WFR	2	No	Gable	8d	Toe-Nail	No	Yes	Yes

Table H.1. Sample Loss Functions for Residential Buildings (continued)

Figure	Loss Type	Walls	Stories	Garage	Roof Shape	Sheathing	Roof/ Wall	Shutters	Upgraded Roof	Secondary Water Resistance
H.108	Building	WFR	2	No	Gable	8d	Strap	No	Yes	Yes
H.109	Building	WFR	2	No	Hip	6d	Toe-Nail	No	Yes	Yes
H.110	Building	WFR	2	No	Hip	6d	Strap	No	Yes	Yes
H.111	Building	WFR	2	No	Hip	8d	Toe-Nail	No	Yes	Yes
H.112	Building	WFR	2	No	Hip	8d	Strap	No	Yes	Yes
H.113	Content	WFR	1	No	Gable	6d	Toe-Nail	No	Yes	Yes
H.114	Content	WFR	1	No	Gable	6d	Strap	No	Yes	Yes
H.115	Content	WFR	1	No	Gable	8d	Toe-Nail	No	Yes	Yes
H.116	Content	WFR	1	No	Gable	8d	Strap	No	Yes	Yes
H.117	Content	WFR	1	No	Hip	6d	Toe-Nail	No	Yes	Yes
H.118	Content	WFR	1	No	Hip	6d	Strap	No	Yes	Yes
H.119	Content	WFR	1	No	Hip	8d	Toe-Nail	No	Yes	Yes
H.120	Content	WFR	1	No	Hip	8d	Strap	No	Yes	Yes
H.121	Content	WFR	2	No	Gable	6d	Toe-Nail	No	Yes	Yes
H.122	Content	WFR	2	No	Gable	6d	Strap	No	Yes	Yes
H.123	Content	WFR	2	No	Gable	8d	Toe-Nail	No	Yes	Yes
H.124	Content	WFR	2	No	Gable	8d	Strap	No	Yes	Yes
H.125	Content	WFR	2	No	Hip	6d	Toe-Nail	No	Yes	Yes
H.126	Content	WFR	2	No	Hip	6d	Strap	No	Yes	Yes
H.127	Content	WFR	2	No	Hip	8d	Toe-Nail	No	Yes	Yes
H.128	Content	WFR	2	No	Hip	8d	Strap	No	Yes	Yes
H.129	Building	WFR	1	No	Gable	6d	Toe-Nail	Yes	Yes	No
H.130	Building	WFR	1	No	Gable	6d	Strap	Yes	Yes	No
H.131	Building	WFR	1	No	Gable	8d	Toe-Nail	Yes	Yes	No
H.132	Building	WFR	1	No	Gable	8d	Strap	Yes	Yes	No
H.133	Building	WFR	1	No	Hip	6d	Toe-Nail	Yes	Yes	No
H.134	Building	WFR	1	No	Hip	6d	Strap	Yes	Yes	No
H.135	Building	WFR	1	No	Hip	8d	Toe-Nail	Yes	Yes	No
H.136	Building	WFR	1	No	Hip	8d	Strap	Yes	Yes	No
H.137	Building	WFR	2	No	Gable	6d	Toe-Nail	Yes	Yes	No
H.138	Building	WFR	2	No	Gable	6d	Strap	Yes	Yes	No
H.139	Building	WFR	2	No	Gable	8d	Toe-Nail	Yes	Yes	No
H.140	Building	WFR	2	No	Gable	8d	Strap	Yes	Yes	No
H.141	Building	WFR	2	No	Hip	6d	Toe-Nail	Yes	Yes	No
H.142	Building	WFR	2	No	Hip	6d	Strap	Yes	Yes	No
H.143	Building	WFR	2	No	Hip	8d	Toe-Nail	Yes	Yes	No
H.144	Building	WFR	2	No	Hip	8d	Strap	Yes	Yes	No
H.145	Content	WFR	1	No	Gable	6d	Toe-Nail	Yes	Yes	No
H.146	Content	WFR	1	No	Gable	6d	Strap	Yes	Yes	No
H.147	Content	WFR	1	No	Gable	8d	Toe-Nail	Yes	Yes	No
H.148	Content	WFR	1	No	Gable	8d	Strap	Yes	Yes	No
H.149	Content	WFR	1	No	Hip	6d	Toe-Nail	Yes	Yes	No
H.150	Content	WFR	1	No	Hip	6d	Strap	Yes	Yes	No

Table H.1. Sample Loss Functions for Residential Buildings (concluded)

Figure	Loss Type	Walls	Stories	Garage	Roof Shape	Sheathing	Roof/ Wall	Shutters	Upgraded Roof	Secondary Water Resistance
H.151	Content	WFR	1	No	Hip	8d	Toe-Nail	Yes	Yes	No
H.152	Content	WFR	1	No	Hip	8d	Strap	Yes	Yes	No
H.153	Content	WFR	2	No	Gable	6d	Toe-Nail	Yes	Yes	No
H.154	Content	WFR	2	No	Gable	6d	Strap	Yes	Yes	No
H.155	Content	WFR	2	No	Gable	8d	Toe-Nail	Yes	Yes	No
H.156	Content	WFR	2	No	Gable	8d	Strap	Yes	Yes	No
H.157	Content	WFR	2	No	Hip	6d	Toe-Nail	Yes	Yes	No
H.158	Content	WFR	2	No	Hip	6d	Strap	Yes	Yes	No
H.159	Content	WFR	2	No	Hip	8d	Toe-Nail	Yes	Yes	No
H.160	Content	WFR	2	No	Hip	8d	Strap	Yes	Yes	No
H.161	Building	WFR	1	No	Gable	6d	Toe-Nail	Yes	Yes	Yes
H.162	Building	WFR	1	No	Gable	6d	Strap	Yes	Yes	Yes
H.163	Building	WFR	1	No	Gable	8d	Toe-Nail	Yes	Yes	Yes
H.164	Building	WFR	1	No	Gable	8d	Strap	Yes	Yes	Yes
H.165	Building	WFR	1	No	Hip	6d	Toe-Nail	Yes	Yes	Yes
H.166	Building	WFR	1	No	Hip	6d	Strap	Yes	Yes	Yes
H.167	Building	WFR	1	No	Hip	8d	Toe-Nail	Yes	Yes	Yes
H.168	Building	WFR	1	No	Hip	8d	Strap	Yes	Yes	Yes
H.169	Building	WFR	2	No	Gable	6d	Toe-Nail	Yes	Yes	Yes
H.170	Building	WFR	2	No	Gable	6d	Strap	Yes	Yes	Yes
H.171	Building	WFR	2	No	Gable	8d	Toe-Nail	Yes	Yes	Yes
H.172	Building	WFR	2	No	Gable	8d	Strap	Yes	Yes	Yes
H.173	Building	WFR	2	No	Hip	6d	Toe-Nail	Yes	Yes	Yes
H.174	Building	WFR	2	No	Hip	6d	Strap	Yes	Yes	Yes
H.175	Building	WFR	2	No	Hip	8d	Toe-Nail	Yes	Yes	Yes
H.176	Building	WFR	2	No	Hip	8d	Strap	Yes	Yes	Yes
H.177	Content	WFR	1	No	Gable	6d	Toe-Nail	Yes	Yes	Yes
H.178	Content	WFR	1	No	Gable	6d	Strap	Yes	Yes	Yes
H.179	Content	WFR	1	No	Gable	8d	Toe-Nail	Yes	Yes	Yes
H.180	Content	WFR	1	No	Gable	8d	Strap	Yes	Yes	Yes
H.181	Content	WFR	1	No	Hip	6d	Toe-Nail	Yes	Yes	Yes
H.182	Content	WFR	1	No	Hip	6d	Strap	Yes	Yes	Yes
H.183	Content	WFR	1	No	Hip	8d	Toe-Nail	Yes	Yes	Yes
H.184	Content	WFR	1	No	Hip	8d	Strap	Yes	Yes	Yes
H.185	Content	WFR	2	No	Gable	6d	Toe-Nail	Yes	Yes	Yes
H.186	Content	WFR	2	No	Gable	6d	Strap	Yes	Yes	Yes
H.187	Content	WFR	2	No	Gable	8d	Toe-Nail	Yes	Yes	Yes
H.188	Content	WFR	2	No	Gable	8d	Strap	Yes	Yes	Yes
H.189	Content	WFR	2	No	Hip	6d	Toe-Nail	Yes	Yes	Yes
H.190	Content	WFR	2	No	Hip	6d	Strap	Yes	Yes	Yes
H.191	Content	WFR	2	No	Hip	8d	Toe-Nail	Yes	Yes	Yes
H.192	Content	WFR	2	No	Hip	8d	Strap	Yes	Yes	Yes

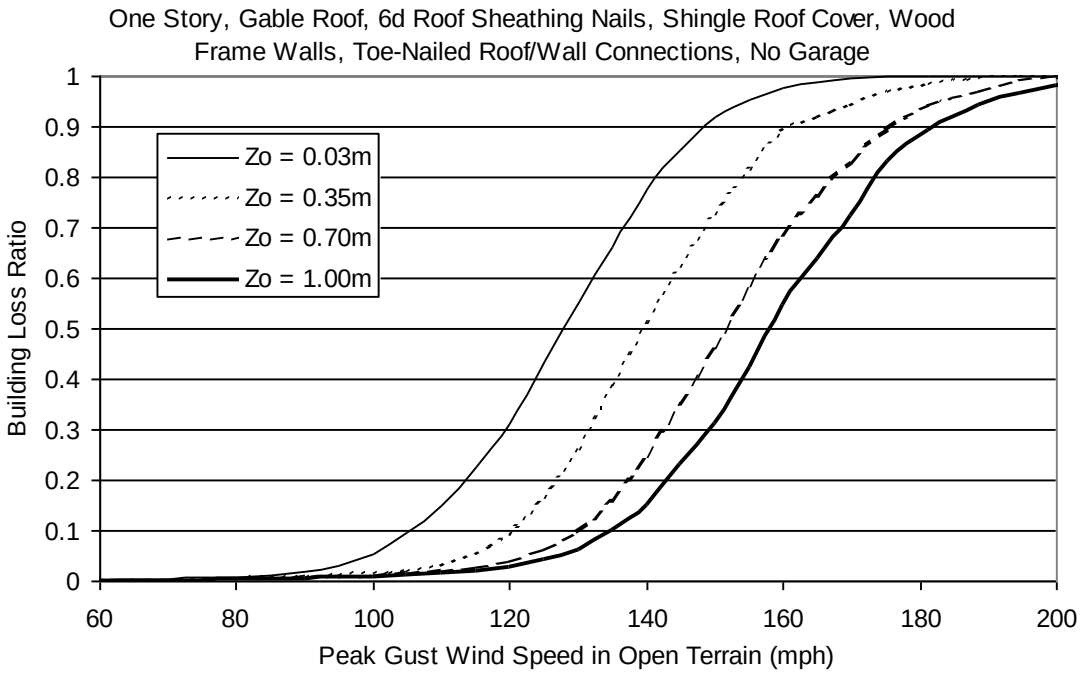

Figure H.1. Building Loss Function for Single Family Residential Building (One Story, 6d Roof Sheathing Nails, Gable Roof, No Garage, Toe-Nailed Roof Wall Connections, Wood Frame).

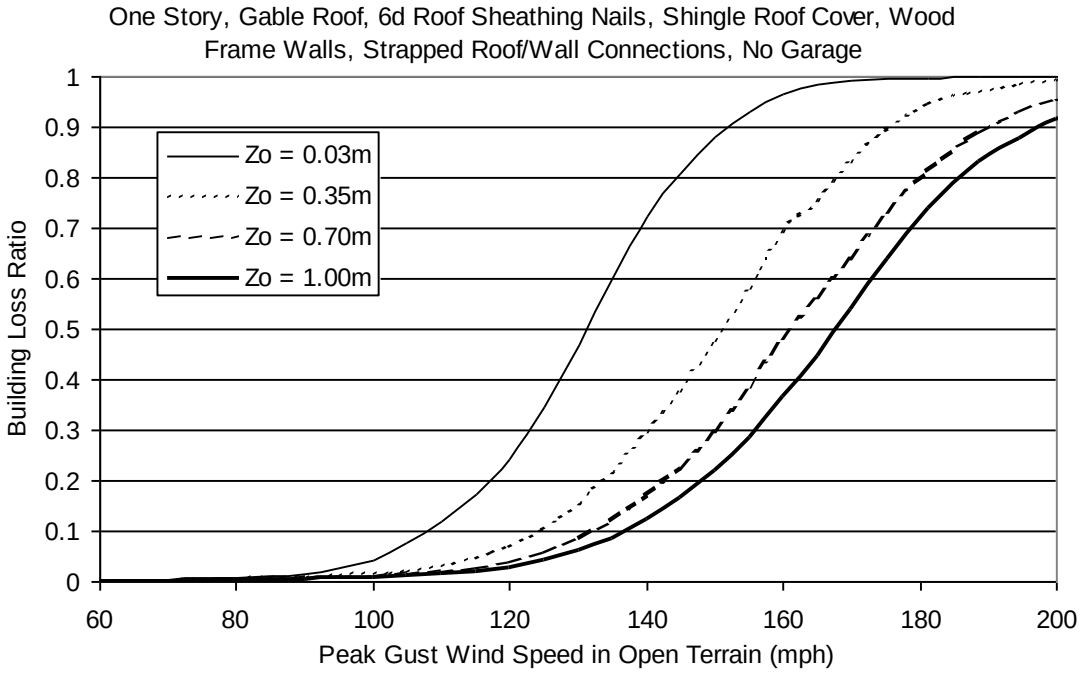

Figure H.2. Building Loss Function for Single Family Residential Building (One Story, 6d Roof Sheathing Nails, Gable Roof, No Garage, Strapped Roof Wall Connections, Wood Frame).

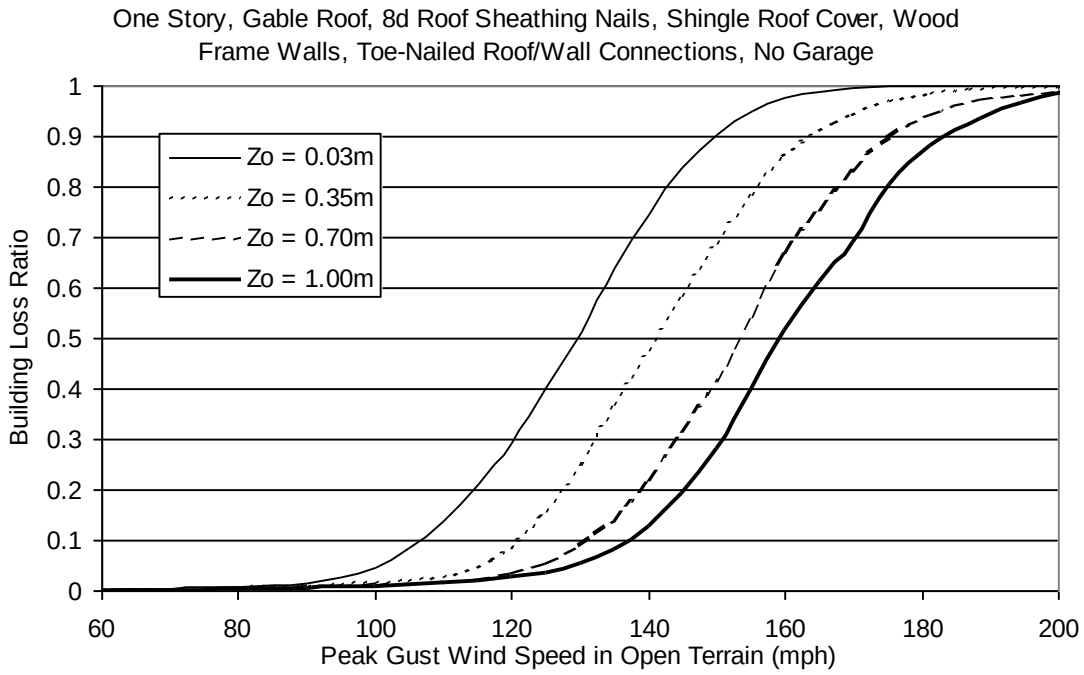

Figure H.3. Building Loss Function for Single Family Residential Building (One Story, 8d Roof Sheathing Nails, Gable Roof, No Garage, Toe-Nailed Roof Wall Connections, Wood Frame).

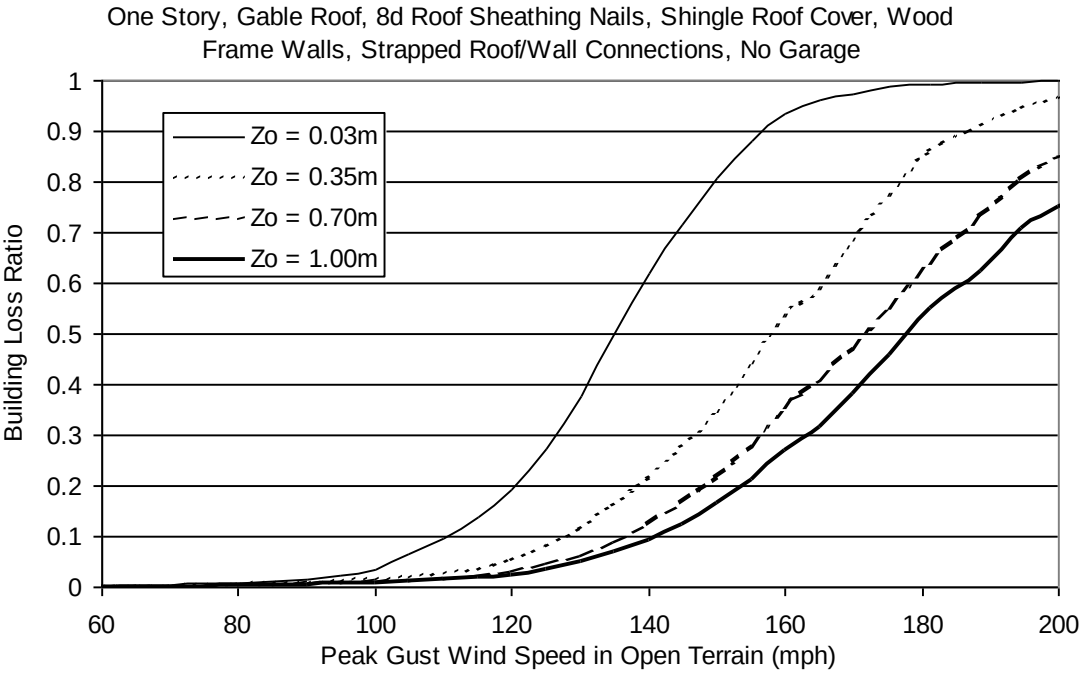

Figure H.4. Building Loss Function for Single Family Residential Building (One Story, 8d Roof Sheathing Nails, Gable Roof, No Garage, Strapped Roof Wall Connections, Wood Frame).

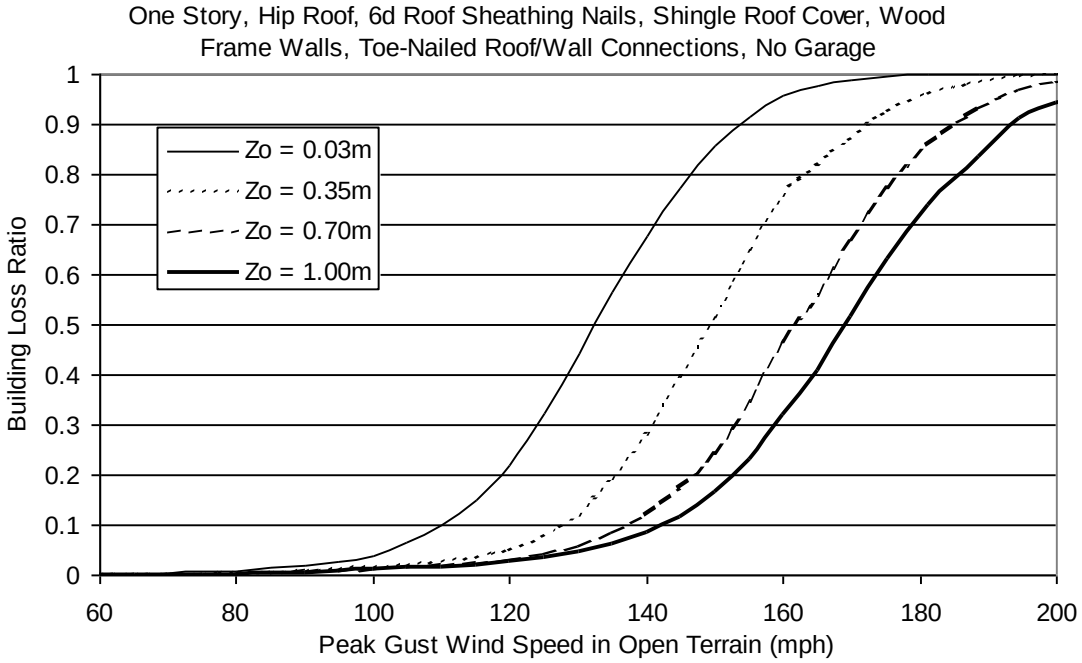

Figure H.5. Building Loss Function for Single Family Residential Building (One Story, 6d Roof Sheathing Nails, Hip Roof, No Garage, Toe-Nailed Roof Wall Connections, Wood Frame).

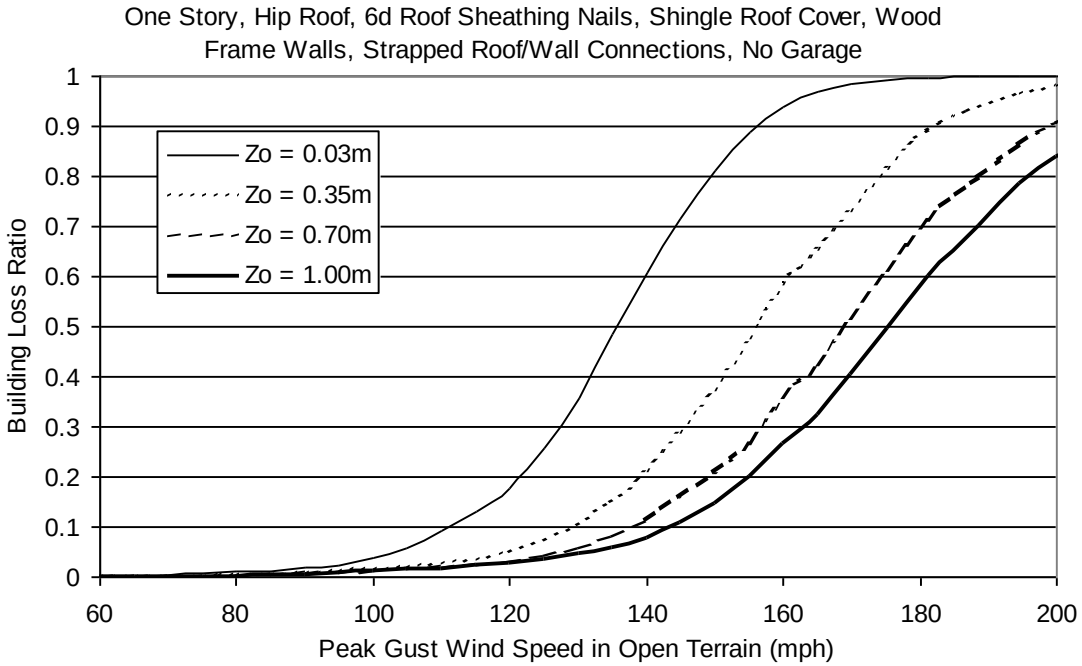

Figure H.6. Building Loss Function for Single Family Residential Building (One Story, 6d Roof Sheathing Nails, Hip Roof, No Garage, Strapped Roof Wall Connections, Wood Frame).

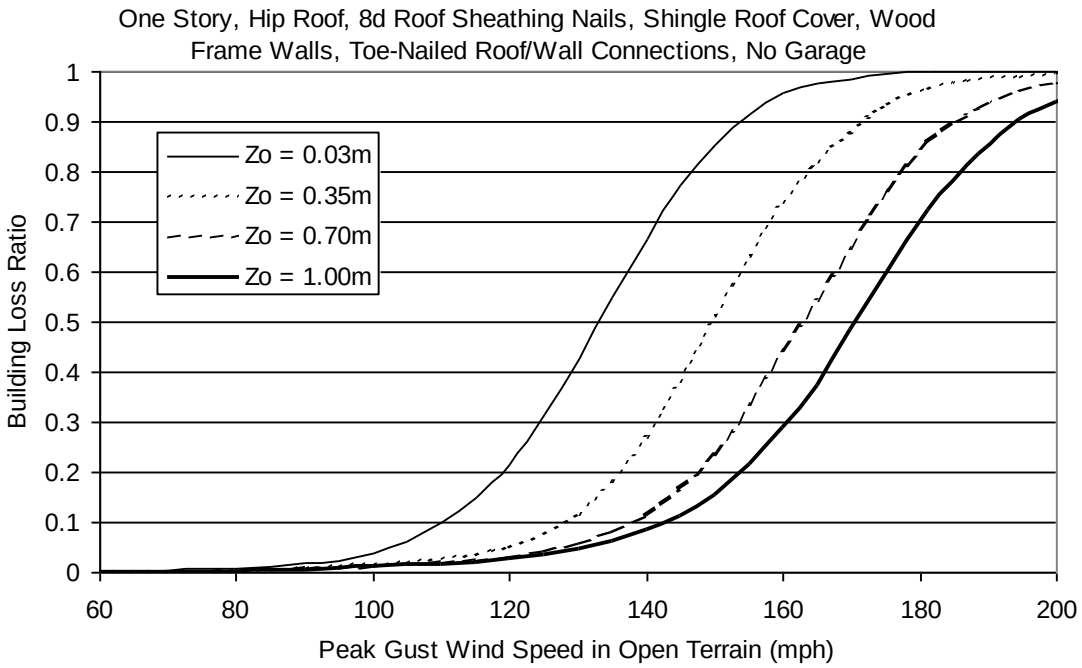

Figure H.7. Building Loss Function for Single Family Residential Building (One Story, 8d Roof Sheathing Nails, Hip Roof, No Garage, Toe-Nailed Roof Wall Connections, Wood Frame).

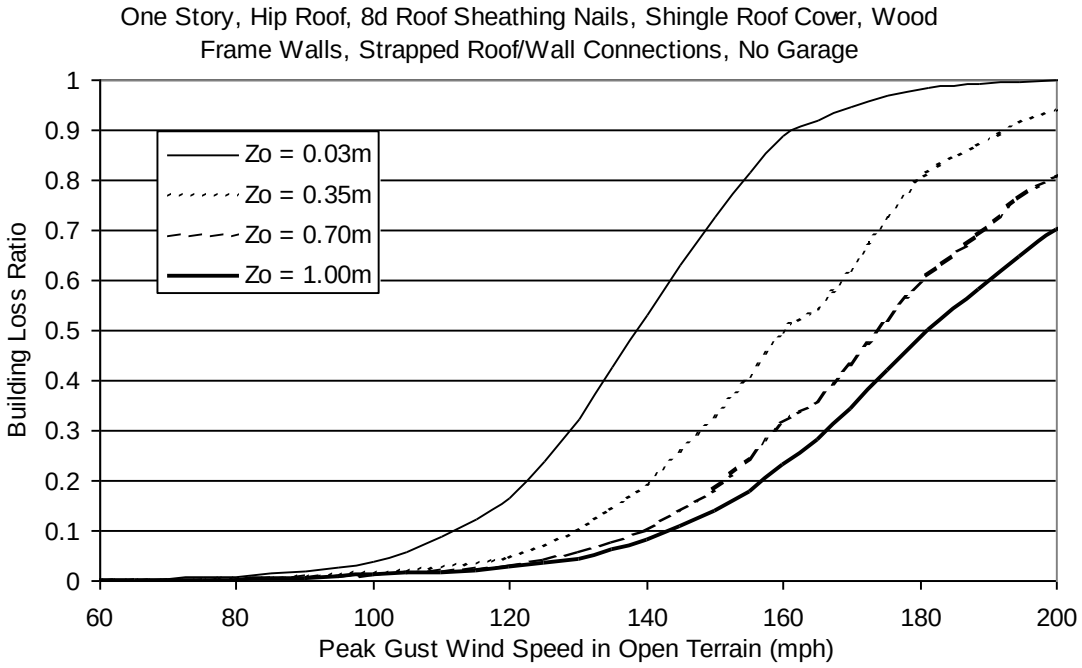

Figure H.8. Building Loss Function for Single Family Residential Building (One Story, 8d Roof Sheathing Nails, Hip Roof, No Garage, Strapped Roof Wall Connections, Wood Frame).

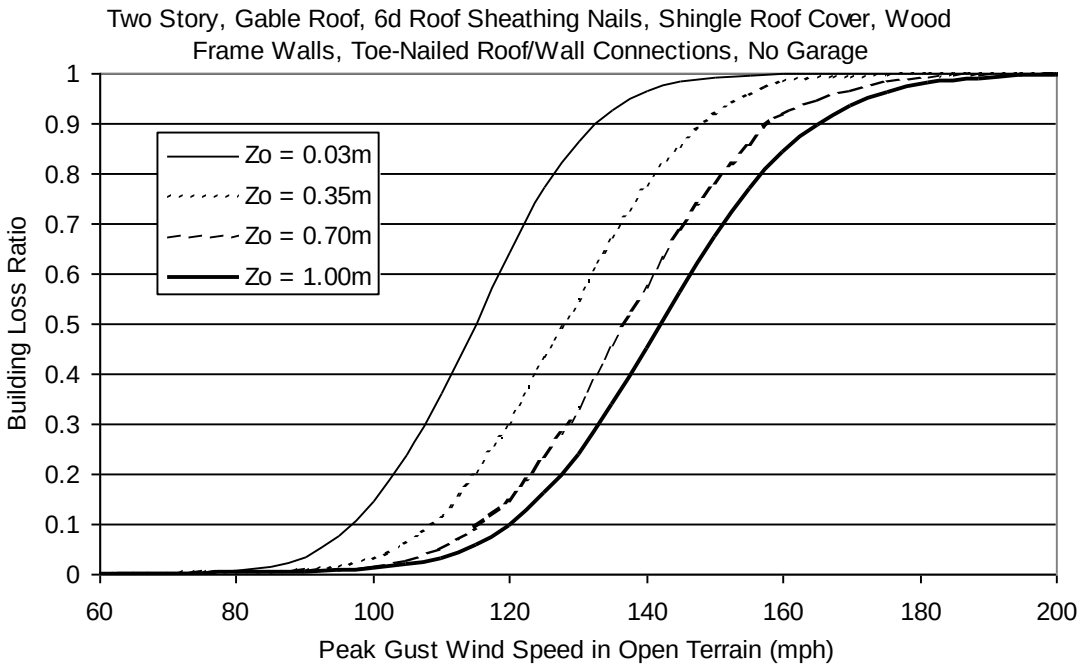

Figure H.9. Building Loss Function for Single Family Residential Building (Two Story, 6d Roof Sheathing Nails, Gable Roof, No Garage, Toe-Nailed Roof Wall Connections, Wood Frame).

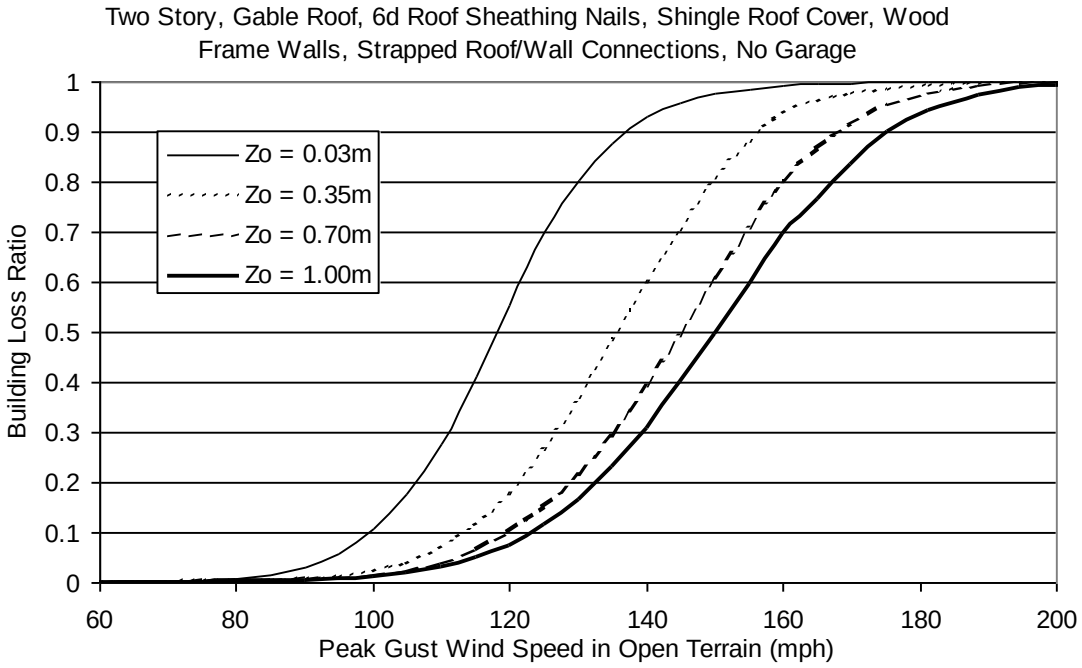

Figure H.10. Building Loss Function for Single Family Residential Building (Two Story, 6d Roof Sheathing Nails, Gable Roof, No Garage, Strapped Roof Wall Connections, Wood Frame).

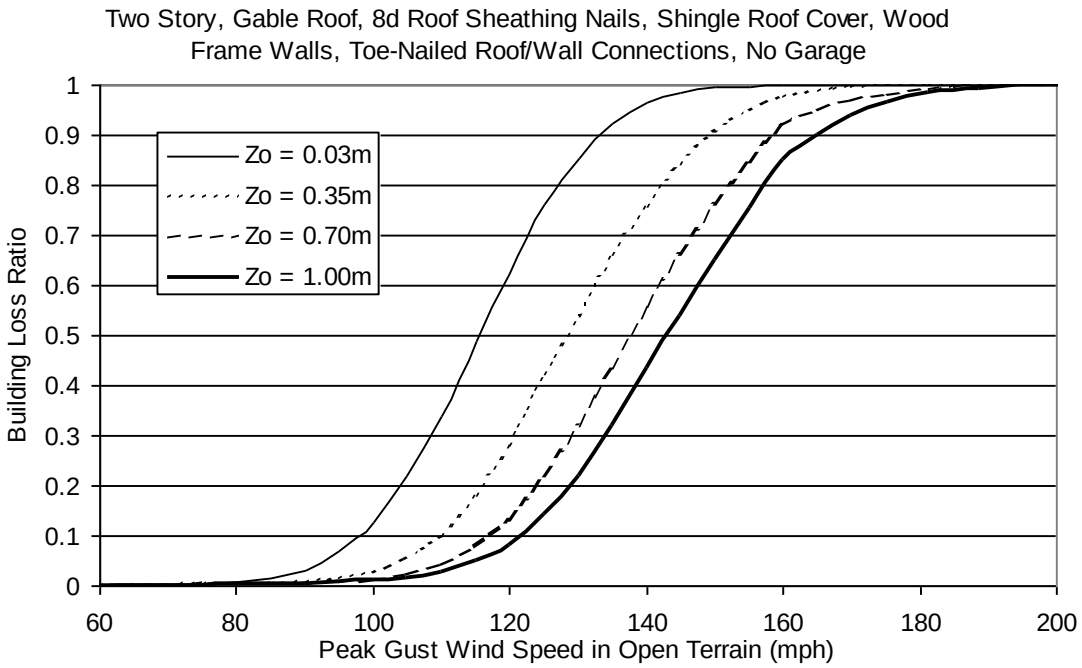

Figure H.11. Building Loss Function for Single Family Residential Building (Two Story, 8d Roof Sheathing Nails, Gable Roof, No Garage, Toe-Nailed Roof Wall Connections, Wood Frame).

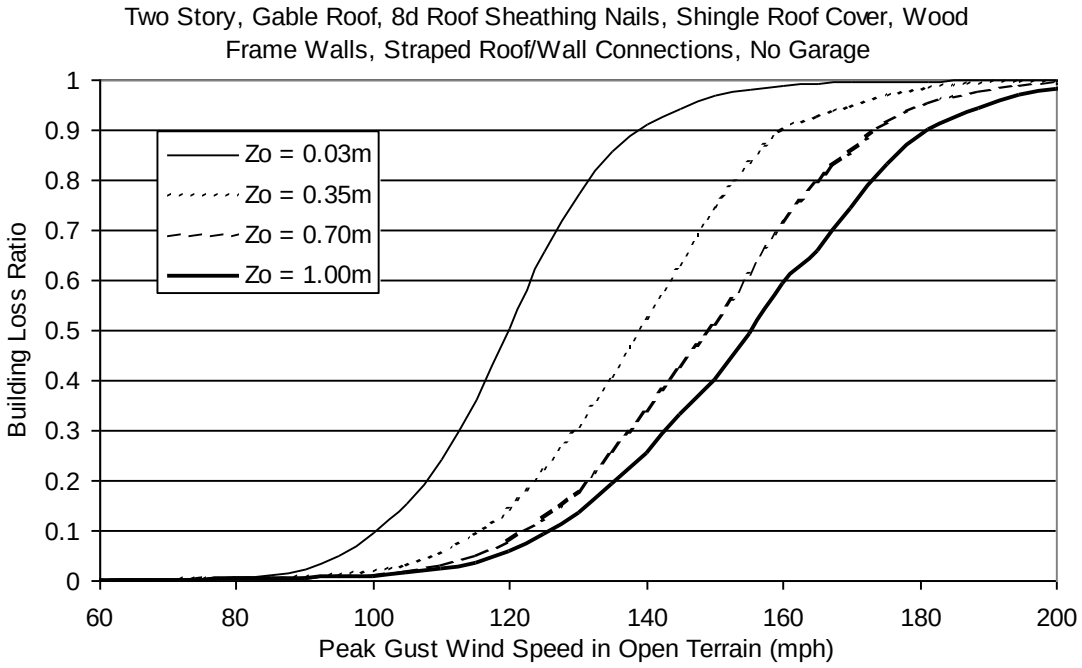

Figure H.12. Building Loss Function for Single Family Residential Building (Two Story, 8d Roof Sheathing Nails, Gable Roof, No Garage, Strapped Roof Wall Connections, Wood Frame).

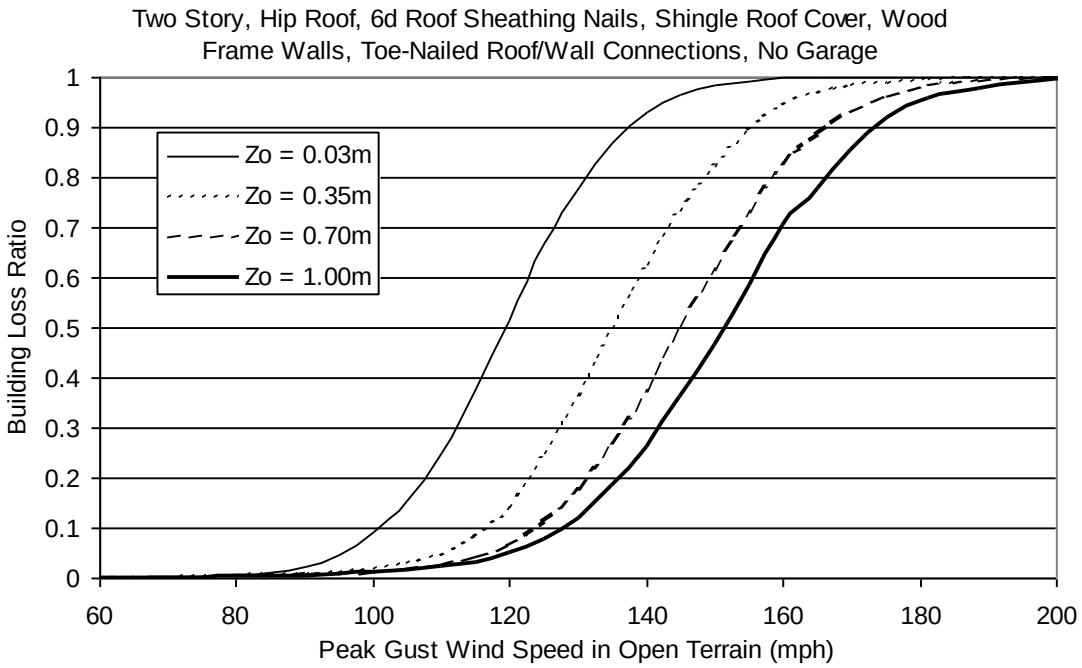

Figure H.13. Building Loss Function for Single Family Residential Building (Two Story, 6d Roof Sheathing Nails, Hip Roof, No Garage, Toe-Nailed Roof Wall Connections, Wood Frame).

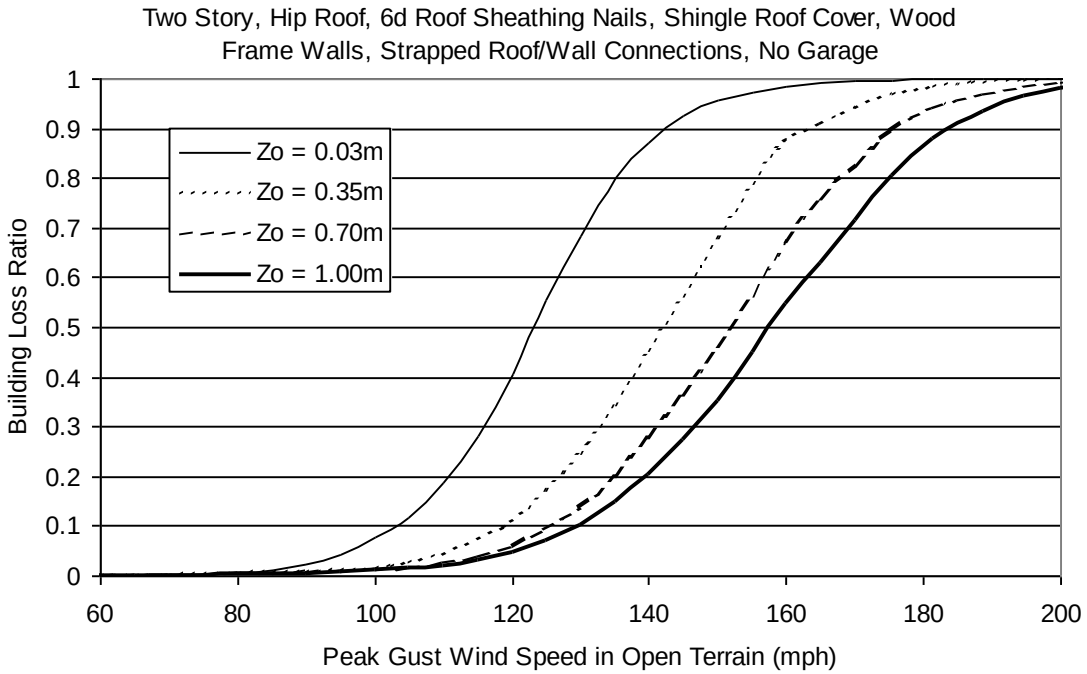

Figure H.14. Building Loss Function for Single Family Residential Building (Two Story, 6d Roof Sheathing Nails, Hip Roof, No Garage, Strapped Roof Wall Connections, Wood Frame).

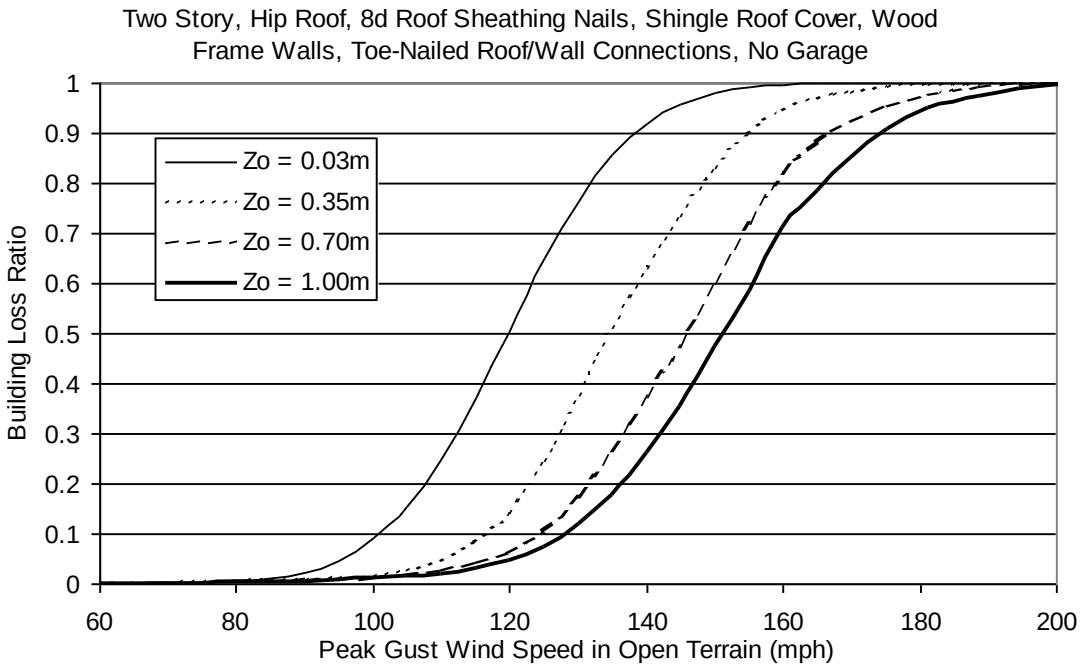

Figure H.15. Building Loss Function for Single Family Residential Building (Two Story, 8d Roof Sheathing Nails, Hip Roof, No Garage, Toe-Nailed Roof Wall Connections, Wood Frame).

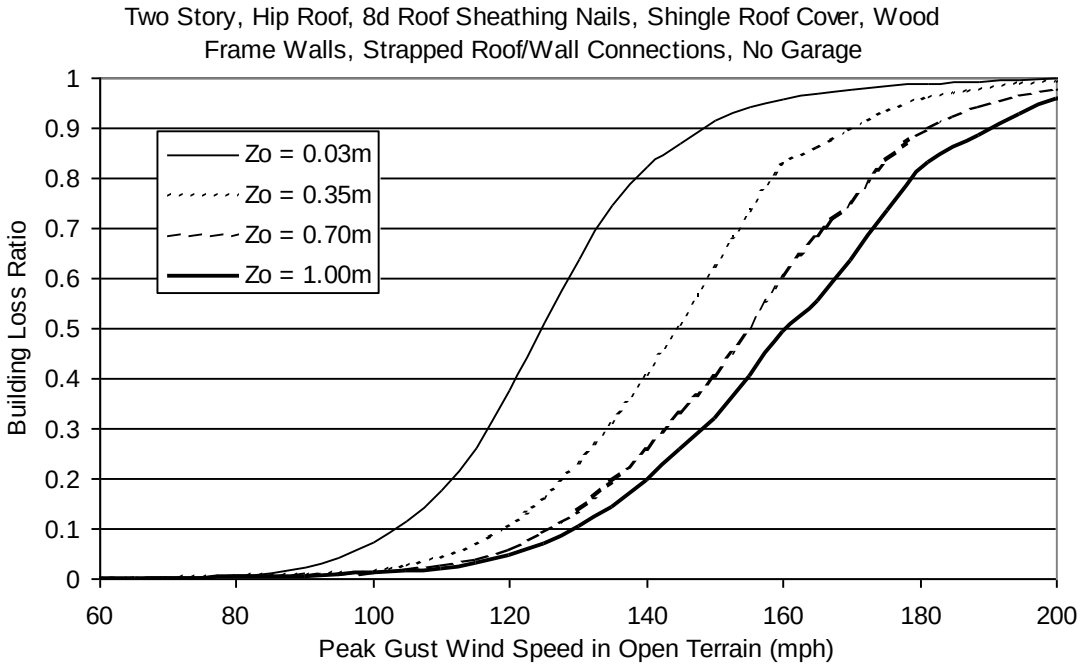

Figure H.16. Building Loss Function for Single Family Residential Building (Two Story, 8d Roof Sheathing Nails, Hip Roof, No Garage, Strapped Roof Wall Connections, Wood Frame).

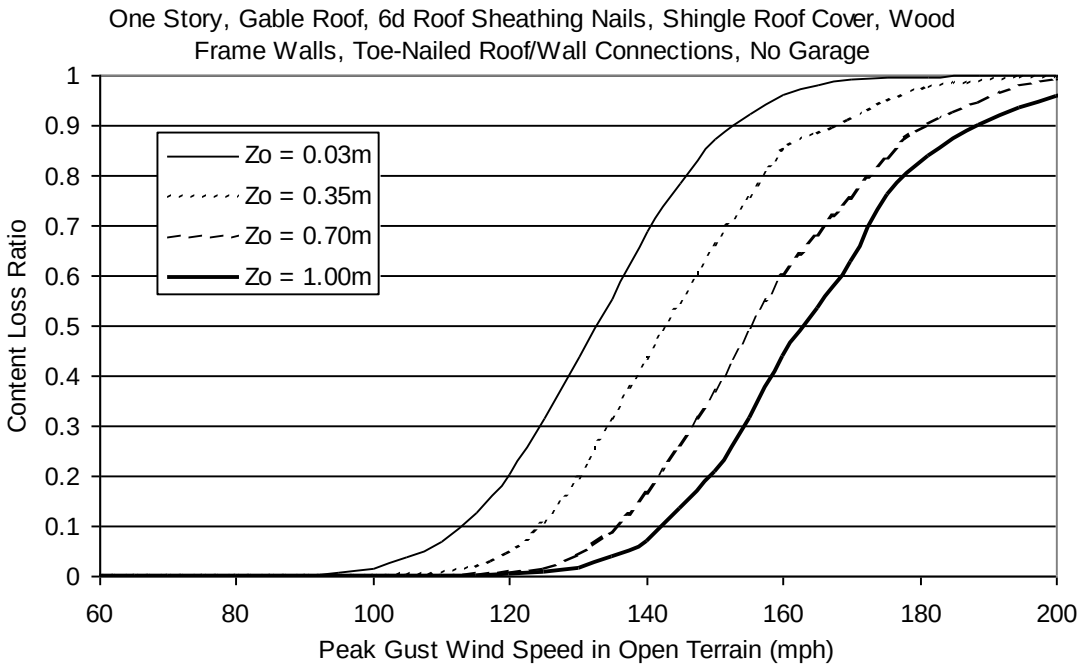

Figure H.17. Content Loss Function for Single Family Residential Building (One Story, 6d Roof Sheathing Nails, Gable Roof, No Garage, Toe-Nailed Roof Wall Connections, Wood Frame).

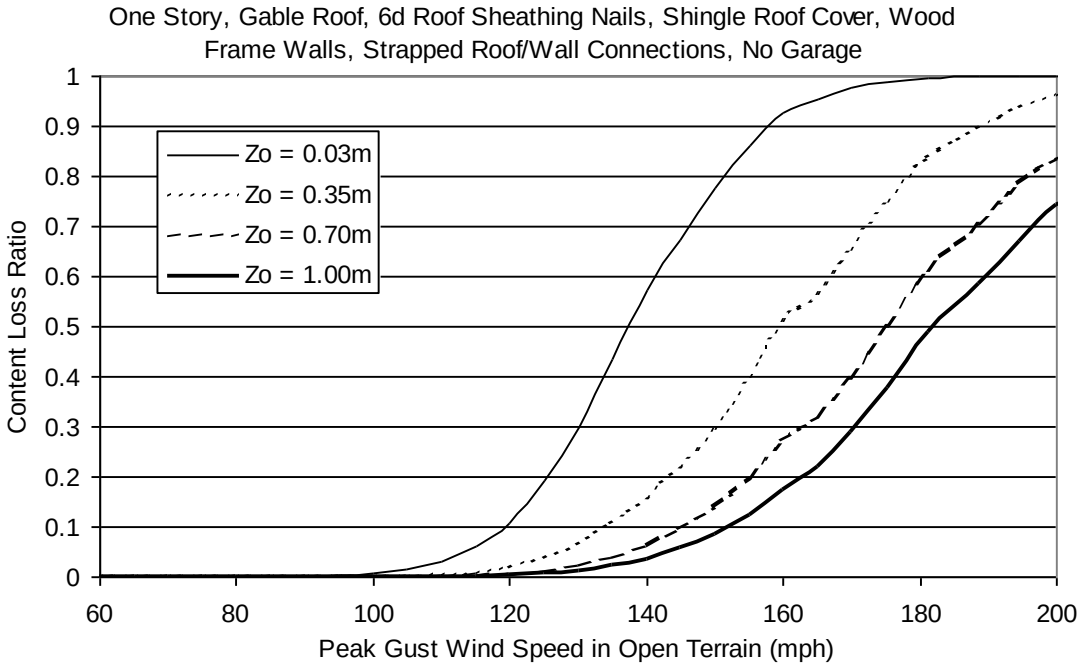

Figure H.18. Content Loss Function for Single Family Residential Building (One Story, 6d Roof Sheathing Nails, Gable Roof, No Garage, Strapped Roof Wall Connections, Wood Frame).

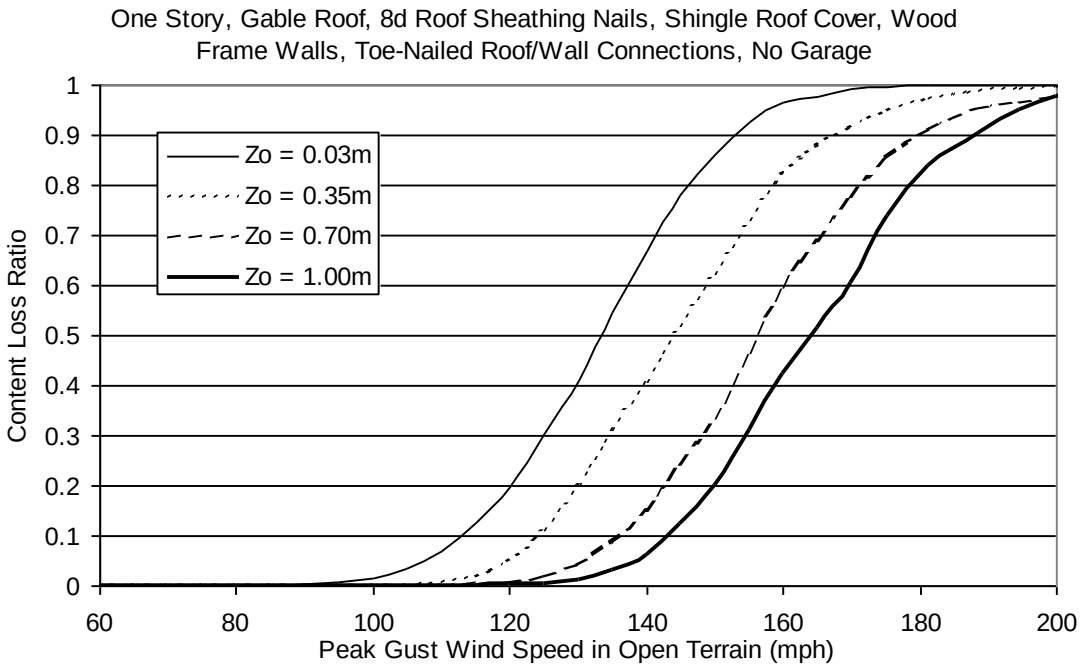

Figure H.19. Content Loss Function for Single Family Residential Building (One Story, 8d Roof Sheathing Nails, Gable Roof, No Garage, Toe-Nailed Roof Wall Connections, Wood Frame).

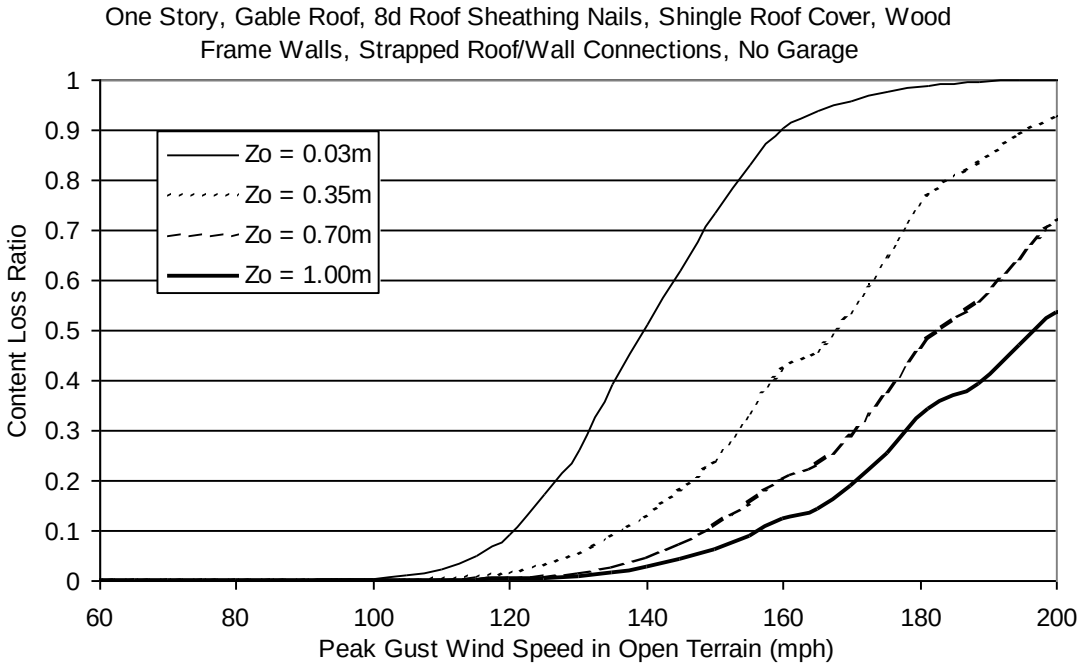

Figure H.20. Content Loss Function for Single Family Residential Building (One Story, 8d Roof Sheathing Nails, Gable Roof, No Garage, Strapped Roof Wall Connections, Wood Frame).

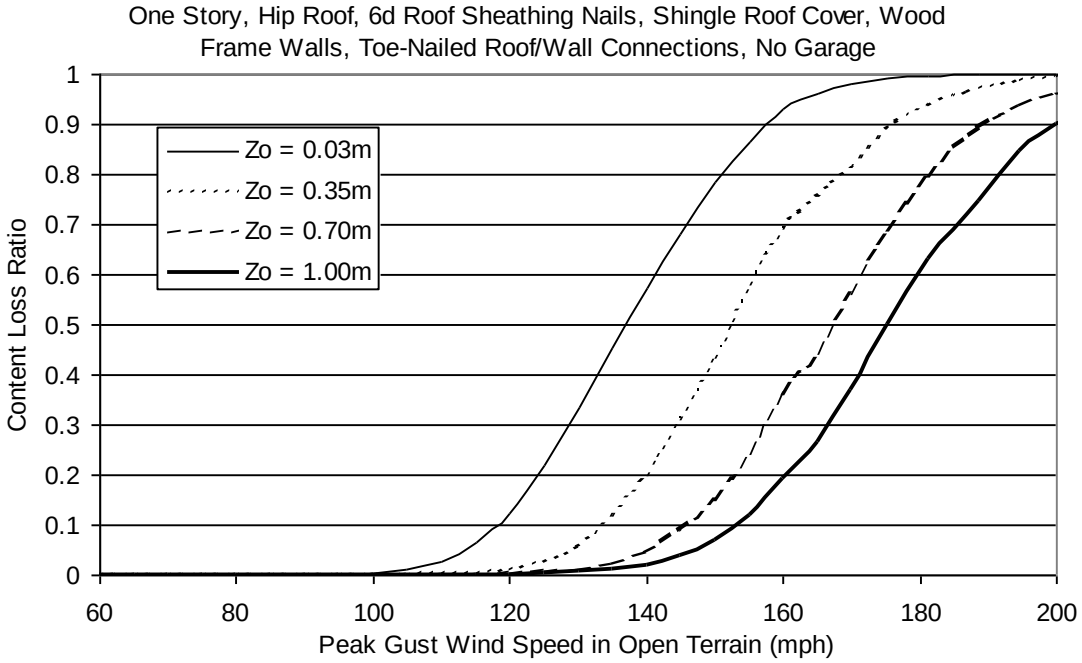

Figure H.21. Content Loss Function for Single Family Residential Building (One Story, 6d Roof Sheathing Nails, Hip Roof, No Garage, Toe-Nailed Roof Wall Connections, Wood Frame).

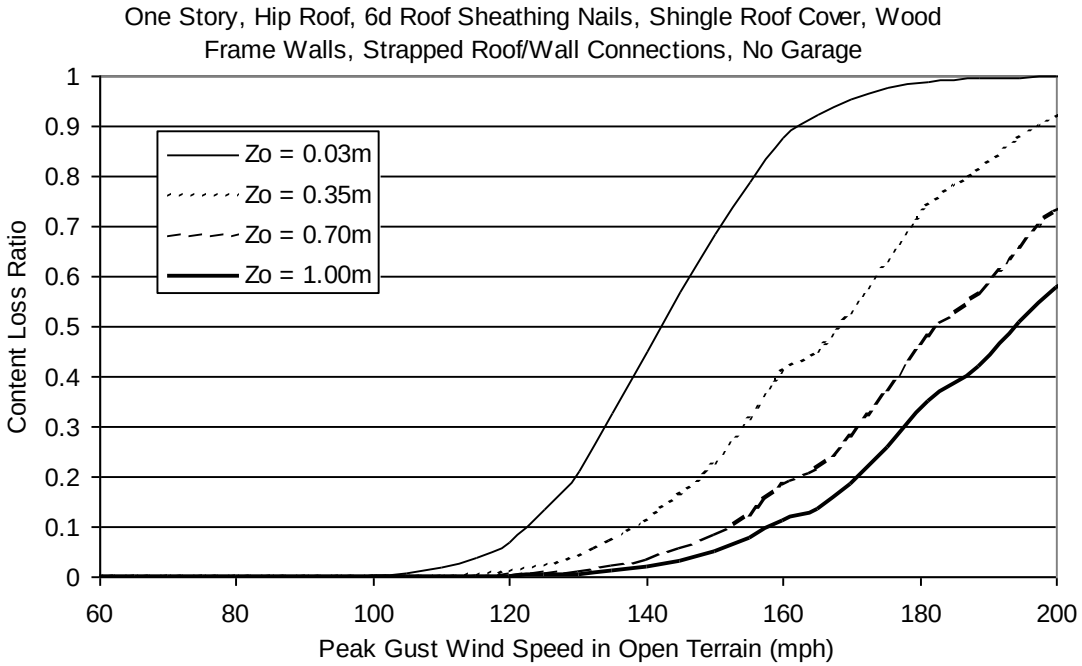

Figure H.22. Content Loss Function for Single Family Residential Building (One Story, 6d Roof Sheathing Nails, Hip Roof, No Garage, Strapped Roof Wall Connections, Wood Frame).

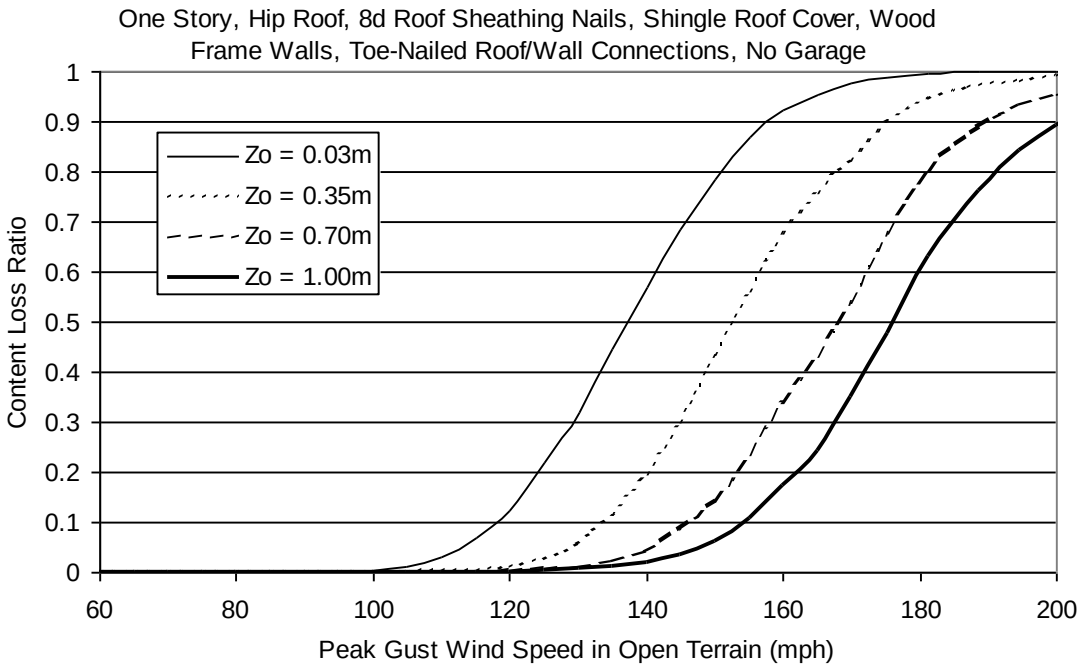

Figure H.23. Content Loss Function for Single Family Residential Building (One Story, 8d Roof Sheathing Nails, Hip Roof, No Garage, Toe-Nailed Roof Wall Connections, Wood Frame).

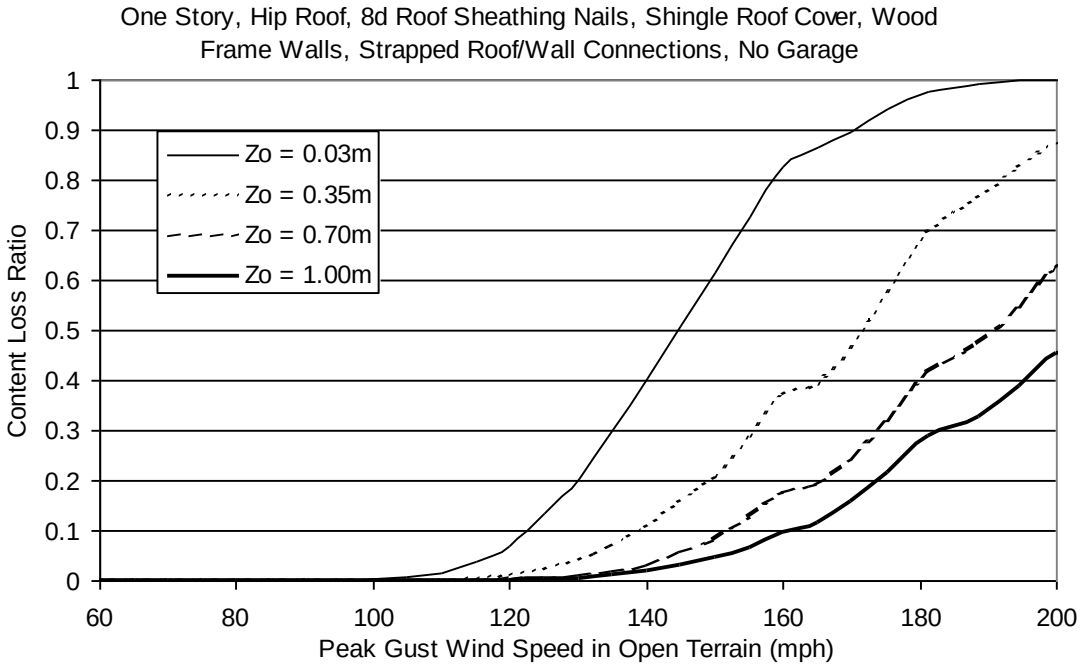

Figure H.24. Content Loss Function for Single Family Residential Building (One Story, 8d Roof Sheathing Nails, Hip Roof, No Garage, Strapped Roof Wall Connections, Wood Frame).

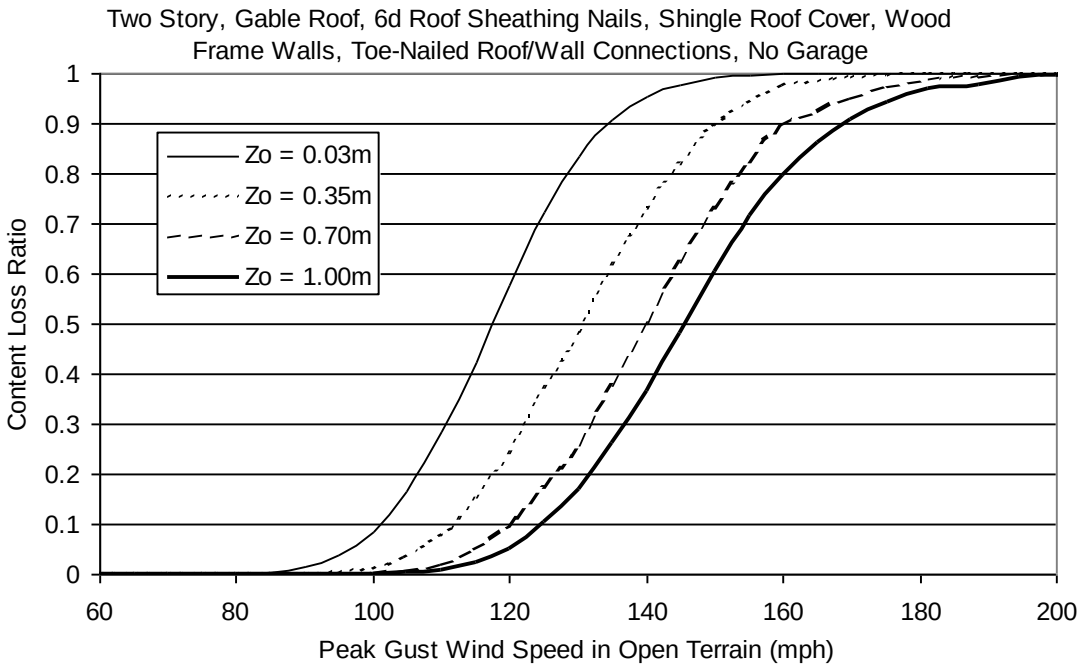

Figure H.25. Content Loss Function for Single Family Residential Building (Two Story, 6d Roof Sheathing Nails, Gable Roof, No Garage, Toe-Nailed Roof Wall Connections, Wood Frame).

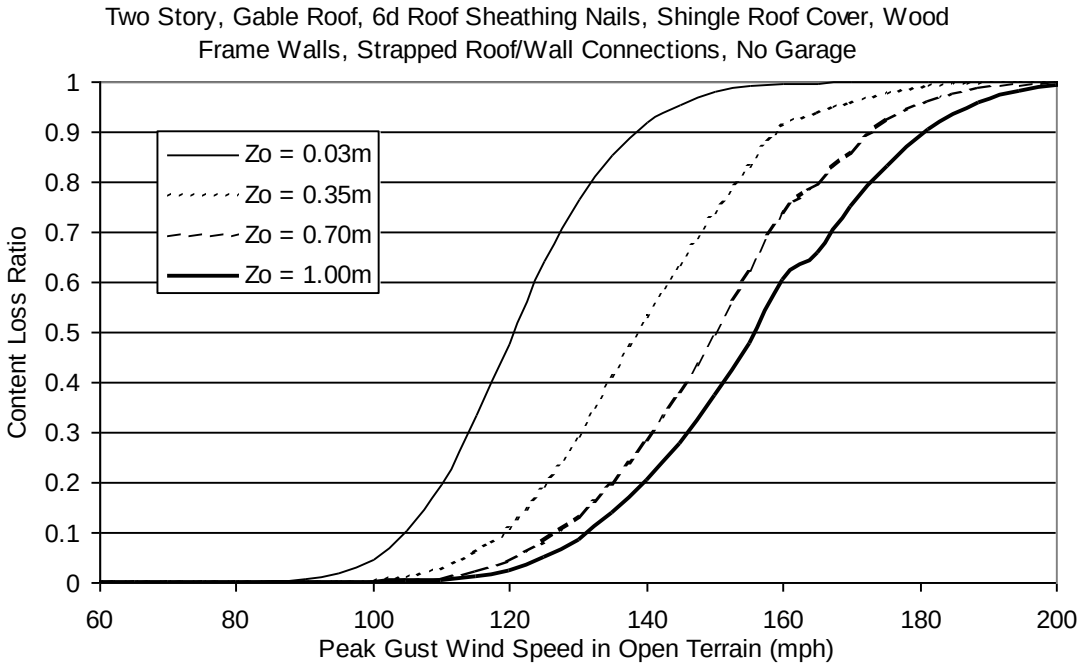

Figure H.26. Content Loss Function for Single Family Residential Building (Two Story, 6d Roof Sheathing Nails, Gable Roof, No Garage, Strapped Roof Wall Connections, Wood Frame).

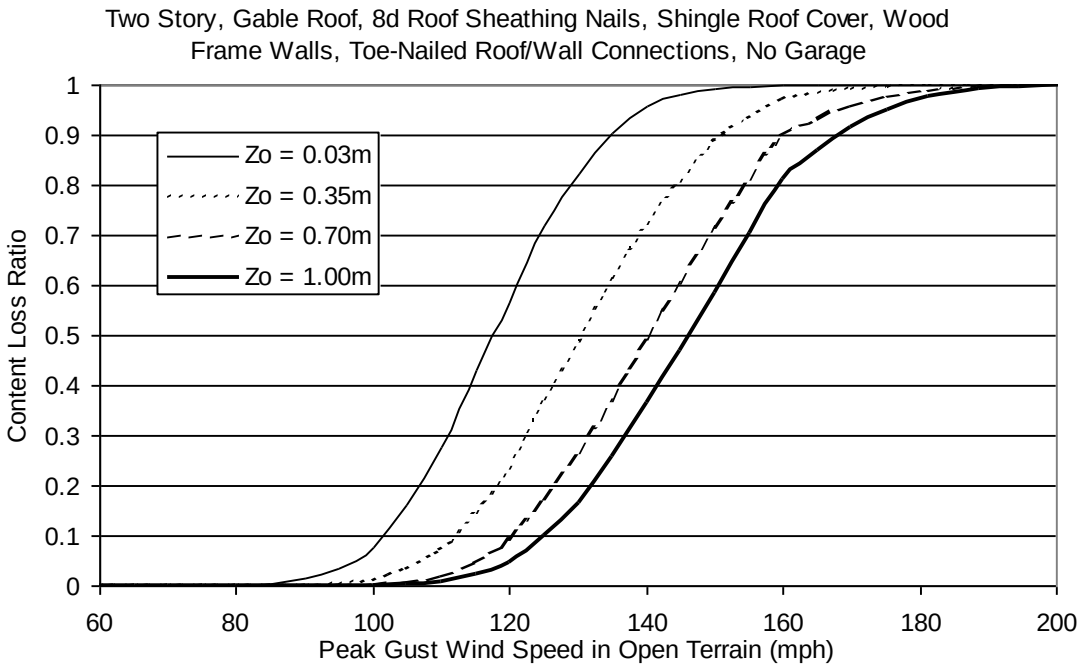

Figure H.27. Content Loss Function for Single Family Residential Building (Two Story, 8d Roof Sheathing Nails, Gable Roof, No Garage, Toe-Nailed Roof Wall Connections, Wood Frame).

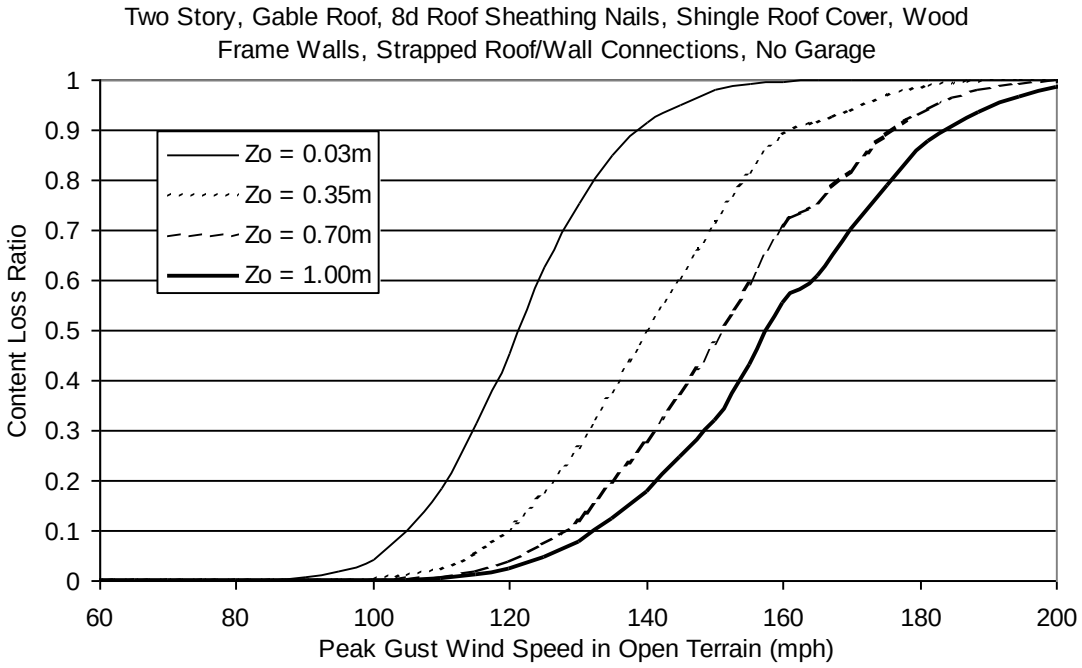

Figure H.28. Content Loss Function for Single Family Residential Building (Two Story, 8d Roof Sheathing Nails, Gable Roof, No Garage, Strapped Roof Wall Connections, Wood Frame).

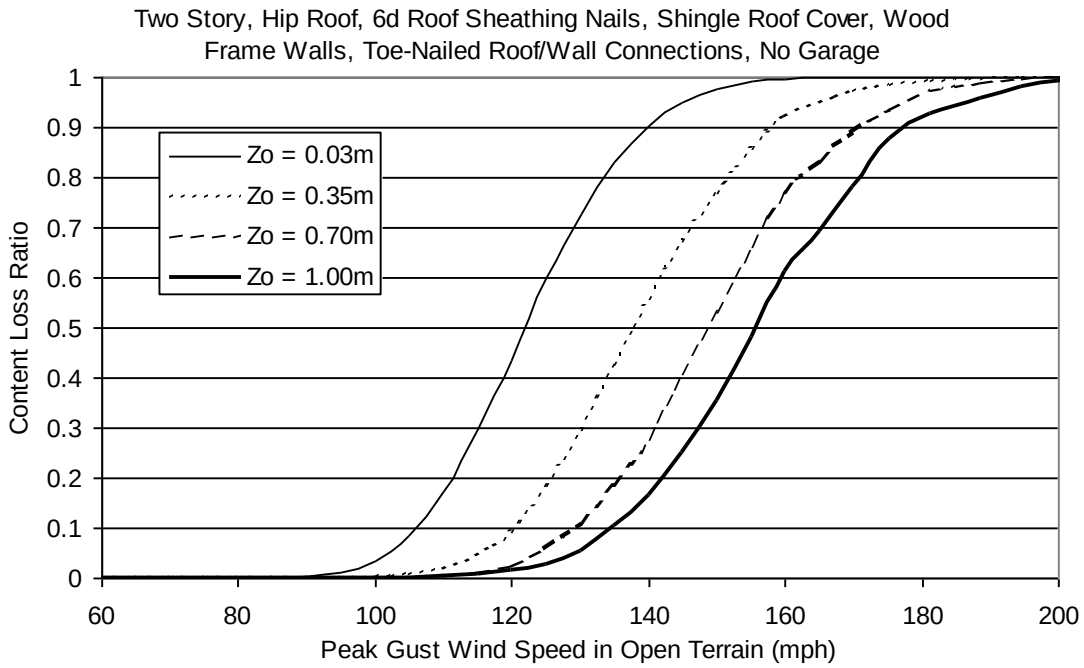

Figure H.29. Content Loss Function for Single Family Residential Building (Two Story, 6d Roof Sheathing Nails, Hip Roof, No Garage, Toe-Nailed Roof Wall Connections, Wood Frame).

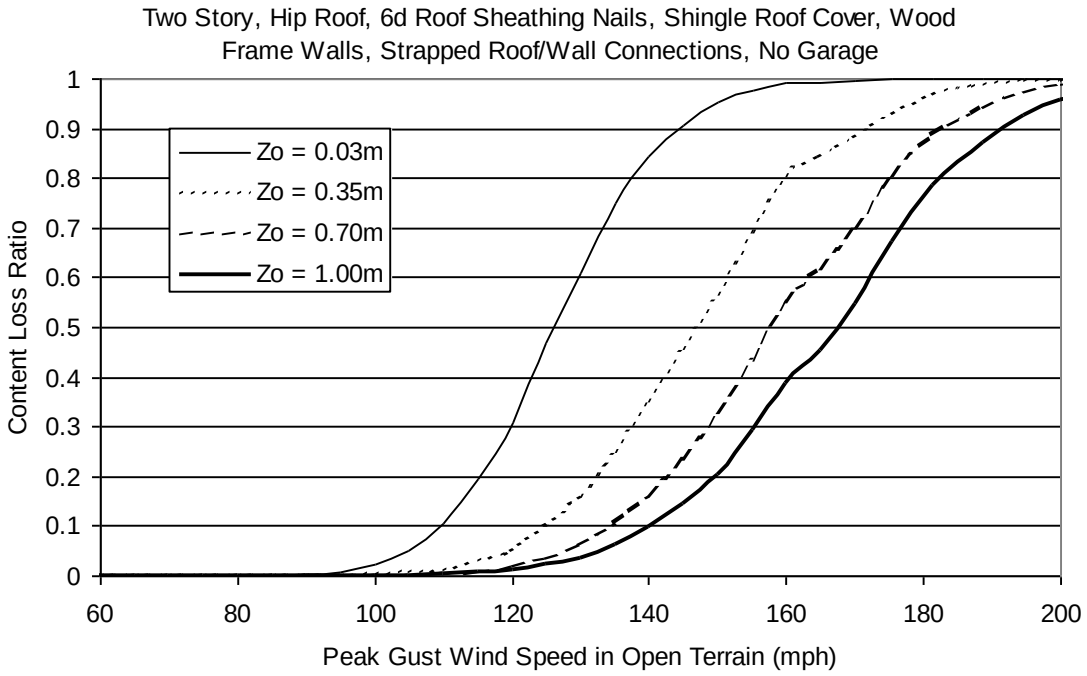

Figure H.30. Content Loss Function for Single Family Residential Building (Two Story, 6d Roof Sheathing Nails, Hip Roof, No Garage, Strapped Roof Wall Connections, Wood Frame).

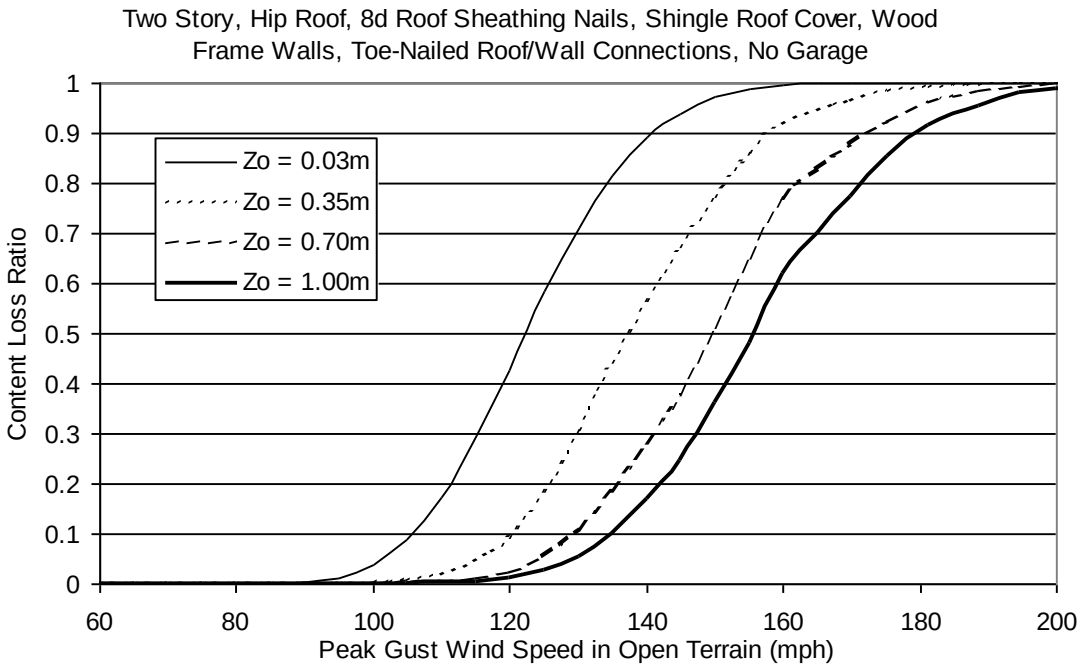

Figure H.31. Content Loss Function for Single Family Residential Building (Two Story, 8d Roof Sheathing Nails, Hip Roof, No Garage, Toe-Nailed Roof Wall Connections, Wood Frame).

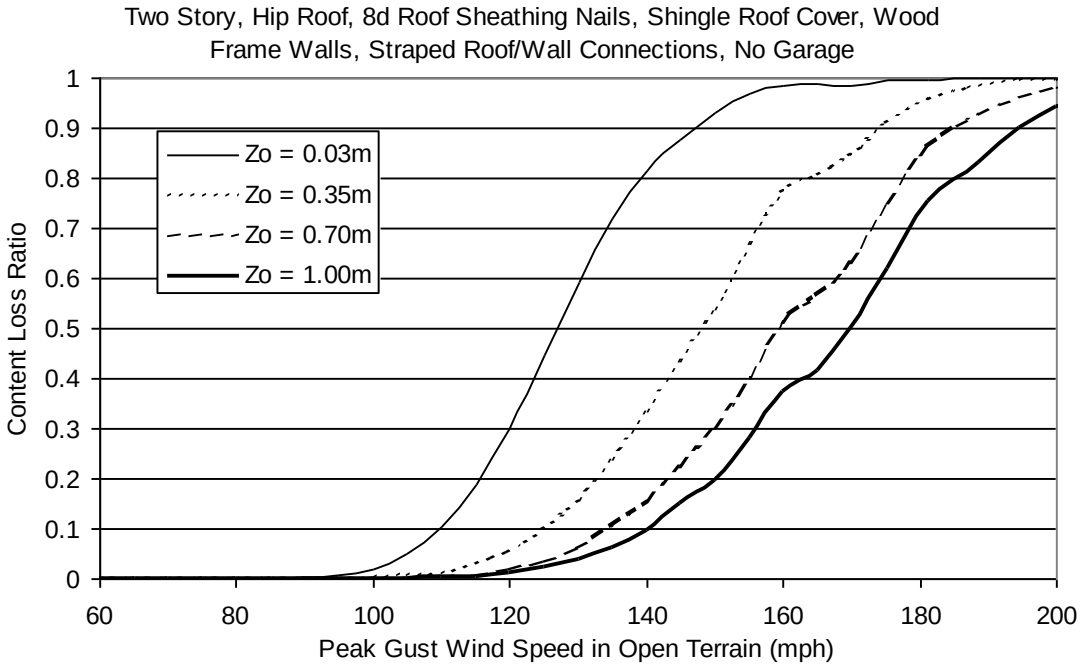

Figure H.32. Content Loss Function for Single Family Residential Building (Two Story, 8d Roof Sheathing Nails, Hip Roof, No Garage, Strapped Roof Wall Connections, Wood Frame).

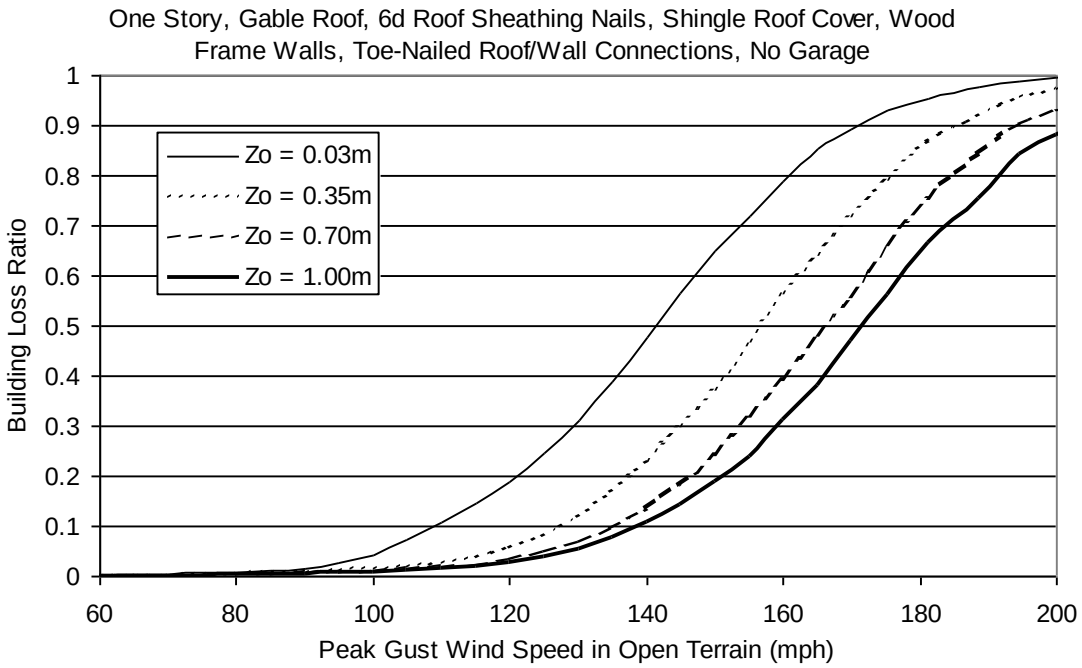

Figure H.33. Building Loss Function for Single Family Residential Building (One Story, 6d Roof Sheathing Nails, Gable Roof, No Garage, Toe-Nailed Roof Wall Connections, Wood Frame, Installed Shutters).

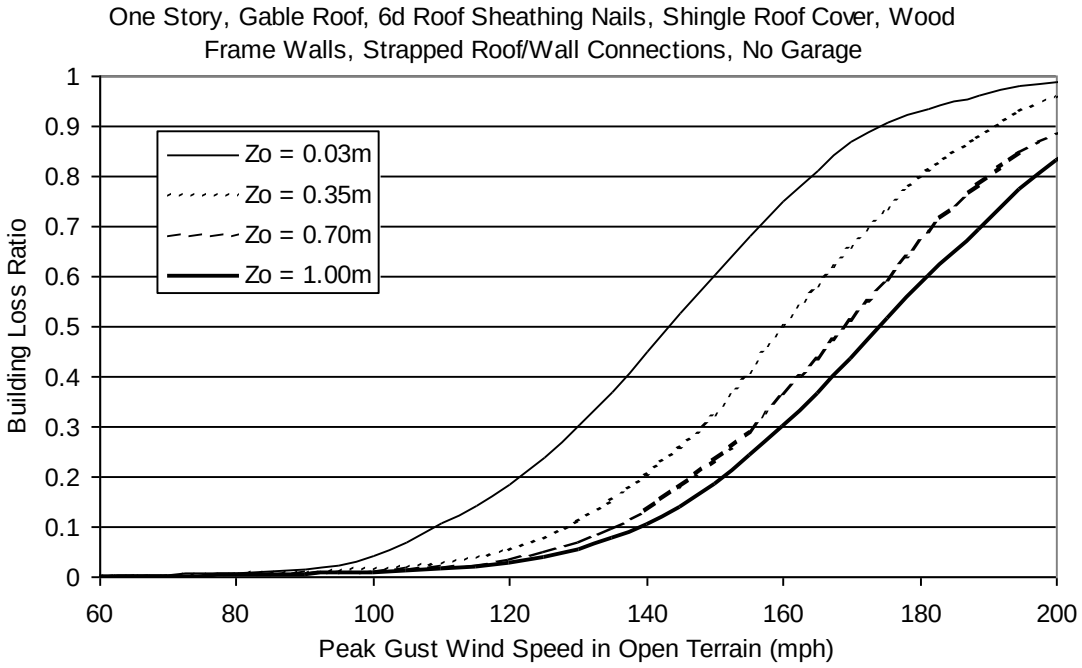

Figure H.34. Building Loss Function for Single Family Residential Building (One Story, 6d Roof Sheathing Nails, Gable Roof, No Garage, Strapped Roof Wall Connections, Wood Frame, Installed Shutters).

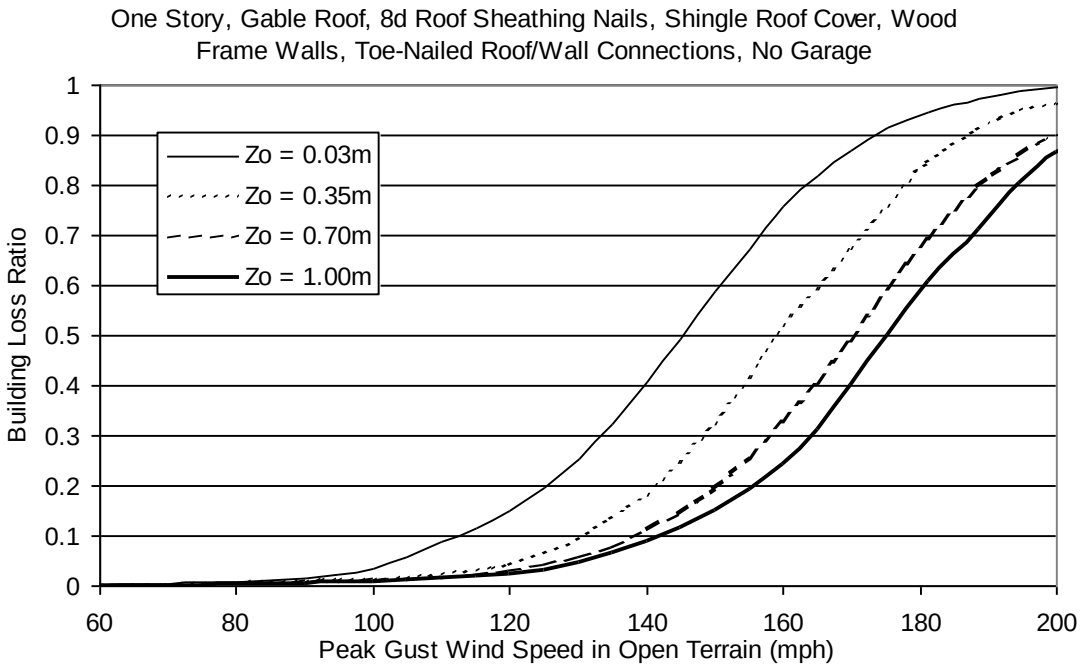

Figure H.35. Building Loss Function for Single Family Residential Building (One Story, 8d Roof Sheathing Nails, Gable Roof, No Garage, Toe-Nailed Roof Wall Connections, Wood Frame, Installed Shutters).

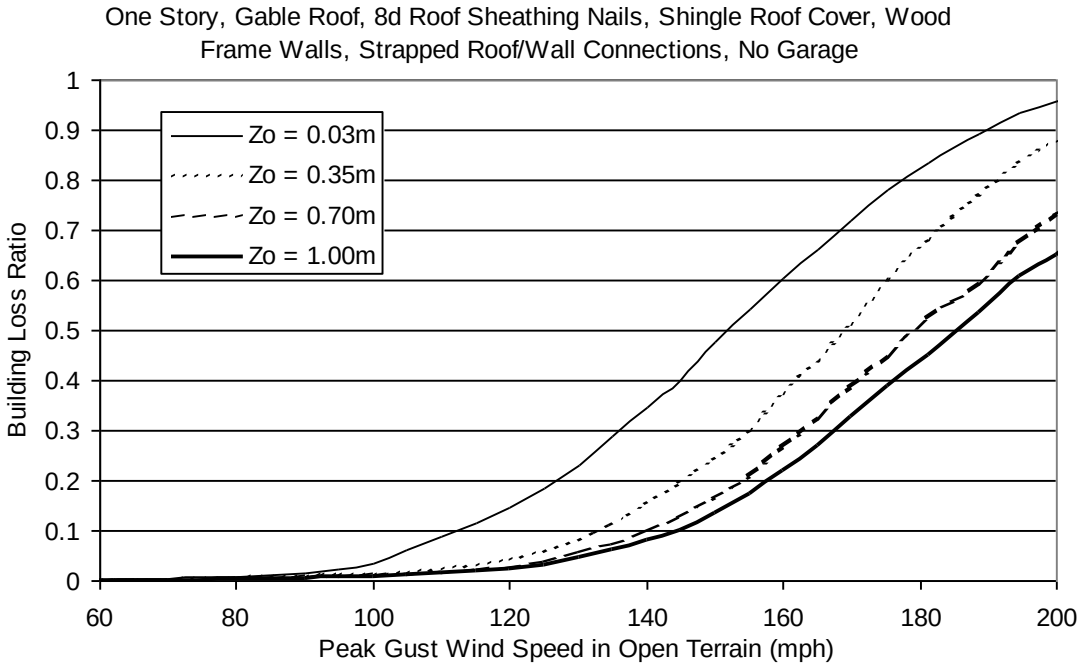

Figure H.36. Building Loss Function for Single Family Residential Building (One Story, 8d Roof Sheathing Nails, Gable Roof, No Garage, Strapped Roof Wall Connections, Wood Frame, Installed Shutters).

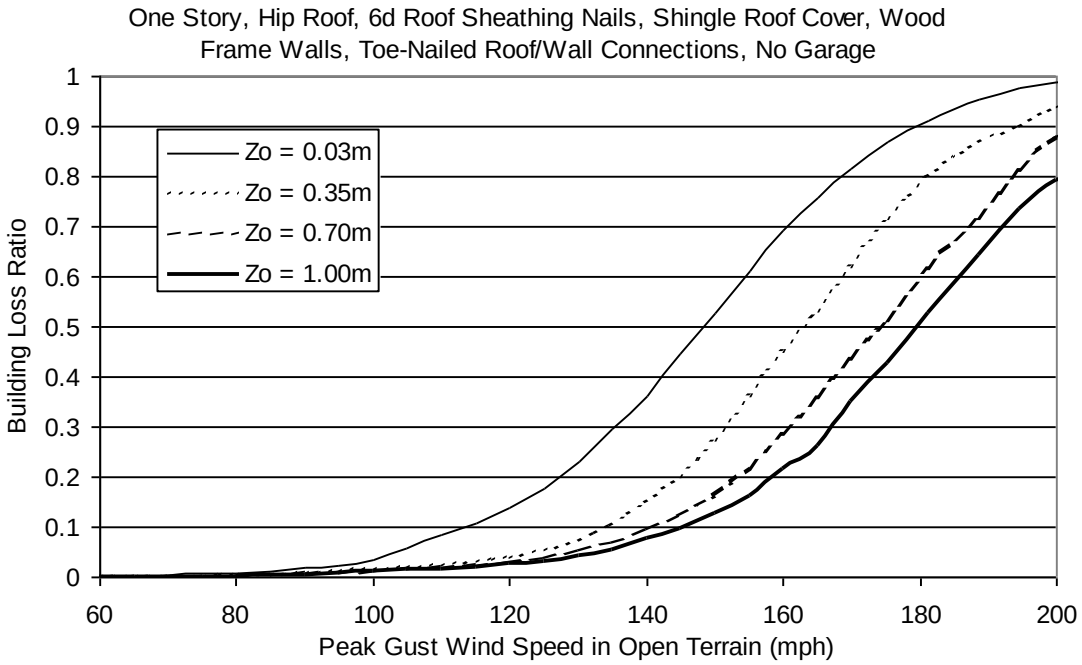

Figure H.37. Building Loss Function for Single Family Residential Building (One Story, 6d Roof Sheathing Nails, Hip Roof, No Garage, Toe-Nailed Roof Wall Connections, Wood Frame, Installed Shutters).

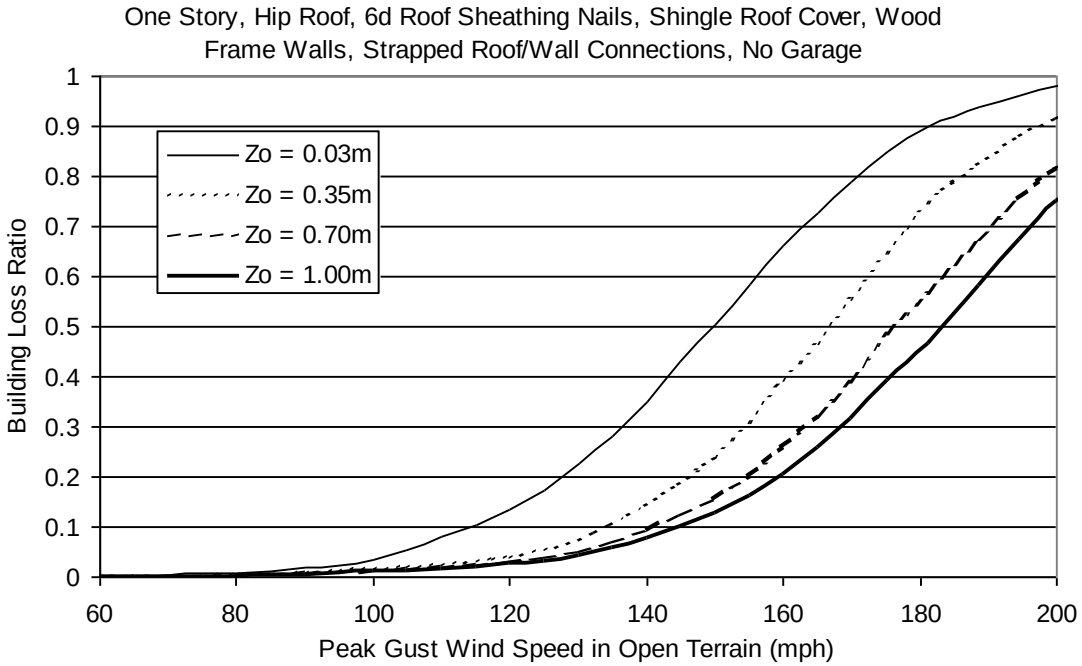

Figure H.38. Building Loss Function for Single Family Residential Building (One Story, 6d Roof Sheathing Nails, Hip Roof, No Garage, Strapped Roof Wall Connections, Wood Frame, Installed Shutters).

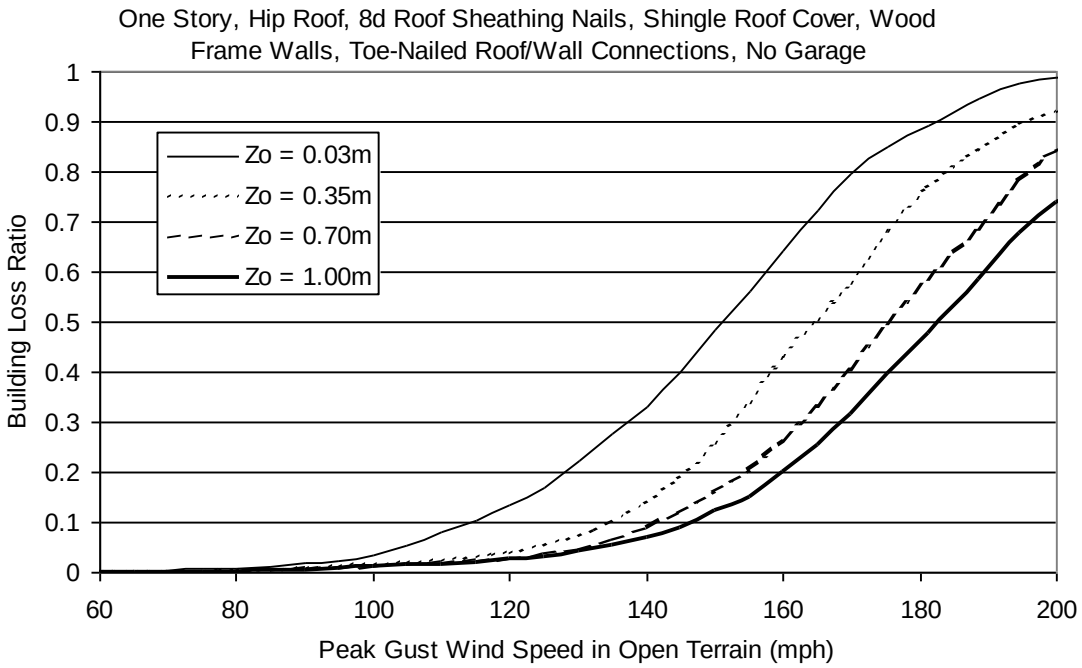

Figure H.39. Building Loss Function for Single Family Residential Building (One Story, 8d Roof Sheathing Nails, Hip Roof, No Garage, Toe-Nailed Roof Wall Connections, Wood Frame, Installed Shutters).

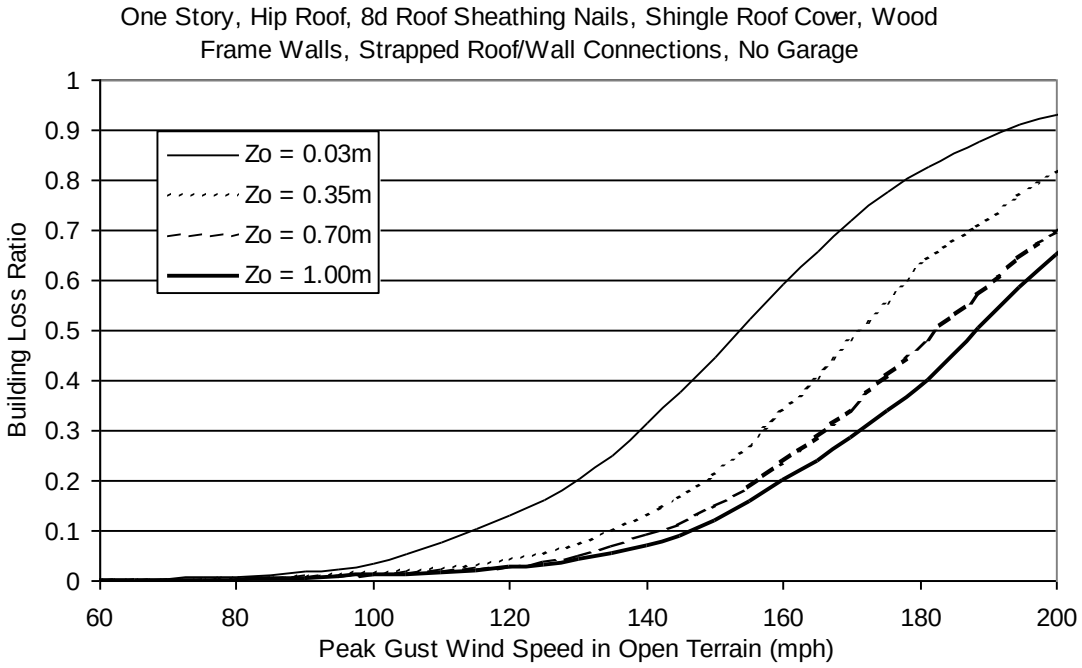

Figure H.40. Building Loss Function for Single Family Residential Building (One Story, 8d Roof Sheathing Nails, Hip Roof, No Garage, Strapped Roof Wall Connections, Wood Frame, Installed Shutters).

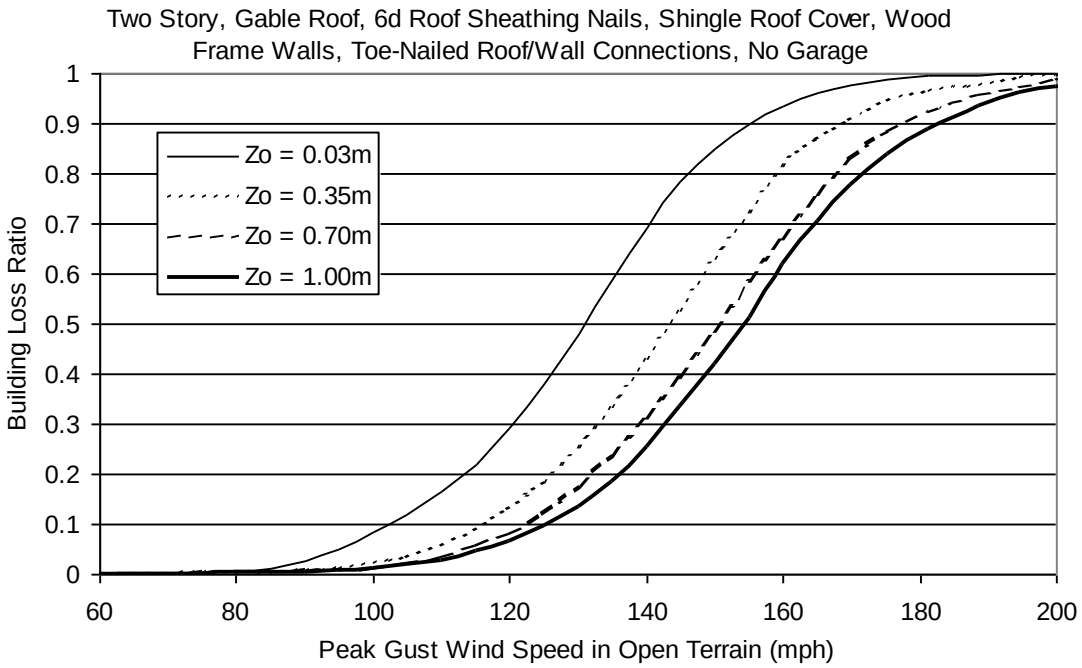

Figure H.41. Building Loss Function for Single Family Residential Building (Two Story, 6d Roof Sheathing Nails, Gable Roof, No Garage, Toe-Nailed Roof Wall Connections, Wood Frame, Installed Shutters).

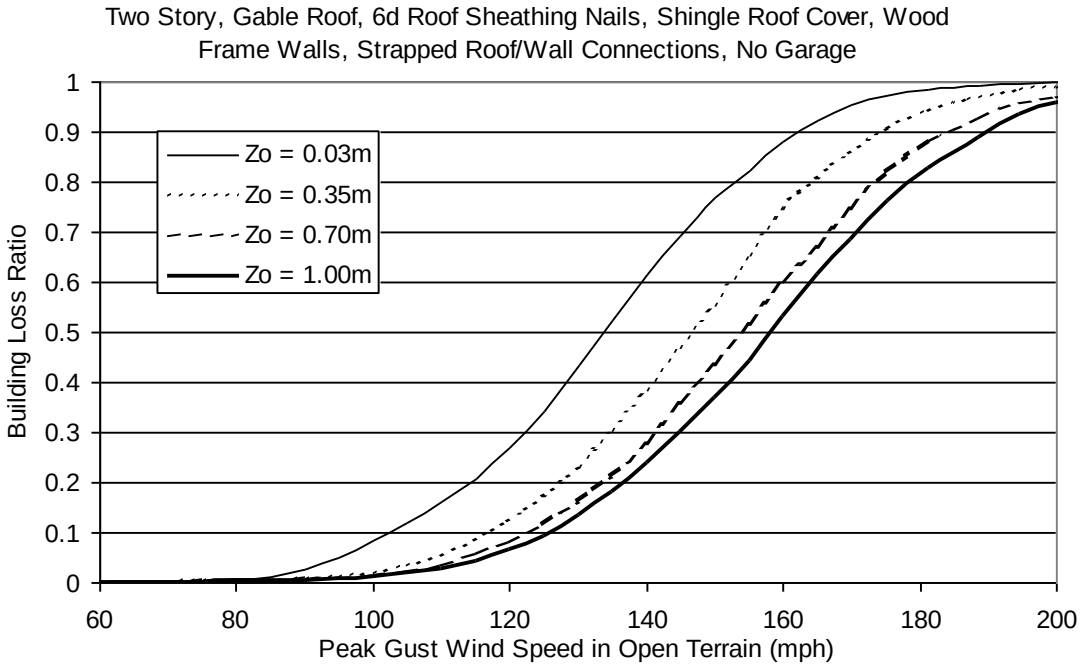

Figure H.42. Building Loss Function for Single Family Residential Building (Two Story, 6d Roof Sheathing Nails, Gable Roof, No Garage, Strapped Roof Wall Connections, Wood Frame, Installed Shutters).

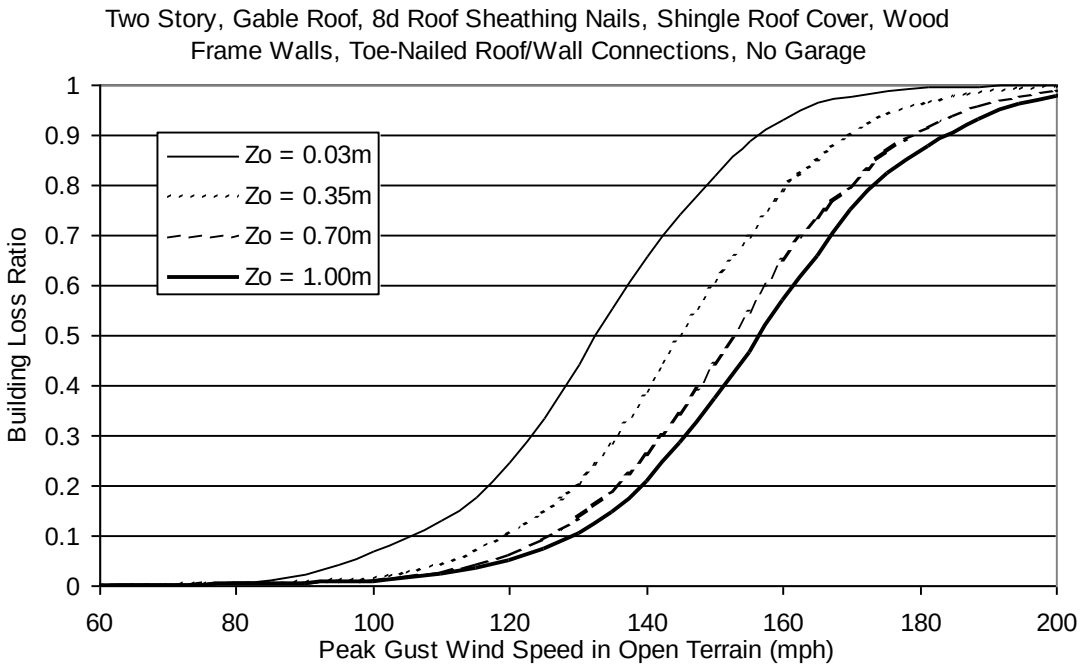

Figure H.43. Building Loss Function for Single Family Residential Building (Two Story, 8d Roof Sheathing Nails, Gable Roof, No Garage, Toe-Nailed Roof Wall Connections, Wood Frame, Installed Shutters).

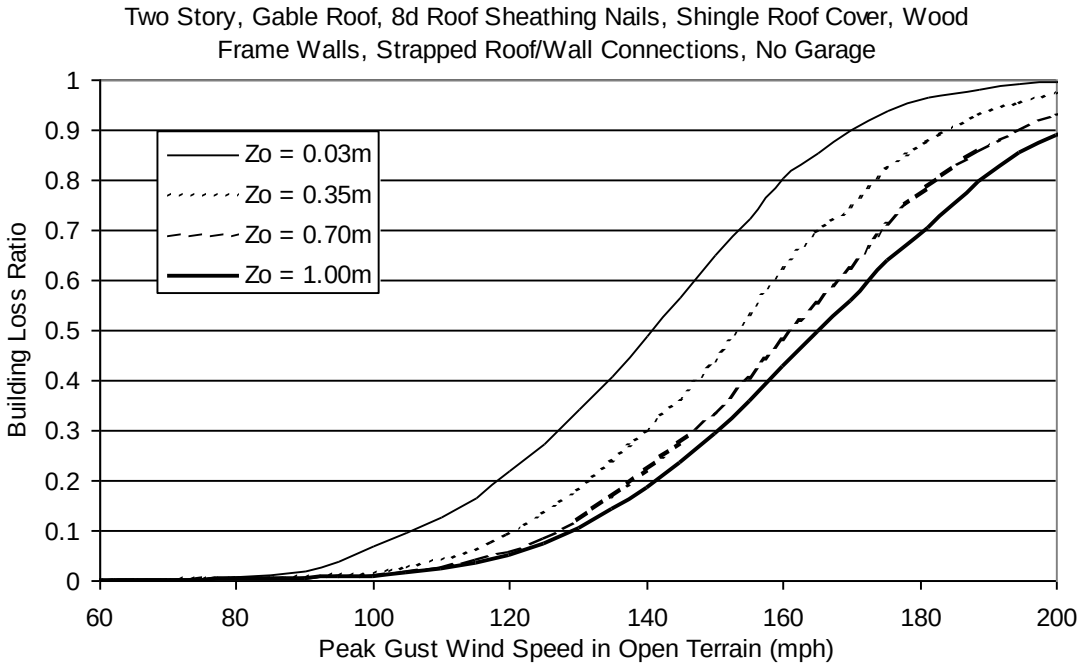

Figure H.44. Building Loss Function for Single Family Residential Building (Two Story, 8d Roof Sheathing Nails, Gable Roof, No Garage, Strapped Roof Wall Connections, Wood Frame, Installed Shutters).

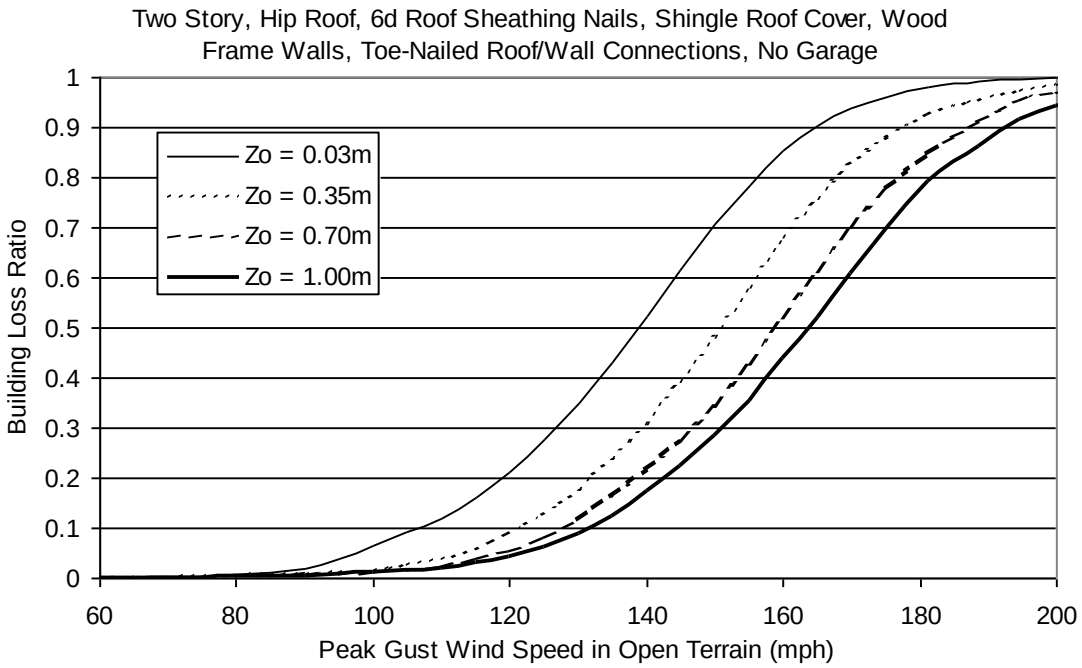

Figure H.45. Building Loss Function for Single Family Residential Building (Two Story, 6d Roof Sheathing Nails, Hip Roof, No Garage, Toe-Nailed Roof Wall Connections, Wood Frame, Installed Shutters).

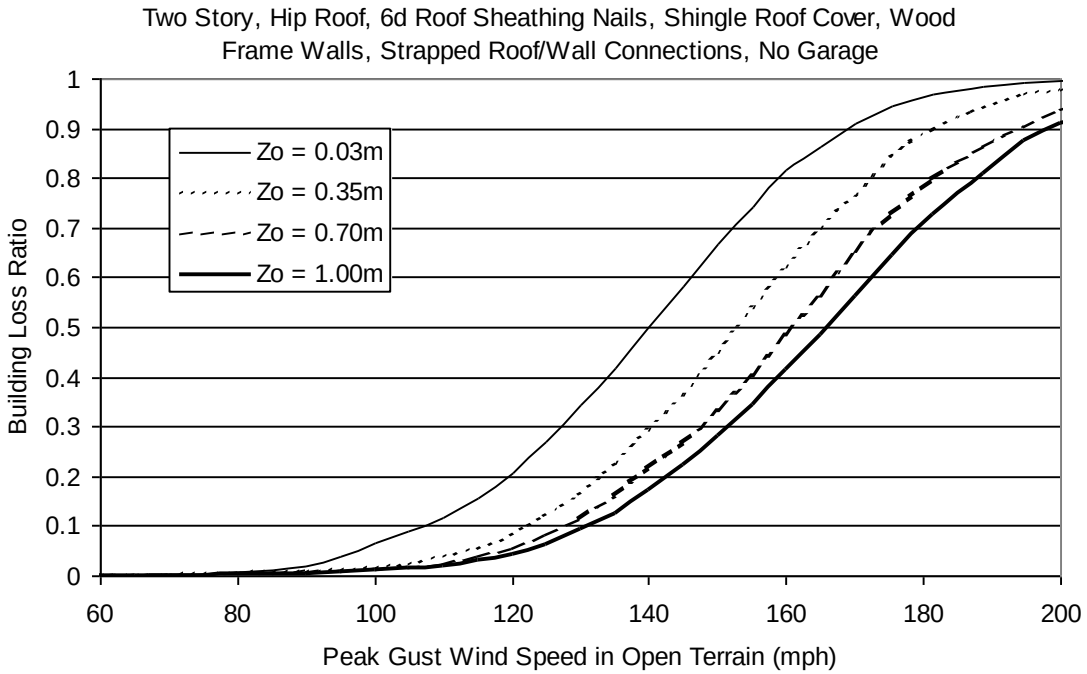

Figure H.46. Building Loss Function for Single Family Residential Building (Two Story, 6d Roof Sheathing Nails, Hip Roof, No Garage, Strapped Roof Wall Connections, Wood Frame, Installed Shutters).

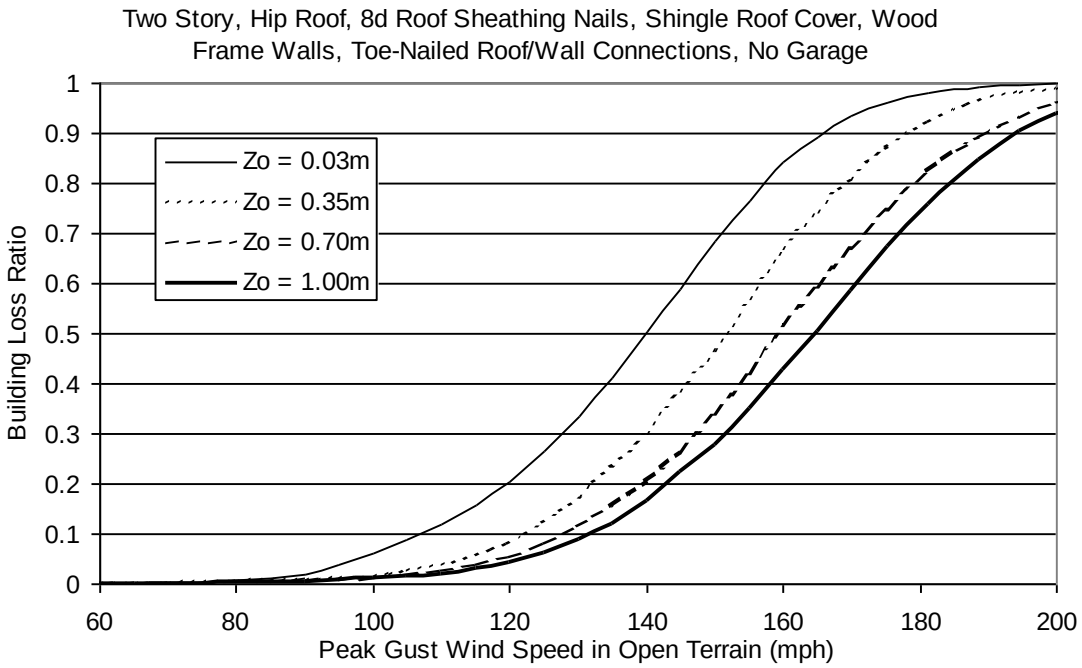

Figure H.47. Building Loss Function for Single Family Residential Building (Two Story, 8d Roof Sheathing Nails, Hip Roof, No Garage, Toe-Nailed Roof Wall Connections, Wood Frame, Installed Shutters).

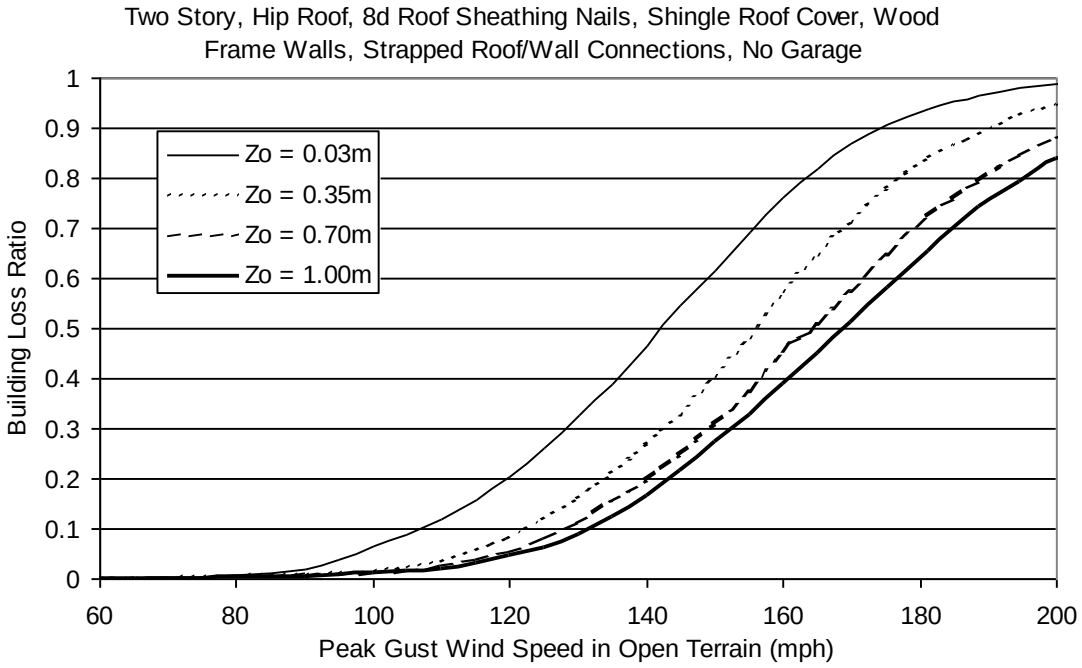

Figure H.48. Building Loss Function for Single Family Residential Building (Two Story, 8d Roof Sheathing Nails, Hip Roof, No Garage, Strapped Roof Wall Connections, Wood Frame, Installed Shutters).

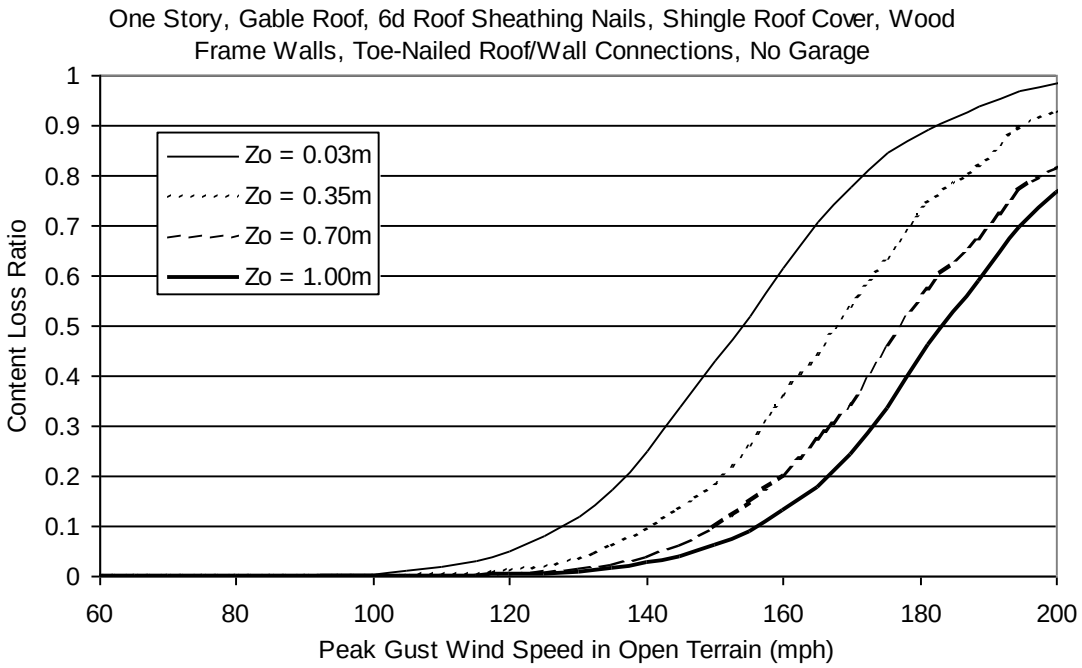

Figure H.49. Content Loss Function for Single Family Residential Building (One Story, 6d Roof Sheathing Nails, Gable Roof, No Garage, Toe-Nailed Roof Wall Connections, Wood Frame, Installed Shutters).

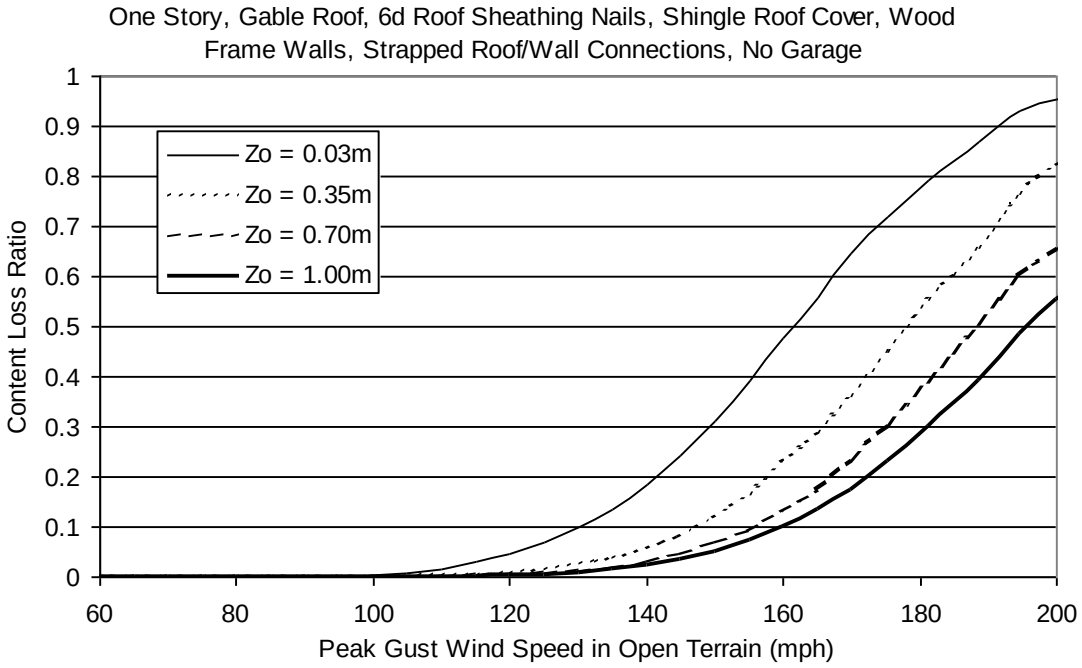

Figure H.50. Content Loss Function for Single Family Residential Building (One Story, 6d Roof Sheathing Nails, Gable Roof, No Garage, Strapped Roof Wall Connections, Wood Frame, Installed Shutters).

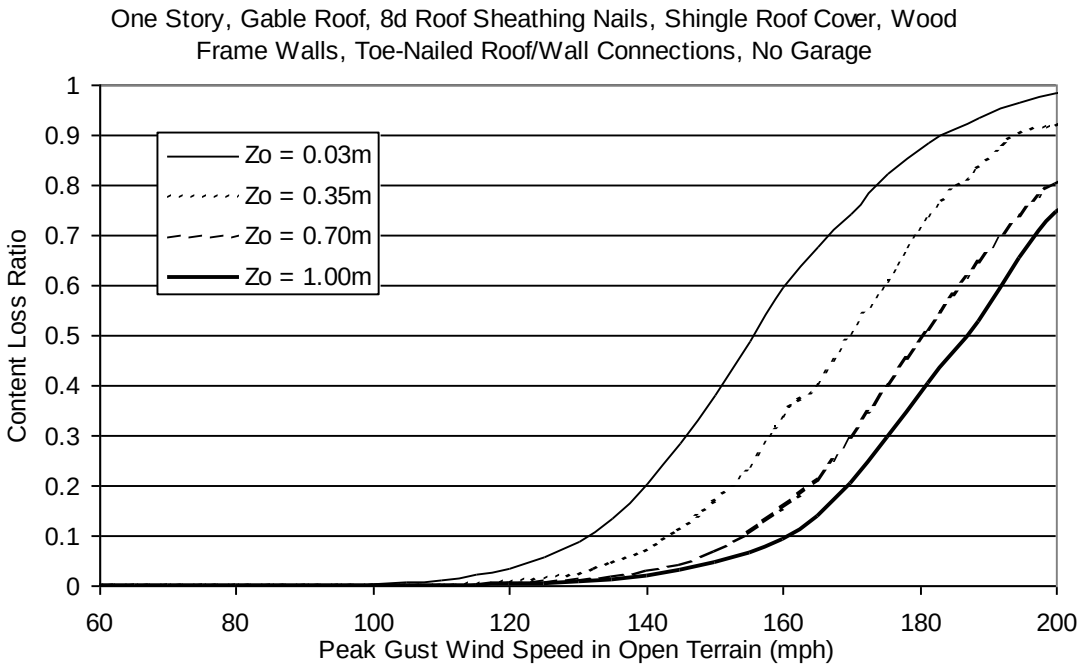

Figure H.51. Content Loss Function for Single Family Residential Building (One Story, 8d Roof Sheathing Nails, Gable Roof, No Garage, Toe-Nailed Roof Wall Connections, Wood Frame, Installed Shutters).

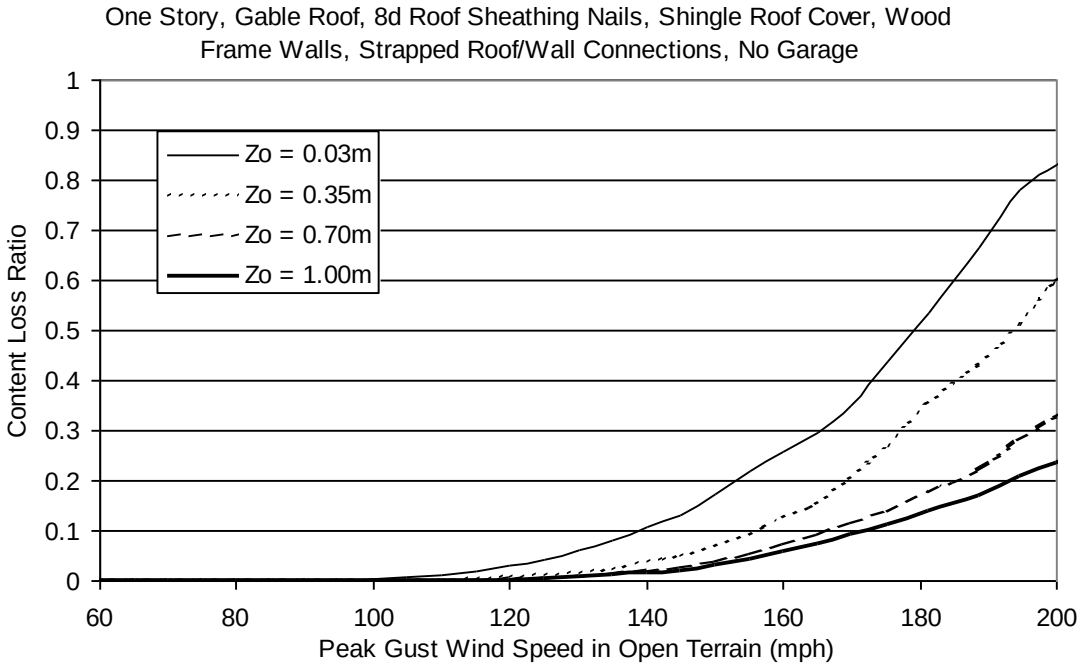

Figure H.52. Content Loss Function for Single Family Residential Building (One Story, 8d Roof Sheathing Nails, Gable Roof, No Garage, Strapped Roof Wall Connections, Wood Frame, Installed Shutters).

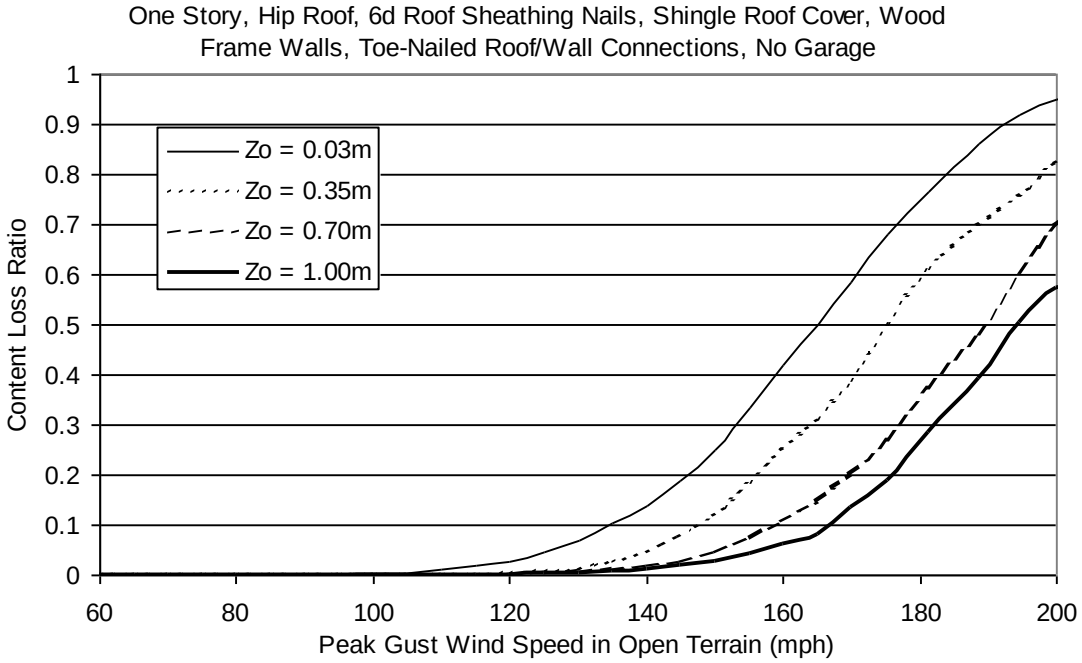

Figure H.53. Content Loss Function for Single Family Residential Building (One Story, 6d Roof Sheathing Nails, Hip Roof, No Garage, Toe-Nailed Roof Wall Connections, Wood Frame, Installed Shutters).

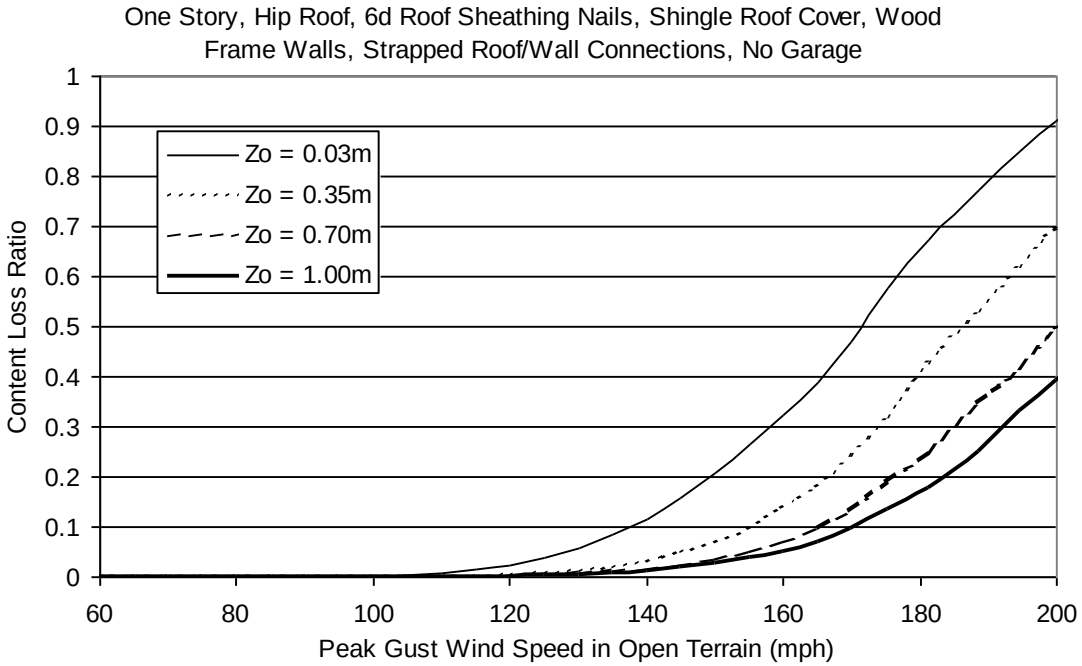

Figure H.54. Content Loss Function for Single Family Residential Building (One Story, 6d Roof Sheathing Nails, Hip Roof, No Garage, Strapped Roof Wall Connections, Wood Frame, Installed Shutters).

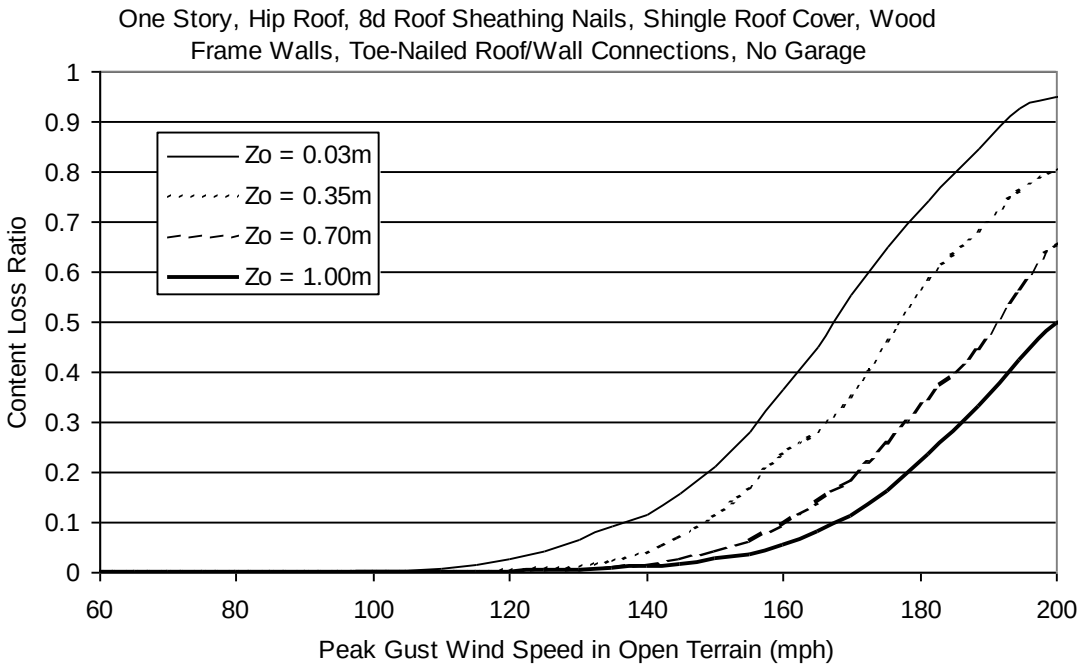

Figure H.55. Content Loss Function for Single Family Residential Building (One Story, 8d Roof Sheathing Nails, Hip Roof, No Garage, Toe-Nailed Roof Wall Connections, Wood Frame, Installed Shutters).

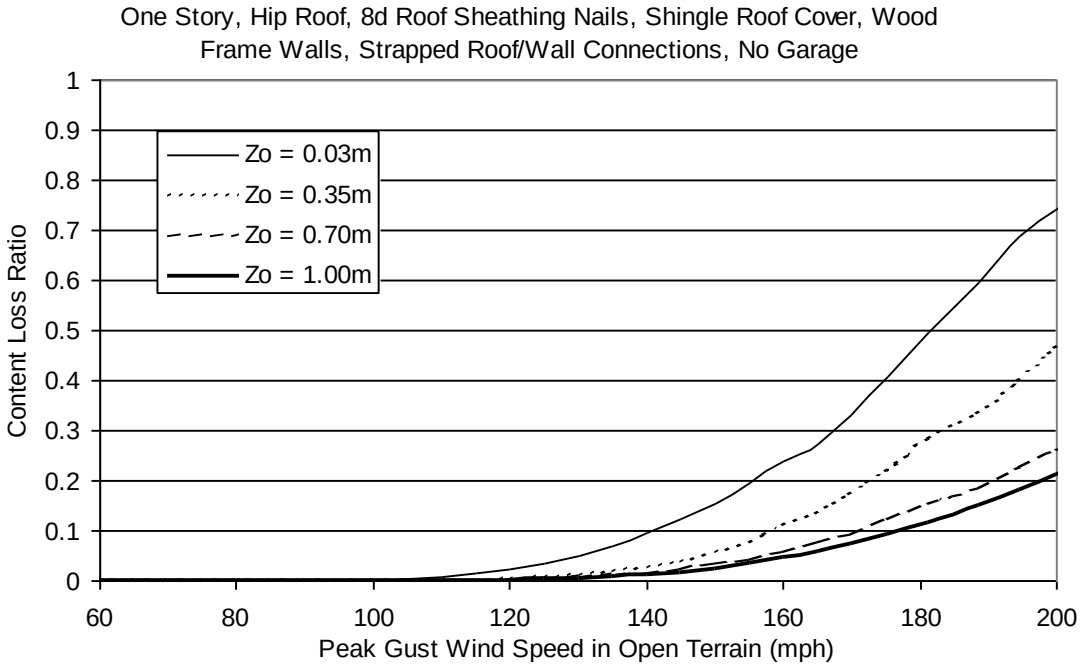

Figure H.56. Content Loss Function for Single Family Residential Building (One Story, 8d Roof Sheathing Nails, Hip Roof, No Garage, Strapped Roof Wall Connections, Wood Frame, Installed Shutters).

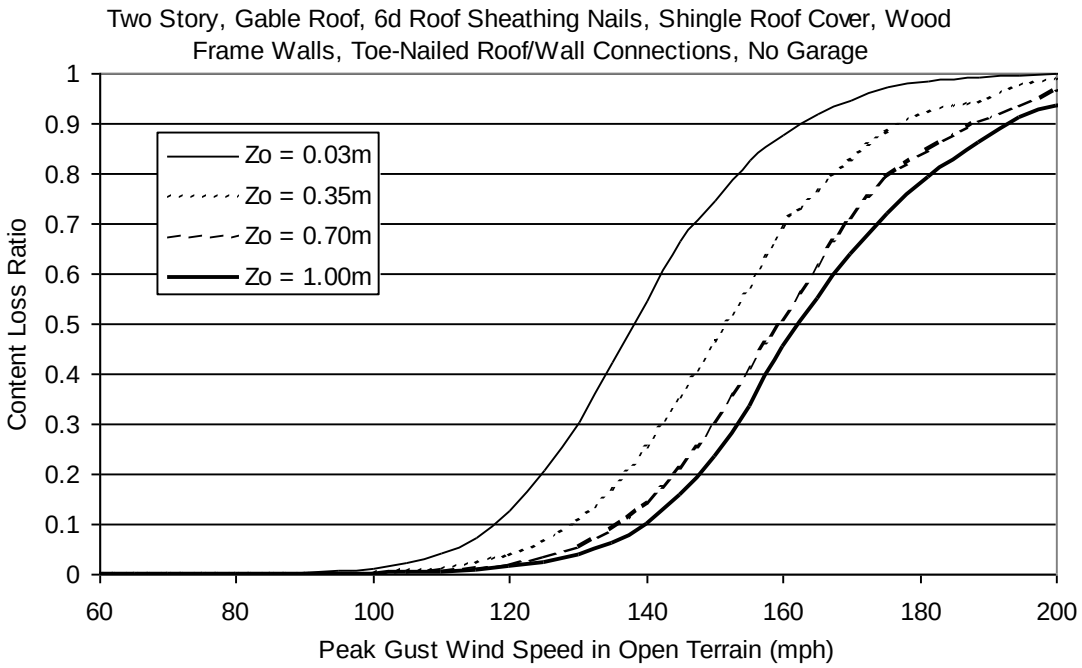

Figure H.57. Content Loss Function for Single Family Residential Building (Two Story, 6d Roof Sheathing Nails, Gable Roof, No Garage, Toe-Nailed Roof Wall Connections, Wood Frame, Installed Shutters).

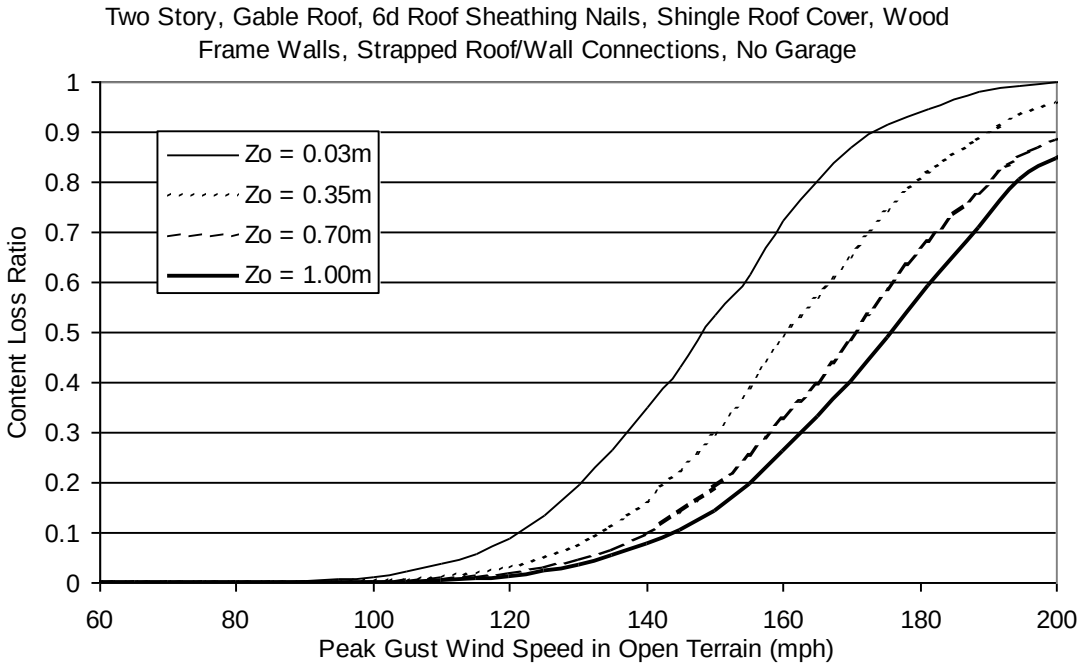

Figure H.58. Content Loss Function for Single Family Residential Building (Two Story, 6d Roof Sheathing Nails, Gable Roof, No Garage, Strapped Roof Wall Connections, Wood Frame, Installed Shutters).

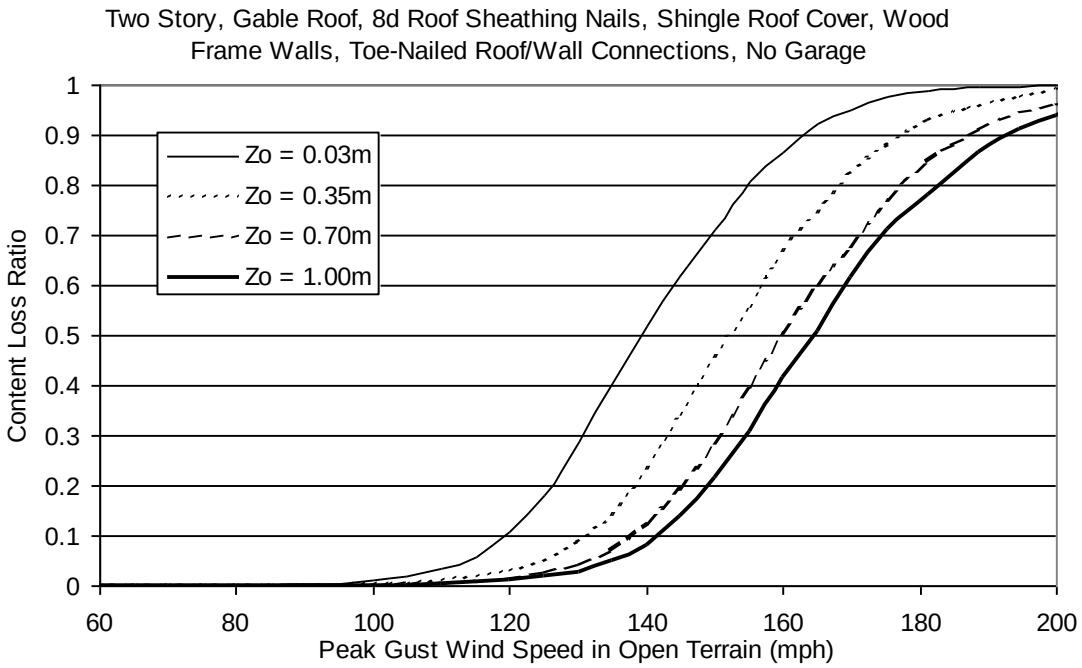

Figure H.59. Content Loss Function for Single Family Residential Building (Two Story, 8d Roof Sheathing Nails, Gable Roof, No Garage, Toe-Nailed Roof Wall Connections, Wood Frame, Installed Shutters).

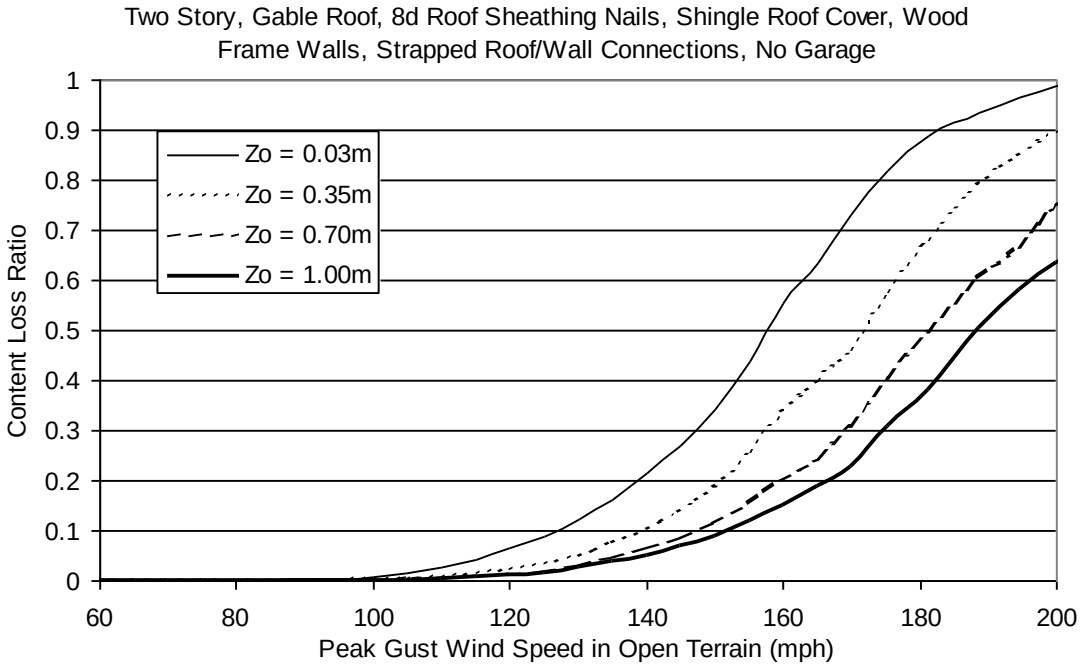

Figure H.60. Content Loss Function for Single Family Residential Building (Two Story, 8d Roof Sheathing Nails, Gable Roof, No Garage, Strapped Roof Wall Connections, Wood Frame, Installed Shutters).

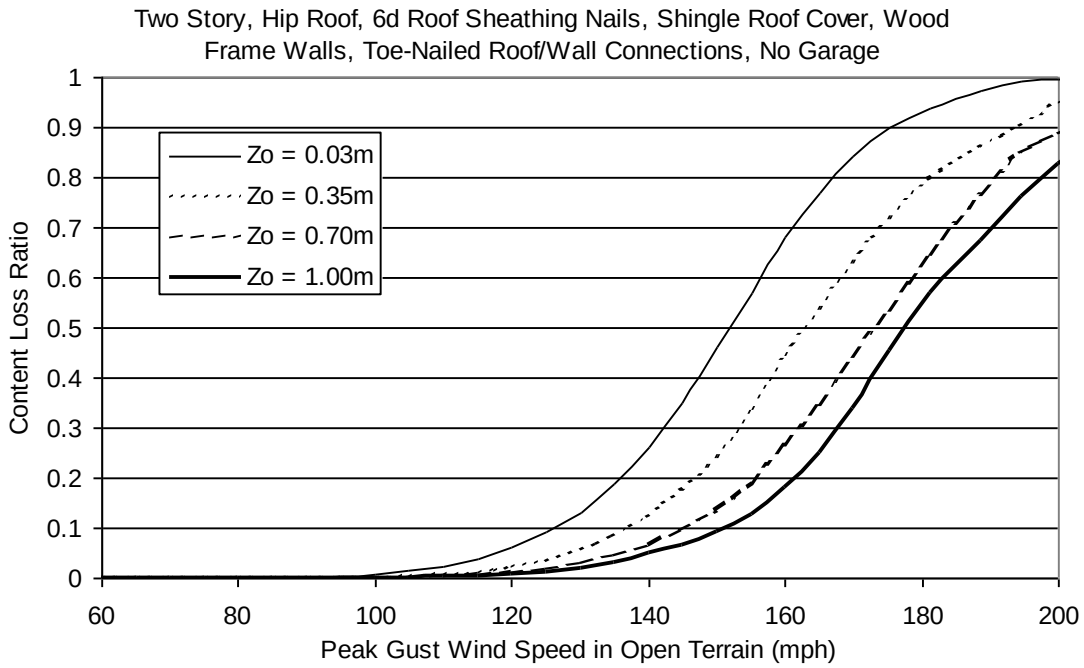

Figure H.61. Content Loss Function for Single Family Residential Building (Two Story, 6d Roof Sheathing Nails, Hip Roof, No Garage, Toe-Nailed Roof Wall Connections, Wood Frame, Installed Shutters).

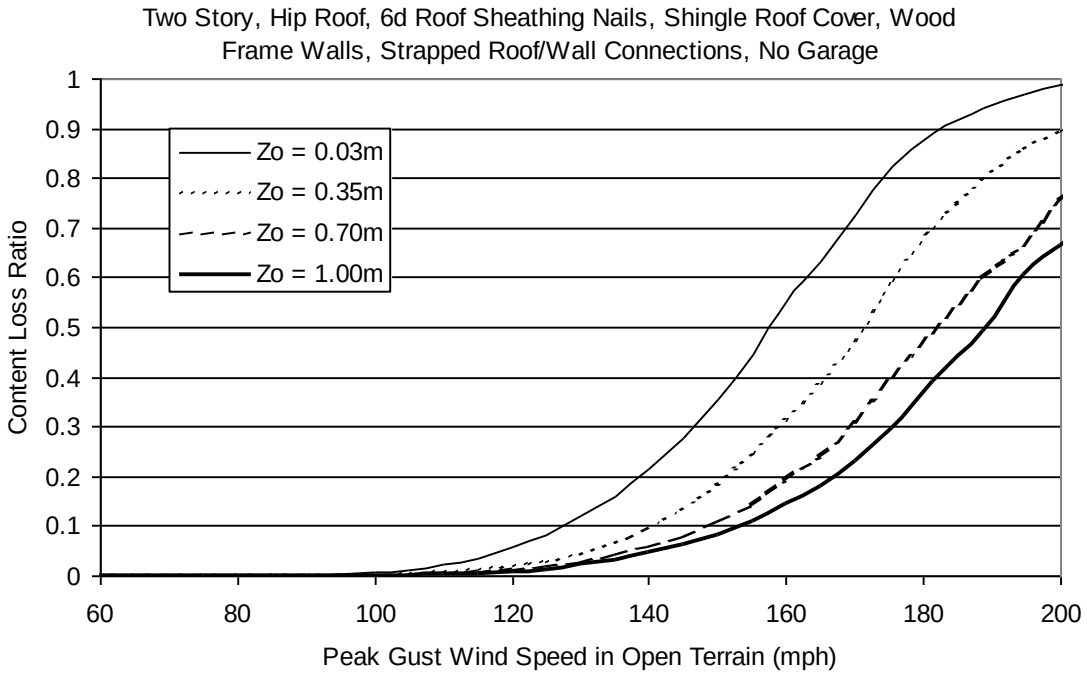

Figure H.62. Content Loss Function for Single Family Residential Building (Two Story, 6d Roof Sheathing Nails, Hip Roof, No Garage, Strapped Roof Wall Connections, Wood Frame, Installed Shutters).

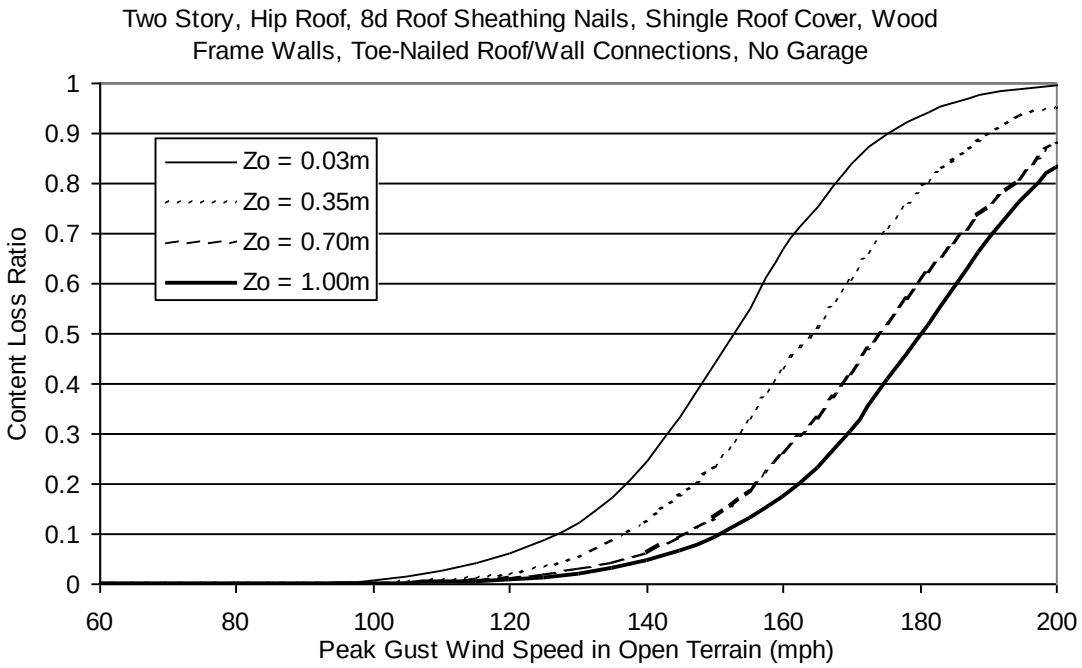

Figure H.63. Content Loss Function for Single Family Residential Building (Two Story, 8d Roof Sheathing Nails, Hip Roof, No Garage, Toe-Nailed Roof Wall Connections, Wood Frame, Installed Shutters).

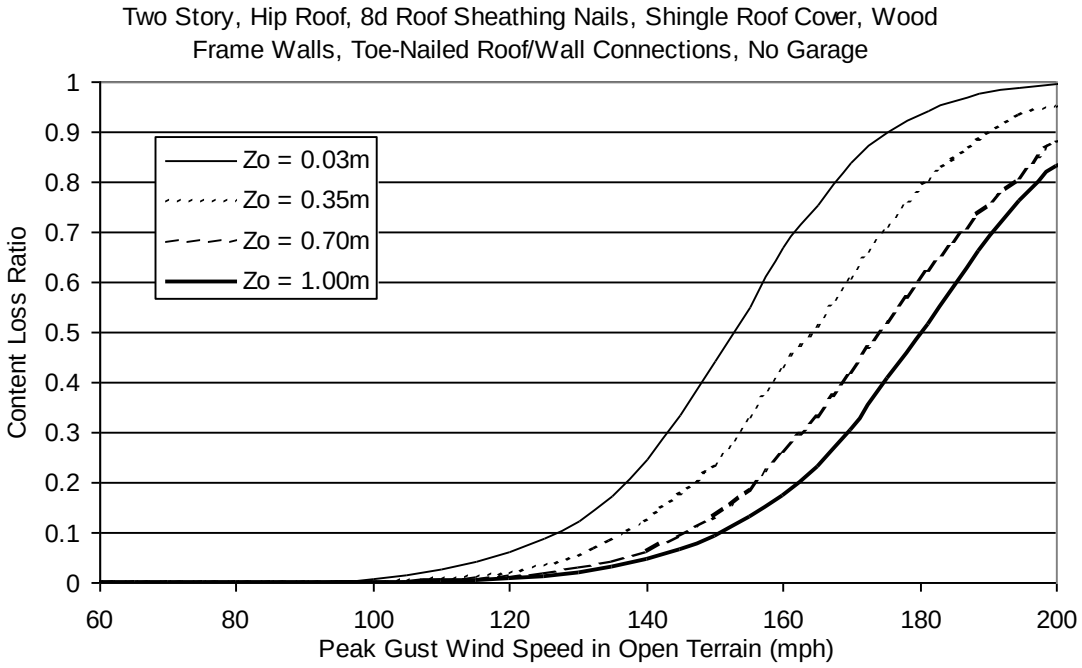

Figure H.64. Content Loss Function for Single Family Residential Building (Two Story, 8d Roof Sheathing Nails, Hip Roof, No Garage, Strapped Roof Wall Connections, Wood Frame, Installed Shutters).

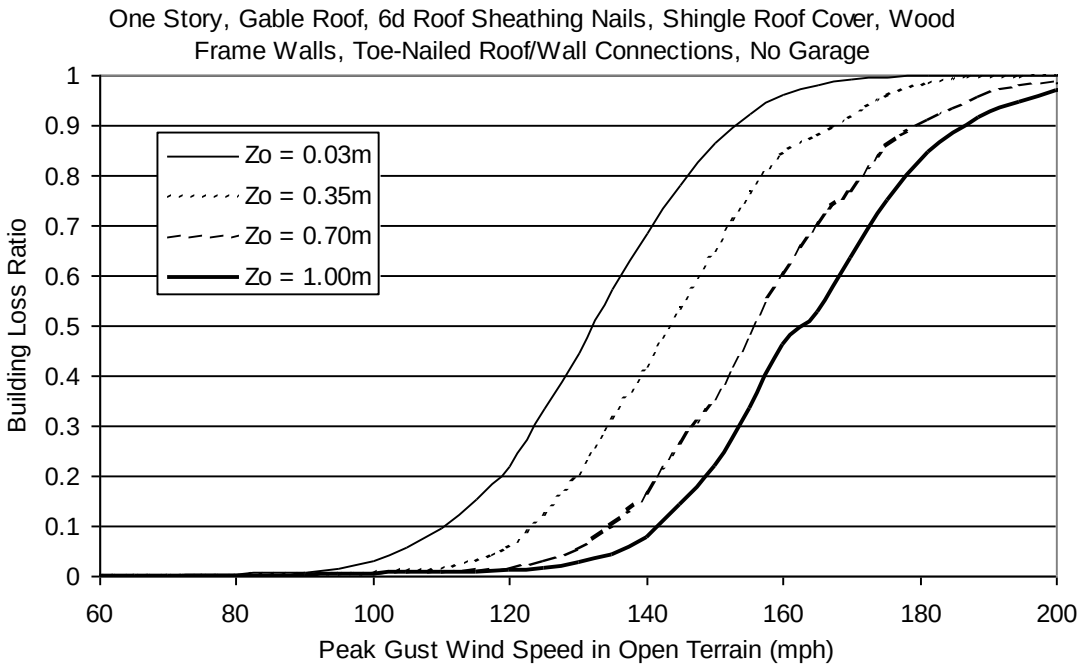

Figure H.65. Building Loss Function for Single Family Residential Building (One Story, 6d Roof Sheathing Nails, Gable Roof, No Garage, Toe-Nailed Roof Wall Connections, Wood Frame, Upgraded Roof).

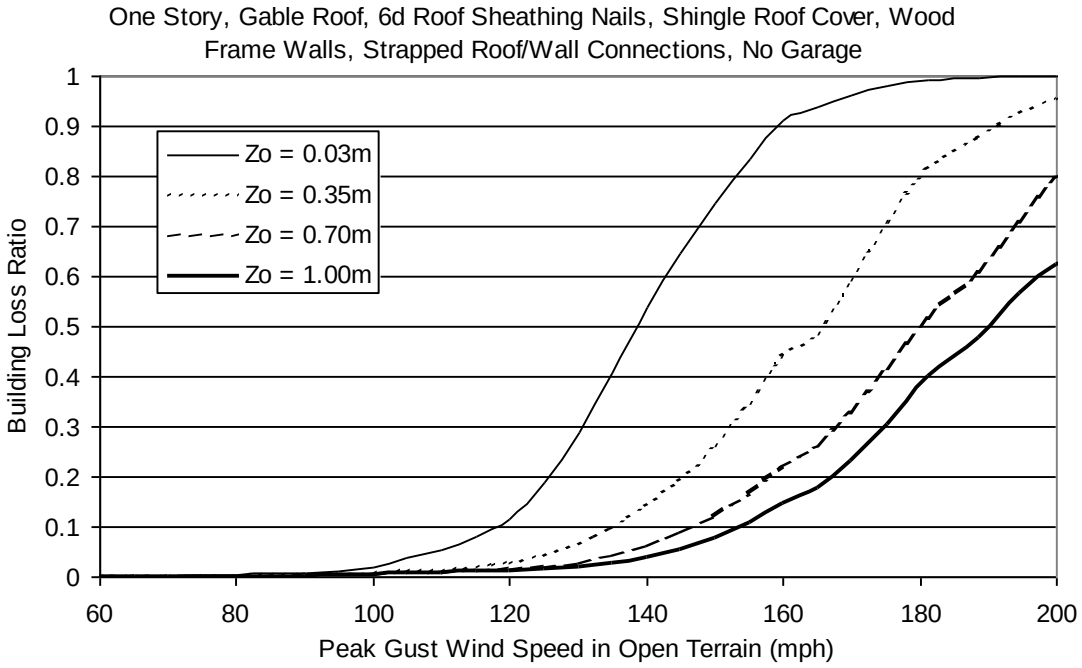

Figure H.66. Building Loss Function for Single Family Residential Building (One Story, 6d Roof Sheathing Nails, Gable Roof, No Garage, Strapped Roof Wall Connections, Wood Frame, Upgraded Roof).

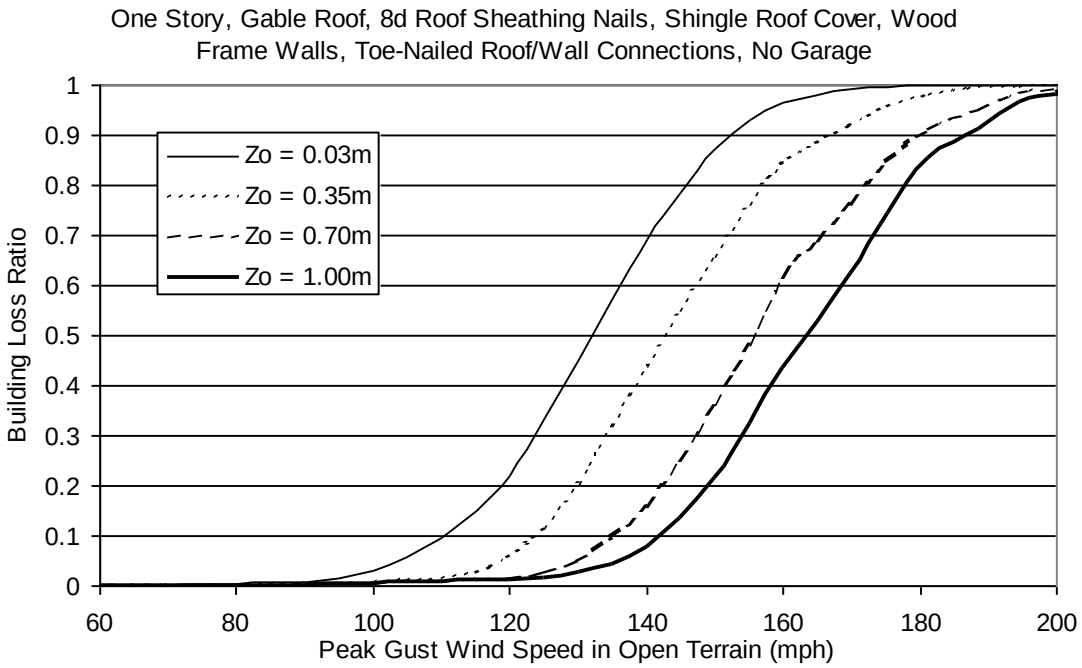

Figure H.67. Building Loss Function for Single Family Residential Building (One Story, 8d Roof Sheathing Nails, Gable Roof, No Garage, Toe-Nailed Roof Wall Connections, Wood Frame, Upgraded Roof).

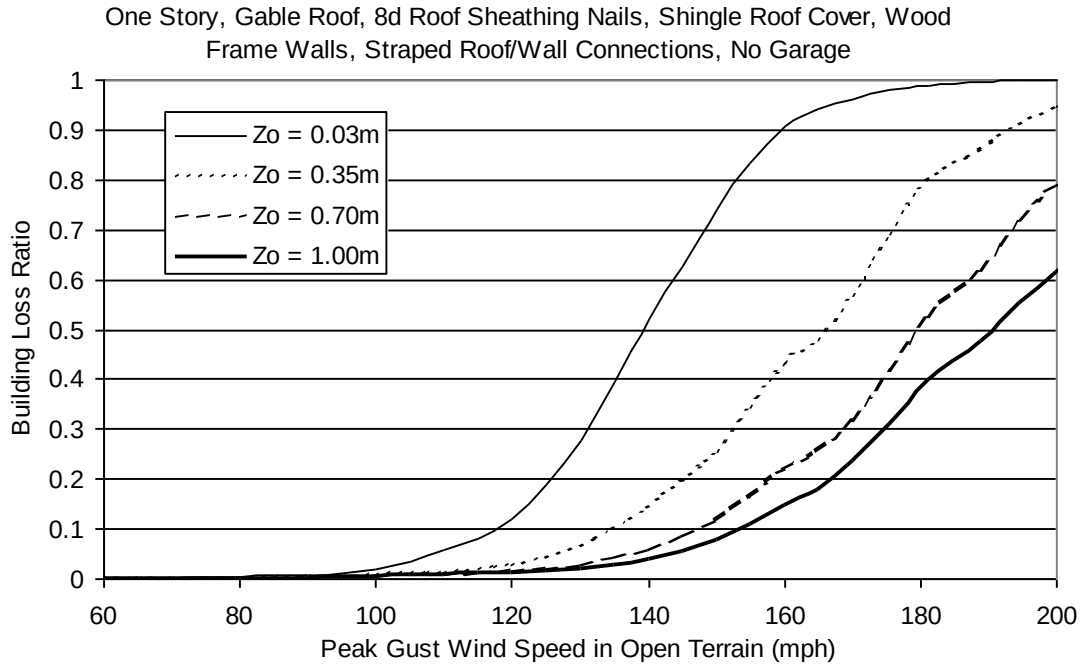

Figure H.68. Building Loss Function for Single Family Residential Building (One Story, 8d Roof Sheathing Nails, Gable Roof, No Garage, Strapped Roof Wall Connections, Wood Frame, Upgraded Roof).

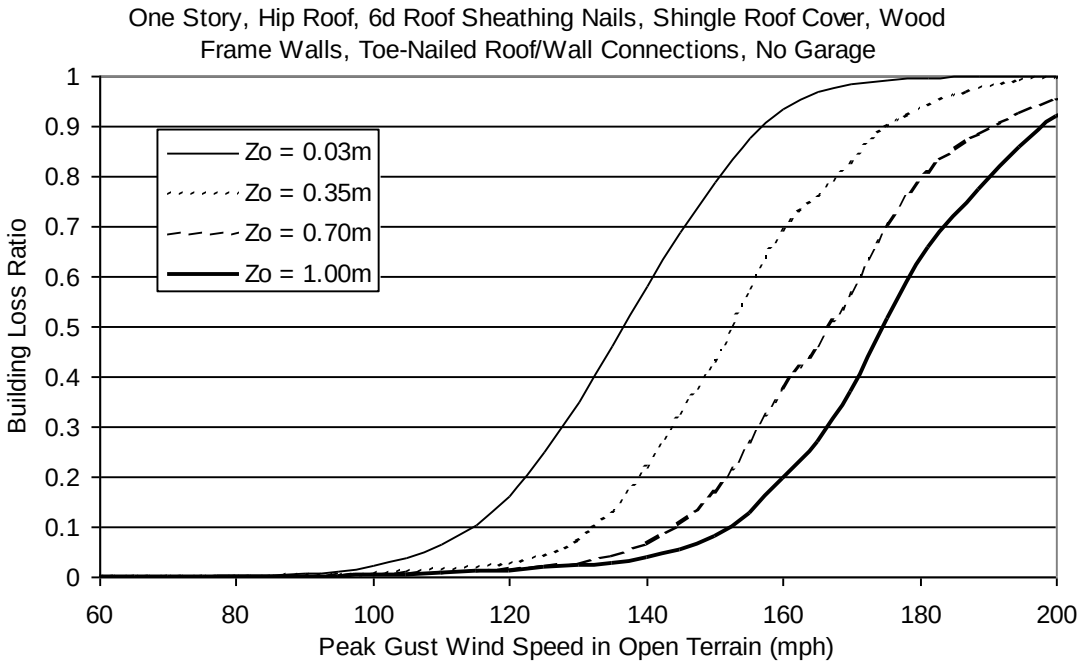

Figure H.69. Building Loss Function for Single Family Residential Building (One Story, 6d Roof Sheathing Nails, Hip Roof, No Garage, Toe-Nailed Roof Wall Connections, Wood Frame, Upgraded Roof).

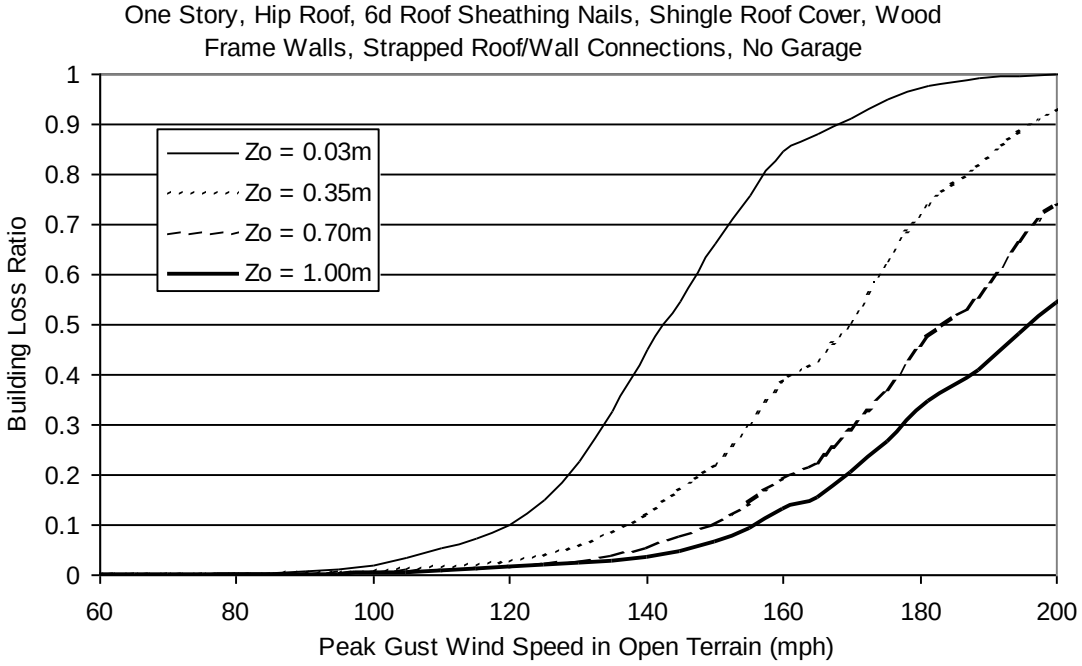

Figure H.70. Building Loss Function for Single Family Residential Building (One Story, 6d Roof Sheathing Nails, Hip Roof, No Garage, Strapped Roof Wall Connections, Wood Frame, Upgraded Roof).

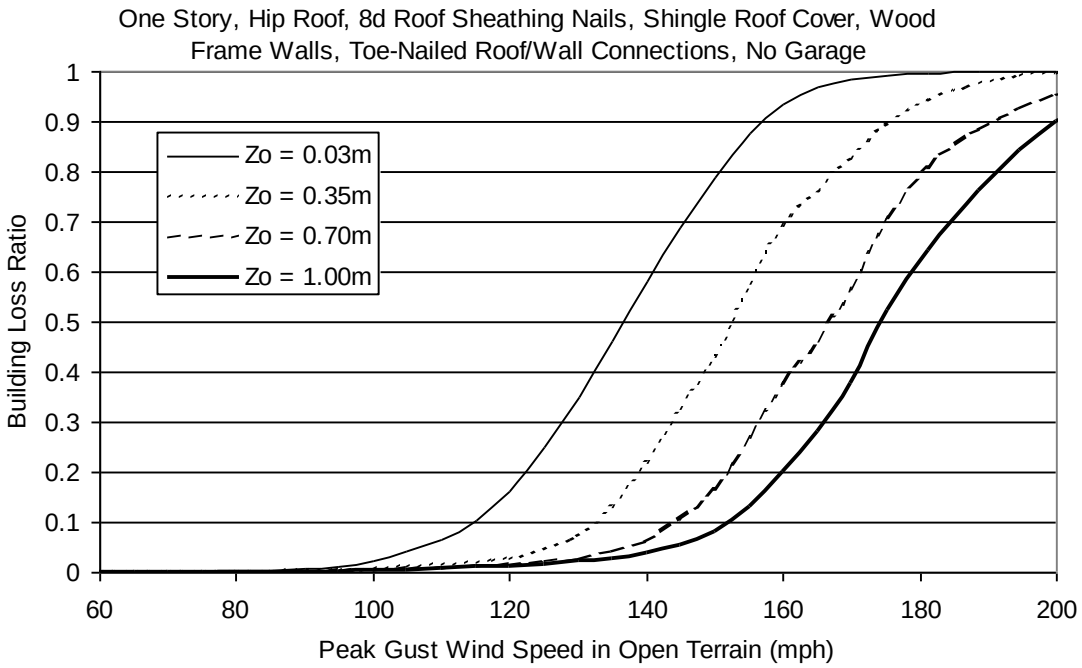

Figure H.71. Building Loss Function for Single Family Residential Building (One Story, 8d Roof Sheathing Nails, Hip Roof, No Garage, Toe-Nailed Roof Wall Connections, Wood Frame, Upgraded Roof).

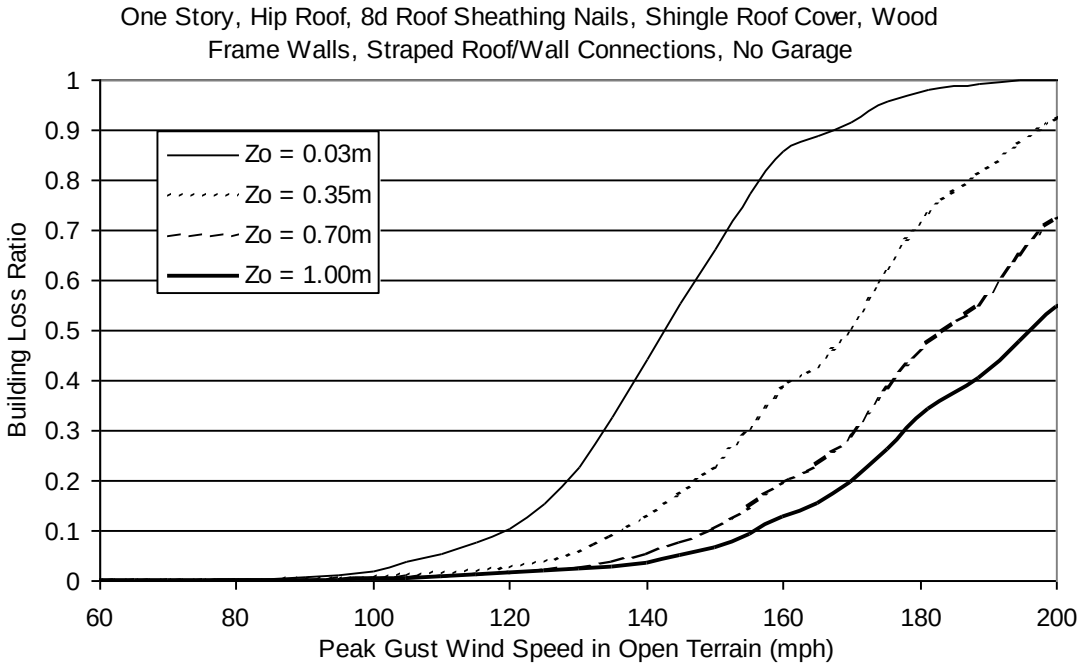

Figure H.72. Building Loss Function for Single Family Residential Building (One Story, 8d Roof Sheathing Nails, Hip Roof, No Garage, Strapped Roof Wall Connections, Wood Frame, Upgraded Roof).

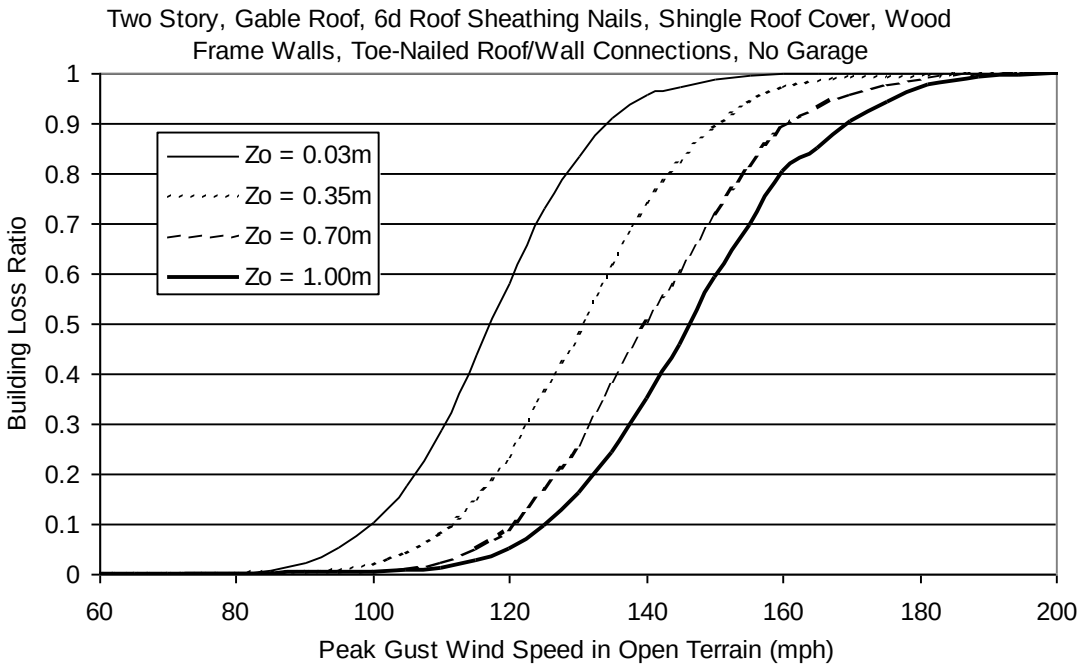

Figure H.73. Building Loss Function for Single Family Residential Building (Two Story, 6d Roof Sheathing Nails, Gable Roof, No Garage, Toe-Nailed Roof Wall Connections, Wood Frame, Upgraded Roof).

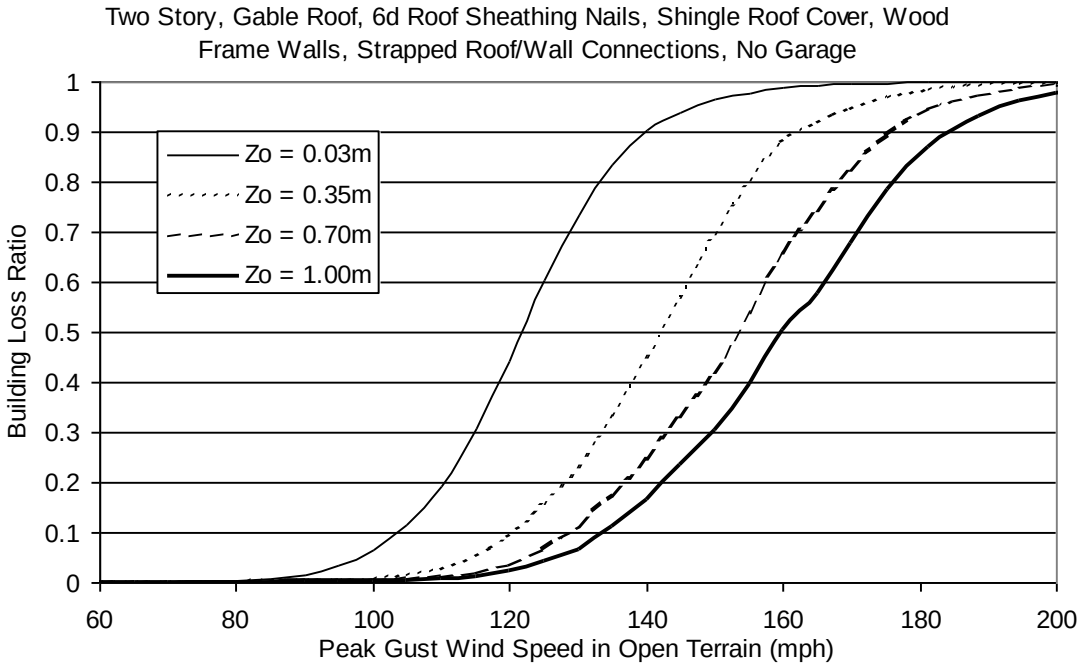

Figure H.74. Building Loss Function for Single Family Residential Building (Two Story, 6d Roof Sheathing Nails, Gable Roof, No Garage, Strapped Roof Wall Connections, Wood Frame, Upgraded Roof).

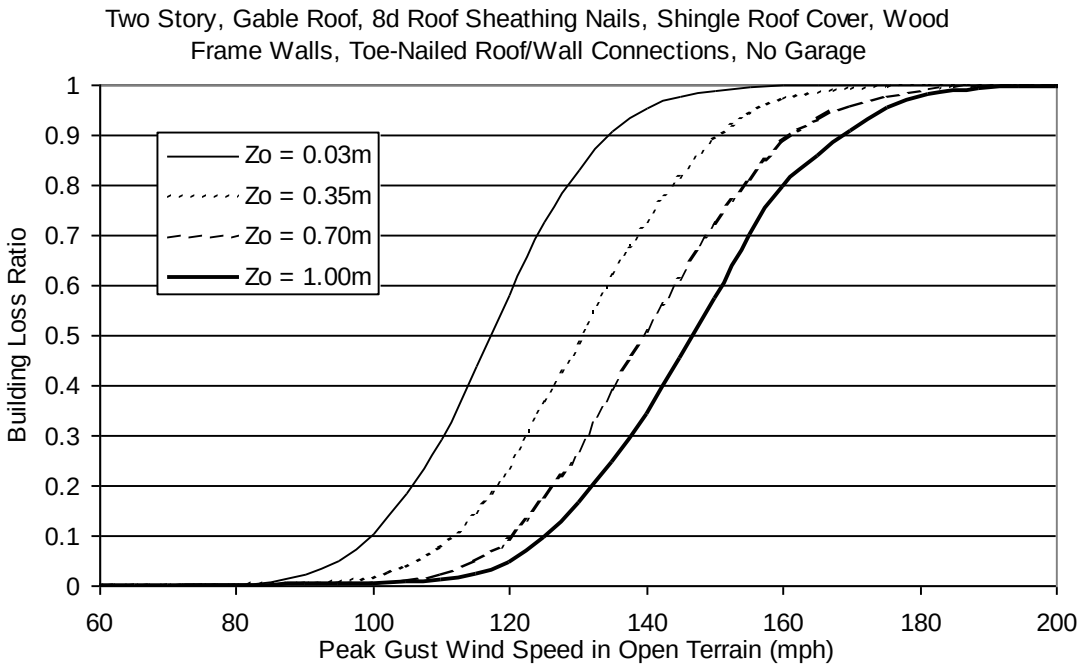

Figure H.75. Building Loss Function for Single Family Residential Building (Two Story, 8d Roof Sheathing Nails, Gable Roof, No Garage, Toe-Nailed Roof Wall Connections, Wood Frame, Upgraded Roof).

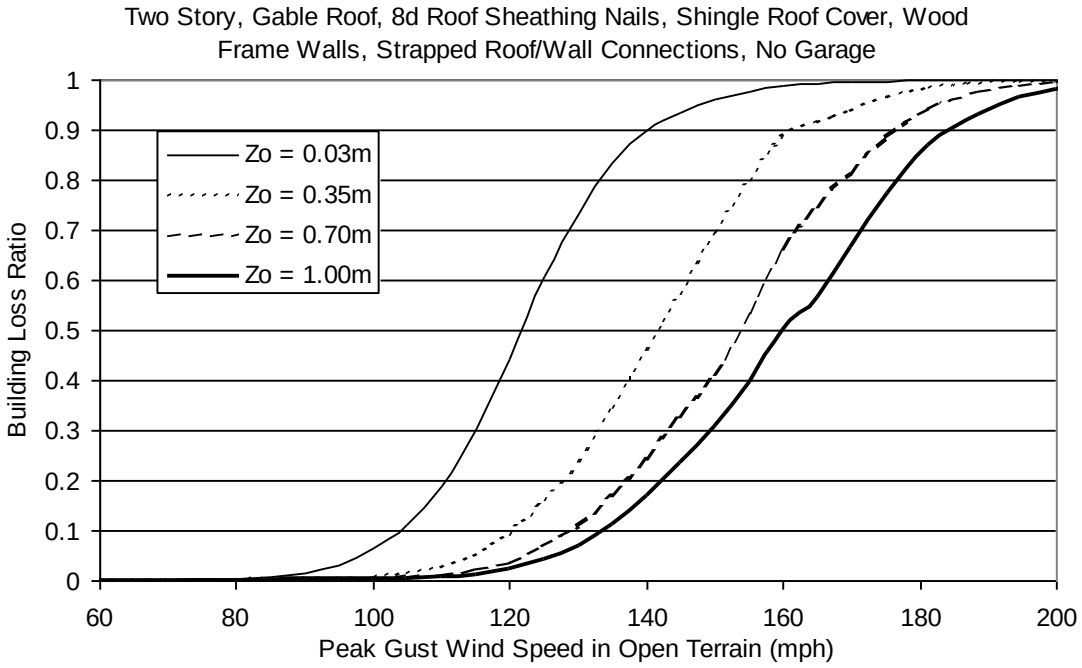

Figure H.76. Building Loss Function for Single Family Residential Building (Two Story, 8d Roof Sheathing Nails, Gable Roof, No Garage, Strapped Roof Wall Connections, Wood Frame, Upgraded Roof).

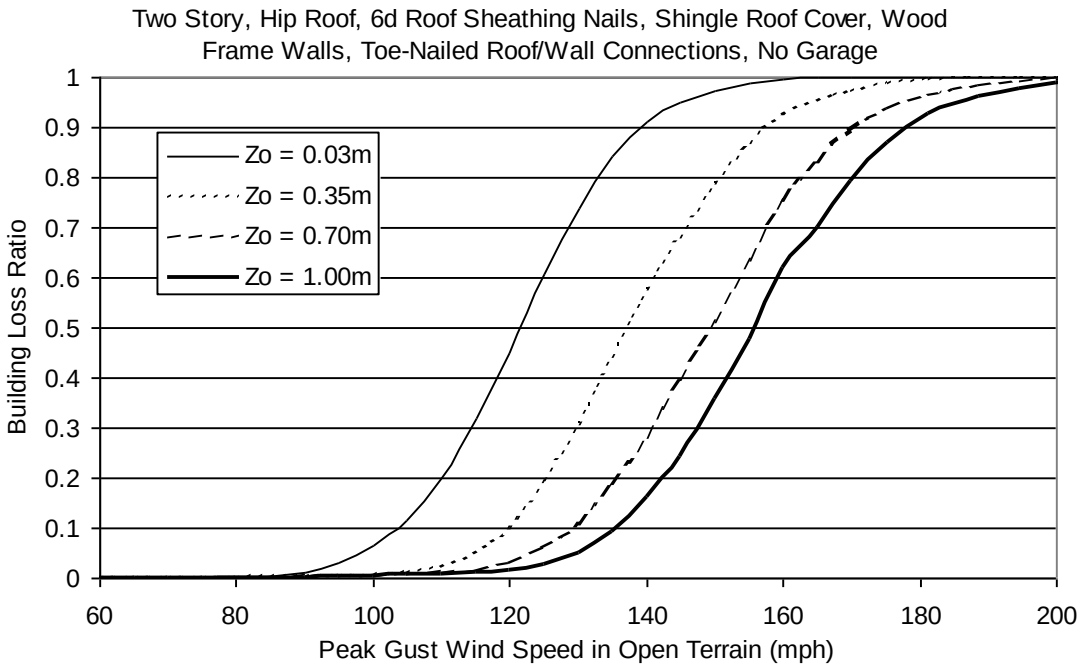

Figure H.77. Building Loss Function for Single Family Residential Building (Two Story, 6d Roof Sheathing Nails, Hip Roof, No Garage, Toe-Nailed Roof Wall Connections, Wood Frame, Upgraded Roof).

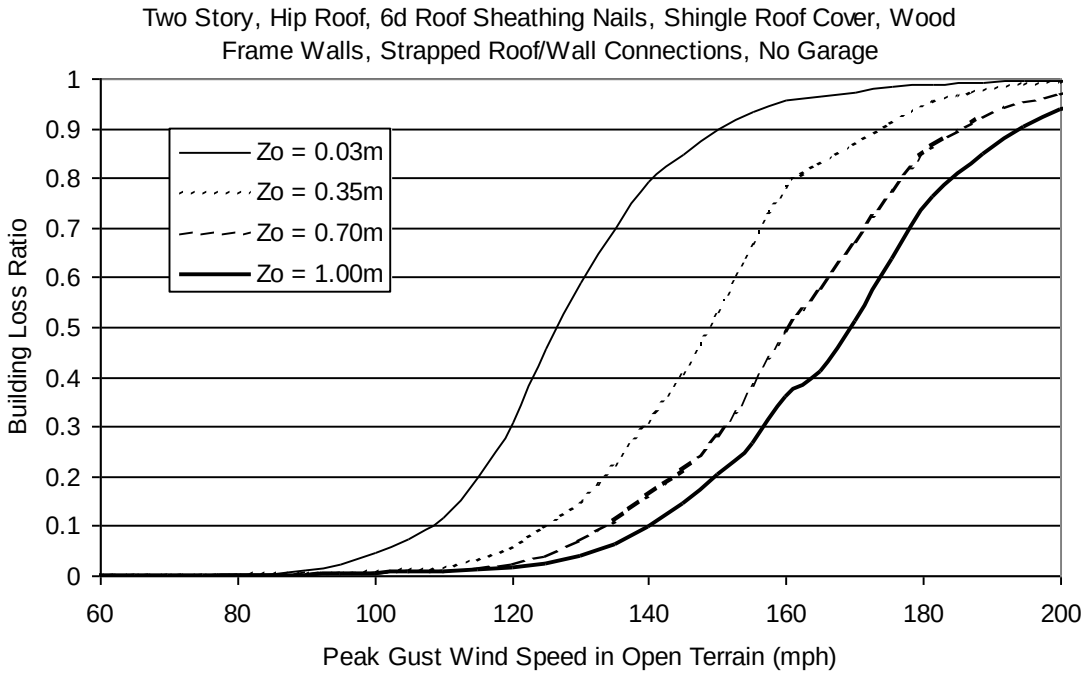

Figure H.78. Building Loss Function for Single Family Residential Building (Two Story, 6d Roof Sheathing Nails, Hip Roof, No Garage, Strapped Roof Wall Connections, Wood Frame, Upgraded Roof).

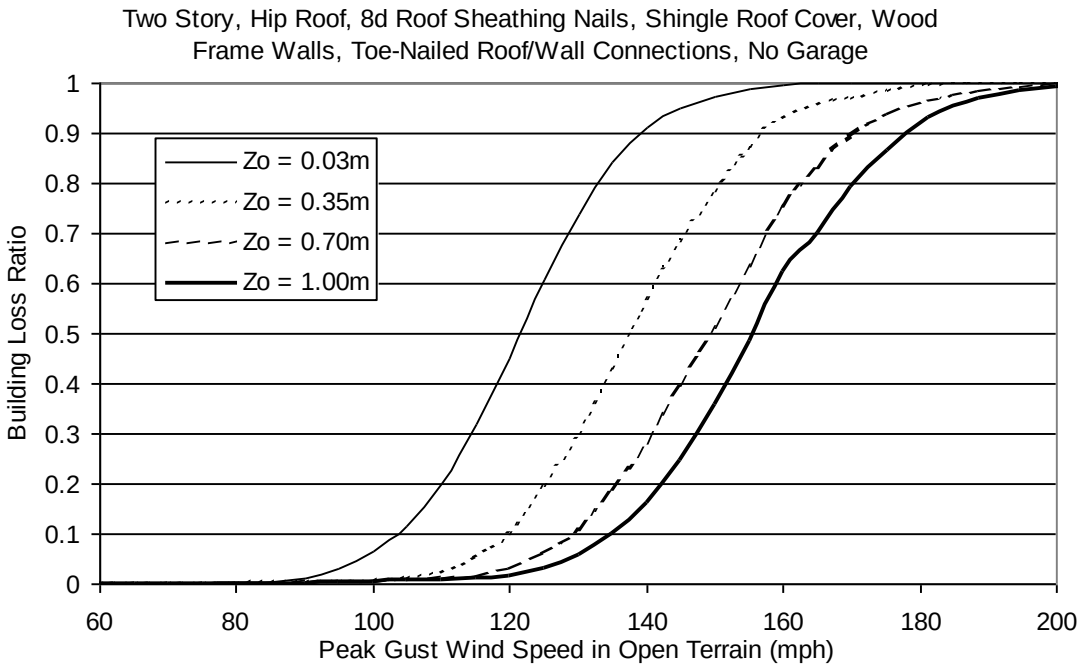

Figure H.79. Building Loss Function for Single Family Residential Building (Two Story, 8d Roof Sheathing Nails, Hip Roof, No Garage, Toe-Nailed Roof Wall Connections, Wood Frame, Upgraded Roof).

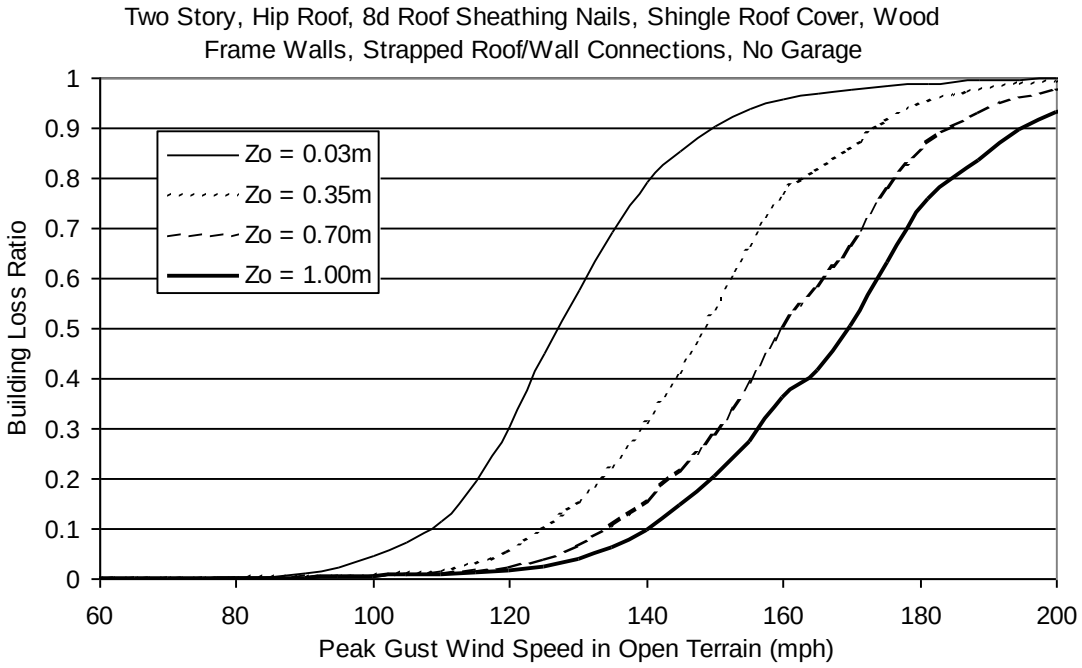

Figure H.80. Building Loss Function for Single Family Residential Building (Two Story, 8d Roof Sheathing Nails, Hip Roof, No Garage, Strapped Roof Wall Connections, Wood Frame, Upgraded Roof).

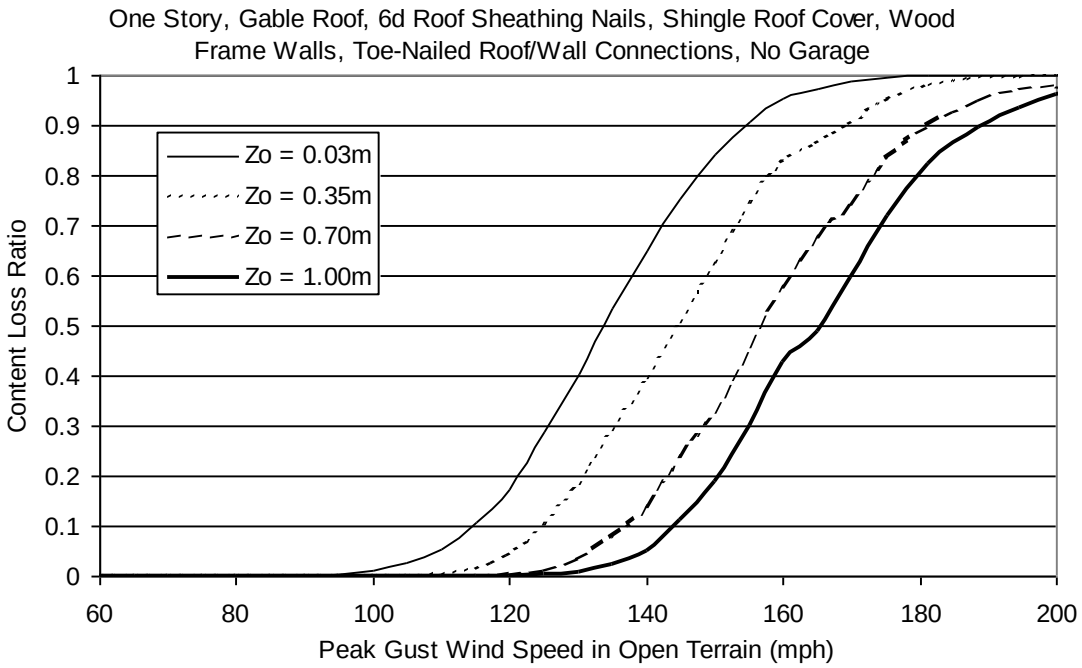

Figure H.81. Content Loss Function for Single Family Residential Building (One Story, 6d Roof Sheathing Nails, Gable Roof, No Garage, Toe-Nailed Roof Wall Connections, Wood Frame, Upgraded Roof).

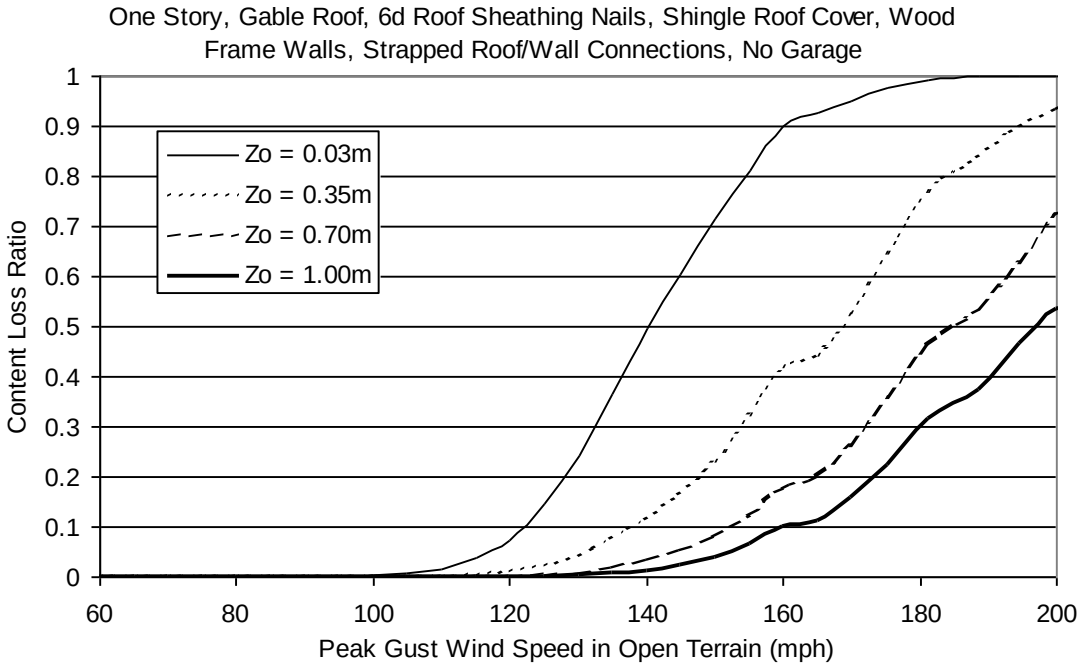

Figure H.82. Content Loss Function for Single Family Residential Building (One Story, 6d Roof Sheathing Nails, Gable Roof, No Garage, Strapped Roof Wall Connections, Wood Frame, Upgraded Roof).

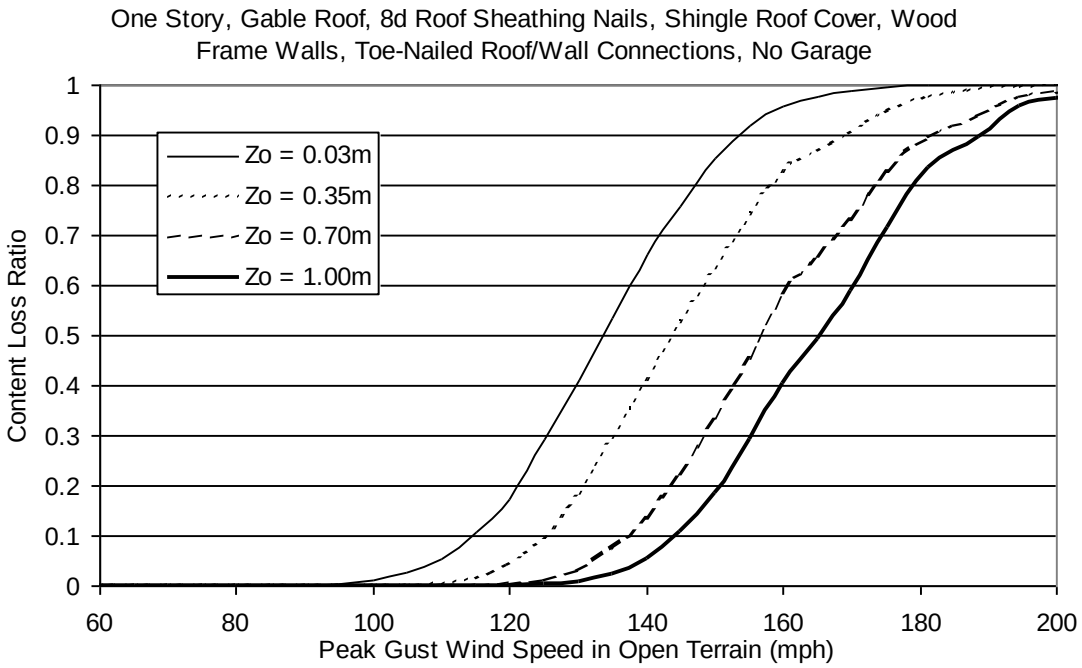

Figure H.83. Content Loss Function for Single Family Residential Building (One Story, 8d Roof Sheathing Nails, Gable Roof, No Garage, Toe-Nailed Roof Wall Connections, Wood Frame, Upgraded Roof).

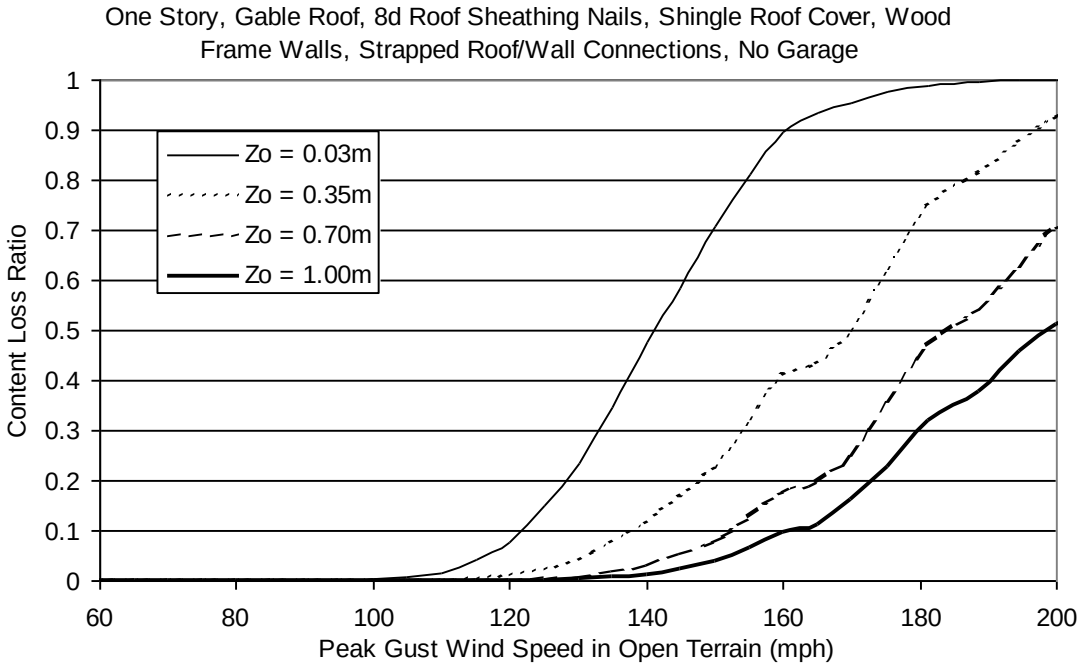

Figure H.84. Content Loss Function for Single Family Residential Building (One Story, 8d Roof Sheathing Nails, Gable Roof, No Garage, Strapped Roof Wall Connections, Wood Frame, Upgraded Roof).

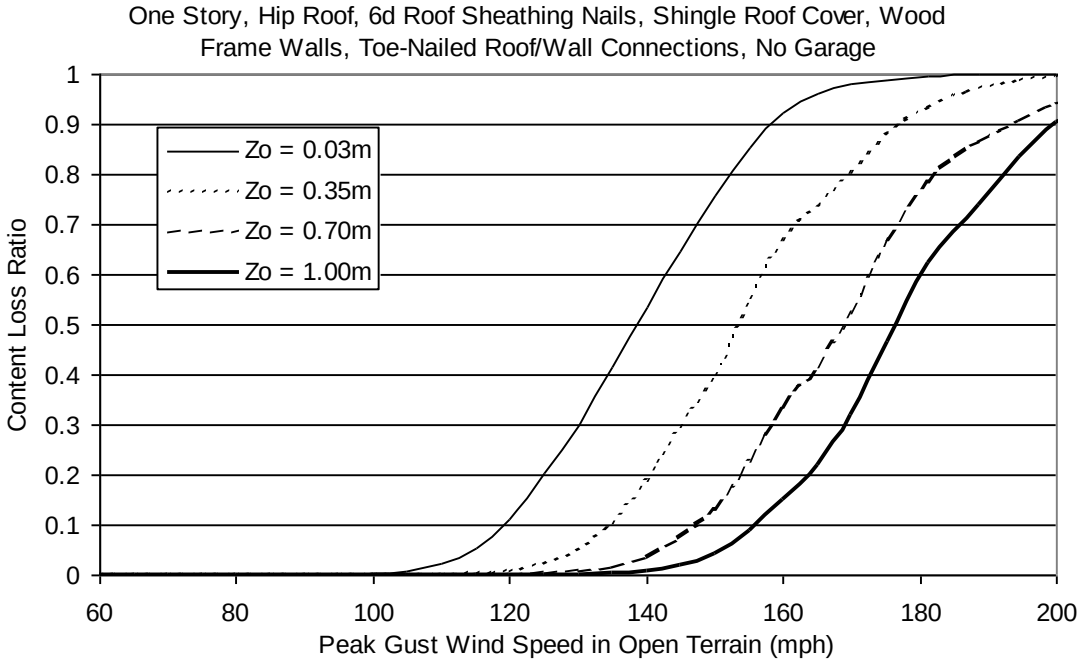

Figure H.85. Content Loss Function for Single Family Residential Building (One Story, 6d Roof Sheathing Nails, Hip Roof, No Garage, Toe-Nailed Roof Wall Connections, Wood Frame, Upgraded Roof).

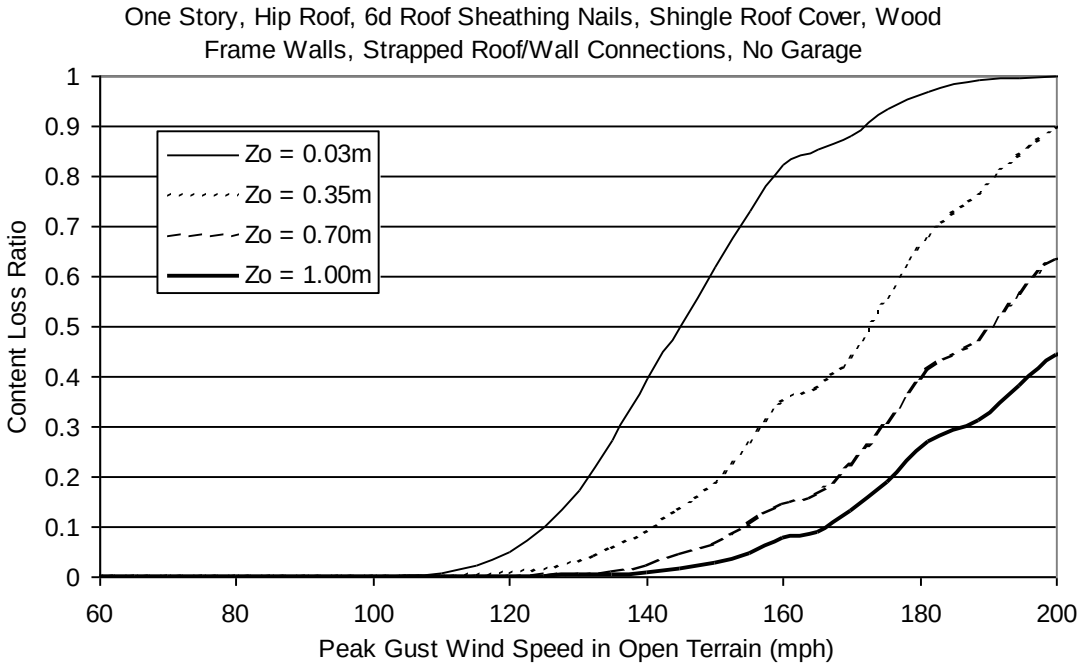

Figure H.86. Content Loss Function for Single Family Residential Building (One Story, 6d Roof Sheathing Nails, Hip Roof, No Garage, Strapped Roof Wall Connections, Wood Frame, Upgraded Roof).

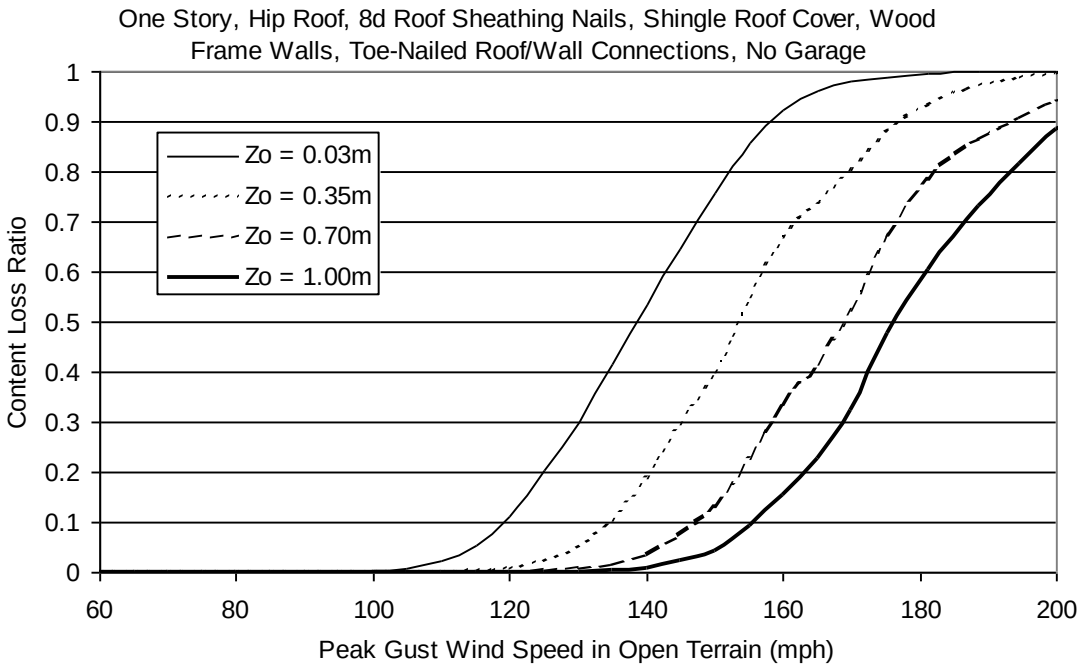

Figure H.87. Content Loss Function for Single Family Residential Building (One Story, 8d Roof Sheathing Nails, Hip Roof, No Garage, Toe-Nailed Roof Wall Connections, Wood Frame, Upgraded Roof).

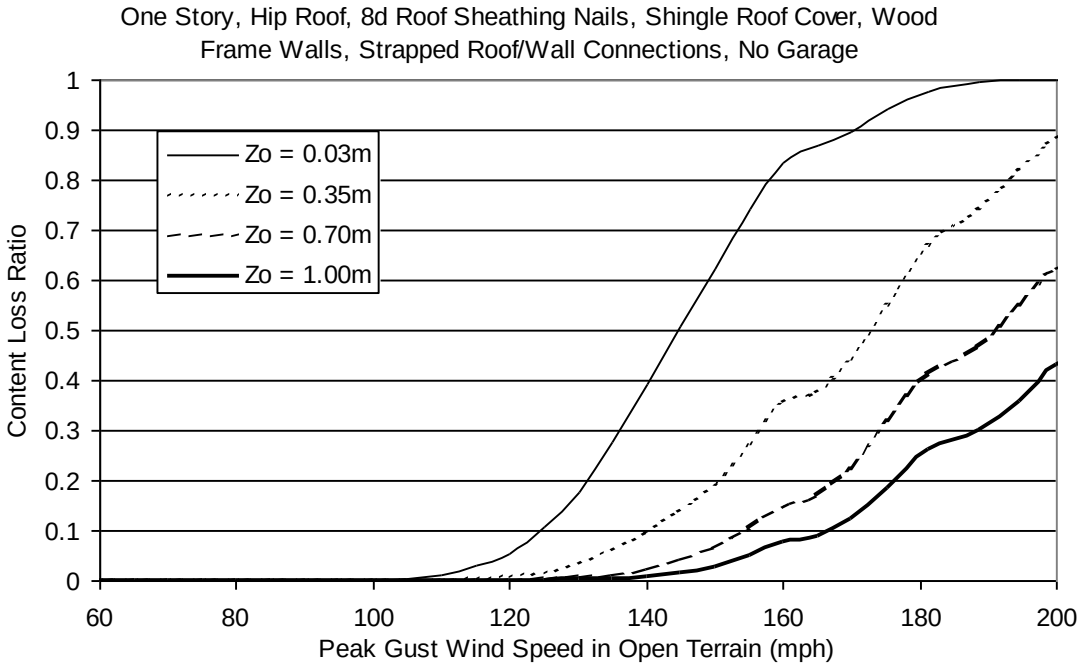

Figure H.88. Content Loss Function for Single Family Residential Building (One Story, 8d Roof Sheathing Nails, Hip Roof, No Garage, Strapped Roof Wall Connections, Wood Frame, Upgraded Roof).

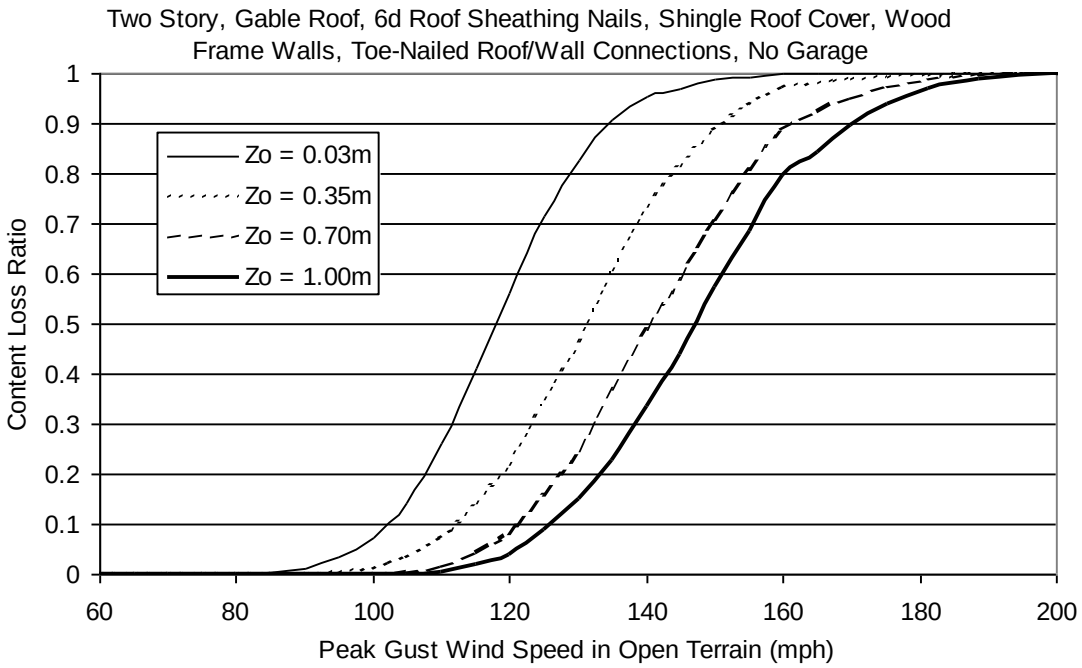

Figure H.89. Content Loss Function for Single Family Residential Building (Two Story, 6d Roof Sheathing Nails, Gable Roof, No Garage, Toe-Nailed Roof Wall Connections, Wood Frame, Upgraded Roof).

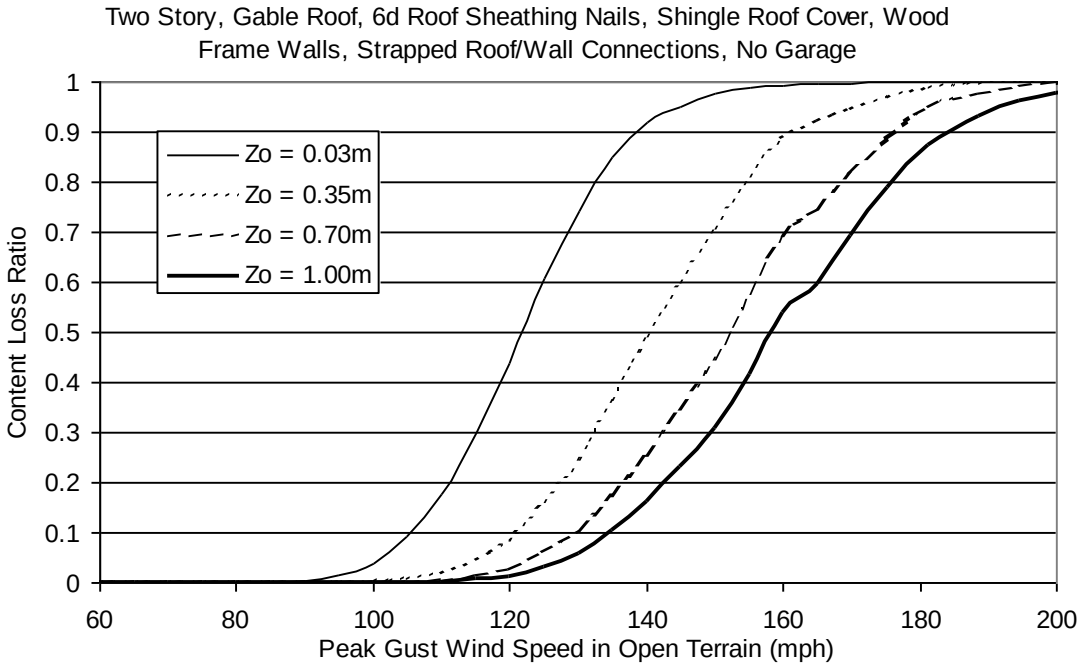

Figure H.90. Content Loss Function for Single Family Residential Building (Two Story, 6d Roof Sheathing Nails, Gable Roof, No Garage, Strapped Roof Wall Connections, Wood Frame, Upgraded Roof).

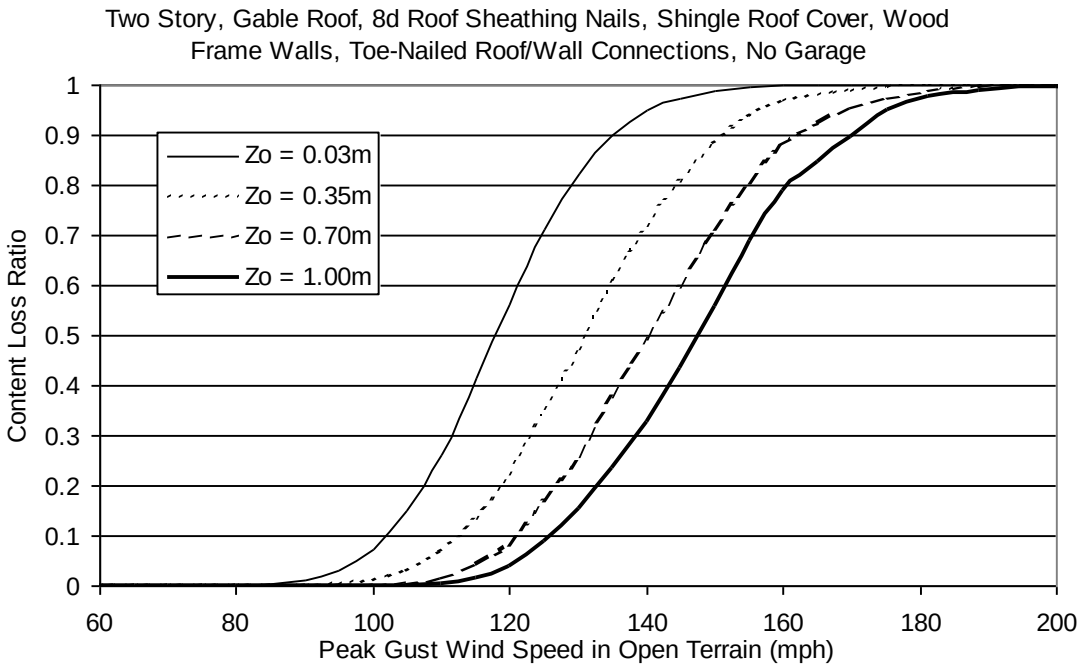

Figure H.91. Content Loss Function for Single Family Residential Building (Two Story, 8d Roof Sheathing Nails, Gable Roof, No Garage, Toe-Nailed Roof Wall Connections, Wood Frame, Upgraded Roof).

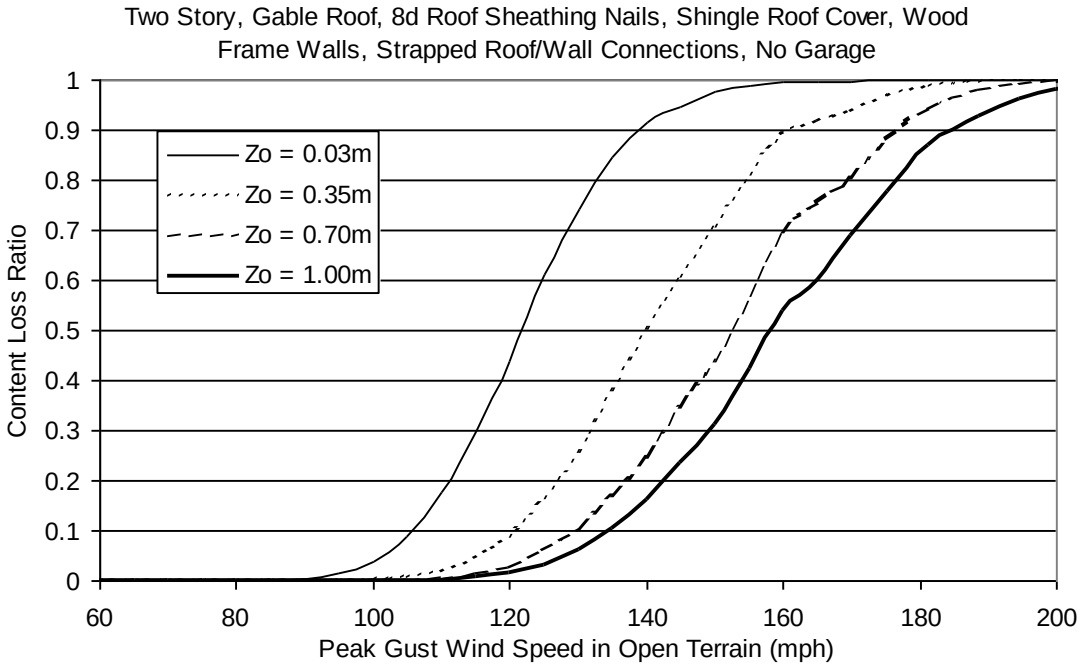

Figure H.92. Content Loss Function for Single Family Residential Building (Two Story, 8d Roof Sheathing Nails, Gable Roof, No Garage, Strapped Roof Wall Connections, Wood Frame, Upgraded Roof).

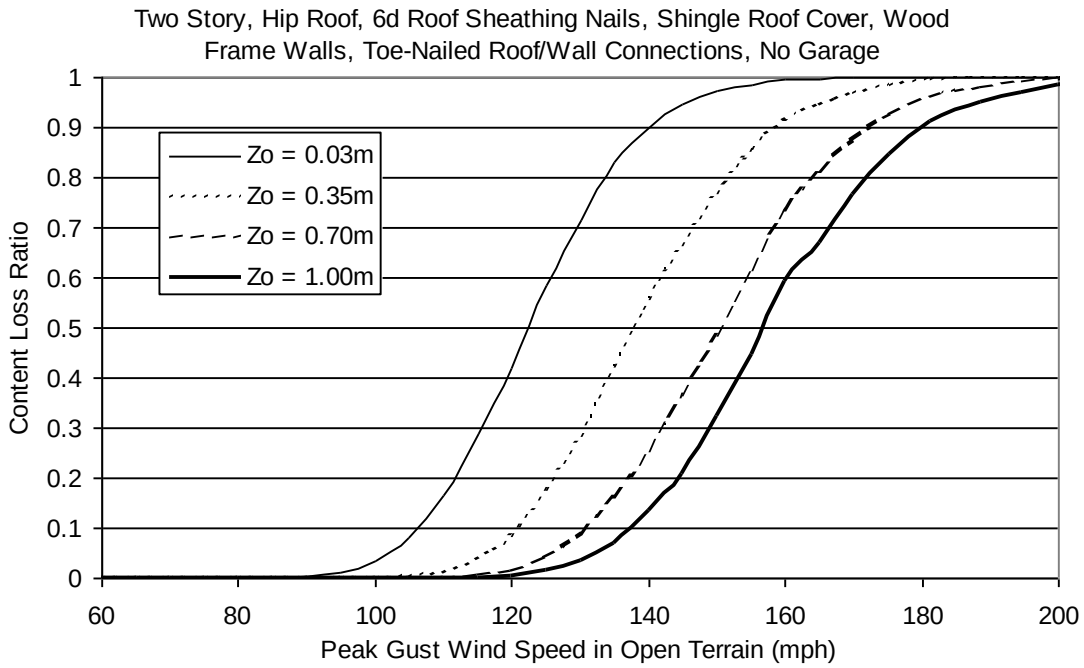

Figure H.93. Content Loss Function for Single Family Residential Building (Two Story, 6d Roof Sheathing Nails, Hip Roof, No Garage, Toe-Nailed Roof Wall Connections, Wood Frame, Upgraded Roof).

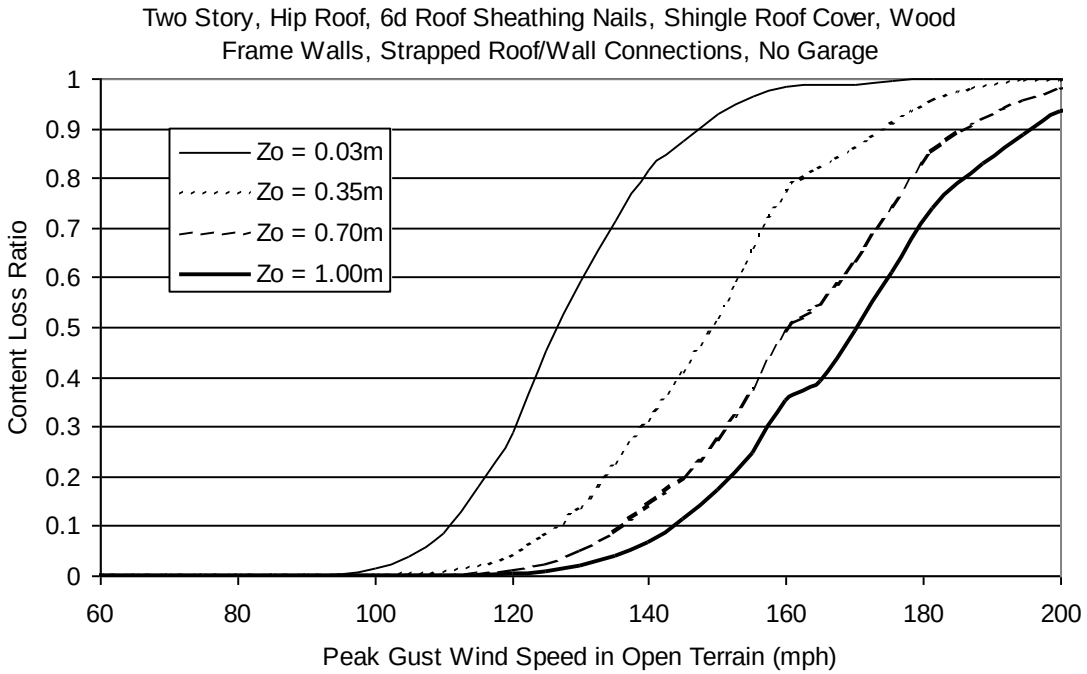

Figure H.94. Content Loss Function for Single Family Residential Building (Two Story, 6d Roof Sheathing Nails, Hip Roof, No Garage, Strapped Roof Wall Connections, Wood Frame, Upgraded Roof).

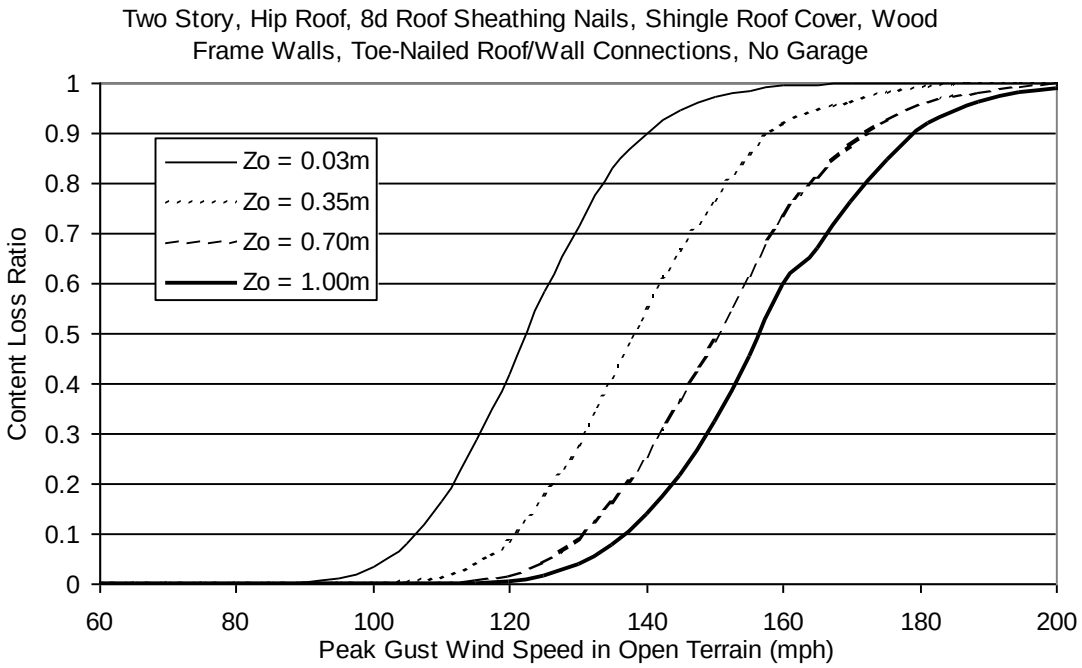

Figure H.95. Content Loss Function for Single Family Residential Building (Two Story, 8d Roof Sheathing Nails, Hip Roof, No Garage, Toe-Nailed Roof Wall Connections, Wood Frame, Upgraded Roof).

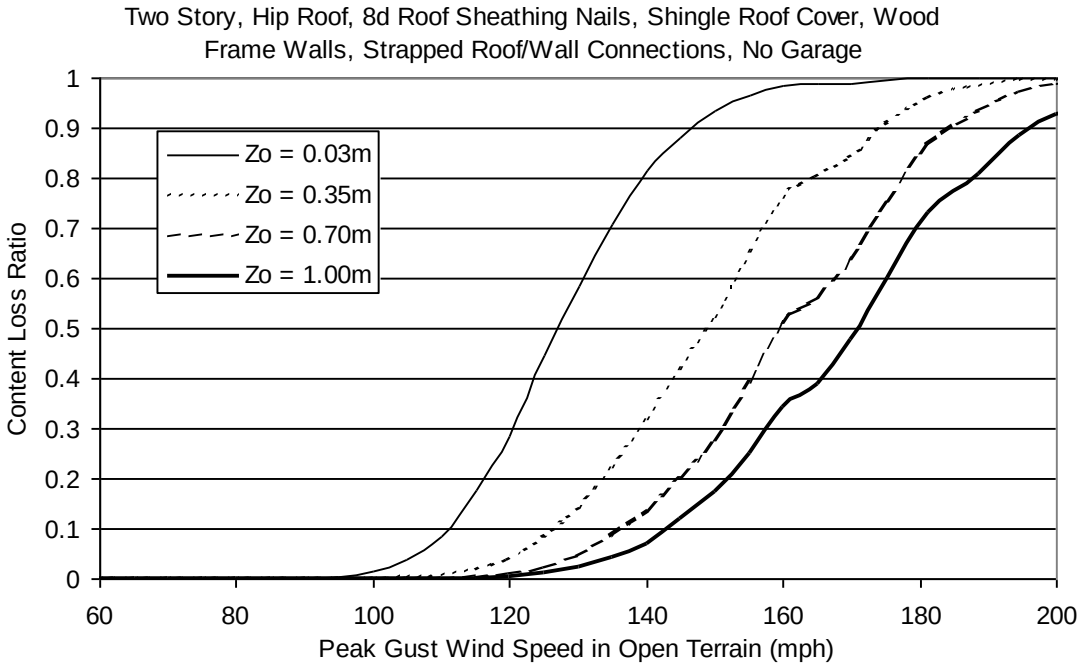

Figure H.96. Content Loss Function for Single Family Residential Building (Two Story, 8d Roof Sheathing Nails, Hip Roof, No Garage, Strapped Roof Wall Connections, Wood Frame, Upgraded Roof).

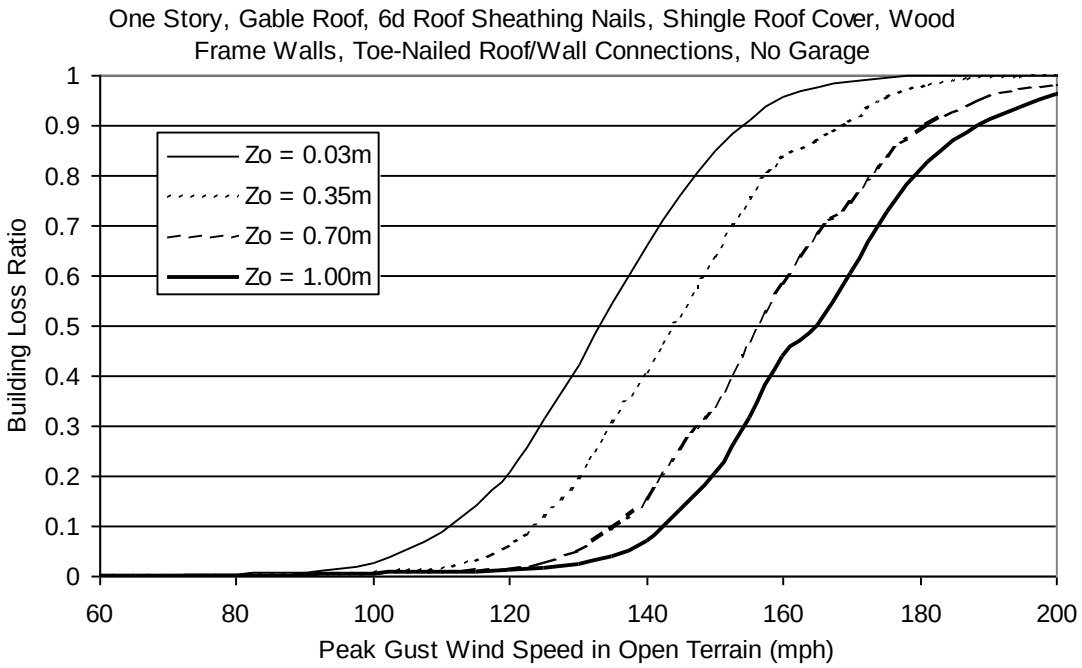

Figure H.97. Building Loss Function for Single Family Residential Building (One Story, 6d Roof Sheathing Nails, Gable Roof, No Garage, Toe-Nailed Roof Wall Connections, Wood Frame, Upgraded Roof and Added Secondary Water Resistance).

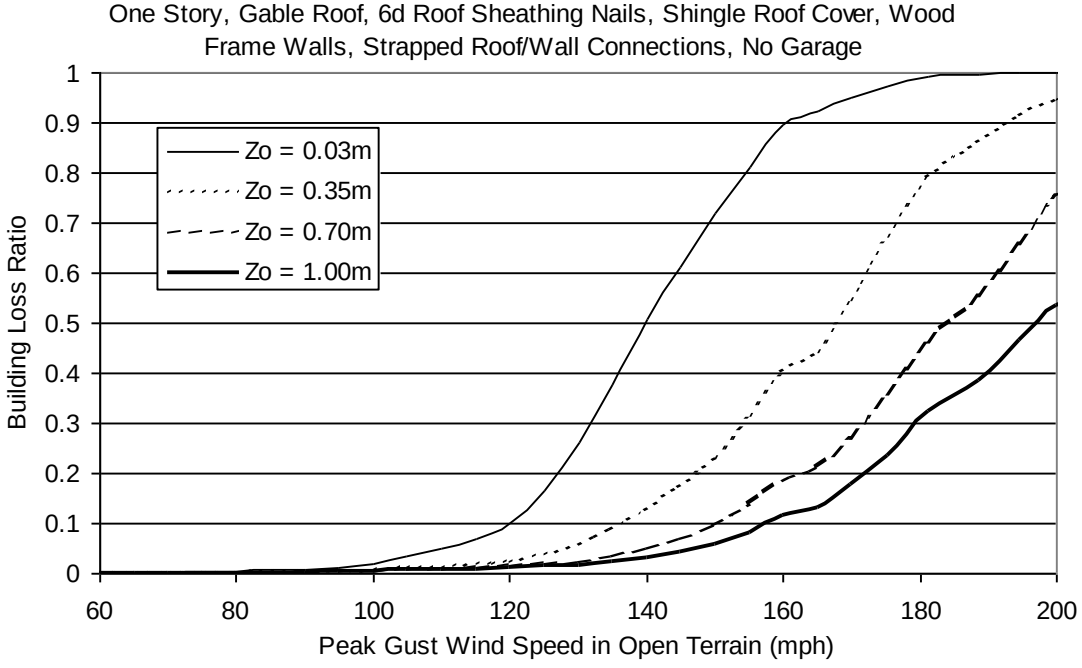

Figure H.98. Building Loss Function for Single Family Residential Building (One Story, 6d Roof Sheathing Nails, Gable Roof, No Garage, Strapped Roof Wall Connections, Wood Frame, Upgraded Roof and Added Secondary Water Resistance).

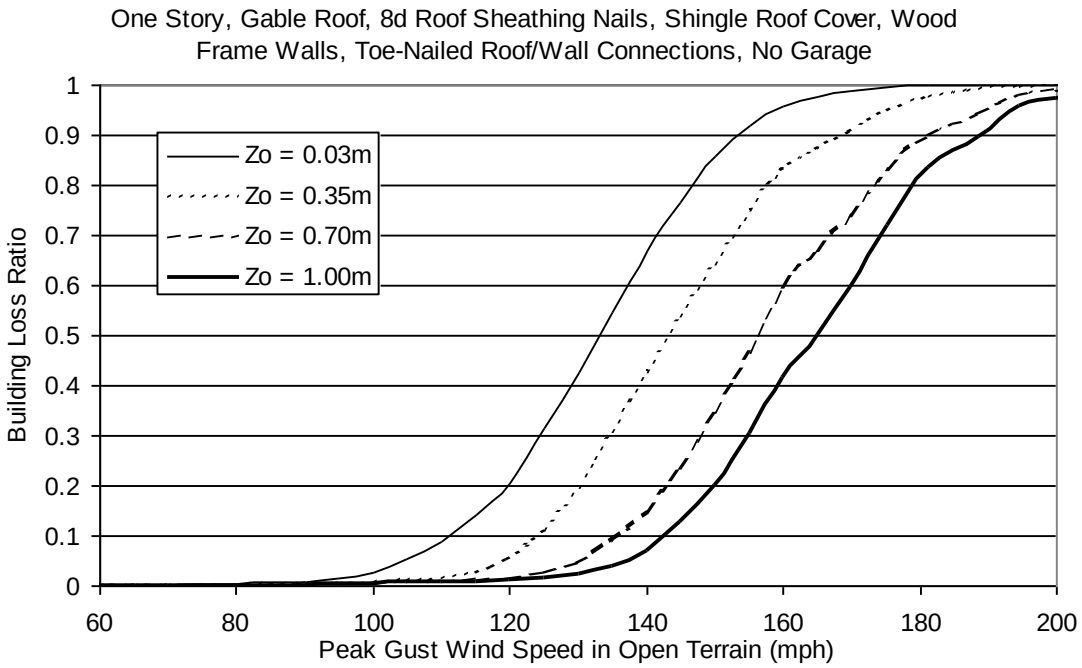

Figure H.99. Building Loss Function for Single Family Residential Building (One Story, 8d Roof Sheathing Nails, Gable Roof, No Garage, Toe-Nailed Roof Wall Connections, Wood Frame, Upgraded Roof and Added Secondary Water Resistance).

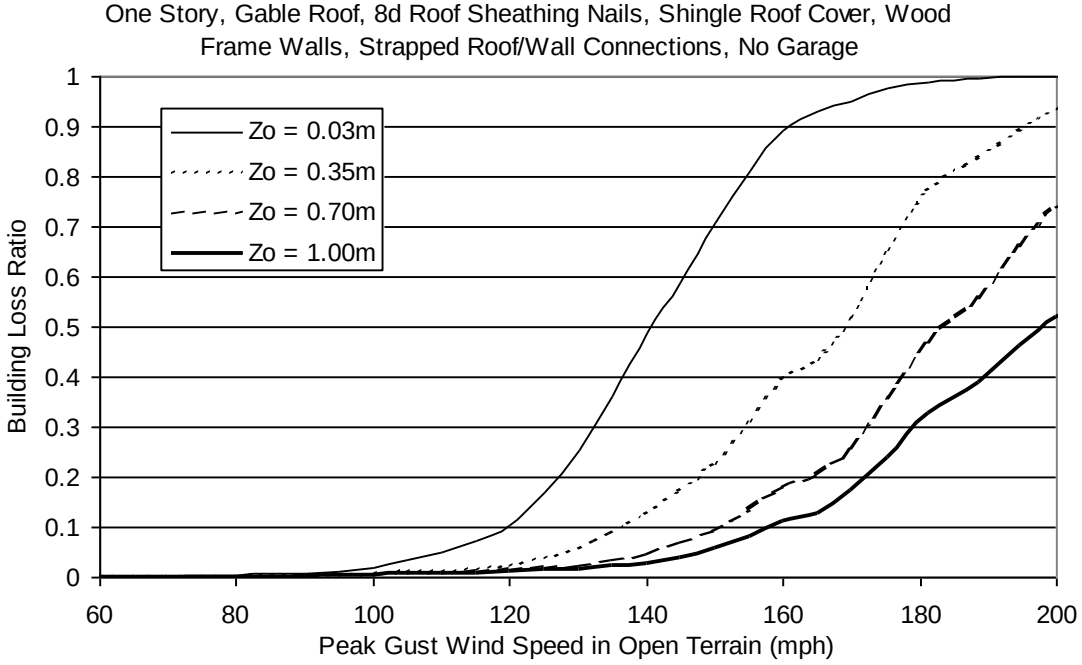

Figure H.100. Building Loss Function for Single Family Residential Building (One Story, 8d Roof Sheathing Nails, Gable Roof, No Garage, Strapped Roof Wall Connections, Wood Frame, Upgraded Roof and Added Secondary Water Resistance).

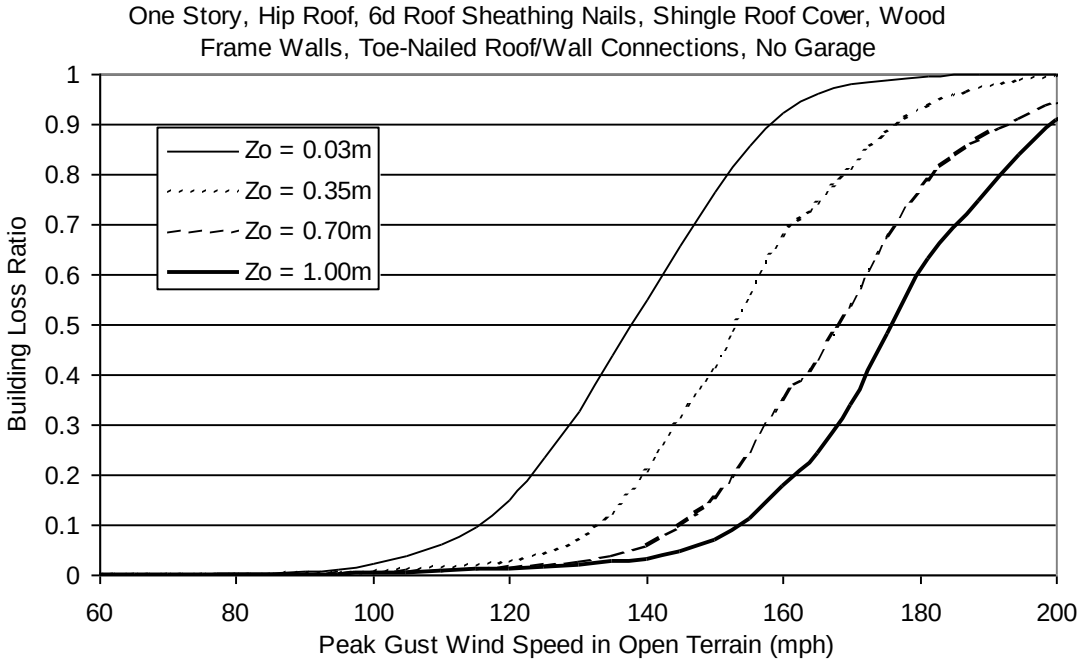

Figure H.101. Building Loss Function for Single Family Residential Building (One Story, 6d Roof Sheathing Nails, Hip Roof, No Garage, Toe-Nailed Roof Wall Connections, Wood Frame, Upgraded Roof and Added Secondary Water Resistance).

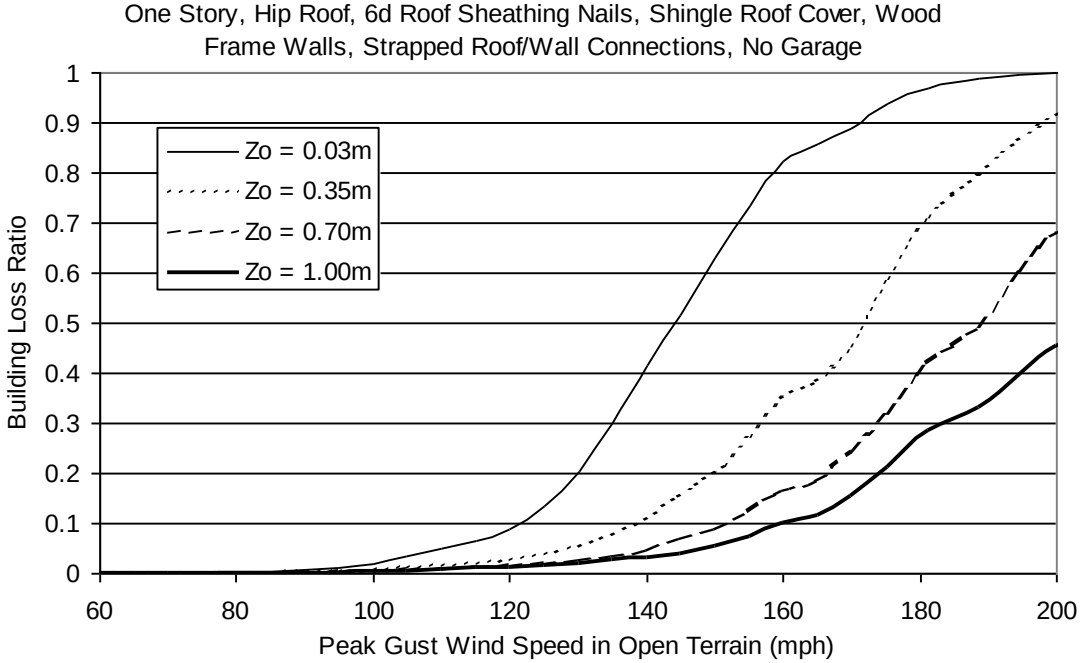

Figure H.102. Building Loss Function for Single Family Residential Building (One Story, 6d Roof Sheathing Nails, Hip Roof, No Garage, Strapped Roof Wall Connections, Wood Frame, Upgraded Roof and Added Secondary Water Resistance).

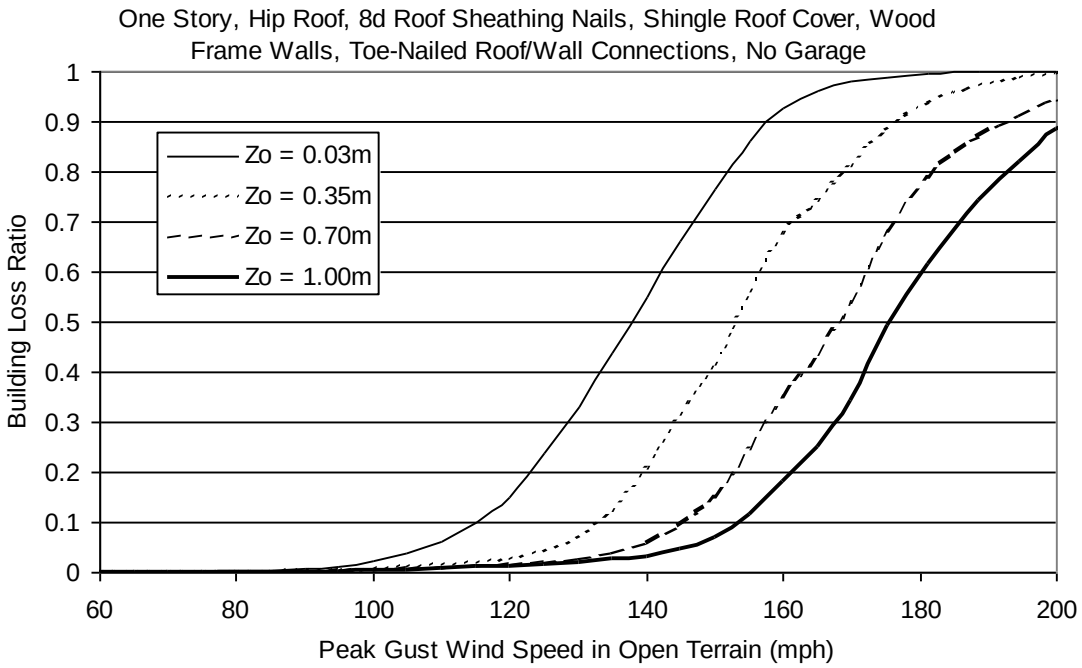

Figure H.103. Building Loss Function for Single Family Residential Building (One Story, 8d Roof Sheathing Nails, Hip Roof, No Garage, Toe-Nailed Roof Wall Connections, Wood Frame, Upgraded Roof and Added Secondary Water Resistance).

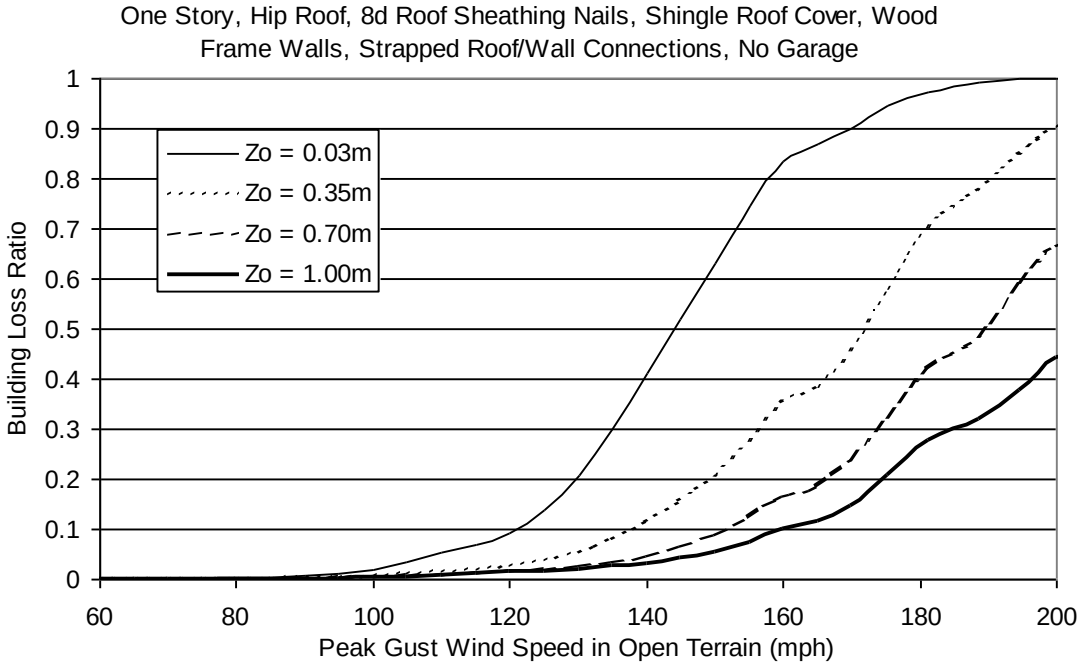

Figure H.104. Building Loss Function for Single Family Residential Building (One Story, 8d Roof Sheathing Nails, Hip Roof, No Garage, Strapped Roof Wall Connections, Wood Frame, Upgraded Roof and Added Secondary Water Resistance).

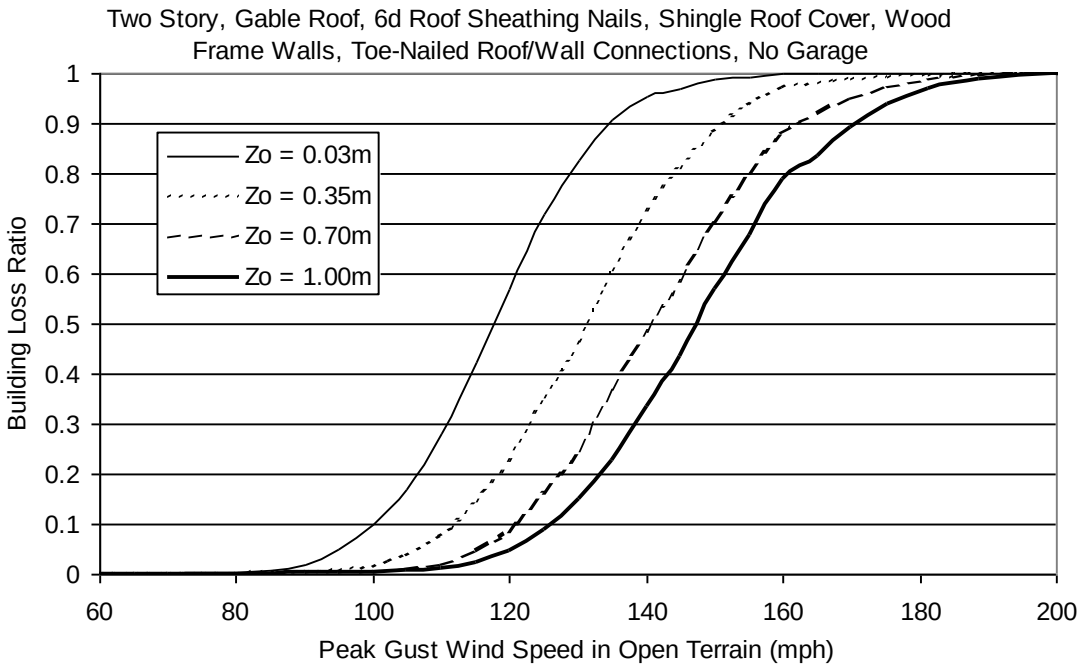

Figure H.105. Building Loss Function for Single Family Residential Building (Two Story, 6d Roof Sheathing Nails, Gable Roof, No Garage, Toe-Nailed Roof Wall Connections, Wood Frame, Upgraded Roof and Added Secondary Water Resistance).

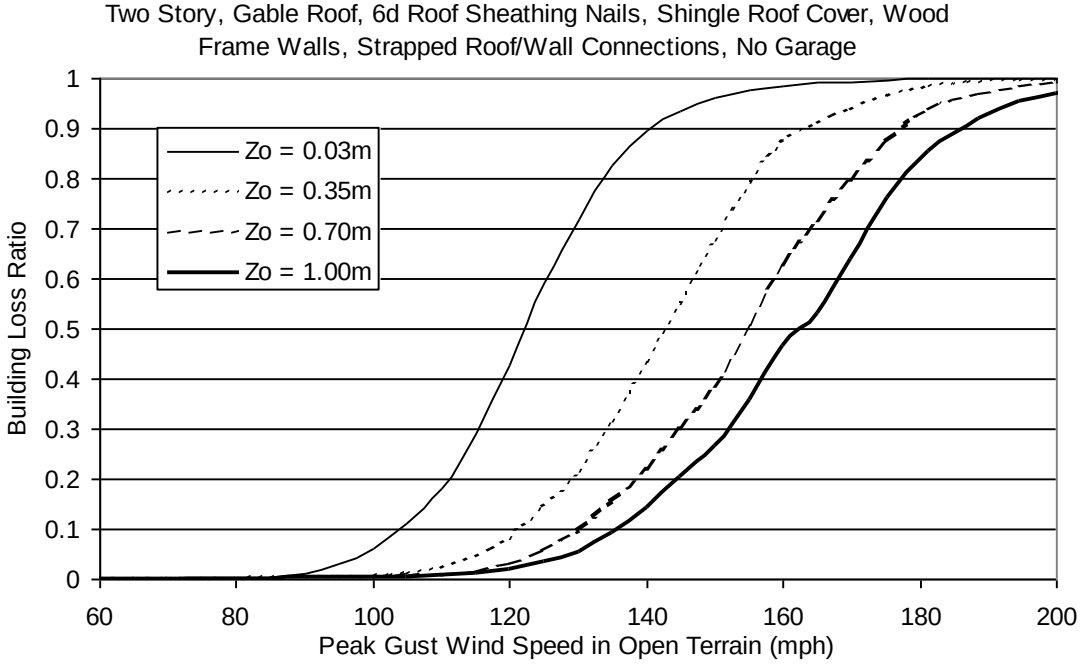

Figure H.106. Building Loss Function for Single Family Residential Building (Two Story, 6d Roof Sheathing Nails, Gable Roof, No Garage, Strapped Roof Wall Connections, Wood Frame, Upgraded Roof and Added Secondary Water Resistance).

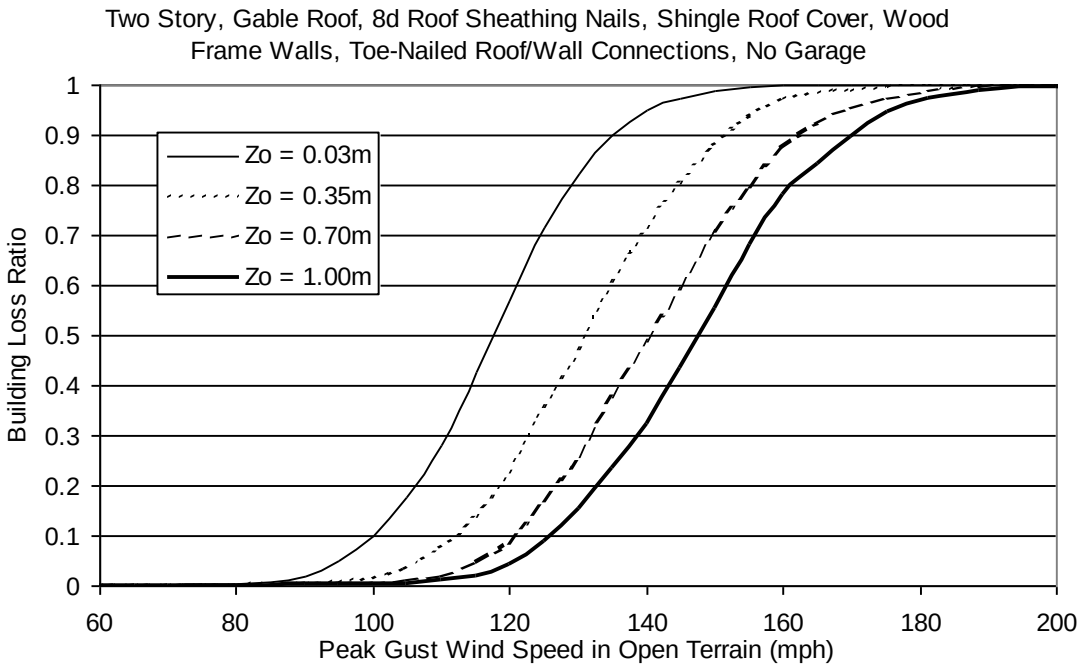

Figure H.107. Building Loss Function for Single Family Residential Building (Two Story, 8d Roof Sheathing Nails, Gable Roof, No Garage, Toe-Nailed Roof Wall Connections, Wood Frame, Upgraded Roof and Added Secondary Water Resistance).

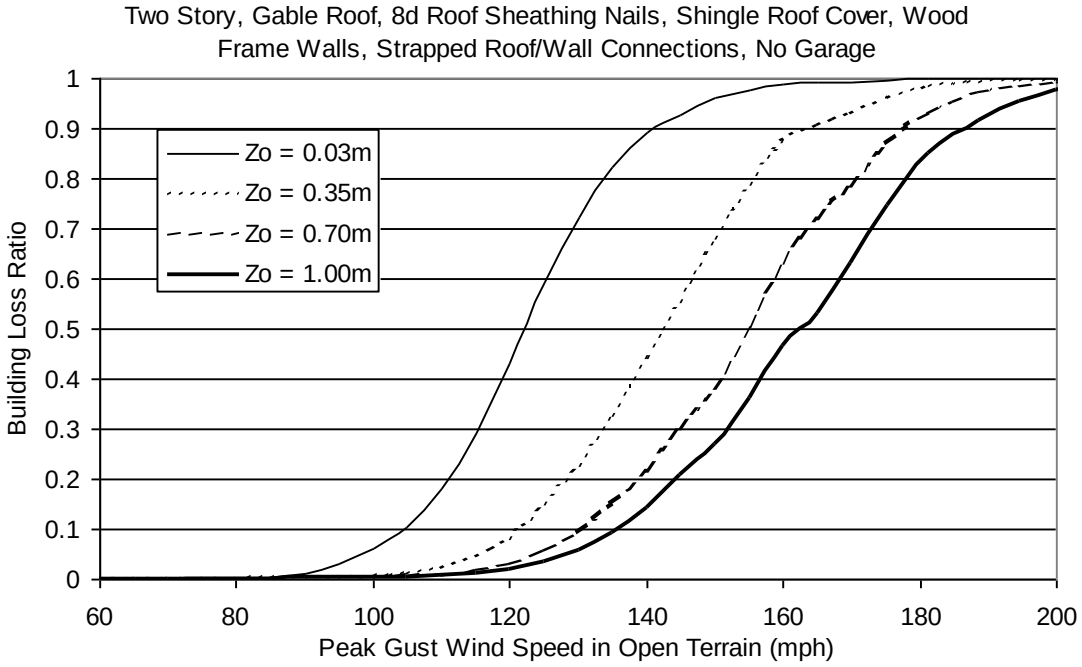

Figure H.108. Building Loss Function for Single Family Residential Building (Two Story, 8d Roof Sheathing Nails, Gable Roof, No Garage, Strapped Roof Wall Connections, Wood Frame, Upgraded Roof and Added Secondary Water Resistance).

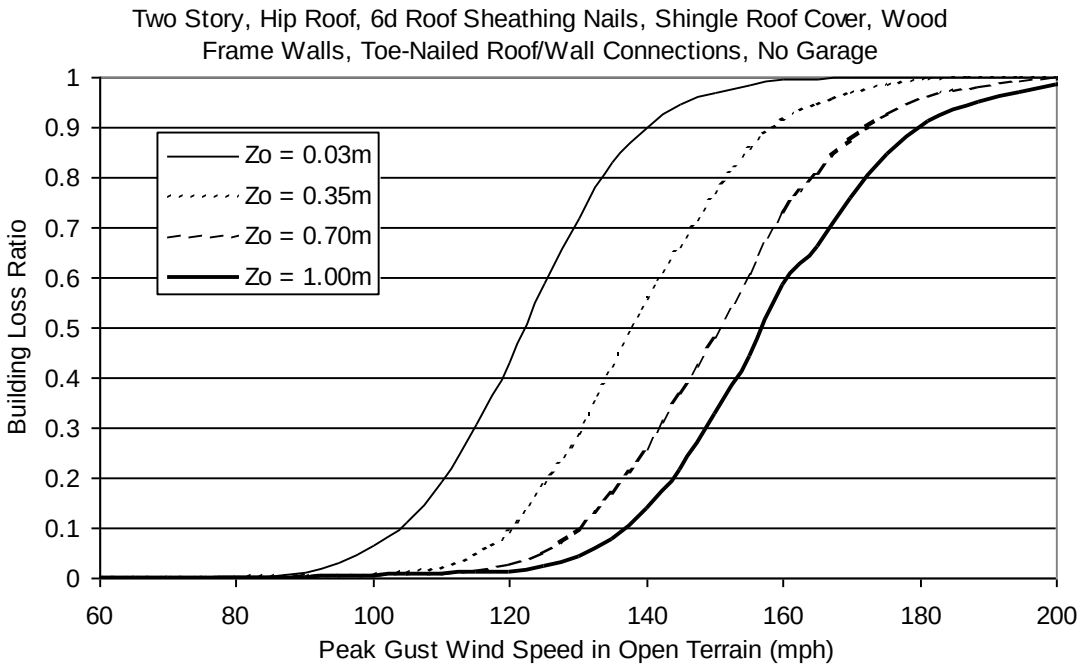

Figure H.109. Building Loss Function for Single Family Residential Building (Two Story, 6d Roof Sheathing Nails, Hip Roof, No Garage, Toe-Nailed Roof Wall Connections, Wood Frame, Upgraded Roof and Added Secondary Water Resistance).

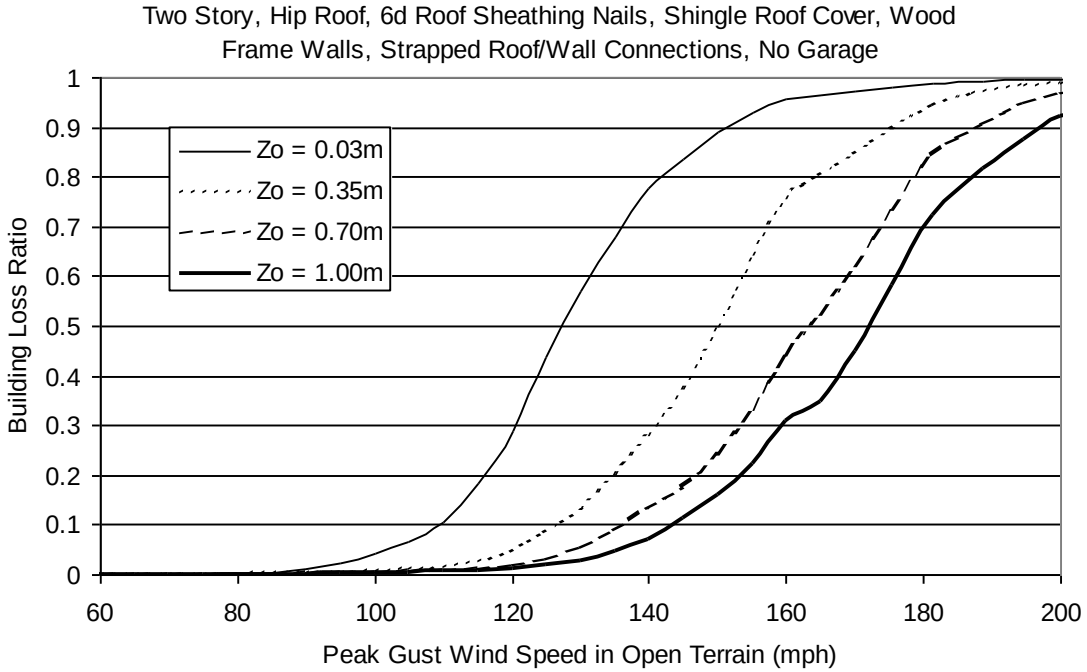

Figure H.110. Building Loss Function for Single Family Residential Building (Two Story, 6d Roof Sheathing Nails, Hip Roof, No Garage, Strapped Roof Wall Connections, Wood Frame, Upgraded Roof and Added Secondary Water Resistance).

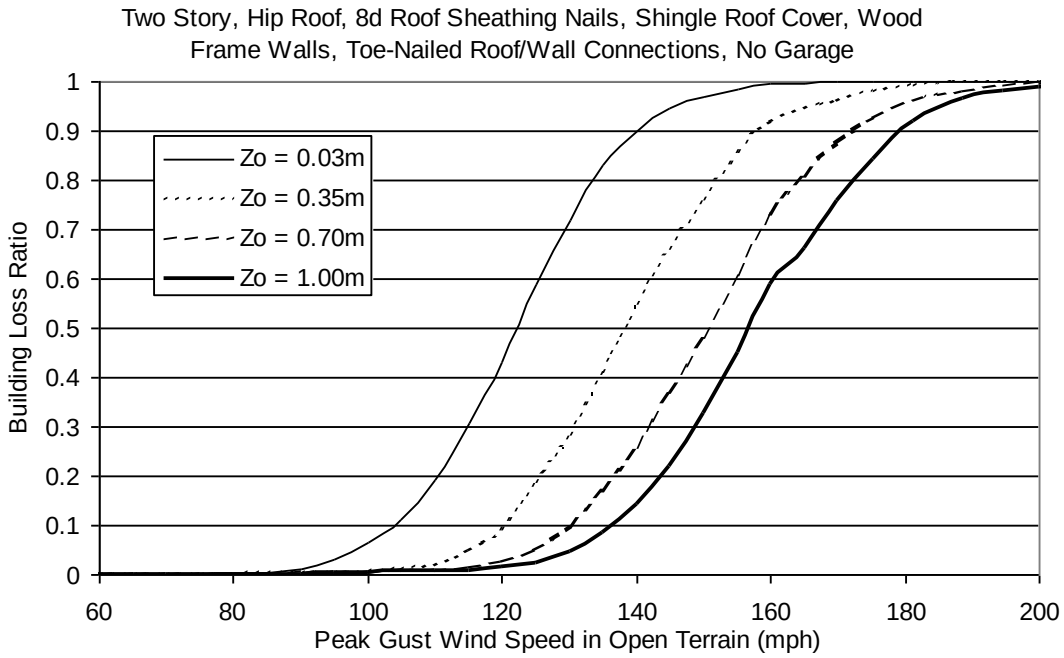

Figure H.111. Building Loss Function for Single Family Residential Building (Two Story, 8d Roof Sheathing Nails, Hip Roof, No Garage, Toe-Nailed Roof Wall Connections, Wood Frame, Upgraded Roof and Added Secondary Water Resistance).

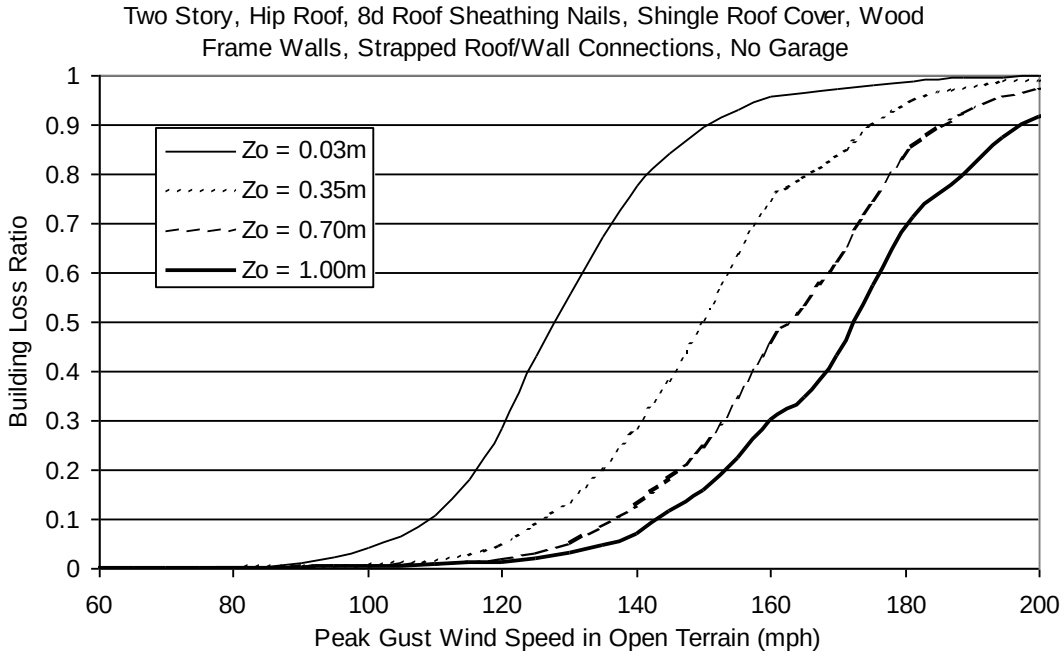

Figure H.112. Building Loss Function for Single Family Residential Building (Two Story, 8d Roof Sheathing Nails, Hip Roof, No Garage, Strapped Roof Wall Connections, Wood Frame, Upgraded Roof and Added Secondary Water Resistance).

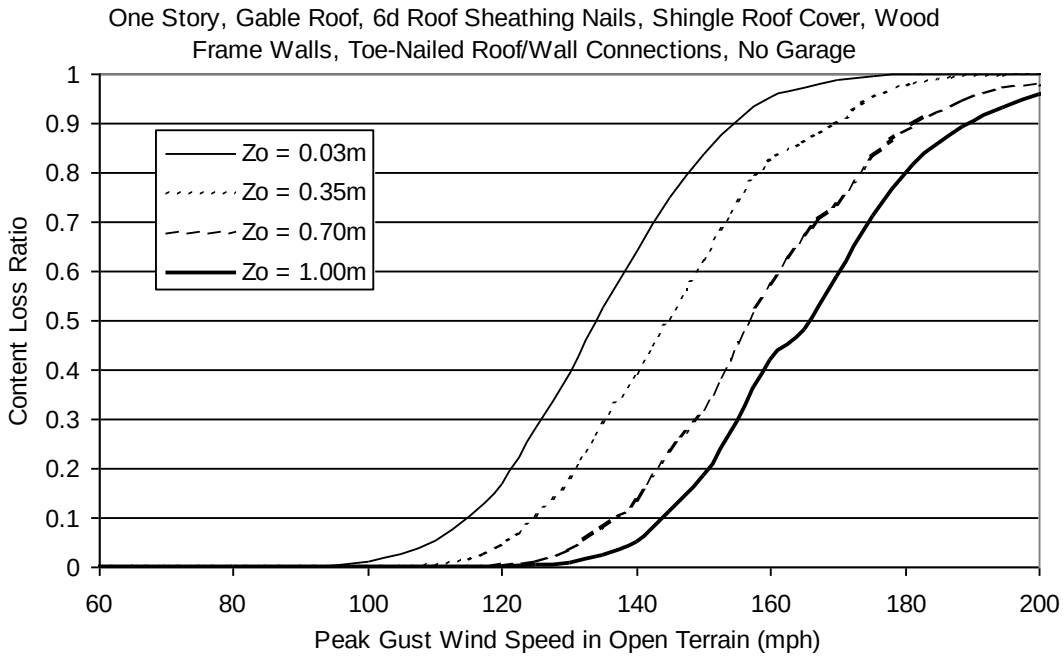

Figure H.113. Content Loss Function for Single Family Residential Building (One Story, 6d Roof Sheathing Nails, Gable Roof, No Garage, Toe-Nailed Roof Wall Connections, Wood Frame, Upgraded Roof and Added Secondary Water Resistance).

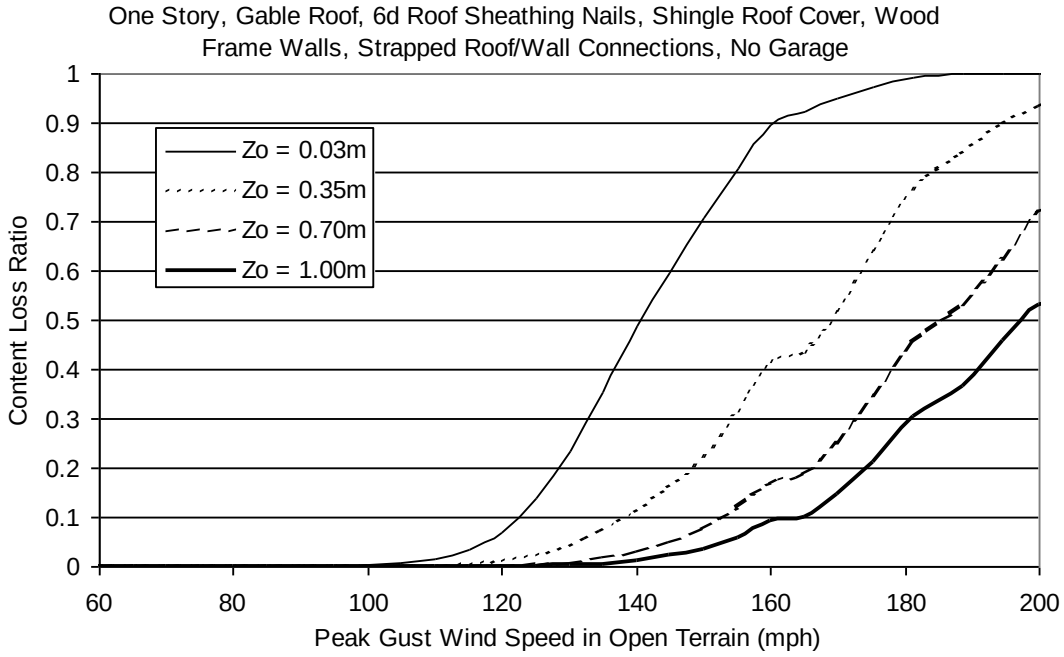

Figure H.114. Content Loss Function for Single Family Residential Building (One Story, 6d Roof Sheathing Nails, Gable Roof, No Garage, Strapped Roof Wall Connections, Wood Frame, Upgraded Roof and Added Secondary Water Resistance).

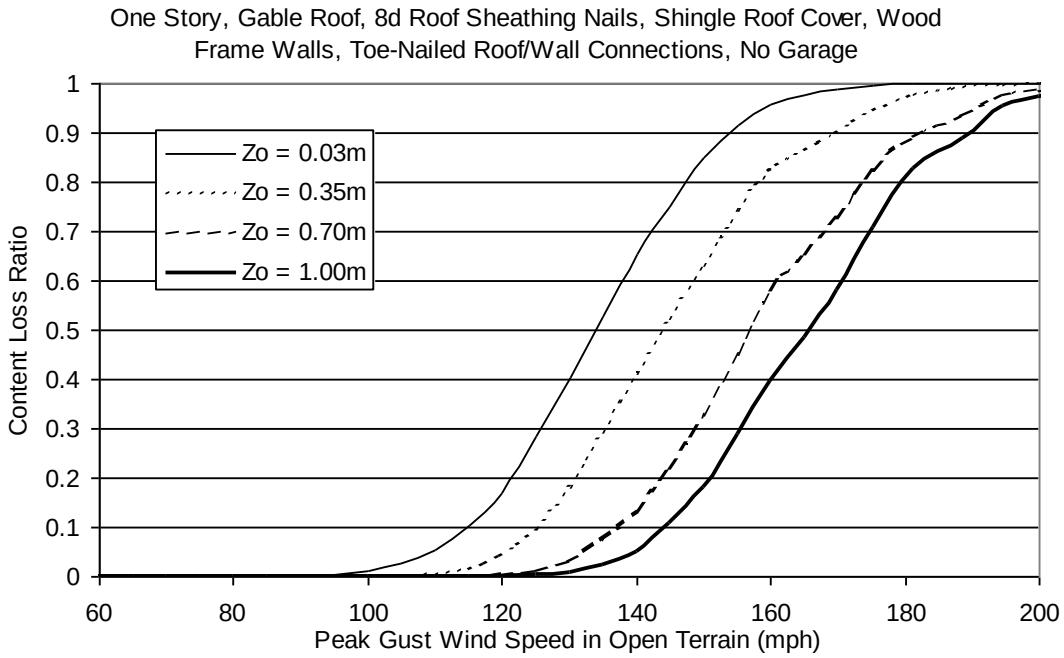

Figure H.115. Content Loss Function for Single Family Residential Building (One Story, 8d Roof Sheathing Nails, Gable Roof, No Garage, Toe-Nailed Roof Wall Connections, Wood Frame, Upgraded Roof and Added Secondary Water Resistance).

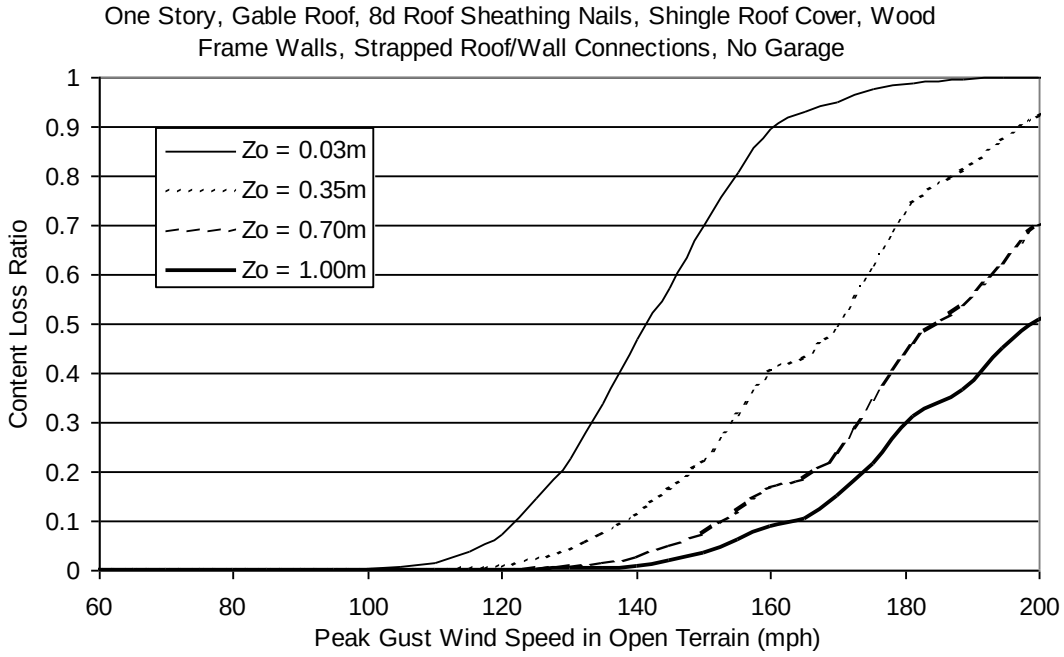

Figure H.116. Content Loss Function for Single Family Residential Building (One Story, 8d Roof Sheathing Nails, Gable Roof, No Garage, Strapped Roof Wall Connections, Wood Frame, Upgraded Roof and Added Secondary Water Resistance).

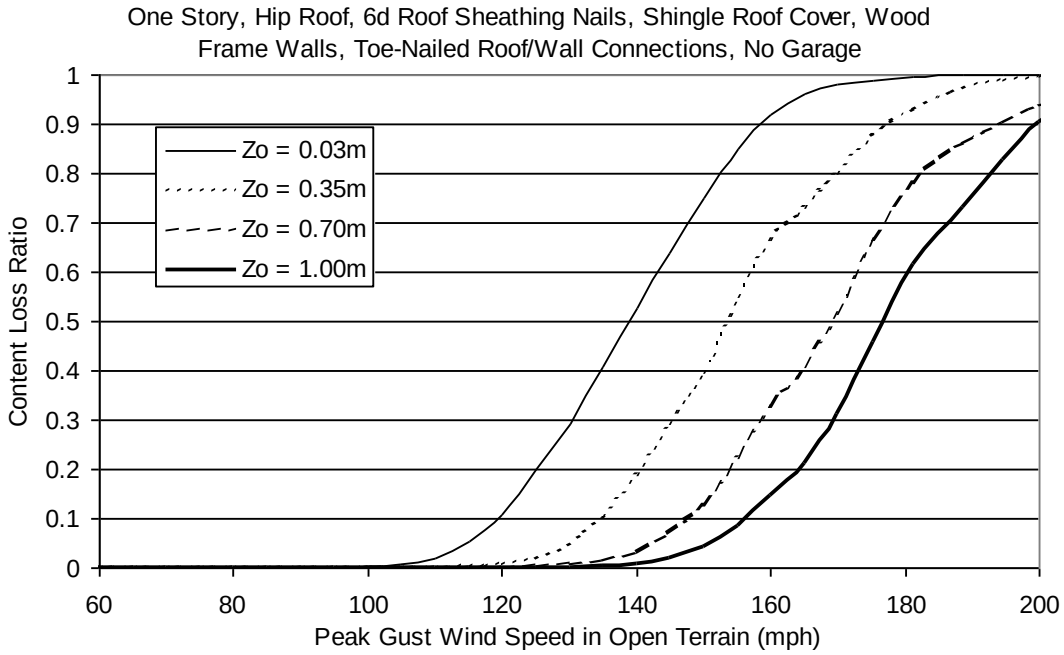

Figure H.117. Content Loss Function for Single Family Residential Building (One Story, 6d Roof Sheathing Nails, Hip Roof, No Garage, Toe-Nailed Roof Wall Connections, Wood Frame, Upgraded Roof and Added Secondary Water Resistance).

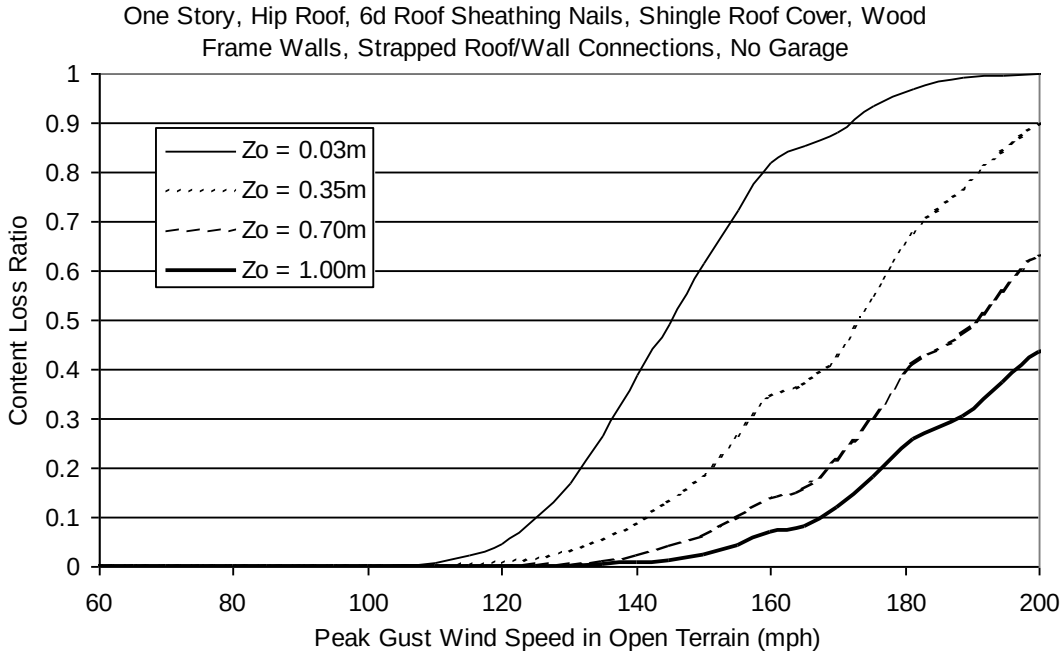

Figure H.118. Content Loss Function for Single Family Residential Building (One Story, 6d Roof Sheathing Nails, Hip Roof, No Garage, Strapped Roof Wall Connections, Wood Frame, Upgraded Roof and Added Secondary Water Resistance).

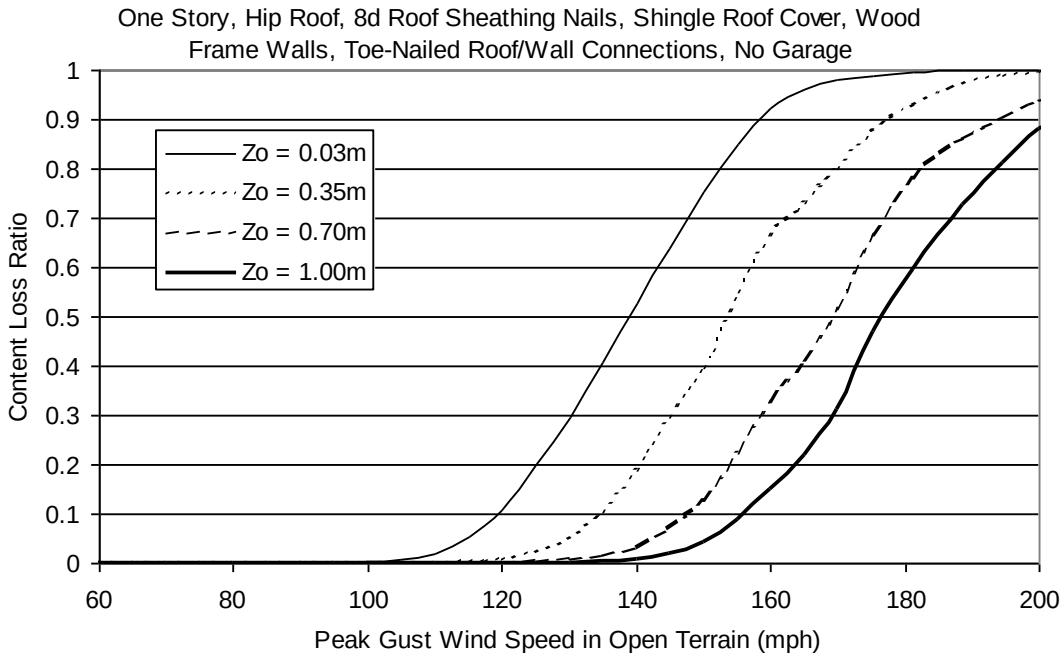

Figure H.119. Content Loss Function for Single Family Residential Building (One Story, 8d Roof Sheathing Nails, Hip Roof, No Garage, Toe-Nailed Roof Wall Connections, Wood Frame, Upgraded Roof and Added Secondary Water Resistance).

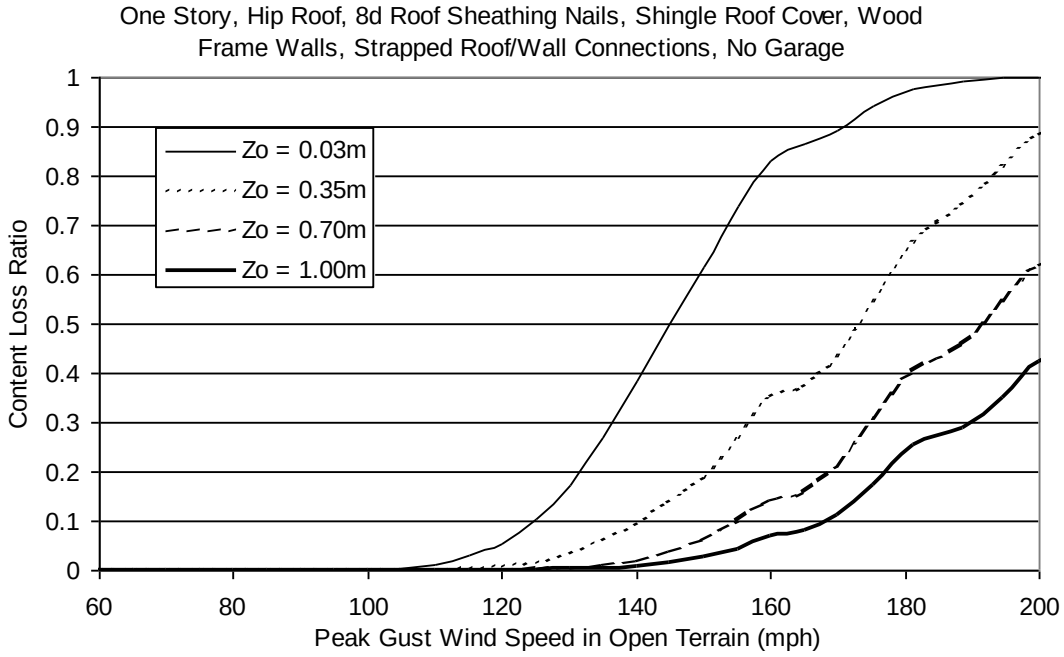

Figure H.120. Content Loss Function for Single Family Residential Building (One Story, 8d Roof Sheathing Nails, Hip Roof, No Garage, Strapped Roof Wall Connections, Wood Frame, Upgraded Roof and Added Secondary Water Resistance).

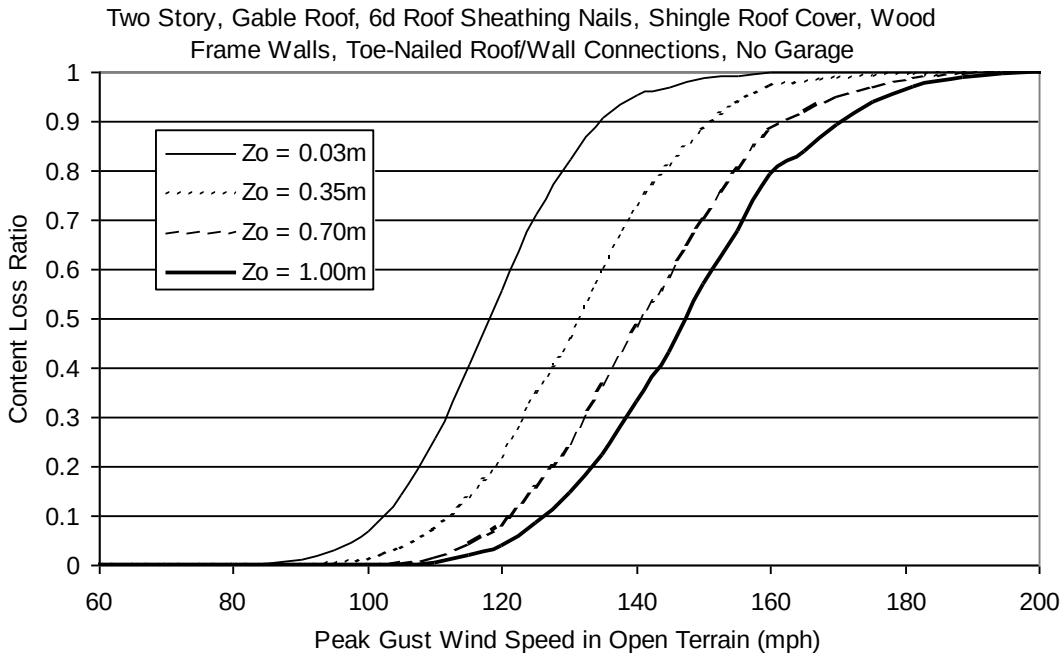

Figure H.121. Content Loss Function for Single Family Residential Building (Two Story, 6d Roof Sheathing Nails, Gable Roof, No Garage, Toe-Nailed Roof Wall Connections, Wood Frame, Upgraded Roof and Added Secondary Water Resistance).

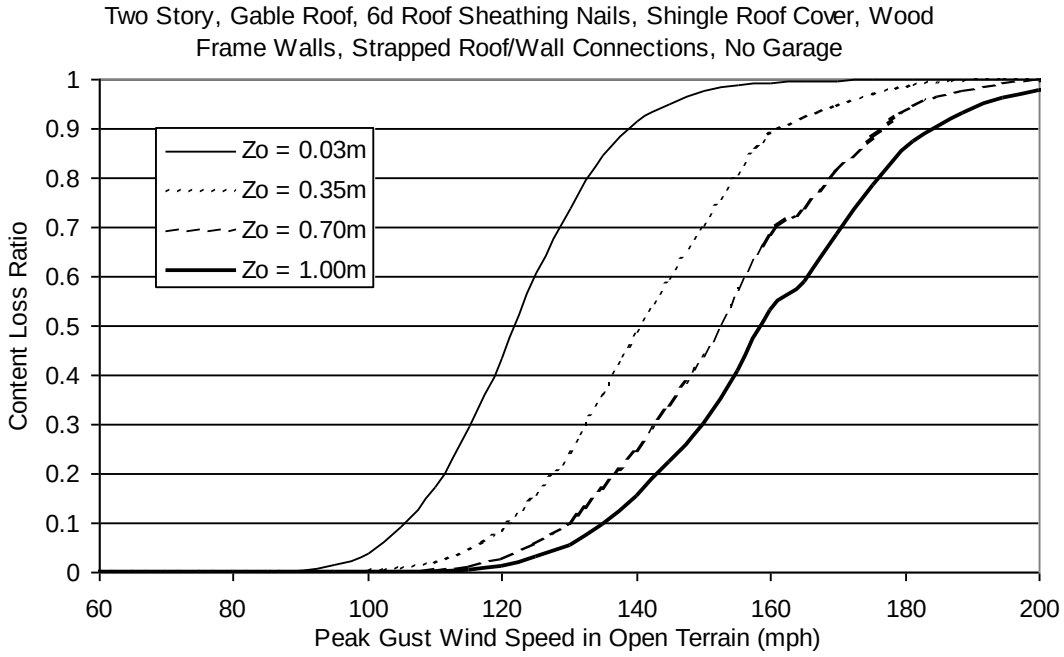

Figure H.122. Content Loss Function for Single Family Residential Building (Two Story, 6d Roof Sheathing Nails, Gable Roof, No Garage, Strapped Roof Wall Connections, Wood Frame, Upgraded Roof and Added Secondary Water Resistance).

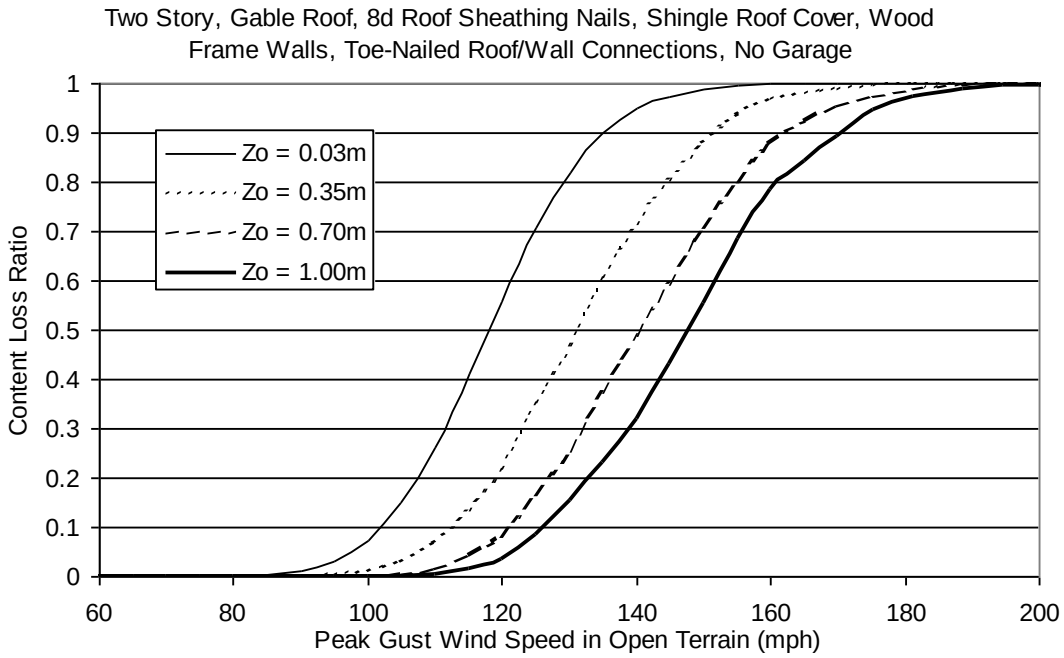

Figure H.123. Content Loss Function for Single Family Residential Building (Two Story, 8d Roof Sheathing Nails, Gable Roof, No Garage, Toe-Nailed Roof Wall Connections, Wood Frame, Upgraded Roof and Added Secondary Water Resistance).

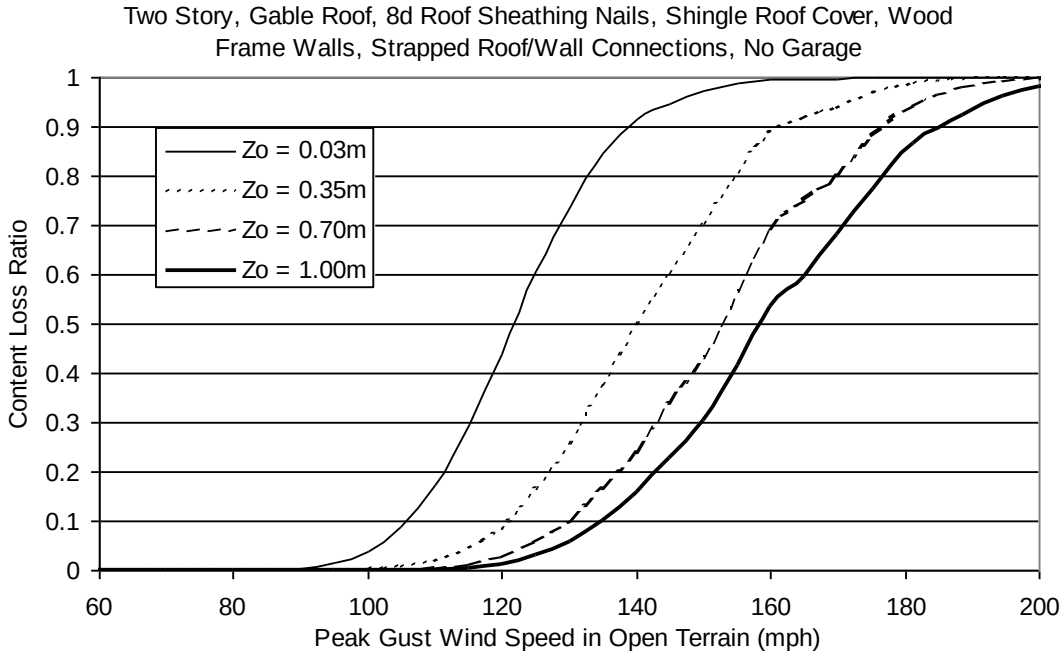

Figure H.124. Content Loss Function for Single Family Residential Building (Two Story, 8d Roof Sheathing Nails, Gable Roof, No Garage, Strapped Roof Wall Connections, Wood Frame, Upgraded Roof and Added Secondary Water Resistance).

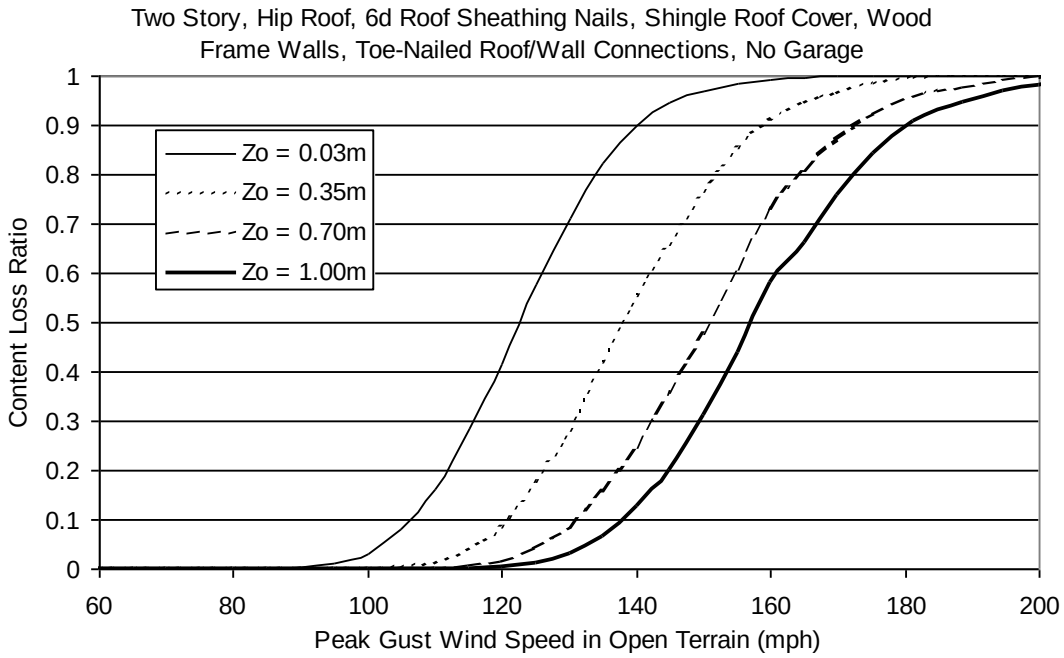

Figure H.125. Content Loss Function for Single Family Residential Building (Two Story, 6d Roof Sheathing Nails, Hip Roof, No Garage, Toe-Nailed Roof Wall Connections, Wood Frame, Upgraded Roof and Added Secondary Water Resistance).

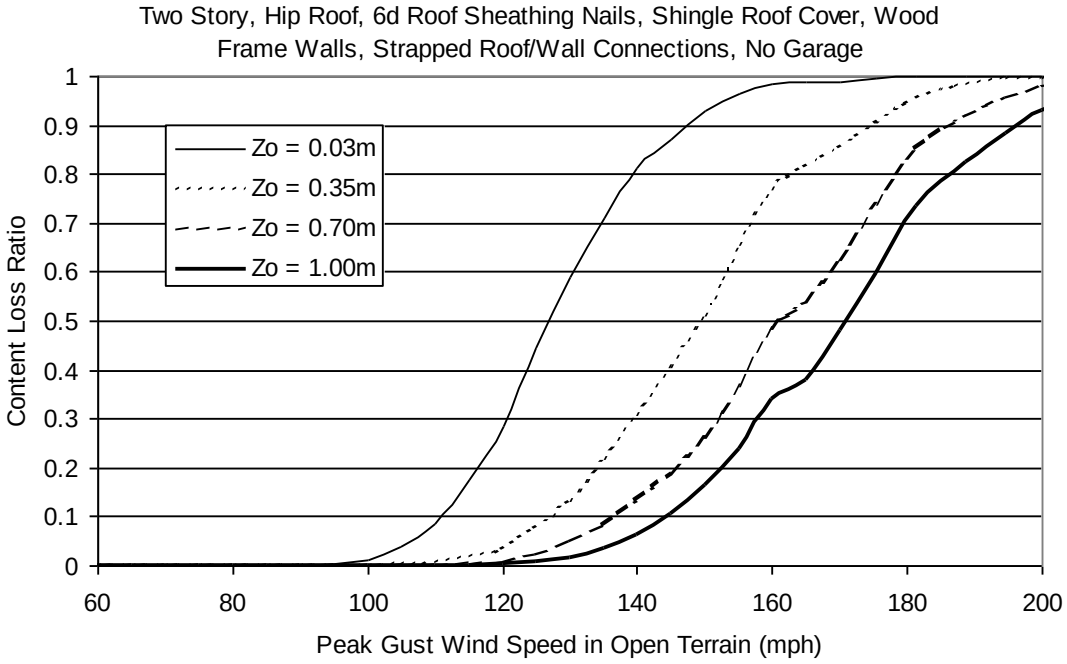

Figure H.126. Content Loss Function for Single Family Residential Building (Two Story, 6d Roof Sheathing Nails, Hip Roof, No Garage, Strapped Roof Wall Connections, Wood Frame, Upgraded Roof and Added Secondary Water Resistance).

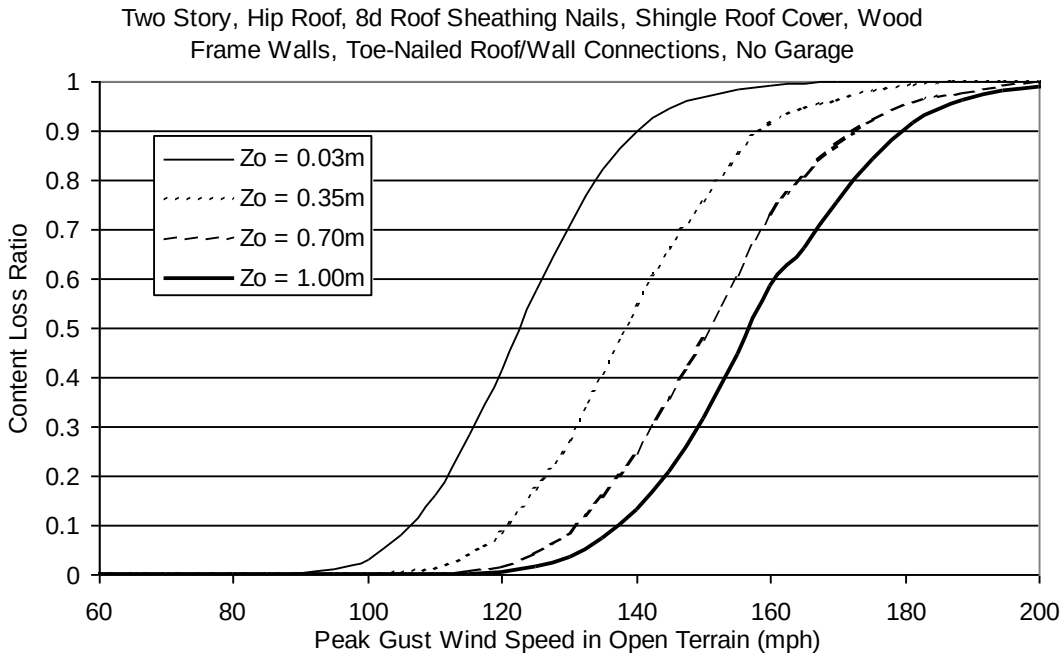

Figure H.127. Content Loss Function for Single Family Residential Building (Two Story, 8d Roof Sheathing Nails, Hip Roof, No Garage, Toe-Nailed Roof Wall Connections, Wood Frame, Upgraded Roof and Added Secondary Water Resistance).

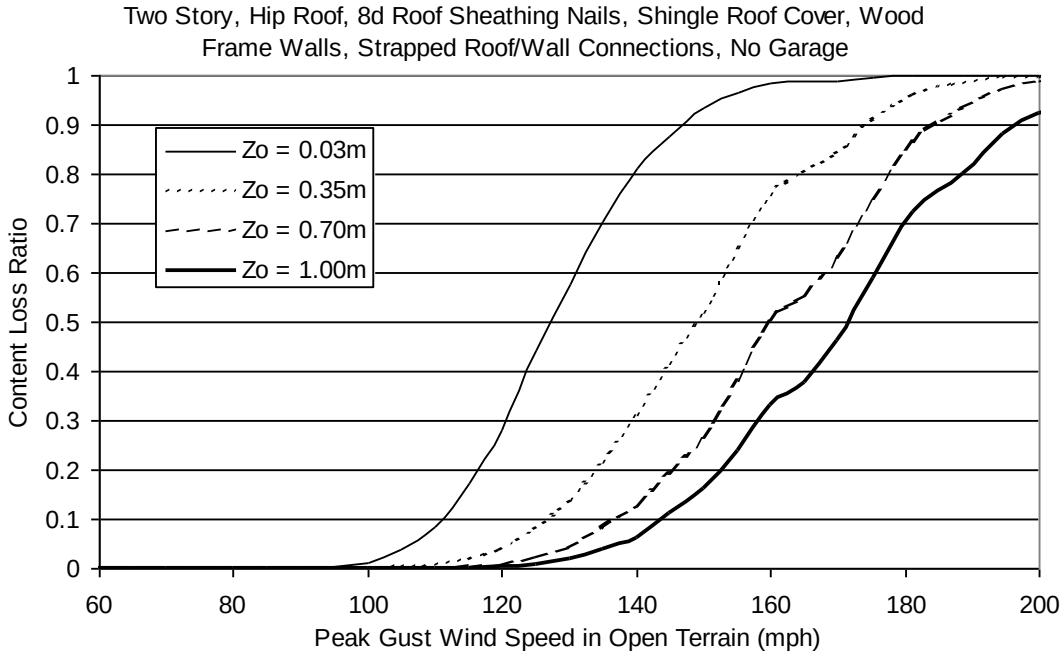

Figure H.128. Content Loss Function for Single Family Residential Building (Two Story, 8d Roof Sheathing Nails, Hip Roof, No Garage, Strapped Roof Wall Connections, Wood Frame, Upgraded Roof and Added Secondary Water Resistance).

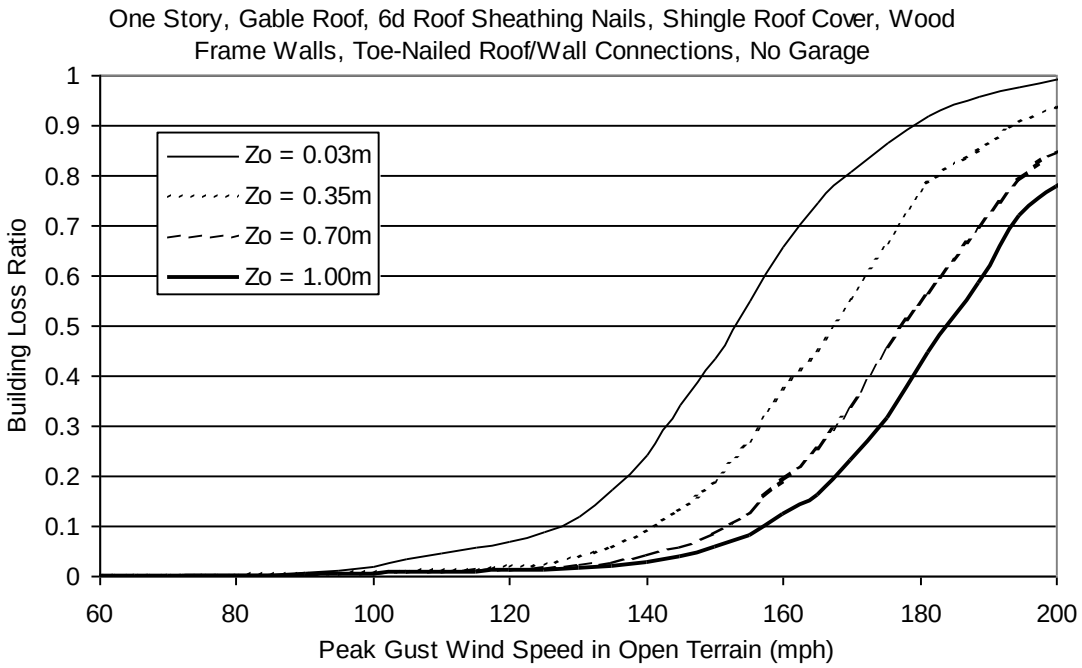

Figure H.129. Building Loss Function for Single Family Residential Building (One Story, 6d Roof Sheathing Nails, Gable Roof, No Garage, Toe-Nailed Roof Wall Connections, Wood Frame, Installed Shutters and Upgraded Roof).

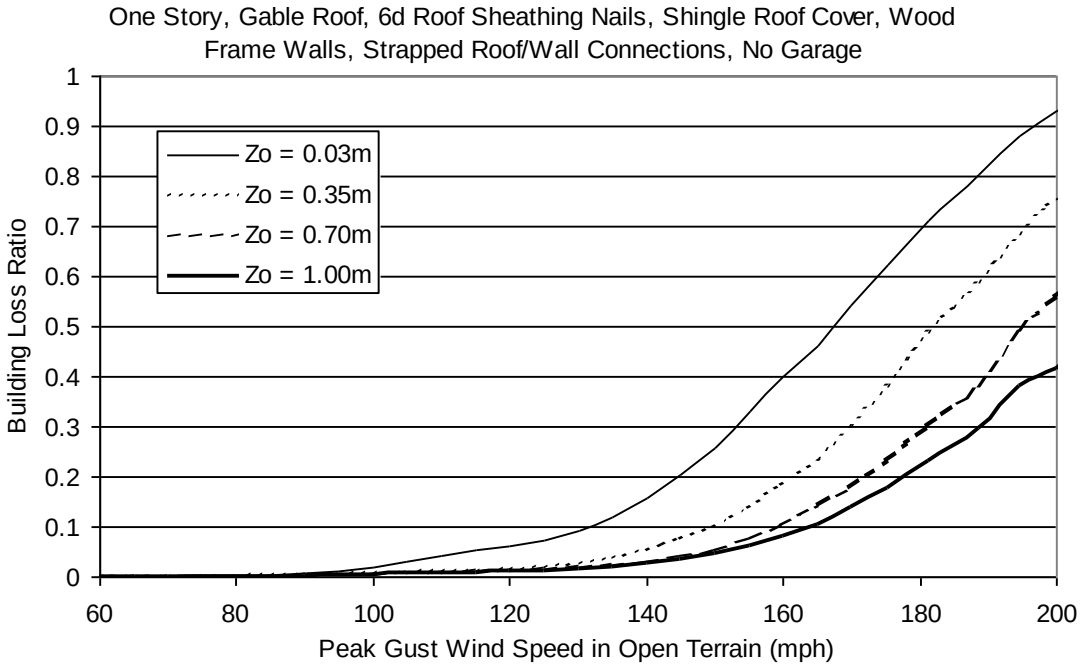

Figure H.130. Building Loss Function for Single Family Residential Building (One Story, 6d Roof Sheathing Nails, Gable Roof, No Garage, Strapped Roof Wall Connections, Wood Frame, Installed Shutters and Upgraded Roof).

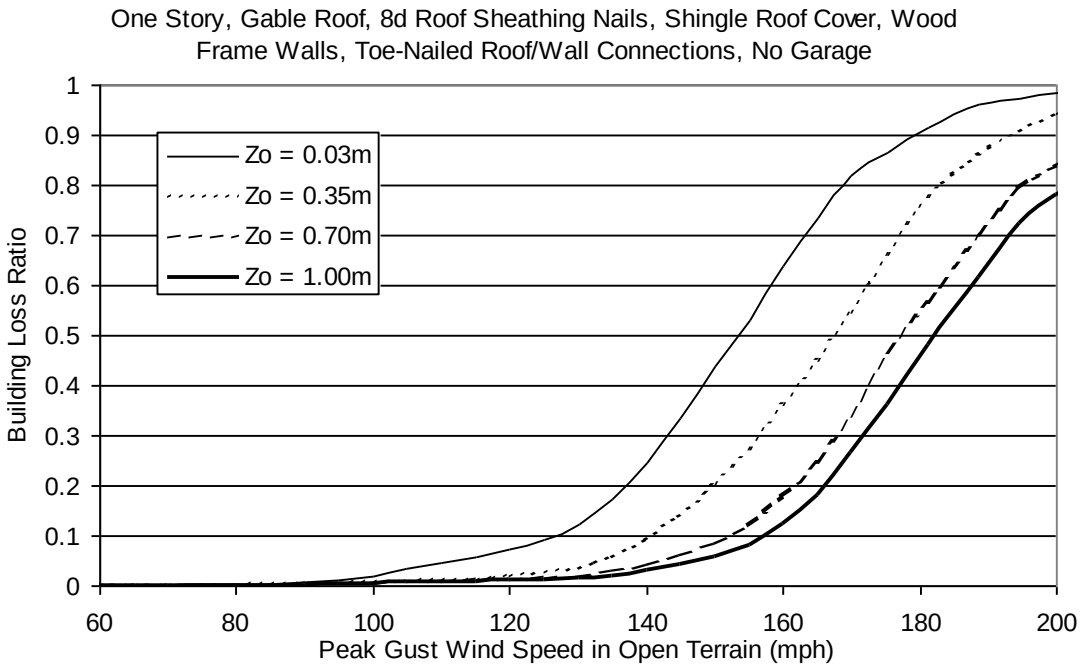

Figure H.131. Building Loss Function for Single Family Residential Building (One Story, 8d Roof Sheathing Nails, Gable Roof, No Garage, Toe-Nailed Roof Wall Connections, Wood Frame, Installed Shutters and Upgraded Roof).

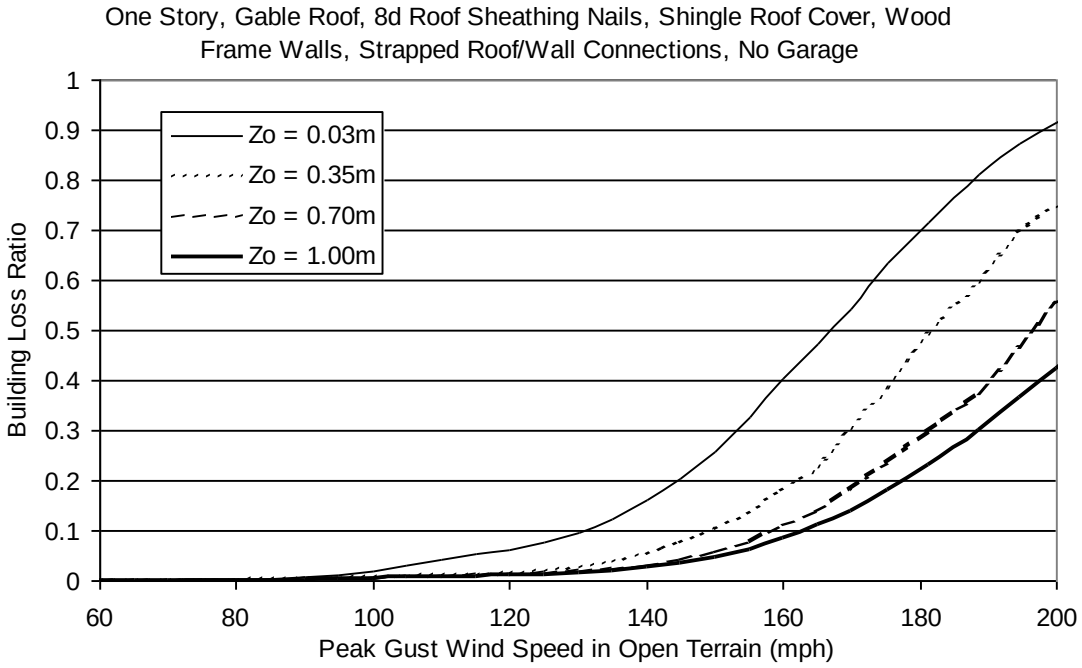

Figure H.132. Building Loss Function for Single Family Residential Building (One Story, 8d Roof Sheathing Nails, Gable Roof, No Garage, Strapped Roof Wall Connections, Wood Frame, Installed Shutters and Upgraded Roof).

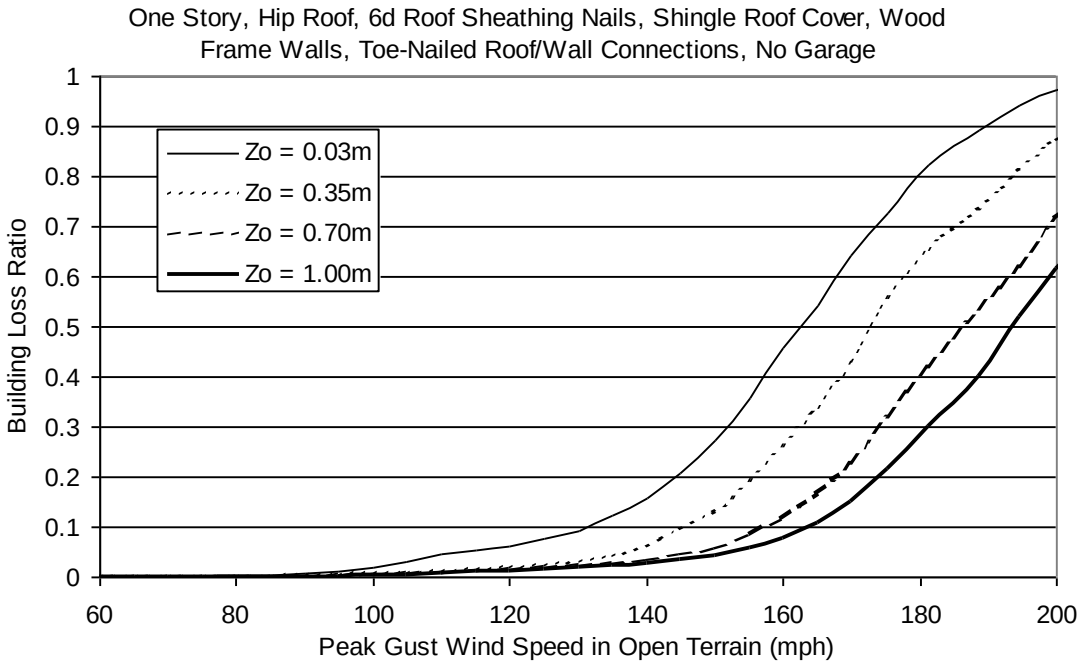

Figure H.133. Building Loss Function for Single Family Residential Building (One Story, 6d Roof Sheathing Nails, Hip Roof, No Garage, Toe-Nailed Roof Wall Connections, Wood Frame, Installed Shutters and Upgraded Roof).

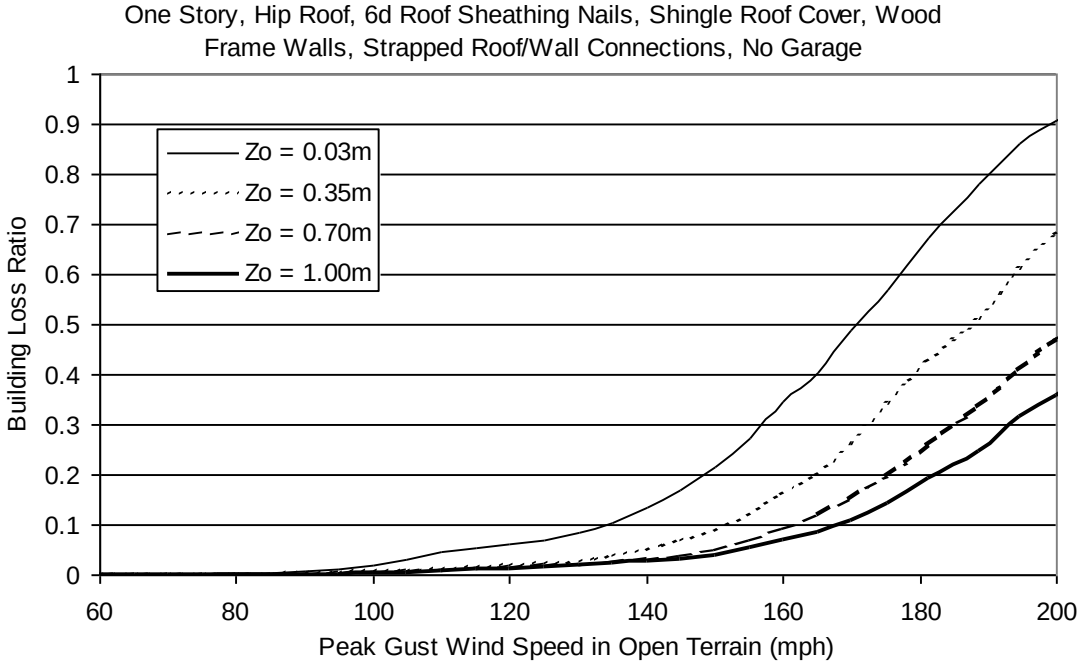

Figure H.134. Building Loss Function for Single Family Residential Building (One Story, 6d Roof Sheathing Nails, Hip Roof, No Garage, Strapped Roof Wall Connections, Wood Frame, Installed Shutters and Upgraded Roof).

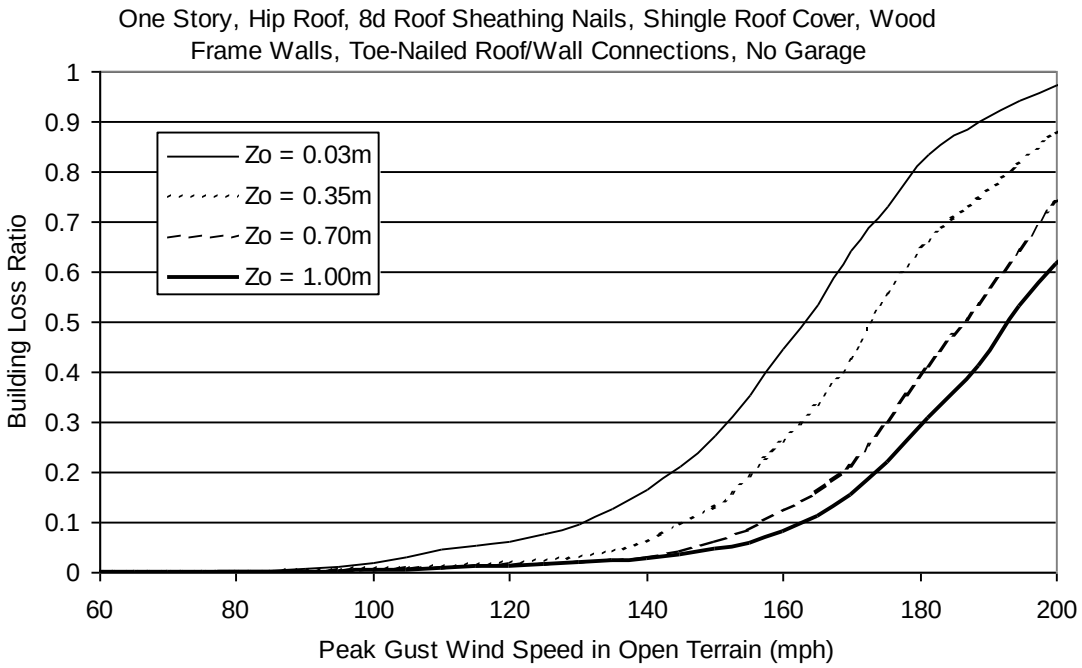

Figure H.135. Building Loss Function for Single Family Residential Building (One Story, 8d Roof Sheathing Nails, Hip Roof, No Garage, Toe-Nailed Roof Wall Connections, Wood Frame, Installed Shutters and Upgraded Roof).

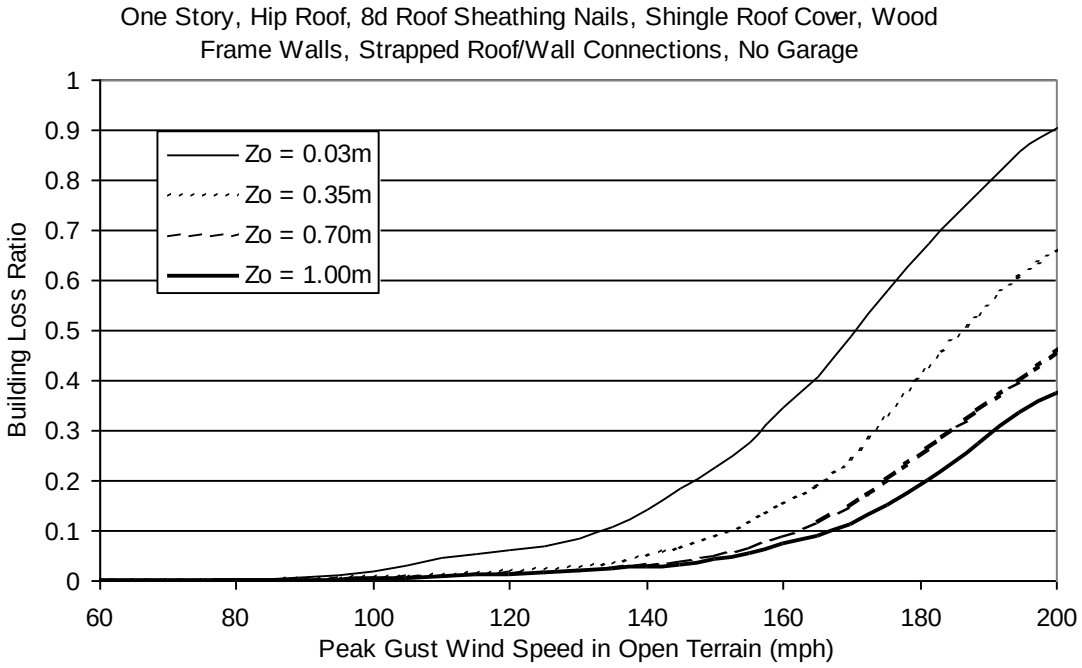

Figure H.136. Building Loss Function for Single Family Residential Building (One Story, 8d Roof Sheathing Nails, Hip Roof, No Garage, Strapped Roof Wall Connections, Wood Frame, Installed Shutters and Upgraded Roof).

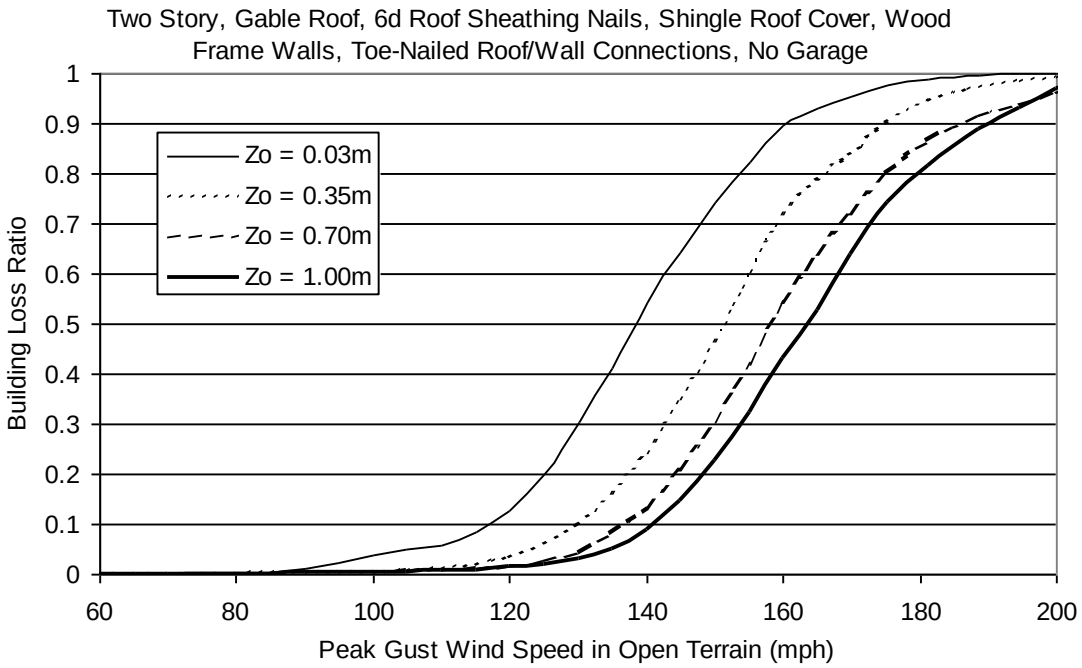

Figure H.137. Building Loss Function for Single Family Residential Building (Two Story, 6d Roof Sheathing Nails, Gable Roof, No Garage, Toe-Nailed Roof Wall Connections, Wood Frame, Installed Shutters and Upgraded Roof).

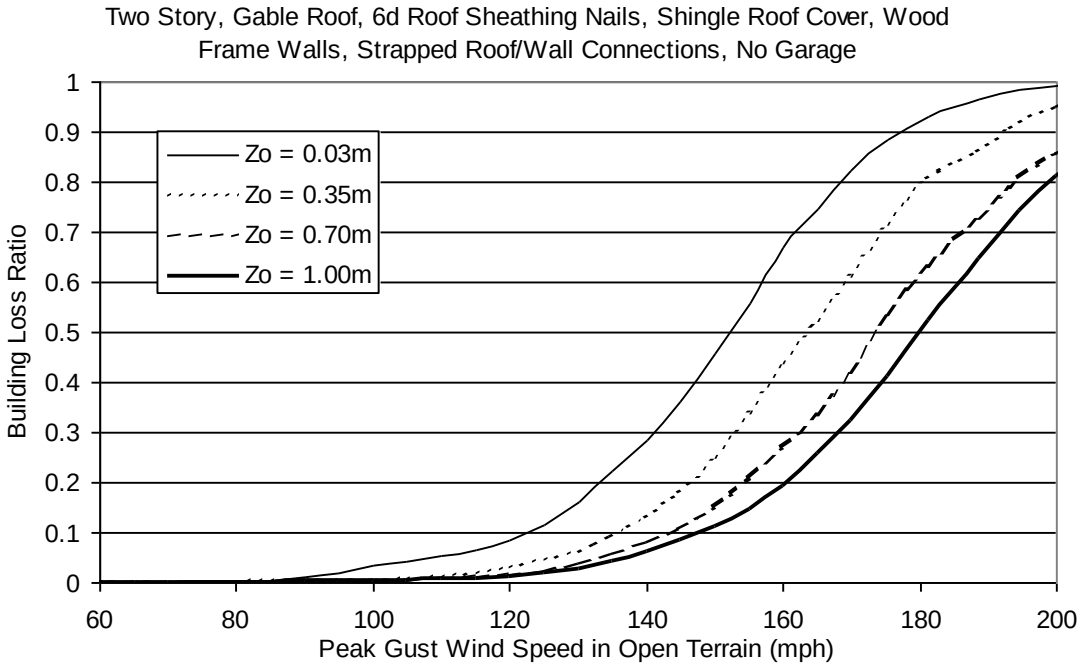

Figure H.138. Building Loss Function for Single Family Residential Building (Two Story, 6d Roof Sheathing Nails, Gable Roof, No Garage, Strapped Roof Wall Connections, Wood Frame, Installed Shutters and Upgraded Roof).

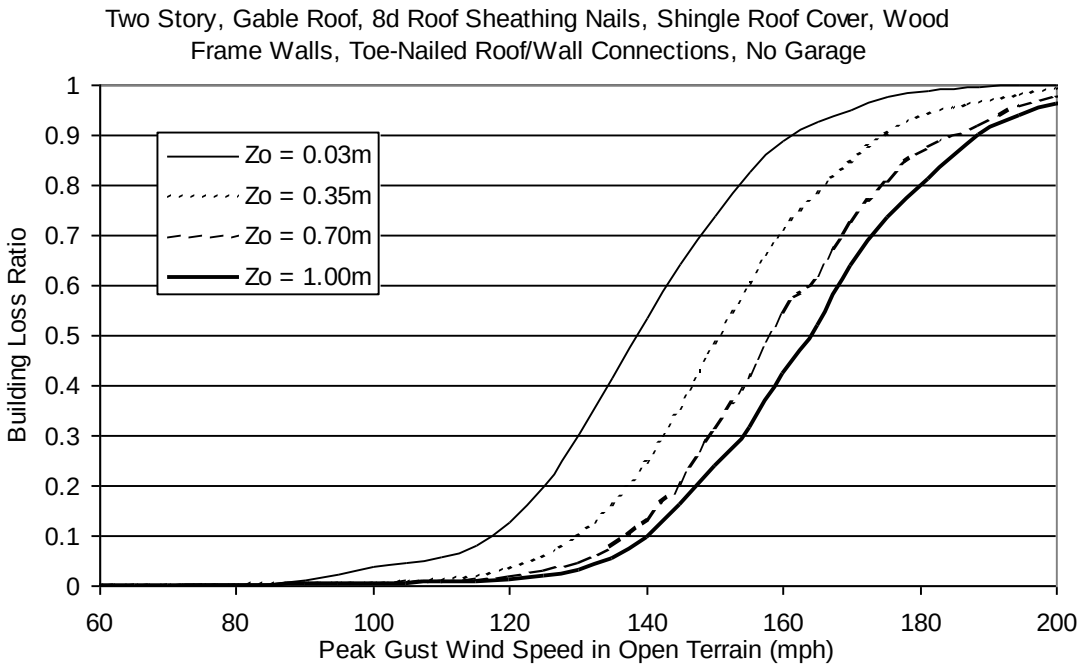

Figure H.139. Building Loss Function for Single Family Residential Building (Two Story, 8d Roof Sheathing Nails, Gable Roof, No Garage, Toe-Nailed Roof Wall Connections, Wood Frame, Installed Shutters and Upgraded Roof).

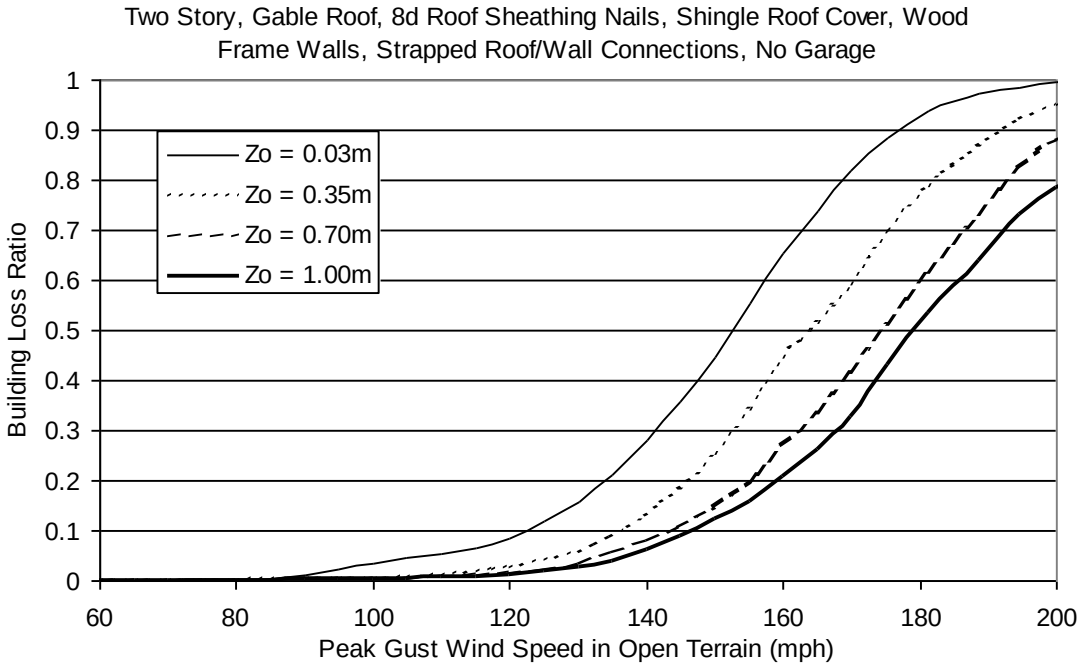

Figure H.140. Building Loss Function for Single Family Residential Building (Two Story, 8d Roof Sheathing Nails, Gable Roof, No Garage, Strapped Roof Wall Connections, Wood Frame, Installed Shutters and Upgraded Roof).

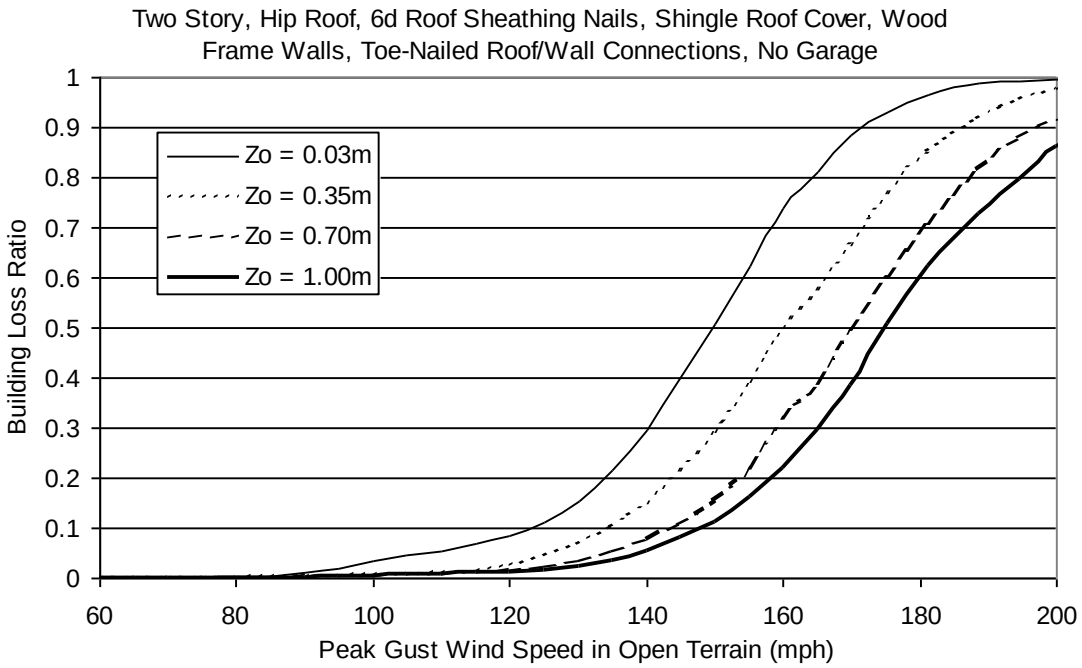

Figure H.141. Building Loss Function for Single Family Residential Building (Two Story, 6d Roof Sheathing Nails, Hip Roof, No Garage, Toe-Nailed Roof Wall Connections, Wood Frame, Installed Shutters and Upgraded Roof).

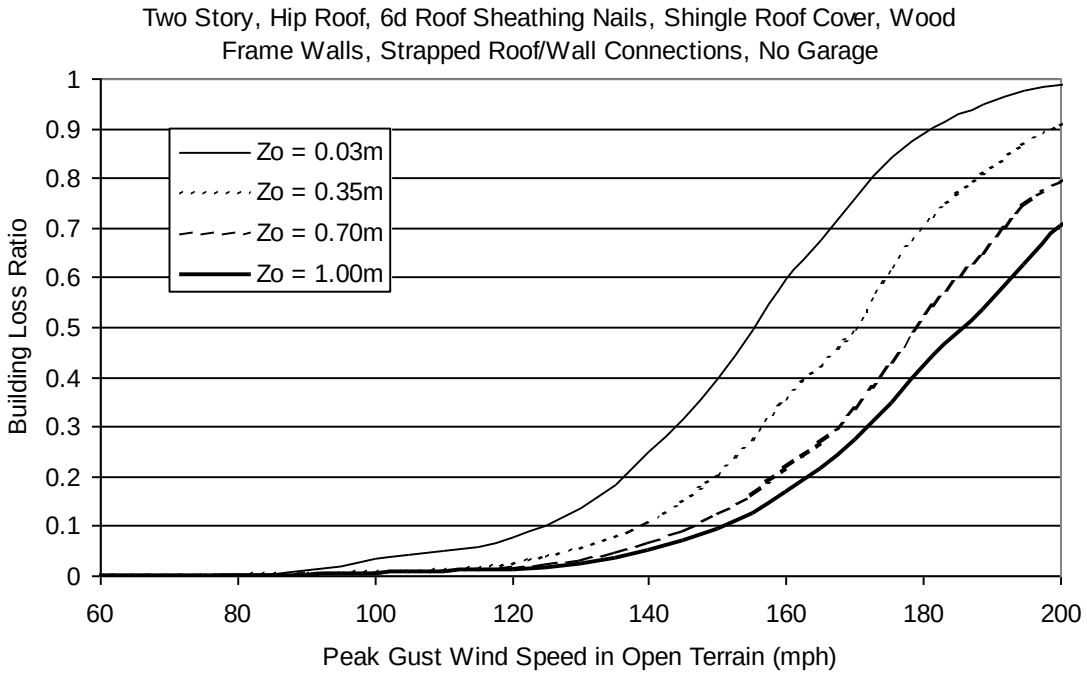

Figure H.142. Building Loss Function for Single Family Residential Building (Two Story, 6d Roof Sheathing Nails, Hip Roof, No Garage, Strapped Roof Wall Connections, Wood Frame, Installed Shutters and Upgraded Roof).

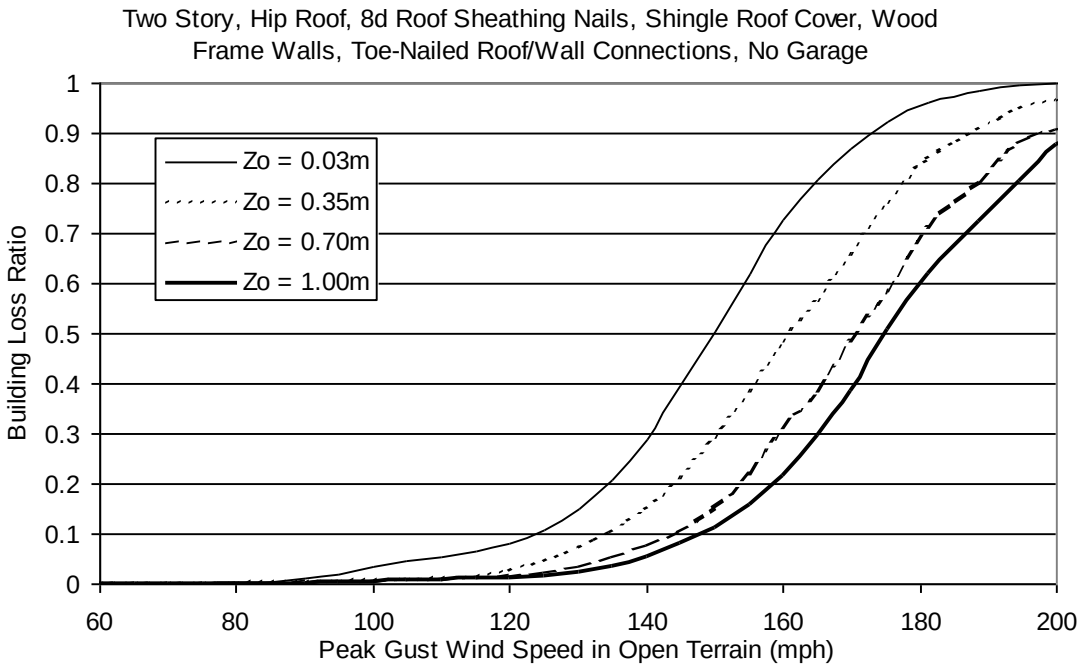

Figure H.143. Building Loss Function for Single Family Residential Building (Two Story, 8d Roof Sheathing Nails, Hip Roof, No Garage, Toe-Nailed Roof Wall Connections, Wood Frame, Installed Shutters and Upgraded Roof).

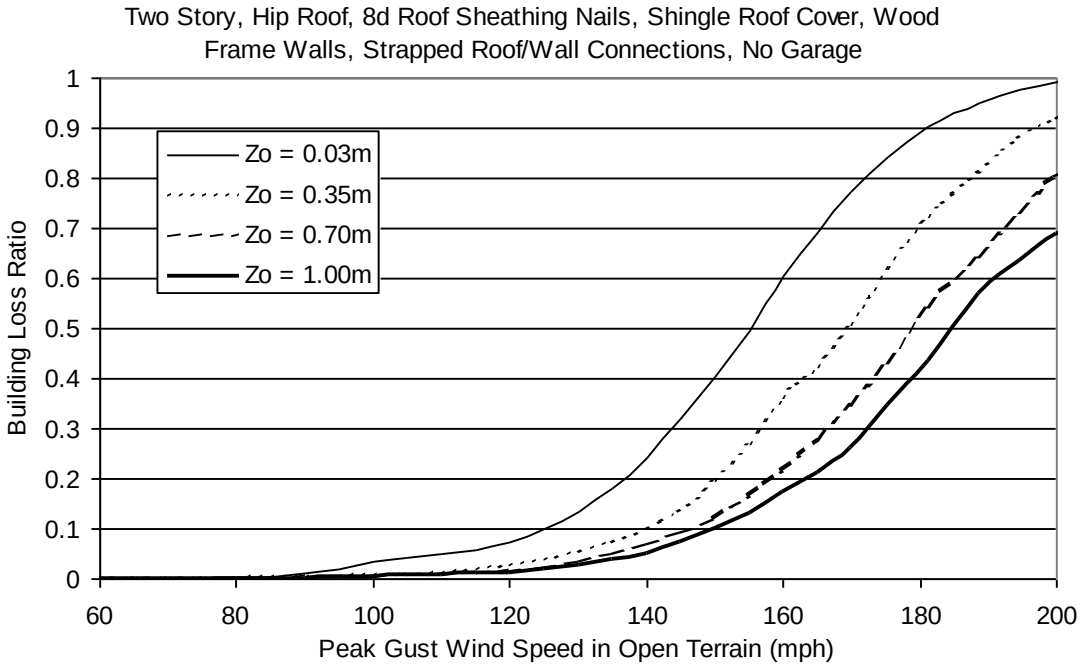

Figure H.144. Building Loss Function for Single Family Residential Building (Two Story, 8d Roof Sheathing Nails, Hip Roof, No Garage, Strapped Roof Wall Connections, Wood Frame, Installed Shutters and Upgraded Roof).

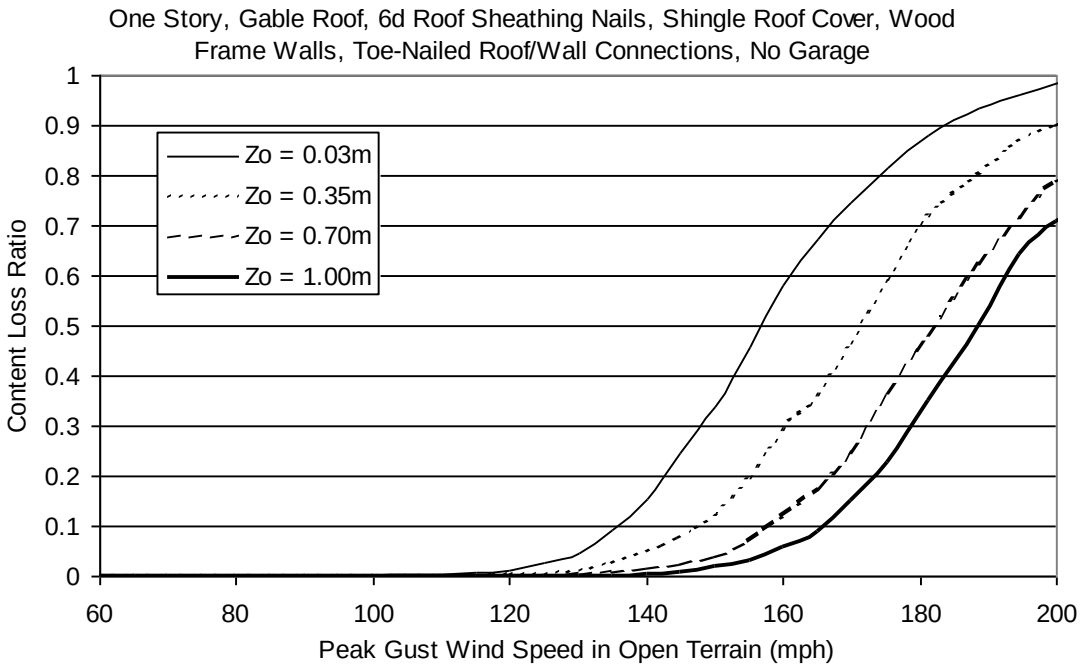

Figure H.145. Content Loss Function for Single Family Residential Building (One Story, 6d Roof Sheathing Nails, Gable Roof, No Garage, Toe-Nailed Roof Wall Connections, Wood Frame, Installed Shutters and Upgraded Roof).

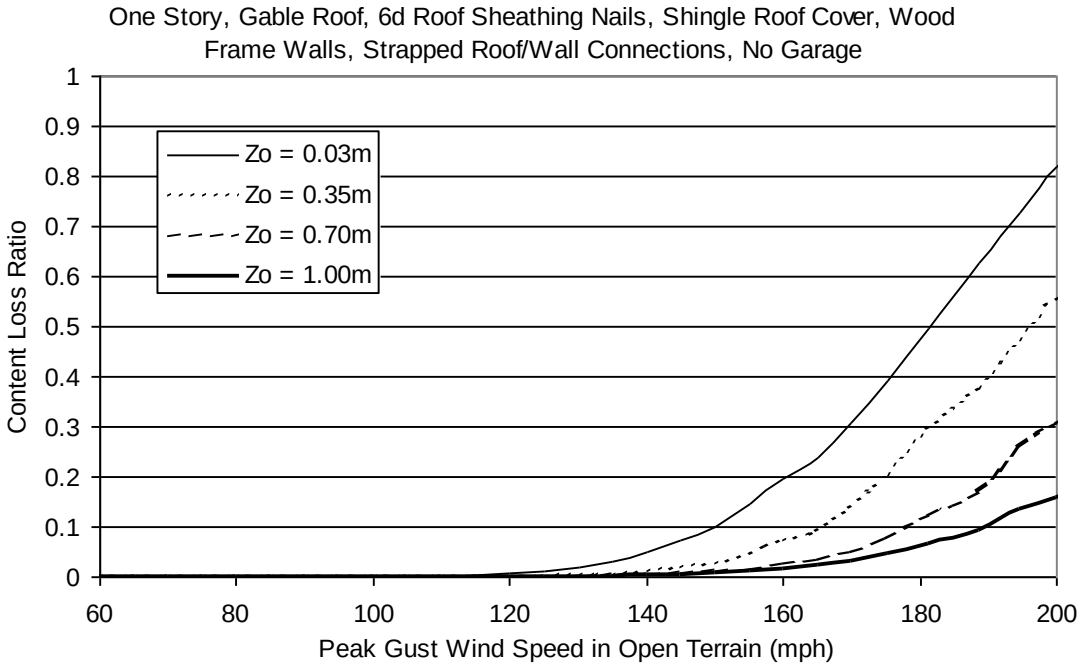

Figure H.146. Content Loss Function for Single Family Residential Building (One Story, 6d Roof Sheathing Nails, Gable Roof, No Garage, Strapped Roof Wall Connections, Wood Frame, Installed Shutters and Upgraded Roof).

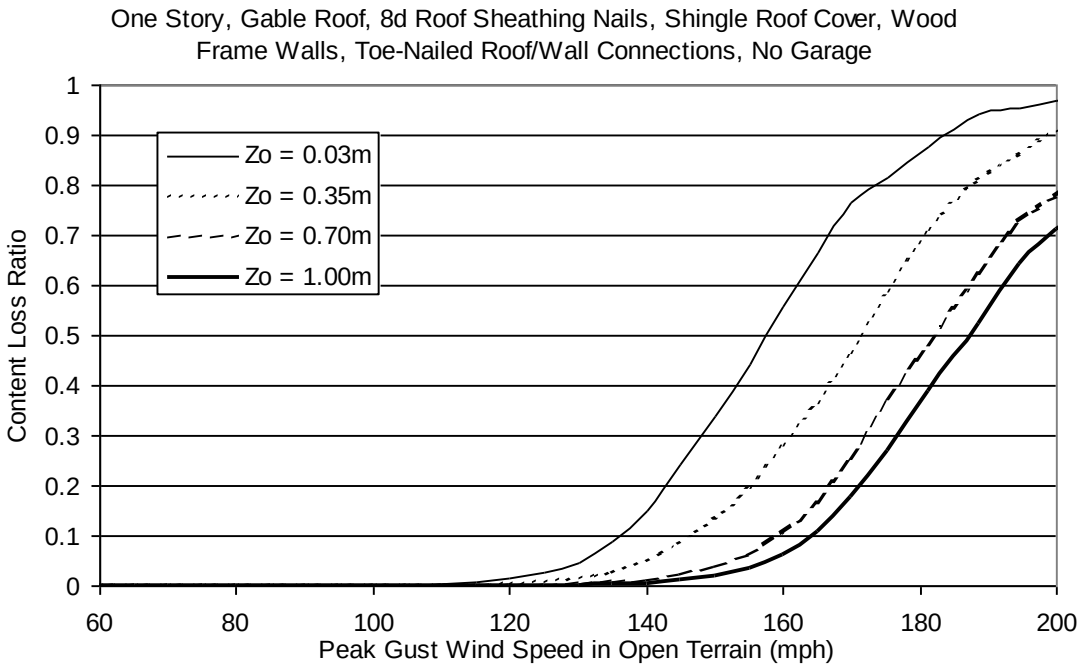

Figure H.147. Content Loss Function for Single Family Residential Building (One Story, 8d Roof Sheathing Nails, Gable Roof, No Garage, Toe-Nailed Roof Wall Connections, Wood Frame, Installed Shutters and Upgraded Roof).

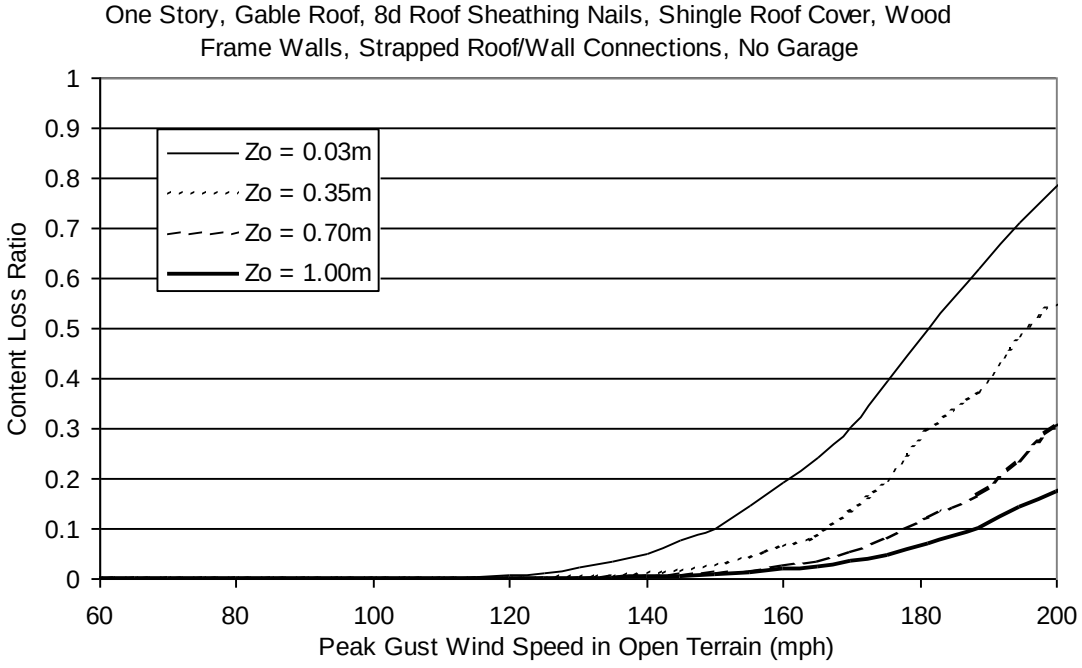

Figure H.148. Content Loss Function for Single Family Residential Building (One Story, 8d Roof Sheathing Nails, Gable Roof, No Garage, Strapped Roof Wall Connections, Wood Frame, Installed Shutters and Upgraded Roof).

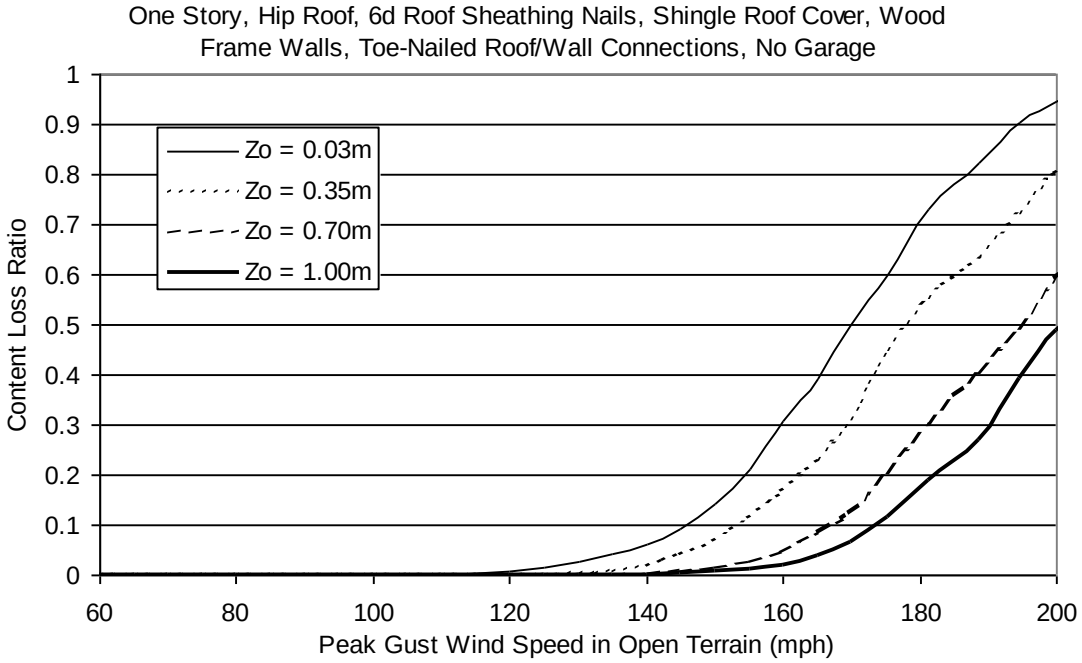

Figure H.149. Content Loss Function for Single Family Residential Building (One Story, 6d Roof Sheathing Nails, Hip Roof, No Garage, Toe-Nailed Roof Wall Connections, Wood Frame, Installed Shutters and Upgraded Roof).

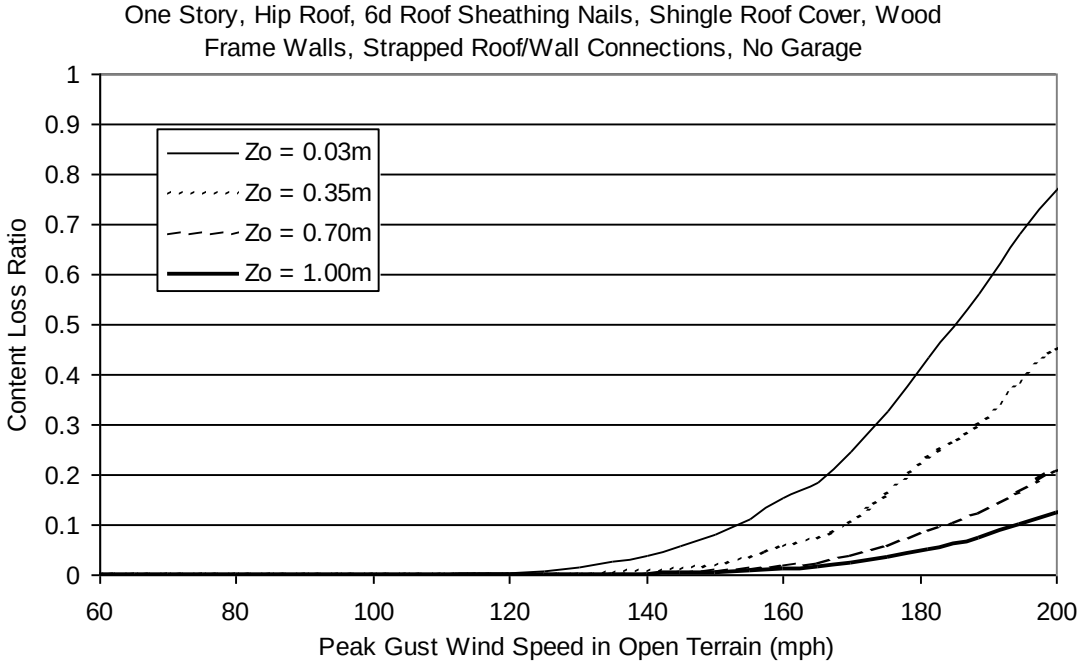

Figure H.150. Content Loss Function for Single Family Residential Building (One Story, 6d Roof Sheathing Nails, Hip Roof, No Garage, Strapped Roof Wall Connections, Wood Frame, Installed Shutters and Upgraded Roof).

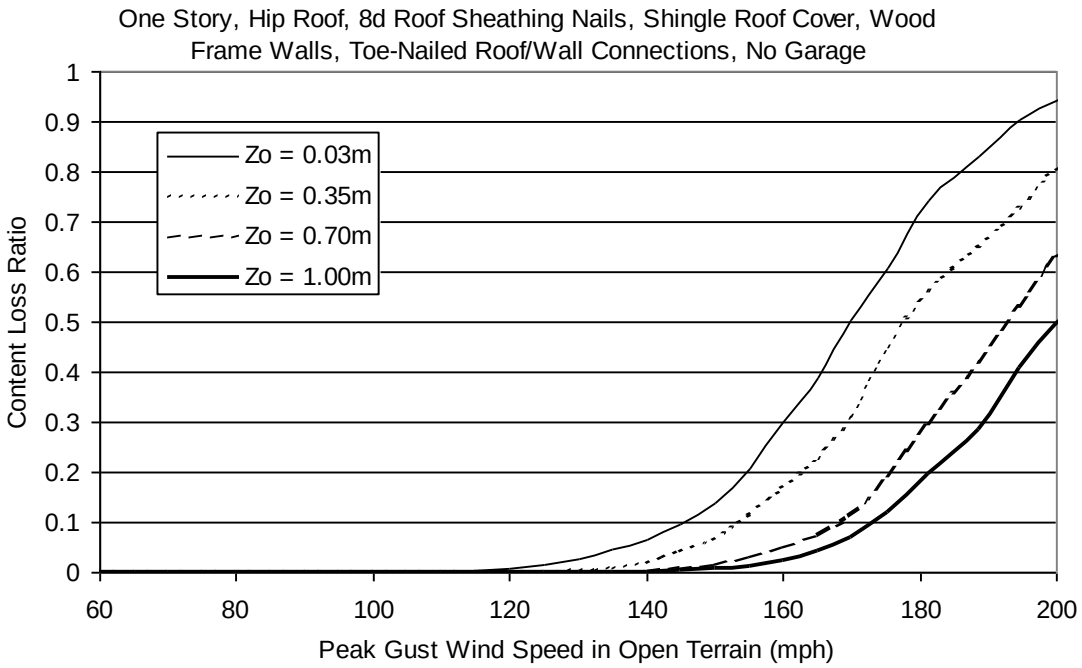

Figure H.151. Content Loss Function for Single Family Residential Building (One Story, 8d Roof Sheathing Nails, Hip Roof, No Garage, Toe-Nailed Roof Wall Connections, Wood Frame, Installed Shutters and Upgraded Roof).

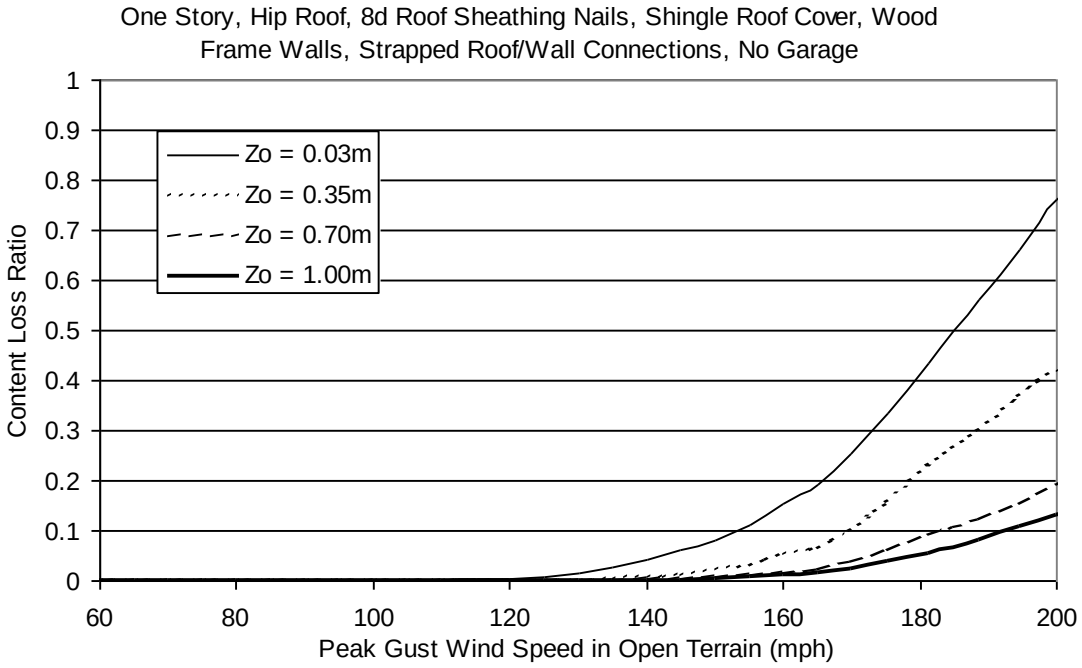

Figure H.152. Content Loss Function for Single Family Residential Building (One Story, 8d Roof Sheathing Nails, Hip Roof, No Garage, Strapped Roof Wall Connections, Wood Frame, Installed Shutters and Upgraded Roof).

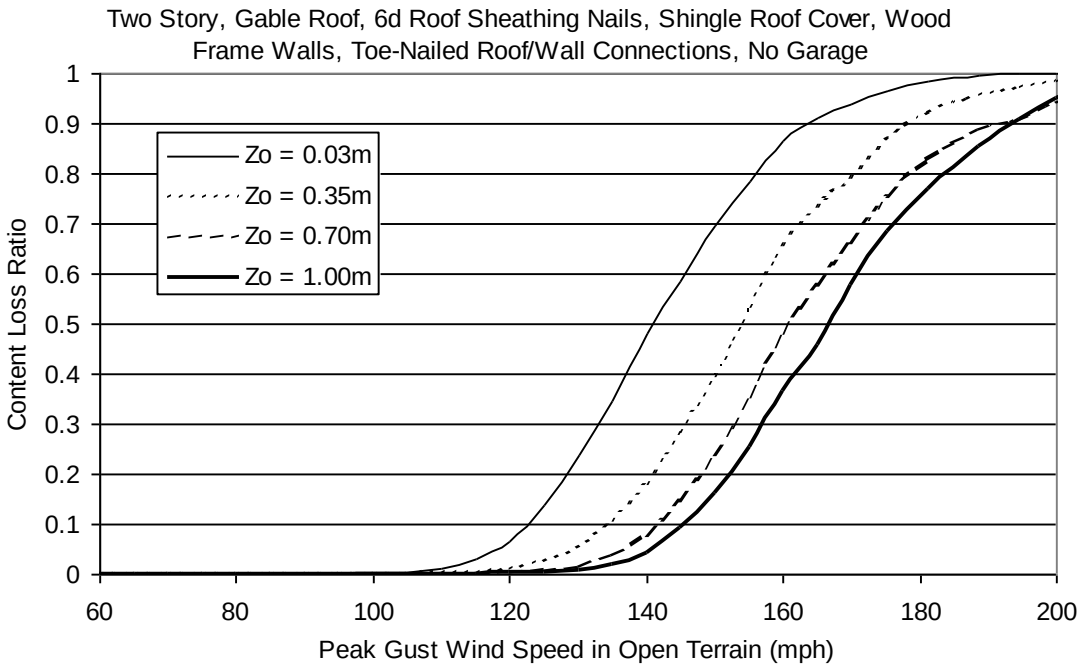

Figure H.153. Content Loss Function for Single Family Residential Building (Two Story, 6d Roof Sheathing Nails, Gable Roof, No Garage, Toe-Nailed Roof Wall Connections, Wood Frame, Installed Shutters and Upgraded Roof).

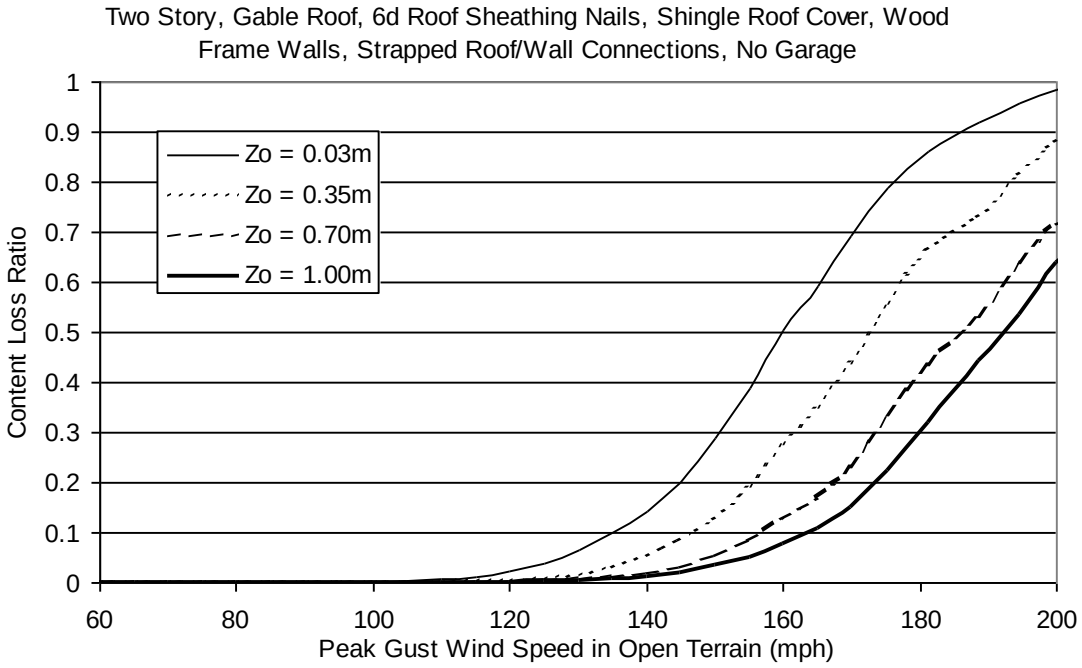

Figure H.154. Content Loss Function for Single Family Residential Building (Two Story, 6d Roof Sheathing Nails, Gable Roof, No Garage, Strapped Roof Wall Connections, Wood Frame, Installed Shutters and Upgraded Roof).

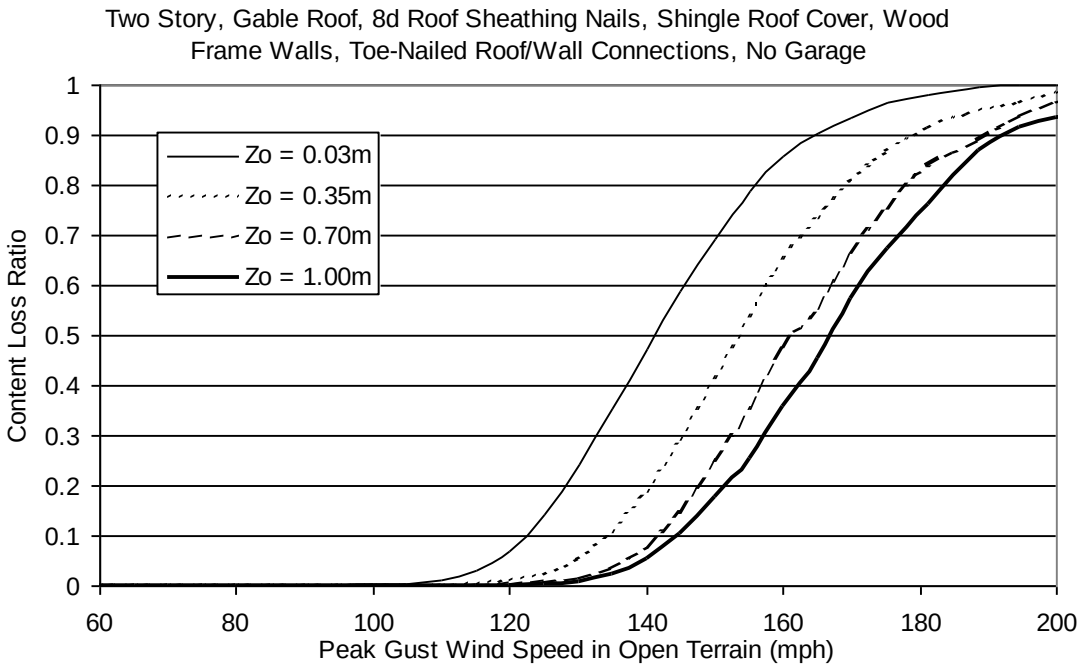

Figure H.155. Content Loss Function for Single Family Residential Building (Two Story, 8d Roof Sheathing Nails, Gable Roof, No Garage, Toe-Nailed Roof Wall Connections, Wood Frame, Installed Shutters and Upgraded Roof).

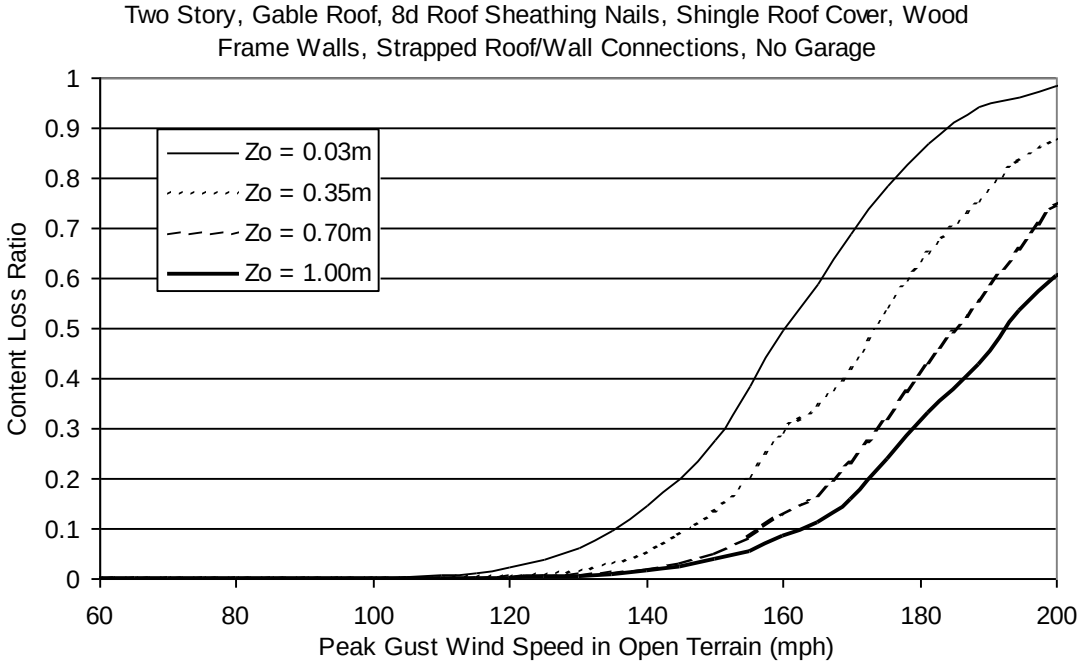

Figure H.156. Content Loss Function for Single Family Residential Building (Two Story, 8d Roof Sheathing Nails, Gable Roof, No Garage, Strapped Roof Wall Connections, Wood Frame, Installed Shutters and Upgraded Roof).

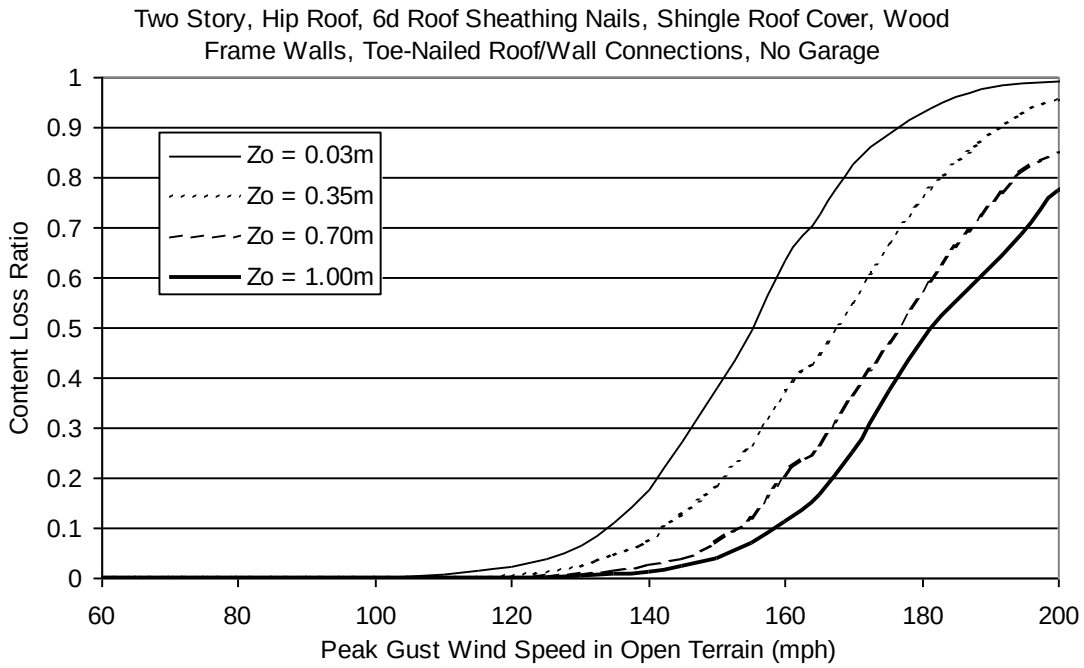

Figure H.157. Content Loss Function for Single Family Residential Building (Two Story, 6d Roof Sheathing Nails, Hip Roof, No Garage, Toe-Nailed Roof Wall Connections, Wood Frame, Installed Shutters and Upgraded Roof).

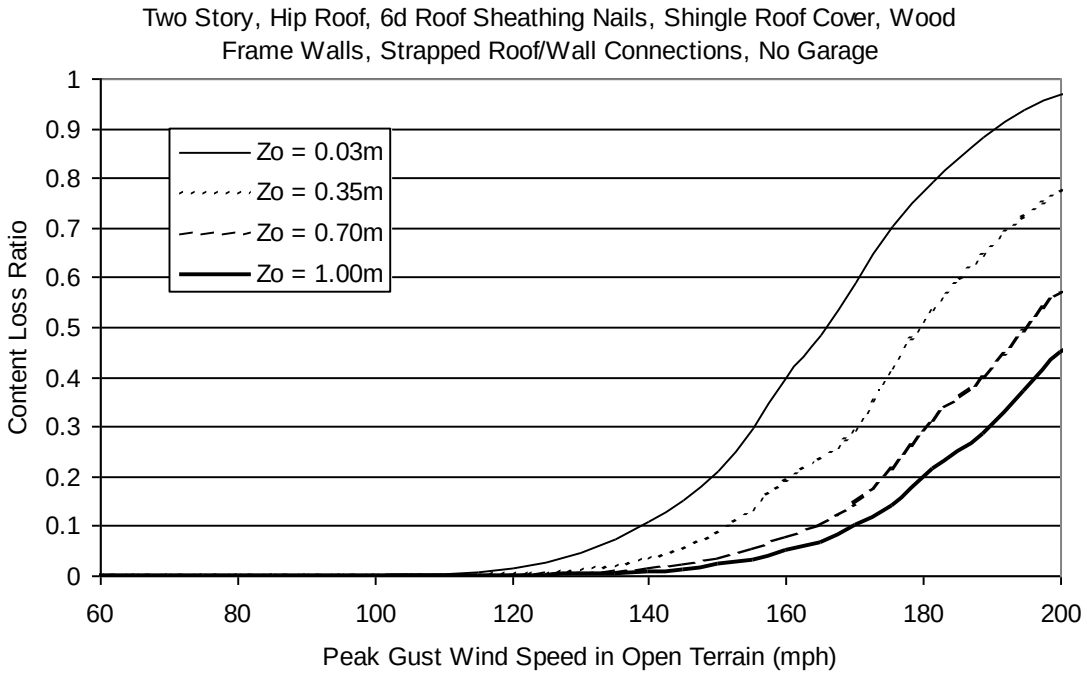

Figure H.158. Content Loss Function for Single Family Residential Building (Two Story, 6d Roof Sheathing Nails, Hip Roof, No Garage, Strapped Roof Wall Connections, Wood Frame, Installed Shutters and Upgraded Roof).

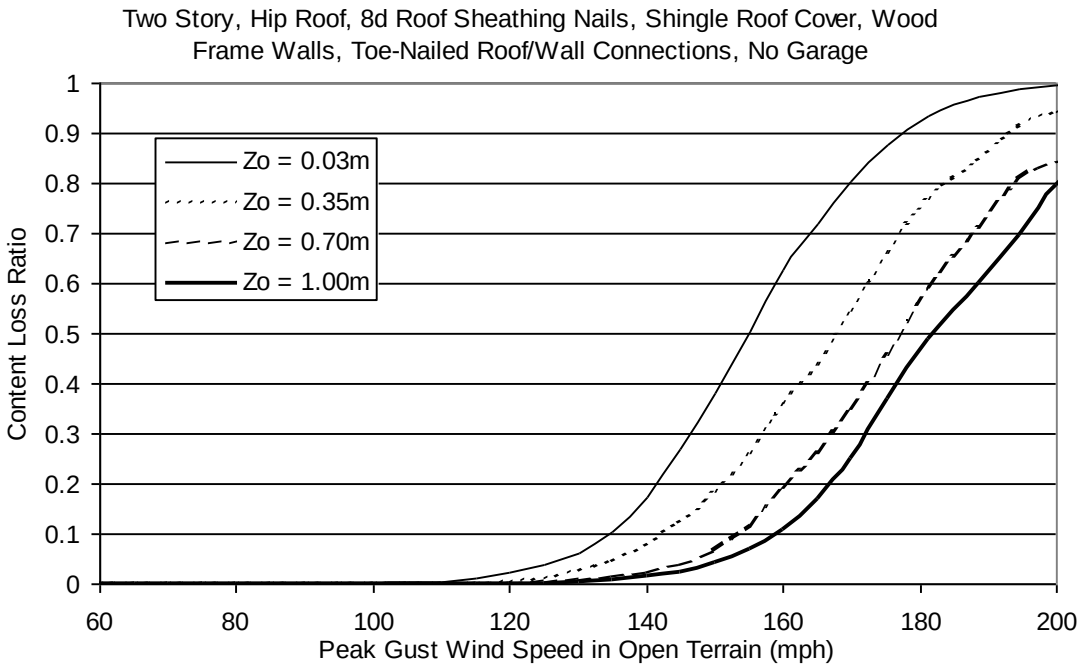

Figure H.159. Content Loss Function for Single Family Residential Building (Two Story, 8d Roof Sheathing Nails, Hip Roof, No Garage, Toe-Nailed Roof Wall Connections, Wood Frame, Installed Shutters and Upgraded Roof).

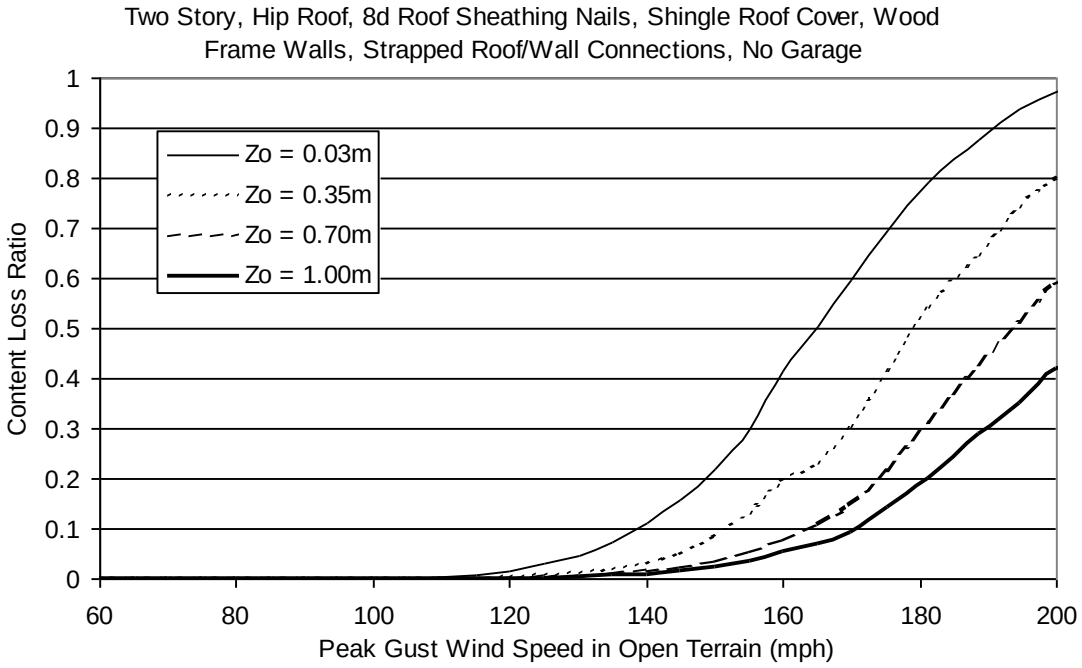

Figure H.160. Content Loss Function for Single Family Residential Building (Two Story, 8d Roof Sheathing Nails, Hip Roof, No Garage, Strapped Roof Wall Connections, Wood Frame, Installed Shutters and Upgraded Roof).

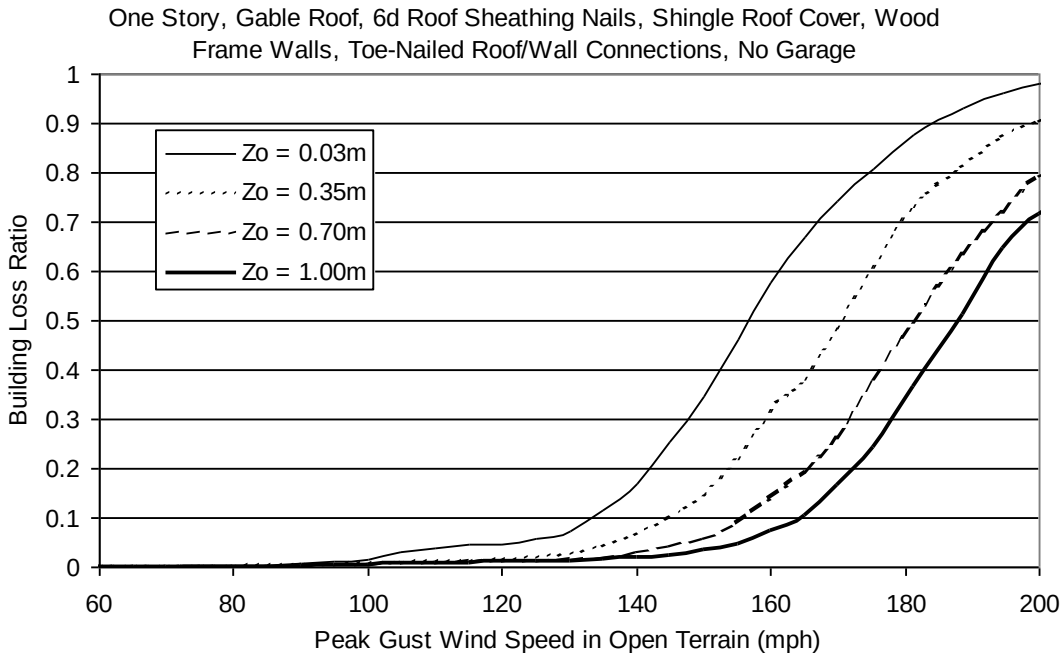

Figure H.161. Building Loss Function for Single Family Residential Building (One Story, 6d Roof Sheathing Nails, Gable Roof, No Garage, Toe-Nailed Roof Wall Connections, Wood Frame, Installed Shutters, Upgraded Roof and Added Secondary Water Resistance).

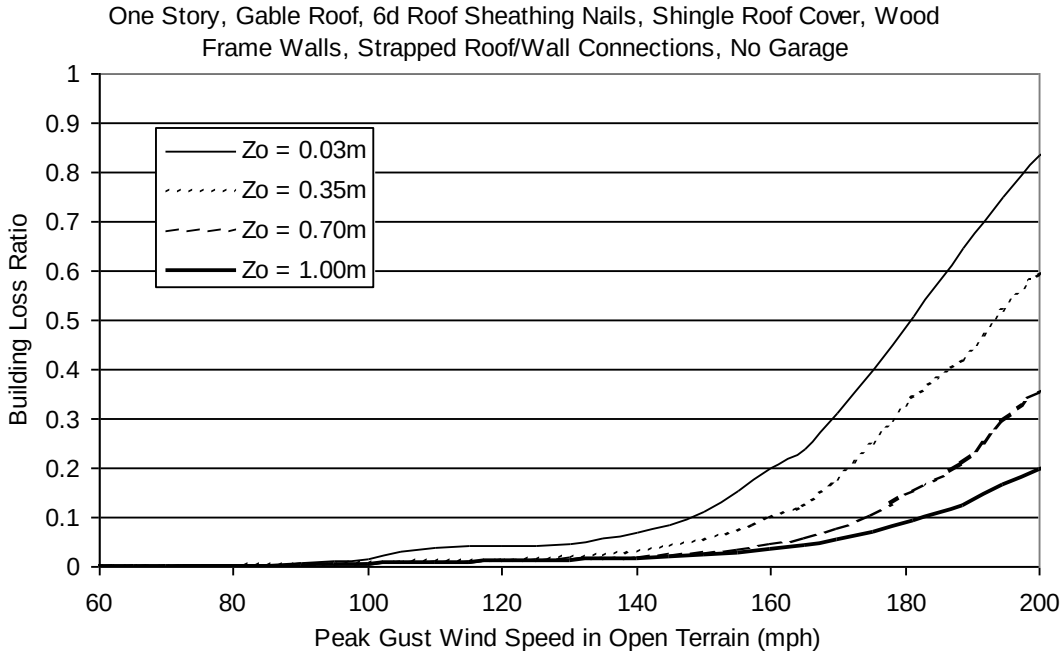

Figure H.162. Building Loss Function for Single Family Residential Building (One Story, 6d Roof Sheathing Nails, Gable Roof, No Garage, Strapped Roof Wall Connections, Wood Frame, Installed Shutters, Upgraded Roof and Added Secondary Water Resistance).

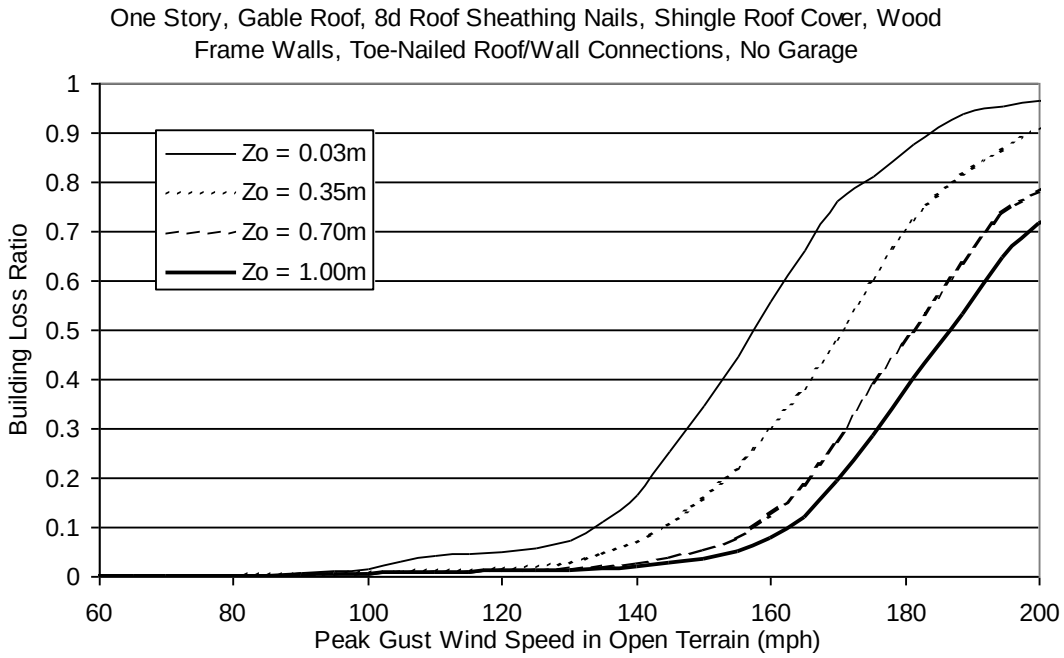

Figure H.163. Building Loss Function for Single Family Residential Building (One Story, 8d Roof Sheathing Nails, Gable Roof, No Garage, Toe-Nailed Roof Wall Connections, Wood Frame, Installed Shutters, Upgraded Roof and Added Secondary Water Resistance).

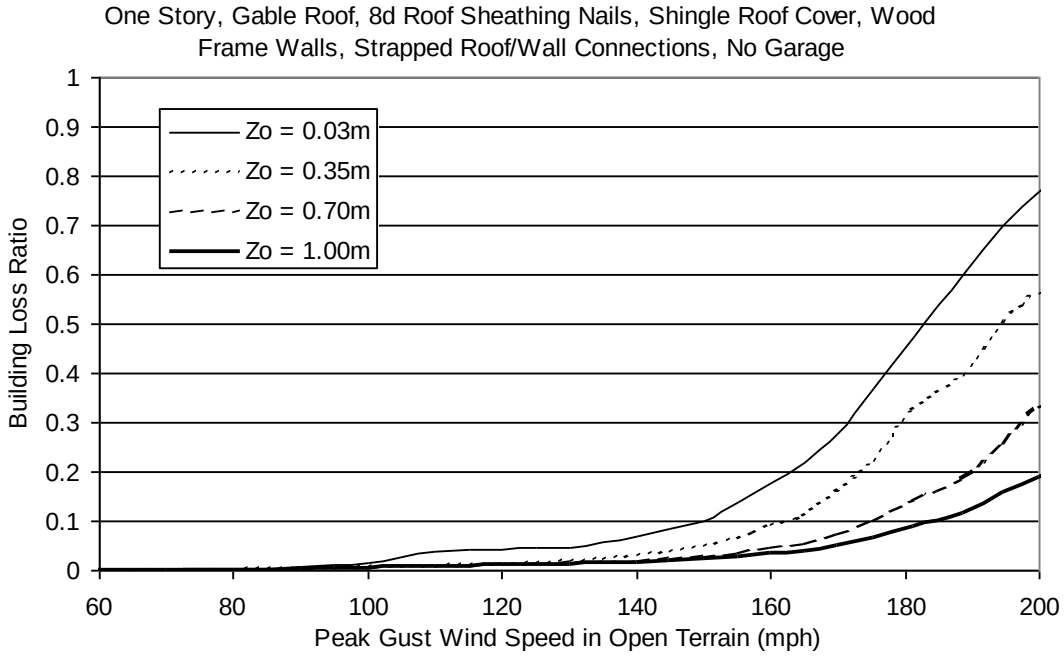

Figure H.164. Building Loss Function for Single Family Residential Building (One Story, 8d Roof Sheathing Nails, Gable Roof, No Garage, Strapped Roof Wall Connections, Wood Frame, Installed Shutters, Upgraded Roof and Added Secondary Water Resistance).

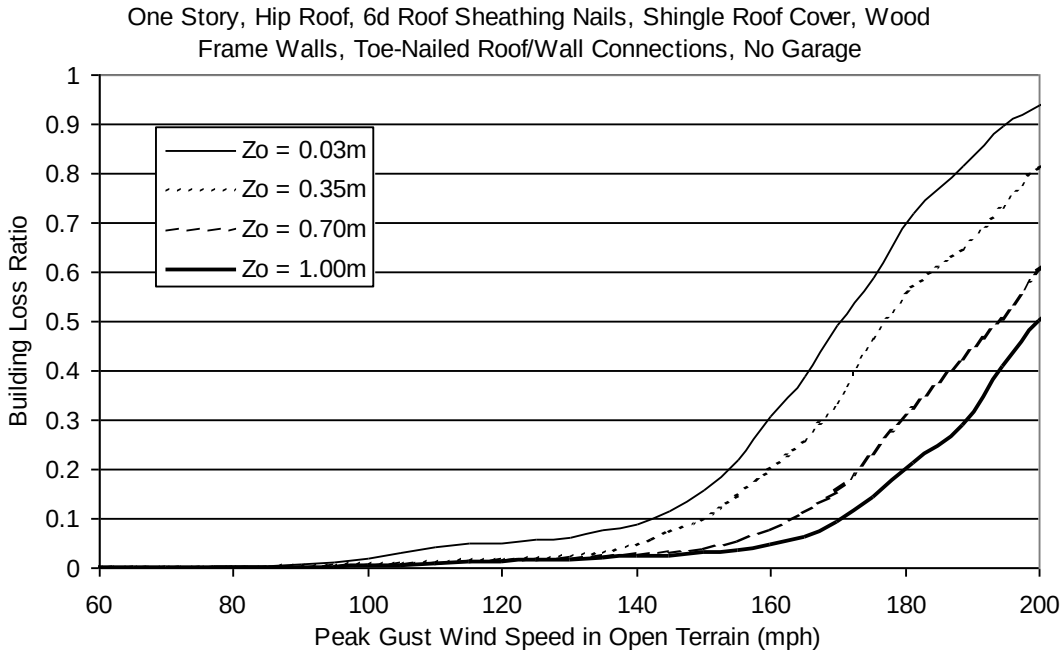

Figure H.165. Building Loss Function for Single Family Residential Building (One Story, 6d Roof Sheathing Nails, Hip Roof, No Garage, Toe-Nailed Roof Wall Connections, Wood Frame, Installed Shutters, Upgraded Roof and Added Secondary Water Resistance).

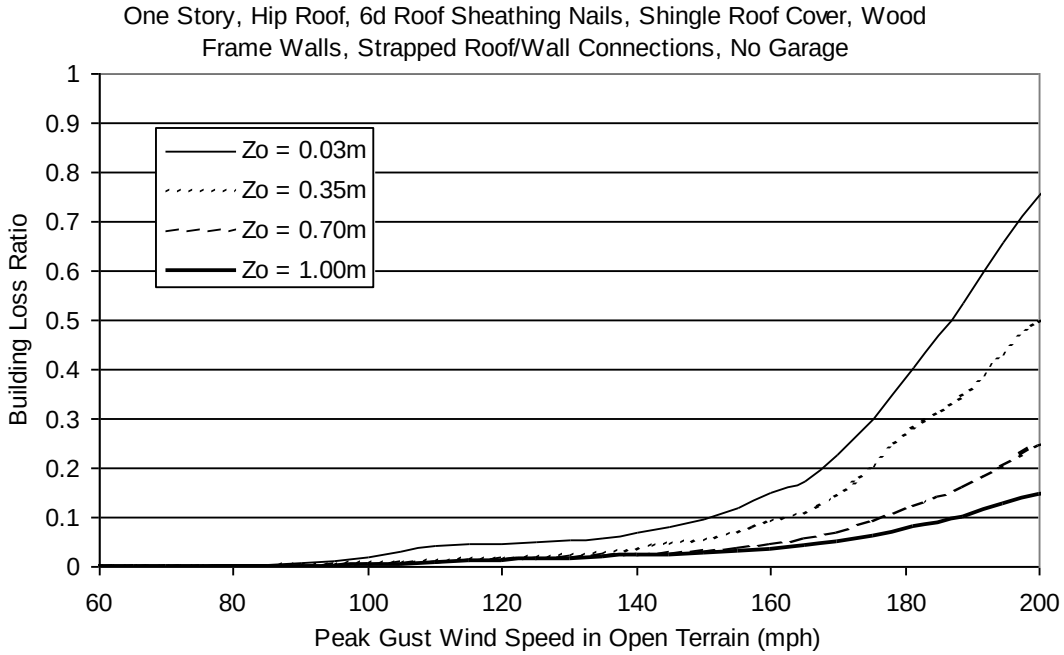

Figure H.166. Building Loss Function for Single Family Residential Building (One Story, 6d Roof Sheathing Nails, Hip Roof, No Garage, Strapped Roof Wall Connections, Wood Frame, Installed Shutters, Upgraded Roof and Added Secondary Water Resistance).

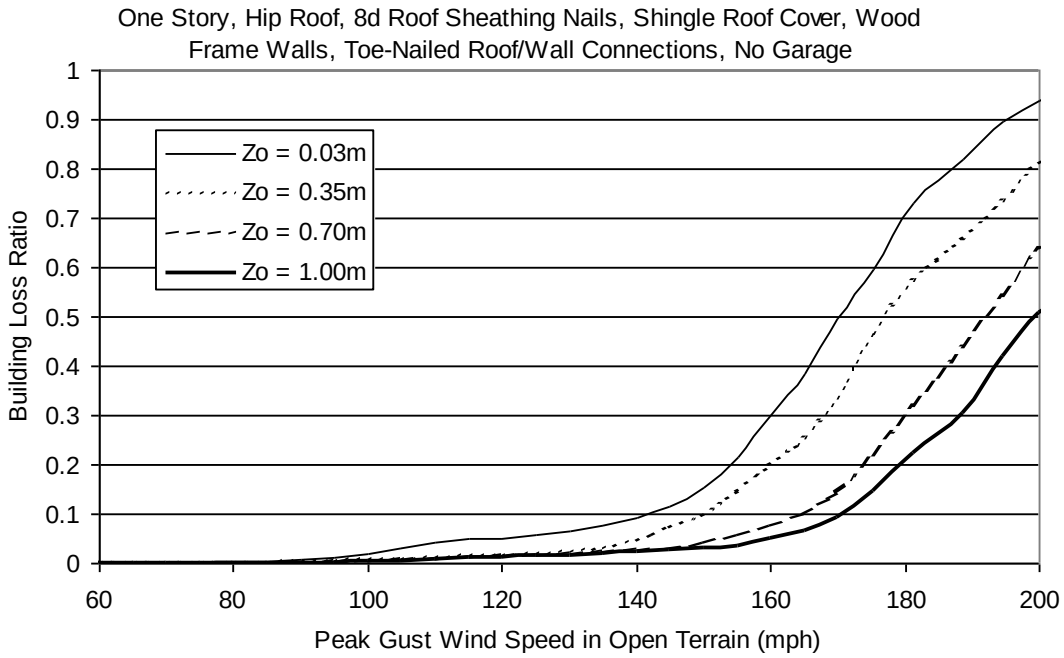

Figure H.167. Building Loss Function for Single Family Residential Building (One Story, 8d Roof Sheathing Nails, Hip Roof, No Garage, Toe-Nailed Roof Wall Connections, Wood Frame, Installed Shutters, Upgraded Roof and Added Secondary Water Resistance).

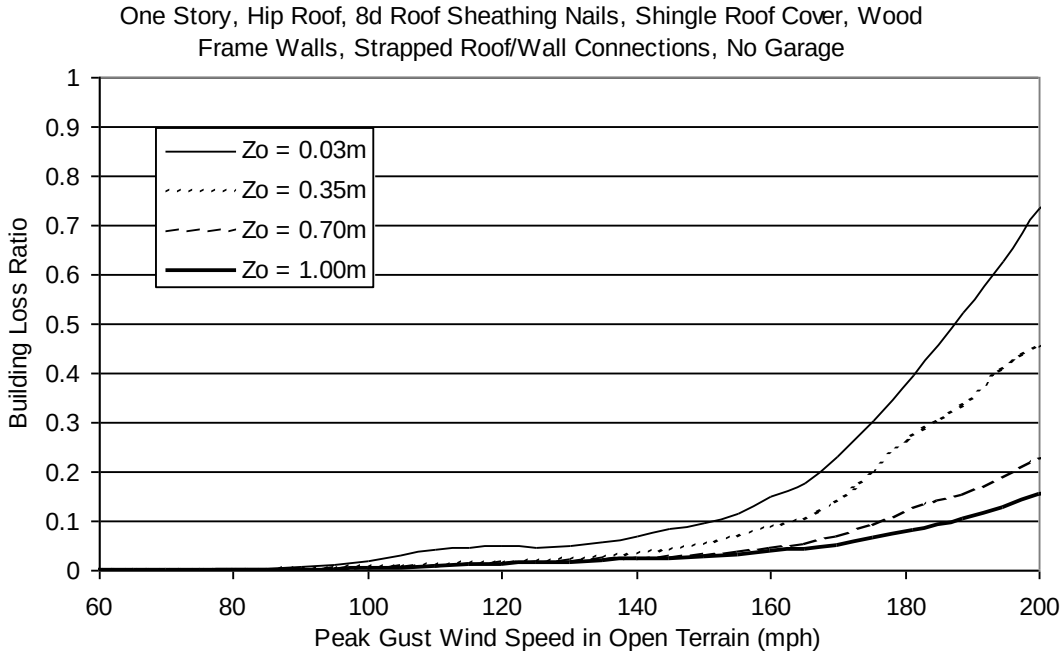

Figure H.168. Building Loss Function for Single Family Residential Building (One Story, 8d Roof Sheathing Nails, Hip Roof, No Garage, Strapped Roof Wall Connections, Wood Frame, Installed Shutters, Upgraded Roof and Added Secondary Water Resistance).

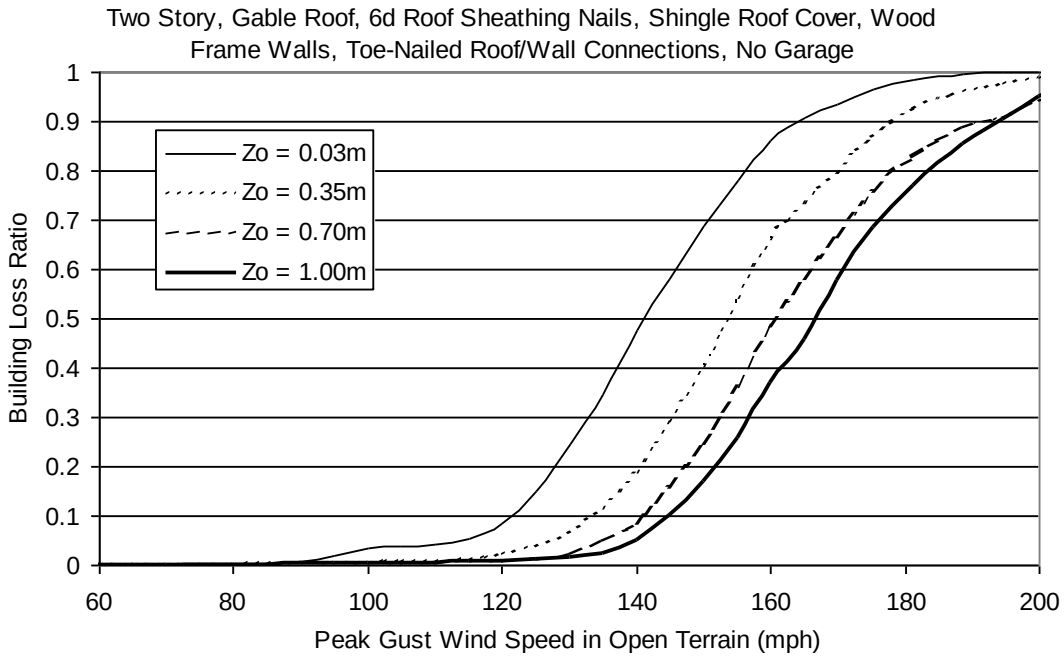

Figure H.169. Building Loss Function for Single Family Residential Building (Two Story, 6d Roof Sheathing Nails, Gable Roof, No Garage, Toe-Nailed Roof Wall Connections, Wood Frame, Installed Shutters, Upgraded Roof and Added Secondary Water Resistance).

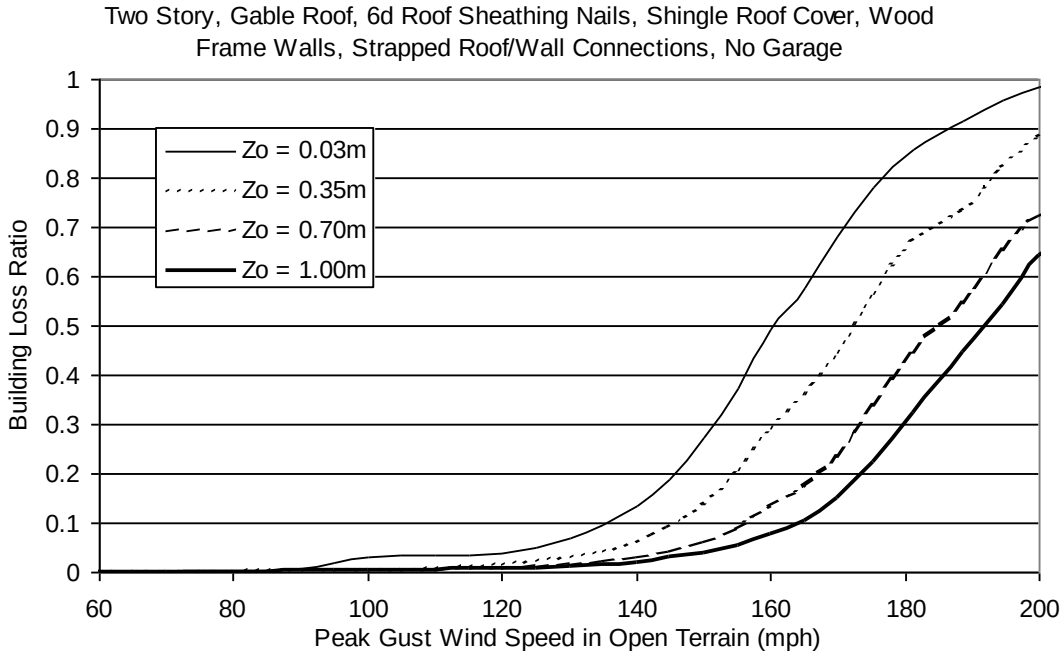

Figure H.170. Building Loss Function for Single Family Residential Building (Two Story, 6d Roof Sheathing Nails, Gable Roof, No Garage, Strapped Roof Wall Connections, Wood Frame, Installed Shutters, Upgraded Roof and Added Secondary Water Resistance).

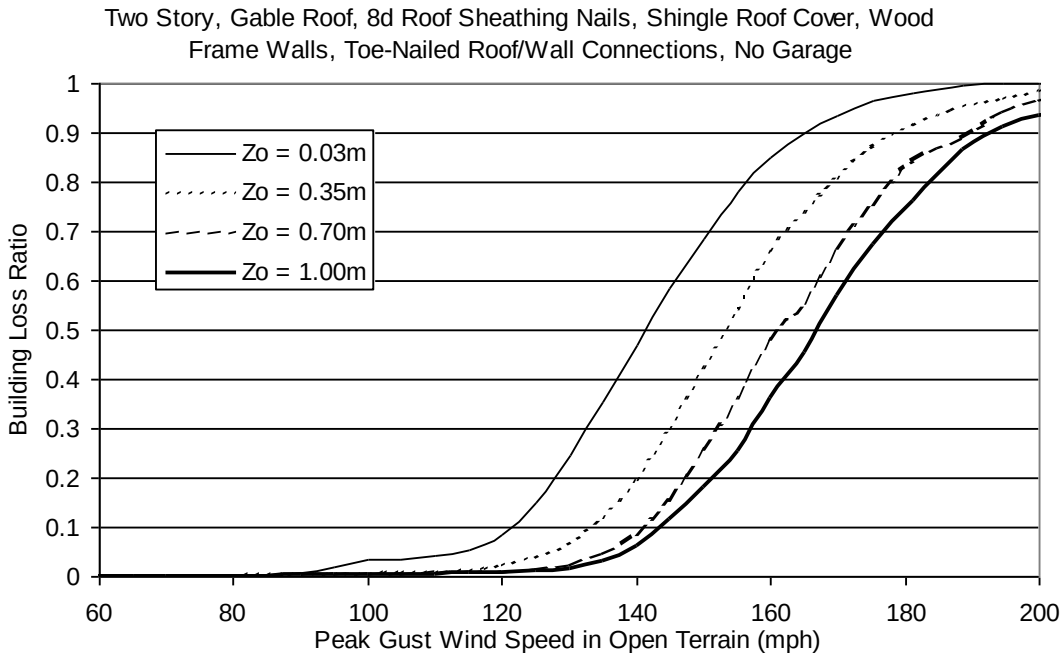

Figure H.171. Building Loss Function for Single Family Residential Building (Two Story, 8d Roof Sheathing Nails, Gable Roof, No Garage, Toe-Nailed Roof Wall Connections, Wood Frame, Installed Shutters, Upgraded Roof and Added Secondary Water Resistance).

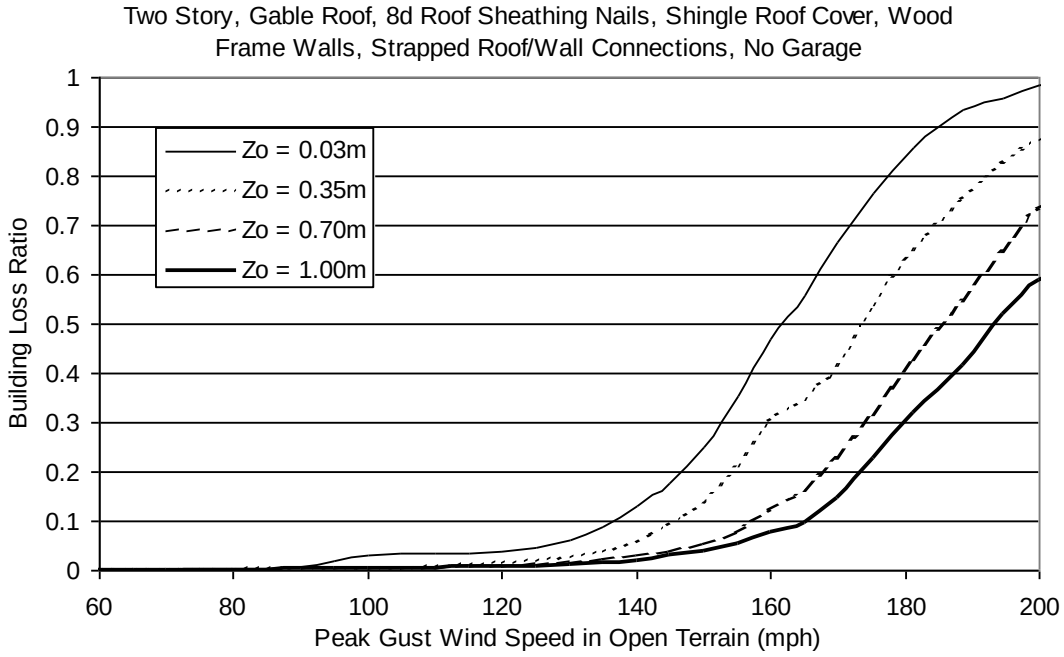

Figure H.172. Building Loss Function for Single Family Residential Building (Two Story, 8d Roof Sheathing Nails, Gable Roof, No Garage, Strapped Roof Wall Connections, Wood Frame, Installed Shutters, Upgraded Roof and Added Secondary Water Resistance).

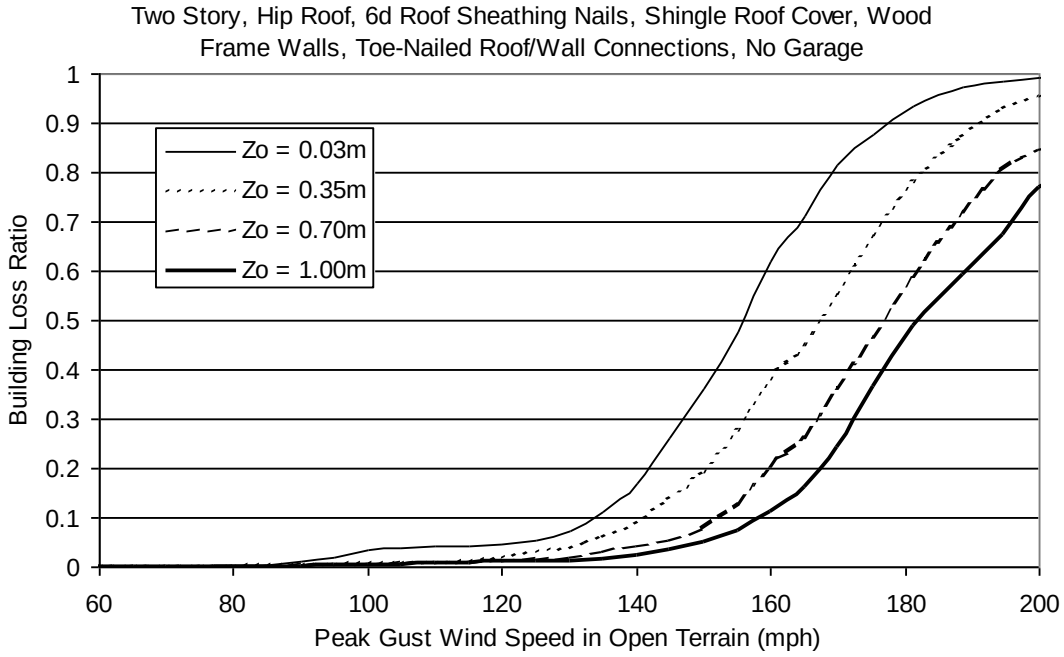

Figure H.173. Building Loss Function for Single Family Residential Building (Two Story, 6d Roof Sheathing Nails, Hip Roof, No Garage, Toe-Nailed Roof Wall Connections, Wood Frame, Installed Shutters, Upgraded Roof and Added Secondary Water Resistance).

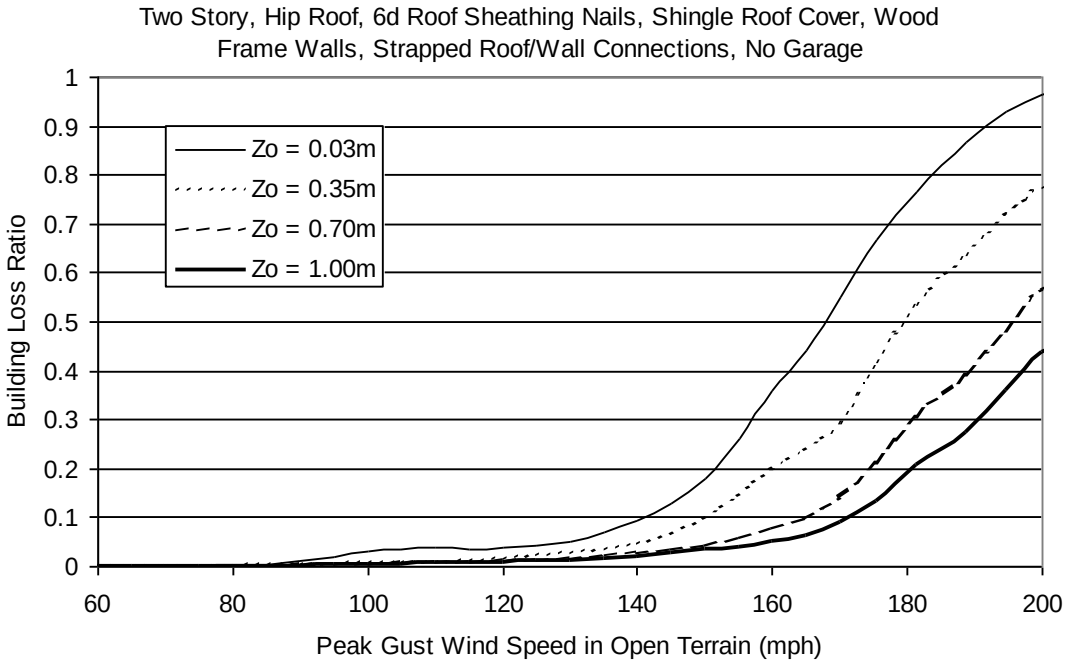

Figure H.174. Building Loss Function for Single Family Residential Building (Two Story, 6d Roof Sheathing Nails, Hip Roof, No Garage, Strapped Roof Wall Connections, Wood Frame, Installed Shutters, Upgraded Roof and Added Secondary Water Resistance).

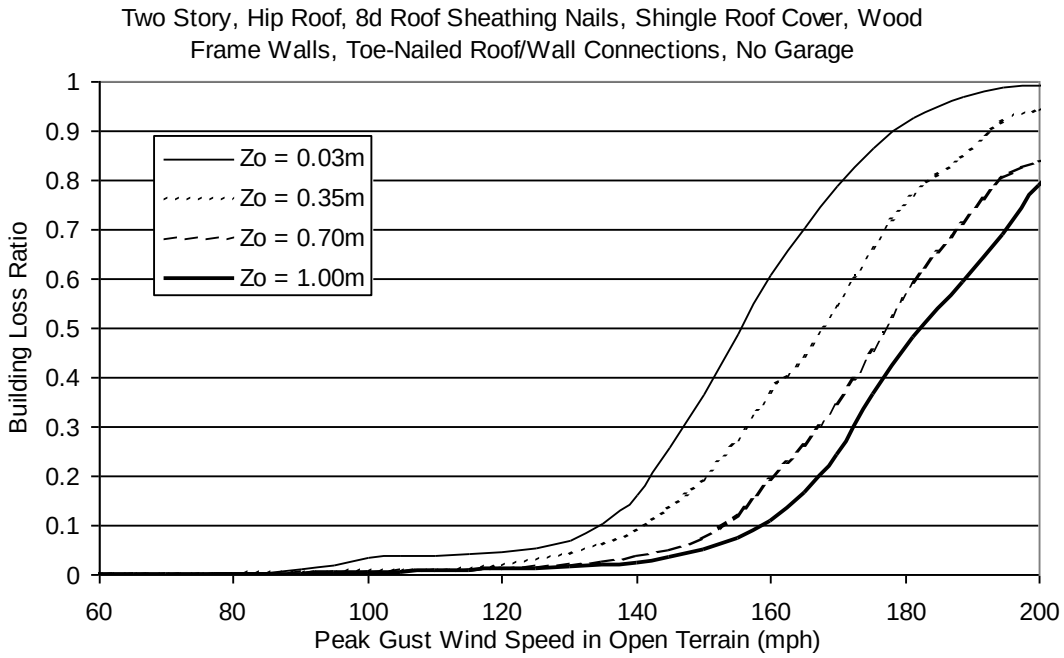

Figure H.175. Building Loss Function for Single Family Residential Building (Two Story, 8d Roof Sheathing Nails, Hip Roof, No Garage, Toe-Nailed Roof Wall Connections, Wood Frame, Installed Shutters, Upgraded Roof and Added Secondary Water Resistance).

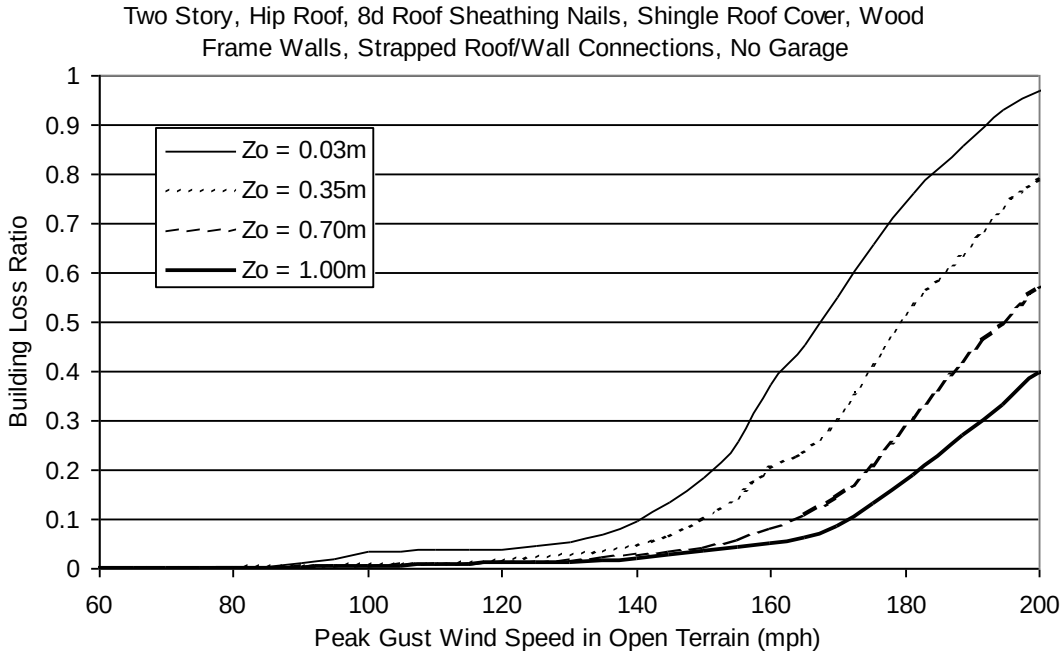

Figure H.176. Building Loss Function for Single Family Residential Building (Two Story, 8d Roof Sheathing Nails, Hip Roof, No Garage, Strapped Roof Wall Connections, Wood Frame, Installed Shutters, Upgraded Roof and Added Secondary Water Resistance).

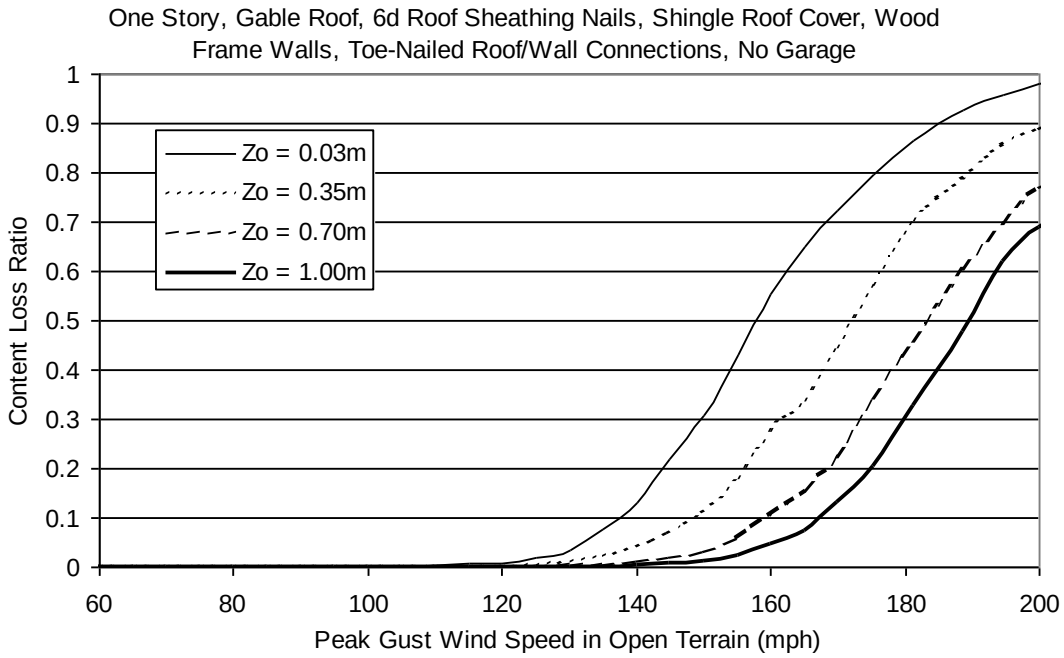

Figure H.177. Content Loss Function for Single Family Residential Building (One Story, 6d Roof Sheathing Nails, Gable Roof, No Garage, Toe-Nailed Roof Wall Connections, Wood Frame, Installed Shutters, Upgraded Roof and Added Secondary Water Resistance).

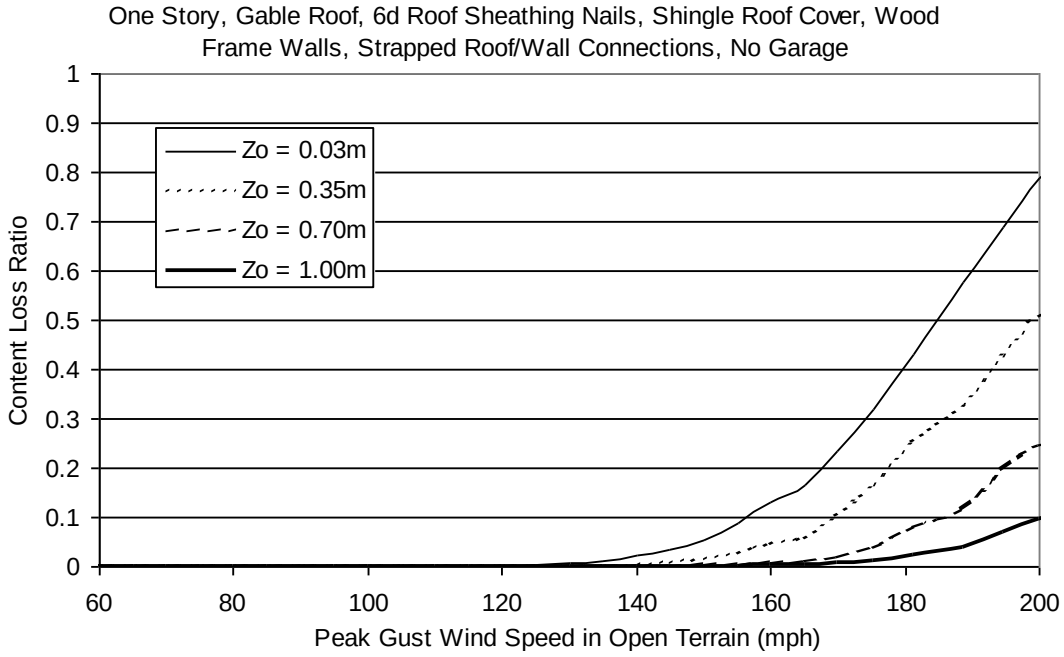

Figure H.178. Content Loss Function for Single Family Residential Building (One Story, 6d Roof Sheathing Nails, Gable Roof, No Garage, Strapped Roof Wall Connections, Wood Frame, Installed Shutters, Upgraded Roof and Added Secondary Water Resistance).

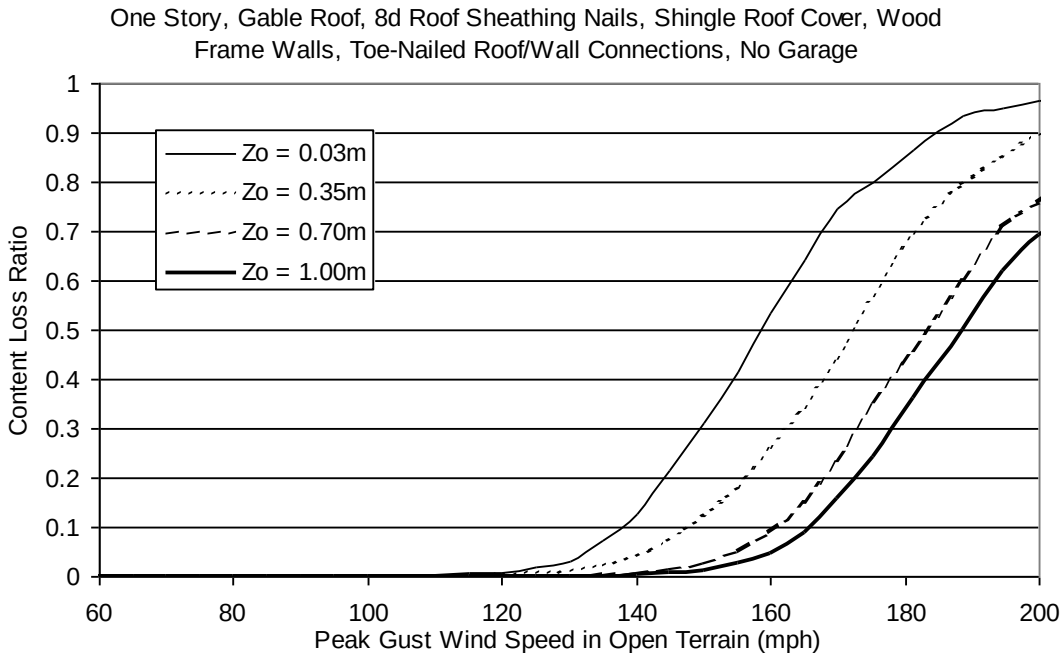

Figure H.179. Content Loss Function for Single Family Residential Building (One Story, 8d Roof Sheathing Nails, Gable Roof, No Garage, Toe-Nailed Roof Wall Connections, Wood Frame, Installed Shutters, Upgraded Roof and Added Secondary Water Resistance).

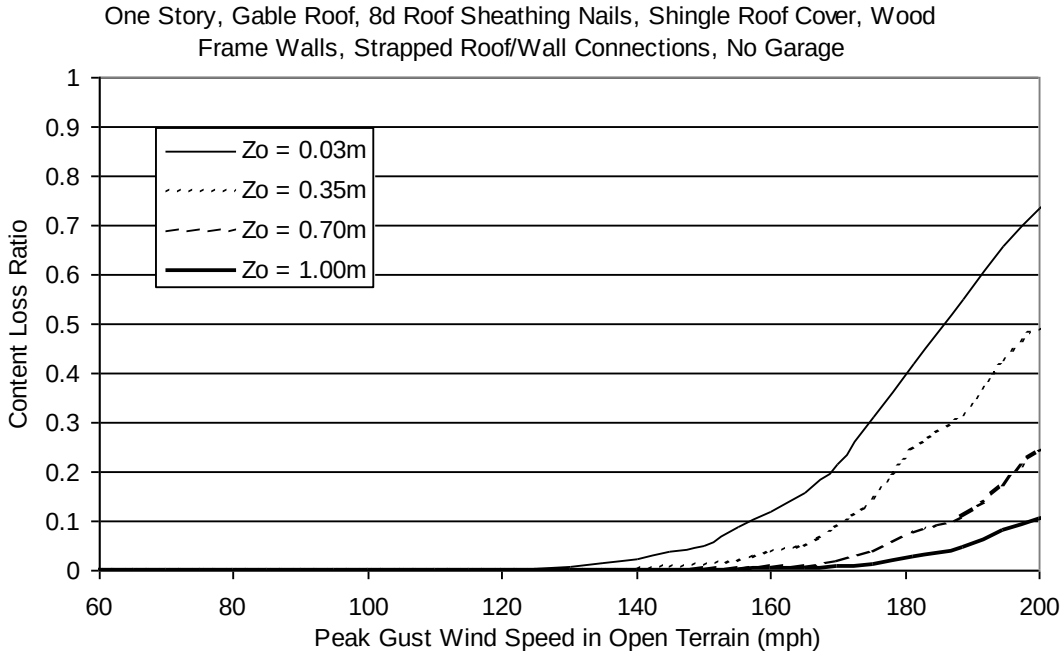

Figure H.180. Content Loss Function for Single Family Residential Building (One Story, 8d Roof Sheathing Nails, Gable Roof, No Garage, Strapped Roof Wall Connections, Wood Frame, Installed Shutters, Upgraded Roof and Added Secondary Water Resistance).

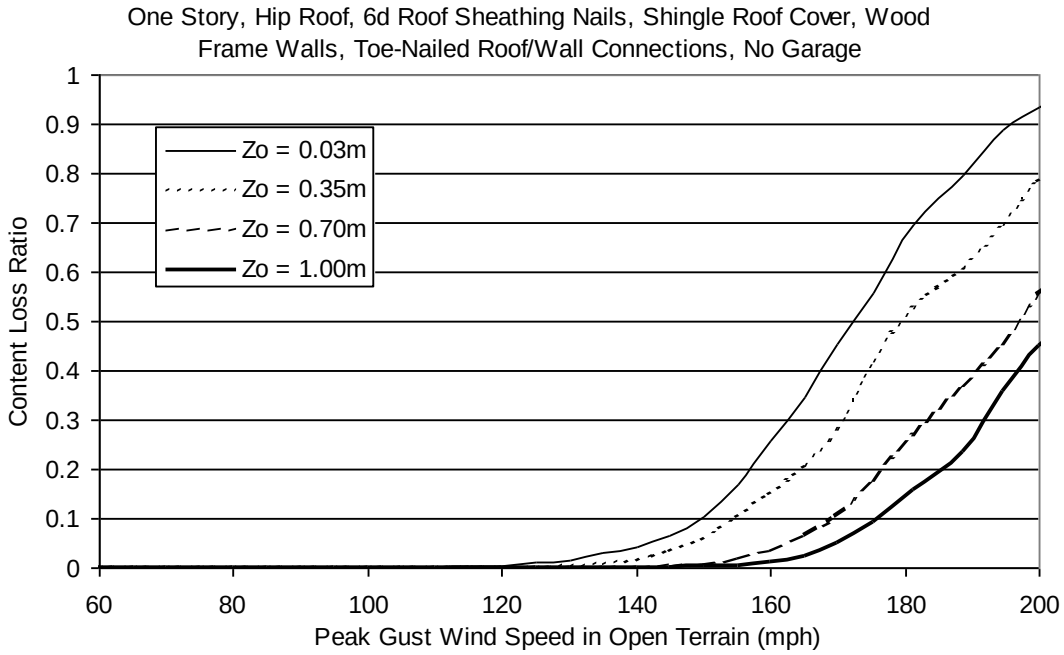

Figure H.181. Content Loss Function for Single Family Residential Building (One Story, 6d Roof Sheathing Nails, Hip Roof, No Garage, Toe-Nailed Roof Wall Connections, Wood Frame, Installed Shutters, Upgraded Roof and Added Secondary Water Resistance).

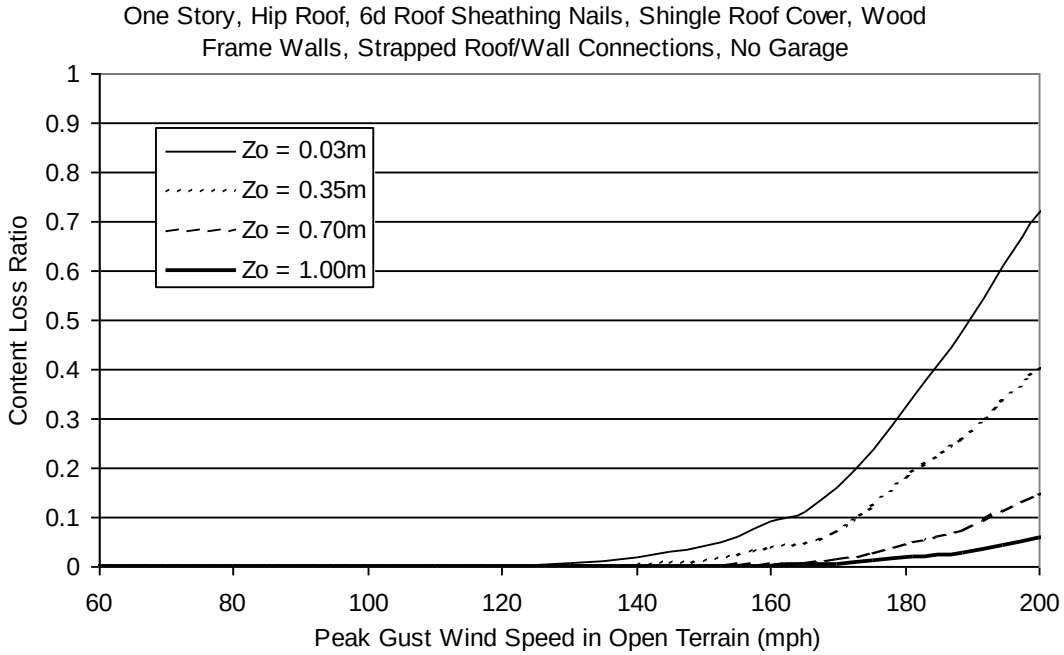

Figure H.182. Content Loss Function for Single Family Residential Building (One Story, 6d Roof Sheathing Nails, Hip Roof, No Garage, Strapped Roof Wall Connections, Wood Frame, Installed Shutters, Upgraded Roof and Added Secondary Water Resistance).

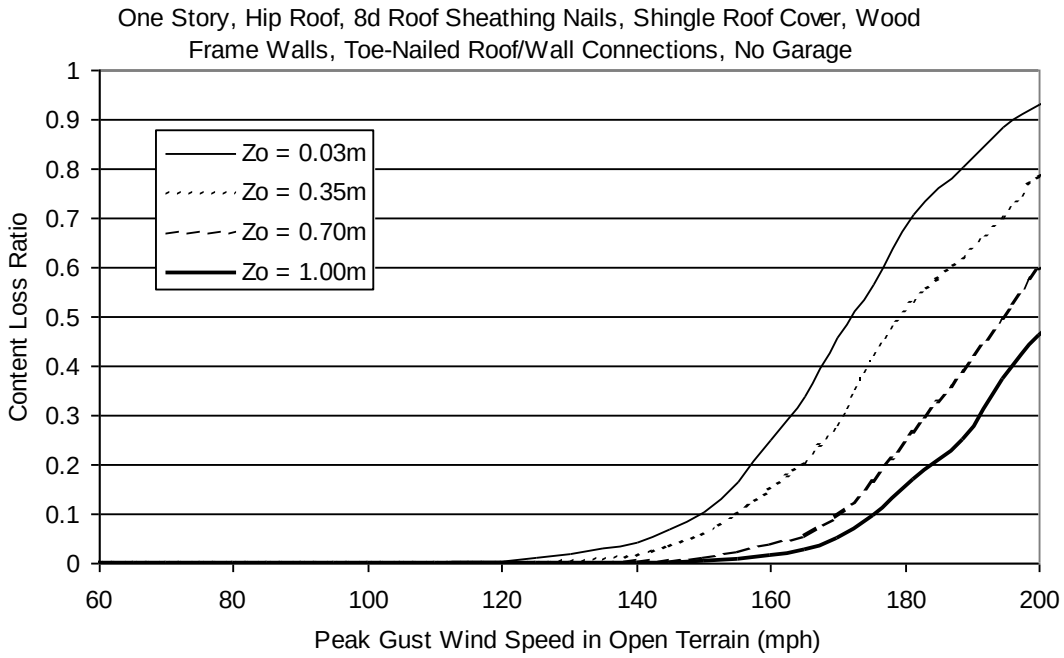

Figure H.183. Content Loss Function for Single Family Residential Building (One Story, 8d Roof Sheathing Nails, Hip Roof, No Garage, Toe-Nailed Roof Wall Connections, Wood Frame, Installed Shutters, Upgraded Roof and Added Secondary Water Resistance).

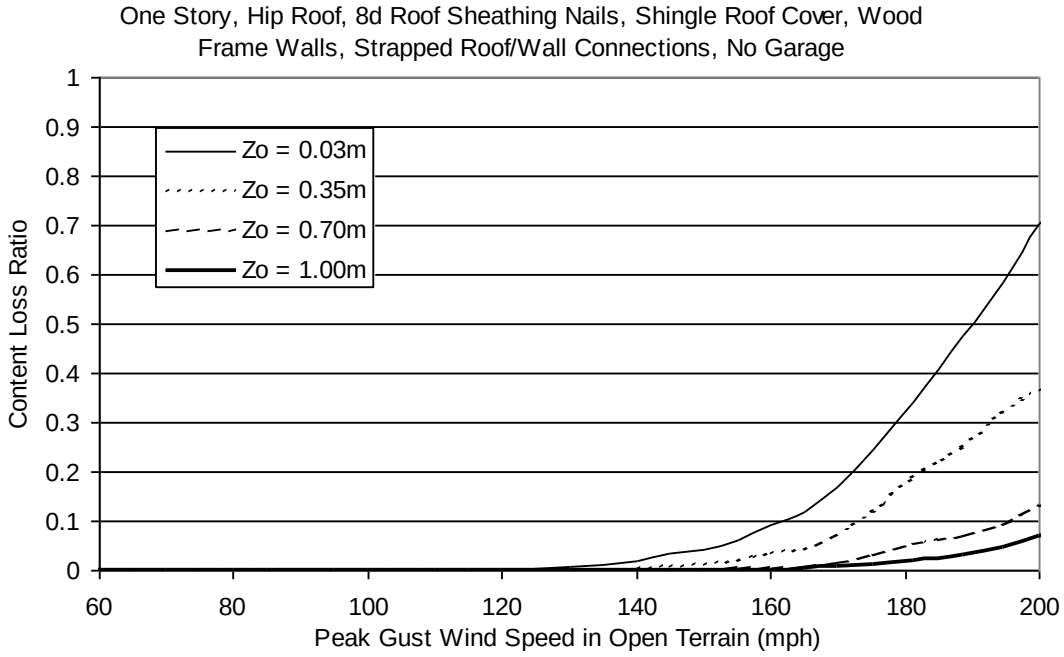

Figure H.184. Content Loss Function for Single Family Residential Building (One Story, 8d Roof Sheathing Nails, Hip Roof, No Garage, Strapped Roof Wall Connections, Wood Frame, Installed Shutters, Upgraded Roof and Added Secondary Water Resistance).

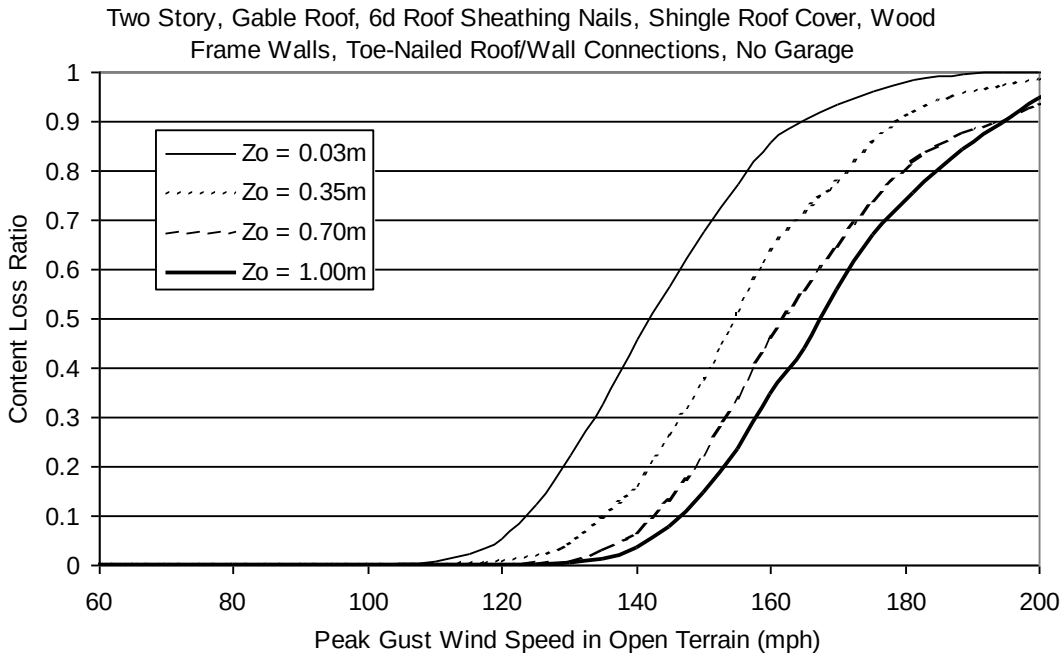

Figure H.185. Content Loss Function for Single Family Residential Building (Two Story, 6d Roof Sheathing Nails, Gable Roof, No Garage, Toe-Nailed Roof Wall Connections, Wood Frame, Installed Shutters, Upgraded Roof and Added Secondary Water Resistance).

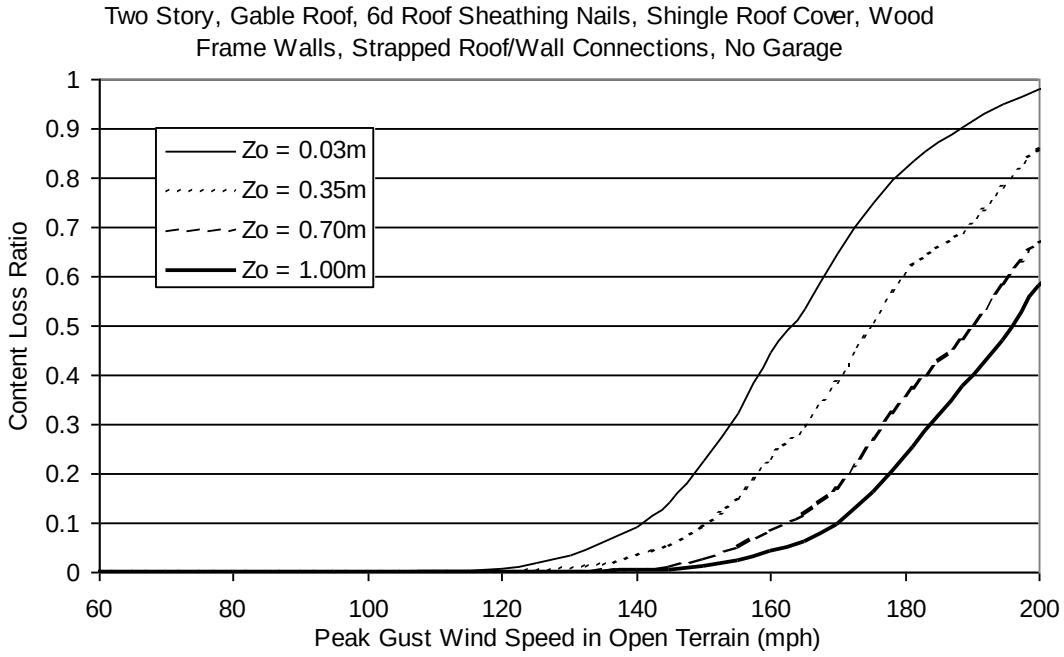

Figure H.186. Content Loss Function for Single Family Residential Building (Two Story, 6d Roof Sheathing Nails, Gable Roof, No Garage, Strapped Roof Wall Connections, Wood Frame, Installed Shutters, Upgraded Roof and Added Secondary Water Resistance).

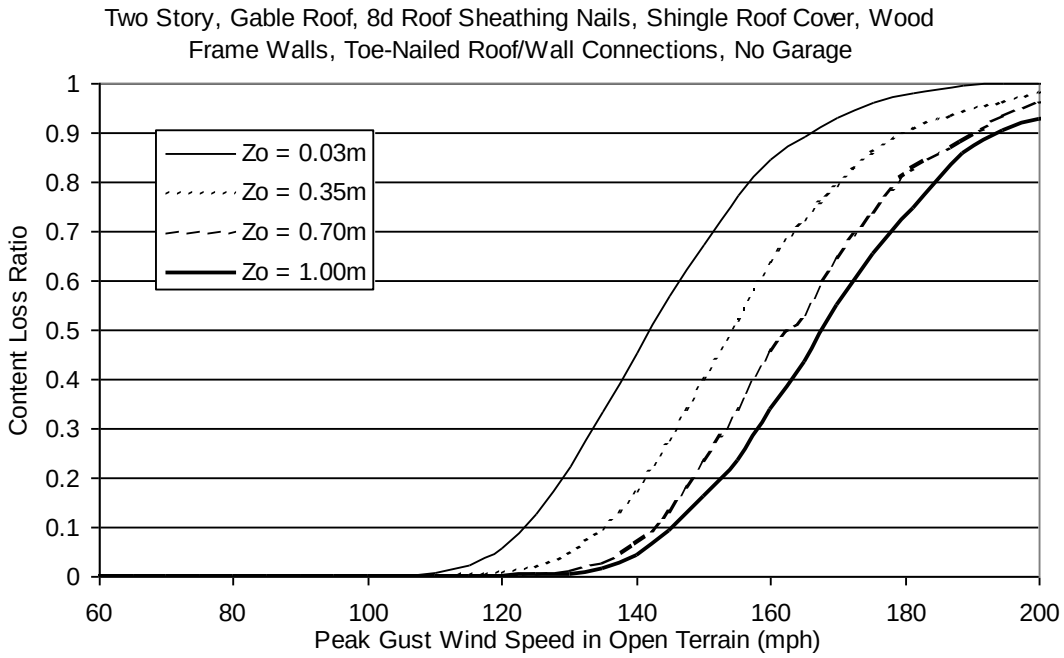

Figure H.187. Content Loss Function for Single Family Residential Building (Two Story, 8d Roof Sheathing Nails, Gable Roof, No Garage, Toe-Nailed Roof Wall Connections, Wood Frame, Installed Shutters, Upgraded Roof and Added Secondary Water Resistance).

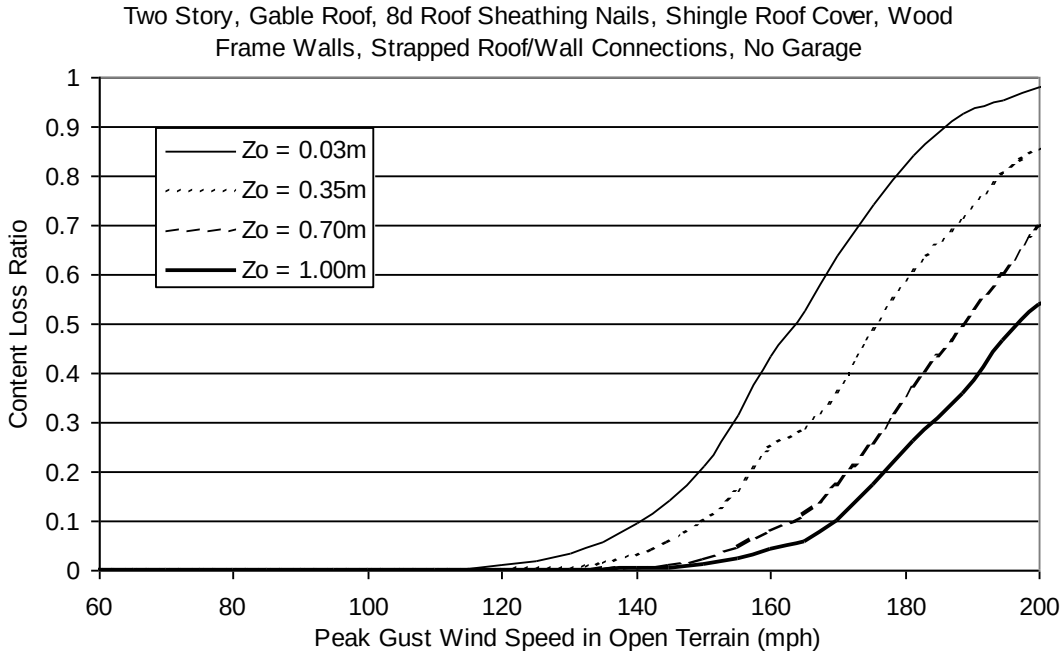

Figure H.188. Content Loss Function for Single Family Residential Building (Two Story, 8d Roof Sheathing Nails, Gable Roof, No Garage, Strapped Roof Wall Connections, Wood Frame, Installed Shutters, Upgraded Roof and Added Secondary Water Resistance).

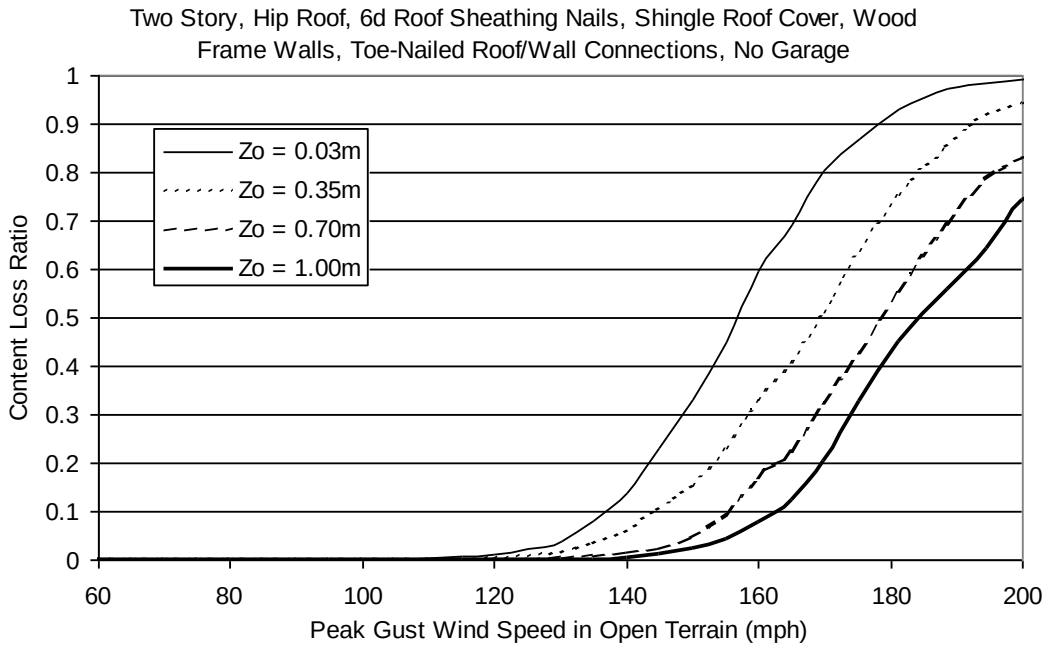

Figure H.189. Content Loss Function for Single Family Residential Building (Two Story, 6d Roof Sheathing Nails, Hip Roof, No Garage, Toe-Nailed Roof Wall Connections, Wood Frame, Installed Shutters, Upgraded Roof and Added Secondary Water Resistance).

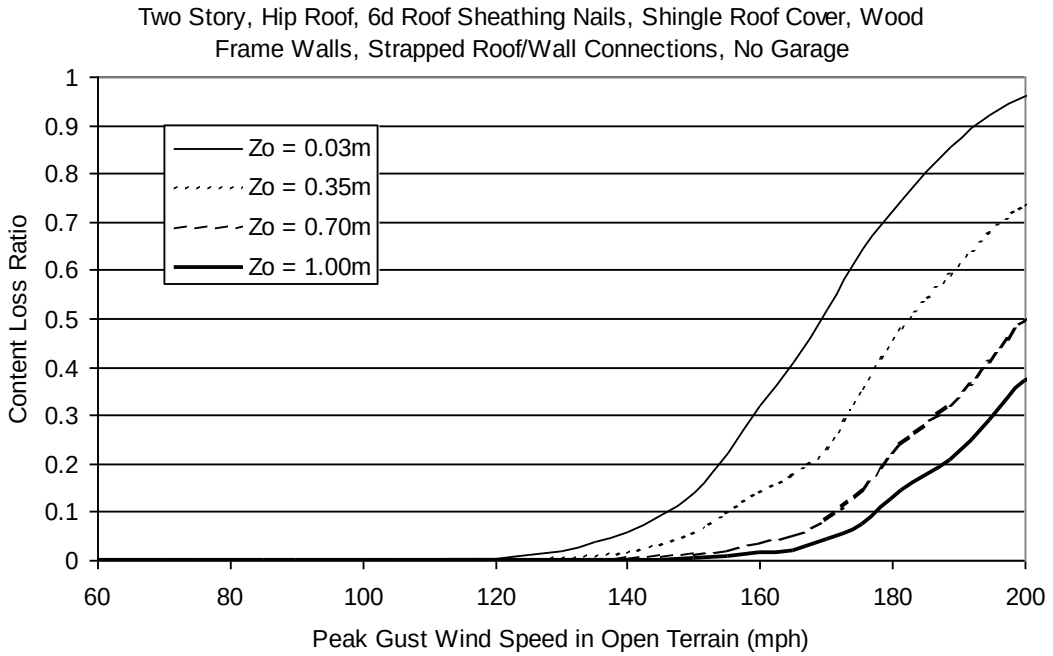

Figure H.190. Content Loss Function for Single Family Residential Building (Two Story, 6d Roof Sheathing Nails, Hip Roof, No Garage, Strapped Roof Wall Connections, Wood Frame, Installed Shutters, Upgraded Roof and Added Secondary Water Resistance).

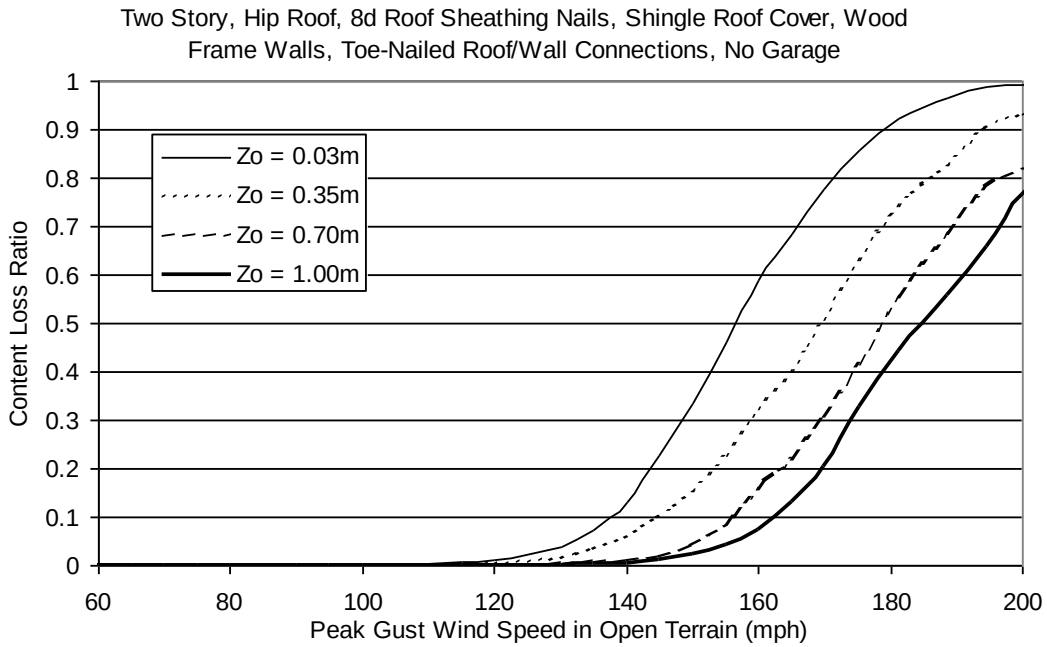

Figure H.191. Content Loss Function for Single Family Residential Building (Two Story, 8d Roof Sheathing Nails, Hip Roof, No Garage, Toe-Nailed Roof Wall Connections, Wood Frame, Installed Shutters, Upgraded Roof and Added Secondary Water Resistance).

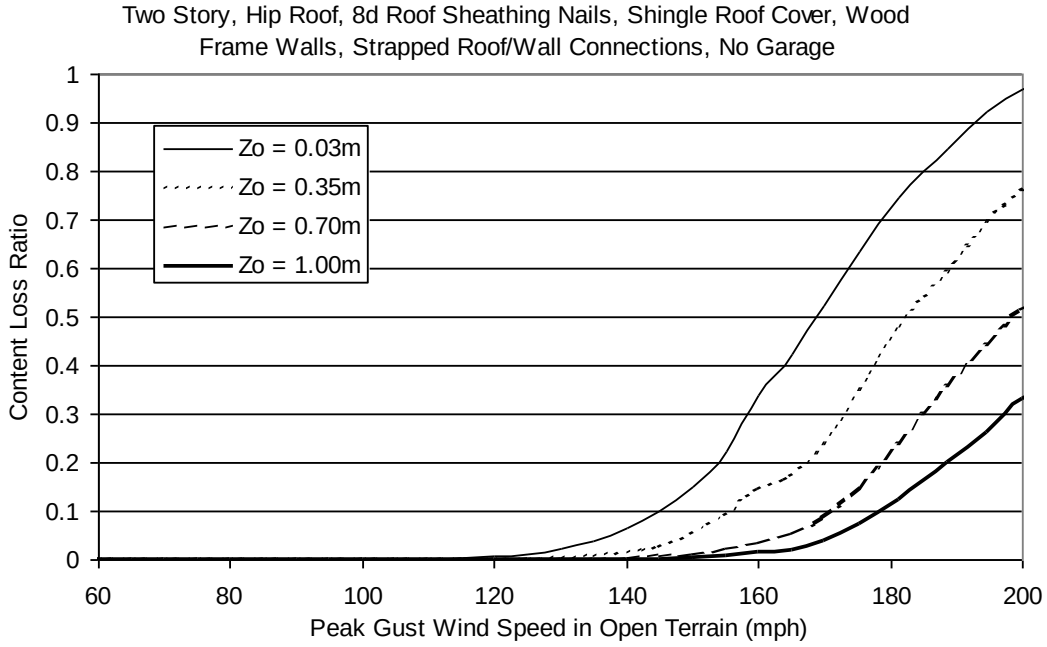

Figure H.192. Content Loss Function for Single Family Residential Building (Two Story, 8d Roof Sheathing Nails, Hip Roof, No Garage, Strapped Roof Wall Connections, Wood Frame, Installed Shutters, Upgraded Roof and Added Secondary Water Resistance)

Appendix I.
Loss Functions for Manufactured Homes

Appendix I.
Loss Functions for Manufactured Homes

This appendix presents loss functions for manufactured homes (see Section 7.8). The loss functions represent either average building loss normalized by building value or average content loss normalized by content value. Therefore, the loss ratios range between 0 and 1 in both cases. Note that the content value is set to 50% of the building value. For a given simulated storm, the building loss ratio and content loss ratio are estimated based on the modeled damage and the largest gust speed over the entire duration of the simulated storm is saved. The loss functions are then computed by averaging the loss ratios associated with the storms producing a maximum gust speed within 5 mph ranges. The average loss ratios (content or building loss) associated with each 5 mph gust speed range are then plotted at the center of that range. Note that the wind speeds are representative of open terrain at 10 m above ground.

Table I.1 lists the figures provided in this appendix.

Table I.1. Loss Functions for Manufactured Homes

Figure	Loss Type
I.1	Building
I.2	Content

1994 HUD – Wind Zone III, Tied Down

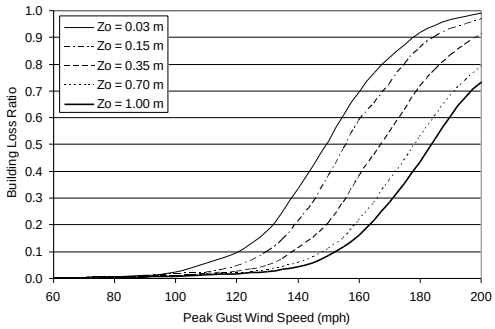

1994 HUD – Wind Zone II, Tied Down

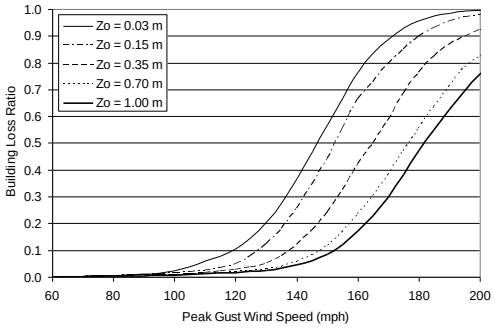

1994 HUD – Wind Zone II, Tied Down

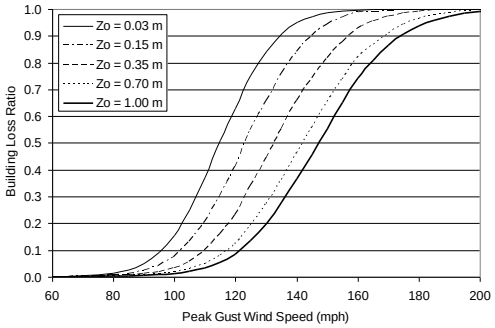

HUD, Tied Down

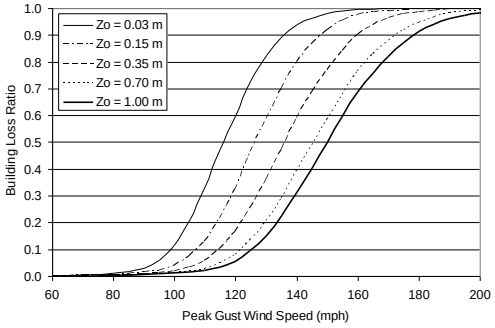

HUD, Not Tied Down

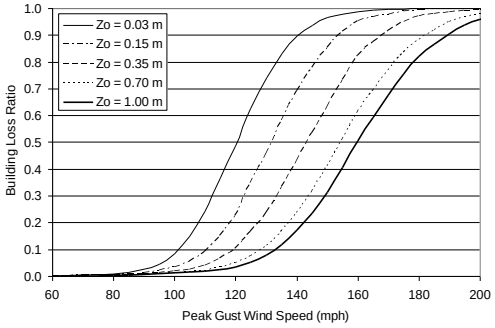

Pre-HUD, Tied Down

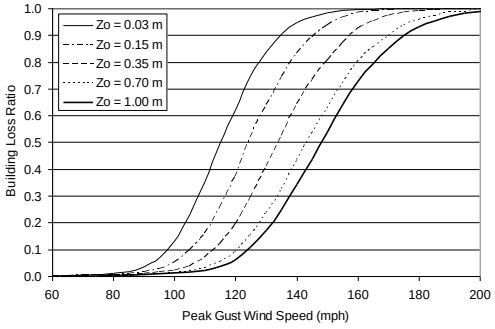

Pre-HUD, Not Tied Down

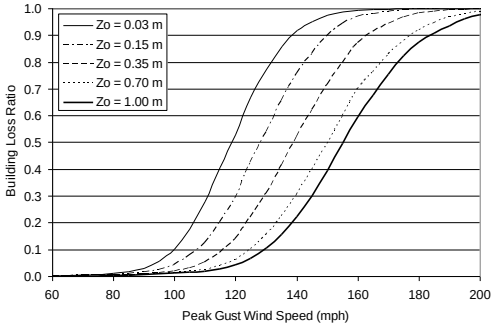

Figure I.1. Building Loss Functions for Manufactured Homes.

1994 HUD – Wind Zone III, Tied Down

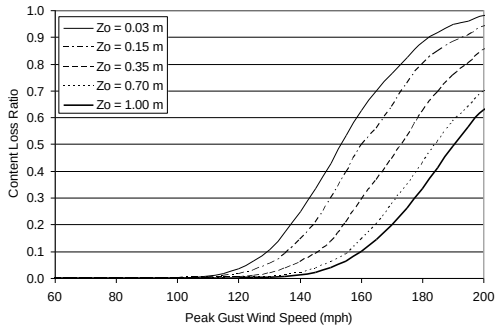

1994 HUD – Wind Zone II, Tied Down

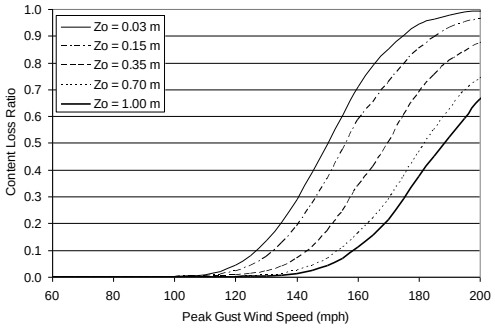

1994 HUD – Wind Zone II, Tied Down

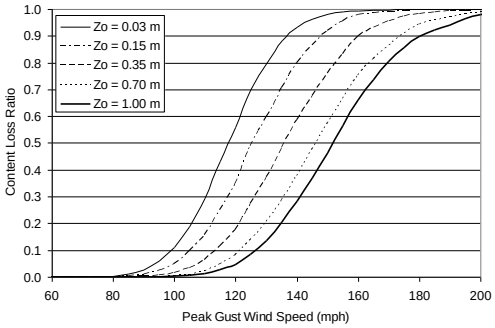

HUD, Tied Down

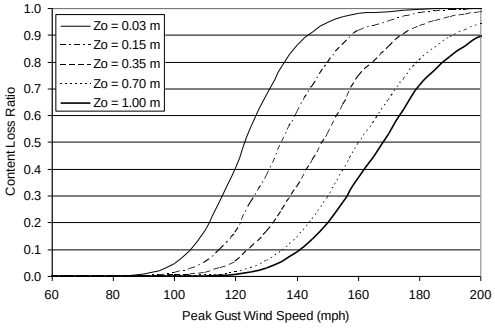

HUD, Not Tied Down

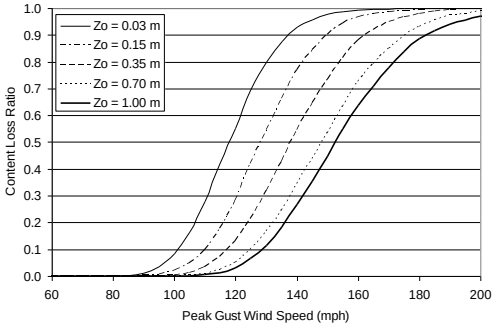

Pre-HUD, Tied Down

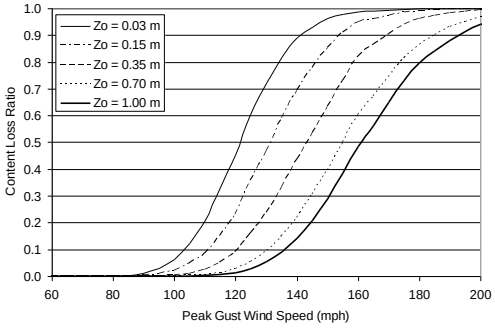

Pre-HUD, Not Tied Down

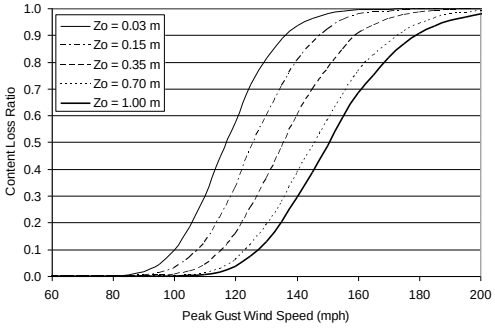

Figure I.2. Content Loss Functions for Manufactured Homes.

Appendix J.
Loss Functions for Marginally- or Non-Engineered Hotel/Motel and Multi-Family Residential Buildings

Appendix J.
Loss Functions for Marginally- or Non-Engineered Hotel/Motel and Multi-Family Residential Buildings

This appendix presents loss functions for marginally-engineered hotel/motel and multi-family residential buildings (see Section 7.10). The loss functions represent either average building loss normalized by building value or average content loss normalized by content value. Therefore, the loss ratios range between 0 and 1 in both cases. Note that the content value is set to 50% of the building value. For a given simulated storm, the building loss ratio and content loss ratio are estimated based on the modeled damage and the largest gust speed over the entire duration of the simulated storm is saved. The loss functions are then computed by averaging the loss ratios associated with the storms producing a maximum gust speed within 5mph ranges. The average loss ratios (content or building loss) associated with each 5 mph gust speed range are then plotted at the center of that range. Note that the wind speeds are representative of open terrain at 10 m above ground.

Table J.1 lists the figures provided in this appendix. Two sets of thirteen figures are shown. The first set of thirteen figures (Figures J.1 through J.13) show building loss ratios and the second set (Figures J.14 through J.26) shown content loss ratios. The first figure in each set of thirteen shows loss results for a one-story building with 8d roof sheathing nails, strapped roof-wall connections, wood frame walls and a gable roof with shingles. The remaining twelve plots in each set show loss results for buildings which are different by a single variable in comparison to the reference building (note that the changed variable is underlined in the figure titles).

Table J.1. Sample Loss Functions for Marginally-Engineered or Non-Engineered Hotel/Motel and Multi-Family Residential Buildings

Figure	Loss Type	Walls	Stories	Sheathing	Roof/ Wall	Roof Shape	Roof Cover
J.1	Building	WFR	1	8d	Strap	Gable	Shingles
J.2	Building	WFR	1	8d	Strap	**Hip**	Shingles
J.3	Building	WFR	1	8d	Strap	**Flat**	**BUR, Average**
J.4	Building	WFR	1	8d	Strap	**Flat**	**BUR, Poor**
J.5	Building	WFR	1	8d	Strap	**Flat**	**EPDM, Average**
J.6	Building	WFR	1	8d	Strap	**Flat**	**EPDM, Poor**
J.7	Building	WFR	1	**6d**	Strap	Gable	Shingles
J.8	Building	WFR	1	8d	**Toe-Nail**	Gable	Shingles
J.9	Building	**URM**	1	8d	Strap	Gable	Shingles
J.10	Building	**RM**	1	8d	Strap	Gable	Shingles
J.11	Building	WFR	**2**	8d	Strap	Gable	Shingles
J.12	Building	WFR	**3**	8d	Strap	Gable	Shingles
J.13	Building	WFR	**4**	8d	Strap	Gable	Shingles

Table J.1. Sample Loss Functions for Marginally-Engineered or Non-Engineered Hotel/Motel and Multi-Family Residential Buildings (concluded)

Figure	Loss Type	Walls	Stories	Sheathing	Roof/ Wall	Roof Shape	Roof Cover
J.14	**Content**	WFR	1	8d	Strap	Gable	Shingles
J.15	Content	WFR	1	8d	Strap	**Hip**	Shingles
J.16	Content	WFR	1	8d	Strap	**Flat**	**BUR, Average**
J.17	Content	WFR	1	8d	Strap	**Flat**	**BUR, Poor**
J.18	Content	WFR	1	8d	Strap	**Flat**	**EPDM, Average**
J.19	Content	WFR	1	8d	Strap	**Flat**	**EPDM, Poor**
J.20	Content	WFR	1	**6d**	Strap	Gable	Shingles
J.21	Content	WFR	1	8d	**Toe-Nail**	Gable	Shingles
J.22	Content	**URM**	1	8d	Strap	Gable	Shingles
J.23	Content	**RM**	1	8d	Strap	Gable	Shingles
J.24	Content	WFR	**2**	8d	Strap	Gable	Shingles
J.25	Content	WFR	**3**	8d	Strap	Gable	Shingles
J.26	Content	WFR	**4**	8d	Strap	Gable	Shingles

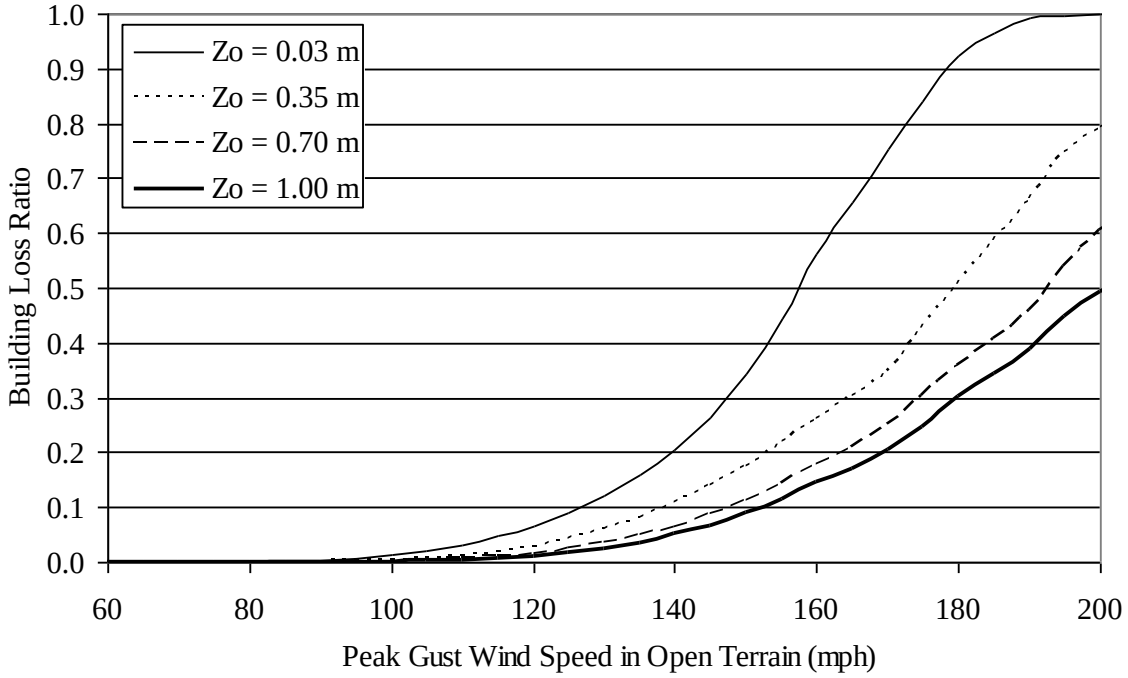

Figure J.1. Building Loss Function – One-Story, 8d Roof Deck Nails, Strapped Roof Trusses, Wood Frame Walls, Gable Roof with Shingles.

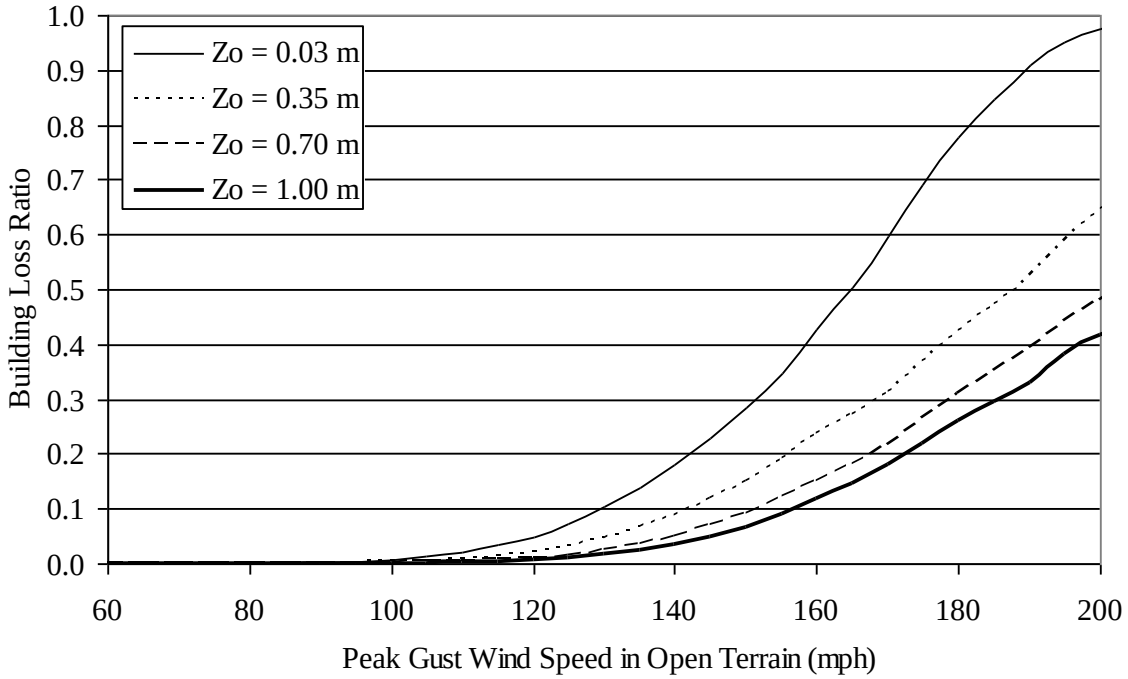

Figure J.2. Building Loss Function – One-Story, 8d Roof Deck Nails, Strapped Roof Trusses, Wood Frame Walls, Hip Roof with Shingles.

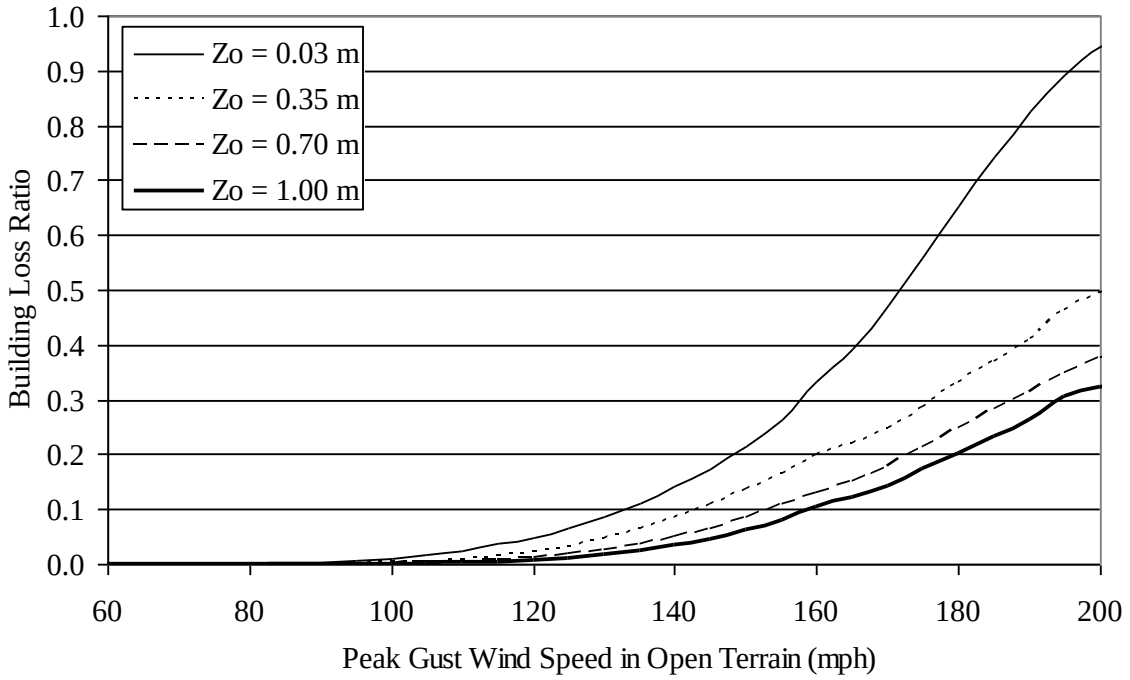

Figure J.3. Building Loss Function – One-Story, 8d Roof Deck Nails, Strapped Roof Trusses, Wood Frame Walls, Flat Roof with Average Quality BUR.

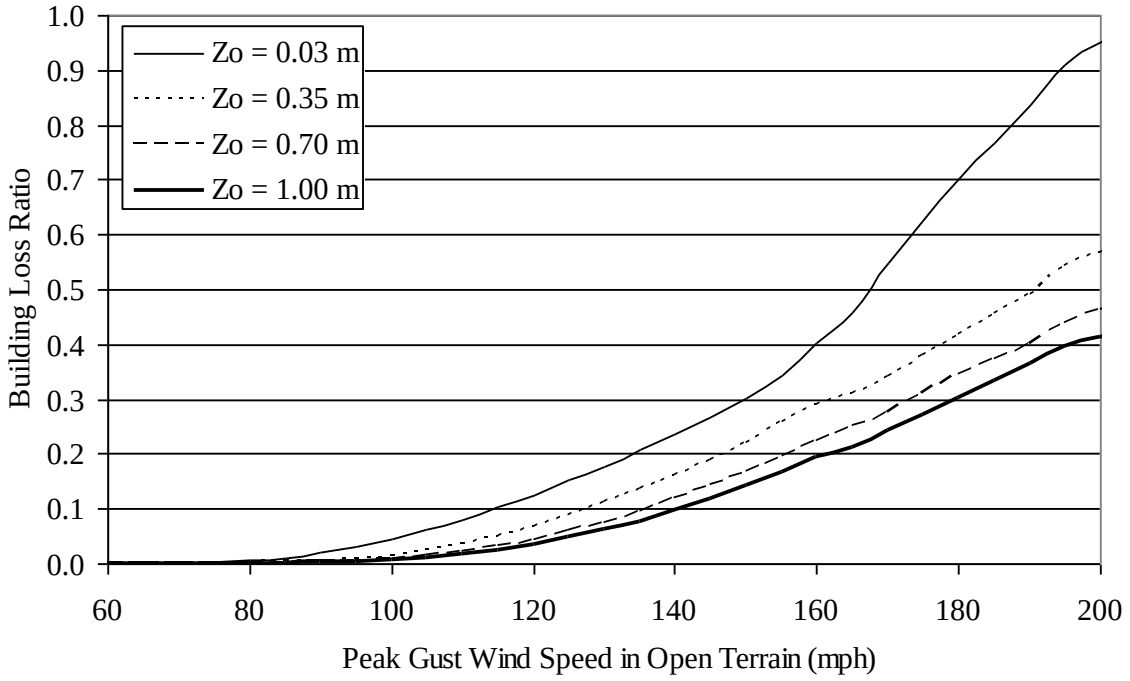

Figure J.4. Building Loss Function – One-Story, 8d Roof Deck Nails, Strapped Roof Trusses, Wood Frame Walls, Flat Roof with Poor Quality BUR.

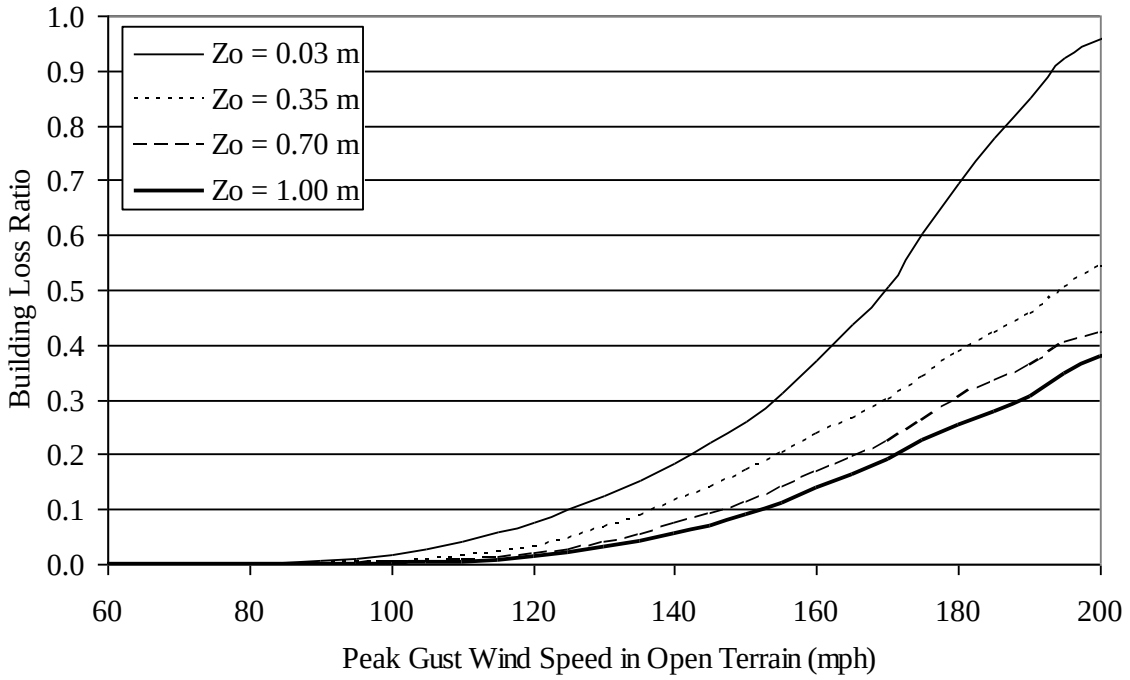

Figure J.5. Building Loss Function – One-Story, 8d Roof Deck Nails, Strapped Roof Trusses, Wood Frame Walls, Flat Roof with Average Quality EPDM.

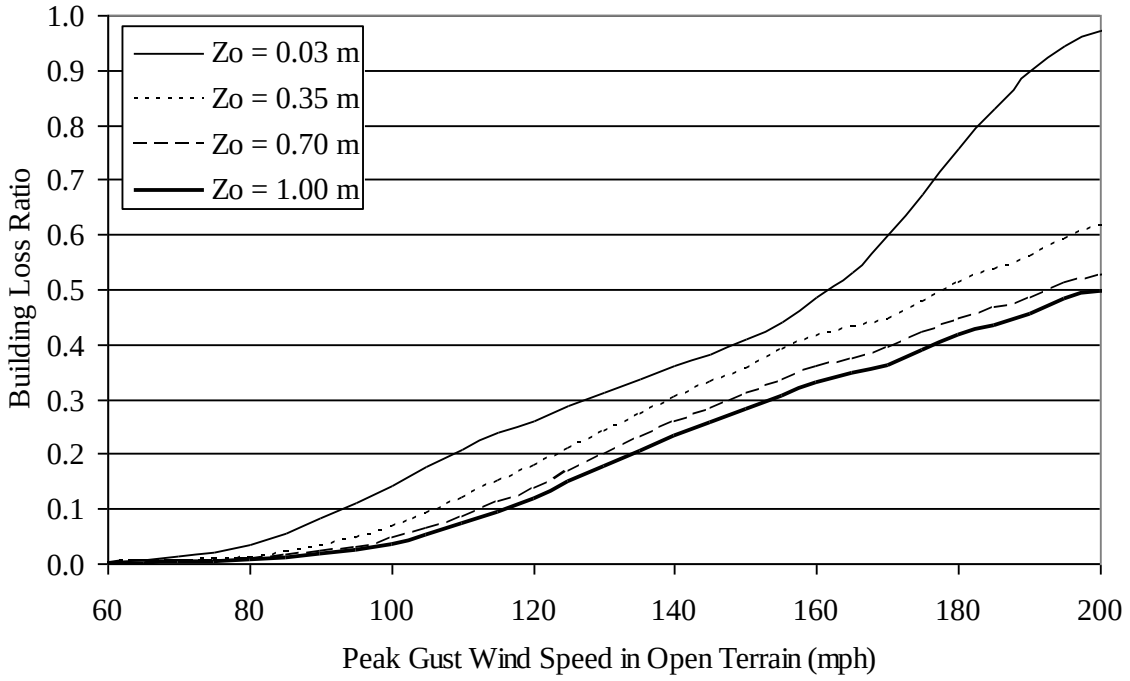

Figure J.6. Building Loss Function – One-Story, 8d Roof Deck Nails, Strapped Roof Trusses, Wood Frame Walls, Flat Roof with Poor Quality EPDM.

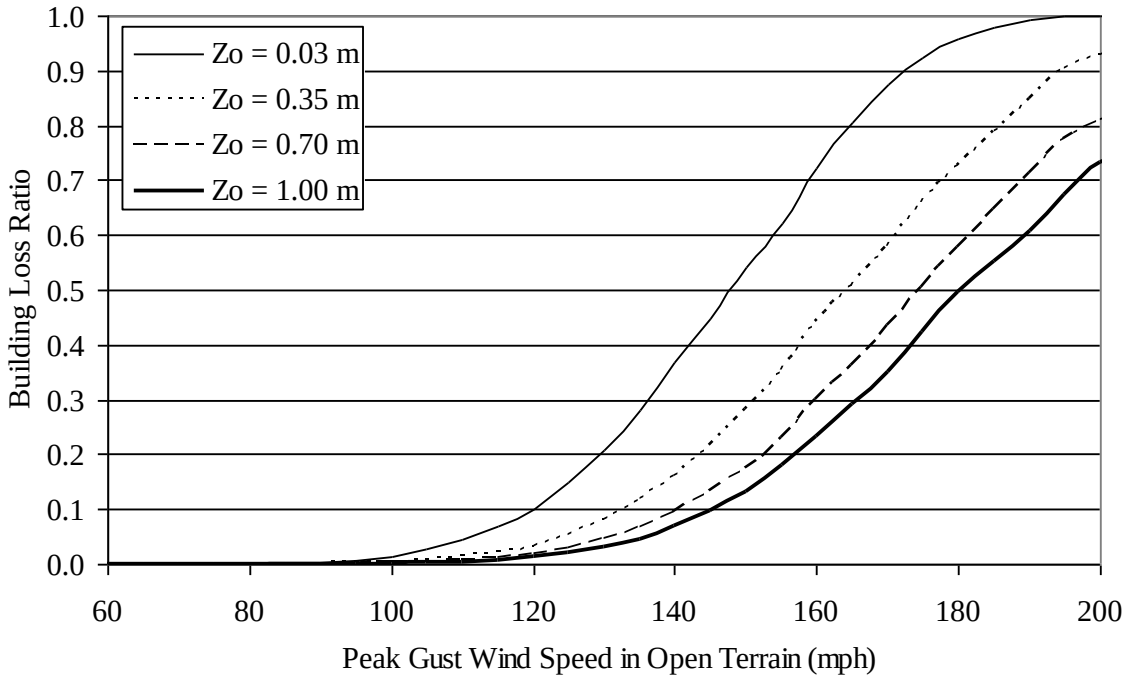

Figure J.7. Building Loss Function – One-Story, 6d Roof Deck Nails, Strapped Roof Trusses, Wood Frame Walls, Gable Roof with Shingles.

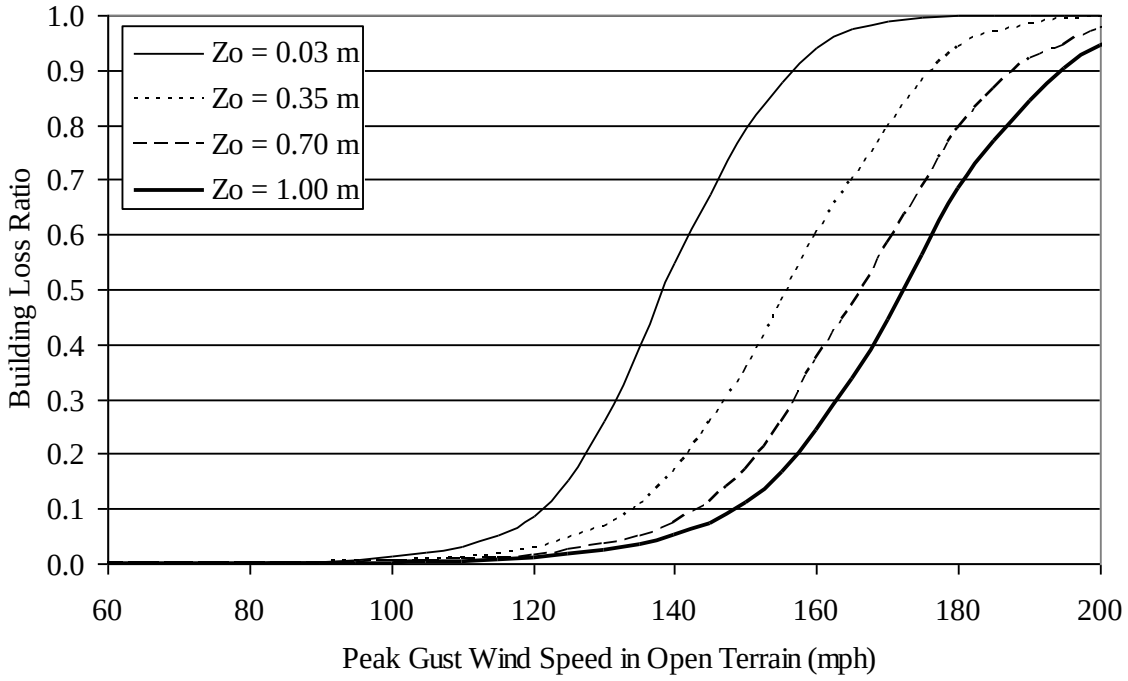

Figure J.8. Building Loss Function – One-Story, 8d Roof Deck Nails, Toe-Nailed Roof Trusses, Wood Frame Walls, Gable Roof with Shingles.

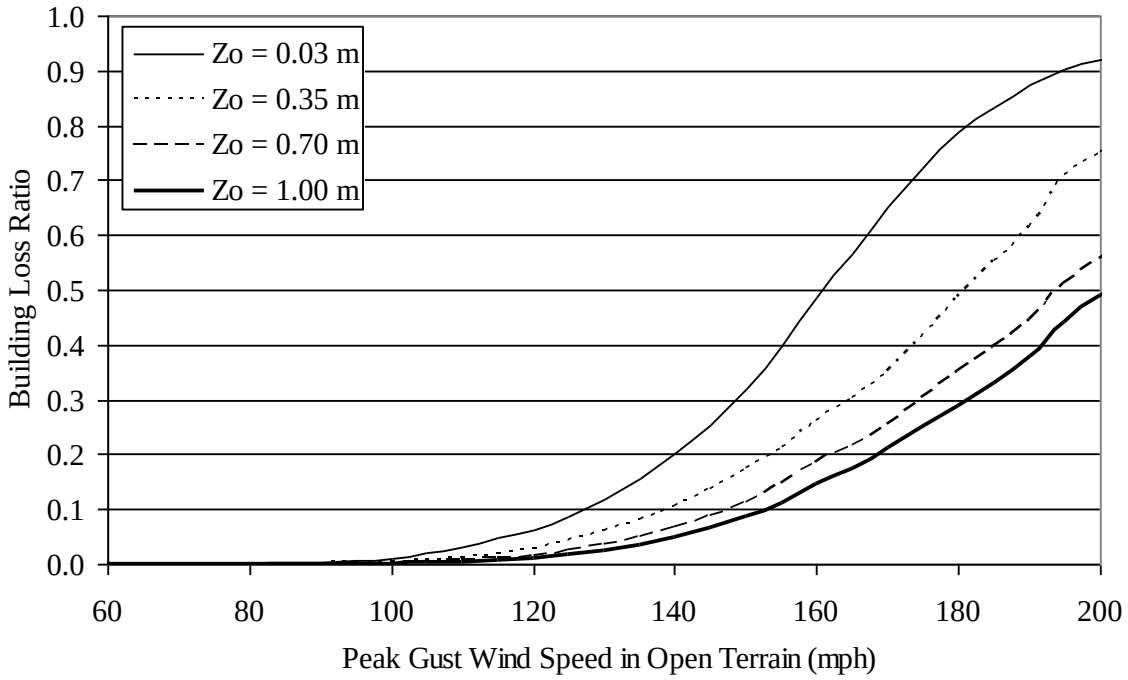

Figure J.9. Building Loss Function – One-Story, 8d Roof Deck Nails, Strapped Roof Trusses, Unreinforced Masonry Walls, Gable Roof with Shingles.

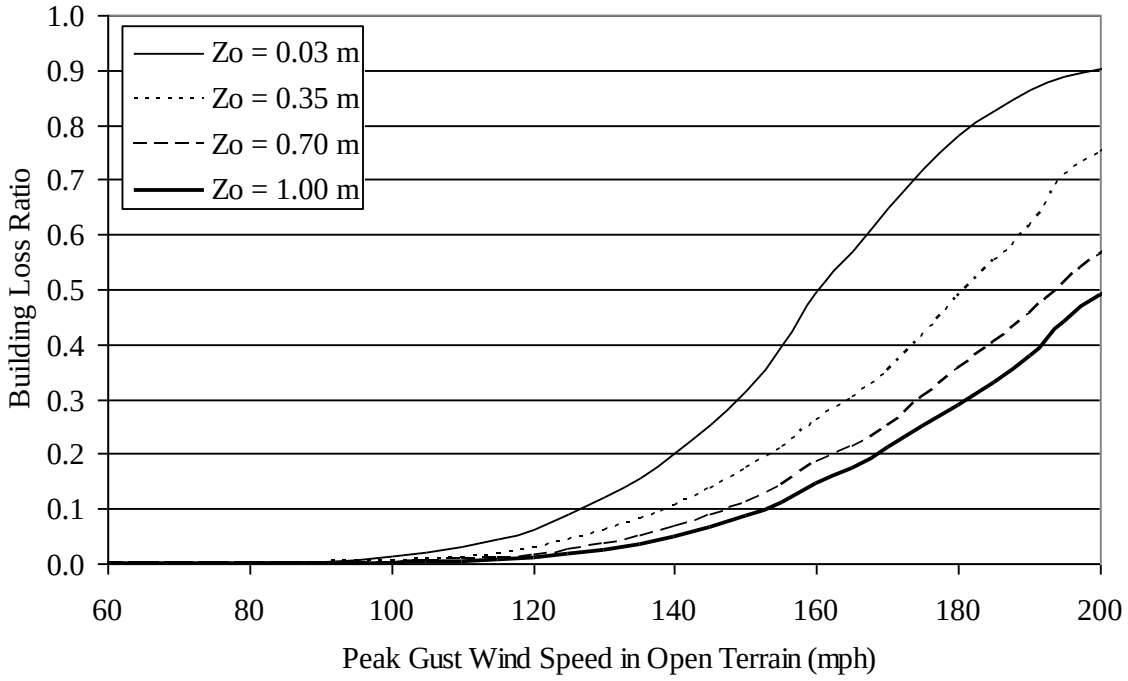

Figure J.10. Building Loss Function – One-Story, 8d Roof Deck Nails, Strapped Roof Trusses, Reinforced Masonry Walls, Gable Roof with Shingles.

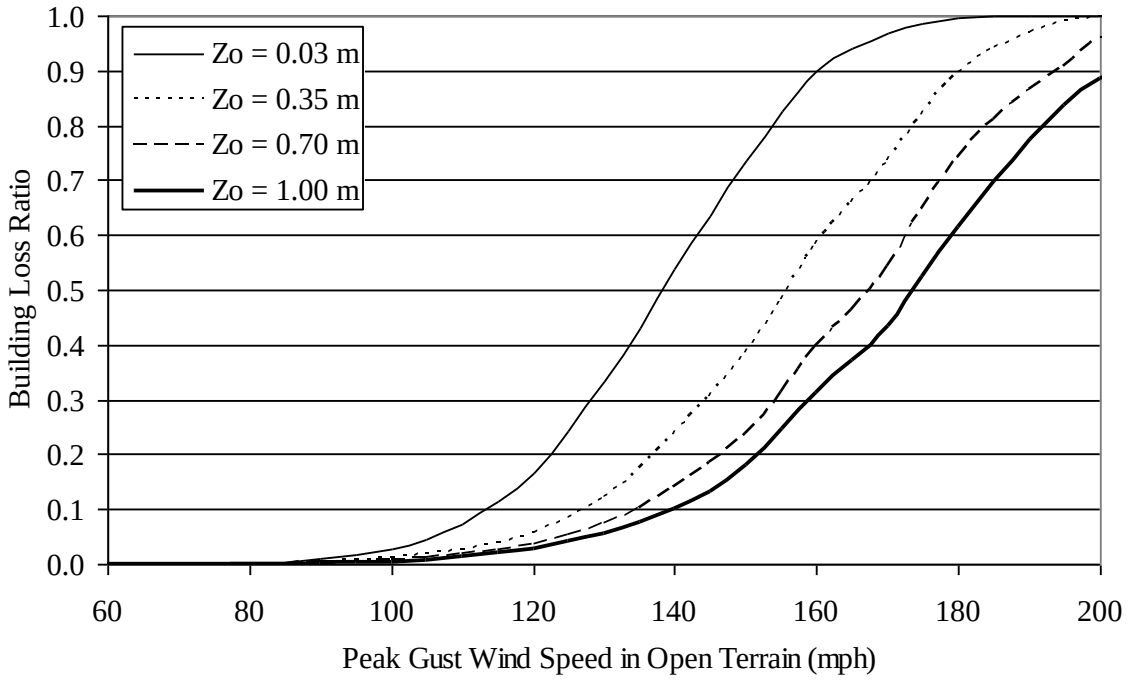

Figure J.11. Building Loss Function – Two-Story, 8d Roof Deck Nails, Strapped Roof Trusses, Wood Frame Walls, Gable Roof with Shingles.

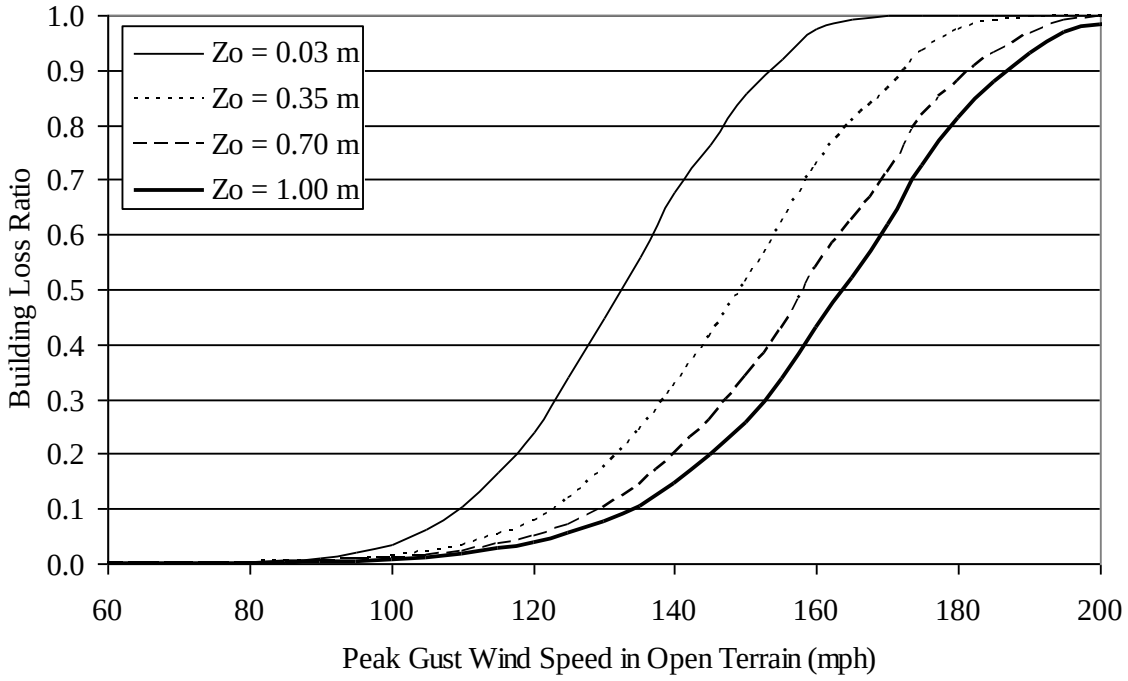

Figure J.12. Building Loss Function – Three-Story, 8d Roof Deck Nails, Strapped Roof Trusses, Wood Frame Walls, Gable Roof with Shingles.

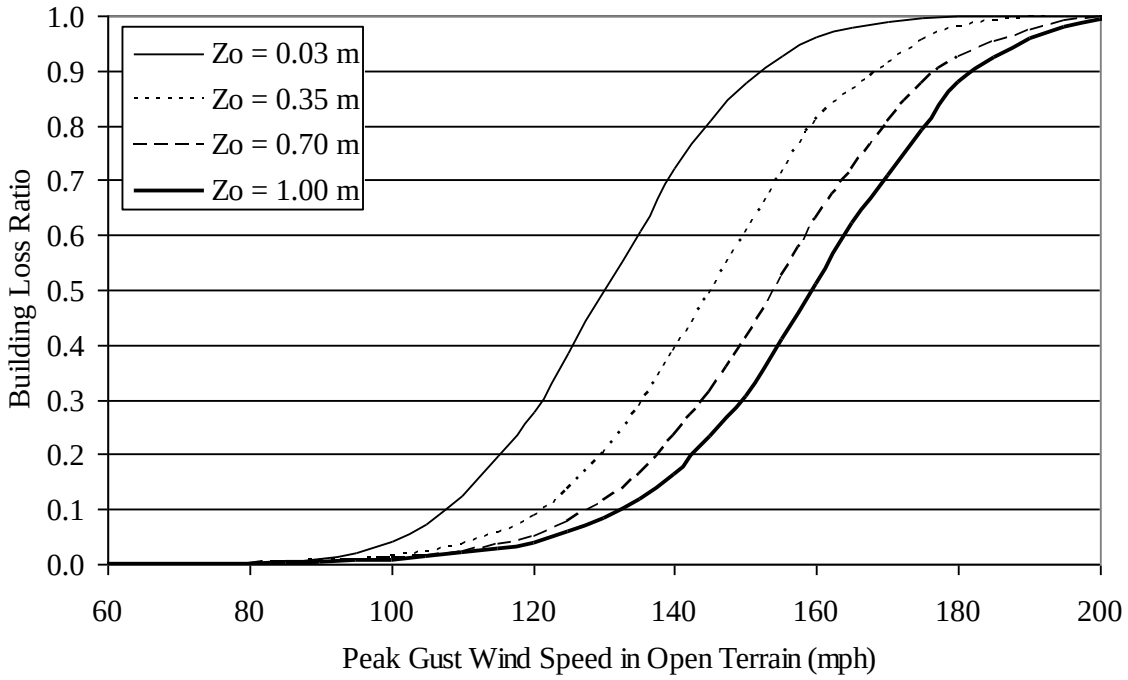

Figure J.13. Building Loss Function – Four-Story, 8d Roof Deck Nails, Strapped Roof Trusses, Wood Frame Walls, Gable Roof with Shingles.

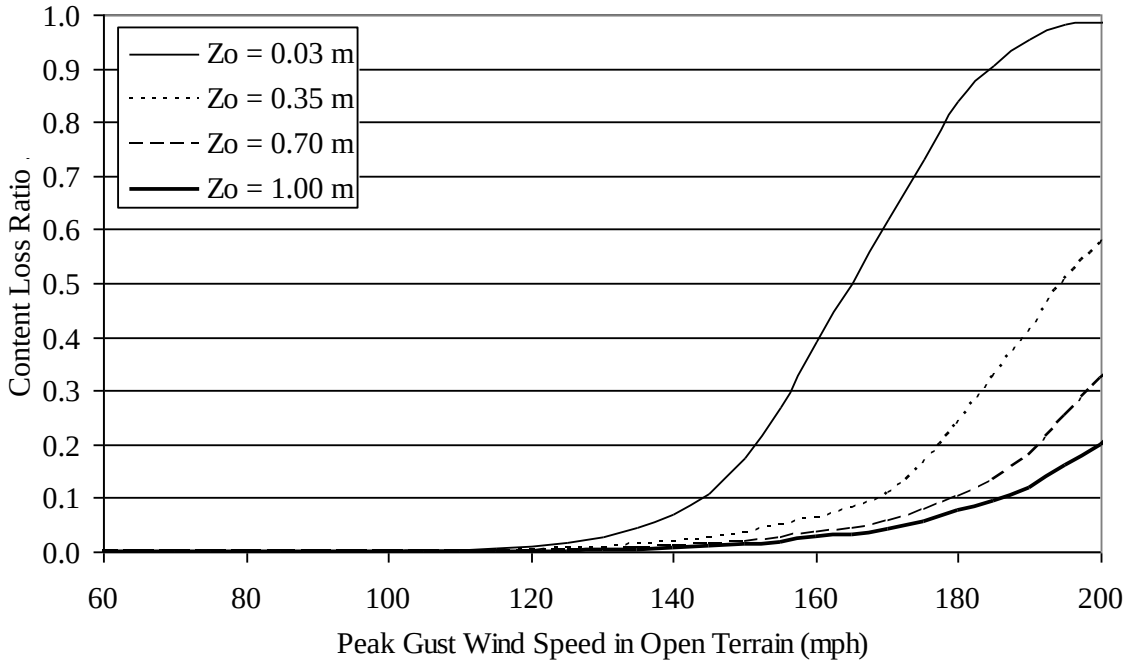

Figure J.14. Content Loss Function – One-Story, 8d Roof Deck Nails, Strapped Roof Trusses, Wood Frame Walls, Gable Roof with Shingles.

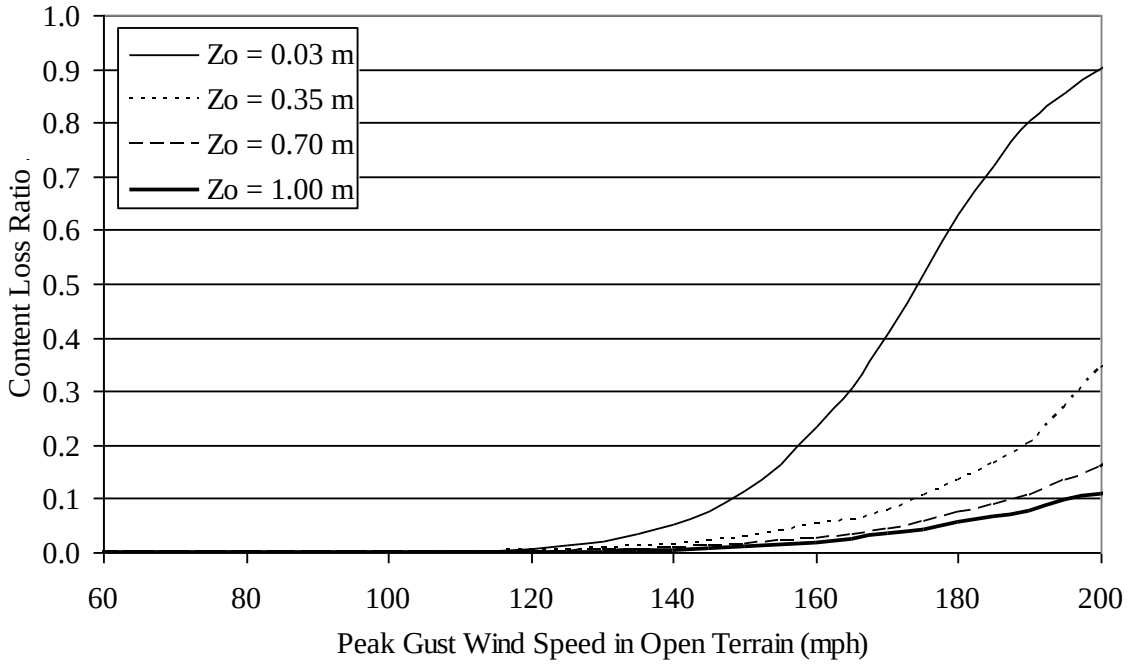

Figure J.15. Content Loss Function – One-Story, 8d Roof Deck Nails, Strapped Roof Trusses, Wood Frame Walls, Hip Roof with Shingles.

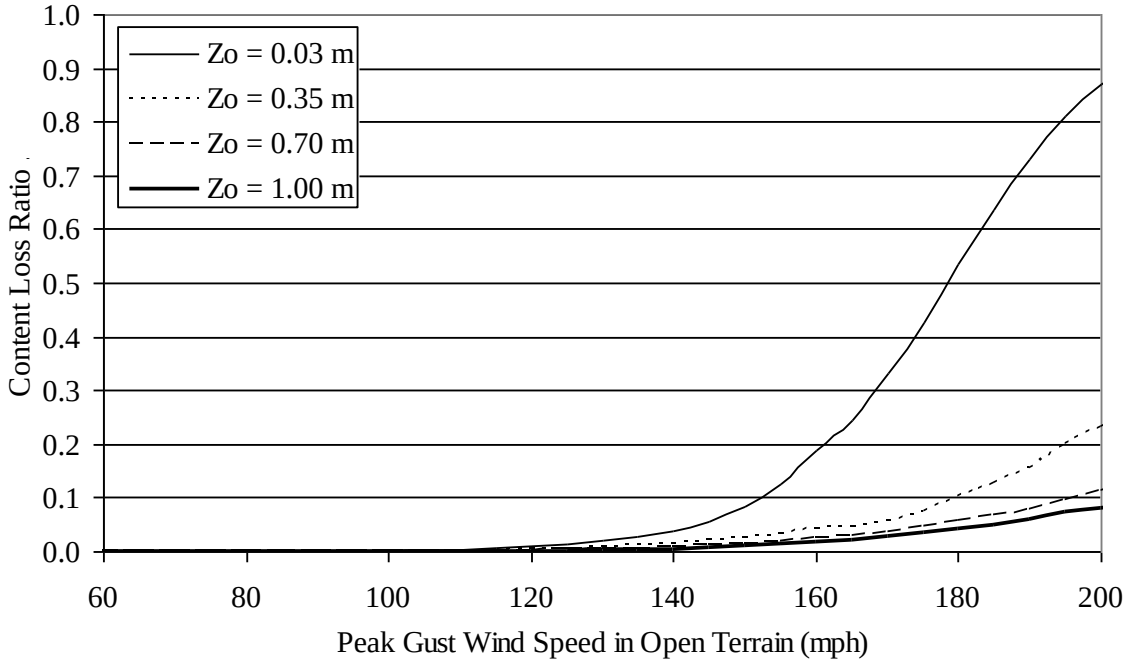

Figure J.16. Content Loss Function – One-Story, 8d Roof Deck Nails, Strapped Roof Trusses, Wood Frame Walls, Flat Roof with Average Quality BUR.

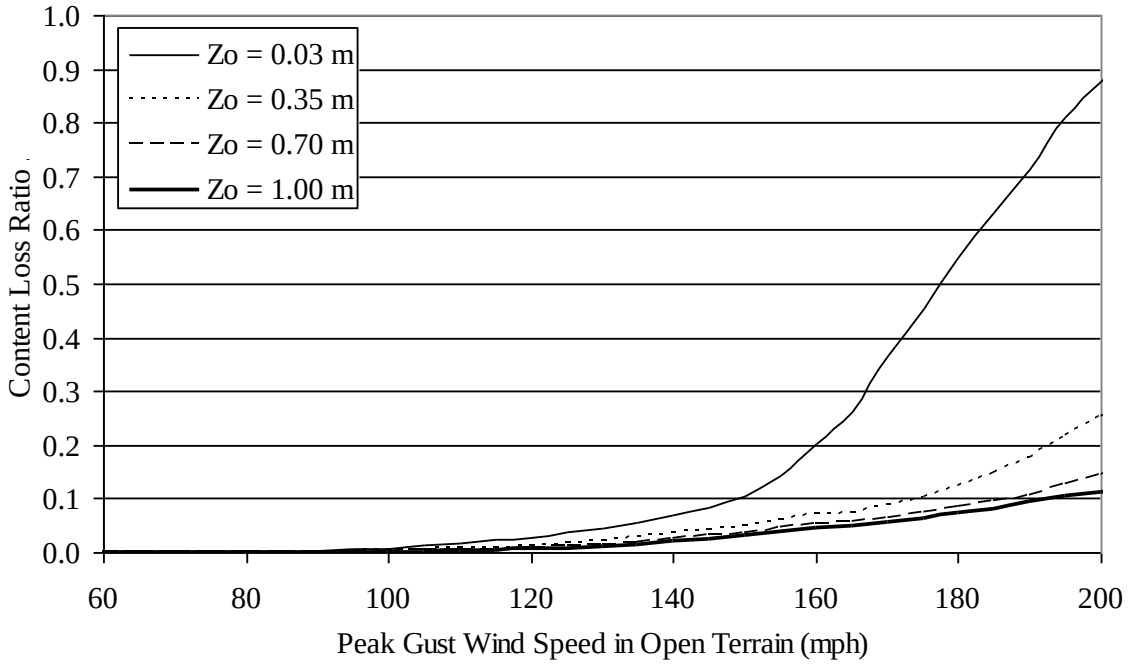

Figure J.17. Content Loss Function – One-Story, 8d Roof Deck Nails, Strapped Roof Trusses, Wood Frame Walls, Flat Roof with Poor Quality BUR.

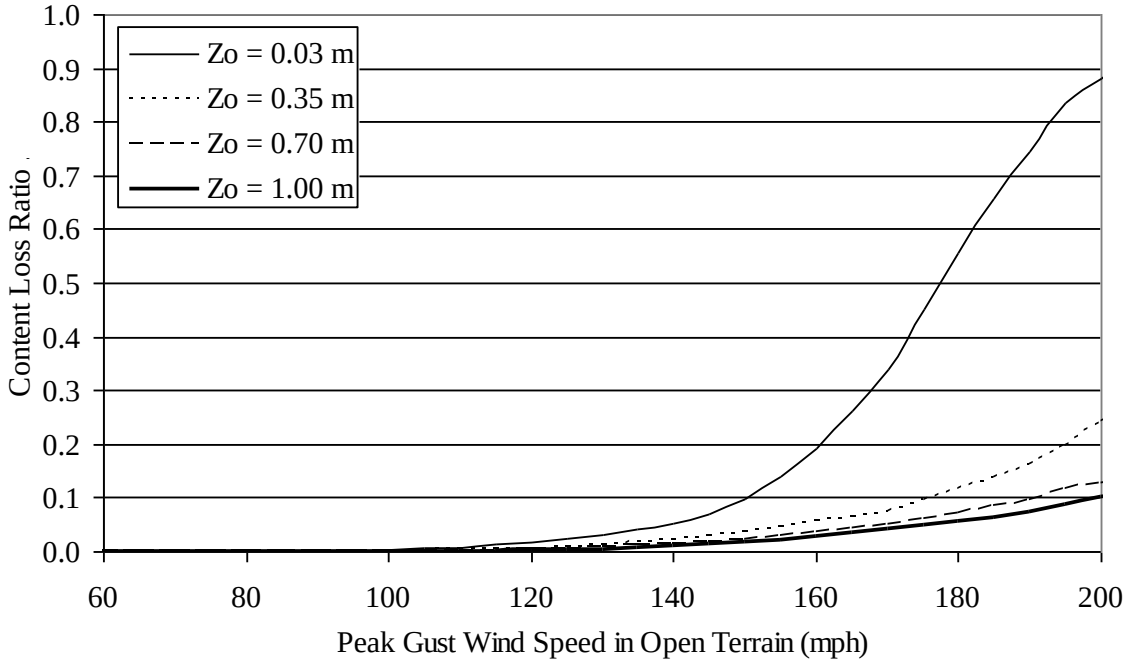

Figure J.18. Content Loss Function – One-Story, 8d Roof Deck Nails, Strapped Roof Trusses, Wood Frame Walls, Flat Roof with Average Quality EPDM.

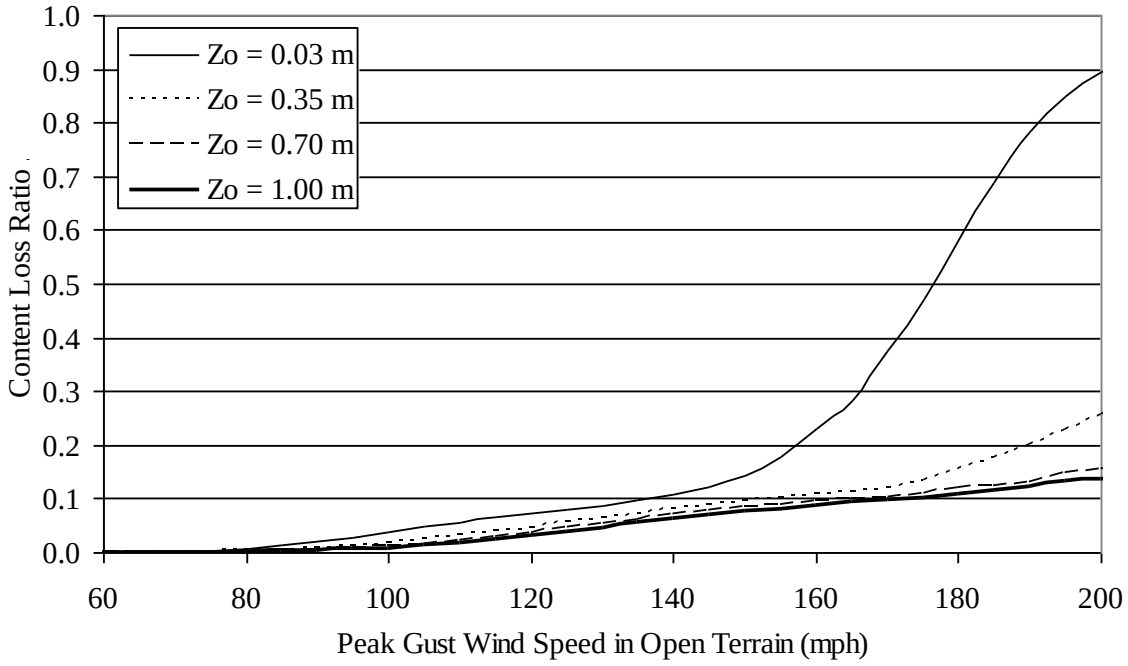

Figure J.19. Content Loss Function – One-Story, 8d Roof Deck Nails, Strapped Roof Trusses, Wood Frame Walls, Flat Roof with Poor Quality EPDM.

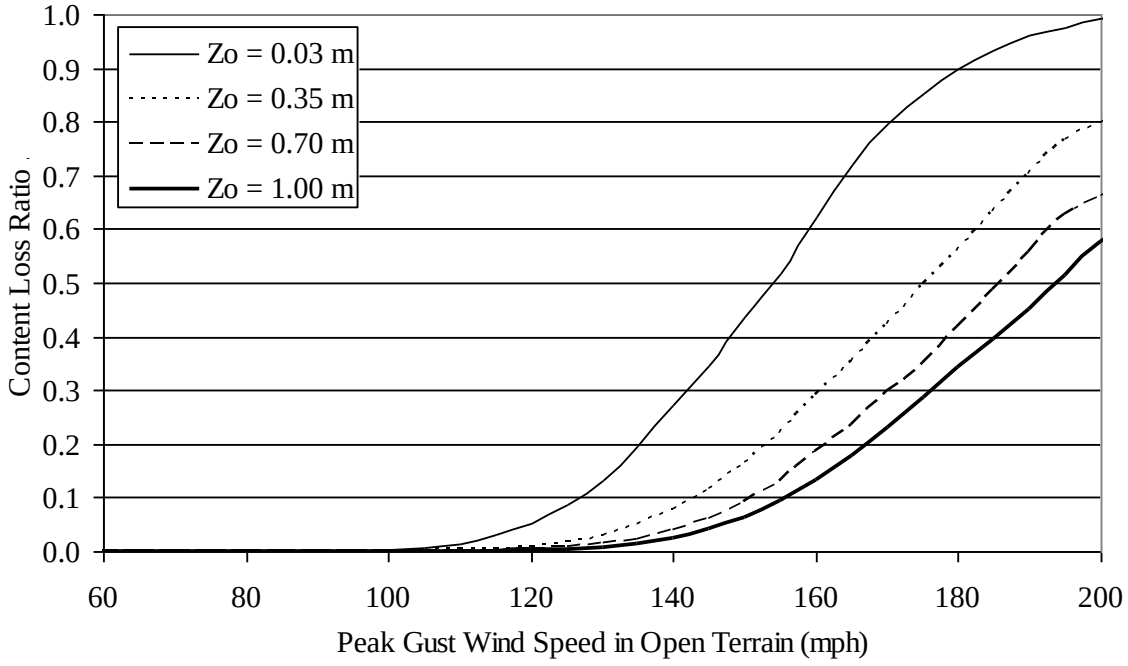

Figure J.20. Content Loss Function – One-Story, 6d Roof Deck Nails, Strapped Roof Trusses, Wood Frame Walls, Gable Roof with Shingles.

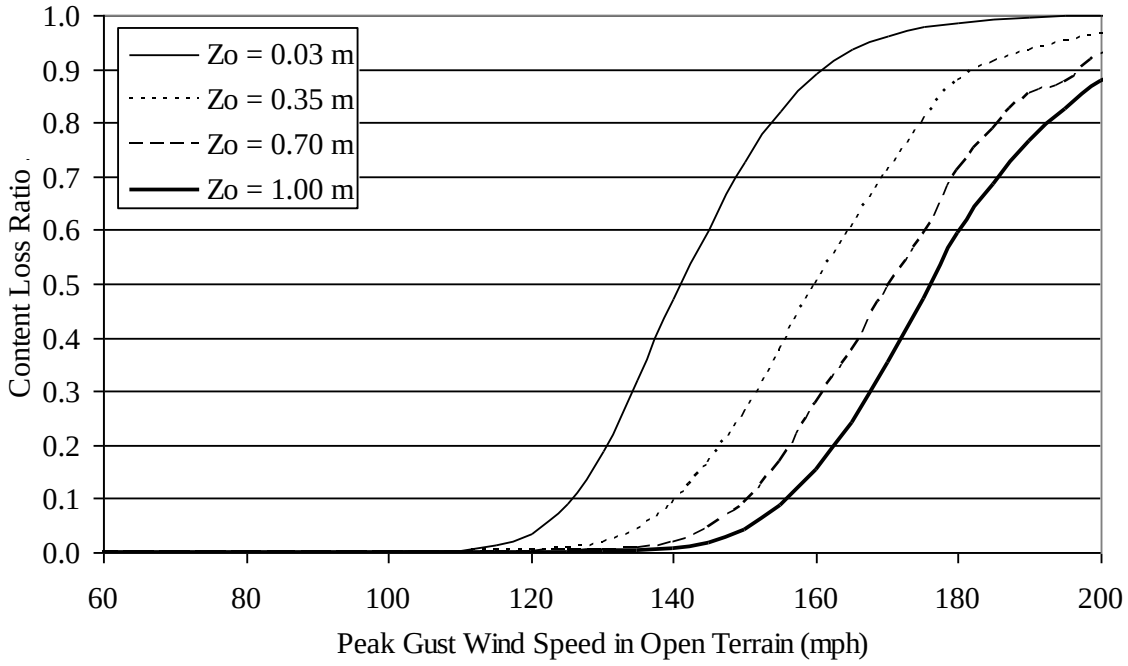

Figure J.21. Content Loss Function – One-Story, 8d Roof Deck Nails, Toe-Nailed Roof Trusses, Wood Frame Walls, Gable Roof with Shingles.

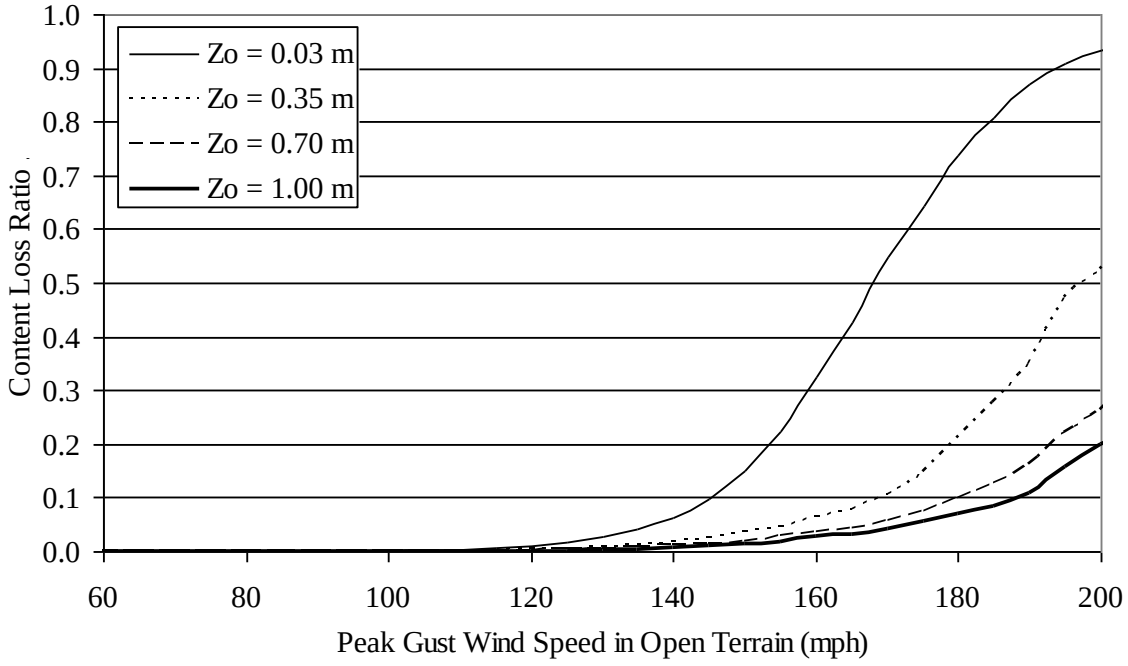

Figure J.22. Content Loss Function – One-Story, 8d Roof Deck Nails, Strapped Roof Trusses, Unreinforced Masonry Walls, Gable Roof with Shingles.

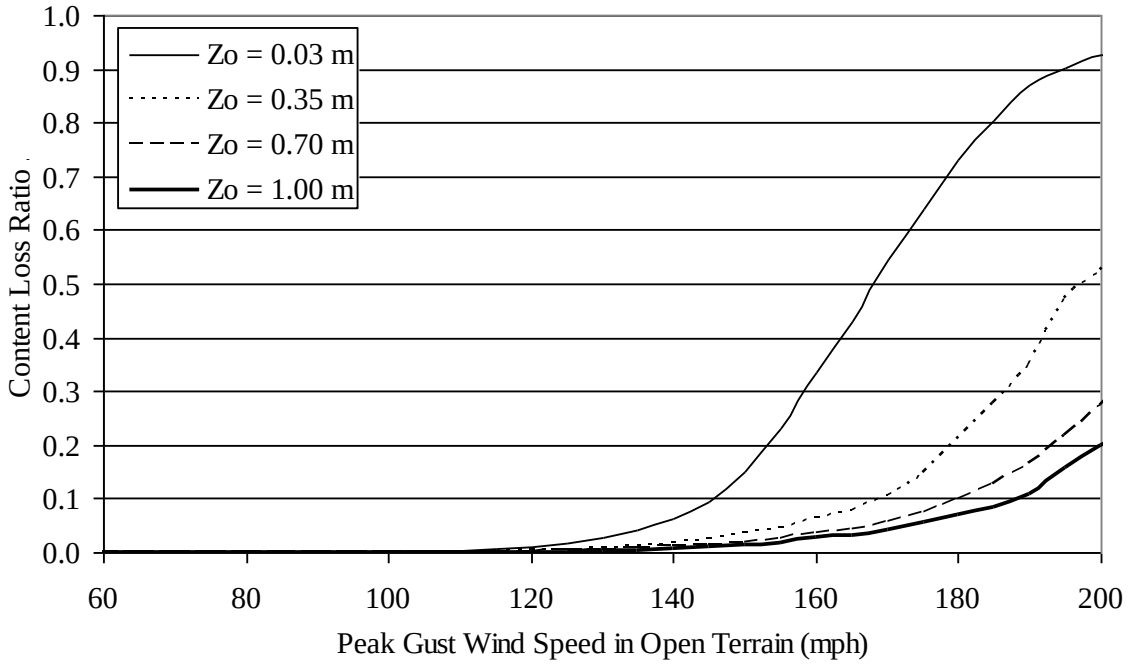

Figure J.23. Content Loss Function – One-Story, 8d Roof Deck Nails, Strapped Roof Trusses, Reinforced Masonry Walls, Gable Roof with Shingles.

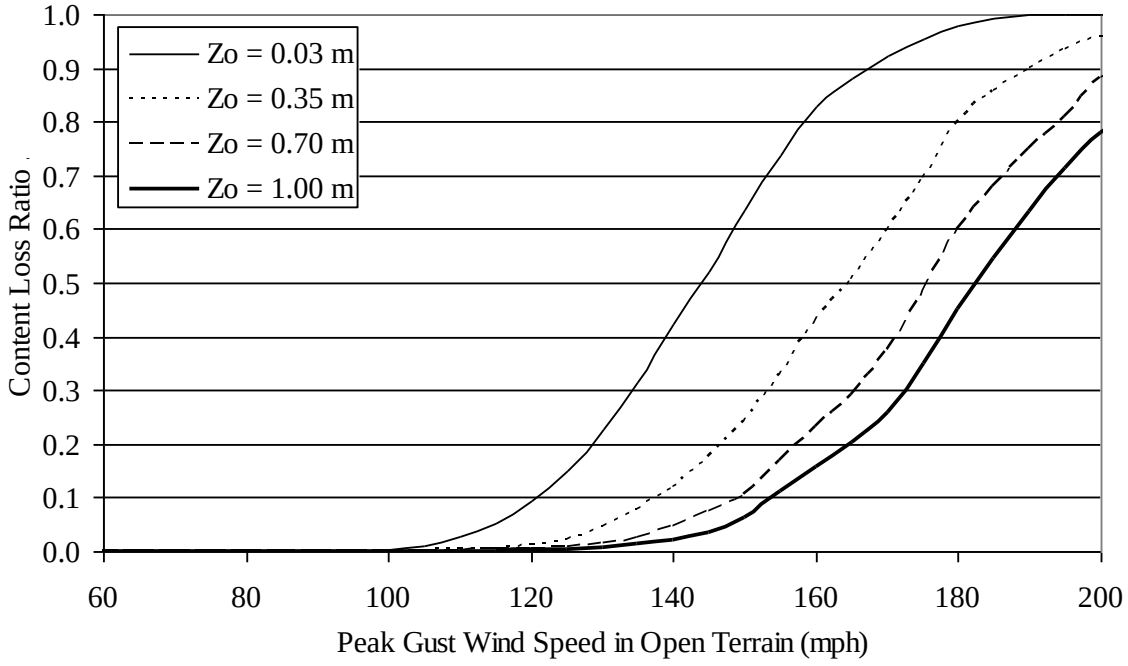

Figure J.24. Content Loss Function – Two-Story, 8d Roof Deck Nails, Strapped Roof Trusses, Wood Frame Walls, Gable Roof with Shingles.

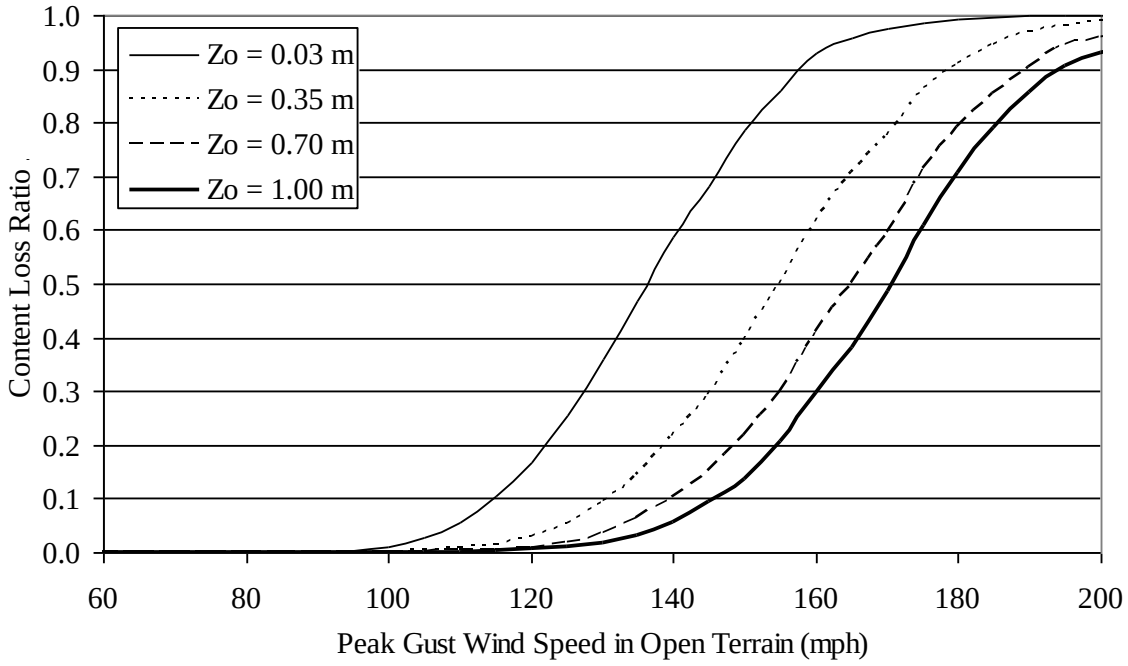

Figure J.25. Content Loss Function – <u>Three-Story</u>, 8d Roof Deck Nails, Strapped Roof Trusses, Wood Frame Walls, Gable Roof with Shingles.

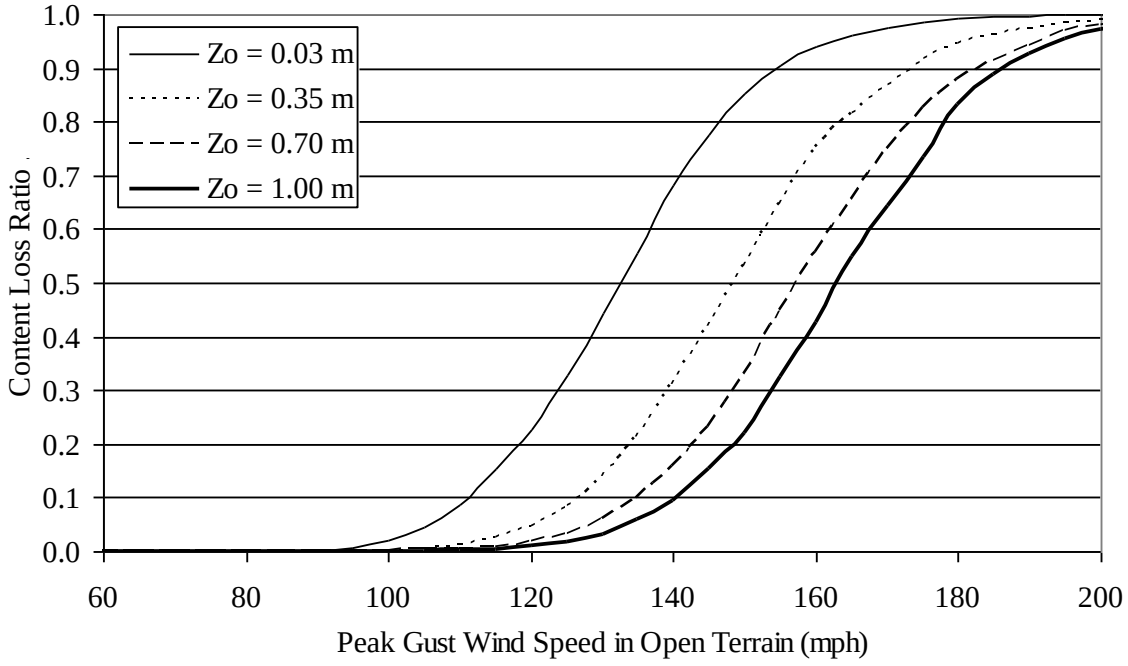

Figure J.26. Content Loss Function – <u>Four-Story</u>, 8d Roof Deck Nails, Strapped Roof Trusses, Wood Frame Walls, Gable Roof with Shingles.

Appendix K.
Loss Functions for Low Rise Masonry Strip Mall Buildings

Appendix K.
Loss Functions for Low Rise Masonry Strip Mall Buildings

This appendix presents loss functions for low rise masonry strip mall buildings (see Section 7.11). The loss functions represent either average building loss normalized by building value or average content loss normalized by content value. Therefore, the loss ratios range between 0 and 1 in both cases. Note that the content value is set to 50% of the building value. For a given simulated storm, the building loss ratio and content loss ratio are estimated based on the modeled damage and the largest gust speed over the entire duration of the simulated storm is saved. The loss functions are then computed by averaging the loss ratios associated with the storms producing a maximum gust speed within 5 mph ranges. The average loss ratios (content or building loss) associated with each 5 mph gust speed range are then plotted at the center of that range. Note that the wind speeds are representative of open terrain at 10 m above ground.

Table K.1 lists the figures provided in this appendix. Figures K.1 through K.18 give example results for the strip mall buildings modeled with a wood roof system. Figures K.19 through K.42 give example results for the strip mall buildings modeled with a steel roof system.

Two sets of nine figures are given for the buildings modeled with a wood roof system. The first set of nine figures (Figures K.1 through K.9) show building loss functions and the second set (Figures K.10 through K.18) show content loss functions. The first figure in each set of nine shows loss results for the 12′ high building with 6 units, 8d roof sheathing nails, strapped roof-wall connections, built-up roof cover, unreinforced masonry walls, and situated in Missile Environment A. The remaining eight plots in each set show loss results for buildings which are different by a single variable in comparison to the reference building (note that the changed variable is underlined in the figure titles).

Two sets of twelve figures are given for the buildings modeled with a metal roof system. The first set of twelve figures (Figures K.19 through K.30) show building loss functions and the second set (Figures K.31 through K.42) show content loss functions. The first figure in each set of twelve shows loss results for the 20′ high building with 6 units, a joist spacing of 6′, metal roof deck fastened with welds, SBCCI roof design criteria, built-up roof cover, unreinforced masonry walls, and situated in Missile Environment A. The remaining eleven plots in each set show loss results for buildings which are different by a single variable in comparison to the reference building (note that the changed variable is underlined in the figure titles).

Table K.1. Sample Loss Functions for Low Rise Masonry Strip Mall Buildings

Figure	Loss Type	Walls	Height	Number of Units	Roof Frame	Frame Spacing	Roof/ Wall	Deck Mat'l.	Deck Attachment	Design Code	Roof Cover	Missile Environ.
K.1	Building	URM	12'	6	Wood	2'	Strap	Wood	8d	-	BUR	A
K.2	Building	URM	12'	6	Wood	2'	Strap	Wood	8d	-	BUR	**B**
K.3	Building	URM	12'	6	Wood	2'	Strap	Wood	8d	-	BUR	**C**
K.4	Building	URM	12'	6	Wood	2'	Strap	Wood	8d	-	BUR	**D**
K.5	Building	URM	12'	6	Wood	2'	Strap	Wood	8d	-	**SPM**	A
K.6	Building	URM	12'	6	Wood	2'	Strap	Wood	**6d**	-	BUR	A
K.7	Building	**RM**	12'	6	Wood	2'	Strap	Wood	8d	-	BUR	A
K.8	Building	URM	12'	6	Wood	2'	**Toe-Nail**	Wood	8d	-	BUR	A
K.9	Building	URM	**20'**	6	Wood	2'	Strap	Wood	8d	-	BUR	A
K.10	Content	URM	12'	6	Wood	2'	Strap	Wood	8d	-	BUR	A
K.11	Content	URM	12'	6	Wood	2'	Strap	Wood	8d	-	BUR	**B**
K.12	Content	URM	12'	6	Wood	2'	Strap	Wood	8d	-	BUR	**C**
K.13	Content	URM	12'	6	Wood	2'	Strap	Wood	8d	-	BUR	**D**
K.14	Content	URM	12'	6	Wood	2'	Strap	Wood	8d	-	**SPM**	A
K.15	Content	URM	12'	6	Wood	2'	Strap	Wood	**6d**	-	BUR	A
K.16	Content	**RM**	12'	6	Wood	2'	Strap	Wood	8d	-	BUR	A
K.17	Content	URM	12'	6	Wood	2'	**Toe-Nail**	Wood	8d	-	BUR	A
K.18	Content	URM	**20'**	6	Wood	2'	Strap	Wood	8d	-	BUR	A
K.19	Building	URM	20'	6	OWSJ	6'	-	Metal	Weld	SBCCI, 100	BUR	A
K.20	Building	URM	20'	6	OWSJ	**4'**	-	Metal	Weld	SBCCI, 100	BUR	A
K.21	Building	URM	20'	**1**	OWSJ	6'	-	Metal	Weld	SBCCI, 100	BUR	A
K.22	Building	URM	**12'**	6	OWSJ	**4'**	-	Metal	Weld	SBCCI, 100	BUR	A
K.23	Building	URM	20'	6	OWSJ	6'	-	Metal	Weld	SBCCI, 100	BUR	**B**
K.24	Building	URM	20'	6	OWSJ	6'	-	Metal	Weld	SBCCI, 100	BUR	**C**
K.25	Building	URM	20'	6	OWSJ	6'	-	Metal	Weld	SBCCI, 100	BUR	**D**
K.26	Building	URM	20'	6	OWSJ	6'	-	Metal	Weld	SBCCI, 100	**SPM**	A
K.27	Building	URM	20'	6	OWSJ	6'	-	Metal	**Weld, 50%**	SBCCI, 100	BUR	A
K.28	Building	URM	20'	6	OWSJ	6'	-	Metal	**Screw**	SBCCI, 100	BUR	A
K.29	Building	URM	20'	6	OWSJ	6'	-	Metal	Weld	**ASCE, 100**	BUR	A
K.30	Building	**RM**	20'	6	OWSJ	6'	-	Metal	Weld	SBCCI, 100	BUR	A
K.31	Content	URM	20'	6	OWSJ	6'	-	Metal	Weld	SBCCI, 100	BUR	A
K.32	Content	URM	20'	6	OWSJ	**4'**	-	Metal	Weld	SBCCI, 100	BUR	A
K.33	Content	URM	20'	**1**	OWSJ	6'	-	Metal	Weld	SBCCI, 100	BUR	A
K.34	Content	URM	**12'**	6	OWSJ	**4'**	-	Metal	Weld	SBCCI, 100	BUR	A
K.35	Content	URM	20'	6	OWSJ	6'	-	Metal	Weld	SBCCI, 100	BUR	**B**
K.36	Content	URM	20'	6	OWSJ	6'	-	Metal	Weld	SBCCI, 100	BUR	**C**
K.37	Content	URM	20'	6	OWSJ	6'	-	Metal	Weld	SBCCI, 100	BUR	**D**
K.38	Content	URM	20'	6	OWSJ	6'	-	Metal	Weld	SBCCI, 100	**SPM**	A
K.39	Content	URM	20'	6	OWSJ	6'	-	Metal	**Weld, 50%**	SBCCI, 100	BUR	A
K.40	Content	URM	20'	6	OWSJ	6'	-	Metal	**Screw**	SBCCI, 100	BUR	A
K.41	Content	URM	20'	6	OWSJ	6'	-	Metal	Weld	**ASCE, 100**	BUR	A
K.42	Content	**RM**	20'	6	OWSJ	6'	-	Metal	Weld	SBCCI, 100	BUR	A

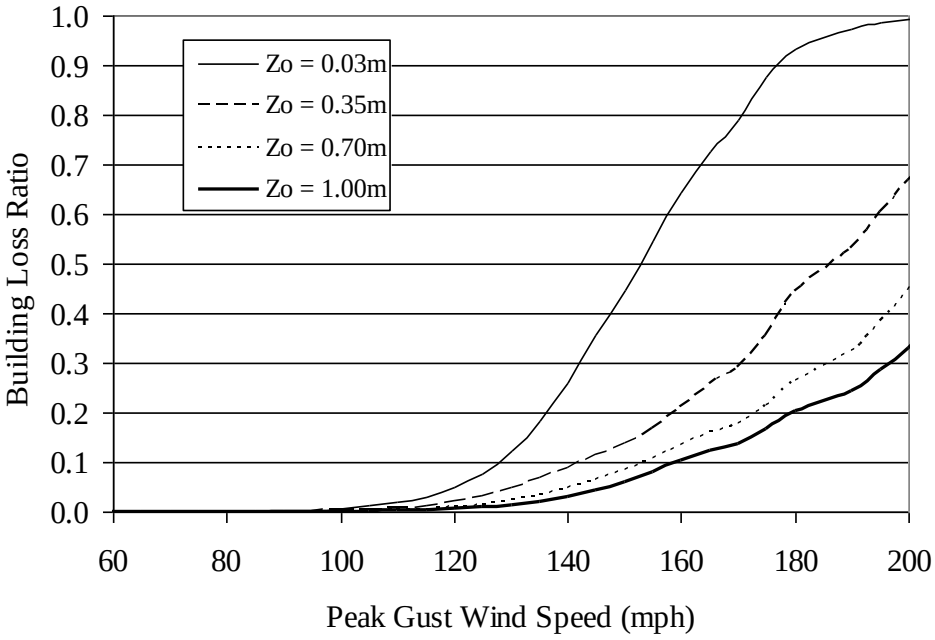

Figure K.1. Building Loss Function – Strip Mall Building A – Height=12′, No. of Units=6, Wood Deck with 8d Nails, Strapped Roof-Wall Connections, Built-up Roof Cover, Unreinforced Masonry Walls, Missile Environment A.

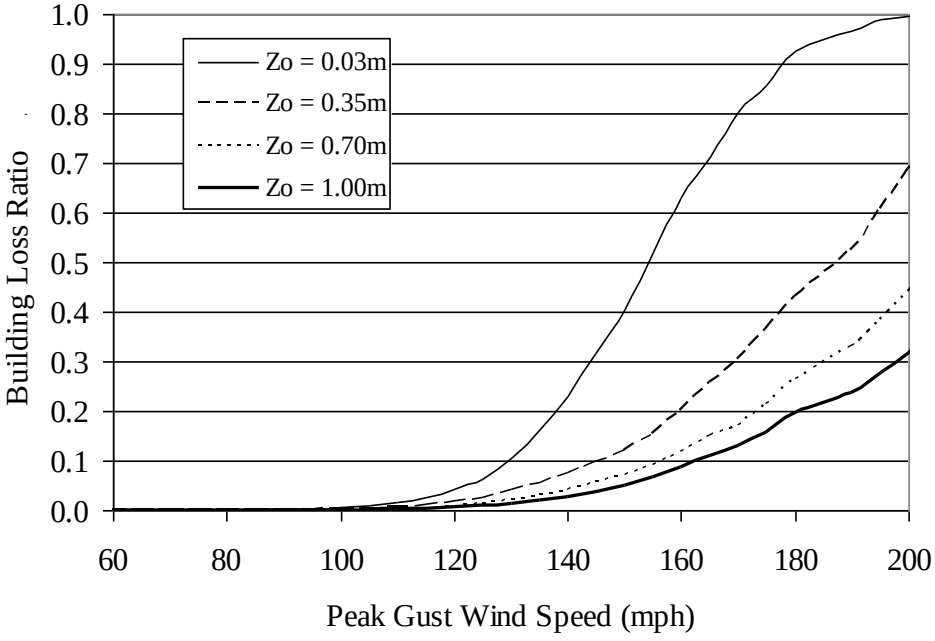

Figure K.2. Building Loss Function – Strip Mall Building A – Height=12′, No. of Units=6, Wood Deck with 8d Nails, Strapped Roof-Wall Connections, Built-up Roof Cover, Unreinforced Masonry Walls, Missile Environment B.

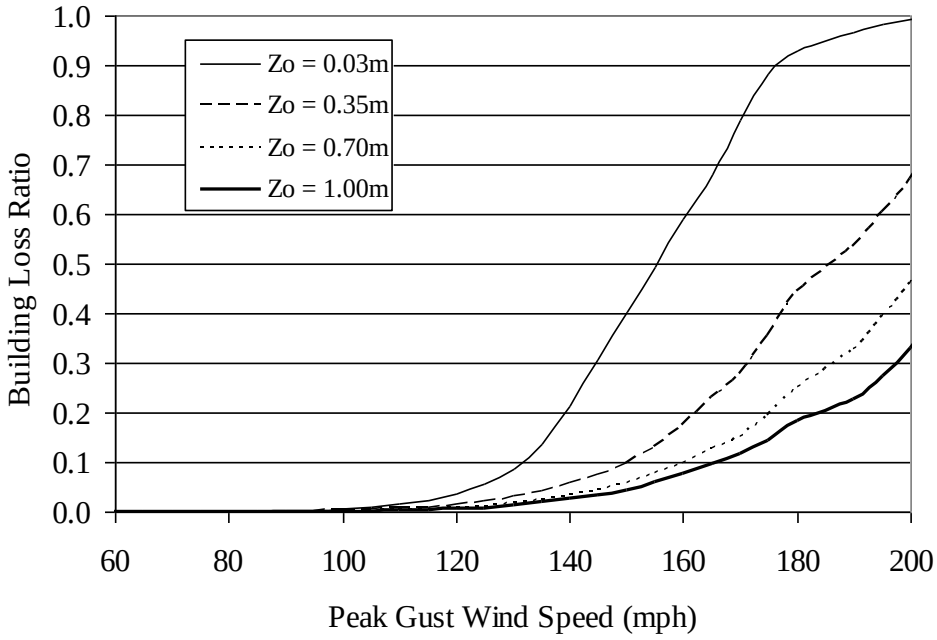

Figure K.3. Building Loss Function – Strip Mall Building A – Height=12′, No. of Units=6, Wood Deck with 8d Nails, Strapped Roof-Wall Connections, Built-up Roof Cover, Unreinforced Masonry Walls, Missile Environment C.

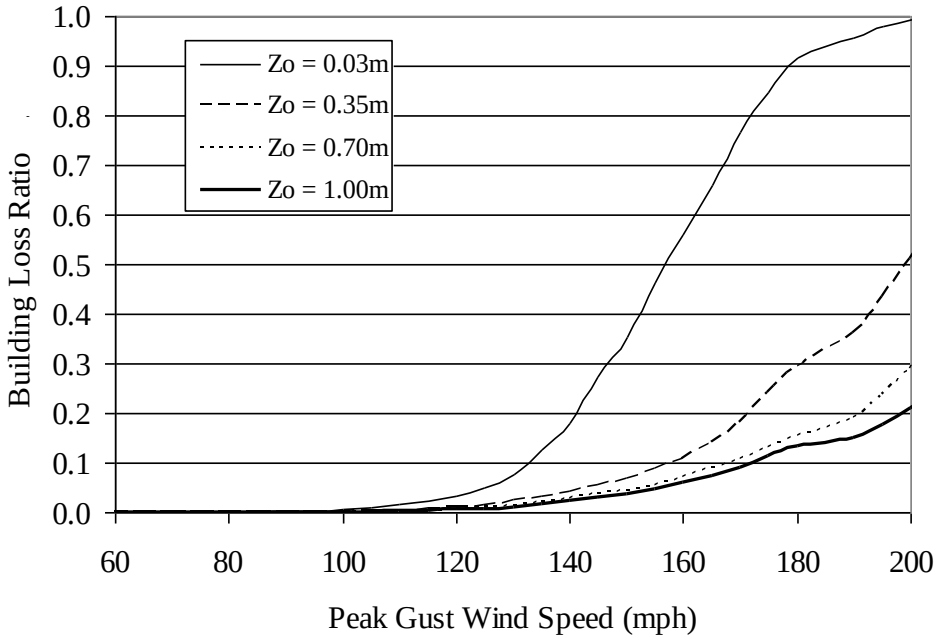

Figure K.4. Building Loss Function – Strip Mall Building A – Height=12′, No. of Units=6, Wood Deck with 8d Nails, Strapped Roof-Wall Connections, Built-up Roof Cover, Unreinforced Masonry Walls, Missile Environment D.

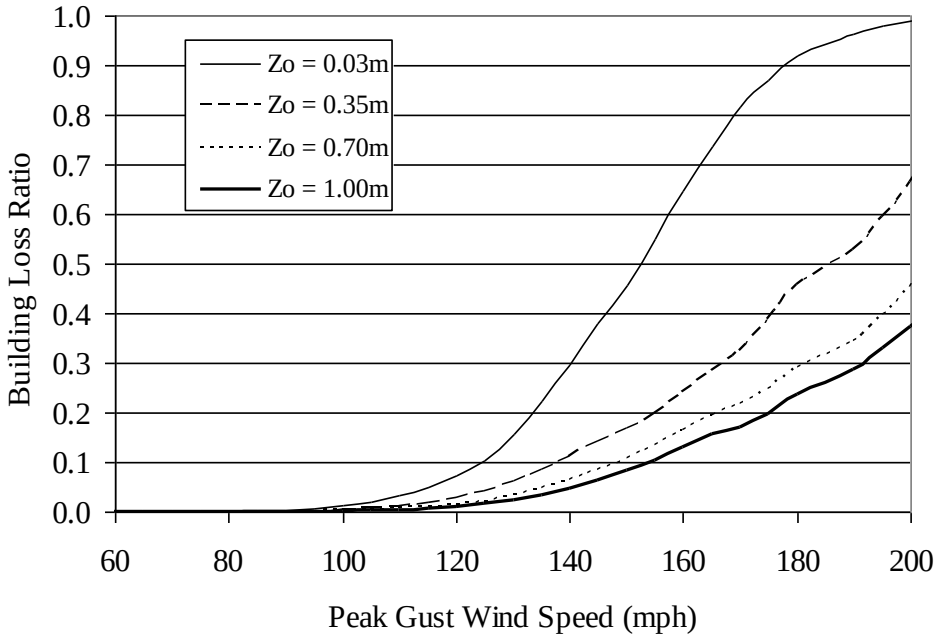

Figure K.5. Building Loss Function – Strip Mall Building A – Height=12′, No. of Units=6, Wood Deck with 8d Nails, Strapped Roof-Wall Connections, Single Ply Membrane Roof Cover, Unreinforced Masonry Walls, Missile Environment A.

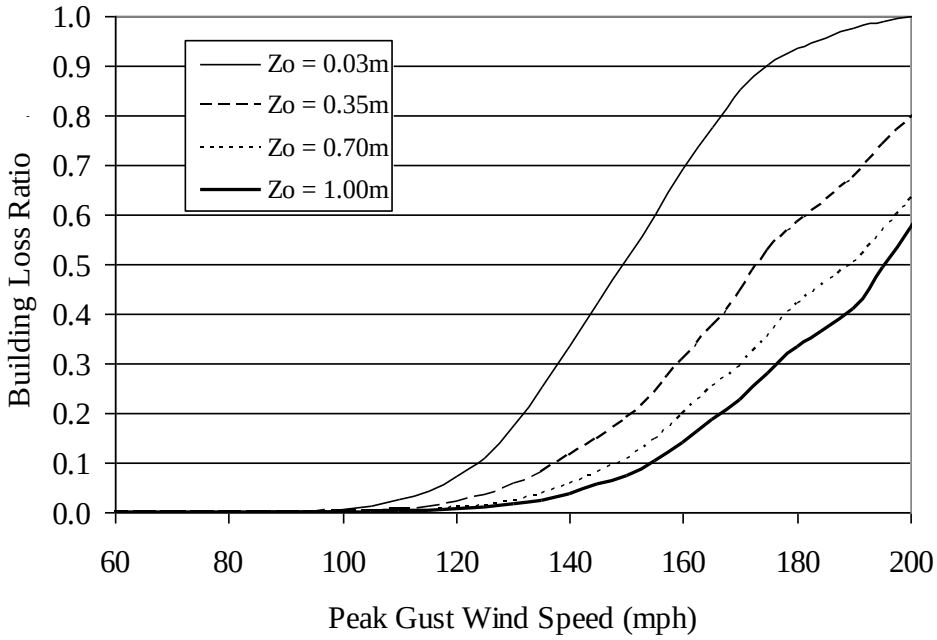

Figure K.6. Building Loss Function – Strip Mall Building A – Height=12′, No. of Units=6, Wood Deck with 6d Nails, Strapped Roof-Wall Connections, Built-up Roof Cover, Unreinforced Masonry Walls, Missile Environment A.

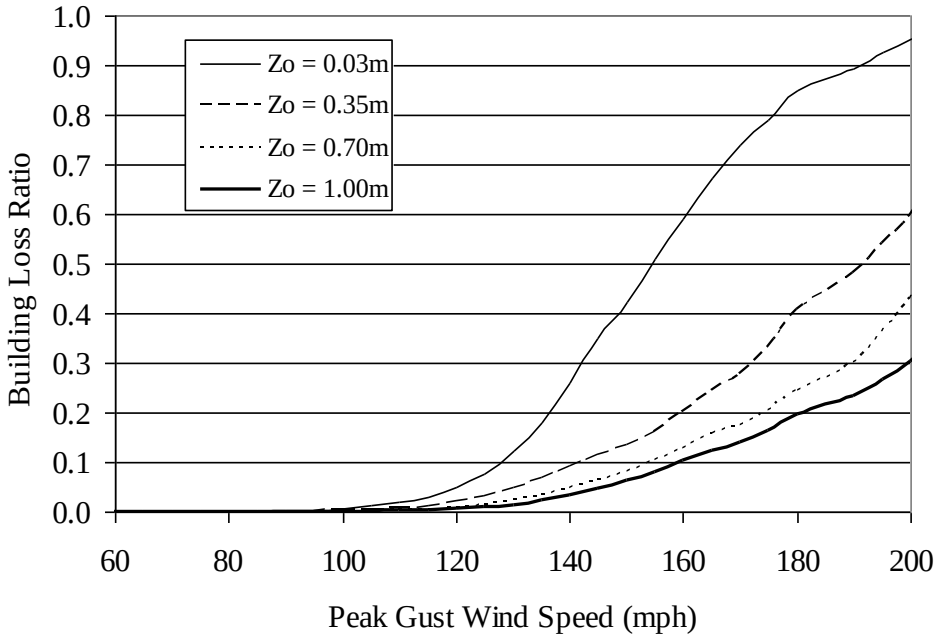

Figure K.7. Building Loss Function – Strip Mall Building A – Height=12′, No. of Units=6, Wood Deck with 8d Nails, Strapped Roof-Wall Connections, Built-up Roof Cover, Reinforced Masonry Walls, Missile Environment A.

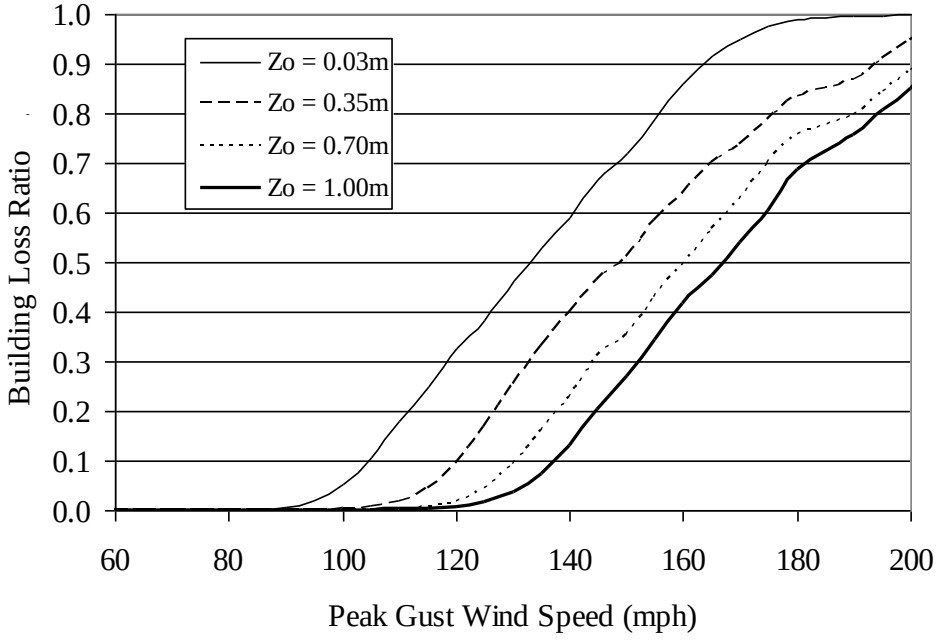

Figure K.8. Building Loss Function – Strip Mall Building A – Height=12′, No. of Units=6, Wood Deck with 8d Nails, Toe-Nailed Roof-Wall Connections, Built-up Roof Cover, Unreinforced Masonry Walls, Missile Environment A.

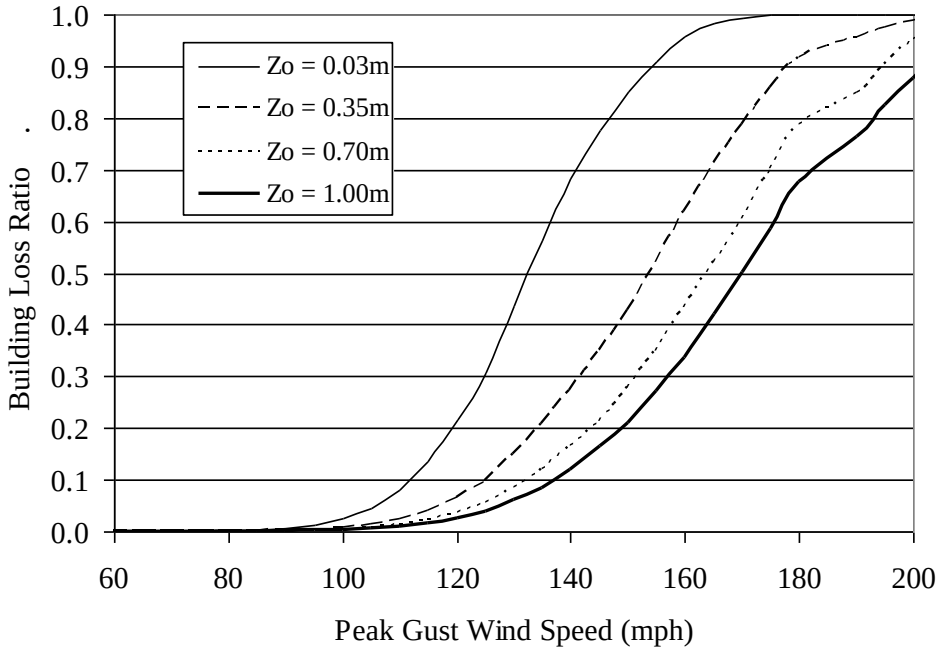

Figure K.9. Building Loss Function – Strip Mall Building B – <u>Height=20′</u>, No. of Units=6, Wood Deck with 8d Nails, Strapped Roof-Wall Connections, Built-up Roof Cover, Unreinforced Masonry Walls, Missile Environment A.

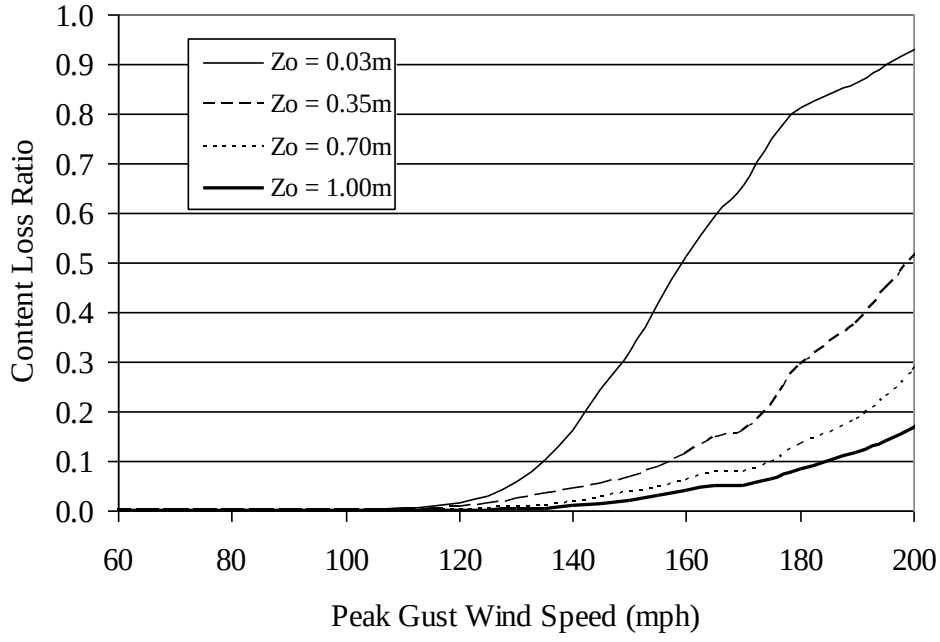

Figure K.10. Content Loss Function – Strip Mall Building A – Height=12′, No. of Units=6, Wood Deck with 8d Nails, Strapped Roof-Wall Connections, Built-up Roof Cover, Unreinforced Masonry Walls, Missile Environment A.

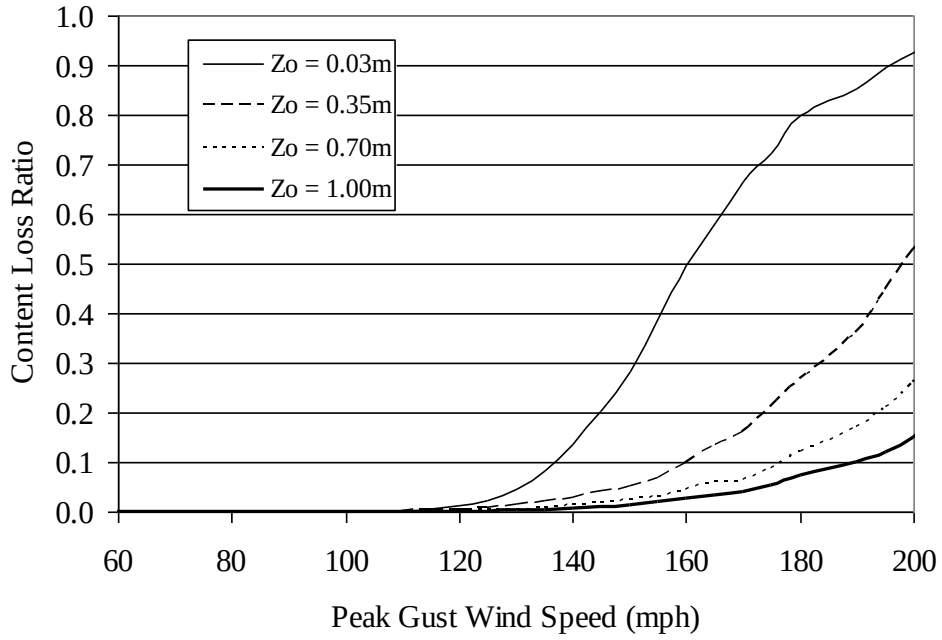

Figure K.11. Content Loss Function – Strip Mall Building A – Height=12′, No. of Units=6, Wood Deck with 8d Nails, Strapped Roof-Wall Connections, Built-up Roof Cover, Unreinforced Masonry Walls, Missile Environment B.

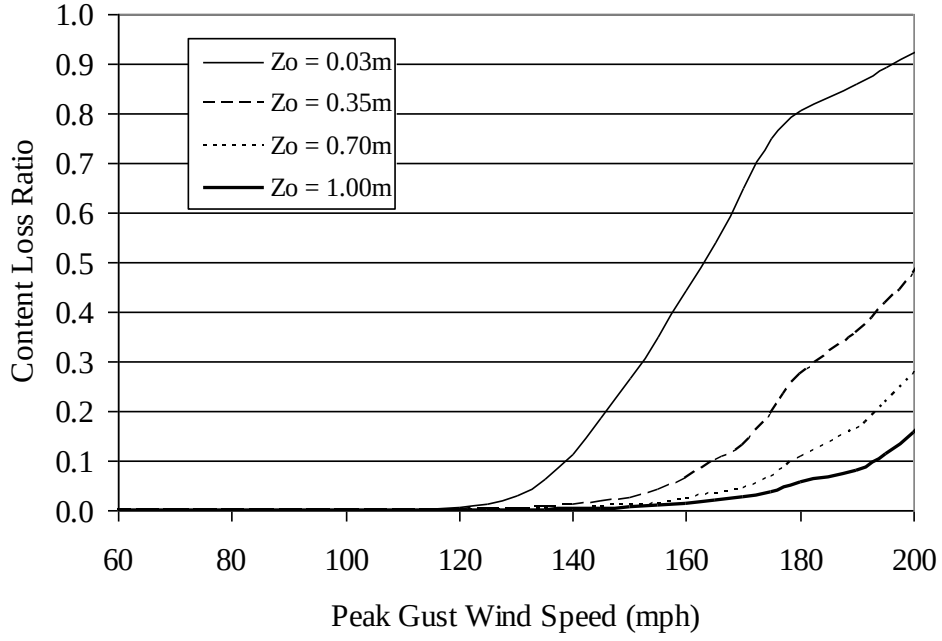

Figure K.12. Content Loss Function – Strip Mall Building A – Height=12′, No. of Units=6, Wood Deck with 8d Nails, Strapped Roof-Wall Connections, Built-up Roof Cover, Unreinforced Masonry Walls, Missile Environment C.

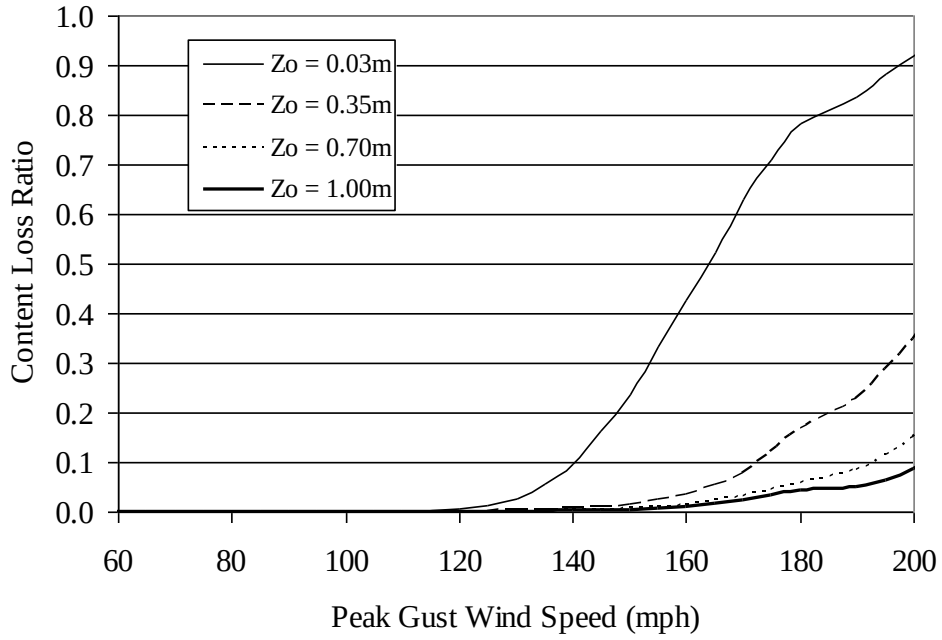

Figure K.13. Content Loss Function – Strip Mall Building A – Height=12′, No. of Units=6, Wood Deck with 8d Nails, Strapped Roof-Wall Connections, Built-up Roof Cover, Unreinforced Masonry Walls, Missile Environment D.

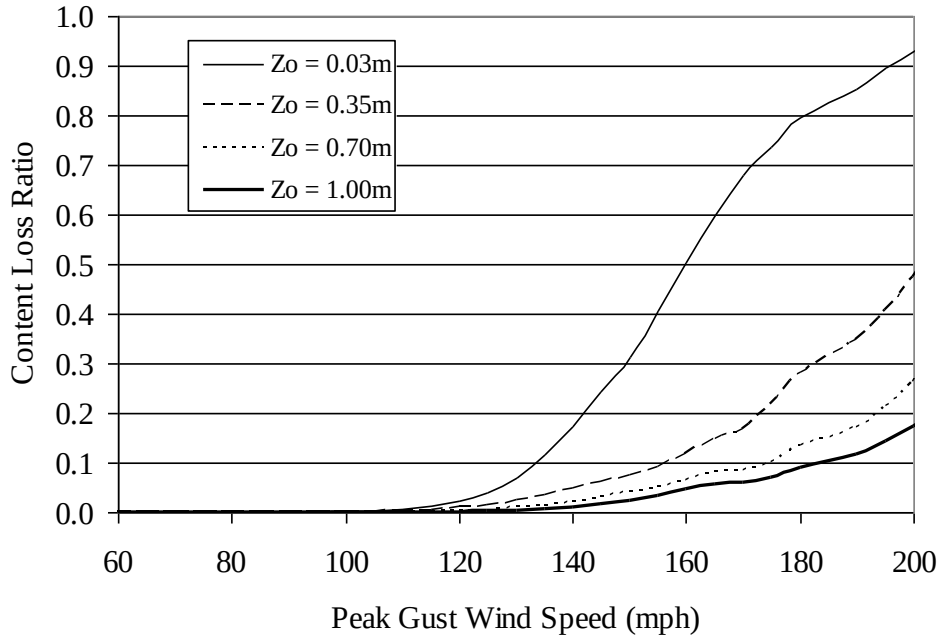

Figure K.14. Content Loss Function – Strip Mall Building A – Height=12′, No. of Units=6, Wood Deck with 8d Nails, Strapped Roof-Wall Connections, Single Ply Membrane Roof Cover, Unreinforced Masonry Walls, Missile Environment A.

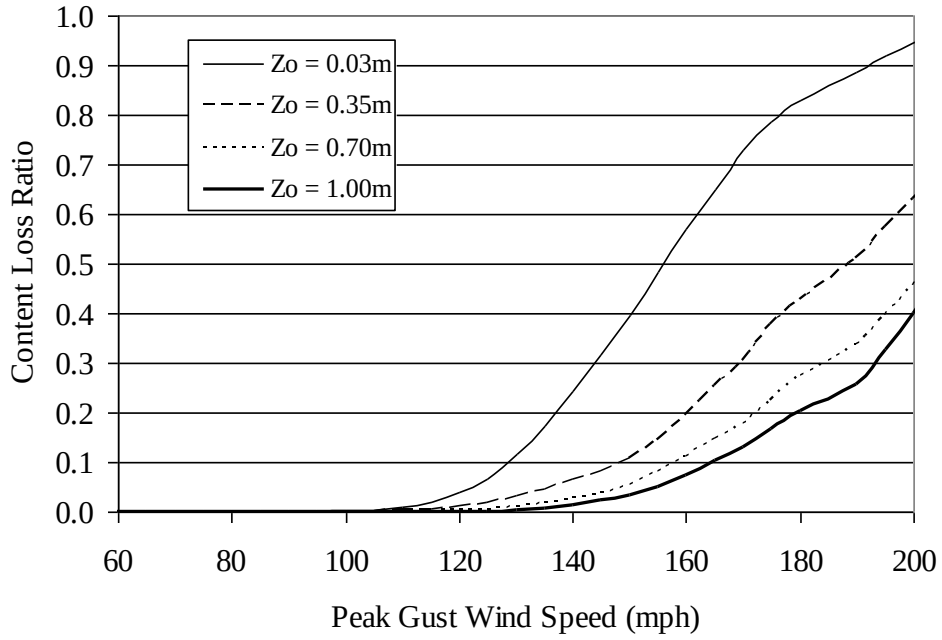

Figure K.15. Content Loss Function – Strip Mall Building A – Height=12′, No. of Units=6, Wood Deck with 6d Nails, Strapped Roof-Wall Connections, Built-up Roof Cover, Unreinforced Masonry Walls, Missile Environment A.

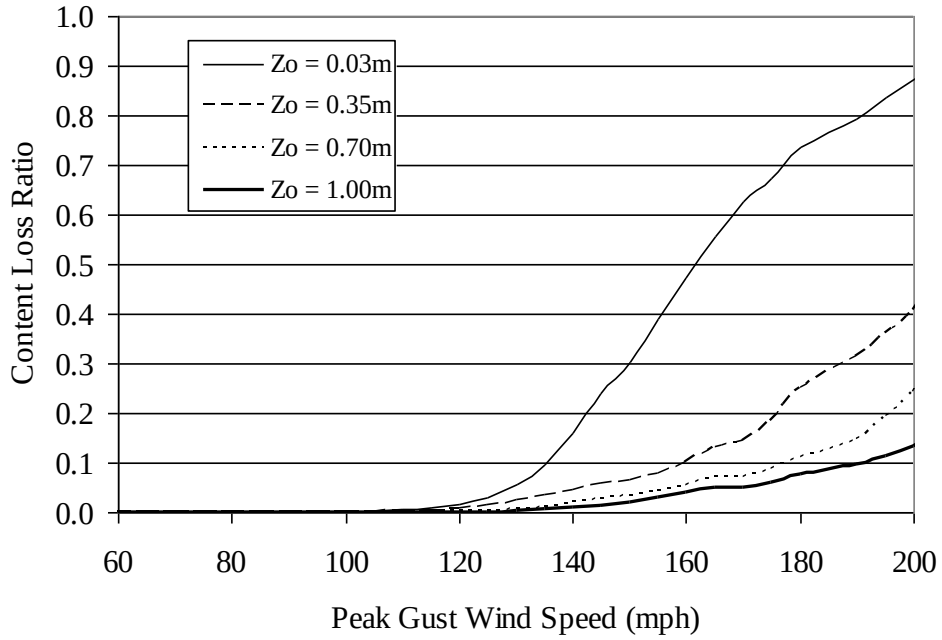

Figure K.16. Content Loss Function – Strip Mall Building A – Height=12′, No. of Units=6, Wood Deck with 8d Nails, Strapped Roof-Wall Connections, Built-up Roof Cover, Reinforced Masonry Walls, Missile Environment A.

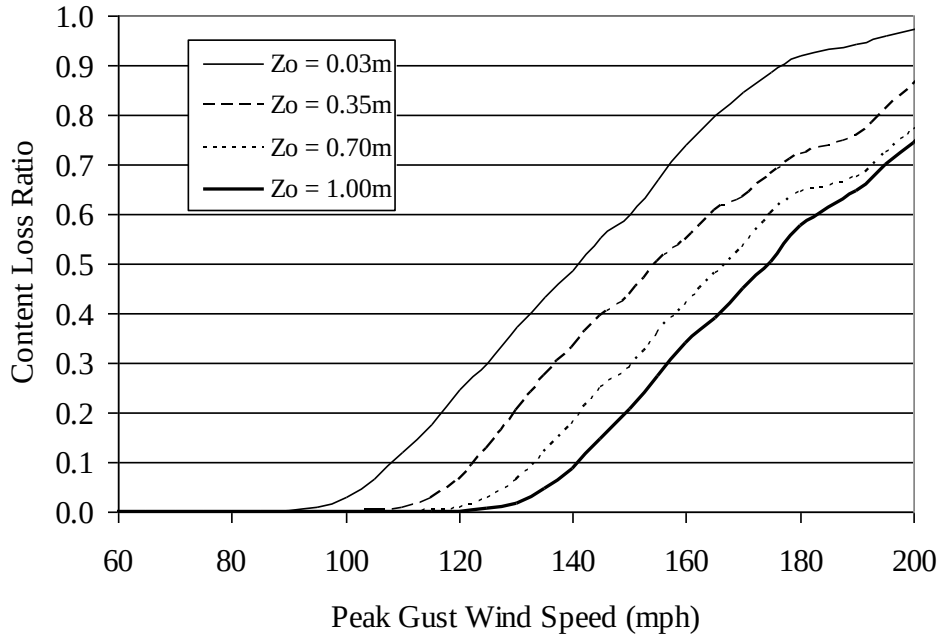

Figure K.17. Content Loss Function – Strip Mall Building A – Height=12′, No. of Units=6, Wood Deck with 8d Nails, Toe-Nailed Roof-Wall Connections, Built-up Roof Cover, Unreinforced Masonry Walls, Missile Environment A.

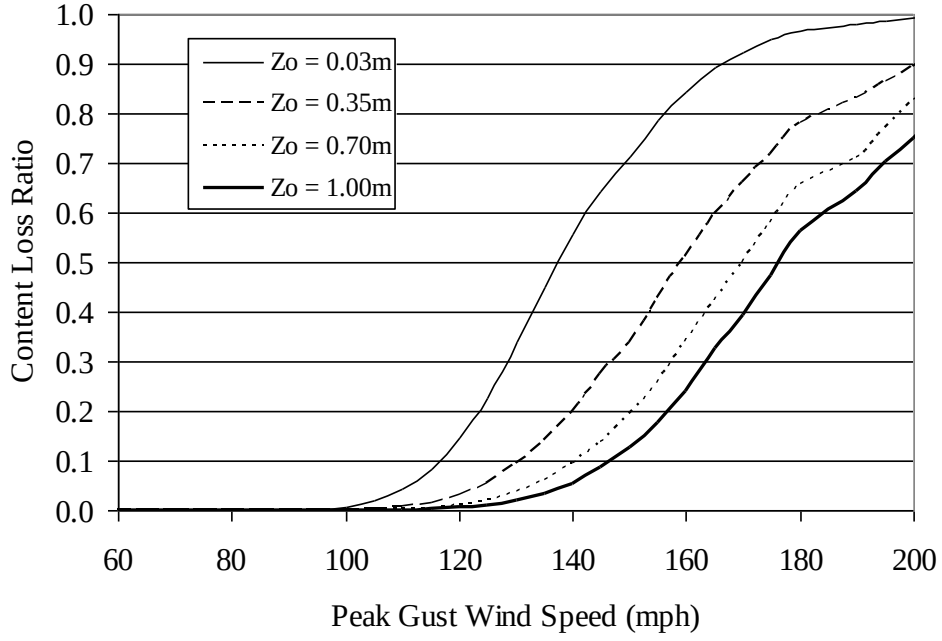

Figure K.18. Content Loss Function – Strip Mall Building B – Height=20′, No. of Units=6, Wood Deck with 8d Nails, Strapped Roof-Wall Connections, Built-up Roof Cover, Unreinforced Masonry Walls, Missile Environment A.

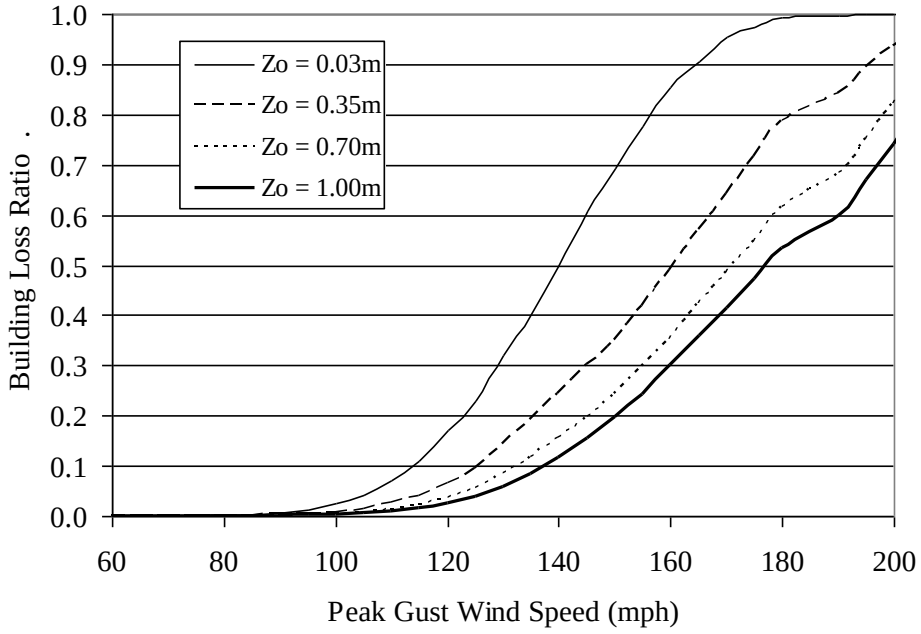

Figure K.19. Building Loss Function – Strip Mall Building C – Height=20′, No. of Units=6, Joist Spacing=6′, Metal Deck Welded to Joists, SBCCI 100 mph Design Criteria, Built-up Roof Cover, Unreinforced Masonry Walls, Missile Environment A.

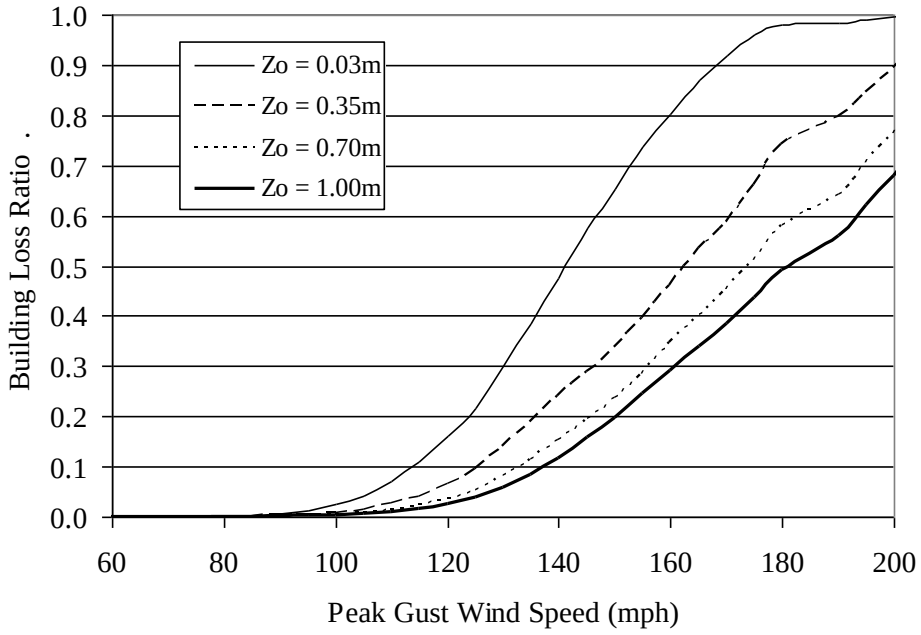

Figure K.20. Building Loss Function – Strip Mall Building B – Height=20′, No. of Units=6, Joist Spacing=4′, Metal Deck Welded to Joists, SBCCI 100 mph Design Criteria, Built-up Roof Cover, Unreinforced Masonry Walls, Missile Environment A.

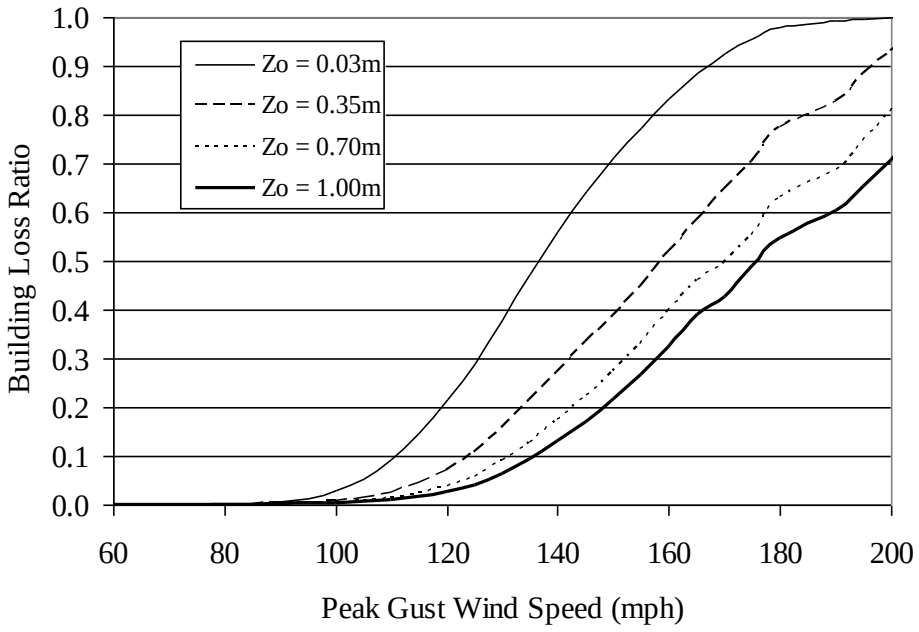

Figure K.21. Building Loss Function – Strip Mall Building D – Height=20′, No. of Units=1, Joist Spacing=6′, Metal Deck Welded to Joists, SBCCI 100 mph Design Criteria, Built-up Roof Cover, Unreinforced Masonry Walls, Missile Environment A.

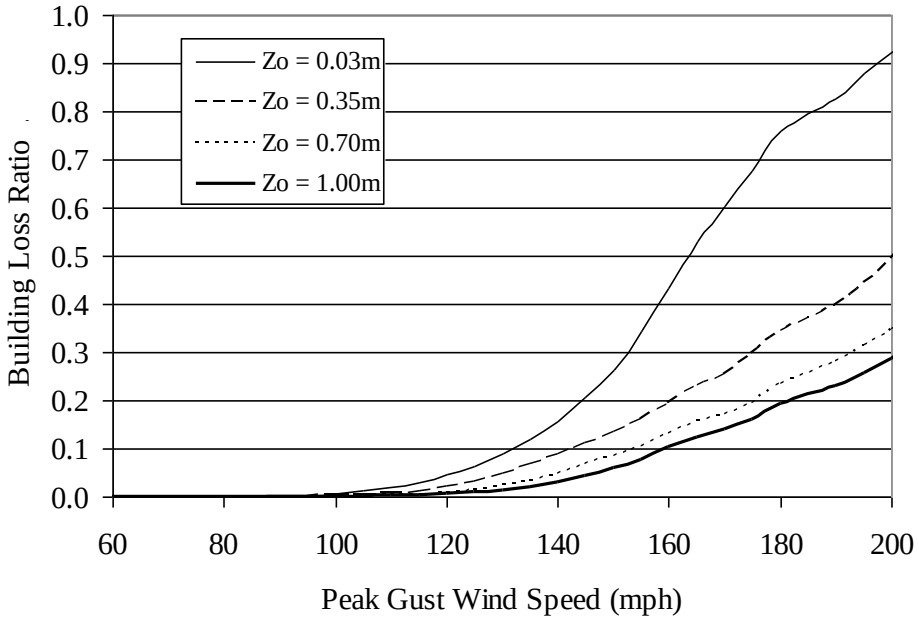

Figure K.22. Building Loss Function – Strip Mall Building A – Height=12′, No. of Units=6, Joist Spacing=4′, Metal Deck Welded to Joists, SBCCI 100 mph Design Criteria, Built-up Roof Cover, Unreinforced Masonry Walls, Missile Environment A.

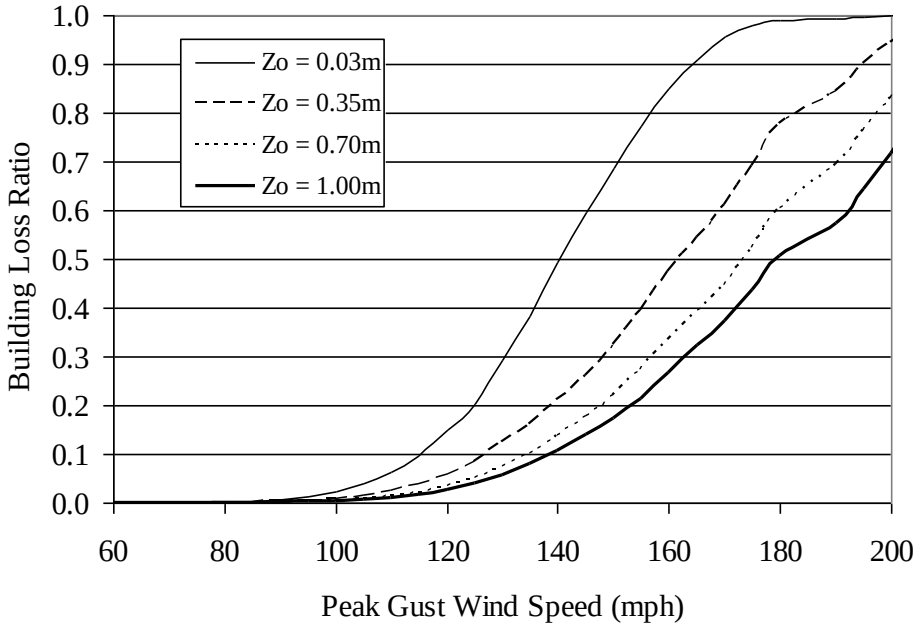

Figure K.23. Building Loss Function – Strip Mall Building C – Height=20′, No. of Units=6, Joist Spacing=6′, Metal Deck Welded to Joists, SBCCI 100 mph Design Criteria, Built-up Roof Cover, Unreinforced Masonry Walls, Missile Environment B.

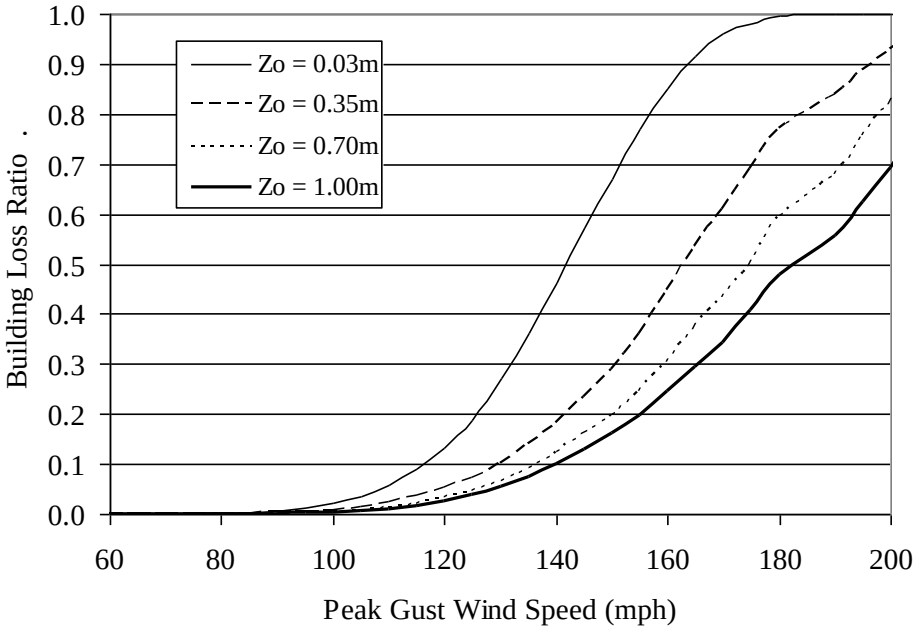

Figure K.24. Building Loss Function – Strip Mall Building C – Height=20′, No. of Units=6, Joist Spacing=6′, Metal Deck Welded to Joists, SBCCI 100 mph Design Criteria, Built-up Roof Cover, Unreinforced Masonry Walls, Missile Environment C.

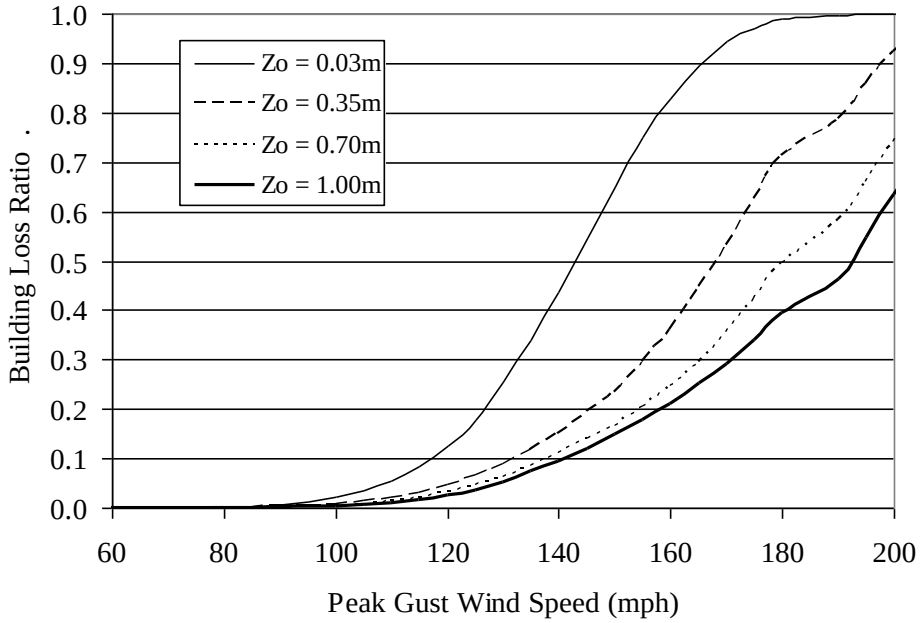

Figure K.25. Building Loss Function – Strip Mall Building C – Height=20′, No. of Units=6, Joist Spacing=6′, Metal Deck Welded to Joists, SBCCI 100 mph Design Criteria, Built-up Roof Cover, Unreinforced Masonry Walls, Missile Environment D.

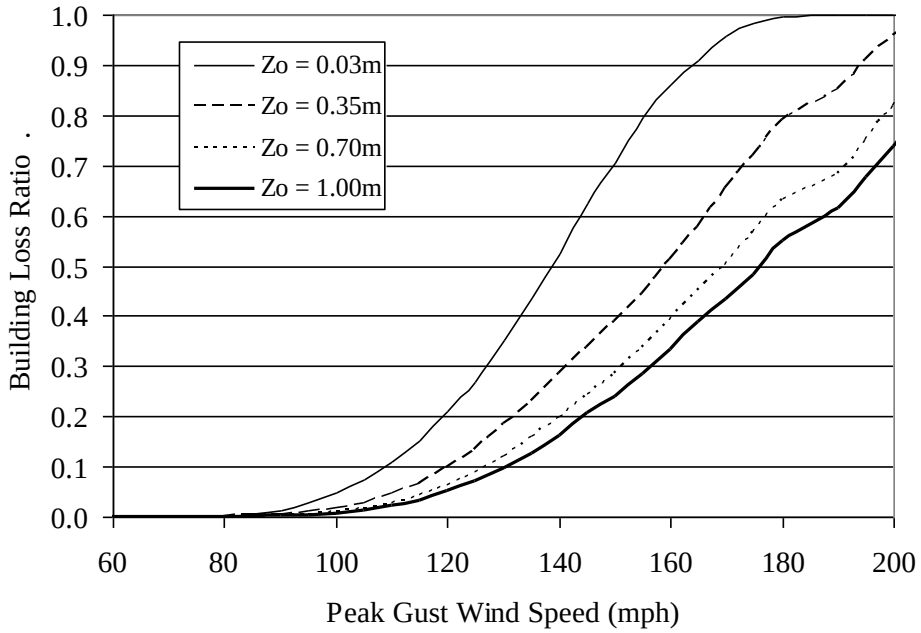

Figure K.26. Building Loss Function – Strip Mall Building C – Height=20′, No. of Units=6, Joist Spacing=6′, Metal Deck Welded to Joists, SBCCI 100 mph Design Criteria, Single Ply Membrane Roof Cover, Unreinforced Masonry Walls, Missile Environment A.

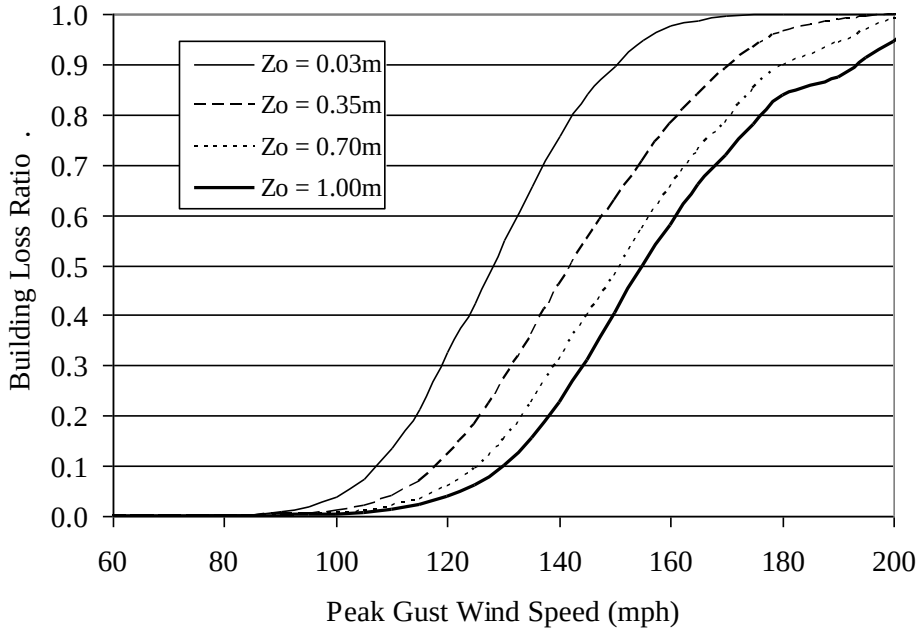

Figure K.27. Building Loss Function – Strip Mall Building C – Height=20′, No. of Units=6, Joist Spacing=6′, Metal Deck Welded to Joists with 50% Reduction in Resistance, SBCCI 100 mph Design Criteria, Built-up Roof Cover, Unreinforced Masonry Walls, Missile Environment A.

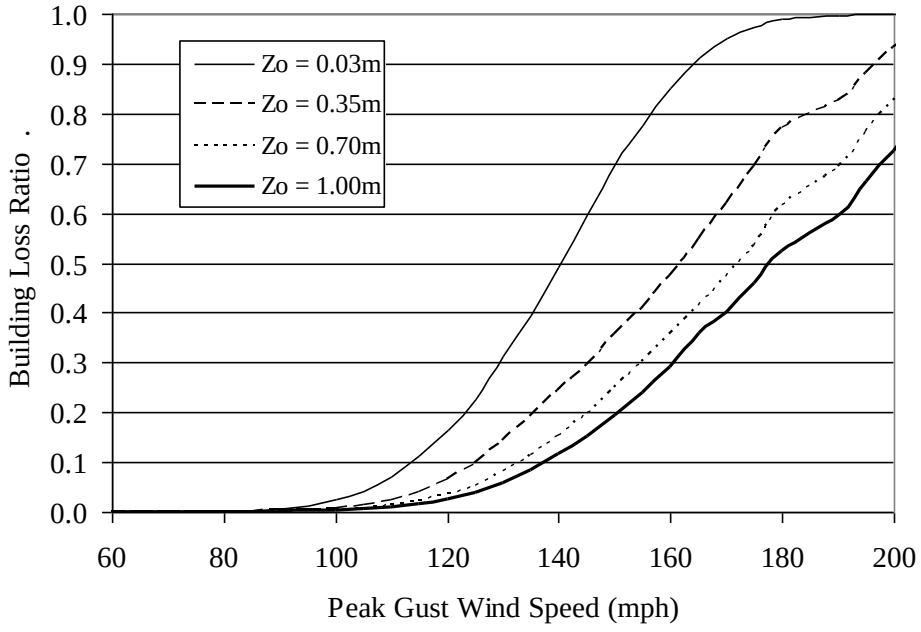

Figure K.28. Building Loss Function – Strip Mall Building C – Height=20′, No. of Units=6, Joist Spacing=6′, Metal Deck Screwed to Joists, SBCCI 100 mph Design Criteria, Built-up Roof Cover, Unreinforced Masonry Walls, Missile Environment A.

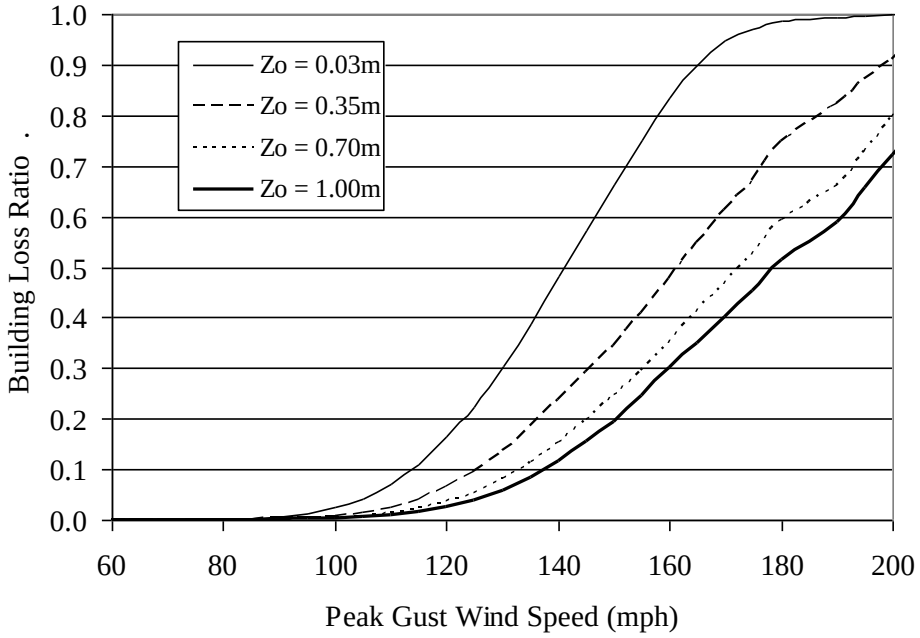

Figure K.29. Building Loss Function – Strip Mall Building C – Height=20′, No. of Units=6, Joist Spacing=6′, Metal Deck Welded to Joists, ASCE 100 mph Design Criteria, Built-up Roof Cover, Unreinforced Masonry Walls, Missile Environment A.

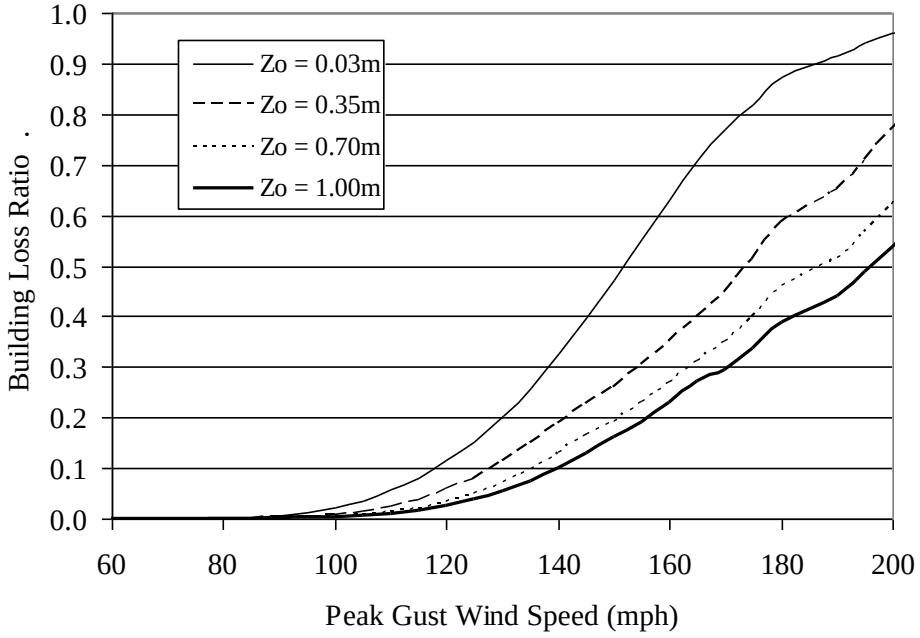

Figure K.30. Building Loss Function – Strip Mall Building C – Height=20′, No. of Units=6, Joist Spacing=6′, Metal Deck Welded to Joists, SBCCI 100 mph Design Criteria, Built-up Roof Cover, Reinforced Masonry Walls, Missile Environment A.

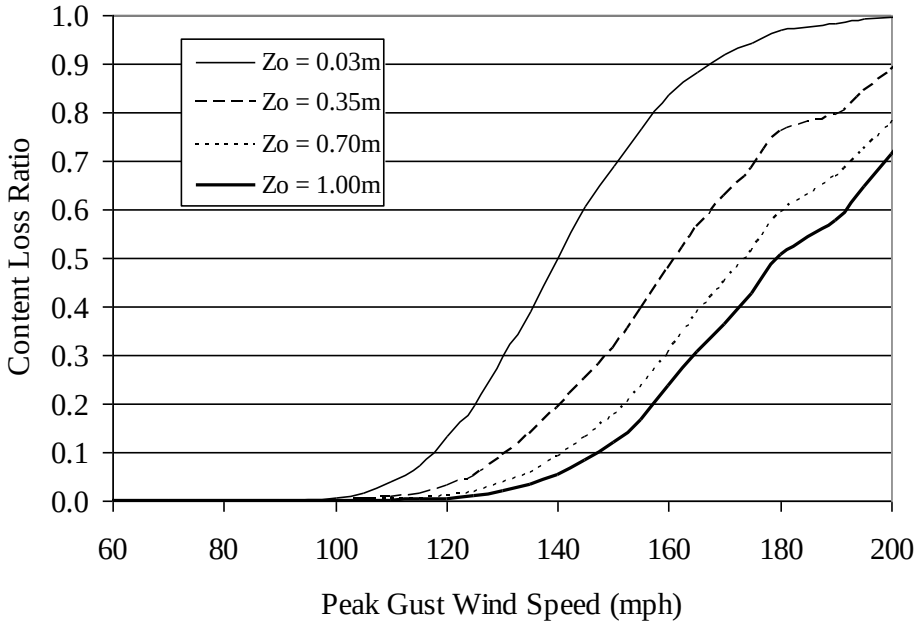

Figure K.31. Content Loss Function – Strip Mall Building C – Height=20′, No. of Units=6, Joist Spacing=6′, Metal Deck Welded to Joists, SBCCI 100 mph Design Criteria, Built-up Roof Cover, Unreinforced Masonry Walls, Missile Environment A.

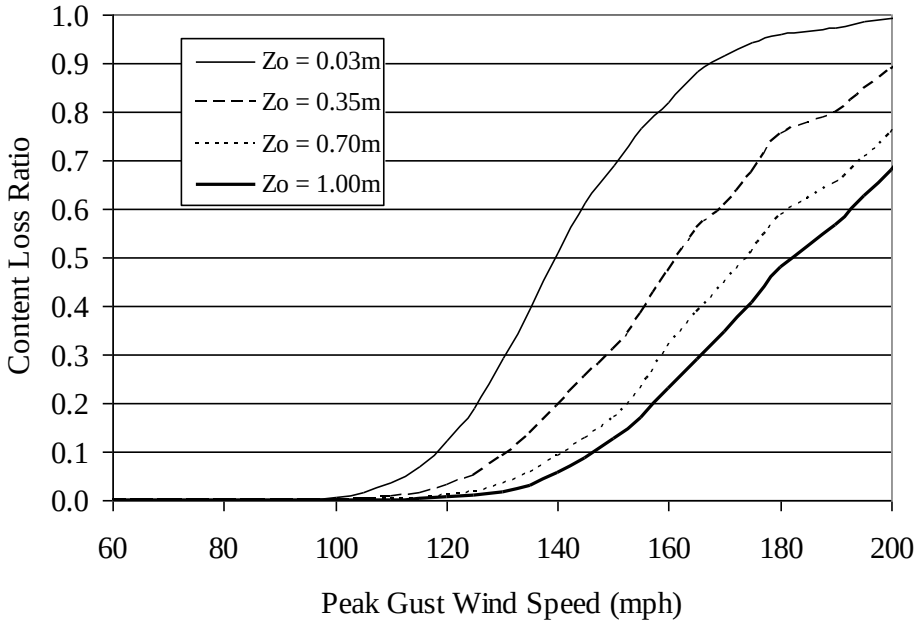

Figure K.32. Content Loss Function – Strip Mall Building B – Height=20′, No. of Units=6, Joist Spacing=4′, Metal Deck Welded to Joists, SBCCI 100 mph Design Criteria, Built-up Roof Cover, Unreinforced Masonry Walls, Missile Environment A.

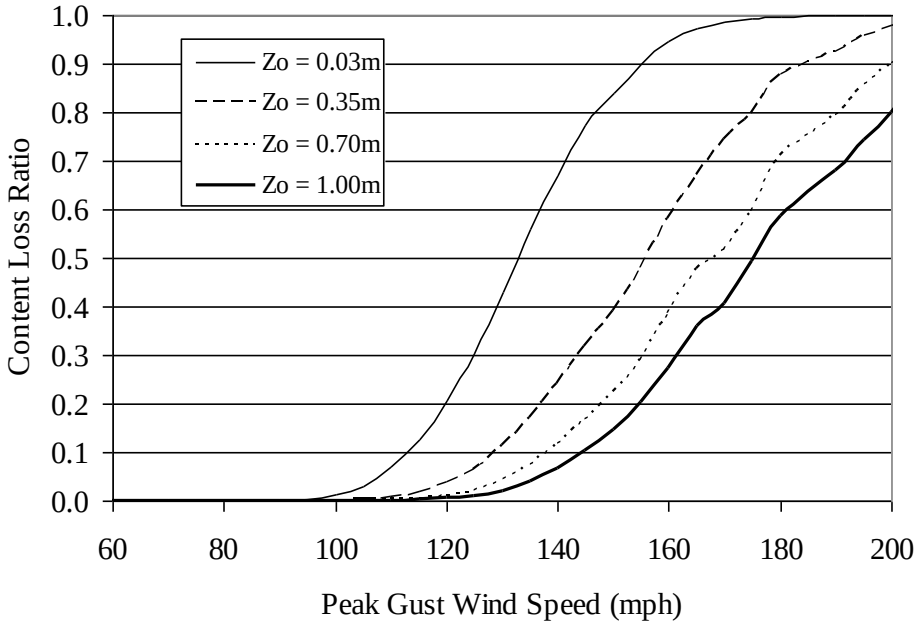

Figure K.33. Content Loss Function – Strip Mall Building D – Height=20′, No. of Units=1, Joist Spacing=6′, Metal Deck Welded to Joists, SBCCI 100 mph Design Criteria, Built-up Roof Cover, Unreinforced Masonry Walls, Missile Environment A.

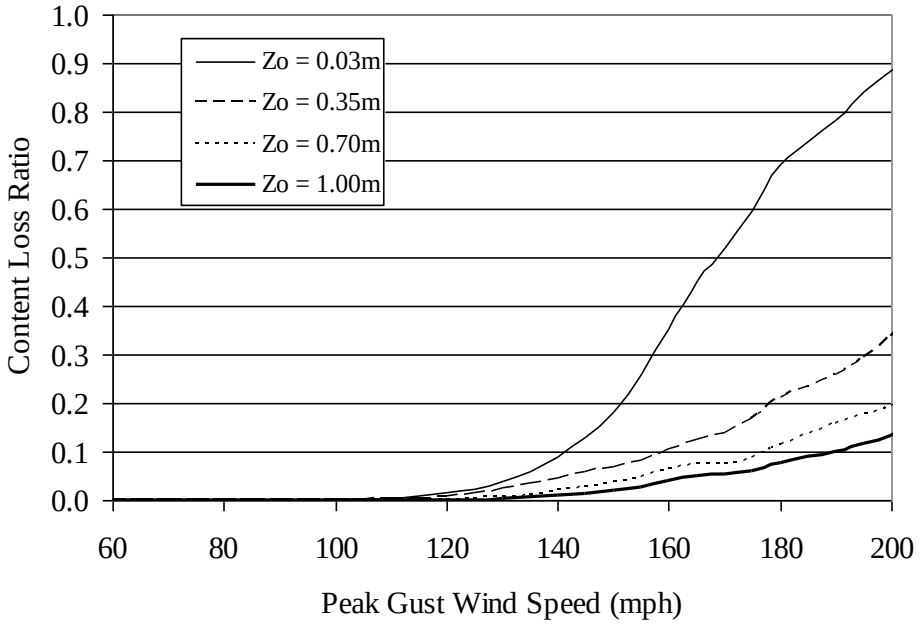

Figure K.34. Content Loss Function – Strip Mall Building A – Height=12′, No. of Units=6, Joist Spacing=4′, Metal Deck Welded to Joists, SBCCI 100 mph Design Criteria, Built-up Roof Cover, Unreinforced Masonry Walls, Missile Environment A.

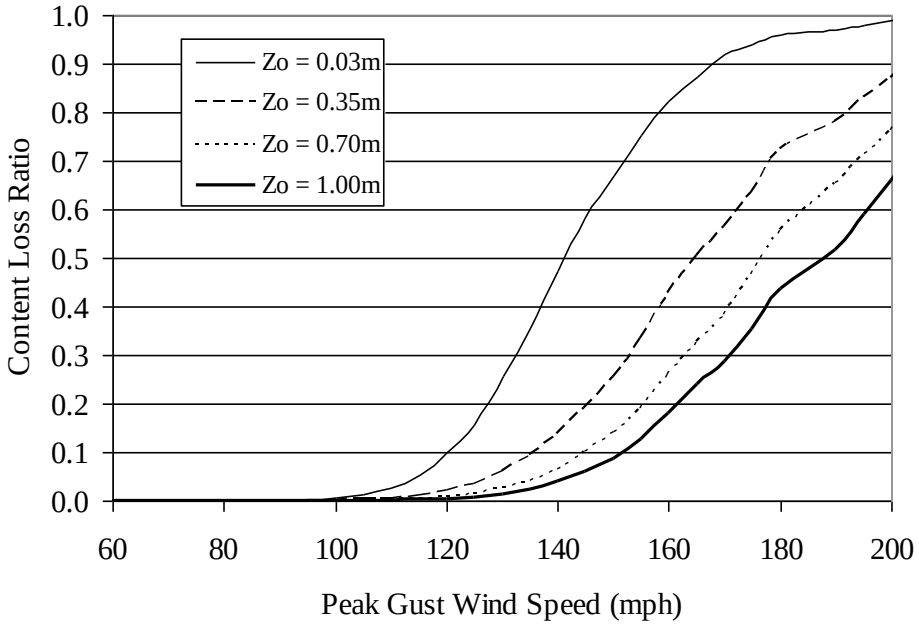

Figure K.35. Content Loss Function – Strip Mall Building C – Height=20′, No. of Units=6, Joist Spacing=6′, Metal Deck Welded to Joists, SBCCI 100 mph Design Criteria, Built-up Roof Cover, Unreinforced Masonry Walls, Missile Environment B.

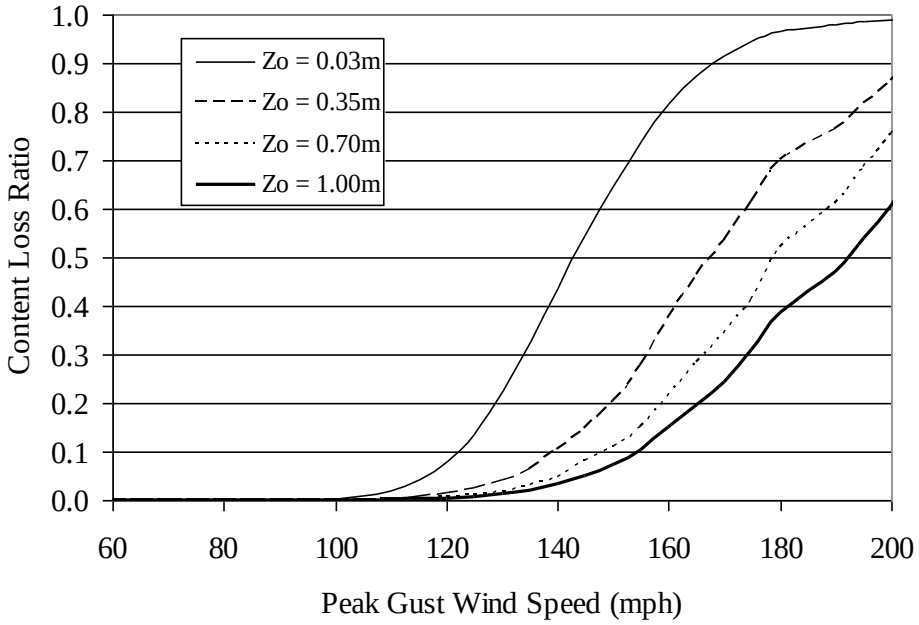

Figure K.36. Content Loss Function – Strip Mall Building C – Height=20′, No. of Units=6, Joist Spacing=6′, Metal Deck Welded to Joists, SBCCI 100 mph Design Criteria, Built-up Roof Cover, Unreinforced Masonry Walls, Missile Environment C.

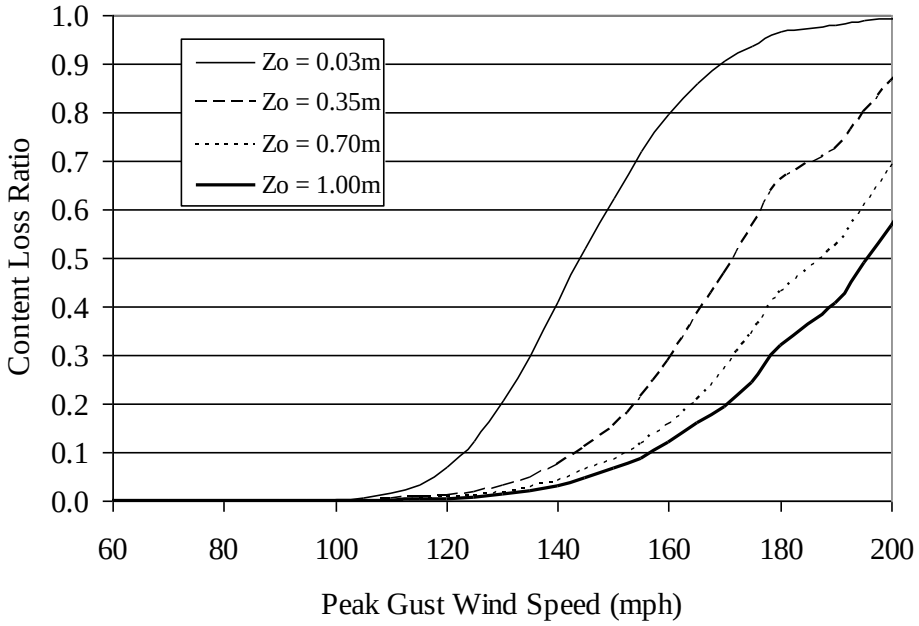

Figure K.37. Content Loss Function – Strip Mall Building C – Height=20′, No. of Units=6, Joist Spacing=6′, Metal Deck Welded to Joists, SBCCI 100 mph Design Criteria, Built-up Roof Cover, Unreinforced Masonry Walls, Missile Environment D.

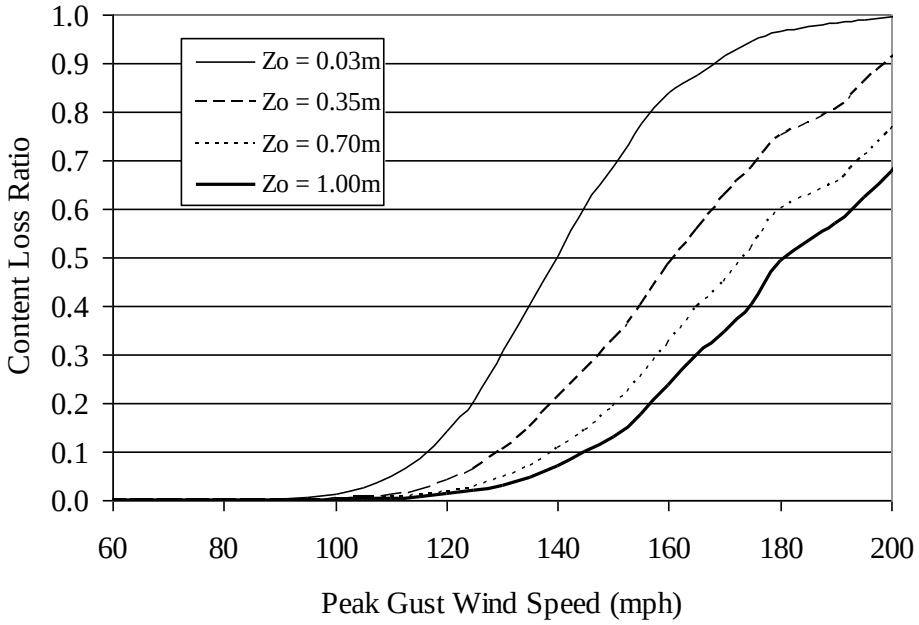

Figure K.38. Content Loss Function – Strip Mall Building C – Height=20′, No. of Units=6, Joist Spacing=6′, Metal Deck Welded to Joists, SBCCI 100 mph Design Criteria, Single Ply Membrane Roof Cover, Unreinforced Masonry Walls, Missile Environment A.

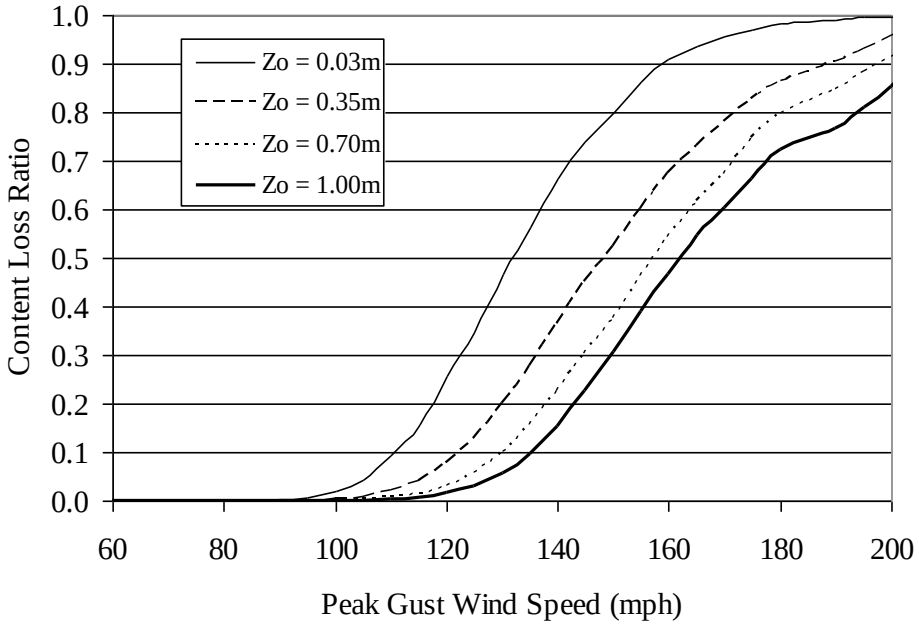

Figure K.39. Content Loss Function – Strip Mall Building C – Height=20′, No. of Units=6, Joist Spacing=6′, Metal Deck Welded to Joists with *50*% Reduction in Resistance, SBCCI 100 mph Design Criteria, Built-up Roof Cover, Unreinforced Masonry Walls, Missile Environment A.

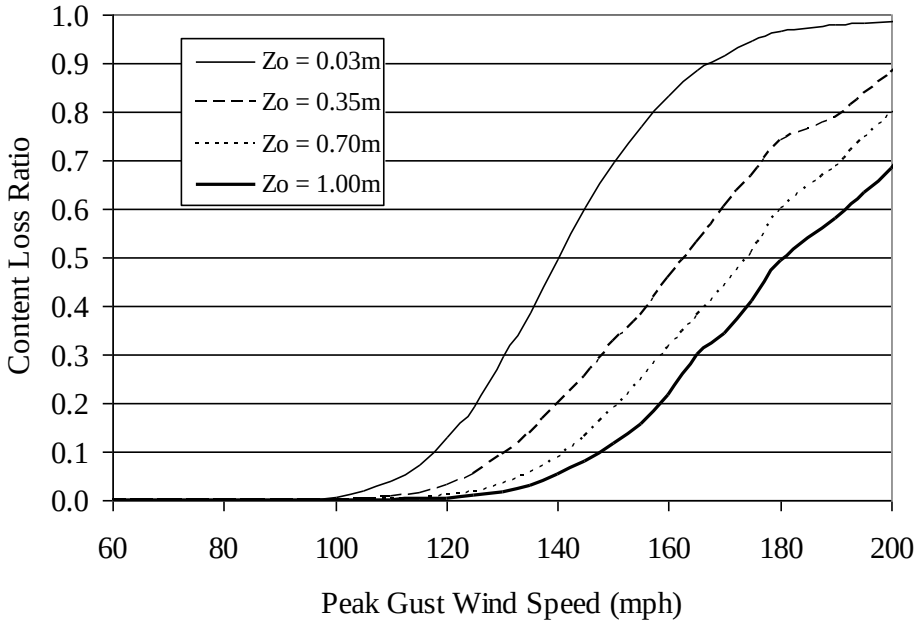

Figure K.40. Content Loss Function – Strip Mall Building C – Height=20′, No. of Units=6, Joist Spacing=6′, Metal Deck Screwed to Joists, SBCCI 100 mph Design Criteria, Built-up Roof Cover, Unreinforced Masonry Walls, Missile Environment A.

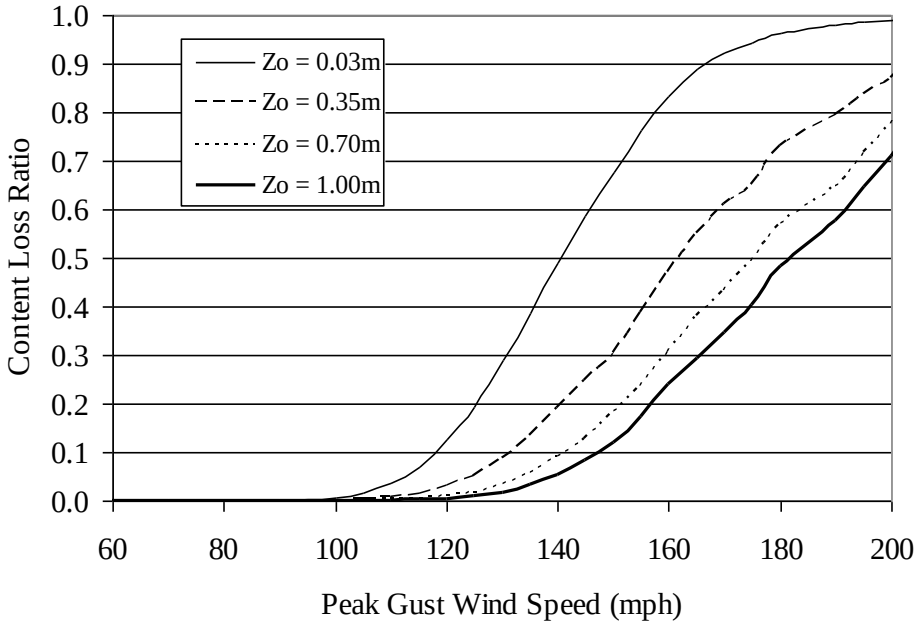

Figure K.41. Content Loss Function – Strip Mall Building C – Height=20′, No. of Units=6, Joist Spacing=6′, Metal Deck Welded to Joists, ASCE 100 mph Design Criteria, Built-up Roof Cover, Unreinforced Masonry Walls, Missile Environment A.

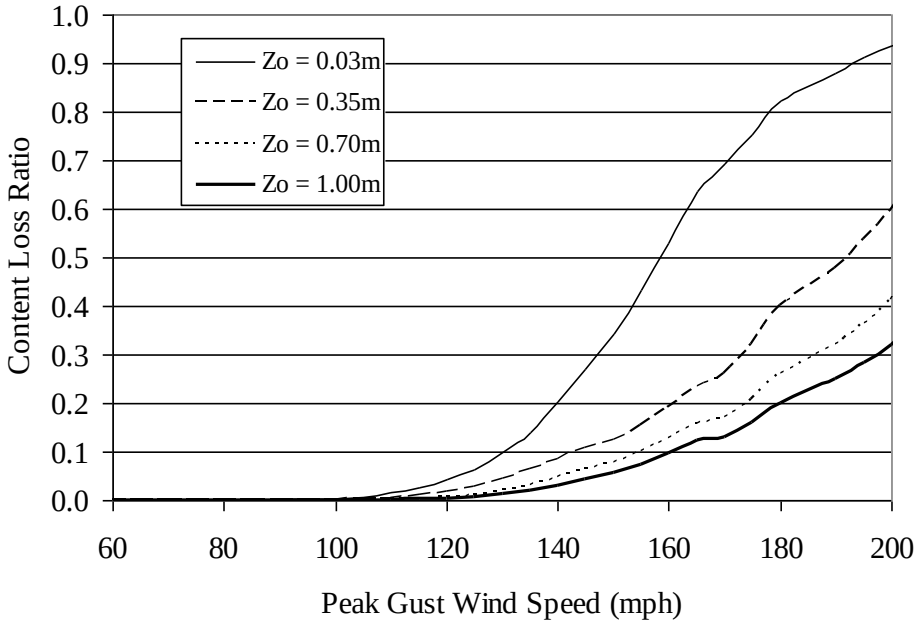

Figure K.42. Content Loss Function – Strip Mall Building C – Height=20′, No. of Units=6, Joist Spacing=6′, Metal Deck Welded to Joists, SBCCI 100 mph Design Criteria, Built-up Roof Cover, Reinforced Masonry Walls, Missile Environment A.

Appendix L.
Loss Functions for Pre-Engineered Metal Buildings

Appendix L.
Loss Functions for Pre-Engineered Metal Buildings

This appendix presents loss functions for pre-engineered metal buildings (see Chapter 7.12). The loss functions represent either average building loss normalized by building value or average content loss normalized by content value. Therefore, the loss ratios range between 0 and 1 in both cases. Note that the content value is set to 50% of the building value. For a given simulated storm, the building loss ratio and content loss ratio are estimated based on the modeled damage and the largest gust speed over the entire duration of the simulated storm is saved. The loss functions are then computed by averaging the loss ratios associated with the storms producing a maximum gust speed within 5 mph ranges. The average loss ratios (content or building loss) associated with each 5 mph gust speed range are then plotted at the center of that range. Note that the wind speeds are representative of open terrain at 10 m above ground.

Table L.1 lists the figures provided in this appendix. Two sets of five figures are given for the metal buildings. The first set of five figures (Figures L.1 through L.5) show building loss functions and the second set (Figures L.6 through L.10) show content loss functions. The first figure in each set of five shows loss results for the small metal building designed using a 100 mph design speed and with no reduction in the metal roof panel capacity. The remaining four plots in each set show loss results for buildings which are different by a single variable in comparison to the reference building (note that the changed variable is underlined in the figure titles).

Table L.1. Sample Loss Functions for Pre-Engineered Metal Buildings

Figure	Loss Type	Model Building	Design Wind Speed	Metal Panel Capacity
L.1	Building	Small	100 mph	Full
L.2	Building	**Medium**	100 mph	Full
L.3	Building	**Large**	100 mph	Full
L.4	Building	Small	**90 mph**	Full
L.5	Building	Small	100 mph	**50%**
L.6	Content	Small	100 mph	Full
L.7	Content	**Medium**	100 mph	Full
L.8	Content	**Large**	100 mph	Full
L.9	Content	Small	**90 mph**	Full
L.10	Content	Small	100 mph	**50%**

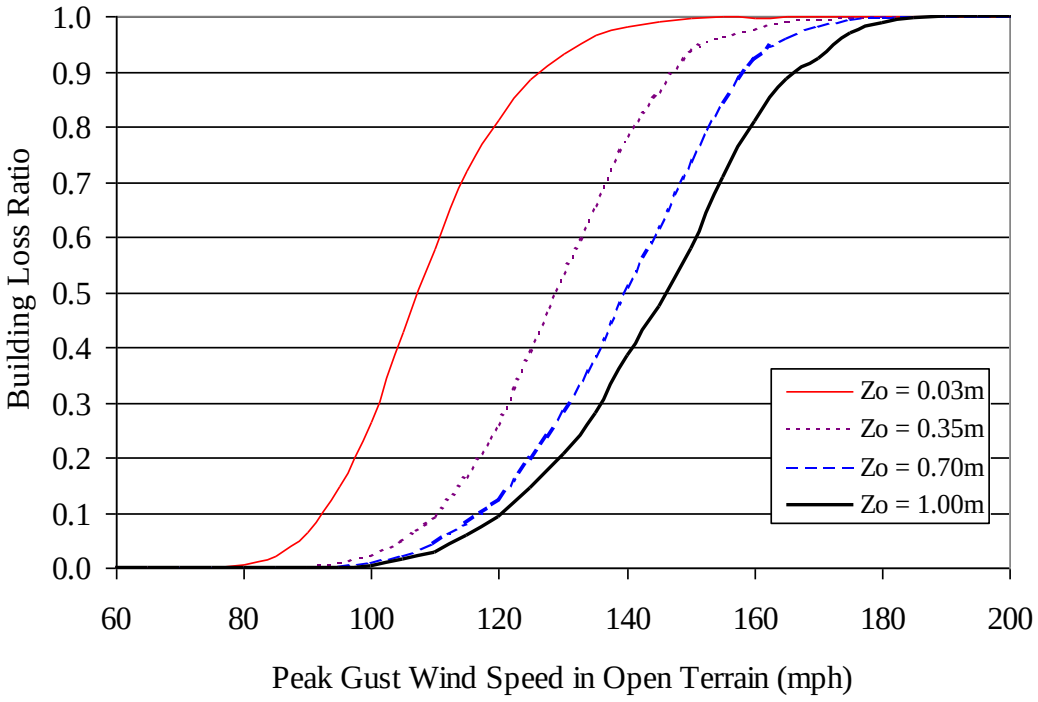

Figure L.1. Building Loss Ratios versus Peak Gust Wind Speed – Small Metal Building, 100 mph Design Speed, No Reduction in Metal Panel Capacity.

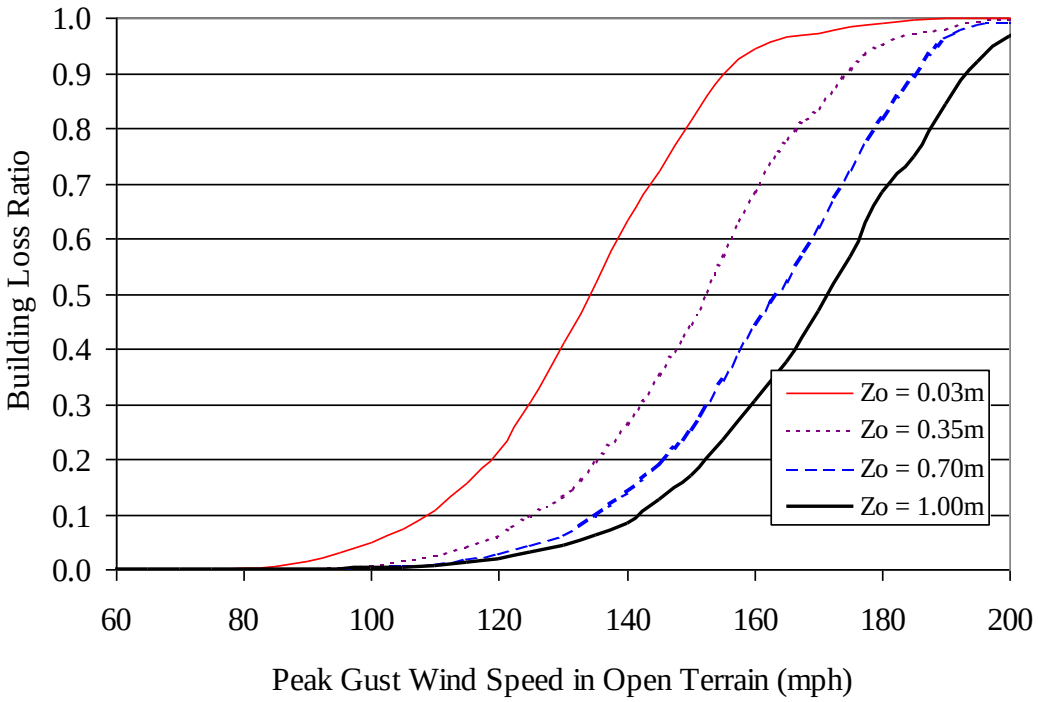

Figure L.2. Building Loss Ratios versus Peak Gust Wind Speed – <u>Medium Metal Building</u>, 100 mph Design Speed, No Reduction in Metal Panel Capacity.

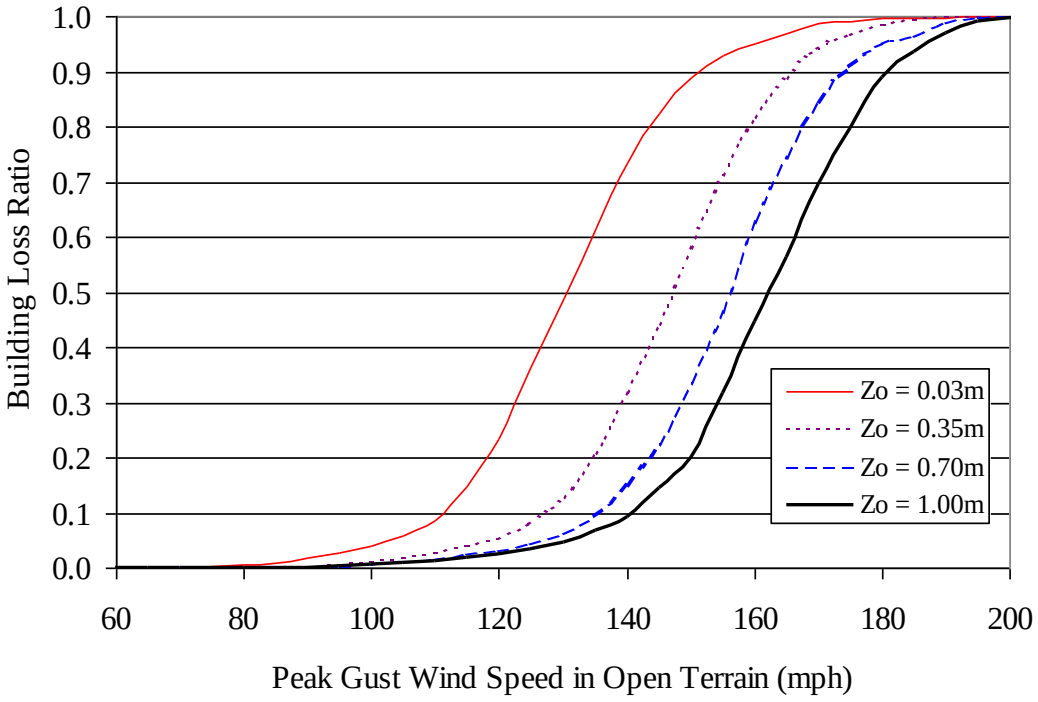

Figure L.3. Building Loss Ratios versus Peak Gust Wind Speed – <u>Large Metal Building</u>, 100 mph Design Speed, No Reduction in Metal Panel Capacity.

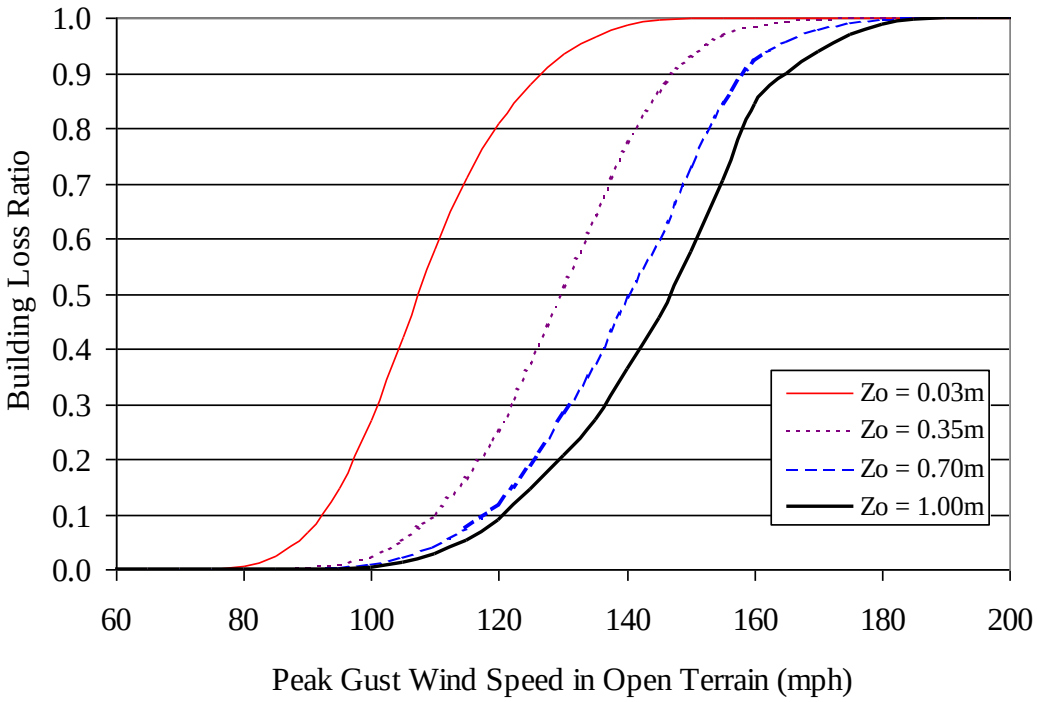

Figure L.4. Building Loss Ratios versus Peak Gust Wind Speed – Small Metal Building, <u>90 mph Design Speed</u>, No Reduction in Metal Panel Capacity.

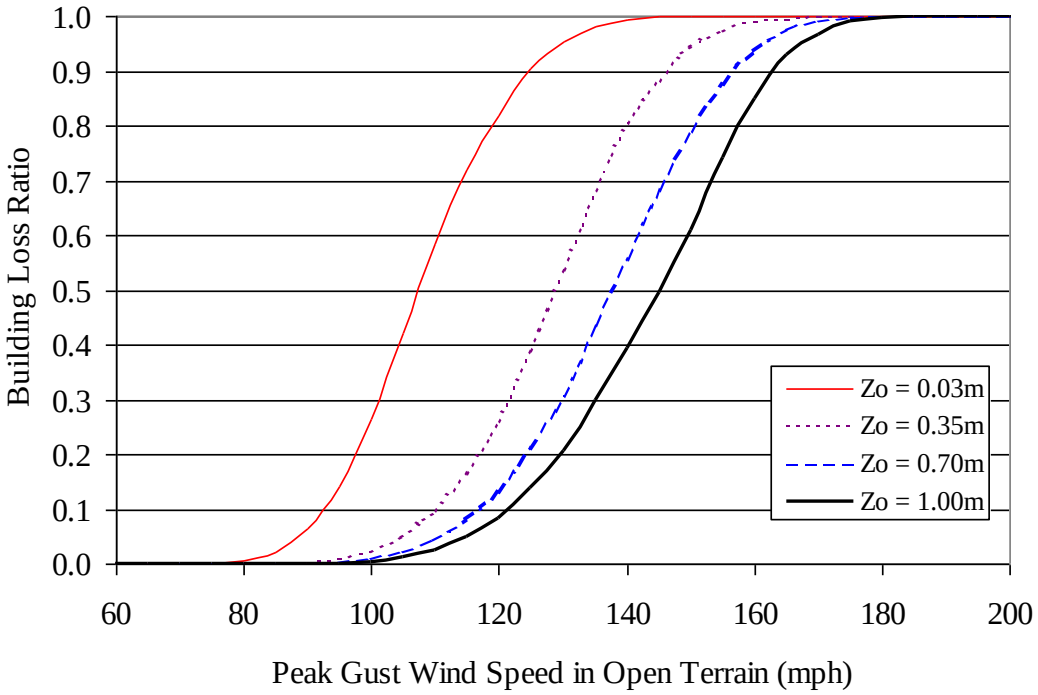

Figure L.5. Building Loss Ratios versus Peak Gust Wind Speed – Small Metal Building, 100 mph Design Speed, 50% Reduction in Metal Panel Capacity.

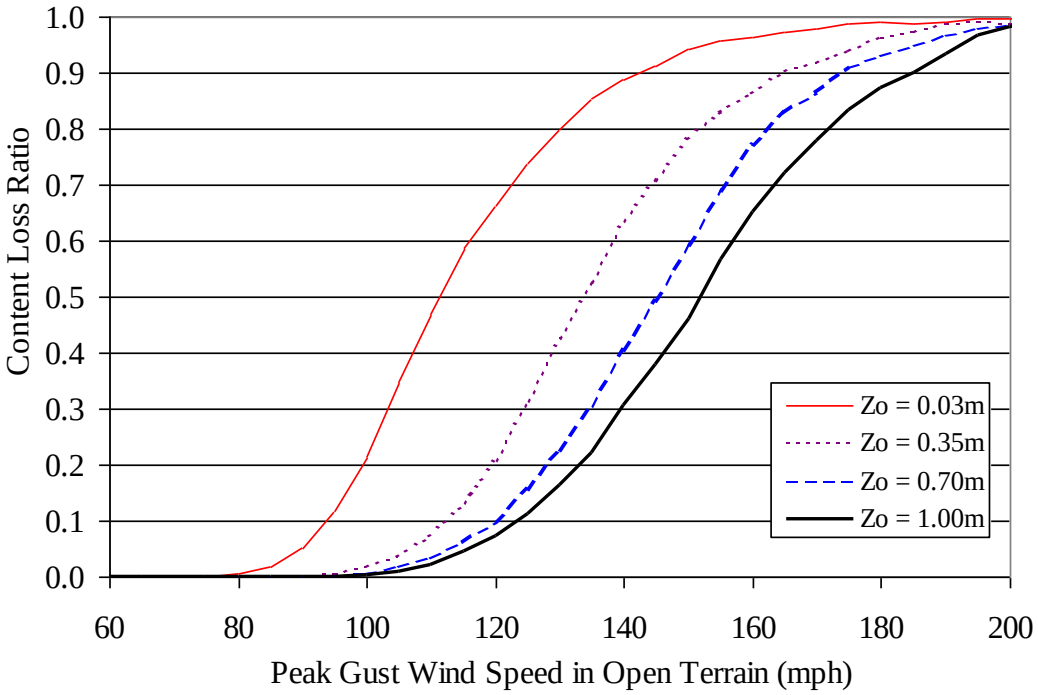

Figure L.6. Content Loss Ratios versus Peak Gust Wind Speed – Small Metal Building, 100 mph Design Speed, No Reduction in Metal Panel Capacity.

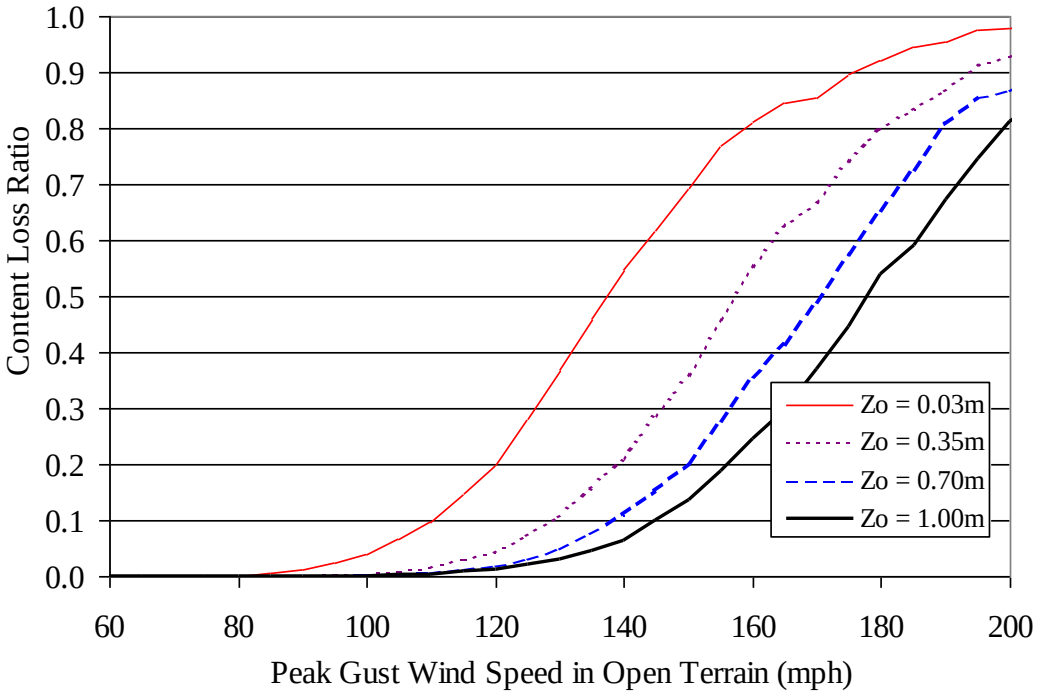

Figure L.7. Content Loss Ratios versus Peak Gust Wind Speed – <u>Medium Metal Building</u>, 100 mph Design Speed, No Reduction in Metal Panel Capacity.

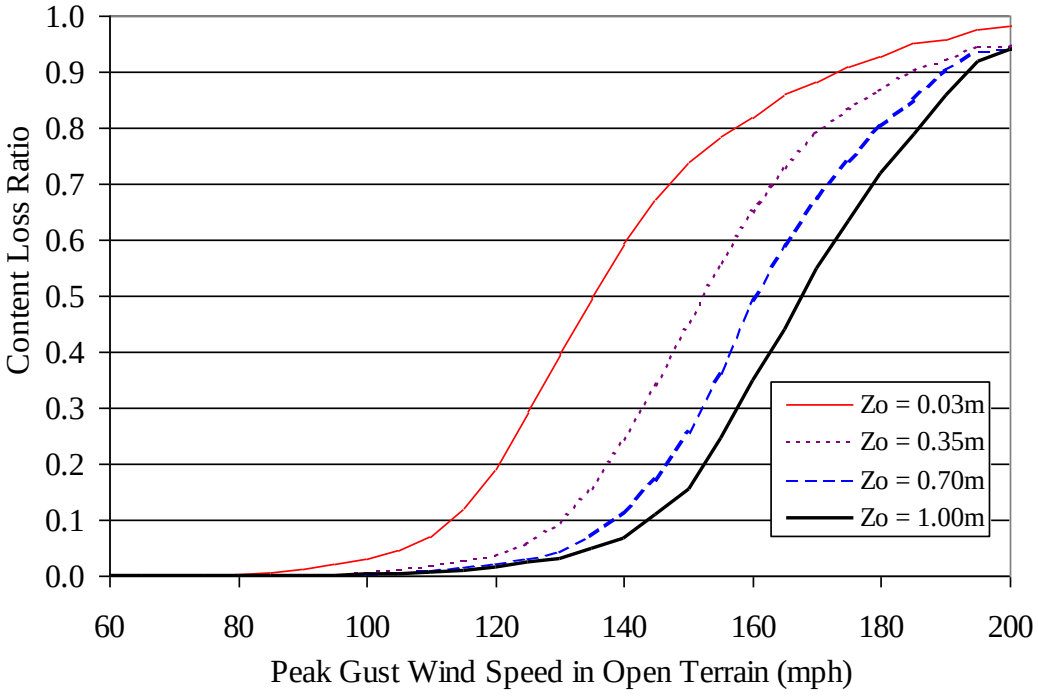

Figure L.8. Content Loss Ratios versus Peak Gust Wind Speed – <u>Large Metal Building</u>, 100 mph Design Speed, No Reduction in Metal Panel Capacity.

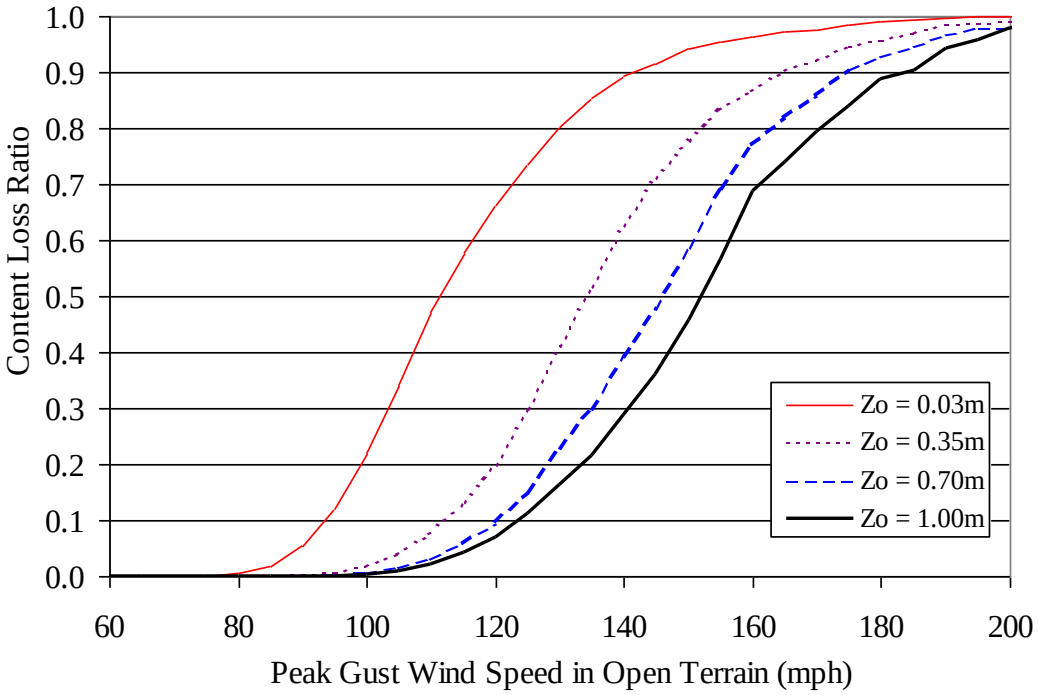

Figure L.9. Content Loss Ratios versus Peak Gust Wind Speed – Small Metal Building, 90 mph Design Speed, No Reduction in Metal Panel Capacity.

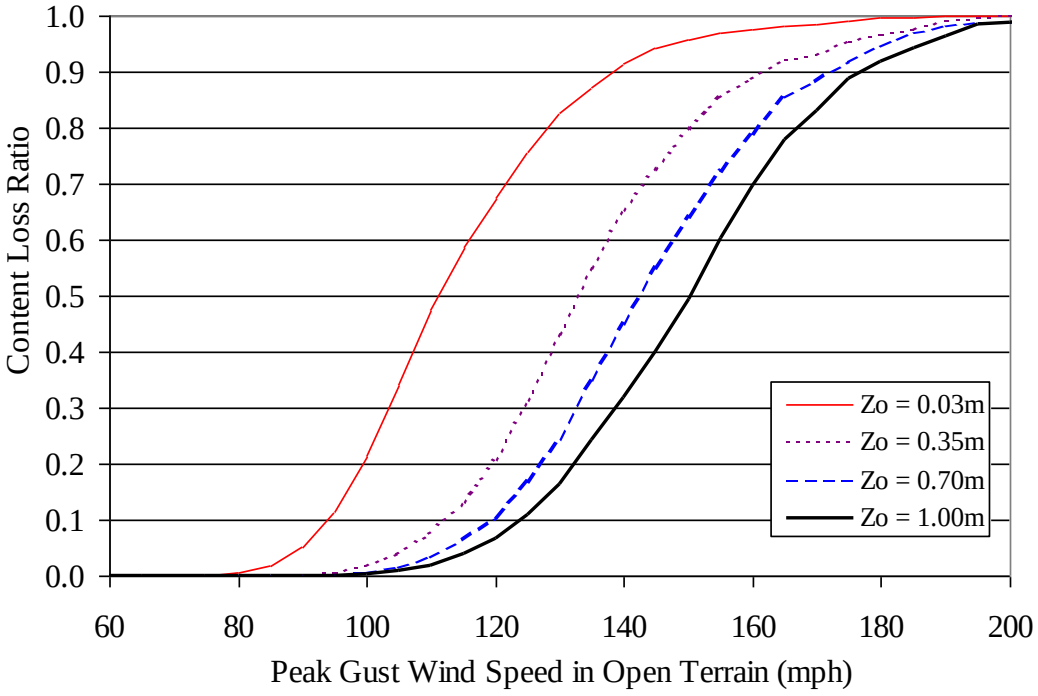

Figure L.10. Content Loss Ratios versus Peak Gust Wind Speed – Small Metal Building, 100 mph Design Speed, 50% Reduction in Metal Panel Capacity.

Appendix M.
Loss Functions for Engineered Residential and Commercial Buildings

Appendix M.
Loss Functions for Engineered Residential and Commercial Buildings

This appendix presents loss functions for engineered residential and commercial buildings (see Section 7.13). The loss functions represent either average building loss normalized by building value or average content loss normalized by content value. Therefore, the loss ratios range between 0 and 1 in both cases. Note that the content value is set to 50% of the building value. For a given simulated storm, the building loss ratio and content loss ratio are estimated based on the modeled damage and the largest gust speed over the entire duration of the simulated storm is saved. The loss functions are then computed by averaging the loss ratios associated with the storms producing a maximum gust speed within 5 mph ranges. The average loss ratios (content or building loss) associated with each 5 mph gust speed range are then plotted at the center of that range. Note that the wind speeds are representative of open terrain at 10 m above ground.

Table M.1 lists the figures provided in this appendix. Loss functions for the two-, five- and eight-story engineered buildings are given in Figures M.1 through M.18, M.19 through M.36 and M.37 through M.54, respectively. Two sets of nine figures are given for each of the two-, five- and eight-story engineered buildings. The first set of nine figures shows building loss functions and the second set shows content loss functions. The first figure in each set of nine shows loss results for the engineered residential building having 33% glazing coverage, a built-up roof cover and situated in Missile Environment A. The remaining eight plots in each set show loss results for buildings which are different by a single variable in comparison to the reference building (note that the changed variable is underlined in the figure titles).

Table M.1. Sample Loss Functions for Engineered Residential and Commercial Buildings

Figure	Loss Type	Stories	Occupancy	Roof Deck	Roof Cover	Glazing	Missile Environ.
M.1	Building	2	Residential	Metal	BUR	33%	A
M.2	Building	2	Residential	Metal	BUR	**20%**	A
M.3	Building	2	Residential	Metal	BUR	**50%**	A
M.4	Building	2	Residential	Metal	**SPM**	33%	A
M.5	Building	2	Residential	Metal	BUR	33%	**B**
M.6	Building	2	Residential	Metal	BUR	33%	**C**
M.7	Building	2	Residential	Metal	BUR	33%	**D**
M.8	Building	2	**Commercial**	Metal	BUR	33%	A
M.9	Building	2	Residential	**Concrete**	BUR	33%	A
M.10	Content	2	Residential	Metal	BUR	33%	A
M.11	Content	2	Residential	Metal	BUR	**20%**	A
M.12	Content	2	Residential	Metal	BUR	**50%**	A
M.13	Content	2	Residential	Metal	**SPM**	33%	A
M.14	Content	2	Residential	Metal	BUR	33%	**B**

Table M.1. Sample Loss Functions for Engineered Residential and Commercial Buildings (concluded)

Figure	Loss Type	Stories	Occupancy	Roof Deck	Roof Cover	Glazing	Missile Environ.
M.15	Content	2	Residential	Metal	BUR	33%	**C**
M.16	Content	2	Residential	Metal	BUR	33%	**D**
M.17	Content	2	**Commercial**	Metal	BUR	33%	A
M.18	Content	2	Residential	**Concrete**	BUR	33%	A
M.19	Building	**5**	Residential	Metal	BUR	33%	A
M.20	Building	5	Residential	Metal	BUR	**20%**	A
M.21	Building	5	Residential	Metal	BUR	**50%**	A
M.22	Building	5	Residential	Metal	**SPM**	33%	A
M.23	Building	5	Residential	Metal	BUR	33%	**B**
M.24	Building	5	Residential	Metal	BUR	33%	**C**
M.25	Building	5	Residential	Metal	BUR	33%	**D**
M.26	Building	5	**Commercial**	Metal	BUR	33%	A
M.27	Building	5	Residential	**Concrete**	BUR	33%	A
M.28	Content	5	Residential	Metal	BUR	33%	A
M.29	Content	5	Residential	Metal	BUR	**20%**	A
M.30	Content	5	Residential	Metal	BUR	**50%**	A
M.31	Content	5	Residential	Metal	**SPM**	33%	A
M.32	Content	5	Residential	Metal	BUR	33%	**B**
M.33	Content	5	Residential	Metal	BUR	33%	**C**
M.34	Content	5	Residential	Metal	BUR	33%	**D**
M.35	Content	5	**Commercial**	Metal	BUR	33%	A
M.36	Content	5	Residential	**Concrete**	BUR	33%	A
M.37	Building	**8**	Residential	Metal	BUR	33%	A
M.38	Building	8	Residential	Metal	BUR	**20%**	A
M.39	Building	8	Residential	Metal	BUR	**50%**	A
M.40	Building	8	Residential	Metal	**SPM**	33%	A
M.41	Building	8	Residential	Metal	BUR	33%	**B**
M.42	Building	8	Residential	Metal	BUR	33%	**C**
M.43	Building	8	Residential	Metal	BUR	33%	**D**
M.44	Building	8	**Commercial**	Metal	BUR	33%	A
M.45	Building	8	Residential	**Concrete**	BUR	33%	A
M.46	Content	8	Residential	Metal	BUR	33%	A
M.47	Content	8	Residential	Metal	BUR	**20%**	A
M.48	Content	8	Residential	Metal	BUR	**50%**	A
M.49	Content	8	Residential	Metal	**SPM**	33%	A
M.50	Content	8	Residential	Metal	BUR	33%	**B**
M.51	Content	8	Residential	Metal	BUR	33%	**C**
M.52	Content	8	Residential	Metal	BUR	33%	**D**
M.53	Content	8	**Commercial**	Metal	BUR	33%	A
M.54	Content	8	Residential	**Concrete**	BUR	33%	A

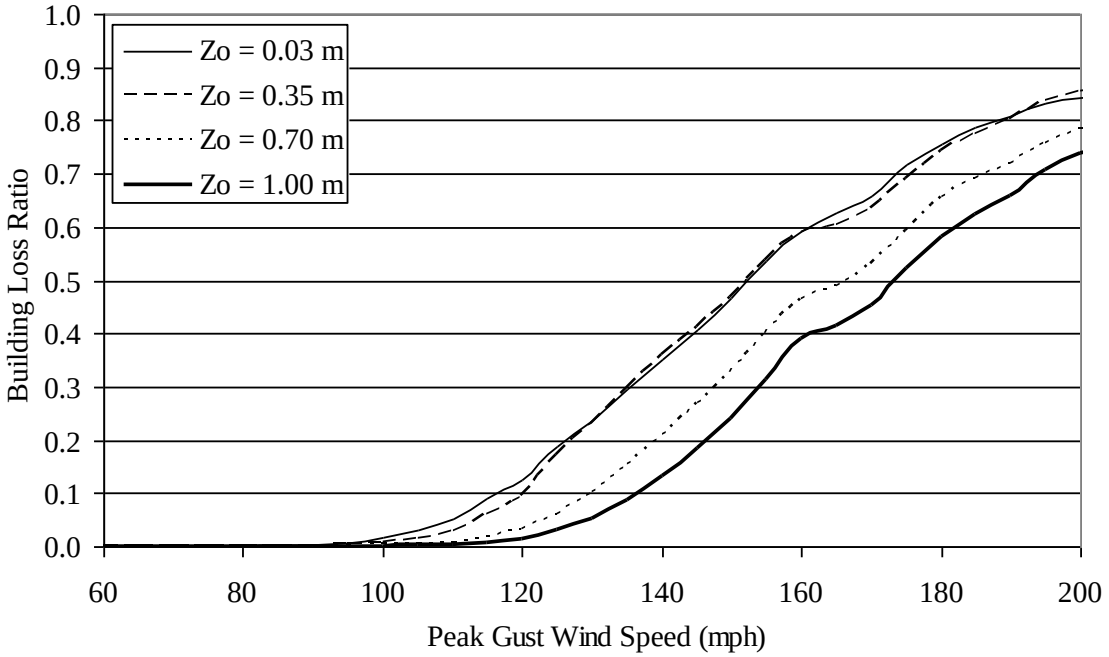

Figure M.1. Building Loss Function – Two-Story Engineered Residential Building – Built-up Roof Cover, 33% Glazing Coverage, Metal Roof Deck, Missile Environment A.

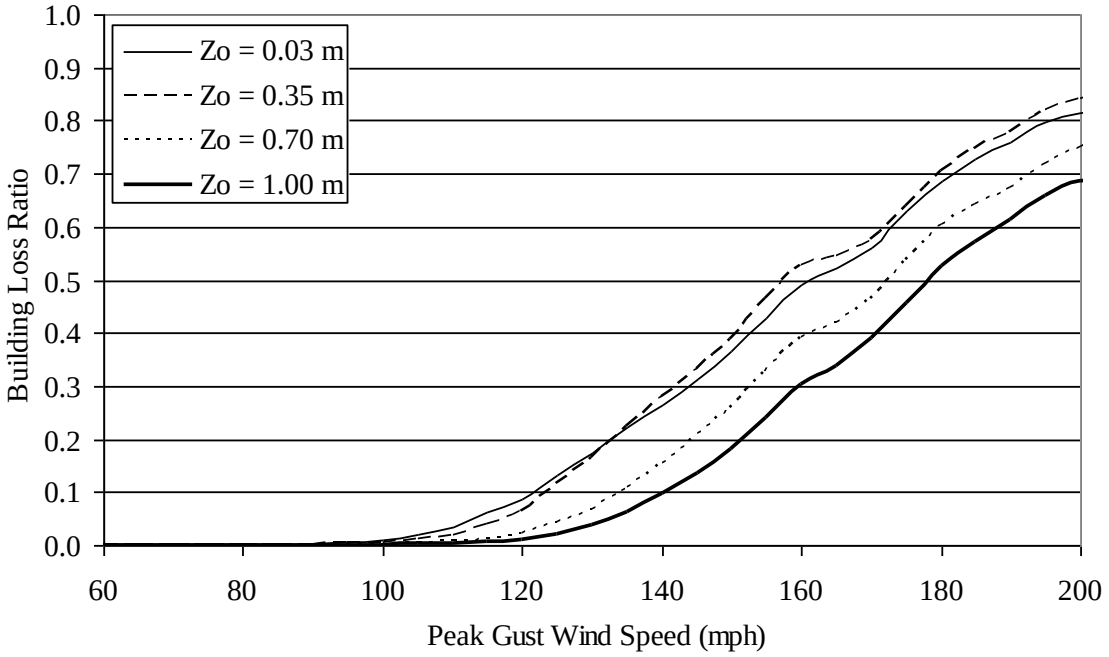

Figure M.2. Building Loss Function – Two-Story Engineered Residential Building – Built-up Roof Cover, 20% Glazing Coverage, Metal Roof Deck, Missile Environment A.

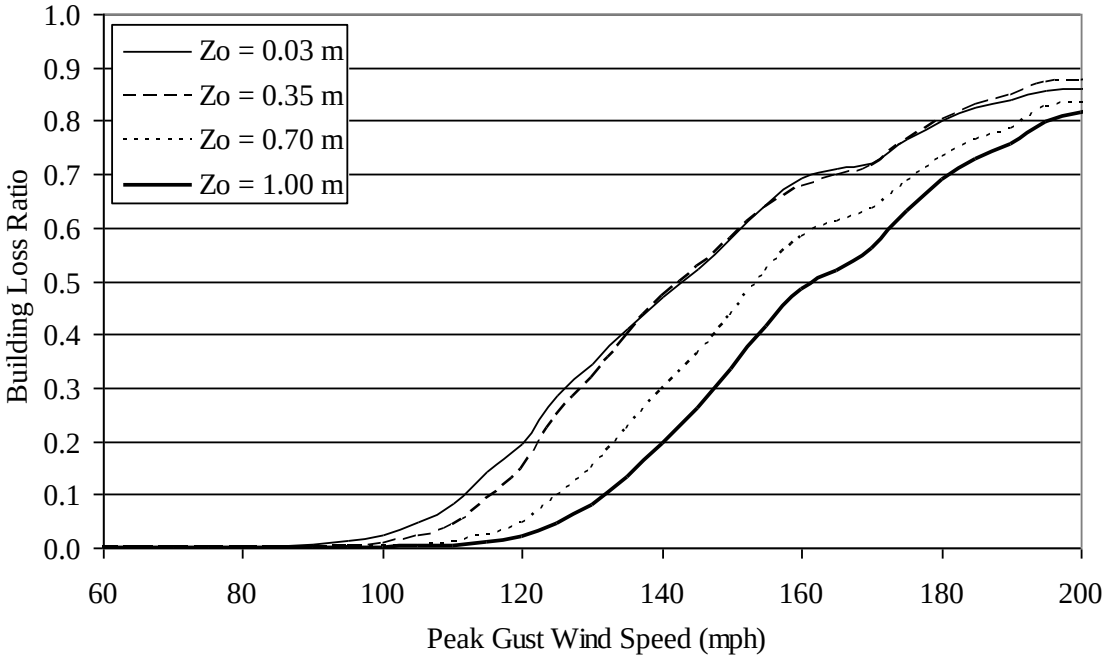

Figure M.3. Building Loss Function – Two-Story Engineered Residential Building – Built-up Roof Cover, 50% Glazing Coverage, Metal Roof Deck, Missile Environment A.

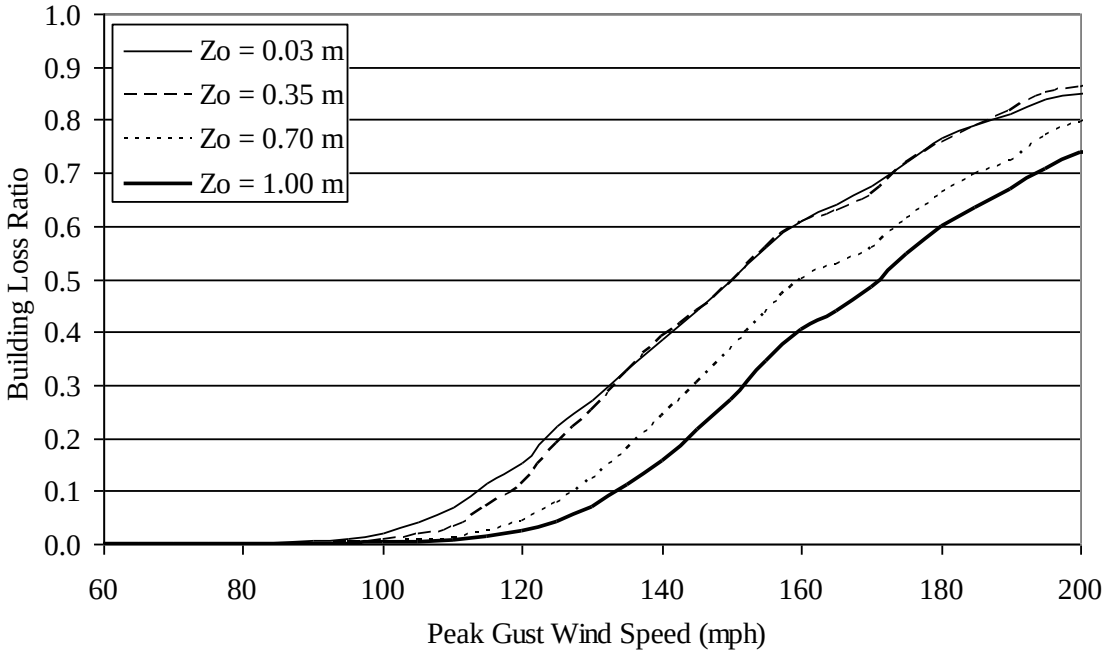

Figure M.4. Building Loss Function – Two-Story Engineered Residential Building – Single Ply Membrane Roof Cover, 33% Glazing Coverage, Metal Roof Deck, Missile Environment A.

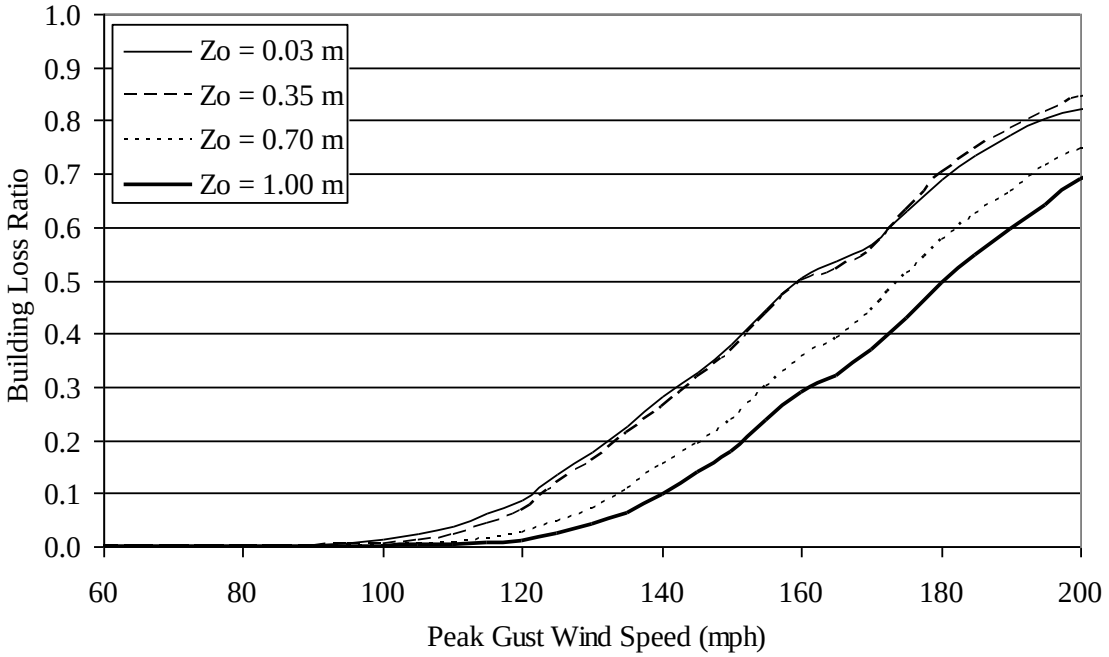

Figure M.5. Building Loss Function – Two-Story Engineered Residential Building – Built-up Roof Cover, 33% Glazing Coverage, Metal Roof Deck, Missile Environment B.

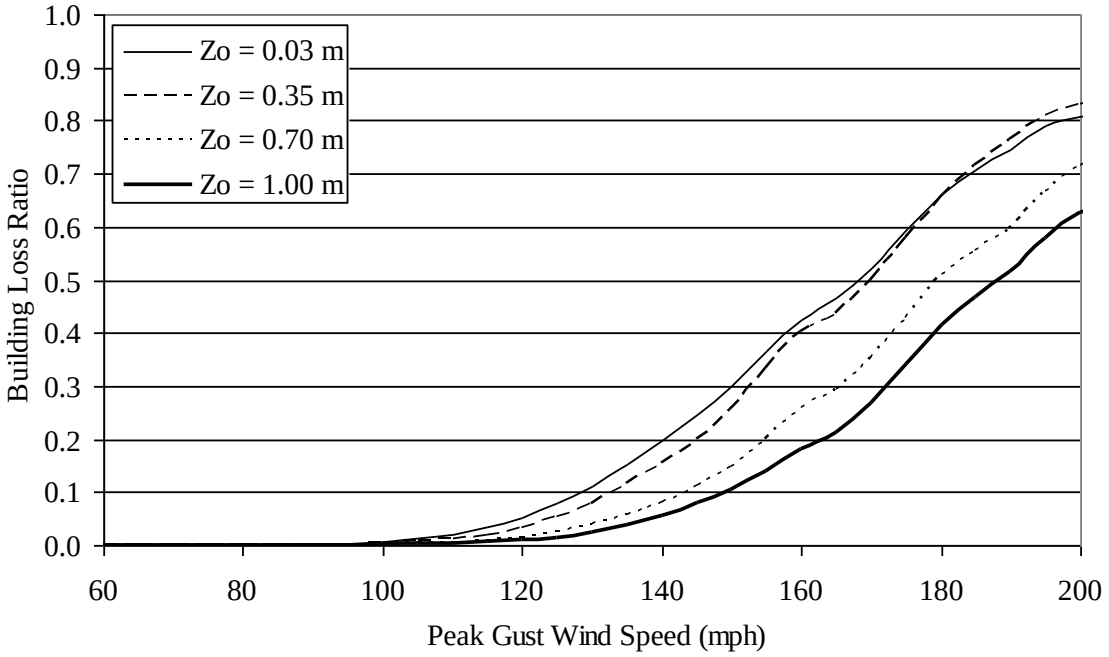

Figure M.6. Building Loss Function – Two-Story Engineered Residential Building – Built-up Roof Cover, 33% Glazing Coverage, Metal Roof Deck, Missile Environment C.

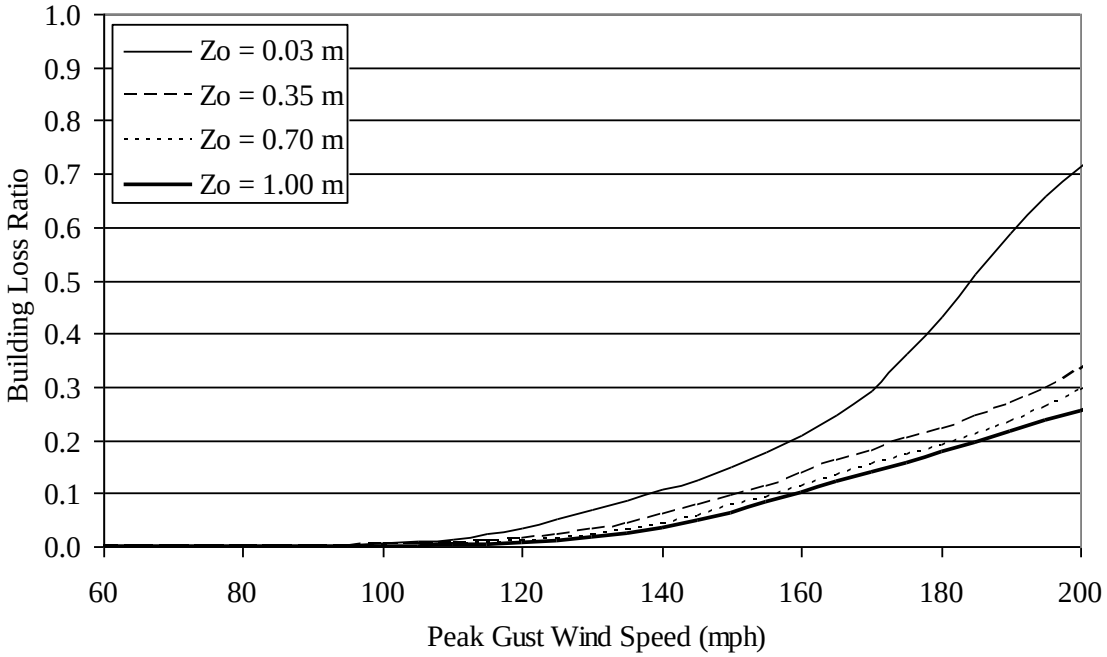

Figure M.7. Building Loss Function – Two-Story Engineered Residential Building – Built-up Roof Cover, 33% Glazing Coverage, Metal Roof Deck, Missile Environment D.

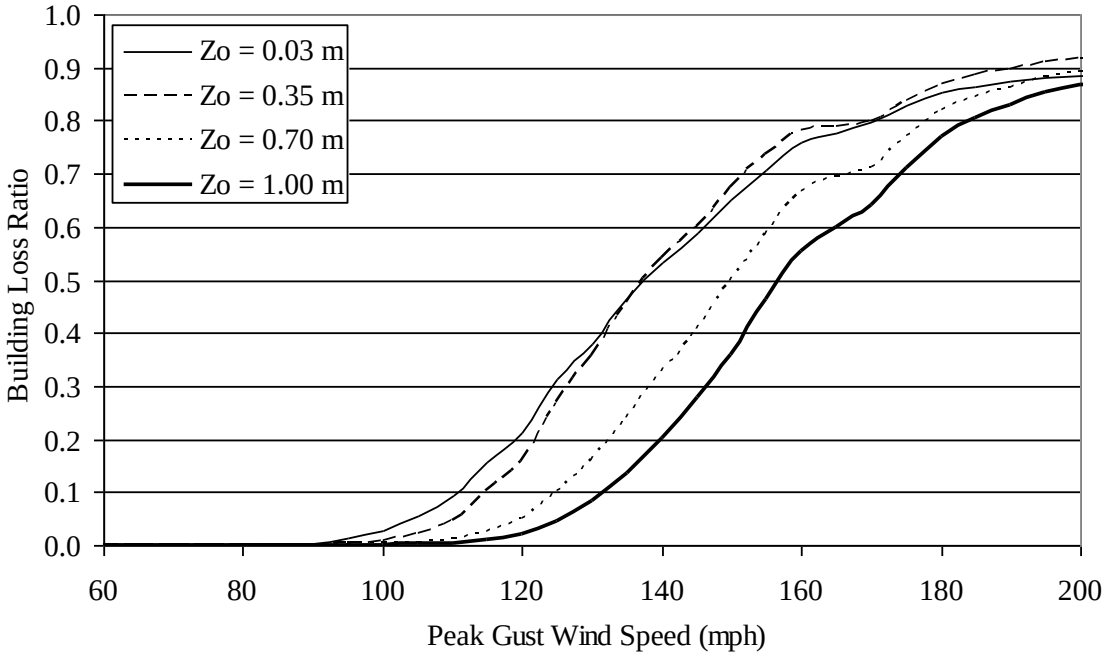

Figure M.8. Building Loss Function – Two-Story Engineered Commercial Building – Built-up Roof Cover, 33% Glazing Coverage, Metal Roof Deck, Missile Environment A.

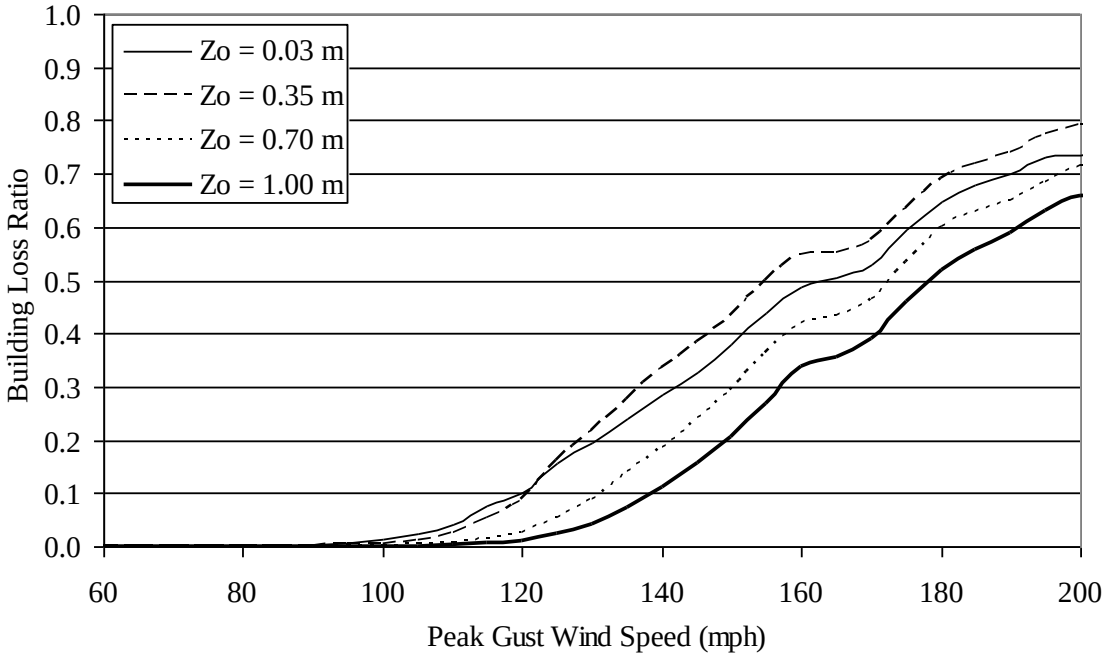

Figure M.9. Building Loss Function – Two-Story Engineered Residential Building – Built-up Roof Cover, 33% Glazing Coverage, Concrete Roof Deck, Missile Environment A.

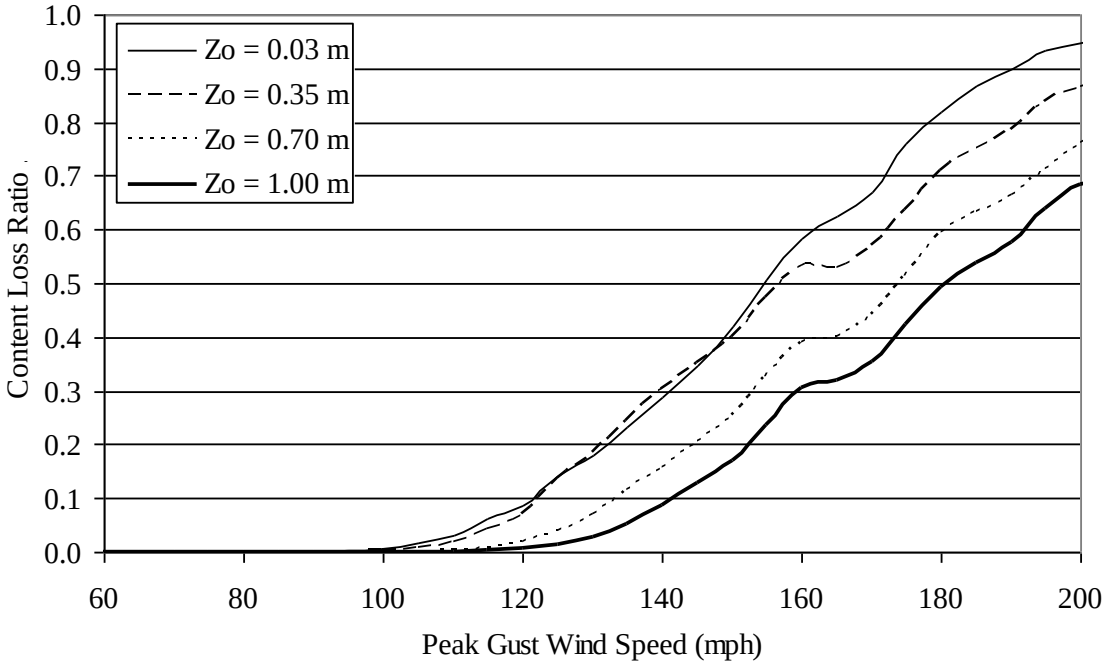

Figure M.10. Content Loss Function – Two-Story Engineered Residential Building – Built-up Roof Cover, 33% Glazing Coverage, Metal Roof Deck, Missile Environment A.

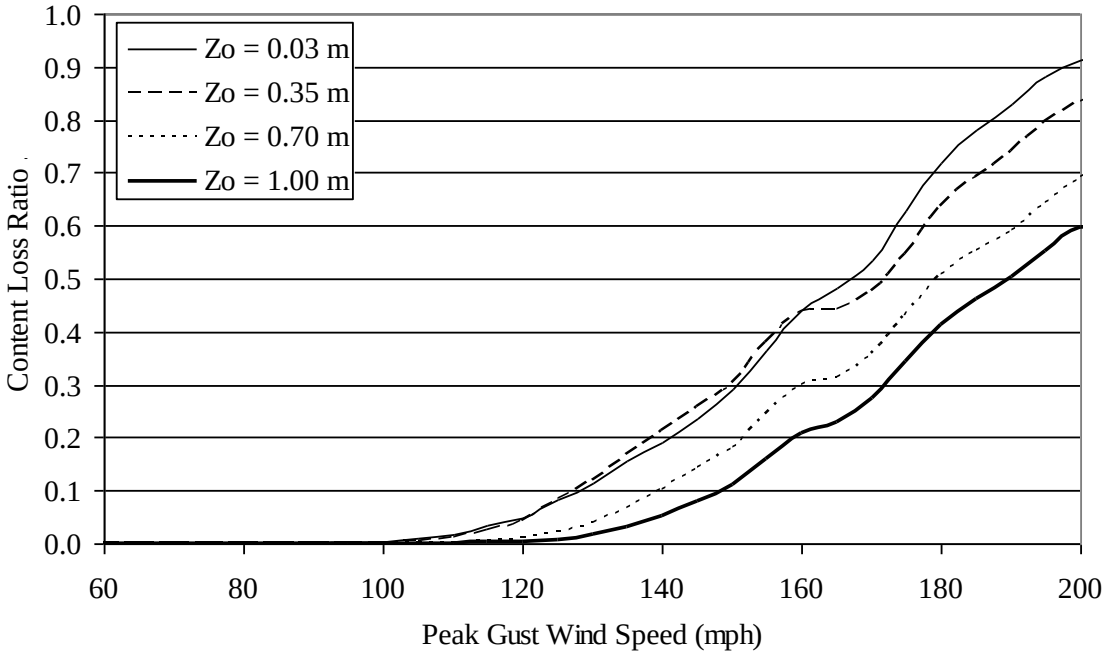

Figure M.11. Content Loss Function – Two-Story Engineered Residential Building – Built-up Roof Cover, 20% Glazing Coverage, Metal Roof Deck, Missile Environment A.

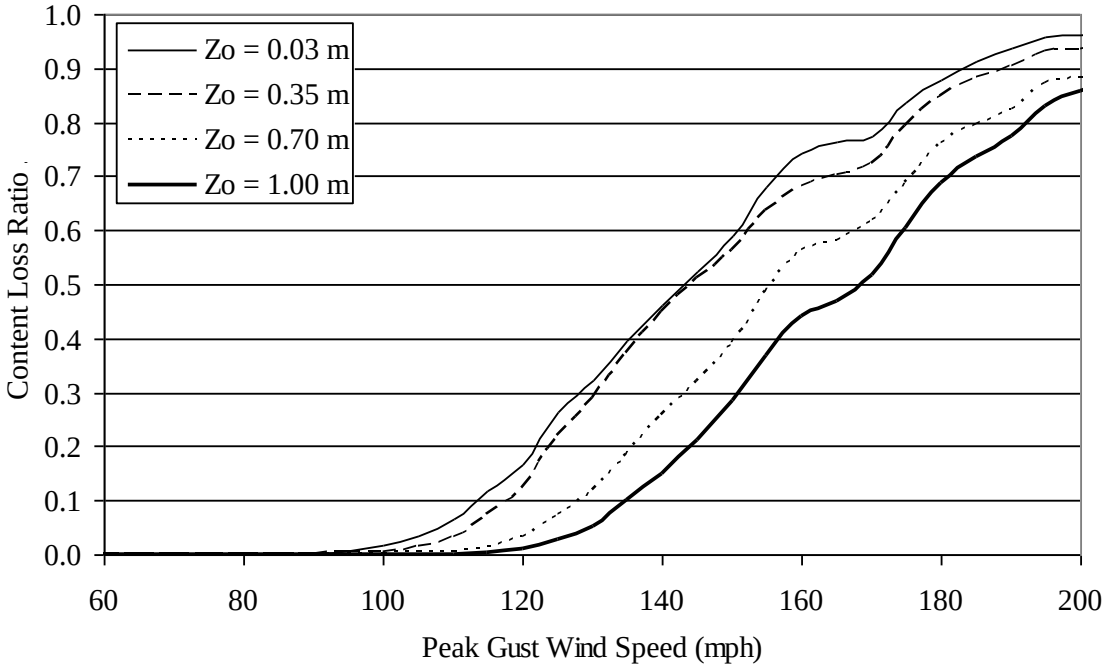

Figure M.12. Content Loss Function – Two-Story Engineered Residential Building – Built-up Roof Cover, 50% Glazing Coverage, Metal Roof Deck, Missile Environment A.

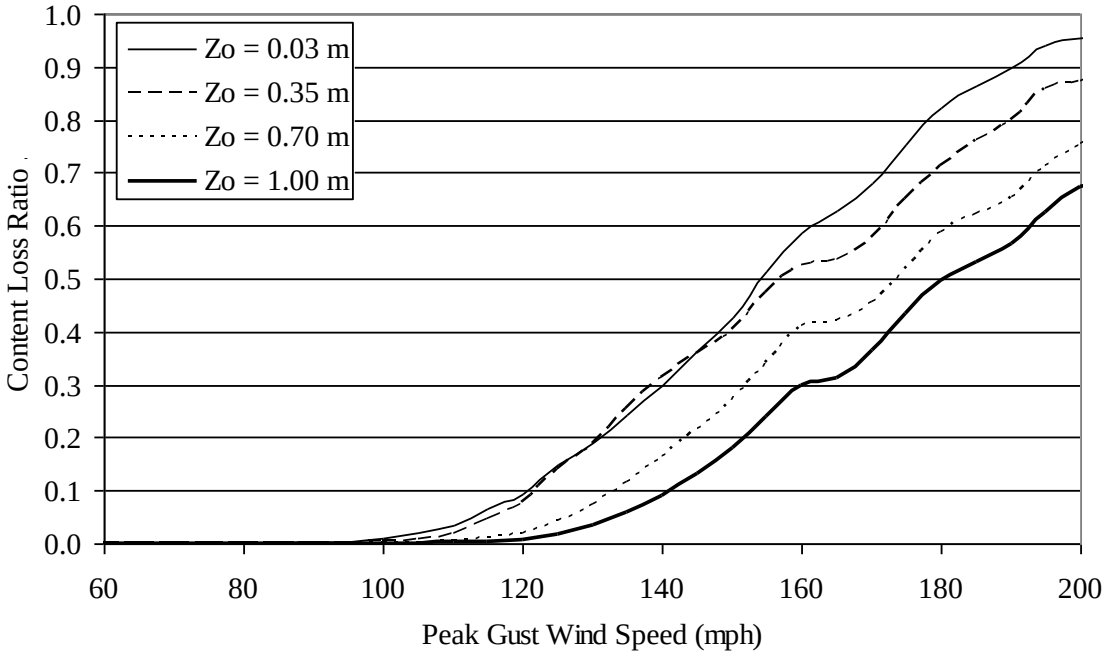

Figure M.13. Content Loss Function – Two-Story Engineered Residential Building – Single Ply Membrane Roof Cover, 33% Glazing Coverage, Metal Roof Deck, Missile Environment A.

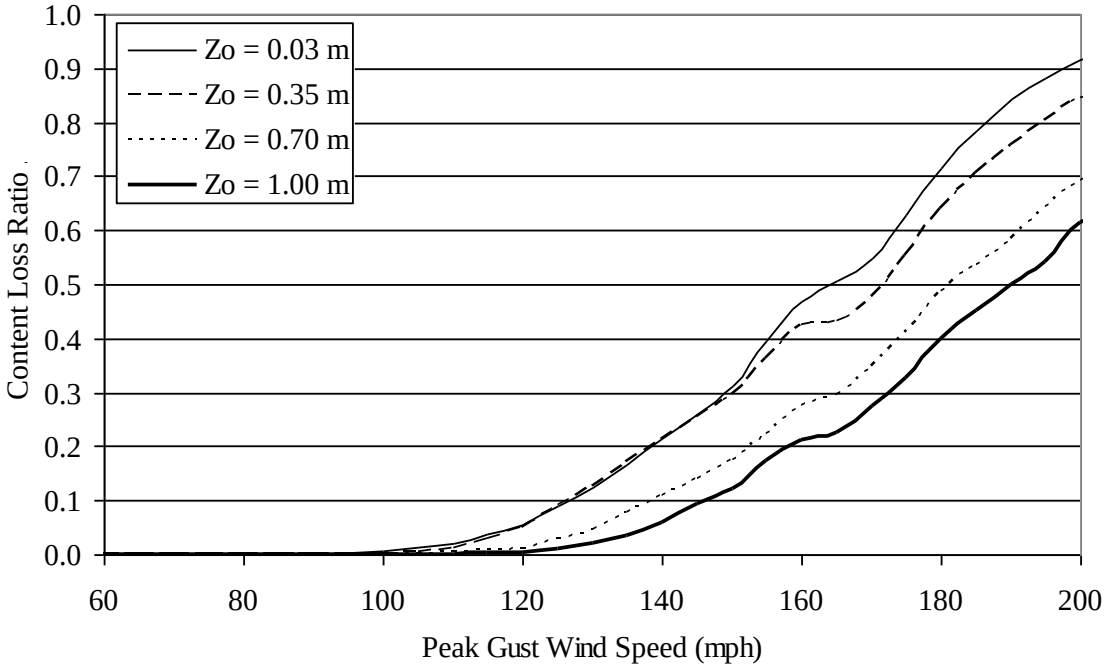

Figure M.14. Content Loss Function – Two-Story Engineered Residential Building – Built-up Roof Cover, 33% Glazing Coverage, Metal Roof Deck, Missile Environment B.

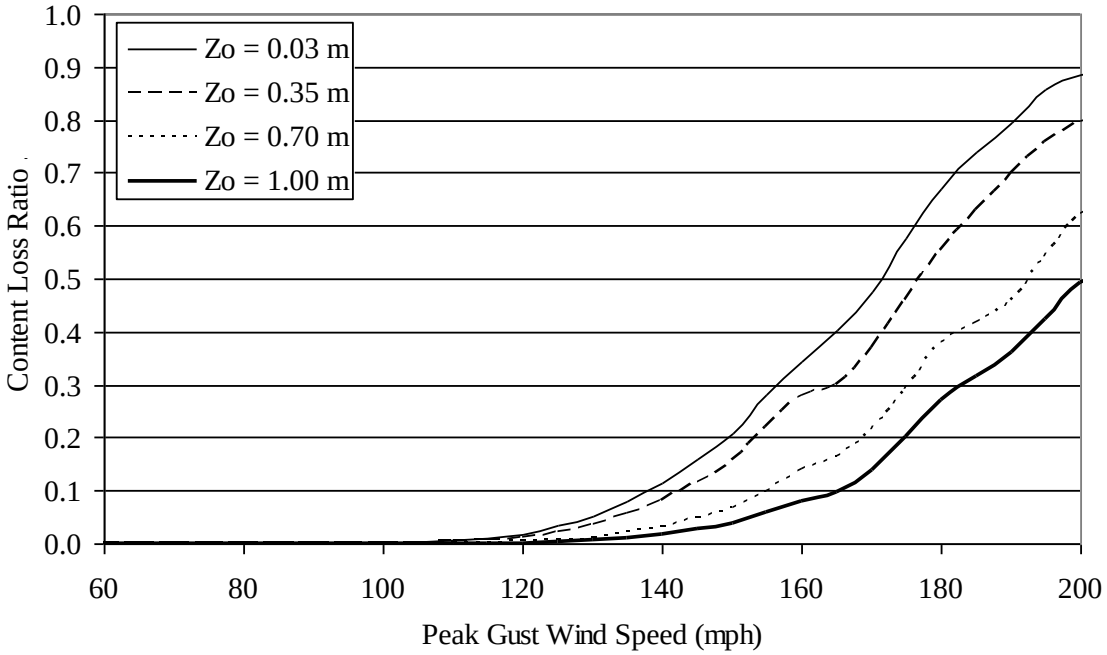

Figure M.15. Content Loss Function – Two-Story Engineered Residential Building – Built-up Roof Cover, 33% Glazing Coverage, Metal Roof Deck, Missile Environment C.

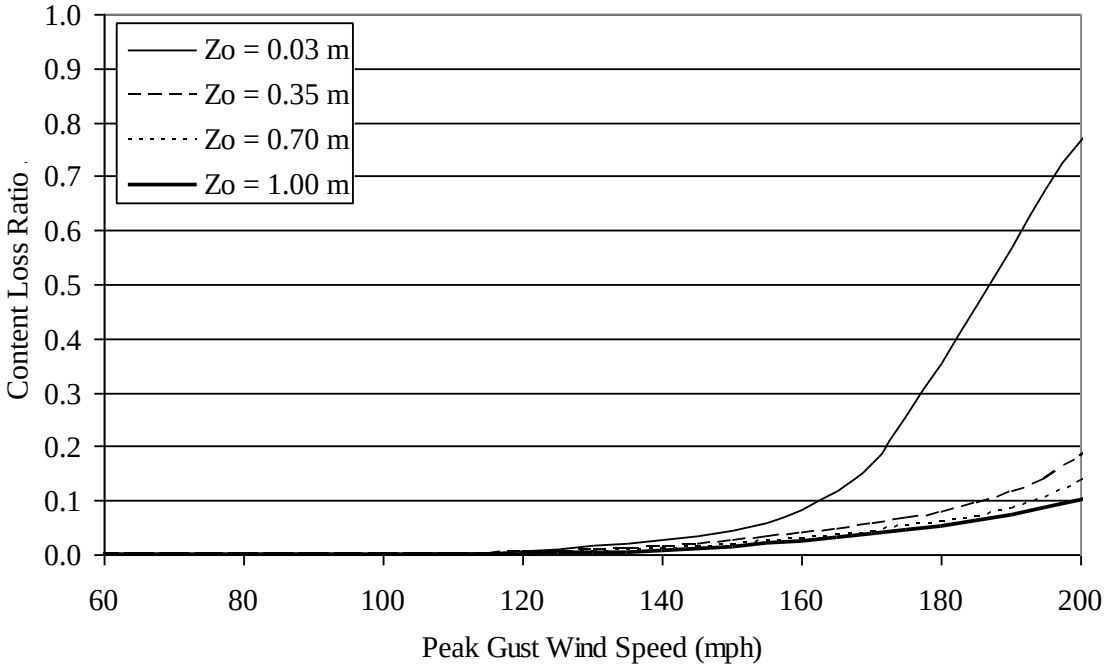

Figure M.16. Content Loss Function – Two-Story Engineered Residential Building – Built-up Roof Cover, 33% Glazing Coverage, Metal Roof Deck, Missile Environment D.

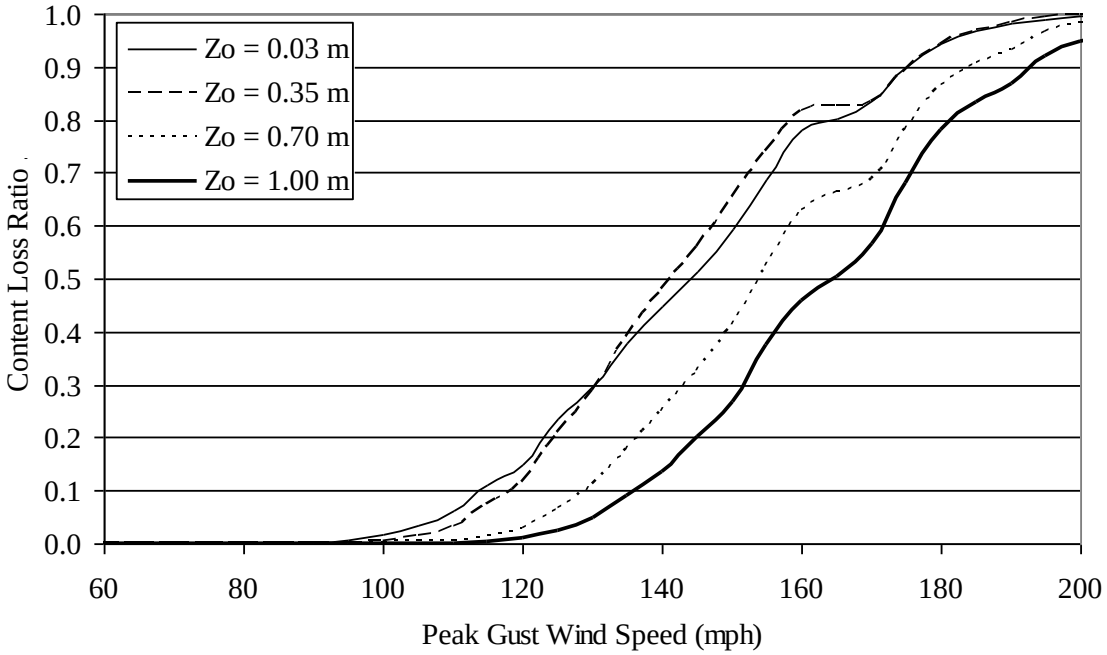

Figure M.17. Content Loss Function – Two-Story Engineered Commercial Building – Built-up Roof Cover, 33% Glazing Coverage, Metal Roof Deck, Missile Environment A.

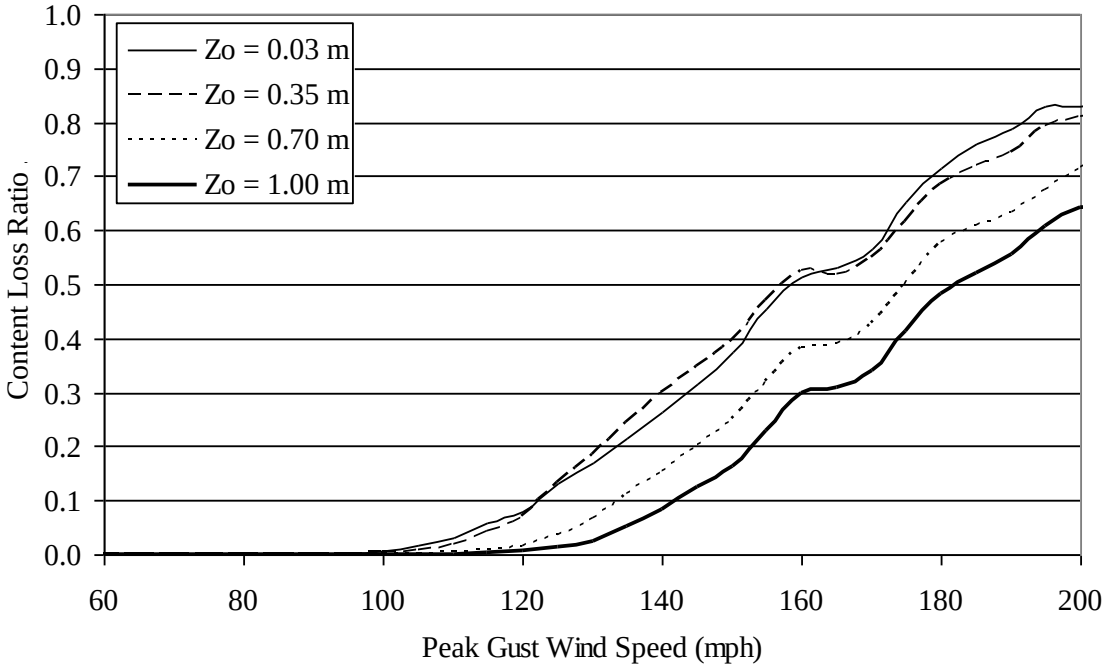

Figure M.18. Content Loss Function – Two-Story Engineered Residential Building – Built-up Roof Cover, 33% Glazing Coverage, Concrete Roof Deck, Missile Environment A.

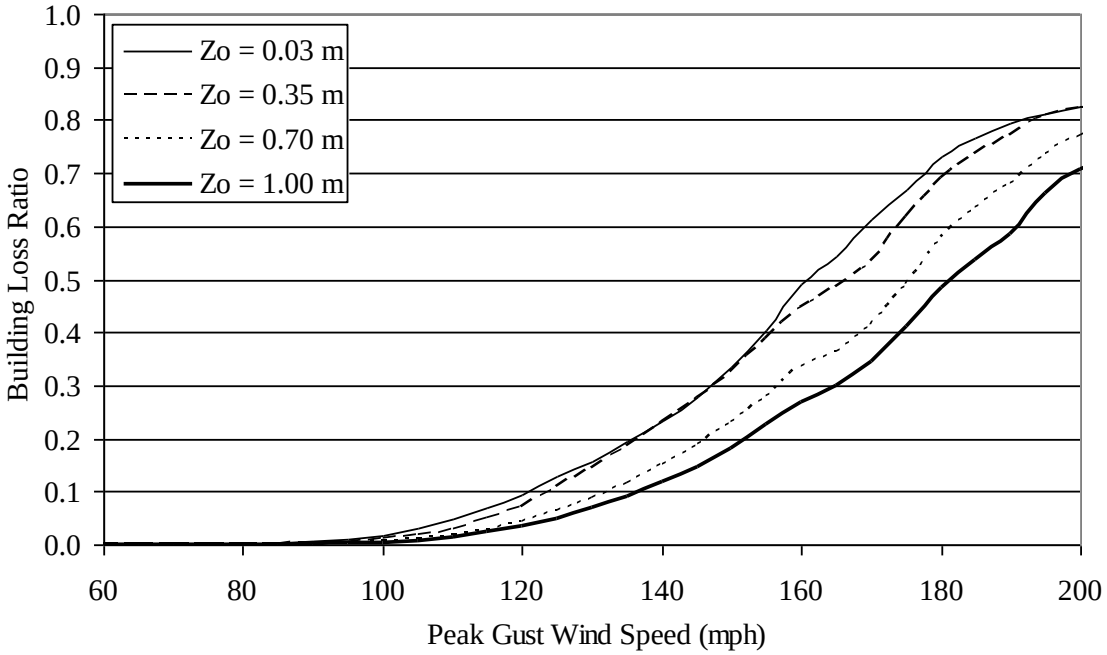

Figure M.19. Building Loss Function – Five-Story Engineered Residential Building – Built-up Roof Cover, 33% Glazing Coverage, Metal Roof Deck, Missile Environment A.

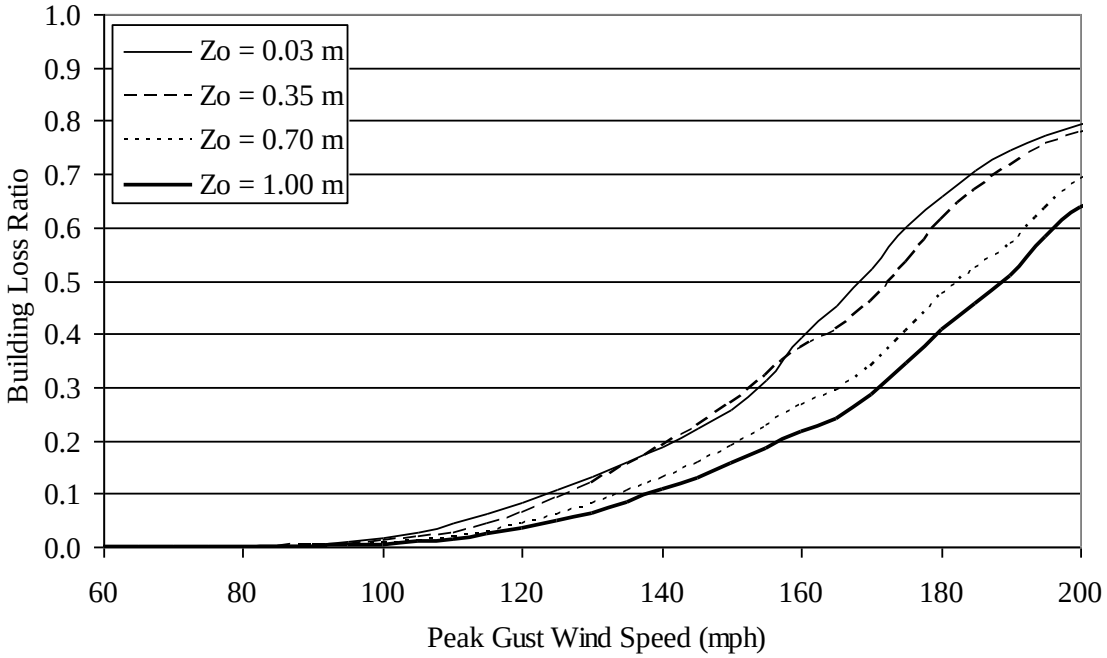

Figure M.20. Building Loss Function – Five-Story Engineered Residential Building – Built-up Roof Cover, <u>20% Glazing Coverage</u>, Metal Roof Deck, Missile Environment A.

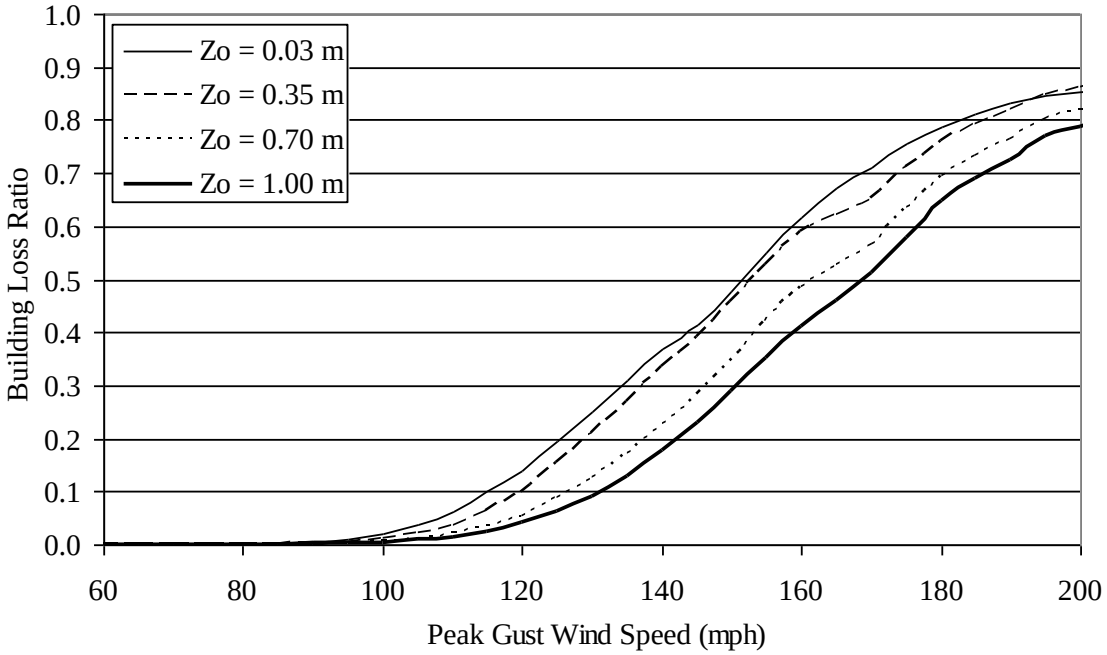

Figure M.21. Building Loss Function – Five-Story Engineered Residential Building – Built-up Roof Cover, 50% Glazing Coverage, Metal Roof Deck, Missile Environment A.

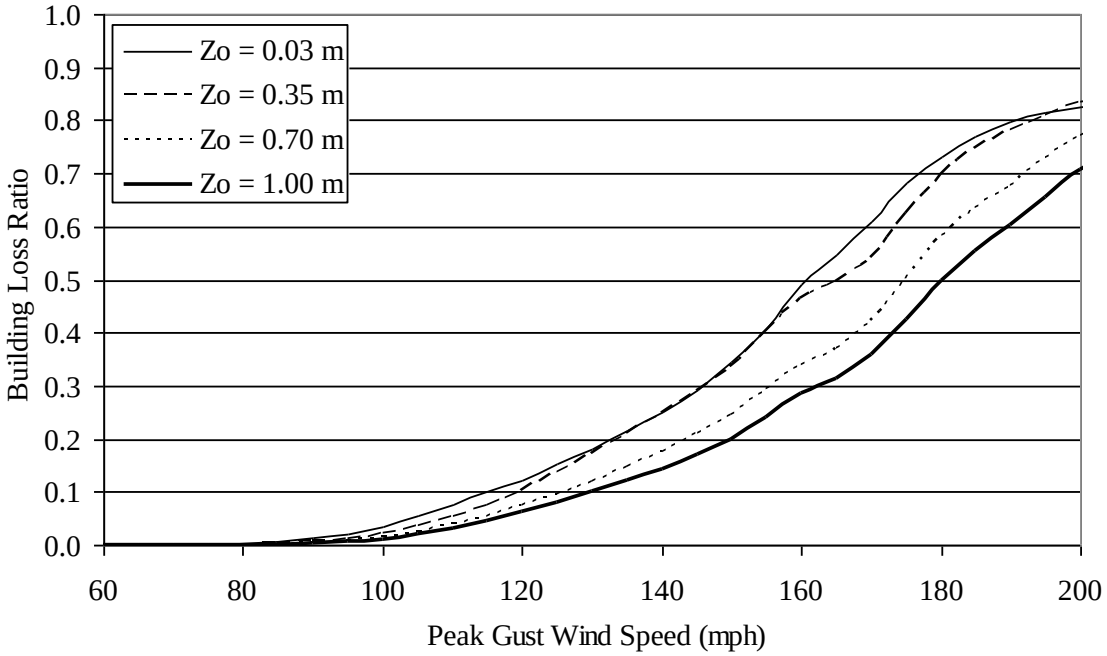

Figure M.22. Building Loss Function – Five-Story Engineered Residential Building – Single Ply Membrane Roof Cover, 33% Glazing Coverage, Metal Roof Deck, Missile Environment A.

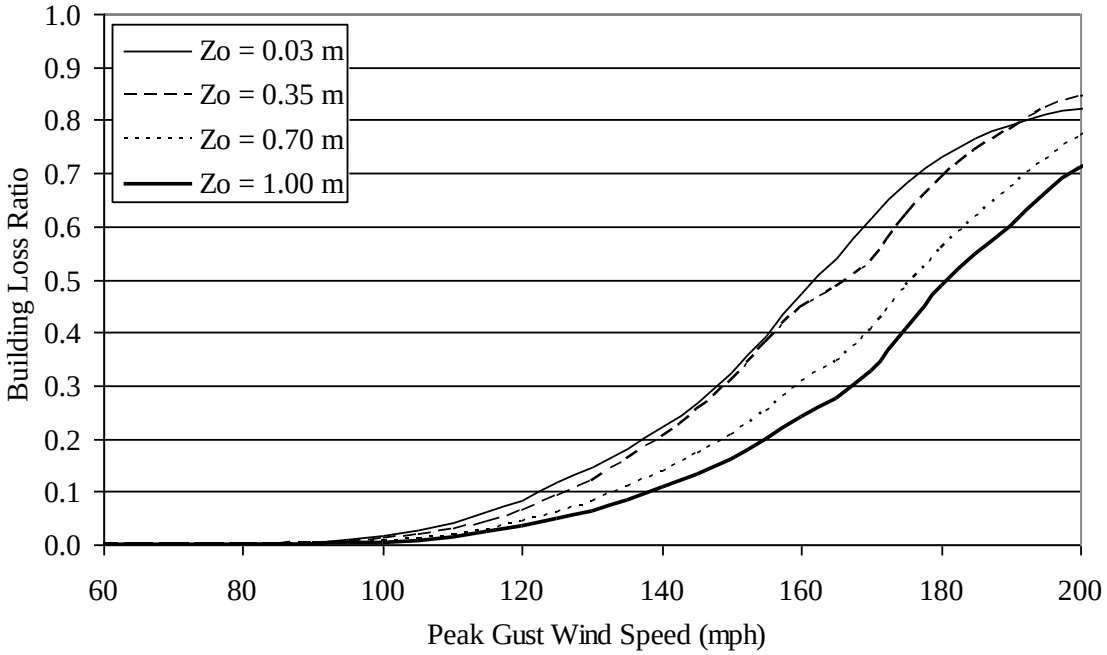

Figure M.23. Building Loss Function – Five-Story Engineered Residential Building – Built-up Roof Cover, 33% Glazing Coverage, Metal Roof Deck, Missile Environment B.

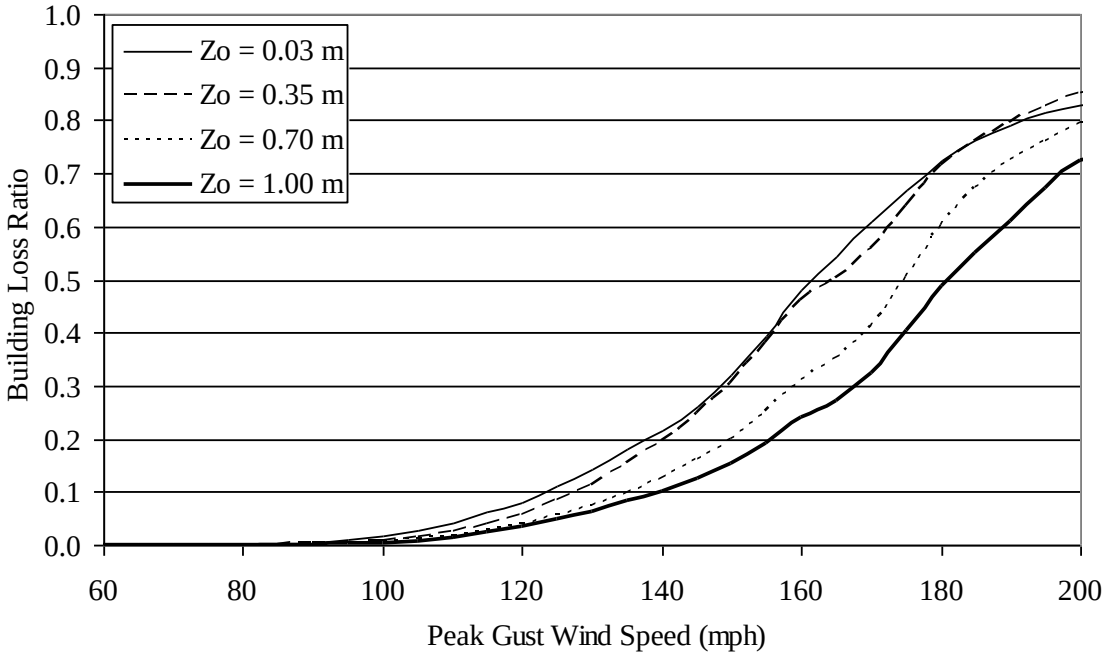

Figure M.24. Building Loss Function – Five-Story Engineered Residential Building – Built-up Roof Cover, 33% Glazing Coverage, Metal Roof Deck, Missile Environment C.

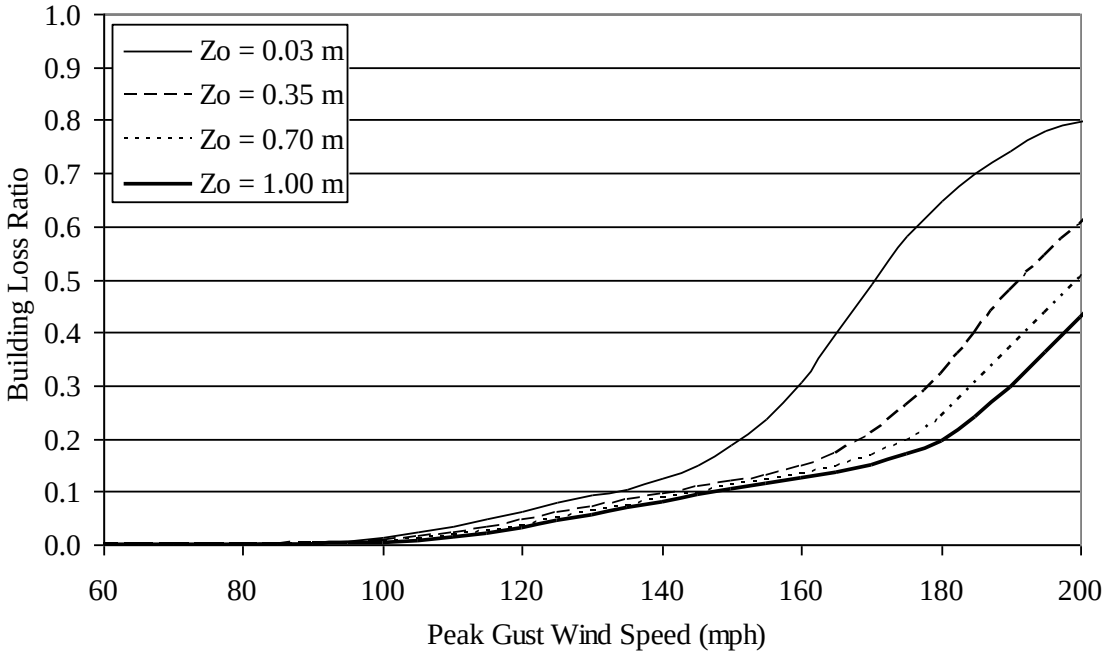

Figure M.25. Building Loss Function – Five-Story Engineered Residential Building – Built-up Roof Cover, 33% Glazing Coverage, Metal Roof Deck, Missile Environment D.

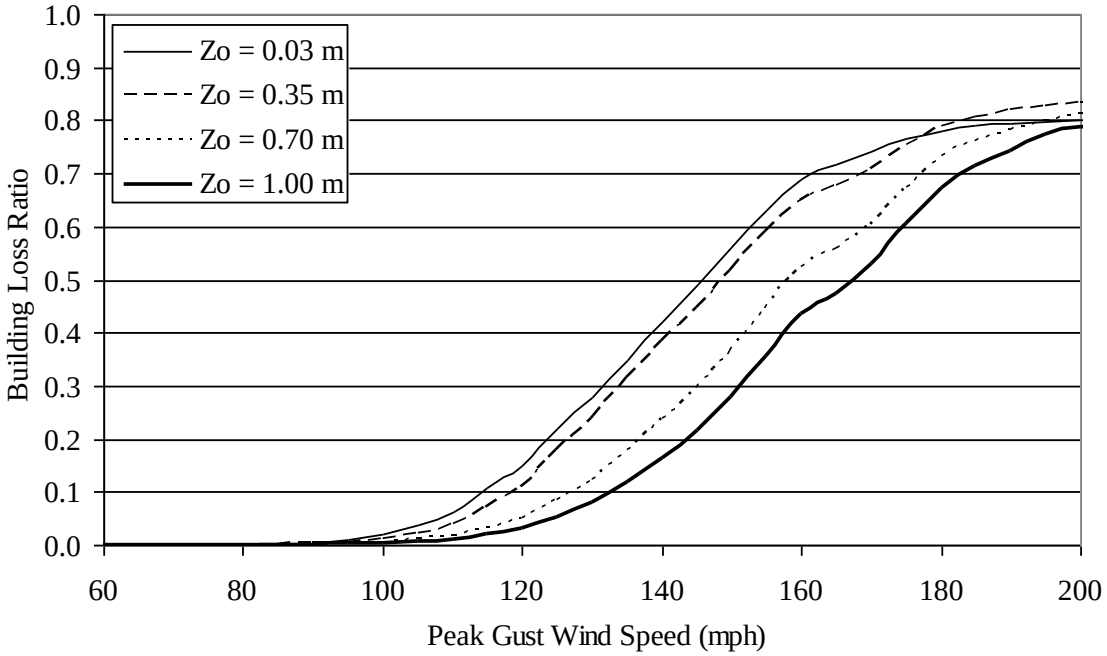

Figure M.26. Building Loss Function – Five-Story Engineered Commercial Building – Built-up Roof Cover, 33% Glazing Coverage, Metal Roof Deck, Missile Environment A.

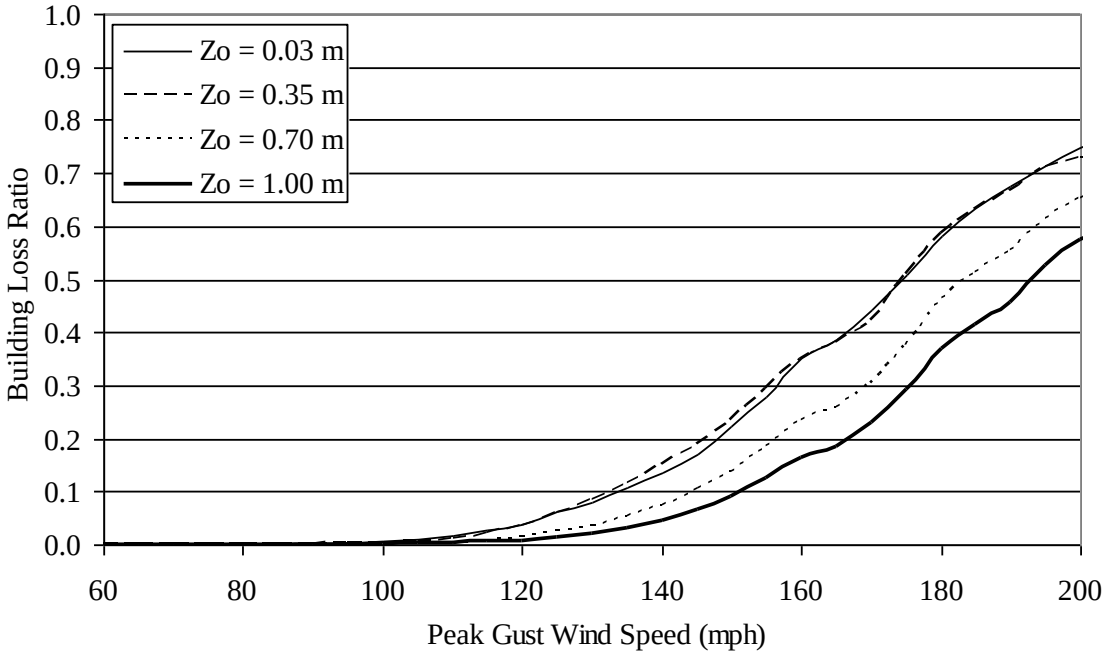

Figure M.27. Building Loss Function – Five-Story Engineered Residential Building – Built-up Roof Cover, 33% Glazing Coverage, Concrete Roof Deck, Missile Environment A.

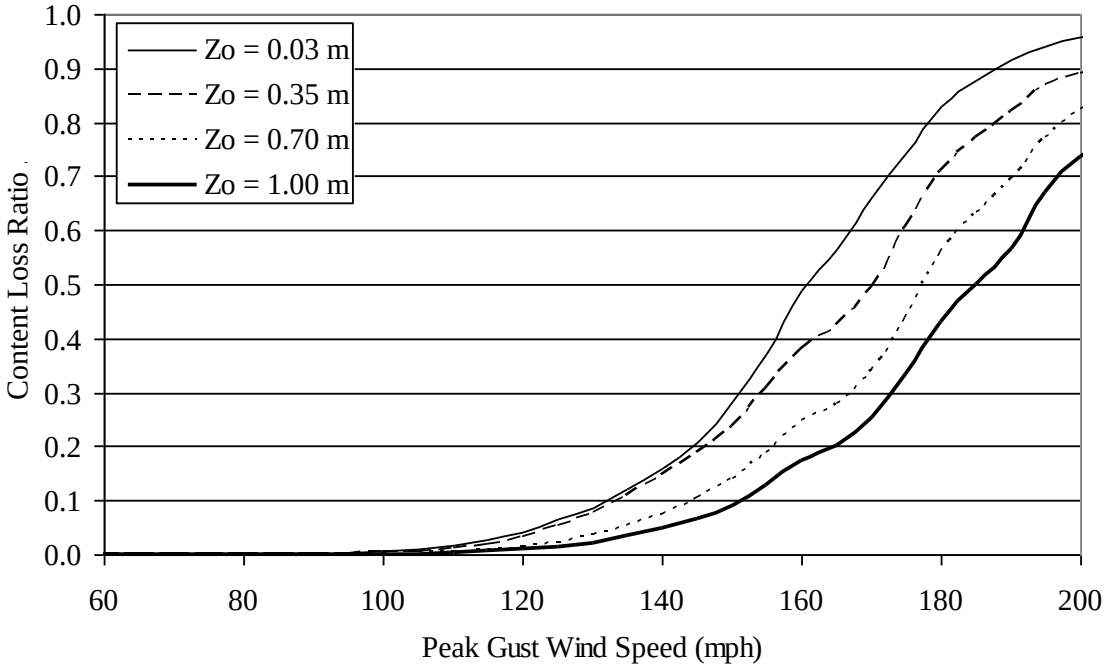

Figure M.28. Content Loss Function – Five-Story Engineered Residential Building – Built-up Roof Cover, 33% Glazing Coverage, Metal Roof Deck, Missile Environment A.

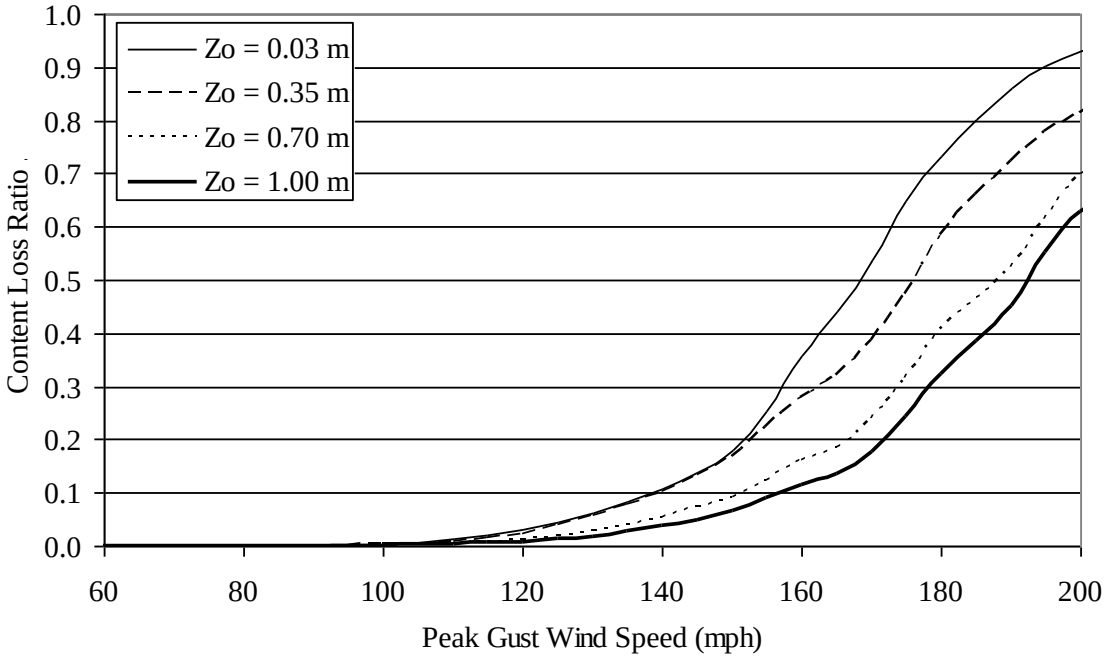

Figure M.29. Content Loss Function – Five-Story Engineered Residential Building – Built-up Roof Cover, 20% Glazing Coverage, Metal Roof Deck, Missile Environment A.

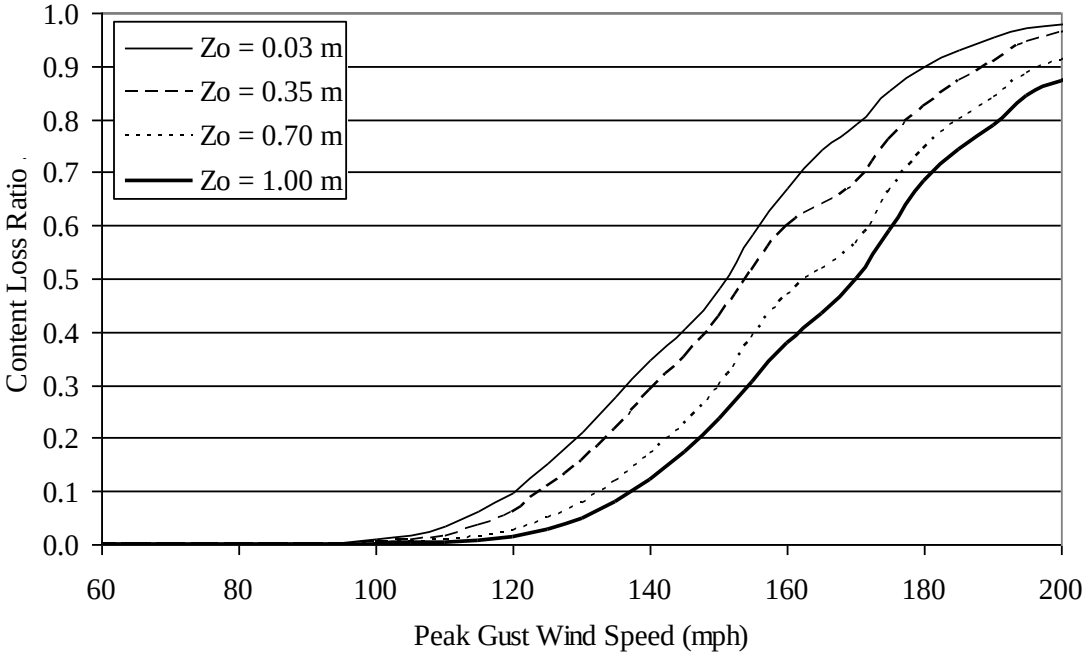

Figure M.30. Content Loss Function – Five-Story Engineered Residential Building – Built-up Roof Cover, 50% Glazing Coverage, Metal Roof Deck, Missile Environment A.

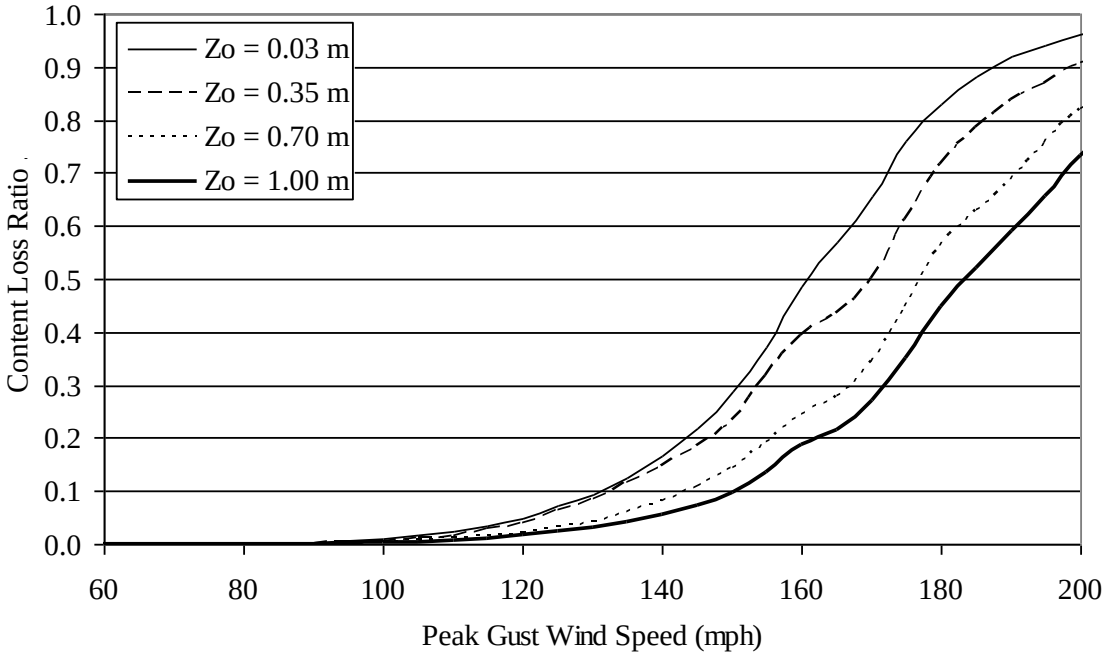

Figure M.31. Content Loss Function – Five-Story Engineered Residential Building – Single Ply Membrane Roof Cover, 33% Glazing Coverage, Metal Roof Deck, Missile Environment A.

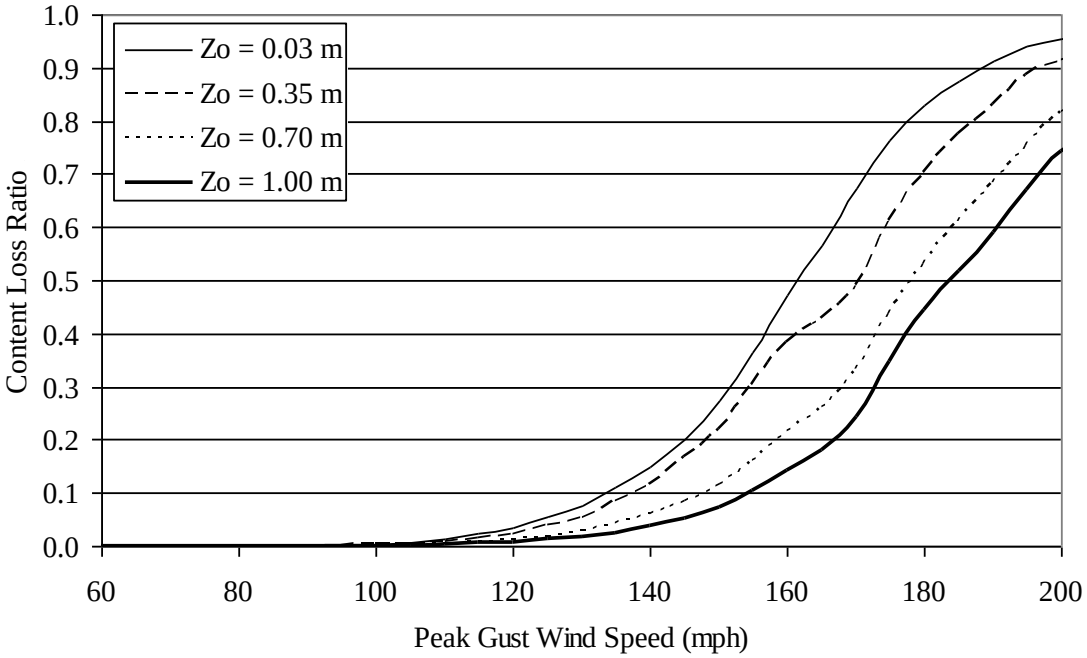

Figure M.31. Content Loss Function – Five-Story Engineered Residential Building – Built-up Roof Cover, 33% Glazing Coverage, Metal Roof Deck, Missile Environment B.

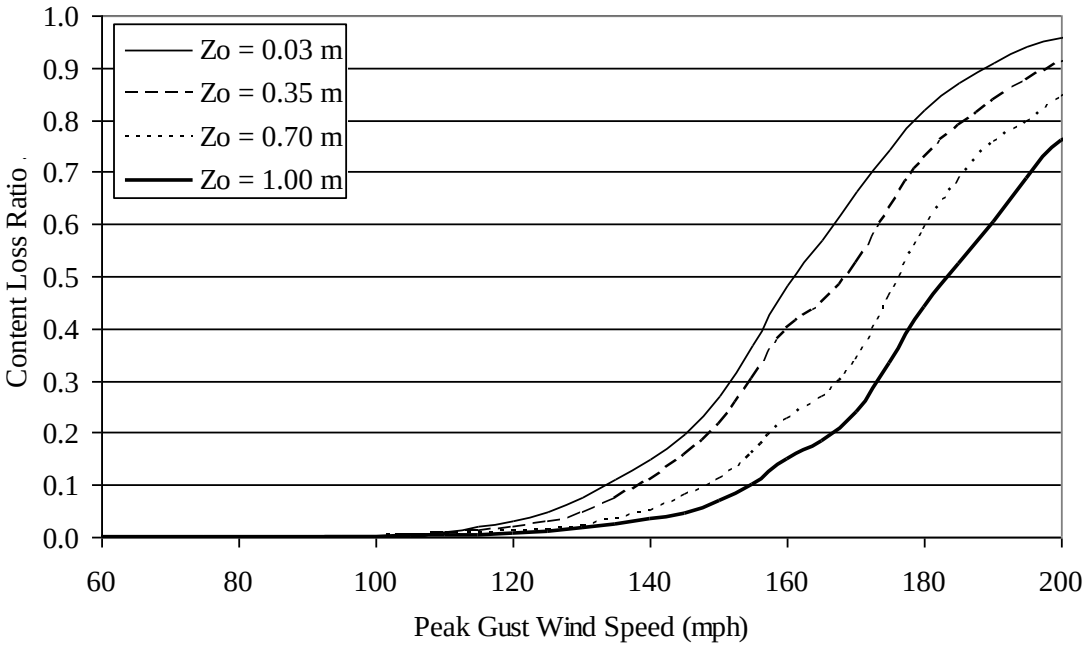

Figure M.33. Content Loss Function – Five-Story Engineered Residential Building – Built-up Roof Cover, 33% Glazing Coverage, Metal Roof Deck, Missile Environment C.

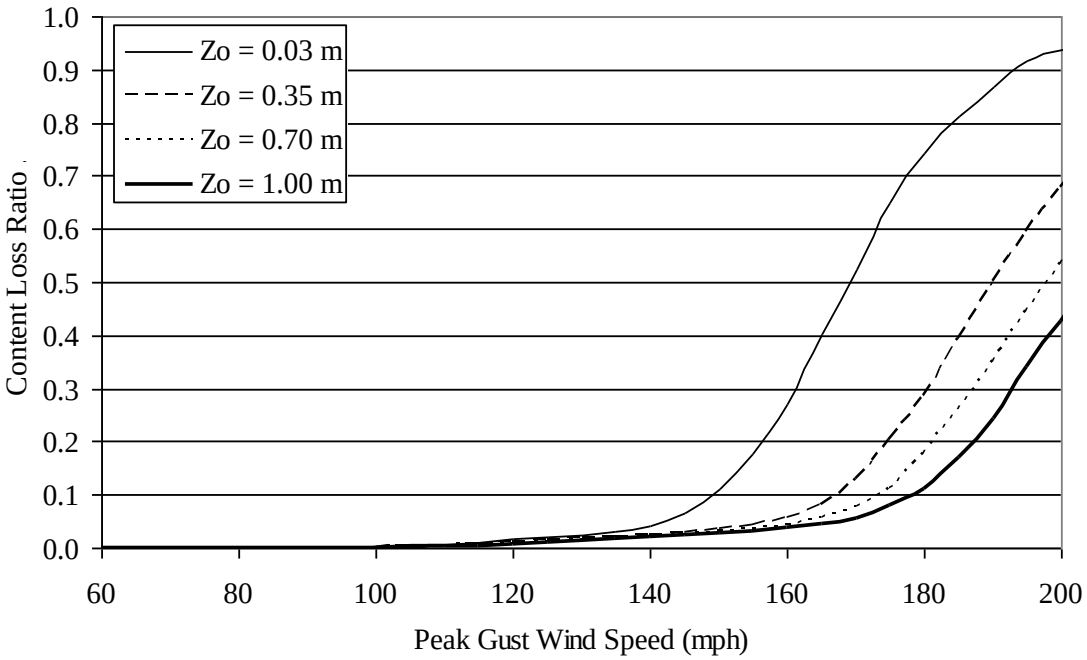

Figure M.34. Content Loss Function – Five-Story Engineered Residential Building – Built-up Roof Cover, 33% Glazing Coverage, Metal Roof Deck, Missile Environment D.

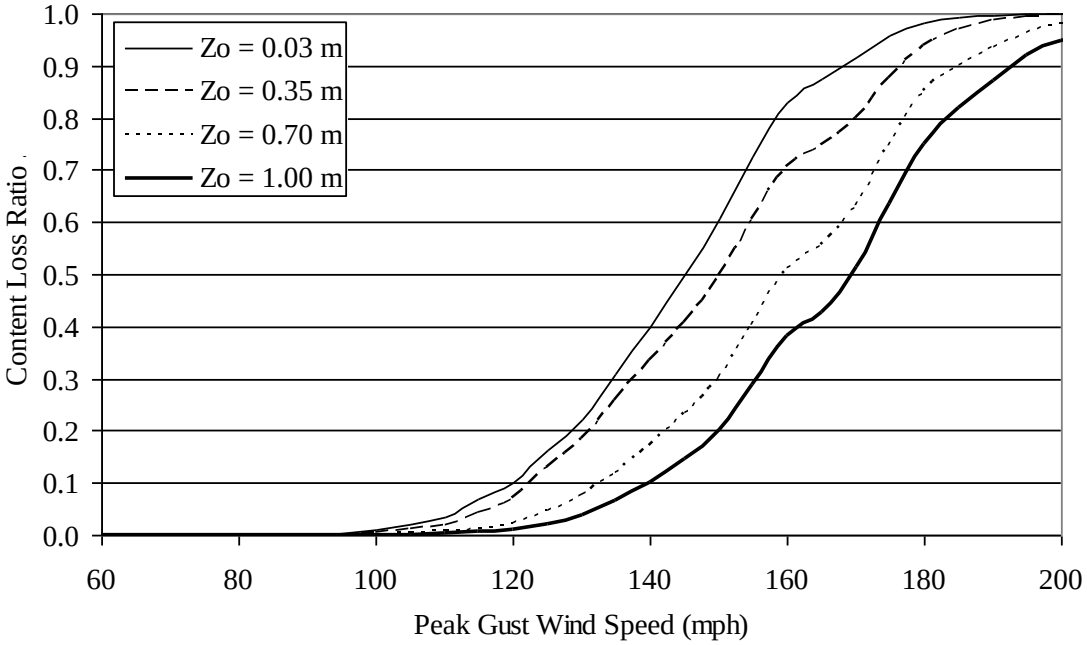

Figure M.35. Content Loss Function – Five-Story Engineered Commercial Building – Built-up Roof Cover, 33% Glazing Coverage, Metal Roof Deck, Missile Environment A.

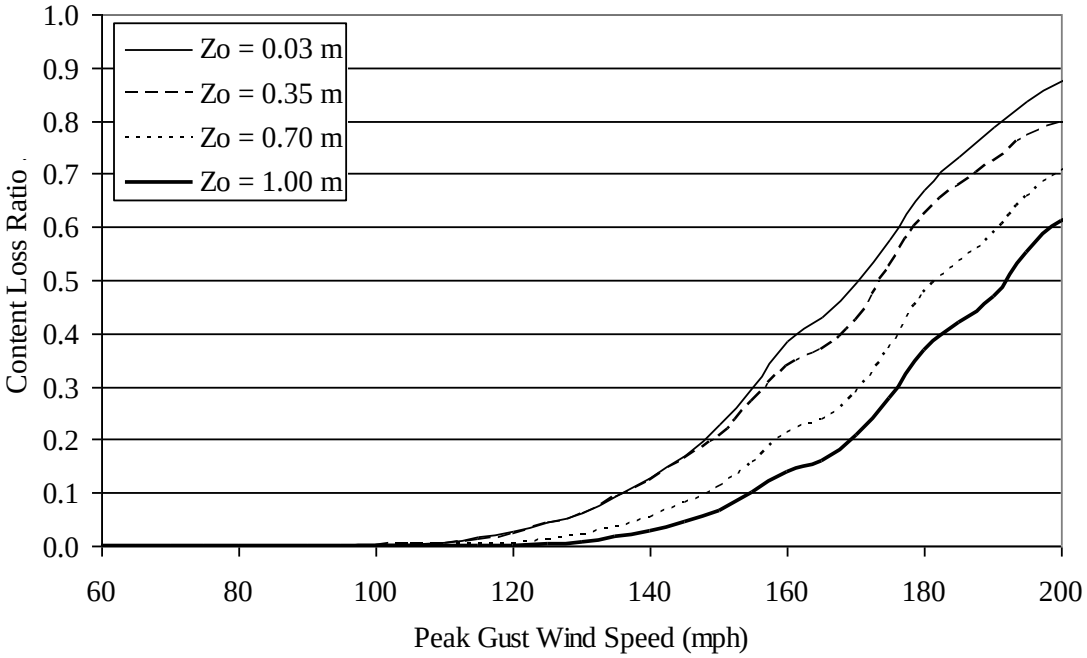

Figure M.36. Content Loss Function – Five-Story Engineered Residential Building – Built-up Roof Cover, 33% Glazing Coverage, Concrete Roof Deck, Missile Environment A.

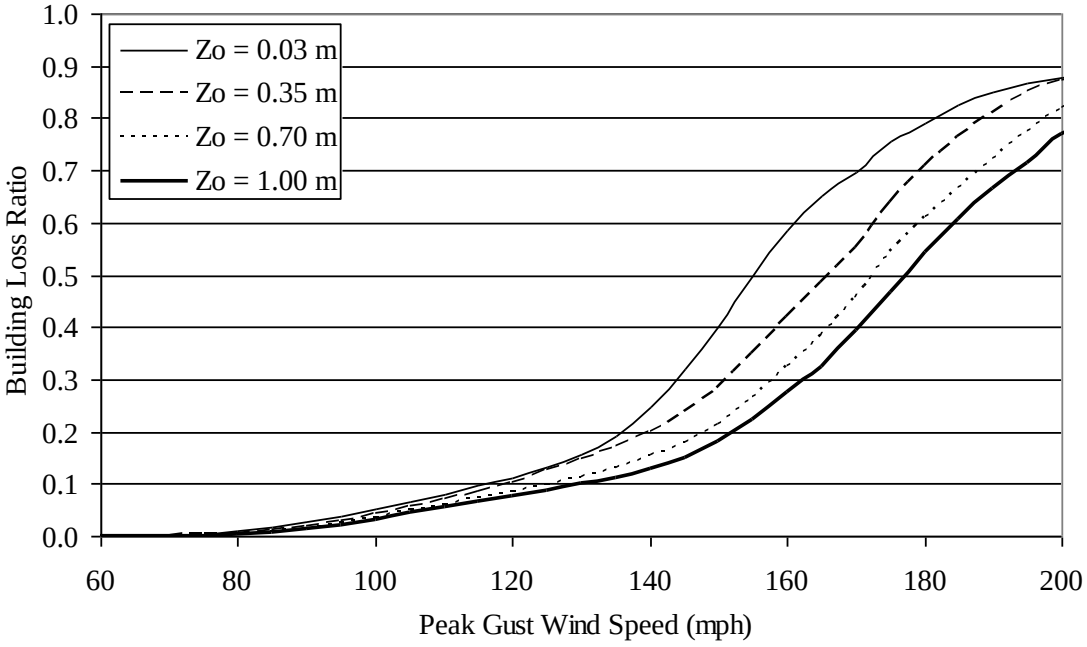

Figure M.37. Building Loss Function – Eight-Story Engineered Residential Building – Built-up Roof Cover, 33% Glazing Coverage, Metal Roof Deck, Missile Environment A.

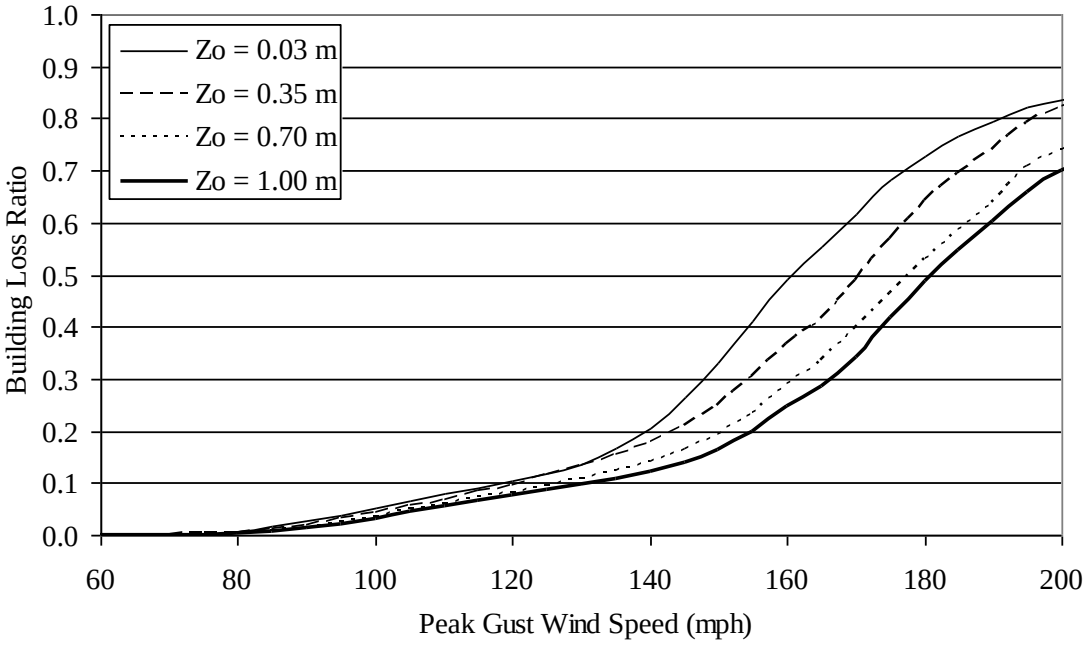

Figure M.38. Building Loss Function – Eight-Story Engineered Residential Building – Built-up Roof Cover, *20*% Glazing Coverage, Metal Roof Deck, Missile Environment A.

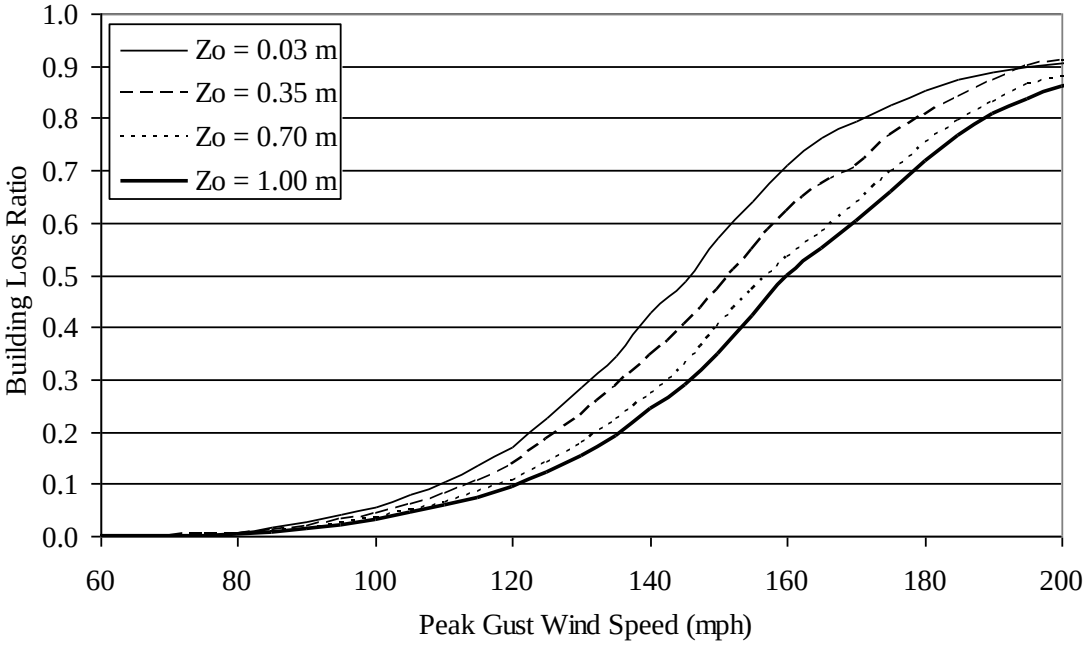

Figure M.39. Building Loss Function – Eight-Story Engineered Residential Building – Built-up Roof Cover, 50% Glazing Coverage, Metal Roof Deck, Missile Environment A.

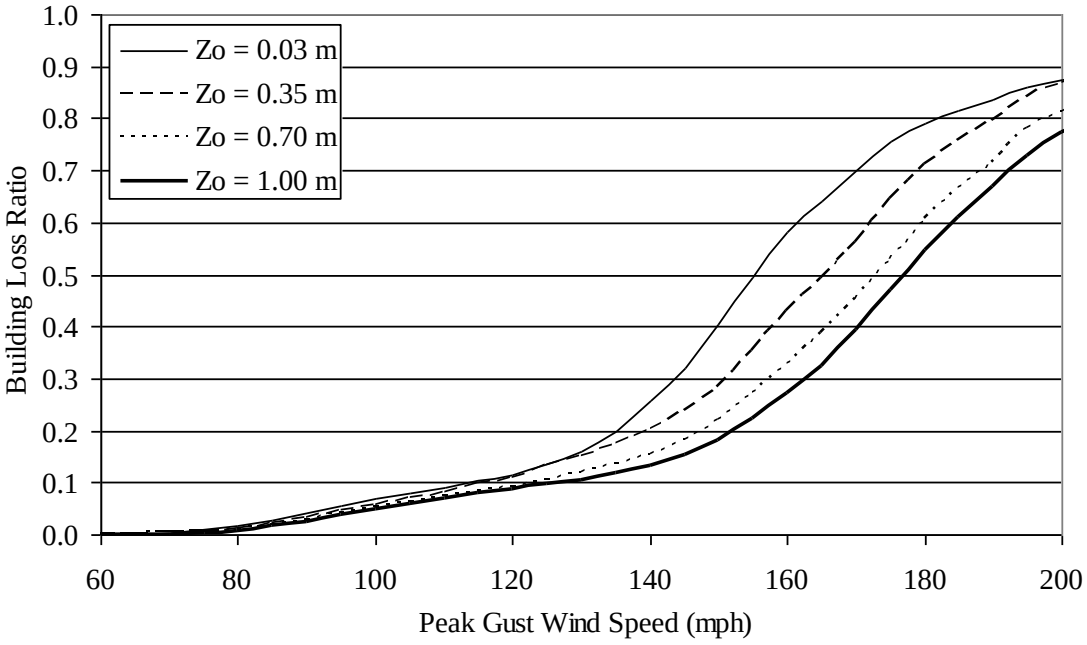

Figure M.40. Building Loss Function – Eight-Story Engineered Residential Building – Single Ply Membrane Roof Cover, 33% Glazing Coverage, Metal Roof Deck, Missile Environment A.

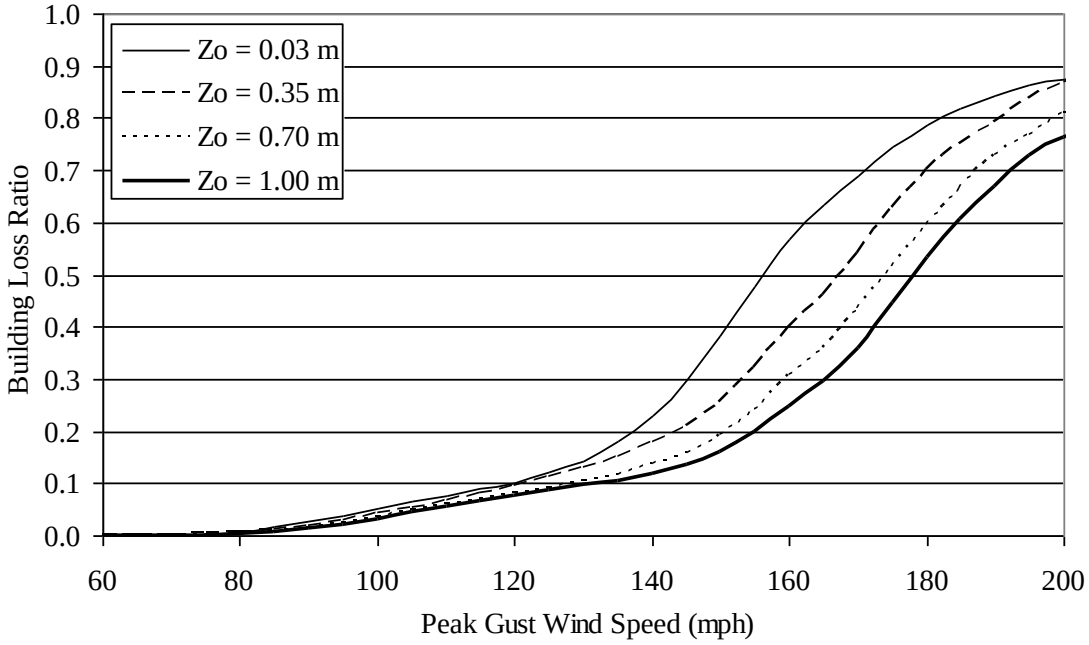

Figure M.41. Building Loss Function – Eight-Story Engineered Residential Building – Built-up Roof Cover, 33% Glazing Coverage, Metal Roof Deck, Missile Environment B.

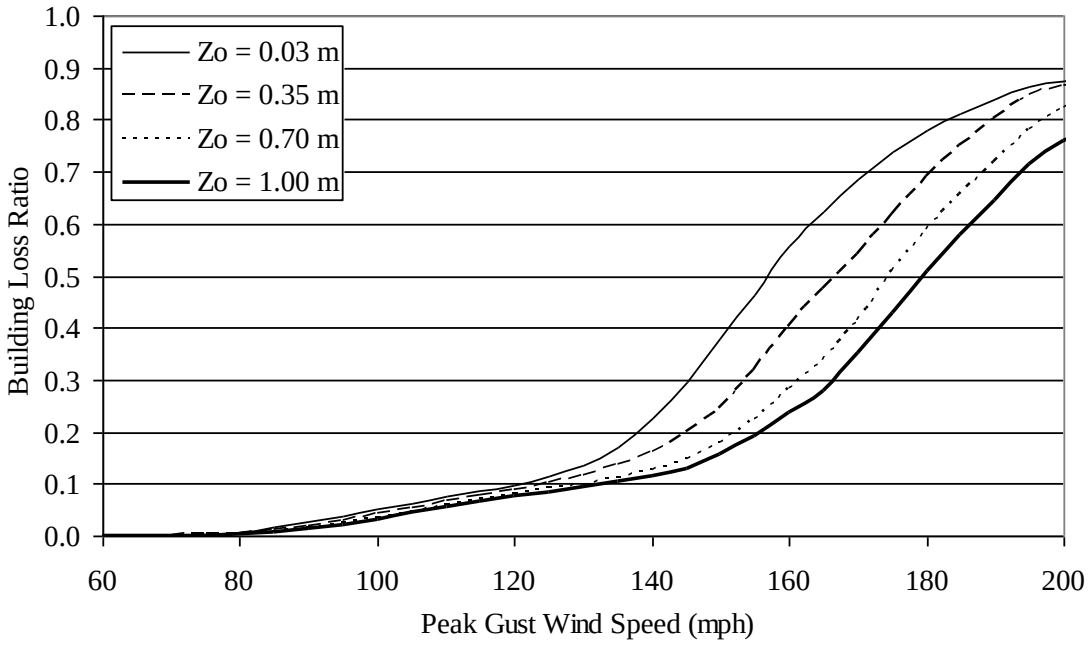

Figure M.42. Building Loss Function – Eight-Story Engineered Residential Building – Built-up Roof Cover, 33% Glazing Coverage, Metal Roof Deck, Missile Environment C.

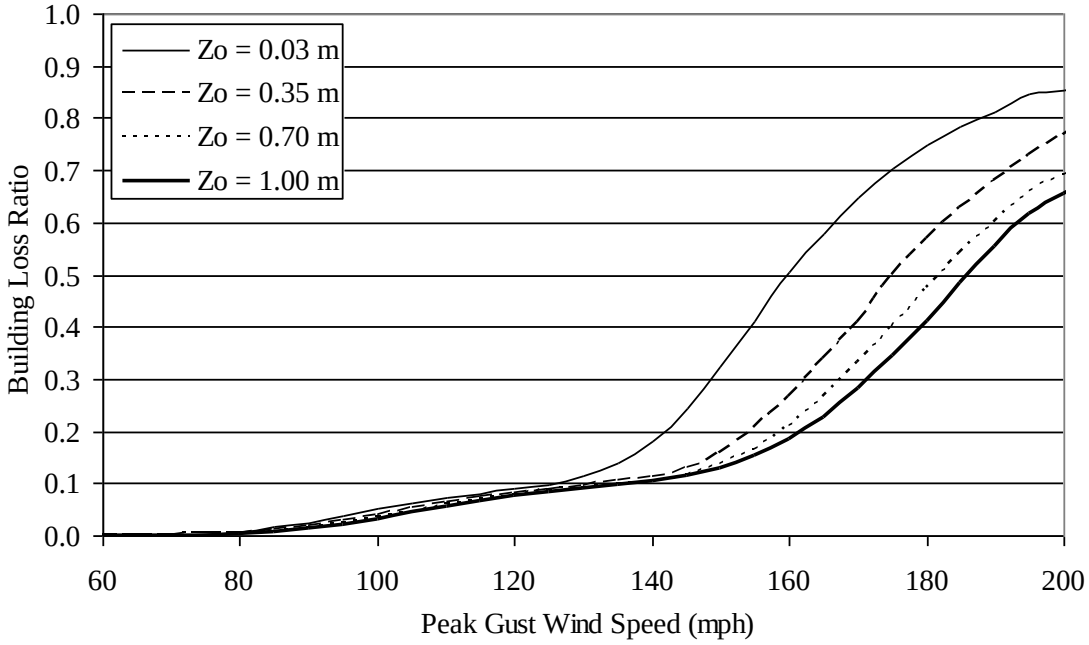

Figure M.43. Building Loss Function – Eight-Story Engineered Residential Building – Built-up Roof Cover, 33% Glazing Coverage, Metal Roof Deck, Missile Environment D.

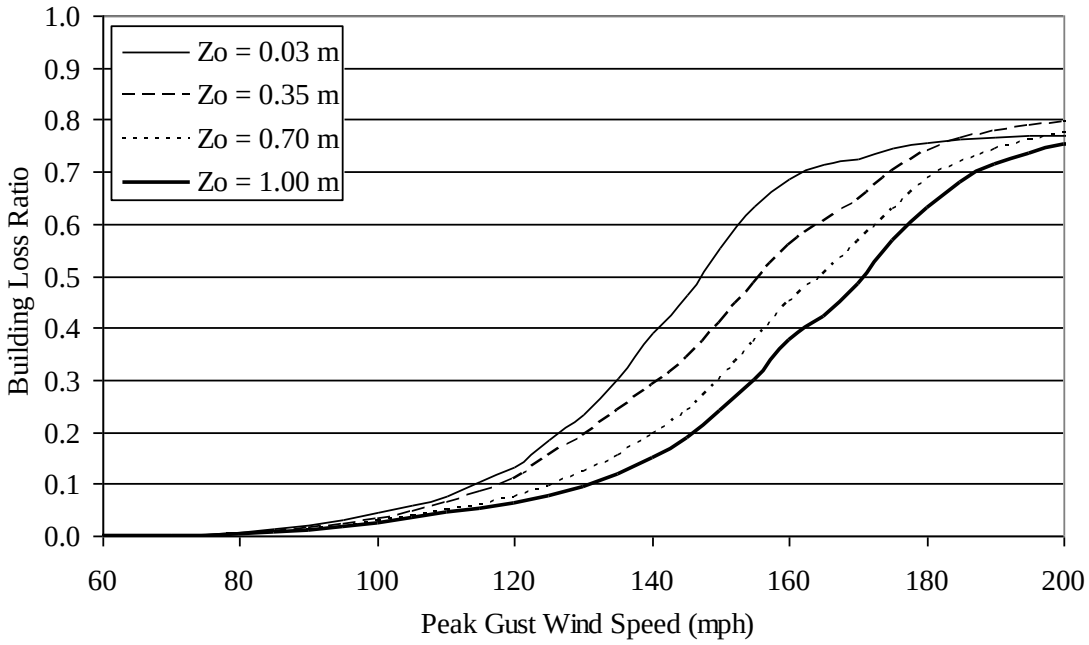

Figure M.44. Building Loss Function – Eight-Story Engineered Commercial Building – Built-up Roof Cover, 33% Glazing Coverage, Metal Roof Deck, Missile Environment A.

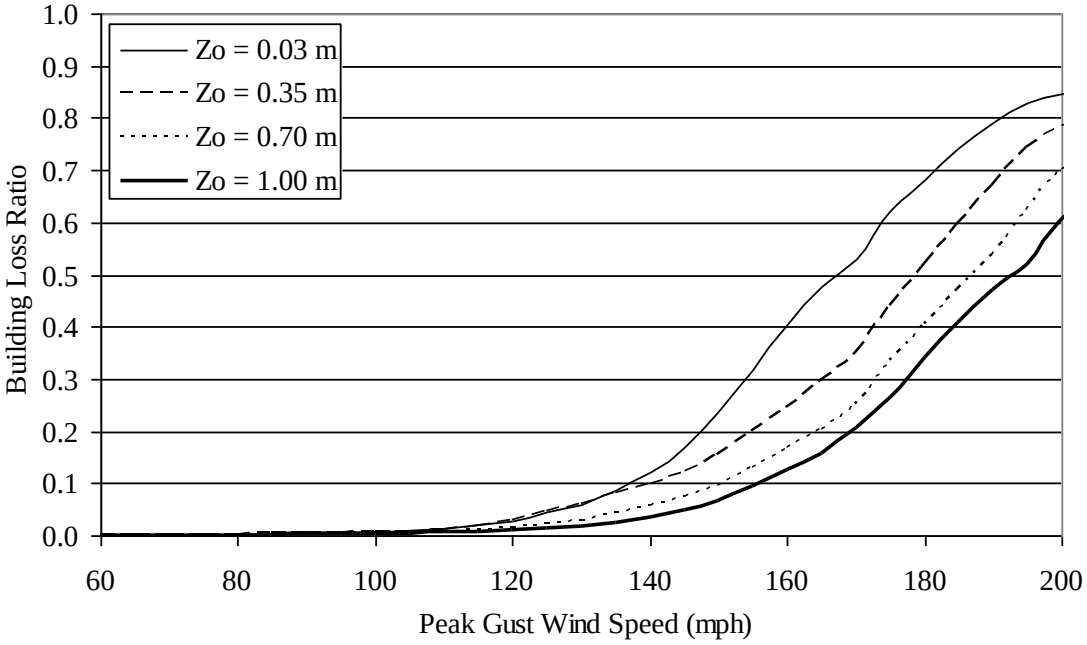

Figure M.45. Building Loss Function – Eight-Story Engineered Residential Building – Built-up Roof Cover, 33% Glazing Coverage, Concrete Roof Deck, Missile Environment A.

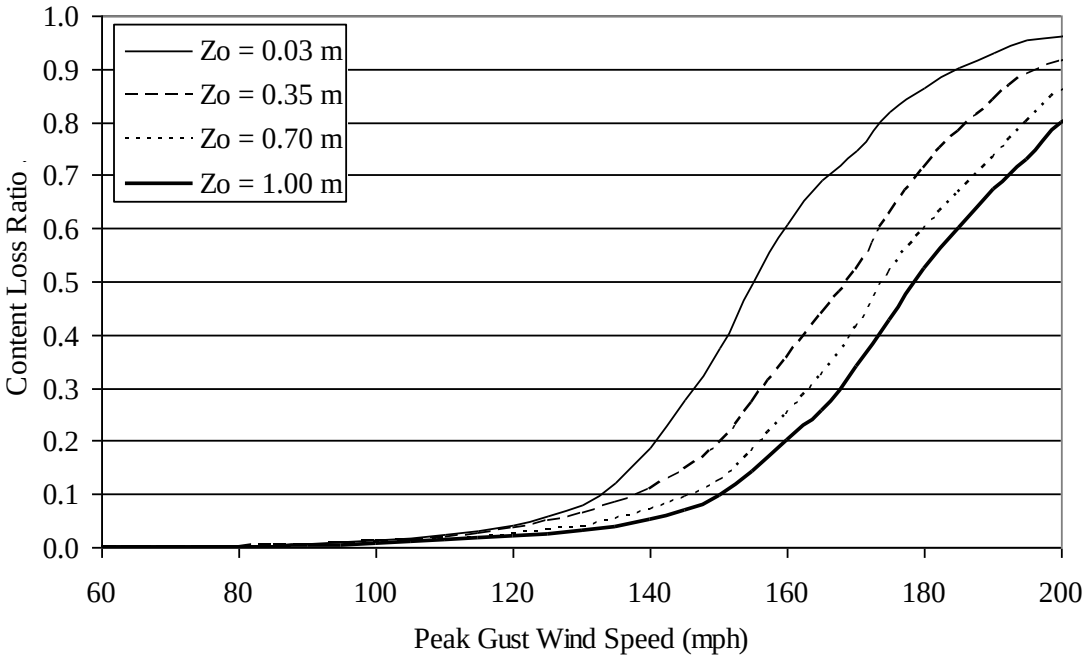

Figure M.46. Content Loss Function – Eight-Story Engineered Residential Building – Built-up Roof Cover, 33% Glazing Coverage, Metal Roof Deck, Missile Environment A.

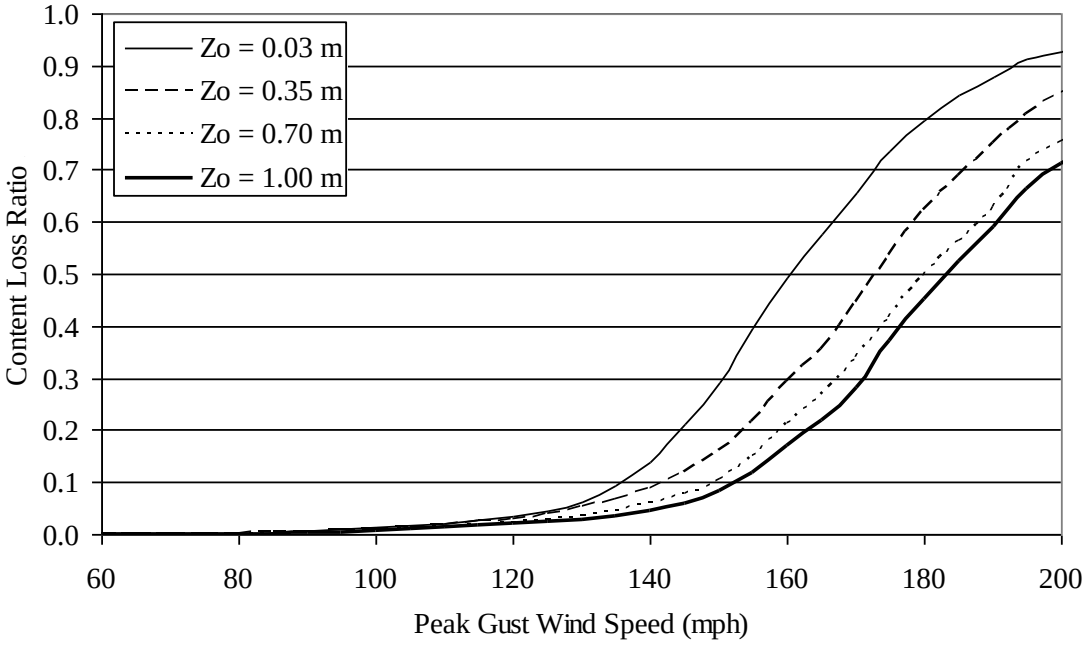

Figure M.47. Content Loss Function – Eight-Story Engineered Residential Building – Built-up Roof Cover, 20% Glazing Coverage, Metal Roof Deck, Missile Environment A.

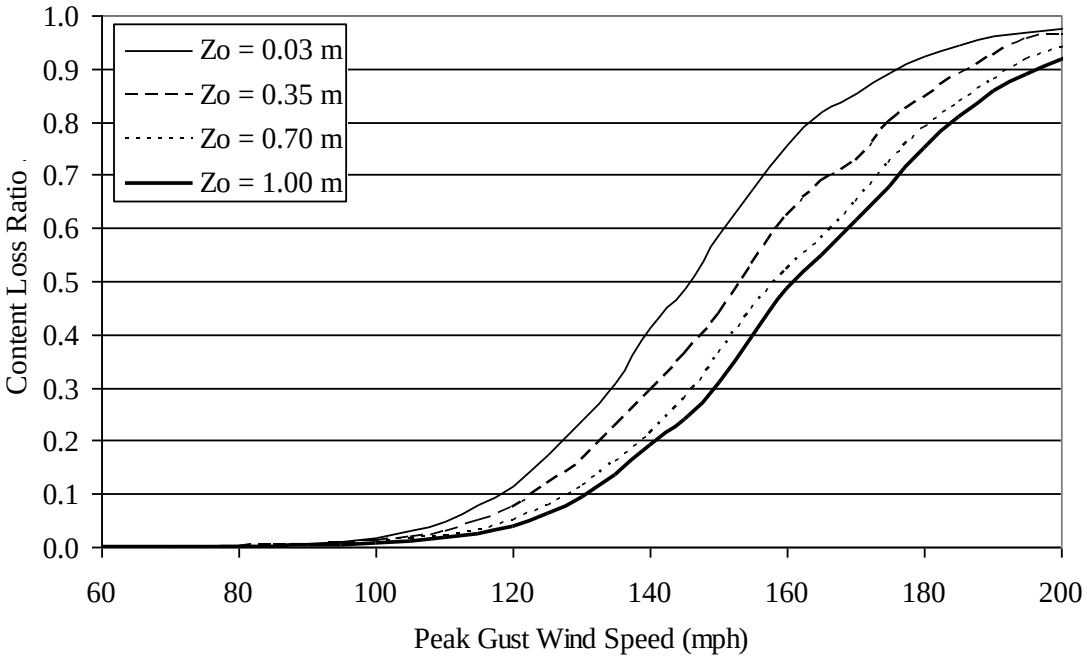

Figure M.48. Content Loss Function – Eight-Story Engineered Residential Building – Built-up Roof Cover, 50% Glazing Coverage, Metal Roof Deck, Missile Environment A.

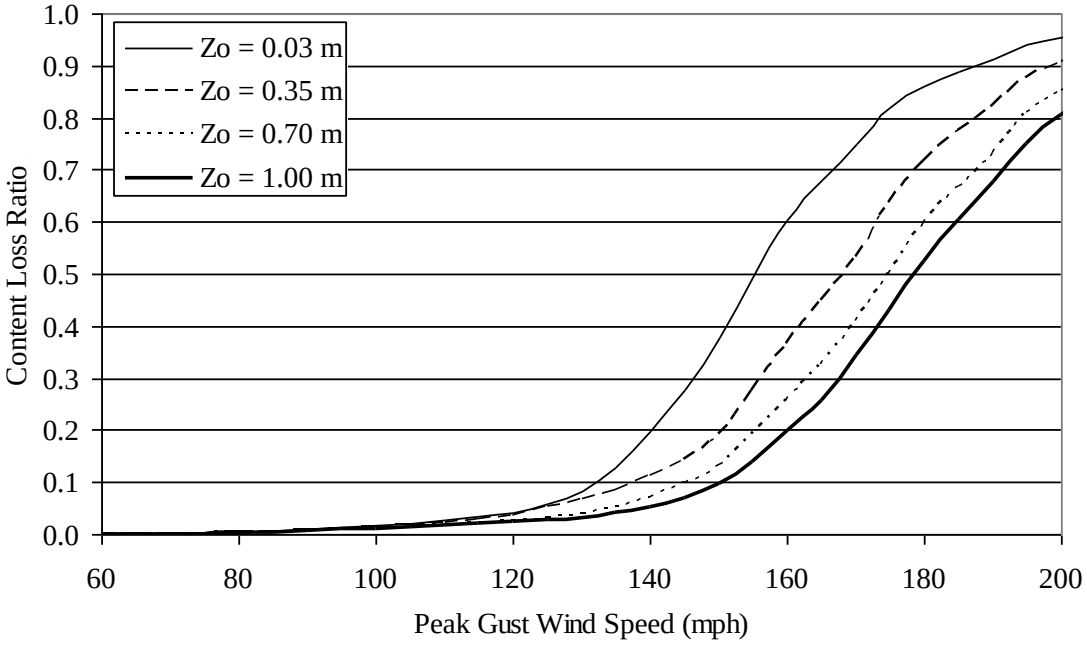

Figure M.49. Content Loss Function – Eight-Story Engineered Residential Building – Single Ply Membrane Roof Cover, 33% Glazing Coverage, Metal Roof Deck, Missile Environment A.

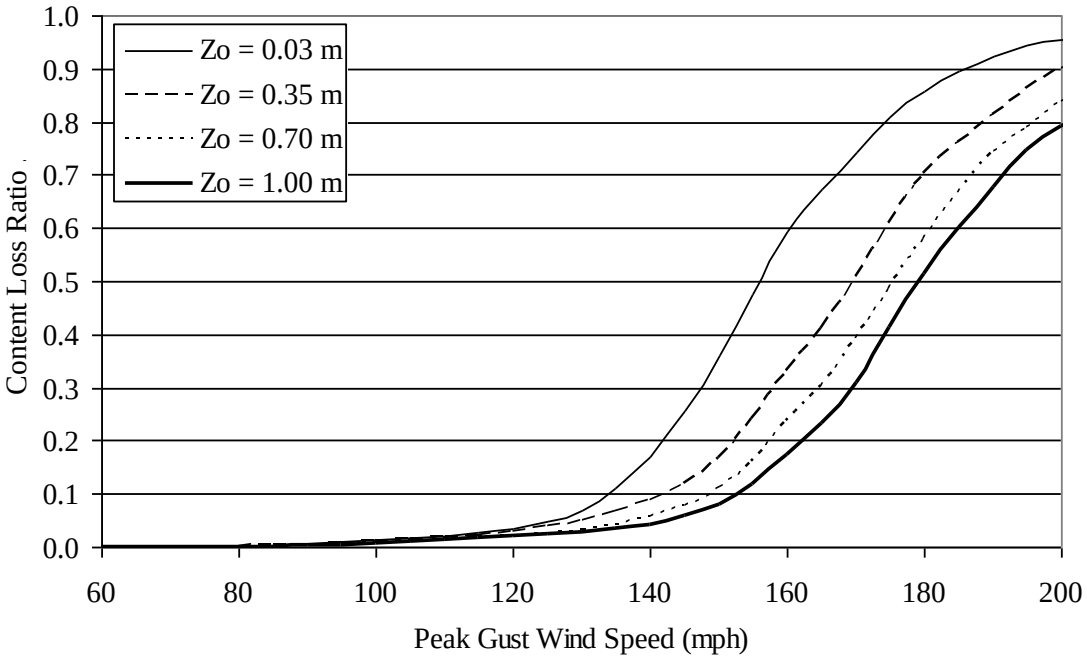

Figure M.50. Content Loss Function – Eight-Story Engineered Residential Building – Built-up Roof Cover, 33% Glazing Coverage, Metal Roof Deck, Missile Environment B.

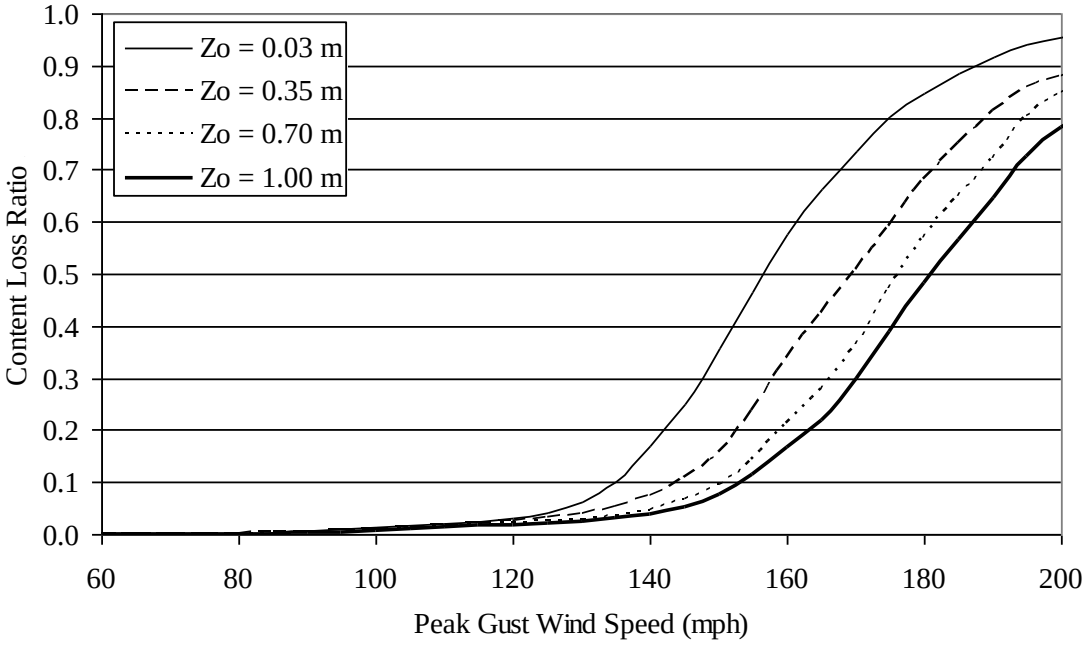

Figure M.51. Content Loss Function – Eight-Story Engineered Residential Building – Built-up Roof Cover, 33% Glazing Coverage, Metal Roof Deck, Missile Environment C.

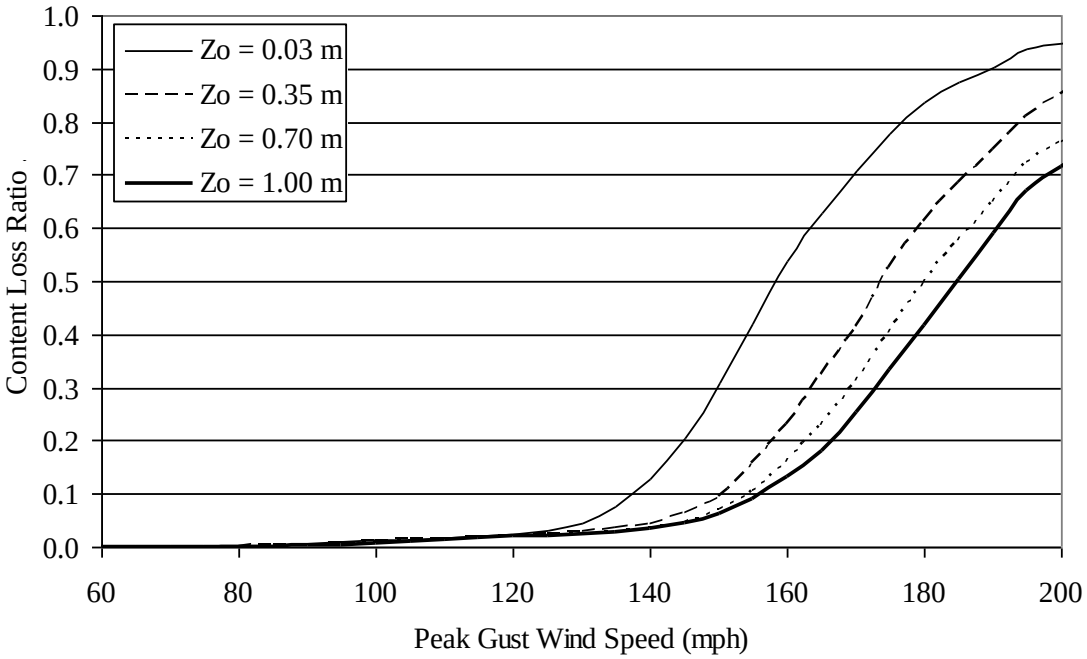

Figure M.52. Content Loss Function – Eight-Story Engineered Residential Building – Built-up Roof Cover, 33% Glazing Coverage, Metal Roof Deck, Missile Environment D.

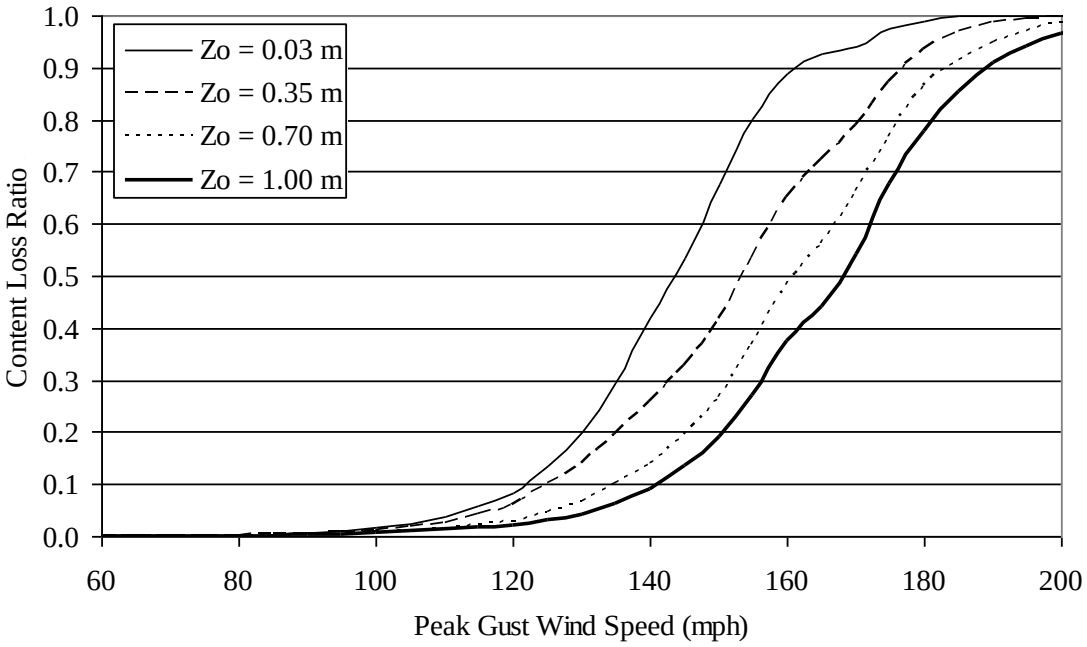

Figure M.53. Content Loss Function – Eight-Story Engineered Commercial Building – Built-up Roof Cover, 33% Glazing Coverage, Metal Roof Deck, Missile Environment A.

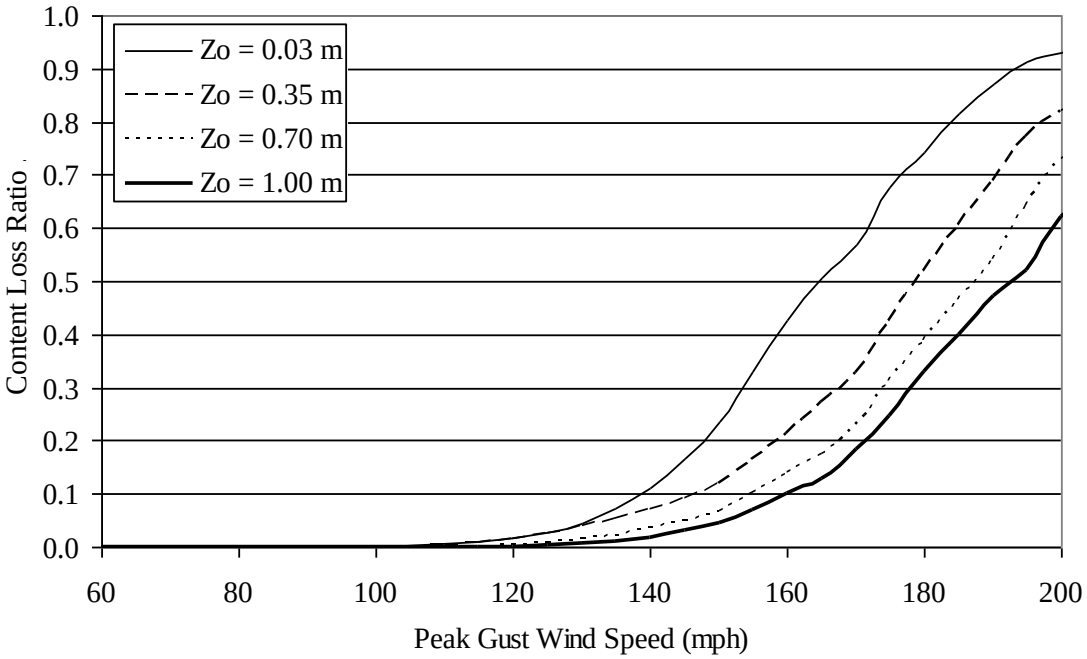

Figure M.54. Content Loss Function – Eight-Story Engineered Residential Building – Built-up Roof Cover, 33% Glazing Coverage, Concrete Roof Deck, Missile Environment A.

Appendix N.
Loss Functions for Industrial Buildings

Appendix N.
Loss Functions for Industrial Buildings

This appendix presents loss functions for industrial buildings (see Section 7.14). The loss functions represent either average building loss normalized by building value or average content loss normalized by content value. Therefore, the loss ratios range between 0 and 1 in both cases. Note that the content value is set to 50% of the building value. For a given simulated storm, the building loss ratio and content loss ratio are estimated based on the modeled damage and the largest gust speed over the entire duration of the simulated storm is saved. The loss functions are then computed by averaging the loss ratios associated with the storms producing a maximum gust speed within 5 mph ranges. The average loss ratios (content or building loss) associated with each 5 mph gust speed range are then plotted at the center of that range. Note that the wind speeds are representative of open terrain at 10 m above ground.

Table N.1 lists the figures provided in this appendix. Two sets of three figures are given for the industrial buildings. The first set of three figures (Figures N.1 through N.3) show building loss functions and the second set (Figures N.4 through N.6) show content loss functions. The first figure in each set of three shows loss results for the industrial building constructed with unreinforced masonry walls, having no reduction in the metal roof deck capacity and situated in Missile Environment A. The remaining two plots in each set show damage state results for buildings which are different by a single variable in comparison to the reference building (note that the changed variable is underlined in the figure titles).

Table N.1. Sample Loss Functions for Industrial Buildings

Figure	Loss Type	Walls	Metal Deck Capacity	Missile Environ.
N.1	Building	URM	Full	A
N.2	Building	**RM**	Full	A
N.3	Building	URM	**50%**	A
N.4	Content	URM	Full	A
N.5	Content	**RM**	Full	A
N.6	Content	URM	**50%**	A

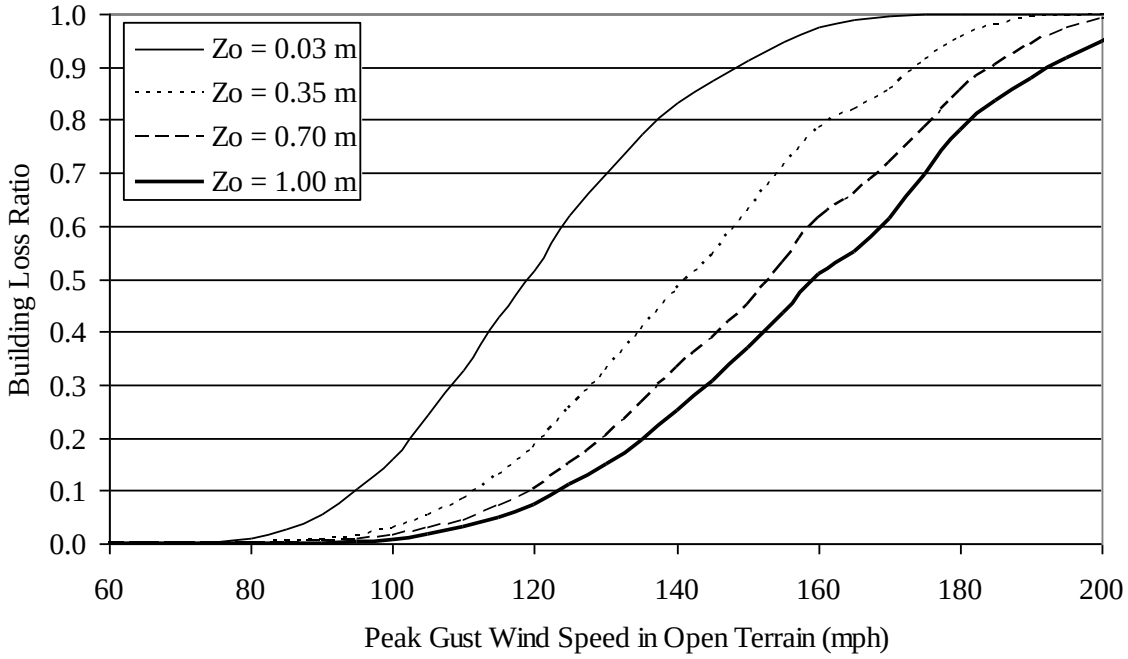

Figure N.1. Building Loss Function – Industrial Building – No Reduction in Metal Deck Capacity, Unreinforced Masonry Walls, Missile Environment A.

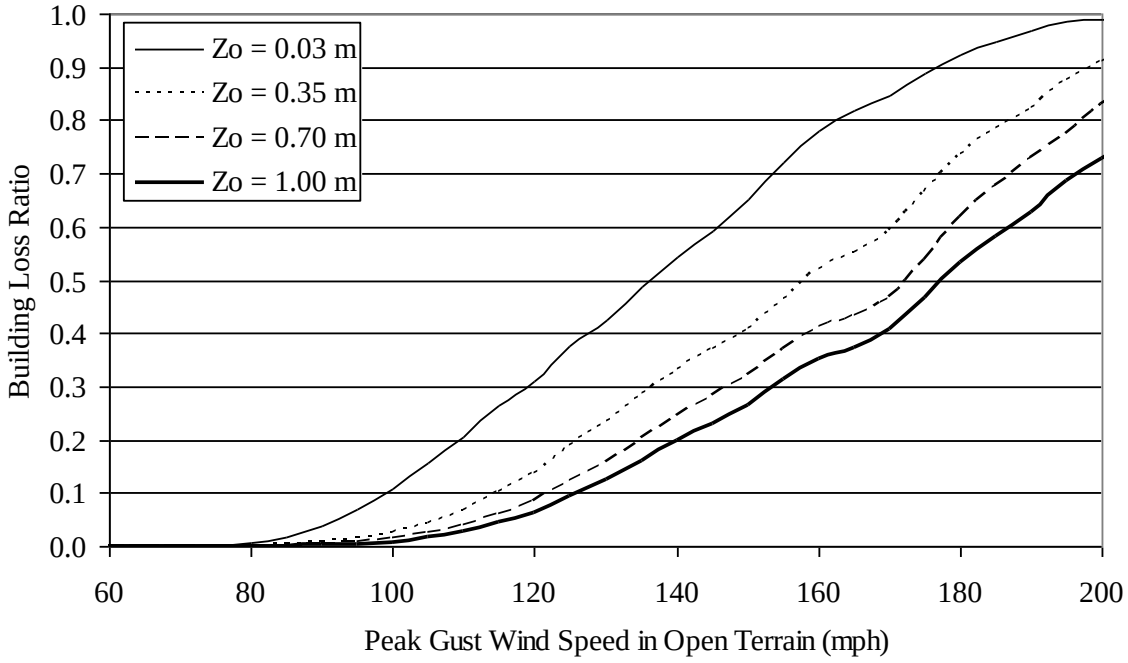

Figure N.2. Building Loss Function – Industrial Building – No Reduction in Metal Deck Capacity, <u>Reinforced Masonry Walls</u>, Missile Environment A.

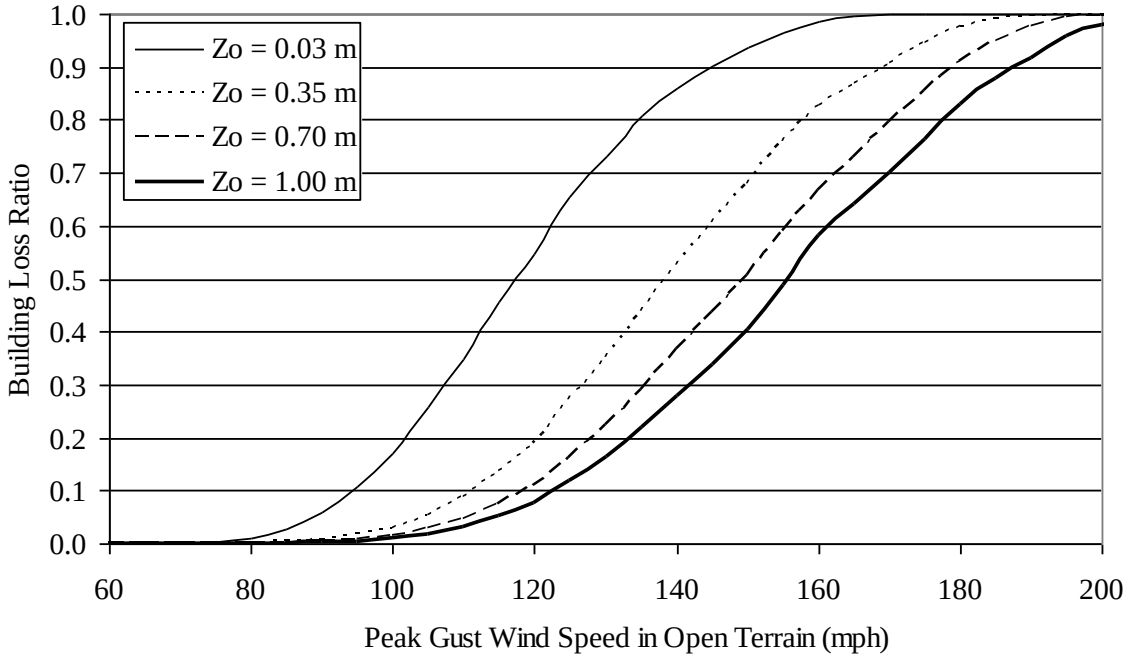

Figure N.3. Building Loss Function – Industrial Building – <u>50% Reduction in Metal Deck Capacity</u>, Unreinforced Masonry Walls, Missile Environment A.

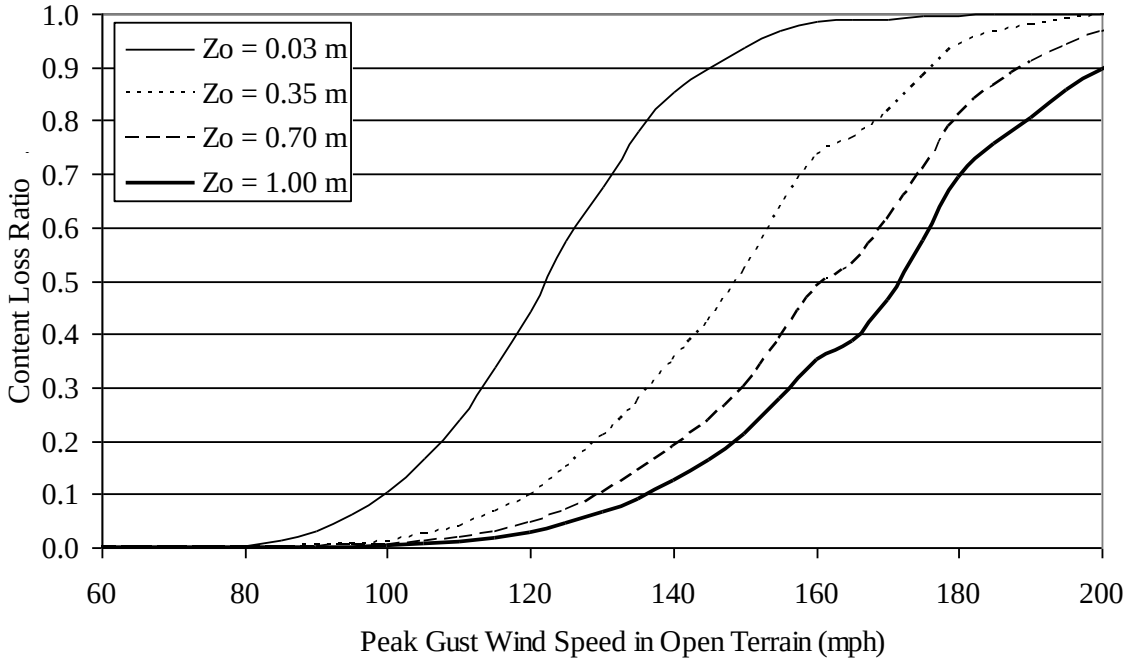

Figure N.4. Content Loss Function – Industrial Building – No Reduction in Metal Deck Capacity, Unreinforced Masonry Walls, Missile Environment A.

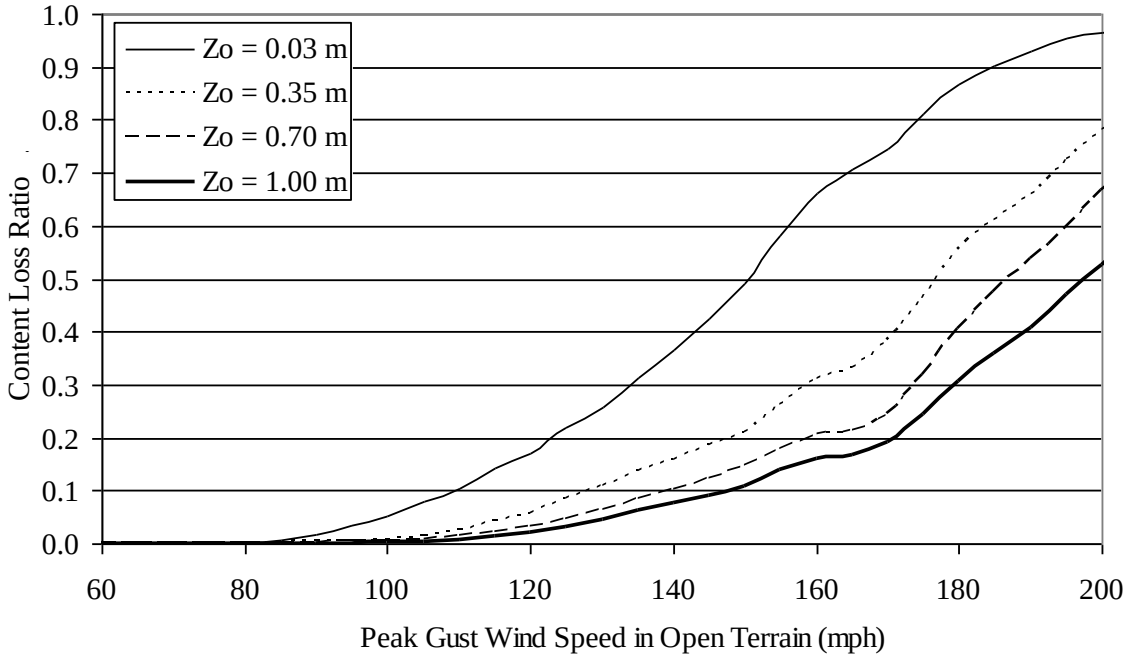

Figure N.5. Content Loss Function – Industrial Building – No Reduction in Metal Deck Capacity, Reinforced Masonry Walls, Missile Environment A.

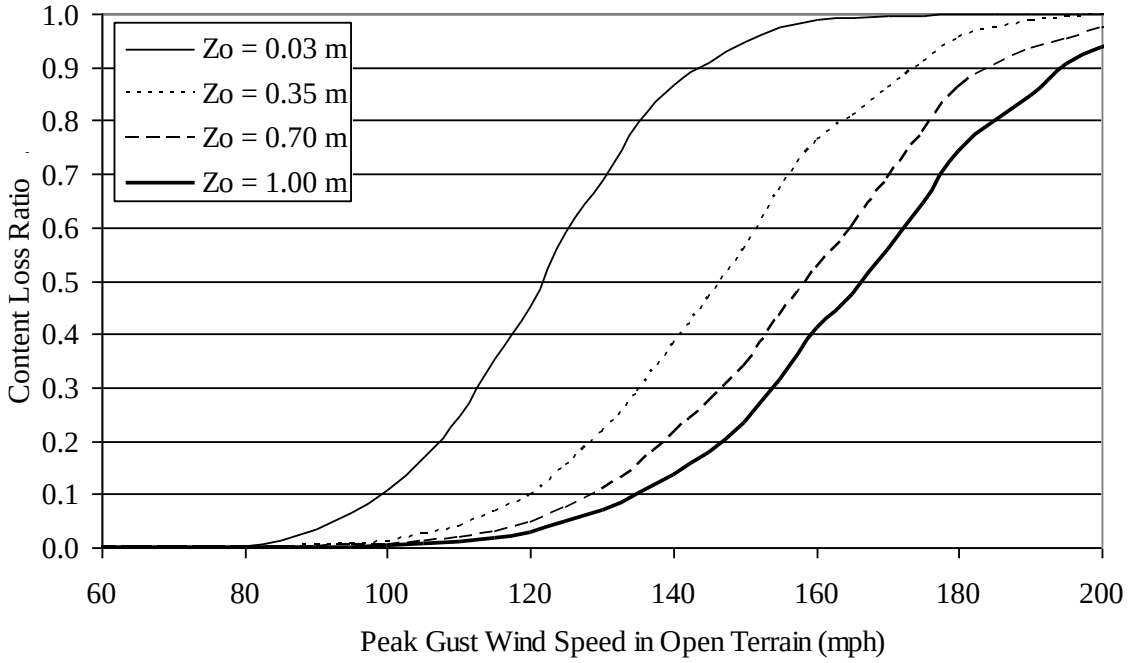

Figure N.6. Content Loss Function – Industrial Building – 50% Reduction in Metal Deck Capacity, Unreinforced Masonry Walls, Missile Environment A.

Appendix O. Comparisons of Modeled and Measured Wind Speeds, Wind Directions, and Pressures for Hurricane Isabel (2003)

This appendix presents comparisons of modeled and observed wind speeds, wind directions, and pressures at multiple locations along the Atlantic Coast of North Carolina and the Chesapeake Bay area during the passage of Hurricane Isabel (2003).

Figure O-1 shows the maximum 10-minute mean wind speeds obtained from three versions of SLOSH model. The first version uses ARA storm track and ARA wind field model (denoted as ARA-TRK-ARA-WD). The second version uses ARA storm track and SLOSH wind field model (denoted as ARA-TRK-SLOSH-WD). The third version uses NOAA best track and SLOSH wind field mode (denoted as NOAA-TRK-ARA-WD). The results are shown for the Pamlico Sound, Norfolk, and Chesapeake Bay SLOSH basins.

Figure O-2 presents the simulated landfall wind field for the Pamlico Sound, Norfolk, and Chesapeake Bay SLOSH basins

Figure O-3 shows a map of the locations of all observing stations as well as the hurricane track. The observed wind speeds and pressures are compared to the simulated wind speeds and pressures from model runs using the ARA-TRK-ARA-WD, ARA-TRK-SLOSH-WD, and NOAA-TRK-ARA-WD models, as shown in Table O-1 and Table O-2.

Figure O-4 presents the comparisons of modeled and observed maximum wind speeds and minimum pressures for Hurricane Isabel. The results indicate that the SLOSH wind field model underestimates the wind speeds, while ARA wind field model slightly overestimates the wind speeds for Hurricane Isabel. The simulated minimum pressures are comparable to the observed data.

Comparisons of the entire modeled and observed time series of mean wind speeds, wind directions, and pressures for all stations, both complete and incomplete, are presented in Figure O-5. The RMS errors of wind speed, wind direction, and pressure are shown in Table O-3.

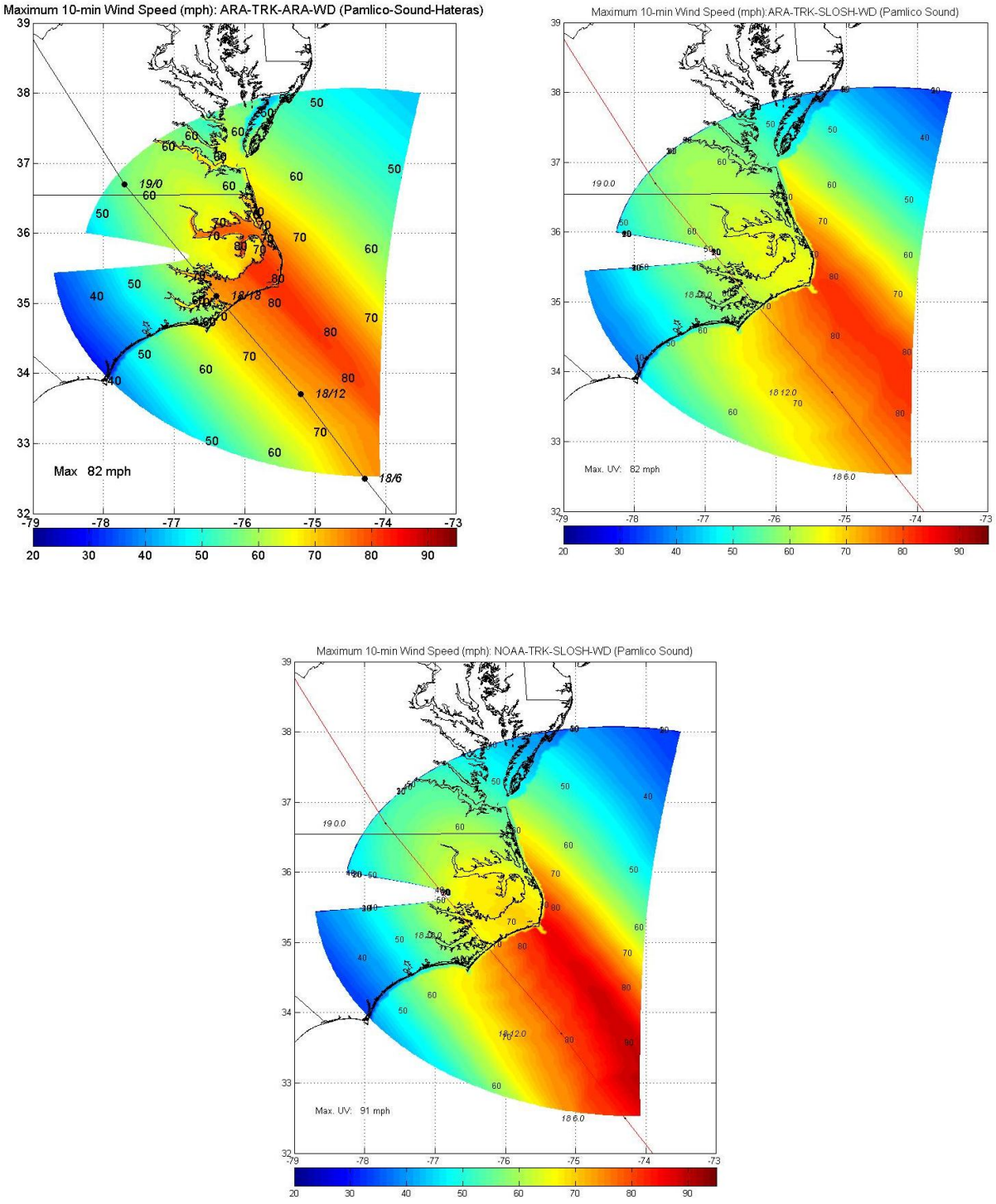

Figure O-1a. Modeled Maximum 10-min Wind Speeds (mph) for Hurricane Isabel (2003) – Pamlico Sound Basin

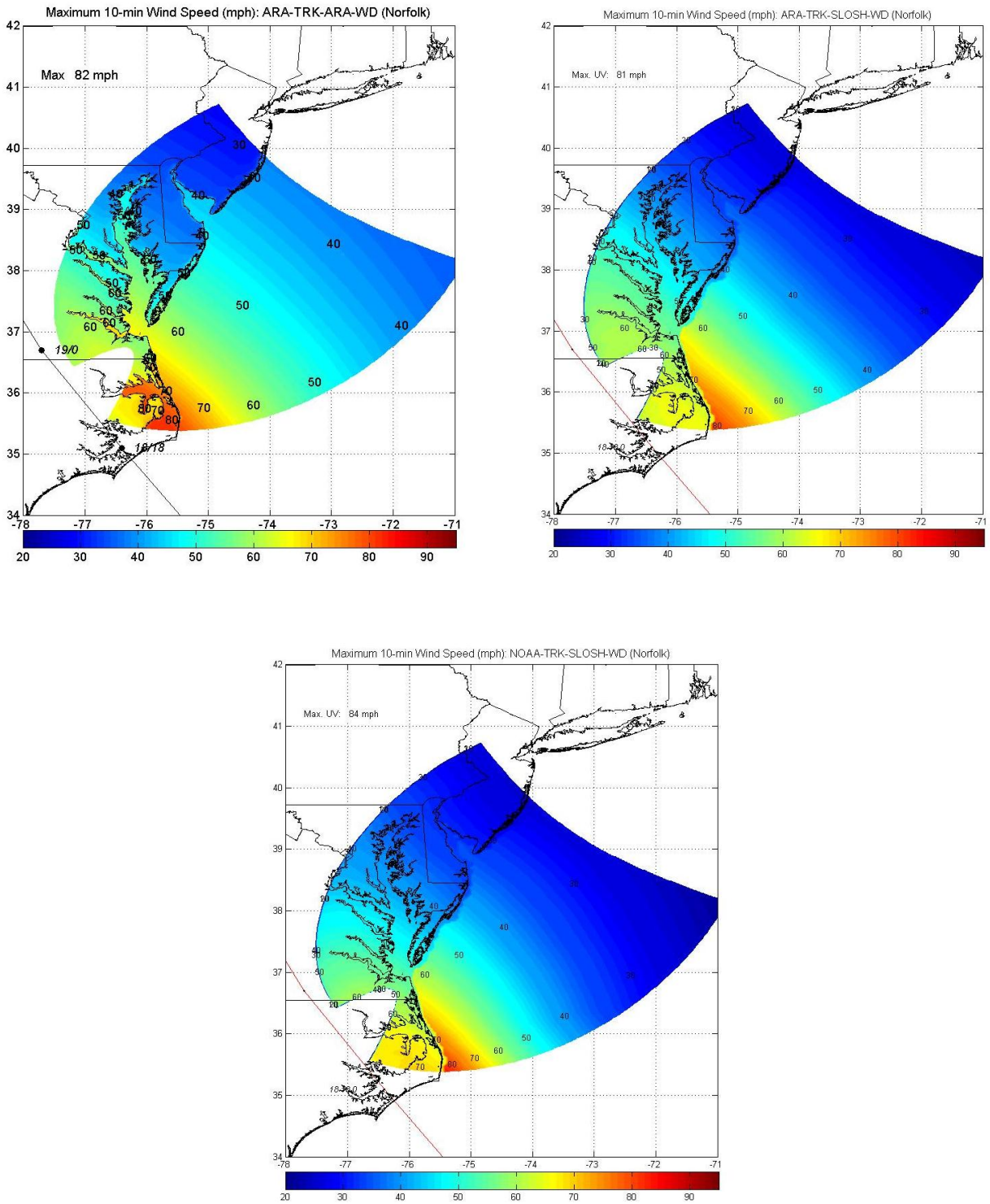

Figure O-1b. Modeled Maximum 10-min Wind Speeds (mph) for Hurricane Isabel (2003) – Norfolk Basin

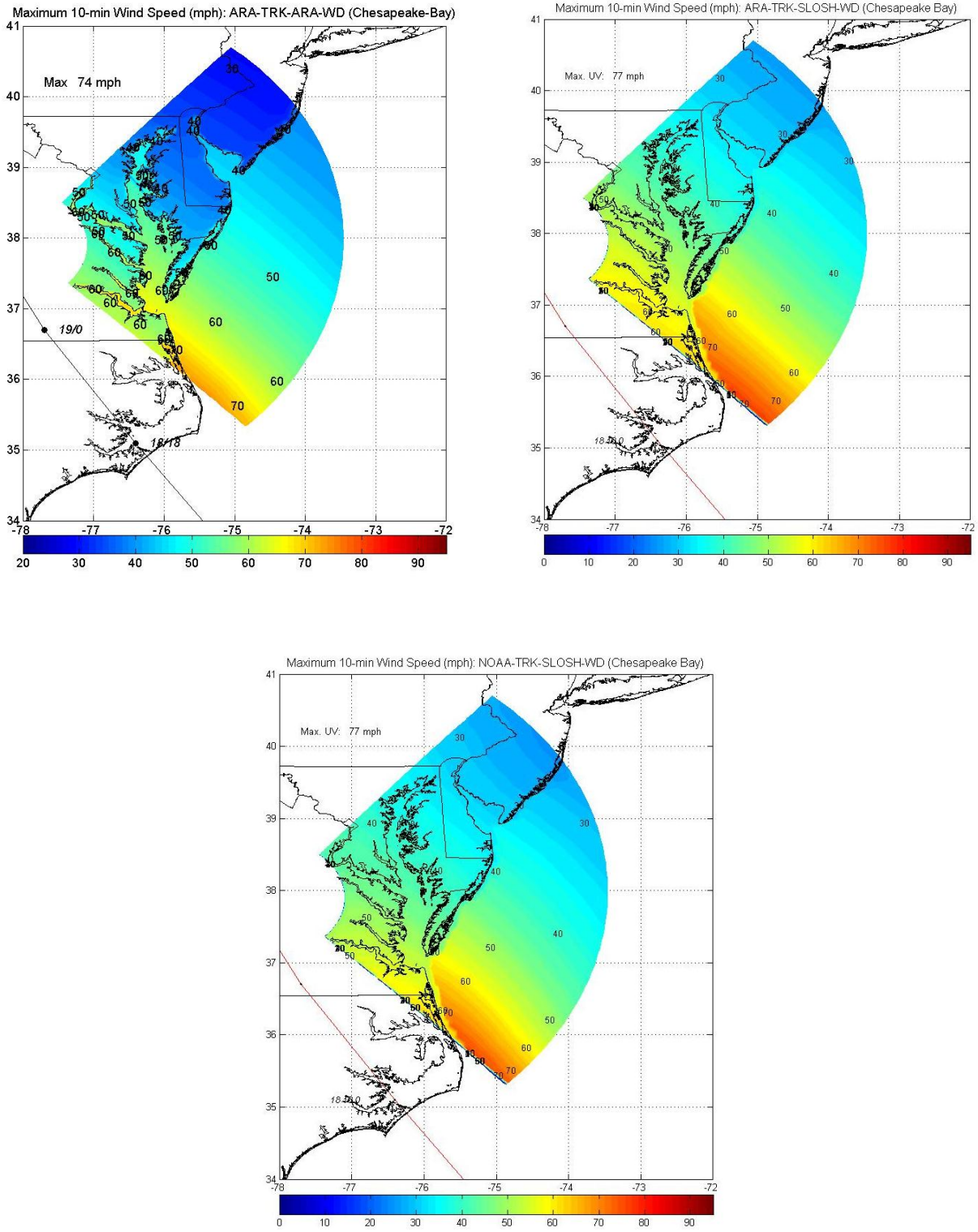

Figure O-1c. Modeled Maximum 10-min Wind Speeds (mph) for Hurricane Isabel (2003) – Chesapeake Bay Basin

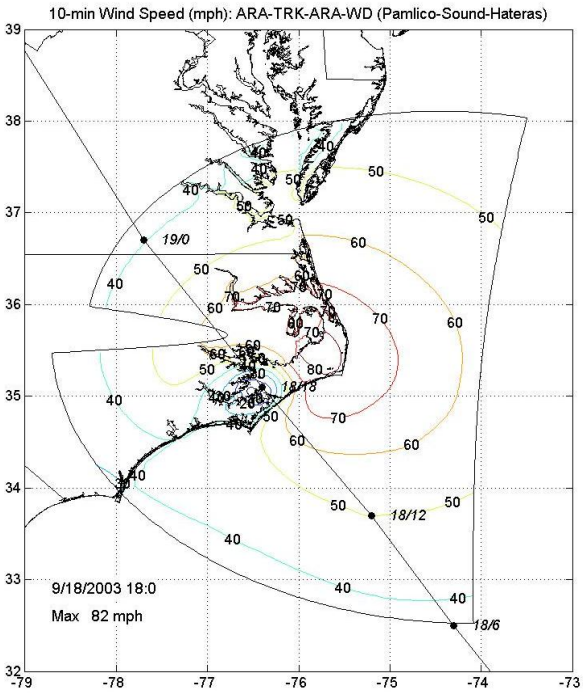

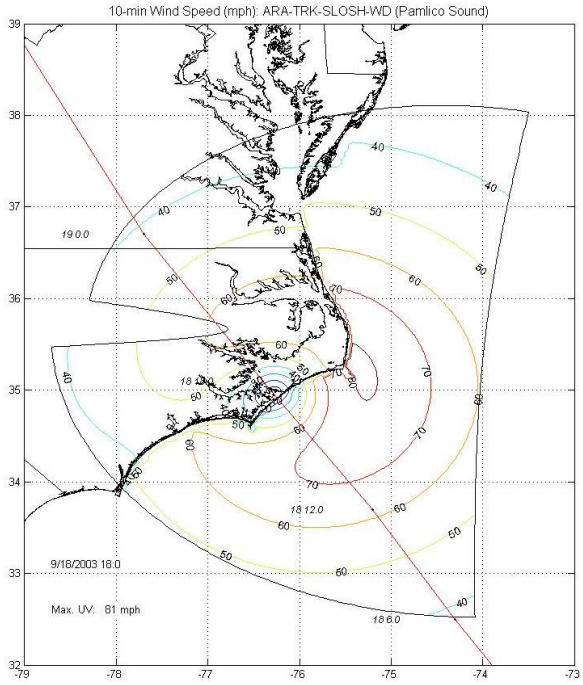

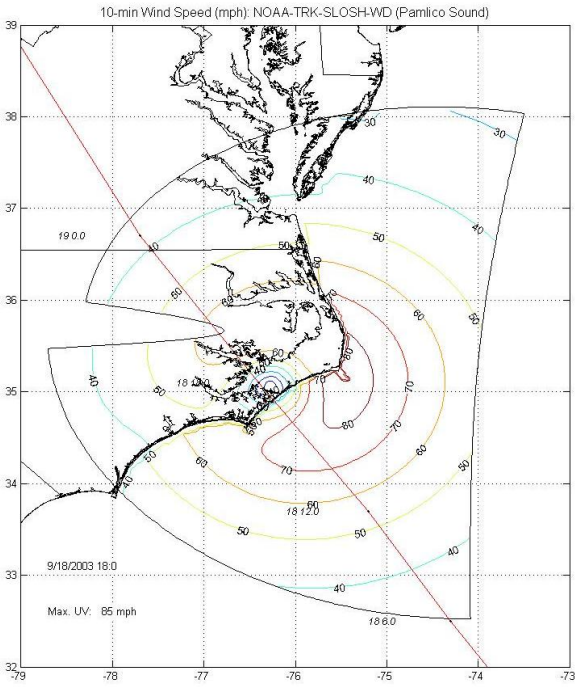

Figure O-2a. Hurricane Isabel (2003) Modeled 10-min Wind Speeds (mph) at Landfall – Pamlico Sound Basin

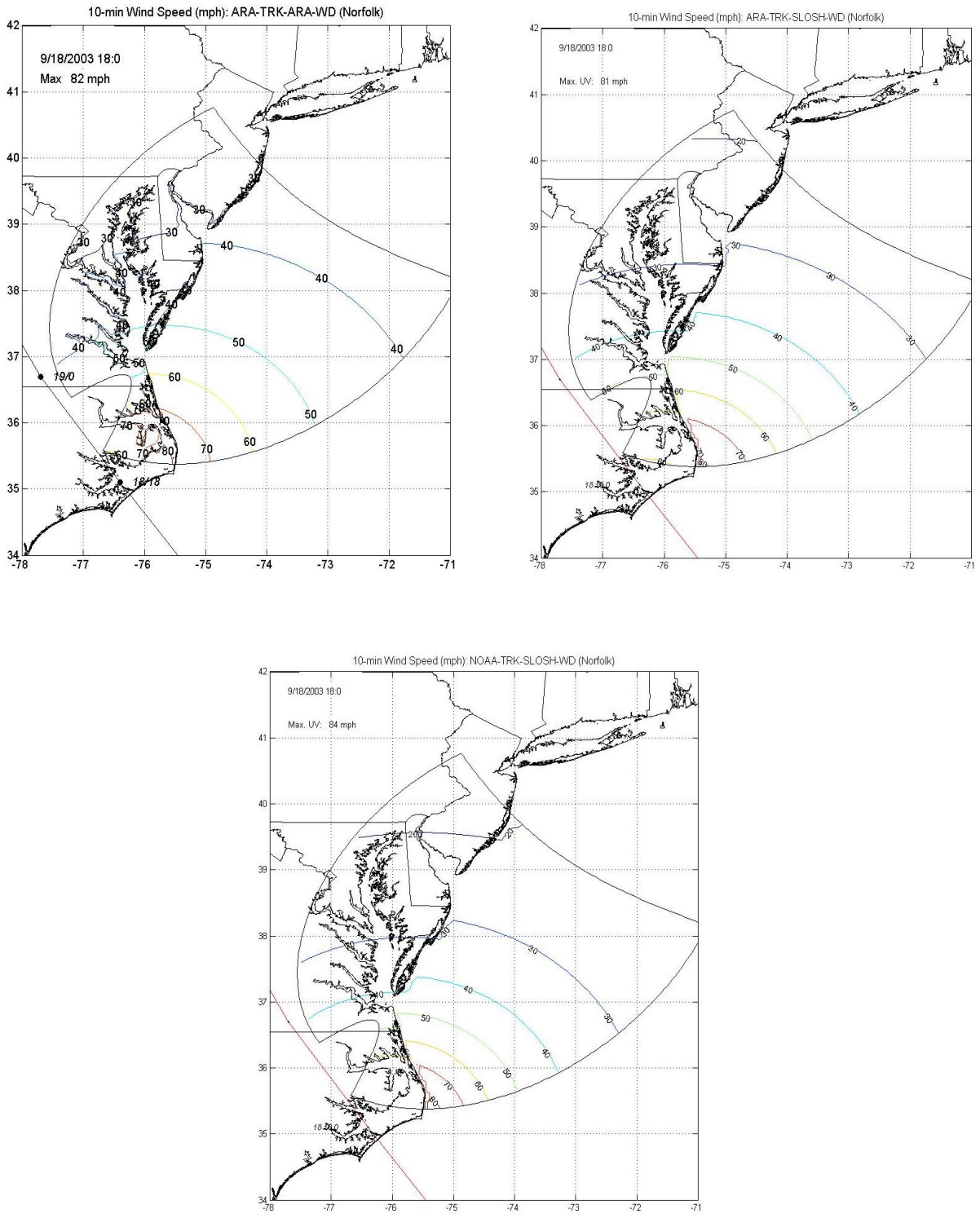

Figure O-2b. Hurricane Isabel (2003) Modeled 10-min Wind Speeds (mph) at Landfall – Norfolk Basin

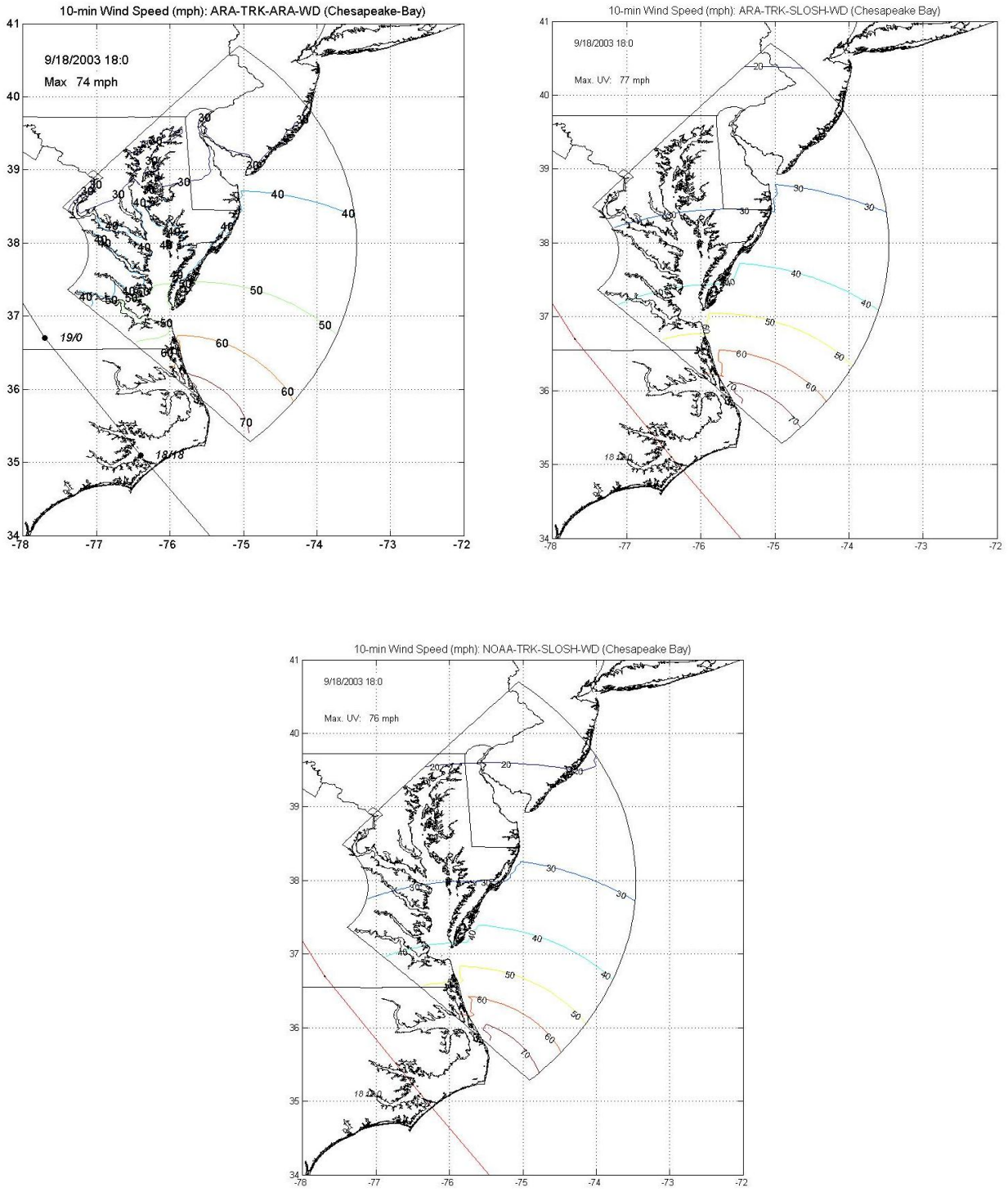

Figure O-2c. Hurricane Isabel (2003) Modeled 10-min Wind Speeds (mph) at Landfall – Chesapeake Bay Basin

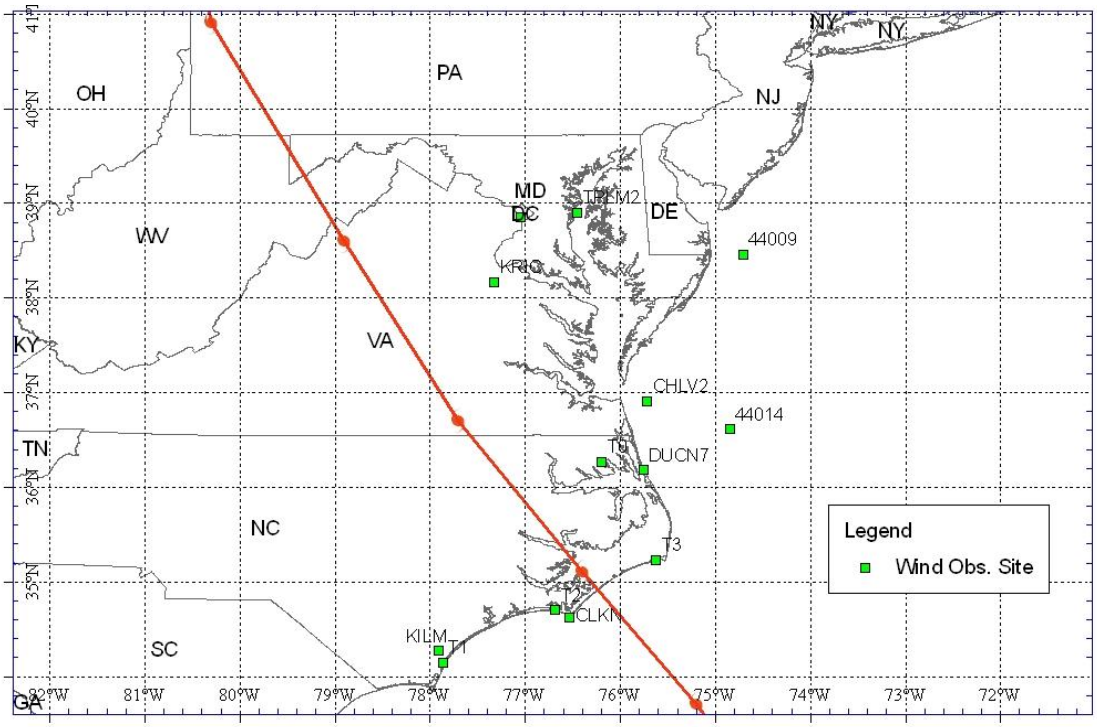

Figure O-3. Wind Observation Locations for Hurricane Isabel

Table O-1. Summary Comparison of Modeled and Observed Maximum 10-min Wind Speeds for Hurricane Isabel

No	Station	Lattitude	Longitude	Max Wind Speed (mph)			
				Obs.	ARA-TRK SLOSH-WD	ARA-TRK ARA-WD	NOAA-TRK SLOSH-WD
1	KILM	34.26670	-77.90030	45.0	40.8	34.1	36.7
2	CLKN	34.62170	-76.52500	67.7	67.3	67.3	68.2
3	FCMP T0	36.26600	-76.18300	59.3	63.1	67.9	62.9
4	FCMP T1	34.14917	-77.85942	34.8	40.2	33.5	36.2
5	FCMP T2	34.69839	-76.67903	54.0	57.0	65.9	58.2
6	FCMP T3	35.23139	-75.62072	66.7	65.6	73.9	69.9
7	DUCN7	36.18000	-75.75000	67.9	61.5	68.3	60.8
8	CHLV2	36.91000	-75.71000	62.7	63.5	62.9	60.1
9	44009	38.46000	-74.70000	45.4	38.1	45.9	36.8
10	44014	36.61000	-74.84000	52.1	56.0	58.1	53.0
11	TPLM2	38.90000	-76.44000	44.2	42.1	51.0	39.2
12	KDCA	38.84722	-77.03444	50.0	45.9	44.1	41.3
13	KRIC	38.16670	-77.31660	42.0	53.3	52.1	45.5

Table O-2. Summary Comparison of Modeled and Observed Minimum Pressures for Hurricane Isabel

No	Station	Lattitude	Longitude	Minimum Central Pressure (mbar)			
				Obs.	ARA-TRK SLOSH-WD	ARA-TRK ARA-WD	NOAA-TRK SLOSH-WD
1	KILM	34.26670	-77.90030	984.4	990.2	991.2	990.0
2	CLKN	34.62170	-76.52500	960.9	964.7	969.7	964.9
3	FCMP T0	36.26600	-76.18300	975.5	980.6	978.6	981.9
4	FCMP T1	34.14917	-77.85942	984.7	991.3	991.9	990.8
5	FCMP T2	34.69839	-76.67903	963.4	967.7	972.5	962.8
6	FCMP T3	35.23139	-75.62072	967.9	974.1	974.9	968.2
7	DUCN7	36.18000	-75.75000	978.7	984.6	982.8	984.4
8	CHLV2	36.91000	-75.71000	985.8	990.9	986.9	990.6
9	44009	38.46000	-74.70000	996.7	999.9	996.0	1006.6
10	44014	36.61000	-74.84000	989.4	994.2	991.9	995.5
11	TPLM2	38.90000	-76.44000	993.4	997.9	993.3	1001.1
12	KDCA	38.84722	-77.03444	992.1	996.7	992.0	999.0
13	KRIC	38.16670	-77.31660	985.3	991.1	986.3	988.0

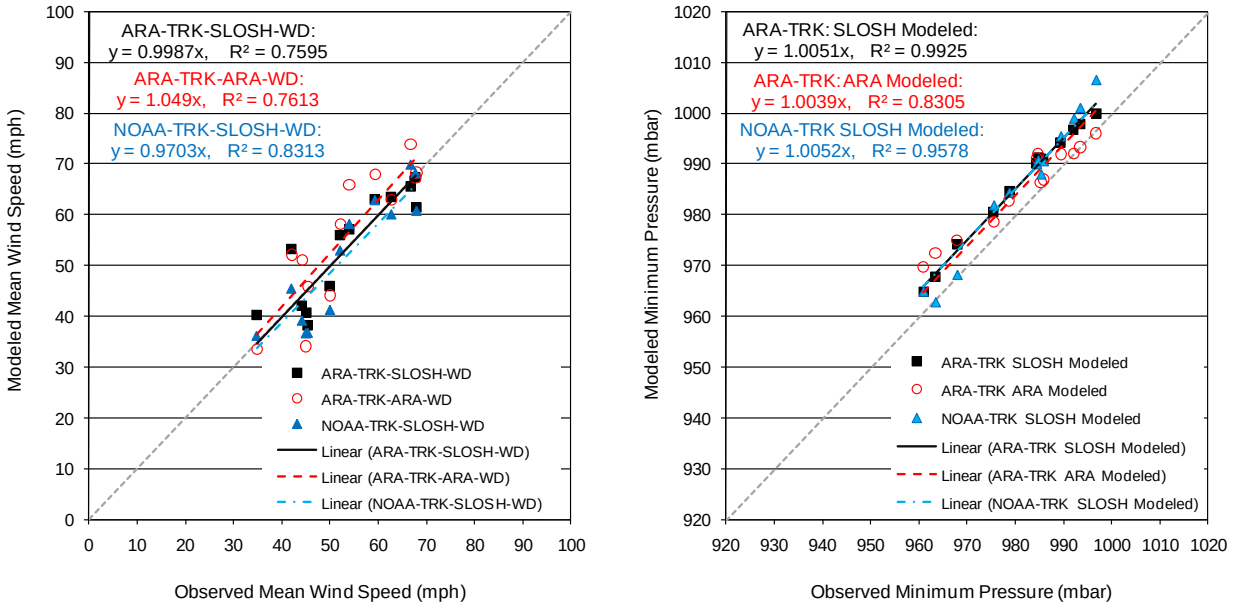

Figure O-4. Comparisons of Modeled and Observed Maximum 10-min Wind Speeds and Minimum Pressures for Hurricane Isabel

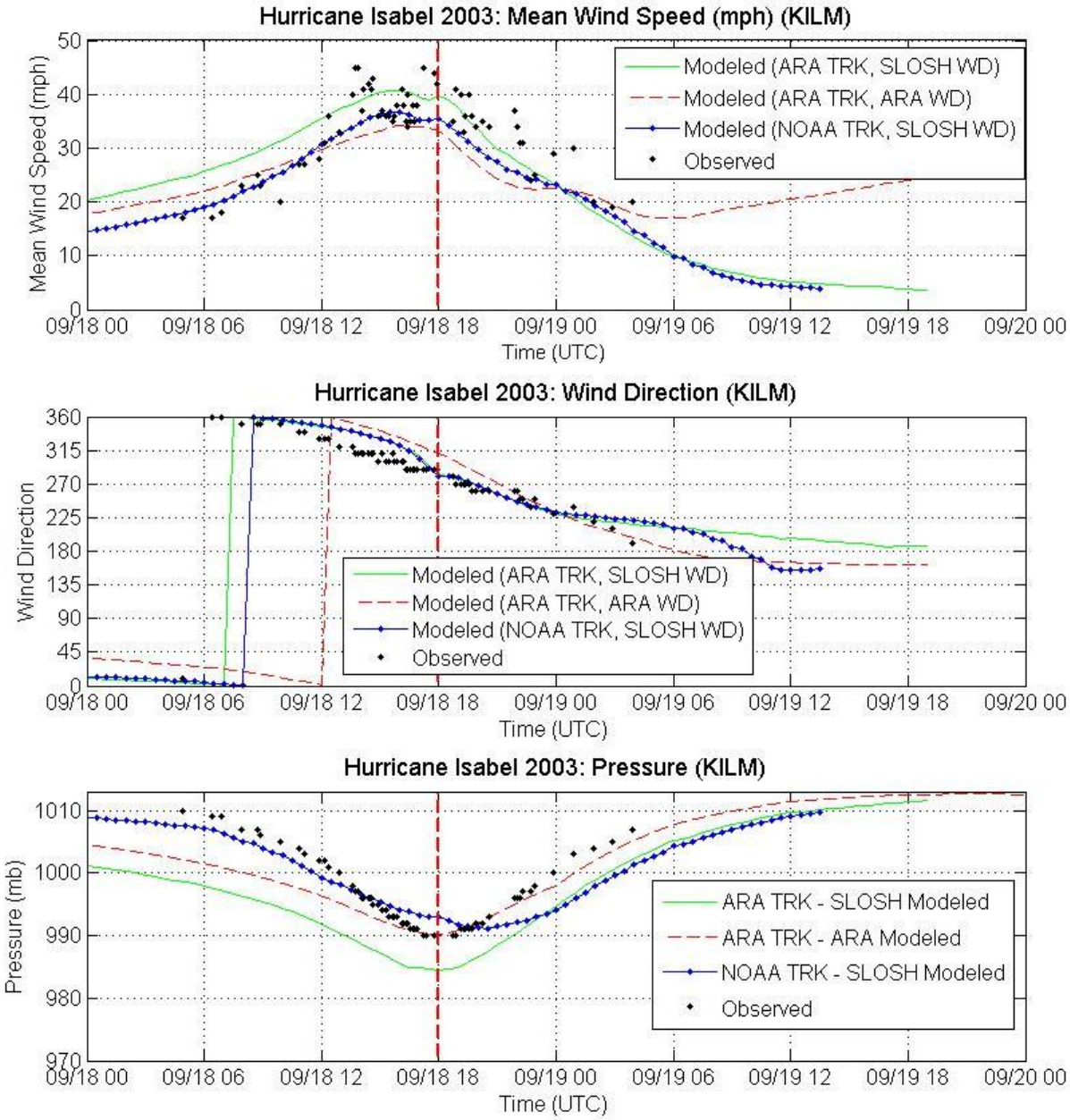

Figure O-5a. Comparisons of Observed and Modeled Time Series Traces of Mean Wind Speeds, Wind Directions, and Pressures for Hurricane Isabel (2003) – KILM

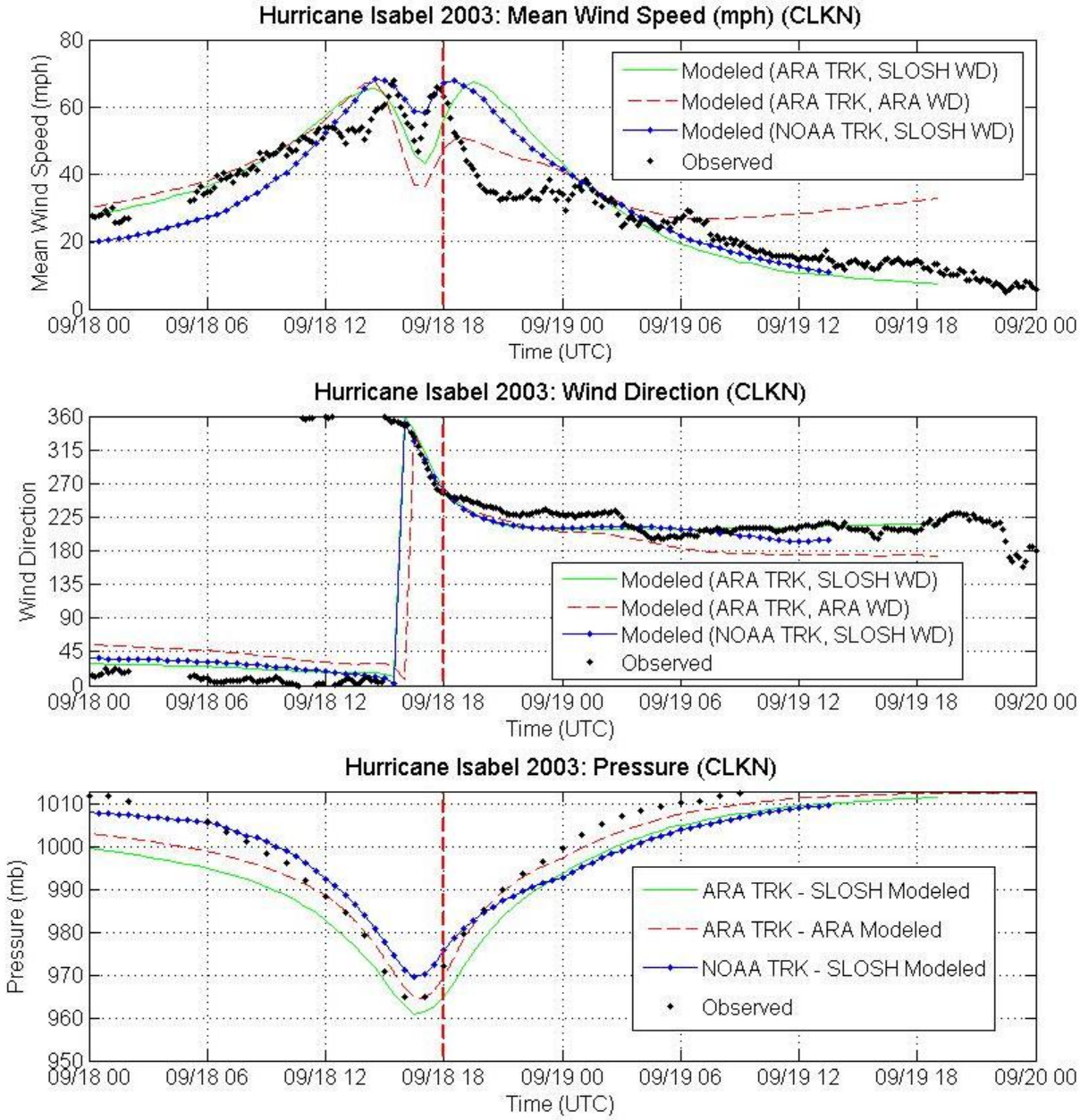

Figure O-5b. Comparisons of Observed and Modeled Time Series Traces of Mean Wind Speeds, Wind Directions, and Pressures for Hurricane Isabel (2003) – CLKN

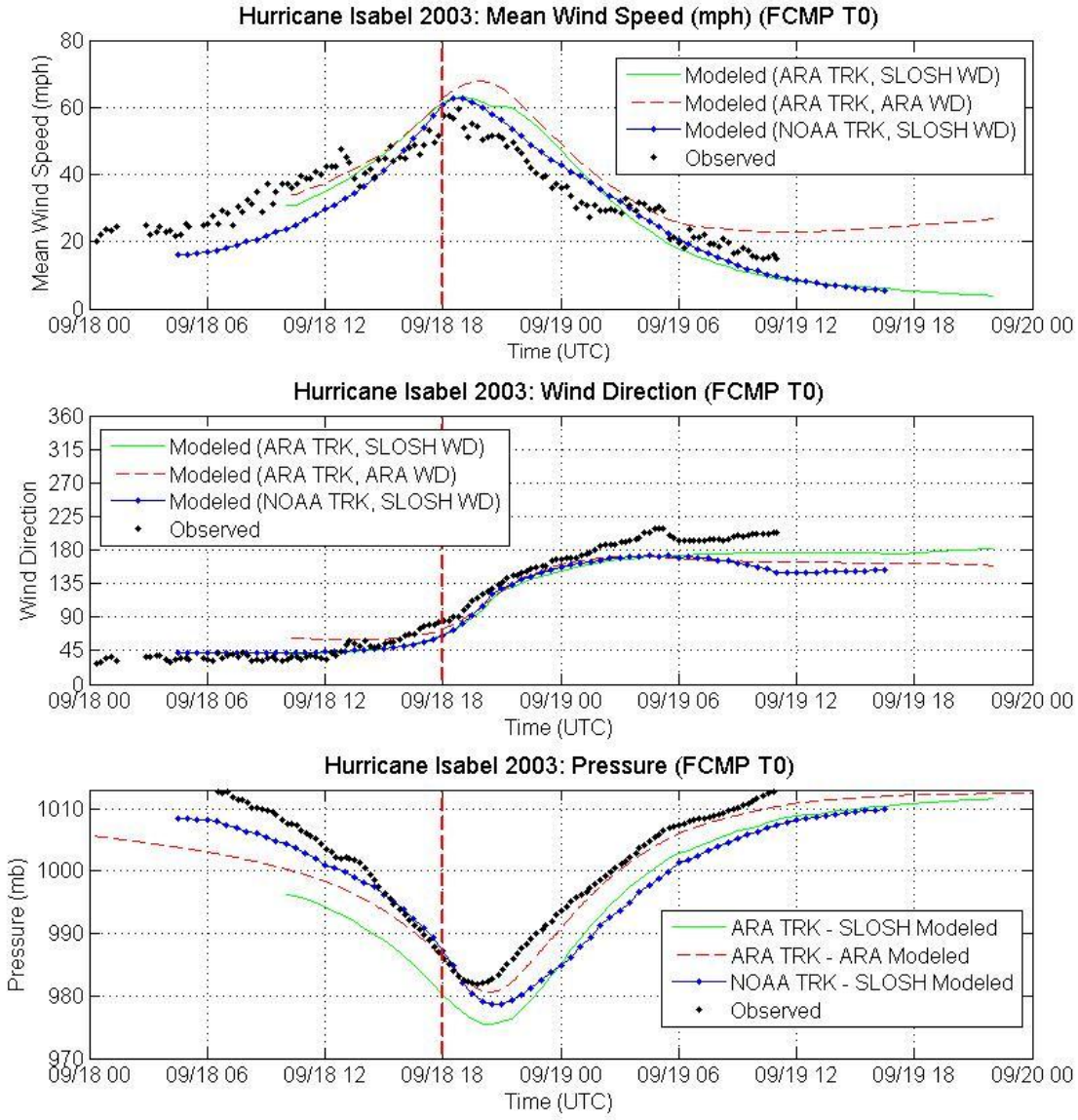

Figure O-5c. Comparisons of Observed and Modeled Time Series Traces of Mean Wind Speeds, Wind Directions, and Pressures for Hurricane Isabel (2003) – FCMP T0

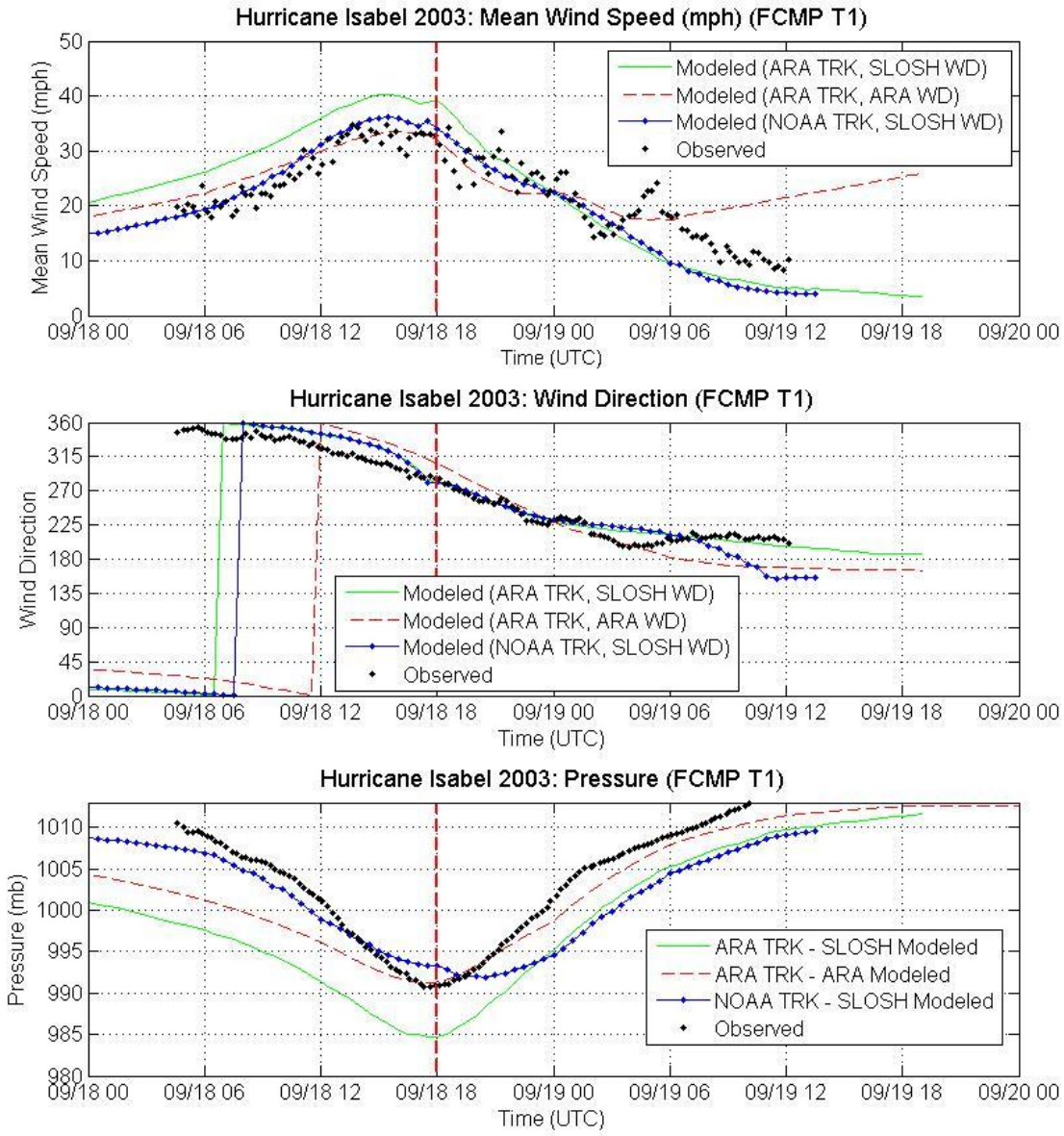

Figure O-5d. Comparisons of Observed and Modeled Time Series Traces of Mean Wind Speeds, Wind Directions, and Pressures for Hurricane Isabel (2003) – FCMP T1

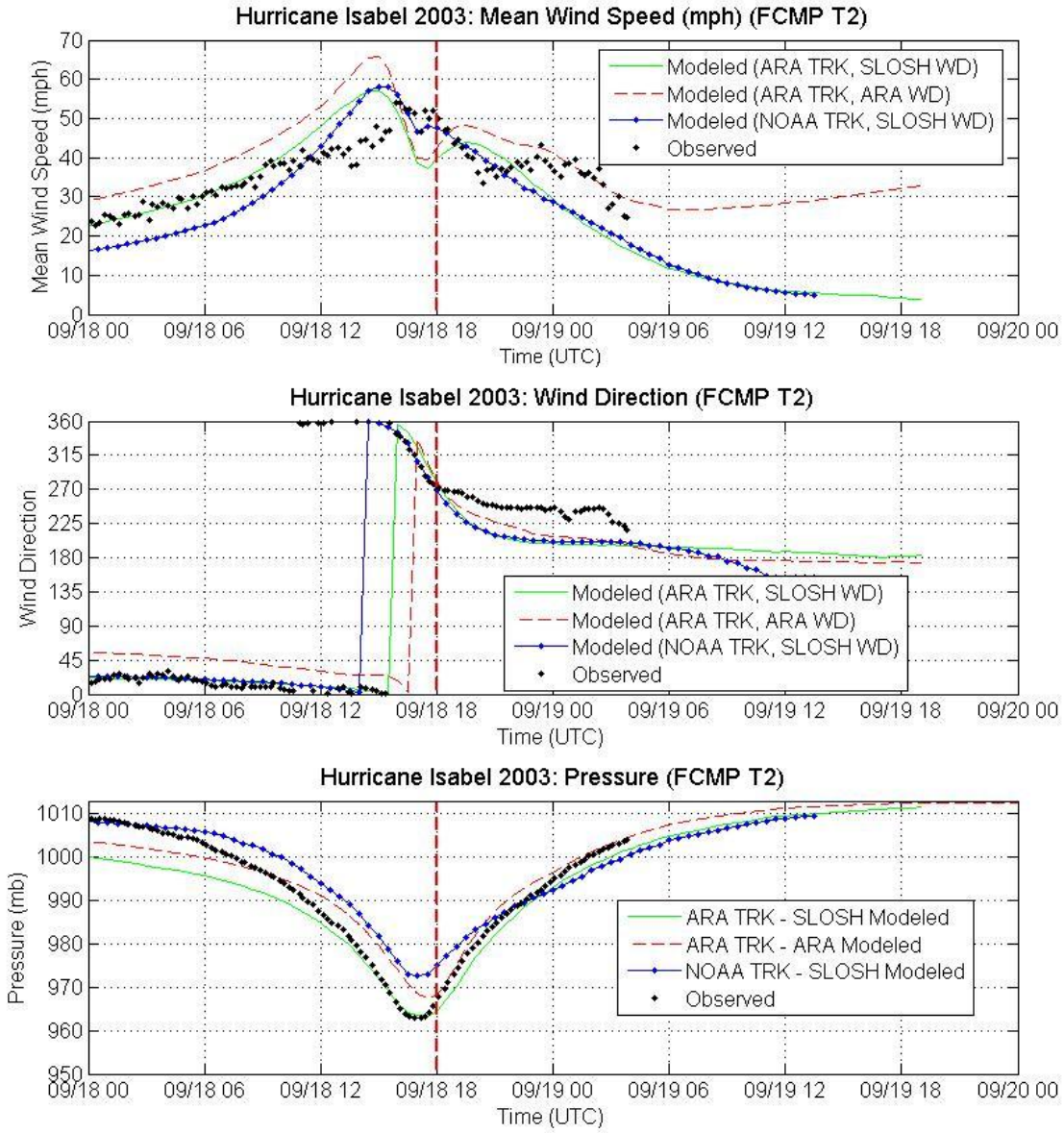

Figure O-5e. Comparisons of Observed and Modeled Time Series Traces of Mean Wind Speeds, Wind Directions, and Pressures for Hurricane Isabel (2003) – FCMP T2

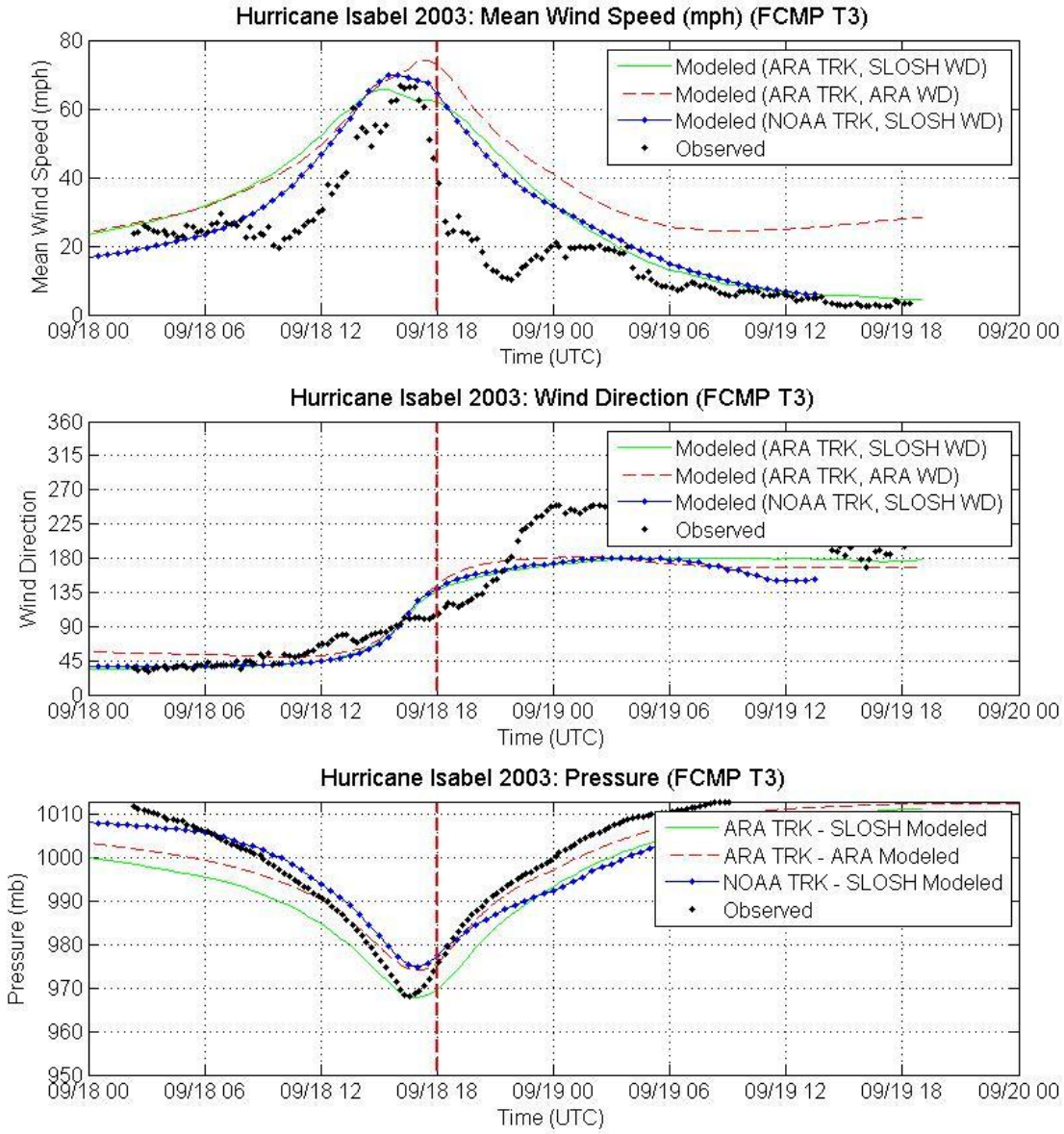

Figure O-5f. Comparisons of Observed and Modeled Time Series Traces of Mean Wind Speeds, Wind Directions, and Pressures for Hurricane Isabel (2003) – FCMP T3

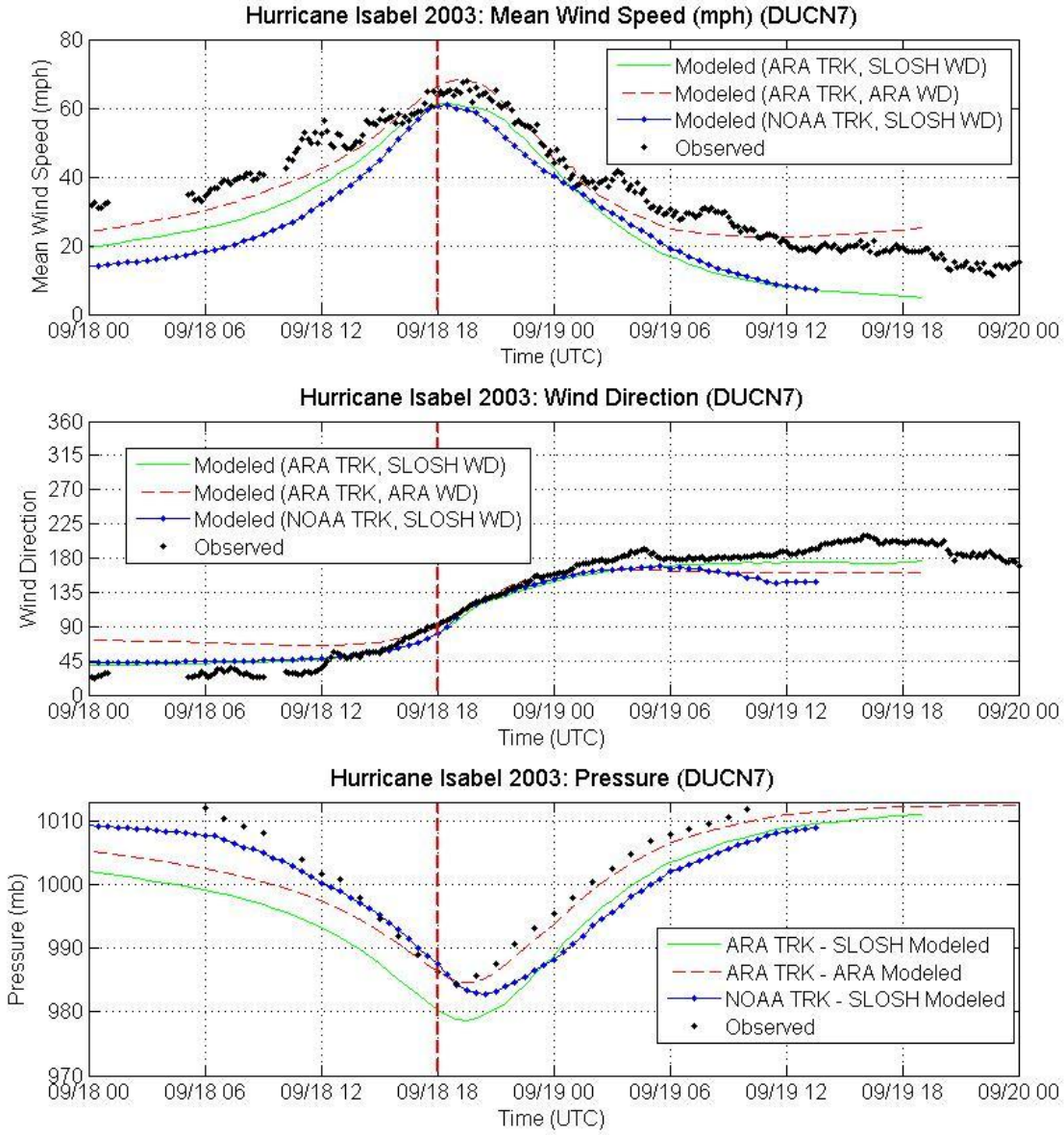

Figure O-5g. Comparisons of Observed and Modeled Time Series Traces of Mean Wind Speeds, Wind Directions, and Pressures for Hurricane Isabel (2003) – DUCN7

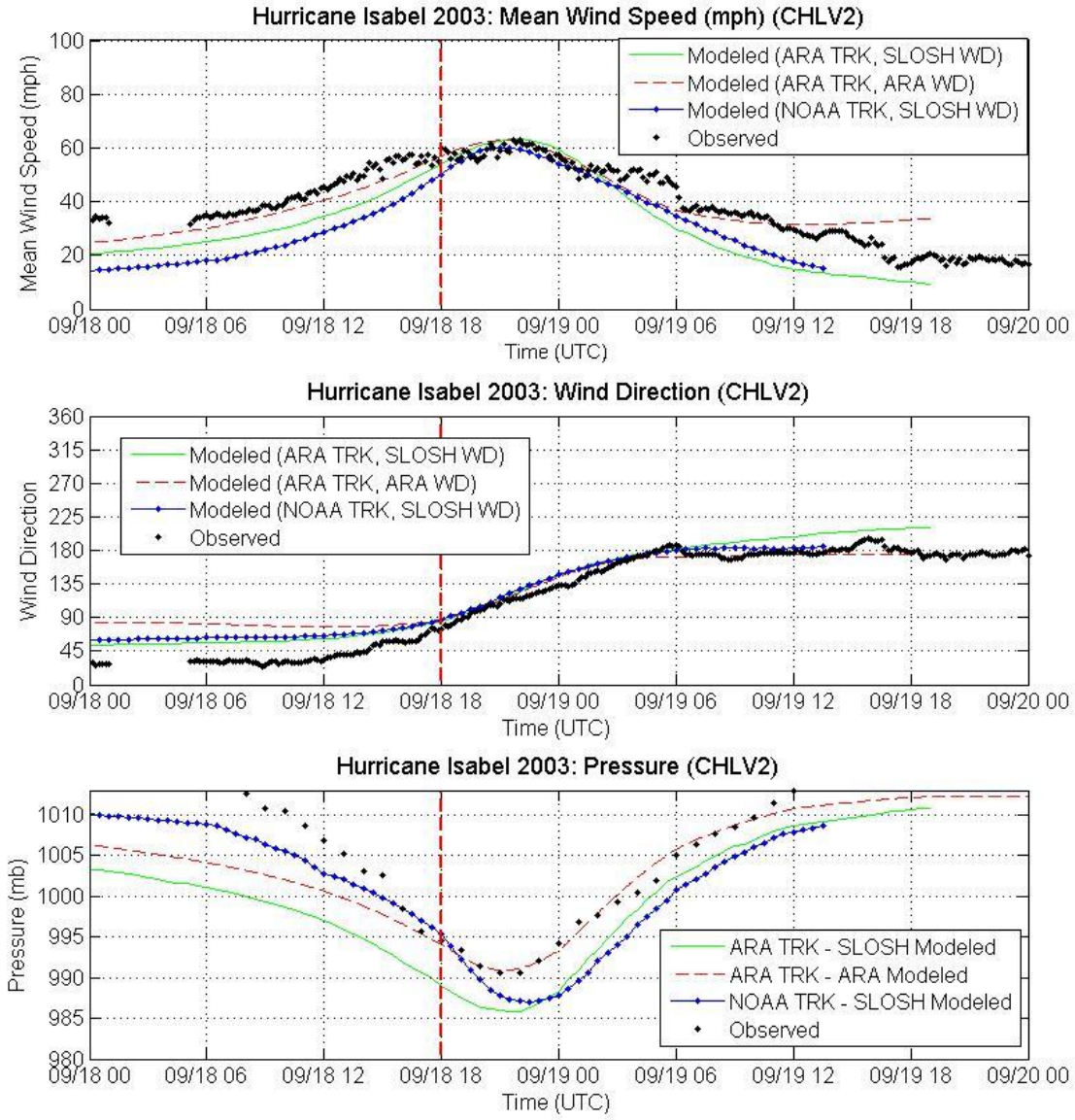

Figure O-5h. Comparisons of Observed and Modeled Time Series Traces of Mean Wind Speeds, Wind Directions, and Pressures for Hurricane Isabel (2003) – CHLV2

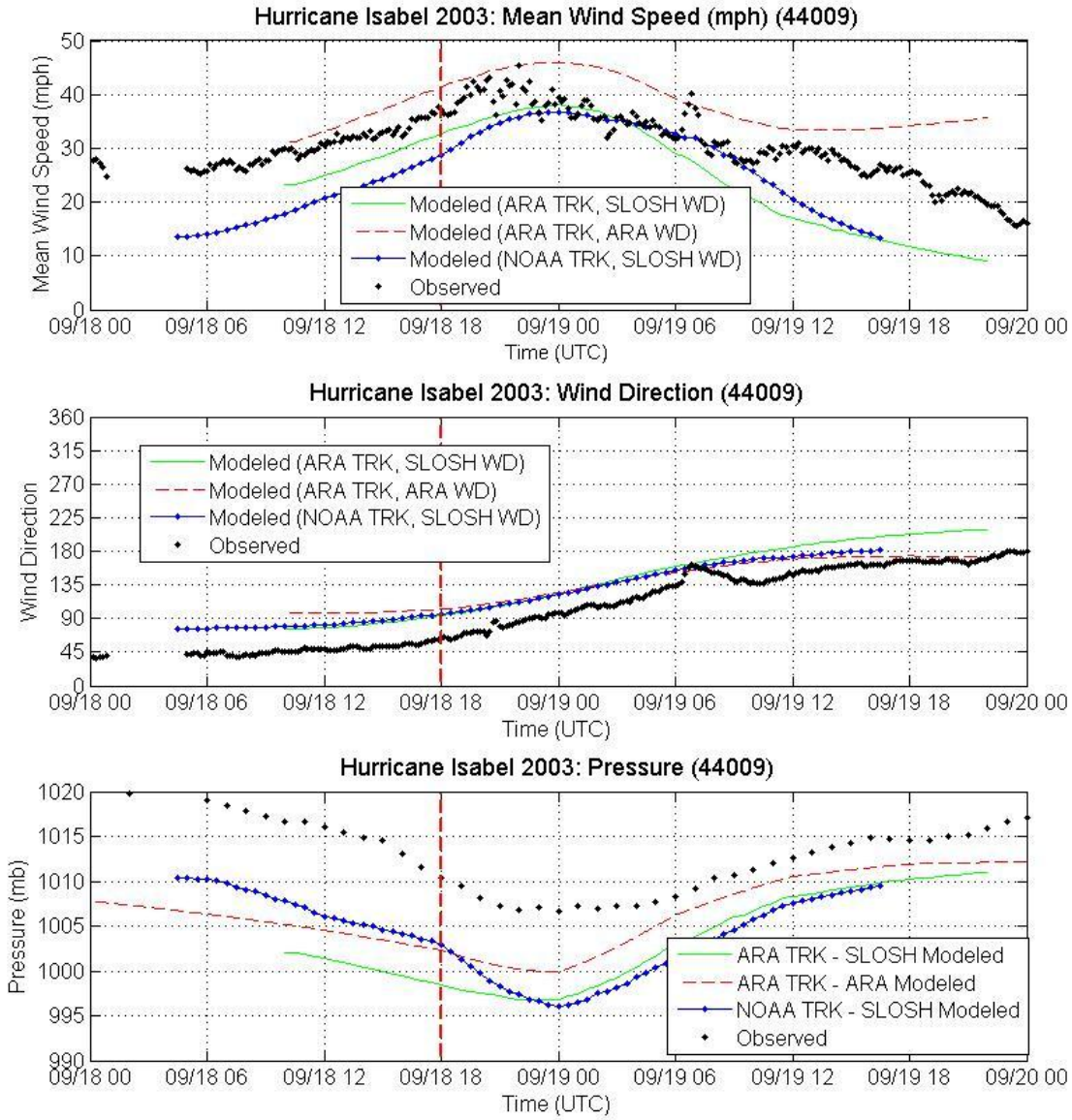

Figure O-5i. Comparisons of Observed and Modeled Time Series Traces of Mean Wind Speeds, Wind Directions, and Pressures for Hurricane Isabel (2003) – 44009

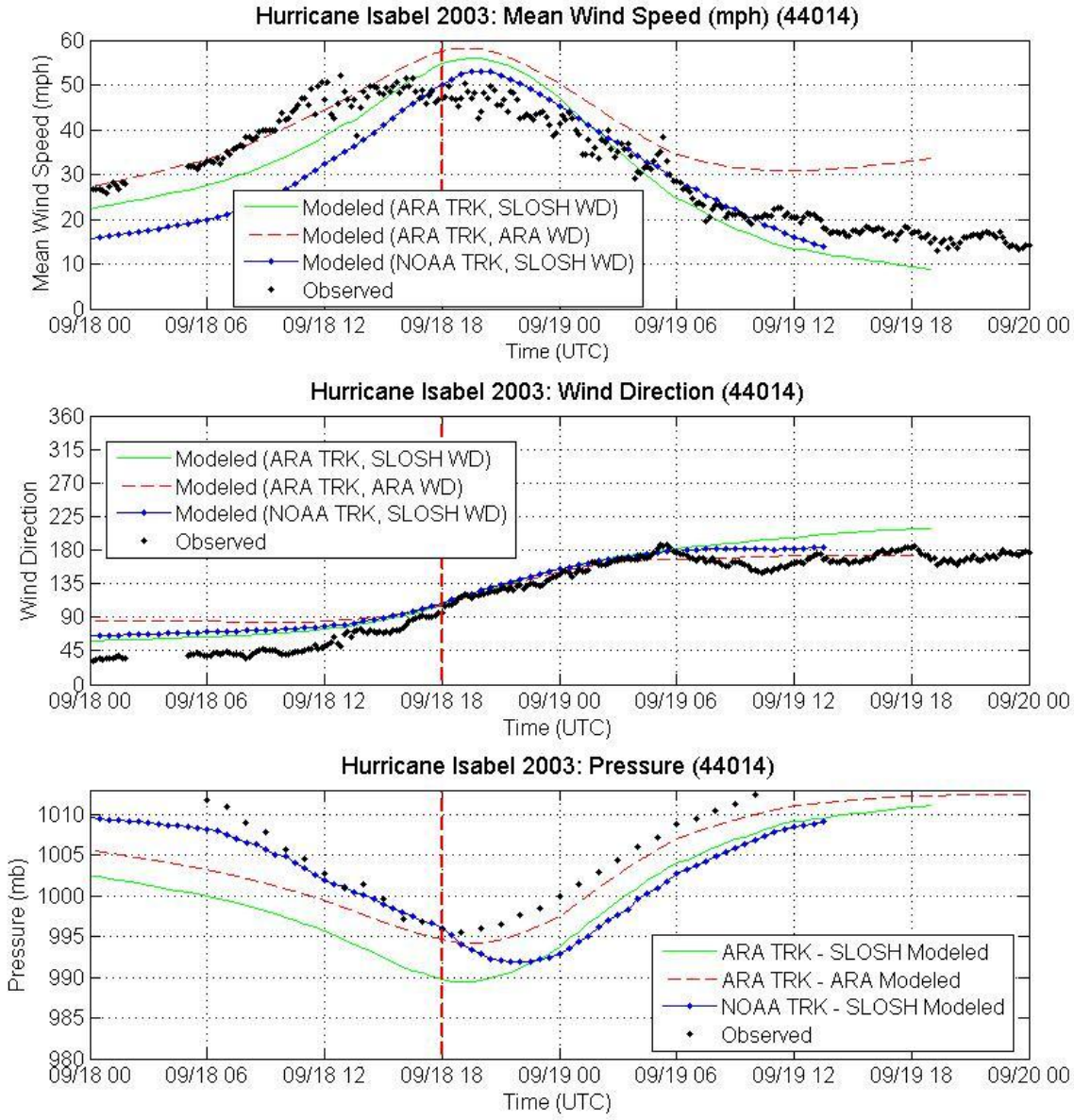

Figure O-5j. Comparisons of Observed and Modeled Time Series Traces of Mean Wind Speeds, Wind Directions, and Pressures for Hurricane Isabel (2003) – 44014

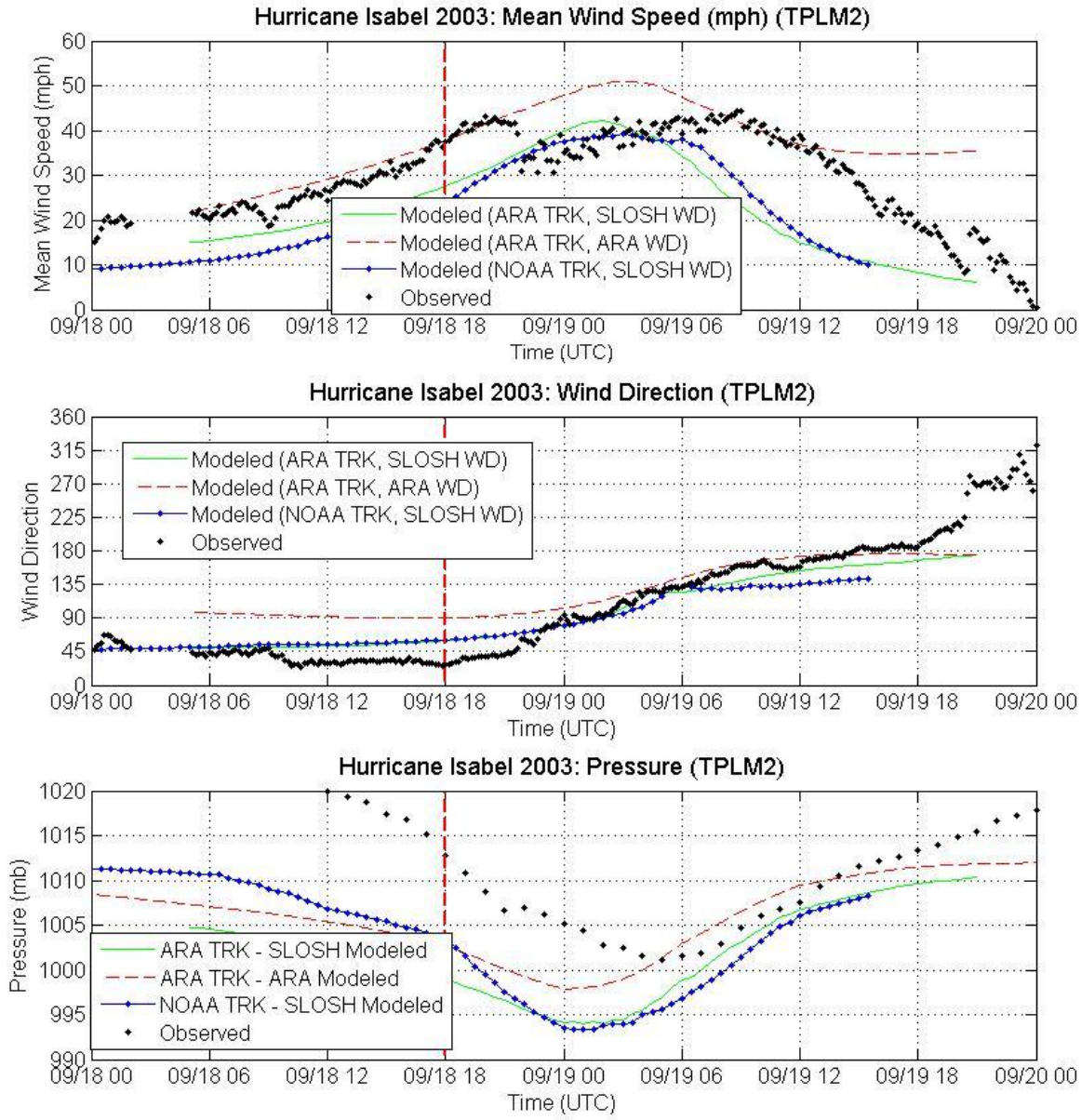

Figure O-5k. Comparisons of Observed and Modeled Time Series Traces of Mean Wind Speeds, Wind Directions, and Pressures for Hurricane Isabel (2003) – TPLM2

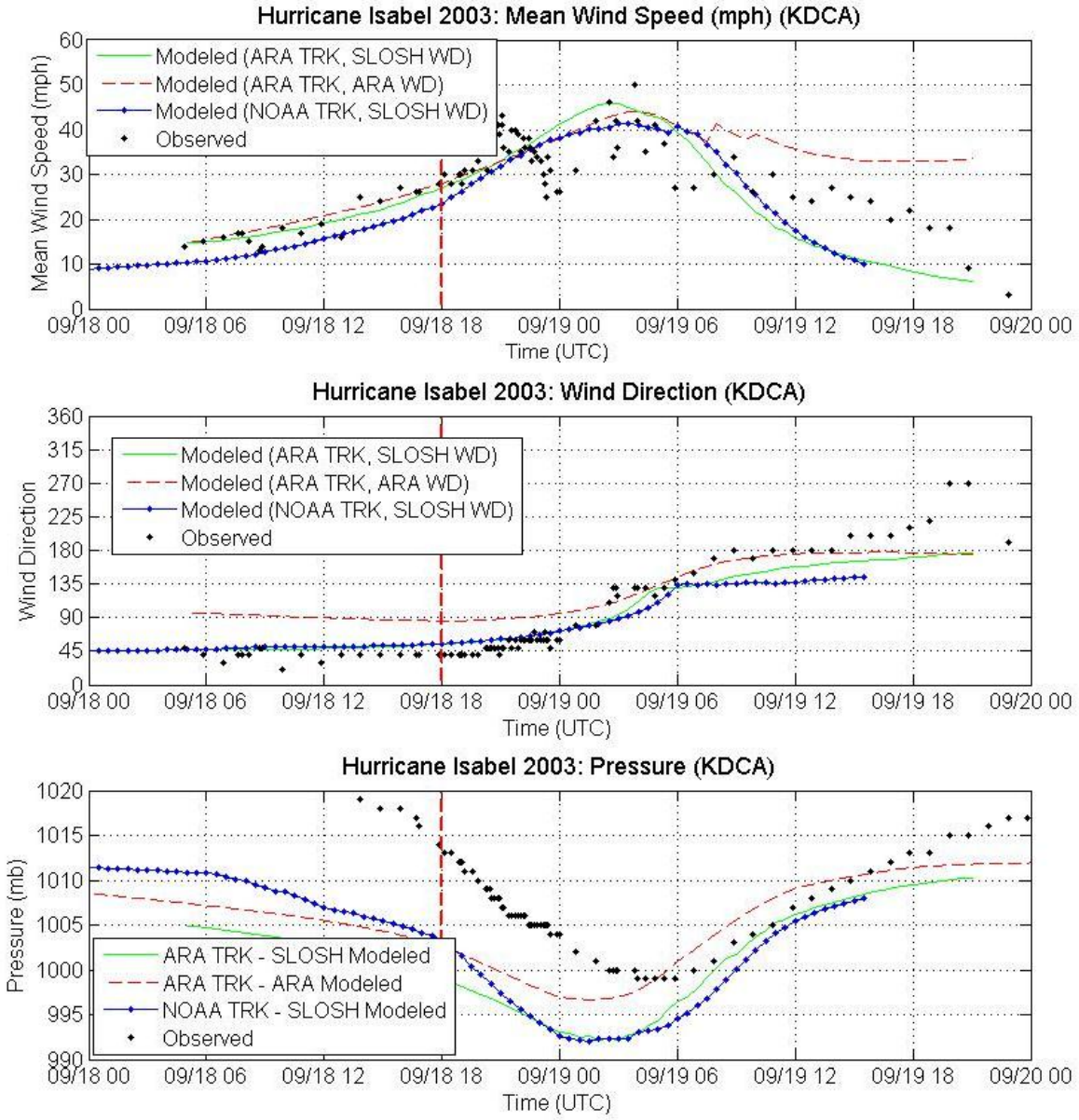

Figure O-5l. Comparisons of Observed and Modeled Time Series Traces of Mean Wind Speeds, Wind Directions, and Pressures for Hurricane Isabel (2003) – KDCA

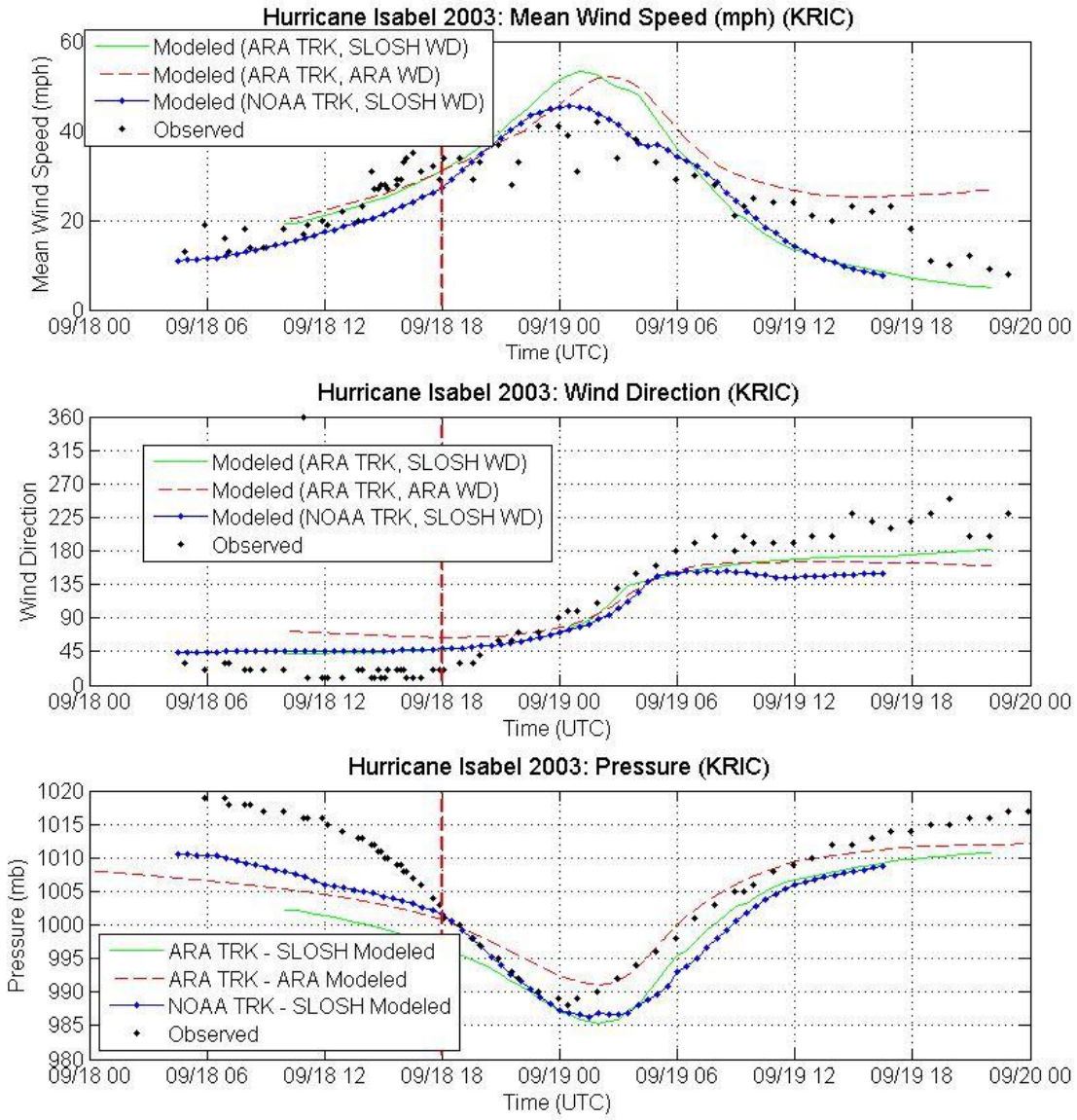

Figure O-5m. Comparisons of Observed and Modeled Time Series Traces of Mean Wind Speeds, Wind Directions, and Pressures for Hurricane Isabel (2003) – KRIC

Table O-3. Error Analysis of Wind Speeds, Wind Directions and Pressures for Hurricane Isabel

Station	Range		Number of Data	Obs		SLOSH-Obs		ARA-Obs		NOAA-Obs	
				Mean	Std	mean	RMS	mean	RMS	mean	RMS
KILM	Wind Speed (mph)	0-20	4	17.8	1.0	5.6	7.5	3.7	4.2	1.0	1.8
		20-40	42	31.9	5.5	1.7	4.9	-3.3	5.2	-1.9	3.9
		40-60	15	42.0	1.9	-3.2	3.8	-9.7	9.9	-7.3	7.6
		all	61	33.5	7.6	0.8	4.9	-4.4	6.6	-3.0	5.0
	Wind Direction (deg)	0-45	1	10.0	0.0	-5.6	5.6	17.5	17.5	-3.5	3.5
		180-225	3	206.7	15.3	12.7	16.4	-0.9	6.8	17.0	19.9
		225-270	12	251.7	10.3	-3.1	9.4	7.3	15.1	-2.2	8.7
		270-315	33	294.2	13.5	17.8	20.5	32.3	32.8	17.6	20.6
		315-360	11	337.3	11.9	12.6	13.8	28.4	28.6	14.0	15.1
		all	60	286.9	51.2	11.7	17.0	24.6	28.1	12.3	17.3
	Pressure (mbar)	989-1030	62	996.5	5.9	-7.2	7.4	-2.2	3.3	-0.7	2.8
		all	62	996.5	5.9	-7.2	7.4	-2.2	3.3	-0.7	2.8
CLKN	Wind Speed (mph)	0-20	29	16.6	1.5	-4.7	4.7	11.4	11.6	-2.8	3.0
		20-40	106	30.7	5.1	4.7	12.1	4.8	6.4	2.1	10.6
		40-60	61	50.1	5.2	4.3	8.9	1.5	8.1	2.6	9.8
		60-80	11	64.0	2.2	-8.1	10.2	-13.3	15.5	1.8	3.5
		all	207	36.2	13.8	2.6	10.4	3.8	8.5	1.5	9.3
	Wind Direction (deg)	0-45	64	8.3	5.2	14.2	14.6	32.5	33.1	17.7	18.7
		180-225	63	207.2	6.0	3.0	6.2	-26.1	28.0	-4.4	12.2
		225-270	56	236.0	9.6	-16.2	18.4	-17.4	19.5	-15.5	17.0
		270-315	5	289.0	15.7	14.1	14.2	5.0	5.1	4.5	5.3
		315-360	18	350.5	10.8	16.3	17.1	26.3	28.2	11.2	15.3
		all	206	168.7	114.7	2.8	14.2	0.0	27.5	1.1	15.9
	Pressure (mbar)	945-965	1	964.9	0.0	-1.9	1.9	2.3	2.3	6.3	6.3
		965-980	5	973.3	6.1	-5.1	5.5	0.0	1.8	4.3	4.7
		980-989	3	986.0	2.0	-5.9	6.0	0.2	0.4	2.5	3.4
		989-1030	26	1005.8	7.7	-7.2	7.6	-3.8	4.4	-4.1	5.4
		all	35	998.3	15.1	-6.6	7.1	-2.7	3.9	-2.0	5.2
FCMP T0	Wind Speed (mph)	0-20	16	17.3	1.7	-5.3	5.5	6.3	6.4	-3.9	4.4
		20-40	42	31.5	5.8	0.6	7.6	5.0	7.9	-0.6	6.9
		40-60	43	47.9	5.2	4.8	8.1	7.3	10.3	1.1	7.4
		all	101	36.2	12.3	1.4	7.5	6.2	8.8	-0.4	6.8
	Wind Direction (deg)	0-45	12	37.0	3.4	4.5	5.3	23.7	24.0	5.7	6.4
		45-90	23	65.5	13.5	-12.3	13.5	-0.5	7.8	-12.2	13.5
		90-135	9	114.4	14.2	-18.5	18.8	-13.4	13.6	-14.0	14.6
		135-180	19	159.8	11.7	-14.6	14.7	-8.1	8.4	-10.2	10.3
		180-225	38	196.1	6.6	-24.0	24.6	-28.3	29.3	-29.8	31.4
		all	101	133.4	62.7	-15.7	18.6	-10.7	20.9	-16.5	21.4
	Pressure (mbar)	980-989	20	984.5	2.2	-7.1	7.2	-1.5	2.2	-2.8	4.1
		989-1030	81	1002.0	6.8	-6.7	7.1	-2.6	3.2	-4.8	5.6
		all	101	998.5	9.3	-6.8	7.1	-2.4	3.1	-4.4	5.3

Table O-3. Error Analysis of Wind Speeds, Wind Directions and Pressures for Hurricane Isabel (Continued)

Station	Range		Number of Data	Obs		SLOSH-Obs		ARA-Obs		NOAA-Obs	
				Mean	Std	mean	RMS	mean	RMS	mean	RMS
FCMP T1	Wind Speed (mph)	0-20	49	14.9	3.7	-1.8	5.8	5.2	6.5	-3.1	5.0
		20-40	78	27.4	4.4	3.8	6.6	-0.4	3.1	0.3	3.7
		all	127	22.6	7.4	1.7	6.3	1.8	4.8	-1.0	4.3
	Wind Direction (deg)	180-225	42	206.0	5.1	3.2	10.4	-23.1	28.0	-7.4	26.6
		225-270	26	243.1	13.7	-0.6	6.1	5.3	13.4	0.9	5.7
		270-315	22	294.7	13.0	10.2	14.2	26.4	26.8	10.1	14.4
		315-360	37	337.8	10.5	14.9	15.4	32.4	32.6	16.5	16.9
		all	127	267.4	55.4	7.0	12.1	7.5	27.0	4.3	19.0
	Pressure (mbar)	989-1030	127	1003.1	7.1	-6.9	7.4	-2.9	3.8	-3.0	4.1
		all	127	1003.1	7.1	-6.9	7.4	-2.9	3.8	-3.0	4.1
FCMP T2	Wind Speed (mph)	20-40	80	32.8	5.3	-1.1	6.5	6.4	7.7	-5.7	7.6
		40-60	32	46.0	4.4	0.6	9.0	5.8	12.2	2.4	7.0
		all	112	36.6	7.8	-0.6	7.3	6.3	9.2	-3.4	7.5
	Wind Direction (deg)	0-45	55	13.7	8.1	1.4	5.1	28.6	29.1	2.1	5.8
		180-225	2	219.5	3.9	-23.4	23.6	-22.1	22.2	-19.9	20.1
		225-270	37	247.6	10.6	-38.6	39.9	-27.7	29.2	-37.2	37.9
		270-315	5	283.7	10.3	11.6	12.8	16.9	18.7	-1.3	3.8
		315-360	13	347.4	15.1	12.7	13.4	32.3	32.5	6.5	9.4
		all	112	145.4	133.8	-10.5	24.0	9.0	29.1	-10.9	22.6
	Pressure (mbar)	945-965	6	963.4	0.6	0.5	0.7	5.8	5.9	9.7	9.7
		965-980	19	972.6	4.6	-1.8	2.3	4.3	5.1	7.5	7.8
		980-989	17	984.6	2.5	-2.3	2.3	3.6	3.7	4.2	5.1
		989-1030	70	1000.4	5.8	-5.2	6.0	-1.2	3.1	0.9	3.4
		all	112	991.3	13.6	-3.9	4.9	0.8	3.8	3.0	5.2
FCMP T3	Wind Speed (mph)	0-20	68	11.5	5.4	8.9	14.1	20.9	22.4	9.0	12.8
		20-40	53	25.6	4.0	14.9	18.1	16.0	20.2	8.7	15.0
		40-60	11	50.0	5.4	12.9	13.3	14.9	15.9	13.7	14.1
		60-80	9	63.7	2.7	-0.5	2.6	6.6	7.7	4.1	5.1
		all	141	23.2	15.9	10.9	15.3	17.7	20.5	8.9	13.5
	Wind Direction (deg)	0-45	27	37.5	3.7	-1.2	3.2	15.5	16.2	0.6	3.2
		45-90	27	65.9	12.9	-15.8	17.1	-8.6	11.6	-16.1	17.5
		90-135	19	110.6	13.0	20.6	23.7	29.7	33.1	24.1	27.3
		135-180	5	157.1	12.5	3.1	10.0	18.3	20.9	6.5	11.7
		180-225	24	212.0	9.8	-34.3	35.5	-40.5	42.1	-43.5	45.7
		225-270	39	238.3	9.0	-61.8	62.7	-62.2	62.5	-68.2	68.9
		all	141	142.3	83.0	-23.3	37.9	-18.1	40.3	-25.7	42.8
	Pressure (mbar)	965-980	17	973.4	4.0	-3.1	3.8	3.2	3.9	4.8	5.2
		980-989	15	985.2	2.7	-6.7	6.9	-0.6	1.5	1.0	3.4
		989-1030	109	1005.6	7.6	-7.6	7.9	-4.1	4.6	-4.3	5.8
		all	141	999.5	13.4	-7.0	7.4	-2.8	4.3	-2.6	5.6

Table O-3. Error Analysis of Wind Speeds, Wind Directions and Pressures for Hurricane Isabel (Continued)

Station	Range		Number of Data	Obs		SLOSH-Obs		ARA-Obs		NOAA-Obs	
				Mean	Std	mean	RMS	mean	RMS	mean	RMS
DUCN7	Wind Speed (mph)	0-20	8	19.1	0.4	-11.6	11.7	3.5	3.5	-11.5	11.5
		20-40	91	32.1	5.6	-12.3	12.8	-4.3	5.2	-13.1	13.8
		40-60	69	51.0	5.7	-7.7	9.2	-3.5	5.6	-11.9	13.3
		60-80	27	63.7	2.0	-4.0	4.4	2.1	2.7	-6.0	6.5
		all	195	42.6	13.7	-9.5	10.7	-2.8	5.0	-11.6	12.8
	Wind Direction (deg)	0-45	45	28.5	4.7	14.5	15.0	39.4	39.9	16.6	17.1
		45-90	32	63.8	13.0	-5.4	7.5	8.1	10.6	-5.1	7.4
		90-135	22	113.7	14.1	-7.2	7.8	-0.4	2.9	-4.4	5.7
		135-180	43	164.2	13.7	-10.5	11.0	-5.7	10.0	-9.0	9.7
		180-225	53	184.0	3.8	-12.2	13.1	-21.7	22.0	-25.2	27.0
		all	195	116.1	64.0	-4.0	11.9	3.2	23.2	-6.3	17.3
	Pressure (mbar)	980-989	4	986.0	1.3	-6.3	6.4	-0.4	0.8	-1.5	2.6
		989-1030	30	1005.1	8.3	-7.7	8.4	-4.0	5.2	-4.6	5.3
		all	34	1002.8	10.0	-7.5	8.2	-3.5	4.9	-4.2	5.0
CHLV2	Wind Speed (mph)	20-40	80	34.5	3.2	-12.0	12.3	-2.4	3.9	-13.0	13.6
		40-60	110	52.0	5.1	-5.8	8.8	-2.6	5.1	-8.7	11.0
		60-80	11	61.4	0.9	0.7	2.3	0.1	1.2	-3.3	4.0
		all	201	45.5	10.2	-7.9	10.2	-2.4	4.5	-10.1	11.9
	Wind Direction (deg)	0-45	62	32.4	4.7	26.6	26.7	47.4	47.8	31.8	31.9
		45-90	29	65.6	11.2	12.7	13.3	18.5	19.6	15.2	15.7
		90-135	34	115.4	13.3	8.7	10.1	7.3	8.5	10.5	11.4
		135-180	67	168.8	10.3	14.6	16.2	1.1	5.0	8.0	8.9
		180-225	9	183.7	3.0	-0.8	7.2	-11.9	12.4	-4.4	5.4
		all	201	103.5	60.0	16.3	18.8	18.3	28.0	16.2	20.0
	Pressure (mbar)	989-1030	34	1004.0	8.3	-6.8	7.8	-3.0	5.1	-4.0	4.5
		all	34	1004.0	8.3	-6.8	7.8	-3.0	5.1	-4.0	4.5
44009	Wind Speed (mph)	20-40	166	32.6	3.8	-5.5	7.1	5.6	6.1	-5.8	7.3
		40-60	17	41.8	1.3	-6.1	6.5	2.5	3.0	-7.4	7.6
		all	183	33.4	4.5	-5.6	7.1	5.3	5.9	-5.9	7.4
	Wind Direction (deg)	45-90	75	59.9	12.5	29.8	29.9	42.6	43.1	32.8	32.9
		90-135	46	109.1	13.0	28.3	28.5	26.2	26.5	25.0	25.2
		135-180	62	151.4	8.8	30.8	32.6	14.7	17.1	19.3	21.2
		all	183	103.2	41.3	29.8	30.5	29.0	32.2	26.3	27.5
	Pressure (mbar)	989-1030	31	1011.0	3.4	-9.1	9.9	-6.0	6.9	-7.9	8.2
		all	31	1011.0	3.4	-9.1	9.9	-6.0	6.9	-7.9	8.2
44014	Wind Speed (mph)	0-20	5	19.5	0.4	-3.4	4.6	11.9	11.9	-0.4	4.0
		20-40	114	29.8	6.7	-3.4	5.3	5.5	7.2	-4.4	8.2
		40-60	88	46.5	2.8	1.1	7.3	5.1	7.6	-3.4	9.4
		all	207	36.6	10.1	-1.5	6.2	5.5	7.5	-3.9	8.7
	Wind Direction (deg)	0-45	42	38.9	3.5	25.1	25.2	45.3	45.4	31.1	31.2
		45-90	41	62.8	13.0	16.6	17.6	25.4	26.9	20.3	21.2
		90-135	37	116.2	14.7	5.4	7.5	4.1	6.6	7.9	9.2
		135-180	82	160.9	9.8	18.5	22.7	4.2	8.7	12.7	15.4
		180-225	5	185.0	2.5	-5.2	5.7	-17.7	17.8	-7.4	7.8
		all	207	109.3	52.5	16.5	20.1	16.2	24.6	16.6	19.9
	Pressure (mbar)	989-1030	35	1005.5	6.6	-7.1	7.5	-3.6	4.5	-4.0	4.7
		all	35	1005.5	6.6	-7.1	7.5	-3.6	4.5	-4.0	4.7

Table O-3. Error Analysis of Wind Speeds, Wind Directions and Pressures for Hurricane Isabel (Continued)

Station	Range		Number of Data	Obs		SLOSH-Obs		ARA-Obs		NOAA-Obs	
				Mean	Std	mean	RMS	mean	RMS	mean	RMS
TPLM2	Wind Speed (mph)	0-20	2	18.8	0.3	-1.6	1.6	7.1	7.1	-5.7	5.7
		20-40	153	31.2	6.0	-7.3	10.9	4.7	6.8	-9.5	11.9
		40-60	52	41.9	1.0	-11.1	12.8	2.4	4.6	-9.6	10.8
		all	207	33.8	7.1	-8.2	11.4	4.2	6.3	-9.5	11.6
	Wind Direction (deg)	0-45	89	34.5	5.3	21.2	22.4	57.7	57.8	22.9	24.0
		45-90	29	64.3	16.8	3.9	9.0	34.6	36.9	5.0	9.5
		90-135	33	112.6	15.4	-3.8	5.9	12.0	12.9	-8.2	10.1
		135-180	51	159.5	11.2	-13.9	14.5	6.5	8.0	-25.9	27.1
		180-225	5	183.2	1.1	-22.0	22.0	-7.8	7.9	-40.8	40.9
		all	207	85.5	54.8	5.1	17.2	33.0	40.9	1.9	22.3
	Pressure (mbar)	989-1030	34	1010.8	7.2	-10.1	11.9	-6.7	9.3	-8.4	9.2
		all	34	1010.8	7.2	-10.1	11.9	-6.7	9.3	-8.4	9.2
KDCA	Wind Speed (mph)	0-20	11	16.1	1.8	0.8	1.9	2.0	2.8	-3.2	3.7
		20-40	54	31.3	4.5	0.7	7.1	3.0	6.3	-0.7	6.6
		40-60	11	42.5	3.0	-2.8	5.7	-3.8	5.7	-5.6	6.7
		all	76	30.7	8.2	0.2	6.4	1.8	5.9	-1.8	6.3
	Wind Direction (deg)	0-45	24	38.3	4.8	13.7	14.6	50.4	50.9	15.2	15.9
		45-90	33	57.6	8.3	6.9	8.7	33.5	34.0	7.1	8.8
		90-135	9	125.6	7.3	-18.4	23.4	-5.5	11.1	-29.3	31.2
		135-180	4	157.5	15.0	-20.1	21.5	-0.6	4.7	-23.6	26.1
		180-225	6	183.3	8.2	-26.0	27.0	-9.2	11.5	-44.1	44.4
		all	76	74.7	47.2	2.0	15.7	29.1	36.7	-0.3	20.5
	Pressure (mbar)	989-1030	68	1007.2	5.8	-10.0	11.0	-6.3	7.9	-8.9	9.4
		all	68	1007.2	5.8	-10.0	11.0	-6.3	7.9	-8.9	9.4
KRIC	Wind Speed (mph)	0-20	3	18.3	1.2	1.9	2.1	3.1	3.2	-1.8	2.0
		20-40	44	28.6	5.1	-0.2	7.7	2.7	6.6	-2.9	7.2
		40-60	3	41.3	0.6	8.9	9.1	5.1	6.1	3.1	3.2
		all	50	28.8	6.3	0.4	7.5	2.9	6.4	-2.5	6.9
	Wind Direction (deg)	0-45	26	17.3	7.8	28.3	28.9	49.1	49.8	29.6	30.3
		45-90	4	65.0	5.8	-6.7	7.5	3.2	4.9	-6.7	7.4
		90-135	5	106.0	15.2	-18.6	19.2	-16.8	17.0	-24.6	24.8
		135-180	2	155.0	7.1	-15.5	15.6	-19.7	19.8	-22.0	22.8
		180-225	11	194.5	11.3	-30.9	32.0	-31.5	32.9	-45.5	46.9
		225-270	1	230.0	0.0	-57.3	57.3	-64.9	64.9	-81.5	81.5
		all	49	85.6	86.3	4.6	28.5	16.5	42.0	0.8	34.9
	Pressure (mbar)	980-989	1	988.0	0.0	-1.2	1.2	4.1	4.1	-1.1	1.1
		989-1030	49	1004.9	8.1	-6.8	8.1	-3.0	5.5	-4.5	5.2
		all	50	1004.5	8.4	-6.7	8.0	-2.8	5.5	-4.4	5.2

Table O-3. Error Analysis of Wind Speeds, Wind Directions and Pressures for Hurricane Isabel (Continued)

Station	Range		Number of Data	Obs		SLOSH-Obs		ARA-Obs		NOAA-Obs	
				Mean	Std	mean	RMS	mean	RMS	mean	RMS
All Stations	Wind Speed (mph)	0-20	195	14.7	4.6	1.1	9.5	11.6	14.7	0.9	8.6
		20-40	1103	31.0	5.5	-2.6	9.8	3.5	7.5	-4.7	9.9
		40-60	512	48.0	5.6	-2.3	9.0	1.3	7.6	-4.8	10.2
		60-80	58	63.3	2.2	-3.3	5.5	-0.5	7.6	-2.4	5.4
		all	1868	35.0	12.4	-2.2	9.4	3.6	8.6	-4.0	9.7
	Wind Direction (deg)	0-45	447	27.1	12.3	16.3	19.4	41.6	43.7	19.1	22.3
		45-90	293	62.5	12.8	9.3	18.8	23.6	30.2	10.9	20.8
		90-135	214	113.3	14.1	6.9	17.6	10.8	17.7	6.4	17.9
		135-180	335	160.7	12.0	8.6	21.1	3.9	10.6	2.3	17.3
		180-225	261	198.4	12.3	-10.4	18.6	-24.9	27.7	-19.7	28.5
		225-270	171	241.2	11.6	-28.4	37.2	-24.9	35.6	-29.2	39.2
		270-315	65	293.2	13.3	14.5	17.6	27.0	28.6	12.6	17.0
		315-360	79	342.2	12.7	14.5	15.3	30.4	31.1	13.3	15.3
		all	1865	133.3	91.2	4.8	21.4	12.1	30.9	3.0	23.5
	Pressure (mbar)	945-965	7	963.6	0.8	0.1	1.0	5.3	5.6	9.2	9.3
		965-980	41	973.0	4.5	-2.7	3.5	3.3	4.3	6.0	6.5
		980-989	60	985.0	2.4	-5.4	6.0	0.4	2.5	0.5	4.1
		989-1030	756	1004.0	7.7	-7.4	8.2	-3.5	5.1	-4.1	5.8
		all	864	1000.9	11.3	-7.0	7.8	-2.9	4.9	-3.2	5.7

Appendix P. Comparisons of Modeled and Measured Wind Speeds, Wind Directions, and Pressures for Hurricane Ivan (2004)

This appendix presents comparisons of modeled and observed wind speeds, wind directions, and pressures at multiple locations along the north central Gulf of Mexico coast and some buoy stations during the passage of Hurricane Ivan (2004).

Figure P-1 shows the maximum 10-minute mean wind speeds obtained from two versions of SLOSH model. The first version uses ARA storm track and ARA wind field model (denoted as ARA-TRK-ARA-WD), and the second version uses ARA storm track and SLOSH wind field model (denoted as ARA-TRK-SLOSH-WD).

Figure P-2 shows the simulated landfall wind field for the Mississippi Gulf Coast, Mobile Bay, Pensacola Bay, Panama City, and Apalachicola Bay SLOSH basins.

Figure P-3 shows a map of the locations of all observing stations as well as the hurricane track. The observed wind speeds and pressures are compared to the simulated wind speeds and pressures from model runs using the ARA-TRK-ARA-WD and ARA-TRK-SLOSH-WD models, as shown in Table P-1 and Table P-2.

Figure P-4 presents the comparisons of modeled and observed maximum wind speeds and minimum pressures for Hurricane Ivan. The results indicate that the SLOSH model slightly overestimates the wind speeds for Hurricane Ivan. The simulated minimum pressures are comparable to the observed data.

Comparisons of the entire modeled and observed time series of mean wind speeds, wind directions, and pressures for all stations, both complete and incomplete, are presented in Figure P-5. The RMS errors of wind speed, wind direction, and central pressure are shown in Table P-3.

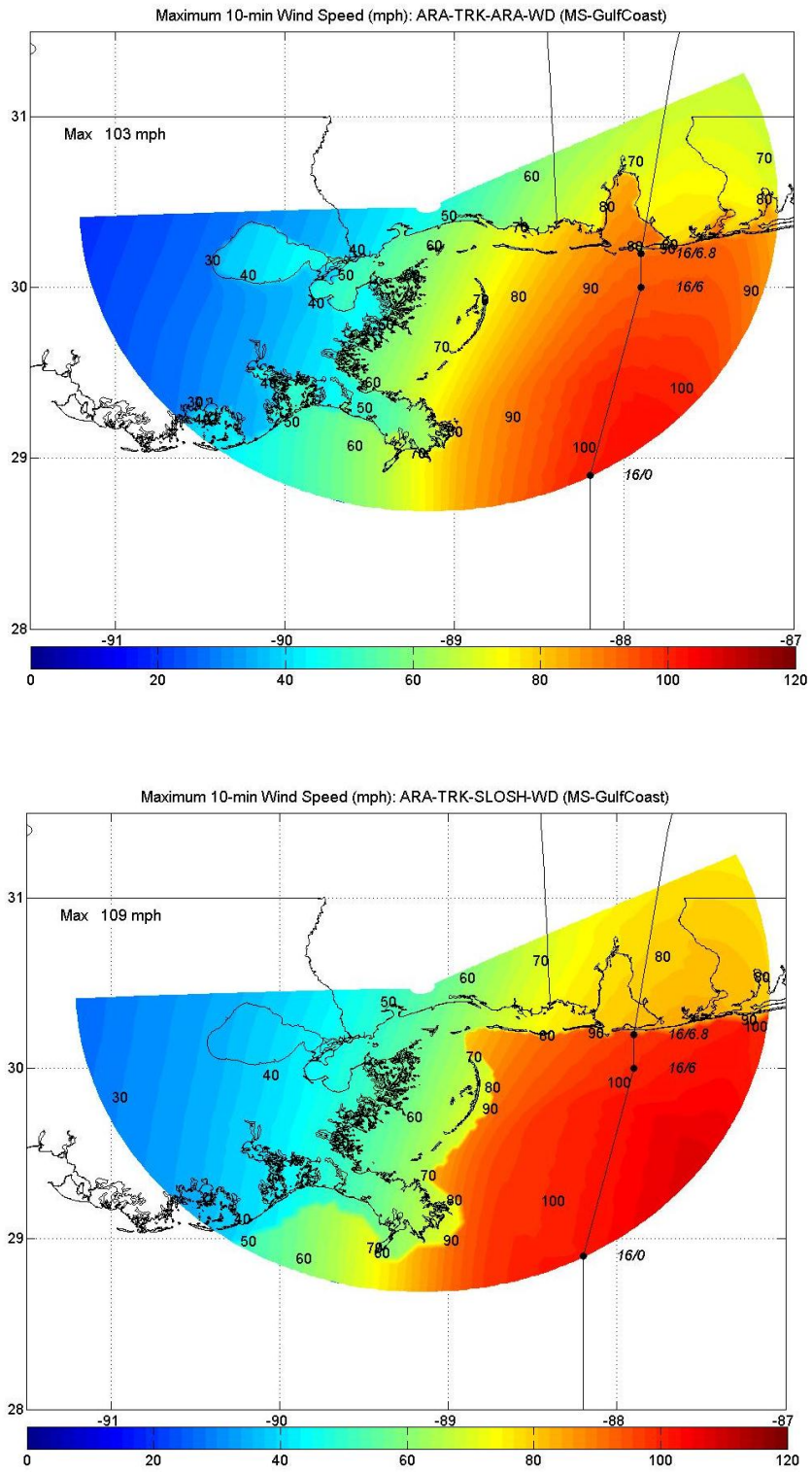

Figure P-1a. Modeled Maximum 10-min Wind Speeds (mph) for Hurricane Ivan (2004) – Mississippi Gulf Coast Basin

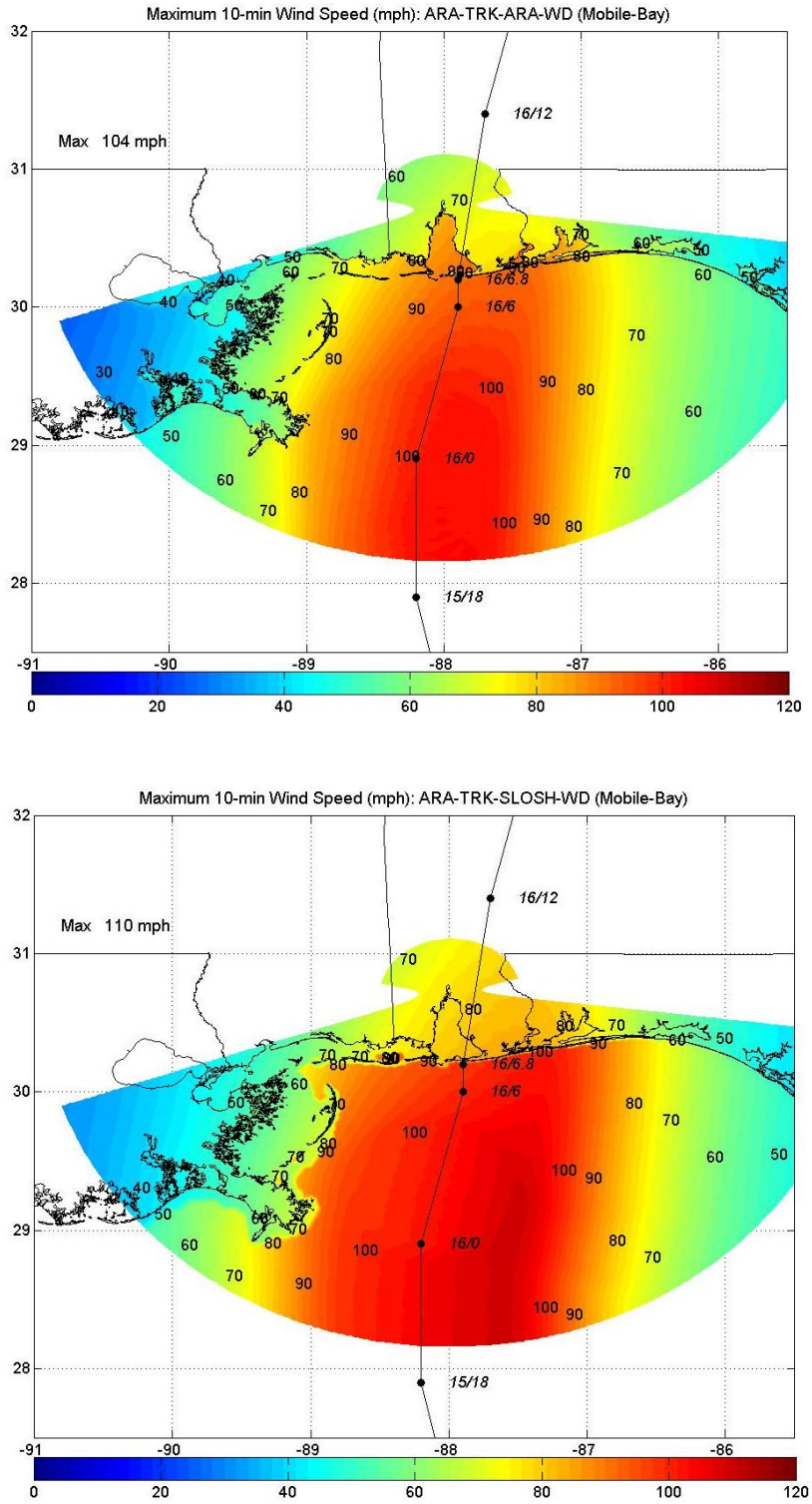

Figure P-1b. Modeled Maximum 10-min Wind Speeds (mph) for Hurricane Ivan (2004) – Mobile Bay Basin

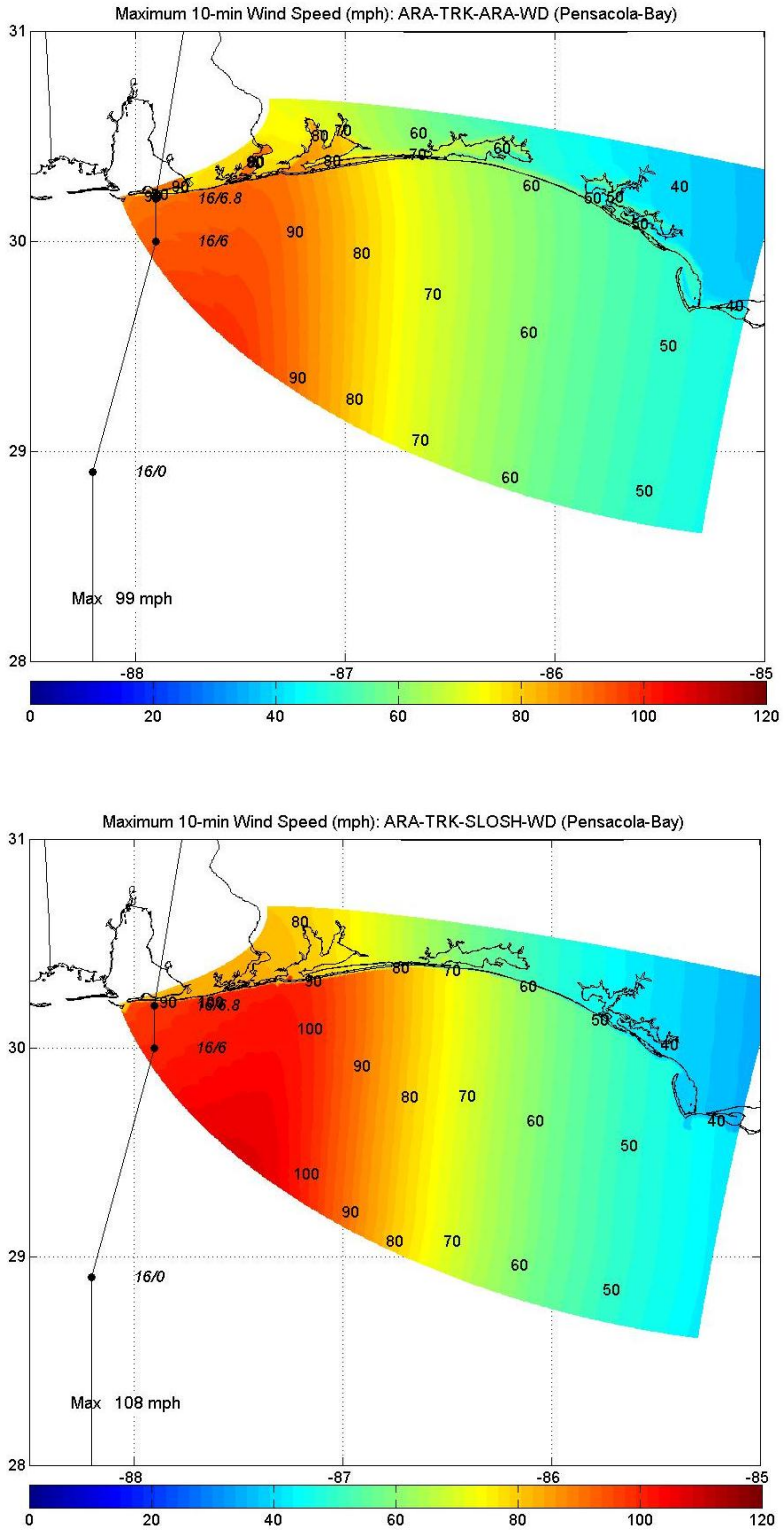

Figure P-1c. Modeled Maximum 10-min Wind Speeds (mph) for Hurricane Ivan (2004) – Pensacola Bay Basin

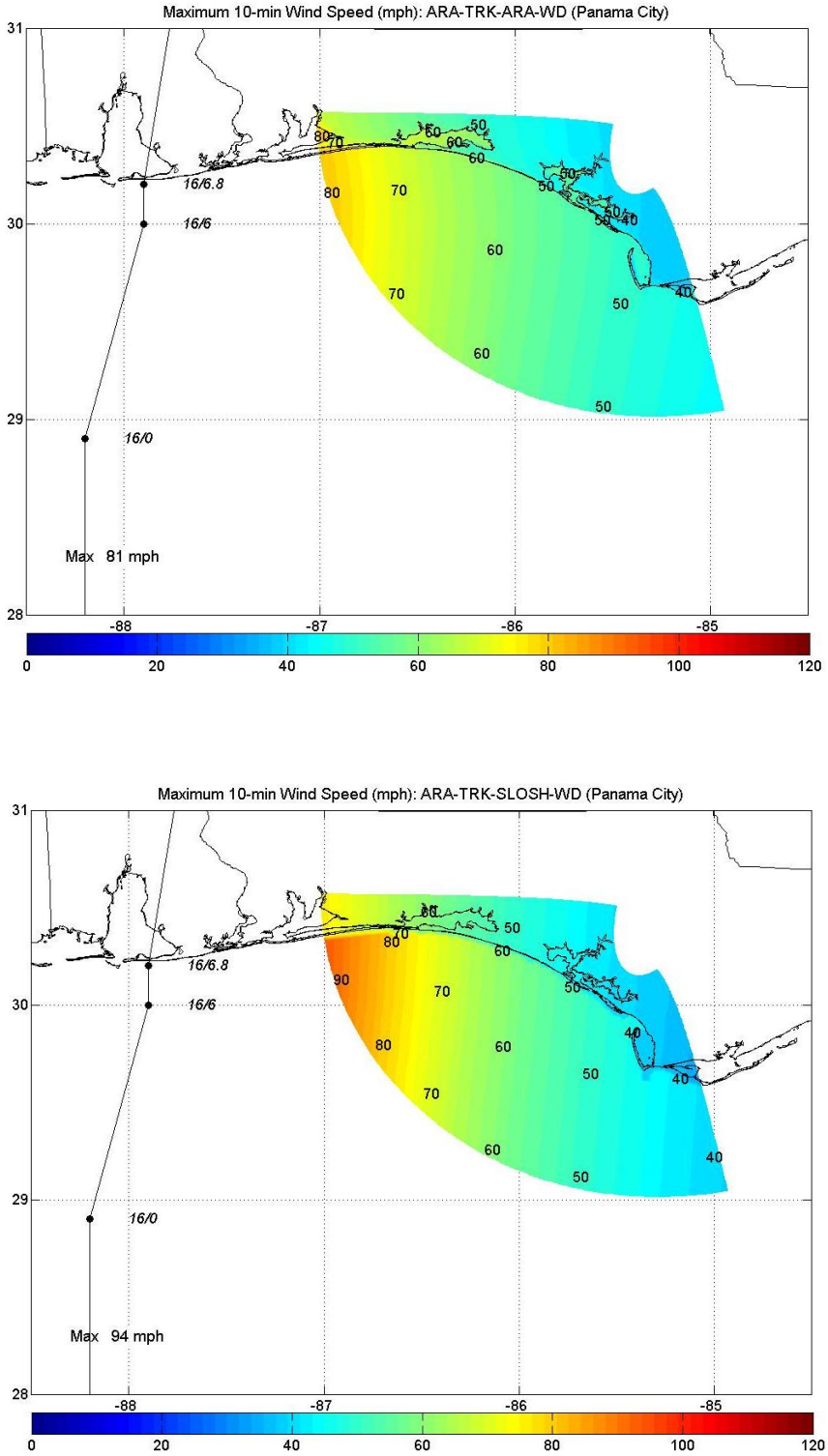

Figure P-1d. Modeled Maximum 10-min Wind Speeds (mph) for Hurricane Ivan (2004) – Panama Bay Basin

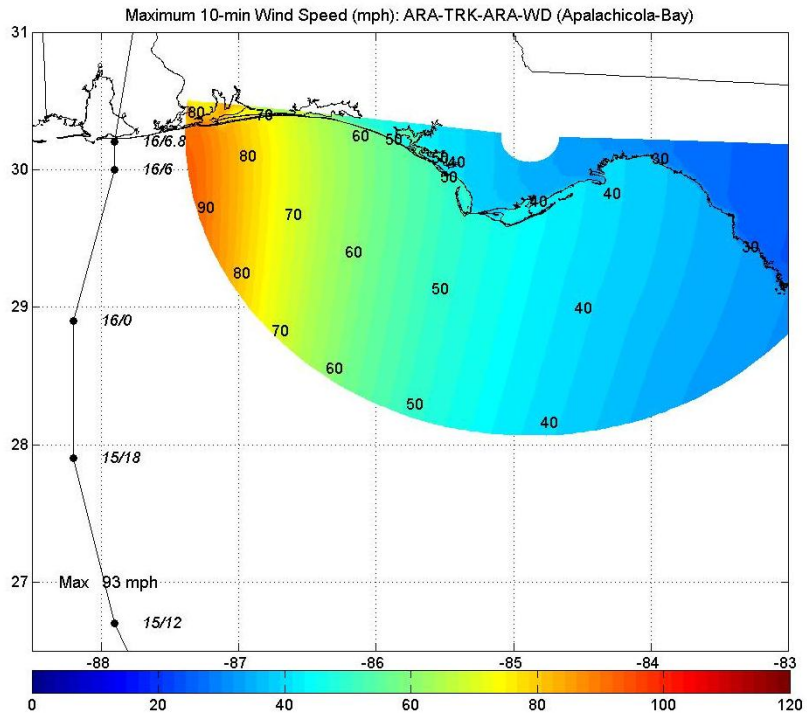

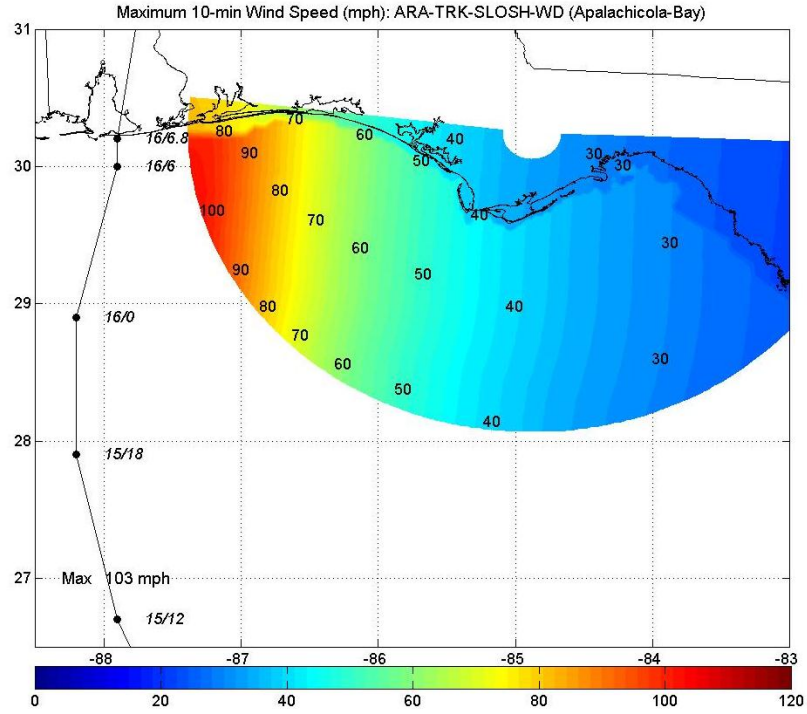

Figure P-1e. Modeled Maximum 10-min Wind Speeds (mph) for Hurricane Ivan (2004) – Apalachicola Bay Basin

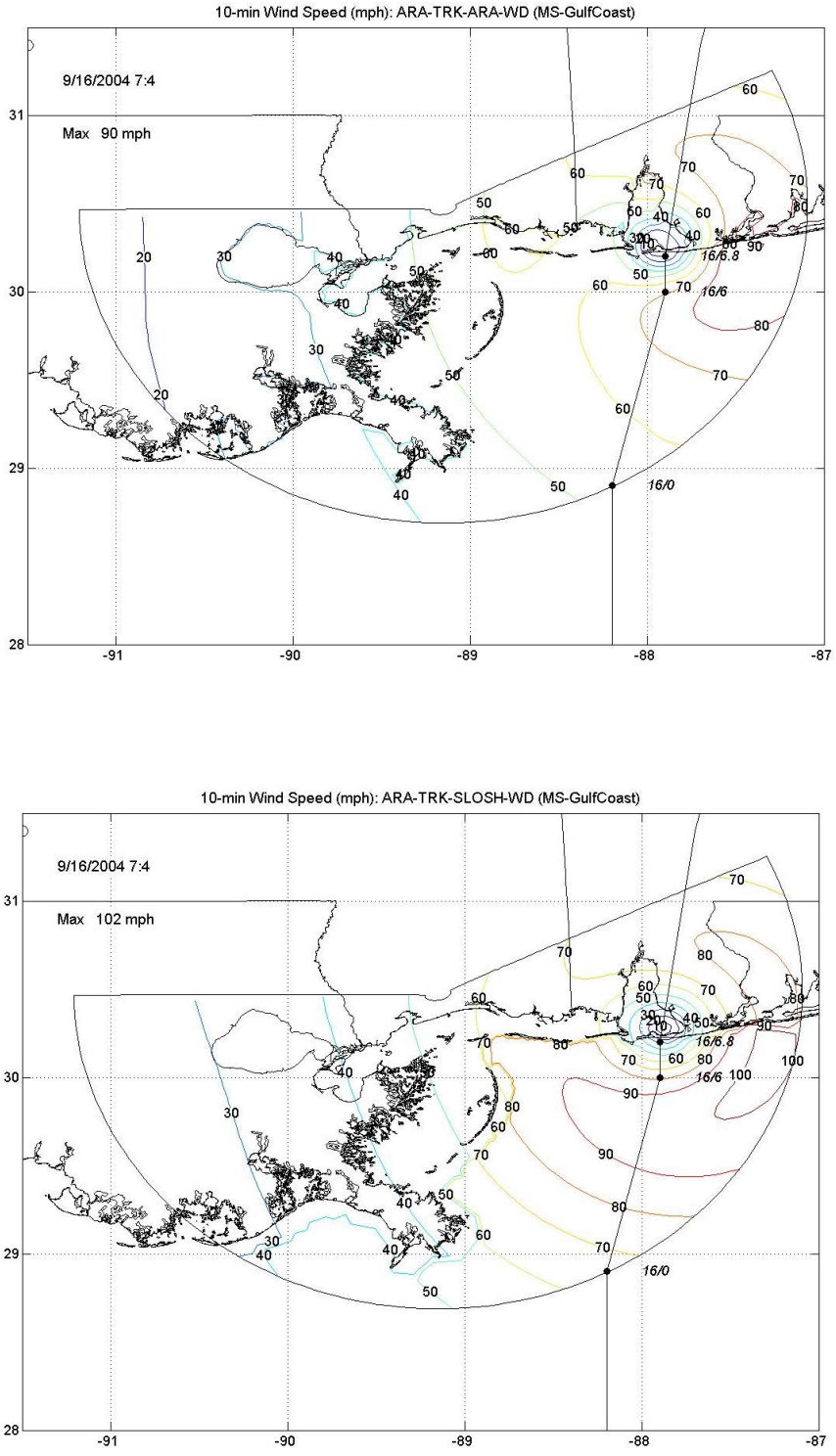

Figure P-2a. Hurricane Ivan (2004) Modeled 10-min Wind Speeds (mph) at Landfall – Mississippi Gulf Coast Basin

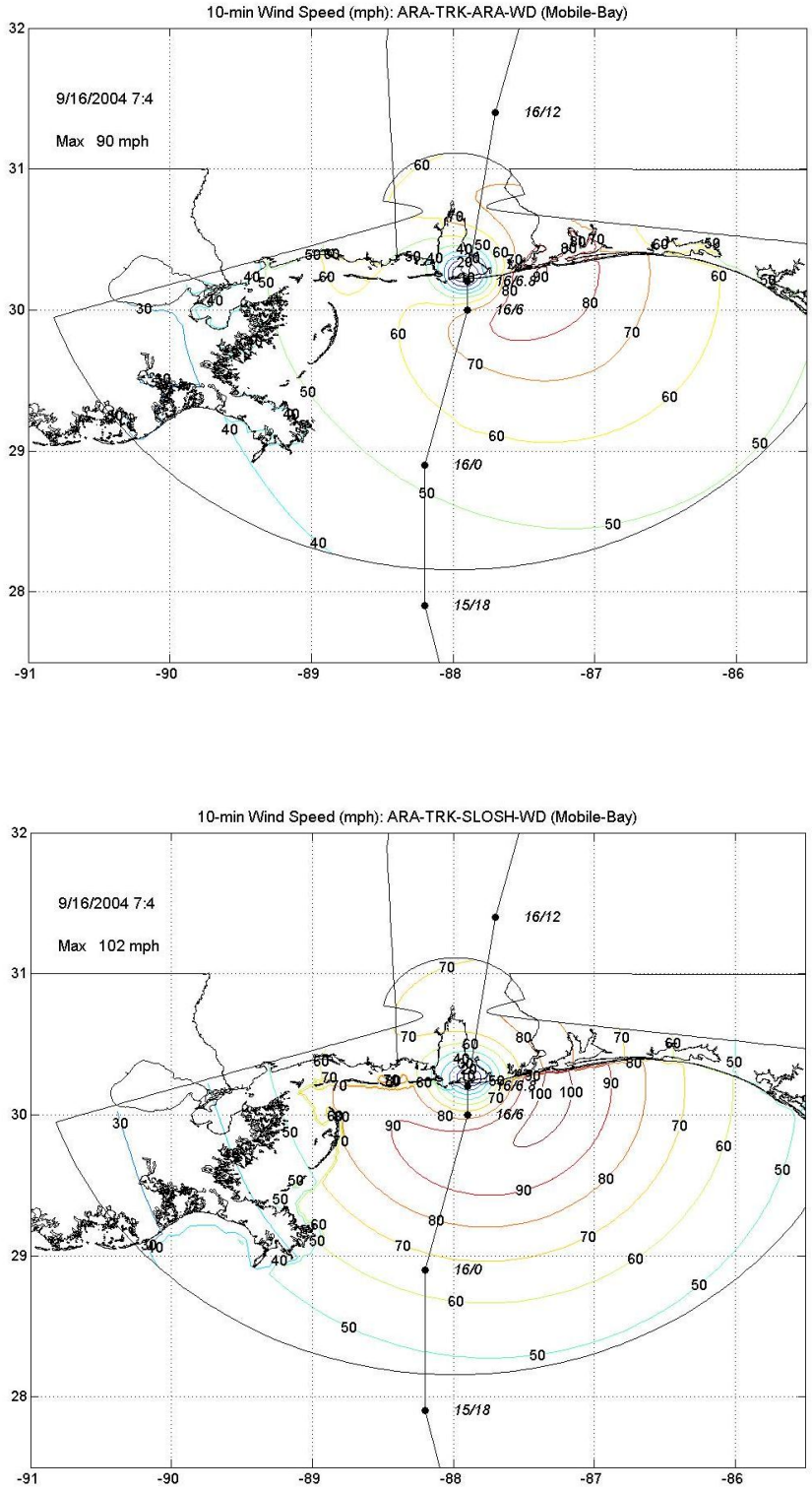

Figure P-2b. Hurricane Ivan (2004) Modeled 10-min Wind Speeds (mph) at Landfall – Mobile Bay Basin

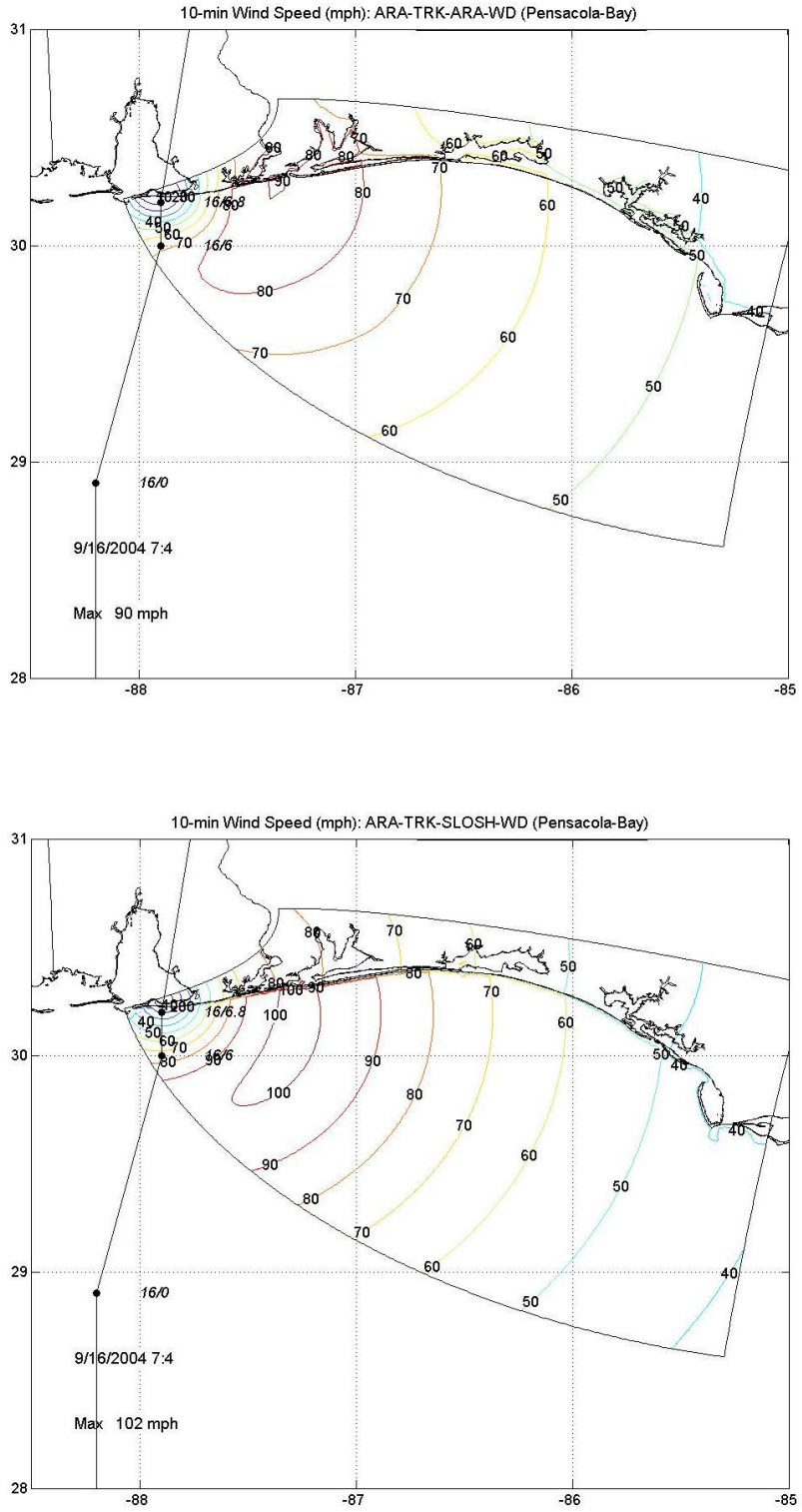

Figure P-2c. Hurricane Ivan (2004) Modeled 10-min Wind Speeds (mph) at Landfall – Pensacola Bay Basin

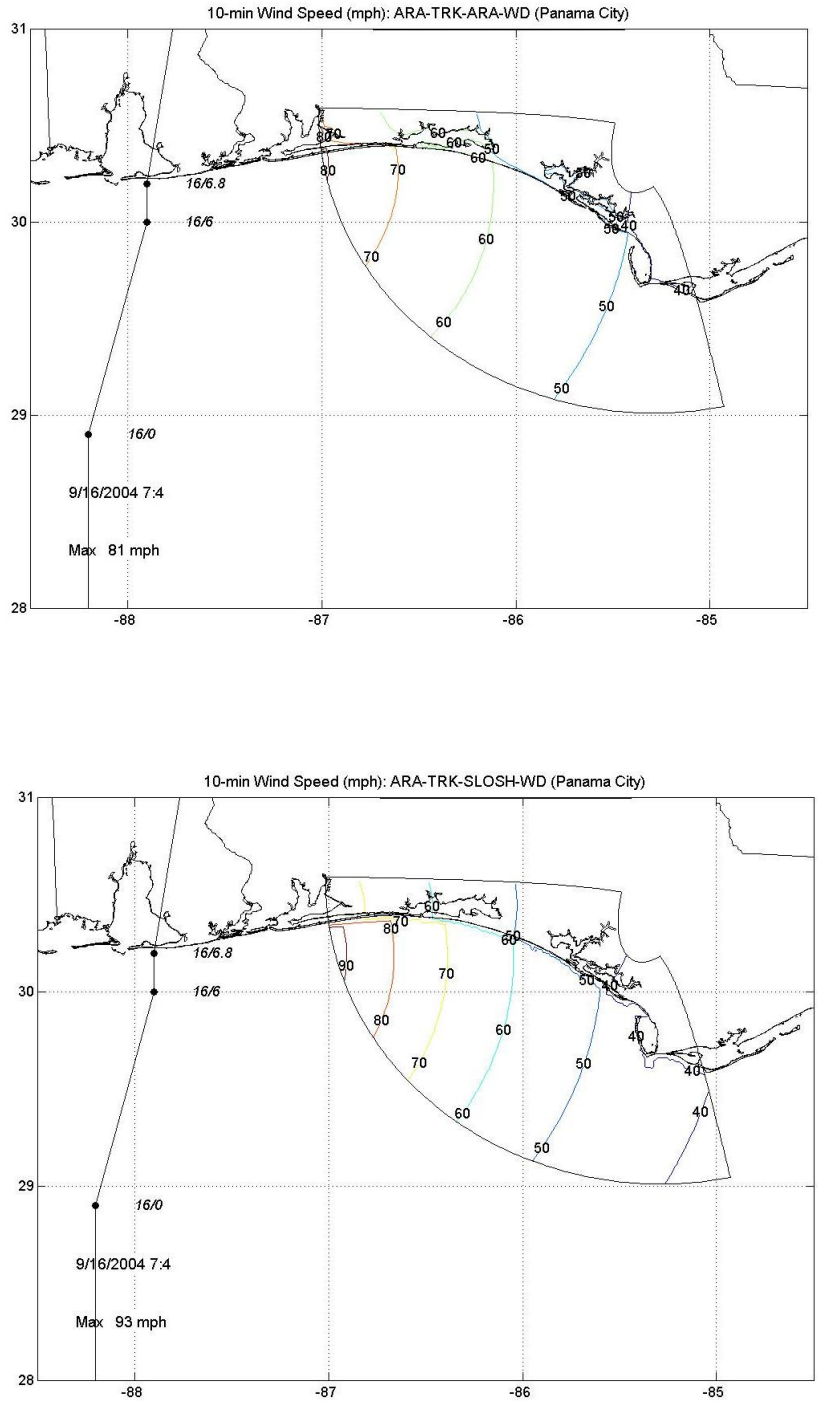

Figure P-2d. Hurricane Ivan (2004) Modeled 10-min Wind Speeds (mph) at Landfall – Panama City Basin

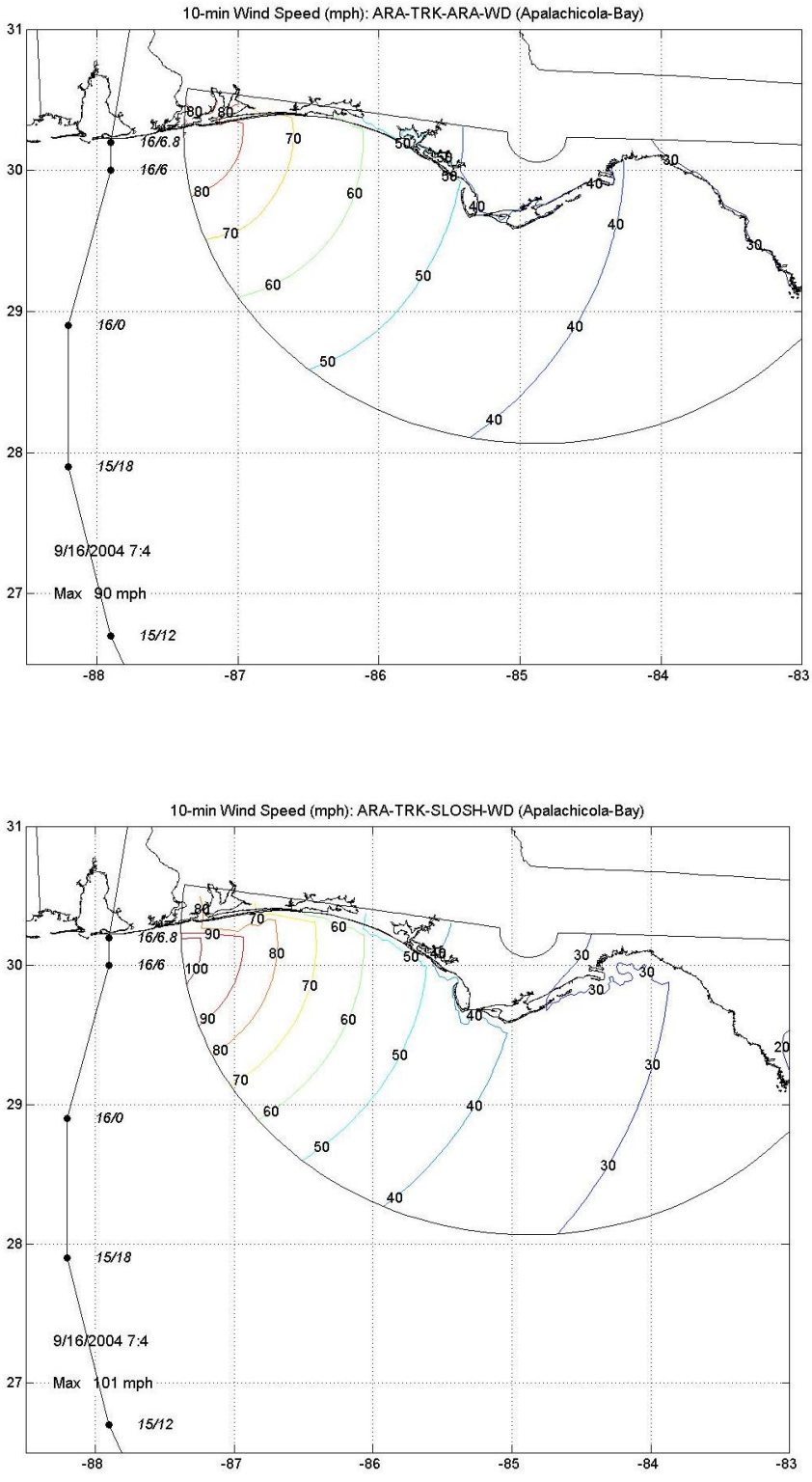

Figure P-2e. Hurricane Ivan (2004) Modeled 10-min Wind Speeds (mph) at Landfall – Apalachicola Bay Basin

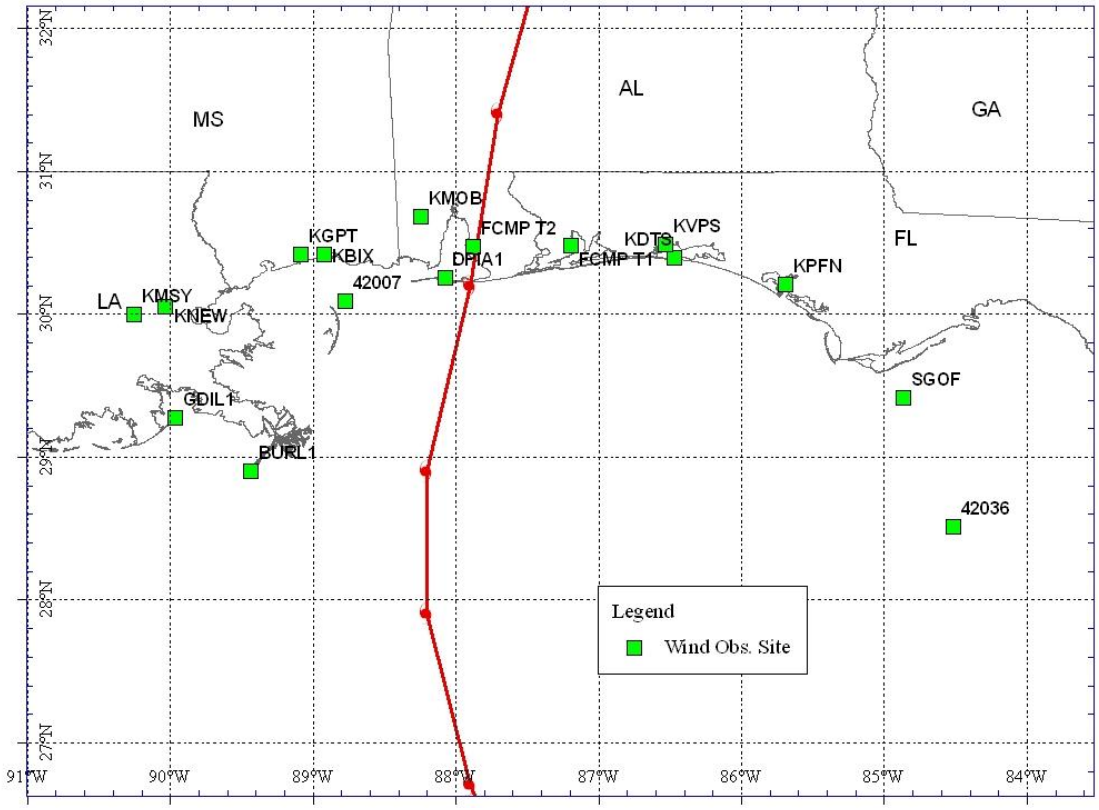

Figure P-3. Wind Observation Locations for Hurricane Ivan

Table P-1. Summary Comparison of Modeled and Observed Maximum 10-min Wind Speeds for Hurricane Ivan

No	name	lat	long	Max Wind Speed (mph)		
				Obs.	ARA-TRK SLOSH-WD	ARA-TRK ARA-WD
1	FCMP T1	30.4793	-87.1869	71.7	80.4	75.3
2	FCMP T2	30.4725	-87.8750	59.0	80.7	74.2
3	KNEW	30.0490	-90.0290	40.0	40.3	43.1
4	KBIX	30.4160	-88.9167	40.0	60.6	53.2
5	KMOB	30.6800	-88.2400	60.0	74.2	66.0
6	KMSY	29.9930	-90.2510	36.0	37.0	32.2
7	KPFN	30.2080	-85.6850	47.0	43.8	44.5
8	42007	30.0900	-88.7700	63.9	85.7	72.7
9	42036	28.5100	-84.5100	42.7	34.3	39.3
10	BURL1	28.9000	-89.4300	72.9	75.1	65.4
11	DPIA1	30.2500	-88.0700	74.6	80.4	88.3
12	GDIL1	29.2700	-89.9600	50.6	44.0	49.7
13	SGOF	29.4100	-84.8600	48.7	38.6	43.7
14	KDTS	30.3940	-86.4670	N/A	60.4	66.5
15	KGPT	30.4120	-89.0810	46.0	56.2	48.5
16	KVPS	30.4833	-86.5253	70.0	61.9	59.3

Table P-2. Summary Comparison of Modeled and Observed Minimum Pressures for Hurricane Ivan

No	name	lat	long	Minimum Central Pressure (mbar)		
				Obs.	ARA-TRK SLOSH-WD	ARA-TRK ARA-WD
1	FCMP T1	30.4793	-87.1869	968.0	971.1	974.5
2	FCMP T2	30.4725	-87.8750	927.1	947.0	949.1
3	KNEW	30.0490	-90.0290	996.0	993.5	996.7
4	KBIX	30.4160	-88.9167	982.0	980.8	984.7
5	KMOB	30.6800	-88.2400	965.0	961.7	966.7
6	KMSY	29.9930	-90.2510	998.0	995.0	998.1
7	KPFN	30.2080	-85.6850	999.0	995.3	997.8
8	42007	30.0900	-88.7700	976.8	974.3	978.3
9	42036	28.5100	-84.5100	1005.0	1000.9	1004.3
10	BURL1	28.9000	-89.4300	983.6	983.6	985.1
11	DPIA1	30.2500	-88.0700	952.7	947.2	948.9
12	GDIL1	29.2700	-89.9600	994.2	992.0	994.0
13	SGOF	29.4100	-84.8600	1005.5	999.6	1002.1
14	KDTS	30.3940	-86.4670	N/A	987.6	990.5
15	KGPT	30.4120	-89.0810	985.0	983.9	987.7
16	KVPS	30.4833	-86.5253	N/A	986.6	989.8

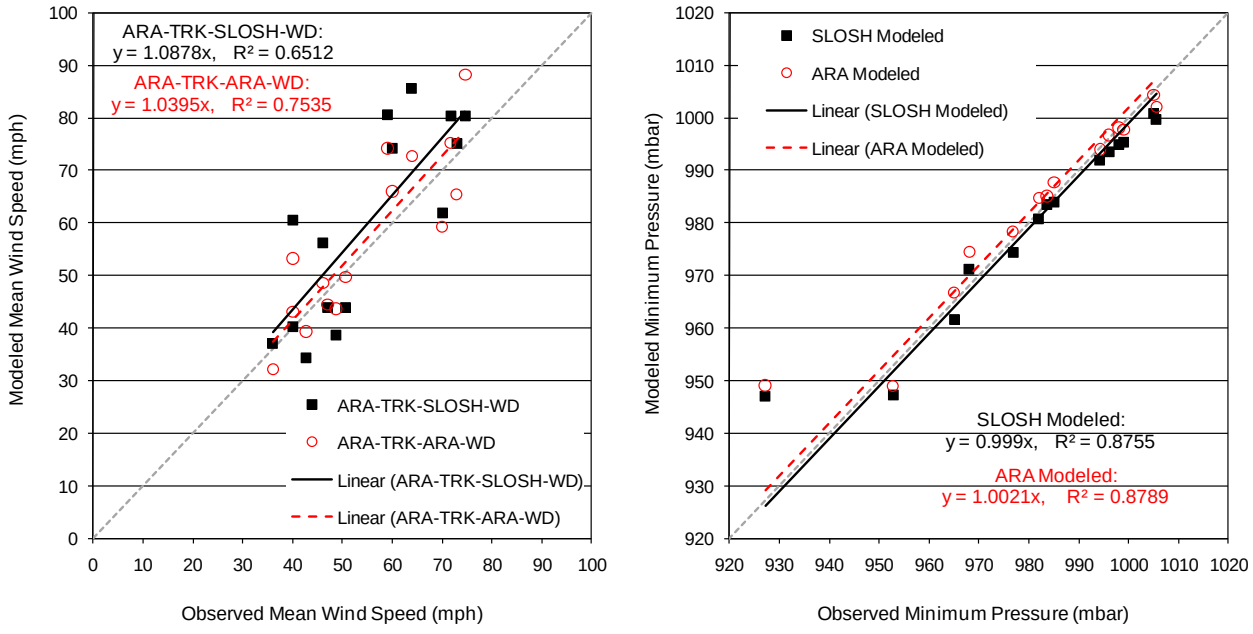

Figure P-4. Comparisons of Modeled and Observed Maximum 10-min Wind Speeds and Minimum Pressures for Hurricane Ivan

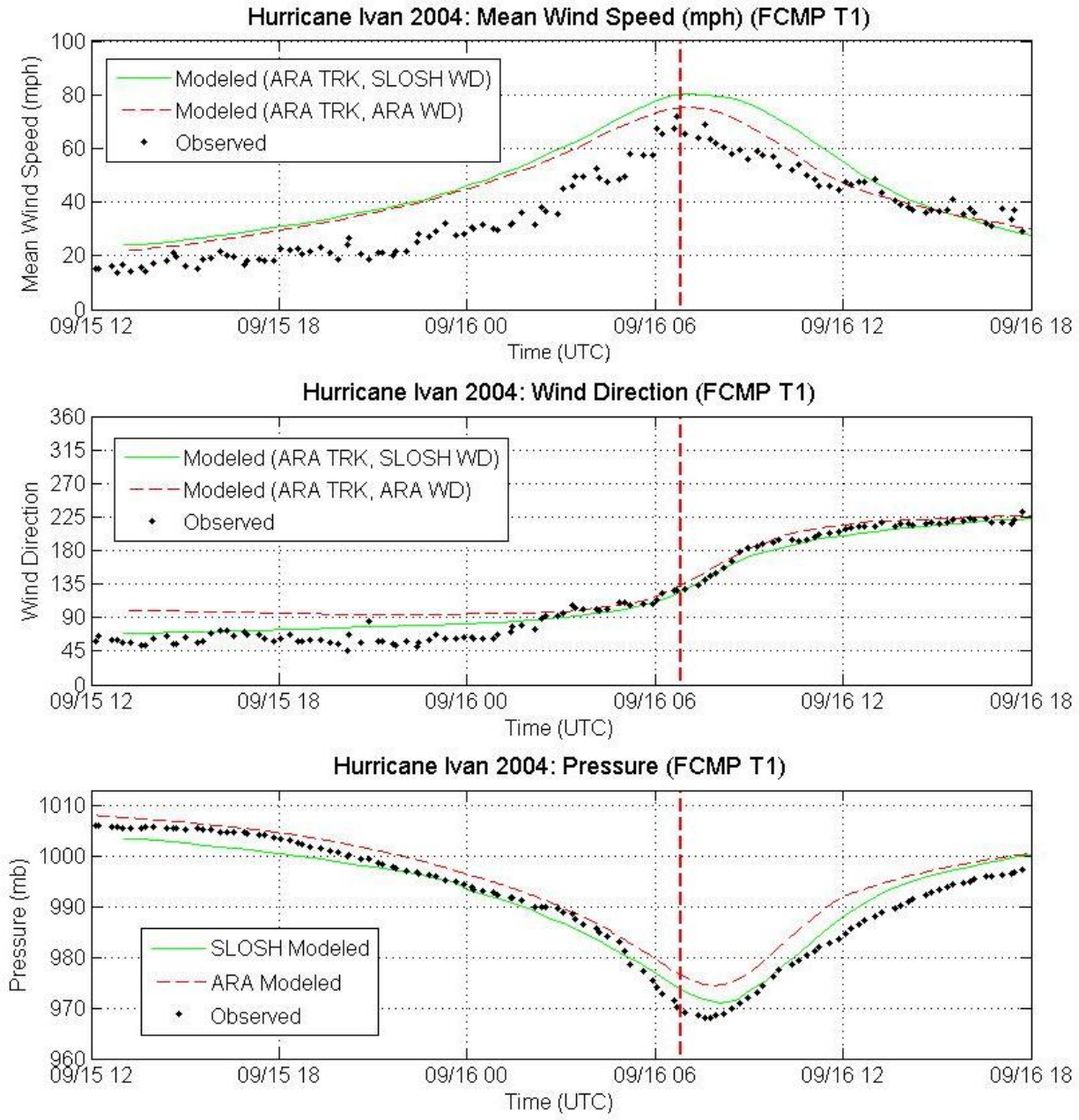

Figure P-5a. Comparisons of Observed and Modeled Time Series Traces of Mean Wind Speeds, Wind Directions, and Pressures for Hurricane Ivan (2004) – FCMP T1

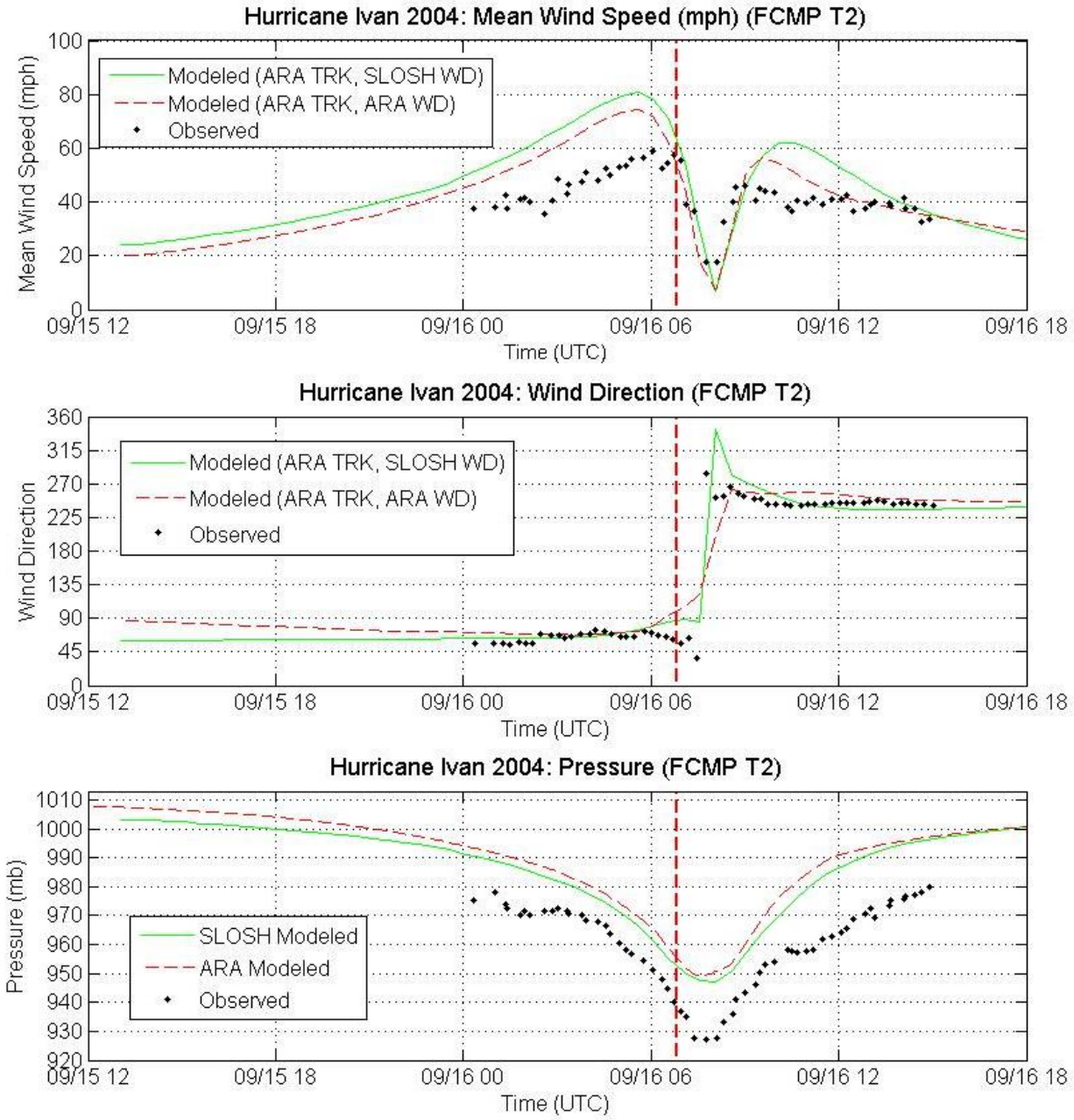

Figure P-5b. Comparisons of Observed and Modeled Time Series Traces of Mean Wind Speeds, Wind Directions, and Pressures for Hurricane Ivan (2004) – FCMP T2

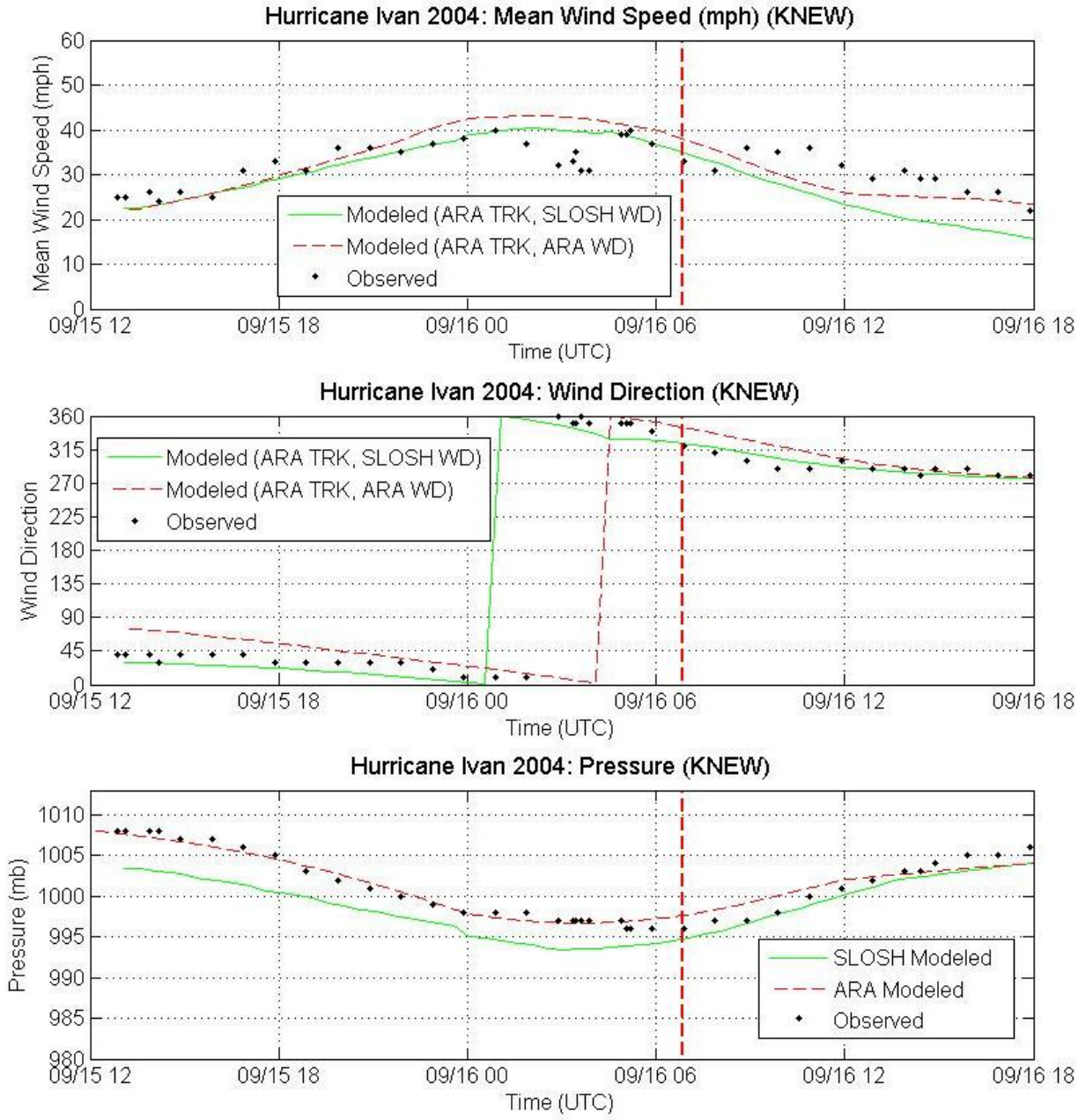

Figure P-5c. Comparisons of Observed and Modeled Time Series Traces of Mean Wind Speeds, Wind Directions, and Pressures for Hurricane Ivan (2004) – KNEW

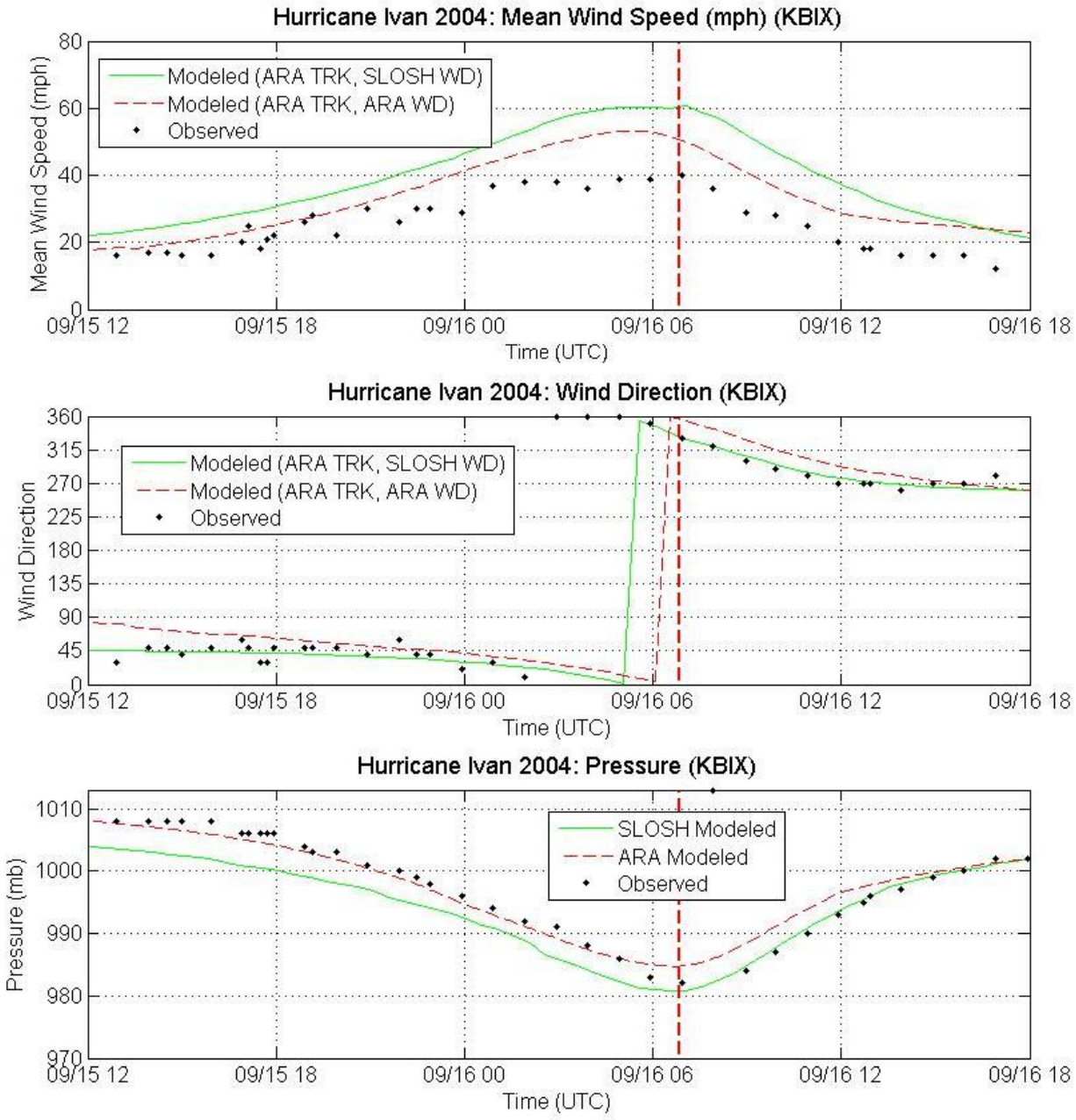

Figure P-5d. Comparisons of Observed and Modeled Time Series Traces of Mean Wind Speeds, Wind Directions, and Pressures for Hurricane Ivan (2004) – KBIX

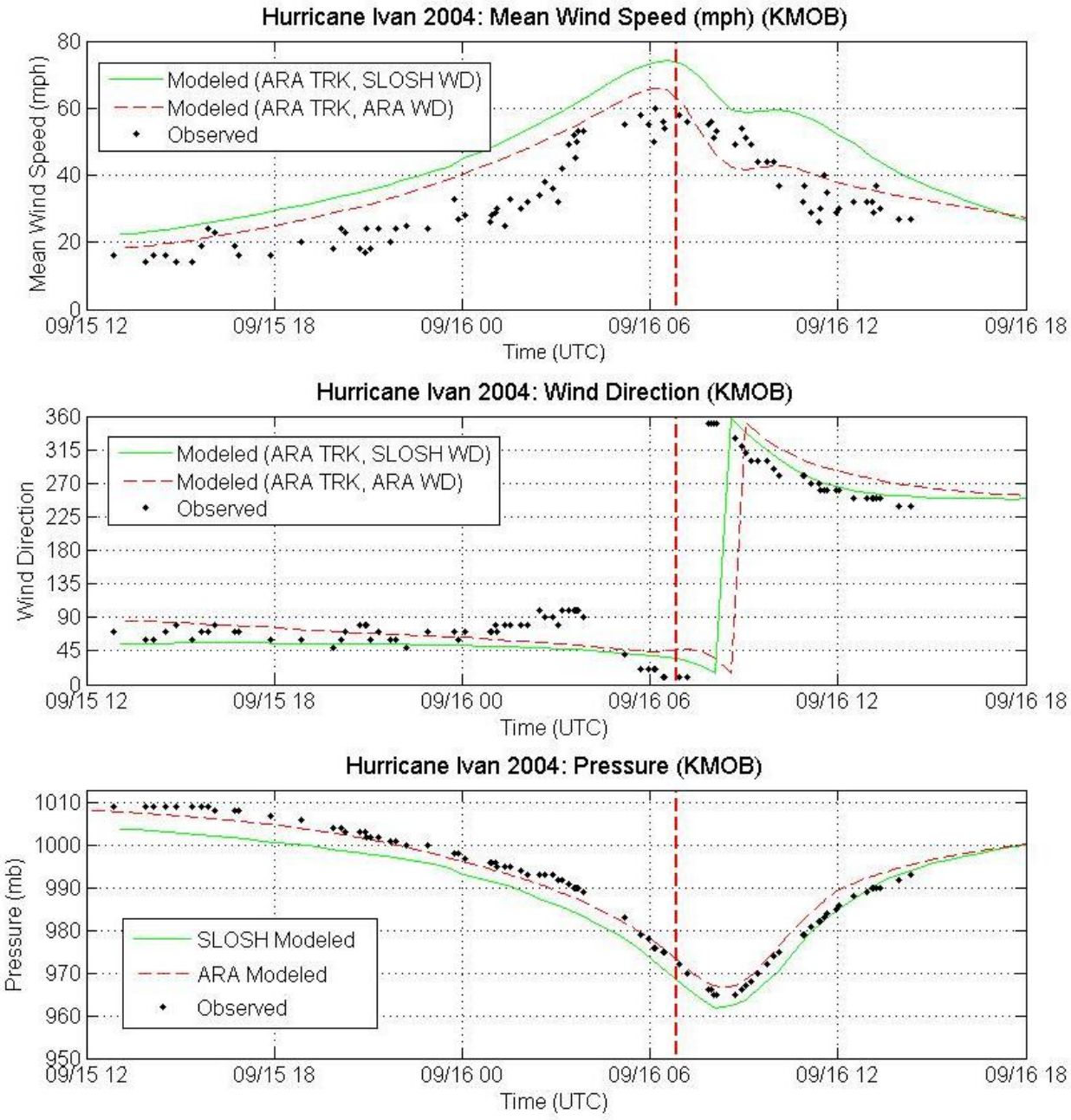

Figure P-5e. Comparisons of Observed and Modeled Time Series Traces of Mean Wind Speeds, Wind Directions, and Pressures for Hurricane Ivan (2004) – KMOB

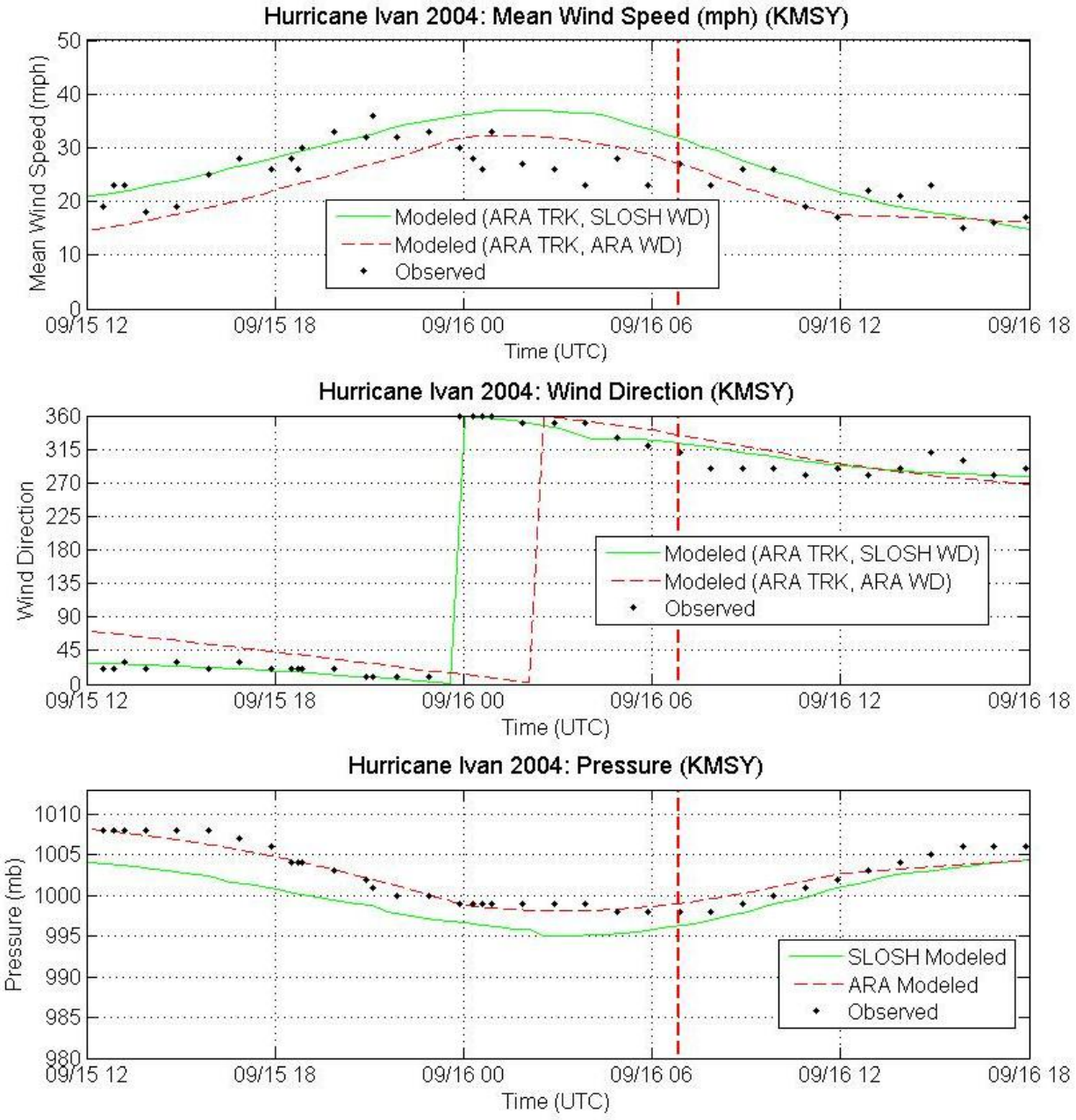

Figure P-5f. Comparisons of Observed and Modeled Time Series Traces of Mean Wind Speeds, Wind Directions, and Pressures for Hurricane Ivan (2004) – KMSY

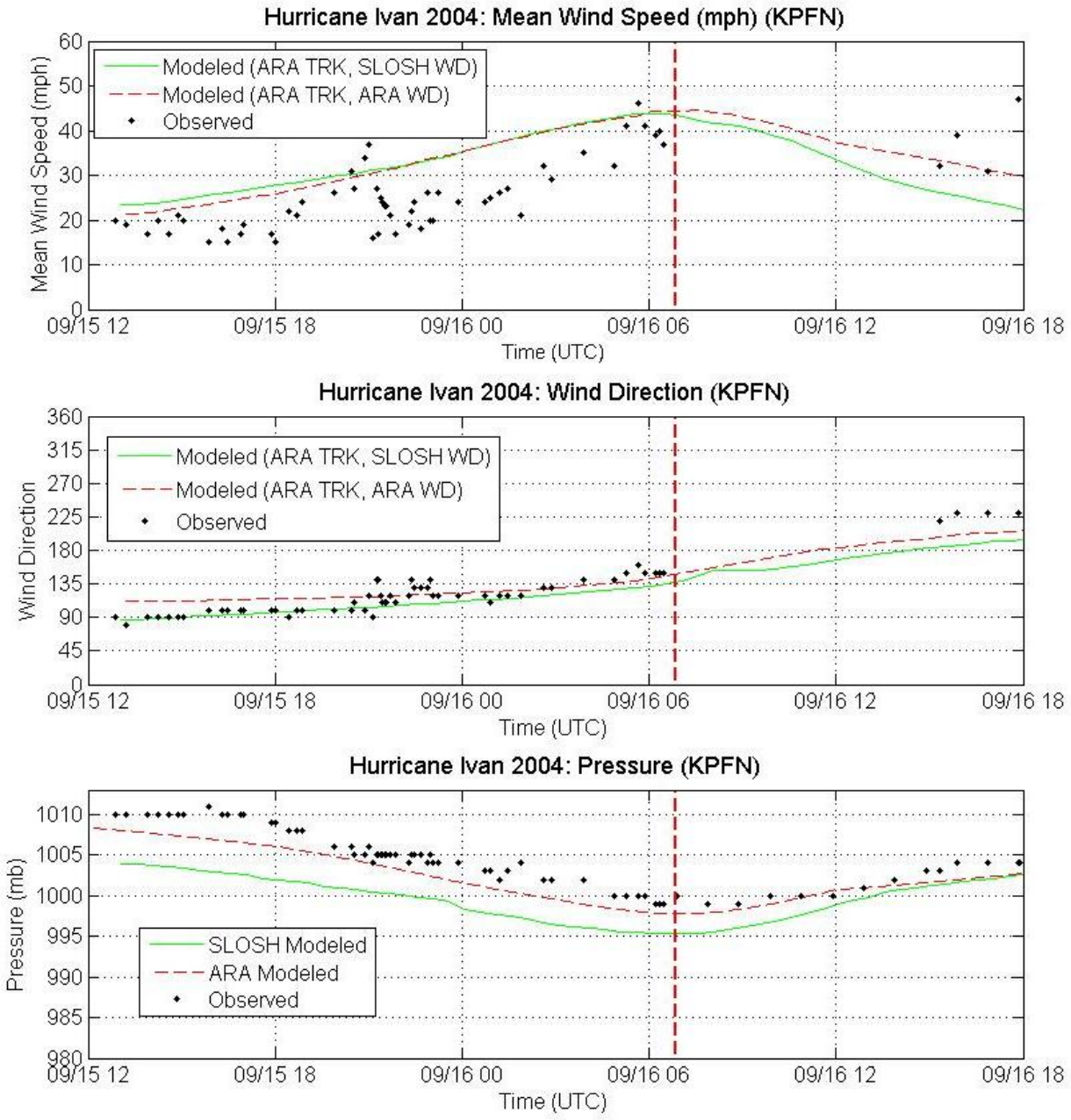

Figure P-5g. Comparisons of Observed and Modeled Time Series Traces of Mean Wind Speeds, Wind Directions, and Pressures for Hurricane Ivan (2004) – KPFN

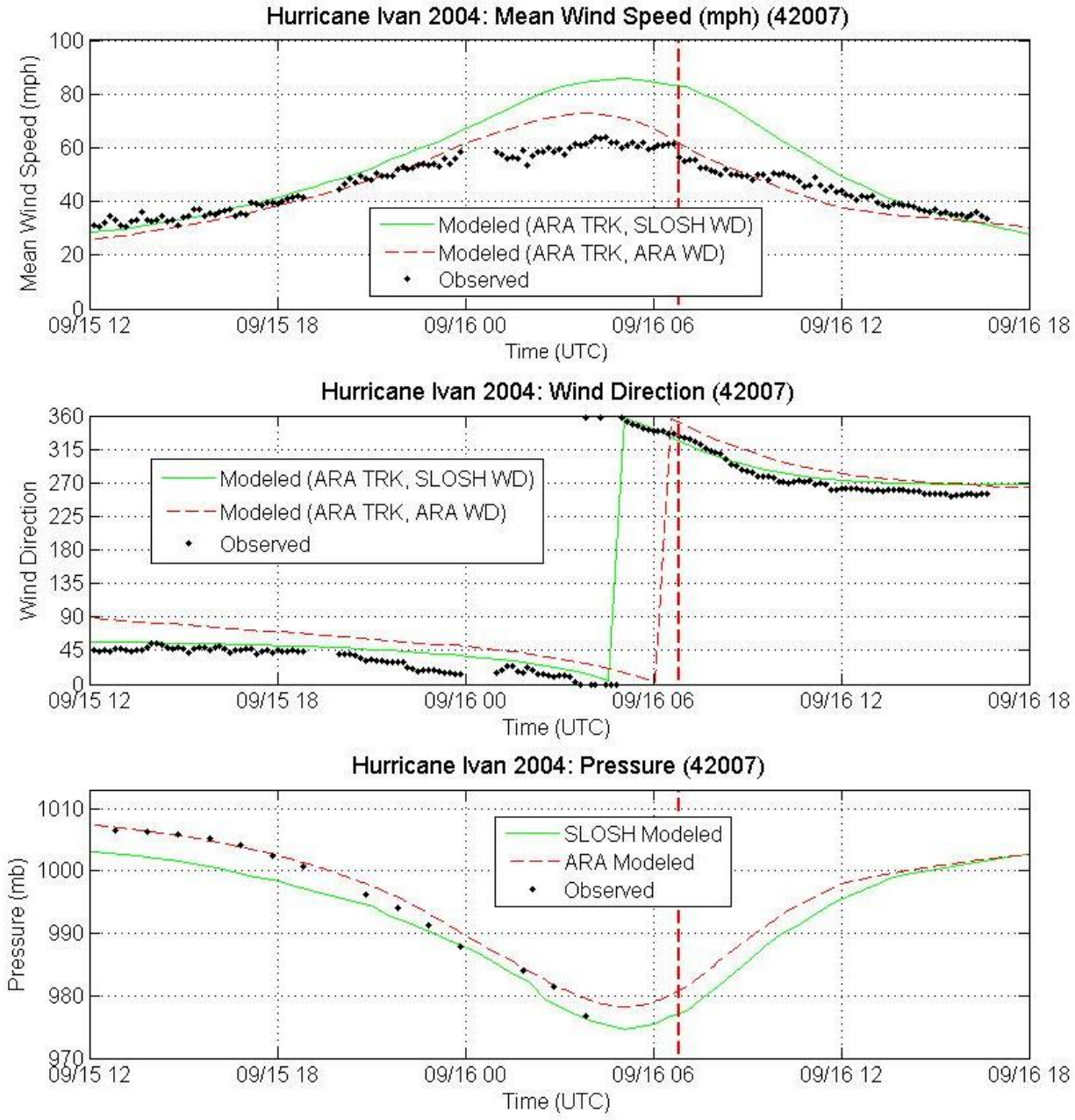

Figure P-5h. Comparisons of Observed and Modeled Time Series Traces of Mean Wind Speeds, Wind Directions, and Pressures for Hurricane Ivan (2004) – 42007

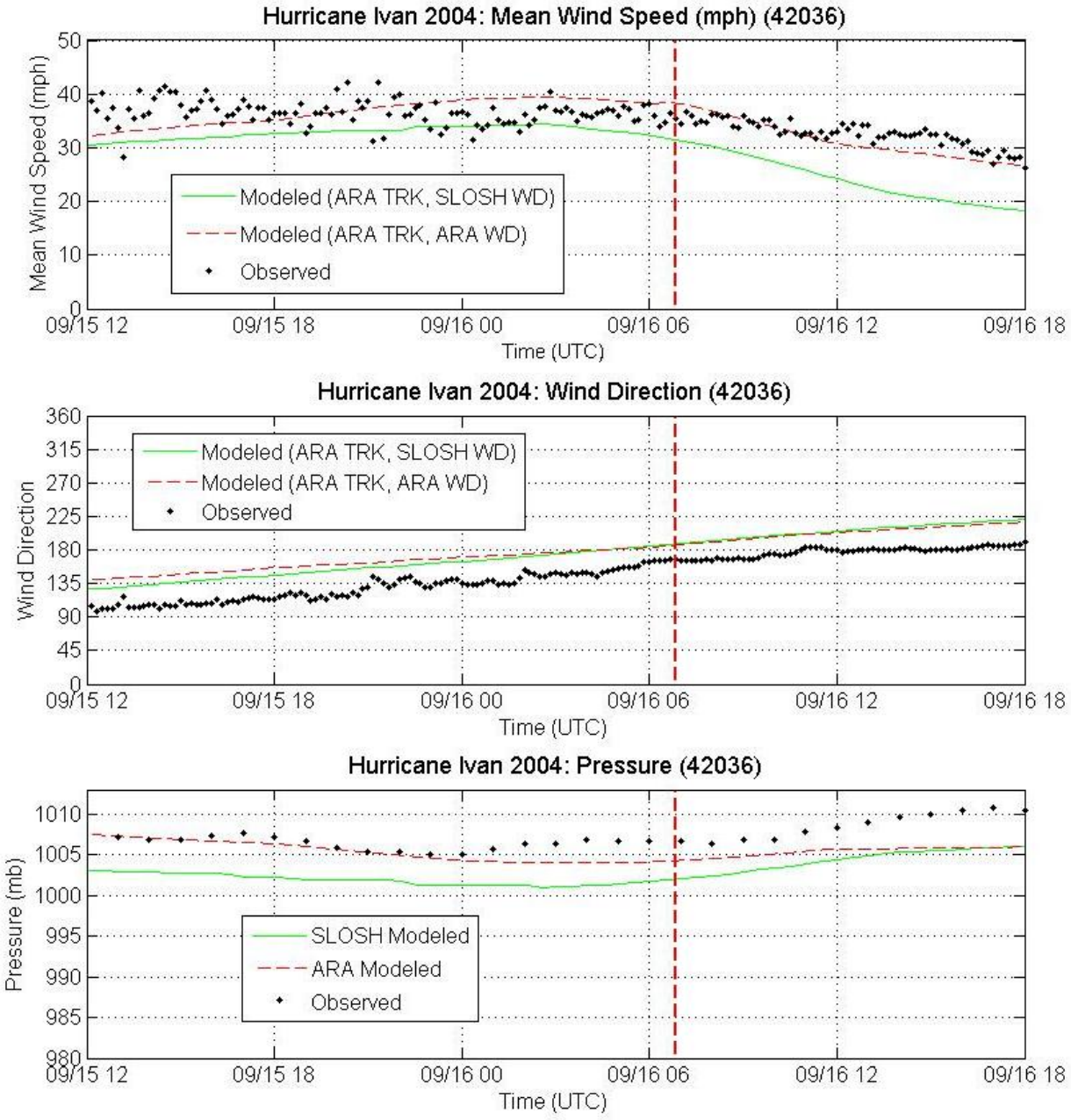

Figure P-5i. Comparisons of Observed and Modeled Time Series Traces of Mean Wind Speeds, Wind Directions, and Pressures for Hurricane Ivan (2004) – 42036

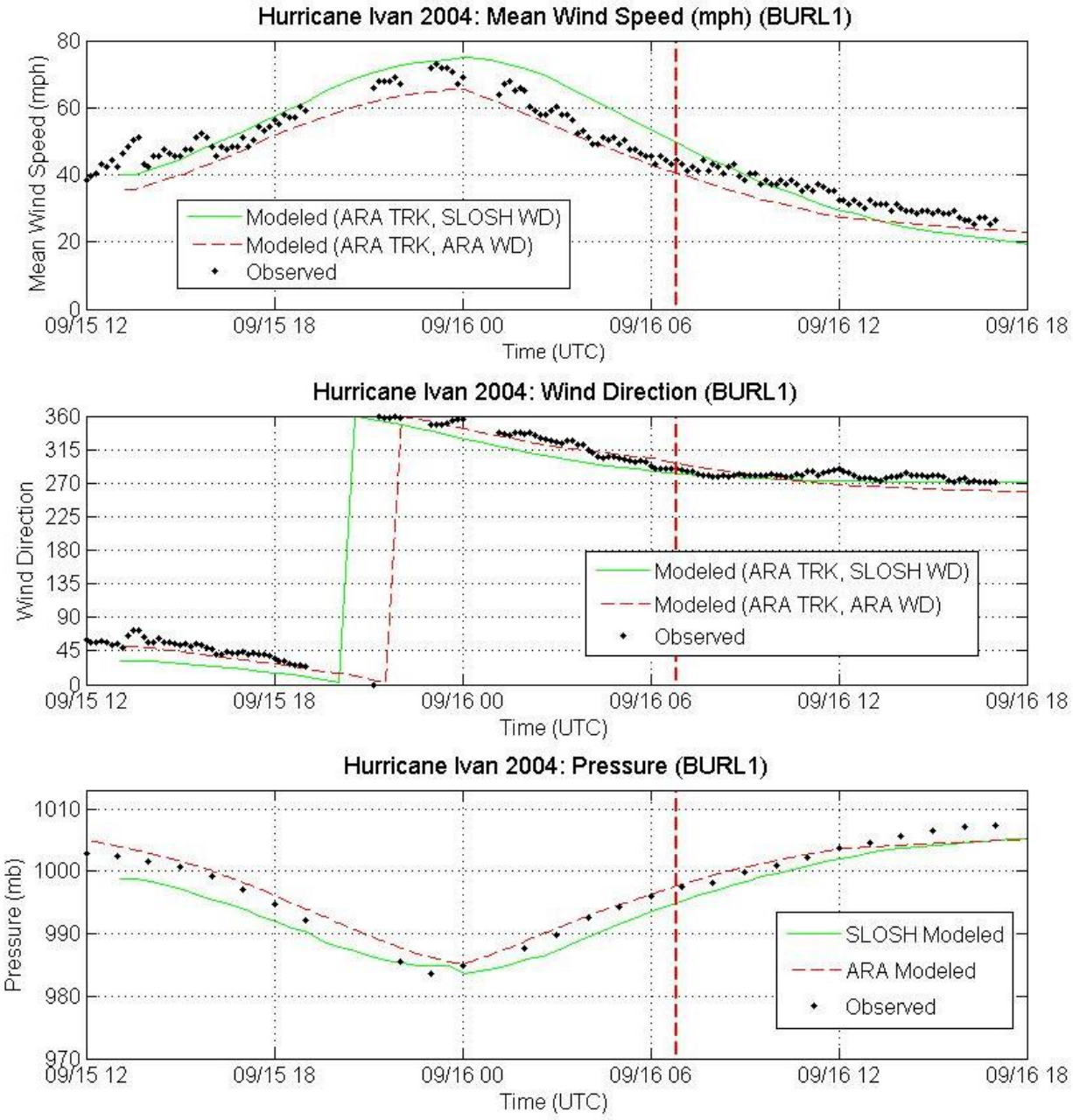

Figure P-5j. Comparisons of Observed and Modeled Time Series Traces of Mean Wind Speeds, Wind Directions, and Pressures for Hurricane Ivan (2004) – BURL1

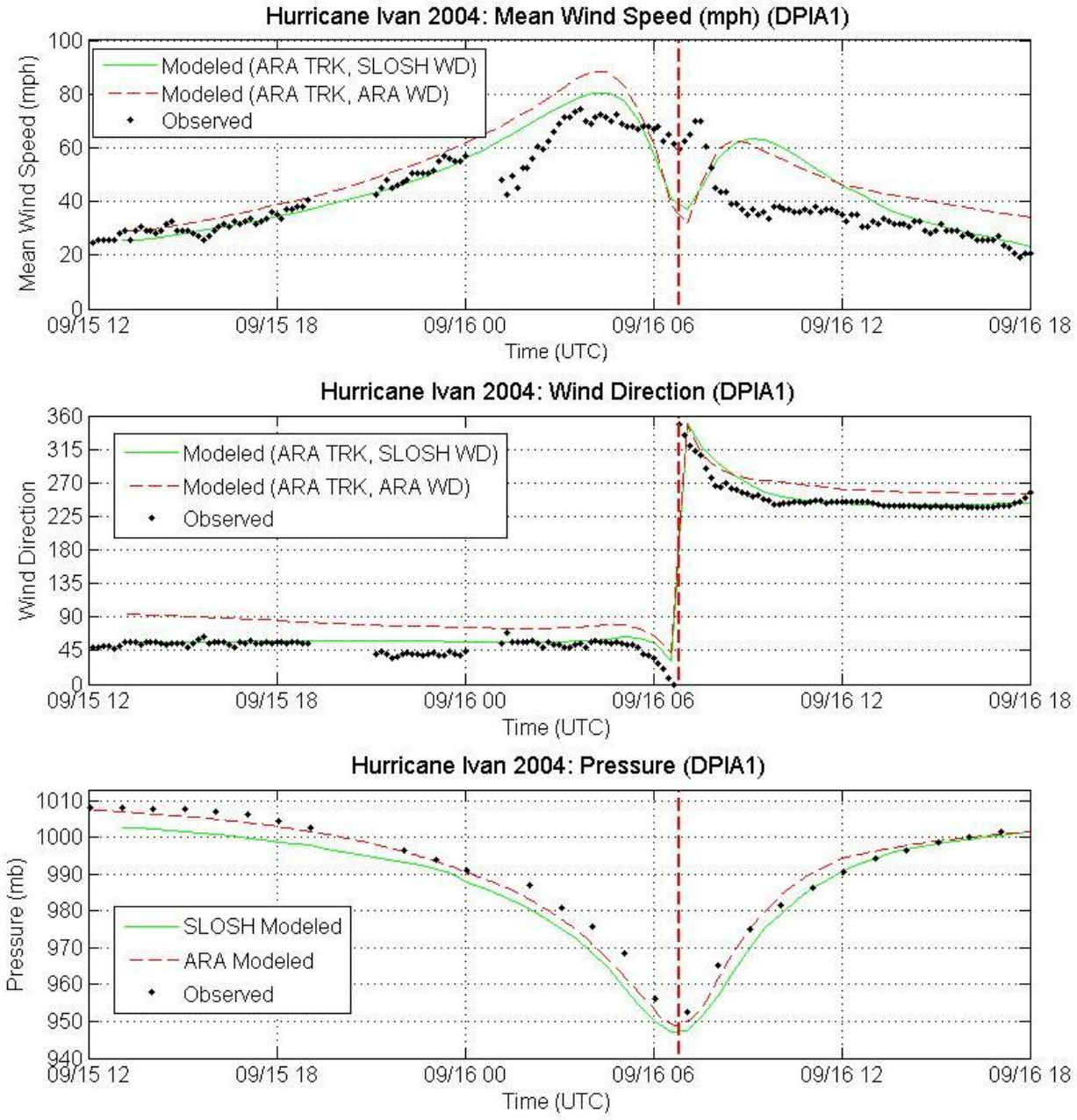

Figure P-5k. Comparisons of Observed and Modeled Time Series Traces of Mean Wind Speeds, Wind Directions, and Pressures for Hurricane Ivan (2004) – DPIA1

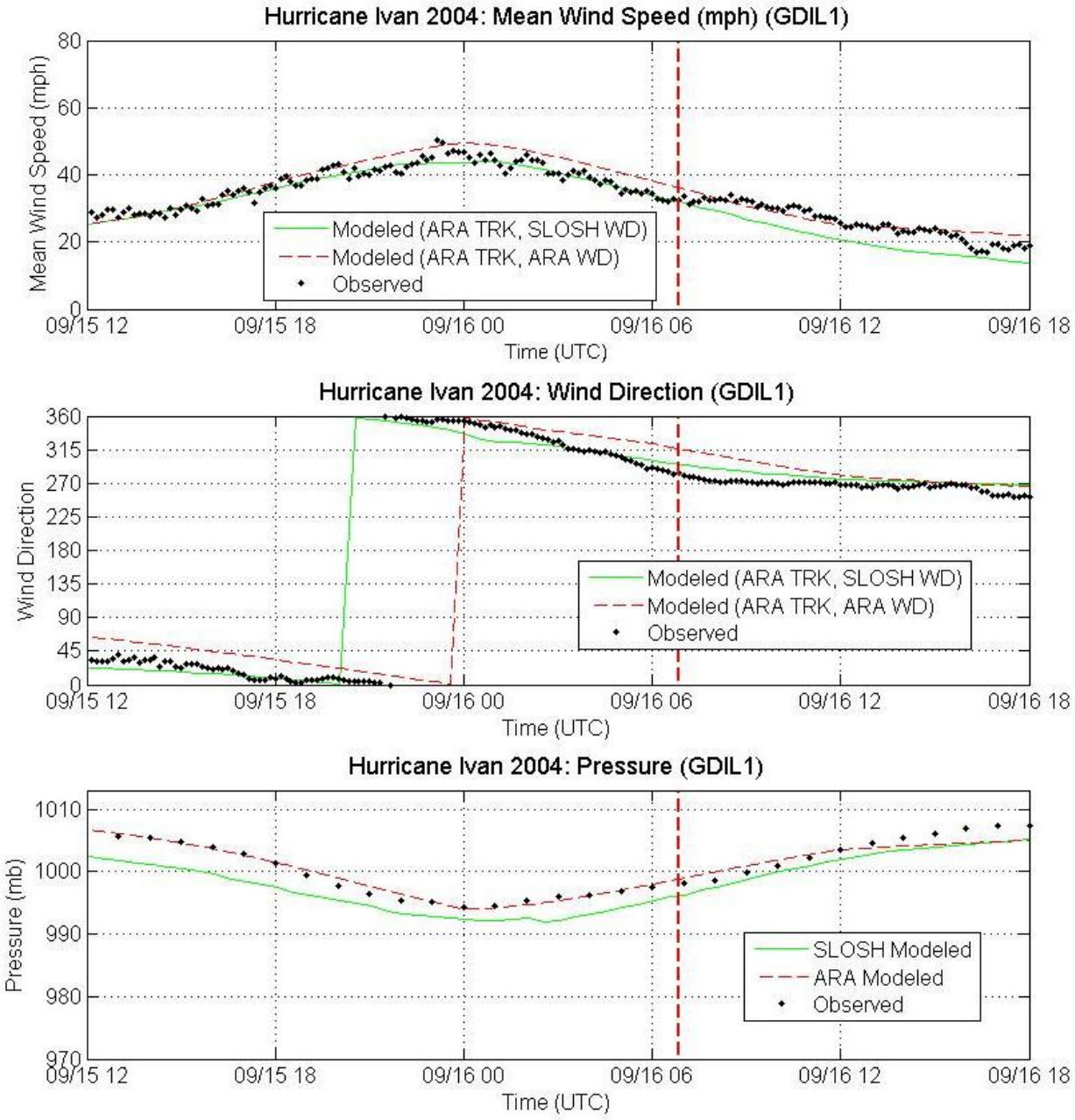

Figure P-5l. Comparisons of Observed and Modeled Time Series Traces of Mean Wind Speeds, Wind Directions, and Pressures for Hurricane Ivan (2004) – GDIL1

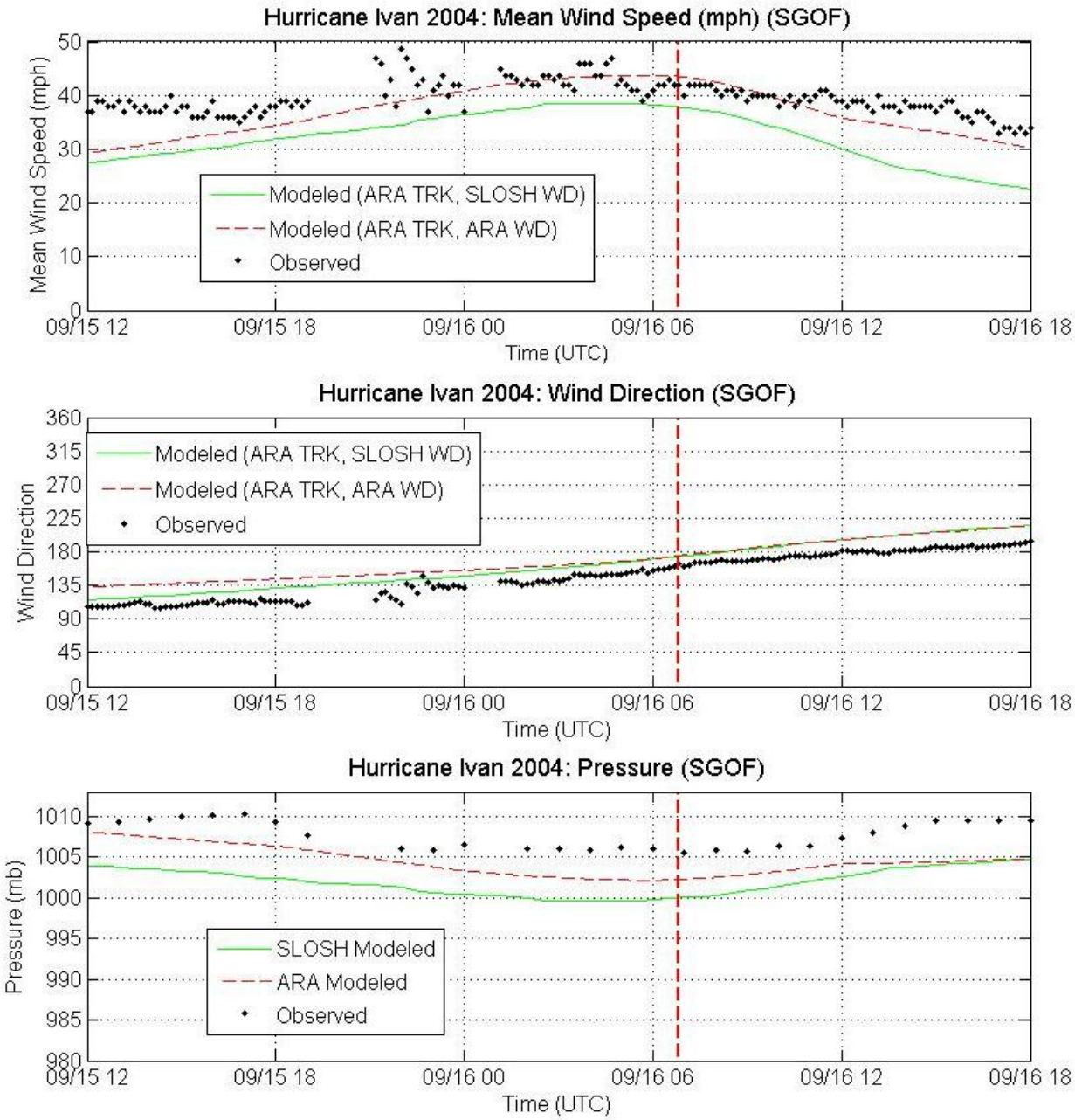

Figure P-5m. Comparisons of Observed and Modeled Time Series Traces of Mean Wind Speeds, Wind Directions, and Pressures for Hurricane Ivan (2004) – SGOF

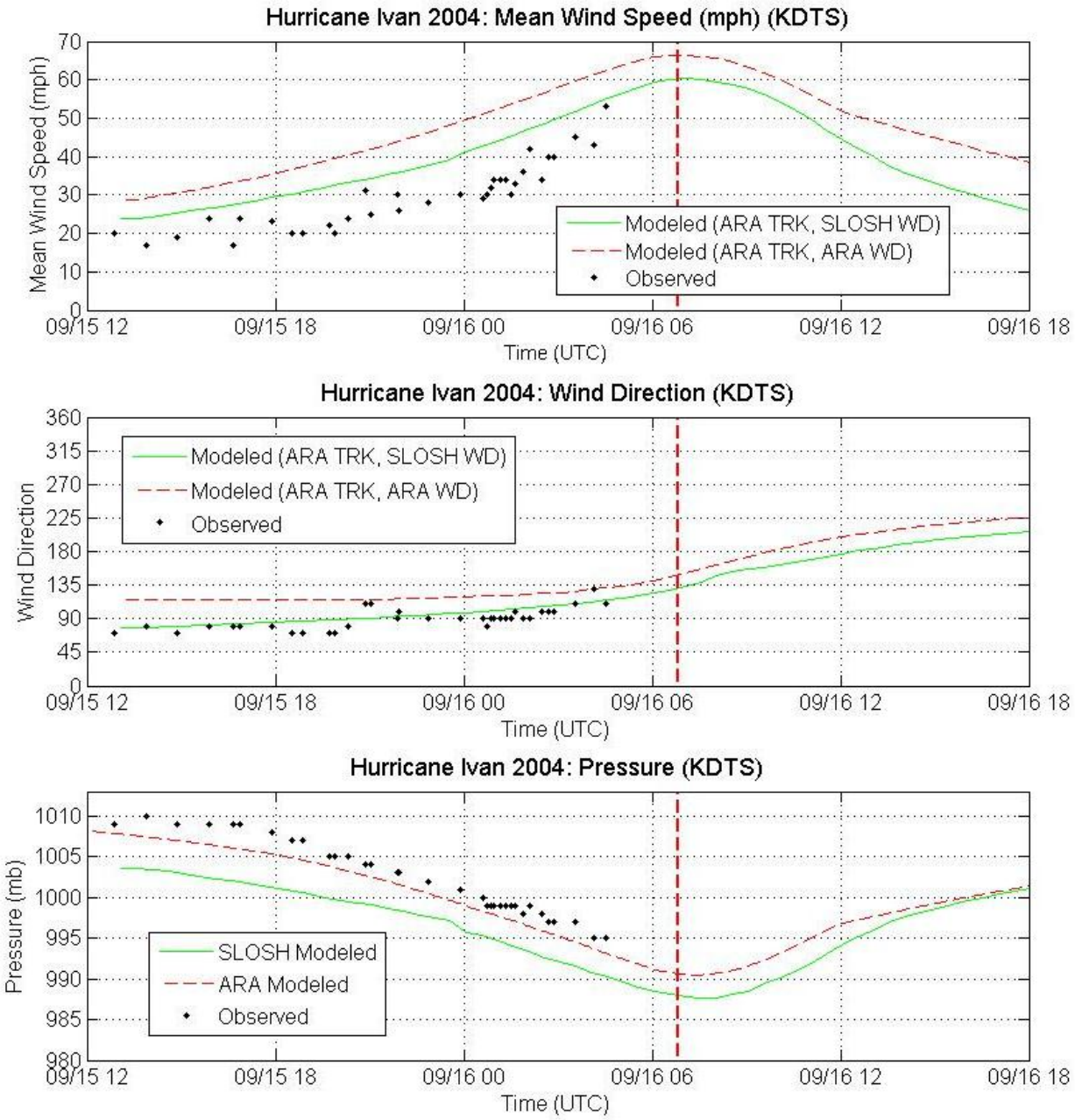

Figure P-5n. Comparisons of Observed and Modeled Time Series Traces of Mean Wind Speeds, Wind Directions, and Pressures for Hurricane Ivan (2004) – KDTS

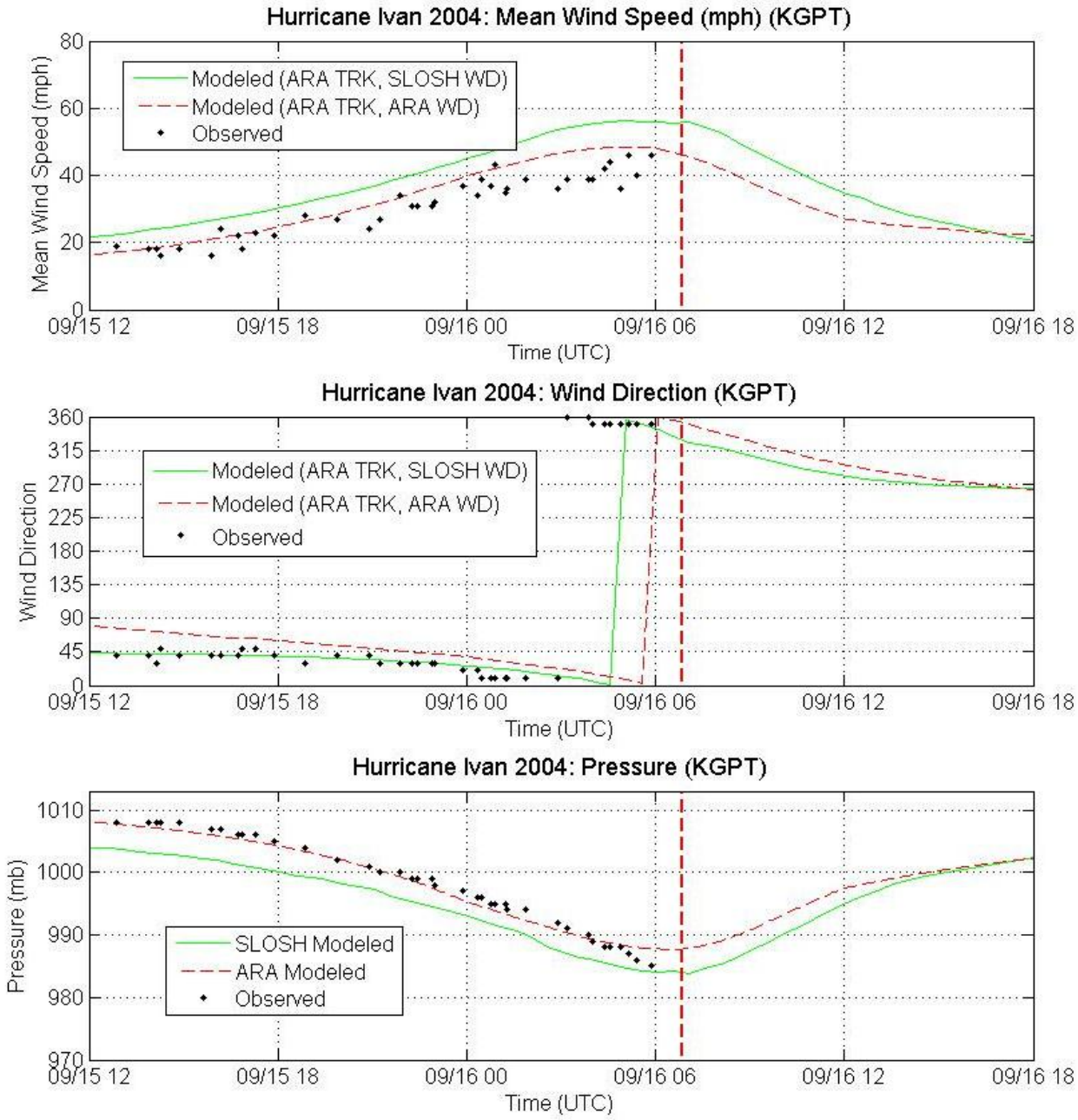

Figure P-5o. Comparisons of Observed and Modeled Time Series Traces of Mean Wind Speeds, Wind Directions, and Pressures for Hurricane Ivan (2004) – KGPT

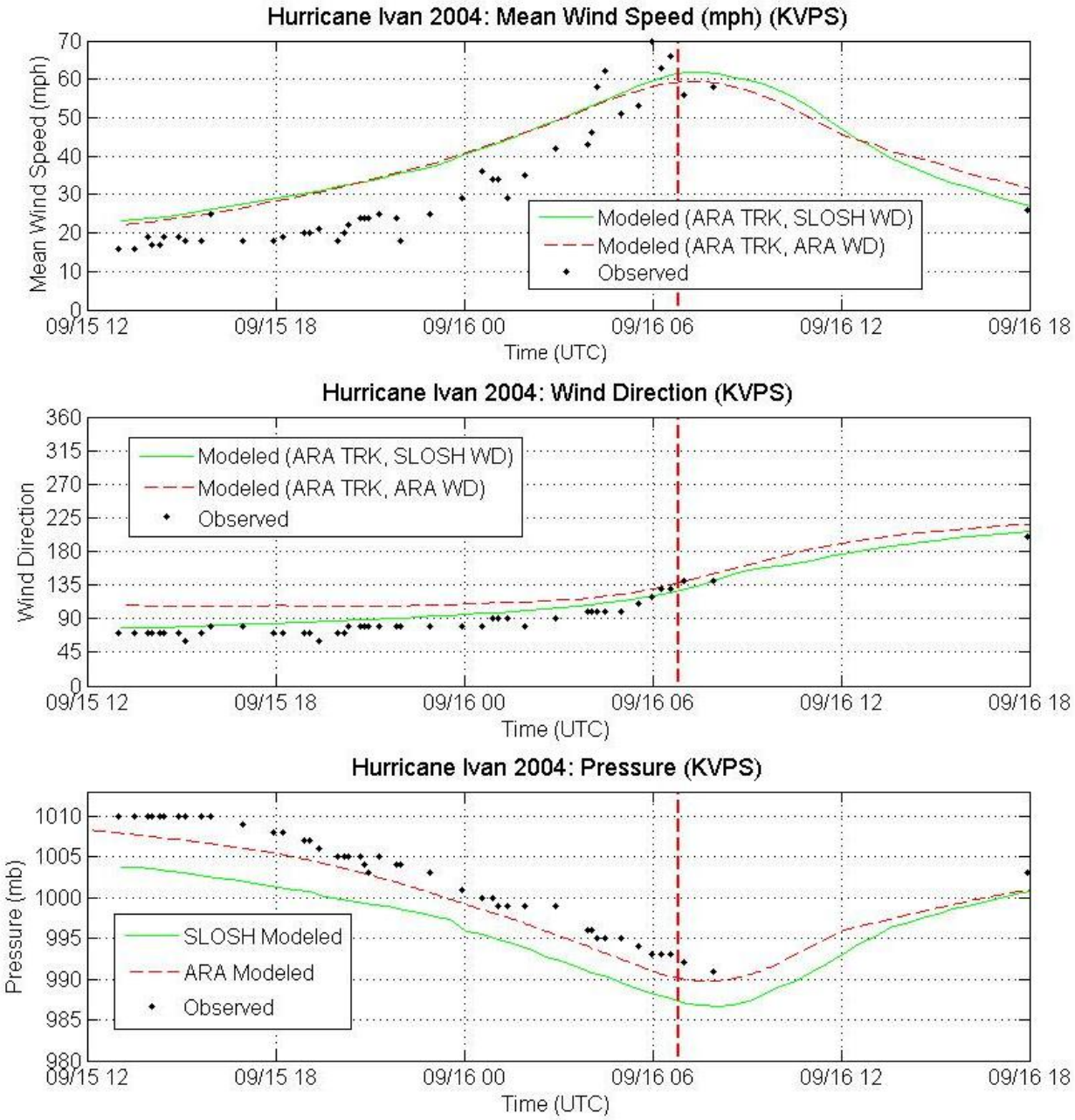

Figure P-5p. Comparisons of Observed and Modeled Time Series Traces of Mean Wind Speeds, Wind Directions, and Pressures for Hurricane Ivan (2004) – KVPS

Table P-3. Error Analysis of Wind Speeds, Wind Directions and Pressures for Hurricane Ivan

Station	Range		Number of Data	Obs		SLOSH-Obs		ARA-Obs	
				Mean	Std	mean	RMS	mean	RMS
FCMP T1	Wind Speed (mph)	0-20	23	13.7	7.6	8.0	9.5	6.8	8.2
		20-40	53	29.3	6.3	9.9	13.1	9.2	12.0
		40-60	34	50.4	5.3	13.2	14.9	7.4	10.2
		60-80	10	65.6	3.4	13.8	14.2	8.5	9.0
		all	120	35.3	16.9	10.8	13.1	8.2	10.6
	Wind Direction (deg)	45-90	53	62.7	8.3	13.9	15.9	33.1	34.2
		90-135	20	109.2	12.3	-4.7	6.3	2.8	5.4
		135-180	6	156.3	13.9	-2.9	5.1	6.2	7.7
		180-225	35	208.9	11.8	-5.4	6.7	5.6	6.7
		225-270	1	232.1	0.0	-10.1	10.1	-5.6	5.6
		all	115	131.6	79.8	3.6	11.6	17.0	23.2
	Pressure (mbar)	965-980	22	972.9	3.8	2.1	2.4	5.5	5.5
		980-989	20	985.1	2.7	0.9	2.7	4.2	5.1
		989-1030	73	998.1	5.3	-0.5	2.4	2.3	2.6
		all	115	991.0	11.1	0.2	2.5	3.2	3.8
FCMP T2	Wind Speed (mph)	0-20	2	17.6	0.3	-3.5	6.6	-6.4	6.8
		20-40	22	37.4	2.1	10.7	14.8	4.7	9.6
		40-60	34	47.2	6.0	15.8	18.8	10.2	13.5
		all	58	42.4	8.2	13.2	17.1	7.5	12.0
	Wind Direction (deg)	0-45	1	37.0	0.0	49.0	49.0	82.1	82.1
		45-90	27	64.4	5.9	5.7	11.1	10.7	17.2
		225-270	29	246.2	5.8	5.9	23.4	5.7	15.1
		270-315	1	283.5	0.0	117.8	117.8	232.5	232.5
		all	58	158.6	93.1	8.5	24.7	13.2	36.0
	Pressure (mbar)	920-945	11	935.7	6.3	15.5	15.8	18.2	18.5
		945-965	19	956.5	5.1	15.2	16.0	19.7	20.4
		965-980	27	972.1	3.4	14.8	15.5	17.3	17.9
		980-989	1	980.1	0.0	16.3	16.3	17.1	17.1
		all	58	960.2	14.7	15.1	15.7	18.3	18.8
KNEW	Wind Speed (mph)	20-40	35	31.8	4.7	-2.0	5.7	0.8	5.2
		40-60	2	40.0	0.0	-1.0	1.1	1.9	2.2
		all	37	31.4	7.1	-1.9	5.5	0.8	5.0
	Wind Direction (deg)	0-45	15	28.7	11.3	-11.7	12.5	20.1	22.9
		270-315	12	290.8	9.0	-0.1	7.5	9.0	15.7
		315-360	8	345.0	10.7	-12.6	15.1	13.1	14.2
		all	35	204.2	145.9	-8.1	11.8	13.9	18.2
	Pressure (mbar)	989-1030	37	1000.9	4.1	-2.6	3.0	0.0	1.0
		all	37	1000.9	4.1	-2.6	3.0	0.0	1.0

Table P-3. Error Analysis of Wind Speeds, Wind Directions and Pressures for Hurricane Ivan (Continued)

Station	Range		Number of Data	Obs		SLOSH-Obs		ARA-Obs	
				Mean	Std	mean	RMS	mean	RMS
KBIX	Wind Speed (mph)	0-20	12	16.3	1.6	11.0	11.4	6.8	7.6
		20-40	23	29.3	6.4	14.3	15.4	7.4	8.7
		40-60	1	40.0	0.0	20.3	20.3	10.5	10.5
		all	36	25.3	8.4	13.3	14.4	7.3	8.4
	Wind Direction (deg)	0-45	10	31.0	9.9	5.1	9.6	22.6	26.6
		45-90	10	52.0	4.2	-10.2	11.7	10.8	14.6
		225-270	1	260.0	0.0	7.7	7.7	19.1	19.1
		270-315	9	277.8	10.9	-0.3	7.8	13.2	19.1
		315-360	3	333.3	15.3	-0.4	0.9	21.0	21.5
		all	33	157.5	134.2	-0.4	9.7	16.6	20.8
	Pressure (mbar)	980-989	6	985.0	2.4	-1.5	2.4	2.1	2.8
		989-1030	31	1001.2	6.0	-4.1	6.8	-1.2	5.1
		all	37	998.6	8.2	-3.7	6.3	-0.7	4.8
KMOB	Wind Speed (mph)	0-20	14	15.4	4.7	10.9	12.0	6.9	8.1
		20-40	43	29.0	4.7	17.4	18.4	9.5	11.0
		40-60	27	51.0	5.0	13.4	14.0	1.5	7.4
		60-80	1	60.0	0.0	13.7	13.7	5.9	5.9
		all	85	34.1	13.9	15.0	16.1	6.5	9.5
	Wind Direction (deg)	0-45	9	17.8	9.7	19.8	21.0	28.0	29.4
		45-90	36	69.2	9.1	-15.6	18.5	0.5	14.4
		90-135	10	97.0	4.8	-49.6	49.9	-43.2	43.5
		225-270	13	252.3	7.3	8.1	8.5	28.0	28.1
		270-315	10	288.0	14.0	15.3	18.9	31.5	32.5
		315-360	6	341.7	13.3	25.2	25.4	44.1	44.3
		all	84	143.4	109.9	-5.5	24.2	9.2	28.0
	Pressure (mbar)	965-980	22	971.7	5.1	-3.4	3.5	1.5	1.7
		980-989	9	983.8	2.2	-1.2	1.9	3.2	3.6
		989-1030	53	998.4	7.0	-4.4	4.9	-1.2	2.1
		all	84	989.8	13.2	-3.8	4.4	0.0	2.2
KMSY	Wind Speed (mph)	0-20	8	17.5	1.5	2.7	3.7	-0.6	1.7
		20-40	29	27.1	3.9	3.0	5.7	-2.0	5.4
		all	37	25.1	5.3	2.9	5.3	-1.7	4.8
	Wind Direction (deg)	0-45	16	19.4	6.8	-1.8	5.3	25.6	28.3
		270-315	12	291.7	10.3	4.1	16.3	5.0	22.3
		315-360	5	340.0	14.1	-3.3	9.3	12.5	14.2
		all	33	187.8	151.0	-0.1	10.5	15.6	23.4
	Pressure (mbar)	989-1030	37	1002.6	3.6	-2.9	3.2	-0.2	1.0
		all	37	1002.6	3.6	-2.9	3.2	-0.2	1.0
KPFN	Wind Speed (mph)	0-20	16	16.0	4.5	10.1	10.9	8.8	9.9
		20-40	38	26.8	5.7	6.1	8.8	6.2	8.3
		40-60	5	43.0	3.2	-3.6	11.2	-2.1	8.1
		all	59	25.2	8.9	6.3	9.6	6.2	8.7
	Wind Direction (deg)	45-90	1	80.0	0.0	7.5	7.5	31.5	31.5
		90-135	41	108.8	13.3	-5.8	9.5	9.5	13.5
		135-180	12	145.8	6.7	-23.6	25.0	-13.0	14.7
		180-225	1	220.0	0.0	-35.2	35.2	-22.0	22.0
		225-270	3	230.0	0.0	-39.2	39.3	-26.7	26.8
		all	58	128.1	45.9	-11.3	17.1	2.8	15.3
	Pressure (mbar)	989-1030	70	1004.5	3.4	-4.7	5.0	-1.8	2.0
		all	70	1004.5	3.4	-4.7	5.0	-1.8	2.0

Table P-3. Error Analysis of Wind Speeds, Wind Directions and Pressures for Hurricane Ivan (Continued)

Station	Range		Number of Data	Obs		SLOSH-Obs		ARA-Obs	
				Mean	Std	mean	RMS	mean	RMS
42007	Wind Speed (mph)	20-40	59	35.5	2.6	-0.7	2.2	-3.3	3.7
		40-60	82	50.6	5.4	12.8	15.6	1.4	6.0
		60-80	20	61.6	1.1	23.1	23.1	8.3	8.8
		all	161	46.4	9.9	9.2	13.8	0.5	5.8
	Wind Direction (deg)	0-45	52	26.7	12.3	14.0	15.1	28.9	29.6
		45-90	30	47.7	2.8	7.0	7.5	31.5	32.0
		225-270	34	258.9	4.2	11.4	11.6	15.7	16.0
		270-315	20	284.6	14.3	5.9	7.9	23.7	24.0
		315-360	19	339.4	12.0	-0.3	6.7	20.8	21.2
		all	155	161.0	132.6	9.2	11.3	24.8	26.0
	Pressure (mbar)	965-980	1	976.8	0.0	-0.4	0.4	2.7	2.7
		980-989	3	984.5	3.3	-1.3	1.8	1.0	1.3
		989-1030	10	1001.2	5.5	-3.3	3.5	0.6	1.0
		all	14	995.9	10.1	-2.7	3.1	0.8	1.3
42036	Wind Speed (mph)	20-40	169	34.8	2.7	-5.4	6.4	0.0	2.9
		40-60	11	41.0	0.7	-8.8	8.9	-5.9	6.2
		all	180	35.2	3.0	-5.6	6.6	-0.4	3.2
	Wind Direction (deg)	90-135	64	114.5	10.0	30.0	30.3	39.4	39.6
		135-180	77	155.7	13.7	25.4	25.8	26.9	27.3
		180-225	39	182.2	2.4	29.7	30.1	26.9	27.3
		all	180	146.8	28.2	28.0	28.4	31.4	32.2
	Pressure (mbar)	989-1030	30	1007.1	1.5	-4.4	4.4	-1.7	2.3
		all	30	1007.1	1.5	-4.4	4.4	-1.7	2.3
BURL1	Wind Speed (mph)	20-40	48	32.0	4.2	-3.9	4.4	-4.8	5.1
		40-60	75	48.8	5.4	3.4	6.5	-4.5	5.5
		60-80	22	67.1	3.7	5.0	5.6	-5.4	5.7
		all	145	46.0	12.6	1.2	5.7	-4.7	5.4
	Wind Direction (deg)	0-45	18	36.4	6.7	-19.0	19.2	-6.6	7.2
		45-90	18	56.9	7.1	-28.1	28.6	-11.1	12.1
		270-315	79	284.1	9.8	-6.2	7.6	-4.6	11.1
		315-360	29	340.5	13.0	-18.6	19.8	-4.8	7.4
		all	144	236.9	112.5	-13.0	16.1	-5.6	10.2
	Pressure (mbar)	980-989	4	985.4	1.7	-0.4	1.2	1.6	1.8
		989-1030	21	999.6	5.2	-2.4	2.5	0.2	1.2
		all	25	997.3	7.1	-2.0	2.3	0.4	1.3

Table P-3. Error Analysis of Wind Speeds, Wind Directions and Pressures for Hurricane Ivan (Continued)

Station	Range		Number of Data	Obs		SLOSH-Obs		ARA-Obs	
				Mean	Std	mean	RMS	mean	RMS
DPIA1	Wind Speed (mph)	0-20	8	2.4	6.8	0.6	1.7	1.9	5.5
		20-40	95	32.1	4.4	6.5	11.7	10.0	12.3
		40-60	35	49.5	5.3	4.4	10.3	9.3	13.4
		60-80	31	67.9	3.9	-2.0	13.3	2.1	16.9
		all	169	40.8	16.9	4.2	11.5	8.0	13.2
	Wind Direction (deg)	0-45	24	37.2	8.1	18.4	18.7	36.2	36.3
		45-90	63	55.0	3.2	2.7	4.7	28.5	29.4
		225-270	67	246.0	9.1	5.9	10.7	19.2	19.7
		270-315	4	296.3	16.2	21.8	22.4	14.0	14.9
		315-360	3	334.3	14.5	21.3	21.4	22.1	22.2
		all	161	153.3	110.2	7.0	11.2	24.3	26.2
	Pressure (mbar)	945-965	2	954.5	2.5	-5.7	5.7	-3.2	3.2
		965-980	4	971.1	5.0	-7.5	7.7	-3.6	4.4
		980-989	4	984.0	3.2	-3.7	4.6	-0.2	3.6
		989-1030	16	1000.5	6.1	-3.2	4.1	-0.4	1.6
		all	26	989.9	16.1	-4.1	5.0	-1.1	2.7
GDIL1	Wind Speed (mph)	0-20	12	18.3	0.9	-3.5	3.7	4.2	4.3
		20-40	122	30.9	5.0	-2.6	3.8	0.8	2.5
		40-60	46	43.4	2.5	-1.1	2.3	3.1	3.7
		all	180	33.3	8.0	-2.3	3.5	1.6	3.0
	Wind Direction (deg)	0-45	57	18.0	12.0	-6.7	8.6	22.4	23.1
		225-270	40	264.0	5.6	8.6	9.6	10.7	12.1
		270-315	46	284.7	15.7	8.7	10.6	25.8	27.0
		315-360	36	344.2	12.5	-11.1	12.5	10.1	11.0
		all	179	207.9	133.1	-0.2	10.2	18.2	20.3
	Pressure (mbar)	989-1030	30	1000.6	4.3	-2.6	2.8	0.0	1.0
		all	30	1000.6	4.3	-2.6	2.8	0.0	1.0
SGOF	Wind Speed (mph)	20-40	105	37.7	1.7	-8.1	8.6	-3.3	4.4
		40-60	57	42.9	1.9	-5.8	6.4	-0.9	3.0
		all	162	39.5	3.1	-7.3	7.9	-2.4	4.0
	Wind Direction (deg)	90-135	56	114.0	8.0	14.7	15.5	28.2	28.5
		135-180	73	157.6	13.9	14.2	14.7	16.6	16.9
		180-225	33	185.2	3.6	21.3	21.4	20.8	20.9
		all	162	148.1	29.0	15.8	16.6	21.5	22.3
	Pressure (mbar)	989-1030	27	1007.6	1.7	-5.7	5.8	-3.2	3.3
		all	27	1007.6	1.7	-5.7	5.8	-3.2	3.3
KDTS	Wind Speed (mph)	0-20	4	13.3	8.9	6.0	7.1	10.0	11.7
		20-40	24	28.0	5.1	9.8	10.3	17.4	17.9
		40-60	6	43.8	4.9	7.2	7.8	15.1	15.4
		all	34	29.1	10.0	8.9	9.6	16.1	16.8
	Wind Direction (deg)	45-90	12	75.8	5.1	10.3	12.7	40.2	40.5
		90-135	21	98.1	10.8	3.4	10.7	23.5	25.2
		all	33	97.9	48.4	5.7	11.3	28.7	31.2
	Pressure (mbar)	989-1030	33	1002.1	4.6	-5.2	5.3	-1.8	1.9
		all	33	1002.1	4.6	-5.2	5.3	-1.8	1.9

Table P-3. Error Analysis of Wind Speeds, Wind Directions and Pressures for Hurricane Ivan (Continued)

Station	Range		Number of Data	Obs		SLOSH-Obs		ARA-Obs	
				Mean	Std	mean	RMS	mean	RMS
KGPT	Wind Speed (mph)	0-20	7	17.6	1.1	7.3	7.6	1.8	2.9
		20-40	25	32.1	5.9	10.4	11.3	4.6	5.9
		40-60	6	43.5	2.3	11.1	11.6	3.7	4.8
		all	38	31.2	9.2	10.0	10.8	3.9	5.3
	Wind Direction (deg)	0-45	26	27.3	12.2	4.5	7.1	21.4	22.9
		45-90	3	50.0	0.0	-9.0	9.1	15.8	16.5
		315-360	7	350.0	0.0	6.9	9.5	18.6	19.2
		all	36	106.1	139.5	4.1	7.9	20.3	21.6
	Pressure (mbar)	980-989	6	987.0	1.3	-2.2	2.3	1.3	1.6
		989-1030	32	1000.1	6.0	-4.1	4.2	-0.9	1.0
		all	38	998.0	7.4	-3.8	4.0	-0.5	1.1
KVPS	Wind Speed (mph)	0-20	14	16.7	4.9	8.1	9.1	7.4	8.6
		20-40	19	26.2	5.2	9.4	9.9	9.7	10.2
		40-60	8	50.9	6.5	5.0	6.3	3.9	5.6
		60-80	4	65.3	3.6	-6.3	6.9	-7.9	8.3
		all	45	31.1	16.7	6.8	8.9	6.4	8.8
	Wind Direction (deg)	45-90	28	73.9	6.3	12.0	13.2	33.7	34.2
		90-135	13	103.8	14.5	6.6	9.3	16.5	18.0
		135-180	2	140.0	0.0	-5.9	8.1	4.1	6.6
		180-225	1	200.0	0.0	7.0	7.0	16.2	16.2
		all	44	94.7	48.2	9.3	11.7	26.3	28.8
	Pressure (mbar)	989-1030	44	1002.5	6.1	-5.5	5.6	-2.2	2.3
		all	44	1002.5	6.1	-5.5	5.6	-2.2	2.3
All Stations	Wind Speed (mph)	0-20	104	17.4	1.5	7.7	9.6	6.5	8.2
		20-40	909	32.4	5.3	1.2	9.2	2.6	7.6
		40-60	429	47.5	5.7	5.8	11.6	2.1	7.9
		60-80	88	65.8	4.1	7.2	14.8	2.0	11.8
		all	1530	37.6	12.0	3.3	10.3	2.7	8.0
	Wind Direction (deg)	0-45	228	26.0	12.7	2.8	13.7	23.5	26.9
		45-90	281	61.2	10.4	1.9	14.0	22.1	28.1
		90-135	225	109.9	12.0	9.2	21.6	21.4	29.1
		135-180	170	155.6	13.7	15.8	21.0	18.7	21.9
		180-225	109	192.2	14.1	15.1	22.1	17.7	20.5
		225-270	188	252.4	10.7	6.8	14.1	14.4	17.9
		270-315	193	285.3	12.5	2.3	13.4	11.3	26.2
		315-360	116	342.0	12.3	-6.9	15.0	11.3	17.2
		all	1510	159.9	105.5	5.6	16.8	18.3	24.8
	Pressure (mbar)	920-945	11	935.7	6.3	15.5	15.8	18.2	18.5
		945-965	21	956.3	5.0	13.2	15.3	17.5	19.5
		965-980	76	972.2	4.1	4.5	9.7	8.0	11.1
		980-989	53	984.9	2.6	-0.4	3.4	3.0	4.5
		989-1030	544	1001.6	5.6	-3.6	4.4	-0.7	2.3
		all	705	994.8	15.0	-1.7	6.1	1.3	6.0

Appendix Q. Comparisons of Modeled and Measured Wind Speeds, Wind Directions, and Pressures for Hurricane Katrina (2005)

This appendix presents comparisons of modeled and observed wind speeds, wind direction, and pressures at multiple locations along the Mississippi Coast and some buoy locations during the passage of Hurricane Katrina (2005).

Figure Q-1 shows the maximum 10-minute mean wind speeds obtained from two versions of SLOSH model. The first version uses ARA storm track and ARA wind field model (denoted as ARA-TRK-ARA-WD), and the second version uses ARA storm track and SLSOH wind field model (denoted as ARA-TRK-SLOSH-WD).

Figure Q-2 shows the simulated wind field for the Mississippi Gulf Coast SLOSH basin. The maximum values of wind speeds are 124 and 107 mph for model run using SLOSH wind field model and model run using ARA wind field model, respectively.

Figure Q-3 shows a map of the locations of all observing stations as well as the hurricane track. The observed wind speeds and pressures are compared to the simulated wind speeds and pressures from model runs using the ARA-TRK-ARA-WD and ARA-TRK-SLOSH-WD models, as shown in Table Q-1 and Table Q-2.

Figure Q-4 presents the comparisons of modeled and observed maximum wind speeds and minimum pressures for Hurricane Katrina. The results indicate that the simulated wind speeds from model runs using ARA-TRK-ARA-WD are more comparable to the observed data than those from model runs using ARA-TRK-SLOSH-WD.

Comparisons of the entire modeled and observed time series of mean wind speeds, wind directions, and pressures for all stations, both complete and incomplete, are presented in Figure Q-5. The RMS errors of wind speed, wind direction, and central pressure are shown in Table Q-3.

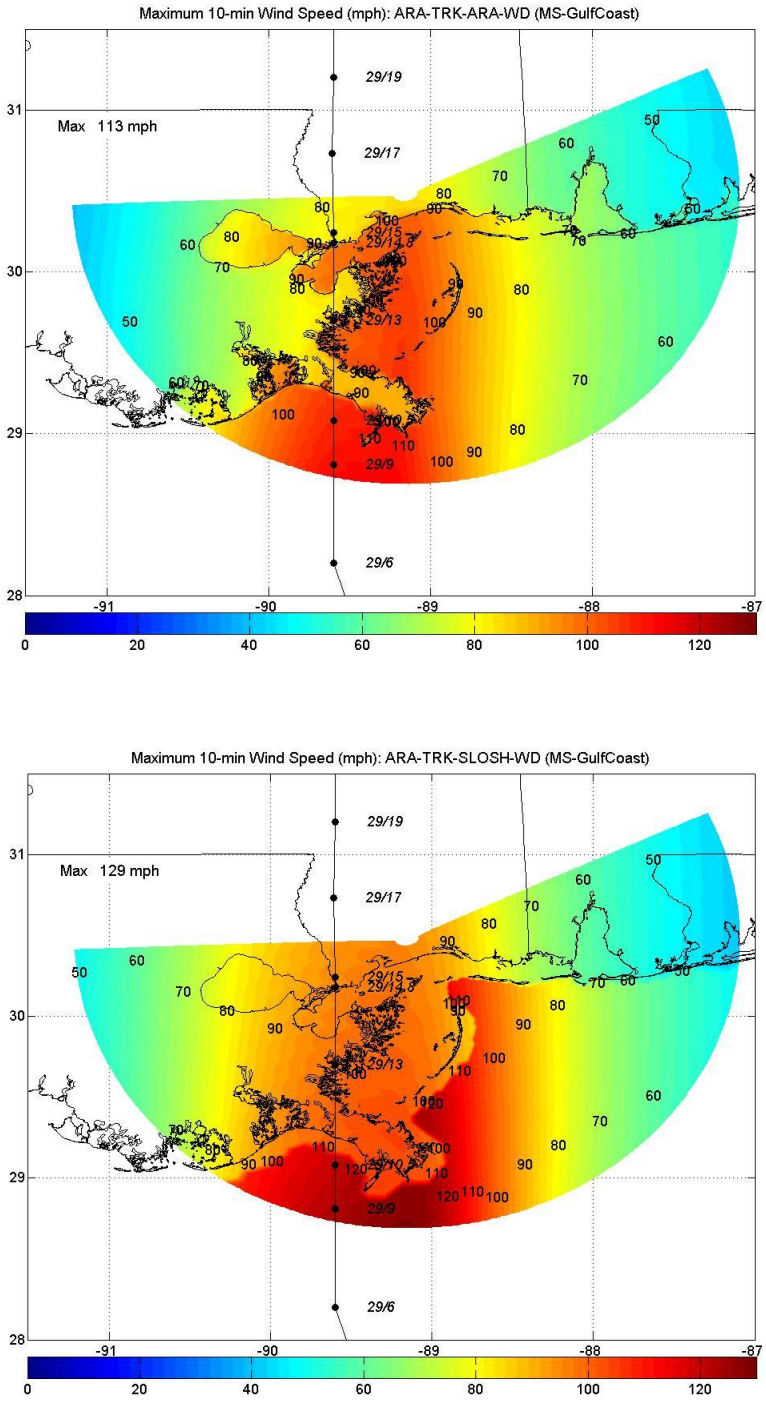

Figure Q-1. Modeled Maximum 10-min Wind Speeds (mph) for Hurricane Katrina (2005) – MS Gulf Coast Basin

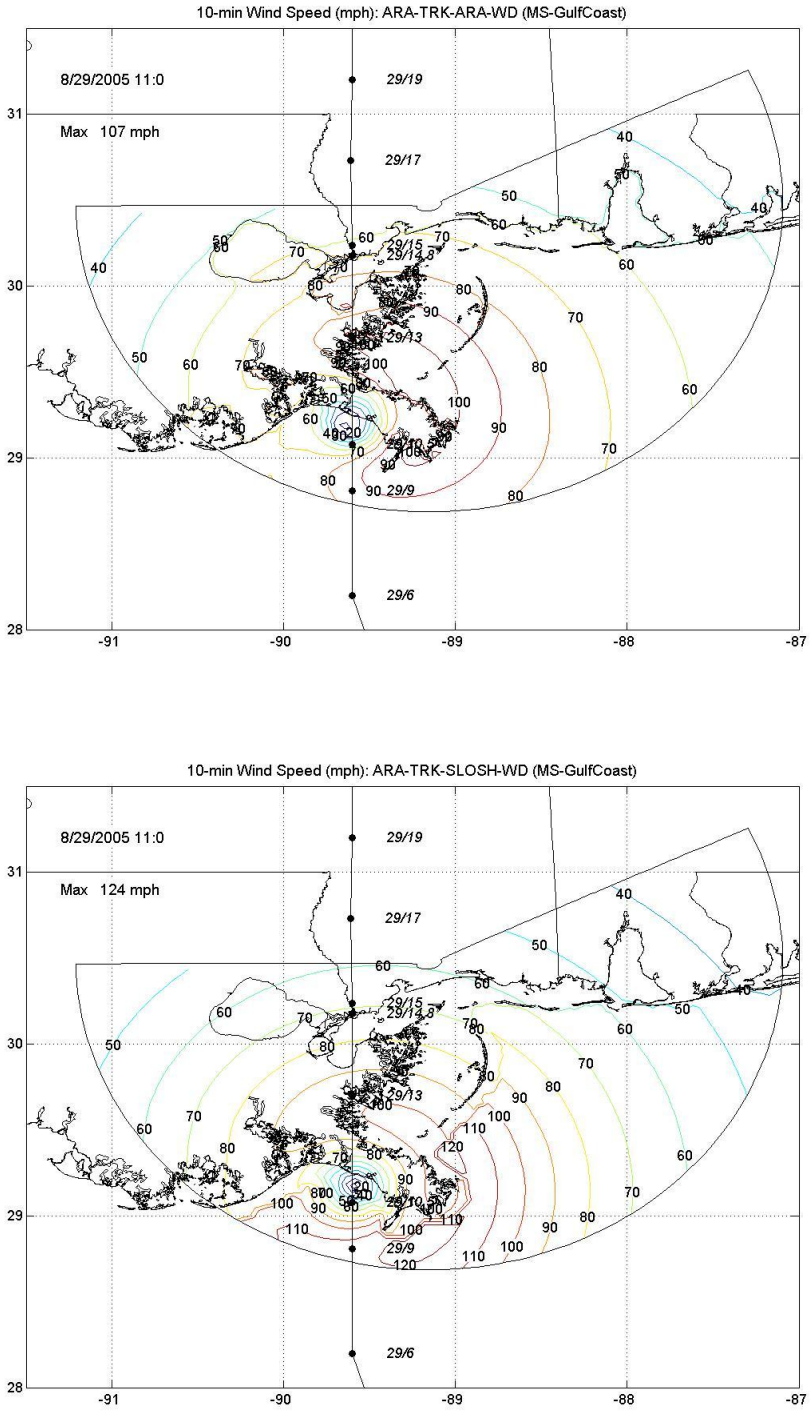

Figure Q-2. Hurricane Katrina (2005) Modeled 10-minWind Speeds (mph) at Landfall – MS Gulf Coast Basin

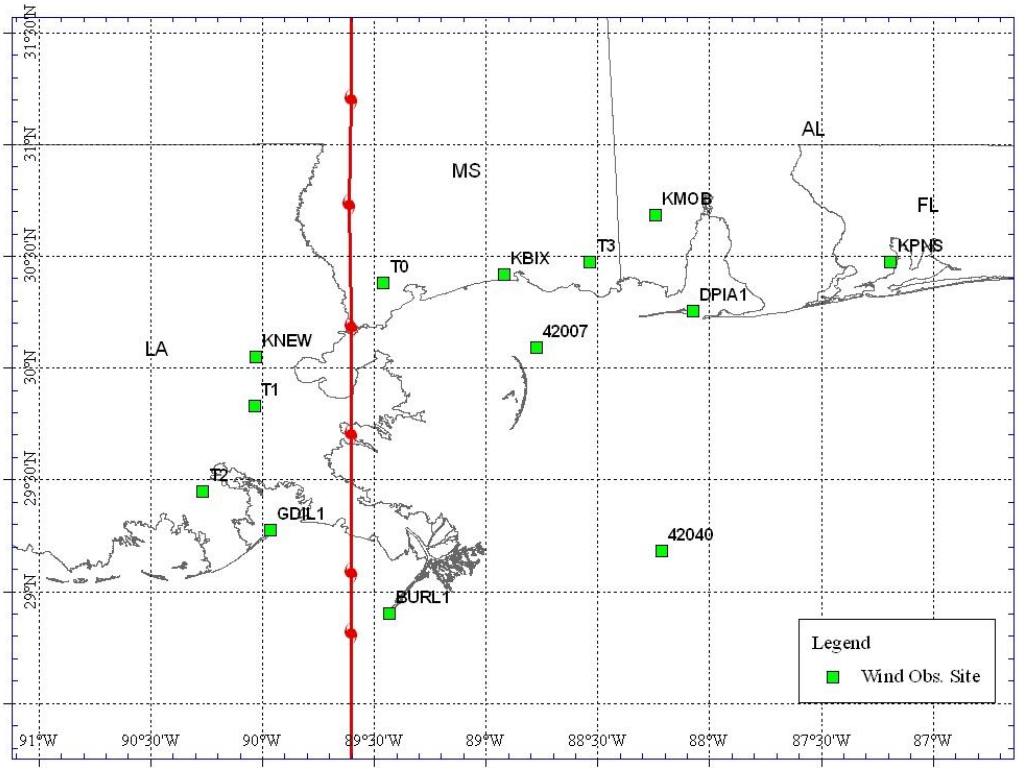

Figure Q-3. Wind Observation Locations for Hurricane Katrina (2005)

Table Q-1. Summary Comparison of Modeled and Observed Maximum 10-min Wind Speeds for Hurricane Katrina

No.	Station Name	lat	long	Max Wind Speed (mph)		
				ARA-TRK-SLOSH-WD	ARA-TRK-ARA-WD	Obs.
1	FCMP T0	30.380080	89.455140	95.6	82.3	N/A
2	FCMP T1	29.825278	-90.031940	88.7	74.7	66.6
3	FCMP T2	29.444000	-90.263000	83.4	70.2	63.1
4	FCMP T3	30.472000	-88.531000	75.8	69.1	65.4
5	KMOB	30.680000	-88.240000	65.8	62	63
6	KPNS	30.473306	-87.187444	43.2	45.8	53
7	DPIA1	30.250000	-88.070000	60.9	69.6	73.5
8	42040	29.180000	-88.210000	80.1	73.1	68.3
9	KNEW	30.049000	90.029000	87.6	79.9	N/A
10	BURL1	28.900000	89.430000	105.8	111.1	N/A
11	42007	30.090000	88.770000	107.4	90.7	N/A
12	KBIX	30.416000	88.916730	90.8	81.7	N/A
13	GDIL1	29.270000	89.960000	94.6	95.7	N/A

Table Q-2. Summary Comparison of Modeled and Observed Minimum Pressures for Hurricane Katrina

No.	Station Name	lat	long	Min Central Pressure (mbar)		
				ARA-TRK-SLOSH-WD	ARA-TRK-ARA-WD	Obs.
1	FCMP T0	30.380080	89.455140	931.7	932.5	N/A
2	FCMP T1	29.825278	-90.031940	947.5	948.8	949.3
3	FCMP T2	29.444000	-90.263000	961.5	961.4	961.1
4	FCMP T3	30.472000	-88.531000	976.3	976.2	978
5	KMOB	30.680000	-88.240000	981.5	981.5	984
6	KPNS	30.473306	-87.187444	992	991.8	995
7	DPIA1	30.250000	-88.070000	984.7	984.1	986.1
8	42040	29.180000	-88.210000	982.8	981.8	979.3
9	KNEW	30.049000	90.029000	948.5	950.2	N/A
10	BURL1	28.900000	89.430000	922.9	920.7	N/A
11	42007	30.090000	88.770000	969.4	969.7	N/A
12	KBIX	30.416000	88.916730	964.3	964.7	N/A
13	GDIL1	29.270000	89.960000	942.5	941.7	944.3

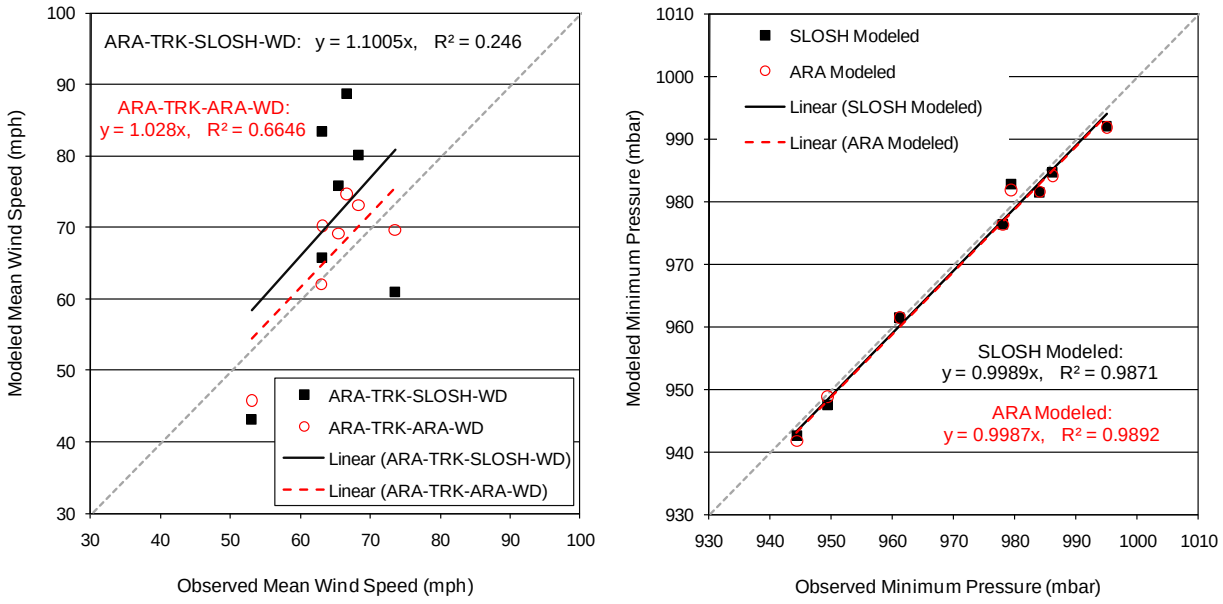

Figure Q-4. Comparisons of Modeled and Observed Maximum 10-min Wind Speeds and Minimum Pressures for Hurricane Katrina

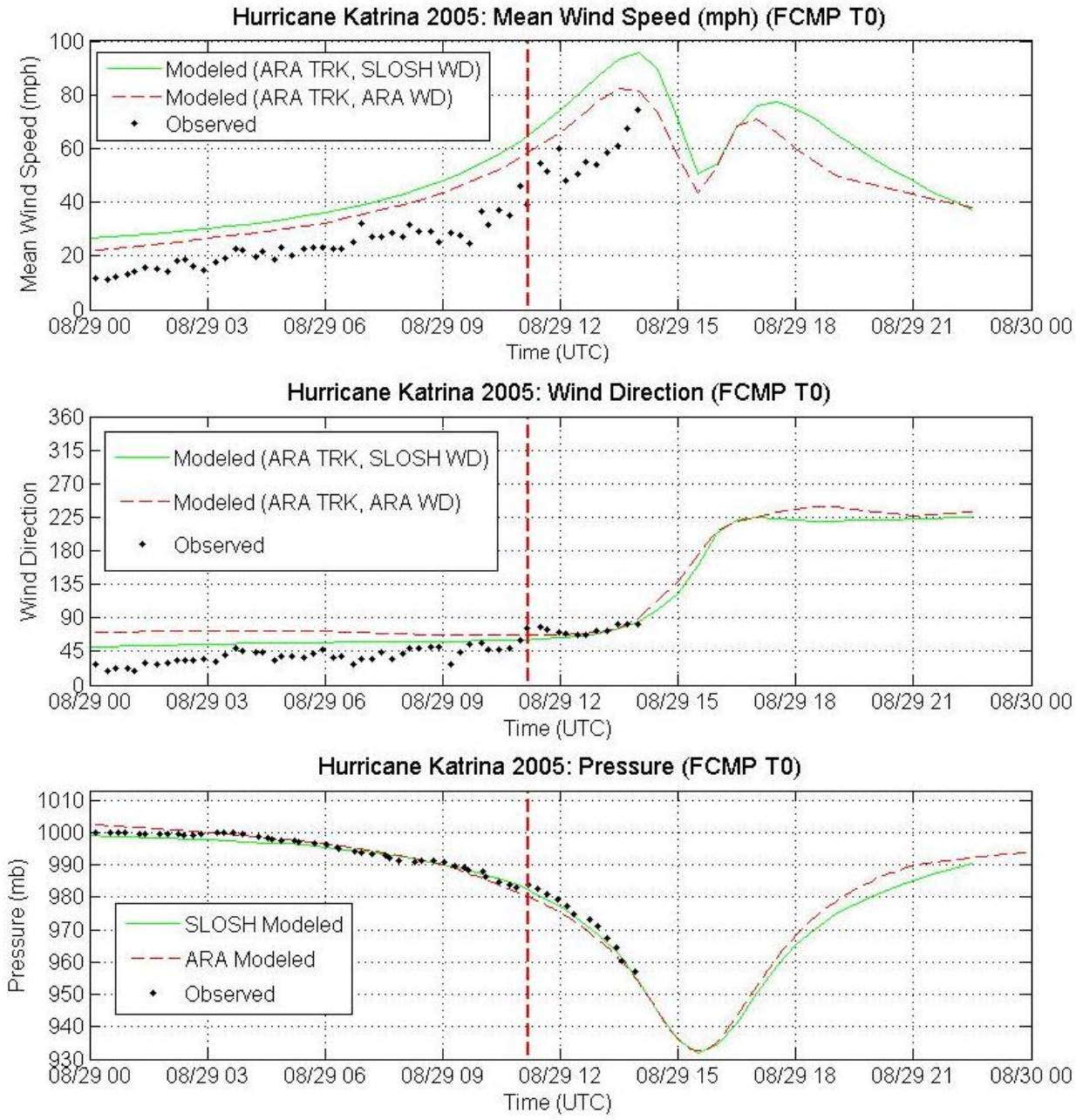

Figure Q-5a. Comparisons of Observed and Modeled Time Series Traces of Mean Wind Speeds, Wind Directions, and Pressures for Hurricane Katrina (2005) – FCMP T0

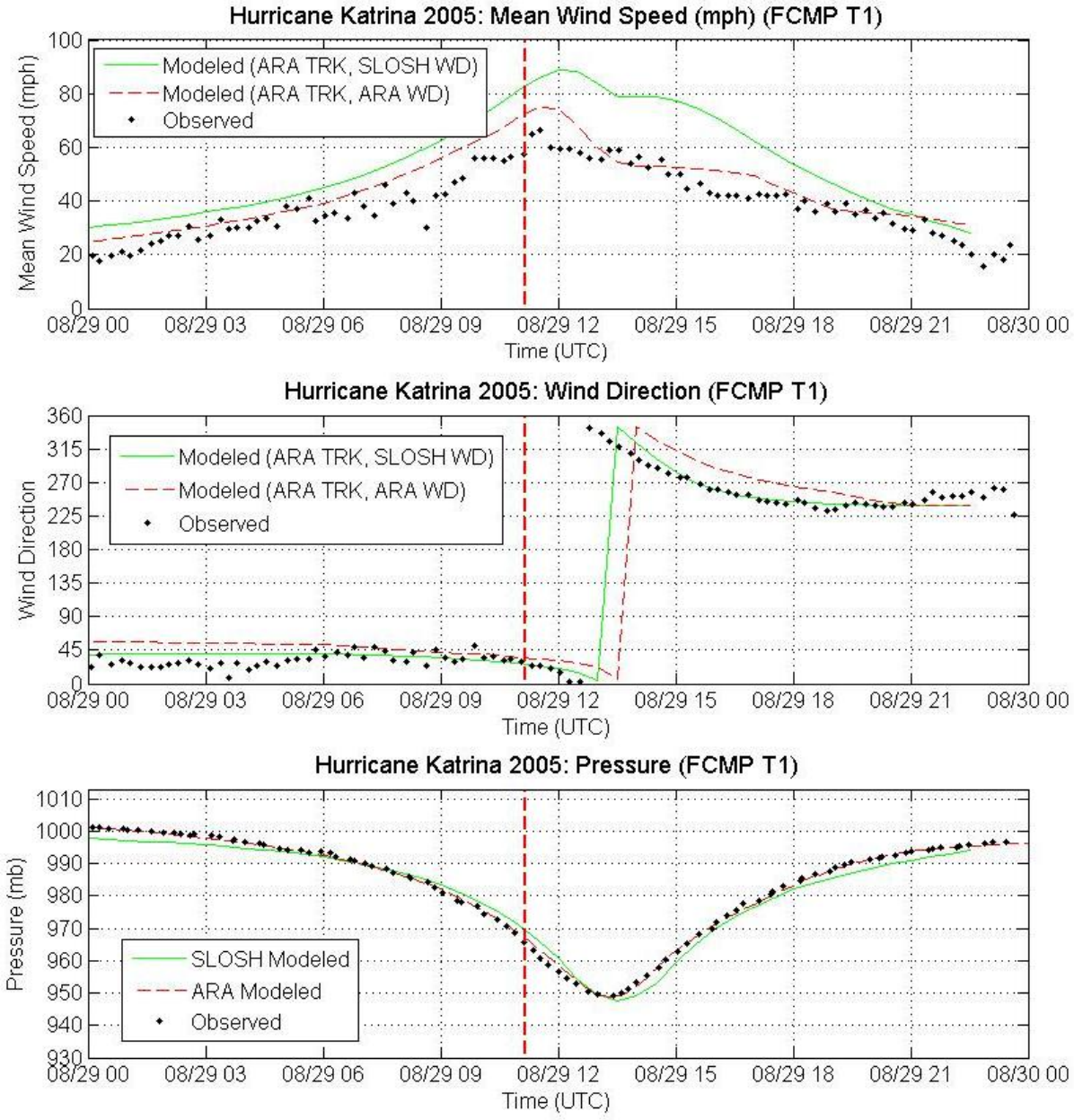

Figure Q-5b. Comparisons of Observed and Modeled Time Series Traces of Mean Wind Speeds, Wind Directions, and Pressures for Hurricane Katrina (2005) – FCMP T1

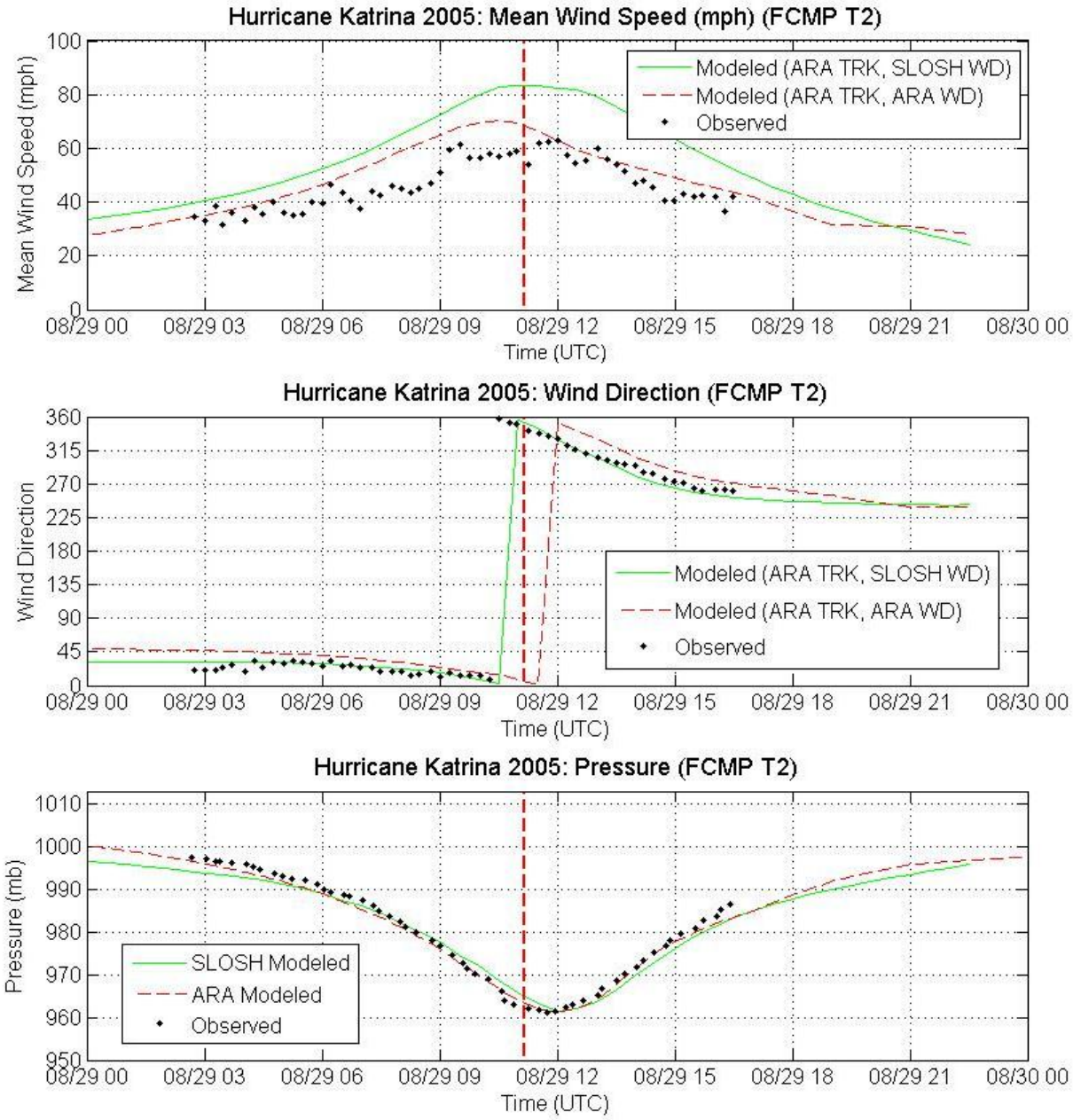

Figure Q-5c. Comparisons of Observed and Modeled Time Series Traces of Mean Wind Speeds, Wind Directions, and Pressures for Hurricane Katrina (2005) – FCMP T2

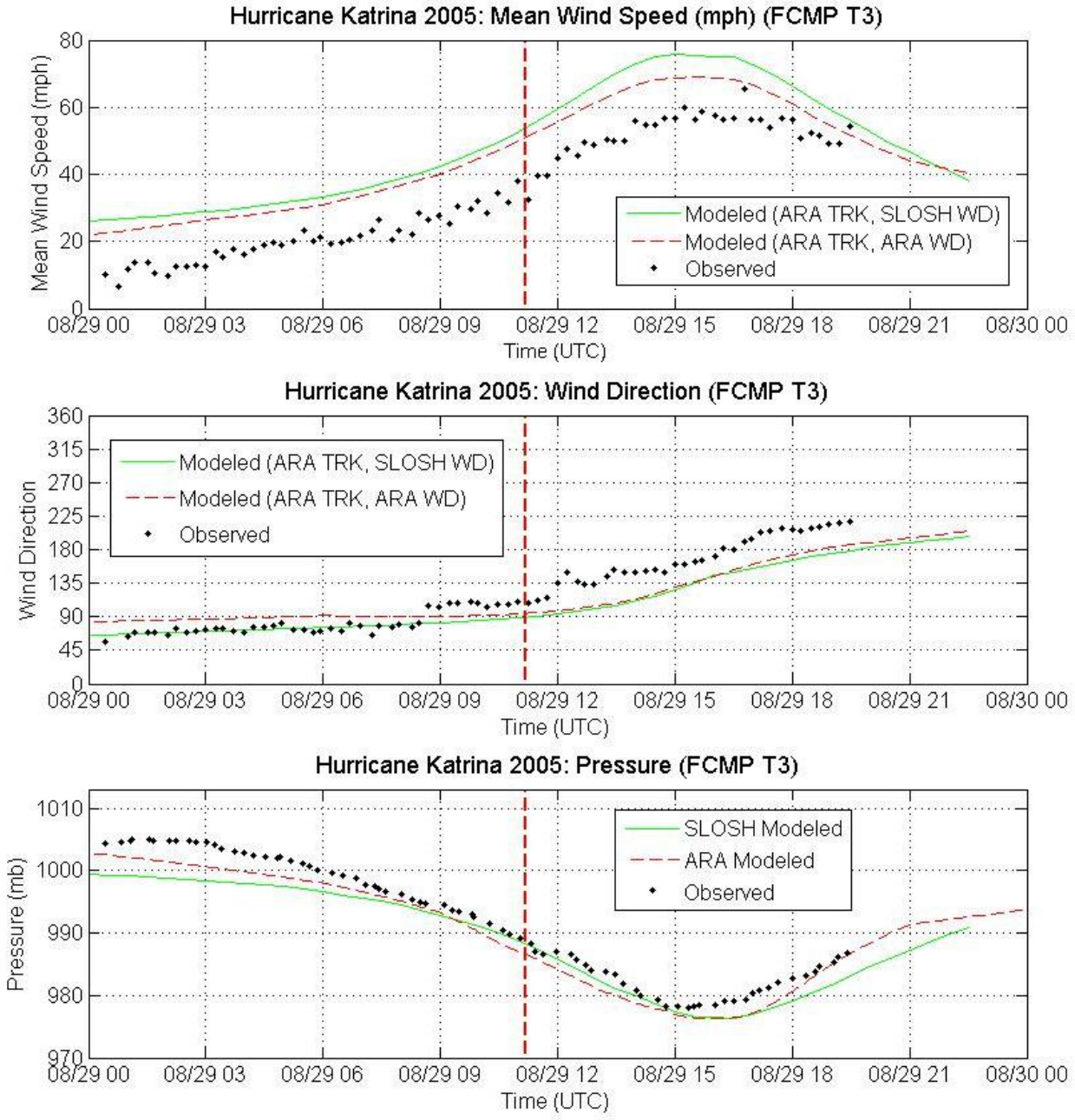

Figure Q-5d. Comparisons of Observed and Modeled Time Series Traces of Mean Wind Speeds, Wind Directions, and Pressures for Hurricane Katrina (2005) – FCMP T3

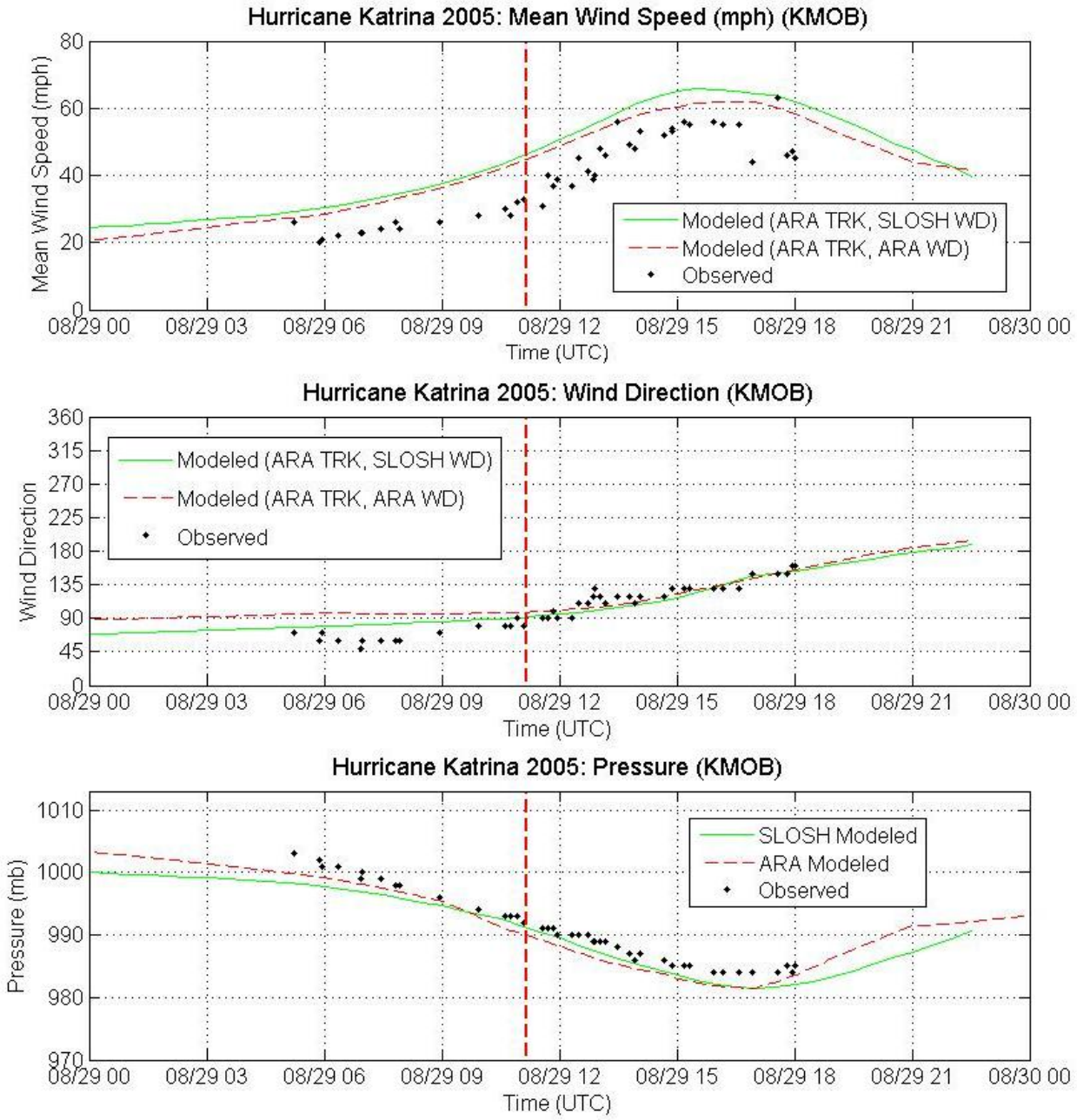

Figure Q-5e. Comparisons of Observed and Modeled Time Series Traces of Mean Wind Speeds, Wind Directions, and Pressures for Hurricane Katrina (2005) – KMOB

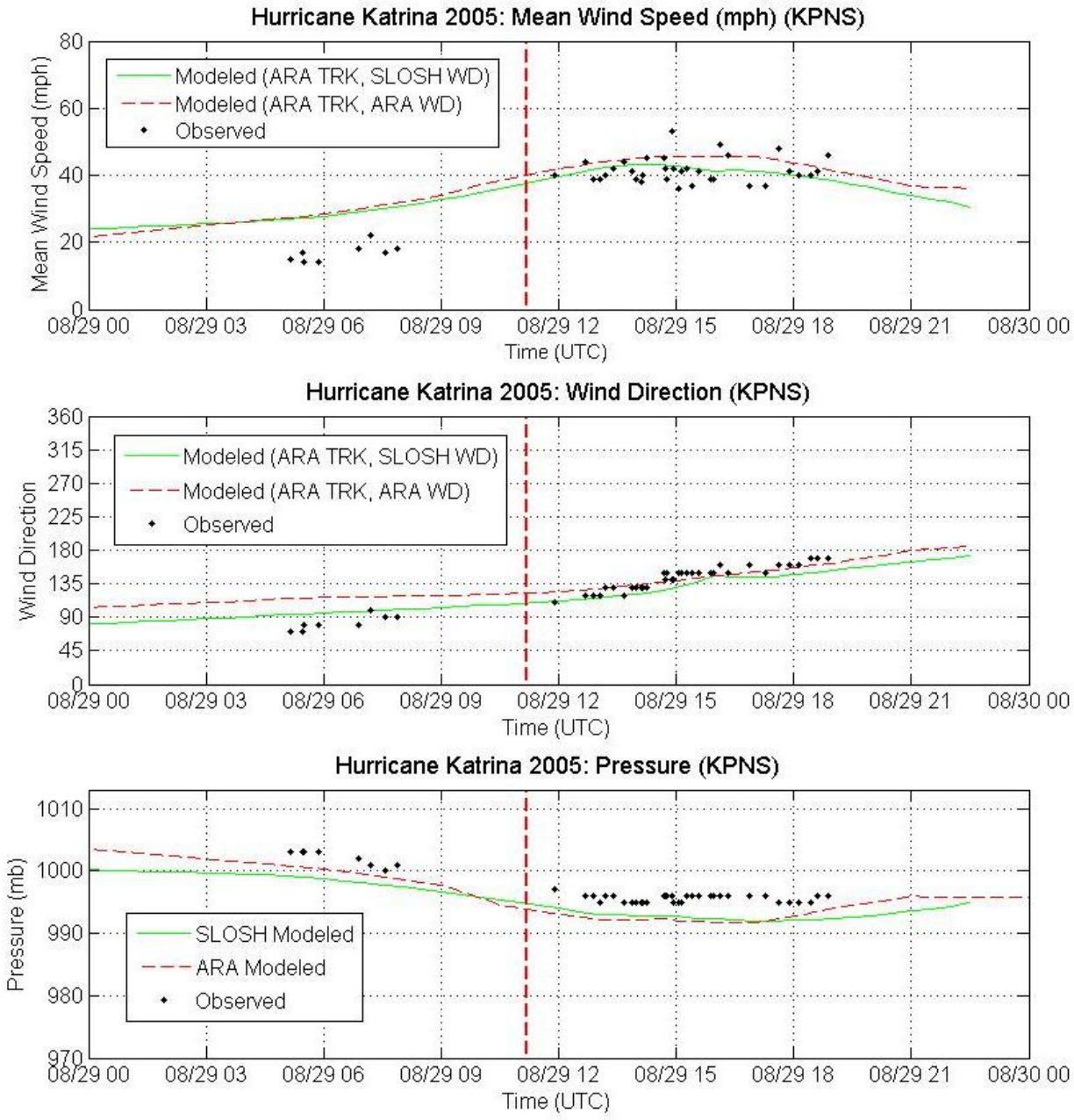

Figure Q-5f. Comparisons of Observed and Modeled Time Series Traces of Mean Wind Speeds, Wind Directions, and Pressures for Hurricane Katrina (2005) – KPNS

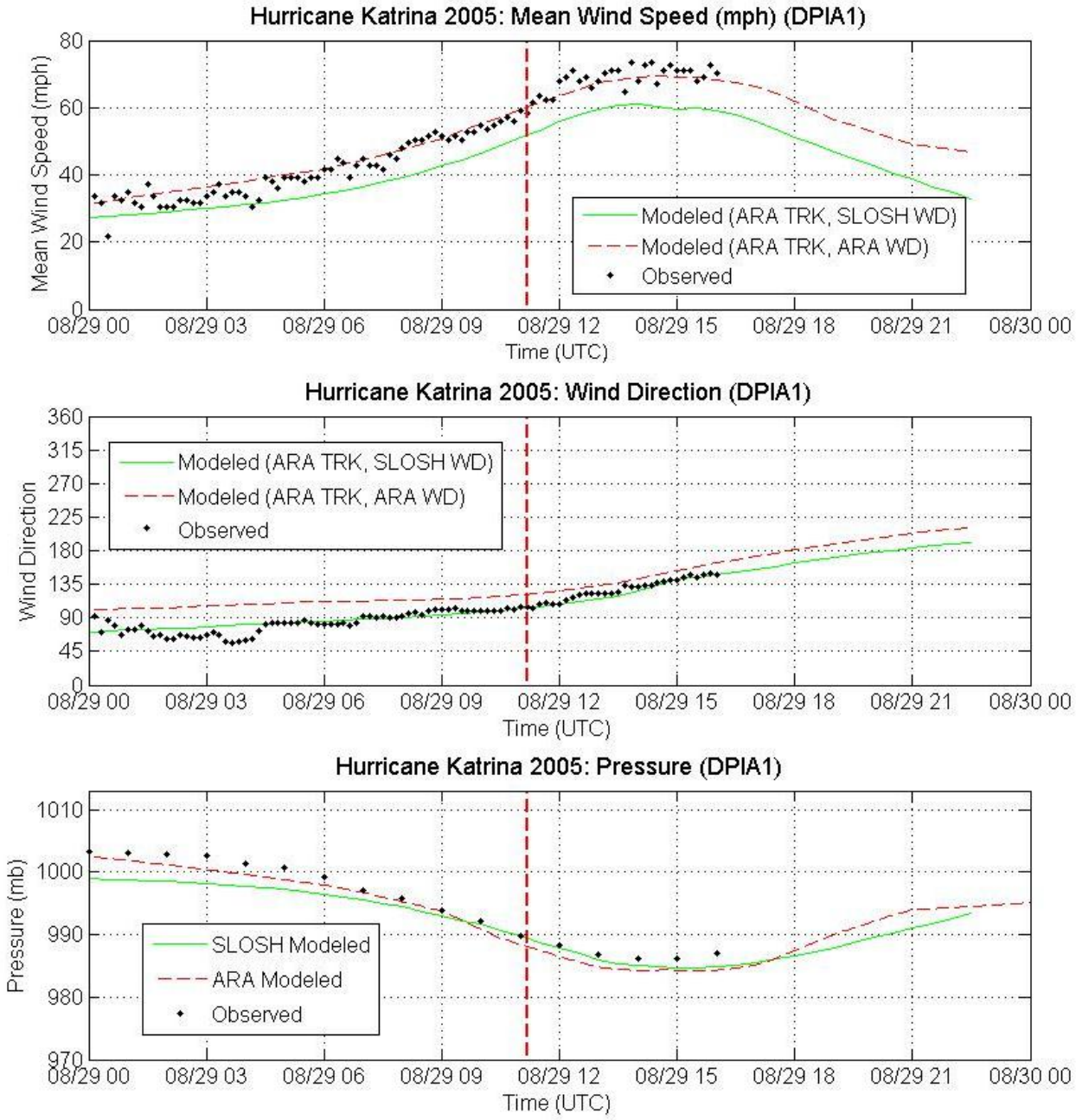

Figure Q-5g. Comparisons of Observed and Modeled Time Series Traces of Mean Wind Speeds, Wind Directions, and Pressures for Hurricane Katrina (2005) – DPIA1

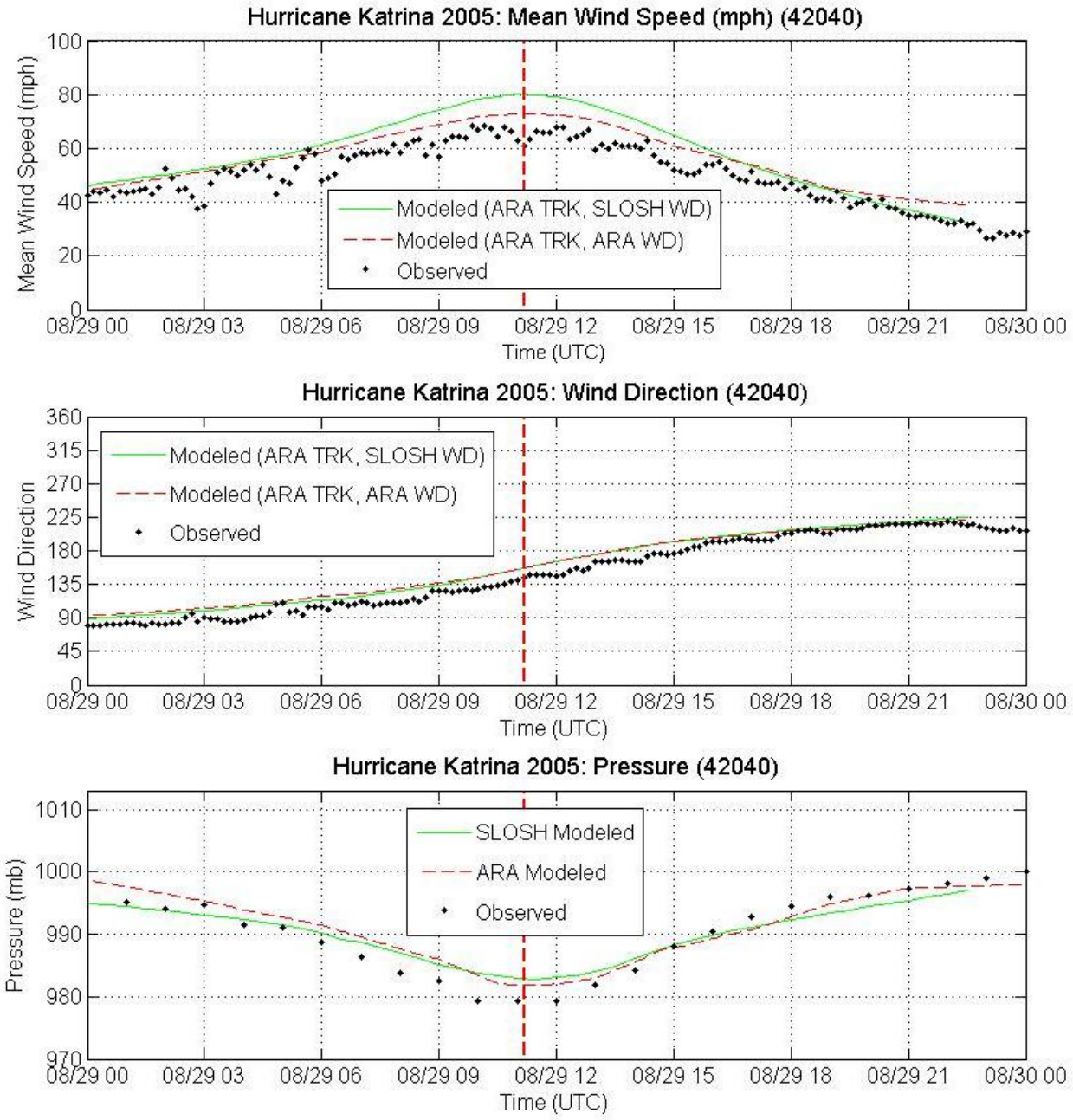

Figure Q-5h. Comparisons of Observed and Modeled Time Series Traces of Mean Wind Speeds, Wind Directions, and Pressures for Hurricane Katrina (2005) – 42040

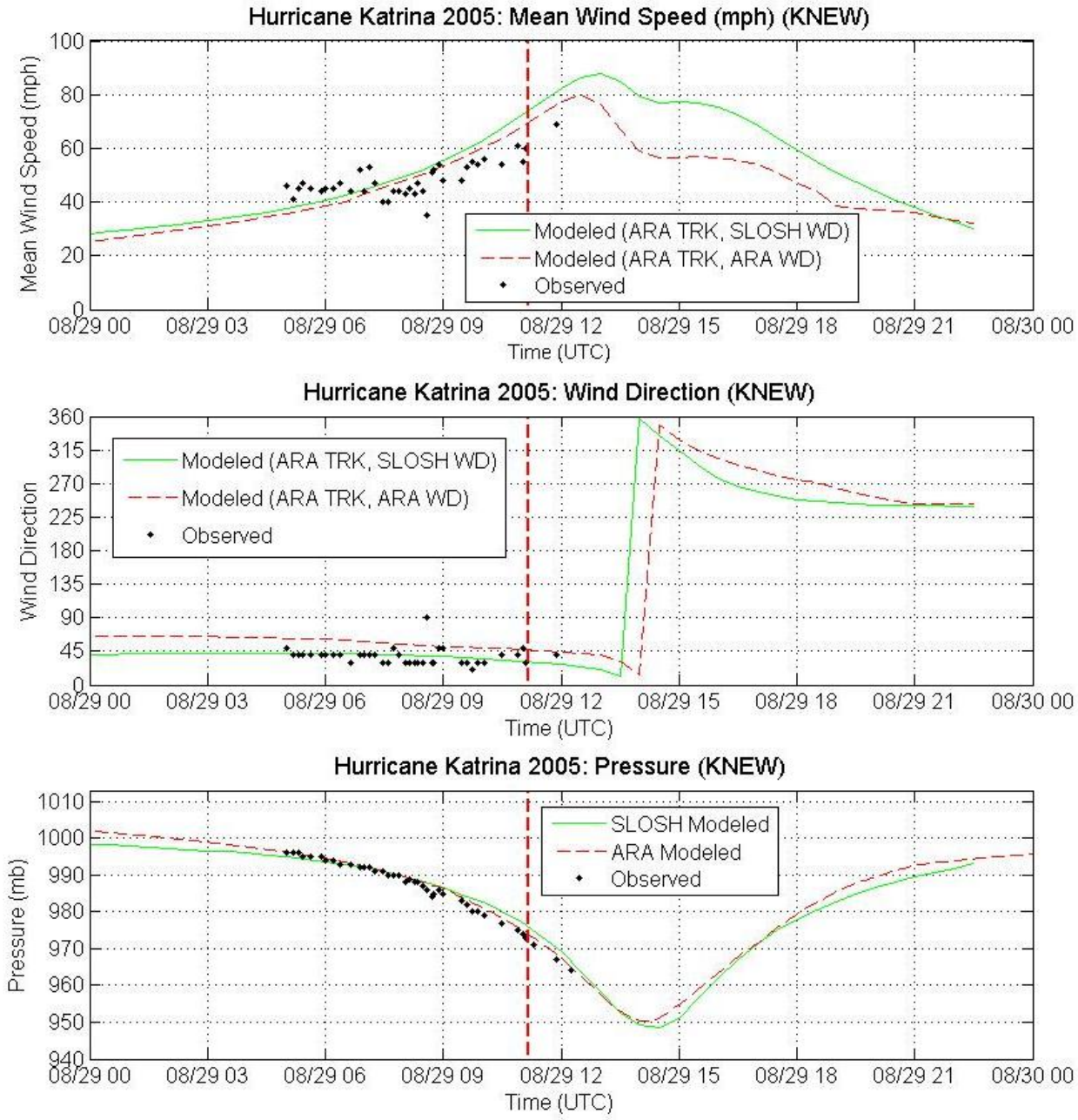

Figure Q-5i. Comparisons of Observed and Modeled Time Series Traces of Mean Wind Speeds, Wind Directions, and Pressures for Hurricane Katrina (2005) – KNEW

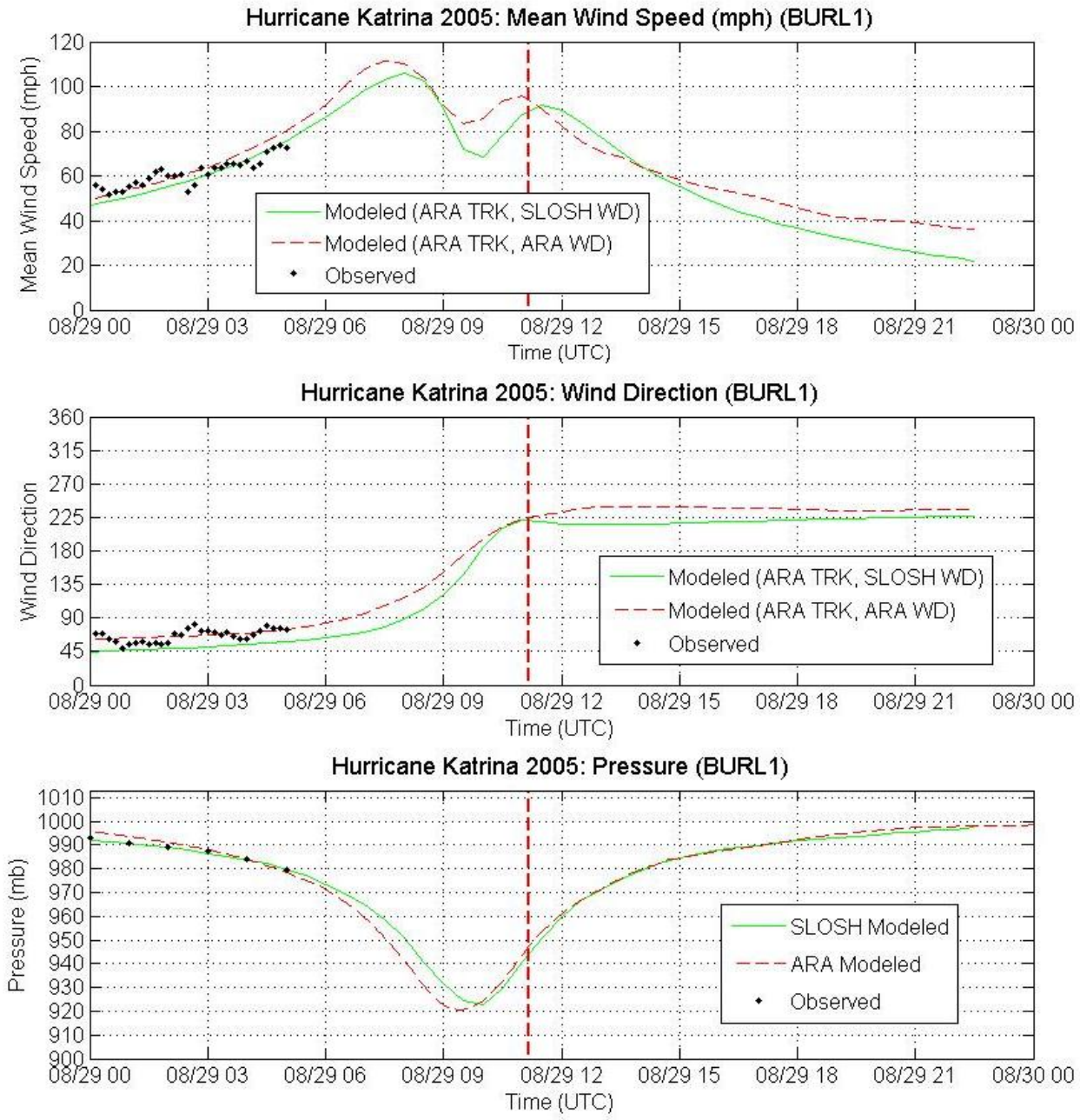

Figure Q-5j. Comparisons of Observed and Modeled Time Series Traces of Mean Wind Speeds, Wind Directions, and Pressures for Hurricane Katrina (2005) – BURL1

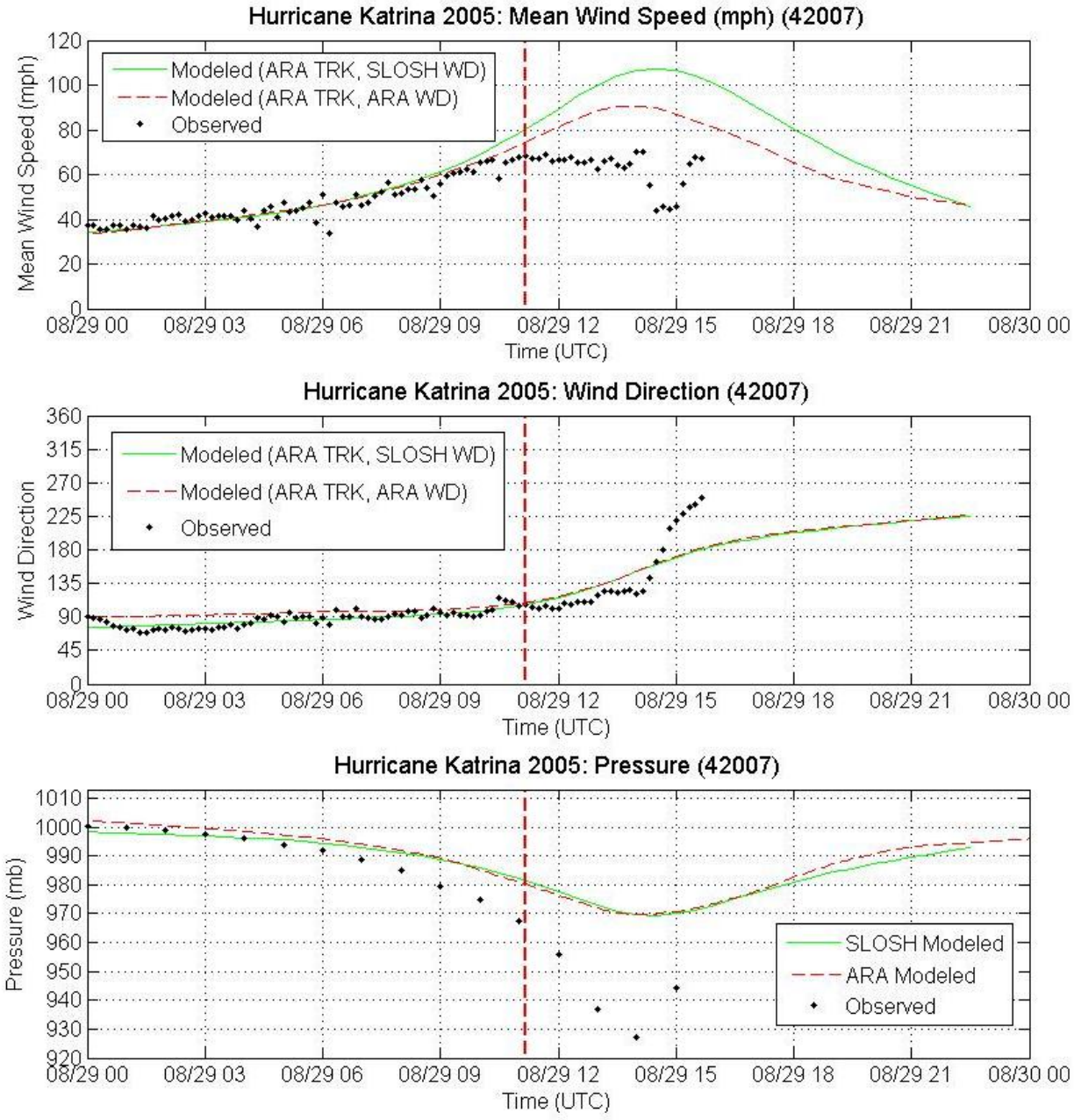

Figure Q-5k. Comparisons of Observed and Modeled Time Series Traces of Mean Wind Speeds, Wind Directions, and Pressures for Hurricane Katrina (2005) – 42007

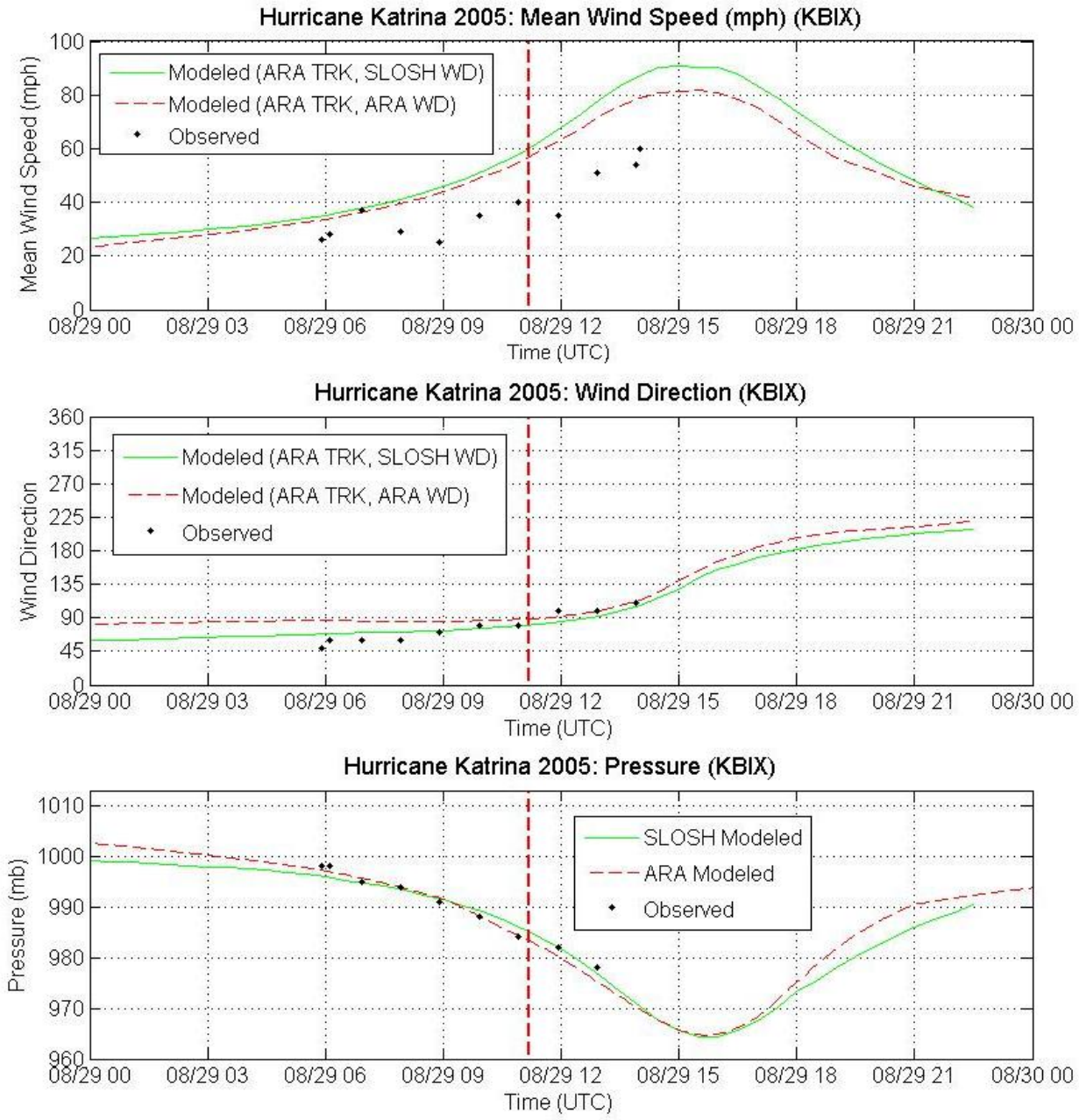

Figure Q-5l. Comparisons of Observed and Modeled Time Series Traces of Mean Wind Speeds, Wind Directions, and Pressures for Hurricane Katrina (2005) – KBIX

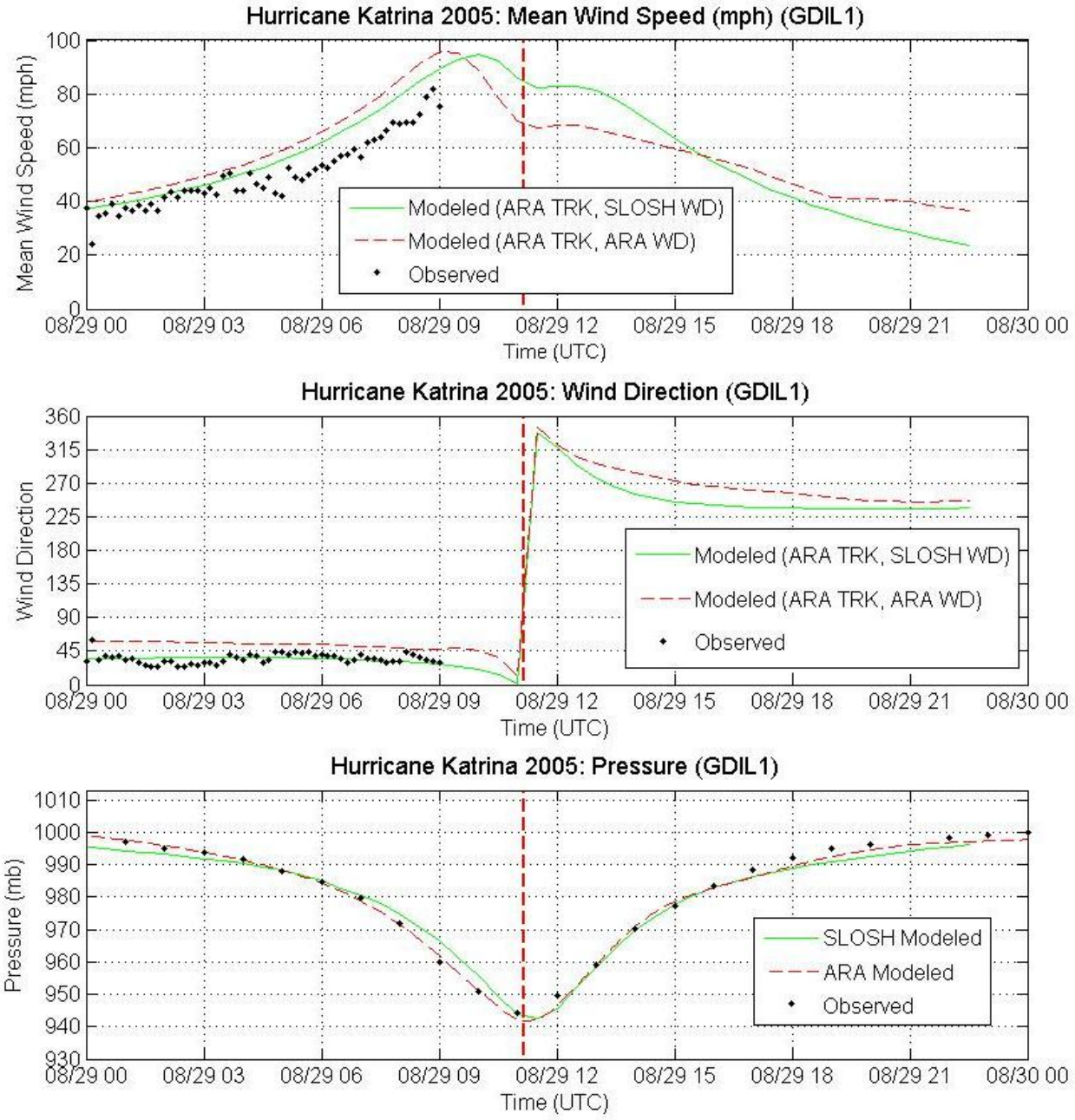

Figure Q-5m. Comparisons of Observed and Modeled Time Series Traces of Mean Wind Speeds, Wind Directions, and Pressures for Hurricane Katrina (2005) – GDIL1

Table Q-3. Error Analysis of Wind Speeds, Wind Directions and Pressures for Hurricane Katrina

Station	Range		Number of Data	Obs		SLOSH-Obs		ARA-Obs	
				Mean	Std	mean	RMS	mean	RMS
FCMP T0	Wind Speed (mph)	0-20	16	15.6	2.8	13.6	13.6	9.6	9.7
		20-40	28	27.4	5.2	16.0	16.9	11.8	12.7
		40-60	9	53.1	4.5	23.5	24.6	15.4	16.7
		60-80	3	67.7	6.8	26.4	26.8	14.0	15.2
		all	56	30.3	15.8	17.1	18.2	11.8	12.8
	Wind Direction (deg)	0-45	31	33.8	7.2	21.7	22.5	37.4	38.1
		45-90	25	62.0	12.9	1.3	8.4	8.1	13.8
		all	56	46.4	17.4	12.6	17.6	24.3	29.8
	Pressure (mbar)	945-965	3	960.6	3.7	-0.7	1.2	-1.6	1.8
		965-980	6	974.0	4.3	-1.7	1.8	-3.3	3.4
		980-989	9	984.6	2.5	-0.3	1.1	-2.0	2.3
		989-1030	38	996.5	3.6	-0.8	1.2	0.7	1.2
		all	56	990.2	11.0	-0.8	1.3	-0.3	1.8
FCMP T1	Wind Speed (mph)	0-20	4	19.0	1.0	12.0	12.0	6.4	6.5
		20-40	45	32.0	5.1	8.7	10.0	3.8	5.8
		40-60	39	49.8	6.9	21.7	22.8	6.3	8.4
		60-80	2	65.8	1.1	19.6	19.6	8.3	8.3
		all	90	39.9	12.0	14.7	17.0	5.1	7.1
	Wind Direction (deg)	0-45	47	28.1	9.2	7.7	11.8	19.1	22.3
		45-90	4	48.6	1.9	-10.8	11.8	-1.4	6.4
		225-270	28	246.3	9.0	-1.3	6.5	12.9	19.8
		270-315	7	289.6	12.1	11.5	14.0	36.9	37.3
		315-360	4	330.4	11.6	25.5	25.5	44.4	44.5
		all	90	130.7	118.0	5.2	11.6	18.8	24.0
	Pressure (mbar)	945-965	16	955.5	4.8	-0.1	3.4	0.6	1.3
		965-980	16	973.0	4.5	0.4	2.4	0.1	0.8
		980-989	15	984.9	2.7	-0.9	1.8	-0.4	0.7
		989-1030	44	995.6	3.6	-2.2	2.5	-0.3	0.5
		all	91	982.8	15.6	-1.2	2.5	-0.1	0.8
FCMP T2	Wind Speed (mph)	20-40	14	35.8	2.3	10.7	11.6	4.9	6.5
		40-60	37	48.6	6.6	20.0	20.7	8.0	9.5
		60-80	5	61.8	1.2	18.9	19.1	1.9	3.9
		all	56	46.6	9.1	17.6	18.7	6.7	8.4
	Wind Direction (deg)	0-45	31	22.2	7.0	2.5	5.5	13.3	14.7
		225-270	5	261.5	1.2	-5.8	6.1	14.3	14.6
		270-315	11	290.9	13.3	-7.3	8.2	17.1	17.6
		315-360	9	337.9	14.2	3.6	4.7	21.1	21.3
		all	56	147.1	142.0	0.0	6.0	15.4	16.5
	Pressure (mbar)	945-965	9	962.5	1.1	1.0	2.0	0.2	1.1
		965-980	19	972.9	4.6	-0.5	1.8	-0.6	0.8
		980-989	13	984.8	2.6	-1.5	1.9	-1.8	2.0
		989-1030	15	994.1	2.6	-2.5	2.6	-1.4	1.5
		all	56	979.7	11.7	-1.0	2.1	-1.0	1.4

Table Q-3. Error Analysis of Wind Speeds, Wind Directions and Pressures for Hurricane Katrina (Continued)

Station	Range		Number of Data	Obs		SLOSH-Obs		ARA-Obs	
				Mean	Std	mean	RMS	mean	RMS
FCMP T3	Wind Speed (mph)	0-20	22	14.8	3.9	14.5	14.7	11.8	12.0
		20-40	24	27.8	6.0	15.2	15.5	12.8	13.1
		40-60	30	53.3	4.1	15.4	16.0	9.7	10.4
		60-80	1	65.4	0.0	8.3	8.3	2.0	2.0
		all	77	34.5	17.3	15.0	15.4	11.2	11.7
	Wind Direction (deg)	45-90	32	72.8	5.6	0.4	4.3	15.8	16.4
		90-135	15	111.3	9.7	-23.6	24.1	-17.1	18.1
		135-180	16	154.6	11.7	-36.2	37.1	-33.3	34.1
		180-225	13	204.8	10.4	-40.4	40.5	-34.0	34.2
		315-360	1	351.4	0.0	74.6	74.6	92.8	92.8
		all	77	123.2	56.6	-17.8	27.5	-8.2	26.9
	Pressure (mbar)	965-980	10	978.6	0.5	-1.7	1.9	-1.9	2.0
		980-989	24	984.1	2.4	-2.2	2.6	-2.1	2.3
		989-1030	43	999.4	4.9	-3.6	4.0	-2.3	2.5
		all	77	991.9	9.5	-2.9	3.4	-2.2	2.4
KMOB	Wind Speed (mph)	20-40	20	28.5	6.1	11.6	12.0	10.1	10.6
		40-60	22	49.3	5.5	11.6	12.2	8.2	9.0
		60-80	1	63.0	0.0	0.5	0.5	-3.0	3.0
		all	43	39.9	12.4	11.3	12.0	8.8	9.7
	Wind Direction (deg)	45-90	14	67.1	9.9	16.7	18.1	29.7	31.0
		90-135	24	114.6	15.3	-6.7	11.8	-2.2	9.7
		135-180	5	154.0	5.5	-3.0	4.7	-2.8	4.7
		all	43	103.7	31.2	1.3	13.6	8.1	19.2
	Pressure (mbar)	980-989	17	985.2	1.2	-1.9	2.0	-2.0	2.1
		989-1030	26	994.3	4.7	-1.9	2.2	-2.2	2.3
		all	43	990.7	5.8	-1.9	2.1	-2.1	2.2
KPNS	Wind Speed (mph)	0-20	7	16.1	1.8	12.3	12.3	13.0	13.1
		20-40	12	36.8	4.8	4.3	4.5	7.1	7.3
		40-60	23	43.2	3.4	-1.6	3.8	1.2	3.5
		all	42	36.8	10.4	2.4	6.3	4.9	7.1
	Wind Direction (deg)	45-90	5	76.0	5.5	19.1	19.5	40.4	40.6
		90-135	15	118.7	14.6	-4.2	8.0	9.8	13.1
		135-180	22	153.6	9.0	-14.2	15.1	-6.7	8.0
		all	42	131.9	28.6	-6.7	13.7	4.8	17.0
	Pressure (mbar)	989-1030	42	996.8	2.6	-3.1	3.2	-3.1	3.2
		all	42	996.8	2.6	-3.1	3.2	-3.1	3.2
DPIA1	Wind Speed (mph)	20-40	37	34.1	3.8	-3.9	4.7	2.4	3.6
		40-60	31	49.6	5.4	-7.6	7.7	0.7	1.8
		60-80	29	68.9	3.4	-10.2	10.5	-1.8	2.9
		all	97	49.5	14.9	-6.9	7.8	0.6	2.9
	Wind Direction (deg)	45-90	40	73.5	9.4	6.1	10.2	33.5	34.5
		90-135	47	107.1	13.1	-5.2	7.8	14.9	15.8
		135-180	10	143.8	4.1	-1.3	2.1	12.3	12.4
		all	97	97.1	25.1	-0.1	8.6	22.3	25.1
	Pressure (mbar)	980-989	5	986.9	0.9	-1.2	1.3	-2.1	2.1
		989-1030	12	998.5	4.7	-2.6	3.1	-1.2	1.4
		all	17	995.0	6.7	-2.2	2.7	-1.5	1.6

Table Q-3. Error Analysis of Wind Speeds, Wind Directions and Pressures for Hurricane Katrina (Continued)

Station	Range		Number of Data	Obs		SLOSH-Obs		ARA-Obs	
				Mean	Std	mean	RMS	mean	RMS
42040	Wind Speed (mph)	20-40	19	35.7	2.8	2.8	5.0	6.5	7.0
		40-60	83	49.9	5.7	6.2	7.6	4.8	5.7
		60-80	34	64.3	2.5	12.0	12.3	6.0	6.4
		all	136	48.6	15.3	6.8	8.5	5.0	5.9
	Wind Direction (deg)	45-90	22	83.1	2.8	12.3	12.7	16.4	16.7
		90-135	42	110.7	12.7	11.0	11.9	14.3	14.9
		135-180	28	158.7	12.9	14.9	15.2	15.0	15.2
		180-225	44	205.0	10.5	5.8	6.4	3.8	5.1
		all	136	158.5	67.8	9.8	11.1	10.8	12.7
	Pressure (mbar)	965-980	3	979.3	0.0	4.0	4.1	3.1	3.2
		980-989	7	985.1	2.7	2.0	2.2	2.2	2.6
		989-1030	13	994.5	2.4	-1.2	1.5	0.4	1.7
		all	23	989.6	6.3	0.5	2.2	1.3	2.2
KNEW	Wind Speed (mph)	20-40	1	35.0	0.0	17.8	17.8	16.1	16.1
		40-60	34	47.5	4.7	2.1	6.9	0.1	6.4
		60-80	3	63.3	4.9	11.8	11.9	7.3	7.4
		all	38	48.4	6.7	3.3	7.9	1.1	6.9
	Wind Direction (deg)	0-45	32	34.7	5.7	4.2	7.1	20.5	21.2
		45-90	5	50.0	0.0	-11.8	12.3	3.7	6.3
		90-135	1	90.0	0.0	-51.3	51.3	-37.3	37.3
		all	38	38.2	11.4	0.7	11.5	16.7	20.5
	Pressure (mbar)	945-965	1	964.0	0.0	2.4	2.4	0.9	0.9
		965-980	7	973.7	3.9	3.3	3.3	1.4	1.5
		980-989	13	984.8	2.8	2.0	2.2	1.5	1.6
		989-1030	19	992.8	2.3	-0.3	0.6	0.2	0.4
		all	40	986.2	8.4	1.1	2.0	0.9	1.2
BURL1	Wind Speed (mph)	40-60	14	55.4	2.7	-3.7	5.0	-0.6	3.5
		60-80	17	65.8	4.1	-0.8	3.7	2.8	4.8
		all	31	61.1	6.3	-2.1	4.3	1.3	4.3
	Wind Direction	45-90	31	66.0	8.4	-15.5	16.9	0.5	6.7
		all	31	66.0	8.4	-15.5	16.9	0.5	6.7
	Pressure (mbar)	965-980	1	979.7	0.0	0.1	0.1	-1.2	1.2
		980-989	2	985.7	2.7	-0.7	0.8	0.3	0.3
		989-1030	3	991.0	2.1	-0.5	0.6	2.4	2.4
		all	6	987.4	4.9	-0.5	0.7	1.1	1.8
42007	Wind Speed (mph)	20-40	17	37.3	1.7	0.4	4.2	0.2	4.4
		40-60	46	47.5	5.6	8.0	21.5	5.4	14.8
		60-80	32	65.8	2.4	22.6	26.4	13.3	15.9
		all	95	51.9	11.5	11.6	21.5	7.1	14.0
	Wind Direction (deg)	45-90	36	79.1	6.4	3.0	6.0	14.2	15.2
		90-135	50	102.7	11.4	2.9	11.1	7.9	11.5
		135-180	2	152.5	14.8	6.6	11.0	8.0	11.9
		180-225	3	202.3	20.1	-35.3	38.0	-33.8	36.6
		225-270	4	239.3	9.1	-62.6	62.8	-61.1	61.3
		all	95	103.7	38.4	-0.9	17.1	6.1	19.0
	Pressure (mbar)	920-945	3	936.1	8.4	34.8	35.5	34.7	35.3
		945-965	1	955.7	0.0	21.9	21.9	20.7	20.7
		965-980	3	973.9	6.1	11.8	12.0	11.2	11.4
		980-989	2	987.0	2.5	5.1	5.1	5.9	6.0
		989-1030	7	997.0	3.1	-0.4	1.7	2.3	2.5
		all	16	977.4	24.2	10.6	17.3	11.7	17.1

Table Q-3. Error Analysis of Wind Speeds, Wind Directions and Pressures for Hurricane Katrina (Continued)

Station	Range		Number of Data	Obs		SLOSH-Obs		ARA-Obs	
				Mean	Std	mean	RMS	mean	RMS
KBIX	Wind Speed (mph)	20-40	7	30.7	4.9	14.0	16.9	11.8	14.7
		40-60	3	48.3	7.4	25.8	26.5	20.0	20.3
		60-80	1	60.0	0.0	27.5	27.5	18.9	18.9
		all	11	38.2	11.9	18.4	21.0	14.7	16.8
	Wind Direction (deg)	45-90	7	65.7	11.3	6.5	9.8	20.6	23.1
		90-135	3	103.3	5.8	-9.7	10.8	-2.5	5.2
		all	10	77.0	20.6	1.6	10.1	13.7	19.6
	Pressure (mbar)	965-980	1	978.0	0.0	-1.2	1.2	-2.7	2.7
		980-989	3	984.7	3.1	1.2	1.4	-0.4	1.0
		989-1030	5	995.2	2.9	-0.9	1.4	-0.1	0.7
		all	9	989.8	7.2	-0.2	1.4	-0.5	1.2
GDIL1	Wind Speed (mph)	20-40	12	35.9	4.0	3.6	4.9	6.3	7.2
		40-60	31	48.3	5.3	5.7	7.2	9.3	10.4
		60-80	11	69.0	5.1	10.7	10.9	16.4	16.6
		80-100	1	81.7	0.0	6.0	6.0	12.6	12.6
		all	55	50.4	12.7	6.2	7.7	10.1	11.4
	Wind Direction (deg)	0-45	54	34.2	5.7	0.2	6.2	20.2	21.4
		45-90	1	60.0	0.0	-25.0	25.0	-1.4	1.4
		all	55	34.7	6.6	-0.2	7.0	19.8	21.2
	Pressure (mbar)	920-945	1	944.3	0.0	-0.5	0.5	-2.1	2.1
		945-965	4	954.9	5.4	1.7	4.5	-0.3	1.8
		965-980	4	974.8	4.5	1.1	1.6	0.2	0.8
		980-989	4	986.3	2.4	-0.6	1.2	-0.9	1.3
		989-1030	9	995.3	2.5	-2.6	2.8	-0.7	1.5
		all	22	980.2	17.4	-0.7	2.8	-0.5	1.4
all stations	Wind Speed (mph)	0-20	49	15.6	3.3	13.7	13.8	10.8	11.1
		20-40	236	32.4	5.7	7.3	10.8	6.6	8.7
		40-60	402	49.2	5.9	8.5	14.7	5.4	9.1
		60-80	139	66.1	3.8	8.8	16.6	6.6	10.3
		80-100	1	81.7	0.0	6.0	6.0	12.6	12.6
		all	827	45.3	14.5	8.5	14.0	6.3	9.3
	Wind Direction (deg)	0-45	195	30.9	8.4	6.5	11.7	21.6	24.2
		45-90	222	71.3	11.2	2.0	11.5	16.7	21.5
		90-135	197	108.7	13.5	-1.5	12.5	7.6	14.1
		135-180	83	154.3	11.3	-5.9	20.2	-1.7	18.5
		180-225	60	204.8	10.8	-6.3	21.4	-6.3	18.4
		225-270	37	247.6	10.2	-8.5	21.5	5.1	27.0
		270-315	18	290.4	12.5	0.0	10.8	24.8	27.0
		315-360	14	336.7	13.6	15.0	24.5	32.9	38.4
		all	826	105.9	72.6	0.5	14.6	12.1	21.0
	Pressure (mbar)	920-945	4	938.1	8.0	26.0	30.7	25.5	30.6
		945-965	34	958.0	5.1	1.1	4.8	0.8	3.8
		965-980	70	974.5	4.5	0.6	3.4	0.0	2.9
		980-989	114	984.9	2.4	-0.7	2.1	-0.9	2.1
		989-1030	275	996.1	4.1	-2.1	2.6	-1.0	2.0
		all	497	987.4	12.7	-0.9	4.0	-0.5	3.6

Appendix R. Comparisons of Modeled and Measured Wind Speeds, Wind Directions, and Pressures for Hurricane Gustav (2008)

This appendix presents comparisons of modeled and observed wind speeds, wind directions and pressures at multiple locations along the north central Gulf of Mexico coast and some buoy stations during the passage of Hurricane Gustav (2008).

Figure R-1 shows the maximum 10-minute mean wind speeds obtained from two versions of SLOSH model. The first version uses ARA storm track and ARA wind field model (denoted as ARA-TRK-ARA-WD), and the second version uses ARA storm track and SLOSH wind field model (denoted as ARA-TRK-SLOSH-WD).

Figure R-2 shows the simulated landfall wind field for Sabine Lake, Vermilion Bay, New Orleans, and Mississippi Gulf Coast SLOSH basins.

Figure R-3 shows map of the locations of all observing stations as well as the hurricane track. The observed wind speeds and pressures are compared to the simulated wind speeds from model runs using the ARA-TRK-ARA-WD and ARA-TRK-SLOSH-WD model, as shown in Table R-1.

Figure R-4 presents the comparisons of modeled and observed maximum wind speeds and minimum pressures for Hurricane Gustav (2008). The results indicate that the simulated wind speeds obtained from ARA wind field model (ARA-TRK-ARA-WD) are comparable to the observed wind speeds, while the SLOSH wind field model (ARA-TRK-SLOSH-WD) overestimates the wind speeds for Hurricane Gustav.

Comparisons of the entire modeled and observed time series of mean wind speeds, wind directions and pressures for all stations, both complete and incomplete, are presented in Figure R-5. The RMS errors of wind speed, wind direction, and pressure are shown in Table R-2.

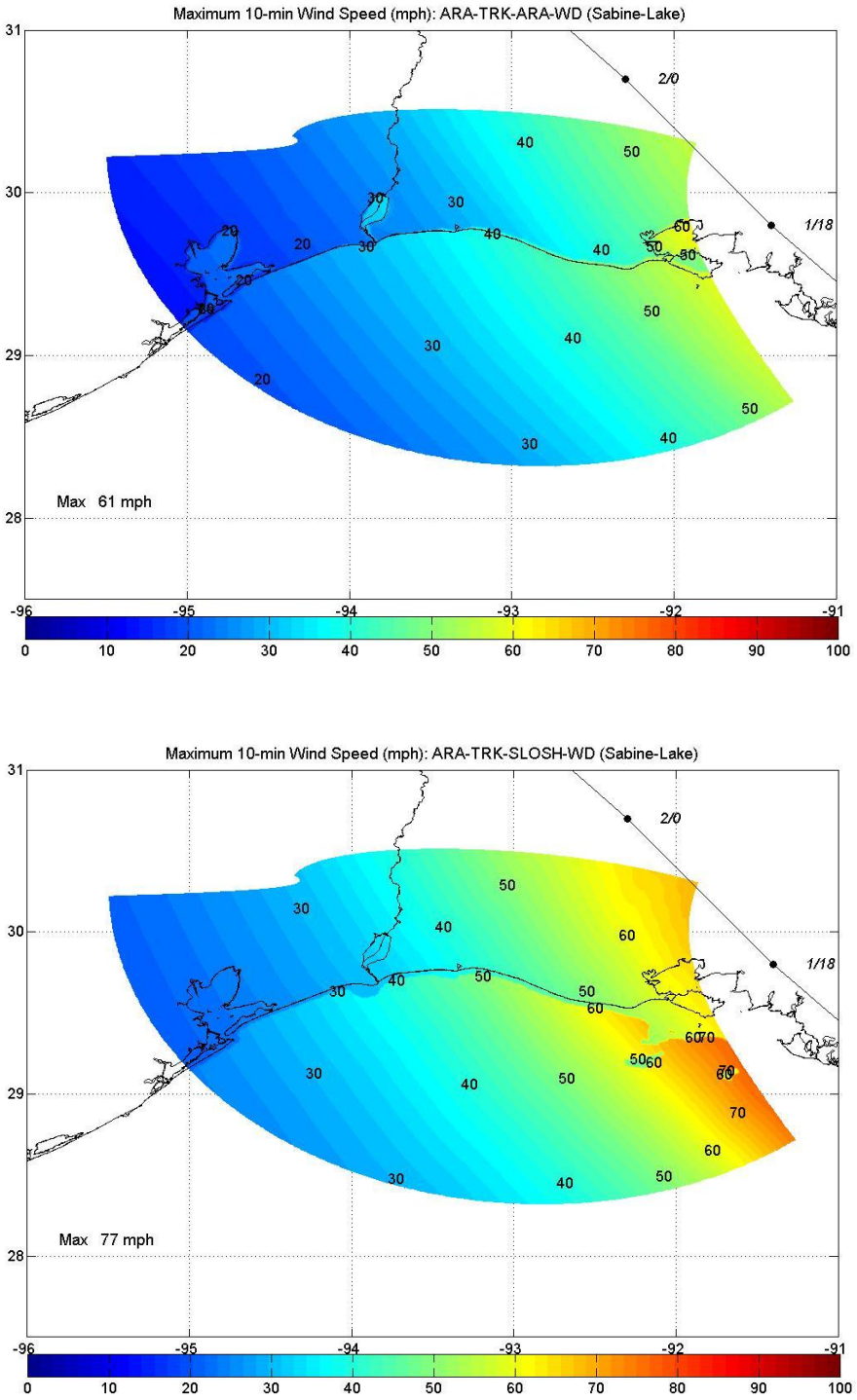

Figure R-1a. Modeled Maximum 10-min Wind Speeds (mph) for Hurricane Gustav (2008) – Sabine Lake Basin

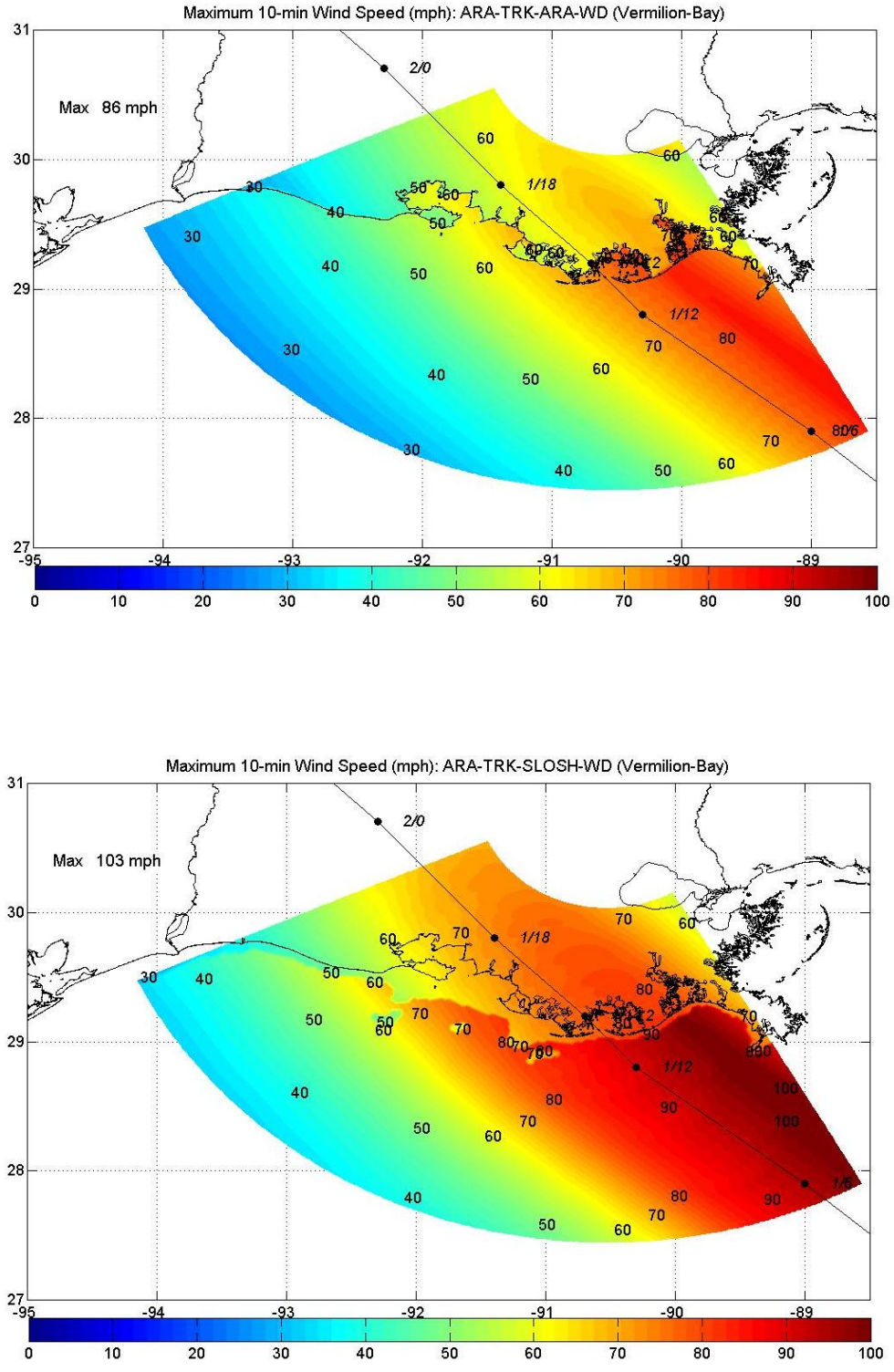

Figure R-1b. Modeled Maximum 10-min Wind Speeds (mph) for Hurricane Gustav (2008) – Vermilion Bay Basin

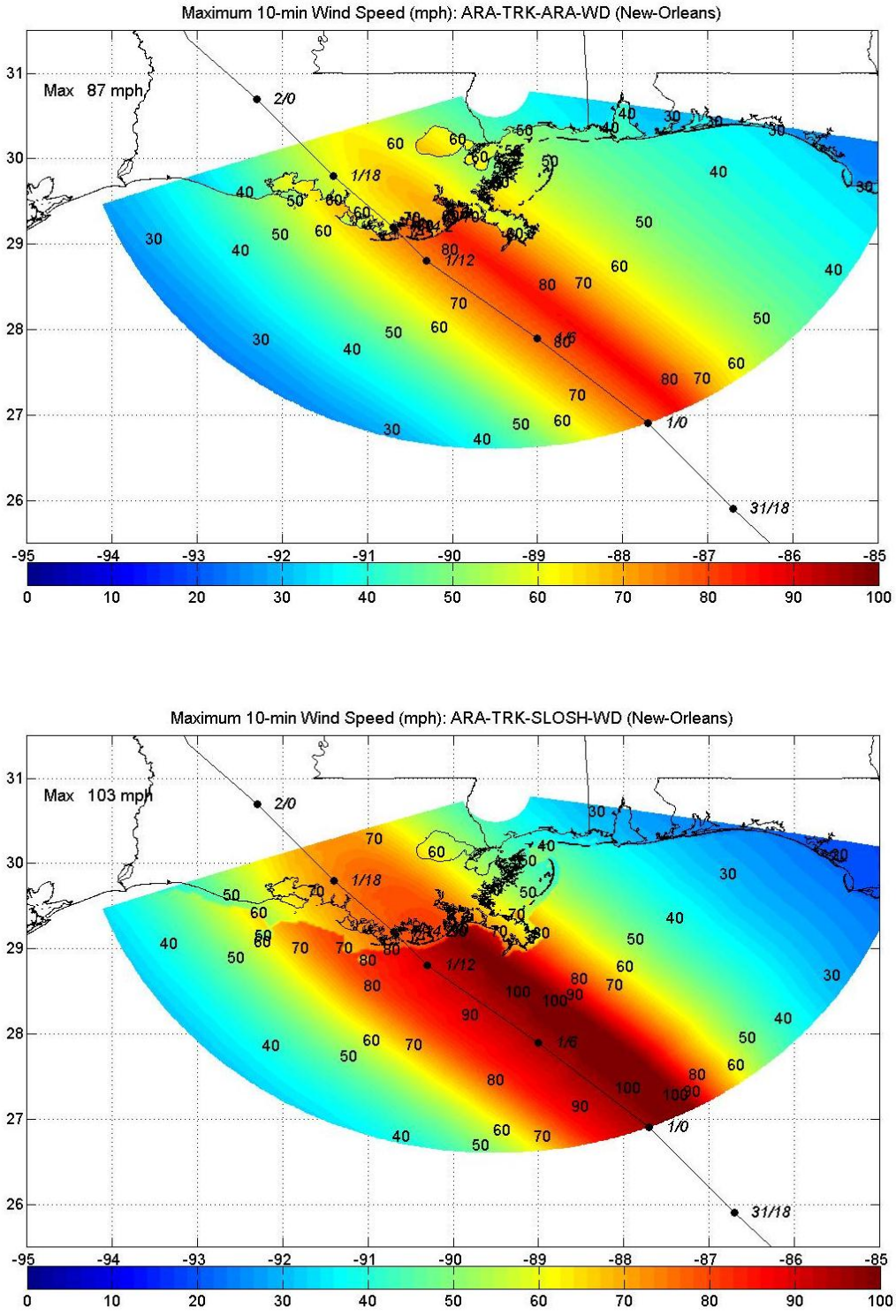

Figure R-1c. Modeled Maximum 10-min Wind Speeds (mph) for Hurricane Gustav (2008) – New Orleans Basin

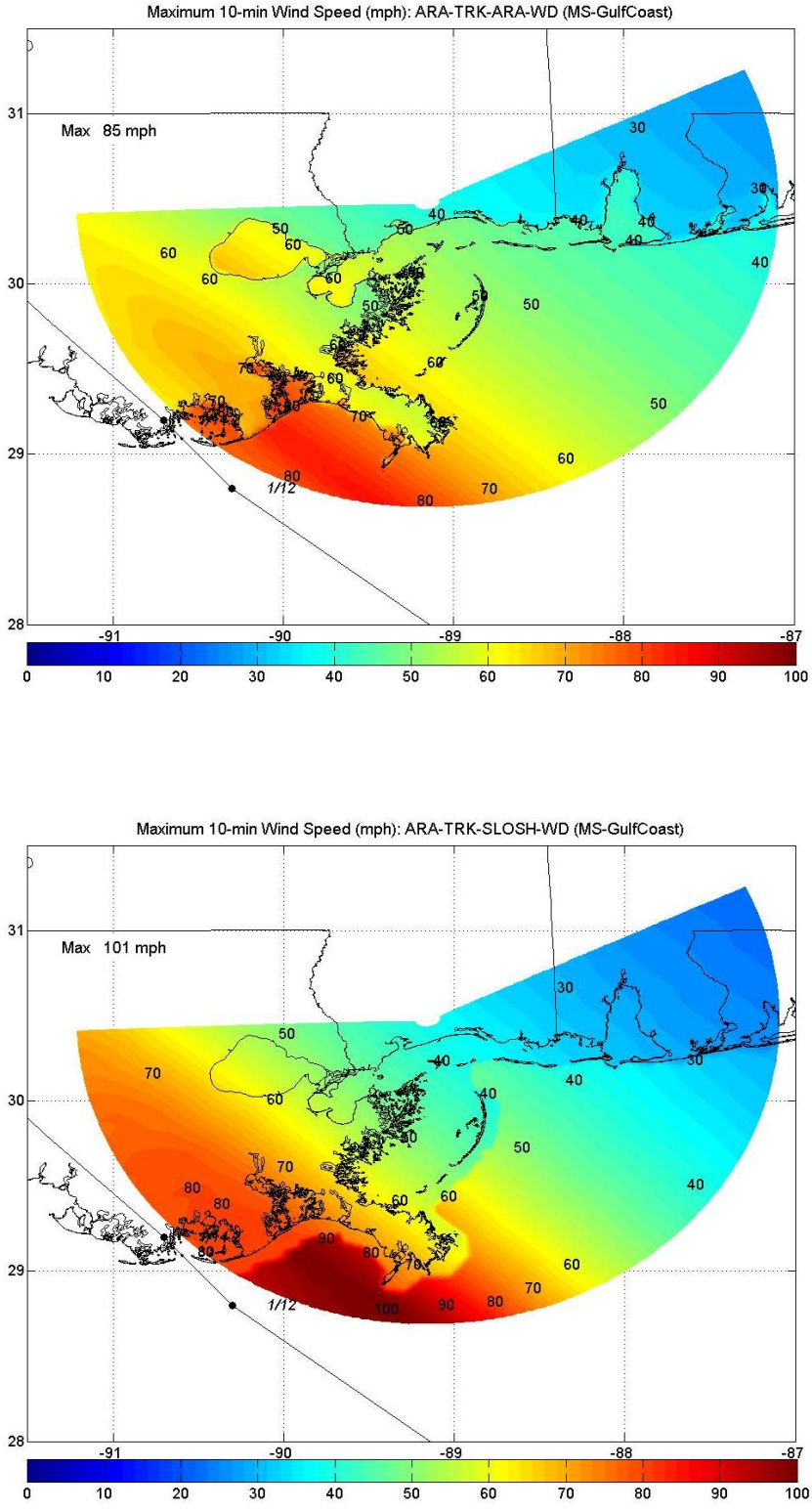

Figure R-1d. Modeled Maximum 10-min Wind Speeds (mph) for Hurricane Gustav (2008) – Mississippi Gulf Coast Basin

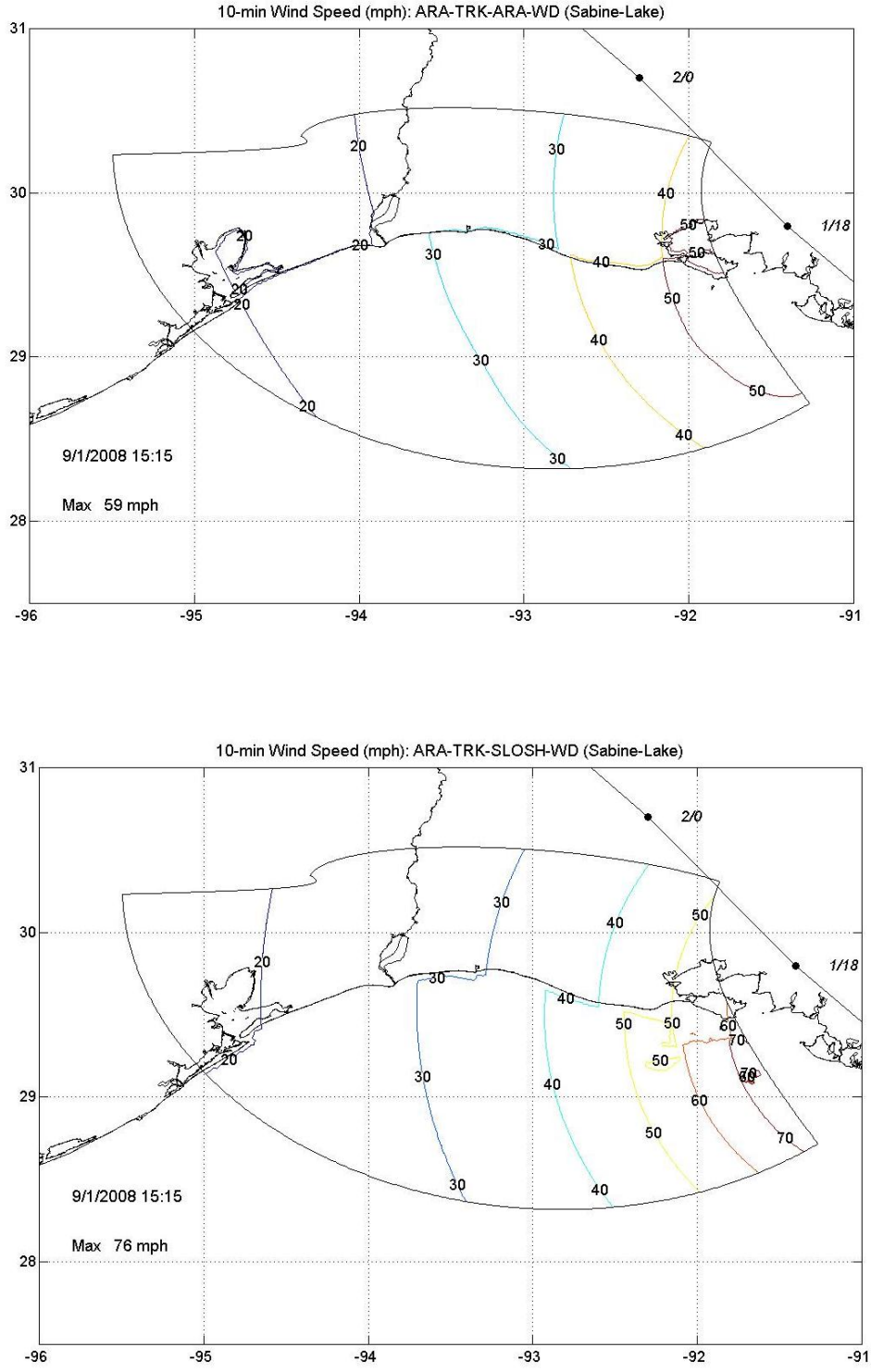

Figure R-2a. Hurricane Gustav (2008) Modeled 10-min Wind Speeds (mph) at Landfall – Sabine Lake Basin

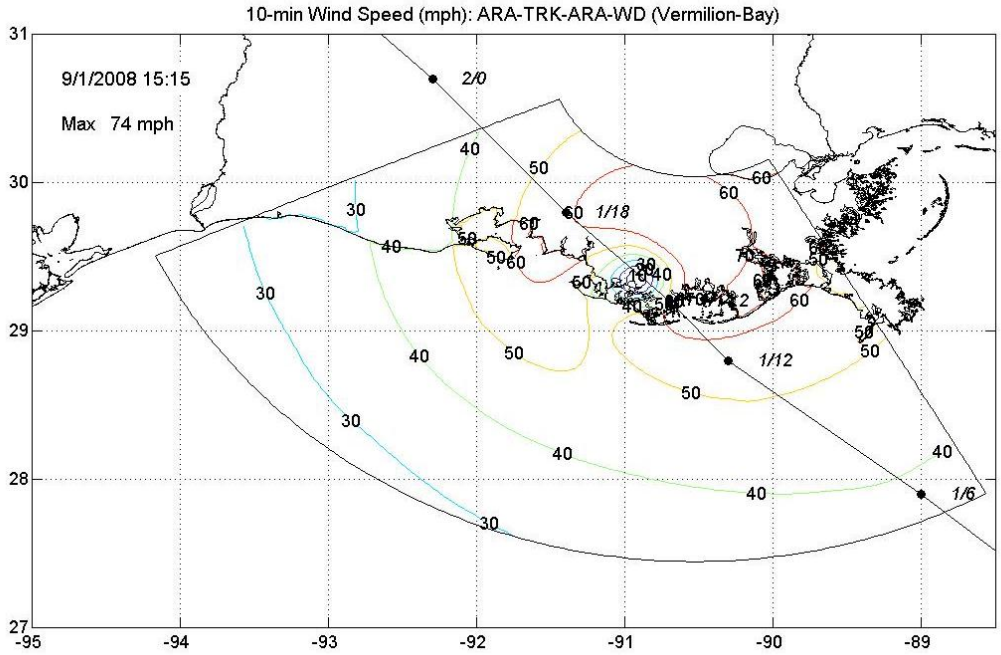

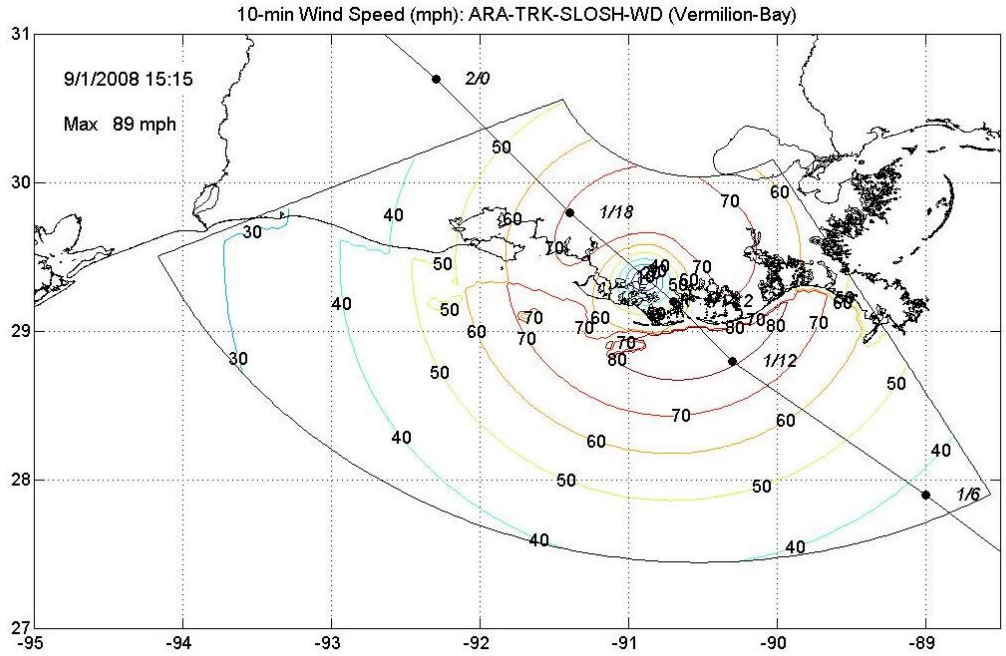

Figure R-2b. Hurricane Gustav (2008) Modeled 10-min Wind Speeds (mph) at Landfall – Vermilion Bay Basin

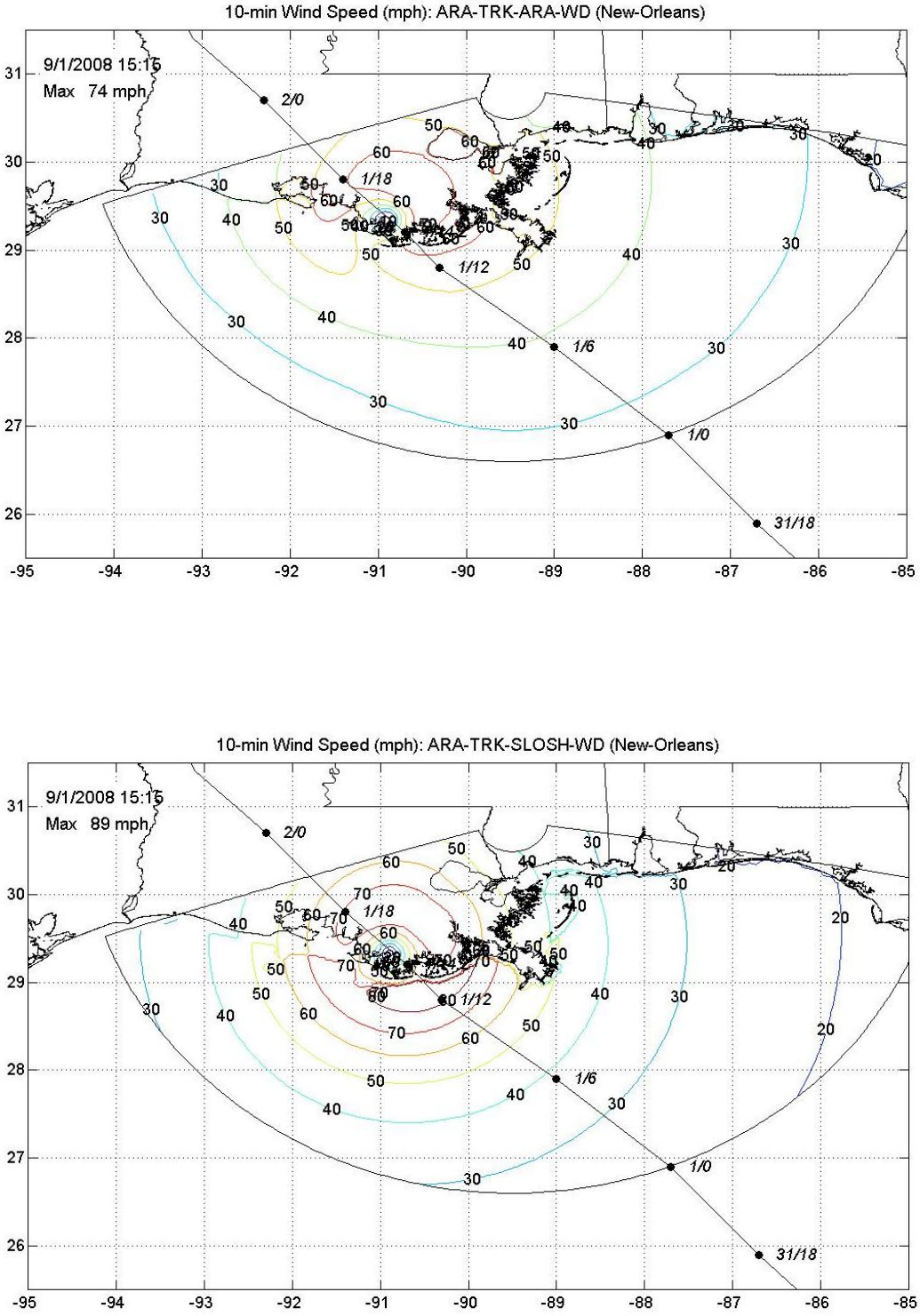

Figure R-2c. Hurricane Gustav (2008) Modeled 10-min Wind Speeds (mph) at Landfall – New Orleans Basin

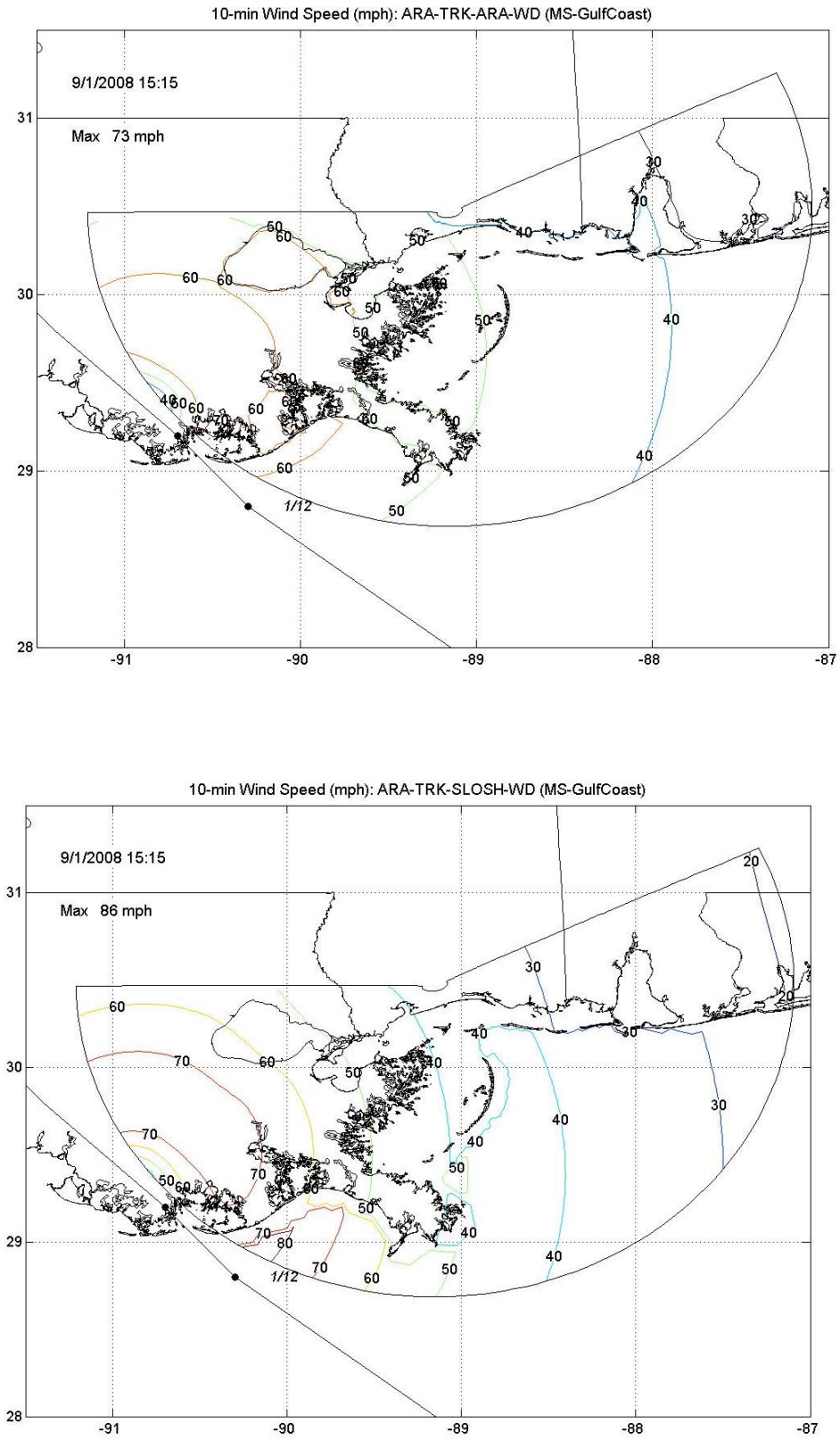

Figure R-2d. Hurricane Gustav (2008) Modeled 10-min Wind Speeds (mph) at Landfall – Mississippi Gulf Coast Basin

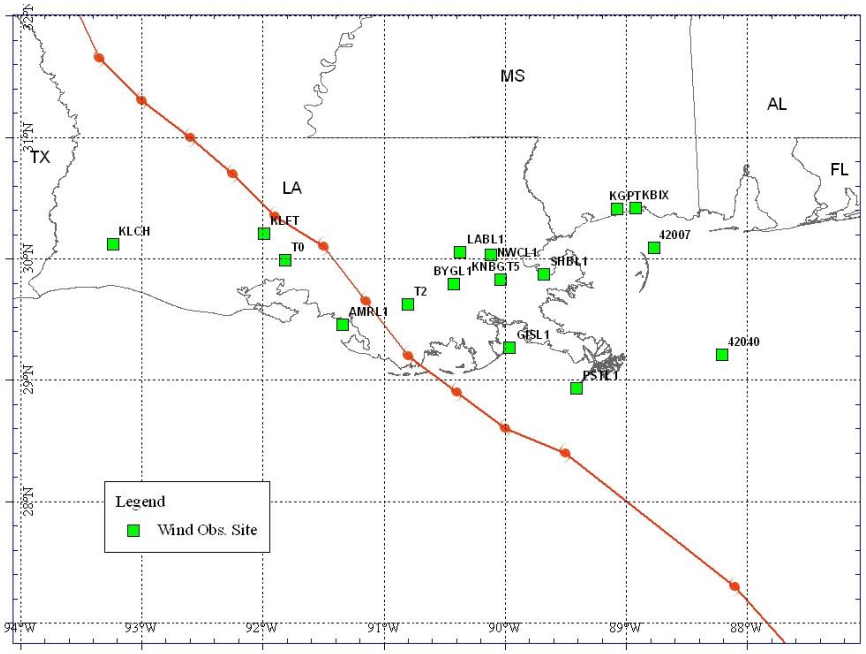

Figure R-3. Wind Observation Locations for Hurricane Gustav

Table R-1. Summary Comparison of Modeled and Observed Maximum 10-min Wind Speeds and Minimum Pressures for Hurricane Gustav

No.	Station Name	lat	long	Max Wind Speed (mph)			Minimum Pressure (mbar)		
				ARA-TRK SLOSH-WD	ARA-TRK ARA-WD	Obs.	SLOSH Modeled	ARA Modeled	Obs.
1	KLCH	30.11667	-93.23333	44.1	33.2	32.0	992.7	993.3	991.0
2	KLFT	30.20000	-91.98333	66.9	53.8	62.0	967.0	967.8	968.0
3	T0	29.98667	-91.81167	68.7	54.3	49.5	965.3	966.6	970.0
4	PSTL1	28.93200	-89.40700	78.5	72.6	82.3	982.1	981.6	976.1
5	GISL1	29.26300	-89.95700	79.5	80.6	67.3	978.1	979.2	976.7
6	AMRL1	29.45000	-91.33800	72.1	67.7	61.1	964.1	965.4	965.2
7	SHBL1	29.86800	-89.67300	55.8	51.9	60.0	993.1	991.9	990.1
8	42040	29.20500	-88.20500	53.1	54.7	52.8	999.1	996.8	993.7
9	NWCL1	30.02700	-90.11300	61.5	55.4	58.9	990.4	989.4	989.8
10	LABL1	30.05000	-90.36800	66.1	59.1	60.6	987.5	986.9	988.8
11	BYGL1	29.78900	-90.42000	74.7	65.2	62.7	982.0	980.9	980.8
12	KGPT	30.40727	-89.07010	38.1	40.0	54.0	1000.1	998.6	1000.0
13	KBIX	30.41600	-88.91670	39.1	45.7	45.0	1002.3	998.4	1001.0
14	T2	29.61828	-90.79608	79.0	66.5	62.6	965.7	965.8	962.0
15	42007	30.09000	-88.76900	46.1	49.7	52.8	1000.1	998.7	996.8
16	KNBG	29.82533	-90.03500	64.6	58.6	46.0	988.8	987.5	989.0
17	T5	29.82512	-90.03305	64.6	58.7	52.0	988.8	987.5	N/A

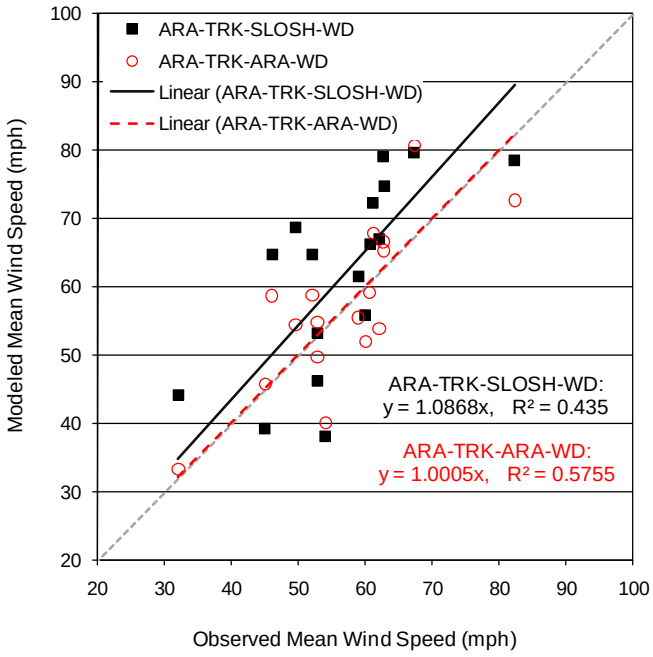

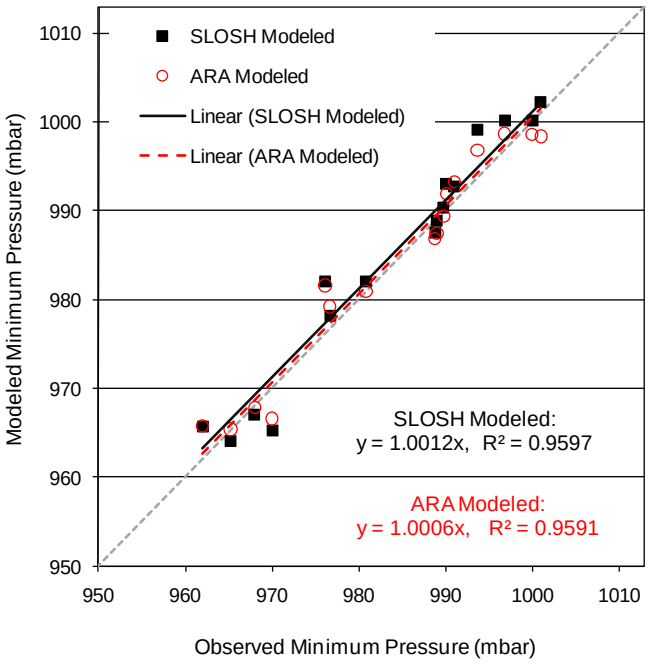

Figure R-4. Comparisons of Modeled and Observed Maximum 10-min Wind Speeds and Minimum Pressures for Hurricane Gustav

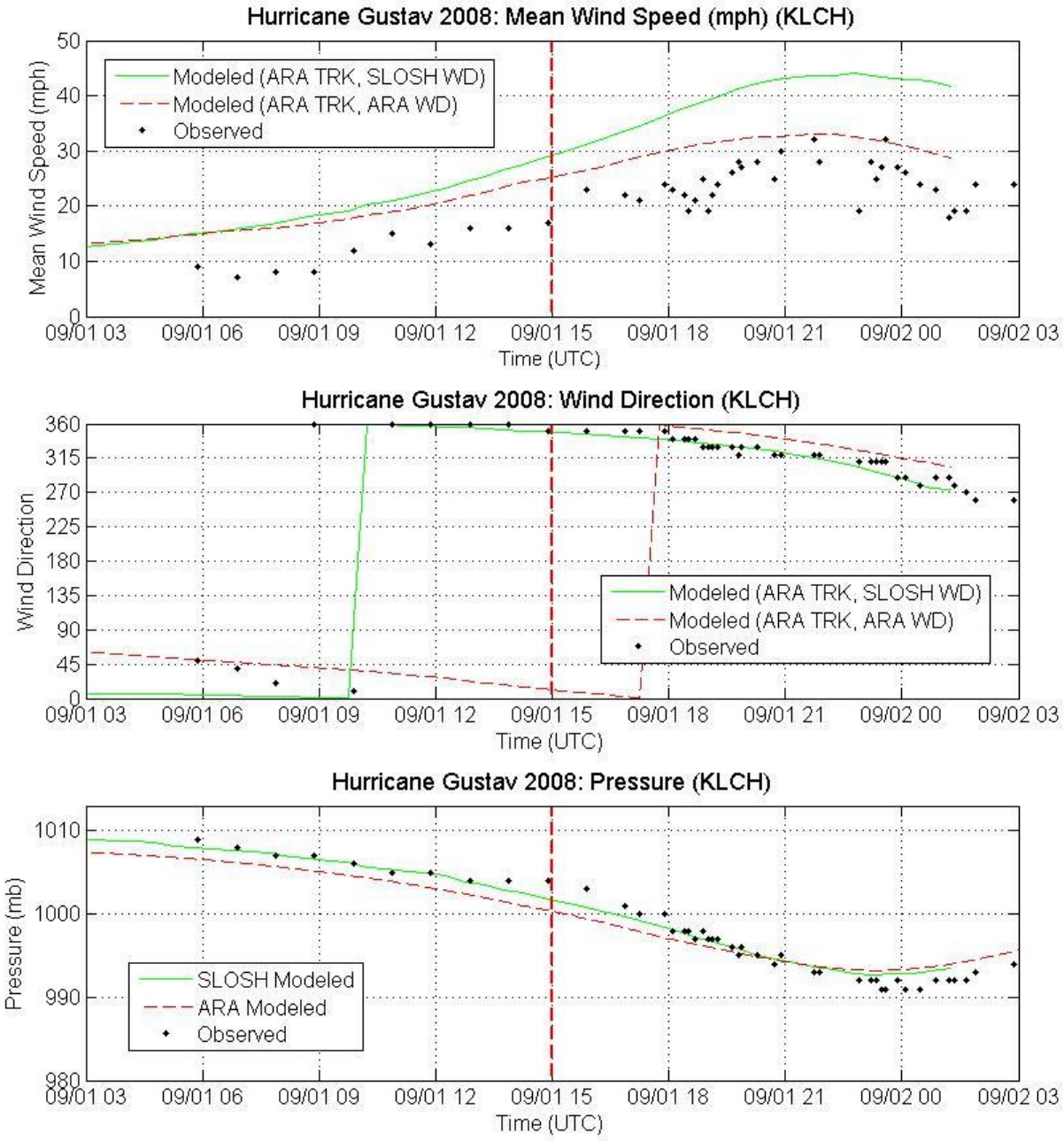

Figure R-5a. Comparisons of Observed and Modeled Time Series Traces of Mean Wind Speeds, Wind Directions, and Pressures for Hurricane Gustav (2008) – KLCH

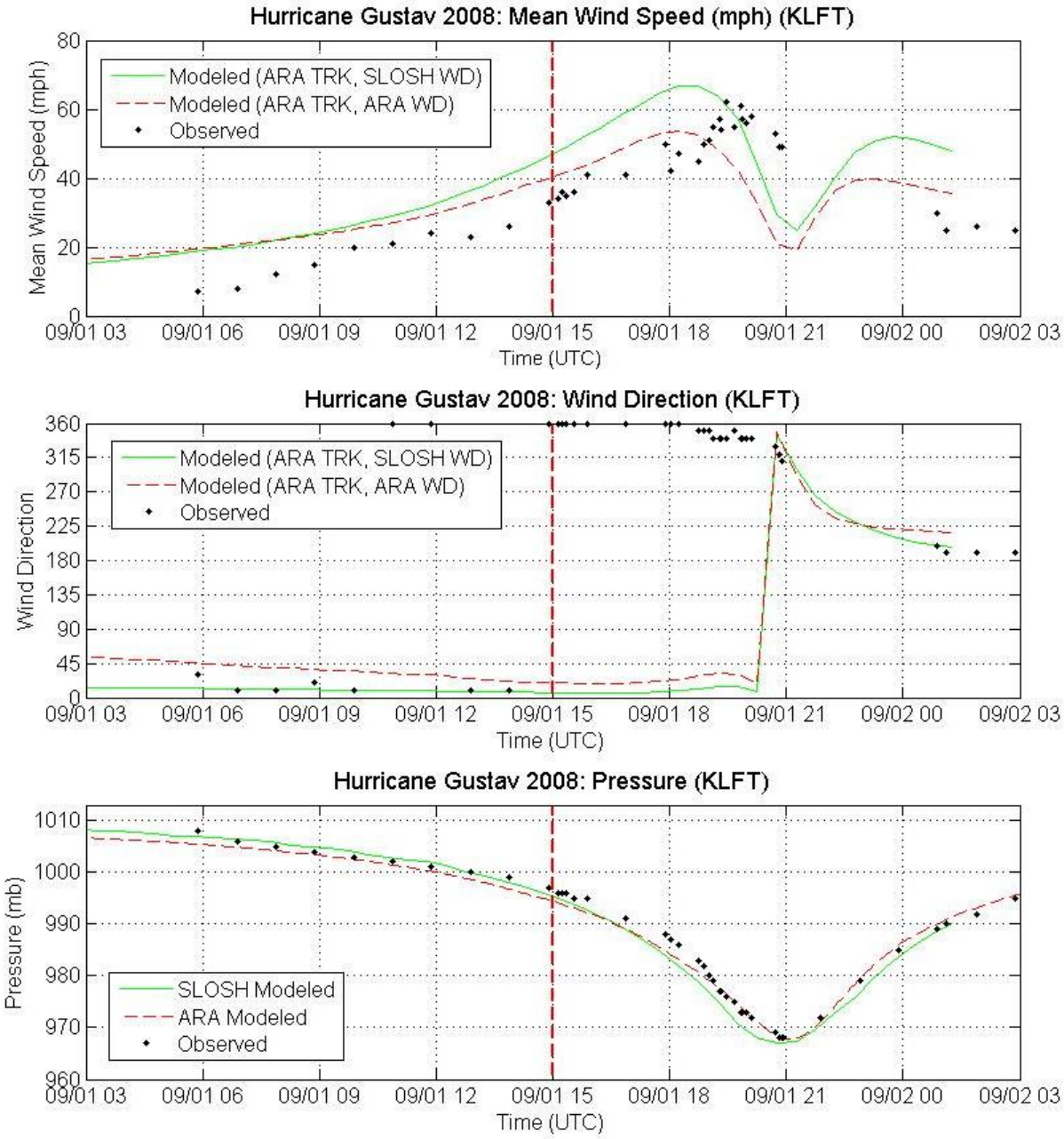

Figure R-5b. Comparisons of Observed and Modeled Time Series Traces of Mean Wind Speeds, Wind Directions, and Pressures for Hurricane Gustav (2008) – KLFT

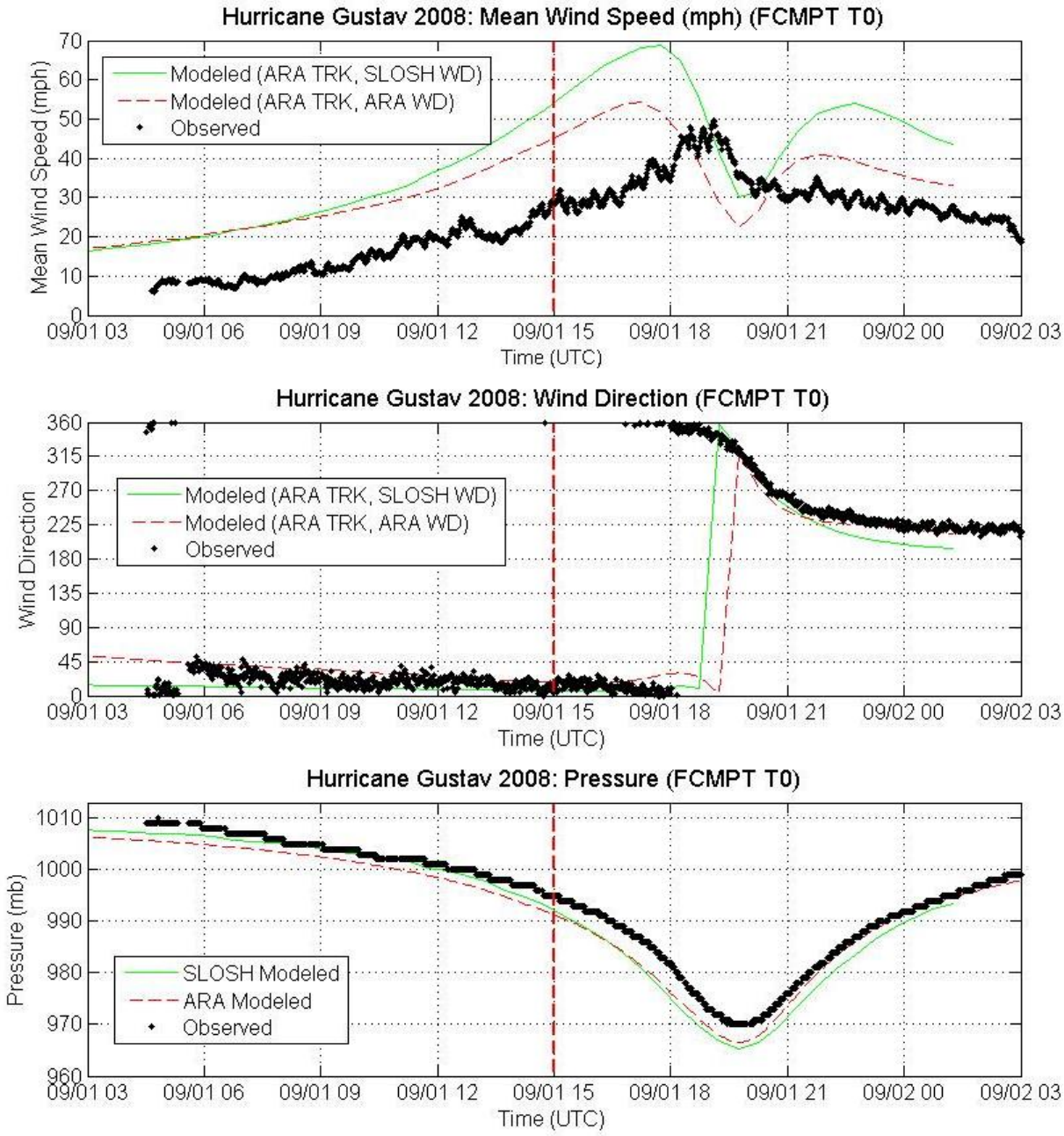

Figure R-5c. Comparisons of Observed and Modeled Time Series Traces of Mean Wind Speeds, Wind Directions, and Pressures for Hurricane Gustav (2008) – FCMP T0

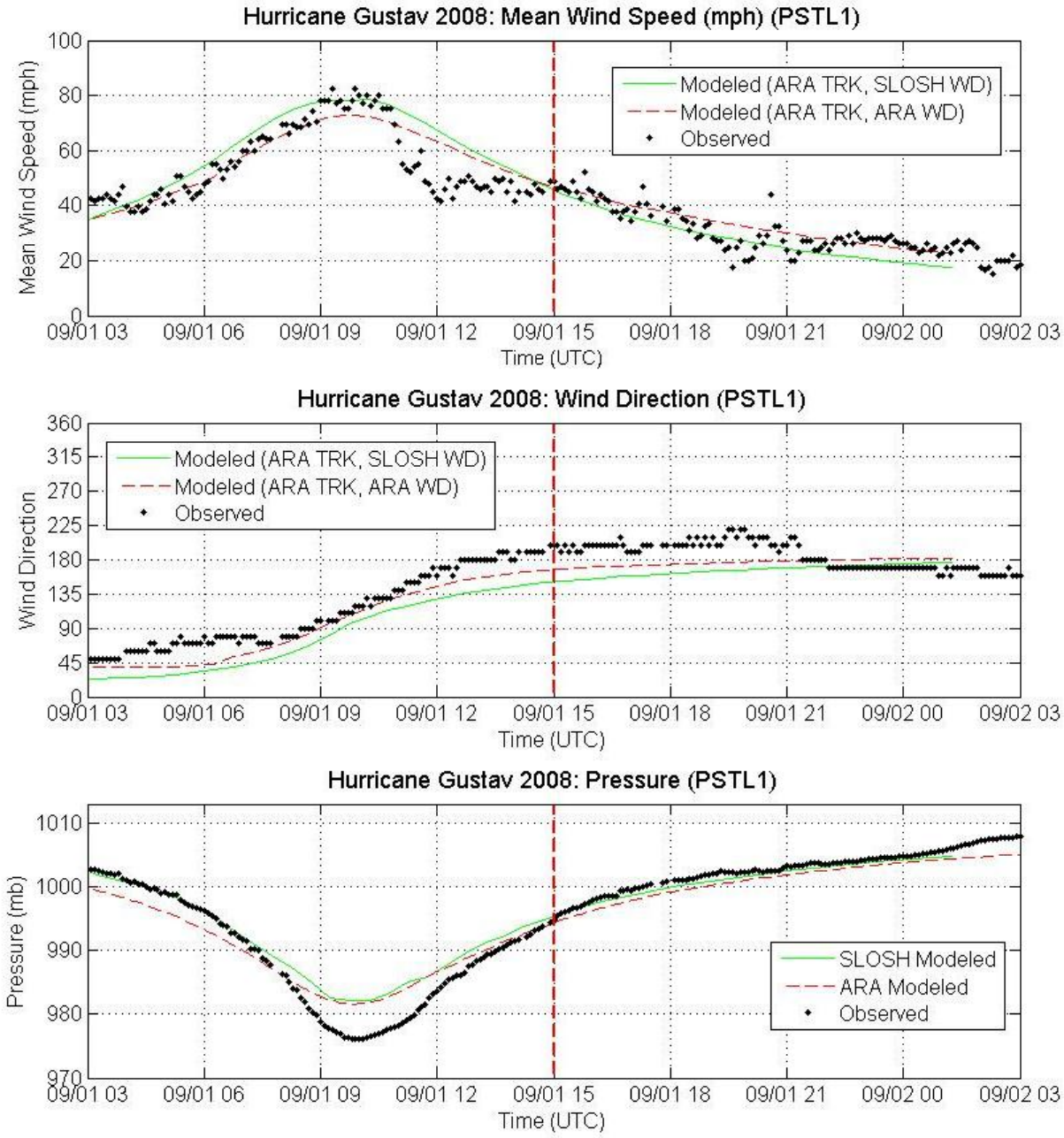

Figure R-5d. Comparisons of Observed and Modeled Time Series Traces of Mean Wind Speeds, Wind Directions, and Pressures for Hurricane Gustav (2008) – PSTL1

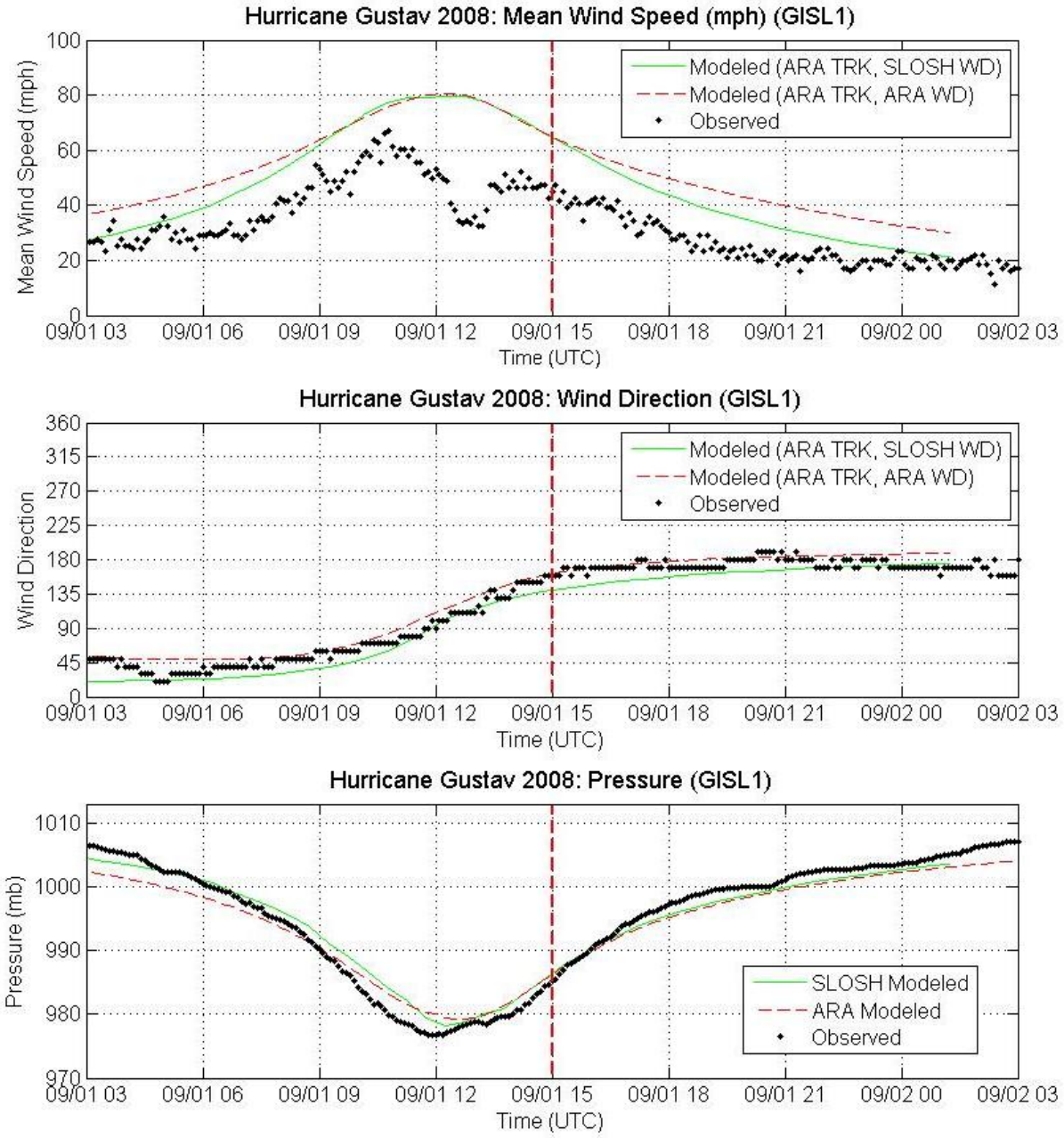

Figure R-5e. Comparisons of Observed and Modeled Time Series Traces of Mean Wind Speeds, Wind Directions, and Pressures for Hurricane Gustav (2008) – GISL1

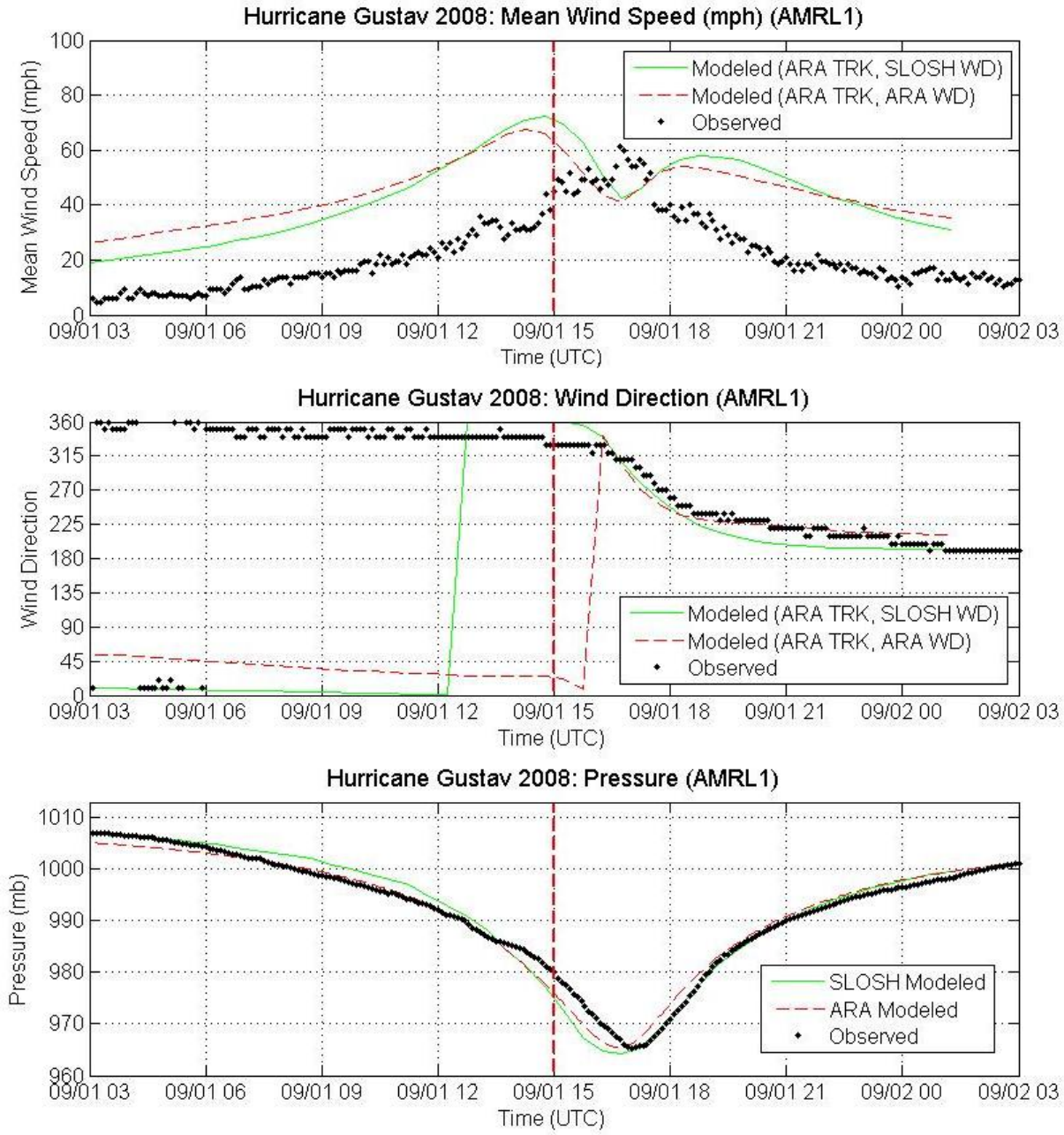

Figure R-5f. Comparisons of Observed and Modeled Time Series Traces of Mean Wind Speeds, Wind Directions, and Pressures for Hurricane Gustav (2008) – AMRL1

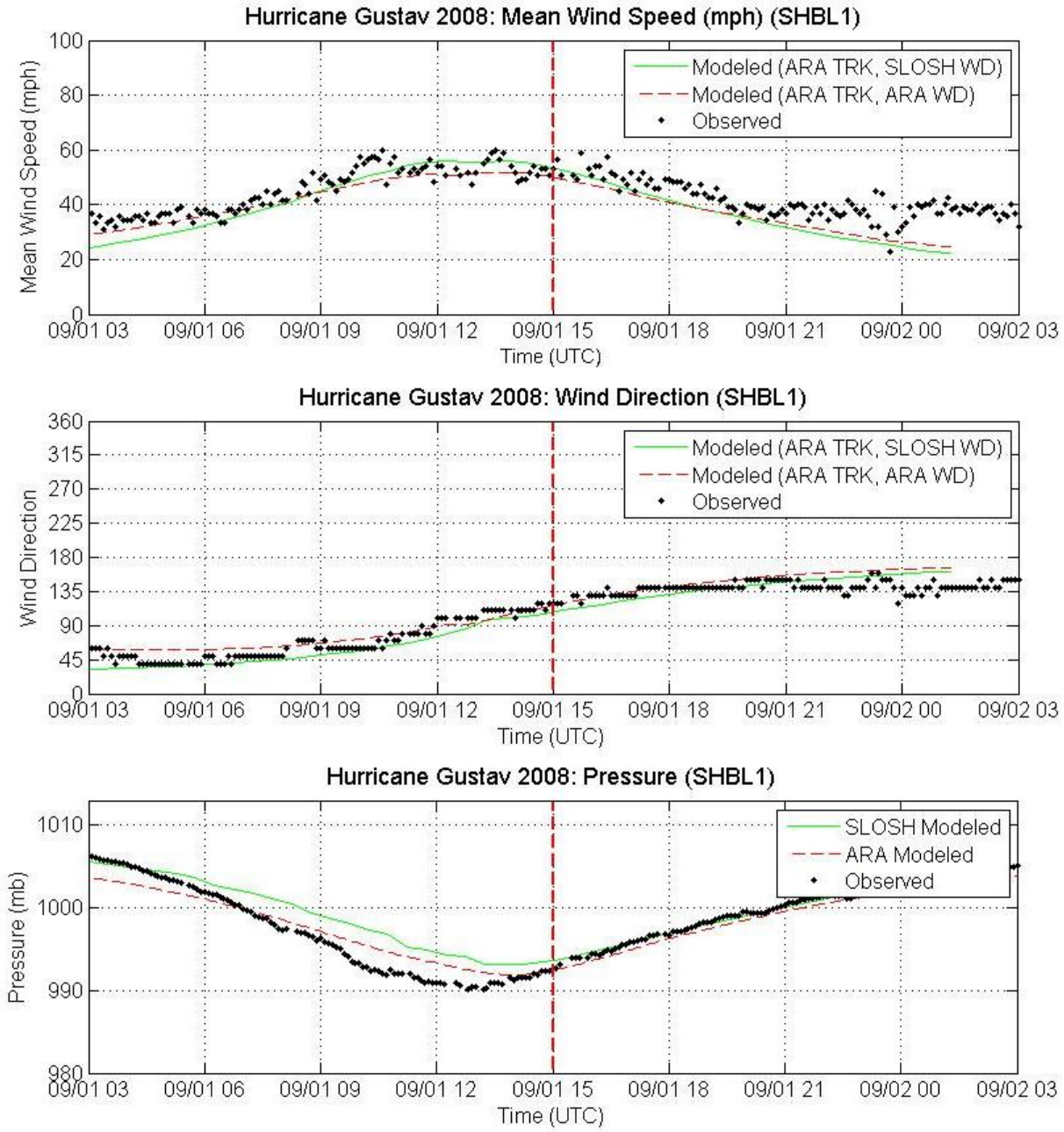

Figure R-5g. Comparisons of Observed and Modeled Time Series Traces of Mean Wind Speeds, Wind Directions, and Pressures for Hurricane Gustav (2008) – SHBL1

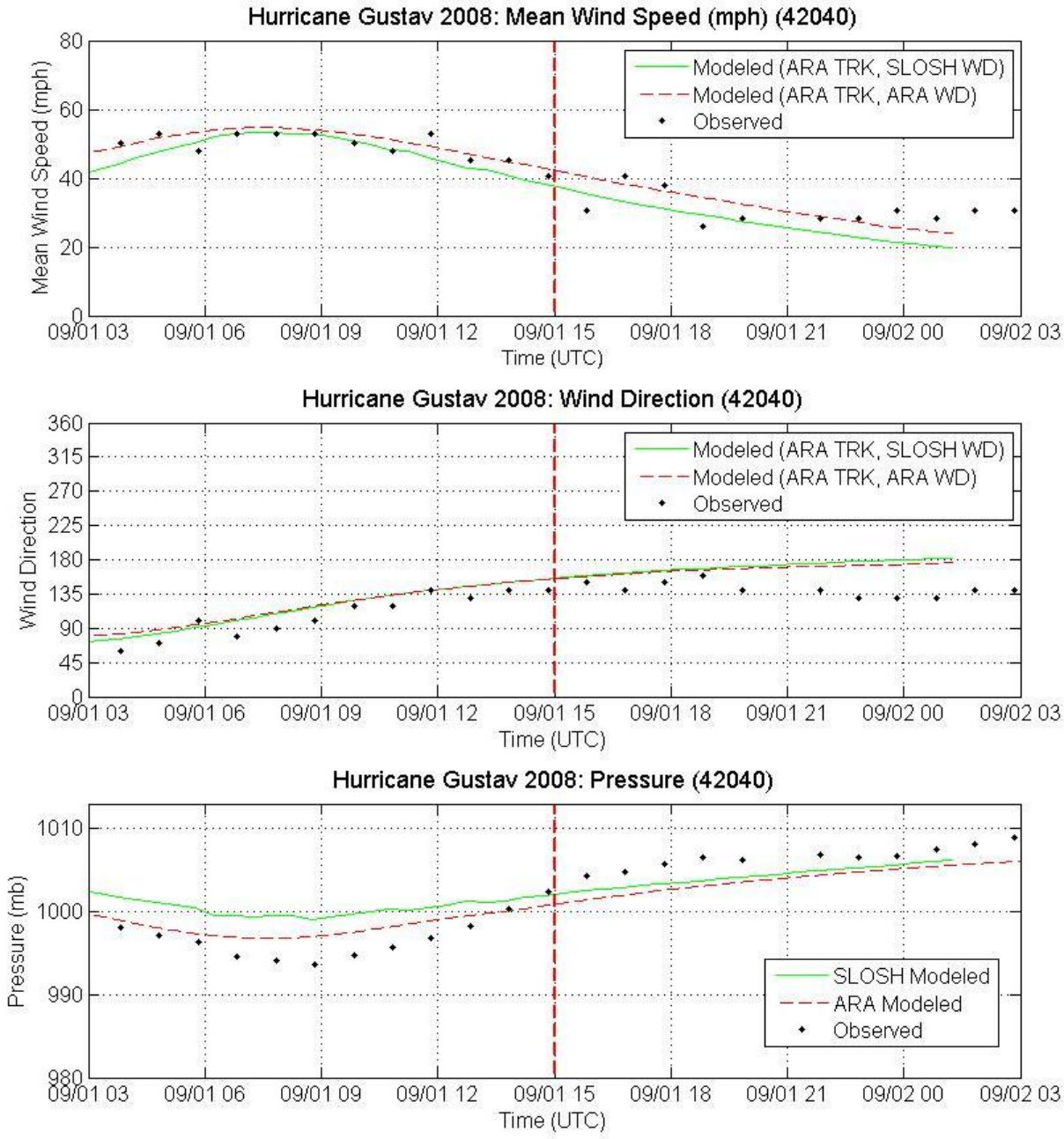

Figure R-5h. Comparisons of Observed and Modeled Time Series Traces of Mean Wind Speeds, Wind Directions, and Pressures for Hurricane Gustav (2008) – 42040

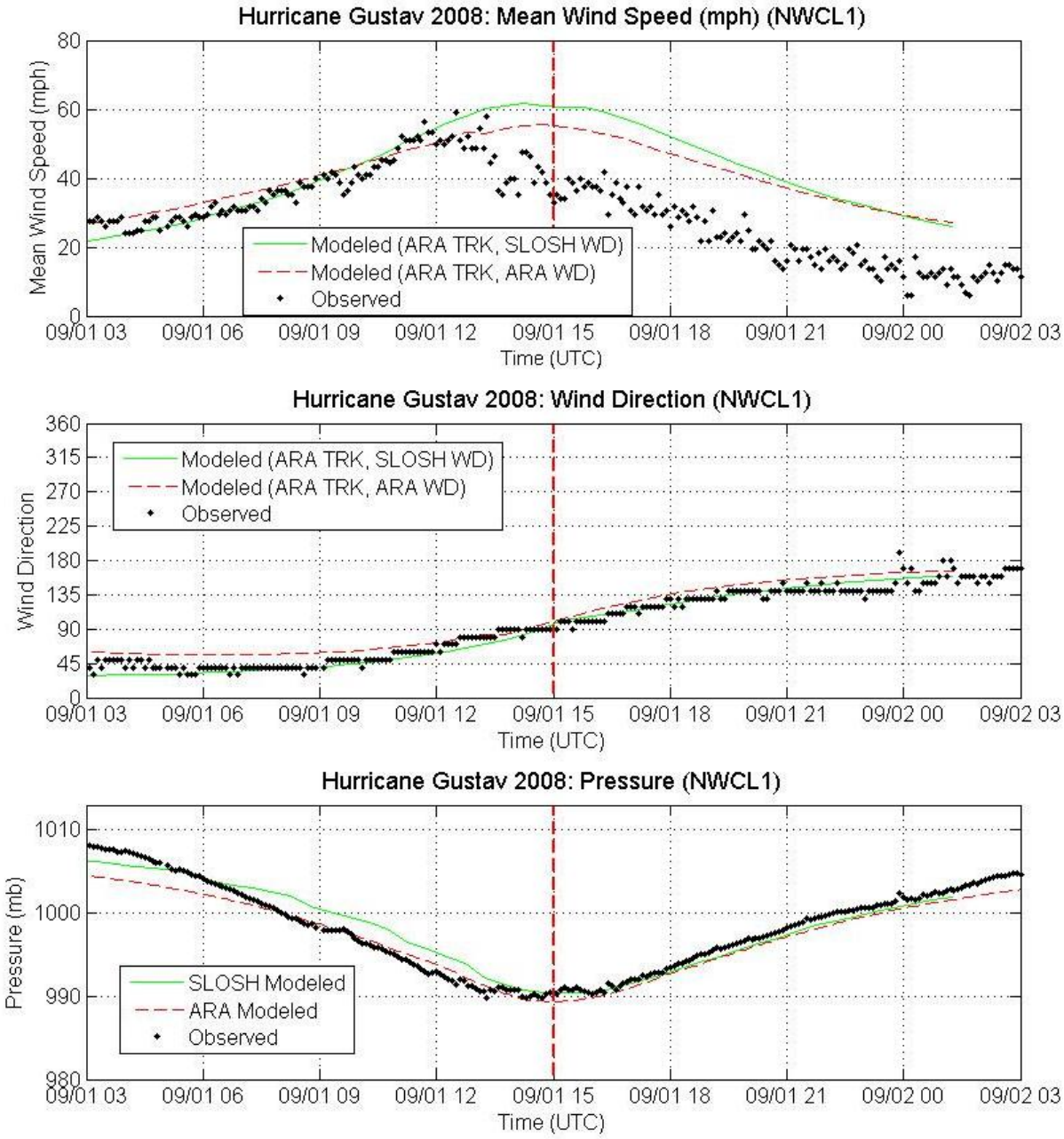

Figure R-5i. Comparisons of Observed and Modeled Time Series Traces of Mean Wind Speeds, Wind Directions, and Pressures for Hurricane Gustav (2008) – NWCL1

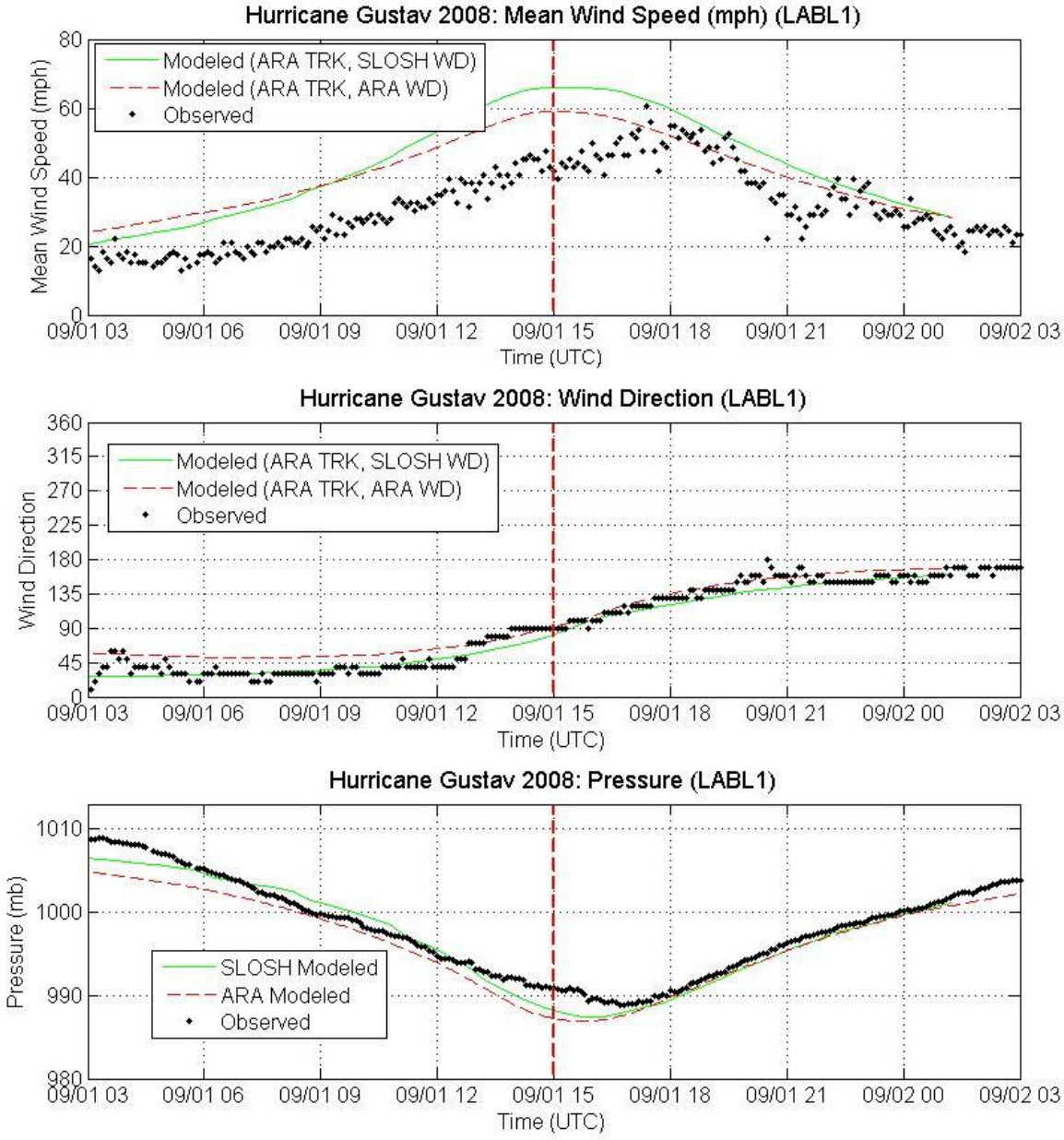

Figure R-5j. Comparisons of Observed and Modeled Time Series Traces of Mean Wind Speeds, Wind Directions, and Pressures for Hurricane Gustav (2008) – LABL1

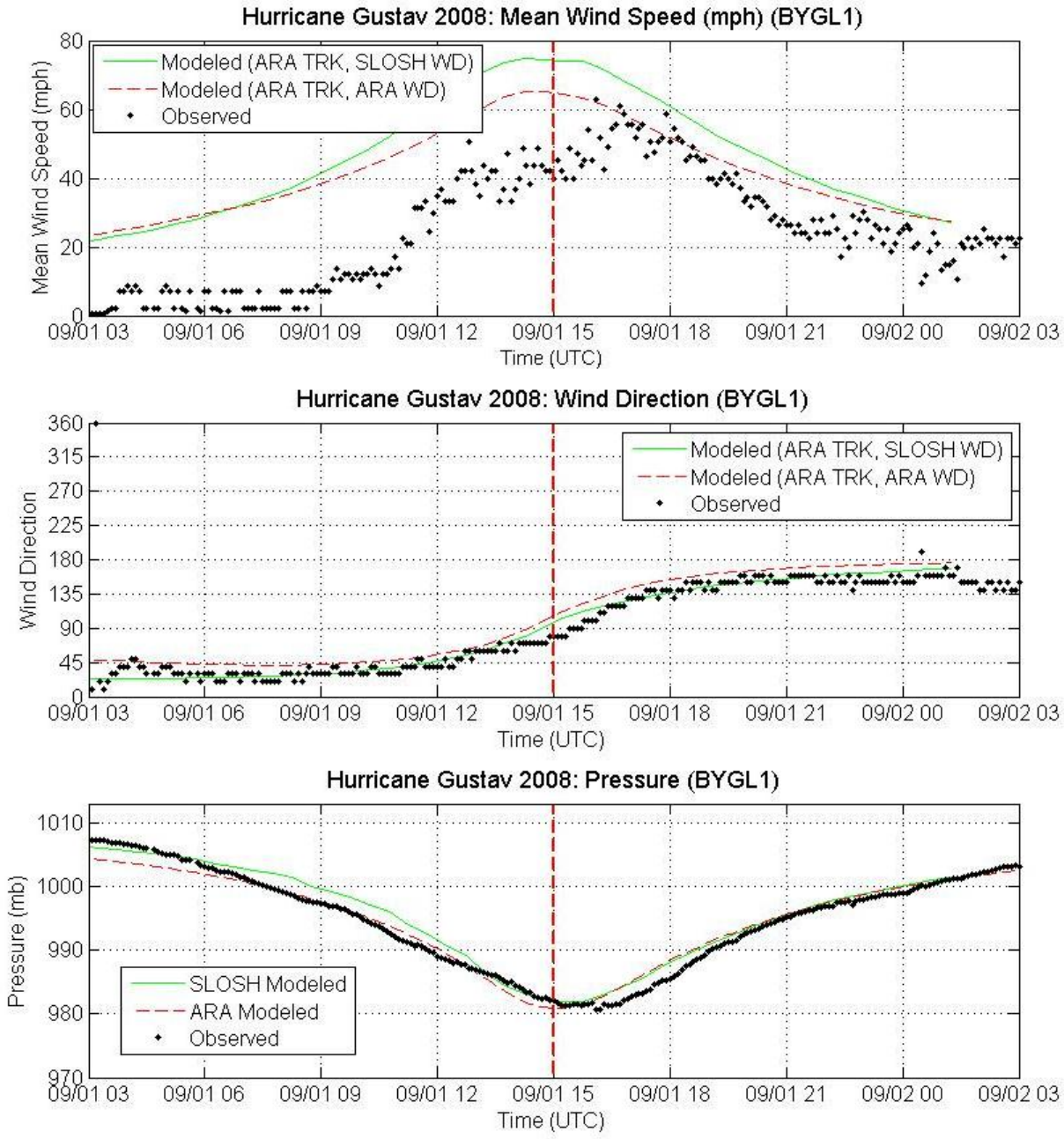

Figure R-5k. Comparisons of Observed and Modeled Time Series Traces of Mean Wind Speeds, Wind Directions, and Pressures for Hurricane Gustav (2008) – BYGL1

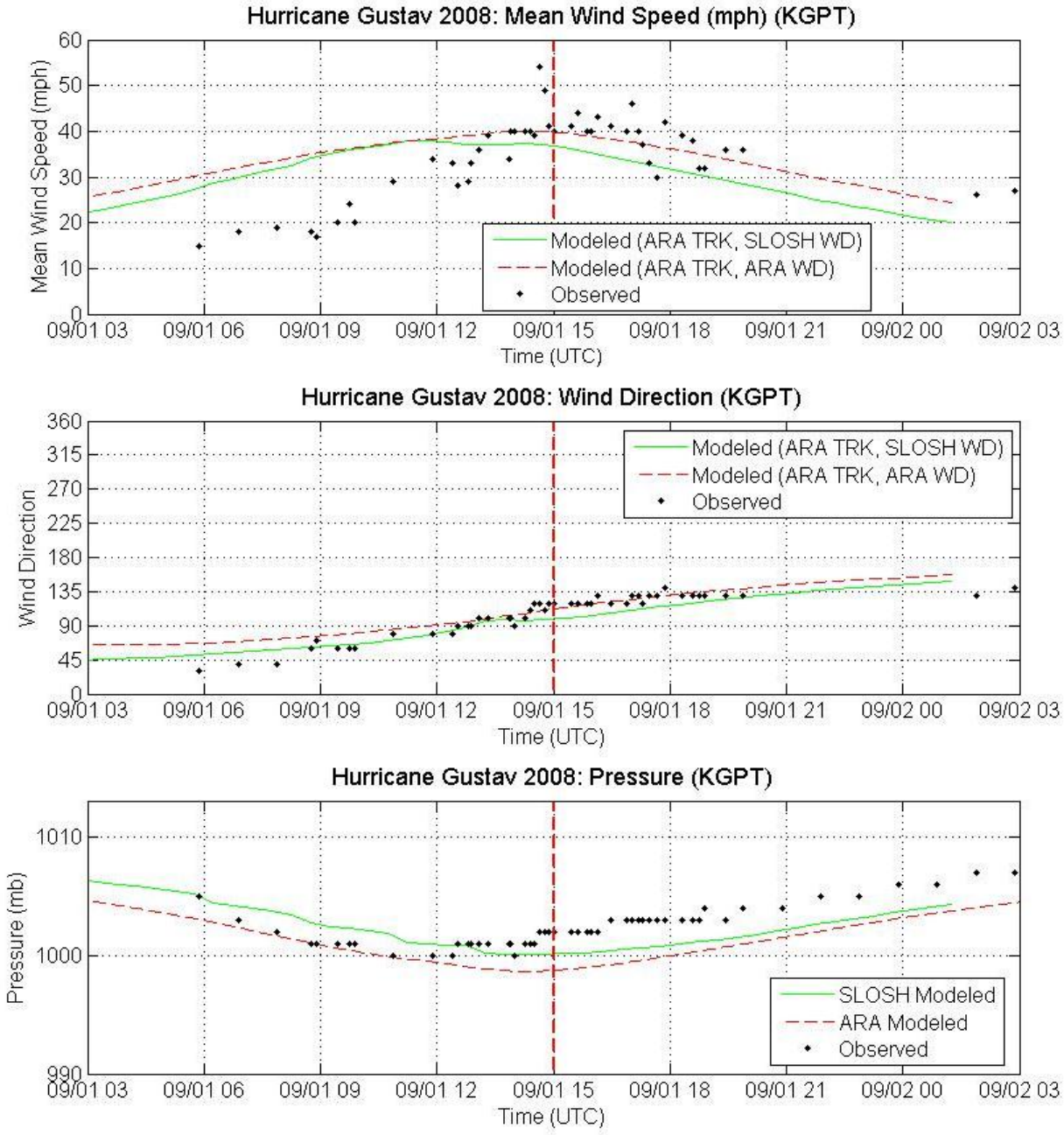

Figure R-5l. Comparisons of Observed and Modeled Time Series Traces of Mean Wind Speeds, Wind Directions, and Pressures for Hurricane Gustav (2008) – KGPT

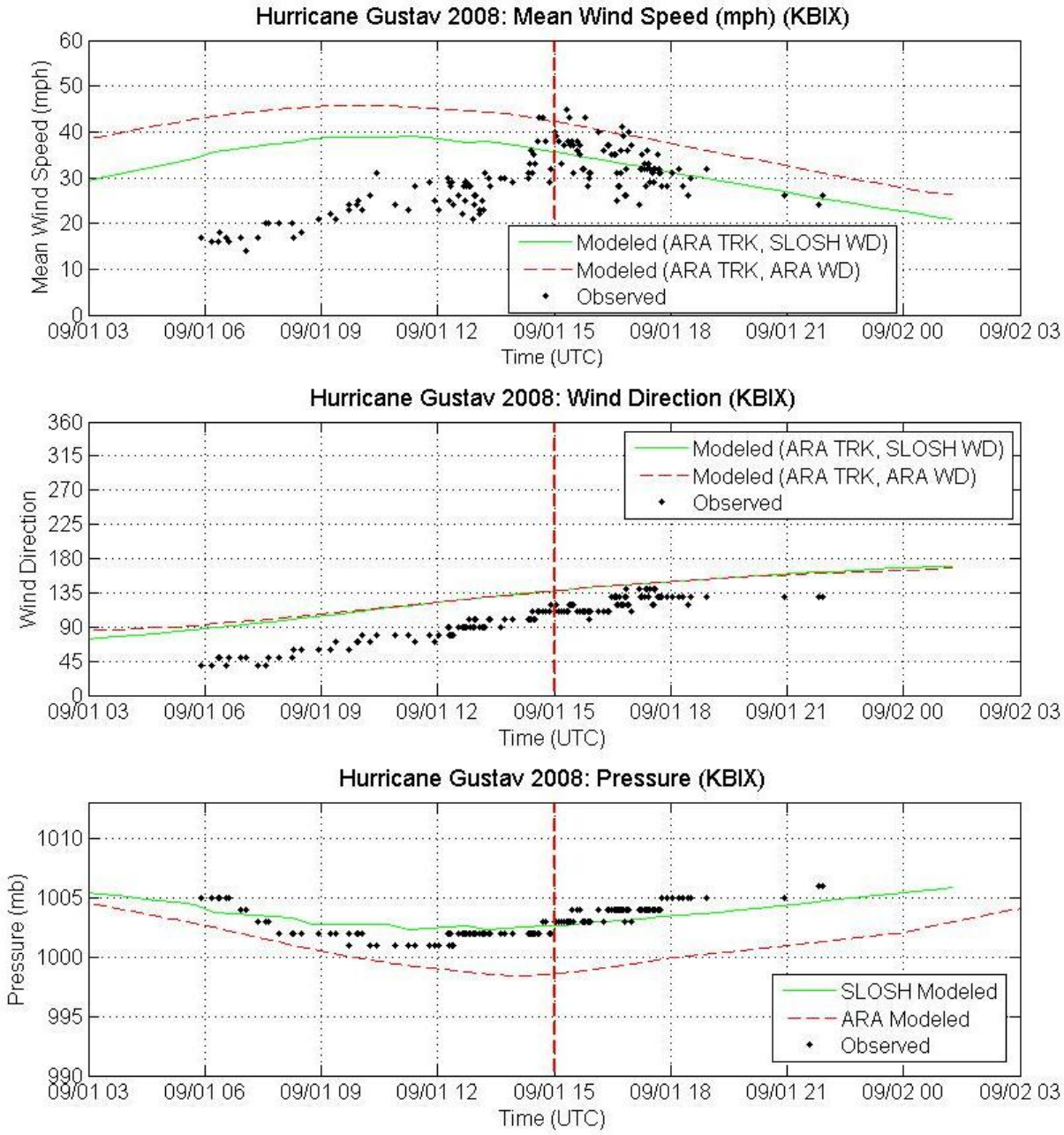

Figure R-5m. Comparisons of Observed and Modeled Time Series Traces of Mean Wind Speeds, Wind Directions, and Pressures for Hurricane Gustav (2008) – KBIX

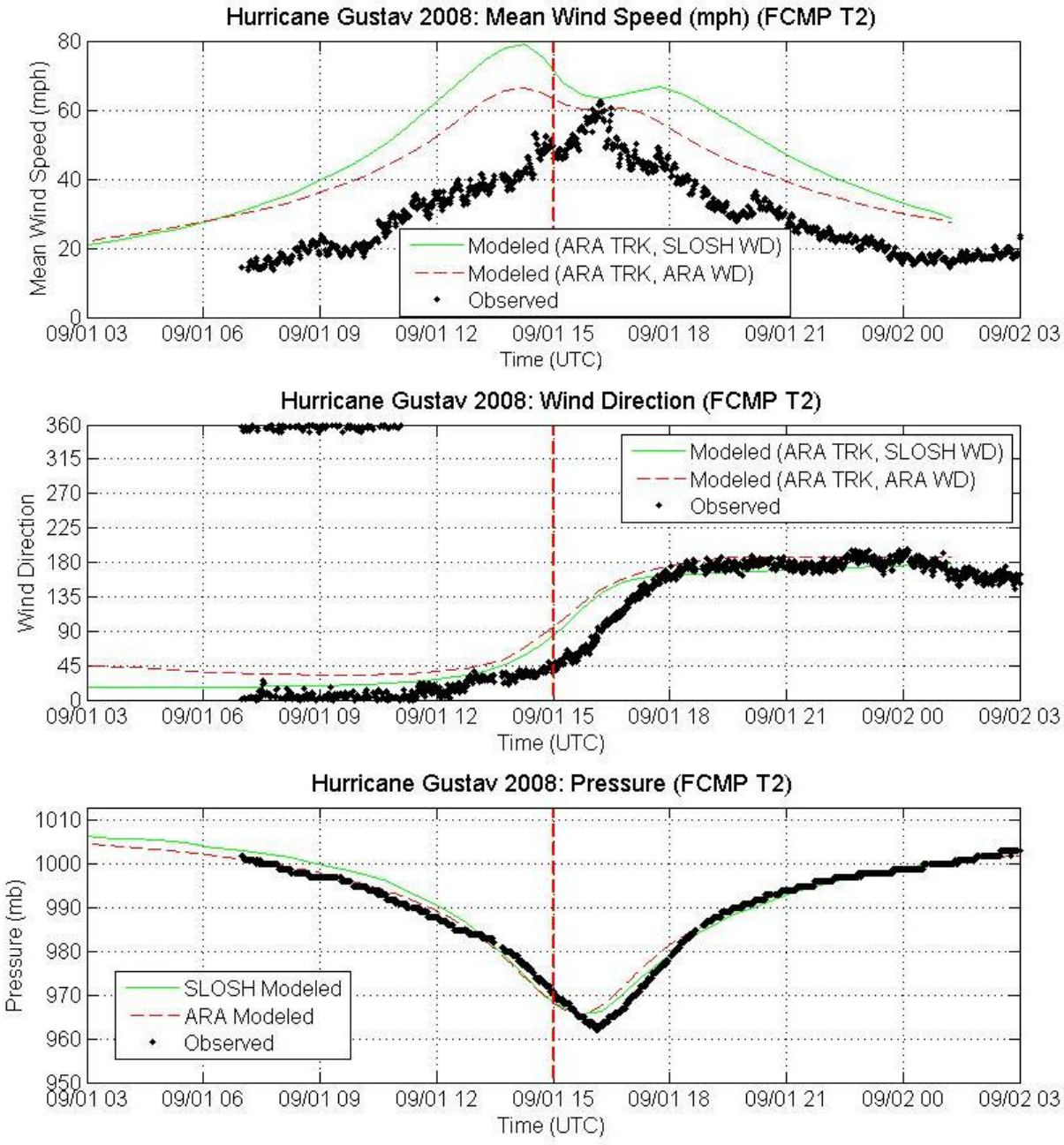

Figure R-5n. Comparisons of Observed and Modeled Time Series Traces of Mean Wind Speeds, Wind Directions, and Pressures for Hurricane Gustav (2008) – FCMP T2

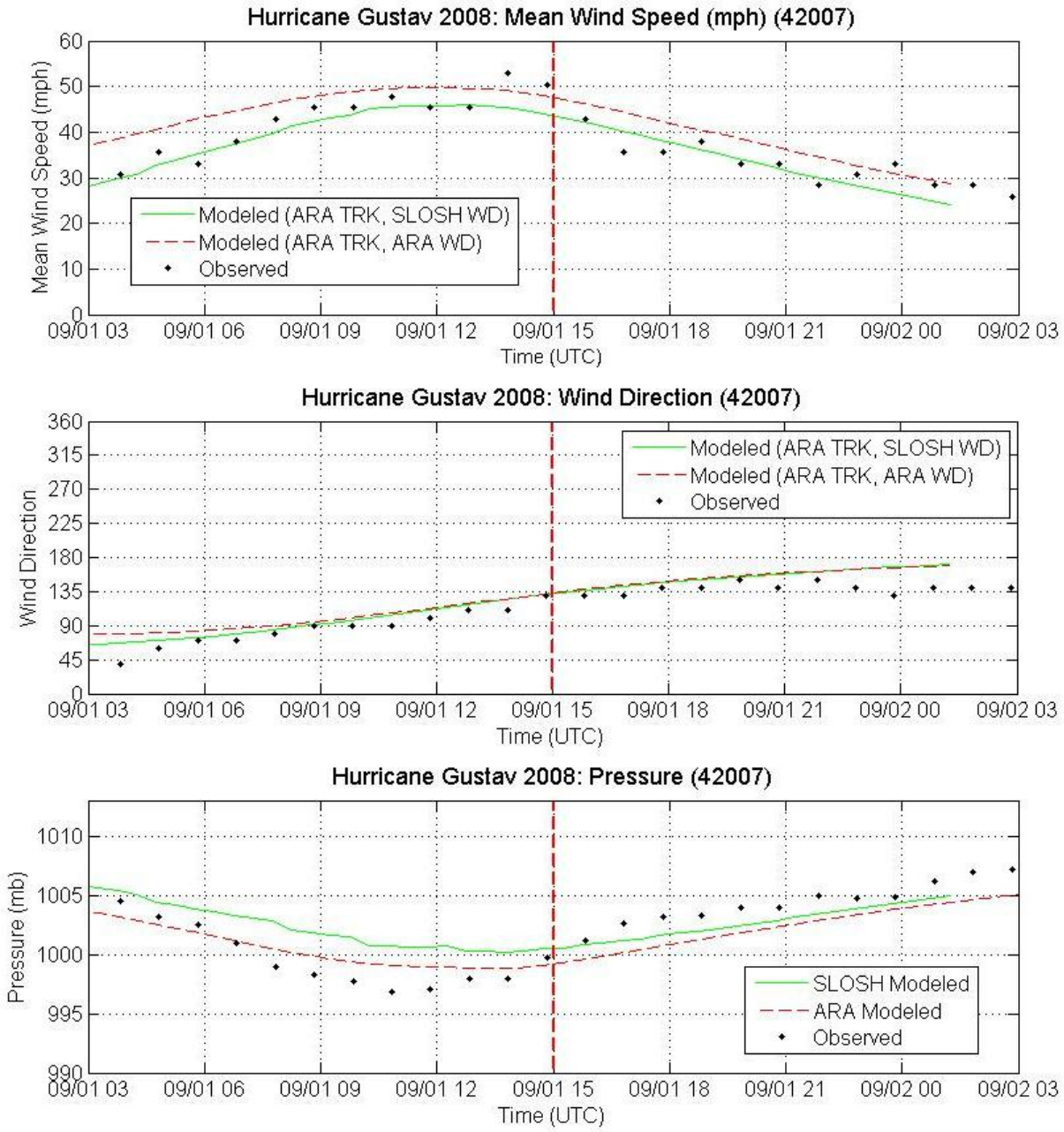

Figure R-5o. Comparisons of Observed and Modeled Time Series Traces of Mean Wind Speeds, Wind Directions, and Pressures for Hurricane Gustav (2008) – 42007

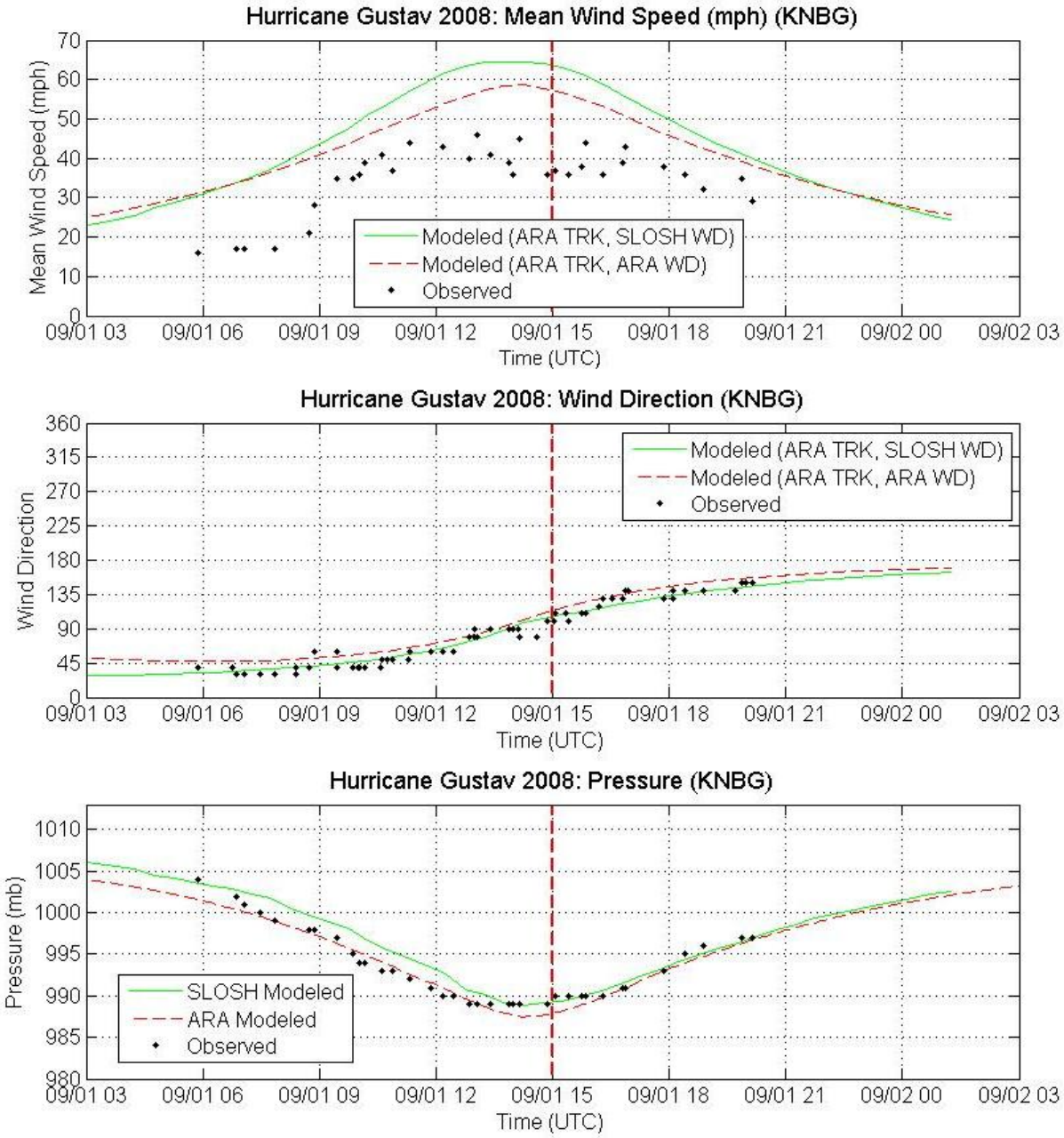

Figure R-5p. Comparisons of Observed and Modeled Time Series Traces of Mean Wind Speeds, Wind Directions, and Pressures for Hurricane Gustav (2008) – KNBG

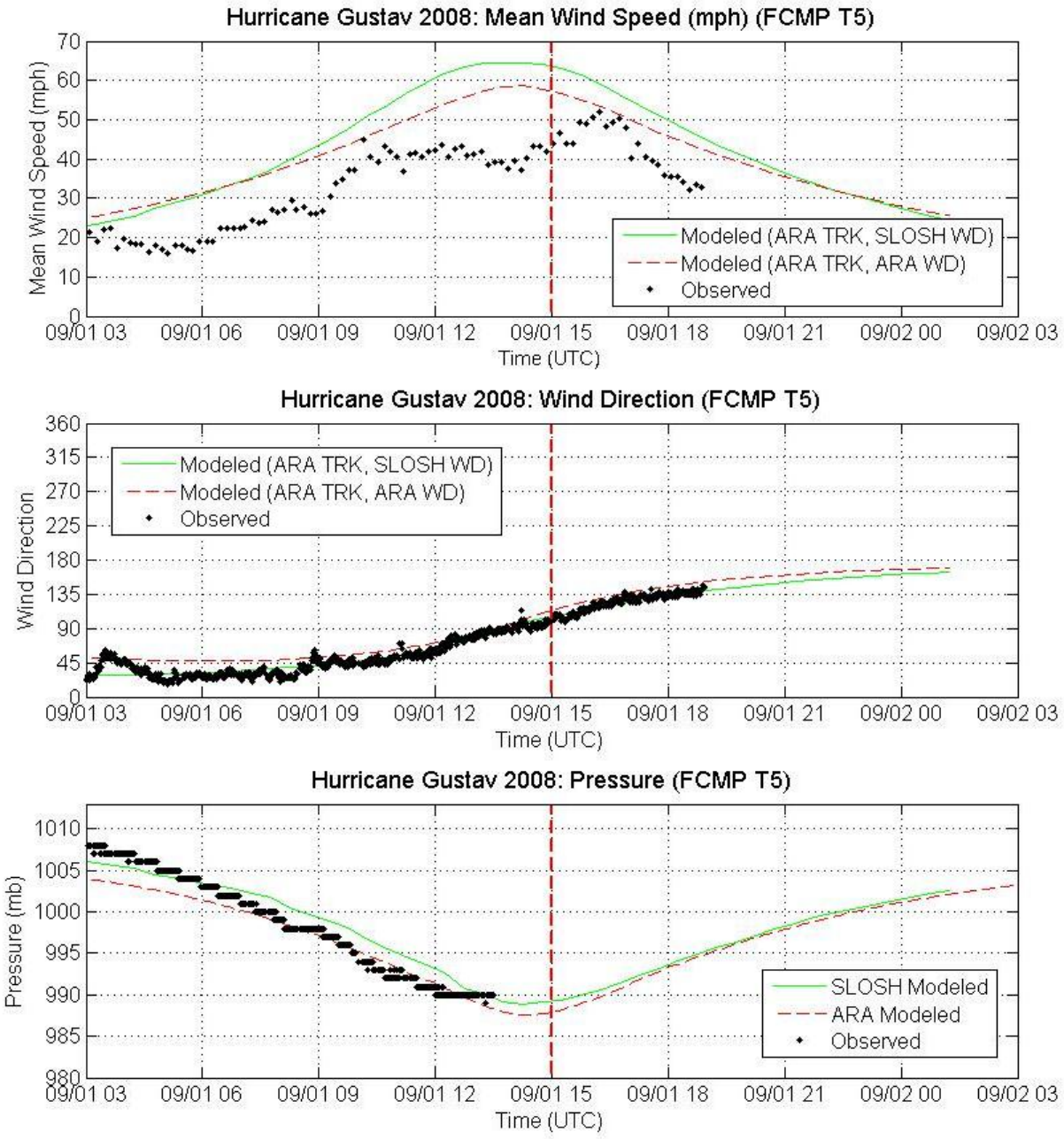

Figure R-5q. Comparisons of Observed and Modeled Time Series Traces of Mean Wind Speeds, Wind Directions, and Pressures for Hurricane Gustav (2008) – FCMP T5

Table R-2. Error Analysis of Wind Speeds, Wind Directions and Pressures for Hurricane Gustav

Station	Range		Number of Data	Obs		SLOSH-Obs		ARA-Obs	
				Mean	Std	mean	RMS	mean	RMS
KLCH	Wind Speed (mph)	0-20	14	14.0	4.5	12.6	14.1	8.5	8.9
		20-40	26	25.5	3.1	14.9	15.1	5.6	6.1
		all	40	21.5	6.6	14.1	14.8	6.6	7.2
	Wind Direction (deg)	0-45	3	23.3	15.3	-21.2	23.8	19.3	21.1
		45-90	1	50.0	0.0	-45.0	45.0	0.5	0.5
		270-315	10	299.0	12.0	-9.2	11.1	17.1	18.5
		315-360	21	334.3	11.2	-1.1	4.9	17.7	18.3
		all	35	298.3	93.2	-6.0	11.8	18.5	20.0
	Pressure (mbar)	989-1030	40	997.9	5.6	0.0	1.0	-0.6	1.8
		all	40	997.9	5.6	0.0	1.0	-0.6	1.8
KLFT	Wind Speed (mph)	0-20	4	10.5	3.7	10.7	10.8	10.9	11.0
		20-40	12	28.6	6.1	13.5	14.2	7.2	7.5
		40-60	18	50.6	5.6	4.9	15.5	-7.7	15.6
		60-80	2	61.5	0.7	-3.6	4.4	-18.5	18.6
		all	36	39.4	16.0	7.9	14.2	-1.3	13.1
	Wind Direction (deg)	0-45	7	14.3	7.9	-4.1	7.8	20.8	22.1
		180-225	2	195.0	7.1	3.7	5.6	21.7	22.2
		270-315	1	310.0	0.0	23.3	23.3	23.0	23.0
		315-360	14	340.7	8.3	27.8	28.5	42.0	43.3
		all	24	274.7	135.0	13.3	19.0	29.6	32.2
	Pressure (mbar)	965-980	15	973.3	3.9	-2.4	2.5	0.1	0.5
		980-989	7	984.4	2.9	-3.5	3.7	-1.9	2.4
		989-1030	18	998.5	5.6	-0.5	1.1	-1.3	1.7
		all	40	986.6	12.4	-1.7	2.3	-0.9	1.6
FCMP T0	Wind Speed (mph)	0-20	452	12.4	4.1	14.6	15.0	13.2	13.3
		20-40	688	29.0	4.5	21.7	23.8	11.4	14.1
		40-60	88	44.3	2.1	6.9	12.4	-7.9	11.0
		all	1228	24.0	10.5	18.0	20.3	10.7	13.6
	Wind Direction (deg)	0-45	769	17.5	9.0	-8.6	12.2	11.1	15.0
		45-90	7	47.3	2.6	-35.2	35.3	-4.8	5.4
		180-225	71	221.1	2.3	-24.0	24.2	-3.3	4.5
		225-270	207	240.5	12.8	-19.4	21.0	-10.5	11.5
		270-315	42	291.1	12.6	-4.4	6.3	-13.7	14.6
		315-360	133	344.6	11.7	15.0	16.5	25.7	29.9
		all	1229	113.4	128.2	-8.7	15.4	7.4	16.5
	Pressure (mbar)	965-980	200	973.7	3.0	-4.7	4.8	-3.2	3.3
		980-989	176	984.5	2.5	-4.7	4.9	-3.0	3.6
		989-1030	861	1000.0	6.2	-1.6	2.0	-2.6	2.8
		all	1237	993.5	11.5	-2.6	3.1	-2.7	3.0

Table R-2. Error Analysis of Wind Speeds, Wind Directions and Pressures for Hurricane Gustav (Continued)

Station	Range		Number of Data	Obs		SLOSH-Obs		ARA-Obs	
				Mean	Std	mean	RMS	mean	RMS
PSTL1	Wind Speed (mph)	0-20	5	19.3	1.0	6.7	7.1	12.1	12.3
		20-40	83	29.4	5.2	-2.9	4.8	1.6	3.8
		40-60	88	46.7	4.1	4.7	10.3	2.9	8.0
		60-80	35	70.5	6.3	4.0	5.1	-2.6	4.0
		80-100	5	81.0	1.2	-2.9	3.1	-8.9	8.9
		all	216	44.1	16.4	1.5	7.6	1.5	6.3
	Wind Direction (deg)	45-90	52	68.1	10.7	-33.4	34.3	-20.7	22.8
		90-135	23	111.3	14.9	-19.9	20.3	-6.2	7.1
		135-180	49	164.9	8.9	-7.4	19.8	2.4	14.3
		180-225	90	196.2	11.2	-38.1	39.5	-25.0	26.7
		225-270	2	261.0	0.0	150.4	152.6	164.9	167.0
		all	216	149.8	54.4	-26.3	35.8	-14.0	27.1
	Pressure (mbar)	965-980	26	977.5	1.2	5.6	5.6	5.0	5.0
		980-989	29	984.8	2.6	2.9	3.0	1.8	2.3
		989-1030	161	999.8	4.5	-0.3	0.8	-1.5	1.8
		all	216	995.1	9.2	0.9	2.3	-0.3	2.5
GISL1	Wind Speed (mph)	0-20	29	18.5	1.2	7.3	8.1	16.2	16.5
		20-40	120	28.5	5.2	12.4	16.2	19.2	20.9
		40-60	66	47.7	5.3	19.7	20.7	20.5	21.3
		60-80	8	62.7	2.7	14.6	15.0	13.5	14.0
		all	223	34.1	12.5	14.0	16.9	19.0	20.3
	Wind Direction (deg)	0-45	39	34.4	6.8	-10.7	12.3	15.4	16.6
		45-90	48	60.2	10.8	-17.3	19.0	6.5	8.7
		90-135	21	110.5	13.6	-1.1	4.8	14.8	15.4
		135-180	78	166.0	8.1	-9.9	14.0	8.7	11.4
		180-225	37	181.9	4.0	-15.8	16.9	1.7	5.2
		all	223	117.6	59.3	-11.8	14.9	8.8	11.7
	Pressure (mbar)	965-980	32	978.3	1.0	1.9	2.3	2.2	2.4
		980-989	33	984.5	2.8	2.2	2.5	1.5	1.8
		989-1030	158	999.7	4.4	-0.7	1.3	-1.9	2.1
		all	223	994.4	9.3	0.1	1.7	-0.8	2.1
AMRL1	Wind Speed (mph)	0-20	124	12.9	4.4	19.8	20.4	24.3	24.4
		20-40	69	29.1	5.5	28.6	29.2	26.4	27.1
		40-60	29	49.2	5.1	6.4	14.5	1.1	10.6
		60-80	1	61.1	0.0	-17.6	17.6	-19.6	19.6
		all	223	22.9	13.7	20.6	22.9	21.7	24.0
	Wind Direction (deg)	0-45	14	12.1	4.3	-3.8	5.5	37.0	37.3
		180-225	47	209.1	9.0	-14.6	16.3	6.9	9.1
		225-270	26	238.8	9.5	-20.8	21.6	-8.1	9.3
		270-315	14	293.6	16.0	-12.4	14.6	-19.1	21.3
		315-360	112	341.7	7.6	19.3	20.0	47.1	48.2
		all	213	278.9	89.9	3.6	18.2	27.5	37.7
	Pressure (mbar)	965-980	39	971.5	4.5	-2.3	3.5	-0.3	3.0
		980-989	40	984.9	2.5	-1.1	2.0	-0.6	1.9
		989-1030	144	998.4	5.3	1.3	1.6	0.1	1.1
		all	223	991.3	11.5	0.2	2.1	-0.1	1.7
SHBL1	Wind Speed (mph)	20-40	83	35.9	2.7	-6.5	7.5	-3.9	5.4
		40-60	127	48.9	5.5	-3.5	6.7	-4.9	6.6
		all	210	43.8	7.8	-4.7	7.1	-4.5	6.2
	Wind Direction (deg)	0-45	21	40.0	0.0	-3.2	3.7	18.1	18.1
		45-90	63	60.0	10.0	-11.0	13.2	6.7	8.8
		90-135	53	117.0	12.6	-5.6	16.3	2.1	15.0
		135-180	73	143.2	5.2	2.3	10.4	10.6	13.9
		all	210	101.3	40.6	-4.2	12.6	8.1	13.4
	Pressure (mbar)	989-1030	210	998.0	4.5	1.2	2.0	-0.1	1.3
		all	210	998.0	4.5	1.2	2.0	-0.1	1.3

Table R-2. Error Analysis of Wind Speeds, Wind Directions and Pressures for Hurricane Gustav (Continued)

Station	Range		Number of Data	Obs		SLOSH-Obs		ARA-Obs	
				Mean	Std	mean	RMS	mean	RMS
42040	Wind Speed (mph)	20-40	8	29.8	3.7	-3.3	5.9	1.4	5.3
		40-60	13	48.6	4.6	-2.4	4.0	0.9	2.5
		all	21	41.5	10.2	-2.7	4.8	1.1	3.8
	Wind Direction (deg)	45-90	3	70.0	10.0	16.8	17.0	21.0	21.2
		90-135	9	116.7	15.8	23.6	30.9	22.5	28.1
		135-180	9	144.4	7.3	16.5	19.7	15.2	18.1
		all	21	121.9	27.9	19.6	24.9	19.2	23.3
	Pressure (mbar)	989-1030	21	1000.8	5.1	1.3	3.3	-0.2	2.3
		all	21	1000.8	5.1	1.3	3.3	-0.2	2.3
NWCL1	Wind Speed (mph)	0-20	47	14.8	3.4	18.1	18.4	17.6	17.8
		20-40	129	31.1	5.3	10.7	16.0	10.1	12.6
		40-60	45	47.9	4.9	5.3	8.0	1.7	5.0
		all	221	31.1	11.8	11.2	15.3	10.0	12.9
	Wind Direction (deg)	0-45	51	38.4	3.7	-4.1	6.3	18.7	19.1
		45-90	54	60.2	11.9	-9.7	11.6	7.9	9.1
		90-135	60	110.0	15.9	0.3	6.8	9.4	11.8
		135-180	53	143.8	7.4	4.8	8.9	14.4	16.0
		180-225	3	183.3	5.8	-25.0	25.8	-17.7	18.7
		all	221	90.4	43.3	-2.4	9.1	12.0	14.4
	Pressure (mbar)	989-1030	221	997.6	5.3	0.3	1.4	-0.8	1.4
		all	221	997.6	5.3	0.3	1.4	-0.8	1.4
LABL1	Wind Speed (mph)	0-20	44	16.6	1.9	9.3	9.7	12.1	12.4
		20-40	114	30.0	5.5	11.9	13.9	9.6	11.4
		40-60	62	46.9	4.2	14.3	16.2	7.2	10.2
		60-80	1	60.6	0.0	1.9	1.9	-6.2	6.2
		all	221	32.2	11.7	12.0	13.8	9.4	11.3
	Wind Direction (deg)	0-45	85	32.1	7.4	2.5	7.7	22.7	23.6
		45-90	22	64.1	12.6	-15.3	18.6	1.8	8.0
		90-135	48	107.7	16.0	-7.8	10.2	2.6	6.6
		135-180	65	153.5	8.2	-6.2	11.1	5.7	9.8
		180-225	1	180.0	0.0	-39.1	39.1	-25.5	25.5
		all	221	88.1	52.6	-4.3	11.1	11.0	16.2
	Pressure (mbar)	980-989	2	988.8	0.0	-0.9	0.9	-1.2	1.2
		989-1030	219	997.6	5.7	-0.6	1.3	-1.6	2.0
		all	221	997.5	5.7	-0.6	1.3	-1.6	2.0
BYGL1	Wind Speed (mph)	0-20	89	7.2	5.1	26.6	27.8	25.5	26.3
		20-40	78	30.1	6.1	18.8	21.7	13.4	15.6
		40-60	52	47.9	5.0	19.1	21.1	9.6	12.8
		60-80	2	61.9	1.1	8.9	8.9	-1.6	1.7
		all	221	25.4	17.4	21.9	24.1	17.3	20.1
	Wind Direction (deg)	0-45	86	30.6	7.6	-0.4	7.6	14.6	16.0
		45-90	34	63.5	10.1	5.6	13.4	14.8	18.1
		90-135	22	113.2	15.5	7.6	10.8	21.0	21.8
		135-180	76	152.0	7.3	2.8	8.4	15.5	16.7
		180-225	1	190.0	0.0	-23.2	23.2	-14.8	14.8
		all	219	89.3	60.5	2.5	9.6	15.8	17.8
	Pressure (mbar)	980-989	68	984.4	2.5	1.2	1.6	0.6	1.8
		989-1030	153	998.3	4.9	1.1	1.6	-0.1	1.3
		all	221	994.0	7.7	1.1	1.6	0.1	1.4

Table R-2. Error Analysis of Wind Speeds, Wind Directions and Pressures for Hurricane Gustav (Continued)

Station	Range		Number of Data	Obs		SLOSH-Obs		ARA-Obs	
				Mean	Std	mean	RMS	mean	RMS
KGPT	Wind Speed (mph)	0-20	5	17.4	1.5	14.1	14.3	15.8	15.9
		20-40	22	32.3	5.6	2.1	7.3	4.9	7.4
		40-60	18	42.3	3.8	-6.7	7.7	-3.3	5.0
		all	45	34.6	9.0	-0.1	8.5	2.8	8.1
	Wind Direction (deg)	0-45	3	36.7	5.8	18.1	18.4	32.6	32.8
		45-90	8	68.8	9.9	0.4	5.6	13.5	14.6
		90-135	33	116.1	14.1	-11.1	13.7	0.0	6.1
		135-180	1	140.0	0.0	-24.2	24.2	-10.3	10.3
		all	45	102.9	28.9	-7.4	13.4	4.3	11.8
	Pressure (mbar)	989-1030	50	1002.3	1.5	-1.0	1.7	-2.3	2.6
		all	50	1002.3	1.5	-1.0	1.7	-2.3	2.6
KBIX	Wind Speed (mph)	0-20	11	16.6	1.1	19.6	19.6	27.4	27.4
		20-40	129	29.7	4.9	5.4	8.5	11.9	13.7
		40-60	9	42.0	1.8	-7.2	7.4	-0.7	1.6
		all	149	29.5	6.6	5.6	9.7	12.3	14.8
	Wind Direction (deg)	0-45	5	40.0	0.0	51.5	51.6	56.1	56.2
		45-90	30	66.0	12.2	42.7	43.0	44.8	45.1
		90-135	105	112.2	14.1	27.9	28.9	27.6	28.5
		135-180	9	140.0	0.0	8.0	8.0	7.8	7.8
		all	149	102.1	26.9	30.5	32.4	30.8	33.1
	Pressure (mbar)	989-1030	149	1003.1	1.2	-0.1	0.9	-3.7	3.8
		all	149	1003.1	1.2	-0.1	0.9	-3.7	3.8
FCMP T2	Wind Speed (mph)	0-20	236	17.3	1.6	17.4	17.8	14.8	15.1
		20-40	561	29.0	5.9	23.5	24.4	15.4	16.1
		40-60	264	47.4	5.1	21.1	22.8	13.3	14.6
		60-80	7	61.5	1.0	2.1	2.4	-1.5	1.8
		all	1068	31.2	11.9	21.4	22.6	14.6	15.5
	Wind Direction (deg)	0-45	355	16.8	13.0	17.1	19.4	28.4	29.8
		45-90	66	60.5	10.5	51.1	51.8	58.8	59.2
		90-135	61	112.0	13.1	37.6	38.2	42.4	42.9
		135-180	311	169.4	9.8	-0.8	8.0	13.4	14.4
		180-225	166	184.7	4.5	-11.9	12.8	2.1	4.8
		315-360	101	356.1	2.4	22.7	22.9	37.2	37.3
		all	1060	132.0	105.8	11.3	21.7	23.6	28.7
	Pressure (mbar)	945-965	37	963.4	0.6	2.8	2.9	3.6	3.8
		965-980	211	971.6	4.4	0.1	2.2	0.9	3.3
		980-989	187	984.6	2.5	0.5	1.9	0.4	1.4
		989-1030	642	995.9	3.4	1.0	2.0	0.2	0.7
		all	1077	988.1	11.1	0.8	2.1	0.5	1.8

Table R-2. Error Analysis of Wind Speeds, Wind Directions and Pressures for Hurricane Gustav (Continued)

Station	Range		Number of Data	Obs		SLOSH-Obs		ARA-Obs	
				Mean	Std	mean	RMS	mean	RMS
42007	Wind Speed (mph)	20-40	13	33.3	3.2	-0.6	2.9	4.9	5.9
		40-60	9	46.5	3.3	-2.6	3.7	1.8	3.3
		all	22	38.7	7.3	-1.4	3.3	3.6	5.0
	Wind Direction (deg)	0-45	1	40.0	0.0	27.2	27.2	38.8	38.8
		45-90	4	70.0	8.2	7.3	7.8	14.7	15.2
		90-135	10	111.0	17.9	11.5	15.1	13.0	15.7
		135-180	7	142.9	4.9	15.4	17.6	15.7	17.5
		all	22	110.5	32.4	12.7	15.7	15.3	17.9
	Pressure (mbar)	989-1030	22	1001.6	3.0	0.8	2.2	-0.5	1.6
		all	22	1001.6	3.0	0.8	2.2	-0.5	1.6
KNBG	Wind Speed (mph)	0-20	4	16.8	0.5	17.4	17.6	17.4	17.4
		20-40	20	34.9	4.4	17.8	19.0	13.2	14.4
		40-60	9	43.0	2.0	17.6	18.0	10.9	11.5
		all	33	34.9	8.5	17.7	18.6	13.1	14.1
	Wind Direction (deg)	0-45	16	36.9	4.8	4.2	6.6	15.2	15.7
		45-90	17	64.7	12.3	1.0	9.8	8.9	12.5
		90-135	20	109.0	16.5	-1.3	6.8	8.2	10.5
		135-180	9	143.3	5.0	-6.1	8.7	6.3	8.5
		all	62	83.2	39.3	0.1	8.0	9.9	12.3
	Pressure (mbar)	989-1030	36	993.4	4.3	1.0	1.6	-0.4	1.0
		all	36	993.4	4.3	1.0	1.6	-0.4	1.0
FCMP T5	Wind Speed (mph)	0-20	17	18.0	1.1	9.8	10.2	11.1	11.3
		20-40	42	30.8	6.4	14.0	15.3	11.3	12.1
		40-60	36	43.9	3.4	15.5	16.4	9.2	10.3
		all	95	33.5	10.5	13.8	15.0	10.5	11.3
	Wind Direction (deg)	0-45	356	31.3	7.1	3.7	7.4	18.0	18.9
		45-90	294	62.3	14.6	-3.5	9.5	6.2	8.6
		90-135	243	114.4	14.8	0.3	5.1	10.7	11.6
		135-180	57	137.9	2.8	-3.1	4.6	9.8	10.4
		all	950	68.6	38.7	0.2	7.5	12.0	14.1
	Pressure (mbar)	989-1030	620	998.5	6.0	1.0	1.8	-1.0	1.9
		all	620	998.5	6.0	1.0	1.8	-1.0	1.9
All Stations	Wind Speed (mph)	0-20	1081	13.8	4.7	16.5	17.5	16.1	17.0
		20-40	2197	29.6	5.4	16.9	20.8	12.1	14.8
		40-60	933	47.1	4.9	11.1	16.7	5.5	12.2
		60-80	56	67.3	6.6	4.7	7.6	-1.0	7.6
		80-100	5	81.0	1.2	-2.9	3.1	-8.9	8.9
		all	4272	30.0	13.3	15.3	19.0	11.5	14.8
	Wind Direction (deg)	0-45	1811	22.8	11.9	0.3	12.9	17.4	20.7
		45-90	703	62.4	12.8	-0.7	23.3	11.4	23.0
		90-135	708	112.9	14.7	6.0	18.2	14.1	20.0
		135-180	797	158.3	14.3	-1.4	10.6	11.3	13.8
		180-225	418	195.9	15.6	-20.4	23.8	-4.3	13.6
		225-270	235	240.5	12.5	-18.1	25.2	-8.7	19.1
		270-315	67	293.1	13.4	-6.4	9.8	-9.7	17.0
		315-360	381	346.1	10.8	17.9	19.6	35.2	38.1
		all	5120	116.1	100.1	-0.5	17.4	13.4	21.5
	Pressure (mbar)	945-965	37	963.4	0.6	2.8	2.9	3.6	3.8
		965-980	523	973.2	4.1	-1.6	3.7	-0.5	3.3
		980-989	542	984.6	2.5	-1.0	3.3	-0.6	2.5
		989-1030	3725	998.6	5.4	0.1	1.8	-1.2	2.0
		all	4827	994.0	10.3	-0.2	2.3	-1.0	2.3

Appendix S. Comparisons of Modeled and Measured Wind Speeds, Wind Directions, and Pressures for Hurricane Ike (2008)

This appendix presents comparisons of modeled and observed wind speeds, wind directions, and pressures at multiple locations along the northwestern part of Gulf of Mexico coast during the passage of Hurricane Ike (2008).

Figure S-1 shows the maximum 10-minute mean wind speeds obtained from two versions of SLOSH model. The first version uses ARA storm track and ARA wind field model (denoted as ARA-TRK-ARA-WD), and the second version uses ARA storm track and SLOSH wind field model (denoted as ARA-TRK-SLOSH-WD).

Figure S-2 shows the simulated landfall wind field for the Galveston Bay, Sabine Lake, Vermilion Bay, and New Orleans SLOSH basins.

Figure S-3 shows a map of the locations of all observing stations as well as the hurricane track. The observed wind speeds are compared to the simulated wind speeds from model runs using ARA-TRK-ARA-WD and ARA-TRK-SLOSH-WD model, as shown in Table S-1 and Table S-2.

Figure S-4 presents the comparisons of modeled and observed maximum wind speeds for Hurricane Ike (2008). The results indicated that the ARA wind field model (ARA-TRK-ARA-WD) slightly overestimates the wind speeds, while the simulated wind speeds obtained from SLOSH wind field model (ARA-TRK-SLOSH-WD) are slightly lower than the observed wind speeds for Hurricane Ike.

Comparisons of the entire modeled and observed time series of mean wind speeds, wind directions, and pressures for all stations, both complete and incomplete, are presented in Figure S-5. The RMS errors of wind speed, wind direction, and pressure are shown in Table S-3.

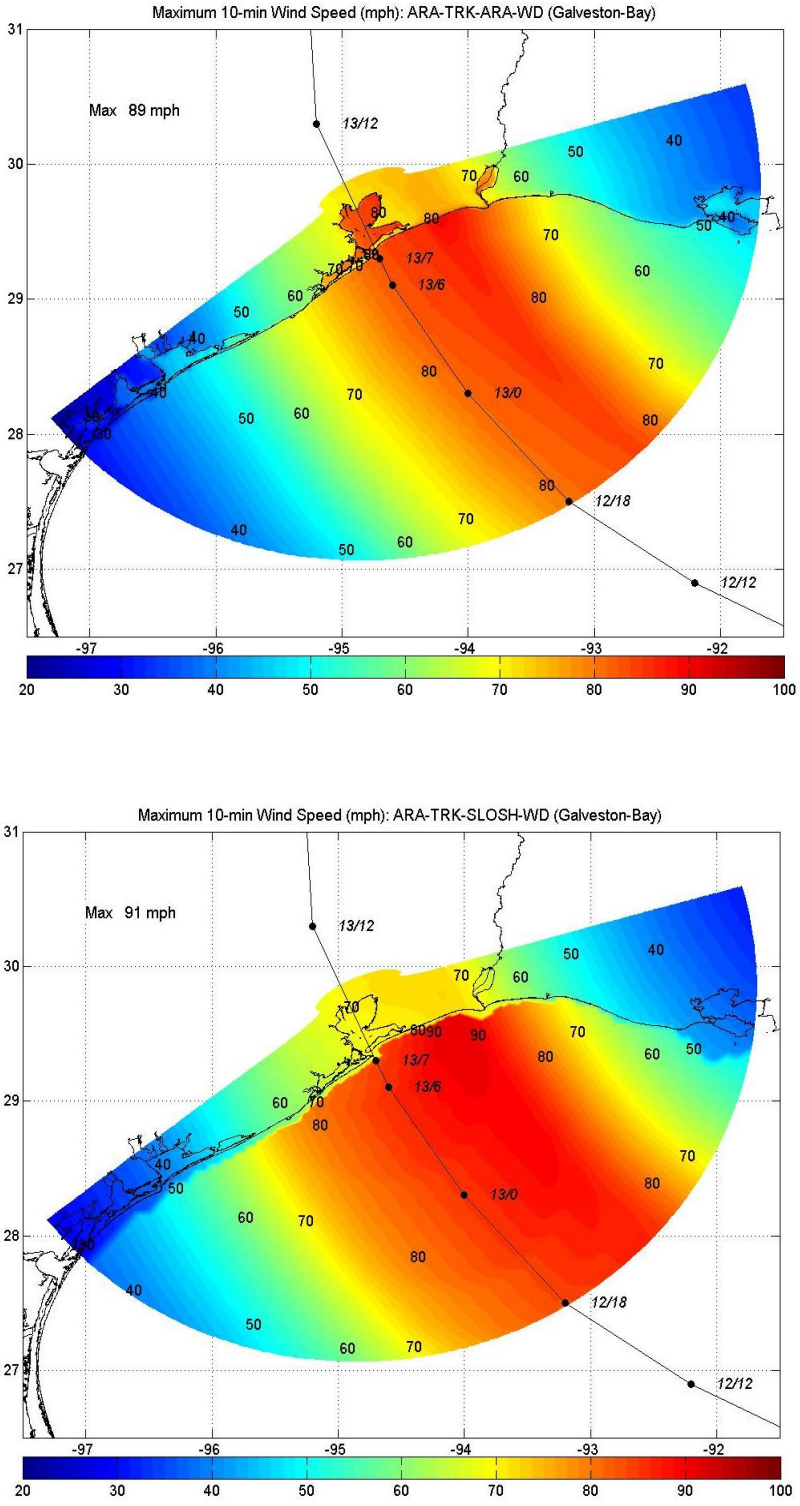

Figure S-1a. Modeled Maximum 10-min Wind Speeds (mph) for Hurricane Ike (2008) – Galveston Bay Basin

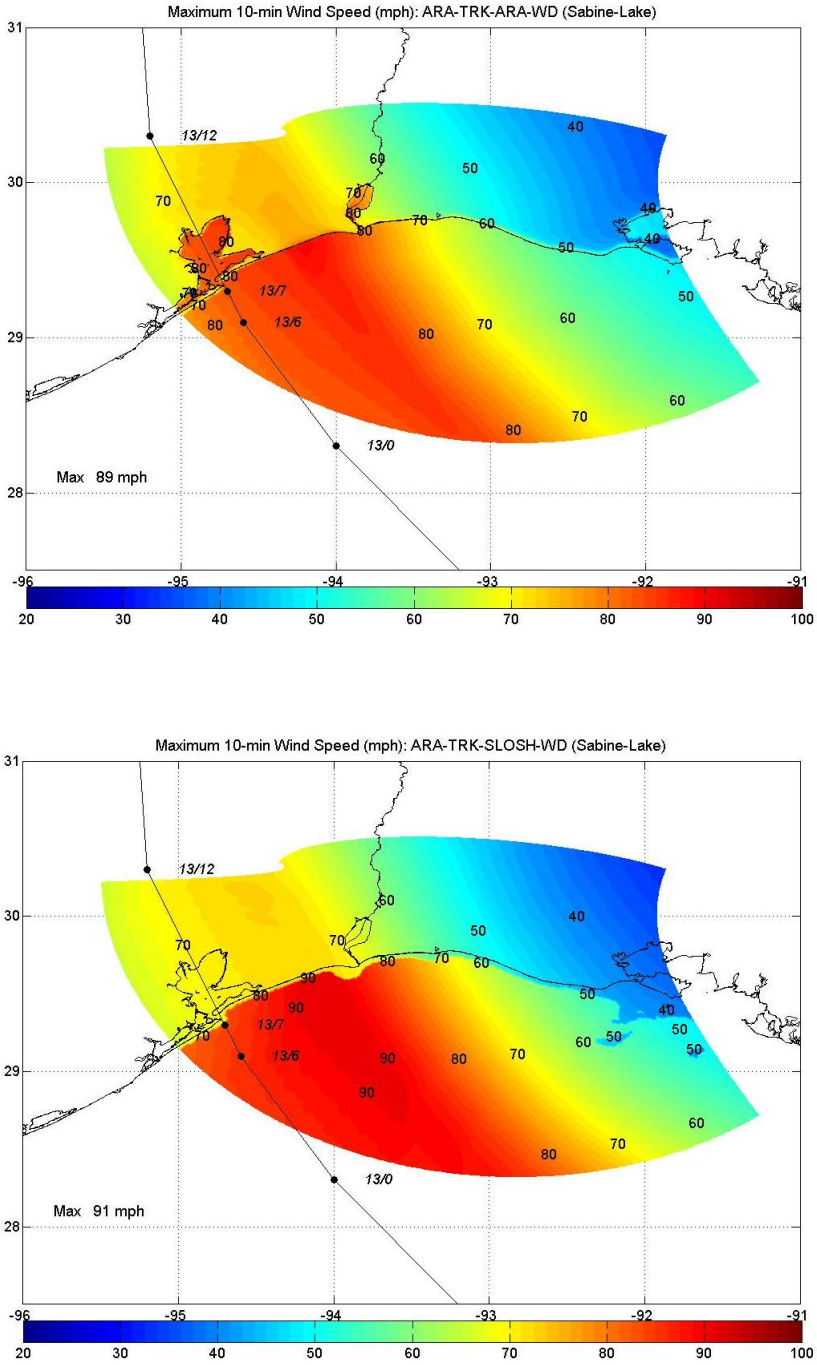

Figure S-1b. Modeled Maximum 10-min Wind Speeds (mph) for Hurricane Ike (2008) – Sabine Lake Basin

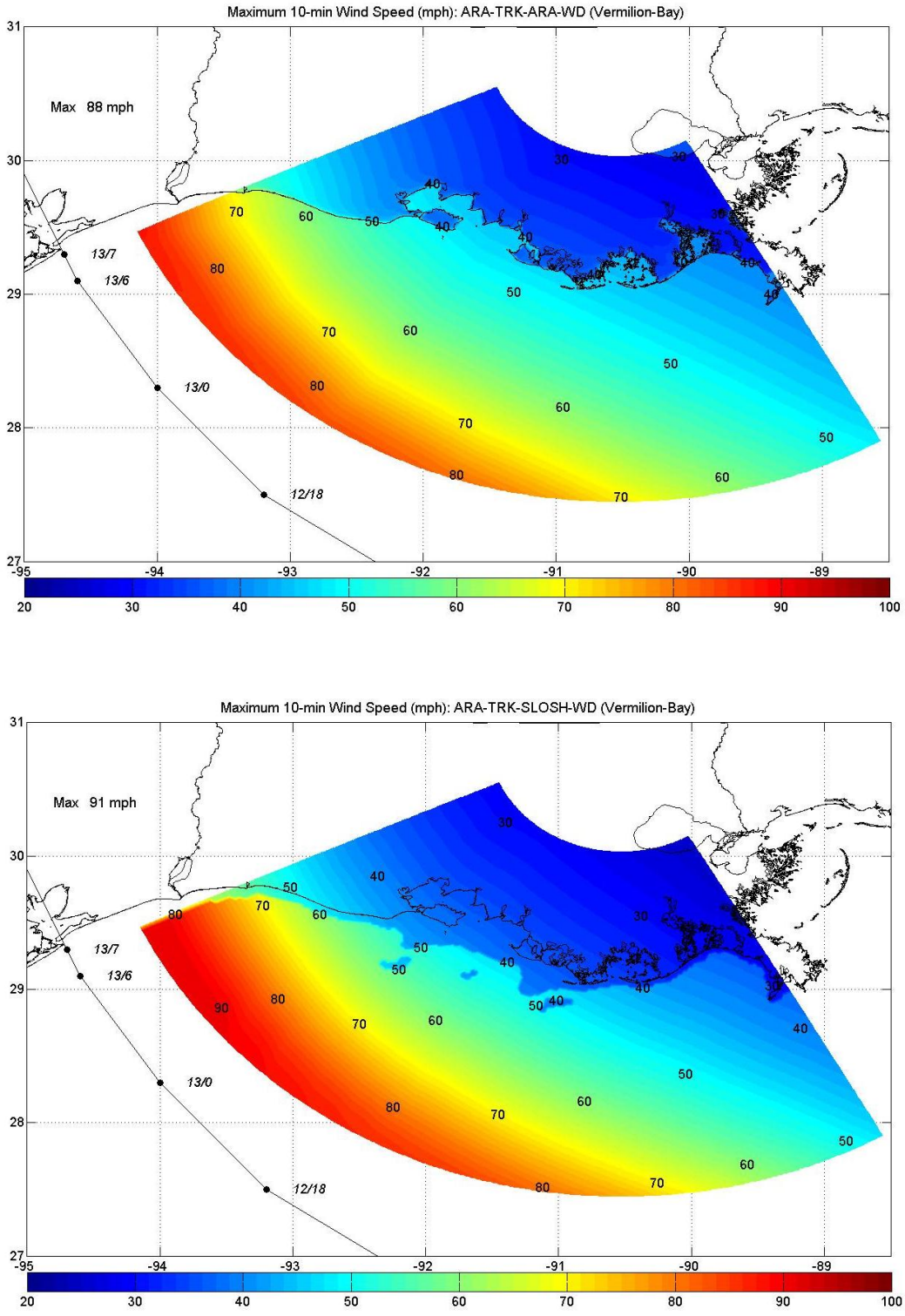

Figure S-1c. Modeled Maximum 10-min Wind Speeds (mph) for Hurricane Ike (2008) – Vermilion Bay Basin

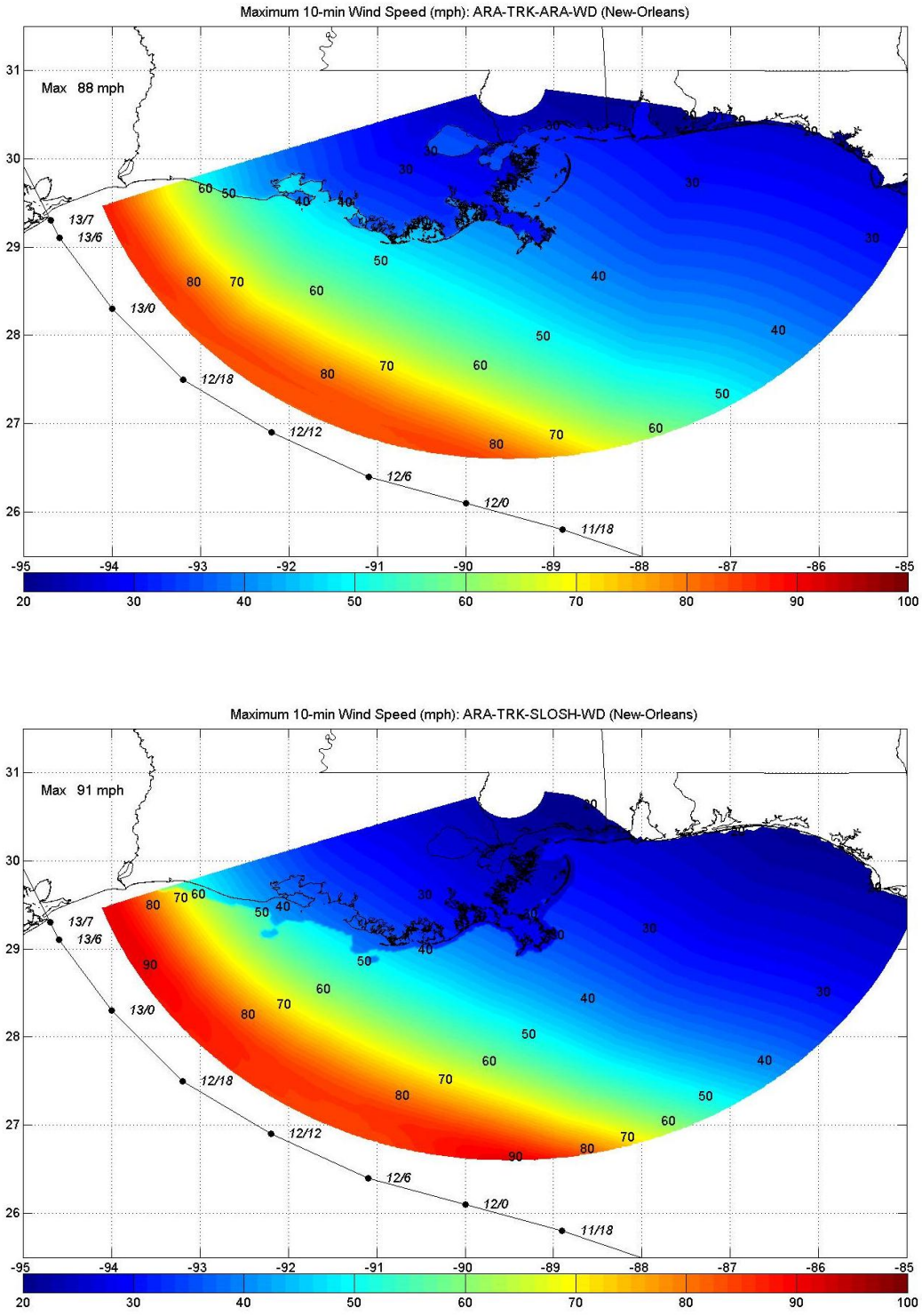

Figure S-1d. Modeled Maximum 10-min Wind Speeds (mph) for Hurricane Ike (2008) – New Orleans Basin

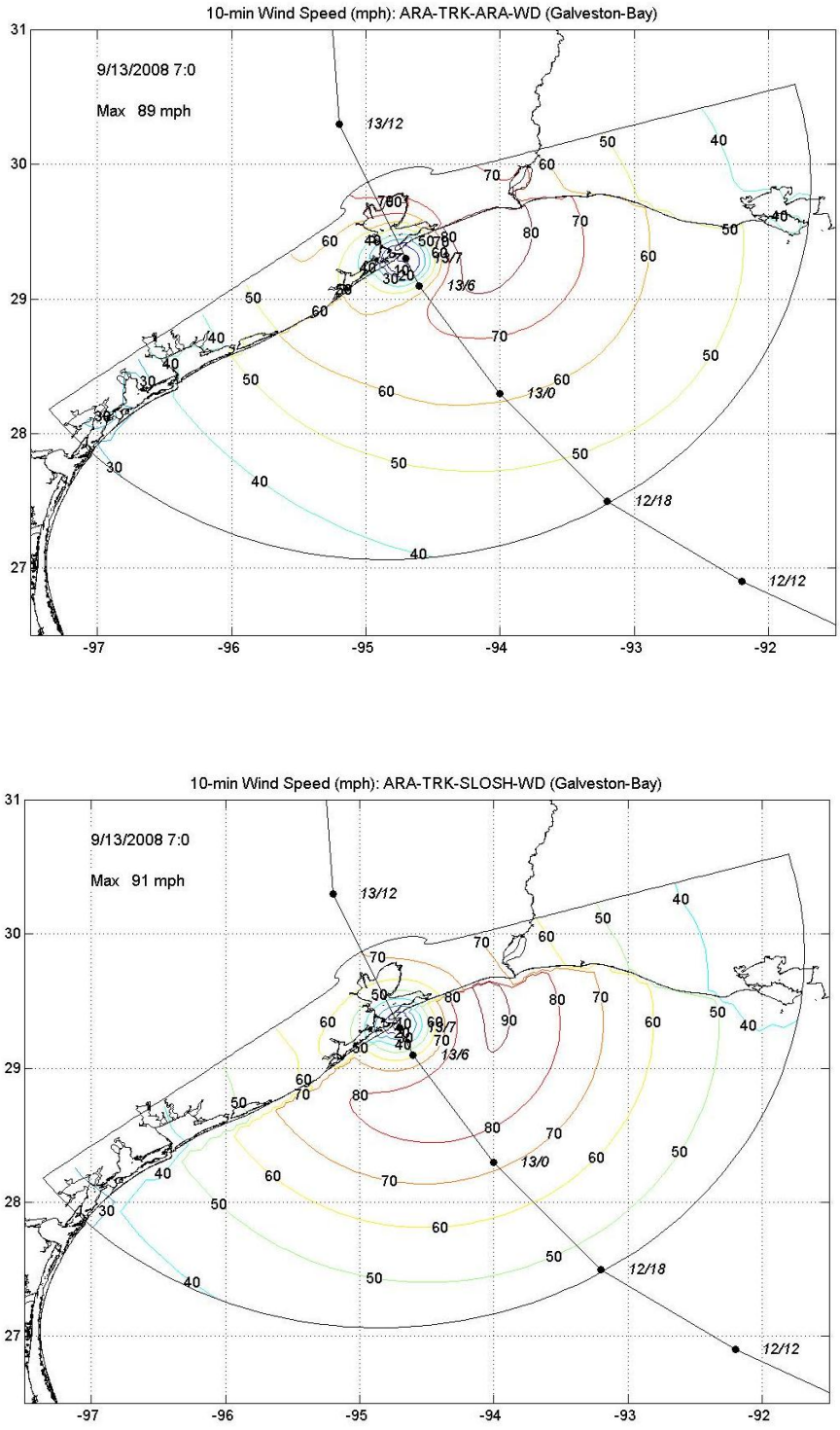

Figure S-2a. Hurricane Ike (2008) Modeled 10-min Wind Speeds (mph) at Landfall – Galveston Bay Basin

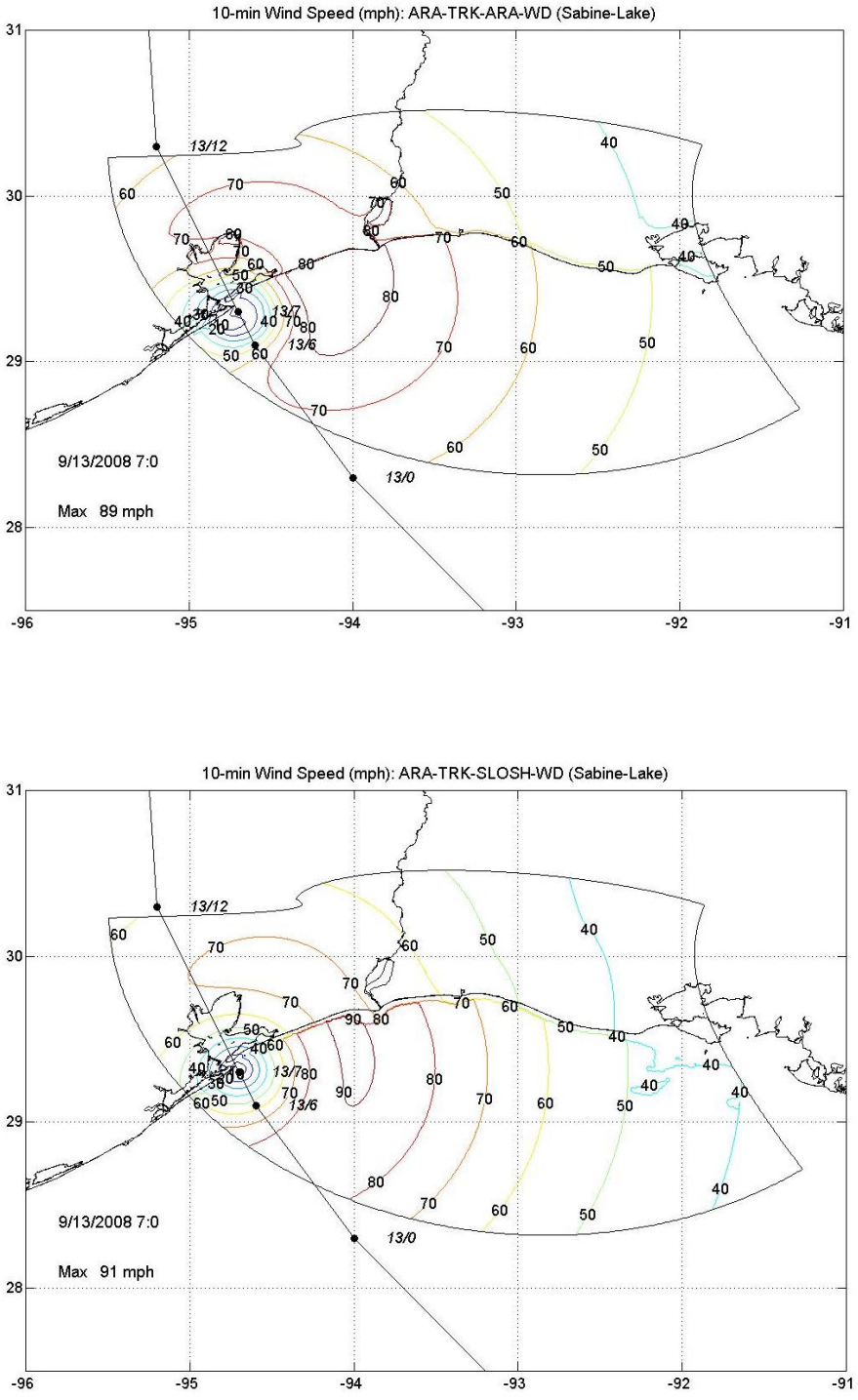

Figure S-2b. Hurricane Ike (2008) Modeled 10-min Wind Speeds (mph) at Landfall – Sabine Lake Basin

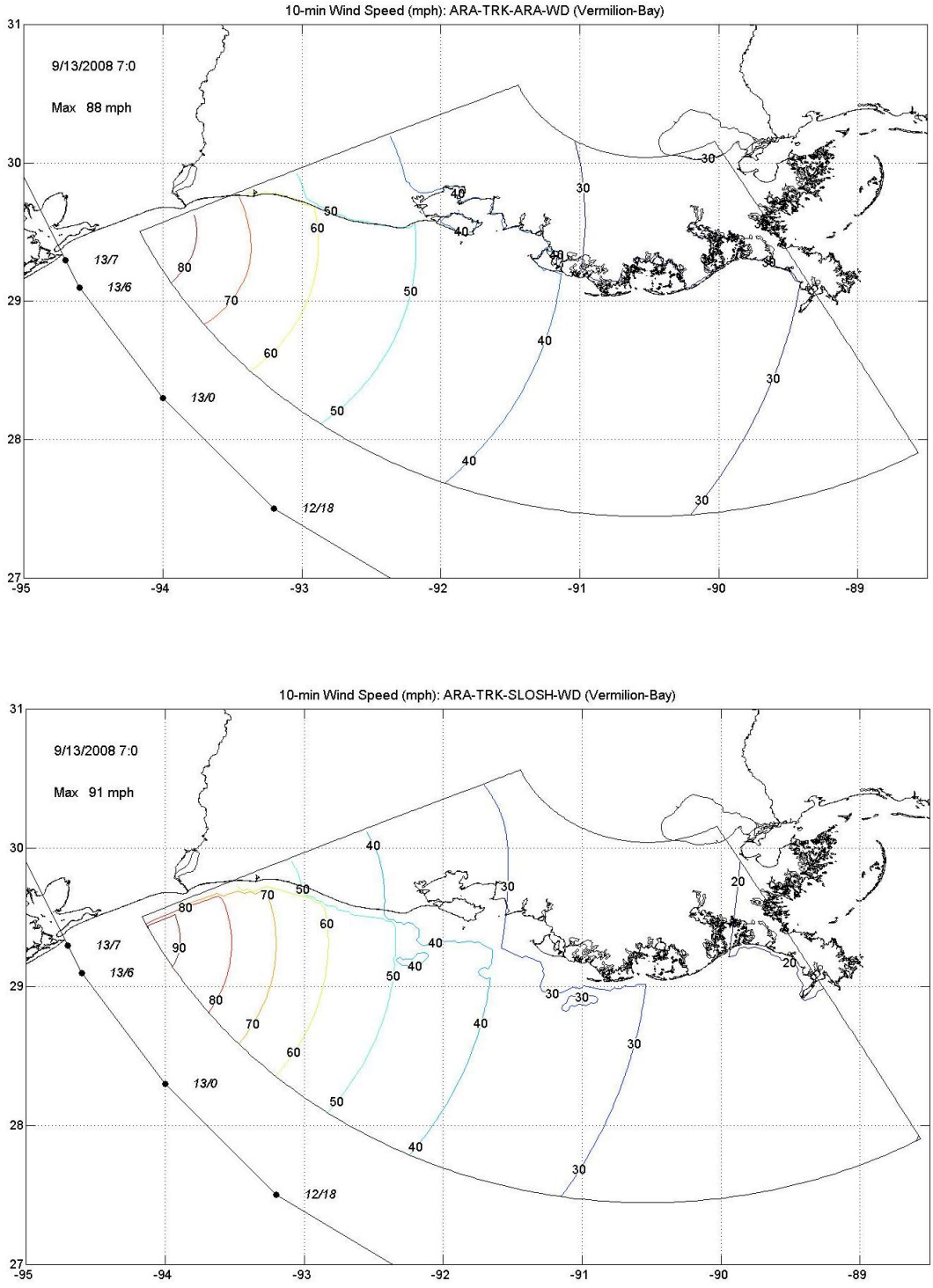

Figure S-2c. Hurricane Ike (2008) Modeled 10-min Wind Speeds (mph) at Landfall – Vermilion Bay Basin

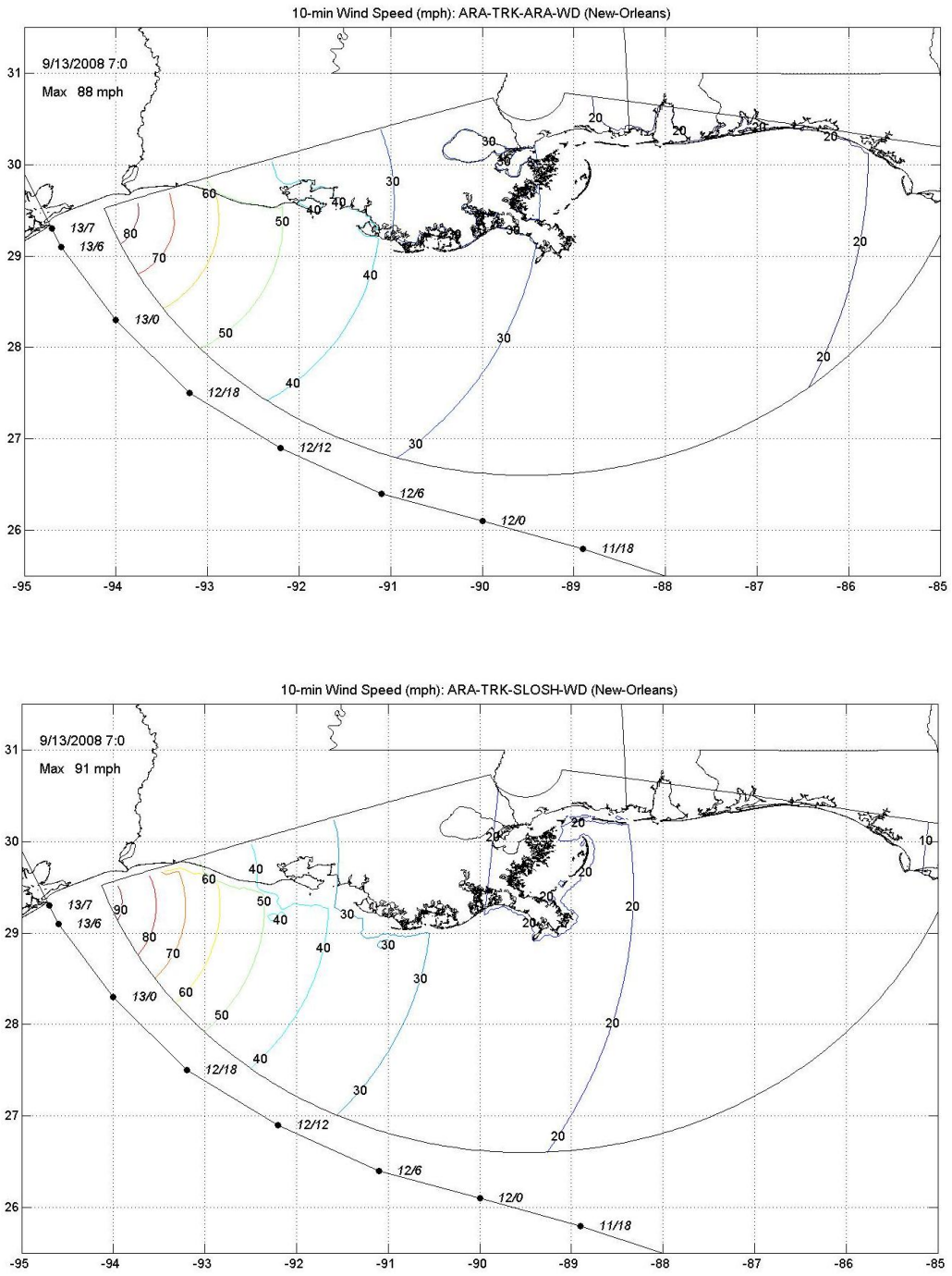

Figure S-2d. Hurricane Ike (2008) Modeled 10-min Wind Speeds (mph) at Landfall – New Orleans Basin

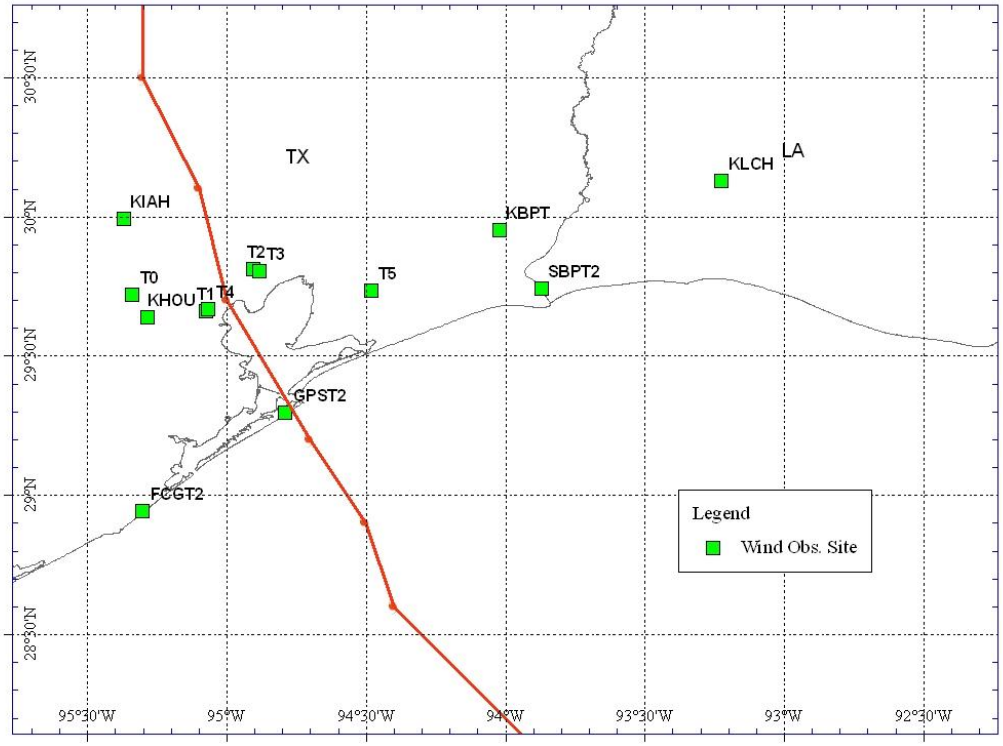

Figure S-3. Wind Observation Locations for Hurricane Ike

Table S-1. Summary Comparison of Modeled and Observed Maximum 10-min Wind Speeds for Hurricane Ike

No.	Station Name	lat	long	Max Wind Speed (mph)		
				ARA-TRK SLOSH-WD	ARA-TRK ARA-WD	Obs.
1	FCMP T0	29.72001	-95.33713	66.5	65.9	60.4
2	FCMP T1	29.65775	-95.07273	68.6	69.2	72.6
3	FCMP T2	29.81197	-94.90158	70.4	72.2	67.9
4	FCMP T3	29.80194	-94.88222	70.5	71.8	70.0
5	FCMP T4	29.66720	-95.06373	68.7	69.4	74.6
6	FCMP T5	29.73254	-94.48130	72.0	74.2	82.2
7	FCGT2	28.94300	-95.30000	61.5	59.8	61.4
8	SBPT2	29.74000	-93.87000	69.0	81.1	70.3
9	GPST2	29.29500	-94.78800	69.2	70.9	62.3
10	KLCH	30.12611	-93.22330	50.8	51.1	49.0
11	KBPT	29.95060	-94.02080	69.6	69.8	72.0
12	KHOU	29.63750	-95.28250	66.6	66.8	N/A
13	KIAH	29.99250	-95.36900	67.2	66.0	N/A

Table S-2. Summary Comparison of Modeled and Observed Minimum Pressures for Hurricane Ike

No.	Station Name	lat	long	Minimum Pressure (mbar)		
				ARA-TRK SLOSH-WD	ARA-TRK ARA-WD	Obs.
1	FCMP T0	29.72001	-95.33713	962.6	963.7	961.0
2	FCMP T1	29.65775	-95.07273	955.0	954.2	954.0
3	FCMP T2	29.81197	-94.90158	953.9	953.7	954.0
4	FCMP T3	29.80194	-94.88222	953.7	953.6	955.0
5	FCMP T4	29.66720	-95.06373	954.6	954.0	954.0
6	FCMP T5	29.73254	-94.48130	960.4	961.9	964.0
7	FCGT2	28.94300	-95.30000	972.4	974.0	971.7
8	SBPT2	29.74000	-93.87000	977.7	981.3	983.0
9	GPST2	29.29500	-94.78800	952.2	950.0	951.7
10	KLCH	30.12611	-93.22330	990.0	993.7	995.0
11	KBPT	29.95060	-94.02080	976.8	981.2	982.0
12	KHOU	29.63750	-95.28250	961.1	962.4	959.0
13	KIAH	29.99250	-95.36900	962.1	961.3	960.0

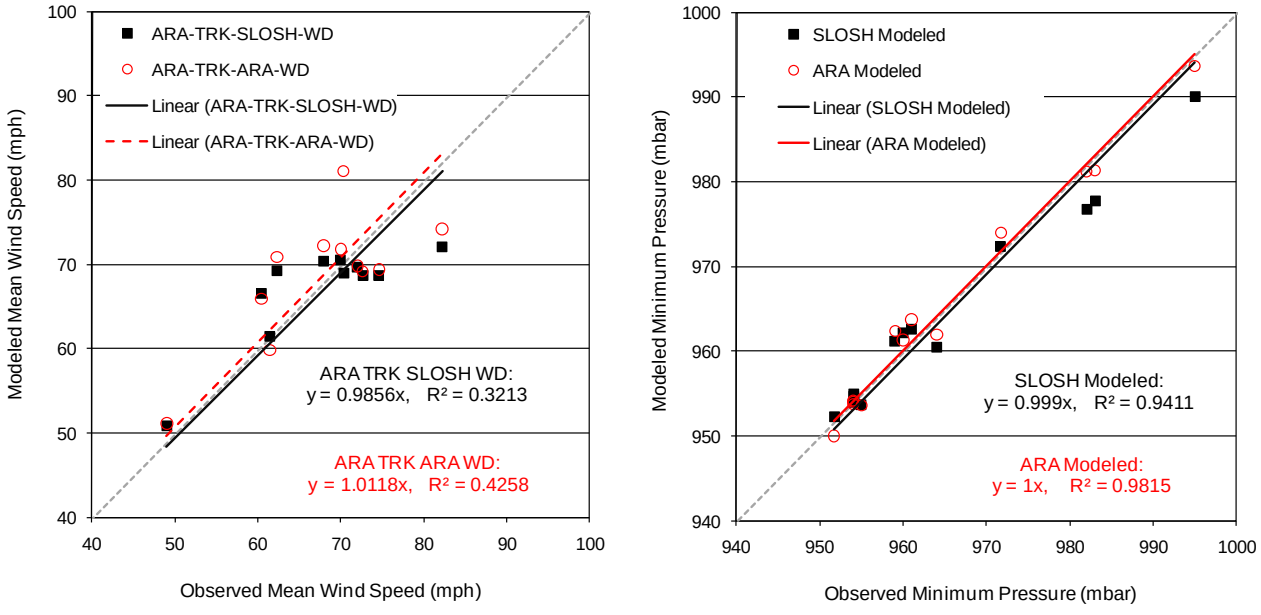

Figure S-4. Comparisons of Modeled and Observed Maximum 10-min Wind Speeds and Minimum Pressures for Hurricane Ike

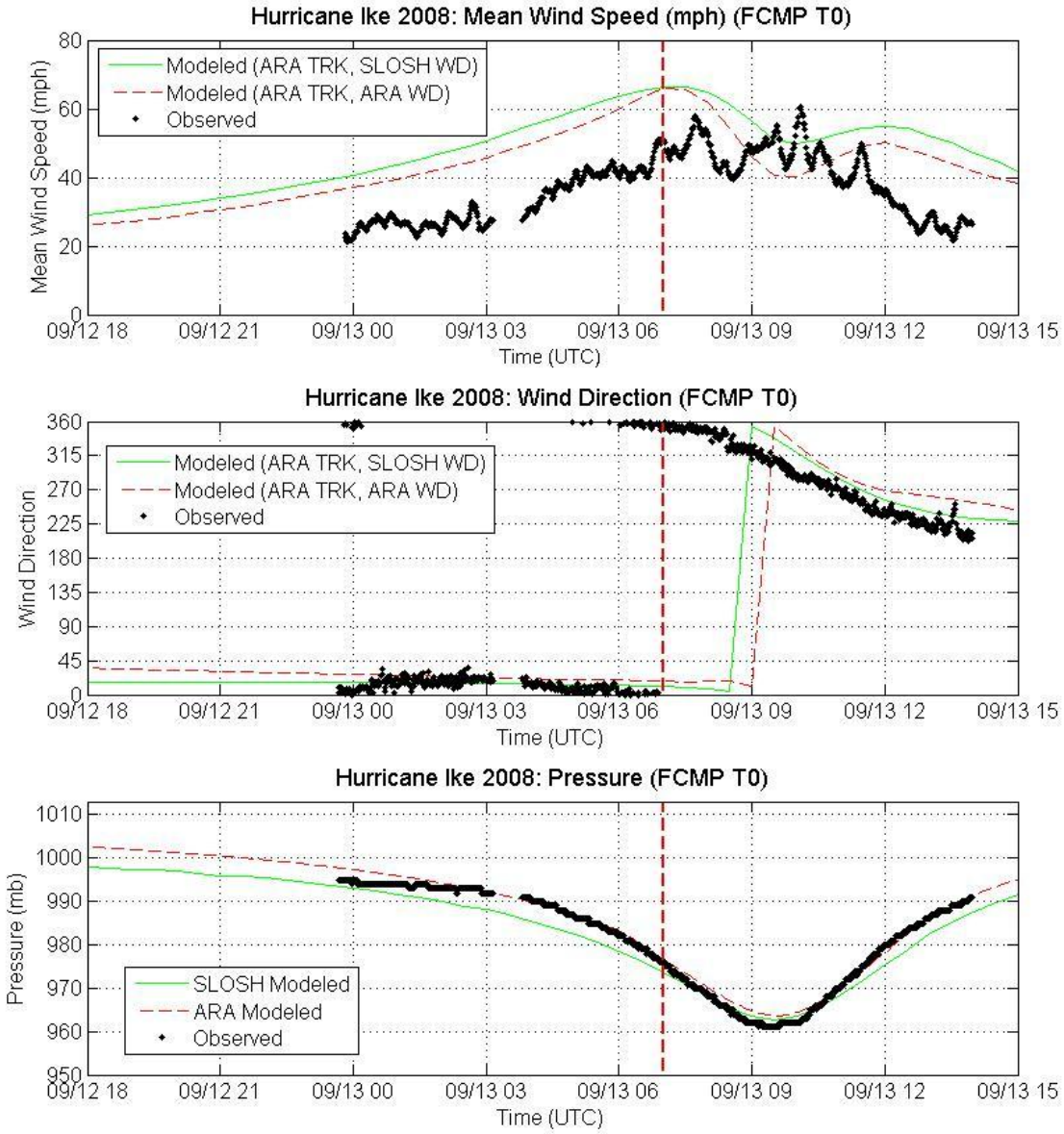

Figure S-5a. Comparisons of Observed and Modeled Time Series Traces of Mean Wind Speeds, Wind Directions, and Pressures for Hurricane Ike (2008) – FCMP T0

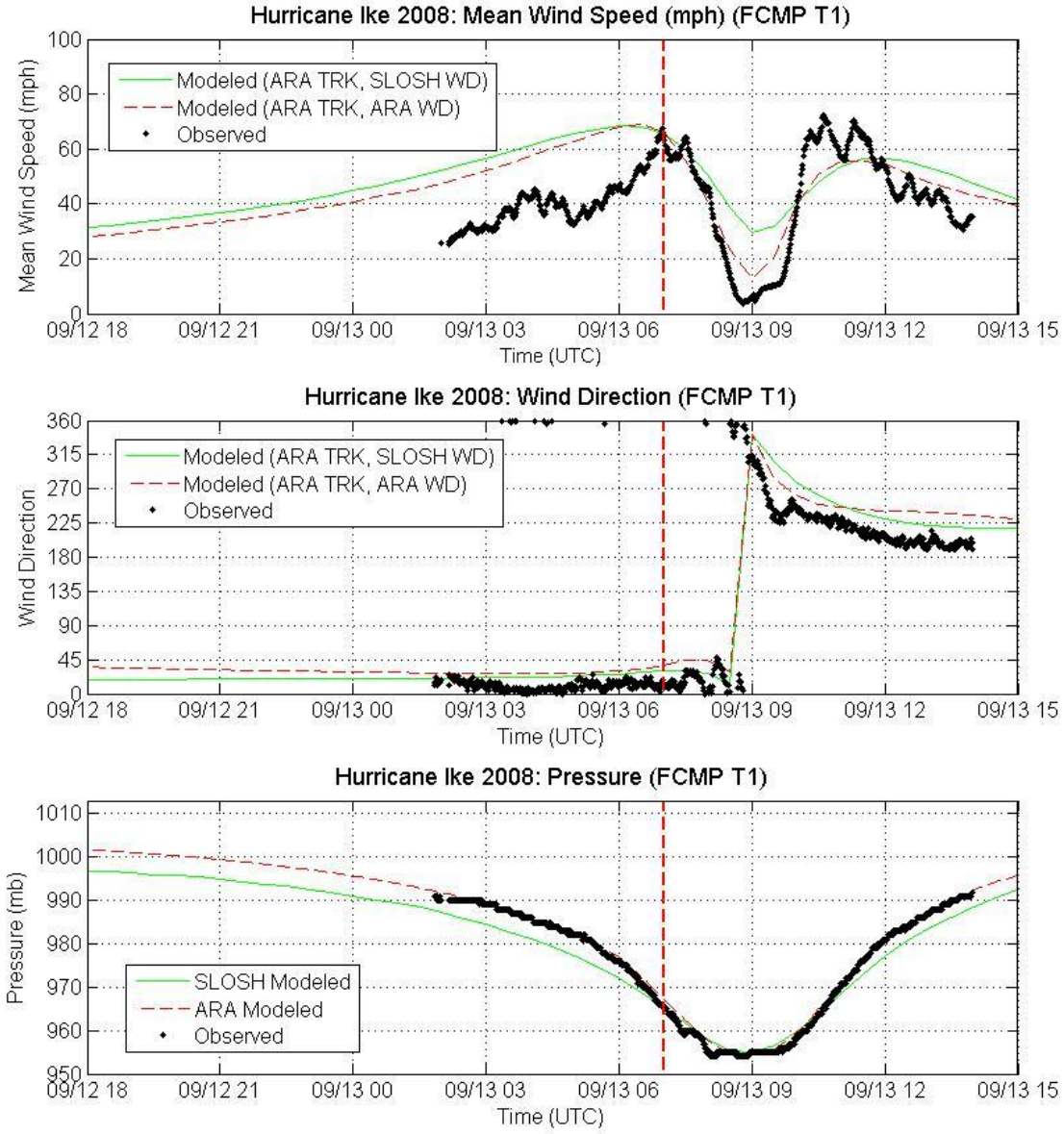

Figure S-5b. Comparisons of Observed and Modeled Time Series Traces of Mean Wind Speeds, Wind Directions, and Pressures for Hurricane Ike (2008) – FCMP T1

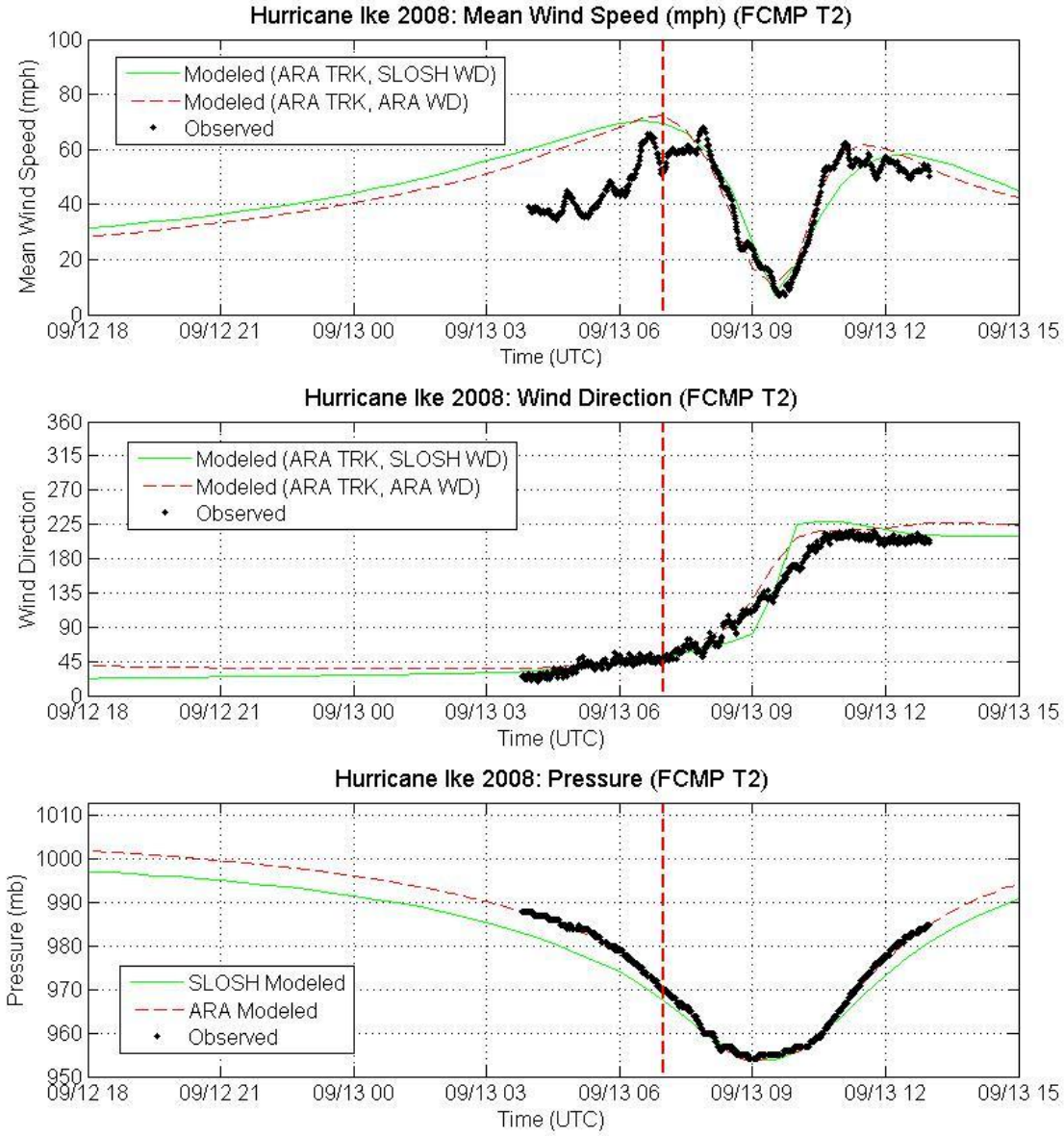

Figure S-5c. Comparisons of Observed and Modeled Time Series Traces of Mean Wind Speeds, Wind Directions, and Pressures for Hurricane Ike (2008) – FCMP T2

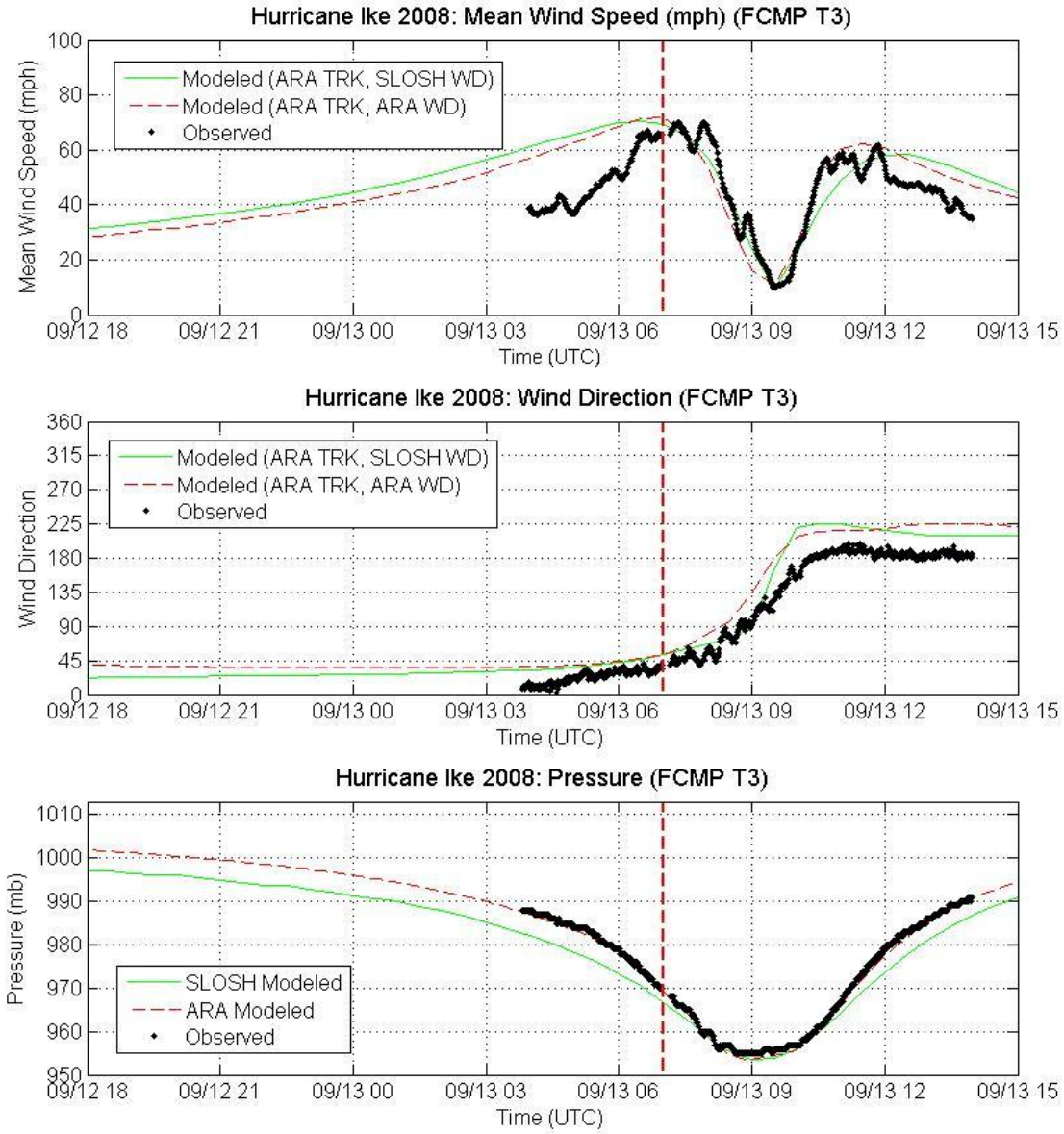

Figure S-5d. Comparisons of Observed and Modeled Time Series Traces of Mean Wind Speeds, Wind Directions, and Pressures for Hurricane Ike (2008) – FCMP T3

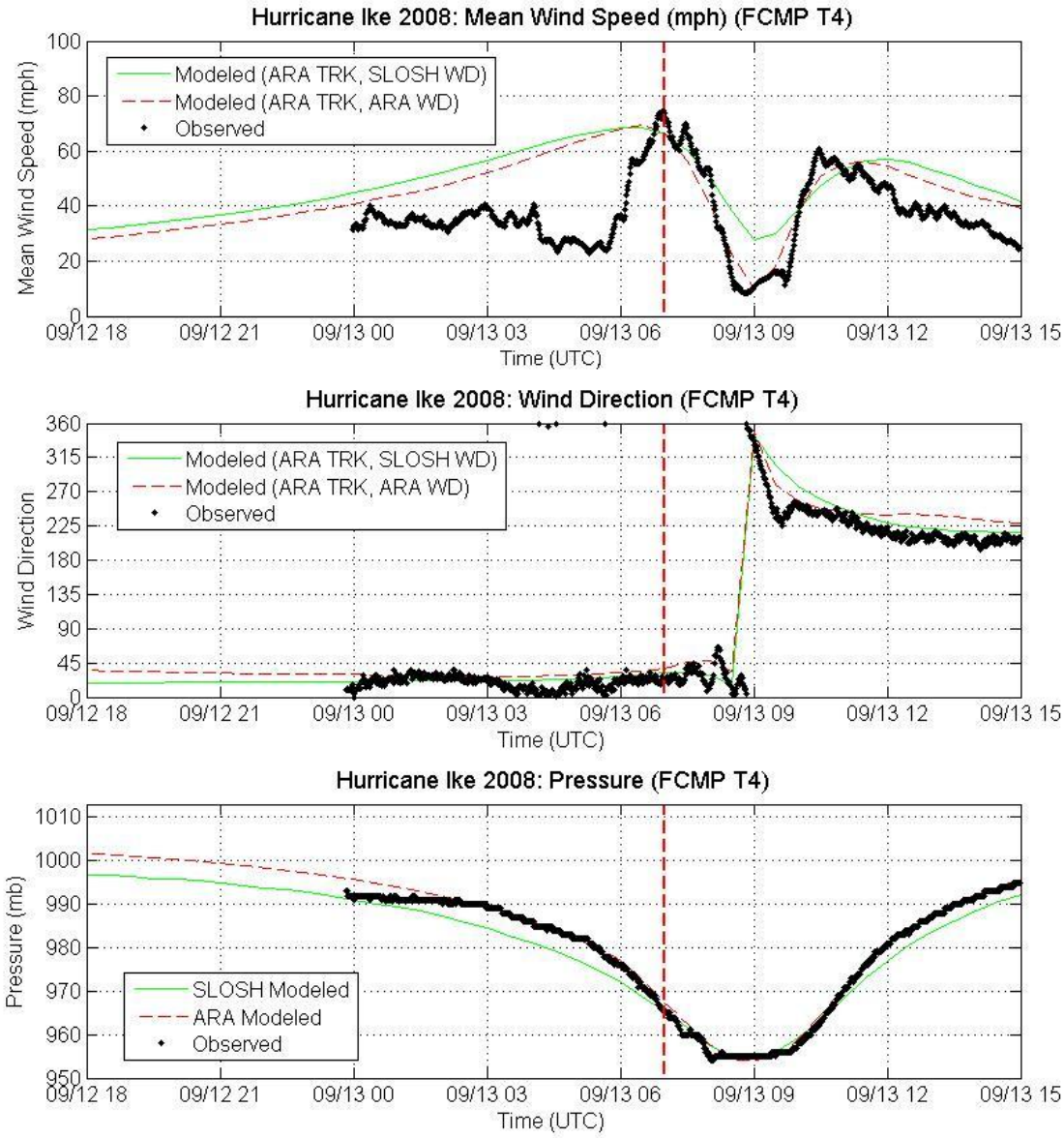

Figure S-5e. Comparisons of Observed and Modeled Time Series Traces of Mean Wind Speeds, Wind Directions, and Pressures for Hurricane Ike (2008) – FCMP T4

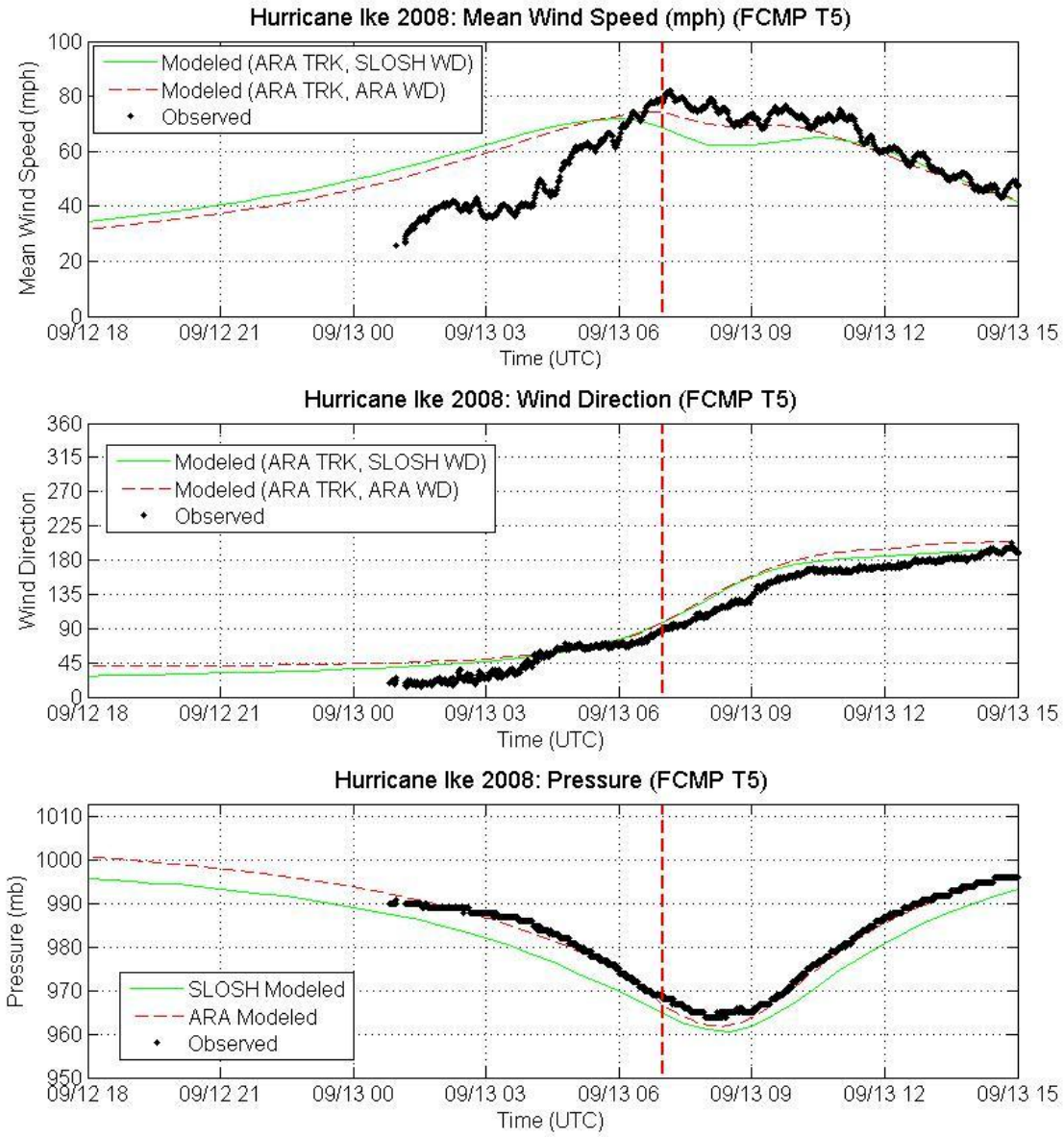

Figure S-5f. Comparisons of Observed and Modeled Time Series Traces of Mean Wind Speeds, Wind Directions, and Pressures for Hurricane Ike (2008) – FCMP T5

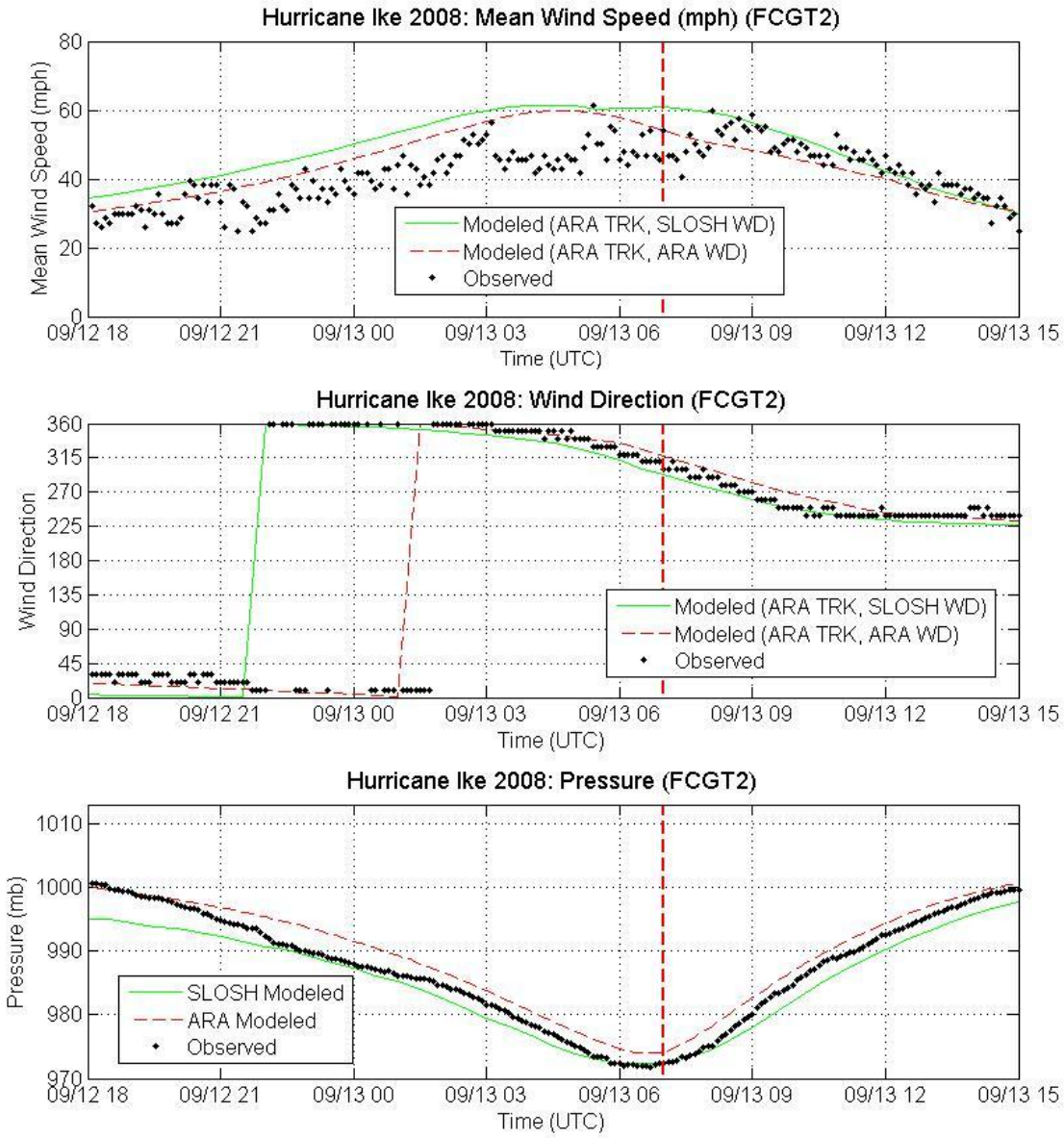

Figure S-5g. Comparisons of Observed and Modeled Time Series Traces of Mean Wind Speeds, Wind Directions, and Pressures for Hurricane Ike (2008) – FCGT2

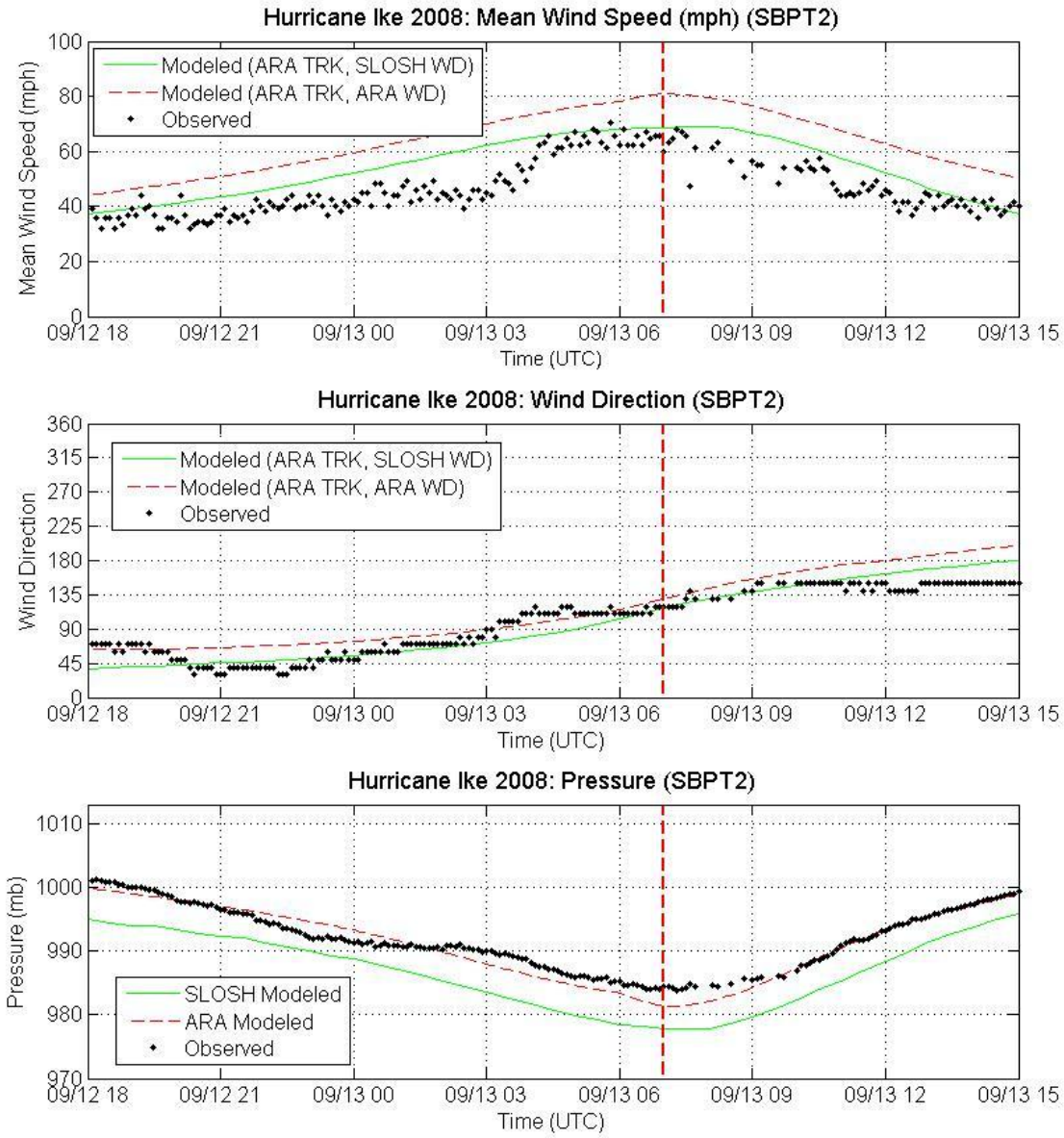

Figure S-5h. Comparisons of Observed and Modeled Time Series Traces of Mean Wind Speeds, Wind Directions, and Pressures for Hurricane Ike (2008) – SBPT2

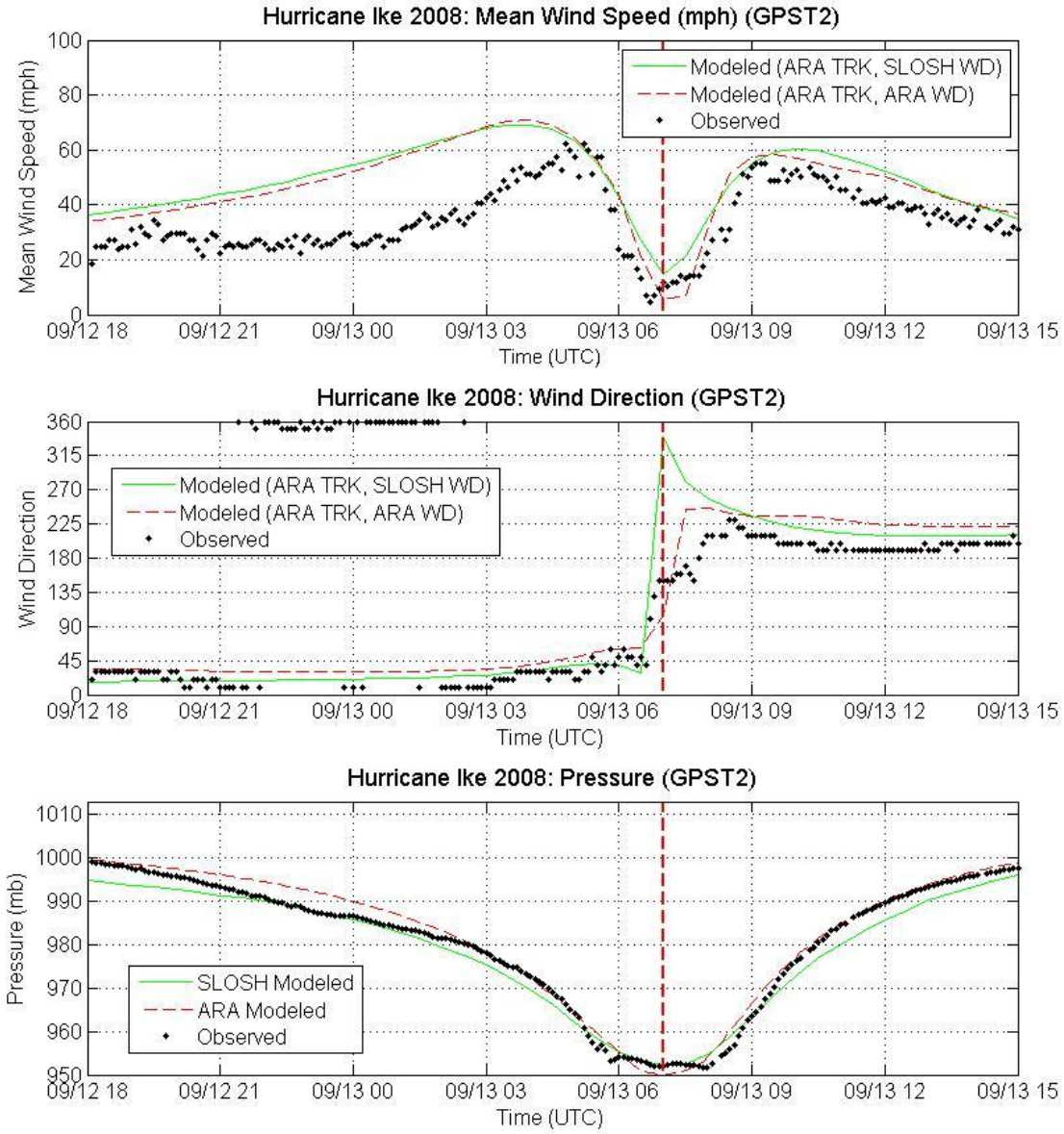

Figure S-5i. Comparisons of Observed and Modeled Time Series Traces of Mean Wind Speeds, Wind Directions, and Pressures for Hurricane Ike (2008) – GPST2

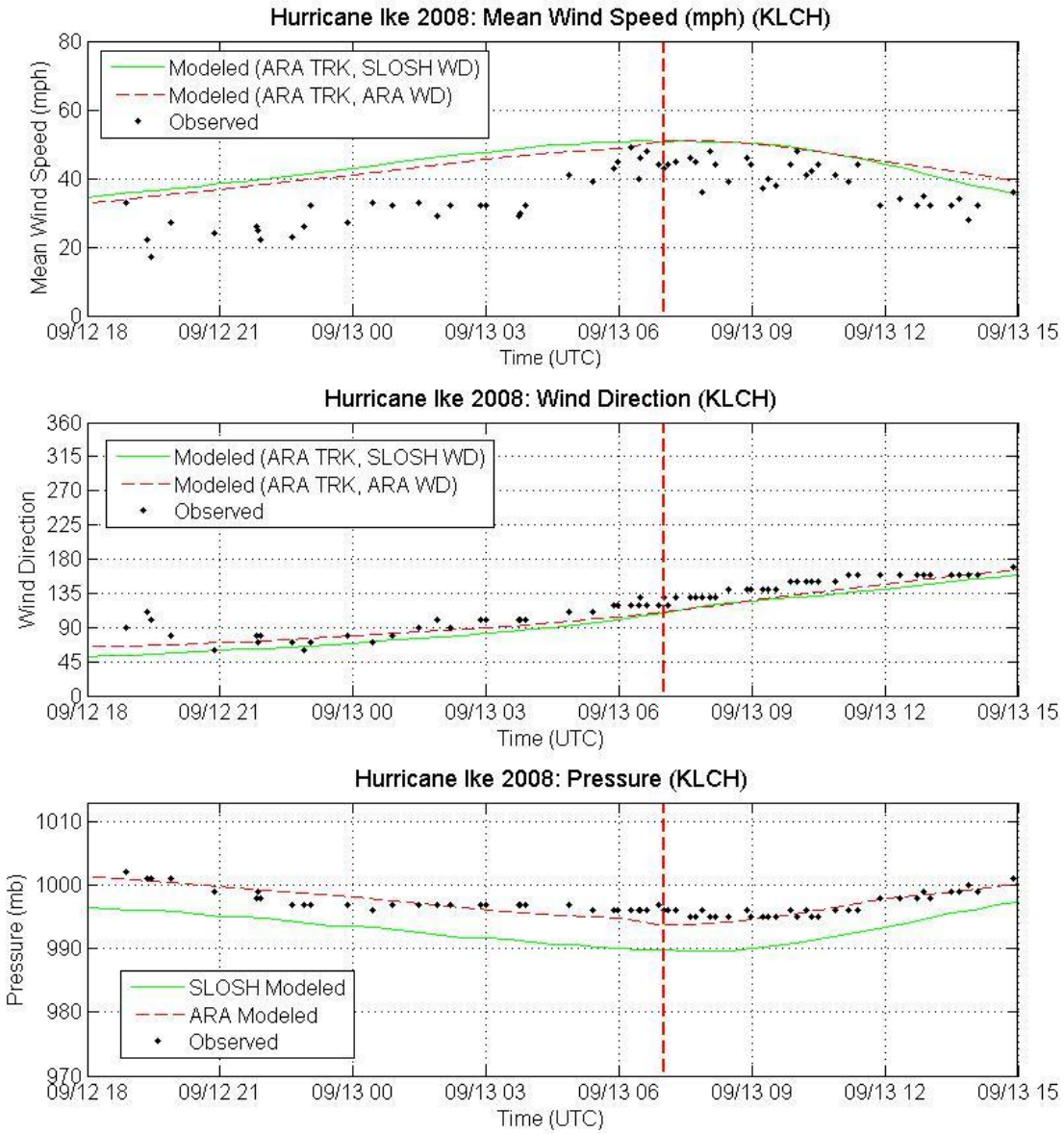

Figure S-5j. Comparisons of Observed and Modeled Time Series Traces of Mean Wind Speeds, Wind Directions, and Pressures for Hurricane Ike (2008) – KLCH

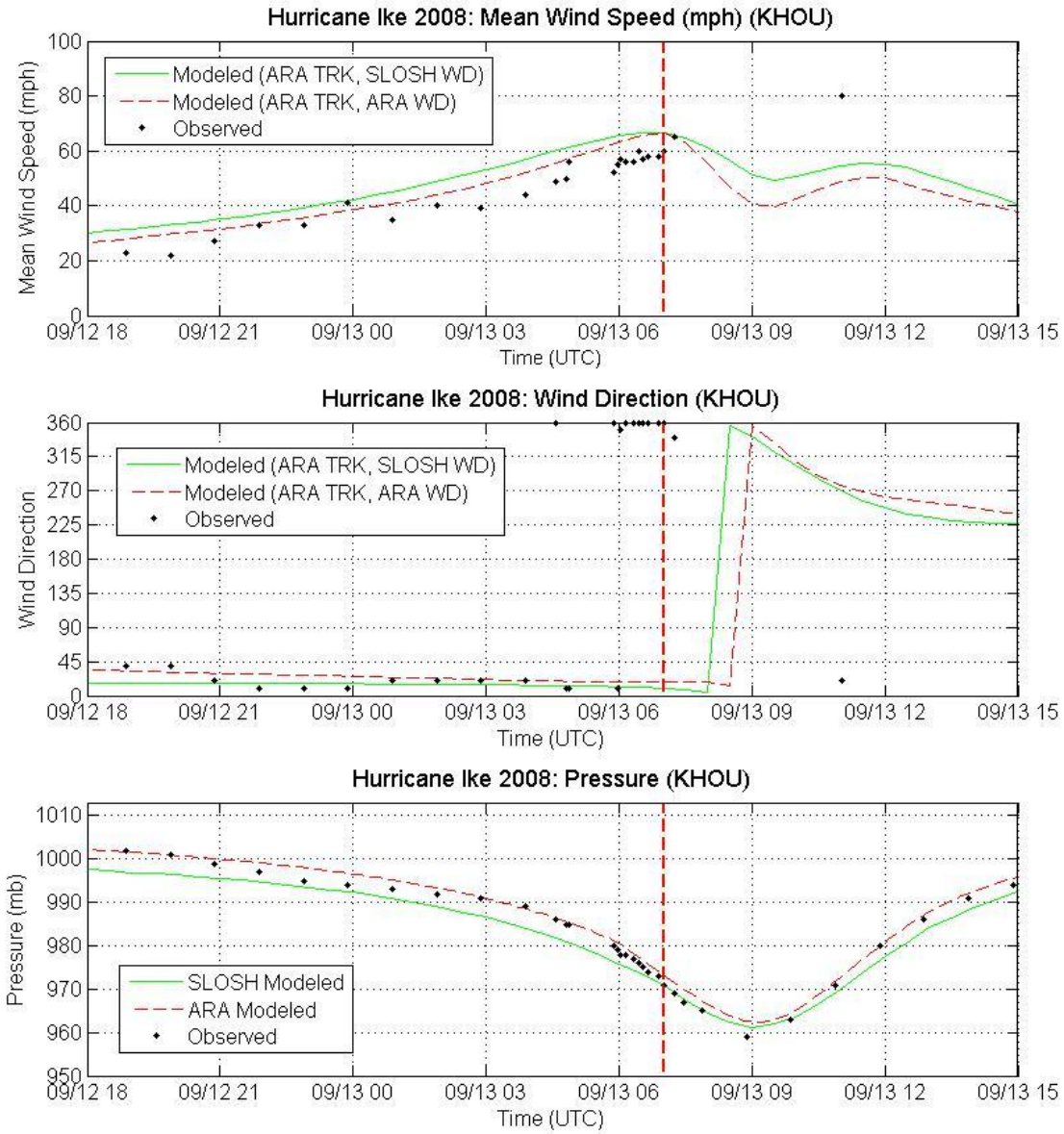

Figure S-5k. Comparisons of Observed and Modeled Time Series Traces of Mean Wind Speeds, Wind Directions, and Pressures for Hurricane Ike (2008) – KHOU

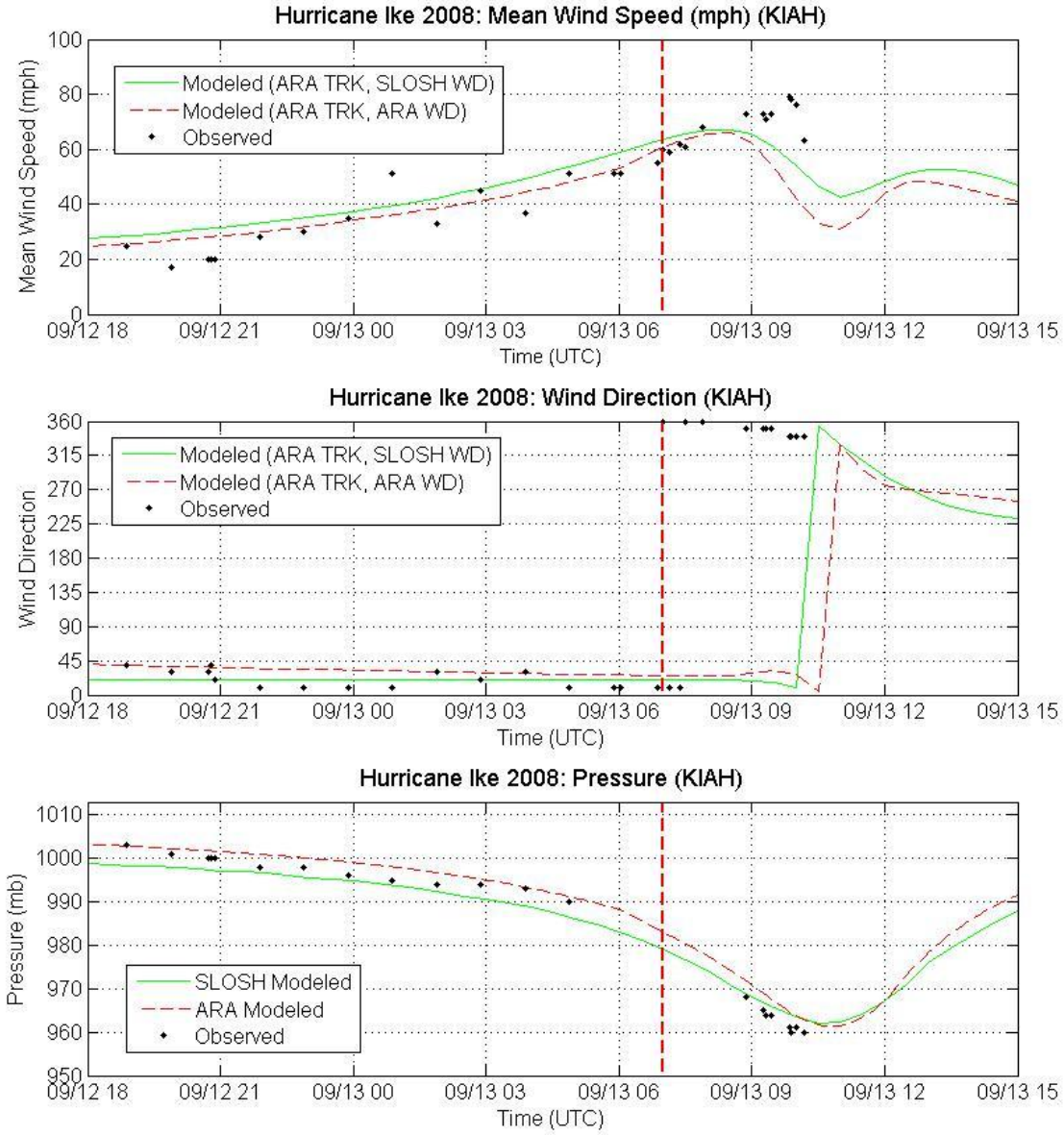

Figure S-5l. Comparisons of Observed and Modeled Time Series Traces of Mean Wind Speeds, Wind Directions, and Pressures for Hurricane Ike (2008) – KIAH

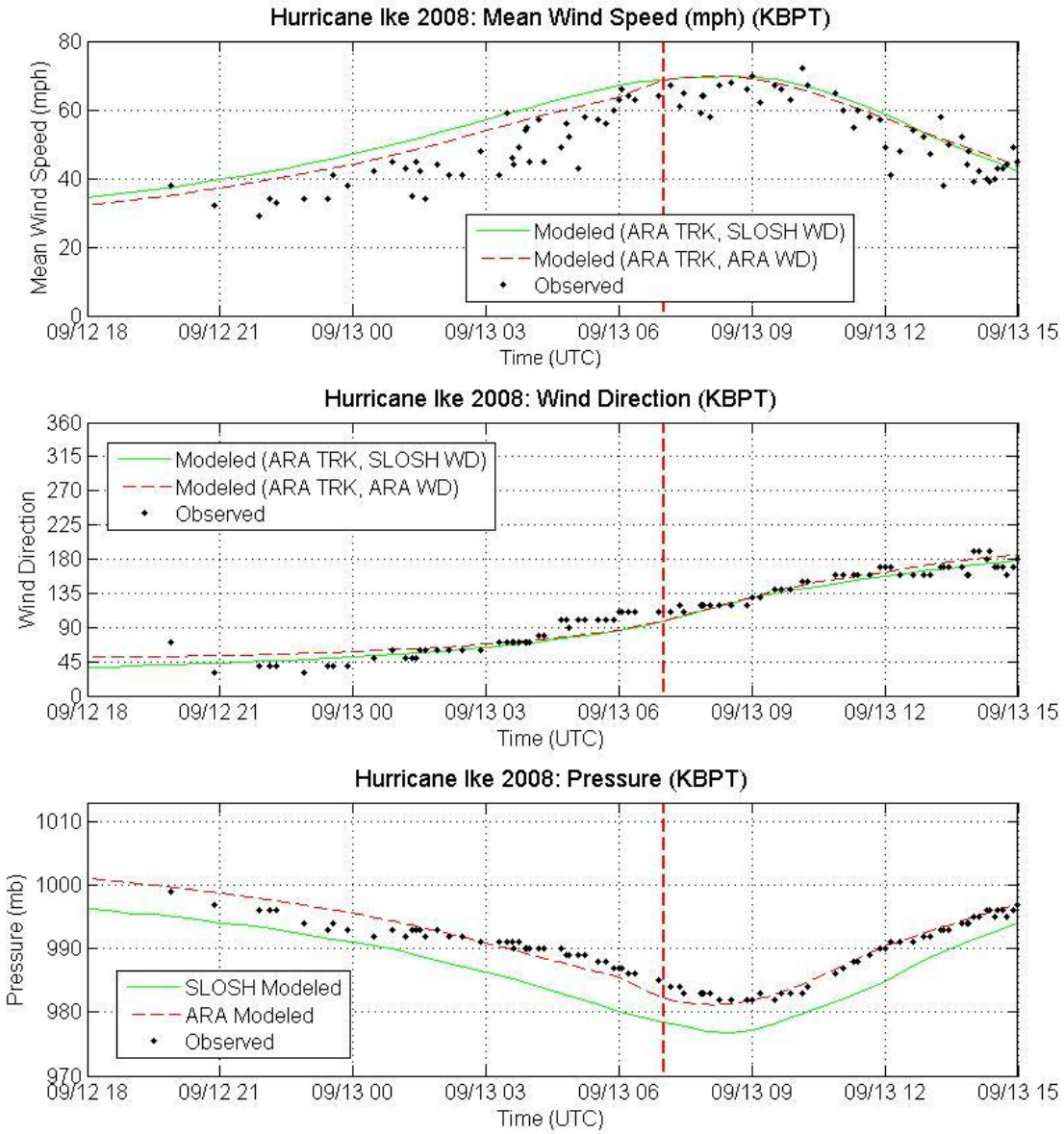

Figure S-5m. Comparisons of Observed and Modeled Time Series Traces of Mean Wind Speeds, Wind Directions, and Pressures for Hurricane Ike (2008) – KBPT

Table S-3. Error Analysis of Wind Speeds, Wind Directions and Pressures for Hurricane Ike

Station	Range		Number of Data	Obs		SLOSH-Obs		ARA-Obs	
				Mean	Std	mean	RMS	mean	RMS
FCMP T0	Wind Speed (mph)	20-40	459	29.7	5.2	20.7	21.1	15.7	16.1
		40-60	349	46.2	4.5	13.0	15.3	7.6	13.3
		60-80	3	60.3	0.1	-10.4	10.4	-19.9	19.9
		all	811	37.0	9.6	17.3	18.8	12.1	15.0
	Wind Direction (deg)	0-45	347	13.1	7.3	1.7	6.9	9.8	11.9
		180-225	47	214.9	5.9	22.0	22.4	43.1	43.3
		225-270	132	241.9	12.2	14.9	16.5	28.2	28.9
		270-315	109	290.5	13.4	25.9	27.0	35.8	37.7
		315-360	179	344.7	13.4	22.0	23.4	32.3	34.1
		all	814	173.3	142.7	12.7	17.6	23.1	27.3
	Pressure (mbar)	945-965	104	962.1	0.9	1.4	1.4	2.4	2.5
		965-980	226	971.8	4.4	-1.7	2.1	0.6	1.3
		980-989	203	984.4	2.6	-4.1	4.1	0.0	0.8
		989-1030	287	992.5	1.9	-3.1	3.4	1.1	1.6
		all	820	981.0	11.2	-2.4	3.1	0.9	1.5
FCMP T1	Wind Speed (mph)	0-20	84	9.3	4.1	24.0	24.2	10.6	10.9
		20-40	229	33.3	4.3	22.5	23.4	17.9	19.4
		40-60	299	48.0	6.0	11.3	14.3	8.5	12.7
		60-80	99	65.0	2.8	-10.6	12.9	-10.1	12.0
		all	711	41.0	16.2	13.3	18.8	9.2	14.9
	Wind Direction (deg)	0-45	377	12.4	7.7	11.2	14.3	18.5	20.3
		45-90	2	46.5	0.7	-26.1	26.1	-8.8	8.8
		180-225	179	203.7	8.7	24.5	24.9	36.9	37.5
		225-270	103	237.2	9.8	39.7	43.0	25.7	28.5
		270-315	23	300.0	11.3	33.9	34.3	30.1	30.6
		315-360	27	351.7	8.1	18.3	20.3	26.7	28.8
		all	711	118.5	116.8	19.6	24.2	24.9	27.5
	Pressure (mbar)	945-965	210	957.4	3.2	1.2	1.5	1.1	1.5
		965-980	171	972.6	4.3	-2.5	2.8	0.8	1.1
		980-989	222	984.5	2.5	-4.4	4.5	0.0	0.5
		989-1030	117	990.0	0.7	-3.9	4.0	0.5	0.7
		all	720	974.7	12.8	-2.2	3.4	0.6	1.1
FCMP T2	Wind Speed (mph)	0-20	63	13.6	4.2	1.4	3.1	1.4	4.1
		20-40	128	33.6	5.8	17.5	21.0	14.0	18.2
		40-60	301	51.8	5.4	7.1	13.1	8.3	12.3
		60-80	49	63.2	2.3	-1.1	8.0	0.9	7.0
		all	541	44.1	15.1	8.1	14.4	8.2	13.0
	Wind Direction (deg)	0-45	131	33.0	7.5	3.1	5.9	6.3	8.4
		45-90	144	57.5	10.9	-4.2	7.0	1.8	8.0
		90-135	66	112.7	13.7	-21.5	25.0	12.8	20.3
		135-180	39	160.0	12.1	31.5	37.9	34.4	34.8
		180-225	170	204.8	6.6	16.8	19.2	14.4	15.9
		all	550	111.1	72.0	4.5	17.7	10.4	15.7
	Pressure (mbar)	945-965	195	957.5	2.7	-0.6	0.9	-0.5	0.8
		965-980	181	972.2	4.5	-3.3	3.5	-0.3	0.7
		980-989	174	983.9	2.4	-5.3	5.3	-0.5	0.7
		all	550	970.7	11.4	-3.0	3.6	-0.4	0.7

Table S-3. Error Analysis of Wind Speeds, Wind Directions and Pressures for Hurricane Ike (Continued)

Station	Range		Number of Data	Obs		SLOSH-Obs		ARA-Obs	
				Mean	Std	mean	RMS	mean	RMS
FCMP T3	Wind Speed (mph)	0-20	44	13.4	3.1	1.2	2.9	1.7	4.4
		20-40	144	34.3	5.4	11.8	17.4	8.2	15.4
		40-60	298	49.3	5.4	7.6	13.5	8.7	11.8
		60-80	105	65.2	2.8	-1.0	6.1	-0.8	7.8
		all	591	45.8	14.4	6.6	13.2	6.4	11.9
	Wind Direction (deg)	0-45	206	24.9	10.1	16.4	17.2	19.3	20.4
		45-90	82	61.8	14.3	6.2	10.4	22.0	24.0
		90-135	48	109.5	12.7	10.7	23.3	41.2	42.8
		135-180	53	161.4	14.4	47.6	48.7	44.8	45.1
		180-225	211	186.3	4.2	30.2	30.8	34.2	34.9
		all	600	105.5	72.0	22.1	26.5	28.9	31.2
	Pressure (mbar)	945-965	191	957.8	2.7	-1.1	1.3	-1.0	1.2
		965-980	170	972.3	4.6	-3.8	4.0	-0.6	0.9
		980-989	205	984.5	2.5	-5.5	5.6	-0.9	1.0
		989-1030	34	989.7	0.7	-4.3	4.3	-0.4	0.5
		all	600	972.8	12.0	-3.6	4.1	-0.8	1.0
FCMP T4	Wind Speed (mph)	0-20	84	12.9	2.9	18.8	19.2	4.9	6.6
		20-40	559	32.9	4.5	21.1	23.2	17.0	20.1
		40-60	193	51.3	5.2	3.3	8.8	2.4	8.5
		60-80	65	66.1	4.3	-2.6	5.4	-3.6	6.4
		all	901	37.4	13.8	15.3	19.7	11.2	16.6
	Wind Direction (deg)	0-45	524	19.9	8.5	3.6	9.7	11.0	14.1
		45-90	10	56.0	6.6	-31.9	32.5	-13.9	15.2
		180-225	214	209.9	6.1	12.8	13.6	27.0	27.5
		225-270	126	241.2	8.3	27.4	33.4	14.8	19.8
		270-315	13	291.1	12.5	34.9	35.6	26.1	26.3
		315-360	20	341.3	13.9	9.8	13.4	14.2	16.2
		all	907	107.7	106.6	9.3	17.0	15.4	19.2
	Pressure (mbar)	945-965	210	957.6	3.0	0.7	1.1	0.8	1.4
		965-980	171	972.6	4.4	-2.6	2.9	0.7	1.1
		980-989	217	984.4	2.4	-4.5	4.6	0.0	0.5
		989-1030	312	991.3	1.4	-3.1	3.3	1.3	1.8
		all	910	978.3	13.4	-2.4	3.2	0.8	1.4
FCMP T5	Wind Speed (mph)	20-40	123	36.1	3.3	23.2	23.4	20.0	20.3
		40-60	280	48.5	6.0	8.0	13.6	6.4	12.3
		60-80	428	70.6	5.6	-5.2	8.7	-2.0	5.5
		80-100	11	81.1	0.6	-13.5	13.5	-7.6	7.7
		all	842	58.3	14.7	3.2	13.5	4.0	11.2
	Wind Direction (deg)	0-45	191	24.6	7.4	20.1	20.6	24.2	24.7
		45-90	183	67.2	9.0	3.8	7.3	3.3	6.5
		90-135	119	110.0	12.8	19.4	20.2	21.7	22.5
		135-180	244	165.4	9.4	13.8	14.1	21.8	22.0
		180-225	114	186.6	5.6	5.9	7.0	16.3	16.9
		all	851	107.8	61.5	12.8	15.1	17.6	19.8
	Pressure (mbar)	945-965	23	964.0	0.0	-3.2	3.2	-2.0	2.0
		965-980	323	970.9	4.8	-4.4	4.5	-1.3	1.6
		980-989	242	984.9	2.6	-6.1	6.1	-1.3	1.5
		989-1030	263	991.6	2.5	-4.2	4.3	-0.1	0.9
		all	851	981.1	9.9	-4.8	4.9	-0.9	1.4

Table S-3. Error Analysis of Wind Speeds, Wind Directions and Pressures for Hurricane Ike (Continued)

Station	Range		Number of Data	Obs		SLOSH-Obs		ARA-Obs	
				Mean	Std	mean	RMS	mean	RMS
FCGT2	Wind Speed (mph)	20-40	89	33.4	4.2	7.1	9.4	3.6	6.2
		40-60	119	47.5	4.3	8.0	10.3	3.5	8.2
		60-80	2	60.7	1.0	-0.8	0.8	-5.8	6.9
		all	210	41.7	8.3	7.5	9.9	3.5	7.4
	Wind Direction (deg)	0-45	57	20.0	8.5	-20.2	21.0	-9.3	10.4
		225-270	62	245.0	7.3	-2.9	22.7	9.7	24.9
		270-315	26	292.3	13.9	-11.9	12.6	12.0	12.7
		315-360	33	339.7	11.3	-11.7	12.3	2.6	6.0
		all	178	222.2	130.7	-10.6	18.0	2.4	15.6
	Pressure (mbar)	965-980	54	975.0	2.6	-0.7	1.1	2.3	2.3
		980-989	60	985.1	2.5	-1.9	2.1	2.4	2.5
		989-1030	96	995.2	3.5	-2.7	3.0	1.6	2.0
		all	210	987.1	8.8	-2.0	2.4	2.0	2.2
SBPT2	Wind Speed (mph)	20-40	51	36.3	2.3	6.4	7.6	14.6	15.2
		40-60	111	46.0	5.1	8.9	10.3	17.9	18.5
		60-80	35	64.3	2.4	3.5	4.3	13.7	14.0
		all	197	46.7	10.1	7.3	8.8	16.3	17.0
	Wind Direction (deg)	0-45	28	37.5	4.4	9.9	11.0	29.9	30.2
		45-90	63	63.8	9.1	-10.3	15.3	9.8	13.7
		90-135	49	112.9	9.4	-14.3	18.6	0.1	10.4
		135-180	57	147.7	4.2	13.7	18.5	32.2	34.6
		all	197	96.5	41.5	-1.5	16.6	16.7	23.7
	Pressure (mbar)	980-989	55	985.8	1.4	-6.1	6.2	-1.7	1.9
		989-1030	142	994.4	3.6	-4.5	4.6	0.0	1.2
		all	197	992.0	5.0	-4.9	5.1	-0.4	1.4
GPST2	Wind Speed (mph)	0-20	18	12.6	4.0	11.7	12.6	3.1	8.2
		20-40	123	29.7	4.9	17.7	19.7	16.2	18.2
		40-60	63	48.9	5.5	11.3	13.4	10.7	13.2
		60-80	2	62.3	0.0	0.1	2.5	1.1	2.8
		all	206	34.4	12.3	15.1	17.3	13.2	16.0
	Wind Direction (deg)	0-45	80	22.0	9.6	2.5	10.3	15.2	17.1
		45-90	7	52.9	4.9	-17.1	17.8	6.2	8.0
		90-135	2	115.0	21.2	-110.9	112.7	-32.1	33.8
		135-180	9	155.6	7.3	-48.9	159.9	25.9	58.8
		180-225	66	198.3	8.5	21.2	24.7	31.0	32.2
		225-270	2	230.0	0.0	14.5	14.6	8.5	8.5
		315-360	10	350.0	0.0	29.7	29.7	40.2	40.2
		all	176	153.4	126.5	8.6	40.0	23.4	28.7
	Pressure (mbar)	945-965	41	955.4	3.9	1.0	1.6	0.8	2.4
		965-980	35	973.3	4.2	-2.7	2.8	0.5	1.1
		980-989	53	984.8	2.6	-1.8	2.4	2.4	2.8
		989-1030	77	994.4	2.9	-2.7	2.9	1.6	2.0
		all	206	980.6	15.0	-1.7	2.6	1.5	2.2

Table S-3. Error Analysis of Wind Speeds, Wind Directions and Pressures for Hurricane Ike (Continued)

Station	Range		Number of Data	Obs		SLOSH-Obs		ARA-Obs	
				Mean	Std	mean	RMS	mean	RMS
KLCH	Wind Speed (mph)	0-20	1	17.0	0.0	19.1	19.1	17.7	17.7
		20-40	37	31.2	4.7	12.0	12.8	11.5	12.0
		40-60	25	44.2	2.5	5.6	6.1	5.3	5.8
		all	63	36.2	7.9	9.6	10.8	9.1	10.2
	Wind Direction (deg)	45-90	11	72.7	7.9	-8.2	11.8	1.6	8.3
		90-135	28	113.6	14.2	-18.8	21.5	-14.7	16.9
		135-180	24	152.9	9.1	-15.6	16.3	-11.0	12.5
		all	63	121.4	31.0	-15.7	18.2	-10.5	14.1
	Pressure (mbar)	989-1030	63	997.0	1.8	-4.7	4.9	-0.4	1.2
		all	63	997.0	1.8	-4.7	4.9	-0.4	1.2
KBPT	Wind Speed (mph)	0-20	-99	-99.0	-99.0	-99.0	-99.0	-99.0	-99.0
		20-40	13	35.2	3.1	9.9	10.9	8.0	9.2
		40-60	51	48.5	6.2	7.3	9.7	5.6	7.8
		60-80	24	64.8	3.1	3.0	4.1	1.9	3.7
		all	88	50.9	10.9	6.5	8.7	5.0	7.1
	Wind Direction (deg)	0-45	8	37.5	4.6	9.7	10.5	18.1	18.6
		45-90	22	64.1	9.1	-2.6	7.6	2.4	6.9
		90-135	26	110.8	10.6	-12.8	15.8	-11.7	14.8
		135-180	28	161.1	9.6	-1.5	8.2	4.7	10.2
		180-225	4	187.5	5.0	-14.1	14.9	-6.4	7.9
		all	88	111.9	47.0	-4.7	11.4	0.0	12.0
	Pressure (mbar)	980-989	29	984.6	2.2	-5.4	5.5	-0.8	1.4
		989-1030	58	992.6	2.4	-4.1	4.3	0.3	1.3
		all	87	989.9	4.5	-4.5	4.7	0.0	1.3
KHOU	Wind Speed (mph)	20-40	7	30.3	6.4	8.8	9.2	5.0	5.6
		40-60	14	52.1	6.3	9.2	9.7	6.5	7.3
		60-80	3	61.7	2.9	4.6	5.3	4.1	5.0
		80-100	1	80.0	0.0	-25.3	25.3	-30.9	30.9
		all	25	48.2	14.1	7.2	10.3	4.3	8.9
	Wind Direction (deg)	0-45	14	18.6	10.3	-11.3	31.2	-1.6	29.2
		315-360	2	345.0	7.1	25.5	25.8	33.3	33.6
		all	16	167.6	171.8	-0.3	25.4	8.3	26.2
	Pressure (mbar)	945-965	2	961.0	2.8	1.2	1.7	2.6	2.8
		965-980	13	973.3	4.5	-1.4	1.8	1.8	1.9
		980-989	6	983.7	2.9	-3.7	3.8	0.5	0.7
		989-1030	12	994.8	4.1	-3.1	3.3	1.2	1.7
		all	33	982.3	11.6	-2.3	2.9	1.4	1.7
KIAH	Wind Speed (mph)	0-20	1	17.0	0.0	12.9	12.9	9.9	9.9
		20-40	9	27.6	6.7	7.9	8.8	4.6	5.7
		40-60	7	51.9	4.3	3.0	7.1	-1.4	6.4
		60-80	12	69.8	6.8	-8.8	13.0	-15.1	20.1
		all	29	50.5	20.1	0.0	10.6	-4.8	13.8
	Wind Direction (deg)	0-45	18	18.9	11.3	1.3	11.0	12.3	15.2
		315-360	8	345.0	5.3	28.7	28.8	42.5	42.6
		all	26	144.1	163.4	10.8	18.5	21.9	26.6
	Pressure (mbar)	945-965	6	961.7	1.9	2.8	2.9	3.6	3.7
		965-980	2	966.5	2.1	1.4	1.4	3.7	3.7
		989-1030	13	997.1	3.8	-2.6	2.8	1.8	2.0
		all	21	984.0	17.3	-0.7	2.7	2.5	2.8

Table S-3. Error Analysis of Wind Speeds, Wind Directions and Pressures for Hurricane Ike (Continued)

Station	Range		Number of Data	Obs		SLOSH-Obs		ARA-Obs	
				Mean	Std	mean	RMS	mean	RMS
All Stations	Wind Speed (mph)	0-20	295	12.1	4.0	13.5	16.9	5.2	7.7
		20-40	1971	32.4	5.1	18.8	21.0	15.2	17.8
		40-60	2110	48.7	5.7	8.8	13.1	7.6	12.2
		60-80	827	67.9	5.5	-4.3	8.6	-2.2	7.9
		80-100	12	81.0	0.6	-14.5	14.9	-9.6	11.6
		all	5215	43.6	15.5	10.7	16.2	8.7	13.9
	Wind Direction (deg)	0-45	1981	19.5	10.4	6.8	13.2	13.8	17.3
		45-90	524	62.8	11.3	-1.3	10.5	6.2	12.4
		90-135	338	111.3	12.5	-1.1	22.9	13.7	24.1
		135-180	454	161.1	11.6	15.5	32.8	24.1	28.9
		180-225	1005	199.7	11.8	19.3	21.9	27.8	30.0
		225-270	425	241.0	10.2	22.0	30.6	20.8	25.7
		270-315	171	292.1	13.5	21.9	27.3	30.7	33.3
		315-360	279	344.8	12.6	17.3	21.9	27.5	31.1
		all	5177	126.2	106.8	11.0	20.6	18.5	23.6
	Pressure (mbar)	945-965	982	958.1	3.3	0.2	1.4	0.4	1.6
		965-980	1346	972.1	4.5	-3.0	3.4	0.0	1.3
		980-989	1466	984.5	2.5	-4.8	5.0	-0.3	1.2
		989-1030	1474	992.5	2.9	-3.6	3.8	0.7	1.5
		all	5268	978.7	12.8	-3.1	3.8	0.2	1.4

Appendix T. Comparison of Observed and Modeled Storm Tides for Hurricane Andrew (1992)

This appendix compares storm tide estimates from SLOSH to high water marks (HWMs) from Hurricane Andrew in Biscayne Bay area of southeastern Florida Hurricane. Andrew made landfall in southern Dade County, Florida at about 0900 UTC August 24, 1992 after passing over Biscayne Bay. The combined effects of storm surge and astronomical tide caused flooding over a large part of extreme southern Florida (Rappaport, 1993).

Observation Data

The U.S. Geological Survey (USGS), in cooperation with the Federal Emergency Management Agency (FEMA), collected HWMs at 336 sites in southern Florida for Hurricane Andrew in 1992 (Murray, 1994). The quality of each mark was assigned a category as Excellent (E), Good (G), Fair (F), or Poor (P). The HWMs assigned as E, G and F are used for this study. There are 156 of such HWMs found. About 42 percent of the these HWMs are denoted as outside HWMs, which generally reflect the combined effect of storm tide and wave set up and run up. The remaining 58 percent are denoted as inside HWMs, generally taken inside buildings where the effects of wave action on water-surface elevations are minimized. All of HWMs are referenced to the National Geodetic Vertical Datum of 1929 (NGVD 1929). The HWMs, surveyed locations, type and quality of marks are shown in Table T-1.

SLOSH Basins and Initial Water Levels

SLOSH basin for Biscayne Bay is used in this study. The initial water level in the basin was selected to match the astronomical tide at the time of landfall. If we let MC represent the estimated difference between the local mean sea level and the reference datum, TE represent the predicted elevation of the astronomical tide above local mean sea level at the time of landfall, and PT represent the difference between the actual tide level and the predicted tide level several days before the storm arrival (i.e., the “tide anomaly”), the initial water level (IH) can be determined using the following equation, as demonstrated in Figure T-1:

$$IH = MC + TE + PT$$

The sea level rise in the Miami area since 1929 is 0.55 feet. In addition, the elevation of the astronomical tide above estimated local mean sea level for the area of Biscayne Bay where Andrew came ashore was 1.3 to 1.5 ft (Murray, 1994). The pre-storm tide anomaly is unavailable. Therefore, the final initial water height for the SLOSH model runs for Hurricane Andrew has been set to 2.0 feet above NGVD 1929.

Methodology

SLOSH is a grid based numerical storm surge model that computes water elevations generated by the wind and pressure forces in tropical cyclones. The time history of the water elevation is saved in individual elements of the basin grid and the maximum value for each grid cell is termed as the Envelope of High Water (EOHW). The observed storm surge elevation was compared to the EOHW in the grid cell that contains the HWM.

For Hurricane Andrew, storm tide validations were carried out with three different run cases: (1) the SLOSH storm track and SLOSH wind field model (denoted as NOAA-TRK-SLOSH-WD), (2) the ARA storm track and SLOSH wind field (denoted as ARA-TRK-SLOSH-WD), and (3) the ARA storm track and ARA wind model (denoted as ARA-TRK-ARA-WD). The simulated values of storm tide were compared to the observed HWMs.

Results

Figure T-2 shows a map of the HWM locations as well as the hurricane track. HWMs in Figure T-2 are compared to the simulated storm tide values based on SLOSH wind model and ARA wind model. The results are listed in Table T-1.

The maximum interior HWM value of 16.9 feet occurred at location 135 on the shoreline Biscayne Bay on the right hand side of the hurricane track. The storm tide estimates produced by the SLOSH at the same location are 14.7 and 12.5 feet for model runs with the ARA storm track combined with the SLOSH wind model and ARA wind model, respectively.

Figures T-3a through T-3d present the comparisons of observed and simulated storm tide values with SLOSH wind model and ARA wind model. Simulated values in Figures T-3a and T-3b are from model runs using the ARA storm track. Simulated values in Figure T-3c are from the model using the SLOSH storm track and the SLOSH wind field model. The comparisons indicate that the SLOSH model overestimates the storm surge for Hurricane Andrew. ARA-TRK-SLOSH-WD and ARA-TRK-ARA-WD produce average overestimates of about 14% and 6%, respectively, as shown in Figures T-3a and T-3b. Comparison of observed HWMs to simulated storm tides using different storm tracks shows that the model run using SLOSH storm track produces better simulations than model run using ARA storm track.

Figures T-3e through T-3g show the comparisons of simulated and observed inside HWMs and outside HWMs. The SLOSH model overestimates the storm tide for both outside HWMs and inside HWMs. It is surprising to see that the overestimates for outside HMWs tend to be larger than the overestimates for inside HMWs even though wave effects are not included in the simulations.

Histograms of the differences (simulated minus observed) were shown in Figure T-4a through T-4c. The error characteristics are indicated in the legend. The mean errors are 1.53, 0.95, and 0.57

feet for model runs of ARA-TRK-SLOSH-WD, ARA-TRK-ARA-WD, and NOAA-TRK-SLOSH-WD, respectively. It should be noted that positive mean errors indicate the SLOSH model overestimates the storm surge for Hurricane Andrew, consistent with the results shown in Figure T-3a through T-3c.

Conclusions

Comparison of observed HWMs to the SLOSH model calculated storm tide in Biscayne Bay showed that the SLOSH model overestimates the storm surge for Hurricane Andrew (1992). Comparison also indicated that the model run using SLOSH storm track produces better simulations than model run using ARA storm track.

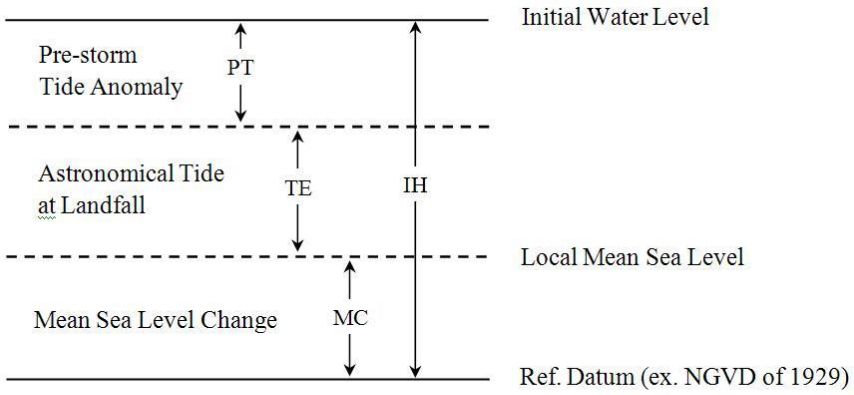

MC: difference between reference datum and local mean sea level

TE: predicted astronomical tide above local mean sea level at the time of landfall

PT: abnormal rise of water level two days before the storm arrival

IH: initial water level above the reference datum

$$IH = MC + TE + PT$$

Figure T-1. Calculation of Initial Water Level

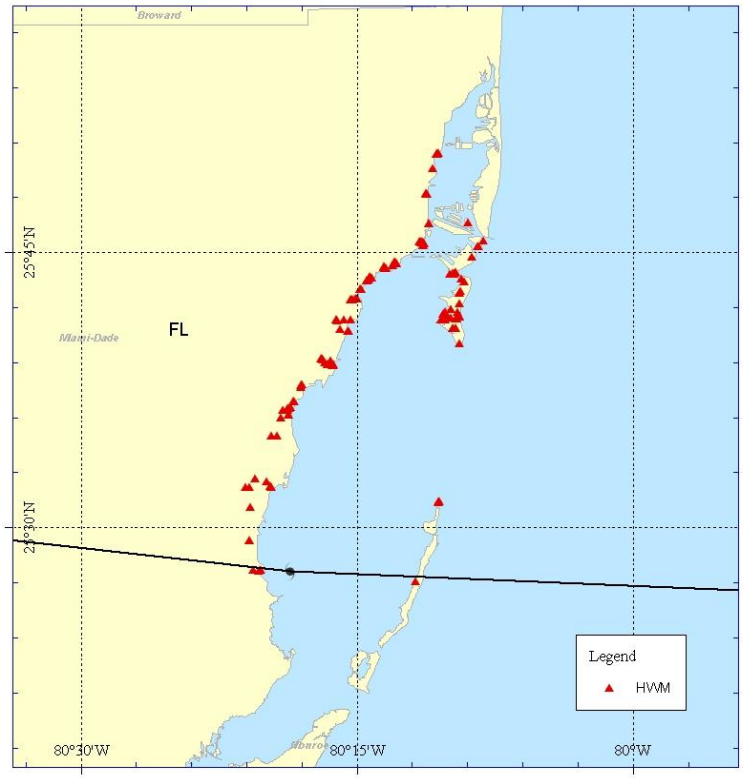

Figure T-2. Coastal High Water Mark Locations for Hurricane Andrew (1992)

Table T-1. Summary of Modeled and Observed Storm Tides (ft NGVD) – Hurricane Andrew

No	Plate No	Mark No	Lat	Lon	Quality Mark	Type Mark	Obs Tide	ARA TRK SLOSH Wind	ARA TRK ARA Wind	SLOSH TRK SLOSH Wind
1	2	1	25.84083	-80.17639	F	O	5.7	4.6	5.2	3.9
2	2	2	25.84028	-80.17694	G	I	5.7	4.6	5.2	3.9
3	2	3	25.84056	-80.17694	G	O	5.7	4.6	5.2	3.9
4	2	4	25.84000	-80.17750	G	O	4.7	4.6	5.2	3.9
5	2	6	25.84000	-80.17806	F	O	5.8	4.6	5.2	3.9
6	2	8	25.82667	-80.18111	E	O	4.2	4.8	5.3	4.0
7	2	25	25.80417	-80.18694	F	O	5.2	6.2	6.5	5.4
8	2	26	25.80389	-80.18694	F	O	5.2	6.2	6.5	5.4
9	2	27	25.80389	-80.18639	F	O	5.3	6.2	6.5	5.4
10	2	28	25.80389	-80.18639	F	O	5.0	6.2	6.5	5.4
11	2	35	25.77806	-80.14944	G	O	4.7	6.9	6.4	5.7
12	2	36	25.77722	-80.18472	F	O	5.3	8.3	8.3	8.1
13	2	37	25.77722	-80.18472	F	O	5.3	8.3	8.3	8.1
14	2	40	25.76139	-80.13528	G	I	8.6	7.0	7.3	5.9
15	2	41	25.75583	-80.13972	G	I	6.6	7.2	7.2	7.0
16	2	42	25.75583	-80.14028	G	O	6.6	7.2	7.2	7.0
17	2	43	25.76056	-80.19306	F	O	7.6	9.3	9.4	8.8
18	2	44	25.76083	-80.19278	G	O	7.7	9.3	9.4	8.8
19	2	45	25.76083	-80.19278	G	I	7.6	9.3	9.4	8.8
20	2	46	25.76028	-80.19139	F	O	7.5	9.3	9.4	8.8
21	2	47	25.76028	-80.19056	E	O	7.5	9.3	9.4	8.8
22	2	48	25.75972	-80.19139	F	O	7.6	9.3	9.4	8.8
23	2	49	25.75944	-80.19028	F	O	8.0	9.3	9.4	8.8
24	2	50	25.75917	-80.19000	E	I	7.5	9.3	9.4	8.8
25	2	51	25.75889	-80.18944	G	I	7.3	9.3	9.4	8.8
26	2	52	25.75861	-80.18944	G	I	7.4	9.3	9.5	8.8
27	2	53	25.75694	-80.18972	E	I	7.8	9.6	9.7	9.0
28	2	54	25.75667	-80.19000	E	I	7.3	9.6	9.7	9.0
29	3	7	25.70889	-80.25028	G	O	9.3	12.2	11.6	10.8
30	3	8	25.70889	-80.25028	E	I	9.1	12.2	11.6	10.8
31	3	9	25.70861	-80.25167	E	I	9.3	12.2	11.6	10.8
32	3	10	25.70778	-80.25417	G	O	9.3	12.2	11.6	10.8
33	3	11	25.70778	-80.25417	E	I	9.3	12.2	11.6	10.8
34	3	12	25.70778	-80.25472	E	I	9.2	12.2	11.6	10.8
35	3	13	25.70778	-80.25583	G	O	9.1	12.2	11.6	10.8
36	3	14	25.70778	-80.25583	E	I	9.3	12.2	11.6	10.8
37	3	15	25.68917	-80.25528	F	O	9.2	12.4	11.8	10.9
38	3	16	25.68944	-80.26194	F	O	9.5	12.5	11.8	11.0
39	3	17	25.68917	-80.26861	E	I	9.3	12.5	11.9	11.0
40	3	18	25.68917	-80.26861	G	O	9.4	12.5	11.9	11.0
41	3	19	25.68861	-80.26750	E	I	9.4	12.5	11.9	11.0
42	3	21	25.67889	-80.25694	F	I	9.0	12.6	11.9	11.0

Table T-1. Summary of Modeled and Observed Storm Tides (ft NGVD) – Hurricane Andrew (Continued)

No	Plate No	Mark No	Lat	Lon	Quality Mark	Type Mark	Obs Tide	ARA TRK SLOSH Wind	ARA TRK ARA Wind	SLOSH TRK SLOSH Wind
43	3	23	25.67917	-80.25806	G	I	9.5	12.6	11.9	11.0
44	3	25	25.68083	-80.26500	E	I	9.3	12.6	11.9	11.1
45	3	28	25.65389	-80.28250	G	O	8.7	13.5	12.2	11.7
46	3	29	25.65389	-80.28194	G	I	8.4	13.5	12.2	11.7
47	3	30	25.65389	-80.28167	G	I	8.6	13.5	12.2	11.7
48	3	31	25.65361	-80.28028	G	I	8.8	13.5	12.1	11.7
49	3	32	25.65194	-80.27361	G	I	8.7	13.3	12.1	11.6
50	3	33	25.64917	-80.27611	G	I	9.8	13.3	12.1	11.6
51	3	34	25.64861	-80.27111	G	I	11.7	13.3	12.1	11.6
52	3	35	25.64833	-80.27222	G	I	9.2	13.3	12.1	11.6
53	3	36	25.64917	-80.27611	G	O	9.8	13.3	12.1	11.6
54	3	37	25.64917	-80.27611	F	O	10.1	13.3	12.1	11.6
55	3	38	25.64806	-80.27111	F	O	10.4	13.3	12.1	11.6
56	3	43	25.63056	-80.29944	G	I	14.6	14.2	12.6	12.5
57	3	45	25.62806	-80.30083	F	I	14.8	14.2	12.6	12.5
58	3	46	25.63000	-80.30056	G	I	15.2	14.2	12.6	12.5
59	3	47	25.65083	-80.27861	G	I	10.2	13.5	12.1	11.7
60	4	1	25.74222	-80.21611	F	O	9.2	10.6	10.7	9.3
61	4	2	25.74167	-80.21528	G	I	9.3	10.6	10.7	9.3
62	4	3	25.74083	-80.21444	F	O	9.1	10.6	10.7	9.3
63	4	4	25.74083	-80.21444	F	O	9.1	10.6	10.7	9.3
64	4	5	25.74056	-80.21417	G	O	9.5	10.6	10.7	9.3
65	4	6	25.73917	-80.21750	G	O	9.1	10.8	10.9	9.5
66	4	7	25.73917	-80.21750	G	I	8.2	10.8	10.9	9.5
67	4	10	25.73778	-80.22528	F	O	9.0	11.2	11.2	10.0
68	4	11	25.73722	-80.22500	G	O	9.4	11.2	11.2	10.0
69	4	12	25.73694	-80.22500	E	I	9.1	11.2	11.2	10.0
70	4	13	25.73694	-80.22500	E	O	9.5	11.2	11.2	10.0
71	4	14	25.73611	-80.22389	G	I	9.9	11.2	11.2	10.0
72	4	15	25.73611	-80.22389	G	I	9.9	11.2	11.2	10.0
73	4	16	25.73639	-80.22472	G	I	9.7	11.2	11.2	10.0
74	4	17	25.73639	-80.22472	G	I	8.5	11.2	11.2	10.0
75	4	20	25.72750	-80.23667	E	I	9.3	11.5	11.4	10.3
76	4	21	25.72750	-80.23667	E	I	9.2	11.5	11.4	10.3
77	4	22	25.72833	-80.23806	E	I	9.6	11.5	11.4	10.3
78	4	23	25.72833	-80.23806	G	I	9.7	11.5	11.4	10.3
79	4	25	25.72583	-80.23944	G	I	9.8	11.7	11.5	10.5
80	4	26	25.72500	-80.24056	F	O	10.8	11.7	11.5	10.5
81	4	27	25.72500	-80.24056	F	O	10.9	11.7	11.5	10.5
82	4	28	25.72500	-80.24111	F	O	9.9	11.7	11.5	10.5
83	4	30	25.71750	-80.24611	G	O	9.7	12.1	11.6	10.7
84	4	31	25.71750	-80.24583	F	O	7.2	12.1	11.6	10.7

Table T-1. Summary of Modeled and Observed Storm Tides (ft NGVD) – Hurricane Andrew (Continued)

No	Plate No	Mark No	Lat	Lon	Quality Mark	Type Mark	Obs Tide	ARA TRK SLOSH Wind	ARA TRK ARA Wind	SLOSH TRK SLOSH Wind
85	4	32	25.71750	-80.24694	G	O	9.7	12.1	11.6	10.7
86	4	33	25.71750	-80.24667	G	O	9.7	12.1	11.6	10.7
87	4	34	25.70889	-80.24917	E	I	9.3	12.2	11.6	10.8
88	4	35	25.74667	-80.14611	G	I	6.5	7.2	5.6	5.0
89	4	37	25.73111	-80.16583	F	O	7.1	8.2	8.3	7.9
90	4	38	25.73250	-80.16083	G	I	6.0	8.2	8.3	7.9
91	4	39	25.73194	-80.16139	G	I	7.2	8.2	8.3	7.9
92	4	40	25.73167	-80.16333	G	I	7.2	8.2	8.3	7.9
93	4	41	25.73111	-80.16222	F	I	7.8	8.2	8.3	7.9
94	4	42	25.72639	-80.15556	G	I	7.4	9.2	7.3	7.6
95	4	43	25.72389	-80.15278	G	I	7.4	7.5	7.3	7.1
96	4	44	25.71528	-80.15611	G	I	7.6	8.2	7.9	7.8
97	4	45	25.71417	-80.15694	G	I	7.3	8.3	8.1	7.7
98	4	46	25.71417	-80.15694	G	I	7.6	8.3	8.1	7.7
99	4	47	25.70417	-80.15694	G	I	7.4	7.7	8.0	7.8
100	4	48	25.69861	-80.16472	G	O	7.1	8.1	8.3	8.0
101	4	49	25.69639	-80.15889	G	O	7.4	7.4	7.7	7.5
102	4	50	25.69639	-80.16972	G	O	8.2	8.7	8.6	8.3
103	4	51	25.69639	-80.16972	G	I	7.5	8.7	8.6	8.3
104	4	52	25.69500	-80.17194	G	O	7.7	9.0	8.6	8.5
105	4	53	25.69500	-80.17194	G	I	7.1	9.0	8.6	8.5
106	4	54	25.68972	-80.17361	G	I	7.6	9.1	8.9	8.5
107	4	55	25.68972	-80.17361	G	O	7.8	9.1	8.9	8.5
108	4	56	25.68972	-80.17361	G	I	7.6	9.1	8.9	8.5
109	4	57	25.68972	-80.16972	F	O	6.9	9.1	8.9	8.5
110	4	58	25.68917	-80.17000	F	O	7.0	9.1	8.9	8.5
111	4	59	25.69083	-80.16750	G	O	6.8	8.7	8.6	8.3
112	4	60	25.69083	-80.16472	G	I	6.4	7.7	7.8	7.6
113	4	61	25.69056	-80.16056	G	O	6.8	7.7	7.8	7.6
114	4	62	25.69056	-80.15944	G	I	6.5	7.7	7.8	7.6
115	4	63	25.69056	-80.15944	G	O	6.6	7.7	7.8	7.6
116	4	64	25.69222	-80.15694	G	I	9.6	7.4	7.7	7.5
117	4	65	25.69222	-80.15694	G	O	9.3	7.4	7.7	7.5
118	4	66	25.69222	-80.15694	G	I	9.5	7.4	7.7	7.5
119	4	67	25.69222	-80.15694	G	O	9.9	7.4	7.7	7.5
120	4	68	25.68139	-80.16306	G	I	5.8	7.9	8.0	7.4
121	4	69	25.68139	-80.16306	F	O	7.5	7.9	8.0	7.4
122	4	70	25.68167	-80.16028	G	I	6.6	7.9	8.0	7.4
123	4	71	25.68167	-80.16028	F	O	6.2	7.9	8.0	7.4
124	4	72	25.66778	-80.15694	G	I	8.7	7.1	6.8	6.1
125	5	9	25.61472	-80.30778	G	I	16.5	14.5	12.7	13.1
126	5	10	25.61528	-80.30694	E	I	16.6	14.5	12.7	13.1

Table T-1. Summary of Modeled and Observed Storm Tides (ft NGVD) – Hurricane Andrew (Continued)

No	Plate No	Mark No	Lat	Lon	Quality Mark	Type Mark	Obs Tide	ARA TRK SLOSH Wind	ARA TRK ARA Wind	SLOSH TRK SLOSH Wind
127	5	11	25.61472	-80.30778	E	I	15.6	14.5	12.7	13.1
128	5	12	25.54500	-80.34222	G	I	15.5	13.6	11.4	12.7
129	5	13	25.61000	-80.30972	E	I	16.2	14.7	12.7	13.3
130	5	14	25.61000	-80.30972	E	I	16.2	14.7	12.7	13.3
131	5	16	25.60889	-80.31111	F	O	16.2	14.7	12.7	13.3
132	5	17	25.60917	-80.31306	G	I	13.2	14.7	12.7	13.3
133	5	20	25.60750	-80.31667	F	I	11.7	14.7	12.5	13.3
134	5	21	25.60778	-80.31250	G	I	16.5	14.7	12.7	13.3
135	5	23	25.60278	-80.31139	F	I	16.9	14.7	12.5	13.3
136	5	24	25.60278	-80.31139	F	O	17.2	14.7	12.5	13.3
137	5	25	25.60028	-80.31833	E	I	14.7	14.7	12.5	13.3
138	5	34	25.58444	-80.32722	E	I	10.1	14.6	11.9	13.1
139	5	35	25.58361	-80.32250	E	I	10.1	14.6	11.9	13.2
140	5	41	25.53750	-80.34750	E	I	10.3	13.3	11.2	12.4
141	5	43	25.54250	-80.33139	F	I	11.8	13.5	11.4	12.7
142	5	44	25.53861	-80.32861	F	O	12.0	13.5	11.3	12.7
143	5	45	25.53861	-80.32861	G	I	12.5	13.5	11.3	12.7
144	5	46	25.53750	-80.32750	E	I	12.6	13.5	11.3	12.7
145	5	48	25.53722	-80.35056	F	O	6.7	13.3	11.0	12.5
146	5	51	25.51917	-80.34639	E	I	8.8	12.9	10.4	11.9
147	6	1	25.52444	-80.17611	G	I	6.9	5.9	5.7	5.4
148	6	2	25.52389	-80.17583	G	I	5.1	5.9	5.7	5.4
149	6	3	25.52472	-80.17556	G	I	4.7	5.9	5.7	5.4
150	7	1	25.48917	-80.34722	F	O	9.7	12.7	9.7	11.7
151	7	2	25.48889	-80.34722	E	I	8.5	12.7	9.7	11.7
152	7	5	25.46250	-80.33750	E	I	6.7	10.2	8.7	9.5
153	7	6	25.46222	-80.33694	E	I	6.9	10.2	8.7	9.5
154	7	7	25.46139	-80.33889	G	I	6.7	10.2	8.7	9.5
155	7	8	25.46167	-80.34389	F	O	6.2	10.6	8.6	8.7
156	8	1	25.45167	-80.19639	E	I	7.3	5.3	5.5	5.3

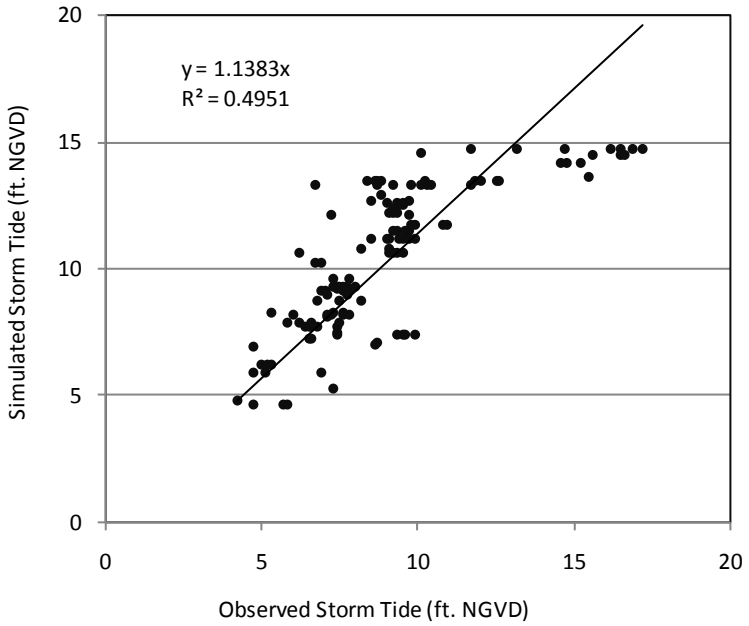

Figure T-3a. Comparison of Simulated and Observed Storm Tide for Hurricane Andrew (ARA Track, SLOSH Wind Field)

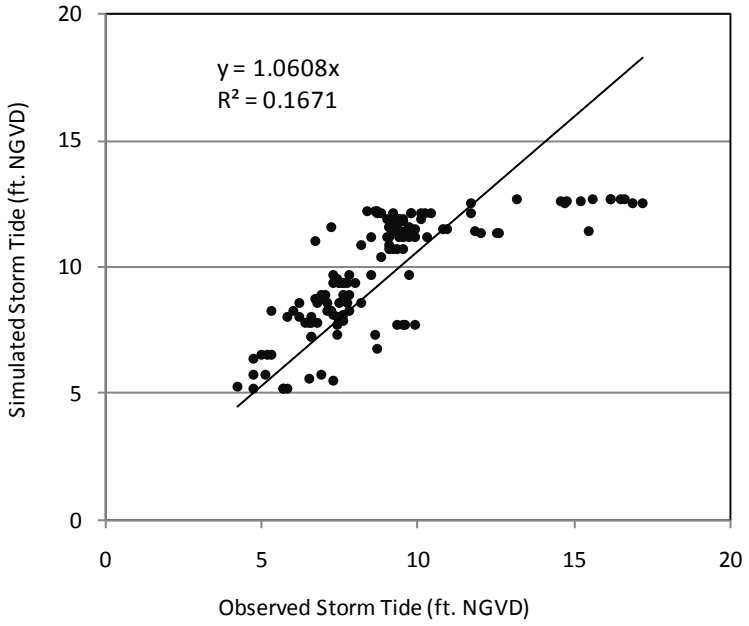

Figure T-3b. Comparison of Simulated and Observed Storm Tide for Hurricane Andrew (ARA Track, ARA Wind Field)

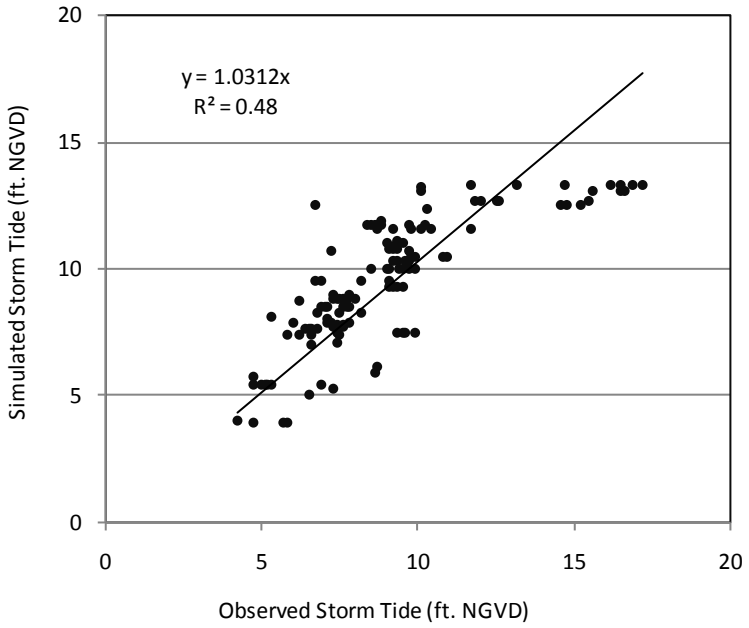

Figure T-3c. Comparison of Simulated and Observed Storm Tide for Hurricane Andrew (SLOSH Track, SLOSH Wind Field)

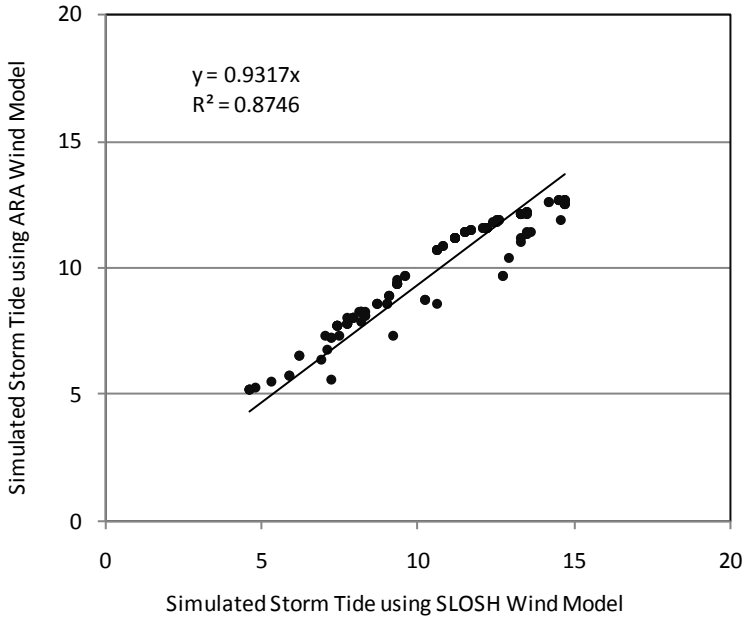

Figure T-3d. Comparison of Simulated Storm Tides for Hurricane Andrew (ARA Track, SLOSH Wind Field vs. ARA Wind Field)

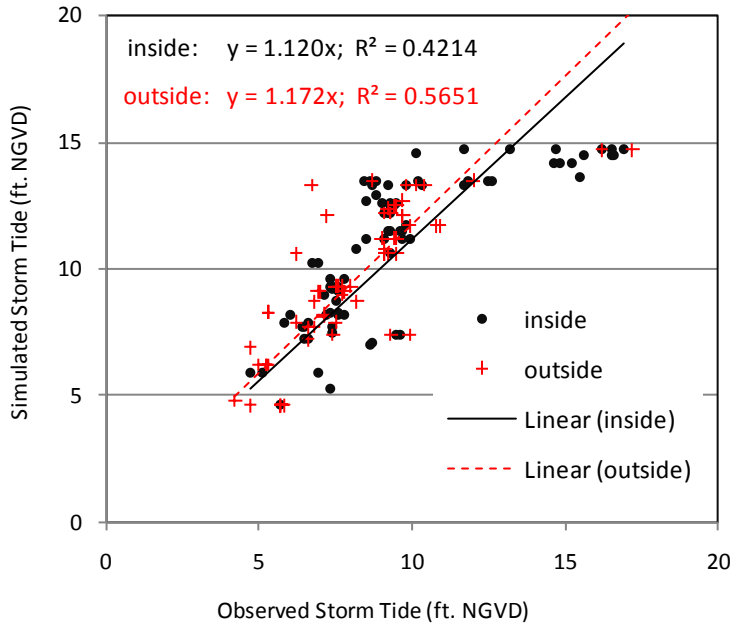

Figure T-3e. Comparison of Simulated and Observed Storm Tide (Inside and Outside) for Hurricane Andrew (ARA Track, SLOSH Wind Field)

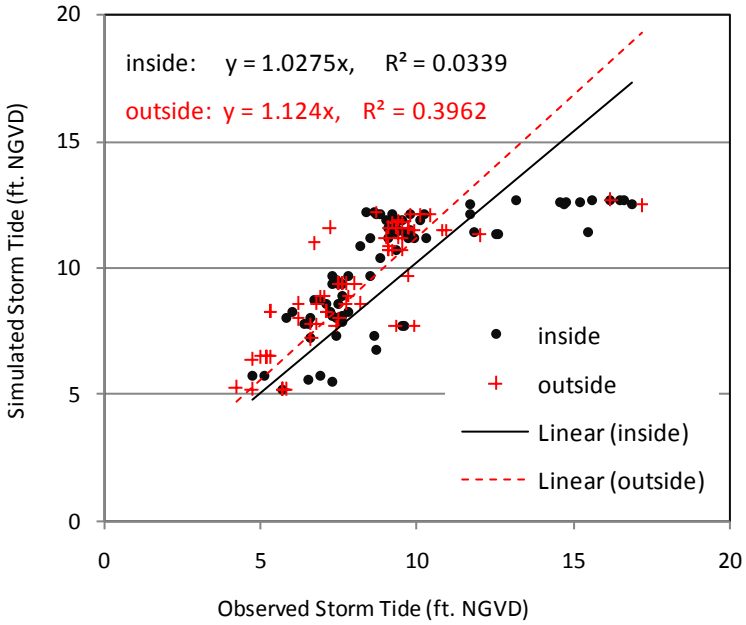

Figure T-3f. Comparison of Simulated and Observed Storm Tide (Inside and Outside) for Hurricane Andrew (ARA Track, ARA Wind Field)

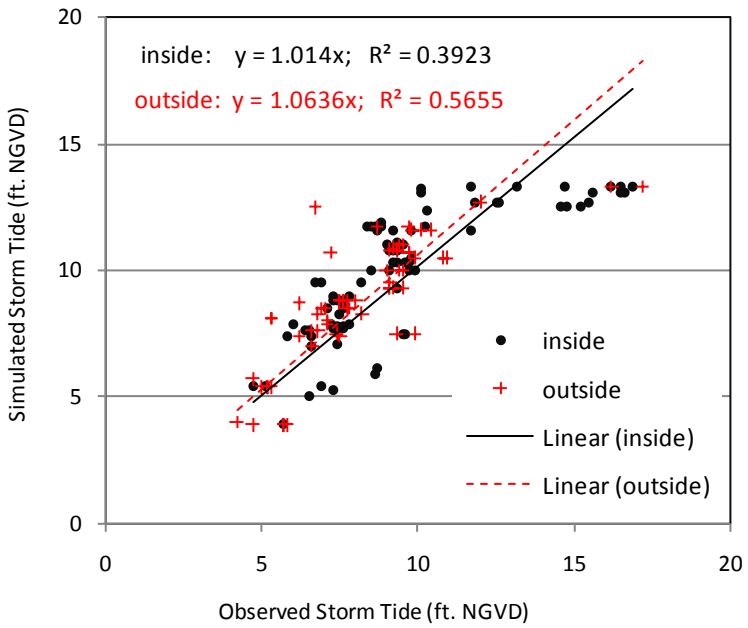

Figure T-3g. Comparison of Simulated and Observed Storm Tide (Inside and Outside) for Hurricane Andrew (SLOSH Track, SLOSH Wind Field)

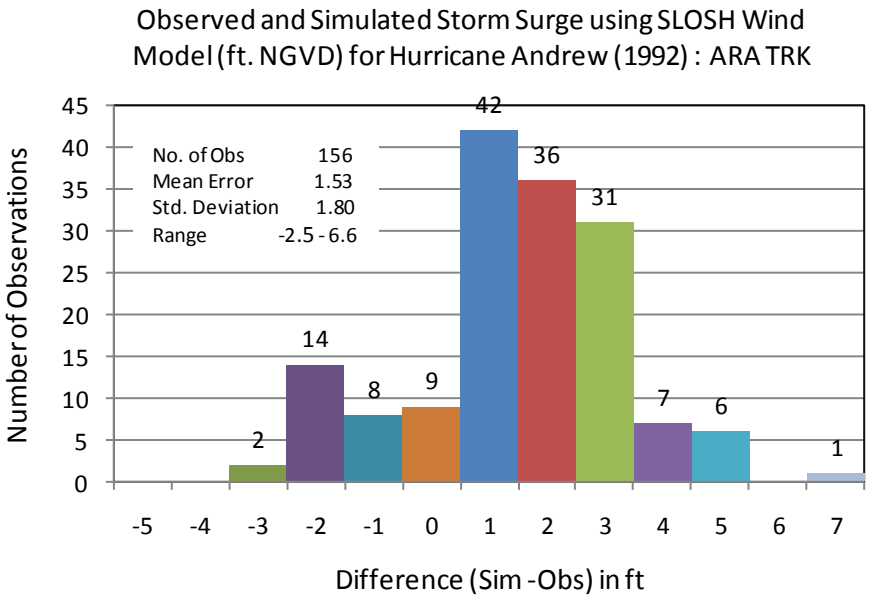

Figure T-4a. Simulated Storm Tide Values minus Observed HWMs for Hurricane Andrew (ARA Track, SLOSH Wind Field)

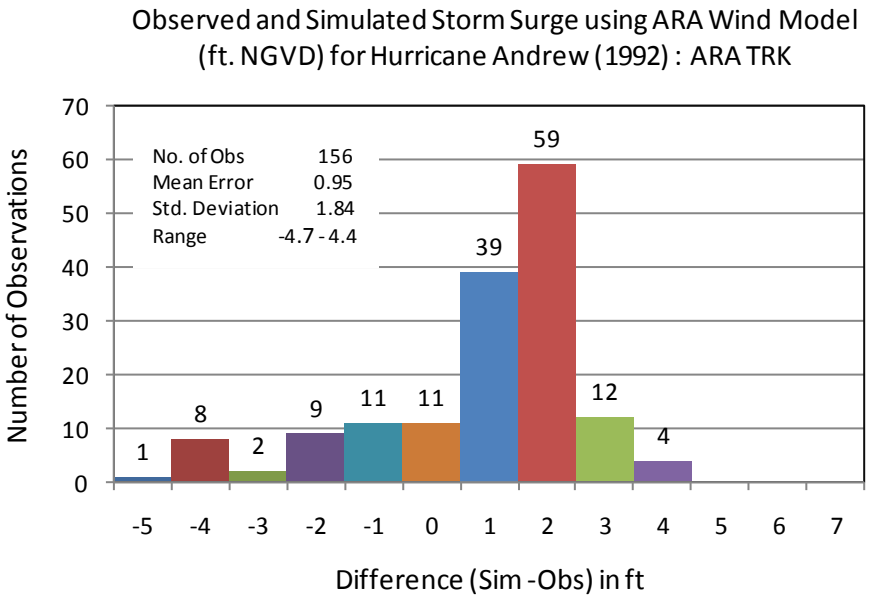

Figure T-4b. Simulated Storm Tide Values minus Observed HWMs for Hurricane Andrew (ARA Track, ARA Wind Field)

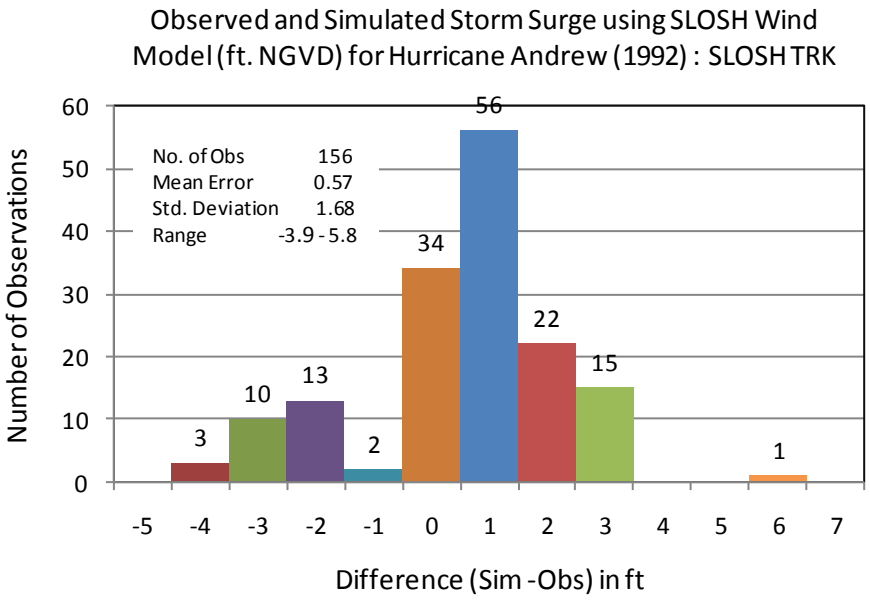

Figure T-4c. Simulated Storm Tide Values minus Observed HWMs for Hurricane Andrew (SLOSH Track, SLOSH Wind Field)

Appendix U. Comparison of Observed and Modeled Storm Tides for Hurricane Isabel (2003)

This appendix compares storm tide estimates from SLOSH to high water marks (HWMs) and tide gauge data from Hurricane Isabel. Isabel made landfall as a Category 2 hurricane near Drum Inlet on the Outer Bankers of North Carolina at about 1730 UTC September 18, 2003 (Beven and Cobb, 2004). The hurricane winds combined with astronomical tide caused storm tides along the coasts from Beaufort, Pamlico Sound and Albemarle Sound in North Carolina northward to central portions of the Chesapeake Bay, Delaware Bay and New Jersey shorelines.

Observation Data

Post-Isabel high water mark surveys were conducted in North Carolina, Virginia and Maryland. The high water marks (HWMs) were assigned a category as surge, wave height and wave run-up, and the quality of each mark was assigned a category as Excellent (E), Good (G), Fair (F), and Poor (P). HWMs assigned as E, G, F and surge flood type were used for this study. There are 110 of such HWMs found. All of HWMs were referenced to the North American Vertical Datum of 1988 (NAVD 88).

Hydrographic records associated with the passage of Hurricane Isabel in 2003 were observed at 23 tide gauges (NOAA, 2003). Five tide gauge records are incomplete due to a malfunction or loss of the gauge; however, they are included in the comparisons because they contain useful information about the initial rise of the water at those locations. Observed HWMs and storm tide hydrographs throughout the impacted area are compared to the results of the SLOSH model runs for same locations based upon Hurricane Isabel input parameters. The tide gauge stations and peak values of storm tide were shown in Table U-1 and Table U-2.

SLOSH Basins and Initial Water Levels

SLOSH basins of Pamlico Sound, Norfolk and Chesapeake Bay are used in the comparisons. The SLOSH model runs use a reference datum of NAVD 1988 for Pamlico Sound basin, and a reference datum of NGVD 1929 for Norfolk basin and Chesapeake Bay basin.

Since 1929, the tide gauges data showed a rise in sea level on the average of about 0.65 feet above NGVD 1929 (-0.35 feet NAVD 1988) at Pamlico Sound, North Carolina. The elevation of the astronomical tide above estimated local mean sea level of 2003 in the area of Pamlico Sound at the time the storm hit the coast was 1.2 feet. In addition, before the arrival of Hurricane Isabel, the tide gauges showed a rise of water, termed as pre-storm tide anomaly, along the coasts of eastern North Carolina, east-central Virginia and Maryland of approximately 0.36 feet above predicted tide levels. Therefore, the final initial water height for the SLOSH model runs in Pamlico Sound basin would be on the average of about 1.2 feet above NAVD 1988.

For the Norfolk basin and Chesapeake Bay basin, the sea level was 0.9 feet above NGVD 1929. The astronomical tide level was 1.0 feet on the outer coast and 0.4 feet inside Chesapeake Bay at the time of hurricane landfall. The pre-storm tide anomaly of 0.36 feet was added to give the final initial water height of 2.3 and 1.7 feet above NGVD 1929 for SLOSH model runs in Norfolk basin and Chesapeake Bay basin, respectively.

Methodology

SLOSH is a grid based numerical storm surge model that computes water elevations generated by the wind and pressure forces in tropical cyclones. The time history of the water elevation is saved in individual elements of the basin grid and the maximum value for each grid cell is termed as the Envelope of High Water (EOHW). The EOHW is compared against observed storm surge data. The observed hydrographic records associated with the passage of Hurricane Isabel (2003) at tide gauges are compared to the SLOSH model-generated storm surge hydrographs in the nearest grid cells.

For Hurricane Isabel storm tide validations were carried out with three different run cases, model run with SLOSH storm track and SLOSH wind field model (NOAA-TRK-SLOSH-WD), model run with ARA storm track and SLOSH wind field (ARA-TRK-SLOSH-WD), model run with ARA storm track and ARA wind model (ARA-TRK-ARA-WD).

All three basins, Pamlico Sound, Norfolk and Chesapeake Bay, are used to validate the storm tide. Where the basins overlap for one observation site, the basin with the minimum distance from the basin center to observation site, usually the basin with smaller grid cells (i.e., finer resolution) at the observation site, is used to compare against observed data.

The observed storm tide data from tide gauges are referenced to the NAVD 1988 datum. For model runs in basins using the NGVD 1929 datum, the simulated storm tide values were converted to NAVD 1988 and compared to the observed data. This conversion was completed using the VERTCON software, developed by the National Geodetic Survey (NGS) office to convert data between different vertical data scales (http://www.ngs.noaa.gov/PC_PROD/VERTCON/).

Results

Figure U-1 shows the HWM and tide gauge locations and hurricane track. The observed storm tide values in Figure U-1 are compared to the simulated storm tide values based on SLOSH wind model and ARA wind model. The results are provided in Table U-1 and Table U-2 and are further discussed below.

Figure U-2 shows the comparisons of the storm track positions and parameters between the NOAA SLOSH storm track and ARA storm track. The central pressure difference at landfall in the ARA track is 57 mbar compared to 52 mbar in the NOAA storm track. The values of radius

to maximum winds (RMW) are 90 and 72 km for ARA storm track and NOAA storm track, respectively.

Figures U-3a through U-3c present the EOHW based upon the ARA storm track and SLOSH wind filed (top left), the ARA storm track and ARA wind model (top right), and the NOAA storm track and SLOSH wind model (bottom). The comparisons show that simulated values of storm tide using ARA track and SLOSH wind model are higher than those using NOAA track and SLOSH wind model, and were lower than those using ARA track and ARA wind model.

Figure U-4 presents the comparisons of observed and simulated storm tide values using different storm tracks and wind models. The comparisons indicate that all three model runs tend to underestimate the storm surge for Hurricane Isabel. As indicated by the slopes of the regression lines, the ARA-TRK-ARA-WD model underestimates the observations by about 11% on average, while the ARA-TRK-SLOSH-WD and the NOAA-TRK-SLOSH-WD models underestimate the storm tide by 42% and 45%, respectively.

Figure U-5 provides histograms of the differences (simulated minus observed). The error characteristics are indicated in the legend. For all data case (HWMs and tide gauge) the mean errors are -2.5, -0.5 and -2.7 feet for model runs with ARA track and SLOSH wind model, ARA track and ARA wind model, NOAA track and SLOSH wind model, respectively. Note that the negative values of the mean error indicate underestimates, consistent with the results shown in Figure U-4.

Observed storm surge hydrographs are compared to the SLOSH model simulated storm surge hydrographs for same locations, as shown in Figure U-6a through U-6x. As an example Figure U-6d shows the comparisons of observed and simulated storm tide at Duck USACE FRF, North Carolina. The simulated maximum values of storm tide are 5.1, 5.1, and 4.3 feet for the ARA-TRK-SLOSH-WD, ARA-TRK-ARA-WD, and NOAA-TRK-SLOSH-WD models, respectively. Each is lower than the observed value of 5.6 feet at the same tide gauge station.

The comparisons indicate that the timing of the simulated peak storm tide is generally in agreement with the observed timing. A notable exception is at the Oregon Inlet Marina, North Carolina site, where the maximum simulated tide occurred at about 1600 UTC September 18 (i.e., 12 hours before the observed storm tide was reached the maximum value at about 0400 UTC September 19), as shown in Figure U-6c. However, the observed storm tide at the two nearest tide sites, Cape Hatteras Fishing Pier and Duck USACE FRF, occurred approximately at the time of hurricane landfall, i.e. 1730 UTC September 18, 2003. This suggests that the times recorded at Oregon Inlet Marina may not have been properly shifted to UTC.

Table U-3 summarizes the RMS error of storm tide for Hurricane Isabel. The results show that the model run with ARA wind field model yields the lowest overall RMS error.

Conclusions

For Hurricane Isabel (2003), comparisons of observed storm tide (110 observed HWMs, 23 tide gauge records) and simulated model storm tide data along the Atlantic coast of North Carolina and Chesapeake Bay area showed that the SLOSH model based upon ARA storm track and ARA wind model calculated the reasonable results.

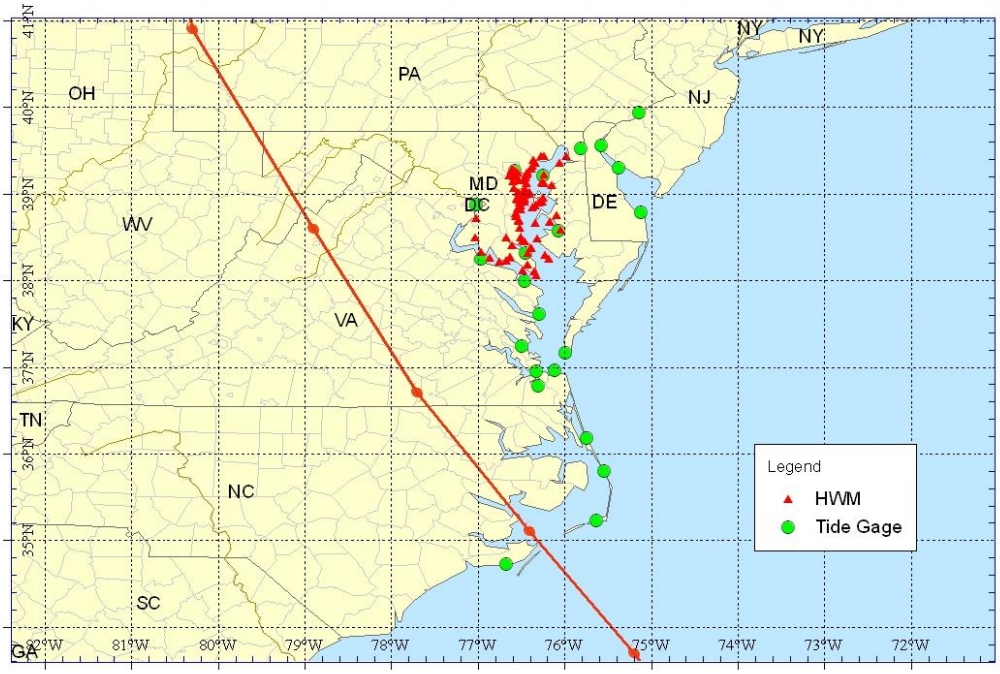

Figure U-1. High Water Mark and Tide Gauge Locations Obtained for Hurricane Isabel

Table U-1. Summary of Modeled and Observed Storm Tides (ft NAVD) – Hurricane Isabel High Water Marks

No	Site ID	County	Survey Lat	Survey Long	HWM Quality	Obs. Storm Tide	ARA TRK SLOSH WD	ARA TRK ARA WD	NOAA TRK SLOSH WD
1	139	St. Mary's	38.234569	-76.678208	Excellent	5.9	4.6	6.2	4.2
2	7	Baltimore	39.282950	-76.596694	Fair	7.6	3.7	6.0	3.7
3	8	Baltimore	39.280817	-76.592464	Fair	7.5	3.7	6.0	3.7
4	10	Baltimore	39.286572	-76.608897	Fair	7.6	3.7	6.0	3.7
5	11	Baltimore	39.283164	-76.611728	Fair	7.4	3.7	6.0	3.7
6	12	Baltimore	39.281575	-76.607167	Fair	5.8	3.7	6.0	3.7
7	14	Anne Arundel	38.977032	-76.484554	Fair	6.5	3.4	5.4	3.3
8	18	Anne Arundel	38.975939	-76.486193	Fair	6.1	3.4	5.4	3.3
9	27	Calvert	38.700709	-76.533286	Fair	7.0	3.2	4.8	3.1
10	28	Calvert	38.709006	-76.530285	Fair	6.1	3.3	4.9	3.2
11	39	Harford	39.404675	-76.356206	Fair	6.4	3.5	6.5	3.5
12	40	Talbot	38.767814	-76.093808	Fair	5.5	3.7	5.9	3.5
13	60	Queen Anne's	38.923169	-76.258756	Fair	1.6	4.2	6.5	4.0
14	61	Queen Anne's	38.922397	-76.256011	Fair	5.6	4.2	6.5	4.0
15	65	Kent	39.106825	-76.143553	Fair	7.4	4.2	7.0	4.0
16	68	Kent	39.136314	-76.251881	Fair	6.7	4.1	6.9	3.9
17	70	Kent	39.229831	-76.234164	Fair	6.4	4.0	7.3	3.9
18	71	Kent	39.370631	-76.063122	Fair	6.4	3.6	7.3	3.4
19	75	Cecil	39.443167	-75.977128	Fair	3.3	3.4	7.4	3.2
20	76	Anne Arundel	39.030463	-76.404262	Fair	7.6	3.3	5.3	3.2
21	78	Anne Arundel	39.006507	-76.406567	Fair	7.2	3.3	5.3	3.2
22	80	Anne Arundel	39.001498	-76.451341	Fair	6.5	3.3	5.2	3.2
23	81	Anne Arundel	38.995103	-76.483059	Fair	6.8	3.4	5.4	3.3
24	82	Anne Arundel	39.006505	-76.512186	Fair	7.0	3.4	5.4	3.3
25	84	Anne Arundel	39.070560	-76.587003	Fair	6.6	3.7	5.8	3.7
26	89	Baltimore	39.282936	-76.597078	Fair	7.5	3.7	6.0	3.7
27	90	Baltimore	39.266875	-76.572708	Fair	6.4	3.7	6.0	3.7
28	91	Baltimore	39.260722	-76.563383	Fair	7.4	3.7	6.0	3.7
29	92	Baltimore	39.261161	-76.559369	Fair	7.6	3.7	6.0	3.7
30	110	Anne Arundel	38.782051	-76.558649	Fair	6.7	3.3	5.0	3.2
31	113	Calvert	38.612842	-76.512665	Fair	6.4	3.1	4.6	3.0
32	115	Calvert	38.500196	-76.503511	Fair	5.6	3.0	4.4	2.9
33	116	Calvert	38.499985	-76.503426	Fair	5.6	3.0	4.4	2.9
34	117	Calvert	38.469584	-76.478529	Fair	6.2	2.9	4.3	2.8
35	120	Calvert	38.379522	-76.391490	Fair	4.6	3.8	5.1	3.5
36	121	Calvert	38.324509	-76.432269	Fair	5.8	4.5	5.8	4.1
37	123	St. Mary's	38.118294	-76.346188	Fair	4.8	4.1	5.3	3.7
38	124	St. Mary's	38.069743	-76.329717	Fair	3.0	4.1	5.2	3.7
39	125	St. Mary's	38.189459	-76.431694	Fair	4.8	4.6	6.2	4.2
40	127	Anne Arundel	39.170533	-76.522736	Fair	7.2	3.4	5.5	3.3
41	135	St. Mary's	38.123556	-76.487915	Fair	6.5	4.2	5.5	3.8
42	136	St. Mary's	38.284199	-76.629500	Fair	7.6	4.6	6.3	4.2
43	137	St. Mary's	38.224229	-76.751216	Fair	7.3	4.5	5.9	4.1
44	144	Baltimore	39.228219	-76.439564	Fair	7.2	3.3	5.6	3.3
45	145	Baltimore	39.202683	-76.446069	Fair	7.1	3.3	5.6	3.3
46	154	Baltimore	39.368189	-76.341019	Fair	7.9	3.4	6.1	3.4
47	156	Anne Arundel	39.221128	-76.639392	Fair	7.5	3.5	5.7	3.5
48	157	Anne Arundel	39.154961	-76.597903	Fair	7.5	3.5	5.7	3.5
49	158	Baltimore	39.209006	-76.583703	Fair	7.4	3.5	5.7	3.5
50	118	Calvert	38.459395	-76.465533	Fair/Good	5.0	2.9	4.3	2.8

Table U-1. Summary of Modeled and Observed Storm Tides (ft NAVD) – Hurricane Isabel High Water Marks (Continued)

No	Site ID	County	Survey Lat	Survey Long	HWM Quality	Obs. Storm Tide	ARA TRK SLOSH WD	ARA TRK ARA WD	NOAA TRK SLOSH WD
51	138	St. Mary's	38.234823	-76.674255	Fair/Good	5.8	4.6	6.2	4.2
52	4	Baltimore	39.331281	-76.368583	Good	7.6	3.4	6.1	3.4
53	6	Baltimore	39.302694	-76.381150	Good	7.5	3.3	5.7	3.3
54	15	Anne Arundel	38.977810	-76.486300	Good	6.3	3.4	5.4	3.3
55	16	Anne Arundel	38.976929	-76.486213	Good	6.4	3.4	5.4	3.3
56	19	Anne Arundel	38.973747	-76.488795	Good	6.3	3.4	5.4	3.3
57	21	Anne Arundel	38.974742	-76.492653	Good	7.3	3.4	5.4	3.3
58	22	Anne Arundel	38.973381	-76.494526	Good	6.6	3.4	5.4	3.3
59	25	Queen Anne's	38.874692	-76.334239	Good	5.6	3.3	5.1	3.1
60	26	Calvert	38.710206	-76.529588	Good	5.7	3.3	4.9	3.2
61	29	Baltimore	39.284931	-76.608286	Good	7.4	3.7	6.0	3.7
62	30	Baltimore	39.279806	-76.589231	Good	7.9	3.7	6.0	3.7
63	31	Baltimore	39.281556	-76.592367	Good	7.7	3.7	6.0	3.7
64	34	Baltimore	39.231092	-76.561444	Good	7.6	3.5	5.7	3.5
65	36	Harford	39.442347	-76.235539	Good	6.9	4.0	7.8	3.8
66	38	Harford	39.446392	-76.266675	Good	7.0	4.1	7.9	3.9
67	42	Talbot	38.672906	-76.338536	Good	5.5	3.1	4.8	3.0
68	43	Talbot	38.681456	-76.170717	Good	5.3	3.7	5.8	3.4
69	44	Talbot	38.682511	-76.173539	Good	5.2	3.7	5.8	3.4
70	45	Talbot	38.593753	-76.050719	Good	5.1	3.3	5.3	2.9
71	47	Dorchester	38.495136	-76.315042	Good	4.1	3.1	4.4	2.9
72	48	Dorchester	38.309553	-76.225544	Good	4.9	4.3	5.7	4.0
73	49	Dorchester	38.256706	-76.177797	Good	4.6	4.0	5.2	3.7
74	51	Baltimore	39.253889	-76.432250	Good	7.4	3.3	5.7	3.3
75	54	Baltimore	39.241719	-76.440492	Good	6.9	3.3	5.7	3.3
76	56	Charles	38.503625	-77.026718	Good	7.3	5.8	7.3	5.2
77	57	Prince George'	38.724332	-77.020229	Good	3.8	4.0	6.6	3.6
78	59	Queen Anne's	38.903394	-76.294875	Good	5.1	3.3	5.2	3.2
79	63	Queen Anne's	38.967567	-76.248019	Good	4.3	4.2	6.5	4.1
80	64	Queen Anne's	38.967744	-76.243706	Good	5.8	4.2	6.5	4.1
81	66	Kent	39.145050	-76.259342	Good	6.9	4.1	6.9	3.9
82	67	Kent	39.141264	-76.260150	Good	6.9	4.1	6.9	3.9
83	69	Kent	39.133186	-76.242667	Good	7.1	4.1	6.9	3.9
84	77	Anne Arundel	39.014537	-76.436321	Good	6.5	3.3	5.3	3.2
85	79	Anne Arundel	39.012943	-76.418172	Good	6.2	3.3	5.3	3.2
86	83	Anne Arundel	39.029843	-76.537815	Good	6.4	3.6	5.6	3.5
87	94	Anne Arundel	38.971707	-76.486813	Good	4.9	3.4	5.4	3.3
88	95	Anne Arundel	38.964110	-76.482280	Good	6.6	3.7	5.5	3.6
89	96	Anne Arundel	38.948085	-76.457693	Good	7.2	3.7	5.5	3.6
90	97	Anne Arundel	38.947686	-76.460961	Good	6.5	3.7	5.5	3.6
91	99	Anne Arundel	38.917146	-76.460095	Good	7.8	3.7	5.5	3.6
92	100	Anne Arundel	38.937495	-76.515338	Good	6.4	3.9	5.8	3.8
93	101	Anne Arundel	38.945932	-76.531956	Good	6.7	3.9	5.8	3.8
94	102	Anne Arundel	38.953121	-76.552311	Good	6.2	3.9	5.8	3.8
95	103	Anne Arundel	38.955129	-76.553978	Good	6.4	3.9	5.8	3.8
96	104	Anne Arundel	38.939165	-76.542592	Good	6.1	3.9	5.8	3.8
97	105	Anne Arundel	38.908158	-76.513910	Good	6.5	3.5	5.3	3.4
98	106	Anne Arundel	38.908606	-76.514349	Good	5.0	3.5	5.3	3.4
99	107	Anne Arundel	38.873816	-76.507739	Good	6.9	3.5	5.3	3.4
100	108	Anne Arundel	38.843359	-76.538899	Good	7.0	3.5	5.2	3.3

Table U-1. Summary of Modeled and Observed Storm Tides (ft NAVD) – Hurricane Isabel High Water Marks (Continued)

No	Site ID	County	Survey Lat	Survey Long	HWM Quality	Obs. Storm Tide	ARA TRK SLOSH WD	ARA TRK ARA WD	NOAA TRK SLOSH WD
101	109	Anne Arundel	38.832507	-76.502916	Good	5.9	3.3	5.1	3.2
102	111	Anne Arundel	38.783202	-76.559240	Good	5.4	3.3	5.0	3.2
103	112	Anne Arundel	38.746220	-76.557582	Good	3.9	3.3	4.9	3.2
104	119	Calvert	38.384088	-76.386661	Good	4.6	3.8	5.1	3.5
105	129	Anne Arundel	39.165400	-76.477869	Good	6.4	3.4	5.5	3.3
106	130	Anne Arundel	39.137150	-76.441686	Good	6.7	3.3	5.4	3.2
107	134	Anne Arundel	39.059469	-76.459219	Good	6.5	3.4	5.4	3.3
108	140	Charles	38.270010	-76.858339	Good	6.3	4.8	6.2	4.3
109	151	Charles	38.510204	-76.678189	Good	5.4	4.7	6.2	4.3
110	152	St. Mary's	38.413091	-76.607701	Good	5.0	5.1	6.5	4.6

Table U-2. Summary of Modeled and Observed Storm Tides (ft NAVD) – Hurricane Isabel Tide Gauges

No	Station Name	Station ID	Lat	Lon	Obs. Tide	ARA TRK SLOSH WD	ARA TRK ARA WD	NOAA TRK SLOSH
1	Beaufort, NC	8656483	34.72000	-76.67000	3.7	2.2	2.7	1.8
2	Cape Hatteras Fishing Pier, NC	8654400	35.22333	-75.63500	N/A	5.5	5.5	5.5
3	Oregon Inlet Marina, NC	8652587	35.79500	-75.54833	4.8	4.9	4.6	4.4
4	Duck USACE FRF, NC	8651370	36.18333	-75.74667	5.6	5.1	5.1	4.3
5	Money Point, Elizabeth River, VA	8639348	36.77833	-76.30167	6.5	5.7	5.9	5.1
6	Sewells Point, VA	8638610	36.94667	-76.33000	6.2	6.4	6.5	5.5
7	Chesapeake Bay Bridge Tunnel, VA	8638863	36.96667	-76.11333	6.7	5.7	5.7	4.8
8	Kiptopeke, Chesapea Bay, VA	8632200	37.16500	-75.98833	4.6	4.7	4.7	4.1
9	Gloucester Point, York River, VA	8637624	37.24667	-76.50000	N/A	6.4	6.9	5.6
10	Windmill Point, VA	8636580	37.61500	-76.29000	N/A	4.4	4.8	3.8
11	Lewisetta, Potomac River, VA	8635750	37.99500	-76.46333	4.6	4.1	5.5	3.8
12	Colonial Beach, Potomac River, VA	8635150	38.25167	-76.96000	N/A	4.9	6.4	4.4
13	Washington, DC	8594900	38.87333	-77.02167	8.9	4.2	7.2	3.7
14	Solomons Island, MD	8577330	38.31667	-76.45167	N/A	4.6	6.0	4.2
15	Cambridge, Choptank River, MD	8571892	38.57333	-76.06833	5.2	3.3	5.4	2.9
16	Annapolis, US Naval Academy, MD	8575512	38.98333	-76.48000	6.4	3.4	5.4	3.3
17	Tolchester Beach, MD	8573364	39.21333	-76.24500	7.0	3.3	7.1	3.2
18	Baltimore, MD	8574680	39.26667	-76.57833	7.3	3.7	6.0	3.7
19	Chesapeake City, MD	8573927	39.52667	-75.81000	7.1	3.5	7.9	3.0
20	Lewes, DE	8557380	38.78167	-75.12000	3.9	2.5	2.8	2.5
21	Reedy Point, DE	8551910	39.55833	-75.57333	5.7	3.3	5.6	3.2
22	Ship John Shoal, NJ	8537121	39.30500	-75.37500	4.8	3.1	4.6	3.0
23	Philadelphia, PA	8545240	39.93333	-75.14167	6.3	2.8	5.4	2.7

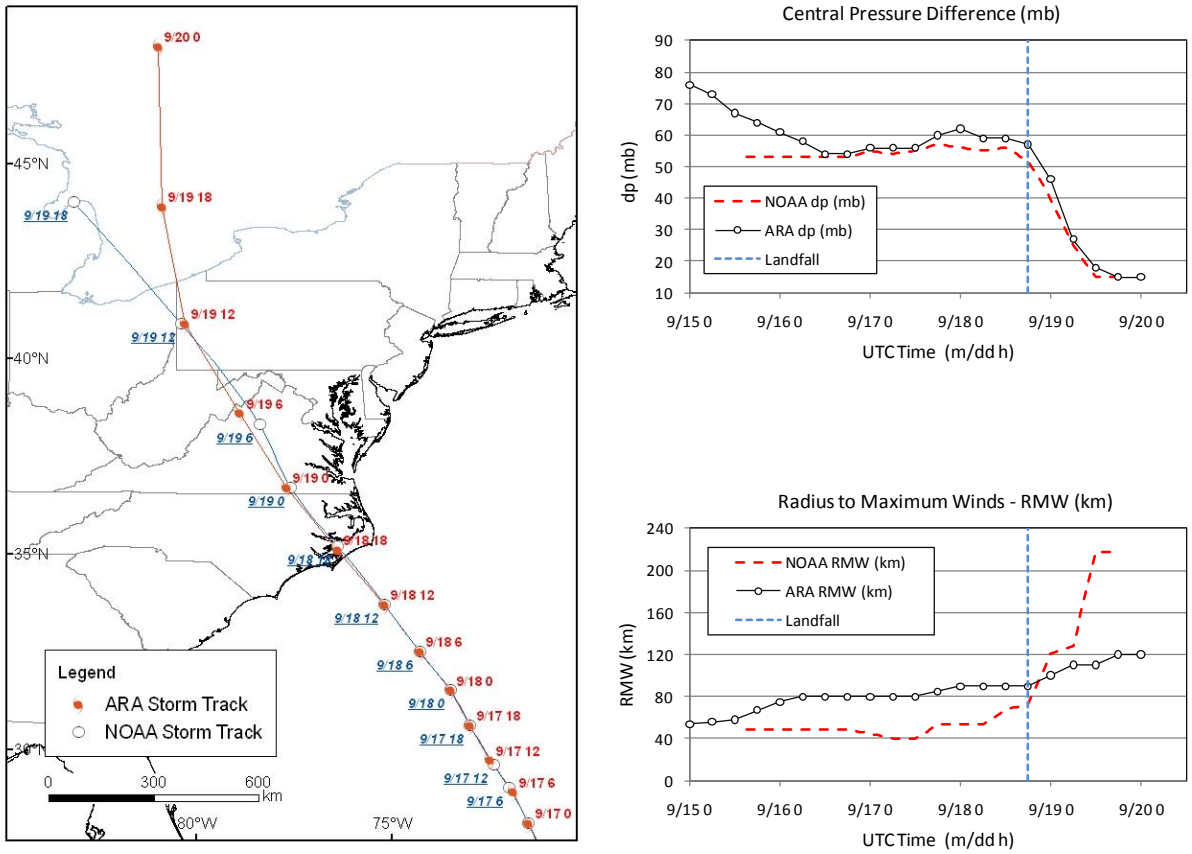

Figure U-2. Comparison of NOAA and ARA Storm Tracks for Hurricane Isabel (2003)

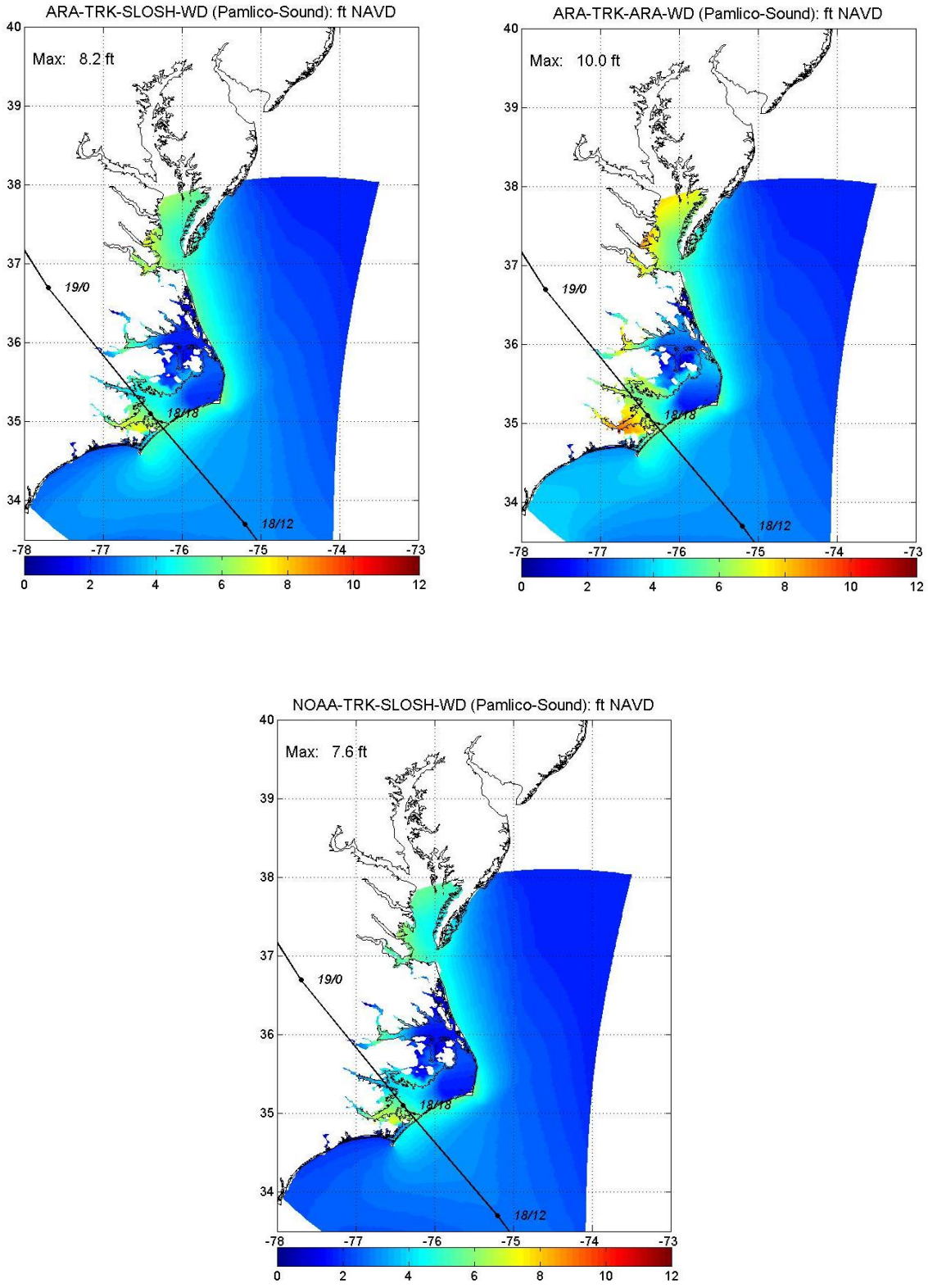

Figure U-3a. Comparison of Simulated Storm Tide Using Different Storm Track and Wind Model for Hurricane Isabel (2003) (Pamlico Sound)

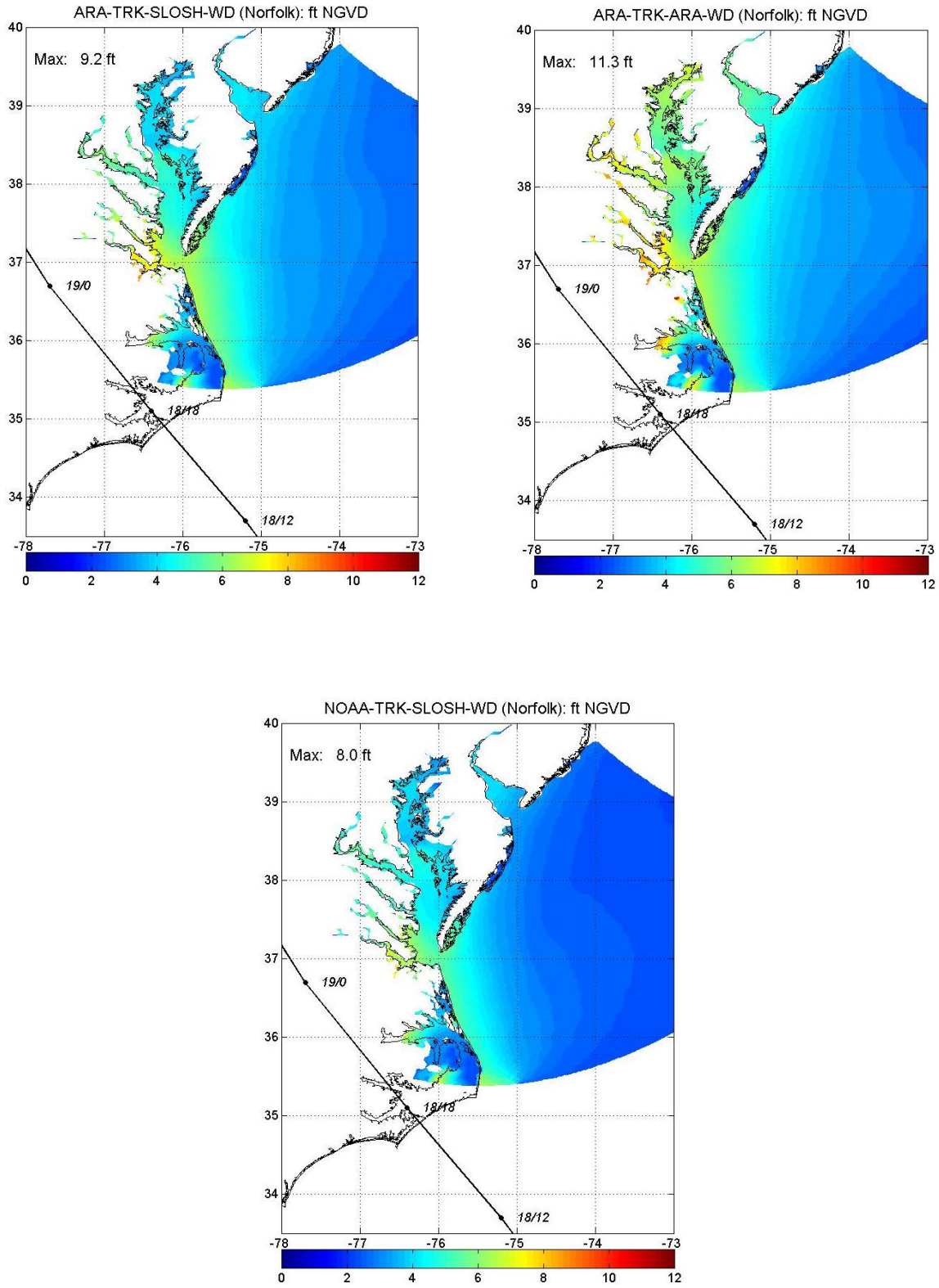

Figure U-3b. Comparison of Simulated Storm Tide Using Different Storm Track and Wind Model for Hurricane Isabel (2003) (Norfolk)

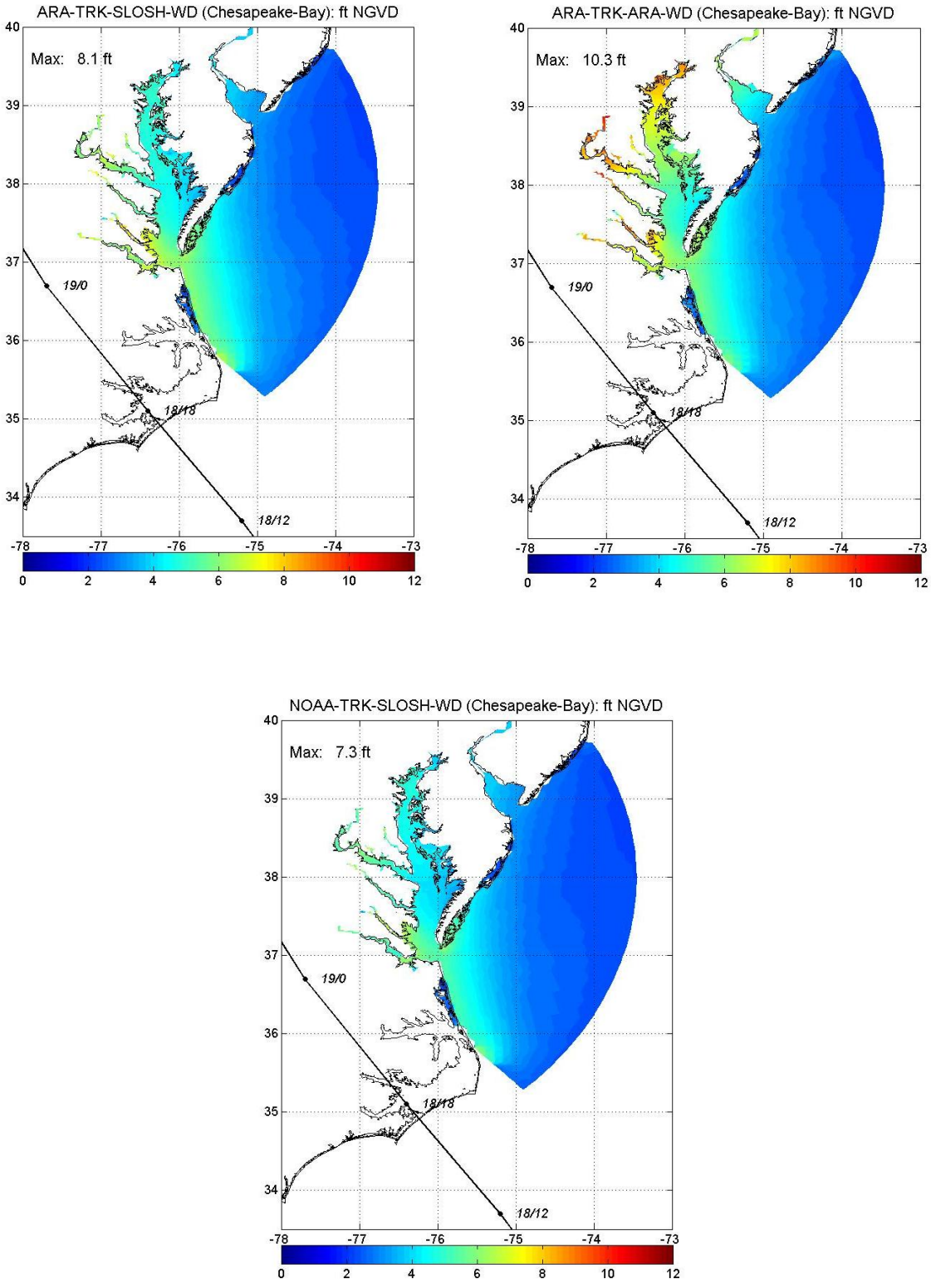

Figure U-3c. Comparison of Simulated Storm Tide Using Different Storm Track and Wind Model for Hurricane Isabel (2003) – Chesapeake Bay

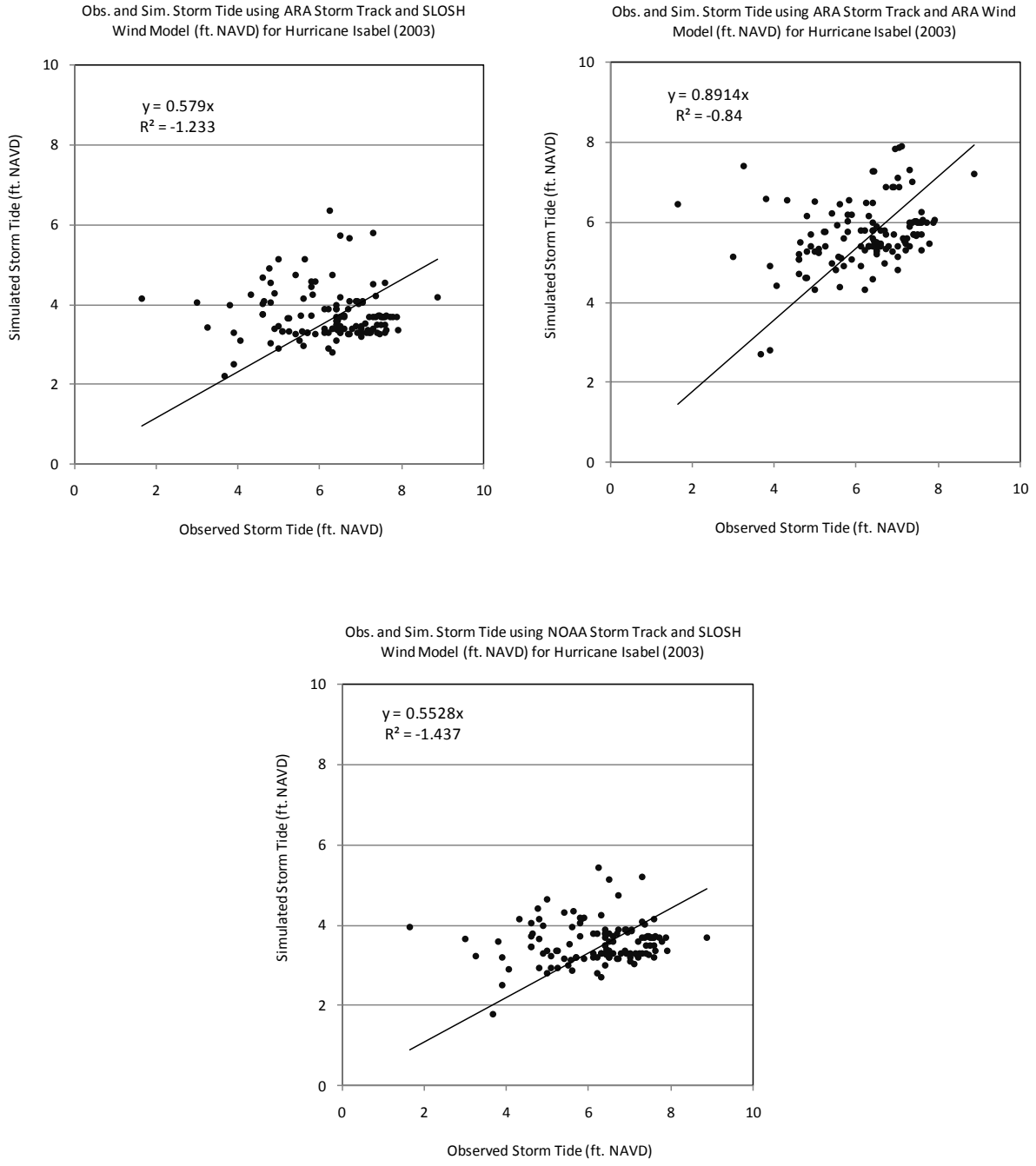

Figure U-4. Comparisons of Simulated and Observed Storm Tide for Hurricane Isabel (2003) – HWM and Tide Gauge

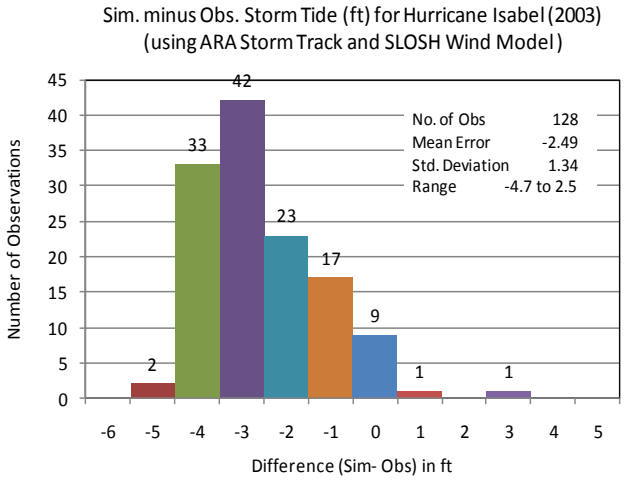

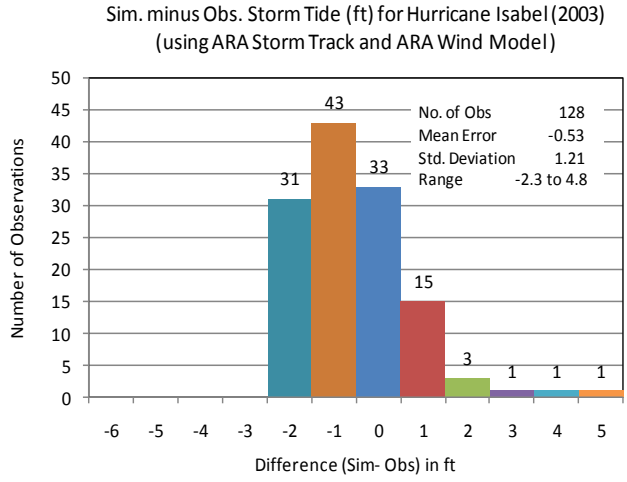

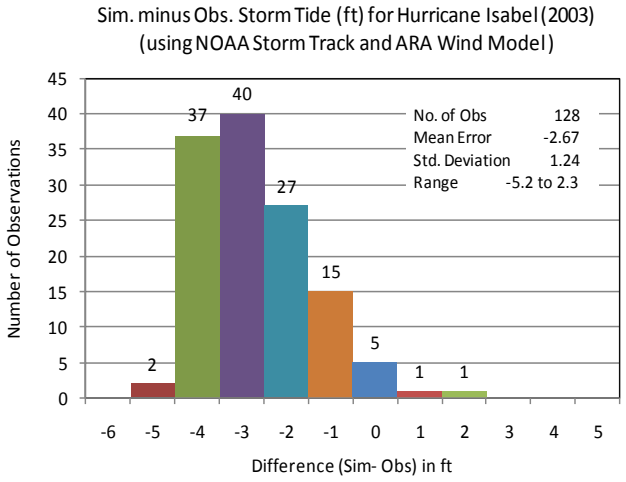

Figure U-5. Simulated Minus Observed Storm Tide (in feet) for Hurricane Isabel (2003) – HWM and Tide Gauge

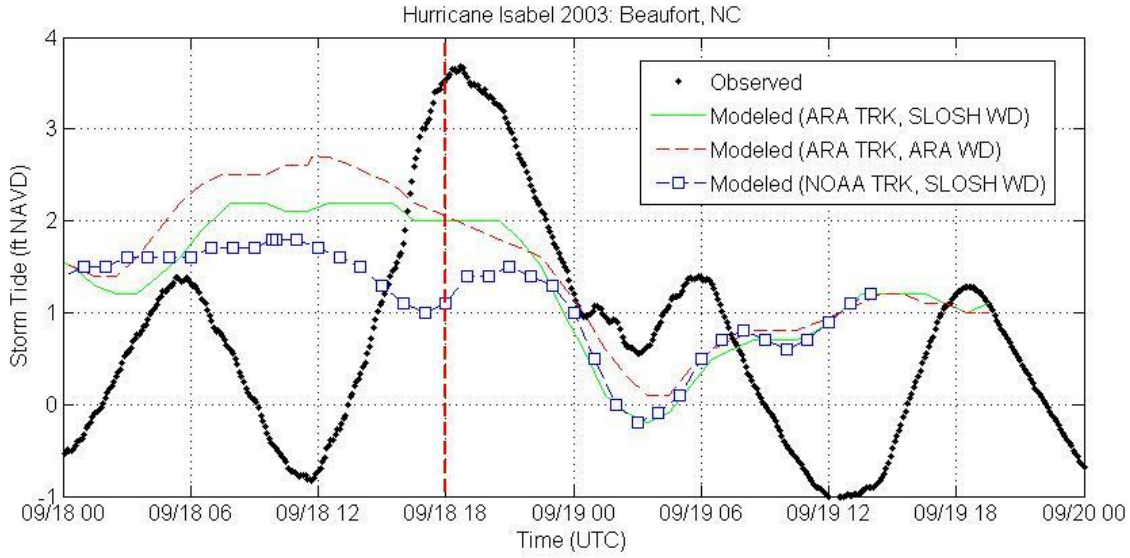

Figure U-6a. Tide gauge record at Beaufort, NC compared to the simulated time histories of storm tide in the SLOSH Grid cell containing the gauge location

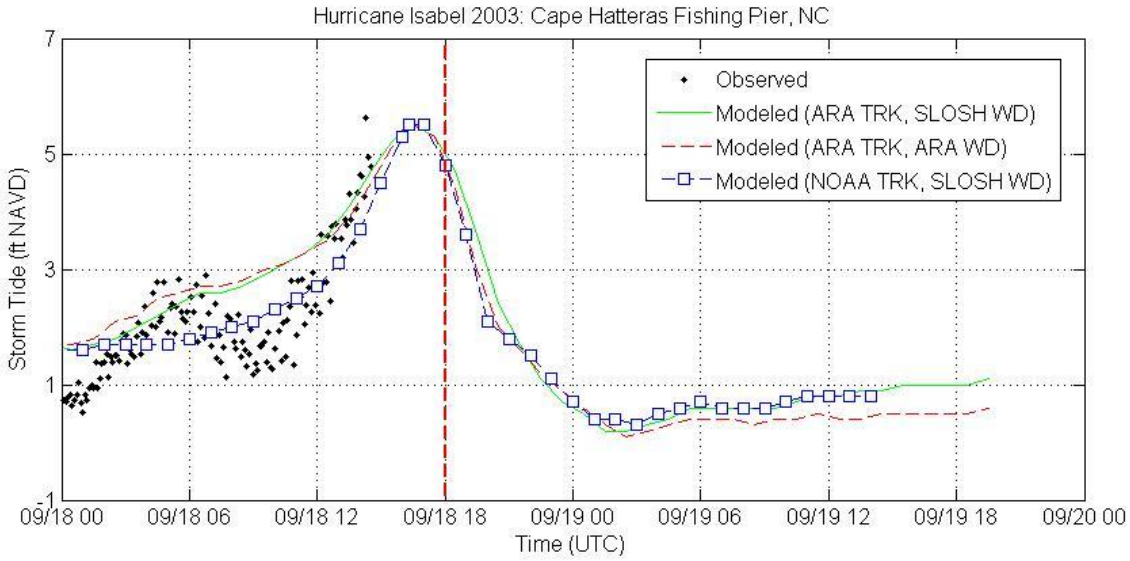

Figure U-6b. Tide gauge record at Cape Hatteras Fishing Pier, NC compared to the simulated time histories of storm tide in the SLOSH Grid cell containing the gauge location

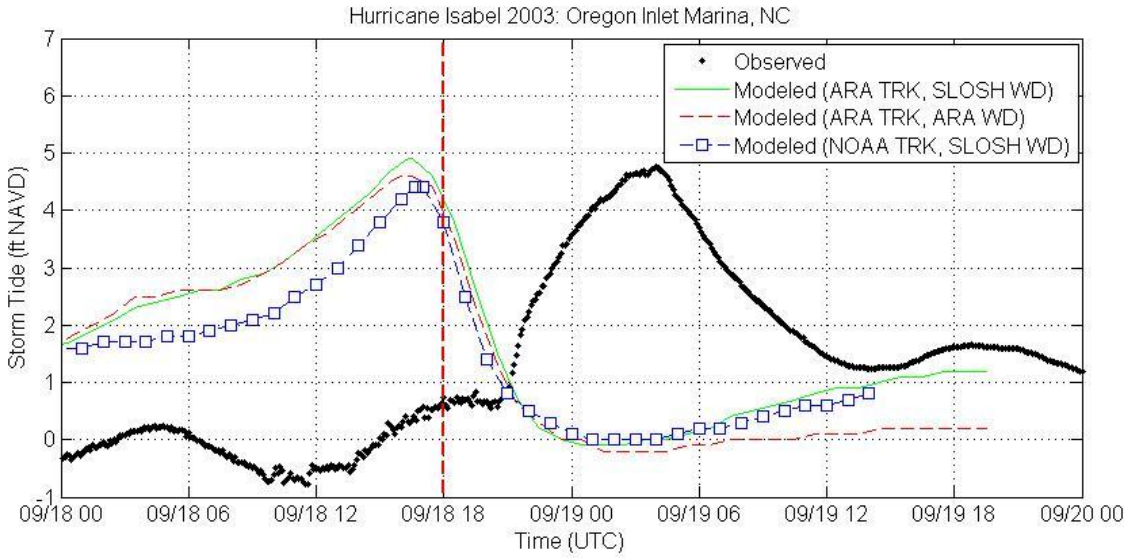

Figure U-6c. Tide gauge record at Oregon Inlet Marina, NC compared to the simulated time histories of storm tide in the SLOSH Grid cell containing the gauge location

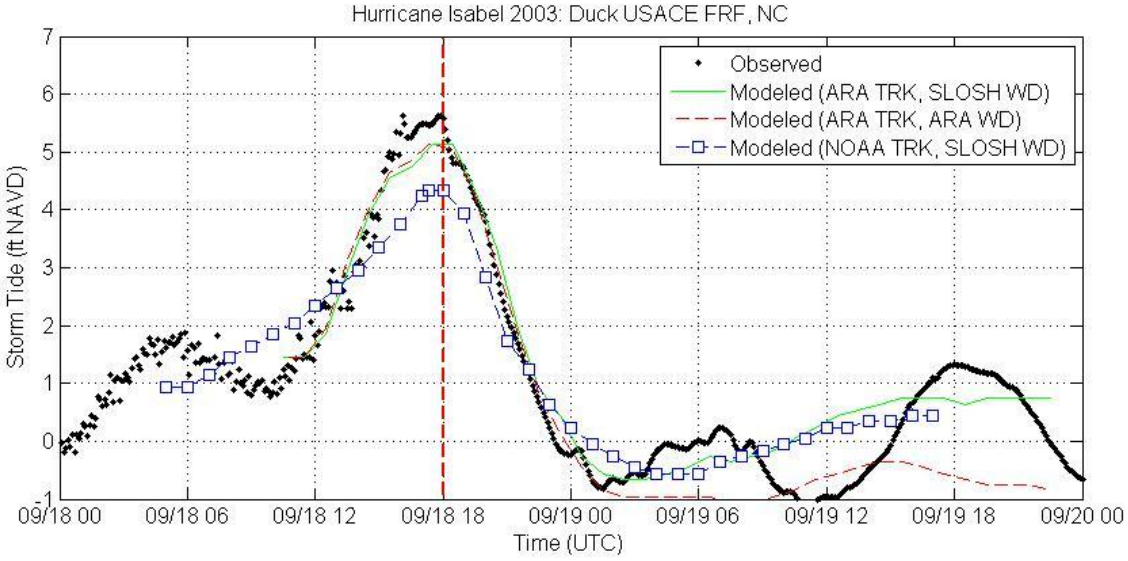

Figure U-6d. Tide gauge record at Duck USACE FRF, NC compared to the simulated time histories of storm tide in the SLOSH Grid cell containing the gauge location

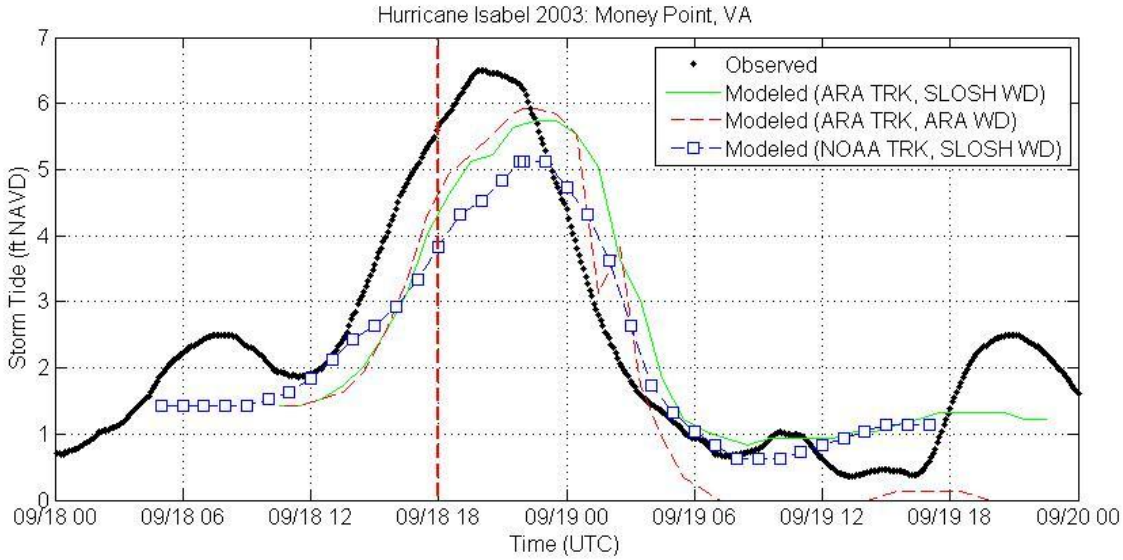

Figure U-6e. Tide gauge record at Money Point, NC compared to the simulated time histories of storm tide in the SLOSH Grid cell containing the gauge location

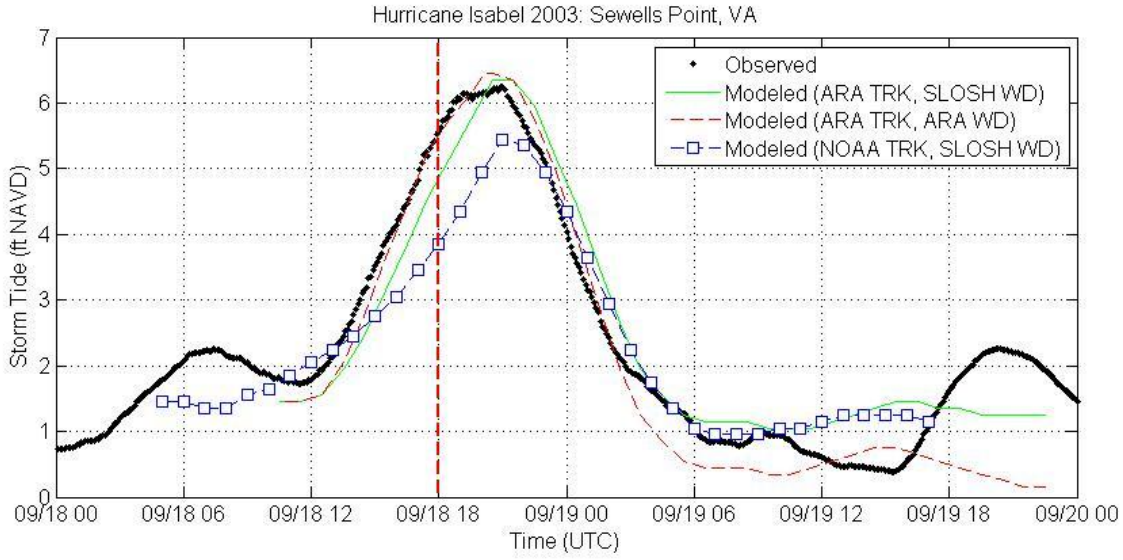

Figure U-6f. Tide gauge record at Sewells Point, VA compared to the simulated time histories of storm tide in the SLOSH Grid cell containing the gauge location

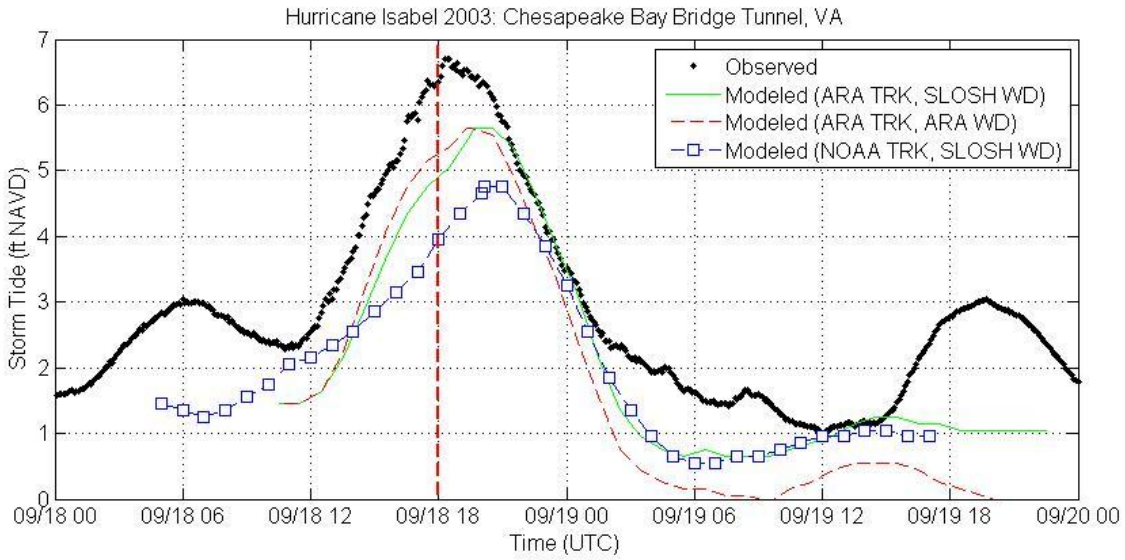

Figure U-6g. Tide gauge record at Chesapeake Bay Bridge Tunnel, VA compared to the simulated time histories of storm tide in the SLOSH Grid cell containing the gauge location

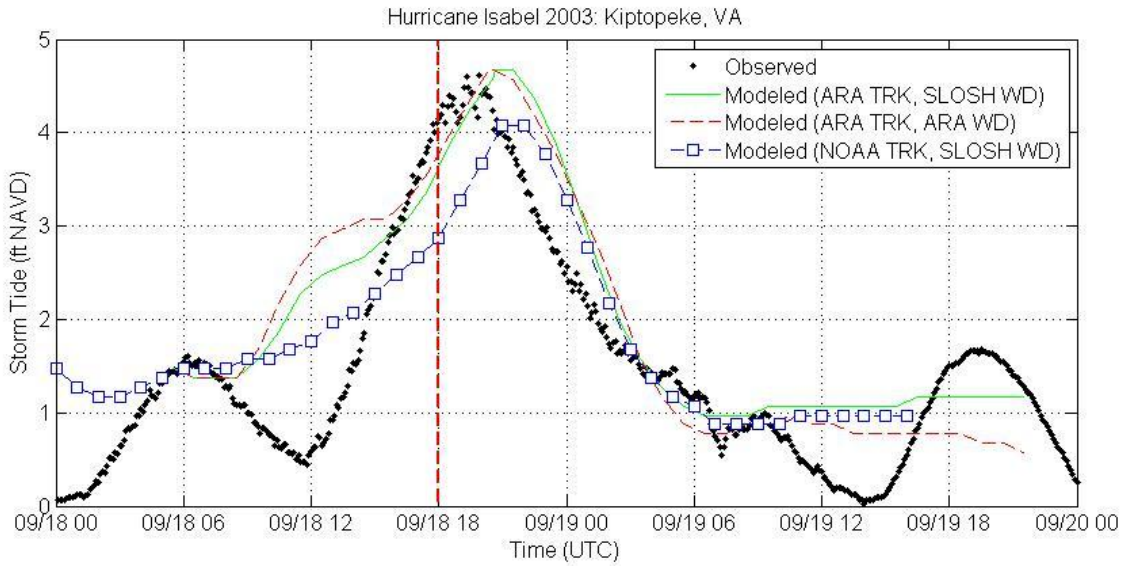

Figure U-6h. Tide gauge record at Kiptopeke, VA compared to the simulated time histories of storm tide in the SLOSH Grid cell containing the gauge location

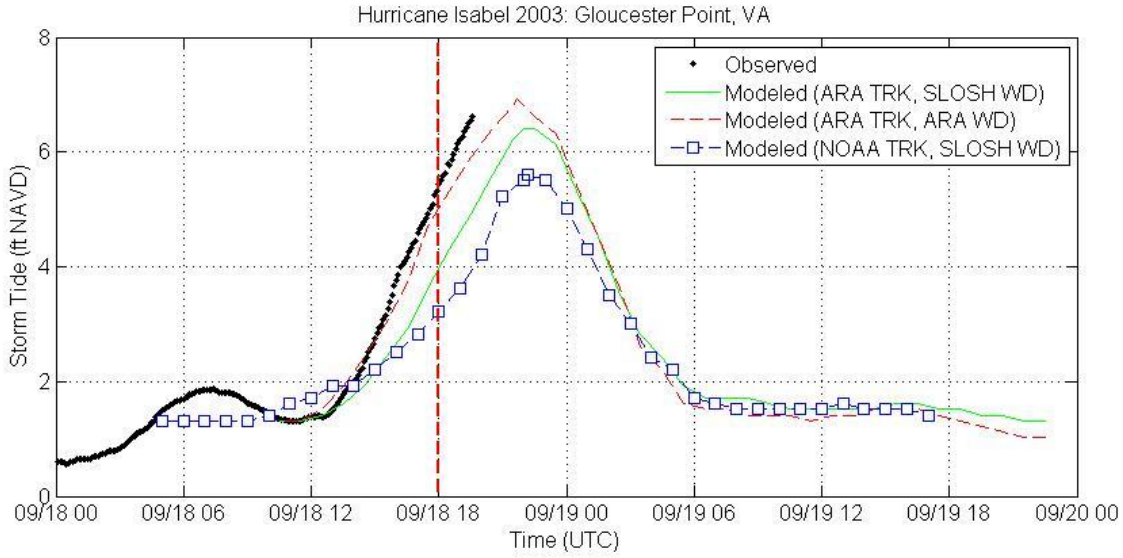

Figure U-6i. Tide gauge record at Gloucester Point, VA compared to the simulated time histories of storm tide in the SLOSH Grid cell containing the gauge location

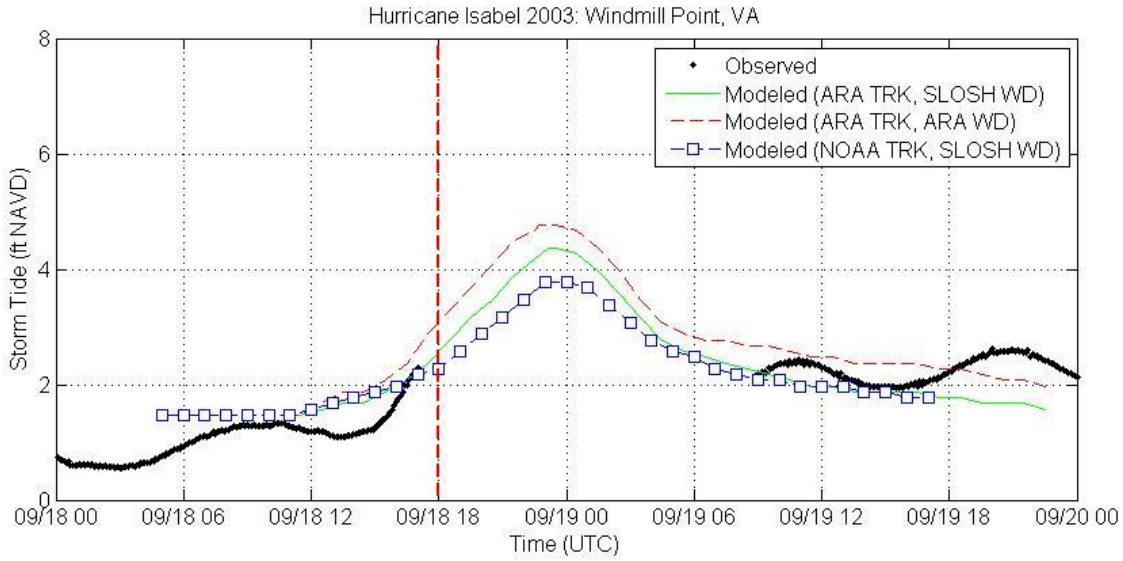

Figure U-6j. Tide gauge record at Windmill Point, VA compared to the simulated time histories of storm tide in the SLOSH Grid cell containing the gauge location

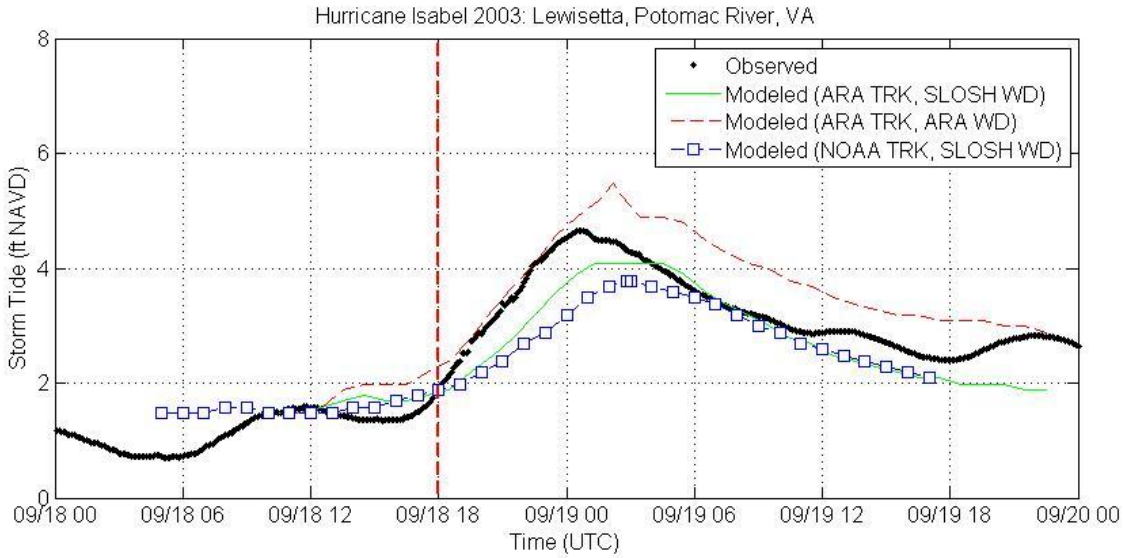

Figure U-6k. Tide gauge record at Lewisetta, Potomac River, VA compared to the simulated time histories of storm tide in the SLOSH Grid cell containing the gauge location

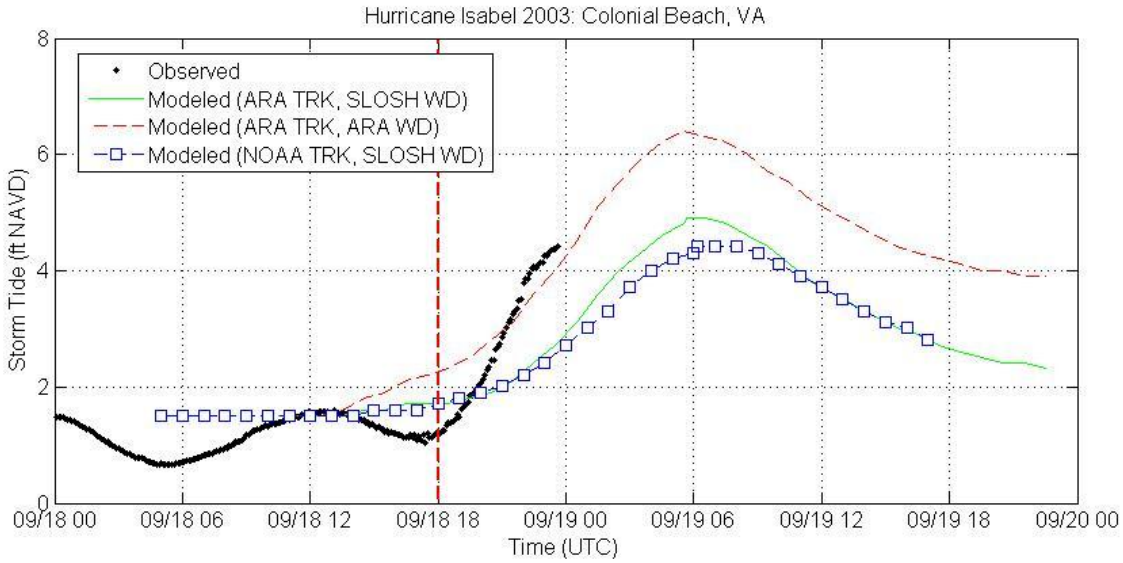

Figure U-6l. Tide gauge record at Colonial Beach, VA compared to the simulated time histories of storm tide in the SLOSH Grid cell containing the gauge location

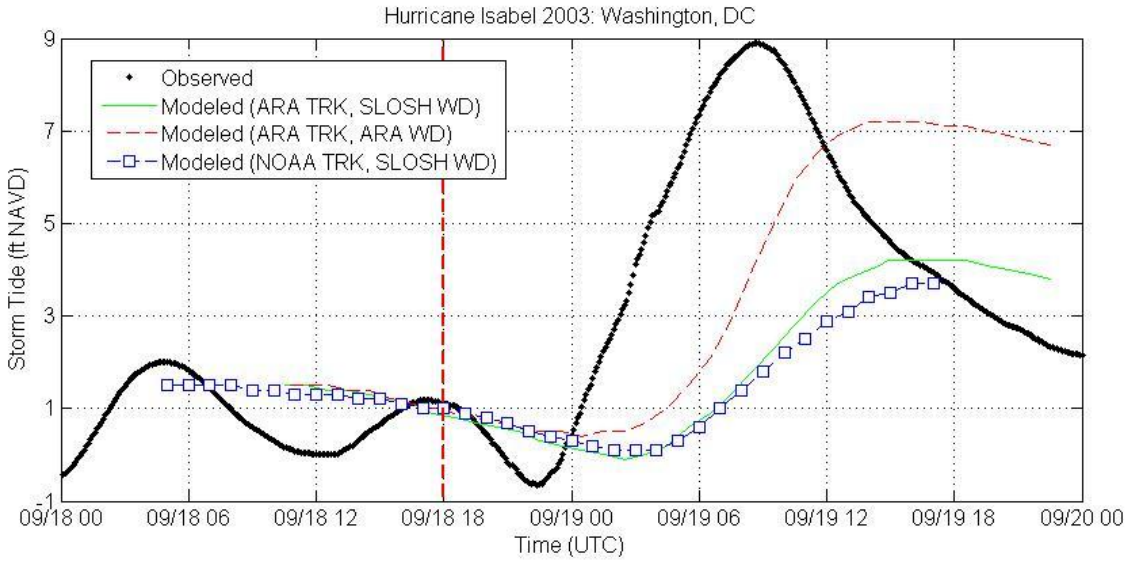

Figure U-6m. Tide gauge record at Washington, DC compared to the simulated time histories of storm tide in the SLOSH Grid cell containing the gauge location

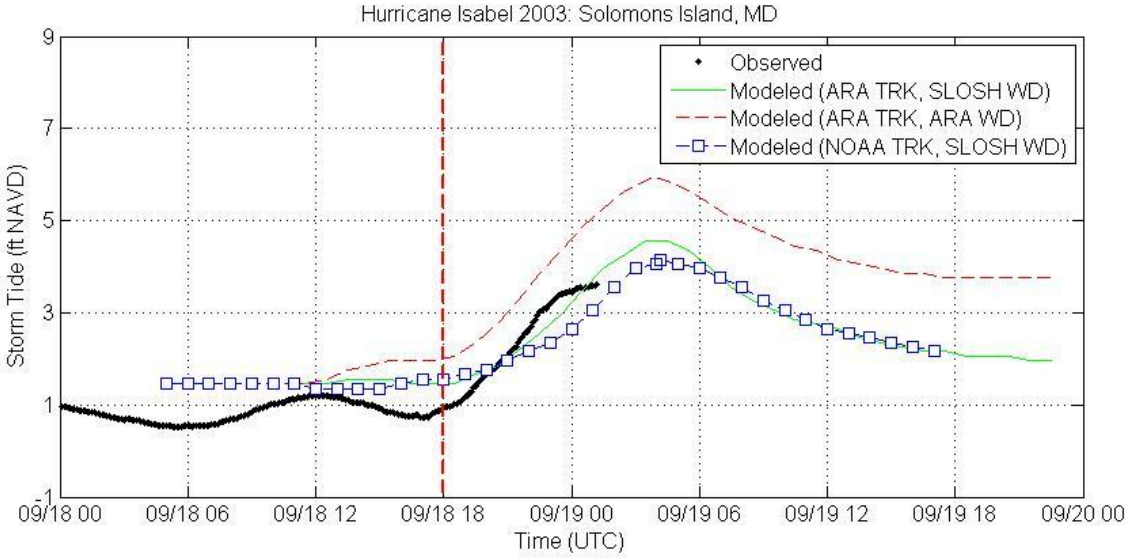

Figure U-6n. Tide gauge record at Solomons Island, MD compared to the simulated time histories of storm tide in the SLOSH Grid cell containing the gauge location

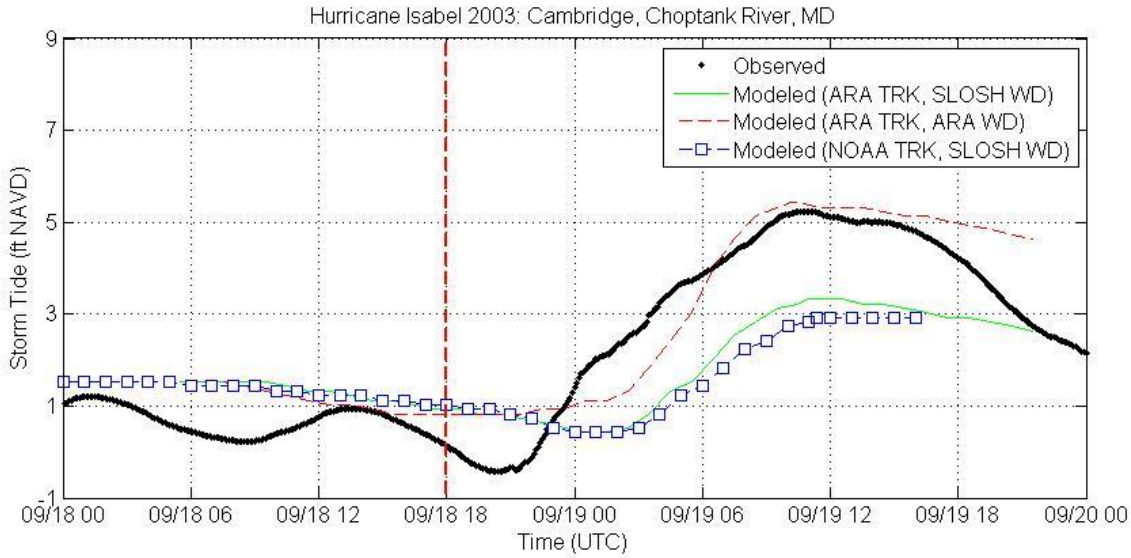

Figure U-6o. Tide gauge record at Cambridge, Choptank River, MD compared to the simulated time histories of storm tide in the SLOSH Grid cell containing the gauge location

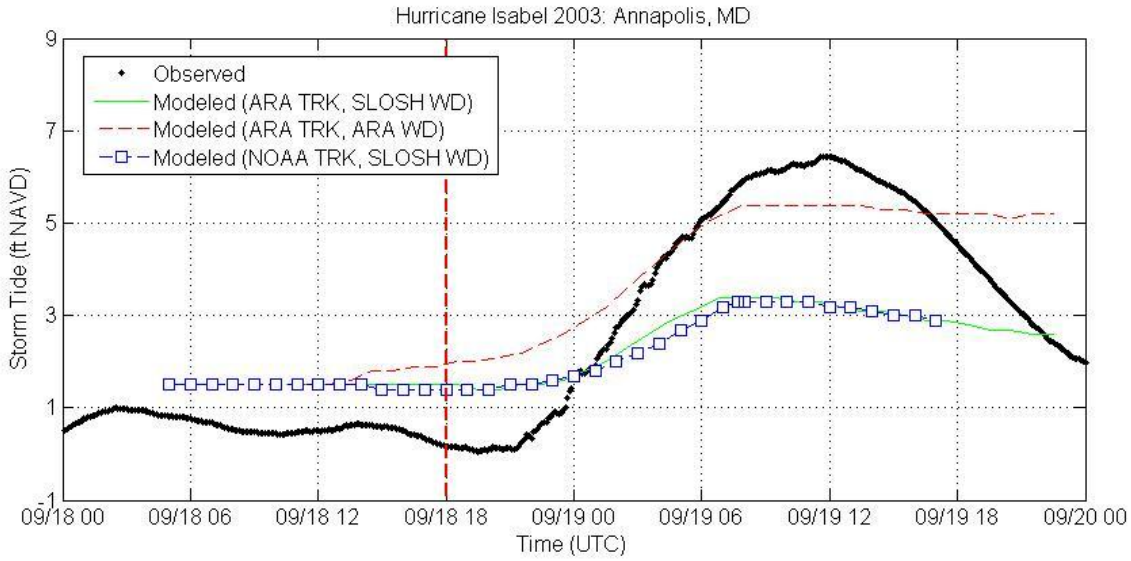

Figure U-6p. Tide gauge record at Annapolis, MD compared to the simulated time histories of storm tide in the SLOSH Grid cell containing the gauge location

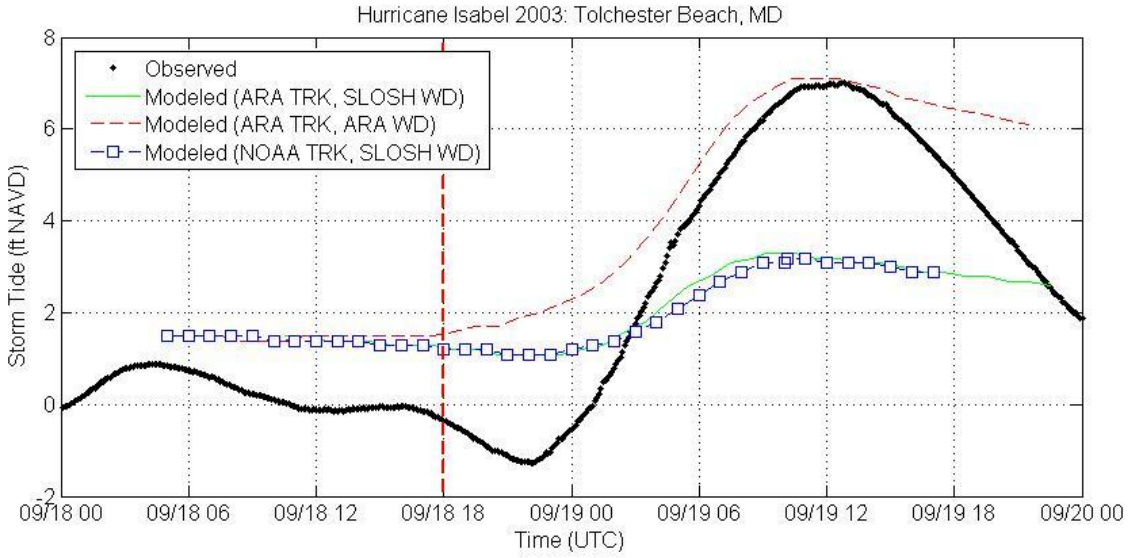

Figure U-6q. Tide gauge record at Tolchester Beach, MD compared to the simulated time histories of storm tide in the SLOSH Grid cell containing the gauge location

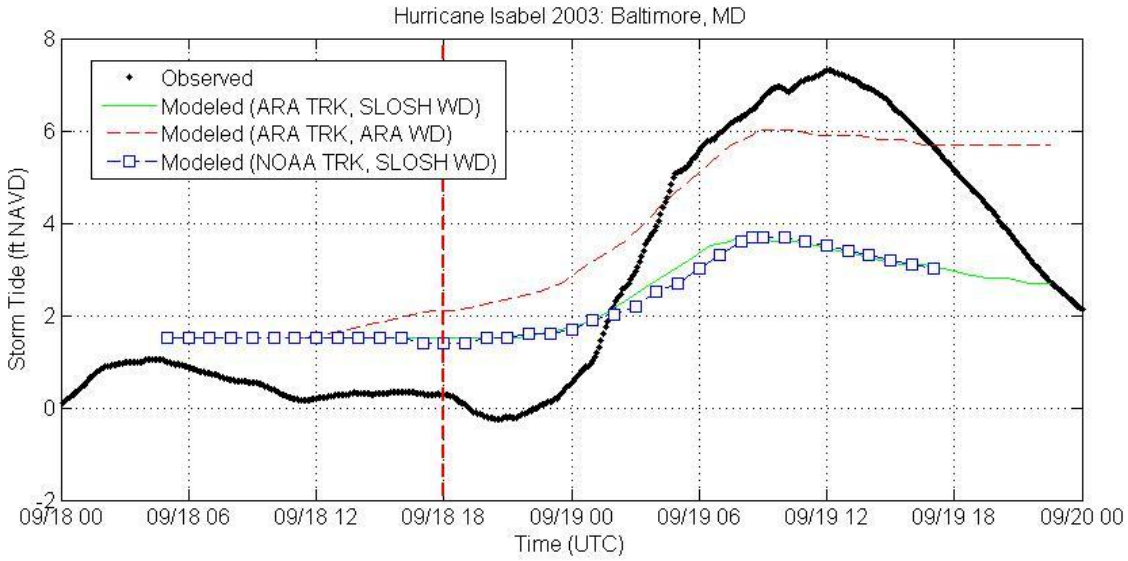

Figure U-6r. Tide gauge record at Baltimore, MD compared to the simulated time histories of storm tide in the SLOSH Grid cell containing the gauge location

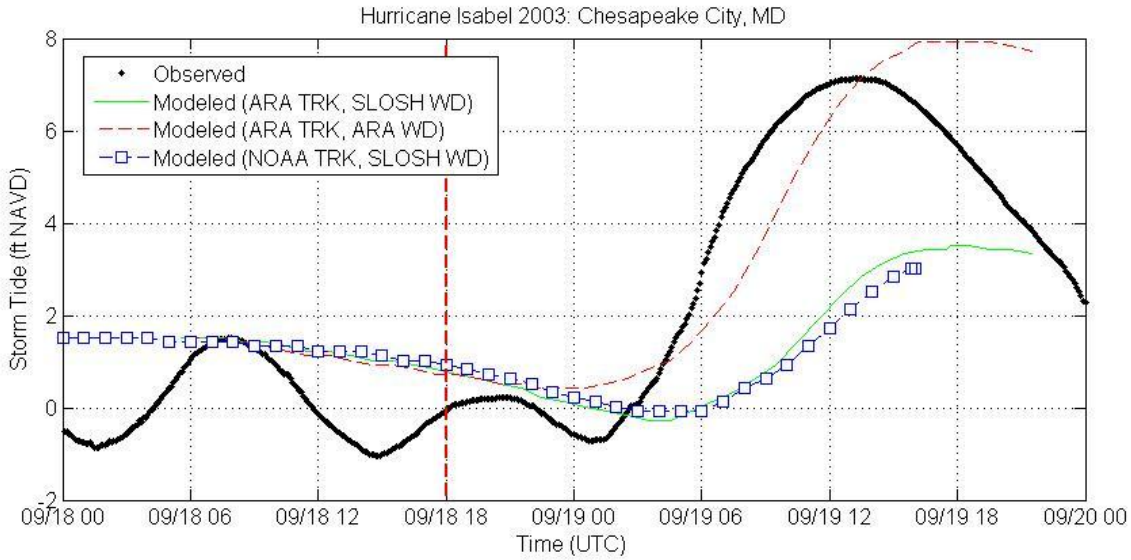

Figure U-6s. Tide gauge record at Chesapeake City, MD compared to the simulated time histories of storm tide in the SLOSH Grid cell containing the gauge location

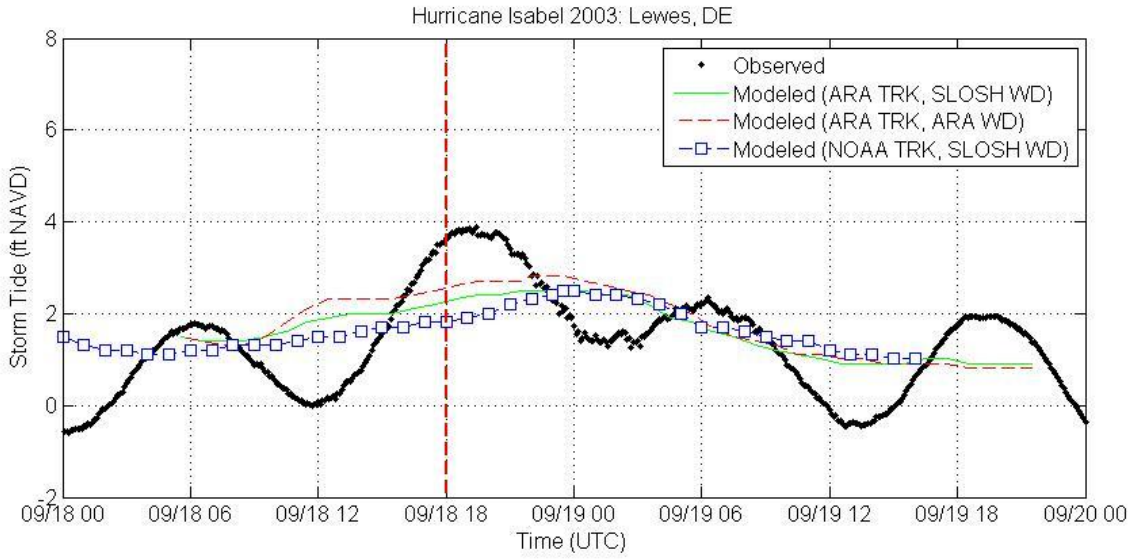

Figure U-6t. Tide gauge record at Lewes, DE compared to the simulated time histories of storm tide in the SLOSH Grid cell containing the gauge location

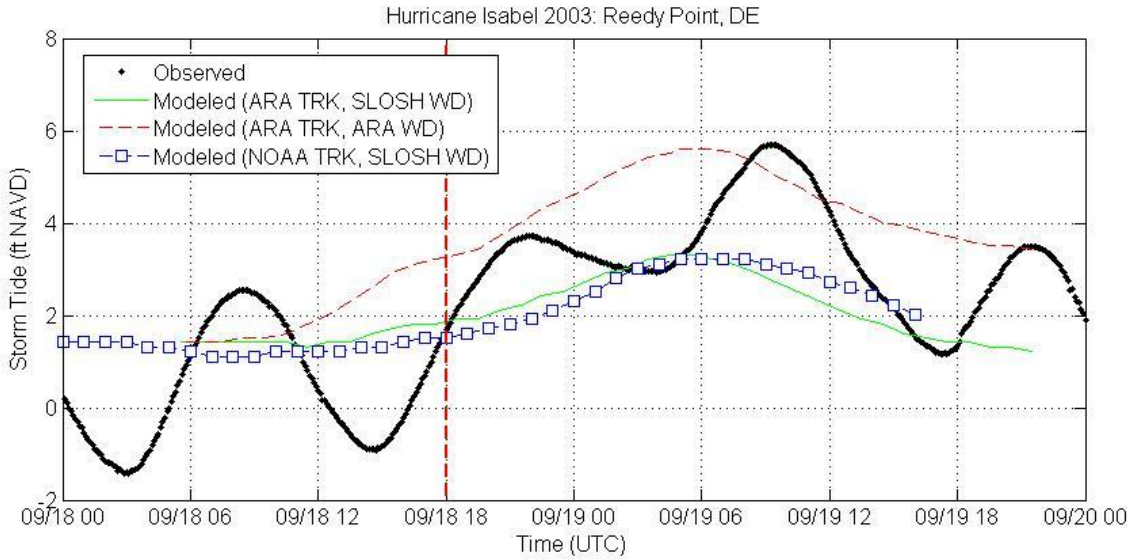

Figure U-6u. Tide gauge record at Reedy Point, DE compared to the simulated time histories of storm tide in the SLOSH Grid cell containing the gauge location

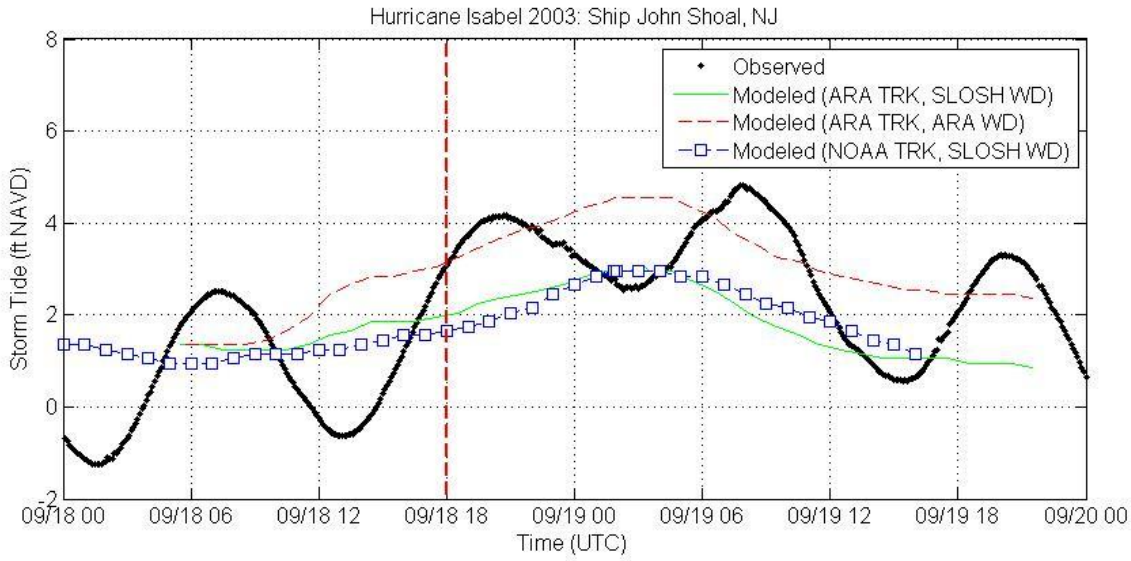

Figure U-6v. Tide gauge record at Ship John Shoal, NJ compared to the simulated time histories of storm tide in the SLOSH Grid cell containing the gauge location

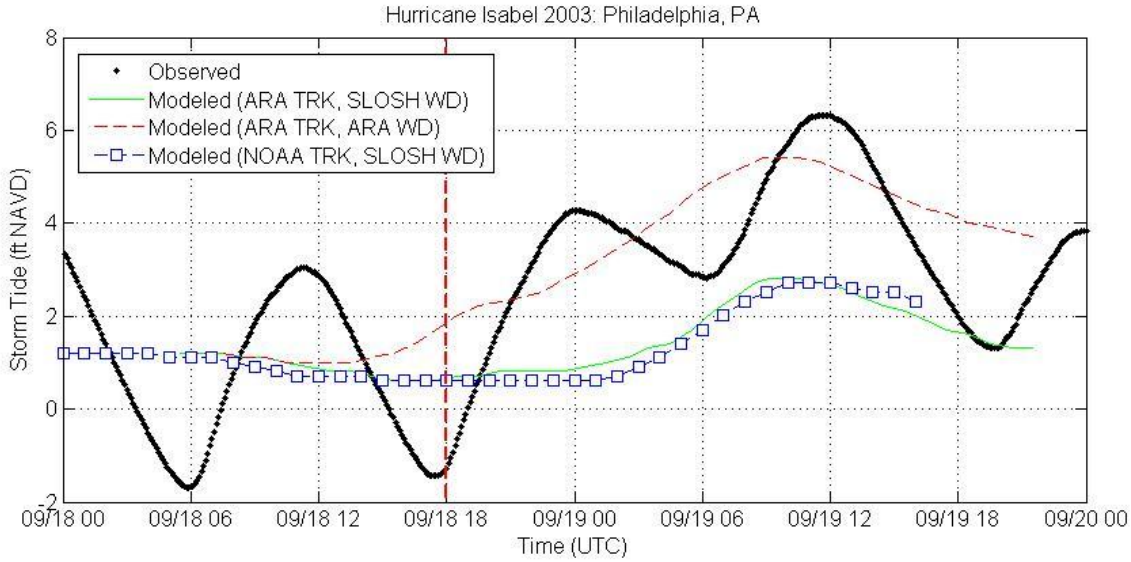

Figure U-6w. Tide gauge record at Philadelphia, PA compared to the simulated time histories of storm tide in the SLOSH Grid cell containing the gauge location

Table U-3. Error Analysis of Storm Tide for Hurricane Isabel

Station	Surge Range	Numer Data	Obs (ft NAVD)		SLOSH-Obs (ft NAVD)		ARA-Obs (ft NAVD)		NOAA-Obs (ft NAVD)	
			Mean	Std	mean	RMS	mean	RMS	mean	RMS
Beaufort, NC	0-3	225	1.1	0.6	0.1	1.0	0.4	1.1	0.0	0.9
	3-6	42	3.4	0.2	-1.4	1.4	-1.4	1.4	-2.1	2.1
	all	267	1.4	1.0	-0.2	1.0	0.1	1.1	-0.4	1.2
Cape Hatteras Fishing Pier, NC	0-3	125	1.8	0.6	0.7	0.8	0.8	0.9	0.2	0.6
	3-6	21	4.0	0.6	0.1	0.4	-0.1	0.4	-0.6	0.7
	all	146	2.1	1.0	0.6	0.8	0.7	0.9	0.1	0.6
Duck USACE FRF, NC	0-3	92	1.3	0.9	0.1	0.4	-0.3	0.7	0.0	0.4
	3-6	66	4.6	0.8	-0.1	0.4	-0.1	0.4	-1.0	1.0
	all	158	2.7	1.9	0.0	0.4	-0.2	0.6	-0.4	0.7
Money Point, Elizabeth River, VA	0-3	194	1.2	0.7	0.4	0.8	-0.4	0.7	0.2	0.5
	3-6	75	4.6	0.9	-0.4	1.3	-0.4	1.2	-0.8	1.2
	6-9	35	6.3	0.1	-1.0	1.1	-0.8	0.9	-1.6	1.7
	all	304	2.6	2.1	0.0	1.0	-0.5	0.9	-0.2	0.9
Sewells Point, VA	0-3	194	1.2	0.7	0.3	0.5	-0.3	0.4	0.3	0.4
	3-6	82	4.5	0.9	-0.1	0.7	0.1	0.3	-0.6	1.0
	6-9	28	6.1	0.1	-0.2	0.4	0.1	0.2	-1.2	1.3
	all	304	2.6	2.0	0.1	0.6	-0.1	0.4	-0.1	0.7
Chesapeake Bay Bridge Tunnel, VA	0-3	183	1.7	0.5	-0.7	0.8	-1.2	1.2	-0.6	0.7
	3-6	85	4.5	0.9	-0.7	0.9	-0.8	0.8	-1.1	1.3
	6-9	36	6.4	0.2	-1.2	1.2	-1.0	1.0	-2.2	2.2
	all	304	3.0	1.8	-0.7	0.9	-1.0	1.1	-0.9	1.2
Kiptopeke, Chesapea Bay, VA	0-3	278	1.2	0.8	0.6	0.8	0.6	0.9	0.4	0.6
	3-6	66	3.9	0.4	0.1	0.6	0.2	0.5	-0.5	0.8
	all	344	1.7	1.3	0.5	0.8	0.5	0.8	0.2	0.7
Gloucester Point, York Rive, VA	0-3	48	1.8	0.5	-0.2	0.3	0.1	0.1	0.1	0.4
	3-6	34	4.6	0.8	-1.3	1.3	-0.4	0.4	-1.7	1.8
	6-9	9	6.4	0.2	-1.6	1.6	-0.6	0.6	-2.6	2.6
	all	91	3.3	1.8	-0.7	0.9	-0.2	0.3	-0.8	1.4

Root Mean Square of Error: $$RMS = \sqrt{\frac{1}{N}\sum_{i=1}^{N}(Sim_i - Obs_i)^2}$$

Table U-3. Error Analysis of Storm Tide for Hurricane Isabel (*Continued*)

Station	Surge Range	Numer Data	Obs (ft NAVD)		SLOSH-Obs (ft NAVD)		ARA-Obs (ft NAVD)		NOAA-Obs (ft NAVD)	
			Mean	Std	mean	RMS	mean	RMS	mean	RMS
Windmill Point, VA	0-3	145	1.8	0.5	0.1	0.3	0.4	0.4	0.1	0.4
	all	145	1.8	0.5	0.1	0.3	0.4	0.4	0.1	0.4
Lewisetta, Potomac River, VA	0-3	165	2.1	0.6	-0.1	0.3	0.5	0.5	-0.1	0.3
	3-6	139	3.8	0.5	-0.3	0.5	0.6	0.7	-0.6	0.8
	all	304	2.9	1.0	-0.2	0.4	0.5	0.6	-0.4	0.6
Colonial Beach, Potomac River, VA	0-3	106	1.5	0.4	0.1	0.4	0.5	0.6	0.1	0.3
	3-6	25	3.9	0.5	-1.5	1.5	-0.3	0.4	-1.6	1.6
	all	131	2.0	1.0	-0.2	0.7	0.3	0.6	-0.2	0.8
Washington, DC	0-3	125	0.8	0.7	0.1	1.1	0.2	1.0	0.1	1.0
	3-6	69	4.7	0.7	-2.2	3.0	0.0	3.1	-2.5	3.1
	6-9	78	7.8	0.9	-5.8	6.0	-3.6	4.2	-6.1	6.2
	all	272	3.8	3.1	-2.2	3.6	-0.9	2.8	-2.3	3.7
Solomons Island, MD	0-3	119	1.3	0.5	0.3	0.5	0.8	0.9	0.3	0.5
	3-6	28	3.4	0.2	-0.2	0.3	1.1	1.1	-0.8	0.8
	all	147	1.7	1.0	0.2	0.4	0.9	0.9	0.1	0.5
Cambridge, Choptank River, MD	0-3	184	0.9	0.8	0.2	1.1	0.3	0.8	0.1	1.1
	3-6	123	4.6	0.6	-1.9	1.9	0.0	0.5	-2.3	2.3
	all	307	2.4	2.0	-0.7	1.5	0.2	0.7	-0.8	1.7
Annapolis, US Naval Academy, MD	0-3	159	0.7	0.7	0.8	1.0	1.4	1.5	0.8	1.0
	3-6	88	5.0	0.8	-2.0	2.1	-0.1	0.3	-2.2	2.2
	6-9	57	6.2	0.1	-3.0	3.0	-0.8	0.8	-3.0	3.0
	all	304	3.0	2.5	-0.7	1.8	0.5	1.1	-0.8	1.9
Tolchester Beach, MD	0-3	34	1.4	0.9	0.2	0.7	1.7	1.8	0.1	0.7
	3-6	52	4.9	0.9	-2.1	2.1	0.8	0.8	-2.3	2.3
	6-9	74	6.7	0.3	-3.5	3.5	0.3	0.3	-3.6	3.6
	all	160	5.0	2.1	-2.2	2.7	0.8	1.0	-2.4	2.8
Baltimore, MD	0-3	132	0.6	0.7	1.1	1.2	1.7	1.7	1.0	1.1
	3-6	48	5.0	0.9	-1.9	2.0	-0.1	0.4	-2.2	2.3
	6-9	91	6.8	0.4	-3.3	3.4	-0.9	1.0	-3.3	3.3
	all	271	3.4	2.9	-0.9	2.3	0.5	1.3	-1.0	2.3
Chesapeake City, MD	0-3	136	0.8	0.7	-0.1	0.9	0.3	0.5	0.0	0.9
	3-6	32	4.7	0.9	-4.3	4.4	-2.0	2.0	-4.4	4.5
	6-9	67	6.8	0.3	-4.5	4.6	-0.4	1.0	-4.9	4.9
	all	235	3.1	2.8	-1.9	3.0	-0.3	1.0	-2.0	3.2
Lewes, DE	0-3	260	1.4	0.8	0.4	0.8	0.6	0.9	0.3	0.7
	3-6	51	3.6	0.3	-1.2	1.2	-0.9	0.9	-1.6	1.6
	all	311	1.7	1.1	0.1	0.9	0.3	0.9	0.0	0.9
Reedy Point, DE	0-3	143	1.9	0.8	-0.1	0.8	0.9	1.5	-0.3	0.8
	3-6	164	4.0	0.9	-1.3	1.6	0.8	1.2	-1.3	1.5
	all	307	3.0	1.4	-0.8	1.3	0.8	1.4	-0.8	1.2
Ship John Shoal, NJ	0-3	174	1.8	0.9	-0.1	0.7	0.9	1.4	-0.1	0.8
	3-6	139	3.9	0.5	-1.5	1.7	-0.1	0.7	-1.5	1.7
	all	313	2.7	1.3	-0.7	1.3	0.5	1.2	-0.7	1.3
Philadelphia, PA	0-3	117	1.9	0.9	-0.8	1.2	0.0	1.3	-1.0	1.3
	3-6	146	4.1	0.8	-2.4	2.5	-0.1	1.0	-2.6	2.7
	6-9	25	6.2	0.1	-3.5	3.5	-1.0	1.0	-3.5	3.5
	all	288	3.4	1.6	-1.9	2.2	-0.1	1.1	-2.0	2.3
All Stations	0-3	3338	1.3	0.8	0.2	0.8	0.4	1.0	0.1	0.8
	3-6	1575	4.3	0.9	-1.3	1.8	0.0	1.1	-1.6	1.9
	6-9	500	6.7	0.7	-3.3	3.8	-1.0	1.8	-3.6	4.0
	all	5413	2.7	2.0	-0.6	1.6	0.1	1.1	-0.7	1.7

Appendix V. Comparison of Observed and SLOSH Model Computed Storm Tides for Hurricane Ivan (2004)

This appendix compares storm tide estimates from SLOSH to high water marks (HWMs) and tide gauge data from Hurricane Ivan. Ivan made landfall as Category 3 hurricane near Gulf Shores, Alabama at about 0650 UTC September 16, 2004, with the strongest winds occurring over a narrow area near the southern Alabama-western Florida panhandle border (Stewart, 2005). The strong hurricane winds combined with astronomical tide caused flooding along the coasts from Destin in the Florida panhandle westward to Mobile Bay/Baldwin County, Alabama.

Observation Data

The U.S. Army Corps of Engineers (USACE) Mobile District collected tide gauge data associated with the passage of Hurricane Ivan at 23 locations (USACE, 2004). HWMs are included at 8 additional sites, with 6 sites labeled as inside and 2 sites labeled as outside HWMs. Time histories of the storm tide along the Gulf Coast for the time period during the storm are available at 7 gauges from the NOAA website (NOAA 2010). Five of these are also locations in the USACE data set. The reference datum for the HWMs and tide gages is NGVD 1929. A total of 33 values of peak water elevation (HWMs and tide gauge data) are shown in Table V-1.

SLOSH Basins and Initial Water Level

The Mississippi Gulf Coast, Mobile Bay, Pensacola Bay, Panama City and Apalachicola Bay SLOSH basins are used in this study. The SLOSH model runs use a reference datum of NGVD 1929 for the MS-Gulf Coast, Panama City, and Apalachicola Bay basins and a reference datum of NAVD 1988 for the Mobile Bay and Pensacola Bay basins.

Since 1929, the tide gages data showed a rise in sea level of about 0.73 feet above NGVD 1929 at Grand Isle, LA. The elevation of the astronomical tide above estimated local mean sea level of 2004 in the area of MS-Gulf Coast at the time the storm hit the coast was 0.38 feet. In addition, before the arrival of Hurricane Ivan, the tide gages showed a rise of water above the predicted tide level (pre-storm tide anomaly) of approximately 0.6 feet. Therefore, the final initial water height for the SLOSH model runs in basin of MS-Gulf Coast will be 1.7 feet above NGVD 1929.

For the Mobile Bay basin, the sea level rise was 0.67 feet. The astronomical tide level was 0.38 feet at the time of hurricane landfall. The pre-storm tide anomaly of 0.6 feet was added to give the final initial water height of 1.7 feet above NAVD 1988. For the Pensacola Bay basin, the sea level rise was 0.41 feet. The astronomical tide level was 0.38 feet at the time of hurricane landfall and the pre-storm tide anomaly of was 0.6 feet. Therefore, the initial water height for SLOSH model runs in Pensacola Bay is 1.4 feet above NAVD 1988.

For the Panama City basin, the sea level rise was 0.18 feet. The elevation of the astronomical tide above estimated local mean sea level at the time the hurricane landfall was 0.19 feet. To take the pre-storm tide anomaly of 0.6 feet into account for the storm tide the SLOSH model simulation is 1.0 feet above NGVD 1929 in the Panama City basin.

For the Apalachicola Bay basin, the sea level was 0.34 feet. The elevation of the astronomical tide above local mean sea level at the time the storm hit the coast was 0.53 feet, and the pre-storm tide anomaly was 0.6 feet. Thus the initial water height is 1.5 feet above NGVD 1929 for SLOSH model run in Apalachicola Bay.

Methodology

SLOSH is a grid based numerical storm surge model that computes water elevations generated by the wind and pressure forces in tropical cyclones. The time history of the water elevation is saved in individual elements of the basin grid and the maximum value for each grid cell is termed as the Envelope of High Water (EOHW). The EOHW is compared against observed storm surge data. The observed hydrographic records associated with the passage of Hurricane Ivan (2004) at tide gauges are compared to the SLOSH model-generated storm surge hydrographs in the nearest grid cells.

Model runs using SLOSH wind model and ARA wind model are compared to the observed data. Where multiple basins contain the same observation site, the basin with minimum distance from the basin center to observation site, usually the basin with smaller grid cells (i.e. finer resolution) at the observation site, is used to compare against observed data.

Results

Figure V-1 shows the HWMs, tide gauge locations and hurricane track. The observed storm tide values in Figure V-1 are compared to the simulated storm tide values based on SLOSH wind model and ARA wind model. The results are provided in Table V-1 and further discussed below.

The maximum storm tide value of 12.9 feet was obtained on the West Bank of Escambia Bay at Highway 90 (Location 20). The SLOSH model produces maximum values of 12.7 and 12.4 feet at this site for the model runs using SLOSH wind model and ARA wind model, respectively.

Figure V-2 presents comparisons of observed and simulated storm tide values with SLOSH wind model and ARA wind model. All simulated values are from model runs using the ARA storm track. The comparisons indicate that both the ARA wind model results and the SLOSH wind model results slightly underestimate the storm surge for Hurricane Ivan.

Histograms of the differences (simulated minus observed) are shown in Figure V-3. The error characteristics are indicated in the legend. The mean errors are -0.35 and -0.25 feet for model

runs with SLOSH wind model and ARA wind model, respectively. The negative values of the mean error are consistent with the results shown in Figure V-2.

Observed storm surge hydrographs from 7 gauge stations are compared to the SLOSH model simulated storm surge hydrographs for same locations, as shown in Figure V-4a through V-4g. Tide gauge record at Pensacola Bay at Pensacola, FL is incomplete because of a malfunction or loss of the gauge.

As an example, Figure V-4c shows the comparison of observed and simulated storm tide at Waveland, MS. The observed maximum storm tide is 4.4 feet, comparable to the simulated value of 4.6 feet with the SLOSH model run using the ARA wind model, and 68% higher than the simulated value of 2.8 feet from the SLOSH model run using the SLOSH wind model. The observed and simulated storm tide values are comparable for tide gauge of Mobile Bay at Dauphin Island, AL, as shown in Figure V-4a. In general, the timing of the simulated peak storm tide is consistent with the timing of the maximum observed storm tides, as shown in Figure V-4a to V-4g.

Comparisons of observed and simulated storm surge hydrographs indicate that the SLOSH model calculated the reasonable results, except for underestimations of about 30% lower values at Panama City Beach, FL for Hurricane Ivan, as shown in Figure V-4f.

Table V-2 summarizes the RMS error of storm tide for Hurricane Ivan. Results show that the model runs with the ARA wind field model generally produce lower mean and RMS errors than the model runs with the SLOSH wind field model.

Conclusions

Comparisons of observed and simulated model storm tide data along the north central Gulf of Mexico coast showed that the SLOSH model calculated the reasonable results. The SLOSH model does a good job in capturing the timing of the peak storm tide. The simulated values of storm tide with model runs using SLOSH wind model and using ARA wind model are comparable for Hurricane Ivan (2004).

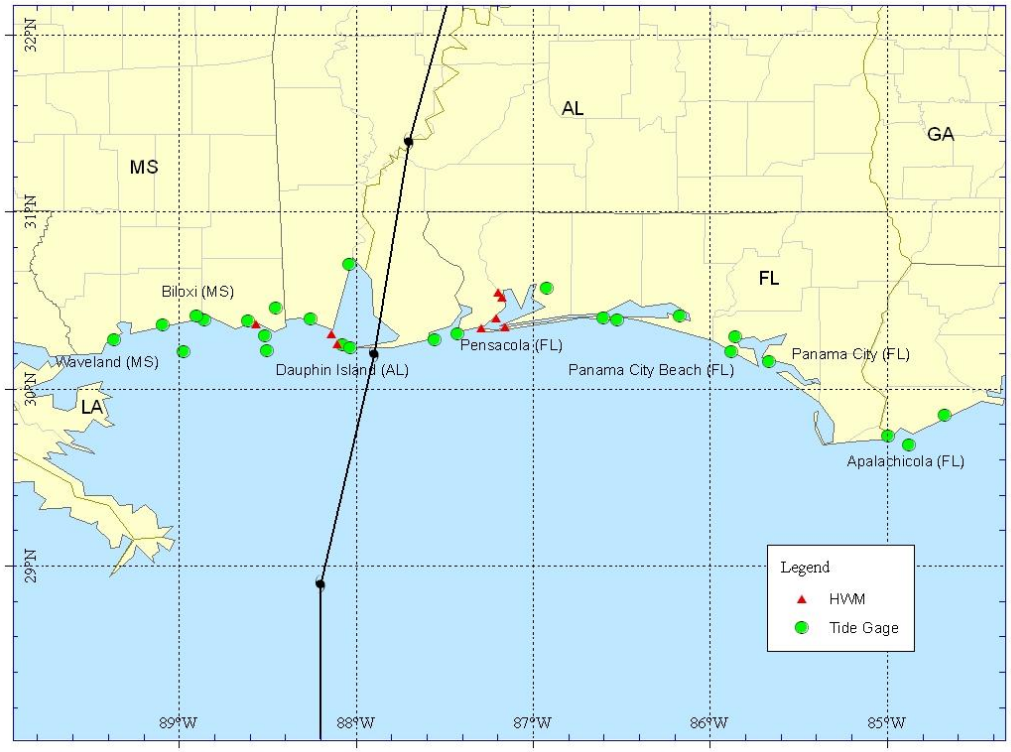

Figure V-1. Tide Gauge Locations during Hurricane Ivan (2004)

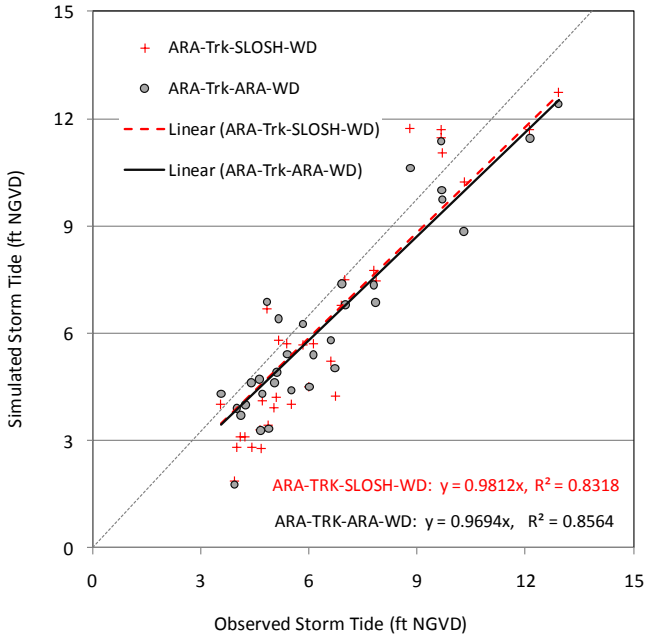

Figure V-2. Comparison of Simulated and Observed Storm Tide for Hurricane Ivan

Table V-1. Summary of modeled and observed storm tide during Hurricane Ivan (2004): ft NGVD

No	Station	Station ID	Lat	Lon	Obs.	Sim. SLOSH wind	Sim. ARA wind
1 [1]	Mississippi Sound at Waveland, MS (USGS)	8747766	30.2806	89.3647	4.4	2.8	4.6
2	Gulfport Harbor at Gulfport, MS (540)		30.3603	89.0908	4.6	3.3	4.7
3	Mississippi Sound at Ship Island		30.2119	88.9719	5.2	5.8	6.4
4	Biloxi Bay at Point Cadet		30.3897	88.8572	4.2	3.1	4.0
5	West Pascagoula River at Hwy 90 at Gautier, MS		30.3828	88.6089	4.1	3.1	3.7
6 [2]	Pascagoula River (NOAA) at Pascagoula, MS		30.3669	88.5633	6.7	4.2	5.0
7	Mississippi Sound at Pascagoula PI- Rear Range		30.2989	88.5144	5.8	5.7	6.3
8	Mississippi Sound at Petit Bois Island		30.2144	88.5056	4.8	6.7	6.9
9	Escatawpa River at I-10 nr Orange Grove, MS		30.4586	88.4514	3.9	1.9	1.8
10	Middle Gage at Bayou LaBatre		30.3986	88.2569	4.7	2.8	3.3
11 [2]	Mobile Bay at Cedar Point, AL		30.3106	88.1383	6.9	6.8	7.4
12 [3]	Dauphin Island Bay at Dauphin Island		30.2583	88.1078	7.8	7.8	7.4
13 [1]	Mobile Bay at Dauphin Island (USCG)	8735180	30.2511	88.0794	7.0	7.5	6.8
14	Mobile River at Mobile, AL		30.7044	88.0394	4.9	3.4	3.3
15	Mobile Bay at Ft Morgan Front Range		30.2333	88.0333	7.9	7.5	6.9
16	Perdido Pass Orange Beach, AL		30.2786	87.5550	8.8	11.7	10.6
17	GIWW at Pensacola Gulf Beach, FL		30.3139	87.4278	9.7	11.7	10.0
18 [3]	Pensacola Bay at Ft. McRee, FL (USCG)		30.3450	87.2897	9.7	11.0	9.7
19 [1]	Pensacola Bay at Pensacola, FL (NOAA)	8729840	30.4033	87.2100	N/A	10.4	9.1
20 [3]	Escambia Bay West Bank at HWY 90		30.5469	87.1942	12.9	12.7	12.4
21 [3]	Escambia Bay West Bank 1.5 miles N of I-10		30.5206	87.1753	12.1	11.7	11.5
22 [3]	GIWW at Gulf Breeze, FL		30.3522	87.1564	10.3	10.2	8.9
23	Yellow River near Milton, FL		30.5711	86.9244	9.7	11.5	11.4
24	Fort Walton Brooks Bridge		30.4000	86.6000	6.1	5.7	5.4
25	DESTIN AT CHOCTAWHACHEE BAY (USCG)		30.3919	86.5258	5.4	5.7	5.4
26	GIWW at Choctawhachee Bay (HWY 331)		30.4119	86.1689	5.5	4.0	4.4
27	GIWW at West Bay, FL (HWY 79)		30.2939	85.8586	6.6	5.2	5.8
28 [1]	St Andrew Bay at Panama City, FL	8729108	30.1528	85.6667	4.7	4.1	4.3
29 [1]	Apalachicola River at Apalachicola, FL	8728690	29.7331	84.9953	5.1	4.2	4.9
30	GIWW at St. George Island, FL		29.6872	84.8769	3.6	4.0	4.3
31	Carrabelle River at Carrabelle, FL		29.8517	84.6758	5.0	3.9	4.6
32 [1]	Biloxi, MS	8744117	30.4117	88.9033	4.0	2.8	3.9
33 [1]	Panama City Beach, FL	8729210	30.2133	85.8783	6.0	4.5	4.5

[1] Tide gauge data from NOAA Tide and Current website, Others from USACE Report;
[2] outside HWM
[3] inside HWM

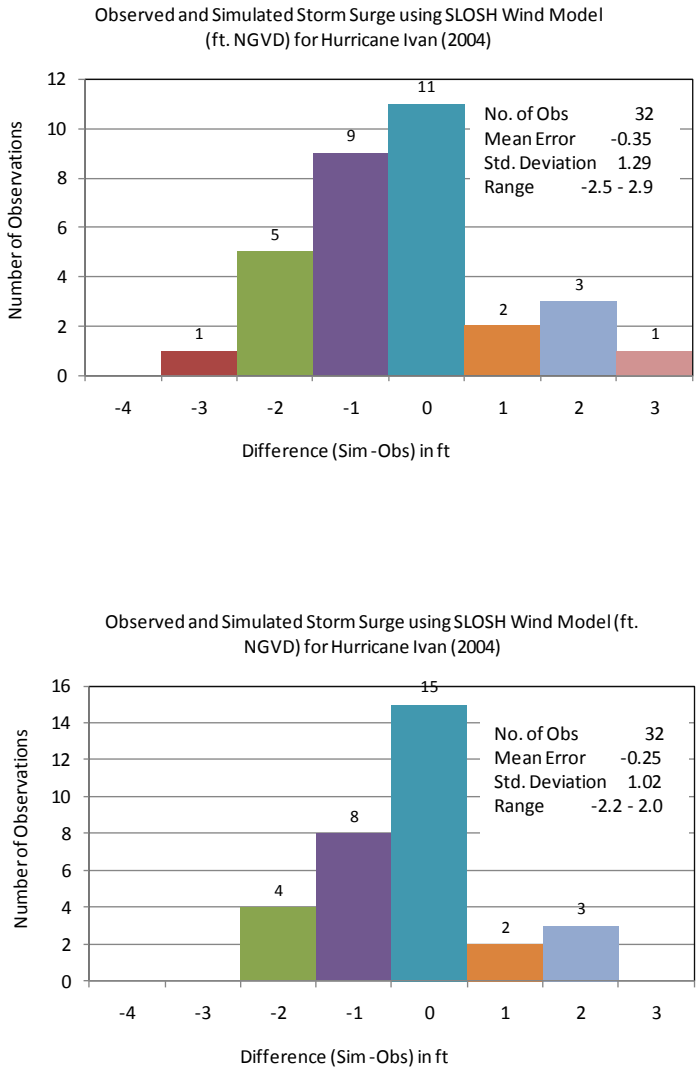

Figure V-3. Simulated Storm Tide Values minus Observed HWMs for Hurricane Ivan

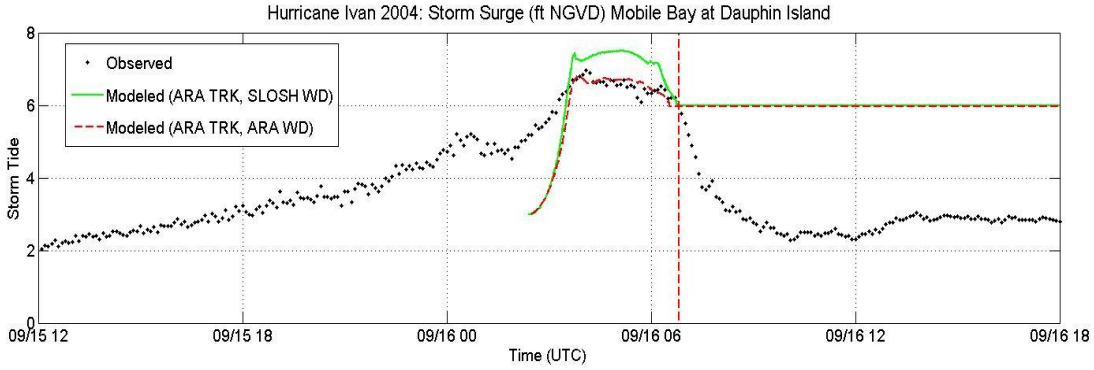

Figure V-4a. Tide gauge record at Dauphin Island, AL compared to the simulated time history of Storm Tide in the SLOSH Grid cell containing the gauge location

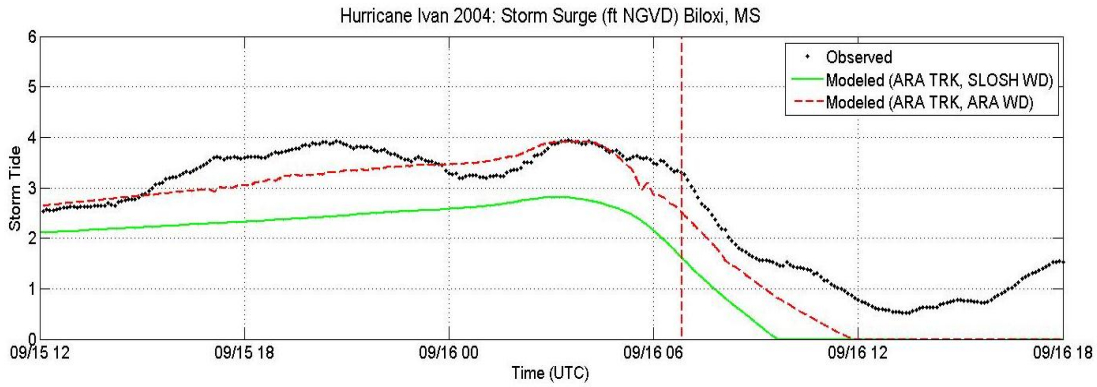

Figure V-4b. Tide gauge record at Biloxi, MS compared to the simulated time history of Storm Tide in the SLOSH Grid cell containing the gauge location

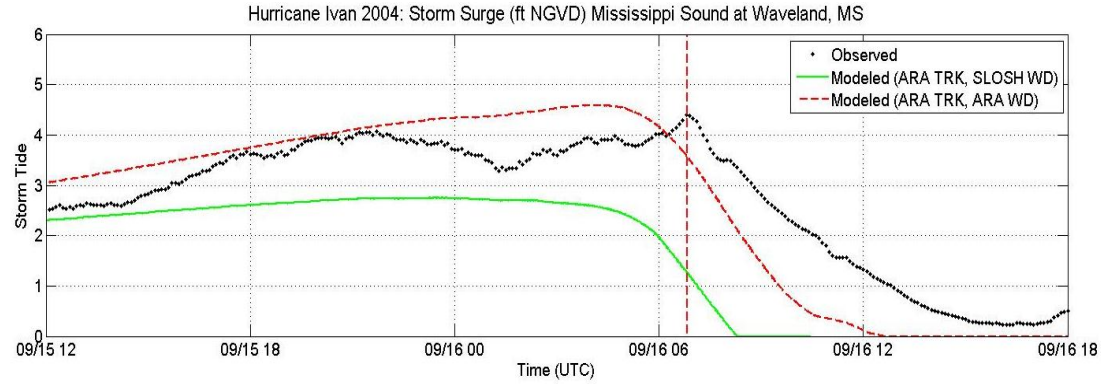

Figure V-4c. Tide gauge record at Waveland, MS compared to the simulated time history of Storm Tide in the SLOSH Grid cell containing the gauge location

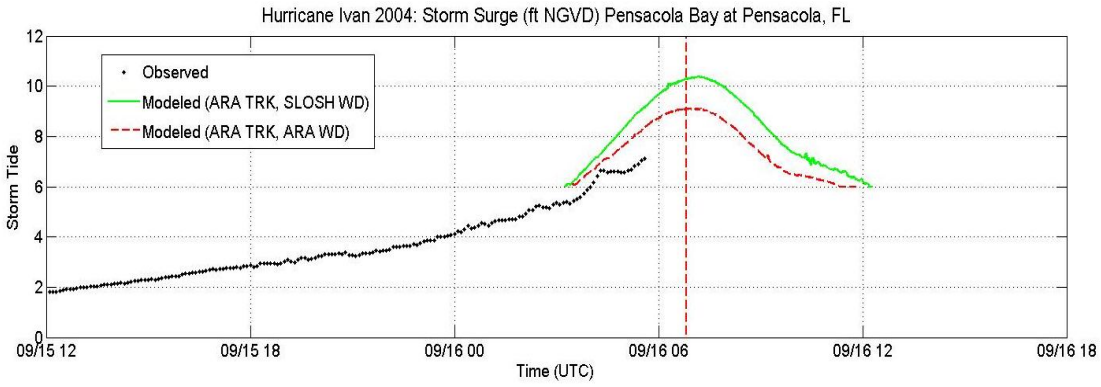

Figure V-4d. Tide gauge record at Pensacola, FL compared to the simulated time history of Storm Tide in the SLOSH Grid cell containing the gauge location

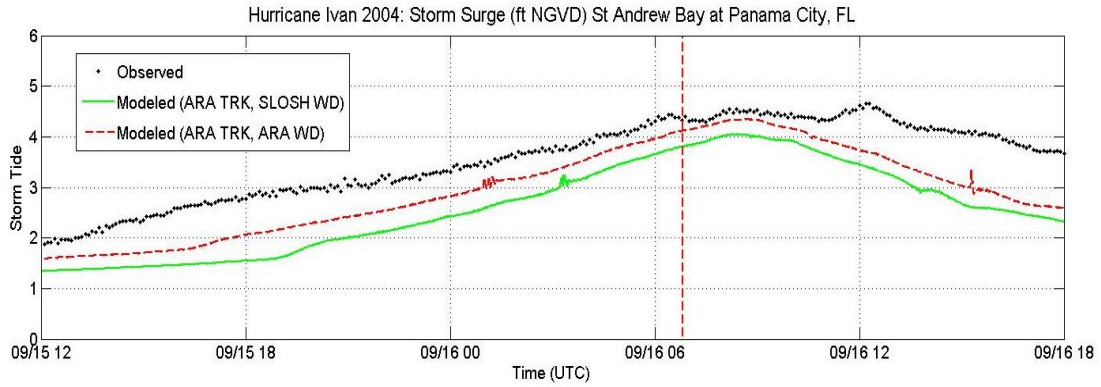

Figure V-4e. Tide gauge record at Panama City, FL compared to the simulated time history of Storm Tide in the SLOSH Grid cell containing the gauge location

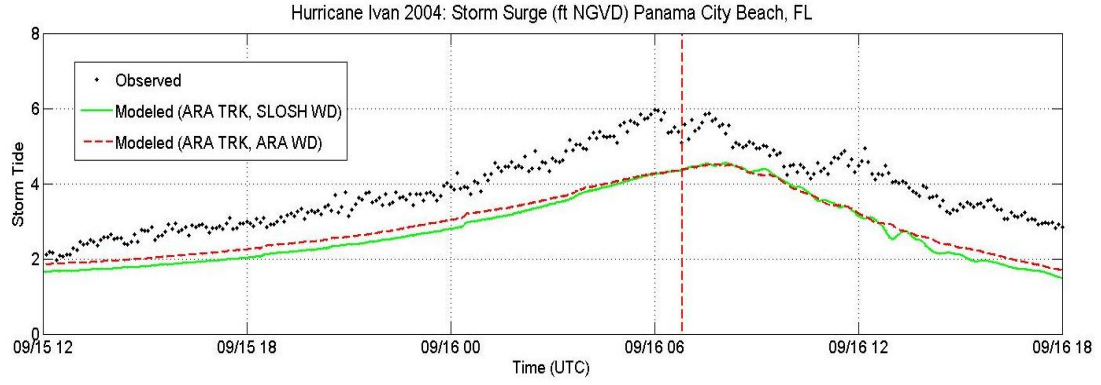

Figure V-4f. Tide gauge record at Panama City Beach, FL compared to the simulated time history of Storm Tide in the SLOSH Grid cell containing the gauge location

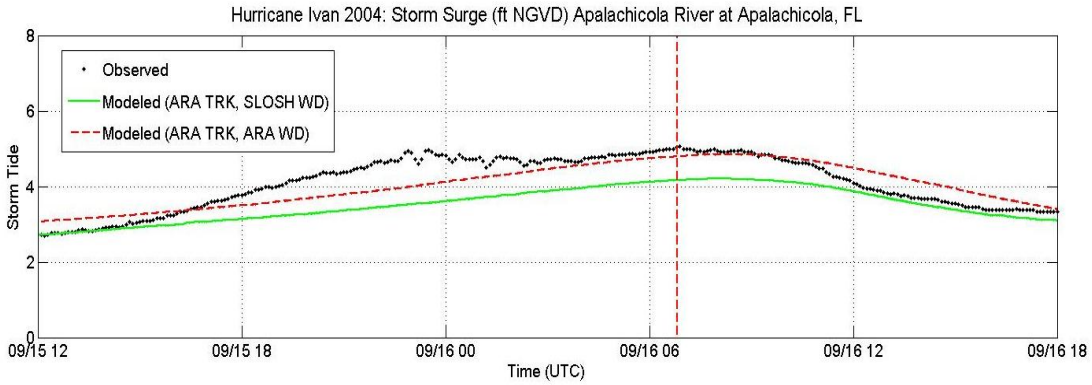

Figure V-4g. Tide gauge record at Apalachicola, FL compared to the simulated time history of Storm Tide in the SLOSH Grid cell containing the gauge location

Table V-2. Error Analysis of Storm Tide for Hurricane Ivan

Station	Surge Range (ft NGVD)	Numer Data	Obs		SLOSH		ARA	
			Mean	Std	mean Err	RMSErr	mean Err	RMSErr
Mississippi Sound at Waveland, MS	0-3	129	1.5	1.0	-1.7	2.0	-0.4	0.9
	3-6	171	3.7	0.3	-1.4	1.6	0.3	0.6
	all	300	2.8	1.3	-1.5	1.8	0.0	0.7
Mobile Bay at Dauphin Island	0-3	92	2.7	0.2	3.3	3.3	3.3	3.3
	3-6	28	4.4	1.1	0.8	2.2	0.7	2.2
	6-9	36	6.5	0.2	0.5	0.7	-0.1	0.4
	all	156	3.9	1.6	2.2	2.7	2.0	2.7
Pensacola Bay at Pensacola	3-6	7	5.6	0.2	0.9	0.9	0.6	0.6
	6-9	16	6.7	0.2	1.5	1.6	0.9	0.9
	all	23	6.3	0.5	1.3	1.4	0.8	0.9
St Andrew Bay at Panama City, FL	0-3	83	2.5	0.3	-1.0	1.0	-0.6	0.7
	3-6	217	3.9	0.5	-0.9	1.0	-0.6	0.7
	all	300	3.5	0.8	-0.9	1.0	-0.6	0.7
Apalachicola River at Apalachicola, FL	0-3	26	2.8	0.1	0.0	0.0	0.3	0.3
	3-6	274	4.2	0.6	-0.6	0.7	-0.1	0.4
	all	300	4.1	0.7	-0.6	0.7	-0.1	0.4
Biloxi, MS	0-3	141	1.5	0.8	-1.1	1.2	-0.6	0.7
	3-6	159	3.6	0.2	-1.1	1.2	-0.3	0.4
	all	300	2.6	1.2	-1.1	1.2	-0.4	0.6
Panama City Beach, FL	0-3	73	2.6	0.3	-0.8	0.9	-0.6	0.7
	3-6	227	4.3	0.8	-1.1	1.2	-1.0	1.1
	all	300	3.9	1.0	-1.1	1.1	-0.9	1.0
all stations	0-3	544	2.1	0.9	-0.4	1.9	0.1	1.5
	3-6	1083	4.0	0.7	-0.9	1.2	-0.3	0.8
	6-9	52	6.5	0.2	0.8	1.1	0.2	0.6
	all	1679	3.5	1.3	-0.7	1.4	-0.2	1.1

Appendix W. Comparison of Observed and SLOSH Model Computed Storm Tides for Hurricane Katrina (2005)

This appendix compares storm tide estimates from SLOSH to high water marks (HWMs) and tide gauge data from Hurricane Katrina. Katrina made landfall as a Category 3 hurricane with estimated maximum sustained winds of 110 knots (127 mph), near Buras, Louisiana at 1110 UTC 29 August, 2005. The strong hurricane winds combined with astronomical tide caused flooding along the Mississippi coast across a swath about 20 miles wide, centered roughly on Bay St. Louis (Knabb, et al. 2005).

Observation Data

The URS Group, Inc. (URS) collected 312 HWM associated with the passage of Hurricane Katrina in coastal and riverine areas of the three Mississippi counties that lie between the Mississippi/Alabama border and the Mississippi/Louisiana border: Hancock, Harrison, and Jackson (FEMA, 2006). Each HWM collected was classified as either a result of coastal flooding (caused by storm surge) or riverine flooding (caused by rainfall). The HWMs designated as coastal flooding were further assigned a category as surge-only, wave height and wave run-up. 242 HWMs assigned as surge-only are used for this study. In addition, the U.S. Geological Survey (USGS) flagged 90 HWMs in Mississippi, assisted by the USACE. All HWMs were surveyed in the North American Vertical Datum of 1988 (NAVD 88).

Time histories of the storm tide along the Mississippi Coast for the time period during the storm are available at 4 gauges from the NOAA website. 3 tide gauge records are incomplete due to a malfunction or loss of the gauge. The HWM-ID, tide gauge stations, and observed storm tide data are shown in Table W-1.

SLOSH Basins and Initial Water Levels

The Mississippi Gulf Coast SLOSH basin covers all of the HWMs observed between the Mississippi/Alabama border and the Mississippi/Louisiana border. The SLOSH model runs use a reference datum of NGVD 1929 for the MS-Gulf Coast basin. The simulated storm tide values are converted to NAVD 1988 for comparison with the observed data. This conversion was completed using the VERTCON software, developed by the National Geodetic Survey (NGS) office to convert data between different vertical data scales (http://www.ngs.noaa.gov/PC_PROD/VERTCON/)

The sea level rise along Mississippi coast from 1929 to 2005 was 0.74 feet, and the predicted elevation of the astronomical tide above local mean sea level at the time of hurricane landfall was 1.0 feet. Finally, a pre-storm tide anomaly (i.e., the difference between the actual and predicted tides) of 1.0 feet was added to give the final initial water height of 2.7 feet above NGVD 1929 for SLOSH runs in the MS-Gulf Coast basin.

Methodology

SLOSH is a grid based numerical storm surge model that computes water elevations generated by the wind and pressure forces in tropical cyclones. The time history of the water elevation is saved in individual elements of the basin grid and the maximum value for each grid cell is termed as the Envelope of High Water (EOHW). The observed storm surge elevation is compared to the EOHW in the nearest grid cells, and the observed hydrographic records associated with the passage of Hurricane Katrina (2005) at tide gauges are compared to the SLOSH model-generated storm surge hydrographs in the nearest grid cells.

Model runs using SLOSH wind model and ARA wind model are carried out, and the simulated storm surge elevations are compared to the observed HWMs and storm tide from tide gauges.

Results

Figure W-1 shows the HWMs, tide gauge locations and hurricane track. The observed storm tide values in Figure W-1 are compared to the simulated storm tide values from model runs using SLOSH wind model and ARA wind model. The results are provided in Table W-1.

The highest coastal HWM elevation of 34.9 feet was found in Pass Christian and represented flooding including wave height (HWM-ID KMSC-20-06), which is significantly higher than the simulated storm tide ranged between 23 and 25 feet along the shoreline in Pass Christian. The maximum observed surge only HWM of 27.2 feet was found in the western portion of the Harrison County (KMSC-04-22, Location 67), where the simulated values of storm tide are 24.4 feet and 23.3 feet for model runs with SLOSH wind model and ARA wind model, respectively.

Figures W-2a and W-2b presented the comparisons of observed and simulated storm tide values using SLOSH wind model and ARA wind model. The comparisons shown in the top left plots are for URS coastal surge only data. The comparisons shown in the top right plots are for the USGS HWMs. The comparisons shown in the bottom plots are for all data (URS surge only and USGS HWMs). All simulated values are from model runs using the ARA storm track.

The comparisons indicate that the model runs using SLOSH wind model tend to slightly overestimate the inside HWMs (surge-only elevations), as shown in Figure W-2a. For model runs using ARA wind field, slight underestimates are found for inside HWMs, as shown in Figure W-2b.

Histograms of the differences (simulated minus observed) were shown in Figures W-3a and W-3b. The error characteristics are indicated in the legend. For all data (URS surge only and USGS HWMs), the mean errors are +0.59 and -0.28 feet for model runs using SLOSH wind model and using ARA wind model, respectively.

Observed storm surge hydrographs from 4 gauge stations are compared to the SLOSH model simulated storm surge hydrographs in Figure W-4a through W-4d.

Figure W-4b shows the comparison of observed and simulated storm tide at Dauphin, AL. The observed maximum storm tide was 6.1 feet, comparable to the simulated value of 7.3 feet with model run using SLOSH wind model and 7.1 feet with model run using ARA wind model. The simulated values are about 16% higher than the observed HWM for this location. According to NOAA, the SLOSH model is generally accurate within plus or minus 20 percent. Comparisons of observed and simulated storm surge hydrographs indicated that the SLOSH model calculated the reasonable results for hurricane Katrina.

The timing of the simulated peak storm tide at Dauphin Island is one to two hours earlier than the observed peak. Tide gauge records at other three stations (Horn Island, Waveland and Biloxi) were incomplete because these gauges malfunctioned before the maximum was reached.

Table W-2 summarizes the RMS error of storm tide for Hurricane Katrina. For this relatively small data set (1 complete record and 3 incomplete records), the SLOSH wind field model tends to produce storm tide RMS errors that are similar to or lower than the storm tide errors produced by the ARA wind field model.

Conclusions

Comparisons of observed and simulated storm tide data along Mississippi coast showed that the model runs using SLOSH wind model slightly overestimated the storm tide, while ARA wind model slightly underestimated the storm tide. The comparisons indicate that the SLOSH model with either the SLOSH or ARA wind model produces reasonable storm tide estimates for Hurricane Katrina.

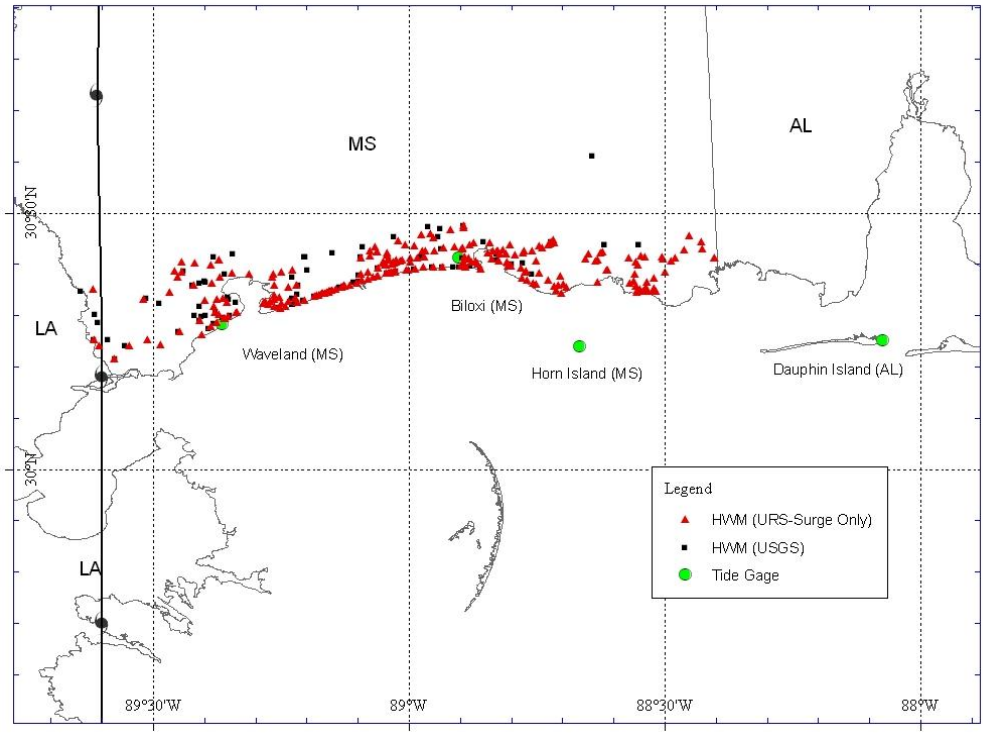

Figure W-1. Tide Gauge Locations and coastal HWMs obtained for Hurricane Katrina (2005)

Table W-1. Observed and Simulated Storm Tide during Hurricane Katrina (2005): ft NAVD

No.	HWM-ID	Flooding-Type	Lat	Lon	Obs. Tide	SLOSH Wind	ARA WIND
URS Team Surveyed Points (Coastal-Surge-Only)							
1	KMSC-02-35	Coastal-SurgeOnly	30.33076	89.37620	20.4	23.7	22.9
2	KMSC-02-36	Coastal-SurgeOnly	30.33342	89.36374	20.6	23.7	22.9
3	KMSC-02-37	Coastal-SurgeOnly	30.31786	89.38075	26.9	23.5	22.8
4	KMSC-02-38	Coastal-SurgeOnly	30.33013	89.39937	21.1	23.7	23.0
5	KMSC-02-39	Coastal-SurgeOnly	30.36259	89.38503	23.8	24.4	23.4
6	KMSC-04-01	Coastal-SurgeOnly	30.24196	89.60566	20.1	18.9	17.8
7	KMSC-04-02	Coastal-SurgeOnly	30.21604	89.57543	19.5	18.9	18.0
8	KMSC-04-03	Coastal-SurgeOnly	30.24389	89.48583	16.6	21.1	20.4
9	KMSC-04-04	Coastal-SurgeOnly	30.26771	89.44931	23.7	22.3	21.5
10	KMSC-04-05	Coastal-SurgeOnly	30.25189	89.51177	20.4	21.1	20.3
11	KMSC-04-06	Coastal-SurgeOnly	30.24011	89.54668	20.1	19.9	18.9
12	KMSC-04-07	Coastal-SurgeOnly	30.35864	89.42138	22.2	24.2	23.4
13	KMSC-05-01	Coastal-SurgeOnly	30.26352	89.40483	19.8	22.4	21.6
14	KMSC-05-02	Coastal-SurgeOnly	30.28597	89.37513	24.4	22.9	22.2
15	KMSC-05-03	Coastal-SurgeOnly	30.29447	89.36120	25.5	23.2	22.4
16	KMSC-05-04	Coastal-SurgeOnly	30.30519	89.33559	25.9	23.6	22.8
17	KMSC-05-09	Coastal-SurgeOnly	30.32481	89.35555	16.3	23.7	22.9
18	KMSC-06-01	Coastal-SurgeOnly	30.37427	89.45183	19.5	24.3	23.4
19	KMSC-06-02	Coastal-SurgeOnly	30.25322	89.61552	18.3	18.9	17.7
20	KMSC-06-05	Coastal-SurgeOnly	30.33179	89.51992	13.1	23.2	22.5
21	KMSC-06-06	Coastal-SurgeOnly	30.34494	89.46735	15.4	23.5	22.8
22	KMSC-06-07	Coastal-SurgeOnly	30.37509	89.37014	25.3	24.8	24.1
23	KMSC-09-01	Coastal-SurgeOnly	30.30616	89.33918	26.7	23.6	22.8
24	KMSC-09-02	Coastal-SurgeOnly	30.29803	89.35445	22.7	23.3	22.6
25	KMSC-09-03	Coastal-SurgeOnly	30.29500	89.36033	25.2	23.2	22.4
26	KMSC-09-04	Coastal-SurgeOnly	30.27923	89.38785	19.6	22.8	22.0
27	KMSC-09-05	Coastal-SurgeOnly	30.28970	89.40986	22.6	22.8	22.0
28	KMSC-09-06	Coastal-SurgeOnly	30.30171	89.37224	22.5	23.3	22.6
29	KMSC-10-55	Coastal-SurgeOnly	30.40173	89.41903	11.6	24.9	23.9
30	KMSC-10-56	Coastal-SurgeOnly	30.40367	89.44528	20.0	24.7	23.6
31	KMSC-10-57	Coastal-SurgeOnly	30.35083	89.61847	11.0	19.8	17.6
32	KMSC-10-58	Coastal-SurgeOnly	30.38575	89.45735	13.6	24.4	23.5
33	KMSC-10-59	Coastal-SurgeOnly	30.38425	89.44432	19.5	24.6	23.6
34	KMSC-10-60	Coastal-SurgeOnly	30.39787	89.38736	21.7	25.3	24.1
35	KMSC-10-61	Coastal-SurgeOnly	30.40831	89.37259	16.0	25.7	24.7
36	KMSC-10-74	Coastal-SurgeOnly	30.38228	89.34681	25.3	24.8	24.0
37	KMSC-10-75	Coastal-SurgeOnly	30.40772	89.37247	20.5	25.7	24.7
38	KMSC-20-02	Coastal-SurgeOnly	30.30594	89.38001	24.5	23.4	22.7
39	KMSC-02-17	Coastal-SurgeOnly	30.45988	88.95763	8.7	19.9	18.9
40	KMSC-02-18	Coastal-SurgeOnly	30.45745	88.97608	15.5	19.8	18.9
41	KMSC-02-19	Coastal-SurgeOnly	30.43836	89.00694	18.7	19.5	18.6
42	KMSC-02-20	Coastal-SurgeOnly	30.42621	88.97374	19.0	19.3	18.4
43	KMSC-02-21	Coastal-SurgeOnly	30.43524	88.99053	18.6	19.5	18.6
44	KMSC-02-22	Coastal-SurgeOnly	30.42547	88.96820	20.4	19.2	19.2
45	KMSC-02-23	Coastal-SurgeOnly	30.42594	88.95002	18.9	19.8	19.4
46	KMSC-02-24	Coastal-SurgeOnly	30.45251	88.95152	12.1	19.9	18.9
47	KMSC-02-25	Coastal-SurgeOnly	30.37490	89.26786	24.6	24.7	23.8

Table W-1. Observed and Simulated Storm Tide during Hurricane Katrina (2005): ft NAVD (Continued)

No.	HWM-ID	Flooding-Type	Lat	Lon	Obs. Tide	SLOSH Wind	ARA WIND
48	KMSC-02-26	Coastal-SurgeOnly	30.35954	89.26345	17.1	24.6	23.7
49	KMSC-02-27	Coastal-SurgeOnly	30.35443	89.23496	24.1	24.7	23.6
50	KMSC-02-28	Coastal-SurgeOnly	30.38095	89.26540	24.7	24.7	23.8
51	KMSC-02-29	Coastal-SurgeOnly	30.38870	89.22745	23.0	25.0	23.8
52	KMSC-03-01	Coastal-SurgeOnly	30.41078	88.88890	20.8	21.0	20.2
53	KMSC-03-02	Coastal-SurgeOnly	30.39468	88.88888	25.8	21.2	20.3
54	KMSC-04-08	Coastal-SurgeOnly	30.31747	89.24256	26.7	24.2	23.2
55	KMSC-04-09	Coastal-SurgeOnly	30.31434	89.25115	25.0	24.2	23.2
56	KMSC-04-10	Coastal-SurgeOnly	30.31707	89.26300	25.0	24.2	23.2
57	KMSC-04-11	Coastal-SurgeOnly	30.32118	89.27509	22.6	24.1	23.2
58	KMSC-04-13	Coastal-SurgeOnly	30.32322	89.28464	22.7	24.1	23.2
59	KMSC-04-14	Coastal-SurgeOnly	30.32760	89.28118	20.9	24.2	23.3
60	KMSC-04-15	Coastal-SurgeOnly	30.32836	89.27141	22.2	24.2	23.3
61	KMSC-04-16	Coastal-SurgeOnly	30.33228	89.26305	24.1	24.3	23.4
62	KMSC-04-17	Coastal-SurgeOnly	30.33945	89.26280	24.9	24.4	23.4
63	KMSC-04-18	Coastal-SurgeOnly	30.33465	89.25411	24.0	24.4	23.4
64	KMSC-04-19	Coastal-SurgeOnly	30.32381	89.24968	22.7	24.3	23.3
65	KMSC-04-20	Coastal-SurgeOnly	30.32795	89.23659	25.5	24.4	23.3
66	KMSC-04-21	Coastal-SurgeOnly	30.33289	89.22254	23.9	24.5	23.3
67	KMSC-04-22	Coastal-SurgeOnly	30.32520	89.21785	27.2	24.4	23.3
68	KMSC-04-23	Coastal-SurgeOnly	30.33024	89.20438	26.3	24.5	23.2
69	KMSC-04-24	Coastal-SurgeOnly	30.35902	89.22022	23.5	24.7	23.6
70	KMSC-04-26	Coastal-SurgeOnly	30.39079	88.86063	23.7	20.7	20.0
71	KMSC-04-27	Coastal-SurgeOnly	30.40653	88.86891	19.7	21.0	20.2
72	KMSC-04-28	Coastal-SurgeOnly	30.40054	88.86520	21.1	21.0	20.2
73	KMSC-04-29	Coastal-SurgeOnly	30.40479	88.87705	20.8	21.0	20.2
74	KMSC-04-30	Coastal-SurgeOnly	30.41131	88.88339	20.6	21.0	20.2
75	KMSC-04-31	Coastal-SurgeOnly	30.41361	88.89200	20.9	20.9	20.1
76	KMSC-04-32	Coastal-SurgeOnly	30.40044	88.89158	20.0	21.0	20.1
77	KMSC-04-33	Coastal-SurgeOnly	30.42906	88.89454	20.6	21.2	20.4
78	KMSC-05-13	Coastal-SurgeOnly	30.34830	89.15094	25.3	24.0	22.9
79	KMSC-05-14	Coastal-SurgeOnly	30.34560	89.15612	25.7	24.0	22.9
80	KMSC-05-15	Coastal-SurgeOnly	30.34279	89.16933	25.9	24.0	22.9
81	KMSC-05-16	Coastal-SurgeOnly	30.33969	89.17612	25.4	24.0	23.0
82	KMSC-05-17	Coastal-SurgeOnly	30.35449	89.13138	25.0	23.9	22.8
83	KMSC-05-18	Coastal-SurgeOnly	30.34489	89.16127	25.2	24.0	22.9
84	KMSC-05-22	Coastal-SurgeOnly	30.34427	89.16534	22.9	24.0	22.9
85	KMSC-05-23	Coastal-SurgeOnly	30.34331	89.17057	25.5	24.0	23.0
86	KMSC-05-24	Coastal-SurgeOnly	30.33977	89.18015	23.9	24.0	23.0
87	KMSC-05-25	Coastal-SurgeOnly	30.33820	89.18391	24.4	24.0	23.0
88	KMSC-05-26	Coastal-SurgeOnly	30.34804	89.15702	23.5	24.0	22.9
89	KMSC-05-27	Coastal-SurgeOnly	30.35217	89.14242	25.5	23.9	22.8
90	KMSC-05-29	Coastal-SurgeOnly	30.35858	89.12723	24.3	23.9	22.8
91	KMSC-06-08	Coastal-SurgeOnly	30.38457	89.25021	23.0	24.8	23.8
92	KMSC-06-09	Coastal-SurgeOnly	30.44620	89.02112	11.7	19.6	18.7
93	KMSC-07-12	Coastal-SurgeOnly	30.37187	89.08016	24.9	23.6	22.4
94	KMSC-07-13	Coastal-SurgeOnly	30.36831	89.09204	23.5	23.6	22.5

Table W-1. Observed and Simulated Storm Tide during Hurricane Katrina (2005): ft NAVD (Continued)

No.	HWM-ID	Flooding-Type	Lat	Lon	Obs. Tide	SLOSH Wind	ARA WIND
95	KMSC-07-14	Coastal-SurgeOnly	30.36349	89.10211	24.5	23.7	22.6
96	KMSC-07-15	Coastal-SurgeOnly	30.35734	89.12641	24.9	23.9	22.8
97	KMSC-07-16	Coastal-SurgeOnly	30.35999	89.11509	24.6	23.8	22.7
98	KMSC-07-17	Coastal-SurgeOnly	30.37402	89.06998	24.8	23.6	22.4
99	KMSC-07-18	Coastal-SurgeOnly	30.37693	89.06202	23.4	23.5	22.3
100	KMSC-07-19	Coastal-SurgeOnly	30.39520	88.93496	23.4	21.9	20.9
101	KMSC-07-20	Coastal-SurgeOnly	30.39546	88.95332	22.2	22.2	21.2
102	KMSC-07-21	Coastal-SurgeOnly	30.39551	88.97295	22.8	22.4	21.4
103	KMSC-07-23	Coastal-SurgeOnly	30.38946	89.00229	23.4	22.7	21.7
104	KMSC-07-24	Coastal-SurgeOnly	30.41490	88.97063	19.3	19.0	18.1
105	KMSC-07-25	Coastal-SurgeOnly	30.41284	88.98297	18.8	19.2	18.3
106	KMSC-07-26	Coastal-SurgeOnly	30.41147	88.99747	19.1	19.2	18.4
107	KMSC-09-08	Coastal-SurgeOnly	30.38181	89.04425	24.2	23.3	22.2
108	KMSC-09-09	Coastal-SurgeOnly	30.38341	89.03777	25.0	23.2	22.1
109	KMSC-09-10	Coastal-SurgeOnly	30.38432	89.03544	23.3	23.2	22.1
110	KMSC-09-11	Coastal-SurgeOnly	30.38601	89.02640	24.7	23.1	22.0
111	KMSC-09-12	Coastal-SurgeOnly	30.38851	89.00598	23.6	22.8	21.7
112	KMSC-09-13	Coastal-SurgeOnly	30.37756	89.06024	23.9	23.5	22.3
113	KMSC-09-14	Coastal-SurgeOnly	30.38362	89.03824	23.2	23.2	22.1
114	KMSC-09-15	Coastal-SurgeOnly	30.38417	89.03160	23.5	23.1	22.1
115	KMSC-09-16	Coastal-SurgeOnly	30.38491	89.02734	23.8	23.1	22.0
116	KMSC-09-17	Coastal-SurgeOnly	30.40344	89.02461	15.5	19.2	18.3
117	KMSC-09-18	Coastal-SurgeOnly	30.40745	89.01324	18.2	19.3	18.4
118	KMSC-09-19	Coastal-SurgeOnly	30.40919	89.02607	18.0	19.3	18.3
119	KMSC-09-20	Coastal-SurgeOnly	30.40245	89.02859	16.6	19.2	18.3
120	KMSC-09-21	Coastal-SurgeOnly	30.40371	89.03096	15.9	19.2	18.3
121	KMSC-09-22	Coastal-SurgeOnly	30.40000	89.03255	15.4	19.2	18.3
122	KMSC-09-23	Coastal-SurgeOnly	30.41028	89.04109	16.6	19.1	18.2
123	KMSC-09-24	Coastal-SurgeOnly	30.41796	89.04281	18.1	18.9	18.0
124	KMSC-09-25	Coastal-SurgeOnly	30.40147	89.04928	16.8	19.1	18.3
125	KMSC-09-26	Coastal-SurgeOnly	30.40390	89.05045	15.1	19.1	18.3
126	KMSC-09-27	Coastal-SurgeOnly	30.39926	89.04690	17.1	19.1	18.3
127	KMSC-09-28	Coastal-SurgeOnly	30.40575	89.01749	18.2	19.3	18.4
128	KMSC-09-29	Coastal-SurgeOnly	30.40435	88.99807	18.6	19.2	18.3
129	KMSC-10-38	Coastal-SurgeOnly	30.46811	88.91872	17.1	19.9	19.0
130	KMSC-10-39	Coastal-SurgeOnly	30.47438	88.89258	15.9	19.9	19.2
131	KMSC-10-42	Coastal-SurgeOnly	30.43185	88.93223	21.1	20.3	19.8
132	KMSC-10-43	Coastal-SurgeOnly	30.43344	88.91097	20.1	20.9	20.3
133	KMSC-10-44	Coastal-SurgeOnly	30.43061	88.89759	20.2	21.2	20.4
134	KMSC-10-51	Coastal-SurgeOnly	30.47108	88.89349	14.6	19.9	19.2
135	KMSC-10-53	Coastal-SurgeOnly	30.43213	88.89518	20.1	21.2	20.4
136	KMSC-10-62	Coastal-SurgeOnly	30.40834	89.03940	19.9	19.2	18.3
137	KMSC-10-63	Coastal-SurgeOnly	30.42241	89.04379	24.6	18.9	18.0
138	KMSC-10-64	Coastal-SurgeOnly	30.42324	89.06337	17.9	18.9	18.0
139	KMSC-10-65	Coastal-SurgeOnly	30.42382	89.06319	19.1	18.9	18.0
140	KMSC-10-66	Coastal-SurgeOnly	30.42677	89.07725	19.3	19.0	18.0
141	KMSC-10-67	Coastal-SurgeOnly	30.41580	89.07594	18.7	19.0	17.9
142	KMSC-10-68	Coastal-SurgeOnly	30.39267	89.06156	18.0	19.0	18.1

Table W-1. Observed and Simulated Storm Tide during Hurricane Katrina (2005): ft NAVD (Continued)

No.	HWM-ID	Flooding-Type	Lat	Lon	Obs. Tide	SLOSH Wind	ARA WIND
143	KMSC-10-69	Coastal-SurgeOnly	30.39842	89.04396	20.0	19.2	18.3
144	KMSC-10-70	Coastal-SurgeOnly	30.38436	89.08097	18.6	18.8	17.9
145	KMSC-10-71	Coastal-SurgeOnly	30.38058	89.09424	18.6	18.7	17.9
146	KMSC-10-72	Coastal-SurgeOnly	30.41131	89.09467	18.0	19.1	17.9
147	KMSC-10-73	Coastal-SurgeOnly	30.38106	89.31298	25.1	24.7	23.9
148	KMSC-15-01	Coastal-SurgeOnly	30.40229	88.89560	20.6	20.9	20.0
149	KMSC-15-02	Coastal-SurgeOnly	30.40077	88.89559	20.5	20.9	20.0
150	KMSC-15-04	Coastal-SurgeOnly	30.39621	88.89695	21.0	21.2	20.3
151	KMSC-15-06	Coastal-SurgeOnly	30.39073	88.98695	25.7	22.6	21.6
152	KMSR-10-19	Coastal-SurgeOnly	30.43398	89.06721	18.2	18.9	18.0
153	KMSC-02-01	Coastal-SurgeOnly	30.41664	88.54711	13.6	15.2	14.7
154	KMSC-02-02	Coastal-SurgeOnly	30.41261	88.56982	14.6	15.2	14.6
155	KMSC-02-03	Coastal-SurgeOnly	30.41459	88.50455	13.0	14.7	14.3
156	KMSC-02-04	Coastal-SurgeOnly	30.41361	88.53962	12.2	14.9	14.4
157	KMSC-02-05	Coastal-SurgeOnly	30.40435	88.55713	12.8	15.0	14.5
158	KMSC-02-06	Coastal-SurgeOnly	30.39791	88.55240	14.7	14.8	14.3
159	KMSC-02-07	Coastal-SurgeOnly	30.40968	88.50395	12.1	14.7	13.6
160	KMSC-02-08	Coastal-SurgeOnly	30.41195	88.47990	11.5	13.8	13.5
161	KMSC-02-09	Coastal-SurgeOnly	30.40595	88.48757	11.7	13.8	13.6
162	KMSC-02-10	Coastal-SurgeOnly	30.34418	88.70230	20.5	16.7	16.1
163	KMSC-02-11	Coastal-SurgeOnly	30.35580	88.69194	16.9	17.2	16.4
164	KMSC-02-12	Coastal-SurgeOnly	30.36135	88.69907	18.4	17.2	16.4
165	KMSC-02-13	Coastal-SurgeOnly	30.35873	88.70924	19.0	17.2	16.7
166	KMSC-02-14	Coastal-SurgeOnly	30.34832	88.71194	19.9	17.2	16.4
167	KMSC-02-15	Coastal-SurgeOnly	30.36806	88.72784	19.2	17.9	17.0
168	KMSC-02-16	Coastal-SurgeOnly	30.37692	88.70432	19.4	17.5	16.7
169	KMSC-02-30	Coastal-SurgeOnly	30.42889	88.46235	10.6	14.1	13.8
170	KMSC-02-31	Coastal-SurgeOnly	30.44342	88.42915	14.2	13.6	13.4
171	KMSC-02-32	Coastal-SurgeOnly	30.36414	88.53526	16.0	14.0	13.5
172	KMSC-02-33	Coastal-SurgeOnly	30.37373	88.52161	14.4	13.8	13.3
173	KMSC-02-34	Coastal-SurgeOnly	30.34688	88.54024	16.7	13.7	13.4
174	KMSC-02-40	Coastal-SurgeOnly	30.38854	88.61455	15.2	15.1	14.5
175	KMSC-02-41	Coastal-SurgeOnly	30.38408	88.49913	14.4	13.5	13.1
176	KMSC-03-05	Coastal-SurgeOnly	30.36482	88.63200	21.1	15.4	14.8
177	KMSC-03-06	Coastal-SurgeOnly	30.39621	88.80012	21.1	20.1	19.2
178	KMSC-03-11	Coastal-SurgeOnly	30.36278	88.75815	18.6	18.9	17.6
179	KMSC-03-12	Coastal-SurgeOnly	30.38672	88.77064	18.8	19.2	18.4
180	KMSC-03-13	Coastal-SurgeOnly	30.37213	88.77929	20.4	19.1	18.3
181	KMSC-03-14	Coastal-SurgeOnly	30.36208	88.56798	17.1	14.2	13.8
182	KMSC-06-11	Coastal-SurgeOnly	30.44082	88.71697	15.3	15.9	15.1
183	KMSC-06-14	Coastal-SurgeOnly	30.41086	88.83805	21.4	21.0	20.4
184	KMSC-06-15	Coastal-SurgeOnly	30.40621	88.82396	20.5	20.5	19.7
185	KMSC-06-16	Coastal-SurgeOnly	30.42288	88.84625	20.7	21.3	20.6
186	KMSC-06-17	Coastal-SurgeOnly	30.39285	88.78132	20.1	19.5	18.7
187	KMSC-06-18	Coastal-SurgeOnly	30.39627	88.80589	21.3	20.1	19.2
188	KMSC-06-19	Coastal-SurgeOnly	30.40467	88.80866	22.4	20.3	19.5
189	KMSC-06-21	Coastal-SurgeOnly	30.35748	88.71583	18.3	17.2	16.4
190	KMSC-06-22	Coastal-SurgeOnly	30.44107	88.72278	16.4	15.9	15.1

Table W-1. Observed and Simulated Storm Tide during Hurricane Katrina (2005): ft NAVD (Continued)

No.	HWM-ID	Flooding-Type	Lat	Lon	Obs. Tide	SLOSH Wind	ARA WIND
191	KMSC-06-23	Coastal-SurgeOnly	30.44107	88.72278	16.4	15.9	15.1
192	KMSC-06-24	Coastal-SurgeOnly	30.44160	88.72324	16.1	15.9	15.1
193	KMSC-06-25	Coastal-SurgeOnly	30.44015	88.72498	18.1	15.9	15.1
194	KMSC-07-01	Coastal-SurgeOnly	30.35175	88.55332	16.9	14.2	13.8
195	KMSC-07-02	Coastal-SurgeOnly	30.35159	88.54808	16.8	14.0	13.5
196	KMSC-07-03	Coastal-SurgeOnly	30.34499	88.55378	18.0	13.7	13.4
197	KMSC-07-04	Coastal-SurgeOnly	30.34772	88.54287	17.2	13.7	13.4
198	KMSC-07-05	Coastal-SurgeOnly	30.34635	88.53315	17.3	13.5	13.1
199	KMSC-07-06	Coastal-SurgeOnly	30.35470	88.53709	16.6	14.0	13.5
200	KMSC-07-07	Coastal-SurgeOnly	30.34685	88.51726	16.8	13.7	13.3
201	KMSC-07-08	Coastal-SurgeOnly	30.35400	88.52187	16.2	13.7	13.3
202	KMSC-07-09	Coastal-SurgeOnly	30.35623	88.55739	20.0	14.2	13.8
203	KMSC-07-10	Coastal-SurgeOnly	30.36605	88.55977	16.7	14.2	13.8
204	KMSC-07-11	Coastal-SurgeOnly	30.37984	88.55891	14.9	14.7	14.1
205	KMSC-07-27	Coastal-SurgeOnly	30.38915	88.61277	14.4	15.1	14.5
206	KMSC-07-29	Coastal-SurgeOnly	30.42380	88.62112	15.2	15.9	15.2
207	KMSC-08-02	Coastal-SurgeOnly	30.41310	88.40328	18.7	12.9	12.9
208	KMSC-08-03	Coastal-SurgeOnly	30.41226	88.40385	19.1	12.9	12.9
209	KMSC-08-04	Coastal-SurgeOnly	30.42943	88.42765	15.0	13.6	13.4
210	KMSC-08-06	Coastal-SurgeOnly	30.40590	88.63450	14.3	15.7	15.0
211	KMSC-08-07	Coastal-SurgeOnly	30.43812	88.72828	15.8	16.9	15.1
212	KMSC-08-08	Coastal-SurgeOnly	30.40731	88.75118	18.9	18.9	16.9
213	KMSC-08-09	Coastal-SurgeOnly	30.38486	88.77394	19.3	19.2	18.4
214	KMSC-08-10	Coastal-SurgeOnly	30.38222	88.74598	19.4	18.5	17.7
215	KMSC-08-11	Coastal-SurgeOnly	30.36800	88.76966	19.7	19.1	18.3
216	KMSC-08-13	Coastal-SurgeOnly	30.36080	88.75180	17.6	18.5	17.6
217	KMSC-10-08	Coastal-SurgeOnly	30.42165	88.62554	14.0	15.7	15.1
218	KMSC-10-09	Coastal-SurgeOnly	30.40764	88.63219	14.4	15.7	15.0
219	KMSC-10-10	Coastal-SurgeOnly	30.40795	88.63200	14.3	15.7	15.0
220	KMSC-10-11	Coastal-SurgeOnly	30.45479	88.45316	7.2	14.2	13.9
221	KMSC-10-20	Coastal-SurgeOnly	30.42525	88.82693	20.1	20.9	20.3
222	KMSC-10-21	Coastal-SurgeOnly	30.42656	88.82743	18.8	20.7	19.8
223	KMSC-10-22	Coastal-SurgeOnly	30.42814	88.81571	19.7	20.6	19.6
224	KMSC-10-23	Coastal-SurgeOnly	30.43701	88.80293	18.4	20.3	19.0
225	KMSC-10-24	Coastal-SurgeOnly	30.42684	88.77556	18.9	21.1	19.6
226	KMSC-10-25	Coastal-SurgeOnly	30.43579	88.74590	21.0	17.2	15.1
227	KMSC-10-28	Coastal-SurgeOnly	30.44763	88.71905	18.9	16.1	15.1
228	KMSC-10-29	Coastal-SurgeOnly	30.44168	88.72179	15.6	15.9	15.1
229	KMSC-10-30	Coastal-SurgeOnly	30.43236	88.73990	17.2	17.2	15.1
230	KMSC-10-31	Coastal-SurgeOnly	30.42692	88.76033	16.5	17.8	16.7
231	KMSC-10-32	Coastal-SurgeOnly	30.42183	88.77750	22.0	21.1	19.6
232	KMSC-10-33	Coastal-SurgeOnly	30.41868	88.79224	22.5	20.3	19.3
233	KMSC-10-34	Coastal-SurgeOnly	30.42037	88.81010	19.5	20.5	19.3
234	KMSC-10-35	Coastal-SurgeOnly	30.42072	88.81079	18.6	20.5	19.3
235	KMSC-10-36	Coastal-SurgeOnly	30.41988	88.82327	20.1	20.9	20.3
236	KMSC-10-45	Coastal-SurgeOnly	30.43872	88.88160	20.9	21.6	20.8
237	KMSC-10-46	Coastal-SurgeOnly	30.42537	88.83599	20.2	21.1	20.5
238	KMSC-10-47	Coastal-SurgeOnly	30.44085	88.84305	21.0	21.4	20.7
239	KMSC-10-48	Coastal-SurgeOnly	30.44251	88.87408	21.4	21.6	20.8
240	KMSC-20-01	Coastal-SurgeOnly	30.34633	88.52309	16.5	13.7	13.3
241	KMSR-10-01	Coastal-SurgeOnly	30.40977	88.65558	14.5	15.8	15.1
242	KMSR-10-02	Coastal-SurgeOnly	30.42073	88.64908	14.5	15.7	15.1

Table W-1. Observed and Simulated Storm Tide during Hurricane Katrina (2005): ft NAVD (Continued)

No.	HWM-ID	Flooding-Type	Lat	Lon	Obs. Tide	SLOSH Wind	ARA WIND
USGS Surveyed Points							
243	KMS_USGS_03	N/A	30.33358	89.51274	13.8	23.2	22.5
244	KMS_USGS_04	N/A	30.35841	89.42297	22.1	24.2	23.4
245	KMS_USGS_05	N/A	30.35798	89.42356	24.7	24.2	23.4
246	KMS_USGS_06	N/A	30.36280	89.40930	20.1	24.4	23.5
247	KMS_USGS_07	N/A	30.36629	89.39846	23.9	24.5	23.6
248	KMS_USGS_08	N/A	30.36577	89.39819	25.4	24.4	23.6
249	KMS_USGS_09	N/A	30.38735	89.44146	19.7	24.6	23.6
250	KMS_USGS_10	N/A	30.41461	89.20379	18.7	25.9	24.3
251	KMS_USGS_11	N/A	30.41521	89.20196	19.0	26.0	24.3
252	KMS_USGS_12	N/A	30.42215	89.14944	27.4	21.1	20.3
253	KMS_USGS_13	N/A	30.43374	89.09012	19.1	19.0	18.0
254	KMS_USGS_14	N/A	30.45448	89.02922	18.8	20.0	19.1
255	KMS_USGS_15	N/A	30.45273	88.94232	16.1	19.9	18.9
256	KMS_USGS_16	N/A	30.44307	88.72214	14.4	15.9	15.1
257	KMS_USGS_17	N/A	30.43746	88.61735	17.3	16.1	15.4
258	KMS_USGS_18	N/A	30.43744	88.61728	16.8	16.1	15.4
259	KMS_USGS_21	N/A	30.61057	88.64169	15.5	14.2	12.6
260	KMS_USGS_23	N/A	30.30016	89.35008	27.0	23.3	22.6
261	KMS_USGS_24	N/A	30.29635	89.36320	26.2	23.2	22.4
262	KMS_USGS_25	N/A	30.32525	89.33803	23.6	23.8	23.1
263	KMS_USGS_26	N/A	30.41956	89.34354	24.8	26.4	25.6
264	KMS_USGS_27	N/A	30.31538	89.25426	24.6	24.2	23.2
265	KMS_USGS_28	N/A	30.31909	89.27284	23.4	24.1	23.2
266	KMS_USGS_29	N/A	30.31987	89.27251	23.7	24.1	23.2
267	KMS_USGS_31	N/A	30.33185	89.35282	25.0	23.8	23.0
268	KMS_USGS_32	N/A	30.33503	89.35384	24.2	23.8	23.1
269	KMS_USGS_33	N/A	30.41209	88.89501	19.7	20.9	20.1
270	KMS_USGS_35	N/A	30.39666	88.87997	21.0	21.0	20.2
271	KMS_USGS_36	N/A	30.39305	88.89166	22.0	21.2	20.3
272	KMS_USGS_37	N/A	30.39527	88.90075	22.5	21.5	20.5
273	KMS_USGS_38	N/A	30.39530	88.91337	22.5	21.6	20.6
274	KMS_USGS_39	N/A	30.39528	88.93399	22.5	21.9	20.9
275	KMS_USGS_40	N/A	30.39399	88.95500	23.1	22.2	21.2
276	KMS_USGS_41	N/A	30.39066	88.99022	23.2	22.6	21.6
277	KMS_USGS_42	N/A	30.42903	88.93747	18.7	20.1	19.7
278	KMS_USGS_43	N/A	30.39060	88.86015	23.6	20.7	20.0
279	KMS_USGS_45	N/A	30.30502	89.37707	23.0	23.3	22.6
280	KMS_USGS_47	N/A	30.41488	89.38075	24.2	25.6	24.7
281	KMS_USGS_48	N/A	30.31793	89.40985	22.3	23.5	22.7
282	KMS_USGS_49	N/A	30.29850	89.40606	22.2	23.1	22.4
283	KMS_USGS_50	N/A	30.30018	89.41819	21.6	23.2	22.4
284	KMS_USGS_51	N/A	30.29923	89.39725	22.4	23.1	22.2
285	KMS_USGS_52	N/A	30.25247	89.58793	18.6	19.2	18.2
286	KMS_USGS_53	N/A	30.25347	89.61565	18.3	18.9	17.7
287	KMS_USGS_54	N/A	30.28663	89.60750	10.9	19.1	17.9

Table W-1. Observed and Simulated Storm Tide during Hurricane Katrina (2005): ft NAVD (Continued)

No.	HWM-ID	Flooding-Type	Lat	Lon	Obs. Tide	SLOSH Wind	ARA WIND
288	KMS_USGS_55	N/A	30.30210	89.61389	8.2	19.1	17.6
289	KMS_USGS_56	N/A	30.32347	89.48797	7.7	23.2	22.5
290	KMS_USGS_57	N/A	30.26839	89.44942	23.6	22.3	21.5
291	KMS_USGS_58	N/A	30.28971	89.40975	23.0	22.8	22.0
292	KMS_USGS_59	N/A	30.27428	89.39050	25.1	22.7	21.9
293	KMS_USGS_60	N/A	30.28424	89.38053	25.3	22.9	22.2
294	KMS_USGS_61	N/A	30.38123	89.35903	25.3	24.8	24.1
295	KMS_USGS_62	N/A	30.37871	89.09765	14.4	18.6	17.9
296	KMS_USGS_63	N/A	30.41418	88.97589	19.2	19.1	18.2
297	KMS_USGS_64	N/A	30.24166	89.55475	19.0	19.9	18.9
298	KMS_USGS_65	N/A	30.21599	89.57525	20.1	18.9	18.0
299	KMS_USGS_66	N/A	30.35769	89.12663	24.8	23.9	22.8
300	KMS_USGS_67	N/A	30.35511	89.13613	25.0	23.9	22.8
301	KMS_USGS_68	N/A	30.34886	89.15049	25.0	23.9	22.9
302	KMS_USGS_69	N/A	30.34234	89.17029	25.0	24.0	23.0
303	KMS_USGS_70	N/A	30.33772	89.18372	24.9	24.0	23.0
304	KMS_USGS_71	N/A	30.32937	89.20655	25.3	24.0	23.1
305	KMS_USGS_72	N/A	30.32576	89.21822	24.5	24.4	23.3
306	KMS_USGS_73	N/A	30.34227	89.21717	23.3	24.5	23.4
307	KMS_USGS_74	N/A	30.33274	89.22839	23.5	24.5	23.3
308	KMS_USGS_75	N/A	30.36459	89.10695	24.3	23.7	22.6
309	KMS_USGS_76	N/A	30.36690	89.09876	24.3	23.6	22.5
310	KMS_USGS_78	N/A	30.38197	89.04237	24.2	23.3	22.2
311	KMS_USGS_79	N/A	30.38432	89.03543	23.9	23.2	22.1
312	KMS_USGS_80	N/A	30.37507	89.22894	23.5	24.9	23.7
313	KMS_USGS_81	N/A	30.35964	89.21695	22.5	24.7	23.6
314	KMS_USGS_82	N/A	30.38888	89.19907	13.4	25.2	23.8
315	KMS_USGS_83	N/A	30.41428	89.09325	16.9	19.1	17.9
316	KMS_USGS_84	N/A	30.39262	89.06110	17.4	19.0	18.1
317	KMS_USGS_85	N/A	30.40259	89.02565	18.8	19.2	18.3
318	KMS_USGS_86	N/A	30.38645	89.02602	23.8	23.1	22.0
319	KMS_USGS_88	N/A	30.44341	88.85492	21.4	21.4	20.7
320	KMS_USGS_89	N/A	30.40902	88.82808	21.3	20.7	19.9
321	KMS_USGS_90	N/A	30.40025	88.79857	21.6	20.1	19.2
322	KMS_USGS_91	N/A	30.40295	88.77714	17.3	19.4	18.5
323	KMS_USGS_92	N/A	30.38160	88.75928	19.1	18.9	18.1
324	KMS_USGS_94	N/A	30.41923	88.82807	20.4	20.9	20.3
325	KMS_USGS_96	N/A	30.32162	89.22731	26.0	24.3	23.2
326	KMS_USGS_98	N/A	30.32183	89.22673	26.1	24.3	23.2
327	KMS_USGS_99	N/A	30.43824	88.55054	11.9	15.3	14.8
328	KMS_USGS_100	N/A	30.43819	88.54988	11.6	15.3	14.8
329	KMS_USGS_102	N/A	30.47278	88.96157	18.9	19.9	19.0
330	KMS_USGS_103	N/A	30.46932	88.93835	18.2	20.0	19.0
331	KMS_USGS_104	N/A	30.47451	88.89256	15.9	19.9	19.2
332	KMS_USGS_105	N/A	30.34752	89.64167	14.8	19.5	17.7
333	Dauphin Island [1]	Tide Gage	30.25000	88.07500	6.1	7.3	7.1
334	Horn Island [1]	Tide Gage	30.23833	88.66667	N/A	13.8	13.1
335	Waveland [1]	Tide Gage	30.28167	89.36667	N/A	22.9	22.2
336	Biloxi [1]	Tide Gage	30.41167	88.90333	N/A	20.8	20.0

[1] Tide gauge data from NOAA Tide and Current website

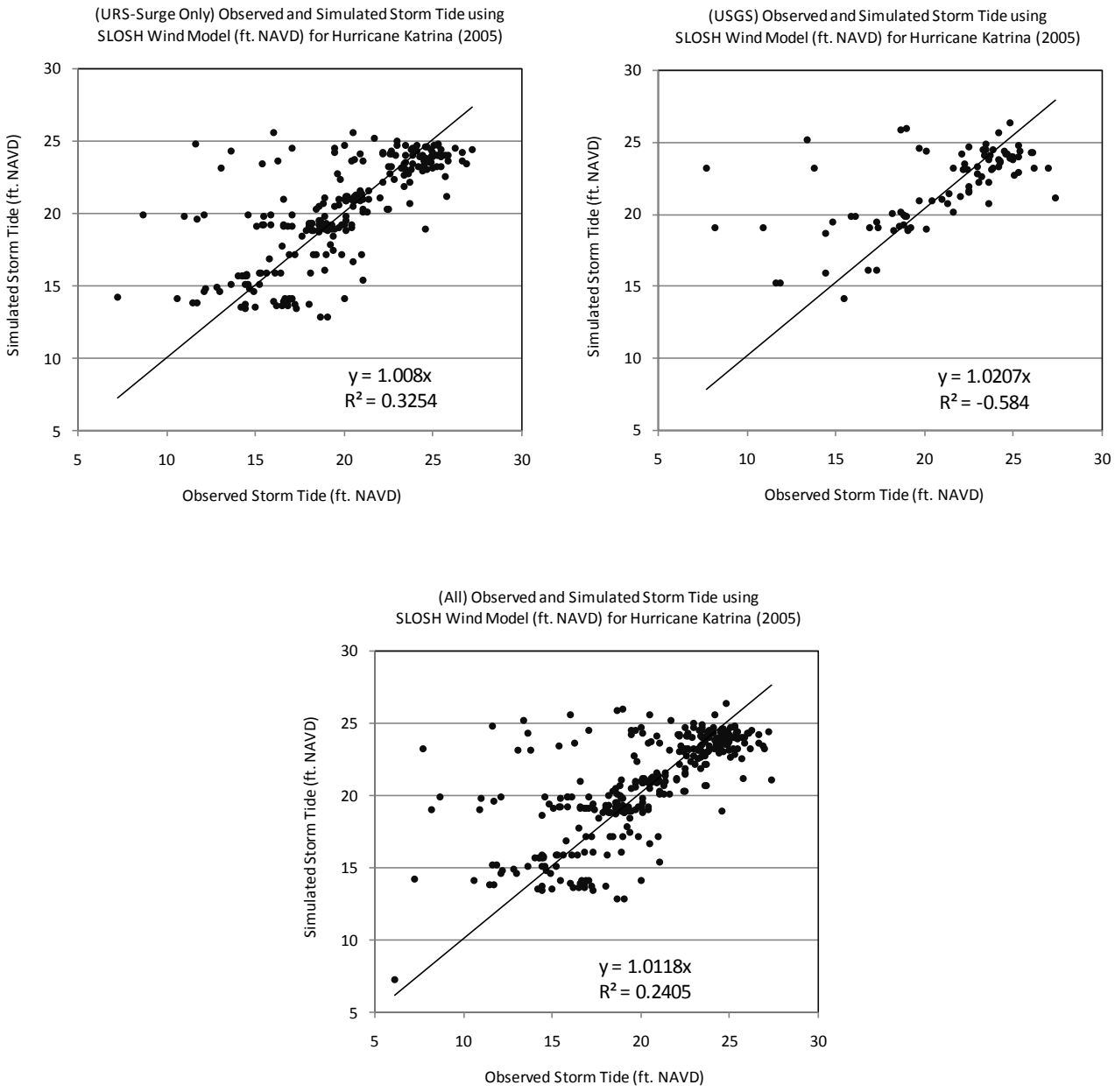

Figure W-2a. Comparison of Simulated and Observed Storm Tide for Hurricane Katrina (SLOSH wind model)

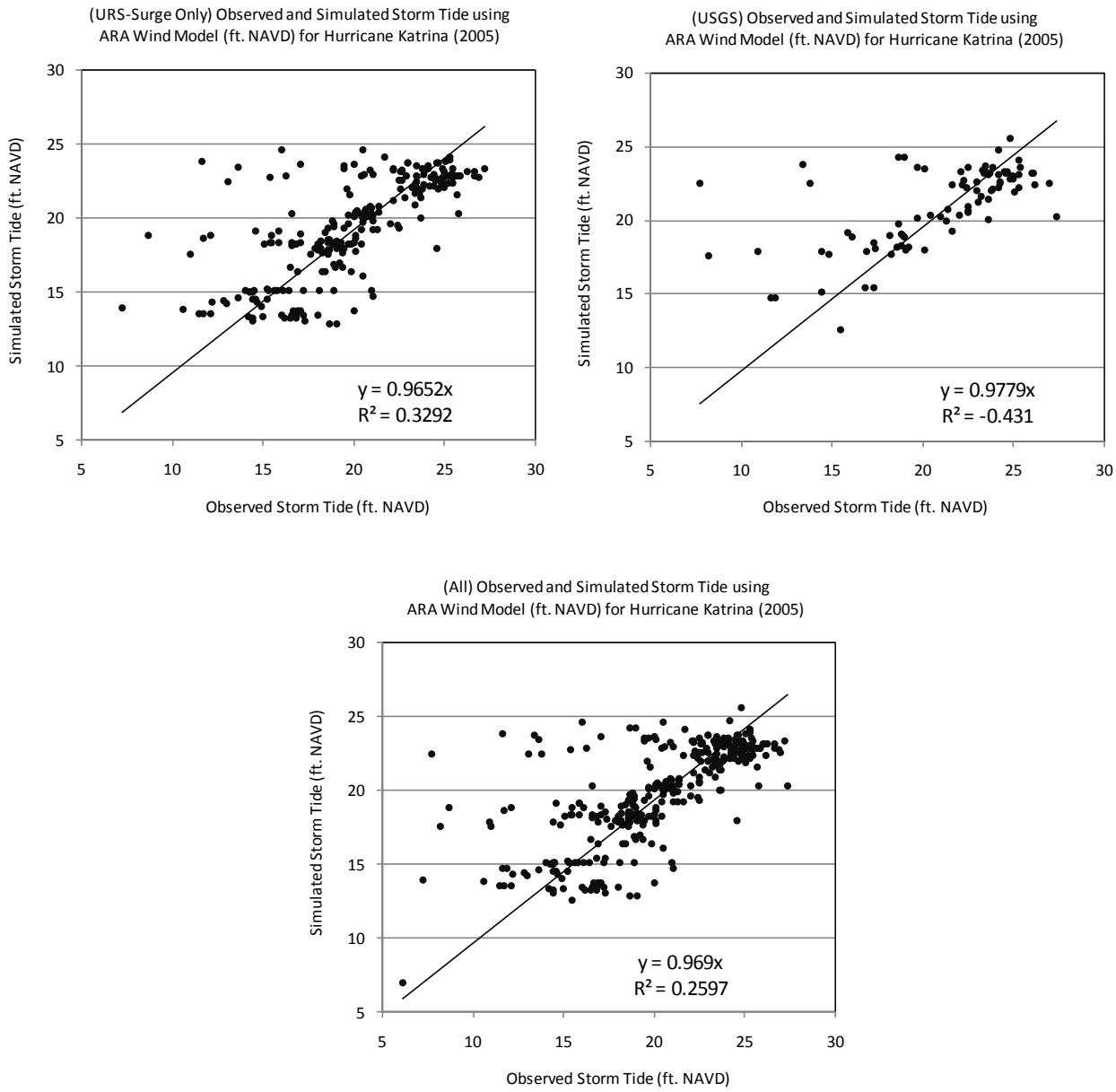

Figure W-2b. Comparison of Simulated and Observed Storm Tide for Hurricane Katrina (ARA wind model)

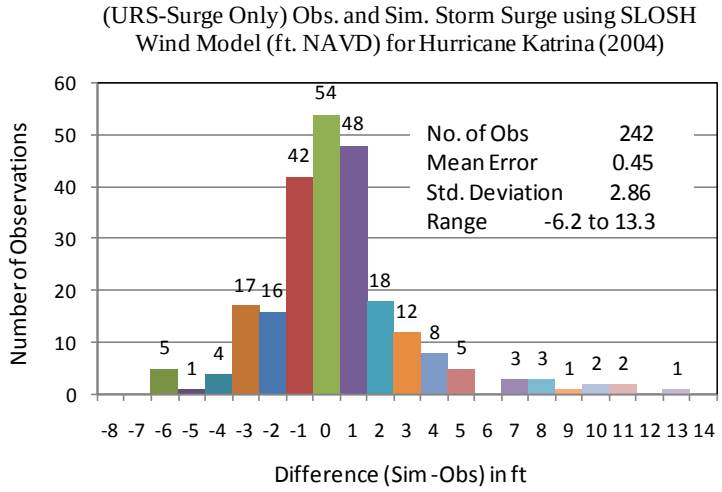

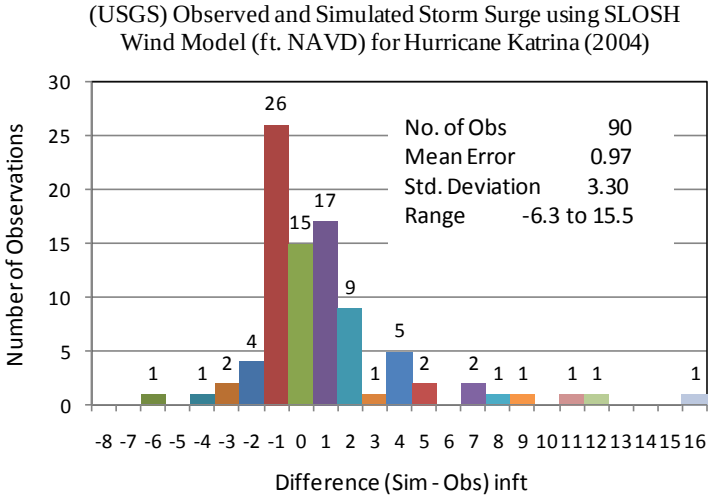

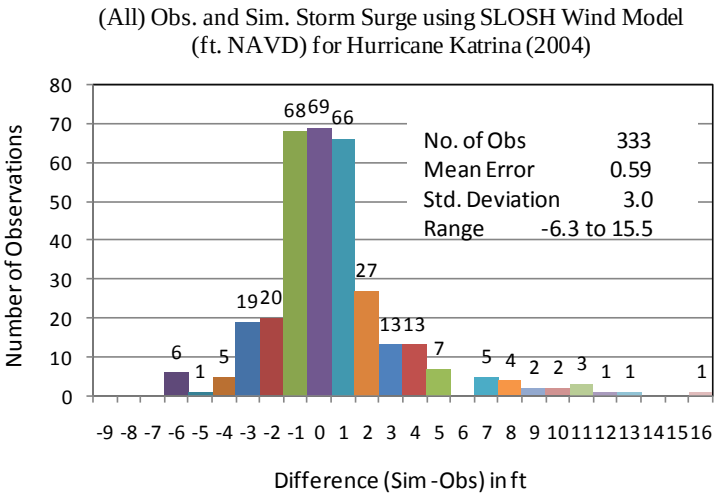

Figure W-3a. Simulated storm tide values minus observed HWMs for Hurricane Katrina (SLOSH Wind Model)

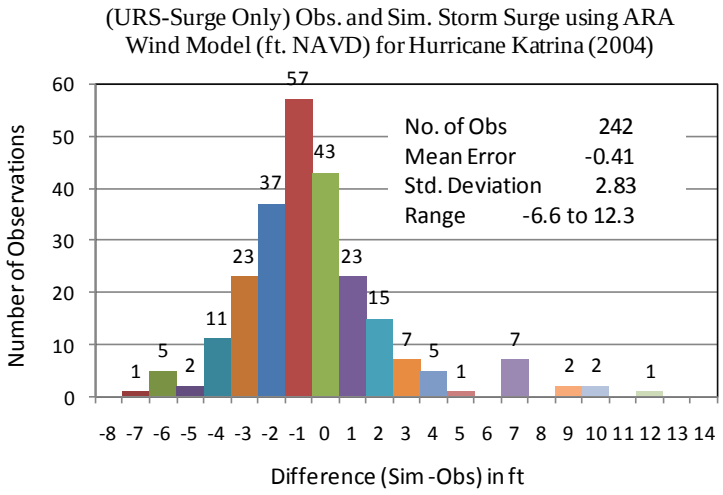

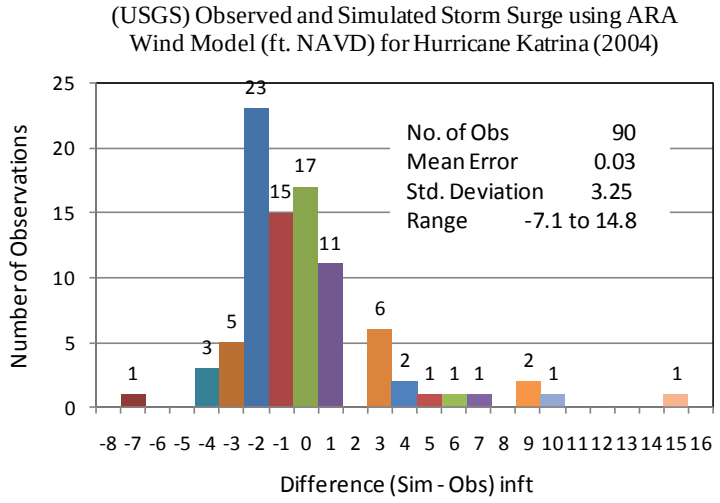

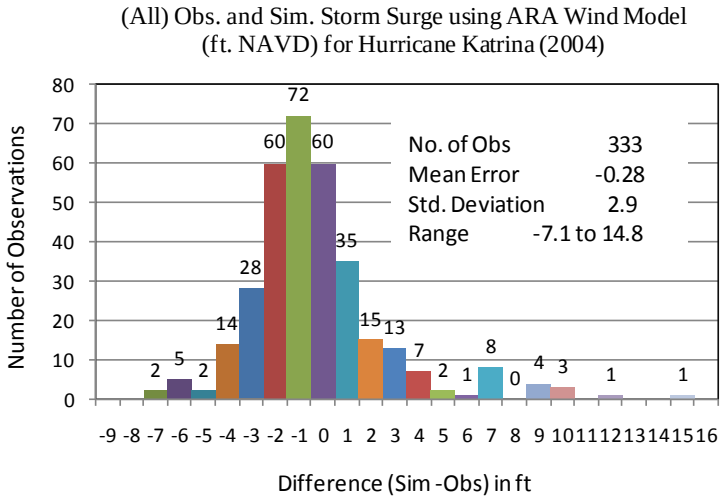

Figure W-3b. Simulated storm tide values minus observed HWMs for Hurricane Katrina (ARA Wind Model)

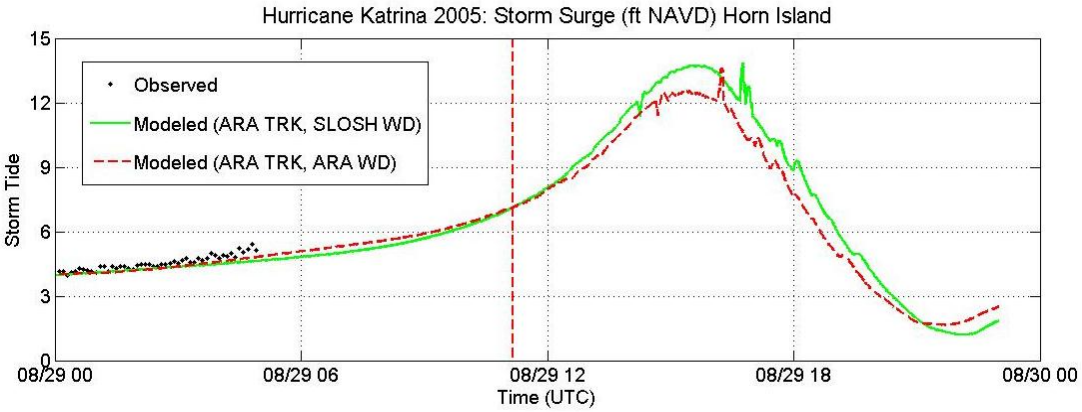

Figure W-4a. Tide gauge record at Horn Island, MS compared to the simulated time history of Storm Tide in the SLOSH Grid cell containing the gauge location

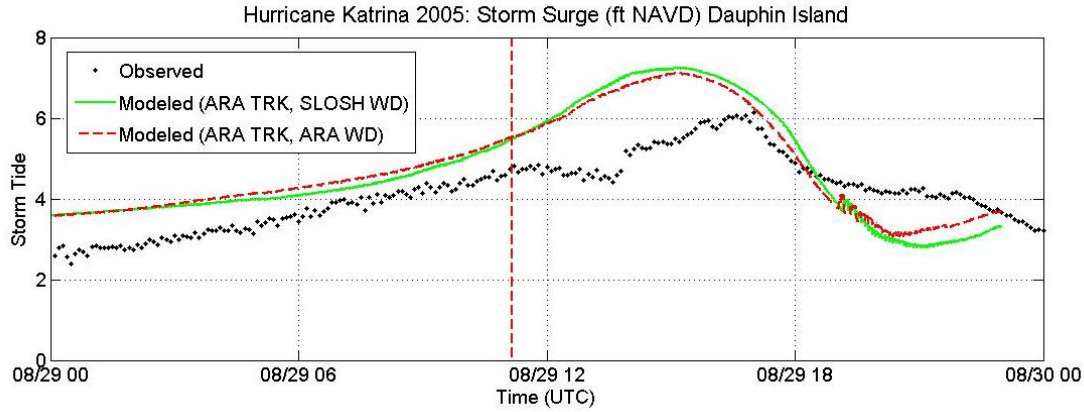

Figure W-4b. Tide gauge record at Dauphin, AL compared to the simulated time history of Storm Tide in the SLOSH Grid cell containing the gauge location

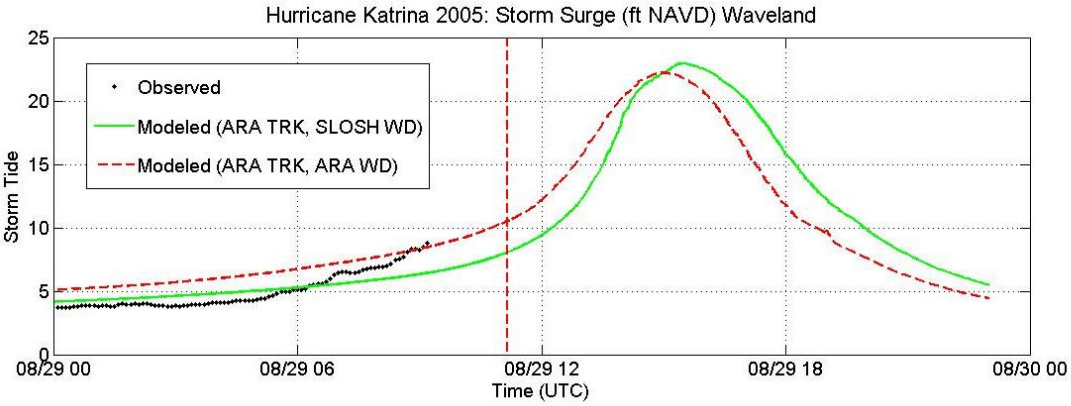

Figure W-4c. Tide gauge record at Waveland, MS compared to the simulated time history of Storm Tide in the SLOSH Grid cell containing the gauge location

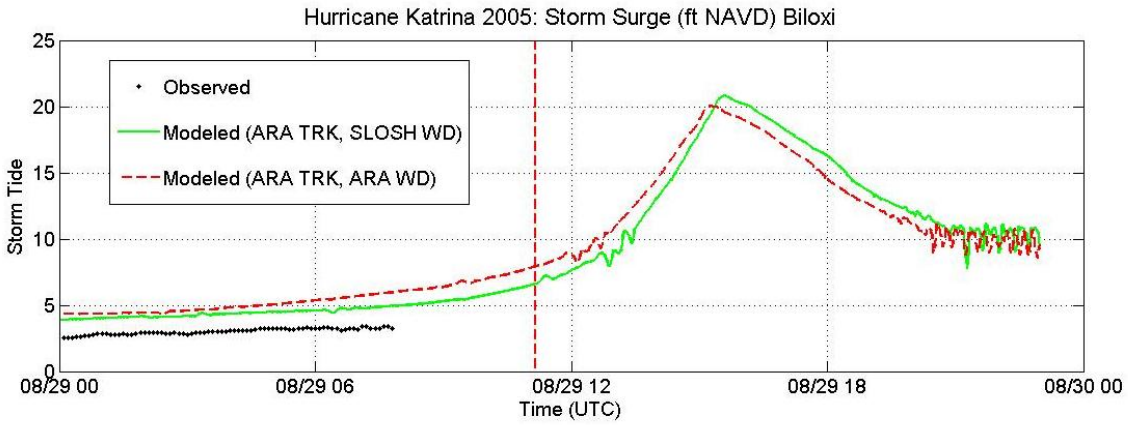

Figure W-4d. Tide gauge record at Biloxi, MS compared to the simulated time history of Storm Tide in the SLOSH Grid cell containing the gauge location

Table W-2. Error Analysis of Storm Tide for Hurricane Katrina

Station	Surge Range	Numer Data	Obs		SLOSH		ARA	
			Mean	Std	mean Err	RMSErr	mean Err	RMSErr
Dauphin Island	0-3	29	2.8	0.1	0.9	0.9	0.9	0.9
	3-6	195	4.3	0.7	0.5	1.1	0.5	1.0
	6-9	6	6.1	0.1	0.7	0.7	0.5	0.5
	all	230	4.2	0.9	0.6	1.0	0.6	1.0
Horn Island	3-6	50	4.5	0.3	-0.3	0.3	-0.2	0.3
	all	50	4.5	0.3	-0.3	0.3	-0.2	0.3
Waveland	3-6	69	4.2	0.6	0.5	0.6	1.7	1.7
	6-9	24	7.2	0.8	-1.3	1.4	0.6	0.7
	all	93	5.0	1.4	0.0	0.8	1.4	1.5
Biloxi	0-3	36	2.8	0.1	1.3	1.3	1.6	1.6
	3-6	43	3.2	0.1	1.4	1.4	2.1	2.1
	all	79	3.0	0.2	1.3	1.3	1.9	1.9
all stations	0-3	65	2.8	0.1	1.1	1.1	1.3	1.4
	3-6	357	4.2	0.7	0.5	1.0	0.8	1.3
	6-9	30	7.0	0.8	-0.9	1.3	0.5	0.6
	all	452	4.2	1.1	0.5	1.0	0.9	1.2

Appendix X. Comparison of Observed and SLOSH Model Computed Storm Tides for Hurricane Gustav (2008)

This appendix compares storm tide estimates from SLOSH to high water marks (HWMs) and tide gauge data from Hurricane Gustav. Gustav made landfall on the coast of Louisiana around 1500 UTC September 1, 2008 as a Category 2 hurricane (Beven and Kimberlain 2008). The hurricane caused widespread storm surge along the northern coast of the Gulf of Mexico, particularly along coast of Louisiana.

Observation Data

Selected surface observations for Hurricane Gustav are given in Beven and Kimberlain (2008). Observed peak storm tides from the National Oceanic Service (NOS) and other stations are given with respect to National Geodetic Vertical Datum of 1929 (NGVD). Only 22 of such observations are found in the report. The details of stations are listed in Table X-1.

Before the landfall of Gustav on Louisiana coast, USGS deployed a mobile monitoring network consisting 124 pressure transducers (i.e., surge sensors) to measure the inland storm surge and coastal flooding due to Gustav. The data obtained from these sensors are reported in Mcghee et al. (2008). The sensor sites were assigned a category as surge, riverine flooding, anthropogenic, and mixed/uncertain. The time histories at 11 surge sites are used for the validation. The water elevations reported for these stations were measured with respect to North American Vertical Datum of 1988 (NAVD).

In addition, 16 tide gauge data provided by Dr. Andrew Kennedy of the University of Notre Dame, as listed in Table X-2, are used for the comparison. The locations of the selected sites are shown in Figure 1 along with the Gustav track obtained from ARA hurricane model.

SLOSH Basins and Initial Water Levels

Four SLOSH basins are selected for the validation study since all of the observation stations/sites listed in Table X-1 and X-2 are located within these basins, and Gustav either crossed these basins or passed nearby. The selected SLOSH basins are Sabine-Lake, Vermilion-Bay, New Orleans and Mississippi Gulf Coast.

The reference datum for the Vermilion Bay and Mississippi Gulf Coast SLOSH basins is NGVD 1929, while the reference datum for the Sabine-Lake and New Orleans basins is NAVD 1988. The average mean sea level change from the year 1929 to the year 2008 is calculated based on several NOAA stations located along the Gulf coast: Grand Isle, Eugene Island, Sabine Pass, Galveston, Freeport, Dauphin Island, Pensacola, Panama City and Apalachicola. The average mean sea level change calculated from these stations is +1.25 ft. Using NOAA tide and currents website (NOAA 2010), the predicted tide level at time of landfall was approximately +0.25 ft.

There was no pre-storm anomaly observed for these stations. Thus, the total initial water level is +1.5 ft-NGVD for the Galveston-Bay and Vermilion-Bay basins and +1.35 ft-NAVD for the Sabine-Lake and New Orleans basins.

Methodology

SLOSH is a grid based numerical storm surge model that computes water elevations generated by the wind and pressure forces in tropical cyclones. The time history of the water elevation is saved in individual elements of the basin grid and the maximum value for each grid cell is termed as the Envelope of High Water (EOHW). The observed storm surge elevation is compared to the EOHW in the nearest grid cells, and the observed hydrographic records associated with the passage of Hurricane Gustav at tide gauges are compared to the SLOSH model-generated storm surge hydrographs in the nearest grid cells.

Model runs using the SLOSH wind model and the ARA wind model are compared to the observed data. Where multiple basins contain the same observation site, the basin with minimum distance from the basin center to observation site, usually the basin with smaller grid cells (i.e. finer resolution) at the observation site, is used to compare against observed data. These values along with the observed values are given in Table X-1 and Table X-2.

Results

Figure X-2 shows the comparisons of observed and simulated storm tide values using SLOSH wind model and ARA wind model. The linear regression line assuming zero intercept is also shown in these figures along with R^2 value and the equation. On average, the SLOSH wind model and ARA wind model produce underestimates of the observed storm tides of 24% and 20%, respectively.

Histograms of the differences (simulated minus observed) are shown in Figure X-3. The error characteristics are indicated in the legend. The mean errors are -0.94 and -0.96 feet for model runs using the SLOSH wind model and the ARA wind model, respectively; however, the range and standard deviation of the ARA wind model errors are substantially smaller than the SLOSH wind model errors.

Figure X-4 shows the time histories of storm tide produced by model runs using SLOSH wind model and ARA wind model compared with the observed data. In general, the magnitudes and timing of the modeled results are in reasonably good agreement with the observations. However, significant underestimates are noted at SSS-LA-ORL-001, SSS-LA-ORL-008, SSS-LA-ORL-013, and Press-13.

Table X-3 summarizes the mean and RMS errors of the storm tide time histories for Hurricane Gustav. The results show that the model runs with ARA wind field model generally produces lower mean errors and lower RMS errors than the model runs using the SLOSH wind model.

Conclusions

For Hurricane Gustav, the SLOSH wind model and ARA wind model produce average underestimates of the observed storm tides of 24% and 20%, respectively. The underestimates are largest at the six locations with observed storm tides in excess of 10 feet. The model runs with ARA wind field model generally produces lower mean time history errors and lower RMS time history errors than the model runs using the SLOSH wind model.

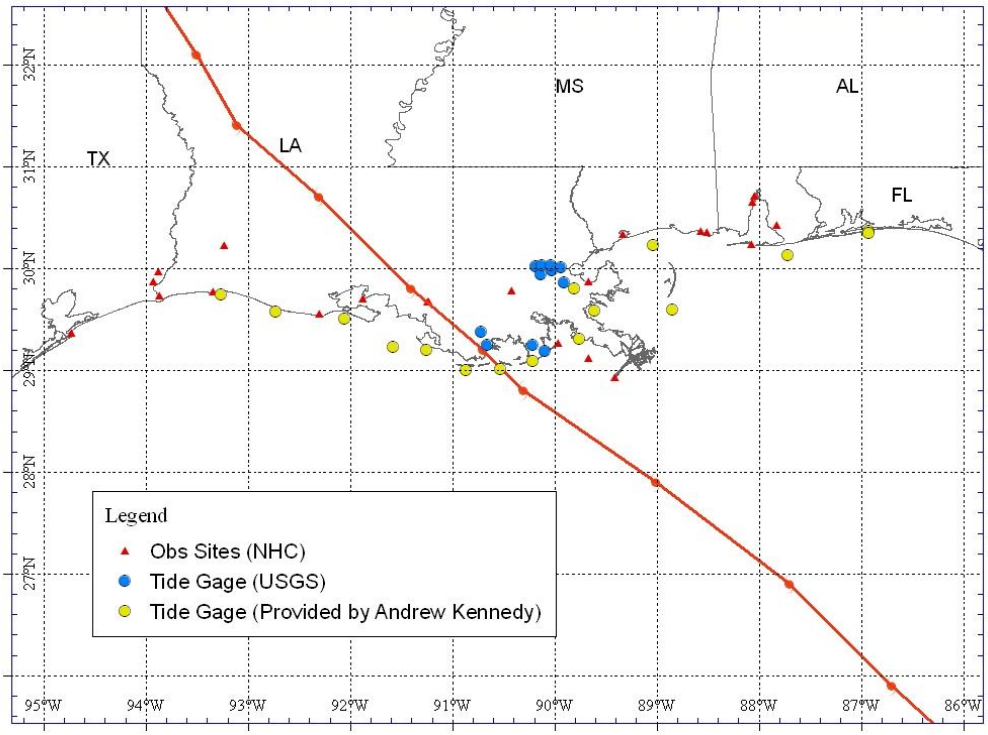

Figure X-1. Locations of the observation stations for Hurricane Gustav (2008)

Table X-1. Summary of modeled and observed storm tide during Hurricane Gustav

No.	Location	Storm Tide (ft NGVD)	ARA-TRK-SLOSH-WD (ft NGVD)	ARA-TRK-ARA-WD (ft NGVD)
1	Amerada Pass, LA (NOS site)	4.8	5.1	3.2
2	Bayou Gauche, LA (NOS site)	1.4	5.4	4.6
3	Calcsieu Pass, LA (NOS site)	3.2	1.4	1.7
4	Grand Isle, LA (NOS site)	5.4	9.2	8.4
5	SW Pass, LA (NOS site)	5.6	4.4	4.0
6	Shell Beach, LA (NOS site)	10.5	7.2	8.7
7	Port Fourchon, LA(NOS site)	4.6	6.1	5.2
8	Tesoro Terminal, LA(NOS site)	2.2	5.1	2.9
9	Cypremort Point, LA (NOS site)	3.2	1.9	1.5
10	Freshwater Canal Rocks, LA(NOS site)	4.0	2.0	2.0
11	Lake Charles, LA (NOS site)	2.8	1.3	1.3
12	Pascagoula NOAA Lab, MS (NOS site)	5.4	3.6	5.0
13	Pascagoula Port Dock E, MS (NOS site)	6.6	4.1	5.0
14	Bay Waveland Yatch Club, MS (NOS site)	10.9	6.3	9.5
15	Dauphin Island, AL	4.2	3.1	3.6
16	Mobile Coast Guard, AL (NOS site)	6.7	2.9	4.1
17	Mobile State Docks, AL (NOS site)	4.9	2.7	3.6
18	Weeks Island, AL (NOS site)	4.1	2.7	3.1
19	Galveston North Jetty, TX (NOS site)	2.8	1.4	1.9
20	Sabine Pass North, TX (NOS site)	2.8	1.4	1.7
21	Port Arthur,TX	2.3	1.4	1.5
22	Rainbow Bridge, TX	2.1	1.3	1.4

Table X-2. Surge sensor site locations during Hurricane Gustav

No	Surge Sensor ID	Lat	Lon	Storm Tide (ft NGVD)	ARA-TRK-ARA-WD (ft NGVD)	ARA-TRK-SLOSH-WD (ft NGVD)
USGS						
1	SSS-LA-JEF-013	30.021210	-90.180430	N/A	N/A	N/A
2	SSS-LA-LAF-006	29.247060	-90.209880	7.0	7.4	8.8
3	SSS-LA-LAF-007	29.187230	-90.090220	7.7	7.9	9.2
4	SSS-LA-ORL-001	29.936750	-90.135430	10.5	7.0	6.2
5	SSS-LA-ORL-002	30.028070	-90.120290	N/A	N/A	N/A
6	SSS-LA-ORL-008	29.980610	-90.022600	12.3	7.4	6.7
7	SSS-LA-ORL-010	30.031820	-90.036580	N/A	N/A	N/A
8	SSS-LA-ORL-013	30.006280	-89.939570	14.7	9.0	7.7
9	SSS-LA-PLA-004	29.863090	-89.908760	N/A	N/A	N/A
10	SSS-LA-TER-024	29.245940	-90.661090	6.5	5.9	7.3
11	SSS-LA-TER-025	29.373170	-90.713000	N/A	N/A	N/A
Tide Gage Data Provided by Andrew Kennedy						
12	Press_1	29.001033	-90.865100	4.8	3.3	4.4
13	Press_2	29.195733	-91.251983	4.9	3.8	5.6
14	Press_4	29.744033	-93.258217	2.5	1.6	1.3
15	Press_5	29.572767	-92.723983	1.9	1.7	1.7
16	Press_6	29.499367	-92.053183	2.4	2.6	4
17	Press_7	29.223983	-91.580117	2.5	2.6	3.7
18	Press_8	29.006917	-90.526300	6.3	4.8	5.6
19	Press_9	29.082633	-90.215167	6.7	7.3	8.3
20	Press_11	29.306183	-89.759817	7.6	7	8.8
21	Press_12	29.590567	-88.844850	4.8	4.4	4.2
22	Press_13	29.580317	-89.605633	13.8	9.6	8.4
23	Press_14	29.798700	-89.802367	8.6	10.5	8.8
24	Press_17	30.229050	-89.029117	8.1	6.6	5.2
25	Press_18	30.365983	-86.921200	3.7	3.1	2.7
26	Press_19	30.127117	-87.715150	3.7	2.7	2.5
27	Press_20	30.341333	-86.919917	3.8	3.1	2.7

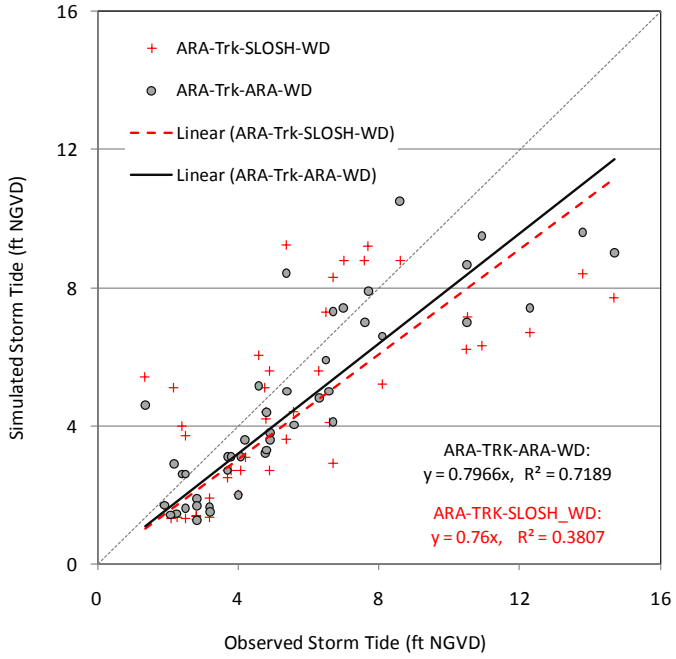

Figure X-2. Comparison of Simulated and Observed Storm Tide for Hurricane Gustav

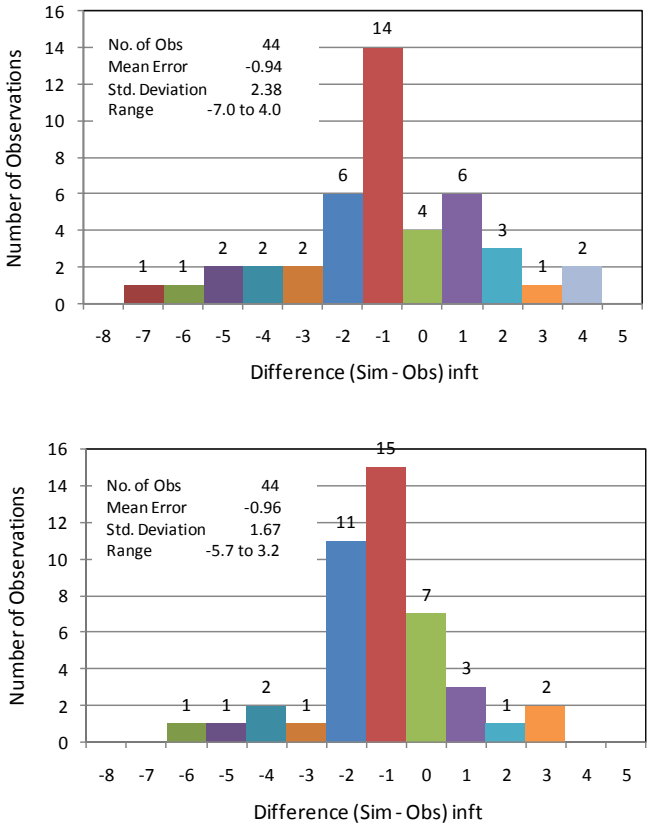

Figure X-3. Simulated storm tide values minus observed storm tide for Hurricane Gustav (2008): (Top, SLOSH wind model; Bottom, ARA wind model)

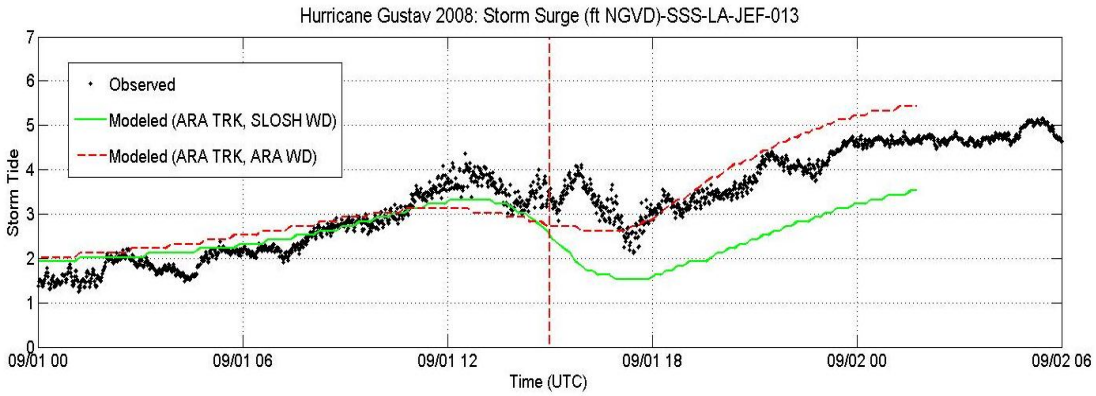

Figure X-4a. Tide gauge record at SSS-LA-JEF-013 compared to the simulated time history of Storm Tide in the SLOSH Grid cell containing the gauge location

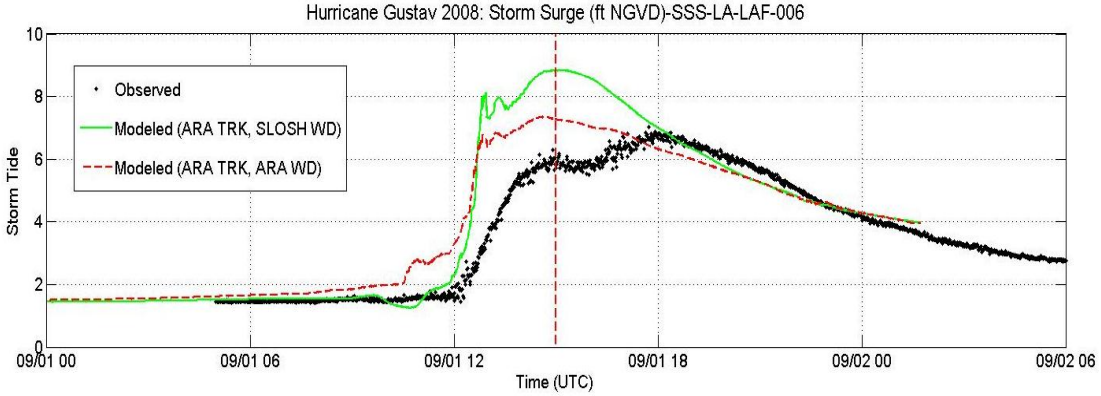

Figure X-4b. Tide gauge record at SSS-LA-LAF-006 compared to the simulated time history of Storm Tide in the SLOSH Grid cell containing the gauge location

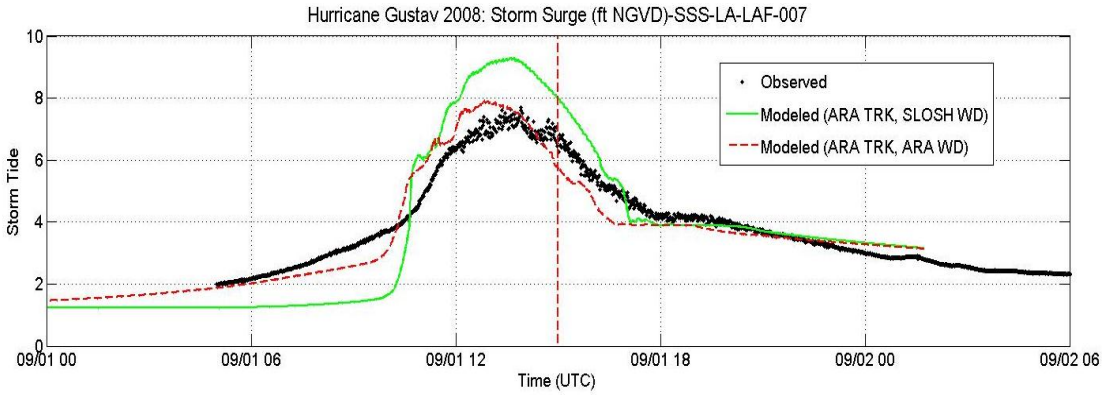

Figure X-4c. Tide gauge record at SSS-LA-LAF-007 compared to the simulated time history of Storm Tide in the SLOSH Grid cell containing the gauge location

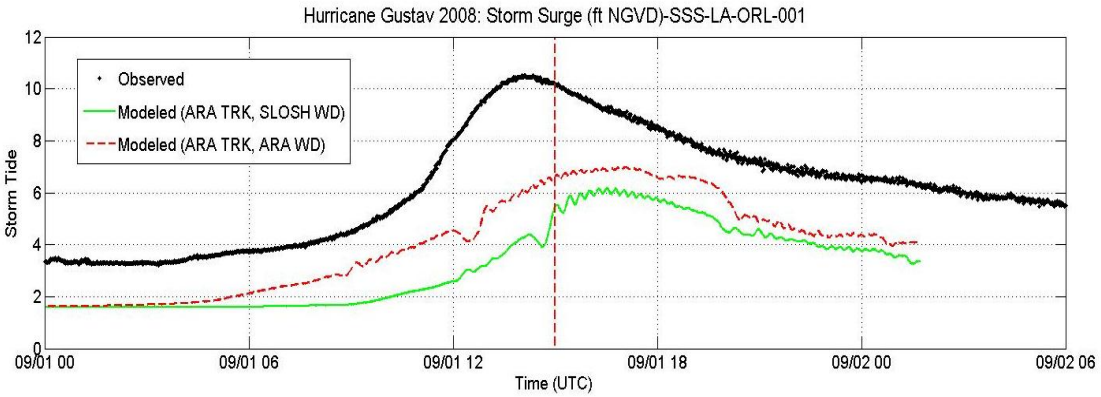

Figure X-4d. Tide gauge record at SSS-LA-ORL-001 compared to the simulated time history of Storm Tide in the SLOSH Grid cell containing the gauge location

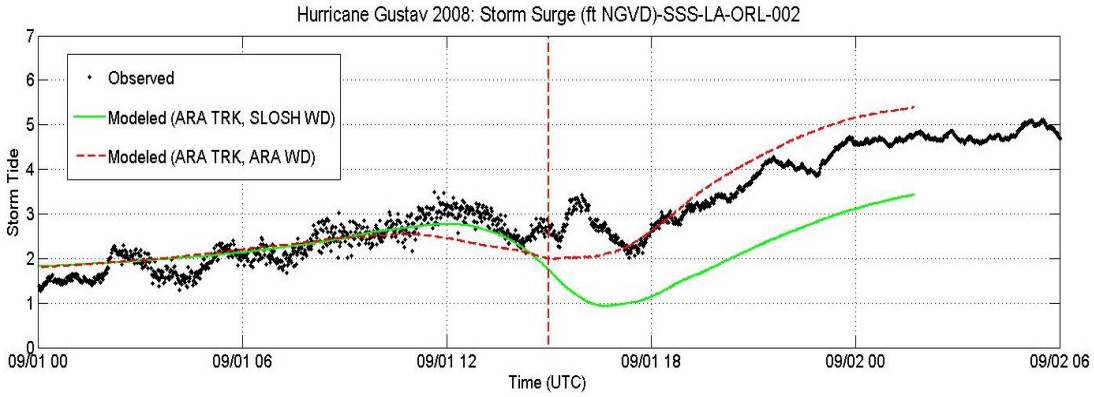

Figure X-4e. Tide gauge record at SSS-LA-ORL-002 compared to the simulated time history of Storm Tide in the SLOSH Grid cell containing the gauge location

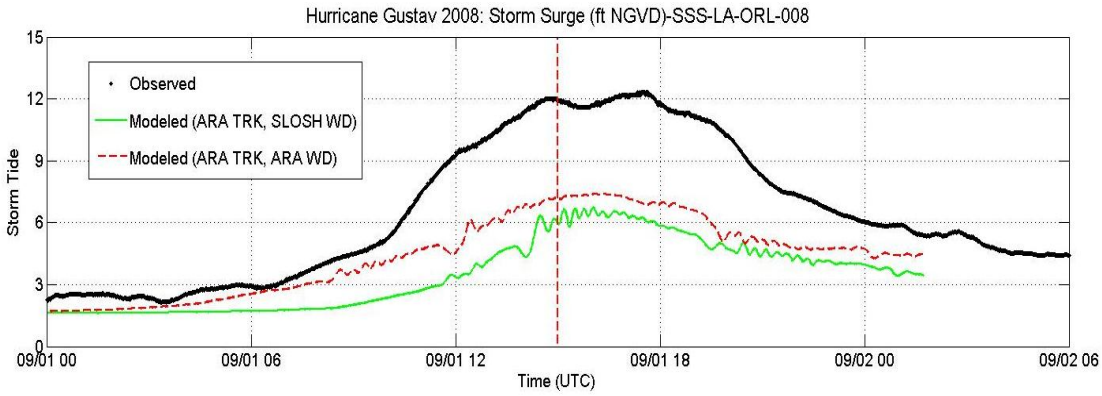

Figure X-4f. Tide gauge record at SSS-LA-ORL-008 compared to the simulated time history of Storm Tide in the SLOSH Grid cell containing the gauge location

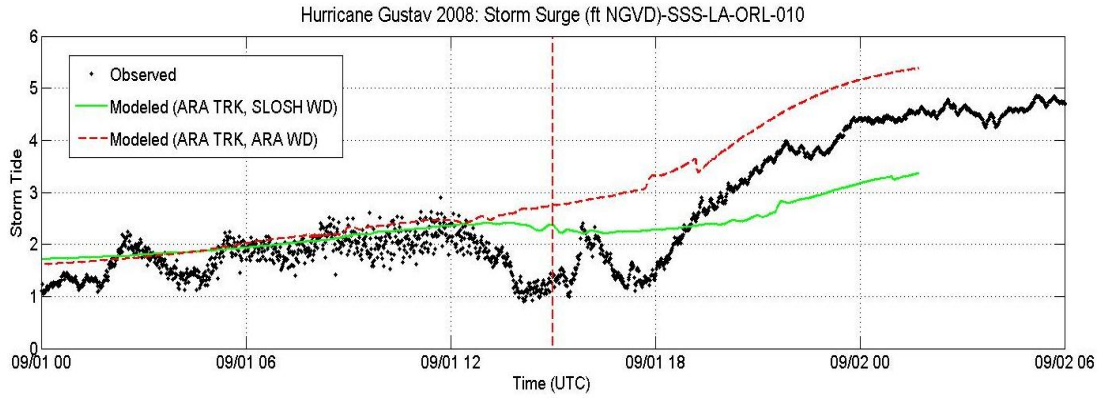

Figure X-4g. Tide gauge record at SSS-LA-ORL-010 compared to the simulated time history of Storm Tide in the SLOSH Grid cell containing the gauge location

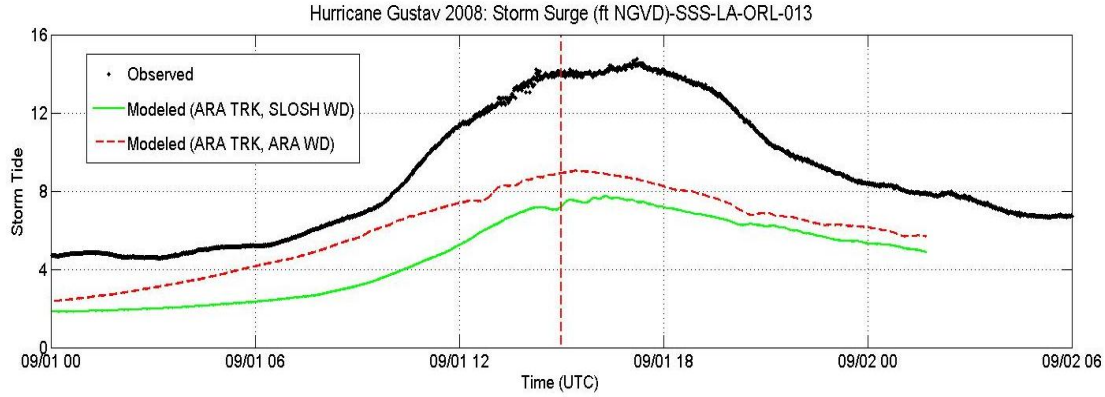

Figure X-4h. Tide gauge record at SSS-LA-ORL-013 compared to the simulated time history of Storm Tide in the SLOSH Grid cell containing the gauge location

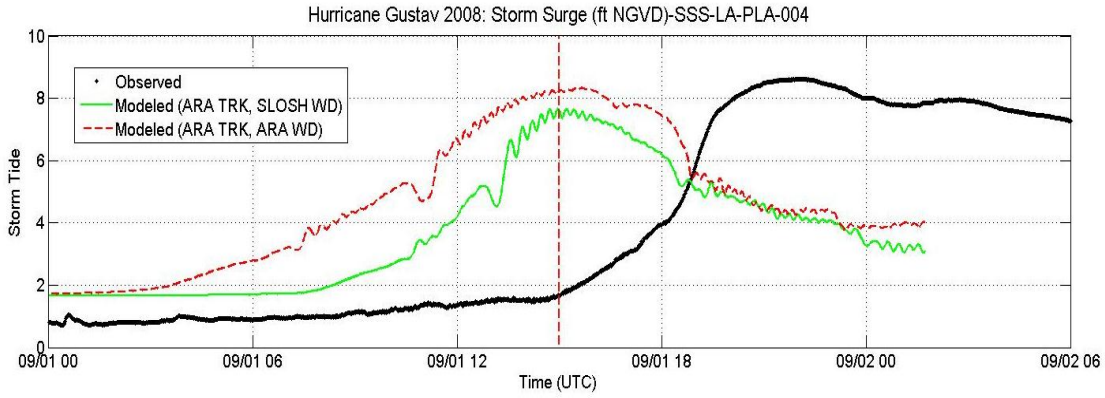

Figure X-4i. Tide gauge record at SSS-LA-PLA-004 compared to the simulated time history of Storm Tide in the SLOSH Grid cell containing the gauge location

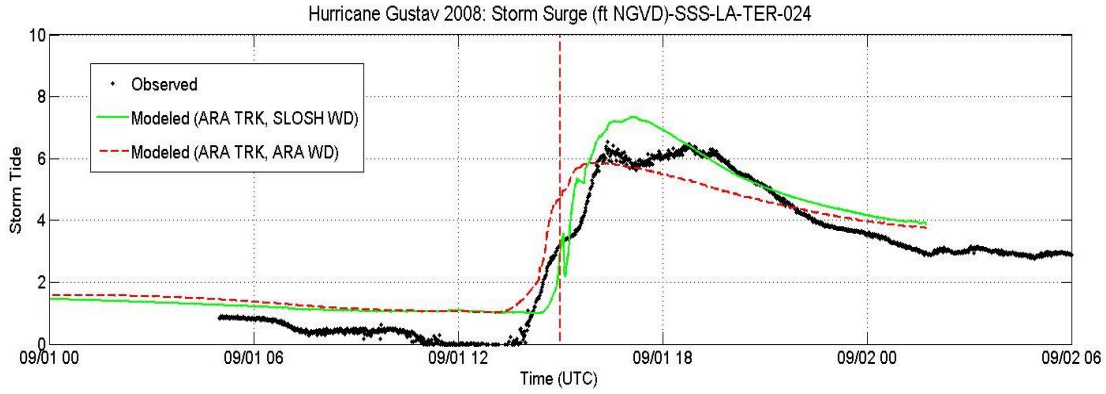

Figure X-4j. Tide gauge record at SSS-LA-TER-024 compared to the simulated time history of Storm Tide in the SLOSH Grid cell containing the gauge location

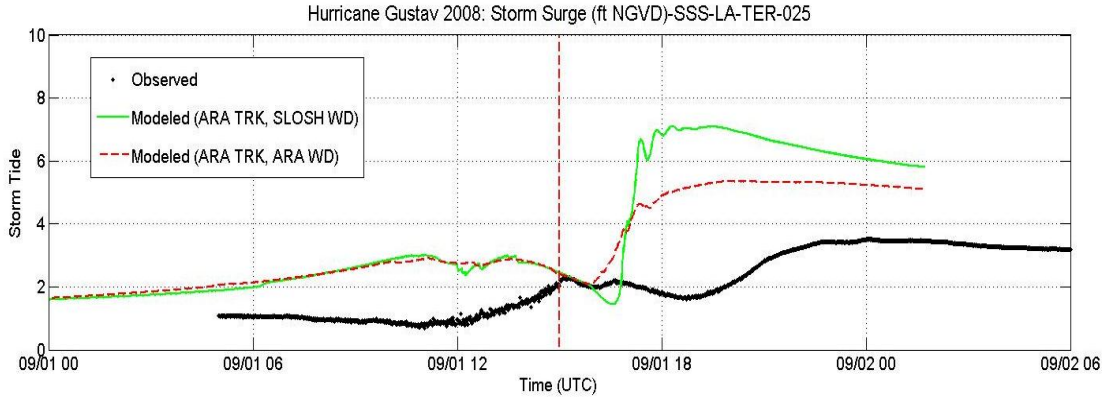

Figure X-4k. Tide gauge record at SSS-LA-TER-025 compared to the simulated time history of Storm Tide in the SLOSH Grid cell containing the gauge location

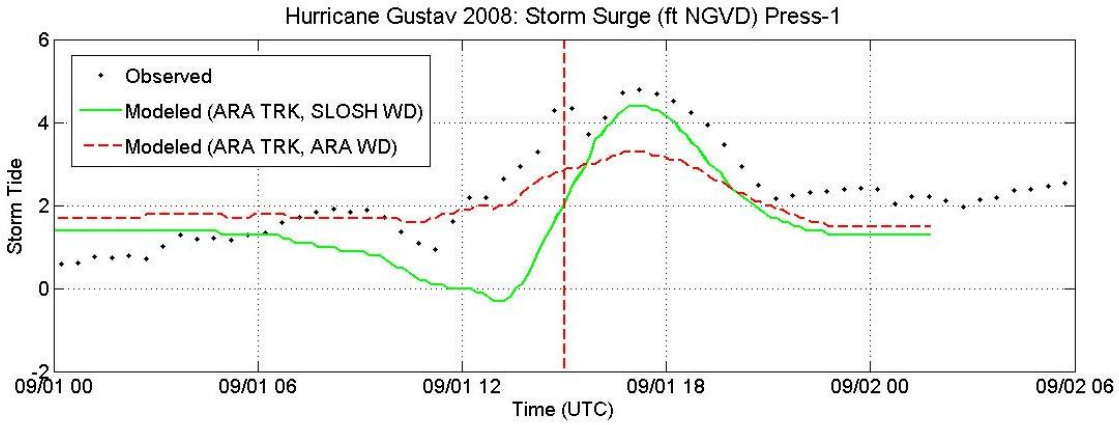

Figure X-4l. Tide gauge record at Press-1 compared to the simulated time history of Storm Tide in the SLOSH Grid cell containing the gauge location

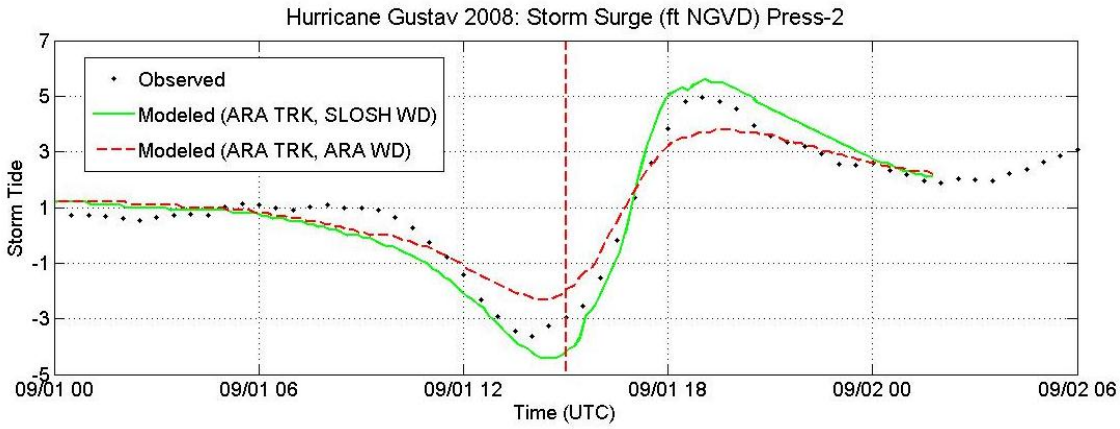

Figure X-4m. Tide gauge record at Press-2 compared to the simulated time history of Storm Tide in the SLOSH Grid cell containing the gauge location

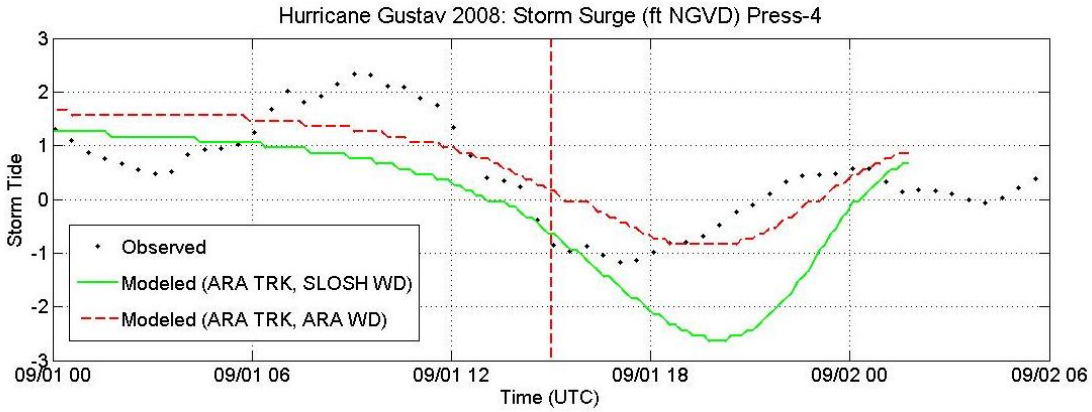

Figure X-4n. Tide gauge record at Press-4 compared to the simulated time history of Storm Tide in the SLOSH Grid cell containing the gauge location

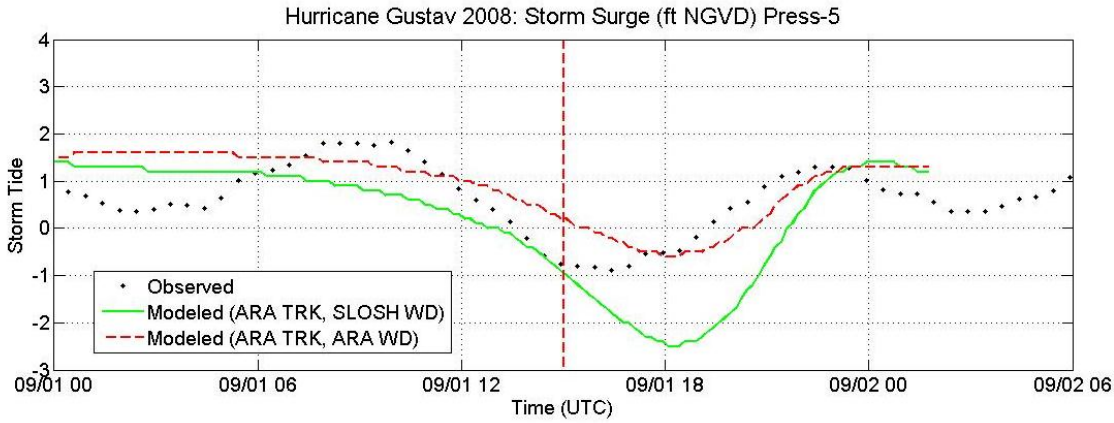

Figure X-4o. Tide gauge record at Press-5 compared to the simulated time history of Storm Tide in the SLOSH Grid cell containing the gauge location

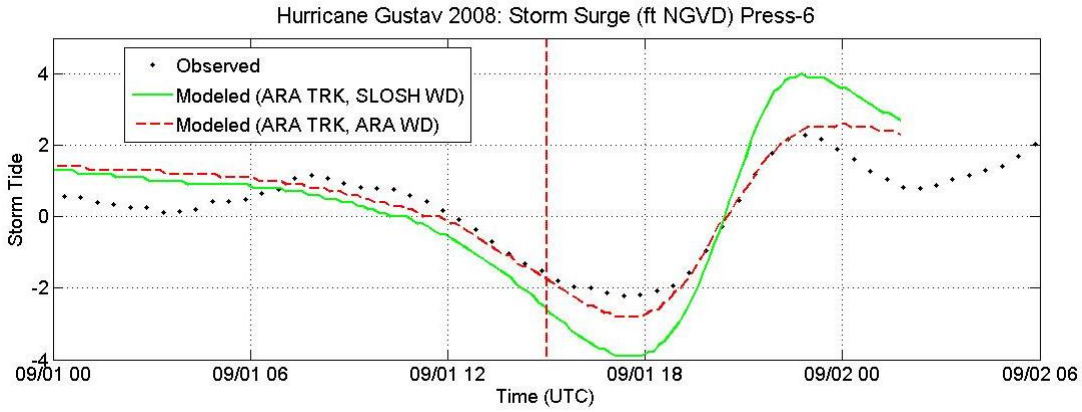

Figure X-4p. Tide gauge record at Press-6 compared to the simulated time history of Storm Tide in the SLOSH Grid cell containing the gauge location

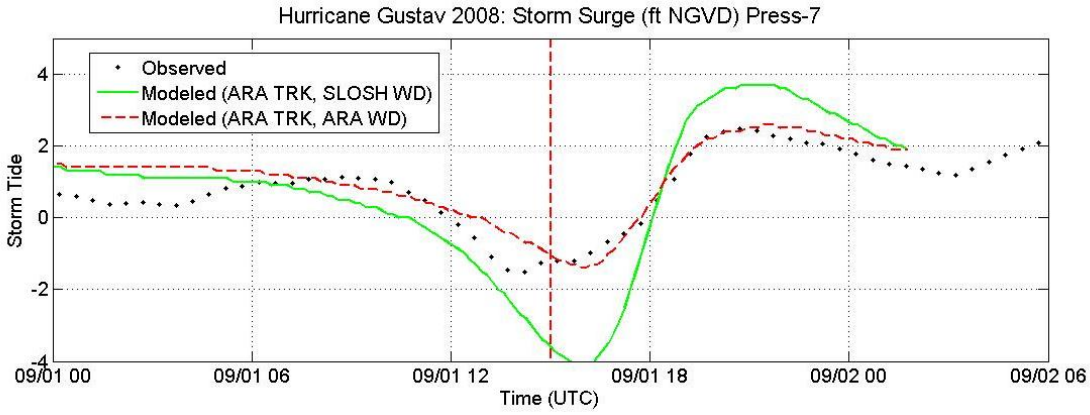

Figure X-4q. Tide gauge record at Press-7 compared to the simulated time history of Storm Tide in the SLOSH Grid cell containing the gauge location

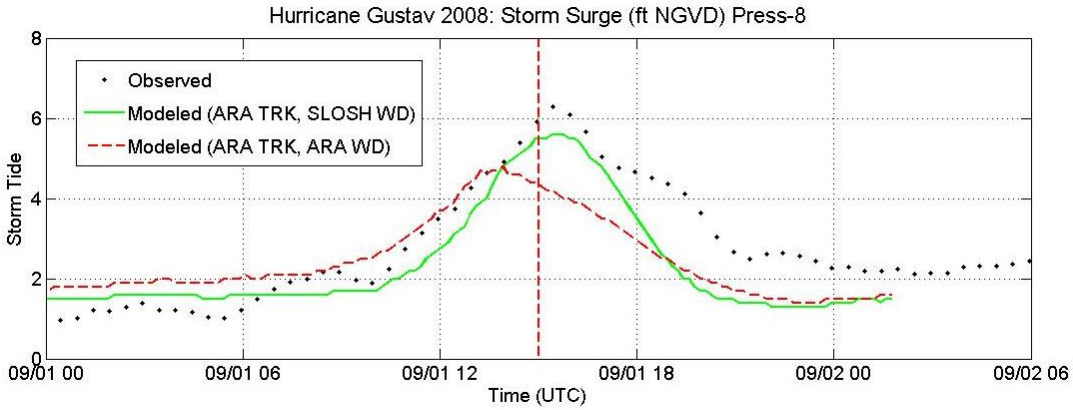

Figure X-4r. Tide gauge record at Press-8 compared to the simulated time history of Storm Tide in the SLOSH Grid cell containing the gauge location

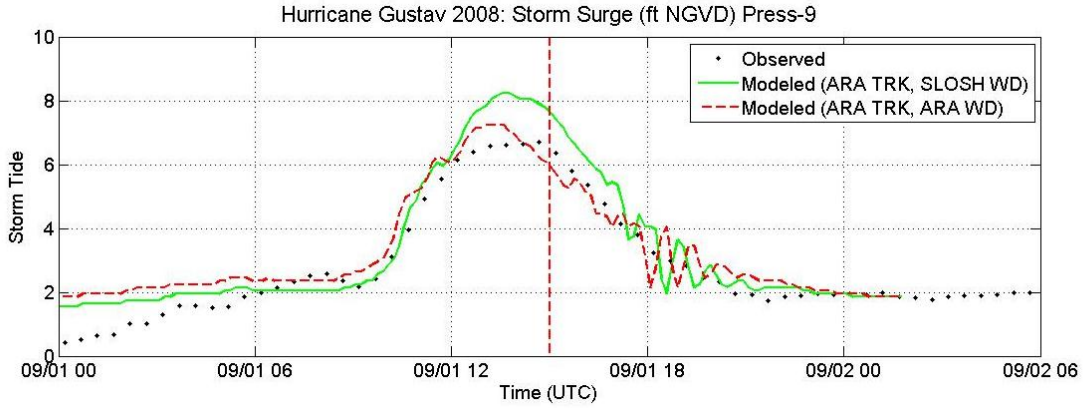

Figure X-4s. Tide gauge record at Press-9 compared to the simulated time history of Storm Tide in the SLOSH Grid cell containing the gauge location

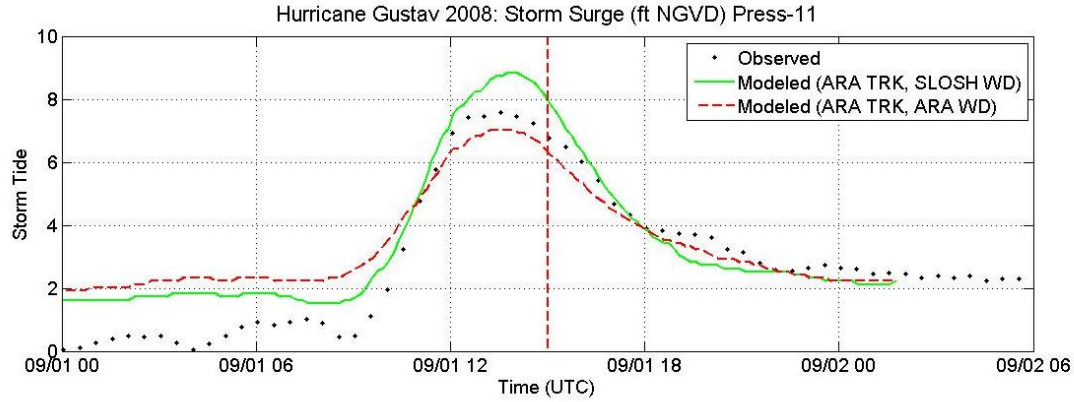

Figure X-4t. Tide gauge record at Press-11 compared to the simulated time history of Storm Tide in the SLOSH Grid cell containing the gauge location

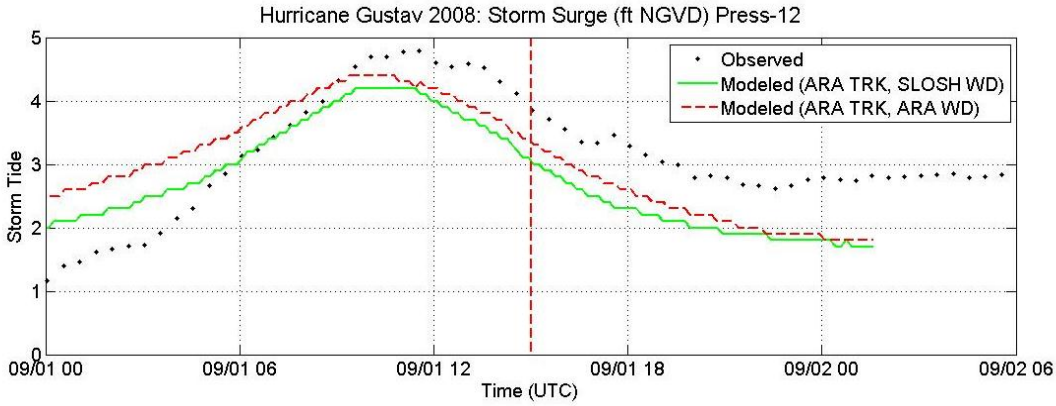

Figure X-4u. Tide gauge record at Press-12 compared to the simulated time history of Storm Tide in the SLOSH Grid cell containing the gauge location

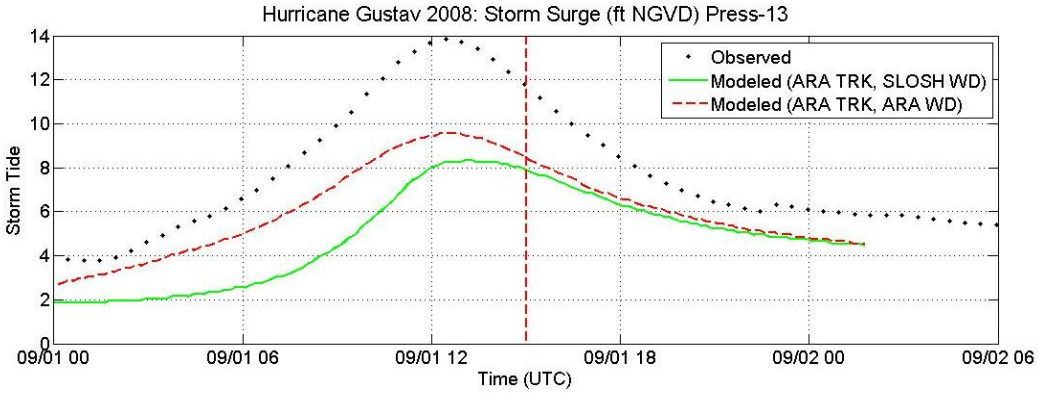

Figure X-4v. Tide gauge record at Press-13 compared to the simulated time history of Storm Tide in the SLOSH Grid cell containing the gauge location

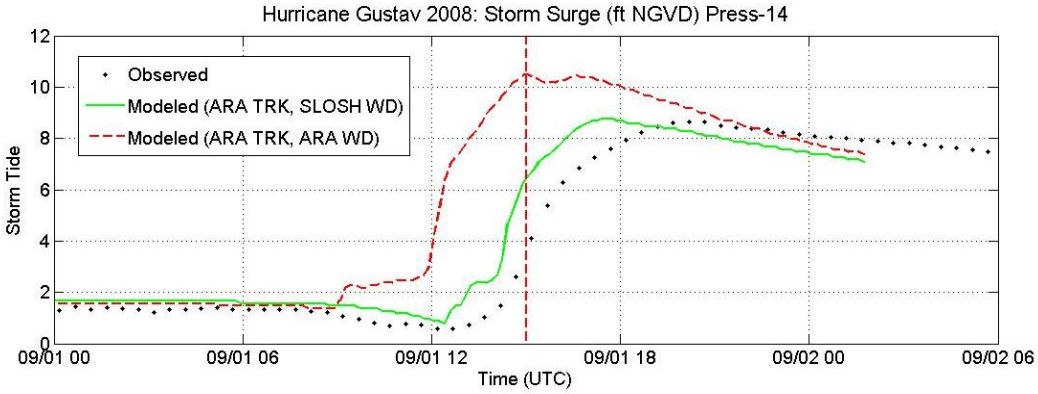

Figure X-4w. Tide gauge record at Press-14 compared to the simulated time history of Storm Tide in the SLOSH Grid cell containing the gauge location

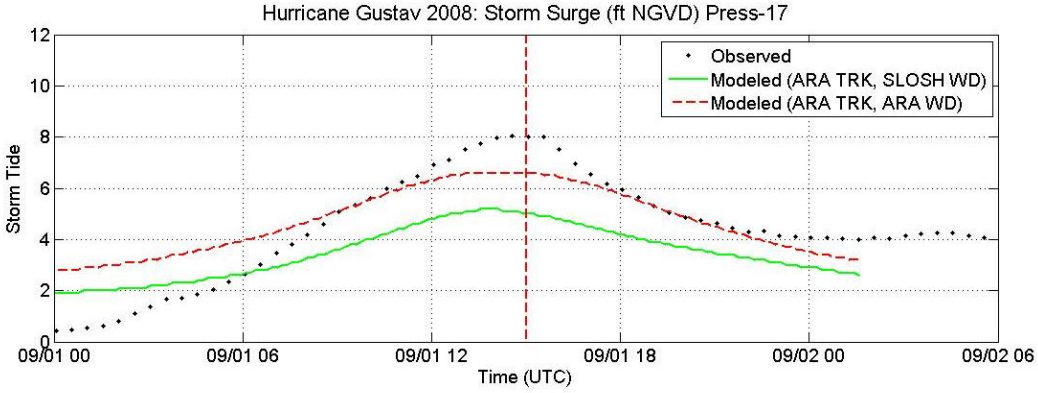

Figure X-4x. Tide gauge record at Press-17 compared to the simulated time history of Storm Tide in the SLOSH Grid cell containing the gauge location

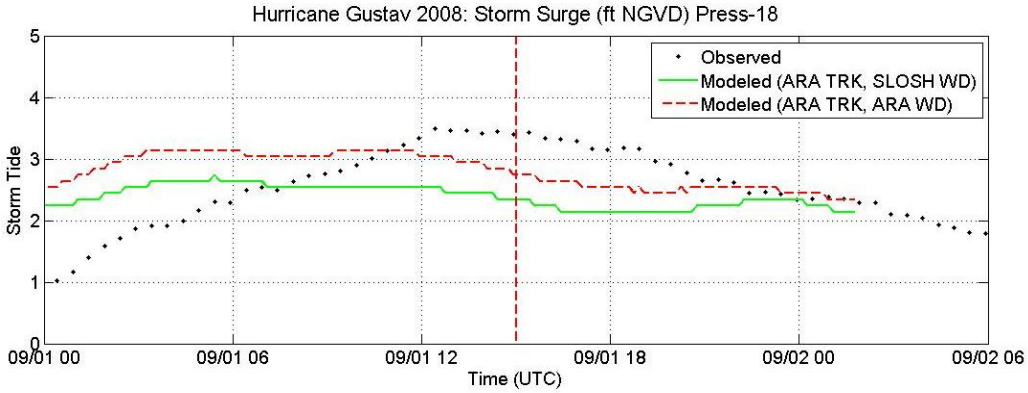

Figure X-4y. Tide gauge record at Press-18 compared to the simulated time history of Storm Tide in the SLOSH Grid cell containing the gauge location

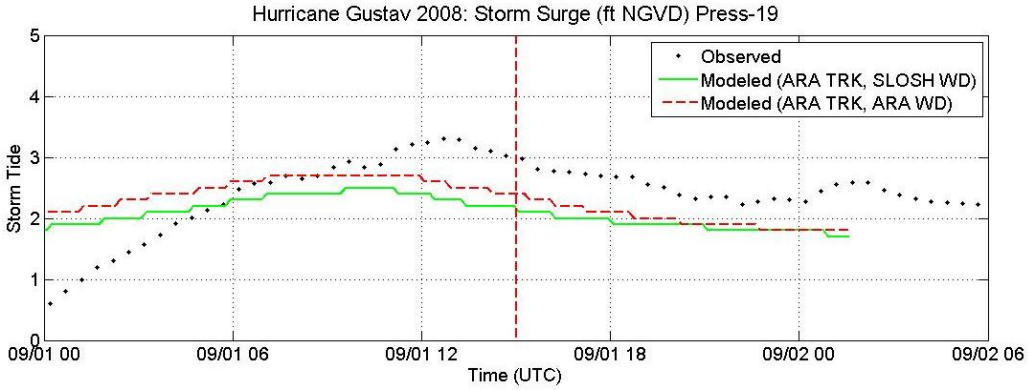

Figure X-4z. Tide gauge record at Press-19 compared to the simulated time history of Storm Tide in the SLOSH Grid cell containing the gauge location

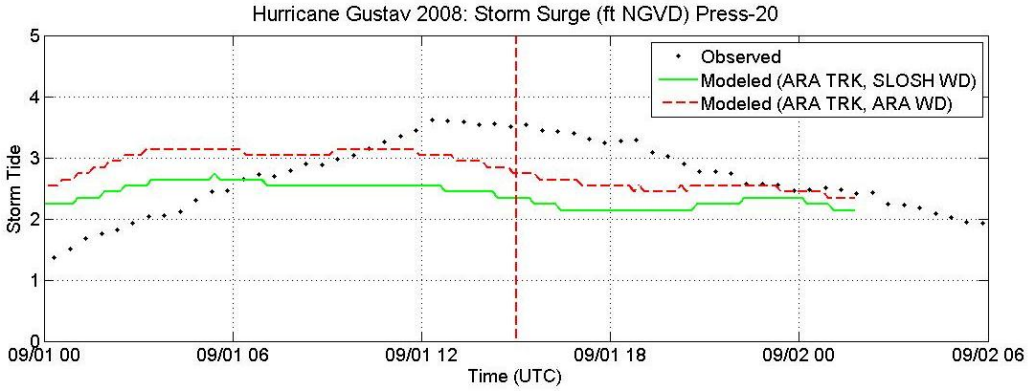

Figure X-4aa. Tide gauge record at Press-20 compared to the simulated time history of Storm Tide in the SLOSH Grid cell containing the gauge location

Table X-3. Error Analysis of Storm Tide for Hurricane Gustav

Station	Surge Range	Numer Data	Obs		SLOSH-Obs (ft NGVD)		ARA-Obs (ft NGVD)	
			Mean	Std	mean	RMS	mean	RMS
SSS-LA-JEF-013	0-3	707	2.2	0.5	0.1	0.5	0.3	0.4
	3-6	839	3.8	0.5	-1.1	1.2	0.0	0.6
	all	1546	3.0	0.9	-0.6	0.9	0.2	0.5
SSS-LA-LAF-006	0-3	466	1.6	0.2	0.2	0.6	0.6	0.9
	3-6	548	4.9	0.8	1.2	2.0	0.7	1.2
	6-9	232	6.4	0.2	0.5	1.0	-0.2	0.5
	all	1246	3.9	2.0	0.7	1.4	0.5	1.0
SSS-LA-LAF-007	0-3	315	2.6	0.3	-0.6	1.0	-0.1	0.3
	3-6	694	4.0	0.7	-0.2	0.9	-0.2	0.6
	6-9	237	6.8	0.4	1.7	1.7	0.2	0.7
	all	1246	4.2	1.5	0.1	1.1	-0.1	0.5
SSS-LA-ORL-001	3-6	655	3.9	0.7	-2.2	2.3	-1.6	1.6
	6-9	621	7.3	0.8	-3.1	3.2	-2.2	2.3
	9-12	269	9.8	0.5	-5.1	5.3	-3.6	3.7
	all	1545	6.3	2.4	-3.1	3.3	-2.2	2.4
SSS-LA-ORL-002	0-3	1009	2.2	0.5	-0.2	0.7	0.0	0.3
	3-6	535	3.8	0.6	-1.3	1.4	0.2	0.7
	all	1544	2.8	0.9	-0.6	1.0	0.1	0.5

(continued on next page)

Table X-3. Error Analysis of Storm Tide for Hurricane Gustav (Continued)

Station	Surge Range	Numer Data	Obs		SLOSH-Obs (ft NGVD)		ARA-Obs (ft NGVD)	
			Mean	Std	mean	RMS	mean	RMS
SSS-LA-ORL-008	0-3	405	2.6	0.2	-0.9	0.9	-0.5	0.6
	3-6	317	4.7	0.9	-2.2	2.3	-1.0	1.0
	6-9	299	7.3	0.8	-3.5	3.6	-2.5	2.6
	9-12	427	10.9	0.9	-5.8	5.8	-4.5	4.5
	12-15	98	12.1	0.1	-6.0	6.0	-5.0	5.0
	all	1546	6.8	3.5	-3.3	3.9	-2.4	3.0
SSS-LA-ORL-010	0-3	1207	1.8	0.4	0.3	0.5	0.6	0.8
	3-6	339	3.9	0.4	-1.0	1.0	0.9	0.9
	all	1546	2.3	1.0	0.0	0.7	0.7	0.8
SSS-LA-ORL-013	3-6	461	5.0	0.3	-2.9	2.9	-1.6	1.6
	6-9	345	7.7	0.9	-3.4	3.5	-1.8	1.9
	9-12	287	10.4	0.9	-4.8	4.9	-3.5	3.6
	12-15	453	13.6	0.7	-6.6	6.6	-5.3	5.3
	all	1546	9.1	3.5	-4.4	4.7	-3.1	3.5
SSS-LAL-PLA-004	0-3	1017	1.2	0.5	2.1	2.8	3.3	3.9
	3-6	126	4.1	0.8	2.0	2.4	3.1	3.4
	6-9	403	8.1	0.5	-4.0	4.1	-3.7	3.8
	all	1546	3.2	3.0	0.5	3.1	1.5	3.8
SSS-LA-TER-024	0-3	483	0.7	0.6	0.5	0.7	0.8	0.8
	3-6	484	4.4	1.0	0.5	0.8	0.2	0.7
	6-9	157	6.2	0.1	0.4	0.6	-0.8	0.8
	all	1124	3.0	2.3	0.5	0.7	0.3	0.8
SSS-LA-TER-025	0-3	982	1.5	0.6	2.1	2.7	1.8	2.0
	3-6	264	3.4	0.1	2.8	2.8	1.9	1.9
	all	1246	1.9	0.9	2.3	2.7	1.8	2.0
Press_1*	0-3	40	1.7	0.7	-0.6	1.1	0.0	0.6
	3-6	12	4.2	0.5	-1.0	1.3	-1.2	1.3
	all	52	2.3	1.2	-0.7	1.2	-0.3	0.8
Press_2*	0-3	31	1.3	0.8	0.0	0.6	0.0	0.5
	3-6	9	4.1	0.7	0.8	0.8	-0.6	0.8
	all	40	1.9	1.4	0.2	0.7	-0.1	0.5
Press_4*	0-3	38.0	1.0	0.7	-0.6	1.0	0.0	0.7
	all	38.0	1.0	0.7	-0.6	1.0	0.0	0.7
Press_5*	0-3	40	1.0	0.5	-0.3	0.9	0.2	0.6
	all	40	1.0	0.5	-0.3	0.9	0.2	0.6
Press_6*	0-3	34	0.9	0.6	0.5	1.0	0.4	0.7
	all	34	0.9	0.6	0.5	1.0	0.4	0.7
Press_7*	0-3	40	1.2	0.7	0.4	0.8	0.3	0.5
	all	40	1.2	0.7	0.4	0.8	0.3	0.5
Press_8*	0-3	32	1.8	0.6	-0.3	0.7	0.1	0.7
	3-6	17	4.4	0.8	-0.9	1.1	-1.0	1.3
	6-9	2	6.2	0.1	-0.6	0.6	-2.1	2.1
	all	51	2.9	1.6	-0.5	0.8	-0.4	1.0

Table X-3. Error Analysis of Storm Tide for Hurricane Gustav (Continued)

Station	Surge Range	Numer Data	Obs		SLOSH-Obs (ft NGVD)		ARA-Obs (ft NGVD)	
			Mean	Std	mean	RMS	mean	RMS
Press_9*	0-3	35	1.8	0.6	0.2	0.5	0.5	0.7
	3-6	10	4.5	1.0	0.6	0.6	0.2	0.6
	6-9	7	6.5	0.2	1.2	1.2	0.1	0.5
	all	52	3.0	1.9	0.4	0.7	0.4	0.6
Press_11*	0-3	30	1.2	1.0	0.7	1.0	1.1	1.4
	3-6	13	4.1	0.8	-0.2	0.5	-0.2	0.4
	6-9	9	7.0	0.5	0.9	0.9	-0.6	0.6
	all	52	2.9	2.4	0.5	0.9	0.5	1.1
Press_12*	0-3	25	2.3	0.6	-0.2	0.8	0.1	0.9
	3-6	27	3.9	0.6	-0.6	0.7	-0.3	0.5
	all	52	3.2	1.0	-0.4	0.7	-0.1	0.7
Press_13*	3-6	12	4.8	0.9	-2.4	2.5	-1.0	1.1
	6-9	20	6.9	0.9	-2.3	2.7	-1.4	1.5
	9-12	10	10.3	0.9	-4.1	4.3	-2.7	2.7
	12-15	9	13.1	0.6	-5.4	5.4	-3.9	3.9
	all	51	8.2	3.1	-3.2	3.6	-2.0	2.3
Press_14*	0-3	30	1.2	0.4	0.5	0.8	1.8	3.2
	3-6	2	4.7	0.9	2.3	2.3	5.6	5.6
	6-9	20	8.0	0.6	-0.1	0.8	0.9	1.6
	all	52	4.0	3.4	0.4	0.9	1.6	2.9
Press_17*	0-3	13	1.4	0.8	0.9	1.0	1.9	2.0
	3-6	25	4.6	0.8	-1.2	1.2	-0.1	0.5
	6-9	14	7.2	0.7	-2.4	2.4	-0.9	1.0
	all	52	4.5	2.3	-1.0	1.6	0.2	1.1
Press_18*	0-3	33	2.3	0.5	0.1	0.5	0.5	0.8
	3-6	18	3.3	0.1	-1.0	1.0	-0.5	0.5
	all	51	2.7	0.6	-0.3	0.7	0.1	0.7
Press_19*	0-3	43	2.3	0.6	-0.2	0.6	0.0	0.6
	3-6	8	3.2	0.1	-0.9	0.9	-0.6	0.6
	all	51	2.4	0.6	-0.3	0.6	-0.1	0.6
Press_20*	0-3	30	2.4	0.4	0.0	0.5	0.4	0.7
	3-6	21	3.4	0.2	-1.0	1.0	-0.6	0.6
	all	51	2.8	0.6	-0.4	0.8	0.0	0.6
all stations	0-3	7085	1.7	0.7	0.6	1.6	0.9	1.8
	3-6	5436	4.2	0.8	-0.7	1.8	-0.1	1.2
	6-9	2366	7.3	0.9	-2.2	3.1	-1.9	2.3
	9-12	993	10.5	0.9	-5.3	5.4	-4.0	4.0
	12-15	560	13.3	0.8	-6.4	6.5	-5.2	5.2
	all	16440	4.3	3.1	-0.8	2.6	-0.3	2.1

* Observed data provided by Andrew Kennedy

Appendix Y. Comparison of Observed and SLOSH Model Computed Storm Tides for Hurricane Ike (2008) Along the Coast of Texas

This appendix compares storm tide estimates from SLOSH to high water marks (HWMs) and tide gauge data from Hurricane Ike. Ike made landfall on the coast of Texas around 0700 UTC September 13, 2008 as a Category 2 hurricane (Berg 2009). The hurricane caused severe storm surge along the northern Gulf Coast of Texas.

Observation data

HWMs were collected from FEMA's Texas Hurricane Ike Coastal High Water Mark (HWM) collection (2008). Only the HWM associated with Coastal Stillwater are considered for the validation study since SLOSH does not compute the rise in water due to wave set up or wave run up. The reference datum for the HWM is NAVD 88.

Before the landfall of Hurricane Ike on Texas coast, the USGS deployed a mobile monitoring network consisting 117 pressure transducers (i.e., surge sensors) at 65 sites to measure the inland storm surge and coastal flooding due to Ike. The data obtained from these sensors are reported in East et al. (2008). The sensor sites were assigned a category as surge, riverine, and beach/wave. The time histories at 20 surge sites are used for this validation study. The water elevations reported for these stations were measured with respect to North American Vertical Datum of 1988 (NAVD).

Hydrographic records associated with the passage of Hurricane Ike were observed at 10 tide gauges (NOAA, 2003). Three tide gauge records are incomplete due to a malfunction or loss of the gauge. In addition, 7 water level records provided by Dr. Andrew Kennedy of the University of Notre Dame are included in the validation.

Observed storm tide data throughout the impacted area are compared to the results of the SLOSH model runs for same locations. The locations of the selected sites are listed in Table Y-1, and shown in Figure Y-1 along with the storm track positions used in the model.

SLOSH Basins and Initial Water Levels

Four SLOSH basins are selected for the validation study since all of the observation stations/sites listed in Table Y-1 are located within these basins, and Ike either crossed these basins or passed nearby. The selected SLOSH basins are: Galveston Bay, Sabine Lake, Vermilion Bay and New Orleans.

The reference datum for the Galveston Bay and Vermilion Bay SLOSH basins is NGVD 1929, while the reference datum for the Sabine Lake and the New Orleans basins is NAVD 1988. The average mean sea level change from the year 1929 to the year 2008 is calculated based on

several NOAA stations located along the Gulf coast: Grand Isle, Eugene Island, Sabine Pass, Galveston, Freeport, Dauphin Island, Pensacola, Panama city and Apalachicola. The average mean sea level change calculated from these stations is +1.25 ft. Using NOAA tide and currents website (NOAA 2010), the predicted tide level at time of landfall was approximately +0.5 ft. A pre-storm tide anomaly of approximately +1.0 ft was observed for some these stations or nearby NOAA stations. Thus, the total initial water level is +2.7 ft-NGVD for the Galveston Bay and Vermilion Bay basins and +2.6 ft-NAVD for the Sabine Lake and New Orleans basins.

Methodology

SLOSH is a grid based numerical storm surge model that computes water elevations generated by the wind and pressure forces in tropical cyclones. The time history of the water elevation is saved in individual elements of the basin grid and the maximum value for each grid cell is termed as the Envelope of High Water (EOHW). The observed storm surge elevation is compared to the EOHW in the nearest grid cells, and the observed hydrographic records associated with the passage of Hurricane Ike at tide gauges are compared to the SLOSH model-generated storm surge hydrographs in the nearest grid cells.

Model runs using the SLOSH wind model and the ARA wind model are compared to the observed data. Where multiple basins contain the same observation site, the basin with minimum distance from the basin center to observation site, usually the basin with smaller grid cells (i.e. finer resolution) at the observation site, is used to compare against observed data. These values along with the observed values are given in Table Y-1.

Results

Figure Y-2 shows the comparisons of observed and simulated storm tide values using the SLOSH wind model and the ARA wind model. Linear regression lines with zero intercepts are also shown in the figure along with R^2 values and the regression equations. On average, the SLOSH wind model and the ARA wind model tend to overestimate the observed data by about 5% and 10%, respectively.

Histograms of the differences (simulated minus observed) were shown in Figure Y-3. The error characteristics were indicated in the legend. The mean errors are +0.4 and +1.1 feet for model runs using SLOSH wind model and using ARA wind model, respectively; however, the standard deviation of the errors from the ARA wind model results are smaller than the standard deviations of the errors from the SLOSH wind model results.

Figure Y-4 shows the time histories obtained for the surge sites using SLOSH-wind model and ARA-wind model and compared with the observed time history. In general, the magnitudes and timing of the modeled results are in reasonably good agreement with the observations. However, significant underestimates are noted at SSS-TX-GAL-001 and SSS-TX-GAL-011, and

significant overestimates are noted at SSS-TX-GAL-019, SSS-TX-JEF-008, and SSS-LA-CAM-003.

Table Y-2 summarizes the mean and RMS errors of the storm tide time histories for Hurricane Ike. The overall results show that the model runs with ARA wind field model produce slightly smaller mean errors and slightly smaller RMS errors than the model runs using the SLOSH wind model.

Conclusions

For Hurricane Ike, the SLOSH wind model and ARA wind model produce average underestimates of the observed storm tides of 5% and 10%, respectively; however, the standard deviation of the errors from the ARA wind model results are smaller than the standard deviations of the errors from the SLOSH wind model results. The model runs with ARA wind field model generally produce slightly smaller mean time history errors and slightly smaller RMS time history errors than the model runs using the SLOSH wind model.

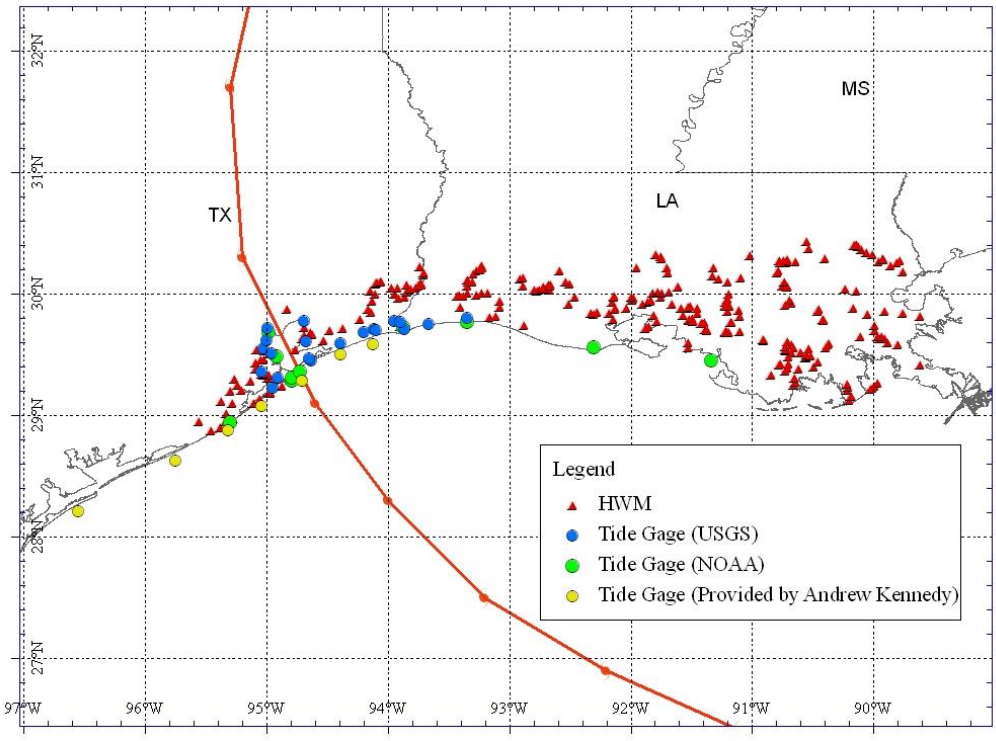

Figure Y-1. Locations of Observation Stations for Hurricane Ike

Table Y-1. Observed and Simulated Storm Tide – Hurricane Ike

FEMA						
No	ID	Lat	Lon	Obs (ft NAVD)	ARA-TRK SLOSH_WD	ARA-TRK ARA_WD
1	353-ITX-02-027	29.30300	-95.26680	6.6	5.9	6.3
2	353-ITX-02-028	29.24790	-95.23630	6.9	5.9	6.3
3	353-ITX-02-029	29.19660	-95.29890	8.8	5.7	6.8
4	353-ITX-02-030	29.11270	-95.37450	5.1	6.1	4.0
5	353-ITX-02-031	28.94900	-95.55530	5.3	2.9	5.3
6	353-ITX-02-032	28.87780	-95.45580	5.5	3.2	6.2
7	353-ITX-02-033	28.89810	-95.38070	7.2	5.8	6.4
8	353-ITX-02-034	28.95060	-95.33840	6.6	3.9	6.9
9	353-ITX-02-035	28.93950	-95.29720	7.3	6.5	7.0
10	353-ITX-02-036	28.94290	-95.29990	7.7	6.4	6.6
11	353-ITX-02-037	28.95380	-95.28200	10.7	6.9	8.0
12	353-ITX-02-038	28.96200	-95.29080	7.7	6.5	8.0
13	353-ITX-04-011	28.93010	-95.31300	8.3	6.6	7.1
14	353-ITX-04-013	28.93540	-95.30380	7.8	6.4	6.6
15	353-ITX-04-014	28.94840	-95.29240	8.0	6.5	7.0
16	353-ITX-04-015	28.96260	-95.27340	9.2	6.9	8.0
17	353-ITX-04-016	29.01360	-95.33080	6.7	5.7	7.2
18	353-ITX-04-017	29.09550	-95.28390	6.3	4.0	4.2
19	353-ITX-04-018	29.20980	-95.21050	6.4	5.9	6.3
20	353-ITX-04-019	29.28450	-95.12940	9.4	8.0	8.0
21	353-ITX-03-001	29.87550	-94.82950	14.8	15.0	15.9
22	353-ITX-03-009	29.65840	-94.68950	13.5	12.9	13.0
23	353-ITX-03-010	29.72820	-94.69020	16.6	15.0	15.0
24	353-ITX-03-011	29.68160	-94.64120	11.6	14.8	14.9
25	353-ITX-03-012	29.66350	-94.62410	15.4	15.5	15.7
26	353-ITX-03-013	29.53800	-94.76140	10.5	11.7	11.7
27	353-ITX-03-015	29.63200	-94.70230	15.3	12.4	12.4
28	353-ITX-03-016	29.61350	-94.53320	14.5	15.5	15.3
29	353-ITX-03-019	29.71490	-94.37550	16.9	19.2	18.4
30	353-ITX-03-020	29.70400	-94.48370	17.5	18.8	18.8
31	353-ITX-02-001	29.09570	-95.10970	10.3	7.6	8.0
32	353-ITX-02-002	29.12990	-95.05850	7.9	8.0	8.3
33	353-ITX-02-004	29.18940	-94.97770	10.8	8.8	9.1
34	353-ITX-02-005	29.24450	-94.87430	10.5	9.7	9.7
35	353-ITX-02-011	29.30730	-94.79410	12.0	11.3	11.4
36	353-ITX-02-014	29.29520	-94.91680	11.9	10.2	10.7
37	353-ITX-02-015	29.30030	-94.91520	11.8	10.2	10.7
38	353-ITX-02-019	29.45780	-95.02100	11.4	10.9	13.7
39	353-ITX-02-020	29.45720	-95.04750	10.4	10.9	13.7
40	353-ITX-02-021	29.43650	-95.09220	10.9	8.7	13.7
41	353-ITX-02-022	29.38100	-95.08910	13.4	8.0	8.8
42	353-ITX-02-023	29.34220	-95.03680	10.3	8.0	8.8
43	353-ITX-02-024	29.30430	-94.98760	12.2	9.3	10.1

Table Y-1. Observed and Simulated Storm Tide – Hurricane Ike (Continued)

No	ID	Lat	Lon	Obs (ft NAVD)	ARA-TRK SLOSH_WD	ARA-TRK ARA_WD
44	353-ITX-02-025	29.33480	-94.97790	10.9	9.2	10.0
45	353-ITX-04-004	29.13150	-95.05880	9.4	8.0	8.3
46	353-ITX-04-008	29.18660	-94.96550	10.7	8.8	9.1
47	353-ITX-04-020	29.33550	-95.02240	10.4	8.0	8.8
48	353-ITX-04-021	29.33710	-95.02440	10.6	8.0	8.8
49	353-ITX-04-029	29.53560	-95.01150	15.4	11.9	13.6
50	353-ITX-04-030	29.51170	-94.97880	15.2	11.9	13.4
51	353-ITX-04-031	29.50070	-94.93470	12.4	11.7	12.7
52	353-ITX-04-022	29.61550	-94.99800	12.8	11.9	13.0
53	353-ITX-04-024	29.56520	-95.01700	12.9	11.8	13.4
54	353-ITX-04-026	29.53860	-95.08510	10.9	9.1	11.6
55	353-ITX-01-006	29.97200	-93.86330	11.8	17.4	16.4
56	353-ITX-01-016	30.09630	-94.09330	11.1	19.7	18.1
57	353-ITX-01-019	29.99640	-93.94980	11.8	18.1	16.8
58	353-ITX-01-020	29.96890	-93.91340	11.5	17.7	16.5
59	353-ITX-03-021	29.87850	-94.16040	9.4	20.8	19.5
60	353-ITX-03-022	29.84940	-94.13500	11.3	19.8	18.5
61	353-ITX-03-023	29.73090	-93.89710	13.0	16.1	14.7
62	353-ITX-03-025	29.79450	-94.22790	13.6	20.1	18.9
63	353-ITX-03-026	29.94340	-94.13020	9.2	21.7	20.3
64	353-ITX-03-027	29.99650	-94.10650	9.6	22.7	21.4
65	353-ITX-03-028	30.08180	-94.09320	11.6	19.5	17.9
66	353-ITX-03-029	30.02790	-94.14910	8.8	24.0	22.6
67	353-ITX-01-008	30.01810	-93.84860	10.2	17.8	16.9
68	353-ITX-01-009	30.01540	-93.83700	13.1	17.7	16.8
69	353-ITX-01-010	30.09150	-93.72680	8.7	17.6	16.7
70	353-ITX-01-011	30.07730	-93.74480	9.6	17.7	16.8
71	353-ITX-01-012	30.07410	-93.72360	9.3	17.4	16.6
72	353-ITX-01-013	30.07480	-93.84930	11.8	18.7	17.9
73	353-ITX-01-014	30.05070	-93.91840	12.9	18.8	17.7
74	353-ITX-01-015	30.09720	-94.06710	10.8	19.6	18.0
75	353-ITX-01-018	30.05350	-93.97350	12.7	19.1	17.8
76	353-ITX-01-021	30.22700	-93.73790	9.9	19.5	18.6
77	353-ITX-01-022	30.15640	-93.70770	7.7	18.3	17.5
78	353-ITX-01-023	30.17740	-93.70740	8.3	18.6	17.7
79	353-ITX-01-024	30.04750	-93.77160	10.8	17.5	16.6
80	353-ITX-01-025	30.06600	-93.74560	9.4	17.6	16.7
81	353-ITX-01-026	30.04520	-93.81390	10.7	18.0	17.2
82	353-ITX-01-027	30.09570	-94.08930	10.9	19.7	18.1
83	353-ITX-01-028	30.09640	-94.05730	11.7	19.5	18.0
84	401-ILA-02-011	30.18980	-92.58980	3.5	4.1	4.2
85	401-ILA-05-005	30.10320	-93.33610	8.7	13.4	12.8
86	401-ILA-05-006	30.11400	-93.34170	9.2	13.5	12.9
87	401-ILA-05-007	30.06590	-93.34840	5.6	13.3	12.7
88	401-ILA-05-013	30.19100	-93.26800	5.5	12.9	12.6

Table Y-1. Observed and Simulated Storm Tide – Hurricane Ike (Continued)

No	ID	Lat	Lon	Obs (ft NAVD)	ARA-TRK SLOSH_WD	ARA-TRK ARA_WD
89	401-ILA-05-014	30.16890	-93.29850	9.2	13.1	12.7
90	401-ILA-05-015	30.10430	-93.30630	9.3	13.3	12.7
91	401-ILA-05-022	30.12960	-92.90770	4.5	9.6	10.1
92	401-ILA-05-027	30.23660	-93.23000	9.6	12.9	12.6
93	401-ILA-05-028	30.21930	-93.22330	8.4	12.8	12.6
94	401-ILA-05-029	30.21100	-93.23560	9.3	12.8	12.5
95	401-ILA-05-030	30.20360	-93.23930	9.2	12.7	12.5
96	401-ILA-05-008	30.00490	-93.34330	8.9	12.9	12.2
97	401-ILA-05-009	29.99070	-93.40920	8.9	13.5	12.8
98	401-ILA-05-010	29.89040	-93.40200	9.7	12.9	11.9
99	401-ILA-05-016	30.01080	-93.22740	7.4	12.0	11.4
100	401-ILA-05-018	29.93820	-93.07970	3.8	10.5	10.0
101	401-ILA-05-019	29.89430	-93.07960	6.1	10.5	9.9
102	401-ILA-05-020	29.81540	-93.11430	8.7	11.1	10.2
103	401-ILA-05-026	29.76480	-93.88100	11.7	16.1	14.3
104	401-ILA-05-031	30.00930	-93.18200	7.0	11.9	11.4
105	401-ILA-05-032	29.98860	-93.26630	9.6	12.3	11.6
106	401-ILA-05-033	29.80850	-93.16550	9.0	11.5	10.6
107	401-ILA-05-038	29.74400	-92.87780	8.0	9.4	8.8
108	401-ILA-05-042	30.02240	-92.76880	3.2	7.9	8.3
109	401-ILA-05-043	30.03210	-92.79260	2.3	8.2	8.5
110	401-ILA-05-044	29.98370	-93.37500	9.4	13.0	12.3
111	401-ILA-05-045	29.98390	-93.42750	8.7	13.6	12.8
112	401-ILA-05-004	30.06940	-92.88420	3.6	9.0	9.4
113	401-ILA-05-023	30.13760	-92.88640	3.5	9.5	10.2
114	401-ILA-02-009	30.08170	-92.50620	3.8	9.2	10.4
115	401-ILA-03-005	30.00060	-91.19320	4.1	2.5	2.5
116	401-ILA-03-006	29.95700	-91.20200	3.1	3.1	3.4
117	401-ILA-03-007	29.90080	-91.18610	2.9	2.9	3.0
118	401-ILA-03-008	29.86640	-91.10810	2.9	2.5	2.5
119	401-ILA-03-012	29.93660	-91.22130	3.1	2.5	2.5
120	401-ILA-05-040	30.03180	-92.75130	3.3	10.8	11.4
121	401-ILA-05-041	30.03770	-92.67180	3.0	10.3	10.8
122	401-ILA-02-002	30.06170	-91.60860	4.7	3.1	3.3
123	401-ILA-02-025	30.05810	-91.60780	5.2	2.7	2.7
124	401-ILA-02-026	29.95190	-91.98490	8.2	8.2	10.3
125	401-ILA-02-027	29.96750	-91.97810	6.4	7.8	10.6
126	401-ILA-02-028	29.94720	-91.98400	8.2	8.2	10.3
127	401-ILA-02-029	29.94900	-91.98860	8.5	8.2	10.3
128	401-ILA-02-030	29.91460	-91.90450	8.4	7.6	9.6
129	401-ILA-02-032	29.93450	-91.86350	7.2	7.5	9.7
130	401-ILA-02-034	29.94970	-91.83590	8.5	7.6	9.8
131	401-ILA-02-035	29.93820	-91.83380	8.1	7.4	9.6
132	401-ILA-02-038	29.82650	-91.80810	8.9	7.0	8.9
133	401-ILA-02-039	29.91450	-91.66220	5.1	2.9	9.3

Table Y-1. Observed and Simulated Storm Tide – Hurricane Ike (Continued)

No	ID	Lat	Lon	Obs (ft NAVD)	ARA-TRK SLOSH_WD	ARA-TRK ARA_WD
134	401-ILA-02-040	29.97890	-91.75390	5.3	7.0	9.3
135	401-ILA-02-041	30.01110	-91.74330	5.5	2.7	2.7
136	401-ILA-02-042	30.01920	-91.68080	4.5	2.7	2.7
137	401-ILA-02-044	30.00600	-91.81700	5.3	7.6	10.4
138	401-ILA-02-045	30.01610	-91.77390	5.0	2.7	2.7
139	401-ILA-01-007	30.21930	-91.31770	5.9	2.6	2.6
140	401-ILA-01-018	30.13480	-91.09320	3.2	2.6	2.6
141	401-ILA-01-019	30.10340	-91.19840	4.3	2.6	2.6
142	401-ILA-01-021	30.12640	-91.27610	3.3	2.6	2.6
143	401-ILA-01-022	30.15020	-91.32780	5.1	2.7	2.9
144	401-ILA-02-010	30.07270	-92.65940	3.3	10.2	10.7
145	401-ILA-05-001	30.07330	-92.66070	4.0	10.2	10.7
146	401-ILA-05-002	30.07520	-92.67710	3.8	10.2	10.7
147	401-ILA-05-003	30.05700	-92.71940	3.3	10.6	11.1
148	401-ILA-02-004	30.21920	-91.95590	8.0	3.0	3.0
149	401-ILA-01-002	30.06910	-90.74990	3.3	3.3	3.9
150	401-ILA-01-013	30.05660	-90.71160	3.4	3.3	3.9
151	401-ILA-01-014	30.05610	-90.71100	3.3	3.3	3.9
152	401-ILA-01-015	29.92240	-90.67200	2.5	3.2	3.4
153	401-ILA-01-016	29.95390	-90.69200	2.4	3.2	3.7
154	401-ILA-01-017	29.91140	-90.72880	2.2	2.4	2.4
155	401-ILA-02-014	30.32430	-91.79000	8.4	2.7	2.7
156	401-ILA-02-017	30.30530	-91.75360	7.4	2.9	2.8
157	401-ILA-02-018	30.29140	-91.74520	7.2	2.9	2.8
158	401-ILA-02-021	30.21800	-91.69790	5.3	3.8	4.0
159	401-ILA-02-022	30.17580	-91.69080	5.5	3.6	3.9
160	401-ILA-03-001	29.81580	-91.10330	3.0	2.5	2.5
161	401-ILA-03-003	29.85570	-91.19800	9.3	4.0	5.5
162	401-ILA-03-004	29.90830	-91.21650	3.1	3.6	5.1
163	401-ILA-03-009	29.76790	-91.16530	2.6	2.7	2.7
164	401-ILA-03-010	29.76400	-91.17580	8.0	4.1	5.8
165	401-ILA-03-011	29.90270	-91.21340	9.7	3.6	5.1
166	401-ILA-02-036	29.73420	-91.85230	9.3	7.1	8.4
167	401-ILA-02-037	29.71430	-91.87690	10.6	7.1	8.3
168	401-ILA-03-056	29.68960	-91.09970	7.3	2.6	2.5
169	401-ILA-03-057	29.68700	-91.18870	6.7	4.6	6.0
170	401-ILA-03-058	29.68280	-91.19230	4.2	4.4	6.0
171	401-ILA-03-059	29.69540	-91.21040	6.9	5.0	5.9
172	401-ILA-03-060	29.69340	-91.21620	6.8	4.2	5.9
173	401-ILA-03-061	29.68540	-91.21880	7.4	4.2	5.9
174	401-ILA-03-062	29.90210	-91.51350	6.7	3.8	4.9
175	401-ILA-03-063	29.87950	-91.45440	4.7	3.8	5.1
176	401-ILA-03-064	29.76440	-91.39400	9.7	4.2	5.6
177	401-ILA-03-065	29.75850	-91.40780	4.8	4.2	5.6
178	401-ILA-03-066	29.71040	-91.38190	5.1	2.3	3.9

Table Y-1. Observed and Simulated Storm Tide – Hurricane Ike (Continued)

No	ID	Lat	Lon	Obs (ft NAVD)	ARA-TRK SLOSH_WD	ARA-TRK ARA_WD
179	401-ILA-03-067	29.70100	-91.37110	6.4	4.6	5.8
180	401-ILA-03-068	29.76220	-91.41930	5.1	2.6	2.5
181	401-ILA-08-029	29.71270	-91.87710	10.2	7.1	8.3
182	401-ILA-08-030	29.77110	-91.78480	8.7	6.9	8.5
183	401-ILA-08-032	29.78820	-91.51900	6.0	5.7	8.0
184	401-ILA-08-034	29.78670	-91.51730	6.9	5.7	8.0
185	401-ILA-08-037	29.82910	-91.56640	6.3	6.0	8.2
186	401-ILA-08-038	29.88700	-91.52270	4.4	3.8	4.9
187	401-ILA-08-039	29.89000	-91.52460	4.0	3.9	4.9
188	401-ILA-08-040	29.84070	-91.45480	5.5	2.5	5.9
189	401-ILA-08-042	29.87950	-91.58580	4.7	6.2	8.6
190	401-ILA-08-044	29.55900	-91.52510	8.1	5.9	6.8
191	401-ILA-08-045	29.60170	-91.52470	6.2	5.9	6.9
192	401-ILA-08-048	29.78740	-91.49530	5.1	5.6	7.9
193	401-ILA-08-049	29.79760	-91.49680	6.7	5.6	7.5
194	401-ILA-08-050	29.77200	-91.48140	5.3	5.4	7.6
195	401-ILA-03-015	29.58530	-90.67740	5.3	4.0	6.1
196	401-ILA-03-016	29.55450	-90.65920	6.0	4.2	6.6
197	401-ILA-03-020	29.51910	-90.67530	6.0	4.4	6.3
198	401-ILA-03-022	29.48220	-90.69830	6.4	4.4	6.2
199	401-ILA-03-023	29.42540	-90.70200	7.1	4.3	5.8
200	401-ILA-03-024	29.39460	-90.71200	7.0	4.3	5.8
201	401-ILA-03-025	29.36890	-90.72310	6.9	4.2	5.7
202	401-ILA-03-026	29.25320	-90.66000	7.6	5.1	6.2
203	401-ILA-03-027	29.27700	-90.64400	7.7	5.0	6.1
204	401-ILA-03-028	29.30470	-90.64800	7.3	4.7	6.0
205	401-ILA-03-029	29.38380	-90.61970	6.9	4.2	5.7
206	401-ILA-03-030	29.47370	-90.55750	3.3	3.8	5.9
207	401-ILA-03-042	29.51330	-90.59600	5.5	4.4	6.4
208	401-ILA-03-043	29.51610	-90.59780	5.5	4.4	6.4
209	401-ILA-03-044	29.53700	-90.71440	4.7	4.0	6.0
210	401-ILA-03-045	29.54470	-90.72340	3.9	4.0	6.0
211	401-ILA-03-046	29.60500	-90.70500	3.9	3.7	5.8
212	401-ILA-03-048	29.56920	-90.72520	4.0	2.4	5.9
213	401-ILA-03-049	29.42820	-90.76440	5.9	3.9	5.5
214	401-ILA-03-050	29.41690	-90.77600	5.7	3.9	5.5
215	401-ILA-03-052	29.33600	-90.84240	5.7	4.1	5.5
216	401-ILA-03-053	29.61630	-90.90220	3.8	2.1	5.3
217	401-ILA-03-054	29.62450	-90.91110	3.9	2.1	5.3
218	401-ILA-05-039	30.04350	-92.70600	4.0	10.5	11.0
219	401-ILA-08-002	29.79390	-92.14490	9.4	8.3	9.6
220	401-ILA-08-004	29.93500	-92.14940	8.0	8.5	10.2
221	401-ILA-08-005	29.88470	-92.12450	8.6	8.6	10.3
222	401-ILA-08-006	29.98350	-92.13600	8.3	8.0	10.0
223	401-ILA-08-007	29.84280	-92.18100	5.4	8.5	9.9

Table Y-1. Observed and Simulated Storm Tide – Hurricane Ike (Continued)

No	ID	Lat	Lon	Obs (ft NAVD)	ARA-TRK SLOSH_WD	ARA-TRK ARA_WD
224	401-ILA-08-008	29.84640	-92.27560	7.4	8.6	9.9
225	401-ILA-08-009	29.83160	-92.30610	5.9	8.6	9.6
226	401-ILA-08-015	29.83860	-92.32820	6.1	8.4	9.6
227	401-ILA-08-017	29.97490	-92.13950	8.1	8.0	10.0
228	401-ILA-08-018	30.04130	-92.72260	3.5	10.6	11.1
229	401-ILA-08-019	30.07130	-92.65710	3.3	10.1	10.6
230	401-ILA-08-020	30.10040	-92.53210	3.6	9.2	10.4
231	401-ILA-08-021	29.91920	-92.51380	3.2	8.6	9.7
232	401-ILA-08-022	29.97820	-92.46210	2.8	8.6	9.8
233	401-ILA-08-025	29.88250	-92.03780	7.8	8.5	10.1
234	401-ILA-08-026	29.87700	-92.12690	9.0	8.6	10.3
235	401-ILA-08-027	29.97510	-91.99400	8.8	8.1	10.6
236	401-ILA-01-006	30.19060	-90.78620	4.1	3.2	5.6
237	401-ILA-01-012	30.17350	-90.78800	3.8	3.3	5.5
238	401-ILA-01-020	30.32140	-91.02090	9.8	3.4	5.1
239	401-ILA-04-020	29.65330	-90.10630	5.2	3.2	4.5
240	401-ILA-04-022	29.88510	-90.16230	4.7	3.1	4.8
241	401-ILA-04-023	30.04200	-90.23540	4.8	4.1	4.9
242	401-ILA-04-025	30.02140	-90.14320	5.3	4.0	4.7
243	401-ILA-06-001	29.23770	-89.99230	4.9	4.2	4.5
244	401-ILA-06-002	29.26260	-89.96210	4.9	4.4	4.7
245	401-ILA-06-004	29.22560	-90.00700	4.7	4.5	4.7
246	401-ILA-06-005	29.21650	-90.02540	5.1	4.2	4.5
247	401-ILA-06-008	29.15550	-90.18340	7.6	4.2	4.5
248	401-ILA-06-009	29.12540	-90.19690	8.3	4.3	4.5
249	401-ILA-06-010	29.15770	-90.17910	8.0	4.4	4.7
250	401-ILA-06-011	29.21120	-90.21980	7.0	4.0	4.3
251	401-ILA-06-013	29.23590	-90.21040	6.7	3.8	4.4
252	401-ILA-06-014	29.25670	-90.21390	5.8	3.8	4.4
253	401-ILA-06-017	29.58920	-90.37020	4.4	3.8	4.4
254	401-ILA-06-018	29.58270	-90.37480	4.4	3.6	3.9
255	401-ILA-06-019	29.55740	-90.38900	4.3	2.6	5.4
256	401-ILA-06-020	29.55270	-90.53460	3.9	2.6	5.4
257	401-ILA-01-005	30.27490	-90.77880	4.4	3.4	5.9
258	401-ILA-07-024	30.43350	-90.54720	3.3	3.5	6.4
259	401-ILA-07-026	30.37660	-90.53720	4.0	3.4	6.3
260	401-ILA-07-028	30.26180	-90.71280	4.6	3.3	5.9
261	401-ILA-07-029	30.28380	-90.70850	4.0	3.3	5.9
262	401-ILA-07-030	30.27320	-90.71050	4.5	3.3	5.9
263	401-ILA-07-031	30.26680	-90.72890	4.4	3.3	5.9
264	401-ILA-07-032	30.27540	-90.73870	4.4	3.3	5.9
265	401-ILA-07-033	30.26100	-90.76370	3.7	3.4	5.7
266	401-ILA-07-034	30.26390	-90.64190	4.5	3.5	5.9
267	401-ILA-04-001	29.63550	-89.95270	3.7	5.1	6.4
268	401-ILA-04-004	29.69900	-89.99130	4.1	5.0	6.3

Table Y-1. Observed and Simulated Storm Tide – Hurricane Ike (Continued)

No	ID	Lat	Lon	Obs (ft NAVD)	ARA-TRK SLOSH_WD	ARA-TRK ARA_WD
269	401-ILA-04-005	29.64810	-89.96290	3.6	5.1	6.4
270	401-ILA-04-006	29.60230	-89.87840	4.3	5.1	6.4
271	401-ILA-04-008	29.41690	-89.61670	6.2	5.2	6.3
272	401-ILA-04-010	29.58610	-89.79720	10.9	5.2	6.5
273	401-ILA-04-011	29.63590	-89.90560	8.1	5.1	6.4
274	401-ILA-04-012	29.74260	-89.98720	8.4	5.0	7.7
275	401-ILA-04-013	29.64840	-89.93570	8.2	5.1	6.4
276	401-ILA-04-014	29.86030	-89.90730	9.0	4.7	5.8
277	401-ILA-04-019	29.83630	-90.04560	5.2	2.6	4.1
278	401-ILA-04-016	29.81990	-89.61120	9.4	5.0	6.5
279	401-ILA-04-017	29.84080	-89.75610	8.8	5.6	6.9
280	401-ILA-06-021	29.78910	-90.42040	3.4	3.6	4.3
281	401-ILA-06-022	29.78240	-90.40480	3.5	3.6	4.3
282	401-ILA-06-024	29.87370	-90.44890	2.7	2.6	2.8
283	401-ILA-06-025	29.86250	-90.45450	2.7	2.6	2.8
284	401-ILA-01-001	30.10180	-90.73490	3.7	3.6	3.9
285	401-ILA-07-001	30.40830	-90.14200	6.6	4.4	6.3
286	401-ILA-07-002	30.34490	-90.05340	6.3	4.3	6.0
287	401-ILA-07-004	30.36570	-90.09590	6.6	4.3	6.0
288	401-ILA-07-006	30.32910	-90.00440	4.7	4.3	5.9
289	401-ILA-07-007	30.26510	-89.95650	5.5	4.2	5.7
290	401-ILA-07-008	30.29120	-89.92790	4.6	4.2	5.9
291	401-ILA-07-009	30.28410	-89.91700	4.9	4.2	5.9
292	401-ILA-07-012	30.27950	-89.78440	4.3	4.1	5.7
293	401-ILA-07-013	30.26110	-89.80330	5.2	4.1	5.7
294	401-ILA-07-014	30.23460	-89.85530	5.1	4.1	5.6
295	401-ILA-07-016	30.18530	-89.75720	4.8	4.0	5.2
296	401-ILA-07-017	30.39430	-90.12030	6.5	4.4	6.2
297	401-ILA-07-018	30.40270	-90.15610	6.6	4.5	6.4
298	401-ILA-07-019	30.39770	-90.15620	6.6	4.4	6.3
299	401-ILA-07-021	30.28970	-90.40140	5.2	3.2	5.8
300	401-ILA-03-031	29.47400	-90.55320	3.9	4.4	5.5
301	401-ILA-03-032	29.48040	-90.55170	4.9	4.4	5.5
302	401-ILA-03-034	29.49920	-90.55120	4.6	4.0	5.6
303	401-ILA-03-037	29.39860	-90.48880	7.5	4.5	5.6
304	401-ILA-03-040	29.43940	-90.46110	7.1	4.3	5.5
305	401-ILA-03-041	29.49050	-90.51980	5.1	4.3	5.5
USGS						
306	SSS-TX-CHA-003	29.604170	-94.675280	12.7	13.1	13.1
307	SSS-TX-CHA-004	29.772780	-94.686940	15.6	14.1	15.0
308	SSS-TX-GAL-001	29.451389	-94.634167	19.1	12.0	12.0
309	SSS-TX-GAL-002	29.465830	-94.648060	13.4	12.6	12.1
310	SSS-TX-GAL-005	29.594440	-94.390280	16.1	15.7	15.0

Table Y-1. Observed and Simulated Storm Tide – Hurricane Ike (Continued)

No	ID	Lat	Lon	Obs (ft NAVD)	ARA-TRK SLOSH_WD	ARA-TRK ARA_WD
311	SSS-TX-GAL-011	29.220830	-94.944720	12.3	9.3	9.5
312	SSS-TX-GAL-016	29.303890	-94.905280	12.5	10.3	10.7
313	SSS-TX-GAL-018	29.355830	-95.040000	10.4	9.0	9.9
314	SSS-TX-GAL-019	29.506390	-94.957780	11.1	11.8	13.0
315	SSS-TX-GAL-022	29.551670	-95.024720	12.3	9.7	13.6
316	SSS-TX-HAR-002	29.620280	-94.998890	12.8	11.7	12.9
317	SSS-TX-HAR-004	29.713060	-94.993330	12.4	11.2	11.7
318	SSS-TX-JEF-001	29.684440	-94.192780	16.7	17.7	16.5
319	SSS-TX-JEF-004	29.710280	-94.116390	16.2	17.5	16.1
320	SSS-TX-JEF-005	29.696940	-94.098330	16.5	17.2	15.9
321	SSS-TX-JEF-006	29.711110	-93.860000	14.4	16.1	14.6
322	SSS-TX-JEF-007	29.773890	-93.942500	12.8	16.8	15.0
323	SSS-TX-JEF-008	29.764720	-93.897780	10.5	16.3	14.4
324	SSS-LA-CAM-001	29.750280	-93.663610	16.5	15.3	13.7
325	SSS-LA-CAM-003	29.804170	-93.348890	10.0	12.9	11.8
NOAA						
No	ID	Lat	Lon	Obs (ft NAVD)	ARA-TRK SLOSH_WD	ARA-TRK ARA_WD
326	Uscg Freeport TX	28.94333	-95.30167	7.9	6.4	6.6
327	Galveston Pleasure Pier TX	29.28500	-94.78833	11.0	11.7	11.7
328	Galveston Pirt TX	29.31000	-94.79333	10.7	11.4	11.4
329	Eagle Point TX	29.48000	-94.91833	12.6	11.9	13.1
330	Sabine Pass North TX	29.72833	-93.87000	14.6	16.0	14.7
331	Calcasieu Pass LA	29.76667	-93.34167	11.9	13.0	11.7
332	Freshwater Cannal Locks LA	29.55500	-92.30500	10.2	9.1	9.2
333	Amerada Pass LA	29.44833	-91.33667	8.5	5.3	5.9
334	Morgans Point TX	29.68167	-94.98500	N/A	11.1	11.9
335	Galveston Bay Entrance TX	29.35833	-94.72500	N/A	12.1	11.8
Nearshore Surge Data Provided by Andrew Kennedy						
No	ID	Lat	Lon	Obs (ft NAVD)	ARA-TRK SLOSH_WD	ARA-TRK ARA_WD
336	S	28.20773	-96.55037	4.8	3.6	4.8
337	U	28.62505	-95.75235	4.9	4.8	5.6
338	V	28.87040	-95.31512	5.9	6.4	6.9
339	W	29.07140	-95.03958	7.7	8.0	8.2
340	X	29.28127	-94.70895	10.3	11.0	10.0
341	Y	29.49643	-94.38840	14.1	13.0	12.0
342	Z	29.58468	-94.12533	15.1	15.0	13.0

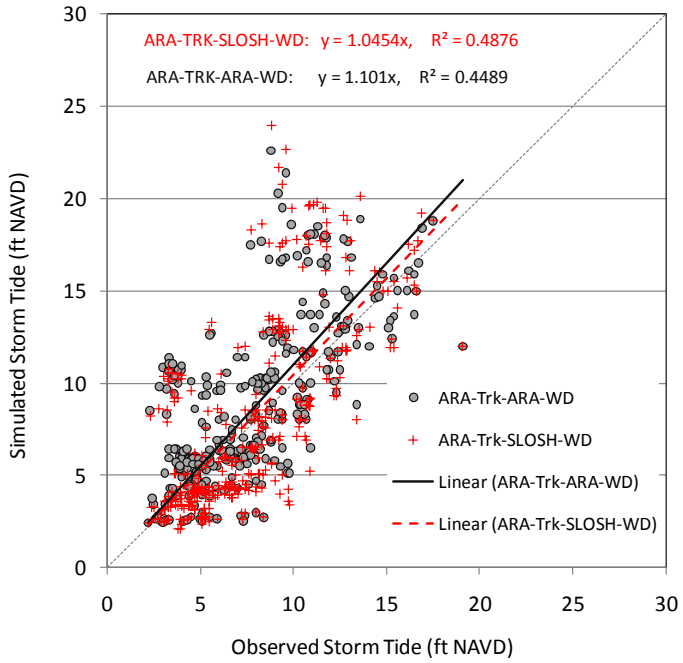

Figure Y-2. Comparison of Simulated and Observed Storm Tide for Hurricane Ike

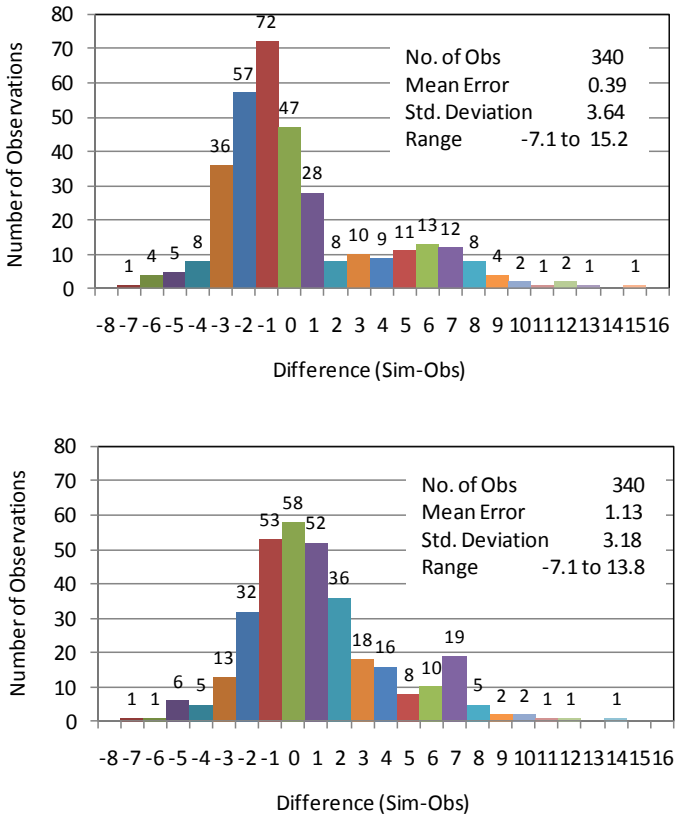

Figure Y-3. Simulated storm tide values minus observed storm tide for Hurricane Ike (2008) (Top, SLOSH wind model; Bottom, ARA wind model)

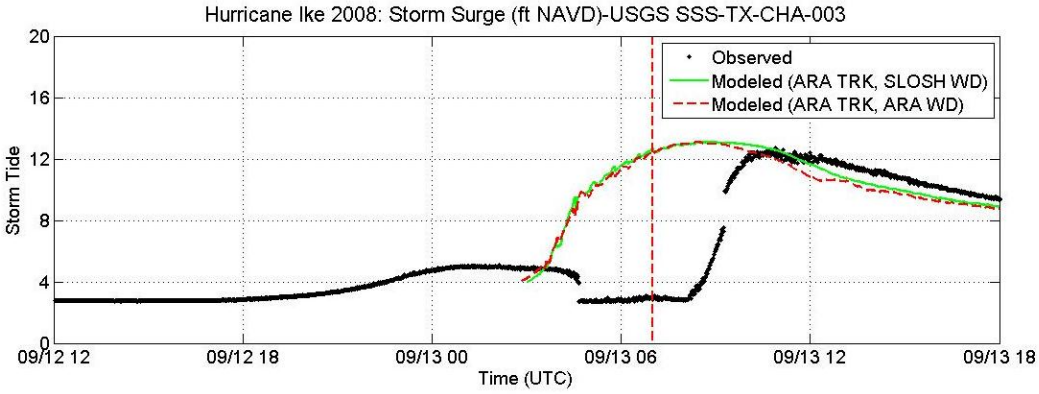

Figure Y-4a. Tide gauge record at SSS-TX-CHA-003 compared to the simulated time history of Storm Tide in the SLOSH Grid cell containing the gauge location

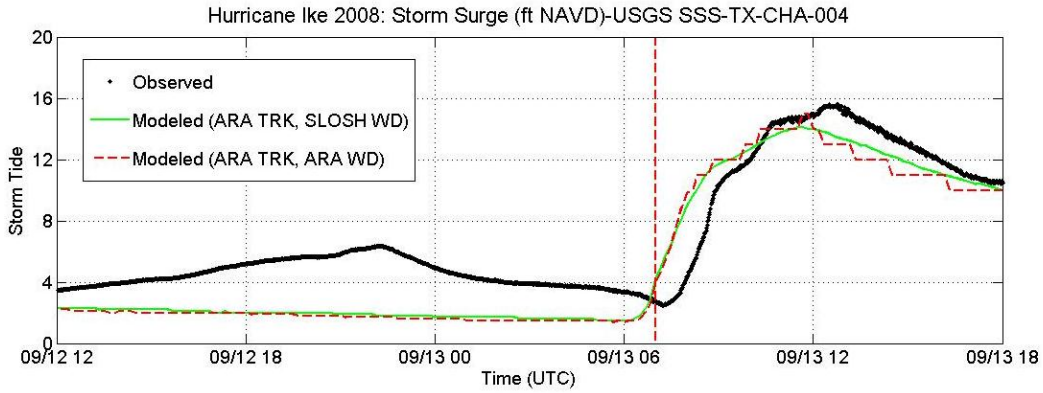

Figure Y-4b. Tide gauge record at SSS-TX-CHA-004 compared to the simulated time history of Storm Tide in the SLOSH Grid cell containing the gauge location

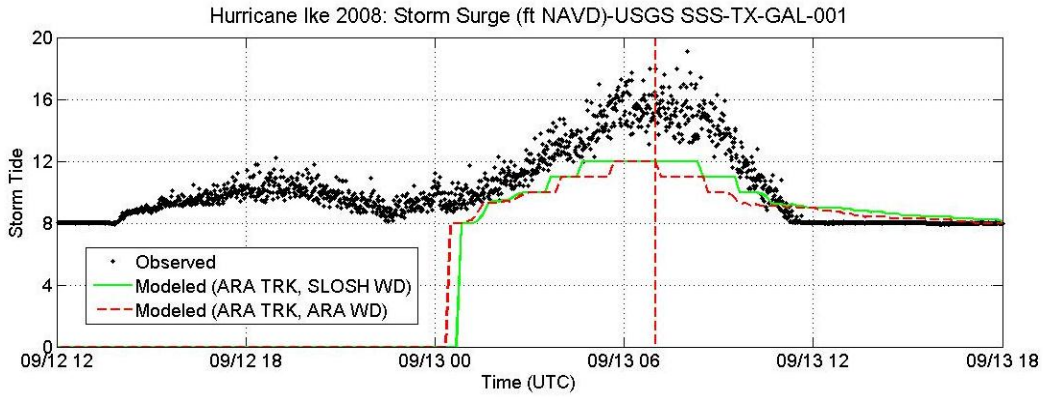

Figure Y-4c. Tide gauge record at SSS-TX-GAL-001 compared to the simulated time history of Storm Tide in the SLOSH Grid cell containing the gauge location

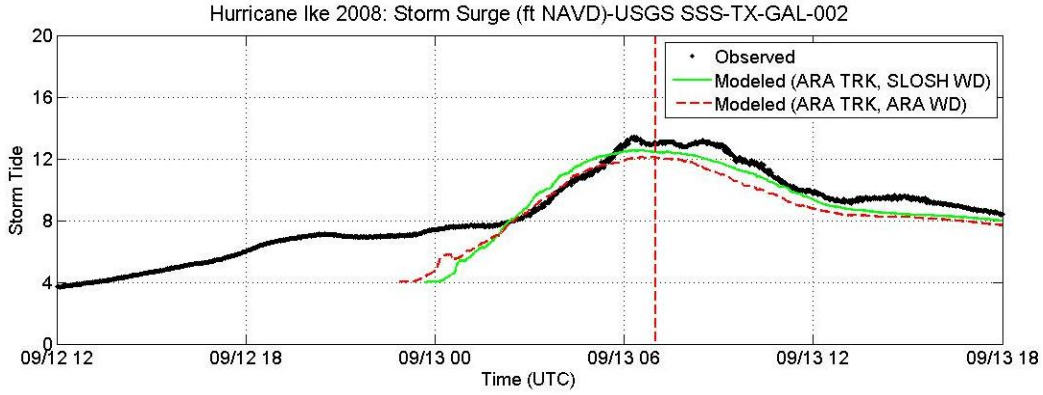

Figure Y-4d. Tide gauge record at SSS-TX-GAL-002 compared to the simulated time history of Storm Tide in the SLOSH Grid cell containing the gauge location

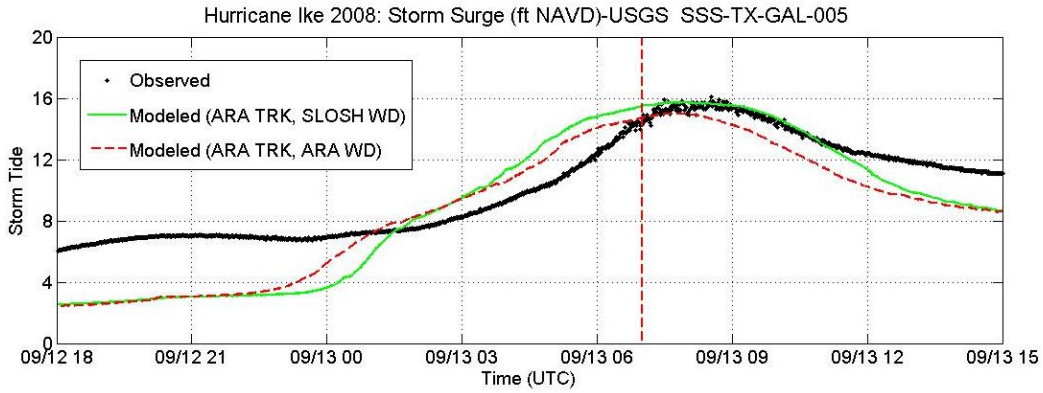

Figure Y-4e. Tide gauge record at SSS-TX-GAL-005 compared to the simulated time history of Storm Tide in the SLOSH Grid cell containing the gauge location

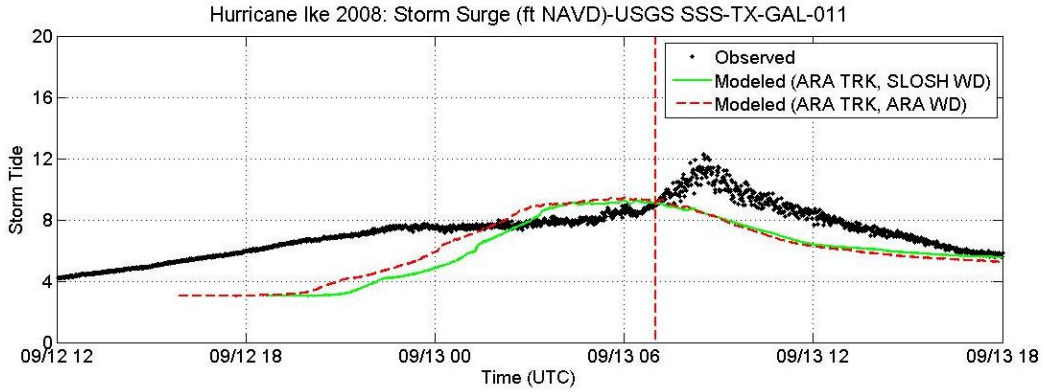

Figure Y-4f. Tide gauge record at SSS-TX-GAL-011 compared to the simulated time history of Storm Tide in the SLOSH Grid cell containing the gauge location

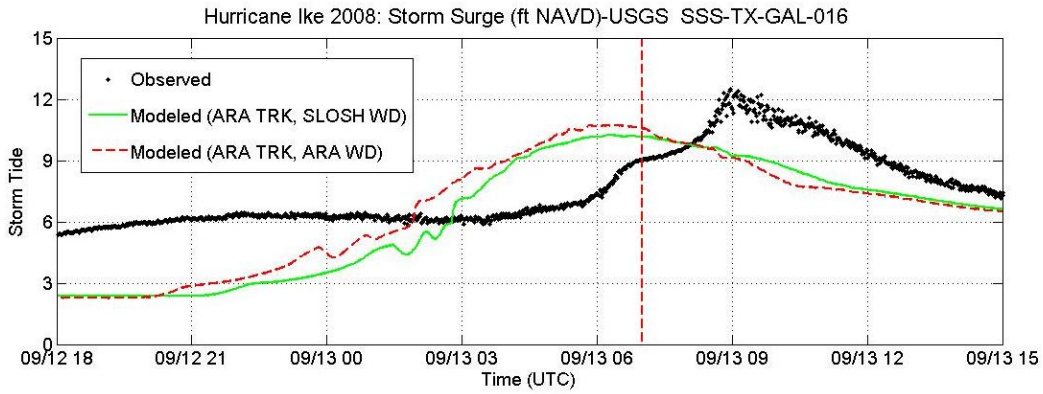

Figure Y-4g. Tide gauge record at SSS-TX-GAL-016 compared to the simulated time history of Storm Tide in the SLOSH Grid cell containing the gauge location

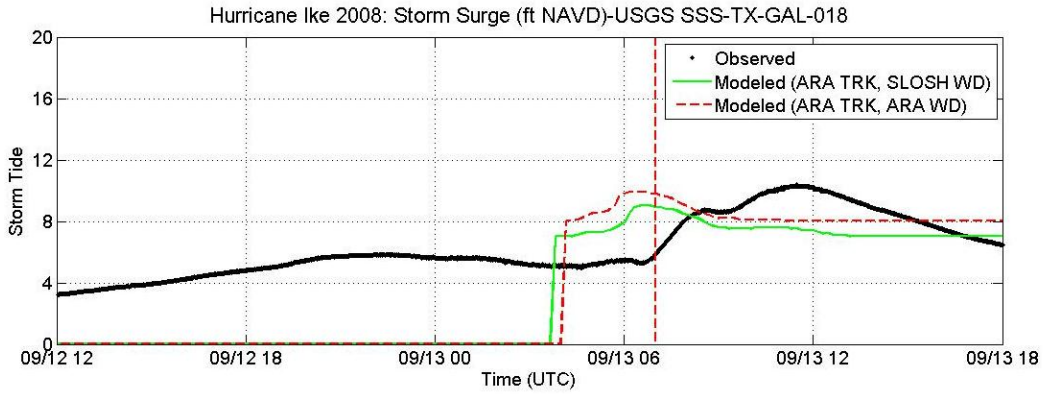

Figure Y-4h. Tide gauge record at SSS-TX-GAL-018 compared to the simulated time history of Storm Tide in the SLOSH Grid cell containing the gauge location

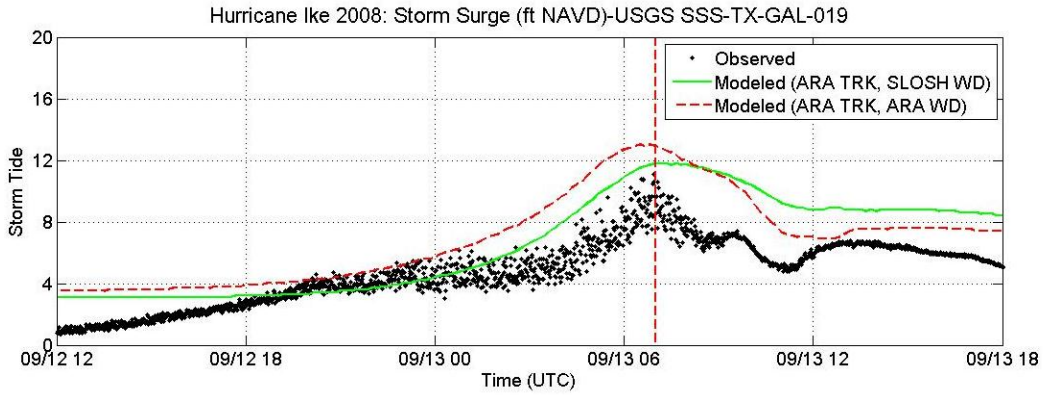

Figure Y-4i. Tide gauge record at SSS-TX-GAL-019 compared to the simulated time history of Storm Tide in the SLOSH Grid cell containing the gauge location

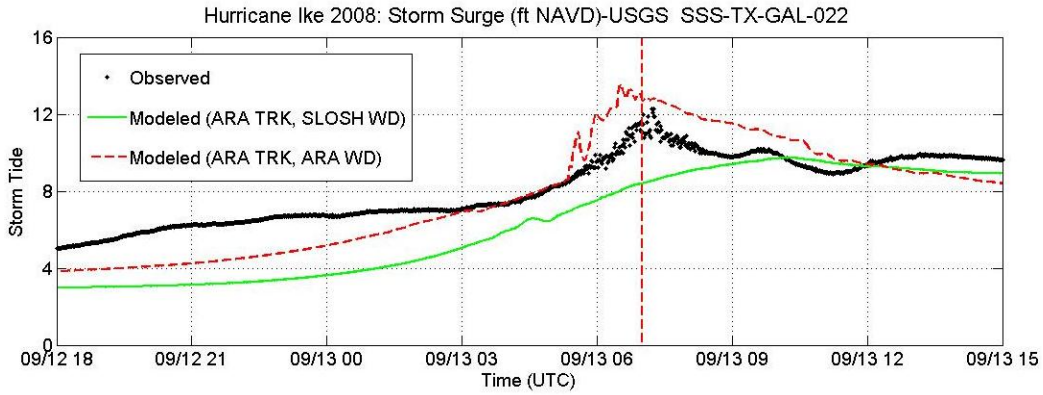

Figure Y-4j. Tide gauge record at SSS-TX-GAL-022 compared to the simulated time history of Storm Tide in the SLOSH Grid cell containing the gauge location

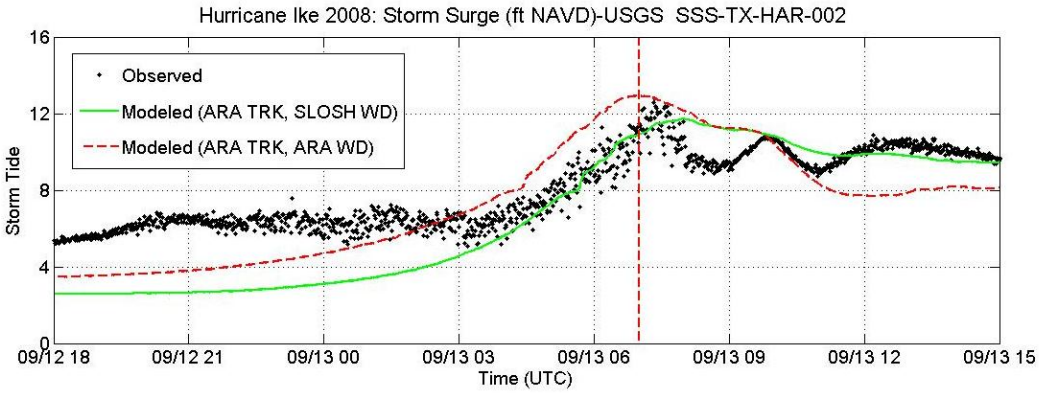

Figure Y-4k. Tide gauge record at SSS-TX-HAR-002 compared to the simulated time history of Storm Tide in the SLOSH Grid cell containing the gauge location

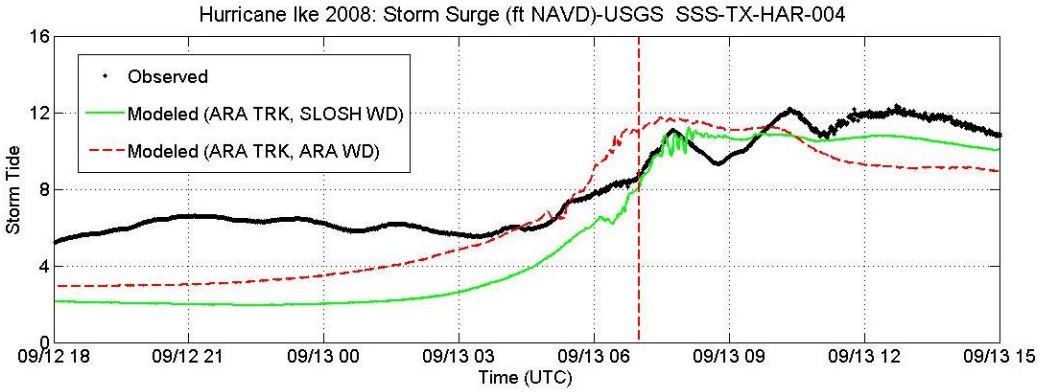

Figure Y-4l. Tide gauge record at SSS-TX-HAR-004 compared to the simulated time history of Storm Tide in the SLOSH Grid cell containing the gauge location

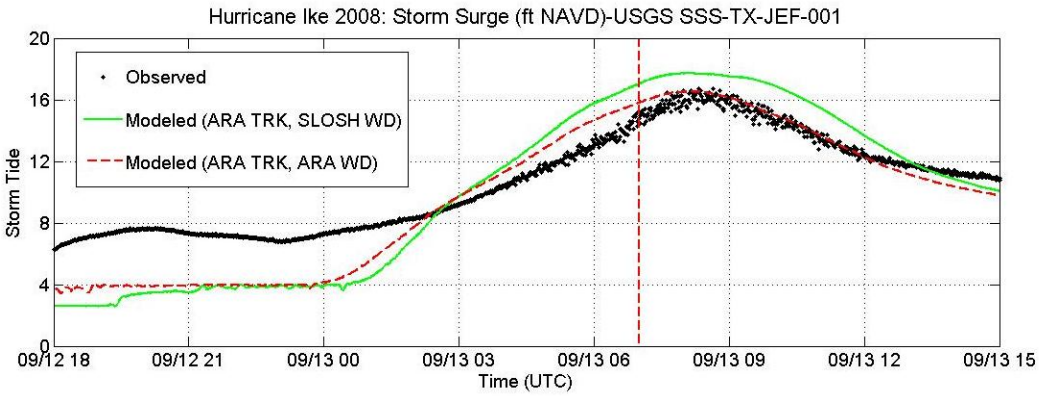

Figure Y-4m. Tide gauge record at SSS-TX-JEF-001 compared to the simulated time history of Storm Tide in the SLOSH Grid cell containing the gauge location

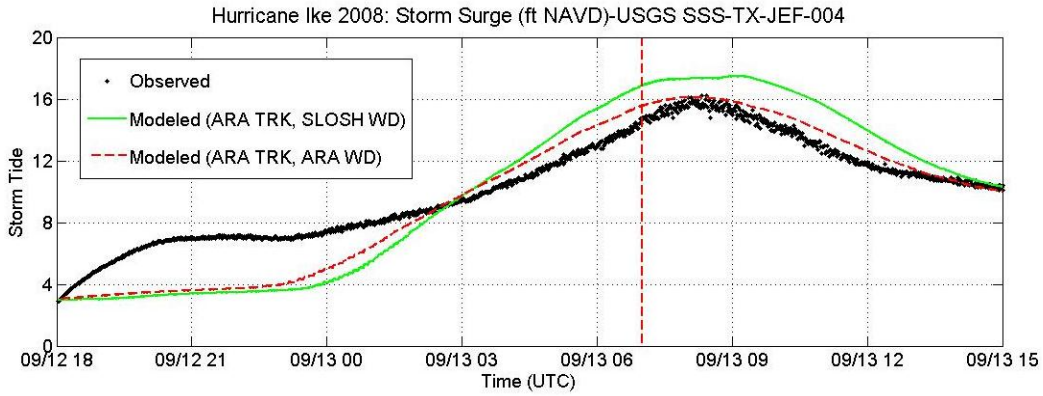

Figure Y-4n. Tide gauge record at SSS-TX-JEF-004 compared to the simulated time history of Storm Tide in the SLOSH Grid cell containing the gauge location

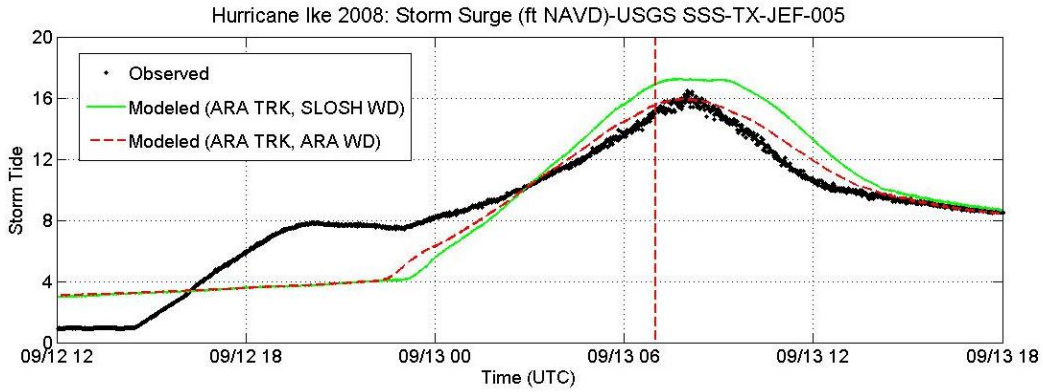

Figure Y-4o. Tide gauge record at SSS-TX-JEF-005 compared to the simulated time history of Storm Tide in the SLOSH Grid cell containing the gauge location

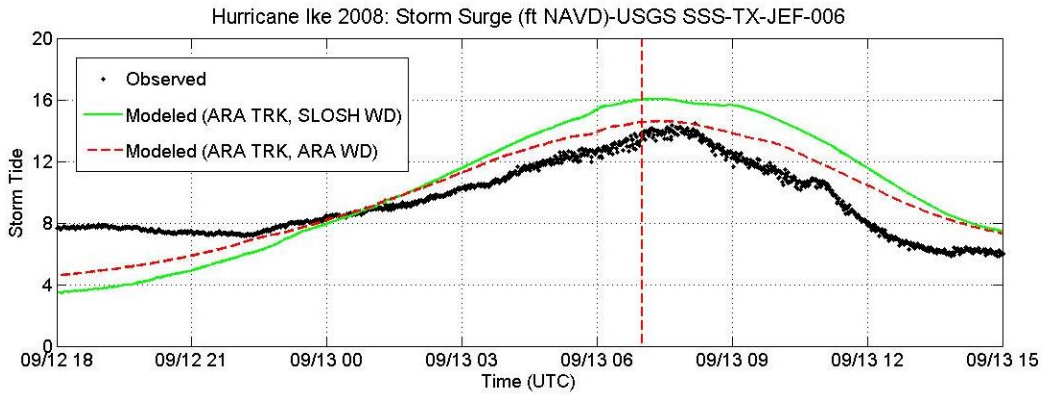

Figure Y-4p. Tide gauge record at SSS-TX-JEF-006 compared to the simulated time history of Storm Tide in the SLOSH Grid cell containing the gauge location

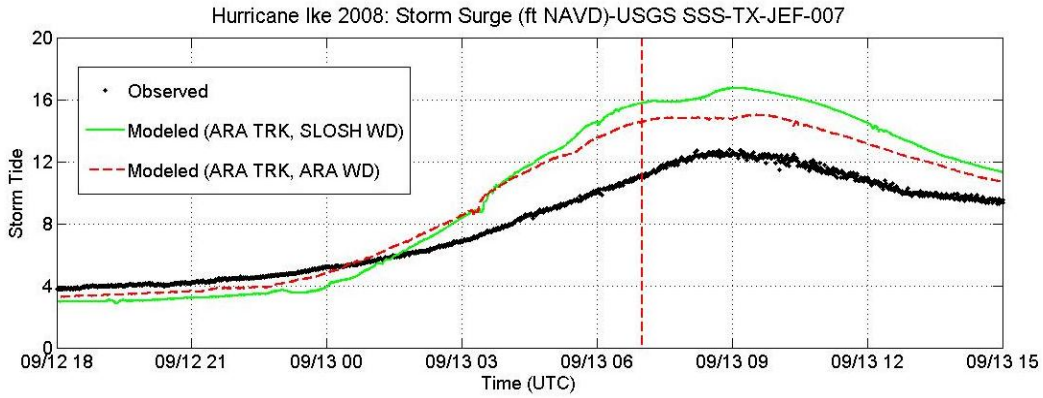

Figure Y-4q. Tide gauge record at SSS-TX-JEF-007 compared to the simulated time history of Storm Tide in the SLOSH Grid cell containing the gauge location

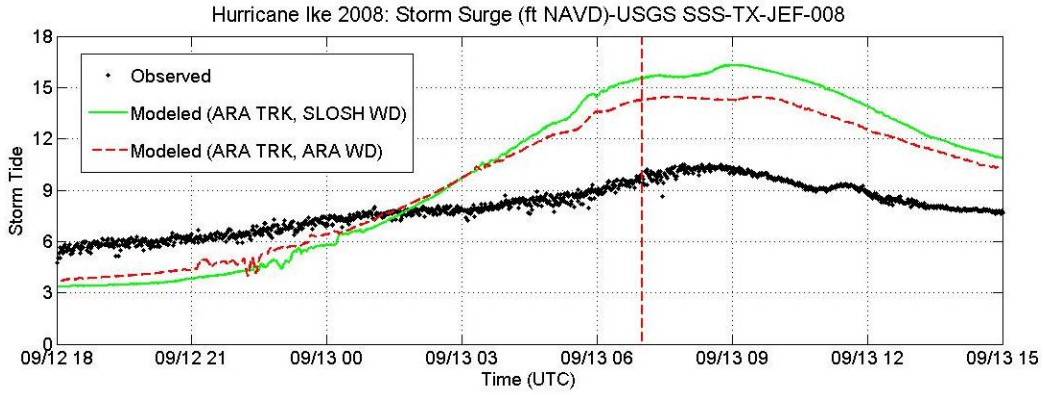

Figure Y-4r. Tide gauge record at SSS-TX-JEF-008 compared to the simulated time history of Storm Tide in the SLOSH Grid cell containing the gauge location

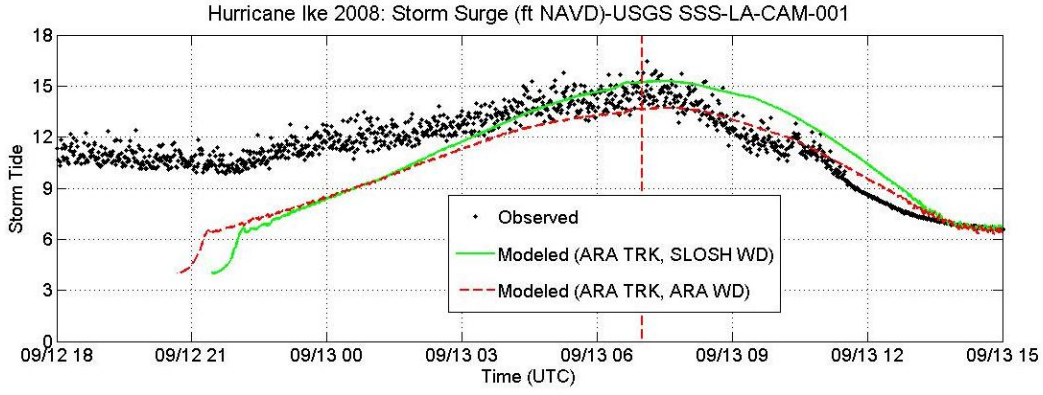

Figure Y-4s. Tide gauge record at SSS-LA-CAM-001 compared to the simulated time history of Storm Tide in the SLOSH Grid cell containing the gauge location

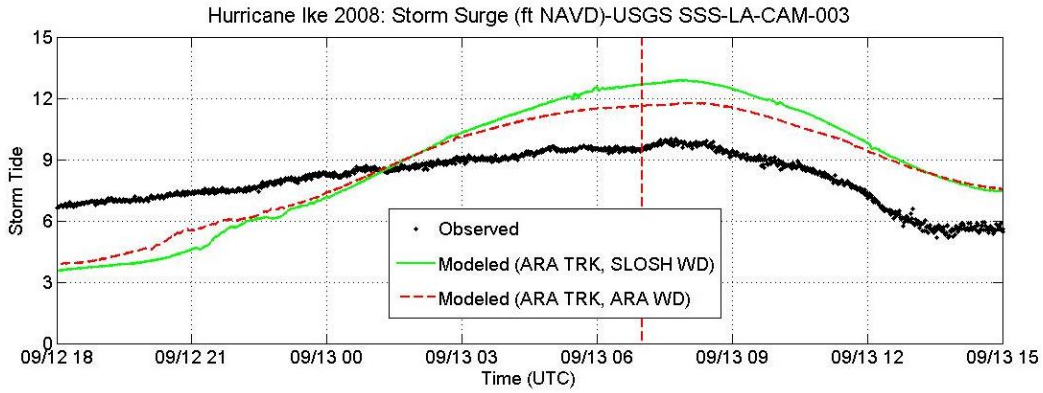

Figure Y-4t. Tide gauge record at SSS-LA-CAM-003 compared to the simulated time history of Storm Tide in the SLOSH Grid cell containing the gauge location

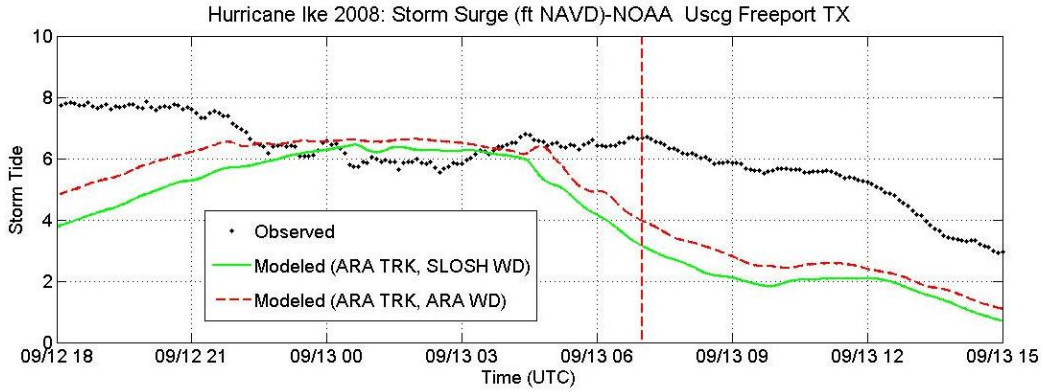

Figure Y-4u. Tide gauge record at Uscg Freeport compared to the simulated time history of Storm Tide in the SLOSH Grid cell containing the gauge location

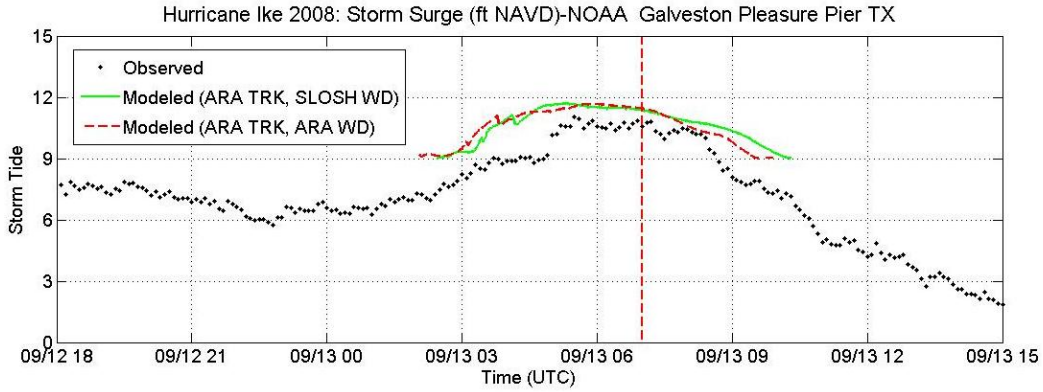

Figure Y-4v. Tide gauge record at Galveston Pleasure Pier compared to the simulated time history of Storm Tide in the SLOSH Grid cell containing the gauge location

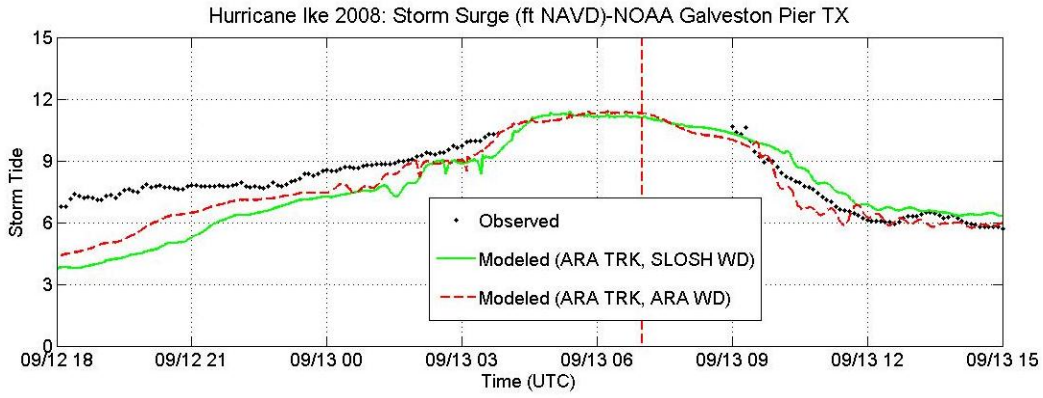

Figure Y-4w. Tide gauge record at Galveston Pier compared to the simulated time history of Storm Tide in the SLOSH Grid cell containing the gauge location

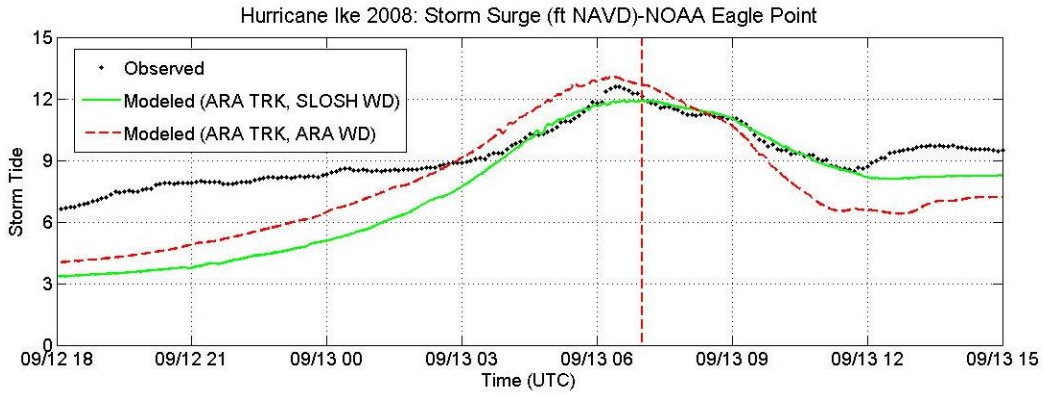

Figure Y-4x. Tide gauge record at Eagle Point compared to the simulated time history of Storm Tide in the SLOSH Grid cell containing the gauge location

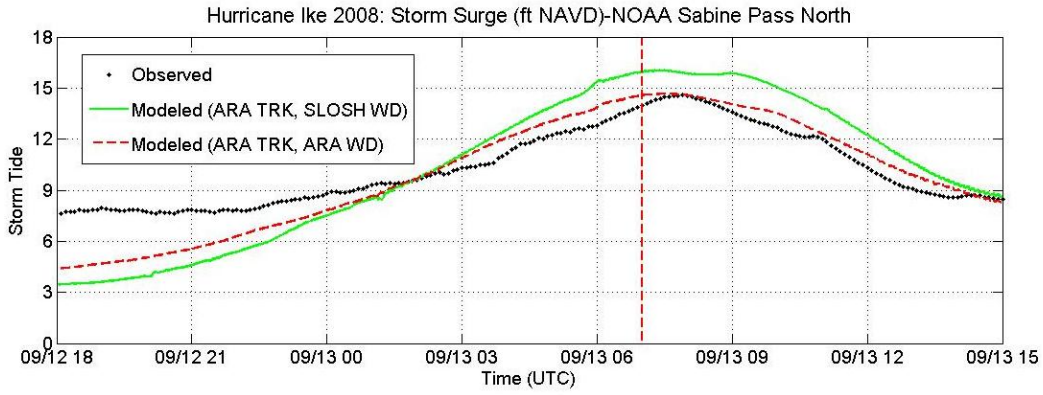

Figure Y-4y. Tide gauge record at Sabine Pass North compared to the simulated time history of Storm Tide in the SLOSH Grid cell containing the gauge location

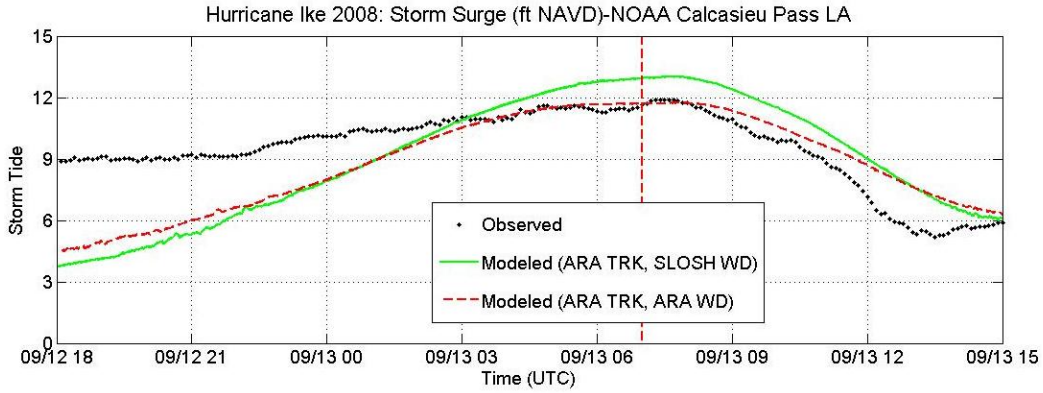

Figure Y-4z. Tide gauge record at Calcasieu Pass compared to the simulated time history of Storm Tide in the SLOSH Grid cell containing the gauge location

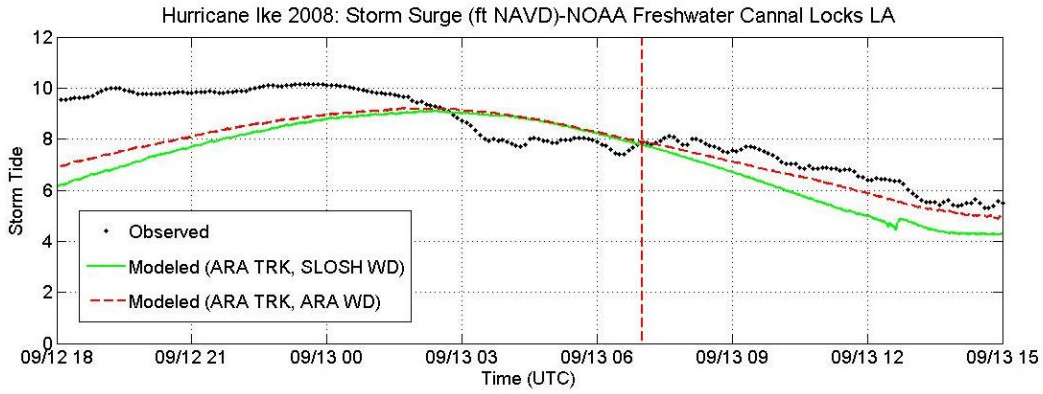

Figure Y-4aa. Tide gauge record at Freshwater Cannel Locks compared to the simulated time history of Storm Tide in the SLOSH Grid cell containing the gauge location

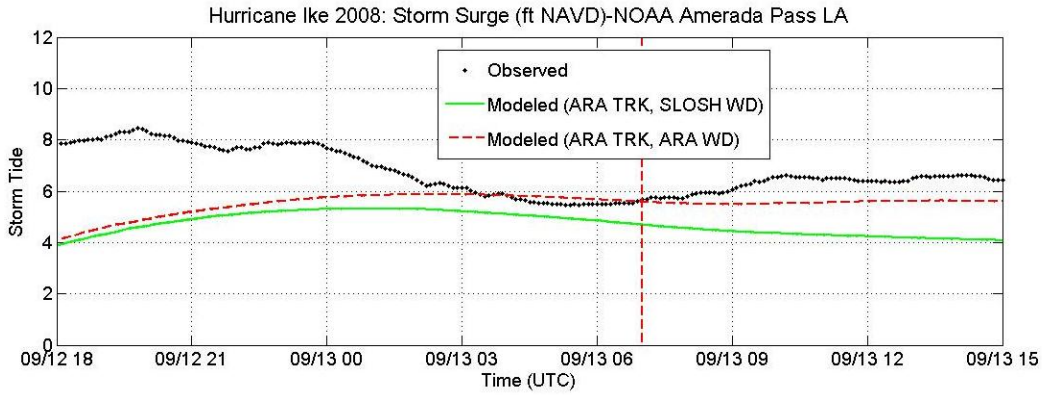

Figure Y-4ab. Tide gauge record at Freshwater Cannel Locks compared to the simulated time history of Storm Tide in the SLOSH Grid cell containing the gauge location

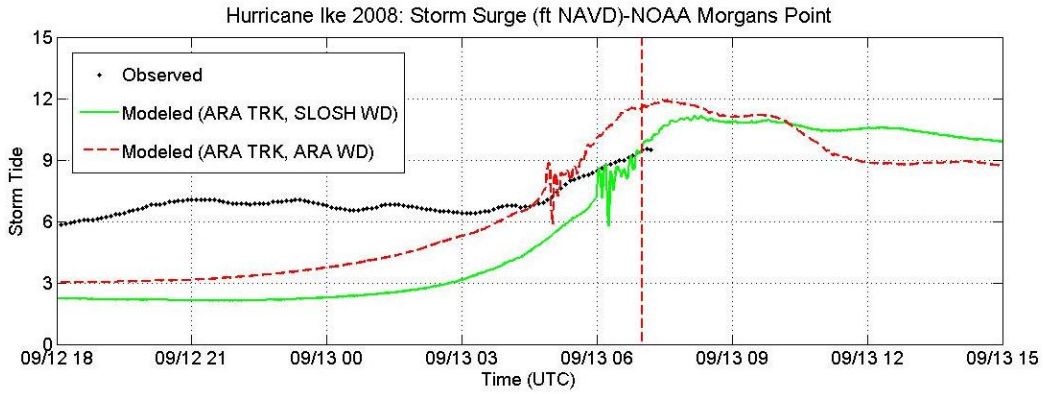

Figure Y-4ac. Tide gauge record at Morgans Point compared to the simulated time history of Storm Tide in the SLOSH Grid cell containing the gauge location

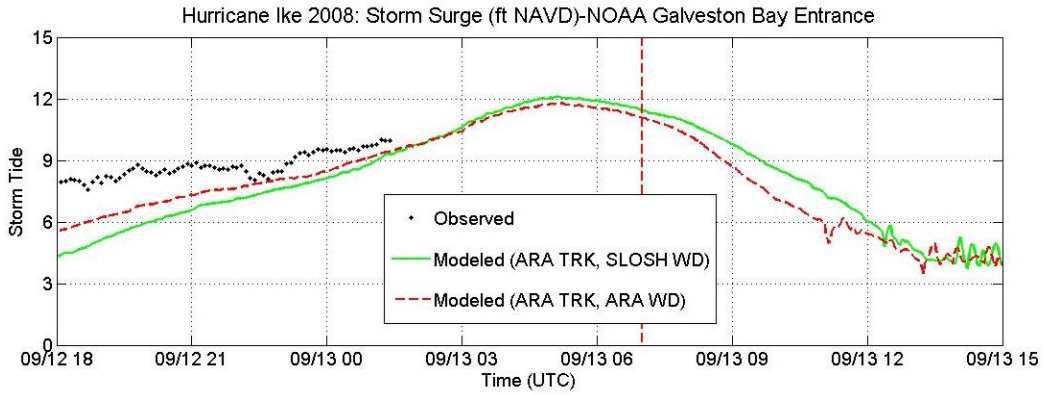

Figure Y-4ad. Tide gauge record at Morgans Point compared to the simulated time history of Storm Tide in the SLOSH Grid cell containing the gauge location

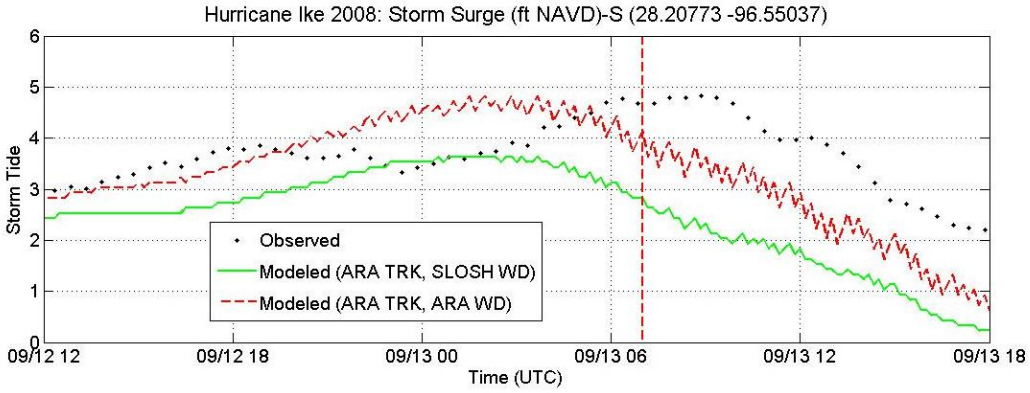

Figure Y-4ae. Tide gauge record at S to the simulated time history of Storm Tide in the SLOSH Grid cell containing the gauge location

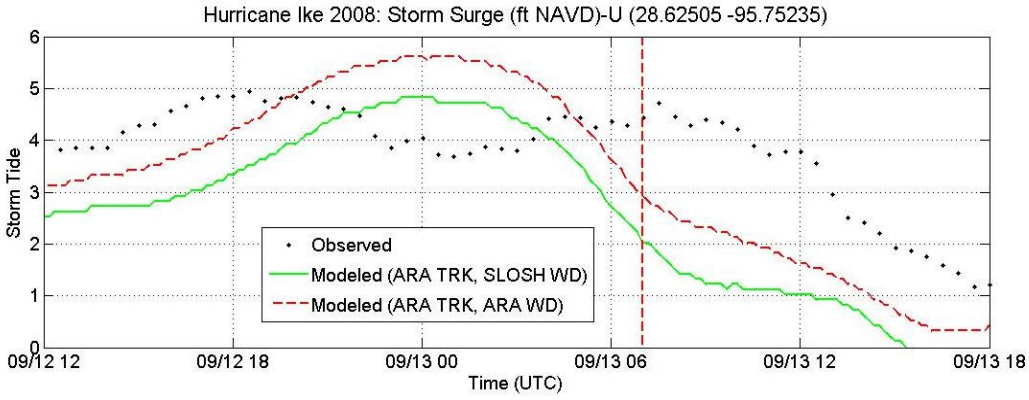

Figure Y-4af. Tide gauge record at U to the simulated time history of Storm Tide in the SLOSH Grid cell containing the gauge location

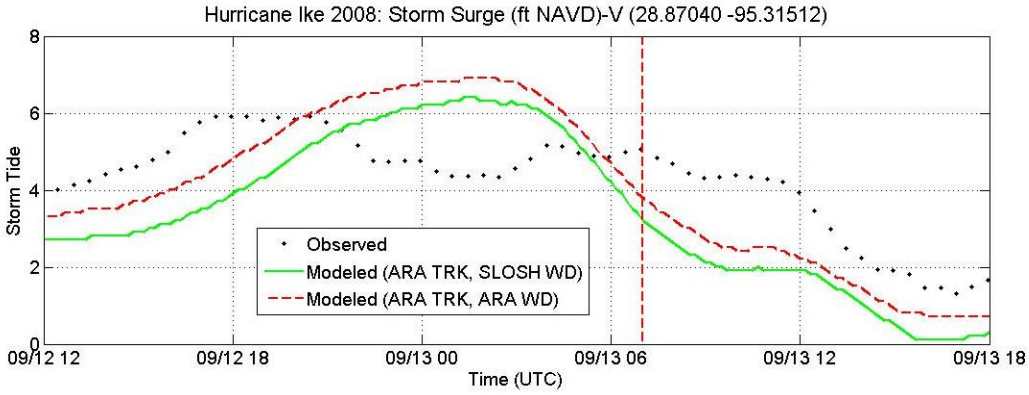

Figure Y-4ag. Tide gauge record at V to the simulated time history of Storm Tide in the SLOSH Grid cell containing the gauge location

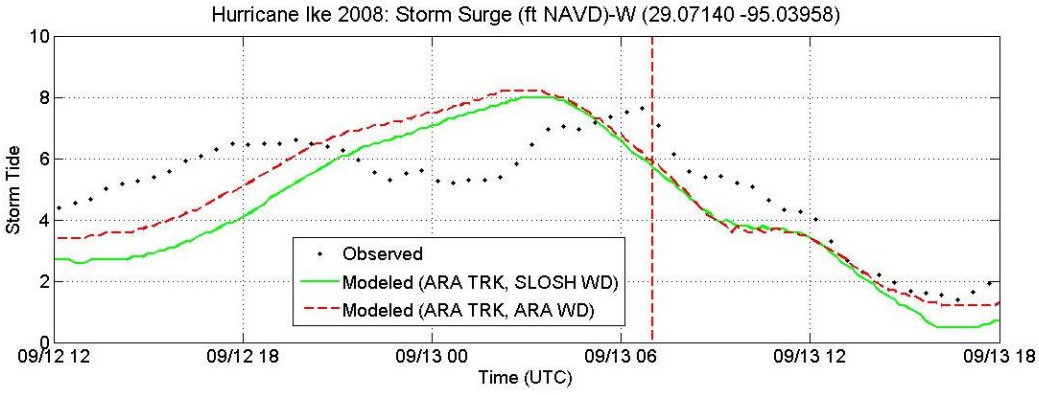

Figure Y-4ah. Tide gauge record at W to the simulated time history of Storm Tide in the SLOSH Grid cell containing the gauge location

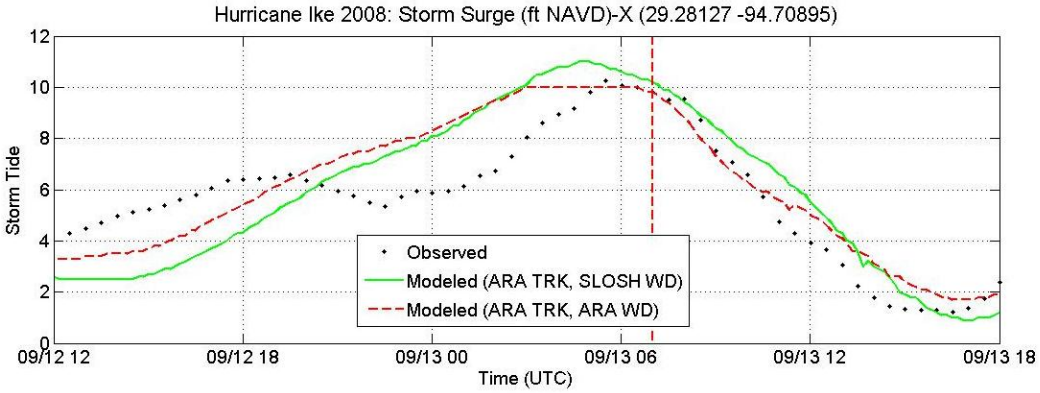

Figure Y-4ai. Tide gauge record at X to the simulated time history of Storm Tide in the SLOSH Grid cell containing the gauge location

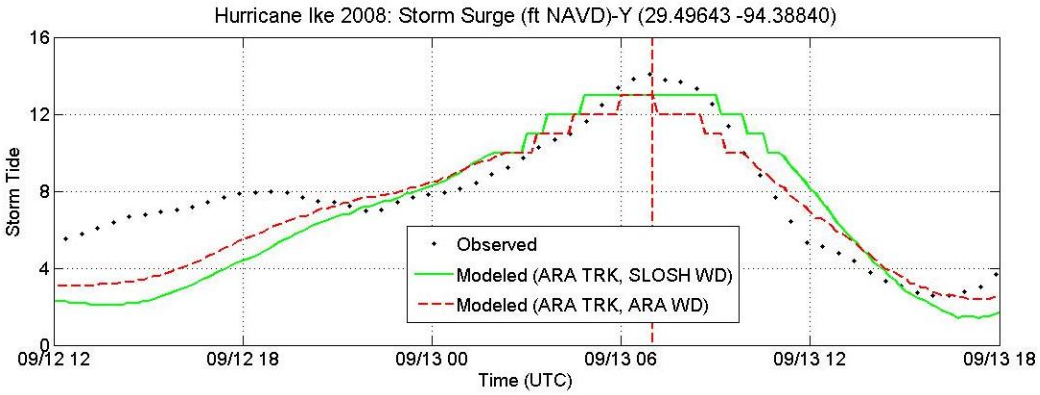

Figure Y-4aj. Tide gauge record at Y to the simulated time history of Storm Tide in the SLOSH Grid cell containing the gauge location

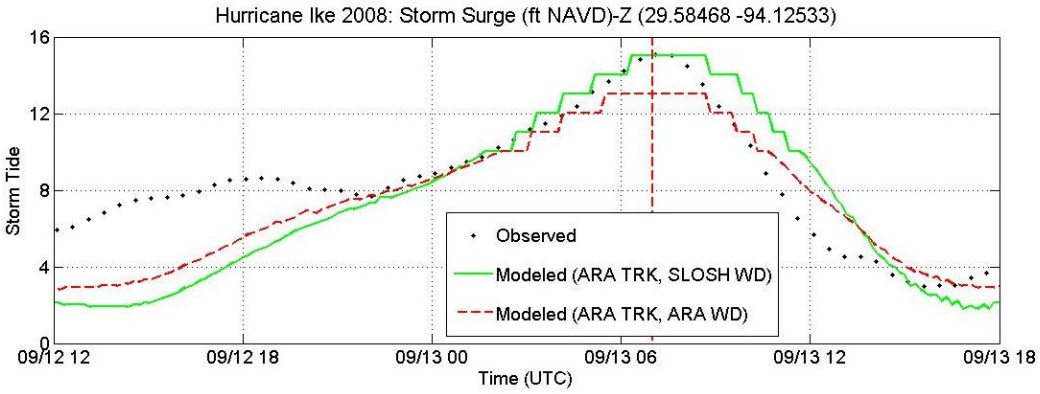

Figure Y-4ak. Tide gauge record at Z to the simulated time history of Storm Tide in the SLOSH Grid cell containing the gauge location

Table Y-2. Error Analysis of Storm Tide for Hurricane Ike

Station	Surge Range	Numer Data	Obs (ft NAVD)		SLOSH-Obs		ARA-Obs	
			Mean	Std	mean	RMS	mean	RMS
SSS-TX-CHA-003	0-3	202	2.8	0.1	8.9	8.9	8.7	8.8
	3-6	157	4.5	0.7	4.2	5.8	4.2	5.7
	6-9	17	6.8	0.5	6.2	6.3	6.1	6.2
	9-12	383	10.7	0.8	-0.4	1.0	-0.7	1.1
	12-15	140	12.2	0.2	0.0	0.5	-0.6	0.8
	all	899	8.0	3.8	2.7	5.0	2.4	4.9
SSS-TX-CHA-004	0-3	53	2.7	0.2	2.1	2.6	1.9	2.5
	3-6	1075	4.4	0.8	-2.2	2.8	-2.3	2.9
	6-9	118	6.4	0.6	-2.7	4.2	-2.7	4.4
	9-12	191	11.0	0.6	0.1	0.8	-0.1	1.1
	12-15	294	13.7	0.9	-0.9	1.1	-1.2	1.6
	15-18	69	15.3	0.2	-1.7	1.7	-2.1	2.2
	all	1800	7.1	4.1	-1.7	2.5	-1.8	2.7
SSS-TX-GAL-001	6-9	676	8.2	0.3	-2.8	5.2	-2.9	5.1
	9-12	734	10.0	0.7	-7.2	8.2	-7.0	8.1
	12-15	251	13.5	0.9	-2.3	2.5	-2.9	3.1
	15-18	135	15.8	0.7	-4.0	4.0	-4.5	4.5
	18-21	4	18.3	0.6	-6.3	6.3	-6.8	6.8
	all	1800	10.3	2.5	-4.6	6.3	-4.7	6.3
SSS-TX-GAL-002	6-9	318	8.1	0.5	-1.1	1.7	-1.0	1.3
	9-12	533	10.0	0.9	-0.4	0.7	-0.8	1.0
	12-15	249	12.9	0.3	-0.7	0.8	-1.2	1.3
	all	1100	10.1	1.8	-0.6	1.1	-1.0	1.2

(continued on next page)

Table Y-2. Error Analysis of Storm Tide for Hurricane Ike (Continued)

Station	Surge Range	Numer Data	Obs (ft NAVD)		SLOSH-Obs		ARA-Obs	
			Mean	Std	mean	RMS	mean	RMS
SSS-TX-GAL-005	6 -9	583	7.14	0.58	-2.46	3.18	-2.12	2.97
	9-12	258	10.90	0.85	0.10	2.37	-0.42	2.13
	12-15	287	13.31	0.93	0.17	1.18	-0.98	1.63
	15-18	132	15.40	0.24	0.19	0.29	-0.80	0.90
	all	1260	10.18	3.16	-1.06	2.48	-1.37	2.39
SSS-TX-GAL-011	3-6	80	5.8	0.1	-0.2	0.3	-0.5	0.5
	6-9	1094	7.5	0.7	-1.5	2.1	-1.1	1.9
	9-12	223	10.0	0.7	-1.9	2.1	-1.9	2.1
	12-15	4	12.2	0.1	-3.7	3.7	-3.8	3.8
	all	1401	7.8	1.3	-1.5	2.1	-1.2	1.9
SSS-TX-GAL-016	3-6	155	5.75	0.19	-2.98	3.21	-2.89	3.30
	6 -9	778	6.80	0.85	-0.80	2.47	-0.26	2.37
	9-12	305	10.22	0.84	-1.35	1.84	-1.59	2.19
	12-15	22	12.17	0.15	-2.91	2.91	-3.13	3.14
	all	1260	7.59	1.86	-1.24	2.45	-0.96	2.48
SSS-TX-GAL-018	3-6	1144	5.0	0.8	-3.6	4.6	-3.6	4.8
	6-9	412	7.8	0.8	-0.4	1.1	0.5	1.1
	9-12	244	9.8	0.4	-2.4	2.5	-1.8	1.8
	all	1800	6.3	2.0	-2.7	3.8	-2.4	3.9
SSS-TX-GAL-019	0-3	406	1.8	0.6	1.3	1.4	1.9	1.9
	3-6	833	4.7	0.8	1.3	2.2	1.9	2.3
	6-9	523	6.9	0.7	3.1	3.2	2.9	3.4
	9-12	38	9.8	0.5	1.8	1.9	3.1	3.1
	all	1800	4.8	2.1	1.9	2.4	2.2	2.6
SSS-TX-GAL-022	3-6	133	5.47	0.29	-2.45	2.47	-1.52	1.53
	6 -9	594	7.05	0.74	-2.43	2.61	-0.94	1.33
	9-12	529	9.91	0.56	-0.90	1.28	0.65	1.38
	12-15	4	12.18	0.15	-3.67	3.67	0.60	0.60
	all	1260	8.10	1.75	-1.80	2.14	-0.33	1.37
SSS-TX-HAR-002	3-6	194	5.65	0.22	-2.49	2.63	-1.12	1.72
	6 -9	536	6.75	0.73	-2.42	2.88	-0.74	2.05
	9-12	515	10.04	0.60	0.25	0.94	-0.26	1.92
	12-15	15	12.27	0.23	-0.86	0.91	0.43	0.48
	all	1260	7.99	1.95	-1.32	2.23	-0.59	1.94
SSS-TX-HAR-004	3-6	293	5.74	0.18	-3.27	3.32	-1.64	1.95
	6 -9	492	6.68	0.71	-3.47	3.70	-1.74	2.65
	9-12	405	10.93	0.80	-0.45	0.92	-0.66	1.81
	12-15	70	12.06	0.09	-1.32	1.32	-2.41	2.53
	all	1260	8.13	2.44	-2.34	2.88	-1.41	2.24

Table Y-2. Error Analysis of Storm Tide for Hurricane Ike (Continued)

Station	Surge Range	Numer Data	Obs (ft NAVD)		SLOSH-Obs		ARA-Obs	
			Mean	Std	mean	RMS	mean	RMS
SSS-TX-JEF-001	6 -9	529	7.44	0.53	-3.25	3.45	-2.71	2.92
	9-12	286	10.90	0.80	0.53	1.07	0.05	0.91
	12-15	279	13.32	0.90	2.05	2.15	0.64	1.00
	15-18	162	15.74	0.46	1.76	1.79	0.40	0.57
	all	1256	10.60	3.12	-0.57	2.59	-0.94	2.01
SSS-TX-JEF-004	0-3	5	2.87	0.07	0.13	0.15	0.19	0.20
	3-6	91	4.68	0.84	-1.64	1.83	-1.47	1.64
	6 -9	415	7.38	0.69	-2.92	3.06	-2.43	2.64
	9-12	359	10.71	0.75	1.01	1.23	0.47	0.64
	12-15	275	13.52	0.87	2.51	2.52	1.05	1.08
	15-18	112	15.48	0.29	1.85	1.88	0.49	0.54
	all	1257	10.18	3.25	-0.08	2.34	-0.50	1.70
SSS-TX-JEF-005	0-3	242	1.3	0.6	1.8	1.9	1.9	1.9
	3-6	124	4.6	0.9	-1.2	1.4	-1.1	1.4
	6-9	564	7.9	0.7	-2.5	2.9	-2.3	2.7
	9-12	483	10.1	0.8	0.8	1.4	0.3	0.7
	12-15	259	13.5	0.9	2.2	2.3	0.8	0.9
	15-18	124	15.5	0.3	1.6	1.7	0.2	0.4
	all	1796	8.7	4.0	0.0	2.2	-0.3	1.8
SSS-TX-JEF-006	3-6	11	5.91	0.05	2.12	2.16	1.89	1.93
	6 -9	633	7.50	0.76	-0.51	2.63	-0.20	1.87
	9-12	354	10.51	0.88	2.11	2.35	1.30	1.37
	12-15	259	13.06	0.67	2.47	2.51	1.05	1.11
	all	1257	9.48	2.37	0.86	2.52	0.50	1.60
SSS-TX-JEF-007	3-6	463	4.58	0.62	-0.93	0.99	-0.39	0.54
	6 -9	197	7.33	0.91	1.97	2.25	2.05	2.20
	9-12	438	10.42	0.81	3.66	3.76	2.59	2.68
	12-15	159	12.34	0.18	4.02	4.03	2.46	2.47
	all	1257	8.03	3.05	1.75	2.85	1.39	2.04
SSS-TX-JEF-008	3-6	124	5.73	0.24	-2.25	2.26	-1.77	1.78
	6 -9	790	7.57	0.81	1.24	3.10	1.14	2.50
	9-12	346	9.70	0.45	5.80	5.81	4.31	4.32
	all	1260	7.97	1.37	2.15	3.98	1.73	3.06
SSS-LA-CAM-001	6 -9	195	7.40	0.70	0.71	1.00	0.36	0.56
	9-12	337	11.01	0.70	-1.45	3.26	-1.66	2.53
	12-15	491	13.34	0.86	-0.28	1.68	-1.22	1.68
	15-18	30	15.41	0.35	-0.45	0.67	-1.93	1.97
	all	1053	11.55	2.41	-0.48	2.22	-1.09	1.88

Table Y-2. Error Analysis of Storm Tide for Hurricane Ike (Continued)

Station	Surge Range	Numer Data	Obs (ft NAVD)		SLOSH-Obs		ARA-Obs	
			Mean	Std	mean	RMS	mean	RMS
SS-LA-CAM-003	3-6	120	5.64	0.17	2.28	2.31	2.35	2.37
	6 -9	753	7.81	0.76	-0.39	2.29	-0.29	1.86
	9-12	385	9.44	0.26	2.66	2.72	1.86	1.88
	all	1258	8.10	1.24	0.80	2.43	0.62	1.92
Uscg Freeport TX	0-3	2	2.95	0.05	-2.20	2.20	-1.81	1.81
	3-6	89	5.18	0.89	-2.06	2.68	-1.66	2.30
	6 -9	119	6.83	0.61	-1.95	2.38	-1.25	1.70
	all	210	6.09	1.14	-2.00	2.51	-1.43	1.98
Galveston Pleasure Pier	6 -9	32	8.24	0.54	1.83	1.89	1.72	1.75
	9-12	42	10.27	0.56	0.97	1.07	0.93	1.07
	all	74	9.39	1.15	1.34	1.48	1.27	1.40
Galveston_Pier	3-6	9	5.85	0.08	0.56	0.57	0.00	0.10
	6 -9	120	7.53	0.85	-1.12	1.83	-0.98	1.25
	9-12	30	9.72	0.50	-0.65	0.85	-0.46	0.57
	all	159	7.85	1.25	-0.93	1.63	-0.83	1.11
Galveston Bay Entrance	6 -9	53	8.39	0.31	-2.19	2.35	-1.39	1.52
	9-12	22	9.57	0.22	-1.15	1.18	-0.82	0.86
	all	75	8.73	0.61	-1.88	2.07	-1.22	1.36
Eagle Point	6 -9	105	8.10	0.60	-2.88	3.14	-2.07	2.29
	9-12	96	10.20	0.88	-0.39	0.76	-0.61	1.71
	12-15	9	12.39	0.16	-0.55	0.57	0.49	0.50
	all	210	9.25	1.43	-1.64	2.28	-1.29	1.99
Morgans Point	3-6	5	5.87	0.08	-3.64	3.64	-2.85	2.85
	6 -9	122	6.93	0.62	-3.69	3.89	-2.06	2.70
	9-12	6	9.38	0.18	-0.05	0.45	2.16	2.17
	all	133	7.00	0.82	-3.53	3.79	-1.90	2.69
Sabine Pass North	6 -9	86	8.18	0.45	-2.06	2.74	-1.52	1.97
	9-12	60	10.22	0.84	0.93	1.31	0.44	0.68
	12-15	64	13.22	0.85	1.99	2.02	0.60	0.68
	all	210	10.30	2.23	0.03	2.19	-0.31	1.37
Calcasieu Pass	3-6	24	5.58	0.21	1.31	1.49	1.47	1.58
	6 -9	31	8.26	0.96	-1.57	3.59	-1.38	3.01
	9-12	155	10.44	0.91	-0.59	2.15	-0.97	1.74
	all	210	9.56	1.84	-0.52	2.36	-0.75	1.97
Freshwater Cannal Locks LA	3-6	20	5.52	0.14	-1.13	1.14	-0.39	0.41
	6 -9	102	7.53	0.62	-0.39	0.99	-0.03	0.62
	9-12	88	9.83	0.24	-1.79	2.01	-1.45	1.63
	all	210	8.30	1.49	-1.05	1.51	-0.66	1.14
Amerada Pass	3-6	57	5.69	0.17	-0.87	0.93	-0.02	0.23
	6 -9	153	7.11	0.74	-2.43	2.55	-1.67	1.98
	all	210	6.72	0.90	-2.01	2.23	-1.22	1.69

Table Y-2. Error Analysis of Storm Tide for Hurricane Ike (Continued)

Station	Surge Range	Numer Data	Obs (ft NAVD)		SLOSH-Obs		ARA-Obs	
			Mean	Std	mean	RMS	mean	RMS
S*	0-3	8	2.5	0.3	-1.7	1.8	-1.0	1.1
	3-6	52	3.9	0.5	-1.1	1.4	-0.2	0.9
	all	60	3.7	0.7	-1.2	1.5	-0.3	0.9
U*	0-3	10	2.0	0.5	-1.8	1.8	-1.3	1.3
	3-6	50	4.2	0.4	-1.1	1.7	-0.3	1.3
	all	60	3.9	0.9	-1.2	1.7	-0.5	1.3
V*	0-3	11	1.9	0.5	-1.3	1.3	-0.9	0.9
	3-6	49	4.8	0.6	-0.7	1.7	-0.1	1.5
	all	60	4.3	1.3	-0.8	1.6	-0.2	1.4
W*	0-3	10	1.9	0.4	-0.7	0.8	-0.3	0.3
	3-6	30	5.1	0.6	-0.4	1.8	0.0	1.6
	6-9	20	6.7	0.5	-0.9	1.5	-0.4	1.1
	all	60	5.1	1.7	-0.6	1.6	-0.2	1.3
X*	0-3	9	1.5	0.3	0.3	0.8	0.8	0.9
	3-6	24	5.0	0.8	0.0	1.9	0.4	1.6
	6-9	19	7.0	0.9	0.4	1.8	0.5	1.5
	9-12	8	9.8	0.4	0.6	0.8	0.0	0.4
	all	60	5.8	2.5	0.3	1.7	0.4	1.3
Y*	0-3	4	2.7	0.1	-0.7	0.8	0.1	0.3
	3-6	11	4.3	1.0	-0.1	2.1	0.0	1.5
	6-9	29	7.5	0.7	-1.4	2.8	-1.0	2.0
	9-12	8	10.5	0.8	1.0	1.1	0.2	0.7
	12-15	8	13.4	0.6	-0.4	0.7	-1.2	1.3
	all	60	7.8	3.1	-0.7	2.2	-0.6	1.6
Z*	0-3	1	3.0	0.0	-0.3	0.3	0.7	0.7
	3-6	12	4.2	1.0	0.2	2.1	0.5	1.6
	6-9	27	7.9	0.7	-2.4	3.6	-1.9	2.7
	9-12	10	10.6	0.9	0.6	1.2	-0.2	0.4
	12-15	8	13.6	0.9	0.6	0.9	-0.9	1.1
	15-18	2	15.0	0.0	0.0	0.0	-2.0	2.0
	all	60	8.5	3.3	-0.9	2.7	-0.9	2.0
All Station	0-3	963	2.0	0.8	2.9	4.4	3.2	4.4
	3-6	5429	4.9	0.8	-1.5	3.1	-1.2	3.1
	6-9	11235	7.4	0.8	-1.3	3.0	-0.8	2.6
	9-12	7871	10.3	0.8	-0.2	3.3	-0.5	3.1
	12-15	3147	13.2	0.9	0.6	2.0	-0.4	1.7
	15-18	766	15.6	0.5	0.1	2.2	-1.0	2.1
	18-21	4	18.3	0.6	-6.3	6.3	-6.8	6.8
	all	29415	8.4	3.1	-0.7	3.0	-0.6	2.8

* Observed data provided by Andrew Kennedy

Appendix T-Y References

Berg, R., 2009: Tropical Cyclone Report- Hurricane Ike (AL092008). National Hurricane Center

Beven II, J. L., and Cobb, H., 2004, Tropical Cyclone Report: Hurricane Isabel, 6-19 September 2003, National Hurricane Center

Beven II, J. L. and Kimberlain, T. B., 2008: Tropical Cyclone Report- Hurricane Gustav (AL072008), National Hurricane Center

East, J. W., Turco, M. J., and Mason, R. R., 2008: Monitoring Inland Storm Surge and Flooding from Ike in Texas and Louisiana, USGS

FEMA, 2006: Final Coastal and Reverie High Water Mark Collection for Hurricane Katrina in Mississippi

FEMA, 2008: Texas Hurricane Ike Rapid Response Coastal High Water Mark Collection

Knabb, R. D., Rhome, J. R., and Brown, D. P., 2005, "Tropical Cyclone Report: Hurricane Katrina, 23 – 30 August 2005", National Hurricane Center

McGhee, B.D., Goree, B.B., Tolett, R.W., and Mason, R. R., 2008. Monitoring Inland Storm Surge and Flooding from Gustav in Texas and Louisiana. U.S. Geological Survey

Murray, M. H., 1994: Storm-tide elevations produced by hurricane Andrew along the southern Florida coasts, USGS

NOAA. 2010: http://tidesandcurrents.noaa.gov/

Rappaport, E., 1993: Preliminary Report: Hurricane Andrew, 16 - 28 August, 1992, National Hurricane Center. (http://www.nhc.noaa.gov/1992andrew.html)

Stewart, S., 2005: Tropical Cyclone Report: Hurricane Ivan, 2 – 24 September, 2004, National Hurricane Center. (http://www.nhc.noaa.gov/2004ivan.shtml)

USACE, Mobile District, Engineering Division and Hydrology and Hydraulics Branch, 2004, Tide Gauge Data for Hurricane Ivan

Appendix Z. Wind Sub-Assembly Loss Tables

Table Z-1. Specific Occupancy, Pre-FIRM Construction

Occupancy	Building Loss	Foundation	Below First Floor	Structure Frame	Roof Cover	Roof Framing	Exterior Wall	Interiors
RES1	10	0.0	0.0	0.0	42.1	0.3	2.4	11.0
RES1	20	0.0	0.0	0.0	66.9	0.5	4.5	23.9
RES1	30	0.0	0.0	0.1	70.9	1.1	5.9	39.2
RES1	40	0.0	0.0	0.3	75.2	1.8	7.8	54.2
RES1	50	0.0	0.0	0.6	77.8	3.0	11.1	68.7
RES1	60	0.0	0.0	1.3	89.0	8.2	17.0	80.8
RES1	70	0.0	0.0	7.0	96.6	16.6	28.9	89.1
RES1	80	0.0	0.0	15.3	100.0	26.2	40.4	97.2
RES1	90	0.0	0.0	24.7	100.0	50.2	61.4	100.0
RES1	100	0.0	0.0	44.3	100.0	100.0	76.2	100.0
RES2	10	0.0	0.0	0.0	46.4	0.2	3.0	11.1
RES2	20	0.0	0.0	0.0	46.4	1.4	4.3	25.3
RES2	30	0.0	0.0	0.1	49.3	3.0	5.6	39.3
RES2	40	0.0	0.0	0.4	57.1	4.8	7.1	52.9
RES2	50	0.0	0.0	0.7	63.7	7.5	10.3	65.9
RES2	60	0.0	0.0	1.7	72.0	14.1	16.9	77.0
RES2	70	0.0	0.0	8.5	83.5	29.1	26.9	84.8
RES2	80	0.0	0.0	19.7	91.5	50.2	40.1	90.3
RES2	90	0.0	0.0	28.6	95.7	64.2	54.8	96.5
RES2	100	0.0	0.0	38.7	100.0	86.6	74.0	100.0
RES3A	10	0.0	0.0	0.0	57.6	10.1	7.3	6.4
RES3A	20	0.0	0.0	0.1	79.7	20.8	17.7	15.1
RES3A	30	0.0	0.0	0.6	86.6	30.2	30.8	24.4
RES3A	40	0.0	0.0	1.5	93.0	42.2	38.9	35.2
RES3A	50	0.0	0.0	2.4	96.0	52.3	47.2	46.6
RES3A	60	0.0	0.0	4.2	98.4	62.6	53.8	58.4
RES3A	70	0.0	0.0	15.0	98.4	72.0	62.1	67.5
RES3A	80	0.0	0.0	25.6	98.9	84.8	67.9	77.3
RES3A	90	0.0	0.0	30.5	100.0	91.4	76.0	88.2
RES3A	100	0.0	0.0	34.3	100.0	100.0	85.2	98.9
RES3B	10	0.0	0.0	0.0	58.1	10.6	5.6	7.1
RES3B	20	0.0	0.0	0.0	80.5	22.7	13.4	16.6
RES3B	30	0.0	0.0	0.2	87.2	33.0	27.0	25.7
RES3B	40	0.0	0.0	0.6	92.3	46.1	36.0	36.3

Occupancy	Building Loss	Foundation	Below First Floor	Structure Frame	Roof Cover	Roof Framing	Exterior Wall	Interiors
RES3B	50	0.0	0.0	1.3	95.8	56.6	44.3	47.7
RES3B	60	0.0	0.0	2.2	98.7	65.4	51.4	59.6
RES3B	70	0.0	0.0	7.1	100.0	73.6	57.9	71.1
RES3B	80	0.0	0.0	17.0	100.0	84.0	63.9	81.3
RES3B	90	0.0	0.0	25.4	100.0	93.4	70.4	91.7
RES3B	100	0.0	0.0	30.6	100.0	100.0	85.1	100.0
RES3C	10	0.0	0.0	0.0	70.4	14.4	5.6	8.1
RES3C	20	0.0	0.0	0.1	87.2	27.5	13.8	17.5
RES3C	30	0.0	0.0	0.2	90.8	35.5	27.9	26.5
RES3C	40	0.0	0.0	0.8	92.8	44.8	35.0	36.6
RES3C	50	0.0	0.0	1.5	93.2	53.1	40.8	46.8
RES3C	60	0.0	0.0	2.4	93.6	60.5	45.6	57.3
RES3C	70	0.0	0.0	10.4	94.0	66.7	53.0	66.4
RES3C	80	0.0	0.0	17.4	94.0	78.7	55.9	76.0
RES3C	90	0.0	0.0	20.2	96.8	87.2	60.5	86.1
RES3C	100	0.0	0.0	22.5	100.0	97.1	67.4	95.8
RES3D	10	0.0	0.0	0.0	70.8	14.4	5.6	8.1
RES3D	20	0.0	0.0	0.1	87.6	28.0	13.6	17.5
RES3D	30	0.0	0.0	0.2	91.6	35.7	28.2	26.5
RES3D	40	0.0	0.0	0.8	93.2	45.3	35.4	36.5
RES3D	50	0.0	0.0	1.5	94.0	53.9	41.0	46.7
RES3D	60	0.0	0.0	2.4	94.4	61.3	46.0	57.1
RES3D	70	0.0	0.0	10.2	94.4	67.7	53.4	66.3
RES3D	80	0.0	0.0	17.5	94.8	79.7	56.7	75.8
RES3D	90	0.0	0.0	20.6	97.2	88.5	61.4	85.8
RES3D	100	0.0	0.0	22.9	100.0	98.7	68.3	95.5
RES3E	10	0.0	0.0	0.0	79.2	16.3	6.2	9.1
RES3E	20	0.0	0.0	0.1	95.2	30.1	14.7	18.9
RES3E	30	0.0	0.0	0.3	97.6	38.1	29.9	28.1
RES3E	40	0.0	0.0	0.8	98.4	47.7	37.3	38.4
RES3E	50	0.0	0.0	1.6	98.4	56.3	43.0	49.0
RES3E	60	0.0	0.0	2.5	98.4	64.0	48.0	59.7
RES3E	70	0.0	0.0	10.5	98.4	70.1	55.4	68.7
RES3E	80	0.0	0.0	18.0	98.4	82.1	58.5	78.1
RES3E	90	0.0	0.0	21.2	100.0	91.2	63.1	88.4
RES3E	100	0.0	0.0	23.5	100.0	100.0	70.3	98.4
RES3F	10	0.0	0.0	0.0	76.8	16.8	2.1	9.9

Occupancy	Building Loss	Foundation	Below First Floor	Structure Frame	Roof Cover	Roof Framing	Exterior Wall	Interiors
RES3F	20	0.0	0.0	0.0	99.2	32.0	6.0	20.1
RES3F	30	0.0	0.0	0.1	100.0	55.2	13.8	29.9
RES3F	40	0.0	0.0	0.3	100.0	75.2	23.3	39.4
RES3F	50	0.0	0.0	0.7	100.0	79.2	34.5	48.7
RES3F	60	0.0	0.0	1.5	100.0	80.8	44.4	58.3
RES3F	70	0.0	0.0	3.1	100.0	81.6	50.5	68.4
RES3F	80	0.0	0.0	8.6	100.0	91.2	50.8	78.8
RES3F	90	0.0	0.0	9.6	100.0	98.4	56.9	89.0
RES3F	100	0.0	0.0	10.7	100.0	100.0	63.4	99.1
RES4	10	0.0	0.0	0.0	64.8	13.6	4.2	9.0
RES4	20	0.0	0.0	0.0	84.8	28.0	11.2	18.2
RES4	30	0.0	0.0	0.2	87.2	38.8	21.9	27.2
RES4	40	0.0	0.0	0.6	88.0	44.4	29.7	36.8
RES4	50	0.0	0.0	1.2	88.8	49.2	36.5	46.5
RES4	60	0.0	0.0	3.5	88.8	54.0	41.8	56.1
RES4	70	0.0	0.0	7.7	88.8	60.8	45.8	65.7
RES4	80	0.0	0.0	10.1	90.4	69.2	49.3	75.5
RES4	90	0.0	0.0	11.1	93.6	79.2	53.3	85.3
RES4	100	0.0	0.0	12.3	100.0	88.0	59.3	94.9
RES5	10	0.0	0.0	0.0	61.6	16.5	4.6	9.7
RES5	20	0.0	0.0	0.1	89.6	32.3	13.5	19.1
RES5	30	0.0	0.0	0.2	94.4	34.7	25.4	28.8
RES5	40	0.0	0.0	0.4	97.6	37.3	36.5	38.7
RES5	50	0.0	0.0	1.1	99.2	43.2	44.9	48.9
RES5	60	0.0	0.0	1.3	100.0	52.3	49.5	59.9
RES5	70	0.0	0.0	1.3	100.0	60.8	51.1	71.6
RES5	80	0.0	0.0	1.3	100.0	67.5	52.1	83.6
RES5	90	0.0	0.0	1.5	100.0	76.0	58.7	94.2
RES5	100	0.0	0.0	2.2	100.0	100.0	83.5	100.0
RES6	10	0.0	0.0	0.0	64.0	8.4	9.1	7.1
RES6	20	0.0	0.0	0.0	84.3	16.8	17.2	16.3
RES6	30	0.0	0.0	0.0	87.5	24.8	26.6	26.0
RES6	40	0.0	0.0	0.0	88.3	35.2	35.2	35.9
RES6	50	0.0	0.0	0.0	89.1	49.2	38.3	46.8
RES6	60	0.0	0.0	0.1	89.6	56.4	43.7	57.4
RES6	70	0.0	0.0	1.0	90.9	60.8	51.1	67.6
RES6	80	0.0	0.0	11.8	92.8	66.4	55.0	77.0

Occupancy	Building Loss	Foundation	Below First Floor	Structure Frame	Roof Cover	Roof Framing	Exterior Wall	Interiors
RES6	90	0.0	0.0	24.2	94.7	72.4	60.2	85.8
RES6	100	0.0	0.0	27.0	100.0	80.8	67.1	95.5
COM1	10	0.0	0.0	0.0	34.7	2.9	6.6	8.6
COM1	20	0.0	0.0	0.2	58.2	12.0	12.6	17.8
COM1	30	0.0	0.0	1.8	73.3	21.4	20.0	27.1
COM1	40	1.7	0.0	3.5	82.4	28.0	25.7	37.2
COM1	50	3.1	0.0	4.1	85.9	31.4	31.8	48.2
COM1	60	3.6	0.0	5.8	89.1	35.5	37.0	59.2
COM1	70	3.7	0.0	7.5	92.2	39.2	44.1	69.9
COM1	80	3.7	0.0	9.0	95.5	45.1	55.8	79.8
COM1	90	3.7	0.0	25.5	96.2	67.0	63.4	86.9
COM1	100	4.3	0.0	28.5	100.0	74.9	70.7	97.0
COM2	10	0.0	0.0	0.0	30.1	4.3	8.2	9.1
COM2	20	0.0	0.0	0.0	47.7	8.7	13.6	21.4
COM2	30	0.0	0.0	0.0	60.6	14.4	20.2	34.0
COM2	40	0.0	0.0	0.0	71.1	30.5	26.3	45.7
COM2	50	0.0	0.0	0.0	82.0	41.0	36.1	57.3
COM2	60	0.0	0.0	3.5	96.7	66.4	41.7	66.2
COM2	70	4.9	0.0	7.1	100.0	72.5	48.9	77.9
COM2	80	8.0	0.0	9.4	100.0	81.8	61.9	89.3
COM2	90	8.8	0.0	27.9	100.0	89.6	73.5	99.9
COM2	100	19.0	0.0	60.1	100.0	100.0	100.0	100.0
COM3	10	0.0	0.0	0.0	40.3	6.4	4.6	7.4
COM3	20	0.0	0.0	0.0	64.0	13.1	8.4	16.9
COM3	30	0.0	0.0	0.0	76.7	18.7	13.7	27.4
COM3	40	0.0	0.0	0.0	82.2	23.5	20.4	38.5
COM3	50	0.0	0.0	0.0	85.9	30.4	27.0	49.8
COM3	60	0.0	0.0	0.0	90.4	39.5	32.2	61.1
COM3	70	0.0	0.0	0.1	95.0	50.4	42.4	71.5
COM3	80	0.0	0.0	4.1	98.3	62.1	53.4	81.3
COM3	90	0.0	0.0	25.5	99.2	71.5	61.8	89.7
COM3	100	0.0	0.0	29.6	100.0	82.7	71.5	100.0
COM4	10	0.0	0.0	0.0	52.0	9.6	5.5	9.9
COM4	20	0.0	0.0	0.0	74.4	16.3	10.9	20.5
COM4	30	0.0	0.0	0.1	83.2	23.5	16.3	31.2
COM4	40	0.0	0.0	0.1	87.2	31.5	22.2	41.9
COM4	50	0.0	0.0	0.3	91.2	40.5	28.8	52.3

Occupancy	Building Loss	Foundation	Below First Floor	Structure Frame	Roof Cover	Roof Framing	Exterior Wall	Interiors
COM4	60	0.2	0.0	1.7	94.4	53.9	33.7	62.7
COM4	70	1.2	0.0	3.1	96.0	62.7	41.6	72.6
COM4	80	1.4	0.0	4.4	97.6	73.3	51.4	81.8
COM4	90	1.6	0.0	15.9	98.4	81.6	57.9	90.3
COM4	100	1.8	0.0	18.0	100.0	92.5	65.7	100.0
COM5	10	0.0	0.0	0.0	44.2	7.1	4.9	8.3
COM5	20	0.0	0.0	0.0	66.6	13.7	8.6	18.1
COM5	30	0.0	0.0	0.0	78.0	19.2	13.6	28.7
COM5	40	0.0	0.0	0.0	82.8	23.6	19.9	39.7
COM5	50	0.0	0.0	0.0	85.6	29.5	26.1	50.5
COM5	60	0.0	0.0	0.0	89.2	37.7	31.0	61.2
COM5	70	0.0	0.0	0.1	93.2	47.9	40.3	71.0
COM5	80	0.0	0.0	3.8	96.0	59.6	51.1	79.9
COM5	90	0.0	0.0	22.8	96.0	68.5	59.0	87.3
COM5	100	0.0	0.0	25.4	100.0	76.4	65.8	97.3
COM6	10	0.0	0.0	0.0	47.2	9.4	5.1	8.6
COM6	20	0.0	0.0	0.0	55.2	13.6	8.3	18.1
COM6	30	0.0	0.0	0.0	60.8	17.0	11.8	27.7
COM6	40	0.0	0.0	0.0	64.8	18.8	15.5	37.4
COM6	50	0.0	0.0	0.0	68.0	21.2	19.7	47.0
COM6	60	0.0	0.0	0.1	72.8	25.2	24.3	56.4
COM6	70	0.0	0.0	0.1	79.2	32.6	31.9	65.4
COM6	80	0.0	0.0	2.5	84.8	41.6	42.1	73.9
COM6	90	0.0	0.0	2.9	95.2	46.8	47.3	83.1
COM6	100	0.0	0.0	3.2	100.0	52.0	52.6	92.4
COM7	10	0.0	0.0	0.0	44.5	7.2	4.9	8.2
COM7	20	0.0	0.0	0.0	66.7	13.6	8.6	17.6
COM7	30	0.0	0.0	0.0	76.5	18.8	13.5	27.4
COM7	40	0.0	0.0	0.0	79.5	23.2	19.5	37.3
COM7	50	0.0	0.0	0.0	81.3	29.2	25.3	47.1
COM7	60	0.0	0.0	0.0	84.5	37.6	30.0	57.1
COM7	70	0.0	0.0	0.2	88.0	47.6	39.1	66.3
COM7	80	0.0	0.0	3.5	90.7	58.0	48.8	75.1
COM7	90	0.0	0.0	21.8	92.0	66.8	56.6	83.4
COM7	100	0.0	0.0	24.2	100.0	74.4	62.9	92.7
COM8	10	0.0	0.0	0.0	46.4	7.7	4.9	8.5
COM8	20	0.0	0.0	0.0	67.4	15.2	8.9	18.7

Occupancy	Building Loss	Foundation	Below First Floor	Structure Frame	Roof Cover	Roof Framing	Exterior Wall	Interiors
COM8	30	0.0	0.0	0.1	78.0	21.3	14.2	29.4
COM8	40	0.0	0.0	0.2	84.0	25.6	20.0	40.4
COM8	50	0.0	0.0	0.3	86.4	30.1	26.1	51.6
COM8	60	0.0	0.0	1.4	90.0	37.6	30.8	62.6
COM8	70	0.0	0.0	2.3	94.4	46.1	38.7	73.1
COM8	80	0.0	0.0	3.7	99.0	60.8	51.3	82.7
COM8	90	0.0	0.0	22.2	99.4	71.2	60.3	90.5
COM8	100	0.0	0.0	26.6	100.0	85.3	72.2	100.0
COM9	10	0.0	0.0	0.0	43.5	3.2	5.4	8.2
COM9	20	0.0	0.0	0.0	59.8	6.8	9.4	18.8
COM9	30	0.0	0.0	0.0	70.1	12.0	13.6	29.7
COM9	40	0.0	0.0	0.1	76.5	14.8	18.7	41.0
COM9	50	0.0	0.0	0.2	81.6	17.6	24.1	52.3
COM9	60	0.0	0.0	0.5	86.2	20.3	30.2	63.5
COM9	70	0.0	0.0	0.9	92.0	24.4	40.0	73.9
COM9	80	0.0	0.0	5.6	95.7	36.9	51.4	82.7
COM9	90	0.0	0.0	13.6	97.8	62.7	60.4	90.2
COM9	100	0.0	0.0	15.8	100.0	73.1	70.4	100.0
COM10	10	0.0	0.0	0.0	0.0	0.0	8.9	24.8
COM10	20	0.0	0.0	0.0	0.0	0.0	26.7	46.9
COM10	30	0.0	0.0	0.0	0.0	0.0	53.3	66.2
COM10	40	0.0	0.0	0.0	0.0	0.0	71.1	88.3
COM10	50	0.0	0.0	0.0	0.0	19.2	100.0	100.0
COM10	60	0.0	0.0	0.0	0.0	99.2	100.0	100.0
COM10	70	0.0	0.0	19.8	0.0	100.0	100.0	100.0
COM10	80	0.0	0.0	39.8	0.0	100.0	100.0	100.0
COM10	90	0.0	0.0	59.8	0.0	100.0	100.0	100.0
COM10	100	13.3	0.0	75.8	0.0	100.0	100.0	100.0
IND1	10	0.0	0.0	0.0	41.0	4.3	5.0	7.3
IND1	20	0.0	0.0	0.0	59.3	10.4	9.1	17.1
IND1	30	0.0	0.0	0.5	69.3	17.9	13.6	27.8
IND1	40	0.0	0.0	0.8	76.0	21.3	18.9	38.9
IND1	50	0.0	0.0	0.8	79.8	34.9	25.4	49.7
IND1	60	1.5	0.0	2.4	83.7	50.1	31.5	60.0
IND1	70	4.2	0.0	4.5	88.2	53.6	37.4	70.6
IND1	80	5.8	0.0	5.9	94.4	64.3	49.0	80.0
IND1	90	6.0	0.0	21.6	97.5	74.4	61.4	89.2

Occupancy	Building Loss	Foundation	Below First Floor	Structure Frame	Roof Cover	Roof Framing	Exterior Wall	Interiors
IND1	100	6.7	0.0	24.0	100.0	83.2	68.7	99.9
IND2	10	0.0	0.0	0.0	38.1	6.1	4.3	6.9
IND2	20	0.0	0.0	0.0	56.7	12.5	7.9	17.3
IND2	30	0.0	0.0	0.0	69.3	17.9	12.7	28.5
IND2	40	0.0	0.0	0.0	77.6	21.8	18.0	40.6
IND2	50	0.0	0.0	0.2	82.6	25.9	23.6	53.1
IND2	60	0.0	0.0	0.8	88.7	31.8	28.9	65.2
IND2	70	0.0	0.0	1.6	95.0	40.1	37.5	76.3
IND2	80	0.0	0.0	4.6	100.0	55.3	50.5	85.6
IND2	90	0.0	0.0	20.6	100.0	67.5	62.1	95.5
IND2	100	0.0	0.0	29.8	100.0	98.3	90.3	100.0
IND3	10	0.0	0.0	0.0	39.3	6.1	4.3	6.8
IND3	20	0.0	0.0	0.0	54.8	12.5	7.9	16.9
IND3	30	0.0	0.0	0.0	65.7	17.6	12.7	27.6
IND3	40	0.0	0.0	0.2	73.2	21.2	17.2	38.9
IND3	50	0.0	0.0	0.4	77.1	24.5	22.2	50.7
IND3	60	0.0	0.0	1.6	82.7	28.9	26.7	62.1
IND3	70	0.0	0.0	3.0	88.7	35.1	33.9	72.8
IND3	80	0.0	0.0	4.8	95.1	50.8	46.5	81.4
IND3	90	0.0	0.0	19.2	98.0	63.1	58.1	90.2
IND3	100	0.0	0.0	22.8	100.0	74.9	69.0	100.0
IND4	10	0.0	0.0	0.0	59.2	9.1	6.4	11.1
IND4	20	0.0	0.0	0.0	75.2	16.8	10.1	24.4
IND4	30	0.0	0.0	0.0	87.6	22.9	14.9	37.8
IND4	40	0.0	0.0	0.0	95.2	26.3	20.6	51.7
IND4	50	0.0	0.0	0.1	98.4	29.3	26.7	65.6
IND4	60	0.0	0.0	0.4	100.0	34.5	32.2	79.3
IND4	70	0.0	0.0	0.6	100.0	43.3	42.0	92.1
IND4	80	0.0	0.0	4.5	100.0	66.4	61.0	100.0
IND4	90	0.0	0.0	25.1	100.0	87.7	80.7	100.0
IND4	100	0.0	0.0	48.0	100.0	100.0	100.0	100.0
IND5	10	0.0	0.0	0.0	43.6	7.0	5.0	8.0
IND5	20	0.0	0.0	0.0	58.0	12.8	8.0	17.8
IND5	30	0.0	0.0	0.0	67.4	17.4	12.2	28.0
IND5	40	0.0	0.0	0.0	72.6	20.2	16.8	38.3
IND5	50	0.0	0.0	0.2	75.6	23.4	21.4	48.9
IND5	60	0.0	0.0	0.5	80.0	28.4	26.0	59.2

Occupancy	Building Loss	Foundation	Below First Floor	Structure Frame	Roof Cover	Roof Framing	Exterior Wall	Interiors
IND5	70	0.0	0.0	0.8	86.0	36.2	34.0	69.0
IND5	80	0.0	0.0	4.2	91.8	49.8	46.0	78.2
IND5	90	0.0	0.0	17.8	94.6	60.4	56.4	87.0
IND5	100	0.0	0.0	19.8	100.0	67.4	62.8	96.9
IND6	10	0.0	0.0	0.0	40.5	6.4	4.5	7.6
IND6	20	0.0	0.0	0.0	66.0	13.5	8.5	18.2
IND6	30	0.0	0.0	0.0	81.8	20.1	14.3	30.4
IND6	40	0.0	0.0	0.0	90.7	25.5	21.6	43.7
IND6	50	0.0	0.0	0.0	96.5	32.6	29.2	57.4
IND6	60	0.0	0.0	0.0	100.0	42.5	35.6	71.4
IND6	70	0.0	0.0	0.1	100.0	55.2	47.2	84.3
IND6	80	0.0	0.0	4.6	100.0	70.2	60.9	95.7
IND6	90	0.0	0.0	32.9	100.0	94.5	82.5	100.0
IND6	100	4.8	4.8	100.0	100.0	100.0	100.0	100.0
AGR1	10	0.0	0.0	0.0	45.9	3.8	6.7	7.6
AGR1	20	0.0	0.0	0.1	74.8	11.4	13.9	18.2
AGR1	30	0.0	0.0	1.5	92.0	22.1	21.8	30.5
AGR1	40	0.0	0.0	2.3	100.0	30.5	32.7	44.8
AGR1	50	0.0	0.0	2.6	100.0	58.4	45.2	55.9
AGR1	60	2.6	0.0	6.1	100.0	83.6	55.3	65.8
AGR1	70	7.5	0.0	11.4	100.0	90.5	62.6	79.1
AGR1	80	10.2	0.0	14.8	100.0	98.3	76.0	92.2
AGR1	90	11.9	0.0	44.5	100.0	100.0	94.6	100.0
AGR1	100	25.0	0.0	93.7	100.0	100.0	100.0	100.0
REL1	10	0.0	0.0	0.0	58.2	7.2	7.8	8.0
REL1	20	0.0	0.0	0.0	81.4	14.9	14.2	19.1
REL1	30	0.0	0.0	0.0	91.8	21.9	22.1	31.3
REL1	40	0.0	0.0	0.0	95.0	29.0	30.6	43.9
REL1	50	0.0	0.0	0.0	96.2	39.7	35.1	56.3
REL1	60	0.0	0.0	0.0	99.2	47.5	40.2	69.4
REL1	70	0.0	0.0	0.3	100.0	56.5	49.4	81.3
REL1	80	0.0	0.0	7.7	100.0	67.1	56.6	91.3
REL1	90	0.0	0.0	18.3	100.0	77.9	65.5	100.0
REL1	100	0.0	0.0	27.2	100.0	100.0	97.4	100.0
GOV1	10	0.0	0.0	0.0	42.8	6.6	4.7	8.1
GOV1	20	0.0	0.0	0.0	62.8	13.4	8.1	18.7
GOV1	30	0.0	0.0	0.0	75.2	18.8	12.8	30.0

Occupancy	Building Loss	Foundation	Below First Floor	Structure Frame	Roof Cover	Roof Framing	Exterior Wall	Interiors
GOV1	40	0.0	0.0	0.0	82.3	22.6	18.5	41.8
GOV1	50	0.0	0.0	0.0	86.1	27.0	24.5	53.9
GOV1	60	0.0	0.0	0.0	91.5	34.0	29.7	65.7
GOV1	70	0.0	0.0	0.1	97.3	43.6	39.1	76.7
GOV1	80	0.0	0.0	3.7	100.0	58.6	52.2	86.5
GOV1	90	0.0	0.0	22.3	100.0	69.6	62.1	94.2
GOV1	100	0.0	0.0	32.1	100.0	100.0	89.3	100.0
GOV2	10	0.0	0.0	0.0	51.6	8.0	5.7	9.7
GOV2	20	0.0	0.0	0.0	70.0	14.8	9.2	20.9
GOV2	30	0.0	0.0	0.0	80.4	20.4	13.9	32.3
GOV2	40	0.0	0.0	0.0	85.2	23.6	19.4	43.6
GOV2	50	0.0	0.0	0.0	87.6	27.6	25.1	55.1
GOV2	60	0.0	0.0	0.0	92.4	34.0	30.1	66.5
GOV2	70	0.0	0.0	0.1	97.6	43.6	39.3	76.9
GOV2	80	0.0	0.0	3.9	100.0	57.6	51.8	85.8
GOV2	90	0.0	0.0	21.2	100.0	67.6	60.7	92.4
GOV2	100	0.0	0.0	26.9	100.0	85.6	77.1	100.0
EDU1	10	0.0	0.0	0.0	46.4	7.2	5.0	8.9
EDU1	20	0.0	0.0	0.0	64.5	13.7	8.2	19.4
EDU1	30	0.0	0.0	0.0	75.5	18.9	12.6	30.2
EDU1	40	0.0	0.0	0.0	81.1	22.3	17.9	41.3
EDU1	50	0.0	0.0	0.0	83.7	26.1	23.5	52.5
EDU1	60	0.0	0.0	0.0	88.3	32.4	28.2	63.4
EDU1	70	0.0	0.0	0.1	93.1	41.1	36.9	73.5
EDU1	80	0.0	0.0	3.1	97.1	55.7	49.2	82.0
EDU1	90	0.0	0.0	21.5	97.1	66.3	58.3	88.6
EDU1	100	0.0	0.0	23.9	100.0	73.9	65.0	98.8
EDU2	10	0.0	0.0	0.0	47.2	7.5	5.3	8.9
EDU2	20	0.0	0.0	0.0	62.8	13.6	8.3	19.0
EDU2	30	0.0	0.0	0.0	72.0	18.1	12.5	29.2
EDU2	40	0.0	0.0	0.0	76.4	21.1	17.4	39.5
EDU2	50	0.0	0.0	0.0	78.8	24.5	22.4	49.8
EDU2	60	0.0	0.0	0.0	82.8	30.4	26.9	60.1
EDU2	70	0.0	0.0	0.1	88.0	38.7	35.4	69.8
EDU2	80	0.0	0.0	3.6	92.8	52.0	47.1	78.4
EDU2	90	0.0	0.0	19.1	93.6	61.9	56.2	85.9
EDU2	100	0.0	0.0	21.3	100.0	68.8	62.5	95.6

Table Z-2. Specific Occupancy, Post-FIRM Construction

Occupancy	Building Loss	Foundation	Below First FLoor	Structure Frame	Roof Cover	Roof Framing	Exterior Wall	Interiors
RES1	10	0.0	0.0	0.0	43.5	0.3	2.5	11.4
RES1	20	0.0	0.0	0.0	69.1	0.5	4.7	24.7
RES1	30	0.0	0.0	0.1	73.4	1.1	6.1	40.6
RES1	40	0.0	0.0	0.3	77.9	1.8	8.1	56.3
RES1	50	0.0	0.0	0.6	80.8	3.2	11.6	71.4
RES1	60	0.0	0.0	1.4	92.3	8.5	17.8	83.9
RES1	70	0.0	0.0	7.4	100.0	17.3	30.8	92.6
RES1	80	0.0	0.0	17.5	100.0	29.0	46.3	100.0
RES1	90	0.0	0.0	29.8	100.0	58.4	74.2	100.0
RES1	100	16.7	16.8	49.8	100.0	100.0	82.5	100.0
RES2	10	0.0	0.0	0.0	47.7	0.2	3.1	11.4
RES2	20	0.0	0.0	0.0	47.7	1.6	4.5	26.1
RES2	30	0.0	0.0	0.1	50.9	3.0	5.8	40.6
RES2	40	0.0	0.0	0.3	59.2	5.0	7.4	54.7
RES2	50	0.0	0.0	0.6	65.9	7.7	10.7	68.1
RES2	60	0.0	0.0	1.5	74.4	14.6	17.6	79.6
RES2	70	0.0	0.0	7.2	86.1	30.1	28.5	87.5
RES2	80	0.0	0.0	17.0	94.1	51.7	42.8	92.9
RES2	90	0.0	0.0	24.8	98.4	65.9	58.6	99.1
RES2	100	0.0	0.0	34.9	100.0	100.0	82.5	100.0
RES3A	10	0.0	0.0	0.0	59.0	10.4	7.5	6.6
RES3A	20	0.0	0.0	0.2	82.1	21.4	18.2	15.6
RES3A	30	0.0	0.0	0.6	89.6	31.2	31.8	25.2
RES3A	40	0.2	0.0	1.5	96.3	43.7	40.3	36.5
RES3A	50	0.4	0.0	2.6	99.5	54.2	48.9	48.3
RES3A	60	0.5	0.0	4.5	100.0	65.1	56.0	60.8
RES3A	70	0.6	0.0	15.7	100.0	75.5	65.1	70.7
RES3A	80	0.6	0.0	27.0	100.0	89.1	71.4	81.3
RES3A	90	0.6	0.0	32.2	100.0	96.3	80.0	93.0
RES3A	100	0.7	0.0	40.0	100.0	100.0	99.5	100.0
RES3B	10	0.0	0.0	0.0	59.5	10.7	5.7	7.2
RES3B	20	0.0	0.0	0.0	82.9	23.4	13.9	17.1
RES3B	30	0.0	0.0	0.2	90.2	34.1	27.9	26.5
RES3B	40	0.0	0.0	0.6	95.7	47.8	37.3	37.6

Occupancy	Building Loss	Foundation	Below First FLoor	Structure Frame	Roof Cover	Roof Framing	Exterior Wall	Interiors
RES3B	50	0.0	0.0	1.4	99.4	58.7	45.9	49.4
RES3B	60	0.0	0.0	2.3	100.0	68.2	53.6	62.1
RES3B	70	0.0	0.0	7.5	100.0	77.0	60.5	74.3
RES3B	80	0.0	0.0	17.8	100.0	88.2	67.0	85.3
RES3B	90	0.0	0.0	26.6	100.0	98.2	74.1	96.5
RES3B	100	0.0	0.0	40.0	100.0	100.0	100.0	100.0
RES3C	10	0.0	0.0	0.0	73.2	14.9	5.9	8.4
RES3C	20	0.0	0.0	0.1	90.8	28.8	14.3	18.2
RES3C	30	0.0	0.0	0.3	95.2	37.1	29.2	27.8
RES3C	40	0.0	0.0	0.8	97.2	46.9	36.7	38.3
RES3C	50	0.0	0.0	1.6	97.6	55.5	42.8	49.1
RES3C	60	0.0	0.0	2.6	98.0	63.5	47.8	60.0
RES3C	70	0.0	0.0	10.8	98.4	69.9	55.6	69.6
RES3C	80	0.0	0.0	18.3	98.8	82.4	58.8	79.7
RES3C	90	0.0	0.0	21.2	100.0	91.5	63.5	90.4
RES3C	100	0.0	0.0	25.1	100.0	100.0	74.9	100.0
RES3D	10	0.0	0.0	0.0	73.6	15.2	5.8	8.4
RES3D	20	0.0	0.0	0.1	91.2	29.1	14.1	18.2
RES3D	30	0.0	0.0	0.3	96.0	37.6	29.4	27.7
RES3D	40	0.0	0.0	0.8	97.6	47.5	37.1	38.2
RES3D	50	0.0	0.0	1.6	98.4	56.3	43.0	49.0
RES3D	60	0.0	0.0	2.5	98.8	64.3	48.2	59.9
RES3D	70	0.0	0.0	10.7	99.2	70.9	56.0	69.5
RES3D	80	0.0	0.0	18.3	99.2	83.7	59.5	79.5
RES3D	90	0.0	0.0	21.6	100.0	93.1	64.4	90.1
RES3D	100	0.0	0.0	25.1	100.0	100.0	74.9	100.0
RES3E	10	0.0	0.0	0.0	83.2	17.1	6.6	9.5
RES3E	20	0.0	0.0	0.1	99.2	31.7	15.4	19.8
RES3E	30	0.0	0.0	0.3	100.0	40.0	31.4	29.6
RES3E	40	0.0	0.0	0.9	100.0	50.1	39.2	40.4
RES3E	50	0.0	0.0	1.7	100.0	59.2	45.3	51.6
RES3E	60	0.0	0.0	2.6	100.0	67.5	50.6	62.9
RES3E	70	0.0	0.0	11.1	100.0	73.9	58.3	72.4
RES3E	80	0.0	0.0	19.0	100.0	86.7	61.7	82.5
RES3E	90	0.0	0.0	22.3	100.0	96.3	66.6	93.3
RES3E	100	0.0	0.0	31.1	100.0	100.0	92.7	100.0
RES3F	10	0.0	0.0	0.0	80.0	16.8	2.1	10.3

Occupancy	Building Loss	Foundation	Below First FLoor	Structure Frame	Roof Cover	Roof Framing	Exterior Wall	Interiors
RES3F	20	0.0	0.0	0.0	100.0	33.6	6.3	21.1
RES3F	30	0.0	0.0	0.1	100.0	57.6	14.5	31.3
RES3F	40	0.0	0.0	0.3	100.0	79.2	24.5	41.3
RES3F	50	0.0	0.0	0.7	100.0	83.2	36.2	51.1
RES3F	60	0.0	0.0	1.5	100.0	84.8	46.6	61.2
RES3F	70	0.0	0.0	3.3	100.0	85.6	53.0	71.8
RES3F	80	0.0	0.0	9.0	100.0	95.2	53.3	82.7
RES3F	90	0.0	0.0	10.1	100.0	100.0	59.7	93.4
RES3F	100	0.0	0.0	14.5	100.0	100.0	85.5	100.0
RES4	10	0.0	0.0	0.0	67.2	14.4	4.4	9.4
RES4	20	0.0	0.0	0.0	88.0	29.2	11.7	19.0
RES4	30	0.0	0.0	0.2	91.2	40.4	22.9	28.5
RES4	40	0.0	0.0	0.6	92.0	46.8	31.0	38.5
RES4	50	0.0	0.0	1.2	92.8	51.6	38.1	48.6
RES4	60	0.0	0.0	3.6	92.8	56.4	43.7	58.8
RES4	70	0.0	0.0	8.1	93.6	63.6	47.9	68.8
RES4	80	0.0	0.0	10.6	94.4	72.8	51.6	79.0
RES4	90	0.0	0.0	11.6	98.4	83.2	55.7	89.3
RES4	100	0.0	0.0	12.9	100.0	92.4	62.0	99.3
RES5	10	0.0	0.0	0.0	64.8	17.3	4.9	10.2
RES5	20	0.0	0.0	0.1	93.6	33.6	14.2	20.0
RES5	30	0.0	0.0	0.2	99.2	36.3	26.7	30.2
RES5	40	0.0	0.0	0.4	100.0	39.2	38.3	40.6
RES5	50	0.0	0.0	1.2	100.0	45.6	47.1	51.4
RES5	60	0.0	0.0	1.3	100.0	54.9	52.1	63.0
RES5	70	0.0	0.0	1.4	100.0	64.0	53.7	75.3
RES5	80	0.0	0.0	1.4	100.0	70.9	54.8	87.8
RES5	90	0.0	0.0	1.6	100.0	79.7	61.7	99.0
RES5	100	0.0	0.0	15.4	100.0	100.0	100.0	100.0
RES6	10	0.0	0.0	0.0	66.9	8.8	9.5	7.4
RES6	20	0.0	0.0	0.0	88.8	17.6	18.2	17.2
RES6	30	0.0	0.0	0.0	92.5	26.4	28.1	27.5
RES6	40	0.0	0.0	0.0	93.3	37.2	37.3	38.1
RES6	50	0.0	0.0	0.0	94.4	52.0	40.6	49.6
RES6	60	0.0	0.0	0.1	94.9	60.0	46.3	60.9
RES6	70	0.0	0.0	1.1	96.3	64.4	54.3	71.8
RES6	80	0.0	0.0	12.5	98.4	70.4	58.4	81.7

Occupancy	Building Loss	Foundation	Below First FLoor	Structure Frame	Roof Cover	Roof Framing	Exterior Wall	Interiors
RES6	90	0.0	0.0	25.8	100.0	77.2	64.1	91.2
RES6	100	0.0	0.0	31.3	100.0	93.6	77.7	100.0
COM1	10	0.0	0.0	0.0	36.2	3.0	6.9	9.0
COM1	20	0.0	0.0	0.2	60.6	12.5	13.1	18.6
COM1	30	0.0	0.0	2.0	76.5	22.4	20.9	28.3
COM1	40	1.9	0.0	3.6	85.9	29.3	26.8	38.8
COM1	50	3.1	0.0	4.3	89.6	32.6	33.1	50.3
COM1	60	3.8	0.0	6.0	93.0	37.1	38.7	61.8
COM1	70	3.9	0.0	7.9	96.3	41.0	46.0	73.1
COM1	80	4.0	0.0	9.3	100.0	47.2	58.4	83.5
COM1	90	4.0	0.0	26.8	100.0	70.4	66.4	91.1
COM1	100	4.9	0.0	32.5	100.0	85.4	80.7	100.0
COM2	10	0.0	0.0	0.0	31.6	4.5	8.6	9.5
COM2	20	0.0	0.0	0.0	50.1	9.0	14.2	22.4
COM2	30	0.0	0.0	0.0	63.9	15.2	21.3	35.8
COM2	40	0.0	0.0	0.0	74.9	32.1	27.7	48.2
COM2	50	0.0	0.0	0.0	86.5	43.3	38.1	60.4
COM2	60	0.0	0.0	3.7	100.0	70.3	44.2	70.1
COM2	70	5.2	0.0	7.5	100.0	76.8	51.8	82.6
COM2	80	8.5	0.0	10.0	100.0	86.5	65.4	94.5
COM2	90	11.0	0.0	34.8	100.0	100.0	91.7	100.0
COM2	100	27.3	0.0	86.4	100.0	100.0	100.0	100.0
COM3	10	0.0	0.0	0.0	41.7	6.7	4.7	7.7
COM3	20	0.0	0.0	0.0	66.4	13.3	8.7	17.5
COM3	30	0.0	0.0	0.0	79.9	19.5	14.3	28.5
COM3	40	0.0	0.0	0.0	85.7	24.5	21.3	40.2
COM3	50	0.0	0.0	0.0	89.9	32.0	28.2	52.1
COM3	60	0.0	0.0	0.0	94.6	41.3	33.8	64.0
COM3	70	0.0	0.0	0.1	99.5	52.8	44.4	74.9
COM3	80	0.0	0.0	4.3	100.0	65.3	56.3	85.6
COM3	90	0.0	0.0	27.0	100.0	75.5	65.3	94.8
COM3	100	0.0	0.0	42.9	100.0	100.0	100.0	100.0
COM4	10	0.0	0.0	0.0	54.4	10.1	5.7	10.4
COM4	20	0.0	0.0	0.0	77.6	16.8	11.4	21.5
COM4	30	0.0	0.0	0.1	87.2	24.5	17.2	32.7
COM4	40	0.0	0.0	0.2	91.2	33.1	23.3	43.9
COM4	50	0.0	0.0	0.3	96.0	42.4	30.2	54.8

Occupancy	Building Loss	Foundation	Below First FLoor	Structure Frame	Roof Cover	Roof Framing	Exterior Wall	Interiors
COM4	60	0.3	0.0	1.8	99.2	56.5	35.4	65.7
COM4	70	1.2	0.0	3.2	100.0	65.6	43.6	76.1
COM4	80	1.6	0.0	4.6	100.0	76.8	53.9	85.8
COM4	90	1.6	0.0	16.6	100.0	85.6	60.8	94.8
COM4	100	2.3	0.0	23.1	100.0	100.0	84.3	100.0
COM5	10	0.0	0.0	0.0	46.0	7.4	5.0	8.6
COM5	20	0.0	0.0	0.0	69.2	14.2	8.9	18.9
COM5	30	0.0	0.0	0.0	81.4	20.1	14.2	29.9
COM5	40	0.0	0.0	0.0	86.6	24.6	20.8	41.5
COM5	50	0.0	0.0	0.0	89.6	30.9	27.3	52.9
COM5	60	0.0	0.0	0.0	93.4	39.5	32.5	64.1
COM5	70	0.0	0.0	0.1	97.6	50.2	42.3	74.3
COM5	80	0.0	0.0	3.9	100.0	62.4	53.5	83.8
COM5	90	0.0	0.0	23.9	100.0	72.0	62.1	91.7
COM5	100	0.0	0.0	29.5	100.0	88.8	76.5	100.0
COM6	10	0.0	0.0	0.0	48.8	9.8	5.3	8.9
COM6	20	0.0	0.0	0.0	57.6	14.2	8.7	18.9
COM6	30	0.0	0.0	0.0	63.2	17.6	12.3	28.9
COM6	40	0.0	0.0	0.0	67.2	19.6	16.3	38.9
COM6	50	0.0	0.0	0.0	70.4	22.2	20.4	48.9
COM6	60	0.0	0.0	0.1	75.2	26.2	25.3	58.8
COM6	70	0.0	0.0	0.1	83.2	34.0	33.2	68.2
COM6	80	0.0	0.0	2.7	88.8	43.4	43.9	77.1
COM6	90	0.0	0.0	3.1	99.2	48.8	49.3	86.7
COM6	100	0.0	0.0	3.3	100.0	54.2	54.9	96.5
COM7	10	0.0	0.0	0.0	46.1	7.6	5.1	8.6
COM7	20	0.0	0.0	0.0	69.3	14.4	8.9	18.3
COM7	30	0.0	0.0	0.0	79.7	19.6	14.0	28.5
COM7	40	0.0	0.0	0.0	82.7	24.0	20.3	38.8
COM7	50	0.0	0.0	0.0	85.1	30.4	26.4	49.2
COM7	60	0.0	0.0	0.0	88.3	39.2	31.3	59.6
COM7	70	0.0	0.0	0.2	92.0	50.0	40.8	69.2
COM7	80	0.0	0.0	3.6	94.7	60.8	51.1	78.5
COM7	90	0.0	0.0	22.8	96.3	70.0	59.3	87.4
COM7	100	0.0	0.0	25.4	100.0	78.4	66.1	97.3
COM8	10	0.0	0.0	0.0	48.2	8.0	5.1	8.8
COM8	20	0.0	0.0	0.0	70.2	15.7	9.3	19.5

Occupancy	Building Loss	Foundation	Below First FLoor	Structure Frame	Roof Cover	Roof Framing	Exterior Wall	Interiors
COM8	30	0.0	0.0	0.1	81.6	22.4	14.9	30.7
COM8	40	0.0	0.0	0.2	87.8	26.7	20.9	42.3
COM8	50	0.0	0.0	0.4	90.4	31.7	27.3	54.0
COM8	60	0.0	0.0	1.5	94.2	39.5	32.2	65.6
COM8	70	0.0	0.0	2.4	99.0	48.5	40.6	76.7
COM8	80	0.0	0.0	3.8	100.0	64.0	53.9	87.0
COM8	90	0.0	0.0	23.4	100.0	75.2	63.5	95.5
COM8	100	0.0	0.0	44.4	100.0	100.0	100.0	100.0
COM9	10	0.0	0.0	0.0	45.3	3.3	5.6	8.5
COM9	20	0.0	0.0	0.0	62.4	7.1	9.7	19.6
COM9	30	0.0	0.0	0.0	73.3	12.5	14.2	31.0
COM9	40	0.0	0.0	0.1	80.0	15.5	19.6	42.9
COM9	50	0.0	0.0	0.2	85.4	18.5	25.2	54.8
COM9	60	0.0	0.0	0.5	90.4	21.2	31.7	66.6
COM9	70	0.0	0.0	1.0	96.5	25.6	42.0	77.6
COM9	80	0.0	0.0	6.0	100.0	38.8	54.0	86.9
COM9	90	0.0	0.0	14.3	100.0	66.0	63.6	95.0
COM9	100	0.0	0.0	20.8	100.0	96.3	92.8	100.0
COM10	10	0.0	0.0	0.0	0.0	0.0	10.0	27.7
COM10	20	0.0	0.0	0.0	0.0	0.0	30.0	52.3
COM10	30	0.0	0.0	0.0	0.0	0.0	60.0	73.8
COM10	40	0.0	0.0	0.0	0.0	0.0	80.0	98.5
COM10	50	0.0	0.0	0.0	0.0	60.0	100.0	100.0
COM10	60	0.0	0.0	10.3	0.0	100.0	100.0	100.0
COM10	70	0.0	0.0	30.8	0.0	100.0	100.0	100.0
COM10	80	0.0	0.0	51.3	0.0	100.0	100.0	100.0
COM10	90	0.0	0.0	71.8	0.0	100.0	100.0	100.0
COM10	100	9.4	0.0	88.2	0.0	100.0	100.0	100.0
IND1	10	0.0	0.0	0.0	42.5	4.5	5.1	7.5
IND1	20	0.0	0.0	0.0	61.6	10.9	9.5	17.8
IND1	30	0.0	0.0	0.4	72.1	18.7	14.1	29.0
IND1	40	0.0	0.0	0.8	79.4	22.4	19.7	40.7
IND1	50	0.0	0.0	0.8	83.4	36.5	26.5	52.0
IND1	60	1.6	0.0	2.8	87.4	52.3	33.0	62.7
IND1	70	4.4	0.0	4.8	92.1	56.0	39.0	73.6
IND1	80	6.0	0.0	6.4	98.4	66.9	51.2	83.4
IND1	90	6.3	0.0	22.4	100.0	78.1	64.4	93.6

Occupancy	Building Loss	Foundation	Below First FLoor	Structure Frame	Roof Cover	Roof Framing	Exterior Wall	Interiors
IND1	100	9.3	0.0	33.2	100.0	100.0	95.1	100.0
IND2	10	0.0	0.0	0.0	39.4	6.3	4.4	7.2
IND2	20	0.0	0.0	0.0	58.9	12.9	8.2	17.9
IND2	30	0.0	0.0	0.0	72.3	18.7	13.2	29.7
IND2	40	0.0	0.0	0.0	81.2	22.9	18.8	42.4
IND2	50	0.0	0.0	0.3	86.6	27.2	24.7	55.6
IND2	60	0.0	0.0	0.8	93.1	33.4	30.3	68.5
IND2	70	0.0	0.0	1.6	99.8	42.2	39.4	80.2
IND2	80	0.0	0.0	4.8	100.0	58.6	53.5	90.8
IND2	90	0.0	0.0	23.2	100.0	76.0	69.8	100.0
IND2	100	4.8	4.8	100.0	100.0	100.0	100.0	100.0
IND3	10	0.0	0.0	0.0	40.6	6.4	4.4	7.0
IND3	20	0.0	0.0	0.0	56.9	12.9	8.2	17.6
IND3	30	0.0	0.0	0.0	68.4	18.4	13.2	28.8
IND3	40	0.0	0.0	0.3	76.4	22.1	17.9	40.6
IND3	50	0.0	0.0	0.3	80.6	25.6	23.2	53.0
IND3	60	0.0	0.0	1.6	86.6	30.3	28.0	65.0
IND3	70	0.0	0.0	3.2	93.0	36.8	35.5	76.3
IND3	80	0.0	0.0	5.1	99.7	53.3	48.7	85.4
IND3	90	0.0	0.0	20.3	100.0	66.5	61.3	95.1
IND3	100	0.0	0.0	30.1	100.0	99.3	91.4	100.0
IND4	10	0.0	0.0	0.0	62.0	9.6	6.7	11.7
IND4	20	0.0	0.0	0.0	79.2	17.7	10.6	25.7
IND4	30	0.0	0.0	0.0	92.4	24.1	15.8	40.0
IND4	40	0.0	0.0	0.0	100.0	27.7	21.8	54.7
IND4	50	0.0	0.0	0.1	100.0	31.2	28.3	69.6
IND4	60	0.0	0.0	0.4	100.0	36.7	34.3	84.3
IND4	70	0.0	0.0	0.7	100.0	46.1	44.7	97.8
IND4	80	0.0	0.0	6.3	100.0	92.4	84.9	100.0
IND4	90	0.0	0.0	33.3	100.0	100.0	100.0	100.0
IND4	100	0.0	0.0	66.7	100.0	100.0	100.0	100.0
IND5	10	0.0	0.0	0.0	45.2	7.4	5.1	8.3
IND5	20	0.0	0.0	0.0	60.4	13.2	8.5	18.6
IND5	30	0.0	0.0	0.0	70.2	18.0	12.8	29.1
IND5	40	0.0	0.0	0.0	75.8	21.2	17.3	40.0
IND5	50	0.0	0.0	0.0	78.8	24.4	22.4	51.0
IND5	60	0.0	0.0	0.4	83.6	29.6	27.2	61.8

Occupancy	Building Loss	Foundation	Below First FLoor	Structure Frame	Roof Cover	Roof Framing	Exterior Wall	Interiors
IND5	70	0.0	0.0	0.8	89.8	37.8	35.5	72.2
IND5	80	0.0	0.0	4.4	96.0	52.2	48.3	81.8
IND5	90	0.0	0.0	18.6	99.2	63.4	59.2	91.3
IND5	100	0.0	0.0	25.8	100.0	87.8	81.9	100.0
IND6	10	0.0	0.0	0.0	42.0	6.6	4.7	7.8
IND6	20	0.0	0.0	0.0	68.6	14.1	8.9	18.9
IND6	30	0.0	0.0	0.0	85.5	21.0	14.9	31.8
IND6	40	0.0	0.0	0.0	95.2	26.7	22.6	45.9
IND6	50	0.0	0.0	0.0	100.0	34.5	30.9	60.7
IND6	60	0.0	0.0	0.0	100.0	45.5	38.0	76.2
IND6	70	0.0	0.0	0.1	100.0	59.0	50.5	90.1
IND6	80	0.0	0.0	5.2	100.0	80.9	70.2	100.0
IND6	90	0.0	0.0	66.7	100.0	100.0	100.0	100.0
IND6	100	23.1	23.2	100.0	100.0	100.0	100.0	100.0
AGR1	10	0.0	0.0	0.0	47.6	4.0	7.0	7.9
AGR1	20	0.0	0.0	0.1	78.1	11.9	14.5	19.1
AGR1	30	0.0	0.0	1.6	96.6	23.3	22.9	32.0
AGR1	40	0.0	0.0	2.5	100.0	32.9	35.3	48.4
AGR1	50	0.0	0.0	2.9	100.0	62.8	48.5	60.0
AGR1	60	2.8	0.0	6.5	100.0	89.2	59.0	70.2
AGR1	70	8.0	0.0	12.1	100.0	96.0	66.5	84.0
AGR1	80	10.9	0.0	15.9	100.0	100.0	81.4	98.7
AGR1	90	17.5	0.0	65.5	100.0	100.0	100.0	100.0
AGR1	100	35.5	0.0	100.0	100.0	100.0	100.0	100.0
REL1	10	0.0	0.0	0.0	60.6	7.5	8.2	8.3
REL1	20	0.0	0.0	0.0	85.2	15.6	14.9	20.0
REL1	30	0.0	0.0	0.0	96.4	23.1	23.2	32.9
REL1	40	0.0	0.0	0.0	100.0	30.6	32.4	46.3
REL1	50	0.0	0.0	0.0	100.0	41.9	37.1	59.4
REL1	60	0.0	0.0	0.0	100.0	50.3	42.6	73.5
REL1	70	0.0	0.0	0.3	100.0	59.9	52.4	86.2
REL1	80	0.0	0.0	8.1	100.0	71.1	60.0	96.8
REL1	90	0.0	0.0	21.6	100.0	92.1	77.4	100.0
REL1	100	0.0	0.0	63.6	100.0	100.0	100.0	100.0
GOV1	10	0.0	0.0	0.0	44.4	7.0	4.9	8.4
GOV1	20	0.0	0.0	0.0	65.5	13.8	8.5	19.5
GOV1	30	0.0	0.0	0.0	78.5	19.8	13.4	31.4

Occupancy	Building Loss	Foundation	Below First FLoor	Structure Frame	Roof Cover	Roof Framing	Exterior Wall	Interiors
GOV1	40	0.0	0.0	0.0	86.1	23.6	19.3	43.8
GOV1	50	0.0	0.0	0.0	90.4	28.4	25.7	56.5
GOV1	60	0.0	0.0	0.0	96.0	35.6	31.1	69.0
GOV1	70	0.0	0.0	0.1	100.0	45.8	41.3	80.8
GOV1	80	0.0	0.0	3.9	100.0	62.0	55.2	91.5
GOV1	90	0.0	0.0	23.6	100.0	73.8	65.7	99.7
GOV1	100	0.0	0.0	63.6	100.0	100.0	100.0	100.0
GOV2	10	0.0	0.0	0.0	53.6	8.4	6.0	10.2
GOV2	20	0.0	0.0	0.0	73.6	15.6	9.7	21.9
GOV2	30	0.0	0.0	0.0	84.4	21.2	14.5	33.8
GOV2	40	0.0	0.0	0.0	89.6	24.8	20.4	45.8
GOV2	50	0.0	0.0	0.0	92.0	28.8	26.3	57.8
GOV2	60	0.0	0.0	0.0	96.8	36.0	31.6	69.8
GOV2	70	0.0	0.0	0.1	100.0	45.6	41.3	80.9
GOV2	80	0.0	0.0	4.1	100.0	60.8	54.5	90.4
GOV2	90	0.0	0.0	22.3	100.0	71.2	64.0	97.3
GOV2	100	0.0	0.0	35.7	100.0	100.0	100.0	100.0
EDU1	10	0.0	0.0	0.0	48.3	7.5	5.2	9.2
EDU1	20	0.0	0.0	0.0	67.5	14.4	8.5	20.2
EDU1	30	0.0	0.0	0.0	78.9	19.9	13.2	31.6
EDU1	40	0.0	0.0	0.0	84.8	23.3	18.8	43.2
EDU1	50	0.0	0.0	0.0	87.7	27.5	24.6	54.9
EDU1	60	0.0	0.0	0.0	92.3	34.0	29.5	66.5
EDU1	70	0.0	0.0	0.1	97.6	43.1	38.7	77.0
EDU1	80	0.0	0.0	3.3	100.0	58.5	51.6	86.0
EDU1	90	0.0	0.0	22.5	100.0	69.7	61.3	93.2
EDU1	100	0.0	0.0	29.6	100.0	91.5	80.5	100.0
EDU2	10	0.0	0.0	0.0	49.2	7.7	5.5	9.3
EDU2	20	0.0	0.0	0.0	65.6	14.1	8.7	19.8
EDU2	30	0.0	0.0	0.0	75.2	18.9	13.0	30.5
EDU2	40	0.0	0.0	0.0	80.0	21.9	18.2	41.3
EDU2	50	0.0	0.0	0.0	82.4	25.9	23.4	52.1
EDU2	60	0.0	0.0	0.0	86.8	31.7	28.1	62.8
EDU2	70	0.0	0.0	0.1	92.0	40.5	37.0	73.0
EDU2	80	0.0	0.0	3.7	96.8	54.7	49.3	82.1
EDU2	90	0.0	0.0	20.1	98.0	65.1	59.0	90.1
EDU2	100	0.0	0.0	22.9	100.0	74.1	67.3	100.0

Table Z-3. General Building Type, Pre-FIRM Construction

General Building Type	Building Loss	Foundation	Below First Floor	Structure Frame	Roof Cover	Roof Framing	Exterior Wall	Interiors
Wood	10	0.0	0.0	0.0	45.8	1.6	2.2	10.3
Wood	20	0.0	0.0	0.1	71.8	3.0	4.2	22.0
Wood	30	0.0	0.0	0.2	76.8	4.6	5.8	35.3
Wood	40	0.0	0.0	0.5	81.4	6.4	8.1	48.5
Wood	50	0.0	0.0	1.0	86.0	9.0	11.4	61.2
Wood	60	0.0	0.0	1.6	96.8	15.4	17.7	72.3
Wood	70	0.0	0.0	2.9	100.0	24.4	29.4	82.0
Wood	80	0.0	0.0	9.2	100.0	37.2	43.1	90.1
Wood	90	0.5	0.0	21.6	100.0	65.2	61.5	94.1
Wood	100	0.7	0.0	28.2	100.0	85.2	80.5	100.0
Concrete	10	0.0	0.0	0.0	92.8	16.0	5.4	9.0
Concrete	20	0.0	0.0	0.1	100.0	31.2	11.4	19.2
Concrete	30	0.0	0.0	0.3	100.0	44.4	18.1	29.3
Concrete	40	0.2	0.0	0.5	100.0	58.4	25.2	39.4
Concrete	50	1.4	0.0	1.5	100.0	76.0	31.5	49.3
Concrete	60	2.8	0.0	2.2	100.0	91.6	38.3	59.2
Concrete	70	3.8	0.0	4.2	100.0	100.0	46.2	68.8
Concrete	80	4.4	0.0	11.9	100.0	100.0	53.7	77.8
Concrete	90	5.0	0.0	13.5	100.0	100.0	60.7	88.0
Concrete	100	5.6	0.0	15.1	100.0	100.0	67.8	98.2
Steel	10	0.0	0.0	0.0	100.0	10.0	5.5	9.1
Steel	20	0.0	0.0	0.1	100.0	21.2	10.4	19.7
Steel	30	0.0	0.0	0.4	100.0	31.6	15.6	30.3
Steel	40	0.2	0.0	0.7	100.0	41.2	20.9	40.8
Steel	50	0.4	0.0	0.8	100.0	51.2	26.8	51.3
Steel	60	0.8	0.0	1.8	100.0	66.4	32.1	61.5
Steel	70	2.8	0.0	3.0	100.0	76.4	38.0	71.7
Steel	80	3.8	0.0	4.9	100.0	92.0	47.7	80.7
Steel	90	4.4	0.0	21.2	100.0	100.0	56.7	87.5
Steel	100	5.0	0.0	23.7	100.0	100.0	63.3	97.7
Masonry	10	0.0	0.0	0.0	69.1	6.4	2.9	9.6
Masonry	20	0.0	0.0	0.1	100.0	13.3	6.0	21.3
Masonry	30	0.0	0.0	0.3	100.0	20.3	10.0	34.3
Masonry	40	0.1	0.0	0.6	100.0	28.5	14.8	47.0
Masonry	50	0.1	0.0	1.0	100.0	39.2	22.4	58.6
Masonry	60	0.2	0.0	2.9	100.0	52.8	31.2	69.2

General Building Type	Building Loss	Foundation	Below First Floor	Structure Frame	Roof Cover	Roof Framing	Exterior Wall	Interiors
Masonry	70	0.7	0.0	5.5	100.0	70.1	41.6	78.8
Masonry	80	1.6	0.0	9.1	100.0	94.4	51.8	87.9
Masonry	90	2.4	0.0	19.6	100.0	100.0	60.4	96.7
Masonry	100	3.5	0.0	28.5	100.0	100.0	87.6	100.0
MH	10	0.0	0.0	0.0	30.7	0.2	1.9	12.4
MH	20	0.0	0.0	0.0	30.7	1.4	2.5	26.9
MH	30	0.0	0.0	0.0	30.7	2.7	3.3	41.3
MH	40	0.0	0.0	0.0	35.2	4.3	4.2	55.3
MH	50	0.0	0.0	0.0	39.2	6.9	6.1	69.0
MH	60	0.0	0.0	0.0	44.8	13.1	10.3	81.4
MH	70	0.0	0.0	0.0	52.8	27.5	18.4	91.4
MH	80	0.0	0.0	0.0	59.2	48.5	30.2	99.6
MH	90	0.0	0.0	0.0	83.7	83.7	56.5	100.0
MH	100	0.0	0.0	0.0	100.0	100.0	90.0	100.0

Table Z-4. General Building Type, Post-FIRM Construction

General Building Type	Building Loss	Foundation	Below First Floor	Structure Frame	Roof Cover	Roof Framing	Exterior Wall	Interiors
Wood	10	0.0	0.0	0.0	49.4	1.8	2.2	10.6
Wood	20	0.0	0.0	0.1	77.6	3.4	4.2	22.9
Wood	30	0.0	0.0	0.2	83.4	5.0	6.0	36.9
Wood	40	0.0	0.0	0.5	88.8	7.0	8.3	50.7
Wood	50	0.0	0.0	0.9	93.8	10.0	11.8	64.1
Wood	60	0.0	0.0	1.5	100.0	17.0	18.4	76.2
Wood	70	0.1	0.0	2.8	100.0	27.4	31.0	86.6
Wood	80	0.1	0.0	8.8	100.0	43.6	48.2	94.3
Wood	90	3.0	0.0	32.6	100.0	74.8	68.0	95.4
Wood	100	3.9	0.0	43.0	100.0	98.6	89.8	100.0
Concrete	10	0.0	0.0	0.0	82.7	14.4	4.4	7.7
Concrete	20	0.0	0.0	0.1	100.0	31.2	10.3	18.1
Concrete	30	0.1	0.0	0.2	100.0	46.8	17.4	29.2
Concrete	40	0.4	0.0	0.4	100.0	62.8	24.8	40.2
Concrete	50	2.0	0.0	1.5	100.0	82.8	31.3	50.8
Concrete	60	4.1	0.0	2.1	100.0	100.0	38.3	61.4
Concrete	70	5.7	0.0	4.2	100.0	100.0	47.3	72.1
Concrete	80	7.7	0.0	13.1	100.0	100.0	56.5	81.4
Concrete	90	8.7	0.0	14.8	100.0	100.0	64.1	92.5
Concrete	100	11.8	0.0	20.0	100.0	100.0	86.4	100.0
Steel	10	0.0	0.0	0.0	100.0	10.8	5.5	9.5
Steel	20	0.0	0.0	0.1	100.0	23.2	10.5	20.7
Steel	30	0.0	0.0	0.4	100.0	34.8	15.7	31.8
Steel	40	0.4	0.0	0.7	100.0	45.6	21.0	42.9
Steel	50	0.6	0.0	0.8	100.0	56.8	27.0	53.9
Steel	60	1.4	0.0	1.7	100.0	73.6	32.3	64.6
Steel	70	4.2	0.0	2.9	100.0	84.8	38.2	75.0
Steel	80	5.8	0.0	4.9	100.0	100.0	48.5	84.4
Steel	90	7.6	0.0	23.3	100.0	100.0	59.6	91.1
Steel	100	9.2	0.0	28.2	100.0	100.0	71.9	100.0
Masonry	10	0.0	0.0	0.0	74.1	6.9	2.9	9.9
Masonry	20	0.0	0.0	0.1	100.0	14.7	6.2	22.5
Masonry	30	0.0	0.0	0.3	100.0	22.7	10.4	36.3
Masonry	40	0.1	0.0	0.6	100.0	31.7	15.3	49.7
Masonry	50	0.3	0.0	1.0	100.0	43.5	23.2	61.9
Masonry	60	0.4	0.0	2.8	100.0	59.5	33.2	72.9

General Building Type	Building Loss	Foundation	Below First Floor	Structure Frame	Roof Cover	Roof Framing	Exterior Wall	Interiors
Masonry	70	1.1	0.0	5.3	100.0	80.3	45.6	82.4
Masonry	80	4.9	0.0	11.1	100.0	100.0	55.1	91.4
Masonry	90	9.7	0.0	25.5	100.0	100.0	62.2	99.9
Masonry	100	14.9	0.0	39.0	100.0	100.0	95.0	100.0
MH	10	0.0	0.0	0.0	32.5	0.2	2.0	12.7
MH	20	0.0	0.0	0.0	32.5	1.4	2.7	27.7
MH	30	0.0	0.0	0.0	32.5	2.9	3.5	42.6
MH	40	0.0	0.0	0.0	37.6	4.6	4.5	57.2
MH	50	0.0	0.0	0.0	42.1	7.4	6.6	71.3
MH	60	0.0	0.0	0.0	47.7	14.1	11.0	84.0
MH	70	0.0	0.0	0.0	56.5	29.4	19.7	94.0
MH	80	0.0	0.0	0.0	69.3	56.8	35.4	100.0
MH	90	0.0	0.0	0.0	93.1	93.0	62.8	100.0
MH	100	0.0	0.0	0.0	100.0	100.0	100.0	100.0

Appendix AA. Flood Sub-Assembly Loss Tables

SOCC or GBT	Pre- or Post-FIRM	Zone	Building Loss	Foundation	Below First Floor	Structure Frame	Roof Covering	Roof Framing	Exterior Walls	Interiors
RES1	Pre	A	0%	0%	0%	0%	0%	0%	0%	0%
RES1	Pre	A	10%	0%	20%	0%	0%	0%	4%	14%
RES1	Pre	A	20%	0%	40%	0%	0%	0%	12%	26%
RES1	Pre	A	30%	0%	60%	0%	0%	0%	21%	37%
RES1	Pre	A	40%	0%	100%	0%	0%	0%	30%	48%
RES1	Pre	A	50%	0%	100%	0%	0%	0%	39%	60%
RES1	Pre	A	60%	0%	100%	0%	0%	0%	47%	74%
RES1	Pre	A	70%	0%	100%	0%	0%	0%	56%	86%
RES1	Pre	A	80%	0%	100%	5%	14%	5%	68%	94%
RES1	Pre	A	90%	5%	100%	26%	27%	26%	83%	96%
RES1	Pre	A	100%	10%	100%	50%	50%	50%	86%	100%
RES1	Post	A	0%	0%	0%	0%	0%	0%	0%	0%
RES1	Post	A	10%	0%	20%	0%	0%	0%	4%	14%
RES1	Post	A	20%	0%	40%	0%	0%	0%	12%	26%
RES1	Post	A	30%	0%	60%	0%	0%	0%	21%	38%
RES1	Post	A	40%	0%	100%	0%	0%	0%	30%	49%
RES1	Post	A	50%	0%	100%	0%	0%	0%	39%	63%
RES1	Post	A	60%	0%	100%	0%	0%	0%	47%	77%
RES1	Post	A	70%	0%	100%	0%	0%	0%	56%	90%
RES1	Post	A	80%	0%	100%	5%	14%	5%	74%	96%
RES1	Post	A	90%	5%	100%	26%	27%	26%	90%	98%
RES1	Post	A	100%	16%	100%	55%	55%	55%	93%	100%
RES1	Pre	CA	0%	0%	0%	0%	0%	0%	0%	0%
RES1	Pre	CA	10%	0%	50%	0%	0%	0%	2%	13%
RES1	Pre	CA	20%	0%	100%	1%	1%	1%	14%	21%
RES1	Pre	CA	30%	0%	100%	6%	6%	6%	22%	32%
RES1	Pre	CA	40%	0%	100%	8%	8%	8%	30%	44%
RES1	Pre	CA	50%	0%	100%	10%	10%	10%	42%	55%
RES1	Pre	CA	60%	1%	100%	13%	13%	13%	51%	66%
RES1	Pre	CA	70%	5%	100%	16%	16%	16%	62%	76%
RES1	Pre	CA	80%	8%	100%	20%	20%	20%	70%	86%
RES1	Pre	CA	90%	13%	100%	24%	24%	24%	78%	98%
RES1	Pre	CA	100%	20%	100%	34%	34%	34%	100%	100%
RES1	Post	CA	0%	0%	0%	0%	0%	0%	0%	0%
RES1	Post	CA	10%	0%	45%	0%	0%	0%	5%	12%

SOCC or GBT	Pre- or Post-FIRM	Zone	Building Loss	Foundation	Below First Floor	Structure Frame	Roof Covering	Roof Framing	Exterior Walls	Interiors
RES1	Post	CA	20%	0%	100%	1%	1%	1%	13%	21%
RES1	Post	CA	30%	0%	100%	2%	2%	2%	24%	33%
RES1	Post	CA	40%	0%	100%	4%	4%	4%	33%	46%
RES1	Post	CA	50%	0%	100%	6%	6%	6%	49%	55%
RES1	Post	CA	60%	0%	100%	8%	8%	8%	60%	67%
RES1	Post	CA	70%	1%	100%	9%	9%	9%	73%	78%
RES1	Post	CA	80%	4%	100%	15%	15%	15%	85%	88%
RES1	Post	CA	90%	8%	100%	24%	24%	24%	90%	98%
RES1	Post	CA	100%	20%	100%	42%	42%	42%	100%	100%
RES2	Pre	A	0%	0%	0%	0%	0%	0%	0%	0%
RES2	Pre	A	10%	0%	9%	0%	0%	0%	3%	13%
RES2	Pre	A	20%	0%	35%	0%	0%	0%	4%	27%
RES2	Pre	A	30%	0%	60%	0%	0%	0%	8%	39%
RES2	Pre	A	40%	0%	79%	0%	0%	0%	16%	51%
RES2	Pre	A	50%	0%	100%	0%	0%	0%	23%	62%
RES2	Pre	A	60%	0%	100%	0%	0%	0%	28%	75%
RES2	Pre	A	70%	0%	100%	0%	0%	0%	35%	88%
RES2	Pre	A	80%	2%	100%	2%	2%	2%	53%	95%
RES2	Pre	A	90%	8%	100%	8%	8%	8%	74%	100%
RES2	Pre	A	100%	12%	100%	20%	20%	20%	100%	100%
RES2	Post	A	0%	0%	0%	0%	0%	0%	0%	0%
RES2	Post	A	10%	0%	6%	0%	0%	0%	7%	12%
RES2	Post	A	20%	0%	35%	0%	0%	0%	10%	25%
RES2	Post	A	30%	0%	60%	0%	0%	0%	18%	37%
RES2	Post	A	40%	0%	80%	0%	0%	0%	22%	50%
RES2	Post	A	50%	0%	100%	0%	0%	0%	30%	62%
RES2	Post	A	60%	0%	100%	0%	0%	0%	36%	75%
RES2	Post	A	70%	0%	100%	0%	0%	0%	42%	88%
RES2	Post	A	80%	2%	100%	3%	3%	3%	50%	99%
RES2	Post	A	90%	9%	100%	9%	9%	9%	79%	100%
RES2	Post	A	100%	21%	100%	24%	24%	24%	100%	100%
RES2	Pre	CA	0%	0%	0%	0%	0%	0%	0%	0%
RES2	Pre	CA	10%	0%	9%	0%	0%	0%	7%	12%
RES2	Pre	CA	20%	0%	35%	0%	0%	0%	10%	25%
RES2	Pre	CA	30%	0%	60%	0%	0%	0%	21%	35%
RES2	Pre	CA	40%	0%	90%	1%	1%	1%	28%	46%
RES2	Pre	CA	50%	0%	100%	2%	2%	2%	34%	57%

SOCC or GBT	Pre- or Post-FIRM	Zone	Building Loss	Foundation	Below First Floor	Structure Frame	Roof Covering	Roof Framing	Exterior Walls	Interiors
RES2	Pre	CA	60%	0%	100%	4%	4%	4%	42%	69%
RES2	Pre	CA	70%	1%	100%	8%	8%	8%	48%	80%
RES2	Pre	CA	80%	3%	100%	10%	10%	10%	57%	91%
RES2	Pre	CA	90%	10%	100%	14%	14%	14%	69%	100%
RES2	Pre	CA	100%	16%	100%	20%	20%	20%	100%	100%
RES2	Post	CA	0%	0%	0%	0%	0%	0%	0%	0%
RES2	Post	CA	10%	0%	3%	0%	0%	0%	7%	12%
RES2	Post	CA	20%	0%	40%	0%	0%	0%	15%	23%
RES2	Post	CA	30%	0%	100%	0%	0%	0%	25%	33%
RES2	Post	CA	40%	0%	100%	1%	1%	1%	31%	46%
RES2	Post	CA	50%	0%	100%	2%	2%	2%	44%	56%
RES2	Post	CA	60%	0%	100%	4%	4%	4%	55%	66%
RES2	Post	CA	70%	1%	100%	8%	8%	8%	60%	78%
RES2	Post	CA	80%	2%	100%	10%	10%	10%	68%	90%
RES2	Post	CA	90%	8%	100%	14%	14%	14%	77%	100%
RES2	Post	CA	100%	19%	100%	25%	25%	25%	100%	100%
RES3A	Pre	A	0%	0%	0%	0%	0%	0%	0%	0%
RES3A	Pre	A	10%	0%	20%	0%	0%	0%	4%	14%
RES3A	Pre	A	20%	0%	40%	0%	0%	0%	12%	26%
RES3A	Pre	A	30%	0%	60%	0%	0%	0%	21%	37%
RES3A	Pre	A	40%	0%	100%	0%	0%	0%	30%	48%
RES3A	Pre	A	50%	0%	100%	0%	0%	0%	39%	60%
RES3A	Pre	A	60%	0%	100%	0%	0%	0%	47%	74%
RES3A	Pre	A	70%	0%	100%	0%	0%	0%	56%	87%
RES3A	Pre	A	80%	0%	100%	5%	14%	5%	68%	95%
RES3A	Pre	A	90%	5%	100%	26%	27%	26%	83%	96%
RES3A	Pre	A	100%	10%	100%	50%	50%	50%	86%	100%
RES3A	Post	A	0%	0%	0%	0%	0%	0%	0%	0%
RES3A	Post	A	10%	0%	20%	0%	0%	0%	4%	14%
RES3A	Post	A	20%	0%	40%	0%	0%	0%	12%	26%
RES3A	Post	A	30%	0%	60%	0%	0%	0%	21%	38%
RES3A	Post	A	40%	0%	100%	0%	0%	0%	30%	49%
RES3A	Post	A	50%	0%	100%	0%	0%	0%	39%	62%
RES3A	Post	A	60%	0%	100%	0%	0%	0%	47%	76%
RES3A	Post	A	70%	0%	100%	0%	0%	0%	56%	89%
RES3A	Post	A	80%	0%	100%	5%	14%	5%	74%	96%
RES3A	Post	A	90%	5%	100%	26%	27%	26%	90%	97%

SOCC or GBT	Pre- or Post-FIRM	Zone	Building Loss	Foundation	Below First Floor	Structure Frame	Roof Covering	Roof Framing	Exterior Walls	Interiors
RES3A	Post	A	100%	15%	100%	53%	53%	53%	93%	100%
RES3A	Pre	CA	0%	0%	0%	0%	0%	0%	0%	0%
RES3A	Pre	CA	10%	0%	50%	0%	0%	0%	2%	13%
RES3A	Pre	CA	20%	0%	100%	1%	1%	1%	14%	22%
RES3A	Pre	CA	30%	0%	100%	6%	6%	6%	22%	33%
RES3A	Pre	CA	40%	0%	100%	8%	8%	8%	30%	45%
RES3A	Pre	CA	50%	0%	100%	10%	10%	10%	42%	55%
RES3A	Pre	CA	60%	1%	100%	13%	13%	13%	51%	67%
RES3A	Pre	CA	70%	5%	100%	16%	16%	16%	62%	76%
RES3A	Pre	CA	80%	8%	100%	20%	20%	20%	70%	87%
RES3A	Pre	CA	90%	13%	100%	24%	24%	24%	78%	98%
RES3A	Pre	CA	100%	20%	100%	34%	34%	34%	100%	100%
RES3A	Post	CA	0%	0%	0%	0%	0%	0%	0%	0%
RES3A	Post	CA	10%	0%	45%	0%	0%	0%	5%	12%
RES3A	Post	CA	20%	0%	100%	1%	1%	1%	13%	21%
RES3A	Post	CA	30%	0%	100%	2%	2%	2%	24%	34%
RES3A	Post	CA	40%	0%	100%	4%	4%	4%	33%	46%
RES3A	Post	CA	50%	0%	100%	6%	6%	6%	49%	56%
RES3A	Post	CA	60%	0%	100%	8%	8%	8%	60%	68%
RES3A	Post	CA	70%	1%	100%	9%	9%	9%	73%	79%
RES3A	Post	CA	80%	4%	100%	15%	15%	15%	85%	88%
RES3A	Post	CA	90%	8%	100%	24%	24%	24%	90%	98%
RES3A	Post	CA	100%	20%	100%	42%	42%	42%	100%	100%
RES3B	Pre	A	0%	0%	0%	0%	0%	0%	0%	0%
RES3B	Pre	A	10%	0%	20%	0%	0%	0%	4%	14%
RES3B	Pre	A	20%	0%	40%	0%	0%	0%	12%	26%
RES3B	Pre	A	30%	0%	60%	0%	0%	0%	21%	38%
RES3B	Pre	A	40%	0%	100%	0%	0%	0%	30%	49%
RES3B	Pre	A	50%	0%	100%	0%	0%	0%	39%	61%
RES3B	Pre	A	60%	0%	100%	0%	0%	0%	47%	74%
RES3B	Pre	A	70%	0%	100%	0%	0%	0%	56%	87%
RES3B	Pre	A	80%	0%	100%	5%	14%	5%	68%	95%
RES3B	Pre	A	90%	5%	100%	26%	27%	26%	83%	96%
RES3B	Pre	A	100%	10%	100%	50%	50%	50%	86%	100%
RES3B	Post	A	0%	0%	0%	0%	0%	0%	0%	0%
RES3B	Post	A	10%	0%	20%	0%	0%	0%	4%	14%
RES3B	Post	A	20%	0%	40%	0%	0%	0%	12%	26%

SOCC or GBT	Pre- or Post-FIRM	Zone	Building Loss	Foundation	Below First Floor	Structure Frame	Roof Covering	Roof Framing	Exterior Walls	Interiors
RES3B	Post	A	30%	0%	60%	0%	0%	0%	21%	38%
RES3B	Post	A	40%	0%	100%	0%	0%	0%	30%	49%
RES3B	Post	A	50%	0%	100%	0%	0%	0%	39%	63%
RES3B	Post	A	60%	0%	100%	0%	0%	0%	47%	76%
RES3B	Post	A	70%	0%	100%	0%	0%	0%	56%	90%
RES3B	Post	A	80%	0%	100%	5%	14%	5%	74%	96%
RES3B	Post	A	90%	5%	100%	26%	27%	26%	90%	98%
RES3B	Post	A	100%	15%	100%	53%	53%	53%	93%	100%
RES3B	Pre	CA	0%	0%	0%	0%	0%	0%	0%	0%
RES3B	Pre	CA	10%	0%	50%	0%	0%	0%	2%	13%
RES3B	Pre	CA	20%	0%	100%	1%	1%	1%	14%	22%
RES3B	Pre	CA	30%	0%	100%	6%	6%	6%	22%	33%
RES3B	Pre	CA	40%	0%	100%	8%	8%	8%	30%	45%
RES3B	Pre	CA	50%	0%	100%	10%	10%	10%	42%	55%
RES3B	Pre	CA	60%	1%	100%	13%	13%	13%	51%	67%
RES3B	Pre	CA	70%	5%	100%	16%	16%	16%	62%	76%
RES3B	Pre	CA	80%	8%	100%	20%	20%	20%	70%	87%
RES3B	Pre	CA	90%	13%	100%	24%	24%	24%	78%	98%
RES3B	Pre	CA	100%	20%	100%	34%	34%	34%	100%	100%
RES3B	Post	CA	0%	0%	0%	0%	0%	0%	0%	0%
RES3B	Post	CA	10%	0%	45%	0%	0%	0%	5%	12%
RES3B	Post	CA	20%	0%	100%	1%	1%	1%	13%	22%
RES3B	Post	CA	30%	0%	100%	2%	2%	2%	24%	34%
RES3B	Post	CA	40%	0%	100%	4%	4%	4%	33%	46%
RES3B	Post	CA	50%	0%	100%	6%	6%	6%	49%	56%
RES3B	Post	CA	60%	0%	100%	8%	8%	8%	60%	68%
RES3B	Post	CA	70%	1%	100%	9%	9%	9%	73%	79%
RES3B	Post	CA	80%	4%	100%	15%	15%	15%	85%	88%
RES3B	Post	CA	90%	8%	100%	24%	24%	24%	90%	98%
RES3B	Post	CA	100%	20%	100%	42%	42%	42%	100%	100%
RES3C	Pre	A	0%	0%	0%	0%	0%	0%	0%	0%
RES3C	Pre	A	10%	0%	20%	0%	0%	0%	4%	11%
RES3C	Pre	A	20%	0%	40%	0%	0%	0%	11%	21%
RES3C	Pre	A	30%	0%	58%	0%	0%	0%	16%	32%
RES3C	Pre	A	40%	0%	100%	0%	0%	0%	26%	41%
RES3C	Pre	A	50%	0%	100%	0%	0%	0%	30%	53%
RES3C	Pre	A	60%	0%	100%	0%	0%	0%	43%	62%

SOCC or GBT	Pre- or Post-FIRM	Zone	Building Loss	Foundation	Below First Floor	Structure Frame	Roof Covering	Roof Framing	Exterior Walls	Interiors
RES3C	Pre	A	70%	0%	100%	0%	0%	0%	49%	73%
RES3C	Pre	A	80%	0%	100%	2%	4%	2%	53%	83%
RES3C	Pre	A	90%	2%	100%	10%	10%	10%	56%	93%
RES3C	Pre	A	100%	8%	100%	20%	20%	20%	68%	100%
RES3C	Post	A	0%	0%	0%	0%	0%	0%	0%	0%
RES3C	Post	A	10%	0%	16%	0%	0%	0%	2%	11%
RES3C	Post	A	20%	0%	40%	0%	0%	0%	9%	23%
RES3C	Post	A	30%	0%	60%	0%	0%	0%	17%	33%
RES3C	Post	A	40%	0%	100%	0%	0%	0%	22%	44%
RES3C	Post	A	50%	0%	100%	0%	0%	0%	26%	56%
RES3C	Post	A	60%	0%	100%	0%	0%	0%	42%	65%
RES3C	Post	A	70%	0%	100%	0%	0%	0%	53%	76%
RES3C	Post	A	80%	0%	100%	1%	5%	1%	62%	87%
RES3C	Post	A	90%	2%	100%	14%	15%	14%	76%	94%
RES3C	Post	A	100%	12%	100%	26%	26%	26%	90%	100%
RES3C	Pre	CA	0%	0%	0%	0%	0%	0%	0%	0%
RES3C	Pre	CA	10%	0%	45%	0%	0%	0%	2%	11%
RES3C	Pre	CA	20%	0%	100%	1%	1%	1%	8%	20%
RES3C	Pre	CA	30%	0%	100%	2%	2%	2%	18%	30%
RES3C	Pre	CA	40%	0%	100%	4%	4%	4%	24%	41%
RES3C	Pre	CA	50%	0%	100%	7%	7%	7%	32%	50%
RES3C	Pre	CA	60%	1%	100%	10%	10%	10%	41%	60%
RES3C	Pre	CA	70%	2%	100%	12%	12%	12%	51%	69%
RES3C	Pre	CA	80%	3%	100%	20%	20%	20%	60%	78%
RES3C	Pre	CA	90%	8%	100%	20%	20%	20%	70%	88%
RES3C	Pre	CA	100%	9%	100%	21%	21%	21%	71%	99%
RES3C	Post	CA	0%	0%	0%	0%	0%	0%	0%	0%
RES3C	Post	CA	10%	0%	45%	0%	0%	0%	4%	11%
RES3C	Post	CA	20%	0%	100%	1%	1%	1%	11%	21%
RES3C	Post	CA	30%	0%	100%	2%	2%	2%	19%	32%
RES3C	Post	CA	40%	0%	100%	3%	3%	3%	26%	43%
RES3C	Post	CA	50%	0%	100%	5%	5%	5%	30%	54%
RES3C	Post	CA	60%	0%	100%	7%	7%	7%	41%	64%
RES3C	Post	CA	70%	1%	100%	8%	8%	8%	52%	74%
RES3C	Post	CA	80%	3%	100%	10%	10%	10%	58%	85%
RES3C	Post	CA	90%	7%	100%	14%	14%	14%	61%	95%
RES3C	Post	CA	100%	12%	100%	35%	35%	35%	75%	100%

SOCC or GBT	Pre- or Post-FIRM	Zone	Building Loss	Foundation	Below First Floor	Structure Frame	Roof Covering	Roof Framing	Exterior Walls	Interiors
RES3D	Pre	A	0%	0%	0%	0%	0%	0%	0%	0%
RES3D	Pre	A	10%	0%	20%	0%	0%	0%	4%	11%
RES3D	Pre	A	20%	0%	40%	0%	0%	0%	11%	21%
RES3D	Pre	A	30%	0%	58%	0%	0%	0%	16%	32%
RES3D	Pre	A	40%	0%	100%	0%	0%	0%	26%	41%
RES3D	Pre	A	50%	0%	100%	0%	0%	0%	30%	53%
RES3D	Pre	A	60%	0%	100%	0%	0%	0%	43%	62%
RES3D	Pre	A	70%	0%	100%	0%	0%	0%	49%	73%
RES3D	Pre	A	80%	0%	100%	2%	4%	2%	53%	83%
RES3D	Pre	A	90%	2%	100%	10%	10%	10%	56%	93%
RES3D	Pre	A	100%	8%	100%	20%	20%	20%	68%	100%
RES3D	Post	A	0%	0%	0%	0%	0%	0%	0%	0%
RES3D	Post	A	10%	0%	16%	0%	0%	0%	2%	11%
RES3D	Post	A	20%	0%	40%	0%	0%	0%	9%	23%
RES3D	Post	A	30%	0%	60%	0%	0%	0%	17%	33%
RES3D	Post	A	40%	0%	100%	0%	0%	0%	22%	44%
RES3D	Post	A	50%	0%	100%	0%	0%	0%	26%	56%
RES3D	Post	A	60%	0%	100%	0%	0%	0%	42%	65%
RES3D	Post	A	70%	0%	100%	0%	0%	0%	53%	76%
RES3D	Post	A	80%	0%	100%	1%	5%	1%	62%	87%
RES3D	Post	A	90%	2%	100%	14%	15%	14%	76%	94%
RES3D	Post	A	100%	12%	100%	26%	26%	26%	90%	100%
RES3D	Pre	CA	0%	0%	0%	0%	0%	0%	0%	0%
RES3D	Pre	CA	10%	0%	45%	0%	0%	0%	2%	11%
RES3D	Pre	CA	20%	0%	100%	1%	1%	1%	9%	21%
RES3D	Pre	CA	30%	0%	100%	2%	2%	2%	10%	32%
RES3D	Pre	CA	40%	0%	100%	3%	3%	3%	15%	43%
RES3D	Pre	CA	50%	0%	100%	6%	6%	6%	24%	53%
RES3D	Pre	CA	60%	1%	100%	9%	9%	9%	32%	62%
RES3D	Pre	CA	70%	2%	100%	12%	12%	12%	43%	72%
RES3D	Pre	CA	80%	3%	100%	14%	14%	14%	57%	81%
RES3D	Pre	CA	90%	7%	100%	17%	17%	17%	61%	91%
RES3D	Pre	CA	100%	15%	100%	20%	20%	20%	73%	100%
RES3D	Post	CA	0%	0%	0%	0%	0%	0%	0%	0%
RES3D	Post	CA	10%	0%	45%	0%	0%	0%	4%	11%
RES3D	Post	CA	20%	0%	100%	1%	1%	1%	11%	21%
RES3D	Post	CA	30%	0%	100%	2%	2%	2%	19%	32%

SOCC or GBT	Pre- or Post-FIRM	Zone	Building Loss	Foundation	Below First Floor	Structure Frame	Roof Covering	Roof Framing	Exterior Walls	Interiors
RES3D	Post	CA	40%	0%	100%	3%	3%	3%	26%	43%
RES3D	Post	CA	50%	0%	100%	5%	5%	5%	30%	54%
RES3D	Post	CA	60%	0%	100%	7%	7%	7%	41%	64%
RES3D	Post	CA	70%	1%	100%	8%	8%	8%	52%	74%
RES3D	Post	CA	80%	3%	100%	10%	10%	10%	58%	85%
RES3D	Post	CA	90%	7%	100%	14%	14%	14%	61%	95%
RES3D	Post	CA	100%	20%	100%	25%	25%	25%	76%	100%
RES3E	Pre	A	0%	0%	0%	0%	0%	0%	0%	0%
RES3E	Pre	A	10%	0%	20%	0%	0%	0%	4%	11%
RES3E	Pre	A	20%	0%	40%	0%	0%	0%	11%	22%
RES3E	Pre	A	30%	0%	58%	0%	0%	0%	16%	32%
RES3E	Pre	A	40%	0%	100%	0%	0%	0%	26%	42%
RES3E	Pre	A	50%	0%	100%	0%	0%	0%	30%	54%
RES3E	Pre	A	60%	0%	100%	0%	0%	0%	43%	64%
RES3E	Pre	A	70%	0%	100%	0%	0%	0%	49%	75%
RES3E	Pre	A	80%	0%	100%	2%	4%	2%	53%	86%
RES3E	Pre	A	90%	2%	100%	10%	10%	10%	56%	95%
RES3E	Pre	A	100%	8%	100%	22%	22%	22%	75%	100%
RES3E	Post	A	0%	0%	0%	0%	0%	0%	0%	0%
RES3E	Post	A	10%	0%	16%	0%	0%	0%	2%	12%
RES3E	Post	A	20%	0%	40%	0%	0%	0%	9%	23%
RES3E	Post	A	30%	0%	60%	0%	0%	0%	17%	34%
RES3E	Post	A	40%	0%	100%	0%	0%	0%	22%	46%
RES3E	Post	A	50%	0%	100%	0%	0%	0%	27%	57%
RES3E	Post	A	60%	0%	100%	0%	0%	0%	44%	67%
RES3E	Post	A	70%	0%	100%	0%	0%	0%	55%	78%
RES3E	Post	A	80%	0%	100%	2%	5%	2%	63%	89%
RES3E	Post	A	90%	2%	100%	15%	15%	15%	77%	96%
RES3E	Post	A	100%	14%	100%	30%	30%	30%	100%	100%
RES3E	Pre	CA	0%	0%	0%	0%	0%	0%	0%	0%
RES3E	Pre	CA	10%	0%	45%	0%	0%	0%	2%	11%
RES3E	Pre	CA	20%	0%	100%	1%	1%	1%	9%	21%
RES3E	Pre	CA	30%	0%	100%	2%	2%	2%	10%	32%
RES3E	Pre	CA	40%	0%	100%	3%	3%	3%	15%	43%
RES3E	Pre	CA	50%	0%	100%	6%	6%	6%	24%	53%
RES3E	Pre	CA	60%	1%	100%	9%	9%	9%	32%	63%
RES3E	Pre	CA	70%	2%	100%	12%	12%	12%	43%	72%

SOCC or GBT	Pre- or Post-FIRM	Zone	Building Loss	Foundation	Below First Floor	Structure Frame	Roof Covering	Roof Framing	Exterior Walls	Interiors
RES3E	Pre	CA	80%	3%	100%	14%	14%	14%	57%	82%
RES3E	Pre	CA	90%	7%	100%	17%	17%	17%	61%	92%
RES3E	Pre	CA	100%	15%	100%	20%	20%	20%	75%	100%
RES3E	Post	CA	0%	0%	0%	0%	0%	0%	0%	0%
RES3E	Post	CA	10%	0%	45%	0%	0%	0%	4%	11%
RES3E	Post	CA	20%	0%	100%	1%	1%	1%	11%	22%
RES3E	Post	CA	30%	0%	100%	2%	2%	2%	19%	33%
RES3E	Post	CA	40%	0%	100%	3%	3%	3%	26%	44%
RES3E	Post	CA	50%	0%	100%	5%	5%	5%	31%	56%
RES3E	Post	CA	60%	0%	100%	7%	7%	7%	41%	66%
RES3E	Post	CA	70%	1%	100%	9%	9%	9%	54%	76%
RES3E	Post	CA	80%	3%	100%	10%	10%	10%	61%	87%
RES3E	Post	CA	90%	7%	100%	14%	14%	14%	66%	97%
RES3E	Post	CA	100%	20%	100%	25%	25%	25%	94%	100%
RES3F	Pre	A	0%	0%	0%	0%	0%	0%	0%	0%
RES3F	Pre	A	10%	0%	0%	0%	0%	0%	3%	11%
RES3F	Pre	A	20%	0%	0%	0%	0%	0%	6%	22%
RES3F	Pre	A	30%	0%	0%	0%	0%	0%	7%	33%
RES3F	Pre	A	40%	0%	0%	0%	0%	0%	10%	44%
RES3F	Pre	A	50%	0%	0%	0%	0%	0%	22%	54%
RES3F	Pre	A	60%	0%	0%	0%	0%	0%	34%	63%
RES3F	Pre	A	70%	0%	0%	0%	0%	0%	46%	72%
RES3F	Pre	A	80%	0%	0%	3%	3%	3%	50%	83%
RES3F	Pre	A	90%	12%	0%	12%	12%	12%	63%	89%
RES3F	Pre	A	100%	25%	0%	15%	15%	15%	66%	100%
RES3F	Post	A	0%	0%	0%	0%	0%	0%	0%	0%
RES3F	Post	A	10%	0%	0%	0%	0%	0%	1%	12%
RES3F	Post	A	20%	0%	0%	0%	0%	0%	3%	24%
RES3F	Post	A	30%	0%	0%	0%	0%	0%	4%	35%
RES3F	Post	A	40%	0%	0%	0%	0%	0%	5%	47%
RES3F	Post	A	50%	0%	0%	0%	0%	0%	7%	59%
RES3F	Post	A	60%	0%	0%	0%	0%	0%	13%	70%
RES3F	Post	A	70%	0%	0%	0%	0%	0%	16%	82%
RES3F	Post	A	80%	0%	0%	3%	3%	3%	27%	91%
RES3F	Post	A	90%	5%	0%	15%	15%	15%	33%	99%
RES3F	Post	A	100%	25%	0%	20%	20%	20%	73%	100%
RES3F	Pre	CA	0%	0%	0%	0%	0%	0%	0%	0%

SOCC or GBT	Pre- or Post-FIRM	Zone	Building Loss	Foundation	Below First Floor	Structure Frame	Roof Covering	Roof Framing	Exterior Walls	Interiors
RES3F	Pre	CA	10%	0%	0%	0%	0%	0%	1%	11%
RES3F	Pre	CA	20%	0%	0%	1%	1%	1%	7%	21%
RES3F	Pre	CA	30%	0%	0%	1%	1%	1%	13%	32%
RES3F	Pre	CA	40%	0%	0%	2%	2%	2%	35%	39%
RES3F	Pre	CA	50%	0%	0%	2%	2%	2%	44%	49%
RES3F	Pre	CA	60%	1%	0%	3%	3%	3%	52%	59%
RES3F	Pre	CA	70%	3%	0%	5%	5%	5%	60%	68%
RES3F	Pre	CA	80%	5%	0%	7%	7%	7%	66%	78%
RES3F	Pre	CA	90%	6%	0%	9%	9%	9%	70%	88%
RES3F	Pre	CA	100%	7%	0%	10%	10%	10%	71%	100%
RES3F	Post	CA	0%	0%	0%	0%	0%	0%	0%	0%
RES3F	Post	CA	10%	0%	0%	1%	1%	1%	1%	12%
RES3F	Post	CA	20%	0%	0%	1%	1%	1%	6%	22%
RES3F	Post	CA	30%	0%	0%	6%	6%	6%	11%	33%
RES3F	Post	CA	40%	0%	0%	7%	7%	7%	18%	43%
RES3F	Post	CA	50%	0%	0%	9%	9%	9%	30%	53%
RES3F	Post	CA	60%	1%	0%	13%	13%	13%	40%	62%
RES3F	Post	CA	70%	8%	0%	18%	18%	18%	50%	71%
RES3F	Post	CA	80%	10%	0%	21%	21%	21%	58%	80%
RES3F	Post	CA	90%	12%	0%	23%	23%	23%	60%	91%
RES3F	Post	CA	100%	14%	0%	25%	25%	25%	74%	100%
RES4	Pre	A	0%	0%	0%	0%	0%	0%	0%	0%
RES4	Pre	A	10%	0%	10%	0%	0%	0%	4%	10%
RES4	Pre	A	20%	0%	30%	0%	0%	0%	7%	20%
RES4	Pre	A	30%	0%	70%	0%	0%	0%	9%	31%
RES4	Pre	A	40%	0%	100%	0%	0%	0%	13%	41%
RES4	Pre	A	50%	0%	100%	0%	0%	0%	27%	49%
RES4	Pre	A	60%	0%	100%	0%	0%	0%	42%	58%
RES4	Pre	A	70%	0%	100%	0%	0%	0%	58%	67%
RES4	Pre	A	80%	0%	100%	2%	2%	2%	64%	77%
RES4	Pre	A	90%	1%	100%	8%	8%	8%	70%	85%
RES4	Pre	A	100%	3%	100%	12%	12%	12%	78%	95%
RES4	Post	A	0%	0%	0%	0%	0%	0%	0%	0%
RES4	Post	A	10%	0%	10%	0%	0%	0%	1%	11%
RES4	Post	A	20%	0%	40%	0%	0%	0%	4%	22%
RES4	Post	A	30%	0%	80%	0%	0%	0%	5%	32%
RES4	Post	A	40%	0%	100%	0%	0%	0%	6%	43%

SOCC or GBT	Pre- or Post-FIRM	Zone	Building Loss	Foundation	Below First Floor	Structure Frame	Roof Covering	Roof Framing	Exterior Walls	Interiors
RES4	Post	A	50%	0%	100%	0%	0%	0%	9%	54%
RES4	Post	A	60%	0%	100%	0%	0%	0%	14%	65%
RES4	Post	A	70%	0%	100%	0%	0%	0%	22%	75%
RES4	Post	A	80%	0%	100%	7%	7%	7%	31%	84%
RES4	Post	A	90%	4%	100%	13%	13%	13%	40%	93%
RES4	Post	A	100%	12%	100%	17%	17%	17%	55%	100%
RES4	Pre	CA	0%	0%	0%	0%	0%	0%	0%	0%
RES4	Pre	CA	10%	0%	20%	0%	0%	0%	2%	10%
RES4	Pre	CA	20%	0%	100%	1%	1%	1%	8%	19%
RES4	Pre	CA	30%	0%	100%	3%	3%	3%	15%	29%
RES4	Pre	CA	40%	0%	100%	5%	5%	5%	25%	38%
RES4	Pre	CA	50%	0%	100%	7%	7%	7%	30%	48%
RES4	Pre	CA	60%	1%	100%	9%	9%	9%	35%	58%
RES4	Pre	CA	70%	2%	100%	13%	13%	13%	40%	67%
RES4	Pre	CA	80%	4%	100%	16%	16%	16%	45%	77%
RES4	Pre	CA	90%	6%	100%	20%	20%	20%	50%	86%
RES4	Pre	CA	100%	10%	100%	25%	25%	25%	55%	95%
RES4	Post	CA	0%	0%	0%	0%	0%	0%	0%	0%
RES4	Post	CA	10%	0%	30%	1%	1%	1%	1%	10%
RES4	Post	CA	20%	0%	100%	4%	4%	4%	8%	20%
RES4	Post	CA	30%	0%	100%	8%	8%	8%	15%	29%
RES4	Post	CA	40%	0%	100%	13%	13%	13%	28%	38%
RES4	Post	CA	50%	0%	100%	16%	16%	16%	38%	48%
RES4	Post	CA	60%	1%	100%	21%	21%	21%	47%	57%
RES4	Post	CA	70%	3%	100%	24%	24%	24%	57%	66%
RES4	Post	CA	80%	5%	100%	27%	27%	27%	64%	76%
RES4	Post	CA	90%	7%	100%	30%	30%	30%	73%	86%
RES4	Post	CA	100%	11%	100%	31%	31%	31%	80%	95%
RES5	Pre	A	0%	0%	0%	0%	0%	0%	0%	0%
RES5	Pre	A	10%	0%	0%	0%	0%	0%	3%	12%
RES5	Pre	A	20%	0%	0%	0%	0%	0%	5%	24%
RES5	Pre	A	30%	0%	0%	0%	0%	0%	7%	36%
RES5	Pre	A	40%	0%	0%	0%	0%	0%	9%	48%
RES5	Pre	A	50%	0%	0%	0%	0%	0%	19%	58%
RES5	Pre	A	60%	0%	0%	0%	0%	0%	31%	68%
RES5	Pre	A	70%	0%	0%	0%	0%	0%	42%	78%
RES5	Pre	A	80%	0%	0%	3%	3%	3%	50%	88%

SOCC or GBT	Pre- or Post-FIRM	Zone	Building Loss	Foundation	Below First Floor	Structure Frame	Roof Covering	Roof Framing	Exterior Walls	Interiors
RES5	Pre	A	90%	5%	0%	8%	8%	8%	60%	97%
RES5	Pre	A	100%	15%	0%	15%	15%	15%	89%	100%
RES5	Post	A	0%	0%	0%	0%	0%	0%	0%	0%
RES5	Post	A	10%	0%	0%	0%	0%	0%	1%	13%
RES5	Post	A	20%	0%	0%	0%	0%	0%	3%	25%
RES5	Post	A	30%	0%	0%	0%	0%	0%	4%	38%
RES5	Post	A	40%	0%	0%	0%	0%	0%	7%	50%
RES5	Post	A	50%	0%	0%	0%	0%	0%	12%	63%
RES5	Post	A	60%	0%	0%	0%	0%	0%	17%	75%
RES5	Post	A	70%	0%	0%	0%	0%	0%	21%	87%
RES5	Post	A	80%	0%	0%	6%	8%	8%	37%	95%
RES5	Post	A	90%	8%	0%	15%	15%	15%	59%	100%
RES5	Post	A	100%	20%	0%	27%	27%	27%	94%	100%
RES5	Pre	CA	0%	0%	0%	0%	0%	0%	0%	0%
RES5	Pre	CA	10%	0%	0%	0%	0%	0%	4%	12%
RES5	Pre	CA	20%	0%	0%	3%	3%	3%	8%	23%
RES5	Pre	CA	30%	0%	0%	5%	5%	5%	10%	34%
RES5	Pre	CA	40%	0%	0%	8%	8%	8%	14%	45%
RES5	Pre	CA	50%	0%	0%	13%	13%	13%	20%	55%
RES5	Pre	CA	60%	4%	0%	17%	17%	17%	26%	65%
RES5	Pre	CA	70%	9%	0%	21%	21%	21%	32%	74%
RES5	Pre	CA	80%	10%	0%	25%	25%	25%	40%	84%
RES5	Pre	CA	90%	20%	0%	28%	28%	28%	46%	94%
RES5	Pre	CA	100%	30%	0%	30%	30%	30%	69%	100%
RES5	Post	CA	0%	0%	0%	0%	0%	0%	0%	0%
RES5	Post	CA	10%	0%	0%	3%	3%	3%	1%	13%
RES5	Post	CA	20%	0%	0%	5%	5%	5%	6%	24%
RES5	Post	CA	30%	0%	0%	10%	10%	10%	11%	34%
RES5	Post	CA	40%	0%	0%	12%	12%	12%	20%	45%
RES5	Post	CA	50%	0%	0%	17%	17%	17%	34%	53%
RES5	Post	CA	60%	1%	0%	19%	19%	19%	46%	63%
RES5	Post	CA	70%	4%	0%	21%	21%	21%	53%	74%
RES5	Post	CA	80%	8%	0%	25%	25%	25%	62%	83%
RES5	Post	CA	90%	13%	0%	28%	28%	28%	69%	93%
RES5	Post	CA	100%	20%	0%	30%	30%	30%	93%	100%
RES6	Pre	A	0%	0%	0%	0%	0%	0%	0%	0%
RES6	Pre	A	10%	0%	0%	0%	0%	0%	3%	11%

SOCC or GBT	Pre- or Post-FIRM	Zone	Building Loss	Foundation	Below First Floor	Structure Frame	Roof Covering	Roof Framing	Exterior Walls	Interiors
RES6	Pre	A	20%	0%	0%	0%	0%	0%	6%	23%
RES6	Pre	A	30%	0%	0%	0%	0%	0%	8%	35%
RES6	Pre	A	40%	0%	0%	0%	0%	0%	11%	46%
RES6	Pre	A	50%	0%	0%	0%	0%	0%	22%	56%
RES6	Pre	A	60%	0%	0%	0%	0%	0%	34%	66%
RES6	Pre	A	70%	0%	0%	0%	0%	0%	47%	75%
RES6	Pre	A	80%	0%	0%	5%	5%	5%	56%	84%
RES6	Pre	A	90%	5%	0%	11%	11%	11%	64%	93%
RES6	Pre	A	100%	10%	0%	21%	21%	21%	75%	100%
RES6	Post	A	0%	0%	0%	0%	0%	0%	0%	0%
RES6	Post	A	10%	0%	0%	0%	0%	0%	1%	13%
RES6	Post	A	20%	0%	0%	0%	0%	0%	3%	25%
RES6	Post	A	30%	0%	0%	0%	0%	0%	4%	37%
RES6	Post	A	40%	0%	0%	0%	0%	0%	5%	50%
RES6	Post	A	50%	0%	0%	0%	0%	0%	15%	60%
RES6	Post	A	60%	0%	0%	0%	0%	0%	28%	70%
RES6	Post	A	70%	0%	0%	0%	0%	0%	39%	81%
RES6	Post	A	80%	0%	0%	4%	4%	4%	43%	92%
RES6	Post	A	90%	4%	0%	11%	11%	11%	54%	100%
RES6	Post	A	100%	14%	0%	25%	25%	25%	100%	100%
RES6	Pre	CA	0%	0%	0%	0%	0%	0%	0%	0%
RES6	Pre	CA	10%	0%	0%	0%	0%	0%	1%	12%
RES6	Pre	CA	20%	0%	0%	3%	3%	3%	7%	22%
RES6	Pre	CA	30%	0%	0%	4%	4%	4%	13%	33%
RES6	Pre	CA	40%	0%	0%	6%	6%	6%	17%	44%
RES6	Pre	CA	50%	0%	0%	9%	9%	9%	21%	54%
RES6	Pre	CA	60%	1%	0%	12%	12%	12%	30%	64%
RES6	Pre	CA	70%	3%	0%	14%	14%	14%	40%	73%
RES6	Pre	CA	80%	7%	0%	17%	17%	17%	51%	82%
RES6	Pre	CA	90%	10%	0%	20%	20%	20%	57%	92%
RES6	Pre	CA	100%	13%	0%	22%	22%	22%	76%	100%
RES6	Post	CA	0%	0%	0%	0%	0%	0%	0%	0%
RES6	Post	CA	10%	0%	0%	1%	1%	1%	1%	12%
RES6	Post	CA	20%	0%	0%	4%	4%	4%	6%	23%
RES6	Post	CA	30%	0%	0%	7%	7%	7%	11%	34%
RES6	Post	CA	40%	0%	0%	10%	10%	10%	21%	44%
RES6	Post	CA	50%	0%	0%	12%	12%	12%	31%	55%

SOCC or GBT	Pre- or Post-FIRM	Zone	Building Loss	Foundation	Below First Floor	Structure Frame	Roof Covering	Roof Framing	Exterior Walls	Interiors
RES6	Post	CA	60%	1%	0%	15%	15%	15%	41%	64%
RES6	Post	CA	70%	2%	0%	18%	18%	18%	51%	74%
RES6	Post	CA	80%	5%	0%	21%	21%	21%	61%	83%
RES6	Post	CA	90%	11%	0%	22%	22%	22%	71%	93%
RES6	Post	CA	100%	15%	0%	27%	27%	27%	97%	100%
COM1	Pre	A	0%	0%	0%	0%	0%	0%	0%	0%
COM1	Pre	A	10%	0%	10%	0%	0%	0%	8%	11%
COM1	Pre	A	20%	0%	30%	0%	0%	0%	17%	22%
COM1	Pre	A	30%	0%	80%	0%	0%	0%	22%	34%
COM1	Pre	A	40%	0%	100%	0%	0%	0%	29%	45%
COM1	Pre	A	50%	0%	100%	0%	0%	0%	38%	57%
COM1	Pre	A	60%	0%	100%	0%	0%	0%	47%	68%
COM1	Pre	A	70%	0%	100%	0%	0%	0%	60%	78%
COM1	Pre	A	80%	0%	100%	9%	9%	9%	70%	87%
COM1	Pre	A	90%	8%	100%	14%	14%	14%	76%	96%
COM1	Pre	A	100%	23%	100%	25%	25%	25%	100%	100%
COM1	Post	A	0%	0%	0%	0%	0%	0%	0%	0%
COM1	Post	A	10%	0%	10%	0%	0%	0%	9%	12%
COM1	Post	A	20%	0%	30%	0%	0%	0%	17%	23%
COM1	Post	A	30%	0%	80%	0%	0%	0%	25%	35%
COM1	Post	A	40%	0%	100%	0%	0%	0%	31%	47%
COM1	Post	A	50%	0%	100%	0%	0%	0%	41%	59%
COM1	Post	A	60%	0%	100%	0%	0%	0%	54%	70%
COM1	Post	A	70%	0%	100%	0%	0%	0%	67%	81%
COM1	Post	A	80%	0%	100%	5%	5%	5%	78%	91%
COM1	Post	A	90%	9%	100%	22%	22%	22%	86%	96%
COM1	Post	A	100%	20%	100%	40%	40%	40%	100%	100%
COM1	Pre	CA	0%	0%	0%	0%	0%	0%	0%	0%
COM1	Pre	CA	10%	0%	20%	0%	0%	0%	2%	12%
COM1	Pre	CA	20%	0%	100%	2%	2%	2%	7%	23%
COM1	Pre	CA	30%	0%	100%	5%	5%	5%	12%	33%
COM1	Pre	CA	40%	0%	100%	8%	8%	8%	29%	43%
COM1	Pre	CA	50%	0%	100%	11%	11%	11%	41%	53%
COM1	Pre	CA	60%	1%	100%	17%	17%	17%	48%	62%
COM1	Pre	CA	70%	3%	100%	22%	22%	22%	53%	72%
COM1	Pre	CA	80%	8%	100%	25%	25%	25%	65%	82%
COM1	Pre	CA	90%	12%	100%	28%	28%	28%	74%	92%

SOCC or GBT	Pre- or Post-FIRM	Zone	Building Loss	Foundation	Below First Floor	Structure Frame	Roof Covering	Roof Framing	Exterior Walls	Interiors
COM1	Pre	CA	100%	16%	100%	31%	31%	31%	89%	100%
COM1	Post	CA	0%	0%	0%	0%	0%	0%	0%	0%
COM1	Post	CA	10%	0%	20%	0%	0%	0%	2%	13%
COM1	Post	CA	20%	0%	100%	1%	1%	1%	5%	24%
COM1	Post	CA	30%	0%	100%	5%	5%	5%	14%	35%
COM1	Post	CA	40%	0%	100%	8%	8%	8%	24%	46%
COM1	Post	CA	50%	0%	100%	12%	12%	12%	34%	56%
COM1	Post	CA	60%	0%	100%	16%	16%	16%	44%	66%
COM1	Post	CA	70%	0%	100%	19%	19%	19%	54%	77%
COM1	Post	CA	80%	0%	100%	22%	22%	22%	64%	88%
COM1	Post	CA	90%	6%	100%	24%	24%	24%	69%	99%
COM1	Post	CA	100%	27%	100%	34%	34%	34%	100%	100%
COM2	Pre	A	0%	0%	0%	0%	0%	0%	0%	0%
COM2	Pre	A	10%	0%	10%	0%	0%	0%	7%	16%
COM2	Pre	A	20%	0%	30%	0%	0%	0%	14%	32%
COM2	Pre	A	30%	0%	80%	0%	0%	0%	21%	47%
COM2	Pre	A	40%	0%	100%	0%	0%	0%	27%	63%
COM2	Pre	A	50%	0%	100%	0%	0%	0%	35%	79%
COM2	Pre	A	60%	0%	100%	0%	0%	0%	44%	94%
COM2	Pre	A	70%	0%	100%	6%	6%	6%	84%	100%
COM2	Pre	A	80%	2%	100%	17%	17%	17%	93%	100%
COM2	Pre	A	90%	16%	100%	50%	50%	50%	100%	100%
COM2	Pre	A	100%	40%	100%	65%	65%	65%	100%	100%
COM2	Post	A	0%	0%	0%	0%	0%	0%	0%	0%
COM2	Post	A	10%	0%	10%	0%	0%	0%	8%	17%
COM2	Post	A	20%	0%	30%	0%	0%	0%	15%	34%
COM2	Post	A	30%	0%	80%	0%	0%	0%	22%	51%
COM2	Post	A	40%	0%	100%	0%	0%	0%	26%	69%
COM2	Post	A	50%	2%	100%	2%	2%	2%	45%	80%
COM2	Post	A	60%	7%	100%	8%	8%	8%	70%	88%
COM2	Post	A	70%	13%	100%	13%	13%	13%	87%	97%
COM2	Post	A	80%	25%	100%	25%	25%	25%	97%	100%
COM2	Post	A	90%	40%	100%	40%	40%	40%	100%	100%
COM2	Post	A	100%	60%	100%	56%	56%	56%	100%	100%
COM2	Pre	CA	0%	0%	0%	0%	0%	0%	0%	0%
COM2	Pre	CA	10%	0%	20%	0%	0%	0%	5%	16%
COM2	Pre	CA	20%	0%	100%	1%	1%	1%	15%	30%

SOCC or GBT	Pre- or Post-FIRM	Zone	Building Loss	Foundation	Below First Floor	Structure Frame	Roof Covering	Roof Framing	Exterior Walls	Interiors
COM2	Pre	CA	30%	0%	100%	2%	2%	2%	30%	44%
COM2	Pre	CA	40%	0%	100%	4%	4%	4%	40%	58%
COM2	Pre	CA	50%	0%	100%	6%	6%	6%	58%	70%
COM2	Pre	CA	60%	1%	100%	9%	9%	9%	67%	84%
COM2	Pre	CA	70%	5%	100%	13%	13%	13%	80%	94%
COM2	Pre	CA	80%	10%	100%	26%	26%	26%	95%	100%
COM2	Pre	CA	90%	32%	100%	37%	37%	37%	100%	100%
COM2	Pre	CA	100%	59%	100%	50%	50%	50%	100%	100%
COM2	Post	CA	0%	0%	0%	0%	0%	0%	0%	0%
COM2	Post	CA	10%	0%	20%	0%	0%	0%	9%	16%
COM2	Post	CA	20%	0%	100%	1%	1%	1%	17%	32%
COM2	Post	CA	30%	0%	100%	3%	3%	3%	32%	46%
COM2	Post	CA	40%	0%	100%	5%	5%	5%	40%	61%
COM2	Post	CA	50%	0%	100%	8%	8%	8%	59%	73%
COM2	Post	CA	60%	1%	100%	11%	11%	11%	67%	88%
COM2	Post	CA	70%	6%	100%	17%	17%	17%	85%	96%
COM2	Post	CA	80%	14%	100%	32%	32%	32%	98%	100%
COM2	Post	CA	90%	37%	100%	40%	40%	40%	100%	100%
COM2	Post	CA	100%	60%	100%	50%	50%	50%	100%	100%
COM3	Pre	A	0%	0%	0%	0%	0%	0%	0%	0%
COM3	Pre	A	10%	0%	10%	0%	0%	0%	8%	12%
COM3	Pre	A	20%	0%	30%	0%	0%	0%	17%	23%
COM3	Pre	A	30%	0%	80%	0%	0%	0%	22%	35%
COM3	Pre	A	40%	0%	100%	0%	0%	0%	29%	47%
COM3	Pre	A	50%	0%	100%	0%	0%	0%	38%	59%
COM3	Pre	A	60%	0%	100%	0%	0%	0%	47%	71%
COM3	Pre	A	70%	0%	100%	0%	0%	0%	60%	82%
COM3	Pre	A	80%	0%	100%	9%	9%	9%	72%	90%
COM3	Pre	A	90%	9%	100%	19%	19%	19%	77%	98%
COM3	Pre	A	100%	30%	100%	35%	35%	35%	90%	100%
COM3	Post	A	0%	0%	0%	0%	0%	0%	0%	0%
COM3	Post	A	10%	0%	10%	0%	0%	0%	9%	12%
COM3	Post	A	20%	0%	30%	0%	0%	0%	17%	25%
COM3	Post	A	30%	0%	80%	0%	0%	0%	25%	37%
COM3	Post	A	40%	0%	100%	0%	0%	0%	31%	49%
COM3	Post	A	50%	0%	100%	0%	0%	0%	41%	62%
COM3	Post	A	60%	0%	100%	0%	0%	0%	54%	74%

SOCC or GBT	Pre- or Post-FIRM	Zone	Building Loss	Foundation	Below First Floor	Structure Frame	Roof Covering	Roof Framing	Exterior Walls	Interiors
COM3	Post	A	70%	0%	100%	0%	0%	0%	67%	86%
COM3	Post	A	80%	0%	100%	9%	9%	9%	88%	94%
COM3	Post	A	90%	10%	100%	21%	21%	21%	91%	100%
COM3	Post	A	100%	40%	100%	36%	36%	36%	100%	100%
COM3	Pre	CA	0%	0%	0%	0%	0%	0%	0%	0%
COM3	Pre	CA	10%	0%	20%	0%	0%	0%	2%	13%
COM3	Pre	CA	20%	0%	100%	1%	1%	1%	7%	24%
COM3	Pre	CA	30%	0%	100%	4%	4%	4%	12%	35%
COM3	Pre	CA	40%	0%	100%	10%	10%	10%	35%	42%
COM3	Pre	CA	50%	0%	100%	13%	13%	13%	44%	54%
COM3	Pre	CA	60%	2%	100%	24%	24%	24%	54%	62%
COM3	Pre	CA	70%	5%	100%	30%	30%	30%	60%	72%
COM3	Pre	CA	80%	11%	100%	34%	34%	34%	71%	81%
COM3	Pre	CA	90%	20%	100%	35%	35%	35%	75%	92%
COM3	Pre	CA	100%	25%	100%	38%	38%	38%	96%	100%
COM3	Post	CA	0%	0%	0%	0%	0%	0%	0%	0%
COM3	Post	CA	10%	0%	20%	0%	0%	0%	8%	13%
COM3	Post	CA	20%	0%	100%	2%	2%	2%	20%	23%
COM3	Post	CA	30%	0%	100%	4%	4%	4%	32%	34%
COM3	Post	CA	40%	0%	100%	8%	8%	8%	38%	46%
COM3	Post	CA	50%	0%	100%	12%	12%	12%	55%	56%
COM3	Post	CA	60%	0%	100%	18%	18%	18%	65%	66%
COM3	Post	CA	70%	1%	100%	26%	26%	26%	75%	76%
COM3	Post	CA	80%	3%	100%	35%	35%	35%	83%	86%
COM3	Post	CA	90%	5%	100%	40%	40%	40%	90%	97%
COM3	Post	CA	100%	20%	100%	54%	54%	54%	100%	100%
COM4	Pre	A	0%	0%	0%	0%	0%	0%	0%	0%
COM4	Pre	A	10%	0%	10%	0%	0%	0%	5%	11%
COM4	Pre	A	20%	0%	30%	0%	0%	0%	10%	22%
COM4	Pre	A	30%	0%	80%	0%	0%	0%	14%	33%
COM4	Pre	A	40%	0%	100%	0%	0%	0%	18%	45%
COM4	Pre	A	50%	0%	100%	0%	0%	0%	23%	56%
COM4	Pre	A	60%	0%	100%	0%	0%	0%	29%	67%
COM4	Pre	A	70%	0%	100%	0%	0%	0%	37%	77%
COM4	Pre	A	80%	0%	100%	10%	10%	10%	45%	86%
COM4	Pre	A	90%	10%	100%	26%	26%	26%	53%	92%
COM4	Pre	A	100%	19%	100%	35%	35%	35%	59%	100%

SOCC or GBT	Pre- or Post-FIRM	Zone	Building Loss	Foundation	Below First Floor	Structure Frame	Roof Covering	Roof Framing	Exterior Walls	Interiors
COM4	Post	A	0%	0%	0%	0%	0%	0%	0%	0%
COM4	Post	A	10%	0%	10%	0%	0%	0%	5%	12%
COM4	Post	A	20%	0%	30%	0%	0%	0%	10%	24%
COM4	Post	A	30%	0%	80%	0%	0%	0%	14%	35%
COM4	Post	A	40%	0%	100%	0%	0%	0%	17%	47%
COM4	Post	A	50%	0%	100%	0%	0%	0%	23%	59%
COM4	Post	A	60%	0%	100%	0%	0%	0%	34%	69%
COM4	Post	A	70%	0%	100%	0%	0%	0%	44%	80%
COM4	Post	A	80%	0%	100%	4%	4%	4%	54%	90%
COM4	Post	A	90%	9%	100%	19%	19%	19%	56%	98%
COM4	Post	A	100%	20%	100%	35%	35%	35%	78%	100%
COM4	Pre	CA	0%	0%	0%	0%	0%	0%	0%	0%
COM4	Pre	CA	10%	0%	20%	0%	0%	0%	6%	11%
COM4	Pre	CA	20%	0%	100%	2%	2%	2%	11%	21%
COM4	Pre	CA	30%	0%	100%	3%	3%	3%	23%	30%
COM4	Pre	CA	40%	0%	100%	5%	5%	5%	30%	40%
COM4	Pre	CA	50%	0%	100%	9%	9%	9%	39%	50%
COM4	Pre	CA	60%	4%	100%	13%	13%	13%	41%	60%
COM4	Pre	CA	70%	8%	100%	18%	18%	18%	48%	70%
COM4	Pre	CA	80%	12%	100%	22%	22%	22%	55%	79%
COM4	Pre	CA	90%	15%	100%	25%	25%	25%	58%	90%
COM4	Pre	CA	100%	22%	100%	27%	27%	27%	66%	100%
COM4	Post	CA	0%	0%	0%	0%	0%	0%	0%	0%
COM4	Post	CA	10%	0%	16%	0%	0%	0%	1%	13%
COM4	Post	CA	20%	0%	100%	2%	2%	2%	5%	23%
COM4	Post	CA	30%	0%	100%	5%	5%	5%	11%	34%
COM4	Post	CA	40%	0%	100%	7%	7%	7%	18%	45%
COM4	Post	CA	50%	0%	100%	13%	13%	13%	23%	56%
COM4	Post	CA	60%	0%	100%	17%	17%	17%	32%	66%
COM4	Post	CA	70%	2%	100%	23%	23%	23%	43%	75%
COM4	Post	CA	80%	6%	100%	28%	28%	28%	51%	84%
COM4	Post	CA	90%	11%	100%	33%	33%	33%	62%	93%
COM4	Post	CA	100%	23%	100%	38%	38%	38%	72%	100%
COM5	Pre	A	0%	0%	0%	0%	0%	0%	0%	0%
COM5	Pre	A	10%	0%	0%	0%	0%	0%	2%	12%
COM5	Pre	A	20%	0%	0%	0%	0%	0%	5%	25%
COM5	Pre	A	30%	0%	0%	0%	0%	0%	7%	37%

SOCC or GBT	Pre- or Post-FIRM	Zone	Building Loss	Foundation	Below First Floor	Structure Frame	Roof Covering	Roof Framing	Exterior Walls	Interiors
COM5	Pre	A	40%	0%	0%	0%	0%	0%	14%	49%
COM5	Pre	A	50%	0%	0%	0%	0%	0%	19%	62%
COM5	Pre	A	60%	0%	0%	0%	0%	0%	25%	74%
COM5	Pre	A	70%	0%	0%	0%	0%	0%	31%	86%
COM5	Pre	A	80%	0%	0%	4%	4%	4%	41%	96%
COM5	Pre	A	90%	5%	0%	17%	17%	17%	62%	100%
COM5	Pre	A	100%	21%	0%	41%	41%	41%	80%	100%
COM5	Post	A	0%	0%	0%	0%	0%	0%	0%	0%
COM5	Post	A	10%	0%	0%	0%	0%	0%	2%	13%
COM5	Post	A	20%	0%	0%	0%	0%	0%	6%	26%
COM5	Post	A	30%	0%	0%	0%	0%	0%	9%	39%
COM5	Post	A	40%	0%	0%	0%	0%	0%	11%	52%
COM5	Post	A	50%	0%	0%	0%	0%	0%	18%	65%
COM5	Post	A	60%	0%	0%	0%	0%	0%	23%	77%
COM5	Post	A	70%	0%	0%	0%	0%	0%	64%	85%
COM5	Post	A	80%	0%	0%	9%	9%	9%	76%	94%
COM5	Post	A	90%	8%	0%	24%	24%	24%	87%	100%
COM5	Post	A	100%	25%	0%	45%	45%	45%	99%	100%
COM5	Pre	CA	0%	0%	0%	0%	0%	0%	0%	0%
COM5	Pre	CA	10%	0%	0%	0%	0%	0%	2%	13%
COM5	Pre	CA	20%	0%	0%	1%	1%	1%	3%	25%
COM5	Pre	CA	30%	0%	0%	4%	4%	4%	7%	36%
COM5	Pre	CA	40%	0%	0%	6%	6%	6%	12%	47%
COM5	Pre	CA	50%	0%	0%	9%	9%	9%	18%	58%
COM5	Pre	CA	60%	1%	0%	10%	10%	10%	23%	70%
COM5	Pre	CA	70%	3%	0%	14%	14%	14%	30%	80%
COM5	Pre	CA	80%	5%	0%	17%	17%	17%	37%	91%
COM5	Pre	CA	90%	8%	0%	21%	21%	21%	48%	100%
COM5	Pre	CA	100%	20%	0%	36%	36%	36%	100%	100%
COM5	Post	CA	0%	0%	0%	0%	0%	0%	0%	0%
COM5	Post	CA	10%	0%	0%	0%	0%	0%	2%	13%
COM5	Post	CA	20%	0%	0%	1%	1%	1%	3%	26%
COM5	Post	CA	30%	0%	0%	4%	4%	4%	8%	37%
COM5	Post	CA	40%	0%	0%	6%	6%	6%	14%	50%
COM5	Post	CA	50%	0%	0%	10%	10%	10%	21%	60%
COM5	Post	CA	60%	1%	0%	12%	12%	12%	25%	72%
COM5	Post	CA	70%	2%	0%	15%	15%	15%	33%	84%

SOCC or GBT	Pre- or Post-FIRM	Zone	Building Loss	Foundation	Below First Floor	Structure Frame	Roof Covering	Roof Framing	Exterior Walls	Interiors
COM5	Post	CA	80%	4%	0%	18%	18%	18%	39%	95%
COM5	Post	CA	90%	10%	0%	24%	24%	24%	75%	100%
COM5	Post	CA	100%	23%	0%	48%	48%	48%	100%	100%
COM6	Pre	A	0%	0%	0%	0%	0%	0%	0%	0%
COM6	Pre	A	10%	0%	0%	0%	0%	0%	1%	10%
COM6	Pre	A	20%	0%	0%	0%	0%	0%	2%	20%
COM6	Pre	A	30%	0%	0%	0%	0%	0%	3%	30%
COM6	Pre	A	40%	0%	0%	0%	0%	0%	4%	40%
COM6	Pre	A	50%	0%	0%	0%	0%	0%	6%	51%
COM6	Pre	A	60%	0%	0%	0%	0%	0%	8%	60%
COM6	Pre	A	70%	0%	0%	0%	0%	0%	10%	70%
COM6	Pre	A	80%	0%	0%	4%	4%	4%	16%	80%
COM6	Pre	A	90%	5%	0%	9%	9%	9%	19%	89%
COM6	Pre	A	100%	6%	0%	10%	10%	10%	21%	98%
COM6	Post	A	0%	0%	0%	0%	0%	0%	0%	0%
COM6	Post	A	10%	0%	0%	0%	0%	0%	1%	10%
COM6	Post	A	20%	0%	0%	0%	0%	0%	3%	21%
COM6	Post	A	30%	0%	0%	0%	0%	0%	5%	31%
COM6	Post	A	40%	0%	0%	0%	0%	0%	7%	42%
COM6	Post	A	50%	0%	0%	0%	0%	0%	8%	52%
COM6	Post	A	60%	0%	0%	0%	0%	0%	9%	62%
COM6	Post	A	70%	0%	0%	0%	0%	0%	13%	73%
COM6	Post	A	80%	1%	0%	6%	6%	6%	24%	82%
COM6	Post	A	90%	5%	0%	11%	11%	11%	34%	90%
COM6	Post	A	100%	7%	0%	15%	15%	15%	36%	100%
COM6	Pre	CA	0%	0%	0%	0%	0%	0%	0%	0%
COM6	Pre	CA	10%	0%	0%	0%	0%	0%	2%	10%
COM6	Pre	CA	20%	0%	0%	3%	3%	3%	6%	20%
COM6	Pre	CA	30%	0%	0%	6%	6%	6%	10%	29%
COM6	Pre	CA	40%	0%	0%	10%	10%	10%	19%	37%
COM6	Pre	CA	50%	0%	0%	14%	14%	14%	23%	46%
COM6	Pre	CA	60%	2%	0%	18%	18%	18%	33%	55%
COM6	Pre	CA	70%	4%	0%	22%	22%	22%	40%	64%
COM6	Pre	CA	80%	8%	0%	28%	28%	28%	49%	72%
COM6	Pre	CA	90%	11%	0%	33%	33%	33%	56%	81%
COM6	Pre	CA	100%	18%	0%	39%	39%	39%	60%	90%
COM6	Post	CA	0%	0%	0%	0%	0%	0%	0%	0%

SOCC or GBT	Pre- or Post-FIRM	Zone	Building Loss	Foundation	Below First Floor	Structure Frame	Roof Covering	Roof Framing	Exterior Walls	Interiors
COM6	Post	CA	10%	0%	0%	0%	0%	0%	1%	10%
COM6	Post	CA	20%	0%	0%	1%	1%	1%	5%	20%
COM6	Post	CA	30%	0%	0%	4%	4%	4%	12%	30%
COM6	Post	CA	40%	0%	0%	9%	9%	9%	23%	39%
COM6	Post	CA	50%	0%	0%	13%	13%	13%	31%	48%
COM6	Post	CA	60%	0%	0%	19%	19%	19%	40%	57%
COM6	Post	CA	70%	0%	0%	23%	23%	23%	49%	67%
COM6	Post	CA	80%	0%	0%	28%	28%	28%	54%	76%
COM6	Post	CA	90%	2%	0%	32%	32%	32%	63%	85%
COM6	Post	CA	100%	8%	0%	34%	34%	34%	68%	94%
COM7	Pre	A	0%	0%	0%	0%	0%	0%	0%	0%
COM7	Pre	A	10%	0%	8%	0%	0%	0%	7%	10%
COM7	Pre	A	20%	0%	24%	0%	0%	0%	15%	19%
COM7	Pre	A	30%	0%	64%	0%	0%	0%	19%	29%
COM7	Pre	A	40%	0%	100%	0%	0%	0%	25%	39%
COM7	Pre	A	50%	0%	100%	0%	0%	0%	33%	49%
COM7	Pre	A	60%	0%	100%	0%	0%	0%	41%	59%
COM7	Pre	A	70%	0%	100%	0%	0%	0%	52%	68%
COM7	Pre	A	80%	0%	100%	3%	3%	3%	63%	77%
COM7	Pre	A	90%	4%	100%	9%	9%	9%	68%	86%
COM7	Pre	A	100%	10%	100%	13%	13%	13%	71%	95%
COM7	Post	A	0%	0%	0%	0%	0%	0%	0%	0%
COM7	Post	A	10%	0%	10%	0%	0%	0%	1%	12%
COM7	Post	A	20%	0%	30%	0%	0%	0%	3%	23%
COM7	Post	A	30%	0%	80%	0%	0%	0%	6%	33%
COM7	Post	A	40%	0%	100%	0%	0%	0%	7%	45%
COM7	Post	A	50%	0%	100%	0%	0%	0%	15%	55%
COM7	Post	A	60%	0%	100%	0%	0%	0%	23%	66%
COM7	Post	A	70%	0%	100%	0%	0%	0%	46%	74%
COM7	Post	A	80%	0%	100%	3%	3%	3%	53%	84%
COM7	Post	A	90%	5%	100%	9%	9%	9%	59%	93%
COM7	Post	A	100%	14%	100%	15%	15%	15%	73%	100%
COM7	Pre	CA	0%	0%	0%	0%	0%	0%	0%	0%
COM7	Pre	CA	10%	0%	20%	0%	0%	0%	1%	11%
COM7	Pre	CA	20%	0%	100%	2%	2%	2%	6%	20%
COM7	Pre	CA	30%	0%	100%	3%	3%	3%	11%	30%
COM7	Pre	CA	40%	0%	100%	5%	5%	5%	30%	38%

SOCC or GBT	Pre- or Post-FIRM	Zone	Building Loss	Foundation	Below First Floor	Structure Frame	Roof Covering	Roof Framing	Exterior Walls	Interiors
COM7	Pre	CA	50%	0%	100%	13%	13%	13%	35%	47%
COM7	Pre	CA	60%	1%	100%	19%	19%	19%	41%	56%
COM7	Pre	CA	70%	4%	100%	25%	25%	25%	50%	64%
COM7	Pre	CA	80%	8%	100%	29%	29%	29%	55%	74%
COM7	Pre	CA	90%	12%	100%	33%	33%	33%	63%	83%
COM7	Pre	CA	100%	17%	100%	38%	38%	38%	69%	92%
COM7	Post	CA	0%	0%	0%	0%	0%	0%	0%	0%
COM7	Post	CA	10%	0%	20%	0%	0%	0%	2%	11%
COM7	Post	CA	20%	0%	100%	2%	2%	2%	5%	21%
COM7	Post	CA	30%	0%	100%	5%	5%	5%	9%	32%
COM7	Post	CA	40%	0%	100%	7%	7%	7%	16%	42%
COM7	Post	CA	50%	0%	100%	11%	11%	11%	21%	53%
COM7	Post	CA	60%	0%	100%	14%	14%	14%	29%	63%
COM7	Post	CA	70%	0%	100%	18%	18%	18%	33%	73%
COM7	Post	CA	80%	1%	100%	22%	22%	22%	40%	83%
COM7	Post	CA	90%	4%	100%	26%	26%	26%	46%	93%
COM7	Post	CA	100%	15%	100%	29%	29%	29%	58%	100%
COM8	Pre	A	0%	0%	0%	0%	0%	0%	0%	0%
COM8	Pre	A	10%	0%	10%	0%	0%	0%	1%	12%
COM8	Pre	A	20%	0%	30%	0%	0%	0%	6%	24%
COM8	Pre	A	30%	0%	80%	0%	0%	0%	9%	35%
COM8	Pre	A	40%	0%	100%	0%	0%	0%	10%	47%
COM8	Pre	A	50%	0%	100%	0%	0%	0%	16%	59%
COM8	Pre	A	60%	0%	100%	0%	0%	0%	21%	70%
COM8	Pre	A	70%	0%	100%	0%	0%	0%	30%	81%
COM8	Pre	A	80%	0%	100%	3%	3%	3%	39%	92%
COM8	Pre	A	90%	4%	100%	10%	10%	10%	56%	100%
COM8	Pre	A	100%	15%	100%	30%	30%	30%	100%	100%
COM8	Post	A	0%	0%	0%	0%	0%	0%	0%	0%
COM8	Post	A	10%	0%	10%	0%	0%	0%	1%	13%
COM8	Post	A	20%	0%	30%	0%	0%	0%	4%	25%
COM8	Post	A	30%	0%	80%	0%	0%	0%	10%	37%
COM8	Post	A	40%	0%	100%	0%	0%	0%	11%	49%
COM8	Post	A	50%	0%	100%	0%	0%	0%	23%	61%
COM8	Post	A	60%	0%	100%	0%	0%	0%	36%	72%
COM8	Post	A	70%	0%	100%	0%	0%	0%	62%	82%
COM8	Post	A	80%	0%	100%	3%	3%	3%	79%	93%

SOCC or GBT	Pre- or Post-FIRM	Zone	Building Loss	Foundation	Below First Floor	Structure Frame	Roof Covering	Roof Framing	Exterior Walls	Interiors
COM8	Post	A	90%	5%	100%	11%	11%	11%	94%	100%
COM8	Post	A	100%	25%	100%	40%	40%	40%	100%	100%
COM8	Pre	CA	0%	0%	0%	0%	0%	0%	0%	0%
COM8	Pre	CA	10%	0%	20%	0%	0%	0%	2%	12%
COM8	Pre	CA	20%	0%	100%	1%	1%	1%	9%	22%
COM8	Pre	CA	30%	0%	100%	3%	3%	3%	16%	33%
COM8	Pre	CA	40%	0%	100%	6%	6%	6%	30%	43%
COM8	Pre	CA	50%	0%	100%	9%	9%	9%	40%	53%
COM8	Pre	CA	60%	1%	100%	11%	11%	11%	50%	64%
COM8	Pre	CA	70%	5%	100%	14%	14%	14%	60%	73%
COM8	Pre	CA	80%	9%	100%	17%	17%	17%	70%	83%
COM8	Pre	CA	90%	11%	100%	21%	21%	21%	80%	93%
COM8	Pre	CA	100%	26%	100%	25%	25%	25%	95%	100%
COM8	Post	CA	0%	0%	0%	0%	0%	0%	0%	0%
COM8	Post	CA	10%	0%	20%	0%	0%	0%	2%	12%
COM8	Post	CA	20%	0%	100%	1%	2%	3%	6%	24%
COM8	Post	CA	30%	0%	100%	3%	3%	3%	12%	35%
COM8	Post	CA	40%	0%	100%	6%	6%	6%	29%	46%
COM8	Post	CA	50%	0%	100%	9%	9%	9%	39%	57%
COM8	Post	CA	60%	1%	100%	11%	11%	11%	49%	68%
COM8	Post	CA	70%	3%	100%	14%	14%	14%	59%	79%
COM8	Post	CA	80%	6%	100%	17%	17%	17%	69%	89%
COM8	Post	CA	90%	11%	100%	21%	21%	21%	79%	98%
COM8	Post	CA	100%	26%	100%	42%	42%	42%	100%	100%
COM9	Pre	A	0%	0%	0%	0%	0%	0%	0%	0%
COM9	Pre	A	10%	0%	10%	0%	0%	0%	1%	13%
COM9	Pre	A	20%	0%	30%	0%	0%	0%	5%	25%
COM9	Pre	A	30%	0%	80%	0%	0%	0%	7%	37%
COM9	Pre	A	40%	0%	100%	0%	0%	0%	8%	50%
COM9	Pre	A	50%	0%	100%	0%	0%	0%	12%	62%
COM9	Pre	A	60%	0%	100%	0%	0%	0%	16%	75%
COM9	Pre	A	70%	0%	100%	0%	0%	0%	23%	87%
COM9	Pre	A	80%	0%	100%	3%	3%	3%	30%	97%
COM9	Pre	A	90%	5%	100%	9%	9%	9%	77%	100%
COM9	Pre	A	100%	25%	100%	28%	28%	28%	100%	100%
COM9	Post	A	0%	0%	0%	0%	0%	0%	0%	0%
COM9	Post	A	10%	0%	10%	0%	0%	0%	1%	13%

SOCC or GBT	Pre- or Post-FIRM	Zone	Building Loss	Foundation	Below First Floor	Structure Frame	Roof Covering	Roof Framing	Exterior Walls	Interiors
COM9	Post	A	20%	0%	30%	0%	0%	0%	4%	26%
COM9	Post	A	30%	0%	80%	0%	0%	0%	8%	38%
COM9	Post	A	40%	0%	100%	0%	0%	0%	9%	51%
COM9	Post	A	50%	0%	100%	0%	0%	0%	19%	63%
COM9	Post	A	60%	0%	100%	0%	0%	0%	29%	75%
COM9	Post	A	70%	0%	100%	0%	0%	0%	51%	86%
COM9	Post	A	80%	0%	100%	3%	3%	3%	71%	95%
COM9	Post	A	90%	11%	100%	15%	15%	15%	90%	100%
COM9	Post	A	100%	27%	100%	42%	42%	42%	100%	100%
COM9	Pre	CA	0%	0%	0%	0%	0%	0%	0%	0%
COM9	Pre	CA	10%	0%	20%	0%	0%	0%	2%	13%
COM9	Pre	CA	20%	0%	100%	1%	1%	1%	7%	23%
COM9	Pre	CA	30%	0%	100%	2%	2%	2%	12%	35%
COM9	Pre	CA	40%	0%	100%	4%	4%	4%	23%	45%
COM9	Pre	CA	50%	0%	100%	8%	8%	8%	33%	56%
COM9	Pre	CA	60%	1%	100%	11%	11%	11%	43%	66%
COM9	Pre	CA	70%	5%	100%	15%	15%	15%	53%	76%
COM9	Pre	CA	80%	11%	100%	18%	18%	18%	63%	85%
COM9	Pre	CA	90%	15%	100%	21%	21%	21%	73%	95%
COM9	Pre	CA	100%	26%	100%	30%	30%	30%	100%	100%
COM9	Post	CA	0%	0%	0%	0%	0%	0%	0%	0%
COM9	Post	CA	10%	0%	20%	0%	0%	0%	2%	13%
COM9	Post	CA	20%	0%	100%	1%	1%	1%	5%	25%
COM9	Post	CA	30%	0%	100%	2%	2%	2%	10%	37%
COM9	Post	CA	40%	0%	100%	8%	8%	8%	25%	46%
COM9	Post	CA	50%	0%	100%	10%	10%	10%	35%	57%
COM9	Post	CA	60%	1%	100%	13%	13%	13%	45%	68%
COM9	Post	CA	70%	5%	100%	17%	17%	17%	55%	78%
COM9	Post	CA	80%	11%	100%	20%	20%	20%	65%	88%
COM9	Post	CA	90%	15%	100%	23%	23%	23%	75%	99%
COM9	Post	CA	100%	26%	100%	42%	42%	42%	100%	100%
COM10	Pre	A	0%	0%	0%	0%	0%	0%	0%	0%
COM10	Pre	A	10%	0%	0%	0%	0%	0%	15%	24%
COM10	Pre	A	20%	0%	0%	0%	0%	0%	20%	49%
COM10	Pre	A	30%	0%	0%	0%	0%	0%	25%	75%
COM10	Pre	A	40%	0%	0%	0%	0%	0%	35%	100%
COM10	Pre	A	50%	6%	0%	6%	0%	6%	86%	100%

SOCC or GBT	Pre- or Post-FIRM	Zone	Building Loss	Foundation	Below First Floor	Structure Frame	Roof Covering	Roof Framing	Exterior Walls	Interiors
COM10	Pre	A	60%	14%	0%	18%	0%	14%	100%	100%
COM10	Pre	A	70%	18%	0%	35%	0%	18%	100%	100%
COM10	Pre	A	80%	25%	0%	52%	0%	25%	100%	100%
COM10	Pre	A	90%	30%	0%	70%	0%	30%	100%	100%
COM10	Pre	A	100%	40%	0%	83%	0%	40%	100%	100%
COM10	Post	A	0%	0%	0%	0%	0%	0%	0%	0%
COM10	Post	A	10%	0%	0%	0%	0%	0%	15%	25%
COM10	Post	A	20%	0%	0%	0%	0%	0%	25%	52%
COM10	Post	A	30%	1%	0%	1%	0%	1%	35%	77%
COM10	Post	A	40%	2%	0%	2%	0%	2%	49%	100%
COM10	Post	A	50%	8%	0%	8%	0%	8%	100%	100%
COM10	Post	A	60%	21%	0%	21%	0%	21%	100%	100%
COM10	Post	A	70%	33%	0%	33%	0%	33%	100%	100%
COM10	Post	A	80%	45%	0%	45%	0%	45%	100%	100%
COM10	Post	A	90%	57%	0%	57%	0%	57%	100%	100%
COM10	Post	A	100%	69%	0%	69%	0%	69%	100%	100%
COM10	Pre	CA	0%	0%	0%	0%	0%	0%	0%	0%
COM10	Pre	CA	10%	0%	0%	0%	0%	0%	15%	24%
COM10	Pre	CA	20%	0%	0%	0%	0%	0%	20%	49%
COM10	Pre	CA	30%	0%	0%	0%	0%	0%	25%	75%
COM10	Pre	CA	40%	0%	0%	0%	0%	0%	35%	100%
COM10	Pre	CA	50%	6%	0%	6%	0%	6%	86%	100%
COM10	Pre	CA	60%	14%	0%	18%	0%	14%	100%	100%
COM10	Pre	CA	70%	18%	0%	35%	0%	18%	100%	100%
COM10	Pre	CA	80%	25%	0%	52%	0%	25%	100%	100%
COM10	Pre	CA	90%	30%	0%	70%	0%	30%	100%	100%
COM10	Pre	CA	100%	40%	0%	83%	0%	40%	100%	100%
COM10	Post	CA	0%	0%	0%	0%	0%	0%	0%	0%
COM10	Post	CA	10%	0%	0%	0%	0%	0%	2%	31%
COM10	Post	CA	20%	0%	0%	0%	0%	1%	5%	60%
COM10	Post	CA	30%	0%	0%	1%	0%	2%	11%	89%
COM10	Post	CA	40%	0%	0%	3%	0%	3%	72%	97%
COM10	Post	CA	50%	0%	0%	13%	0%	13%	100%	100%
COM10	Post	CA	60%	0%	0%	29%	0%	29%	100%	100%
COM10	Post	CA	70%	3%	0%	44%	0%	44%	100%	100%
COM10	Post	CA	80%	9%	0%	59%	0%	59%	100%	100%
COM10	Post	CA	90%	12%	0%	74%	0%	74%	100%	100%

SOCC or GBT	Pre- or Post-FIRM	Zone	Building Loss	Foundation	Below First Floor	Structure Frame	Roof Covering	Roof Framing	Exterior Walls	Interiors
COM10	Post	CA	100%	15%	0%	88%	0%	88%	100%	100%
IND1	Pre	A	0%	0%	0%	0%	0%	0%	0%	0%
IND1	Pre	A	10%	0%	10%	0%	0%	0%	1%	13%
IND1	Pre	A	20%	0%	30%	0%	0%	0%	5%	25%
IND1	Pre	A	30%	0%	80%	0%	0%	0%	7%	37%
IND1	Pre	A	40%	0%	100%	0%	0%	0%	8%	50%
IND1	Pre	A	50%	0%	100%	0%	0%	0%	12%	62%
IND1	Pre	A	60%	0%	100%	0%	0%	0%	16%	75%
IND1	Pre	A	70%	0%	100%	0%	0%	0%	23%	87%
IND1	Pre	A	80%	0%	100%	2%	2%	2%	40%	97%
IND1	Pre	A	90%	5%	100%	11%	11%	11%	82%	100%
IND1	Pre	A	100%	22%	100%	38%	38%	38%	100%	100%
IND1	Post	A	0%	0%	0%	0%	0%	0%	0%	0%
IND1	Post	A	10%	0%	10%	0%	0%	0%	1%	13%
IND1	Post	A	20%	0%	30%	0%	0%	0%	4%	26%
IND1	Post	A	30%	0%	80%	0%	0%	0%	8%	39%
IND1	Post	A	40%	0%	100%	0%	0%	0%	9%	52%
IND1	Post	A	50%	0%	100%	0%	0%	0%	19%	64%
IND1	Post	A	60%	0%	100%	0%	0%	0%	29%	76%
IND1	Post	A	70%	0%	100%	0%	0%	0%	51%	87%
IND1	Post	A	80%	0%	100%	2%	2%	2%	74%	97%
IND1	Post	A	90%	11%	100%	15%	15%	15%	100%	100%
IND1	Post	A	100%	28%	100%	50%	50%	50%	100%	100%
IND1	Pre	CA	0%	0%	0%	0%	0%	0%	0%	0%
IND1	Pre	CA	10%	0%	20%	0%	0%	0%	2%	13%
IND1	Pre	CA	20%	0%	100%	1%	1%	1%	7%	23%
IND1	Pre	CA	30%	0%	100%	2%	2%	2%	12%	35%
IND1	Pre	CA	40%	0%	100%	4%	4%	4%	23%	46%
IND1	Pre	CA	50%	0%	100%	8%	8%	8%	33%	57%
IND1	Pre	CA	60%	1%	100%	11%	11%	11%	44%	67%
IND1	Pre	CA	70%	4%	100%	13%	13%	13%	55%	77%
IND1	Pre	CA	80%	9%	100%	16%	16%	16%	66%	87%
IND1	Pre	CA	90%	12%	100%	18%	18%	18%	77%	97%
IND1	Pre	CA	100%	20%	100%	42%	42%	42%	100%	100%
IND1	Post	CA	0%	0%	0%	0%	0%	0%	0%	0%
IND1	Post	CA	10%	0%	20%	0%	0%	0%	2%	13%
IND1	Post	CA	20%	0%	100%	1%	1%	1%	5%	25%

SOCC or GBT	Pre- or Post-FIRM	Zone	Building Loss	Foundation	Below First Floor	Structure Frame	Roof Covering	Roof Framing	Exterior Walls	Interiors
IND1	Post	CA	30%	0%	100%	2%	2%	2%	10%	37%
IND1	Post	CA	40%	0%	100%	5%	5%	5%	25%	48%
IND1	Post	CA	50%	0%	100%	9%	9%	9%	36%	60%
IND1	Post	CA	60%	1%	100%	13%	13%	13%	47%	70%
IND1	Post	CA	70%	3%	100%	18%	18%	18%	55%	81%
IND1	Post	CA	80%	9%	100%	20%	20%	20%	66%	91%
IND1	Post	CA	90%	12%	100%	24%	24%	24%	80%	100%
IND1	Post	CA	100%	27%	100%	55%	55%	55%	100%	100%
IND2	Pre	A	0%	0%	0%	0%	0%	0%	0%	0%
IND2	Pre	A	10%	0%	10%	0%	0%	0%	1%	15%
IND2	Pre	A	20%	0%	30%	0%	0%	0%	4%	29%
IND2	Pre	A	30%	0%	80%	0%	0%	0%	6%	43%
IND2	Pre	A	40%	0%	100%	0%	0%	0%	7%	58%
IND2	Pre	A	50%	0%	100%	0%	0%	0%	11%	72%
IND2	Pre	A	60%	0%	100%	0%	0%	0%	25%	84%
IND2	Pre	A	70%	0%	100%	0%	0%	0%	42%	95%
IND2	Pre	A	80%	0%	100%	17%	17%	17%	60%	100%
IND2	Pre	A	90%	16%	100%	40%	40%	40%	71%	100%
IND2	Pre	A	100%	20%	100%	60%	60%	60%	100%	100%
IND2	Post	A	0%	0%	0%	0%	0%	0%	0%	0%
IND2	Post	A	10%	0%	10%	0%	0%	0%	1%	16%
IND2	Post	A	20%	0%	30%	0%	0%	0%	3%	31%
IND2	Post	A	30%	0%	80%	0%	0%	0%	7%	46%
IND2	Post	A	40%	0%	100%	0%	0%	0%	8%	61%
IND2	Post	A	50%	0%	100%	0%	0%	0%	16%	76%
IND2	Post	A	60%	0%	100%	0%	0%	0%	25%	90%
IND2	Post	A	70%	0%	100%	0%	0%	0%	54%	99%
IND2	Post	A	80%	0%	100%	10%	10%	10%	90%	100%
IND2	Post	A	90%	10%	100%	49%	49%	49%	100%	100%
IND2	Post	A	100%	32%	100%	65%	65%	65%	100%	100%
IND2	Pre	CA	0%	0%	0%	0%	0%	0%	0%	0%
IND2	Pre	CA	10%	0%	20%	0%	0%	0%	1%	15%
IND2	Pre	CA	20%	0%	100%	1%	1%	1%	6%	27%
IND2	Pre	CA	30%	0%	100%	3%	3%	3%	11%	41%
IND2	Pre	CA	40%	0%	100%	6%	6%	6%	21%	52%
IND2	Pre	CA	50%	0%	100%	11%	11%	11%	35%	63%
IND2	Pre	CA	60%	1%	100%	17%	17%	17%	45%	73%

SOCC or GBT	Pre- or Post-FIRM	Zone	Building Loss	Foundation	Below First Floor	Structure Frame	Roof Covering	Roof Framing	Exterior Walls	Interiors
IND2	Pre	CA	70%	4%	100%	24%	24%	24%	55%	82%
IND2	Pre	CA	80%	9%	100%	28%	28%	28%	65%	92%
IND2	Pre	CA	90%	18%	100%	31%	31%	31%	87%	100%
IND2	Pre	CA	100%	25%	100%	55%	55%	55%	100%	100%
IND2	Post	CA	0%	0%	0%	0%	0%	0%	0%	0%
IND2	Post	CA	10%	0%	20%	0%	0%	0%	8%	14%
IND2	Post	CA	20%	0%	100%	3%	3%	3%	12%	27%
IND2	Post	CA	30%	0%	100%	8%	8%	8%	21%	39%
IND2	Post	CA	40%	0%	100%	11%	11%	11%	31%	52%
IND2	Post	CA	50%	0%	100%	15%	15%	15%	43%	65%
IND2	Post	CA	60%	0%	100%	19%	19%	19%	53%	77%
IND2	Post	CA	70%	0%	100%	23%	23%	23%	64%	89%
IND2	Post	CA	80%	0%	100%	28%	28%	28%	77%	100%
IND2	Post	CA	90%	13%	100%	44%	44%	44%	100%	100%
IND2	Post	CA	100%	50%	100%	49%	49%	49%	100%	100%
IND3	Pre	A	0%	0%	0%	0%	0%	0%	0%	0%
IND3	Pre	A	10%	0%	10%	0%	0%	0%	1%	13%
IND3	Pre	A	20%	0%	30%	0%	0%	0%	4%	26%
IND3	Pre	A	30%	0%	80%	0%	0%	0%	6%	39%
IND3	Pre	A	40%	0%	100%	0%	0%	0%	7%	52%
IND3	Pre	A	50%	0%	100%	0%	0%	0%	11%	65%
IND3	Pre	A	60%	0%	100%	0%	0%	0%	15%	78%
IND3	Pre	A	70%	0%	100%	0%	0%	0%	21%	90%
IND3	Pre	A	80%	0%	100%	8%	8%	8%	28%	100%
IND3	Pre	A	90%	12%	100%	22%	22%	22%	64%	100%
IND3	Pre	A	100%	20%	100%	42%	42%	42%	100%	100%
IND3	Post	A	0%	0%	0%	0%	0%	0%	0%	0%
IND3	Post	A	10%	0%	10%	0%	0%	0%	1%	14%
IND3	Post	A	20%	0%	30%	0%	0%	0%	3%	28%
IND3	Post	A	30%	0%	80%	0%	0%	0%	7%	41%
IND3	Post	A	40%	0%	100%	0%	0%	0%	8%	55%
IND3	Post	A	50%	0%	100%	0%	0%	0%	16%	68%
IND3	Post	A	60%	0%	100%	0%	0%	0%	25%	81%
IND3	Post	A	70%	0%	100%	0%	0%	0%	43%	92%
IND3	Post	A	80%	0%	100%	11%	11%	11%	63%	99%
IND3	Post	A	90%	13%	100%	31%	31%	31%	80%	100%
IND3	Post	A	100%	24%	100%	60%	60%	60%	100%	100%

SOCC or GBT	Pre- or Post-FIRM	Zone	Building Loss	Foundation	Below First Floor	Structure Frame	Roof Covering	Roof Framing	Exterior Walls	Interiors
IND3	Pre	CA	0%	0%	0%	0%	0%	0%	0%	0%
IND3	Pre	CA	10%	0%	20%	0%	0%	0%	1%	13%
IND3	Pre	CA	20%	0%	100%	2%	2%	2%	6%	24%
IND3	Pre	CA	30%	0%	100%	4%	4%	4%	11%	37%
IND3	Pre	CA	40%	0%	100%	6%	6%	6%	21%	48%
IND3	Pre	CA	50%	0%	100%	11%	11%	11%	31%	58%
IND3	Pre	CA	60%	1%	100%	18%	18%	18%	41%	67%
IND3	Pre	CA	70%	6%	100%	23%	23%	23%	51%	77%
IND3	Pre	CA	80%	11%	100%	32%	32%	32%	58%	85%
IND3	Pre	CA	90%	17%	100%	42%	42%	42%	68%	93%
IND3	Pre	CA	100%	24%	100%	50%	50%	50%	80%	100%
IND3	Post	CA	0%	0%	0%	0%	0%	0%	0%	0%
IND3	Post	CA	10%	0%	20%	0%	0%	0%	2%	14%
IND3	Post	CA	20%	0%	100%	2%	2%	2%	4%	26%
IND3	Post	CA	30%	0%	100%	4%	4%	4%	8%	39%
IND3	Post	CA	40%	0%	100%	6%	6%	6%	30%	49%
IND3	Post	CA	50%	0%	100%	11%	11%	11%	39%	60%
IND3	Post	CA	60%	1%	100%	18%	18%	18%	52%	69%
IND3	Post	CA	70%	6%	100%	23%	23%	23%	63%	79%
IND3	Post	CA	80%	11%	100%	32%	32%	32%	70%	88%
IND3	Post	CA	90%	17%	100%	42%	42%	42%	74%	97%
IND3	Post	CA	100%	30%	100%	50%	50%	50%	100%	100%
IND4	Pre	A	0%	0%	0%	0%	0%	0%	0%	0%
IND4	Pre	A	10%	0%	0%	0%	0%	0%	1%	15%
IND4	Pre	A	20%	0%	0%	0%	0%	0%	6%	30%
IND4	Pre	A	30%	0%	0%	0%	0%	0%	9%	45%
IND4	Pre	A	40%	0%	0%	0%	0%	0%	10%	61%
IND4	Pre	A	50%	0%	0%	0%	0%	0%	16%	76%
IND4	Pre	A	60%	0%	0%	0%	0%	0%	21%	90%
IND4	Pre	A	70%	0%	0%	0%	0%	0%	55%	100%
IND4	Pre	A	80%	0%	0%	17%	17%	17%	90%	100%
IND4	Pre	A	90%	8%	0%	37%	37%	37%	100%	100%
IND4	Pre	A	100%	25%	0%	57%	57%	57%	100%	100%
IND4	Post	A	0%	0%	0%	0%	0%	0%	0%	0%
IND4	Post	A	10%	0%	0%	0%	0%	0%	1%	17%
IND4	Post	A	20%	0%	0%	0%	0%	0%	4%	33%
IND4	Post	A	30%	0%	0%	0%	0%	0%	10%	49%

SOCC or GBT	Pre- or Post-FIRM	Zone	Building Loss	Foundation	Below First Floor	Structure Frame	Roof Covering	Roof Framing	Exterior Walls	Interiors
IND4	Post	A	40%	0%	0%	0%	0%	0%	11%	65%
IND4	Post	A	50%	0%	0%	0%	0%	0%	23%	80%
IND4	Post	A	60%	0%	0%	0%	0%	0%	36%	95%
IND4	Post	A	70%	0%	0%	2%	2%	2%	97%	100%
IND4	Post	A	80%	0%	0%	26%	26%	26%	100%	100%
IND4	Post	A	90%	9%	0%	47%	47%	47%	100%	100%
IND4	Post	A	100%	26%	0%	65%	65%	65%	100%	100%
IND4	Pre	CA	0%	0%	0%	0%	0%	0%	0%	0%
IND4	Pre	CA	10%	0%	0%	0%	0%	0%	2%	15%
IND4	Pre	CA	20%	0%	0%	1%	1%	1%	9%	29%
IND4	Pre	CA	30%	0%	0%	4%	4%	4%	16%	42%
IND4	Pre	CA	40%	0%	0%	8%	8%	8%	25%	54%
IND4	Pre	CA	50%	0%	0%	11%	11%	11%	35%	65%
IND4	Pre	CA	60%	2%	0%	15%	15%	15%	45%	76%
IND4	Pre	CA	70%	9%	0%	18%	18%	18%	55%	88%
IND4	Pre	CA	80%	11%	0%	23%	23%	23%	65%	98%
IND4	Pre	CA	90%	25%	0%	35%	35%	35%	95%	100%
IND4	Pre	CA	100%	35%	0%	55%	55%	55%	100%	100%
IND4	Post	CA	0%	0%	0%	0%	0%	0%	0%	0%
IND4	Post	CA	10%	0%	0%	0%	0%	0%	8%	15%
IND4	Post	CA	20%	0%	0%	2%	2%	2%	10%	31%
IND4	Post	CA	30%	0%	0%	6%	6%	6%	14%	44%
IND4	Post	CA	40%	0%	0%	9%	9%	9%	32%	55%
IND4	Post	CA	50%	0%	0%	14%	14%	14%	33%	69%
IND4	Post	CA	60%	2%	0%	19%	19%	19%	44%	80%
IND4	Post	CA	70%	5%	0%	27%	27%	27%	52%	89%
IND4	Post	CA	80%	8%	0%	33%	33%	33%	61%	100%
IND4	Post	CA	90%	18%	0%	48%	48%	48%	80%	100%
IND4	Post	CA	100%	25%	0%	67%	67%	67%	100%	100%
IND5	Pre	A	0%	0%	0%	0%	0%	0%	0%	0%
IND5	Pre	A	10%	0%	0%	0%	0%	0%	2%	11%
IND5	Pre	A	20%	0%	0%	0%	0%	0%	12%	22%
IND5	Pre	A	30%	0%	0%	0%	0%	0%	18%	32%
IND5	Pre	A	40%	0%	0%	0%	0%	0%	20%	43%
IND5	Pre	A	50%	0%	0%	0%	0%	0%	32%	54%
IND5	Pre	A	60%	0%	0%	0%	0%	0%	42%	64%
IND5	Pre	A	70%	0%	0%	0%	0%	0%	60%	74%

SOCC or GBT	Pre- or Post-FIRM	Zone	Building Loss	Foundation	Below First Floor	Structure Frame	Roof Covering	Roof Framing	Exterior Walls	Interiors
IND5	Pre	A	80%	0%	0%	6%	6%	6%	80%	83%
IND5	Pre	A	90%	9%	0%	18%	18%	18%	89%	90%
IND5	Pre	A	100%	15%	0%	20%	20%	20%	100%	100%
IND5	Post	A	0%	0%	0%	0%	0%	0%	0%	0%
IND5	Post	A	10%	0%	0%	0%	0%	0%	3%	12%
IND5	Post	A	20%	0%	0%	0%	0%	0%	10%	23%
IND5	Post	A	30%	0%	0%	0%	0%	0%	23%	34%
IND5	Post	A	40%	0%	0%	0%	0%	0%	25%	45%
IND5	Post	A	50%	0%	0%	0%	0%	0%	35%	57%
IND5	Post	A	60%	0%	0%	0%	0%	0%	48%	68%
IND5	Post	A	70%	0%	0%	0%	0%	0%	63%	78%
IND5	Post	A	80%	0%	0%	6%	6%	6%	75%	88%
IND5	Post	A	90%	5%	0%	10%	10%	10%	92%	98%
IND5	Post	A	100%	25%	0%	30%	30%	30%	100%	100%
IND5	Pre	CA	0%	0%	0%	0%	0%	0%	0%	0%
IND5	Pre	CA	10%	0%	0%	0%	0%	0%	6%	11%
IND5	Pre	CA	20%	0%	0%	2%	2%	2%	18%	21%
IND5	Pre	CA	30%	0%	0%	5%	5%	5%	20%	31%
IND5	Pre	CA	40%	0%	0%	7%	7%	7%	30%	42%
IND5	Pre	CA	50%	0%	0%	11%	11%	11%	40%	51%
IND5	Pre	CA	60%	1%	0%	14%	14%	14%	50%	61%
IND5	Pre	CA	70%	4%	0%	18%	18%	18%	60%	71%
IND5	Pre	CA	80%	8%	0%	21%	21%	21%	70%	80%
IND5	Pre	CA	90%	10%	0%	26%	26%	26%	75%	90%
IND5	Pre	CA	100%	13%	0%	28%	28%	28%	80%	100%
IND5	Post	CA	0%	0%	0%	0%	0%	0%	0%	0%
IND5	Post	CA	10%	0%	0%	0%	0%	0%	5%	11%
IND5	Post	CA	20%	0%	0%	2%	2%	2%	13%	22%
IND5	Post	CA	30%	0%	0%	5%	5%	5%	28%	33%
IND5	Post	CA	40%	0%	0%	7%	7%	7%	38%	43%
IND5	Post	CA	50%	0%	0%	11%	11%	11%	46%	54%
IND5	Post	CA	60%	1%	0%	14%	14%	14%	56%	64%
IND5	Post	CA	70%	4%	0%	18%	18%	18%	66%	74%
IND5	Post	CA	80%	8%	0%	21%	21%	21%	76%	84%
IND5	Post	CA	90%	11%	0%	26%	26%	26%	86%	94%
IND5	Post	CA	100%	18%	0%	42%	42%	42%	100%	100%
IND6	Pre	A	0%	0%	0%	0%	0%	0%	0%	0%

SOCC or GBT	Pre- or Post-FIRM	Zone	Building Loss	Foundation	Below First Floor	Structure Frame	Roof Covering	Roof Framing	Exterior Walls	Interiors
IND6	Pre	A	10%	0%	10%	0%	0%	0%	5%	16%
IND6	Pre	A	20%	0%	30%	0%	0%	0%	10%	32%
IND6	Pre	A	30%	0%	80%	0%	0%	0%	16%	48%
IND6	Pre	A	40%	0%	100%	0%	0%	0%	21%	64%
IND6	Pre	A	50%	0%	100%	0%	0%	0%	28%	80%
IND6	Pre	A	60%	0%	100%	0%	0%	0%	35%	96%
IND6	Pre	A	70%	0%	100%	13%	13%	13%	65%	100%
IND6	Pre	A	80%	2%	100%	30%	30%	30%	100%	100%
IND6	Pre	A	90%	18%	100%	50%	50%	50%	100%	100%
IND6	Pre	A	100%	30%	100%	75%	75%	75%	100%	100%
IND6	Post	A	0%	0%	0%	0%	0%	0%	0%	0%
IND6	Post	A	10%	0%	10%	0%	0%	0%	1%	19%
IND6	Post	A	20%	0%	30%	0%	0%	0%	3%	37%
IND6	Post	A	30%	0%	80%	0%	0%	0%	7%	54%
IND6	Post	A	40%	0%	100%	0%	0%	0%	8%	73%
IND6	Post	A	50%	0%	100%	0%	0%	0%	16%	90%
IND6	Post	A	60%	0%	100%	0%	0%	0%	62%	98%
IND6	Post	A	70%	0%	100%	14%	14%	14%	100%	100%
IND6	Post	A	80%	7%	100%	41%	41%	41%	100%	100%
IND6	Post	A	90%	15%	100%	70%	70%	70%	100%	100%
IND6	Post	A	100%	41%	100%	75%	75%	75%	100%	100%
IND6	Pre	CA	0%	0%	0%	0%	0%	0%	0%	0%
IND6	Pre	CA	10%	0%	20%	0%	0%	0%	5%	16%
IND6	Pre	CA	20%	0%	100%	2%	2%	2%	9%	30%
IND6	Pre	CA	30%	0%	100%	6%	6%	6%	14%	45%
IND6	Pre	CA	40%	0%	100%	9%	9%	9%	21%	59%
IND6	Pre	CA	50%	0%	100%	14%	14%	14%	31%	72%
IND6	Pre	CA	60%	1%	100%	18%	18%	18%	41%	85%
IND6	Pre	CA	70%	4%	100%	24%	24%	24%	51%	96%
IND6	Pre	CA	80%	8%	100%	34%	34%	34%	76%	100%
IND6	Pre	CA	90%	20%	100%	47%	47%	47%	100%	100%
IND6	Pre	CA	100%	25%	100%	80%	80%	80%	100%	100%
IND6	Post	CA	0%	0%	0%	0%	0%	0%	0%	0%
IND6	Post	CA	10%	0%	20%	0%	0%	0%	5%	16%
IND6	Post	CA	20%	0%	100%	2%	2%	2%	11%	33%
IND6	Post	CA	30%	0%	100%	6%	6%	6%	18%	48%
IND6	Post	CA	40%	0%	100%	9%	9%	9%	25%	63%

SOCC or GBT	Pre- or Post-FIRM	Zone	Building Loss	Foundation	Below First Floor	Structure Frame	Roof Covering	Roof Framing	Exterior Walls	Interiors
IND6	Post	CA	50%	0%	100%	14%	14%	14%	36%	77%
IND6	Post	CA	60%	1%	100%	18%	18%	18%	50%	90%
IND6	Post	CA	70%	4%	100%	25%	25%	25%	65%	100%
IND6	Post	CA	80%	10%	100%	39%	39%	39%	100%	100%
IND6	Post	CA	90%	25%	100%	57%	57%	57%	100%	100%
IND6	Post	CA	100%	35%	100%	82%	82%	82%	100%	100%
AGR1	Pre	A	0%	0%	0%	0%	0%	0%	0%	0%
AGR1	Pre	A	10%	0%	0%	0%	0%	0%	2%	22%
AGR1	Pre	A	20%	0%	0%	0%	0%	0%	18%	38%
AGR1	Pre	A	30%	0%	0%	0%	0%	0%	28%	58%
AGR1	Pre	A	40%	0%	0%	0%	0%	0%	38%	76%
AGR1	Pre	A	50%	0%	0%	0%	0%	0%	60%	90%
AGR1	Pre	A	60%	0%	0%	0%	0%	0%	100%	100%
AGR1	Pre	A	70%	2%	0%	30%	30%	30%	100%	100%
AGR1	Pre	A	80%	8%	0%	55%	55%	55%	100%	100%
AGR1	Pre	A	90%	19%	0%	75%	75%	75%	100%	100%
AGR1	Pre	A	100%	24%	0%	100%	100%	100%	100%	100%
AGR1	Post	A	0%	0%	0%	0%	0%	0%	0%	0%
AGR1	Post	A	10%	0%	0%	0%	0%	0%	12%	21%
AGR1	Post	A	20%	0%	0%	0%	0%	0%	21%	42%
AGR1	Post	A	30%	0%	0%	0%	0%	0%	35%	61%
AGR1	Post	A	40%	0%	0%	0%	0%	0%	49%	80%
AGR1	Post	A	50%	0%	0%	0%	0%	0%	65%	100%
AGR1	Post	A	60%	2%	0%	14%	14%	14%	100%	100%
AGR1	Post	A	70%	12%	0%	35%	35%	35%	100%	100%
AGR1	Post	A	80%	16%	0%	60%	60%	60%	100%	100%
AGR1	Post	A	90%	23%	0%	85%	85%	85%	100%	100%
AGR1	Post	A	100%	35%	0%	100%	100%	100%	100%	100%
AGR1	Pre	CA	0%	0%	0%	0%	0%	0%	0%	0%
AGR1	Pre	CA	10%	0%	0%	0%	0%	0%	10%	19%
AGR1	Pre	CA	20%	0%	0%	1%	1%	1%	18%	38%
AGR1	Pre	CA	30%	0%	0%	4%	4%	4%	27%	53%
AGR1	Pre	CA	40%	0%	0%	8%	8%	8%	40%	69%
AGR1	Pre	CA	50%	0%	0%	14%	14%	14%	55%	82%
AGR1	Pre	CA	60%	1%	0%	19%	19%	19%	65%	97%
AGR1	Pre	CA	70%	6%	0%	30%	30%	30%	88%	100%
AGR1	Pre	CA	80%	10%	0%	52%	52%	52%	100%	100%

SOCC or GBT	Pre- or Post-FIRM	Zone	Building Loss	Foundation	Below First Floor	Structure Frame	Roof Covering	Roof Framing	Exterior Walls	Interiors
AGR1	Pre	CA	90%	21%	0%	73%	73%	73%	100%	100%
AGR1	Pre	CA	100%	33%	0%	90%	90%	90%	100%	100%
AGR1	Post	CA	0%	0%	0%	0%	0%	0%	0%	0%
AGR1	Post	CA	10%	0%	0%	0%	0%	0%	10%	20%
AGR1	Post	CA	20%	0%	0%	1%	1%	1%	20%	41%
AGR1	Post	CA	30%	0%	0%	9%	9%	9%	30%	56%
AGR1	Post	CA	40%	0%	0%	12%	12%	12%	42%	75%
AGR1	Post	CA	50%	0%	0%	18%	18%	18%	60%	88%
AGR1	Post	CA	60%	1%	0%	27%	27%	27%	74%	100%
AGR1	Post	CA	70%	6%	0%	40%	40%	40%	100%	100%
AGR1	Post	CA	80%	16%	0%	60%	60%	60%	100%	100%
AGR1	Post	CA	90%	25%	0%	80%	80%	80%	100%	100%
AGR1	Post	CA	100%	39%	0%	95%	95%	95%	100%	100%
REL1	Pre	A	0%	0%	0%	0%	0%	0%	0%	0%
REL1	Pre	A	10%	0%	10%	0%	0%	0%	9%	16%
REL1	Pre	A	20%	0%	30%	0%	0%	0%	17%	30%
REL1	Pre	A	30%	0%	80%	0%	0%	0%	28%	45%
REL1	Pre	A	40%	0%	100%	0%	0%	0%	38%	59%
REL1	Pre	A	50%	0%	100%	0%	0%	0%	50%	75%
REL1	Pre	A	60%	0%	100%	0%	0%	0%	66%	89%
REL1	Pre	A	70%	0%	100%	4%	4%	4%	80%	100%
REL1	Pre	A	80%	5%	100%	21%	21%	21%	100%	100%
REL1	Pre	A	90%	23%	100%	38%	38%	38%	100%	100%
REL1	Pre	A	100%	45%	100%	56%	56%	56%	100%	100%
REL1	Post	A	0%	0%	0%	0%	0%	0%	0%	0%
REL1	Post	A	10%	0%	10%	0%	0%	0%	11%	17%
REL1	Post	A	20%	0%	30%	0%	0%	0%	18%	33%
REL1	Post	A	30%	0%	80%	0%	0%	0%	30%	48%
REL1	Post	A	40%	0%	100%	0%	0%	0%	49%	62%
REL1	Post	A	50%	0%	100%	0%	0%	0%	55%	80%
REL1	Post	A	60%	0%	100%	0%	0%	0%	66%	95%
REL1	Post	A	70%	0%	100%	11%	11%	11%	93%	100%
REL1	Post	A	80%	6%	100%	32%	32%	32%	100%	100%
REL1	Post	A	90%	13%	100%	55%	55%	55%	100%	100%
REL1	Post	A	100%	27%	100%	72%	72%	72%	100%	100%
REL1	Pre	CA	0%	0%	0%	0%	0%	0%	0%	0%
REL1	Pre	CA	10%	0%	20%	0%	0%	0%	10%	15%

SOCC or GBT	Pre- or Post-FIRM	Zone	Building Loss	Foundation	Below First Floor	Structure Frame	Roof Covering	Roof Framing	Exterior Walls	Interiors
REL1	Pre	CA	20%	0%	100%	1%	1%	1%	20%	28%
REL1	Pre	CA	30%	0%	100%	5%	5%	5%	30%	40%
REL1	Pre	CA	40%	0%	100%	11%	11%	11%	40%	51%
REL1	Pre	CA	50%	0%	100%	17%	17%	17%	50%	63%
REL1	Pre	CA	60%	5%	100%	21%	21%	21%	66%	73%
REL1	Pre	CA	70%	11%	100%	27%	27%	27%	77%	82%
REL1	Pre	CA	80%	18%	100%	31%	31%	31%	88%	92%
REL1	Pre	CA	90%	27%	100%	37%	37%	37%	99%	100%
REL1	Pre	CA	100%	50%	100%	56%	56%	56%	100%	100%
REL1	Post	CA	0%	0%	0%	0%	0%	0%	0%	0%
REL1	Post	CA	10%	0%	20%	0%	0%	0%	10%	16%
REL1	Post	CA	20%	0%	100%	1%	1%	1%	21%	30%
REL1	Post	CA	30%	0%	100%	5%	5%	5%	35%	42%
REL1	Post	CA	40%	0%	100%	11%	11%	11%	40%	55%
REL1	Post	CA	50%	0%	100%	17%	17%	17%	55%	67%
REL1	Post	CA	60%	5%	100%	21%	21%	21%	66%	79%
REL1	Post	CA	70%	13%	100%	27%	27%	27%	80%	86%
REL1	Post	CA	80%	18%	100%	31%	31%	31%	86%	100%
REL1	Post	CA	90%	30%	100%	46%	46%	46%	97%	100%
REL1	Post	CA	100%	43%	100%	65%	65%	65%	100%	100%
GOV1	Pre	A	0%	0%	0%	0%	0%	0%	0%	0%
GOV1	Pre	A	10%	0%	10%	0%	0%	0%	1%	13%
GOV1	Pre	A	20%	0%	30%	0%	0%	0%	6%	26%
GOV1	Pre	A	30%	0%	80%	0%	0%	0%	9%	39%
GOV1	Pre	A	40%	0%	100%	0%	0%	0%	10%	52%
GOV1	Pre	A	50%	0%	100%	0%	0%	0%	16%	65%
GOV1	Pre	A	60%	0%	100%	0%	0%	0%	21%	78%
GOV1	Pre	A	70%	0%	100%	0%	0%	0%	50%	88%
GOV1	Pre	A	80%	1%	100%	18%	18%	18%	89%	88%
GOV1	Pre	A	90%	6%	100%	22%	22%	22%	95%	100%
GOV1	Pre	A	100%	26%	100%	40%	40%	40%	100%	100%
GOV1	Post	A	0%	0%	0%	0%	0%	0%	0%	0%
GOV1	Post	A	10%	0%	10%	0%	0%	0%	1%	14%
GOV1	Post	A	20%	0%	30%	0%	0%	0%	4%	28%
GOV1	Post	A	30%	0%	80%	0%	0%	0%	10%	41%
GOV1	Post	A	40%	0%	100%	0%	0%	0%	11%	55%
GOV1	Post	A	50%	0%	100%	0%	0%	0%	23%	68%

SOCC or GBT	Pre- or Post-FIRM	Zone	Building Loss	Foundation	Below First Floor	Structure Frame	Roof Covering	Roof Framing	Exterior Walls	Interiors
GOV1	Post	A	60%	0%	100%	0%	0%	0%	61%	78%
GOV1	Post	A	70%	0%	100%	0%	0%	0%	83%	89%
GOV1	Post	A	80%	0%	100%	9%	9%	9%	89%	100%
GOV1	Post	A	90%	6%	100%	35%	35%	35%	100%	100%
GOV1	Post	A	100%	13%	100%	67%	67%	67%	100%	100%
GOV1	Pre	CA	0%	0%	0%	0%	0%	0%	0%	0%
GOV1	Pre	CA	10%	0%	20%	0%	0%	0%	9%	12%
GOV1	Pre	CA	20%	0%	100%	2%	2%	2%	17%	23%
GOV1	Pre	CA	30%	0%	100%	4%	4%	4%	24%	35%
GOV1	Pre	CA	40%	0%	100%	6%	6%	6%	38%	46%
GOV1	Pre	CA	50%	0%	100%	14%	14%	14%	46%	55%
GOV1	Pre	CA	60%	2%	100%	23%	23%	23%	53%	65%
GOV1	Pre	CA	70%	6%	100%	33%	33%	33%	66%	72%
GOV1	Pre	CA	80%	10%	100%	40%	40%	40%	70%	82%
GOV1	Pre	CA	90%	15%	100%	44%	44%	44%	72%	93%
GOV1	Pre	CA	100%	25%	100%	51%	51%	51%	80%	100%
GOV1	Post	CA	0%	0%	0%	0%	0%	0%	0%	0%
GOV1	Post	CA	10%	0%	20%	0%	0%	0%	9%	13%
GOV1	Post	CA	20%	0%	100%	2%	2%	2%	21%	24%
GOV1	Post	CA	30%	0%	100%	4%	4%	4%	30%	37%
GOV1	Post	CA	40%	0%	100%	6%	6%	6%	40%	49%
GOV1	Post	CA	50%	0%	100%	14%	14%	14%	50%	59%
GOV1	Post	CA	60%	2%	100%	23%	23%	23%	61%	68%
GOV1	Post	CA	70%	5%	100%	32%	32%	32%	67%	78%
GOV1	Post	CA	80%	10%	100%	40%	40%	40%	74%	86%
GOV1	Post	CA	90%	12%	100%	41%	41%	41%	79%	100%
GOV1	Post	CA	100%	30%	100%	55%	55%	55%	100%	100%
GOV2	Pre	A	0%	0%	0%	0%	0%	0%	0%	0%
GOV2	Pre	A	10%	0%	0%	0%	0%	0%	10%	11%
GOV2	Pre	A	20%	0%	0%	0%	0%	0%	18%	23%
GOV2	Pre	A	30%	0%	0%	0%	0%	0%	29%	33%
GOV2	Pre	A	40%	0%	0%	0%	0%	0%	38%	44%
GOV2	Pre	A	50%	0%	0%	0%	0%	0%	46%	56%
GOV2	Pre	A	60%	0%	0%	0%	0%	0%	52%	68%
GOV2	Pre	A	70%	0%	0%	0%	0%	0%	66%	78%
GOV2	Pre	A	80%	0%	0%	16%	16%	16%	74%	84%
GOV2	Pre	A	90%	5%	0%	18%	18%	18%	77%	96%

SOCC or GBT	Pre- or Post-FIRM	Zone	Building Loss	Foundation	Below First Floor	Structure Frame	Roof Covering	Roof Framing	Exterior Walls	Interiors
GOV2	Pre	A	100%	25%	0%	35%	35%	35%	80%	100%
GOV2	Post	A	0%	0%	0%	0%	0%	0%	0%	0%
GOV2	Post	A	10%	0%	0%	0%	0%	0%	10%	12%
GOV2	Post	A	20%	0%	0%	0%	0%	0%	20%	23%
GOV2	Post	A	30%	0%	0%	0%	0%	0%	29%	35%
GOV2	Post	A	40%	0%	0%	0%	0%	0%	37%	48%
GOV2	Post	A	50%	0%	0%	0%	0%	0%	47%	60%
GOV2	Post	A	60%	0%	0%	0%	0%	0%	52%	72%
GOV2	Post	A	70%	0%	0%	0%	0%	0%	62%	84%
GOV2	Post	A	80%	0%	0%	8%	8%	8%	73%	93%
GOV2	Post	A	90%	7%	0%	16%	16%	16%	84%	100%
GOV2	Post	A	100%	26%	0%	40%	40%	40%	100%	100%
GOV2	Pre	CA	0%	0%	0%	0%	0%	0%	0%	0%
GOV2	Pre	CA	10%	0%	0%	0%	0%	0%	10%	11%
GOV2	Pre	CA	20%	0%	0%	3%	3%	3%	20%	21%
GOV2	Pre	CA	30%	0%	0%	7%	7%	7%	27%	31%
GOV2	Pre	CA	40%	0%	0%	10%	10%	10%	36%	42%
GOV2	Pre	CA	50%	0%	0%	16%	16%	16%	40%	52%
GOV2	Pre	CA	60%	3%	0%	22%	22%	22%	55%	60%
GOV2	Pre	CA	70%	8%	0%	25%	25%	25%	60%	70%
GOV2	Pre	CA	80%	11%	0%	32%	32%	32%	66%	80%
GOV2	Pre	CA	90%	14%	0%	35%	35%	35%	75%	90%
GOV2	Pre	CA	100%	17%	0%	40%	40%	40%	80%	100%
GOV2	Post	CA	0%	0%	0%	0%	0%	0%	0%	0%
GOV2	Post	CA	10%	0%	0%	0%	0%	0%	10%	12%
GOV2	Post	CA	20%	0%	0%	3%	3%	3%	20%	23%
GOV2	Post	CA	30%	0%	0%	7%	7%	7%	30%	33%
GOV2	Post	CA	40%	0%	0%	10%	10%	10%	35%	45%
GOV2	Post	CA	50%	0%	0%	13%	13%	13%	46%	56%
GOV2	Post	CA	60%	3%	0%	21%	21%	21%	52%	65%
GOV2	Post	CA	70%	8%	0%	26%	26%	26%	60%	74%
GOV2	Post	CA	80%	11%	0%	31%	31%	31%	65%	85%
GOV2	Post	CA	90%	14%	0%	37%	37%	37%	70%	95%
GOV2	Post	CA	100%	19%	0%	42%	42%	42%	99%	100%
EDU1	Pre	A	0%	0%	0%	0%	0%	0%	0%	0%
EDU1	Pre	A	10%	0%	10%	0%	0%	0%	4%	12%
EDU1	Pre	A	20%	0%	30%	0%	0%	0%	8%	23%

SOCC or GBT	Pre- or Post-FIRM	Zone	Building Loss	Foundation	Below First Floor	Structure Frame	Roof Covering	Roof Framing	Exterior Walls	Interiors
EDU1	Pre	A	30%	0%	80%	0%	0%	0%	15%	34%
EDU1	Pre	A	40%	0%	100%	0%	0%	0%	20%	46%
EDU1	Pre	A	50%	0%	100%	0%	0%	0%	24%	58%
EDU1	Pre	A	60%	0%	100%	0%	0%	0%	28%	70%
EDU1	Pre	A	70%	0%	100%	0%	0%	0%	34%	82%
EDU1	Pre	A	80%	0%	100%	3%	3%	3%	41%	92%
EDU1	Pre	A	90%	5%	100%	12%	12%	12%	50%	100%
EDU1	Pre	A	100%	20%	100%	35%	35%	35%	77%	100%
EDU1	Post	A	0%	0%	0%	0%	0%	0%	0%	0%
EDU1	Post	A	10%	0%	10%	0%	0%	0%	4%	11%
EDU1	Post	A	20%	0%	30%	0%	0%	0%	8%	22%
EDU1	Post	A	30%	0%	80%	0%	0%	0%	15%	32%
EDU1	Post	A	40%	0%	100%	0%	0%	0%	20%	43%
EDU1	Post	A	50%	0%	100%	0%	0%	0%	24%	55%
EDU1	Post	A	60%	0%	100%	0%	0%	0%	28%	66%
EDU1	Post	A	70%	0%	100%	0%	0%	0%	34%	77%
EDU1	Post	A	80%	0%	100%	7%	7%	7%	41%	86%
EDU1	Post	A	90%	7%	100%	14%	14%	14%	50%	94%
EDU1	Post	A	100%	22%	100%	32%	32%	32%	55%	100%
EDU1	Pre	CA	0%	0%	0%	0%	0%	0%	0%	0%
EDU1	Pre	CA	10%	0%	20%	0%	0%	0%	5%	12%
EDU1	Pre	CA	20%	0%	100%	1%	1%	1%	8%	23%
EDU1	Pre	CA	30%	0%	100%	4%	4%	4%	12%	34%
EDU1	Pre	CA	40%	0%	100%	6%	6%	6%	22%	44%
EDU1	Pre	CA	50%	0%	100%	12%	12%	12%	30%	53%
EDU1	Pre	CA	60%	4%	100%	18%	18%	18%	41%	61%
EDU1	Pre	CA	70%	8%	100%	24%	24%	24%	50%	70%
EDU1	Pre	CA	80%	13%	100%	29%	29%	29%	62%	79%
EDU1	Pre	CA	90%	19%	100%	33%	33%	33%	70%	88%
EDU1	Pre	CA	100%	20%	100%	34%	34%	34%	75%	100%
EDU1	Post	CA	0%	0%	0%	0%	0%	0%	0%	0%
EDU1	Post	CA	10%	0%	20%	0%	0%	0%	5%	11%
EDU1	Post	CA	20%	0%	100%	1%	1%	1%	8%	21%
EDU1	Post	CA	30%	0%	100%	4%	4%	4%	12%	32%
EDU1	Post	CA	40%	0%	100%	6%	6%	6%	23%	42%
EDU1	Post	CA	50%	0%	100%	12%	12%	12%	28%	51%
EDU1	Post	CA	60%	4%	100%	18%	18%	18%	38%	60%

SOCC or GBT	Pre- or Post-FIRM	Zone	Building Loss	Foundation	Below First Floor	Structure Frame	Roof Covering	Roof Framing	Exterior Walls	Interiors
EDU1	Post	CA	70%	8%	100%	24%	24%	24%	44%	69%
EDU1	Post	CA	80%	13%	100%	29%	29%	29%	50%	79%
EDU1	Post	CA	90%	19%	100%	33%	33%	33%	56%	88%
EDU1	Post	CA	100%	20%	100%	34%	34%	34%	62%	99%
EDU2	Pre	A	0%	0%	0%	0%	0%	0%	0%	0%
EDU2	Pre	A	10%	0%	10%	0%	0%	0%	1%	11%
EDU2	Pre	A	20%	0%	30%	0%	0%	0%	6%	21%
EDU2	Pre	A	30%	0%	80%	0%	0%	0%	9%	32%
EDU2	Pre	A	40%	0%	100%	0%	0%	0%	10%	43%
EDU2	Pre	A	50%	0%	100%	0%	0%	0%	16%	53%
EDU2	Pre	A	60%	0%	100%	0%	0%	0%	21%	64%
EDU2	Pre	A	70%	0%	100%	0%	0%	0%	35%	72%
EDU2	Pre	A	80%	0%	100%	3%	3%	3%	46%	83%
EDU2	Pre	A	90%	3%	100%	6%	6%	6%	57%	90%
EDU2	Pre	A	100%	10%	100%	10%	10%	10%	70%	100%
EDU2	Post	A	0%	0%	0%	0%	0%	0%	0%	0%
EDU2	Post	A	10%	0%	10%	0%	0%	0%	1%	11%
EDU2	Post	A	20%	0%	30%	0%	0%	0%	4%	22%
EDU2	Post	A	30%	0%	80%	0%	0%	0%	10%	33%
EDU2	Post	A	40%	0%	100%	0%	0%	0%	11%	44%
EDU2	Post	A	50%	0%	100%	0%	0%	0%	23%	55%
EDU2	Post	A	60%	0%	100%	0%	0%	0%	34%	65%
EDU2	Post	A	70%	0%	100%	0%	0%	0%	45%	75%
EDU2	Post	A	80%	0%	100%	4%	4%	4%	56%	85%
EDU2	Post	A	90%	5%	100%	10%	10%	10%	68%	94%
EDU2	Post	A	100%	15%	100%	25%	25%	25%	80%	100%
EDU2	Pre	CA	0%	0%	0%	0%	0%	0%	0%	0%
EDU2	Pre	CA	10%	0%	20%	0%	0%	0%	2%	11%
EDU2	Pre	CA	20%	0%	100%	1%	1%	1%	9%	20%
EDU2	Pre	CA	30%	0%	100%	3%	3%	3%	16%	30%
EDU2	Pre	CA	40%	0%	100%	5%	5%	5%	23%	40%
EDU2	Pre	CA	50%	0%	100%	8%	8%	8%	31%	50%
EDU2	Pre	CA	60%	4%	100%	12%	12%	12%	40%	59%
EDU2	Pre	CA	70%	9%	100%	16%	16%	16%	51%	68%
EDU2	Pre	CA	80%	14%	100%	19%	19%	19%	60%	77%
EDU2	Pre	CA	90%	19%	100%	21%	21%	21%	69%	86%
EDU2	Pre	CA	100%	20%	100%	24%	24%	24%	75%	96%

SOCC or GBT	Pre- or Post-FIRM	Zone	Building Loss	Foundation	Below First Floor	Structure Frame	Roof Covering	Roof Framing	Exterior Walls	Interiors
EDU2	Post	CA	0%	0%	0%	0%	0%	0%	0%	0%
EDU2	Post	CA	10%	0%	20%	0%	0%	0%	4%	11%
EDU2	Post	CA	20%	0%	100%	1%	1%	1%	11%	21%
EDU2	Post	CA	30%	0%	100%	3%	3%	3%	18%	31%
EDU2	Post	CA	40%	0%	100%	5%	5%	5%	23%	42%
EDU2	Post	CA	50%	0%	100%	8%	8%	8%	34%	52%
EDU2	Post	CA	60%	4%	100%	12%	12%	12%	44%	61%
EDU2	Post	CA	70%	9%	100%	16%	16%	16%	53%	70%
EDU2	Post	CA	80%	14%	100%	19%	19%	19%	63%	80%
EDU2	Post	CA	90%	19%	100%	21%	21%	21%	69%	90%
EDU2	Post	CA	100%	21%	100%	24%	24%	24%	75%	100%
Wood	Pre	A	0%	0%	0%	0%	0%	0%	0%	0%
Wood	Pre	A	10%	0%	10%	0%	0%	0%	1%	14%
Wood	Pre	A	20%	0%	30%	0%	0%	0%	3%	27%
Wood	Pre	A	30%	0%	80%	0%	0%	0%	5%	40%
Wood	Pre	A	40%	0%	100%	0%	0%	0%	5%	54%
Wood	Pre	A	50%	0%	100%	0%	0%	0%	8%	68%
Wood	Pre	A	60%	0%	100%	0%	0%	0%	11%	81%
Wood	Pre	A	70%	0%	100%	0%	0%	0%	25%	91%
Wood	Pre	A	80%	0%	100%	6%	6%	6%	48%	97%
Wood	Pre	A	90%	6%	100%	13%	13%	13%	74%	100%
Wood	Pre	A	100%	15%	100%	29%	29%	29%	100%	100%
Wood	Post	A	0%	0%	0%	0%	0%	0%	0%	0%
Wood	Post	A	10%	0%	10%	0%	0%	0%	1%	15%
Wood	Post	A	20%	0%	30%	0%	0%	0%	3%	29%
Wood	Post	A	30%	0%	80%	0%	0%	0%	6%	43%
Wood	Post	A	40%	0%	100%	0%	0%	0%	9%	57%
Wood	Post	A	50%	0%	100%	0%	0%	0%	14%	70%
Wood	Post	A	60%	0%	100%	0%	0%	0%	24%	82%
Wood	Post	A	70%	0%	100%	0%	0%	0%	31%	95%
Wood	Post	A	80%	0%	100%	11%	11%	11%	55%	100%
Wood	Post	A	90%	6%	100%	20%	20%	20%	88%	100%
Wood	Post	A	100%	25%	100%	40%	40%	40%	100%	100%
Wood	Pre	CA	0%	0%	0%	0%	0%	0%	0%	0%
Wood	Pre	CA	10%	0%	20%	0%	0%	0%	10%	12%
Wood	Pre	CA	20%	0%	100%	1%	1%	1%	18%	22%
Wood	Pre	CA	30%	0%	100%	6%	6%	6%	25%	32%

SOCC or GBT	Pre- or Post-FIRM	Zone	Building Loss	Foundation	Below First Floor	Structure Frame	Roof Covering	Roof Framing	Exterior Walls	Interiors
Wood	Pre	CA	40%	0%	100%	9%	9%	9%	31%	44%
Wood	Pre	CA	50%	0%	100%	13%	13%	13%	41%	54%
Wood	Pre	CA	60%	3%	100%	21%	21%	21%	49%	62%
Wood	Pre	CA	70%	9%	100%	29%	29%	29%	56%	71%
Wood	Pre	CA	80%	16%	100%	36%	36%	36%	60%	81%
Wood	Pre	CA	90%	22%	100%	42%	42%	42%	69%	90%
Wood	Pre	CA	100%	27%	100%	51%	51%	51%	70%	100%
Wood	Post	CA	0%	0%	0%	0%	0%	0%	0%	0%
Wood	Post	CA	10%	0%	20%	0%	0%	0%	10%	12%
Wood	Post	CA	20%	0%	100%	1%	1%	1%	20%	22%
Wood	Post	CA	30%	0%	100%	6%	6%	6%	27%	34%
Wood	Post	CA	40%	0%	100%	9%	9%	9%	33%	46%
Wood	Post	CA	50%	0%	100%	13%	13%	13%	44%	56%
Wood	Post	CA	60%	3%	100%	21%	21%	21%	57%	64%
Wood	Post	CA	70%	9%	100%	29%	29%	29%	62%	74%
Wood	Post	CA	80%	16%	100%	36%	36%	36%	69%	83%
Wood	Post	CA	90%	22%	100%	42%	42%	42%	75%	92%
Wood	Post	CA	100%	27%	100%	51%	51%	51%	85%	100%
Steel	Pre	A	0%	0%	0%	0%	0%	0%	0%	0%
Steel	Pre	A	10%	0%	0%	0%	0%	0%	1%	12%
Steel	Pre	A	20%	0%	0%	0%	0%	0%	3%	24%
Steel	Pre	A	30%	0%	0%	0%	0%	0%	5%	35%
Steel	Pre	A	40%	0%	0%	0%	0%	0%	5%	48%
Steel	Pre	A	50%	0%	0%	0%	0%	0%	8%	59%
Steel	Pre	A	60%	0%	0%	0%	0%	0%	11%	71%
Steel	Pre	A	70%	0%	0%	0%	0%	0%	26%	79%
Steel	Pre	A	80%	0%	0%	6%	6%	6%	51%	84%
Steel	Pre	A	90%	8%	0%	14%	14%	14%	66%	91%
Steel	Pre	A	100%	16%	0%	21%	21%	21%	70%	100%
Steel	Post	A	0%	0%	0%	0%	0%	0%	0%	0%
Steel	Post	A	10%	0%	0%	0%	0%	0%	1%	13%
Steel	Post	A	20%	0%	0%	0%	0%	0%	2%	25%
Steel	Post	A	30%	0%	0%	0%	0%	0%	5%	37%
Steel	Post	A	40%	0%	0%	0%	0%	0%	6%	49%
Steel	Post	A	50%	0%	0%	0%	0%	0%	12%	61%
Steel	Post	A	60%	0%	0%	0%	0%	0%	31%	69%
Steel	Post	A	70%	0%	0%	0%	0%	0%	42%	79%

SOCC or GBT	Pre- or Post-FIRM	Zone	Building Loss	Foundation	Below First Floor	Structure Frame	Roof Covering	Roof Framing	Exterior Walls	Interiors
Steel	Post	A	80%	0%	0%	10%	10%	10%	68%	83%
Steel	Post	A	90%	7%	0%	17%	17%	17%	86%	90%
Steel	Post	A	100%	15%	0%	20%	20%	20%	88%	100%
Steel	Pre	CA	0%	0%	0%	0%	0%	0%	0%	0%
Steel	Pre	CA	10%	0%	0%	0%	0%	0%	9%	10%
Steel	Pre	CA	20%	0%	0%	1%	1%	1%	15%	21%
Steel	Pre	CA	30%	0%	0%	3%	3%	3%	24%	30%
Steel	Pre	CA	40%	0%	0%	7%	7%	7%	33%	40%
Steel	Pre	CA	50%	0%	0%	11%	11%	11%	42%	49%
Steel	Pre	CA	60%	4%	0%	16%	16%	16%	51%	58%
Steel	Pre	CA	70%	7%	0%	21%	21%	21%	60%	66%
Steel	Pre	CA	80%	11%	0%	27%	27%	27%	69%	75%
Steel	Pre	CA	90%	16%	0%	31%	31%	31%	78%	84%
Steel	Pre	CA	100%	21%	0%	38%	38%	38%	86%	92%
Steel	Post	CA	0%	0%	0%	0%	0%	0%	0%	0%
Steel	Post	CA	10%	0%	0%	0%	0%	0%	9%	11%
Steel	Post	CA	20%	0%	0%	1%	1%	1%	15%	22%
Steel	Post	CA	30%	0%	0%	3%	3%	3%	24%	32%
Steel	Post	CA	40%	0%	0%	7%	7%	7%	33%	42%
Steel	Post	CA	50%	0%	0%	11%	11%	11%	42%	52%
Steel	Post	CA	60%	4%	0%	16%	16%	16%	51%	61%
Steel	Post	CA	70%	7%	0%	21%	21%	21%	60%	70%
Steel	Post	CA	80%	11%	0%	27%	27%	27%	69%	79%
Steel	Post	CA	90%	16%	0%	31%	31%	31%	78%	88%
Steel	Post	CA	100%	21%	0%	38%	38%	38%	86%	96%
Concrete	Pre	A	0%	0%	0%	0%	0%	0%	0%	0%
Concrete	Pre	A	10%	0%	0%	0%	0%	0%	1%	12%
Concrete	Pre	A	20%	0%	0%	0%	0%	0%	3%	24%
Concrete	Pre	A	30%	0%	0%	0%	0%	0%	5%	35%
Concrete	Pre	A	40%	0%	0%	0%	0%	0%	5%	48%
Concrete	Pre	A	50%	0%	0%	0%	0%	0%	8%	59%
Concrete	Pre	A	60%	0%	0%	0%	0%	0%	11%	71%
Concrete	Pre	A	70%	0%	0%	0%	0%	0%	26%	79%
Concrete	Pre	A	80%	0%	0%	2%	2%	2%	51%	85%
Concrete	Pre	A	90%	3%	0%	8%	8%	8%	66%	92%
Concrete	Pre	A	100%	8%	0%	13%	13%	13%	79%	100%
Concrete	Post	A	0%	0%	0%	0%	0%	0%	0%	0%

SOCC or GBT	Pre- or Post-FIRM	Zone	Building Loss	Foundation	Below First Floor	Structure Frame	Roof Covering	Roof Framing	Exterior Walls	Interiors
Concrete	Post	A	10%	0%	0%	0%	0%	0%	1%	13%
Concrete	Post	A	20%	0%	0%	0%	0%	0%	3%	26%
Concrete	Post	A	30%	0%	0%	0%	0%	0%	6%	38%
Concrete	Post	A	40%	0%	0%	0%	0%	0%	7%	51%
Concrete	Post	A	50%	0%	0%	0%	0%	0%	15%	63%
Concrete	Post	A	60%	0%	0%	0%	0%	0%	39%	72%
Concrete	Post	A	70%	0%	0%	0%	0%	0%	54%	82%
Concrete	Post	A	80%	0%	0%	3%	3%	3%	79%	90%
Concrete	Post	A	90%	2%	0%	8%	8%	8%	87%	100%
Concrete	Post	A	100%	25%	0%	30%	30%	30%	100%	100%
Concrete	Pre	CA	0%	0%	0%	0%	0%	0%	0%	0%
Concrete	Pre	CA	10%	0%	0%	0%	0%	0%	8%	10%
Concrete	Pre	CA	20%	0%	0%	1%	1%	1%	17%	20%
Concrete	Pre	CA	30%	0%	0%	3%	3%	3%	26%	30%
Concrete	Pre	CA	40%	0%	0%	6%	6%	6%	33%	40%
Concrete	Pre	CA	50%	0%	0%	11%	11%	11%	41%	49%
Concrete	Pre	CA	60%	1%	0%	15%	15%	15%	50%	58%
Concrete	Pre	CA	70%	3%	0%	19%	19%	19%	59%	67%
Concrete	Pre	CA	80%	7%	0%	23%	23%	23%	65%	77%
Concrete	Pre	CA	90%	11%	0%	26%	26%	26%	73%	86%
Concrete	Pre	CA	100%	15%	0%	29%	29%	29%	74%	97%
Concrete	Post	CA	0%	0%	0%	0%	0%	0%	0%	0%
Concrete	Post	CA	10%	0%	0%	0%	0%	0%	8%	11%
Concrete	Post	CA	20%	0%	0%	1%	1%	1%	17%	23%
Concrete	Post	CA	30%	0%	0%	3%	3%	3%	26%	34%
Concrete	Post	CA	40%	0%	0%	6%	6%	6%	33%	45%
Concrete	Post	CA	50%	0%	0%	11%	11%	11%	41%	55%
Concrete	Post	CA	60%	1%	0%	15%	15%	15%	50%	65%
Concrete	Post	CA	70%	3%	0%	19%	19%	19%	59%	75%
Concrete	Post	CA	80%	7%	0%	23%	23%	23%	65%	86%
Concrete	Post	CA	90%	11%	0%	26%	26%	26%	73%	96%
Concrete	Post	CA	100%	25%	0%	35%	35%	35%	94%	100%
Masonry	Pre	A	0%	0%	0%	0%	0%	0%	0%	0%
Masonry	Pre	A	10%	0%	10%	0%	0%	0%	0%	15%
Masonry	Pre	A	20%	0%	30%	0%	0%	0%	3%	29%
Masonry	Pre	A	30%	0%	80%	0%	0%	0%	4%	43%
Masonry	Pre	A	40%	0%	100%	0%	0%	0%	4%	58%

SOCC or GBT	Pre- or Post-FIRM	Zone	Building Loss	Foundation	Below First Floor	Structure Frame	Roof Covering	Roof Framing	Exterior Walls	Interiors
Masonry	Pre	A	50%	0%	100%	0%	0%	0%	7%	72%
Masonry	Pre	A	60%	0%	100%	0%	0%	0%	9%	86%
Masonry	Pre	A	70%	0%	100%	0%	0%	0%	22%	97%
Masonry	Pre	A	80%	0%	100%	15%	15%	15%	38%	100%
Masonry	Pre	A	90%	6%	100%	26%	26%	26%	68%	100%
Masonry	Pre	A	100%	16%	100%	34%	34%	34%	100%	100%
Masonry	Post	A	0%	0%	0%	0%	0%	0%	0%	0%
Masonry	Post	A	10%	0%	10%	0%	0%	0%	0%	15%
Masonry	Post	A	20%	0%	30%	0%	0%	0%	2%	30%
Masonry	Post	A	30%	0%	80%	0%	0%	0%	4%	44%
Masonry	Post	A	40%	0%	100%	0%	0%	0%	5%	59%
Masonry	Post	A	50%	0%	100%	0%	0%	0%	10%	73%
Masonry	Post	A	60%	0%	100%	0%	0%	0%	26%	84%
Masonry	Post	A	70%	0%	100%	0%	0%	0%	36%	96%
Masonry	Post	A	80%	0%	100%	15%	15%	15%	55%	100%
Masonry	Post	A	90%	5%	100%	34%	34%	34%	74%	100%
Masonry	Post	A	100%	25%	100%	44%	44%	44%	100%	100%
Masonry	Pre	CA	0%	0%	0%	0%	0%	0%	0%	0%
Masonry	Pre	CA	10%	0%	20%	0%	0%	0%	1%	15%
Masonry	Pre	CA	20%	0%	100%	1%	1%	1%	4%	27%
Masonry	Pre	CA	30%	0%	100%	3%	3%	3%	7%	41%
Masonry	Pre	CA	40%	0%	100%	5%	5%	5%	13%	53%
Masonry	Pre	CA	50%	0%	100%	8%	8%	8%	33%	59%
Masonry	Pre	CA	60%	1%	100%	13%	13%	13%	47%	68%
Masonry	Pre	CA	70%	2%	100%	17%	17%	17%	58%	78%
Masonry	Pre	CA	80%	4%	100%	21%	21%	21%	67%	88%
Masonry	Pre	CA	90%	6%	100%	25%	25%	25%	75%	98%
Masonry	Pre	CA	100%	17%	100%	31%	31%	31%	100%	100%
Masonry	Post	CA	0%	0%	0%	0%	0%	0%	0%	0%
Masonry	Post	CA	10%	0%	20%	0%	0%	0%	8%	13%
Masonry	Post	CA	20%	0%	100%	1%	1%	1%	12%	26%
Masonry	Post	CA	30%	0%	100%	3%	3%	3%	20%	37%
Masonry	Post	CA	40%	0%	100%	5%	5%	5%	29%	49%
Masonry	Post	CA	50%	0%	100%	8%	8%	8%	37%	61%
Masonry	Post	CA	60%	1%	100%	13%	13%	13%	44%	73%
Masonry	Post	CA	70%	3%	100%	17%	17%	17%	53%	84%
Masonry	Post	CA	80%	5%	100%	21%	21%	21%	61%	95%

SOCC or GBT	Pre- or Post-FIRM	Zone	Building Loss	Foundation	Below First Floor	Structure Frame	Roof Covering	Roof Framing	Exterior Walls	Interiors
Masonry	Post	CA	90%	10%	100%	30%	30%	30%	79%	100%
Masonry	Post	CA	100%	24%	100%	45%	45%	45%	100%	100%
MH	Pre	A	0%	0%	0%	0%	0%	0%	0%	0%
MH	Pre	A	10%	0%	9%	0%	0%	0%	3%	13%
MH	Pre	A	20%	0%	35%	0%	0%	0%	4%	27%
MH	Pre	A	30%	0%	60%	0%	0%	0%	8%	39%
MH	Pre	A	40%	0%	79%	0%	0%	0%	16%	51%
MH	Pre	A	50%	0%	100%	0%	0%	0%	23%	62%
MH	Pre	A	60%	0%	100%	0%	0%	0%	28%	75%
MH	Pre	A	70%	0%	100%	0%	0%	0%	35%	88%
MH	Pre	A	80%	2%	100%	2%	2%	2%	53%	95%
MH	Pre	A	90%	8%	100%	8%	8%	8%	74%	100%
MH	Pre	A	100%	12%	100%	20%	20%	20%	100%	100%
MH	Post	A	0%	0%	0%	0%	0%	0%	0%	0%
MH	Post	A	10%	0%	6%	0%	0%	0%	7%	12%
MH	Post	A	20%	0%	35%	0%	0%	0%	10%	25%
MH	Post	A	30%	0%	60%	0%	0%	0%	18%	37%
MH	Post	A	40%	0%	80%	0%	0%	0%	22%	50%
MH	Post	A	50%	0%	100%	0%	0%	0%	30%	62%
MH	Post	A	60%	0%	100%	0%	0%	0%	36%	75%
MH	Post	A	70%	0%	100%	0%	0%	0%	42%	88%
MH	Post	A	80%	2%	100%	3%	3%	3%	50%	99%
MH	Post	A	90%	9%	100%	9%	9%	9%	79%	100%
MH	Post	A	100%	21%	100%	24%	24%	24%	100%	100%
MH	Pre	CA	0%	0%	0%	0%	0%	0%	0%	0%
MH	Pre	CA	10%	0%	9%	0%	0%	0%	7%	12%
MH	Pre	CA	20%	0%	35%	0%	0%	0%	10%	25%
MH	Pre	CA	30%	0%	60%	0%	0%	0%	21%	35%
MH	Pre	CA	40%	0%	90%	1%	1%	1%	28%	46%
MH	Pre	CA	50%	0%	100%	2%	2%	2%	34%	57%
MH	Pre	CA	60%	0%	100%	4%	4%	4%	42%	69%
MH	Pre	CA	70%	1%	100%	8%	8%	8%	48%	80%
MH	Pre	CA	80%	3%	100%	10%	10%	10%	57%	91%
MH	Pre	CA	90%	10%	100%	14%	14%	14%	69%	100%
MH	Pre	CA	100%	16%	100%	20%	20%	20%	100%	100%
MH	Post	CA	0%	0%	0%	0%	0%	0%	0%	0%
MH	Post	CA	10%	0%	3%	0%	0%	0%	7%	12%

SOCC or GBT	Pre- or Post-FIRM	Zone	Building Loss	Foundation	Below First Floor	Structure Frame	Roof Covering	Roof Framing	Exterior Walls	Interiors
MH	Post	CA	20%	0%	40%	0%	0%	0%	15%	23%
MH	Post	CA	30%	0%	100%	0%	0%	0%	25%	33%
MH	Post	CA	40%	0%	100%	1%	1%	1%	31%	46%
MH	Post	CA	50%	0%	100%	2%	2%	2%	44%	56%
MH	Post	CA	60%	0%	100%	4%	4%	4%	55%	66%
MH	Post	CA	70%	1%	100%	8%	8%	8%	60%	78%
MH	Post	CA	80%	2%	100%	10%	10%	10%	68%	90%
MH	Post	CA	90%	8%	100%	14%	14%	14%	77%	100%
MH	Post	CA	100%	19%	100%	25%	25%	25%	100%	100%